

# 66<sup>th</sup> Annual Meeting

of the International Society of Electrochemistry

4-9 October, 2015  
Taipei, Taiwan

Green Electrochemistry for  
Tomorrow's Society



# PROGRAM



<http://annual66.ise-online.org>  
e-mail: [events@ise-online.org](mailto:events@ise-online.org)



# The 66<sup>th</sup> Annual Meeting of the International Society of Electrochemistry

Green Electrochemistry for Tomorrow's Society  
4-9 October 2015, Taipei, Taiwan

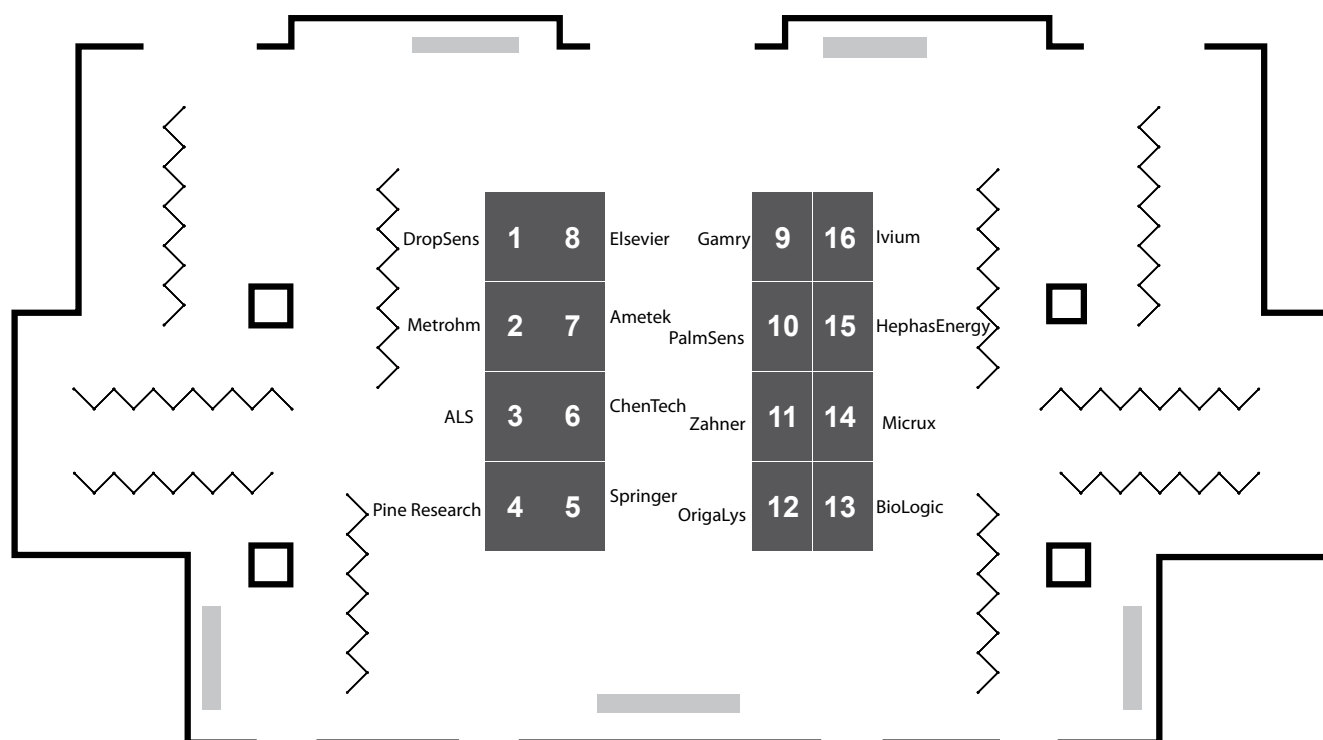
Organized with the contribution of ECSTW   
The Electrochemical Society of Taiwan

## Contents List

Organizing Committee .....	v
Symposium Organizers .....	vi-vii
Tutorial Lectures .....	viii
Author Workshop .....	viii
Plenary Lectures .....	ix
Prize Winners .....	x-xii
ISE Society Meetings .....	xiii
Poster Sessions .....	xiv
General Information .....	inside front cover
Registration Hours during the Meeting .....	inside front cover
On Site Registration Fees .....	inside front cover
Lunches .....	inside front cover
Coffee Breaks .....	inside front cover
Internet Service .....	inside front cover
Accompanying Persons .....	inside front cover
Publications .....	xv
Social Program: Receptions, Excursions and Banquet .....	xv-xvi
Oral Presentation Program	
Monday, 5 October – Friday, 9 October .....	1
Poster Presentation Program - All Symposia .....	81
Author Index .....	140
ISE Society Information .....	159
Poster Plan Session 1 - Monday (Symposia <b>1, 2, 3</b> ) .....	173
Poster Plan Session 2 - Tuesday (Symposia <b>5, 6, 8, 9, 11, 18</b> ) .....	174
Poster Plan Session 3 - Wednesday (Symposia <b>4, 7, 10, 12, 13, 14, 15, 16, 17</b> ) .....	175
Week Schedule .....	176
Symposium Schedule and Floor Plan .....	back cover



## Exhibitor booths



## Exhibition Hours

Monday:	09:30-20:00
Tuesday:	09:30-17:30
Wednesday:	09:30-12:30
Thursday:	09:30-17:30
Friday:	09:30-12:00



## Sponsors



Bureau of Foreign Trade



Ministry of Foreign Affairs  
Republic of China (Taiwan)



Department of Information  
and Tourism



Ministry of Science and Technology



National Taiwan University  
of Science and Technology



Star Alliance



World Scientific Publishing

## Exhibitors



Elsevier



Gamry Instruments



DropSens



IVIUM Technologies



ALS Co. Ltd



Metrohm Autolab



Pine Research Instrumentation



Bio-Logic



Springer



HephasEnergy Co. Ltd.



Origalys



Micrux Fluidic S.L.



PalmSens



Ametek/Princeton/Solartron



Zahner elektrik GmbH&Co



Chen Tech Electric




## Welcome Address

On behalf of the Executive Committee of ISE, the Organizing Committee and Symposium Organizers, we warmly welcome you to Taipei and look forward to your participation in the 66th Annual Meeting of the ISE, “**Green Electrochemistry for Tomorrow’s Society**”, from October 4th to October 9th, 2015. Taipei is the capital city of Taiwan. It was first inhabited by the Ketagalan Tribe hundreds of years ago and now has evolved into an international and high-tech city. Located not far from beautiful coast, Taipei is full of great natural beauty including Maokong, Yangmingshan and hot springs. Taipei is also home to various world-famous architectural or cultural landmarks such as National Palace Museum, Taipei 101, Hsing Tian Kong, Longshan Temple, etc. We hope that you will discover the versatile cultures and experience the Taiwanese hospitality, friendship and vibrant life here. You should definitely reserve some time to walk along the lovely city, explore museums, enjoy the hot springs, stroll down in night markets, have a gentle foot massage, taste a variety of local or fusion cuisine, or simply sip a cup of tea for spiritual tranquility.

Taiwan has a strong tradition in electrochemistry, and scientists in this field have shown significant contribution to academic researches and industrial applications. Nevertheless, the Electrochemical Society of Taiwan (ECSTw) was just founded in 2013 and became one of regional ISE representatives in 2014. The 66th ISE annual meeting is the first ISE conference held ever in Taiwan, but you will expect more ISE conferences hosted by Taiwan in future.

The theme of the 66th ISE annual meeting is planned to address the growing needs for sustainable materials, technologies, processes and applications ranging from energy, environments to food and healthcare in our society. The meeting consists of 18 Symposia sponsored by all Divisions of the ISE. The Symposia organizers have paid a particular attention to preparation of the scientific program to emphasize the most pressing and emerging issues of the field as well as to outline the likely future directions of its development.

“66” means “great success, running smoothly” in local culture. Regardless of all the efforts extended by the Organizing committee, Symposia organizers and Executive Committee so far, the Meeting cannot truly succeed without your participation. We, therefore, sincerely hope that your particular contribution to the scientific program and fruitful discussion will make the 66th Annual ISE Meeting successful and memorable. Finally, we also hope the provided platform and distributed information during the meeting would generate new breakthroughs and in turn furnish a springboard for innovative ideas, future cooperation and new friendship.



*Chair and Secretary General, Organizing Committee, ISE Annual Meeting 2015*



## Organizing Committee

**Christian Amatore, *France***

**Susana Cordoba de Torresi, *Brazil***

**Bing Joe Hwang, *Taiwan (Chair)***

**Manuela Rueda, *Spain***

**Wei-nien Su, *Taiwan (Secretary General)***

**Zhongqun Tian, *China***

**Bernard Tribollet, *France***

**Wei-Ta Tsai, *Taiwan***

**Chi-Chao Wan, *Taiwan***

**Nae-Lih Wu, *Taiwan***

## Symposium Organizers

- Symposium 1: New Directions in Analytical Electrochemistry**  
Lin-Chi Chen (Coordinator), National Taiwan University, Taiwan  
Meng-Jiy Wang, National Taiwan University of Science and Technology, Taiwan  
Alison Downard, University of Canterbury, New Zealand  
Daniel Mandler, The Hebrew University of Jerusalem, Israel
- Symposium 2: Electrochemical Aspects of Biological Systems: Theory, Experiment and Applications**  
Damien Arrigan (Coordinator), Curtin University, Australia  
Shen-Ming Chen, National Taipei University of Technology, Taiwan  
Elena Ferapontova, Aarhus University, Denmark  
Mei-Jywan Syu, National Cheng Kung University, Taiwan
- Symposium 3: Batteries for Tomorrow's World**  
Robert Kostecki (Coordinator), Lawrence Berkeley National Laboratory, USA  
She-Huang Wu (Co-coordinator), Tatung University, Taiwan  
Kuniaki Tatsumi, National Inst. of Advanced Industrial Science & Technology, Japan  
Fu-Ming Wang, National Taiwan University of Science and Technology, Taiwan
- Symposium 4: Advances in Fuel Cells from Materials to Systems**  
Hiroyuki Uchida (Coordinator), University of Yamanashi, Japan  
Lorenz Gubler (Co-coordinator), Paul Scherrer Institute, Switzerland  
Kuan-Zong Fung, National Cheng Kung University, Taiwan  
Kuei-Hsien Chen, Institute of Atomic and Molecular Sciences, Taiwan  
Yu-Lin Kuo, National Taiwan University of Science and Technology, Taiwan
- Symposium 5: Novel Insights to Electrochemical Capacitors**  
Hsi-Sheng Teng (Coordinator), National Cheng Kung University, Taiwan  
Chi-Chang Hu (Co-coordinator), National Tsing Hua University, Taiwan  
Elzbieta Frackowiak (Coordinator), Poznan University of Technology, Poland  
Masashi Ishikawa, Kansai University, Japan  
Frédéric Favier, CNRS University of Montpellier 2, France
- Symposium 6: New Progress in Electrochemical Solar Cells**  
Ladislav Kavan (Coordinator), J. Heyrovsky Inst. Physical Chemistry, Czech Republic  
Anders Hagfeldt, Uppsala University, Sweden  
Kuo-Chuan Ho, National Taiwan University, Taiwan  
Jih-Jen Wu, National Cheng Kung University, Taiwan
- Symposium 7: Electrodeposition - The Frontier Approach in Material Science and Nanofabrication**  
Stanko Brankovic (Coordinator), University of Houston, USA  
Massimo Innocenti, University of Florence, Italy  
Nosang Myung, University of California, USA  
Wei-Ping Dow, National Chung Hsing University, Taiwan  
Ming-Der Ger, National Defense University, Taiwan
- Symposium 8: Corrosion and Passivity**  
Nick Birbilis (Coordinator), Monash University, Australia  
Dirk Engelberg, University of Manchester, UK  
Shinji Fujimoto, Osaka University, Japan  
Jing-Chie Lin, National Central University, Taiwan  
Chao-Sung Lin, National Taiwan University, Taiwan
- Symposium 9: Electrocatalytic Materials**  
Kotaro Sasaki (Coordinator), Brookhaven National Laboratory, USA  
Andrew Lin, Chang Gung University, Taiwan  
Chen-Hao Wang, National Taiwan University of Science & Technology, Taiwan  
Anthony Kucernak, Imperial College London, UK

**Symposium 10: Electrochemical Technology: New Challenges for a More Competitive Economy**

Juan Manuel Peralta-Hernandez (Coordinator), CIATEC, Mexico  
Shi-Chern Yen (Co-coordinator), National Taiwan University, Taiwan  
Manuel Andres Rodrigo, Universidad de Castilla-la-Mancha, Spain  
Alex Peng, Industrial Technology Research Institute, Taiwan

**Symposium 11: New Important Frontiers in Molecular Electrochemistry**

Jirí Ludvík (Coordinator), J. Heyrovský Inst of Physical Chemistry, Czech Republic  
Chun-Hsien Chen (Co-coordinator), National Taiwan University, Taiwan  
Olivier Buriez, CNRS UMR ENS, France  
Flavio Maran, University of Padova, Italy  
Armando Pombeiro, Instituto Superior Tecnico, Portugal

**Symposium 12: Physical Electrochemistry: Spectroscopic, Structural, and Theoretical Investigations of the Electrified Interface**

Andrea Russell (Coordinator), University of Southampton, UK  
Axel Gross, Ulm University, Germany  
Ifan Stephens, Technical University of Denmark, Denmark  
Jyh-Chiang Jiang, National Taiwan University of Science and Technology, Taiwan  
Yuh-Lang Lee, National Cheng Kung University, Taiwan

**Symposium 13: Molecular Systems for Energy Conversion**

Jay Wadhawan (Coordinator), The University of Hull, UK  
Carlos Eduardo Frontana Vazquez, CIDETEQ, Mexico  
Nathan Lawrence, Schlumberger Cambridge Research, UK  
Bluse Ching-Hsing Chen, National Taiwan Univ. Science and Technology, Taiwan

**Symposium 14: Modeling, Design and Characterization of Nanostructured, Electroactive and Multifunctional Materials**

Francesco Paolucci (Coordinator), University of Bologna, Italy  
Pawel J. Kulesza, University of Warsaw, Poland  
Renato Seeber, University of Modena and Reggio Emilia, Italy  
Chin-Lung Kuo, National Taiwan University, Taiwan  
Shirley Meng, University of California San Diego, USA

**Symposium 15: Electrochemical Engineering from a Quantum Description to the Plant Modeling: Experiments and Design across Length Scales**

Alejandro A. Franco (Coordinator), CNRS-University of Picardie, France  
Hung-Lung Chou (Co-coordinator), National Taiwan Univ. Science & Techn, Taiwan  
François Lapique, CNRS and University of Lorraine, France  
Jaeyoung Lee, Gwangju Institute of Science and Technology, Korea

**Symposium 16: Supramolecular Electrochemistry for Analysis, Medicine and Biological Sciences**

Marilia Goulart (Coordinator), Federal University of Alagoas, Brazil  
Stéphane Arbault, University of Bordeaux 1, Pessac, France  
Renata Bilewicz, University of Warsaw, Warsaw, Poland  
Hsien-Chang Chang, National Cheng Kung University, Tainan City, Taiwan  
Chii-Wann Lin, National Taiwan University, Taipei, Taiwan

**Symposium 17: Novel in Situ in Operando Methods**

Hector Abruna (Coordinator), Cornell University, Ithaca, USA  
Patrick Unwin, University of Warwick, Coventry, UK  
Anthony Kucernak, Imperial College London, London, UK  
Michael Eikerling, Simon Fraser University, Burnaby, Canada  
Shawn D. Li, National Taiwan University of Science and Technology, Taipei, Taiwan  
Ming Chang Yang, National Cheng Kung University, Tainan City, Taiwan

**Symposium 18: General Session**

Justin Gooding (Coordinator), The University of New South Wales, Sydney, Australia  
Juan M. Feliu, University of Alicante, Alicante, Spain  
Nae-Lih Wu, National Taiwan University, Taipei, Taiwan  
Liang-Yih Chen, National Taiwan University of Science and Technology, Taipei, Taiwan

---

## Tutorial Lectures and Workshop

---

**Sunday, 4 October 2015**

**Location: TICC**

Taipei International Convention Center

13:30 to 17:00

---

### Tutorial 1

---

**Room 201 AB**

#### Fundamental Aspects and Applications of Cu Electrodeposition

**Rohan Akolkar**, *Case Western Reserve University, USA*

**Peter Broekmann**, *University of Bern, Switzerland*

13:30 to 17:00

---

### Tutorial 2

---

**Room 201 EF**

#### Principles and Applications of in situ in Operando Methods in Electrochemistry

**Neeraj Sharma**, *The University of New South Wales, Australia*

**Bluse Ching-Hsing Chen**, *National Taiwan University of Science and Technology, Taiwan*

13:30 to 17:00

---

### EA Workshop

---

**Room 101 C**

#### Electrochimica Acta / ISE author workshop

**Robert Hillman**, *Editor-in-Chief Electrochimica Acta, University of Leicester, United Kingdom*

15:00 to 15:15

Coffee break



---

## Plenary Lectures

---

**Location: Plenary Hall**

---

### Monday, 5 October 2015



08:15 to 09:15

**Tomokazu Matsue**

*(Tohoku University, Japan)*

Electrochemical Imaging with Micro/Nanoelectrode Systems

### Tuesday, 6 October 2015



08:15 to 09:15

**Hongjie Dai**

*(Stanford University, USA)*

Novel Materials for Renewable Energy

### Wednesday, 7 October 2015



08:15 to 09:15

**Li-Jun Wan**

*(Chinese Academy of Sciences, China)*

Nanomaterials for Energy Conversion and Storage: Structure Design and In-Situ Monitoring

### Thursday, 8 October 2015



08:15 to 09:15

**Martin Winter**

*(Münster University, Germany)*

Neglected, Forgotten or Unimportant? Inactive Materials in Lithium Ion Batteries

### Friday, 9 October 2015



08:15 to 09:15

**Alan Bond**

*(Monash University, Australia)*

A Voltammetric Odyssey: From Homogeneous Dropping Mercury to Heterogeneous Macro and Nano Electrodes; From the Manual Era to Advanced Automated High Speed Computation

---

## ISE Prize Winners 2014

---

### Electrochimica Acta Gold Medal



**Alan Bond**, *Monash University, Australia*

08:15 to 09:15, Friday, 9 October 2015, Plenary Lecture, Plenary Hall

**A Voltammetric Odyssey: From Homogeneous Dropping Mercury to Heterogeneous Macro and Nano Electrodes; From the Manual Era to Advanced Automated High Speed Computation**

The Electrochimica Acta Gold Medal was awarded to Alan Bond for his outstanding and diverse contributions to electrochemical science, spanning innovation in electrochemical techniques, fundamental mechanistic insights and novel materials and media.

### Brian Conway Prize for Physical Electrochemistry



**Masatoshi Osawa**, *Hokkaido University, Japan*

09:30 to 10:10, Monday, 5 October 2015, Symposium 12, Room 101C

**Surface-Enhanced Infrared Absorption Spectroscopy (SEIRAS): Shedding Light on The Electrochemical Interface**

The Brian Conway Prize for Physical Electrochemistry was awarded to Prof. Masatoshi Osawa in recognition of his pioneering work on the development of in situ, time-resolved Surface-Enhanced Infrared Absorption Spectroscopy (SEIRAS).

### Jaroslav Heyrovsky Prize for Molecular Electrochemistry



**Flavio Maran**, *Padova University, Italy*

14:00 to 14:40, Thursday, 8 October 2015, Symposium 11, Room 201D

**Molecular Electrochemistry: from Protons to Electrons, from Molecules to Molecular Nanoclusters**

The Jaroslav Heyrovsky Prize for Molecular Electrochemistry was awarded to Flavio Maran, Padova University, Italy, in recognition of his outstanding contributions to molecular electrochemistry, particularly mechanistic aspects on organic systems and hybrid systems constituted by molecule-like monolayer-protected gold nanoclusters.

### Tajima Prize



**Yu-Guo Guo**, *Chinese Academy of Sciences, China*

09:30 to 10:10, Thursday, 8 October 2015, Symposium 3, Room 201AB

**Advanced Cathodes and Metallic Anodes for Next-Generation Rechargeable Batteries**

The Tajima Prize was awarded to Yu-Guo Guo in recognition of his research activity in electrochemical energy storage with batteries, ion/electron storage and transport in nanoscaled systems kinetics and thermodynamics of nanostructured energy materials.

---

## ISE Prize Winners 2014

---

### Bioelectrochemistry Prize of ISE Division 2



**James Rusling**, *University of Connecticut, USA*

09:30 to 10:10, Monday, 5 October 2015, Symposium 2, Room 101D

**From Protein Film Bioelectrochemistry to Biomedical Devices and Diagnostics**

The Bioelectrochemistry Prize of ISE Division 2 was awarded to James Rusling in recognition of his research activity on thin biosystems for bioelectrochemical applications, direct electron transfer with proteins, bioelectrochemical catalysis, and detection of cancer biomarkers.

### Hans-Jürgen Engell Prize



**Fabio La Mantia**, *Ruhr-Universität Bochum, Germany*

10:10 to 10:30, Tuesday, 6 October 2015, Symposium 3, Room 201AB

**Aqueous Zinc-Ion Batteries based on Prussian Blue Derivatives**

The Hans-Jürgen Engell Prize was awarded to Fabio La Mantia for his excellent contribution to electrochemical materials science in the field of Li-ion batteries.

### Early Career Analytical Electrochemistry Prize of ISE Division 1



**Jan Vacek**, *Palacky University, Olomouc, Czech Republic*

09:30 to 10:10, Thursday 8 October 2015, Symposium 1, Room 103

**Electrochemistry of Membrane Proteins**

The Early Career Analytical Electrochemistry Prize of ISE Division 1 was awarded to Dr. Jan Vacek for his work on new electrochemical methodologies for the analysis of biopolymer interactions and structural modifications, and on electroanalysis of biomolecules.

### ISE Prize for Environmental Electrochemistry



**Sergi Garcia-Segura**, *Barcelona University, Spain*

14:00 to 14:20, Monday 5 October 2015, Symposium 10, Room 101B

**Electrochemical Processes Based on Fenton's Reaction for Wastewater Treatment. An Eco-Friendly, Efficient and Affordable Technology: Then, Now and Tomorrow**

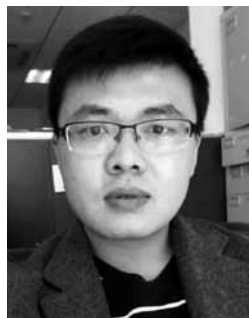
The ISE Prize on Environmental Electrochemistry was awarded to Sergi Garcia Segura in recognition of his contributions on the use of electrochemical advanced oxidation processes for wastewater treatment.

---

## ISE Prize Winners 2014

---

### ISE Prize for Applied Electrochemistry



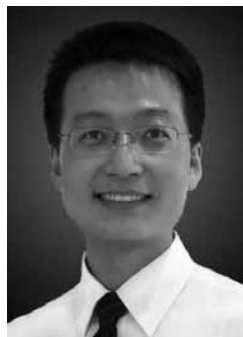
**Yonggang Wang**, *Key Laboratory of Molecular Catalysis, China*

10:30 to 10:50, Monday, 5 October 2015, Symposium 3, Room 201AB

#### **Aqueous Li (or Na)-ion Batteries for Grid-scale Energy Storage**

The ISE Prize for Applied Electrochemistry was awarded to Yonggang Wang for discovery and characterization of new materials, and invention of energy storage devices.

### Oronzio and Niccolò De Nora Foundation Young Author Prize



**Peng Bai**, *Massachusetts Institute of Technology, USA*

16:40 to 17:00, Thursday, 8 October 2015, Symposium 3, Room 201C

#### **A Solid-Electrolyte-Enabled Lithium-Bromine Flow Battery**

The Oronzio and Niccolò De Nora Young Author Prize was awarded to Bai Peng, author of the article “Statistical kinetics of phase-transforming nanoparticles in LiFePO<sub>4</sub> porous electrodes”, *Electrochimica Acta* 89 (2013) 644– 651 (co-author Guangyu Tian).

### Electrochimica Acta Travel Award Winners 2015

**Wenjing Hong**, *Switzerland*

**Klaus Mathwig**, *the Netherlands*

### ISE Travel Award Winners 2015

**Tso-Fu Mark Chang**, *Japan*

**Marta Costa Figueiredo**, *the Netherlands*

**Javier Llanos**, *Spain*

**Jian-Feng Li**, *China*

**Xiaopeng Li**, *Germany*

**Justus Masa**, *Germany*

**Joaquin Rodriguez-Lopez**, *USA*

**Min-Hsin Yeh**, *USA*



---

## ISE Society Meetings

---

### **Sunday, 4 October 2015**

#### **Opening Ceremony**

17:00 to 18:00 › Plenary Hall

### **Monday, 5 October 2015**

#### **Division Officers Luncheon Meeting**

12:50 to 13:50 › Room 201C

#### **Regional Representatives Luncheon Meeting**

12:50 to 13:50 › Room 201D

### **Tuesday, 6 October 2015**

#### **Council Meeting**

12:50 to 13:50 › Room 201AB

### **Thursday, 8 October 2015**

#### **General Assembly**

11:10 to 12:10 › Plenary Hall

#### **Division Meetings**

12:50 to 13:50

**Division 1 Analytical Electrochemistry › Room 101D**

**Division 2 Bioelectrochemistry › Room 101B**

**Division 3 Electrochemical Energy Conversion and Storage › Room 101C**

**Division 4 Electrochemical Materials Science › Room 102**

**Division 5 Electrochemical Process Engineering and Technology › Room 101A**

**Division 6 Molecular Electrochemistry › Room 201D**

**Division 7 Physical Electrochemistry › Room 201C**

### **Friday, 9 October 2015**

#### **Closing Ceremony**

12:30 to 12:50 › Plenary Hall

*See room locations on back cover*

---

## Poster presentation session 1 - Monday

---

Symposia: 1, 2, 3

Poster set-up Monday: 08:30-10:30 *See poster locations map on page 173*

Poster take-down Monday: 18:00-19:00

**Poster Presentation: Monday, 5 October: 10:50-12:30** (Banquet Hall - 3F)

---

## Poster presentation session 2 - Tuesday

---

Symposia: 5, 6, 8, 9, 11, 18

Poster set-up Tuesday: 08:30-10:30 *See poster locations map on page 174*

Poster take-down Tuesday: 18:00-19:00

**Poster Presentation: Tuesday, 6 October: 10:50-12:30** (Banquet Hall - 3F)

---

## Poster presentation session 3 - Wednesday

---

Symposia: 4, 7, 10, 12, 13, 14, 15, 16, 17

Poster set-up Wednesday: 08:30-10:30 *See poster locations map on page 175*

Poster take-down Thursday: 14:00-16:00

**Poster Presentation: Wednesday, 7 October: 10:50-12:30** (Banquet Hall - 3F)

..

---

## General Information

---

### Publications

A special issue of the Society's journal, *Electrochimica Acta*, is planned based on selected original contributions made at the conference. Selection will be made by an international editorial Committee comprising the following Editors and Guest Editors, one for each of the Symposia in which the meeting is articulated:

Symposium 1 Alison Downard, Symposium 2 Elena Ferapontova, Symposium 3 Robert Kostecki, Symposium 4 Lorenz Gubler, Symposium 5 Chi-Chang Hu, Symposium 6 Ladislav Kavan, Symposium 7 Wei Ping Dow, Symposium 8 Nick Birbilis, Symposium 9 Kotaro Sasaki, Symposium 10 Manuel Andres Rodrigo, Symposium 11 Flavio Maran, Symposium 12 Andrea Russell, Symposium 13 Carlos Eduardo Frontana, Symposium 14 Pawel J. Kulesza, Symposium 15 François Lapicque, Symposium 16 Renata Bilewicz, Symposium 17 Michael Eikerling. The Special Issues Editor, Sergio Trasatti, will co-ordinate the action of the editorial Committee and will be directly responsible for the review procedure. The Special Issue is planned to accommodate ca. 170 papers.

**Submission only on invitation of one of the Guest Editors.**

**Submission timespan: 10 October 2015 - 10 January 2016**

---

## Social Program

---

### RECEPTIONS

#### Welcome Reception

**Sunday, 4 October 2015, 18:00-20:00**

After the Opening Ceremony on floor 1F of the Taipei International Convention Center (TICC)

#### Monday Reception

**Monday, 5 October 2015, 18:40-20:00** on floor 3F in the Taipei International Convention Center (TICC)

#### Tuesday Social Event – Ge Zai Xi (Taiwanese Opera)

(Sponsored by Bureau of Foreign Trade, Ministry of Economic Affairs)

**Tuesday, 6 October 2015, 20:00-21:00**

At the National Taiwan Arts Education Center / No. 47, Nanhai Road, Taipei City

Ticket: US\$ 10.00 had to be booked online during registration

Transportation: MRT Danshui Line (Line 2) to Chiang Kai-Shek Memorial Hall (Exit at No. 1 or 2)

Songshan-Xindian Line (Line 3) to Xiaonamen (Exit at No. 3) [http://www.arte.gov.tw/eng/vist\\_train.asp](http://www.arte.gov.tw/eng/vist_train.asp)

Please check map on inside backcover.

#### Ming Hwa Yuan Arts & Cultural Group

##### About Ge Zai Xi (Taiwanese Opera)

Ge Zai Xi (Taiwanese Opera) is the only performing art form that originated within Taiwan. Because of its origin as folk entertainment, the development and expression of Ge Zai Xi are free from restraints and strict rules of other more formal and traditional performing arts. This all embracing characteristic allowed Ge Zai Xi to develop over the past hundred year into a unique and constantly evolving performing art form which includes fusion of Beijing opera, Gaojia opera, Nanguan and Beiguan as well as modern drama to name a few.

#### Thursday Banquet

**Thursday, 8 October 2015, 19:00**

At the Taipei World Trade Center Club on the 33rd floor. Only 3 walking minutes from the conference center.

<http://www.twtclub.com.tw/en/aboutus.html>

Price: US\$70.00

*Places are limited.*

*All tickets for the Banquet are nonrefundable.*

## EXCURSIONS

### Wednesday, 7 October

You can choose among 6 different excursions that will be organized by Lion Travel on Wednesday afternoon, 7 October 2015. The excursions will depart from the Taipei International Convention Center. Excursions should be pre-booked. Details can be found on the website <http://annual66.isc-online.org/excursions.html>

#### All excursions

Include: Bus rental fee (including Tip for driver), English speaking tour guide.

Travel insurance: NT\$5,000,000 travel industry liability insurance & NT\$200,000 accident medical insurance.

Exclude: Personal expense and meals (Lunch and Dinner)

Special Offer: One bottle of Water and Souvenir

Minimum booking for each tour: 16 persons

#### 1) Tour 1 : Creative Park and Village

Departure from TICC at 13:00

Return at approx 17h10

Price: NTD 1,390 = EUR 40 /per person

#### 2) Tour 2 : Culture of Temples

Departure from TICC at 13:00

Return at approx 17h00

NTD 1,390 = EUR 40 /per person

#### 3) Tour 3 : Culture of Hot Spring

Departure from TICC at 13:00

Return at approx 17h10

NTD 1,390 = EUR 40 /per person

#### 4) Tour 4 : Yingge, Sanxia Ceramics and Temple Tour

Departure from TICC at 13:00

Return at approx 17h00

NTD 1,390 = EUR 40 /per person

#### 5) Tour 5 : Exploring Northern Taiwan !

##### Jiufen Old Street, Gold Waterfall

Departure from TICC at 13:00

Return at approx 17h00

NTD 1,390 = EUR 40 /per person

#### 6) Tour 6 : Culture of Lanyang, Yilan

Departure from TICC at 13:00

Return at approx 18h00

Price: NTD 1,590 = €43/ per person

# Oral presentation program





ROOMS:		101A	101B	101C	101D	102	103	201AB	201EF	201C	201D
SYMPOSIUM	s05	s10	s12	s02	s04	s17	s03	s09	s13/s06	s16	
Plenary Lecture: Tomokazu Matsue (Plenary Hall)											
08:15 - 09:15											
09:30 - 09:50	Katsuhiko Naoi	Guohua Chen	Masa. Osawa	James Rusling	Kenichiro Ota Akimitsu Ishihara	Zhi-You Zhou Yi-Fan Huang	Petr Novak	Piotr Zelenay	Nam-Gyu Park Xinhua Zhong	Olivier Burtiez J. Juhaniewicz	
09:50 - 10:10											
10:10 - 10:30	G. Zheng Chen	Miguel Sandoval	Ye Wang	Benoît Piro	Ch. Hyuck Choi	Long Huang	Minoru Inaba	Yuto Miyahara	Yu-Tung Yin	R. Daniel Little	
10:30 - 10:50	Chinwe Ikpo	Tsu. Hoshino	Kun Jiang	Xing-Hua Xia	Xiaodong Yang	Fabian Kubannek	Yonggang Wang	Federico Tasca	Liang-Che Chen		
10:50 - 11:10	Coffee Break										
11:10 - 11:30											
11:30 - 11:50											
11:50 - 12:10											
12:10 - 12:30											
12:30 - 12:50											
12:50 - 13:10											
13:10 - 13:30											
13:30 - 14:00											
14:00 - 14:20	Yury Gogotsi	S. García-Segura Ricardo Salazar	H. Ogasawara	Sean Elliott Ross Milton	Zidong Wei Hsin-Chih Huang	Karl Mayrhofer	Zemp. Ogumi	Denis Kramer Shuihua Tang	Chen-Yu Yeh Hyunwo. Seo	Rich. McCreery	
14:20 - 14:40											
14:40 - 15:00	E. Frackowiak	N. E. Flores Tapia	K. A. Stoerzinger	Seiya Tsujimura	Jin-Song Hu	Bin Ren	Xuejie Huang	H. Koshikawa	Qingh. Zhang	Ping Yu	
15:00 - 15:20	Olivier Crosnier	Ign. González	R. Jinnouchi	Matteo Duca	Tim. Peckham	San. Rondinini	Franz. Mueller	Kotaro Sasaki	Mark. Zukalova	Serge Cosnier	
15:20 - 15:40	Christ. Lethien	B. K. Körbahti	Andy Wain	Ad. De Andrade	Dario Dekel	Eric Sorte	Alvin Wu	Ming Zhou	Jinbao Zhang	Pawel Krynsinski	
15:40 - 16:00	Hiroshi Inoue	Minghua Zhou	M. Figueiredo	Paul Bernhardt	Jingshuai Yang	Sarah Day	Eunseog Cho	YuYe Tong	Kuan-JiuH Lin	D. Matyszcwska	
16:00 - 16:20	Abdulc. Yavuz	Ali Farhat	Sunny Hy		Yu Yang	Simon Thiele	Andrew Gewirth	Justus Masa	Ladislav Kavan	Lars Jeuken	
16:20 - 16:40	Coffee Break										
16:40 - 17:00	Daniel Bélanger	Yunny Meas	Zhong-Qun Tian	Alain Walcarlus	P. Lettenmeier	Mario El Kazzi	Mark Orazem	Atsun. Ikezawa	Peter Deák	Rich. Compton	
17:00 - 17:20	Keryn Lian		Masato Tominaga	Elisabeth Lojou	Yeh-Hung Lai	Misun Hong	Wei Kong Pang	Samuel Perry	Flor. Le Formal		
17:20 - 17:40	Yuan Chen	K. Petrov	Shino Sato	Enrico Marsili	Lin Gan	Yosh. Uchimoto	J. M. Paz-Garcia	Lior Elbaz	Pauline Bornoz	Enno Käthehöhn	
17:40 - 18:00	Peihua Huang	Hui-Wen Lin	Juan M. Feliu	M. Karaskiewicz	Ken. Ozoemena	Neeraj Sharma	Klaus Wedlich	Ci. Zafferoni	Yan-Gu Lin	Marcin Opallo	
18:00 - 18:20	Wat. Sugimoto	Olivier Lefebvre	Robert Hillman	Lo Gorton	K. Boni. Kokoh	Hector Abruna	S. Pradanawati	Daniel Scherson	Maur. Schieda	Hua Cui	
18:20 - 18:40	Dah-Shy. Tsai	K. Kawaguchi	K. Motobayashi	W. Schuhmann	Wenjing Zhang		Jianbo Zhang	Minhua Shao	Kenji Sakamaki	Fred Lisdat	
18:40 - 20:00	Reception										

# Monday, 5 October 2015 - Morning

## Plenary Lecture

**Room : Plenary Hall**

*Chaired by:* Ken-ichiro Ota

08:15 to 09:15

**Tomokazu Matsue** (WPI-Advanced Institute for Materials Research, Tohoku University, Sendai, Japan)

[Electrochemical Imaging with Micro/Nanoelectrode Systems](#)

## Symposium 2: Electrochemical Aspects of Biological Systems: Theory, Experiment and Applications

**Room : 101D**

*Chaired by:* Renata Bilewicz and Karen Monsalve

09:30 to 10:10 Keynote **Bioelectrochemistry Prize of ISE Division 2**

**James Rusling** (Chemistry, University of Connecticut, Storrs, USA)

[From Protein Film Bioelectrochemistry to Biomedical Devices and Diagnostics](#)

10:10 to 10:30

**Benoît Piro** (Chemistry, University Paris Diderot, Lab. ITODYS, Ivry-sur-Seine, France), Malika Souada, Steve Reisberg, Guillaume Anquetin, Vincent Noël, Minh-Chau Pham

[Label-free Electrochemical Detection of Prostate-Specific Antigen based on Nucleic Acid Aptamer](#)

10:30 to 10:50

**Xing-Hua Xia** (School of Chemistry and Chemical Engineering, Nanjing University, Nanjing, China)

[Manipulation of biomolecular functions at electrode surfaces via surface modification](#)

10:50 to 11:10

Coffee Break

## Symposium 3: Batteries for Tomorrow's World

**Room : 201AB**

*Chaired by:* Robert Kostecki

09:30 to 10:10 Keynote

**Petr Novak** (Paul Scherrer Institut, Electrochemical Energy Storage Section, Villigen PSI, Switzerland), Peter Bleith, Rosa Robert, Tsuyoshi Sasaki, Claire Villevieille

[How to Understand the Electrochemistry of Battery Materials?](#)

10:10 to 10:30 Invited

**Minoru Inaba** (Department of Molecular Chemistry and Biochemistry, Doshisha University, Kyotanabe, Japan), Rin Masuhara, Yusuke Shimizu, Michihiro Hashinokuchi, Takayuki Doi

[Highly Concentrated Electrolytes for 5-V Cathodes](#)

10:30 to 10:50 Invited **ISE Prize for Applied Electrochemistry**

**Yonggang Wang** (Department of Chemistry, Fudan University, Shanghai, China), Yongyao Xia

[Aqueous Li \(or Na\)-ion Batteries for Grid-scale Energy Storage](#)

10:50 to 11:10

Coffee Break

## Symposium 4: Advances in Fuel Cells from Materials to Systems

Room : 102

Chaired by: Kenichiro Ota

09:30 to 09:50 Invited

**Kenichiro Ota** (Green Hydrogen Research Center, Yokohama National University, Yokohama, Japan), Koichi Matsuzawa, Shigenori Mitsushima, Akimitsu Ishihara

[Challenges of NPGM Oxide Cathode for PEFCs](#)

09:50 to 10:10

**Akimitsu Ishihara** (Institute of Advanced Sciences, Yokohama National University, Yokohama, Japan), Makoto Hamazaki, Tomoaki Hayashi, Yuko Tamura, Yuji Kohno, Koichi Matsuzawa, Shigenori Mitsushima, Hideto Imai, Kenichiro Ota

[Proposal of Oxide-Based Compounds as Non-Platinum Group Metals and Carbon-Free Cathodes for Polymer Electrolyte Fuel Cells](#)

10:10 to 10:30

**Chang Hyuck Choi** (Department of Interface Chemistry and Surface Engineering, Max-Planck-Institut für Eisenforschung, Düsseldorf, Germany), Karl Mayrhofer

[Operando degradation studies of Fe-N-C catalysts in acid electrolyte](#)

10:30 to 10:50

**Xiaodong Yang** (College of Chemistry and Chemical Engineering, Xiamen University, Xiamen, China)

[Liquid Fuel Cells with Polymer Fiber Membrane and Non-precious Metal Catalysts](#)

10:50 to 11:10

Coffee Break

## Symposium 5: Novel Insights to Electrochemical Capacitors

Room : 101A

Chaired by: Chi-Chang Hu

09:30 to 10:10 Keynote

**Katsuhiko Naoi** (Department of Applied Chemistry, Tokyo University of Agriculture & Technology, Tokyo, Japan)

["Nanohybrid Capacitor" -Future Projection for Gen.II Supercapacitors-](#)

10:10 to 10:30 Invited

**George Zheng Chen** (Department of Chemical and Environmental Engineering, University of Nottingham Ningbo China, Ningbo, China)

[On Combined Capacitive and Nernstian Mechanisms for Improved Electrochemical Energy Storage](#)

10:30 to 10:50

**Chinwe Ikpo** (Chemistry, University of the Western Cape, Cape Town, South Africa), Ntuthuko Hlongwa, Kenneth Ozoemena, Emmanuel Iwuoha, Natasha Ross, Miranda Ndipingwi, Myra Nzaba, Milua Masikini, Nolubabalo Matinise, Nomxolisi Dywili, Priscilla Baker

[Lithium Manganese Phosphate-gold Nanoparticles Composite as an Efficient Lithium Ion Electrochemical Capacitor](#)

10:50 to 11:10

Coffee Break

---

## Symposium 9: Electrocatalytic Materials

---

**Room : 201EF**

*Chaired by:* Kotaro Sasaki

09:30 to 10:10 Keynote

**Piotr Zelenay** (Materials Physics and Applications Division, Los Alamos National Laboratory, Los Alamos, USA)

[Non-Precious Metal Catalysts for Oxygen Reduction: Accomplishments and Challenges](#)

10:10 to 10:30

**Yuto Miyahara** (Graduate School of Engineering, Kyoto University, Kyoto, Japan), Kohei Miyazaki, Tomokazu Fukutsuka, Takeshi Abe

[Catalytic Activities of Perovskite-type Oxide Thin Films and Single Crystals as Oxygen Electrodes in Alkaline Media](#)

10:30 to 10:50

**Federico Tasca** (Department of Chemistry of Materials, University of Santiago of Chile, Santiago, Chile), Javier Recio, Jose Zagal, Nataly Silva, Carmen Castro, Cesar Zuñiga, Maria Oyarzun

[O<sub>2</sub> Reduction at Graphite Electrodes Modified with MN<sub>4</sub> Macrocyclic Complexes and Pyridine Grafted Carbon Nanotubes](#)

10:50 to 11:10

Coffee Break

---

## Symposium 10: Electrochemical Technology: New Challenges for a More Competitive Economy

---

**Room : 101B**

*Chaired by:* Geoff Kelsall and Philippe Vernoux

09:30 to 10:10 Keynote

**Guohua Chen** (Department of Chemical and Biomolecular Engineering, The Hong Kong University of Science and Technology, Hong Kong, China), Ping Geng

[Magnéli Ti<sub>4</sub>O<sub>7</sub> Modified Ceramic Membrane for Electrically-assisted Filtration with Antifouling Property](#)

10:10 to 10:30

**Miguel Sandoval** (Department of Chemical Engineering, University of Guanajuato, Guanajuato, Mexico), Rosalba Fuentes, José L. Nava, Israel Rodríguez

[Fluoride Removal from Drinking Water by Electrocoagulation in a Continuous Filter Press Reactor coupled to a Flocculator and Clarifier](#)

10:30 to 10:50

**Tsuyoshi Hoshino** (Japan Atomic Energy Agency, Japan Atomic Energy Agency, 2-166 Obuchi, Omotedate, Rokkasho-mura, Japan)

[Development of Lithium Recovery Technique from Seawater by using Innovative Electrodialysis with Lithium Ionic Superconductor](#)

10:50 to 11:10

Coffee Break

## Symposium 12: Physical Electrochemistry: Spectroscopic, Structural, and Theoretical Investigations of the Electrified Interface

**Room : 101C**

*Chaired by:* Masatoshi Osawa and Ifan Stephens

### 09:30 to 10:10 Keynote **Brian Conway Prize for Physical Electrochemistry**

**Masatoshi Osawa** (Catalysis Research Center, Hokkaido University, Sapporo, Japan)

[Surface-Enhanced Infrared Absorption Spectroscopy \(SEIRAS\): Shedding Light on The Electrochemical Interface](#)

10:10 to 10:30

**Ye Wang** (Department of Chemistry, Fudan University, Shanghai, China), Wen-Bin Cai

[Enhanced Electrocatalysis of Ethanol on Dealloyed Pd-Ni-P Film in Alkaline Media: an Infrared Spectroelectrochemical Investigation](#)

10:30 to 10:50

**Kun Jiang** (Department of Chemistry, Fudan University, Shanghai, China), Sylvain Brimaud, Wen-Bin Cai, R. Jürgen Behm

[C1 Molecule Adsorption-Dissociation on Pt and Cu-modified Pt Electrode Surfaces](#)

10:50 to 11:10

Coffee Break

## Symposium 13: Molecular Systems for Energy Conversion

**Room : 201C**

*Chaired by:* Nam-Gyu Park and Xinhua Zhong

09:30 to 09:50 Invited

**Nam-Gyu Park** (School of Chemical Engineering and Dept. of Energy Science, Sungkyunkwan University, Suwon, Korea)

[Methodologies for 20% Efficient Perovskite Solar Cells](#)

09:50 to 10:10

**Xinhua Zhong** (Institute of Applied Chemistry, East China University of Science and Technology, Shanghai, China)

[Ligand Induced Self-Assembly for High Efficiency Quantum Dot Sensitized Cells](#)

10:10 to 10:30

**Yu-Tung Yin** (Department of Chemical Engineering, National Taiwan University of Science and Technology, Taipei City, Taiwan)

[Impedance Spectroscopic Analysis of Organic-Inorganic Hybrid Perovskite Solar Cell under Different Architectures](#)

10:30 to 10:50

**Liang-Che Chen** (Chemical Engineering, National Cheng Kung University, Tainan, Taiwan) Te-Fu Yeh, Chiao-Yi Teng, Hsisheng Teng

[Graphene Oxide Quantum Dots for Photon Energy Conversion](#)

10:50 to 11:10

Coffee Break



---

## Symposium 16: Supramolecular Electrochemistry for Analysis, Medicine and Biological Sciences

---

**Room : 201D**

*Chaired by:* Marilia Goulart and Hsien-Chang Chang

09:30 to 09:50 Invited

**Olivier Buriez** (Ecole Normale Supérieure, CNRS, Paris, France)

[Contribution of Electrochemistry to Investigate the Solubilization and Transport Through Suspended Membranes of Redox Active Molecules](#)

09:50 to 10:10

**Joanna Juhaniewicz** (Faculty of Chemistry, University of Warsaw, Warsaw, Poland), Dorota Konarzewska, Michal Jamroz, Slawomir Sek

[Application of Natural Cationic Peptides as Potential Antibacterial Agents](#)

10:10 to 10:50 Keynote

**R. Daniel Little** (Chemistry and Biochemistry, University of California Santa Barbara, Santa Barbara, USA), Seung Joon Yoo, Sebastian Herold, Long-Ji Li, Cheng-Chu Zeng

[A Recyclable Reaction Medium: Applications to Oxidative and Reductive Organic Electrochemical Transformations](#)

10:50 to 11:10

Coffee Break

---

## Symposium 17: Novel in Situ in Operando Methods

---

**Room : 103**

*Chaired by:* Michael Eikerling and Ming-Chang Yang

09:30 to 09:50

**Zhi-You Zhou** (Department of Chemistry, Xiamen University, Xiamen, China), Yu-Hao Hong, Tian Sheng, Jian-Long Lin, Jie Ren, Sheng-Pei Chen, Shi-Gang Sun

[Electrooxidation mechanism of NH<sub>3</sub> on Pt by in situ FTIR reflection spectroscopy](#)

09:50 to 10:10

**Yi-Fan Huang** (Chemistry, Leiden University, Leiden, Netherlands), Marc T.M. Koper

[In-situ identification of electrochemical oxidation of Pt\(111\) and Pt\(100\) by Raman spectroscopy assisted by DFT calculation](#)

10:10 to 10:30

**Long Huang** (College of Chemistry and Chemical Engineering, Xiamen University, Xiamen, China), Eric Sorte, Yuye Tong, Shi-Gang Sun

[In-situ <sup>13</sup>C NMR spectroscopy study of ethanol electro-oxidation on Pt and PtRu](#)

10:30 to 10:50

**Fabian Kubannek** (Institute of Energy and Process Systems Engineering, TU Braunschweig, Braunschweig, Germany), Ulrike Krewer

[From Quantitative Differential Electrochemical Mass Spectrometry Experiments to Electrochemical Surface Reaction Models](#)

10:50 to 11:10

Coffee Break

# Monday, 5 October 2015 - Afternoon

MONDAY PM

## Symposium 2: Electrochemical Aspects of Biological Systems: Theory, Experiment and Applications

Room : 101D

Chaired by: Liza Rassaei, Mei-Jywan Syu and Jan Vacek

14:00 to 14:20 Invited

**Sean Elliott** (Department of Chemistry, Boston University, Boston, USA), Kathryn Bewley, Evan Judd, Kelly Walsh, Lindsey Walker

[Diversity and Electrocatalysis by Multi-heme Cytochromes c](#)

14:20 to 14:40

**Ross Milton** (Department of Chemistry, University of Utah, Salt Lake City, USA), David Hickey, Sofiene Abdellaoui, Koun Lim, Boxuan Tan

[Naphthoquinone Derivatives as Low-Potential Electron Mediators of FAD-Dependent Glucose Dehydrogenase](#)

14:40 to 15:00

**Seiya Tsujimura** (Faculty of Pure and Applied Sciences, University of Tsukuba, Tsukuba, Japan)

[Biocathode based on a MgO-template Carbon Electrode Modified with ABTS and Bilirubin Oxidase](#)

15:00 to 15:20

**Matteo Duca** (Department of Chemistry, University of Oxford, Oxford, United Kingdom), Justin Weeks, Justin Fedor, Joel Weiner, Kylie Vincent

[Electrocatalytic cascades driven by enzymes and metal nanoparticles on carbon supports: the reduction of nitrate to ammonia at neutral pH](#)

15:20 to 15:40

**Adalgisa De Andrade** (Chemistry, FFCLRP/USP, Universidade de São Paulo, Ribeirao Preto, Brazil), Sidney Aquino-Neto, David Hickey, Ross Milton, Shelley Minter

[High Current Density Bioanodes for Ethanol Oxidation using PQQ-dependent Enzymes](#)

15:40 to 16:20 Keynote

**Paul Bernhardt** (School of Chemistry and Molecular Biosciences, University of Queensland, Brisbane, Australia)

[Molybdenum Enzyme Electrochemistry](#)

16:20 to 16:40

Coffee Break

16:40 to 17:00 Invited

**Alain Walcarius** (LCPME - CNRS, CNRS and Lorraine University, Villers-les-Nancy, France)

[Bioelectrocatalysis with sol-gel biocomposite layers deposited onto porous electrodes](#)

17:00 to 17:20

**Elisabeth Lojou** (BIP-CNRS, CNRS-AMU, Marseille, France), Anne de Poulpique, Karen Monsalve, Christian Kjaergaard, Ed Solomon, Nicolas Mano

[Thermostable enzymes for biofuel cells: wiring strategies and inhibitor influence](#)

17:20 to 17:40

**Enrico Marsili** (Singapore Centre on Life Sciences Engineering, Nanyang Technological University, Singapore, Singapore), Abeed Fatima Binti Mohidin Batcha, Kannan Palanisamy, Carlo Santoro, Maria Yung, Thomas Seviour, Jamie Hinks, Federico Lauro

[Detection of semivolatile organic compounds \(VOCs\) in wastewater through current output of electrochemically active bacteria](#)

17:40 to 18:00

**Maciej Karaskiewicz** (College of Inter-Faculty Individual Studies in Mathematics, University of Warsaw, Warsaw, Poland), Jerzy Rogalski, Renata Bilewicz, Jacek Lipkowski

[Probing Laccase Immobilization on Modified Gold Electrodes and Conformational Changes by Surface-Enhanced Infrared Absorption Spectroscopy](#)

18:00 to 18:20

**Lo Gorton** (Dept. of Biochemistry and Structural Biology, Lund University, Lund, Sweden)

[Electrochemical Communication between Photosynthetic Membranes/Cells and Electrodes](#)

18:20 to 18:40

**Wolfgang Schuhmann** (Analytical Chemistry, Center for Electrochemical Sciences, Ruhr-Universität Bochum, Bochum, Germany), Adrian Ruff, Piyanut Pinyou, Sabine Alsaoub, Fangyuan Zhao, Francesco Lopez, Stefan Barwe, Nikola Markovic, Corina Andronescu, Nicolas Plumeré

[Redox polymers @ bioelectrochemistry. From biosensors to biofuel cells and self-powered bioelectrochemical devices](#)

---

## Symposium 3: Batteries for Tomorrow's World

---

**Room : 201AB**

*Chaired by:* Petr Novak

14:00 to 14:40 Keynote

**Zempachi Ogumi** (Office of Society-Academia Collaboration for Innovation, Kyoto University, Gokasho, Uji, Japan), Hajime Arai, Yoshiharu Uchimoto

[Reactions in cathode positive composite electrode by using synchrotron X-ray](#)

14:40 to 15:00 Invited

**Xuejie Huang** (Institute of Physics, Chinese Academy of Sciences, Beijing, China)

[High Voltage Cathode Materials  \$\text{LiNi}\_{0.5}\text{Mn}\_{1.5}\text{O}\_4\$  for Li-ion Batteries](#)

15:00 to 15:20

**Franziska Mueller** (Helmholtz Institute Ulm, Karlsruhe Institute of Technology, Ulm, Germany), Dominic Bresser, Ulderico Ulissi, Stefano Passerini

[Advanced Anode Materials combining Conversion & Alloying Energy Storage Mechanism for Lithium-Ion Batteries](#)

15:20 to 15:40

**Alvin Wu** (R&D, Underwriters Laboratories Taiwan Co., Ltd., Taipei, Taiwan)

[Explore the Failure Mechanism in Lithium-ion Batteries by Forensic Analysis Techniques](#)

15:40 to 16:00

**Eunseog Cho** (Samsung Advanced Institute of Technology, Samsung Electronics, Suwon, Korea), Kihong Kim, Changhoon Jung, Hyo Sug Lee, Kyoungmin Min, Woo Sung Jeon, Gyeong-Su Park, Jaikwang Shin

[The role of the oxygen in the  \$\text{Li}\_2\text{MnO}\_3\$  cathode material for the Li-ion batteries](#)

16:00 to 16:20

**Andrew Gewirth** (Chemistry, University of Illinois, Urbana, USA)

[Electrochemical Stiffness in Lithium Ion Batteries](#)

16:20 to 16:40

Coffee Break

16:40 to 17:00

**Mark E. Orazem** (Department of Chemical Engineering, University of Florida, Gainesville, USA), Salim Erol

[The Influence of Anomalous Diffusion on the Impedance Response of  \$\text{LiCoO}\_2/\text{C}\$  Batteries](#)

17:00 to 17:20

**Wei Kong Pang** (Bragg Institute, Australian Nuclear Science and Technology Organisation, Kirrawee DC, Australia), Vanessa K. Peterson

[Characterisation of Electrode Materials for Li-Ion Batteries Using Operando Neutron Powder Diffraction](#)

17:20 to 17:40

**Juan Manuel Paz-Garcia** (Division of Solid Mechanics, Lund University, Lund, Sweden), Oluwadamilola O. Taiwo, Paul R. Shearing, Donal Finegan, Rajmund Mokso, Erika Tudisco, Matti Ristinmaa, Stephen Hall

[Electrochemical-mechanical Coupled Phenomena in Silicon-based Li-ion Batteries Using X-ray Tomographic Characterization](#)

17:40 to 18:00

**Klaus Wedlich** (Institute of Energy and Climate Research (IEK-3), Forschungszentrum Jülich, Jülich, Germany), Carsten Korte, Detlef Stolten

[Investigation of the growth of a SEI-like surface layer on LiNi<sub>0.5</sub>Mn<sub>1.5</sub>O<sub>4</sub> high voltage cathodes](#)

18:00 to 18:20

**Sylvia Ayu Pradanawati** (Graduate Institute of Applied Science, National Taiwan University of Science and Technology, Taipei, Taiwan), Fu-Ming Wang

[In-Situ Observation of Solid Electrolyte Interphase \(SEI\) Formation in Electrochemical Surface Plasma Resonance \(EC-SPR\)](#)

18:20 to 18:40 Invited

**Jianbo Zhang** (Dept of Automotive Engineering, Tsinghua University, Beijing, China), Jun Huang, Zhe Li

[Characterizing Interfacial and Bulk Phase Processes in LIB Using EIS](#)

---

## Symposium 4: Advances in Fuel Cells from Materials to Systems

---

**Room : 102**

*Chaired by:* Dario Dekel and Timothy J. Peckham

14:00 to 14:20

**Zidong Wei** (School of Chemistry and Chemical Engineering, Chongqing University, Chongqing, China), Wei Ding, Li Li, Siguo Chen, Xueqiang Qi

[Pt-free Catalyst for Oxygen Reduction Reaction in Fuel Cells](#)

14:20 to 14:40

**Hsin-Chih Huang** (Department of Materials Science and Engineering, National Taiwan University of Science and Technology, Taipei, Taiwan), Sun-Tang Chang, Chen-Hao Wang, Li-Chyong Chen, Kuei-Hsien Chen

[High Activity Pyrolyzed Iron-FA as Potential Pt-Substitute for Oxygen Reduction Reaction](#)

14:40 to 15:00

**Jin-Song Hu** (Institute of Chemistry, Chinese Academy of Sciences, Beijing, China), Zidong Wei, Li-Jun Wan

[Designing Efficient Nanocatalysts for Oxygen Reduction Reaction](#)

15:00 to 15:20 Invited

**Timothy J. Peckham** (Department of Chemistry, Simon Fraser University, Burnaby, Canada), Andrew G. Wright, Owen D. Thomas, Mahesh P. Kulkarni, Kristen J.W.Y. Soo, Steven Holdcroft

[Membranes with Potential AAEMFC Applications: Structure-Property Relationships of Methylated Poly\(benzimidazole\)s](#)

15:20 to 15:40 Invited

**Dario Dekel** (Chemical Engineering, Technion - Israel Institute of Technology, Haifa, Israel)

[Review of the Latest Advances and Current Challenges of Anion Exchange Membrane Fuel Cell Technology](#)

15:40 to 16:00

**Jingshuai Yang** (Department of Chemistry, Northeastern University, Shenyang, China)

[Preparation and Properties of PTFE Reinforced Novel Anion Exchange Membranes Based on Silane Crosslinked Imidazolium Containing Poly\(2,6-dimethyl-1,4-phenylene oxide\)](#)

16:00 to 16:20

**Yu Yang** (Department of Materials Science and Technology, Nagaoka University of Technology, Nagaoka, Japan), Sayoko Shironita, Kunio Nakatsuyama, Kenichi Souma, Minoru Umeda

[Corrosion Characteristics of Ni-free Nitriding Stainless Steel as Bipolar Plate Material for PEFC](#)

16:20 to 16:40

Coffee Break

16:40 to 17:00

**Philipp Lettenmeier** (Institute of Engineering Thermodynamics, German Aerospace Center, Stuttgart, Germany), Rainey Wang, Rami Abouatallah, Aldo Saul Gago, Kaspar Andreas Friedrich

[Durable MEAs for PEM electrolyser systems operating at high current densities](#)

17:00 to 17:20

**Yeh-Hung Lai** (Fuel Cell Research and Development, General Motors Company, Pontiac, USA), Corey P Schaffer

[Shorting in Proton Exchange Membrane Fuel Cells](#)

17:20 to 17:40

**Lin Gan** (Division of Energy and Environment, Graduate School at Shenzhen, Tsinghua University, Shenzhen, China), Chunhua Cui, Fabio Dionigi, Peter Strasser

[Shaped Pt Bimetallic Nanoparticles: Linking the Anisotropic Growth to the Electrocatalytic Properties](#)

17:40 to 18:00

**Kenneth Ozoemena** (Materials Science and Manufacturing, Council for Scientific and Industrial Research (CSIR), Pretoria, South Africa)

[Novel Pd-Fe-Co Core-Core-Shell Anode Nanocatalyst in Alkaline Anion-Exchange Membrane Alcohol Fuel Cells](#)

18:00 to 18:20

**Kouakou Boniface Kokoh** (Chemistry, University of Poitiers / IC2MP, Poitiers, France), Roberta Alvarenga Isidoro, Elisabete Inacio Santiago, Nihat Ege Sahin, Teko W. Napporn

[Effective Pd-based Electrode Nanomaterials for H<sub>2</sub>/O<sub>2</sub> Solid Polymer Electrolyte Fuel Cells](#)

18:20 to 18:40

**Wenjing (Angela) Zhang** (Department of Energy Conversion and Storage, Technical University of Denmark, Ros, Denmark), Debora Marani, Rafael Hubert Silva, Rebecka Maria Larsen Wercheister, Kent Kammer Hansen, Vincenzo Esposito

[Electrospun Nanofiber Catalysts for Green Technology](#)

## Symposium 5: Novel Insights to Electrochemical Capacitors

Room : 101A

*Chaired by:* George Zheng Chen, Yury Gogotsi, Kwang-Bum Kim and Katsuhiko Naoi

14:00 to 14:40 Keynote

**Yury Gogotsi** (Drexel University, Materials Science and Engineering, A.J. Drexel Nanomaterials , Philadelphia, USA)

[Two-Dimensional Materials and Electrode Architectures for Capacitive and Pseudocapacitive Energy Storage](#)

14:40 to 15:00 Invited

**Elzbieta Frackowiak** (Institute of Chemistry and Technical Electrochemistry, Poznan University of Technology, Poznań, Poland), Adam Kolodziej, Krzysztof Fic

[Towards Green Aqueous Capacitors with Chitin as Binder](#)

15:00 to 15:20

**Olivier Crosnier** (CNRS - IMN, University of Nantes, Nantes, France), Nicolas Goubard, Frédéric Favier, Christophe Payen, Philippe Leone, Thierry Brousse

[FeWO<sub>4</sub> as a new high volumetric capacitance material for aqueous electrochemical supercapacitors](#)

15:20 to 15:40

**Christophe Lethien** (IEMN - RS2E, Université Lille, Villeneuve d'ascq, France), Kevin Brousse, Etienne Eustache, Peihua Huang, Camille Douard, Barbara Daffos, Pierre Louis Taberna, Jean Le Bideau, Thierry Brousse, Patrice Simon

[On chip 3D pseudocapacitive and carbon based electrochemical microsupercapacitors at the wafer level](#)

15:40 to 16:00

**Hiroshi Inoue** (Applied Chemistry, Osaka Prefecture University, Sakai, Japan), Kentaro Konishi, Eiji Higuchi, Masanobu Chiku

[Electrochemical Characterization of an Aqueous Hybrid Capacitor with Zinc and Activated Carbon Electrodes](#)

16:00 to 16:20

**Abdulcabbar Yavuz** (Department of Chemistry, University of Leicester, Leicester, United Kingdom), Robert Hillman, Karl S. Ryder

[Ion Exchange Optimization of Polyaniline Films in Deep Eutectic Solvents for Supercapacitor Application](#)

16:20 to 16:40

Coffee Break

16:40 to 17:00 Invited

**Daniel Bélanger** (Chimie, Université du Québec à Montréal, Montréal, Canada), Galyna Shul

[New materials for electrochemical capacitors](#)

17:00 to 17:20 Invited

**Keryn Lian** (Department of Materials Science and Engineering, University of Toronto, Toronto, Canada), Matthew Genovese, Yeewei Foong

[Design and Modification of Inorganic/Organic Polyoxometalates-Carbon Pseudocapacitive Electrodes](#)

17:20 to 17:40 Invited

**Yuan Chen** (School of Chemical and Biomedical Engineering, Nanyang Technological University, Singapore, Singapore)

[Micro-supercapacitors based on carbon hybrid fibers](#)

17:40 to 18:00

**Peihua Huang** (CIRIMAT, Université Paul Sabatier, Toulouse, France), Kevin Brousse, Christophe Lethien, Marc Respaud, Yury Gogotsi, Pierre-Louis Taberna, Patrice Simon

[On-chip Carbide Derived Carbon Thin Films for Microsupercapacitors](#)

18:00 to 18:20 Invited

**Wataru Sugimoto** (Center for Energy and Environmental Science, Shinshu University, Ueda, Japan), Sho Makino

[Pseudocapacitance of ruthenium oxide in buffered solutions](#)

18:20 to 18:40

**Dah-Shyang Tsai** (Chemical Engineering Department, National Taiwan University of Science and Technology, Taipei, Taiwan)

[Structure and Capacity of a Tin-Copper-CNT Composite Anode and its Lithium Ion Hybrid Capacitor Performance](#)

---

## Symposium 6: New Progress in Electrochemical Solar Cells

---

**Room : 201C**

*Chaired by:* Kuei-Hsien Chen, Ib Chorkendorff, Florian Le Formal and Chen-Yu Yeh

14:00 to 14:20 Keynote

**Chen-Yu Yeh** (Chemistry, National Chung Hsing University, Taichung, Taiwan)

[Recent Progress of Porphyrin-Sensitized Solar Cells](#)

14:20 to 14:40

**Hyunwoong Seo** (Information Science and Electrical Engineering, Kyushu University, Fukuoka, Japan), Min-Kyu Son, Shinji Hashimoto, Naho Itagaki, Kazunori Koga, Masaharu Shiratani

[Novel polymer counter electrode of dye-sensitized solar cells](#)

14:40 to 15:00

**Qinghong Zhang** (State Key Laboratory for Modification of Chemical Fibers, Donghua University, Shanghai, China)

[Some Chemical Routes to Form Compact Films of Dye-sensitized Solar Cells](#)

15:00 to 15:20

**Marketa Zukalova** (Electrochemical Materials, J. Heyrovsky Institute of Physical Chemistry, AS CR, Prague, Czech Republic), Ladislav Kavan, Milan Bousa, Zdenek Bastl, David Havlicek

[Sol-gel TiO<sub>2</sub> blocking layers for dye-sensitized and perovskite solar cells: Electrochemical properties and electrochemical doping](#)

15:20 to 15:40

**Jinbao Zhang** (Chemistry, Uppsala University, Uppsala, Sweden), Nick Vlachopoulos, Erik Johansson, Mohamed Jouini, Gerrit Boschloo, Anders Hagfeldt

[In-situ Photoelectrochemical Polymerization Approach For Efficient Solid-state Dye Sensitized Solar Cells](#)

15:40 to 16:00

**Kuan-Jiuh Lin** (Department of Chemistry, National Chung-Hsing University, Taichung, USA), Yin-Cheng Yen

[Plasmon-Induced Efficiency Enhancement on Dye-Sensitized Solar Cell by a TNW-AuNP Layer](#)

16:00 to 16:20

**Ladislav Kavan** (Electrochemical Materials, J. Heyrovsky Institute of Physical Chemistry, Prague 8, Czech Republic), Zuzana Vlckova-Zivcova, Hana Krysova, Petr Cigler, Paul Liska, Shaik M. Zakeeruddin, Michael Grätzel

[Novel Cathode and Photocathode Materials for Dye-Sensitized Solar Cells](#)

16:20 to 16:40

Coffee Break

16:40 to 17:00 Invited

**Peter Deák** (BCCMS, University of Bremen, Bremen, Germany), Jolla Kullgren, Balint Aradi, Thomas Frauenheim, Ladislav Kavan

[Resolving the Controversy about the Band Alignment between Rutile and Anatase: the Role of OH<sup>-</sup>/H<sup>±</sup> Adsorption](#)



17:00 to 17:20 Invited

**Florian Le Formal** (Institute of Chemical Science and Engineering (LIMNO), Ecole Polytechnique Federale de Lausanne, Lausanne, Switzerland), Mathieu Prévot, Xiaoyun Yu, Wiktor S. Bourée, Nestor Guizarro, Kevin Sivula

[Solution-Processed Nanostructured p-type Photocathodes for Solar Hydrogen Production](#)

17:20 to 17:40

**Pauline Borno** (Institute of Chemistry and Chemical Engineering, École Polytechnique Fédérale de Lausanne, Lausanne, Switzerland), Mathieu Prévot, Xavier Jeanbourquin, Kevin Sivula

[An Organic Semiconductor as a Photoanode for Solar Water Splitting](#)

17:40 to 18:00

**Yan-Gu Lin** (Scientific Research Division, National Synchrotron Radiation Research Center, Hsinchu, Taiwan), Hong-Jhe Lin, Yu-Chang Lin

[Earth-Abundant Materials for Photocatalytic Water splitting](#)

18:00 to 18:20

**Mauricio Schieda** (Institute of Materials Research, Helmholtz-Zentrum Geesthacht, Geesthacht, Germany), Herman Kriegel, Iris Herrmann-Geppert, Aafke C. Bronneberg, Deirdre L. Olynick, Thomas Klassen

[Solar Water Splitting With Nanoimprinted Model Photoelectrodes](#)

18:20 to 18:40

**Kenji Sakamaki** (Department of Chemistry, Fukushima College, National Institute of Technology, Iwaki, Japan), Ryoko Kato, Haruka Endo, Masataka Sato, Yoichi Kamo

[Photoelectrochemical Zero Bias Hydrogen Generation with a Novel Three Compartment Cell for Decreasing Theoretical and Total Water Electrolysis Voltage \(10\)](#)

---

## Symposium 9: Electrocatalytic Materials

---

**Room : 201EF**

*Chaired by:* Chia-Ying Chiang, Daniel Scherson, Atsushi Iwanaga and YuYe Tong

14:00 to 14:20 Invited

**Denis Kramer** (Engineering Materials, University of Southampton, Southampton, United Kingdom), Tobias Binniger, Emiliana Fabbri, Thomas Justus Schmidt

[Theoretical Thoughts on Electronic Interactions between Metallic Electrocatalysts and Oxide Supports](#)

14:20 to 14:40

**Shuihua Tang** (School of Materials Science and Engineering, Southwest Petroleum University, Chengdu, China), Haixin Huangfu, Yuxiao Deng, Leping Sui, Zhen Dai, Zhentao Zhu, Xiaolong Qin, Jiawei Yuan

[High-Performance Electrocatalyst for Oxygen Reduction Derived from Riboflavin and Iron](#)

14:40 to 15:00

**Hiroyuki Koshikawa** (Department of Applied Chemistry, The University of Tokyo, Tokyo, Japan), Kazuhide Kamiya, Shuji Nakanishi, Kazuhito Hashimoto

[Heat-treated 3,5-diamino-1,2,4-triazole/graphene Hybrid Functions as an Oxygen Reduction Electrocatalyst with High Activity and Stability](#)

15:00 to 15:20

**Kotaro Sasaki** (Chemistry Department, Brookhaven National Laboratory, Upton, USA), Kurian Kuttijiel, Dong Su, Lijun Wu, Yimei Zhu, Radoslaw Adzic

[Gold-promoted structurally ordered intermetallic palladium cobalt nanoparticles for the oxygen reduction reaction](#)

15:20 to 15:40

**Ming Zhou** (Chemistry, The University of Hong Kong, Hong Kong, China), Kwong-Yu Chan

[Highly Active and Stable Iron-nitrogen-doped Carbon with Hollow-core-mesoporous-shell \(HCMS\) Structure for Oxygen Reduction Reaction](#)



15:40 to 16:00

**YuYe Tong** (Chemistry, Georgetown University, Washington, USA), Yanyan Wang

[Unexpected Good Deed of a Traditional Poison: Sulfur-Adsorption Enhanced Activity and Stability of Pt for Oxygen Reduction Reaction](#)

16:00 to 16:20

**Justus Masa** (Analytical Chemistry and Center for Electrochemical Sciences, Ruhr-Universitaet Bochum, Bochum, Germany), Wei Xia, Anqi Zhao, Martin Muhler, Wolfgang Schuhmann

[Electrocatalysis of oxygen reduction and water oxidation using metal oxides embedded in nitrogen-doped carbon](#)

16:20 to 16:40

Coffee Break

16:40 to 17:00

**Atsunori Ikezawa** (Graduate School of Engineering, Kyoto University, Kyoto, Japan), Kohei Miyazaki, Tomokazu Fukutsuka, Takeshi Abe

[Investigations of Triple Phase Boundary Regions in Bifunctional Air Electrodes Using Partially Immersed Platinum Electrodes](#)

17:00 to 17:20

**Samuel Perry** (Chemistry, University of Southampton, Southampton, United Kingdom), Guy Denuault

[Determination of Oxygen Binding Energy from Simple Amperometric Experiments and its Application Towards the Evaluation of Novel Materials for the Oxygen Reduction Reaction](#)

17:20 to 17:40

**Lior Elbaz** (Chemistry, Bar Ilan University, Ramat-Gan, Israel), Zeev Gross, Naomi Levi, Atif Mahammed

[Electroreduction of Oxygen with Brominated Metallo-Corroles](#)

17:40 to 18:00

**Claudio Zafferoni** (Department of Chemistry Ugo Schiff, University of Florence, Florence, Italy), Giulia Tuci, Giuliano Giambastiani, Massimo Innocenti

[Bimetallic catalysts and metal-free catalysts for ORR](#)

18:00 to 18:20

**Daniel Scherson** (Chemistry, Case Western Reserve University, Cleveland, USA), Adriel Jebaraj, Nicholas Georgescu

[On The Effects of Bromide Adsorption on the Rates of Redox Reactions](#)

18:20 to 18:40 Invited

**Minhua Shao** (Department of Chemical and Biomolecular Engineering, Hong Kong University of Science and Technology, Hong Kong, China)

[Size, Shape and Morphology Effects on Catalytic Activity of Oxygen Reduction Reaction](#)

## Symposium 10: Electrochemical Technology: New Challenges for a More Competitive Economy

**Room : 101B**

*Chaired by:* Guohua Chen and Onofrio Scialdone

### 14:00 to 14:20 Invited **ISE Prize for Environmental Electrochemistry**

**Sergi Garcia-Segura** (Chemistry, Universidade Federal do Rio Grande do Norte, Natal, Brazil), Enric Brillas

[Electrochemical Processes Based on Fenton's Reaction for Wastewater Treatment. An Eco-Friendly, Efficient and Affordable Technology: Then, Now and Tomorrow](#)

### 14:20 to 14:40 Invited

**Ricardo Salazar** (Química de los Materiales, Universidad de Santiago de Chile, Santiago, Chile)

[Remediation of bovine slurry wastewater using electrochemical advances oxidation process.](#)

### 14:40 to 15:00

**Nelly Esther Flores Tapia** (Química Física, University of Barcelona, Barcelona, Spain), Enric Brillas, Ignacio Sirés, Pere Cabot, Rosa Rodríguez, José Garrido, Francisco Centellas

[Comparison of trans-cinnamic and trans-ferulic acids degradation by advanced oxidation processes](#)

### 15:00 to 15:20 Invited

**Ignacio González** (Universidad Autónoma Metropolitana-Iztapalapa, Chemistry, México, Mexico), Odín Rodríguez-Nava, Miguel Angel Arellano-González, Anne Claire Texier

[Removal of emerging pollutants and biodegradable organic matter from wastewater by combined electrochemical -biological processes](#)

### 15:20 to 15:40 Invited

**Bahadır K. Körbahti** (Mersin University, Chemical Engineering Department, Mersin University, Mersin, Turkey)

[Electrochemical Processes for Green Environment: the emerging technology in wastewater treatment](#)

### 15:40 to 16:00 Invited

**Minghua Zhou** (College of Environmental Science and Engineering, Nankai University, Tianjin, China), Liang Ma, Weilu Yang, Gengbo Ren, Fangke Yu

[Flow-through Electrochemical Cells for Efficient Dye Removal](#)

### 16:00 to 16:20

**Ali Farhat** (Advanced Water Management Centre, University of Queensland, Brisbane, Australia), Stephan Tait, Jurg Keller, Jelena Radjenovic

[Role of Sulfate and Persulfate Ions in Electrochemical Oxidation of Persistent Organics at a Boron-doped Diamond Anode](#)

### 16:20 to 16:40

Coffee Break

### 16:40 to 17:20 Keynote

**Yunny Meas** (Research and Development, CIDETEQ, Pedro Escobedo, Mexico), Alejandro Medel, Georgina Zuñiga, José A. Ramírez

[Novel Electrochemical Prototype for the Treatment of Spent Caustic from Hydrocarbon Industry and its Industrial Scaling](#)

### 17:20 to 17:40

**Konstantin Petrov** (Electrocatalysis, IEES-BAS, Sofia, Bulgaria), Venko Beshkov, Elena Razkazova, Djamal Uzun

[A method for the simultaneous cleansing of H<sub>2</sub>S and SO<sub>2</sub>](#)

### 17:40 to 18:00

**Hui-Wen Lin** (Advanced Water Management Centre, The University of Queensland, Brisbane, Australia), Korneel Rabaey, Jurg Keller, Zhiguo Yuan, Ilje Pikaar

[Simultaneous scaling-free electrochemical production of caustic and oxygen from domestic wastewater for sulfide control in sewers](#)

18:00 to 18:20

**Olivier Lefebvre** (Department of Civil and Environmental Engineering, National University of Singapore, Singapore, Singapore), Emmanuel Mousset, Muhammad Syafiq Bin Ahmad, Zuxin Wang

[Graphene-based electrodes: a new promising material for a more competitive electro-Fenton technology](#)

18:20 to 18:40

**Kenji Kawaguchi** (Organization for Research Initiatives and Development, Doshisha University, Kyo-tanabe, Kyoto, Japan), Masatsugu Morimitsu

[Reaction Selectivity of IrO<sub>2</sub>-Ta<sub>2</sub>O<sub>5</sub> Nano-Amorphous Hybrid Catalysts for Oxygen Evolution and Metal Oxide Deposition](#)

---

## Symposium 12: Physical Electrochemistry: Spectroscopic, Structural, and Theoretical Investigations of the Electrified Interface

---

**Room : 101C**

*Chaired by:* Hirohito Ogasawara, Kelsey A. Stoerzinger and Juan M. Feliu

14:00 to 14:40 Keynote

**Hirohito Ogasawara** (2SUNCAT ctr for Interface Science and Catalysis, SLAC National Accelerator Laboratory, Menlo Park, USA), Daniel Friebe, Anders Nilsson

[Operando X-ray Studies of Electrocatalysis](#)

14:40 to 15:00 Invited

**Kelsey A. Stoerzinger** (Department of Materials Science & Engineering, Massachusetts Institute of Technology, Cambridge, USA), Wesley T. Hong, Yueh-Lin Lee, Livia Giordano, Yang Shao-Horn

[Molecular Insight into Wetted Oxide Surfaces and Oxygen Electrocatalysis](#)

15:00 to 15:20 Invited

**Ryosuke Jinnouchi** (Material Design Lab., Toyota Central R&D Labs., Inc., Nagakute, Japan), Kensaku Kodama, Eishiro Toyoda, Kenji Kudo, Naoki Kitano, Naoki Hasegawa, Yu Morimoto

[Atomistic Simulations for Designing High-Performance Electrode Materials for Polymer Electrolyte Fuel Cells](#)

15:20 to 15:40

**Andy Wain** (Materials Division, National Physical Laboratory, Teddington, United Kingdom)

[Mapping Oxygen Reduction at Individual Nanostructures Using High-Resolution Electrochemical-Topographical Imaging](#)

15:40 to 16:00

**Marta Figueiredo** (Leiden Institute of Chemistry, Leiden University, Leiden, Netherlands), Marc T.M. Koper

[CO<sub>2</sub> electroreduction products and intermediates in organic solvents](#)

16:00 to 16:20

**Sunny Hy** (Department of Chemical Engineering, National Taiwan University of Science and Technology, Taipei, Taiwan), Felix Felix, Bing-Joe Hwang

[Designing In Situ Solid Electrolyte Interphase Studies using Surface-enhanced Raman Spectroscopy](#)

16:20 to 16:40

Coffee Break

16:40 to 17:00

**Zhong-Qun Tian** (Chemistry Department, Xiamen University, Xiamen, China), Meng Zhang, William Valenzuela, Runwen Yan, Songyuan Ding, Juan Perez, De-Yin Wu, Bingwei Mao, Juan M. Feliu,

[Extending Shell-isolated Nanoparticle-enhanced Raman Spectroscopy to Study Ordered/Disordered](#)

[Adsorption of \(Bi\)sulfate on Au Single Crystal Electrodes](#)

17:00 to 17:20

**Masato Tominaga** (Graduate School of Science and Technology, Kumamoto University, Kumamoto, Japan), Yudai Nagahama, Yuto Yatsugi[Raman Spectroscopic Detection of Electrochemical Oxidative Reaction of Single-Walled Carbon Nanotubes](#)

17:20 to 17:40

**Shino Sato** (Department of Chemistry, Faculty of Science, Hokkaido University, Sapporo, Japan), Kohei Uosaki, Kei Murakoshi, Katsuyoshi Ikeda[Interface control in a chemically modified electrode for overpotential reduction](#)

17:40 to 18:00

**Juan M. Feliu** (Physical Chemistry, University of Alicante, Alicante, Spain), Paula Sebastian, Ricardo Martinez-Hincapie, Andrea Sandoval, Victor Climent[Laser induced temperature jump investigation of the interface between Pt single crystals in contact with ionic liquids](#)

18:00 to 18:20

**Robert Hillman** (Department of Chemistry, University of Leicester, Leicester, United Kingdom), Rachel Sapstead, Virginia Ferreira, Karen Smith, Karl S. Ryder, Emma Smith, Nina-Juliane Steinke, Robert Dalglish[Dynamic In Situ Neutron Reflectivity Studies of Metal Electrodeposition and Alloy Formation in Ionic Liquid Media](#)

18:20 to 18:40

**Kenta Motobayashi** (Catalysis Research Center, Hokkaido University, Sapporo, Japan), Kazuya Minami, Ken-ichi Uchida, Naoya Nishi, Tetsuo Sakka, Masatoshi Osawa[Potential-Dependent Behavior of Ionic Liquid \[BMIM\]\[TfSA\] with Additives on a Gold Electrode Studied by Surface-Enhanced Infrared Absorption Spectroscopy](#)

---

## Symposium 16: Supramolecular Electrochemistry for Analysis, Medicine and Biological Sciences

---

**Room : 201D***Chaired by:* Stephane Arbault and Olivier Buriez

14:00 to 14:40 Keynote

**Richard McCreery** (Department of Chemistry, University of Alberta, Edmonton, Canada), Adam Bergren, Nikola Pekas, Oleksii Ivanshenko, Jerry Fereiro, Bryan Szeto[Charge Transport Through Molecules Acting as “Supramolecular” Electronic Devices](#)

14:40 to 15:00

**Ping Yu** (Institute of Chemistry, Chinese Academy of Sciences, Beijing, China), Lanqun Mao[Imidazolium-Based Supramolecular Ionic Material and Its Application in Biosensing and Electronic Device](#)

15:00 to 15:20 Invited

**Serge Cosnier** (Department of Molecular Chemistry, Grenoble Alpes University-CNRS, Grenoble, France)[Supramolecular Biological Assemblies for Biosensors and Biofuel Cells](#)

15:20 to 15:40

**Pawel Kryszinski** (Faculty of Chemistry, University of Warsaw, Warsaw, Poland), Dorota Nieciecka, Aleksandra Joniec[Magnetic Nanoparticles and Magnetoliposomes as Anticancer Drug Carriers](#)

15:40 to 16:00

**Dorota Matyszewska** (Faculty of Chemistry, University of Warsaw, Warsaw, Poland), Renata Bilewicz, Jan Biernat[Interactions of Anticancer Drug and Adducts of the Drug with Carbon Nanotubes with Model Biological Membranes – Langmuir-Blodgett and Electrochemical Studies](#)

16:00 to 16:20 Invited

**Lars Jeuken** (School of Biomedical Sciences, University of Leeds, Leeds, United Kingdom)

[Lipid-Membrane Modified Electrodes to Study Respiratory Membrane Enzymes and their Complexes in a Native-Like Lipid Environment](#)

16:20 to 16:40

Coffee Break

16:40 to 17:20 Keynote

**Richard Compton** (Chemistry, Oxford University, Oxford, United Kingdom)

[Nano Impacts: Recent Advances](#)

17:20 to 17:40

**Enno Kätelhön** (Department of Chemistry, Physical and Theoretical Chemistry, University of Oxford, Oxford, United Kingdom), Shaltiel Eloul, Christopher Batchelor-McAuley, Kristina Tschulik, Richard Compton

[First-Passage Statistics in Nanoelectrochemistry: Applications to Nano-Impacts](#)

17:40 to 18:00 Invited

**Marcin Opallo** (Department of Electrode Processes, Institute of Physical Chemistry Polish Academy of Sciences, Warszawa, Poland), Joanna Dolinska, Palanisamy Kannan, Volodymyr Sashuk, Janusz Sobczak, Zbigniew Kaszkur, Wojciech Lisowski, Martin Jonsson Niedziolka

[Electrocatalytic glucose oxidation in suspension and film consisting charged Au and Pt nanoparticles](#)

18:00 to 18:20

**Hua Cui** (Department of Chemistry, University of Science and Technology of China, Hefei, China), Hongli Zhang, Zhili Han

[One-step Supermolecule Assembly of N-\(aminobutyl\)-N-\(ethylisoluminol\) Functionalized Gold Nanodots on Multiwalled Carbon Nanotubes and Their Applications to Sensors](#)

18:20 to 18:40

**Fred Lisdat** (Biosystems Technology, Institute of Applied Life Sciences, Technical University Wildau, Wildau, Germany), S. Feifel, R. McGovern, P. Crowley, Roland Ludwig

[Artificial protein architectures on electrodes](#)

---

## Symposium 17: Novel in Situ in Operando Methods

---

**Room : 103**

*Chaired by:* Fu-Ming Wang and Patrick Unwin

14:00 to 14:40 Keynote

**Karl Mayrhofer** (Department of Interface Chemistry and Surface Engineering, Max-Planck-Institut for Iron Research, Düsseldorf, Germany), Serhiy Cherevko, Jan-Philip Grote, Chang-Hyuck Choi, Aleksandar Zeradjanin, Nejc Hodnik, Claudio Baldizzone, Simon Geiger

[In-situ investigation of catalyst degradation](#)

14:40 to 15:00

**Bin Ren** (Department of Chemistry, Xiamen University, Xiamen, China), Cheng Zong, Chanjuan Chen, Meng Zhang

[Electrochemical Surface-Enhanced Raman Microscopy \(EC-SERM\)](#)

15:00 to 15:20

**Sandra Rondinini** (Department of Chemistry, Università degli Studi di Milano, Milano, Italy), Paolo Ghigna, Elisabetta Achilli, Alberto Vertova, Cristina Locatelli, Francesco D'Acapito

[Combined Ionic Diffusion and Faradaic Reactions in Electrodeposited Highly Hydrated Amorphous Iridium Oxide by in-operando Dispersive XAS Investigation](#)

15:20 to 15:40

**Eric Sorte** (Department of Chemistry, Georgetown University, Washington DC, USA), YuYe Tong[Innovations in In situ Electrochemical Nuclear Magnetic Resonance](#)

15:40 to 16:00

**Sarah Day** (Diamond Light Source, Diamond Light Source, Didcot, United Kingdom), Annabelle Baker, Chiu Tang[A Long Duration Experiment Facility for the Study of Battery Materials Using In Situ Synchrotron X-Ray Powder Diffraction](#)

16:00 to 16:20

**Simon Thiele** (Institute of Microsystems Engineering (IMTEK), University of Freiburg, Freiburg, Germany)[Multi-scale tomographic analysis of fuel cells, batteries and electrolyzers](#)

16:20 to 16:40

Coffee Break

16:40 to 17:00

**Mario El Kazzi** (Electrochemical Energy Storage Section (PSI), Paul Scherrer Institut (PSI), Villigen, Switzerland), Daniel Streich, Petr Novak[Complementary Operando XPS and Raman Spectroscopy of Ggraphite Cycled in Ionic Liquids](#)

17:00 to 17:20

**Misun Hong** (Byon Initiative Research Unit (IRU), RIKEN, Wako, Japan), Hee Cheul Choi, Hye Ryung Byon[In Situ Visualization of  \$\text{Li}\_2\text{O}\_2\$  Decomposition for a  \$\text{Li}-\text{O}\_2\$  Battery Using Electrochemical Atomic Force Microscopy \(ECAFM\)](#)

17:20 to 17:40

**Yoshiharu Uchimoto** (Graduate School of Human and Environmental Studies, Kyoto University, Kyoto, Japan), Yuki Orikasa[Operando synchrotron X-ray analysis for investigation of electrode property of lithium ion battery cathode](#)

17:40 to 18:00

**Neeraj Sharma** (School of Chemistry, UNSW Australia, Sydney, Australia)[The time and current-resolved evolution of sodium location and distribution in electrodes of sodium-ion batteries](#)

18:00 to 18:40 Keynote

**Hector Abruña** (Chemistry and Chemical Biology, Cornell University, Ithaca, USA)[Operando Methods for the Characterization Energy Materials](#)



ROOMS:	101A	101B	101C	101D	102	103	201AB	201EF	201C	201D	S.Lounge	
	101A	101B	101C	101D	102	103	201AB	201EF	201C	201D	S.Lounge	
SYMPOSIUM	s05	s10	s12	s02	s04/s15	s7/s01	s03	s09	s06/s03	s16/s08	s15	
08:15 - 09:15					Plenary Lecture: Hongjie Dai (Plenary Hall)							
09:30 - 09:50	Kwang-Bum Kim	Geoff Kelsall	Enrique Herrero	Dedhen Jian	S. Kumaraguru	Nikolay Dimitrov	George Crabtree	Jong-Sung Yu	Ib Chorkendorff	Renata Bilewicz	F. Sauvage	
09:50 - 10:10			I. Katsounaros	T. Yasukawa					Kuei-Hsien Chen	Olga Swiech	Hye Jin Lee	
10:10 - 10:30	D. Rochefort	A. d. I. Consuegra	Jian-Feng Li	Christine Kranz	Alexandra Patru	Natasa Vasiljevic	Fabio La Mantia	Candice Rassie	Marcel Schreier	Alexander Kuhn	F. Sekli Belaidi	
10:30 - 10:50	Tavo Romann	Jesus Iniesta	A. Mukkannan		Maxi Frei	S. Brankovic	Yuping Wu	Yan-Xia Jiang	Yi-June Huang		Ivan Kondov	
10:50 - 11:10	Coffee Break											
11:10 - 11:30												
11:30 - 11:50												
11:50 - 12:10												
12:10 - 12:30												
12:30 - 12:50												
12:50 - 13:10												
13:10 - 13:30												
13:30 - 14:00												
14:00 - 14:20	Etsuro Iwama	Javier Llanos	Jan Rossmelisl	Langqun Mao	Bongjin Simon Mun	Osamu Niwa	Takeshi Abe	Dangsheng Su	Yi Cui	Oliver Chyan		
14:20 - 14:40	Wan-Yu Tsai	Henry Bergmann					M. V. Reddy	Kamiya Kazuhide	D. Battybekuly	Jun-Seob Lee		
14:40 - 15:00	Tu-Ting Weng	Onofrio Socialdone	Katharina Krischer	Shen-Ming Chen	Byungchan Han	Andreas Lesch	Shuijiang Ding	Deli Wang	Xiaogang Zhang	Peter Keedh		
15:00 - 15:20	Chung-Ting Tsai	Emmanuel Mousset	A. Bandarenka	Nicolas Mano	G. Ramos-Sanchez	S. Chandra	Alejandro A. Franco	Bart Geboes	A. Mentbayeva	Xavier Feaugas		
15:20 - 15:40	Krzysztof Fic	Tsuyoshi Ochiai	F. Calle-Vallejo	Stephane Arbault	Trung Van Nguyen	S. Daniele	A. Lewandowski	Ifan Stephens	Heng-Liang Wu	D. Veys-Renaux		
15:40 - 16:00	Laura Coustan	Philippe Vernoux	Ali Malek	Libuse Trnkova	Tetsuya Mashio	Yukihiko Shintani	A. Ponrouch	Silver Sepp	Jason Fang	Hans-H. Strehblow		
16:00 - 16:20	Pawel Jezowski	C. A. Martinez-Huit.		A-M Oliveira-B.			Kolja Beltrop		Matthew Lacey			
16:20 - 16:40	Coffee Break											
16:40 - 17:00	Yongyao Xia	Takayuki Homma	S. Panahian Jand	A. Bondarenko	Daniel Brandell	Jyh-Myng Zen	Atsuo Yamada	Sandra Temmel	Yong Yang	Nadine Pebere		
17:00 - 17:20	Frédéric Favier	Priscilla Baker	Qingji Zou	Daliborka Jambrec	Christine Frayret	Grzegorz Lisak		Kensaku Kodama	Arianna Moretti	I-Wen Huang		
17:20 - 17:40	Soo-Gil Park	Nick Daems	Shen Ye	Karen Monsalve	P. Kaghazchi	Christopher Brett	Shirley Meng	Qingli Hao	Elie Paillard	Hiroaki Tsuchiya		
17:40 - 18:00	Soshi Shiraishi	G. Martin Haarberg	Ove Oll	Shaiahan Siraj	Yinghui Yin	Ch. A. Gunawan	Jie Li	Gert Göransson	N. Bonnet-M.	Koji Fushimi		
18:00 - 18:20	Jong-Huy Kim	Tom Breugelmanns	Matej Velicky	Bongkyu Kim	Seunghwa Lee	M. Castaño-A.	Ha-Kyung Roh	Adriano Gomes	Satoshi Fujiki	Khurram Shahzad		
18:20 - 18:40	JunHui Jeong	C. M Fernandez M.	Katsuyoshi Ikeda	Rachel Gao	Hyungjun Kim		Masashi Okubo	Pawel J. Kulesza	Yuebin Yang	Pei-Yu Lai		
20:00	Chinese Opera											



# Tuesday, 6 October 2015 - Morning

---

## Plenary Lecture

**Room : Plenary Hall**

*Chaired by:* Bing Joe Hwang

08:15 to 09:15

**Hongjie Dai** (Stanford University, Stanford, USA)

[Novel Materials for Renewable Energy](#)

---

## Symposium 2: Electrochemical Aspects of Biological Systems: Theory, Experiment and Applications

**Room : 101D**

*Chaired by:* Sofiene Abdellaoui and Vera Essmann

09:30 to 09:50

**Dechen Jiang** (School of Chemistry and Chemical Engineering, Nanjing University, Nanjing, China)

[Luminol Electrochemical-luminescence for Single Cell Analysis](#)

09:50 to 10:10

**Tomoyuki Yasukawa** (Graduate School of Material Science, University of Hyogo, Ako, Japan), Yuki Minakuchi, Hironobu Hatanaka, Fumio Mizutani

[Negative dielectrophoretic separation of cells based on the expression of specific surface antigen](#)

10:10 to 10:50 Keynote

**Christine Kranz** (Institute of Analytical and Bioanalytical Chemistry, University of Ulm, Ulm, Germany), Corinna Frey, Alexander Eifert, Holger Barth, Boris Mizaikoff

[Investigation of pore forming proteins in supported lipid membranes](#)

10:50 to 11:10

Coffee Break

## Symposium 3: Batteries for Tomorrow's World

Room : 201AB

Chaired by: Atsuo Yamada

09:30 to 10:10 Keynote

**George Crabtree** (Joint Center for Energy Storage Research (JCESR), Argonne National Laboratory, Argonne, USA)

[The Joint Center for Energy Storage Research \(JCESR\): A New Paradigm for Energy Storage Research](#)

10:10 to 10:30 Invited **Hans-Jürgen Engell Prize**

**Fabio La Mantia** (Analytical Chemistry, Ruhr-Universität Bochum, Bochum, Germany)

[Aqueous Zinc-Ion Batteries based on Prussian Blue Derivatives](#)

10:30 to 10:50

**Yuping Wu** (College of Energy, Nanjing Tech University, Nanjing, China), Zheng Chang, Yanfang Wang

[New Concept Aqueous Rechargeable Batteries with High Energy Densities](#)

10:50 to 11:10

Coffee Break

## Symposium 4: Advances in Fuel Cells from Materials to Systems

Room : 102

Chaired by: Hiroyuki Uchida

09:30 to 10:10 Keynote

**Swami Kumaraguru** (Fuel Cell Activities, General Motors, Pontiac, USA), Jingxin Zhang, Wenbin Gu, Balsu Lakshmanan, Mark Mathias

[PEMFC Cathode Performance and Durability Challenges at Low Platinum Loading](#)

10:10 to 10:30

**Alexandra Patru** (Electrochemistry Laboratory, Paul Scherrer Institut, Villigen, Switzerland), Johannes Biesdorf, Antoni Forner Cuenca, Emiliana Fabbri, Pierre Boillat, Thomas Justus Schmidt

[Performance and Stability of New Oxide Catalyst Supports under PEFC Operating Conditions](#)

10:30 to 10:50

**Maxi Frei** (IMTEK, Department of Microsystems Engineering, University of Freiburg, Freiburg, Germany), Johannes Erben

[Fabrication of platinum electrodes with high roughness factor using a 3D-support](#)

10:50 to 11:10

Coffee Break

---

## Symposium 5: Novel Insights to Electrochemical Capacitors

---

**Room : 101A**

*Chaired by:* Masashi Ishikawa

09:30 to 10:10 Keynote

**Kwang-Bum Kim** (Department of Material Science and Engineering, Yonsei University, Seoul, Korea), Sang-Hoon Park, Hyun-Kyung Kim, Hee Chang Youn, Myeong-Seong Kim, Suk-Woo Lee

[Graphene-based Nanomaterials for Energy Storage Devices](#)

10:10 to 10:30

**Dominic Rochefort** (Chemistry, Universite de Montreal, Montreal, Canada), Han Jin Xie, Bruno Gelinas

[On the Performance and Self-Discharge of a Redox-Active Electrolyte Supercapacitor Based on an Ionic Liquid Modified with Ferrocene](#)

10:30 to 10:50

**Tavo Romann** (Institute of Chemistry, University of Tartu, Tartu, Estonia), Erik Anderson, Ove Oll, Piret Pikma, Enn Lust

[High Voltage Graphene Capacitor Technology](#)

10:50 to 11:10

Coffee Break

---

## Symposium 6: New Progress in Electrochemical Solar Cells

---

**Room : 201C**

*Chaired by:* Peter Deák

09:30 to 09:50 Invited

**Ib Chorkendorff** (Department of Physics, Technical University of Denmark, Kongen Lyngby, Denmark)

[The Challenge of Interfacing Catalysts, Protection layers, and Semiconductors in a Tandem Device](#)

09:50 to 10:10 Invited

**Kuei-Hsien Chen** (IAMS, Academia Sinica, Taipei, Taiwan)

[Graphene Oxides Based Photocatalyst for Solar Fuels](#)

10:10 to 10:30

**Marcel Schreier** (Institute of Chemical Sciences and Engineering, Swiss Federal Institute of Technology Lausanne (EPFL), Lausanne, Switzerland), T. M. Aufar Kari, Laura Curvat, Thomas Moehl, Fabrizio Giordano, Antonio Abate, Jingshan Luo, Matthew T. Mayer, Michael Grätzel

[Efficient sunlight-driven reduction of CO<sub>2</sub> to fuels based on Cu<sub>2</sub>O and perovskite absorbers](#)

10:30 to 10:50

**Yi-June Huang** (Department of Chemical Engineering, National Taiwan University, Taipei, Taiwan), Miao-Syuan Fan, Chun-Ting Li, Chuan-Pei Lee, R. Vittal, Kuo-Chuan Ho

[A Low<sub>i</sub> VCost Counter Electrode with a MoSe<sub>2</sub>/PEDOT:PSS Composite Catalytic Film for Dye-Sensitized Solar Cells](#)

10:50 to 11:10

Coffee Break

## Symposium 7: Electrodeposition - The Frontier Approach in Material Science and Nanofabrication

**Room : 103**

*Chaired by:* Stanko Brankovic and Natasa Vasiljevic

09:30 to 10:10 Keynote

**Nikolay Dimitrov** (Chemistry, Binghamton University - SUNY, Binghamton, USA)

[Advances in the Growth of Metals and Alloys Assisted by a Monolayer Amount of UPD Atoms](#)

10:10 to 10:30 Invited

**Natasa Vasiljevic** (School of Physics, University of Bristol, Bristol, United Kingdom), Benjamin Rawlings, Michael P. Mercer, Zakiya Al Amri

[Surface Limited Redox Replacement Design of Pt Bimetallic Nanostructures](#)

10:30 to 10:50 Invited

**Stanko Brankovic** (Electrical and Computer Engineering, University of Houston, Houston, USA), Ela Bulut, Donjun Wu, Hasan Kilic

[SLRR of UPD Monolayers – Fundamental Aspects and Interplay of UPD, Reaction Kinetics, and Nucleation](#)

10:50 to 11:10

Coffee Break

## Symposium 9: Electrocatalytic Materials

**Room : 201EF**

*Chaired by:* Chen-Hao Wang

09:30 to 10:10 Keynote

**Jong-Sung Yu** (Department of Energy Systems Engineering, Daegu Gyeongbuk Institute of Science and technology (DGIST), Daegu, Korea), Dea-Soo Yang, Min Young Song, Kiran Pal Singh, Fatemeh Razmjooei  
Heteroatom-Doped Porous Carbon as Electrocatalyst: Surface Properties and Electrocatalytic Activity

10:10 to 10:30

**Candice Rassie** (Chemistry, University of the Western Cape, Cape Town, South Africa), Lindsay Wilson, Priscilla Baker, Emmanuel Iwuoha

[Microscopic and Electrochemical Signatures of Copper-poly\(propyleneimine\) Metallodendrimer System](#)

10:30 to 10:50

**Yan-Xia Jiang** (Department of Chemistry, Xiamen University, Xiamen, China), Bin-Wei Zhang, Shi-Gang Sun

[Pt<sub>3</sub>Ni intermetallic with Pt-rich surface supported on porous carbon as a high efficient electrocatalyst for oxygen reduction reaction](#)

10:50 to 11:10

Coffee Break

---

## Symposium 10: Electrochemical Technology: New Challenges for a More Competitive Economy

---

**Room : 101B**

*Chaired by:* Juan Manuel Peralta-Hernández and Carlos Ponce de Leon

09:30 to 10:10 Keynote

**Geoff Kelsall** (Department of Chemical Engineering, Imperial College London, London, United Kingdom), Nick Farandos, Anna Hankin, Lisa Kleiminger

[Electrode Structural Effects on Solid Oxide Electrolyser Performance](#)

10:10 to 10:30

**Antonio de Lucas Consuegra** (Chemical Engineering, Castilla La Mancha, Ciudad Real, Spain), Jesús Gonzalez-Cobos, Victor Rico, Agustín Gonzalez-Elipe, Jose Luis Valverde

[Hydrogen production and storage by coupling of catalysis and electrochemistry](#)

10:30 to 10:50

**Jesus Iniesta** (Physical Chemistry and Institute of Electrochemistry, Alicante University, Alicante, Spain), Leticia Garcia-Cruz, Vicente Montiel, Conchi Ania

[Electrocatalytic properties of Cu-/Ni-loaded nanoporous carbons for the electrooxidation of alcohols](#)

10:50 to 11:10

Coffee Break

---

## Symposium 12: Physical Electrochemistry: Spectroscopic, Structural, and Theoretical Investigations of the Electrified Interface

---

**Room : 101C**

*Chaired by:* Aliaksandr Bandarenka and Ana Sofia Varela

09:30 to 09:50

**Enrique Herrero** (Instituto de Electroquímica, Universidad de Alicante, Alicante, Spain), Valentin Briega-Martos, Adolfo Ferre-Vilaplana

[Effect of Acetonitrile Adsorption on the ORR on Platinum Single Crystal Electrodes. A Combined Electrochemical, Spectroscopic and DFT Study](#)

09:50 to 10:10

**Ioannis Katsounaros** (Leiden Institute of Chemistry, Leiden Universiteit, Leiden, Netherlands), Pietro P. Lopes, Dusan Strmcnik, Andrew Gewirth, Marc T.M. Koper, Nenad M. Markovic

[Electrochemical Oxidation of Ammonia on Pt\(100\) in Alkaline Solutions](#)

10:10 to 10:30

**Jian-Feng Li** (Chemistry, Xiamen University, Xiamen, China), Chao-Yu Li, Jin-Chao Dong, Xi Jin

[Electrochemical Shell-Isolated Nanoparticle-Enhanced Raman Spectroscopy \(EC-SHINERS\)](#)

10:30 to 10:50

**Azhagurajan Mukkannan** (Frontier Institute for Interdisciplinary Sciences, Tohoku University, Sendai, Japan), Takashi Itoh

[Direct observation of electrochemical processes at single atomic layer: an advanced optical microscopy study](#)

10:50 to 11:10

Coffee Break

## Symposium 15: Electrochemical Engineering from a Quantum Description to the Plant Modeling: Experiments and Design across Length Scale

**Room : South Lounge**

*Chaired by:* Alejandro A. Franco

09:30 to 09:50 Invited

**Frédéric Sauvage** (Laboratoire de Réactivité et Chimie des Solides, CNRSUMR7314, Université de Picardie Jules Verne, Amiens, France)

[Solid electrolyte interphase formation in dye-sensitized solar cells: where experimental ends and modeling could start](#)

09:50 to 10:10 Invited

**Hye Jin Lee** (Chemistry, Kyungpook National University, Daegu, Korea)

[Electrochemistry with Nanobioconjugates and Soft Interfaces for Sensing Applications](#)

10:10 to 10:30

**Fadhila Sekli Belaidi** (Micro-Nano-Bio-Technologie, LAAS-CNRS, Toulouse, France), William Tiddi, Matthieu Polverel, Gabriel Lemercier, Venkata Suresh Reddy Vajrala, Dodzi Zigah, Neso Sojic, Jérôme Launay, Pierre Temple-Boyer, Stephane Arbault

[Arrays of Microwells Equipped with a Recessed Ring Nanoelectrode and a Disk Microelectrode for Nanoelectrochemistry Investigations](#)

10:30 to 10:50

**Ivan Kondov** (Steinbuch Centre for Computing, Karlsruhe Institute of Technology, Eggenstein-Leopoldshafen, Germany), Patrick Faubert, Claas Müller, Holger Reinecke

[Modelling, Simulation and Characterization of Electrocatalytic Oxygen Reduction on Cr-modified Ni Surfaces](#)

10:50 to 11:10

Coffee Break

## Symposium 16: Supramolecular Electrochemistry for Analysis, Medicine and Biological Sciences

**Room : 201D**

*Chaired by:* Chii-Wann Lin and Francesco Paolucci

09:30 to 09:50

**Renata Bilewicz** (Faculty of Chemistry, University of Warsaw, Warsaw, Poland), Ewa Nazaruk, Monika Szlezak, Ehud M. Landau

[Lyotropic cubic phase gels and nanoparticles for drug delivery: tuning drug diffusion and sustained release from the mesophase](#)

09:50 to 10:10

**Olga Swiech** (Faculty of Chemistry, University of Warsaw, Warsaw, Poland), Ewelina Kurowicka, Agata Krzak, Maciej Majdecki, Marcin Kruszewski, Renata Bilewicz

[Application of New Conjugate of Cyclodextrin and Lipoic Acid in pH-Sensitive, Multifunctional Drug Carriers](#)

10:10 to 10:50 Keynote

**Alexander Kuhn** (ENSCBP, University Bordeaux, Pessac, France), Thittaya Yutthalekha, Chularat Wattanakit, Yémima Bon Saint Côme, Veronique Lapeyre, Philippe A. Bopp, Matthias Heim, Sudarat Yadnum, Somkiat Nokbin, Chompunuch Warakulwit, Jumras Limtrakul

[Supramolecular Enantioselective Recognition at Mesoporous Chiral Metal Surfaces](#)

10:50 to 11:10

Coffee Break

# Tuesday, 6 October 2015 - Afternoon

## Symposium 1: New Directions in Analytical Electrochemistry

Room : 103

Chaired by: J. Justin Gooding; Yi-Tao Long

### 14:00 to 14:40 Keynote

**Osamu Niwa** (Biomedical Research Institute, National Institute of Advanced Industrial Sci. and Tech., Tsukuba, Japan), Dai Kato, Tomoyuki Kamata, Daiki Kato, Shunsuke Shiba, Shigeru Hirono, Eisuke Kuraya, Masashi Kunitake, Naoto Yamaguchi, Hiroshi Imaya

[Hybrid carbon film electrodes for electroanalytical applications](#)

### 14:40 to 15:00

**Andreas Lesch** (Laboratory of Physical and Analytical Electrochemistry, École Polytechnique Fédérale de Lausanne, Lausanne, Switzerland), Fernando Cortés-Salazar, Sunny Maye, Véronique Amstutz, Philippe Tacchini, Hubert Girault

[Nano-Hydrogel Modified Carbon Nanotubes Electrodes for Antioxidant Monitoring in Complex Samples](#)

### 15:00 to 15:20

**Shaneel Chandra** (School of Biological and Chemical Sciences, The University of the South Pacific, Suva, Fidji), Wycliff Tupiti

[Gold nanoparticles-modified physically small carbon sensors towards sensitive and selective As\(III\) detection in aquatic samples](#)

### 15:20 to 15:40

**Salvatore Daniele** (Molecular Sciences and Nanosystems, University Cà Foscari Venice, Venice, Italy), Alberto Citron, Dario Battistel, Carlo Bragato, Daniele Veclani

[Disk Shaped Platinum Nanoelectrodes with Unexpected High Surface Area for the Detection of Hydrogen Peroxide](#)

### 15:40 to 16:00

**Yukihiro Shintani** (School of Science and Engineering, Waseda University, Tokyo, Japan)

[All-solid-State pH Sensor utilizing Termination-controlled Boron-doped Diamond Surface as pH-sensitive/pH-less-sensitive Interface](#)

### 16:20 to 16:40

Coffee Break

### 16:40 to 17:00 Invited

**Jyh-Myng Zen** (Chemistry, National Chung Hsing University, Taichung, Taiwan)

[An Easily Applicable Green Method for Real Sample Analysis Based on Disposable Gas Sensor](#)

### 17:00 to 17:20

**Grzegorz Lisak** (Chemical Engineering, Process Chemistry Centre, Laboratory of Analytical Chemistry, Åbo Akademi, Åbo-Turku, Finland), Jingwen Cui, Sylwia Strzałkowska, Thomas Arnebrant, Tautgirdas Ruzgas, Johan Bobacka

[Analytical Applications of Paper and Textiles in Microfluidic Sampling and Sample Handling Integrated with Electrochemical Sensors](#)

### 17:20 to 17:40

**Christopher Brett** (Department of Chemistry, University of Coimbra, Coimbra, Portugal), Madalina M. Barsan, Melinda David, Monica Florescu

[Self-Assembled Layer-by-Layer Architectures for Electrochemical Sensors and Biosensors](#)

17:40 to 18:00

**Christian Andre Gunawan** (School of Chemistry, The University of New South Wales, Sydney, Australia),  
Richard Gondosiswanto, Mengchen Ge, Chuan Zhao

[Salt-on-a-chip: Miniaturized Ionic Liquid Systems](#)

18:00 to 18:20

**Mario Castaño-Álvarez** (R&D, Micrux Technologies, Oviedo, Spain), Ana Fernández-la-Villa, Diego F. Pozo-Ayuso, Jorge Elizalde, María Tijero

[Novel Microfluidic Electrochemical Sensors for Thin-Layer based Flow Analysis Systems](#)

TUESDAY PM

## Symposium 2: Electrochemical Aspects of Biological Systems: Theory, Experiment and Applications

**Room : 101D**

*Chaired by:* Damien Arrigan and Ross Milton

14:00 to 14:40 Keynote

**Lanqun Mao** (Institute of Chemistry, Chinese Academy of Sciences, Beijing, China)

[Enabling Bioelectrochemistry for In Vivo Analysis](#)

14:40 to 15:00

**Shen-Ming Chen** (Department of Chemical Engineering and Biotechnology, National Taipei University of Technology, Taiwan), Chelladurai Karuppiah, Rajkumar Devasenathipathy, Selvakumar Palanisamy, Verappan Mani

[Synthesis and Characterization of carbon based nanocomposites and its electrocatalytic activity towards biomolecules and hazardous pollutants](#)

15:00 to 15:20

**Nicolas Mano** (CRPP- UPR 8641, Bordeaux, Pessac, France), Anne Sophie Michardière, Cintia Mateo-Mateo, Sébastien Gounel, Isabelle Ly, Philippe Poulin

[Wet spun Bio-electronic fibers of imbricated enzymes and carbon nanotubes for efficient microelectrodes](#)

15:20 to 15:40

**Stéphane Arbault** (Institute of Molecular Sciences - CNRS, University of Bordeaux, PESSAC, France), Emmanuel Suraniti, Salem Ben-Amor, Pauline Landry, Michel Rigoulet, Eric Fontaine, Serge Bottari, Anne Devin, Neso Sojic, Nicolas Mano

[Monitoring Electrochemically the Early Events of Hydrogen Peroxide Production by Mitochondria](#)

15:40 to 16:00

**Libuse Trnkova** (Department of Chemistry, Faculty of Science, Masaryk University, Brno, Czech Republic), Iveta Pilarova

[DNA Heptamers with Different Central Trinucleotide Sequences Studied by Electrochemical and Spectral Methods](#)

16:00 to 16:20

**Ana Maria Oliveira-Brett** (Chemistry Department, University of Coimbra, University of Coimbra, Coimbra, Portugal), A.M. Chiorcea-Paquim, T.A. Enache

[Amyloid  \$\beta\$  Peptides Nanostructures: Voltammetric and Atomic Force Microscopy Characterization](#)

16:20 to 16:40

Coffee Break

16:40 to 16:50

**Alexandra Bondarenko** (Institut des sciences et ingénierie chimiques, Ecole polytechnique fédérale de Lausanne, Lausanne, Switzerland), Tzu-En Lin, Horst Pick, Andreas Lesch, Fernando Cortés-Salazar, Hubert Girault

[Scanning electrochemical microscopy of adherent melanoma cells: alive, fixed and permeabilized](#)



16:50 to 17:00

**Daliborka Jambrec** (Analytical Chemistry - Center for Electrochemical Sciences, Ruhr University Bochum, Bochum, Germany), Magdalena Gebala, Fabio La Mantia, Wolfgang Schuhmann

[Diving into the Mechanism of Potential-Assisted ssDNA Immobilization](#)

17:00 to 17:10

**Vera Essmann** (Analytical Chemistry - Center for Electrochemical Science, Ruhr-Universität Bochum, Bochum, Germany), Yasin Ugur Kayran, Daliborka Jambrec, Adrian Ruff, Stefanie Grützke, Wolfgang Schuhmann

[Facile optimization of gold nanostructures for high SERS intensity by means of bipolar electrochemistry](#)

17:10 to 17:20

**Karen Monsalve** (Bioenergetics and Protein Engineering, Mediterranean Institute of Microbiology-CNRS, Marseille, France), Alan Le Goff, Nicolas Mano, Cristina Gutierrez-Sanchez, Jean-Yves Lojou, Elisabeth Lojou

[H<sub>2</sub>/O<sub>2</sub> Biofuel Cells: Macro-structured Conductive Supports to Enhance Power Cell Performances](#)

17:20 to 17:30

**Shajahan Siraj** (Department of Chemistry and Biomolecular Sciences, Macquarie University, Sydney, Australia)

[Hydrogenated and 4-Sulfobenzene Modified Conical-tip Carbon Electrodes with Antifouling Property for Sensitive Detection of Dopamine](#)

17:30 to 17:40

**Bongkyu Kim** (School of Environmental Science and Engineering, Gwangju Institute of Science and Technology, Gwangju, Korea), Yooseok Lee, Jisu Kim, In Seop Chang

[Commercialization Strategies of Microbial Fuel Cells: Prevention of Voltage reversal in Stackable Approach](#)

17:40 to 17:50

**Rachel Gao** (Chemistry, University of Southampton, Southampton, United Kingdom), Sarah A. Goodchild, Philip Bartlett

[Anthraquinone Labelled DNA for Direct Detection and Discrimination of Closely Related DNA Targets](#)

17:50 to 18:00

**Chun-Hao Su** (Department of Chemical Engineering, National Taiwan University, Taipei, Taiwan), Chung-Wei Kung, Kuo-Chuan Ho, Ying-Chih Liao

[Fabrication of Uniform Metal-organic Framework Thin Film via Inkjet Printing Technology and its Application as a Nitrite Sensor](#)

18:00 to 18:10

**Yung-Chun Lin** (Chemistry, University of Southampton, Southampton, United Kingdom), James Richardson, Tom Brown, Philip Bartlett

[Surface-Enhanced Raman Spectroscopic study of a DNA Beacon Probe Immobilized at a Au Electrode](#)

18:10 to 18:20

**Xiaochun Tian** (College of Chemistry & Chemical Engineering, Xiamen University, Xiamen, China), Ranran Wu, Zhiyong Zheng, Feng Zhao, Yan-Xia Jiang, Shi-Gang Sun

[Electron Transfer effect on the Bioluminescence of Shewanella Woodyi](#)

18:20 to 18:30

**Makoto Togami** (Graduate School of Science and Technology, Kumamoto University, Kumamoto, Japan), Aiko Sasaki, Masato Tominaga

[Acceleration of Laccase Bioelectrocatalysis at Carbon Nanotube Interface Modified with Steroid-Type Biosurfactants](#)

## Symposium 3: Batteries for Tomorrow's World

Room : 201AB

Chaired by: Minoru Inaba

14:00 to 14:20 Invited

**Takeshi Abe** (Graduate School of Engineering, Kyoto University, Kyoto, Japan), Shohei Maruyama, Kohei Miyazaki

[Rate Determining Factors at Graphite Electrodes- from charge transfer resistances to ion transport resistances -](#)

14:20 to 14:40 Invited

**M. V. Reddy** (Materials Science & Engg and Physics, National University of Singapore, Singapore, Singapore)

[Novel V-containing cathode materials for Li-ion Batteries](#)

14:40 to 15:00

**Shuji Ding** (Department of Applied Chemistry, Xi'an Jiaotong University, Xi'an, China)

[The Design and Preparation of Multi-dimensional Nanostructured Materials and electrochemical storage](#)

15:00 to 15:20

**Alejandro A. Franco** (Laboratoire de Réactivité et Chimie de Solides (LRCS), Université de Picardie Jules Verne & CNRS, Amiens, France), Garima Shukla, Matias A. Quiroga, Kan-Hao Xue, Trong-Khoa Nguyen, Guillaume Blanquer, Yinghui Yin

[Computational data mining to boost the next generation batteries R&D: the composite electrode architecture](#)

15:20 to 15:40

**Andrzej Lewandowski** (Faculty of Chemical Technology, Poznan University of Technology, Poznan, Poland)

[Li-ion battery operation limits](#)

15:40 to 16:00

**Alexandre Ponrouch** (QES, ICMAB-CSIC, Bellaterra, Spain), Carlos Frontera, Fanny Bardé, M. Rosa Palacín

[Towards a rechargeable battery technology based on calcium](#)

16:00 to 16:20

**Kolja Beltrop** (MEET Battery Research Centre, WWU, University of Münster, Münster, Germany), Martin Winter, Tobias Placke

[Does Size really Matter? New Insights into the Intercalation Behavior of Anions into a Graphite Based Positive Electrode](#)

16:20 to 16:40

Coffee Break

16:40 to 17:20 Keynote

**Atsuo Yamada** (Department of Chemical System Engineering, The University of Tokyo, Tokyo, Japan), Masashi Okubo, Prabeer Barpanda, Shin-ichi Nishimura, Sai-Cheong Chung, Gosuke Oyama, Yuya Suzuki

[Alluaudite  \$\text{Na}\_{2+2x}\text{Fe}\_{2-x}\(\text{SO}\_4\)\_3\$  as 3.8 V Sodium Battery Cathode](#)

17:20 to 17:40 Invited

**Shirley Meng** (Sustainable Power and Energy Center, University of California San Diego, La Jolla, USA), Chuze Ma, Judith Alvarado, Jing Xu, Haodong Liu

[Designing and optimizing novel electrode materials for rechargeable Na-ion batteries with high energy and low cost](#)

17:40 to 18:00

**Jie Li** (MEET Battery Research Center/Institute of Physical Chemistry, University of Muenster, Muenster, Germany), Jun Wang, Xin He, Haidong Liu, Tim Risthaus, Tim Risthaus

[Synthesis and electrochemistry performance of  \$\text{Na}\[\text{FeTi}\]\text{O}\_4\$  as anode material for sodium-ion batteries](#)

18:00 to 18:20

**Ha-Kyung Roh** (Department of Material Science and Engineering, Yonsei University, Seoul, Korea), Hyun-Kyung Kim, Myeong-Seong Kim, Kwang Chul Roh

[One-pot synthesis of NaTi<sub>2</sub>\(PO<sub>4</sub>\)<sub>3</sub>/rGO nanocomposite for sodium-ion batteries](#)

18:20 to 18:40

**Masashi Okubo** (Department of Chemical System Engineering, The University of Tokyo, Tokyo, Japan), Satoshi Kajiyama, Xianfen Wang, Hiroki Inuma, Ryohei Morita, Kazuma Gotoh, Atsuo Yamada

[Flexible MXene Nanosheets: Negative Electrode Materials for Lithium-Ion and Sodium-Ion Batteries](#)

---

## Symposium 3: Batteries for Tomorrow's World

---

**Room : 201C**

*Chaired by:* Xuejie Huang

14:00 to 14:20 Invited

**Yi Cui** (Department of Materials Science and Engineering, Stanford University, Stanford, USA)

[Materials Design for Lithium-Sulfur Batteries](#)

14:20 to 14:40

**Dauren Batyrbekuly** (Institute of Batteries, Institute of Batteries, Astana, Kazakhstan), Almagul Mentbayeva, Yongguang Zhang, Indira Kurmanbayeva, Kuralay Korzhynbayeva

[Reinforced composite gel-polymer electrolytes for lithium-sulfur batteries](#)

14:40 to 15:00

**Xiaogang Zhang** (College of Material Science and Engineering, Nanjing University of Aeronautics and Astronautics, Nanjing, China), Guiyin Xu, Bing Ding, Hui Dou, Ping Nie, Jin Pan

[Insights into the Absorption Mechanism of Carbon Nanotube Paper-Titanium Dioxide as a Multifunctional Barrier for Lithium-Sulfur Batteries](#)

15:00 to 15:20

**Almagul Mentbayeva** (Institute of Batteries, Institute of Batteries, Nazarbayev University, Astana, Kazakhstan), Aishuak Konarov, Ayaulym Belgibayeva, Toru Hara, Nurzhan Umirov, Zagipa Bakenova

[Free standing sulfur-composite cathode for lithium-sulfur batteries](#)

15:20 to 15:40

**Heng-Liang Wu** (Department of Chemistry, University of Illinois Urbana-Champaign, Urbana, USA), Laura A. Huff, Andrew Gewirth

[In-situ Raman Spectroscopy and EQCM study of Lithium-Sulfur Batteries](#)

15:40 to 16:00

**Jason Fang** (Material and Chemical Research Laboratories, Industrial Technology Research Institute, Hsinchu, Taiwan)

[A High Energy, Long-life Li-S Battery Enabled by Mille-Feuille Structure Electrode](#)

16:00 to 16:20

**Matthew Lacey** (Department of Chemistry - Ångström Laboratory, Uppsala University, Uppsala, Sweden), Anurag Yalamanchili, Viking Oesterlund, Fabian Jeschull, Julia Maibach, Carl Tengstedt, Kristina Edström, Daniel Brandell

[Self-Discharge and Cycling Stability in the Li-S System: Where Every Cell Component Plays a Role](#)

16:20 to 16:40

Coffee Break

16:40 to 17:00 Invited

**Yong Yang** (Chemistry, Xiamen University, Xiamen, China), Sihui Wang, Xuehang Wu, Shouding Li, Jianghuai Guo, Yixiao Li

[Enhancing electrochemical performance of layered oxide cathode materials for Li/Na ion batteries](#)

17:00 to 17:20

**Yuebin Yang** (Department of Chemical and Biomolecular Engineering, The Hong Kong University of Science and Technology, Hong Kong, China), Hui Xu

[Carbonized Polydopamine/Sulfur Composite with One-Dimensional Structure for High Performance Lithium Sulfur Batteries](#)

17:20 to 17:40

**Elie Paillard** (Helmholtz Institute Muenster, Forschungszentrum Juelich, Muenster, Germany), Lorenzo Grande, Marija Kirchhöfer, Irene Osada, Stephan Koch, Stefano Passerini

[Ionic Liquids and Polymer Electrolytes for Li-metal Batteries](#)

17:40 to 18:00

**Nadège Bonnet-Mercier** (Byon Initiative Research Unit (IRU), RIKEN, Wakoshi, Japan), Raymond Wong, Hye Ryung Byon

[Understanding Na-O<sub>2</sub> Electrochemistry in Non-aqueous Na-O<sub>2</sub> Batteries](#)

18:00 to 18:20

**Satoshi Fujiki** (AR-3, Samsung R&D Institute Japan, 2-1-11, Semba Nishi, Minoh City, Japan)

[Development of a high energy density sulfide-based all-solid-state battery](#)

---

## Symposium 5: Novel Insights to Electrochemical Capacitors

---

**Room : 101A**

*Chaired by:* Masayuki Morita, Soo-Gil Park, Patrice Simon and Wataru Sugimoto

14:00 to 14:20

**Etsuro Iwama** (Applied Chemistry, Tokyo University of Agriculture and Technology, Tokyo, Japan), Takumi Furuhashi, Yuta Abe, Keita Okazaki, Shintaro Aoyagi, Junichi Miyamoto, Wako Naoi, Katsuhiko Naoi

[Ultrafast Electrochemical Characteristics of nc-TiO<sub>2</sub> \(B\)/Nanocarbon Composites for Hybrid Capacitor System](#)

14:20 to 14:40

**Wan-Yu Tsai** (CIRIMAT, Université Paul Sabatier, Toulouse, France), John M. Griffin, Alexander C. Forse, Clare P. Grey, Pierre-Louis Taberna, Patrice Simon

[In-situ Electrochemical Quartz Crystal Microbalance \(EQCM\) Study of Ion Dynamics and Charge Storage Mechanism for Supercapacitors](#)

14:40 to 15:00

**Tu-Ting Weng** (Department of Chemical Engineering, National Taiwan University, Taipei, Taiwan), H.A. Pan, R. C. Lee, T.Y. Huang, Y. Chu, J.F. Lee, H.S. Sheu, Nae-Lih Wu

[Spatially Confined MnO<sub>2</sub> Nanostructure Enabling Long-Term Reversible Two-Electron Transfer in Mixed Pseudocapacitor-Battery Electrode](#)

15:00 to 15:20

**Chung-Ting Tsai** (Research and Development, China Steel Chemical Corporation, Kaohsiung, Taiwan), Jing-Mei Li, Chi-Shyan Mai, Sen-Tsan Shen, Ming-Da Fang

[The influence of Pore Size Distribution and surface area both are analyzed by QSDFT on capacitance and ESR of EDLC consists of activated carbon from coal tar pitch](#)

15:20 to 15:40

**Krzysztof Fic** (Institute of Chemistry and Technical Electrochemistry, Poznan University of Technology, Poznan, Poland), Jakub Menzel, Elzbieta Frackowiak

[Faradaic and Non-faradaic Interactions at the Electrode/Electrolyte Interface in Electrochemical Capacitors](#)

15:40 to 16:00

**Laura Coustan** (ICGM-AIME, Institut Charles Gerhardt, UMR 5253 CNRS, Université Montpellier, Montpellier, France), Vanessa Armel, Frederic Jaouen, Frédéric Favier

[Metal Organic Frameworks as precursors of porous carbon materials for supercapacitor applications](#)

16:00 to 16:20

**Pawel Jezowski** (Institute of Chemistry and Technical Electrochemistry, Poznan University of Technology, Poznan, Poland), Olivier Crosnier, Thierry Brousse, François Béguin

[New materials for in-situ pre-lithiation of the graphite anode in lithium ion capacitor](#)

16:20 to 16:40

Coffee Break

16:40 to 17:00 Invited

**Yongyao Xia** (Chemistry, Fudan University, Shanghai, China), Yanfang Song, Dandan Zhou

[Nitrogen-doped Mesoporous Carbon for Supercapacitor Application](#)

17:00 to 17:20 Invited

**Frédéric Favier** (Institut Charles Gerhardt Montpellier, UMR 5253 CNRS Université de Montpellier, Montpellier, France), Peng-Cheng Gao, Laura Coustan, Wan-Yu Tsai, Carlos Pérez, Patricia Russo, Yury Gogotsi, Nicola Pinna, Patrice Simon

[Graphene-based Electrochemical Capacitors](#)

17:20 to 17:40 Invited

**Soo-Gil Park** (Industrial Engineering Chemistry, Chungbuk National University, Cheongju, Korea), Joeng-Jin Yang, Han-Joo Kim, Young-Jae Yuk

[Electrochemical Characteristics of Composite Materials as Carbon & Metal Oxide for Hybrid Capacitor](#)

17:40 to 18:00 Invited

**Soshi Shiraishi** (Gunma University, Graduate School of Science and Technology, Kiryu, Japan), Yasuyoshi Shiraishi, Hiroyuki Fujimoto

[Graphite-Fluoride Lithium Hybrid Capacitor](#)

18:00 to 18:20 Invited

**Jong-Huy Kim** (Energy Storage Research Lab., Korea Institute of Energy Research, Daejeon, Korea), Young-Joon Oh, Jung-Joon Yoo, Yong-Il Kim, Jae-Kook Yoon

[Oxygen Functional Groups of Incompletely Reduced Graphene Oxides for a Thin-film Electrode of Supercapacitor](#)

18:20 to 18:40

**JunHui Jeong** (Material Science and Engineering, Yonsei Univ., Seoul, Korea), Hyun-Kyung Kim, Suk-Woo Lee

[Fabrication of Graphene Microspheres for High Performance Supercapacitor Applications](#)

## Symposium 8: Corrosion and Passivity

Room : 201D

Chaired by: Dirk Engelberg and Shinji Fujimoto

14:00 to 14:20

**Oliver Chyan** (Department of Chemistry, University of North Texas, Denton, USA)

[Micro-pattern Corrosion Screening on Bimetallic Corrosion for Microelectronic Application](#)

14:20 to 14:40

**Jun-Seob Lee** (Graduate School of Chemical Sciences and Engineering, Hokkaido University, Sapporo, Japan), Yuichi Kitagawa, Takayuki Nakanishi, Yasuchika Hasegawa, Koji Fushimi

[Passivation Behavior of Type-316L Stainless Steel in the Presence of Hydrogen Sulfide Ions Generated from Liquid-Phase Ion Gun](#)

14:40 to 15:00

**Peter Keech** (Nuclear Waste Management Organization, Toronto, Canada), Sridhar Ramamurthy, Rachel Partovi-Nia, Jian Chen, Rebecca Jacklin, David Shoesmith

[Copper Coatings for Used Nuclear Fuel Containers: Corrosion Testing](#)

15:00 to 15:20

**Xavier Feaugas** (La Rochelle University, LaSIE UMR 7356 CNRS, La Rochelle University, La Rochelle, France), Niusha Shakibi Nia, Matthieu Lagarde, Juan Creus, Catherine Savall

[Electrochemical behavior of electrodeposited Ni-W nanostructured alloys](#)

15:20 to 15:40

**Delphine Veys-Renaux** (Institut Jean Lamour, Université de Lorraine, CNRS, Vandoeuvre les Nancy, France), Emmanuel Rocca, Nouha M'hiri, Solenn Reguer, Irina Ioannou, Mohammed Ghoul

[Corrosion inhibition of steel by flavonoid model molecules: naringin, neohesperidin, rutin](#)

15:40 to 16:20 Keynote

**Hans-Henning Strehblow** (Institute of Physical Chemistry, Heinrich-Heine-Universitaet-Duesseldorf, Duesseldorf, Germany)

[The Investigation of Passivity of Metals Studied by Surface Analytical Methods, a Review](#)

16:20 to 16:40

Coffee Break

16:40 to 17:00 Invited

**Nadine Pebere** (CIRIMAT, CNRS, Toulouse, France), Fatah Chiter, Corinne Lacaze-Dufaure, Sabrina Marcelin, Hao Tang

[Corrosion Inhibition of Pure Aluminium by 8-Hydroxyquinoline: Combined Electrochemical and DFT Studies](#)

17:00 to 17:20

**I-Wen Huang** (Materials Science and Engineering, The Ohio State University, Columbus, USA), Rudolph Buchheit

[Assessing Uniform Corrosion of Aluminum Alloys 2024-T3, 6061-T6, and 7075-T6 in Aqueous Immersion Conditions](#)

17:20 to 17:40

**Hiroaki Tsuchiya** (Division of Materials and Manufacturing Science, Osaka University, 2-1 Yamada-oka, Suita, Japan), Min-Su Kim, Toshiaki Erami, Yuki Otani, Shinji Fujimoto

[Alloy Anodization in Fluoride-Containing Electrolytes](#)

17:40 to 18:00 Invited

**Koji Fushimi** (Faculty of Engineering, Hokkaido University, Sapporo, Japan), Haruya Ikeyama, Yuichi Kitagawa, Takayuki Nakanishi, Yasuchika Hasegawa, Mikito Ueda, Toshiaki Ohtsuka

[Photo-electrochemical Degradation of Anodized Titanium Surface Observed using EIS and Ellipso-microscopy](#)

18:00 to 18:20

**Khurram Shahzad** (Graduate School of Chemical Sciences and Engineering, Hokkaido University, Sapporo, Japan)

[Influence of water concentration on growth efficiency of barrier-type anodic film on magnesium](#)

18:20 to 18:40

**Pei-Yu Lai** (Materials Science and Engineering, National Taiwan University of Science and Technology, Taipei, Taiwan), Jinn P. Chu, Bing-Joe Hwang

[Metallic Glass Coatings for Aluminum Current Collectors – Corrosion Inhibition](#)

---

## Symposium 9: Electrocatalytic Materials

---

Room : 201EF

*Chaired by:* Kensaku Kodama, Dangsheng Su, Sandra Temmel and Jong-Sung Yu

14:00 to 14:20 Invited

**Dangsheng Su** (Shenyang National Laboratory for Materials Science, Institute of Metal Research, Chinese Academy of Science, Shenyang, China)

[Investigation of the Structure of Fe–N–C Complexes for Oxygen Reduction Reactions](#)

14:20 to 14:40

**Kamiya Kazuhide** (Department of Applied Chemistry, The University of Tokyo, Tokyo, Japan), Ryo Kamai, Kazuhito Hashimoto, Shuji Nakanishi

[Platinum-modified Covalent Triazine Frameworks as Methanol-tolerant Oxygen Reduction Electrocatalysts](#)

14:40 to 15:00

**Deli Wang** (School of Chemistry and Chemical Engineering, Huazhong University of Science and Technology, Wuhan, China), Jing Zhu, Sufen Liu, Jie Wang, Zexing Wu

[Novel Structured Pt-Based Intermetallic Electrocatalysts for ORR](#)

15:00 to 15:20

**Bart Geboes** (Research Group Advanced Reactor Technology (ART), University of Antwerp, Antwerp, Belgium), Jon Ustarroz, Kadir Sentosun, Sara Bals, Annick Hubin, Tom Breugelmans

[Activity and Stability of Electrodeposited Nanoporous Catalysts towards the Oxygen Reduction Reaction](#)

15:20 to 15:40

**Ifan Stephens** (Physics, Technical University of Denmark, Kongens Lyngby, Denmark), Maria Escudero-Escribano, Ulrik Grønbjerg, Vladimir Tripkovic, Jakob Schiøtz, Jan Rossmeisl, Ib Chorkendorff

[Tuning the activity and stability of Pt for oxygen reduction by means of the lanthanide contraction](#)

15:40 to 16:00

**Silver Sepp** (Institute of Chemistry, University of Tartu, Tartu, Estonia), Jaak Nerut, Kersti Vaarmets, Indrek Tallo, Enn Lust

[Performance of PEMFC Half Cells Prepared Using Hierarchical Microporous-Macroporous Carbon Supported Pt-Catalyst](#)

16:20 to 16:40

Coffee Break

16:40 to 17:00

**Sandra Temmel** (General Energy Department, ETH Zürich/ Paul-Scherrer-Institute, Villigen, Switzerland), Emiliana Fabbri, Daniele Pergolesi, Thomas Lippert, Thomas Justus Schmidt

[Investigation of ORR activity of strained thin film Pt electrocatalyst produced by pulsed laser deposition](#)

17:00 to 17:20

**Kensaku Kodama** (Fuel Cell System Laboratory, Toyota Central R&D Labs. Inc., Nagakute, Japan), Ryosuke Jinnouchi, Naoko Takahashi, Hajime Murata, Yu Morimoto

[ORR activities of Au-Modified Stepped Pt Single Crystal Electrodes](#)



17:20 to 17:40

**Qingli Hao** (School of Chemical Engineering, Nanjing University of Science and Technology, Nanjing, China),  
Wu Lei, Lei Lu, Xifeng Xia

[Synthesis of CoFe<sub>2</sub>O<sub>4</sub>/ Nitrogen-doped Graphene and its Catalytic Performance for ORR](#)

17:40 to 18:00

**Gert Göransson** (Department of Chemistry and Molecular Biology, University of Gothenburg, Gothenburg, Sweden), Elisabet Ahlberg, Alexander Björling

[A study of the Formation of Co<sub>1-x</sub>Fe<sub>x</sub>S<sub>2</sub> in Microwave Synthesis and its Electrocatalytic Properties towards Oxygen Reduction and Hydrogen Evolution](#)

18:00 to 18:20

**Adriano Gomes** (Department of Chemistry and Molecular Biology, University of Gothenburg, Gothenburg, Sweden), Zareen Abbas, Nina Simic, Mats Wildlock, Elisabet Ahlberg

[Electrochemical Water Reduction in Highly Concentrated Electrolytes: Theory and Experiments](#)

18:20 to 18:40

**Pawel J. Kulesza** (Department of Chemistry, University of Warsaw, Warsaw, Poland)

[Development and Characterization of Nanostructured Multifunctional Materials for Photoelectrochemical and Electrocatalytic Reduction of Carbon Dioxide and Water Splitting](#)

---

## Symposium 10: Electrochemical Technology: New Challenges for a More Competitive Economy

---

**Room : 101B**

*Chaired by:* Ignacio González and Ricardo Salazar

14:00 to 14:20 Invited

**Javier Llanos** (Department of Chemical Engineering, University of Castilla-la Mancha, Ciudad Real, Spain), Sabri Kalkan, Alexandra Raschitor, Bahadır K. Körbahti, Pablo Cañizares, Manuel Andres Rodrigo

[Development of Reactive Ion Exchange Membranes for Electro-Disinfection](#)

14:20 to 14:40

**Henry Bergmann** (FB 6 & 7, Anhalt University, Köthen/Anh., Germany), Wido Schmidt, Jens Hartmann

[On the necessity of field studies for direct electrochemical drinking water disinfection](#)

14:40 to 15:00 Invited

**Onofrio Scialdone** (Dipartimento di ingegneria chimica, gestionale, informatica, Università degli Studi di Palermo, Palermo, Italy), Adriana D'Angelo, Alessandro Galia, Simona Sabatino, Fabrizio Vicari

[Abatement of pollutants in water by different electrochemical approaches](#)

15:00 to 15:20

**Emmanuel Mousset** (Civil and Environmental Engineering, National University of Singapore (NUS), Singapore, Singapore), Zuxin Wang, Olivier Lefebvre

[Towards a More Competitive Advanced Electrochemical Technology: New Carbon-Based Electrodes Combination for Wastewater Treatment](#)

15:20 to 15:40

**Tsuyoshi Ochiai** (Photocatalyst Group, Kanagawa Academy of Science and Technology, Kawasaki, Japan), Mio Hayashi, Shoko Tago, Kazuo Hirota, Takeshi Kondo, Kazuhito Satomura, Akira Fujishima

[Flexible Pinpoint Electrolysis Unit by Using of Boron-doped Diamond Powder \(BDDP\) Based Polymer Composites for Dental Treatments](#)

15:40 to 16:00 Invited

**Philippe Vernoux** (IRCELYON, CNRS, Villeurbanne, France)

[Electrochemical activation of environmental catalysis](#)



16:00 to 16:20

**Carlos Alberto Martinez-Huitle** (Institute of Chemistry, Federal University of Rio Grande do Norte, NATAL, Brazil), Ana S. dos Santos Fajardo, Maiara Barbosa Ferreira, Rui C. Martins, Djalma Ribeiro da Silva, Rosa M. Quinta-Ferreira

[Electrochemical Sequential Flow Reactors for removing Textile Dyes Using Different Anodes](#)

16:20 to 16:40

Coffee Break

16:40 to 17:00 Invited

**Takayuki Homma** (Applied Chemistry, Waseda University, Tokyo, Japan), Yingying Sun, Masahiro Kunimoto, Mikiko Saito, Masahiro Yanagisawa

[In situ Analysis of Electrochemical Fabrication Processes Using Raman Spectroscopy with Plasmonic Sensors](#)

17:00 to 17:20

**Priscilla Baker** (Chemistry, University of the Western Cape, Bellville, South Africa), Meryck Ward, Euodia Hess, Stephen Mailu, Christopher Sunday, Milua Masikini, Emmanuel Iwuoha

[Electrochemical protocols for measurement of polycyclic aromatic hydrocarbons in environmental samples](#)

17:20 to 17:40

**Nick Daems** (Centre for Surface Chemistry and Catalysis, K.U. Leuven, Heverlee, Belgium), Jonatan Wouters, Ivo Vankelecom, Paolo Pescarmona

[Non-noble metal-containing doped graphitic carbons as electrocatalysts for the cogeneration of electricity and aniline.](#)

17:40 to 18:00

**Geir Martin Haarberg** (Materials Science and Engineering, Norwegian University of Science and Technology, Trondheim, Norway), Junli Xu

[Sustainable Electrolysis for Electrowinning and Electrorefining of Metals in Molten Salts and Aqueous Electrolytes](#)

18:00 to 18:20

**Tom Breugelmans** (Research group Advanced Reactor Technology (ART), University of Antwerp, Hoboken, Belgium), Bart Vanrenterghem, Bart Geboes, Jon Ustarroz, Sara Bals, Annick Hubin

[Influence of the morphology of electrodeposited nanoparticles on their activity for the cyclisation reaction of allyl 2-bromobenzyl](#)

18:20 to 18:40

**Carmen Maria Fernandez Marchante** (Chemical Engineering, University of Castilla La Mancha, Ciudad Real, Spain), Yeray Asensio, Eduardo Penteado, Iciar Begoña Montes, Marcelo Zaiat, Justo Lobato, Pablo Cañizares, Ernesto Gonzalez, Manuel Andres Rodrigo

[Influence of electrode material on microbial fuel cell treating a synthetic and a winery wastewater](#)

## Symposium 12: Physical Electrochemistry: Spectroscopic, Structural, and Theoretical Investigations of the Electrified Interface

**Room : 101C**

*Chaired by:* Federico Calle-Vallejo, Axel Gross, Katharina Krischer, Jan Rossmeisl

14:00 to 14:40 Keynote Invited

**Jan Rossmeisl** (Department of Chemistry, University of Copenhagen, København, Denmark)

[Special Sites in Electrocatalysis](#)

14:40 to 15:00

**Katharina Krischer** (Physik-Department, Technische Universität München, Garching bei München, Germany), Philipp Bauer, Munir Salman, Antoine Bonnefont

[Peculiar Excitation Waves during CO Electrooxidation on Pt Electrodes in an Electrochemical Flow Cell](#)

15:00 to 15:20 Invited

**Aliaksandr Bandarenka** (Department of Physics, Technische Universität München, Garching, Germany)

[Oxygen Electroreduction at Non-uniform Pt Surfaces: From Model Electrodes to Nanostructured Catalysts](#)

15:20 to 15:40 Invited

**Federico Calle-Vallejo** (Laboratoire de Chimie, ENS Lyon, Lyon, France), Jakub Timoczko, Viktor Colic, Quang Huy Vu, Marcus D. Pohl, Karina Morgenstern, David Loffreda, Philippe Sautet, Wolfgang Schuhmann, Aliaksandr Bandarenka

[Designing Better Electrocatalysts by Simply Counting Surface nearest Neighbors](#)

15:40 to 16:00

**Ali Malek** (Department of Chemistry, Simon Fraser University, Burnaby, Canada), Mohammad J. Eslamibidgoli, Michael Eikerling

[DFT Study of Surface Charging Effects on Oxygen Covered Pt\(111\)](#)

16:20 to 16:40

Coffee Break

16:40 to 17:00

**Sara Panahian Jand** (Institut für Chemie und Biochemie, Freie Universität Berlin, Berlin, Germany), Payam Kaghazchi

[Theoretical Simulation of Solid Electrolyte Interphases](#)

17:00 to 17:20

**Qingli Zou** (Mechanical and Automation Engineering, The Chinese University of Hong Kong, Shatin, Hong Kong, China), Yi-Chun Lu

[Influence of Electrolyte on Sulfur Redox Reactions: Combined RRDE and in situ UV-VIS Studies](#)

17:20 to 17:40

**Shen Ye** (Catalysis Research Center, Hokkaido University, Sapporo, Japan), Yu Qiao

[In-situ Study of Oxygen Reduction in DMSO Solution](#)

17:40 to 18:00

**Ove Oll** (Institute of Chemistry, University of Tartu, Tartu, Estonia), Tavo Romann, Enn Lust

[An Infrared Study of the Few-Layer Graphene | Ionic Liquid Interface: Correlation between Electronic and Ionic Surface Structure](#)

18:00 to 18:20

**Matej Velicky** (School of Chemistry, University of Manchester, Manchester, United Kingdom), Peter S. Toth, Mark A. Bissett, Ian A. Kinloch, Konstantin S. Novoselov, Robert A.W. Dryfe

[Electrochemistry of Two-Dimensional Materials](#)

18:20 to 18:40

**Katsuyoshi Ikeda** (Graduate School of Engineering, Nagoya Institute of Technology, Nagoya, Japan)

[Surface enhanced Raman observation of molecular adsorbates on atomic local surface sites](#)

## Symposium 15: Electrochemical Engineering from a Quantum Description to the Plant Modeling: Experiments and Design across Length Scale

**Room : 102**

*Chaired by:* Jaeyoung Lee

14:00 to 14:40 Keynote Invited

**Bongjin Simon Mun** (Gwangju Institute of Science and Technology, Gwangju, Korea)

[Development of Ambient Pressure XPS and its Applications to Electrochemistry](#)

14:40 to 15:00

**Byungchan Han** (Chemical and Biomolecular Engineering, Yonsei university, Seoul, Korea), Seunghyo Noh

[Multi-scale Computational Design of Multi-functional Catalyst Materials for Fuel Cells Beyond Conventional Bulk Pt](#)

15:00 to 15:20

**Guadalupe Ramos-Sanchez** (Departamento de Química, Universidad Autónoma Metropolitana, Mexico City, Mexico)

[A multi-scale model to account for the electrochemical response of the oxygen reduction reaction on highly active graphene nanosheets in alkaline conditions](#)

15:20 to 15:40 Invited

**Trung Van Nguyen** (Chemical and Petroleum Engineering, University of Kansas, Lawrence, USA)

[Water Management in Proton Exchange Membrane Fuel Cells by Materials Design and Engineering](#)

15:40 to 16:20 Keynote

**Tetsuya Mashio** (Research Division, Nissan Motor Co., Ltd., Yokosuka, Japan), Atsushi Ohma, Takashi Tokumasu

[Analysis of PEMFC Catalyst Layers from Fabrication Process to Performance](#)

16:20 to 16:40

Coffee Break

16:40 to 17:00

**Daniel Brandell** (Department of Chemistry, Uppsala University, Uppsala, Sweden), Shruti Srivastav, Matthew Lacey

[Combined Finite Element Modelling and EIS Studies for SoC Indication in Rechargeable Li-Ion Batteries](#)

17:00 to 17:20 Invited

**Christine Frayret** (UFR des Sciences, LRCS-CNRS UMR 7314, Université de Picardie Jules Verne, Amiens, France), Daniele Tomerini, Carlo Gatti, Yann Danten

[Catalyzing Innovation in Organic Battery Electrodes from Computational Modelling](#)

17:20 to 17:40 Invited

**Payam Kaghazchi** (Physikalische und Theoretische Chemie, Freie Universität Berlin, Berlin, Germany)

[Theoretical Study of Lithium-Sulfur Battery Cathodes](#)

17:40 to 18:00

**Yinghui Yin** (Laboratoire de Réactivité et Chimie des Solides (LRCS), Université de Picardie Jules Verne & CNRS, Amiens, France), Guillaume Blanquer, Matias A. Quiroga, Alejandro A. Franco

[Boosting Lithium Air Batteries from a Multiscale Modeling Approach](#)

18:00 to 18:20

**Seunghwa Lee** (School of Environmental Science and Engineering, Gwangju Institute of Science and Technology, Gwangju, Korea), Hansaem Jang, Jaeyoung Lee

[The pH Effect on the Electrochemical Reduction of Carbonate Species over Metal Oxide Electrodes](#)

18:20 to 18:40

**Hyungjun Kim** (Graduate School of EEWS, Korea Advanced Institute of Science and Technology, Daejeon, Korea), Hyung-Kyu Lim, Hyeyoung Shin

[Toward efficient electrochemical conversion of CO<sub>2</sub>: catalyst design accelerated by simulation-based screening](#)

Wednesday, 7 October 2015

ROOMS:	101A	101B	101C	101D	102	103	201AB	201EF	201C	201D
	101A	101B	101C	101D	102	103	201AB	201EF	201C	201D
SYMPOSIUM	s05	s10	s07	s02	s04	s01	s03	s09	s03	s08
08:15 - 09:15	Plenary Lecture: Li-Jun Wan (Plenary Hall)									
09:30 - 09:50	Thierry Brousse	C. Ponce de Leon	Chih Chen	Y. Takahashi	Eiichi Yasumoto	J. Justin Gooding	Claude Delmas	Lin Zhuang	Fridolin Röder	Bernard Tribollet
09:50 - 10:10		Mitsuru Wakisaka		Ming-Chang Yang	Tae-Hyun Yang				Fabian Jeschull	
10:10 - 10:30	Andrea Balducci	Min-Hsin Yeh	Rohan Akolkar	Woonsup Shin	Michael Fleige	Emmanuel Iwuoha	Shou-Yu Shen	Junliang Zhang	Po-Han Lee	Yu-Min Chen
10:30 - 10:50	Sonia Dsoke	Laura Valero	Atsushi Kitada		Hiroki Habazaki	Sabine Szunerits	Shinya Suzuki	Wei Xing	Nan Lin	Sara Munktel
10:50 - 11:10	Coffee Break									
11:10 - 11:30										
11:30 - 11:50										
11:50 - 12:10										
12:10 - 12:30										

# Wednesday, 7 October 2015 - Morning

---

## Plenary Lecture

Room : Plenary Hall

*Chaired by:* Zhong-Qun Tian

08:15 to 09:15

**Li-Jun Wan** (Institute of Chemistry, Chinese Academy of Sciences, Beijing, China)

[Nanomaterials for Energy Conversion and Storage: Structure Design and In-Situ Monitoring](#)

---

## Symposium 1: New Directions in Analytical Electrochemistry

Room : 103

*Chaired by:* Osamu Niwa and Patrick Unwin

09:30 to 10:10 Keynote

**J. Justin Gooding** (School of Chemistry, The University of New South Wales, Sydney, Australia), Moinul Choudhury, Simone Ciampi, Stephen G. Parker, Ying Yang, Roya Tavallaie, Leila Zarei, Vinicius Goncales

[Light Activated Electrochemistry: A strategy for performing voltammetry on a monolithic surface where you want, when you want with micron scale spatial resolution](#)

10:10 to 10:30

**Emmanuel Iwuoha** (Department of Chemistry, SensorLab, University of Western Cape, Cape Town, South Africa)

[Biocompatible Quantum Dots and Conducting Polymer Nanocomposites in Disease Signalling Biosensors](#)

10:30 to 10:50 Invited

**Sabine Szunerits** (IEMN, University Lille, Villeneuve d'Ascq, France)

[Reduced graphene oxide modified electrodes: from glucose sensing to electrochemical delivery of insulin](#)

10:50 to 11:10

Coffee Break

## Symposium 2: Electrochemical Aspects of Biological Systems: Theory, Experiment and Applications

**Room : 101D**

*Chaired by:* Alexandra Bondarenko and Shen-Ming Chen

09:30 to 09:50

**Yasufumi Takahashi** (WPI-AIMR, Tohoku University, Sendai, Japan), Sen Mustafa, Hiroki Ida, Hitoshi Shiku, Tomokazu Matsue

[Improving the Electrochemical Measurement Sensitivity of SECM-SICM by using Pt Electrodeposited Carbon Nanoelectrode](#)

09:50 to 10:10

**Ming-Chang Yang** (Department of Chemical Engineering, National Cheng Kung University, Tainan, Taiwan), Yi-Kai Chih, Ya-Yun Zhan

[Nitrogen-doped Carbon Electrodes for Simultaneous Detection of Dopamine, Uric Acid and Ascorbic Acid](#)

10:10 to 10:50 Keynote

**Woonsup Shin** (Department of Chemistry, Sogang University, Seoul, Korea)

[Development of Drug Delivery Devices Based on Nongassing Electroosmotic Pump](#)

10:50 to 11:10

Coffee Break

## Symposium 3: Batteries for Tomorrow's World

**Room : 201AB**

*Chaired by:* Yong Yang

09:30 to 10:10 Keynote

**Claude Delmas** (ICMCB, CNRS, Pessac, France)

[An Overview of the Behavior of Overlithiated  \$\text{Li}\(\text{Li}, \text{Mn}, \text{Co}, \text{Ni}\)\text{O}\_2\$  Layered Oxides In Lithium-ion Batteries](#)

10:10 to 10:30

**Shou-Yu Shen** (College of Chemistry and Chemical Engineering, Xiamen University, Xiamen, China)

[Superior electrochemical performance of Li-rich  \$\text{Li}\_{1.188}\text{Ni}\_{0.198}\text{Co}\_{0.087}\text{Mn}\_{0.553}\text{O}\_2\$  cathode material by coating Li-La-Zr-O solid electrolyte](#)

10:30 to 10:50

**Shinya Suzuki** (Department of Applied Chemistry, School of Engineering, The University of Tokyo, Tokyo, Japan), Masaru Miyayama

[Electrode properties of the restacked  \$\text{MnO}\_2\$ -based nanosheets with vacancy defects](#)

10:50 to 11:10

Coffee Break

## Symposium 3: Batteries for Tomorrow's World

Room : 201C

Chaired by: K. Zaghib

09:30 to 09:50

**Fridolin Röder** (Institute of Energy and Process Systems Engineering, Technical University of Braunschweig, Braunschweig, Germany), Ulrike Krewer

[Fundamental Analysis of Lithium-ion Battery Performance and Degradation in Context of Particle Size Distribution](#)

09:50 to 10:10

**Fabian Jeschull** (Department of Chemistry, Ångström Laboratory, Uppsala University, Uppsala, Sweden), Matthew Lacey, Daniel Brandell

[Functional Binders - SEI Formers, Dispersants and Local Electrolyte Components](#)

10:10 to 10:30

**Po-Han Lee** (Department of Materials Engineering, Tatung University, Taipei City, Taiwan), She-huang Wu

[Unexpected Cycle Aging of a Commercial 18650 Cell](#)

10:30 to 10:50

**Nan Lin** (Institute of Energy and Process Systems Engineering, TU Braunschweig, Braunschweig, Germany), Ulrike Krewer

[Novel Electrochemical-Thermal Modeling for Lithium-ion Battery Design based on a Fast Reduced P2D Electrochemical Model](#)

10:50 to 11:10

Coffee Break

WEDNESDAY AM

## Symposium 4: Advances in Fuel Cells from Materials to Systems

Room : 102

Chaired by: Hiroyuki Uchida

09:30 to 09:50 Invited

**Eiichi Yasumoto** (Corporate Engineering Division, Appliances Company, Panasonic Corporation, 3-1-1 Yagumo-naka-machi, Moriguchi City, Japan), Masataka Ozeki

[Evolution of "ENE-FARM" and the Activities for the Market Expansion in Panasonic](#)

09:50 to 10:10 Invited

**Tae-Hyun Yang** (Fuel Cell Research Center, Korea Institute of Energy Research, Daejeon, Korea), Young-Jun Sohn, Minjin Kim, Seung-Gon Kim

[Design and Development of a Fuel Cell Power Module for High Altitude and Long Endurance Unmanned Aerial Vehicles](#)

10:10 to 10:30

**Michael Fleige** (Department of Chemistry and Nano-Science Center, University of Copenhagen, Copenhagen, Denmark), Gustav Wiberg, Matthias Arenz

[RDE system for ORR measurements at elevated \(>100 °C\) temperature and pressure conditions](#)

10:30 to 10:50

**Hiroki Habazaki** (Faculty of Engineering, Hokkaido University, Sapporo, Japan)

[Oxygen Reduction Activity and Durability of Pt Electrocatalysts Supported on Platelet Carbon Nanofibers](#)

10:50 to 11:10

Coffee Break

## Symposium 5: Novel Insights to Electrochemical Capacitors

**Room : 101A**

*Chaired by:* Elzbieta Frackowiak

09:30 to 10:10 Keynote

**Thierry Brousse** (Institut des Matériaux Jean Rouxel (IMN), Université de Nantes, Nantes, France), Mylène Brachet, Jean Le Bideau, Dorian Gaboriau, Gérard Bidan, Pascal Gentile, Said Sadki

[Ionogels as safe and thermally stable electrolytes for macro and micro electrochemical capacitors](#)

10:10 to 10:30

**Andrea Balducci** (Helmholtz Institute Ulm, Helmholtz Institute Ulm - Karlsruhe Institute of Technology, Ulm, Germany), Christoph Schütter, Sebastian Pohlmann, Claudia Ramirez-Castro, Tamara Husch, Martin Korth

[Innovative conducting salts and solvents for advanced electrochemical double layer capacitors](#)

10:30 to 10:50

**Sonia Dsoke** (ECM, ZSW, Ulm, Germany), Tong Zhang, Bettina Fuchs, Marco Secchiaroli, Serife Kaymaksiz, Margret Wohlfahrt-Mehrens

[Combination of Li-salt-based electrolytes with activated carbon electrodes for the development of hybrid battery-supercapacitors](#)

10:50 to 11:10

Coffee Break

WEDNESDAY AM

## Symposium 7: Electrodeposition - The Frontier Approach in Material Science and Nanofabrication

**Room : 101C**

*Chaired by:* Dow Wei-Ping and Shu-Hua Cheng

09:30 to 10:10 Keynote

**Chih Chen** (Materials Science and Engineering, National Chiao Tung Univ, Hsin-chu, Taiwan)

[Electrodeposition of Highly \(111\)-oriented Nanotwinned Cu and its Application](#)

10:10 to 10:30 Invited

**Rohan Akolkar** (Chemical and Biomolecular Engineering, Case Western Reserve University, Cleveland, USA), Chang-Jung Hsueh, Dai Shen, Mirko Antloga, Craig Virnelson, Uziel Landau, Mark DeGuire

[A Novel Titanium Electrowinning Process Using Specialized Segmented Diaphragms](#)

10:30 to 10:50

**Atsushi Kitada** (Department of Materials Science and Engineering, Kyoto University, Kyoto, Japan), Yuu Kang, Kai Nakamura, Kazuhiro Fukami, Kuniaki Murase

[Room Temperature Electrodeposition of Elemental Magnesium and Aluminum from Glyme-Based Electrolytes](#)

10:50 to 11:10

Coffee Break



---

## Symposium 8: Corrosion and Passivity

---

**Room : 201D**

*Chaired by:* Mark E. Orazem

09:30 to 10:10 Keynote

**Bernard Tribollet** (UMR8235 LISE, UPMC - CNRS, Paris, France), Sara Chakri, Isabelle Frateur, Frederic Kanoufi, Eliane Sutter, Vincent Vivier

[Analysis by EIS of Cathodic Reactions on Carbon Steel in Aerated Solution at pH 13](#)

10:10 to 10:30

**Yu-Min Chen** (Department of Chemical Engineering, University of Florida, Gainesville, USA), Mark E. Orazem

[Analysis of Corrosion Behavior of ASTM A416 Steel by Electrochemical Impedance Spectroscopy](#)

10:30 to 10:50

**Sara Munktel** (Department of Chemistry - Ångström Laboratory, Uppsala Universitet, Uppsala, Sweden), Leif Nyholm, Fredrik Björefors

[Towards high-throughput Corrosion Screening using Bipolar Electrochemistry](#)

10:50 to 11:10

Coffee Break

---

## Symposium 9: Electrocatalytic Materials

---

**Room : 201EF**

*Chaired by:* Shawn D. Lin

09:30 to 10:10 Keynote

**Lin Zhuang** (Department of Chemistry, Wuhan University, Wuhan, China)

[Alkaline polymer electrolyte fuel cells: materials and catalysis](#)

10:10 to 10:30 Invited

**Wei Xing** (State Key Laboratory of Electroanalytical Chemistry, Changchun Institute of Applied Chemistry, Jilin, China), Jianbing Zhu, Junjie Ge, Changpeng Liu, Meiling Xiao

[Exploration of efficient low-platinum and non-platinum catalysts for oxygen reduction reaction](#)

10:30 to 10:50

**Atif Koca** (Chemical Engineering Department, Marmara University, Istanbul, Turkey), Mehmet Aydemir, Duygu Akyüz, Burag Agopcan, Cevat Sarioğlu, M. Kasim Sener, Fatma K. Albayrak

[Electrocatalytic and Photocatalytic Hydrogen Production](#)

10:50 to 11:10

Coffee Break

---

## Symposium 10: Electrochemical Technology: New Challenges for a More Competitive Economy

---

**Room : 101B**

*Chaired by:* Carlos Alberto Martinez-Huitle and Henry Bergmann

09:30 to 09:50 Invited

**Carlos Ponce de Leon** (Faculty of Engineering and the Environment, University of Southampton, Southampton, United Kingdom), Rachel D. McKerracher, Horacio A. Figueredo-Rodriguez, Frank C Walsh

[A Bifunctional Air Electrode Catalyzed by Transition Metal Ferricyanide Derivatives for an Iron-air battery](#)

09:50 to 10:10

**Mitsuru Wakisaka** (Fuel Cell Nanomaterials Center, University of Yamanashi, Kofu, Japan), Masashi Kunitake

[Direct Electrochemical Hydrogenation of Aromatic Molecules at Pt Electrode in Microemulsion Electrolyte Solution](#)

10:10 to 10:30

**Min-Hsin Yeh** (School of Materials Science and Engineering, Georgia Institute of Technology, Atlanta, USA), Long Lin, Zhong Lin Wang

[Motion-driven Electrochromic Reactions for Self-powered Smart Window System](#)

10:30 to 10:50

**Laura Valero** (Research Electronics Departament, Universidad Autónoma Del Estado de México, Toluca, Mexico), Toribio Fernández Otero, Eduardo Rodríguez, Angel Estévez

[Validation of Polymeric artificial muscles with a Proportional- Integral control system](#)

10:50 to 11:10

Coffee Break



ROOMS:		101A	101B		101C		101D	102	103	201AB		201EF	201C	201D
SYMPOSIUM		s05	s18	s07	s14	s04	s01	s03	s09	s03	s08/s11			
08:15 - 09:15		Plenary Lecture: Martin Winter (Plenary Hall)												
09:30 - 09:50	François Béguin	Yann Leroux	Peter Broekmann	Masa-aki Haga	Shengli Chen	Jan Vacek	Yu-Guo Guo	Li-Chyong Chen	Nae-Lih Wu	Yudai Yamamoto				
09:50 - 10:10	Takashi Kakiuchi	Kazuo Kondo	I. A. Rutkowska	Yujia Deng	Guy Denuault	Judith Rishpon	Louise Frenck	Ana Sofia Varela	Laurence Hardwick	Achim W. Hassel				
10:10 - 10:30	Mathieu Salanne	Jeyab. Chinnaya	Wei-Yang Zeng	Kim Daasbjerg	Anthony Kucernak	Tzu-En Lin	Hang Su	Ida Hjorth	Sven Uhlenbruck	En-Hou Han				
10:30 - 10:50	Teresa A. Centeno	Chu-Chi Liu												
10:50 - 11:10		Coffee Break												
11:10 - 11:30		General Assembly 11:10 to 12:10 (Plenary Hall)												
11:30 - 11:50														
11:50 - 12:10														
12:10 - 12:30														
12:30 - 12:50														
12:50 - 13:10		Division 5 Meeting		Division 2 Meeting		Division 3 Meeting		Division 1 Meeting		Division 4 Meeting		Division 7 Meeting		Division 6 Meeting
13:10 - 13:50														
13:50 - 14:00														
14:00 - 14:20	John R. Miller	Alexander Oleinick	Jon Ustarroz	Y. Tateyama	Yu Morimoto	Fethi Bedioui	K. Zaghib	Jun Maruyama	Gao Liu	Flavio Mara				
14:20 - 14:40	Hsisheng Teng	A. Fernández-Ia-V.	Philip Bartlett	Louzhen Fan		Jan Clausmeyer		Yan Shen	Xiaopeng Li					
14:40 - 15:00	Masashi Ishikawa	Ying Wan	Lu Chen	Xingxing Chen	Kuan-Wen Wang	Yu-Chen Chang	Kisuk Kang	Sho Fujita	Hiroyuki Usui	Dongil Lee				
15:00 - 15:20	Patrice Simon	Conchi Ania	Tso-Fu Mark Chang	A. Minguzzi	Tilman Jurzinsky	Angelika Holzinger	Reinhold Koch	Xi Cheng	Qihui Wu	M. F. Guedes da S.				
15:20 - 15:40	Indrek Tallo	Maria Cuartero	Jinqiu Zhang	J. Rodriguez-Lop.	Sayoko Shironita	Ahmed Abdo	Michael Palmer	Wenting Xu	Yingshun Li	Eric Labbe				
15:40 - 16:00	Masayuki Morita	S. Moraes Silva	Zenglin Wang	Michael Holzinger	Evgeniy Gribov	Patrick Unwin	Jagabandhu Patra	Juan Manriquez	Selina Tillmann	James Y. Becker				
16:00 - 16:20	Juhan Lee	Jen-Yuan Wang	Chiao-Chien Wei		Fen Guo		Ji Su Chae	Ruud Kortlever	Leiting Zhang	Zhifeng Ding				
16:20 - 16:40		Coffee Break												
16:40 - 17:00	Chi-Chang Hu	A. Gomis-Bereng.	Ryoichi Aogaki	Giovanni Valenti	Jianguo Liu	Raymond Wong	Chun-Ting Li	Peng Bai	Kazuhiro Chiba					
17:00 - 17:20	Panel Discussion about Novel Insights to Electrochemical Capacitors	Leigh Aldous	Po-Fan Chan	Kristina Tschulik	Byungchan Bae	Gunther Wittstock	O. S. Mendoza-H.	Fabio Dionigi	Edgar Ventosa					
17:20 - 17:40		Dan Nguyen Dang	Iwao Mogi	Line Koefoed	Kwong-Yu Chan	Jie Zhang	Hai-Jung Peng	C. M. Sanchez-S.	Jee-Jay Chen	Jingxian Yu				
17:40 - 18:00		Zhang Dalei	Alex. Vaskevich	Stefania Rapino	Michael Eikerling	Yi-Tao Long	Xiaoyu Liu	L. Tamasauskaite	Georgios Nikiforidis	Chengchu Zeng				
18:00 - 18:20		Miikka Jokinen	Yao-Lin Tsai	M. A. Vorotyntsev	S. Shanmugam	Jung-Chi Wang	Han Wang	Luis F. Arenas	Jiri Ludvik	Wenrong Yang				
18:20 - 18:40				S. Cordoba de Tor.										
19:00		Banquet												

# Thursday, 8 October 2015 - Morning

---

## Plenary Lecture

**Room : Plenary Hall**

*Chaired by:* Nae-Lih Wu

08:15 to 09:15

**Martin Winter** (MEET Battery Research Center/Institute of Physical Chemistry, University of Muenster/Helmholtz Institute Muenster HI MS, Muenster, Germany), Dennis Gallus, Ralf Wagner, Marius Amereller, Johannes Kasnatscheew, Elisabeth Kraemer, Steffen Krueger, Xin Qi, Ji Lie, Isidora Cekic-Laskovic

[Neglected, Forgotten or Unimportant? Inactive Materials in Lithium Ion Batteries](#)

---

## Symposium 1: New Directions in Analytical Electrochemistry

**Room : 103**

*Chaired by:* Fethi Bedioui and Gunther Wittstock

09:30 to 10:10 Keynote **Early Career Analytical Electrochemistry Prize of ISE Division 1**

**Jan Vacek** (Department of Medical Chemistry and Biochemistry, Palacky University, Olomouc, Czech Republic)

[Electrochemistry of Membrane Proteins](#)

10:10 to 10:30

**Judith Rishpon** (Molecular Microbiology and Biotechnology, Tel-Aviv University, Tel-Aviv, Israel)

[Combined Tyrosinase \(A Multi-Potent Enzyme\) and Electrodes Modified with nanoparticles for Fast and Highly Sensitive Environmental Monitoring and Medical Diagnostics](#)

10:30 to 10:50

**Tzu-En Lin** (Chemistry and Chemical Engineering, Ecole Polytechnique Fédérale de Lausanne, Lausanne, Switzerland), Fernando Cortés-Salazar, Andreas Lesch, Alexandra Bondarenko, Hubert Girault

[Cancer Stage Identification by Scanning Electrochemical Microscopy: Investigation of Tyrosinase inside Melanoma Tissues](#)

10:50 to 11:10

Coffee Break

---

## Symposium 3: Batteries for Tomorrow's World

---

**Room : 201AB**

*Chaired by:* Claude Delmas

### 09:30 to 10:10 Keynote **Tajima Prize**

**Yu-Guo Guo** (Institute of Chemistry, Chinese Academy of Sciences (CAS), Beijing, China)

[Advanced Cathodes and Metallic Anodes for Next-Generation Rechargeable Batteries](#)

10:10 to 10:30

**Louise Frenck** (Environmental Energy Technologies Division, Lawrence Berkeley National Laboratory, Berkeley, USA), Renaud Bouchet, Philippe Stevens, Nitash Balsara

[Study of ceramic-polymer/lithium interface for lithium air batteries](#)

10:30 to 10:50

**Hang Su** (College of Energy & School of Energy Research, Xiamen University, Xiamen, China)

[Hierarchical Mn<sub>2</sub>O<sub>3</sub> Hollow Microspheres of high performance as Anode of LIBs and XANES studies of Conversion Reaction Mechanism](#)

10:50 to 11:10

Coffee Break

---

## Symposium 3: Batteries for Tomorrow's World

---

**Room : 201C**

*Chaired by:* Yong Joon Park

09:30 to 09:50 Invited

**Nae-Lih WU** (Department of Chemical Engineering, National Taiwan University, Taipei, Taiwan), Fu-Sheng Li, Yu-Shiang Wu, Jacky Chou, Martin Winter

[Research on Polymeric Artificial Solid-Electrolyte-Interphase for Enhanced Performance of Li-ion Battery Anodes](#)

09:50 to 10:10 Invited

**Laurence Hardwick** (Chemistry, University of Liverpool, Liverpool, United Kingdom), Vivek Padmanabhan, Richard Nichols

[In situ infrared spectroscopy on gold substrates to track film formation and intermediates in Li-ion and Li-air electrolytes](#)

10:10 to 10:30

**Sven Uhlenbruck** (Institute of Energy and Climate Research (IEK-1), Forschungszentrum Jülich GmbH, Jülich, Germany), Hans-Gregor Gehrke, Sandra Lobe, Chih-Long Tsai, Christian Dellen, Aiko Bünting, Martin Bitzer, Jürgen Dornseiffer, Tim Van Gestel, Olivier Guillon

[Manufacturing and Performance of solid-state thin-film batteries](#)

10:50 to 11:10

Coffee Break

## Symposium 4: Advances in Fuel Cells from Materials to Systems

Room : 102

Chaired by: Shengli Chen

09:30 to 09:50 Invited

**Shengli Chen** (Chemistry Department, Wuhan University, Wuhan, China), Junxiang Chen, Yuwen Liu

[Nature of Active Sites and Origin of Large Overpotential of the Oxygen Reduction Reaction on Pt\(111\) Surface](#)

09:50 to 10:10

**Yujia Deng** (Department of Chemistry, University of Copenhagen, Copenhagen, Denmark), Matthias Arenz, Gustav K.H. Wiberg

[The Steady State coverage of oxygenated species on Platinum and its influence on the Oxygen Reduction and Hydrogen Oxidation Reaction in acid electrolyte](#)

10:10 to 10:30

**Guy Denuault** (Chemistry, University of Southampton, Southampton, United Kingdom), Samuel Perry

[Amperometric Study of the Oxygen Reduction Reaction on Oxide Free Metals: Evidence for the Reduction of Pre-adsorbed Dioxide and its Dependence on the Metal Substrate](#)

10:30 to 10:50

**Anthony Kucernak** (Chemistry, Imperial College London, London, United Kingdom), Matthew Markiewicz, Christopher Zalitis, Christopher Zalitis, Matthew Markiewicz

[Is the Tafel approximation sufficient to predict electrocatalyst performance in polymer electrolyte fuel cells?](#)

10:50 to 11:10

Coffee Break

## Symposium 5: Novel Insights to Electrochemical Capacitors

Room : 101A

Chaired by: Frédéric Favier

09:30 to 10:10 Keynote

**François Béguin** (Institute of Chemistry and Technical Electrochemistry, Poznan University of Technology, Poznan, Poland), Patryk Przygocki, Qamar Abbas, Paula Ratajczak

[The aqueous electrochemical capacitor: a high energy alternative solution to organic electrolyte-based systems](#)

10:10 to 10:30 Invited

**Mathieu Salanne** (Laboratoire PHENIX / Maison de la Simulation, UPMC / CNRS, Paris, France), Clarisse Pean, Celine Merlet, Benjamin Rotenberg, Paul Madden, Pierre-Louis Taberna, Barbara Daffos, Patrice Simon, Yury Gogotsi, Matthieu Haefele, David Limmer, David Chandler

[The Electric Double Layer has a Life of its Own](#)

10:30 to 10:50 Invited

**Teresa A. Centeno** (Coal, Science and Environment, Instituto Nacional del Carbón-CSIC, Oviedo, Spain), Belén Lobato, Gelines Moreno-Fernández, Andrea Balducci

[Physico-Chemical Features of Carbons and their Behavior in Electrochemical Capacitors](#)

10:50 to 11:10

Coffee Break

## Symposium 7: Electrodeposition - The Frontier Approach in Material Science and Nanofabrication

**Room : 101C**

*Chaired by:* Rohan Akolkar and Dow Wei-Ping

09:30 to 09:50 Invited

**Peter Broekmann** (Department of Chemistry and Biochemistry, University of Bern, Bern, Switzerland), Hai Nguyen, Valentine Grimaudo, Pavel Moreno-Garcia, David Lechner, Florian Stricker, Andreas Riedo, Peter Wurz

[Combining Superfill and Leveling Capabilities: New Hybrid Polymers for Advanced Damascene Applications](#)

09:50 to 10:10 Invited

**Kazuo Kondo** (Ch.E., Osaka Prefecture University, Sakai, Japan), Van Ha

[Extremely Fast Filling by V-shape TSV and Cu\(I\)thiolate accumulation](#)

10:10 to 10:30

**Wei-Yang Zeng** (Chemical Engineering, National Chung Hsing University, Taichung, Taiwan), Wei-Ping Dow

[Using Graphene as a Conducting Layer and Barrier Layer for high aspect ratio Through Silicon Via Filling](#)

10:30 to 10:50

**Chu-Chi Liu** (Chemical Engineering, National Chung Hsing University, Taichung, Taiwan), Wei-Ping Dow

[Microvia filling in an Acidic Copper Planting Bath with Insoluble Anodes](#)

10:50 to 11:10

Coffee Break

THURSDAY AM

## Symposium 8: Corrosion and Passivity

**Room : 201D**

*Chaired by:* Koji Fushimi

09:30 to 09:50

**Yudai Yamamoto** (Graduate School of Chemical Sciences and Engineering, Hokkaido University, Sapporo, Japan), Misako Jin, Yuichi Kitagawa, Takayuki Nakanishi, Yasuchika Hasegawa, Koji Fushimi

[Local Measurement of Hydrogen Diffusion in Steel Sheet](#)

09:50 to 10:10 Invited

**Achim Walter Hassel** (CD Laboratory COMBOX, Johannes Kepler University Linz, Linz, Austria)

[Corrosion studies using non radioactive isotopes of H, Zn and Fe](#)

10:10 to 10:50 Keynote

**En-Hou Han** (Institute of Metal Research, Chinese Academy of Sciences, Shenyang, China), En-Hou Han, Jianqiu Wang, Xinqiang Wu, Zhiming Zhang

[Corrosion Electrochemistry and Surface Film Properties of Alloy 690 in High Temperature Pressurized Water](#)

10:50 to 11:10

Coffee Break



---

## Symposium 9: Electrocatalytic Materials

---

**Room : 201EF**

*Chaired by:* Chen-Hao Wang and Lin Zhuang

09:30 to 10:10 Keynote

**Li-Chyong Chen** (Center for Condensed Matter Sciences, National Taiwan University, Taipei, Taiwan), Kuei-Hsien Chen, Hsin-Cheng Hsu, He-yun Du, Indrajit Shown, Hsin-Chih Huang, Yu-Chung Chang, Chen-Hao Wang, Sung-Tung Chang

[Macrocyclics, Graphene Oxides-based Nano-catalysts, and Related Hybrids for Fuel Cells and Solar Fuels](#)

10:10 to 10:30

**Ana Sofia Varela** (Chemical Engineering, TU-Berlin, Berlin, Germany), Wen Ju, Peter Strasser

[CO<sub>2</sub> Electroreduction on Heteroatom-doped Carbon Catalyst](#)

10:30 to 10:50

**Ida Hjorth** (Chemical Engineering, Norwegian University of Technology and Science, Trondheim, Norway), Navaneethan Muthuswamy, De Chen

[Effects from modifying carbon nanofiber supports on metal nanoparticle catalyzed CO<sub>2</sub> reduction](#)

10:50 to 11:10

Coffee Break

---

## Symposium 14: Modeling, Design and Characterization of Nanostructured, Electroactive and Multifunctional Materials

---

**Room : 101D**

*Chaired by:* Michael Holzinger

09:30 to 09:50

**Masa-aki Haga** (Department of Applied Chemistry, Chuo University, 1-13-27 Ksuga, Bunkyo-ku, Japan), Hiroaki Ozawa, Takumi Nagashima

[Photoelectrochemical Response of Hetero-layer Films Composed of Redox-active Ru Complexes: Charge Trapping and Memory Effect](#)

09:50 to 10:10

**Iwona A. Rutkowska** (Department of Chemistry, University of Warsaw, Warsaw, Poland), Pawel J. Kulesza

[Development of Multifunctional Materials Composed of Selected Noble Metal and Metal Oxide Nanostructures for Efficient Electrocatalytic Oxidation of Small Organic Molecules](#)

10:10 to 10:50 Keynote

**Kim Daasbjerg** (Department of Chemistry, Aarhus University, Aarhus, Denmark)

[Novel Hybrid Materials Prepared from Polymer Brushes and Graphene](#)

10:50 to 11:10

Coffee Break

---

## Symposium 18: General Session

---

**Room : 101B**

*Chaired by:* Juan M. Feliu

09:30 to 09:50

**Yann Leroux** (Institut des Sciences Chimiques de Rennes, CNRS - Université de Rennes 1, Rennes Cedex, France), Sébastien Lhenry, Christophe Orain, Françoise Conan, Nathalie Cosquer, Nicolas Le Poul, Yves Le mest, Olivia Reinaud, Philippe Hapiot

[Locally Self-induced “electro-click” onto self-assembled monolayer: Evidence for surface self-catalysis propagation.](#)

09:50 to 10:10

**Takashi Kakiuchi** (Department of Chemistry of Functional Molecules, Konan University, Kobe, Japan), Masahiro Yamamoto

[Single ion activity, pH, liquid junction potential, and the essence of electrochemistry: in response to “A pH centenary” by Robert de Levie](#)

10:10 to 10:30

**Jeyabharathi Chinnaya** (Institute of Biochemistry, University of Greifswald, Greifswald, Germany), Paula Ahrens, Ulrich Hasse, Fritz Scholz

[Does a link between multiple oxidation peaks of gold oxide formation and exposed crystal planes exist on polycrystalline gold?](#)

10:50 to 11:10

Coffee Break

# Thursday, 8 October 2015 - Afternoon

## Symposium 1: New Directions in Analytical Electrochemistry

Room : 103

Chaired by: Sabine Szunerits; Jan Vacek

14:00 to 14:20

**Fethi Bedioui** (CNRS UTCBS 8258-Chimie ParisTech, Chimie ParisTech, Paris, France), Gonzalo Ramirez, Sophie Griveau, Minerva Alvaro, Silvia Gutierrez-Granados

[In Vivo Electrochemical Assessment of Possible Melatonin Effect on Nitric Oxide Production From Kidneys of Sub-Acute Lead Treated Rats](#)

14:20 to 14:40

**Jan Clausmeyer** (Analytische Chemie, Center for Electrochemical Sciences, Ruhr-Universität Bochum, Bochum, Germany), Yanjun Zhang, Miriam Marquitan, Ainara López Córdoba, Yuri Korchev, Wolfgang Schuhmann

[Amperometric Nanosensors and Field-Effect Transistors for Extra- and Intracellular Chemical Analysis](#)

14:40 to 15:00

**Yu-Chen Chang** (Chemical Engineering, National Taiwan University of Science and Technology, Taipei, Taiwan), Yi-Ting Chen, Guan-Lin Chen, Kuo-Chuan Ho, Wei-Hung Chiang

[Controllable Synthesis of Heteroatom-Doped Carbon Nanotubes under Atmospheric Pressure and Their Electrocatalytic Ability to L-cysteine](#)

15:00 to 15:20

**Angelika Holzinger** (Institute of Analytical and Bioanalytical Chemistry, University Ulm, Ulm, Germany), Peter Knittel, Jong Seok Moon, Christine Kranz

[AFM Tip-integrated Antimony Electrodes for pH Detection](#)

15:20 to 15:40

**Ahmed (Galal) Abdo** (Department of Chemistry, Faculty of Science - Kuwait University, Kuwait, Kuwait), Ekram El-Ads, Asmaa Ibrahim, Youssuf Mohamed, Nada Atta

[Electrochemistry and Determination of Some Biomedical and Biological Molecules at Carbon –Based Ionic Liquid Crystals Composite Electrodes](#)

15:40 to 16:00 Invited

**Patrick Unwin** (Department of Chemistry, University of Warwick, Coventry, United Kingdom)

[Making Movies: Next Generation Electrochemical Imaging](#)

16:20 to 16:40

Coffee Break

16:40 to 17:20 Keynote

**Gunther Wittstock** (Department of Chemistry, Carl von Ossietzky University of Oldenburg, Oldenburg, Germany), Heinz Bültel, Fabian Peters, Julian Schwenzel, Patrick Schwager, Daniela Fenske

[Microelectrochemical in situ observation of battery electrodes](#)

17:20 to 17:40 Invited

**Jie Zhang** (Chemistry, Monash University, Melbourne, Australia), Kiran Bano, Si-Xuan Guo, Alan Bond

[Determination of Fast Electrode Kinetics Using Fourier Transformed Large Amplitude AC Voltammetry](#)

17:40 to 18:00

**Yi-Tao Long** (Department of Chemistry, East China University of Science and Technology, Shanghai, China)

[Ubiquinones: understanding electrochemistry from solution to surface](#)

## Symposium 3: Batteries for Tomorrow's World

Room : 201AB

Chaired by: Takeshi Abe

14:00 to 14:40 Keynote

**K. Zaghib** (Institut de Recherche d'Hydro-Québec, Varennes, Canada), P. Hovington, M. Lagacé, A. Guerfi, P. Bouchard, A. Mauger, C. M. Julien, M. Armand

[New Lithium Metal Polymer Solid State Battery for an Ultrahigh Energy: Nano C-LiFePO<sub>4</sub> versus Nano Li<sub>1.2</sub>V<sub>3</sub>O<sub>8</sub>](#)

14:40 to 15:00 Invited

**Kisuk Kang** (Department of Materials Science and Engineering, Seoul National University, Seoul, Korea), Kyu-Young Park

[Olivine with zero anti-site defect and three dimensional lithium diffusion paths](#)

15:00 to 15:20

**Reinhold Koch** (RP06, TUM Create Ltd., Singapore, Singapore), Andreas Jossen

[On the Influence of Mechanical Compression on the Impedance of Aged LiFePO<sub>4</sub> - Graphite Cells](#)

15:20 to 15:40

**Michael Palmer** (Chemistry, University Of Southampton, Southampton, United Kingdom), John R. Owen, Andrew Hector

[In-situ XRD of High Voltage Lithium Insertion Electrodes](#)

15:40 to 16:00

**Jagabandhu Patra** (Institute of Materials Science & Engineering, National Central University, Taoyuan, Taiwan), Prem Prakash Dahiya, Jason Fang, Yu-Wei Lin, Chung-Jen Tseng, S. Basu, S. B. Majumder, Jeng-Kuei Chang

[Electrochemical Performance of 0.5Li<sub>2</sub>MnO<sub>3</sub>-0.5Li\(Mn<sub>0.375</sub>Ni<sub>0.375</sub>Co<sub>0.25</sub>\)O<sub>2</sub> Composite Cathode Using Pyrrolidinium-based Ionic Liquid Electrolytes](#)

16:00 to 16:20

**Ji Su Chae** (Energy & Environmental Division, Korea Institute of Ceramic Engineering & Technology, Jinju-si, Korea), Sun-Min Park, Won-Sub Yoon

[Understanding the Improved Electrochemical Properties of Li<sub>2</sub>O-2B<sub>2</sub>O<sub>3</sub> Coated LiNi<sub>0.5</sub>Mn<sub>1.5</sub>O<sub>4</sub> for Lithium-ion Batteries](#)

16:20 to 16:40

Coffee Break

16:40 to 17:00

**Raymond Wong** (Byon Initiative Research Unit, RIKEN, Wako, Japan), Hye Ryung Byon

[The Role of Defects and Oxygen Functionalities in Carbon Nanotube-based electrodes for the Lithium-oxygen Battery](#)

17:00 to 17:20

**Omar Samuel Mendoza-Hernandez** (Department of Materials Science and Technology, Nagaoka University of Technology, Nagaoka, Japan), Shuichi Taniguchi, Yuki Maruyama, Hiroaki Ishikawa, Yoshitsugu Sone, Minoru Umeda

[Thermal Runaway Behavior of 18650 Li-ion Cells Before and After Storage Degradation at High Temperature](#)

17:20 to 17:40

**Hai-Jung Peng** (Electrochemical Energy Storage Section, Paul Scherrer Institute, Villigen PSI, Switzerland), Sigita Urbonaitė, Claire Villevieille, Hannes Wolf, Klaus Leitner, Petr Novak

[Consequences of Electrolyte Degradation for the Electrochemical Performance of NCM Battery Materials](#)

17:40 to 18:00

**Xiaoyu Liu** (Chemistry Department, Fudan University, Shanghai, China)

[Surface phase transformation and CaF<sub>2</sub> coating for enhanced electrochemical performance of Li-rich Mn-based Cathodes](#)

18:00 to 18:20

**Jung-Chi Wang** (Graduate Institute of Applied Science and Technology, National Taiwan University of Science and Technology, Taipei, Taiwan), Fu-Ming Wang

[Forward and reverse differential-pulse applied in the formation of solid electrolyte interface with constant temperature addition in lithium ion battery](#)

## Symposium 3: Batteries for Tomorrow's World

**Room : 201C**

*Chaired by:* T. Richard Jow

14:00 to 14:20 Invited

**Gao Liu** (Energy Storage and Distributed Resources Division, Lawrence Berkeley National Laboratory, Berkeley, USA), Hui Zhao, Zhe Jia, Sang-Jae Park

[Functional Conductive Polymer Binders Enabled High-stability Cycling of Alloy Anodes](#)

14:20 to 14:40

**Xiaopeng Li** (Institute of Physics, Martin-Luther-Universität Halle-Wittenberg, Halle, Germany), Ralf Wehrspohn

[High performance mesoporous metallurgical silicon nanowire anode for lithium ion batteries](#)

14:40 to 15:00

**Hiroyuki Usui** (Graduate School of Engineering, Tottori University, Tottori, Japan), Masahito Nomura, Hiroki Nishino, Masatoshi Kusatsu, Tadatoshi Murota, Hiroki Sakaguchi

[Gadolinium silicide/silicon composite anode for next-generation lithium-ion battery](#)

15:00 to 15:20

**Qihui Wu** (Chemistry, Quanzhou Normal University, Quanzhou, China)

[Ge@GeO<sub>2</sub> core@shell nanoparticles/multi-layer carbon composites as anode materials for lithium-ion batteries](#)

15:20 to 15:40

**Yingshun Li** (School of Energy and Environment, City University of Hong Kong, Hong Kong, China), Jieqing He, Hui Zhou, Wenpei Kang, Denis Y. W. Yu

[Enhancing cycling stability of tin dioxide anode for lithium-ion batteries with a stretchable polyimide matrix](#)

15:40 to 16:00

**Selina Tillmann** (MEET Battery Research Center, University of Muenster, Muenster, Germany), Daniel Hermida Merino, Martin Winter, Isidora Cekic-Laskovic, Katja Loos

[Block Copolymer-Templates for the Design of Three-Dimensional Interpenetrating Current Collectors for Submicrostructured Electrodes](#)

16:00 to 16:20

**Leiting Zhang** (Department of Chemical and Biomolecular Engineering, The Hong Kong University of Science and Technology, Hong Kong, China), Jean-Marie Tarascon, Guohua Chen

[Impact of Relative Humidity on Sulfate-based Cathode Materials](#)

16:20 to 16:40

Coffee Break

16:40 to 17:00 **Oronzio and Niccolò De Nora Foundation Young Author Prize**

**Peng Bai** (Chemical Engineering, Massachusetts Institute of Technology, Cambridge, USA), Martin Z. Bazant

[A Solid-Electrolyte-Enabled Lithium-Bromine Flow Battery](#)

17:00 to 17:20

**Edgar Ventosa** (Department of Analytical Chemistry, University of Bochum, Bochum, Germany), Cristina Flox, Joan Ramon Morante, Wolfgang Schuhmann

[Semi-solid flow battery: an emerging electrochemical system](#)

17:20 to 17:40

**Jee-Jay Chen** (Chemical Engineering, University of Michigan - Ann Arbor, Ann Arbor, USA), Mark Barteau  
[Polyoxometalates for Non-aqueous Redox Flow Battery Applications](#)

17:40 to 18:00

**Georgios Nikiforidis** (Byon Initiative Research Unit (IRU), RIKEN, Wako, Japan), Hye Ryung Byon  
[Improvements in the aqueous lithium-iodine battery](#)

18:00 to 18:20

**Luis F. Arenas** (Faculty of Engineering and the Environment, University of Southampton, Southampton, United Kingdom), Carlos Ponce de Leon, Frank C. Walsh  
[Advances on the Zinc-Cerium Redox Flow Battery for Energy Storage](#)

---

## Symposium 4: Advances in Fuel Cells from Materials to Systems

---

**Room : 102**

*Chaired by:* Byungchan Bae and Yu Morimoto

14:00 to 14:40 Keynote

**Yu Morimoto** (Sustainable Energy & Environment Dept., Toyota Central R&D Labs., Inc., Nagakute, Japan), Masanori Inaba, Shuhei Yoshino, Masao Shibata, Tatsuya Hatanaka  
[Alternative PEFC Catalysts for Future Commercial FCVs](#)

14:40 to 15:00

**Kuan-Wen Wang** (Institute of Materials Science and Engineering, National Central University, Taoyuan, Taiwan), Jeng-Han Wang, Yu-Ting Liang  
[The Performance and Stability of the Oxygen Reduction Reaction on Pt/Vbased Nanorods: An Experimental and Computational Study](#)

15:00 to 15:20

**Tilman Jurzinsky** (Applied Electrochemistry, Fraunhofer Institute for Chemical Technology, Pfaffzettel, Germany), Carsten Cremers, Karsten Pinkwart, Jens Tübke  
[A DEMS Study on the Influence of Ag Add-Atoms on Pd-based Catalysts for Methanol Oxidation in Alkaline Environment](#)

15:20 to 15:40

**Sayoko Shironita** (Department of Materials Science and Technology, Nagaoka University of Technology, Nagaoka, Japan), Kazutaka Sato, Kazuma Yoshitake, Minoru Umeda  
[Pt-Ru/C Anode Performance of Polymer Electrolyte Fuel Cell under Carbon Dioxide Atmosphere](#)

15:40 to 16:00

**Evgeniy Gribov** (Group of Adsorption & catalytic processes for fuel cells, Boreskov Institute of Catalysis, Novosibirsk, Russia), Aleksey Kuznetsov, Viktor Golovin, Dmitriy Krasnikov, Vladimir Kuznetsov, Aleksey Okunev  
[The Oxygen Electroreduction Reaction Performance of Pt Catalysts Supported on Commercial Blacks and Nanostructured Carbons: Multiwall Nanotubes and Nanofibers](#)

16:00 to 16:20

**Fen Guo** (College of Materials Science and Chemical Engineering, Harbin Engineering University, Harbin, China), Dianxue Cao, Ke Ye, Kui Cheng, Mengmeng Du, Dongming Zhang  
[Preparation of Ni-Co Nanowire Arrays Anode Electrocatalyst and the Performance of Direct Urea-Hydrogen Peroxide Fuel Cell](#)

16:20 to 16:40

Coffee Break

16:40 to 17:00

**Jianguo Liu** (College of Engineering and Applied Sciences, Nanjing University, Nanjing, China), Jin Xie, Zhigang Zou

[Well-ordered Ru@Pt Core-shell Nanocatalysts with Tunable Composition and Enhanced Electrocatalytic Properties](#)

17:00 to 17:20

**Byungchan Bae** (Fuel Cell Laboratory, Korea Institute of Energy Research, Yuseong-gu, Daejeon, Korea)

[Development of Sulfonated Poly\(Arylene Ether Sulfone\) Multi-Block Membranes for PEMFC Application](#)

17:20 to 17:40

**Kwong-Yu Chan** (Department of Chemistry, The University of Hong Kong, Pokfulam Road, Hong Kong, China)

[Ion Exchange Polymer Threaded in MOF as a Potential Electrolyte with Fast Exchange and High Selectivity](#)

17:40 to 18:00

**Michael Eikerling** (Department of Chemistry, Simon Fraser University, Burnaby, Canada), Mahdi Ghelichi, Pierre-Eric Alix Melchy

[Modeling of Structure Formation and Fracturing in Polymer Electrolyte Membranes](#)

18:00 to 18:20

**Sangaraju Shanmugam** (Energy Systems Eng, DGIST, Daegu, Korea), Kriangsak Ketpang

[Development of Composite Electrolyte Membranes for Polymer Electrolyte Fuel cells Operating at Low Humidity](#)

---

## Symposium 5: Novel Insights to Electrochemical Capacitors

---

**Room : 101A**

*Chaired by:* Thierry Brousse, François Béguin, Daniel Bélanger and Teresa A. Centeno

14:00 to 14:20 Invited

**John R. Miller** (JME, Inc. and Case Western Reserve University, JME, Inc. and Case Western Reserve University, Beachwood, USA)

[Valuing Electrochemical Capacitor Technology](#)

14:20 to 14:40

**Hsisheng Teng** (Chemical Engineering, National Cheng Kung University, Tainan, Taiwan), Wei Hsieh, Hsin-Chieh Huang

[Facile Simulation of Electric Double-Layer Capacitance Based on Helmholtz Models](#)

14:40 to 15:00 Invited

**Masashi Ishikawa** (Chemistry and Materials Engineering, Kansai University, Japan), Masaki Yamagata

[Advanced Auxiliary Materials in EDLC for Enhancing Power and Energy](#)

15:00 to 15:20 Invited

**Patrice Simon** (CIRIMAT, Université Paul Sabatier, Toulouse, France), Barbara Daffos, Wan Yu Tsai, Peihua Huang, Kevin Brousse, Pierre-Louis Taberna

[Recent advances on the understanding of ion adsorption/transfer in nanoporous carbon electrodes: application to supercapacitors](#)

15:20 to 15:40

**Indrek Tallo** (Institute of Chemistry, University of Tartu, Tartu, Estonia), Ester Tee, Enn Lust, Thomas Thomberg, Heisi Kurig, Alar Jänes

[Surprisingly Large Improvements in SiC-CDC Based EDLC via Simple CO<sub>2</sub> Activation Method](#)

15:40 to 16:00 Invited

**Masayuki Morita** (Department of Applied Chemistry, Graduate School of Science, Yamaguchi University, Ube, Japan), Takuma Izumi, Yuya Noguchi, Masahiro Tokita, Kenta Fujii, Nobuko Yoshimoto

[Influences of Residual Water in Porous Carbon Electrodes on Their Cycling Behavior in Organic Electrolyte Solutions](#)

16:00 to 16:20

**Juhan Lee** (Energy Materials Group, INM - Leibniz Institute for New Materials, Saarbruecken, Germany), Daniel Weingarth, Volker Presser

[Hybrid capacitors for moderate energy storage and high power applications: double layer formation and soluble redox couples](#)

16:20 to 16:40

Coffee Break

16:40 to 17:00 Invited

**Chi-Chang Hu** (Department of Chemical Engineering, National Tsing Hua University, Hsinchu, Taiwan), Arturas Adomkevicius, Shin-Ming Li, Tzu-Man Ou

[Preparation and characterization of Mn oxide-based composites for high-performance asymmetric supercapacitors](#)

17:00 to 18:20

**Panel Discussion about Novel Insights to Electrochemical Capacitors**

---

## Symposium 7: Electrodeposition - The Frontier Approach in Material Science and Nanofabrication

---

**Room : 101C**

*Chaired by:* Alexander Vaskevich

14:00 to 14:20

**Jon Ustarroz** (Electrochemical and Surface Engineering (SURF), Vrije Universiteit Brussel, Brussels, Belgium), El Amine Mernissi Cherigui, Bart Geboes, Kadir Sentosun, Pieter Bouckennoog, Herman Terryn, Sara Bals, Tom Breugelmans, Annick Hubin

[Electrodeposition of Electrocatalytic Nanostructures from Aqueous Solutions and Deep Eutectic Solvents: Aggregative Growth](#)

14:20 to 14:40

**Philip Bartlett** (Chemistry, University of Southampton, Southampton, United Kingdom)

[Electrodeposition of Nanowires and Nanostructures from Supercritical Fluids](#)

14:40 to 15:00

**Lu Chen** (Chemistry Department, Monash University, Melbourne, Australia), Mike Horne, Alan Bond, Jie Zhang

[Room Temperature Electrodeposition of Metallic Magnesium from Ethylmagnesiumbromide/Tetrahydrofuran and Ionic Liquid Mixtures](#)

15:00 to 15:20 Invited

**Tso-Fu Mark Chang** (Precision and Intelligence Laboratory, Tokyo Institute of Technology, Yokohama, Japan), Wei-Hao Lin, Chun-Yi Chen, Yung-Jung Hsu, Chi-Chang Hu, Tatsuo Sato, Masato Sone

[Conducting Electrochemical Deposition Reactions in Supercritical Carbon Dioxide Emulsified Electrolyte](#)

15:20 to 15:40

**Jinqiu Zhang** (School of Chemical Engineering and Technology, Harbin Institute of Technology, Harbin, China), Xing Gu, Peixia Yang, Maozhong An

[Electrodeposition Process of Ni-Ga Bimetallic Catalyst in BMIm-OTf Ionic Liquid Electrolyte](#)



15:40 to 16:00

**Zenglin Wang** (School of Chemistry and Chemical Engineering, Shaanxi Normal University, Xi'an, China),  
Shaojun Ren, Zhanwu Lei

[Investigation Nitrogen Heterocyclic Compounds as Levelers for Electroplating Cu Filling by Electrochemical Method and Quantum Chemical Calculation](#)

16:00 to 16:20

**Chiao-Chien Wei** (Wet Deposition, BASF AP, Taoyuan, Taiwan), Eric Chou, Shih-Ming Lin, Steve Shih

[Bottom-up Filling of Damascene Trenches with Cobalt by Electroplating Process](#)

16:20 to 16:40

Coffee Break

16:40 to 17:00

**Ryoichi Aogaki** (Electronic Engineering, Polytechnic University, Tokyo, Japan), Ryoichi Morimoto, Miki Asanuma, Iwao Mogi, Atushi Sugiyama, Makoto Miura, Yoshinobu Oshikiri, Yusuke Yamauchi

[Chloride Effect on Chiral Catalytic Activity in Magneto-electrodeposition](#)

17:00 to 17:20

**Po-Fan Chan** (Chemical Engineering, National Chung Hsing University, Taichung, Taiwan), Wei-Ping Dow

[The Spontaneous Potential Oscillations in a Galvanostatic Copper Electrodeposition](#)

17:20 to 17:40

**Iwao Mogi** (Institute for Materials Research, Tohoku University, Sendai, Japan), Ryoichi Aogaki, Kazuo Watanabe

[Chirality Induction by Galvanostatic Magneto-electrodeposition](#)

17:40 to 18:00

**Alexander Vaskevich** (Materials and Interfaces, Weizmann Institute of Science, Rehovot, Israel), Mariano Susman, Israel Rubinstein

[Chemical Deposition and Galvanic Replacement of Morphologically Controlled Cu<sub>2</sub>O Nanoparticle Films](#)

18:00 to 18:20

**Yao-Lin Tsai** (Chemical Engineering, National Chung Hsing University, Taichung, Taiwan), Wei-Ping Dow

[Using Cu Nanoparticles as Catalysts of Electroless Copper Deposition for Metallization of a Printed Circuit Board](#)

---

## Symposium 9: Electrocatalytic Materials

---

**Room : 201EF**

*Chaired by:* Fabio Dionigi, Anthony Kucernak, Jun Maruyama and Yan Shen

14:00 to 14:20 Invited

**Jun Maruyama** (Environmental Technology Research Division, Osaka Municipal Technical Research Institute, Osaka, Japan), Tsutomu Shinagawa

[Catalyst Layer Structures for Enhancement of Redox Reactions of Oxovanadium Ions](#)

14:20 to 14:40

**Yan Shen** (Wuhan National Laboratory for Optoelectronics, HuaZhong University of Science and Technology, Wuhan, China)

[Self-Supported Co<sub>4</sub>FeP Nanosheet Arrays Supported on Carbon Cloth: An Efficient Catalyst for Electrochemical Hydrogen Evolution](#)

14:40 to 15:00

**Sho Fujita** (Chemical and Energy Engineering, Yokohama National University, 240-8501 Yokohama, Japan), Koichi Matsuzawa, Yuji Kohno, Ikuo Nagashima, Yoshio Sunada, Akiyoshi Manabe, Yoshinori Nishiki, Shigenori Mitsushima

[Property of Oxide Film and Activity of Li<sub>x</sub>Ni<sub>2-x</sub>O<sub>2</sub>/Ni Anode for Alkaline Water Electrolysis](#)

15:00 to 15:20

**Xi Cheng** (Electrochemistry Laboratory, Paul Scherrer Institute, Villigen PSI, Switzerland), Emiliana Fabbri, Maarten Nachtegaal, Raphael Haumont, Thomas Justus Schmidt

[Oxygen evolution reaction: correlation between electronic property and OER activity for  \$\text{La}\_{1-x}\text{Sr}\_x\text{CoO}\_3\$  \( \$x=0, 0.2, 0.4, 0.6, 0.8, 1\$ \) perovskite oxides](#)

15:20 to 15:40

**Wenting Xu** (Department of Materials Science and Engineering, Norwegian University of Science and Technology, Trondheim, Norway), Geir Martin Haarberg, Svein Sunde

[Electrochemical Performance of Oxygen Evolving Anodes in Sulphate Electrolyte for Copper Electrowinning](#)

15:40 to 16:00

**Juan Manriquez** (Department of Research, Cideteq, Pedro Escobedo, Mexico)

[Electrocatalytic oxidation of urea on Ni\(II\)cyclam-modified nanoparticulate  \$\text{TiO}\_2\$  anodes for promoting the  \$\text{H}\_2\$  evolution on Pt counterelectrodes](#)

16:00 to 16:20

**Ruud Kortlever** (Catalysis and Surface Chemistry, Leiden University, Leiden, Netherlands), Ines Peters, Collin Balemans, Meital Shviro, Youngkook Kwon, David Zitoun, Marc T.M. Koper

[Electrochemical  \$\text{CO}\_2\$  Reduction on Pd-based Bimetallic Catalysts](#)

16:20 to 16:40

Coffee Break

16:40 to 17:00

**Chun-Ting Li** (Chemical Engineering, National Taiwan University, Taipei, Taiwan), Chuan-Pei Lee, I-Ting Chiu, Kuo-Chuan Ho

[Earth Abundant Iron Diselenide Nanorod Arrays as the Flexible Electro-Catalytic Counter Electrode for Dye-Sensitized Solar Cells](#)

17:00 to 17:20

**Fabio Dionigi** (Department of Chemical Engineering, Technische Universität Berlin, Berlin, Germany), Tobias Reier, Zarina Pawolek, Manuel Gliech, Peter Strasser

[Activity and Selectivity of NiFe Layered Double Hydroxide Electrocatalyst for Seawater Electrolysis](#)

17:20 to 17:40

**Carlos M. Sanchez-Sanchez** (Laboratoire Interfaces et Systèmes Electrochimiques (LISE), CNRS UMR8235 - Sorbonne Universités, UPMC Univ Paris 06, Paris, France), Florin A. Hanc-Scherer, Enrique Herrero

[Electrochemical  \$\text{CO}\_2\$  Reduction at Platinum Surface Structured Electrodes in Room Temperature Ionic Liquids](#)

17:40 to 18:00

**Loreta Tamasauskaite-Tamasiunaite** (Department of Catalysis, Center for Physical Sciences and Technology, Vilnius, Lithuania), Ausrine Zabielaite, Svetlana Lichusina, Agne Matuseviciute, Dijana Simkunaite, Algirdas Selskis, Eugenijus Norkus

[Investigation of Hydrazine Oxidation at Co Fiber Structure Decorated with Pt Nanoparticles](#)

18:00 to 18:20

**Han Wang** (Department of Chemistry, Fudan University, Shanghai, China), Han Wang, Wen-Bin Cai

[Pt \(Pd\) Monolayer on Au Formed by One-Pot Chemical Process with Enhanced Electrocatalytic Performance on Ethanol Oxidation](#)

## Symposium 11: New Important Frontiers in Molecular Electrochemistry

**Room : 201D**

*Chaired by:* Chun-hsien Chen, Toshio Fuchigami, Jiri Ludvik and Armando Pombeiro

### 14:00 to 14:40 Keynote **Jaroslav Heyrovsky Prize for Molecular Electrochemistry**

**Flavio Maran** (Chemistry, University of Padova, Padova, Italy)

[Molecular Electrochemistry: from Protons to Electrons, from Molecules to Molecular Nanoclusters](#)

14:40 to 15:00

**Dongil Lee** (Department of Chemistry, Yonsei University, Seoul, Korea)

[Electrochemistry of Atomically Precise Metal Nanoclusters](#)

15:00 to 15:20 Invited

**M. Fátima C. Guedes da Silva** (Centro de Química Estrutural, Instituto Superior Técnico, Universidade de Lisboa, Lisboa, Portugal)

[Electron-transfer Induced Reactions in Ru and Sn Complexes with Biological Activity](#)

15:20 to 15:40

**Eric Labbe** (Departement de Chimie, Ecole Normale Supérieure, Paris, France), Jose de Jesus Cazaes-Marinero, Olivier Buriez, Christian Amatore, Gerard Jaouen, Hui Zhi Shirley Lee, Pascal Pigeon, Siden Top, Weng Kee Leong

[An electrochemical overview of the oxidative chemistry of ferrocenophanic and ruthenocene antiproliferative drugs](#)

15:40 to 16:00

**James Y. Becker** (Chemistry, Ben-Gurion University of the Negev, Beer Sheva, Israel), Tatiana Golub

[The Effect of Ring-Size on the Anodic Oxidation of Cyclic Amides](#)

16:00 to 16:20 Invited

**Zhifeng Ding** (Chemistry, The University of Western Ontario, London, Canada)

[Electrochemiluminescence of Quantum Dots and Clusters](#)

16:20 to 16:40

Coffee Break

16:40 to 17:20 Keynote

**Kazuhiro Chiba** (Applied Biological Science, Tokyo University of Agriculture and Technology, Tokyo, Japan), Takao Shoji, Yohei Okada, Shokaku Kim

[Anodic Synthesis of Unnatural Peptide and Nucleic Acid Derivatives](#)

17:20 to 17:40

**Jingxian Yu** (Department of Chemistry, The University of Adelaide, Adelaide, Australia), John Horsley, Andrew Abell

[Tunable Peptide-Based Molecular Wires: Experimental Evidence and Theoretical Insights](#)

17:40 to 18:00

**Chengchu Zeng** (College of Life-Science & Bioengineering, Beijing University of Technology, Beijing, China), Nanning Lu, Longji Li

[Electrochemically Induced Friedel-Crafts Arylation of Chalcone Epoxides and Enamides by Organic Redox Mediators](#)

18:00 to 18:20

**Jiri Ludvik** (Molecular Electrochemistry, J. Heyrovský Institute of Physical Chemistry ASCR, Prague, Czech Republic), Tomas Mikysek, Hana Kvapilova, Frantisek Josefik

[Oxaborine and Triazaborine Chromophores, Electrochemical and Theoretical Study](#)

18:20 to 18:40

**Wenrong Yang** (School of Life and Environmental Sciences, Deakin University, Waurn Pond, Australia)

[Real-time Electrochemical Monitoring Covalent Bond Formation in Solution via Nanoparticle-Electrode Collisions](#)

## Symposium 14: Modeling, Design and Characterization of Nanostructured, Electroactive and Multifunctional Materials

**Room : 101D**

*Chaired by:* Line Koefoed and Stefania Rapino

14:00 to 14:20 Invited

**Yoshitaka Tateyama** (International Center for Materials Nanoarchitectonics, National Institute for Materials Science, Tsukuba, Japan), Keisuke Ushirogata, Keitaro Sodeyama, Yukihiro Okuno

[DFT-MD Study on Formation Processes of Solid Electrolyte Interphase at Negative Electrode Interfaces in Lithium-Ion Battery](#)

14:20 to 14:40

**Louzhen Fan** (Department of Chemistry, Beijing Normal University, Beijing, China), Xiaoyun Tan, Ruihua Guo

[Electrochemical Synthesis of Red Fluorescent Graphene Quantum Dots for the Bioimaging Platform](#)

14:40 to 15:00

**Xingxing Chen** (School of Chemical Engineering, University of Science and Technology Liaoning, Anshan, China), Justus Masa, Alexander Botz, Daniela Wintrich, Wolfgang Schuhmann

[Evaluation of Bifunctional Electrocatalysts for Oxygen Reduction and Evolution by Means of Scanning Electrochemical Microscopy \(SECM\)](#)

15:00 to 15:20

**Alessandro Minguzzi** (Dipartimento di Chimica, Università degli Studi di Milano, Milan, Italy), Elisabetta Achilli, Francesco D'Acapito, Alberto Naldoni, Francesco Malara, Cristina Locatelli, Alberto Vertova, Paolo Ghigna

[Observation of Charge Transfer Cascade in  \$\alpha\$ -Fe<sub>2</sub>O<sub>3</sub>/IrO<sub>2</sub> Photoanodes by In-Operando X-Rays Absorption Spectroscopy](#)

15:20 to 15:40

**Joaquin Rodriguez-Lopez** (Department of Chemistry, University of Illinois at Urbana-Champaign, Urbana, USA), Jingshu Hui, Richa Bhargava, Xuan Zhou, Adam J. Chinderle

[The Impact of Short-Range Electronic Interactions on the Electrochemical Activity of Single- and Few-Layer Graphene](#)

15:40 to 16:20 Keynote

**Michael Holzinger** (Département de Chimie Moléculaire (DCM), University of Grenoble Alpes - CNRS, Grenoble, France)

[Graphene and Carbon Nanotubes for Bioelectrochemical applications](#)

16:20 to 16:40

Coffee Break

16:40 to 17:00 Invited

**Giovanni Valenti** (Chemistry G. Ciamician, University of Bologna, Bologna, Italy), Alessandro Boni, Tiziano Montini, Massimo Marcaccio, Stefania Rapino, Paolo Fornasiero, Maurizio Prato, Francesco Paolucci

[Co-axial Nanostructures for CO<sub>2</sub> Conversion: Synergic Effects between Carbon Nanotubes and Metal Oxides](#)

17:00 to 17:20

**Kristina Tschulik** (Chemistry, University of Oxford, Oxford, United Kingdom), Richard Compton

[Nano-Impacts – Studying Magnetic Field Effects on Single Magnetite Nanoparticles in Solution](#)

17:20 to 17:40

**Line Koefoed** (Department of Chemistry and iNANO, Aarhus University, Aarhus C, Denmark), Kyoko Shimizu, Steen Uttrup Pedersen, Kim Daasbjerg, Alexander Kuhn, Dodzi Zigah

[Simultaneous Covalent Assembling of Two Different Organic Films on Glassy Carbon Using Bipolar Electrochemistry](#)

17:40 to 18:00

**Stefania Rapino** (Department of Chemistry G. Ciamician, University of Bologna, Bologna, Italy), Emanuele Treossi, Vincenzo Palermo, Massimo Marcaccio, Francesco Zerbetto, Francesco Paolucci

[Scanning Electrochemical Microscopy for Probing the Properties of 2D Materials](#)

18:00 to 18:20

**Mikhail A. Vorotyntsev** (Chemistry Department, D. Mendeleev University of Chemical Technology of Russia, Moscow, Russia), Dmitry V. Konev, Olga I. Istakova, Olga A. Sereda, Maria A. Chamraeva, Charles H. Devillers

[Spectroelectrochemistry in the Course of Oxidative Electrolysis as a Tool to Determine the Molecular Structure of Electroactive Polymer Based on Mg\(II\) Porphine](#)

18:20 to 18:40

**Susana Cordoba de Torresi** (Instituto de Quimica, Universidade de São Paulo, São Paulo, Brazil), Fabian A. Cerda Pastrian, Andreson Marques, Pedro H.C. Camargo

[Tuning the electrocatalytic properties of Cu<sub>2</sub>O nanoparticles by controlling size and geometry](#)

---

## Symposium 18: General Session

---

**Room : 101B**

*Chaired by:* Leigh Aldous and Yann Leroux

14:00 to 14:20

**Alexander Oleinick** (Departement de Chimie, CNRS-ENS-UPMC UMR 8640 PASTEUR, Paris, France), Oleksii Sliusarenko, Irina Svir, Christian Amatore

[Validating a Central Approximation in Theories of Regular and Random Electrochemical Electrode Arrays](#)

14:20 to 14:40

**Ana Fernández-la-Villa** (R&D, Micrux Technologies, Oviedo, Spain), Diego F. Pozo-Ayuso, Mario Castaño-Álvarez

[New Strategies to Manufacture Low-cost Thin-film MicroElectrode Arrays for Electroanalysis](#)

14:40 to 15:00

**Ying Wan** (School of Mechanical Engineering, Nanjing University of Science and Technology, Nanjing, China), Pengjuan Wang, Yan Su

[Surface-Initiated Enzymatic Polymerization Based Signal Amplification Strategies for Sensitivity Improvement of Electrochemical DNA Sensors](#)

15:00 to 15:20

**Conchi Ania** (INCAR, CSIC, Oviedo, Spain), Alicia Gomis-Berenguer, Naiara Hernández-Ibañez, Jesus Iniesta

[Conductive mesoporous carbon electrodes for biosensing applications](#)

15:20 to 15:40

**Maria Cuartero** (Department of Inorganic and Analytical Chemistry, University of Geneva, Geneva, Switzerland), Gaston Crespo, Eric Bakker

[Thin Layer Ionophore-Based Membranes Electrochemically modulated by Poly\(3-octylthiophene\) for Multianalyte Detection](#)

15:40 to 16:00

**Saimon Moraes Silva** (Chemistry, The University of New South Wales, Sydney, Australia), Roya Tavallaie, Muhammed Alam, J. Justin Gooding

[Electrochemical Characterization of Gold-Coated Magnetic Nanoparticles as 'Dispersible Electrodes'](#)

16:00 to 16:20

**Jen-Yuan Wang** (Physics Division, Institute of Nuclear Energy Research, Taoyuan, Taiwan), Tse-Chuan Chou, Lin-Chi Chen, Kuo-Chuan Ho

[Amperometric Detection of Hemoglobin A1c using a Poly\(3-aminophenylboronic acid\) Thin Film with Binding-Induced Ion Flux Blocking](#)

16:20 to 16:40 Coffee Break

16:40 to 17:00

**Alicia Gomis-Berenguer** (Procesos químicos en energía y medio ambiente, Instituto nacional del carbón (INCAR-CSIC), Oviedo, Spain), Verónica Celorrio, David J. Fermín, Jesus Iniesta, Conchi O. Ania

[A glance at the photoelectrochemical response of nanoporous carbon/semiconductor electrodes](#)

17:00 to 17:20

**Leigh Aldous** (School of Chemistry, The University of New South Wales, The University of New South Wales, Sydney, Australia), Wuan Xin Teh, Trang Quynh To, Sean Cadogan

[Ferrocenium triiodide ionic liquids: Synthesis, electron transfer and their \(thermo\)electrochemical waste heat harvesting properties](#)

17:20 to 17:40

**Dan Nguyen Dang** (UR ABTE - EA 4651 & CRISMAT UMR6508 CNRS, IUT de Caen, Univ. Caen Basse-Normandie, Caen, France), Stéphanie Gascoin, Cosmelina G. Da Silva, Richard Retoux, Benoît Riffault, Daniel Chateigner, Otavio Gil

[Volume Synthesis of Calcareous Deposit on Carbon Steel in Natural Seawater: Effect of Two-Step Applied Potential Waveform](#)

17:40 to 18:00

**Zhang Dalei** (College of Mechanical and Electronic Engineering, China University of Petroleum, Qingdao, China)

[Wire Beam Electrode Technique for Investigation Galvanic Corrosion Behavior between Zinc and Carbon Steel](#)

18:00 to 18:20

**Miikka Jokinen** (Department of Chemistry, Aalto University, Espoo, Finland), José A. Manzanares, Kyösti Kontturi, Lasse Murtoimäki

[Thermal membrane potential - Application to thermoelectric power generation](#)



ROOMS:		101A	101B	101C	101D	102	103	201AB	201EF	201C	201D
SYMPOSIUM	s09	s18	s07	s14	s04	s01	s03	s09	s03	s11	
08:15 - 09:15	Plenary Lecture: Alan Bond (Plenary Hall)										
09:30 - 09:50	Chuan Zhao	Aicheng Chen	Shuehlin Yau	Enrico Veriato	Nguyen Minh	Gaston Crespo	T. Richard Jow	Chia-Ying Chiang	Helmut Balttruschat	Wenjing Hong	
09:50 - 10:10	Dejin Zang		Andrew Lodge	Guobao Xu	Aziz Nechache	Daniel Mandler		Atif Koca	James T. Frith	Toshio Fuchigami	
10:10 - 10:30	Wei-Fu Chen	A. I. Mardare	W. Schwarzacher	Kenta Imai	Anne Hauch	Damien Arigan	Liwei Zhao	Petr Krtil	Guoqing Wang	J-M. Saveant	
10:30 - 10:50	Zhaoxiong Xi	Micheal Scanlon	Marco Musiani	Joanna Dolinska	Sergey Rashkeev	Lin-Chi Chen	K. Tsunashima	Daniel Guay	Jing-Hua Tian		
10:50 - 11:10	Coffee Break										
11:10 - 11:30	Lindsay Wilson	Sung-Wook Kim	Damian Kowalski	Gyeong S. Hwang	L. Fernandez Macia	Zhang Meining	W. Wieczorek	Wen-Bin Cai	Masaki Yamagata	Joanne Tory	
11:30 - 11:50	Erika Bustos		Jianming Li		Junfu Bu		K. Uta Schwenke	Chr. Engelbrekt	Fu-Ming Wang	Xinsheng Zhang	
11:50 - 12:10	Xue Leng		H. Kazimierzak	S. Cordoba de T.			A. M. Haregewoin	Kobra Ghobadi	Masahiro Shimizu	Hiroyuki Ueda	
12:10 - 12:30	Chen-Hao Wang		Derck Schlettwein	Herenilton Oliveira			Chao Xu	Cheng-Lan Lin	Seung Sik Hwang		
Closing Ceremony 12:30 to 12:50 (Plenary Hall)											



# Friday, 9 October 2015 - Morning

---

## Plenary Lecture

**Room : Plenary Hall**

*Chaired by:* Justin Gooding

### 09:15 to 09:15 **Electrochimica Acta Gold Medal**

**Alan Bond** (Chemistry, Monash University, Clayton, Australia)

[A Voltammetric Odyssey: From Homogeneous Dropping Mercury to Heterogeneous Macro and Nano Electrodes: From the Manual Era to Advanced Automated High Speed Computation](#)

---

## Symposium 1: New Directions in Analytical Electrochemistry

**Room : 103**

*Chaired by:* Jyh-Myng Zen and Jie Zhang

09:30 to 09:50

**Gaston Crespo** (Inorganic and Analytical Chemistry, University of Geneva, Geneva, Switzerland), Majid Ghahraman Afshar, Eric Bakker

[Selective Proton Pump for Thin Layer Chemical Modulations](#)

09:50 to 10:10

**Daniel Mandler** (Institute of Chemistry, Hebrew University of Jerusalem, Jerusalem, Israel), Shlomit Kraus, Netta Bruchiel-Spanier, Yamit Pisman, Maria Hitrik

[Nanoparticles Imprinted Polymers \(NIP\): Speciation of Nanoparticles](#)

10:10 to 10:30

**Damien Arrigan** (NRI & Chemistry, Curtin University, Perth, Australia), Yang Liu, Masniza Sairi, Gregor Neusser, Christine Kranz

[Achieving diffusional independence in arrays of liquid-liquid nanointerfaces: improving the electroanalytical performance](#)

10:30 to 10:50

**Lin-Chi Chen** (Department of Bio-Industrial Mechatronics Engineering, National Taiwan University, Taipei, Taiwan), Chieh-Wen Yao, Chia-Hao Chang, Chih-Hao Chen, Che-Lun Chang, Hung-Yun Liao

[Stability-enhanced Screen-Printed Ion-Selective Electrodes \(SPISEs\) for Plant Factory and Smart Farming Applications](#)

10:50 to 11:10

Coffee Break

11:10 to 11:30

**Zhang Meining** (Department of Chemistry, Renmin University of China, Beijing, China)

[Patterning of Microelectrode Array with soft lithography for Biological Sensing](#)

## Symposium 3: Batteries for Tomorrow's World

Room : 201AB

Chaired by: She-huang Wu

09:30 to 10:10 Keynote

**T. Richard Jow** (Energy and Power Division, U.S. Army Research Laboratory, Adelphi, USA), Jan Allen, Joshua Allen, Samuel Delp, Jeffrey Wolfenstine

[Challenges and Progress in Developing High Voltage Li-ion Batteries](#)

10:10 to 10:30

**Liwei Zhao** (Elements Strategy Initiative for Catalysts and Batteries, Kyoto University, Fukuoka, Japan), Shigeto Okada

[A comparison of the thermal stability of electrolytes for Li- and Na-ion batteries](#)

10:30 to 10:50

**Katsuhiko Tsunashima** (Department of Materials Science, National Institute of Technology, Wakayama College, Wakayama, Japan), Hayato Fujimoto, Hsien Hau Wang, Larry Curtiss, Khalil Amine, Youhei Mizuguchi

[Electrochemical Behavior of Oxygen in Phosphonium Ionic Liquids as Electrolytes for Lithium Air Batteries](#)

10:50 to 11:10

Coffee Break

11:10 to 11:30 Invited

**W. Wieczorek** (Faculty of Chemistry, Warsaw University of Technology, Warsaw, Poland), M. Dranka, J. Zachara, Marek Marcinek, L. Niedzicki, M. Kalita, Anna Bitner-Michalska, G. P. Jankowski, Z. Zukowska

[Studies on ionic transport in liquid and polymeric electrolytes based on novel organic salts](#)

11:30 to 11:50

**K. Uta Schwenke** (Technical Electrochemistry, Technische Universität München, Garching bei München, Germany), Sophie Solchenbach, Benjamin Strehle, Michael Metzger, Stefano Meini, Julien Demeaux, Brett L. Lucht, Hubert A. Gasteiger

[The impact of CO<sub>2</sub> evolved from the reduction of VC and FEC during the formation cycle of lithium-ion batteries](#)

11:50 to 12:10

**Atetegeb Meazah Haregewoin** (Chemical Engineering, National Taiwan University of Science and Technology, Taipei, Taiwan)

[Design of Sulfur Based Electrolyte Additives for Advanced Lithium-ion Batteries](#)

12:10 to 12:30

**Chao Xu** (Department of Chemistry-Angström Laboratory, Uppsala University, Uppsala, Sweden), Fredrik Lindgren, Bertrand Philippe, Mihaela Gorgoi, Fredrik Björefors, Kristina Edström, Torbjörn Gustafsson

[Improved Performance of Silicon Anode for Li-Ion Batteries: Understanding the Surface Modification Mechanism of Fluoroethylene Carbonate as an Effective Electrolyte Additive](#)

---

## Symposium 3: Batteries for Tomorrow's World

---

**Room : 201C**

*Chaired by:* Gao Liu

09:30 to 09:50

**Helmut Baltruschat** (Chemistry, University of Bonn, Bonn, Germany), Christoph Bondué

[Oxygen Reduction and Evolution for Li-Air batteries: Role of the Electrocatalyst](#)

09:50 to 10:10

**James T. Frith** (Chemistry, University of Southampton, Southampton, United Kingdom), Luyi Yang, Nuria Garcia-Araez, John R. Owen

[Homogeneous Catalysts for Li-Oxygen Cells](#)

10:10 to 10:30

**Guoqing Wang** (School of Materials Science and Engineering, Zhejiang University, Hangzhou, China), Shuangyu Liu, Jian Xie, Fangfang Tu, Shichao Zhang, Tiejun Zhu, Gaoshao Cao, Xinbing Zhao

[RuO<sub>2</sub>-nanoparticles-coated  \$\delta\$ -MnO<sub>2</sub> as efficient catalytic cathode for high-performance Li-O<sub>2</sub> batteries](#)

10:30 to 10:50

**Jing-Hua Tian** (School of Energy, Soochow University, Suzhou, China), Yujiao Xu, Yue Fu, Jin Wang, Ruizhi Yang

[Synthesis and Catalytic Activity of Ni Doped CoFe<sub>2</sub>O<sub>4</sub> Hollow Nanospheres as Bi-functional Catalysts for Lithium Air Batteries](#)

10:50 to 11:10

Coffee Break

11:10 to 11:30

**Masaki Yamagata** (Faculty of Chemistry, Materials and Bioengineering, Kansai University, Suita, Japan), Yukiko Matsui, Takuya Takahashi, Satoshi Uchida, Masashi Ishikawa

[How to make an ideal electrolyte based on bis\(trifluorosulfonyl\)imide-based ionic liquid for lithium-ion and lithium-sulfur batteries](#)

11:30 to 11:50

**Fu-Ming Wang** (Graduate Institute of Applied Science and Technology, National Taiwan University of Science and Technology, Taipei, Taiwan)

[Self Terminated Oligomer Branched Architecture \(STOBA\) in lithium ion battery](#)

11:50 to 12:10

**Masahiro Shimizu** (Chemistry and Biotechnology, Tottori University, Tottori, Japan), Hiroyuki Usui, Hiroki Sakaguchi

[Application of ionic liquid electrolytes to Si electrode as a Li-ion battery anode](#)

12:10 to 12:30

**Seung Sik Hwang** (Energy Lab, Samsung Advanced Institute of Technology, Samsung Electronic, Suwon-si, Korea), Jun-Hwang Ku, Jae-Man Choi

[Lithium Containing Polymeric Binder for Improved Performance of Li-Ion Batteries](#)

## Symposium 4: Advances in Fuel Cells from Materials to Systems

Room : 102

Chaired by: Anne Hauch and Nguyen Minh

09:30 to 09:50 Invited

**Nguyen Minh** (Center for Energy Research, University of California, San Diego, La Jolla, USA)

[Solid Oxide Fuel Cells - A Clean and Efficient Energy Technology for the Future](#)

09:50 to 10:10

**Aziz Nechache** (Division of Physical Sciences and Engineering, King Abdullah University of Science and Technology (KAUST), Thuwal, Saudi Arabia), Samir Boulfrad, Mark Cassidy, Enrico Traversa, John T.S. Irvine

[Study of LSCM-CGO-Ni Anode Characteristics by Electrochemical Impedance Spectroscopy](#)

10:10 to 10:30

**Anne Hauch** (Department of Energy Conversion and Storage, Technical University of Denmark, Roskilde, Denmark), Karen Brodersen, Peter Stanley Jørgensen, Ming Chen

[Ni/YSZ Electrodes Optimized for Stability at High Electrolysis Current Density](#)

10:30 to 10:50

**Sergey Rashkeev** (Theory, Modeling & Simulation, Qatar Environment & Energy Research Institute, Doha, Qatar), Michael Glazoff, Stephen Herring

[Towards Control of Major Degradation Processes in Solid Oxide Electrolysis Cells](#)

10:50 to 11:10

Coffee Break

11:10 to 11:30

**Lucia Fernandez Macia** (Electrochemical and Surface Engineering group, Vrije Universiteit Brussel, Brussels, Belgium), Dries Van Laethem, Sigelinde Steenberge, Diederik Depla, Johan Deconinck, Annick Hubin

[Advanced EIS Study of the Ionic Conduction in Nanocrystalline Yttrium-Doped Ceria](#)

11:30 to 11:50

**Junfu Bu** (Department of Materials Science and Engineering, KTH Royal Institute of Technology, Stockholm, Sweden), Pär Jönsson, Zhe Zhao

[BaZr<sub>x</sub>Ce<sub>0.8-x</sub>Y<sub>0.2</sub>O<sub>3-δ</sub> \(x = 0.5, 0.6, 0.7\) Proton Conductors Prepared by Spark Plasma Sintering](#)

## Symposium 7: Electrodeposition - The Frontier Approach in Material Science and Nanofabrication

Room : 101C

Chaired by: Nikolay Dimitrov and Andrew Gewirth

09:30 to 09:50 Invited

**Shuehlin Yau** (Chemistry, National Central University, Zhongli, Taiwan)

[In situ Scanning Tunneling Microscopy Imaging Self-Assembled Monolayers of Mercaptoacetic Acid and Cupric Ion on Au\(111\) Electrode](#)

09:50 to 10:10

**Andrew Lodge** (Department of Chemistry, University of Southampton, Southampton, United Kingdom), Calum Robertson, Andrew Hector

[The Synthesis and Characterisation of Mesoporous Silica Films for use in Supercritical Fluid Electrodeposition](#)

10:10 to 10:30

**W. Schwarzacher** (Physics, University of Bristol, Bristol, United Kingdom), R. J. Brooke, Chengjun Jin, D. S. Szumski, R. J. Nichols, Bingwei Mao, K. S. Thygesen

[A Ni - 4,4'-bipyridine - Ni single-molecule electrochemical transistor](#)

10:30 to 10:50

**Marco Musiani** (IENI, CNR, Padova, Italy), Sandro Cattarin, Nicola Comisso, Paolo Guerriero, Luca Mattarozzi, Enrico Verlato

[Oxygen Bubble Templated Anodic Deposition of Porous PbO<sub>2</sub>](#)

10:50 to 11:10

Coffee Break

11:10 to 11:30

**Damian Kowalski** (Laboratoire de Recherche en Nanosciences, University of Reims Champagne-Ardenne, Reims, France)

[TiO<sub>2</sub> Nanotubes with Wide Spacing – a Platform for Electrodeposited Nanostructures](#)

11:30 to 11:50

**Jianming Li** (Research Institute of Petroleum Exploration & De, PetroChina, Beijing, China), Jin Xu, Xiaoqi Wang, Liang Sun, Songtao Wu

[Characterization of the microstructure of reservoirs using electrodeposition method](#)

11:50 to 12:10

**Honorata Kazimierzak** (Institute of Metallurgy and Materials Science, Polish Academy of Sciences, Krakow, Poland), Agnieszka Hara, Piotr Ozga

[Electrodeposition of Zn-Mn-Mo layers from citrate solutions](#)

12:10 to 12:30

**Derck Schlettwein** (Institute of Applied Physics, Justus-Liebig-University Giessen, Giessen, Germany), Martina Stumpp, Thi Hai Quyen Nguyen, Christian Lupo

[Interplay of Different Reaction Pathways in the Pulsed Galvanostatic Deposition of ZnO](#)

---

## Symposium 9: Electrocatalytic Materials

---

**Room : 101A**

*Chaired by:* Lindsay Wilson and Dejin Zang

09:30 to 09:50

**Chuan Zhao** (School of Chemistry, The University of New South Wales, Sydney, Australia), Xunyu Lu, Changlong Xiao

[Three Dimensional Precious Metal Free Electrocatalysts for Water Splitting](#)

09:50 to 10:10

**Dejin Zang** (Chemistry, University of Strasbourg, Institute of Chemistry, Strasbourg, France), Antoine Bonnefont, Laurent Ruhlmann

[Porphyrin-Polyoxometalates@Pt Modified Electrodes for Electrocatalytic Hydrogen Evolution Reaction](#)

10:10 to 10:30

**Wei-Fu Chen** (Chemistry Department, Brookhaven National Laboratory, Upton, USA), Kotaro Sasaki, Jonathan Schneider, Chiu-Hui Wang, James Muckerman, Etsuko Fujita

[Nitride-Stabilized Tungsten Carbide Electrocatalysts for Hydrogen Evolution Reaction](#)

10:30 to 10:50

**Zhaoxiong Xie** (Department of Chemistry, Xiamen University, Xiamen, China), Qiaoli Chen, Haixin Lin, Yanyan Jia, Zhenming Cao, Yaqi Jiang, Lansun Zheng

[Supersaturation Dependent Evolution of Nanocrystal Surfaces and its Application in the Synthesis of Noble Metal Nanocatalysts with Enhanced Electrocatalytic Properties](#)

10:50 to 11:10 Coffee Break

11:10 to 11:30

**Lindsay Wilson** (Chemistry, University of the Western Cape, Cape Town, South Africa), Candice Rassie, Priscilla Baker, Emmanuel Iwuoha

[Electrochemical Responses of Transglutaminase Immunosensor Developed on a Polypyrrole-Cobalt \(II\) Salicyladiimine Dendritic Composite Material](#)

11:30 to 11:50

**Erika Bustos** (Science, Centro de Investigación y Desarrollo Tecnológico en Electroq, Querétaro, Mexico), Rosa Herrada, Oswaldo Cuevas, Federico Manríquez, Alejandro Medel, Igancio Sirés

[Electrocatalytic Effect of IrO<sub>2</sub>-Ta<sub>2</sub>O<sub>5</sub>/Ti in the Electrochemical Degradation of Phenanthrene, Naphthalene and Fluoranthene in Wastewater from the Electrokinetic Treatment of Polluted Soil by Hydrocarbons](#)

11:50 to 12:10

**Xue Leng** (School of Chemistry and Molecular Biosciences, the University of Queensland, Brisbane, Australia)

[Reduction Induced Surface Amorphization Enhances Oxygen Evolution Reaction Activity in Co<sub>3</sub>O<sub>4</sub>](#)

12:10 to 12:30

**Chen-Hao Wang** (Department of Materials Science and Engineering, National Taiwan University of Science and Technology, Taipei, Taiwan), Vuri Ayu Setyowati, Hsin-Chih Huang

[Effect of Iron Precursor on Oxygen Reduction Reaction of Fe-N-C Catalyst in PEMFC](#)

---

## Symposium 9: Electrocatalytic Materials

---

**Room : 201EF**

*Chaired by:* Christian Engelbrekt and Petr Krtil

09:30 to 09:50

**Chia-Ying Chiang** (Department of Chemical Engineering, National Taiwan University of Science and Technology, Taipei, Taiwan), Po-Tso Ting

[Multi-Components Amorphous Metal-Oxides Catalysts for Oxygen Evolution Reaction](#)

09:50 to 10:10

**Cheng-Lan Lin** (Department of Chemical and Materials Engineering, Tamkang University, New Taipei City, Taiwan), Ju-Yu Yeh

[Preparation and Characterization of Platinum Nanoparticles Supported on Silica-Carbon Black Nanocomposites for Methanol Oxidation Reaction](#)

10:10 to 10:30

**Petr Krtil** (Electrocatalysis, J. Heyrovsky Institute of Physical Chemistry, Prague, Czech Republic), Tatsuya Hiratoko, Hana Hoffmannova, Jonathan Mueller, Timo Jacob

[Dynamics of Pt/Ru Based Alloy Catalysts in Formate Oxidation Process – a DFT and In-Situ XAS Approach](#)

10:30 to 10:50

**Daniel Guay** (Énergie, Matériaux, Télécommunications, INRS, Varennes, Canada), Claudie Roy, Sébastien Garbarino, Ifan Stephens, Ib Chorkendorff

[Electroreduction of CO on mesoporous Cu and oxide-derived mesoporous Cu electrodes](#)

10:50 to 11:10

Coffee Break

11:10 to 11:30

**Wen-Bin Cai** (Department of Chemistry, Fudan University, Shanghai, China), Kun Jiang, Ye Wang

[Bridging across Electrocatalytic Performances of Nanomaterials & Interfacial Species Evolution with Realtime ATR-IR Spectroscopy](#)

11:30 to 11:50

**Christian Engelbrekt** (Department of Chemistry, Technical University of Denmark, Lyngby, Denmark),  
Nedjeljko Seselj, Jens Ulstrup, Jingdong Zhang

[Facile synthesis of starch-scaffolded bimetallic Au-Pt nanostructure and electrocatalysis](#)

11:50 to 12:10

**Kobra Ghobadi** (Chemistry, Yazd University, Yazd, Iran (Islamic Republic of)), Hamid Reza Zare, Hossein Khoshro, Alireza Gorji, Abbas Ali Jafari

[A Study of the Catalytic Activity of a Schiff Base Ligand on Electrochemical Reduction of Carbon Dioxide: Indirect Electrocatalytic Synthesis of Isonicotinic Acid](#)

---

## Symposium 11: New Important Frontiers in Molecular Electrochemistry

---

**Room : 201D**

*Chaired by:* Olivier Buriez, Kazuhiro Chiba, Flavio Mara and Jean-Michel Saveant

09:30 to 09:50

**Wenjing Hong** (Department of Chemistry and Biochemistry, University of Bern, Bern, Switzerland), Masoud Baghernejad, Cancan Huang, Thomas Wandlowski

[Break Junction under Electrochemical Gating: Fermi-level Tuning and Redox Manipulation](#)

09:50 to 10:10

**Toshio Fuchigami** (Department of Electronic Chemistry, Tokyo Institute of Technology, Yokohama, Japan), Shinsuke Inagi

[Selective Electrochemical Fluorination of Organic Molecules and Macromolecules Using Poly\(HF\) Salt Ionic Liquids](#)

10:10 to 10:50 Keynote

**Jean-Michel Saveant** (Chemistry, Université Paris Diderot (Paris 7), Paris 13, France)

[Current Issues in Molecular Catalysis Illustrated by Iron Porphyrins as Catalysts of the CO<sub>2</sub>-to-CO Electrochemical Conversion](#)

10:50 to 11:10 Coffee Break

11:10 to 11:30

**Joanne Tory** (Chemistry, University of Reading, Reading, United Kingdom), František Hartl

[Transition Metal  \$\alpha\$ -Diimine Carbonyl Complexes for Electrocatalytic CO<sub>2</sub> Reduction](#)

11:30 to 11:50

**Xinsheng Zhang** (Department of Chemical Reaction Engineering, East China University of Science and Technology, Shanghai, China), Ling Jin, Dongfang Niu

[Action Mechanism of Quaternary Ammonium Compound in the Electroreduction of Oxalic Acid to Glyoxylic Acid](#)

11:50 to 12:10

**Hiroyuki Ueda** (Graduate School of Science and Technology, Kumamoto University, Kumamoto, Japan), Katsuhiko Nishiyama, Soichiro Yoshimoto

[Influence of Cations on the Control of the Multiple Redox States of Fullerene at the Ionic Liquid Electrochemical Interface](#)

## Symposium 14: Modeling, Design and Characterization of Nanostructured, Electroactive and Multifunctional Materials

**Room : 101D**

*Chaired by:* Masa-aki Haga and Alessandro Minguzzi

09:30 to 09:50 Invited

**Enrico Verlato** (IENI-CNR, CNR, Padova, Italy), Simona Barison, Wenyan He, Didier Floner, Florence Fourcade, Abdeltif Amrane, Florence Geneste, Marco Musiani

[Deposition of Ag Nanostructures on Ni-based 3D Electrodes and their Application as Electrocatalysts](#)

09:50 to 10:10

**Guobao Xu** (State Key Laboratory of Electroanalytical Chemistry, Changchun Institute of Applied Chemistry, Chinese Academy of, Changchun, China), Jianping Lai, Wenxin Niu, Ling Zhang

[Shape-Controlled and Size-Controlled Synthesis of Metal Nanocrystals and Their Electrochemical Applications](#)

10:10 to 10:30

**Kenta Imai** (Department of Chemistry, University of Bologna, Bologna, Italy), Giovanni Valenti, Elena Villani, Massimo Marcaccio, Luca Prodi, Francesco Paolucci

[Effect of Electrode Surface-State Change on Electrogenenerated Chemiluminescence from a Ruthenium-Doped Silica Nanoparticle](#)

10:30 to 10:50

**Joanna Dolinska** (Department of Electrode Processes, Institute of Physical Chemistry Polish Academy of Sciences, Warsaw, Poland), Arunraj Chidambaram, Zahra Taleat, Witold Adamkiewicz, Wojciech Lisowski, Michalina Iwan, Barbara Palys, Volodymyr Sashuk, Tomasz Andryszewski, Marcin Opallo, Liza Rassaei

[Electrocatalytic Oxidation of Biologically Active Compoundson MoS<sub>2</sub> Nanopetal Stacks Decorated with Carbon or Gold Nanoparticles](#)

10:50 to 11:10

Coffee Break

11:10 to 11:50 Keynote

**Gyeong S. Hwang** (McKetta Department of Chemical Engineering, University of Texas at Austin, Austin, USA)

[Understanding and Predicting the Photocatalytic Properties of Bismuth Vanadate from First Principles](#)

11:50 to 12:10

**Herenilton Oliveira** (Chemistry, Universidade de São Paulo, Ribeirão Preto, Brazil), Jane Machado

[Preparation, Characterization, and Electrochemical Properties of Monolith Glass-like Carbon-Silica Composites](#)



---

## Symposium 18: General Session

---

**Room : 101B**

*Chaired by:* Micheal Scanlon and Neeraj Sharma

09:30 to 10:10 Keynote

**Aicheng Chen** (Department of Chemistry, Lakehead University, Thunder Bay, Canada)

[Palladium-Based Nanomaterials: Synthesis and Electrochemical Applications](#)

10:10 to 10:30

**Andrei Ionut Mardare** (Institut for Chemical Technology of Inorganic Materials, Johannes Kepler University Linz, Linz, Austria), Christian Siket, Cezarina Cela Mardare, Siegfried Bauer, Achim Walter Hassel

[Dynamics of Interfacial Oxide Formation during Anodization of Valve Metal Superimposed Ultra-Thin Films](#)

10:30 to 10:50

**Micheal Scanlon** (Department of Chemistry & Tyndall National Institute, University College Cork, Cork, Ireland), Andres Molina Osorio

[Functionalization of Conductive Carbon Supports at Water/Oil Interfaces with Non-Precious Metal Hydrogen Evolution Catalysts](#)

10:50 to 11:10

Coffee Break

11:10 to 11:30

**Sung-Wook Kim** (Nuclear Fuel Cycle Process Development Group, Korea Atomic Energy Research Institute, Daejeon, Korea), Eun-Young Choi, Wooshin Park, Hun Suk Im, Jin-Mok Hur

[Conductive Ceramics as O<sub>2</sub>-Evolving Anodes for Electrolytic Reduction of Metal Oxides](#)



# Poster presentation program



## Symposium 1: New Directions in Analytical Electrochemistry

### Analytes

s01-001

**Shu-Hua Cheng** (Department of Applied Chemistry, National Chi Nan University, Nantou Hsien, Taiwan), Yen-Hua Liao, Ya-Ling Su

[Electrochemical Determination of Bisphenol A at Conducting Poly\(diallyldimethylammonium chloride\) Film-Modified Preanodized Screen-Printed Carbon Electrodes](#)

s01-002

**Xiaorong Gan** (School of Environmental Science and Technology, Dalian University of Technology, Dalian, China)

Highly Sensitive Electrochemical Sensor for Cu (II) Ions Based on Three-dimensional Porous  $H_xTiS_2$  Nanosheet-polyaniline

s01-003

**Huangxian Ju** (State Key Laboratory of Analytical Chemistry for Life Science, Nanjing University, Nanjing, China)

Amplified Electrochemical Analysis of DNA and Proteins

s01-004

**Akira Kotani** (School of Pharmacy, Tokyo University of Pharmacy and Life Sciences, Tokyo, Japan), Mizuki Watanabe, Kazuhiro Yamamoto, Fumiyo Kusu, Hideki Hakamata

High-performance Liquid Chromatography with Electrochemical Detection for Determining a Ratio of Eicosapentaenoic Acid to Arachidonic Acid in Human Plasma

s01-005

**Si-Ping Wang** (Chang Gung University, Taoyuan, Taiwan), Trav Huang, Andrew S. Lin

Study of the Electrochemical Oxidation of Dissolved Carbon Monoxide in Acidic and Alkaline Electrolytes by Using and Fabricated Au-Microelectrode

### Data analysis

s01-006

**RyeoYun Hwang** (Graduate School of Analytical Science & Technology, Chungnam National University, Daejeon, Korea), Oc Hee Han, Young-Seok Byun

Multiple On-line NMR System Development to Detect Electrochemical Reactions of Direct Alcohol Fuel Cells

s01-007

**Jan Vacek** (Department of Medical Chemistry and Biochemistry, Palacky University, Olomouc, Czech Republic), Jan Hrbac, Vladimir Halouzka, Libuse Trnkova

eL-Chem Viewer: A Freeware Package for the Analysis of Electrochemical Data

### Electrodes

s01-008

**Fethi Bedioui** (CNRS UTCBS 8258-Chimie ParisTech, Chimie ParisTech, Paris, France), Amandine Calmet, Sophie Griveau, Virginie Lair, Michel Cassir, Abdelilah Amar, Eliane Sutter, Philippe Brunswick

Corrosion behavior of biocompatible stainless steels in physiological medium for application to non-invasive diagnosis of small fiber neuropathies

s01-009

**Jan Clausmeyer** (Analytische Chemie, Center for Electrochemical Sciences, Ruhr-Universität Bochum, Bochum, Germany), Justus Masa, Edgar Ventosa, Wolfgang Schuhmann

Investigation of Single Ni(OH)<sub>2</sub> Nanoparticles: Electrocatalysis and Energy Storage at Ultrafast Mass Transport

s01-010

**Yingchun Li** (Pharmacy, School of Pharmacy, Shihezi University, Shihezi, China), Jie Liu, Han Song, Jiang Liu, Lu Zhang

Ultrasensitive electrochemical sensing of metronidazole using molecularly imprinted polymer decorated hollow nickel nanospheres on carbon nanotubes

s01-011

**Huei-Ping Liou** (Chemical and Materials Engineering, Chang Gung University, Tao-Yuan, Taiwan), Chia-Liang Sun

Microwave-Assisted Synthesis of Graphene Oxide Nanoribbons Using Green Chemistry for the Electrochemical Detection

s01-012

**Yanyan Song** (Research Center for Analytical Sciences, College of Sciences, Northeastern University, Yanyan Song, China), Tongtong Li

Cocoon Silk-Derived Carbon Nanospheres: Highly Activated Metal-Free Electrocatalysts for Reduction of Dissolved Oxygen and Glucose Sensing

s01-013

**Chia-Liang Sun** (Dept. of Chem. and Mater. Eng., Chang Gung University, Tao-Yuan, Taiwan), Chun-Hao Su, Jhing-Jhou Wu, Chen-Fu Pan

Synthesis of Short or Holey Graphene Oxide Nanoribbons for the Electrochemical Detection of Biomarkers

s01-014

**Takami Tsukuma** (Dept of Science of Environment and Mathematical Modeling, Doshisha University, Kyotanabe, Japan), Masatsugu Morimitsu

A Novel Electrochemical Sensing of Hydrogen Phosphate Ion with RuO<sub>2</sub>-Ta<sub>2</sub>O<sub>5</sub> Mixed Oxide

s01-015

**Giovanni Valenti** (Chemistry G. Ciamician, University of Bologna, Bologna, Italy), Martina Zangheri, Sandra Sansaloni, Mara Mirasoli, Alain Penicaud, Aldo Roda, Francesco Paolucci

Transparent Carbon Nanotube Network for Efficient Electrochemiluminescence Device

s01-016

**Guor-Tzo Wei** (Chemistry and Biochemistry, National Chung Cheng University, Chiayi, Taiwan)

The Modification of Screen-printed Carbon Electrodes with Polymerized Ionic Liquid Composites for Chemical Analysis

s01-017

**Yavuz Yardým** (Analytical Chemistry, Yüzüncü Yıl University, Faculty of Pharmacy, Van, Turkey), Metin Celebi, Abdulkadir Levent, Zühre Sentürk, Aydin Yigit

Using Graphene-Nafion Composite Film Modified Glassy Carbon Electrode for the Simultaneous Determination of Paracetamol, Aspirin and Caffeine in Pharmaceutical Formulations

s01-018

**Mingzhong Zou** (Condensed Matter Physics, Fujian Normal University, Fuzhou, China), Wenyu Yang, Xiang Chen, Guiying Zhao, Jiaxin Li, Yingbin Lin, Zhigao Huang

Suppression of degradation of lithium ion batteries for LiFePO<sub>4</sub>@C batteries by nano Si surface modification

## Techniques

s01-019

**Gan-Zuei Chang** (Department of Chemistry, University of Oxford, Oxford, United Kingdom), Robert Jacobs, Kylie Vincent

*In situ* ATR-IR spectroelectrochemical study of the deactivation of Pd/C catalysts used in DFAFC by common impurities found in formic acid

s01-020

**Guy Denuault** (Chemistry, University of Southampton, Southampton, United Kingdom), Ana Cristina Perdomo Marin

An *in-situ* Microelectrode Study of the Sea Surface Microlayer: Experimental and Theoretical Challenges

s01-021

**Ertugrul Keskin** (Analytical Chemistry, Adiyaman University, Faculty of Pharmacy, Adiyaman, Turkey), Yavuz Yardim, Abdulkadir Levent, Zuhre Senturk

Electrochemical determination of Norepinephrine by adsorptive stripping voltammetry using a boron doped diamond electrode

s01-022

**Genxi Li** (Department of Biochemistry, Nanjing University, Nanjing, China), Hao Li, Yue Huang, Luming Wei, Weiwei Li, Xiaoli Zhu

Fabrication of Electrochemical Biosensor by Using Peptide as a New Kind of Recognition Element

s01-023

**Samuel Perry** (Chemistry, University of Southampton, Southampton, United Kingdom), Guy Denuault

Normalised Sampled-Current Voltammetry at Microdisc Electrodes: Kinetic Information from Pseudo Steady State to Steady State Voltammetry

s01-024

**Yukihiro Shintani** (School of Science and Engineering, Tokyo, Japan)

Characterization of Polycrystalline Doped-diamond Electrolyte-solution-gate Field-effect Transistor pH Sensor with/without Termination Control

s01-025

**Simon Theil** (ZSW - Ulm, Zentrum für Sonnenenergie und Wasserstoffforschung, Ulm, Germany), Margret Wohlfahrt-Mehrens

Investigation of cell aging by analysis of electrolyte decomposition *via* gas chromatography

s01-026

**Her Shuang Toh** (Department of Chemistry, Oxford University, Oxford, United Kingdom), Richard Compton

'Nano-impacts': An Electrochemical Technique for Nanoparticle Sizing in Optically Opaque Solutions

s01-027

**Yavuz Yardým** (Analytical Chemistry, Yüzüncü Yıl University, Faculty of Pharmacy, Van, Turkey)

Square-Wave Adsorptive Stripping Voltammetric Determination of Resveratrol Using Boron-Doped Diamond Electrode in the Presence of Hexadecyl Trimethyl Ammonium Bromide

s01-028

**Chuan Zhao** (School of Chemistry, The University of New South Wales, Sydney, Australia), Asim Khan

Oxygen Reduction Reactions in Ionic Liquids-Based Mixture Electrolytes for High Performance Rechargeable Li-O<sub>2</sub> Batteries

s01-029

**Javier Izquierdo Pérez** (Institute of Analytical and Bioanalytical Chemistry, University of Ulm, Ulm, Germany), B. Mizaikoff, C. Kranz

[An Analytical Platform for the Characterization of Electrochemical Processes at AuNPs-Modified BDD Electrodes](#)

s01-030

**Omotayo Arotiba** (Applied Chemistry, University of Johannesburg, Johannesburg, South Africa) Olayiwola Idris, Nonhlangabezo Mabuba

[Dealing with Interferences in the Electrochemical Detection of Arsenic – a Complexometric Masking Approach](#)

## Symposium 2: Electrochemical Aspects of Biological Systems: Theory, Experiment and Applications

### Bio-device

s02-001

**Stefania Rapino** (Chemistry Department G. Ciamician, University of Bologna, Bologna, Italy), Mirella Trinei, Matteo Iurlo, Eleonora Ussano, Alice Soldà, Giovanni Valenti, Pier-Giuseppe Pelicci, Francesco Paolucci, Massimo Marcaccio, Marco Giorgio

Development of an Electrochemically Based Rapid, Low-cost and Spreadable Assay for Heart Injury and Cancer Related Pathologies

s02-002

**Mistuo Sano** (Precision and Intelligence Laboratory, Tokyo Institute of Technology, Yokohama, Japan), Yuma Tahara, Chun-Yi Chen, Tomoko Hashimoto, Hiromichi Kurosu, Masato Sone

Pd Catalyzation and Electroless Deposition of Ni on Textile Using Supercritical Carbon Dioxide

### Biochip

s02-003

**Ausra Baradoke** (Department of Nanoengineering, Center for Physical Sciences and Technology, Vilnius, Lithuania), Aneta Radzevic, Raimonda Celiesiute, Ramunas Valiokas, Rasa Pauliukaite

Graphene Electrodes for Electrochemical Detection of Biomarkers

### Bioelectrocatalysis

s02-004

**Sofiene Abdellaoui** (Chemistry, University of Utah, Salt Lake City, USA)

New enzymes for the hybrid enzymatic and organic electrocatalytic cascade for the complete oxidation of glycerol

s02-005

**Fred Lisdat** (Biosystems Technology, Institute of Applied Life Sciences, Technical University Wildau, Wildau, Germany), J. Gladisch, D. Sarauli, B. Schulz

Electrospun, conductive polymer fleeces as electrode materials for enhanced bioelectrocatalysis

### Biofuel

s02-006

**Adalgisa De Andrade** (Chemistry, FFCLRP/USP, Universidade de São Paulo, Ribeirao Preto, Brazil), Sidney Aquino-Neto, Ana L. R. L. Zimbardi, Franciane P. Cardoso, Lais B. Crepaldi, Rosa R.P.M. Furriel

Biocathodes Using a Laccase from *Pycnoporus sanguineus* and their Potential Application in Methanol/O<sub>2</sub> Biofuel Cell

s02-007

**Isao Shitanda** (Department of Pure and Applied Chemistry, Tokyo University of Science, Chiba, Japan), Saki Nohara, Seiya Tsujimura, Yoshinao Hoshi, Masayuki Itagaki

Fabrication of Paper-based Disk-shaped Glucose Biofuel Array

### Biointerface

s02-008

**Eun Joong Kim** (Department of Chemistry, Seoul National University, Seoul, Korea), Taek Dong Chung

Fabrication of Artificial Synaptic Interfaces Using Engineered Synaptic Adhesion Proteins

s02-009

**Alexander Vaskevich** (Materials and Interfaces, Weizmann Institute of Science, Rehovot, Israel), Tatyana B. Bendikov, Ortal Bachar, Frolov Ludmila, Israel Rubinstein

Effect of Nanoscale Surface Morphology on Biorecognition Using Localized Surface Plasmon Resonance (LSPR) Spectroscopy

**Biosensor**

s02-010

**Jingyi Chen** (College of Chemistry and Chemical Engineering, Jiangxi Normal University, Nanchang, China)  
An Ultrasensitive pH-Switchable Electrochemical Immunosensing based on Integrated 3D-KSCs Electrode as Singal Collector and AuNPs-Ab<sub>2</sub>-GOD-ConA as Tracing Tag for Assay of CEA

s02-011

**Shengyuan Deng** (School of Environmental and Biological Engineering, Nanjing University of Science and Technology, Nanjing, China)  
Label-Free Biomimetic Electrocatalysis-Induced Precipitation for Ultrasensitive Bioanalysis

s02-012

**Juan He** (College of Chemistry and Chemical Engineering, Jiangxi Normal University, Nanchang, China), Li Wang  
The GOD/Cu-Hemin Metal Organic Frameworks Nanocomposites for Glucose Sensing

s02-013

**Bang-De Hong** (Department of Chemical and Materials Engineering, National Kaohsiung University of Applied Sciences, Kaohsiung City, Taiwan), Chien-Liang Lee  
Defective graphene flake-supported Pd nanocubes as electrochemical glucose sensor

s02-014

**Shih-Han Huang** (Graduate Institute of Applied Science and Technology, National Taiwan University of Science and Technology, Taipei, Taiwan), Fu-Ming Wang  
Ultra-sensitive electrochemical electrode developed for ovarian cancer

s02-015

**Yuki Igaki** (Graduate School of Material Science, University of Hyogo, Ako, Japan), Fumio Mizutani, Tomoyuki Yasukawa  
Measurement of oxygen consumption of contracting C<sub>2</sub>C<sub>12</sub> myotube using scanning electrochemical microscopy

s02-016

**Bohdan Josypcuk** (Biomimetic Electrochemistry, J. Heyrovsky Institute of Physical Chemistry, Prague, Czech Republic), Oksana Josypcuk  
Biosensors with Electrochemical Detection at High Negative Potentials in Flow Systems

s02-017

**Yingchun Li** (Pharmacy, School of Pharmacy, Shihezi University, Shihezi, China), Han Song, Jie Liu, Lu Zhang, Jiang Liu, Yuan Liu  
Ultrasensitive and selective electrochemical sensor for dopamine determination based on novel supportless nanoporous Au-Ag alloy microrod

s02-018

**Ya-Yi Liang** (Department of Chemical and Materials Engineering, National Chin-Yi University of Technology, Taichung, Taiwan), Yung-Chien Luo, Jing-Shan Do  
Preparation and characterization of amperometric monoenzyme creatinine biosensor based on creatinine deiminase/PANI-PSSMA/Au/Al<sub>2</sub>O<sub>3</sub> electrode

s02-019

**Ming Jie Lin** (Department of Bio-industrial Mechatronics Engineering, National Chung Hsing University, Taichung, Taiwan), Ching Chou Wu  
Effect of the ratio of poly-L-lysine/glucose oxidase/ferricyanide composite on the sensing properties of second generation blood glucose sensors

s02-020

**Yang Liu** (Department of Chemistry, Tsinghua University, Beijing, China)  
Electrodeposited NiCo bimetallic nanoparticles decorated reduced graphene oxide for highly sensitive and selective determination of dopamine

s02-021

**Aimi Suzuki** (Materials Science, Faculty of Pure and Applied Sciences, University of Tsukuba, Tsukuba, Japan), Kazuki Murata, Seiya Tsujimura  
Characterization of Glucose Oxidase-Redox Hydrogel on MgO-templated Carbon Electrode



s02-022

**Junko Tanaka** (Research & Development Group, Hitachi, Ltd., Tokyo, Japan), Yu Ishige, Masao Kamahori  
Direct detection for ratio of concentrations of HbA1c to total hemoglobin with potentiometric immunoassay

s02-023

**Nozomu Tsuruoka** (Division of Material Science, Pure and Applied Sciences, University of Tsukuba, Tsukuba, Japan), Kazuki Murata, Seiya Tsujimura  
Glucose Biosensor based on a Glassy Carbon Electrode Modified with Poly(methylene green) and FAD-dependent Glucose Dehydrogenase

s02-024

**Shih-Han Wang** (Department of Chemical Engineering, I-Shou University, Kaohsiung City, Taiwan), Yi-Han Yen, Jing-Hwei Wang, Ming-Der Ger  
Improvement of Electrochemical Biosensor Performance for Hydrogen Peroxide Sensing Based on Iridium Nanoparticles Modified Graphene Oxide

s02-025

**Mikito Yasuzawa** (Department of Chemical Science and Technology, Tokushima University, Tokushima, Japan), Jiang Li, Masahiro Uchimar, Shunsuke Isoai, Yusuke Fuchiwaki  
Fabrication of Low Invasive Glucose Sensor for Continuous Glucose Monitoring

s02-026

**Yongchun Zhu** (Chemistry, Institute of Energy and Environment Catalysis, Shenyang Normal University, Shenyang, China), Jie Hao, Jianqiao Lang, Nan Xiao, Amin Bao  
Amperometric bromide biosensor based on graphite powder composite electrode modified with leaf paste of natural amaranth induced by spaying KBr aqueous solution

## Electron transfer

s02-027

**Xiao-Yuan Liu** (Department of Chemistry, East China University of Science and Technology, Shanghai, China)  
Electrochemistry-controlled Photo-induced Electron Transfer in Ubiquinone-based Systems

s02-028

**Galina Pankratova** (Department of Biochemistry and Structural Biology, Lund University, Lund, Sweden), Kamrul Hasan, Donal Leech, Lars Hederstedt, Lo Gorton  
Electrochemical Study of the Extracellular Electron Transfer of *Enterococcus faecalis* to Electrodes

s02-029

**Rasa Pauliukaite** (Department of Nanoengineering, Center for Physical Sciences and Technology, Vilnius, Lithuania), Raimonda Celiesiute, Aneta Radzevic, Tomas Rakickas, Zivile Ruzele, Sarunas Vaitekonis, Tautvydas Venckus  
Application of Polyfolates to the Development of Enzymatic Biosensors

## Membrane

s02-030

**Osamu Shirai** (Graduate School of Agriculture, Kyoto University, Kyoto, Japan), Yoshinari Takano, Yuki Kitazumi, Kenji Kano  
Propagation of the change in the membrane potential -Electrochemical elucidation on nerve conduction-

## Nanobiotechnology

s02-031

**Ewelina Zabost** (Faculty of Chemistry, University of Warsaw, Warsaw, Poland), Wioletta Liwińska, Agnieszka Kowalczyk, Zbigniew Stojek  
Multicomponent hydrogel/aptamer-based nanofibers and nanoparticles for storing and release of intercalators and genetic material

**Nucleic acid**

s02-032

**Wioletta Liwińska** (Faculty of Chemistry, University of Warsaw, Warsaw, Poland), Ewelina Zabost, Zbigniew Stojek

Nanoparticles designed from hydrogels and DNA in triple hybridisation process for improved storing and release of intercalators

**Protein**

s02-033

**Shengyuan Deng** (School of Environmental and Biological Engineering, Nanjing University of Science and Technology, Nanjing, China), Xubo Ji, Peng Xin, Dan Shan

An Electrogenerated Chemiluminescence Approach for the Assay of Zinc Finger Proteins (EGR1)

s02-034

**Sin-Cih Sun** (Department of Chemistry, Tunghai University, Taichung, Taiwan), Yuan-Hao Hsu, Min-Chieh Chuang

Interaction between Ferric/Ferrous Cytochrome c and Cardiolipin: An Electrochemical and Quartz Crystal Microbalance with Dissipation Study

**Techniques**

s02-035

**Christian Andre Gunawan** (School of Chemistry, The University of New South Wales, Sydney, Australia), Ekaterina Nam, Pall Thordarson, Chuan Zhao

Scanning Electrochemical Microscopy of Switchable Redox Enzyme Cascades

---

**Symposium 3: Batteries for Tomorrow's World**


---

**Li-ion and beyond li-ion battery systems**

s03-001

**Iain Aldous** (Stephenson Institute for Renewable Energy, University of Liverpool, Liverpool, United Kingdom), Laurence Hardwick

Adventures in Dioxygen Electrochemistry

s03-002

**Hajime Arai** (Kyoto University, Gokasho, Uji, Japan), Akiyoshi Nakata, Masaki Ono, Tadashi Kakeya, Tomokazu Yamane, Katsutoshi Fukuda, Hajime Tanida, Miwa Murakami, Yoshiharu Uchimoto, Zempachi Ogumi

Rechargeability of Zinc Electrodes Evaluated by *In Situ* Analysis

s03-003

**Arenst Andreas Arie** (Chemical Engineering, Parahyangan Catholic University, Bandung, Indonesia), Inez Devina, Ratna Frida Susanti, Hary Devianto, Martin Halim, Joong Kee Lee

Preparation and Electrochemical Performance of Turpentine Oil Derived Carbon Nanohorns as Anode Materials for Lithium-Ion Batteries

s03-004

**Arenst Andreas Arie** (Chemical Engineering, Parahyangan Catholic University, Bandung, Indonesia), Susan Olivia Limarta, Hans Kristianto, Martin Halim, Joong Kee Lee

Rice Husks Based Nanosilica as Anode Materials for Lithium-Ion Batteries

s03-005

**Chika Baba** (Dept of Sci of Environment and Mathematical Modeling, Doshisha University, Kyotanabe, Japan), Kenji Kawaguchi, Masatsugu Morimitsu

A High Energy Density of MH/Air Secondary Battery Using A<sub>2</sub>B<sub>7</sub> Type of Hydrogen Storage Alloys

s03-006

**Kolja Beltrop** (MEET Battery Research Center, WWU, University of Münster, Münster, Germany), Paul Meister, Olga Fromm, Martin Winter, Tobias Placke

Electrochemical Intercalation of Anions into Graphite – The Role of Anion Structure and Solvent Properties

s03-007

**Andrea Boschini** (Applied Physics, Chalmers University of Technology, Gothenburg, Sweden), Patrik Johansson  
Characterization of Sodium Based Ternary Polymer Electrolytes

s03-008

**Daniel Brandell** (Department of Chemistry, Uppsala University, Uppsala, Sweden), Bing Sun, Jonas Mindemark  
A Renaissance for Solid Polymer Electrolyte through Alternative Host Materials: Polycarbonates

s03-009

**Solveig Böhme** (Chemistry, Ångström Uppsala University, Uppsala, Sweden), Kristina Edström, Leif Nyholm  
Electrochemical behaviour of tin(IV) oxide electrodes in lithium-ion batteries at high potentials

s03-010

**Fei-Fei Cao** (College of Sciences, Huazhong Agricultural University, Wuhan, China)  
Facile Synthesis of CuO Nanochains as Anode Materials for Lithium-Ion Batteries

s03-011

**Suman Chae** (Materials Science and Engineering, Kunsan National University, Kunsan, Korea), Joongpyo Shim, Gyungse Park, Ho-Jung Sun

The Effects of Substrates on the Phase Formation Behavior and the Electrochemical Properties of  $\text{Li}_2\text{MnSiO}_4$  Cathode Thin Films Deposited by RF Sputtering for Thin Film Batteries

s03-012

**Chia-Chin Chang** (Department of Greenery Technology, National University of Tainan, Tainan, Taiwan), Li-Chia Chen, Yung-Der Juang

Effect of nano sized tin composite on graphite as anode for lithium ion battery

s03-013

**Chia-Chin Chang** (Department of Greenery Technology, National University of Tainan, Tainan, Taiwan), Tsan-Yao Chen, Pin-Chin Wu, Po-Wei Yang, Yu-Fan Chen, Chih-Wei Hu, Yen-Fa Liao

*In-Situ* X-ray Diffraction on the Lithium-Ion Migrating in Micro-Porous Separator

s03-014

**Long Chen** (Department of Chemistry, Fudan University, Shanghai, China), Wangyu Li, Zhaowei Guo, Yonggang Wang, Congxiao Wang, Yongyao Xia

Aqueous Lithium-Ion Batteries Using  $\text{O}_2$  Self-elimination Polyimides Electrodes

s03-015

**Jian Chen** (Dalian National Laboratory of Clean Energy, Dalian Institute of Chemical Physics, CAS, Dalian, China), Shifeng Yang, Jiao Zhao, Panpan Su, Qihua Yang, Can Li

High Energy Density Electrode Materials Prepared with Metal-Organic Coordination-Polymers for the Applications in LIBs

s03-016

**Hsun-Yi Chen** (Bio-Industrial Mechatronics Engineering, National Taiwan University, Taipei, Taiwan), Chih-Wei Chang, Dong-Yi Chao

Buffer Effects of Electrolyte Additives on Lead-Acid Flow Batteries

s03-017

**Rui Di** (Graduate School of Engineering, Kyoto University, Kyoto, Japan), Kohei Miyazaki, Tomokazu Fukutsuka, Takeshi Abe

Anion Conductivities of Positively-charged Hydroxides with One-dimensional Channel Framework

s03-018

**Chil Hoon Doh** (Battery Research Center, KERI, Korea Electrotechnology Research Institute, Changwon, Korea), You Jin Lee, Adnan Yaqub, Min Ji Hwang, Jeong Hee Choi, Hae Young Choi

Low Temperature Performances of  $\text{LiNi}_{0.6}\text{Co}_{0.2}\text{Mn}_{0.2}\text{O}_2$ /graphite Batteries

s03-019

**Xiaoli Dong** (Department of Chemistry, Fudan University, Shanghai, China), Yonggang Wang, Yongyao Xia  
Re-building Daniell Cell with a Li-ion Exchange Film

s03-020

**Jason Fang** (Material and Chemical Research Laboratories, Industrial Technology Research Institute, Hsinchu, Taiwan)

High Energy Solid State Battery

s03-021

**Tsukasa Gejo** (Dept of Science of Environment and Mathematical Modeling, Doshisha University, Kyotanabe, Japan), Shintaro Terui, Masatsugu Morimitsu

High Capacity and High Energy Density of Air Secondary Battery Using Metal Hydride Negative Electrode

s03-022

**Masashi Hattori** (Graduate School of Human and Environmental Studies, Kyoto University, Kyoto, Japan), Kentaro Yamamoto, Koji Nakanishi, Takuya Mori, Titus Mase, Yuki Orikasa, Yukinori Koyama, Zempachi Ogumi, Yoshiharu Uchimoto

Operando X-ray absorption spectroscopic study on magnesium metal anode reaction for magnesium rechargeable battery

s03-023

**Ping He** (College of Engineering & Applied Sciences, Nanjing University, Nanjing, China)

Enabling Catalytic Oxidation of  $\text{Li}_2\text{O}_2$  at Liquid-Solid Interface: A Successful Evolution for an Aprotic  $\text{Li-O}_2$  Battery

s03-024

**Min Young Hong** (Graduate School of Knowledge-based Technology and Energy, Korea Polytechnic University, Siheung-si, Korea), Hyojin Jung, Ji Heon Ryu

Improvement of High-Temperature Performance of the  $\text{LiMn}_2\text{O}_4$  Positive Electrode by the Addition of  $\text{Li}_3\text{PO}_4$

s03-025

**Hui-Yu Hong** (Department of Chemical Engineering, National Taiwan University of Science and Technology, Taipei, Taiwan), Chao-Yen Kuo, Jian-Ting Chin, Chen-Jui Huang, Men-Che Tsai, Bing-Joe Hwang

Interaction between Carbon Defects and Polysulfides in Lithium Sulfur Battery

s03-026

**Shang-Chieh Hou** (Department of Materials Science and Engineering, National Cheng Kung University, Tainan, Taiwan), Chia-Chin Chang, Jow-Lay Huang, Shun-Min Yang

Characterizations and electrochemical properties of high energy mechanical milled Si as anode for Li-ion batteries

s03-027

**Tien-Hsiang Hsueh** (Physics Division, Institute of Nuclear Energy Research, Taoyuan, Taiwan), Chi-Hung Su, Der-Jun Jan, Yuh-Jenq Yu, Yuan-Ruei Jheng

Island-like deposition of lithium manganese oxide spinel ( $\text{LiMn}_2\text{O}_4$ ) in all-solid-state thin film lithium ion battery

s03-028

**Ling Huang** (College of Chemistry and Chemical Engineering, Xiamen University, Xiamen, China)

Tuning structure and *in situ* XRD characterization of Li-rich layered cathode Materials for lithium ion batteries

s03-029

**Meiqi Huang** (Graduate School of Engineering, Kyoto University, Kyoto, Japan), Tomokazu Fukutsuka, Kohei Miyazaki, Akitoshi Hayashi, Masahiro Tatsumisago, Takeshi Abe

Interfacial Lithium-ion Transfer between Graphite Negative Electrode and Sulfide Solid Electrolyte

s03-030

**Sunhyung Jurng** (Department of Chemical and Biological Engineering, Seoul National University, Seoul, Korea), Hyun-seung Kim, Jae Gil Lee, Ji Heon Ryu, Seung M. Oh

Low Temperature Characteristics of Surface Film Derived from Elemental Sulfur Additive on Graphite Negative Electrode

s03-031

**Takehisa Kato** (Department of Materials, Physics and Energy Engineering, Nagoya University, Nagoya, Japan), Shinya Iwasaki, Yuta Yamamoto, Munekazu Motoyama, Yasutoshi Iriyama

Oxide-Based All-Solid-State Rechargeable Lithium Batteries with  $\text{LiNi}_{1/3}\text{Mn}_{1/3}\text{Co}_{1/3}\text{O}_2$ -Glass Ceramic Solid Electrolyte Composite Prepared by Aerosol Deposition

s03-032

**Tomáš Kazda** (Department of Electrical and Electronic Technology, Brno University of Technology, Brno, Czech Republic), Jirí Vondrák, Marie Sedlářková, Andrea Fedorková Straková, Marek Slávik, Pavel Eudek

Influence of the Used Carbons and Binders to the Electrochemical Properties of Li-S Cathode

s03-033

**Nam Seon Kim** (R&D Center, Aekyung Chemical Company, Daejeon, Korea), Soo Jung Kim, Dae Won Park, Gwang Sik Choi

The High Performance Silicon Anodes Including New Water Based Binder in Lithium Ion Batteries

s03-034

**Dong-Wan Kim** (School of Civil, Environmental and Architectural Engineering, Korea University, Seoul, Korea), Gwang-Hee Lee, Joosun Kim

Three Dimensional Cu/C/Ge Heterostructured Electrodes for High-performance Li ion Batteries

s03-035

**Jongjung Kim** (Department of Chemical and Biological Engineering, Seoul National University, Seoul, Korea)

Failure mechanism of SiO negative electrode during high temperature storage

s03-036

**Duri Kim** (Graduate School of Knowledge-based Technology and Energy, Korea Polytechnic University, Siheung-si, Korea), Mina You, Ji Heon Ryu

Effect of Electrode Composition on the Electrochemical Performance of the MnO Negative Electrode Materials for Li-ion Batteries

s03-037

**Toshio Kimura** (Department of Materials, Physics and Energy Engineering, Nagoya University, Nagoya, Japan), Munekazu Motoyama, Yasutoshi Iriyama

*In-Situ* SEM Observations of Li Plating/Stripping Reactions through Li-Pt Alloying on a LiPON Electrolyte

s03-038

**Lingbin Kong** (School of Materials Science and Engineering, Lanzhou University of Technology, Lanzhou, China), Yang Li, Maocheng Liu, Xixin Wang, Ming Shi, Jinbei Liu, Long Kang

Template-free synthesis of porous  $\text{Co}_3\text{O}_4$ @C hierarchical structure for high performance lithium-ion batteries

s03-039

**Chao-Yen Kuo** (Department of Chemistry, Institute of Nuclear Energy Research, Taoyuan, Taiwan), Heng-Wei Chiang, Chien-Hong Lin, Hwa-Jou Wei, Bing-Joe Hwang

Application of Amorphous Carbon-Coated Electrodes in Vanadium Redox Flow Battery

s03-040

**Liang-Yin Kuo** (Department of Chemical Engineering, National Taiwan University of Science and Technology, Taipei, Taiwan)

Highly Stable Sn-C Nanocomposite as an Anode Material for Lithium ion Batteries

s03-041

**Song-Zhu Kure-Chu** (Department of Chemistry and Bioengineering, Iwate University, Morioka, Japan), Haruki Sakuyama, Hitoshi Yashiro, Kuniaki Sasaki, Hiroyo Segawa, Kenji Wada, Satoru Inoue

Facile Formation of 3D Nanoporous Anodic  $\text{TiO}_2$ -TiN Composite Films as Anode Materials for Lithium Rechargeable Batteries

s03-042

**Matthew Lacey** (Department of Chemistry, Ångström Laboratory, Uppsala University, Uppsala, Sweden), Kristina Edström, Daniel Brandell

Detailed “Mapping” of Internal Resistance in Li-S Batteries

s03-043

**Chen-Hsuan Lai** (Materials Science and Engineering, National Dong Hwa University, Hualien, Taiwan), Ing-Song Yu, Fa-Hsing Yeh

Silicon-carbon anode by plasma enhanced chemical vapor deposition for lithium-ion batteries

s03-044

**Jae Gil Lee** (Department of Chemical and Biological Engineering, Seoul National University, Seoul, Korea), Jongjung Kim, Jeong Beom Lee, Hosang Park, Tae-jin Lee, Ji Heon Ryu, Seung M. Oh

A quantitative analysis on the failure mechanism of nano-Si electrode and the effect of fluoroethylene carbonate

s03-045

**Won Jae Lee** (Battery Research Center, KERI, Korea Electrotechnology Research Institute, Changwon, Korea), Yong Hwan Gwon, Seong Ju Sim, You Jin Lee, Doo Hun Kim, Chil Hoon Doh

The performance of All Solid State Li ion Battery with Composite Sulfide Solid Electrolyte

s03-046

**Zhaohui Li** (Chemistry, Xiangtan University, Xiangtan, China), Kailing Sun, Can Peng, Xiaozhen Xiao, Gangtie Lei

Hybrid  $V_2O_5/C$  coated Li- rich manganese-based solid solution and its improved electrochemical properties

s03-047

**Zhaohui Li** (Chemistry, Xiangtan University, Xiangtan, China), Wenjun Li, Chenlu Yang, Xiaozhen Xiao, Gangtie Lei

A batwing-like  $SiO_2/PVdF-g-PMMA$  membrane for high-performance lithium-ion batteries

s03-048

**Jun-Tao Li** (College of Energy, Xiamen University, Xiamen, China), Jie Liu, Zhan-Yu Wu, Tao Zhang, Ling Huang, Shi-Gang Sun

Guar Gum as the Binder for Si Anode of Lithium-Ion Battery

s03-049

**Ximeng Li** (Graduate School of Engineering, Kyoto university, Kyoto, Japan), Shohei Maruyama, Kohei Miyazaki, Tomokazu Fukutsuka, Takeshi Abe

Ion Transport in Graphite Composite Electrode

s03-050

**Chi-Ying Vanessa Li** (Dept of Chemistry, The University of Hong Kong, Hong Kong, China), Ching-Kit Ho, Zhao-Feng Deng, Kwong-Yu Chan

Durable Mesoporous Core-Shell Lithium Titanate-Carbon Composite as Anode in Lithium ion Batteries

s03-051

**Biao Li** (College of Engineering, Peking University, Beijing, China), Huijun Yan, Li An, Hang Wei, Jin Ma

Tuning the Electronic Structure of Layered Oxides Electrodes for Reversible Anionic Redox in Lithium Ion Batteries

s03-052

**Zhuojian Liang** (Mechanical and Automation Engineering, The Chinese University of Hong Kong, Hong Kong, China), Yi-Chun Lu

Probing the Oxygen Evolution Efficiency of Redox Mediator-Catalyzed Lithium-Oxygen Batteries using On-Line Electrochemical Mass Spectrometer

s03-053

**Haibo Lin** (College of Chemistry, Jilin University, Changchun, China), Wenli Zhang, Jian Yin, Zheqi Lin, Haiyan Lu, Yue Wang, Jinpeng Bao, Tingting Liu

3D Hierarchical Porous Carbon Derived from Lignin with Enhanced Lithium Storage Capability

s03-054

**Wei-Ren Liu** (Department of Chemical Engineering, Chung Yuan Christian University, Taoyuan City, Taiwan), Ji-Xuan Fu, Wei-Ting Wong

Temperature Effects on Porous  $ZnCo_2O_4$  Anode for Lithium-ion Batteries

s03-055

**Chunling Liu** (School of Chemical and Chemical Engineering, Shaanxi Normal University, Xi'an, China), Jing Ma, Chaofan Yun, Wang Wang, Xueqian Wang, Wensheng Dong

Self-healing Sn composite lithium-ion battery electrode with high capacity and good cycling stability

s03-056

**Wei-Ren Liu** (Department of Chemical Engineering, Chung Yuan Christian University, Chung Li, Taiwan), Yu-Cheng Liu, Nae-Lih Wu

Effects of  $\text{Al}^{3+}/\text{Cl}^-$  co-doping on the electrochemical properties of  $\text{Li}_{1.2}\text{Ni}_{0.4}\text{Mn}_{0.6}\text{O}_{2.2}$  cathode materials for lithium ion batteries

s03-057

**Wei-Ren Liu** (Department of Chemical Engineering, Chung Yuan Christian University, Chung Li, Taiwan), Jeng-Shin Lu, Yu-Chian Shie

Binder Effects and Architecture Design of Si-based Composite Anode for Li-ion batteries

s03-058

**Haimei Liu** (College of Environmental and Chemical Engineering, Shanghai University of Electric Power, Shanghai, China)

Studies of Non-metal Elements Doped Carbon Coated Electrode Materials of Lithium (Sodium) Ion Batteries

s03-059

**Yi-Hung Liu** (Department of Greenery Technology, National University of Tainan, Tainan, Taiwan), Tomoaki Takasaki, Kazuya Nishimura, Masahiro Yanagida, Tetsuo Sakai

Development of Lithium Ion Batteries Using Fiber-Type Current Collectors

s03-060

**Nicholas Loeffler** (Helmholtz Institute Ulm (HIU), Karlsruhe Institute of Technology (KIT), Ulm, Germany), Guk-Tae Kim, Diogo Vieira Carvalho, Stefano Passerini

Environmentally friendly binders for lithium ion batteries

s03-061

**Mechthild Luebke** (University College London, London, United Kingdom), Zhaolin Liu, Ian Johnson, Jawwad Darr

The Benefits of Hydrothermal Flow Reactors for High Power and High Energy Lithium-ion Battery Electrode Materials

s03-062

**Xu-Feng Luo** (Institute of Materials Science and Engineering, National Central University, Taoyuan, Taiwan), Chueh-Han Wang, Cheng-Hsien Yang, Jeng-Kuei Chang

Physiochemical characteristics of graphene nanosheets affecting their electrochemical  $\text{Na}^+$  storage properties

s03-063

**Wen Ma** (Graduate School of Engineering, Kyoto University, Kyoto, Japan), Kohei Miyazaki, Fukutsuka Tomakazu, Takeshi Abe

Electrochemical Properties of Surface-treated Hard Carbon Electrode

s03-064

**Sladjana Martens** (Institut für Informatik VI, Technische Universität München, Garching, Germany), Lukas Seidl, Jiwei Ma, Ehab Mostafa, Huinan Si, Xinping Qiu, Ulrich Stimming, Oliver Schneider

Towards the mechanism of  $\text{Mg}^{2+}$ -ions intercalation into  $\text{V}_2\text{O}_5$  as the cathode material

s03-065

**Yukiko Matsui** (Faculty of Chemistry, Materials and Bioengineering, Kansai University, Suita, Japan), Takuya Takahashi, Satoshi Uchida, Masaki Yamagata, Masashi Ishikawa

Composite positive electrode using sulfur/micro porous carbon for high-performance lithium-sulfur battery

s03-066

**Ralph Nicolai Nasara** (Department of Materials Science and Engineering, National Cheng Kung University, Tainan, Taiwan), Kuan-Wei Lu, Yen-Ting Pan, Ping-chun Tsai, Wei-chih Lin, Chung-Ta Ni, Shih-kang Lin, Kuan-Zong Fung

A modified RAPET approach to  $\text{Li}_4\text{Ti}_5\text{O}_{12}$  defect spinel nanoparticles as anode material for lithium ion batteries

s03-067

**Chung-Ta Ni** (Materials Science and Engineering, National Cheng Kung University, Tainan, Taiwan), Shu-Yi Tsai, Kuan-Zong Fung, Wei-Zhi Lin

Observation of Spinel Formation on Capacity Fading of Li-rich Layer-structured Cathode Materials

s03-068

**Nadya Nissaulya** (Chemical Engineering, National Taiwan University of Science and Technology, Taipei, Taiwan), Chong-Shyan Chern, Fu-Ming Wang

Synthesis and Characteristics of Hyper-Branched Oligomer Directly Coated on High Voltage Cathode Material in Lithium Ion Battery

s03-069

**Yong Joon Park** (Department of Advanced Materials Engineering, Kyonggi University, Suwon, Korea), Seon Hye Yoon, Chan Kyu Lee

Enhanced Li-air batteries using redox mediator

s03-070

**Kyu-Young Park** (Department of Materials Science and Engineering, Seoul National University, Seoul, Korea), Inchul Park, Hyungsub Kim, Gabin Yoon, Hyeok-Jo Gwon, Yongbeom Choa, Young Soo Yun

Olivine with zero anti-site defect and three dimensional lithium diffusion paths

s03-071

**Tobias Placke** (MEET Battery Research Center, University of Muenster, Muenster, Germany), Haiping Jia, Britta Vortmann, Martin Winter

Nanostructured  $\text{ZnFe}_2\text{O}_4$ -based anodes for lithium-ion batteries – Novel synthesis route and analytical study on metal dissolution

s03-072

**Alexandre Ponrouch** (QES, ICMAB-CSIC, Bellaterra, Spain), M. Rosa Palacín

On the high and low temperature performances of Na-ion batteries: Hard carbon as a case study

s03-073

**M. V. Reddy** (Materials Science & Eng. and Physics, National University of Singapore, Singapore)

Electrochemical studies of binary oxides,  $\text{MO}_2$  (M= Ti, Mn, Mo, Ru)

s03-074

**William Richardson** (Department of Electrochemistry, University of Southampton, Southampton, United Kingdom), Nuria Garcia-Araez

Identifying Solution Based Catalysts for the Lithium Oxygen Battery

s03-075

**Fumihiko Sagane** (Department of Electronics and Materials Science, Shizuoka University, Hamamatsu, Japan)

Synthesis of  $\text{NaTi}_2(\text{PO}_4)_3$  Thin-film and Electrochemical Behavior in Aqueous Solutions

s03-076

**Hideyuki Sano** (Dept of Science of Environment and Mathematical Modeling, Doshisha University, Kyotanabe, Japan), Masatsugu Morimitsu

A Novel Air Electrode Comprising Core-Shell Particles for MH/Air Secondary Battery

s03-077

**Lukas Seidl** (Physik Department, Technische Universität München, Garching, Germany), Luis Flacke, Sladjana Martens, Ulrich Stimming, Oliver Schneider

*In-Situ* EC-STM, EQCM and EIS studies of interfacial processes in Na ion battery electrolytes

s03-078

**Dane Sotta** (Department of Electricity and Hydrogen for Transportation, CEA, Grenoble, France), Alice Robba, Sophie Chazelle, Marianne Chami, Séverine Jouanneau-Si Larbi

Polymer Binders Evaluation for Improved Lithium-ion Batteries Positive Electrodes *via* Water-based Processing Route

s03-079

**Kazuhiro Soutome** (Department of Biomolecular Functional Engineering, Ibaraki University, Ibaraki, Japan), Kenta Iwasawa, Mika Shiraishi, Risa Shiraishi, Mikka Nishitani-Gamo, Toshihiro Ando, Mika Eguchi

Electrochemical characteristics of a  $\text{Li}_4\text{Ti}_5\text{O}_{12}$ /Marimo carbon composite

s03-080

**Shintaro Terui** (Dept of Science of Environment and Mathematical Modeling, Doshisha University, Kyotanabe, Japan), Masatsugu Morimitsu

Development of Air Electrode with  $\text{Bi}_2\text{Ir}_2\text{O}_{7-z}$  Nano-catalyst for MH/Air Secondary Battery



s03-081

**Xuan Minh Tran** (Department of Fine Chemical Engineering & Applied Chemistry, Chungnam National University, Daejeon, Korea), Dan Thien Nguyen, Seung-wan Song

Electrochemical Studies of Tin Film Model Electrode for Magnesium-ion Batteries

s03-082

**Chih-Long Tsai** (Institute of Energy and Climate Research, IEK-1, Forschungszentrum Juelich GmbH, Juelich, Germany), Christian Dellen, Hans-Gregor Gehrke, Sandra Lobe, Sven Uhlenbruck, Olivier Guillon

All-solid-state Li Battery using garnet structure Ta-substituted  $\text{Li}_7\text{La}_3\text{Zr}_2\text{O}_{12}$  as solid electrolyte

s03-083

**Shu-Yi Tsai** (Department of Materials Science and Engineering, National Cheng Kung University, Tainan, Taiwan), Chung-Ta Ni, Kuan-Zong Fung

Processing and Characterization of  $\text{Li}_4\text{Ti}_5\text{O}_{12}$  (LTO) Spinel Thin -Film for Li Battery Applications

s03-084

**Satoshi Uchida** (Chemistry and Materials Engineering, Kansai University, Suita, Japan), Masaki Yamagata, Masashi Ishikawa

Low-Temperature Operation Performance of LiFSI-Based Low EC Content Electrolyte with Specific Solvation State

s03-085

**Sigita Urbonaite** (Electrochemistry Laboratory, Paul Scherrer Institute, Villigen PSI, Switzerland), Petr Novak

Search for Perfect Carbonaceous Sulphur Hosts for Li-S Batteries

s03-086

**Lina Wang** (Department of Chemistry, Fudan University, Shanghai, China), Yonggang Wang, Yongyao Xia

A high performance lithium-ion sulfur battery based on a  $\text{Li}_2\text{S}$  cathode using dual-phase electrolyte

s03-087

**Chueh-Han Wang** (Institute of Materials Science and Engineering, National Central University, Taoyuan, Taiwan), Xu-Feng Luo, Cheng-Hsien Yang, Jeng-Kuei Chang

$\text{Na}_{0.44}\text{MnO}_2$ -VHard Carbon Sodium-Ion Battery using N-propyl-N-methylpyrrolidinium Bis(fluorosulfonyl)imide Ionic Liquid Electrolyte

s03-088

**Guoqing Wang** (School of Materials Science and Engineering, Zhejiang University, Hangzhou, China), Shuangyu Liu, Jian Xie, Fangfang Tu, Huiying Yang, Shichao Zhang, Tiejun Zhu, Gaoshao Cao, Xinbing Zhao

Au-nanocrystals-decorated  $\delta\text{-MnO}_2$  as efficient catalytic cathode for high-performance Li- $\text{O}_2$  batteries

s03-089

**Jian-Hua Wu** (Graduate Institute of Applied Science and Technology, National Taiwan University of Science and Technology, Taipei, Taiwan), Fu-Ming Wang

Electrochemical performance of lithium-rich ( $\text{Li}_{1.2}\text{Ni}_{0.2}\text{Mn}_{0.6}\text{O}_2$ ) high-capacity cathode of lithium battery modified with fluorine-benzimidazole-based Li salt addition in electrolyte

s03-090

**Yi-Shiuan Wu** (Battery Research Center of Green Energy, Ming Chi University of Technology, New Taipei City, Taiwan)

A novel PVDF-HFP/PET/PVDF-HFP composite membrane by electrospinning and solution-casting techniques for  $\text{LiFePO}_4$  lithium-ion batteries

s03-091

**Shohei Yamaguchi** (Dept. of Science of Environment and Mathematical Modeling, Doshisha University, Kyotanabe, Japan), Masatsugu Morimitsu

Output Performance of MH/Air Secondary Battery using  $\text{Bi}_2\text{Ru}_2\text{O}_{7-z}$  Catalyst in Positive Electrode

s03-092

**Jun Yang** (Department of Chemistry, Fudan University, Shanghai, China), Mengyan Hou, Yongyao Xia  
Improving the Cycling Performance of the Layered Ni-Rich Oxide Cathode by Introducing the Low-Content  $\text{Li}_2\text{MnO}_3$

s03-093

**Chun-Chen Yang** (Battery Research Center of Green Energy, Ming Chi University, New Taipei City, Taiwan), Jer-Huan Jang, Jia-Rong Jiang  
Synthesis and Characterization of  $\text{LiFePO}_4$  Composite Cathode Material Modified with *in-situ* Graphene and Solid-State Electrolyte

s03-094

**Jung Hoon Yang** (Energy Efficiency Research Division, Korea Institute of Energy Research, Daejeon, Korea)  
In-Situ Electrochemical Analysis for Electrolyte in Vanadium Redox Flow Battery

s03-095

**Wenyu Yang** (College of Physics and Energy, Fujian Normal University, Fuzhou, China)  
Suppression of degradation of lithium ion batteries for  $\text{LiFePO}_4/\text{C}$  batteries by nano Si surface modification

## Modeling and characterization

s03-096

**Juichi Arai** (Technical Center, Yamaha Motor Co., Ltd., Iwata, Japan)  
Physical Model Simulation for Degradation of Li-ion Battery

s03-097

**Wonyoung Chang** (Center of Energy Convergence, Korea Institute of Science and Technology, Seoul, Korea), Sooyeon Hwang, Woo-Sung Choi, Kim Seung Min, Young Sun Shin, Byung-Won Choi, Kyung Yoon Chung, Eric Stach, Heon-Cheol Shin  
Investigation of the Degradation Mechanism of  $\text{Li}_x\text{Ni}_y\text{Mn}_z\text{Co}_{1-y-z}\text{O}_2$  Cathode Materials for Lithium Ion Batteries

s03-098

**Kezheng Chen** (Graduate School of Human and Environment Studies, Kyoto University, Kyoto, Japan)  
Temperature Dependence of Effective Ionic Conductivity in Composite Electrode of Lithium Ion Battery

s03-099

**Shoma Ida** (Graduate School of Human and Environmental Studies, Kyoto University, Kyoto, Japan), Yuki Orikasa, Hideyuki Komatsu, Koji Kitada, Yukinori Koyama, Zempachi Ogumi, Yoshiharu Uchimoto  
Simulation Analysis of Reaction Distribution in  $\text{LiFePO}_4$  Composite Electrodes

s03-100

**Jaehyang Jeong** (Department of Printed Electronics Engineering, Sunchon National University, Sunchon, Korea), Myoungho Pyo  
Highly crosslinked graphene framework for tin dioxide anodes of excellent lithium-storage capability and cyclability

s03-101

**Boram Koo** (Department of Energy Systems Research, Ajou University, Suwon, Korea), Jaeshin Yi  
Thermal modeling of a lithium-ion battery module for hybrid electric vehicle applications

s03-102

**Robert Kostecki** (Energy Storage and Distributed Resources, Lawrence Berkeley National Laboratory, Berkeley, USA), Maurice Ayache, Simon Lux, Ivan Lucas  
Near-Field Optical Spectroscopy and Imaging of the SEI Layer on Sn, Si and Graphite Li-ion Anodes

s03-103

**Fyodor Malchik** (Chemical, Al-Farabi Kazakh National University, Almaty, Kazakhstan), Andrey Kurbatov  
Study of the kinetic of  $\text{LiFePO}_4$  oxidation in aqueous solutions

s03-104

**Takuya Mori** (Graduate School of Human and Environmental Studies, Kyoto University, Kyoto, Japan), Kazufumi Otani, Toshiyuki Munesada, Kentaro Yamamoto, Titus Masese, Yuki Orikasa, Koji Ohara, Katsutoshi Fukuda, Yukinori Koyama, Toshiyuki Nohira, Rika Hagiwara, Zempachi Ogumi, Yoshiharu Uchimoto  
Dynamics of the Phase Transition Behavior of the  $\text{LiFePO}_4$  Investigated by Time-resolved X-ray Diffraction at Various Temperatures

s03-105

**Hao-Ting Peng** (Chemical Engineering, Tatung University, Taipei, Taiwan), Pei-Sin Yin, Jeng-Yu Lin  
High-performance lithium-ion batteries based on  $\text{C Li}_4\text{Ti}_{4.95}\text{Al}_{0.05}\text{O}_{12}$  anode materials

s03-106

**Neeraj Sharma** (School of Chemistry, UNSW Australia, Sydney, Australia)  
The structural evolution of cathode materials in the current generation of commercial lithium-ion batteries

### Novel electrode materials and electrode/electrolyte interfaces - theory

s03-107

**Gaukhar Askarova** (Chemistry and Chemical Technology, Al-Farabi Kazakh National University, Almaty, Kazakhstan)  
Development of Charge Transport Model in Composite Polymer Electrolytes

s03-108

**Heng-Wei Chiang** (Department of Chemistry, Institute of Nuclear Energy Research, Taoyuan, Taiwan), Chao-Yen Kuo, Chien-Hong Lin  
Modified Carbon Felt *via* a Facile Oxidation Treatment as an Efficient Electrode for a Vanadium Redox Flow Battery

s03-109

**Yu-Ju Chien** (Chemical Engineering, National Tsing Hua University, Hsin-Chu City, Taiwan)  
Synthesis of Ternary Spinel Iron-Cobalt-Nickel Oxide/Carbon Black Composites as a High-Performance Bifunctional Electrocatalyst for Rechargeable Zinc-Air Batteries

s03-110

**Josh Y. Z. Chiou** (Department of Materials Engineering, Tatung University, Taipei, Taiwan), Shou-Huang Su  
Structural Effects of Spinel  $\text{LiMn}_{1.5}\text{Ni}_{0.5}\text{O}_4$  on Their Electrochemical Properties

s03-111

**Ahmad Fauzan Adziimaa** (Graduate Institute of Applied Science and Technology, National Taiwan University of Science and Technology, Taipei, Taiwan), Fu-Ming Wang  
Combination effects of graphene oxide as carbon black and maleimide as electrolyte additive in lithium ion batteries

s03-112

**Giyanto Giyanto** (Graduate Institute of Applied Science and Technology, National Taiwan University of Science and Technology, Taipei, Taiwan), Fu-Ming Wang  
The electronegativity effects of maleimide based electrolyte additives in SEI formation of lithium ion battery

s03-113

**Xiaoyan Hu** (Chemistry Department, Xiamen University, Xiamen, China), Bingwei Mao  
*In-situ* STM characterization of ionic liquids on Au(111) and HOPG electrodes in the presence of lithium salt

s03-114

**Xiao Huang** (Department of Chemistry, BMC, Uppsala University, Uppsala, Sweden), Li Yang, Maria Stromme, Adolf Gogoll, Martin Sjödin  
Synthesis and Redox Properties of Thiophene-Terephthalate Building Blocks for Low Potential Conducting Redox Polymers

s03-115

**Hyuntak Jo** (Energy Science and Technology, Chungnam National University, Daejeon, Korea), Xuan Minh Tran, Dan-Thien Nguyen, Hyo Ki Hwang, Kil Ku Kang, Seung-Wan Song  
Correlation between Interfacial Reaction Behavior and Cycling Characteristics of Silicon-based Anodes in Li-ion Batteries

s03-116

**Shingo Kaneko** (Research Institute for Engineering, Kanagawa University, Yokohama, Japan), Yuichi Sato, Futoshi Matsumoto, Junwei Zheng, Decheng Li

Size-regulated Precursor-Based Synthesis of Lithium-Rich Layered Cathode Material Deriving High Rate Capability

s03-117

**Donghyun Kil** (Department of Chemical and Biomolecular Engineering, Yonsei University, Seoul, Korea), Hansung Kim

Development of short-termed and highly effective graphite felt surface treatment process for all-vanadium redox flow battery applications

s03-118

**Joon soo Kim** (Advanced Materials and Devices Laboratory, Korea Institute of Energy Research, Daejeon, Korea), Bo yun Jang, Jin Seok Lee, Jeong Boon Koo, Jeong Eun Lee

Synthesis of Si Nanoparticles by Atmospheric Microwave Plasma

s03-119

**Richard Kloepsch** (MEET Battery Research Center, University of Muenster, Muenster, Germany), Jatinkumar Rana, Gerhard Schumacher, John Banhart, Martin Winter, Jie Li

Investigation of surface and bulk structural modifications in Li/Mn-rich cathode materials of Li-ion batteries using X-ray absorption spectroscopy

s03-120

**Hwa Jin Lee** (School of Chemical Engineering, University of Ulsan, Ulsan, Korea), Seul Lee, Eun-Suok Oh

Application of modified rosin-derivatives as promising adhesives for lithium titanium oxide electrodes in lithium ion batteries

s03-121

**Tae-jin Lee** (Department of Chemical and Biological Engineering, Seoul National University, Seoul, Korea), Taeho Yoon, Jiwon Jung, Jiyong Soon, Jae Gil Lee, Ji Heon Ryu

A comparative study on Li<sup>+</sup> ion migration characteristics in the interphases of positive and negative electrodes

s03-122

**Jeong Beom Lee** (Department of Chemical and Biological Engineering, Seoul National University, Seoul, Korea), Janghyuk Moon, Oh B. Chae, Ji Heon Ryu, Maenghyo Cho, Kyeongjae Cho, Seung M. Oh

Combined Theoretical *Ab-initio* and Experimental Study on LiVO<sub>3</sub>, A Novel Conversion-type Negative Electrode for Lithium-ion Batteries

s03-123

**Shih-kang Lin** (Department of Materials Science and Engineering, National Cheng Kung University, Tainan, Taiwan), Ping-chun Tsai, Wen-Dung Hsu

*Ab initio*-aided Li<sub>4</sub>Ti<sub>5</sub>O<sub>12</sub> defect spinel electrode materials designs for durable lithium ion batteries

s03-124

**Arailym Nurpeisova** (Graduate School of Energy Science and Technology, Chungnam National University, Daejeon, Korea), Da-In Park, Sung-Soo Kim

SEI stabilizer agent epicyanohydrin for cathodes used in LIBs

s03-125

**Sangki Park** (Department of Chemical and Biomolecular Engineering, Yonsei University, Seoul, Korea), Hansung Kim

Polypyrrole as the Coating Agent and Nitrogen Precursor for the Fabrication of Nitrogen-Doped Graphite Felts as Positive Electrode for a Vanadium Redox Flow Battery

s03-126

**Hao-Ting Peng** (Chemical Engineering, Tatung University, Taipei, Taiwan), Cheng-Yao Lee, She-huang Wu, Jeng-Yu Lin

Effects of electrolyte additive on the electrochemical properties of lithium-ion batteries based on Li<sub>4</sub>Ti<sub>5</sub>O<sub>12</sub> anode materials

s03-127

**Joaquin Rodriguez-Lopez** (Department of Chemistry, University of Illinois at Urbana-Champaign, Urbana, USA), Elena Catalina Montoto Blanco, Jingshu Hui, Nagarjuna Gavvalapalli, Etienne Chenard, Kevin Cheng, Timothy Lichtenstein, Jeffrey Moore

Redox Active Polymers: Pursuing a Size-Selective Strategy for High Performance Non-Aqueous Redox Flow Batteries

s03-128

**Hayate Saito** (IMRAM, Tohoku University, Sendai, Japan), Daiki Komatsu, Takaaki Tomai, Itaru Honma  
Capacity enhancement of semi-solid flow capacitor using quinonic compounds

s03-129

**Sébastien Sallard** (Electrochemistry Laboratory, Paul Scherrer Institut, Villigen-PSI, Switzerland), Sebastian Schmidt, Denis Sheptyakov, Petr Novak, Claire Villevieille  
Lithium iron methylene diphosphonate, a new organic-inorganic hybrid material for Li-ion batteries.

s03-130

**Selina Tillmann** (MEET Battery Research Center, University of Muenster, Muenster, Germany), Martin Winter, Isidora Cekic-Laskovic  
Electrodeposition of Silicon for the Preparation of Submicrostructured Electrodes

s03-131

**Roberto Torresi** (Instituto de Química, Universidade de São Paulo, São Paulo, Brazil), Vitor L. Martins, Nédher Sanchez-Ramirez, Mauro C. C. Ribeiro  
Transport properties of Li<sup>+</sup> Mixtures in Two Phosphonium Containing Ionic Liquids

s03-132

**Gang Wang** (School of Chemistry and Chemical Engineering, Shihezi University, Shihezi City, China), Yongtao Zuo, Jun Peng, Gang Li, Feng Yu, Bin Dai, Xuhong Guo  
Hybridization of graphene sheets and carbon-coated Fe<sub>3</sub>O<sub>4</sub> hollow nanoparticles as a high-performance anode material for lithium-ion batteries

s03-133

**Gang Wang** (School of Chemistry and Chemical Engineering, Shihezi University, Shihezi City, China), Jun Peng, Yongtao Zuo, Gang Li, Feng Yu, Bin Dai, Xuhong Guo  
*In situ* polyol-assisted synthesis of Zn<sub>2</sub>SnO<sub>4</sub> nanocrystals/graphene nanohybrid as high-performance anode for Li-ion batteries

s03-134

**Nan Hung Yeh** (Graduate Institute of Applied Science and Technology, National Taiwan University of Science and Technology, Taipei, Taiwan), Lyu Ye Yang, Fu-Ming Wang  
Next generation of Self Terminated Oligomer Branched Architecture (STOBA) in Li-rich (Li<sub>1.2</sub>Ni<sub>0.2</sub>Mn<sub>0.6</sub>O<sub>2</sub>) high capacity cathode material of lithium ion battery

s03-135

**Aishui Yu** (Chemistry Department, Fudan University, Shanghai, China)  
Three-Dimensional Activated Porous Carbon /Sulfur Composites as Cathode Materials for Lithium-Sulfur Batteries

s03-136

**Ludan Zhang** (Chemistry, Fudan University, Shanghai, China)  
Carbon-coated Na<sub>3</sub>V<sub>2</sub>(PO<sub>4</sub>)<sub>3</sub> Nanocomposite as a Novel High Rate Cathode Material for Aqueous Sodium Ion Batteries

s03-137

**Qianyu Zhang** (Key Laboratory of Renewable Energy, Guangzhou Institute of Energy Conversion, Chinese Academy of Sciences, Guangzhou, China), Chuying Ouyang, Lingzhi Zhang  
W<sup>6+</sup>&Br-codoped Li<sub>4</sub>Ti<sub>5</sub>O<sub>12</sub> Anodes with Super Rate Performance

s03-138

**Wenli Zhang** (College of Chemistry, Jilin University, Changchun, China), Jian Yin, Zheqi Lin, Haibo Lin, Haiyan Lu, Yue Wang, Jinpeng Bao, Tingting Liu  
Mechanisms of Activated Carbon in Lead-Carbon Battery

s03-139

**Haoliang Zhong** (Guangzhou Institute of Energy Conversion, Chinese Academy of Sciences, Guangzhou, China), Lingzhi Zhang  
Carboxymethyl Chitosan/Poly(ethylene oxide) as a Water Soluble Blend Binder for 5 V LiNi<sub>0.5</sub>Mn<sub>1.5</sub>O<sub>4</sub> Cathodes with Improved Cycle Stability in Li-Ion Batteries

s03-140

**Dauren Batyrbekuly** (Institute of Batteries, Institute of Batteries, Astana, Kazakhstan), Almagul Mentbayeva, Yongguang Zhang, Indira Kurmanbayeva, Kuralay Korzhynbayeva, Zhumabai Bakenov  
Reinforced composite gel-polymer electrolytes for lithium-sulfur batteries

## Symposium 4: Advances in Fuel Cells from Materials to Systems

### Ageing and degradation

s04-001

**Daniel Garcia** (Electrochemical Energy Technology, Deutsches Zentrum für Luft- und Raumfahrt (DLR), Stuttgart, Germany)

Comparison of the Degradation process during the bus application loading cycling in PEMFC

s04-002

**Misako Ikeyama** (Graduate School of Engineering, Oita University, Oita, Japan), Taro Kinumoto, Sawaka Kitayama, Miki Matsuoka, Tomoki Tsumura, Masahiro Toyoda

IL-FE-SEM Study for Ambience Dependence of Degradation of Pt/C Catalyst

s04-003

**Timothy J. Peckham** (Department of Chemistry, Simon Fraser University, Burnaby, Canada), Lida Ghassemzadeh, Thomas Weissbach, Xiaoyan Luo, Steven Holdcroft

Structure and Property Changes of PFSA Ionomer Upon Exclusive Reaction with HO and H Radicals

s04-004

**Mirosław Stygar** (Faculty of Materials Science and Ceramics, AGH University of Science and Technology, Krakow, Poland), Juliusz Dabrowa, Tomasz Brylewski

Oxidation kinetics and microstructure of oxide products formed on the Crofer 22APU ferritic stainless steel in a dual atmosphere

s04-005

**Lung-Yu Sung** (Energy storage Department, Industrial Technology Research Institute, Hsinchu, Taiwan)

Effects of H<sub>3</sub>PO<sub>4</sub> leaching on the performance and degradation of high temperature-proton exchange membrane fuel cells

### Direct alcohol fuel cells

s04-006

**Patricia Corradini** (Instituto de Química de São Carlos, Universidade de São Paulo, São Carlos, Brazil), Nathalia Santos, Valdecir Paganin, Ermete Antolini, Joelma Perez

Synthesis and characterization of electrocatalysts PtSnEu/C for anode in direct alcohol fuel cell

s04-007

**Lin Gan** (Division of Energy and Environment, Graduate school at Shenzhen, Tsinghua University, Shenzhen, China), Lingyi Peng, Hao Yang, Jia Li, Hongda Du

Role of Interfaces of Au@Pt Nanoparticles in the Electrocatalysis of Alcohol Oxidation

s04-008

**Xuan Zhang** (College of Chemistry, Chemical Engineering & Biotechnology, Donghua University, Shanghai, China), Jia-Wei Zhang, Bei Zhang

Improving the Electrocatalytic Activity of Binary Alloy Cu<sub>x</sub>Pd<sub>y</sub> for Methanol Oxidation Reaction by Tailoring Chemical Composition

### Electrolysis

s04-009

**Tae-Hyun Yang** (Fuel Cell Research Center, Korea Institute of Energy Research, Daejeon, Korea), Young-Jun Sohn, Minjin Kim

Simulated Design of High-altitude Long-endurance Unmanned Aerial Vehicles using Regenerative Fuel Cell Systems

### Fuel cell and electrolysis membranes and separators

s04-010

**Min-Hsing Chang** (Mechanical Engineering, Tatung University, Taipei, Taiwan), Sheng-Wei Huang

Fabrication of Anode Microporous Layer with Carbon Nanotubes and its Effect on Proton Exchange Membrane Fuel Cell Performance

s04-011

**Ping-Yen Chen** (Materials Science and Engineering, National Taiwan University of Science and Technology, Taipei, Taiwan)

Novel Polybenzimidazoles Containing Bulky Side Groups for High-temperature Polymer Electrolyte Membranes Fuel Cell Applications

s04-012

**Nick Daems** (Centre for Surface Chemistry and Catalysis, K.U. Leuven, Heverlee, Belgium), Sam Milis, Paolo Pescarmona, Ivo Vankelecom

Synthesis of membrane electrode assemblies for proton-exchange membrane fuel cells

s04-013

**Ronghuan He** (Department of Chemistry, College of Sciences, Northeastern University, Shenyang, China), Yixin Xu, Jingshuai Yang

Cross-Linked Imidazolium-Based Anion Exchange Membranes

s04-014

**Xiangnan He** (Chemistry, Northeastern University, Shenyang, China)

Bi-imidazolium Cation Crosslinked Poly(2,6-dimethyl-1,4-phenylene oxide) Anion Exchange Membranes for Fuel Cell Application

s04-015

**Wang Hsiang-Cheng** (School of Defense Science, CCIT, National Defense University, Taoyuan, Taiwan), Ger Ming-Der, Lu Chen-En

Improvement on corrosion resistance and conductivity by electroplated coatings on aluminum 5052 bipolar plate of proton exchange membrane fuel cell

s04-016

**Taro Kimura** (Graduate School of Medicine and Engineering, University of Yamanashi, Kofu, Japan), Masanori Hara, Junji Inukai, Makoto Uchida, Manai Shimada, Hideaki Ono, Shigefumi Shimada, Kenji Miyatake, Masahiro Watanabe

Anion-conductive areas on anion exchange membranes analyzed by current-sensing atomic force microscopy under controlled conditions

s04-017

**Dong-Hoon Lee** (Green Materials Research Group, Youngin, Korea), Eun-Su Lee, Nayoung Kim, Moo-Seok Lee

Development of Nanofiber Reinforced PEM Impregnated with Hydrocarbon Polymer Electrolytes

s04-018

**Hyejin Lee** (Fuel Cell Laboratory, Korea Institute of Energy Research (KIER), Daejeon, Korea), Byungchan Bae

Proton Conducting Composite Membranes with Improved Oxidative Stability for PEMFC

s04-019

**Sojeong Lee** (Fuel Cell Laboratory, Daejeon, Korea), Byungchan Bae

Crosslink-free highly sulfonated multi-block poly(arylene ether sulfone) multi-block membranes for PEMFC

s04-020

**Shih-Wei Lee** (Materials Science and Engineering, National Taiwan University of Science and Technology, Taipei, Taiwan), Jin-An Wu, Kuei-Hsien Chen

Novel Poly(ether sulfones) with Clustered Sulfonic Groups for PEMFC Applications at Various Relative Humidity

s04-021

**Kwangjin Oh** (Energy Systems Engineering, Daegu Gyeongbuk Institute of Science and Technology, Daegu, Korea)

Synthesis of sulfonated block copolymer for polymer electrolyte fuel cells operating at intermediate temperature

s04-022

**Gyu-Hyeon Oh** (Department of Environmental Engineering, Sangmyung University, Cheonan, Korea), Mun-Sik Shin, Moon-Sung Kang, Jin-Soo Park

Effects of Solvents for Dispersion Solutions on Membrane-Electrode Assembly for Proton Exchange Membrane Fuel Cells – Overvoltage and Durability

s04-023

**Mun-Sik Shin** (Department of Environmental Engineering, Sangmyung University, Cheonan, Korea), Jin-Soo Park

The Porous Polyimide Membranes Derived from Diamine Monomer Containing Benzimidazole Unit for High Temperature Fuel Cells

s04-024

**Mun-Sik Shin** (Department of Environmental Engineering, Sangmyung University, Cheonan, Korea), Moon-Sung Kang, Jin-Soo Park

Preparation and Characterization of Anion Conducting Ionomer Binder based on Quaternized Polybenzimidazole for Solid Alkaline Fuel Cells

## Fuel cell electrocatalysis

s04-025

**Koki Baba** (Department of Biomolecular Functional Engineering, Ibaraki University, Ibaraki, Japan), Mika Shiraishi, Risa Shiraishi, Mikka Nishitani-Gamo, Toshihiro Ando, Mika Eguchi

Enhancement of polymer electrolyte fuel cell performance using a Marimo carbon

s04-026

**Antoinette Boreave** (Chemistry, CNRS, Villeurbanne, France), Foteini M. Sapountzi, Michail N. Tsampas, Chunhua Zhao, Laurence Retailleau, Dario Montinaro, Philippe Vernoux

Triode Operation for Enhancing the Performance of H<sub>2</sub>S-Poisoned SOFCs for CH<sub>4</sub> Steam Reforming

s04-027

**Kuo-Wei Chiang** (Department of Chemical Engineering and Materials Science, Yuan Ze University, Taoyuan, Taiwan), Bo-Syun Cheng, Ken-Ming Yin

Mathematical Model of Non-Uniform Cathode Catalytic Layer on the Performance of PEMFC

s04-028

**Xiaoqiang Cui** (School of Materials Science and Engineering, Jilin University, Changchun, China)

Plasmonic Induced Inhibition and Enhancement of the Electrocatalytic Activity for Ethanol Oxidation on Pd/Au Hetero-Nanoraspberries

s04-029

**He-yun Du** (Center for Condensed Matter Sciences, National Taiwan University, Taipei, Taiwan), Li-Chyong Chen, Kuei-Hsien Chen, Chen-Hao Wang

Enhanced Proton Conductivity of Polybenzimidazole Membranes Synthesized *via* Direct-casting Process for High Temperature Fuel Cells

s04-030

**Kazuma Furuhashi** (Department of Biomolecular Functional Engineering, Ibaraki University, Hitachi, Japan), Mika Shiraishi, Risa Shiraishi, Mikka Nishitani-Gamo, Toshihiro Ando, Mika Eguchi

Electrochemical characterization of Marimo carbon supported Pt–Pd

s04-031

**Daniel Garcia** (Institut für Technische Thermodynamik, Deutsches Zentrum für Luft und Raumfahrt (DLR), Stuttgart, Germany), Beatriz Martinez, J.L Castillo, Kaspar Andreas Friedrich, P.L Garcia-Ybarra

Characterization of ultra-low loading MEAs fabricated by electrospray deposition

s04-032

**Valentina Grippo** (Faculty of Chemistry, University of Warsaw, Warsaw, Poland), Roland Ludwig, Renata Bilewicz

Comparison of fuel cells based on different cathode and anode enzymes

s04-033

**Makoto Hamazaki** (Green Hydrogen Research Center, Yokohama National University, Yokohama, Japan), Akimitsu Ishihara, Yuji Kohno, Koichi Matsuzawa, Shigenori Mitsushima, Kenichiro Ota

Evaluation of durability of titanium-niobium oxides mixed with Ti<sub>4</sub>O<sub>7</sub> as non-precious metals and carbon-free cathodes for PEFC in sulfuric acid at 80°C

s04-034

**Akari Hayashi** (International Research Center for Hydrogen Energy, Kyushu University, Fukuoka, Japan), Yasuto Minamida, Zhiyun Noda, Kazunari Sasaki

Development of a cathode material for durable PEFC through the encapsulation of Pt into carbon mesopores



s04-035

**Hsiao-Chun Huang** (Department of Chemical Engineering, National Taiwan University of Science and Technology, Taipei, Taiwan), Chun-Jern Pan, Wei-Nien Su, Bing-Joe Hwang

Conductive oxide supported Co<sub>3</sub>O<sub>4</sub> nanocomposite as robust catalysts for oxygen reduction and evolution reaction

s04-036

**Xuan Jian** (College of Chemistry and Chemical Engineering, Taiyuan University of Technology, Taiyuan, China), Xian Liu, Huimin Yang, Zhenhai Liang

Graphene-Carbon Nanofibers Composite Film As a Highly Active Catalyst Support for Formic Acid Electrooxidation

s04-037

**Nozomi Kawakami** (Department of Chemical Engineering, National Institute of Technology, Nara College, Yamatokoriyama, Japan), Hirohisa Yamada, Takanori Kobayashi, Zyun Siroma, Katsumi Katakura, Minoru Inaba

Fundamental Studies on Oxygen Reduction Reaction and Hydrogen Peroxide Reduction Reaction with RRDE Technique

s04-038

**Marika Muto** (Graduate School of Environmental Science, Hokkaido University, Sapporo, Japan), Masaru Kato, Ichizo Yagi

Copper-Incorporated Carbon Catalysts for Oxygen Reduction Reaction

s04-039

**Tsukasa Nagai** (Research Institute of Electrochemical Energy, AIST, Osaka, Japan), Shin-ichi Yamazaki, Naoko Fujiwara, Masafumi Asahi, Zyun Siroma, Tsutomu Ioroi

Metalloporphyrin-Modified Perovskite-Type Oxide for Cathode Catalyst in Alkaline Fuel Cell

s04-040

**Aziz Nechache** (Division of Physical Sciences and Engineering, King Abdullah University of Science and Technology (KAUST), Thuwal, Saudi Arabia), Samir Boulfrad, Shahid P. Shafi, Enrico Traversa

La<sub>0.2</sub>Sr<sub>0.25</sub>Ca<sub>0.45</sub>Ti<sub>1-x</sub>yNb<sub>x</sub>Ni<sub>y</sub>O<sub>3</sub> as Potential Anode Material for IT-SOFCs

s04-041

**Yao Nie** (School of Chemistry and Chemical Engineering, Chongqing University, Chongqing, China), Siguo Chen, Wei Ding, Xiaohong Xie, Yun Zhang, Zidong Wei

Pt/C Trapped in Activated Graphitic Carbon Layers as a Highly Durable Electrocatalyst for Oxygen Reduction Reaction

s04-042

**Kazuma Shinozaki** (Chemistry, Colorado School of Mines, Golden, USA), Shyam Kocha

Rotating Disk Electrode Studies on the Effect of Nafion on the Oxygen Reduction Reaction for Pt/C and Pt Alloy/C

s04-043

**Ryo Shirasaka** (Chemical Engineering, Tokyo National College of Technology, Hachioji, Japan), Sakumi Aoyagi, Hidenobu Shiroishi, Keiji Nagai, Hiraku Ota, Mikka Nishitani-Gamo

Effect of dispersion methods on oxygen reduction and ammonia oxidation activity for a MWCNT supported Pt catalyst

s04-044

**Hidenobu Shiroishi** (Chemical Science and Engineering, Tokyo National College of Technology, Hachioji, Japan), Genki Horiguchi, Yu Chikaoka, Masato Uehara, Naoki Matsuda

Synthesis of Pt Nanoparticles using Microbubble-assisted Low-Voltage Low Frequency Solution Plasma Processing

s04-045

**Yuko Tamura** (Green Hydrogen Research Center, Yokohama National University, Yokohama, Japan), Akimitsu Ishihara, Yuji Kohno, Koichi Matsuzawa, Shigenori Mitsushima, Kenichiro Ota

Titanium-niobium oxides as non-platinum cathodes for polymer electrolyte fuel cells

**Oxygen evolution/reduction reactions**

s04-046

**Wei Ding** (School of Chemistry and Chemical Engineering, Chongqing University, Chongqing, China), Wei Li, Guangping Wu, Li Li, Siguo Chen, Xueqiang Qi, Zidong Wei

Shape Fixing *via* Salt Recrystallization: A Morphology-Controlled Approach to Convert Nanostructured Polymer to Carbon Nanomaterial as a High Active Catalyst for Oxygen Reduction Reaction

s04-047

**Monika Góral-Kurbiel** (Jerzy Haber Institute of Catalysis and Surface Chemistry PAS, Kraków, Poland), Alicja Drelinkiewicz, Robert Kosydar, Jacek Gurgul, Beata Dembińska, Pawel J. Kulesza, Elzbieta Bielańska, M. Ruggiero

The Effect of Nafion Ionomer on Electroactivity of Palladium-Polypyrrole Catalysts for Oxygen Reduction Reaction

s04-048

**Tomoaki Hayashi** (Green Hydrogen Research Center, Yokohama National University, Yokohama, Japan), Akimitsu Ishihara, Yuji Kohno, Koichi Matsuzawa, Shigenori Mitsushima, Kenichiro Ota

Kinetics of oxygen reduction reaction on titanium oxide-based catalysts prepared from oxy-titanium tetra-pyrazino-porphyrizine in acidic media

s04-049

**Zi-Jun Lin** (Institute of Materials Science and Engineering, National Central University, Taoyuan, Taiwan), Hong-Shou Chen, Yu-Ting Liang, Kuan-Wen Wang

The Effect of Heat-Treatment on the Oxygen Reduction Reaction Activity of Carbon-Supported PtCoAg Electrocatalysts

s04-050

**Yuta Nabae** (Department of Organic and Polymeric Materials, Tokyo Institute of Technology, Meguro-ku, Japan), Teruaki Hayakawa, Hideharu Niwa, Yoshihisa Harada, Masaharu Oshima, Atsushi Matsunaga, Ayano Isoda, Kazuhisa Tanaka

Synthesis and Characterization of Carbon-Based Non-Precious-Metal Cathode Catalysts from Polyimide Fine Particles

s04-051

**Chen-Yu Tsai** (Department of Chemical Engineering, National Taiwan University of Science and Technology, Taipei, Taiwan), Yi-Chen Wu, Men-Che Tsai, Chun-Jern Pan

Preparation of Highly Conductive TiO<sub>2</sub> Supported Pt Catalyst and Its Electrochemical Performance

**Physical electrochemistry**

s04-052

**Yongli Zheng** (Hefei National Laboratory for Physical Sciences at Microscale, University of Science and Technology of China, Hefei, China), Yanxia Chen, Zhengda He, Jie Wei

The Degradation of Oxygen Reduction Activity at Stepped Platinum Surfaces in Acidic Media

s04-053

**Yongli Zheng** (Hefei National Laboratory for Physical Sciences at Microscale, University of Science and Technology of China, Hefei, China), Yao Yao, Dong Mei, Yanxia Chen

Oxygen reduction reaction on Au@Pt nanoparticles and Au(100) electrode

**Solid oxide cells**

s04-054

**Junfu Bu** (Department of Materials Science and Engineering, KTH Royal Institute of Technology, Stockholm, Sweden), Pär Jönsson, Zhe Zhao

The Effect of NiO on the Conductivities of BaZr<sub>x</sub>Ce<sub>0.8-x</sub>Y<sub>0.2</sub>O<sub>3-δ</sub> (x = 0.5, 0.6, 0.7, 0.8) Proton Conductors

s04-055

**Zhao Hui** (Chemistry, Heilongjiang University, Harbin, China)

Electrochemical performance of double perovskite Pr<sub>2</sub>NiMnO<sub>6</sub> as cathode for intermediate temperature solid oxide fuel cells

s04-056

**I-Ming Hung** (Department of Chemical Engineering and Materials Science, Yuan Ze University, Taoyuan, Taiwan), Hao-Ying Cheng, Sheng-Wei Lee, Jeng-Kuei Chang, Jing-Chie Lin, Jason Shian-Ching Jang, Chuan Li, Chi-Shiung Hsi

Synthesis and Characterization of High Temperature Proton Conductor  $\text{Sr}(\text{Ce}_{0.6}\text{Zr}_{0.4})\text{O}_{3-\delta}$  co-doped with Indium and Yttrium

s04-057

**Sou Ikeda** (Department of Hydrogen Energy Systems, Kyushu University, Fukuoka, Japan), Shota Kotake, Hironori Nakajima, Tatsumi Kitahara

Mass Transfer Analysis of Anode-Supported Honeycomb Solid Oxide Fuel Cells

s04-058

**Yuya Kitaguchi** (Chemical Engineering, National Institute of Technology, Nara College, Yamatokoriyama, Japan), Hirohisa Yamada, Katsumi Katakura

Study on Ion conductivity of Mg-Al Layered Double Hydroxides prepared by electrochemical co-precipitation method

s04-059

**Aditya Maheshwari** (Institute of Inorganic Chemistry, University of Muenster, Muenster, Germany), Hans-Dieter Wiemhöfer

A Novel Approach to Develop MIEC material:  $\text{CeO}_2\text{-ZrO}_2$  composite

s04-060

**Chung-Ta Ni** (Materials Science and Engineering, National Cheng Kung University, Tainan, Taiwan), Shu-Yi Tsai, Kuan-Zong Fung, Yu-Cheng Su, Han-Lung Liu

Structural Stability of Mixed Conducting  $\text{La}_{0.8}\text{Ca}_{0.2}\text{Fe}_{1-x}\text{Co}_x\text{O}_3$  ( $x=0\sim0.4$ ) Perovskite in Different Atmospheres

s04-061

**Chung-Ta Ni** (Research Center for Energy Technology and Strategy, National Cheng Kung University, Tainan City, Taiwan), Shu-Yi Tsai, Kuan-Zong Fung, Hsin-Chia Ho

Effect of Thermal Effect on Phase Transformation of Plasma Sprayed Protective Oxides on SOFC Metallic Interconnects

s04-062

**Masanori Ochi** (Applied Physics, Tokyo University of Science, Tokyo, Japan), Shohei Yamaguchi, Takaaki Suetsugu, Naoya Suzuki, Kinya Kawamura, Takashi Tsuchiya, Masaki Kobayashi, Hiroshi Kumigashira, Tohru Higuchi

Structural and Electrical properties of Ru-doped  $\text{BaCe}_{0.90}\text{Y}_{0.10}\text{O}_{3-\delta}$  Thin Film

s04-063

**Mirosław Stygar** (Faculty of Materials Science and Ceramics, AGH University of Science and Technology, Krakow, Poland), Waldemar Tejchman, Juliusz Dabrowa, Tomasz Brylewski

Preparation and structural and electrical properties of calcium-doped and nickel-doped yttrium chromate(III)

s04-064

**Shu-Yi Tsai** (Research Center for Energy Technology and Strategy, National Cheng Kung University, Tainan City, Taiwan), Kuan-Zong Fung, Chung-Ta Ni, Yu-Fan Chang

Effect of Composite Cathode on Polarization Reduction for Solid Oxide Fuel Cells based on Microstructure and Ion-Conduction Consideration

## Symposium 5: Novel Insights to Electrochemical Capacitors

### Edl capacitor

s05-001

**Mohammad BinSabt** (Chemistry, Faculty of Science, Kuwait University, Kuwait, Kuwait), Ahmed Abdel Nazeer, Ahmed Galal

Effect of Nickel Oxide Type on the Electrochemical Behavior of Nickel-Graphene Oxide Hybrid – Towards Electrochemical Capacitor

s05-002

**Hsiu-Chuan Chien** (Chemical Engineering, National Tsing Hua University, Hsin-Chu City, Taiwan)

Buffer Effect on Electrolytes towards Supercapacitors Application

s05-003

**Hui Dou** (College of Material Science and Engineering, Nanjing University of Aeronautics and Astronautics, Nanjing, China), Guiyin Xu, Qi Sheng, Bing Ding, Aixiu Wang, Zhi Chang

Porous Carbon Nanofiber with Phosphorus and Nitrogen Dual-Doping for High Performance Supercapacitors

s05-004

**Hsin-Chieh Huang** (Department of Chemical Engineering, National Cheng Kung University, Tainan, Taiwan), Hsisheng Teng

Facile Fabrication of High-Performance All-Solid-State Micro-supercapacitors through Laser Micromachining

s05-005

**Pawel Jezowski** (Institute of Chemistry and Technical Electrochemistry, Poznan University of Technology, Poznan, Poland), François Béguin

Activated carbon electrode expansion during EDL charging in various salt aqueous electrolytes

s05-006

**Ick-Jun Kim** (Battery Research Center, Korea Electrotechnology Research Institute, Changwon Si, Korea)

Effects of joule-heating on the activated carbon for improved electric double layer capacitor

s05-007

**Chunling Liu** (School of Chemistry and Chemical Engineering, Shaanxi Normal University, Xi'an, China), Yana Li, Li Wang, Fajun Xia, Tong Yang, Wensheng Dong

Ordered mesoporous carbon nitride as an electrode material for high performance electrochemical capacitors

s05-008

**Jiayun Liu** (Environmental Engineering, Donghua University, Shanghai, China), Miao Lu, Jianmao Yang, Jian Cheng, Wenshu Cai, Zhubiao Xiong

Asymmetric Capacitors to Improve the Charge Efficiency of the Capacitive Deionization

s05-009

**Mahmoud Mohamed Mahmoud Ahmed** (Graduate Institute of Applied Science and Technology, NTUST, Taipei, Taiwan), Toyoko Imae, Masaki Ujihara

Nondestructive production of magnetic graphene towards energy applications

s05-010

**Sung June Park** (Department of Energy Systems Research, Ajou University, Suwon, Korea), Jaeshin Yi, Kyung-Seok Min, Jongrak Choi, Ha-Young Lee

Thermal modeling of an ultracapacitor module for automotive applications

s05-011

**Hsiao-Hsuan Shen** (Chemical Engineering, Tsing Hua University, Hsin Chu, Taiwan)

Criteria of Activated Carbon Electrical Double-Layer Capacitors in Propylene Carbonate-Based Electrolyte

s05-012

**Sheng Sian Yang** (Chemical Engineering, National Taipei University of Technology, Taipei, Taiwan), Jun-Ming Chiu, Chao-Chi Tu, Lu-Yin Lin

The Simple Method for Synthesis of the Nickel Foam-supported graphene with High Surface Area for Supercapacitors

**Electrolytes (organic, aqueous & ionic)**

s05-013

**Jaanus Eskusson** (Faculty of Science and Technology, University of Tartu, Institute of Chemistry, Tartu, Estonia), Alar Jänes, Enn Lust

Influence of 1,2-Dimethoxyethane Additive on the Electrochemical Characteristics of EMImTFSI Based Electrolytes for Supercapacitors

s05-014

**Paula Ratajczak** (Institute of Chemistry and Technical Electrochemistry, Poznan University of Technology, Poznan, Poland), Piotr Gajewski, François Béguin

Optimizing the high cell potential performance of AC/AC supercapacitors based on two aqueous electrolytes

s05-015

**Paula Ratajczak** (Institute of Chemistry and Technical Electrochemistry, Poznan University of Technology, Poznan, Poland), Adam Slesinski, Elzbieta Frackowiak, François Béguin

Performance improvement of AC/AC capacitors in aqueous medium through selection of current collectors

s05-016

**Tsukasa Ueda** (Applied Chemistry, Tokyo University of Agriculture and Technology, Tokyo, Japan), Kenji Oshima, Natsuki Miyashita, Shinichi Seto, Etsuro Iwama, Wako Naoi, Katsuhiko Naoi

Li<sub>4</sub>Ti<sub>5</sub>O<sub>12</sub> / Activated Carbon Hybrid Capacitor for High Voltage Operation

s05-017

**Cheng-Hsien Yang** (Institute of Materials Science & Engineering, National Central University, Taoyuan, Taiwan), Po-Ling Huang, Xu-Feng Luo, Chueh-Han Wang, Chi Li, Yi-Hsuan Wu, Jeng-Kuei Chang

Holey Graphene Nanosheets with Surface Oxygen-containing Groups for High Supercapacitor Performance in Ionic Liquid Electrolyte

**Pseudocapacitors & hybrids**

s05-018

**Arturas Adomkevicius** (Department of Chemical Engineering, National Tsing Hua University/The University of Liverpool, Hsin-Chu city, Taiwan), Chi-Chang Hu, Laurence Hardwick

Synthesis and Characterisation of Sodium ion Pre-intercalated Manganese Oxide for High Performance Asymmetric Supercapacitors

s05-019

**Esther Baek** (Electronic Materials Engineering, Kwangwoon University, Seoul, Korea), Jeong Hyun Lee, Hong-Ki Kim

Superior power and energy density based on hybrid electrodes of Activated carbon-H<sub>2</sub>Ti<sub>12</sub>O<sub>25</sub> anode for hybrid supercapacitor

s05-020

**Jun-Ming Chiu** (Chemical Engineering, National Taipei University of Technology, Taipei, Taiwan)

Synthesis of Cobalt Sulfide Hydrangea Macrophylla Nanostructures with High Charge-Accumulation Surface Area for Supercapacitors

s05-021

**Chaopeng Fu** (Department of Materials, University of Oxford, Oxford, United Kingdom), Patrick Grant

Low-cost and high performance supercapacitors based on up-cycled industrial mill scale

s05-022

**Qiu Jiang** (Material Science and Engineering, KAUST, Thuwal, Saudi Arabia), Narendra Kurra, Husam Alshareef

A General Strategy for the Fabrication of High Performance Microsupercapacitors

s05-023

**Lingbin Kong** (School of Materials Science and Engineering, Lanzhou University of Technology, Lanzhou, China), Xuejing Ma, Weibin Zhang, Yongchun Luo, Long Kang

Nanocrystalline vanadium trioxide as negative electrodes for asymmetric supercapacitors

s05-024

**Seung-Hwan Lee** (Electronic Materials Engineering, Kwangwoon University, Seoul, Korea), Hyeong Jong Choi, Jin Hyeon Kim

Improved electrochemical performance of hybrid supercapacitor using highly dispersed Carbon-AlPO<sub>4</sub> binary coated H<sub>2</sub>Ti<sub>12</sub>O<sub>25</sub> as anode

s05-025

**Yang Li** (Materials Science, Shanghai Second Polytechnic University, Shanghai, China), Jing Li, Huaqing Xie

Hydrothermal prepared Al-doped  $\alpha$ -MnO<sub>2</sub> nanotube and its electrochemical performances for supercapacitors

s05-026

**Jeng-Yu Lin** (Department of Chemical Engineering, Tatung University, Taipei City, Taiwan), Chao-Shuan Dai, Pei-Yi Chien, Shu-Wei Chou, Tsung-Wu Lin

Nickel sulfide/carbon nanotube nanocomposites as cathode materials for hybrid supercapacitors

s05-027

**Yu Wei Lin** (High Power Energy Storage Materials and Devices, Industrial Technology Research Institute, Hsinchu, Taiwan), Jun Long Li, Chung Hsiang Chao, Li Duan Tsai, Jason Fang

An Energy Enhanced, Long-Life Supercabattery Based on High Discharge Efficiency Hybrid Electrodes

s05-028

**Xiaoxia Liu** (Chemistry, Northeastern University, Shenyang, China), Li-Jie Sun, Ming-Hua Bai

Electrochemical Co-deposition of Polyaniline with Inorganic Oxides for Pseudocapacitive Application

s05-029

**Zong-Huai Liu** (School of Materials Science and Engineering, Shaanxi Normal University, Xian, China), Yun Long Bai, Gai Ni Zhang, Li Ping Kang, Zhi Bin Lei

Design and fabrication of supercapacitor electrodes with good rate performance from hole grapheme nanosheets

s05-030

**Alina Pruna** (Faculty of Physics, University of Bucharest, Bucharest, Romania), Qi Shao, Juan Antonio Zapien, Antonio Ruotolo

Effect of ZnO on Capacitive Properties of Core / Hybrid Shell Arrays

s05-031

**Muniyandi Rajkumar** (Chemical Engineering, National Tsing Hua University, Hsinchu, Taiwan)

Enhancing Ultrahigh Loading with High Areal Specific Capacitance in Nickel–Cobalt Double Hydroxides/CNT composites for Supercapacitor Device

s05-032

**Ashis Kumar Satpati** (Analytical Chemistry Division, Bhabha Atomic Research Centre, Mumbai, India), M. K. Dey

Hydrothermally Prepared Reduced Graphene Oxide and Manganese Oxide Nano Rod Composite Materials for Supercapacitor Applications

s05-033

**Indrajit Shown** (Institute of Atomic and Molecular Sciences, Academia Sinica, Taipei, Taiwan), Abhijit Ganguly, Li-Chyong Chen, Kuei-Hsien Chen

Design and development of direct-growth *in-situ* doped Polypyrrole on carbon cloth as a high performance flexible supercapacitor

s05-034

**Chao-Chi Tu** (Department of Chemical Engineering and Biotechnology, National Taipei University of Technology, Taipei, Taiwan), Sheng-Sian Yang, Jun-Ming Chiu, Lu-Yin Lin

*In-situ* Polymerization of Pyrrole in MoS<sub>2</sub> Nanosheets as Highly Conductive Materials with Large Surface Area for Supercapacitors

s05-035

**Chuan Xia** (Materials Science & Engineering, King Abdullah University of Science & Technology, Jeddah, Saudi Arabia), Wei Chen, Xianbin Wang, Mohamed Hedhili, Nini Wei, Husam Alshareef

Polyaniline-RuO<sub>2</sub> Core-Shell Nanostructured Arrays for Very Stable and High Performance Pseudocapacitors

s05-036

**Sainan Yang** (College of Materials Science and Chemical Engineering, Harbin Engineering University, Harbin, China), Yiju Li, Dianxue Cao, Guiling Wang  
Reduced Graphene Oxide Decorated on MnO<sub>2</sub> Nanoflakes Grew on C/TiO<sub>2</sub> Nanowire Arrays for Supercapacitor

s05-037

**Nobuko Yoshimoto** (Graduate School of Science and Engineering, Yamaguchi University, Ube, Japan), In-Tae Kim, Nobuo Kouda, Masayuki Morita  
Synthesis and Electrochemical Analysis of Electrodeposited MnO<sub>2</sub>/C Composite Electrode for Supercapacitors

s05-038

**Zi fan Zeng** (Department of Materials Science, Sichuan University, Cheng Du, China), Ji liang Zhu, Xiao hong Zhu, Xi Liu, Chuang Kou, Fang yuan Xie  
Ni(OH)<sub>2</sub> Nanowires with High Performance as Supercapacitor Electrode *via* Cathodic Electrodeposition

s05-039

**Yaping Zhao** (College of Chemistry, Chemical Engineering & Biotechnology, Donghua University, Shanghai, China), Hong Zhao, Caihong Liu, Bingzheng Song, Zaisheng Cai  
Pulse Electropolymerization Synthesis of Polypyrrole Layers on Multiwalled Carbon Nanotubes coated Cotton Fabrics

### Redox active species

s05-040

**Shintaro Aoyagi** (Department of Applied Chemistry, Tokyo University of Agriculture and Technology, Tokyo, Japan), Takumi Furuhashi, Yuta Abe, Keita Okazaki, Junichi Miyamoto, Etsuro Iwama, Wako Naoi, Katsuhiko Naoi  
V-rated "Nanohybrid Supercapacitor" utilizing Ultrafast b-axis-controlled TiO<sub>2</sub> (B) Nanocrystals

s05-041

**Kazuaki Kisu** (Department of Applied Chemistry, Tokyo University of Agriculture and Technology, Tokyo, Japan), Shota Nakashima, Yuki Sakai, Etsuro Iwama, Yuki Orikasa, Patrick Rozier, Wako Naoi, Patrice Simon, Katsuhiko Naoi  
Detailed Analysis on Carbon-Nested Ultrafast nano-LiFePO<sub>4</sub> Prepared by Means of Ultracentrifugation for Hybrid EES

s05-042

**Jakub Menzel** (Institute of Chemistry and Technical Electrochemistry, Poznan University of Technology, Poznan, Poland), Krzysztof Fic, Elzbieta Frackowiak  
Improving energy performance of electrochemical capacitors by combining redox reaction with hydrogen storage phenomena

s05-043

**Prakash Ramakrishnan** (Energy Systems Engineering, Daegu Gyeongbuk Institute of Science & Technology (DGIST), Daegu, Korea), Sangaraju Shanmugam  
Electrochemical Performance of Nitrogen Doped Nano-channel Carbon Structures in Redox Electrolyte Supported Supercapacitor

## Symposium 6: New Progress in Electrochemical Solar Cells

### Dye sensitized solar cell

s06-001

**Taame Abraha Berhe** (Graduate Institute of Applied Science and Technology, National Taiwan University of Science and Technology, Taipei, Taiwan)

Laser Induced Degradation Study of  $\text{CH}_3\text{NH}_3\text{PbI}_3$  Light Harvesting Oih-Perovskite Semiconductor

s06-002

**I-Ting Chiu** (Department of Chemical Engineering, National Taiwan University, Taipei, Taiwan), Chun-Ting Li, Chuan-Pei Lee, Pei-Yu Chen, Kuo-Chuan Ho

Highly Efficient Cobalt Selenide Hierarchical Nano-Wall for the Electro-Catalytic Counter Electrodes in Dye-Sensitized Solar Cells

s06-003

**Zheng-Chang Huang** (Chemical Engineering, Tatung University, Taipei, Taiwan)

Pt-free counter electrode of  $\text{NiCo}_2\text{S}_4$  by two step dip-coating as dye-sensitized solar cells

s06-004

**Chun-Ting Li** (Chemical Engineering, National Taiwan University, Taipei, Taiwan), Chuan-Pei Lee, Chun-Ting Li, Miao-Syuan Fan, Yi-June Huang, Ling-Yu Chang, Jiang-Jen Lin, Kuo-Chuan Ho

Microemulsion-assisted Zinc Oxide Synthesis: Morphology Control and its Applications in Photoanodes of Dye-Sensitized Solar Cells

s06-005

**Gerald Ensang Timuda** (Energy Sciences, Tokyo Institute of Technology, Yokohama-shi, Japan), Runbang Tao, Keiko Waki

Electrochemical Analysis of Dye Sensitized Solar Cell Employing Indoline-based and Ruthenium-based Dye Combined with Volatile and Non-Volatile Solution-based Electrolyte

s06-006

**Yu-Hao Tseng** (Department of Chemical Engineering, National Taiwan University, Taipei, Taiwan), Miao-Syuan Fan, Chuan-Pei Lee, Chun-Ting Li, Ming-Chou Chen, Kuo-Chuan Ho

Efficient Quasi-Solid-State Dye-Sensitized Solar Cells with Novel Polymeric Ionic Liquids

### Nanostructured semiconductors

s06-007

**Yen-Chun Chuan Sun** (Chemical Engineering, National Tsing Hua University, Hsinchu, Taiwan)

A Novel Preparation Method for Titanium Dioxide in the Rutile Phase for Electrochemical Photocatalytic Applications

s06-008

**Kai-Chieh Tsai** (Department of Chemical Engineering, National Taiwan University of Science and Technology, Taipei, Taiwan), Hsin-Fu Teng, Wei-Nien Su, Bing-Joe Hwang

Surface Textured Silicon Photocathode for  $\text{H}_2$  Production Improves Photoelectrochemical Water Splitting efficiency

s06-009

**Shu-Yi Tsai** (Department of Materials Science and Engineering, National Cheng Kung University, Tainan, Taiwan), Chung-Ta Ni, Kuan-Zong Fung

Infrared transparent  $\text{NiCo}_2\text{O}_4$  thin film as a Front Electrode for Solar Cells

s06-010

**Nan Zhang** (Chemistry, Xiamen University, Xiamen, China), Changjian Lin, Miaoqiang Lv, Meidan Ye, Dajiang Zheng

Rutile  $\text{TiO}_2$  Nanosheet Arrays on Thermally Oxidized  $\text{TiO}_2$  Blocking Layer for Enhancing Efficiency of Perovskite Solar Cells



**Photovoltaic**

s06-011

**Wahyu Diyatmika** (Materials Science and Engineering, National Taiwan University of Science and Technology, Taipei, Taiwan), Lingjun Xue, Jinn P. Chu

Thin film metallic glass as a diffusion barrier for flexible CIGS solar cell on stainless steel substrate: A feasibility study

**Solar energy conversion**

s06-012

**Yen-Jhih Chen** (Department of Chemical Engineering, National Taiwan University of Science and Technology, Taipei City, Taiwan)

Fabrication of Ti doping Hematite Nanotubes Arrays Photoanode *via* Anodic Electrodeposition for Solar Water Splitting

s06-013

**Ramona Gutkowski** (Analytical Chemistry - Center of Electrochemical Science, Ruhr-Universität Bochum, Bochum, Germany), Kirill Sliozberg, Wolfgang Schuhmann

Improvement of the photoelectrocatalytic performance of BiVO<sub>4</sub> by metal doping and co-catalyst decoration using an optical scanning droplet cell

s06-014

**Tsung-Yeh Ho** (Department of Chemical Engineering, National Taiwan University of Science and Technology, Taipei City, Taiwan)

The Study of Carrier Transport/Transfer Mechanism inside CZTS/MS(M=Zn, Cd, Cu)/TiO<sub>2</sub> Nanorods for Solar Water Splitting

s06-015

**Moon-Sung Kang** (Department of Environmental Engineering, Sangmyung University, Cheonan, Korea), Hye-Rin Kim

Performance Enhancement of Perovskite-based Solar Cells with TiO<sub>2</sub> Scaffold by Optimizing Electron-Hole Transport

s06-016

**Jan Macak** (Center of Materials and Nanotechnologies, University of Pardubice, Pardubice, Czech Republic), Milos Krbal, Filip Bures

Hybrid Photoelectrochemical Systems Based on Self-Organized TiO<sub>2</sub> Nanotubes and Novel Chromophores

s06-017

**Wu Zhi** (College of Chemistry and Chemical Engineering, Xiamen University, Xiamen, China), Changjian Lin

Bi<sub>2</sub>S<sub>3</sub> Nanoparticle Modified TiO<sub>2</sub> Nanotube Arrays for High Efficiency of Photoelectrochemical Hydrogen Production

## Symposium 7: Electrodeposition - The Frontier Approach in Material Science and Nanofabrication

### Additives

s07-001

**Satoru Watanabe** (Faculty of Science and Technology, Tokyo University of Science, Noda, Japan), Isao Shitanda, Yoshinao Hoshi, Tatsuo Aikawa, Masayuki Itagaki

Intelligent Self-lubricant Composite Nickel Coating based on Phase Transition of Polystyrene and Polymethyl Methacrylate Particles

### Alloy deposition

s07-002

**Mao-Chun Hung** (Chemical Engineering, National Chung Hsing University, Taichung, Taiwan), Po-Fan Chan, Wei-Ping Dow, Hsiao-Yen Lee, Yi-Sheng Lin, Ping-Feng Yang

Effect of Plating Additives on Microstructure and Properties of Electrodeposited Ni-Fe Alloy

s07-003

**Sho Kawamura** (Department of Applied Material and Life Science, Graduate School of Engineering, Kanto Gakuin University, Yokohama-shi, Japan), Nobuaki Watanabe, Ichiro Koiwa

Pulse Electroplating of Cu-Mo Alloy @Film @Using Disodium Molybdate

s07-004

**Tomio Nagayama** (Surface Finishing Technology Lab., Kyoto Municipal Inst. of Industrial Technology and Culture, Kyoto, Japan), Takayo Yamamoto, Toshihiro Nakamura

Mechanical properties of electrodeposited Fe-Ni alloys in the Invar composition range

s07-005

**Toshihiro Nakamura** (Surface Finishing Technology Lab., Kyoto Municipal Institute of Industrial Tech. and Culture, Kyoto, Japan), Takayo Yamamoto, Tomio Nagayama

Contact Resistance of Thin Gold Overlay on Cu-Sn Alloy Electrodeposits with Various Compositions

s07-006

**Yu-Sheng Wang** (Department of Medicinal and Applied Chemistry, Kaohsiung Medical University, Kaohsiung, Taiwan)

Voltammetric Study and Electrodeposition of Zinc in N-butyl-N-methylpyrrolidinium Bis(trifluoromethanesulfonyl)imide Room Temperature Ionic Liquid

s07-007

**Takayo Yamamoto** (Surface Finishing Technology Lab., Kyoto Municipal Institute of Industrial Tech. and Culture, Kyoto, Japan), Tomio Nagayama, Toshihiro Nakamura

Fabrication of the three-dimensional micro structure by Fe-Ni alloy electroforming process -Effect of saccharin concentration-

s07-008

**Sachio Yoshihara** (Department of Material and Environmental Chemistry, Utsunomiya University, Utsunomiya, Japan), Wataru Oikawa, Yoshifusa Ishikawa, Kazuyoshi Suzuki, Daisuke Suzuki

Application of Amorphous Alloy Plating to Various Industrial Fields

### Bi-polar electrodeposition

s07-009

**Shih-I. Wen** (Chemical Engineering, National Chung Hsing University, Taichung, Taiwan), Wei-Ping Dow

Using Copolymers as Suppressors in a Copper Plating Bath for Through-Hole Filling

### Electroless deposition

s07-010

**Chih-I. Hsu** (School of Defense Science, National Defense University, Taoyuan, Taiwan), Wang Gao-Liang, Ger Ming-Der, Hou Kung-Hsu

Properties of electroless Ni-P/BN(h) composite coatings at elevated temperatures

s07-011

**Xinyu Liu** (Chemical and Biomolecular Engineering, Case Western Reserve University, Cleveland, USA), Xun Zhan, Frank Ernst, Rohan Akolkar, Werner Richtering

Electroless Deposition of Amorphous Nickel-Tungsten-Phosphorus Alloys with Superior Resistance to Crystallization

s07-012

**Tzu-Hsuan Tsai** (Department of Materials and Mineral Resources Engineering, National Taipei University of Technology, Taipei, Taiwan), Yu-Pei Shih

Recovery of Nanosilver from Si-Wafer Manufacturing Wastes

s07-013

**Yaping Zhao** (College of Chemistry, Chemical Engineering & Biotechnology, Donghua University, Shanghai, China), Hong Zhao, Caihong Liu, Bingzheng Song, Zaisheng Cai

Electromagnetic Shielding Polyamide Fabrics prepared by Electroless Ni Plating with Chitosan-Nickel Complexes Activation

## Nucleation

s07-014

**Atsushi Iwanaga** (Elemental Technology R&D, Y Lab, Furukawa, Japan), Hisayoshi Matsushima, Satoshi Miyazawa, Shinichi Nagano

Numerical Simulation of Current Density Distribution between Vertical Cu Electrode

s07-015

**Peter Keech** (Nuclear Waste Management Organization, Toronto, Canada), Peter Lin, Neil Mahalanobis

Electrodeposited Copper Coatings for Used Fuel Containers

s07-016

**Kai Nakamura** (Materials Science and Engineering, Kyoto University, Kyoto, Japan), Atsushi Kitada, Kazuhiro Fukami, Kuniaki Murase

Characterization of  $\text{AlCl}_3$ /Diglyme Solution for Aluminum Electrodeposition

s07-017

**Jon Ustarroz** (Electrochemical and Surface Engineering (SURF), Vrije Universiteit Brussel, Brussels, Belgium), El Amine Mernissi Cherigui, Pieter Bouckennooge, Kadir Sentosun, Mesfin Haile Mammé, Herman Terryn, Sara Bals, Annick Hubin

Electrodeposition of Nickel Nanostructures from Deep Eutectic Solvents: New Insights into Nucleation and Growth Mechanisms

## Thin films

s07-018

**Chun-Yi Chen** (Precision and Intelligence Laboratory, Tokyo Institute of Technology, Yokohama, Japan), Xun Luo, Tso-Fu Mark Chang, Masato Sone

Effect of Supercritical Carbon Dioxide on Crystal Structure of Electrodeposited Cobalt Films

s07-019

**Caimei Fan** (College of Chemistry and Chemical Engineering, Taiyuan University of Technology, Taiyuan, China), Yingyuan Hu, Rui Li, Xiaoming Mao

One-step Synthesis of Porous BiOBr Film from Bi Plate *Via* Electrochemical Method

s07-020

**Yuya Ito** (Department of Applied Material and Life Science, Graduate School of Engineering, Kanto Gakuin University, Yokohama-shi, Japan), Ichiro Koiwa, Nobuaki Watanabe

Control of Crystal Orientation of Electrodeposited Aluminum Films from Bath Using  $\text{DMSO}_2$  as a Solvent

s07-021

**Ichiro Koiwa** (Department of Applied Chemistry, College of Science and Engineering, Kanto Gakuin University, Yokohama-shi, Japan), Nobuaki Watanabe, Akihiro Yamamoto, Kenta Chokki, Kazuhiro Yabe

$\text{Zn-AlO}_x(\text{OH})_y$  Composite Films Prepared from Non-Suspended Solution by Electrochemical Technique

s07-022

**Song-Zhu Kure-Chu** (Department of Chemistry and Bioengineering, Iwate University, Morioka, Japan), Toru Ogasawara, Hitoshi Yashiro, Kuniaki Sasaki

Thermal Stability and Sulfidizing Resistance of High Reflective Sn/Ag<sub>3</sub>Sn-based Films Electrodeposited on Cu

s07-023

**Chia Wen Liao** (Chung-Cheng Institute of Technology, National Defense University, Taoyuan, Taiwan), Kung Hsu Hou, Ming-Der Ger

Characterization of the Cr-C-Si<sub>3</sub>N<sub>4</sub> Composite Coatings Electroplated from a Trivalent Chromium Bath

s07-024

**Cheng-Lan Lin** (Department of Chemical and Materials Engineering, Tamkang University, New Taipei City, Taiwan), Kuen-Yi Ding

Electrostatic Field-Assisted Direct Potentiostatic and Pulse-Potential Electrodeposition of Prussian Blue Films

s07-025

**Kuniaki Murase** (Department of Materials Science and Engineering, Kyoto University, Kyoto, Japan), Yusuke Seki, Tsutomu Shinagawa, Atsushi Kitada, Kazuhiro Fukami

Electrodeposition of Cu<sub>2</sub>O from Aqueous Lactate Solutions - Studies on Copper(II) Complexes in Alkaline Deposition Baths

s07-026

**Yusuke Okamura** (IMRAM, Tohoku University, Sendai, Japan), Itaru Honma

Electrodeposition of mono-layer graphene from carboxylic acid under hydrothermal condition

s07-027

**Liza Rassaei** (Chemical Engineering, Delft University of Technology, Delft, Netherlands), Hanan Al-Kutubi, Jorge Gascon, Ernst Sudholter, Hamid Reza Zafarani, Alla Dikhtiarenko

Synthesis of ZIF-8 metal organic framework thin film on ZnO nanorods

s07-028

**Mei-Jywan Syu** (Chemical Engineering, National Cheng Kung University, Tainan, Taiwan), Yan-Di Tseng

Amperometric Detection of Bilirubin *via* A Room-Temperature Ionic Liquid-Imprinted Polymer Composite Electrode

s07-029

**Takuya Tokuda** (Graduate School of Advanced Integrated Science, Chiba University, Chiba-shi, Inage-ku, Yayoi-cho, Japan), Dan Takamura, Katsuyoshi Hoshino

Electrochemical preparation of novel metal-like lustrous films

s07-030

**Pu-Wei Wu** (Materials Science and Engineering, National Chiao Tung University, Hsinchu, Taiwan), Po-Chun Chen, Chia-Yun Hsu, Shih-Cheng Chou, Aniruddha Joi, Yezdi Dordi, Jyh-Fu Lee

Electrodeposition of CuMn thin film from a nonaqueous electrolyte

s07-031

**Yu-Beom Yeon** (Department of Advanced Materials Chemistry, Korea University, Sejong Special Self-Governing City, Korea), Viswanathan Saji

Electrodeposition of Copper, Indium, Gallium and Selenium on Molybdenum Investigated by Voltammetry, X-Ray Diffraction, and Scanning Electron Microscopy/Energy Dispersive Spectroscopy

s07-032

**Claudio Zafferoni** (Department of Chemistry Ugo Schiff, Florence, Italy), Serena Cinotti, Francesco Di Benedetto, Andrea Giaccherini, Giordano Montegrossi, Annalisa Guerri, Francesco Carlà, Roberto Felici, Massimo Innocenti

Synthesis and characterization of metal sulfides for solar devices

## Symposium 8: Corrosion and Passivity

### Corrosion

s08-001

**Silviu Drob** (Electrochemistry and Corrosion, Institute of Physical Chemistry Ilie Murgulescu, Bucuresti, Romania), Cora Vasilescu, Jose Maria Calderon Moreno, Petre Osiceanu

A New Dental Alloy with Improved Properties: Its Corrosion Resistance in Various Conditions Simulating Oral Cavity Environment

s08-002

**I-Wen Huang** (Materials Science and Engineering, The Ohio State University, Columbus, USA), Rudolph Buchheit

Assessing and Predicting Concurrent Uniform Corrosion of Aluminum Alloys as a Function of pH, Temperature, Time, and [Cl<sup>-</sup>]

s08-003

**Jia-Lin Jhan** (Department of Chemical Engineering and Materials Science, Yuan Ze University, Taoyang, Taiwan), Leo Chau-Kuang Liao

Corrosion of Indium Tin Oxide Films in SiO<sub>2</sub> Solutions

s08-004

**Katsutoshi Nakayama** (Graduate School of Chemical Sciences and Engineering, Hokkaido University, Sapporo, Japan), Etsushi Tsuji, Yoshitaka Aoki

Fabrication of super-liquid-repellent aluminum mesh with chemical etching/anodizing

s08-005

**Mikhail Pletnev** (Innovative, Izevsk State Technical University, Izhevsk, Russia)

Comparative analysis of the anodic dissolution of iron at low and high over potentials

s08-006

**Britta Schafstaller** (BTT-SF, Atotech Deutschland, Berlin, Germany), Mathias Wuensche, Sebastian Weissbrod, Grigory Vazhenin, Constanze Donner

Au Immersion on mid NiP Substrates – Balance between NiP Dissolution and Au-Adhesion properties

s08-007

**Maria Stepanova** (Materials Science and Engineering, Norwegian University of Science and Technology, Trondheim, Norway), Otto Lunder, Jan Halvor Nordlien, Kemal Nisancioglu

Corrosion resistance of zinc diffusion layers on aluminium

### *In-situ* corrosion measurements

s08-008

**Thangaraj Balusamy** (Materials Recycling Design Group, NIMS, Tsukuba, Japan)

Evaluation of the corrosion behaviour of epoxy coated carbon steel at the damaged zone in saturated Ca(OH)<sub>2</sub> with varying concentration of chloride ions by localized electrochemical impedance spectroscopy

s08-009

**Lin Niu** (Department of Chemistry, Shandong University, Jinan, China), Xiaoping Han, Yu Liu, Weiwei Zhang, Rui Ma, Shuai Li, Tong Li

Local Electrochemical Study on the Effect of Residual Stresses on Localized Corrosion Susceptibility of Type 316 Stainless Steels

s08-010

**Bo Zhao** (Research and Development Center, China Special Equipment Inspection And Research Institute, Beijing, China), Zhiyong Liu, Cuiwei Du, Xiaogang Li, Binan Shou, Tong Xu

Influence of Crevice Thickness to Corrosion Behavior of API X80 Steel under Disbonded Coating in Acid Soil Environment

**Passive films**

s08-011

**Ahmed Galal** (Chemistry, Kuwait University, Kuwait, Kuwait), Mohammad BinSabt, Kamal Shalabi, Faizah Al-Kharafi

Protection of Al93Mg7 Alloy against Corrosion in NaCl Containing Solutions Using Silane and Silane-Graphene Films

s08-012

**Shun-Yi Jian** (Department of Materials Science and Engineering, National Taiwan University, Taipei, Taiwan), Yueh-Lien Lee, Chao-Sung Lin

Electrochemical Corrosion Behavior of Permanganate Conversion Coating on AZ31B Magnesium Alloys - Long Term Evaluation by EIS

s08-013

**Chengqiang Ren** (School of Materials Science and Engineering, Southwest Petroleum University, Chengdu, China), Ye Peng, Jiameng Li, Jingsi Hu, Bo Liu, Li Liu

Electrochemical Investigation on Passivation Characteristic of P110 Steel in Alkaline Solution

s08-014

**Emmanuel Rocca** (Institut Jean Lamour UMR CNRS, Université de Lorraine, Vandoeuvre Les Nancy, France), Joffrey Tardelli

Electrochemical properties of  $\eta$ -MgZn<sub>2</sub> phase in sulfuric acid : anodizing behavior at high potential

s08-015

**Cora Vasilescu** (Electrochemistry and Corrosion, Institute of Physical Chemistry Ilie Murgulescu, Bucuresti, Romania), Silviu Drob, Silviu Preda, Jose Maria Calderon Moreno, Petre Osiceanu

Passive Film Characterization on New Ternary Ti-Ta-Zr Alloy Surface

s08-016

**Delphine Veys-Renaux** (Institut Jean Lamour, Université de Lorraine, CNRS, Vandoeuvre les Nancy, France), Emmanuel Rocca, Khadoudj Guessoum

Zinc anodizing at high voltage in alkaline media

---

## Symposium 9: Electrocatalytic Materials

---

**Electrocatalytic materials**

s09-001

**Nathalia Abe Santos** (Instituto de Química de São Carlos, Universidade de São Paulo, São Carlos, Brazil), Patricia Gon Corradini, Joelma Perez

Study of ethanol electro-oxidation on PtNd/C and PtSnNd/C: stability test and FTIR

s09-002

**Ludwig Asen** (Fakultät für Chemie, Technische Universität München, Garching, Germany), Ehab Mostafa, Wenbo Ju, Sladjana Martens, Ulrich Heiz, Ulrich Stimming, Oliver Schneider

Electrodeposition of Novel Materials as ORR Catalysts for MEAs

s09-003

**Helmut Baltruschat** (Chemistry, University of Bonn, Bonn, Germany), Hatem M.A. Amin, Sevda Ayata

Synergistic Electrocatalytic Effects on Oxides + Ag - Electrodes for Oxygen Reduction and Evolution

s09-004

**Ausra Baradoke** (Department of Nanoengineering, Center for Physical Sciences and Technology, Vilnius, Lithuania), Isabel Pastoriza-Santos, Elisa Gonzalez-Romero

Ruthenium Nanocomposites for Electrochemical Detection: Design and Modification of Graphene Electrodes for Biosensors

s09-005

**Stefan Barwe** (Analytical Chemistry – Center for Electrochemical Science, Ruhr-Universität Bochum, Bochum, Germany), Stefan Klink, Wolfgang Schuhmann

A poly(benzoxazine) as binder matrix for OER catalysts derived from Prussian blue analogue precursors

s09-006

**Jiajin Bi** (Graduate School of Engineering, Yokohama National University, Yokohama, Japan), Koichi Matsuzawa, Yuji Kohno, Shigenori Mitsushima

Catalytic Activity and Durability for Oxygen Evolution on LaNiO<sub>3</sub>/Ni for Alkaline Water Electrolysis under Potential Cycling

s09-007

**Stanko Brankovic** (Electrical and Computer Engineering, University of Houston, Houston, USA), Qiuyi Yuan, Hieu Doan, Lars Grabow

Structure vs. Properties Relation in Novel RuPt Core-Edge Catalyst Nanoclusters

s09-008

**Cheng-Chuan Chen** (Department of Bio-Industrial Mechatronics Engineering, National Taiwan University, Taipei City, Taiwan)

Pd-based bimetallic nanocatalysts for alkaline glucose electrooxidation and fuel cells application

s09-009

**Qiaoli Chen** (Department of Chemistry, Xiamen University, Xiamen, China), Zhaoxiong Xie

Synthesis of Excavated Trioctahedral Au<sup>+</sup>CPd Alloy Nanocrystals with Tunable Composition for Electro-Oxidation of Ethanol

s09-010

**Yuan Chen** (School of Chemical and Biomedical Engineering, Nanyang Technological University, Singapore, Singapore)

Bacteria Derived Carbon as High-Performance Electrocatalysts

s09-011

**Kui Cheng** (College of Material Science and Chemical Engineering, Harbin Engineering University, Harbin, China)

Design and fabrication Co<sub>3</sub>O<sub>4</sub>-based electrode and its application for H<sub>2</sub>O<sub>2</sub> electroreduction

s09-012

**Nan-Kuang Chou** (Department of Chemical and Materials Engineering, National Kaohsiung University of Applied Sciences, Kaohsiung City, Taiwan), Meng-Shan Hsieh, Chien-Liang Lee

Different-sized truncated Pd nanocubes for glucose electrooxidation

s09-013

**Martín Dávila** (Fisicoquímica, Benemérita Universidad Autónoma de Puebla, Puebla, Mexico)

Electrochemical Oxidation of Dibenzothiophene and Dibenzothiophene Sulphone

s09-014

**Ali Ehsani** (Chemistry, Qom University, Qom, Iran)

Physioelectrochemical properties and catalytic activity of green synthesized metal oxide nanoparticles and conductive polymer composite film

s09-015

**Makoto Eto** (Graduate School of Engineering, Oita University, Oita, Japan), Taro Kinumoto, Kohei Ono, Tomoki Tsumura, Masahiro Toyoda

Oxygen Evolution Reaction Behavior of Vapor Grown Carbon Fiber and the Loading Effect of LaMnO<sub>3</sub> in KOH Aqueous Solution

s09-016

**Miao-Syuan Fan** (Department of Chemical Engineering, National Taiwan University, Taipei, Taiwan), Chuan-Pei Lee, Chun-Ting Li, Yi-June Huang, R. Vittal, Kuo-Chuan Ho

Molybdenum Disulfide/Nitrogen-Doped Graphene Composite as an Electrocatalytic Material for Dye-Sensitized Solar Cells

s09-017

**Lucia Fernandez Macia** (Electrochemical and Surface Engineering Group, Vrije Universiteit Brussel, Brussels, Belgium), Bart Geboes, Jon Ustarroz, Laurens Stevaert, Tom Breugelmans, Annick Hubin

A Reliable and Quantitative Characterization of Electrocatalysts Towards the Oxygen Reduction Reaction from LSV/RDE Experiments

s09-018

**Kobra Ghobadi** (Chemistry, Yazd University, Yazd, Iran), Hamid Reza Zare, Hossein Khoshro, Alireza Gorji, Abbas Ali Jafari

Electrocatalytic Synthesis of Cinnamic Acid by Reaction of Electrocatalytic Activated CO<sub>2</sub> with Phenylacetylene

s09-019

**Kristoffer Hedenstedt** (Chemistry and Molecular Biology, University of Gothenburg, Gothenburg, Sweden), Elisabet Ahlberg, Nina Simic, Mats Wildlock

Electrochemical Investigation of Water Reduction on Goethite, Lepidocrocite and Mild Steel in Slightly Alkaline Electrolyte

s09-020

**Takahiro Hirai** (Dept of Science of Environment and Mathematical Modeling, Doshisha University, Kyotanabe, Japan), Tian Zhang, Masatsugu Morimitsu

Composition, Structure, and Kinetics of RuO<sub>2</sub>-Ta<sub>2</sub>O<sub>5</sub>/Ti Anode for Oxygen Evolution in H<sub>2</sub>SO<sub>4</sub> Solutions

s09-021

**Huin-Ning Huang** (Department of Chemical Engineering, National Taiwan University of Science and Technology, Taipei, Taiwan), Wei-Hung Chiang

Synthesis of Metal Nanoparticle/Graphene Nanocomposites using Atmospheric-Pressure-Microplasma-Assisted Electrochemistry

s09-022

**Yi-June Huang** (Department of Chemical Engineering, National Taiwan University, Taipei, Taiwan), Chuan-Pei Lee, Miao-Syuan Fan, Chun-Ting Lee, R. Vittal, Kuo-Chuan Ho

A Pt-Free Counter Electrode based on Novel Cobalt Diselenide Architectures for Dye-Sensitized Solar Cells

s09-023

**Eunkyoung Hwang** (School of Integrative Engineering, Chung-Ang University, Seoul, Korea), Soo-Kil Kim, Sung Hoon Hong, Jihui Choi, Jin Yeung Kim, Hoyoung Kim

Electrocatalysts for CO<sub>2</sub>-C<sub>1</sub> Fuel Inter-conversion

s09-024

**Suyeon Hyun** (Energy Systems Engineering, Daegu Gyeongbuk Institute of Science & Technology (DGIST), Daegu, Korea), Vignesh Ahilan

Porous Co<sub>3</sub>V<sub>2</sub>O<sub>8</sub> Nanostructures as Promising Electrocatalyst for Oxygen Evolution Reaction in Alkaline Medium

s09-025

**Yukiko Ishimura** (Dept of Science of Environment and Mathematical Modeling, Doshisha University, Kyotanabe, Japan), Kenji Kawaguchi, Masatsugu Morimitsu

Oxygen Reduction on RuO<sub>2</sub>-Ta<sub>2</sub>O<sub>5</sub> Mixed Oxide Catalyst in Alkaline Solution

s09-027

**Hwakyeung Jeong** (Chemistry, Chungbuk National University, Cheongju, Korea)

Electrodeposition of Nanoflake Pd Structures: Structure-Dependent Wettability and SERS Activity

s09-028

**Abdel-Nasser Kawde** (Chemistry, King Fahd University of Petroleum and Minerals, Dhahran, Saudi Arabia)

Successful Strategies to Overcome the Carbon Electrodes Surfaces Fouling of Phenols

s09-029

**Jin Yeong Kim** (School of Integrative Engineering, Chung-Ang University, Seoul, Korea), Jihui Choi, Sung Hoon Hong, Hoyoung Kim, Eunkyoung Hwang, Soo-Kil Kim

Ru/M Bi-layered Oxide Catalysts for Oxygen Evolution Reaction (OER) in Acidic Water Splitting



s09-030

**Seulki Kim** (Department of Applied Chemistry, Konkuk University, Chungju, Korea), Changhyun Lee, Noseung Myung

Synthesis of Pt-CuO Composite *via* Electrodeposition Followed by Galvanic Replacement-Heat Treatment and Its Application to Non-Enzymatic Glucose Sensor

s09-031

**Joosun Kim** (High-Temperature Energy Materials Research Center, Korea Institute of Science and Technology, Seoul, Korea), Donghyun Bae, Miyoung Yoon, Eunseok Kwon, Seunghwan Lee, Jooho Moon, Hyunjung Shin

Catalytic Performance and Characterization of Iron Oxide-Based Composite Catalyst for Reduction of CO<sub>2</sub>

s09-032

**Shuhei Kimura** (Dept of Science of Environment and Mathematical Modeling, Doshisha University, Kyotanabe, Japan), Kenji Kawaguchi, Masatsugu Morimitsu

Effects of Precursor Solution on Morphology and Catalytic Activity of RuO<sub>2</sub>-based Ti anode for Oxygen Evolution

s09-033

**Anthony Kucernak** (Chemistry, Imperial College London, London, United Kingdom)

New palladium phosphide catalysts for fuel cell relevant reactions

s09-034

**Kousuke Kumamoto** (Dept of Science of Environment and Mathematical Modeling, Doshisha University, Kyotanabe, Japan), Tian Zhang, Masatsugu Morimitsu

Effects of Composition of Amorphous IrO<sub>2</sub>-Ta<sub>2</sub>O<sub>5</sub> Coatings on Oxygen Evolution in Alkaline Solutions

s09-035

**Dong Wook Lee** (Department of Chemical and Biomolecular Engineering, Yonsei University, Seoul, Korea), Woong Hee Lee, Hansung Kim

Enhancement on ORR Activity of N-Doped Carbon Catalysts Derived from Melamine Based Polymer

s09-036

**Seunghwa Lee** (School of Environmental Science and Engineering, Gwangju Institute of Science and Technology, Gwangju, Korea), Jaeyoung Lee

On The Role of Cl<sup>-</sup> : Synergistic Effects with Cu<sub>2</sub>O for The Electroreduction of CO<sub>2</sub> to Multi-Carbon Fuels

s09-037

**Andreas Lesch** (Laboratory of Physical and Analytical Electrochemistry, École Polytechnique Fédérale de Lausanne, Lausanne, Switzerland), Victor Costa Bassetto, Hubert Girault

Preparing electrocatalysts for energy conversion by inkjet printing and photonic curing in one fabrication process

s09-038

**Philipp Lettenmeier** (Institute of Engineering Thermodynamics, German Aerospace Center, Stuttgart, Germany), Schwan Hosseiny, Li Wang, Aldo Saul Gago, Kaspar Andreas Friedrich

Synthesis and Characterization of Highly Active Ir Nanoparticles for Oxygen Evolution Reaction in Acid Media

s09-039

**Xiaoheng Liu** (College of Chemical Engineering, Nanjing University of Science and Technology, Nanjing, China), Wei Chen

One-step Hydrothermal Route to Fabricate Novel ZnIn<sub>2</sub>S<sub>4</sub>/g-C<sub>3</sub>N<sub>4</sub> Heterojunction Photocatalysts with Highly-efficient Visible Light Response

s09-040

Cancelled

s09-041

**Nai-Chang Lo** (Chemistry, National Cheng Kung University, Tainan, Taiwan)

Electrochemical Formation of Cu Nanoparticles in Tributyl-Methylammonium bis((trifluoromethyl)sulfonyl)imide Room-Temperature Ionic Liquid

s09-042

**Juan Manriquez** (Department of Research, Cideteq, Pedro Escobedo, Mexico)

Orange II mineralization on C-modified nanoparticulate TiO<sub>2</sub> cathodes able for producing OH• radicals through the O<sub>2</sub> reduction which is simultaneously generated on a grade 2 Ti anode *via* the H<sub>2</sub>O oxidation

s09-043

**Yu-Xiang Mao** (Department of Chemical Engineering, National Taiwan University of Science and Technology, Taipei, Taiwan), Chun-Jern Pan, Men-Che Tsai, Wei-Nien Su, Bing-Joe Hwang

Ni-based bimetallic nanoparticles as active and durable catalysts towards hydrogen oxidation reaction

s09-044

**Jun Maruyama** (Environmental Technology Research Division, Osaka Municipal Technical Research Institute, Osaka, Japan), Takahiro Hasegawa, Satoshi Iwasaki, Tomoko Fukuhara, Yuki Orikasa, Yoshiharu Uchimoto

Carbonaceous Thin Film Coating with Fe–N<sub>4</sub> Site for Enhancement of Dioxovanadium Ion Reduction

s09-045

**Kenji Matsumae** (Engineering, Yokohama National University, Yokohama, Japan), Kohei Nagai, Yuji Kohno, Koichi Matsuzawa, Shigenori Mitsushima

Degradation of IrO<sub>2</sub>-Ta<sub>2</sub>O<sub>5</sub> / Ti anode with toluene contamination

s09-046

**Hisayoshi Matsushima** (Faculty of Engineering, Hokkaido University, Sapporo, Japan), Shota Shibuya, Ryota Ogawa, Mikito Ueda

Kinetic Isotope Effect on Hydrogen Evolution and Oxidation Reaction

s09-047

**Eugenijus Norkus** (Department of Catalysis, Center for Physical Sciences and Technology, Vilnius, Lithuania), Jane Jaciauskiene, Kestutis Prusinskas, Irena Stalnioniene, Loreta Tamasauskaite-Tamasiunaite, Dordi Yezdi, Aniruddha Joi

The Use of Environmentally-Friendly Natural Polyols as Cu(II) Ligands in Electroless Copper Plating Processes

s09-048

**Eugenijus Norkus** (Department of Catalysis, Center for Physical Sciences and Technology, Vilnius, Lithuania), Loreta Tamasauskaite-Tamasiunaite, Zita Sukackiene, Aldona Balciunaite, Algirdas Selskis

Gold Nanoparticles Modified Cobalt-Boron-Copper and Cobalt-Boron-Tungsten-Copper as Electrocatalysts for Borohydride Oxidation

s09-049

**Lidia Jagoda Opuchlik** (Faculty of Chemistry, University of Warsaw, Warsaw, Poland), Renata Bilewicz

Anisotropic gold nanoplates – characterization and application in catalysis

s09-050

**Ali Riza Ozkaya** (Chemistry Department, Marmara University, Istanbul, Turkey), Zuhail Yazar, Mehmet Piskin, Zafer Odabas

Redox properties and electrocatalytic oxygen reducing performances of various novel metal phthalocyanines

s09-051

**Chien-Yeh Pan** (Department of Applied Chemistry, National Chiao Tung University, Taipei, Taiwan), Chia-Kan Hao, Chi-Shen Lee

Metal-doped Pyrochlore as Novel Anode Material for Intermediate Solid Oxide Fuel Cell

s09-052

**Jun Peng** (Faculty of Chemistry, Northeast Normal University, Key Laboratory of Polyoxometalate Science of Ministry of Education, Changchun, China)

Assembly of hybrids based on Keggin POMs and Co-tris(imidazolyl) complexes with bifunctional electrocatalytic activities

s09-053

**Morihiro Saito** (Department of Applied Chemistry, Tokyo University of Agriculture and Technology, Koganei-shi, Japan), Shinpei Kosaka, Chiaki Tsukada, Hiroshi Suzuki, Hidenobu Shiroishi, Yumi Tanaka, Shiro Seki

New Air Electrode Catalysts Based on Mn Oxide Nanosheet/Nanocarbon Composite Materials for Li Air Batteries

s09-054

**Yanyan Song** (College of Science, Northeastern University, Shenyang, China), Zhida Gao, Patrik Schmuki  
Carbon Cladded TiO<sub>2</sub> Nanotubes Enabling Highly Defined RuO<sub>2</sub> Decoration for Efficient Supercapacitor Performance

s09-055

**Yung-Tao Sung** (Chemical Engineering, National Taipei University of Technology, Taipei, Taiwan), Jun-Ming Chiu, Chao-Chi Tu  
Improved Visible-light Photoelectrochemical Water Oxidation using Titanium Dioxide /Antimony Trisulfide Heterojunction Structure

s09-056

**Hogiartha Sutiono** (Chemical Engineering, National Taiwan University of Science and Technology, Taipei, Taiwan), Ching-Hsiang Chen, Wei-Nien Su, Liang-Yih Chen, Bing-Joe Hwang  
A Shortcut: Core (Rutile) – Shell (Anatase) Nanorods for Highly Efficient Solar Water-Splitter

s09-057

**Takuma Suzuki** (Department of Pure and Applied Chemistry, Tokyo University of Science, Noda, Japan), Yoshinao Hoshi, Isao Shitanda, Masayuki Itagaki  
Motion control of TiO<sub>2</sub>/Pt/Au nanomotor by UV light irradiation

s09-058

**Loreta Tamasauskaite-Tamasiunaite** (Department of Catalysis, Center for Physical Sciences and Technology, Vilnius, Lithuania), Gilius Kisielius, Teofilis Kilmonis, Aldona Balciunaite, Ina Stankeviciene, Aldona Jagminiene, Agne Matuseviciute, Eugenijus Norkus  
Preparation of Graphene Supported PtCoMo by Electroless Deposition

s09-059

**Dong-Ying Tzou** (Chemical Engineering and Materials Science, Yuan Ze University, Chung-Li, Taiwan), Chien-Te Hsieh, Yu-Fu Chen, Jen-Hao Hsueh  
Graphene and Carbon Nanotube Composites as Electrode Materials for Electrochemical Capacitors in Organic Electrolyte

s09-060

**Dong-Ying Tzou** (Department of Chemical Engineering and Materials Science, Yuan Ze University, Chung-Li, Taiwan)  
Synthesis of MnO<sub>2</sub>/Carbon Composites as Electrode Materials for Supercapacitors

s09-061

**Yusuke Ujino** (Dept of Science of Environment and Mathematical Modeling, Doshisha University, Kyotanabe, Japan), Kenji Kawaguchi, Masatsugu Morimitsu  
Formation and Electrochemical Behaviors of RuO<sub>2</sub>-Ta<sub>2</sub>O<sub>5</sub> Coating on Pb Substrate for Oxygen Evolution

s09-062

**Shan-Yu Wang** (Chemical Engineering, National Taiwan University of Science and Technology, Taipei, Taiwan), Yan-Sheng Li, Wei-Hung Chiang  
Controllable Synthesis of Metal Nanoparticle/Graphene Nanoribbon Composites

s09-063

**Chen-Hao Wang** (Department of Materials Science and Engineering, National Taiwan University of Science and Technology, Taipei, Taiwan), Yu-Chen Shih, Yu-Chung Chang, Ning-Yih Hsu, Yi-Sin Chou  
Functionalization of Carbon Felt as Catalytic Material for Vanadium Redox Flow Battery

s09-064

**Yu-Ching Weng** (Department of Chemical Engineering, Feng Chia University, Taichung, Taiwan), Wei-Fen Xiong  
Screening of Ru-based Electrocatalysts for Oxygen Reduction by Scanning Electrochemical Microscopy

s09-065

**Lindsay Wilson** (Chemistry, University of the Western Cape, Cape Town, South Africa), Candice Rassie, Priscilla Baker, Emmanuel Iwuoha  
Electrochemical Responses of Transglutaminase Immunosensor Developed on a Polypyrrole-Cobalt (II) Salicyladiimine Dendritic Composite Material

s09-066

**Ching Chou Wu** (Department of Bio-Industrial Mechatronics Engineering, National Chung Hsing University, Taichung, Taiwan), Ming Yuan Lee

Fabrication of nanostructured copper phosphate electrodes for the detection of  $\alpha$ -amino acids

s09-067

**Yi-Shan Wu** (Department of Chemical and Materials Engineering, National Kaohsiung University of Applied Sciences, Kaohsiung City, Taiwan), Chien-Liang Lee

Electrophoretic deposition of graphene sheets on porous nickel foam as effective catalysts for oxygen evolution reaction and hydrogen peroxide sensor

s09-068

**Ke Ye** (College of Materials Science and Chemical Engineering, Harbin Engineering University, Harbin, China), Dianxue Cao, Hongyu Zhang, Long Yang, Xin Wang, Kui Cheng

Three-dimensional Nickel Film Electrodeposited on Porous Carbon Sponge: High Catalytic Performance and Low-cost Anode for Urea Electro-oxidation in Alkaline Medium

s09-069

**Hiromu Yoshida** (Department of Material Chemistry, Graduate School of Engineering, Kyoto University, Kyoto, Japan)

Fundamental Studies on Electrochemical Oxidative Properties of a Gold Nanoparticle-Attached Palladium Electrode

s09-070

**Sawaguchi Yuki** (Science and Engineering, Yokohama National University, Yokohama, Japan), Yasutomo Takakuwa, Kensaku Nagasawa, Yuji Kohno, Koichi Matsuzawa, Shigenori Mitsushima

Polarization for a toluene hydrogenation electrolyzer with various concentration of toluene feed

s09-071

**Xinsheng Zhang** (Department of Chemical Reaction Engineering, East China University of Science and Technology, Shanghai, China), Rensheng Zhong, Dongfang Niu

The effect of surface functional groups of carbon nanofiber on oxygen reduction reaction

s09-072

**Ming Zhou** (Chemistry, The University of Hong Kong, Hong Kong, China), Kwong-Yu Chan

RuO<sub>2</sub> nanoparticles loaded well-defined iron-nitrogen doped mesoporous core-shell carbon spheres as an effective cathode for rechargeable lithium-oxygen battery

---

## Symposium 10: Electrochemical Technology: New Challenges for a More Competitive Economy

---

### Electrochemical technology

s10-001

**Henry Bergmann** (FB 6 & 7, Anhalt University, Köthen, Anh., Germany)

On the continuity of chlorine production during electrochemical water disinfection

s10-002

**Roel Bisselink** (Water Treatment, TNO, Zeist, Netherlands), Mathias Panjer

Indium recovery from secondary sources by electrowinning

s10-003

**Roel Bisselink** (Water Treatment, TNO, Zeist, Netherlands), Lourens Feenstra

Electrochemical synthesis of hydrogen peroxide coupled with UV-C for the oxidation of endocrine disruptor compounds

s10-004

**Erika Bustos** (Science, Centro de Investigación y Desarrollo Tecnológico en Electroq, Querétaro, Mexico), Maribel Pérez-Corona, José Alberto García, Gabor Taller, Dorothy Polgár, Zsuzsana Plank

The Cone Penetration Test and 2D Imaging Resistivity as Tools to Simulate the Distribution of Hydrocarbon in Soil

s10-005

**Miao-Syuan Fan** (Department of Chemical Engineering, National Taiwan University, Taipei, Taiwan), Ling-Yu Chang, Chuan-Pei Lee, R. Vittal, Jiang-Jen Lin, Kuo-Chuan Ho

Synthesis of a Novel Polymeric Ionic Liquid for Electrochromic Device Application

s10-006

**Ali Farhat** (Advanced Water Management Centre, University of Queensland, Brisbane, Australia), Stephan Tait, Jurg Keller, Jelena Radjenovic

Removal of Persistent Organic Contaminants by Electrochemically Activated Sulfate

s10-007

**Carmen Maria Fernandez Marchante** (Chemical Engineering, University of Castilla La Mancha, Ciudad Real, Spain), Manuel Andres Rodrigo, Carolina Risco, Cristina Sáez, Rubén López-Vizcaíno, Pablo Cañizares, Vicente Navarro

Electrokinetic remediation of natural soil polluted with the herbicide 2,4-D

s10-008

**Sergi Garcia-Segura** (Chemistry, Universidade Federal do Rio Grande do Norte, Natal, Brazil), Amison Rick Lopes da Silva, Gustavo Rodrigues de Oliveira, Carlos Alberto Martinez-Huitle

Electrochemical Oxidation of 2-Naphthol on BDD Anodes: Dissolved Oxygen Participation, Mechanism and Theoretical Calculations

s10-009

**Li Guan** (Chemical & Environmental Engineering, The University of Nottingham, Nottingham, United Kingdom), George Zheng Chen

Intact Recovery of Carbon Nanotubes from their Conducting Polymer Composites *via* Selective Fenton-Oxidation

s10-010

**Lianhuan Han** (Department of Chemistry, Xiamen University, Xiamen, China)

A Novel Processing Method and Simulation Based on Confined Etching Layer Technique

s10-011

**Yosuke Imanishi** (Graduate School of Human and Environmental Studies, Kyoto University, Kyoto, Japan), Tatsuma Yahara, Tatsuro Haruki, Yuki Orikasa, Yoshiharu Uchimoto

Development of Intermediate Temperature Fuel Cells using Methylcyclohexane Organic Hydride Fuel

s10-012

**Ye-Jin Jeong** (Department of Environmental Engineering, Sangmyung University, Cheonan, Korea), Chan-Soo Kim, Nam-Jo Jeong, Jin-Soo Park

Effect of Simulated Foulants on Membrane Fouling in Reverse Electrodialysis

s10-013

**Babak Khalaghi** (Department of Materials Science and Engineering, Norwegian University of Science and Technology, Trondheim, Norway)

Supplying of Methane through Porous Carbon Anodes during Aluminium Electrolysis

s10-014

**Jong-Hoon Kim** (Electrical Engineering, Power Electronics Lab, Ajou University, Suwon, Korea), Jung-Nam Lee, Chung-Yul Yoo

Toward Cost Effectiveness of Alkaline Water Electrolysis for Hydrogen Economy

s10-015

**Javier Llanos** (Department of Chemical Engineering, University of Castilla-la Mancha, Ciudad Real, Spain), F. L. Souza, Cristina Sáez, M.V. Lanza, Pablo Cañizares, Manuel Andres Rodrigo

Coupling Wind Turbines and PV Panels to Electrochemical Processes: Treatment of Wastewater and Soil Polluted with Herbicides

s10-016

**Paulo Olivi** (Departamento de Química, FFCLRP, Universidade de São Paulo, Ribeirão Preto, Brazil), Cláudio Castro

Electrochemical oxidation of Disperse Yellow 3 dye using BDD electrodes

s10-017

**Juan Manuel Paz-Garcia** (Division of Solid Mechanics, Lund University, Lund, Sweden), Maria Villen-Guzman, Jose M. Rodriguez-Maroto, Cesar Gomez-Lahoz, Matti Ristinmaa, Stephen Hall

Electrokinetic Remediation of Lead-contaminated Carbonate-rich Soil

s10-018

**Carlos Ponce de Leon** (Faculty of Engineering and the Environment, University of Southampton, Southampton, United Kingdom), I. Ishita, Vanessa M. Vasconcelos, Marcos R.V. Lanza, José L. Nava

Electrochemical degradation of RB-5 dye by anodic oxidation, Electro-Fenton and by combining anodic oxidation-electro-Fenton in a filter-press flow cell

s10-019

**Ricardo Salazar** (Química de los Materiales, Universidad de Santiago de Chile, Santiago, Chile)

Degradation of Industrial Textile Dye Disperse Red BG by electro-oxidation: Role of Anode, pH and Supporting Electrolyte

s10-020

**Onofrio Scialdone** (Dipartimento di Ingegneria Chimica, Gestionale, Informatica, Università degli Studi di Palermo, Palermo, Italy), Alessandro Galia, Simona Sabatino

Electrochemical reduction of carbon dioxide to formic acid at tin cathode in divided and undivided cells: Effect of operating parameters

s10-021

**Kazuya Takeuchi** (Dept of Science of Environment and Mathematical Modeling, Doshisha University, Kyotanabe, Japan), Kenji Kawaguchi, Masatsugu Morimitsu

A Challenge to Synthesize  $\text{Bi}_2\text{Ir}_2\text{O}_{7-z}$ -based Hybrid Oxide for Oxygen Reduction

s10-022

**Po-Chih Tsai** (Graduate Institute of Applied Science and Technology, National Taiwan University of Science and Technology, Taipei, Taiwan), Bing-Joe Hwang, Wei-Nien Su, Hsin-Fu Deng

Metal Ion Additive Effect on the Morphology of Silicon Etching

s10-023

**Elisama Vieira dos Santos** (Institute of Chemistry, Federal University of Rio Grande do Norte, Natal, Brazil), Cristina Sáez, Pablo Cañizares, Manuel Andres Rodrigo, Carlos Alberto Martinez-Huitle

Extraction Agents for Removing Petroleum from Soil and Application of Electrolysis to Treat Washing Fluid

s10-024

**Elisama Vieira dos Santos** (Institute of Chemistry, Federal University of Rio Grande do Norte, Natal, Brazil),  
Cristina Sáez, Carlos Alberto Martinez-Huitle, Pablo Cañizares, Manuel Andres Rodrigo

Combined soil washing and CDEO for the removal of oxyfluorfen from soils

s10-025

**Jiade Wang** (Environmental Engineering Center, Zhejiang University of Technology, Haangzhou, China),  
Mingming Zhou, Guolong Huang, Yongping Gan

Simultaneous Removal of COD and Ammonia Nitrogen using a Novel Electro-oxidation Reactor

s10-026

**Masafumi Yasuno** (Dept of Science of Environment and Mathematical Modeling, Doshisha University,  
Kyotanabe, Japan), Kenji Kawaguchi, Masatsugu Morimitsu

Development of Air Electrode Material Comprising Nano-oxide on Ni for MH/Air Secondary Battery

s10-027

**Min-Hsin Yeh** (School of Materials Science and Engineering, Georgia Institute of Technology, Atlanta, USA),  
Hengyu Guo, Long Lin, Zhen Wen, Zhaoling Li, Chenguo Hu, Zhong Lin Wang

Integrated Bundle Structure of Rolling Free Standing Triboelectric Nanogenerators and its Applications in  
Self-powered Copper Collecting Electrochemical system *via* Harvesting Hydropower

s10-028

**Chung-Yul Yoo** (Advanced Materials & Devices Laboratory, Korea Institute of Energy Research, Daejeon,  
Korea), Dae Sik Yun, Jong Hoon Joo, Ji Haeng Yu, Jong-Nam Kim, Hyung-Chul Yoon

Solid State Ammonia Synthesis – Present State and Perspective

s10-029

**Hsin-Fu Yu** (Department of Chemical Engineering, National Taiwan University, Taipei, Taiwan), Jen-Yuan  
Wang, Min-Chuan Wang, Der-Jun Jan, You-Shiang Lin, Man-kit Leung, Kuo-Chuan Ho

A High Contrast Complementary Electrochromic Device with Sub-second Response Time

s10-030

**Antonio de Lucas Consuegra** (Chemical Engineering, Castilla La Mancha, Ciudad Real, Spain), Nuria  
Gutierrez-Guerra, Jesús Gonzalez-Cobos, Juan Carlos Serrano-Ruiz, José Luis Valverde

Electrochemical modification of Ni catalyst with alkali ionic conductors for CO<sub>2</sub> hydrogenation

## Symposium 11: New Important Frontiers in Molecular Electrochemistry

### Electrochemistry of new organometallic and coordination compounds

s11-001

**Masafumi Asahi** (Department of Energy and Environment, AIST, Ikeda, Japan), Shin-ichi Yamazaki, Zyun Siroma, Naoko Fujiwara, Tsukasa Nagai, Shinobu Itoh, Tsutomu Ioroi

Substituent Effects on Electrochemical Properties and Oxygen Reduction Reaction Activity of Copper Complexes

s11-002

**Zhaohui Huo** (Chemistry, Université de Strasbourg, Laboratoire d'Electrochimie, Strasbourg, France)

Original Porphyrin – Polyoxometalate Copolymers: Application for the Photocurrent Generation

s11-003

**Klaus Mathwig** (Groningen Research Institute of Pharmacy, University of Groningen, Groningen, Netherlands), Hamid Reza Zafarani, Sahana Sarkar, J. Matthäus Speck, Heinrich Lang, Serge Lemay, Oliver G. Schmidt

Potential-Dependent Electrochemical Spectroscopy of Multiferrocenylthiophenes in a Nanogap Sensor

s11-004

**Derck Schlettwein** (Institute of Applied Physics, Justus-Liebig-University Giessen, Giessen, Germany), Juliane Weissbecker, Andrei Loas, Sergiu M. Gorun

Influence of Decreased Intermolecular Coupling on the Electrochromic Switching-Rate of Substituted Phthalocyanine Thin Films

### Electron transfer

s11-005

**Carlos Frontana** (Investigacion, Centro de Investigacion y Desarrollo Tecnológico en Electroq, Pedro Escobedo, Mexico), Eduardo Martinez-Gonzalez

Electronic Structure Effects on Electron Transfer Controlled Hydrogen Bonding in Substituted Dinitrobenzene Electrogenated Anions As Receptors for 1,3-Diethylurea

### Molecular electrochemistry

s11-006

**John Horsley** (Chemistry, University of Adelaide, Adelaide, Australia)

The Correlation of Electrochemical Measurements and Molecular Junction Conductance Simulations in  $\beta$ -Strand Peptides

s11-007

**Cancan Huang** (Department of Chemistry and Biochemistry, University of Bern, Bern, Switzerland)

Tuning of charge transport in single molecule with the chemical and electrochemical methods

s11-008

**Miangang Li** (Chemistry Department, Xiamen University, Xiamen, China), Li Chen, Yunxin Zhong, Jiawei Yan, Bingwei Mao

Investigation of Electrode Reaction at Well-Defined Electrochemical Interfaces in Ionic Liquids

s11-009

**Hsin-Che Lu** (Department of Chemical Engineering, National Taiwan University, Taipei, Taiwan), Ting-Hsiang Chang, Chung-Wei Kung, Sheng-Yuan Kao, Kuo-Chuan Ho

The Influence of Alkyl Chain Length of Viologens on the Performance of Their Electrochromic Devices

s11-010

**Jiri Ludvik** (Molecular Electrochemistry, J. Heyrovský Institute of Physical Chemistry ASCR, Prague, Czech Republic), Alan Liska

Structure-controlled Electrochemical Reduction of mono- and di-, nitro or nitroso Calix[4]arenes

s11-011

**Suzaliza Mustafar** (Chemistry, University of Tokyo, Tokyo, Japan), Kuo-Hui Wu, Kenji Takada, Ryojun Toyoda, Ryota Sakamoto, Hiroshi Nishihara

Synthesis of a  $\pi$ -conjugated porphyrin polymer film on electrode by electrooxidation of 5,15-di(4-aminophenyl)-10,20-diphenylporphyrinatozinc(II)



s11-012

**Laurent Ruhlmann** (Chemistry, Université de Strasbourg, Laboratoire d'Electrochimie, Strasbourg, France)  
Electrosynthesis Processes Based on Oxidative Couplings of Porphyrins for the Formation of  
Supramolecular Assemblies

s11-013

**Li Yang** (Department of Engineering Sciences, Uppsala University, Uppsala, Sweden), Xiao Huang, Adolf  
Gogoll, Maria Strømme, Martin Sjödin  
Terephthalate Functionalized Conducting Redox Polymers: Organic Anode Materials for Energy Storage

## Redox catalysis

s11-014

**Jingyuan Chen** (Department of Applied Physics, University of Fukui, Fukui, Japan), Wenwen Li, Koichi Aoki  
Catalytic reduction of dioxygen by ferrous hemin over formation of ferrous hemin -O<sub>2</sub> adduct

---

## Symposium 12: Physical Electrochemistry: Spectroscopic, Structural, and Theoretical Investigations of the Electrified Interface

---

### *In situ* spectroscopy (infrared, Raman, SHG, SFG, X-ray)

s12-001

**Jin-Chao Dong** (Chemistry, Xiamen University, Xiamen, China), Du-Hong Chen, Yue Li, Jin-Hui Meng, Yang  
Zhao, Chao-Yu Li, Jian-Feng Li  
*In-Situ* Monitoring the Electrocatalytic Reaction Processes at Platinum Single Crystal Electrode Using  
SHINERS

s12-002

**Kingo Itaya** (Frontier Institute for Interdisciplinary Sciences, Tohoku University, Sendai, Japan), Azhagurajan  
Mukkannan  
Application of an Ultra-high Resolution Optical Microscopy ~Imaging of Fast Reactions with Single  
Atomic Step Resolution~

s12-003

**Masaru Kato** (Faculty of Environmental Earth Science, Hokkaido University, Sapporo, Japan), Ken'ichi  
Kimijima, Mari Shibata, Hideo Notsu, Kazuya Ogino, Kiyoshi Inokuma, Narumi Ohta, Hiromitsu Uehara, Yohei  
Uemura, Nobuhisa Oyaizu, Tadashi Ohba, Satoru Takakusagi, Kiyotaka Asakura, Ichizo Yagi  
*In Situ* X-ray Absorption Fine Structure Spectroscopy of Dinuclear Copper Catalyst under Oxygen  
Reduction Reaction Conditions

s12-004

**Jan Philipp Kollender** (Institute for Chemical Technology of Inorganic Materials, Johannes Kepler University  
Linz, Linz, Austria), Andrei Ionut Mardare, Achim Walter Hassel  
*In-situ* monitoring of metal dissolution during anodisation of Al and Ti

s12-005

**Kamila Lepicka** (Department of Physical Chemistry of Supramolecular Complexes, Institute of Physical  
Chemistry Polish Academy of Sciences, Gdańsk, Poland), Piotr Pieta, Pawel Borowicz, Alexey Popov,  
Włodzimierz Kutner  
Spectroelectrochemical characterization of a salicilidene Ni(II) redox conducting polymer for  
supercapacitors

s12-006

**Shawn D. Lin** (Chemical Engineering, National Taiwan University of Science and Technology, Taipei, Taiwan),  
Bing-Joe Hwang, Yaw-Terng Chern  
*In Situ* DRIFTS Analysis of SEI formation over Cathodes at Elevated Temperature

s12-007

**Kei Murakoshi** (Department of Chemistry, Hokkaido University, Sapporo, Japan), Yumi Wakisaka, Mai Takase, Hiro Minamimoto, Satoshi Yasuda

Optical Force Applied to Molecules at Nanogap of Metal Nanodimer

s12-008

**Martin Pfaffeneder-Kmen** (Department of Physical Chemistry, University of Vienna, Vienna, Austria)

The Redox Behaviour of Graphene Oxide: A Spectroelectrochemical Study

s12-009

**Bin Ren** (Department of Chemistry, Xiamen University, Xiamen, China), Zhi-Cong Zeng, Sheng-Chao Huang, Teng-Xiang Huang, Jin-Hui Zhong, Mao-Hua Li, Xiang Wang

Electrochemical Tip-Enhanced Raman Spectroscopy (EC-TERS)

s12-010

**Manuela Rueda** (Department of Physical Chemistry, University of Seville, Seville, Spain), Francisco Prieto, Julia Alvarez-Malmaro, Jose M. Ors

ATR-SEIRAS and Electrochemical Study of the Tautomeric Equilibrium of Adsorbed Thymine on Gold Electrodes

s12-011

**Ken-ichi Uchida** (Catalysis Research Center, Hokkaido University, Sapporo, Japan), Kenta Motobayashi, Kazuya Minami, Naoya Nishi, Tetsuo Sakka, Masatoshi Osawa

Potential-Dependent Structure of [BMIM]<sub>(1-x)</sub>Li<sub>x</sub>[FSA] on a Gold Electrode: A Surface-Enhanced Infrared Study

s12-012

**De-Yin Wu** (College of Chemistry and Chemical Engineering, Xiamen University, Xiamen, China), Yuan-Fei Wu, Zhong-Qun Tian

Electrochemical Adsorption and Surface-Enhanced Raman Spectroscopy on Nanostructured Electrodes

s12-013

**Momo Yaguchi** (Section of Interfacial Chemistry, Catalysis Research Center, Sapporo, Japan), Marc T.M. Koper, Masatoshi Osawa

Electrocatalysis of Formic Acid Oxidation on Gold and Platinum: Where Does the Crucial Activity Difference Come From?

## Physical electrochemistry

s12-014

**Niloofer Ghanbari** (Electrochemical Materials Research, Solar and Hydrogen Energy Research (ZSW), Ulm, Germany), Thomas Waldmann, Peter Axmann, Michael Kasper, Margret Wohlfahrt-Mehrens

Glow Discharge Optical Emission Spectroscopy Used for Film Formation Studies on Graphite Electrodes

s12-015

**Enrique Herrero** (Institute of Electrochemistry, University of Alicante, Alicante, Spain), Carlos Busó-Rogero, Jose Solla-Gullon, Francisco J. Vidal-Iglesias, Juan M. Feliu

Tailoring properties of Pt nanoparticles electrocatalysts towards ethanol oxidation: surface-structure, particles dispersion and pH effect

s12-016

**Yuta Kitada** (IMRAM, Tohoku University, Sendai, Japan), Naoka Nagamura, Ryosuke Taniki, Itaru Honma

X-ray spectroscopic analyses of electronic states on quinone-based cathode materials for Li-ion batteries

s12-017

**Fei Li** (Department of Chemistry, School of Science, Xi'an Jiaotong University, Xi'an, China), Li Ma, Han Zhou, Shuli Xin, Chunhui Xiao, Shujiang Ding

Imaging of electrocatalytical activities of mixed transition metal oxides for oxygen reduction reaction with scanning electrochemical microscopy

s12-018

**Vladimír Mareček** (Department of Biomimetic Electrochemistry, J. Heyrovský Institute of Physical Chemistry of the CAS, Prague, Czech Republic), Oksana Josypczuk, Karel Holub

Noise and AC impedance analysis of ion transfer kinetics at the micro liquid/liquid interface

s12-019

**Armando Pombeiro** (Centro de Quimica Estrutural, Instituto Superior Tecnico, Lisboa, Portugal), Anirban Karmakar, Luísa Martins, M. Fátima C. Guedes da Silva, Susanta Hazra

Electrochemical behaviour of new 3-aminopyrazine-2-carboxylate Fe(III)-complexes

s12-020

**Yuma Takeuchi** (Department of Chemistry, Faculty of Science, Hokkaido University, Sapporo, Japan), Kohei Uosaki, Kei Murakoshi, Katsuyoshi Ikeda

Nanoparticle-assisted electrochemical formation of ferrocenethiol-monolayer nanodots

s12-021

**De-Yin Wu** (College of Chemistry and Chemical Engineering, Xiamen University, Xiamen, China), Ran Pang, Zhong-Qun Tian

Adsorption and Photocatalytic Hydrogen Evolution Reactions of Water on Silver and Gold Cathodes: DFT and SERS Study

### Structural studies (XRD, STM, AFM)

s12-022

**Xavier Feaugas** (LaSIE UMR CNRS 7356, University of La Rochelle, La Rochelle, France)

Potentiostatic pulse technique to investigate the hydrogen diffusion and trapping into subsurface of nickel single crystal (100)

s12-023

**Yi-Hsien Lu** (Institute of Physics, Academia Sinica, Taipei, Taiwan), Chih-Wen Yang, Chung-Kai Fang, Hsien-Chen Ko, Ing-Shouh Hwang

Observation of Gas Structures at the Interface between a Hydrophobic Electrode and Water Using Atomic Force Microscopy

s12-024

**Jan Macak** (Center of Materials and Nanotechnologies, University of Pardubice, Pardubice, Czech Republic), Petr Knotek, Hanna Sopha, Milos Krbal, Jan Subrt, Mariana Klementova

Self-Organized TiO<sub>2</sub> Nanotubes: Influence of Ti substrates

s12-025

**D. William A. Morton** (School of Electronic and Electrical Engineering, University of Leeds, Leeds, United Kingdom), A. Giles Davies, Christoph Walti

Electrochemical interrogation of the structure of self-assembled monolayers on nanofabricated metallic nanowires

### Theoretical models

s12-026

**Junxiang Chen** (Department of Chemistry, Wuhan University, Wuhan, China)

On the origin of the greatly different kinetics of the hydrogen electrode reactions on Pt in acid and alkaline media

s12-027

**Yu-cheng Chuang** (Department of Materials Science and Engineering, National Cheng Kung University, Tainan, Taiwan), Ping-chun Tsai, Shih-kang Lin

*Ab initio* lattice stability of the  $x\text{Li}_2\text{MnO}_3 \cdot (1-x)\text{Li}(\text{Ni}_{1/3}\text{Mn}_{1/3}\text{Co}_{1/3})\text{O}_2$  composite-layered cathode materials for lithium-ion batteries

s12-028

**Oksana Limanovskaya** (Urals Federal University, Ekaterinburg, Russia), Valentin Nekrasov, Andrey Suzdaltsev, Andrey Khramov, Yuriy Zaikov

Modeling of quasi-stationary process at the Platinum anode in the KF–NaF–AlF<sub>3</sub>–Al<sub>2</sub>O<sub>3</sub>

## Symposium 13: Molecular Systems for Energy Conversion

### Electrodes materials

s13-001

**Abdullah Al Mayouf** (Chemistry, King Saud University, Riyadh, Saudi Arabia), Mohamed Ali Ghanem, Maged Naji Shaddad, Prabhakarn Arunachalam, Mansour Al Hoshan, Mark T. Weller, Frank Marken

Photoelectrochemical characterization of ZnLaTaON based electrodes for water oxidation reaction

## Symposium 14: Modeling, Design and Characterization of Nanostructured, Electroactive and Multifunctional Materials

### Composites

s14-001

**Katarzyna Krukiewicz** (Department of Physical Chemistry and Technology of Polymers, Silesian University of Technology, Gliwice, Poland), John Bulmer, Dawid Janas, Krzysztof Koziol, Jerzy Zak

Nucleation and Growth of PEDOT on the Surface of Horizontally Aligned Carbon Nanotubes

### Electroactive materials

s14-002

**Rajendranath Kirankumar** (Medicinal and Applied Chemistry, Kaohsiung Medical University, Kaohsiung, Taiwan)

Electropolymerized Carbazole-Containing Ionic Liquid

s14-003

**Jing-Ting Liao** (Materials Science and Engineering, National Cheng Kung University, Tainan, Taiwan), Sin-Syu Liao

Electrical Characteristics of Raw Si-based Powders for Li-ion Electrode by Kelvin Probe Force Microscopy (KPFM) and Electrostatic Force Microscopy (EFM)

s14-004

**Mikhail A. Vorotyntsev** (Chemistry Department, D. Mendeleev University of Chemical Technology of Russia, Moscow, Russia), Dmitry V. Konev, Olga I. Istakova, Dinara K. Khayrullina

Study of Effect of Various Solvents on the Electropolymerization Process of Mg(II) Porphine and Electroactive Properties of Polyporphine Films

### Electrocatalysis

s14-005

**Li Li** (School of Chemistry and Chemical Engineering, Chongqing University, Chongqing, China), Yao Nie, Siguo Chen, Wei Ding, Xueqiang Qi, Feng Shi, Zidong Wei

Insight into the effect of oxygen vacancy concentration on the catalytic performance of MnO<sub>2</sub>

**Functional and nanostructured materials**

s14-006

**Jung Sang Cho** (Department of Materials Science and Engineering, Korea University, Seoul, Korea)  
Advanced Anode Material with Bubble-Nanorod-Structured Metal Oxide-Carbon Composite Nanofibers

s14-007

**Jooyoun Jeong** (Department of Chemical Engineering, Pohang University of Science and Technology (POSTECH), Pohang, Korea), Seongbeen Kim, Yongchai Kwon  
Mesocellular Carbon based Electrodes for High-Performance Vanadium Redox Flow Battery

s14-008

**Joonhee Kang** (Energy systems Engineering, DGIST, Daegu, Korea), Byungchan Han  
First principles study of thermal stability of LiNiO<sub>2</sub> materials coated with ultrathin amorphous Al<sub>2</sub>O<sub>3</sub> layers

s14-009

**Yann Leroux** (Institut des Sciences Chimiques de Rennes, CNRS - Université de Rennes 1, Rennes Cedex, France), Philippe Hapiot  
Nanostructured Monolayers on Carbon Substrates

s14-010

**Aiping Liu** (Center for Optoelectronics Materials and Devices, Zhejiang Sci-Tech University, Hangzhou, China)  
GO/rGO Microelectrode Arrays with Adjustable Electrochemical Activity and Biocompatibility for Highly Sensitive Detection of Hydrogen Peroxide Released by Living Cells

s14-011

**Hiro Minamimoto** (Department of Applied Chemistry, Graduate School of Engineering, Osaka University, Osaka, Japan), Haruyasu Irie, Taro Uematsu, Tetsuya Tsuda, Akihito Imanishi, Shu Seki, Susumu Kuwabata  
Fabrication of 3D Micro/Nano-Polymer and Metal Structures in Room-Temperature Ionic Liquid by Electron Beam Irradiation

s14-012

**Herenilton Oliveira** (Chemistry, Universidade de São Paulo, Ribeirão Preto, Brazil), Laura Novais, Raíssa Camargo, Paulo Noronha Filho  
Glassy Polymeric Carbon/Fe<sub>x</sub>C<sub>y</sub> and Carbon/Co<sub>x</sub>C<sub>y</sub> Nanocomposites: Electrochemical and Magnetic Properties

s14-013

**Emmanuel Rocca** (Institut Jean Lamour UMR CNRS, Université de Lorraine, Vandoeuvre Les Nancy, France), Hadri Faiz, François Mirambet, Solenn Reguer  
Electrochemical properties of nano functionalized iron oxyhydroxide: strategies for the corrosion protection of rusted steels

s14-014

**Jinju Song** (Materials Science and Engineering, Chonnam National University, Gwangju, Korea), Jihyeon Gim, Sungjin Kim, Jeonggeun Jo, Joseph Paul Baboo, Seokhun Kim, Sohyun Park, Dongyun Kim  
Pyro-Synthesis of Functional Nanocrystals

s14-015

**Lu-Hsiang Yin** (Chemical Engineering, National Taiwan University, Taipei, Taiwan), Sheng-Yuan Kao, Chung-Wei Kung, Ting-Hsiang Chang, Kuo-Chuan Ho  
An Electrochromic Copolymer with One-dimensional Nanowire Arrays

**Materials electrosynthesis**

s14-016

**Na Tian** (Department of Chemistry, Xiamen University, Xiamen, China), Jia-Huan Du, Shi-Gang Sun  
Electrochemical shape transformation of Pt nanocrystals with high-index facets

**Molecular architectures**

s14-017

**Laurence Hardwick** (Chemistry, University of Liverpool, Liverpool, United Kingdom), Scott Lewis, Ming Liu, Linjiang Chen, Iain Aldous, Marc Little, Sam Chong, Andy Cooper  
Understanding Proton Conductivity within Porous Organic Cage Networks

**Nanoparticles**

s14-018

**C. Y. Ho** (Mechanical Engineering, Hwa Hsia University of Technology, New Taipei, Taiwan), B.C. Chen, M. Y. Wen, Y. H. Tsai, H. H. Ku

Electrical Heating Effect of Carbon Nanoparticles as Electrodes in the Charging Process

s14-019

**Hongjiao Li** (Chemistry Department, Technische Universität München, Munich, Germany), Yunchang Liang, Wenbo Ju, Marian D. Rötzer, Florian F. Schweinberger, Ulrich Stimming, Ueli Heiz, Oliver Schneider

Activity and Stability of Pt Clusters supported on Au(111) for Electro-oxidation of Formic Acid

s14-020

**Shuo Liu** (College of Chemistry and Chemical Engineering, Xiamen University, Xiamen, China)

Electrochemical Reaction of Single Nanoparticle

s14-021

**Mesfin Haile Mamme** (Research Group Electrochemical and Surface Engineering, Vrije Universiteit Brussel, Brussels, Belgium), El Amine Mernissi Cherigui, Olga Dolgikh, Jon Ustarroz, Herman Terry, Johan Deconinck

A Finite Element Simulation of the Electrochemical Growth of Single Nanoparticle

**Organic-inorganic and polymer-inorganic hybrids**

s14-022

**Chien-Hong Lin** (Chemistry Division, Institute of Nuclear Energy Research, Longtan, Taiwan)

Amino-Silica Modified Nafion Membrane for Vanadium Redox Flow Battery

---

## Symposium 15: Electrochemical Engineering from a Quantum Description to the Plant Modeling: Experiments and Design across Length Scale

---

**Design**

s15-001

**Hung-Lung Chou** (Graduate Institute of Applied Science and Technology, National Taiwan University of Science and Technology, Taipei, Taiwan)

Combined Experiment and DFT Investigations of Catalytic Activities into Pt-based Electrocatalysts for Fuel Cell Applications

s15-002

**Alejandro A. Franco** (Laboratoire de Réactivité et Chimie de Solides (LRCS), Université de Picardie Jules Verne & CNRS, Amiens, France), Kan-Hao Xue, Claude Guery, Patrik Johansson, Mathieu Morcrette

A flexible framework for solving transport in lithium sulfur batteries

s15-003

**Hyung-Kyu Lim** (Graduate School of EEWS, Korea Advanced Institute of Science and Technology, Daejeon, Korea), Hyungjun Kim

Discover a Role of Ionic-Liquid in Electrochemical CO<sub>2</sub> Reduction by Using QM/MM Method

s15-004

**Yinghui Yin** (Laboratoire de Réactivité et Chimie des Solides (LRCS), Université de Picardie Jules Verne, Amiens, France), Matias A. Quiroga, Alejandro A. Franco

Multiparadigm Simulation of Electrochemical Energy Devices: The Fuel Cell Membrane Degradation

## Experiments

s15-005

**Hye Youn Han** (Chemistry, Kyungpook National University, Daegu, Korea), Farhana Sharmin Diba, Hye Jin Lee

Electrochemical Studies at an Interface between Two Immiscible Electrolyte Solutions for CO<sub>2</sub> Reduction

s15-006

**Changbin Im** (Ertl Center for Electrochemistry and Catalysis, Gwangju Institute of Science and Technology, Gwangju, Korea), Jae Kwang Lee, Jaeyoung Lee

Synthesis of High Ionic Conductive L<sub>7</sub>La<sub>3</sub>Zr<sub>2</sub>O<sub>12</sub> Solid Electrolyte by a Sol-gel Process

---

## Symposium 16: Supramolecular Electrochemistry for Analysis, Medicine and Biological Sciences

---

### Inclusion complexes

s16-001

**Mei-Jywan Syu** (Chemical Engineering, National Cheng Kung University, Tainan, Taiwan), Yao-Wei Hsu

On the Synthesis of Zinc-Tetrapyrrolylporphine Complex for the Electrochemical Recognition of Bilirubin in Serum

### Molecular recognition

s16-002

**Yu Cheng** (Dept. Biomedical Engineering, National Cheng Kung University, Tainan, Taiwan)

A Rapid Detection of Biomarkers Applied by Electrochemical Biosensor Accelerated with an AC Electrokinetic Manipulation

s16-003

**Flavio Maran** (Chemistry, University of Padova, Padova, Italy), Anna Pellattiero, Federico Polo, Giuseppe Toffoli, Aline S. C. Fabricio, Massimo Gion

Ultrasensitive Electrochemical Detection of the Cancer Biomarker CA19.9

s16-004

**Manuela Rueda** (Department of Physical Chemistry, University of Seville, Seville, Spain), Julia Alvarez-Malmagro, Francisco Prieto

DNA Bases Co-Adsorption at Gold Electrodes. An *in-situ* FT-IR Spectro-Electrochemical Study

### Redox therapy, drug carriers

s16-005

**Marilia Goulart** (Instituto de Química e Biotecnologia, Universidade Federal de Alagoas, Maceio, Brazil), Thaissa Silva, Camila Vasconcelos, Fabricia Ferreira, Chaquip Netto, Paulo Costa

The Yin-Yang Nature of Biologically Active Pterocarpanquinones: ROS Release and Alkylating Ability also Revealed by Electrochemistry

s16-006

**Katarzyna Krukiewicz** (Department of Physical Chemistry and Technology of Polymers, Silesian University of Technology, Gliwice, Poland), Tomasz Jarosz, Barbara Bednarczyk-Cwynar, Piotr Ruszkowski, Jerzy Zak

Local Delivery of Biologically Active Compounds Based on Conjugated Polymer Matrices

### Self-assembly

s16-007

**Hiromi Yoda** (Graduate School of Engineering, Kanagawa Institute of Technology, Atsugi, Japan), Ayumi Koike-Takeshita

Application of GroEL Complexes as Nano-sized Cargo

## Symposium 17: Novel in Situ in Operando Methods

### Energy materials and electrocatalysts

s17-001

**Patrick Faubert** (Department of Microsystems Engineering – IMTEK, Albert-Ludwigs-University, Freiburg, Germany), Ivan Kondov, Claas Müller, Holger Reinecke, Peter Smyrek, Johannes Pröll, Wilhelm Pfleging  
Analysis of the Surface Structure and Catalytic Behavior of Cr-modified Ni Surfaces for Fuel Cells

s17-002

**Tzu-Ho Wu** (Chemistry, University of Liverpool, Liverpool, United Kingdom), Jia-Cing Chen, Chun-Tsung Hsu, Laurence Hardwick  
Cation Effect on Ni(OH)<sub>2</sub> Phase Transformation

### In-situ microscopy and spectroscopy

s17-003

**Ju-Hsiang Cheng** (Department of Chemical Engineering, National Taiwan University of Science and Technology, Taipei City, Taiwan), Ming-Hsien Lin, Chun-Yi Wu, Chun-Chieh Wang, Yen-Fang Song, Bing-Joe Hwang  
A Study on the Hollow Cubic SnO<sub>2</sub> as Anode Material for Lithium-ion Battery by Transmission X-ray Microscopy

s17-004

**Yi-Ting Hsieh** (Department of Chemistry, National Cheng Kung University, Tainan, Taiwan)  
Electrodeposition of Cu-Sn Hexagonal Tubes from Room Temperature Ionic Liquid and its *In-Situ* Scanning Electron Microscopy Study

s17-005

**Chen-Yuan Lu** (Materials Science and Engineering, National Cheng Kung University, Tainan, Taiwan), Yu-Lun Cheng  
Investigation of Solid Electrolyte Interface of Silicon Electrode in Li-ion Batteries by Dual-Electrode Scanning Probe

### Multi-technique approaches

s17-006

**Nicolas Jäckel** (Energy Materials, INM- Leibnitz-Institute for New Materials, Saarbrücken, Germany), Nethanel Shpigel, Sergey Sigalov, Mikhael D. Levi, Daniel Weingarth, Doron Aurbach, Volker Presser  
*In-situ* monitoring of elastic properties of common binders in Lithium ion batteries *via* electrochemical quartz microbalance with dissipation and dilatometry

### Structural transformations

s17-007

**Keiji Shimoda** (Office of Society-Academia Collaboration for Innovation, Kyoto University, Uji, Japan), Miwa Murakami, Hideyuki Komatsu, Hajime Arai, Yoshiharu Uchimoto, Zempachi Ogumi  
*In situ* and *ex situ* NMR observation of delithiation/lithiation behavior of LiNi<sub>0.5</sub>Mn<sub>1.5</sub>O<sub>4</sub>



---

## Symposium 18: General Session

---

### Analytical electrochemistry

s18-001

**Ching-Hsiang Chen** (Graduate Institute of Applied Science and Technology, National Taiwan University of Science and Technology, Taipei City, Taiwan), Agnes Purwidyantri, Bing-Joe Hwang, Ya-Chung Tian, Chi-Hui Cheng, Chao-Sung Lai

Fabrication of AuNPs Array on ITO electrode *via* Nanospheres Lithography and its DNA Sensing Applications

s18-002

**Arturo-de-Jesus García-Mendoza** (Analytical Chemistry, Universidad Nacional Autonoma de Mexico, Mexico City, Mexico), Adrián De-Santiago-Zárate, José-Alejandro Baeza-Reyes

Minimal instrumentation electroanalytical experimental approach

s18-003

**Arturo-de-Jesus García-Mendoza** (Analytical Chemistry, Universidad Nacional Autonoma de Mexico, Mexico City, Mexico), Julio-César Aguilar-Cordero

Construction and evaluation of reference electrodes for imidazolium-based ionic liquids. An analytical description

s18-004

**Abdulkadir Levent** (Analytical Chemistry, Batman University, Batman, Turkey)

Simultaneous Determination of Ascorbic Acid, Epinephrine and Uric Acid by Differential Pulse Voltammetry on a Disposable Pencil Graphite Electrode

s18-005

**Abdulkadir Levent** (Analytical Chemistry, Batman University, Batman, Turkey)

Simultaneous Determination of Ascorbic acid, Norepinephrine and Uric acid by Differential Pulse Voltammetry on a Disposable Pencil Graphite Electrode in the Pharmaceutical Formulations and Human Urine Samples

s18-006

**Adeline Loo** (Division of Chemistry & Biological Chemistry, SPMS, NTU, Nanyang Technological University, Singapore, Singapore), Alessandra Bonanni, Adriano Ambrosi, Martin Pumera

Molybdenum Disulfide (MoS<sub>2</sub>) Nanoflakes as Inherently Electroactive Labels for DNA Hybridization Detection

s18-007

**Masakuni Takahashi** (Chemical Engineering, Tokyo National College of Technology, Hachioji, Japan), Hidenobu Shiroishi, Genichiro Nakamura, Tatsuhiko Okada

Evaluation of oxygen reduction properties by ring-disk flow electrode

s18-008

**Wei Zhe Teo** (Chemistry & Biological Chemistry, Nanyang Technological University, Singapore, Singapore), Martin Pumera

Fate of Silver Nanoparticles in Natural Waters; Integrative Use of Conventional and Electrochemical Analytical Techniques

s18-009

**Tadaharu Ueda** (Applied Science, Kochi University, Kochi, Japan), Takashi Okumura, Yukino Tanaka, Saki Akase, Mina Taniguchi, Tomoko Shimamura, Hiroyuki Ukeda

Development of New Electrochemical Evaluation Method for Antioxidant Capacity with Polyoxometalates as Potential Probes

s18-010

**Hiroyuki Ueda** (Graduate School of Science and Technology, Kumamoto University, Kumamoto, Japan), Katsuhiko Nishiyama, Soichiro Yoshimoto

Electrochemical Redox Behavior of Cobaltocenium in Imidazolium-based Ionic Liquids with Various Alkyl Chain Length

s18-011

**Colin Hong An Wong** (Division of Chemistry & Biological Chemistry, SPMS, NTU, Nanyang Technological University, Singapore, Singapore), Zdenek Sofer, Marie Kubešová, Jan Kucera, Stanislava Matejková, Martin Pumera

Inadvertent contamination of graphene materials: Synthetic routes introduce a whole spectrum of unanticipated metallic elements

s18-012

**Guan Xiao-Rui** (China University of Petroleum, Qingdao, China), Zhang Dalei, Jin You-hai, Wang Jian-jun  
Electrochemical Characterization and Molecular Dynamics Simulation on Corrosion Inhibition of Quinoline

## Bioelectrochemistry

s18-013

**Seung-Ryong Kwon** (Chemistry, Seoul National University, Seoul, Korea), Sung Yul Lim, Taek Dong Chung  
Reverse Electrodialysis (RED) as a New Electrical Power Source for a Drug Delivery System

s18-014

**Pu-Wei Wu** (Materials Science and Engineering, National Chiao Tung University, Hsinchu, Taiwan), Chai-Wei Chung, Yong-Min Chen, Po-Chun Chen  
Multilayer Deposition of Iridium Oxide for Biocompatible Stimulating Electrode Application

## Electrochemical energy conversion and storage

s18-015

**Hao Huang** (Department of Engineering Sciences, Uppsala University, Uppsala, Sweden), Christoffer Karlsson, Rikard Emanuelsson, Maria Strømme, Adolf Gogoll, Martin Sjödin  
Quinone Based Polypyrroles for Energy Storage Materials

s18-016

**Moon-Sung Kang** (Department of Environmental Engineering, Sangmyung University, Cheonan, Korea), Do-Hyeong Kim, Eun-Hye Jang, Yu-Jin Kim, Jin-Soo Park  
Optimization of Ionomer Membrane Characteristics for High Performance Reverse Electrodialysis

s18-017

**Zhenhai Liang** (College of Chemistry and Chemical Engineering, Taiyuan University of Technology, Taiyuan, China), Xian Liu, Xuan Jian, Huimin Yang  
A Novel Photoelectrocatalytic Approach for Regenerating NaOH by a BiOCl/bipolar Membrane Sandwich Structure

s18-018

**Yingbin Lin** (College of Physics and Energy, Fujian Normal University, Fuzhou, China), Zhigao Huang  
Synthesis and Electrochemical Performances of Hollow Spherical  $\text{Li}_4\text{Ti}_5\text{O}_{12}$  for Lithium Ion Batteries

s18-019

**Shohei Suzuki** (Department of Life Science and Sustainable Chemistry, Faculty of Engineering, Tokyo Polytechnic University, Atsugi, Kanagawa, Japan), Masaru Ogasawara, Noritoshi Nanbu  
Physical and Electrochemical Properties of Quaternary Ammonium Compounds in Highly Concentrated Solutions

## Electrochemical materials science

s18-020

**Aicheng Chen** (Department of Chemistry, Lakehead University, Thunder Bay, Canada), Suresh Konda, Cassandra Ostrom, Brian Adams, Robert Asmussen  
Synthesis and Electrochemical FTIR Study of Nanoporous Palladium-Based Bimetallic Catalysts

s18-021

**Jin Cui** (MESA+ Institute for Nanotechnology, University of Twente, Enschede, Netherlands), Klaus Mathwig, Serge Lemay  
Concentration Rectification in Nanofluidic Transducers

s18-022

**Alex Yong Sheng Eng** (Chemistry and Biological Chemistry, Nanyang Technological University, Singapore, Singapore), Adriano Ambrosi, Zdenek Sofer, Petr Simek, Martin Pumera

Electrochemistry of Transition Metal Dichalcogenides: Dependence on Composition and Exfoliation Method

s18-023

**Robert Hillman** (Department of Chemistry, University of Leicester, Leicester, United Kingdom), Rachel Sapstead, Natalie Corden, Emma Palin

Electrochromic Copolymer Film Deposition for Visualization of Latent Fingerprints on Stainless Steel Surfaces

s18-024

**Jia-Lin Jhan** (Department of Chemical Engineering and Materials Science, Yuan Ze University, Taoyang, Taiwan), Leo Chau-Kuang Liao, Po-Chin Tseng

Effects of constant on-off current pulse on the properties of Cu<sub>2</sub>O films fabricated by electrochemical deposition method

s18-025

**Masahiro Kobayashi** (Chemical Engineering, Tokyo National College of Technology, Hachioji, Japan), Hidenobu Shiroishi, Masahiko Kijima, Yumi Tanaka, Jun Kuwano

Synthesis of nanoparticle-type new proton conductor made from d-glucose by a hydrothermal method

s18-026

**Hsueh Ming Liu** (Chemistry, National Central University, Taoyuan City, Taiwan), Cheng-Gang Wu, Diganta Saikia, Hsien-Ming Kao

Synthesis and Characterization of Polyether Diamine based Organic-Inorganic Hybrid Solid Electrolyte for Electrochromic Devices

s18-027

**Hsueh Ming Liu** (Chemistry, National Central University, Taoyuan City, Taiwan), Kwo-Wei Lou, Diganta Saikia, Hsien-Ming Kao

Synthesis, Structure Characterization, Electrical and Thermodynamic Properties of Comb Structured Organic-Inorganic Hybrid Solid Polymer Electrolytes

s18-028

**Toshiyuki Matsunaga** (Academia Collaboration for Innovation, Kyoto University, Kyoto, Japan), Hideyuki Komatsu, Keiji Shimoda, Taketoshi Minato, Masao Yonemura, Takashi Kamiyama, Shunsuke Kobayashi, Takeharu Koto, Tsukasa Hirayama, Yuichi Ikuhara, Hajime Arai, Yoshio Ukyo, Yoshiharu Uchimoto, Zempachi Ogumi

Significant cation mixing in the transition-metal layer of Li<sub>2</sub>MnO<sub>3</sub>

s18-029

**Masaru Ogasawara** (Department of Life Science and Sustainable Chemistry, Faculty of Engineering, Tokyo Polytechnic University, Atsugi, Kanagawa, Japan), Shouhei Suzuki, Noritoshi Nanbu

Relative Permittivities of Binary Solvent Mixtures

s18-030

**Kayato Ooya** (Chemical Engineering, Tokyo National College of Technology, Hachioji, Japan), Hidenobu Shiroishi, Morihiro Saito, Yumi Tanaka

Characteristics of an intermediate-temperature fuel cell using proton conductive ZrO<sub>2</sub>-1.6P<sub>2</sub>O<sub>5</sub>-doped ZnO-2P<sub>2</sub>O<sub>5</sub> hybrid electrolyte

## Electrochemical process engineering and technology

s18-031

**Kazuhisa Azumi** (Graduate School of Engineering, Hokkaido University, Sapporo, Japan), Hayato Yoshikawa, Kazunori Suetake

Electrochemical CO<sub>2</sub> Reduction in EMIN-TFSI Ionic Liquid

s18-032

**Gha-Young Kim** (Nuclear Fuel Cycle Process Development, Korea Atomic Energy Research Institute, Daejeon, Korea), Jisun Shin, Si-Hyung Kim, Do-Hee Ahn, Seungwoo Paek

Actinide Recovery using Anode-Liquid Cathode Module for Pyroprocessing

s18-033

**Do-Hyeong Kim** (Department of Environmental Engineering, Sangmyung University, Cheonan, Korea), Eun-Hye Jang, Jin-Soo Park, Moon-Sung Kang

Development of Novel Bipolar Membranes for Efficient Electro-Adsorptive Deionization

s18-034

**Do-Hyeong Kim** (Department of Environmental Engineering, Sangmyung University, Cheonan, Korea), Yu-Jin Kim, Jin-Soo Park, Moon-Sung Kang

Determination of optimal design parameters for preparing ion-exchange membranes for efficient redox flow batteries

s18-035

**Jooyul Lee** (Electrochemistry Department, Korea Institute of Materials Science, Changwon, Korea), Yongsoo Jeong

Manufacturing of Micro Probe Tip through Ni Alloys Electroplating

s18-036

**Jau-Kai Wang** (Applied Chemistry and Material Science, Fooyin University, Kaohsiung, Taiwan), Yan-Ru Wang, Ying-Ting Wang

A study on Supercritical Electrolytic Polishing Process for Stainless steel substrates

s18-037

**Jen-Yuan Wang** (Physics Division, Institute of Nuclear Energy Research, Taoyuan, Taiwan), Min-Chuan Wang, Hsin-Fu Yu, Der-Jun Jan, Kuo-Chuan Ho

A Flexible all-solid-state Electrochromic Device with Polymeric Crystal Composite Electrolyte and WO<sub>3</sub>/NiO Complementary System

## Physical electrochemistry

s18-038

**B.C. Chen** (Chinese Medicine, Buddhist Dalin Tzu Chi General Hospital, Chiayi, Taiwan), C. Y. Ho, H. H. Ku, M. Y. Wen, W. C. Wu, Y. H. Tsai

Electrical Current-Induced Thermal Characteristics in a Carbon Nanotube

s18-039

**Keiichi Nishihata** (Advanced Engineering Faculty, National Institute of Technology, Wakayama College, Wakayama, Japan), Katsuhiko Tsunashima, Masahiko Matsumiya

Preparation and Physicochemical Properties of Room-Temperature Phosphonium Ionic Liquids Based on Tetracyanoborate Anion

s18-040

**Marcin Opallo** (Department of Electrode Processes, Institute of Physical Chemistry Polish Academy of Sciences, Warszawa, Poland), Justyna Jedraszko, Wojciech Nogala, Wojciech Adamiak, Saustin Dongmo, Gunther Wittstock, Hubert Girault

(Electro)catalysis at Room Temperature Ionic Liquid/Water Interface: H<sub>2</sub>O<sub>2</sub> Generation

s18-041

**Wei Wang** (College of Chemistry and Chemical Engineering, Xiamen University, Xiamen, China), Fang-Fang Wang, Jie Zhang, Bao-Fa Su, Dongping Zhan, Zhong-Qun Tian

Quantifying Surface Diffusion by Nanoelectrode



# Author Index

How to read the Author Index: s08-017 = Poster number  
(Thu s13)16:00 = Oral presentation day, symposium, time

## A

- Abate, Antonio, (Tue s06)10:10  
 Abbas, Qamar, (Thu s05)09:30  
 Abbas, Zareen, (Tue s09)18:00  
 Abdel Nazeer, Ahmed, s05-001  
 Abdellaoui, Sofiene, (Mon s02)14:20, s02-004  
 Abe Santos, Nathalia, s09-001  
 Abe, Takeshi, (Mon s09)10:10, (Mon s09)16:40, (Tue s03)14:00, s03-017, s03-029, s03-049, s03-063  
 Abe, Yuta, (Tue s05)14:00, s05-040  
 Abell, Andrew, (Thu s11)17:20  
 Abouattallah, Rami, (Mon s04)16:40  
 Abruna, Hector, (Mon s17)18:00  
 Achilli, Elisabetta, (Mon s17)15:00, (Thu s14)15:00  
 Adamiak, Wojciech, s18-040  
 Adamkiewicz, Witold, (Fri s14)10:30  
 Adams, Brian, s18-020  
 Adomkevicius, Arturas, (Thu s05)16:40, s05-018  
 Adzic, Radoslav, s09-061, (Mon s09)15:00  
 Agopcan, Burag, s09-035, (Fri s09)09:50  
 Aguilar-Cordero, Julio-César, s18-003  
 Ahilan, Vignesh, s09-024  
 Ahlberg, Elisabet, (Tue s09)17:40, (Tue s09)18:00, s09-019, s09-020  
 Ahn, Do-Hee, s18-032  
 Ahrens, Paula, (Thu s18)10:10  
 Aikawa, Tatsuo, s07-001  
 Akase, Saki, s18-009  
 Akolkar, Rohan, (Wed s07)10:10, s07-011  
 Akyüz, Duygu, (Fri s09)09:50, s09-035  
 Al Amri, Zakia, (Tue s07)10:10  
 Al-Kharafi, Faizah, s08-011  
 Al-Kutubi, Hanan, s07-027  
 Alam, Muhammed, (Thu s18)15:40  
 Albayrak, Fatma K., (Fri s09)09:50, s09-035  
 Aldous, Iain, s03-001, s14-017  
 Aldous, Leigh, (Thu s18)17:00  
 Al Hoshan, Mansour, s13-001  
 Allen, Jan, (Fri s03)09:30  
 Allen, Joshua, (Fri s03)09:30  
 AlMayouf, Abdullah, s13-001  
 Alsaoub, Sabine, (Mon s02)18:20  
 Alshareef, Husam, s05-022, s05-035  
 Alvarado, Judith, (Tue s03)17:20  
 Alvarez-Malmagro, Julia, s12-010, s16-004  
 Alvaro, Minerva, (Thu s01)14:00  
 Amar, Abdelilah, s01-008  
 Amatore, Christian, (Thu s18)14:00, (Thu s11)15:20  
 Ambrosi, Adriano, s18-006, s18-022  
 Amereller, Marius, (Thu s0)08:15  
 Amin, Hatem M.A., s09-003  
 Amine, Khalil, (Fri s03)10:30  
 Amrane, Abdelatif, (Fri s14)09:30  
 Amstutz, Véronique, (Tue s01)14:40  
 An, Li, s03-051  
 An, Maozhong, (Thu s07)15:20  
 Anderson, Erik, (Tue s05)10:30  
 Ando, Toshihiro, s03-079, s04-025, s04-030  
 Andronesu, Corina, (Mon s02)18:20  
 Andryszewski, Tomasz, (Fri s14)10:30  
 Ania, Conchi, (Tue s10)10:30, (Thu s18)15:00, (Thu s18)16:40  
 Anquetin, Guillaume, (Mon s02)10:10  
 Antloga, Mirko, (Wed s07)10:10  
 Antolini, Ermete, s04-006  
 Aogaki, Ryoichi, (Thu s07)16:40, (Thu s07)17:20  
 Aoki, Koichi, s11-014  
 Aoki, Yoshitaka, s08-004  
 Aoyagi, Sakumi, s04-043  
 Aoyagi, Shintaro, (Tue s05)14:00, s05-040  
 Aquino-Neto, Sidney, (Mon s02)15:20, s02-006  
 Aradi, Balint, (Mon s06)16:40  
 Arai, Hajime, (Mon s03)14:00, s03-002, s17-007, s18-028  
 Arai, Juichi, s03-096  
 Arbault, Stephane, (Tue s15)10:10, (Tue s02)15:20  
 Arellano-González, Miguel Angel, (Mon s10)15:00  
 Arenas, Luis F., (Thu s03)18:00, s03-099  
 Arenz, Matthias, (Wed s04)10:10, (Thu s04)09:50  
 Arie, Arenst Andreas, s03-003, s03-004  
 Armand, M., (Thu s03)14:00  
 Armel, Vanessa, (Tue s05)15:40  
 Arnebrant, Thomas, (Tue s01)17:00  
 Arrigan, Damien, (Fri s01)10:10  
 Arunachalam, Prabhakarn, s13-001  
 Asahi, Masafumi, s04-039, s11-001  
 Asakura, Kiyotaka, s12-003  
 Asanuma, Miki, (Thu s07)16:40  
 Asen, Ludwig, s09-002  
 Asensio, Yeray, (Tue s10)18:20  
 Askarova, Gaukhar, s03-107  
 Asmussen, Robert, s18-020  
 Atta, Nada, (Thu s01)15:20  
 Aurbach, Doron, s17-006  
 Axmann, Peter, s12-014  
 Ayache, Maurice, s03-102  
 Ayata, Sevda, s09-003  
 Aydemir, Mehmet, (Fri s09)09:50, s09-035  
 Ayu Pradanawati, Sylvia, (Mon s03)18:00  
 Azumi, Kazuhisa, s18-031
- ## B
- Baba, Chika, s03-005  
 Baba, Koki, s04-025  
 Bachar, Ortal, s02-009  
 Bae, Byungchan, (Thu s04)17:00, s04-018, s04-019  
 Bae, Donghyun, s09-031  
 Baek, Esther, s05-019  
 Baeza-Reyes, José-Alejandro, s18-002  
 Baghernejad, Masoud, (Fri s11)09:30  
 Bai, Ming-Hua, s05-028  
 Bai, Peng, (Thu s03)16:40, s03-006  
 Bai, Yunlong, s05-029  
 Bakenova, Zagipa, (Tue s03)15:00  
 Baker, Annabelle, (Mon s17)15:40  
 Baker, Priscilla, (Mon s05)10:30, (Tue s09)10:10, (Tue s10)17:00, (Fri s09)11:10, s09-058, s09-065  
 Bakker, Eric, (Thu s18)15:20, (Fri s01)09:30  
 Balciunaite, Aldona, s09-048, s09-058  
 Baldizzzone, Claudio, (Mon s17)14:00  
 Balducci, Andrea, (Wed s05)10:10, (Thu s05)10:30  
 Balemans, Collin, (Thu s09)16:00  
 Bals, Sara, (Tue s09)15:00, (Tue s10)18:00, (Thu s07)14:00, s07-017, s10-004  
 Balsara, Nitash, (Thu s03)10:10  
 Baltruschat, Helmut, (Fri s03)09:30, s09-003  
 Balusamy, Thangaraj, s08-008  
 Bandarenka, Aliaksandr, (Tue s12)15:00, (Tue s12)15:20  
 Banhart, John, s03-119  
 Bano, Kiran, (Thu s01)17:20  
 Bao, Amin, s02-026  
 Bao, Jinpeng, s03-053, s03-138  
 Baradoke, Ausra, s02-003, s09-004  
 Barbosa Ferreira, Maiara, (Tue s10)16:00  
 Bardé, Fanny, (Tue s03)15:40  
 Barison, Simona, (Fri s14)09:30  
 Barpanda, Prabeer, (Tue s03)16:40  
 Barsan, Madalina M., (Tue s01)17:20  
 Barteau, Mark, (Thu s03)17:20  
 Barth, Holger, (Tue s02)10:10  
 Bartlett, Philip, (Tue s02)17:40, (Tue s02)18:00, (Thu s07)14:20  
 Barwe, Stefan, (Mon s02)18:20, s09-005  
 Bastl, Zdenek, (Mon s06)15:00  
 Basu, S., (Thu s03)15:40  
 Batchelor-McAuley, Christopher, (Mon s16)17:20  
 Battistel, Dario, (Tue s01)15:20  
 Batyrbekuly, Dauren, (Tue s03)14:20, s03-140  
 Bauer, Philipp, (Tue s12)14:40  
 Bauer, Siegfried, (Fri s18)10:10  
 Bazant, Martin Z., (Thu s03)16:40, s03-006  
 Becker, James Y., (Thu s11)15:40  
 Bedioui, Fethi, (Thu s01)14:00, s01-008  
 Bednarczyk-Cwynar, Barbara, s16-006  
 Béguin, François, (Tue s05)16:00, (Thu s05)09:30, s05-005, s05-014, s05-015  
 Behm, R. Jürgen, (Mon s12)10:30  
 Bélanger, Daniel, (Mon s05)16:40  
 Belgibayeva, Ayaulym, (Tue s03)15:00  
 Beltrop, Kolja, (Tue s03)16:00, s03-006  
 Ben-Amor, Salem, (Tue s02)15:20  
 Bendikov, Tatyana B., s02-009  
 Bergmann, Henry, (Tue s10)14:20, s10-001  
 Bergren, Adam, (Mon s16)14:00  
 Berhe, Taame Abraha, s06-001  
 Bernhardt, Paul, (Mon s02)15:40  
 Beshkov, Venko, (Mon s10)17:20  
 Bewley, Kathryn, (Mon s02)14:00  
 Bhargava, Richa, (Thu s14)15:20  
 Bi, Jiajin, s09-006

- Bidan, Gérard, (*Wed s05*)09:30  
 Bielańska, Elzbieta, *s04-047*  
 Biernat, Jan, (*Mon s16*)15:40  
 Biesdorf, Johannes, (*Tue s04*)10:10  
 Bilewicz, Renata, (*Mon s16*)15:40,  
 (*Mon s02*)17:40, (*Tue s16*)09:30,  
 (*Tue s16*)09:50, *s04-032*, *s09-049*  
 Binninger, Tobias, (*Mon s09*)14:00  
 BinSabt, Mohammad, *s05-001*, *s08-011*  
 Binti Mohidin Batcha, Abeed Fatima,  
 (*Mon s02*)17:20  
 Bisselink, Roel, *s10-002*, *s10-003*  
 Bissett, Mark A., (*Tue s12*)18:00  
 Bitner-Michalska, Anna, (*Fri s03*)11:10  
 Bitzer, Martin, (*Thu s03*)10:10, *s03-087*  
 Björefors, Fredrik, (*Wed s08*)10:30,  
 (*Fri s03*)12:10  
 Björling, Alexander, (*Tue s09*)17:40,  
*s09-020*  
 Blanquer, Guillaume, (*Tue s03*)15:00,  
 (*Tue s15*)17:40  
 Bleith, Peter, (*Mon s03*)09:30  
 Bobacka, Johan, (*Tue s01*)17:00  
 Böhme, Solveig, *s03-009*  
 Bohn, Paul, (*Tue s01*)16:00  
 Boillat, Pierre, (*Tue s04*)10:10  
 Bon Saint Côme, Yémima, (*Tue s16*)10:10  
 Bonanni, Alessandra, *s18-006*  
 Bond, Alan, (*Thu s07*)14:40,  
 (*Thu s01*)17:20, (*Fri*)08:15  
 Bondarenko, Alexandra, (*Tue s02*)16:40,  
 (*Thu s01*)10:30  
 Bondue, Christoph, (*Fri s03*)09:30  
 Boni, Alessandro, (*Thu s14*)16:40  
 Bonnefont, Antoine, (*Tue s12*)14:40,  
 (*Fri s09*)09:50  
 Bonnet-Mercier, Nadège, (*Tue s03*)17:40  
 Bopp, Philippe A., (*Tue s16*)10:10  
 Boreave, Antoinette, *s04-026*  
 Bornoz, Pauline, (*Mon s06*)17:20  
 Borowicz, Pawel, *s12-005*  
 Boschini, Andrea, *s03-007*  
 Boschloo, Gerrit, (*Mon s06*)15:20  
 Bottari, Serge, (*Tue s02*)15:20  
 Botz, Alexander, (*Thu s14*)14:40  
 Bouchard, P., (*Thu s03*)14:00  
 Bouchet, Renaud, (*Thu s03*)10:10  
 Bouckenooge, Pieter, (*Thu s07*)14:00,  
*s07-017*  
 Boulfrad, Samir, (*Fri s04*)09:50, *s04-040*  
 Bourée, Wiktor S., (*Mon s06*)17:00  
 Bousa, Milan, (*Mon s06*)15:00  
 Brachet, Mylène, (*Wed s05*)09:30  
 Bragato, Carlo, (*Tue s01*)15:20  
 Brandell, Daniel, (*Tue s03*)16:00,  
 (*Tue s15*)16:40, (*Wed s03*)09:50,  
*s03-008*, *s03-030*, *s03-042*  
 Brankovic, Stanko, (*Tue s07*)10:30,  
*s09-007*  
 Bresser, Dominic, (*Mon s03*)15:00,  
*s03-120*  
 Brett, Christopher, (*Tue s01*)17:20  
 Breugelmans, Tom, (*Tue s09*)15:00,  
 (*Tue s10*)18:00, (*Thu s07*)14:00,  
*s09-017*, *s10-004*  
 Briega-Martos, Valentin, (*Tue s12*)09:30  
 Brillas, Enric, (*Mon s10*)14:00,  
 (*Mon s10*)14:40  
 Brimaud, Sylvain, (*Mon s12*)10:30  
 Brodersen, Karen, (*Fri s04*)10:10  
 Broekmann, Peter, (*Thu s07*)09:30  
 Bronneberg, Aafke C., (*Mon s06*)18:00  
 Brooke, R. J., (*Fri s07*)10:10  
 Brousse, Kevin, (*Mon s05*)15:20,  
 (*Mon s05*)17:40, (*Thu s05*)15:00  
 Brousse, Thierry, (*Mon s05*)15:00,  
 (*Mon s05*)15:20, (*Tue s05*)16:00,  
 (*Wed s05*)09:30  
 Brown, Tom, (*Tue s02*)18:00  
 Bruchiel-Spanier, Netta, (*Fri s01*)09:50  
 Brunswick, Philippe, *s01-008*  
 Brylewski, Tomasz, *s04-004*, *s04-063*  
 Bu, Junfu, (*Fri s04*)11:30, *s04-054*  
 Buchheit, Rudolph, (*Tue s08*)17:00,  
*s08-002*  
 Bülter, Heinz, (*Thu s01*)16:40  
 Bünting, Aiko, (*Thu s03*)10:10, *s03-087*  
 Bulmer, John, *s14-001*  
 Bulut, Ela, (*Tue s07*)10:30  
 Bures, Filip, *s06-016*  
 Buriez, Olivier, (*Mon s16*)09:30,  
 (*Thu s11*)15:20  
 Busó-Rogero, Carlos, *s12-015*  
 Bustos, Erika, (*Fri s09*)11:30, *s10-004*  
 Byon, Hye Ryung, (*Mon s17*)17:00,  
 (*Tue s03*)17:40, (*Thu s03*)16:40,  
 (*Thu s03*)17:40  
 Byun, Young-Seok, *s01-006*
- C**  
 Cabot, Pere, (*Mon s10*)14:40  
 Cadogan, Sean, (*Thu s18*)17:00  
 Cai, Wen-Bin, (*Mon s12*)10:10,  
 (*Mon s12*)10:30, (*Thu s09*)18:00,  
 (*Fri s09*)11:10, *s09-074*  
 Cai, Wenshu, *s05-008*  
 Cai, Zaisheng, *s05-039*, *s07-013*  
 Calderon Moreno, Jose Maria, *s08-001*,  
*s08-015*  
 Calle-Vallejo, Federico, (*Tue s12*)15:20  
 Calmet, Amandine, *s01-008*  
 Camargo, Pedro H.C., (*Fri s14*)11:50  
 Camargo, Raissa, *s14-012*  
 Cañizares, Pablo, (*Tue s10*)14:00,  
 (*Tue s10*)18:20, *s10-007*, *s10-015*,  
*s10-023*, *s10-024*  
 Cao, Dianxue, (*Thu s04*)16:00, *s05-036*,  
*s09-068*  
 Cao, Fei-Fei, *s03-010*  
 Cao, Gaoshao, (*Fri s03*)10:10, *s03-088*  
 Cao, Zhenming, (*Fri s09*)10:30, *s09-080*  
 Cardoso, Franciane P., *s02-006*  
 Carlà, Francesco, *s07-032*  
 Cassidy, Mark, (*Fri s04*)09:50  
 Cassir, Michel, *s01-008*  
 Castaño-Álvarez, Mario, (*Tue s01*)18:00,  
 (*Thu s18*)14:20  
 Castillo, J.L., *s04-031*  
 Castro, Carmen, (*Mon s09*)10:30  
 Castro, Cláudio, *s10-016*  
 Cattarin, Sandro, (*Fri s07*)10:30  
 Cazares-Marín, Jose de Jesus,  
 (*Thu s11*)15:20  
 Cekic-Laskovic, Isidora, (*Thu*)08:15,  
 (*Thu s03*)15:40, *s03-130*  
 Celebi, Metin, *s01-017*  
 Celiesiute, Raimonda, *s02-003*, *s02-029*  
 Celorrio, Verónica, (*Thu s18*)16:40  
 Centellas, Francisco, (*Mon s10*)14:40  
 Centeno, Teresa A., (*Thu s05*)10:30  
 Cerda Pastrian, Fabian A., (*Fri s14*)11:50  
 Chae, Ji Su, (*Thu s03*)16:00  
 Chae, Oh B., *s03-122*  
 Chae, Suman, *s03-011*  
 Chakri, Sara, (*Wed s08*)09:30  
 Chami, Marianne, *s03-078*  
 Chamraeva, Maria A., (*Thu s14*)18:00  
 Chan, Kwong-Yu, (*Mon s09*)15:20,  
 (*Thu s04*)17:20, *s03-050*, *s09-072*  
 Chan, Po-Fan, (*Thu s07*)17:00, *s07-002*  
 Chandler, David, (*Thu s05*)10:10  
 Chandra, Shaneel, (*Tue s01*)15:00  
 Chang, Che-Lun, (*Fri s01*)10:30  
 Chang, Chia-Chin, *s03-012*, *s03-013*,  
*s03-026*  
 Chang, Chia-Hao, (*Fri s01*)10:30  
 Chang, Chih-Wei, *s03-016*  
 Chang, Gan-Zuei, *s01-019*  
 Chang, In Seop, (*Tue s02*)17:30  
 Chang, Jeng-Kuei, (*Thu s03*)15:40,  
*s03-062*, *s03-087*, *s04-056*, *s05-017*  
 Chang, Ling-Yu, *s06-004*, *s10-005*  
 Chang, Min-Hsing, *s04-010*  
 Chang, Sun-Tang, (*Mon s04*)14:20  
 Chang, Sung-Tung, (*Thu s09*)09:30  
 Chang, Ting-Hsiang, *s11-009*, *s14-015*  
 Chang, Tso-Fu Mark, (*Thu s07*)15:00,  
*s07-018*  
 Chang, Wonyoung, *s03-097*  
 Chang, Yu-Chen, (*Thu s01*)14:40  
 Chang, Yu-Chung, (*Thu s09*)09:30,  
*s09-063*  
 Chang, Yu-Fan, *s04-064*  
 Chang, Zheng, (*Tue s03*)10:30  
 Chang, Zhi, *s05-003*  
 Chao, Chung Hsiang, *s05-027*  
 Chao, Dong-Yi, *s03-016*  
 Chateigner, Daniel, (*Thu s18*)17:20  
 Chazelle, Sophie, *s03-078*  
 Chen, Aicheng, (*Fri s18*)09:30, *s18-020*  
 Chen, B.C., *s14-018*, *s18-038*  
 Chen, Chanjuan, (*Mon s17*)14:40  
 Chen, Cheng-Chuan, *s09-008*  
 Chen, Chih, (*Wed s07*)09:30  
 Chen, Chih-Hao, (*Fri s01*)10:30  
 Chen, Ching-Hsiang, *s09-056*, *s18-001*  
 Chen, Chun-Yi, (*Thu s07*)15:00, *s02-002*,  
*s07-018*  
 Chen, De, (*Thu s09*)10:30  
 Chen, Du-Hong, *s12-001*  
 Chen, George Zheng, (*Mon s05*)10:10,  
*s10-009*  
 Chen, Guan-Lin, (*Thu s01*)14:40  
 Chen, Guohua, (*Mon s10*)09:30,  
 (*Thu s03*)16:00  
 Chen, Hong-Shou, *s04-049*  
 Chen, Hsun-Yi, *s03-016*  
 Chen, Jee-Jay, (*Thu s03*)17:20  
 Chen, Jia-Cing, *s17-002*  
 Chen, Jian, (*Tue s08*)14:40, *s03-015*  
 Chen, Jingyi, *s02-010*  
 Chen, Jingyuan, *s11-014*  
 Chen, Junxiang, (*Thu s04*)09:30, *s12-026*  
 Chen, Kezheng, *s03-098*  
 Chen, Kuei-Hsien, (*Mon s04*)14:20,  
 (*Tue s06*)09:50, (*Thu s09*)09:30,  
*s04-020*, *s04-029*, *s05-033*  
 Chen, Li, *s11-008*

- Chen, Li-Chia, *s03-012*  
 Chen, Li-Chyong, (*Mon s04*)14:20,  
*(Thu s09)*09:30, *s04-029*, *s05-033*  
 Chen, Liang-Yih, *s09-056*  
 Chen, Lin-Chi, (*Thu s18*)16:00,  
*(Fri s01)*10:30  
 Chen, Linjiang, *s14-017*  
 Chen, Long, *s03-014*  
 Chen, Lu, (*Thu s07*)14:40  
 Chen, Ming, (*Fri s04*)10:10  
 Chen, Ming-Chou, *s06-006*  
 Chen, Pei-Yu, *s06-002*  
 Chen, Ping-Yen, *s04-011*  
 Chen, Po-Chun, *s07-030*, *s18-014*  
 Chen, Qiaoli, (*Fri s09*)10:30, *s09-009*,  
*s09-080*  
 Chen, Shen-Ming, (*Tue s02*)14:40  
 Chen, Sheng-Pei, (*Mon s17*)09:30  
 Chen, Shengli, (*Thu s04*)09:30  
 Chen, Siguo, (*Mon s04*)14:00, *s04-041*,  
*s04-046*, *s14-005*  
 Chen, Tsan-Yao, *s03-013*  
 Chen, Wei, *s05-035*, *s09-039*  
 Chen, Wei-Fu, (*Fri s09*)10:10  
 Chen, Xiang, *s01-018*  
 Chen, Xingxing, (*Thu s14*)14:40  
 Chen, Yanxia, *s04-052*, *s04-053*  
 Chen, Yen-Jhih, *s06-012*  
 Chen, Yi-Ting, (*Thu s01*)14:40  
 Chen, Yong-Min, *s18-014*  
 Chen, Yu-Fan, *s03-013*  
 Chen, Yu-Fu, *s09-059*  
 Chen, Yu-Min, (*Wed s08*)10:10  
 Chen, Yuan, (*Mon s05*)17:20, *s09-010*  
 Chenard, Etienne, *s03-127*  
 Cheng, Bo-Syun, *s04-027*  
 Cheng, Chi-Hui, *s18-001*  
 Cheng, Hao-Ying, *s04-056*  
 Cheng, Jian, *s05-008*  
 Cheng, Ju-Hsiang, *s17-003*  
 Cheng, Kevin, *s03-127*  
 Cheng, Kui, (*Thu s04*)16:00, *s09-011*,  
*s09-068*  
 Cheng, Shu-Hua, *s01-001*  
 Cheng, Xi, (*Thu s09*)15:00  
 Cheng, Yu, *s16-002*  
 Cheng, Yu-Lun, *s17-005*  
 Cherevko, Serhiy, (*Mon s17*)14:00  
 Chern, Chong-Shyan, *s03-068*  
 Chern, Yaw-Terng, *s12-006*  
 Chiang, Chia-Ying, (*Fri s09*)09:30,  
*s09-012*  
 Chiang, Heng-Wei, *s03-039*, *s03-108*  
 Chiang, Kuo-Wei, *s04-027*  
 Chiang, Wei-Hung, (*Thu s01*)14:40,  
*s09-021*, *s09-062*  
 Chiba, Kazuhiro, (*Thu s11*)16:40  
 Chidambaram, Arunraj, (*Fri s14*)10:30  
 Chien, Hsiu-Chuan, *s05-002*  
 Chien, Pei-Yi, *s05-026*  
 Chien, Yu-Ju, *s03-109*  
 Chih, Yi-Kai, (*Wed s02*)09:50  
 Chikaoka, Yu, *s04-044*  
 Chiku, Masanobu, (*Mon s05*)15:40  
 Chin, Jian-Ting, *s03-025*  
 Chinderle, Adam J., (*Thu s14*)15:20  
 Chinnaya, Jeyabharathi, (*Thu s18*)10:10  
 Chiorcea-Paquim, A.M., (*Tue s02*)16:00  
 Chiou, Josh Y. Z., *s03-110*  
 Chiter, Fatah, (*Tue s08*)16:40  
 Chiu, I-Ting, (*Thu s09*)16:40, *s06-002*,  
*s09-043*  
 Chiu, Jun-Ming, *s05-012*, *s05-020*,  
*s05-034*, *s09-055*  
 Cho, Eunseog, (*Mon s03*)15:40  
 Cho, Jung Sang, *s14-006*  
 Cho, Kyeongjae, *s03-122*  
 Cho, Maenghyo, *s03-122*  
 Choa, Yongbeom, *s03-070*  
 Choi, Byung-Won, *s03-097*  
 Choi, Chang Hyuck, (*Mon s04*)10:10,  
*(Mon s17)*14:00  
 Choi, Eun-Young, (*Fri s18*)11:10  
 Choi, Gwang Sik, *s03-033*  
 Choi, Hae Young, *s03-018*  
 Choi, Hee Cheul, (*Mon s17*)17:00  
 Choi, Hyeong Jong, *s05-024*  
 Choi, Jae-Man, (*Fri s03*)12:10  
 Choi, Jeong Hee, *s03-018*  
 Choi, Jihui, *s09-023*, *s09-029*  
 Choi, Jongrak, *s05-010*  
 Choi, Woo-Sung, *s03-097*  
 Chokki, Kenta, *s07-021*  
 Chong, Sam, *s14-017*  
 Chorkendorff, Ib, (*Tue s06*)09:30,  
*(Tue s09)*15:20, (*Fri s09*)10:30  
 Chou, Eric, (*Thu s07*)16:00  
 Chou, Hung-Lung, *s15-001*  
 Chou, Jacky, (*Thu s03*)09:30  
 Chou, Nan-Kuang, *s09-012*  
 Chou, Shih-Cheng, *s07-030*  
 Chou, Shu-Wei, *s05-026*  
 Chou, Tse-Chuan, (*Thu s18*)16:00  
 Chou, Yi-Sin, *s09-063*  
 Choudhury, Moinul, (*Wed s01*)09:30  
 Chu, Jinn P., (*Tue s08*)18:20, *s06-011*  
 Chu, Y., (*Tue s05*)14:40  
 Chuan Sun, Yen-Chun, *s06-007*  
 Chuang, Min-Chieh, *s02-034*  
 Chuang, Yu-cheng, *s12-027*  
 Chung, Chai-Wei, *s18-014*  
 Chung, Kyung Yoon, *s03-097*  
 Chung, Sai-Cheong, (*Tue s03*)16:40  
 Chung, Taek Dong, *s02-008*, *s18-013*  
 Chyan, Oliver, (*Tue s08*)14:00  
 Ciampi, Simone, (*Wed s01*)09:30  
 Cigler, Petr, (*Mon s06*)16:00  
 Cinotti, Serena, *s07-032*  
 Citron, Alberto, (*Tue s01*)15:20  
 Clausmeyer, Jan, (*Thu s01*)14:20, *s01-009*  
 Climent, Victor, (*Mon s12*)17:40  
 Colic, Viktor, (*Tue s12*)15:20  
 Comisso, Nicola, (*Fri s07*)10:30  
 Compton, Richard, (*Mon s16*)16:40,  
*(Mon s16)*17:20, (*Thu s14*)17:00,  
*s01-026*  
 Conan, Françoise, (*Thu s18*)09:30  
 Cooper, Andy, *s14-017*  
 Corden, Natalie, *s18-023*  
 Cordoba de Torresi, Susana, (*Fri s14*)11:50  
 Corradini, Patricia, *s04-006*  
 Cortés-Salazar, Fernando, (*Tue s01*)14:40,  
*(Tue s02)*16:40, (*Thu s01*)10:30  
 Cosnier, Serge, (*Mon s16*)15:00  
 Cosquer, Nathalie, (*Thu s18*)09:30  
 Costa Bassetto, Victor, *s09-037*  
 Costa, Paulo, *s16-005*  
 Coustan, Laura, (*Tue s05*)15:40,  
*(Tue s05)*17:00  
 Crabtree, George, (*Tue s03*)09:30  
 Cremers, Carsten, (*Thu s04*)15:00  
 Crepaldi, Lais B., *s02-006*  
 Crespo, Gaston, (*Thu s18*)15:20,  
*(Fri s01)*09:30  
 Creus, Juan, (*Tue s08*)15:00  
 Crosnier, Olivier, (*Mon s05*)15:00,  
*(Tue s05)*16:00  
 Crowley, P., (*Mon s16*)18:20  
 Cuartero, Maria, (*Thu s18*)15:20  
 Cuevas, Oswaldo, (*Fri s09*)11:30  
 Cui, Chunhua, (*Mon s04*)17:20  
 Cui, Hua, (*Mon s16*)18:00  
 Cui, Jin, *s18-021*  
 Cui, Jingwen, (*Tue s01*)17:00  
 Cui, Xiaoliang, *s04-028*  
 Cui, Yi, (*Tue s03*)14:00  
 Curtiss, Larry, (*Fri s03*)10:30  
 Curvat, Laura, (*Tue s06*)10:10  
**D**  
 D'Acapito, Francesco, (*Mon s17*)15:00,  
*(Thu s14)*15:00  
 D'Angelo, Adriana, (*Tue s10*)14:40  
 Da Silva, Cosmelina G., (*Thu s18*)17:20  
 Daasbjerg, Kim, (*Thu s14*)10:10,  
*(Thu s14)*17:20  
 Dabrowa, Juliusz, *s04-004*, *s04-063*  
 Daems, Nick, (*Tue s10*)17:20, *s04-012*  
 Daffos, Barbara, (*Mon s05*)15:20,  
*(Thu s05)*10:10, (*Thu s05*)15:00  
 Dahiya, Prem Prakash, (*Thu s03*)15:40  
 Dai, Bin, *s03-132*, *s03-133*  
 Dai, Chao-Shuan, *s05-026*  
 Dai, Hongjie, (*Tue s08*)15:15  
 Dai, Zhen, (*Mon s09*)14:20  
 Dalgliesh, Robert, (*Mon s12*)18:00  
 Daniele, Salvatore, (*Tue s01*)15:20  
 Danten, Yann, (*Tue s15*)17:00  
 Darr, Jawwad, *s03-061*  
 David, Melinda, (*Tue s01*)17:20  
 Davies, A. Giles, *s12-025*  
 Dávila, Martín, *s09-013*  
 Day, Sarah, (*Mon s17*)15:40  
 De Andrade, Adalgisa, (*Mon s02*)15:20,  
*s02-006*  
 de lucas Consuegra, Antonio,  
*(Tue s10)*10:10, *s10-030*  
 de Poulpique, Anne, (*Mon s02*)17:00  
 De-Santiago-Zárate, Adrián, *s18-002*  
 Deák, Peter, (*Mon s06*)16:40  
 Deconinck, Johan, (*Fri s04*)11:10, *s14-021*  
 DeGuire, Mark, (*Wed s07*)10:10  
 Dekel, Dario, (*Mon s04*)15:20  
 Dellen, Christian, (*Thu s03*)10:10,  
*s03-082*, *s03-087*  
 Delmas, Claude, (*Wed s03*)09:30  
 Delp, Samuel, (*Fri s03*)09:30  
 Dembińska, Beata, *s04-047*  
 Demeaux, Julien, (*Fri s03*)11:30  
 Deng, Hsin-Fu, *s10-022*  
 Deng, Shengyuan, *s02-011*, *s02-033*  
 Deng, Yujia, (*Thu s04*)09:50  
 Deng, Yuxiao, (*Mon s09*)14:20  
 Deng, Zhao-Feng, *s03-050*  
 Denuault, Guy, (*Mon s09*)17:00,  
*(Thu s04)*10:10, *s01-020*, *s01-023*  
 Depla, Diederik, (*Fri s04*)11:10



- Devasenathipathy, Rajkumar, (Tue s02)14:40  
 Devianto, Hary, s03-003  
 Devillers, Charles H., (Thu s14)18:00  
 Devin, Anne, (Tue s02)15:20  
 Devina, Inez, s03-003  
 Dey, M. K., s05-032  
 Di Benedetto, Francesco, s07-032  
 Di, Rui, s03-017  
 Diba, Farhana Sharmin, s15-005  
 Dikhtiarenko, Alla, s07-027  
 Dimitrov, Nikolay, (Tue s07)09:30  
 Ding, Bing, (Tue s03)14:40, s03-097, s05-003  
 Ding, Kuen-Yi, s07-024  
 Ding, Shuijiang, (Tue s03)14:40, s12-017  
 Ding, Songyuan, (Mon s12)16:40  
 Ding, Wei, (Mon s04)14:00, s04-041, s04-046, s14-005  
 Ding, Zhifeng, (Thu s11)16:00  
 Dionigi, Fabio, (Mon s04)17:20, (Thu s09)17:00  
 Diyatmika, Wahyu, s06-011  
 Do, Jing-Shan, s02-018  
 Doan, Hieu, s09-007  
 Doh, Chil Hoon, s03-018, s03-045  
 Doi, Takayuki, (Mon s03)10:10  
 Dolgikh, Olga, s14-021  
 Dolinska, Joanna, (Mon s16)17:40, (Fri s14)10:30  
 Dong, Jin-Chao, (Tue s12)10:10, s12-001,  
 Dong, Wensheng, s03-055, s05-007  
 Dong, Xiaoli, s03-019  
 Dongmo, Saustin, s18-040  
 Donner, Constanze, s08-006  
 Dordi, Yezdi, s07-030  
 Dornseiffer, Jürgen, (Thu s03)10:10, s03-087  
 dos Santos Fajardo, Ana S., (Tue s10)16:00  
 Dou, Hui, (Tue s03)14:40, s03-097, s05-003  
 Douard, Camille, (Mon s05)15:20  
 Dow, Wei-Ping, (Thu s07)10:10, (Thu s07)10:30, (Thu s07)17:00, (Thu s07)18:00, s07-002, s07-009  
 Dranka, M., (Fri s03)11:10  
 Drelinkiewicz, Alicja, s04-047  
 Drob, Silviu, s08-001, s08-015  
 Dryfe, Robert A.W., (Tue s12)18:00  
 Dsoke, Sonia, (Wed s05)10:30  
 Du, Cuiwei, s08-010  
 Du, He-yun, (Thu s09)09:30, s04-029  
 Du, Hongda, s04-007  
 Du, Jia-Huan, s14-016  
 Du, Mengmeng, (Thu s04)16:00  
 Duca, Matteo, (Mon s02)15:00  
 Dywili, Nomxolisi, (Mon s05)10:30
- E**  
 Edström, Kristina, (Tue s03)16:00, (Fri s03)12:10, s03-009, s03-042  
 Eguchi, Mika, s03-079, s04-025, s04-030  
 Ehsani, Ali, s09-014  
 Eifert, Alexander, (Tue s02)10:10  
 Eikerling, Michael, (Tue s12)15:40, (Thu s04)17:40  
 El Kazzi, Mario, (Mon s17)16:40  
 El-Ads, Ekram, (Thu s01)15:20  
 Elbaz, Lior, (Mon s09)17:20  
 Elizalde, Jorge, (Tue s01)18:00
- Elliott, Sean, (Mon s02)14:00  
 Eloul, Shaltiel, (Mon s16)17:20  
 Emanuelsson, Rikard, s18-015  
 Enache, T.A., (Tue s02)16:00  
 Endo, Haruka, (Mon s06)18:20  
 Eng, Alex Yong Sheng, s18-022  
 Engelbrekt, Christian, (Fri s09)11:30  
 Erami, Toshiaki, (Tue s08)17:20  
 Erben, Johannes, (Tue s04)10:30  
 Ernst, Frank, s07-011  
 Erol, Salim, (Mon s03)16:40  
 Escudero-Escribano, Maria, (Tue s09)15:20  
 Eskusson, Jaanus, s05-013  
 Eslamibidgoli, Mohammad J., (Tue s12)15:40  
 Esposito, Vincenzo, (Mon s04)18:20  
 Essmann, Vera, (Tue s02)17:00  
 Estévez, Angel, (Wed s10)10:30  
 Eto, Makoto, s09-015  
 Eudek, Pavel, s03-032  
 Eustache, Etienne, (Mon s05)15:20
- F**  
 Fabbri, Emiliana, (Mon s09)14:00, (Tue s04)10:10, (Tue s09)16:40, (Thu s09)15:00  
 Fabricio, Aline S. C., s16-003  
 Faiz, Hadri, s14-013  
 Fan, Caimei, s07-019  
 Fan, Louzhen, (Thu s14)17:40  
 Fan, Miao-Syuan, (Tue s06)10:30, s06-004, s06-006, s09-016, s09-022, s10-005  
 Fang, Chung-Kai, s12-023  
 Fang, Jason, (Tue s03)15:40, (Thu s03)15:40, s03-020, s05-027  
 Fang, Ming-Da, (Tue s05)15:00  
 Farandos, Nick, (Tue s10)09:30  
 Farhat, Ali, (Mon s10)16:00, s10-006  
 Faubert, Patrick, (Tue s15)10:30, s17-001  
 Fauzan Adziimaa, Ahmad, s03-111  
 Favier, Frédéric, (Mon s05)15:00, (Tue s05)15:40, (Tue s05)17:00  
 Feaugas, Xavier, (Tue s08)15:00, s12-022  
 Fedor, Justin, (Mon s02)15:00  
 Fedorková Straková, Andrea, s03-032  
 Feenstra, Lourens, s10-003  
 Feifel, S., (Mon s16)18:20  
 Felici, Roberto, s07-032  
 Feliu, Juan M., (Mon s12)16:40, (Mon s12)17:40, s12-015  
 Felix, Felix, (Mon s12)16:00  
 Fenske, Daniela, (Thu s01)16:40  
 Fereiro, Jerry, (Mon s16)14:00  
 Fermín, David J., (Thu s18)16:40  
 Fernandez Macia, Lucia, (Fri s04)11:10, s09-017  
 Fernandez Marchante, Carmen Maria, (Tue s10)18:20, s10-007  
 Fernández Otero, Toribio, (Wed s10)10:30  
 Fernández-la-Villa, Ana, (Tue s01)18:00, (Thu s18)14:20  
 Ferre-Vilaplana, Adolfo, (Tue s12)09:30  
 Ferreira, Fabricia, s16-005  
 Ferreira, Virginia, (Mon s12)18:00  
 Fic, Krzysztof, (Mon s05)14:40, (Tue s05)15:20, s05-042  
 Figueiredo, Marta, (Mon s12)15:40
- Figueredo-Rodriguez, Horacio A., (Wed s10)09:30  
 Finegan, Donal, (Mon s03)17:20  
 Flacke, Luis, s03-077  
 Fleige, Michael, (Wed s04)10:10  
 Floner, Didier, (Fri s14)09:30  
 Flores Tapia, Nelly Esther, (Mon s10)14:40  
 Florescu, Monica, (Tue s01)17:20  
 Flox, Cristina, (Thu s03)17:00  
 Fontaine, Eric, (Tue s02)15:20  
 Foong, Yeewei, (Mon s05)17:00  
 Fornasiero, Paolo, (Thu s14)16:40  
 Forner Cuenca, Antoni, (Tue s04)10:10  
 Forse, Alexander C., (Tue s05)14:20  
 Foster, Erick, (Fri s01)11:30  
 Fourcade, Florence, (Fri s14)09:30  
 Frackowiak, Elzbieta, (Mon s05)14:40, (Tue s05)15:20, s05-015, s05-042  
 Franco, Alejandro A., (Tue s03)15:00, (Tue s15)17:40, s15-002, s15-004  
 Frateur, Isabelle, (Wed s08)09:30  
 Frauenheim, Thomas, (Mon s06)16:40  
 Frayret, Christine, (Tue s15)17:00  
 Frei, Maxi, (Tue s04)10:30  
 Frenck, Louise, (Thu s03)10:10  
 Frey, Corinna, (Tue s02)10:10  
 Friebe, Daniel, (Mon s12)14:00  
 Friedrich, Kaspar Andreas, (Mon s04)16:40, s04-031, s09-038  
 Frith, James T., (Fri s03)09:50  
 Fromm, Olga, s03-006  
 Frontana, Carlos, s11-005  
 Frontera, Carlos, (Tue s03)15:40  
 Fu, Chaopeng, s05-021  
 Fu, Ji-Xuan, s03-054  
 Fu, Yue, (Fri s03)10:30  
 Fuchigami, Toshio, (Fri s11)09:50  
 Fuchiwaki, Yusuke, s02-025  
 Fuchs, Bettina, (Wed s05)10:30  
 Fuentes, Rosalba, (Mon s10)10:10  
 Fujii, Kenta, (Thu s05)15:40  
 Fujiki, Satoshi, (Tue s03)18:00  
 Fujimoto, Hayato, (Fri s03)10:30  
 Fujimoto, Hiroyuki, (Tue s05)17:40  
 Fujimoto, Shinji, (Tue s08)17:20  
 Fujishima, Akira, (Tue s10)15:20  
 Fujita, Etsuko, (Fri s09)10:10  
 Fujita, Sho, (Thu s09)14:40  
 Fujiwara, Naoko, s04-039, s11-001  
 Fukami, Kazuhiro, (Wed s07)10:30, s07-016, s07-025  
 Fukuda, Katsutoshi, s03-002, s03-104  
 Fukuhara, Tomoko, s09-044  
 Fukutsuka, Tomokazu, (Mon s09)10:10, (Mon s09)16:40, s03-017, s03-029, s03-049  
 Fung, Kuan-Zong, s03-066, s03-067, s03-083, s04-060, s04-061, s04-064, s06-009  
 Furriel, Rosa R.P.M., s02-006  
 Furuhashi, Kazuma, s04-030  
 Furuhashi, Takumi, (Tue s05)14:00, s05-040  
 Fushimi, Koji, (Tue s08)14:20, (Tue s08)17:40, (Thu s08)09:30
- G**  
 Gaboriau, Dorian, (Wed s05)09:30  
 Gago, Aldo Saul, (Mon s04)16:40, s09-038  
 Gajewski, Piotr, s05-014

- Galal, Ahmed, (*Thu s01*)15:20, s05-001, s08-011
- Galia, Alessandro, (*Tue s10*)14:40, s10-020
- Gallus, Dennis, (*Thu*)08:15
- Gan, Lin, (*Mon s04*)17:20, s04-007
- Gan, Xiaorong, s01-002
- Gan, Yongping, s10-025
- Ganguly, Abhijit, s05-033
- Gao, Peng-Cheng, (*Tue s05*)17:00
- Gao, Rachel, (*Tue s02*)17:40
- Gao, Zhida, s09-054
- Garbarino, Sébastien, (*Fri s09*)10:30
- Garcia, Daniel, s04-001, s04-031
- García, José Alberto, s10-004
- Garcia-Araez, Nuria, (*Fri s03*)09:50, s03-074
- Garcia-Cruz, Leticia, (*Tue s10*)10:30
- García-Mendoza, Arturo-de-Jesus, s18-002, s18-003
- Garcia-Segura, Sergi, (*Mon s10*)14:00, s10-008
- Garcia-Ybarra, P.L., s04-031
- Garrido, José, (*Mon s10*)14:40
- Gascoin, Stéphanie, (*Thu s18*)17:20
- Gascon, Jorge, s07-027
- Gasteiger, Hubert A., (*Fri s03*)11:30
- Gatti, Carlo, (*Tue s15*)17:00
- Gavvalapalli, Nagarjuna, s03-127
- Ge, Junjie, (*Wed s09*)10:30
- Ge, Mengchen, (*Tue s01*)17:40
- Gebala, Magdalena, (*Tue s02*)16:50
- Geboes, Bart, (*Tue s09*)15:00, (*Tue s10*)18:00, (*Thu s07*)14:00, s09-017, s10-004
- Gehrke, Hans-Gregor, (*Thu s03*)10:10, s03-082, s03-087
- Geiger, Simon, (*Mon s17*)14:00
- Gejo, Tsukasa, s03-021
- Gelinas, Bruno, (*Tue s05*)10:10
- Geneste, Florence, (*Fri s14*)09:30
- Geng, Ping, (*Mon s10*)09:30
- Genovese, Matthew, (*Mon s05*)17:00
- Gentile, Pascal, (*Wed s05*)09:30
- Georgescu, Nicholas, (*Mon s09*)18:00
- Ger, Ming-Der, s02-024, s04-015, s07-010, s07-023
- Gewirth, Andrew, (*Mon s03*)16:00, (*Tue s12*)09:50, (*Tue s03*)15:20
- Ghahraman Afshar, Majid, (*Fri s01*)09:30
- Ghanbari, Niloofar, s12-014
- Ghanem, Mohamed Ali, s13-001
- Ghassemzadeh, Lida, s04-003
- Ghelichi, Mahdi, (*Thu s04*)17:40
- Ghigna, Paolo, (*Mon s17*)15:00, (*Thu s14*)15:00
- Ghobadi, Kobra, (*Fri s09*)11:50, s09-018
- Ghoul, Mohammed, (*Tue s08*)15:20
- Giaccherini, Andrea, s07-032
- Giambastiani, Giuliano, (*Mon s09*)17:40
- Giffin, Guinevere A., (*Tue s03*)17:00
- Gil, Otavio, (*Thu s18*)17:20
- Gim, Jihyeon, s14-014
- Gion, Massimo, s16-003
- Giordano, Fabrizio, (*Tue s06*)10:10
- Giordano, Livia, (*Mon s12*)14:40
- Giorgio, Marco, s02-001
- Girault, Hubert, (*Tue s01*)14:40, (*Tue s02*)16:40, (*Thu s01*)10:30, s09-037, s18-040
- Giyanto, Giyanto, s03-112
- Gladisch, J., s02-005
- Glazoff, Michael, (*Fri s04*)10:30
- Gliech, Manuel, (*Thu s09*)17:00
- Göransson, Gert, s09-020, (*Tue s09*)17:40
- Gogoll, Adolf, s03-114, s11-013, s18-015
- Gogotsi, Yury, (*Mon s05*)14:00, (*Mon s05*)17:40, (*Tue s05*)17:00, (*Thu s05*)10:10
- Golovin, Viktor, (*Thu s04*)15:40
- Golub, Tatiana, (*Thu s11*)15:40
- Gomes, Adriano, (*Tue s09*)18:00
- Gomez-Lahoz, Cesar, s10-017
- Gomis-Berenguer, Alicia, (*Thu s18*)15:00, (*Thu s18*)16:40
- Gon Corradini, Patricia, s09-001
- Goncales, Vinicius, (*Wed s01*)09:30
- Gondosiswanto, Richard, (*Tue s01*)17:40
- Gonzalez, Ernesto, (*Tue s10*)18:20
- González, Ignacio, (*Mon s10*)15:00
- Gonzalez-Cobos, Jesús, (*Tue s10*)10:10, s10-030
- Gonzalez-Elipse, Agustín, (*Tue s10*)10:10
- Gonzalez-Romero, Elisa, s09-004
- Goodchild, Sarah A., (*Tue s02*)17:40
- Gooding, J. Justin, (*Wed s01*)09:30, (*Thu s18*)15:40
- Góral-Kurbiel, Monika, s04-047
- Gorgoi, Mihaela, (*Fri s03*)12:10
- Gorji, Alireza, (*Fri s09*)11:50, s09-018
- Gorton, Lo, (*Mon s02*)18:00, s02-028
- Gorun, Sergiu M., s11-004
- Gotoh, Kazuma, (*Tue s03*)18:20
- Goubard, Nicolas, (*Mon s05*)15:00
- Goulart, Marilia, s16-005
- Gounel, Sébastien, (*Tue s02*)15:00
- Grabow, Lars, s09-007
- Grätzel, Michael, (*Mon s06*)16:00, (*Tue s06*)10:10
- Grande, Lorenzo, (*Tue s03*)17:20, s03-069
- Grant, Patrick, s05-021
- Grey, Clare P., (*Tue s05*)14:20
- Gribov, Evgeniy, (*Thu s04*)15:40
- Griffin, John M., (*Tue s05*)14:20
- Grimaudo, Valentine, (*Thu s07*)09:30
- Grippio, Valentina, s04-032
- Griveau, Sophie, (*Thu s01*)14:00, s01-008
- Gross, Zeev, (*Mon s09*)17:20
- Grote, Jan-Philip, (*Mon s17*)14:00
- Grützke, Stefanie, (*Tue s02*)17:00
- Grønberg, Ulrik, (*Tue s09*)15:20
- Gu, Wenbin, (*Tue s04*)09:30
- Gu, Xing, (*Thu s07*)15:20
- Guan, Li, s10-009
- Guan, Xiao-Rui, s18-012
- Guay, Daniel, (*Fri s09*)10:30
- Guedes da Silva, M. Fátima C., (*Thu s11*)15:00, s12-019
- Guerfi, A., (*Thu s03*)14:00
- Guerri, Annalisa, s07-032
- Guerriero, Paolo, (*Fri s07*)10:30
- Guery, Claude, s15-002
- Guessoum, Khadoudj, s08-016
- Guijarro, Nestor, (*Mon s06*)17:00
- Guillon, Olivier, (*Thu s03*)10:10, s03-082, s03-087
- Gunawan, Christian Andre, (*Tue s01*)17:40, s02-035
- Guo, Fen, (*Thu s04*)16:00
- Guo, Hengyu, s10-027
- Guo, Jianghuai, (*Tue s03*)16:40
- Guo, Ruihua, (*Thu s14*)17:40
- Guo, Si-Xuan, (*Thu s01*)17:20
- Guo, Xuhong, s03-132, s03-133
- Guo, Yu-Guo, (*Thu s03*)09:30
- Guo, Zhaowei, s03-014
- Gurgul, Jacek, s04-047
- Gustafsson, Torbjörn, (*Fri s03*)12:10
- Gutierrez-Granados, Silvia, (*Thu s01*)14:00
- Gutierrez-Guerra, Nuria, s10-030
- Gutierrez-Sanchez, Cristina, (*Tue s02*)17:10
- Gutkowski, Ramona, s06-013
- Gwon, Hyeok-Jo, s03-070
- Gwon, Yong Hwan, s03-045
- ## H
- Ha, Van, (*Thu s07*)09:50
- Haarberg, Geir Martin, (*Tue s10*)17:40, (*Thu s09*)15:20
- Habazaki, Hiroki, (*Wed s04*)10:30
- Haeffele, Matthieu, (*Thu s05*)10:10
- Haga, Masa-aki, (*Thu s14*)09:30
- Hagfeldt, Anders, (*Mon s06*)15:20
- Hagiwara, Rika, s03-104
- Hakamata, Hideki, s01-004
- Halim, Martin, s03-003, s03-004
- Hall, Stephen, (*Mon s03*)17:20, s10-017
- Halouzka, Vladimir, s01-007
- Hamazaki, Makoto, (*Mon s04*)09:50, s04-033
- Han, Byungchan, (*Tue s15*)14:40, s14-008
- Han, Donghoon, (*Fri s01*)11:30
- Han, En-Hou, (*Thu s08*)10:10, (*Thu s08*)10:10
- Han, Hye Youn, s15-005
- Han, Lianhuan, s10-010
- Han, Oc Hee, s01-006
- Han, Xiaoping, s08-009
- Han, Zhili, (*Mon s16*)18:00
- Hanc-Scherer, Florin A., (*Thu s09*)17:20, s09-060
- Hankin, Anna, (*Tue s10*)09:30
- Hansen, Kent Kammer, (*Mon s04*)18:20
- Hao, Chia-Kan, s09-051
- Hao, Jie, s02-026
- Hao, Qingli, (*Tue s09*)17:20
- Hapiot, Philippe, (*Thu s18*)09:30, s14-009
- Hara, Agnieszka, (*Fri s07*)11:50, s07-004
- Hara, Masanori, s04-016
- Hara, Toru, (*Tue s03*)15:00
- Harada, Yoshihisa, s04-050
- Hardwick, Laurence, (*Thu s03*)09:50, s03-001, s05-018, s14-017, s17-002
- Haregewoin, Atetegeb Meazah, (*Fri s03*)11:50
- Hartl, František, (*Fri s11*)11:10
- Hartmann, Jens, (*Tue s10*)14:20
- Haruki, Tatsuro, s10-011
- Hasan, Kamrul, s02-028
- Hasegawa, Naoki, (*Mon s12*)15:00
- Hasegawa, Takahiro, s09-044
- Hasegawa, Yasuchika, (*Tue s08*)14:20, (*Tue s08*)17:40, (*Thu s08*)09:30
- Hashimoto, Kazuhito, (*Mon s09*)14:40, (*Tue s09*)14:20
- Hashimoto, Shinji, (*Mon s06*)14:20
- Hashimoto, Tomoko, s02-002
- Hashinokuchi, Michihiro, (*Mon s03*)10:10

- Hasse, Ulrich, (*Thu s18*)10:10  
 Hassel, Achim Walter, (*Thu s08*)09:50,  
 (*Fri s18*)10:10, *s12-004*  
 Hatanaka, Hironobu, (*Tue s02*)09:50  
 Hatanaka, Tatsuya, (*Thu s04*)14:00  
 Hattori, Masashi, *s03-022*  
 Hauch, Anne, (*Fri s04*)10:10  
 Haumont, Raphael, (*Thu s09*)15:00  
 Havlicek, David, (*Mon s06*)15:00  
 Hayakawa, Teruaki, *s04-050*  
 Hayashi, Akari, *s04-034*  
 Hayashi, Akitoshi, *s03-029*  
 Hayashi, Mio, (*Tue s10*)15:20  
 Hayashi, Tomoaki, (*Mon s04*)09:50,  
*s04-048*  
 Hazra, Susanta, *s12-019*  
 He, Jieqing, (*Thu s03*)15:20  
 He, Juan, *s02-012*  
 He, Ping, *s03-023*  
 He, Ronghuan, *s04-013*  
 He, Wenyan, (*Fri s14*)09:30  
 He, Xiangnan, *s04-014*  
 He, Xin, (*Tue s03*)17:40  
 He, Zhengda, *s04-052*  
 Hector, Andrew, (*Thu s03*)15:20,  
 (*Fri s07*)09:50  
 Hedenstedt, Kristoffer, *s09-019*  
 Hederstedt, Lars, *s02-028*  
 Hedhili, Mohamed, *s05-035*  
 Heim, Matthias, (*Tue s16*)10:10  
 Heiz, Ueli, *s14-019*  
 Heiz, Ulrich, *s09-002*  
 Hermida Merino, Daniel, (*Thu s03*)15:40  
 Hernández-Ibañez, Naiara, (*Thu s18*)15:00  
 Herold, Sebastian, (*Mon s16*)10:10  
 Herrada, Rosa, (*Fri s09*)11:30  
 Herrero, Enrique, (*Tue s12*)09:30,  
 (*Thu s09*)17:20, *s09-060*, *s12-015*  
 Herring, Stephen, (*Fri s04*)10:30  
 Herrmann-Geppert, Iris, (*Mon s06*)18:00  
 Hess, Euodia, (*Tue s10*)17:00  
 Hickey, David, (*Mon s02*)14:20,  
 (*Mon s02*)15:20  
 Higuchi, Eiji, (*Mon s05*)15:40  
 Higuchi, Tohru, *s04-062*  
 Hillman, Robert, (*Mon s05*)16:00,  
 (*Mon s12*)18:00, *s18-023*  
 Hinks, Jamie, (*Mon s02*)17:20  
 Hirai, Takahiro, *s09-020*  
 Hiratoko, Tatsuya, (*Fri s09*)10:10  
 Hirayama, Tsukasa, *s18-028*  
 Hirono, Shigeru, (*Tue s01*)14:00  
 Hirota, Kazuo, (*Tue s10*)15:20  
 Hitrik, Maria, (*Fri s01*)09:50  
 Hjorth, Ida, (*Thu s09*)10:30  
 Hlongwa, Ntuthuko, (*Mon s05*)10:30  
 Ho, C. Y., *s14-018*, *s18-038*  
 Ho, Ching-Kit, *s03-050*  
 Ho, Hsin-Chia, *s04-061*  
 Ho, Kuo-Chuan, (*Tue s06*)10:30,  
 (*Tue s02*)17:50, (*Thu s01*)14:40,  
 (*Thu s18*)16:00, (*Thu s09*)16:40,  
*s06-002*, *s06-004*, *s06-006*, *s09-016*,  
*s09-022*, *s09-043*, *s10-005*, *s10-029*,  
*s11-009*, *s14-015*, *s18-037*  
 Ho, Tsung-Yeh, *s06-014*  
 Hodnik, Nejc, (*Mon s17*)14:00  
 Hoffmannova, Hana, (*Fri s09*)10:10  
 Holdcroft, Steven, (*Mon s04*)15:00,  
*s04-003*  
 Holub, Karel, *s12-018*  
 Holzinger, Angelika, (*Thu s01*)15:00  
 Holzinger, Michael, (*Thu s14*)15:40  
 Homma, Takayuki, (*Tue s10*)16:40  
 Hong, Bang-De, *s02-013*  
 Hong, Hui-Yu, *s03-025*  
 Hong, Min Young, *s03-024*  
 Hong, Misun, (*Mon s17*)17:00  
 Hong, Sung Hoon, *s09-023*, *s09-029*  
 Hong, Wenjing, (*Fri s11*)09:30  
 Hong, Wesley T., (*Mon s12*)14:40  
 Hong, Yu-Hao, (*Mon s17*)09:30  
 Honma, Itaru, *s03-128*, *s07-026*, *s12-016*  
 Horiguchi, Genki, *s04-044*  
 Horne, Mike, (*Thu s07*)14:40  
 Horsley, John, (*Thu s11*)17:20, *s11-006*  
 Hoshi, Yoshinao, *s02-007*, *s07-001*,  
*s09-057*  
 Hoshino, Katsuyoshi, *s07-029*  
 Hoshino, Tsuyoshi, (*Mon s10*)10:30  
 Hosseiny, Schwan, *s09-038*  
 Hou, Kung Hsu, *s07-010*, *s07-023*  
 Hou, Mengyan, *s03-092*  
 Hou, Shang-Chieh, *s03-026*  
 Hovington, P., (*Thu s03*)14:00  
 Hrbac, Jan, *s01-007*  
 Hsi, Chi-Shiung, *s04-056*  
 Hsieh, Chien-Te, *s09-059*  
 Hsieh, Meng-Shan, *s09-012*  
 Hsieh, Wei, (*Thu s05*)14:20  
 Hsieh, Yi-Ting, *s17-004*  
 Hsu, Chia-Yun, *s07-030*  
 Hsu, Chih-I., *s07-010*  
 Hsu, Chun-Tsung, *s17-002*  
 Hsu, Hsin-Cheng, (*Thu s09*)09:30  
 Hsu, Ning-Yih, *s09-063*  
 Hsu, Wen-Dung, *s03-123*  
 Hsu, Yao-Wei, *s16-001*  
 Hsu, Yuan-Hao, *s02-034*  
 Hsu, Yung-Jung, (*Thu s07*)15:00  
 Hsueh, Chang-Jung, (*Wed s07*)10:10  
 Hsueh, Jen-Hao, *s09-059*  
 Hsueh, Tien-Hsiang, *s03-027*  
 Hu, Chenguo, *s10-027*  
 Hu, Chi-Chang, (*Thu s07*)15:00,  
 (*Thu s05*)16:40, *s05-018*  
 Hu, Chih-Wei, *s03-013*  
 Hu, Jin-Song, (*Mon s04*)14:40  
 Hu, Jingsi, *s08-013*  
 Hu, Xiaoyan, *s03-113*  
 Hu, Yingyuan, *s07-019*  
 Huang, Cancan, (*Fri s11*)09:30, *s11-007*  
 Huang, Chen-Jui, *s03-025*  
 Huang, Guolong, *s10-025*  
 Huang, Hao, *s18-015*  
 Huang, Hsiao-Chun, *s04-035*  
 Huang, Hsin-Chieh, (*Thu s05*)14:20,  
*s05-004*  
 Huang, Hsin-Chih, (*Mon s04*)14:20,  
 (*Thu s09*)09:30, (*Fri s09*)12:10,  
*s09-072*  
 Huang, Huin-Ning, *s09-021*  
 Huang, I-Wen, (*Tue s08*)17:00, *s08-002*  
 Huang, Jow-Lay, *s03-026*  
 Huang, Jun, (*Mon s03*)18:20  
 Huang, Ling, *s03-028*, *s03-048*  
 Huang, Long, (*Mon s17*)10:10  
 Huang, Meiqi, *s03-029*  
 Huang, Peihua, (*Mon s05*)15:20,  
 (*Mon s05*)17:40, (*Thu s05*)15:00  
 Huang, Po-Ling, *s05-017*  
 Huang, Sheng-Chao, *s12-009*  
 Huang, Sheng-Wei, *s04-010*  
 Huang, Shih-Han, *s02-014*  
 Huang, T. Y., (*Tue s05*)14:40  
 Huang, Teng-Xiang, *s12-009*  
 Huang, Trav, *s01-005*  
 Huang, Xiao, *s03-114*, *s11-013*  
 Huang, Xuejie, (*Mon s03*)14:40  
 Huang, Yi-Fan, (*Mon s17*)09:50  
 Huang, Yi-June, (*Tue s06*)10:30, *s06-004*,  
*s09-016*, *s09-022*  
 Huang, Yue, *s01-022*  
 Huang, Zheng-Chang, *s06-003*  
 Huang, Zhigao, *s01-018*, *s18-018*  
 Huangfu, Haixin, (*Mon s09*)14:20  
 Hubin, Annick, (*Tue s09*)15:00,  
 (*Tue s10*)18:00, (*Thu s07*)14:00,  
 (*Fri s04*)11:10, *s07-017*, *s09-017*,  
*s10-004*  
 Huff, Laura A., (*Tue s03*)15:20  
 Hui, Jingshu, (*Thu s14*)15:20, *s03-127*  
 Hui, Zhao, *s04-055*  
 Hung, I-Ming, *s04-056*  
 Hung, Mao-Chun, *s07-002*  
 Huo, Zhaohui, *s11-002*  
 Hur, Jin-Mok, (*Fri s18*)11:10  
 Husch, Tamara, (*Wed s05*)10:10  
 Hwang, Bing-Joe, (*Mon s12*)16:00,  
 (*Tue s08*)18:20, *s03-025*, *s03-039*,  
*s04-035*, *s06-008*, *s09-043*, *s09-056*,  
*s10-022*, *s12-006*, *s17-003*, *s18-001*  
 Hwang, Eunkyong, *s09-023*, *s09-029*  
 Hwang, Gyeong S., (*Fri s14*)11:10  
 Hwang, Hyo Ki, *s03-115*  
 Hwang, Ing-Shouh, *s12-023*  
 Hwang, Min Ji, *s03-018*  
 Hwang, RyeoYun, *s01-006*  
 Hwang, Seung Sik, (*Fri s03*)12:10  
 Hwang, Sooyeon, *s03-097*  
 Hy, Sunny, (*Mon s12*)16:00,  
 Hyun, Suyeon, *s09-024*  
**I**  
 Ibrahim, Asmaa, (*Thu s01*)15:20  
 Ida, Hiroki, (*Wed s02*)09:30, *s02-008*  
 Ida, Shoma, *s03-099*  
 Igaki, Yuki, *s02-015*  
 Inuma, Hiroki, (*Tue s03*)18:20  
 Ikeda, Katsuyoshi, (*Mon s12*)17:20,  
 (*Tue s12*)18:20, *s12-020*  
 Ikeda, Sou, *s04-057*, *s04-057*  
 Ikeyama, Haruya, (*Tue s08*)17:40  
 Ikeyama, Misako, *s04-002*  
 Ikezawa, Atsunori, (*Mon s09*)16:40  
 Ikpo, Chinwe, (*Mon s05*)10:30  
 Ikuhara, Yuichi, *s18-028*  
 Im, Changbin, *s15-006*  
 Im, Hun Suk, (*Fri s18*)11:10  
 Imae, Toyoko, *s05-009*  
 Imai, Hideto, (*Mon s04*)09:50  
 Imai, Kenta, (*Fri s14*)10:10  
 Imanishi, Akihito, *s14-011*  
 Imanishi, Yosuke, *s10-011*  
 Imaaya, Hiroshi, (*Tue s01*)14:00  
 Inaba, Masanori, (*Thu s04*)14:00  
 Inaba, Minoru, (*Mon s03*)10:10, *s04-037*

- Inagi, Shinsuke, (*Fri s11*)09:50  
 Iniesta, Jesus, (*Tue s10*)10:30,  
 (*Thu s18*)15:00, (*Thu s18*)16:40  
 Innocenti, Massimo, (*Mon s09*)17:40,  
*s07-032*  
 Inokuma, Kiyoshi, *s12-003*  
 Inoue, Hiroshi, (*Mon s05*)15:40  
 Inoue, Satoru, *s03-041*  
 Inukai, Junji, *s04-016*  
 Ioannou, Irina, (*Tue s08*)15:20  
 Ioroi, Tsutomu, *s04-039, s11-001*  
 Irie, Haruyasu, *s14-011*  
 Iriyama, Yasutoshi, *s03-031, s03-037*  
 Irvine, John T.S., (*Fri s04*)09:50  
 Ishige, Yu, *s02-022*  
 Ishihara, Akimitsu, (*Mon s04*)09:30,  
 (*Mon s04*)09:50, *s04-033, s04-045,*  
*s04-048*  
 Ishikawa, Hiroaki, (*Thu s03*)17:00  
 Ishikawa, Masashi, (*Thu s05*)14:40,  
 (*Fri s03*)11:10, *s03-065, s03-084*  
 Ishikawa, Yoshifusa, *s07-008*  
 Ishimura, Yukiko, *s09-025*  
 Ishita, I., *s10-018*  
 Isidoro, Roberta Alvarenga,  
 (*Mon s04*)18:00  
 Isoai, Shunsuke, *s02-025*  
 Isoda, Ayano, *s04-050*  
 Istakova, Olga I., (*Thu s14*)18:00, *s14-004*  
 Itagaki, Masayuki, *s02-007, s07-001,*  
*s09-057*  
 Itagaki, Naho, (*Mon s06*)14:20  
 Itaya, Kingo, *s12-002*  
 Ito, Yuya, *s07-020*  
 Itoh, Shinobu, *s11-001*  
 Itoh, Takashi, (*Tue s12*)10:30  
 Iurlo, Matteo, *s02-001*  
 Ivanshenko, Oleksii, (*Mon s16*)14:00  
 Iwama, Etsuro, (*Tue s05*)14:00, *s05-016,*  
*s05-040, s05-041*  
 Iwan, Michalina, (*Fri s14*)10:30  
 Iwanaga, Atsushi, *s07-014*  
 Iwasaki, Satoshi, *s09-044*  
 Iwasaki, Shinya, *s03-031*  
 Iwasawa, Kenta, *s03-079*  
 Iwuoha, Emmanuel, (*Mon s05*)10:30,  
 (*Tue s09*)10:10, (*Tue s10*)17:00,  
 (*Wed s01*)10:10, (*Fri s09*)11:10,  
*s09-058, s09-065*  
 Izumi, Takuma, (*Thu s05*)15:40
- J**  
 Jönsson, Pär, (*Fri s04*)11:30, *s04-054*  
 Jaciauskiene, Jane, *s09-047*  
 Jacklin, Rebecca, (*Tue s08*)14:40  
 Jacob, Timo, (*Fri s09*)10:10  
 Jacobs, Robert, *s01-019*  
 Jäckel, Nicolas, *s17-006*  
 Jänes, Alar, (*Thu s05*)15:20, *s05-013*  
 Jafari, Abbas Ali, (*Fri s09*)11:50, *s09-018*  
 Jagminiene, Aldona, *s09-058*  
 Jambrec, Daliborka, (*Tue s02*)16:50,  
 (*Tue s02*)17:00  
 Jamroz, Michal, (*Mon s16*)09:50  
 Jan, Der-Jun, *s03-027, s10-029, s18-037*  
 Janas, Dawid, *s14-001*  
 Jang, Bo yun, *s03-118*  
 Jang, Eun-Hye, *s18-016, s18-033*  
 Jang, Hansaem, (*Tue s15*)18:00  
 Jang, Jason Shian-Ching, *s04-056*  
 Jang, Jer-Huan, *s03-093*  
 Jankowski, G. P., (*Fri s03*)11:10  
 Jaouen, Frederic, (*Tue s05*)15:40  
 Jaouen, Gerard, (*Thu s11*)15:20  
 Jarosz, Tomasz, *s16-006*  
 Jeanbourquin, Xavier, (*Mon s06*)17:20  
 Jebaraj, Adriel, (*Mon s09*)18:00  
 Jedraszko, Justyna, *s18-040*  
 Jeon, Woo Sung, (*Mon s03*)15:40  
 Jeong, Hwakyung, *s09-026, s09-027*  
 Jeong, Jaehyang, *s03-100*  
 Jeong, Jooyoun, *s14-007*  
 Jeong, Jun-Hui, (*Tue s05*)18:20  
 Jeong, Nam-Jo, *s10-012*  
 Jeong, Sangsik, (*Tue s03*)17:00  
 Jeong, Ye-Jin, *s10-012*  
 Jeong, Yongsoo, *s18-035*  
 Jeschull, Fabian, (*Tue s03*)16:00,  
 (*Wed s03*)09:50, *s03-030*  
 Jeuken, Lars, (*Mon s16*)16:00  
 Jezowski, Pawel, (*Tue s05*)16:00, *s05-005*  
 Jhan, Jia-Lin, *s08-003, s18-024*  
 Jheng, Yuan-Ruei, *s03-027*  
 Ji, Xubo, *s02-033*  
 Jia, Haiping, *s03-071*  
 Jia, Yanyan, (*Fri s09*)10:30, *s09-080*  
 Jia, Zhe, (*Thu s03*)14:00  
 Jian, Shun-Yi, *s08-012*  
 Jian, Xuan, *s04-036, s18-017*  
 Jiang, Dechen, (*Tue s02*)09:30  
 Jiang, Jia-Rong, *s03-093*  
 Jiang, Kun, (*Mon s12*)10:30,  
 (*Fri s09*)11:10  
 Jiang, Qiu, *s05-022*  
 Jiang, Yan-Xia, (*Tue s09*)10:30,  
 (*Tue s02*)18:10  
 Jiang, Yaqi, (*Fri s09*)10:30, *s09-080*  
 Jin, Chengjun, (*Fri s07*)10:10  
 Jin, Ling, (*Fri s11*)11:30  
 Jin, Misako, (*Thu s08*)09:30  
 Jin, Xi, (*Tue s12*)10:10  
 Jin, You-hai, *s18-012*  
 Jinnouchi, Ryosuke, (*Mon s12*)15:00,  
 (*Tue s09*)17:00  
 Jo, Hyuntak, *s03-115*  
 Jo, Jeongeun, *s14-014*  
 Johansson, Erik, (*Mon s06*)15:20  
 Johansson, Patrik, *s03-007, s15-002*  
 Johnson, Ian, *s03-061*  
 Joi, Aniruddha, *s07-030, s09-047*  
 Jokinen, Miikka, (*Thu s18*)18:00  
 Joniec, Aleksandra, (*Mon s16*)15:20  
 Jonsson Niedziolka, Martin,  
 (*Mon s16*)17:40  
 Joo, Jong Hoon, *s10-028*  
 Josefik, Frantisek, (*Thu s11*)18:00  
 Joseph Paul, Baboo, *s14-014*  
 Jossen, Andreas, (*Thu s03*)15:00  
 Josypcuk, Bohdan, *s02-016*  
 Josypcuk, Oksana, *s02-016, s12-018*  
 Jouanneau Si Larbi, Séverine, *s03-078*  
 Jouini, Mohamed, (*Mon s06*)15:20  
 Jow, T. Richard, (*Fri s03*)09:30  
 Ju, Huangxian, *s01-003*  
 Ju, Wen, (*Thu s09*)10:10  
 Ju, Wenbo, *s09-002, s14-019*  
 Juang, Yung-Der, *s03-012*  
 Judd, Evan, (*Mon s02*)14:00  
 Juhaniewicz, Joanna, (*Mon s16*)09:50  
 Julien, C. M., (*Thu s03*)14:00  
 Jung, Changhoon, (*Mon s03*)15:40  
 Jung, Hyojin, *s03-024*  
 Jung, Jiwon, *s03-121*  
 Jurng, Sunhyung, *s03-030*  
 Jurzinsky, Tilman, (*Thu s04*)15:00  
 Jørgensen, Peter Stanley, (*Fri s04*)10:10
- K**  
 Kätelhön, Enno, (*Mon s16*)17:20  
 Kaghazchi, Payam, (*Tue s12*)16:40,  
 (*Tue s15*)17:20  
 Kajiyama, Satoshi, (*Tue s03*)18:20  
 Takeya, Tadashi, *s03-002*  
 Kakiuchi, Takashi, (*Thu s18*)09:50  
 Kalita, M., (*Fri s03*)11:10  
 Kalkan, Sabri, (*Tue s10*)14:00  
 Kamahori, Masao, *s02-022*  
 Kamai, Ryo, (*Tue s09*)14:20  
 Kamata, Tomoyuki, (*Tue s01*)14:00  
 Kamiya, Kazuhide, (*Mon s09*)14:40  
 Kamiyama, Takashi, *s18-028*  
 Kamo, Yoichi, (*Mon s06*)18:20  
 Kaneko, Shingo, *s03-116*  
 Kang, Joonhee, *s14-008*  
 Kang, Kil Ku, *s03-115*  
 Kang, Kisuk, (*Thu s03*)14:40  
 Kang, Liping, *s05-029*  
 Kang, Long, *s03-038, s05-023*  
 Kang, Moon-Sung, *s04-022, s04-024,*  
*s06-015, s18-016, s18-033, s18-034*  
 Kang, Wenpei, (*Thu s03*)15:20  
 Kang, Yuu, (*Wed s07*)10:30  
 Kannan, Palanisamy, (*Mon s16*)17:40  
 Kano, Kenji, *s02-030*  
 Kanoufi, Frederic, (*Wed s08*)09:30  
 Kao, Hsien-Ming, *s18-026, s18-027*  
 Kao, Sheng-Yuan, *s11-009, s14-015*  
 Karaskiewicz, Maciej, (*Mon s02*)17:40  
 Kari, T. M. Aufar, (*Tue s06*)10:10  
 Karlsson, Christoffer, *s18-015*  
 Karmakar, Anirban, *s12-019*  
 Karuppiiah, Chelladurai, (*Tue s02*)14:40  
 Kasnatscheew, Johannes, (*Thu s08*)15  
 Kasper, Michael, *s12-014*  
 Kaszkur, Zbigniew, (*Mon s16*)17:40  
 Katakura, Katsumi, *s04-037, s04-058*  
 Kato, Dai, (*Tue s01*)14:00  
 Kato, Daiki, (*Tue s01*)14:00  
 Kato, Masaru, *s04-038, s12-003*  
 Kato, Ryoko, (*Mon s06*)18:20  
 Kato, Takehisa, *s03-031*  
 Katsounaros, Ioannis, (*Tue s12*)09:50  
 Kavan, Ladislav, (*Mon s06*)15:00,  
 (*Mon s06*)16:00, (*Mon s06*)16:40  
 Kawaguchi, Kenji, (*Mon s10*)18:20,  
*s03-005, s09-025, s09-032, s09-061,*  
*s10-012, s10-021, s10-026*  
 Kawakami, Nozomi, *s04-037*  
 Kawamura, Kinya, *s04-062*  
 Kawamura, Sho, *s07-003*  
 Kawde, Abdel-Nasser, *s09-028*  
 Kaymaksiz, Serife, (*Wed s05*)10:30  
 Kayran, Yasin Ugur, (*Tue s02*)17:00  
 Kazda, Tomáš, *s03-032*  
 Kazimierzczak, Honorata,  
*s07-004(Fri s07)11:50*  
 Kazuhide, Kamiya, (*Tue s09*)14:20  
 Keech, Peter, (*Tue s08*)14:40, *s07-015*

- Keller, Jurg, (*Mon s10*)16:00,  
(*Mon s10*)17:40, *s10-006*  
Kelsall, Geoff, (*Tue s10*)09:30  
Keskin, Ertugrul, *s01-021*  
Ketpang, Kriangsak, (*Thu s04*)18:00  
Khalaghi, Babak, *s10-013*  
Khan, Asim, *s01-028*  
Khayrullina, Dinara K., *s14-004*  
Khoshro, Hossein, (*Fri s09*)11:50, *s09-018*  
Khranov, Andrey, *s12-028*  
Kijima, Masahiko, *s18-025*  
Kil, Donghyun, *s03-117*  
Kilic, Hasan, (*Tue s07*)10:30  
Kilmonis, Teofilus, *s09-058*  
Kim, Bongkyu, (*Tue s02*)17:30  
Kim, Chan-Soo, *s10-012*  
Kim, Do-Hyeong, *s18-016*, *s18-033*,  
*s18-034*  
Kim, Dong-Wan, *s03-034*  
Kim, Dongyun, *s14-014*  
Kim, Doo Hun, *s03-045*  
Kim, Duri, *s03-036*  
Kim, Eun Joong, *s02-008*  
Kim, Gha-Young, *s18-032*  
Kim, Guk-Tae, *s03-060*  
Kim, Han-Joo, (*Tue s05*)17:20  
Kim, Hansung, *s03-117*, *s03-125*, *s09-035*  
Kim, Hong-Ki, *s05-019*  
Kim, Hoyoung, *s09-023*, *s09-029*  
Kim, Hye-Rin, *s06-015*  
Kim, Hyun-Kyung, (*Tue s05*)09:30,  
(*Tue s03*)18:00, (*Tue s05*)18:20,  
*s03-076*  
Kim, Hyun-seung, *s03-030*  
Kim, Hyungjun, (*Tue s15*)18:20, *s15-003*  
Kim, Hyungsub, *s03-070*  
Kim, Ick-Jun, *s05-006*  
Kim, In-Tae, *s05-037*  
Kim, Jin Hyeon, *s05-024*  
Kim, Jin Yeong, *s09-029*  
Kim, Jin Yeung, *s09-023*  
Kim, Jisu, (*Tue s02*)17:30  
Kim, Jong-Hoon, *s10-014*  
Kim, Jong-Huy, (*Tue s05*)18:00  
Kim, Jong-Nam, *s10-028*  
Kim, Jongjung, *s03-035*, *s03-044*  
Kim, Joon soo, *s03-118*  
Kim, Joosun, *s03-034*, *s09-031*  
Kim, Kihong, (*Mon s03*)15:40  
Kim, Kwang-Bum, (*Tue s05*)09:30  
Kim, Min-Su, (*Tue s08*)17:20  
Kim, Minjin, (*Wed s04*)09:50, *s04-009*  
Kim, Myeong-Seong, (*Tue s05*)09:30,  
(*Tue s03*)18:00, *s03-076*  
Kim, Nam Seon, *s03-033*  
Kim, Nayoung, *s04-017*  
Kim, Seokhun, *s14-014*  
Kim, Seongbeen, *s14-007*  
Kim, Seulki, *s09-030*  
Kim, Seung-Gon, (*Wed s04*)09:50  
Kim, Shokaku, (*Thu s11*)16:40  
Kim, Si-Hyung, *s18-032*  
Kim, Soo Jung, *s03-033*  
Kim, Soo-Kil, *s09-023*, *s09-029*  
Kim, Sung-Soo, *s03-124*  
Kim, Sung-Wook, (*Fri s18*)11:10  
Kim, Sungjin, *s14-014*  
Kim, Yong-Il, (*Tue s05*)18:00  
Kim, Yu-Jin, *s18-016*, *s18-034*  
Kimijima, Ken'ichi, *s12-003*  
Kimura, Shuhei, *s09-032*  
Kimura, Taro, *s04-016*  
Kimura, Toshio, *s03-037*  
Kinloch, Ian A., (*Tue s12*)18:00  
Kinumoto, Taro, *s04-002*, *s09-015*  
Kirankumar, Rajendranath, *s14-002*  
Kirchhöfer, Marija, *s03-069*,  
(*Tue s03*)17:20  
Kisieliu, Gilius, *s09-058*  
Kisu, Kazuaki, *s05-041*  
Kitada, Atsushi, (*Wed s07*)10:30, *s07-016*,  
*s07-025*  
Kitada, Koji, *s03-099*  
Kitada, Yuta, *s12-016*  
Kitagawa, Yuichi, (*Tue s08*)14:20,  
(*Tue s08*)17:40, (*Thu s08*)09:30  
Kitaguchi, Yuya, *s04-058*  
Kitahara, Tatsumi, *s04-057*  
Kitano, Naoki, (*Mon s12*)15:00  
Kitayama, Sawaka, *s04-002*  
Kitazumi, Yuki, *s02-030*  
Kjaergaard, Christian, (*Mon s02*)17:00  
Klassen, Thomas, (*Mon s06*)18:00  
Kleiminger, Lisa, (*Tue s10*)09:30  
Klementova, Mariana, *s12-024*  
Klink, Stefan, *s09-005*  
Kloepsch, Richard, *s03-119*  
Knittel, Peter, (*Thu s01*)15:00  
Knotek, Petr, *s12-024*  
Ko, Hsien-Chen, *s12-023*  
Kobayashi, Masahiro, *s18-025*  
Kobayashi, Masaki, *s04-062*  
Kobayashi, Shunsuke, *s18-028*  
Kobayashi, Takanori, *s04-037*  
Koca, Atif, (*Fri s09*)09:50, *s09-035*  
Koch, Reinhold, (*Thu s03*)15:00  
Koch, Stephan, (*Tue s03*)17:20, *s03-069*  
Kocha, Shyam, *s04-042*  
Kodama, Kensaku, (*Mon s12*)15:00,  
(*Tue s09*)17:00  
Koefoed, Line, (*Thu s14*)17:20  
Körbahti, Bahadır K., (*Mon s10*)15:20,  
(*Tue s10*)14:00  
Koga, Kazunori, (*Mon s06*)14:20  
Kohno, Yuji, (*Mon s04*)09:50,  
(*Thu s09*)14:40, *s04-033*, *s04-045*,  
*s04-048*, *s09-006*, *s09-045*, *s09-070*  
Koike-Takeshita, Ayumi, *s16-007*  
Koiwa, Ichiro, *s07-003*, *s07-020*, *s07-021*  
Kokoh, Kouakou Boniface,  
(*Mon s04*)18:00  
Kollender, Jan Philipp, *s12-004*  
Kolodziej, Adam, (*Mon s05*)14:40  
Komatsu, Daiki, *s03-128*  
Komatsu, Hideyuki, *s03-099*, *s17-007*,  
*s18-028*  
Konarov, Aishuak, (*Tue s03*)15:00  
Konarzewska, Dorota, (*Mon s16*)09:50  
Konda, Suresh, *s18-020*  
Kondo, Kazuo, (*Thu s07*)09:50  
Kondo, Takeshi, (*Tue s10*)15:20  
Kondov, Ivan, (*Tue s15*)10:30, *s17-001*  
Konev, Dmitry V., (*Thu s14*)18:00, *s14-004*  
Kong, Lingbin, *s03-038*, *s05-023*  
Konishi, Kentaro, (*Mon s05*)15:40  
Kontturi, Kyösti, (*Thu s18*)18:00  
Koo, Boram, *s03-101*  
Koo, Jeong Boon, *s03-118*  
Koper, Marc T.M., (*Mon s17*)09:50,  
(*Mon s12*)15:40, (*Tue s12*)09:50,  
(*Thu s09*)16:00, *s12-013*  
Korchev, Yuri, (*Thu s01*)14:20  
Korte, Carsten, (*Mon s03*)17:40  
Korth, Martin, (*Wed s05*)10:10  
Kortlever, Ruud, (*Thu s09*)16:00  
Korzhybayeva, Kuralay, (*Tue s03*)14:20  
Kosaka, Shinpei, *s09-053*  
Koshikawa, Hiroyuki, (*Mon s09*)14:40  
Kostecki, Robert, *s03-102*  
Kosydar, Robert, *s04-047*  
Kotake, Shota, *s04-057*  
Kotani, Akira, *s01-004*  
Koto, Takeharu, *s18-028*  
Kou, Chuang, *s05-038*  
Kouda, Nobuo, *s05-037*  
Kowalczyk, Agnieszka, *s02-031*  
Kowalski, Damian, (*Fri s07*)11:10  
Koyama, Yukinori, *s03-022*, *s03-099*,  
*s03-104*  
Koziol, Krzysztof, *s14-001*  
Kraemer, Elisabeth, (*Thu*)08:15  
Kramer, Denis, (*Mon s09*)14:00  
Kranz, Christine, (*Tue s02*)10:10,  
(*Thu s01*)15:00, (*Fri s01*)10:10  
Krasnikov, Dmitriy, (*Thu s04*)15:40  
Kraus, Shlomit, (*Fri s01*)09:50  
Krbal, Milos, *s06-016*, *s12-024*  
Krewer, Ulrike, (*Mon s17*)10:30,  
(*Wed s03*)09:30, (*Wed s03*)10:30  
Kriegel, Herman, (*Mon s06*)18:00  
Krischer, Katharina, (*Tue s12*)14:40  
Kristianto, Hans, *s03-004*  
Krtil, Petr, (*Fri s09*)10:10  
Krueger, Steffen, (*Thu*)08:15  
Krukiewicz, Katarzyna, *s14-001*, *s16-006*  
Kruszewski, Marcin, (*Tue s16*)09:50  
Krysinski, Pawel, (*Mon s16*)15:20  
Krysova, Hana, (*Mon s06*)16:00  
Krzak, Agata, (*Tue s16*)09:50  
Ku, H. H., *s14-018*, *s18-038*  
Ku, Jun-Hwang, (*Fri s03*)12:10  
Kučera, Jan, *s18-011*  
Kubannek, Fabian, (*Mon s17*)10:30  
Kubešová, Marie, *s18-011*  
Kucernak, Anthony, (*Thu s04*)10:30,  
*s09-033*  
Kudo, Kenji, (*Mon s12*)15:00  
Kuhn, Alexander, (*Tue s16*)10:10,  
(*Thu s14*)17:20  
Kulesza, Pawel J., (*Tue s09*)18:20,  
(*Thu s14*)09:50, *s04-047*  
Kulkarni, Mahesh P., (*Mon s04*)15:00  
Kullgren, Jolla, (*Mon s06*)16:40  
Kumamoto, Kousuke, *s09-034*  
Kumaraguru, Swami, (*Tue s04*)09:30  
Kumigashira, Hiroshi, *s04-062*  
Kung, Chung-Wei, (*Tue s02*)17:50,  
*s11-009*, *s14-015*  
Kunimoto, Masahiro, (*Tue s10*)16:40  
Kunitake, Masashi, (*Tue s01*)14:00,  
(*Wed s10*)09:50  
Kuo, Chao-Yen, *s03-025*, *s03-039*, *s03-108*  
Kuo, Liang-Yin, *s03-040*  
Kuraya, Eisuke, (*Tue s01*)14:00  
Kurbatov, Andrey, *s03-103*  
Kure-Chu, Song-Zhu, *s03-041*, *s07-022*  
Kurig, Heisi, (*Thu s05*)15:20

Kurmanbayeva, Indira, (*Tue s03*)14:20  
 Kurosu, Hiromichi, *s02-002*  
 Kurowicka, Ewelina, (*Tue s16*)09:50  
 Kurra, Narendra, *s05-022*  
 Kusatsu, Masatoshi, (*Thu s03*)14:40  
 Kusu, Fumiyo, *s01-004*  
 Kutner, Wlodzimierz, *s12-005*  
 Kuttiyiel, Kurian, (*Mon s09*)15:00,  
*s09-061*  
 Kuwabata, Susumu, *s14-011*  
 Kuwano, Jun, *s18-025*  
 Kuznetsov, Aleksey, (*Thu s04*)15:40  
 Kuznetsov, Vladimir, (*Thu s04*)15:40  
 Kvapilova, Hana, (*Thu s11*)18:00  
 Kwon, Eunseok, *s09-031*  
 Kwon, Seung-Ryong, *s18-013*  
 Kwon, Yongchai, *s14-007*  
 Kwon, Youngkook, (*Thu s09*)16:00

## L

- La Mantia, Fabio, (*Tue s03*)10:10,  
 (*Tue s02*)16:50  
 Labbe, Eric, (*Thu s11*)15:20  
 Lacaze-Dufaure, Corinne, (*Tue s08*)16:40  
 Lacey, Matthew, (*Tue s03*)16:00,  
 (*Tue s15*)16:40, (*Wed s03*)09:50,  
*s03-030, s03-042*  
 Lagacé, M., (*Thu s03*)14:00  
 Lagarde, Matthieu, (*Tue s08*)15:00  
 Lai, Chao-Sung, *s18-001*  
 Lai, Chen-Hsuan, *s03-043*  
 Lai, Jianping, (*Fri s14*)09:50  
 Lai, Pei-Yu, (*Tue s08*)18:20  
 Lai, Yeh-Hung, (*Mon s04*)17:00  
 Lair, Virginie, *s01-008*  
 Lakshmanan, Balsu, (*Tue s04*)09:30  
 Landau, Ehud M., (*Tue s16*)09:30  
 Landau, Uziel, (*Wed s07*)10:10  
 Landry, Pauline, (*Tue s02*)15:20  
 Lang, Heinrich, *s11-003*  
 Lang, Jianqiao, *s02-026*  
 Lanza, M.V., *s10-015*  
 Lanza, Marcos R.V., *s10-018*  
 Lapeyre, Veronique, (*Tue s16*)10:10  
 Launay, Jérôme, (*Tue s15*)10:10  
 Lauro, Federico, (*Mon s02*)17:20  
 Le Bideau, Jean, (*Mon s05*)15:20,  
 (*Wed s05*)09:30  
 Le Formal, Florian, (*Mon s06*)17:00  
 Le Goff, Alan, (*Tue s02*)17:10  
 Le Mest, Yves, (*Thu s18*)09:30  
 Le Poul, Nicolas, (*Thu s18*)09:30  
 Lechner, David, (*Thu s07*)09:30  
 Lee, Chan Kyu, *s03-069*  
 Lee, Changhyun, *s09-030*  
 Lee, Cheng-Yao, *s03-126*  
 Lee, Chi-Shen, *s09-051*  
 Lee, Chien-Liang, *s02-013, s09-012,*  
*s09-067*  
 Lee, Chuan-Pei, (*Tue s06*)10:30,  
 (*Thu s09*)16:40, *s06-002, s06-004,*  
*06-006, s09-016, s09-022, s09-043,*  
*s10-005*  
 Lee, Chun-Ting, *s09-022*  
 Lee, Dong Wook, *s09-035*  
 Lee, Dong-Hoon, *s04-017*  
 Lee, Dongil, (*Thu s11*)14:40  
 Lee, Eun-Su, *s04-017*  
 Lee, Gwang-Hee, *s03-034*  
 Lee, Ha-Young, *s05-010*  
 Lee, Hsiao-Yen, *s07-002*  
 Lee, Hui Zhi Shirley, (*Thu s11*)15:20  
 Lee, Hwa Jin, *s03-120*  
 Lee, Hye Jin, (*Tue s15*)09:50, *s15-005*  
 Lee, Hyejin, *s04-018*  
 Lee, Hyo Sug, (*Mon s03*)15:40  
 Lee, J.F., (*Tue s05*)14:40  
 Lee, Jae Gil, *s03-030, s03-044, s03-121*  
 Lee, Jae Kwang, *s15-006*  
 Lee, Jaeyoung, (*Tue s15*)18:00, *s09-036,*  
*s15-006*  
 Lee, Jeong Beom, *s03-044, s03-122*  
 Lee, Jeong Eun, *s03-118*  
 Lee, Jeong Hyun, *s05-019*  
 Lee, Jin Seok, *s03-118*  
 Lee, Joong Kee, *s03-003, s03-004*  
 Lee, Jooyul, *s18-035*  
 Lee, Juhan, (*Thu s05*)16:00  
 Lee, Jun-Seob, (*Tue s08*)14:20  
 Lee, Jung-Nam, *s10-014*  
 Lee, Jyh-Fu, *s07-030*  
 Lee, Ming Yuan, *s09-066*  
 Lee, Moo-Seok, *s04-017*  
 Lee, Po-Han, (*Wed s03*)10:10, *s03-106*  
 Lee, R. C., (*Tue s05*)14:40  
 Lee, Seul, *s03-120*  
 Lee, Seung-Hwan, *s05-024*  
 Lee, Seunghwa, (*Tue s15*)18:00, *s09-036*  
 Lee, Seunghwan, *s09-031*  
 Lee, Sheng-Wei, *s04-056*  
 Lee, Shih-Wei, *s04-020*  
 Lee, Sojeong, *s04-019*  
 Lee, Suk-Woo, (*Tue s05*)09:30,  
 (*Tue s05*)18:20  
 Lee, Tae-jin, *s03-044, s03-121*  
 Lee, Won Jae, *s03-045*  
 Lee, Woong Hee, *s09-035*  
 Lee, Yoosok, (*Tue s02*)17:30  
 Lee, You Jin, *s03-018, s03-045*  
 Lee, Yueh-Lien, *s08-012*  
 Lee, Yueh-Lin, (*Mon s12*)14:40  
 Leech, Donal, *s02-028*  
 Lefebvre, Olivier, (*Mon s10*)18:00,  
 (*Tue s10*)15:00, *s10-015*  
 Lei, Gangtie, *s03-046, s03-047*  
 Lei, Wu, (*Tue s09*)17:20  
 Lei, Zhanwu, (*Thu s07*)15:40  
 Lei, Zhibin, *s05-029*  
 Leitner, Klaus, (*Thu s03*)17:20  
 Lemay, Serge, *s11-003, s18-021*  
 Lemercier, Gabriel, (*Tue s15*)10:10  
 Leng, Xue, *s09-040* (*Fri s09*)11:50  
 Leone, Philippe, (*Mon s05*)15:00  
 Leong, Weng Kee, (*Thu s11*)15:20  
 Lepicka, Kamila, *s12-005*  
 Leroux, Yann, (*Thu s18*)09:30, *s14-009*  
 Lesch, Andreas, (*Tue s01*)14:40,  
 (*Tue s02*)16:40, (*Thu s01*)10:30,  
*s09-037*  
 Lethien, Christophe, (*Mon s05*)15:20,  
 (*Mon s05*)17:40  
 Lettenmeier, Philipp, (*Mon s04*)16:40,  
*s09-038*  
 Leung, Man-kit, *s10-029*  
 Levent, Abdulkadir, *s01-017, s01-021,*  
*s18-004, s18-005*  
 Levi, Mikhael D., *s17-006*  
 Levi, Naomi, (*Mon s09*)17:20  
 Lewandowski, Andrzej, (*Tue s03*)15:20  
 Lewis, Scott, *s14-017*  
 Lhenry, Sébastien, (*Thu s18*)09:30  
 Li, Biao, *s03-051*  
 Li, Can, *s03-015*  
 Li, Chao-Yu, (*Tue s12*)10:10, *s12-001*  
 Li, Chi, *s05-017*  
 Li, Chi-Ying Vanessa, *s03-050*  
 Li, Chuan, *s04-056*  
 Li, Chun-Ting, (*Tue s06*)10:30,  
 (*Thu s09*)16:40, *s06-002, s06-004,*  
*s06-006, s09-016, s09-043*  
 Li, Decheng, *s03-116*  
 Li, Fei, *s12-017*  
 Li, Fu-Sheng, (*Thu s03*)09:30  
 Li, Gang, *s03-132, s03-133*  
 Li, Genxi, *s01-022*  
 Li, Hao, *s01-022*  
 Li, Hongjiao, *s14-019*  
 Li, Jia, *s04-007*  
 Li, Jiameng, *s08-013*  
 Li, Jian-Feng, (*Tue s12*)10:10, *s12-001*  
 Li, Jiang, *s02-025*  
 Li, Jianming, (*Fri s07*)11:30  
 Li, Jiaxin, *s01-018*  
 Li, Jie, (*Tue s03*)17:40, *s03-119*  
 Li, Jing, *s05-025*  
 Li, Jing-Mei, (*Tue s05*)15:00  
 Li, Jun Long, *s05-027*  
 Li, Jun-Tao, *s03-048*  
 Li, Li, (*Mon s04*)14:00, (*Thu s03*)10:30,  
*s04-046, s14-005*  
 Li, Long-Ji, (*Mon s16*)10:10,  
 (*Thu s11*)17:40  
 Li, Mao-Hua, *s12-009*  
 Li, Miangang, *s11-008*  
 Li, Rui, *s07-019*  
 Li, Shin-Ming, (*Thu s05*)16:40  
 Li, Shouding, (*Tue s03*)16:40  
 Li, Shuai, *s08-009*  
 Li, Tong, *s08-009*  
 Li, Tongtong, *s01-012*  
 Li, Wangyu, *s03-014*  
 Li, Wei, *s04-046*  
 Li, Weiwei, *s01-022*  
 Li, Wenjun, *s03-047*  
 Li, Wenwen, *s11-014*  
 Li, Xiaogang, *s08-010*  
 Li, Xiaopeng, (*Thu s03*)14:20  
 Li, Ximeng, *s03-049*  
 Li, Yan-Sheng, *s09-062*  
 Li, Yana, *s05-007*  
 Li, Yang, *s03-038, s05-025*  
 Li, Yiju, *s05-036*  
 Li, Yingchun, *s01-010, s02-017*  
 Li, Yingshun, (*Thu s03*)15:20  
 Li, Yixiao, (*Tue s03*)16:40  
 Li, Yue, *s12-001*  
 Li, Zhaohui, *s03-046, s03-047*  
 Li, Zhaoling, *s10-027*  
 Li, Zhe, (*Mon s03*)18:20  
 Lian, Keryn, (*Mon s05*)17:00  
 Liang, Ya-Yi, *s02-018*  
 Liang, Yu-Ting, (*Thu s04*)14:40, *s04-049*  
 Liang, Yunchang, *s14-019*  
 Liang, Zhenhai, *s04-036, s18-017*  
 Liang, Zhuojian, *s03-052*  
 Liao, Chia Wen, *s07-023*  
 Liao, Hung-Yun, (*Fri s01*)10:30  
 Liao, Jing-Ting, *s14-003*

- Liao, Sin-Syu, *s14-003*  
 Liao, Yen-Fa, *s03-013*  
 Liao, Yen-Hua, *s01-001*  
 Liao, Ying-Chih, (*Tue s02*)17:50  
 Liao, Leo Chau-Kuang, *s08-003, s18-024*  
 Lichtenstein, Timothy, *s03-127*  
 Lichusina, Svetlana, (*Thu s09*)17:40, *s09-067*  
 Lie, Ji, (*Thu*)08:15  
 Lim, Hyung-Kyu, (*Tue s15*)18:20, *s15-003*  
 Lim, Koun, (*Mon s02*)14:20  
 Lim, Sung Yul, *s18-013*  
 Limanovskaya, Oksana, *s12-028*  
 Limarta, Susan Olivia, *s03-004*  
 Limmer, David, (*Thu s05*)10:10  
 Limtrakul, Jumras, (*Tue s16*)10:10  
 Lin, Andrew S., *s01-005*  
 Lin, Chao-Sung, *s08-012*  
 Lin, Cheng-Lan, (*Wed s09*)09:50, *s07-024*  
 Lin, Chien-Hong, *s03-039, s03-108, s14-022*  
 Lin, Haibo, *s03-053, s03-138*  
 Lin, Haixin, (*Fri s09*)10:30, *s09-080*  
 Lin, Hong-Jhe, (*Mon s06*)17:40  
 Lin, Hui-Wen, (*Mon s10*)17:40  
 Lin, Jeng-Yu, *s03-105, s03-126, s05-026*  
 Lin, Jian-Long, (*Mon s17*)09:30  
 Lin, Jiang-Jen, *s06-004, s10-005*  
 Lin, Jing-Chie, *s04-056*  
 Lin, Kuan-Jiuh, (*Mon s06*)15:40  
 Lin, Long, (*Wed s10*)10:10, *s10-027*  
 Lin, Lu-Yin, *s05-012, s05-034*  
 Lin, Ming Jie, *s02-019*  
 Lin, Ming-Hsien, *s17-003*  
 Lin, Nan, (*Wed s03*)10:30  
 Lin, Peter, *s07-015*  
 Lin, Shawn D., *s12-006*  
 Lin, Shih-kang, *s03-066, s03-123, s12-027*  
 Lin, Shih-Ming, (*Thu s07*)16:00  
 Lin, Tsung-Wu, *s05-026*  
 Lin, Tzu-En, (*Tue s02*)16:40, (*Thu s01*)10:30  
 Lin, Wei-chih, *s03-066*  
 Lin, Wei-Hao, (*Thu s07*)15:00  
 Lin, Wei-Zhi, *s03-067*  
 Lin, Yan-Gu, (*Mon s06*)17:40  
 Lin, Yi-Sheng, *s07-002*  
 Lin, Yingbin, *s01-018, s18-018*  
 Lin, You-Shiang, *s10-029*  
 Lin, Yu Wei, (*Thu s03*)15:40, *s05-027*  
 Lin, Yu-Chang, (*Mon s06*)17:40  
 Lin, Yung-Chun, (*Tue s02*)18:00  
 Lin, Zheqi, *s03-053, s03-138*  
 Lin, Zi-Jun, *s04-049*  
 Lindgren, Fredrik, (*Fri s03*)12:10  
 Liou, Huei-Ping, *s01-011*  
 Lipkowski, Jacek, (*Mon s02*)17:40  
 Lippert, Thomas, (*Tue s09*)16:40  
 Lisak, Grzegorz, (*Tue s01*)17:00  
 Lisdat, Fred, (*Mon s16*)18:20, *s02-005*  
 Liska, Alan, *s11-010*  
 Liska, Paul, (*Mon s06*)16:00  
 Lisowski, Wojciech, (*Mon s16*)17:40, (*Fri s14*)10:30  
 Little, Marc, *s14-017*  
 Little, R. Daniel, (*Mon s16*)10:10  
 Liu, Aiping, *s14-010*  
 Liu, Bo, *s08-013*  
 Liu, Caihong, *s05-039, s07-013*  
 Liu, Changpeng, (*Wed s09*)10:30  
 Liu, Chu-Chi, (*Thu s07*)10:30  
 Liu, Chunling, *s03-055, s05-007*  
 Liu, Gao, (*Thu s03*)14:00  
 Liu, Haidong, (*Tue s03*)17:40  
 Liu, Haimei, *s03-058*  
 Liu, Han-Lung, *s04-060*  
 Liu, Haodong, (*Tue s03*)17:20  
 Liu, Hsueh-Ming, *s18-026, s18-027*  
 Liu, Jiang, *s01-010, s02-017*  
 Liu, Jianguo, (*Thu s04*)16:40  
 Liu, Jianyun, *s05-008*  
 Liu, Jie, *s01-010, s02-017, s03-048*  
 Liu, Jinbei, *s03-038*  
 Liu, Li, *s08-013*  
 Liu, Maocheng, *s03-038*  
 Liu, Ming, *s14-017*  
 Liu, Shuangyu, (*Fri s03*)10:10, *s03-088*  
 Liu, Shuo, *s14-020*  
 Liu, Sufen, (*Tue s09*)14:40  
 Liu, Tingting, *s03-053, s03-138*  
 Liu, Wei-Ren, *s03-054, s03-056, s03-057*  
 Liu, Xi, *s05-038*  
 Liu, Xian, *s04-036, s18-017*  
 Liu, Xiao-Yuan, *s02-027*  
 Liu, Xiaoheng, *s09-039*  
 Liu, Xiaoxia, *s05-028*  
 Liu, Xiaoyu, (*Thu s03*)17:40  
 Liu, Xinyu, *s07-011*  
 Liu, Xuan, (*Thu s03*)10:30  
 Liu, Yang, (*Fri s01*)10:10, *s02-020*  
 Liu, Yi-Hung, *s03-059*  
 Liu, Yu, *s08-009*  
 Liu, Yu-Cheng, *s03-056*  
 Liu, Yuan, *s02-017*  
 Liu, Yuwen, (*Thu s04*)09:30  
 Liu, Zhaolin, *s03-061*  
 Liu, Zhiyong, *s08-010*  
 Liu, Zong-Huai, *s05-029*  
 Liwińska, Wioletta, *s02-031, s02-032*  
 Llanos, Javier, (*Tue s10*)14:00, *s10-015*  
 Lo, Nai-Chang, *s09-041*  
 Loas, Andrei, *s11-004*  
 Lobato, Belén, (*Thu s05*)10:30  
 Lobato, Justo, (*Tue s10*)18:20  
 Lobe, Sandra, (*Thu s03*)10:10, *s03-082, s03-087*  
 Locatelli, Cristina, (*Mon s17*)15:00, (*Thu s14*)15:00  
 Lodge, Andrew, (*Fri s07*)09:50  
 Loeffler, Nicholas, *s03-060*  
 Loffreda, David, (*Tue s12*)15:20  
 Lojou, Elisabeth, (*Mon s02*)17:00, (*Tue s02*)17:10  
 Lojou, Jean-Yves, (*Tue s02*)17:10  
 Long, Yi-Tao, (*Thu s01*)17:40  
 Loo, Adeline, *s18-006*  
 Loos, Katja, (*Thu s03*)15:40  
 Lopes da Silva, Amison Rick, *s10-008*  
 Lopes, Pietro P., (*Tue s12*)09:50  
 López Córdoba, Ainara, (*Thu s01*)14:20  
 Lopez, Francesco, (*Mon s02*)18:20  
 López-Vizcaíno, Rubén, *s10-007*  
 Lou, Kwo-Wei, *s18-027*  
 Lu, Chen-En, *s04-015*  
 Lu, Chen-Yuan, *s17-005*  
 Lu, Haiyan, *s03-053, s03-138*  
 Lu, Hsin-Che, *s11-009*  
 Lu, Jeng-Shin, *s03-057*  
 Lu, Kuan-Wei, *s03-066*  
 Lu, Lei, (*Tue s09*)17:20  
 Lu, Miao, *s05-008*  
 Lu, Nanning, (*Thu s11*)17:40  
 Lu, Xunyu, (*Fri s09*)09:30  
 Lu, Yi-Chun, (*Tue s12*)17:00, *s03-052*  
 Lu, Yi-Hsien, *s12-023*  
 Lucas, Ivan, *s03-102*  
 Lucht, Brett L., (*Fri s03*)11:30  
 Ludmila, Frolov, *s02-009*  
 Ludvik, Jiri, (*Thu s11*)18:00, *s11-010*  
 Ludwig, Roland, (*Mon s16*)18:20, *s04-032*  
 Luebke, Mechthild, *s03-061*  
 Lunder, Otto, *s08-007*  
 Luo, Jingshan, (*Tue s06*)10:10  
 Luo, Xiaoyan, *s04-003*  
 Luo, Xu-Feng, *s03-062, s03-087, s05-017*  
 Luo, Xun, *s07-018*  
 Luo, Yongchun, *s05-023*  
 Luo, Yung-Chien, *s02-018*  
 Lupo, Christian, (*Fri s07*)12:10, *s07-029*  
 Lust, Enn, (*Tue s05*)10:30, (*Tue s09*)15:40, (*Tue s12*)17:40, (*Thu s05*)15:20, *s05-013, s09-062*  
 Lux, Simon, *s03-102*  
 Lv, Miaoqiang, *s06-010*  
 Ly, Isabelle, (*Tue s02*)15:00
- ## M
- M'hiri, Nouha, (*Tue s08*)15:20  
 Ma, Chaoxiong, (*Fri s01*)11:30  
 Ma, Chuze, (*Tue s03*)17:20  
 Ma, Jin, *s03-051*  
 Ma, Jing, *s03-055*  
 Ma, Jiwei, *s03-064*  
 Ma, Li, *s12-017*  
 Ma, Liang, (*Mon s10*)15:40  
 Ma, Rui, *s08-009*  
 Ma, Wen, *s03-063*  
 Ma, Xuejing, *s05-023*  
 Macak, Jan, *s06-016, s12-024*  
 Machado, Jane, (*Fri s14*)12:10  
 Madden, Paul, (*Thu s05*)10:10  
 Mahalanobis, Neil, *s07-015*  
 Mahammed, Atif, (*Mon s09*)17:20  
 Maheshwari, Aditya, *s04-059*  
 Mahmoud Ahmed, Mahmoud Mohamed, *s05-009*  
 Mai, Chi-Shyan, (*Tue s05*)15:00  
 Maibach, Julia, (*Tue s03*)16:00  
 Mailu, Stephen, (*Tue s10*)17:00  
 Majdecki, Maciej, (*Tue s16*)09:50  
 Majumder, S. B., (*Thu s03*)15:40  
 Makino, Sho, (*Mon s05*)18:00  
 Malara, Francesco, (*Thu s14*)15:00  
 Malchik, Fyodor, *s03-103*  
 Malek, Ali, (*Tue s12*)15:40  
 Mamme, Mesfin Haile, *s07-017, s14-021*  
 Manabe, Akiyoshi, (*Thu s09*)14:40  
 Mandler, Daniel, (*Fri s01*)09:50  
 Mani, Verappan, (*Tue s02*)14:40  
 Mano, Nicolas, (*Mon s02*)17:00, (*Tue s02*)15:00, (*Tue s02*)15:20, (*Tue s02*)17:10  
 Manríquez, Federico, (*Fri s09*)11:30  
 Manriquez, Juan, (*Thu s09*)15:40, *s09-042*  
 Manzanares, José A., (*Thu s18*)18:00  
 Mao, Bingwei, (*Mon s12*)16:40, (*Fri s07*)10:10, *s03-113, s11-008*

- Mao, Lanqun, (*Mon s16*)14:40,  
(*Tue s02*)14:00
- Mao, Xiaoming, *s07-019*
- Mao, Yu-Xiang, *s09-043*
- Maran, Flavio, (*Thu s11*)14:00, *s16-003*
- Marani, Debora, (*Mon s04*)18:20
- Marcaccio, Massimo, (*Thu s14*)14:20,  
(*Thu s14*)16:40, (*Fri s14*)10:10,  
*s02-001*
- Marcelin, Sabrina, (*Tue s08*)16:40
- Marcinek, Marek, (*Fri s03*)11:10
- Mardare, Andrei Ionut, (*Fri s18*)10:10,  
*s12-004*
- Mardare, Cezarina Cela, (*Fri s18*)10:10
- Marecek, Vladimír, *s12-018*
- Marken, Frank, *s13-001*
- Markiewicz, Matthew, (*Thu s04*)10:30
- Markovic, Nenad M., (*Tue s12*)09:50
- Markovic, Nikola, (*Mon s02*)18:20
- Maroni, Fabio, (*Tue s03*)17:00
- Marques, Andreson, (*Fri s14*)11:50
- Marquitan, Miriam, (*Thu s01*)14:20
- Marsili, Enrico, (*Mon s02*)17:20
- Martens, Sladjana, *s03-064*, *s03-077*,  
*s09-002*
- Martinez, Beatriz, *s04-031*
- Martinez-Gonzalez, Eduardo, *s11-005*
- Martinez-Hincapie, Ricardo,  
(*Mon s12*)17:40
- Martinez-Huitl, Carlos Alberto,  
(*Tue s10*)16:00, *s10-008*, *s10-023*,  
*s10-024*
- Martins, Luisa, *s12-019*
- Martins, Rui C., (*Tue s10*)16:00
- Martins, Vitor L, *s03-131*
- Maruyama, Jun, (*Thu s09*)14:00, *s09-044*
- Maruyama, Shohei, (*Tue s03*)14:00,  
*s03-049*
- Maruyama, Yuki, (*Thu s03*)17:00
- Masa, Justus, (*Mon s09*)16:00,  
(*Thu s14*)14:40, *s01-009*
- Masese, Titus, *s03-022*, *s03-104*
- Mashio, Tetsuya, (*Tue s15*)15:40
- Masikini, Milua, (*Mon s05*)10:30,  
(*Tue s10*)17:00
- Masuhara, Rin, (*Mon s03*)10:10
- Matějková, Stanislava, *s18-011*
- Mateo-Mateo, Cintia, (*Tue s02*)15:00
- Mathias, Mark, (*Thu s04*)09:30
- Mathwig, Klaus, *s11-003*, *s18-021*
- Matinise, Nolubabalo, (*Mon s05*)10:30
- Matsuda, Naoki, *s04-044*
- Matsue, Tomokazu, (*Mon*)08:15,  
(*Wed s02*)09:30, *s02-008*
- Matsui, Yukiko, (*Fri s03*)11:10, *s03-065*
- Matsumae, Kenji, *s09-045*
- Matsumiya, Masahiko, *s18-039*
- Matsumoto, Futoshi, *s03-116*
- Matsunaga, Atsushi, *s04-050*
- Matsunaga, Toshiyuki, *s18-028*
- Matsuoka, Miki, *s04-002*
- Matsushima, Hisayoshi, *s07-014*, *s09-046*
- Matsuzawa, Koichi, (*Mon s04*)09:30,  
(*Mon s04*)09:50, (*Thu s09*)14:40,  
*s04-033*, *s04-045*, *s04-048*, *s09-006*,  
*s09-045*, *s09-070*
- Mattarozzi, Luca, (*Fri s07*)10:30
- Matuseviciute, Agne, (*Thu s09*)17:40,  
*s09-058*, *s09-067*
- Matyszewska, Dorota, (*Mon s16*)15:40
- Mauger, A., (*Thu s03*)14:00
- Maye, Sunny, (*Tue s01*)14:40
- Mayer, Matthew T., (*Tue s06*)10:10
- Mayrhofer, Karl, (*Mon s04*)10:10,  
(*Mon s17*)14:00
- McCreery, Richard, (*Mon s16*)14:00
- McGovern, R., (*Mon s16*)18:20
- McKerracher, Rachel D., (*Wed s10*)09:30
- Meas, Yunny, (*Mon s10*)16:40
- Medel, Alejandro, (*Mon s10*)16:40,  
(*Fri s09*)11:30
- Mei, Dong, *s04-053*
- Meini, Stefano, (*Fri s03*)11:30
- Meining, Zhang, (*Fri s01*)11:10
- Meister, Paul, *s03-006*
- Melchy, Pierre-Eric Alix, (*Thu s04*)17:40
- Mendoza-Hernandez, Omar Samuel,  
(*Thu s03*)17:00
- Meng, Jin-Hui, *s12-001*
- Meng, Shirley, (*Tue s03*)17:20
- Mentbayeva, Almagul, (*Tue s03*)14:20,  
(*Tue s03*)15:00
- Menzel, Jakub, (*Tue s05*)15:20, *s05-042*
- Mercer, Michael P., (*Tue s07*)10:10
- Merlet, Celine, (*Thu s05*)10:10
- Mernissi Cherigui, El Amine,  
(*Thu s07*)14:00, *s07-017*, *s14-021*
- Metzger, Michael, (*Fri s03*)11:30
- Michardière, Anne Sophie, (*Tue s02*)15:00
- Mikysek, Tomas, (*Thu s11*)18:00
- Milis, Sam, *s04-012*
- Miller, John R., (*Thu s05*)14:00
- Milton, Ross, (*Mon s02*)14:20,  
(*Mon s02*)15:20
- Min, Kyoungmin, (*Mon s03*)15:40
- Min, Kyung-Seok, *s05-010*
- Minakuchi, Yuki, (*Tue s02*)09:50
- Minami, Kazuya, (*Mon s12*)18:20, *s12-011*
- Minamida, Yasuto, *s04-034*
- Minamimoto, Hiro, *s12-007*, *s14-011*
- Minato, Taketoshi, *s18-028*
- Mindemark, Jonas, *s03-008*
- Minguzzi, Alessandro, (*Thu s14*)15:00
- Minh, Nguyen, (*Fri s04*)09:30
- Minteer, Shelley, (*Mon s02*)15:20
- Mirambet, François, *s14-013*
- Mirasoli, Mara, *s01-015*
- Mitsushima, Shigenori, (*Mon s04*)09:30,  
(*Mon s04*)09:50, (*Thu s09*)14:40,  
*s04-033*, *s04-045*, *s04-048*, *s09-006*,  
*s09-045*, *s09-070*
- Miura, Makoto, (*Thu s07*)16:40
- Miyahara, Yuto, (*Mon s09*)10:10
- Miyamoto, Junichi, (*Tue s05*)14:00,  
*s05-040*
- Miyashita, Natsuki, *s05-016*
- Miyatake, Kenji, *s04-016*
- Miyayama, Masaru, (*Wed s03*)10:30
- Miyazaki, Kohei, (*Mon s09*)10:10,  
(*Mon s09*)16:40, (*Tue s03*)14:00,  
*s03-017*, *s03-029*, *s03-049*, *s03-063*
- Miyazawa, Satoshi, *s07-014*
- Mizaikoff, Boris, (*Tue s02*)10:10
- Mizuguchi, Youhei, (*Fri s03*)10:30
- Mizutani, Fumio, (*Tue s02*)09:50, *s02-015*
- Moehl, Thomas, (*Tue s06*)10:10
- Mogi, Iwao, (*Thu s07*)16:40,  
(*Thu s07*)17:20
- Mohamed, Youssuf, (*Thu s01*)15:20
- Mokso, Rajmund, (*Mon s03*)17:20
- Molina Osorio, Andres, (*Fri s18*)10:30
- Monsalve, Karen, (*Mon s02*)17:00,  
(*Tue s02*)17:10
- Montegrossi, Giordano, *s07-032*
- Montes, Iciar Begoña, (*Tue s10*)18:20
- Montiel, Vicente, (*Tue s10*)10:30
- Montinaro, Dario, *s04-026*
- Montini, Tiziano, (*Thu s14*)16:40
- Montoto Blanco, Elena Catalina, *s03-127*
- Moon, Janghyuk, *s03-122*
- Moon, Jong Seok, (*Thu s01*)15:00
- Moon, Jooho, *s09-031*
- Moore, Jeffrey, *s03-127*
- Moraes Silva, Saimon, (*Thu s18*)15:40
- Morante, Joan Ramon, (*Thu s03*)17:00
- Morcrette, Mathieu, *s15-002*
- Moreno-Fernández, Gelines,  
(*Thu s05*)10:30
- Moreno-Garcia, Pavel, (*Thu s07*)09:30
- Morgenstern, Karina, (*Tue s12*)15:20
- Mori, Takuya, *s03-022*, *s03-104*
- Morimitsu, Masatsugu, (*Mon s10*)18:20,  
*s01-014*, *s03-005*, *s03-021*, *s03-076*,  
*s03-080*, *s03-091*, *s09-020*, *s09-025*,  
*s09-032*, *s09-034*, *s09-061*, *s10-012*,  
*s10-021*, *s10-026*
- Morimoto, Ryoichi, (*Thu s07*)16:40
- Morimoto, Yu, (*Mon s12*)15:00,  
(*Tue s09*)17:00, (*Thu s04*)14:00
- Morita, Masayuki, (*Thu s05*)15:40,  
*s05-037*
- Morita, Ryohei, (*Tue s03*)18:20
- Morton, D. William A., *s12-025*
- Mostafa, Ehab, *s03-064*, *s09-002*
- Motobayashi, Kenta, (*Mon s12*)18:20,  
*s12-011*
- Motoyama, Munekazu, *s03-031*, *s03-037*
- Mousset, Emmanuel, (*Mon s10*)18:00,  
(*Tue s10*)15:00, *s10-015*
- Muckerman, James, (*Fri s09*)10:10
- Müller, Claas, (*Tue s15*)10:30, *s17-001*
- Mueller, Franziska, (*Mon s03*)15:00,  
*s03-120*
- Mueller, Jonathan, (*Fri s09*)10:10
- Muhler, Martin, (*Mon s09*)16:00
- Mukkannan, Azhagurajan, (*Tue s12*)10:30,  
*s12-002*
- Mun, Bongjin Simon, (*Tue s15*)14:00
- Munesada, Toshiyuki, *s03-104*
- Munktell, Sara, (*Wed s08*)10:30
- Murakami, Miwa, *s03-002*, *s17-007*
- Murakoshi, Kei, (*Mon s12*)17:20, *s12-007*,  
*s12-020*
- Murase, Kuniaki, (*Wed s07*)10:30,  
*s07-016*, *s07-025*
- Murata, Hajime, (*Tue s09*)17:00
- Murata, Kazuki, *s02-021*, *s02-023*
- Murota, Tadatoshi, (*Thu s03*)14:40
- Murtomäki, Lasse, (*Thu s18*)18:00
- Musiani, Marco, (*Fri s14*)09:30,  
(*Fri s07*)10:30
- Mustafa, Sen, (*Wed s02*)09:30, *s02-008*
- Mustafar, Suzaliza, *s11-011*
- Muthuswamy, Navaneethan,  
(*Thu s09*)10:30
- Muto, Marika, *s04-038*
- Myung, Noseung, *s09-030*



**N**

- Nabae, Yuta, *s04-050*  
 Nachtegaal, Maarten, (*Thu s09*)15:00  
 Nagahama, Yudai, (*Mon s12*)17:00  
 Nagai, Keiji, *s04-043*  
 Nagai, Kohei, *s09-045*  
 Nagai, Tsukasa, *s04-039, s11-001*  
 Nagamura, Naoka, *s12-016*  
 Nagano, Shinichi, *s07-014*  
 Nagasawa, Kensaku, *s09-070*  
 Nagashima, Ikuo, (*Thu s09*)14:40  
 Nagashima, Takumi, (*Thu s14*)09:30  
 Nagayama, Tomio, *s07-004, s07-005, s07-007*  
 Nakajima, Hironori, *s04-057*  
 Nakamura, Genichiro, *s18-007*  
 Nakamura, Kai, (*Wed s07*)10:30, *s07-016*  
 Nakamura, Toshihiro, *s07-004, s07-005, s07-007*  
 Nakanishi, Koji, *s03-022*  
 Nakanishi, Shuji, (*Mon s09*)14:40, (*Tue s09*)14:20  
 Nakanishi, Takayuki, (*Tue s08*)14:20, (*Tue s08*)17:40, (*Thu s08*)09:30  
 Nakashima, Shota, *s05-041*  
 Nakata, Akiyoshi, *s03-002*  
 Nakatsuyama, Kunio, (*Mon s04*)16:00  
 Nakayama, Katsutoshi, *s08-004*  
 Naldoni, Alberto, (*Thu s14*)15:00  
 Nam, Ekaterina, *s02-035*  
 Nanbu, Noritoshi, *s18-019, s18-029*  
 Naoi, Katsuhiko, (*Mon s05*)09:30, (*Tue s05*)14:00, *s05-016, s05-040, s05-041*  
 Naoi, Wako, (*Tue s05*)14:00, *s05-016, s05-040, s05-041*  
 Napporn, Teko W., (*Mon s04*)18:00  
 Nasara, Ralph Nicolai, *s03-066*  
 Nava, José L., (*Mon s10*)10:10, *s10-018*  
 Navarro, Vicente, *s10-007*  
 Nazaruk, Ewa, (*Tue s16*)09:30  
 Ndipingwi, Miranda, (*Mon s05*)10:30  
 Nechache, Aziz, (*Fri s04*)09:50, *s04-040*  
 Nekrasov, Valentin, *s12-028*  
 Nerut, Jaak, (*Tue s09*)15:40, *s09-062*  
 Netto, Chaquip, *s16-005*  
 Neusser, Gregor, (*Fri s01*)10:10  
 Nguyen, Dan-Thien, *s03-081, s03-115*  
 Nguyen Dang, Dan, (*Thu s18*)17:20  
 Nguyen, Hai, (*Thu s07*)09:30  
 Nguyen, Thi Hai Quyen, (*Fri s07*)12:10, *s07-029*  
 Nguyen, Trong-Khoa, (*Tue s03*)15:00  
 Nguyen, Trung Van, (*Tue s15*)15:20  
 Ni, Chung-Ta, *s03-066, s03-067, s03-083, s04-060, s04-061, s04-064, s06-009*  
 Nichols, Richard, (*Thu s03*)09:50, (*Fri s07*)10:10  
 Nie, Ping, (*Tue s03*)14:40, *s03-097*  
 Nie, Yao, *s04-041, s14-005*  
 Nieciecka, Dorota, (*Mon s16*)15:20  
 Niedzicki, L., (*Fri s03*)11:10  
 Nikiforidis, Georgios, (*Thu s03*)17:40  
 Nilsson, Anders, (*Mon s12*)14:00  
 Nisancioglu, Kemal, *s08-007*  
 Nishi, Naoya, (*Mon s12*)18:20, *s12-011*  
 Nishihara, Hiroshi, *s11-011*  
 Nishihata, Keiichi, *s18-039*  
 Nishiki, Yoshinori, (*Thu s09*)14:40  
 Nishimura, Kazuya, *s03-059*  
 Nishimura, Shin-ichi, (*Tue s03*)16:40  
 Nishino, Hiroki, (*Thu s03*)14:40  
 Nishitani-Gamo, Mikka, *s03-079, s04-025, s04-030, s04-043*  
 Nishiyama, Katsuhiko, (*Fri s11*)11:50, *s18-010*  
 Nissaulya, Nadya, *s03-068*  
 Niu, Dongfang, (*Fri s11*)11:30, *s09-071*  
 Niu, Lin, *s08-009*  
 Niu, Wenxin, (*Fri s14*)09:50  
 Niwa, Hideharu, *s04-050*  
 Niwa, Osamu, (*Tue s01*)14:00  
 Noda, Zhiyun, *s04-034*  
 Noël, Vincent, (*Mon s02*)10:10  
 Nogala, Wojciech, *s18-040*  
 Noguchi, Yuya, (*Thu s05*)15:40  
 Noh, Seunghyo, (*Tue s15*)14:40  
 Nohara, Saki, *s02-007*  
 Nohira, Toshiyuki, *s03-104*  
 Nokbin, Somkiat, (*Tue s16*)10:10  
 Nomura, Masahito, (*Thu s03*)14:40  
 Nordlien, Jan Halvor, *s08-007*  
 Norkus, Eugenijus, (*Thu s09*)17:40, *s09-047, s09-048, s09-058, s09-067*  
 Noronha Filho, Paulo, *s14-012*  
 Notsu, Hideo, *s12-003*  
 Novais, Laura, *s14-012*  
 Novak, Petr, (*Mon s03*)09:30, (*Mon s17*)16:40, (*Thu s03*)17:20, *s03-085, s03-129*  
 Novoselov, Konstantin S., (*Tue s12*)18:00  
 Nurpeissova, Arailym, *s03-124*  
 Nyholm, Leif, (*Wed s08*)10:30, *s03-009*  
 Nzaba, Myra, (*Mon s05*)10:30
- O**  
 Ochi, Masanori, *s04-062*  
 Ochiai, Tsuyoshi, (*Tue s10*)15:20  
 Odabas, Zafer, *s09-050*  
 Oesterlund, Viking, (*Tue s03*)16:00  
 Ogasawara, Hirohito, (*Mon s12*)14:00  
 Ogasawara, Masaru, *s18-019, s18-029*  
 Ogasawara, Toru, *s07-022*  
 Ogawa, Ryota, *s09-046*  
 Ogino, Kazuya, *s12-003*  
 Ogumi, Zempachi, (*Mon s03*)14:00, *s03-002, s03-022, s03-099, s03-104, s17-007, s18-028*  
 Oh, Eun-Suok, *s03-120*  
 Oh, Gyu-Hyeon, *s04-022*  
 Oh, Kwangjin, *s04-021*  
 Oh, Seung M., *s03-030, s03-044, s03-122*  
 Oh, Young-Joon, (*Tue s05*)18:00  
 Ohara, Koji, *s03-104*  
 Ohba, Tadashi, *s12-003*  
 Ohma, Atsushi, (*Tue s15*)15:40  
 Ohta, Narumi, *s12-003*  
 Ohtsuka, Toshiaki, (*Tue s08*)17:40  
 Oikawa, Wataru, *s07-008*  
 Okada, Shigeto, (*Fri s03*)10:10  
 Okada, Tatsuhiro, *s18-007*  
 Okada, Yohei, (*Thu s11*)16:40  
 Okamura, Yusuke, *s07-026*  
 Okazaki, Keita, (*Tue s05*)14:00, *s05-040*  
 Okubo, Masashi, (*Tue s03*)16:40, (*Tue s03*)18:20  
 Okumura, Takashi, *s18-009*  
 Okunev, Aleksey, (*Thu s04*)15:40  
 Okuno, Yukihiro, (*Thu s14*)14:00  
 Oleinick, Alexander, (*Thu s18*)14:00  
 Oliveira, Herenilton, (*Fri s14*)12:10, *s14-012*  
 Oliveira-Brett, Ana Maria, (*Tue s02*)16:00  
 Olivi, Paulo, *s10-016*  
 Oll, Ove, (*Tue s05*)10:30, (*Tue s12*)17:40  
 Olynick, Deirdre L., (*Mon s06*)18:00  
 Ono, Hideaki, *s04-016*  
 Ono, Kohei, *s09-015*  
 Ono, Masaki, *s03-002*  
 Ooya, Kayato, *s18-030*  
 Opallo, Marcin, (*Mon s16*)17:40, (*Fri s14*)10:30, *s18-040*  
 Opuchlik, Lidia Jagoda, *s09-049*  
 Orain, Christophe, (*Thu s18*)09:30  
 Orazem, Mark E., (*Mon s03*)16:40, (*Wed s08*)10:10  
 Orikasa, Yuki, (*Mon s17*)17:20, *s03-022, s03-099, s03-104, s05-041, s09-044, s10-011*  
 Ors, Jose M., *s12-010*  
 Osada, Irene, (*Tue s03*)17:20, *s03-069*  
 Osawa, Masatoshi, (*Mon s12*)09:30, (*Mon s12*)18:20, *s12-011, s12-013*  
 Oshikiri, Yoshinobu, (*Thu s07*)16:40  
 Oshima, Kenji, *s05-016*  
 Oshima, Masaharu, *s04-050*  
 Osiceanu, Petre, *s08-001, s08-015*  
 Ostrom, Cassandra, *s18-020*  
 Ota, Hiraku, *s04-043*  
 Ota, Kenichiro, (*Mon s04*)09:30, (*Mon s04*)09:50, *s04-033, s04-045, s04-048*  
 Otani, Kazufumi, *s03-104*  
 Otani, Yuki, (*Tue s08*)17:20  
 Ou, Tzu-Man, (*Thu s05*)16:40  
 Ouyang, Chuying, *s03-137*  
 Owen, John R., (*Thu s03*)15:20, (*Fri s03*)09:50  
 Oyaizu, Nobuhisa, *s12-003*  
 Oyama, Gosuke, (*Tue s03*)16:40  
 Oyarzun, Maria, (*Mon s09*)10:30  
 Ozawa, Hiroaki, (*Thu s14*)09:30  
 Ozeki, Masataka, (*Wed s04*)09:30  
 Ozga, Piotr, (*Fri s07*)11:50, *s07-004*  
 Ozkaya, Ali Riza, *s09-050*  
 Ozoemena, Kenneth, (*Mon s05*)10:30, (*Mon s04*)17:40
- P**  
 Padmanabhan, Vivek, (*Thu s03*)09:50  
 Paek, Seungwoo, *s18-032*  
 Paganin, Valdecir, *s04-006*  
 Paillard, Elie, (*Tue s03*)17:20, *s03-069*  
 Palacín, M. Rosa, (*Tue s03*)15:40, *s03-072*  
 Palanisamy, Kannan, (*Mon s02*)17:20  
 Palanisamy, Selvakumar, (*Tue s02*)14:40  
 Palermo, Vincenzo, (*Thu s14*)14:20  
 Palin, Emma, *s18-023*  
 Palmer, Michael, (*Thu s03*)15:20  
 Palys, Barbara, (*Fri s14*)10:30  
 Pan, Chen-Fu, *s01-013*  
 Pan, Chien-Yeh, *s09-051*  
 Pan, Chun-Jern, *s04-035, s04-051, s09-043*  
 Pan, H.A., (*Tue s05*)14:40  
 Pan, Jin, (*Tue s03*)14:40, *s03-097*  
 Pan, Yen-Ting, *s03-066*  
 Panahian Jand, Sara, (*Tue s12*)16:40  
 Pang, Ran, *s12-021*

- Pang, Wei Kong, (*Mon s03*)17:00  
Panjer, Mathias, *s10-002*  
Pankratova, Galina, *s02-028*  
Paolucci, Francesco, (*Thu s14*)14:20, (*Thu s14*)16:40, (*Fri s14*)10:10, *s01-015*, *s02-001*  
Park, Da-In, *s03-124*  
Park, Dae Won, *s03-033*  
Park, Gyeong-Su, (*Mon s03*)15:40  
Park, Gyeongse, *s03-011*  
Park, Hosang, *s03-044*  
Park, Inchul, *s03-070*  
Park, Jin-Soo, *s04-022*, *s04-023*, *s04-024*, *s10-012*, *s18-016*, *s18-033*, *s18-034*  
Park, Kyu-Young, (*Thu s03*)14:40, *s03-070*  
Park, Nam-Gyu, (*Mon s13*)09:30  
Park, Sang-Hoon, (*Tue s05*)09:30  
Park, Sang-Jae, (*Thu s03*)14:00  
Park, Sangki, *s03-125*  
Park, Sohyun, *s14-014*  
Park, Soo-Gil, (*Tue s05*)17:20  
Park, Sun-Min, (*Thu s03*)16:00  
Park, Sung June, *s05-010*  
Park, Wooshin, (*Fri s18*)11:10  
Park, Yong Joon, *s03-069*  
Parker, Stephen G., (*Wed s01*)09:30  
Partovi-Nia, Rachel, (*Tue s08*)14:40  
Passerini, Stefano, (*Mon s03*)15:00, (*Tue s03*)17:00, (*Tue s03*)17:20, *s03-060*, *s03-069*, *s03-120*  
Pastoriza-Santos, Isabel, *s09-004*  
Patra, Jagabandhu, (*Thu s03*)15:40  
Patru, Alexandra, (*Tue s04*)10:10  
Pauliukaite, Rasa, *s02-003*, *s02-029*  
Pawolek, Zarina, (*Thu s09*)17:00  
Payen, Christophe, (*Mon s05*)15:00  
Paz-Garcia, Juan Manuel, (*Mon s03*)17:20, *s10-017*  
Pean, Clarisse, (*Thu s05*)10:10  
Pebere, Nadine, (*Tue s08*)16:40  
Peckham, Timothy J., (*Mon s04*)15:00, *s04-003*  
Pedersen, Steen Uttrup, (*Thu s14*)17:20  
Pekas, Nikola, (*Mon s16*)14:00  
Pelicci, Pier-Giuseppe, *s02-001*  
Pellattiero, Anna, *s16-003*  
Peng, Can, *s03-046*  
Peng, Hai-Jung, (*Thu s03*)17:20  
Peng, Hao-Ting, *s03-105*, *s03-126*  
Peng, Jun, *s03-132*, *s03-133*, *s09-052*  
Peng, Lingyi, *s04-007*  
Peng, Ye, *s08-013*  
Penicaud, Alain, *s01-015*  
Penteado, Eduardo, (*Tue s10*)18:20  
Perdomo Marin, Ana Cristina, *s01-020*  
Pérez, Carlos, (*Tue s05*)17:00  
Perez, Joelma, *s04-006*, *s09-001*  
Perez, Juan, (*Mon s12*)16:40  
Pérez-Corona, Maribel, *s10-004*  
Pergolesi, Daniele, (*Tue s09*)16:40  
Perry, Samuel, (*Mon s09*)17:00, (*Thu s04*)10:10, *s01-023*  
Pescarmona, Paolo, (*Tue s10*)17:20, *s04-012*  
Peters, Fabian, (*Thu s01*)16:40  
Peters, Ines, (*Thu s09*)16:00  
Peterson, Vanessa K., (*Mon s03*)17:00  
Petrov, Konstantin, (*Mon s10*)17:20  
Pfaffeneder-Kmen, Martin, *s12-008*  
Pflöging, Wilhelm, *s17-001*  
Pham, Minh-Chau, (*Mon s02*)10:10  
Philippe, Bertrand, (*Fri s03*)12:10  
Pick, Horst, (*Tue s02*)16:40  
Pieta, Piotr, *s12-005*  
Pigeon, Pascal, (*Thu s11*)15:20  
Pikaar, Ilje, (*Mon s10*)17:40  
Pikma, Piret, (*Tue s05*)10:30  
Pilarova, Iveta, (*Tue s02*)15:40, *s02-032*  
Pinkwart, Karsten, (*Thu s04*)15:00  
Pinna, Nicola, (*Tue s05*)17:00  
Pinyou, Piyanut, (*Mon s02*)18:20  
Piro, Benoît, (*Mon s02*)10:10  
Piskin, Mehmet, *s09-050*  
Pisman, Yamit, (*Fri s01*)09:50  
Placke, Tobias, (*Tue s03*)16:00, *s03-006*, *s03-071*  
Plank, Zsuzsana, *s10-004*  
Pletnev, Mikhail, *s08-005*  
Plumeré, Nicolas, (*Mon s02*)18:20  
Pohl, Marcus D., (*Tue s12*)15:20  
Pohlmann, Sebastian, (*Wed s05*)10:10  
Polgár, Dorothy, *s10-004*  
Polo, Federico, *s16-003*  
Polverel, Matthieu, (*Tue s15*)10:10  
Pombeiro, Armando, *s12-019*  
Ponce de Leon, Carlos, (*Wed s10*)09:30, (*Thu s03*)18:00, *s03-099*, *s10-018*  
Ponrouch, Alexandre, (*Tue s03*)15:40, *s03-072*  
Popov, Alexey, *s12-005*  
Poulin, Philippe, (*Tue s02*)15:00  
Pozo-Ayuso, Diego F., (*Tue s01*)18:00, (*Thu s18*)14:20  
Prato, Maurizio, (*Thu s14*)16:40  
Preda, Silviu, *s08-015*  
Presser, Volker, (*Thu s05*)16:00, *s17-006*  
Prévot, Mathieu, (*Mon s06*)17:00, (*Mon s06*)17:20  
Prieto, Francisco, *s12-010*, *s16-004*  
Prodi, Luca, (*Fri s14*)10:10  
Pröll, Johannes, *s17-001*  
Pruna, Alina, *s05-030*  
Prusinskas, Kestutis, *s09-047*  
Przygocki, Patryk, (*Thu s05*)09:30  
Pumera, Martin, *s18-006*, *s18-008*, *s18-011*, *s18-022*  
Purwidyantri, Agnes, *s18-001*  
Pyo, Myoungcho, *s03-100*
- Q**  
Qi, Xin, (*Thu*)08:15  
Qi, Xueqiang, (*Mon s04*)14:00, *s04-046*, *s14-005*  
Qiao, Yu, (*Tue s12*)17:20  
Qin, Xiaolong, (*Mon s09*)14:20  
Qiu, Xinping, *s03-064*  
Quinta-Ferreira, Rosa M., (*Tue s10*)16:00  
Quiroga, Matias A., (*Tue s03*)15:00, (*Tue s15*)17:40, *s15-004*
- R**  
Rötzer, Marian D., *s14-019*  
Rabaey, Korneel, (*Mon s10*)17:40  
Radjenovic, Jelena, (*Mon s10*)16:00, *s10-006*  
Radzevic, Aneta, *s02-003*, *s02-029*  
Rajkumar, Muniyandi, *s05-031*  
Rakickas, Tomas, *s02-029*  
Ramakrishnan, Prakash, *s05-043*  
Ramamurthy, Sridhar, (*Tue s08*)14:40  
Ramirez, Gonzalo, (*Thu s01*)14:00  
Ramírez, José A., (*Mon s10*)16:40  
Ramirez-Castro, Claudia, (*Wed s05*)10:10  
Ramos-Sanchez, Guadalupe, (*Tue s15*)15:00  
Rana, Jatinkumar, *s03-119*  
Rapino, Stefania, (*Thu s14*)14:20, (*Thu s14*)16:40, *s02-001*  
Raschitor, Alexandra, (*Tue s10*)14:00  
Rashkeev, Sergey, (*Fri s04*)10:30  
Rassaei, Liza, (*Fri s14*)10:30, *s07-027*  
Rassie, Candice, (*Tue s09*)10:10, (*Fri s09*)11:10, *s09-058*, *s09-065*  
Ratajczak, Paula, (*Thu s05*)09:30, *s05-014*, *s05-015*  
Rawlings, Benjamin, (*Tue s07*)10:10  
Razkazova, Elena, (*Mon s10*)17:20  
Razmjooei, Fatemeh, (*Tue s09*)09:30  
Recio, Javier, (*Mon s09*)10:30  
Reddy, M. V., (*Tue s03*)14:20, *s03-073*  
Reguer, Solenn, (*Tue s08*)15:20, *s14-013*  
Reier, Tobias, (*Thu s09*)17:00  
Reinaud, Olivia, (*Thu s18*)09:30  
Reinecke, Holger, (*Tue s15*)10:30, *s17-001*  
Reisberg, Steeve, (*Mon s02*)10:10  
Ren, Bin, (*Mon s17*)14:40, *s12-009*  
Ren, Chengqiang, *s08-013*  
Ren, Gengbo, (*Mon s10*)15:40  
Ren, Jie, (*Mon s17*)09:30  
Ren, Shaojun, (*Thu s07*)15:40  
Respaud, Marc, (*Mon s05*)17:40  
Retailleau, Laurence, *s04-026*  
Retoux, Richard, (*Thu s18*)17:20  
Ribeiro da Silva, Djalma, (*Tue s10*)16:00  
Ribeiro, Mauro C. C., *s03-131*  
Richardson, James, (*Tue s02*)18:00  
Richardson, William, *s03-074*  
Richtering, Werner, *s07-011*  
Rico, Victor, (*Tue s10*)10:10  
Riedo, Andreas, (*Thu s07*)09:30  
Riffault, Benoît, (*Thu s18*)17:20  
Rigoulet, Michel, (*Tue s02*)15:20  
Risco, Carolina, *s10-007*  
Rishpon, Judith, (*Thu s01*)10:10  
Risthaus, Tim, (*Tue s03*)17:40  
Ristinmaa, Matti, (*Mon s03*)17:20, *s10-017*  
Robba, Alice, *s03-078*  
Robert, Rosa, (*Mon s03*)09:30  
Robertson, Calum, (*Fri s07*)09:50  
Rocca, Emmanuel, (*Tue s08*)15:20, *s08-014*, *s08-016*, *s14-013*  
Rocheffort, Dominic, (*Tue s05*)10:10  
Roda, Aldo, *s01-015*  
Rodrigo, Manuel Andres, (*Tue s10*)14:00, (*Tue s10*)18:20, *s10-007*, *s10-015*, *s10-023*, *s10-024*  
Rodrigues de Oliveira, Gustavo, *s10-008*  
Rodríguez, Eduardo, (*Wed s10*)10:30  
Rodríguez, Israel, (*Mon s10*)10:10  
Rodríguez, Rosa, (*Mon s10*)14:40  
Rodríguez-Lopez, Joaquin, (*Thu s14*)15:20, *s03-127*  
Rodriguez-Maroto, Jose M., *s10-017*  
Rodríguez-Nava, Odín, (*Mon s10*)15:00  
Röder, Fridolin, (*Wed s03*)09:30  
Rogalski, Jerzy, (*Mon s02*)17:40  
Roh, Ha-Kyung, *s03-076*(*Tue s03*)18:00  
Roh, Kwang Chul, (*Tue s03*)18:00,

- s03-076  
Romann, Tavo, (*Tue s05*)10:30,  
(*Tue s12*)17:40  
Rondinini, Sandra, (*Mon s17*)15:00  
Ross, Natasha, (*Mon s05*)10:30  
Rossmeisl, Jan, (*Tue s12*)14:00,  
(*Tue s09*)15:20  
Rotenberg, Benjamin, (*Thu s05*)10:10  
Roy, Claudie, (*Fri s09*)10:30  
Rozier, Patrick, s05-041  
Rubinstein, Israel, (*Thu s07*)17:40, s02-009  
Rueda, Manuela, s12-010, s16-004  
Ruff, Adrian, (*Mon s02*)18:20,  
(*Tue s02*)17:00  
Ruggiero, M., s04-047  
Ruhlmann, Laurent, (*Fri s09*)09:50,  
s11-012  
Ruotolo, Antonio, s05-030  
Rusling, James, (*Mon s02*)09:30  
Russo, Patricia, (*Tue s05*)17:00  
Ruszkowski, Piotr, s16-006  
Rutkowska, Iwona A., (*Thu s14*)09:50  
Ruzele, Zivile, s02-029  
Ruzgas, Tautgirdas, (*Tue s01*)17:00  
Ryder, Karl S., (*Mon s05*)16:00,  
(*Mon s12*)18:00  
Ryu, Ji Heon, s03-024, s03-030, s03-036,  
s03-044, s03-121, s03-122
- S**  
Sabatino, Simona, (*Tue s10*)14:40, s10-020  
Sadki, Said, (*Wed s05*)09:30  
Sáez, Cristina, s10-007, s10-015, s10-023,  
s10-024  
Sagane, Fumihiko, s03-075  
Sahin, Nihat Ege, (*Mon s04*)18:00  
Saikia, Diganta, s18-026, s18-027  
Sairi, Masniza, (*Fri s01*)10:10  
Saito, Hayate, s03-128  
Saito, Mikiko, (*Tue s10*)16:40  
Saito, Morihiro, s09-053, s18-030  
Saji, Viswanathan, s07-031  
Sakaguchi, Hiroki, (*Thu s03*)14:40,  
(*Fri s03*)11:50  
Sakai, Tetsuo, s03-059  
Sakai, Yuki, s05-041  
Sakamaki, Kenji, (*Mon s06*)18:20  
Sakamoto, Ryota, s11-011  
Sakka, Tetsuo, (*Mon s12*)18:20, s12-011  
Sakuyama, Haruki, s03-041  
Salanne, Mathieu, (*Thu s05*)10:10  
Salazar, Ricardo, (*Mon s10*)14:20, s10-019  
Sallard, Sébastien, s03-129  
Salman, Munir, (*Tue s12*)14:40  
Sanchez-Ramirez, Nédher, s03-131  
Sanchez-Sanchez, Carlos M.,  
(*Thu s09*)17:20, s09-060  
Sandoval, Andrea, (*Mon s12*)17:40  
Sandoval, Miguel, (*Mon s10*)10:10  
Sano, Hideyuki, s03-076  
Sano, Mistuo, s02-002  
Sansaloni, Sandra, s01-015  
Santiago, Elisabete Inacio, (*Mon s04*)18:00  
Santoro, Carlo, (*Mon s02*)17:20  
Santos, Nathalia, s04-006  
Sapountzi, Foteini M., s04-026  
Sapstead, Rachel, (*Mon s12*)18:00,  
s18-023  
Sarioğlu, Cevat, (*Fri s09*)09:50, s09-035  
Sarauli, D., s02-005  
Sarkar, Sahana, s11-003  
Sasaki, Aiko, (*Tue s02*)18:20  
Sasaki, Kazunari, s04-034  
Sasaki, Kotaro, (*Mon s09*)15:00,  
(*Fri s09*)10:10, s09-061  
Sasaki, Kuniaki, s03-041, s07-022  
Sasaki, Tsuyoshi, (*Mon s03*)09:30  
Sashuk, Volodymyr, (*Mon s16*)17:40,  
(*Fri s14*)10:30  
Sato, Kazutaka, (*Thu s04*)15:20  
Sato, Masataka, (*Mon s06*)18:20  
Sato, Shino, (*Mon s12*)17:20  
Sato, Tatsuo, (*Thu s07*)15:00  
Sato, Yuichi, s03-116  
Satomura, Kazuhito, (*Tue s10*)15:20  
Satpati, Ashis Kumar, s05-032  
Sautet, Philippe, (*Tue s12*)15:20  
Sauvage, Frédéric, (*Tue s15*)09:30  
Savall, Catherine, (*Tue s08*)15:00  
Saveant, Jean-Michel, (*Fri s11*)10:10  
Scanlon, Micheal, (*Fri s18*)10:30  
Schaffer, Corey P., (*Mon s04*)17:00  
Schafsteller, Britta, s08-006  
Scherson, Daniel, (*Mon s09*)18:00  
Schieda, Mauricio, (*Mon s06*)18:00  
Schjötz, Jakob, (*Tue s09*)15:20  
Schlettwein, Derck, (*Fri s07*)12:10,  
s07-029, s11-004  
Schmidt, Oliver G., s11-003  
Schmidt, Sebastian, s03-129  
Schmidt, Thomas Justus, (*Mon s09*)14:00,  
(*Tue s04*)10:10, (*Tue s09*)16:40,  
(*Thu s09*)15:00  
Schmidt, Wido, (*Tue s10*)14:20  
Schmuki, Patrik, s09-054  
Schneider, Jonathan, (*Fri s09*)10:10  
Schneider, Oliver, s03-064, s03-077,  
s09-002, s14-019  
Scholz, Fritz, (*Thu s18*)10:10  
Schreier, Marcel, (*Tue s06*)10:10  
Schütter, Christoph, (*Wed s05*)10:10  
Schuhmann, Wolfgang, (*Mon s09*)16:00,  
(*Mon s02*)18:20, (*Tue s12*)15:20,  
(*Tue s02*)16:50, (*Tue s02*)17:00,  
(*Thu s01*)14:20, (*Thu s14*)14:40,  
(*Thu s03*)17:00, s01-009, s06-013,  
s09-005  
Schulz, B., s02-005  
Schumacher, Gerhard, s03-119  
Schwager, Patrick, (*Thu s01*)16:40  
Schwarzacher, W., (*Fri s07*)10:10  
Schweinberger, Florian F., s14-019  
Schwenke, K. Uta, (*Fri s03*)11:30  
Schwenzel, Julian, (*Thu s01*)16:40  
Scialdone, Onofrio, (*Tue s10*)14:40,  
s10-020  
Sebastian, Paula, (*Mon s12*)17:40  
Secchiaroli, Marco, (*Wed s05*)10:30  
Sedlářková, Marie, s03-032  
Segawa, Hiroyo, s03-041  
Seidl, Lukas, s03-064, s03-077  
Sek, Slawomir, (*Mon s16*)09:50  
Seki, Shiro, s09-053  
Seki, Shu, s14-011  
Seki, Yusuke, s07-025  
Sekli Belaidi, Fadhila, (*Tue s15*)10:10  
Selskis, Algirdas, (*Thu s09*)17:40, s09-048,  
s09-067  
Sener, M. Kasım, (*Fri s09*)09:50, s09-035  
Sentosun, Kadir, (*Tue s09*)15:00,  
(*Thu s07*)14:00, s07-017  
Sentürk, Zühre, s01-017, s01-021  
Seo, Hyunwoong, (*Mon s06*)14:20  
Sepp, Silver, (*Tue s09*)15:40, s09-062  
Sereda, Olga A., (*Thu s14*)18:00  
Serrano-Ruiz, Juan Carlos, s10-030  
Seselj, Nedjeljko, (*Fri s09*)11:30  
Seto, Shinichi, s05-016  
Setyowati, Vuri Ayu, (*Fri s09*)12:10,  
s09-072  
Seung Min, Kim, s03-097  
Seviour, Thomas, (*Mon s02*)17:20  
Shaddad, Maged Naji, s13-001  
Shafi, Shahid P., s04-040  
Shahzad, Khurram, (*Tue s08*)18:00  
Shakibi Nia, Niusha, (*Tue s08*)15:00  
Shalabi, Kamal, s08-011  
Shan, Dan, s02-033  
Shanmugam, Sangaraju, (*Thu s04*)18:00,  
s05-043  
Shao, Minhua, (*Mon s09*)18:20  
Shao, Qi, s05-030  
Shao-Horn, Yang, (*Mon s12*)14:40  
Sharma, Neeraj, (*Mon s17*)17:40, s03-106  
Shearing, Paul R., (*Mon s03*)17:20  
Shen, Dai, (*Wed s07*)10:10  
Shen, Hsiao- Hsuan, s05-011  
Shen, Sen-Tsan, (*Tue s05*)15:00  
Shen, Shou-Yu, (*Wed s03*)10:10  
Shen, Yan, (*Thu s09*)14:20  
Sheng, Qi, s05-003  
Sheng, Tian, (*Mon s17*)09:30  
Sheptyakov, Denis, s03-129  
Sheu, H.S., (*Tue s05*)14:40  
Shi, Feng, s14-005  
Shi, Ming, s03-038  
Shiba, Shunsuke, (*Tue s01*)14:00  
Shibata, Mari, s12-003  
Shibata, Masao, (*Thu s04*)14:00  
Shibuya, Shota, s09-046  
Shie, Yu-Chian, s03-057  
Shih, Steve, (*Thu s07*)16:00  
Shih, Yu-Chen, s09-063  
Shih, Yu-Pei, s07-012  
Shiku, Hitoshi, (*Wed s02*)09:30, s02-008  
Shim, Joongpyo, s03-011  
Shimada, Manai, s04-016  
Shimada, Shigefumi, s04-016  
Shimamura, Tomoko, s18-009  
Shimizu, Kyoko, (*Thu s14*)17:20  
Shimizu, Masahiro, (*Fri s03*)11:50  
Shimizu, Yusuke, (*Mon s03*)10:10  
Shimoda, Keiji, s17-007, s18-028  
Shin, Heon-Cheol, s03-097  
Shin, Hyeyoung, (*Tue s15*)18:20  
Shin, Hyunjung, s09-031  
Shin, Jaikwang, (*Mon s03*)15:40  
Shin, Jisun, s18-032  
Shin, Mun-Sik, s04-022, s04-023, s04-024  
Shin, Woonup, (*Wed s02*)10:10  
Shin, Young Sun, s03-097  
Shinagawa, Tsutomu, (*Thu s09*)14:00,  
s07-025  
Shinozaki, Kazuma, s04-042  
Shintani, Yukihiro, (*Tue s01*)15:40,  
s01-024

- Shirai, Osamu, *s02-030*  
 Shiraishi, Mika, *s03-079, s04-025, s04-030*  
 Shiraishi, Risa, *s03-079, s04-025, s04-030*  
 Shiraishi, Soshi, *(Tue s05)17:40*  
 Shiraishi, Yasuyoshi, *(Tue s05)17:40*  
 Shirasaka, Ryo, *s04-043*  
 Shiratani, Masaharu, *(Mon s06)14:20*  
 Shiroishi, Hidenobu, *s04-043, s04-044, s09-053, s18-007, s18-025, s18-030*  
 Shironita, Sayoko, *(Mon s04)16:00, (Thu s04)15:20*  
 Shitanda, Isao, *s02-007, s07-001, s09-057*  
 Shoesmith, David, *(Tue s08)14:40*  
 Shoji, Takao, *(Thu s11)16:40*  
 Shou, Binan, *s08-010*  
 Shown, Indrajit, *(Thu s09)09:30, s05-033*  
 Shpigel, Nethanel, *s17-006*  
 Shukla, Garima, *(Tue s03)15:00*  
 Shul, Galyna, *(Mon s05)16:40*  
 Shviro, Meital, *(Thu s09)16:00*  
 Si, Huinan, *s03-064*  
 Sigalov, Sergey, *s17-006*  
 Siket, Christian, *(Fri s18)10:10*  
 Silva, Nataly, *(Mon s09)10:30*  
 Silva, Rafael Hubert, *(Mon s04)18:20*  
 Silva, Thaissa, *s16-005*  
 Sim, Seong Ju, *s03-045*  
 Simek, Petr, *s18-022*  
 Simic, Nina, *(Tue s09)18:00, s09-019*  
 Simkunaite, Dijana, *(Thu s09)17:40, s09-067*  
 Simon, Patrice, *(Mon s05)15:20, (Mon s05)17:40, (Tue s05)14:20, (Tue s05)17:00, (Thu s05)10:10, (Thu s05)15:00, s05-041*  
 Singh, Kiran Pal, *(Tue s09)09:30*  
 Siraj, Shajahan, *(Tue s02)17:20*  
 Sirés, Ignacio, *(Mon s10)14:40, (Fri s09)11:30*  
 Siroma, Zyun, *s04-037, s04-039, s11-001*  
 Sivula, Kevin, *(Mon s06)17:00, (Mon s06)17:20*  
 Sjödin, Martin, *s03-114, s11-013, s18-015*  
 Slávik, Marek, *s03-032*  
 Slesinski, Adam, *s05-015*  
 Sliozberg, Kirill, *s06-013*  
 Sliusarenko, Oleksii, *(Thu s18)14:00*  
 Smith, Emma, *(Mon s12)18:00*  
 Smith, Karen, *(Mon s12)18:00*  
 Smyrek, Peter, *s17-001*  
 Sobczak, Janusz, *(Mon s16)17:40*  
 Sodeyama, Keitaro, *(Thu s14)14:00*  
 Sofer, Zdeněk, *s18-011, s18-022*  
 Sohn, Young-Jun, *(Wed s04)09:50, s04-009*  
 Sojic, Neso, *(Tue s15)10:10, (Tue s02)15:20*  
 Solchenbach, Sophie, *(Fri s03)11:30*  
 Soldà, Alice, *s02-001*  
 Solla-Gullon, Jose, *s12-015*  
 Solomon, Ed, *(Mon s02)17:00*  
 Son, Min-Kyu, *(Mon s06)14:20*  
 Sone, Masato, *(Thu s07)15:00, s02-002, s07-018*  
 Sone, Yoshitsugu, *(Thu s03)17:00*  
 Song, Bingzheng, *s05-039, s07-013*  
 Song, Han, *s01-010, s02-017*  
 Song, Jinju, *s14-014*  
 Song, Min Young, *(Tue s09)09:30*  
 Song, Seung-Wan, *s03-081, s03-115*  
 Song, Yanfang, *(Tue s05)16:40*  
 Song, Yanyan, *s01-012, s09-054*  
 Song, Yen-Fang, *s17-003*  
 Soo, Kristen J.W.Y., *(Mon s04)15:00*  
 Soon, Jiyong, *s03-121*  
 Sopha, Hanna, *s12-024*  
 Sorte, Eric, *(Mon s17)10:10, (Mon s17)15:20*  
 Sotta, Dane, *s03-078*  
 Souada, Malika, *(Mon s02)10:10*  
 Souma, Kenichi, *(Mon s04)16:00*  
 Soutome, Kazuhiro, *s03-079*  
 Souza, F. L., *s10-015*  
 Speck, J. Matthäus, *s11-003*  
 Srivastav, Shruti, *(Tue s15)16:40*  
 Stach, Eric, *s03-097*  
 Stalnioniene, Irena, *s09-047*  
 Stankeviciene, Ina, *s09-058*  
 Steenberge, Sigelinde, *(Fri s04)11:10*  
 Steinke, Nina-Juliane, *(Mon s12)18:00*  
 Stepanova, Mariia, *s08-007*  
 Stephens, Ifan, *(Tue s09)15:20, (Fri s09)10:30*  
 Stevaert, Laurens, *s09-017*  
 Stevens, Philippe, *(Thu s03)10:10*  
 Stimming, Ulrich, *s03-064, s03-077, s09-002, s14-019*  
 Stoerzinger, Kelsey A., *(Mon s12)14:40*  
 Stojek, Zbigniew, *s02-031, s02-032*  
 Stoltz, Detlef, *(Mon s03)17:40*  
 Strasser, Peter, *(Mon s04)17:20, (Thu s09)10:10, (Thu s09)17:00*  
 Strehblow, Hans-Henning, *(Tue s08)15:40*  
 Strehle, Benjamin, *(Fri s03)11:30*  
 Streich, Daniel, *(Mon s17)16:40*  
 Stricker, Florian, *(Thu s07)09:30*  
 Strmcnik, Dusan, *(Tue s12)09:50*  
 Stromme, Maria, *s03-114, s11-013, s18-015*  
 Strzałkowska, Sylwia, *(Tue s01)17:00*  
 Stumpp, Martina, *(Fri s07)12:10, s07-029*  
 Stygar, Mirosław, *s04-004, s04-063*  
 Su, Bao-Fa, *s18-041*  
 Su, Chi-Hung, *s03-027*  
 Su, Chun-Hao, *(Tue s02)17:50, s01-013*  
 Su, Dangsheng, *(Tue s09)14:00*  
 Su, Dong, *(Mon s09)15:00, s09-061*  
 Su, Hang, *(Thu s03)10:30*  
 Su, Panpan, *s03-015*  
 Su, Shou-Huang, *s03-110*  
 Su, Wei-Nien, *s04-035, s06-008, s09-043, s09-056, s10-022*  
 Su, Ya-Ling, *s01-001*  
 Su, Yan, *(Thu s18)14:40*  
 Su, Yu-Cheng, *s04-060*  
 Subrt, Jan, *s12-024*  
 Sudholter, Ernst, *s07-027*  
 Suetake, Kazunori, *s18-031*  
 Suetsugu, Takaaki, *s04-062*  
 Sugimoto, Wataru, *(Mon s05)18:00*  
 Sugiyama, Atushi, *(Thu s07)16:40*  
 Sui, Leping, *(Mon s09)14:20*  
 Sukackiene, Zita, *s09-048*  
 Sun, Bing, *s03-008*  
 Sun, Chia-Liang, *s01-011, s01-013*  
 Sun, Ho-Jung, *s03-011*  
 Sun, Kailing, *s03-046*  
 Sun, Li-Jie, *s05-028*  
 Sun, Liang, *(Fri s07)11:30*  
 Sun, Shi-Gang, *(Mon s17)09:30, (Mon s17)10:10, (Tue s09)10:30, (Tue s02)18:10, s03-048, s14-016*  
 Sun, Sin-Cih, *s02-034*  
 Sun, Yingying, *(Tue s10)16:40*  
 Sunada, Yoshio, *(Thu s09)14:40*  
 Sunday, Christopher, *(Tue s10)17:00*  
 Sunde, Svein, *(Thu s09)15:20*  
 Sung, Lung-Yu, *s04-005*  
 Sung, Yung-Tao, *s09-055*  
 Suraniti, Emmanuel, *(Tue s02)15:20*  
 Susanti, Ratna Frida, *s03-003*  
 Susman, Mariano, *(Thu s07)17:40*  
 Sutiono, Hogiarta, *s09-056*  
 Sutter, Eliane, *(Wed s08)09:30, s01-008*  
 Suzdaltsev, Andrey, *s12-028*  
 Suzuki, Aimi, *s02-021*  
 Suzuki, Daisuke, *s07-008*  
 Suzuki, Hiroshi, *s09-053*  
 Suzuki, Kazuyoshi, *s07-008*  
 Suzuki, Naoya, *s04-062*  
 Suzuki, Shinya, *(Wed s03)10:30*  
 Suzuki, Shohei, *s18-019, s18-029*  
 Suzuki, Takuma, *s09-057*  
 Suzuki, Yuya, *(Tue s03)16:40*  
 Svir, Irina, *(Thu s18)14:00*  
 Swiech, Olga, *(Tue s16)09:50*  
 Syafiq Bin Ahmad, Muhammad, *(Mon s10)18:00, s10-015*  
 Syu, Mei-Jywan, *s07-028, s16-001*  
 Szeto, Bryan, *(Mon s16)14:00*  
 Szlezak, Monika, *(Tue s16)09:30*  
 Szumski, D. S., *(Fri s07)10:10*  
 Szunerits, Sabine, *(Wed s01)10:30*
- ## T
- Taberna, Pierre-Louis, *(Mon s05)15:20, (Mon s05)17:40, (Tue s05)14:20, (Thu s05)10:10, (Thu s05)15:00*  
 Tacchini, Philippe, *(Tue s01)14:40*  
 Tago, Shoko, *(Tue s10)15:20*  
 Tahara, Yuma, *s02-002*  
 Tait, Stephan, *(Mon s10)16:00, s10-006*  
 Taiwo, Oluwadamilola O., *(Mon s03)17:20*  
 Takada, Kenji, *s11-011*  
 Takahashi, Masakuni, *s18-007*  
 Takahashi, Naoko, *(Tue s09)17:00*  
 Takahashi, Takuya, *(Fri s03)11:10, s03-065*  
 Takahashi, Yasufumi, *(Wed s02)09:30, s02-008*  
 Takakusagi, Satoru, *s12-003*  
 Takakuwa, Yasutomo, *s09-070*  
 Takamura, Dan, *s07-029*  
 Takano, Yoshinari, *s02-030*  
 Takasaki, Tomoaki, *s03-059*  
 Takase, Mai, *s12-007*  
 Takeuchi, Kazuya, *s10-021*  
 Takeuchi, Yuma, *s12-020*  
 Taleat, Zahra, *(Fri s14)10:30*  
 Taller, Gabor, *s10-004*  
 Tallo, Indrek, *(Tue s09)15:40, (Thu s05)15:20, s09-062*  
 Tamasauskaite-Tamasiunaite, Loreta, *(Thu s09)17:40, s09-047, s09-048, s09-058, s09-067*  
 Tamura, Yuko, *(Mon s04)09:50, s04-045*  
 Tan, Boxuan, *(Mon s02)14:20*  
 Tan, Xiaoyun, *(Thu s14)17:40*  
 Tanaka, Junko, *s02-022*

- Tanaka, Kazuhisa, *s04-050*  
 Tanaka, Yukino, *s18-009*  
 Tanaka, Yumi, *s09-053, s18-025, s18-030*  
 Tang, Chiu, (*Mon s17*)15:40  
 Tang, Hao, (*Tue s08*)16:40  
 Tang, Shuihua, (*Mon s09*)14:20  
 Tanida, Hajime, *s03-002*  
 Taniguchi, Mina, *s18-009*  
 Taniguchi, Shuichi, (*Thu s03*)17:00  
 Taniki, Ryosuke, *s12-016*  
 Tao, Runbang, *s06-005*  
 Tarascon, Jean-Marie, (*Thu s03*)16:00  
 Tardelli, Joffrey, *s08-014*  
 Tasca, Federico, (*Mon s09*)10:30  
 Tateyama, Yoshitaka, (*Thu s14*)14:00  
 Tatsumisago, Masahiro, *s03-029*  
 Tavalalaie, Roya, (*Wed s01*)09:30, (*Thu s18*)15:40  
 Tee, Ester, (*Thu s05*)15:20  
 Teh, Wuan Xin, (*Thu s18*)17:00  
 Tejchman, Waldemar, *s04-063*  
 Temmel, Sandra, (*Tue s09*)16:40  
 Temple-Boyer, Pierre, (*Tue s15*)10:10  
 Teng, Chiao-Yi, *s13-002*  
 Teng, Hsin-Fu, *s06-008*  
 Teng, Hsisheng, (*Thu s05*)14:20, *s05-004, s13-002*  
 Tengstedt, Carl, (*Tue s03*)16:00  
 Teo, Wei Zhe, *s18-008*  
 Terryn, Herman, (*Thu s07*)14:00, *s07-017, s14-021*  
 Terui, Shintaro, *s03-021, s03-080*  
 Texier, Anne Claire, (*Mon s10*)15:00  
 Theil, Simon, *s01-025*  
 Thiele, Simon, (*Mon s17*)16:00  
 Thomas, Owen D., (*Mon s04*)15:00  
 Thomborg, Thomas, (*Thu s05*)15:20  
 Thordarson, Pall, *s02-035*  
 Thygesen, K. S., (*Fri s07*)10:10  
 Tian, Jing-Hua, (*Fri s03*)10:30  
 Tian, Na, *s14-016, s14-016*  
 Tian, Xiaochun, (*Tue s02*)18:10  
 Tian, Ya-Chung, *s18-001*  
 Tian, Zhong-Qun, (*Mon s12*)16:40, *s12-012, s12-021, s18-041*  
 Tiddi, William, (*Tue s15*)10:10  
 Tijero, María, (*Tue s01*)18:00  
 Tillmann, Selina, (*Thu s03*)15:40, *s03-130*  
 Timoczko, Jakub, (*Tue s12*)15:20  
 Timuda, Gerald Ensang, *s06-005*  
 Ting, Po-Tso, *s09-012*(*Fri s09*)09:30  
 To, Trang Quynh, (*Thu s18*)17:00  
 Toffoli, Giuseppe, *s16-003*  
 Togami, Makoto, (*Tue s02*)18:20  
 Toh, Her Shuang, *s01-026*  
 Tokita, Masahiro, (*Thu s05*)15:40  
 Tokuda, Takuya, *s07-029*  
 Tokumasu, Takashi, (*Tue s15*)15:40  
 Tomai, Takaaki, *s03-128*  
 Tomakazu, Fukutsuka, *s03-063*  
 Tomerini, Daniele, (*Tue s15*)17:00  
 Tominaga, Masato, (*Mon s12*)17:00, (*Tue s02*)18:20  
 Tong, YuYe, (*Mon s17*)10:10, (*Mon s17*)15:20, (*Mon s09*)15:40  
 Top, Siden, (*Thu s11*)15:20  
 Torresi, Roberto, *s03-131*  
 Tory, Joanne, (*Fri s11*)11:10  
 Toth, Peter S., (*Tue s12*)18:00  
 Toyoda, Eishiro, (*Mon s12*)15:00  
 Toyoda, Masahiro, *s04-002, s09-015*  
 Toyoda, Ryojun, *s11-011*  
 Tran, Xuan Minh, *s03-081, s03-115*  
 Traversa, Enrico, (*Fri s04*)09:50, *s04-040*  
 Treossi, Emanuele, (*Thu s14*)14:20  
 Tribollet, Bernard, (*Wed s08*)09:30  
 Trinei, Mirella, *s02-001*  
 Tripkovic, Vladimir, (*Tue s09*)15:20  
 Trnkova, Libuse, (*Tue s02*)15:40, *s01-007, s02-032*  
 Tsai, Chen-Yu, *s04-051*  
 Tsai, Chih-Long, (*Thu s03*)10:10, *s03-082, s03-087*  
 Tsai, Chung-Ting, (*Tue s05*)15:00  
 Tsai, Dah-Shyang, (*Mon s05*)18:20  
 Tsai, Kai-Chieh, *s06-008*  
 Tsai, Li Duan, *s05-027*  
 Tsai, Men-Che, *s03-025, s04-051, s09-043*  
 Tsai, Ping-chun, *s03-066, s03-123, s12-027*  
 Tsai, Po-Chih, *s10-022*  
 Tsai, Shu-Yi, *s03-067, s03-083, s04-060, s04-061, s04-064, s06-009*  
 Tsai, Tzu-Hsuan, *s07-012*  
 Tsai, Wan-Yu, (*Tue s05*)14:20, (*Tue s05*)17:00, (*Thu s05*)15:00  
 Tsai, Y. H., *s14-018, s18-038*  
 Tsai, Yao-Lin, (*Thu s07*)18:00  
 Tsampas, Michael N., *s04-026*  
 Tschulik, Kristina, (*Mon s16*)17:20, (*Thu s14*)17:00  
 Tseng, Chung-Jen, (*Thu s03*)15:40  
 Tseng, Po-Chin, *s18-024*  
 Tseng, Yan-Di, *s07-028*  
 Tseng, Yu-Hao, *s06-006*  
 Tsuchiya, Hiroaki, (*Tue s08*)17:20  
 Tsuchiya, Takashi, *s04-062*  
 Tsuda, Tetsuya, *s14-011*  
 Tsuji, Etsushi, *s08-004*  
 Tsujimura, Seiya, (*Mon s02*)14:40, *s02-007, s02-021, s02-023*  
 Tsukada, Chiaki, *s09-053*  
 Tsukuma, Takami, *s01-014*  
 Tsumura, Tomoki, *s04-002, s09-015*  
 Tsunashima, Katsuhiko, (*Fri s03*)10:30, *s18-039*  
 Tsuruoka, Nozomu, *s02-023*  
 Tu, Chao-Chi, *s05-012, s05-034, s09-055*  
 Tu, Fangfang, (*Fri s03*)10:10, *s03-088*  
 Tuci, Giulia, (*Mon s09*)17:40  
 Tudisco, Erika, (*Mon s03*)17:20  
 Tübke, Jens, (*Thu s04*)15:00  
 Tupiti, Wycliff, (*Tue s01*)15:00  
 Tzou, Dong-Ying, *s09-059, s09-060*
- U**  
 Uchida, Ken-ichi, (*Mon s12*)18:20, *s12-011*  
 Uchida, Makoto, *s04-016*  
 Uchida, Satoshi, (*Fri s03*)11:10, *s03-065, s03-084*  
 Uchimarui, Masahiro, *s02-025*  
 Uchimoto, Yoshiharu, (*Mon s03*)14:00, (*Mon s17*)17:20, *s03-002, s03-022, s03-099, s03-104, s09-044, s10-011, s17-007, s18-028*  
 Ueda, Hiroyuki, (*Fri s11*)11:50, *s18-010*  
 Ueda, Mikito, (*Tue s08*)17:40, *s09-046*  
 Ueda, Tadaharu, *s18-009*  
 Ueda, Tsukasa, *s05-016*  
 Uehara, Hiromitsu, *s12-003*  
 Uehara, Masato, *s04-044*  
 Uematsu, Taro, *s14-011*  
 Uemura, Yohei, *s12-003*  
 Uhlenbruck, Sven, (*Thu s03*)10:10, *s03-082, s03-087*  
 Ujihara, Masaki, *s05-009*  
 Ujino, Yusuke, *s09-061*  
 Ukedo, Hiroyuki, *s18-009*  
 Ukyo, Yoshio, *s18-028*  
 Ulissi, Ulderico, (*Mon s03*)15:00, *s03-120*  
 Ulstrup, Jens, (*Fri s09*)11:30  
 Umeda, Minoru, (*Mon s04*)16:00, (*Thu s04*)15:20, (*Thu s03*)17:00  
 Umirov, Nurzhan, (*Tue s03*)15:00  
 Unwin, Patrick, (*Thu s01*)15:40  
 Uosaki, Kohei, (*Mon s12*)17:20, *s12-020*  
 Urbonaite, Sigita, (*Thu s03*)17:20, *s03-085*  
 Ushirogata, Keisuke, (*Thu s14*)14:00  
 Ussano, Eleonora, *s02-001*  
 Ustarroz, Jon, (*Tue s09*)15:00, (*Tue s10*)18:00, (*Thu s07*)14:00, *s07-017, s09-017, s10-004, s14-021*  
 Usui, Hiroyuki, (*Thu s03*)14:40, (*Fri s03*)11:50  
 Uzun, Djamal, (*Mon s10*)17:20
- V**  
 Vaarmets, Kersti, (*Tue s09*)15:40, *s09-062*  
 Vacek, Jan, (*Thu s01*)09:30, *s01-007*  
 Vaitekonis, Sarunas, *s02-029*  
 Vajrala, Venkata Suresh Reddy, (*Tue s15*)10:10  
 Valenti, Giovanni, (*Thu s14*)16:40, (*Fri s14*)10:10, *s01-015, s02-001*  
 Valenzuela, William, (*Mon s12*)16:40  
 Valero, Laura, (*Wed s10*)10:30  
 Valiokas, Ramunas, *s02-003*  
 Valverde, José Luis, (*Tue s10*)10:10, *s10-030*  
 Van Gestel, Tim, (*Thu s03*)10:10, *s03-087*  
 Van Laethem, Dries, (*Fri s04*)11:10  
 Vankelecom, Ivo, (*Tue s10*)17:20, *s04-012*  
 Vanrenterghem, Bart, (*Tue s10*)18:00, *s10-004*  
 Varela, Ana Sofia, (*Thu s09*)10:10  
 Vasconcelos, Camila, *s16-005*  
 Vasconcelos, Vanessa M., *s10-018*  
 Vasilescu, Cora, *s08-001, s08-015*  
 Vasiljevic, Natasa, (*Tue s07*)10:10  
 Vaskevich, Alexander, (*Thu s07*)17:40, *s02-009*  
 Vazhenin, Grigory, *s08-006*  
 Veclani, Daniele, (*Tue s01*)15:20  
 Velicky, Matej, (*Tue s12*)18:00  
 Venckus, Tautvydas, *s02-029*  
 Ventosa, Edgar, (*Thu s03*)17:00, *s01-009*  
 Verlato, Enrico, (*Fri s14*)09:30, (*Fri s07*)10:30  
 Vernoux, Philippe, (*Tue s10*)15:40, *s04-026*  
 Vertova, Alberto, (*Mon s17*)15:00, (*Thu s14*)15:00  
 Veys-Renaux, Delphine, (*Tue s08*)15:20, *s08-016*  
 Vicari, Fabrizio, (*Tue s10*)14:40  
 Vidal-Iglesias, Francisco J., *s12-015*  
 Vieira Carvalho, Diogo, *s03-060*  
 Vieira dos Santos, Elisama, *s10-023, s10-024*

Villani, Elena, (*Fri s14*)10:10  
 Villen-Guzman, Maria, *s10-017*  
 Villeveille, Claire, (*Mon s03*)09:30,  
*(Thu s03)*17:20, *s03-129*  
 Vincent, Kylie, (*Mon s02*)15:00, *s01-019*  
 Virmelson, Craig, (*Wed s07*)10:10  
 Vittal, R., (*Tue s06*)10:30, *s06-004*,  
*s09-016*, *s09-022*, *s10-005*  
 Vivier, Vincent, (*Wed s08*)09:30  
 Vlachopoulos, Nick, (*Mon s06*)15:20  
 Vlkova-Zivcova, Zuzana, (*Mon s06*)16:00  
 Vondrák, Jiří, *s03-032*  
 Vorotyntsev, Mikhail A., (*Thu s14*)18:00,  
*s14-004*  
 Vortmann, Britta, *s03-071*  
 Vu, Quang Huy, (*Tue s12*)15:20

**W**  
 Wada, Kenji, *s03-041*  
 Wagner, Ralf, (*Thu*)08:15  
 Wain, Andy, (*Mon s12*)15:20  
 Waki, Keiko, *s06-005*  
 Wakisaka, Mitsuru, (*Wed s10*)09:50  
 Wakisaka, Yumi, *s12-007*  
 Walcarius, Alain, (*Mon s02*)16:40  
 Waldmann, Thomas, *s12-014*  
 Walker, Lindsey, (*Mon s02*)14:00  
 Walsh, Frank C., (*Wed s10*)09:30,  
*(Thu s03)*18:00, *s03-099*  
 Walsh, Kelly, (*Mon s02*)14:00  
 Walti, Christoph, *s12-025*  
 Wan, Li-Jun, (*Mon s04*)14:40, (*Wed*)08:15  
 Wan, Ying, (*Thu s18*)14:40  
 Wandlowski, Thomas, (*Fri s11*)09:30  
 Wang, Aixiu, *s05-003*  
 Wang, Chen-Hao, (*Mon s04*)14:20,  
*(Thu s09)*09:30, (*Fri s09*)12:10,  
*s04-029*, *s09-063*, *s09-072*  
 Wang, Chiu-Hui, (*Fri s09*)10:10  
 Wang, Chueh-Han, *s03-062*, *s03-087*,  
*s05-017*  
 Wang, Chun-Chieh, *s17-003*  
 Wang, Congxiao, *s03-014*  
 Wang, Deli, (*Tue s09*)14:40  
 Wang, Fang-Fang, *s18-041*  
 Wang, Fu-Ming, (*Mon s03*)18:00,  
*(Thu s03)*18:00, (*Fri s03*)11:30,  
*s02-014*, *s03-068*, *s03-089*, *s03-111*,  
*s03-112*, *s03-134*  
 Wang, Gang, *s03-132*, *s03-133*  
 Wang, Gao-Liang, *s07-010*  
 Wang, Guiling, *s05-036*  
 Wang, Guoqing, (*Fri s03*)10:10, *s03-088*  
 Wang, Han, (*Thu s09*)18:00, *s09-074*  
 Wang, Hsiang-Cheng, *s04-015*  
 Wang, Hsien Hau, (*Fri s03*)10:30  
 Wang, Jau-Kai, *s18-036*  
 Wang, Jen-Yuan, (*Thu s18*)16:00, *s10-029*,  
*s18-037*  
 Wang, Jeng-Han, (*Thu s04*)14:40  
 Wang, Jiade, *s10-025*  
 Wang, Jian-jun, *s18-012*  
 Wang, Jianqiu, (*Thu s08*)10:10  
 Wang, Jie, (*Tue s09*)14:40  
 Wang, Jin, (*Fri s03*)10:30  
 Wang, Jing-Hwei, *s02-024*  
 Wang, Jun, (*Tue s03*)17:40  
 Wang, Jung-Chi, (*Thu s03*)18:00  
 Wang, Kuan-Wen, (*Thu s04*)14:40,

*s04-049*  
 Wang, Li, *s02-012*, *s05-007*, *s09-038*  
 Wang, Lina, *s03-086*  
 Wang, Min-Chuan, *s10-029*, *s18-037*  
 Wang, Pengjuan, (*Thu s18*)14:40  
 Wang, Rainey, (*Mon s04*)16:40  
 Wang, Shan-Yu, *s09-062*  
 Wang, Shih-Han, *s02-024*  
 Wang, Si-Ping, *s01-005*  
 Wang, Sihui, (*Tue s03*)16:40  
 Wang, Wang, *s03-055*  
 Wang, Wei, *s18-041*  
 Wang, Xianbin, *s05-035*  
 Wang, Xianfen, (*Tue s03*)18:20  
 Wang, Xiang, *s12-009*  
 Wang, Xiaoqi, (*Fri s07*)11:30  
 Wang, Xin, *s09-068*  
 Wang, Xixin, *s03-038*  
 Wang, Xueqian, *s03-055*  
 Wang, Yan-Ru, *s18-036*  
 Wang, Yanfang, (*Tue s03*)10:30  
 Wang, Yanyan, (*Mon s09*)15:40  
 Wang, Ye, (*Mon s12*)10:10, (*Fri s09*)11:10  
 Wang, Ying-Ting, *s18-036*  
 Wang, Yonggang, (*Mon s03*)10:30,  
*s03-014*, *s03-019*, *s03-086*  
 Wang, Yu-Sheng, *s07-006*  
 Wang, Yue, *s03-053*, *s03-138*  
 Wang, Zenglin, (*Thu s07*)15:40  
 Wang, Zhong Lin, (*Wed s10*)10:10,  
*s10-027*  
 Wang, Zuxin, (*Mon s10*)18:00,  
*(Tue s10)*15:00, *s10-015*  
 Warakulwit, Chompunuch, (*Tue s16*)10:10  
 Ward, Meryck, (*Tue s10*)17:00  
 Watanabe, Kazuo, (*Thu s07*)17:20  
 Watanabe, Masahiro, *s04-016*  
 Watanabe, Mizuki, *s01-004*  
 Watanabe, Nobuaki, *s07-003*, *s07-020*,  
*s07-021*  
 Watanabe, Satoru, *s07-001*  
 Wattanakit, Chularat, (*Tue s16*)10:10  
 Wedlich, Klaus, (*Mon s03*)17:40  
 Weeks, Justin, (*Mon s02*)15:00  
 Wehrspohn, Ralf, (*Thu s03*)14:20  
 Wei, Chiao-Chien, (*Thu s07*)16:00  
 Wei, Guor-Tzo, *s01-016*  
 Wei, Hang, *s03-051*  
 Wei, Hwa-Jou, *s03-039*  
 Wei, Jie, *s04-052*  
 Wei, Luming, *s01-022*  
 Wei, Nini, *s05-035*  
 Wei, Zidong, (*Mon s04*)14:00,  
*(Mon s04)*14:40, *s04-041*, *s04-046*,  
*s14-005*  
 Weiner, Joel, (*Mon s02*)15:00  
 Weingarth, Daniel, (*Thu s05*)16:00,  
*s17-006*  
 Weissbach, Thomas, *s04-003*  
 Weissbecker, Julianne, *s11-004*  
 Weissbrod, Sebastian, *s08-006*  
 Weller, Mark T., *s13-001*  
 Wen, M. Y., *s14-018*, *s18-038*  
 Wen, Shih-I., *s07-009*  
 Wen, Zhen, *s10-027*  
 Weng, Tu-Ting, (*Tue s05*)14:40  
 Weng, Yu-Ching, *s09-064*  
 Wercheister, Rebecka Maria Larsen,  
*(Mon s04)*18:20

Wiberg, Gustav  
 Wiberg, Gustav K.H., (*Wed s04*)10:10,  
*(Thu s04)*09:50  
 Wieczorek, W., (*Fri s03*)11:10  
 Wiemhöfer, Hans-Dieter, *s04-059*  
 Wildlock, Mats, (*Tue s09*)18:00, *s09-019*  
 Wilson, Lindsay, (*Tue s09*)10:10,  
*(Fri s09)*11:10, *s09-058*, *s09-065*  
 Winter, Martin, (*Tue s03*)16:00,  
*(Thu)*08:15, (*Thu s03*)09:30,  
*(Thu s03)*15:40, *s03-006*, *s03-071*,  
*s03-119*, *s03-130*  
 Wintrich, Daniela, (*Thu s14*)14:40  
 Wittstock, Gunther, (*Thu s01*)16:40,  
*s18-040*  
 Wohlfahrt-Mehrens, Margret,  
*(Wed s05)*10:30, *s01-025*, *s12-014*  
 Wolf, Hannes, (*Thu s03*)17:20  
 Wolfenstine, Jeffrey, (*Fri s03*)09:30  
 Wong, Colin Hong An, *s18-011*  
 Wong, Raymond, (*Tue s03*)17:40,  
*(Thu s03)*16:40  
 Wong, Wei-Ting, *s03-054*  
 Wouters, Jonatan, (*Tue s10*)17:20  
 Wright, Andrew G., (*Mon s04*)15:00  
 Wu, Alvin, (*Mon s03*)15:20  
 Wu, Cheng-Gang, *s18-026*  
 Wu, Ching Chou, *s02-019*, *s09-066*  
 Wu, Chun-Yi, *s17-003*  
 Wu, De-Yin, (*Mon s12*)16:40, *s12-012*,  
*s12-021*  
 Wu, Donjun, (*Tue s07*)10:30  
 Wu, Guangping, *s04-046*  
 Wu, Heng-Liang, (*Tue s03*)15:20  
 Wu, Jhing-Jhou, *s01-013*  
 Wu, Jian-Hua, *s03-089*  
 Wu, Jin-An, *s04-020*  
 Wu, Kuo-Hui, *s11-011*  
 Wu, Lijun, (*Mon s09*)15:00, *s09-061*  
 Wu, Nae-Lih, (*Tue s05*)14:40,  
*(Thu s03)*09:30, *s03-056*  
 Wu, Pin-Chin, *s03-013*  
 Wu, Pu-Wei, *s07-030*, *s18-014*  
 Wu, Qihui, (*Thu s03*)15:00  
 Wu, Ranran, (*Tue s02*)18:10  
 Wu, She-huang, (*Wed s03*)10:10, *s03-106*,  
*s03-126*  
 Wu, Songtao, (*Fri s07*)11:30  
 Wu, Tzu-Ho, *s17-002*  
 Wu, W. C., *s18-038*  
 Wu, Xinqiang, (*Thu s08*)10:10  
 Wu, Xuehang, (*Tue s03*)16:40  
 Wu, Yi-Chen, *s04-051*  
 Wu, Yi-Hsuan, *s05-017*  
 Wu, Yi-Shan, *s09-067*  
 Wu, Yi-Shiuan, *s03-090*  
 Wu, Yu-Shiang, (*Thu s03*)09:30  
 Wu, Yuan-Fei, *s12-012*  
 Wu, Yuping, (*Tue s03*)10:30  
 Wu, Zexing, (*Tue s09*)14:40  
 Wu, Zhan-Yu, *s03-048*  
 Wuensche, Mathias, *s08-006*  
 Wurz, Peter, (*Thu s07*)09:30

**X**  
 Xia, Chuan, *s05-035*  
 Xia, Fajun, *s05-007*  
 Xia, Wei, (*Mon s09*)16:00  
 Xia, Xifeng, (*Tue s09*)17:20  
 Xia, Xing-Hua, (*Mon s02*)10:30

Xia, Yongyao, (*Mon s03*)10:30,  
(*Tue s05*)16:40, *s03-014*, *s03-019*,  
*s03-086*, *s03-092*  
Xiao, Changlong, (*Fri s09*)09:30  
Xiao, Chunhui, *s12-017*  
Xiao, Meiling, (*Wed s09*)10:30  
Xiao, Nan, *s02-026*  
Xiao, Xiaozhen, *s03-046*, *s03-047*  
Xie, Fang yuan, *s05-038*  
Xie, Han Jin, (*Tue s05*)10:10  
Xie, Huaqing, *s05-025*  
Xie, Jian, (*Fri s03*)10:10, *s03-088*  
Xie, Jin, (*Thu s04*)16:40  
Xie, Xiaohong, *s04-041*  
Xie, Zhaoxiong, (*Fri s09*)10:30, *s09-009*,  
*s09-080*  
Xin, Peng, *s02-033*  
Xin, Shuli, *s12-017*  
Xing, Wei, (*Wed s09*)10:30  
Xiong, Wei-Fen, *s09-064*  
Xiong, Zhubiao, *s05-008*  
Xu, Chao, (*Fri s03*)12:10  
Xu, Guiyin, (*Tue s03*)14:40, *s03-097*,  
*s05-003*  
Xu, Guobao, (*Fri s14*)09:50  
Xu, Hui, (*Tue s03*)18:20  
Xu, Jin, (*Fri s07*)11:30  
Xu, Jing, (*Tue s03*)17:20  
Xu, Junli, (*Tue s10*)17:40  
Xu, Tong, *s08-010*  
Xu, Wei, (*Fri s01*)11:30  
Xu, Wenting, (*Thu s09*)15:20  
Xu, Yixin, *s04-013*  
Xu, Yujiao, (*Fri s03*)10:30  
Xue, Kan-Hao, (*Tue s03*)15:00, *s15-002*  
Xue, Lingjun, *s06-011*

## Y

Yabe, Kazuhiro, *s07-021*  
Yadnum, Sudarat, (*Tue s16*)10:10  
Yagi, Ichizo, *s04-038*, *s12-003*  
Yaguchi, Momo, *s12-013*  
Yahara, Tatsuma, *s10-011*  
Yalamanchili, Anurag, (*Tue s03*)16:00  
Yamada, Atsuo, (*Tue s03*)16:40,  
(*Tue s03*)18:20  
Yamada, Hirohisa, *s04-037*, *s04-058*  
Yamagata, Masaki, (*Thu s05*)14:40,  
(*Fri s03*)11:10, *s03-065*, *s03-084*  
Yamaguchi, Naoto, (*Tue s01*)14:00  
Yamaguchi, Shohei, *s03-091*, *s04-062*  
Yamamoto, Akihiro, *s07-021*  
Yamamoto, Kazuhiro, *s01-004*  
Yamamoto, Kentaro, *s03-022*, *s03-104*  
Yamamoto, Masahiro, (*Thu s18*)09:50  
Yamamoto, Takayo, *s07-004*, *s07-005*,  
*s07-007*  
Yamamoto, Yudai, (*Thu s08*)09:30  
Yamamoto, Yuta, *s03-031*  
Yamane, Tomokazu, *s03-002*  
Yamauchi, Yusuke, (*Thu s07*)16:40  
Yamazaki, Shin-ichi, *s04-039*, *s11-001*  
Yan, Huijun, *s03-051*  
Yan, Jiawei, *s11-008*  
Yan, Runwen, (*Mon s12*)16:40  
Yanagida, Masahiro, *s03-059*  
Yanagisawa, Masahiro, (*Tue s10*)16:40  
Yang, Cheng-Hsien, *s03-062*, *s03-087*,  
*s05-017*  
Yang, Chenlu, *s03-047*  
Yang, Chih-Wen, *s12-023*  
Yang, Chun-Chen, *s03-093*  
Yang, Dea-Soo, (*Tue s09*)09:30  
Yang, Hao, *s04-007*  
Yang, Huimin, *s04-036*, *s18-017*  
Yang, Huiying, *s03-088*  
Yang, Jianmao, *s05-008*  
Yang, Jingshuai, (*Mon s04*)15:40, *s04-013*  
Yang, Joeng-Jin, (*Tue s05*)17:20  
Yang, Jun, *s03-092*  
Yang, Jung Hoon, *s03-094*  
Yang, Li, *s03-114*, *s11-013*  
Yang, Long, *s09-068*  
Yang, Luyi, (*Fri s03*)09:50  
Yang, Lyu Ye, *s03-134*  
Yang, Ming-Chang, (*Wed s02*)09:50  
Yang, Peixia, (*Thu s07*)15:20  
Yang, Ping-Feng, *s07-002*  
Yang, Po-Wei, *s03-013*  
Yang, Qihua, *s03-015*  
Yang, Ruizhi, (*Fri s03*)10:30  
Yang, Sainan, *s05-036*  
Yang, Sheng Sian, *s05-012*, *s05-034*  
Yang, Shifeng, *s03-015*  
Yang, Shun-Min, *s03-026*  
Yang, Tae-Hyun, (*Wed s04*)09:50, *s04-009*  
Yang, Tong, *s05-007*  
Yang, Weilu, (*Mon s10*)15:40  
Yang, Wenrong, (*Thu s11*)18:20  
Yang, Wenyu, *s01-018*, *s03-095*  
Yang, Xiaodong, (*Mon s04*)10:30  
Yang, Ying, (*Wed s01*)09:30  
Yang, Yong, (*Tue s03*)16:40  
Yang, Yu, (*Mon s04*)16:00  
Yang, Yuebin, (*Tue s03*)17:00  
Yao, Chieh-Wen, (*Fri s01*)10:30  
Yao, Yao, *s04-053*  
Yaqub, Adnan, *s03-018*  
Yardym, Yavuz, *s01-017*, *s01-021*, *s01-027*  
Yashiro, Hitoshi, *s03-041*, *s07-022*  
Yasuda, Satoshi, *s12-007*  
Yasukawa, Tomoyuki, (*Tue s02*)09:50,  
*s02-015*  
Yasumoto, Eiichi, (*Wed s04*)09:30  
Yasuno, Masafumi, *s10-026*  
Yasuzawa, Mikito, *s02-025*  
Yatsugi, Yuto, (*Mon s12*)17:00  
Yau, Shuehlin, (*Fri s07*)09:30  
Yavuz, Abdulcabbar, (*Mon s05*)16:00  
Yazar, Zuhail, *s09-050*  
Ye, Ke, (*Thu s04*)16:00, *s09-068*  
Ye, Meidan, *s06-010*  
Ye, Shen, (*Tue s12*)17:20  
Yeh, Chen-Yu, (*Mon s06*)14:00  
Yeh, Fa-Hsing, *s03-043*  
Yeh, Ju-Yu, (*Wed s09*)09:50  
Yeh, Min-Hsin, (*Wed s10*)10:10, *s10-027*  
Yeh, Nan Hung, *s03-134*  
Yeh, Te-Fu, *s13-002*  
Yen, Yi-Han, *s02-024*  
Yen, Yin-Cheng, (*Mon s06*)15:40  
Yeon, Yu-Beom, *s07-031*  
Yezdi, Dordi, *s09-047*  
Yi, Jaeshin, *s03-101*, *s05-010*  
Yigit, Aydin, *s01-017*  
Yin, Jian, *s03-053*, *s03-138*  
Yin, Ken-Ming, *s04-027*  
Yin, Lu-Hsiang, *s14-015*

Yin, Pei-Sin, *s03-105*  
Yin, Yinghui, (*Tue s03*)15:00,  
(*Tue s15*)17:40, *s15-004*  
Yin, Yu-Tung, (*Mon s13*)10:10, *s13-002*  
Yoda, Hiromi, *s16-007*  
Yonemura, Masao, *s18-028*  
Yoo, Chung-Yul, *s10-014*, *s10-028*  
Yoo, Jung-Joon, (*Tue s05*)18:00  
Yoo, Seung Joon, (*Mon s16*)10:10  
Yoon, Gabin, *s03-070*  
Yoon, Hyung-Chul, *s10-028*  
Yoon, Jae-Kook, (*Tue s05*)18:00  
Yoon, Miyoung, *s09-031*  
Yoon, Seon Hye, *s03-069*  
Yoon, Taeho, *s03-121*  
Yoon, Won-Sub, (*Thu s03*)16:00  
Yoshida, Hiromu, *s09-069*  
Yoshihara, Sachio, *s07-008*  
Yoshikawa, Hayato, *s18-031*  
Yoshimoto, Nobuko, (*Thu s05*)15:40,  
*s05-037*  
Yoshimoto, Soichiro, (*Fri s11*)11:50,  
*s18-010*  
Yoshino, Shuhei, (*Thu s04*)14:00  
Yoshitake, Kazuma, (*Thu s04*)15:20  
You, Mina, *s03-036*  
Youn, Hee Chang, (*Tue s05*)09:30  
Yu, Aishui, *s03-135*  
Yu, Denis Y. W., (*Thu s03*)15:20  
Yu, Fangke, (*Mon s10*)15:40  
Yu, Feng, *s03-132*, *s03-133*  
Yu, Hsin-Fu, *s10-029*, *s18-037*  
Yu, Ing-Song, *s03-043*  
Yu, Ji Haeng, *s10-028*  
Yu, Jingxian, (*Thu s11*)17:20  
Yu, Jong-Sung, (*Tue s09*)09:30  
Yu, Ping, (*Mon s16*)14:40  
Yu, Xiaoyun, (*Mon s06*)17:00  
Yu, Yuh-Jenq, *s03-027*  
Yuan, Jiawei, (*Mon s09*)14:20  
Yuan, Qiuyi, *s09-007*  
Yuan, Zhiguo, (*Mon s10*)17:40  
Yuk, Young-Jae, (*Tue s05*)17:20  
Yuki, Sawaguchi, *s09-070*  
Yun, Chaofan, *s03-055*  
Yun, Dae Sik, *s10-028*  
Yun, Young Soo, *s03-070*  
Yung, Maria, (*Mon s02*)17:20  
Yutthalekha, Thittaya, (*Tue s16*)10:10

## Z

Zabielaite, Ausrine, (*Thu s09*)17:40,  
*s09-067*  
Zabost, Ewelina, *s02-031*, *s02-032*  
Zachara, J., (*Fri s03*)11:10  
Zafarani, Hamid Reza, *s07-027*, *s11-003*  
Zafferoni, Claudio, (*Mon s09*)17:40,  
*s07-032*  
Zagal, Jose, (*Mon s09*)10:30  
Zaghib, K., (*Thu s03*)14:00  
Zaiat, Marcelo, (*Tue s10*)18:20  
Zaikov, Yuriy, *s12-028*  
Zaino Jr., Lawrence, (*Fri s01*)11:30  
Zak, Jerzy, *s14-001*, *s16-006*  
Zakeeruddin, Shaik M., (*Mon s06*)16:00  
Zalitis, Christopher, (*Thu s04*)10:30  
Zang, Dejin, (*Fri s09*)09:50  
Zangheri, Martina, *s01-015*  
Zapien, Juan Antonio, *s05-030*  
Zare, Hamid Reza, (*Fri s09*)11:50, *s09-018*

- Zarei, Leila, (*Wed s01*)09:30  
 Zen, Jyh-Myng, (*Tue s01*)16:40  
 Zeng, Chengchu, (*Mon s16*)10:10, (*Thu s11*)17:40  
 Zeng, Wei-Yang, (*Thu s07*)10:10  
 Zeng, Zhi-Cong, *s12-009*  
 Zeng, Zi fan, *s05-038*  
 Zeradjanin, Aleksandar, (*Mon s17*)14:00  
 Zerbetto, Francesco, (*Thu s14*)14:20  
 Zhan, Dongping, *s18-041*  
 Zhan, Xun, *s07-011*  
 Zhan, Ya-Yun, (*Wed s02*)09:50  
 Zhang, Bei, *s04-008*  
 Zhang, Bin-Wei, (*Tue s09*)10:30  
 Zhang, Dalei, (*Thu s18*)17:40, *s18-012*  
 Zhang, Dongming, (*Thu s04*)16:00  
 Zhang, Gaini, *s05-029*  
 Zhang, Hongli, (*Mon s16*)18:00  
 Zhang, Hongyu, *s09-068*  
 Zhang, Jia-Wei, *s04-008*  
 Zhang, Jianbo, (*Mon s03*)18:20  
 Zhang, Jie, (*Thu s07*)14:40, (*Thu s01*)17:20, *s18-041*  
 Zhang, Jinbao, (*Mon s06*)15:20  
 Zhang, Jingdong, (*Fri s09*)11:30  
 Zhang, Jingxin, (*Tue s04*)09:30  
 Zhang, Jinqiu, (*Thu s07*)15:20  
 Zhang, Leiting, (*Thu s03*)16:00  
 Zhang, Ling, (*Fri s14*)09:50  
 Zhang, Lingzhi, *s03-137*, *s03-139*  
 Zhang, Lu, *s01-010*, *s02-017*  
 Zhang, Ludan, *s03-136*  
 Zhang, Meng, (*Mon s17*)14:40, (*Mon s12*)16:40  
 Zhang, Nan, *s06-010*  
 Zhang, Qianyu, *s03-137*  
 Zhang, Qinghong, (*Mon s06*)14:40  
 Zhang, Shichao, (*Fri s03*)10:10, *s03-088*  
 Zhang, Tao, *s03-048*  
 Zhang, Tian, *s09-020*, *s09-034*  
 Zhang, Tong, (*Wed s05*)10:30  
 Zhang, Weibin, *s05-023*  
 Zhang, Weiwei, *s08-009*  
 Zhang, Wenjing (Angela), (*Mon s04*)18:20  
 Zhang, Wenli, *s03-053*, *s03-138*  
 Zhang, Xiaogang, (*Tue s03*)14:40, *s03-097*  
 Zhang, Xinsheng, (*Fri s11*)11:30, *s09-071*  
 Zhang, Xuan, *s04-008*  
 Zhang, Yanjun, (*Thu s01*)14:20  
 Zhang, Yongguang, (*Tue s03*)14:20, *s04-041*  
 Zhang, Yun, *s04-041*  
 Zhang, Zhiming, (*Thu s08*)10:10  
 Zhao, Anqi, (*Mon s09*)16:00  
 Zhao, Bo, *s08-010*  
 Zhao, Chuan, (*Tue s01*)17:40, (*Fri s09*)09:30, *s01-028*, *s02-035*  
 Zhao, Chunhua, *s04-026*  
 Zhao, Fangyuan, (*Mon s02*)18:20  
 Zhao, Feng, (*Tue s02*)18:10  
 Zhao, Guiying, *s01-018*  
 Zhao, Hong, *s05-039*, *s07-013*  
 Zhao, Hui, (*Thu s03*)14:00  
 Zhao, Jiao, *s03-015*  
 Zhao, Liwei, (*Fri s03*)10:10  
 Zhao, Wenzhi, (*Thu s03*)10:30  
 Zhao, Xinbing, (*Fri s03*)10:10, *s03-088*  
 Zhao, Yang, *s12-001*  
 Zhao, Yaping, *s05-039*, *s07-013*  
 Zhao, Zhe, (*Fri s04*)11:30, *s04-054*  
 Zheng, Dajiang, *s06-010*  
 Zheng, Junwei, *s03-116*  
 Zheng, Lansun, (*Fri s09*)10:30, *s09-080*  
 Zheng, Yongli, *s04-052*, *s04-053*  
 Zheng, Zhiyong, (*Tue s02*)18:10  
 Zhi, Wu, *s06-017*  
 Zhong, Haoxiang, *s03-139*  
 Zhong, Jin-Hui, *s12-009*  
 Zhong, Rensheng, *s09-071*  
 Zhong, Xinhua, (*Mon s13*)09:50  
 Zhong, Yunxin, *s11-008*  
 Zhou, Dandan, (*Tue s05*)16:40  
 Zhou, Han, *s12-017*  
 Zhou, Hui, (*Thu s03*)15:20  
 Zhou, Ming, (*Mon s09*)15:20, *s09-072*  
 Zhou, Minghua, (*Mon s10*)15:40  
 Zhou, Mingming, *s10-025*  
 Zhou, Xuan, (*Thu s14*)15:20  
 Zhou, Zhi-You, (*Mon s17*)09:30  
 Zhu, Ji liang, *s05-038*  
 Zhu, Jianbing, (*Wed s09*)10:30  
 Zhu, Jing, (*Tue s09*)14:40  
 Zhu, Tiejun, (*Fri s03*)10:10, *s03-088*  
 Zhu, Xiao hong, *s05-038*  
 Zhu, Xiaoli, *s01-022*  
 Zhu, Yimei, (*Mon s09*)15:00, *s09-061*  
 Zhu, Yongchun, *s02-026*  
 Zhu, Zhentao, (*Mon s09*)14:20  
 Zhuang, Lin, (*Wed s09*)09:30  
 Zigah, Dodzi, (*Tue s15*)10:10, (*Thu s14*)17:20  
 Zimbardi, Ana L. R. L., *s02-006*  
 Zitoun, David, (*Thu s09*)16:00  
 Zong, Cheng, (*Mon s17*)14:40  
 Zou, Mingzhong, *s01-018*  
 Zou, Qingli, (*Tue s12*)17:00  
 Zou, Zhigang, (*Thu s04*)16:40  
 Zukalova, Marketa, (*Mon s06*)15:00  
 Zukowska, Z., (*Fri s03*)11:10  
 Zuñiga, Cesar, (*Mon s09*)10:30  
 Zuñiga, Georgina, (*Mon s10*)16:40  
 Zuo, Yongtao, *s03-132*, *s03-133*



# The International Society of Electrochemistry



The International Society of Electrochemistry (ISE) was founded in 1949 by leading European and American electrochemists to serve the growing needs of electrochemistry. At that time only a handful of scientists were members of the society – known as CITCE (Comité International de Thermodynamique et Cinétique Electrochimiques). Since then ISE has evolved and comprises now more than 3500 individual members, from 72 countries, and is organized in 44 Regional Sections. Both industrialised and developing countries from all five continents are represented. ISE is, therefore, a truly world-wide organisation. ISE is a non-profit-making organisation with its seat in Lausanne, Switzerland.

The International Society of Electrochemistry (ISE) is devoted to the advancement of electrochemical science and technology through the promotion of international contacts and the dissemination of scientific knowledge. For this ISE organises Annual and Topical Meetings which are held in different countries each year and which cover a wide range of current topics in fundamental and applied electrochemistry. The activities of ISE include the sponsoring of regional meetings, and of special meetings of limited participation devoted to particular subjects. A scientific journal, *Electrochimica Acta*, is edited by ISE and supplied to its members at a special rate. Individuals, non-profit organisations, industrial companies and learned societies may become members of ISE. The administration of ISE is done by an Executive Committee, periodically elected by all members. The Regional Representatives together with the Division Officers form the ISE Council which advises the Executive Committee. The scientific activities of ISE are grouped into Scientific Divisions. They are organised and co-ordinated by the Committee of Division Officers headed by the President Elect. Upon joining ISE each member indicates his/her divisional interests.

The history of the International Society of Electrochemistry (ISE) is described in a series of articles published in Volume 45 of *Electrochimica Acta* and available on the web site of the Society (<http://www.ise-online.org/geninfo/history.php>).

## Why you should join ISE

ISE membership provides a number of advantages which can be summarized as follows:

- Individual members can get reduced subscription rates for the following journals:  
*Electrochimica Acta* (online),  
*Journal of Electroanalytical Chemistry* (online),  
*Electrochemistry Communications* (online),  
*Bioelectrochemistry* (online),  
*Journal of Power Sources* (online),  
*Journal of Applied Electrochemistry* (print),  
*Electroanalysis* (print),  
*Journal of Solid State Electrochemistry* (print) for personal use.  
There is also a Discounted Package available consisting of the *Journal of Electroanalytical Chemistry*, *Electrochemistry Communications*, and *Bioelectrochemistry* (online).
- Reduced registration fees at ISE Meetings
- Access to the "members restricted area" of the ISE website
- Access to the full membership directory with all members addresses

## How to become an ISE member

Becoming an ISE member is simple: you will find a Membership Application Form on the Society web site (at the address: [http://members.ise-online.org/members/new\\_members.php](http://members.ise-online.org/members/new_members.php)), which you can fill in and submit online. In the application form you will have to select up to three Divisions and indicate two sponsoring ISE members. Should it be difficult for you finding these sponsors, please write to the Executive Secretary of the Society Dr. M. Musiani, e-mail: [m.musiani@ieni.cnr.it](mailto:m.musiani@ieni.cnr.it).

## Membership fees

Individual yearly membership fees are 40 EUR for members above 30 years of age, and 10 EUR for members of age 30 or less and for Emeritus members.



---

## ISE Organization

---

### Executive Committee

The Executive Committee is entrusted with the management of the Society.

### ISE Office

The ISE Office performs all administrative tasks related to the operation of the Society. It is located in Switzerland, and managed by an Executive Secretary.

The ISE Office serves as the primary contact for members and non-members.

### Division Officers

The scientific activities of ISE are grouped into seven Scientific Divisions and a New Topics Committee. The divisions are headed by a Chairperson assisted by a Past Chair, a Chair Elect and two Vice Chairs. Their role is to promote and represent the scientific interests of the division and its members, for example through contributing to the organization of Annual, Topical and other Society meetings.

### Regional Representatives

In each country or group of countries having fifteen members or more, a national or regional section of ISE may be formed. Each section has a Regional Representative.

### Council

The ISE Council is an Advisory Body. The voting members of the Council consist of three Officers from each Division and all the Regional Representatives. All persons constituting the Council are elected by the members of the Society.

### Scientific Meetings Committee

The Scientific Meetings Committee plans and oversees the organization and sponsorship of scientific meetings within the broad field of electrochemistry.

### Fellows Nominating Committee

The Fellows Nominating Committee is a standing committee which proposes names to the Executive Committee for the title of ISE Fellow. It is also responsible for identifying candidates for honorary membership.

### Publications Committee

The Publication Committee, a standing committee of ISE, acts as an advisory board to the Executive Committee on publication matters.



## ISE Executive Committee

### President

**Christian Amatore**, Paris, France (2015-2016)

Representation of ISE. Chairperson of Executive Committee, Council and General Assembly

### President Elect

**Philip N. Bartlett**, Southampton (2015-2016)

Chairperson of Committee of Division Officers. Coordination of scientific program of future Annual Meetings, supervision of Division Officers' activities

### Immediate Past President

**Hasuck Kim**, Seoul, Korea (2015-2016)

Chairperson of Executive Committee in the absence of the President

### Vice Presidents

**Justin Gooding**, Sidney, Australia (2013-2015)

Responsible for relations with other Societies

**Plamen Atanasov**, Albuquerque, NM, USA (2015-2017)

Responsible for Corporate and Corporate Sustaining Members

**Katharina Krischer**, München, Germany (2015-2017)

Responsible for Educational Activities in ISE

**Yunny Meas**, CIDETEQ, Querétaro, Mexico (2014-2016)

Responsible for Regional Sections

### Secretary General

**Manuela Rueda** (2015-2017)

#### *General tasks*

Ensuring continuity and efficiency of scientific policy. Coordination of tasks of Vice Presidents.

Identification of new developments in electrochemistry and possible new scientific and nonscientific activities. Scientific matters not handled by the President or President Elect.

#### *Tasks in collaboration with ISE Office*

Ensuring that constitution, bylaws, guidelines, schedules etc. are observed. Preparation of Annual Reports.

Collection of information for newsletters and coordination of actions.

#### *Annual and Topical ISE Meetings*

Coordination of Meetings (location, time, topics). Representative of Executive Committee and advisor to Local Organising Committees for nonscientific matters (location, facilities, control of financial planning, schedule, publicity).

### Treasurer

**Bernard Tribollet**, Paris, France (2014-2016)

Responsible for the administration and the management of the assets and property of the Society, preparation of budgets and financial reports, financial planning, investment policy, supervision of financial matters of Annual and Topical ISE Meetings.

### Executive Secretary

**Marco Musiani**, Padova, Italy (2014-2018)

Responsible for maintaining the ISE calendar, assisting with organizing the business and financial arrangements for Annual and Topical Meetings, organising committee appointments, assisting the Secretary General with Society elections, recruiting new members, and co-ordinating Executive Committee meetings. Drafts ISE documents, acts as web page editor, maintains ISE archives and records, and serves as the contact person for members (particularly at ISE meetings).



## Scientific Divisions of ISE

### Division 1 – ANALYTICAL ELECTROCHEMISTRY

Experimental and theoretical aspects of the analytical process in which electrochemistry has a role, including sample collection / processing, separation, and species identification and quantitation.

Chair: F. Bedioui, Past Chair: A. Downard, Chair Elect: D. Mandler, Vice-Chairs: P. Baker and J. Pingarron

### Division 2 – BIOELECTROCHEMISTRY

Aspects of electrochemistry and electroanalysis characterizing biological processes at the molecular level and relevant to the mechanisms of biological regulation of cells.

Chair: R. Bilewicz, Past Chair: W. Shin, Chair Elect: F. Lisdat, Vice-Chairs: D. Arrigan and E. Lojou

### Division 3 – ELECTROCHEMICAL ENERGY CONVERSION AND STORAGE

Experimental and theoretical aspects of electrochemistry in which the goal is the interconversion of energy between different forms or the storage of energy, including the processes themselves and materials used for these purposes.

Chair: S. Passerini, Past Chair: D. Jones, Chair Elect: R. Kostecki, Vice-Chairs: F. Soavi and H. Uchida

### Division 4 – ELECTROCHEMICAL MATERIALS SCIENCE

Aspects of materials science in which electrochemistry is part of the synthesis, processing, surface treatment, corrosion, characterization or modeling of new or existing materials, or in which electrochemistry is the user of such materials.

Chair: Chair: S. Brankovic, Past Chair: M. Ryan, Chair Elect: G. Zangari, Vice-Chairs: N. Birbilis and M. Vorotyntsev

### Division 5 – ELECTROCHEMICAL PROCESS ENGINEERING AND TECHNOLOGY

Experimental and theoretical aspects and applications of electrochemistry in which engineering issues play a significant role, including scale-up and reactor design.

Chair: J. Peralta-Hernandez, Past Chair: F. Lapicque, Chair Elect: K. Bouzek, Vice-Chairs: S. Mitsushima and M. Rodrigo

### Division 6 – MOLECULAR ELECTROCHEMISTRY

Structural and mechanistic aspects of electrode processes of inorganic, metallorganic and organic substances; synthetic applications.

Chair: F. Paolucci, Past Chair: M. Goulart, Chair Elect: O. Buriez, Vice-Chairs: C. Frontana and G. Xu

### Division 7 – PHYSICAL ELECTROCHEMISTRY

Experimental, theoretical and computational aspects of electrochemistry, alone or in conjunction with other methods, relevant to interfaces and conductive media; this shall include physicochemical nature, structure and dynamics from the molecular to the macroscopic level.

Chair: A. Russell, Past Chair: M. Eikerling, Chair Elect: A. Gewirth, Vice-Chairs: M. Arenz and Y. Chen

### New Topics Committee

The New Topics Committee identifies interesting and relevant scientific and technological subjects not covered by the ISE Divisions. It has tasks similar to those of a Division, except that it may have several and changing technical priorities.

Chair: P. Unwin, Past Chair: T. Jacob, Chair-Elect: N.J. Tao



## Regional Representatives

Argentina:	A.E. Bolzan	2015-2017	2nd term
Australia-NZealand:	C. Hogan	2015-2017	1st term
Austria:	W. Kautek	2013-2015	2nd term
Belgium:	C. Buess-Herman	2013-2015	2nd term
Brazil:	H. Varela	2015-2017	1st term
Bulgaria:	E. Slavcheva	2015-2017	1st term
Canada:	G. Jerkiewicz	2013-2015	1st term
Caribbean Region:	J. Calderon	2014-2016	1st term
Chile:	R. Salazar	2013-2015	1st term
China:	S.G. Sun	2013-2015	1st term
Croatia:	M. Kraljic-Rokovic	2015-2017	1st term
Czech Republic:	M. Hromadova	2013-2015	2nd term
Denmark:	Qingfeng Li	2015-2017	2nd term
Estonia:	E. Härk	2014-2016	1st term
Finland:	B. Wilson	2014-2016	1st term
France:	N. Pébère	2014-2016	2nd term
Germany:	H. Baltruschat	2015-2017	2nd term
Greece:	S. Bebelis	2013-2015	2nd term
Hungary:	L. Peter	2014-2016	2nd term
India:	S.K. Aggarwal	2014-2016	1st term
Iran:	M.A.A. Ensafi	2013-2015	1st term
Ireland:	E. Marsili	2013-2015	2nd term
Israel:	N. Eliaz	2015-2017	1st term
Italy:	S. Cattarin	2013-2015	1st term
Japan:	S. Kuwabata	2014-2016	1st term
Korea:	I.-H. Yeo	2013-2015	2nd term
Lithuania:	R. Pauliukaite	2014-2016	1st term
Mexico:	C. Frontana	2015-2017	2nd term
Netherlands:	M. Van Brussel	2013-2015	2nd term
Norway:	S. Sunde	2013-2015	2nd term
Poland:	M. Skompska	2013-2015	1st term
Portugal:	J.M. Palma Correia	2015-2017	2nd term
Romania:	M. Ungureanu	2015-2017	1st term
Russia:	M. Vorotyntsev	2013-2015	1st term
Serbia:	A. Dekanski	2014-2016	1st term
South Africa:	K. Ozoemena	2013-2015	2nd term
Spain:	E. Herrero	2014-2016	1st term
Sweden:	F. Björefors	2013-2015	2nd term
Switzerland:	E. Bakker	2013-2015	1st term
Taiwan:	B.J. Hwang	2015-2017	1st term
Turkey:	M.S. Yazici	2014-2016	1st term
Ukraine:	O. Linyucheva	2013-2015	2nd term
United Kingdom:	T. Albrecht	2014-2016	2nd term
USA:	G. Botte	2015-2017	1st term



---

## Corporate and Corporate Sustaining Members of ISE

---

Ametek  
Apple Inc.  
Bio-Logic SAS  
Crown Battery Manufacturing  
DropSens, S.L.  
Gamry Instruments  
Google  
Metrohm Autolab BV  
PalmSens BV  
Permascand AB  
Sensolytics GmbH  
Scribner Associates, Inc.  
Tanaka Kikinzoku Kogyo K.K.  
Zahner-elektrik GmbH & Co KG

Central Electrochemical Research Institute  
Paul Scherrer Institute, Switzerland  
Sokolsky Institute of Organic Catalysis and Electrochemistry, Russia

---

## Co-operation with other Societies

---

*ISE is an Associated Organization of IUPAC and has co-operation agreements with:*

- Bioelectrochemical Society (The)
- Chinese Society of Electrochemistry
- Deutsche Gesellschaft für Galvano- und Oberflächentechnik (DGO)
- Electrochemical Division of the Italian Chemical Society
- Electrochemical Society (The)
- Electrochemical Society of Japan
- Electrochemistry and Electroanalytical Division of the Brazilian Chemical Society
- Electrochemistry Group of the French Society of Chemistry
- European Federation of Corrosion
- Fachgruppe Angewandte Elektrochemie der Gesellschaft Deutscher Chemiker  
(Section Applied Electrochemistry of the Society of German Chemists)
- Korean Electrochemical Society
- Mexican Electrochemical Society
- Royal Society of Chemistry (The)
- Sociedad Iberoamericana de Electroquímica
- Society for Electroanalytical Chemistry (The)



---

## ISE Honorary Members

---

Honorary Members are appointed by the Executive Committee, after consultation with the Council, primarily in recognition of their contribution to ISE. The total number at any time is limited to ten.

The first Honorary Member of ISE, appointed in the year 2003, was **Otmar Dossenbach**, Treasurer of the Society for 21 years (1980-2000) and Executive Secretary for 2 years (2001-2002).

Two new Honorary Members were appointed in the year 2004: **Roger Parsons** and **Sergio Trasatti**, former Presidents of the Society.

Three Honorary Members were appointed in the year 2005: **Ron Armstrong**, former Editor-in-Chief of *Electrochimica Acta* for 18 years, **Elton Cairns** and **Dieter Landolt**, former Presidents of the Society,

One Honorary Member was appointed in the year 2011: **Sharon Roscoe**, former Secretary General of the Society.

---

## ISE Fellows

---

In recognition of their scientific or technical contributions to electrochemistry, the Society may confer on individual members the distinction of ISE Fellowship. Such ISE Fellows are appointed by the Executive Committee after consultation with the Council. The appointment does not carry with it automatic life-time ISE membership.

The present Fellows of ISE are:

H. Abruña	J. Heinze	Z. Samec
R. Adzic	R. Hillman	R. Savinell
A. Aldaz	B.J. Hwang	E. Savinova
R. Alkire	G. Inzelt	D. Schiffrin
Ph. Alongue	K. Itaya	W. Schmickler
C. Amatore	Y. Ito	P. Schmuki
D. Aurbach	H. Ju	F. Scholz
P. Bartlett	A. Jutand	W. Schuhmann
R. J. Behm	T. Kakiuchi	B. Scrosati
A. Bond	A. Karyakin	A. Shukla
E. Cairns	H. Kim	U. Stimming
A. Chen	M. Koper	S. Sun
C. Comninellis	A. Kornyshev	Z. Tian
R. Compton	C. Lamy	J. Ulstrup
S. Cosnier	O. Lev	P. Unwin
P. Delahay	J. Lipkowski	K. Uosaki
C. Fan	D. Macdonald	C. Vayenas
W.R. Fawcett	D. Mandler	M. Watanabe
J. Feliu	P. Marcus	A. Wieckowski
C. Gabrielli	R.A. Marcus	G. Wilson
E. Gileadi	N. Markovic	M. Winter
H. Girault	J. McBreen	J. Zagal
L. Gorton	R. Nichols	J. Zhang
R. Guidelli	T. Osaka	
P. Hapiot	M. Osawa	



## Society Awards

### Electrochimica Acta Gold Medal

The Electrochimica Acta Gold Medal may be awarded every two years to the person judged to have made the most significant contribution to electrochemistry in recent years.

### Frumkin Memorial Medal

The Frumkin Memorial Medal may be given once every two years. It recognises the outstanding contribution of a living individual over his/her life in the field of fundamental electrochemistry.

### Prix Jacques Tacussel

The Prix Jacques Tacussel may be awarded every two years to a person who has made important contributions to an electrochemical technique.

### Katsumi Niki Prize for Bioelectrochemistry

The Katsumi Niki Prize for Bioelectrochemistry may be awarded every two years to a scientist who has made an important contribution to the field of bioelectrochemistry.

### Bioelectrochemistry Prize of ISE Division 2

The Bioelectrochemistry Prize of ISE Division 2 may be awarded every two years to a scientist who has made an important contribution to the field of bioelectrochemistry.

### Brian Conway Prize for Physical Electrochemistry

The Brian Conway Prize for Physical Electrochemistry may be awarded every two years, in recognition of the most successful achievements in Physical Electrochemistry in recent years.

### Alexander Kuznetsov Prize for Theoretical Electrochemistry

The Kuznetsov Prize is awarded every two years to a living individual who has made groundbreaking contribution to the theory of electrochemical phenomena.

### Jaroslav Heyrovsky Prize for Molecular Electrochemistry

The Jaroslav Heyrovsky Prize for Molecular Electrochemistry, supported by ISE Division 6, may be awarded annually to a scientist who has made an important contribution to the field of molecular electrochemistry in the last 5 years.

### Tajima Prize

The Tajima Prize recognises the contributions made by younger electrochemists. Candidates must be less than 40 years old. An award may be made every year. The decision of the Award Committee will be based on published work.

### Hans-Jürgen Engell Prize

The Hans-Jürgen Engell Prize may be awarded annually to a young electrochemist on the basis of published work in the field of corrosion, electrodeposition or surface treatment.

### Oronzio and Niccolò De Nora Foundation Young Author Prize

The Oronzio and Niccolò De Nora Foundation Young Author Prize may be awarded annually to a scientist of less than 30 years for the best paper published in the ISE society journal in the calendar year preceding the award.

### ISE Prize for Environmental Electrochemistry

The ISE Prize for Environmental Electrochemistry may be awarded annually to a scientist of less than 35 years of age on January 1 of the year of the award, for recent application-oriented achievements in the field of environmental electrochemistry.

### ISE Prize for Applied Electrochemistry

The ISE Prize for Applied Electrochemistry may be awarded annually to a scientist of less than 35 years of age on January 1 of the year of the award, for recent achievements in the field of applied electrochemistry.

### Early Career Analytical Electrochemistry Prize of Division 1

The Early Career Analytical Electrochemistry Prize of ISE Division 1, sponsored by OrigaLys, may be awarded annually to a scientist of less than 35 years of age on January 1st of the year of the award in recognition of her/his recent achievements in Analytical Electrochemistry.

### Electrochimica Acta and ISE Travel Award for Young Electrochemists

The Electrochimica Acta Travel Awards for Young Electrochemists are aimed at favouring the participation of young electrochemists in the ISE Annual Meetings. The applicants must be ISE members. They must have obtained their Ph.D. not earlier than 6 years before the deadline for applications.





---

## ISE Sponsored Meeting Information

---

### What is an ISE sponsored meeting?

You may have noticed that scientific meetings in the field of electrochemistry are often labelled “ISE sponsored Meeting”. What does this mean? In addition to organizing its own meetings, such as the Annual and Topical Meetings, ISE may sponsor other international scientific meetings in the area of electrochemistry. ISE sponsorship is intended to be a sign of quality for the meeting.

### What are the requirements for ISE sponsorship?

ISE requires that the scientific quality of the meeting reaches the standard of its own meetings. It is desirable that the advisory board consists of ISE members, as far as possible. The meeting must be open to all ISE members.

### Who decides?

The decision is normally taken by the officers of the ISE Division in whose field of interest the topic of the meeting lies. ISE Division Officers should be involved in the organisation of the meeting. The ISE Executive Committee decides on the sponsorship for meetings of general interest.

### What are the obligations of the organizers?

The organizers have to publicise the ISE sponsorship in all the official documents related to the meeting (announcements, program, website etc.). At the meeting, a representative of ISE must be allowed to say a few words on behalf of the Society, and ISE must have the opportunity to advertise. After the meeting, the organizers should submit a short report to ISE to be published on the ISE website.

### What do the organizers receive from ISE?

ISE publishes announcements and reports of ISE sponsored meetings on its website. The ISE Office can organize, free of charge, mailings to all, or a group of ISE members. In appropriate cases, there may be a special issue of *Electrochimica Acta* associated with these meetings. Decisions about special issues are made by the Editor-in-Chief.

### What about money?

ISE sponsorship of a meeting does not necessarily include a financial contribution from ISE. The sponsoring Division(s) may use its funds to support such a meeting. The level of financial contribution will be determined by the Division(s), but a typical sum may be 500 Euros.

### How to apply for ISE sponsorship?

If you would like to have the scientific meeting you are organizing sponsored by ISE, please send an e-mail to the ISE Office, at least one year in advance of the time of the meeting, and attach a completely filled in sponsor request form. This form can be found on the ISE website at: <http://ise-online.org/sponsmeet/info.php>. The decision will be taken by the Officers of the sponsoring Division(s), or by the Executive Committee, and the ISE Office will inform the applicant.

---

## ISE Regional Student Meetings

---

Graduate Students who are members of ISE and intend to organize a Regional Student Meeting can apply for ISE financial support. Applications submitted by Graduate Students jointly with their supervisors or with other senior members of the staff of their university are also acceptable, but it is expected that the students will be engaged in the organizational aspects of the meeting as much as possible. Regional Student Meetings are typically one-day meetings involving graduate students active in the geographic area where the meeting takes place. The format of the meeting (oral presentations, posters, discussion sessions, other) is autonomously decided by the organizers who will be responsible for securing a venue and collecting registrations. No registration fee should be requested, if financially possible. When the Regional Student Meeting is associated to a larger ISE-sponsored meeting taking place in the same venue, the application must provide clear indication on the connections between the two events and must clearly describe the independent activities reserved to student participants. No later than one month after the meeting, the organizer(s) will send to the ISE Office a report on the event, including the names and the e-mail addresses of the participants. The student participants will be invited to apply for ISE membership. A report giving an overview of the meeting, accompanied by suitable pictures if available, will be posted on the ISE website under Student Activities.

Applications for ISE support must be sent by e-mail to the ISE Office, with a copy to the Regional Representative of the country where the meeting is organized, 3-12 months before the meeting date, using the application form. The local ISE Regional Representative, if requested, will assist the potential meeting organizer in the preparation of the application. Applications will be analyzed by a committee consisting of (i) ISE Immediate Past President (ii) ISE Secretary General, (iii) ISE Treasurer, (iv) ISE Vice President responsible for Educational Activity and (v) ISE Vice President responsible for Regional Sections. The response will be communicated to the applicant and to the relevant Regional Representative no later than 1 month after the application submission.

The maximum financial support will be 600 €; the expected use of the funds must be specified in the application. Co-sponsoring by other Societies and/or institutions is possible.

# PalmSens<sup>3</sup>

Potentiostat / Galvanostat / Impedance Analyzer



- ✓  $\pm 5.000$  V dc-potential range
- ✓  $\pm 8.0$  V compliance voltage
- ✓ current ranges from pA up to 10 mA (8 ranges)
- ✓ frequency range of 100  $\mu$ Hz to 50 kHz
- ✓ ac- amplitude range of 1 mV to 0.3 V (rms)

Visit **[www.palmsens.com](http://www.palmsens.com)**

for more information about PalmSens and our other instruments:

- embedded potentiostats;
- multi-channel potentiostats;
- multiplexers;
- and more...



**PalmSens**

Compact Electrochemical Interfaces

# **DROPSENS**

Innovative Technology for Miniaturised Electrochemistry



## **SPELEC**

**SPECTROELECTROCHEMISTRY  
INSTRUMENT**

- ONE INSTRUMENT
- ONE SOFTWARE



## **ECL**

**ELECTROCHEMILUMINESCENCE  
INSTRUMENT**

- ONE SOFTWARE
- VERY EASY SET UP
- FULLY SYNCHRONIZED LUMINESCENCE  
& ELECTROCHEMICAL MEASUREMENTS

## **PORTABLE POTENTIOSTATS/GALVANOSTATS**



**STAT8000**



**STAT400**



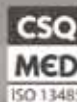
**DROPSTAT**

## **SCREEN-PRINTED ELECTRODES**



ISO 9001:2008

[www.dropsens.com](http://www.dropsens.com)  
[info@dropsens.com](mailto:info@dropsens.com)



ISO 13485

# *The Most Flexible Multichannel Potentiostat*



***Keep everything in a single chassis or undock your channels and move them closer to your cell.***

***Closer to cell = Shorter cell cables = Better results.***

- Up to 5 A per Channel
- EIS to 1 MHz at >99% Accuracy on Every Channel
- Fully Isolated from Earth Ground
- Independent, Simultaneous Measurements
- Undock Individual Channels for Flexible Placement

***Now with the NEW***  
**INTERFACE5000**



# **GAMRY**

INSTRUMENTS

[www.gamry.com](http://www.gamry.com)



# Battery Cycling System series

Now a complete family...

BCS-815 10 A

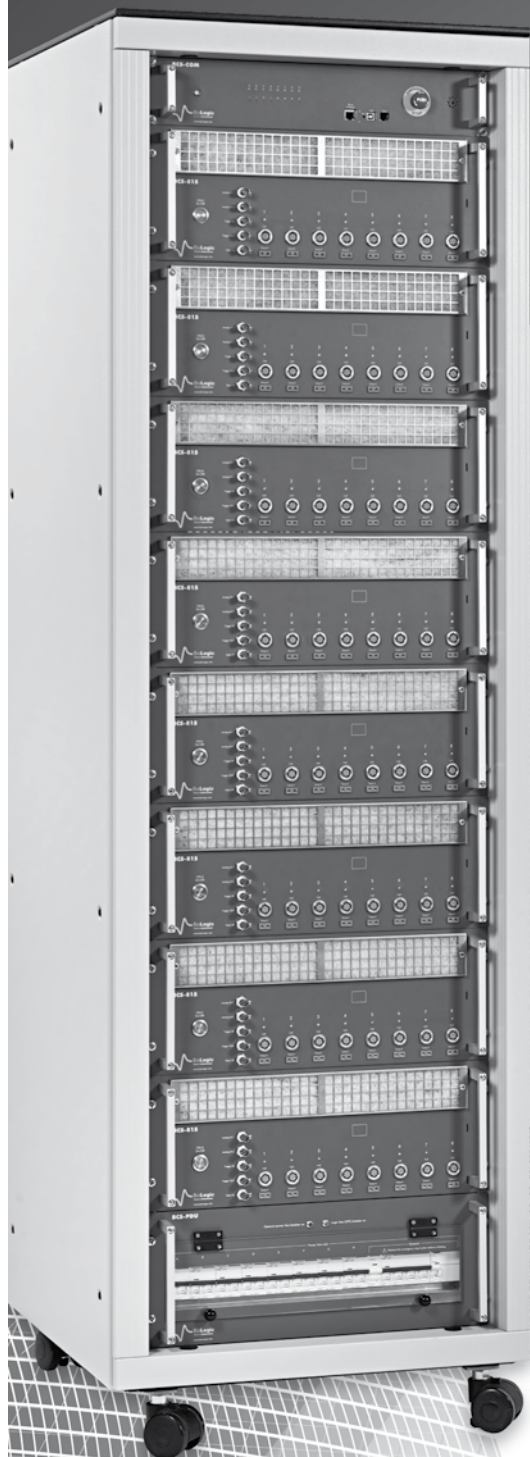
**NOW**

BCS-810 1 A

BCS-805 100 mA

The potential  
to do more...

- High quality EIS: Full scan from 10 kHz to 10 mHz
- 18-bit A/D converter (40  $\mu$ V resolution)
- HPC measurement down to 6.3 ppm
- Modularity from few  $\mu$ A to 120 A
- Voltage measurement from 0 V to 9 V
- Module mixing BCS 805, 810 & 815



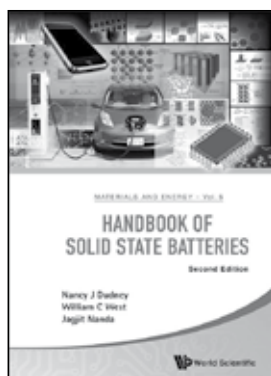
For further information:



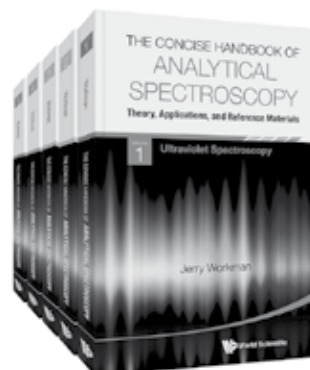
Bio-Logic SAS  
1, rue de l'Europe  
38640 Claix - France  
Phone: +33 476 98 68 31

[www.bio-logic.info](http://www.bio-logic.info)

**Highly Recommended**



edited by **Nancy J Dudley** (Oak Ridge National Laboratory, USA),  
**William C West** (Nagoya University, Japan) &  
**Jagjit Nanda** (Oak Ridge National Laboratory, USA)  
9789814651899 US\$235

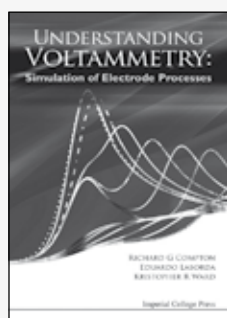


by **Jerry Workman**  
(Unity Scientific, USA & National University, USA)  
9789814508056 US\$1480 US\$1280  
Intro Offer till Mar 31, 2016

**New & Bestselling Titles**



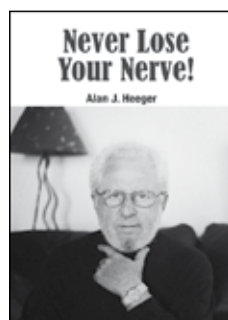
edited by **George S Wilson**  
(University of Kansas, USA) &  
**Adrian C Michael**  
(University of Pittsburgh, USA)  
978-981-4619-76-9 US\$165



by **Richard G Compton** (Oxford),  
**Eduardo Laborda** (Oxford & University  
of Murcia, Spain) &  
**Kristopher R Ward** (Oxford)  
9781783263233 US\$58



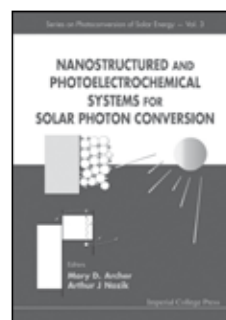
by **Andreas Manz** (KIST Europe, Germany),  
**Petra S Dittrich** (ETH Zürich, Switzerland),  
**Nicole Pamme** (University of Hull, UK) &  
**Dimitri Iossifidis** (AMALVA S.A., Athens, Greece)  
978-1-78326-671-5 US\$84  
978-1-78326-672-2 (pbk) US\$48



by **Alan J Heeger** (UC Santa Barbara)  
978-981-4704-85-4 US\$58  
978-981-4704-86-1 (pbk) US\$28



edited by **Francis D'Souza** (University  
of North Texas, USA) & **Karl M Kadish**  
(University of Houston, USA)  
978-981-4678-90-2 US\$330 US\$295  
Intro Offer till Dec 31, 2015



edited by **Mary D Archer**  
(Imperial College, UK) &  
**Arthur J Nozik**  
(National Renewable Energy Laboratory, USA)  
978-1-86094-255-6 US\$282

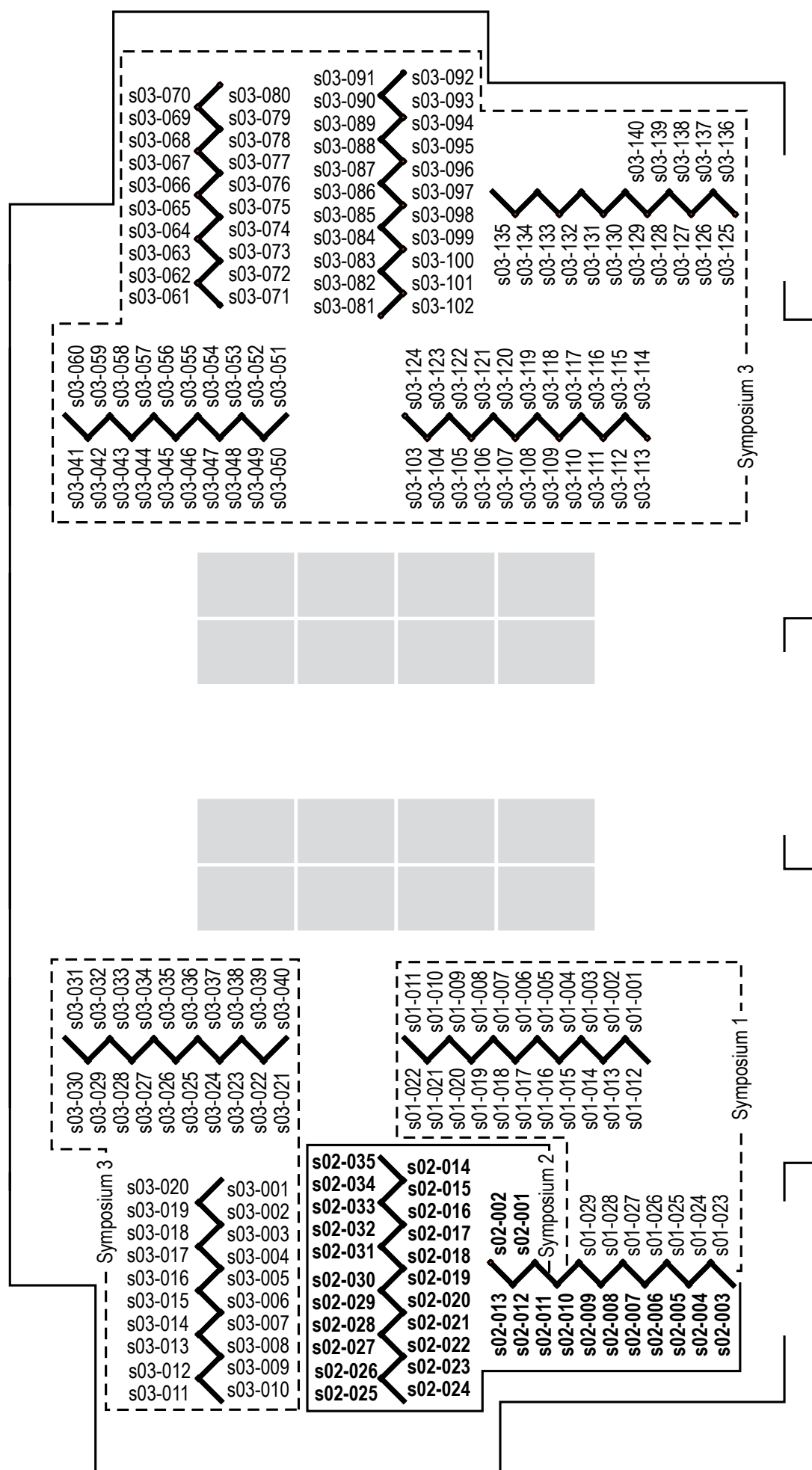
## Poster plan of poster presentation session 1 - Monday

Symposia: 1, 2, 3

Poster set-up Monday: 08:30-10:30

Poster take-down Monday: 18:00-19:00

Poster Presentation: Monday, 5 October: 10:50-12:30



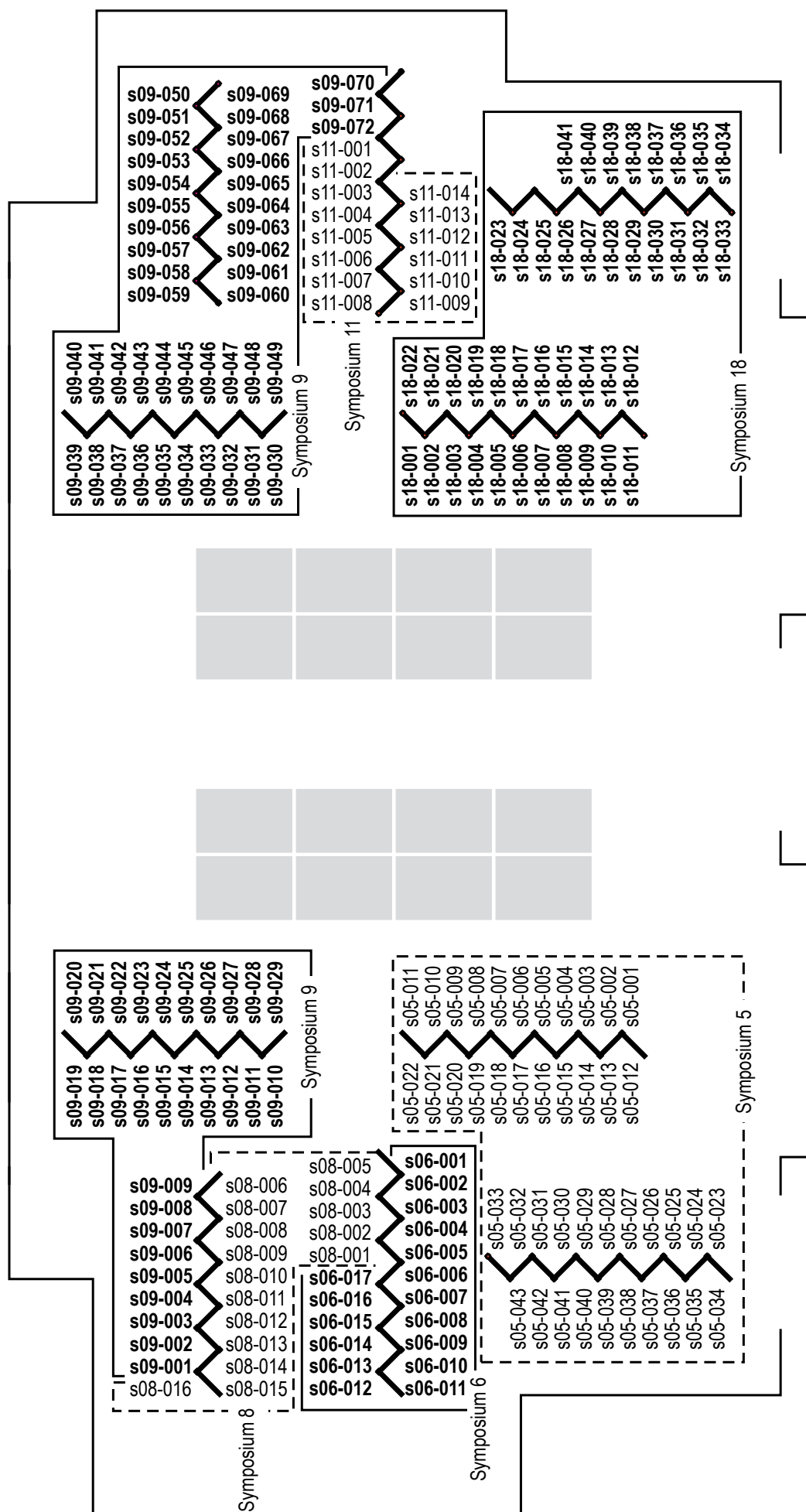
## Poster plan of poster presentation session 2 - Tuesday

Symposia: 5, 6, 8, 9, 11, 18

Poster set-up Tuesday: 08:30-10:30

Poster take-down Tuesday: 18:00-19:00

Poster Presentation: Tuesday, 6 October: 10:50-12:30





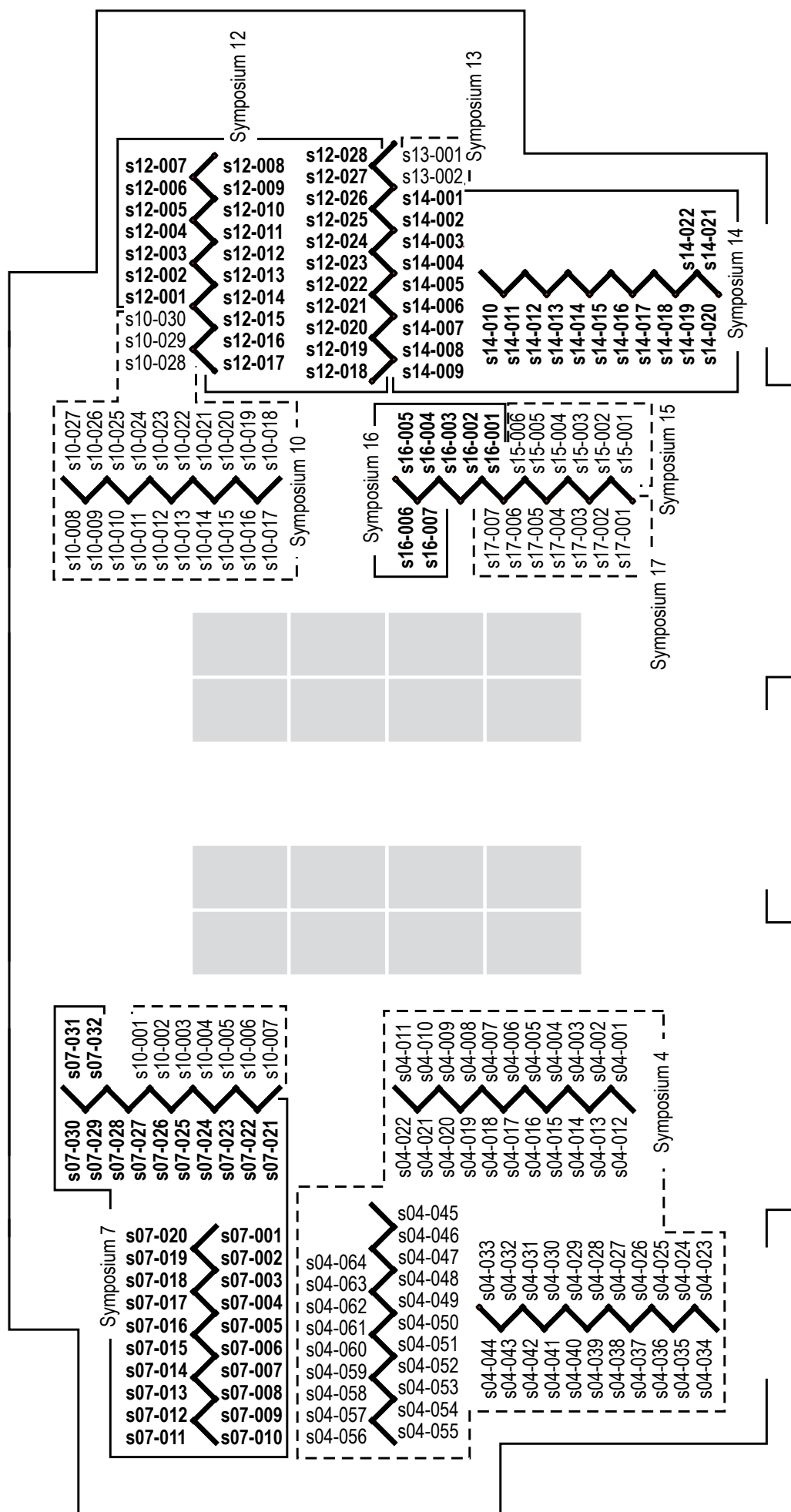
## Poster plan of poster presentation session 3 - Wednesday

Symposia: 4, 7, 10, 12, 13, 14, 15, 16, 17

Poster set-up Wednesday: 08:30-10:30

Poster take-down Thursday: 14:00-16:00

Poster Presentation: Wednesday, 7 October: 10:50-12:30



## Week schedule

	SUNDAY	MONDAY	TUESDAY	WEDNESDAY	THURSDAY	FRIDAY
08:15 - 09:15		Plenary Lecture	Plenary Lecture	Plenary Lecture	Plenary Lecture	Plenary Lecture
09:30 - 09:50						
09:50 - 10:10		Oral presentations	Oral presentations	Oral presentations	Oral presentations	Oral presentations
10:10 - 10:30						
10:30 - 10:50						
10:50 - 11:10		Coffee Break	Coffee Break	Coffee Break	Coffee Break	Coffee Break
11:10 - 11:30					11:10 - 12:10 General Assembly	
11:30 - 11:50		Poster Session 1	Poster Session 2	Poster Session 3		Oral presentations
11:50 - 12:10						
12:10 - 12:30					Lunch	
12:30 - 12:50		Lunch	Lunch			Closing Ceremony
12:50 - 13:50		12:50 -13:50 Division+Reg.Rep. meetings	12:50 - 13:50 Council meeting		12:50 - 13:50 Division meetings	
13:50 - 14:00						
14:00 - 14:20						
14:20 - 14:40						
14:40 - 15:00						
15:00 - 15:20		Oral presentations	Oral presentations		Oral presentations	
15:20 - 15:40	Tutorials & Workshop					
15:40 - 16:00						
16:00 - 16:20				Excursions		
16:20 - 16:40		Coffee Break	Coffee Break		Coffee Break	
16:40 - 17:00						
17:00 - 17:20						
17:20 - 17:40	Opening Ceremony	Oral presentations	Oral presentations		Oral presentations	
17:40 - 18:00						
18:00 - 18:20						
18:20 - 18:40	Welcome Reception					
18:40 - 19:00		Reception				
19:00 - 20:00					Banquet	
			Taiwanese Opera			

## **Novel Materials for Renewable Energy**

Hongjie Dai  
*Stanford University, USA*

This talk will review our recent work on advancing new types of electrocatalysts and batteries for renewable energy applications. I will talk about achieving high performance electrocatalysts for water splitting including HER and OER. We have developed a novel Ni/NiO heterostructured hydrogen evolution reaction (HER) catalyst with near zero overpotential. The nanoscale nickel oxide/nickel NiO/Ni hetero-structures formed on carbon nanotube sidewalls are highly effective electrocatalysts for hydrogen evolution reaction with activity similar to Pt with near zero overpotential in HER onset in basic solutions. A novel approach to stabilize the catalyst will be presented. We have also developed a NiFe layered double hydroxide (NiFe LDH) oxygen evolution reaction (OER) catalyst with  $\sim 250\text{mV}$  overpotential, which was among the most active OER catalyst in basic solutions. The NiFe LDH exhibited higher OER catalytic activity and stability than commercial Ir based catalysts. Using the highly active Ni/NiO HER and NiFe LDH catalyst, we achieved water splitting using low voltages  $< 1.5$  volt, making it possible to make an electrolyzer for hydrogen and oxygen gas generation running on a single AAA alkaline battery cell. Lastly, I will present our latest development of rechargeable Al ion battery. The past, present and future of Al ion batteries will be discussed.

# Nanomaterials for Energy Conversion and Storage: Structure Design and In-Situ Monitoring

Li-Jun Wan

*Institute of Chemistry, Chinese Academy of Sciences (CAS), Beijing 100190, P.R. China*

e-mail: wanlijun@iccas.ac.cn

With the increasing demand for efficient and economic energy conversion and storage, advanced solar cells, fuel cells, rechargeable batteries with high efficiency have attracted more and more attention. Nanostructured materials are currently of interest for such devices because of their high surface area, novel size effects, significantly enhanced performance, and so on.<sup>1</sup> Here, we reports our recent progress of nanostructure designs for advanced electrode materials as well as in-situ monitoring techniques of electrode/electrolyte interfaces in these systems,<sup>2,3</sup> including the following aspects.

(i) Nanostructured electrocatalysts for fuel cells: To lower the cost of Pt catalysts, various Pt nanostructures and binary catalysts have been proposed.<sup>4</sup> Hanging Pt hollow nanocrystal assemblies on graphene could further improve the electrocatalytic performance of Pt nanocatalysts.<sup>5</sup>

(ii) Nano/micro hierarchical electrode materials for Li-ion & Li-S batteries: The performances of lithium batteries are hindered by the specific capacities and kinetics of electrode materials.<sup>1,2</sup> Hierarchically nano/micro-structured anode and cathode materials with improved electrochemical performance have been designed and synthesized.<sup>6</sup> Nanocarbon networks are suggested to be good solutions for promoting the kinetics of electrode materials used in Li-ion and Li-S batteries.<sup>2,7,8</sup> To address the surface/interface issue of nanomaterials, we also discuss carbon and carbon-free nanocoatings for nanostructured electrode materials.<sup>9,10</sup>

(iii) In-situ monitor: Reactions taking place on the electrode/electrolyte interface, such as surface film formation accompanied by electrolyte decomposition and deterioration of the host structure of electrode materials, play an important role in the performance and calendar-life characteristics of batteries. Several in-situ monitoring techniques, including in-situ ECSTM, and in-situ ECAFM, have been developed for the direct observation and characterization of the formation of SEI on graphite anode, Si nanowire anode, and  $\text{LiNi}_{0.5}\text{Mn}_{1.5}\text{O}_4$  cathode during the Li-ion battery operation.<sup>11,12</sup>

## References

- [1] Yu-Guo Guo, Jin-Song Hu, Li-Jun Wan, *Adv. Mater.*, 2008, 20, 2878-2887
- [2] Sen Xin, Yu-Guo Guo, Li-Jun Wan, *Acc. Chem. Res.*, 2012, 45, 1759-1769
- [3] Yan Jiang, Xing Zhang, Qian-Qing Ge, Bin-Bin Yu, Yu-Gang Zou, Wen-Jie Jiang, Wei-Guo

- Song, Li-Jun Wan, Jin-Song Hu, *Nano Lett.*, 2014, 14, 365-372
- [4] Han-Pu Liang, Hui-Min Zhang, Jin-Song Hu, Yu-Guo Guo, Li-Jun Wan, Chun-Li Bai, *Angew. Chem. Int. Ed.*, 2004, 43, 1540-1543
- [5] Yu-Ping Xiao, Shuo Wan, Xing Zhang, Jin-Song Hu, Zi-Dong Wei, Li-Jun Wan, *Chem. Commun.*, 2012, 48, 10331 – 10333
- [6] An-Min Cao, Jin-Song Hu, Han-Pu Liang, Li-Jun Wan, *Angew. Chem. Int. Ed.*, 2005, 44, 4391-4395
- [7] Sen Xin, Lin Gu; Na-Hong Zhao; Ya-Xia Yin; Long-Jie Zhou, Yu-Guo Guo, Li-Jun Wan, *J. Am. Chem. Soc.*, 2012, 134, 18510-18513.
- [8] Ding-Jiang Xue, Sen Xin, Yang Yan, Ke-Cheng Jiang, Ya-Xia Yin, Yu-Guo Guo, Li-Jun Wan, *J. Am. Chem. Soc.* 2012, 134, 2512–2515
- [9] Yong-Qing Wang, Lin Gu, Yu-Guo Guo, Hong Li, Xiao-Qing He, Susumu Tsukimoto, Yuichi Ikuhara, Li-Jun Wan, *J. Am. Chem. Soc.* 2012, 134, 7874–7879
- [10] Wei Zhang, Zi-Xiang Chi, Wen-Xin Mao, Rong-Wen Lu, An-Min Cao, Li-Jun Wan, *Angew. Chem. Int. Ed.*, 2014, 53, 12766-17365
- [11] Xing-Rui Liu, Xin Deng, Ran-Ran Liu, Hui-Juan Yan, Yu-Guo Guo, Dong Wang, Li-Jun Wan, *ACS Appl. Mater. Interfaces*, 2014, 6, 20317–20323
- [12] Ran-Ran Liu, Xin Deng, Xing-Rui Liu, Hui-Juan Yan, An-Min Cao, Dong Wang, *Chem. Commun.*, 2014, 50, 15756-15759



Dr. Li-Jun Wan is a Professor at Institute of Chemistry, Chinese Academy of Sciences (ICCAS), Director of CAS key laboratory of molecular nanostructure and nanotechnology, Director of Beijing National Laboratory for Molecular Science, and Chairman of Academic Committee of ICCAS.

Dr. Wan graduated from Dalian University of Technology in 1982, and received his Ph.D from Tohoku University of Japan in 1996. His research focuses on (1) the study of single molecule, molecular reaction and molecular assembly on solid surface by chemical environment and electrochemical scanning probe microscopy, and (2) nanomaterials and their applications in energy conversion/storage and environmental protection such as for Li-ion battery, fuel cell, solar cell, and water processing. He published more than 300 peer-reviewed papers in the journals including Nat. Comm., PNAS, JACS, Angew. Chem., and Adv. Mater. He serves as Members of Editorial Board and International Editorial Advisory Board such as Science China Chemistry, JACS, Acc. Chem. Res., Angew. Chem., ChemComm., Adv. Mater., and Associate Editor of JACS. His main awards include: Chemistry Award, TWAS (the Academy of Sciences for the Developing World); 2<sup>nd</sup>-Class National Natural Science Award, China; Natural Science Award, Beijing and Prize for Scientific and Technological Progress by The HO LEUNG HO LEE Foundation. He is an elected member of CAS, Fellow of TWAS, Fellow of Royal Chemical Society. He is elected as Vice-President of Chinese Chemical Society and President of Chinese Society of Electrochemistry.

# Electrochemical Imaging with Micro/Nanoelectrode Systems

Tomokazu Matsue

*WPI-Advanced Institute for Materials Research (WPI-AIMR), Tohoku University  
Aramaki 6-6-11-605, Aoba, Sendai 980-8579, Japan  
[matsue@bioinfo.che.tohoku.ac.jp](mailto:matsue@bioinfo.che.tohoku.ac.jp)*

Electrochemical imaging is not popular as compared with conventional imaging methods based on optical measurements. Since there have been increasing demands for visualization of local electrochemical phenomena, several imaging technologies based on electrochemical measurements have been proposed so far. There are two basic ways to realize electrochemistry-based imaging [1]. One is to use a scanning probe to pick up localized electrochemical reaction to visualize the surfaces. The other is imaging based on microelectrode arrays to obtain multi-point electrochemical signals to give images.

The most frequently-used tool in the former category is a scanning electrochemical microscope (SECM) [2] and related systems. SECM equips a micro/nanoelectrode scanning probe to acquire information on electrochemical property of surfaces without physical contact. The distance control between the probe and sample has been a big challenge to improve the temporal resolution and sensitivity. We have incorporated an ion-conductance feedback control in SECM system (SECM-SICM) for simultaneous noncontact imaging of the topography and electrochemical signals [3]. SECM-SICM acquired high-resolution topographic images of live cells together with the map of their electrochemical signals. We also developed voltage-switching mode scanning electrochemical microscopy (VSM-SECM) for high-resolution bioimaging [4]. Recently we modified these systems and combined with a scanning electrochemical cell microscopy (SECCM) to fabricate NanoSECCM. This system was applied to visualize localized electrochemical property of battery materials [5].

Electrochemical imaging can also be realized by using microelectrode arrays. The conventional array consists of an array of electrodes with the same number of corresponding bonding pads. This method is easy to implement from a technological point of view; however, the number of individually addressable electrodes is limited since sufficient space for bond pads is not available in surrounding areas. To solve this problem, we developed a novel devices based on electrochemical measurements of redox cycling (LRC) [6]. The LRC was induced on a planar device with row and column electrodes [7]. The crossing points of the row and column electrodes served as the measurements points with limited number of bonding pads for external connection. The LRC devices with microwells at individual measurement points were applied for imaging of gene expression from single cells and high-throughput detection of differentiation of embryonic stem cells [8]. A CMOS-based Bio-LSI with an array of microelectrodes was also fabricated for rapid, highly-sensitive, comprehensive analysis and imaging of biomaterials [9].

- [1] T. Matsue, *Bull. Chem. Soc., Jp.*, 2012, 85, 545; *Anal. Sci.*, 2013, 29, 171.
- [2] A. J. Bard and M. V. Mirkin, ed., "Scanning Electrochemical Microscopy", 2001, Marcel Dekker, New York.
- [3] Y. Takahashi et al., *J. Am. Chem. Soc.*, 2010, 132, 10118; *Angew. Chem. Int. Ed.*, 2011, 50, 9638.
- [4] Y. Takahashi et al., *PNAS*, 2012, 109, 11540.
- [5] Y. Takahashi et al., *Nature Commun.*, 2014, 5, 6450.
- [6] Z. Lin et al., *Anal. Chem.*, 2008, 80, 6830; *Angew. Chem. Int. Ed.*, 2009, 48, 2044
- [7] K. Ino et al., *Anal. Chem.*, 2014, 86, 2989; *Lab. Chip.*, 2014, 14, 787.
- [8] K. Ino et al., *Angew. Chem. Int. Ed.*, 2012, 51, 6648.
- [9] K. Y. Inoue et al., *Lab Chip*, 2012, 12, 3481; *Lab. Chip.*, 2015, 15, 848.

# Neglected, Forgotten or Unimportant? Inactive Materials in Lithium Ion Batteries

D. Gallus, R. Wagner, M. Amereller, J. Kasnatscheew, E. Kraemer, S. Krueger, X. Qi, J. Li,  
I. Cekic-Laskovic, and M. Winter

*MEET Battery Research Center, Institute of Physical Chemistry, University of Muenster, Corrensstraße 46, DE-48149 Münster, Germany*

*Helmholtz Institute Muenster (HI MS) 'Ionics in Energy Storage'*

*E-mail: [martin.winter@uni-muenster.de](mailto:martin.winter@uni-muenster.de); [m.winter@fz-juelich.de](mailto:m.winter@fz-juelich.de)*

Today, it is widely accepted that materials research in the field of electrochemical energy storage has to follow a system approach as the interactions between active materials, the electrolyte, the separator, and the various inactive materials are of similar or even higher importance as the properties and performance parameters of the individual materials only. Surprisingly, apart from a more recent interest in electrolytes, still inactive materials are considered as commodity within the scientific community and the important influence of the interactions between anode and cathode is mostly neglected.

In this presentation, we will discuss the influence of so-called 'inactive' materials on the performance of lithium ion batteries. Apart from electrolyte considerations, we will discuss (i) the so-called Al current collector corrosion, which is actually an anodic dissolution reaction of the non-noble metal aluminum [1,2], (ii) the influence of the conductive filler on lithium ion battery performance [3,4], and (iii) how reactions at the anode deteriorate the cathode performance [5].

## References

- [1] Krämer, E.; Passerini, S.; Winter, M., *ECS Electrochem. Lett.*, **2012**, 1(5), C1 - C3.
- [2] Krämer, E.; Schedlbauer, T.; Hoffmann, B.; Terborg, L.; Nowak, S.; Gores, H.J.; Passerini, S.; Winter, M., *Journal of The Electrochemical Society*, **2012**, *J. Electrochem. Soc.* **2013**, 160 (2), A356 - A360.
- [3] Qi, X.; Blizanac, B.; DuPasquier, A.; Placke, T.; Meister, P.; Oljace, M.; Li, J.; Winter, M.; *Phys. Chem. Chem. Phys.*, **2014**, 15, 25306 - 25313.
- [4] Qi, X.; Blizanac, B.; DuPasquier, A.; Oljaca, M.; Li, J.; Winter, M.; *Carbon*, **2013**, 64, 334 - 340.
- [5] Krüger, S.; Klöpsch, R.; Li, J.; Nowak, S.; Passerini, S.; Winter, M.; *J. Electrochem. Soc.*, **2013**, 160 (4), A542 - A548.



# **A Voltammetric Odyssey: From Homogeneous Dropping Mercury to Heterogeneous Macro and Nano Electrodes; From the Manual Era to Advanced Automated High Speed Computation**

Alan M. Bond

*School of Chemistry, Monash University, Clayton Vic 3800, Australia  
alan.bond@monash.edu*

At the start of my career as an electrochemist, the technique of polarography, using a dropping mercury electrode, dominated the field of voltammetry. As an apprentice, I learned how to measure current that oscillated with the growth and fall of the mercury drop using a galvanometer, apply potential with a rheostat/potentiometer and point by point construct and analyse current -potential- time curves. At that time, almost all aspects of the voltammetric experiment involved a manual manipulation of some kind. In contrast, some 40 years later, the dropping mercury electrode is essentially obsolete due to occupational health concerns (rational?). In its place, a plethora of electrode materials are now available that are often heterogeneous in nature and range in size from discs of cm diameter down to the nanometre dimension and high speed computers govern most aspects of now highly automated instrumentation and data analysis.

So what have I achieved and observed in my career? During my voltammetric odyssey, with inspiration and help from co-workers, I undertook my PhD studies on vacuum lines with Teflon dropping mercury electrode and used a Tesler coil to create dropping mercury electrode made from Kel-F. These non-glass materials allowed polarographic studies to be made in anhydrous HF and the reduction of metal fluorides to be achieved for the first time. This was followed by a substantial period of interest in microelectrodes made in numerous shapes from organometallic paints and in disc form by use of Wollaston wire and skilled glassblowing. Near steady state studies with and without added supporting electrolyte and other advances were implemented with the microelectrodes. The use of AC methods in my laboratories commenced with simple superimposition of a sinewave onto the DC waveform used in classical voltammetry. Now sophisticated forms of Fourier transform aided methodology, combined with advanced forms of data analysis are routine and evolution from “log plot” analysis of data to advanced data optimisation methods using high speed computers has occurred. Instrumentation has also developed spectacularly. My career has bridged the manual analogue to digital era. The latter has progressed from a laboratory computer to the early microprocessors with 2K memory and hand assembled programming and now to parallel processing with an array of computers that are part of recent developments in our version of large amplitude Fourier Transformed AC voltammetry. Of course the theory can now accommodate many nuances that were impossible to implement at the start of my career. Nowadays, it can be anticipated that most reasonable mechanisms can be simulated using commercially available software packages.

In this lecture, a voltammetric odyssey will be presented from my perspective. There are many aspects of the present day “modus operandi” that are revolutionary, but in some ways it is difficult to understand why the best electrode for theory-experiment comparisons, the dropping microelectrode, is now confined to a vague memory. I will conclude by noting that use of this electrode might well enable far deeper understanding to be made on the nature of double layer and mass transport in ionic liquids than has emerged from studies with theory-experiment comparisons using modern electrodes. This is an area where theory may have outstripped experiments and where obtaining high quality fundamentally important data with heterogeneous electrode has proved to be problematic?

The above represents the past and the present, but what about the future? The lecture will conclude with crystal ball gazing as to voltammetric advances that might be introduced in the next decade. Of course I also acknowledge with pleasure the contributions from many outstanding electrochemists with whom I have collaborated during my career. It is fellow electrochemists who have consolidated some of my crazy ideas into reality and provided much of the inspiration that has made my award of the 2014 ISE Electrochimica Acta Gold Medal possible.

# The Investigation of Passivity of Metals Studied by Surface Analytical Methods, a Review

Hans-Henning Strehblow

Heinrich-Heine-Universitaet-Duesseldorf

Universitaetsstr. 01, D-40225 Duesseldorf

[henning@uni-duesseldorf.de](mailto:henning@uni-duesseldorf.de), [hstrehblow@gmail.com](mailto:hstrehblow@gmail.com)

The passivity of metals has been studied since more than 200 years with chemical and electrochemical methods. When commercial Ultra High Vacuum systems were available with an efficient specimen transfer in the mid-seventies, X-ray Photoelectron Spectroscopy (XPS) and Ion Scattering Spectroscopy (ISS and RBS) were applied to study the chemistry of passive layers. A specimen transfer without contact to the laboratory atmosphere excluded the contamination of the surface and uncontrolled oxide growth. Later the development of Scanning Methods (STM, SFM) and Synchrotron Methods (XAS and XRD) allowed a reliable *in situ* investigation of the atomic structure of these surface films. The chemical and structural changes could be investigated with a systematical variation of the environmental parameters like the electrode potential, the composition of the solution and metal, as well as the changes with time from the millisecond range up to hours or days. In this lecture an overview of the achievements of these methods and the results for several metals and their alloys are given as examples.

Passivity of metals is determined by thermodynamic and kinetic parameters, which involves the chemical properties of the metals and their oxides and hydroxides as well as the influence of the electrolyte. Passivating oxide films have usually a complicated multilayer structure with the lower valent cations inside and the higher valent cations outside. The duplex passive films on copper or iron substrates are good examples. For alloys more noble components remain at the metal/oxide interface whereas the reactive components form the oxide layer like in the case of aluminum with a small copper content as can be shown by RBS depth profiles. If both components are reactive, both are present within the oxide, but one of them is often seriously enriched like for Cr-Fe or Cr-Ni alloys. Here the extremely slow dissolution kinetics of  $\text{Cr}^{3+}$ -ions at the oxide/electrolyte interface are the cause for their enrichment within the passive layer in acidic electrolytes, which easily can be shown by XPS and ISS depth profiles. In alkaline solutions Fe(III)oxide remains at the outer surface due to its small solubility for high pH values. The slow dissolution- and reaction-kinetics of  $\text{Cr}^{3+}$  within an oxide- or a chloride-matrix are also the cause for the excellent resistance of pure Cr to halide attack or its beneficial addition to other metals to withstand pitting by halides.

The atomic structure of the passive layers may be visualized directly by STM. Usually a film gets more protective with aging which goes along with the development of a crystalline structure. Often there exists an epitaxial relationship between the oxide film and the metal substrate and the details of the changes of the metal surface are ruled by its orientation, as can be seen by the anodic oxidation of copper for different crystal orientations. Detailed changes may be followed by *in situ* STM with time for small driving forces, i.e. only a small overpotential for oxide formation. Similarly the reduction of an oxide layer can be studied with time resolution. For Co (0001) surfaces this has been examined with various intermediate structures of  $\text{Co}(\text{OH})_2$  species moving on the metal surface and their final integration as Co atoms into the metal terrace with a decoration of its steps by  $\text{Co}(\text{OH})_2$  trimers. In situ XAS studies of metal oxidation and reduction allows even the determination of the near range order of disordered or amorphous oxide films. Investigations have been performed of Cu deposits on Pt clusters by XAS in transmission. The investigation of oxide growth on bulk metals requires a grazing incidence geometry with angles below total reflection of the X-ray beam for a sufficient suppression of the contribution of the substrate metal to the XAS signal. Examples for silver oxide formation on Ag are presented with  $\text{Ag}_2\text{O}$ - and AgO-formation according to the applied electrode potential. Dissolving species in front of an electrode in solution may be investigated by XAS in transmission with the X-ray beam passing close to the metal surface.

# Ionogels as safe and thermally stable electrolytes for macro and micro electrochemical capacitors

Thierry Brousse<sup>a,b</sup>, Mylène Brachet<sup>a,b</sup>, Jean Le Bideau<sup>a,b</sup>, Dorian Gaboriau<sup>c,d</sup>, Gérard Bidan<sup>c,d</sup>, Pascal Gentile<sup>c,d</sup>, Said Sadki<sup>c,d</sup>

<sup>a</sup>Institut des Matériaux Jean Rouxel (IMN), Université de Nantes, CNRS,  
2, rue de la Houssinière, BP32229, 44322 Nantes Cedex 3, France

<sup>b</sup>Réseau sur le Stockage Electrochimique de l'Energie (RS2E), CNRS FR 3459

<sup>c</sup>CEA Grenoble/ INAC/ SPrAM (UMR 5819 (CEA,CNRS, UJF)/ LEMOH

<sup>d</sup>CEA Grenoble/ INAC/ SP2M (UMR-E CEA/UJF)/ SiNaPS  
CEA/INAC Grenoble 17 rue des Martyrs, 38054-Grenoble, FRANCE,

thierry.brousse@univ-nantes.fr

Electrochemical Double Layer Capacitors (EDLCs), so called supercapacitors, are now used in a large variety of applications, such as start & stop modules in cars. In these devices organic solvents are often used that may present some hazard for the users. Thus, alternative electrolytes such as room temperature ionic liquids (RTILs) have been envisioned. In micro-supercapacitors ( $\mu$ SCs), the use of liquid electrolytes is prohibited since there might be some leakage. Additionally,  $\mu$ SCs need to be implemented in microelectronic circuits which are often designed using a reflow soldering process, i.e. an annealing at 250°C for few tens of seconds. Thus, the use of volatile solvents is forbidden. RTILs have a fair ionic conductivity and a broad temperature operating range, without flammability. They can also be confined in a host matrices, which prevents from leakage, in which their liquid state properties are maintained. Such ionogel,<sup>1</sup> could enable to increase the safety of energy storage devices such as EDLCs. Furthermore, ionogels for which host network is made solely of mesoporous silica can solve the thermal stability issue when reflow soldering process is used.

In this communication, we will evidence the interest of ionogel electrolytes in various EDLCs designs, namely standard EDLCs using two symmetric high loading activated carbon electrodes<sup>2</sup> (Fig. 1), and microsupercapacitors using silicon nanowires/nanotrees electrodes. The electrochemical performance (energy and power densities, long term cycling, temperature behavior) will be compared to that of their liquid based equivalent and some perspectives will be given for future devices.

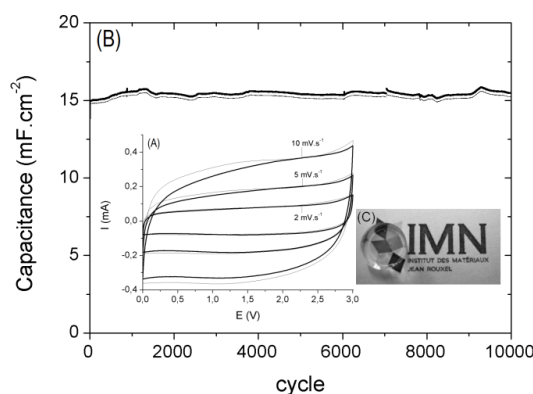


Fig.1 : (A) CVs (0 to 3V) at 2, 5 and 10mV.s<sup>-1</sup> of activated carbon based EDLCs using ionogel (—) and RTIL (---) electrolytes. (B) Long term cycling behaviour of EDLC with Ionogel electrolyte : charge(—) and discharge (---) capacitances obtained with CCGC (I=1mA.cm<sup>-2</sup>). (C) 1 cm Ø transparent ionogel.

## References :

1. "Deconstructing ionic liquids in ionogels: enhanced ionic liquid properties for solid devices" A. Guyomard-Lack, P.-E. Delannoy, N. Dupré, B. Humbert, J. Le Bideau, Phys. Chem. Chem. Phys. 16 (2014) 23639-23645
2. All Solid-State Symmetrical Activated Carbon Electrochemical Double Layer Capacitors Designed with Ionogel Electrolyte, M. Brachet, T. Brousse, J. Le Bideau, ECS Electrochemistry Letters, 3 (2014) A112-A115.

# Microelectrochemical in situ observation of battery electrodes

G. Wittstock,<sup>1</sup> H. Bülter,<sup>1</sup> F. Peters,<sup>2</sup> J. Schwenzel,<sup>2</sup> P. Schwager,<sup>1,2</sup> D. Fenske<sup>2</sup>

<sup>1</sup> Carl von Ossietzky University of Oldenburg, Department of Chemistry, D-26111 Oldenburg, Germany  
<sup>2</sup> Fraunhofer Institute for Manufacturing Technology and Advanced Materials IFAM, Wiener Strasse 12,

D-28359 Bremen, Germany  
gunther.wittstock@uni-oldenburg.de

In our society Li ion batteries are widely used. Intensive research is conducted on next generation batteries such as metal-air batteries. The requirements of high energy density dictate the use of very high (oxidizing) or very low (reducing) potential. These extreme potentials can cause molecular compounds to undergo electron transfer reactions at the interfaces. This is well documented for lithium-ion batteries, where a solid electrolyte interphase (SEI) between the lithiated graphite electrode and the electrolyte is formed by the decomposition of electrolyte components mainly during the first charging process. This layer is critical for the performance and safety of the Li ion batteries [1]. This talk will review a number of approaches to understand charge transport across SEI by using concepts of microelectrochemistry in particular scanning electrochemical microscopy (SECM).

Characterization of the SEI is a challenge, because of the variety of chemically similar components and enclosed electrolyte species. Furthermore, *ex situ* analysis of the SEI requires separation and isolation of the SEI, which may change the content and the structure of the SEI [2]. Recently we used the feedback mode of scanning electrochemical microscopy (SECM) to investigate *in situ* the electron transport at the lithiated graphite (Figure) [3]. 2,5-di-*tert*-butyl-1,4-dimethoxy benzene was identified as an useful SECM mediator providing sufficient stability and sensitivity to study passivation properties of SEI. All measurements were conducted under open circuit conditions. The SECM results show gradual and significant short-term *spatiotemporal* changes of the SEI properties and demonstrate the dynamic and spontaneous behavior of SEI formation, damage and reformation under open circuit conditions above lithiated graphite anodes. The results emphasize that *spatiotemporal* changes of the passivating SEI properties are highly localized and occur preferentially in between the gaps of graphite particles. Significant short-term *spatiotemporal* changes of the SEI properties clarify that electrolyte reduction still occurs after SEI formation at localized spots.

Using a related setup for the investigation of lithium-air batteries, gas permeation through a gas-diffusion electrode (GDE) into a Li<sup>+</sup>-containing electrolyte has been studied in order to understand pore blocking vs. electrode coating by lithium oxides during the operation of lithium-air batteries [4]. The GDE was positioned between an Ar-O<sub>2</sub> and an Ar atmosphere. The passivation of the local detector electrode was avoided by the use of a pulse program that contained a cleaning step for the microelectrode. The difference in O<sub>2</sub> partial pressure was the driving force for the transport of O<sub>2</sub> through the wetted pore structure of the GDE. Depending on the potential of the GDE, O<sub>2</sub> enters the organic electrolyte or is completely consumed in the GDE. In this way it was possible to detect the build up of concentration gradients in the electrolyte above an GDE in organic electrolytes in dependence of the operation characteristics of the air cathode. Intermediates of the oxygen electrode have been detected but the chemical identification of such short lived intermediates remains challenging.

[1] S. Krueger, R. Kloeppsch, J. Li, S. Nowak, S. Passerini, M. Winter, J. Electrochem. Soc. 160 (2013) A542.

[2] P. Verma, P. Maire, P. Novak, Electrochim. Acta 55 (2010) 6332.

[3] H. Bülter, F. Peters, J. Schwenzel, G. Wittstock, Angew. Chem. Int. Ed. 53 (2014) 10531.

[4] P. Schwager, D. Fenske, G. Wittstock, J. Electroanal. Chem. 740 (2015) 82.

# Hybrid carbon film electrodes for electroanalytical applications

Osamu Niwa<sup>1,3</sup>, Dai Kato<sup>1</sup>, Tomoyuki Kamata<sup>1,2</sup>, Daiki Kato<sup>3</sup>, Shunsuke Shiba<sup>3</sup>, Shigeru Hirono<sup>4</sup>,  
Eisuke Kuraya<sup>5,6</sup>, Masashi Kunitake<sup>5</sup>, Naoto Yamaguchi<sup>7</sup>, Hiroshi Imai<sup>7</sup>

<sup>1</sup>National Institute of Advanced Industrial Science and Technology, Central 6, 1-1-1 Higashi, Tsukuba,  
Ibaraki, 305-8566, Japan<sup>1</sup>, Chiba Institute of Technology<sup>2</sup>, University of Tsukuba<sup>3</sup>, JVC Afty<sup>4</sup>  
Corporation, Kumamoto University<sup>5</sup>, Okinawa National College of  
Technology<sup>6</sup>, Riken Keiki Co., Ltd.<sup>7</sup>

niwa.o@aist.go.jp

The electrochemical performance of carbon film electrodes can be widely controlled depending upon surface termination or doping of other atoms such as oxygen, nitrogen, fluorine and various metals. We have been studying nanocarbon film electrodes formed by various sputtering techniques<sup>1,2</sup>. The surfaces of the carbon films are electrochemically or plasma treated to introduce oxygen and fluorine containing groups on to the surfaces. As we reported previously, electrochemically treated carbon film becomes hydrophilic by significant increase in the surface oxygen concentration<sup>3</sup>. This hydrophilic and very flat surface of the carbon film is advantageous to measure relatively large biomolecules such as oligonucleotides. The carbon film can detect the amount of all the bases in the single stranded DNA and successfully demonstrated SNPs and DNA methylation analysis<sup>4,5</sup> because the adsorption of biomolecules can be significantly suppressed.

A nitrogen-doped nanocarbon film electrodes with mixed sp<sup>2</sup> and sp<sup>3</sup> bonds formed using ECR sputtering method has a very smooth surface with an average roughness of 0.1 to 0.2 nm, which is almost independent of nitrogen concentration<sup>6</sup>. The oxygen and hydrogen peroxide (H<sub>2</sub>O<sub>2</sub>) reduction potentials at N-ECR carbon film electrode shifted about 0.3 and 0.15 V (vs. Ag/AgCl), respectively, and the peak height of H<sub>2</sub>O<sub>2</sub> is greatly increased similar to well known carbon alloy materials<sup>8</sup>.

We previously reported electrochemically stable fluorinated nanocarbon film by CF<sub>4</sub> plasma treatment that had an sp<sup>2</sup> and sp<sup>3</sup> hybrid bonds<sup>9</sup>. The contact angle of the film surface increased from 72 to 93 degree after surface fluorination. We employed the fluorinated carbon film electrode to selectively detect hydrophobic antioxidants in foods and drinks. The film electrode shows fast electron transfer for hydrophobic  $\alpha$ -tocopherol. In contrast, electrochemical responses for hydrophilic antioxidants such as ascorbic acid were effectively suppressed at the fluorinated film electrode<sup>10</sup>. These properties allowed us to achieve selective and quantitative measurements of hydrophobic antioxidants with maintaining the suppression for the responses of hydrophilic antioxidants in the analyte solution. The fluorinated nanocarbon film was also applied for selective electrochemical reaction of ferrocene against Fe<sup>2+</sup>/Fe<sup>3+</sup> redox couple, which could be applied electrochemical amplification of electrochemical biosensor for lipopolysaccharide (LPS).

Metal nanoparticles embedded carbon film electrode was developed by co-sputtering of metal and carbon because of low intermiscibility between metals and carbon. The Pt nanoparticles dispersed carbon electrodes can be applied for stable detection of hydrogen peroxide<sup>11</sup>. We formed Pt nanoparticles embedded carbon film on the surface of porous Teflon film and successfully applied for continuous monitoring of HCl and HBr gas. More recently, we fabricated Ni/Cu nanoalloys embedded carbon film electrode using unbalanced magnetron (UBM) co-sputtering of Ni, Cu and carbon. The improved sensitivity and repeatability was realized for detecting clinical sugar markers such as D-manitol by high electrocatalytic activity of Ni/Cu nanoalloy compared with bulk metal electrodes.

## References

- (1) Niwa O. et al., *J. Am. Chem. Soc.*, **2006**, 128, 7144.
- (2) Kamata T. et al., *Diamond Relat. Mater.* **2014**, 49, 25.
- (3) Sekioka N. et al., *Carbon*, **2008**, 46, 1918.
- (4) Kato D. et al., *Angew. Chem. Int. Ed.*, **2008**, 47, 6681.
- (5) Kato D. et al., *J. Am. Chem. Soc.*, **2008**, 130, 3716.
- (6) Kamata T., *Anal. Chem.*, **2013**, 85, 9845.
- (7) T. Kamata et al., *Anal. Sci.* submitted
- (8) Ozaki, J. et al., *Electrochim Acta*, **2010**, 55, 1864.
- (9) Ueda A. et al., *Carbon*, **2009**, 47, 1943.
- (10) Kuraya E. et al., *Anal. Chem.*, **2015**, 87, 1489.
- (11) You, T. et al., *Anal. Chem.*, **2003**, 75, 2080.

# From Protein Film Bioelectrochemistry to Biomedical Devices and Diagnostics

James F. Rusling,<sup>†,‡,§,∅</sup>

<sup>†</sup>*Department of Chemistry, 55 North Eagleville Road, Storrs, Connecticut 06269*, <sup>‡</sup>*Institute of Materials Science, University of Connecticut, Storrs, Connecticut 06269*, <sup>§</sup>*Department of Cell Biology, University of Connecticut Health Center, Farmington, Connecticut 06032*

<sup>∅</sup>*School of Chemistry, National University of Ireland at Galway, Ireland*  
[James.Rusling@uconn.edu](mailto:James.Rusling@uconn.edu)

My electrochemical career began at Wyeth Labs in Philadelphia in the 1970s and continued in Prof. Petr Zuman's lab. In the early 1990s, Dr. Ala Nassar and I began to develop protein film voltammetry for direct electron transfer involving heme enzymes like cyt P450s in thin lipid films. Dr. Yuri Lvov later joined our group as a senior scientist and with Prof. John Schenkman at our health center we began to work on cyt P450s and their enzyme reactions in thin layer-by-layer (LbL) polyelectrolyte films, which were much more stable and ultrathin. We demonstrated electrochemically driven enzyme activities of human cyt P450s the same or better than the NADPH-activated enzyme system in solution. With Dr. Sadagopan Krishnan, we later developed the first electrochemically-driven cyt P450 films that followed the natural redox cycle by using cyt P450s in film of polyelectrolytes and microsomal cyt P450 reductase. We also showed that voltammetry could reveal mechanistic details of cyt P450-reductase interactions.

These bioelectrochemistry efforts eventually led to applications to toxicity screening. The link is that cyt P450s and other metabolic enzymes often make toxic metabolites that react with DNA and these metabolites are known as genotoxic species. Schenkman and I and our students developed arrays combining DNA, a Ru-dye polymer and metabolic enzymes using LbL technology in which increased levels of electrochemiluminescence (ECL) for damaged DNA, and thus were able to measure relative rates of DNA damage from a metabolized chemical. Our most advanced version is a microfluidic array that performs cell-free in vitro metabolic genotoxicity screening of pollutants and drugs using enzymes from four different organs. We also developed analogous high-throughput approaches to assessing metabolite-related DNA damage using LC-MS/MS to complement the electrochemical arrays.

Our expertise in film fabrication on electrodes coupled with the nanomaterials skills of Prof. Fotios Papadimitrakopoulos led to projects in microfluidic immunoarray development for protein-based cancer diagnostics. We found that nanostructured sensor arrays coupled with microfluidics and massively multilabeled particles for detection provide very high sensitivity for multiple proteins using amperometric and electrochemiluminescent (ECL) detection. We recently automated one of these approaches, and are working on additional automated immunoarrays based on 3D printing.

# Nano Impacts: Recent Advances

Richard G Compton

*Oxford University, United Kingdom*

*Department of Chemistry, Physical and Theoretical Chemistry Laboratory*

*South Parks Road, Oxford, OX1 3QZ*

*Richard.compton@chem.ox.ac.uk*

Recent progress in the electrochemical study of single nanoparticles by means of the nano-impacts approach will be surveyed and evaluated

The design of electrodes and nano-impacts methodology allowing the electrochemical sizing of nanoparticles as small as 4nm will be described, and shown to be applicable to nanoparticle concentrations as low as 0.1 pM.

Contrasts will be drawn between experiments conducted on ensembles of nanoparticle, as in nanoparticle modified electrodes, and the behavior contrasted seen for single nanoparticle experiments. Important factors include the change of mass transport regime, altered apparent electrochemical reversibility and the incomplete 'stripping' seen for aggregated nanoparticles.

The role of surface charge on the observed electrochemical behavior will be explored with reference to experiments carried out using indigo nanoparticles in weakly supported aqueous electrolytes.

Experiments with diverse types of nanoparticles will be reported, namely metallic (Ag, Cu, Ni, Au), metal oxides ( $\text{Fe}_3\text{O}_4$ ), organic (indigo and oil blue) and polymeric (poly-N-vinyl carbazole) as well as studies on single drug encapsulating liposomes.

Electro-catalytic processes occurring during nano-impacts of soft nanoparticles will be discussed with reference to the reduction of oxygen mediated via attomole quantities of vitamin B12 present in single nano-droplets.

Finally a speculative electrochemical perspective on the origins of the toxicity of silver nanoparticles will be offered.

## References

"The electrochemical detection and characterization of silver nanoparticles", Y Zhou, N V Rees and R G Compton, *Angewandte Chemie International Edition*, 50, 2011, 4219

"Electrochemical sizing of organic nanoparticles", W Cheng, X Zhou and R G Compton, *Angewandte Chemie International Edition*, 52, 2013, 12980

"Electrochemical observation of single collision events: fullerene nanoparticles", E J E Stuart, K Tschulik, C Batchelor-McAuley and R G Compton, *ACS Nano*, 8, 2014, 7648

"Doping of single polymeric nanoparticles", X Zhou, W Cheng and R G Compton, *Angewandte Chemie International Edition*, 53, 2014, 12587

"Investigation of single drug encapsulating liposomes using the nano-impact method, W Cheng and R G Compton, , *Angewandte Chemie International Edition*, 53, 2014, 13928

"Oxygen reduction mediated via single nanodroplets containing attomoles of vitamin B12: Electro-catalytic nano-impacts", W Cheng and R G Compton, *Angewandte Chemie International Edition*, 2015, in press

"Why are silver nanoparticles more toxic than bulk silver? Towards understanding the dissolution and toxicity of silver nanoparticles", C Batchelor-McAuley, K Tschulik, C C M Neumann, E Laborda and R



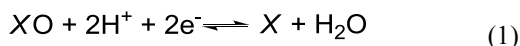


# Molybdenum Enzyme Electrochemistry

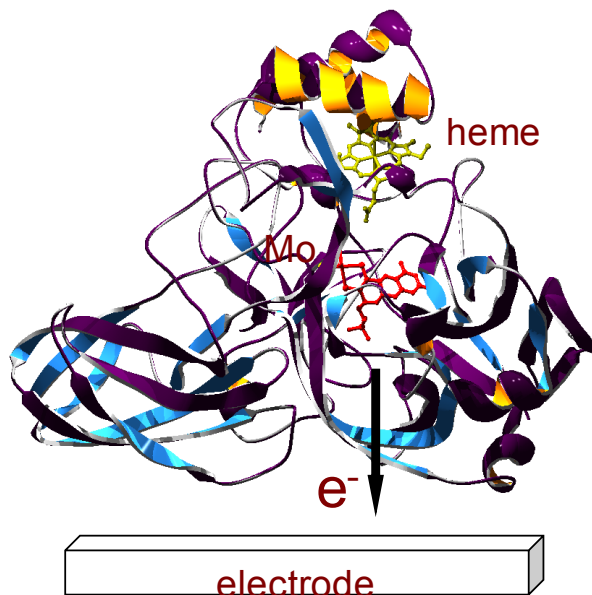
Paul V. Bernhardt

*School of Chemistry and Molecular Biosciences,  
University of Queensland, Brisbane 4072, Australia  
p.bernhardt@uq.edu.au*

The mononuclear Mo enzymes comprise a diverse but coherent family of oxidoreductases that typically catalyse coupled two-electron, O-atom transfer reactions and are found in all forms of life. The reductases and oxidases/dehydrogenases are equally represented amongst the mononuclear Mo enzymes *i.e.* eq. 1 may proceed either to the left or right depending on the enzyme.



Like all redox active enzymes, an external electron donor or acceptor is necessary to sustain catalysis. Integration of the Mo enzyme with an electrical circuit is central to the transition from native function to an artificial bioelectronic device. There are two main ways that this can be done: direct electron transfer between the enzyme and the electrode or indirectly *via* mediators that relay electrons between the electrode and the enzyme. Both approaches have their merits and their shortcomings. Above all else, electronic communication with the enzyme must be achieved without compromising stability, reactivity of selectivity.



Some recent results from our lab will be presented where we apply different approaches to these remarkable enzymes in an effort to exploit the high selectivity and reactivity of these interesting systems toward the development of biosensors.

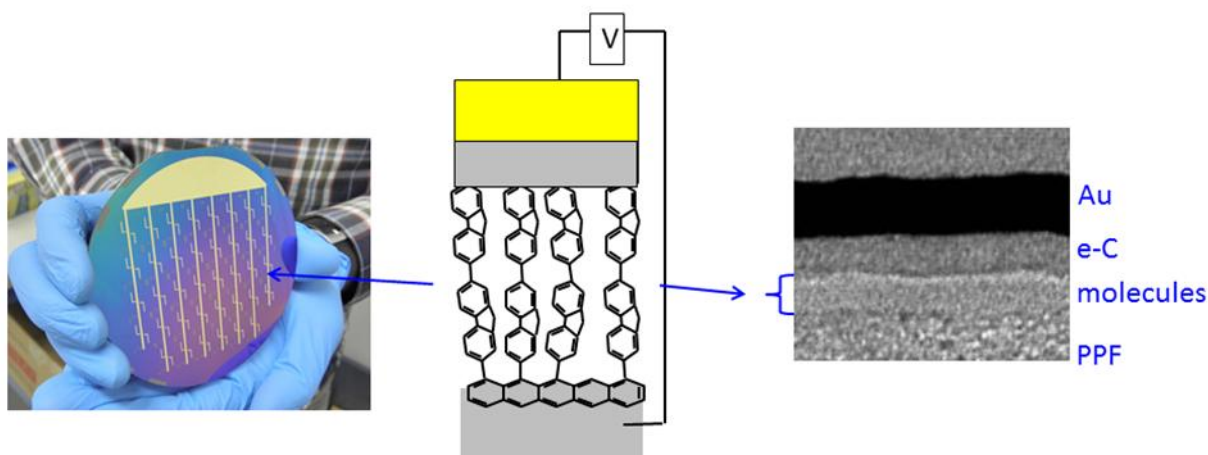
## References

1. Bernhardt, P.V. *Chem. Commun.*, **2011**, 47, 1663-1673.
2. Kalimuthu, P.; Kappler, U.; Bernhardt, P. V. Catalytic voltammetry of the molybdoenzyme sulfite dehydrogenase from *Sinorhizobium meliloti*. *J. Phys. Chem. B* **2014**, 118, 7091-7099.
3. Kalimuthu, P.; Fischer-Schrader, K.; Schwarz, G.; Bernhardt, P. V. A sensitive and stable amperometric nitrate biosensor employing *Arabidopsis thaliana* nitrate reductase. *J. Biol. Inorg. Chem.* **2015**, 20, 385-393.

# Charge Transport Through Molecules Acting as “Supramolecular” Electronic Devices

Richard L. McCreery<sup>1,2</sup>, Adam Bergren<sup>2</sup>, Nikola Pekas<sup>2</sup>, Oleksii Ivashenko<sup>1</sup>, Jerry Fereiro<sup>1</sup>, Bryan Szeto<sup>2</sup>  
University of Alberta<sup>1</sup>, National Institute for Nanotechnology<sup>2</sup>  
11421 Saskatchewan Dr  
Edmonton, Alberta  
Canada T6G 2M9  
mccreery@ualberta.ca

The molecular junction (MJ) is not generally described as “supramolecular”, but it definitely qualifies, since it consists of molecules bonded covalently in parallel between two conducting contacts. We study “all carbon” molecular junctions made by covalent bonding of aromatic molecules to flat, conducting, sp<sup>2</sup> carbon surfaces, then vapor depositing disordered sp<sup>2</sup> carbon to make a conducting “top contact”. Such MJs can be incorporated into electronic circuit consisting of conventional semiconductor components to realize functions not possible with silicon. Electron transport across 1-20 nm differs fundamentally from that in standard semiconductors and thicker organic films, and often involves quantum mechanical tunneling. When molecular orbitals have suitable energies, field ionization can generate charge carriers, and transport may occur across distances much too long for tunneling. Ultraviolet photoelectron spectroscopy and photocurrent measurements from illuminated molecular junctions permit direct determination of energy levels in molecular junctions, often simultaneously with electronic conduction. Molecular junctions also produce light during current flow, indicating significant “ballistic” transport without inelastic scattering. A potential commercial application of molecular junctions in audio processing will also be described and demonstrated.



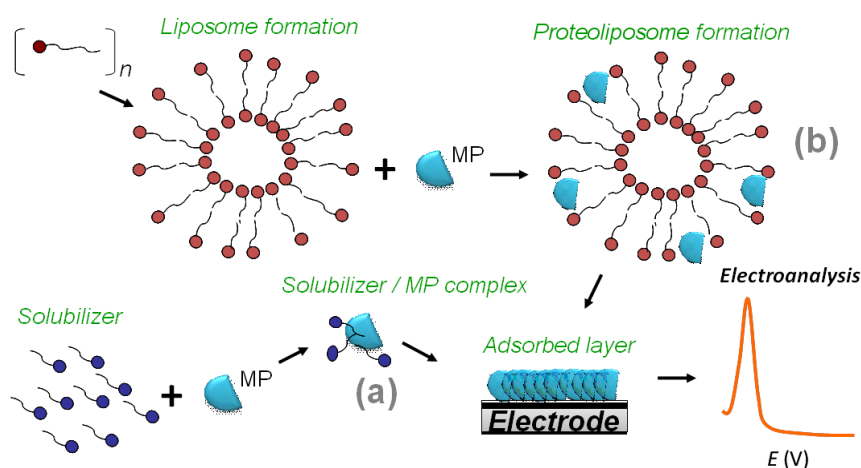
- (1) Yan, H.; Bergren, A. J.; McCreery, R.; Della Rocca, M. L.; Martin, P.; Lafarge, P.; Lacroix, J. C. Activationless charge transport across 4.5 to 22 nm in molecular electronic junctions, *Proceedings of the National Academy of Sciences* **2013**, 110, 5326.
- (2) McCreery, R.; Yan, H.; Bergren, A. J. A Critical Perspective on Molecular Electronic Junctions: There is Plenty of Room in the Middle, *Physical Chemistry Chemical Physics* **2013**, 15, 1065.
- (3) Fereiro, J. A.; Kondratenko, M.; Bergren, A. J.; McCreery, R. L.; Internal Photoemission in Molecular Junctions: Parameters for Interfacial Barrier Determinations; *J. Am. Chem. Soc.* **2015**, 137, 1296.
- (4) Sayed, S. Y.; Fereiro, J. A.; Yan, H.; McCreery, R. L.; Bergren, A. J. Charge transport in molecular electronic junctions: Compression of the molecular tunnel barrier in the strong coupling regime, *Proceedings of the National Academy of Sciences* **2012**, 109, 11498.

# Electrochemistry of Membrane Proteins

Jan Vacek

Department of Medical Chemistry and Biochemistry, Faculty of Medicine and Dentistry, Palacky University, Hnevotinska 3, 775 15 Olomouc, Czech Republic  
e-mail: jan.vacek@upol.cz

Membrane proteins (MPs) are proteins associated with the membranes of a cell or separated organelles. It has been estimated that ~30% of all genes in most genomes encode MPs. For this reason, MPs are interesting target molecules in current biochemical research and hence the search for novel methodologies for studying MPs is important in the investigation of their structure and function. In this contribution, a procedure for measuring the intrinsic electroactivity of MPs using mercury and carbon electrodes is described. MPs were analysed after their (a) solubilisation by non-ionic detergents or selected ionic liquids and/or (b) reconstitution into liposomes. The formed species, solubilized proteins (cf. a) or proteoliposomes (cf. b), were adsorbed onto electrode surfaces and typical anodic and cathodic protein peaks were monitored:



The electrochemical responses reflected the concentration of the studied MPs in the samples and the changes in electrochemical peaks indicate the structural changes in the MPs resulting from ligands binding to them. Na/K ATPase (ubiquitous, sodium/potassium pump), uncoupling proteins (components of mitochondrial membranes), protein f1t103 (bacterial periplasmic protein) and cytochromes c (small heme proteins associated with the inner membrane of the mitochondria) were used as model MPs. The applicability of intrinsic electroactivity measurement for MP research is discussed in general, especially in the context of studying the interactions of MPs with detergents, lipids, solid surfaces and binding ligands such as drugs, toxins and various prooxidant agents.

## References

- J. Vacek, M. Zatloukalova, M. Havlikova, J. Ulrichova, M. Kubala, *Electrochem. Commun.*, 27, 104–107, 2013
- M. Zatloukalova, E. Orolinova, M. Kubala, J. Hrbac, J. Vacek, *Electroanalysis*, 24, 1758–1765, 2012
- M. Huliciak, J. Vacek, M. Sebela, E. Orolinova, J. Znaleziona, M. Havlikova, M. Kubala, *Biochem. Pharmacol.*, 83, 1507–1513, 2012
- R. Vecerkova, L. Hernychova, P. Dobes, J. Vrba, B. Josypcuk, M. Bartosik, J. Vacek, *Anal. Chim. Acta* 830, 23–31, 2014
- J. Vacek, M. Zatloukalova, J. Vrba, M. Kubala, *Electrochim. Acta* 126, 31–36, 2014
- M. Havlikova, M. Zatloukalova, J. Ulrichova, P. Dobes, J. Vacek, *Anal. Chem.* 87, 1757–1763, 2015
- M. Kubala, J. Geleticova, M. Huliciak, M. Zatloukalova, J. Vacek, M. Sebela, *Biomed. Pap.* 158, 194–200, 2014

## Acknowledgement

This work was supported by the Czech Science Foundation (project No. 14-08032S) and by the Ministry of Education, Youth and Sports of the Czech Republic, project No. LD14033 (COST Action EU-ROS, BM1203).

# How to Understand the Electrochemistry of Battery Materials?

Petr Novák, Peter Bleith, Rosa Robert, Tsuyoshi Sasaki\*, Claire Villevieille

Paul Scherrer Institute, Electrochemistry Laboratory

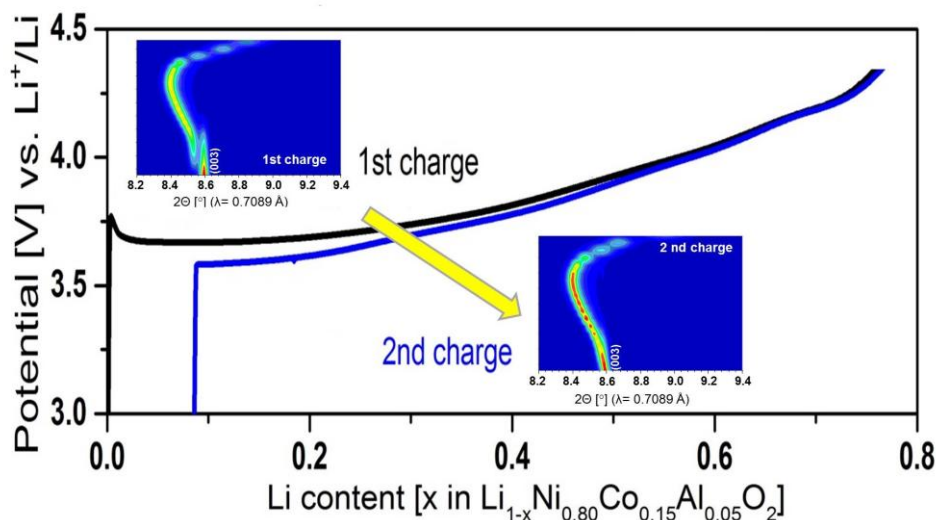
CH-5232 Villigen PSI, Switzerland

\*Toyota Central R&D Labs. Inc., Nagakute, Japan

petr.novak@psi.ch; novakp@ethz.ch

Lithium-ion batteries (LIBs) are now considered to be the most available power sources for portable devices. The next generation of high-end rechargeable batteries will still rely on lithium-ion host materials. Later, post-lithium-ion systems, at first Li/S, are expected to enter the market. But oxides and, more generally, inorganic solid materials reacting reversibly with lithium, will remain the backbone of the future battery systems. Clearly, independently of the technology, understanding the fundamental properties of battery materials and the interactions of these materials with their environment will be the key to further improvements in energy density, safety, and life time of batteries.

In the presentation, focus will be on some interesting effects related to lithium insertion and deinsertion, recently identified in industrially used metal oxide electrodes like NCA,  $\text{Li}(\text{Ni},\text{Co},\text{Al})\text{O}_2$  and LFP,  $\text{LiFePO}_4$ . The data on NCA suggest an unknown irreversible activation of the material in the first electrochemical cycle which seems to be a combination of an irreversible two-phase transition and a reversible solid solution reaction mechanism. Understanding the difference in the reaction pathways that NCA undergoes in the first and subsequent cycles provides further insights into the irreversible charge “loss” between the first charge and discharge. For LFP we found an obvious “memory effect” in the charging curve after a shallow depth of charge and discharge. In contrast to Ni-Cd and Ni-MH batteries, the memory effect of LFP appears already after only one partial cycle. The understanding of the memory effect is highly essential for the exact estimation of the SOC and the effective use of LIBs based on LFP. Additionally, this notable behavior gives us a strong hint to make the real charge/discharge reaction mechanism and kinetics of  $\text{LiFePO}_4$  clear. Moreover,  $\text{LiFePO}_4$  is described to be a phase separating material when cycled under low current density conditions. But *in situ* synchrotron X-ray diffraction under ultra-high rate alternating current and medium rate direct current density excitation revealed a continuous but current-dependent solid-solution regime of  $\text{LiFePO}_4$  and  $\text{FePO}_4$ . In another example, the reaction with lithium of metal titanium oxyphosphates ( $\text{M}_{0.5}\text{TiOPO}_4$ ) will be discussed. These oxyphosphates are a family of isostructural materials exhibiting an unexpectedly high specific charge. The reaction mechanism upon lithiation and delithiation was therefore investigated using a combination of XAS,  $^{31}\text{P}$ -NMR, XRD, EDX, and electrochemical techniques. Surprisingly, the oxyphosphate materials react, through several steps, via a combination of insertion and conversion processes, the reaction mechanism being dependent on the (transition) metal in the structure.



Contour plots of the intensity, at selected  $2\theta$  regions, and corresponding galvanostatic plot for synchrotron data for the first and second charge of NCA to  $4.3 \text{ V Li}^+/\text{Li}$ .

# Supramolecular Enantioselective Recognition at Mesoporous Chiral Metal Surfaces

Alexander Kuhn<sup>1</sup>, Thittaya Yutthalekha<sup>1,2</sup>, Chularat Wattanakit<sup>1,2</sup>, Yémima Bon Saint Côme<sup>1</sup>, Veronique Lapeyre<sup>1</sup>, Philippe A. Bopp<sup>1</sup>, Matthias Heim<sup>1</sup>, Sudarat Yadnum<sup>1,2</sup>, Somkiat Nokbin<sup>2</sup>, Chompunuch Warakulwit<sup>2</sup>, Jumras Limtrakul<sup>2</sup>

<sup>1</sup>Univ. de Bordeaux, CNRS, ISM, UMR 5255, 16 Avenue Pey Berland, FR-33607 Pessac, France

<sup>2</sup>Department of Chemistry, and NANOTEC Center for Nanoscale Materials Design for Green Nanotechnology, Kasetsart University, Bangkok 10900, Thailand  
kuhn@enscbp.fr

Chirality is widespread in natural systems, and reproducing chiral recognition artificially is a major scientific challenge, especially because of the various potential applications ranging from catalysis to sensing and separation science. In this context, molecular imprinting is a well-known approach for generating materials with enantioselective properties, and it has been successfully employed using polymers [1]. However it is particularly difficult to synthesize chiral metal matrices by this method. We report here, for the first time, the elaboration of chiral imprinted mesoporous metal, obtained by the electrochemical reduction of platinum salts in the presence of a liquid crystal phase [2] and chiral template molecules [3]. The porous platinum retains a chiral character after removal of the template molecules. A matrix obtained in this way exhibits a large active surface area due to its mesoporosity, and most importantly also shows a very significant discrimination between two enantiomers, when they are studied using these materials as electrodes in Differential Pulse Voltammetry. Recently it has been possible to extend the concept even to the recognition of enantiomers which are different from the imprinted ones in terms of chemical composition. This is possible due to the geometric nature of the chiral recognition process [4].

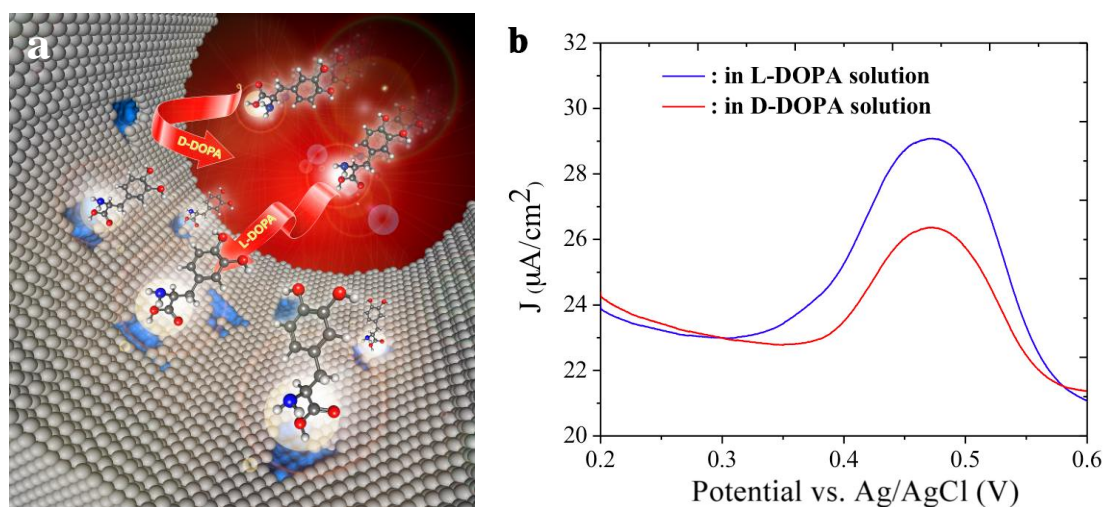


Figure a) Scheme illustrating the inside of a chiral imprinted mesopore, b) Differential Pulse Voltammetry signal of a mesoporous electrode that has been imprinted with L-DOPA

## References:

- [1] K. Haupt, A. Linares, M. Bompert, B. Bui, in *Molecular Imprinting*, Vol. 325 (Ed.: K. Haupt), Springer Berlin Heidelberg, 2012, pp. 1-28.
- [2] G. S. Attard, P. N. Bartlett, N. R. B. Coleman, J. M. Elliott, J. R. Owen, J. H. Wang, *Science* 278 (1997) 838
- [3] C. Wattanakit, Y. Bon Saint Côme, V. Lapeyre, P. A. Bopp, M. Heim, S. Yadnum, S. Nokbin, C. Warakulwit, J. Limtrakul, A. Kuhn, *Nat. Comm.* (2014) 5:3325
- [4] T. Yutthalekha, C. Warakulwit, J. Limtrakul, A. Kuhn, *Electroanalysis* (2015) in press

## **In-situ investigation of catalyst degradation**

S. Cherevko, S. Geiger, N. Hodnik, G. Keeley, C. Choi, C. Baldizzone, J. Grote, A. Zeradjanin, K.J.J. Mayrhofer

*Department of Interface Chemistry and Surface Engineering, Max-Planck-Institut für Eisenforschung, Max-Planck-Strasse 1, 40237 Düsseldorf, Germany  
mayrhofer@mpie.de*

Continuous electrochemical flow reactors for efficient conversion of electrical energy into chemicals and vice versa, i.e. fuel cells and electrolyzers, become increasingly important considering energy sustainability and environmental concerns. The electrocatalyst materials, which constitute the core of electrochemical energy conversion devices, however are still a bottleneck for their efficiency. While the optimization of kinetics of electrocatalysts has been widely explored, the highly important stability of the materials is less studied. In this presentation I will demonstrate how fundamental investigations of electrocatalyst stability can be performed online and in parallel to activity determination, and what can be learned from these studies for large scale applications. The focus will be on the recent methodological developments from our group, in particular the scanning flow cell (SFC) coupled to online analytics, which also allows for combinatorial analysis. The potential of this approach will be demonstrated by results on the essential oxygen electrochemistry on noble metal catalysts as used in low-temperature fuel cells and electrolyzers.

1. Katsounaros, I.; Cherevko, S.; Zeradjanin, A.R.; Mayrhofer, K.J.J.; *Oxygen Electrochemistry as a Cornerstone for Sustainable Energy Conversion; Angewandte Chemie – International Edition* 2014, 53, 102 – 121.
2. Topalov, A.A.; Cherevko, S.; Zeradjanin, A.R.; Meier, J.C.; Katsounaros, I.; Mayrhofer, K.J.J.; *Towards a comprehensive understanding of platinum dissolution in acidic media; Chemical Science*, 2014, 5, 631-638.
3. Cherevko, S.; Topalov, A.A.; Zeradjanin, A.R.; Katsounaros, I.; Mayrhofer, K.J.J.; *Gold dissolution: towards understanding of noble metal corrosion; RSC Advances* 2013, 3, 16516-16527.

## **Title in Times Roman 14 point – Upper and Lower Case**

Presenting author, Co-Authors

*Affiliation*

*Address*

*e-mail address*

These instructions are an example of what a properly prepared meeting abstract should look like. Proper column and margin measurements are indicated.

The abstract **should not exceed ONE PAGE** of text, references, tables and figures. Abstracts exceeding this limit may be cut without consideration of content after the first page.

Type the title single-spaced in 14-point Times Roman bold, upper and lower case and NOT in ALL CAPITAL letters.

Type the author(s) name(s) single-spaced in 10-point Times Roman regular.

Type the affiliation(s) and address(es) single-spaced in 10-point Times Roman italic.

Type the body of the abstract text (including references and tables) single-spaced in 10-point Times Roman regular.

**Paper Size: A4 (21.0 x 29.7 cm)**

### **Margins**

Top: 30.0 mm

Bottom: 30.0 mm

Sides: 30.0 mm



# Enabling Bioelectrochemistry for In Vivo Analysis

Lanqun Mao

*Beijing National Laboratory for Molecular Sciences, Key Laboratory of Living Biosystems, Institute of Chemistry, the Chinese Academy of Sciences, Beijing 100190, China.*

*Tel: 86-10-62646525. E-mail: lqmao@iccas.ac.cn*

To understand the molecular basis of brain functions, researchers would like to be able to quantitatively monitor the levels of neurochemicals in the extracellular fluid in vivo. However, the chemical and physiological complexity of the central nervous system (CNS) presents challenges for the development of these analytical methods. We herein demonstrated a new strategy for in vivo analysis based on bioelectrochemistry by rationally design and careful construction the surface/interface chemistry.

We used the redox nature of neurochemicals at the electrode/electrolyte interface to establish a basis for monitoring specific neurochemicals. Carbon nanotubes provide an electrode/electrolyte interface for the selective oxidation of ascorbate, and we have developed both in vivo voltammetry and an online electrochemical detecting system for continuously monitoring this molecule in the CNS. By using the CNT-based OECS, we compared the dynamic regional changes of extracellular ascorbate level in four different brain regions 1 h after global cerebral ischemia induced by two-vessel occlusion (2-VO). We also compared the change in the level of ascorbate in the different ischemia model (i.e., two-vessel occlusion (2-VO) and left middle cerebral artery occlusion (LMCAO) in striatum. We also demonstrated the validity of the OECS for ascorbate detection as a platform for in vivo evaluation of neuroprotective efficiency of antioxidants by studying the dynamic change of hippocampal ascorbate during the acute period of cerebral ischemia and its responses to intravenous administration of antioxidants including ascorbate and glutathione.

Although  $\text{Ca}^{2+}$  and  $\text{Mg}^{2+}$  are involved in a number of neurochemical signaling processes, they are still difficult to detect in the CNS. These divalent cations can enhance electrocatalytic oxidation of NADH at an electrode modified with toluidine blue O. We used this property to develop online electrochemical detection systems for simultaneous measurements of  $\text{Ca}^{2+}$  and  $\text{Mg}^{2+}$  and for continuous selective monitoring of  $\text{Mg}^{2+}$  in the CNS.

We have also harnessed biological schemes for neurosensing in the brain to design other monitoring systems. By taking advantage of the distinct reaction properties of dopamine (DA), we have developed a nonoxidative mechanism for DA sensing and a system that can potentially be used for continuously sensing of DA release. Using “artificial peroxidase” (Prussian blue) to replace a natural peroxidase (horseradish peroxidase, HRP), our online system can simultaneously detect basal levels of glucose and lactate. By substituting oxidases with dehydrogenases, we have used enzyme-based biosensing schemes to develop a physiologically relevant system for detecting glucose and lactate in rat brain. Because of their unique optical properties and modifiable surfaces, gold nanoparticles (Au-NPs) have provided a platform of colorimetric assay for in vivo cerebral glucose quantification. We designed and modified the surfaces of Au-NPs and then used a sequence of reactions to produce hydroxyl radicals from glucose.



# Alternative PEFC Catalysts for Future Commercial FCVs

Masanori Inaba, Shuhei Yoshino, Masao Shibata, Tatsuya Hatanaka and Yu Morimoto\*

*Toyota Central Research and Development Labs., Inc.*

*41-1 Yokomichi, Nagakute 480-1192 Japan*

*\*Corresponding author email address: [morimoto@mosk.tytlabs.co.jp](mailto:morimoto@mosk.tytlabs.co.jp)*

Toyota Motor Co. has started commercialization of FCV MIRAI to general public In Japan in November, 2014 and will do so in Europe and US in 2015. Although it is an epoch-making accomplishment resulting from long and hard efforts by many scientists and engineers, further development is necessary for wider commercialization. One of the most important technological areas is the electrode catalyst. Pt or Pt based alloys (e.g. Pt-Co for MIRAI) , which is almost exclusively used, can provide sufficient efficiency and power but also poses cost and degradation issues, the latter of which can be avoided by system-based approaches, which, however, cause additional cost issues.

An alternative electrode catalyst is extended thin-film Pt, which was firstly introduced by 3M as NSTF[1], which is totally different from that of the conventional Pt/C electrode: low platinum surface area ( $10 - 25 \text{ cm}^2\text{Pt}/\text{cm}^2$ ), nonconductive substrate, and no ionomer contained. Although NSTF electrodes showed higher efficiency and power density than conventional Pt/C electrodes under suitable operating conditions[2], it has been reported that they tend to show larger performance loss under dry or wet conditions[3].

In this communication, after a short introduction on the present status and challenges on the catalysts, we present our research on thin film electrodes mainly for revealing their general features.

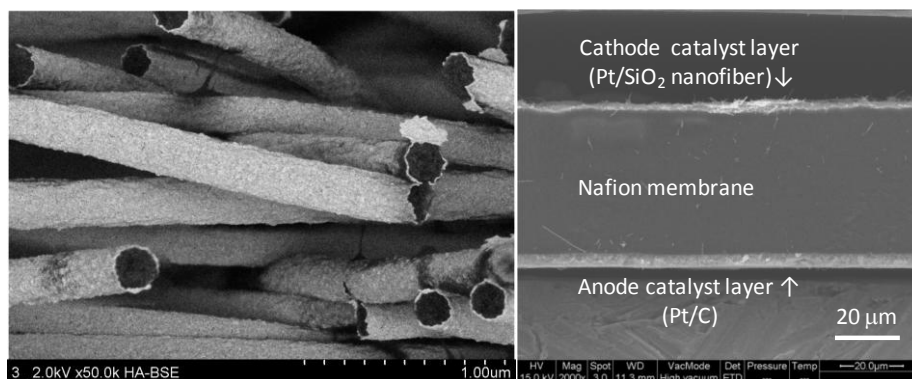


**Figure 1 Pt-coated SiO<sub>2</sub> electrode(left) and its MEA(right)**

Figure 1 shows an ALD-Pt on electrospun SiO<sub>2</sub> fibre electrode and a membrane-electrode-assembly using it for the cathode. The MEA exhibited comparable performance with the conventional Pt/C cell under 80°C, 100%RH condition in spite of the much smaller electrochemical surface area (ECSA), it showed poor performance under overly dry or wet conditions. The overvoltage was analyzed and some countermeasures were examined.

## References

- [1] M. K. Debe in Handbook of Fuel Cells –Fundamentals, Technology and Applications, W. Vielstich, A. Lamm, H. A. Gasteiger, Editors, Ch. 45, John Wiley & Sons (2003)
- [2] A. Kongskanand et al., J. Electrochem. Soc., 158(2011)B1286
- [3] P. K. Sinha et al., J. Electrochem. Soc., 158(2011)B831

# Heteroatom-Doped Porous Carbon as Electrocatalyst: Surface Properties and Electrocatalytic Activity

Dea-Soo Yang, Min Young Song, Kiran Pal Singh, Fatemeh Razmjooei and Jong-Sung Yu

*Department of Energy Systems Engineering, Daegu Gyeongbuk Institute of Science and technology (DGIST),  
Daegu, 711-873, Republic of Korea, Fax: (+82)53-785-6409, E-mail: [jsyu@dgist.ac.kr](mailto:jsyu@dgist.ac.kr)*

Fuel cells have received a plethora of attention because of their high energy conversion efficiency, low pollution, low operating temperature, high power density, and wide range of applications. Oxygen reduction reaction (ORR) takes place usually on Pt or Pt alloys loaded on carbon support, but their large-scale commercial application has been precluded mainly by the high cost and low durability of the requisite noble metal electrocatalyst [1]. Heteroatom-doped carbon catalysts, due to their high stability, excellent electrocatalytic performance, and economic viability over costly Pt-based catalysts are being pioneered as a suitable alternative [2,3]. Heteroatoms such as N, P and S are most common elements doped into carbon framework for electrochemical reactions.

Although the heteroatom-doped porous carbon materials have evolved as one of best possible solutions in this regard, the probable synergy of heteroatom doping and textural properties has not been well investigated yet in details. Active species, conductivity, porous structure and surface area are the key factors affecting overall electrocatalytic activity of carbon-based electrocatalysts [4]. In this work, we report a noble technique to synthesize highly conductive and microporous N and S-doped carbon from polyaniline (PANI) via a simple hydrothermal method followed by carbonization in presence of iodine. Iodine treatment removes large amount of attached oxygen and other heteroatoms, and as a consequence increases the carbon content. Therefore, the iodine treatment decreases catalytically active heteroatom doping level, which is unfavorable for oxygen reduction reaction (ORR), but at the same time, significantly increases the electrical conductivity, which is beneficial for ORR [5]. In particular, iodine-treated carbonized PANI (CPANI) shows exceptionally high conductivity, about 3 times that of untreated CPANI. Iodine treatment is also found to enhance the micropore surface area of the PANI during carbonization without using any activating agent. Electrocatalytic study indicates that amazingly the activity of the iodine-treated sample is found to be much better than that of untreated sample. This remarkable upsurge in activity is mainly attributed to the high increase in conductivity and surface area of the iodine-treated sample. The ORR activity is discussed in terms of heteroatom content, surface area, porous structure, and conductivity of the carbon [4-6]. This convenient innovative approach can open up a window for the designing of highly efficient future fuel cell electrocatalysts.

## References

1. B. Fang, M. S. Kim, J. H. Kim, J. -S. Yu, *Acc. Chem. Res.* 46 (2013) 1397.
2. G. Wu, K. L. More, C. M. Johnston, P. Zelenay, *Science* 332 (2011) 443.
3. D. S. Yang, D. Bhattacharjya, S. Inamdar, J. Park, J. -S. Yu, *J. Am. Chem. Soc.* 134 (2012) 16127.
4. D.S. Yang, S. Chaudhari, K. P. Rajesh, J. -S. Yu, *ChemCatChem* 6 (2014) 1236.
5. K. P. Singh, M. Y. Song, J.-S. Yu, *J. Mater. Chem. A* 2 (2014) 18115.
6. D.-S. Yang, M. Y. Song, K. P. Singh, J.-S. Yu, *Chem. Commun.* 51 (2015) 2450.

# A Recyclable Reaction Medium: Applications to Oxidative and Reductive Organic Electrochemical Transformations

R. Daniel Little,<sup>a</sup> Seung Joon Yoo,<sup>a</sup> Sebastian Herold,<sup>b</sup> Long-Ji Li,<sup>c</sup> Cheng-Chu Zeng,<sup>c</sup>

<sup>a</sup> *Department of Chemistry & Biochemistry, University of California Santa Barbara*

<sup>b</sup> *Graduate School Materials Science in Mainz, Germany*

<sup>c</sup> *Beijing University of Technology*

*little@chem.ucsb.edu*

The need for a supporting electrolyte in preparative scale electrosynthetic processes is clear. Several years ago, Yoo and Little initiated an effort one of whose goals was to devise a conveniently prepared and reusable reaction medium that avoided the use of a traditional supporting electrolyte.

Yoo's successes and the nature of the reaction medium, a so-called composite dispersion, will be described.[1] Its applicability to a variety of different oxidative transformations and its extension to reductive processes will be presented. An electrohydrocyclization that was previously used in the synthesis of a sesquiterpene called sterpurene will be revisited within the context of the new reaction medium.[2] The challenges associated with a) extending the scope of the chemistry to more challenging reductive processes, b) the problems encountered, c) the insights obtained, and d) the "solution(s)" devised will be highlighted.

## References

- [1] Yoo, S. J.; Li, Long-Ji; Zeng, C-C.; Little, R. D. *Angew. Chem. Int. Ed.* **2015**, 127, 3815
- [2] Moëns, L.; Baizer, M. M.; Little, R. D. *J. Org. Chem.* **1986**, 51, 4497

# Graphene-based Nanomaterials for Energy Storage Devices

Kwang-Bum Kim, Sang-Hoon Park, Hyun-Kyung Kim,  
Hee Chang Youn, Myeong-Seong Kim and Suk-Woo Lee  
*Department of Material Science and Engineering, Yonsei University,  
50 Yonsei-ro, Seodaemun-gu, Seoul 120-749, Republic of Korea.  
TEL: +82-2-365-7745*

## Abstract

Graphene, a one-atom-thick, two-dimensional (2D)  $sp^2$  carbon structure, has attracted considerable interest as a next-generation electrode material. This can be attributed to a number of interesting properties of graphene, such as its good mechanical/chemical stability, high electrical/thermal conductivity, and a large surface area (over  $2630\text{ m}^2\text{g}^{-1}$ ) due to its high surface-to-volume ratio. The combination of these unique physical and chemical properties means that graphene has significant potential to act as either an electrochemically active material in itself or as a conductive carbon template suitable for use in energy storage devices such as supercapacitors and Li-ion batteries.<sup>1-3</sup> At the same time, metal oxide/graphene nanocomposites are also of considerable interest for electrochemical energy storage applications owing to their outstanding properties. These excellent properties of metal oxide/graphene nanocomposites are generated from synergistic combination of graphene with metal oxide on the nanometer scale.<sup>1-3</sup> In this study, we report on the synthesis and electrochemical characterization of graphene and metal oxide/graphene nanocomposites for energy storage applications.

## References

1. H.C Youn, J.P Jegal, S.H Park, H.K Kim, H.S Park, K.C Roh, K.B Kim, *ACS Nano* **2014**, 8, 2279
2. H.K Kim, S.H Park, S.B Yoon, C.W Lee, J.H Jeong, K.C Roh, K.B Kim *Chem. Mater* **2014**, 26, 4838
3. S.H Park, S.B Yoon, H.K Kim, J.T Han, H.W Park, J Han, S.M Yun, H.G Jeong, K.C Roh, K.B Kim, *Sci. Rep.*, **2014**, 4, 6118

# Investigation of pore forming proteins in supported lipid membranes

Christine Kranz<sup>1</sup>, Corinna Frey<sup>1</sup>, Alexander Eifert<sup>1</sup>, Holger Barth<sup>2</sup>, Boris Mizaikoff<sup>1</sup>

<sup>1</sup>*Institute of Analytical and Bioanalytical Chemistry, University of Ulm, Albert-Einstein-Allee 11, 89081 Ulm, Germany*

<sup>2</sup>*Institute of Pharmacology and Toxicology, University of Ulm, Albert-Einstein-Allee 11, 89081 Ulm, Germany*

E-mail: [christine.kranz@uni-ulm.de](mailto:christine.kranz@uni-ulm.de)

Molecular transport on a cellular level plays a crucial role within the human body, and entails shuttling specific molecules and ions through the cell membrane via specific protein pores or ion channels. As natural membranes are exceedingly complex and exist in a variety of composition, artificial membranes such as lipid bilayers and supported lipid bilayers are frequently used as surrogates to investigate fundamental transport processes. To study such transport phenomena, electrochemical methods, in particular scanning electrochemical microscopy (SECM) [1,2] using nano-sized electrodes or ion selective micropipettes are highly attractive.

Here, we present electrochemical studies using cyclic voltammetry and combined atomic force – scanning electrochemical microscopy (AFM-SECM) to characterize transport through pore-forming proteins titrated into solid-supported lipid layers. As a model system, the trypsin-activated transport component C2IIa produced by *Clostridium botulinum* bacteria is investigated. The clostridium botulinum C2 toxin is a binary toxin using receptor-mediated endocytosis, and a C2IIa-mediated translocation of its C2I enzymatic component into the cytosol of mammalian cells, thereby developing the toxic effect within the cell after activation [3]. C2IIa forms heptameric pores, which are selective for cations and voltage dependent, and which spontaneously incorporate into lipid bilayers.

Gold-substrate-supported lipid bilayers (SLB) were formed via 1-octadecanethiol (ODT) and 1-palmitoyl-2-oleoyl-sn-glycero-3-phosphocholine (POPC). Bulk cyclic voltammetry experiments were performed to characterize the individual steps of the biomimetic layer formation, and the C2IIa pore incorporation. To investigate that the transmembrane transport is selectively induced by C2IIa pore incorporation, the antidote chloroquine was added to block the immobilized pores [4]. In addition, AFM-SECM was evaluated as a novel tool for monitoring the formation of pores by recording AFM-SECM approach curves at AFM tip-integrated conical Pt/C composite electrodes [5]. Experimental challenges and technological potential of characterizing the formation and transport properties of protein pores will be discussed in this contribution.

[1] S. Amemiya, A. J. Bard, *Anal. Chem.*, 72 (2000) 4940.

[2] J. Kim, A. Izadyar, N. Nioradze, S. Amemiya, *J. Amer. Chem. Soc.*, 135 (2013) 2321.

[3] H. Barth, K. Aktories, *Eur. J. Cell Biol.*, 90 (2011) 944.

[4] A. Schmid, R. Benz, I. Just, K. Aktories, *J. Biol. Chem.*, 269 (1994) 16706.

[5] P. Knittel, M. Higgins, C. Kranz, *Nanoscale* 6 (2014) 2255.

# **Light Activated Electrochemistry: A strategy for performing voltammetry on a monolithic surface where you want, when you want with micron scale spatial resolution**

Moinul Choudhury, Simone Ciampi, Stephen G. Parker, Ying Yang, Roya Tavallaie, Leila Zarei, Vinicius Goncales, J. Justin Gooding

*School of Chemistry and Australian Centre for NanoMedicine, The University of New South Wales, Sydney, 2052, Australia*

*E-mail: [justin.gooding@unsw.edu.au](mailto:justin.gooding@unsw.edu.au)*

Light and electrodes have a long history with spectroelectrochemistry, electrochemiluminescence and photovoltaics. Here we exploit light shined on an electrode to locally activate the electrode surface to allow Faradaic electrochemistry to occur on the illuminated spot only. To achieve this, first an oxide free silicon electrode is modified with a self-assembled monolayer of 1,8-nonadiyne which protects the surface against oxidation. Subsequently a redox species is attached to the surface, either a ferrocene derivative for n-type silicon or an anthraquinone derivative for p-type silicon. Provided the silicon is in the depletion at the potential at which the oxidation/reduction of the redox species occurs, then no electrochemistry is observed in the dark. Upon illumination distinct Faradaic electrochemistry is observed. We show this electrochemistry can be confined to 50  $\mu\text{m}$  with backside illumination and 30  $\mu\text{m}$  with frontside illumination. Subsequently, using SECM we show that the surface bound redox species can be used as a mediator to detect redox species in solution. We next show that we can detect DNA hybridization and form DNA electrode arrays (an example of reading electrochemical information from the electrode surface) and show that we can write conducting polymers to the surface. Finally we demonstrate an application for the capture and localized release of cells from the surface.

## **Alkaline polymer electrolyte fuel cells: materials and catalysis**

Lin Zhuang\*

*Department of Chemistry, Wuhan University, Wuhan 430072, China  
lzhuang@whu.edu.cn*

In this invited keynote lecture, I will talk about the recent research progress on alkaline polymer electrolyte fuel cells (APEFC), a promising new branch of the fuel cell family. The following topics will include:

- ✧ The state-of-the-art of alkaline polymer electrolytes
- ✧ Hydrogen oxidation reaction (HOR) catalysts in alkaline media
- ✧ Nonprecious metal catalysts for oxygen oxidation reaction (ORR) in alkaline media
- ✧ The performance and challenge of APEFC.

## Analysis by EIS of Cathodic Reactions on Carbon Steel in Aerated Solution at pH 13

B. Tribollet<sup>1,2</sup>, S. Chakri<sup>1,2</sup>, I. Frateur<sup>1,2</sup>, F. Kanoufi<sup>3</sup>, E. Sutter<sup>1,2</sup>, V. Vivier<sup>1,2</sup>

1- CNRS, UMR 8235, Laboratoire Interfaces et Systèmes Electrochimiques, France

2- Sorbonne Universités, UPMC Univ Paris 06, UMR 8235, LISE, F-75005, France

3- Univ. Paris Diderot, Sorbonne Paris Cité, ITODYS, UMR CNRS 7086, 15 rue J.A. Baif, 75013 Paris, France

*bernard.tribollet@upmc.fr*

At pH 13, the carbon steel is passivated at the corrosion potential and the oxide layer is reduced at more cathodic potential. The transition potential between a carbon steel electrode coated by an oxide layer and a bare (*i.e.* oxide-free) electrode is difficult to determine by electrochemical measurements, but surface reflectivity measurements clearly show that transition.

In aerated solution, the oxygen reduction is a pure kinetic reaction at the corrosion potential but it is under mixed control at more cathodic potential, and finally the reaction is under pure mass transport control on the diffusion plateau and at very cathodic potential. For the lowest cathodic potentials, the water reduction occurs and must be added in parallel with the oxygen reduction.

From the corrosion potential ( $\sim -0.65$  V/SME) down to the cathodic potential limit ( $-1.70$  V/SME), the electrochemical impedance (EIS) data obtained with a C15 carbon steel electrode in aerated 0.1 M NaOH solution were analyzed considering for the cathodic reaction(s):

- oxygen reduction on the oxide-coated electrode with a pure kinetic control,
- oxygen reduction on the oxide-coated electrode with a mixed control,
- oxygen reduction on the bare electrode with a mixed control,
- oxygen reduction on the bare electrode with a pure mass transport limitation,
- oxygen reduction with a pure mass transport limitation and water reduction on the bare electrode.

The evolution with potential of the different kinetic parameters obtained from the fitting procedure is in agreement with the proposed models. In particular, the values of the oxide layer thickness deduced from EIS data are similar to those estimated from surface reflectivity measurements.



# Novel Electrochemical Prototype for the Treatment of Spent Caustic from Hydrocarbon Industry and its Industrial Scaling

A. Medel\*, G. Zuñiga, J. A. Ramírez, Yunny Meas\*

*Centro de Investigación y Desarrollo Tecnológico en Electroquímica, S.C., Parque Tecnológico, Querétaro-Sanfandila, P.O. Box 064-76703 Pedro Escobedo, QRO, México. Phone: +52-442-211-6000, Fax: +52-442-211-6001*

*\*email: yunnymeas@cideteq.mx; amedel@cideteq.mx*

*Oral presentation: Symposium 10:*

*Electrochemical Technology: New Challenges for a More Competitive Economy*

The spent caustic generated by the hydrocarbon industry is an extremely toxic aqueous residue, with a concentration of phenolic compounds in the range 10,000-30,600 mg L<sup>-1</sup>. The high and irreparable damage to the environment, as well as human health risk, posed by the inadequate disposal and treatment of spent caustic requires the development of new and efficient processes in order to achieve its treatment and destruction up to CO<sub>2</sub> and water. In this symposium we present the development of a new electrochemical process based on the use of Boron Doped Diamond (BDD), MO<sub>x</sub>/Ti and Graphite. The study conducted is the result of a grand research project, divided into separate phases, beginning with the development of a methodology for BDD activation [1], as well as of exhaustive characterization and micro-electrolysis tests of water produced [2] and spent caustic [3], ending with the scaling and fabrication of a prototype with a potential for industrial use. To carry out this project and to drive the use of electrochemical technology through the use of the BDD, each research phase, as well as the optimization of the operation variables, was carried out by means of the construction and implementation of a specialized infrastructure. At a laboratory level, the optimization of the operation variables was based on the analysis of the hydroxyl radical ( $\bullet\text{OH}_a$ ). The grade of mineralization of the phenolic compounds and its toxicity was evaluated by means of total organic carbon (TOC) analysis and use of the luminescent bacteria *Vibrio fischeri* (photobacterium phosphoreum). When comparing the efficiency of treatment with BDD with regard to the use of MO<sub>x</sub>/Ti and Graphite, in terms of the chemical oxygen demand (COD), percentages of 90 and 60-80% were obtained. The results obtained are discussed based on the production of different electro-generated oxidizing agents in addition to  $\bullet\text{OH}_a$  and simple electron transfer processes. Strategically, the evaluation of the prototype developed was carried out using MO<sub>x</sub>/Ti electrodes in order to evaluate and validate the potential use of the process of electrochemical conversion of phenolic compounds present in spent caustics, before proceeding to their total destruction or electrochemical incineration using BDD electrodes. Additionally, through the development of this new electrochemical process [3], 10% of the hydrocarbons present could be recovered, in this way causing a positive economic impact in the petrochemical industry by reducing the elevated costs of disposing of spent caustic and/or by salvaging the raw materials. The magnitude of this project and its importance is not only reflected in the reduction of costs for the petrochemical sector but also, and of even greater importance, in the elimination of the potential environmental impact and human health risk that a spill of spent caustic represents.

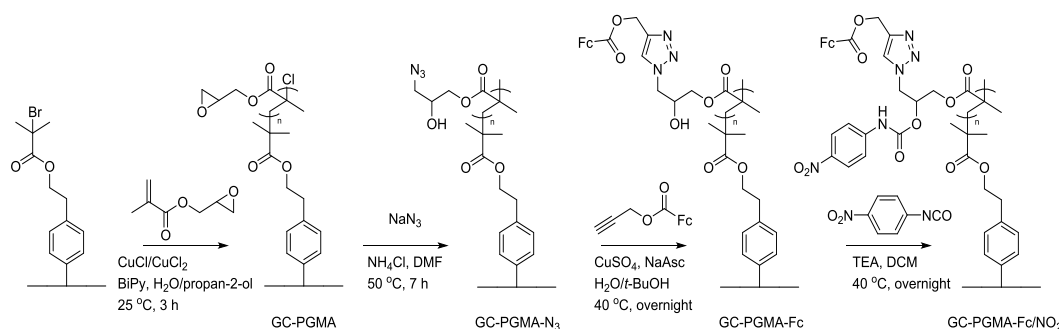
- [1] A. Medel, E. Bustos, L. M. Apátiga, and Y. Meas, Surface activation of C-sp<sup>3</sup> in Boron-Doped Diamond Electrode, *Electrocatalysis-US* 4 (2013) 189.
- [2] A. Medel, E. Bustos, K. Esquivel, L. A. Godínez, and Y. Meas, Electrochemical Incineration of Phenolic Compounds from the Hydrocarbon Industry using Boron Doped Diamond Electrodes, *Int. J. Photoenergy* 2012 (2012) 1.
- [3] A. Medel, E. Méndez, J. L. Hernández, J. A. Ramírez, J. Cárdenas, R. F. Frausto, L.A. Godínez, E. Bustos, and Y. Meas, Novel Electrochemical Treatment of Spent Caustic from the Hydrocarbon Industry using Ti/BDD, *Int. J. Photoenergy* (2015).

# Novel Hybrid Materials Prepared from Polymer Brushes and Graphene

Kim Daasbjerg

Carbon Dioxide Activation Center (CADIAC), Interdisciplinary Nanoscience Center, and Department of Chemistry, Aarhus University  
Gustav Wieds Vej 14, 8000 Aarhus, Denmark  
kdaa@chem.au.dk

Our recent research efforts are concerned with the development of surface modification tools as applied to the study of polymer brushes, coatings, hybrid materials, and composites. Functionalization of various substrates is of interest in many research fields, including life science<sup>1</sup> and molecular electronics.<sup>2</sup> One of the technologies employed in our group is construction of covalently attached polymer brushes from electrochemically modified surfaces,<sup>3,4</sup> where the covalent linkage is pertinent to ensure a high durability of the interfaces. In particular, the possibility of introducing new technologies for coating purposes seems appealing.<sup>5</sup> Polymeric systems containing a reactive side chain such as poly(glycidyl methacrylate) (PGMA) brushes are highly promising, in that the epoxide group readily reacts with various nucleophiles to provide further functionalization. Recently, we demonstrated that PGMA brushes grown by surface-initiated atom transfer radical polymerization (ATRP) on glassy carbon could be used as a versatile chemical platform for the construction of dual-functionalized organic films (Scheme 1).<sup>6</sup>



**Scheme 1.** Poly(glycidyl methacrylate) Brushes Grown by ATRP from Electrochemically Modified Glassy Carbon Followed by Chemical Modifications to Create Dual-Functional and Electrochemically Addressable Polymer Brushes.<sup>6</sup>

In this context, we have also considered graphene as substrate material due to its exceptional strength and barrier abilities. This may be exploited to improve the properties of a polymer matrix, once the graphene through functionalization is made compatible with the matrix.<sup>7</sup> In fact, a controlled electrochemical carboxylation of graphene provides a straightforward way of forming new hybrid materials via carboxylate groups as linker units.<sup>8</sup>

## References

- 1) Jonkheijm, P.; Weinrich, D.; Schröder, H.; Niemeyer, C. M.; Waldmann, H. *Ang. Chem. Int. Ed.* **2008**, *47*, 9618–9647.
- 2) McCreery, R. L. *Chem. Rec.* **2012**, *12*, 149–163.
- 3) Iruthayaraj, J.; Chernyy, S.; Lillethorup, M.; Ceccato, M. Røn, T.; Hinge, M.; Kingshott, P.; Besenbacher, F.; Pedersen, S. U.; Daasbjerg, K. *Langmuir* **2011**, *27*, 1070–1078.
- 4) Chernyy, S.; Iruthayaraj, J.; Ceccato, M.; Hinge, M.; Pedersen, S. U.; Daasbjerg, K. *J. Polym. Sci., Part A: Polym. Chem.* **2012**, *50*, 4465–4475.
- 5) Shimizu, K.; Malmos, K.; Spiegelhauer, S.-A.; Hinke, J.; Holm, A. H.; Pedersen, S. U.; Daasbjerg, K.; Hinge, M. *Int. J. Adhes. Adhes.* **2014**, *51*, 1–12.
- 6) Lillethorup, M.; Shimizu, K.; Plumeré, N.; Pedersen, S. U.; Daasbjerg, K. *Macromolecules* **2014**, *47*, 5081–5088.
- 7) Lillethorup, M.; Kongsfelt, M.; Ceccato, M.; Jensen, B. B. E.; Jørgensen, B. Pedersen, S. U.; Daasbjerg, K. *Small* **2014**, *10*, 922–934.
- 8) Bjerglund, E.; Kongsfelt, M.; Shimizu, K.; Jensen, B. B. E.; Koefoed, L.; Ceccato, M.; Skrydstrup, T.; Pedersen, S. U.; Daasbjerg, K. *Langmuir*, **2014**, *30*, 6622–6628.

# Advances in the Growth of Metals and Alloys Assisted by a Monolayer Amount of UPD Atoms

Nikolay Dimitrov

*Department of Chemistry*

*Binghamton University - SUNY, P.O. Box 6000, Binghamton, NY 13902-6000,*

*e-mail: dimitrov@binghamton.edu*

In the realm of ever increasing importance of nanotechnology, the deposition of ultrathin metal / alloy layers with perfect structure and unique functionality becomes an objective of paramount importance. Aiming at epitaxial metal deposition in solution a pioneering work in the beginning of this century of Sieradzki et al. introduced the defect mediated growth (DMG) [1] and surfactant mediated growth (SMG) [2] as first electrochemical approaches where underpotentially deposited (UPD) atoms were intended to mediate the growth of ultra thin and continuous metal layers. In both methods, potentially controlled protocols ensure efficient manipulation of the UPD mediated deposition kinetics. Later on work of Dimitrov's and Stickney's groups described in details the development of new method for epitaxial thin film growth referred to as surface limited redox replacement (SLRR). This method inspired by a pioneering work of Brankovic et al. realizes as a "building block" reaction the replacement of a pre-deposited sacrificial (in most cases UPD) metal by the growing metal. Successive recurrence of this step results in coformal metal deposition. Work constituting advances in the field was done in understanding and first principle modelling of the SLRR protocol. Most recently, the SLRR development was extended to the application of all-electroless approaches for carrying out the SLRR (ESLRR). Finally, an effort is ongoing to utilize the power of UPD mediated functionalization for the design and development of a new generation of potent catalysts with applications in energy storage and generation. While the work of different research groups has been spread over the growth of a variety of metals including Cu, Ag, Pd, Pt and Ru as well as some of their alloys by DMG, SMG, SLRR, and ESLRR, no systematic comparison of growth regimes, resulting structure, morphology, thickness control, efficiency, limitations and/ or drawbacks has ever been presented for those approaches.

In the beginning of this presentation an overview of DMG, SMG, SLRR and ESLRR will first be presented. A comparison of the proposed mechanism will be made with emphasis on the ability of those methods to produce epitaxial, flat and uniform deposits. In the course of this comparison illustrations will be provided with results, illustrating the advantages and limitations of these deposition approaches in the growth of Ag and Cu thin films on Au (111) substrates. To support the discussion, on the approaches employed, results of electrochemical, in-situ scanning tunneling microscopy (STM), X-ray Photoelectron Spectroscopy characterization experiments will be presented and compared.

In the second part, the applicability of SLRR and ESLRR in the growth of Pt and Pt-based alloys on Au (111) substrate will be discussed. Experimentally demonstrated will be the SLRR growth of Pt layers with controllable thickness taking place in "shuttling" chamber, flow cell, and "one-pot" configuration. Open circuit potentiometry during the replacement reaction will be shown as a way to control the completion of each deposition event. Anodic stripping of the entire multilayer will be used for determining the overall film thickness. Cyclic Voltammetry and STM will be employed to characterize the growth of Pt and Pt-alloy layers with up to 10 nm thickness. High-resolution STM results and modelling concepts underlying the foundation of the proposed approaches will shed light on the mechanistic aspects associated with the nature of growth by redox exchange at a monolayer level.

In the third component of this presentation an overview of recent work on the design of potent catalysts with application in energy production and storage will be presented. This will include the use of SLRR approach for coating nanoparticles and continuous nanoporous metal layers with ultra thin films of metal / alloy with specific functionality. Successful outcome of this coating renders the final product catalytically active. In this part, a brief description will be provided also on the direct use of SLRR based protocols for the smart design of bimetallic alloy and/or core shell clusters with application in the most commonly used reactions in the field of fuel-cell catalysis. The discussion on the synthetic component of all relevant activities will be concluded with demonstration of results of testing of accordingly developed catalysts. Finally, a glimpse into the future of this rapidly developing field will be also provided.

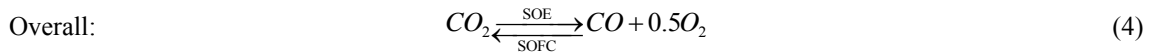
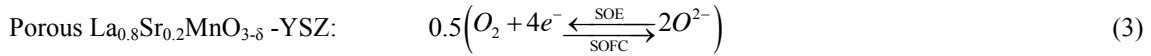
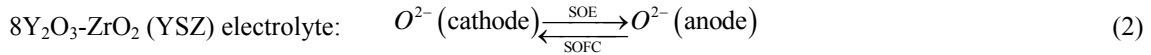
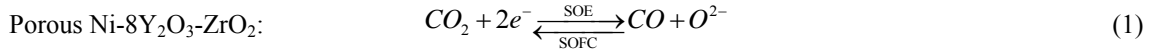
## **References:**

*Details on most of the activities in this presentation could be found in relevant works of R. Adzic et al, S. Brankovic et al, N. Dimitrov et al, T. Moffat et al, J. Stickney et al, and N. Vasiljevic et al.*

# Electrode Structural Effects on Solid Oxide Electrolyser Performance

N. Farandos, A. Hankin, G.H. Kelsall, L. Kleiminger  
 Department of Chemical Engineering, Imperial College London  
 South Kensington, London SW7 2AZ, UK  
 g.kelsall@imperial.ac.uk

Energy conversion efficiencies of solid oxide fuel cells (SOFCs) and electrolyser (SOEs) operating at  $> 600^\circ\text{C}$ , can be increased principally by increasing densities of triple phase boundaries (electrode | electrolyte | reactant gas in pores) where reactions such as  $\text{CO}_2$  and / or  $\text{H}_2\text{O}$  splitting occur:



SOFCs and SOEs with infiltrated-scaffold composite electrode structures have been shown to have greater densities of triple phase boundaries (TPBs), and enhanced control of particle size and porosity compared with structures derived from powder mixing [1]. However, methods that fabricate reproducible, tailored scaffolds with micrometre length scales have yet to be reported. Hence, we are developing 3D printing ('additive manufacturing'), using a Ceradrop X-Series inkjet printer with multi-nozzle print heads, to fabricate reproducible, structured metal oxide frameworks with ca.  $50\ \mu\text{m}$  lateral and  $< 1\ \mu\text{m}$  vertical resolutions, prior to sintering. Ultimately, this should enable fabrication of percolated (porous) cathode | (non-porous) electrolyte | (porous) anode structures more reproducibly and with greater definition than hitherto, to achieve increased energy conversion performances. The reproducible geometries will also enable more facile comparison of experimental data and model predictions [2].

One prerequisite is the development of stable dispersions ('inks') of sub-micrometre sized metal oxide particles (i.e.  $(\text{ZrO}_2)_{0.92}(\text{Y}_2\text{O}_3)_{0.08}$ , NiO,  $\text{La}_{1-x}\text{Sr}_x\text{MnO}_{3-\delta}$ ) in liquid phases with suitable solids fractions and physical properties, to enable printing of the functional layers of SOFCs/SOEs (Fig.1). However, geometries of electrode | electrolyte structures are subject to limitations imposed by the requirement to minimise the spatial distributions of potential and current densities. Hence, results will also be presented for predictions (Fig.2) of those parameters, modelled using finite element software, together with preliminary current density-potential difference data for a printed SOE.

Firstly, yttria-stabilized zirconia (YSZ) particles were deposited onto a planar YSZ-NiO substrate, as precursors to a thin (ca.  $10\text{-}30\ \mu\text{m}$ ) gas-tight electrolyte (Fig. 1), formed by heating the green structure to ca.  $600^\circ\text{C}$  to burn out organics used to stabilise ink particles against aggregation, then sintered at ca.  $1450^\circ\text{C}$ .

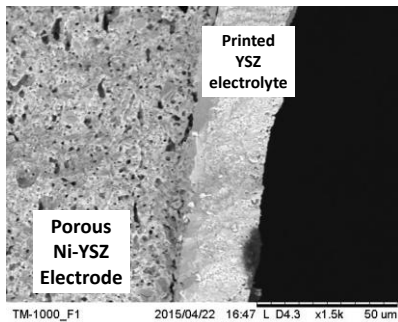


Fig. 1. YSZ particles printed onto YSZ-NiO substrate, then sintered to a ca.  $30\ \mu\text{m}$  gas-tight electrolyte

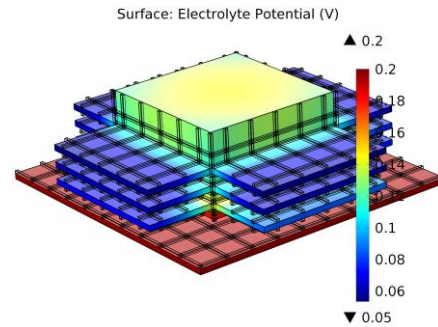


Fig. 2. Finite element predictions of potential distribution on 'infiltrated' Ni-YSZ scaffold electrode.

## References

1. M. Kishimoto, M. Lomberg, E. Ruiz-Trejo, N.P. Brandon, J. Power Sources, 266 (2014) 291-5.
2. U. Doraswami, et al., Solid State Ionics, 192 (2011) 494-500.

## Analysis of PEMFC Catalyst Layers from Fabrication Process to Performance

Tetsuya Mashio,<sup>a,b,\*</sup> Atsushi Ohma,<sup>a</sup> Takashi Tokumasu<sup>b</sup>

<sup>a</sup> Advanced Materials Laboratory, Research Division, Nissan Motor Co., Ltd.,  
1 Natsushima-cho, Yokosuka-shi, Kanagawa 237-8523, Japan

<sup>b</sup> Tohoku University, Institute of Fluid Science,  
2-1-1 Katahira, Aoba-ku, Sendai, Miyagi, 980-8577, Japan  
t-mashio@mail.nissan.co.jp

Polymer electrolyte membrane fuel cells (PEMFCs) are promising power sources for the automotive use. Cost reduction is the primary concern associated with commercialization of fuel cell electric vehicles (FCEVs). The reduction of Pt usage in catalyst layers (CLs) without sacrificing power density is indispensable for the cost reduction of PEMFCs. CL is random porous media, which generally consists of Pt deposited on carbon supports and proton conducting ionomer. The proton conducting ionomer is essential for proton transport, while excess amount of ionomer hinders both reactant gas transport and electrochemical reaction.[1-3] The structure optimization of ionomer is highly desired in order to reduce Pt usage in CLs. Despite the importance of optimizing ionomer structure, morphology of ionomer in CLs and the mechanism of how ionomer structure is formed during the fabrication processes are still controversial due to the difficulty of experimental analysis.

We have been analyzing the structure and properties of CLs from characterization and modeling aspects, in order to understand the microstructure formation during fabrication process and its influence on performance.[4] In the presentation, challenges and update of the CL analysis in Nissan will be introduced with experimental data and simulation results.

- [1] A. Ohma, T. Mashio, K. Sato, H. Iden, Y. Ono, K. Sakai, K. Akizuki, S. Takaichi, K. Shinohara, *Electrochim. Acta* 56, 10832 (2011).
- [2] H. Iden, A. Ohma, *J. Electroanal. Chem.* 693, 34 (2013).
- [3] Y. Furuya, H. Iden, T. Mashio, A. Ohma, K. Shinohara, *221st ECS Meeting abstr.* 1522, Seattle, USA (2012).
- [4] S. Takahashi, T. Mashio, N. Horibe, K. Akizuki, A. Ohma, *ChemElectroChem*, submitted (2015)

## Reactions in cathode positive composite electrode by using synchrotron X-ray

Zempachi Ogumi\*, Hajime Arai\*, Yoshiharu Uchimoto\*\*

*\*office of Society-Academia Collaboration for Innovation*

*Kyoto University, Gokasho Uji, 611-0011 Japan*

*\*\*Graduate School of Human and Environmental Science*

*Kyoto University, Yoshida, Kyoto, 606 Japan*

*Ogumi@scl.kyoto-u.ac.jp*

There remain some issues for lithium ion batteries (LIBs) to grow in the application to advanced vehicles. Durability is the most important one among them because that gives a great impact on safety and cost.

Most of LIBs are composed of composite electrodes as positive and negative electrodes. Uniform reactions through the composite electrode lead LIB to the highest performance. Even very uniform distribution of their composition including porosity causes the reaction distribution along the thickness of the composite electrode due to electric and ionic conductivities.

Some researchers have published simulation results of reaction distribution in composite electrodes, but reports of distribution measurements, especially on operand *in situ* measurements are very limited. Synchrotron radiation X-ray is a very powerful tool to examine a reaction distribution in composite electrodes. The authors have devised some methods to measure operand *in situ* reaction distributions. The figure shows reaction distribution on the surface of composite electrodes of  $\text{LiFePO}_4$  at different AB contents.

### Acknowledgment

This work was supported by RISING of NEDO.

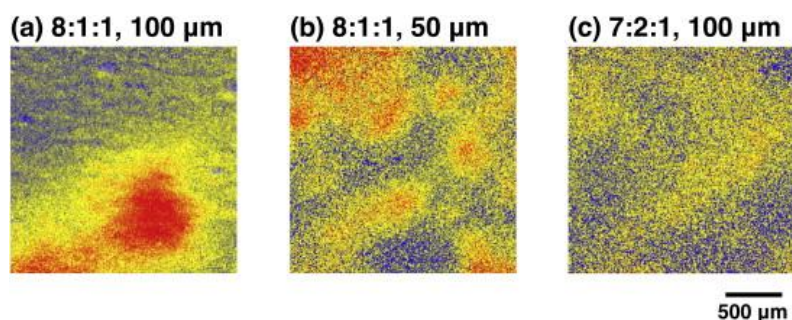


Fig. Comparison of reaction distributions for cathodes fabricated under different preparation conditions. The weight ratios of LFP, acetylene black, and polyvinylidene difluoride and the applied thickness of the cathode mixture are given.

J. Power Sources, 269 (2014), 994-999.

# “Nanohybrid Capacitor” -Future Projection for Gen.II Supercapacitors-

Katsuhiko Naoi<sup>1), 2), 3)\*</sup> and Wako Naoi<sup>2), 3)</sup>

<sup>1</sup>Department of Applied Chemistry, <sup>2</sup>Advanced Capacitor Research Center,  
Tokyo Univ. of Agriculture & Technology, Koganei, Tokyo 184-8588, Japan  
<sup>3</sup>Division of Arts & Sciences, K & W Inc., Kunitachi, Tokyo 186-0002, Japan

\*E-mail: k-naoi@cc.tuat.ac.jp

To meet growing demands for electric automotive and regenerative energy storage applications, researchers all over the world have sought to increase the energy density of electrochemical capacitors. Hybridizing battery and capacitor electrodes can overcome the energy density limitation of the conventional electrochemical capacitors because they employ both the system of a battery-like (redox) and a capacitor-like (double-layer) electrode, producing a larger working voltage and capacitance. However, to balance such asymmetric systems, the rates for the redox portion must be substantially increased to the levels of double-layer process, which presents a significant challenge.

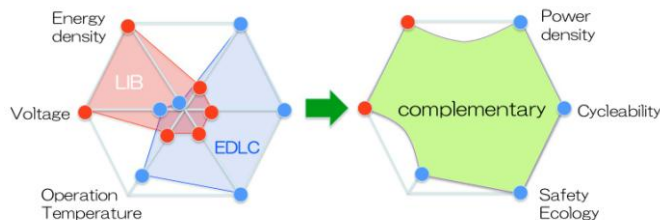
An in situ material processing technology called “ultracentrifuging (UC) treatment” has been used to prepare a novel ultrafast  $\text{Li}_4\text{Ti}_5\text{O}_{12}$  (LTO) nanocrystal electrode for capacitive energy storage. In the present paper, the author will describe an extremely high performance supercapacitor that utilizes highly optimized “nano-nano-LTO/carbon composites” prepared via the UC treatment. The UC-treated LTO nanocrystals are grown as either nanosheets or nanoparticles, and both have hyperlinks to two types of nanocarbons: carbon nanofibers and supergrowth (single-walled) carbon nanotubes. The spinel structured LTO has been prepared with two types of hyperdispersed carbons. The UC treatment at 75000G stoichiometrically accelerates the in situ sol-gel reaction, hydrolysis followed by polycondensation, and further forms, anchors, and grafts the nanoscale LTO precursors onto the carbon matrices. The mechano-chemical sol-gel reaction is followed by a short heat-treatment process in vacuo. This immediate treatment with heat is very important for achieving optimal crystallization, inhibiting oxidative decomposition of carbon matrices, and suppressing agglomeration.

Such nanocrystal composites can store and deliver energy at the highest rate attained to this date. The charge-discharge profiles indicate a very high-sustained capacity of 80 mAh/g at an extremely high rate of 1200 C. Using this ultrafast material, we assembled a hybrid device called a “Nanohybrid capacitor” that consists of a Faradaic Li- intercalating LTO electrode and a non-Faradaic AC electrode employing an ion adsorption-desorption process. The “nanohybrid capacitor” cell has demonstrated remarkable energy, power, and cycleability performance as an electrochemical capacitor electrode. It also exhibits the same ion adsorption-desorption process rates as those of standard activated carbon electrodes in electrochemical capacitors.

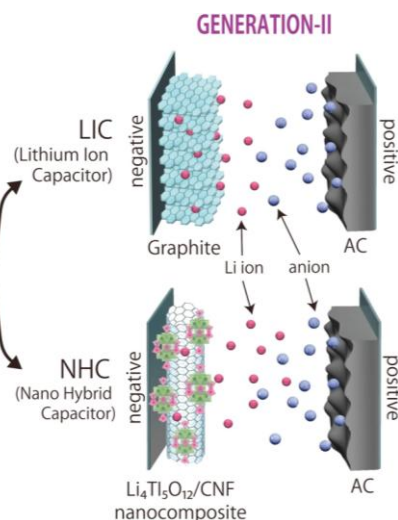
The new-generation “Nanohybrid capacitor” technology produced more than triple the energy density of a conventional electrochemical capacitor. Moreover, the synthetic simplicity of the high-performance nanostructures makes it possible to scale them up for large-volume material production and further applications in many other electrochemical energy storage devices.

## References

- [1] K. Naoi, *Fuel Cells*, 10, 825 (2010).
- [2] K. Hata, D.N. Futaba, K. Mizuno, T. Namai, M. Yumura, S. Iijima, *Science*, 306, 1362 (2004).



- [3] K. Naoi, S. Ishimoto, J. Miyamoto, W. Naoi, *Energy & Environmental Science*, 5, 9363 (2012).
- [4] K. Naoi, W. Naoi, S. Aoyagi, J. Miyamoto, T. Kamino, *Accounts Chem. Res.*, 46, 1075 (2013).



# **Development of Drug Delivery Devices Based on Nongassing Electroosmotic Pump**

Woonsup Shin

*Department of Chemistry and Interdisciplinary Program of Integrated Biotechnology, Sogang University, Seoul  
121-742, Republic of Korea  
[shinws@sogang.ac.kr](mailto:shinws@sogang.ac.kr)*

Electrochemistry is known to be a key transducing technology between chemical energy and electrical energy. Electroosmosis is a phenomenon which the fluid moves upon applying electric field through capillary or porous ceramic membrane. This is a rare example where electrochemistry is utilized for a mechanical transducer. Electroosmotic pumps are the simplest among all the pumps, consisting of two electrodes separated by a porous membrane, but its practical use has been hindered by the use of platinum electrode. On platinum the pumped solution keeps being electrolyzed to produce  $O_2$  from anode and  $H_2$  from the cathode and the bubbles are easily trapped in the membrane to make the flow irregular. Even the co-production of  $O_2$  and  $H_2$  makes the system unsafe in the closed loop. The use of electrochemical reaction such as  $Ag/Ag_2O$  could substitute the reactions on the platinum electrode to operate the pump non-gassing with higher efficiency. It also enabled the pump battery-operable. The pump is now currently used to develop drug pumps such as insulin patch pump and implantable morphine pump.



# Corrosion Electrochemistry and Surface Film Properties of Alloy 690 in High Temperature Pressurized Water

En-Hou Han, Jianqiu Wang, Xinqiang Wu, Zhiming Zhang  
*Institute of Metal Research, Chinese Academy of Sciences*  
62 Wencui Road, Shenyang 110016, China  
ehhan@imr.ac.cn

The steam generator tubing of pressurized water reactors (PWRs) are fabricated by nickel-based alloy 690 during last 20 years since their superior resistance to general corrosion and stress corrosion cracking in the primary side of the nuclear reactor. It was generally recognized that the nucleation and propagation of localized corrosion was strongly related to the properties of the oxide film formed on the metal surface. A considerable number of investigations have been devoted to the identification of the oxide film. However, the oxide film formed in high temperature water is difficult to be characterized. The objective of this work was to investigate the electrochemical behavior and the oxide film properties of alloy 690 in high temperature pressurized water, to understand the corrosion mechanisms, to improve the corrosion properties of alloy 690 and to insure the lifetime of steam generator.

The effects of dissolved oxygen (DO) and hydrogen (DH), pH of solution, surface finishing of material, and even Zn injection into the solution on the electrochemical behavior and the oxide film properties of alloy 690 in high temperature pressurized water by means of in-situ potentiodynamic polarization measurements, electrochemical impedance spectra (EIS), Mott–Schottky (MS) plots, ex-situ X-ray photoelectron spectroscopy (XPS), scanning electron microscopy (SEM), transmission electron microscopy (TEM) and Grazing incidence X-ray diffraction (GIXRD) in Synchrotron Radiation Facility (SSRF) analysis. The related growth mechanisms of the oxide films were also discussed.

The alloy 690TT samples were exposed in pure and the primary water of PWRs at 325°C and 15 MPa. The change in water chemistry from pure to primary water was found to vary the film structure from duplex to triple layer, and lead to change in the morphology of NiO on the surface. The increased pH and solution conductivity of primary water also accelerate the dissolution of Cr species and enhance the electrochemical corrosion. The Ni-rich and Cr depleted inner layer formed under both water chemistries is porous and not protective. Under higher DO, the oxide film mainly consisted of outer spinel particles and porous NiO base layer. A thin Cr-rich film gradually develops with decreasing DO. Fe and Ni levels in the film decrease while Cr level increases concomitantly. The film preformed under low DO becomes much thicker when immersed under high DO, with gradual development of spinel particles and NiO base layer. The surface roughness and micro-hardness decreased gradually from the ground to mechanical polished and electro polished surfaces. The grains in the near-surface layers of the ground and mechanical polished surfaces had been refined and the residual strains were also very high with parallel dislocation lines. The thickness of the superficial cold-worked layers decreased gradually from the ground surfaces to polished surfaces. The oxide morphologies and oxidation rate depended greatly on the surface states of samples. Cold-working by grinding treatments could benefit the outward diffusion of metallic atoms and the nucleation of surface oxides and then accelerate the growth of surface oxide films. With Zn injection in the solution,  $\text{ZnCr}_2\text{O}_4$  and  $\text{ZnFe}_2\text{O}_4$  were formed in the inner and outer layers of the oxide films on Alloy 690, respectively, through exchange reactions between  $\text{Zn}^{2+}$  and  $\text{Fe}^{2+}/\text{Ni}^{2+}$ .

# Advanced Cathodes and Metallic Anodes for Next-Generation Rechargeable Batteries

Yu-Guo Guo\*

*Institute of Chemistry, Chinese Academy of Sciences (CAS)*

*Beijing 100190, P. R. China*

*e-mail: ygguo@iccas.ac.cn*

Next-generation rechargeable batteries with high energy densities are the most important cutting-edge science and technology [1-3]. Among various candidates, rechargeable lithium batteries using metallic Li or Na as the anodes, and chalcogen elements (O, S, Se, etc.) as the cathodes are most promising [1-3]. Here, we report our recent progress in this field covering Li-S, Li-Se, room-temperature Na-S, Na-Se, as well as Mg(-ion) batteries [4-9]. We show that rational design of these cathode materials could play an important role in improving the performance of these rechargeable metal batteries. We report the electrochemistry of chalcogen elements (S, Se, Te) with different allotropies (cyclic and chain-like molecules). Especially, we report our recent progress on the electrochemical deposition/dissolution processes, and the evolution of interfacial chemical composition and structure of the metallic Li anodes, as well as Li-S and Li-Se pouch cells (2~10 Ah).

## References

- [1] S. Xin, Y.G. Guo, L.J. Wan, *Acc. Chem. Res.* **2012**, *45*, 1759
- [2] Y.X. Yin, S. Xin, Y.G. Guo, L.J. Wan, *Angew. Chem. Int. Edit.* **2013**, *52*, 13186
- [3] C.-P. Yang, Y.-X. Yin, Y.-G. Guo, *J. Phys. Chem. Lett.*, **2015**, *6*, 256
- [4] S. Xin, L. Gu, N.H. Zhao, Y.X. Yin, L.J. Zhou, Y.G. Guo, L.J. Wan, *J. Am. Chem. Soc.* **2012**, *134*, 18510
- [5] Y. You, X.Q. Yu, Y.X. Yin, K.W. Nam, Y.G. Guo, *Nano Res.*, **2015**, *8*, 117
- [6] N. Wu, Z.Z. Yang, H.R. Yao, Y.X. Yin, Y.G. Guo, *Angew. Chem. Int. Ed.*, **2015**, DOI: 10.1002/anie.201501005, in press
- [7] S. Xin, Y.-X. Yin, Y.-G. Guo, L.-J. Wan, *Adv. Mater.*, **2014**, *26*, 1261
- [8] C.-P. Yang, S. Xin, Y.-X. Yin, H. Ye, J. Zhang, Y.-G. Guo, *Angew. Chem. Int. Edit.* **2013**, *52*, 8363
- [9] C.-P. Yang, Y.-X. Yin, Y.-G. Guo, L.-J. Wan, *J. Am. Chem. Soc.* **2015**, *137*, 2215

# Surface-Enhanced Infrared Absorption Spectroscopy (SEIRAS): Shedding Light on The Electrochemical Interface

Masatoshi Osawa

*Catalysis Research Center, Hokkaido University*

*N21W10, Kita-ku, Sapporo 001-0021, Japan*

*osawam@cat.hokudai.ac.jp*

Surface-enhanced infrared absorption (SEIRA) is an effect in which infrared absorption of molecular species on metal surfaces is greatly enhanced.<sup>1</sup> This effect is similar to surface-enhanced Raman scattering (SERS) in nature, but there are some differences between them. The most important is that SEIRA is applicable not only to coinage metals but also to transition metals including Pt and Pt group metals. From this point of view, SEIRAS has wider applications than SERS in principle. Unfortunately, however, the enhancing mechanism of IR absorption has not been fully understood yet. In this talk, a new theoretical model for SEIRAS, an extended version of an old one,<sup>2</sup> will be presented first and, on the basis of the theoretical consideration, it will be discussed how SEIRAS experiments should be designed and what can we obtained from SEIRA spectra.

## References

1. M. Osawa, *Bull. Chem. Soc. Jpn.* **70**, 2861 (1997),
2. M. Osawa, K. Ataka, K. Yoshii, and Y. Niahikawa, *Appl. Spectrosc.*, **47**, 1497 (1993).

# The aqueous electrochemical capacitor: a high energy alternative solution to organic electrolyte-based systems

Patryk Przygocki, Qamar Abbas, Paula Ratajczak, François Béguin

Poznan University of Technology, Institute of Chemistry and Technical Electrochemistry, Berdychowo 4, 60-965 Poznan, Poland

[francois.beguin@put.poznan.pl](mailto:francois.beguin@put.poznan.pl)

Activated carbon (AC) based electrochemical capacitors in organic (TEABF<sub>4</sub>/acetonitrile) and aqueous (KOH and H<sub>2</sub>SO<sub>4</sub>) electrolytes have been extensively investigated during the last decade. However, due to the environmentally unfriendly character of the former and low operating cell potential of the later, alternative electrolytes are desirable. Recently, capacitors based on salt aqueous electrolyte e.g., 1 mol L<sup>-1</sup> Li<sub>2</sub>SO<sub>4</sub> (pH = 6.5), capable of operating up to 1.5 - 2 V have been reported [1-3]. Such high cell potential is realized owing to the high over-potential for di-hydrogen evolution at the negative AC electrode [2]. Besides, high capacitance (C) was demonstrated by realizing AC/AC capacitors in aqueous solution of potassium iodide, owing to hybridization between the I<sup>-</sup>/I<sub>2</sub> redox positive electrode and the typical EDL negative one. However, in this electrolyte, the cell potential (U) is limited to 1.2 V [4]. This presentation will show strategies based on aqueous electrolyte optimization for simultaneously enhancing cell potential, capacitance and operating temperature range.

An aqueous mixture of 2 mol L<sup>-1</sup> manganese sulfate (MnSO<sub>4</sub>) and 0.5 mol L<sup>-1</sup> potassium iodide (KI) with pH = 3 has been used in order to get synergy between the I<sup>-</sup>/I<sub>2</sub> redox couple at the positive electrode and high cell potential allowed by MnSO<sub>4</sub>. Galvanostatic two-electrode cell experiments up to potential of 1.5 V demonstrate that the addition of KI to MnSO<sub>4</sub> results in enhanced cell capacitance of 93 F g<sup>-1</sup> compared to 41 F g<sup>-1</sup> for MnSO<sub>4</sub> (Fig. 1a). Interestingly, the presence of iodide improves the cycle life under potentiostatic floating at 1.5 V for 120 hours, where the capacitor exhibits constant capacitance of ~55 F g<sup>-1</sup> and low resistance of 2 Ω (Fig. 1b). Experiments in two-electrode cells with a reference electrode show that, at pH = 3, the I<sup>-</sup>/I<sub>2</sub> redox couple is highly active at the positive AC electrode with a small potential window, while the negative AC electrode mainly exhibits an EDL behavior, determining the overall capacitive performance of the system. The AC/AC capacitor based on the MnSO<sub>4</sub> + KI electrolyte displays comparable energy density at 0.2 A g<sup>-1</sup> current load to the one using the same carbon in TEABF<sub>4</sub>/acetonitrile.

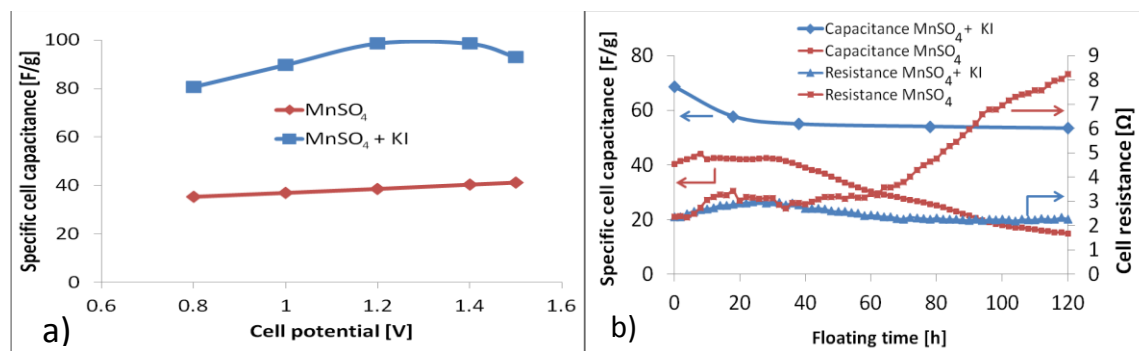


Fig. 1 AC/AC capacitors in 2 mol L<sup>-1</sup> MnSO<sub>4</sub> and 2 mol L<sup>-1</sup> MnSO<sub>4</sub> + 0.5 mol L<sup>-1</sup> KI: (a) Specific cell capacitance vs. cell potential; (b) specific cell capacitance and cell resistance during floating at 1.5 V.

MnSO<sub>4</sub> and MnSO<sub>4</sub> + KI aqueous electrolytes containing an antifreezing additive have been further designed and implemented in the AC/AC capacitor, demonstrating possible operation down to -30°C. The mechanisms playing in the system when temperature is reduced will be discussed.

- [1] L. Demarconnay, E. Raymundo, F. Béguin, *Electrochem. Comm.* 12 (2010) 1275.
- [2] Q. Gao, L. Demarconnay, E. Raymundo-Pinero, F. Béguin, *Energy Environ. Sci.*, 2012, **5**, 9611-9617.
- [3] P. Ratajczak, K. Jurewicz, P. Skowron, Q. Abbas, F. Béguin, *Electrochim. Acta*, 2014, **130**, 344-350.
- [4] J. Menzel, K. Fic, M. Meller, E. Frąckowiak, *J. App. Electrochem.*, 2014, **44**, 439-445

# Development of Ambient Pressure XPS and its Applications to Electrochemistry

Bongjin Simon Mun

*Gwangju Institute of Science and Technology*

*123 Cheomdangwariro, Gwangju, Korea*

*bsmun@gist.ac.kr*

X-ray photoelectron spectroscopy (XPS) is one of the major tools in the fields of surface chemistry due to its excellent capabilities in studying surface chemical and electronic properties. However, due to the short inelastic attenuation lengths of photoelectrons, as well as the requirement of high vacuum in the electron spectrometer, only the model studies or ex-situ systems have been carried out, and thus creating so-called “pressure-gap”. In an effort to bridge this pressure-gap, the ambient pressure x-ray photoelectron spectroscopy (AP-XPS) has been continuously developed and now puts a new road map in the world of surface science with use of synchrotron radiation facility. [1]

In this presentation, the basic principles and the latest instrumental developments of AP-XPS will be presented. Also, the applications of AP-XPS to several practical systems will be given, including electrochemical system. Now, with the use of high-energy photon source, it becomes possible to run *in-situ* analysis of liquid/solid interface under operating condition.

## Reference

[1] Bongjin Simon Mun, Hiroshi Kondoh, Zhi Liu, Phil N. Ross Jr., Zahid Hussain, *Current Trends of Surface Science and Catalysis*, Springer, 2014, edited by Jeong Young Park

# Graphene and Carbon Nanotubes for Bioelectrochemical applications

Michael Holzinger

University of Grenoble-Alpes – CNRS  
Département de Chimie Moléculaire, UMR 5250  
570 rue de la Chimie, BP 53  
38041 Grenoble, France  
michael.holzinger@ujf-grenoble.fr

Due to the increasing need to monitor health and environment in real time and to energize small electronic devices, new materials are under extensive investigations. Between others, carbon nanotubes (CNTs) and graphene are promising alternatives as building blocks in bioelectrochemical devices due to their unique electrical, mechanical properties, biocompatibility and high specific surface. In the past years, we focused the development of biosensors and biofuel cells based on such carbon nanostructures<sup>[1-3]</sup>. Our efforts in this domain aim the construction of nano-architecture at molecular scale associating different nano-objects via organic or organo-metallic connectors to immobilize redox enzymes<sup>[4]</sup>. Furthermore, our efforts focus redox enzyme wiring on nanotubes and graphene to enable direct electron transfer (DET)<sup>[5, 6]</sup>.

Particular interesting results were obtained by electropolymerization of pyrrole- or pyrene derivatives onto the CNT sidewalls to obtain highly functional nanostructured carbon receptors<sup>[7]</sup>. Such CNT modified electrodes offer a high specific surface with an excellent accessibility for the anchoring of proteins via affinity interactions<sup>[1]</sup>.

The possibility to generate electrical power *via* living organisms directed biofuel cell research towards glucose biofuel cells (GBFC) since the two required compounds (glucose and oxygen) are present in both, vegetal and body fluids. In this vein, the first implantation of a biofuel cell in the rat abdomen have paved the way for future applications of biofuel cells for continuous supply of implanted electronic devices such as pacemakers, insulin pumps, etc<sup>[8]</sup>. However, in spite of this promising evolution, there are still some issues to be resolved before enzymatic biofuel cells become competitive in practical applications. Two critical obstacles are short lifetime and poor power density, where both are related to enzyme stability, electron transfer rate, and enzyme loading. Our proposed design of bioelectrodes for enzymatic biofuel cells is based on a highly porous 3D nanostructured scaffold that allows high enzyme loading in a protective environment while allowing optimal flow of the “fuel” and oxygen containing solution<sup>[4]</sup>. Furthermore, this biofuel cell setup could successfully be implanted inside a rat and delivered sufficient power out of the rat’s extra cellular body liquids to light a LED and a digital thermometer<sup>[9]</sup>. However, even when some milestones could be overcome, some critical issues are still to resolve like long term stability and power output. In this context, some alternative approaches to optimize the electron transfer are presented.

- [1] M. Singh, M. Holzinger, M. Tabrizian, S. Winters, N. C. Berner, S. Cosnier, G. S. Duesberg, *Journal of the American Chemical Society* **2015**, 137, 2800.
- [2] M. Singh, M. Holzinger, M. Tabrizian, S. Cosnier, *Carbon* **2015**, 81, 731.
- [3] A. Zebda, C. Gondran, A. Le Goff, M. Holzinger, P. Cinquin, S. Cosnier, *Nature Communications* **2011**, 2, 370.
- [4] B. Reuillard, A. Le Goff, C. Agnès, M. Holzinger, A. Zebda, C. Gondran, K. Elouarzaki, S. Cosnier, *Physical Chemistry Chemical Physics* **2013**, 15, 4892.
- [5] N. Lalaoui, A. Le Goff, M. Holzinger, M. Mermoux, S. Cosnier, *Chemistry – A European Journal* **2015**, 21, 3198.
- [6] M. Bourourou, K. Elouarzaki, N. Lalaoui, C. Agnès, A. Le Goff, M. Holzinger, A. Maaref, S. Cosnier, *Chemistry - A European Journal* **2013**, 19, 9371.
- [7] R. Haddad, M. Holzinger, R. Villalonga, A. Neumann, J. Roots, A. Maaref, S. Cosnier, *Carbon* **2011**, 49, 2571.
- [8] P. Cinquin, C. Gondran, F. Giroud, S. Mazabrard, A. Pellissier, F. Boucher, J.-P. Alcaraz, K. Gorgy, F. Lenouvel, S. Mathé, P. Porcu, S. Cosnier, *PLoS ONE* **2010**, 5, e10476.
- [9] A. Zebda, S. Cosnier, J.-P. Alcaraz, M. Holzinger, A. Le Goff, C. Gondran, F. Boucher, F. Giroud, K. Gorgy, H. Lamraoui, P. Cinquin, *Sci. Rep.* **2013**, 3, 1516.

# Electrodeposition of Highly (111)-oriented Nanotwinned Cu and Its Application

Chih Chen<sup>1</sup>, Chien-min Liu<sup>1</sup>, Chia-Ling Lu<sup>1</sup>, Kuan-Neng Chen<sup>2</sup>, K. N. Tu<sup>3</sup>

<sup>1</sup>Department of Materials Science and Engineering,

National Chiao Tung University, Hsinchu, Taiwan 30010, Republic of China

<sup>2</sup>Department of Electronics Engineering,

National Chiao Tung University, Hsinchu, Taiwan 30010, Republic of China

<sup>3</sup>Department of Materials Science and Engineering,

University of California at Los Angeles, Los Angeles, California 90095, USA

E-mail: [chih@mail.nctu.edu.tw](mailto:chih@mail.nctu.edu.tw) (C. Chen)

## Abstract:

In this talk, we will present electrodeposition of highly oriented [111] Cu grains with densely packed nanotwins by DC and AC with a high stirring rate. Nearly 100% of the surface grains are [111] oriented. With the [111] oriented and nanotwinned Cu (nt-Cu), we can control the growth of Cu<sub>6</sub>Sn<sub>5</sub> intermetallics in the microbumps of 3D IC packaging. Therefore, a uniform microstructure in a large number of microbumps of controlled orientation can be obtained. Electron backscatter diffraction (EBSD) was employed to analyze the statistical distributions of surface grain orientations and the grain boundaries of the Cu and the Cu<sub>6</sub>Sn<sub>5</sub>. The results indicate that 96% of the columnar Cu grains have less than 10 degrees of misalignment with respect to

the [111] direction. In addition, EBSD orientation image maps for the  $\text{Cu}_6\text{Sn}_5$  compounds show a preferred orientation near the (0001) plane of the  $\text{Cu}_6\text{Sn}_5$ . The oriented nt-Cu can eliminate the Kirkendall voids during the solid-state aging in Cu-Sn reactions. In addition, with high diffusivity of Cu atoms on the (111) surfaces, Cu-to-Cu direct bonding can be achieved below 200°C at a compressive stress of 114 psi held for 30 min at  $10^{-3}$  torr, or at 150°C at for 60 min. The details will be presented in the conference.



# Macrocyclics, Graphene Oxides-based Nano-catalysts, and Related Hybrids for Fuel Cells and Solar Fuels

Li-Chyong Chen<sup>1</sup>, Kuei-Hsien Chen<sup>1,2</sup>, Hsin-Cheng Hsu<sup>1,3</sup>, He-Yun Du<sup>1</sup>, Indrajit Shown<sup>2</sup>, Hsin-Chih Huang<sup>3</sup>, Yu-Chung Chang<sup>3</sup>, Chen-Hao Wang<sup>3</sup>, and Sung-Tung Chang<sup>4</sup>

1. Center for Condensed Matter Sciences, National Taiwan University, Taipei, Taiwan

2. Institute of Atomic and Molecular Sciences, Academia Sinica, Taipei, Taiwan

3. Department of Materials Science and Engineering, National Taiwan University of Science and Technology, Taipei, Taiwan

4. National Synchrotron Radiation Research Center, Hsin-Chu, Taiwan

Correspondent postal address: Center for Condensed Matter Sciences, National Taiwan University,  
No.1, Roosevelt Road, Section 4, Taipei, 10617, Taiwan  
E-mail address: chenlc@ntu.edu.tw, Tel: 886-2-33665249

## Abstract

Catalysts play a critical role in solar fuels and fuel cells. Not only there are only a few materials that function well enough, be it measured by the power/energy output, oxygen reduction reaction (ORR) activity, hydrocarbon fuels-production rate, selectivity and durability, *etc.*; but also, most of the champion catalysts reported so far is not earth-abundant or costly in process. In this talk, selective case studies on energy-conversion that utilizes low-cost nanostructures as their key components will be presented. Two different systems will be highlighted: (1) novel macrocyclic compounds to replace the precious metal-catalysts for fuel cells [1-3], and (2) photo-catalysts based on graphene oxides and their hybrids with MoS<sub>2</sub>, and Cu nanoparticles for CO<sub>2</sub> conversion [4-5]. It should be noted that exploration of the macrocyclic compounds as functional electro-catalysts was stimulated by biomimetic concept, *i.e.*, the principle learned from the nature. Whereas photo-catalytic conversion of CO<sub>2</sub> to hydrocarbons, the so-called artificial photosynthesis, makes possible simultaneous solar energy harvesting and CO<sub>2</sub> reduction, two birds with one stone for the energy and environmental issues. In addition to the usual microstructural characterizations, various synchrotron-radiation spectroscopic techniques, including XAS, XANES, and EXAFS, were also employed for studying the binding and electronic structures of these nano-structures, wherever appropriate. I will address how the spectroscopic techniques may help answering some key questions in their catalytic activity and conversion performance.

## References:

- [1] S. T. Chang, C. H. Wang, H. Y. Du, H. C. Hsu, C. M. Kang, C. C. Chen, S. C. Yen, W. F. Huang, L. C. Chen, M. C. Lin, and K. H. Chen, *Energ. Environ. Sci.* 5, 5305 (2012).
- [2] H. C. Huang, I. Shown, S. T. Chang, H. C. Hsu, H. Y. Du, M. C. Kuo, K. T. Wong, S. F. Wang, C. H. Wang, L. C. Chen and K. H. Chen, *Adv. Func. Mater.* 22, 3500 (2012).
- [3] H. C. Huang, C. H. Wang, I. Shown, S. T. Chang, H. C. Hsu, H. Y. Du, L. C. Chen, K. H. Chen, *J. Mater. Chem. A* 1, 14692 (2013).
- [4] H. C. Hsu, I. Shown, H. Y. Wei, Y. C. Chang, H. Y. Du, Y. G. Lin, C. H. Wang, L. C. Chen, Y. C. Lin and K. H. Chen, *Nanoscale* 5, 262 (2013).
- [5] I. Shown, H. C. Hsu, Y. C. Chang, C. H. Lin, P. Roy, A. Ganguly, C. H. Wang, J. Chang, C. I. Wu, L. C. Chen, K. H. Chen, *Nano Lett.* 14, 6097 (2014).

# Anodic Synthesis of Unnatural Peptide and Nucleic Acid Derivatives

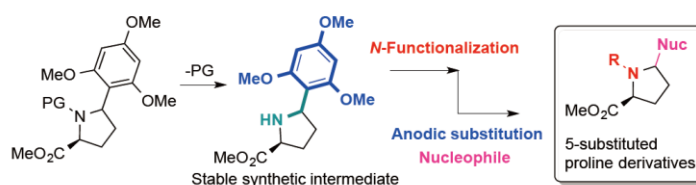
Kazuhiro CHIBA, Takao SHOJI, Yohei Okada, Shokaku KIM

Department of Applied Biological Science  
Tokyo University of Agriculture and Technology  
3-5-8 Saiwai-cho, Fuchu, Tokyo 183-8509, Japan  
[chiba@cc.tuat.ac.jp](mailto:chiba@cc.tuat.ac.jp)

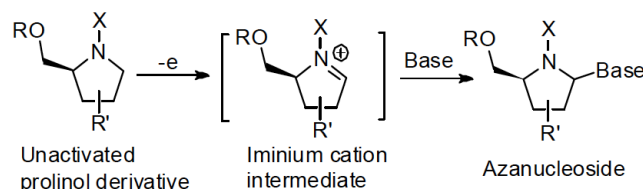
Although the anodic  $N$ - $\alpha$  C-H activation of  $N$ -carbonyl bonds is attractive for the synthesis of artificial proline analogues, there are significant limitations for further diversification in both the  $N$ -terminal and  $C$ -terminal directions. These limitations arise from the relatively high oxidation potential of  $N$ -carbonyl bonds, and the structural vulnerability associated with leaving groups at 5-position of proline. The electrochemical conversions cannot be directly applied to proline derivatives including the lower oxidation potential peptide side chain, protecting group and other functional units as compared with that of  $N$ -carbonyl bonds. Furthermore, replacement reactions in the  $N$ -terminal direction involving the deprotection of a proline  $N$ -protected with a 5-methoxy, trifluoroethoxy or acetoxy group generate unstable intermediates containing the hemiaminal ether bond; these intermediates decompose before they can engage in the subsequent reaction.

To address these problems, we explored viable electrochemical strategies for diversifying 5-substituted proline derivatives. Specifically, considering aspects of the oxidation potential and the lack of the stability, we sought to introduce a phenyl group as the leaving moiety: this intermediate should be stable as it avoids the *germinal* diheterolytic linkage. We then assumed that anodic oxidation of 5-trimethoxyphenyl proline would transiently form the radical cation, thus triggering C-C bond cleavage to deliver the  $N$ -acyl iminium cation and the phenyl radical. The resulting cation would couple with nucleophiles to provide 5-substituted proline derivatives. Furthermore, incorporation of electron-donating substituents into the phenyl group would lower the oxidation potential, thus enabling the use of various nucleophiles.

We therefore achieved anodic modification reactions of proline derivatives using the 2,4,6-trimethoxyphenyl moiety as a leaving group. 2,4,6-Trimethoxyphenyl at the 5-position of proline is stable during deprotection of the  $N$ - and  $C$ - termini and the subsequent modification reaction. Furthermore, the anodic substitution reaction proceeded *via* carbon-carbon bond cleavage at a lower oxidation potential due to the electron-donating property of the trimethoxy substituents.



In addition to the modification of prolyl peptides, we have developed a highly efficient synthetic method for azanucleosides, which allows the installation of various nucleophiles, including protected nucleobases, into prolinol derivatives directly and exclusively at the 5-position. The  $\text{LiClO}_4\text{-CH}_3\text{NO}_2$  system anodically converted prolinol derivatives to the corresponding iminium cation intermediates, which were stabilized and efficiently trapped by various nucleophiles. The applicability and limitations of this system are currently under investigation.



## References

- Shoji T.; Kim S.; Yamamoto K.; Kawai, T.; Okada, Y.; Chiba, K., *Org. Lett.*, **2014**, *16* (24), 6404–6407.
- Kim S., Shoji T.; Kitano Y.; Chiba K., *Chem. Comm.*, **2013**, *49*, 6525–6527.



# **The Joint Center for Energy Storage Research (JCESR): A New Paradigm for Energy Storage Research**

George Crabtree

*Director, Joint Center for Energy Storage Research (JCESR)*

*University of Illinois at Chicago*

*845 W Taylor St, Chicago IL USA 60607*

*Argonne National Laboratory, 9700 S. Cass Ave, Argonne IL USA 60439*

*crabtree@anl.gov*

The Joint Center for Energy Storage Research (JCESR) pursues high performance, low cost beyond lithium ion electricity storage that will transform transportation and the electricity grid. JCESR will leave three legacies:

- a library of fundamental knowledge of the materials and phenomena of energy storage at the atomic and molecular level
- two prototypes, one for the grid and one for transportation, that, when scaled to manufacturing will be able to deliver five times the energy density at one-fifth the cost
- a new paradigm for battery R&D that combines discovery science, battery design, research prototyping and manufacturing collaboration in a single highly interactive organization, accelerates the pace of discovery and innovation and significantly shortens the time from discovery to commercialization.

An introduction to JCESR's vision, mission and legacies will be followed by research highlights from UIC illustrating its advances in fundamental science and the promising pathways to transformational battery designs and prototypes.

This work was supported as part of the Joint Center for Energy Storage Research, an Energy Innovation Hub funded by the U.S. Department of Energy, Office of Science, Basic Energy Sciences

# Molecular Electrochemistry: from Protons to Electrons, from Molecules to Molecular Nanoclusters

Flavio Maran

*Department of Chemistry, University of Padova  
via Marzolo 1, 35131 Padova, Italy  
flavio.maran@unipd.it*

Molecular electrochemistry is a discipline embracing topics such as electron-transfer (ET) induced transformation of molecules, associated chemical reactions, control of long-range and mediated ET reactions, and electrochemistry on electrodes and modified electrodes. The focus is always on molecular aspects. By following the steps of my mentor, the late Professor Elio Vianello, my initial research concerned organic electrochemistry and the kinetics and mechanism of proton-transfer reactions associated with the electrode processes. Analysis of self-protonation reactions allowed developing an original method for determining the  $pK_a$  of weak acids in *N,N*-dimethylformamide<sup>1</sup> and obtain crucial information on the very elusive  $\alpha$ -lactam intermediate.<sup>2</sup> My research gradually shifted toward the study of the mechanisms of dissociative ETs. For the first time, it was possible to: observe a quadratic activation – driving force relationship in the direct electroreduction of peroxides;<sup>3</sup> prove that peroxides undergo nonadiabatic dissociative ETs;<sup>4,5</sup> detect the continuous transition between concerted and stepwise heterogeneous ETs;<sup>6</sup> show that stepwise dissociative ETs may proceed very slowly through formation of loose radical anions;<sup>7</sup> establish a quantitative relationship between heterogeneous and homogeneous ET kinetics in a very wide intrinsic-barrier range.<sup>8</sup> Molecular electrochemistry proved to be very powerful also to study the distance effect on ET reactions.<sup>9</sup> My current interest is mostly on applying similar concepts and methodologies to the study of monolayer-protected gold nanoclusters. For gold cores of less than 1.5 nm, these clusters display truly molecular features, including very nice electrochemical behavior in organic solvents.<sup>10,11</sup> Some of their oxidation states can be used as efficient homogeneous ET mediators.<sup>10,12</sup> Very recently, we showed that heterogeneous ET provides a very efficient tool for assessing the structure of such protecting but not-so shielding monolayers.<sup>13</sup>

1. Maran, F.; Celadon, D.; Severin, M. G.; Vianello, E. *J. Am. Chem. Soc.* **1991**, *113*, 9320.
2. Maran, F. *J. Am. Chem. Soc.* **1993**, *115*, 6557.
3. Antonello, S.; Musumeci, M.; Wayner, D. D. M.; Maran, F. *J. Am. Chem. Soc.* **1997**, *119*, 9541.
4. Workentin, M.; Maran, F.; Wayner, D. D. M. *J. Am. Chem. Soc.* **1995**, *117*, 2120.
5. Antonello, S.; Formaggio, F.; Moretto, A.; Toniolo, C.; Maran, F. *J. Am. Chem. Soc.* **2001**, *123*, 9577.
6. Antonello, S.; Maran, F. *J. Am. Chem. Soc.* **1999**, *121*, 9668.
7. Antonello, S.; Benassi, R.; Gavioli, G.; Taddei, F.; Maran, F. *J. Am. Chem. Soc.* **2002**, *124*, 7529.
8. Meneses, A. B.; Antonello, S.; Arévalo, M. C.; González, C. C.; Sharma, J.; Wallette, A. N.; Workentin, M. S.; Maran, F. *Chem. Eur. J.* **2007**, *13*, 7983.
9. Antonello, S.; Maran, F. *Chem. Soc. Rev.* **2005**, *34*, 418.
10. Antonello, S.; Holm, A. H.; Instuli, E.; Maran, F. *J. Am. Chem. Soc.* **2007**, *129*, 9836.
11. Antonello, S.; Perera, N. V.; Ruzzi, M.; Gascón, J. A.; Maran, F. *J. Am. Chem. Soc.* **2013**, *135*, 15585.
12. Antonello, S.; Hesari, M.; Polo, F.; Maran, F. *Nanoscale* **2012**, *17*, 5333.
13. Antonello, S.; Arrigoni, G.; Dainese, T.; De Nardi, M.; Parisio, G.; Perotti, L.; René, A.; Venzo, A.; Maran, F. *ACS Nano* **2014**, *8*, 2788.

# Operando X-ray Studies of Electrocatalysis

Anders Nilsson<sup>1,2</sup>, Daniel Friebe<sup>2</sup> and Hirohito Ogasawara<sup>2</sup>

<sup>1</sup>*Division of Chemical Physics, Department of Physics, AblaNova University Center, Stockholm University, SE-106 91 Stockholm, Sweden*

*And*

<sup>2</sup>*SUNCAT ctr for Interface Science and Catalysis, SLAC National Accelerator Laboratory, 2575 Sand Hill Road, MS 31, Menlo Park, CA 94070, USA*

We will demonstrate how electron and x-ray spectroscopy can be used to address fundamental questions regarding the reaction mechanism and active sites of the Oxygen Reduction Reaction (ORR), Oxygen Evolution Reaction (OER) and Hydrogen Evolution Reaction (HER). We have developed in-situ XPS capabilities using a membrane assembly where either the anode or cathode side is exposed to a differential pumped environments where direct measurements of the changes in the catalyst and various reaction intermediates can be probed during ORR on Pt, OER on IrO<sub>2</sub> and HER conditions for MoS<sub>2</sub>. We have also recently conducted high-energy resolution fluorescence detection (HERFD) studies of the Fe and Ni K-edges under OES conditions in the highly active Ni-Fi oxyhydroxides to determine the nature of the active sites. In particular we observe that Fe encounter an extremely strained local geometry when Ni undergoes a transformation from the 2+ to 3+ state.

# Understanding and Predicting the Photocatalytic Properties of Bismuth Vanadate from First Principles

Gyeong S. Hwang

*McKetta Department of Chemical Engineering, University of Texas at Austin*

*1 University Station C0400, Austin, Texas 78712, U.S.A.*

*gshwang@che.utexas.edu*

Renewable sources of energy are increasingly needed and solar production of hydrogen fuel from water offers significant potential to contribute to these needs. Bismuth vanadate ( $\text{BiVO}_4$ ) has received much interest as a promising visible-light-active photocatalyst for water splitting and pollutant decomposition. However, some fundamental aspects of its photocatalysis remain still unclear, including phase-dependent activity, doping effect, and surface reactivity. For instance, molecular mechanisms underlying the oxidative water splitting into molecular oxygen and proton are largely unexplored. In addition, charge localization and transport in  $\text{BiVO}_4$  and its effects on the photocatalytic performance need to be further explored. This talk will focus on discussing our recent findings from extensive first-principles calculations regarding the underlying mechanisms of the oxygen evolution reaction as well as the localization and transport of excess charge carriers. The improved understanding may offer important guidance for the rational design of photocatalytic materials.

# AN OVERVIEW OF THE BEHAVIOR OVERLITHIATED Li(Li,Mn,Co,Ni)O<sub>2</sub> LAYERED OXIDES IN LITHIUM-ION BATTERIES

**C. Delmas<sup>1</sup>, H. Koga<sup>1,2</sup>, L. Croguennec<sup>1</sup>, M. Ménétrier<sup>1</sup>, S. Belin<sup>3</sup>, C. Genevois<sup>4</sup> and F. Weill<sup>1</sup>**

<sup>1</sup> ICMCB-CNRS, Université de Bordeaux, IPB-ENSCBP, 87 avenue Schweitzer, 33608 Pessac cedex, France

<sup>2</sup> TOYOTA MOTOR EUROPE NV/SA, Hoge Wei 33, B-1930 Zaventem, Belgium

<sup>3</sup> Synchrotron Soleil - L'orme des Merisiers Saint Aubin, Gif-sur-Yvette, F-91192, France

<sup>4</sup> GPM, Université de Rouen, avenue de l'Université, BP12, 76801 Saint Etienne du Rouvray

Contact author : C. Delmas     delmas@icmcb-bordeaux.cnrs.fr

The materials belonging to the (1-x)LiMO<sub>2</sub>.xLi<sub>2</sub>MnO<sub>3</sub> system (M = Ni, Co) exhibit the largest capacity among all other layered oxides. These materials are overlithiated layered oxides (Li<sub>1</sub>(Li<sub>y</sub>Mn<sub>1-y-u-t</sub>Co<sub>u</sub>Ni<sub>t</sub>O<sub>2</sub>) with a significant amount of lithium in the transition metal site. Depending on the starting composition, Mn ions can be tri- or tetravalent while Ni ions can be di- or trivalent. In the literature there is a strong debate about the existence of a solid solution or the presence of a composite structure. The structure of the obtained material depends on the composition and on the conditions of the thermal treatment. The cationic distribution is strongly related to the difference in charge and ionic radius.

A very general study of the synthesis and of the electrochemical characterization of the Li<sub>1.20</sub>Mn<sub>0.54</sub>Co<sub>0.13</sub>Ni<sub>0.13</sub>O<sub>2</sub> phase has been undertaken for several years in our lab. In order to have a better overview of its behavior a systematic study has been also carried out by chemical deintercalation. All the structural, electrochemical and physical characterizations show that these materials are very similar to those electrochemically obtained.

During the first charge, when all cations are oxidized to the tetravalent state, an overcharge of the cell leads to a structural modification that can be schematically described as a Li<sub>2</sub>O extraction occurs that cannot explain alone the oxidation process. Either oxidation of cations to a higher oxidation state or of oxygen is required. All experiments to detect cation oxidation state higher than four failed, so the oxidation of oxygen has been considered.

The contribution of oxygen to the redox activity in this material family is considered from several years. It was suggested in 2009 by Koyama *et al.* from first principle calculation in Li<sub>2</sub>MnO<sub>3</sub> [1], then by Kikkawa *et al.* in their Mossbauer study of the Li<sub>1.2</sub>Mn<sub>0.4</sub>Fe<sub>0.4</sub> phase [2] and more recently by Ito *et al.* from an XAS study on the Li<sub>1.20</sub>Mn<sub>0.56</sub>Co<sub>0.07</sub>Ni<sub>0.17</sub>O<sub>2</sub> phase [3]. In our lab we have clearly shown its occurrence in the case of the electrochemical (or chemical) cycling of the Li<sub>1.20</sub>Mn<sub>0.54</sub>Co<sub>0.13</sub>Ni<sub>0.13</sub>O<sub>2</sub> phase [4-5]. Sathiya *et al.* [6] also confirmed it in the case of the Li<sub>2</sub>Ru<sub>1-y</sub>Sn<sub>y</sub>O<sub>3</sub> system.

In order to clarify the mechanism which is involved during the overcharge a systematic study has been carried using chemical analysis, X-ray and neutron diffraction, in operando XAS, very high-resolution electron microscopy and Raman diffraction. During the high voltage plateau in the first cycle, there is a partial densification on the external part of the particles followed by an oxygen oxidation in the bulk of the lattice without oxygen migration. This redox process is completely reversible in discharge. The contribution of nickel and cobalt and oxygen reduction leads to the huge specific capacity of this material family.

A general overview of all reactions mechanisms will be presented.

## References:

- [1] Y. Koyama, I. Tanaka, M. Nagao, R. Kanno, J. Power Sources, **189** (2009) 798.
- [2] J. Kikkawa, T. Akita, M. Takuchi, K. Tatsumi and M. Kohyama; J. Electrochem. Soc., **158**(6) A760-A768 (2011).
- [3] A. Ito, Y. Sato, T. Sanada, M. Hatano, H. Horie, Y. Ohsawa, J. Power Sources, **196** (2011) 6828.
- [4] H. Koga, L. Croguennec, M. Ménétrier, P. Mannessiez, K. Dohil, S. Belin, L. Bourgeois, E. Suard F. Weill, C. Delmas; J. Electrochem Soc., **160**(6) A786-A792 (2013)
- [5] H. Koga, L. Croguennec, M. Ménétrier, P. Mannessiez, F. Weill and C. Delmas ; J. P. Sources, **236**, 250-258 (2013)
- [6] M. Sathiya, G. Rousse, K. Ramesha, C.P. Laisa, H. Vezin, M.T. Sougrati, M.-L. Doubilet, D. Foix, D. Gonbeau, W. Walker, A.S. Prakash, M. Ben Hassine, L. Dupont and J.M. Tarascon, Nature Mat. July 2013.



## **Special Sites in Electrocatalysis**

Jan Rossmeisl

*Department of Chemistry, University of Copenhagen  
Universitetsparken 5, 2100, København Ø, Denmark.  
jan.rossmeisl@chem.ku.dk*

So far most electrocatalyst has been designed only based on reactivity of the surface. This single parameter is not sufficient to optimize the activity and selectivity. This means that activities and selectivity can only be optimized to a certain point. The activity as function of the surface reactivity is often represented in volcano curves. Electrocatalytic activity and selectivity is ultimately determined by the atomic and electronic structure of the catalyst surface. By controlling the atomic structure of the catalyst surface it is possible provide more parameters besides the reactivity to tune activity and selectivity beyond the normally limits. I will show some examples on atomic scale design of special electrocatalytic sites for oxygen evolution and oxygen reduction for better selectivity and activity.

# Operando Methods for the Characterization Energy Materials

Héctor D. Abruña

*Department of Chemistry and Chemical Biology*

*Director, Energy Materials Center at Cornell*

*Baker Laboratory, Cornell University*

*Ithaca, New York 14853-1301*

*hda1@cornell.edu*

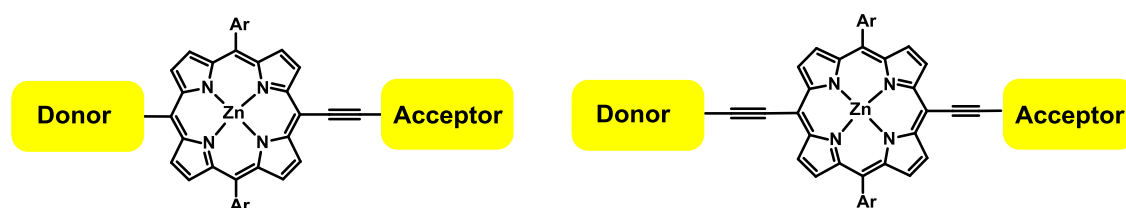
This presentation will deal with the development of *operando* methods for the study and characterization of fuel cell and battery materials. The presentation will begin with a brief overview of the methods employed. Particular emphasis will be placed on the use of X-ray diffraction (XRD) and X-ray absorption spectroscopy (XAS), transmission electron microscopy (TEM) under active potential control, confocal Raman and differential electrochemical mass spectrometry (DEMS). The utility of these methods will be illustrated by selected examples including the use of Ge nanowires as lithium ion battery anodes, spectroscopic studies of Li/S batteries and the use of DEMS to characterize electrolyte systems for LIBs. The use of operando TEM will be illustrated by studies of fuel cell catalyst degradation and coalescence and lithiation/de-lithiation dynamics of  $\text{LiFePO}_4$  via energy-filtered TEM. The presentation will conclude with an assessment of future directions.

## Recent Progress of Porphyrin-Sensitized Solar Cells

Chen-Yu Yeh, Hsien-Hsin Chou, Chi-Lun Mai, Hsuan-Wei Lee, Sudhir Kamani, Guan-Jie Fang, Chia-Wei Hsu

Department of Chemistry, National Chung Hsing University, Taichung, Taiwan  
250 Kuo-Kuang Rd., Taichung 402, Taiwan  
cyyeh@dragon.nchu.edu.tw

Porphyrin dyes with a push-pull framework have been prepared and used in dye-sensitized solar cells (DSSC), their spectral, electrochemical and photovoltaic properties were investigated. The photovoltaic measurements show that **YD2-o-C8** achieves a record power conversion efficiency ~12% using Co(II)/Co(III) as the electrolyte. When **YD2-o-C8** is co-sensitized with an organic dye **Y123**, the device gives a power conversion efficiency of 12.3% under standard AM 1.5 sunlight, and 13.1% under AM 1.5 solar light of 500 W m<sup>-2</sup> intensity. In **YD2-o-C8**, The hydrophobic alkoxy chains at the *ortho*-positions of the *meso*-phenyls suppress molecular aggregation and successfully block the approach of the electrolyte to the surface of TiO<sub>2</sub> to reduce charge recombination, giving an improved *V<sub>oc</sub>* and the power conversion efficiency. Based on the structure of **YD2-o-C8**, a new porphyrin **GY50** with more red-shifted absorption has been synthesized. The device of **GY50** gives a power conversion efficiency of 12.75% under standard AM 1.5 sunlight. To improve the long term stability of the devices, pyridine-type anchors have been tested. It was demonstrated that 2-carboxypyridine is an efficient and stable anchoring group as **MH1** showed better cell performance and long-term stability than **YD2-o-C8** under light soaking conditions. We found that introduction of push and pull units to *meso*-positions is demonstrated to be achievable. Furthermore, bulky donors are compatible with cobalt-based electrolytes and yield high *V<sub>oc</sub>*, long alkyl chains at *meso*-phenyls successfully reduce dye aggregation and decrease charge recombination rate, and the benzoic acid acceptor is superior to the cyanoacrylic acid counterpart. These push-pull porphyrin dyes are promising candidates for highly efficient DSSC.



### References:

1. Yella, A.; Mai, C.-L.; Zakeeruddin, S. M.; Chang, S.-N.; Hsieh, C.-H.; Yeh, C.-Y.; Graetzel, M. *Angew. Chem. Int. Ed.*, 2014, 53, 2973.
2. Yella, A.; Lee, H.-W.; Tsao, H. N.; Yi, C.; Chandiran, A. K.; Nazeeruddin, M.; Diao, E. W.-G.; Yeh, C.-Y.; Zakeeruddin, S. M.; Graetzel, M., *Science*, 2011, 334, 629.

# Two-Dimensional Materials and Electrode Architectures for Capacitive and Pseudocapacitive Energy Storage

Y. Gogotsi

*A.J. Drexel Nanomaterials Institute and Department of Materials Science and Engineering, Drexel University, Philadelphia, PA, 19104, USA*

Electrical energy storage is a key challenge because our daily life depends on numerous electronic devices. Moreover, with miniaturization of electronics, penetration of wireless devices into our homes and clothes, wide use of sensor networks and widely anticipated “internet of things”, there is a major effort to develop miniature, but powerful storage devices. To satisfy the growing demand, new concepts must be formulated that will lead to a new generation of sustainable, affordable and safe energy storage technologies that will approach the theoretical limits for electrochemical storage and deliver electrical energy rapidly and efficiently [1]. Two-dimensional (2D) materials [2], including graphene [3], layered transition metal oxides (e.g.,  $\text{MoO}_3$  [4]) and carbides (MXenes –  $\text{Ti}_3\text{C}_2$ ,  $\text{V}_2\text{C}$ ,  $\text{Ti}_2\text{C}$ , etc. [5]) offer a unique opportunity to produce thin or thick films with high volumetric capacitance and energy density, because 2D sheets can be packed denser than activated carbon or metal oxide particles, still providing accessibility for electrolyte. 2D particles can also be printed onto a variety of surfaces and assembled into flexible films without a polymer binder. However, when the lateral dimensions of particles become large and the electrode thickness increases, diffusion may limit the energy storage. To overcome those diffusional limitations, 2D particles can be separated by one- or zero-dimensional particles (e.g., carbon nanotubes or onion-like carbon). By combining double-layer and pseudocapacitive (surface and fast intercalation redox processes) energy storage, it is possible to increase the capacitance well beyond conventional double-layer capacitors. Nitrogen-functionalized graphene, as well as transition metal compounds show capacitance values approaching 500 F/g or 1000 F/cm<sup>3</sup> [5]. Planar architectures that increase the volumetric energy density of electrodes also allow the use of very thin separators or replacing separators by a thin film of gel electrolyte, as no piercing by large particles or sharp tubes/rods is possible. MXenes films having metallic conductivity or highly conducting graphene papers can be used to build current-collector free devices, further increasing the storage per unit of volume or weight.

1. Y. Gogotsi, What nano can do for energy storage, *ACS Nano*, **8** (6) 5369-5371 (2014)
  2. M. Naguib, Y. Gogotsi, Synthesis of two-dimensional materials by selective extraction, *Accounts of Chemical Research*, **48** (1), 128-135 (2015)
  3. W.-Y. Tsai, R. Lin, S. Murali, L. L. Zhang, J. K. McDonough, R. S. Ruoff, P.-L. Taberna, Y. Gogotsi, P. Simon, Outstanding performance of activated graphene based supercapacitors in ionic liquid electrolyte from –50 to 80 °C, *Nano Energy*, **2** (3), 403-411 (2013)
  4. X. Xiao, Z. Peng, C. Chen, C. Zhang, M. Beidaghi, Z. Yang, N. Wu, Y. Huang, L. Miao, Y. Gogotsi, J. Zhou, Freestanding  $\text{MoO}_{3-x}$  nanobelt/carbon nanotube films for Li-ion intercalation pseudocapacitors, *Nano Energy*, **9**, 355-363 (2014)
  5. M. Ghidui, M. R. Lukatskaya, M.-Q. Zhao, Y. Gogotsi, M. W. Barsoum, Conductive two-dimensional titanium carbide ‘clay’ with high volumetric capacitance, *Nature*, **516**, 78–81 (2014)
-

# PEMFC Cathode Performance and Durability Challenges at Low Platinum Loading

Swami Kumaraguru, Jingxin Zhang, Wenbin Gu, Balsu Lakshmanan and Mark Mathias

*General Motors Fuel Cell Activities  
895 Joslyn Avenue, Pontiac MI 48340  
swami.kumaraguru@gm.com*

Cost of the fuel cell system is one of the biggest challenges towards commercialization of fuel cell electric vehicles. Platinum-based catalysts can contribute a significant percentage of the cost at high production volumes. Platinum loading levels of 0.4 mg<sub>Pt</sub>/cm<sup>2</sup> to 0.2 mg<sub>Pt</sub>/cm<sup>2</sup> for cathode catalyst layer can be achieved by a combination of advances in dispersed Pt catalyst (both Pt and Pt alloy) and efficient use of ionomer in the electro-catalyst layer. Further efforts to reduce Pt loading to <0.1 mg<sub>Pt</sub>/cm<sup>2</sup> requires significant improvements on both performance and durability front. On the performance front, the desired high current density operation (>1.5 A/cm<sup>2</sup>) is severely limited by the presence of local oxygen transport resistance<sup>1-2</sup>. While the mechanism of local oxygen transport resistance is still unclear, it is resistive in nature and the thin ionomer film encapsulating the Pt particles is widely considered to be the source. On the durability front, in addition to traditional degradation mechanisms such as Oswald ripening and non-noble metal dissolution (Co in case of PtCo nanoparticle catalysts), the lower roughness factor (available Pt surface area cm<sup>2</sup><sub>Pt</sub>/cm<sup>2</sup><sub>geometric</sub>) at low loading is very sensitive to contamination from both within the cell<sup>3</sup> and from external sources<sup>4</sup>. Some of the voltage loss from contamination is reversible. The lecture will focus on the above mentioned challenges and provide recommendations for areas of research.

## References

- [1] T.A.Greszler, D.A.Caulk, P.Sinha, J.Electrochem. Soc., 159(12), F831, 2012.
- [2] N.Nonoyoma, S.Okazaki, A.Weber, Y.Ikoji, T.Yoshida, J. Electrochem. Soc., 158(4), B416, 2011.
- [3] J.Zhang, B.Litteer, F. Coms, R.Makharia, J.Electrochem. Soc., 159 (7), F287, 2012.
- [4] X. Chenga, Z. Shi, N.Glass, L. Zhang, J Zhang, D. Song, Z. Liu, H. Wang, Jun Shen, J.Power Sources, 165, 739, 2007.

# Challenges and Progress in Developing High Voltage Li-ion Batteries

T. Richard Jow, Jan L. Allen, Joshua L. Allen, Samuel A. Delp, Jeffrey B. Wolfenstine  
U.S. Army Research Laboratory  
2800 Powder Mill Road, Adelphi, MD 20783, U.S.A.  
t.r.jow.civ@mail.mil

The demand for more compact power sources for portable electronic devices and vehicles applications drives the development of more energy dense lithium-ion (Li-ion) batteries beyond what are available today. The use of high voltage cathodes to increase the energy density is one approach that has been actively pursued. The high voltage cathodes considered include 4.7 V spinel  $\text{LiNi}_{0.5}\text{Mn}_{1.5}\text{O}_4$  (LNMO) and 4.8 V lithium cobalt phosphate  $\text{LiCoPO}_4$  (LCP), versus  $\text{Li/Li}^+$ . However, this approach has encountered difficulties including most notably capacity fading and low coulombic efficiency (CE) in the baseline electrolyte made of  $\text{LiPF}_6$  in alkyl carbonate solvent mixtures. What are the issues? Oxidation of electrolyte at high voltages has been considered as a major one<sup>1,2</sup>. The dissolution of transition metal, highly reactive electrode surfaces at high voltage, and structure instability of the delithiated state of the high voltage cathodes have also been considered<sup>2</sup>.

On the electrolyte front, the use of fluorinated solvents with the expectation that could make the electrolyte more oxidatively stable was pursued<sup>3</sup> for resolving the issues of the LNMO/graphite cells. The use of fluorinated and non-fluorinated additives was also pursued<sup>4,5</sup>. Capacity retention was improved using fluorinated solvents or additives. On the cathode front, a partial substitution of Ni by doping of Fe, Cr and Ga in LNMO,  $\text{LiNi}_{0.5-x}\text{M}_x\text{Mn}_{1.5}\text{O}_4$  ( $\text{M} = \text{Cr, Fe, and Ga, } x=0.08$ ), results in improvement in capacity retention compared to the non-substituted LNMO<sup>6</sup>. The improvement in either electrolyte or electrode itself results in the improvement in capacity retention and CE of LNMO/graphite cells.

For LCP electrode, 0.6 Li utilization could be achieved for each LCP when cycled against Li and faded fast with the capacity retention only at 53% at the 10th cycle in the baseline electrolyte<sup>7</sup>. No improvement in capacity or capacity retention was observed even when the advanced high voltage electrolyte was employed. However, significant improvement in capacity realization and capacity retention were observed by Allen et al.<sup>8</sup> in partial substitution of Co by Fe in LCP even without using high voltage electrolyte. Further improvement was made using high voltage electrolyte<sup>8</sup>.

The above example strongly indicates that improvements in electrode materials and electrolytes need to go hand in hand for the cell level improvements for meeting the needs of tomorrow. This paper will review the recent efforts and present the progresses made in the development of high voltage Li-ion batteries.

## References

1. O. Borodin, W. Behl, and T. R. Jow, Oxidative Stability and Initial Decomposition Reactions of Carbonate, Sulfone and Alkyl Phosphate-Based Electrolytes, *J. Phys. Chem. C*, 2013, 117, 8661-8682.
2. D. Lu, M. Xu, L. Zhou, A. Garsuch, B. L. Lucht, Failure Mechanism of Graphite/ $\text{LiNi}_{0.5}\text{Mn}_{1.5}\text{O}_4$  Cells at High Voltage and Elevated Temperature, *J. Electrochem. Soc.*, 2013, 160 (5), A3138-A3143.
3. L. Hu, Z. Zhang, K. Amine, Fluorinated electrolytes for Li-ion battery: An FEC-based electrolyte for high voltage  $\text{LiNi}_{0.5}\text{Mn}_{1.5}\text{O}_4$ /graphite couple, *Electrochem. Comm.*, 35 (2013), 76-79.
4. A. v. Cresce, K. Xu, "Electrolyte Additive in Support of 5 V Li Ion Chemistry," *J. Electrochem. Soc.*, 2011, 158(3), A337-A342.
5. S. A. Delp, J. L. Allen and T. R. Jow, Investigation of Electrolyte Additives with  $\text{LiNi}_{0.5}\text{Mn}_{1.5}\text{O}_4$ /Graphite Cells at High Temperature, *ECS Trans.*, 2014, 58(48), 111-118.
6. A. Manthiram, Materials Challenges and Opportunities of Lithium Ion Batteries, *Phys. Chem. Lett.*, 2011, 2, 176-184.
7. J. Wolfenstine, U. Lee, B. Poesse and J. L. Allen, Effect of oxygen partial pressure on the discharge capacity of  $\text{LiCoPO}_4$ , *J. Power Sources*, 2005, 144, 226.
8. J. L. Allen, T. R. Jow, J. Wolfenstine, Improved Cycle Life of Fe-substituted  $\text{LiCoPO}_4$ , *J. Power Sources*, 2011, 196, 8656.

# Alluaudite $\text{Na}_{2+2x}\text{Fe}_{2-x}(\text{SO}_4)_3$ as 3.8 V Sodium Battery Cathode

Atsuo Yamada,<sup>1,2</sup> Masashi Okubo,<sup>1,2</sup> Prabeer Barpanda,<sup>1,2</sup> Shin-ichi Nishimura,<sup>1,2</sup>

Sai-Cheong Chung,<sup>1,2</sup> Gosuke Oyama,<sup>1</sup> Yuya Suzuki<sup>1</sup>

Department of Chemical System Engineering, School of Engineering, The University of Tokyo, Hongo 7-3-1, Bunkyo-ku, Tokyo 113-8656, Japan

<sup>2</sup>Unit of Elements Strategy Initiative for Catalysts & Batteries (ESICB), Kyoto University, Japan  
yamada@chemsys.t.u-tokyo.ac.jp

Rechargeable lithium batteries have ushered the wireless revolution over last two decades and are now matured to enable green automobiles. However, the growing concern on scarcity and large-scale applications of Li-resources have steered effort to realize sustainable sodium-ion batteries, Na and Fe being abundant and low cost charge-carrier and redox center respectively. However, their performance is limited owing to low operating voltage and sluggish kinetics. Here, we report a hitherto-unknown material with entirely new composition and structure with the first *alluaudite*-type sulfate framework,  $\text{Na}_{2+2x}\text{Fe}_{2-x}(\text{SO}_4)_3$ , registering the highest ever  $\text{Fe}^{3+}/\text{Fe}^{2+}$  redox potential at 3.8 V (vs. Na, and hence 4.1V vs. Li) along with very fast rate kinetics. Rare-metal-free sodium-ion rechargeable battery system compatible with the present lithium-ion battery is now in realistic scope without sacrificing high energy density and high power, and paves way for discovery of new earth-abundant sustainable cathodes for large-scale batteries.

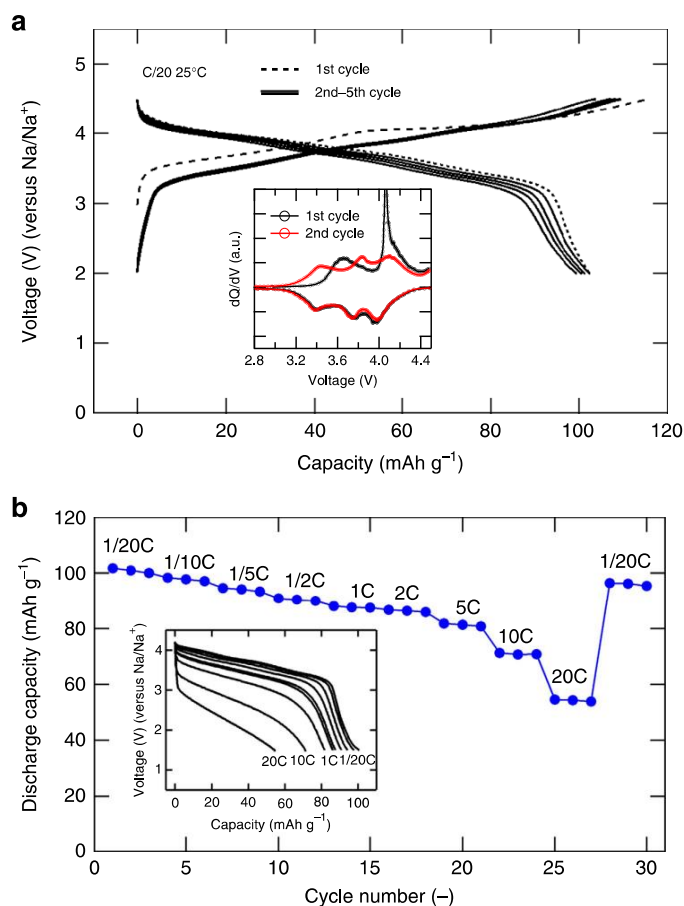


Figure 1. Electrode properties of *Alluaudite*  $\text{Na}_{2+2x}\text{Fe}_{2-x}(\text{SO}_4)_3$

## Reference

- [1] P. Barpanda, *et al.*, & A. Yamada, *Nature Comm.*, **2014**, 5, 4358.
- [2] J. Ming, *et al.*, & A. Yamada, *Electrochem. Comm.*, **2015**, 51, 19.
- [3] G. Oyama *et al.*, & A. Yamada, *ChemElectroChem.*, **2015**, DOI: 10.1002/celec.201500036

# New Lithium Metal Polymer Solid State Battery for an Ultrahigh Energy: Nano C-LiFePO<sub>4</sub> versus Nano Li<sub>1.2</sub>V<sub>3</sub>O<sub>8</sub>

P. Hovington <sup>†</sup>, M. Lagacé <sup>†</sup>, A. Guerfi <sup>†</sup>, P. Bouchard <sup>†</sup>, A. Mauger <sup>‡</sup>, C. M. Julien <sup>§</sup>, M. Armand <sup>||</sup>, and K. Zaghib <sup>‡†</sup>

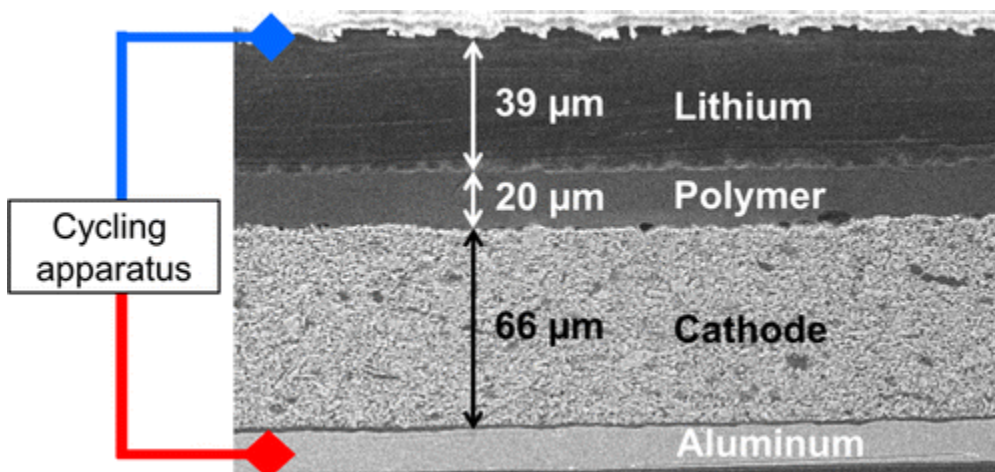
<sup>†</sup> Institut de Recherche d'Hydro-Québec (IREQ), 1800 Bd Lionel-Boulet, Varennes, Quebec J3X 1S1 Canada

<sup>‡</sup> Sorbonne Universités, UPMC Univ Paris 06, Institut de Minéralogie, de Physique des Matériaux et de Cosmochimie (IMPMC), CNRS UMR 7590, 4 place Jussieu, F-75005 Paris, France

<sup>§</sup> Sorbonne Universités, UPMC Univ Paris 06, Physicochimie des Électrolytes et Nanosystèmes Interfaciaux (PHENIX), CNRS UMR 8234, 4 place Jussieu, F-75005 Paris, France

<sup>||</sup> CIC Energigune, Parque Tecnológico de Alava, Albert Einstein 48, Ed. CIC, 01510 Miñano, Spain

Novel lithium metal polymer solid state batteries with nano C-LiFePO<sub>4</sub> and nano Li<sub>1.2</sub>V<sub>3</sub>O<sub>8</sub> counter-electrodes (average particle size 200 nm) were studied for the first time by in situ SEM and impedance during cycling ( Fig. 1). The kinetics of Li-motion during cycling is analyzed self-consistently together with the electrochemical properties. We show that the cycling life of the nano Li<sub>1.2</sub>V<sub>3</sub>O<sub>8</sub> is limited by the dissolution of the vanadium in the electrolyte, which explains the choice of nano C-LiFePO<sub>4</sub> (1300 cycles at 100% DOD): with this olivine, no dissolution is observed. In combination with lithium metal, at high loading and with a stable SEI an ultrahigh energy density battery was thus newly developed in our laboratory.





## Magnéli Ti<sub>4</sub>O<sub>7</sub> Modified Ceramic Membrane for Electrically-assisted Filtration with Antifouling Property

Ping Geng, Guohua Chen \*

*Department of Chemical and Biomolecular Engineering, The Hong Kong University of Science and Technology, Clear Water Bay, Kowloon, Hong Kong, China*

E-mail address: kechengh@ust.hk

### Abstract

Antifouling tubular Al<sub>2</sub>O<sub>3</sub> microfiltration membranes were successfully developed with a Magnéli Ti<sub>4</sub>O<sub>7</sub> modified inner layer to enhance filtration performance coupling with external electricity. The Magnéli Ti<sub>4</sub>O<sub>7</sub> layer was obtained by first dip-coating a layer of TiO<sub>2</sub> and then reducing this layer at 1050°C in H<sub>2</sub> atmosphere. The fabricated Ti<sub>4</sub>O<sub>7</sub> layer exhibited the conductivity of over 200 S·cm<sup>-1</sup> with particle size of 200 - 300 nm, average pore diameter of 350 nm and contact angle of 0°. The antifouling performance of tubular Ti<sub>4</sub>O<sub>7</sub>/Al<sub>2</sub>O<sub>3</sub> membrane was evaluated through a home-made cross-flow electrically-assisted membrane filtration module for the treatment of three typical feed solutions that are known to foul easily, namely, oily wastewater, humic acid (HA), and bovine serum albumin (BSA). During membrane filtrations, the permeate fluxes of Ti<sub>4</sub>O<sub>7</sub>/Al<sub>2</sub>O<sub>3</sub> composite membranes at around critical electrical potentials could maintain over 90% of their initial values after 1 h, in contrast to the low values obtained with the uncoated Al<sub>2</sub>O<sub>3</sub> membranes, 15.6% for oily wastewater, 62.7% for HA and 41.6% for BSA. Meanwhile, the permeate quality was also improved correspondingly, with oil, HA and BSA rejections increased from 95.8, 2.0 and 18.1% of uncoated Al<sub>2</sub>O<sub>3</sub> membranes to 97.9, 96.2 and 76.1% of Ti<sub>4</sub>O<sub>7</sub>/Al<sub>2</sub>O<sub>3</sub> membranes respectively. The total energy consumed by the electrically-assisted filtration of oily wastewater at around critical electrical potential in 1 h has decreased 44% in comparison with uncoated Al<sub>2</sub>O<sub>3</sub> membrane in term of kW·h per m<sup>3</sup> permeate. For HA and BSA, the total energies also decreased over 57 and 20% compared with corresponding ultra- or nano-filtration membranes, which are commonly used for HA and BSA rejections, at the same average permeate fluxes in 1 h. Therefore, the designed electrically-assisted filtration process with Magnéli Ti<sub>4</sub>O<sub>7</sub> modified membrane provides a promising alternative for ceramic membrane filtrations with antifouling property, good permeate quality and low maintenance cost.

**Keywords:** Electrically-assisted filtration, membrane antifouling, Magnéli titanium sub-oxides, wastewater treatment, bovine serum albumin.

# Palladium-Based Nanomaterials: Synthesis and Electrochemical Applications

Aicheng Chen  
Department of Chemistry, Lakehead University  
955 Oliver Road, Thunder Bay, Ontario P7B 5E1, Canada  
achen@lakeheadu.ca

Palladium (Pd) is well known for its remarkable capacity for hydrogen absorption/adsorption, and is broadly used as a primary catalyst for the low temperature reduction of automobile pollutants, hydrogenation reactions, hydrogen purification, petroleum cracking, and a wide range of electrochemical applications. The main drawback of Pd, much like platinum, is its exorbitant cost. Over the last several years, the price of Pd has increased and is expected to continue to rise as interest in this material expands. Thus, there is an urgent need for the design of advanced catalysts to reduce the amount of noble metals required, while increasing their activity and stability.

In this talk, a number of methods for the synthesis of Pd based nanomaterials, as well as the impacts of their dimensions, morphologies and compositions toward various electrochemical applications are presented and compared. Fabrication strategies primarily include physical synthesis techniques, hydrothermal methods, electrochemical deposition, and other processes, such as electroless deposition, microemulsion, and photochemically assisted synthesis. The chemical and catalytic properties of Pd and Pd-based nanomaterials for electrochemical purposes, including fuel cells, hydrogen purification and storage, gas sensors, biosensors, capacitors and the degradation of pollutants are also discussed. Hydrogen storage remains one of the most challenging prerequisites to overcome toward the realization of a hydrogen based economy. Recent advancements are highlighted regarding palladium based nanomaterials for hydrogen storage, as well as the effects of hydrogen spillover on various adsorbents.

With increasing environmental concerns and the accelerated depletion of fossil fuels, there will be a significant demand for the development of advanced technologies for environmental remediation, as well as for the production of alternative energy conversion and storage devices. In the biomedical sector, the growing need for point of care, real-time quantitative detection and monitoring will drive the emergence of innovative sensing devices and systems. The design and implementation of high-performance Pd-based nanomaterials are anticipated to expand considerably over the next decade.

Mis en forme : Gauche : 3 cm, Droite : 3 cm, Haut : 3 cm,  
Bas : 3 cm

# Making Movies: Next Generation Electrochemical Imaging

Patrick R. Unwin<sup>1</sup>, Dmitry Momotenko<sup>1</sup>, Kim M. McKelvey<sup>1</sup>, Chang-Hui Chen<sup>1</sup>, Leon Jacobse<sup>2</sup>, Yang-Rae Kim<sup>1</sup>, Aleix G. Güell<sup>1</sup>, Anatolii S. Cuharuc<sup>1</sup>, Guohui Zhang<sup>1</sup>, Sze-yin Tan<sup>1</sup>, Stanley C. S. Lai<sup>3</sup>, Marc T. M. Koper<sup>2</sup>

<sup>1</sup>*Department of Chemistry, University of Warwick  
Coventry CV4 7AL, UK*

<sup>2</sup>*Leiden Institute of Chemistry, Leiden University, P.O. Box 9502, 2300 RA Leiden, The Netherlands*

<sup>3</sup>*MESA+ Institute for Nanotechnology, University of Twente, PO Box 217, 7500 AE Enschede, The Netherlands*

*p.r.unwin@warwick.ac.uk*

Compared to other scanning probe microscopy techniques, scanning electrochemical probe microscopy (SEPM) methods suffer seriously from slow image acquisition rates. The timescale of obtaining just one image is often tens of minutes and there are examples where a single image has taken several hours to record. This makes SEPMs impractical for recording more than one or a few snapshots on a particular system and severely limits the amount of dynamic information accessible (activity maps as a function of potential or time), while also raising issues about changes that might occur at the electrode surface (and tip) during such long experiments.

In this contribution, we present two distinct strategies for greatly enhancing the dynamic information content and data throughput in electrochemical imaging experiments. These approaches are illustrated with scanning electrochemical cell microscopy (SECCM, e.g. [1–5]), a powerful multifunctional droplet-based SEPM, but the principles are easily extended to other techniques such as scanning electrochemical microscopy (SECM) and its variants. First, we describe **voltammetric imaging** in which a voltammogram is recorded at every pixel making up an image. Data can be represented as movies (hundreds of frames) of current (over a surface region) at a series of potentials and are highly revealing of subtle variations in electrode activity. We illustrate this concept through studies of outer sphere electron transfer at graphite and graphene, and hydrazine oxidation at platinum. We compare electrochemical images with microscopic and nanoscopic electrode structure in the same area, deduced from atomic force microscopy, Raman microscopy and electron backscatter diffraction. This **multimicroscopy** approach is highly revealing and we show how this general approach provides information on structure-activity that would be lost in both macroscopic measurements and conventional (fixed potential) SEPM.

A second approach is the development of a **high-speed imaging** for the acquisition of a series of high-resolution images at unprecedented rates approaching 4 s per frame. Thus, within less than 10 minutes, > 100 images at different driving forces can be obtained with better resolution (1000 pixels/μm<sup>2</sup>) than in conventional SEPM. This approach is illustrated with studies of model array electrodes, individual carbon nanotubes and catalytic nanoparticles. Together, these studies provide preliminary proof of concept data and a platform for next generation electrochemical imaging. This will see the emergence of SEPMs as truly dynamic techniques, with **electrochemical movies** providing a powerful new way to probe, visualise and understand electrochemical systems.

Some of this work has been partly supported by a European Research Council Advanced Investigator Grant to PRU (ERC-2009-AdG 247143-QUANTIF).

## References

1. Ebejer, N.; Schnippering, M.; Colburn, A. W.; Edwards, M. A.; Unwin, P. R. *Anal. Chem.* **2010**, *82*, 9141-9145.
2. Ebejer, N.; Güell, A. G.; Lai, S. C. S.; McKelvey, K.; Snowden, M. E.; Unwin, P. R. *Annu. Rev. Anal. Chem.* **2013**, *6*, 329-351.
3. Lai, S. C. S.; Patel, A. N.; McKelvey, K.; Unwin, P. R. *Angew. Chem. Int. Ed.* **2012**, *51*, 5405-5408.
4. Güell, A. G.; Ebejer, N.; Snowden, M. E.; Macpherson, J. V.; Unwin, P. R. *J. Am. Chem. Soc.* **2012**, *134*, 7258-7261.
5. Aaronson, B. D. B.; Chen, C.-H.; Li, H.; Koper, M. T. M.; Lai, S. C. S.; Unwin, P. R. *J. Am. Chem. Soc.* **2013**, *135*, 3873-3880.

# Ubiquinones: understanding electrochemistry from solution to surface

Yi-Tao Long\*

Key Laboratory for Advanced Materials & Department of Chemistry, East China University of Science and Technology, 130 Meilong Road, Shanghai, 200237, P. R. China.

yitaolong@gmail.com

Quinones are ubiquitous in nature and constitute an important class of natural evolutionary redox molecules. It is well known that quinone fulfill a universal and possibly unique function in electron transfer and energy conservation systems. Ubiquinones are the central cofactors in the enzymatic reaction of the electron-transport system that couples the transfer of electrons to the generation of trans-membrane electrochemical proton gradients that drive the production of adenosine triphosphate in photosynthesis and respiration.

Researches on ubiquinone are not only for better understanding its electrochemical properties, but also for developing ubiquinone-based biomolecular systems to study its biological functions. We have been focusing on ubiquinone from synthesis, electrochemistry and applications and attempt to construct biomimetic systems to mimic the functions of quinone in photosystem II and respiration.<sup>1,2,3</sup>

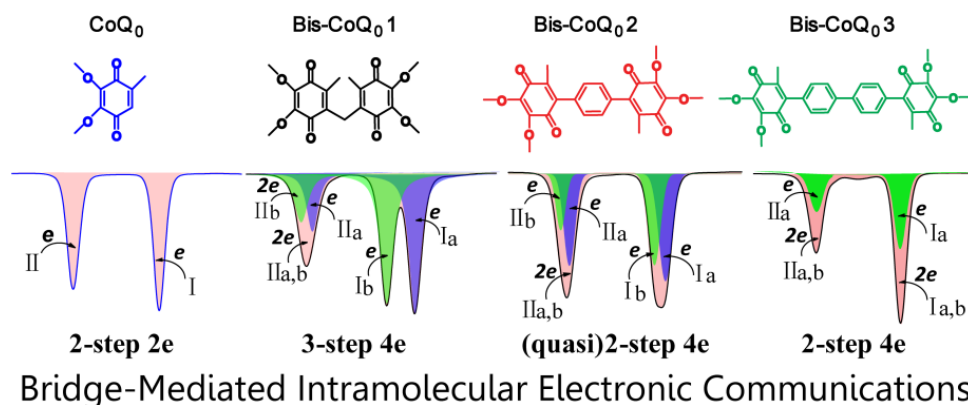


**Figure 1** Chemical structures and electrochemical properties of ubiquinone-based compounds.

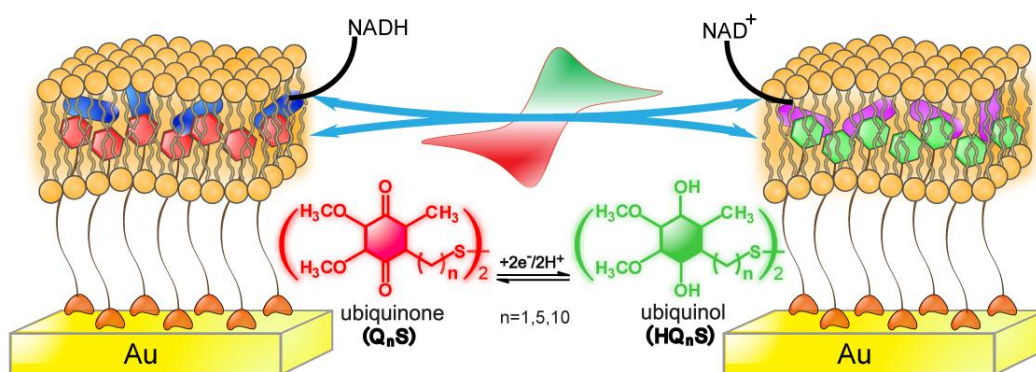


**Figure 2** Electron Transfer Process between Ubiquinone and NADH

## REFERENCES

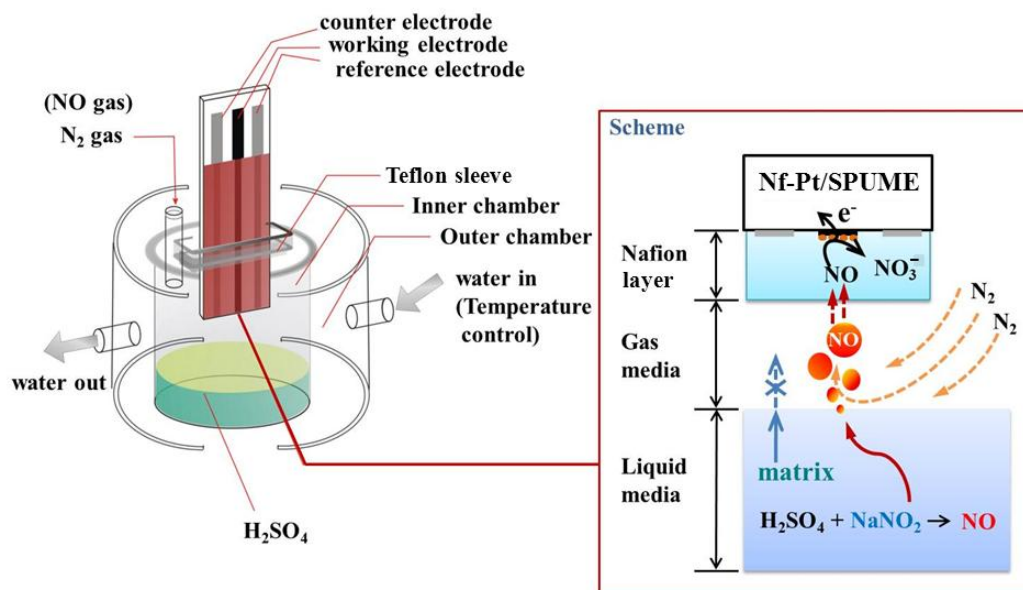
1. X. W. Wang, Y. T. Long et al, *Chem. Asian J.* **6**, 1064–1073 (2011).
2. W. Ma, Y. T. Long et al., *J. Am. Chem. Soc.* **133**, 12366-12369 (2011).
3. L. -X. Qin, Y.-T. Long et al., *Chem.-Eur. J.* **17**, 5262-5271 (2011).

# An Easily Applicable Green Method for Real Sample Analysis Based on Disposable Gas Sensor

Jyh-Myng Zen

*Department of Chemistry, National Chung Hsing University  
250 Kuo Kuang Road, Taichung, Taiwan  
jmzen@dragon.nchu.edu.tw*

We have developed novel electrochemical gas sensors based on electrochemical deposition of high catalytic metal particles (e.g., Pt, Pd) on screen-printed carbon ultramicroelectrode (SPUME). An efficient mass transfer effect of ultramicroelectrode facilitates for electrochemical reduction of metals. Homogeneous size and distribution of metal nanoparticles can be easily decorated at the surface of carbon ultramicroelectrode without either protective or capped agents. The as-prepared Pt/SPUME was then applied for the development of sensitive nitric oxide, formaldehyde, formic acid and hydrogen peroxide gas sensors can be achieved. The system can also be applied to develop hydroxyl radical, glycerol and triglyceride sensors as well. By using a reaction involving acid and nitrite, in-situ evaluation of NO gas can be carried out in an inert atmosphere and sensing in the gas phase. This new approach was successfully demonstrated for the determination of nitrite in food samples such as sausage and vegetable by standard addition method and the results were compared with the classical spectroscopic method to verify the analytical applicability of the method. These promising analytical performances open new possibilities for easy and selective determination of nitrite and nitric oxide in environmental and biological samples.

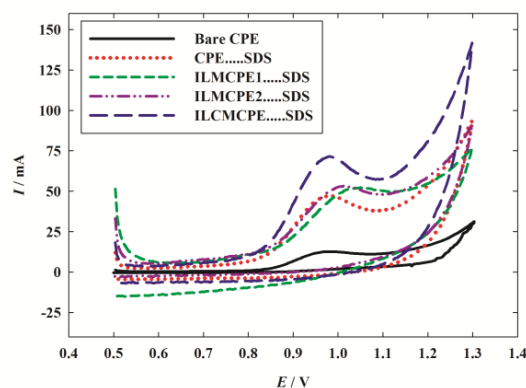
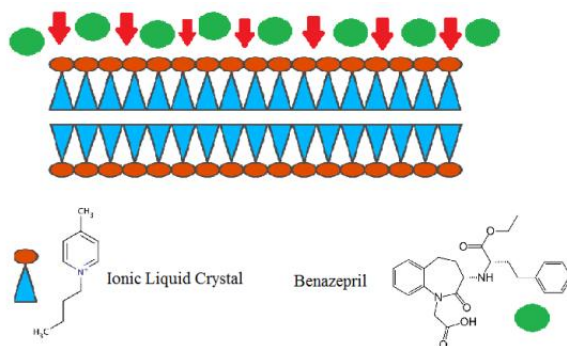


## Electrochemistry and Determination of Some Biomedical and Biological Molecules at Carbon – Based Ionic Liquid Crystals Composite Electrodes

Nada F. Atta, Ekram H. El-Ads, Asmaa H. Ibrahim, Youssuf Mohamed, Ahmed Galal

Department of Chemistry, Faculty of Science, Cairo University, 12613 Giza, Egypt, Tel.: +20 0237825266; fax: +20 0235727556, e-mail: [anada@sci.cu.edu.eg](mailto:anada@sci.cu.edu.eg)

The electrochemistry of some organic molecules of biomedical and biological importance is studied using a novel ionic liquid crystals (ILC) carbon composite electrode. ILC are materials that represent green media with remarkable chemical and physical properties. ILC mimic the natural bio-based ionic liquid crystals such as cell membranes structures. Thus a noticeable increase in surface ordering and excellent increase in electrical conductivity resulted in enhanced electron transfer mediation for the electrochemical oxidation process of the studied compounds. Thus, ionic liquid crystal [(1-Butyl-1-methylpiperidinium hexafluorophosphate)] was hybridized with carbon in presence of sodium dodecyl sulfate (ILCMCPE....SDS) for studying the electrochemical behavior of some neurotransmitters and drugs. Cyclic voltammetry, electrochemical impedance spectroscopy and chronoamperometry were used to determine the electrochemical behavior, diffusion coefficients, and electrical characteristics of the electrode. Surface morphology and structure were determined using atomic force microscopy (AFM), field-emission scanning electron microscopy (FE-SEM/EDAX) and surface enhanced Raman spectroscopy (SERS). Examples of studied compounds are Dopamine, Enoxacin, Benazepril hydrochloride, etc. The enhancement of charge transfer was ascertained by the high diffusion coefficients determined at the electrode surface and detection limits in the order of nano-molar quantities were achieved.



Ionic liquid crystals mimic the natural bio-based

ionic liquid crystals such as cell membranes structures in their interactions with drugs.

Cyclic voltammograms (CV) of  $1.0 \times 10^{-3}$  mol L<sup>-1</sup> of EN in B-R buffer pH 7.4 at scan rate 100 mVs<sup>-1</sup> recorded at different working electrodes (bare CP (solid line), CPE....SDS(dotted line), ILMCPE1....SDS (small dashed line) , ILMCPE2....SDS(dashed dotted line) and ILMCPE....SDS(large dashed line).

**Acknowledgement:** The Support of Cairo University (Egypt) is highly appreciated through the office of Vice President for Research and Graduate Studies.

# AFM Tip-integrated Antimony Electrodes for pH Detection

Angelika Holzinger<sup>1</sup>, Peter Knittel<sup>1</sup>, Jong Seok Moon<sup>2</sup>, Christine Kranz<sup>1</sup>

<sup>1</sup>*Institute of Analytical and Bioanalytical Chemistry, University of Ulm, Albert-Einstein-Allee 11, 89081 Ulm, Germany*

<sup>2</sup>*former address: School of Chemistry and Biochemistry, Georgia Institute of Technology, Atlanta, GA 30332-0400, USA*

*E-mail (presenting author): angelika.holzinger@uni-ulm.de*

*E-mail (corresponding author): christine.kranz@uni-ulm.de*

Mapping local pH changing plays an important role in interfacial reactions such as enzyme reactions, metabolic microbial processes and corrosion science. Solid-state metal-metal oxide electrodes especially iridium (Ir) oxide and antimony (Sb) oxide have been widely used for pH sensing [1]. Mapping of localized pH changes have been demonstrated using scanning electrochemical microscopy (SECM) with micro-sized Sb [2] and Ir microelectrodes [3]. In this contribution, we present atomic force microscopy (AFM) tip-integrated solid-state pH sensors. Commercially available silicon nitride AFM probes were modified with a Sb layer and insulated with Parylene C by polymer vapor deposition. The electrochemical active area was exposed by subsequent focused ion beam (FIB) milling (Fig.1). Calibration of the obtained probes in Tris(hydroxymethyl)aminomethane (Tris) buffer showed approximate a Nernstian slope (53mV/pH) in the range of 2-10 pH. When used for AFM imaging, the topography of the sample surface and local pH changes can be recorded simultaneously. The pH was detected by means of open circuit potential (OCP) against Ag/AgCl reference electrode (Fig. 2).

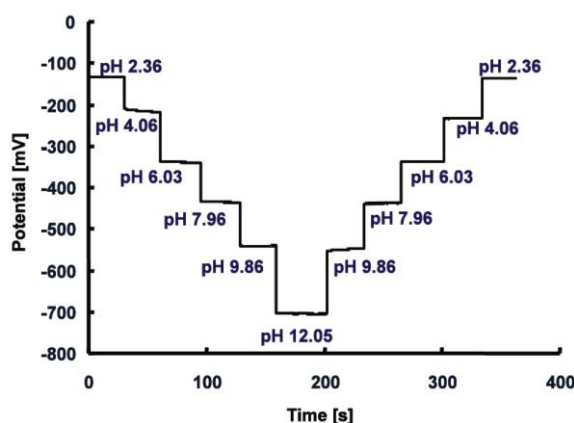


Fig.2: pH calibration (measurement of open circuit potential against Ag/AgCl reference electrode) in 0.05M Tris buffer.

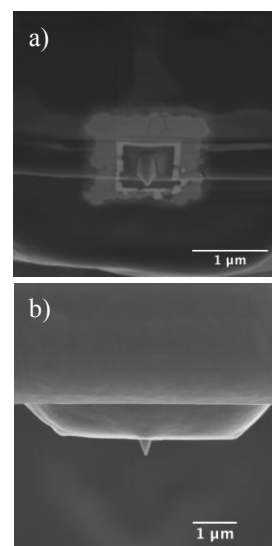


Fig.1: Scanning electron micrograph of a modified AFM-SECM probe: a) 56° tilted view of electrode area surrounding the tip and b) side view.

To demonstrate the potential of such probes for combined imaging, the pH change during the dissolution of a calcite microcrystal in aqueous solution was investigated as model sample [4]. The microcrystals were embedded in a photoresist (SU-8). First results towards simultaneous detection of pH and topography of calcite microcrystal by AFM-SECM are presented.

- [1] S. Glab, A. Hulanicki, G. Edwall, F. Ingman, Metal-metal oxide and metal oxide electrodes as pH sensors Crit. Rev. Anal. Chem., 21, 1 (1989) 29.
- [2] B. Horrocks, M. V. Mirkin, D. T. Pierce, A. J. Bard, G. Nagy, K. Toth, Scanning electrochemical microscopy, 19. Ion-selective potentiometric microscopy Anal. Chem. 65 (1993) 1213.
- [3] D. O. Wipf, F. Ge, T. W. Spaine, J. W. Baur, Microscopic measurement of pH with iridium oxide microelectrodes Anal. Chem. 72 (2000) 4921.
- [4] B. P. Nadappuram, K. McKelvey, R. Al Botros, A. W. Colburn, P. R. Unwin, Fabrication and characterization of dual function nanoscale pH-scanning ion conductance microscopy (SICM) probes for high resolution pH mapping Anal. Chem. 85, 17 (2013) 8070.



# Amperometric Nanosensors and Field-Effect Transistors for Extra- and Intracellular Chemical Analysis

Jan Clausmeyer,<sup>a</sup> Yanjun Zhang,<sup>b</sup> Miriam Marquitan,<sup>a</sup> Ainara López Córdoba,<sup>b</sup> Yuri Korchev,<sup>b</sup> Wolfgang Schuhmann<sup>a</sup>

<sup>a</sup> *Analytische Chemie – Center for Electrochemical Sciences (CES), Ruhr-Universität Bochum, Universitätsstrasse 150, 44780 Bochum, Germany*

<sup>b</sup> *Department of Medicine, Imperial College London, London W12 0NN, United Kingdom  
jan.clausmeyer@rub.de*

During periods of environmental stress, cells produce significant levels of reactive oxygen species (ROS), which damage cell structures and may lead to various pathological conditions. For the analysis of cell physiology in relation to ROS production we report the use of needle-type carbon nanoelectrodes functionalized with platinum as well as Prussian Blue to comprise sensitive amperometric nanosensors for the detection of oxygen<sup>1</sup> and hydrogen peroxide<sup>2</sup>, respectively. The amperometric probes are inserted into single living neurons and HEK cells to measure biologically relevant oxygen species in real time and with minimal perturbation of the cell function due to the small dimensions of the probes.

In order to enhance the sensitivity and versatility of nanobiosensors we show the fabrication of highly sensitive field-effect transistor (FET) probes based on double-barrel carbon electrodes. By depositing polypyrrole (PPy) across the two individually addressable nanoelectrodes a conductive nanojunction is generated. The resulting FET shows excellent sensitivity towards pH changes. Modifying the transistor gate with hexokinase yields a high-sensitivity nanobiosensor for the detection of ATP.

The spear-like shape of the probe allows to position the sensor in proximity to cells and perform real-time chemical analysis with high spatial resolution. We measure the acidification of the cell microenvironment typical of cancer cells. Moreover, the FET nanobiosensors can monitor spatial gradients of ATP released from melanoma cells and cardiomyocytes into the solution and detect the ATP release of a single cell as the response to chemical and physical stimuli.

## References

- (1) Actis, P.; Tokar, S.; Clausmeyer, J.; Babakinejad, B.; Mikhaleva, S.; Cornut, R.; Takahashi, Y.; López Córdoba, A.; Novak, P.; Shevchuck, A. I.; Dougan, J. A.; Kazarian, S. G.; Gorelkin, P. V.; Erofeev, A. S.; Yaminsky, I. V.; Unwin, P. R.; Schuhmann, W.; Klenerman, D.; Rusakov, D. A.; Sviderskaya, E. V.; Korchev, Y. E. *ACS Nano*. **2014**, *8*, 875–884.
- (2) Clausmeyer, J.; Actis, P.; López Córdoba, A.; Korchev, Y. E.; Schuhmann, W. *Electrochem. Commun.* **2014**, *40*, 28–30.



# **All-solid-State pH Sensor utilizing Termination-controlled Boron-doped Diamond Surface as pH-sensitive/pH-less-sensitive Interface**

Yukihiro Shintani<sup>1,2</sup>, Kotaro Ogawa<sup>2</sup>, Hiroshi Kwarada<sup>1</sup>

*1 School of Science and Engineering Waseda University, 3-4-1 Okubo, Shinjuku-ku, Tokyo, 169-8555, Japan*

*2 Research and Business Development Dept., Innovation Center, Yokogawa Electric Corporation  
2-9-32 Nakacho, Musashino-shi, Tokyo, 180-8750, Japan  
shintani@toki.waseda.jp*

A glass-type pH electrode is a well-established pH sensor because it has a standard of construction and application. Its remaining disadvantage is mainly due to a solution-containing reference Ag/AgCl electrode. To overcome its problem, there is an interest in the replacement of the Ag/AgCl reference electrode by solid-state reference electrode. Though a variety of considerable efforts were undertaken for years, an all-solid-state pH sensor has not still not commercialized. Here, we applied a differential boron-doped diamond field effect transistor (FET) sensor to realize an all-solid-state pH device. A termination-controlled boron-doped diamond surface was successfully applied for the electrolyte - solution-gate FET (SGFET). To control pH sensitivity, a partially amino-and/or oxygen-terminated, a partially fluorine-terminated, and a hydrogen-terminated diamond SGFET sensor was evaluated. The oxygen-terminated SGFET had pH sensitivity of up to 40 mV/pH, whereas, a fluorine-terminated diamond SGFET had pH sensitivity of down to 4 mV/pH. The characteristics of differential SGFET measurement were studied by using a partially oxygen-terminated SGFET as pH-sensitive FET(ISFET) and a fluorine-terminated SGFET as reference FET(REFET), where a Pt electrode was employed as quasi-reference electrode.

# Disk Shaped Platinum Nanoelectrodes with Unexpected High Surface Area for the Detection of Hydrogen Peroxide

Alberto Citron, Dario Battistel, Carlo Bragato, Daniele Veciani, Salvatore Daniele  
*Department of Molecular Sciences and Nano systems, University Cà Foscari Venice, Calle Larga S.  
Marta 2137, 30123 Venice, Italy  
sig@unive.it*

The unique properties of nanoelectrodes such as high mass transport rate, fast electrochemical responses, rapid potential switching, small RC constants, and the ability to perform measurements in highly resistive solutions, have resulted in their application in a wide range of research areas, including fundamental electrochemical research, neurobiology and single cell studies, as well as in scanning electrochemical microscopy. Reproducible nanoelectrode fabrication with highly controlled electrode geometry can be achieved by pulling metal micro-wires into glass capillaries with the help of a laser pipette puller. In this way, gold, carbon, silver and platinum nanodisk electrodes have been fabricated. Among them, flat platinum or platinized metal/carbon nanoelectrodes have been mostly employed for the detection of reactive nitrogen and oxygen (ROS) species outside and inside a variety of biological cells. For ROS, and in particular for  $\text{H}_2\text{O}_2$ , platinum displays catalytic activity, which can further be enhanced by increasing the real surface area by modification of the geometrical area of the electrode with platinum black or mesoporous platinum films. Interestingly is to note that, by following proper procedures for the modification of the micro- and nano-electrode surface, the higher real surface area does not affect the general above mentioned properties of the small electrodes.

In a recent paper, it has been reported that platinum nanoelectrodes, prepared by the laser puller methodology, have displayed an effective (i.e., real) surface area ( $A_R$ ) much higher than that of the corresponding geometric surface area ( $A_G$ ). This was found by recording cyclic voltammograms in sulfuric acid solutions over the potential window where adsorption of hydrogen and oxygen species occurs. In this way, flat disk shaped platinum nanoelectrodes with a roughness factor ( $R_F = A_R/A_G$ ) as high as 800 has been found. This implies that, with these nanoelectrodes, electrode processes of surface sensitive electroactive species, such as  $\text{H}_2\text{O}_2$ , should be less affected by kinetic hindering.

In this paper we report on the voltammetric behaviour of a series of platinum nanoelectrodes, having radii over the range 15 – 1000 nm, in aqueous solutions containing  $\text{H}_2\text{O}_2$  over a wide concentration range in phosphate buffer media. The disk shaped nanoelectrodes were fabricated by pulling platinum wires into quartz capillaries. These electrodes, investigated in sulphuric acid solutions, displayed unexpected very high surface area ( $R_F$  up to a few thousands), which depended on the disk radius of the nanoelectrode. In particular, it was found that the lower was the electrode radius, the higher the  $R_F$  value. Also, the measurements performed with the nanoelectrodes in aqueous solutions containing  $\text{H}_2\text{O}_2$  in phosphate buffer media showed steady-state voltammetric responses, whose current values were much larger than those predicted on the basis of the geometric surface area and mass transport coefficient of the flat nanoelectrode. Moreover, steady-state currents for both the oxidation and reduction process of  $\text{H}_2\text{O}_2$  were linear over a wide concentration range (0.1mM – 30 mM). These results were explained as due to the higher  $R_F$  value of the nanoelectrodes, which, as for mesoporous or platinised nanoelectrodes, allowed overcoming the kinetic hindering that usually affects the electrode process of  $\text{H}_2\text{O}_2$  at flat platinum surface. Comparative measurements performed either in sulphuric acid or  $\text{H}_2\text{O}_2$  containing aqueous solutions with a classical polished platinum microelectrode 12.5  $\mu\text{m}$  radius supported the above hypothesis.

# Self-Assembled Layer-by-Layer Architectures for Electrochemical Sensors and Biosensors

Christopher M.A. Brett<sup>1</sup>, Madalina M. Barsan<sup>1</sup>, Melinda David<sup>2,3</sup>,  
Monica Florescu<sup>3</sup>

<sup>1</sup>*Department of Chemistry, Faculty of Sciences and Technology, University of Coimbra,  
3004-535 Coimbra, Portugal*

<sup>2</sup>*Facultatea de Fizica, Universitatea din Bucuresti, Magurele 077125, Romania*

<sup>3</sup>*Facultatea de Medicina, Universitatea Transilvania din Brasov,  
Brasov 500019, Romania  
cbrett@ci.uc.pt*

New self-assembled layer-by-layer (LbL) strategies for constructing thin, multilayer electrochemical sensors and biosensors have the potential to improve analyte access to the reaction sites and reduce the diffusion time of the analytes and reaction products, whilst also increasing sensor robustness. Self-assembly by electrostatic attraction as deposition methodology enables organised and stable architectures to be formed with less use of reagents in thin multilayer platforms. Such approaches have yet to be extensively exploited.

In recent work, carbon nanotubes (CNT) and graphene (G), as well as their nitrogen-doped analogues, have been investigated as electrode modifier materials, including in conjunction with redox polymers, as ways to enhance sensor performance. Doping CNT or G with nitrogen can increase the electronic conductivity, as already shown for nitrogen-doped CNT [1] and nitrogen-doped graphene (NG) which can catalyse important biologically-relevant reactions such as enzyme co-factor regeneration [2].

The advantages of the LbL technique for enzyme immobilization in chitosan matrices with CNT or G as electrical bridges have been investigated. Multilayer films containing glucose oxidase (GOx) together with NG dispersed in the biocompatible positively-charged polymer chitosan ( $\text{chit}^+(\text{NG} + \text{GOx})$ ), together with the negatively charged polymer poly(styrene sulfonate),  $\text{PSS}^-$  have been prepared [3], growth monitored by a quartz crystal microbalance and the benefits of nitrogen doping demonstrated. Characterisation of the films was done by cyclic voltammetry, electrochemical impedance spectroscopy and scanning electron microscopy.

The introduction of functional groups into CNT or G, by acidic or basic treatment, increases the specific capacitance and hydrophilicity which in turn influences the multilayer structure. These aspects have been investigated and the best functionalized carbon nanomaterial of the four for construction of a biosensor assembly incorporating glucose oxidase in the positively charged chitosan, with  $\text{PSS}^-$  as negatively charged layer, identified as basic functionalized graphene and acid-functionalised CNT; four bilayers lead to the best biosensor performance. Characterisation by voltammetric techniques and electrochemical impedance after deposition of each bilayer, sensor stability, and comparison with other glucose biosensors was carried out and will be discussed.

## References

- [1]. M.M. Barsan, R.C. Carvalho, Y. Zhong, X. Sun, C.M.A. Brett, *Electrochim. Acta*, 85 (2012) 203.
- [2]. M.M. Barsan, K.P. Prathish, X. Sun, C.M.A. Brett, *Sens. Actuators B*, 203 (2014) 579.
- [3]. M.M. Barsan, M. David, M. Florescu, L. Tugulea, C.M.A. Brett, *Bioelectrochemistry*, 99 (2014) 46.

# Biocompatible Quantum Dots and Conducting Polymer Nanocomposites in Disease Signalling Biosensors

E.I. Iwuoha

SensorLab, University of Western Cape,  
Department of Chemistry, P. Bag X17, Bellville, Cape Town, 7535, South Africa  
eiwuoha@uwc.ac.za

As biochemical species that indicate the occurrence or the severity of a disease, biomarkers and their detection have become very important in disease therapy. Notwithstanding the benefits of disease treatment with drugs, there is currently an intensified research work world-wide in several fields of study, focused on the development of novel diagnostic methods for early detection and screening of diseases such as cancers. Nanobiosensor systems for the detection of disease biomarkers were constructed at the University of Western Cape SensorLab by the incorporation of biological signaling elements onto biocompatible quantum dots<sup>1,2</sup> and conducting polymer nanocomposites<sup>3-6</sup>. Cancer disease biomarkers sensor to be presented include breast cancer genosensor for human epidermal growth factor receptor-2 (Her2/Neu oncogene) and coeliac disease immunosensor for anti-tissue transglutaminase antibody biomarker for gluten intolerance autoimmune disorder<sup>7</sup>. Other systems are DNA aptamer-based estrogen disrupting affinity sensor, 17 $\beta$ -estradiol receptorsens devised from estrogen receptor  $\alpha$ -recombinant protein (ER- $\alpha$ ) bio-sensitiser and quantum dots genosensors for telomerase reverse transcriptase RNA cancer biomarker. Stress signaling biosensor based on the determination of nitric oxide with a novel arabidopsis flavin monooxygenase<sup>8</sup> bioelectrode is also included in the presentation.

## References

- [1]. P. M. Ndangili *et al.* and E.I. Iwuoha; *J. Electroanal Chem*, 2011, 653, 67–74.
- [2]. J.C. Kemmegne-Mbougouen *et al.* and E.Iwuoha; *Inter J. Electrochem Sci*, 2014, 9, 478-492.
- [3]. R.F. Ajayi *et al.* and E.I. Iwuoha; *Electrochim Acta*, 2014, 128, 149–155.
- [4]. A.A. Baleg *et al.* and E.I. Iwuoha; *Electrochim Acta*, 2014, 128, 448–457.
- [5]. C.E. Sunday *et al.* and E.I. Iwuoha; *Electrochim Acta*, 2014, 128, 128–137.
- [6]. A. Venkatanarayanan, *et al.* and E. I. Iwuoha, *Electrochem Comm*, 2013, 31, 116–119.
- [7]. N. West *et al.* and E.I. Iwuoha; *J. Bioactive Compat Pol*, 2013, 28, 167-177.
- [8]. T. Mulaudzi *et al.* and E. Iwuoha; *FEBS Letters*, 2011, 585, 2693-2697.

# Nanoparticles Imprinted Polymers (NIP): Speciation of Nanoparticles

Daniel Mandler, Shlomit Kraus, Netta Bruchiel-Spanier, Yamit Pisman, Maria Hitrik  
*Institute of Chemistry, The Hebrew University of Jerusalem*  
*Jerusalem 9190401, Israel*  
[daniel.mandler@mail.huji.ac.il](mailto:daniel.mandler@mail.huji.ac.il)

Nanotoxicity is a new discipline, which requires the development of appropriate tools for determination of nanoobjects such as nanoparticles (NPs). These tools are also crucial for monitoring the interactions between nanoobjects and organisms. These interactions are affected by the core, size, shape, and stabilizing shell of the objects. Hence, speciation of NPs, is becoming of utmost importance. There are known approaches for measuring single particles based on their size. However, simple, miniature and inexpensive sensors for specific NPs detection based on the criteria mentioned above are not available yet.

We will present a new concept for selective recognition of NPs by a polymeric matrix imprinted with the same NPs. This approach can be classified as nanoparticle imprinted polymer (NIP) in analogy to the well-known concept of molecularly imprinted polymers (MIP)] in which the molecular analyte is imprinted in a polymer by polymerization of proper monomers with which it chemically associates. The removal of the template forms complementary cavities capable of selective recognition of the analyte.

We have shown that the NIP concept works in three different systems. The first<sup>1</sup> is based on forming a polyaniline matrix that extracted Au NPs stabilized by citrate to form NIPs, which showed high selectivity based on the size of the NPs. The Au NPs were removed by electrochemical oxidation to form voids that were used as size exclusion matrix. Moreover, we showed that increasing the thickness of the matrix by deposition of multilayers increased the selectivity. The second system<sup>2</sup> was assembled using cellulose acetate in which hydrophobic Au NPs were incorporated. This system showed selectivity based on the thickness of the NPs shell. In the third system<sup>3</sup> a different strategy was used. Namely, the NP were first attached to the surface and then the free area was filled with molecular species, such as oleic acid. The latter wrapped the Au NPs, which were further removed. The reuptake process showed again high selectivity toward Au and Ag NPs of the same size and shape as initially imprinted.

In conclusion, we have developed a new and promising approach for sensing nanoparticles based on their size, structure and shell based on imprinting thin films.

1. S. Kraus-Ophir, J. Witt, G. Wittstock; D. Mandler; *Angew. Chem. Int. Ed.* 2014, 53, 294-298
2. N. Bruchiel-Spanier and D. Mandler, *ChemElectroChem*, <http://dx.doi.org/10.1002/celc.201402407>
3. M. Hitrik, Y. Pisman, G. Wittstock and D. Mandler, in preparation

# Stability-enhanced Screen-Printed Ion-Selective Electrodes (SPISEs) for Plant Factory and Smart Farming Applications

Chieh-Wen Yao, Chia-Hao Chang, Chih-Hao Chen, Che-Lun Chang, Hung-Yun Liao, and  
Lin-Chi Chen\*

*Department of Bio-Industrial Mechatronics Engineering, National Taiwan University  
 No.1, Sec. 4, Roosevelt Rd., Da'an Dist., Taipei City 10617, Taiwan (R.O.C.)*

*\*E-mail: [chenlinchi@ntu.edu.tw](mailto:chenlinchi@ntu.edu.tw)*

Modern farming systems, such as plant factory, vertical farming, and information technology-based smart farming, have been developed worldwide recently to cope with food security and safety issues in response to the rapid growth of population (especially in urban areas) and CO<sub>2</sub> emission. This emerging sustainable topic provides electrochemical ion-selective electrodes (ISEs) promising opportunities and niches in future crop cultivation quality control. Viewing cost and size disadvantages of traditional ISEs, our lab has devoted to research and develop novel screen-printed ISEs (SPISEs) technology for real-time or off-line sensing the essential macro-elemental ions (K<sup>+</sup>, Ca<sup>2+</sup>, Mg<sup>2+</sup>, NH<sub>4</sub><sup>+</sup>, NO<sub>3</sub><sup>-</sup>, SO<sub>4</sub><sup>2-</sup>, and PO<sub>4</sub><sup>2-</sup>) for plant growth. In addition to small size, low cost, easy for mass production, and all solid state, our SPISEs also feature a stability-enhancing ion-to-electron transducer (IET) layer in between the ion-selective membrane (ISM) and carbon paste electrode (CPE). Thus, the SPISEs are able to eliminate the potential instability problem (potential drift) in long-term hydroponic nutrient monitoring (Fig. 1). This is because that the IET layer can prevent the formation of a penetrated “water layer” during long-term in-solution monitoring that hinders ion-to-electron transduction between ISM and CPE and decreases ISE sensitivity and selectivity. Meanwhile, the IET layer itself made of an electroactive material can facilitate the ion-to-electron transduction. In this presentation, we will discuss how to select an IET layer material from a list of carbon nanomaterials and conducting polymers, such as amino-modified MWCNT, MWCNT-ester, polypyrrole, polythiophene and poly-o-aminophenol according to water layer test (Fig. 2), charge-transfer resistance estimation, double-layer capacitance measurement, and contact angle characterization. Besides, we will present the sensitivity, selectivity, response time characteristics of a panel of SPISEs based on an ideal poly-o-aminophenol IET layer. We will also show the practical use of SPISEs for hydroponic nutrient sensing in combination with our homemade electronic reader that can transmit the ion-sensing data simultaneously to a smart phone via a Bluetooth module. With this presentation, we will demonstrate how classical ISEs are reshaped for green electrochemistry for tomorrow's society.

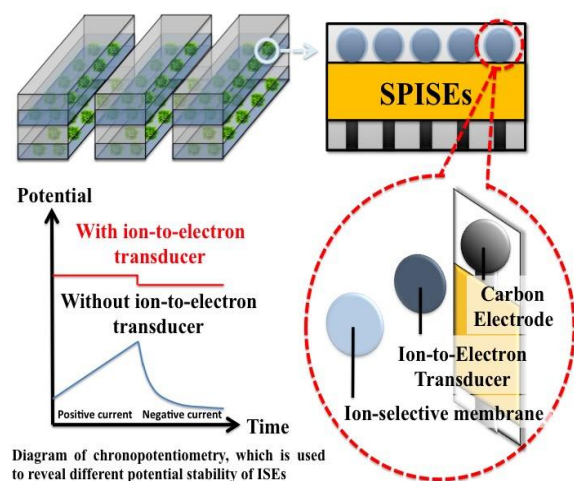


Fig. 1 Idea of stability-enhanced SPISE for plant nutrient monitoring in a modern farming system

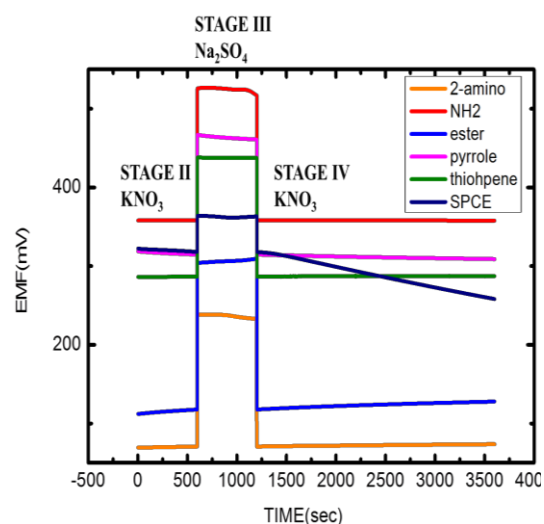


Fig. 2 Water layer test of different IET layer materials for a NO<sub>3</sub><sup>-</sup> SPISE

# Novel Microfluidic Electrochemical Sensors for Thin-Layer based Flow Analysis Systems

Ana Fernández-la-Villa<sup>1</sup>, Diego F. Pozo-Ayuso<sup>1</sup>, Jorge Elizalde<sup>2</sup>, María Tijero<sup>2</sup>, Mario Castaño-Álvarez<sup>1\*</sup>

<sup>1</sup>*MicruX Technologies. Severo Ochoa Bldg. Julián Clavería s/n, Floor -1, Room 4 & 6, 33006 Oviedo (Asturias) SPAIN.*

<sup>2</sup>*IK4-IKERLAN. P<sup>o</sup> JM<sup>a</sup> Arizmendiarieta 2, 20500 Arrasate (Gipuzkoa) SPAIN*

*\*[mcastano@micruxfluidic.com](mailto:mcastano@micruxfluidic.com)*

Electrochemical sensors as well as microfluidic platforms are of increasing interest for the development of novel smart analytical tools for Lab-on-a-Chips (LOC) or Point-of-Care (POC) systems. The integration in a single device of microfluidics and electrochemical sensors could pave the way to enhance the miniaturization, portability, automation as well as throughput of multiplexing analysis for several applications.

In this sense, thin-film microtechnologies enable the fabrication of metal-based (micro)electrodes with high precision and resolution in a cost-effective way. Moreover, these technologies are also suitable for the development and integration of microfluidic stages in the same device. Thus, a single microfluidic device with integrated electrochemical sensors could be developed by using an optimized photolithographic process.

In this work, a simple microfluidic chip with integrated (micro)electrodes has been designed, manufactured and evaluated. The new microfluidic electrochemical sensor has been designed for using in a flow injection analysis (FIA) system with a thin-layer approach. The basic layout of the microfluidic sensor is shown in **Figure 1**.

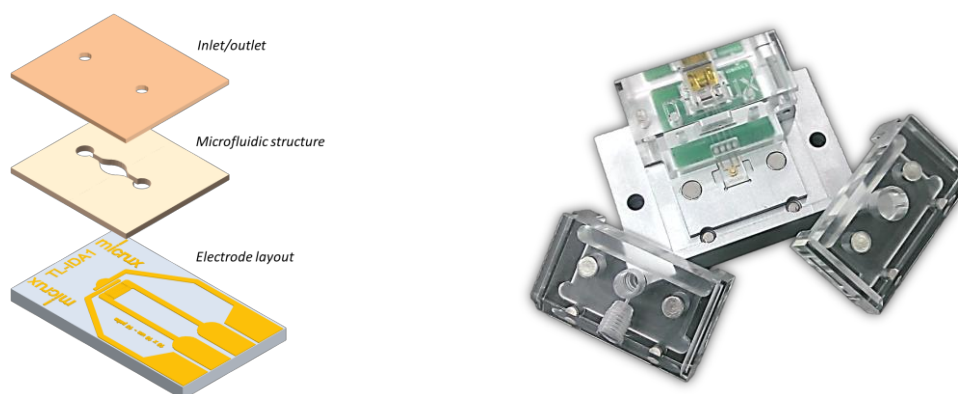


**Figure 1.** Basic layout of the microfluidic electrochemical sensor and AIO platform for using the chips

The full-integrated chips consist of a glass substrate in which the (micro)electrodes are manufactured. Two different electrode approaches were designed; a basic **three-electrode system** (SE) and an **interdigitated microelectrode array** (IDA). A SU-8 resin layer is used for the construction of the microfluidic structure on the glass substrate with the electrodes. Finally, a SU-8 film is used as cover with the inlet/outlet for closing the microfluidic structure, getting the final integrated chip.

The new microfluidic sensor was coupled to a basic flow system by using an innovative multipurpose interface: **All-in-One** (AIO) platform (**Figure 1**). A special add-on, including an inlet and outlet, was developed for integrating the new chip in the FIA system and performing the electrochemical measurements. Thus, the novel thin-layer based flow system enable an excellent control of the fluids through the electrodes, decreasing the use of sample (<20  $\mu$ L) and reagents, but keeping a high sensitivity with very low dead-volume.

The performance of the new microfluidic electrochemical sensors has been evaluated with different phenolic compounds in the FIA system.

*This work has been supported by the Spanish Ministry of Economy and Competitiveness under project RTC-2014-1496-1 (RETOS-COLABORACIÓN)*

# Determination of Fast Electrode Kinetics Using Fourier Transformed Large Amplitude AC Voltammetry

Jie Zhang, Kiran Bano, Si-Xuan Guo and Alan M. Bond

School of Chemistry and Australian Research Council Centre of Excellence for Electromaterials Science,  
Monash University, Clayton, Victoria 3800, Australia  
*Jie.zhang@monash.edu*

Measurement of fast electrode kinetics close to the reversible limit is subject to substantial uncertainties. The concept of using an internal reference for the determination of fast electrode kinetics to minimize the uncertainties has been developed and applied to the Fourier transformed large amplitude AC voltammetry. Kinetic parameters (i.e. electron transfer rate constant,  $k^0$ , and electron transfer coefficient,  $\alpha$ ) do not influence the voltammetric characteristics of a reversible process. Consequently, when the reversible process is employed as an internal reference, predetermined experimental parameters, such as electrode area ( $A$ ), concentration ( $C$ ), diffusion coefficient ( $D$ ) and uncompensated resistance ( $R_u$ ), which often encounter uncertainties, can be reliably and conveniently calibrated based on theory-experiment comparisons. Then, the new  $A$ ,  $C$ ,  $D$  and  $R_u$  values can be used for the determination of electrode kinetics associated the process of interest through theory-experimental comparison exercises with  $k^0$  and  $\alpha$  as the unknown parameters. In this way, the impact of systematic errors in the parameters  $A$ ,  $C$ ,  $D$  and  $R_u$  on the measurement of electrode kinetics near the reversible limit is significantly diminished. Application of this method is demonstrated with respect to electron transfer kinetics associated with oxidation of tetrathiafulvalene (TTF), where the  $\text{TTF}^{0/+}$  process is used as a reversible internal reference for the measurement of the quasi-reversible kinetics of the  $\text{TTF}^{+/2+}$  process. The more generalized concept of an internal reference is also demonstrated by use of the  $\text{Fc}^{0/+}$  ( $\text{Fc}$  = ferrocene) reversible process as an internal reference for measurement of the kinetics of the  $\text{Cc}^{+/0}$  ( $\text{Cc}^+$  = cobaltocenium) process. Via the internal reference approach, heterogeneous charge transfer rate constants of  $0.55 \text{ cm s}^{-1}$  was obtained for the  $\text{TTF}^{+/2+}$  process at a glassy carbon electrode and  $2.7 \text{ cm s}^{-1}$  for the  $\text{Cc}^{+/0}$  one at a carbon fiber microelectrode in acetonitrile (0.1 M  $\text{Bu}_4\text{NPF}_6$ ).

## References:

1. Guo, S.-X.; Bond, A.M.; Zhang, J. *Rev. Polarogr.* **2015**, in press.
2. Bano, K.; Zhang, J.; Bond, A.M. Unwin, P.R.; Macpherson, J.V. *J. Phys. Chem. C* in press.
3. Bano, K.; Zhang, J.; Bond, A.M. *J. Phys. Chem. C* **2014**, *118*, 9560-9569.
4. Bond, A.M.; Bano, K.; Adeel, S.; Martin, L.L.; Zhang, J. *ChemElectroChem* **2014**, *1*, 99-107.
5. Bano, K.; Nafady, Ayman; Zhang, J.; Bond, A.M. *J. Phys. Chem. C* **2011**, *115*, 24153-24163.
6. Zhang, J.; Guo, S.-X.; Bond, A.M. *Anal. Chem.* **2007**, *79*, 2276-2288.
7. Bond, A.M.; Duffy, N.W.; Guo, S.-X.; Zhang, J.; Elton, D. *Anal. Chem.* **2005**, *77*, 186A-195A.



# Patterning of Microelectrode Array with soft lithography for Biological Sensing

Meining Zhang

*Department of Chemistry, Renmin University of China, Beijing 100872, China*

*e-mail mnzhang@ruc.edu.cn*

Biological analysis, environmental monitoring, food safety and disease diagnosis require sensitive, low-cost and multiplex assay. Microelectrode array (MEA) could meet these requirements and has been receiving significant attention because of its advantages such as higher sensitivity (versus macroelectrode) benefited from the enhanced mass transportation, improved signal-to-noise ratio and larger current response (versus microelectrode). So far, the fabrication of regular MEA has been accomplished mainly by depositing an insulating layer on a macroelectrode surface and then making patterned holes in this layer with photolithography, which were often prohibitively expensive and time-consuming. Soft lithography has been proved to be a rapid and cost-effective method to form and transfer patterns and structures. Our group commits to develop various soft lithography for fabricating MEA. We reproducibly fabricated regular Au band MEA with hydrogel etching and proposed a new technique to fabricate reduced graphene oxide (rGO)-based MEA with microtransfer molding. The developed MEA showed a lower detection limit and a larger current density for the detection of biological compounds, such as  $\text{H}_2\text{O}_2$ , dopamine, as compared with the macroscopic electrode.

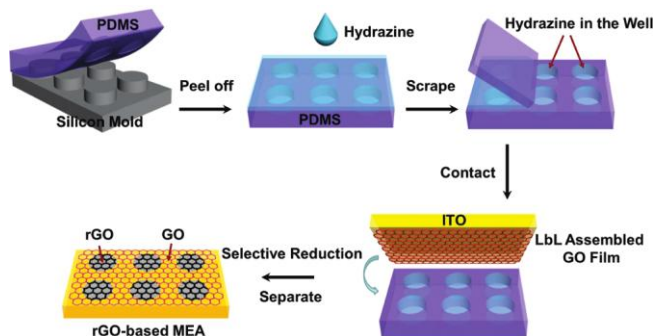


Figure 1 Schematic illustration of the procedures for fabrication of rGO-based MEA.

ACKNOWLEDGMENT: We gratefully acknowledge the financial support from National Natural Science Foundation of China (Grant 21175151)

## REFERENCES

1. B. D. Gates, Q. Xu, M. Stewart, D. Ryan, C. G. Willson and G. M. Whitesides, *Chem. Rev.*, 105: 1171-1196(2005).
2. X. Tang, D. Zhao, J. He, F. Li, J. Peng and M. Zhang, 85: *Anal. Chem.*, 1711-1718 (2013).
3. F. Li, M. Xue, X. Ma, M. Zhang and T. Cao, *Anal. Chem.*, 83: 6426-6430 (2011).
4. J. He, X. Ma, Y. Zhu, F. Li, X. Tang, X. Zhang and M. Zhang. *Electrochem. Commun.*, 3:67-70 (2013)

# Controllable Synthesis of Heteroatom-Doped Carbon Nanotubes under Atmospheric Pressure and Their Electrocatalytic Ability to L-cysteine

Yu-Chen Chang<sup>1</sup>, Yi-Ting Chen<sup>2</sup>, Guan-Lin Chen<sup>1</sup>, Kuo-Chuan Ho<sup>2</sup>, Wei-Hung Chiang<sup>1</sup>

<sup>1</sup>Department of Chemical Engineering, National Taiwan University of Science and Technology, Taipei 10607, Taiwan

<sup>2</sup>Department of Chemical Engineering, National Taiwan University, Taipei 10617, Taiwan  
No.43, Sec. 4, Keelung Rd., Da'an Dist., E2-510, Taipei 106, Taiwan (R.O.C.)  
whchiang0102@gmail.com

L-cysteine (L-cys), a sulfur containing amino acid, plays a crucial role in regulating the biological activity of certain proteins, peptides and enzymes. Low level of L-cys is related to myriad of diseases, including slow growth in children, lethargy, liver damage, loss of muscle and fat, skin lesions, and weakness. However, current L-cys sensing techniques require intensive pretreatments, purifications with low sensitivity. As a result, developing a relatively easy, selective and sensitive L-cys biosensor in physiological study and clinical diagnosis is highly demanded. Recent works have suggested that heteroatom-doped carbon nanomaterials such as carbon nanotubes (CNTs) and graphenes as novel materials with exceptional properties for electrochemical applications including energy storage and electrochemical sensing. However, current synthesis methods of heteroatom-doped carbon nanomaterials usually involve complicated vacuum systems, making it difficult to enable industrial-scale production. Therefore, the development of a controllable synthesis of heteroatom-doped carbon nanomaterials at atmospheric pressure will lead to important advances on both scientific studies and innovation applications.

Here we demonstrate an atmospheric-pressure, solution-assisted optimized substitution method to produce heteroatom-doped CNTs with varying heteroatoms including B, P, and S. Pristine multi-walled CNTs (MWCNTs) synthesized using a water-assisted chemical vapor deposition (CVD) were used as starting materials. The heteroatom-doped CNTs were then produced by heating the mixture of heteroatom precursor and MWCNTs under argon (Ar) atmosphere from 400 to 1200°C for 1 to 4 hour at atmospheric pressure. Systematic micro Raman intensity ratio ( $I_D/I_G$ ) of the D- and the G- bands indicated the density of defects which induced by heteroatom doping. S-CNTs possess more defects than others and from 2D-band shift, B-CNTs behave more like n-type semiconductor (Fig. 1(a)). Extensive X-ray photoelectron spectroscopy (XPS) indicated that the heteroatoms were successfully doped into the  $sp^2$  graphene lattice of CNTs. The electrical conductance was improved by heteroatom doping (Fig. 2(b)). We found that heteroatom concentrations in the nanotubes could be tuned by controlling the reaction temperature and time. Furthermore, thin-film electrical conductance characterization using a four-point probe method confirmed the electrical conductance of the as-prepared heteroatom-doped CNTs.

Electrochemical characterization shows different performances among B-CNT, P-CNT and S-CNT in Fig. 1(c). The results show that B-CNT possesses the best electrocatalytic ability. It has the lowest overpotential and the highest current density. P-CNT, although does not have an obvious oxidation peak, still shows a relatively large current density. As for S-CNT, the result shows there is nearly no difference between S-CNT and pristine CNT.

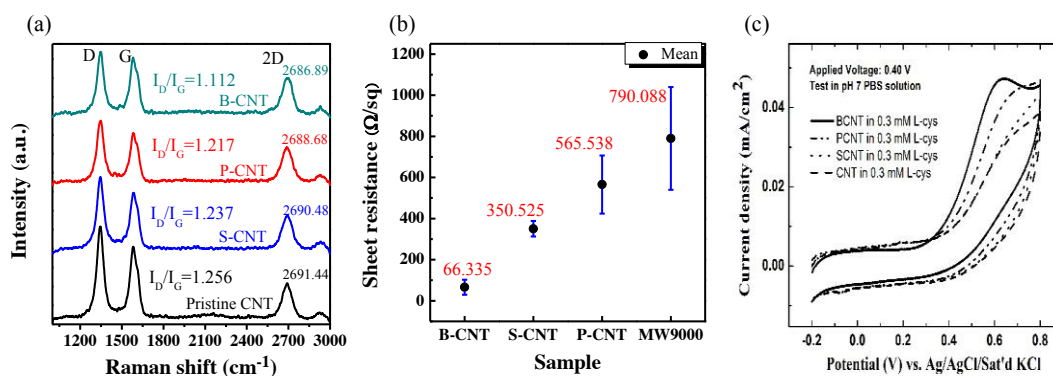


Figure 1. (a) Raman spectra of different atoms doped CNT by solution-assisted substitution method. (b) Resistance of conductive thin-film (PVDF) fabricated by different atoms doped CNT. (c) Cyclic voltammetry of pristine CNT (dash), S-CNT (dot), P-CNT (dash dot dot) and B-CNT (solid).

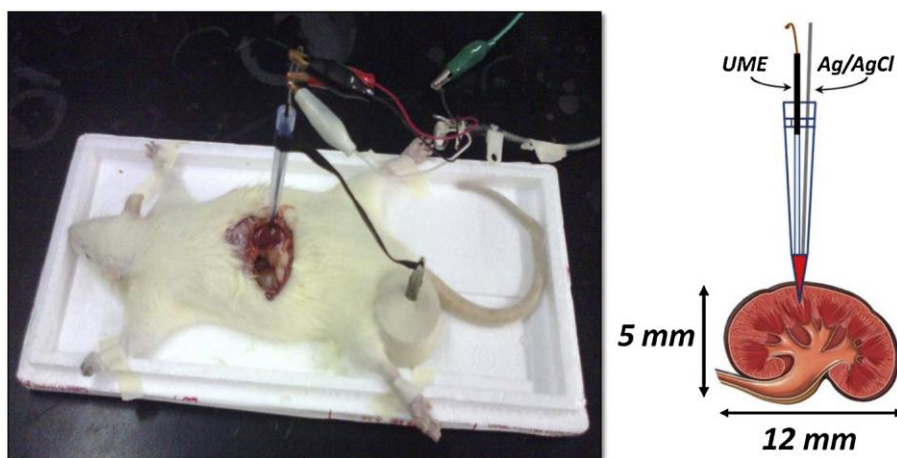
# In Vivo Electrochemical Assessment of Possible Melatonin Effect on Nitric Oxide Production From Kidneys of Sub-Acute Lead Treated Rats

Gonzalo Ramirez-Garcia<sup>1,2</sup>, Sophie Griveau<sup>1</sup>, Minerva Martínez-Alfaro<sup>2</sup>, Silvia Gutierrez-Granados<sup>2</sup> and Fethi Bedioui<sup>1</sup>

<sup>1</sup> *Unité de Technologies Chimiques et Biologiques pour la Santé, PSL Research University, Chimie ParisTech, Paris, 75005, France*

<sup>2</sup> *Departamento de Química, Universidad de Guanajuato, Guanajuato, 36000, Mexico  
(fethi.bedioui@chimie-paristech.fr)*

Nitric oxide (NO) is known to be implicated in various renal diseases induced by lead poisoning and recent works have shown the effect of some antioxidants in reducing the toxic effects of lead. Melatonin is attractive for its direct and indirect antioxidant effects; furthermore it is naturally produced in mammals, including humans. Recently, it has been shown that melatonin attenuates the toxic effects of sub-acute lead intoxication in kidneys without altering NO metabolites concentration. This work demonstrates the use of nickel tetrasulfonated phthalocyanine/polyphenol-modified ultramicroelectrodes to monitor in vivo and in situ changes of NO within rat kidneys. NO itself was detected directly and in real-time inside the kidney of lead and melatonin treated rats after induction by L-arginine. The results indicate that NO production decreases in lead treated rats, likewise in co-treated with melatonin rats. In addition, melatonin administration did not affect the production of NO respect to the control. By means of these experiments was verified that melatonin does not alters NO production in kidneys during sub-acute lead intoxication (1).



(1) G. Ramirez-Garcia, M. Martinez-Alfaro, S. Gutierrez-Granados, A. Alatorre-Ordaz, S. Griveau, F. Bedioui, *Electrochim. Acta* 166 (2015) 88-92

# **Combined Tyrosinase (A Multi-Potent Enzyme) and Electrodes Modified with nanoparticles for Fast and Highly Sensitive Environmental Monitoring and Medical Diagnostics**

Judith Rishpon, Michal Mossberg  
*Tel-Aviv University*  
*Ramat-Aviv, Israel*  
*Judithri@Tauex.tau.ac.il*

Tyrosinase is a copper-containing enzyme present in plant and animal tissues that catalyzes the production of melanin and other pigments from tyrosine by oxidation. Tyrosinase plays a dominant role in environmental monitoring, food control and medical diagnostic due to its affinity for aromatic compounds nominates.

Dense arrays of self-assembled nanostructures are highly important for the fabrication of high-performance sensors of large surface area. The diphenylalanine (FF), the core recognition motif of the  $\beta$ -amyloid polypeptide, self assembles into discrete nanotubes (Peptide nanotubes, PNTs). Carbon nanotubes (CNTs), were discovered earlier, and are being used extensively for many years in electrochemical biosensors, due to their excellent mechanical and electrical properties and good stability.

We have developed a sensitive and fast biosensor for phenolic compounds using the enzyme Tyrosinase as bio recognition element. Screen printed working electrodes were modified with numerous nano particles (carbon nano tubes and various peptide nano tubes) and we investigated their contribution on the biosensor sensitivity. It was evident from the conducted amperometric experiments, that the modified electrodes had a significantly higher signal, compared to the untreated electrode.

We investigate the inhibition of Tyrosinase using several pesticides. Nano particles modifications were applied on the electrode and studied. In order to monitor environmental contaminants which serve as Tyrosinase inhibitors, we used a microflow system and immobilized Tyrosinase on modified Nanoparticles screen printed electrodes. Our data shows highly sensitive detection (nM range) of parathion, dichlorovos, diazinon and other pesticides.

In addition, a new electrochemical method of detecting and diagnosing melanoma based on melanoma biomarker was developed and its feasibility demonstrated. The method is based on an electrochemical biosensor platform comprised of a special biochip and device, performing a multi-channel amperometric detection of the enzymatic activity of tyrosinase, an enzyme biomarker of melanoma. The newly developed biosensor platform is able to electrochemically detect Tyrosinase activity in fresh biopsy samples. This bioelectrochemical detection method is rapid, yielding results within minutes from biopsy removal. Using "as is" biopsy samples, without pre-treatment, simplifies the process, saves time and reduces cost and labor dramatically.

In conclusion, the Tyrosinase electrochemical biosensors present exciting opportunities for on-site sensitive monitoring of environmental and food contaminants. The cancer diagnostic tools may pave the way towards decentralized clinical applications.

# Selective Proton Pump for Thin Layer Chemical Modulations

Gastón A. Crespo, Majid Ghahraman Afshar and Eric Bakker  
Department of Inorganic and Analytical Chemistry,  
University of Geneva, Quai Ernest-Ansermet 30, CH-1205 Geneva.  
gaston.crespo@unige.ch

We report on a general concept based on a selective electrochemical ion pump used for creating concentration perturbations in thin layer samples (~40  $\mu\text{L}$ ). As a first example, protons are released from a selective polymeric membrane actuator and the resulting pH is assessed potentiometrically with a second membrane placed directly opposite. By applying a constant potential modulation for 30-s, an induced proton concentration of up to 350 mM may be realized. This concept may become an attractive tool for in-situ titrations without the need for sampling, since the thin layer eventually re-equilibrates with the bulk sample. Acid-base titrations of NaOH and  $\text{Na}_2\text{CO}_3$  are demonstrated. The determination of total alkalinity in a river water sample is carried out, giving levels (23.1 mM) comparable to that obtained by standard methods (23.6 mM). The concept may be easily extended to other ions (cations, anions, polyions) and may become attractive for environmental and clinical applications.

Concentration gradients can be modulated in the entire thin layer sample, by applying either an external current or potential to an appropriate ion-transferring element placed (i.e., ion-selective membrane) in contact with the solution. Aiming to demonstrate this idea, we report here on a new fundamental concept that imposes a controlled and selective proton release on a thin layer sample with subsequent potentiometric readout. The thin layer eventually re-equilibrates with a solution of larger volume, allowing one to achieve repeated localized titrations without sampling or volumetric delivery.

Figure 1 schematically shows the thin layer titration concept for a strong acid-base pair (i.e., HCl-NaOH). The electrochemical cell is composed of two key elements, the hydrogen ion actuator and the pH detector. The thin layer solution is delimited by the flat geometry of both elements. The proton pump is a fast diffusive hydrogen ion-selective membrane that acts as a working electrode (WE) in a three-electrode cell with the respective counter (CE) and reference electrode ( $\text{RE}_1$ ) placed outside of the thin layer. The applied potential or the applied current is controlled by a potentiostat/galvanostat that allows the current to flow between the working and the counter electrode while the potential is simultaneously measured between the working and the reference electrode. Opposite to the actuator, a less diffusive pH responsive membrane based on poly(vinylchloride) is located (detector). This membrane is measured at zero-current against a second reference electrode ( $\text{RE}_2$ ) in the outside solution. As expected for a pH probe, the potential readout is linear with pH according to the Nernst equation. This electrochemical configuration combines dynamic and equilibrium electrochemistry bridged by a thin layer sample.

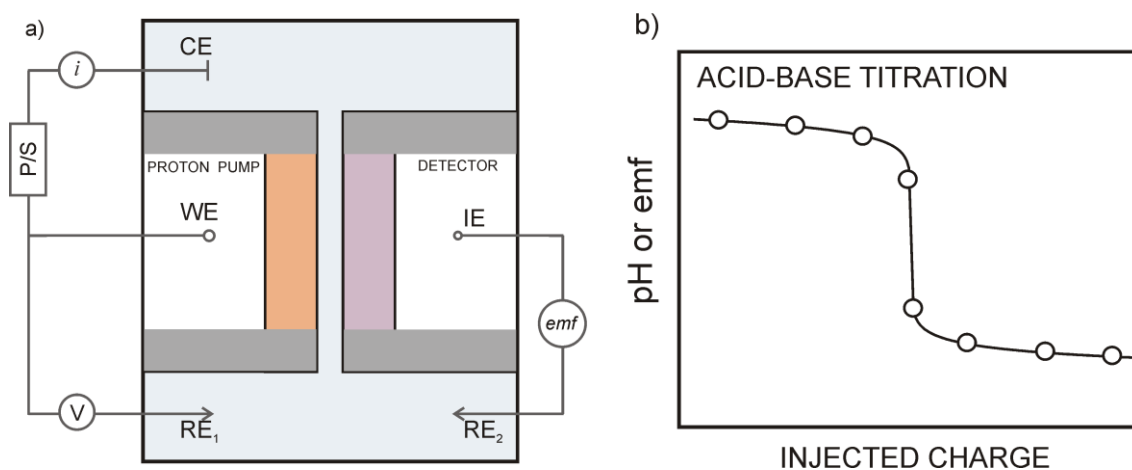


Figure 1 - Schematic illustration of the reported concept. a) Electrochemical cell composed of proton pump and detector proton selective membrane M1 (orange) and M2 (purple), respectively. WE: working electrode, RE: commercial reference electrode, CE: Pt rod, IE: indicator electrode, V: potential reader, i: current reader, P/S: power supply, emf: potentiometer. b) Acid-base titration output signal.

# Gold nanoparticles-modified physically small carbon sensors towards sensitive and selective As(III) detection in aquatic samples

Wycliff Tupiti, Shaneel Chandra

*School of Biological and Chemical Sciences, The University of the South Pacific, Private Mail Bag, Suva  
FIJI*

*chandra\_s@usp.ac.fj*

We present in this work for the first time, new physically small gold nanoparticles-modified carbon electrodes (typically 2  $\mu\text{m}$  diameter and 4  $\mu\text{m}$  axial length) that are capable of rapid and sensitive detection applied towards As(III) detection in aquatic samples have been developed. As is a Group 15 metalloid prevalent in trace levels in the natural environment [1]. In natural waters, it can exist in two different oxidation states depending on the environment and the ratio of As(V) to As(III) in natural water is usually 0.1:1 to 10:1, although As(V) is thermodynamically favored [2].

Arsenic species behave differently in terms of mobility, bioavailability, toxicity, and thus arsenic speciation information is required to understand its biogeochemical cycling and potential toxicity of waters [3]. Its toxic form is As(III) and it is therefore useful to be able to measure this form of the element.

A common challenge in the study of As(III) using conventional carbon-based electrodes is that the species is largely undetected in the absence of surface modification. In this regard, modifications of the carbon surface with gold nanoparticles or gold-based sensors have been previously demonstrated to work successfully. However these have largely focused on using either gold nanoparticles onto conventional glassy carbon electrodes [4], gold nanoparticles with multi-walled carbon nanotubes on glassy carbon electrodes [2], gold wire [3], or gold microwire housed inside polythene tube [5] for instance, which have employed sensing tips greater than those reported in this study.

Physically small carbon electrodes with nanometer dimensions were prepared in our laboratory and characterized prior to and following modification with gold nanoparticles modification were used to selectively detect As(III) in aquatic samples. The electrochemical behaviour of several redox systems including hexamineruthenium(III) chloride, potassium ferricyanide and sulphuric acid was studied to characterize the modified electrodes. The findings from these studies, together with the performance of the electrodes in As(III) detection in aquatic samples will be reported.

## References

- [1] Wilson, S. C.; Lockwood, P. V.; Ashley, P. M.; Tighe, M. (2010) The chemistry and behaviour of antimony in the soil environment with comparisons to arsenic: A critical review, *Environ. Pollut.*, 158 (5), 1169-1181.
- [2] Xiao, L.; Wildgoose, G. G.; Compton, R. G. (2008) Sensitive electrochemical detection of arsenic (III) using gold nanoparticle modified carbon nanotubes via anodic stripping voltammetry, *Anal. Chim. Acta.*, 620 (1-2), 44-49.
- [3] Gibbon-Walsh, K.; Salaün, P.; van den Berg, C. M.G. (2010), Arsenic speciation in natural waters by cathodic stripping voltammetry, *Anal. Chim. Acta.*, 662 (1), 1-8.
- [4] Dai, X.; Nekrassova, O.; Hyde, M. E.; Compton, R.G. (2004), Anodic Stripping Voltammetry of Arsenic (III) Using Gold Nanoparticle-Modified Electrodes, *Anal. Chem.*, 76 (19), 5924-5929.
- [5] Salaün, P.; Planer-Friedrich, B.; van den Berg, C. M.G. (2007), Inorganic arsenic speciation in water and seawater by anodic stripping voltammetry with a gold microelectrode, *Anal. Chim. Acta.*, 585 (2), 312-322.

# Salt-on-a-chip: Miniaturized Ionic Liquid Systems

Christian Andre Gunawan, Richard Gondosiswanto, Mengchen Ge, Chuan Zhao  
*School of Chemistry, The University of New South Wales*  
*Kensington Campus, Sydney, New South Wales, 2052*  
*christian.gunawan@unsw.edu.au*

Lab-on-a-chip and miniaturized systems have gained significant interest due to dramatic differences in material at the micron-nano scale realm including, material conservation, rapid response or reaction time, and for some cases high product yield.<sup>1,2</sup> Nevertheless, in order to fully exploit their chemistry, solvent volatility problems have to be solved and the reproducibility need to be improved and simplified.<sup>3</sup>

Ionic liquids (ILs) are a class of solvents that typically have negligible vapor pressure with excellent thermal and chemical stability.<sup>4</sup> They have demonstrated applications in many fields of science including electrochemistry. However, the use of ionic liquids in macro scale is often not efficient owing to their poor mass transport as a result of intrinsic high viscosities.

We show in this presentation our effort in fabrication of extremely small ionic liquid drops and microstructures as open, “wall-less” microreactors and sensors on a chip surface that can be part of an electrochemical or spectroscopic system. The micropatterned ionic liquid droplets have been demonstrated as ‘open’ micro-electrochemical cells and photoreactors for microfabrication of metals and charge transfer complexes, substrates for immobilisation of protein forming biological microarray and as membrane-free high-performance amperometric gas sensor array. The results suggest that miniaturised ionic liquid systems can provide a versatile platform for novel applications of ionic liquids.

## References:

- (1) Hogan, J. *Nature* **2006**, *442*, 351.
- (2) Dubois, P.; Marchand, G.; Fouillet, Y.; Berthier, J.; Douki, T.; Hassine, F.; Gmouh, S.; Vaultier, M. *Anal. Chem.* **2006**, *78*, 4909.
- (3) Christian, A. G.; Mengchen, G.; Chuan, Z. *Nature Communications* **2014**, *5*.
- (4) Freemantle, M. *An Introduction to Ionic Liquids*; Royal Society of Chemistry, 2010.

# Achieving diffusional independence in arrays of liquid-liquid nanointerfaces: improving the electroanalytical performance

Damien W. M. Arrigan,<sup>1,\*</sup> Yang Liu,<sup>1</sup> Masniza Sairi,<sup>1</sup> Gregor Neusser<sup>2</sup> and Christine Kranz<sup>2</sup>

<sup>1</sup>Nanochemistry Research Institute, Department of Chemistry, Curtin University, GPO Box U1987, Perth, WA 6845, Australia

<sup>2</sup>Institute of Analytical and Bioanalytical Chemistry, University of Ulm, Albert-Einstein-Allee 11, 89081 Ulm, Germany

e-mail: d.arrigan@curtin.edu.au

Electrochemistry at the interface between two immiscible electrolyte solutions (ITIES) provides a simple route to detect non-redox-active ions. Amperometry or voltammetry at the ITIES enables detection of a range of targets, ranging from inorganic ions [1] to biological macromolecules [2]. Miniaturised ITIES, to the microscale and nanoscale [3], have been explored in recent years to achieve an improved sensing and detection capability, e.g. in terms of sensitivity, limits of detection and stability. While the currents are reduced in line with the interface size, current densities are increased due to the enhanced mass transport from radial diffusion. This low current is overcome by use of arrays of micro- or nano-ITIES, which then brings into question design features such as separations between individual elements in the array so as to achieve diffusional independence. In the recent years we have prepared nano-ITIES arrays using electron beam lithography [4] and focused ion-beam milling [5], to create nanopores in membranes at which the ITIES can be formed. FIB offers scope for rapid prototyping of arrays, while EBL is excellent for patterning of large arrays in parallel.

In this work, independent radial diffusion at arrayed nanoITIES was examined. The nanoITIES were formed at nanopores fabricated by FIB milling of silicon nitride (SiN) membranes, which enabled preparation of nanopore array designs with different ratios of pore centre-to-centre distance ( $r_c$ ) and pore radius ( $r_a$ ). These five array designs were used to form arrays of nanoITIES and the transfer of tetrapropylammonium across the water – 1,6-dichlorohexane interface was employed to examine the mass transport effects of the array designs. It was found that the diffusion-limited current for ion transfer increased with the value of  $r_c/r_a$ , reaching a plateau at the theoretical current expected for radial diffusion to an array of non-interacting inlaid interfaces. This indicates that mass transport at the individual nanoITIES was greatly enhanced due to the decreased overlap of diffusion zones at adjacent nanointerfaces. Furthermore, the electroanalytical performance parameters of sensitivity and limit of detection were shown to be at their best when larger  $r_c/r_a$  ( $\geq 56$ ) values were employed. On the basis of these experimental findings, the development of arrayed nanoITIES devices for electrochemical sensing can be improved.

[1] Z. Samec, E. Samcova, H.H. Girault, *Talanta*, 2004, 63, 21.

[2] D.W.M. Arrigan, *Annu. Rep. Prog. Chem., Sect. C: Phys. Chem.*, 2013, 109, 167.

[3] S. Liu, Q. Li, Y. Shao, *Chem. Soc. Rev.*, 2011, 40, 2236.

[4] M.D. Scanlon, J. Strutwolf, A. Blake, D. Iacopino, A.J. Quinn, D.W.M. Arrigan, *Anal. Chem.*, 2010, 82, 6115.

[5] M. Sairi, N. Chen-Tan, G. Neusser, C. Kranz, D.W.M. Arrigan, *ChemElectroChem*, 2015, 2, 98.



# Cancer Stage Identification by Scanning Electrochemical Microscopy: Investigation of Tyrosinase inside Melanoma Tissues

*Tzu-En Lin, Fernando Cortés-Salazar, Andreas Lesch, Alexandra Bondarenko, and Hubert H. Girault*  
*Ecole Polytechnique Fédérale de Lausanne, Laboratoire d'Electrochimie Physique et Analytique*  
*Station 6, CH-1015 Lausanne, Switzerland*  
*tzu-en.lin@epfl.ch*

Melanoma is one of the most lethal cutaneous malignancies that strikes thousands of people around the world. Indeed, the survival rate depends on the stage of the cancer when it is diagnosed. Therefore, the early diagnosis and unequivocal identification of cancer stages are of high relevance. Since the appearance of melanomas often resembles moles, for its further identification, the microscopic analysis by immunohistochemistry (IHC), fluorescence in situ hybridization (FISH), or comparative genomic hybridization (CGH) are usually performed to confirm the diagnosis[1, 2]. Unfortunately, the read-out of IHC by fluorescent staining, which is one of the most employed methods, could be affected by autofluorescence and photobleaching, leading to wrong diagnosis.

In contrast, electrochemistry has shown to provide efficient tools for the monitoring of malignant tumors by the precise detection of cancer biomarkers, while avoiding common limitations found in optical techniques (*e.g.* sample background, oxygen concentration or light scattering). Scanning electrochemical microscopy (SECM) is a useful scanning tool since it enables the localization of target biomolecules with a high spatial resolution. With this aim, we employed SECM for mapping precisely the presence of the melanoma biomarker tyrosinase. The electrochemical detection of tyrosinase on skin tissue samples from melanoma patients was performed by a sandwich immunoassay readout by SECM (Fig. 1a).

We will demonstrate that we have not only been able to detect the overexpression of tyrosinase on melanoma tissues, but also to differentiate melanoma stages based on the distinct tyrosinase immunopositivity that characterizes each melanoma stage [3]. Implementation and optimization of the proposed approach, as well as, the SECM read out of melanoma tissues will be presented (Fig. 1b). Furthermore, envisioning the possibility of converting SECM as a quick electrochemical screening tool of malignant melanoma, soft linear arrays of microelectrodes have been employed for high throughput analysis. We demonstrate that SECM coupled with immunoassay strategies provides a promising approach for better diagnosis and understanding of the spatial distribution of tyrosinase, and generally it offers great possibilities to study a wider variety of processes on cancer tissues in a reliable manner.

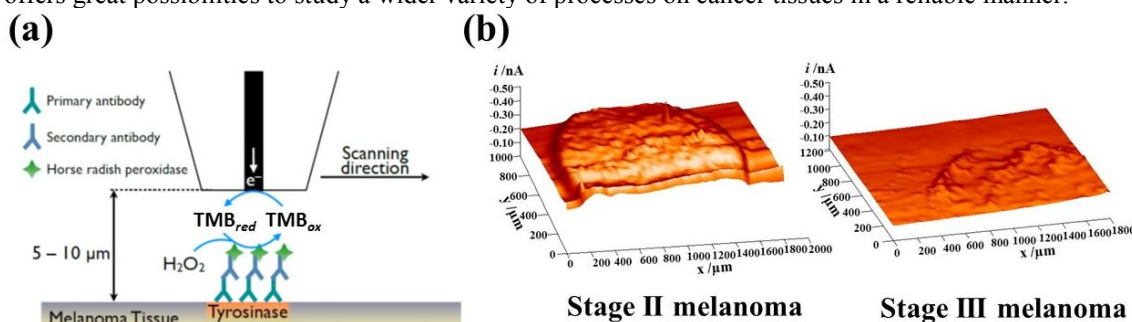


**Fig. 1.** (a) Schematic representation of tyrosinase detection in melanoma by SECM. (b) SECM images of a stage II and III melanoma tissue.

- [1] Z. Jehan, S. Uddin, K. S Al-Kuraya, In-situ hybridization as a molecular tool in cancer diagnosis and treatment, *Curr. Med. Chem.* 19 (2012) 3730-8.
- [2] G. Palmieri, P. Sarantopoulos, R. Barnhill, A. Cochran, *Molecular Pathology of Melanocytic Skin Cancer*, Skin Cancer, Springer, 2014, pp. 59-74.
- [3] G.F. Hofbauer, J. Kamarashev, R. Geertsen, R. Böni, R. Dummer, Tyrosinase immunoreactivity in formalin- fixed, paraffin- embedded primary and metastatic melanoma: frequency and distribution, *Journal of cutaneous pathology* 25 (1998) 204-9.

**Acknowledgements:** Taiwan Government for the 2013 MOE Technologies Incubation Scholarship.

# Nano-Hydrogel Modified Carbon Nanotubes Electrodes for Antioxidant Monitoring in Complex Samples

Andreas Lesch,<sup>a,#</sup> Fernando Cortés-Salazar,<sup>a</sup> Sunny Maye,<sup>a</sup> Véronique Amstutz,<sup>a</sup> Philippe Tacchini,<sup>b</sup> Hubert H. Girault<sup>a</sup>

<sup>a</sup> École Polytechnique Fédérale de Lausanne, Lausanne, Switzerland

<sup>b</sup> Edel for Life, Lausanne, Switzerland

# andreas.lesch@epfl.ch

The rapid, reliable and low-cost monitoring of the global antioxidant (AO) content in several biological fluids such as blood bags or beverages is of great interest in the human health sector as well as in the food industry. By transforming excess reactive oxygen species into harmless compounds, AOs can counterbalance oxidative stress conditions. Knowing the AO concentration can provide information about the status of the AO defense system, which is mainly composed of enzymes, metal chelators, drugs and dietary AOs such as ascorbic acid.

One approach to measure directly the AO concentration is by using voltammetric methods. However, biological samples consist usually of complex sample matrices that can influence the electrode surface and consequently the measured signal. Recently, we have demonstrated the batch production of disposable, stand alone carbon nanotubes (CNTs) sensors on polyimide by multi-layer inkjet printing.<sup>[1]</sup> These electrodes showed highly reproducible and homogeneous active electrode areas presenting a quasi-reversible electrochemical behavior adequate for amperometric sensing. Relevant sample information are mathematically extracted from the linear sweep voltammograms and an antioxidant power is determined by using a pseudo-titration concept.<sup>[1]</sup>

Herein, we present a strategy to cover the CNT electrodes with a nanometer thin layer of a polyacrylamide (PA) hydrogel (Fig. 1) which is generated by the simultaneous inkjet printing and UV photopolymerization of self-made inks containing the monomer acrylamide and the cross-linker *N,N'*-methylene-bis-acrylamide in the presence of a photoinitiator and catalyst.<sup>[2]</sup> Within the ink formulation a pre-polymerization step has been introduced to adjust the viscosity of the ink and to enhance the rate of polymerization leading to very stable nano-hydrogel/ CNT electrodes that can be used without pre-treatment. We characterized those PA-modified CNT electrodes optically and electrochemically and applied them for the direct AO monitoring in untreated red wine, fresh orange juice containing pulp and fibers and also in erythrocyte concentrates. In comparison to bare CNT and carbon paste electrodes (CPEs), the nanometric PA coating can compensate for matrix effects showing lower potentials and higher measured currents.

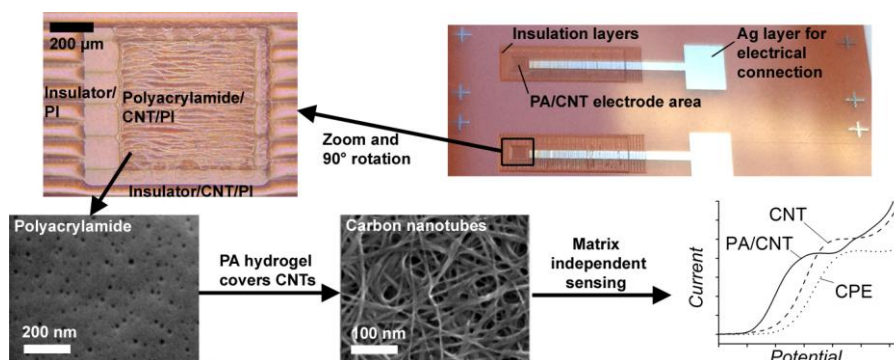


**Figure 1.** Fully inkjet-printed, nano-polyacrylamide hydrogel/CNT electrodes for matrix independent antioxidant monitoring.

## References:

- [1] A. Lesch, F. Cortés-Salazar, M. Prudent, J. Delobel, S. Rastgar, N. Lion, J.-D. Tissot, P. Tacchini, H. H. Girault, *J. Electroanal. Chem.* **2014**, 61, 717-718.
- [2] A. Lesch, F. Cortés-Salazar, V. Amstutz, P. Tacchini, H. H. Girault, *Anal. Chem.* **2015**, 87, 1026–1033.

# Analytical Applications of Paper and Textiles in Microfluidic Sampling and Sample Handling Integrated with Electrochemical Sensors

Grzegorz Lisak<sup>1</sup>, Jingwen Cui<sup>1</sup>, Sylwia Strzałkowska<sup>2</sup>, Thomas Arnebrant<sup>3</sup>, Tautgirdas Ruzgas<sup>3</sup>, Johan Bobacka<sup>1</sup>

<sup>1</sup>Åbo Akademi University, Johan Gadolin Process Chemistry Centre, c/o Laboratory of Analytical Chemistry, Biskopsgatan 8, FIN- 20500 Åbo-Turku, Finland

<sup>2</sup>University of Warsaw, Department of Chemistry, Pasteura 1, 02-093 Warsaw, Poland

<sup>3</sup>Department of Biomedical Sciences, Faculty of Health and Society, Biofilms- Research Centre for Biointerfaces, Malmö University, 20506 Malmö, Sweden  
email address: grzegorz.lisak@gmail.com

Potentiometric sensing utilizing paper- and textile-based microfluidic sampling was applied and evaluated for the determination of clinically ( $\text{Na}^+$ ,  $\text{K}^+$ ,  $\text{Cl}^-$ ), industrially and environmentally ( $\text{Cd}^{2+}$ ,  $\text{Pb}^{2+}$  and pH) relevant analytes. In this technological design, calibration solutions and samples were absorbed into sampling substrates (paper, textile). The potentiometric sensors (ion-selective electrodes and reference electrode) were pressed against that substrate while the micro volumes of absorbed liquid closed electric circuit between the two electrodes allowing electrochemical detection of ions. All-solid-state ion-selective electrodes coupled with reference electrode were successfully applied in electrochemical sensing utilizing paper- and textile-based microfluidic sampling. In this method, the sampling substrate acts simultaneously as a sampling unit and as a sample container [1, 2, 3].

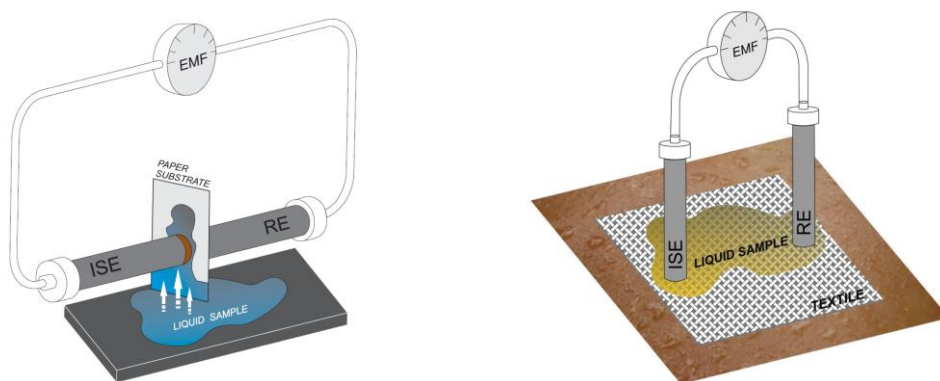


Figure 1. Illustration of the potentiometric setup utilizing paper-based (left) and textile-based sampling (right).

As illustrated in Figure 1, the study was done in two sampling modes: paper substrate kept vertical or parallel to the sample surface. Various sampling substrates were investigated for the use in a wide spectrum of applications. Microfluidic sampling was investigated by using paper substrates including three ashless filter papers with different pore size, hospital cotton tissue, dirt-free tissue paper and delicate task wipes. The studied textile substrates included cotton, polyamide, polyester and their blends with elastane. Various samples, such as ground water, moisten soil, food products and artificial serum were used to validate new possibilities for direct chemical analysis of small-volume samples.

## References:

- [1] J. Cui, G. Lisak, S. Strzałkowska, J. Bobacka, *Analyst*, 139 (2014) 2133.
- [2] G. Lisak, J. Cui, J. Bobacka, *Sensors and Actuators B*, 207 (2015) 933.
- [3] G. Lisak, T. Arnebrant, T. Ruzgas, J. Bobacka, submitted (December 2014) to *Analytica Chimica Acta*.

# Reduced graphene oxide modified electrodes: from glucose sensing to electrochemical delivery of insulin

Sabine Szunerits

*Institut d'Electronique, de Microélectronique et de Nanotechnologie (CNRS UMR8520), Université Lille 1, Cité Scientifique, avenue Poincaré, BP 60069, 59652 Villeneuve d'Ascq, France*

[Sabine.Szunerits@iri.uni-lille1.fr](mailto:Sabine.Szunerits@iri.uni-lille1.fr)

Diabetes has been assigned next to cancer, cardiovascular and chronic respiratory diseases as the most leading cause of death and disability. A close monitoring of blood glucose concentrations plays a significant role in the diagnostics and prevention of diabetes and tremendous efforts have been put into the development of blood glucose sensors.<sup>1</sup> In this presentation, a special focus will be given on the use of reduced graphene oxide (rGO) nanohybrids for the sensitive sensing of glucose in an enzyme free manner.<sup>2,3</sup> Boronic acid modified rGO as well as electrophoretically formed rGO/Ni(OH)<sub>2</sub> were used for this purpose and their fabrication and sensing characteristics will be discussed.

Moreover, reduced graphene oxide matrixes have shown additionally compliant with efficient insulin loading and release.<sup>4</sup> In type 1 diabetes, absolute deficiency of insulin production results from massive auto-immune destruction of pancreatic beta cells. For this reason, the main therapy consists in delivering exogenous insulin. The treatment methods require numerous daily injections of insulin administered by subcutaneous needle injection, insulin pen and catheters connected to insulin pumps. In this presentation, the advantage of flexible electrodes modified with reduced graphene and loaded with insulin, to electrically trigger insulin release over time will be presented. A special focus will be on the development of insulin-impregnated conductive matrixes and the influence of potential and current on the biological activity of released insulin.

## References

1. (a) J. Wang, Chem. Rev. 2008, 108, 814-825; (b) N.S. Olivier, C. Toumazou, A. E. Casse, D. G. Johnston, Diabet. Med. 2009, 26, 197-210.
2. Q. Wang, I. Kaminska, J. Niedziolka-Jonsson, M; Opallo, M. Li, R. Boukherroub, S. Szunerits, Biosensors and Bioelectronics, 2013, 50, 331-337.
3. P. Subramanian, J. Niedziolka-Jonsson, A. Lesniewski, Q. Wang, M. Li, R. Boukherroub, S. Szunerits, J. Mater. Chem A, 2014, 2, 5525-5533.
4. K. Turcheniuk, M. Khanal, A. Montorina, P. Subramanian, A. Barras, V. Zaitsev, V. Kuncer, A. Leca, A. Martoriati, K. Cailliau, J.-F. Bodart, R. Boukherroub, S. Szunerits, RSC Adv. 2014, 4 (2) 865-875.

# Highly Sensitive Electrochemical Sensor for Cu (II) Ions Based on Three-dimensional Porous $\text{H}_x\text{TiS}_2$ Nanosheet-polyaniline

Xiaorong Gan, Huimin Zhao\*

Key Laboratory of Industrial Ecology and Environmental Engineering (Ministry of Education, China),  
School of Environmental Science and Technology, Dalian University of Technology, Dalian, 116024,  
China.

e-mail : zhaohuim@dlut.edu.cn

Heavy metal ions as harmful pollutants in the biosphere can result in toxicology and cellular effects even though the human body suffered from chronic exposure<sup>[1]</sup>. Thereinto, abnormal levels of copper ions may greatly damage the liver or kidney of the organisms and cause a series of diseases. Therefore, it is still desirable to develop novel and reliable methods for sensitive and selective assaying of copper ions. Traditional methods for  $\text{Cu}^{2+}$  detection have some limitations such as time-consuming sample pretreatment and sophisticated instrumentation skills. In contrast, electrochemical sensors as emerging technologies showed many advantages for heavy metal ions due to their excellent sensitivity, short analysis time, portability and low cost. Until now, the reported strategies for constructing electrochemical sensors have been developed mainly based on the signal simplification using nanomaterials, enzymes and aptamers etc.

In the study, based on the strong coordination between the nitrogen atoms in polyaniline (PANI) and the transition metal centers of metal dichalcogenides<sup>[2]</sup>, we first synthesized three types of different morphology and structures of hydric titanium disulfide ultrathin ( $\text{H}_x\text{TiS}_2$ ) nanosheet-PANI nanocomposites with different mass ratios of  $\text{H}_x\text{TiS}_2$  nanosheet vs. aniline monomer (1:3.5, 1:1.5 and 1:0.5, respectively), and investigated their electrochemical performances. It was found that the incorporation of  $\text{H}_x\text{TiS}_2$  nanosheets as a suitable substrate can regulate the growth of PANI on the surface of  $\text{H}_x\text{TiS}_2$  nanosheets. As the mass ratio of  $\text{H}_x\text{TiS}_2$  nanosheet vs. aniline monomer was 1:1.5, the obtained nanocomposites showed three-dimensional (3D) porous architectures which were composed of the interconnected  $\text{H}_x\text{TiS}_2$  nanosheets with the help of polymerization reactions of aniline. The nanocomposites modified glass carbon electrode (GCE) showed higher interfacial charge transfer rate, better stability and lower overpotential of  $\text{Cu}^{2+}$  detection than those of other  $\text{H}_x\text{TiS}_2$  nanosheet-PANI nanocomposites. Based on the 3D porous nanocomposites, we developed a novel electrochemical sensor to directly detect trace amount of  $\text{Cu}^{2+}$  by square wave anodic stripping voltammetry (SWASV), and discovered that its high selectivity was contributed to the coordination interaction between  $\text{Cu}^{2+}$  and the nitrogen atoms of the imine moieties in PANI. In addition, the electrochemical sensor exhibited a high sensitivity with a detection limit of 0.7 nM (S/N=3) and a linear range from 25 nM to 5  $\mu\text{M}$  under optimal conditions. The high sensitivity was due to the high conductivity of both PANI and  $\text{H}_x\text{TiS}_2$  nanosheets and the unique 3D porous architectures. The as-formed electrochemical sensor showed good potential in  $\text{Cu}^{2+}$  detection in situ in real water.

This work was supported by National Natural Science Foundation of China (No. 21277016) and the Research Project of Chinese Ministry of Education (No. 113017A).

## References

- [1] Sayadi, M. H.; Rezaei, M. R.; Rezaei, A. *Environ. Monit. Assess.* **2015**, *187*, 4110-4121.
- [2] Tang, H. J.; Wang, J. Y.; Yin, H. J.; Zhao, H. J.; Wang, D.; Tang, Z. Y. *Adv. Mater.* **2014**, *27*, 1117-1123.

# Amplified Electrochemical Analysis of DNA and Proteins

Huangxian Ju

State Key Laboratory of Analytical Chemistry for Life Science, Department of Chemistry, Nanjing University, Nanjing 210093, P. R. China.  
*e-mail address:* hxju@nju.edu.cn

In last two years, we continued to bring nanotechnology and molecular biological technology into the design of electrochemical biosensing strategies, which led to a series of amplified methods for sensitive detection of DNA and protein.

Two porphyrin-encapsulated metal-organic frameworks were used as electrochemical catalytic probes to couple with the designed molecular switches for electrochemical DNA sensing.<sup>1a,b</sup> With gold nanoparticle catalyzed silver deposition and surface circular strand-replacement polymerization, a DNA detection method was proposed.<sup>1c</sup> Two electrochemiluminescent DNA sensors were designed by using carbon nitride nanosheet as emitter for loading of hemin labeled single-stranded DNA and hybridization with a molecular beacon to form hemin/G-quadruplex architecture for signal inhibition.<sup>1d,e</sup> The photoelectrochemical platforms with quantum dot-functionalized porous ZnO nanosheets and catalytic hairpin assembly-programmed porphyrin-DNA complex were also developed for DNA detection.<sup>1f,g</sup> A highly selective detection method for microRNA was presented based on distance-dependent electrochemiluminescence resonance energy transfer between CdTe nanocrystals and Au nanoclusters.<sup>2</sup>

Four electrochemical immunoassay methods for detection small molecules and tumor markers were developed by nanostructure assembly of host-guest linked gold nanorod superstructure,<sup>3a</sup>  $\beta$ -cyclodextrin-functionalized AuPd bimetallic nanoprobe,<sup>3b</sup> platinum nanodendrite functionalized graphene nanosheets,<sup>3c</sup> and nanogold/mesoporous carbon foam-mediated silver.<sup>3d</sup> Three ultrasensitive immunoassay based on electrochemiluminescent quenching of quantum dots along with new quenching mechanisms were designed.<sup>4</sup> More recently, three ratiometric electrochemical proximity assay methods for sensitive one-step protein detection was proposed.<sup>5a,b,c</sup> And an amplified electrochemical immunosensing method for protein biomarker was developed through target-driven triple-binding formation of MNzyme.<sup>5d</sup>

## References:

1. a) Anal. Chem. 87, 3957-63 (2015); b) Biosens. Bioelectron. 10.1016/j.bios.2015.04.046; c) Biosens. Bioelectron. 39, 199-203 (2013); d) Biosens. Bioelectron. BIOS-D-15-00184, in revision; e) Nanoscale 5, 5435-41 (2013); f) Nanoscale 6, 2710-17 (2014); g) Anal. Chem. 10.1021/acs.analchem.5b00888.
2. Biosens. Bioelectron. 51, 431-36 (2014).
3. a) Biosens. Bioelectron. 45, 195-200 (2013); b) Anal. Chem. 85, 6505-10 (2013); c) J. Mater. Chem. B 1, 5347-52 (2013); Biosens. Bioelectron., 52, 153-58 (2014).
4. J. Mater. Chem. C 1, 299-306 (2013); Chem. Commun. 49, 2106-08 (2013); Anal. Chem. 85, 5390-6 (2013).
5. a) Sci. Rep. 4, 4360 (2014); b) Anal. Chem. 86, 7494-9 (2014); c) Biosens. Bioelectron. 66, 345-9 (2015); d) Anal. Chem. 87, 1694-700 (2015).

## Acknowledgements

We gratefully acknowledge National Basic Research Program (2010CB732400), and National Natural Science Foundation of China (21135002, 21121091).

# **Characterization of Polycrystalline Doped-diamond Electrolyte-solution-gate Field-effect Transistor pH Sensor with/without termination control**

Yukihiro Shintani<sup>1,2</sup>, Kotaro Ogawa<sup>2</sup>, Hiroshi Kawarada<sup>1</sup>

*1 School of Science and Engineering Waseda University, 3-4-1 Okubo, Shinjuku-ku, Tokyo, 169-8555, Japan*

*2 Research and Business Development Dept., Innovation Center, Yokogawa Electric Corporation*

*2-9-32 Nakacho, Musashino-shi, Tokyo, 180-8750, Japan  
shintani@toki.waseda.jp*

A rapid sensing of pH in solution is of great interest for chemical industry. A glass-type electrode becomes the de facto global standard for pH sensing device, and it is widely used in laboratory and manufacturing process. However, in addition to its instability in fluorine-containing solution such as hydrofluoric acid, an alkaline error is known as serious issue. Furthermore, the glass-type electrode possesses fragile nature and difficulties in miniaturization. Thus, alternative pH electrode is still desirable. A diamond is an excellent candidate since it has wide electrochemical potential window, superior robustness, highly flexible surface modification, and high chemical inactivity. In our previous study, an electrolyte-solution-gate field-effect transistor (SGFET) utilizing a non-doped diamond surface as gate channel was sensitive to various ions, and the diamond termination control can led to the adjustment of pH sensitivity. Here, we proposed a polycrystalline boron-doped diamond channel solution-gate FET. A hydrogen-terminated boron-doped layer was formed on a non-doped diamond film on Si substrate by CVD deposition, and it was employed as SGFET gate channel whose pH sensitivity was down to 10mV/pH. To evaluate pH sensitivity of various diamond terminations, the hydrogen-terminated boron-doped diamond channels were changed to oxygen- termination by UV-ozone treatment, and fluorine-termination by ICPRIE. Fluorine-terminated diamond SGFETs were less-sensitive to pH, whereas, diamond SGFET with partially oxygen-terminated gate surface was sensitive to pH up to 40 mV/pH.

# Investigation of cell aging by analysis of electrolyte decomposition via gas chromatography

Simon Theil, Margret Wohlfahrt-Mehrens  
ZSW-Zentrum für Sonnenenergie- und Wasserstoff-Forschung  
Helmholtzstrasse 8, D-89081 Ulm, Germany  
*simon.theil@zsw-bw.de*

The electrochemical performance of lithium ion batteries can be highly influenced by electrolyte degradation. On the one hand, solvent decomposition is, in case of graphite anodes, intended to build up the SEI. On the other hand it can result in several negative effects, such as pressure build-up because of gaseous decomposition products, loss of lithium due to formation of organic lithium salts, excessive filming on anode and cathode resulting in higher resistance and drying-out of the cell. Most of the decomposition reactions lead to byproducts which are soluble in the electrolyte. By analysing those byproducts it is possible to draw conclusions about the type and quantity of electrolyte decomposition.

For electrolyte analysis we used a Headspace gas chromatography (HS-GC) method due to its high sensitivity to low boiling species and its applicability for LiPF<sub>6</sub> containing electrolyte. The experiments have been performed by aging pouch full cells.

The work mainly focused on two parts of the electrolyte decomposition: Firstly on monitoring the consumption of the well known additive vinylene carbonate (VC), secondly on analysis of the byproducts resulting from solvent decomposition.

The aim was to investigate the type and amount of decomposition during formation as well as during long term aging. Monitoring VC consumption in the first charge of the formation gave information about the build up of the SEI in terms of anode potential, graphite surface and electrolyte composition.

Analysing electrolyte decomposition after storage or long term cycling via gas chromatography could be correlated with several conditions and parameters of the cell. Firstly the influence of electrode balancing and current density, leading to different degrees of lithium plating was investigated. Secondly the effect of the applied potential window, set by the cut-off voltage or changed by switching to different active materials, could be analysed. Furthermore, those experiments have been performed with electrolytes containing different solvent and different amount of additives. The correlation of the change of the electrochemical performance with the electrolyte decomposition led to a deeper understanding of the link between cell aging and electrolyte degradation.

**Acknowledgments:** Financial support from Deutsche Forschungsgemeinschaft (DFG, Functional materials and material analysis for lithium high power batteries, PAK 177) and Bundesministerium für Wirtschaft und Energie (BMW, Project NP-LiB, Förderkennzeichen 01MX12047B) is gratefully acknowledged.



# **Suppression of degradation of lithium ion batteries for $\text{LiFePO}_4\text{@C}$ batteries by nano Si surface modification**

Wenyu Yang, Xiang Chen, Mingzhong Zou, Guiying Zhao, Jiaxin Li, Yingbin Lin, Zhigao Huang\*

College of Physics and Energy, Fujian Normal University, Fujian Provincial Key Laboratory of Quantum Manipulation and New Energy Materials, Fuzhou, 350117, China

**Abstract:** Si nanoparticles are deposited uniformly on the  $\text{LiFePO}_4\text{@C}$  electrode by a spray technique. And the effect of Si incorporation on the electrochemical performances of  $\text{LiFePO}_4\text{@C}$  18650 cylindrical cells is investigated systematically by charge-discharge testing, cyclic voltammograms, AC impedance spectroscopy, respectively. At the same time, the aging and degradation of those cells have been studied. Non-destructive electrochemical methods were used to examine the capacity loss, voltage drop, resistance change, lithium loss, and active material loss during the life testing. The measuring results of the cycle life indicated that the capacity loss was strongly influenced by the rate, temperature, surface modification and discharge states (DOS). Especially, nano Si surface modification suppresses greatly the degradation of those cells. Moreover, the rate, temperature, time, and surface modification dependences of the cycle life were discussed.

# Dealing with Interferences in the Electrochemical Detection of Arsenic – a Complexometric Masking Approach

O.A. Arotiba<sup>a,b</sup>, O.A. Idris<sup>a</sup>, N. Mabuba<sup>a</sup>

<sup>a</sup> *Department of Applied Chemistry, University of Johannesburg, Doornfontein 2028, South Africa*

<sup>b</sup> *Centre for Nanomaterials Science Research, University of Johannesburg, South Africa*  
oarotiba@uj.ac.za

Arsenic, a highly toxic element, has been known to cause many adverse health effects such as dermal changes, gastrointestinal disorder, respiratory impairment, and cancer in human<sup>1</sup>. Contamination of ground water by arsenic has been documented in several countries, where arsenic in drinking water was above the guide line value of the maximum concentration of arsenic in water, which is 10 ppb by the World Health Organisation<sup>2</sup>. The detection of arsenic (III) using stripping voltammetry is a very sensitive, simple and plausible route in comparison to other classical methods such as atomic absorption spectroscopy and inductively couple plasma. However, this electrochemical technique is hampered by few interferences especially copper which gives a false increase in arsenic concentration<sup>3</sup>. In the bid to tackle this copper interference, we present the square wave anodic stripping voltammetric (SWASV) determination of As (III) in the presence of Cu (II) using aqueous ammonia as a complexing agent. Gold nanoparticle (AuNPs) were electrochemically deposited on a glassy carbon electrode (GCE) using cyclic voltammetry to form GCE-AuNP electrode. The modified electrode was electrochemically characterised in  $[\text{Fe}(\text{CN})_6]^{3-/4-}$  redox probe. Arsenic (III) with and without Cu (II) was detected using SWASV. Ammonia solution was then added to the arsenic solution with and without copper while the voltammetric responses were recorded. Our results showed that ammonia was able to selectively mask Cu (II) in the As (III) solution by forming a complex. A detection limit of ca 5 ppb for As (III) in the presence of Cu (II) ion of was calculated. This approach was used for real samples with excellent recovery. This method was further validated by comparing it to inductively coupled plasma technique where a good correlation was observed. Our work such presents a simple and novel way of dealing with interferences in heavy metal sensing using stripping voltammetry.

## References

1. L. Cai, Z. Xud, P. Baoc, M. He, L. Douc, L. Chend, Y. Zhouc and Y. Zhuc. Multivariate and geostatistical analyses of the spatial distribution and sources of arsenic and heavy metals in agricultural soils in Shunde, Southeast China. *Journal of Geochemical Exploration* 148 (2015) 189-195.
2. T. Sorga, A. Chen and L. Wang. Arsenic species in drinking water wells in the USA with high arsenic concentrations. *Water research* 48 (2014) 156-169.
3. T. Ndlovu, B. Mamba, S. Sampath, R. Krause and O.A Arotiba. Voltammetric detection of arsenic on a bismuth modified exfoliated graphite. *Electrochimica Acta* 128 (2014) 48-53.

# Microwave-Assisted Synthesis of Graphene Oxide Nanoribbons Using Green Chemistry for the Electrochemical Detection

Huei-Ping Liou<sup>1</sup> and Chia-Liang Sun<sup>1\*</sup>

<sup>1</sup> Department of Chemical and Materials Engineering, Chang Gung University,  
Kwei-Shan, Tao-Yuan 333, Taiwan

\*E-mail address: sunchialiang@gmail.com

## Abstract

The process to create graphene nanoribbons (GNRs) from carbon nanotubes (CNTs) can be divided into several categories, including wet chemical methods, physicochemical methods, intercalation exfoliation, catalytic approaches, electrical methods, and so on. In many of the published examples, microwave heating has been shown to dramatically reduce reaction time, increase product yields, and enhance product purities by reducing unwanted side reactions compared with conventional heating methods. [1, 2] Following the trend of eco-conscious, using various methods to reduce the use of chemicals which would pollute the environment in any process is of great interests to scientists. In this study, we demonstrated that the addition of  $\text{KNO}_3$  besides  $\text{KMnO}_4$  can reduce the use of  $\text{H}_2\text{SO}_4$  volume in our microwave-assisted process. Transmission electron microscopy (TEM) were used to examine the morphology and structure of our products. i.e. graphene oxide nanoribbons (GONRs), using much less acid than that in the original recipe. Figure 1 illustrated the core-shell CNT/GONR heterostructure. [1] Furthermore, GONRs were adopted to modify the glassy carbon (GC) electrodes for the electrochemical detection of ascorbic acid (AA), dopamine (DA) and uric acid (UA). After reducing  $\text{H}_2\text{SO}_4$  volume down to 40 %, cyclic voltammograms in Figure 2 showed the similar anodic oxidation currents of AA using GONRs fabricated by the early and green recipes.

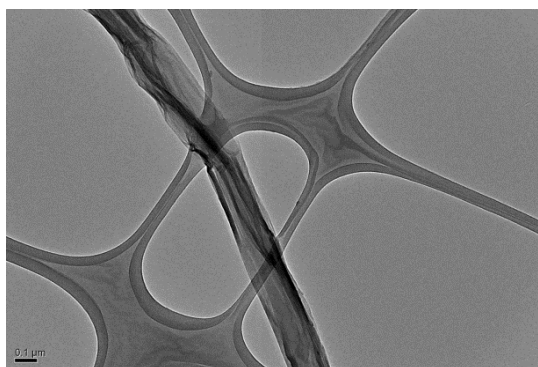


Fig. 1 TEM images of GONR

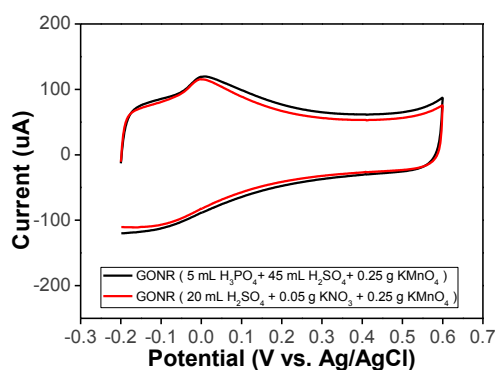


Fig. 2 The cyclic voltammograms of GONRs derived from the early and green recipes for the detection of AA in 0.1 M PBS.

- [1] C. L. Sun, C. T. Chang, H. H. Lee, J. Zhou, J. Wang, T.K. Sham, W. F. Pong, ACS Nano, 2011, 5, 7788.  
[2] H. M. Kingston, S. J. Haswell, Microwave-Enhanced Chemistry: Fundamentals, Sample Preparation, and Applications; ACS Publication: Washington DC, 1997.

**Keywords:** graphene nanoribbon, microwave reactor, ascorbic acid, dopamine, uric acid

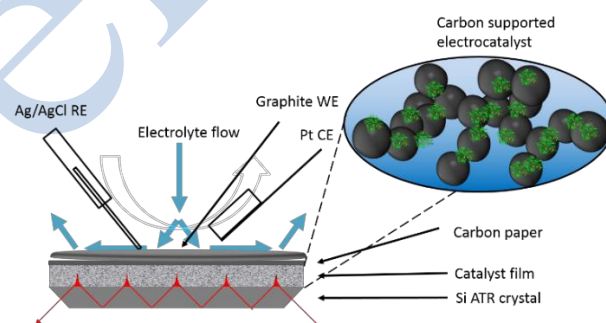
# ***In situ* ATR-IR spectroelectrochemical study of the deactivation of Pd/C catalysts used in DFAFC by common impurities found in formic acid**

Gary G.-Z. Chang<sup>1</sup>, Robert M.J. Jacobs<sup>1</sup> and Kylie A. Vincent<sup>1</sup>

<sup>1</sup>*Department of Chemistry, University of Oxford, Inorganic Chemistry Laboratory, South Park Road, Oxford, OX1 3QR*

*Email: gan-zuei.chang@chem.ox.ac.uk*

Direct formic acid fuel cells (DFAFC) offer the possibility for power generation from oxidation of a liquid fuel, coupled to O<sub>2</sub> reduction.<sup>[1]</sup> The oxidation of formic acid is also of interest for study because it provides a simplified model for methanol oxidation. Platinum has good activity for formic acid oxidation and the mechanism of this reaction has been studied intensively,<sup>[1]</sup> but adsorption of CO (CO<sub>ads</sub>) from dehydration of formic acid on Pt presents a major challenge because CO<sub>ads</sub> poisons surface sites and high overpotentials are needed to activate its oxidative removal. Palladium is considered as an excellent option to replace platinum-based electrocatalysts due to lack of CO<sub>ads</sub> from the dehydration pathway.<sup>[1]</sup> However, a slow deactivation of Pd during formic acid oxidation has been observed by numerous research groups, for example, reference<sup>[2]</sup>. The proposed reasons for deactivation of Pd catalysts include surface poisoning adsorbates such as formate, bicarbonate, carbon dioxide and sulphuric anions.<sup>[3]</sup> Impurities in formic acid have also been suggested as a cause of deactivation of Pd/C by formation of CO<sub>ads</sub> from trace acetic acid, methanol and ethanol in industrial and reagent grade formic acid.<sup>[4]</sup> In this study, we demonstrate the use of a new Attenuated Total Reflectance (ATR)-IR spectroelectrochemical approach<sup>[5]</sup> to investigate electro-oxidation of different purities of formic acids on carbon supported Pd (60 % on XC-72, Premetek). Poisoning by CO was not observed during electrocatalytic oxidation of HPLC grade formic acid. However, IR peaks which have previously been assigned as multi-bonded CO (CO<sub>M</sub>) and hollow-bonded CO (CO<sub>H</sub>) were observed during oxidation of reagent grade formic acid, and CO<sub>ads</sub> was also observed for HPLC grade formic acid 'spiked' with 100 ppm ethanol, methanol or acetic acid. This supports the suggestion that deactivation of Pd/C during formic acid oxidation arises from organic impurities in the fuel.



## **References**

- [1] K. Jiang, H. Zhang, and W. Cai, *Phys. Chem. Chem. Phys.*, 2014, 2, 20360–20376.
- [2] X. Yu and P. G. Pickup, *J. Power Sources*, 2009, 187, 493–499.
- [3] X. Yu and P. G. Pickup, *Electrochem. commun.*, 2009, 11, 1012–1014.
- [4] Mikołajczuk, Borodzinski, P. Kedzierzawski, L. Stobinski, B. Mierzwa, and R. Dziura, *Appl. Surf. Sci.*, 257, 8211–8214.
- [5] Hidalgo, R., Ash, P.A., Healy, A.J., Vincent, K.A. *Angew. Chemie Int Ed. Eng.*, 2015, DOI: 10.1002/anie.201502338R1.

# Investigation of Single Ni(OH)<sub>2</sub> Nanoparticles: Electrocatalysis and Energy Storage at Ultrafast Mass Transport

Jan Clausmeyer, Justus Masa, Edgar Ventosa, Wolfgang Schuhmann

Analytische Chemie – Center for Electrochemical Sciences (CES), Ruhr-Universität Bochum,  
Universitätsstrasse 150, 44780 Bochum, Germany  
jan.clausmeyer@rub.de

Analysis of single micro- or nanometric objects such as catalytically active nanoparticles reveals information not accessible to classical techniques developed for studying their statistical ensembles. Nanoelectrodes are a versatile tools to perform non-ensemble measurements.<sup>1,2</sup>

Ni(OH)<sub>2</sub> is a well-known catalyst for the oxygen evolution reaction (OER) and also commonly used for energy storage in aqueous batteries. We demonstrate the use of carbon nanoelectrodes for the study of the electrochemical properties of single Ni(OH)<sub>2</sub> nanoparticles. The nanoelectrodes fabricated from pyrolytic decomposition of butane inside of quartz capillaries are tunable in size from 1 nm to several 100 nm.<sup>3,4</sup>

Ni(OH)<sub>2</sub> was electrochemically deposited on the needle-type nanoelectrodes of a few nm in diameter, resulting in the formation of single Ni(OH)<sub>2</sub> nanoparticles.

Compared to classical techniques, this method provides very high mass transport rates, by far exceeding those obtained in rotating disk experiments. Thus, electrode kinetics may be studied at high overpotentials and at current densities as high as 10<sup>4</sup> A cm<sup>-2</sup>. High turnover numbers approaching 1000 s<sup>-1</sup> were found.

For the characterization of battery materials, the diffusion of charge carriers in solution of porous paste electrodes may become the limiting factor and hinder the analysis of the intrinsic properties of the material. Due to the fast mass transport at single nanoparticles electrodes, the influence of diffusion in solution is negligible.

We investigated the pseudo-capacitive contribution to the energy storage in nickel hydroxide, in which case the diffusion in solution becomes more problematic. We found that, even at small particles sizes, the reaction is mainly limited by the diffusion of charge carriers in the bulk of the material, since the pseudo-capacitive contribution appeared to be relatively small and constant for all particle size.

## References

- (1) Xiao, X.; Bard, A. J. *J. Am. Chem. Soc.* **2007**, *129*, 9610-9612 .
- (2) Chen, S.; Kucernak, A. *J. Phys. Chem. B* **2004**, *108*, 3262-3276.
- (3) Actis, P.; Tokar, S.; Clausmeyer, J.; Babakinejad, B.; Mikhaleva, S.; Cornut, R.; Takahashi, Y.; López Córdoba, A.; Novak, P.; Shevchuck, A. I.; Dougan, J. A.; Kazarian, S. G.; Gorelkin, P. V.; Erofeev, A. S.; Yaminsky, I. V.; Unwin, P. R.; Schuhmann, W.; Klenerman, D.; Rusakov, D. A.; Sviderskaya, E. V.; Korchev, Y. E. *ACS Nano*. **2014**, *8*, 875–884.
- (4) Clausmeyer, J.; Actis, P.; López Córdoba, A.; Korchev, Y. E.; Schuhmann, W. *Electrochem. Commun.* **2014**, *40*, 28–30.

# Transparent Carbon Nanotube Network for Efficient Electrochemiluminescence Device

Giovanni Valenti,<sup>a</sup> Martina Zangheri,<sup>a</sup> Sandra E. Sansaloni,<sup>a, b</sup> Mara Mirasoli,<sup>a</sup> Alain Penicaud,<sup>b</sup> Aldo Roda,<sup>a</sup> Francesco Paolucci<sup>a</sup>

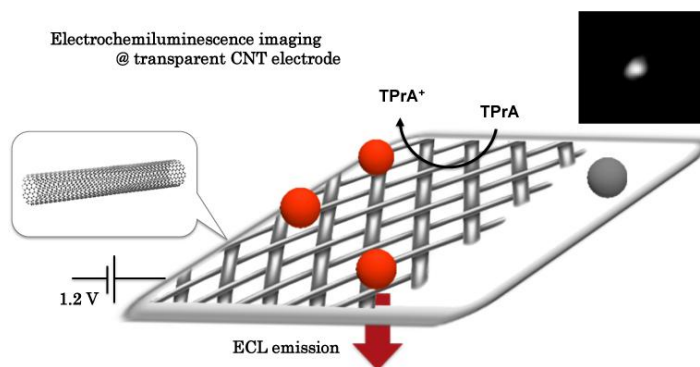
<sup>a</sup> Department of Chemistry "G. Ciamician" University of Bologna, via Selmi 2, 40126 Bologna, Italy

<sup>b</sup> CNRS, Centre de Recherche Paul Pascal (CRPP), Pessac, France

e-mail: g.valenti@unibo.it

Electrochemically generated chemiluminescence (ECL), also called electrochemiluminescence, is a luminescence induced by an electrochemical stimulus.<sup>[1]</sup> As an analytical technique, it possesses several advantages over photoluminescence and chemiluminescence, in particular for (bio)sensor applications.<sup>[2]</sup> The electrochemically-induced way to generate luminescence signal allows to obtain sensors with low background signal and high sensitivity, good temporal and spatial resolution, robustness, versatility, and low cost. The peculiar analytical performances in terms of high detectability of conventional chemiluminescence (CL) are retained and, in addition, the electrochemical trigger of the reaction allows controlling the time and position of light emission from ECL probes. These properties make ECL systems particularly attractive also for microscopy imaging techniques in biological tissue sections or single cells, such as *in situ* hybridization (ISH) and immunohistochemistry (IHC). In this context, the nanostructured materials such as carbon nanotubes (CNTs) and graphene are particularly promising for sensing applications.<sup>[3]</sup>

Here we present the application of optically transparent electrodes based on carbon nanotubes to ECL, demonstrating the electrocatalytic superiority of such materials *vis-à-vis* ITO electrodes. CNTs electrodes are excellent material for ECL application thanks to the very favourable overpotential of amine oxidation that represents the rate-determining step for the signal generation in both research systems and commercial instrumentation. The employ of carbon nanotubes resulted in a ten times higher emission efficiency compared to commercial transparent ITO electrodes. Finally, we demonstrate as a proof of principle that our CNT device can be used for ECL imaging in which micro-beads were used to mimic a real biological sample, such as single cell visualization.



## References

- [1] a) A. J. Bard, in *Electrogenerated Chemiluminescence*, Marcel Dekker, New York, **2004**; b) M. M. Richter, *Chem. Rev.*, **2004**, *104*, 3003-3036 ; c) E. Rampazzo, S. Bonacchi, D. Genovese, R. Juris, M. Marcaccio, M. Montalti, F. Paolucci, M. Sgarzi, G. Valenti, N. Zaccheroni, L. Prodi, *Coord. Chem. Rev.* **2012**, *256*, 1664 – 1681.
- [2] a) R. J. Forster, P. Bertoncello, T. E. Keyes, *Annu. Rev. Anal. Chem.*, **2009**, *2*, 359; b) L. Z. Hu, G. B. Xu, *Chem. Soc. Rev.*, **2010**, *39*, 3275-3304.
- [3] V. Zamolo, G. Valenti, E. Venturelli, O. Chaloin, M. Marcaccio, S. Boscolo, V. Castagnola, S. Sosa, F. Berti, G. Fontanive, M. Poli, A. Tubaro, A. Bianco, F. Paolucci, M. Prato, *ACS Nano*, **2012**, *6*, 9, 7989–7997.

# Ultrasensitive electrochemical sensing of metronidazole using molecularly imprinted polymer decorated hollow nickel nanospheres on carbon nanotubes

Jie Liu, Han Song, Jiang Liu, Lu Zhang, Yingchun Li\*,  
Key Laboratory of Xinjiang Phytomedicine Resources of Ministry of Education, School of  
Pharmacy, Shihezi University, Shihezi, Xinjiang, 832000  
e-mail address: yingchunli@shzu.edu.cn

## Abstract

A novel electrochemical sensor for detecting metronidazole (MNZ) is developed by using hybrid recognition elements of multi-walled carbon nanotubes (MWCNTs) modified with hollow nickel nanospheres (HNNSs) and electropolymerized molecularly imprinted polymer (MIP) on glassy carbon electrodes (GCE). The composite of HNNSs and MWCNTs, serving as the loading platform for MIP film, is introduced for the purpose of double signal-enhancement by raising surface area and electron transport ability, while MIP affords selectivity for specific recognition of MNZ. The morphology of the hybrid materials were observed by scanning electron microscope (SEM) and the properties of the sensor (MIP/HNNSs-MWCNTs/GCE) were examined by cyclic voltammetry (CV) and electrochemical impedance spectroscopy (EIS). In MNZ determination, MIP/HNNSs-MWCNTs/GCE displayed dynamic linear range from  $2 \times 10^{-15}$  mol L<sup>-1</sup> to  $8.0 \times 10^{-13}$  mol L<sup>-1</sup> with a remarkably low detection limit of  $6.67 \times 10^{-16}$  mol L<sup>-1</sup> (S/N=3), superb selectivity in discriminating MNZ from its structural analogues and good anti-interference ability towards several co-existing substances. The detection limit of MNZ is lower than any reports than we can find. In addition, the sensor showed some favorable features such as simple preparation and good stability. Detection of MNZ in pharmaceutical dosage form and in fish tissue has been successfully carried out without complicated separation treatment.

**Keywords** metronidazole, molecularly imprinted polymer, hollow nickel nanospheres, multi-walled carbon nanotubes, electrochemical sensor

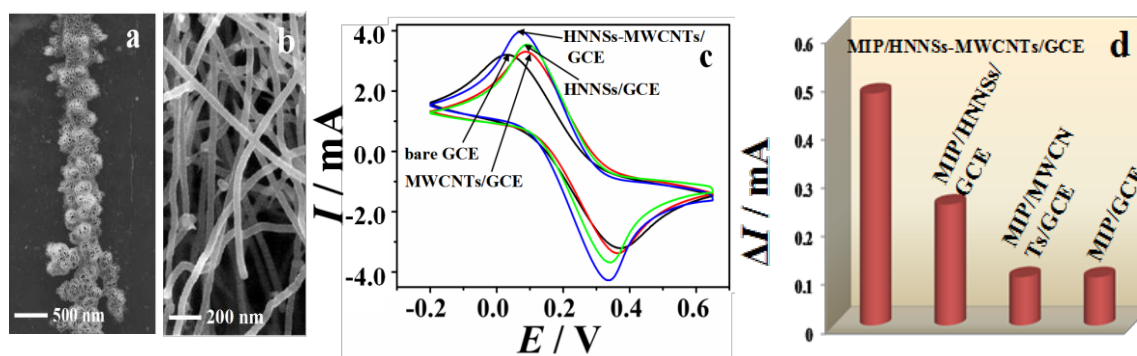


**Fig. 1** SEM photo of (a) HNNSs-MWCNTs/GCE and (b) MWCNTs/GC. (c) Cyclic voltammograms of different electrodes in the solution of  $0.05 \text{ mol L}^{-1} [\text{Fe}(\text{CN})_6]^{3-/4-}$  and  $0.1 \text{ mol L}^{-1} \text{KNO}_3$  at a scan rate of  $100 \text{ mV s}^{-1}$ . (d) Comparison of sensing response of four electrodes in detecting MNZ at the same concentration.

## References

1. Y.C. Li, Y. Liu, J. Liu, J. Liu, H. Tang, C. Cao, D. Zhao, Y. Ding, Sci. Rep. 5 (2015) 1-8.
2. Y. Liu, J. Liu, H. Tang, J. Liu, B. B. Xu, F. Yu, Y.C. Li, Sensor. Actuator. B: Chem. 206 (2015) 647-652.
3. J. Liu, H. Song, J. Liu, Y. Liu, L. Li, H. Tang, Y.C. Li, Talanta. 134 (2015) 761-767.



# Multiple On-line NMR System Development to Detect Electrochemical Reactions of Direct Alcohol Fuel Cells

Ryeo Yun Hwang<sup>1,2</sup>, Young-Seok Byun<sup>1,2</sup> and Oc Hee Han<sup>1,2,3,\*</sup>

<sup>1</sup>Western Seoul Center, Korea Basic Science Institute, Seoul 120-140, Korea

<sup>2</sup>Graduate School of Analytical Science & Technology, Chungnam National University, Daejeon 305-764, Korea

<sup>3</sup>Department of Chemistry & Nano Sciences, College of Natural Sciences, Ewha Womans University, Seoul 120-140, Korea

ryhwang@kbsi.re.kr

For the efficient generation of electricity out of direct methanol fuel cells (DMFCs), it is essential to eliminate or, at least, to reduce the loss of fuel due to fuel crossing from anodes to cathodes. In this sense, the in situ/on line investigation of fuel cell exhausts would be the first step to solve the problem. The results of this kind of investigation often have limitations with a focus on a single side of the system, therefore, not providing simultaneous detection of chemicals in the fuel cell exhausts of both electrodes. In contrast, this work reports the chemical detection for anode and cathode exhausts using the on-line Nuclear Magnetic Resonance (NMR) system (**Figure 1**) developed for detection of multiple samples at the same time. We used two dimensional <sup>2</sup>H-NMR spectroscopy to observe chemicals present in the liquid anode and cathode exhausts of DMFCs. Our results demonstrate that application of this on-line NMR system can be extended to other chemical systems with multiple chemical flows such as the flow batteries and the combinatorial chemical systems.

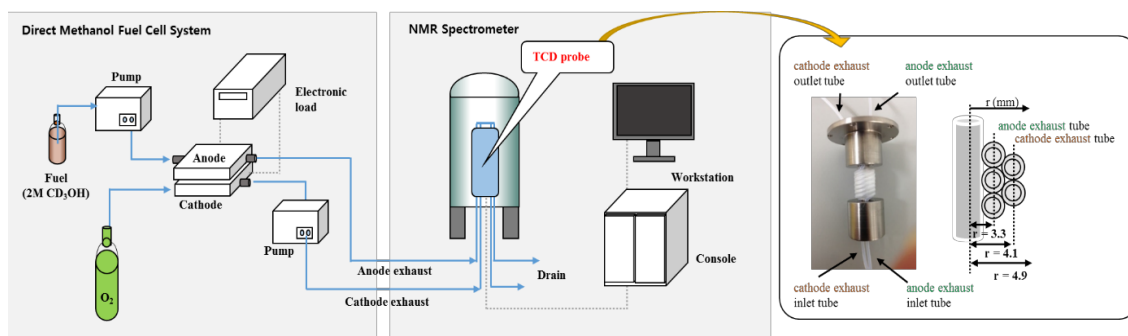


**Figure 1.** Schematic of the DMFC on-line NMR system that detects anode & cathode exhausts of a flat type DMFC with a toroid cavity detector (TCD) NMR probe. The inset on the right shows the photograph of the dumbbell-shape central conductor, wrapped in two layers of tubings, of a TCD (left) and the schematic diagram of the central conductor wrapped in two layers of tubing filled with exhausts (right).

**Acknowledgments.** This work was supported by the KBSI grants (T34419 & T35419) to O. H. Han.



# Oxygen Reduction Reactions in Ionic Liquids-Based Mixture Electrolytes for High Performance Rechargeable Li-O<sub>2</sub> Batteries

Asim Khan and Chuan Zhao

School of Chemistry, The University of New South Wales, Sydney, NSW 2052, Australia  
chuan.zhao@unsw.edu.au

Li-O<sub>2</sub> batteries can offer high energy densities at low cost and are promising candidates for future energy storage and energy conversion devices. However, the technology is still at research and development stages and extensive efforts are required to address numerous problems related to discharge/charge cycles to make it commercially successful [1]. In Li-O<sub>2</sub> batteries, the cathode reaction i.e. the oxygen reduction reaction (ORR) is of a great importance and is greatly influenced by the type of electrocatalysts and electrolytes [2]. The nature of electrolyte plays a critical role in the performance/cycle life of Li-O<sub>2</sub> cell. Decomposition of electrolytes by the attack of reactive reduction products leads to the formation of lithium alkylcarbonates and lithium carbonate that greatly reduces the performance/cycle life of Li-O<sub>2</sub> batteries.

Because of their unique properties like non-volatility, non-flammability, thermal stability and good electrochemical stability, ionic liquids have been considered as an electrolyte for Li-O<sub>2</sub> batteries. The ORR has been studied in a range of aprotic and protic ionic liquids [2, 3] as well as in organic solvents such as dimethyl sulfoxide (DMSO), acetonitrile, and dimethyl formamide (DMF) [4]. However, there are very few studies have been carried out for ORR in ionic liquids based mixed electrolytes. The addition of ionic liquids into aprotic organic solvent can possibly lower the overpotential for the oxidation of discharge products and enhances the stability against the attack of superoxide [5, 6].

In this presentation, the oxygen reduction-oxidation processes are investigated in a range of ionic liquid based mixed electrolytes in the presence and absence of Li<sup>+</sup>. Compared to pure organic electrolytes, the ionic liquid based mixed electrolytes exhibit higher conductivity, diffusion and oxygen solubility. Cyclic voltammetry results show that the mixed electrolyte had better retention of cathodic current after several cycles than the pure organic electrolytes. The results show that both cations and anions of ionic liquids have significant effect on ORR mechanism, and the optimized mixed electrolyte can result in improved cell cycling performance.

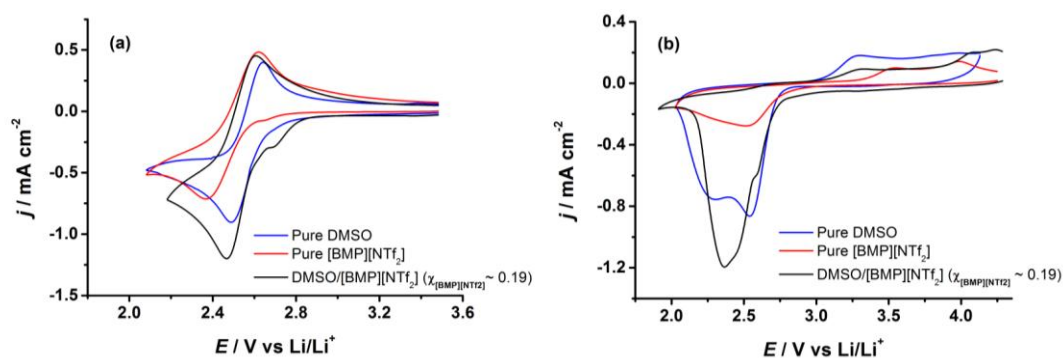


Figure 1: Cyclic voltammograms of ORR on Au electrode in different electrolytes (a) in the presence of 0.1 M TBAPF<sub>6</sub> and (b) in the presence of 0.25 M LiNTf<sub>2</sub>. Scan rate 0.1 V s<sup>-1</sup>.

- [1] P.G. Bruce, S.A. Freunberger, L.J. Hardwick, J.-M. Tarascon, Nat. Mater., 11 (2012) 19.
- [2] R.G. Evans, O.V. Klymenko, S.A. Saddoughi, C. Hardacre, R.G. Compton, J. Phys. Chem. B, 108 (2004) 7878.
- [3] A. Khan, X. Lu, L. Aldous, C. Zhao, J. Phys. Chem. C, 117 (2013) 18334.
- [4] J.D. Wadhawan, P.J. Welford, H.B. McPeak, C.E.W. Hahn, R.G. Compton, Sensors and Actuators B: Chemical, 88 (2003) 40.
- [5] L. Cecchetto, M. Salomon, B. Scrosati, F. Croce, J. Power Sources, 213 (2012) 233.
- [6] A. Khan, C. Zhao, Electrochem. Comm., 49 (2014) 1.

# Electrochemical determination of Norepinephrine by adsorptive stripping voltammetry using a boron doped diamond electrode

Ertugrul Keskin<sup>1</sup>, Yavuz Yardım<sup>2</sup>, Abdulkadir Levent<sup>3</sup>, Zühre Şentürk<sup>4</sup>

<sup>1</sup>Adıyaman University, Faculty of Pharmacy, Department of Analytical Chemistry, 02040 Adıyaman, Turkey

<sup>2</sup>Yüzüncü Yıl University, Faculty of Pharmacy, Department of Analytical Chemistry, 65080 Van, Turkey

<sup>3</sup>Batman University, Health Services Vocational College, 72100 Batman, Turkey

<sup>4</sup>Yüzüncü Yıl University, Faculty of Science, Department of Analytical Chemistry, 65080 Van, Turkey

keskinertugrul@hotmail.com

The electrochemical analysis of biomolecules has been intensively investigated in recent years. Among these biomolecules, norepinephrine (NE, 4,5- $\beta$ -trihydroxy phenethylamine), also called noradrenaline, is a catecholamine with multiple roles including those as an endogenous hormone secreted by the adrenal medulla and a neurotransmitter in the central nervous system. Medically it is used in those with severe hypotension. It does this by increasing vascular tone (tension of vascular smooth muscle) through  $\alpha$ -adrenergic receptor activation. On the other hand, it is a drug belonging to the stimulants that are on the World Anti-Doping Agency's 2005 Prohibited List. Owing to its important effects in human system, its illegal use by athletes and its therapeutic use, the novel and perspective analytical methods providing rapid, sensitive and reliable detection and determination of NE are important for medical diagnostic tests, for industrial quality control or for doping controls. Its electrochemical detection has been the focus of research for electroanalytical scientists and neurochemists, and some modified electrodes have been used to determine NE [1-3].

This work aims to throw a more light upon its redox behavior at surface of boron doped diamond electrode without any modification by using cyclic and adsorptive stripping voltammetry and to establish a methodology for its rapid determination. The cyclic voltammogram in Britton-Robinson buffer, pH 2.0 showed a couple of redox peaks with the potential value of the anodic and the cathodic (reverse) peaks of +0.852 and +0.174 V (vs. Ag/AgCl), respectively. The experimental conditions affecting the adsorptive stripping behavior were studied in terms of pH of various supporting electrolyte, accumulation variables and square-wave parameters by means of pulse voltammetric techniques due to the well-resolved signal. Using square-wave stripping mode, the compound yielded a well-defined voltammetric response in Britton-Robinson buffer, pH 2.0 at +0.835 V (vs. Ag/AgCl) (a pre-concentration step being carried out at open-circuit condition for 60 s). A linear calibration graph was obtained in the concentration range of 1 to 40  $\mu\text{g mL}^{-1}$  ( $4.9 \times 10^{-6} \text{ M} - 2.0 \times 10^{-4} \text{ M}$ ). A detection limit of 0.254  $\mu\text{g mL}^{-1}$  ( $1.2 \times 10^{-6} \text{ M}$ ) and relative standard deviation of 2.6% for a concentration level of 10  $\mu\text{g mL}^{-1}$  (n: 12) were calculated. As an example, the practical applicability of the proposed method was tested for the determination of this compound in a commercially available ampoule sample which contains NE acid tartrate. The results obtained were statistically analyzed and compared with those obtained by applying the high-performance liquid chromatographic method with diode-array detection.

## Acknowledgements

This research was funded by the Scientific Research Projects Presidency of Yüzüncü Yıl University (2013-ECZ-B007).

## References

1. H. Dong, S. Wang, A. Liu, J.J. Galligan, G.M. Swain, M.D. Hawley, *J. Electroanal. Chem.* 632 (2009) 20.
2. M. Mazloum-Ardakani, H. Beitollahi, B. Ganjipour, H. Naeimi, *Int. J. Electrochem. Sci.* 5 (2010) 531.
3. M. Ansari, S. Kazemi, M.A. Khalilzadeh, H. Karimi-Maleh, M.B.P. Zalousi, *Int. J. Electrochem. Sci.* 8 (2013) 1938.

# Synthesis of Short or Holey Graphene Oxide Nanoribbons for the Electrochemical Detection of Biomarkers

Chia-Liang Sun<sup>1\*</sup>, Chun-Hao Su<sup>1</sup>, Jhing-Jhou Wu<sup>1</sup>, and Chen-Fu Pan<sup>1</sup>

<sup>1</sup> *Department of Chemical and Materials Engineering, Chang Gung University,  
Kwei-Shan, Tao-Yuan 333, Taiwan*

*\*E-mail address: sunchialiang@gmail.com*

In the first part of this presentation, we plan to demonstrate the microwave-assisted synthesis of short graphene oxide nanoribbons (GONRs) through unzipping cut multiwalled carbon nanotubes (MWCNTs). [1, 2] Transmission electron microscopy and dynamic light scattering spectroscopy were used to examine the length, size, and morphology, i.e. unzipping level, of our various products. The nanotube core and nanoribbon shell can be observed from short GONRs via a modified unzipping recipe. Then the short GONRs were adopted to modify the glassy carbon electrode for the electrochemical detection of ascorbic acid (AA), uric acid (UA), and dopamine (DA). Compared to other nanomaterials, cyclic voltammograms of short GONRs show higher anodic oxidation currents for AA, UA, and DA. The detection limits of three analytes are 26, 98, and 24 nM, respectively, in amperometric current-time measurements. Especially, the sensitivity for DA is improved to be  $40.86 \mu\text{A} \mu\text{M}^{-1} \text{cm}^{-2}$ . The improved detection signals are due to the increased active sites of the open ends of short GONRs. Moreover, the width side of short GONRs could be more active than their length side. All above-mentioned results reveal that the short GONRs can provide a novel platform for electrochemically biomarker detection of Parkinson's disease. In the second part of this presentation, we plan to demonstrate the synthesis of holey GONRs (hGONRs) with the help of a facile thermal treatment. The improved electrochemical properties of hGONRs will be shown and correlated with their morphologies.

**Keywords :** graphene oxide nanoribbon, multiwalled carbon nanotube, unzipping, ascorbic acid, dopamine, uric acid

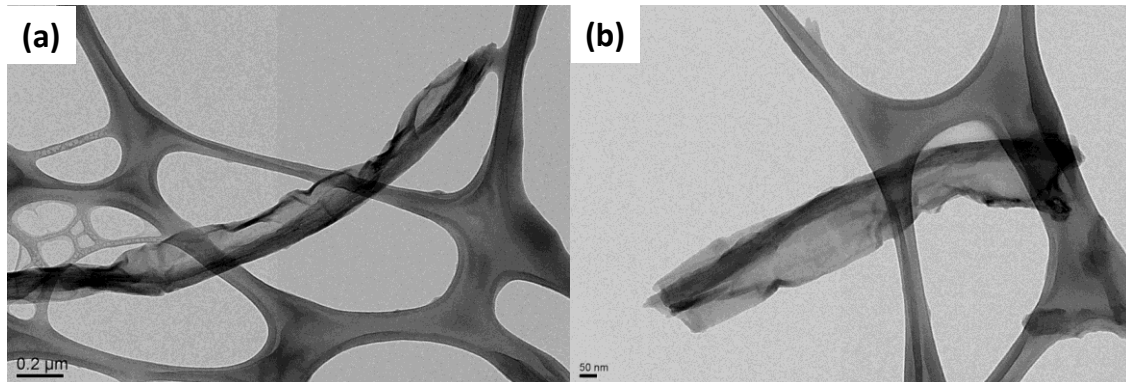


Figure 1. Low magnification transmission electron microscopy images of a single (a) GONR and a single (b) short GONR. [2]

## References

1. C. L. Sun, C. T. Chang, H. H. Lee, J. Zhou, J. Wang, T. K. Sham, W. F. Pong, *ACS Nano* **5**, 7788 (2011).
2. C. L. Sun, C. H. Su, J. J. Wu, *Biosens. Bioelectron.* **67**, 327 (2015).

# Fabrication of Electrochemical Biosensor by Using Peptide as a New Kind of Recognition Element

Hao Li<sup>a</sup>, Yue Huang<sup>a</sup>, Luming Wei<sup>a</sup>, Weiwei Li<sup>a</sup>, Xiaoli Zhu<sup>b</sup>, Genxi Li<sup>a,b,\*</sup>

(<sup>a</sup> State Key Laboratory of Pharmaceutical Biotechnology, Department of Biochemistry, Nanjing University, Nanjing, 210093; <sup>b</sup> Laboratory of Biosensing Technology, School of Life Sciences, Shanghai University, Shanghai 200444; E-mail: genxili@nju.edu.cn)

Over the last decade, artificially synthesized targeting ligands, particularly aptamer, have gradually evolved into a powerful tool of molecular recognition, not inferior to the biologically generated antibodies. In the meantime, it should be noted that short functional peptide, frequently acting as therapeutic and biomedical agent, can target many kinds of protein-ligand interactions, thus peptide may also be used as recognition element for the development of electrochemical biosensors. Therefore, some functional peptides have been recently constructed and employed in the lab of the authors, through electrode surface self-assembly, to form sensitive biosensing interfaces for protein detection. In these biosensor designs, the peptide motifs of protein recognition, metal ion coordination, and several other biochemical functions have been assembled and combined to construct multi-functional peptide-based probes, while some protein sensing interfaces have been preliminarily optimized to suit the need of clinical detection of disease marker proteins.

As is well known, peptide is the structural element composing the complex functional structure of a protein molecule. To some extent, peptide also possesses the chemical and conformational diversity of a protein molecule, which enables interaction with a myriad of partners ranging from bio-active small molecules, biological macromolecules, all the way to synthesized nanomaterial or even macroscopic surfaces of metal and glasses. Among these interactions, many a peptide-ligand recognition is potentially exploitable for biosensor design. On the one hand, the many protein-targeting peptide sequences screened out and rationally designed during the last few decades can provide a rich reservoir for the design of sensing probes for protein detection. On the other, peptides having molecular partners beyond protein molecules can furnish these protein-targeting peptide probes with more diverse biosensing functions such as signal conversion and amplified signal readout. Therefore, many peptide-based biosensing interfaces have been designed and fabricated in our lab for the electrochemical detection of different types of protein targets. For instance, based on the "host-guest" inclusion of peptide side chain groups into synthetic macrocyclic host, the coordination of metal ion by short 3-mer peptides, and the bioconjugation of therapeutic function groups to peptides, several electrochemical biosensors have been developed for the detection of disease markers in cancer of various origins, as well as in Alzheimer's disease. Furthermore, by conjugating the small-molecule peptide probe with some kinds of macromolecules, the modified peptide probe can be used together with the original probe to electrochemically study the relationship between the number of nitrated amino acids and functional state of the target proteins.

In the above biosensor designs, electrochemical techniques can control and fine-tune the micro-environment of the peptide probes on the sensing interfaces, such as the oxidative/reductive status, ion strength near the surface layer, which in turn determines the peptide-ligand interactions of the biosensing process. These electrochemically controlled biosensing peptides and sensitive interfaces have extended the scope of design for protein biosensor and its application in clinical protein detection. Taking the chance to participate in the great event of the 66th ISE Annual Meeting, the authors would like to share the ideas of the typical strategies for the fabrication of some electrochemical biosensors by using peptide as a new kind of recognition element.

1. H. Li, Y. Huang, B. Zhang, X. Pan, X. Zhu, G. Li, *Anal Chem*, 2014, 86 (24): 12138-12142.
2. H. Xie, H. Li, Y. Huang, X. Wang, Y. Yin, G. Li, *ACS Appl. Mater. Interfaces*, 2014, 6: 459-463.
3. H. Li, Y. Huang, B. Zhang, D. Yang, X. Zhu, G. Li, *Theranostics*, 2014; 4: 701-707.
4. Y. Yu, H. Li, B. Zhang, X. Pan, X. Zhu, Y. Ding, G. Li, *ACS Appl. Mater. Interfaces*, 2015, 2015, 7: 4401-4405.

# Study of the Electrochemical oxidation of Dissolved Carbon monoxide in Acidic and Alkaline electrolytes by Using and Fabricated Au-Microelectrode

Robin Wang, Trav Huang, Andrew S. Lin

*Department of Chemical and Materials Engineering, Chang Gung University,  
Taoyuan, Taiwan  
E-mail: andrew@mail.cgu.edu.tw*

## Abstract

In this study, gold (Au) was used to study the electrochemical oxidation of dissolved carbon monoxide (CO) in acidic or alkaline electrolytes. The experimental results indicate that gold micro-electrode or gold clusters on micro-electrode may measure limiting currents without using rotating disk electrode approaches. Microelectrode is defined as having at least one dimension of an electrode in the micrometers and the characteristics of these electrodes is as following (i) small amounts of current (ii) small electrode area and (iii) measurements of limiting currents without forced convections.

The electrochemical oxidation of dissolved carbon monoxide (CO) on Au-RDE is mainly diffusion-controlled processes at the potentials greater than 0.6 V (vs. RHE) in acidic electrolyte and 0 V (vs. RHE) in alkaline electrolyte, respectively. Fabricated Au-microelectrode is used to study the rates of mass transfer of the dissolved carbon monoxide (CO) electro-catalysis in acidic and alkaline system. The limiting currents of microelectrode measurements indicated the forced convection phenomena with no rotating disk electrode needed. The onset potentials of gold micro-electrode indicate the electro-catalytic effects on the electrochemical oxidation of dissolved CO.

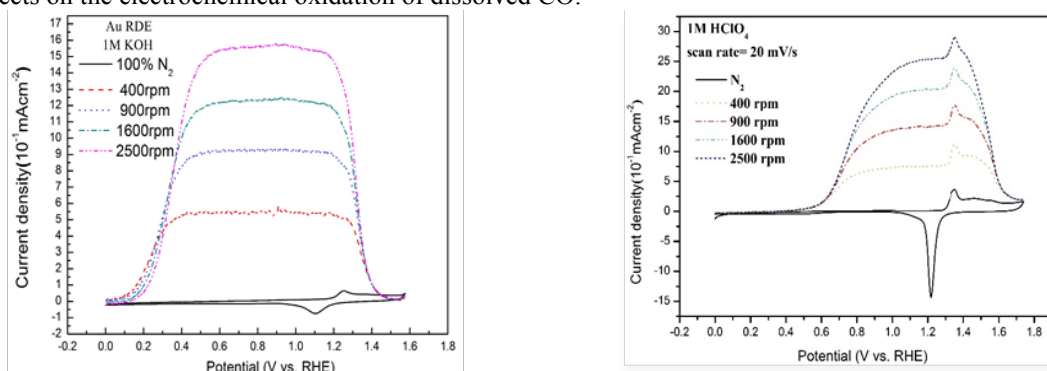


Fig.1 Cyclic voltammetry of solution phase CO oxidation on rotating gold disk electrode in 1M KOH (left) and 1M HClO<sub>4</sub> (right) in various rotating speeds (400 to 2500 rpm) with sweep rate of 20 mV/s.

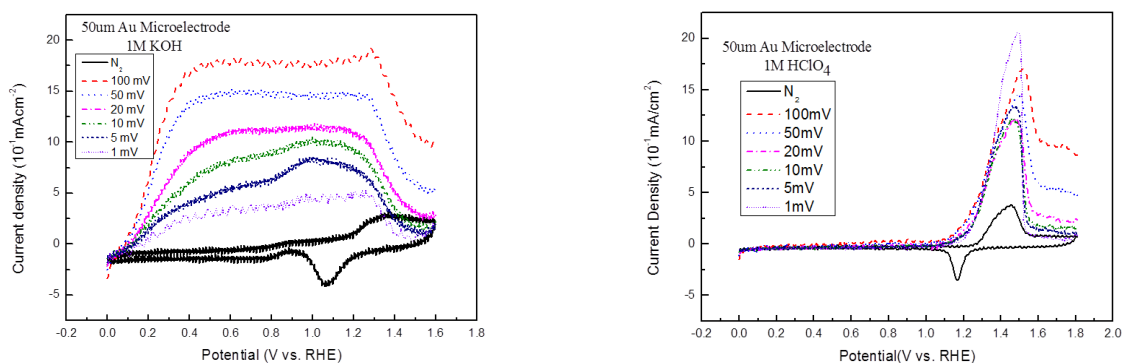


Fig.2 Cyclic voltammetry of solution phase CO oxidation on fabricated gold micro-electrode of 50  $\mu\text{m}$  in 1M KOH (left) and in 1M HClO<sub>4</sub> (right) in various sweep rates of 1 to 100 mV/s.

# A Novel Electrochemical Sensing of Hydrogen Phosphate Ion with RuO<sub>2</sub>-Ta<sub>2</sub>O<sub>5</sub> Mixed Oxide

Takami Tsukuma<sup>1</sup> and Masatsugu Morimitsu<sup>\*1,2</sup>

<sup>1</sup>Department of Science of Environment and Mathematical Modeling,

<sup>2</sup>Department of Environmental Systems Science

Doshisha University

1-3 Tatara-miyakodani, Kyotanabe, Kyoto 610-0394, Japan

\*E-mail: mmorimit@mail.doshisha.ac.jp

Detection and quantification of phosphorus is needed in environmental, medical, and agricultural fields in addition to food, drink, and drug, while the method is limited to the visible spectroscopy in combination with a chemical reaction between phosphorus and molybdenum, *i.e.*, molybdenum blue method. A electrochemical sensor would be one of the possible options for phosphorus sensing, and some literatures [1,2] has mentioned oxide catalysts to quantify phosphorus concentration in aqueous solutions by measuring redox potential or oxidation current, although it is still needed to improve the sensitivity, selectivity, concentration range, and response time. In this work, the development of a novel catalyst for electrochemical sensing of phosphorus was done, in which the target is hydrogen phosphate ions, HPO<sub>4</sub><sup>2-</sup>. For this purpose, we focused on RuO<sub>2</sub>-Ta<sub>2</sub>O<sub>5</sub> mixed oxides which can be prepared by thermal decomposition of a precursor solution and can be changed in crystallographic structure and composition by modifying the metal contents in the precursor solution and thermal decomposition temperature. The results present very unique properties on electrochemical catalytic activity of the mixed oxide to HPO<sub>4</sub><sup>2-</sup> and an excellent possibility for the novel material of the detecting electrode for electrochemical hydrogen phosphate sensors.

RuO<sub>2</sub>-Ta<sub>2</sub>O<sub>5</sub> mixed oxides were prepared by thermal decomposition of precursor solutions containing Ru (III) and Ta (V). The Ru mole ratio was changed from 30 mol% to 80 mol% and thermal decomposition was carried out at a temperature from 260 °C to 500 °C. The characterization of the coatings was done with XRD and SEM. Electrochemical measurements by cyclic voltammetry and chronoamperometry were performed using a conventional three-electrode cell and KCl solutions with or without various concentration of HPO<sub>4</sub><sup>2-</sup>.

XRD and SEM measurements revealed that the crystallographic structure of RuO<sub>2</sub>-Ta<sub>2</sub>O<sub>5</sub> mixed oxides became amorphous with decreasing thermal decomposition temperature and lowering Ru mole ratio. Cyclic voltammograms indicated that HPO<sub>4</sub><sup>2-</sup> was oxidized at 0.8 V or more vs. KCl sat. Ag/AgCl followed by the diffusion-limited current which increased with the concentration of HPO<sub>4</sub><sup>2-</sup>, so that the oxidation of HPO<sub>4</sub><sup>2-</sup> occurs on RuO<sub>2</sub>-Ta<sub>2</sub>O<sub>5</sub> coatings. The oxidation current was also examined by chronoamperometry, and the data at different concentrations of HPO<sub>4</sub><sup>2-</sup> are summarized in Fig. 1. It is clear that the oxidation current density is linear to the concentration, in which the linear region is found in a wide range from 10<sup>-6</sup> mol/L to 10<sup>-2</sup> mol/L. This result is quite important, because RuO<sub>2</sub>-Ta<sub>2</sub>O<sub>5</sub> catalyst can present the constant sensitivity which is independent of the concentration range, even though chloride ions, a typical ion of specific absorption, are contained in the test solution. Therefore, this work has proven that HPO<sub>4</sub><sup>2-</sup> can be electrochemically detected and quantified with the novel electrocatalyst, RuO<sub>2</sub>-Ta<sub>2</sub>O<sub>5</sub>, prepared by thermal decomposition.

In this paper, more detailed results on the effects of the composition and thermal decomposition temperature in oxide preparation on the catalytic activity to HPO<sub>4</sub><sup>2-</sup> will be presented.

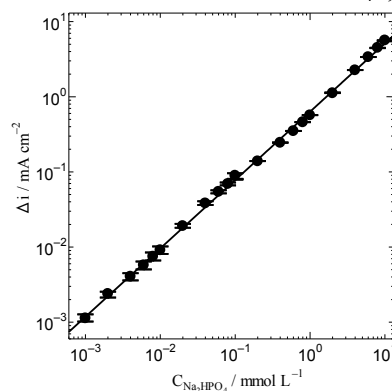


Figure.1 Relationship between the HPO<sub>4</sub><sup>2-</sup> concentration and the oxidation current density measured with RuO<sub>2</sub>-Ta<sub>2</sub>O<sub>5</sub> catalysts.

## References

- [1] Y. Shimizu, S. Takase, T. Kidosaki, *Journal of Sensor Technology*, pp. 95-101 (2012).
- [2] Y. Shimizu, S. Takase, T. Matsumoto, *Electrochemistry*, Vol. 78, No. 2, pp. 150-152 (2010).

# Normalised Sampled-Current Voltammetry at Microdisc Electrodes: Kinetic Information from Pseudo Steady State to Steady State Voltammetry

Samuel C. Perry, Guy Denuault  
University of Southampton  
University Road, Southampton SO17 1BJ, UK  
scp2g08@soton.ac.uk

In sampled-current voltammetry (SCV), current transients acquired after stepping the potential along the redox wave of interest are sampled at a fixed time to produce a sigmoidal current-potential curve akin to a pseudo steady state voltammogram. Repeating the sampling for different times yields a family of SCVs. In this way, multiple SCVs can be recorded from the same collection of current transients.

The concept is used to describe the current-time-potential relationship at planar electrodes, but is rarely employed as an electroanalytical method except in normal pulse voltammetry, where the chronoamperograms are sampled once to produce a single voltammogram. Here we combine the unique properties of microdisc electrodes with SCV (MSCV) and report a simple protocol to analyse and compare the MSCVs irrespective of sampling time. This is particularly useful for microelectrodes where cyclic voltammograms change shape as the mass transport regime evolves from planar diffusion at short times to hemispherical diffusion at long times. We also combine MSCV with a conditioning waveform to produce voltammograms where each data point is recorded with the same electrode history and demonstrate that the waveform is crucial to obtaining reliable MSCVs below 100 ms.

To facilitate qualitative analysis of the voltammograms, we convert the current-potential data recorded at different time scales into a unique sigmoidal curve by normalising MSCVs by the theoretical diffusion controlled current<sup>1</sup>, which clearly highlights kinetic complications. To qualitatively model the MSCVs, we derive an analytical expression which accounts for the diffusion regime and kinetic parameters. The procedure is validated with the reduction of  $[\text{Ru}(\text{NH}_3)_6]^{3+}$ , a model one electron outer sphere process, and applied to the derivation of the kinetic parameters for the reduction of  $\text{Fe}^{3+}$  and ferricyanide on Pt microdiscs<sup>2</sup>. The methodology reported here is easily implemented on computer controlled electrochemical workstations as a new electroanalytical method to exploit the unique properties of microelectrodes, in particular at short times.

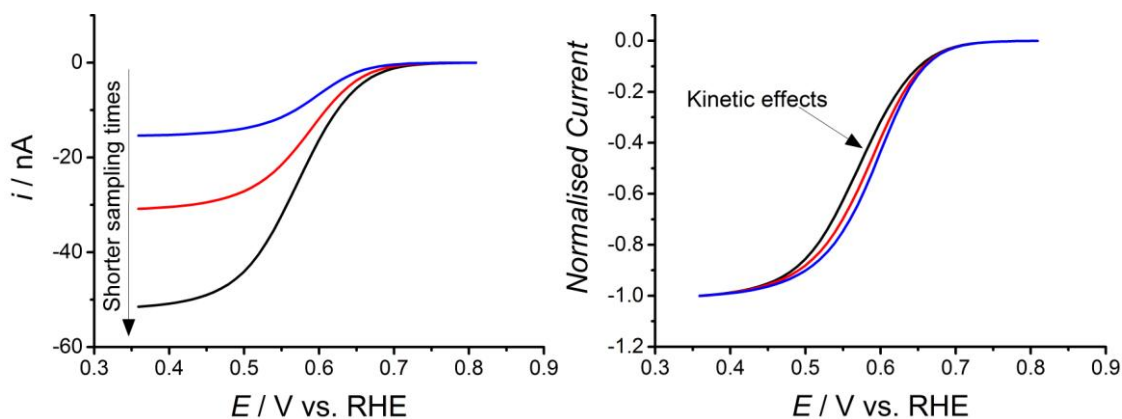


Figure 1: Sampled current voltammograms at a microdisc electrode (MSCV) showing the increase in current as the sampling time is shortened (left) and the kinetics effects revealed by the normalisation procedure (right)<sup>2</sup>.

- (1) Mahon, P. J.; Oldham, K. B. *Analytical Chemistry* **2005**, 77, 6100.
- (2) Perry, S. C.; Al Shandoudi, L. M.; Denuault, G. *Analytical Chemistry*, **2014**, 86, 9917 - 9923

# The Modification of Screen-printed Carbon Electrodes with Polymerized Ionic Liquid Composites for Chemical Analysis

Sheng-Huang Wu, Yi-Jhong Chen, Yi-Yu Chen, Yang Hsiao, Guor-Tzo Wei

*Department of Chemistry and Biochemistry, National Chung Cheng University*

*168 Univ. Rd., Min-Hsiung, Chiayi 62102, TAIWAN*

*chegtwtw@ccu.edu.tw*

The use of ionic liquids for electrode modification has been widely reported recently<sup>1</sup>. Ionic liquids are good media to dissolve/suspense nanomaterials<sup>2-3</sup>. In this study, we used ionic liquids to immobilize nano-materials on the electrode surface and form a disposable composite-material modified screen-printed carbon electrode for electrochemical analysis. With the conductive ability of ionic liquids, it can effectively enhance the electron transfer and improve the detection sensitivity. The results demonstrate the potential of ionic liquid as the platform of chemical modify electrode.

In the first example of the study, multi-walled carbon nanotubes (MWCNT) and graphene (reduced graphene oxide, RGO) were added to the mixture of two ionic liquid monomers ([C<sub>4</sub>VIM][PF<sub>6</sub>] and [C<sub>9</sub>(VIM)<sub>2</sub>][PF<sub>6</sub>]<sub>2</sub>), and dropped coating this mixture on the surface of screen printed carbon electrode (SPCE). With thermal polymerized, nano-carbon ionic liquid composite modified SPCEs (CNT-PIL-SPCE and RGO-PIL-SPCE) were created. Due to the large surface area of CNT and RGO, the currents of CNT-PIL-SPCE and RGO-PIL-SPCE are greater than bare SPCE. In addition, the reactive potential is lower. Due to the robustness of the electrode, we were able to use flow injection analysis (FIA) for the analysis of adenine and guanine with CNT-PIL-SPCE. The detection limits are 1.93  $\mu$ M and 1.37  $\mu$ M (S/N=3) for adenine and guanine, respectively. RGO-PIL-SPCE was used for the determination of 2-mercaptoethanol (2-ME) and 3-Mercaptopropionic acid (3-MPA), the detection limits are 8.03  $\mu$ M and 1.22  $\mu$ M (S/N=3) for 2-ME and 3-MPA, respectively.

In the second example of the study, Ag nanoparticles were incorporated into the poly-ionic liquid modified screen printed carbon electrode to form an AgNP-PIL-SPCE electrode. We used cyclic nitramine explosive, HMX (Octahydro-1,3,5,7-tetranitro-1,3,5,7-tetrazocine), as a model compound to demonstrate that AgNP-PIL-SPCE electrode has catalytic activity of non-aromatic explosive. Since AgNP-PIL-SPCE has high stability, we were able to employ flow injection analysis for HMX analysis. The detection limit of HMX is about 10  $\mu$ M (S/N=3).

## References:

1. M. Opallo, A. Lesniewski, J. Electroanal. Chem., 2011, 656, 2.
2. T. Fukushima1, A. Kosaka, Y. Ishimura, T. Yamamoto, T. Takigawa, N. Ishii, T. Aida, Science, 2003, 300, 2072.
3. G. Wei, Z. Yang, C. Lee, H. Yang, C. Wang, J. AM. CHEM. SOC. 2004, 126, 5036.



# An in-situ Microelectrode Study of the Sea Surface Microlayer: Experimental and Theoretical Challenges

Guy Denuault, Ana Cristina Perdomo Marin  
University of Southampton  
University Road, Southampton SO17 1BJ, UK  
gd@soton.ac.uk

We will describe and discuss experimental results obtained with microelectrodes and scanning electrochemical microscopy (SECM) during an investigation of the sea surface microlayer (SML), a complex medium at the interface between bulk sea water and the atmosphere. Although the SML plays a key role in ocean-atmosphere exchanges, its thickness, structure and composition are still poorly understood, primarily because appropriate sampling and analytical methods are still lacking. While some defined the SML as the upper 1 mm of the surface oceans others determined its thickness to be circa 50  $\mu\text{m}$ . In some instances it is described as a multilayer stratified medium, in others it is considered as a continuous medium. Its precise composition is particularly difficult to determine but it is known to consist of a mixture of inorganic (various salts including heavy metals, dust particulates, etc...), organic (natural lipids, fatty acids) and biological (extra cellular matrix, bacteria, microalgae, etc...) matter. As a result, its properties, e.g. viscosity, pH, oxygen and  $\text{CO}_2$  solubility, are thought to vary across the layer.

Our aim is to develop a new analytical approach to study the SML and since sampling of the medium is a challenge we opted to employ microelectrodes and SECM to perform in-situ electroanalytical measurements. To facilitate the interpretation of results during the development of the analytical protocol, we carried out experiments with a range of synthetic SML and used redox mediators to probe the properties of the medium. We used the SECM to position the microelectrode tip at various positions within and below the SML and performed voltammetry and chronoamperometry at each location. Approach curves were also recorded. Exploiting the properties of microdisc electrodes, chronoamperograms were analysed to simultaneously extract the diffusion coefficient<sup>1</sup> and concentration of the redox mediator at each tip location. Using nanostructured PdH microdisc electrodes developed in our group<sup>2-4</sup> attempts were also made to record pH transients at different depths when varying the partial pressure of  $\text{CO}_2$  above the SML.

This presentation will describe the experimental and theoretical challenges encountered during the study.

- (1) Denuault, G.; Mirkin, M. V.; Bard, A. J. *J. Electroanal. Chem.* **1991**, 308, 27-38.
- (2) Imokawa, T.; Williams, K. J.; Denuault, G. *Anal. Chem.* **2006**, 78, 265-271.
- (3) Serrapede, M.; Denuault, G.; Sosna, M.; Pesce, G. L.; Ball, R. J. *Anal. Chem.* **2013**, 85, 8341-8346.
- (4) Serrapede, M.; Pesce, G. L.; Ball, R. J.; Denuault, G. *Anal. Chem.* **2014**, 86, 5758-5765.

# Electrochemical Determination of Bisphenol A at Conducting Poly(diallyldimethylammonium chloride) Film-Modified Preanodized Screen-Printed Carbon Electrodes

Yen Hua Liao, Ya-Ling Su, Shu-Hua Cheng\*

*Department of Applied Chemistry, National Chi Nan University,*

*Nantou Hsien 54561, Taiwan*

[shcheng@ncnu.edu.tw](mailto:shcheng@ncnu.edu.tw)

Bisphenol A (BPA) is widely known as a toxic endocrine-disrupting compound. In this study, a selective electrochemical sensor based on medium exchange procedure was developed for the determination of BPA. A conducting film-modified preanodized screen-printed carbon electrode (SPCE\*) was prepared, using 0.2% poly(diallyldimethylammonium chloride) film (PDDA). The surface characteristics of the obtained electrode were characterized by field emission scanning electron microscopy (FE-SEM), X-ray photoelectron spectroscopy (XPS), Fourier-Transform infrared spectrometer (FTIR), and atomic force microscope (AFM) experiments. The SPCE\*/PDDA contains highly abundant nitrogen functionality, and was found to be hydrophilic to adsorb anion strongly and hence increase the detection sensitivity. The proposed sensor exhibited a linear response to BPA in the range of 1 to 20  $\mu\text{M}$  in pH 9.0 buffer solution under the optimized differential pulse voltammetry (DPV). The method sensitivity and detection limit ( $S/N=3$ ) are 9.15  $\mu\text{A}/\mu\text{M}$  and 0.4  $\mu\text{M}$ , respectively. A simple medium-exchange procedure was developed for the selective determination of BPA in complex real samples by the use of the SPCE\*/PDDA. The recovery of spiked BPA in Tamsui River (Taiwan) and fresh milk samples was studied using standard addition method.

## References:

1. J.-M. Lin, Y.-L. Su, W.-T. Chang, W.-Y. Su, S.-H. Cheng, *Electrochimica Acta*, 149 (2014) 65.
2. Y. Zhang, Y. Cheng, Y. Zhou, B. Li, W. Gu, X. Shi, Y. Xian, *Talanta*, 107 (2013) 211.
3. Z. Zheng, Y. Du, Z. Wang, Q. Feng, C. Wang, *Analyst*, 138 (2013) 693.
4. R. Cai, W. Rao, Z. Zhang, F. Long, Y. Yin, *Analytical Methods*, 6 (2014) 1590.

# Corrosion behavior of biocompatible stainless steels in physiological medium for application to non-invasive diagnosis of small fiber neuropathies

Amandine Calmet <sup>a,b</sup>, Abdelilah Amar <sup>b</sup>, Sophie Griveau <sup>b</sup>, Virginie Lair <sup>a</sup>, Eliane Sutter <sup>c</sup>, Philippe Brunswick <sup>d</sup>, Fethi Bedioui <sup>b</sup>, Michel Cassir <sup>a</sup>

<sup>a</sup> PSL Research University, Chimie Paristech-CNRS, Institut de Recherche de Chimie de Paris, 11 rue Pierre et Marie Curie, F-75231 Paris Cedex 05, France

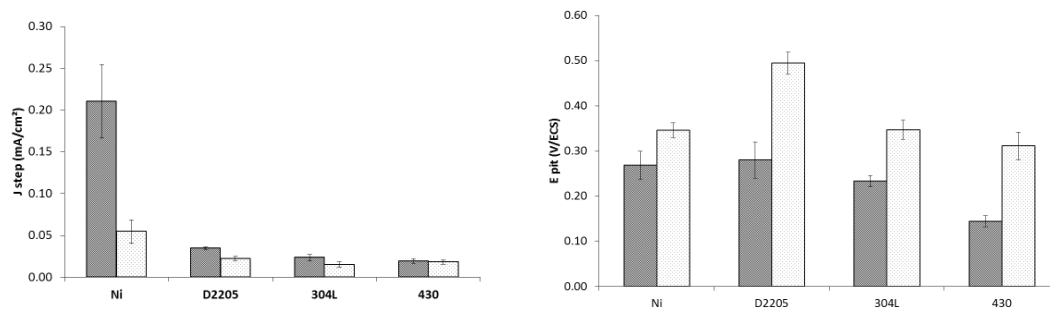
<sup>b</sup> PSL Research University, Chimie ParisTech, Unité de Technologies Chimiques et Biologiques pour la Santé, 75005 Paris, France

<sup>c</sup> Sorbonne Universités, UPMC Univ Paris 06, UMR 8235, Laboratoire Interfaces et Systèmes Electrochimiques, 75005, Paris, France

<sup>d</sup> IMPETO Medical, 17 rue Campagne Première, F-75014 Paris, France

([fethi.bedioui@chimie-paristech.fr](mailto:fethi.bedioui@chimie-paristech.fr))

Small fiber neuropathy is a dysfunction caused by diseases such as type II diabetes and cystic fibrosis. This disease can be detected rapidly using a non-invasive device, Sudoscan<sup>TM</sup> technology (Impeto Medical Inc.). This technology is based on measurements of the electrochemical conductance of the skin *via* the imposition of low amplitude voltages between electrodes applied to the skin and measuring the low current generated. The output measurement is related to the sweat composition associated to glands innervations and their permeability to chloride and proton ions. In order to acquire deeper understanding on the mechanisms occurring at the electrodes and optimize the sensitivity of the instrument, *in vitro* electrochemical experiments were performed in mimetic electrolytic solutions of sweat. The present work was dedicated to the analysis of the electrochemical behavior of different biocompatible stainless steels and, more precisely, their resistance to the pitting corrosion in sweat mimicking electrolyte at pH 7, and using chloride concentrations varying between 36 and 120 mM and carbonate as buffer. Their behavior was compared to that of nickel that was initially used as sensing electrode in the technology and thus serves as reference material. Despite the low chloride concentrations, the corrosion behaviors of stainless steel were markedly different. AISI 430T is not sensitive to chloride concentrations in sweat concentration range so that this stainless steel cannot be used for the Sudoscan<sup>TM</sup> technology. Duplex 2205 and AISI 430 can be good substitutes to 304L as these materials are more sensitive to chloride variations and at lower potentials in comparison to 304L. Among the materials investigated, the best substitute appears to be stainless steel 430



Right: Histogram showing the evolution of the current at the passivity plateau  $J_{step}$  as a function of the material electrode and NaCl concentration. Grey: 120 mM, Light grey: 36 mM. Left: Histogram showing the evolution of the pitting potential  $E_{pit}$  as a function of the electrode material and NaCl concentration. Grey: 120 mM, Light grey: 36 mM

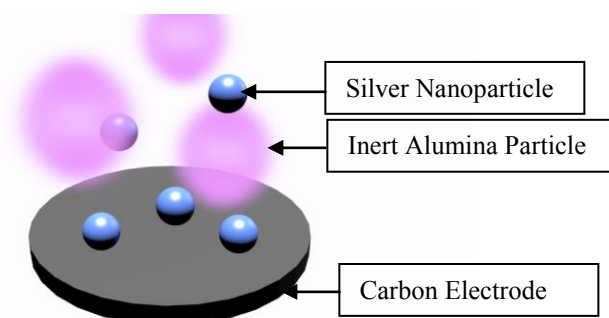
# **‘Nano-impacts’: An Electrochemical Technique for Nanoparticle Sizing in Optically Opaque Solutions**

Her Shuang Toh, Richard G. Compton

Oxford University

Department of Chemistry, Physical and Theoretical Chemistry Laboratory, Oxford University, South Parks Road, Oxford, OX1 3QZ, United Kingdom

her.toh@keble.ox.ac.uk



Typical laser-dependent methods such as nanoparticle tracking analysis (NTA) and dynamic light scattering (DLS) are not able to detect nanoparticles in an optically opaque medium due to scattering or absorption of light. In this talk, the electrochemical technique of ‘nano-impacts’ is used to detect nanoparticles in solution in the presence of high levels of alumina particulates causing a milky white suspension.

Anodic particle coulometry (via ‘nano-impacts’) is a novel technique developed within the last 20 years which works on the basis of recording single nanoparticle-electrode impact events through electrochemistry.<sup>[1]</sup> These events are recorded through the electrochemical signal generated by the redox reaction of the nanoparticle. In this talk, citrate capped silver nanoparticle diffuses under Brownian motion and hits the carbon microelectrode held at a suitable oxidising potential. Thus, the silver nanoparticle is oxidised into silver(I) ions, generating a current ‘spike’ which is observed in the chronoamperogram recorded. Through the use of Faraday’s first law, the size of the nanoparticle can be estimated via Equation 1.<sup>[2-3]</sup>

$$R_{NP} = \sqrt[3]{\frac{3QA_r}{4\pi F\rho}} \quad (1)$$

where  $R_{NP}$  is the nanoparticle radius,  $Q$  is the total charge passed under a single ‘spike’,  $A_r$  is the atomic molecular mass of silver of  $107.9 \text{ g mol}^{-1}$ ,  $F$  is the Faraday constant and  $\rho$  is the density of silver of  $10.5 \times 10^6 \text{ g m}^{-3}$ . Therefore, if the opacity is caused by inert particles, this technique is capable of differentiating between the redox active nanoparticles and the inert particulates.

Using this method, silver nanoparticles were successfully detected and sized in the model opaque medium containing high concentration of alumina particulates. The nanoparticles are sized to be  $13.8 \pm 2.2 \text{ nm}$  via the electrochemical method and it compares well with the results obtained transmission electron microscopy (TEM) ( $14.6 \pm 2.1 \text{ nm}$ ), an ex situ method for nanoparticle size determination. Therefore, the ability to use the ‘nano-impacts’ method in media unmeasurable to competitor techniques confers a significant advantage on the electrochemical approach.

## References

- [1] N. V. Rees, *Electrochem. Commun.* **2014**, *43*, 83-86.
- [2] Y.-G. Zhou, N. V. Rees, R. G. Compton, *Angew. Chem. Int. Ed.* **2011**, *50*, 4219-4221.
- [3] E. J. F. Dickinson, N. V. Rees, R. G. Compton, *Chem. Phys. Lett.* **2012**, *528*, 44-48.

# High-performance Liquid Chromatography with Electrochemical Detection for Determining a Ratio of Eicosapentaenoic Acid to Arachidonic Acid in Human Plasma

Akira Kotani, Mizuki Watanabe, Kazuhiro Yamamoto, Fumiyo Kusu, Hideki Hakamata  
School of Pharmacy, Tokyo University of Pharmacy and Life Sciences  
1432-1 Horinouchi, Hachioji, Tokyo 192-0392 JAPAN  
kotani@toyaku.ac.jp

Eicosapentaenoic acid (EPA) and docosahexaenoic acid (DHA), classified in  $\omega$ -3 polyunsaturated fatty acids (PUFAs), are essential for growth and development, and play an important role in the prevention and treatment of inflammatory and cardiovascular diseases. Recently, it is reported that a ratio of EPA to arachidonic acid (AA) in plasma can be a biomarker for cardiovascular events in a general clinical practice. Gas chromatography with mass spectrometry (GC-MS) and high-performance liquid chromatography with fluorescent detection (HPLC-FL) are applied to determine plasma PUFAs, however, in these methods, the cleanup and derivatization procedures are essential to perform sensitive and selective determination of PUFAs in a real sample analysis. Thus, using simpler sample preparation procedures, a sensitive and selective analytical method for determining PUFAs without derivatization is highly desirable from a practical viewpoint. We had developed a voltammetric method using 3,5-di-*tert*-butyl-1,2-benzoquinone (DBBQ) for determining plasma free fatty acids, showing to be quite sensitive and selective for the acid determination without derivatization of acids. In the present study, an HPLC with electrochemical detection (HPLC-ECD) system was fabricated to determine PUFAs in human plasma. Moreover, the present HPLC-ECD was applied to determine a ratio of EPA to AA in human subject.

The HPLC-ECD was comprised of a degasser, two pumps, a manual sample injector, a column (Develosil C<sub>30</sub>-XG-3, 3  $\mu$ m), an electrochemical detector, and a recorder. An acetonitrile-water mixture (80:20) and that containing 2.0 mmol/L DBBQ and 20 mmol/L lithium perchlorate served as the mobile phase and the DBBQ solution, respectively. The mobile phase and DBBQ solution were made to flow at the rates of 0.03 mL/min and 0.1 mL/min, respectively. A healthy adult male subject was studied upon receipt of his informed consent. The protocol and the subject's informed consent were approved by the Institutional Human Research Committee of Tokyo University of Pharmacy and Life Sciences before commencement of the trial. The blood of 0.1 mL was collected by a finger pricked with a lancing device, and then heparinized blood was separated by centrifugation to obtain plasma. Forty microliter of plasma with nonanoic acid (internal standard) was mixed with 0.4-mL diethyl ether, and PUFAs in plasma were extracted into the diethyl ether phase. The collected diethyl ether was dried completely by nitrogen stream to obtain the lipid residue, which was then dissolved in a 40- $\mu$ L acetonitrile-water mixture (80:20) to prepare a test solution. A 5  $\mu$ L aliquot of test solution was injected into the C<sub>30</sub> column maintained at 30°C, and the eluate was allowed to merge with the DBBQ solution stream to mix together in a mixing tube, and then each PUFA was detected at -0.2 V vs. Ag/AgCl in the electrochemical detector.

The chromatographic peaks of EPA, DHA, nonanoic acid, and AA were observed within 35 min, and these peak heights were found to be proportional to each PUFA concentration, ranging from 0.75  $\mu$ mol/L to 0.1 mmol/L ( $r > 0.998$ ) in all cases. The detection limit of the concentration of each PUFA was 0.23  $\mu$ mol/L. Standard solution of each PUFA at 50  $\mu$ mol/L was determined six times with relative standard deviation (RSD) of less than 3.3%. To estimate an accuracy and precision in the present HPLC-ECD, determinations of PUFAs in human control serum were carried out. The concentration of EPA, DHA, and AA was 10.4, 16.4, and 129  $\mu$ mol/L, respectively, and the repeatability was less than 3.3% RSD. The recovery rate ( $n = 6$ ) of the PUFA for the spiked human control serum in all cases was more than 99.2% and its RSD was less than 5.5%. These results show that the HPLC-ECD method is characterized by higher reproducibility, indicating that the present HPLC-ECD method provides accurate measurements of PUFAs in human serum and plasma. Blood specimen was collected from a healthy human subject subsequent to a fasting for 11 hr, and determination of PUFAs in the human plasma was performed. The concentrations of EPA, DHA, and AA were 4.4, 17.4, and 30.3  $\mu$ mol/L, respectively, thus the ratio of EPA to AA in the human subject was 0.15.

In conclusion, the present HPLC-ECD would be a powerful analytical method for determining ratio of EPA to AA in plasma because it is able to detect PUFAs without the derivatization of acids and the procedure for the sample preparation using a small blood sample would be facile.

# eL-Chem Viewer: A Freeware Package for the Analysis of Electrochemical Data

Jan Hrbac,<sup>a</sup> Vladimir Halouzka,<sup>b</sup> Libuse Trnkova,<sup>a</sup> Jan Vacek<sup>b</sup>

<sup>a</sup>*Department of Chemistry, Masaryk University, Kamenice 5, Brno 625 00, Czech Republic*

<sup>b</sup>*Department of Medical Chemistry and Biochemistry, Faculty of Medicine and Dentistry, Palacky University, Hnevotinska 3, 775 15 Olomouc, Czech Republic  
e-mail: jan.hrbac@upol.cz, jan.vacek@upol.cz*

In electrochemical sensing, a number of voltammetric or amperometric curves are obtained which are subsequently processed, typically by evaluating peak currents and peak potentials or wave heights and half-wave potentials, frequently after background correction. Transformations of voltammetric data can help to extract specific information, e.g., the number of transferred electrons, and can reveal aspects of the studied electrochemical system, e.g., the contribution of adsorption phenomena. In this contribution, we introduce a LabView-based software package, 'eL-Chem Viewer', which is for the analysis of voltammetric and amperometric data, and enables their post-acquisition processing using semiderivative, semiintegral, derivative, integral and elimination procedures. The software supports the single-click transfer of peak/wave current and potential data to spreadsheet software, a feature that greatly improves productivity when constructing calibration curves, trumpet plots and performing similar tasks. eL-Chem Viewer is freeware and can be downloaded from **[www.lchem.cz/elchemviewer.htm](http://www.lchem.cz/elchemviewer.htm)**.

## Reference

J. Hrbac, V. Halouzka, L. Trnkova, J. Vacek, eL-Chem Viewer: A Freeware Package for the Analysis of Electroanalytical Data and Their Post-Acquisition Processing, *Sensors* 14, 13943-13954, 2014

## Acknowledgement

This work was supported by the Czech Science Foundation (project No. 14-08032S), by the Ministry of Education, Youth and Sports of the Czech Republic, project No. LD14033 (COST Action EU-ROS, BM1203), by the Project Postdoc I, reg. No. CZ.1.07/2.3.00/30.0009, KONTAKT II (LH 13050) of the Ministry of Education, Youth and Sports of the Czech Republic, by the student grant IGA\_PrF\_2014032 from Palacky University, and by the Project No. FR-TI4/457 of the Ministry of Industry and Trade of the Czech Republic.

# Square-Wave Adsorptive Stripping Voltammetric Determination of Resveratrol Using Boron-Doped Diamond Electrode in the Presence of Hexadecyl Trimethyl Ammonium Bromide

Yavuz Yardım

*Yüzüncü Yıl University, Faculty of Pharmacy, Department of Analytical Chemistry, 65080 Van,  
Yavuzyardim2002@yahoo.com*

Resveratrol (3,4',5-Trihydroxy-*trans*-stilbene), is a stilbenoid, a type of natural phenol, and a phytoalexin produced naturally by several plants in response to injury or when the plant is under attack by pathogens such as bacteria or fungi . As phenolic compound, resveratrol contributes to the antioxidant potential of red wine and thereby may play a role in the prevention of human cardiovascular diseases. Resveratrol has been shown to modulate the metabolism of lipids, and to inhibit the oxidation of low-density lipoproteins and the aggregation of platelets. Moreover, as phytoestrogen, resveratrol may provide cardiovascular protection. This compound also possesses anti-inflammatory and anticancer properties [1].

In the present paper, a sensitive electroanalytical methodology for the determination of resveratrol using adsorptive stripping voltammetry at a boron-doped diamond (BDD) electrode is presented. In cyclic voltammetry, resveratrol shows one irreversible and adsorption-controlled oxidation peak on BDD electrode. The voltammetric results indicate that in the presence of sodium Hexadecyl trimethyl ammonium bromide (CTAB) the BDD electrode remarkably enhances the oxidation of resveratrol which leads to improvement of peak current with shift of peak potential to less positive values. Using square-wave stripping mode, the compound yielded a well-defined voltammetric response in 0.1 M HNO<sub>3</sub> solution, containing 100  $\mu$ M CTAB at +0.74 V (vs. Ag/AgCl) (after 60 s accumulation at open-circuit condition). Two linear calibration graphs were obtained in the concentration range of 0.025 to 1.0  $\mu$ g mL<sup>-1</sup> ( $1.09 \cdot 10^{-7}$ - $4.38 \cdot 10^{-6}$  M) and 2.5 to 60 ( $1.09 \cdot 10^{-5}$ - $2.63 \cdot 10^{-4}$  M). A detection limit of 0.0063  $\mu$ g mL<sup>-1</sup> ( $2.76 \cdot 10^{-8}$  M), and relative standard deviation of 2.39% for a concentration level of 2.5  $\mu$ g mL<sup>-1</sup> (n = 8) were calculated. As an example, the practical applicability of BDD electrode was tested with the measurement of resveratrol in the dietary supplement products.

[1] L. Fremont, Life Sciences 66 (2000) 663.

# Using Graphene-Nafion Composite Film Modified Glassy Carbon Electrode for the Simultaneous Determination of Paracetamol, Aspirin and Caffeine in Pharmaceutical Formulations

Aydın Yiğit<sup>1</sup>, Yavuz Yardım<sup>1</sup>, Metin Çelebi<sup>2</sup>, Abdulkadir Levent<sup>3</sup>, Zühre Şentürk<sup>4</sup>

<sup>1</sup>Yüzüncü Yıl University, Faculty of Pharmacy, Department of Analytical Chemistry, 65080 Van, Turkey

<sup>2</sup>Yüzüncü Yıl University, Faculty of Science, Department of Inorganic Chemistry, 65080 Van, Turkey

<sup>3</sup>Batman University, Health Services Vocational College, 72100 Batman, Turkey

<sup>4</sup>Yüzüncü Yıl University, Faculty of Science, Department of Analytical Chemistry, 65080 Van, Turkey

E-mail: yavuzyardim2000@yahoo.com

Paracetamol (PAR) / aspirin (ASA) / caffeine (CAF) is a combination drug for the treatment of pain, especially tension headache and migraine. However, an overdose of these mixing drugs may induce nausea, seizures, diarrhea, abdominal pain, vomiting, sweating, confusion or an irregular heartbeat. Thus, their determination in trace quantities is of great importance.

In this study, the electrochemical behaviors of PAR, ASA and CAF on a graphene-nafion (GR-NF) nanocomposite modified glassy carbon electrode (GCE) were investigated by cyclic voltammetry (CV), and adsorptive stripping square-wave voltammetry (AdSSWV).

When a comparative study was carried out employing AdSSWV for PAR, ASA and CAF on bare GCE, GR/GCE and GR-NF/GCE, it could be observed that the best results for both peak current and peak potential were obtained from the GR-NF/GCE (Figure 1). The oxidation peak currents of the three compounds on this electrode were linearly dependent on PAR, ASA and CAF concentrations in the ranges of 0.00125–0.25  $\mu\text{g mL}^{-1}$ , 0.05–5  $\mu\text{g mL}^{-1}$  and 0.05–10  $\mu\text{g mL}^{-1}$  in the individual detection of each component, respectively. By simultaneously changing the concentrations of PAR, ASA and CAF, their electrochemical oxidation peaks appeared at 0.66, 1.04 and 1.45 V, and good linear current responses were obtained in the concentration ranges of 0.00125–0.075  $\mu\text{g mL}^{-1}$ , 0.15–3  $\mu\text{g mL}^{-1}$  and 0.05–2  $\mu\text{g mL}^{-1}$  with the detection limits of 0.00014, 0.0074 and 0.0064  $\mu\text{g mL}^{-1}$ , respectively. The proposed electrochemical sensor was successfully applied for quantifying PAR, ASA and CAF in commercial pharmaceutical formulations without any sample pretreatment. The prepared modified electrode showed several advantages, such as a simple preparation method, high sensitivity, very low detection limits and excellent reproducibility.

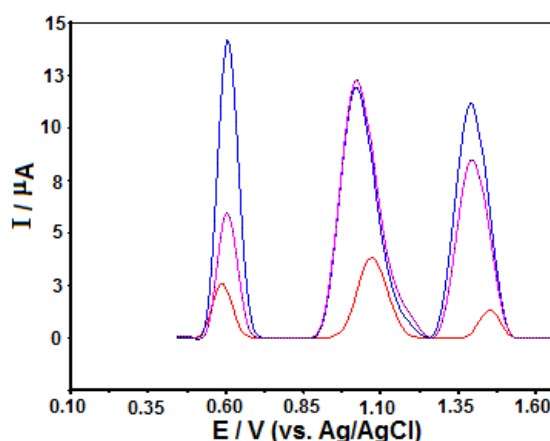


**Figure 1.** SW stripping voltammograms of PAR, ASA and CAF (from left to right) in phosphate buffer (pH 2.5) at GCE (red line), GR/GCE (purple line) and GR-NF/GCE (blue line).  $t_{\text{acc}}=60\text{s}$  at open circuit condition; SWV parameters: frequency, 50 Hz; scan increment, 8 mV; pulse amplitude, 30 mV.

## Acknowledgements

This research was funded by the Scientific and Technological Research Council of Turkey (TUBITAK) (Project number: KBAG114Z405).



# Cocoon Silk-Derived Carbon Nanospheres: Highly Activated Metal-Free Electrocatalysts for Reduction of Dissolved Oxygen and Glucose Sensing

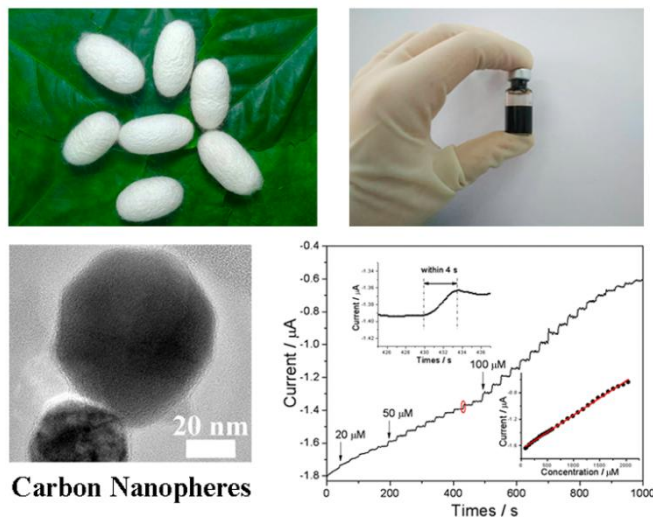
Tongtong Li, Yanyan Song\*

*Research Center for Analytical Sciences, College of Sciences, Northeastern University  
Wenhua Road 3-11, Shenyang 110004, China  
yysong@mail.neu.edu.cn*

In this work, we reported an N-doped porous carbon fiber by calcination of cocoon silk, which is world-widely abundant and has high nitrogen content. Using a simple nitric acid activation of the porous carbon fibers, the carbon nanospheres (CNS) with a diameter of 20-60 nm were achieved. Due to their abundant oxygen-rich groups and nitrogen content, the obtained CNS exhibited excellent electrocatalytic activity and long-term stability towards the reduction of dissolved oxygen at a low operating potential. The modified electrode based on CNS film displayed a linear range from 5.1 to 64.8  $\mu\text{M}$  and detection limit of 0.15  $\mu\text{M}$ . Considering the excellent electrocatalytic activity of the CNS toward the reduction of oxygen, the CNS were further applied in the construction of glucose amperometric biosensor using glucose oxidase as a model. The proposed glucose biosensor showed fast response (within 4 s), good stability and satisfied selectivity for glucose detection with a wide linear range from 79.7 to 2038.9  $\mu\text{M}$ , and a detection limit of 39.1  $\mu\text{M}$ . This work demonstrates the feasibility of CNS modified electrode in sensing application, and provides an effective approach to prepare CNS-based amperometric biosensors.

## Acknowledgements

This work was supported by the National Natural Science Foundation of China (No. 21322504, 11174046, 21275026), the Fundamental Research Funds for the Central Universities (N140505001, N140504006).



## Detection of semivolatile organic compounds (VOCs) in wastewater through current output of electrochemically active bacteria

Abeed Fatima Binti Mohidin Batcha, Kannan Palanisamy, Carlo Sntoro, Maria Yung, Thomas Seviour, Jamie Hinks, Federico Lauro and Enrico Marsili  
Singapore Centre on Environmental Life Sciences Engineering, Nanyang Technological University,  
60 Nanyang Drive, 637551 Singapore  
emarsili@ntu.edu.sg

Volatile and semi-volatile organic compounds (VOCs) are pollutants of concern, because they can be toxic to both microorganisms and humans. While some VOCs like N-methyl-2-pyrrolidone or dibutyl phthalate can be easily degraded in sludge and sewage water [1] or in the soil [2], other like 2,5-pyrrolidinedione, 1-methyl are poorly characterized in terms of their toxicity and environmental impacts. Semi-volatile VOCs are common organic solvents and are found in wastewater from electronics and textile industry. At concentration as low as 10-100 mg L<sup>-1</sup>, VOCs contribute to failure of used water treatment processes either through direct inhibition of biomass or because they are not degraded during biological treatment and are discharged in the effluent. Environmental, low cost detection of VOC is highly desirable in Singapore, because of its widely spread sewage network. Current methods for VOC detection are costly and often require off-line analysis. These shortcomings make current technology incompatible with distributed environmental VOC sensing.

Bioelectrochemical systems (BESs) represent an emerging technology that exploits so-called electroactive bacteria (EABs) to catalyze redox reactions at solid electrodes. The anodic current produced in BESs depends on the fitness of viable EABs in the device. Therefore, BESs can be used to sense toxic chemicals, as the latter decrease the vitality of the EAB community in the anodic chamber and hence current output. EABs capable of electron transfer to solid state electrodes are commonly encountered in used water and a BES that maintain a constant current output can be deployed with minimum material cost. In this study, we adopted screen printed graphite electrode coated with carbon nanotubes. EABs grown on these high surface electrodes produce high and stable current after few hours from inoculation.

We present results for amperometric detection of selected VOC in *Pseudomonas aeruginosa* and *Escherichia coli* pure cultures. Exogenous redox mediators (e.g., riboflavin, pyocyanin, AQDS and HNQ) were added to increase the current output and therefore the sensitivity to VOCs. Chronoamperometry was performed at oxidative potential (0.2 V vs. Ag/AgCl) on screen printed graphite electrodes coated with carbon nanotubes. In this setup, VOC detection limit was <25 ppm and response time was <1 min. The linear response range was 0-300 ppm for most of the VOC investigated. While the specificity of the proposed sensor requires further investigation (ongoing), this represent the first step for the development of genetically engineered community capable of high sensitivity and high selectivity VOC detection.

[1] ST Chow and TL Ng, 1983, *Water Res* 17, 117.

[2] W Den FH Ko, and TY Huang, 2002, *IEEE Trans Semicond Manufact* 15, 540.

# High Current Density Bioanodes for Ethanol Oxidation using PQQ-dependent Enzymes

Sidney Aquino Neto<sup>1</sup>, David P. Hickey<sup>2</sup>, Ross D. Milton<sup>2</sup>, Adalgisa R. De Andrade<sup>1</sup>, Shelley D. Minteer<sup>2</sup>

<sup>1</sup> Departamento de Química, Faculdade de Filosofia Ciências e Letras de Ribeirão Preto, Universidade de São Paulo, Ribeirão Preto, SP, Brazil

<sup>2</sup> Departments of Chemistry and Materials Science and Engineering, University of Utah, Salt Lake City, Utah 84112

netaoaquino@yahoo.com.br

Among the various alternative technologies for efficient energy conversion that have been developed over the past few decades, the use of enzymes immobilized onto the surface of electrodes as the main catalyst in biological fuel cells has been extensively reported. In this work, we explore the bioelectrooxidation of ethanol using PQQ-dependent alcohol and aldehyde dehydrogenase (ADH and AldDH) enzymes for biofuel cell applications. The bioanode architectures were designed in both direct electron transfer (DET) and mediated electron transfer (MET) mechanisms employing high surface area materials such as multi-walled carbon nanotubes (MWCNTs) and MWCNT-decorated gold nanoparticles along with different immobilization techniques. From the different polymeric matrices tested (tetrabutyl ammonium bromide (TBAB)-modified Nafion; octyl-modified linear polyethyleneimine (C8-LPEI); and cellulose) in DET studies, the modified Nafion membrane provided the best electrical communication between enzymes and the electrode surface, with catalytic currents as high as  $16.8 \pm 2.1 \mu\text{A cm}^{-2}$ . Considering the MET studies, the redox polymer 1,1'-dimethylferrocene-modified linear polyethyleneimine (FcMe<sub>2</sub>-C<sub>3</sub>-LPEI) provided the best electrochemical response. Using this polymer, the electrochemical assays conducted in the presence of MWCNTs and MWCNTs-Au indicated a  $J_{\text{max}}$  of  $781 \pm 59 \mu\text{A cm}^{-2}$  and  $925 \pm 68 \mu\text{A cm}^{-2}$ , respectively. Overall, from the results here obtained, DET using the PQQ-dependent ADH and AldDH still lacks of high current density generated, while the bioanodes that operate via MET employing Fc-modified LPEI redox polymers show efficient energy conversion capability.

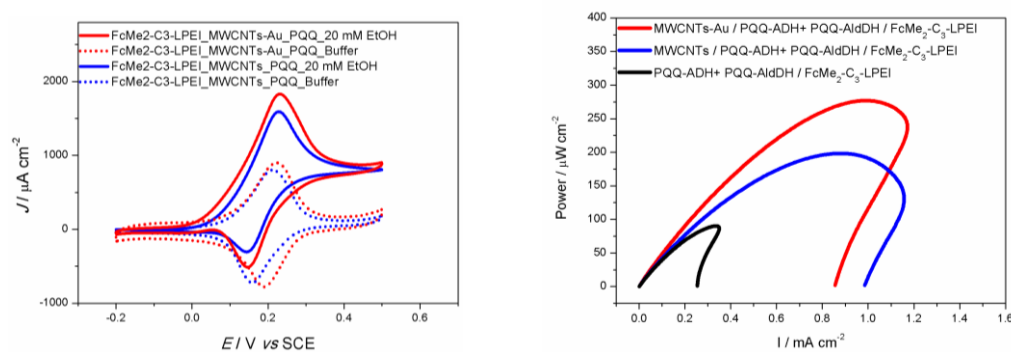


Figure 1. Representative cyclic voltammograms of the bioanodes based on FcMe<sub>2</sub>-C<sub>3</sub>-LPEI prepared with MWCNTs or MWCNTs-Au in the absence and in the presence of 20 mM ethanol (left) and power density curves obtained in ethanol/O<sub>2</sub> biofuel cell tests (right).

# Luminol Electrochemical-luminescence for Single Cell Analysis

Dechen Jiang

*School of Chemistry and Chemical Engineering, Nanjing University  
22 Hankou Rd, Nanjing, Jiangsu, 210092  
dechenjiang@nju.edu.cn*

Electrochemical imaging of single living cells suffers limitations owing to low throughput associated with scanning electrochemical microscopy, and to undesirably high detection limit associated with surface-plasmon-resonance-based electrochemical imaging techniques. In our group, luminol electrochemiluminescence (ECL) was applied for the imaging of hydrogen peroxide in single living cells with a spatial resolution of 0.8  $\mu\text{m}$ , thus establishing a novel electrochemical imaging technique for single cells with high analysis throughput and low detection limit. The technique was expanded to image surface-confined molecules by coupling the reaction of the molecules with their corresponding oxidase to generate hydrogen peroxide. Using this strategy, active membrane cholesterol was imaged in single cells, which could not be achieved using fluorescent assay. Compared with fluorescence assay that needed design the specific probe for each molecule, our ECL imaging strategy was universal for more molecules with the aid of commercial oxidases, and can distinguish the molecules with different chemical activity at cells. This success in ECL imaging of single living cells opens a new field in the imaging of biological samples.

## Reference

1. R. M. Wightman, Science 2006, 311, 1570-1574.
2. S. Amemiya, A. J. Bard, F. R. F. Fan, M. V. Mirkin, P. R. Unwin, Annu.Rev. Anal. Chem, 2008, 1, 95-131.
3. C. X. Tian, J. Y. Zhou, Z. Q. Wu, D. J. Fang, D. C. Jiang, Anal Chem, 2014, 86, 678-684.

# DNA Heptamers with Different Central Trinucleotide Sequences Studied by Electrochemical and Spectral Methods

Iveta Pilarova <sup>a</sup>, Libuse Trnkova <sup>a,b</sup>

<sup>a</sup>*Department of Chemistry, Faculty of Science, Masaryk University, Kamenice 5, Brno 625 00, Czech Republic*

<sup>b</sup>*Central European Institute of Technology, Brno, University of Technology, Technicka 3058/10, 616 00 Brno, Czech Republic e-mail: [libuse@chemi.muni.cz](mailto:libuse@chemi.muni.cz)*

Monitoring the relationship between a structure and the corresponding electrochemical response is very important not only from the aspect of the knowledge of dynamic structural changes to the charged interface (electrode surface, membrane, surface of the gel), but also in terms of proper evaluation of the electrochemical signals for potential biosensors. This relationship was studied for the case of short DNA fragments, the heptamer d(GCGAAGC) with its analogs carrying different trinucleotide sequences in the center of the molecule (XXX = AAA, CCC, GGG or TTT) and hexamers of d(GCGAGC) type with different dinucleotide sequences. All fragments were investigated by spectral methods (CD and UV spectra) and electrochemical methods (cyclic and linear sweep voltammetry, polyacrylamide gel electrophoresis). For deeper understanding of DNA heptamers and hexamers behavior on the electrode surface (mercury and carbon) the elimination voltammetric procedure (EVP) for reduction and oxidation responses was used. The EVP indicated strong adsorption of reduced form of guanine on a mercury electrode (readable peak-counterpeak signal). Our results showed that (i) the central triplet GAA or AAA dramatically stabilizes DNA heptamers, (ii) a stem-loop configuration is not supported by CCC or TTT sequences, instead, these heptamers adopt bimolecular duplex forms, and finally (iii) in the case of GGG sequence a very stable supramolecular G - quadruplex is formed. In the next experiments, we compared DNA and RNA fragments. DNA heptamers and hexamers provided double oxidation peaks (GI and GII) while RNA analogs provide only a single G peak. Based on this fact, DNA or RNA fragments can be quickly and inexpensively distinguished.

## References

- [1] I. Pilarova, I. Kejnovska, M. Vorlickova, L. Trnkova, Dynamic Structures of DNA Heptamers with Different Central Trinucleotide Sequences Studied by Electrochemical and Spectral Methods *Electroanalysis*, 26 (2014) 2118.
- [2] L. Trnkova, Application of Elimination Voltammetry with Linear Scan in Bioelectrochemistry, in: V. Adam and R. Kizek (Eds.), *Utilizing of Bioelectrochemical and Mathematical Methods in Biological Research*, Ch. 4, Signpost, India 2007, p.51.
- [3] J. Hrbac, V. Halouzka, L. Trnkova, J Vacek, eL-Chem Viewer: A Freeware Package for the Analysis of Electroanalytical Data and Their Post-Acquisition Processing, *Sensors* 14 (2014) 13943.

## Acknowledgement

This research was supported by the CEITEC – Central European Institute of Technology Project CZ. 1.05/1.1.00/02.0068, by the projects: MUNI/A/0972/2013 and LH 13053 KONTAKT II of the Ministry of Education, Youth and Sports of the Czech Republic.

# Nitrogen-doped Carbon Electrodes for Simultaneous Detection of Dopamine, Uric Acid and Ascorbic Acid

Ming-Chang Yang, Yi-Kai Chih, and Ya-Yun Zhan

Department of Chemical Engineering, National Cheng Kung University

University Rd. 1, East District, Tainan, Taiwan 70101

mcyang@mail.ncku.edu.tw

Dopamine (DA), uric acid (UA) and ascorbic acid (AA) are important biomolecules in human bodies. Previous studies have proven that many diseases are associated with their concentrations. Abnormal secretion of DA can lead to schizophrenia and Parkinson's disease. High concentrations of UA can lead to hyperuricemia, gout, and other diseases. AA is a powerful antioxidant that is effective against the superoxide radical, the hydroxyl radical. The content of AA in biological fluids can be prevented cancer, diabetes and hepatic disease. Monitoring the concentrations of DA, UA and AA in blood or urine is an effective early warning sign for central nervous system or kidney diseases.

Two nitrogen-doped carbon materials were successfully applied to detect DA, UA and AA simultaneously in this report. For the first material, graphene oxide (GO) was synthesized from graphite powder by a modified Hummers method. Polyvinylpyrrolidone (PVP) was then mixed with GO dispersion in water. After heat treatment in oven, the thermally reduced GO was doped with nitrogen (NGO). The carbon material is coated on glassy carbon electrode with binder of Nafion. The differential pulse voltammogram (DPV) showed the detection peaks for DA, UA and AA are well separated (fig. 1). The heat treatment condition played important effect on the detection ability. Other effects of the preparation condition on the sensing behaviors will be reported.

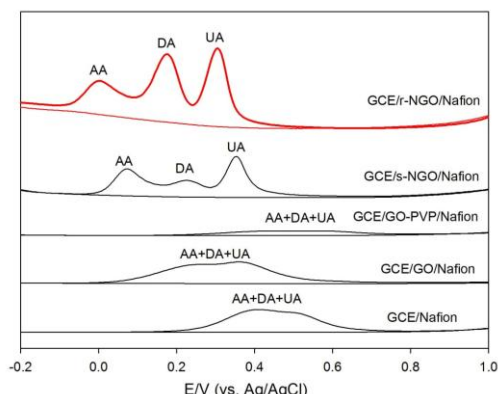


Fig. 1 DPVs for GCE/r-NGO-Nafion electrode and other electrodes in 0.1M PBS (pH 7.0) containing 10  $\mu$ M DA, 180  $\mu$ M UA and 1,000  $\mu$ M AA.

For the second material, dopamine was first polymerized on zinc oxide nanoparticles. After pyrolysis in nitrogen atmosphere, mesoporous carbon material formed with nitrogen doping. Hollow-type mesoporous carbon with nitrogen doping formed after template removal. The carbon material was coating on electrode and showed good peak separation for DA, UA and AA (fig. 2). The amount of ink for coating affected the sensing ability. Other effects of the preparation conditions on the sensing behaviors will be also reported.

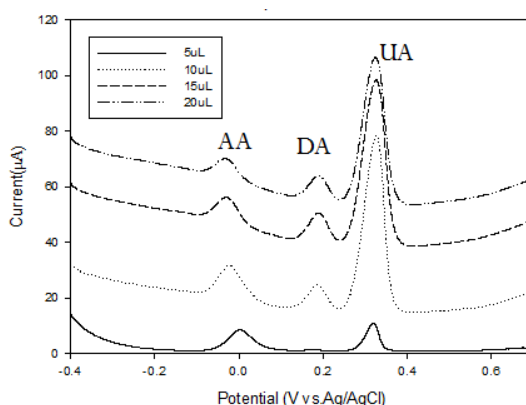


Fig. 2 DPVs for nitrogen-doped hollow mesoporous carbon in 0.1M PBS (pH 7.0) containing 10  $\mu$ M DA, 90  $\mu$ M UA and 500  $\mu$ M AA.

# Surface-Enhanced Raman Spectroscopic study of a DNA Beacon Probe Immobilized at a Au Electrode

Yung-Chun Lin<sup>1</sup>, James Richardson<sup>2</sup>, Tom Brown<sup>2</sup> and Philip N. Bartlett<sup>1</sup>

<sup>1</sup>Chemistry, University of Southampton, Southampton, SO17 1BJ, UK.

<sup>2</sup>Department of Chemistry, University of Oxford, Chemistry Research Laboratory, 112 Mansfield Road, Oxford, OX1 3TA, UK.

yl46g11@soton.ac.uk

The conformational changes of oligonucleotides at charged surfaces are a core issue in the development of biosensors<sup>1-3</sup>. In the present work we used a 35 mer beacon probe having a 7 mer self-complementary region at both termini. The beacon probe was labeled with Texas Red at the 3' end as a Raman label and attached to the gold surface through three cyclic disulfides at the 5' end together with mercaptohexanol to passivate the surface. Electrochemical and Raman measurements were made simultaneously on sphere segment void (SSV)<sup>4</sup> SERS active surfaces. On scanning the potential two overlapping potential regions show distinct reversibility in the SER spectra. On the first cathodic cycle the mercaptohexanol reductively desorbs [2] around -0.7 V leading to a restructuring of the immobilised oligonucleotide which is seen in the SER spectra which then stabilise on repeated cycling. Over the potential region from -0.3 to -0.9 V vs. Ag/AgCl, the surface structure contained desorbed mercaptohexanol reorganized the packing structure with beacon probe to form a quasi-stable self-assembly monolayer on the surface<sup>2</sup>. This observation provides insight into the behavior of the immobilized DNA on a mercaptohexanol-passivated electrode that is of benefit to DNA biosensor working at negative potentials.

Mis en forme : Non Surlignage

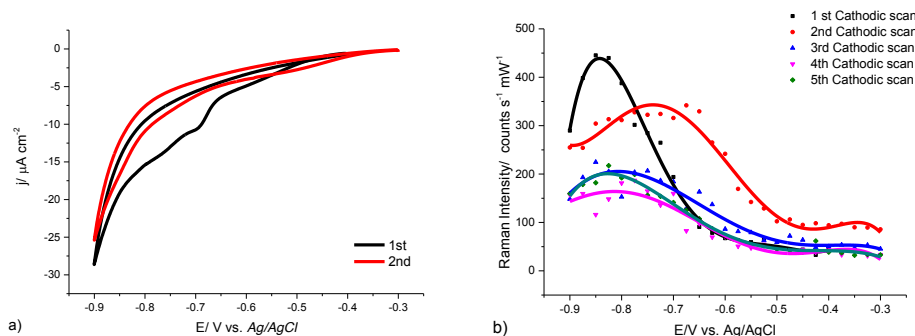


**Figure.** Five consecutive scans from -0.3 to -0.9 V vs. Ag/AgCl and back recorded at 1 mV/s for a DNA beacon probe immobilized at a gold SSV surface together with mercaptohexanol. a) The voltammetric response (only the first two scans are shown for clarity; b) the corresponding variation in the intensity of Texas Red band in the SER spectrum at  $1500 \text{ cm}^{-1}$ .

## References

1. Mahajan, S.; Richardson, J.; Brown, T.; Bartlett, P. N. *J. Am. Chem. Soc.* **2008**, *130*, 15589.
2. Josephs, E.; Ye, T. *Nano Lett.* **2012**, *12*, 5255.
3. Kaiser, W.; Rant, U. *J. Am. Chem. Soc.* **2010**, *132*, 7935.

4. Mahajan, S.; Cole, R. M.; Soares, B. F.; Pelfrey, S. H.; Russell, A. E.; Baumberg, J. J.; Bartlett, P. N. *J. Phys. Chem. C* **2009**, *113*, 9284.



# Fabrication of Uniform Metal-organic Framework Thin Film via Inkjet Printing Technology and its Application as a Nitrite Sensor

Chun-Hao Su, Chung-Wei Kung, Kuo-Chuan Ho<sup>\*1</sup>, and Ying-Chih Liao<sup>\*2</sup>  
*Department of Chemical Engineering, National Taiwan University, Taipei, Taiwan*  
*Address: No. 1, Sec. 4, Roosevelt Rd., Taipei 10617, Taiwan (R.O.C.)*  
*e-mail address<sup>\*1</sup>: kcho@ntu.edu.tw*  
*e-mail address<sup>\*2</sup>: liaoy@ntu.edu.tw*

Nitrite in physiological systems can form nitrosamines by interacting with amines, which are toxic and carcinogenic substances, and thus brings serious problems, such as eutrophications and many potential hazards to human health [1-2]. Therefore, accurate determination of nitrite is important to reduce human health risks. Many techniques have been developed for determining nitrite, such as flow injection analysis, colorimetric method, chemiluminescence, and electrochemical analysis. Recently, metal-organic frameworks (MOF), [3] a class of three-dimensional (3D) porous materials constructed of organic linkers and metal-based nodes, have shown their great potential in electrochemical applications due to their ultrahigh surface area, regular nanostructured pores, and high permanent porosity.

In this study, we fabricate a thin film MOF sensor for nitrite based on inkjet printing technology. First, specific MOF-525 nanocubes with high electrocatalytic activity toward nitrite oxidation is synthesized and categorized by size. With proper ink formulation and particle suspension, MOF-525 inks are inkjet-printed to form uniform thin films on gold electrodes to find the optimal size for nitrite sensing. The sensitivity, stability and repeatability with potential applications of the printed sensors will be carefully examined to demonstrate the feasibility of printed sensors for quick and accurate determination of nitrite.

## References

1. S.R.Carpenter, N.F.Caraco, D.L.Correll, R.W.Howarth,A.N.Sharpley,V.H.Smith,Ecol.Appl., 8,559–568(1998).
2. S.S.Mirvish, Cancer Lett.,93, 17–48 (1995).
3. C.-W. Kung, T.-H. Chang, L.-Y. Chou, J. T. Hupp,O. K. Farha and K.-C. Ho, Chem. Commun.,51,2414-2417(2015).

# Anthraquinone labelled DNA for direct detection and discrimination of closely related DNA targets

Rachel Gao<sup>a</sup>, Sarah A. Goodchild<sup>b</sup> and Phillip N. Bartlett<sup>a</sup>

<sup>a</sup>*School of Chemistry, University of Southampton, Southampton, SO17 1BJ*

<sup>b</sup>*DSTL, Porton Down, Salisbury, Wiltshire, SP4 0JQ*

*rg805@soton.ac.uk*

A novel detection approach using immobilised DNA probes labelled with Anthraquinone (AQ) as an electrochemically active reporter moiety has been successfully developed as a new, simple, reliable method for the detection of DNA. This method represents a step forward in DNA detection as it can discriminate between multiple nucleotide polymorphisms within target DNA strands without the need for any additional reagents, reporters or processes such as melting of DNA strands. The detection approach utilises single stranded DNA probes immobilised on gold surfaces labelled at the distal terminus with AQ. The effective immobilisation has been monitored using techniques such as AC impedance and Raman spectroscopy. Simple voltammetry techniques (Differential Pulse Voltammetry, Cyclic Voltammetry) are then used to monitor the reduction potential of the AQ before and after the addition of complementary strand of target DNA. A reliable relationship between the shift in reduction potential and the number of base pair mismatch has been established and can be used to discriminate between DNA from highly related pathogenic organisms of clinical importance. This indicates that this approach may have great potential to be exploited within biosensor kits for detection and diagnosis of pathogenic organisms in Point of Care devices.

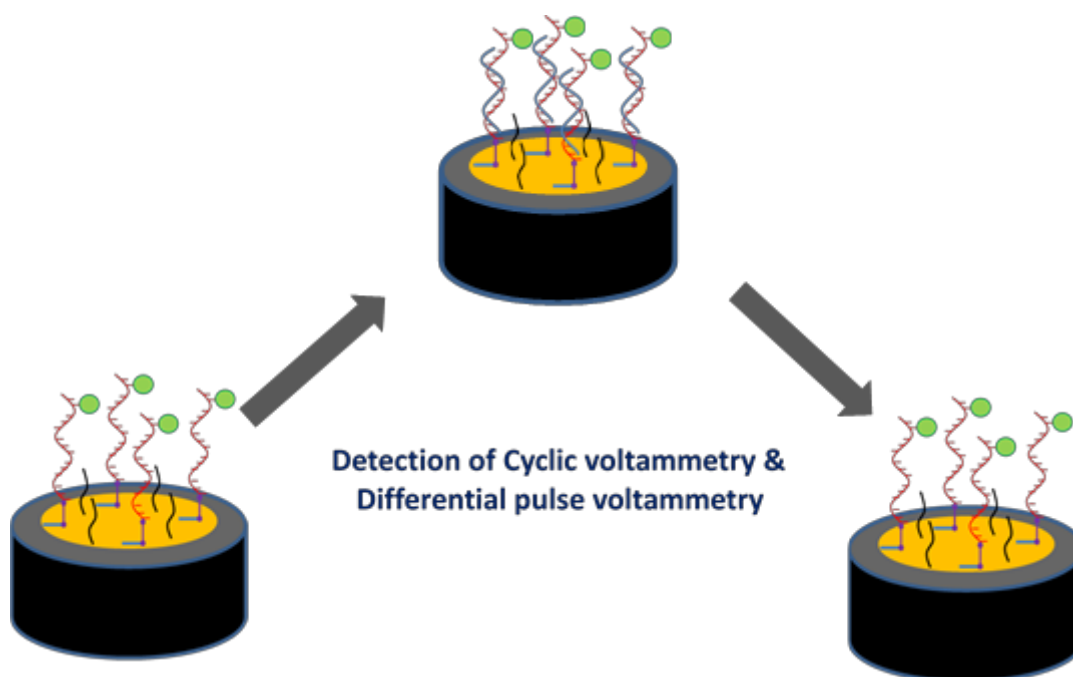


**Figure 1.** DNA hybridisation detection process.

# Electrochemical Communication between Photosynthetic Membranes/Cells and Electrodes

Lo Gorton<sup>1</sup>, Kamrul Hasan<sup>1</sup>, Galina Pankratova<sup>1</sup>, Dónal Leech<sup>2</sup>, Cecilia Hägerhäll<sup>1</sup>, Sinan Cem Emek<sup>1</sup>, Per-Åke Albertsson<sup>1</sup>, Hans-Erik Åkerlund<sup>1</sup>, Yusuf Dilgin<sup>3</sup>, Michael A. Packer<sup>4</sup>, Eva Sperling<sup>1</sup>, Peter ÓConghaile<sup>2</sup>, Huseyin Bekir Yildiz<sup>5</sup>, Dmitrii Pankratov<sup>6</sup>, Sergey Shleev<sup>6</sup>

<sup>1</sup> Lund University, P.O.Box 124, SE-221 00 Lund, Sweden, <sup>2</sup> National University of Ireland Galway, Galway, Ireland, <sup>3</sup> Çanakkale Onsekiz Mart University, Çanakkale, Turkey, <sup>4</sup> Cawthron Institute, 98 Halifax Street, Nelson, New Zealand, <sup>5</sup> KTO Karatay University, 42020 Konya, Turkey, <sup>6</sup> Malmö University, 20560 Malmö, Sweden

Lo.Gorton@biochemistry.lu.se

Electrochemical transfer communication between bacterial cells/biological membranes and electrodes can usually be obtained through the use of freely diffusing monomeric redox mediators. Previously we have, however, also shown that flexible osmium redox polymers can work as efficient mediators for a number of both Gram– as well as Gram+ bacteria and electrodes, clearly showing that the mediator does not need to pass the inner membrane to be able to shuttle the charge between the cells and the electrode [1,2]. As a continuation of our work on bacterial cells [3-8] we have now turned to various photosynthetic organisms/membrane systems. Here we report on electrochemical communication between whole viable photosynthetic bacterial cells (*Rhodobacter capsulatus* [9,10] and *Leptolyngbia* sp. [11].) as well as with eukaryote systems (thylakoid membranes from spinach [12,13], the eukaryote unicellular algae *Paulschulzia pseudovolvox* [14]) and electrodes through the use of osmium redox polymers. Here we also report on how to increase the efficiency of the charge transfer from the photosynthetic reaction centres to the electrode as well as to increase the stability of the system.

- [1] K. Hasan, S. A. Patil, D. Leech, L. Gorton, *Biochem. Soc. Rev.*, **40** (2012) 1330-1335.
- [2] S. A. Patil, C. Hägerhäll, L. Gorton, *Bioanal. Rev.*, **4** (2012) 159–192.
- [3] I. Vostiar, E. E. Ferapontova, L. Gorton, *Electrochem. Commun.*, **6** (2004) 621-626
- [4] S. Timur, B. Haghighi, J. Tkac, N. Pazarlioglu, A. Telefoncu, L. Gorton, *Bioelectrochemistry*, **71** (2007) 38-45.
- [5] S. Timur, U. A. Kirgoz, D. Odaci, L. Gorton, *Electrochem. Commun.*, **9** (2007) 1810–1815.
- [6] S. Alferov, V. Coman, Tobias Gustavsson, A. Reshetilov, C. von Wachenfeldt, C. Hägerhäll, L. Gorton, *Electrochim. Acta*, **54** (2009) 4979-4984.
- [7] V. Coman, T. Gustavsson, A. Finkelsteinas, C. von Wachenfeldt, C. Hägerhäll, L. Gorton, *J. Am. Chem. Soc.*, **131** (2009) 16171-16176.
- [8] S. A. Patil, K. Hasan, D. Leech, C. Hägerhäll, L. Gorton, *Chem. Commun.*, **48** (2012) 10183–10185.
- [9] K. Hasan, S. A. Patil, K. Gorecki, C. Hägerhäll, L. Gorton, *Bioelectrochemistry*, **93** (2013) 30–36.
- [10] K. Hasan, K. V. Raghava Reddy, V. Eßmann, K. Górecki, P. ÓConghaile, W. Schuhmann, D. Leech, C. Hägerhäll, L. Gorton, *Electroanalysis*, **27** (2015) 118–127 .
- [11] K. Hasan, H. B. Yildiz, E. Sperling, P. ÓConghaile, M. A. Packer, D. Leech, C. Hägerhäll, L. Gorton, *Physical Chemistry Chemical Physics*, **16** (2014) 24676-24680.
- [12] K. Hasan, Y. Dilgin, S. Cem Emek, M. Tavahodi, H.-E. Åkerlund, P.-Å. Albertsson, L. Gorton, *ChemElectroChem*, **1** (2014) 131–139.
- [13] H. Hamidi, K. Hasan, S. C. Emek, Y. Dilgin, H.-E. Åkerlund, P.-Å. Albertsson, D. Leech, L. Gorton, *ChemSusChem*, **8** (2015) 990-993.
- [14] K. Hasan, E. Çevik, E. Sperling, M. A. Packer, D. Leech, L. Gorton, *in manuscript*.

# Commercialization Strategies of Microbial Fuel Cells: Prevention of Voltage reversal in Stackable Approach

Bongkyu Kim, Yooseok Lee, Jisu Kim, In Seop Chang

*School of Environmental Science and Engineering, Gwangju Institute of Science and Technology (GIST)  
261 Cheomdan-gwagiro, Buk-gu, Gwangju 500-712, Korea  
b.kim0602@gmail.com, ischang@gist.ac.kr*

Microbial fuel cell system (MFCs) is a source technique for bio-electrochemical system (BES) including biosensors, bio-energy system, and especially bioelectronics device such as microbial electrolysis cell, microbial electro-synthesis cell, and microbial desalination cell and so on [1]. The MFCs is a device that produce bio-electricity by converting chemical energy to generate electricity with microbial metabolism [2]. Thus, the MFCs is also belongs to one part of the fuel cell. The biggest difference between the MFC and the typical fuel cell is the use of living organisms which is electrogenic bacteria as anodic catalysis to produce electron on anode [3]. For this reason, the advantage of the MFCs is use of a wide range of environment-friendly energy source, e.g., organic/inorganic compound in lake water, muds, wastewater, and sludge etc. On the other hand, a current production aspect is extremely low compared to the typical proton exchange membrane fuel cell (PEMFC) due to low anodic kinetic activity of the living organism. In addition, the working voltage of MFCs is also not enough that is around 0.2 ~ 0.5 V. Hence, to commercialize the MFCs, increases of currents as well as voltages are necessary [4]. To meet the needs, stack system has been frequently tried in MFCs with power management system. However, when the MFCs are connected as serially, a voltage reversal is seriously occurred which is the voltage of unit cell connected in series is reversed [5]. In this situation, the reversed unit cell is not working as galvanic cell, and it is working as electrolysis cell. In the PEMFC, the voltage reversal is generated mainly by fuel starvation and fuel crossover. However, in the MFCs, the voltage reversal is mainly occurred by unbalance of unit cells' performances, especially kinetic difference of unit cells. The voltage reversal is more magnified at scale-up of MFCs for commercialization. Therefore in this paper, to understand the reason of voltage reversal in MFCs, and also to prevent the voltage reversal, multiple electrode MFC was designed [6] and assistance current method was suggested with controlling current system [7].

- [1] B. E. Logan, B. Hamelers, R. Rozendal, U. Schröder, J. Keller, S. Freguia, *et al.*, "Microbial fuel cells: methodology and technology," *Environmental science & technology*, vol. 40, pp. 5181-5192, 2006.
- [2] B. H. Kim, D. H. Park, P. K. Shin, I. S. Chang, and H. J. Kim, "Anode, cathode, microbial catalyst," ed: Google Patents, 1999.
- [3] B. H. Kim, I. S. Chang, and G. M. Gadd, "Challenges in microbial fuel cell development and operation," *Applied Microbiology and Biotechnology*, vol. 76, pp. 485-494, 2007.
- [4] D. Kim, J. An, B. Kim, J. K. Jang, B. H. Kim, and I. S. Chang, "Scaling-Up Microbial Fuel Cells: Configuration and Potential Drop Phenomenon at Series Connection of Unit Cells in Shared Anolyte," *ChemSusChem*, vol. 5, pp. 1086-1091, 2012.
- [5] J. An and H. S. Lee, "Occurrence and Implications of Voltage Reversal in Stacked Microbial Fuel Cells," *ChemSusChem*, vol. 7, pp. 1689-1695, 2014.
- [6] B. Kim, J. An, D. Kim, T. Kim, J. K. Jang, B.-G. Lee, *et al.*, "Voltage increase of microbial fuel cells with multiple membrane electrode assemblies by in series connection," *Electrochemistry Communications*, vol. 28, pp. 131-134, 2013.
- [7] B. Kim, B. G. Lee, B. H. Kim, and I. S. Chang, "Assistance Current Effect for Prevention of Voltage Reversal in Stacked Microbial Fuel Cell Systems," *ChemElectroChem*, 2015.

# Hydrogenated and 4-Sulfobenzene Modified Conical-tip Carbon Electrodes with Antifouling Property for Sensitive Detection of Dopamine

Shajahan Siraj, Danny K. Y. Wong

*Department of Chemistry and Biomolecular Science, Macquarie University*

*Sydney, NSW 2109, Australia*

*shajahan.siraj@students.mq.edu.au*

In this work, we report the development and application of physically small conical-tip carbon electrodes (approximately 2  $\mu\text{m}$  diameter and 15  $\mu\text{m}$  axial length), consisting of a hydrophobic surface that was grafted with a 4-sulfobenzene layer, as an antifouling sensor to the detection of the neurotransmitter dopamine. During detection of dopamine *in vivo*, amphiphilic proteins, peptides and lipids present in extracellular fluid can easily adsorb on an electrode surface and cause fouling. This surface barrier prevents dopamine from making contact with the electrode for electron transfer reaction, yielding a slowly diminishing transient detection signal. This may then give rise to results that are less meaningful. In our work, we exploit a hydrophobic carbon surface, achieved by hydrogenating the carbon electrode using an *n*-butylsilane reduction method, to discourage adsorption of the amphiphilic species. In addition, a bonus is that the hydrophobic surface was found to be unfavourable for the oxidation of ascorbic acid, which is often a major interfering agent during dopamine detection. However, after hydrogenation, slower dopamine oxidation kinetics were observed at these modified electrodes, resulting in a 13% decrease of the dopamine oxidation current. This is also supported by an increase in the charge transfer resistance of dopamine at the hydrophobic electrode compared to that at a bare electrode, as determined by electrochemical impedance spectroscopy. Next, a 4-sulfobenzene layer was immobilised on the electrode to introduce negatively charged groups for electrostatic attraction towards positively charged dopamine (under physiological pH) and thus increase the electron transfer kinetics of dopamine at the electrode. In characterising the modified electrodes, we observed a 4% increase in the reduction current of  $[\text{Ru}(\text{NH}_3)_6]^{3+}$  and a 4% increase in the oxidation current of dopamine owing to enhanced adsorption of the analytes on the grafted sulfobenzene layer. More significantly, the fabricated electrodes retained 87% sensitivity to dopamine after being incubated in a synthetic fouling solution containing 1.0% (v/v) caproic acid (a lipid), 4% (w/v) bovine serum albumin and 0.01% (w/v) cytochrome c (both are proteins), and 0.002% (w/v) human fibrinopeptide B (a peptide) for 30 min. In contrast, hydrogenated electrodes were found to retain only 65% sensitivity in dopamine detection under identical experimental conditions. These results support minimal fouling at the fabricated electrodes *in vitro*.

# Probing Laccase Immobilization on Modified Gold Electrodes and Conformational Changes by Surface-Enhanced Infrared Absorption Spectroscopy

Maciej Karaskiewicz, Jerzy Rogalski, Renata Bilewicz, Jacek Lipkowski  
College of Inter-Faculty Individual Studies in Mathematics  
and Natural Sciences, University of Warsaw  
93 Zwirki i Wigury Street, Warsaw  
mkaraskiewicz@chem.uw.edu.pl

Reduction of oxygen catalysed by blue-copper oxidases (e.g. laccase) is a common reaction applied in biofuel cells [1]. Therefore, better understanding of enzyme electrode reaction and orientation of laccase on the electrode may have great impact on the efficiency of oxygen reduction and, as a result, on the biofuel cell characteristics. There are several techniques suitable for in-depth studies of structural changes of enzymes *in-situ*. One of them is surface-enhanced infrared absorption spectroscopy (SEIRAS) combined with the electrochemical techniques. They allow to probe adsorption and conformational changes at various potentials [2]. In our work, laccase molecules were adsorbed on modified carbon nanotubes (CNTs). SEIRAS spectra of laccase adsorbed on CNTs recorded in the presence and absence of oxygen show sharp changes in intensity of Amide I and Amide II bands depending on potential, suggesting strong structural changes of  $\alpha$ -helix and minor  $\beta$ -sheet region of laccase molecule. It has been shown that gold electrodes covered with modified carbon nanotubes have completely different properties for the immobilization of enzymes compared to the SAM systems reported elsewhere [3]. It has been proven that a favorable environment for the immobilization of enzymes are carbon nanotubes and the amide I band of such a system occurs at a wavenumber, characteristic for the main, secondary and tertiary structure of laccase  $\beta$ -sheet. Synchronous spectra obtained by two-dimensional correlation spectroscopy, in argon and oxygen saturated solutions, show that laccase conformational changes take place mainly in the vicinity of active sites, which is the area of the  $\alpha$ -helix.

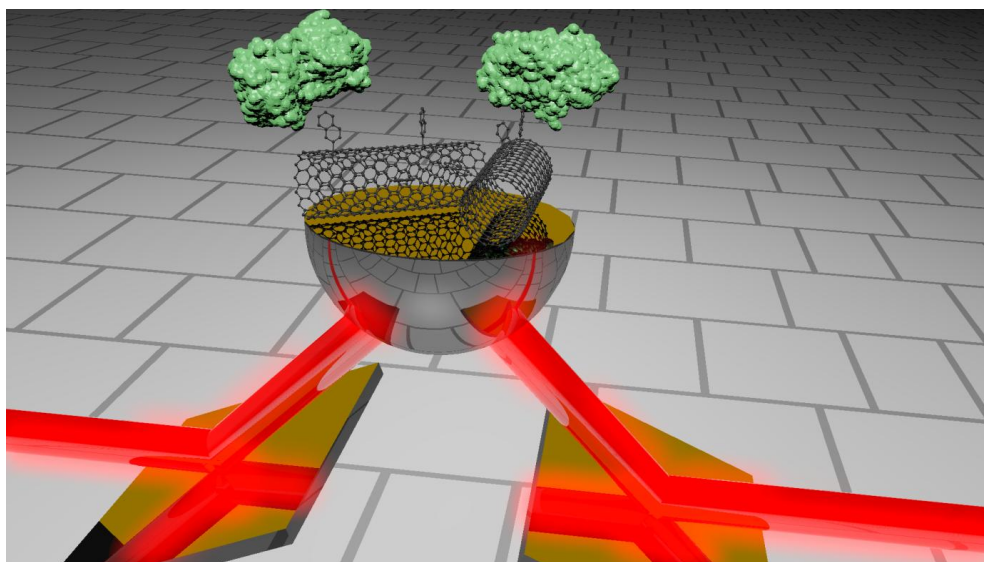


Fig. Scheme of described SEIRA system and thin film of gold modified with CNTs and laccase.

## References:

- [1] K. Stolarczyk; M. Kizling; D. Majdecka; K. Zelechowska; J. F. Biernat; J. Rogalski; R. Bilewicz, *J. Power Sources* 249 (2014) 263.
- [2] C. Zou; M. Larisika; G. Nagy; J. Srajer; Ch. Oostenbrink; X. Cheng; W. Knoll; B. Liendberg; Ch. Nowak *J. Phys. Chem. B* 117 (2013) 9606.
- [3] G. Gupta; V. Rajendran; P. Atanassov, *Electroanalysis*, 16 (2004) 1182.

# Bioelectrocatalysis with sol-gel biocomposite layers deposited onto porous electrodes

Alain WALCARIUS

*Laboratoire de Chimie Physique et Microbiologie pour l'Environnement (LCPME)  
UMR 7564 CNRS – Université de Lorraine, 405, rue de Vandoeuvre, 54600 Villers-les-Nancy, France  
alain.walcarius@univ-lorraine.fr*

Sol-gel-derived silica-based materials offer attractive features (rigid three-dimensional framework ensuring fast mass transport, ease of modification with a variety of organo-functional groups, host for various reactants, including biomolecules), which can be advantageously exploited in electrochemistry, at the condition to be manufactured in a controlled way ensuring a close contact to an electrode surface (e.g., as thin films of uniform morphology and homogeneous composition). Sol-gel thin films on electrodes are usually prepared by dip- or spin-coating, for which film formation occurs via solvent evaporation and concomitant condensation of the precursors. The approach operates quite well but it is basically restricted to deposition onto flat surfaces only (it may suffer from some drawbacks when applied to the modification of high surface area porous electrodes, such as pore blocking). On the other hand, sol-gel matrices are attractive hosts for enzymes owing to their excellent biocompatibility and thanks to the soft conditions associated to sol-gel processing. On that basis, significant developments appeared in the past on the use of sol-gel materials for elaborating electrochemical biosensors [1].

It will be discussed here how the electrochemically-assisted generation of bio-doped sol-gel films on highly porous electrodes with large surface areas constitutes an attractive method for bioelectrocatalysis purposes, notably for applications as electrochemical bioreactors for the production of fine chemicals. This will be exemplified here on the basis of dehydrogenase-type enzymes.

Functionalized silica thin films can be generated via an electrochemically-driven deposition method implying a local electrochemical tuning of pH at the electrode/solution interface to induce precursor condensation in a controlled way [2,3]. This approach is compatible with biomolecule encapsulation while maintaining its biological activity [4,5]. It can be applied to uniform deposition onto nanostructured electrodes such as macroporous gold [4] or assemblies of electrospun platinum fibers [5]. This strategy has been applied for the design of bioelectrocatalytic reactors made of dehydrogenase-based sol-gel films deposited over large area porous electrodes [6-9]. They were also molecularly engineered in the same time to include the co-factors and mediators necessary to build reagent-free electrochemical bioreactors [7-9]. Once again, electrochemistry was particularly attractive as it constitutes a unique way to deposit such biohybrids as uniform thin films onto non-flat surfaces of complex geometry (e.g., carbon felt electrodes, nanotubes assemblies, ordered macroporous electrodes), which are essential to get reactors with high yields and good operational stability [10].

- 
- [1] J. Wang, *Anal. Chim. Acta* 1999, 399, 21.
  - [2] R. Shacham, D. Avnir, D. Mandler, *Adv. Mater.* 1999, 11, 384.
  - [3] E. Sibottier, S. Sayen, F. Gaboriaud, A. Walcarius, *Langmuir* 2006, 22, 8366.
  - [4] F. Qu, R. Nasraoui, M. Etienne, Y. Bon Saint Côme, A. Kuhn, J. Lenz, J. Gajdzik, R. Hempelmann, A. Walcarius, *Electrochem. Commun.* 2011, 13, 138.
  - [5] I. Mazurenko, M. Etienne, R. Ostermann, B. Smarsly, O. Tananaiko, V. Zaitsev, A. Walcarius, *Langmuir* 2011, 27, 7140.
  - [6] Z. Wang, M. Etienne, G.-W. Kohring, Y. Bon Saint Côme, A. Kuhn, A. Walcarius, *Electrochim. Acta* 2011, 56, 9032.
  - [7] Z. Wang, M. Etienne, F. Quilès, G.-W. Kohring, A. Walcarius, *Biosens. Bioelectron.* 2012, 32, 111.
  - [8] Z. Wang, M. Etienne, S. Pöller, W. Schuhmann, G.-W. Kohring, V. Mamane, A. Walcarius, *Electroanalysis* 2012, 24, 376.
  - [9] Z. Wang, M. Etienne, V. Urbanova, G.-W. Kohring, A. Walcarius, *Anal. Bioanal. Chem.* 2013, 405, 3899.
  - [10] I. Mazurenko, W. Ghach, G.-W. Kohring, C. Despas, A. Walcarius, M. Etienne, *Bioelectrochem.* 2015, 104, 65.

# Biocathode based on a MgO-template Carbon Electrode Modified with ABTS and Bilirubin Oxidase

Seiya Tsujimura, Kazuki Murata

Division of Materials Science, Faculty of Pure and Applied Sciences, University of Tsukuba

1-1-1 Tennodai, Tsukuba, Ibaraki 305-8573, Japan

seiya@ims.tsukuba.ac.jp

Bilirubin oxidase (BOD) from *Myrothecium verrucaria* is one of the most widely used bioelectrocatalysts for the four-electron oxygen reduction reaction (ORR) under neutral pH conditions [1]. The interfacial electron transfer rate depends on the electron transfer distance between the electrode surface and the enzyme electrochemically active site, and the magnitude of the maximum catalytic current depends on the effective surface area available for the electrochemical reaction involving BOD. Therefore, when a mesoporous carbon electrode such as MgO-templated carbon (MgOC) [2] is used, BOD showed as high catalytic current density as 6 mA per geometric surface area, without a mediator on the rotating disk voltammetry at pH 5, 8000 rpm (Figure 1(A)). In order to improve the cathode performance, surface modifications were also exploited to enhance interfacial electron transfer from the electrode surface to the active site of BOD, or by loading BOD onto the surface by providing suitable attractive interactions. For example, enhanced catalytic current and stability of the BOD were reported on the electrode modified with 6-amino-2-naphthoic acid or bilirubin [3,4]. Meanwhile, in this study, by simply applying a solution consisting of a mixture of BOD and 2,2'-Azinobis(3-ethylbenzothiazolin-6-sulfonate) (ABTS) to the porous carbon, both of these compounds can be adsorbed on the electrode surface. The ABTS molecules can be adsorbed on the surface of MgOC and shows very stable redox behavior without undergoing a disproportionation, which would cause the degradation of these molecules. The maximum catalytic current increased twice in the presence of ABTS across a wide pH range (Figure 1(B)). The pH-dependence of the oxygen reduction voltammogram revealed that the ABTS adsorbed on the electrode surface accelerated the direct and mediated electron transfer rates by improving the orientation of BOD on the carbon surface or enhancing enzyme loading favorable for the electron transfer, and by mediating the electron transfer from the electrode to the electro-active site of BOD. We will also present a gas-diffusion type biocathode using MgOC with PTFE as a binder based on BOD/ABTS system.

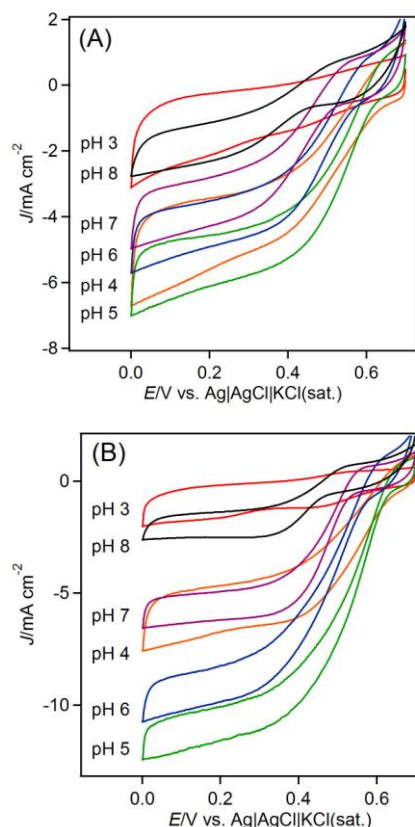


**Fig. 1.** Rotating cyclic voltammograms for the ORR on BOD-MgOC-E (A) and BOD/ABTS-MgOC-E (B) at pH 3.0, 4.0, 5.0, 6.0, 7.0, and 8.0 under O<sub>2</sub>-saturated conditions at 25 °C at 8000 rpm. Scan rate: 5 mV s<sup>-1</sup>.

## References:

- [1] S. Tsujimura et al., J. Electroanal. Chem., 496, 69-75 (2001).
- [2] S. Tsujimura et al., J. Am. Chem. Soc., 136, 14432-14437 (2014).
- [3] L. dos Santos et al., Phys. Chem. Chem. Phys., 12, 13962-13974 (2010).
- [4] J.A. Cracknell et al., Dalton Trans., 40, 6668-6675 (2011).



# Negative dielectrophoretic separation of cells based on the expression of specific surface antigen

Tomoyuki Yasukawa, Yuki Minakuchi, Hironobu Hatanaka, Fumio Mizutani  
Graduate School of Material Science, University of Hyogo  
3-2-1 Kouto, Kamigori, Ako, Hyogo 678-1297, Japan  
E-mail: yasu@sci.u-hyogo.ac.jp

**Introduction:** The expression patterns of surface antigens on cells are related to various diseases and differentiation. We have been applied dielectrophoresis (DEP) to fabricate the particle and cell pattern and applied particle manipulation for rapid and simple immunosensing. Recently, we also applied the combination of positive DEP (p-DEP) and negative DEP (n-DEP) to capture the specific cells by immunoreactions and separate the cells with specific surface antigen from a cell population. The use of this system enabled the rapid (3 min) and simple (label free) discrimination of specific cells. However, the cell binding efficiency was approximately half due to the use of a cell suspension medium with relatively low conductivity in which immunoreactivity is low. Unfortunately, no living cell experienced the attractive force of p-DEP in the higher conductivity region within the used frequency region (10 kHz–10 MHz). In this presentation, we employed n-DEP to fabricate two different cell patterns by switching the applied voltage and applied the method to discriminate and separate cells with a target antigen with high binding efficiency.

**Experiment methods:** Figure 1 depicts the method for detecting the surface antigen. The suspension of HL-60 cells with CD33 antigen was introduced into the device consisted of an upper indium tin oxide (ITO) electrode and a lower ITO-interdigitated band array (ITO-IDA) electrode. The surface of the ITO-IDA electrode substrate was modified with the anti-CD 33 antibody. When AC voltage is applied between the upper ITO and lower ITO-IDA electrodes, the cells accumulate at the gap regions between the IDA bands by n-DEP, thereby accelerating the capture of cells with the target antigen via an immunoreaction. After the applied voltage for band B was switched off, electric fields disappeared between the upper ITO and band B and appeared between bands A and B, thereby leading to the formation of relatively weak electric field areas above band B. Thus, unbound cells were removed from the gap region to the area above band B to form another line pattern. The ratio of the captured cell density (cell binding efficiency) was calculated from the optical images of the two different patterns.

**Results and discussion:** Cells dispersed randomly in the channel and rapidly accumulated in the gap area between the bands within 5 s due to the repulsive force of n-DEP. We removed the cells accumulated in the gap by switching the voltage of band B to zero 60 s after cells had accumulated. When the cells accumulated in the gap modified with anti-CD33, some cells moved to the area above band B, whereas others remained even after the band B voltage was switched to zero. In contrast, almost all cells moved to the area above band B after voltage was switched to zero, and cells accumulated in the gap modified with non-specific anti-mouse IgG. These results indicate that the cells with CD33 surface antigens reacted with the antibodies to be irreversibly captured at that position. Cell binding efficiency was estimated from the steady-state value and was  $68.3 \pm 3.2\%$ . Moreover, the swing of accumulated cells allowed further improvement of cell binding efficiency ( $83.9 \pm 1.4\%$ ). Times as short as 60 s and 30 s were required to capture the cells with immunoreactions and to remove unbound cells, respectively. Therefore, cells with CD33 cell surface antigens could be rapidly identified from the cell suspension with high binding efficiency by spatial separation based on an immunoreaction and manipulation by n-DEP.

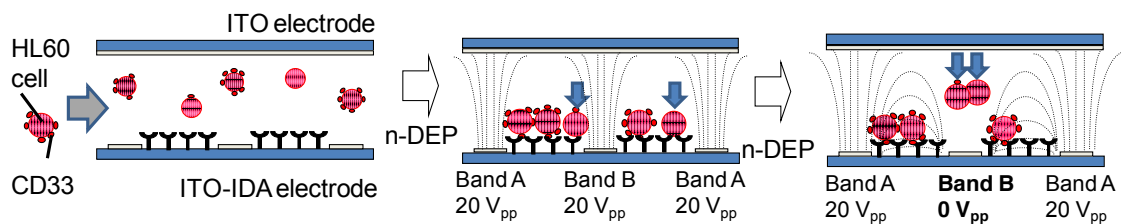


Fig. 1 Discrimination of cells with specific surface antigens using n-DEP manipulation.

# Redox polymers @ bioelectrochemistry. From biosensors to biofuel cells and self-powered bioelectrochemical devices

Wolfgang Schuhmann<sup>1</sup>, Adrian Ruff<sup>1</sup>, Piyanut Pinyou<sup>1</sup>, Sabine Alsaoub<sup>1</sup>, Fangyuan Zhao<sup>1</sup>, Francesca Lopez<sup>1</sup>, Stefan Barwe<sup>1</sup>, Nikola Markovic<sup>1</sup>, Corina Andronesu<sup>2</sup>, Nicolas Plumeré<sup>3</sup>

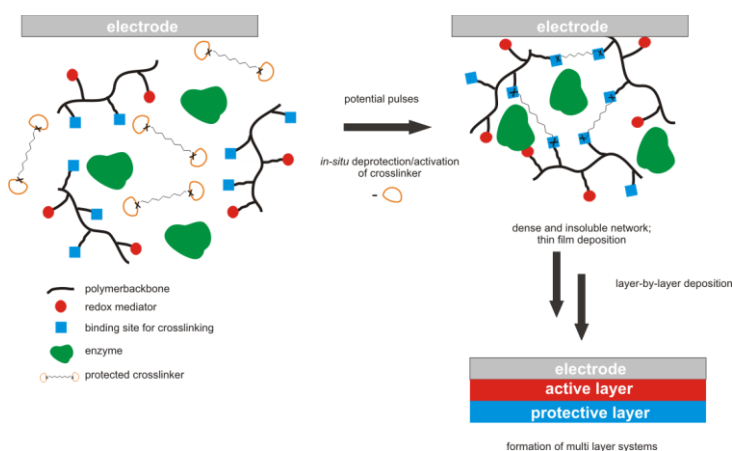
<sup>1</sup> Analytical Chemistry – Center for Electrochemical Sciences (CES); Ruhr-Universität Bochum; Universitätsstr. 150; D-44780 Bochum, Germany

<sup>2</sup> Advanced Polymer Materials Group; University “Politehnica” of Bucharest; 1-7, Gh. Polizu Street, Bucharest, Romania

<sup>3</sup> Center for Electrochemical Sciences (CES) – Molecular Nanostructures; Ruhr-Universität Bochum; Universitätsstr. 150; D-44780 Bochum, Germany  
wolfgang.schuhmann@rub.de

Wiring of redox enzymes to electrodes surfaces is of key for optimization of properties of biosensors, biofuel cells and bioelectrochemical devices. Besides the adaptation of the formal potential of the polymer bound redox relay to the active site of the polymer-integrated biological recognition element, the properties of the polymer backbone itself, the swelling properties, the permeability for substrate and products, restricting the access of potentially interfering compounds and adding suitable anti-interference layers is of high importance. Moreover, strategies for non-manual immobilization of all components in a highly reproducible way even allowing the formation of complex bioelectrochemically active layers is becoming increasingly important.

In this contribution, we suggest a new strategy for the rational build-up of complex sensor architectures using the previously reported electrochemically induced activation of bifunctional crosslinkers by cleaving off the protecting groups [1]. By careful design of the redox polymers using novel strategies for achieving more uniform molecular-weight distribution together with high loading of the redox relay and crosslinkable sites a new generation of bioelectrodes was achieved. Examples will include the protection



of sensitive enzymes within redox polymers, the design of biofuel cells with high open circuit voltage and high power densities, the use of these type of biofuel cells in self-powered bioelectrochemical devices e.g. for glucose determination or antibiotic determination in milk. The self-powered bioelectrochemical devices were further extended to instrument free bioelectrochemical devices by converting the biocatalytic current into an optical read-out capability.

[1] S. Pöller, D. Koster, W. Schuhmann, *Electrochem. Commun.* **34** (2013) 327-330. Stabilizing redox polymer films by electrochemically induced crosslinking.

**Acknowledgement:** This work was supported by the EC in the framework of PITN-GA-2013-607793 “Bioenergy”, the Cluster of Excellence RESOLV (EXC 1069) and the Deutsch-Israelische Projektkooperation (DIP); “Nanoengineered optoelectronics with biomaterials and bioinspired assemblies” both funded by the Deutsche Forschungsgemeinschaft (DFG). F. Z. is grateful for the support by the China Scholarship Council (CSC). P. P. is grateful for the support by the German Academic Exchange Service (DAAD). CA is grateful to the Sectoral Operational Programme Human Resources Development 2007-2013 of the Ministry of European Funds through the Financial Agreement POSDRU/159/1.5/S/132397. Moreover, the fruitful cooperation with Olaf Rüdiger, Wolfgang Lubitz (MPI-CEC, Mülheim, Germany), Volker Hartmann, Marc M. Novaczyk, Matthias Rögner (Plant Physiology, Ruhr-University Bochum, Germany), Ulla Wollenberger, Silke Leimkühler (Potsdam University, Germany), Christophe Léger (Marseille, France), Roland Ludwig (BOKU Vienna, Austria) is gratefully acknowledged.

# Acceleration of Laccase Bioelectrocatalysis at Carbon Nanotube Interface Modified with Steroid-Type Biosurfactants

Makoto Togami<sup>1</sup>, Aiko Sasaki<sup>1</sup>, Masato Tominaga<sup>1, 2\*</sup>

<sup>1</sup>Graduate School of Science and Technology, Kumamoto University, Kumamoto 860-8555, Japan

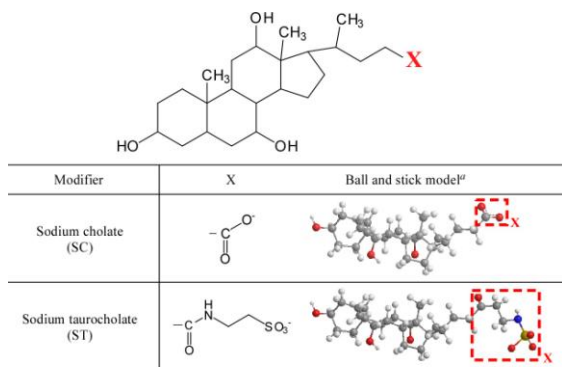
<sup>2</sup>Kumamoto Institute for Photo-Electro Organics (Phoenix), Kumamoto 862-0901, Japan

\*masato@gpo.kumamoto-u.ac.jp

Direct electron transfer (DET) reaction between multicopper oxidases, especially laccase (Lac) and bilirubin oxidase, and a carbon electrode has been widely studied as fuel cell electrode for oxygen reduction in an enzymatic bio-cathode. Great effort has been directed toward studying the design of electrode interface to be given suitable enzyme molecular orientation for the DET reaction. The electrode interface modified with an organic compound such as anthracene has gave the enhanced bioelectrocatalytic current of Lac.<sup>1</sup> Here, we present acceleration of the DET of Lac with the interface of single-walled carbon nanotubes (SWCNTs) modified with steroid-type biosurfactants.<sup>2</sup>

Sodium cholate (SC) and sodium taurocholate (ST) were used as a steroid-type biosurfactant. SWCNTs were synthesized onto a gold surface as described in previous reports.<sup>3</sup> Immediately after synthesis, the fresh SWCNT electrodes were immersed into 0.1 wt% SC or ST aqueous solutions for 24 hrs (Fig. 1). After rinsed gently, the modified SWCNT electrodes were immersed into 0.1 mol dm<sup>-3</sup> acetate buffer solution (pH 5) containing 10 μmol dm<sup>-3</sup> Lac for 30 min. A 1.0 mol dm<sup>-3</sup> phosphate-citrate buffer solution (pH 3.0) was used as an electrolyte solution, and was purged with high-purity argon before taking measurements.

The surface concentrations of the adsorbed Lac at SC-, ST-modified and none-modified SWCNT surfaces were evaluated to be 2.4, 2.3, and 2.2 pmol cm<sup>-2</sup>, respectively, which were less than monolayer level. The onset potentials at which the Lac started to catalyze the electrochemical reduction of O<sub>2</sub> at SC- and ST-SWCNTs, were 0.998 and 0.977 V (vs. NHE) respectively, which were higher than that observed at none-modified SWCNTs (Fig. 2). From the analysis of steady-state current density ( $j_a$ ) using the adsorption model given by  $j_a = nFk_c\Gamma_a / (1 + (k_c/k_f) + (k_b/k_f))$ ,  $k_f = k^\circ \exp[-\alpha(nF/RT)(E^\circ - E^\circ)]$ ,  $k_b = k^\circ \exp[(1-\alpha)(nF/RT)(E^\circ - E^\circ)]$  ( $n=1$ ,  $k_c=2600$  s<sup>-1</sup>,  $E^\circ=0.925$  V,  $T=298.15$ ),<sup>4</sup> the  $k^\circ$  values were determined to be 3000 and 1500 s<sup>-1</sup> at the SC- and ST-SWCNTs, respectively.<sup>2</sup> On the other hand, the  $k^\circ$  value at none-modified SWCNTs was 400 s<sup>-1</sup>.



<sup>a</sup> The 3D structures are optimized.

Fig. 1 Chemical structures of steroid-type biosurfactants.

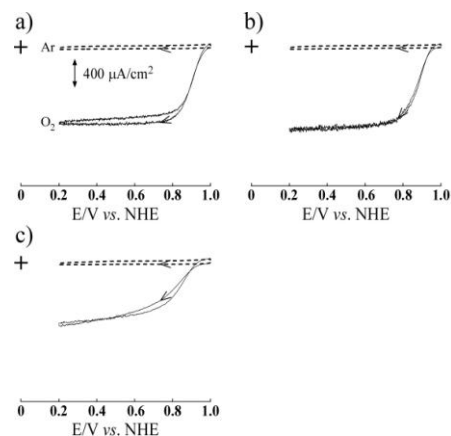


Fig. 2 Cyclic voltammograms at the a) SC-, b) ST-, and c) none-modified SWCNTs. Potential sweep rate: 10 mV s<sup>-1</sup>.

1. C. Blanford, R. S. Heath, F. A. Armstrong, *Chem. Commun.* **17** (2007) 1710.
2. M. Tominaga, A. Sasaki, M. Togami, *Anal. Chem.*, to be submitted.
3. M. Tominaga, S. Sakamoto, H. Yamaguchi, *J. Phys. Chem. C* **116** (2012) 9498.
4. S. Tsujimura, K. Kano, T. Ikeda, *J. Electroanal. Chem.* **576** (2005) 113.

# Naphthoquinone Derivatives as Low-Potential Electron Mediators of FAD-Dependent Glucose Dehydrogenase

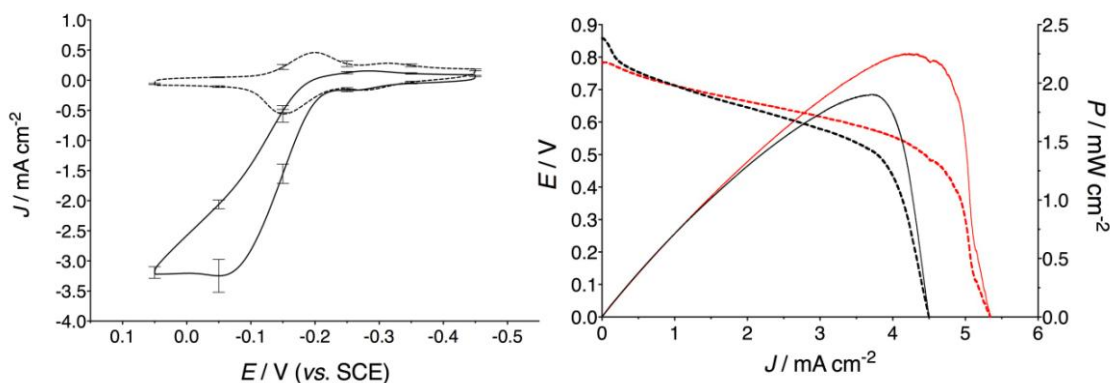
Ross D. Milton<sup>a</sup>, David P. Hickey<sup>a</sup>, Sofiene Abdellaoui<sup>a</sup>, Koun Lim<sup>a</sup>, Boxuan Tan<sup>a</sup> and Shelley D. Minter<sup>a</sup>

<sup>a</sup>Department of Chemistry, University of Utah, 315 S 1400 E Rm 2020, Salt Lake City, Utah, 84112, USA.  
minter@chem.utah.edu

Flavin adenine dinucleotide-dependent glucose dehydrogenase (FAD-GDH) is rapidly emerging as an alternative glucose-oxidizing enzyme for enzymatic fuel cell (EFC) applications.<sup>1, 2</sup> The FAD cofactor has a relatively low redox potential (in comparison to heme-based and PQQ-dependent enzymes). Furthermore, FAD-GDH has the added benefit over its commonly used counterpart, glucose oxidase (GOx), of not undergoing the parasitic reduction of O<sub>2</sub> to H<sub>2</sub>O<sub>2</sub>, which can be troublesome in EFC applications.<sup>3</sup> Unfavorable electron transfer competition at the bioanode and dissolved O<sub>2</sub> depletion (important for most enzymatic O<sub>2</sub>-reducing cathodes) can be avoided.

Recent works have demonstrated how the use of FAD-GDH can be useful in high-power EFC applications. Maximum current densities of 100 mA cm<sup>-2</sup> have been reported with the use of an osmium-based redox hydrogel at +0.7 V (vs. Ag/AgCl),<sup>4</sup> although efforts must be made to obtain high current densities at potentials which are applicable to EFC technology.

This paper presents a range of naphthoquinone analogues that are capable of mediating electron transfer between FAD-GDH and carbon electrodes, with onset potentials ranging between -425 to -150 mV (vs. SCE), at pH 7.4. A naphthoquinone derivative was rationally designed to yield a naphthoquinone redox hydrogel and direct enzyme labeling. Both methods demonstrated large catalytic current densities at low onset potentials. When coupled with an O<sub>2</sub>-reducing biocathode (bilirubin oxidase, direct electron transfer-type) the glucose/O<sub>2</sub> EFC possessed a large open-circuit potential (OCP) of 0.864 mV and was able to deliver a maximum current density of 5.4 mW cm<sup>-2</sup>. The EFC reached its maximum power density (2.3 mW cm<sup>-2</sup>) at 0.55 V.



1. M. N. Zafar, N. Beden, D. Leech, C. Sygmund, R. Ludwig and L. Gorton, *Anal. Bioanal. Chem.*, 2012, **402**, 2069-2077.
2. I. Osadebe and D. Leech, *ChemElectroChem*, 2014, **1**, 1988-1993.
3. R. D. Milton, F. Giroud, A. E. Thumser, S. D. Minter and R. C. T. Slade, *Phys. Chem. Chem. Phys.*, 2013, **15**, 19371-19379.
4. S. Tsujimura, K. Murata and W. Akatsuka, *J. Am. Chem. Soc.*, 2014, **136**, 14432-14437.

## Diversity and Electrocatalysis by Multi-heme Cytochromes *c*

Sean J. Elliott, Kathryn D. Bewley, Evan T. Judd, Lindsey M. Walker and Kelly A. Walsh

*Boston University*

*Department of Chemistry, 590 Commonwealth Ave., Boston, MA 02215*

*elliott@bu.edu*

Cytochromes *c* (cyts *c*) are heme-bearing redox-active proteins that have at least one covalently tethered protoporphyrin IX cofactor that is attached to the protein via two cysteine (Cys) residues found in a CXXCH sequence motif. Multi-heme cytochromes *c* contain multiple heme cofactors, where the resulting metalloproteins have been implicated in long-range electron transfer in “electronic” microbes and as multi-electron redox catalysts. Here, a series of vignettes depicting the trials and tribulations using protein electrochemistry and bioinformatics will be presented in the context of bacterial cytochromes *c*, spanning tetraheme cytochrome *c*<sub>554</sub> and its orthologs, to more complex enzymes such pentaheme cytochrome *c* nitrite reductase from *Shewanella oneidensis*. In the case of orthologs of cytochrome *c*<sub>554</sub>, a presumed core protein-fold and placement of four heme cofactors has been analyzed in the context the remarkable ability of *Nitrosomonas europaea* cyt *c*<sub>554</sub> to engage in apparent cooperative electron transfer across the protein structure. Using a recombinant *Ne* cyt *c*<sub>554</sub> construct, and newly discovered orthologs of this metalloprotein family, we examine the issues surrounding cooperativity – ie, how Nature takes two one-electron units and persuades them to do two-electron chemistry. Interfacial electron transfer rate and inter-cofactor arrangement are key determinants in whether cooperativity is observed or not. In the case of cytochrome *c* nitrite reductase (ccNiR), complex electrocatalytic signatures of the enzyme reducing nitrite will be used to address the mechanism of ccNiR catalysis. We find that despite the pentaheme nature of the enzyme, electrocatalysis proceeds in via a series of one-electron steps, and that only some of these steps are linked to proton-transfers. A series of mutations in close proximity to the active site allows for determining  $pK_a$  values for the catalytic electron transfer steps, and yields a new view of the multi-electron chemistry catalyzed by the enzyme in action. Here, the proposed mechanism of nitrite reduction to ammonia will be evaluated in the context of the electrocatalytic data. Finally, efforts to understand the diversity of reactivity observed in multiheme cytochromes *c* will be presented. Although multi-heme cytochromes *c* contain multiple CXXCH motifs, the diversity of their function (provide either specific redox partners, general electron transfer pathways, or catalysts for either oxidative or reductive chemistries) has yet to be understood in a rigorous way. Here, we will examine this diversity in the context of a sequence similarity network approach, and correlating the bioinformatics analysis to known redox properties.

# Electrocatalytic cascades driven by enzymes and metal nanoparticles on carbon supports: the reduction of nitrate to ammonia at neutral pH

Matteo Duca<sup>a,\*</sup>, Justin R. Weeks<sup>b</sup>, Justin G. Fedor<sup>b</sup>, Joel H. Weiner<sup>b</sup>, Kylie A. Vincent<sup>a</sup>

<sup>a</sup> Department of Chemistry, University of Oxford, Inorganic Chemistry Laboratory, South Parks Road, Oxford OX1 3QR, United Kingdom

<sup>b</sup> Department of Biochemistry, 474 Medical Science Building, University of Alberta, Edmonton, Alberta T6G 2H7, Canada

\*matteo.duca@chem.ox.ac.uk

The treatment of nitrate-laden wastewater is a key challenge in Environmental Sciences, calling for improved methods for the selective removal of this polluting ion.

The electrochemical reduction of nitrate is severely limited by a series of significant drawbacks[1]: low catalytic activity at neutral pH (typical of wastewater), and at low concentrations, or interference by other solution species which adsorb more strongly. These limitations do not affect biological catalysts, such as the enzyme nitrate reductase (Nar); direct electrochemistry has been demonstrated for one (*E. coli* NarGHI) immobilized onto a graphite electrode [2]. In this way, NarGHI functions as an electrocatalyst for the reduction of nitrate in a broad pH range ( $5 < \text{pH} < 9$ ) and at sub-millimolar concentrations. The reduction of nitrite is the following step in denitrification, occurring at noble metal electrodes even at neutral pH, but with diminishing catalytic activity at pH values in the range 6-8.

In this study, NarGHI and noble metal nanoparticles have been combined to assemble a composite electrode capable of reducing nitrate to ammonia at neutral pH [3]. NarGHI is immobilized onto high-surface area carbon particles, mixed with commercial carbon-supported Pt, Rh or Pd nanoparticles and deposited onto a pyrolytic graphite “edge” electrode (PGE), thus allowing potential control of the two catalysts simultaneously. When this composite electrode is immersed in a pH 6.1 phosphate buffer solution containing 1 mM NaNO<sub>3</sub>, NarGHI selectively performs the reaction  $\text{NO}_3^- \rightarrow \text{NO}_2^-$  at a potential close to 0.1 V vs SHE. As the potential is decreased, NO<sub>2</sub><sup>-</sup> produced *in situ* can be further reduced to NH<sub>4</sub><sup>+</sup> by the metal nanoparticles. ATR-IR spectroscopy has been used to study intermediates in the catalyst layer, while rotating-ring disk and photometric methods have been employed to study the product distribution after constant-potential reduction and how it is affected by varying the ratio of the two catalysts.

This study opens up a new approach to the fabrication of composite electrode able to overcome the intrinsic limitations of the individual catalysts used.

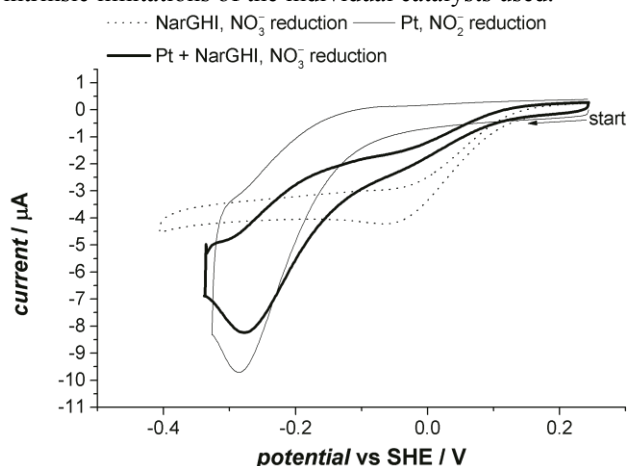


**Figure 1:** dotted line, cyclic voltammogram of NO<sub>3</sub><sup>-</sup> reduction to NO<sub>2</sub><sup>-</sup> at NarGHI immobilized on carbon and deposited on PGE. Thin line: cyclic voltammogram of NO<sub>2</sub><sup>-</sup> reduction (400 μM) to NH<sub>4</sub><sup>+</sup> at Pt nanoparticles on PGE. **Bold** cascade catalysis of NO<sub>3</sub><sup>-</sup> to NH<sub>4</sub><sup>+</sup> at NarGHI + Pt deposited on a PGE electrode.

Electrolyte 100 mM phosphate buffer, pH 6.1, + 1 mM NaNO<sub>3</sub>.  $\nu = 10 \text{ mV s}^{-1}$ .

[1] M. Duca, M.T.M. Koper, Powering denitrification: the perspectives of electrocatalytic nitrate reduction, *Energy Environ. Sci.*, 5 (2012) 9726-9742.

[2] S.J. Elliott, K.R. Hoke, K. Heffron, M. Palak, R.A. Rothery, J.H. Weiner, F.A. Armstrong, Voltammetric studies of the catalytic mechanism of the respiratory nitrate reductase from *Escherichia coli*: How nitrate reduction and inhibition depend on the oxidation state of the active site, *Biochemistry*, 43 (2004) 799-807.

[3] M. Duca *et al*, submitted for publication

# **Wet spun Bio-electronic fibers of imbricated enzymes and carbon nanotubes for efficient microelectrodes**

Anne-Sophie Michardière, Cintia Mateo-Mateo, Sébastien Gounel, Isabelle Ly, Philippe Poulin and  
Nicolas Mano

*CNRS, CRPP, UPR 8641, F-33600 Pessac, France and Univ. Bordeaux, CRPP, UPR 8641, F-33600  
Pessac, France  
mano@crpp-bordeaux.cnrs.fr*

The electrical connection of enzymes and microelectrodes is usually achieved via the direct deposition of biomolecules at the electrode surface. Optimization of this interface can be done either by using conductive nanomaterials such as carbon nanotubes, by adding shuttles of electrons and/or by tuning the geometry of the electrode. However, immobilized enzymes remain essentially located at the outer surface of the electrode, limiting therefore the current density of the devices.

We developed a single step and scalable fiber wet-spinning approach that allows the fabrication of microfibers into which enzymes and carbon nanotubes are imbricated in the core of the fiber. Their efficiency is tested against the enzymatic reduction of O<sub>2</sub> using bilirubin oxidases (BODs) as enzyme. The delicate combination and formulation of CNTs and BODs allowed the development of a new wet spinning process to produce efficient enzymatic hybrid bioelectronics for the reduction of O<sub>2</sub>. A 7 fold increase in current density is reached compared to conventional coating method while preserving all the advantages of microelectrodes in terms of miniaturization and spatio-temporal resolution. This significant improvement is ascribed to the large amount of enzyme immobilized in the core of the fibers.

The present approach could also be extended to other enzymes and finally the scalability of the fiber wet-spinning method would be a valuable advantage for future applications.



# Monitoring Electrochemically the Early Events of Hydrogen Peroxide Production by Mitochondria

E. Suraniti<sup>1</sup>, S. Ben-Amor<sup>2</sup>, P. Landry<sup>1</sup>, M. Rigoulet<sup>3</sup>, E. Fontaine<sup>4</sup>, S. Bottari<sup>4</sup>,  
A. Devin<sup>3</sup>, N. Sojic<sup>2</sup>, N. Mano<sup>1</sup>, S. Arbault<sup>2</sup>

1. CNRS, Centre de Recherche Paul Pascal, UPR 8641, University of Bordeaux, 33600 Pessac, FRANCE

2. University of Bordeaux, Institute of Molecular Sciences, CNRS UMR 5255, Analytical NanoSystems Group, ENSCBP, 33607 Pessac, FRANCE

3. University of Bordeaux, Institute of Cell Biochemistry and Genetics, CNRS UMR 5095, 33077 Bordeaux, FRANCE

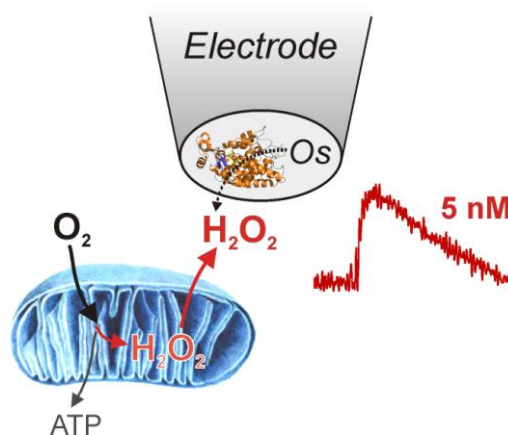
4. University Grenoble-Alpes, Laboratory of fundamental and applied Bioenergetics, INSERM U1055, 38400 Saint Martin d'Hères, FRANCE  
[stephane.arbault@u-bordeaux.fr](mailto:stephane.arbault@u-bordeaux.fr)

Mitochondria are the site of metabolic transformation of organic substrates into the energetic ATP. The respiratory chain couples electron transfers to proton transport used by ATP synthases (namely, the OXPHOS process). The final electron acceptor of the respiratory chain is oxygen converted into water. However, it is demonstrated that the respiratory chain is also producing reactive oxygen species (ROS), involved either in signaling pathways or in oxidative stress. Dysregulation of mitochondria metabolism leads to severe pathological processes (myopathies, neurodegenerative diseases...).

We have developed an electrochemical biosensor to monitor quantitatively and kinetically the production of a ROS, hydrogen peroxide, by mitochondria. Our approach consist in embedding horseradish peroxidase (HRP) in a cross-linked 3D-polymer matrix bearing mobile osmium-based redox ( $\text{Os}^+ / \text{Os}^{2+}$ ) moieties. We optimized the ratio between components (HRP/polymer/cross-linker) and the whole loading on electrode surface, so as to reach high analytical performances: specific amperometric detection of  $\text{H}_2\text{O}_2$  at +0 V vs. Ag/AgCl, 1 nM LOD for  $\text{H}_2\text{O}_2$ , and a linear response over 5 concentration-decades.

These bioelectrodes allowed monitoring the release of  $\text{H}_2\text{O}_2$  by mitochondria (yeast origin) under several conditions (phosphorylating, inhibited respiration...). We report the detection of two concomitant regimes of  $\text{H}_2\text{O}_2$  release: large fluxes (hundreds of nM) under complex III-blockade, and bursts of a few nanomolars and few min.-duration immediately following mitochondria activation. These bursts of  $\text{H}_2\text{O}_2$  match superoxide flashes observed by fluorescence, and can be assigned to the role of mitochondria as the central hub of redox signaling in cells.

**Figure:** Detection principle of Hydrogen peroxide release by mitochondria during oxidative phosphorylation. Nanomolar bursts of  $\text{H}_2\text{O}_2$  by energized mitochondria were detected (red curve on right) owing to a bioelectrode (HRP/Osmium based redox polymer/carbon electrode).



**References:** Suraniti E. et al., *Bioelectrochemistry* **2012**, 88, 65-69; Ben-Amor S. et al., *Electroanalysis*, **2013**, 173, 656; Ben-Amor S. et al., *Electrochimica Acta*, **2014**, 126, 171; Suraniti E. et al., *Angewandte Chemie*, **2014**, 126, 6773



# Electron transfer effect on the bioluminescence of *Shewanella woodyi*

Xiaochun Tian<sup>1</sup>, Ranran Wu<sup>2</sup>, Zhiyong Zheng<sup>2</sup>, Feng Zhao<sup>2\*</sup>, Yanxia Jiang<sup>1\*</sup>, Shigang Sun<sup>1</sup>

<sup>1</sup>State Key Laboratory of Physical Chemistry of Solid Surfaces, Department of Chemistry, College of Chemistry and Chemical Engineering, Xiamen University  
422 SiMing south Road, Xiamen, FuJian 361005, China

<sup>2</sup>Institute of Urban Environment, Chinese Academy of Sciences  
1799 Jimei Road, Xiamen, FuJian 361021, China

[yxjiang@xmu.edu.cn](mailto:yxjiang@xmu.edu.cn); [fzhao@iue.ac.cn](mailto:fzhao@iue.ac.cn)

Bioluminescence is the light emitted by living organism via some reactions<sup>[1]</sup>. The bacterial luminescence mechanism was proposed that the luciferase can oxidize the reduced form of flavin mononucleotide (FMNH<sub>2</sub>) using molecular oxygen to generate blue-green light, as shown in equation 1<sup>[2]</sup>. Therefore, FMNH<sub>2</sub> is one of the key substrates for the bioluminescence production. It is widely accepted that the fully oxidized flavin (FMN) can be reduced to FMNH<sub>2</sub> in “one step” with a 2e<sup>-</sup>/2H<sup>+</sup> reduction by applying a reducing potential in aqueous media<sup>[3]</sup>. Therefore, we supposed that the bioluminescence may be affected by the redox reaction of FMNH<sub>2</sub> controlled by electrode.



Herein, *Shewanella woodyi*<sup>[4]</sup> was cultured in 2216E medium at 25°C with 150 rpm shaking. The growth curve and luminance were recorded by OD<sub>600nm</sub> and fluorescent imaging system, respectively. As shown in Fig.1(a), *S. woodyi* showed the highest luminescence when it was cultured for 30 h which corresponds to the beginning of stable phase. *S. woodyi* is electrochemical active bacterium based on CV results. Besides, the electrochemical bioluminescence response of *Shewanella woodyi* was successfully regulated on the ITO/suspension interface at the potential range of -0.6 V ~ 0.4 V, which can reduce and oxidize FMN to FMNH<sub>2</sub> along with the change of potential.

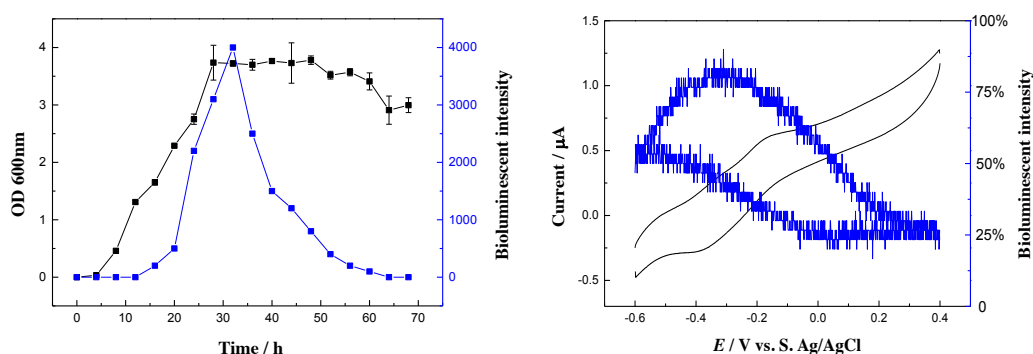


**Figure 1** (a) growth curve and bioluminescent intensity of *Shewanella woodyi* cultured at 25°C (b) CV and corresponding electrochemical bioluminescence response of the bacterial suspension which cultured for 28 h.

This work was supported by National Science Foundation of China (Grant No. 21273180).

## References

- [1]. H.F. Tsai, Y.C. Tsai, S. Yagur-Kroll, N. Palevsky, S. Belkin, J.Y. Cheng, Water pollutant monitoring by a whole cell array through lens-free detection on CCD, Lab on a Chip, 15 (2015) 1472-1480.
- [2]. K.H. Nealson, J.W. Hastings, Bacterial bioluminescence: its control and ecological significance, Microbiological Reviews, 43 (1979) 496-518.
- [3]. S.L.J. Tan, J.M. Kan, R.D. Webster, Differences in Proton-Coupled Electron-Transfer Reactions of Flavin Mononucleotide (FMN) and Flavin Adenine Dinucleotide (FAD) between Buffered and Unbuffered Aqueous Solutions, The Journal of Physical Chemistry B, 117 (2013) 13755-13766.
- [4]. J.C. Makemson, N.R. Fulayfil, W. Landry, L.M. Van Ert, C.F. Wimpee, E.A. Widder, J.F. Case, *Shewanella woodyi* sp. nov., an Exclusively Respiratory Luminous Bacterium Isolated from the Alboran Sea, International Journal of Systematic Bacteriology, 47 (1997) 1034-1039.

# Manipulation of biomolecular functions at electrode surfaces via surface modification

Xing-Hua Xia

*State Key Laboratory of Analytical Chemistry for Life Science, School of Chemistry and Chemical Engineering, Nanjing University, Nanjing 210093, China  
e-mail: xhxia@nju.edu.cn*

Immobilization of proteins and enzymes on electrode surfaces plays an important role in determining the orientation, conformation, direct electron transfer and related biocatalytic activity. We used surface enhanced infrared absorption spectroscopy (SEIRAS) and electrochemical techniques studied the influence of surface properties on adsorption, orientation, conformation and related DET and biocatalytic activity of immobilized proteins.

First, the adsorption kinetics of cytochrome c on a nanostructured gold film will be discussed. Following the evolution of amide I and amide II bands with time, the adsorption kinetics of the protein can be explained by the Freundlich model. Then, COOH, OH and CH<sub>3</sub>-terminated thiols have been self-assembled on the nanostructured Au films. With COOH-terminated SAM, the surface electric field can be manipulated by pH, and the influence of electric field on the DET of cytochrome c on this SAM was studied. We then used the OH and CH<sub>3</sub>-terminated SAMs to immobilize cytochrome c and studied the influence of surface wettability on the DET of cytochrome c. It showed that DET of cytochrome c occurs when the heme plane is parallel to the hydrophilic SAM/gold surface, while it is forbidden if the heme plane is perpendicular to the hydrophobic SAM/gold surface, although the secondary structure of immobilized cyt c is the same on both SAMs.

## References:

1. (a) Jin B. et al. *J. Phys. Chem. C*, 2012, 116: 13038; (b) Jin B. et al. *Langmuir*, 2012, 28: 9460.
2. (a) Hua B.Y. et al. *Chem. Commun.*, 2012, 48: 2316; (b) Wang G.X. et al. *Chem. Commun.*, 2012, 48:10859; (c) Wang G. X. et al. *Chem. Commun.* 2015, 51: 689.
3. (a) Xu J.Y. et al. *Langmuir*, 2012, 28: 17564; (b) Xu J.Y. et al. *Chem. Commun.*, 2012, 48: 3052.
4. (a) Wu Z.Q. et al. *Anal. Chem.*, 2012, 84: 10586; (b) Zhao Y. et al. *Anal. Chem.*, 2013, 85: 1053.

# **Synthesis and Characterization of carbon based nanocomposites and its electrocatalytic activity towards biomolecules and hazardous pollutants**

**Shen-Ming Chen\*, Chelladurai Karuppiyah, Rajkumar Devasenathipathy, Selvakumar Palanisamy, Verappan Mani**

Electroanalysis and Bioelectrochemistry Lab, Department of Chemical Engineering and Biotechnology, National Taipei University of Technology, 1, Sec. 3, Chung-Hsiao E. Rd., Taipei, 10608, Taiwan, R.O.C.  
[smchen78@ms15.hinet.net](mailto:smchen78@ms15.hinet.net)

## **Abstract**

Graphene (GR) based nanocomposites are very effective electrocatalyst towards biomolecules and toxic pollutants because of their stability, high mass transfer and relatively large surface areas. The electrode materials were characterized by cyclic voltammetry, X-ray photoelectron spectroscopy, high-resolution transmission electron microscopy, field-emission scanning electron microscopy, energy-dispersive X-ray spectroscopy and X-ray diffraction studies. Firstly, GR/cobalt oxide nanoparticles ( $\text{Co}_3\text{O}_4\text{-NP}_s$ ) have been used for the immobilization of glucose oxidase (GOx) to construct the glucose biosensor and also developed  $\text{H}_2\text{O}_2$  sensor. The prepared GR nanosheets/polyethyleneimine/gold nanoparticles (GNS/PEI/AuNPs) composite film exhibited excellent electrocatalytic activity towards the selective determination of dopamine in the presence of ascorbic acid and also demonstrated for the determination of dopamine in human urine samples. In addition, the electrodeposition of calcium ions cross linked pectin (CCLP) stabilized AuNPs on GR modified electrode have significantly enhanced electrocatalytic ability towards oxidation of hydrazine. The fabricated GR based nanocomposites have shown excellent analytical parameters towards biomolecules and toxic pollutants.

# Improving the Electrochemical Measurement Sensitivity of SECM-SICM by using Pt Electrodeposited Carbon Nanoelectrode

Takahashi, Yasufumi<sup>1,2,3</sup>; Mustafa, Sen<sup>2</sup>; Ida, Hiroki<sup>2</sup>; Shiku, Hitoshi<sup>2</sup>; Matsue, Tomokazu<sup>1,2</sup>  
<sup>1</sup>WPI-Advanced Institute for Materials Research, Tohoku University Sendai, Miyagi 980-8576, Japan  
<sup>2</sup>Graduate School of Environmental Studies, Tohoku University, Sendai, Miyagi 980-8576, Japan  
<sup>3</sup>PRESTO, JST, Kawaguchi, Saitama 332-0012, Japan  
 takahashi@bioinfo.che.tohoku.ac.jp

Scanning electrochemical microscopy (SECM) uses an electrode tip for detecting electroactive chemical species and is an effective tool for the investigation of the localized chemical properties of sample surfaces and interfaces. We have developed nanoelectrode and electrode-sample distance control system to improve SECM resolution<sup>1,2,3</sup>, and to insert the electrode into cell for intracellular measurement<sup>4</sup>. Although SECM imaging with nanoelectrode provides high spatial resolution, chemical sensitivity is usually lost. The amperometric detection of 1  $\mu\text{M}$  of electroactive species by using a 3  $\mu\text{m}$  radius microelectrode produces about 1 pA current level, which is limit of the electrochemical detection for conventional current amplifier. To perform a highly sensitive electrochemical measurement while maintaining the spatial resolution of the SECM, it is necessary to increase the size of the electrode locally.

Here, we report the size controllable Pt electrochemical deposition electrode to improve sensitivity of electrochemical measurement. For electrode accurate position control, we used ion current feedback distance control, which is used in a scanning ion conductance microscopy (SICM). We compared a bare carbon electrode with Pt-deposited electrode based on the electrochemical sensitivity and imaging quality<sup>5</sup>. Figure 1 shows the images of immunocytochemically stained EGFR proteins on A431 cells. The current response of SECM image with the Pt-deposited electrode was almost 6 times larger than that for the bare carbon electrode. This result indicates the Pt-deposited electrode is useful to image of low concentration chemical around a single cell.

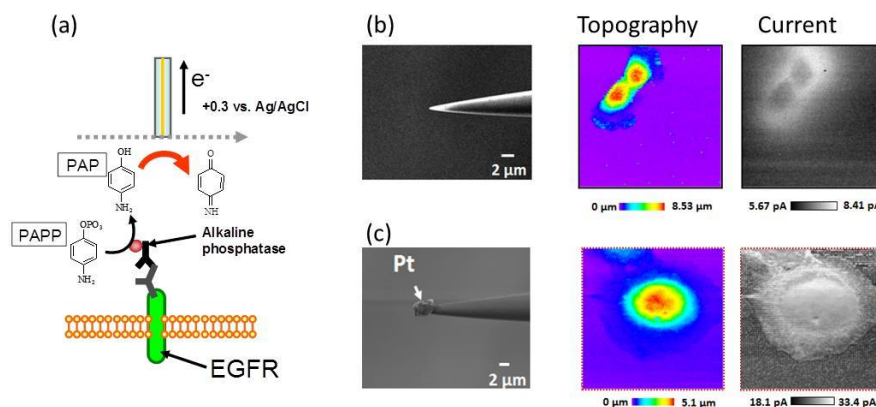


Figure 1 (a) Schematic illustration membrane protein imaging using SECM. SEM images of (b) bare carbon and (c) Pt-deposited electrode probe ( $-10$  nA of final deposition current) in 1 mM of  $\text{FcCH}_2\text{OH}$ +PBS. Topographic and electrochemical images of A431 cells in 4.7 mM PAPP using (b) bare carbon and (c) Pt-deposited probes. SECM and SICM electrodes were held at +0.3 and +0.2 V vs Ag/AgCl, respectively. (The scanned areas are (b)  $80 \times 80 \mu\text{m}$  and (c)  $50 \times 50 \mu\text{m}$ .)

1. Y. Takahashi, et al., *J. Am. Chem. Soc.* **132**, 10118 (2010).
2. Y. Takahashi, et al., *Angew. Chem. Int. Ed.* **50**, 9638 (2011).
3. Y. Takahashi, et al., *Proc. Natl. Acad. Sci. U. S. A.* **109**, 11540 (2012).
4. P. Actis, Y. Takahashi, et al., *Acs Nano* **8**, 875 (2014).
5. M. Sen, Y. Takahashi, et al., *Anal. Chem.* **87**, 3484 (2015).

# Thermostable enzymes for biofuel cells: wiring strategies and inhibitor influence

E. Lojou<sup>1</sup>, A. de Poulpiquet<sup>1</sup>, K. Monsalve<sup>1</sup>, C. Kjaergaard<sup>2</sup>, E. Solomon<sup>2</sup>, N. Mano<sup>3</sup>

<sup>1</sup> *Bioénergétique et Ingénierie des Protéines, CNRS-AMU, 31, ch. Aiguier, 13009 Marseille, France*

<sup>2</sup> *Department of Chemistry, Stanford University, Stanford, California 94305, United States*

<sup>3</sup> *CNRS, CRPP, UPR 8641, 33600 Pessac, France*  
*lojou@imm.cnrs.fr*

Hydrogen enzymatic biofuel cells (EBFC) are based on hydrogenases and multicopper oxidases for H<sub>2</sub> oxidation and O<sub>2</sub> reduction, respectively. Their development just emerged because of the recent identification and characterization of hydrogenases able to tolerate oxygen while being efficient H<sub>2</sub> oxidizers. We especially identified in the ancestral bacterium *Aquifex aeolicus* a hyperthermophile hydrogenase tolerant to O<sub>2</sub> and insensitive to CO [1]. Based on this hydrogenase and *Myrothecium verrucaria* bilirubin oxidase (BOD), both covalently grafted on carbon nanotubes, we designed two years ago a hydrogen EBFC delivering 300  $\mu\text{W}\cdot\text{cm}^{-2}$  [2]. This first biodevice allowed defining the main limitations to be overcome before enabling practical applications. On one hand, enhancement of the amount of electrically connected hydrogenases was required. On the other hand, there was a need for a thermostable O<sub>2</sub>-reducing enzyme in order to take benefit of the hyperthermophily of *A. aeolicus* hydrogenase.

We present in this work a new generation of H<sub>2</sub>/O<sub>2</sub> EBFC able to deliver more than 1 mW/cm<sup>2</sup> over a temperature range from 30 to 70°C. These performances are linked to the direct wiring of two thermostable enzymes in fishbone nanofiber mesoporous films, i.e. *A. aeolicus* hydrogenase and *Bacillus pumilus* BOD [3-5]. We discuss the performances of this EBFC as a function of carbon nanostructure, mass transport, temperature and pH.

Thanks to an efficient direct electron transfer between *B. pumilus* and carbon nanofiber-modified electrode, we investigate the catalytic mechanism of O<sub>2</sub> reduction in the presence of NaCl, and discuss the conditions of formation of an enzyme state only active after being reduced at low potentials [6]. Because BODs have been preferred to chloride sensitive laccases to be used for the elaboration of biocathodes, these new findings will have consequences for other devices than hydrogen EBCFs such as sugars/O<sub>2</sub> implantable biofuel cells.

[1] A. de Poulpiquet et al., ChemElectroChem 1 (2014) 1724

[2] A. Ciaccafava et al., Electrochem. Com., 23 (2012) 25

[3] A. de Poulpiquet et al., Phys. Chem. Chem. Phys., 16 (2014) 1366.

[4] N. Mano et al., Biosensors and Bioelectronics 50 (2013) 478

[5] A. de Poulpiquet et al., Electrochem. Com., 42 (2014) 72.

[6] A. de Poulpiquet et al., in preparation

# **Amyloid $\beta$ Peptides Nanostructures: Voltammetric and Atomic Force Microscopy Characterization**

Ana Maria Oliveira-Brett, A.M. Chiorcea-Paquim, T.A. Enache  
*Department of Chemistry, University of Coimbra, 3004-535 Coimbra, Portugal*  
*brett@ci.uc.pt*

Alzheimer's disease (AD), the most common form of dementia, is an incurable, progressive, and terminal neurodegenerative disease. The AD brain histopathology is characterized by the presence of intracellular neurofibrillary tangles of hyperphosphorylated tau proteins and by extracellular amyloid plaques containing a mixture of amyloid  $\beta$  ( $A\beta$ ) peptides of approximately 40 amino acids, having different N- and C- termini, generated from a larger amyloid  $\beta$  protein precursor ( $A\beta$ PP) through proteolytic cleavage of  $\beta$  and  $\gamma$  secretases.

Since  $A\beta$  peptides participate in redox reactions in the extracellular medium, the aim of the present study was the investigation of the  $A\beta$  peptides direct electron transfer processes.

Different length, native and mutant,  $A\beta$  monomer structures were systematically studied by cyclic and differential pulse voltammetry, at a glassy carbon electrode, and by AFM, on the surface of highly oriented pyrolytic graphite, to elucidate the redox behavior and the adsorption mechanisms, with respect to the  $A\beta$  peptides ability to form protofibrils and fibrils, to large aggregated structures.

The  $A\beta$  monomers,  $A\beta$ 01-40 and  $A\beta$ 01-42, contain five electroactive residues: three histidines (H6, H13 and H14), one tyrosine (Y10) and one methionine (M35).

At physiological pH 7.4 the most easily detected amino acid was tyrosine, followed by histidine. Methionine oxidation occurred at a higher potential.

The investigation of the  $A\beta$  peptides direct electrochemical oxidation mechanisms, in solution and adsorbed at the electrode surface, provided valuable insights into biological redox reactions of this class of molecules, resulting in a better understanding of mechanisms in which different fragments and mutants aggregate at different rates and by different pathways.

Atomic force microscopy was capable of characterising features at single-molecular level, providing additional information about the  $A\beta$  peptides fibrillation process.

# Label-free Electrochemical Detection of Prostate-Specific Antigen based on Nucleic Acid Aptamer

B. Piro, M. Souada, S. Reisberg, G. Anquetin, V. Noël, M.C. Pham  
Univ. Paris Diderot, Sorbonne Paris Cité, ITODYS, UMR 7086 CNRS,  
15 rue J-A de Baïf, 75205 Paris Cedex 13, France  
piro@univ-paris-diderot.fr

For detection and quantification of proteins such as prostate specific antigen (PSA, a biomarker of prostate cancer) with high affinity and specificity, immunosensors have been thoroughly investigated. However, if the immunologic approach is mature, non-immunologic ones were poorly investigated. Recently, nucleic aptamers (nucleic acid strands having recognition properties toward other molecules than DNA, such as organic molecules or proteins) appeared as promising alternatives to antibodies, due to their ease of production. Aptamers were initially developed for targeting cancer cells; they only appeared in the literature dedicated to analytical chemistry in the middle of the 2000s. Since, most works have focused on a model protein, thrombin. Among various transduction techniques, electrochemistry has been extensively investigated using redox labels, redox intercalators or even label-free, but there is still very few literature dealing with PSA. The first publication on PSA detection used nanostructured mesoporous electrodes, a biotin-streptavidin immobilizing strategy and hexacyanoferrate added in solution as redox reporter, with a LoD in the  $\text{ng mL}^{-1}$  range [1]. Another work reported a sandwich-type electrochemical biosensor based on gold electrodes modified with aptamers. The captured PSA was then derivatized with gold nanoparticles carrying a redox tag, followed by voltammetric detection. A sub-picomolar LoD was determined for this elaborated multi-step procedure [2].

We report in this work a label-free electrochemical aptasensor (no need to add redox label or redox molecule in solution) featuring a DNA aptamer having an excellent affinity for PSA ( $K_D$  in the nM range) [3]. The immobilized redox reporter is a quinone-modified electrode onto which the anti-PSA aptamer is grafted. PSA being a significantly heavier molecule than the aptamer, its capture hinders the polymer/electrolyte interface, therefore causes a decrease of the redox current intensity (“signal-off”), measured by Square Wave Voltammetry. This current decrease is specific for PSA above a limit of quantification in the  $\text{ng mL}^{-1}$  range ( $\sim 300$  pM). We have shown that this can be switched to a current increase (“signal-on”) by subsequent hybridization of the aptamer with its complementary DNA strand added in solution, which breaks PSA-aptamer interactions. This *on-off* procedure is a way to estimate the specificity of the system in order to avoid false positives. The PSA-aptamer dissociation constant  $K_D$ , of ca. 2.6 nM, was determined by this electrochemical method.

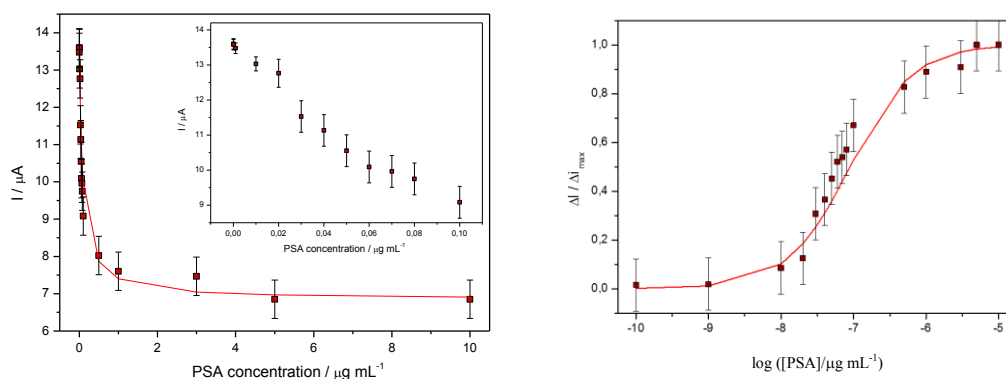


**Figure 1.** (a) Peak current of SWVs in PBS of a poly(JUG-co-JUGA)/Apta electrode as a function of PSA concentration (Inset: concentrations from 1 to 100  $\text{ng mL}^{-1}$ ). (b) Corresponding isotherm giving  $K_D = 2.6$  nM ( $89$   $\text{ng mL}^{-1}$ ) for PSA concentrations from 1  $\text{ng mL}^{-1}$  to 10  $\mu\text{g mL}^{-1}$ . Pulse height 50 mV, scan increment 2 mV, 12.5 Hz. Curves correspond to fit with the Langmuir isotherm.

- [1] Liu, B., Lu, L., Hua, E., Jiang, S., Xie, G., **2012**. *Microchimica Acta* 178, 163–170  
[2] Xia, N., Deng, D., Zhang, L., Yuan, B., Jing, M., Du, J., Liu, L., **2013**. *Biosens. Bioelectron.* 43, 155–159  
[3] Savory, N., Abe, K., Sode, K., Ikebukuro, K., **2010**. *Biosens. Bioelectron.* 26, 1386-1391

# H<sub>2</sub>/O<sub>2</sub> biofuel cells: Macro-structured conductive supports to enhance power cell performances

Monsalve Karen,<sup>a</sup> Le Goff Alan,<sup>b</sup> Mano Nicolas,<sup>c</sup> Gutierrez-Sanchez Cristina,<sup>a</sup> Lojou Jean-Yves,<sup>d</sup>  
Lojou Elisabeth<sup>a</sup>

<sup>a</sup> BIP, UMR 7281, CNRS-AMU, 31 chemin Joseph Aiguier, 13009 Marseille, France

<sup>b</sup> Univ. Grenoble Alpes, DCM, UMR 5250, 38000 Grenoble, France

<sup>c</sup> Univ. Bordeaux, CRPP, UPR 8641, 33600 Pessac, France

<sup>d</sup> IS2, 26 chemin Joseph Aiguier 13009 Marseille, France

kmonsalve@imm.cnrs.fr

Enzymatic H<sub>2</sub>/O<sub>2</sub> biofuel cells (BFC) recently emerged as attractive devices for small power applications [1]. In this “green” fuel cell, biocatalysts would replace chemical catalysts both at the anodic and cathodic sides. We previously identified and purified a hyperthermophile [NiFe] hydrogenase with outstanding properties compared to classical [NiFe] hydrogenases. We proved it is very efficient for oxidizing H<sub>2</sub> over a large range of temperatures from 25 to 80 °C and is tolerant to O<sub>2</sub> and completely insensitive to CO [2]. Coupled to a very efficient cathode based on the thermostable bilirubin oxidase from *Bacillus pumilus* (Bp BOD), a BFC was recently designed delivering 1.5 mW.cm<sup>-2</sup> at 0.6 V over a range of temperature from 30 to 80 °C [3].

One of the main challenges to enzymatic biofuel cells is to achieve higher performances and stability in order to become a self-sufficiency source of energy. H<sub>2</sub>/O<sub>2</sub> biofuel cells based on fish bone carbon nanofibers (CNFs) have proved that three main key challenges on enzyme immobilization have to be overcome: 1- Carbon nanofiber film stability on planar graphite electrodes which limits the available interacting surface; 2- substrate transport limitation through the mesoporous material; and 3- stability of the bio hybrid over time [3]. Recently we explored two different ways to overcome of these limitations of biofuel cell set-ups. We showed that gold nanoparticle can serve as efficient platforms for hydrogenase immobilization [4]. The long-term stability of the biohybrid was shown to be enhanced. We also designed a H<sub>2</sub>/O<sub>2</sub> BFC with an air-breathing cathode [5]. We present in this work, new strategies based on enzymes entrapped in carbon felt-based materials which act as enzyme host matrices with no need of additional electron collector. Microscopy and electrochemical probes experiments will be carried out to characterize the carbon support. Catalytic oxidation of H<sub>2</sub> and reduction of O<sub>2</sub> will be analyzed using electrochemistry in terms of enzyme grafting, influence of carbon material modification with different nano-materials and biopolymers. Electrochemical analysis of the biohybrid stability will be linked to quantification of enzyme release and/or denaturation. Finally, we will develop a H<sub>2</sub>/O<sub>2</sub> BFC demonstrator with the power cell efficiency required to feed a wireless electronic device.

## References

- (1) A. de Poulpique et al., *ChemElectroChem*, (2014), 1, 1724-1750
- (2) M. Guiral et al., *Adv. Microbial. Physiol.*, (2012), 61, 125-194
- (3) A. de Poulpique et al., *Electrochem. Com.*, (2014), 42, 72-74
- (4) K. Monsalve et al., *Bioelectrochem.* (2015), to be published
- (5) N. Lalaoui et al., *Chem. Comm.* (2015) DOI :10.1039/C5CC02166A



# Facile optimization of gold nanostructures for high SERS intensity by means of bipolar electrochemistry

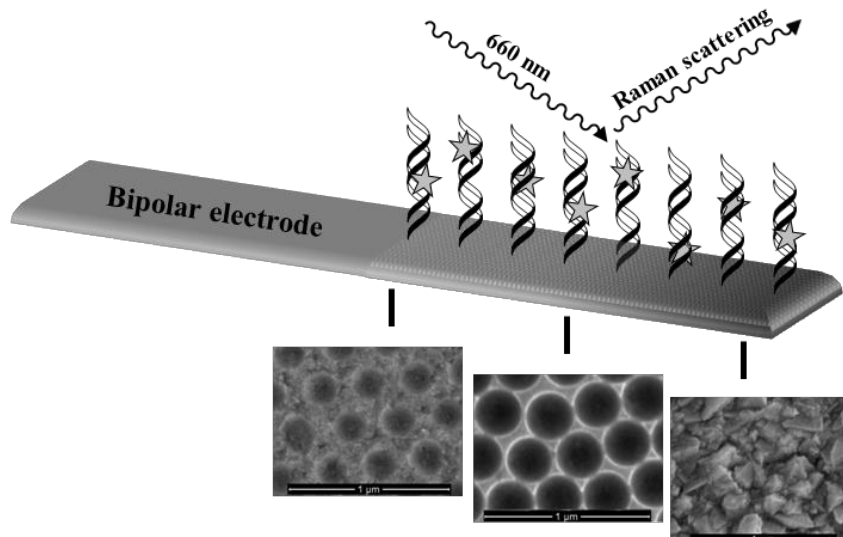
Vera Eßmann, Yasin Uğur Kayran, Daliborka Jambrec, Adrian Ruff, Stefanie Grützke, Wolfgang Schuhmann

Analytical Chemistry - Center for Electrochemical Sciences (CES); Ruhr-Universität Bochum, Universitätsstr. 150; 44780 Bochum; Germany  
vera.essmann@rub.de

Surface enhanced Raman spectroscopy (SERS) is a very powerful and versatile analytical tool able to detect even single molecules.<sup>1</sup> When inducing surface plasmons at a metal surface with light, Raman signals can be intensified due to an amplification of the localized electric field. The enhancement occurs predominantly at so-called “hot spots” such as nanoscale junctions between suitable metallic structures like silver or gold nanoparticles or -voids.

Here, we present a simple and fast approach for the fabrication and selection of nanostructures that lead to very high SERS intensities by means of bipolar electrochemistry. The process is based on the preparation of a size gradient of gold nanovoids on a single electrode (see figure). First, the gold electrode was coated with a 2D crystal of polystyrene (PS) nanobeads using a Langmuir trough. Then a potential gradient across the nanobead-modified surface enables wireless and gradual electrodeposition of gold leading to a gradient of nanovoid sizes after removal of the PS beads. This allows for the determination of the optimal nanostructures and thus the optimal deposition potential for highest SERS signals by using only a single bipolar electrode. A correlation between the nanovoid dimensions and the SERS intensity was observed employing an adsorbed Raman reporter molecule.

Furthermore, the nanovoid SERS substrates were evaluated with respect to the detection of DNA hybridization. In dependence on the nanovoid characteristics, double-stranded DNA could be distinguished from the single-stranded probe DNA via a label-free approach using a Raman-active DNA intercalator.<sup>2</sup>



Schematic illustration of the size gradient of nanovoids on a gold surface and the label-free approach for detection of dsDNA via SERS.

## References

- (1) Nie, S., Emory, S. R. Probing single molecules and single nanoparticles by surface-enhanced Raman scattering. *Science* **1997**, 275, 1102–1106.
- (2) Grützke, S., Abdali, S., Schuhmann, W., Gebala, M. Detection of DNA hybridization using electrochemical impedance spectroscopy and surface enhanced Raman scattering. *Electrochemistry Communications* **2012**, 19, 59–62.

# Diving into the Mechanism of Potential-Assisted ssDNA Immobilization

Daliborka Jambrec<sup>a</sup>, Magdalena Gebala<sup>b</sup>, Fabio La Mantia<sup>c</sup>, Wolfgang Schuhmann<sup>a</sup>

<sup>a</sup> Analytical Chemistry – Center for Electrochemical Sciences (CES), Ruhr-Universität Bochum, Universitätsstr. 150, 44780 Bochum, Germany

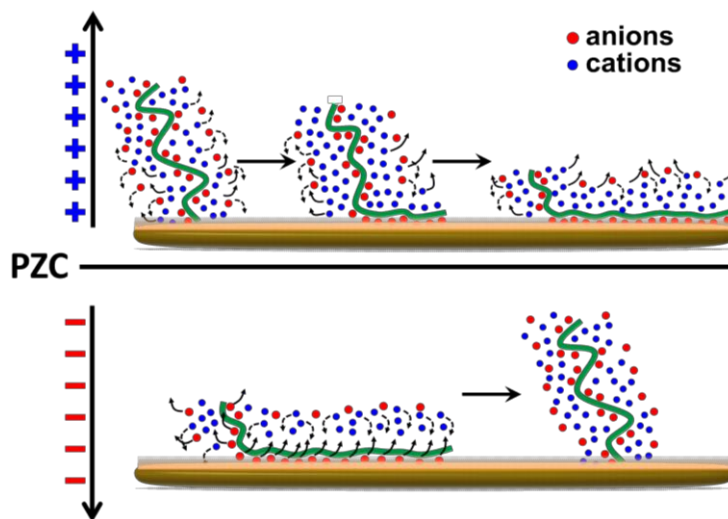
<sup>b</sup> Stanford School of Medicine, dept. Biochemistry, Beckman Center, B465, 270 W. Campus Dr. MC: 5307 Stanford, CA 94305; U.S.A.

<sup>c</sup> Semiconductor and Energy Conversion – Center for Electrochemical Sciences; Ruhr-Universität Bochum, Universitätsstr. 150; D-44780 Bochum; Germany  
daliborka.jambrec@ruhr-uni-bochum.de

During the course of the DNA immobilization process on gold surfaces via the incubation of the DNA, grafting of subsequent strands becomes energetically unfavourable due to the increasing electrostatic repulsion between the strands. Consequently, depending on the desired DNA coverage, the immobilization process using the incubation method can last from a couple of hours to days. We present a new potential-assisted immobilization method that overcomes this limitation and significantly accelerates the immobilization process by pulse-type modulation of the potential applied to the electrode surface during the immobilization process.

The manipulation of the DNA in the vicinity of electrified interfaces by potentials applied to the electrode surface is attracting increasing attention<sup>1</sup>. It was reported that potentials more positive than the potential of zero charge (pzc) cause bending of the grafted DNA towards the surface, while negative potentials favor an upright orientation of the immobilized DNA strands<sup>2</sup>. Furthermore, previous attempts aiming at the potential-assisted DNA immobilization itself, which took pzc into consideration, referred to the pzc of the bare electrode<sup>3</sup>. It was reported, that due to the applied potential the DNA strands are attracted or repelled during the course of the immobilization process.

We will present a new model for the potential-assisted immobilization of DNA at gold electrodes that considers the role of counterions surrounding the DNA, the distance from the electrode surface to which applied potentials have an effect and the shift of the pzc during the course of the immobilization due to the surface modification with DNA. Furthermore, we show the importance of choosing suitable potentials with respect to the pzc to obtain the optimal immobilization yield. By taking into account the proposed model, we obtained a highly reproducible potential-assisted immobilization method that is much more efficient and much faster than the standard incubation method.



- [1] Rant U., Arinaga K., Fujita S., Yokoyama N., Abstreiter G., Tornow M., *Nano Lett.* 2004, 4, 2441-2445.
- [2] Kelley S., Barton J., Jackson N., McPherson L., Potter A., Spain E., Allen M. and Hill M., *Langmuir* 1998, 14, 6781-6784.
- [3] Quan X., Heiskanen A., Tenje M., Biosen A., *Electrochem. Comm.* 2014, 48, 111-114.

# Scanning electrochemical microscopy of adherent melanoma cells: alive, fixed and permeabilized

Alexandra Bondarenko,<sup>a</sup> Tzu-En Lin,<sup>a</sup> Horst Pick,<sup>b</sup> Andreas Lesch,<sup>a</sup> Fernando Cortés-Salazar<sup>a</sup> and Hubert H. Girault<sup>a</sup>

<sup>a</sup> Laboratoire d'Electrochimie Physique et Analytique (LEPA), EPFL, Lausanne, Switzerland

<sup>b</sup> Laboratoire de Chimie Physique des Polymères et Membranes (LCPPM), EPFL, Lausanne, Switzerland  
alexandra.bondarenko@epfl.ch

Scanning electrochemical microscopy (SECM) is a surface reactivity characterization technique based on an electrochemical signal recorded at a probe positioned or scanned in close proximity to a substrate<sup>1</sup>. Thanks to its high spatial resolution and versatility, SECM has demonstrated to be a useful tool for the electrochemical imaging and intracellular investigation of different living cells types including mammalian cells<sup>2</sup>. However, the interpretation of the experimental data obtained from living cells can be difficult due to i) cell to cell variability in terms of metabolic activities and simultaneously occurring different biological processes, ii) possible dynamic morphological changes of cells due to cell mobility and iii) experimental time restrictions (e.g. experimental buffer solutions and redox mediators can be toxic for cells during long term experiments). Alternatively, working with fixed cells (e.g. after treatment with paraformaldehyde and/or methanol) leads to the elimination of biological activity of adherent cells, but opens the opportunity to access more easily the preserved cellular ultrastructure as well as proteins, carbohydrates and other bio-active moieties in their original spatial organization within the cells. Whereas paraformaldehyde crosslinks cellular proteins but does not permeabilize the plasma membrane, methanol fixation is based on proteins precipitation and partial dissolution of lipids resulting in membrane pores formation<sup>3</sup>. The paraformaldehyde fixation can be used for SECM to investigate the topography or the passive transport of the redox mediator through the membrane in a constant height scanning mode for any type of redox mediators while the methanol fixation can open the intracellular compartment to be analyzed by the scanning ultramicroelectrode (Figure 1a).

In this contribution, different melanoma cell lines representing progressive stages of skin cancer development (SBC12, non-invasive radial growth phase; WM115, vertical growth phase; WM239, metastatic) were studied by SECM in the feedback mode. The data were collected for living cells, cells fixed with formaldehyde and cells fixed with methanol. Depending on the employed cell fixation procedure cells were able to provide both positive and negative feedback by using the same redox mediator based on the ability of the redox mediator to access the intracellular space and to react with electrochemical active species (Figure 1b). For a better understanding the nature of the feedback signal, the influence of the redox mediator type (charged or non-charged), the ultramicroelectrode size and the probe translation speed were investigated. Furthermore, the permeabilization of cell membranes during the methanol fixation process was employed to compare the tyrosinase expression in different melanoma cell lines by immunostaining. With this aim, fixed melanoma cells were incubated with primary antibodies (Ab) and secondary Ab conjugated with horseradish peroxidase. The enzymatic activity was then readout by SECM in the substrate generation – tip collection mode.

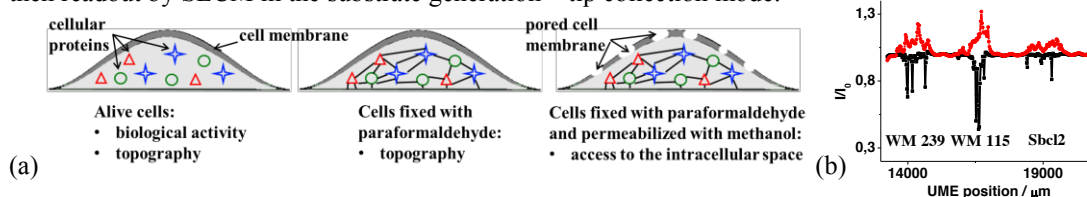


**Figure 1.** (a) Schematic representation of cells fixation with formaldehyde and methanol and the information which can be obtained during the SECM experiments in each case and (b) electrochemical signal recorded during line-scans above the same cells fixed with formaldehyde (black) and methanol (red) using 1 mM  $\text{K}_3\text{IrCl}_6$  as redox mediator. The current  $I$  was normalized by the current  $I_0$  above the Petri dish surface. The working distance  $d$  was equal to 25  $\mu\text{m}$ . Exp. Conditions: applied potential at a Pt UME 1 V; diameter 25  $\mu\text{m}$ , RG 3.5, CE Pt, QRE Ag.

The authors are thankful to the SNSF from Switzerland for the support through the project No. IZERZO\_142236/1.

## References:

- (1) Bard, A. J.; Fan, F. F.; Kwak, J.; Lev, O. *Anal. Chem.* **1989**, *61*, 132–138.
- (2) Bard, A. J.; Mirkin, M. V. *Scanning Electrochemical Microscopy*; second.; CRC Press, 2012; p. 670.
- (3) Watkins, S. *Curr. Protoc. Cytom.* **2009**, 12.16.1–12.16.10.

# **Preparation and characterization of amperometric monoenzyme creatinine biosensor based on creatinine deiminase/PANI-PSSMA/Au/Al<sub>2</sub>O<sub>3</sub> electrode**

Ya-Yi Liang<sup>1</sup>, Yung-Chien Luo<sup>2</sup>, Jing-Shan Do<sup>1\*</sup>

<sup>1</sup>*Department of Chemical and Materials Engineering, National Chin-Yi University of Technology, Taichung, Taiwan 411, ROC*

<sup>2</sup>*Department of Chemical and Materials Engineering, Tunghai University, Taichung, Taiwan 407, ROC*

*\* E-mail of corresponding author: jsdo@ncut.edu.tw*

The level of creatinine in human serum is an important and useful indicator for monitoring the function of people's kidney. Many creatinine biosensors have been developed based on tri-enzyme system for converting creatinine to creatine, creatine to sarcosine and sarcosine to glycerine with the various enzymes [1]. The tri-enzyme creatinine biosensor is designed to sensing the level of oxygen consumed or hydrogen peroxide generated in enzyme reactions. However, the level of creatinine can be determined by analysis the concentration of ammonium ion (product of enzymatic hydrolysis of creatinine by creatinine deiminase) for the monoenzymatic creatinine biosensor [1]. Using PANI (polyaniline)-Nafion/Au/Al<sub>2</sub>O<sub>3</sub> prepared by cyclic voltammetry (CV) with cycle number of 5 as sensing electrode, the sensitivity of ammonium ion sensor is obtained to be 100.4  $\mu\text{A mM}^{-1}$ . The nano-structured PANI-PSSMA (poly(styrene sulfonate-co-maleic acid)/Au/Al<sub>2</sub>O<sub>3</sub> prepared by chronopotentiometric technique is also used to sensing the concentration of ammonium ion. The sensitivity of amperometric ammonium ion sensor is increased by increasing the amount of PSSMA and decreasing temperature for preparing PANI-PSSMA composite film. The maximum sensitivity of amperometric ammonium ion sensor based on PANI-PSSMA/Au/Al<sub>2</sub>O<sub>3</sub> is found to be 126.2  $\mu\text{A mM}^{-1}$ . The amperometric monoenzyme creatinine biosensing electrodes are fabricated by immobilizing creatinine deiminase onto PANI-Nafion/Au/Al<sub>2</sub>O<sub>3</sub> and nano-structured PANI-PSSMA/Au/Al<sub>2</sub>O<sub>3</sub>. The surface morphologies of the sensing electrode are analyzed by FESEM. The sensing properties of monoenzyme creatinine amperometric biosensors are systematically investigated in this work.

## **References**

- [1] A. Radomska, E. Bodenszac, S. Głab, R. Koncki, Creatinine biosensor based on ammonium ion selective electrode and its application in flow-injection analysis, *Talanta* 64 (2004) 603–608.

# Fabrication of Low-Invasive Type Biosensor for Continuous Glucose Monitoring

Mikito Yasuzawa,<sup>1,\*</sup> Jiang Li,<sup>1</sup> Masahiro Uchimaru,<sup>1</sup> Yusuke Isoai,<sup>1</sup> Yusuke Fuchiwaki<sup>2</sup>

<sup>1</sup> Department of Chemical Science and Technology, The University of Tokushima,  
Tokushima 770-8506, Japan

<sup>2</sup> Health Research Institute, National Institute of Advanced Industrial Science and Technology  
Takamatsu, Kagawa 761-0395, Japan  
yasuzawa@tokushima-u.ac.jp

Recently, several types of implantable glucose sensors for continuous glucose monitoring (CGM) are available in the market and have provided significant benefit on the management of diabetic health care. The big advantage of CGM is that it will present not only the point of glucose degree but also its trend. The recognition of distinct rising or lowering of blood glucose may lead to an opposite treatment even the glucose level was same on its point. Moreover, daily trend observation is useful for the evaluation and improvement of individual pharmacotherapy. However, since sensor device of CGM at a present day requires a length of 1 cm to be inserted in skin, development of lower invasive CGM system is expected for the improvement of diabetic patients' quality of life.

In this study, a fine needle tube type glucose sensor, which has sensing region at the tip of a fine tapered electrode, was proposed. Since the sensing region is at the tip of tapered electrode, it only requires the sensor tip to be implanted in the tissue for glucose monitoring. In other words, it can be possible to perform as a patch type sensor, which impresses the user as a sticking sensor instead of a implanting sensor. Fine platinum-iridium alloy wire with a diameter of 0.17 mm was placed inside the tapered PEEK tube and glucose oxidase (GOx) was immobilized on the surface of platinum electrode by using the combination of electrodeposition and electropolymerization technique, which was similar to the procedure proposed by Wilson's group [1,2]. Glucose sensor properties of the obtained GOx-immobilized electrode were evaluated mainly by in vitro measurement.

The response current of the obtained electrode increased with increasing concentration of glucose up to 21.6 mM. Response current provided good linear relationship with glucose concentration. Correlation coefficient of 0.988 was obtained ranging up to 21.6 mM. Variation of response in time on the prepared electrode was investigated for two weeks. The response of the electrode was measured at 40°C and stored in phosphate buffer at 4°C when not in use. After an initial increase of response current for few days, the electrode provided stable response current.

## Acknowledgment

This study was supported in part by a Grant-in-Aid for Scientific Research (C) No. 24500510 from Japan Society for the Promotion of Sciences (JSPS).

## References

- [1] N. Matsumoto, X. Chen and G. S. Wilson, *Anal. Chem.*, **74** (2002) 362.
- [2] X. Chen, N. Matsumoto, Y. Hu and G. S. Wilson, *Anal. Chem.*, **74** (2002) 368.

# Improvement of Electrochemical Biosensor Performance for Hydrogen Peroxide Sensing Based on Iridium Nanoparticles Modified Graphene Oxide

<sup>1</sup>Shih-Han Wang\*, <sup>1</sup>Yi-Han Yen, <sup>1</sup>Jing-Hwei Wang and <sup>2</sup>Ming-Der Ger

<sup>1</sup>Department of Chemical Engineering, I-Shou University

No.1, Sec. 1, Syuecheng Rd., Kaohsiung City 840, Taiwan

<sup>2</sup>Department of Chemical and Materials Engineering, Chung Cheng Institute

Technology National Defense University, No.75, Shiyuan Rd., Daxi Township, Taoyuan, Taiwan

shwang@isu.edu.tw

Hydrogen peroxide is an important marker in the biomedical reactions, and it is a kind of electroactive species which could be detected using electrochemical techniques. In the previous studies, graphene-based material has been extensively applied for electrochemical sensors [1], and it showed high sensitivity. In order to improve the selectivity, some electrocatalysts were introduced for lower the operating potential such as Pr, Au and Ir [2]. Although graphene-based materials are promising for sensing, it is not so easy to deposit metal onto the surface due to the lack of functional group for the reaction.

In this study, the high functional group density of graphene oxide was exploited as the substrate for the nanoparticles deposition. A highly sensitive nonenzymatic hydrogen peroxide ( $H_2O_2$ ) sensor was fabricated based on Iridium Nanoparticle/Graphene Oxide (Ir NP/GO) nanocomposites. The nanocomposites were rapidly synthesized via a one-step hydrothermal technique. The synthesized composites were characterized by X-ray diffraction (XRD), transmission electron microscopy (TEM), Fourier Transform Infrared Spectroscopy (FTIR) and X-ray photoelectron spectroscopy (XPS).

The TEM results indicated that Ir nanoparticles (IrNPs) distributed on the graphene surface uniformly with the average diameter of around 2.0 nm. We have found the operating potential of IrNP/GO was lower than that of GO. It implied the decorated IrNP catalyzed  $H_2O_2$  electrochemical oxidation reaction. It also showed high sensitivity to  $H_2O_2$  at low concentration and the detection limit was lower than 0.1 nM. Since the oxidation state might altered the morphology of IrNP/GO and the sensing performance, the effect of the oxidation state was studied. The sensitivity, reproducibility and the selectivity were evaluated. On the other hand, the effect of pH value and operating temperature was accessed as well in the sensing process. A highly sensitive platform of IrNP-GO for  $H_2O_2$  sensing was developed successfully.

## Acknowledgement

The financial support from the Ministry of Science and Technology, Taiwan, R.O.C. (MOST 103-2221-E-214 -053 - ) was acknowledged.

## References

1. C. L.Sun, H.H. Lee, J.M.Yang, C.C. Wu, Biosensors and Bioelectronics **26**(8), 3450–34 (2011).
2. Y. Zhang, M. Janyasuoab, C.W. Liu, P.Y. Lin, K.W. Wang, j. Xu and C. C. Liu, International Journal of Electrochemistrty, 410846 (2012)

# Development of an Electrochemically Based Rapid, Low-cost and Spreadable Assay for Heart Injury and Cancer Related Pathologies

S. Rapino<sup>a,b</sup>, M. Trinei<sup>b</sup>, E. Ussano<sup>a</sup>, M. Iurlo<sup>a</sup>, A. Soldà<sup>a,b</sup>, G. Valenti<sup>a</sup>, M. Iurlo<sup>a</sup>, M. Marcaccio<sup>a</sup>, F. M. P.G. Pelicci<sup>b</sup>, F. Paolucci<sup>a</sup>, M. Giorgio<sup>b</sup>

*a: Dipartimento di Chimica "G. Ciamician" Università di Bologna, via Selmi 2, 40126 Bologna, ITALY*

*b: IEO Dipartimento di Oncologia Sperimentale, Istituto Europeo di Oncologia, Via Adamello 16, 20139 Milano, ITALY*

[stefania.rapino3@unibo.it](mailto:stefania.rapino3@unibo.it)

Early and fast diagnosis and prognosis of heart injury and cancer pathologies are of paramount importance for a successful treatment of the diseases. Furthermore, cancer related pathologies, also caused by anticancer treatment, are determinant in cancer patient survival. Several molecular markers of heart damage and cancer are emerging and electrochemical driven trapping, detection and signal transduction of biomarkers have proven to be profitably employed in the development of sensing biochips and assays.

For instance, cytochrome c (cyt c) is an inner mitochondrial membrane (IMM) protein, which plays an important role in oxidative phosphorylation. This protein is not detectable in healthy patients' blood but it has been demonstrated that during some diseases, which involves the cellular apoptosis, cyt c is released [1]. In particular, cyt c is released from cellular membrane as a consequence of the treatment of infarction.[2] A fast monitoring of cyt c concentration can help to control the progression and extension of the heart injury guiding the therapeutic actions.

In this view, there is an urgent need to develop biochips/sensors/devices for the rapid detection of markers, such as cyt c, in very early stages of the diseases to evaluate the state and to operate with fast bedside therapies.

Herein, we show some strategies based on optimized chemical affinity for the trapping and the detection of disease markers and for signal amplification.

[1] V.E. Kagan et al., Free Radical Biol. Med. 2009, 46, 1439-1453

[2] G. Marenzi et al., Am. J. Cardiol. 2010, 106, 1443-1449

# Nanoparticles designed from hydrogels and DNA in triple hybridization process for improved storing and release of intercalators

Wioletta Liwinska\*, Zbigniew Stojek, Ewelina Zabost\*\*,

*Faculty of Chemistry, University of Warsaw*

*Pasteura 1, 02-093 Warsaw, Poland*

*\*wchmielowiec@chem.uw.edu.pl, \*\*ezabost@chem.uw.edu.pl*

Recent focus in the field of micro- and nano-sized targeted drug delivery systems, in strategies of its pre-formulation and formulation, is highly oriented on creation of systems for poorly soluble and/or highly unstable substances; reporting it to be the significant arena in pharmaceutical research. [1] Polymer and hydrogel-based materials with incorporated aptamer oligonucleotides are recently present as a particularly promising line for design of targeted delivery systems. These materials have been successfully proposed for several biomedical applications due to its unique dynamical structural properties such: the complementarity rule, denaturation, annealing, hybridization, conformation. [2,3]

In our work, we would like to present the synthesis and optimization steps needed for preparation of nanostructure materials designed from PNIPA, PAA, PEG hydrogels and DNA oligonucleotides; for improved delivery of selected anticancer drug – doxorubicin (DOX) and Symadex (C-1311). We synthesized nanostructured hydrogel-based lattices with noncovalently entrapped native ssDNA and dsDNA, as well, several kinds of thermoresponsive nano- and –microparticles with covalently attached selected DNA sequences. The synthesis procedure was carried out by free radical polymerization of the 5' ended acrylic group modified two DNA strands and attachment of third DNA strands to both covalently attached DNA in hybridization process. The physicochemical parameters of new materials as: the amount of incorporated DNA, pore distribution, sizes, zeta potentials, were tested. The main goal was investigations of the ability of particular networks to store and release of doxorubicin, before and after initiation of structural changes of oligonucleotides and volume transition of lattices in function of hyperthermia routinely used in cancer treatment.

## References:

- [1] G. Karwal, P. Kaur, R.Kakkar, H. Rao, Int. J. Nat. Prod. Science 1, (2012), 38.
- [2] A. Mukerjee, AP, Ranjan, J K., Vishwanatha, Curr. Med. Chem., 19 (2012) 3714.
- [3] E Zabost, W. Chmielowiec, T. Rapecki, M. Karbarz, Z. Stojek, Electrochem. Commun. 40,(2014) 50.



# Multicomponent hydrogel/aptamer-based nanofibers and nanoparticles for storing and release of intercalators and genetic material

Ewelina Zabost\*, Wioletta Liwinskaa, Agnieszka Kowalczyk, Zbigniew Stojek  
*Faculty of Chemistry, University of Warsaw*  
*Pasteura 1, 02-093 Warsaw, Poland*  
*\* ezabost@chem.uw.edu.pl*

The ultimate goal in cancer therapy remains focused on the development of treatment modalities that effectively kill tumor cells without harming normal cells. Thus, novel strategies for targeted cancer therapy are in great demand for effective cancer treatment. [1] The rapid development of multifunctional theranostic materials for biomedical applications show promising potential in cancer therapy. [2] Most of presented in literature nanomaterials can nonspecifically accumulate in cancer tissue through the enhanced permeability and retention (EPR) effect, that is, by passive targeting, albeit with limited dosage and selectivity. [3] Recently, the active, cell-specific targeting of nanomaterials has begun to represent a potentially powerful technology in cancer treatment. Active targeting is achieved by conjugating nanomaterials with targeting ligands that bind to overexpressed antigens or receptors on the target cells. [4]

In our work we would like to propose the construction of several nanosized and regular materials based on selected hydrogel lattices, metallic nanoparticles and covalently and noncovalently introduced oligonucleotide aptamers. We would like to expand the synthesis ways and optimization steps needed for preparation of multicomponent drug delivery system with incorporated DNA and improved delivery properties.

The first way of synthesis involves the application of charge controlled coaxial core-shell electrospinning process for creation of thin micro- and nanocomposites of PLCL/PNIPA/DNA/Au NPs. During electrospinning of polylactide-co -caprolactone (PLCL) polymer and thermoresponsive PNIPA hydrogel composites, selected oligonucleotides and neat and modified Au NPs were introduced into composited. The modification of Au NPs involved covalent and noncovalent attachment of DNA aptamers and selected antitumor drug – doxorubicin. Doxorubicin (Dox) was attached by covalent bonding sensitive to tumor environment, as well, was noncovalently entrapped in DNA structures. We investigated the release profiles of Dox-modified Au NPs from PLCL nanofibers, by spectroscopic (UV-Vis, CD) and electrochemical techniques (CV, SWV) and in vitro experiments (HeLa, Insulinoma and Glioma cells). The morphology of composites was inspected by TEM, SEM and optical microscopy.

Second way assume the introduction of particular conformations of selected aptamers into PAM and PNIPA hydrogel networks, for formation of multicomponent nanoparticles and storing of Dox and releasing of it after initiation of structural changes of aptamers and volume phase transition of lattices. Second kind of lattices was synthesized with Au NPs with attached Dox. The DNA-based biomaterials were characterized by a strong increase in guanine and adenine anodic currents that starts at physiological temperature. [5] The structural alterations were used as a control element in the releasing of doxorubicin. Doxorubicin was slowly released by using a minor temperature increase as it is routinely done in hyperthermia. The binding strength, the rate of release of Dox and the composite properties were examined using voltammetry, SEM and ICP-MS.

- [1] A. Mukerjee, A.P. Ranjan, J.K. Vishwanatha, *Curr. Med. Chem.* 19 (2012) 3714.
- [2] L. Eun-Kyung Lim, K. Taekhoon Kim, P. Soonmyung, H. Seungjoo Haam, H. Yong-Min, L. Kwangyeol, *Chem. Rev.*, 115 (2015) 327.
- [3] S. Bamrungsap, Z. Zhao, T. Chen, L. Wang, C. Li, T. Fu, W. Tan, *Nanomedicine*, 7 (2012) 1253.
- [4] Tan, W., Wang, H., Chen, Y., Zhang, X., Zhu, H., Yang, C., Yang, R. & Liu, C., *Trends Biotechnol.* 29 (2011) 634.
- [5] E. Zabost, W. Chmielowiec, T. Rapecki, M. Karbarz, Z. Stojek, *Electrochem. Commun.* 42 (2014) 50.

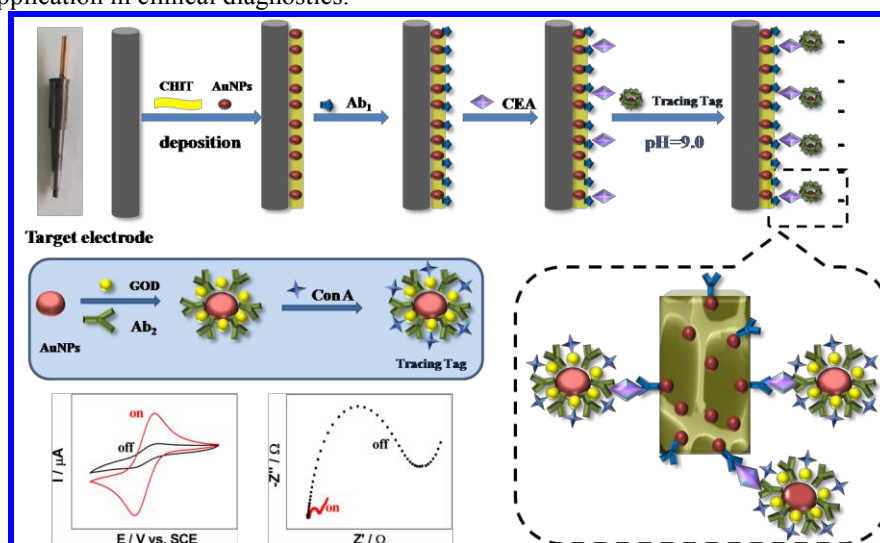
# An Ultrasensitive pH-Switchable Electrochemical Immunosensing based on Integrated 3D-KSCs Electrode as Singal Collector and AuNPs-Ab<sub>2</sub>-GOD-ConA as Tracing Tag for Assay of CEA

Jingyi Chen, Yonghai Song, and Li Wang

Key Laboratory of Functional Small Organic Molecule, Ministry of Education, Key Laboratory of Chemical Biology, Jiangxi Province, College of Chemistry and Chemical Engineering, Jiangxi Normal University, Nanchang, 330022, China.

[lwangsy2003@hotmail.com](mailto:lwangsy2003@hotmail.com)

**Abstract:** A novel ultrasensitive immunsensor for detection of the tumor biomarker, carcinoembryonic antigen (CEA), was developed by using AuNPs-Ab<sub>2</sub>-glucose oxidase (GOD)-Concanavalin A (Con A) as pH-switchable immunosensing probe and BSA-Ab<sub>1</sub>/chitosan (CHIT)-AuNPs/integrated three-dimensional macroporous carbon (3D-KSCs) derived from kenaf stem electrode as signal collector based on a sandwich-type assay mode. After a sandwich immunoreaction, the quantitative capture of AuNPs-Ab<sub>2</sub>-GOD-ConA on CEA/BSA-Ab<sub>1</sub>/CHIT-AuNPs/integrated 3D-KSCs electrode could greatly hinder Fe(CN)<sub>6</sub><sup>3-/4-</sup> electron transfer to make cyclic voltammograms response decrease and electrochemical impedance spectroscopy signal greatly increase. The electron transfer hindering of Fe(CN)<sub>6</sub><sup>3-/4-</sup> not only resulted from the increase of modified layer but also the electrostatic repulsion between Fe(CN)<sub>6</sub><sup>3-/4-</sup> and the negatively charged AuNPs-Ab<sub>2</sub>-GOD-ConA. The integrated 3D-KSCs electrode as signal collector not only provided a large specific surface area to load a large number of Ab<sub>1</sub> but also enhanced the mass transfer. As a consequence, the proposed immunsensor could detect CEA with a linear range of 5 pg mL<sup>-1</sup> to 50 ng mL<sup>-1</sup> and a detection limit down to 1.3 pg mL<sup>-1</sup>. In addition, the immunosensor had low cost, satisfactory reproducibility, stability and acceptable reliability. Thus, this method might provide a potential application in clinical diagnostics.



**Scheme 1.** Schematic illustrating of the pH-switchable immunosensor fabrication and sandwich-type immunoassay procedure.

## References

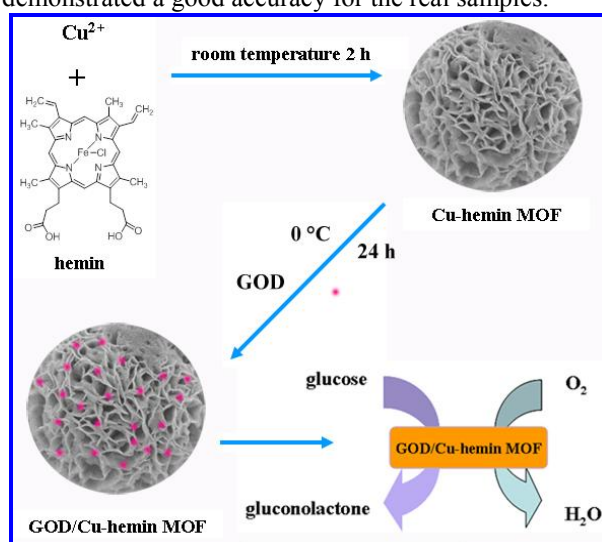
- [1] B. Jeong, R. Akter, O.H. Han, C.K. Rhee, M.A. Rahman, Increased electrocatalyzed performance through dendrimer-encapsulated gold nanoparticles and carbon nanotube-assisted multiple bienzymatic labels: highly sensitive electrochemical immunosensor for protein detection, *Anal. Chem.*, 85 (2013) 1784-1791.
- [2] J. Miao, X. Wang, L. Lu, P. Zhu, C. Mao, H. Zhao, Y. Song, J. Shen, Electrochemical immunosensor based on hyperbranched structure for carcinoembryonic antigen detection, *Biosens. Bioelectron.*, 58 (2014) 9-16.
- [3] J. Zhou, L. Du, L. Zou, Y. Zou, N. Hu, P. Wang, An ultrasensitive electrochemical immunosensor for carcinoembryonic antigen detection based on staphylococcal protein A—Au nanoparticle modified gold electrode, *Sens. Actuators, B*, 197 (2014) 220-227.

# The GOD/Cu-Hemin Metal Organic Frameworks Nanocomposites for Glucose Sensing

Juan He, Yonghai Song and Li Wang\*

College of Chemistry and Chemical Engineering, Jiangxi Normal University, 99 Ziyang Road, Nanchang 330022, People's Republic of China  
[yhsong@jxnu.edu.cn](mailto:yhsong@jxnu.edu.cn)

**Abstract:** Hemin as a member of iron porphyrin was first used alone as metalloligands to fabricate metal-organic-framework (MOF). In our study, a novel 3D mesoporous metal-metalloporphyrin MOF (Cu-hemin MOF) as peroxidase mimetic has been firstly demonstrated by a simple and facile one-step method in aqueous solution, which has owned a pretty morphology like flower-ball and enjoy a better water-stably. Based on this, glucose oxidase (GOD) has been successfully immobilized into Cu-hemin MOF for glucose detection based on the consumption and reduction reaction of  $O_2$  to obtain a large detection linear range. The GOD/Cu-hemin MOF nanocomposites could be used to achieve glucose detection directly with a wide linear range from 9.10  $\mu M$  to 30.0 mM, and the limit detection has been estimated to be as low as 2.73  $\mu M$ . Moreover, it was also successfully applied to the detection of glucose under coexistence of human serum, which demonstrated a good accuracy for the real samples.



**Scheme 1.** A schematic representation of synthesis and detection mechanism of GOD/Cu-hemin MOF.

## References

- [1] Y. Yu, Z. Chen, S. He, B. Zhang, X. Li, M. Yao, Direct electron transfer of glucose oxidase and biosensing for glucose based on PDDA-capped gold nanoparticle modified graphene/multi-walled carbon nanotubes electrode, *Biosens. Bioelectron.*, 52 (2014) 147-152.
- [2] Y. Song, H. Liu, Y. Wang, L. Wang, A novel bi-protein bio-interphase of cytochrome c and glucose oxidase: Electron transfer and electrocatalysis, *Electrochim. Acta*, 93 (2013) 17-24.
- [3] M. Zhao, Y. Gao, J. Sun, F. Gao, Mediatorless glucose biosensor and direct electron transfer type glucose/air biofuel cell enabled with carbon nanodots, *Anal. Chem.*, 87 (2015) 2615-2622.
- [4] P. Ling, J. Lei, L. Zhang, H. Ju, Porphyrin-Encapsulated Metal–Organic Frameworks as Mimetic Catalysts for Electrochemical DNA Sensing via Allosteric Switch of Hairpin DNA, *Anal. Chem.*, 87 (2015) 3957-3963.

# **Fabrication of Artificial Synaptic Interfaces Using Engineered Synaptic Adhesion Proteins**

Eun Joong Kim and Taek Dong Chung\*

*Department of Chemistry, Seoul National University*

*Gwanak-ro 599, Gwanak-gu, Seoul 151-747, Korea*

*E-mail: tdchung@snu.ac.kr*

In the nervous system, a neuron communicates with another to transmit neural information via synapses. Synaptic transmission for chemical neurotransmitters as well as electrical signals takes place in the synaptic clefts, which are gap junctions between pre- and postsynaptic boutons. The formation and function of synapse involve synaptic cell adhesion molecules (CAMs) localized at the synaptic site. In order to induce synapses between synthetic surfaces and neuronal cells and thereby construct artificial synaptic interfaces, we engineered well-known postsynaptic CAMs, i.e. neuroligin-1 (NL1), neuroligin-2 (NL2), and slitrk-3 (SL3), which were tagged with the fluorescent protein and biotin. The NL1 immobilized on microbead substrates were co-cultured with rat hippocampal neurons, and retained strong preference to the excitatory presynaptic differentiation. In addition, the artificial synapses formed by the NL1 beads maintained regardless of the developmental stages of cultured neuronal cells. While the NL2 and SL3 microbeads induced the strengthened inhibitory presynaptic differentiation when only contacted with the mature neurons. Such artificially induced synapses are reconstituted on the desired positions in the microchannel-guided patterns so that we were able to detect neurotransmitters and electrical signals. The artificial synaptic interface in this work is expected to serve as not only unprecedented electrochemical cell but novel neural interface at which biological nerve cell and electronic circuit exchange information with each other.

# Propagation of the change in the membrane potential -Electrochemical elucidation on nerve conduction-

Osamu Shirai, Yoshinari Takano, Yuki Kitazumi, and Kenji Kano  
Division of Applied Life Sciences, Graduate School of Agriculture, Kyoto University  
Sakyo, Kyoto 606-8502, Japan  
shiraio@kais.kyoto-u.ac.jp

Conduction mechanism of an action potential along a nerve axon was investigated by use of liquid membrane cells. Propagation of the change in a potential difference between two aqueous phases (W1 and W2) across a liquid membrane ( $E_{W1-W2}$ ) was elucidated based on the knowledge of voltammetry for the ion transfer at the interface of two immiscible electrolyte solutions [1,2]. We used a system coupling three liquid membrane cells which were composed of two aqueous phases and a 1,2-dichloroethane solution phase to analyze the change in the membrane potentials of the potential-sending and potential-receiving cells (potential-sending: cells S and Ap, potential-receiving: cell Rec). The ionic composition of the potential-sending cell (S) was identical to that of the receiving cell (Rec), and that of another potential-sending cell (Ap) was different from that of cell Rec. Thus, the membrane potential of cell S or Rec and that of cell Ap mimicked a rest and an action potentials, respectively, observed in the nerve transmission. When the connection of cell Rec was switched from cell S to cell Ap, the change in the membrane potential was caused with the circulating current in the cell system. The properties for the propagation of the change in the membrane potential depend on the ratio of the magnitude of the limiting current at cell Ap versus that at cell Rec. The limiting current observed at the interface, of which the potential difference varies in cell Rec and corresponds to the threshold, and the magnitude of the limiting current at the interface, of which the potential difference varies in cell Ap, reflects the potency of the propagation of the action potential. The potential differences at every interface are controlled by the ion transfers and the circulating current flowed to keep the electroneutrality of every phase.

The influence of some capacitors or some electric resistors on the propagation of the change in the membrane potential was investigated by setting some capacitors or some resistors in the electric circuit [3]. Changing the connection of cell Rec from cell S to cell Ap, the membrane potential of cell Rec varied from the rest potential to a different membrane potential that is close to the action potential. The delay and decrement of the propagation of the change in the membrane potential was observed by setting capacitors or resistors in the electric circuit. It is thought that the change in the membrane potential was reduced by both the potential drop prompted by generation of the circulating current and that the delay of the propagation was caused by the electric charging of the capacitor in analogy with the propagation of the action potential in the nerve transmission.

In order to construct a cell system composed of the cells having the roles of  $K^+$  and  $Na^+$  channels in nerve cells, the cells of which the membrane potentials were determined by the transfer of  $K^+$  and  $Na^+$ , respectively, were prepared. The membrane potential of cell S or Rec at zero current corresponds to the rest potential, and that of cell Ap at the zero current corresponds to the action potential. By coupling multiple Ap cells through the electric relays which begin to work at the membrane potential more than the threshold, the directionality of the propagation of the action potential was investigated. We succeeded in reproducing the propagation of the action potential like the nerve conduction.

1. N. Ueya, O. Shirai, Y. Kushida, S. Tsujimura, and K. Kano, *J. Electroanal. Chem.*, **2012**, 673, 8.
2. Y. Kushida, O. Shirai, Y. Kitazumi, and K. Kano, *Bull. Chem. Soc. Jpn.*, **2014**, 87, 110.
3. Y. Kushida, O. Shirai, Y. Kitazumi, and K. Kano, *Electroanalysis*, **2014**, 26, 1858.

# Interaction between Ferric/Ferrous Cytochrome *c* and Cardiolipin: An Electrochemical and Quartz Crystal Microbalance with Dissipation Study

Sin-Cih Sun, Yuan-Hao Hsu, Min-Chieh Chuang

*Department of Chemistry, Tunghai University*

*No. 1727, Sec. 4, Taiwan Blvd., Taichung 40704, Taiwan*

*sandy79325@gmail.com*

Cytochrome *c* (cyt *c*), a protein inherent with a redox-centered heme in ferric/ferrous states, locates in the mitochondrial intermembrane space in eukaryotic cells. The oxidation state of heme regulates structure of cyt *c* and its affinity to electron transport complexes, in which the ferric cyt *c* tends to bind to complex III and the ferrous cyt *c* associates with complex IV. Approximate 15% of the positively charged cyt *c* associates with the mitochondrial cardiolipin (CL) in homeostatic conditions [1] and function as a peroxidase to promote CL oxidation which is referred as an early step towards apoptosis [2]. Although ferric and ferrous cyt *c* have been shown to form complexes with CL, the exact mechanism leading to apoptosis in connection to oxidation state of cyt *c* remains unresolved.

We performed electrochemical techniques to interrogate effect of redox switch (cyt *c*) upon the interaction between cyt *c* and CL. Cyt *c* was functionalized on a carboxylic- and hydroxyl-groups terminated self-assembled monolayer on gold electrode by electrostatic and hydrophobic attraction. Cyclic voltammogram reveals that the formal potentials acquired from both ferric and ferrous cyt *c* shifted to less positive potential (by 19.5 and 15 mV) upon the association with CL. The potential separation of redox waves also increased upon the cyt *c*-CL association. The results correlated with the conclusion obtained in AC voltammetric experiments wherein the ferric cyt *c* exhibited a potential shift (24.1 mV), remarkably greater than 9.2 mV of ferrous cyt *c*, inferring a substantial structural change of ferric cyt *c* upon the association with CL. A molecular modeling also suggested a more perpendicular orientation of heme-plane (in the adsorbed ferrous cyt *c*) to the electrode surface.

The cyt *c*-CL interaction was further interrogated using Quartz Crystal Microbalance with Dissipation monitoring (QCM-D). The mass the ferric cyt *c* adsorbed onto a phosphatidylcholine (PC)/CL (4:1 in molar ratio) lipid bilayer was 2.4-fold greater than the ferrous one which, however, represented greater shear modulus ( $\mu = 1.44 \times 10^3$  Pa) for the binding of cyt *c* to CL. The *D-f* plot revealed different slopes given by ferrous and ferric cyt *c*, presumably ascribed to distinct adsorption kinetics. The ferric cyt *c* displayed two linear regimes with different slopes containing the initial part having a greater slope and the second one giving a slope same with ferrous cyt *c* throughout the adsorption.

Reference:

[1] Kalanxhi, E. and Wallace, C. J., *Biochem J* (2007) 407, 179-187.

[2] Kagan, V. E. et al., *Free Radical Bio Med* (2009) 46, 1439-1453.

# Electrodeposited NiCo bimetallic nanoparticles decorated reduced graphene oxide for highly sensitive and selective determination of dopamine

Yang Liu, Wenyan Zhang

Department of Chemistry, Beijing Key Laboratory for Microanalytical Methods and Instrumentation,  
Tsinghua University, Beijing 100084, P. R. China  
e-mail: liu-yang@mail.tsinghua.edu.cn

Bimetallic nanoparticles, composed of two chemically distinct metals, have aroused extensive interests due to their unique optical, electronic, and especially catalytic properties. The bimetallic-NP-based catalysts often show superior catalytic activity compared with the homologous monometallic counterparts, arising from the synergistic effects of both moieties. However, the aggregation and coalescence of the bimetallic nanoparticles generally reduces the catalytic activity and surface area, which limits its application in biosensing. Because of the huge surface area, high conductivity, and rich physical and chemical functionalities, graphene has been proofed to be a remarkable nanosupport to stabilize nanoparticle with high activity. In this work, a uniform reduced graphene oxide thin film was firstly prepared by a electrochemical deposition, and NiCo bimetallic nanoparticles were anchored on reduced graphene oxide (rGO) by a dual potential electrochemical deposition method (NiCo/rGO). Compared to the single component of NiCo or rGO, the NiCo bimetallic nanoparticles were well dispersed. NiCo/rGO composite modified glassy carbon electrode (GCE) exhibits excellent electrocatalytic activity of dopamine (DA) which plays a significant role in human meta-bolic, renal, cardiovascular, central nervous and hormonal systems and was various detection approaches has been developed. Under optimal condition, the electrochemical biosensor displays high sensitivity toward DA detection. A good linear relationship between the current and the concentration of DA was obtained in the range of 1  $\mu\text{M}$  to 100  $\mu\text{M}$  with A detection limit of 50 nM ( $S/N = 3$ ). In addition, the NiCo/rGO based electrochemical sensor showed excellent selectivity toward DA detection in the presence of ascorbic acid (AA), uric acid (UA) and other interference reagents, and was applied for the DA detection of human serum samples. The results demonstrate the developed approach provides a promising strategy to improve the sensitivity and selectivity of electrochemical biosensors in the application of clinical diagnostics.

## References

- [1] A.K. Geim, K.S. Novoselov, *Nat. Mater.*, 6 (2007) 183-186.
- [2] J.D. Fowler, M.J. Allen, V.C. Tung, Y. Yang, R.B. Kaner, B.H. Weiller, *Acs Nano*, 3 (2009) 301-306.
- [3] C.-L. Sun, H.-H. Lee, J.-M. Yang, C.-C. Wu, *Biosensor. Bioelectron.*, 26 (2011) 3450-3455.
- [4] Y. Liu, X. Dong, P. Chen, *Chem. Soc. Rev.*, 41 (2012) 2283-2307.
- [5] J.N. Tiwari, K. Nath, S. Kumar, R.N. Tiwari, K.C. Kemp, N.H. Le, D.H. Youn, J.S. Lee, K.S. Kim, *Nat. Commun.*, 4 (2013).

# Effect of Nanoscale Surface Morphology on Biorecognition Using Localized Surface Plasmon Resonance (LSPR) Spectroscopy

Alexander Vaskevich,<sup>1</sup> Tatyana B. Bendikov,<sup>2</sup> Ortal Bahar,<sup>1</sup> Ludmila Frolov,<sup>1</sup> Israel Rubinstein<sup>1</sup>

Departments of <sup>1</sup>Materials and Interfaces and <sup>2</sup>Chemical Research Support,  
Weizmann Institute of Science, Rehovot 7610001, Israel  
alexander.vaskevich@weizmann.ac.il

The surface nanoscale morphology has been generally recognized as one of the major parameters determining the properties of adsorbed biological molecules, in cases such as organization of ssDNA on Au nanoparticles (NPs) and nanorods (NRs), proteins on silica and gold NPs, the secondary structure of peptides, the structure of protein corona, oligomerization of surface-bound proteins, and NP-cell interaction.

Metal nanostructures supporting excitation of localized surface plasmons present a unique situation encompassing controllable nanoscale morphology which can be varied over a wide range of shapes and curvatures, from several to hundreds of nm, providing sensitivity of the spectral response that can be tuned to the properties of the environment in the vicinity of the nanostructured surface.

High-resolution scanning electron microscopy (HRSEM) imaging of polyelectrolyte multilayers, adsorbed proteins and immobilized oligo-DNA strands shows formation of rather uniform shells on Au nano-islands (Figure 1). Preparation of morphologically stable LSPR transducers based on Au island films with variable average island size provides a convenient platform for studying the influence of the surface curvature on the organization of biomolecules on surfaces presenting a controlled morphology. We explored the possibility of quantifying the morphology-dependent LSPR response for immobilization and interaction of oligonucleotides and immunoassay using a simple core-shell model which allowed quantification of the optical response.<sup>1,2</sup>

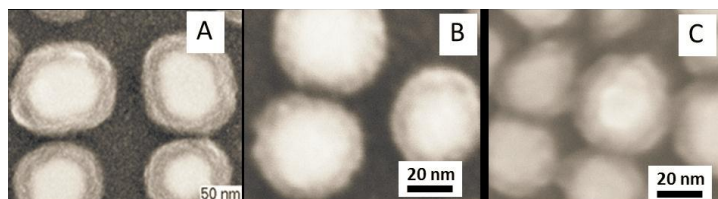


Figure 1. HRSEM images of Au nano-island films coated with (A) a polyelectrolyte multilayer, (B) immobilized 8-His BLIP, and (C) immobilized oligo-DNA (43 bases). Samples B and C were stained before imaging.<sup>3</sup>

Studies of immobilization and hybridization of ss oligo-DNA showed the applicability of a core-shell model to the analysis of immobilization of thiolated and amine-terminated ssDNA, as well as hybridization of ss-DNA on LSPR transducers with variable average island diameter (15–32 nm). Comparison of the model and the experimental data showed a near quantitative correspondence using the effective layer thickness as a single fitting parameter.

We found that the activity of rabbit IgG or anti-rabbit IgG adsorbed directly on the Au surface was preserved over the entire range of island sizes. Binding of anti-rabbit IgG to rabbit IgG on the smallest Au islands was suppressed compared to the larger islands, possibly associated with the similarity in size between the small islands and the IgG proteins. The same antigen-antibody system was tested using indirect binding of the recognition IgG layer to the Au surface via covalent attachment to a pre-assembled monolayer of a linker thiol-NHS. We found that binding of anti-rabbit IgG to covalently tethered rabbit IgG receptor layer shows substantially larger optical response compared to the respective changes associated with binding of the first protein layer. This intriguing observation, not seen in the case of directly adsorbed rabbit IgG receptor layer, suggests a greater than 1:1 antigen-antibody binding ratio on the surface.

## References

- [1] Vaskevich, A.; Rubinstein, I. Localized surface plasmon resonance (LSPR) transducers based on random evaporated gold island films: Properties and sensing applications, in *Nanoplasmonic Sensors*; Dmitriev, A., Ed.; Springer Publishing: NY, 2012, p. 333.
- [2] Kedem, O.; Vaskevich, A.; Rubinstein, I. Critical Issues in Localized Plasmon Sensing, *J. Phys. Chem. C* 118 (2014) 8227–8244.
- [3] Bendikov, T. A.; Rabinkov, A.; Karakouz, T.; Vaskevich, A.; Rubinstein, I. Biological sensing and interface design in gold island film based localized plasmon transducers. *Anal. Chem.* 80 (2008) 7487-7498.



# Ultrasensitive electrochemical sensor for dopamine determination based on novel supportless nanoporous Au-Ag alloy microrod

Han Song, Jie Liu, Lu Zhang, Jiang Liu, Yuan Liu, Ying-Chun Li\*

Key Laboratory of Xinjiang Phytomedicine Resources of Ministry of Education, School of Pharmacy, Shihezi University, Shihezi, Xinjiang, 832000

e-mail address: yingchunli@shzu.edu.cn

## Abstract

Dopamine (DA) is a catecholamine neurotransmitter of significant biologic interest, for its demonstration of the treatment of the central nervous system disorders, such as schizophrenia and Parkinson's disease. Hence, accurate and sensitive determination of DA is vitally important in the diagnosis of various mental diseases. In this work, we develop a novel freestanding metallic microrod as working electrode for highly sensitive and selective electrochemical detection of trace DA. The electrode was facilely fabricated via first dealloying of smooth Au-Ag alloy microrod (AMR) into nanoporous Au-Ag alloy microrod (NPAMR) and further modification with electropolymerized molecularly imprinted polymer (MIP). The 3D open and continuous nanoporous structure of the supportless microrod provides large specific surface area and the outer MIP layer imparts recognition ability of DA molecules to the sensor. Therefore, the outstanding determination performance of the as-prepared sensor arises from coupling the amplification feature of NPAMR with the superior selectivity of MIP. Moreover, the fact that the microrod is able to work without the assistance of a commercial electrode simplifies the construction of sensor system and lowers the cost. Influencing factors including dealloying time, pH value and molar ratio of monomer to template molecule during electropolymerization process were optimized. Under the optimal conditions, a linear range from  $2 \times 10^{-13}$  to  $2 \times 10^{-8}$  mol L<sup>-1</sup> for measuring DA was obtained with a detection limit of  $7.63 \times 10^{-14}$  mol L<sup>-1</sup> (S/N=3), which is lower than the data from all the reported DA sensors we can find. In addition, the MIP-modified electrode (MIP/NPAMR) was successfully employed to test DA in biological samples.

**Keywords** Molecularly imprinted polymer; Nanoporous alloy microrod; Electrochemical sensor; Trace measurement

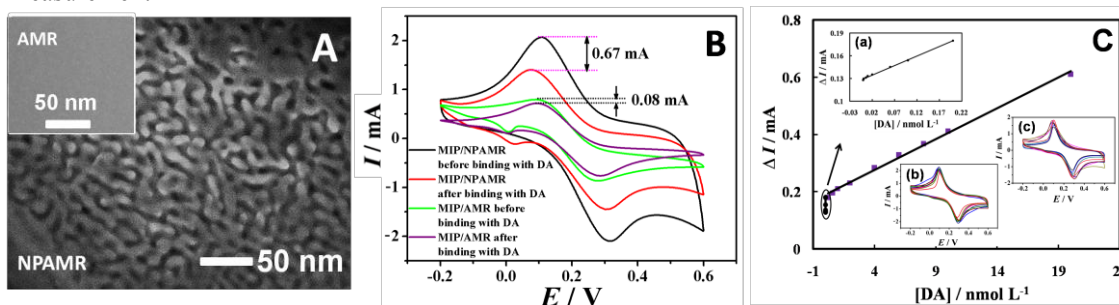


**Fig. 1** (A) SEM image of NPAMR and AMR (Inset). (B) Comparison of two differently modified sensors before and after binding with  $2 \times 10^{-8}$  mol L<sup>-1</sup> DA at a scan rate of 100 mV s<sup>-1</sup> in 0.05 mol L<sup>-1</sup> [Fe(CN)<sub>6</sub>]<sup>3-/4-</sup>. (C) Calibration curve for DA detection correlating reduction peak current shift with DA concentration by using MIP/NPAMR. The inset (a) is magnified curve in low concentration range and the inset (b) and (c) show typical cyclic voltammograms of sensor in response to DA.

## References

1. B. Liu, H. Lian, J. Yin, X. Sun, *Electrochim. Acta* 75 (2012) 108-114
2. J. Liu, L. Zhang, H. Song, Y. Liu, Y. C. Li, J. Sep. Sci. DOI: 10.1002/jssc.201401248
3. Y.C. Li, Y. Liu, J. Liu, J. Liu, H. Tang, C. Cao, D. Zhao, Y. Ding, *Sci. Rep.* 5 (2015) 7699.
4. Y. Liu, J. Liu, H. Tang, J. Liu, B.B. Xu, F. Yu, Y.C. Li, *Sensor. Actuator. B: Chem.* 206 (2015) 647-652.

# Fabrication of Paper-based Disk-shaped Glucose Biofuel Array

Isao Shitanda<sup>1,2</sup>, Saki Nohara<sup>1</sup>, Seiya Tsujimura<sup>3</sup>, Yoshinao Hoshi<sup>1,2</sup>, Masayuki Itagaki<sup>1,2</sup>

<sup>1</sup>*Department of Pure and Applied Chemistry, Faculty of Science and Technology, Tokyo University of Science Noda, Chiba 278-8510, Japan.*

<sup>2</sup>*Research Institute for Science and Technology, Tokyo University of Science, 2641 Yamazaki, Noda, Chiba 278-8510, Japan.*

<sup>3</sup>*Division of Materials Sciences, Faculty of Pure and Applied Sciences, University of Tsukuba, 1-1-1 Tennodai, Tsukuba, Ibaraki, 305-8573, Japan.*

*E-mail address: shitanda@rs.noda.tus.ac.jp (I. Shitanda)*

There are a lot of attentions of wearable electrochemical devices for monitoring vital signs such as concentration of glucose. We previously reported a screen-printed paper-based flexible biofuel cell based on glucose oxidase and bilirubin oxidase with high disposability and biocompatibility<sup>1</sup>. The fabricated biofuel cell (BFC) exhibited a remarkable power output of  $0.12 \text{ mW cm}^{-2}$ .

In the present study, we developed a high-power paper-based glucose biofuel cell array for self-powered wearable health-monitoring devices. The device is expected to be put on a diaper to generate electricity from the glucose contained in urine, and can wirelessly send information such as glucose- and electrolyte-concentrations. Figure 1 shows the schematic illustration of the present biofuel cell array.

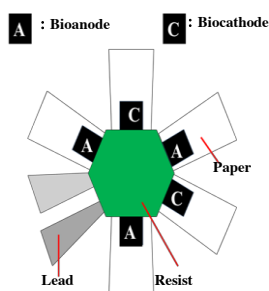


Fig. 1 Schematic illustration of a disk-shaped paper-based biofuel array

The maximum power of the present biofuel array was about  $400 \mu\text{W}$ . The device may find application in health-check systems, thereby decreasing the burden of the nursing staff in a nursing home and similar medical care facilities. In this presentation, we introduce the structure and characteristics of the present biofuel cell array in detail.

## Acknowledgement

This work was partially supported by JSPS KAKENHI 70434024 Grant (I. Shitanda) and the Iwatani Foundation (I. Shitanda).

# Ultra-Sensitive Electrochemical electrode developed for ovarian cancer

Shih-Han Huang<sup>1</sup>, Fu-Ming Wang<sup>1,2\*</sup>

<sup>1</sup>Graduate Institute of Applied Science and Technology, National Taiwan University of Science and Technology

<sup>2</sup>Sustainable Energy Center, National Taiwan University of Science and Technology

43 Keelung Road, Section 4, Taipei 10607, Taiwan

Correspondence: mccabe@mail.ntust.edu.tw

Enzyme-linked immune-sorbent assay (ELISA) is a traditional clinical analysis. The assay system utilizes a monoclonal antibody, which directs against a distinct antigenic determinant on the intact CA125 molecule and is used for solid phase immobilization. A rabbit anti-CA125 antibody conjugated to horseradish peroxidase (HRP) is in the antibody-enzyme conjugate solution. The test sample is allowed to react simultaneously with the two antibodies, resulting in the CA125 molecules are being sandwiched between the solid phase and enzyme-linked antibodies. The minimum detectable concentration of CA125 in this assay is estimated to be 5 U/ml. According to the previous research, decreasing the detection limit and increasing analytical sensitive are our study goal [1].

In this study, an electrochemical immunosensor established on graphene sheet (GS) has been developed. Graphene sheet is used to immobilize the mediator thionine (TH), secondary anti-CA125 antibody (Ab2), and gold nanoparticles. The resulting nanostructure (GS-TH-AuNPs-Ab2) is able to use as the label for the immunosensor. By immobilizing primary anti-CA125 antibody (Ab1) and cancer antigen 125 (CA125) onto the nanostructure, the working electrode is constructed by coating the nanostructure on the glassy carbon electrode (GCE) [2]. In order to increase the detecting accuracy of ovarian cancer, multiplexed tumor markers (CA125, CA153) on sandwich-format electrochemical immunosensor are also fabricated [3].

Figure 1 shows our result in differential pulse voltammetry (DPV) measurement. Green line represents the solution only with gold nanoparticles (AuNPs) and reveals two typical peaks, indicating the electron transfer in the electrochemical reaction. When coated with graphene (black line), one of the peaks becomes weak and shows that the oxygen functional group might affect the electron transfer. After adding mediator thionine (red line), the peak turns clearly; it proves mediator can make the signal stronger. Finally we added bovine serum albumin (BSA), the peak becomes small (blue line) due to the BSA is covered on the electrode and inhibits the electron transfer.

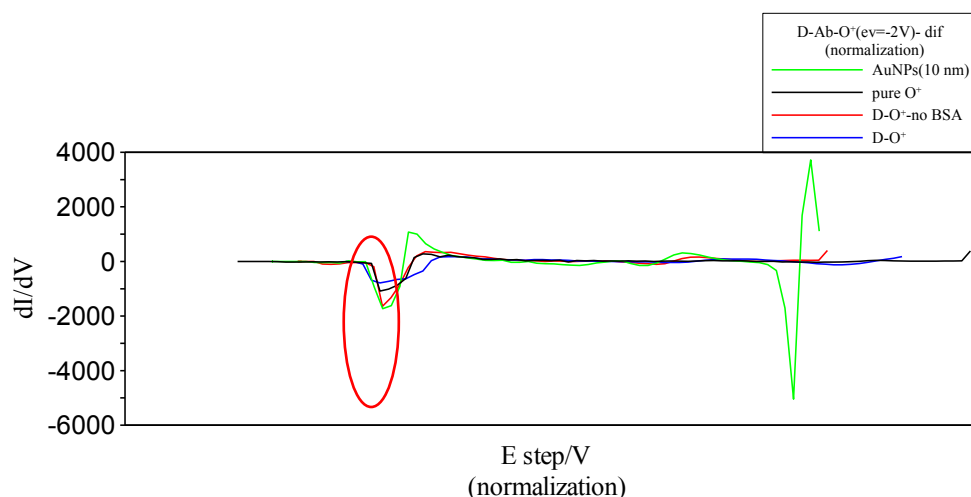


Figure 1 Normalized DPV curves of ultra-sensitive electrodes

## Reference

- [1] Clin Cancer Res. 2006 April 1; 12(7 Pt 1): 2117-2124. doi:10.1158/1078-0432.CCR-05-2007.
- [2] M. Yang, A. Javadib, H. Lia, S. Gongc, Biosensors and Bioelectronics 26 (2010) 560.
- [3] X. J., Z. Liu, N. Liu, Z. Man, Biosensors and Bioelectronics 53 (2014) 160.

# Pd Catalyzation and Electroless Deposition of Ni on Textile Using Supercritical Carbon Dioxide

Mitsuo Sano<sup>1</sup>, Yuma Tahara<sup>2</sup>, Tso-Fu Mark Chang<sup>1,3,\*</sup>, Chun-Yi Chen<sup>1,3</sup>, Tomoko Hashimoto<sup>2</sup>, Hiromichi Kurosu<sup>2</sup>, Masato Sone<sup>1,3</sup>

<sup>1</sup>*Precision and Intelligence Laboratory, Tokyo Institute of Technology, 4259 Nagatsuta, Midori-ku, Yokohama 226-8503, Japan*

<sup>2</sup>*Department of Clothing Environmental Science, Nara Women's University, Kitauoya Higashimachi, Nara 630-8506, Japan*

<sup>3</sup>*CREST, Japan Science and Technology Agency, 4259 Nagatsuta, Midori-ku, Yokohama 226-8503, Japan*  
*chang.m.aa@m.titech.ac.jp*

Wearable device is an advanced technology that can be applied in various fields. For example, the wearable sensor can prevent “drink & driving” by sensing alcohol from the human body before initiation of a car’s engine. Sportswear equipped with a wearable sensor can contribute dramatically to progress of sports science. One of the challenging points in wearable device is deposition of electrical-conductive, usually metallic, materials on the textile. In comparison with other metal deposition methods such as sputtering and evaporation, electroless deposition is the most promising technology at the industrial level because of its simple operation and low cost process. Therefore, study on fabrication of fibers coated with metallic materials by electroless deposition has attracted much attention. However, there are still some problems needed to be improved in electroless plating. First, a pretreatment process is usually needed, and the pretreatment process is performed with toxic substance [1]. In this case, the toxic substance raises concerns for practical use of the fibers in clothing. Second, the fibers can be damaged or even lost because the pretreatment is performed with a strong acid. Third, adherence of the metallic coating on the fibers still needs to be improved.

In previous studies, we have proposed a supercritical CO<sub>2</sub> catalyzation (SCC) method with organo Pd complex followed by an electroless plating method with supercritical CO<sub>2</sub> emulsified electrolyte (ELP-SCE) to improve coverage and adherence of Ni on a Kapton® polyimide film [2-4]. Supercritical fluid is any substance at a temperature and pressure above its critical point. Surface tension of supercritical CO<sub>2</sub> is extremely low, and diffusivity is very high. Therefore, it can improve transfer of materials into very fine space. We believe the SCC and ELP-SCE can also be applied in electroless plating of Ni-P on textile to eliminate the concerns of the toxic chemicals used in the pretreatment and improve adhesion of the Ni-P coating on the textile.

The textile used in this study is Nylon 6,6 fiber. No pretreatment was conducted in this study. The catalyzation was either a conventional method with a PdCl<sub>2</sub>/SnCl<sub>2</sub> mixture solution (CONV-cat) or in the SCC with bis (2,4-pentandionato)-palladium. The catalyzation temperature was 353 K, and pressure for the SCC is 15 MPa. After the catalyzation process, either a conventional electroless plating (CONV-ELP) or ELP-SCE was performed. The reaction temperature was 353 K for both of the plating methods, and pressure of 15 MPa was used for the ELP-SCE. Surface of the Ni-P coatings was observed by an optical microscope and a SEM.

The coated Ni-P by the CONV-cat and the CONV-ELP had many pin-holes and did not show outline of the textile but fused into rough structure. This comes from the individual nodule growth of the Ni-P nuclei during the electroless deposition process. Ni-P coating by the SCC and the CONV-ELP showed rough Ni coating on surface of each fiber, and many peered-off parts were observed. On the other hand, uniform Ni coating on the surface of each fiber was obtained by the SCC and the EP-SCE. These results demonstrate that the SCC is effective to impregnate the Pd catalysts into the fibers and the EP-SCE can inhibit the nodule growth of Ni-P. Thus, the method proposed in this study can metallize surface of each fibers in the textile and has potential to give some functions on textiles.

## Reference:

- [1] T. Miyamura, J. Koike, *Mater. Sci. Eng. A*, **445–446** (2007) 620.
- [2] B.H. Woo, M. Sone, A. Shibata, C. Ishiyama, K. Masuda, M. Yamagata, Y. Higo, *Microelectron. Eng.*, **86** (2009) 1179.
- [3] B.H. Woo, M. Sone, A. Shibata, C. Ishiyama, K. Masuda, M. Yamagata, Y. Higo, *Surf. Coat. Technol.*, **203** (2009) 1971.
- [4] B.H. Woo, M. Sone, A. Shibata, C. Ishiyama, S. Edo, M. Tokita, J. Watanabe, Y. Higo, *Surf. Coat. Technol.*, **204** (2010) 1785.

# Electrochemistry-controlled Photo-induced Electron Transfer in Ubiquinone-based Systems

Xiao-Yuan Liu, Yi-Tao Long\*

Key Laboratory for Advanced Materials & Department of Chemistry, East China University of Science and Technology, 130 Meilong Road, Shanghai, 200237, P. R. China.

xiaoyuanliu@mail.ecust.edu.cn

In photosynthesis process, photo-induced electron from excited state of  $P_{680}$  in photosystem II (PSII) is transferred along an electron transport chain via three mobile carriers (plastoquinone, plastocyanin and ferredoxin) to fulfill the synthesis process of adenosine triphosphate (ATP) and the reduction of carbon dioxide, where the photo-induced electron transfer (PET) plays an essential role.<sup>1-3</sup>

To research the PET processes, we designed and synthesized a ubiquinone-based triphenylamine compound (TPA-CoQ<sub>0</sub>) to research the PET from optical studies and Density Functional Theory (DFT) calculations. In TPA-CoQ<sub>0</sub>, triphenylamine and ubiquinone acts as electron acceptor, respectively. Ubiquinone undergoes two-step two-electron redox process, which could fine-tune the PET process from triphenylamine moiety to ubiquinone group.

The optical studies indicate the PET process could be fine-tuned via redox processes of ubiquinone and the system exhibits switched “off/on” and “off/on” fluorescent properties between TPA-CoQ<sub>0</sub> and TPA-H<sub>2</sub>CoQ<sub>0</sub>. The DFT calculations demonstrate that the changed LUMO orbitals of ubiquinone/hydroquinone are ascribed to the switched PET processes.

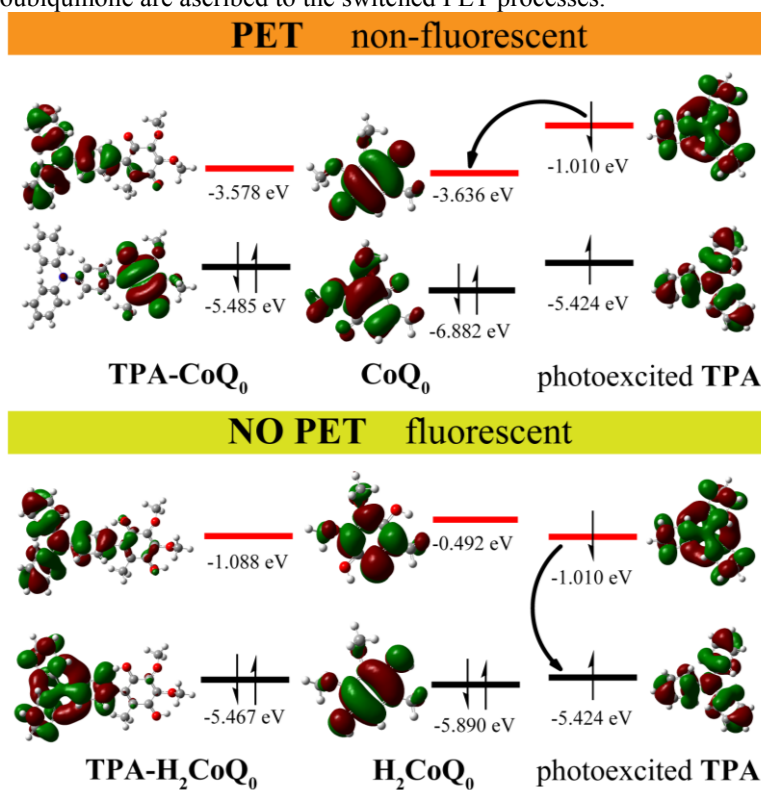


**Figure.1** The frontier molecular orbital energy diagrams.

## REFERENCES

1. Emerson, R., Chalmers, R. & Cederstrand, C. *Proc. Natl. Acad. Sci. U. S. A.* **43**, 133-143 (1957).
2. Nonella, M. *J. Phys. Chem. B* **102**, 4217-4225 (1998).
3. Bauer, A., Westkamper, F., Grimme, S. & Bach, T. *Nature* **436**, 1139-1140 (2005).

# Defective graphene flake-supported Pd nanocubes as electrochemical glucose sensor

Bang-De Hong, Chien-Liang Lee\*

*Department of Chemical and Materials Engineering, National Kaohsiung University of Applied Sciences  
No. 415, Chien Kung Rd., Kaohsiung 807, Taiwan  
e-mail address: [cl\\_lee@kuas.edu.tw](mailto:cl_lee@kuas.edu.tw); [cl\\_lee@url.com.tw](mailto:cl_lee@url.com.tw)*

Defective graphene flakes (DGFs) is of interesting for the effect in an electrocatalytic process. Previously, we reported a sonoelectrochemical method to rapidly prepared defective grapene flakes (DGF<sub>SECM</sub>) and observed the domination of physical defects on the surfaces of these DGF<sub>SECM</sub> as compared to defective grapene flakes prepared via a chemical reduction method (DGF<sub>CM</sub>) [1]. In this study, the DGF<sub>SECM</sub> and DGF<sub>CM</sub> were used to support these 10 nm Pd nanocubes, forming defective graphene flake-supported Pd nanocubes, successfully used as catalysts for non-enzymatic D-glucose sensor. Compared with the DGF<sub>CM</sub> systems, the DGF<sub>SECM</sub> system has a higher electrochemically real surface area and greater catalytic activity on glucose oxidation. Additionally, there were two linear current-responses relationships for the sensitivities on the DGF<sub>SECM</sub>, DGF<sub>CM</sub> system and DGF-free Pd nanocubes. The DGF<sub>SECM</sub>-supported Pd nanocubes showed the higher sensitivities of  $74 \mu\text{A}\cdot\text{mM}^{-1}\cdot\text{cm}^{-2}$  from 0.25 mM to 5 mM and  $45.86 \mu\text{A}\cdot\text{mM}^{-1}\cdot\text{cm}^{-2}$  from 5 mM to 20 mM. The data in the selective tests depicted that DGF<sub>SECM</sub>-supported Pd nanocubes as compared to DGF-free Pd nanocubes showed remarkable tolerance to foreign ascorbic acid and uric acid, for which DGF<sub>CM</sub>-supported Pd nanocubes had slight current. The low deviation by serum sample analyses further confirmed the potential of DGF<sub>SECM</sub>-supported Pd nanocubes as a glucose sensor.

## References:

- [1] C.-W. Chen, Z.-T. Liu, Y.-Z. Zhang, J.-S.Y. Ye, C.-L. Lee, Sonoelectrochemical intercalation and exfoliation for the preparation of defective graphene sheets and their application as nonenzymatic H<sub>2</sub>O<sub>2</sub> sensors and oxygen reduction catalysts, RSC Advances 5(2015) 21988-21998.

# Direct detection for ratio of concentrations of HbA1c to total hemoglobin with potentiometric immunoassay

Junko Tanaka, Yu Ishige, and Masao Kamahori

Research & Development Group, Hitachi, Ltd.

1-280, Higashi-koigakubo, Kokubunji-shi, Tokyo, 185-8601 Japan

The increasing number of diabetes patients is resulting in the rise of health care costs. Earlier treatment for patients in the diabetes mellitus preliminary group is considered one of the best ways to suppress the rise of costs in the future. While blood glucose level reflects the severity of diabetes, it is not the best indicator for screening because it fluctuates, even on a daily basis. HbA1c, hemoglobin glycosylated by glucose in the blood, reflects the average blood glucose level for past 1–2 months, so it is considered the gold standard for determining the treatment of diabetes.

Conventionally, HbA1c has been determined by the HPLC method with ion exchange or affinity columns to separate HbA1c from other hemoglobin. Therefore, HbA1c (%), which is the ratio of concentration of HbA1c to total Hb (hemoglobin), is used as the HbA1c indicator. The HPLC method can determine HbA1c (%) directly but requires large and expensive instruments. Antibody-based immunoassay and enzyme-based enzymatic assay methods, which do not require large instruments, are increasingly available to clinical laboratories, but these methods require a separate measurement of total hemoglobin content in the samples and a calculation of the ratio of HbA1c to total Hb. In this study, we developed a potentiometric immunosensor with a direct measurement method for HbA1c (%) measurement to simplify the measurement system.

The developed potentiometric immunosensor is shown in Fig. 1. The target molecules are captured by capture antibodies and a sandwich of the captured antibody-target-labeled antibodies is formed. Alkaline phosphatase as the labeling enzyme hydrolyzes ascorbic acid phosphate (AsA-P) and produces ascorbic acid (AsA). AsA reacts with ferricyanide and produces ferrocyanide. Since redox potential follows the ratio of ferricyanide and ferrocyanide as the Nernst equation, the amount of produced ferrocyanide that is proportional to the amount of captured target can be obtained by measuring the potential of the electrode located nearby. The proposed scheme for HbA1c (%) detection is shown in Fig. 2. Anti-Hb and anti-HbA1c antibodies were used for capture and labeled antibodies, respectively. The capture antibodies capture a certain portion of Hb maintaining HbA1c (%) in the sample blood. The enzyme-labeled antibodies detect only HbA1c in captured Hb. As a result, the HbA1c (%) can be directly measured without Hb measurement. The results of HbA1c (%) measurement using our developed potentiometric immunosensor showed good correlation between certified and experimental values of HbA1c (%) (Fig. 3).

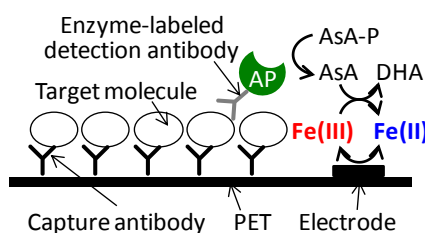


Fig. 1 Potentiometric immunosensor.

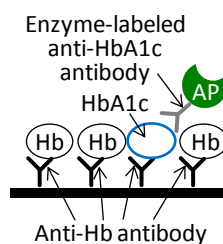


Fig. 2 Proposed scheme for HbA1c% detection.

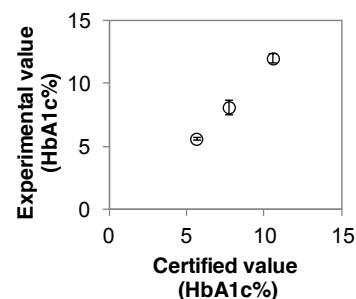


Fig. 3 Experimental results.

# Electrospun, conductive polymer fleeces as electrode materials for enhanced bioelectrocatalysis

J. Gladisch<sup>1</sup>, D. Sarauli<sup>1</sup>, B. Schulz<sup>2</sup>, F. Lisdat<sup>1</sup>

*1- Biosystems Technology, Institute of Applied Life Sciences, Technical University Wildau, Germany,*

*2-Institute of Chemistry, University of Potsdam, Germany*

*e-mail: flisdat@th-wildau.de*

Polyanillines as conductive polymers have found widespread applications in the area of biosensors. By sulfonation of the polymers properties such as solubility and conductivity at neutral pH values can be significantly improved [1]. It is already known that by combining sulfonated polyanillines with PQQ-dependent glucose dehydrogenase (PQQ-GDH) efficient enzyme electrodes with direct electron transfer can be prepared [2,3].

In electrochemical sensors the surface and the surface area are critical parameters influencing strongly the overall performance. Several techniques and materials have been applied in the last couple of years in order to enhance the surface area available for fixation of the biocomponent and signal generation. A rather young technique for this field of application is the electrospinning process. Here polymeric fleeces with rather thin polymer fibers down to about 100nm can be prepared.

In this study the electrospinning technique was intended to be combined with the conductive properties of sulfonated polyanillines and to exploit the potential of direct electron transfer from the substrate reduced enzyme PQQ-GDH to polyaniline. In order to spin the polymer into fibers the sulfonated polyaniline was mixed with polyacrylonitrile. In this mixture different sulfonated polyanillines have been tested. Conditions can be found in order to obtain a homogeneous coverage of ITO electrodes. Within the polymer fleeces a sufficient conductivity can be ensured by the polyaniline polymers used. PQQ-GDH can thus not only be immobilized on the polymeric fiber network, but can also be connected with the electrode. In the presence of the enzyme substrate consequently a catalytic current was obtained. The efficiency was found to depend on the substitution pattern on the polyaniline chain used. For the best system bioelectrocatalysis started near the redox potential of the enzymes redox center.

With this study it could be shown that bioelectrocatalysis with electrospun matrices is feasible.

[1] Jaymand M. Prog. Polym. Sci. 38(9) (2013) 1287-1306.

[2] Sarauli D., Xu, C, Dietzel B., Schulz, B., Lisdat F., Acta Biomaterialia 9(9) (2013) 8290-8298.

[3] Sarauli, D., Peters K., Xu C., Schulz B., Fattakhova-Rohlfing D., Lisdat F.,  
ACS Applied Materials & Interfaces 6 (20) (2014) 17887-17893.



# Measurement of oxygen consumption of contracting C2C12 myotube using scanning electrochemical microscopy

Yuki Igaki, Fumio Mizutani, and Tomoyuki Yasukawa  
Graduate School of Material Science, University of Hyogo  
3-2-1 Koto Kamigori Ako Hyogo 678-1297, Japan  
Ri14p002@stkt.u-hyogo.ac.jp

## 1. Introduction

C2C12 myoblast is a mouse skeletal muscle cell line with a differentiation potential to myotube with a contraction property, which have been used to investigate skeletal muscle physiology and functions of muscle. Oxygen consumption which reflects the respiration activity of cells is useful as an indicator for the cellular metabolism. Scanning electrochemical microscopy (SECM) has been used to investigate the respiration and metabolic activities of individual living cells. SECM measurement allows to the non-invasive determination of oxygen and imaging of oxygen distribution in the vicinity of a targeted cell. In this study, the reduction currents of oxygen were monitored by Pt microelectrode tip positioned close above an inspected myotube to detect an oxygen consumption of contractile myotubes.

## 2. Material and method

C2C12 myoblasts were cultured on a dish (60 mm diameter) treated with collagen in a growth medium of Dubecco's modified Eagle's medium (DMEM) containing 10% fetal bovine serum at 37°C, under a 5% CO<sub>2</sub>. Myoblasts were then cultured in DMEM containing 2% horse serum and 1 nM insulin for inducing the differentiation into myotubes. An electric pulse stimulation were applied to myotubes appeared four days after changing medium by using cover of cell culture dish with Au wire electrodes (1.0 mm diameter, 40 mm distance). The contraction was induced by applying electric pulses with the voltage of 0.7 Vmm<sup>-1</sup>, the frequency of 1.0 Hz with the pulse duration time of 2.0 ms by using the Au electrodes for 2.5 h. The microelectrode was positioned at 50 µm away from a dish surface in 25.0 mM HEPES buffer containing 5.0 mM KCl, 1.8 mM CaCl<sub>2</sub>, and 140 mM NaCl adjusted at pH7.6 by NaOH. The average height of the differentiated myotubes was 40 µm. The potential of -0.4 V was applied to the microelectrode to detect the reduction current of oxygen.

## 3. Results and discussion

After electric pulses were applied for 2.5 h, myotubes contracted immediately after the electric pulse was applied and returned to its original shape within 200 ms. The beating of myotubes was synchronized with the periodic pulses from 0.017 Hz (1 min<sup>-1</sup>) to 5.0 Hz, while no beating was observed by applying electric pulses beyond 5.0 Hz. Figure 1 show the current responses for oxygen at Pt microelectrode that was placed 10 µm above the myotube (300 µm length, 30 µm width) upon electric pulses by Au wire electrodes. when the electric pulses with 1.0 Hz were applied to induce the contraction of the myotube for 2 min, the reduction current immediately decreased and reached an almost steady-state in 30 s, indicating that the concentration of oxygen around the myotube decreased due to the consumption of oxygen by the increase of the respiration activity. The reduction current returned to its original level within approximately 30 s, when the application of pulses was turned off. When the electric pulses with 0.5 Hz were applied for 2 min, the reduction current also decreased to reach a steady-state. However, the decrease of the reduction current by applying electric pulses with 0.5 Hz is half that with 1.0 Hz. These results indicate that the increase of the oxygen consumption by the respiration of single myotubes per single pulse would be constant.

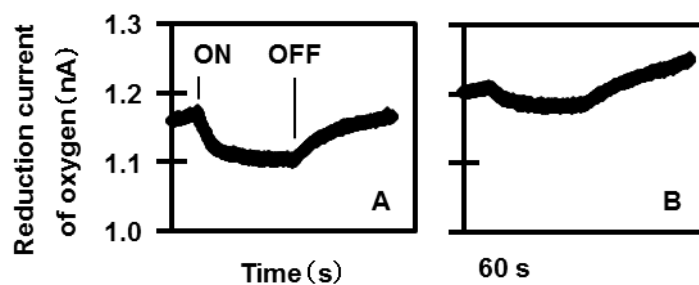


Fig.1. Current responses of oxygen upon electric pulses by Au wire electrodes. Frequencies of applied pulse were set at (A) 1 Hz and (B) 0.5 Hz. Therefore, microelectrochemistry based on the SECM can be applied to monitor the oxygen consumption of contractile myotubes

# Characterization of Glucose Oxidase-Redox Hydrogel on MgO-templated Carbon Electrode

Aimi Suzuki, Kazuki Murata, Seiya Tsujimura\*,

Division of Materials Science, Faculty of Pure and Applied Sciences, University of Tsukuba

1-1-1 Tennodai, Tsukuba, Ibaraki 305-8573, Japan

seiya@ims.tsukuba.ac.jp

A redox hydrogel electrode in which enzymes are wired with an Os-complex water-soluble redox polymer with a crosslinker on the electrode allows for glucose electrooxidation current densities on flat glassy carbon (GC) electrodes as high as a few milliamperes per centimeter squared at 37 °C. In most cases, electron transfer within the hydrogel film would be the rate-limiting step. To overcome this issue, one approach is introducing a porous carbon scaffold to form an ultrathin hydrogel film and reduce the electron transfer distance. Our group developed a pore-size-controlled carbon material, MgO-templated carbon (MgOC) [1], as a hydrogel scaffold. The hydrogel-coated MgOC (38-nm-diameter mesopores)-modified electrode with deglycosylated flavin adenine dinucleotide-dependent glucose dehydrogenase exhibited greater than 200 mA cm<sup>-2</sup> at 37 °C and a hydrogel loading of 1600 µg cm<sup>-2</sup> [2]. The design of a hierarchical electrode structure would be a very promising approach for the development of hydrogel electrodes for the applications of continuous blood-sugar-level monitoring and biofuel cells.

On the basis of the hierarchical structure-controlled MgOC electrode, we used Glucose Oxidase (GOx from *Aspergillus niger*), which is commercially available and the most widely used enzyme, as an electrocatalyst to produce a high and stable glucose oxidation current. The MgOC used in this study was kindly provided by Toyo Tanso (CNobel®, Japan) with an average pore diameter of 38 nm and a narrow pore-size distribution. The MgOC was modified on a glassy carbon disk electrode (GC-E, 3-mm diameter, BAS, Japan) by electrophoretic deposition (EPD) as follows: MgOC particles were electrodeposited on GC-E by applying a DC voltage at 50 V between these two carbon substrates for 60 s in acetonitrile containing MgOC and poly (vinylidene difluoride). The electrode was dried in air at room temperature. A biocatalyst solution including GOx, poly (1-vinylimidazole) complexed with [Os(bipyridine)<sub>2</sub>Cl] (PVI-Os), and poly (ethylene glycol) diglycidyl ether, was placed by a syringe onto the MgOC-modified electrode (MgOC-E), which was made hydrophilic by plasma oxidation before modifying the hydrogel. PVI-Os was synthesized and partially quaternized to improve water solubility. After modifying the hydrogel, the electrode was dried at 4 °C for 18 h.

Figure 1 shows the cyclic voltammograms for the hydrogel electrode using the MgOC and GC electrodes in the presence of 500 mM of glucose with a total hydrogel loading of 800 µg cm<sup>-2</sup> at 37 °C. The glucose oxidation current for the MgOC-hydrogel electrode was 63 ± 2 mA cm<sup>-2</sup>, which was 13 times higher than that for the GC-E. To the best of our knowledge, this is the first time that such high current densities are reported using GOx as an electrocatalyst. The steady-state current of the MgOC-E reached 0.85 V, which would be due to the solution resistance at a high current.

We will also represent a dependence of the glucose oxidation current on the hydrogel loading, and stabilities of the continuous current responses of the hydrogel electrodes on the MgOC-E, compared to that on the GC-E.

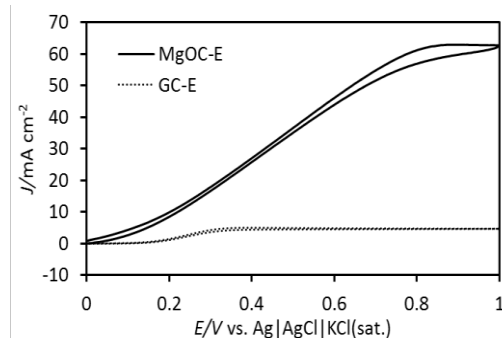


Figure 1. Cyclic voltammograms for glucose oxidation on the MgOC-E (solid curve) and GC-E (dotted curve); total hydrogel loading of 800 µg cm<sup>-2</sup>, 500 mM of glucose, 100 mM of phosphate buffer, pH 7.0, 37 °C, 8000 rpm, 20 mV s<sup>-1</sup>.

## Reference:

[1] Murata, K., Akatsuka, W., Tsujimura, S., *Chem. Lett.*, 43, 928-930 (2014).

[2] Tsujimura S., Murata K., Akatsuka W., *J. Am. Chem. Soc.*, 136, 14432-14437 (2014).

# New enzymes for the hybrid enzymatic and organic electrocatalytic cascade for the complete oxidation of glycerol

Sofiène Abdellaoui<sup>a</sup>, David P. Hickey<sup>a</sup>, Matthew S. McCamant<sup>a</sup>, Matthew S. Sigman<sup>a</sup> and Shelley D. Minteer<sup>a</sup> <sup>a</sup>Department of Chemistry, University of Utah, 315 S 1400 E, Salt Lake City, Utah, 84112, USA.  
Sofiène.abdellaoui@gmail.com

The complete electrochemical oxidation of the biofuel, glycerol, to CO<sub>2</sub> using a hybrid enzymatic and organic catalytic system has been demonstrated<sup>1</sup>. This system combines an organic catalyst, 4-amino-(2,2,6,6-Tetramethylpiperidin-1-yl)oxy (TEMPO-NH<sub>2</sub>) with oxalate oxidase (OxOx), resulting in the complete electrochemical oxidation of glycerol at a carbon electrode (Figure 1). This hybrid approach consists of five initial oxidative steps (by TEMPO), resulting in the oxidation of glycerol to mesoxalic acid (**1** → **6**, Figure 1). A combination of OxOx and TEMPO then facilitates the oxidation of mesoxalic (**6**) acid to glyoxalic acid (**7**), oxalic acid (**8**), and finally, CO<sub>2</sub>.

Nevertheless, this system is partly limited, by the weak overlap in pH profiles of OxOx and TEMPO, the first working at acidic pH (pH 4.0) and the latter preferring alkaline pH. Moreover, the electrons generated in the cascade reaction by enzymatic oxidative steps are not mediated to the electrode (4 / 16 electrons) and the OxOx substrate range is limited.

In order to improve this system, we are investigating new enzymes to replace OxOx. Like this latter, Oxalate decarboxylase (Oxdc) belongs to the cupin superfamily of proteins and incorporates mononuclear manganese ions coordinated by four amino acids<sup>2,3</sup>. This enzyme is able to transform oxalate to formate and CO<sub>2</sub>, with O<sub>2</sub> acting as a unique cofactor which can be used to catalyze a side oxidation reaction with o-phenylenediamine<sup>4</sup> or 2,2'-azino-bis(3-ethylbenzothiazoline-6-sulphonic acid) (ABTS). Therefore, efforts have been focused on screening redox mediators which could be coupled with this enzyme. Otherwise, preliminary results with the OxOx of *Bacillus subtilis* expressed in *E. coli* have shown that this enzyme has a residual activity with other substrates, such as mesoxalic acid and glyoxalic acid. The direct evolution of Oxdc could be performed to yield new enzymes with improved activity, broader substrate range and pH range.

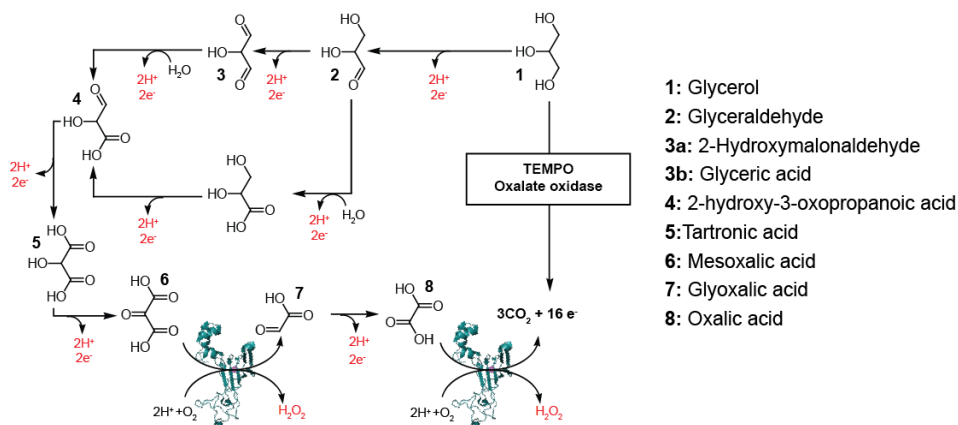


**Figure 1:** Electrocatalytic Oxidation Cascade of Glycerol by TEMPO and Oxalate Oxidase<sup>1</sup>

- (1) Hickey, D. P.; McCamant, M. S.; Giroud, F.; Sigman, M. S.; Minteer, S. D. *Journal of the American Chemical Society* **2014**, *136*, 15917.
- (2) Moomaw, E. W.; Angerhofer, A.; Moussatche, P.; Ozarowski, A.; Garcia-Rubio, I.; Richards, N. G. J. *Biochemistry* **2009**, *48*, 6116.
- (3) Tanner, A.; Bowater, L.; Fairhurst, S. A.; Bornemann, S. *Journal of Biological Chemistry* **2001**, *276*, 43627.
- (4) Emiliani, E.; Bekes, P. *Archives of biochemistry and biophysics* **1964**, *105*, 488.

# Graphene Electrodes for Electrochemical Detection of Biomarkers

Aušra Baradokė, Aneta Radzevič, Raimonda Celiešiūtė, Ramūnas Valiokas, Rasa Pauliukaite  
Department of Nanoengineering, *Center for Physical Sciences and Technology, Savanorių ave 231,*  
*LT-0200 Vilnius, Lithuania*  
*ausra.baradoke@ftmc.lt*

Electrochemical detection of biomarkers is a promising strategy for the next generation of diagnostic methods and instrumentation [1]. Graphene is a rather new material which is widely used for many application, including electroanalysis. Graphene electrodes modified with specific antibodies for target protein have been already demonstrated and they are in particular interesting as low-cost, disposable biosensors for point-of-care applications [2].

Nevertheless, preparation of graphene modified electrodes is a challenging task due to aggregation of graphene flakes [3]. Therefore, we have been developing graphene oxide modified electrodes on different supports and currently we are focusing on functional fabrication of such electrodes [4]. We have employed the thin film processes and prepared electrodes by the spin-coating technique from graphene oxide suspensions in aqueous chitosan solutions. We analyzed in detail the resulting electrode morphology by applying optical and atomic force microscopy.

Also, we demonstrated that an inkjet printing system can be used for stable immobilization of capture antibodies on the electrode surface, which, in turn, could be pre-structured by other microfabrication techniques. We have investigated the electrode characteristics by means of electrochemical measurements, including cyclic and square wave voltammetries as well as electrochemical impedance spectroscopy, and we discuss these results in comparison with other similar electrode systems.

## References

- [1] J. Wang, *Biosen. Bioelectron.*, 2006, 21, 1887.
- [2] M. Pumera, *Mater. Today*, 2011, 14, 308.
- [3] R. Celiešiūtė, G. Grincienė, Š. Vaitekūnis, T. Venckus, T. Rakickas, R. Pauliukaite, *Chemija*, 2013, 24, 296.
- [4] R. Celiešiūtė, R. Trusovas, G. Račiukaitis, G. Niaura, V. Švedas, Ž. Ruželė, R. Pauliukaite, *Electrochim. Acta*, 2014, 132, 265.

# Glucose Biosensor based on a Glassy Carbon Electrode Modified with Poly(methylene green) and FAD-dependent Glucose Dehydrogenase

Nozomu Tsuruoka, Kazuki Murata, Seiya Tsujimura,  
Division of Material Science, Faculty of Pure and Applied Sciences, University of Tsukuba  
1-1-1 Tennodai, Tsukuba, Ibaraki 305-8573, Japan,  
seiya@ims.tsukuba.ac.jp

## [Introduction]

Enzyme modified electrodes for electrochemical glucose-oxidation have been used to improve the QOL of diabetic people with less pain, complications, and anxiety. Recently increasing number of glucose sensors utilize flavin adenine dinucleotide (FAD) dependent glucose dehydrogenase (FAD-GDH)[1] as a catalyst which requires appropriate redox mediator to assist electron transfer from the enzyme to electrode. The majority of personal blood glucose sensors are based on disposable enzyme electrode test strip using diffusional mediator such as ferricyanide or ferrocene. Meanwhile, continuous glucose monitoring (CGM) system gathers increasing attentions to get a more complete picture of the glucose levels, which can lead to better glucose control. For the construction of CGM system, it is essential to jointly immobilize the enzyme and mediator on an electrode surface for a long period. Redox hydrogel technology using osmium redox polymer pioneered by Heller [2] allows a fast electron exchange and stable sensor response; however, it has a drawback in cost. To develop an immobilized redox mediator, we focused on methylene green, which can be electropolymerized by potential cycling on glassy carbon electrode [3]. In this paper, we exploit an electropolymerized methylene green as a redox mediator for FAD-GDH.

## [Experimental]

Methylene green (MG) was polymerized electrochemically onto a glassy carbon (GC) electrode, 3mm in diameter, by cycling the applied potential between  $-0.4$  and  $1.2$  V vs. Ag|AgCl at scan rate  $50$  mV/sec for  $10\sim30$  cycles in a  $100$  mM, pH  $7$  phosphate buffer solution containing  $100$  mM  $\text{NaNO}_3$  and  $1$  mM MG.  $0.5$   $\mu\text{L}$  aliquot of  $4.5$  mM FAD-GDH solution was dropped onto the poly(methylene green) (PMG)-modified GC electrode. The solvent was allowed to evaporate and then the surface was covered with a dialysis membrane. The glucose oxidation current by FAD-GDH on PMG-modified GC was measured with stirring in a  $100$  mM phosphate buffer by chronoamperometry at  $0.5$  V. All experiment was carried out in an oxygen-free solution, platinum wire were used as the counter electrode.

## [Results and Discussion]

Dotted line in Figure 1 (1) shows cyclic voltammogram (CV) of PMG-modified on GC electrode in the absence of FAD-GDH, which shows PMG was successfully modified on GC [3]. Solid line shows the catalytic CV for glucose oxidation by FAD-GDH. This result indicates PMG modified on GC worked as a redox mediator for FAD-GDH. Figure 1 (2) shows the typical time dependence of the catalytic current on successive addition of  $0.2$  mM glucose to a neutral buffer solution. The catalytic current reached its limiting value within  $60$  sec and increased with successive glucose injection. The response is liner over the investigated range from  $0$  to  $1.0$  mM glucose.

## [Reference]

- [1] S.Tsujimura *et al.*, *Biosci.Biotech.Biochem.*, **70** 654-659 (2006)
- [2] A. Heller, *J. Phys. Chem.*, **96** 3579-3587 (1992)
- [3] R.A.Rincon *et al.*, *Electroanalysis*, **22** 799-806 (2010)

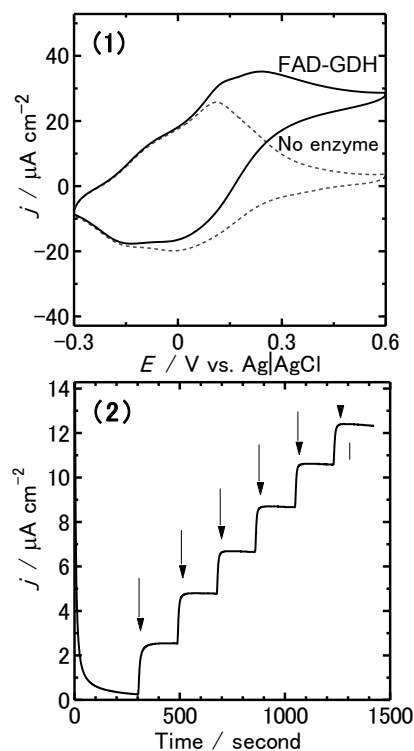


Fig.1. (1) Cyclic voltammograms of PMG-modified electrode in the presence(solid line) and absence(dotted line) of FAD-GDH in a pH  $7$  phosphate buffer containing  $100$  mM glucose. (2) Constant potential electrolysis of glucose by FAD-GDH and PMG-modified electrode at  $0.5$  V. At the points indicated by the arrows, a glucose stock solution was successively added at final concentration of  $0.2$ ,  $0.4$ ,  $0.6$ ,  $0.8$ ,  $1.0$ , and  $1.2$  mM.

# Effect of the ratio of poly-L-lysine/glucose oxidase/ferricyanide composite on the sensing properties of second generation blood glucose sensors

Ming-Jie Lin, Cing-Chou Wu

Department of Bio-industrial Mechatronics Engineering, National Chung Hsing University

No. 250 Kuo-Kuang Rd. Taichung, Taiwan 402

y4ky5k@yahoo.com.tw

Using ferricyanide ( $\text{Fe}(\text{CN})_6^{-3}$ ) as a mediator for glucose oxidase (GOx) to catalyze glucose is the most popular strategy in the development of blood-glucose biosensor. Generally, increase of  $\text{Fe}(\text{CN})_6^{-3}$  concentration can improve the catalytic rate of GOx for glucose, but over-added  $\text{Fe}(\text{CN})_6^{-3}$  may affect the micro environment around GOx, resulting in the deactivation of GOx with a short lifetime. In the study, poly-L-lysine (PLL) was used as polycations to entrap and counterbalance the negatively charged GOx and  $\text{Fe}(\text{CN})_6^{-3}$  on NaOH-preanodized screen printed carbon electrodes (named  $\text{SPCE}_{\text{NaOH}}$ ). The effect of the ratio of poly-L-lysine/GOx/ $\text{Fe}(\text{CN})_6^{-3}$  composite on the calibration curves of glucose sensors was showed in Fig. 1. The ratio of GOD: $\text{Fe}(\text{CN})_6^{-3}$  (0.5 mM:9.5 mM) entrapped by 5 mM PLL presented the larger sensitivity and catalytic rate, as shown in the Fig. 1(a). Moreover, the sensitivity, the linear range and the catalytic rate increased with the number of coating layer. Furthermore, the sensitivity can be promoted with the increase of PLL concentration (Fig. 1(b)). When the concentration of PLL and  $\text{Fe}(\text{CN})_6^{-3}$  simultaneously increased to 50 mM and 99.5 mM, the sensitivity of biosensors was as high as  $132.83 \pm 13.63 \text{ nA/mM mm}^2$ . The results indicate that the optimal ratio of PLL/ $\text{Fe}(\text{CN})_6^{-3}$ /GOD composite permits the glucose biosensors to exhibit the better catalytic rate of GOD and sensitivity.

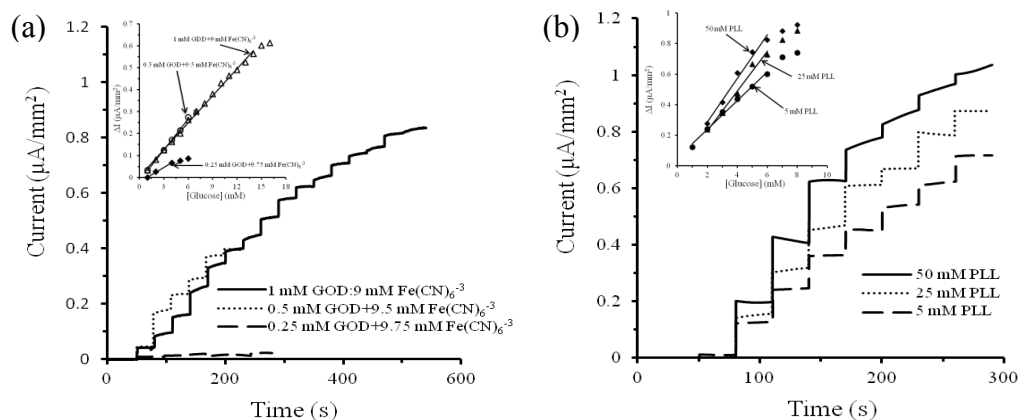


**Fig. 1** Chronoamperometry of  $\text{SPCE}_{\text{NaOH}}$  coated by 5 mM PLL and the three kind of GOD: $\text{Fe}(\text{CN})_6^{-3}$  ratio (0.25 mM:9.75 mM, 0.5 mM:9.5 mM, 1 mM:9 mM) (a) and coated by the composite of 0.5 mM GOx, 9.5 mM  $\text{Fe}(\text{CN})_6^{-3}$  and three kind of PLL concentration (5, 25, 50 mM) (b). The inset shows the corresponding calibration curves.

[1]H. Katano, K. Uematsu, H. T. Ikeda, T. Tsukatani, Anal. Sci. 25 (2009) 1077.

# An Electrogenenerated Chemiluminescence Approach for the Assay of Zinc Finger Proteins (EGR1)

Shengyuan Deng, Xubo Ji, Peng Xin, and Dan Shan\*

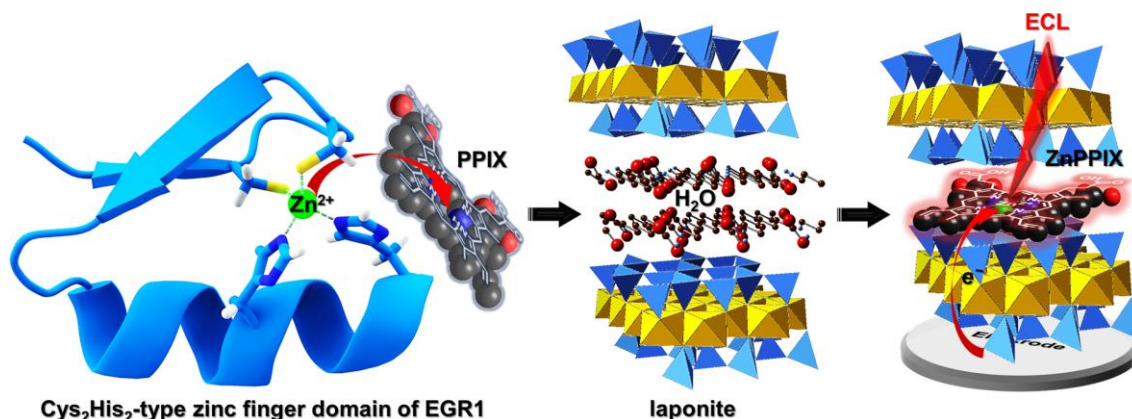
*Sino–French Laboratory of Biomaterials and Bioanalytical Chemistry*

*School of Environmental and Biological Engineering, Nanjing University of Science and Technology*

*200 Xiaolingwei, Xuanwu District, Nanjing 210094, P. R. China*

[sydeng@njust.edu.cn](mailto:sydeng@njust.edu.cn), [danshan@njust.edu.cn](mailto:danshan@njust.edu.cn)

Early growth response protein 1 (EGR1), as a characteristic example of zinc finger proteins, acts as a transcription factor in eukaryotic cells, mediating protein-protein interactions. Here, a novel electrochemiluminescence (ECL)-based protocol for EGR1 assay was developed with a new eco-friendly emitter: nanoclay-supported zinc *proto*-porphyrin IX (ZnPPIX) (**Scheme 1**). It stimulates an intense monochromic ECL irradiation at 644 nm in the aqueous solution with the dissolved oxygen as an endogenous coreactant. This ECL derivation was rationalized via hyphenated spectroscopy and theoretical calculation. To promote hydrophilicity and solid-state immobilization of porphyrins, the lamellar artificial laponite was employed as a nanocarrier owing to its large specific area without the black-body effect. The facile exfoliation of laponite produced quality monolayered nanosheets and facilitated the adsorption and flattening of PPIX upon the surface, resulting in a highly efficient ECL emission. Based on the release of  $\text{Zn}^{2+}$  in zinc finger domains of EGR1 upon contact with the ECL-inactive PPIX, which was monitored by circular dichroism and UV-absorption, a sensitive  $\text{Zn}^{2+}$ -selective electrode for the "signal-on" detection of EGR1 was prepared with a detection limit down to  $0.48 \text{ pg mL}^{-1}$  and a linearity over 6 orders of magnitude. The proposed porphyrin-based ECL system thus infused fresh blood into the traditional family of ECL nanoemitters, showing great promise in bioassays of structural Zn(II) proteins and zinc finger-binding nucleotides.



**Scheme 1.** Schematic illustration of a typical protocol for the ECL assay of zinc finger proteins.

## References

- [1] Mali, P.; Yang, L. H.; Esvelt, K. M.; Aach, J.; Guell, M.; DiCarlo, J. E.; Norville, J. E.; Church, G. M. *Science* **2013**, *339*, 823–826.
- [2] Liu, X. G.; Zhang, P.; Bao, Y.; Han, Y. M.; Wang, Y.; Zhang, Q.; Zhan, Z. Z.; Meng, J.; Li, Y. K.; Li, N. *Proc. Nat. Acad. Sci. USA* **2013**, *110*, 11097–11102.
- [3] Wang, H. Y.; Yang, H.; Shivalila, C. S.; Dawlaty, M. M.; Cheng, A. W.; Zhang, F.; Jaenisch, R. *Cell* **2013**, *153*, 910–918.

# Application of Polyfolates to the Development of Enzymatic Biosensors

Raimonda Celiešiūtė, Aneta Radzevič, Tomas Rakickas, Živilė Ruželė, Šarūnas Vaitekoniš,  
Tautvydas Venckus, Rasa Pauliukaite  
*Department of Nanoengineering, Center for Physical Sciences and Technology*  
*Savanoriu Ave. 231, LT-02300 Vilnius, Lithuania*  
*pauliukaite@ftmc.lt*

Enzymatic electrochemical biosensors are fast and selective tool for analyte analysis. However, their sensitivity and stability is still problematic and require improvements. In order to extend the lifetime of an enzymatic electrochemical biosensor, natural materials as mediators are preferred to be used in the development of these biosensors.

Recently, it has been shown that some vitamins, in particular, folic acid (vitamin B<sub>9</sub>) can be polymerized and used as redox mediator as well as conducting polymer in electrochemical biosensing [1,2]. The polymerization efficiency of folic acid depends significantly on solution pH and supporting electrolyte. It has been found that Cl<sup>-</sup> accelerates polymerization of vitamin B<sub>9</sub> [1,2]. The most stable electrochemically grown polymer was obtained when it is deposited from pH 2.0 [1]. However, such biosensor showed a poor sensitivity. The sensitivity of the biosensor has been increased when polyfolate was electrosynthesized from phosphate buffer saline solution, pH 5.0 [2]. In order to increase its stability, the polyfolate has been covered with graphene-chitosan composite layer, which was optimized previously [3].

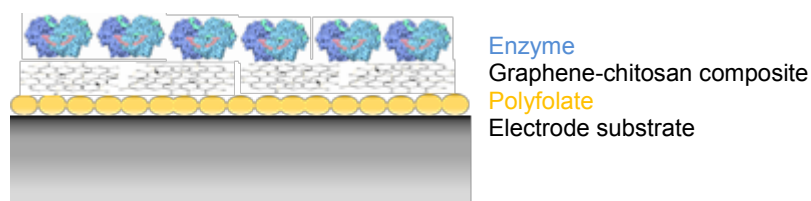


Fig. 1. Scheme of a biosensor design

The similar strategy was applied to the development of other enzymatic biosensors based on oxidases (Fig. 1). This approach has been attempted with such enzymes as glucose oxidase, xanthine oxidase, alcohol oxidase, glutamate oxidase and cholesterol oxidase. All these biosensors were successfully developed using the same design, however, their analytical parameters and stability differ significantly; this will be discussed in the presentation.

## References

1. R. Celiešiūtė, T. Venckus, Š. Vaitekoniš, R. Pauliukaite, *Electrochim. Acta*, 138 (2014) 62.
2. T. Venckus, R. Celiešiūtė, A. Radzevič, T. Rakickas, Š. Vaitekoniš, Ž. Ruželė, R. Pauliukaite, *Electroanalysis*, 26 (2014) 2273.
3. R. Celiešiūtė, R. Trusovas, G. Račiukaitis, G. Niaura, V. Švedas, Ž. Ruželė, R. Pauliukaite, *Electrochim. Acta*, 132 (2014) 265.



# Biosensors with Electrochemical Detection at High Negative Potentials in Flow Systems

Bohdan Josypčuk, Oksana Josypčuk

*J. Heyrovsky Institute of Physical Chemistry of AS CR, v.v.i.*

*Department of Biomimetic Electrochemistry*

*Doležskova 2155, 182 23 Prague, Czech Republic*

*josypcuk@jh-inst.cas.cz*

High selectivity and sensitivity are great advantages of biosensors with electrochemical detection. Electrochemical detection in flow analysis is widely used especially in connection with biosensors. Detection (working) electrode is the basic element and the sole source of analytical signal in electrochemical methods. Depending on properties of the analyte and on conditions of measurements a suitable electrode material must be chosen. Electrodes of gold, platinum or of other, mostly noble metals, are used for work in positive potential range and for analyte oxidation. Electrodes of various types of carbon are suitable for measurements not only at positive potentials, but also at moderately negative ones. The best possibilities for performing electroreduction processes, particularly at high negative potentials, provide mercury and amalgam electrodes. High hydrogen overvoltage on these materials allows to work in aqueous solutions up to  $-2$  V.

Incorporation of pure mercury electrodes in flow systems and especially for biosensors preparation is complicated due to mechanical instability of the mercury drop, and therefore the Hg-electrodes are practically not used for this purpose. Construction of solid and paste amalgam electrodes is not different from electrodes of other materials suitable for flow analysis [1]. The very useful advantage of solid amalgams is the possibility to prepare electrodes of required size and shape. The silver solid amalgam (AgSA) detectors were used for work in wall-jet and thin-layer arrangement of an electrolytic cell. Introduction of tubular AgSA-detector substantially simplified the design of flow electrochemical cell and increased the reliability and reproducibility of measurements [2].

Sensitivity of the enzyme biosensors depends on the area covered by the enzyme. Classical solid detection electrodes have a relatively small surface which can be enlarged by use of an enzymatic reactor. The large surface of the enzymatic reactor can be provided by various porous or powdered materials. The reactor is placed in flow system in front of the detector. In this case, the biosensor consists of two separate parts: the enzymatic reaction takes place in the reactor and the detector then registers either some product of enzymatic reaction or, e.g., decrease/increase of oxygen concentration in the solution [3]. Recently, we have prepared silver solid amalgam as a suitable porous material and we have used this material for preparation of the enzymatic reactor with a large surface [3]. The flow biosensors based on the minireactor filled by powdered silver solid amalgam covered by enzyme were constructed and tested for the first time [4]. Enzymes ascorbate oxidase, glucose oxidase, sarcosine oxidase, catalase, tyrosinase and laccase were used to test the biosensors. Reactor with enzyme modified porous amalgam or amalgam powder can be substituted in a few seconds by reactor with other enzyme, and it is possible to immediately start measurement of an appropriate analyte. The fabricated silver amalgam tubular detector in a flow system allowed the use of highly negative potentials, which significantly increased the current response and consequently the sensitivity of the determinations. Using high negative potential allows to measure such compounds reduction of which on other electrodes is not possible. The suggested procedure for preparing the biosensors is universal and suitable for covalent attachment of various substances containing  $-NH_2$  group to the amalgam surface.

**Acknowledgements:** This work was financially supported by Grant Agency of the Czech Republic (Grants P206/11/1638 and P208/12/1645).

## References

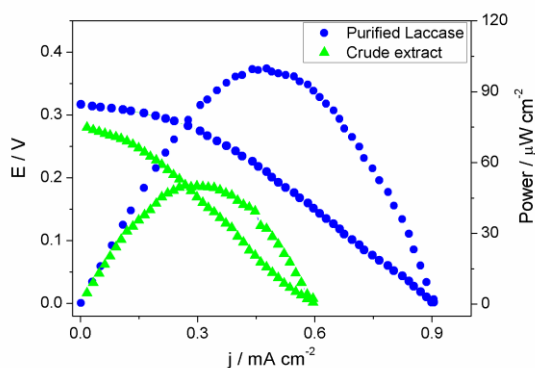
- [1] B. Josypchuk and J. Barek, *Crit. Rev. Anal. Chem.* **2009**, 39, 189.
- [2] O. Josypchuk, J. Barek, and B. Josypchuk, *Electroanalysis* **2012**, 24, 2230.
- [3] B. Josypčuk, J. Barek, and O. Josypčuk, *Anal. Chim. Acta* **2013**, 778, 24.
- [4] O. Josypčuk, J. Barek, and B. Josypčuk, *Electroanalysis* **2014**, 26, 1729.

# Biocathodes Using a Laccase from *Pycnoporus sanguineus* and their Potential Application in Methanol/O<sub>2</sub> Biofuel cell

A. R. de Andrade, S. Aquino Neto, A. L. R. L. Zimbardi, F. P. Cardoso, L. B. Crepaldi, R. P. M. Furriel

*Departamento de Química da Faculdade de Filosofia, Ciências e Letras de Ribeirão Preto,  
Universidade de São Paulo  
Avenida Bandeirantes, 3900, Ribeirão Preto, São Paulo, Brazil  
ardandra@ffclrp.usp.br*

We prepared and characterized biocathodes for a methanol/O<sub>2</sub> biofuel cell using the crude extract and a purified laccase from a strain of *Pycnoporus sanguineus* (PyS). The biocathode assembly was achieved by immobilizing either the enzymes in the crude extract or the purified laccase with polyamidoamine (PAMAM) dendrimers on top of a polypyrrole matrix containing entrapped 2,2'-azino-bis{3-ethylbenzothiazoline-6-sulfonate} (ABTS) species as the redox mediator. The kinetic characterization of the biocathodes showed that samples prepared with either the crude extract or the purified laccase retained ABTS oxidation activity after the immobilization procedure. The electrochemical activity of the biocathodes was verified by cyclic voltammetry experiments in the absence and in the presence of dissolved oxygen. The biofuel cell tests showed that the biocathodes were able to furnish maximum power densities of 51.2 and 99.8  $\mu\text{W cm}^{-2}$  for the samples prepared with the crude extract and the purified enzyme, respectively. Moreover, it was observed that both biocathodes tested displayed a very similar loss in power performance as a function of time, reaching 60% of the initial activity after 60 days. Overall, the laccase-based biocathodes prepared are able to achieve high electrochemical active and stable biomaterials.



Polarization and power density curves: (▲) crude extract (●)purified laccase from PyS, in acetate buffer pH 4.5, containing 0.1 mol L<sup>-1</sup> methanol.

Acknowledgements: This work was supported by FAPESP, CNPq, and CAPES.

# Scanning Electrochemical Microscopy of Switchable Redox Enzyme Cascades

Christian Andre Gunawan, Ekaterina Nam, Pall Thordarson, Chuan Zhao  
*School of Chemistry, The University of New South Wales  
Kensington Campus, Sydney, New South Wales, 2052  
christian.gunawan@unsw.edu.au*

In the past decades there have been substantial efforts devoted to the development of method to control activity of redox proteins and enzymes. However, most proposed systems suffer from one major shortcoming.<sup>1-3</sup> That is, once the enzymatic cascade has been initiated after introducing all the necessary substrates, it is difficult to control and study the catalytic activity of individual enzymes, and it is almost impossible to modulate or switch off the cascade.<sup>4,5</sup>

We are developing a novel strategy for temporal and spatial control of redox enzymes cascade by either photochemical and/or electrochemical stimuli. This will be achieved by utilizing metallo-bisterpyridine (M(X)tpy<sub>2</sub>) as redox-active chromophores. This chromophore can be excited at specific wavelength and/or redox potential. The chromophore is bioconjugated to redox active protein or enzymes, which will enable them to function as a switch to control the redox activity.

This presentations concern several aspects of the cascade construct including, surface modification by using self-assembled monolayers (SAMs). Organothiols on gold or organosilane/organophosphonic acid on glass, coupled with soft lithography to achieve microscale patterns with high fidelity. Click chemistry of the ruthenium(II)bis(terpyridine) bioconjugate, followed by reconstitution of the cytochrome *c* redox co-factor and cytochrome *c* peroxidase on the surface. Scanning electrochemical microscopy will then be employed to analyze the activity of the surface-bound cascade with and without the external photo/electrochemical stimuli.

## References:

- (1) Zhou, J.; Campbell, C.; Heller, A.; Bard, A. J. *Anal. Chem.* **2002**, *74*, 4007.
- (2) Willner, I.; Katz, E. *Angew. Chem. Int. Ed.* **2003**, *42*, 4576.
- (3) Wilhelm, T.; Wittstock, G. *Langmuir* **2002**, *18*, 9485.
- (4) Riklin, A.; Katz, E.; Wiliner, I.; Stocker, A.; Bückmann, A. F. *Nature* **1995**, *376*, 672.
- (5) Zhao, C.; Wittstock, G. *Anal. Chem.* **2004**, *76*, 3145.

# Amperometric bromide biosensor based on graphite powder composite electrode modified with leaf paste of natural *amaranth* induced by spaying KBr aqueous solution

Yongchun Zhu, Jie Hao, Jianqiao Lang, NanXiao, Amin Bao,  
Institute of energy and environment catalysis, Shenyang Normal University  
253 Huanghe street Huanggu District Shenyang Liaoning China  
e-mail Yongchunzhu@126.com

According to biochemical reaction of enzyme or other biological units and targets we build up biosensors[1]. Can we build up a biological unit for a given target? The answer is yes. Here we present an example to show creating biunit for bromide biosensor by target-inducing plant secretion. As we known amaranthine existing abundantly in *amaranth* plants is an antioxidant, and can be used in catalytic spectrophotometric detection of bromide[2]. But natural *amaranth* leaf is not suitable to build up a tissue paste biosensor [3]. In this work, natural *amaranth* plants were schematically treated by spaying lower concentration of potassium bromide aqueous solution to induce the secretory compound for bromide detection. After the induction process, the *amaranth* leaf paste was used to build up a plant paste modified graphite powder composite electrode.

Fig.1 shows the induced *amaranth* paste modified electrode gives a unique electrochemical oxidation behavior in differential pulse voltammetric curve (A1), but the uninduced plant leaf paste modified electrode gives a broadened oxidation peak with lower oxidation peak potentials(A3), while the nearby plant paste modified electrode gives a similar peak with smaller peak current as induced one(A2). Under the suitable experimental conditions, the oxidation current was inverse to the logarithm of bromide concentration in the range of  $1.0 \times 10^{-16} \sim 1.0 \times 10^{-9}$  M with two lines and the minimum detection limit of  $1.0 \times 10^{-16}$  M. The biosensor was applied in the detection of bromide in fresh seaweed with reasonable results. The idea can be used to build up other target biosensors from various biosystems to create some suitable biounits.

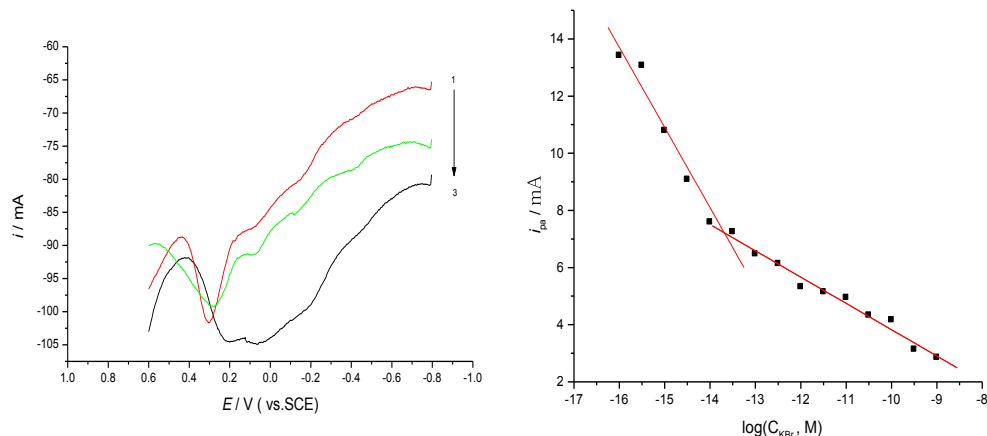


Fig.1 DPV curves of *amaranth* leaf paste modified electrodes (A) and working curve for bromide detection. 1, leaf from an *amaranth* induced by bromide; 2, from the nearby plant; 3, from the plant without induced.

## Reference

1. D.A., Stenger, W., Guenter, G., Edward, W., Keefer, K.M., Shaffer, J.D., Andreadis, W., Ma, J. J., Pancrazio, Trends in Biotechnology 19 (8) (2001) 304-309.
2. S., Uchiyama, G.A., Rechnitz, Analytical Letters, 20(3) (1978) 451-470.
3. C. PANG, Y. ZHU, H. GAO, Y. Dong J. Lu, Analyst, 136 (4) (2011) 841-846.

# Electrochemical Study of the Extracellular Electron Transfer of *Enterococcus faecalis* to Electrodes

Galina Pankratova<sup>a</sup>, Kamrul Hasan<sup>a</sup>, Donal Leech<sup>b</sup>, Lars Hederstedt<sup>a</sup>, and  
Lo Gorton<sup>a</sup>

<sup>a</sup>*Lund University, Lund, Sweden*

<sup>b</sup>*National University of Ireland Galway, Galway, Ireland*  
*galina.pankratova@biochemistry.lu.se*

*Enterococcus faecalis* is a gram positive bacterium, being a part of the natural microflora that inhabits the gastrointestinal tracts of mammals. It grows by fermentation with lactic acid as the main end product and can use more than 30 carbohydrates as substrates. This bacterium is a facultative anaerobe and aerobic respiration depends on the presence of heme, which serves as a cofactor for cytoplasmic catalase [1] and membrane bound cytochrome *bd* oxidase [2]. *Enterococcus faecalis* does not require heme to grow and lacks the genes to synthesize it but is able to take up heme or its analogues from the environment. When the cells are supplied with heme, an oxygen minimal respiratory chain is built up, including several NADH dehydrogenases, a demethylmenaquinol pool in the membrane and the heme-dependent cytochrome *bd* oxidase [3]. The bacterial cells were “wired” with an osmium containing redox polymer to facilitate electron transfer from the cells to the electrode in the presence of a substrate [4].

The aim of this study was to investigate the role of each of the respiratory chain components and according to this to find out the mechanism of the extracellular electron transfer from the bacterial cells and the redox polymer modified electrode.

In this connection the wild type as well as three different strains of *Enterococcus faecalis* with different mutations within the electron transport chain were investigated using cyclic voltammetry and chronoamperometry under flow injection conditions and different experimental and culture conditions to find out possible ways which the electrons follow from the cell to the electrode.

This work was financially supported by the European Commission (project “BIOENERGY” FP7-PEOPLE-2013-ITN-607793) and the Swedish Research Council (project 2014-5908).

[1] L. Frankenberg, M. Brugna, and L. Hederstedt, *J. Bacteriol.*, 184, **2002**, 6351-6.

[2] L. Winstedt, L. Frankenberg, L. Hederstedt, and C. von Wachenfeldt, *J. Bacteriol.*, 182, **2000**, 3863-6.

[3] T. W. Ritchey, and H. W. Seeley, *J. Gen. Microbiol.*, 85 (2), **1974**, 220-228

[4] K. Hasan, S. A. Patil, D. Leech, C. Hägerhäll, and L. Gorton, *Biochem. Soc. Transact.*, 40, **2012**, 1330-1335.

# Label-Free Biomimetic Electrocatalysis-Induced Precipitation for Ultrasensitive Bioanalysis

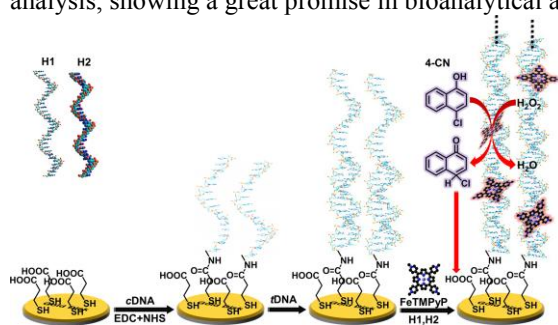
Peixin Yuan, Shengyuan Deng, Xubo Ji, Peng Xin, Dan Shan\*

School of Environmental and Biological Engineering, Nanjing University of Science and Technology

No.200 Xiaolingwei, Xuanwu District, Nanjing 210094, P.R. China

[sydeng@njust.edu.cn](mailto:sydeng@njust.edu.cn), [danshan@njust.edu.cn](mailto:danshan@njust.edu.cn)

The pursuit of more specific and sensitive signals is a perpetual goal for modern biosensors. Here we proposed a novel label-free strategy of biomimetic electrocatalysis-induced precipitation (BEP) based on the electrochemistry-coupled surface plasmon resonance (*e*-SPR) technique for ultrasensitive detection of DNA (Scheme 1). The protocol starts with the modification of gold disk with peptide nucleic acid as capture probe (*c*DNA). After the association of immobilized *c*DNA with target DNA (*t*DNA), the hybridization chain reaction (HCR) was triggered by the introduction of mutual partial complementary primers (H1,H2) to elongate the terminal into nanoscale duplex. As the electro-active iron porphyrins could intercalate into the grooves of double-stranded DNA (*ds*DNA) scaffold, multiple positive-charged Fe<sup>III</sup> *meso-tetra*(*N*-methyl-4-pyridyl)porphine (FeTMPyP) were under potentiostatic adsorption into porphyrin-*ds*DNA complex. Given FeTMPyP a highly efficient electrocatalyst for peroxide reduction, its groove binding as a biomimetic cofactor was validated possessing a high electrocatalytic activity with fast catalytic kinetics and stability. Using 4-chloro-1-naphthol (4-CN) as a proton donor, the electrocatalytic reduction of H<sub>2</sub>O<sub>2</sub> would oxidize it into insoluble benzo-4-chlorohexadienone, the mass of which instantaneously deposited on heterogeneous interface and aroused significant signal amplification of SPR response (Figure 1). The SPR increment was proportional to the concentration of *t*DNA, thus an ultrasensitive *e*-SPR-based DNA assay was developed with a *sub*-femtomolar detection limit. The proposed electrochemical methodology breaks the bottleneck of sensitivity in conventional SPR-based DNA analysis, showing a great promise in bioanalytical applications.



**Scheme 1.** Schematic illustration of the fabrication of *e*-SPR-based DNA assay.

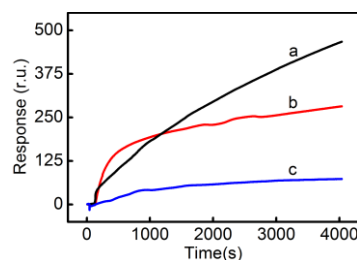


**Figure 1.** The *e*-SPR response over time to 1.0 pM (a), 1.0 fM (b), and 0 M (c) *t*DNA in 10 mM pH 7.4 phosphate buffer saline.

# Materials Design for Lithium-Sulfur Batteries

Yi Cui,

*Department of Materials Science and Engineering, Stanford University.  
Stanford Institute for Materials and Energy Sciences, SLAC National Accelerator Laboratory.  
yicui@stanford.edu*

Rechargeable batteries have been a great success in powering consumer electronics. There has been a recent strong interest in applying rechargeable batteries to vehicle electrification and grid-scale storage. Novel battery chemistries are necessary for enabling these opportunities although they also present significant fundamental materials challenges. Here I will present our research progress on Li-S batteries, including understanding of  $\text{Li}_x\text{S}$  interaction with materials and designing nanomaterials for encapsulation and selective deposition of  $\text{Li}_x\text{S}$  species. We demonstrated excellent performance of Li-S batteries.

# Designing and optimizing novel electrode materials for rechargeable

## Na-ion batteries with high energy and low cost

Chuze Ma, Judith Alvarado, Jing Xu, Haodong Liu and Y. Shirley Meng

Sustainable Power and Energy Center, University of California San Diego

La Jolla, CA 92093, USA

With the pressing needs for economically feasible and environmentally benign energy storage technologies, Na-ion batteries have re-captured the attentions of the scientific communities due to its natural abundance and broad distribution. In this talk, we report our recent work on P2 and O3 types of layered Na transition metal (TM) oxides,  $\text{Na}_x[\text{Li}_y\text{Ni}_z\text{Mn}_{1-y-z}]\text{O}_2$  ( $0 < x, y, z < 1$ ), working as cathode materials in Na-ion batteries. In these compounds, the intercalation in the TM slabs and 2-D transportation of Na-ions occur concomitant with TM redox change during cycling. By identifying the interplay among structural evolution, electronic transition, and electrochemical reactions, the optimized composition is designed and significant improvement in battery performance is achieved. In addition to the cathode study, we have performed a systematic investigation on  $\text{Na}_2\text{Ti}_3\text{O}_7$  as anode in Na-ion batteries, since it is able to provide 177 mAh/g specific capacity at an ultra low voltage, 0.3 V. A new phase is identified upon full discharge. We have also optimize the material for better cycling retention and rate performance. The Na-ion full cell fabricated by our group with the two electrode materials above successfully demonstrates high voltage and reversibility, indicating a bright future for Na-ion batteries.

**Keywords:** novel electrodes; intercalation mechanism; Na-ion battery



# A Solid-Electrolyte-Enabled Lithium-Bromine Flow Battery

Peng Bai, Martin Z. Bazant

Massachusetts Institute of Technology

77 Massachusetts Avenue, Cambridge, Massachusetts 02139, USA

[pengbai@mit.edu](mailto:pengbai@mit.edu)

Water-stable solid electrolyte has become an enabling material for novel aqueous lithium-air batteries,<sup>1</sup> and hybrid-electrolyte lithium redox batteries,<sup>2</sup> in which lithium metal anode can be paired with various aqueous cathodes/catholytes via a nonaqueous-solid-aqueous hybrid electrolyte.<sup>2</sup> Here, we design and fabricate a lithium-bromine flow battery with the lithium ion conducting glass ceramic (LICGC) from Ohara, Inc. The proof-of-concept battery with a flat catalyst-free graphite electrode can discharge at 9mW/cm<sup>2</sup> with highly concentrated bromine catholytes, which in principle could provide a specific energy of 791.8 Wh/kg, superior to many existing cathode materials and catholytes. Scanning electron microscopy images reveal that both the organic electrolyte and the bromine electrolyte corrode the solid electrolyte plate quickly, leading to nanoporous pathways that can percolate through the plate, thus limiting the cell performance and lifetime. Further impedance analysis of samples immersed in different catholytes for two weeks confirms the deterioration of the conductivities of both the grains and grain boundaries. With improved solid electrolytes or membraneless flow designs, the lithium-bromine system could enable electric vehicles, by providing a critical high-power mode to high-energy-density (but otherwise low-power) lithium-air batteries.

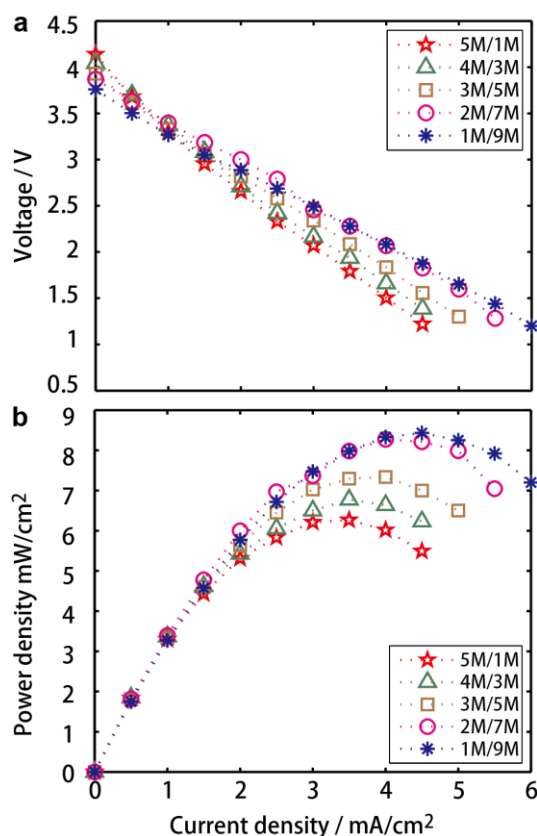


Figure 1. Polarization curves obtained from 5-min Galvanostatic discharging with different catholytes (a) and the corresponding power output (b).

## Reference

1. T. Zhang, N. Imanishi, Y. Shimonishi, A. Hirano, Y. Takeda, O. Yamamoto and N. Sammes, *Chemical Communications*, 2010, **46**, 1661-1663.
2. Y. R. Wang, P. He and H. S. Zhou, *Adv Energy Mater*, 2012, **2**, 770-779.

# Functional Conductive Polymer Binders Enabled High-stability Cycling of Alloy Anodes

Gao Liu, Hui Zhao, Zhe Jia, Sang-Jae Park  
Lawrence Berkeley National Laboratory  
1 Cyclotron Rd., Berkeley, CA 94720, USA  
gliu@lbl.gov

A class of new functional conductive polymers is developed for electrochemical energy storage applications. Contrasting other polymer binders, these binders have tailored electronic structure, adhesive functional groups, and controlled polarity for ion transport. This class of materials is suitable as binders for high capacity alloy anode materials. Materials with high lithium storage capacity, such as Si and Sn based alloys, have recently been extensively studied for their applications as lithium-ion battery anodes. However, the large-volume change associated with lithiation and delithiation of these materials severely hinders the practical application. The functional conductive polymer binders maintain conductivity and mechanical integrity during the battery operation, implementing the conceptual idea of combining binding, electron conducting and ion conducting into one material to significantly improve the electrode cycling performance.

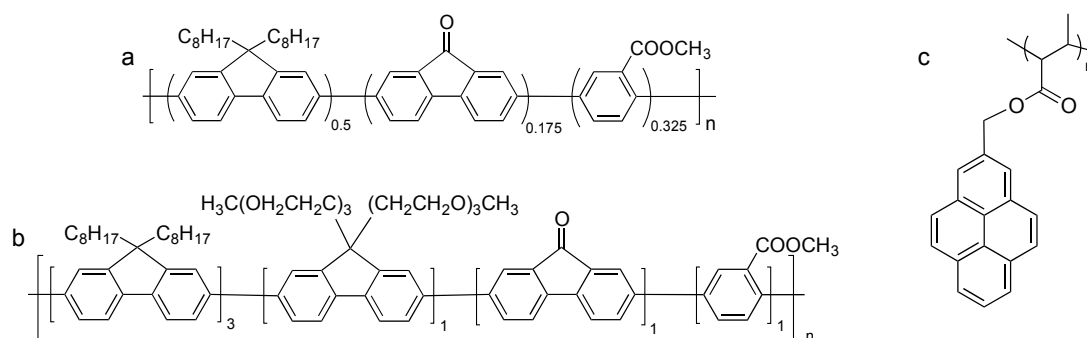


Figure 1. Molecular structure of the functional conductive polymer binders. a. First generation. b. Second generation. c. Third generation

We will cover the theory to develop the functional conductive polymer binders for Si and Sn alloy, three generations of the conductive polymer binders from our laboratory (Figure 1), and discuss the electric conductivity, adhesion and ion transport functionalities in these binders. Different Si based materials such as Si nanomaterial and SiO micron size materials are also used with these binders to fabricate electrode, and their performance characteristics reported. Electrode architectures are also very important for functional binders and alloy materials. The talk will also cover develop Si and conductive polymer electrode architectures including Si/binder composite particles, and in situ formation of Si network in the electrode. Conductive polymers with Sn materials system in lithium and Sodium ion batteries will also be discussed.

## References

1. Sangjae Park, Hui Zhao, Guo Ai, Cheng Wang, Xiangyun Song, Neslihan Yuca, Vincent S. Battaglia, Wanli Yang, and Gao Liu, Side-chain conducting and phase-separated polymeric binders for high performance silicon anodes in lithium-ion batteries. *J. Am. Chem. Soc.* **2015**, 137, 2565-2571.
2. Mingyan Wu, Xiangyun Song, Xiaosong Liu, Vincent Battaglia, Wanli Yang, and Gao Liu, Manipulating the polarity of conductive polymer binders for Si-based anodes in lithium ion batteries. *J. Mater. Chem. A* **2015**, 3, 3651-3658.
3. Wu, M.; Xiao, X.; Vukmirovic, N.; Xun, S.; Das, P. K.; Song, X.; Olade-Velasco, P.; Wang, D.; Weber, A. Z.; Wang, L.-W.; Battaglia, V. S.; Yang, W.; Liu, G.; Toward an Ideal Polymer Binder Design for High-Capacity Battery Anodes. *J. Am. Chem. Soc.* **2013**, 135, 12048-12056.
4. Liu, G.; Xun, S.; Vukmirovic, N.; Song, X.; Olalde-Velasco, P.; Zheng, H.; Battaglia, V. S.; Wang, L.; Yang, W, Polymers with Tailored Electronic Structure for High Capacity Lithium Battery Electrodes, *Adv. Mater.* **2011**, 23, 4679-4683.

# Self Terminated Oligomer Branched Architecture (STOBA) in lithium ion battery

Fu-Ming Wang<sup>1,2\*</sup>

<sup>1</sup>Graduate Institute of Applied Science and Technology, National Taiwan University of Science and Technology

<sup>2</sup>Sustainable Energy Center, National Taiwan University of Science and Technology  
43 Keelung Road, Section 4, Taipei 10607, Taiwan

Correspondence: mccabe@mail.ntust.edu.tw

Lithium ion battery provides high energy and power density that uses into portable electronics and electric vehicle; however, the safety is a big issue and cannot be guaranteed due to different habits of users. In order to improve the safety performance of battery, a new technology called Self Terminated Oligomer Branched Architecture (STOBA) had been developed [1]. The STOBA is used to prevent the direct contact between anode and cathode when the battery suffers short problem. According to the literature [1], STOBA is an oligomer that homogeneously disperses into cathode slurry and electrochemically forms solid electrolyte interface (SEI) on cathode's surface. This SEI provides further isolated polymerization behavior in order to inhibit the decomposition of cathode material while battery gets short.

In this study, second generation of STOBA has been created. Figure 1 shows that the second generation of STOBA is polymerized by BMI/BTA oligomer (1<sup>st</sup> generation STOBA) and poly(phenylsiloxane) (PhSLX). The PhSLX is used to enhance the thermal and electrochemical stability of STOBA. In accordance with the results, this 2<sup>nd</sup> generation STOBA not only maintains high safety performance, but the cycle-ability at high temperature also increases.

The second generation of STOBA is a highly potential additive for application in electric vehicle.

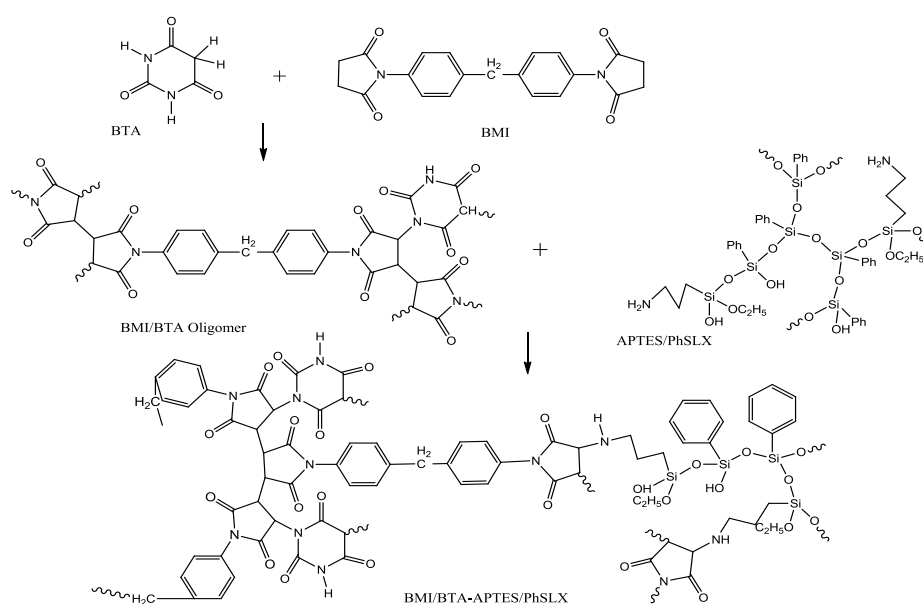


Figure 1 The reaction mechanism of the self-polymerized branched oligomer additive.

## References

- [1] Fu-Ming Wang *et al.*, J. Membrane Sci. 368 (2011) 165.

# Oxygen Reduction and Evolution for Li-Air batteries: Role of the Electrocatalyst

Christoph Bondü, Christoph Molls, Philipp Reinsberg, Martina Hegemann, Helmut Baltruschat  
*University of Bonn*  
*Roemerstrasse 164, 53117 Bonn*  
*baltruschat@uni-bonn.de*

It is generally accepted that oxygen reduction in aprotic solvents leads to superoxide or peroxide, depending on the cation present. Since no bond breaking is occurring here, a dependence of the reaction on the electrocatalyst material is not expected.

We have carried out a detailed study involving differential electrochemical mass spectrometry (DEMS), electrochemical quartz crystal microbalance (EQCM) and the rotating disc electrode (RRDE) using a variety of smooth model electrodes (different noble metals and glassy carbon) and found marked differences on different materials. E.g., during oxygen reduction in a  $\text{Li}^+$  containing DMSO, reduction to super oxide and peroxide occur in well separated potential regions, whereas on Rh reduction occurs in a 2 electron process (as demonstrated by DEMS) in the whole reduction region. In the presence of Li, only a part of the formed reduction product ( $\text{Li}_2\text{O}_2$ ) is deposited on the electrode, another part is dissolved in the electrolyte:

From the deposit, oxygen can be evolved, the amount of which also depends on the electrode material. Whereas on Pt and Rh the oxidation occurs in only one oxidation peak (which is paralleled by oxygen evolution) close to the equilibrium potential, on Au three peaks are observed in a wide potential range. Astonishingly, no weight changes are observed by EQCM during oxygen evolution.

Comparative experiments in  $\text{Mg}^{2+}$  and other cation - containing electrolytes will also be presented.

Acknowledgement: Funding of this project by the BMBF (LuLi - project 03X4624A and Mg - Luft, 03SF0447A) is gratefully acknowledged.

1. C. J. Bondue, A. A. Abd-El-Latif, H. P. and H. Baltruschat, J. Electrochemical Soc. 162 (2015) A479-A487

# ***In situ* infrared spectroscopy on gold substrates to track film formation and intermediates in Li-ion and Li-air electrolytes**

Laurence Hardwick\*, Vivek Padmanabhan and Richard Nichols

*Department of Chemistry, Stephenson Institute for Renewable Energy, University of Liverpool,  
Liverpool, L69 7ZF, UK*

*\*hardwick@liverpool.ac.uk*

The main challenge for *in situ* infrared spectroscopy is to isolate the bands you wish to observe from the background bands arising from, for example the electrolyte. *In situ* attenuated total reflection surface-enhanced infrared absorption spectroscopy (ATR-SEIRAS) is particularly attractive for such spectroelectrochemical experiments [1]. ATR-SEIRAS uses a property of total internal reflection resulting in an evanescent wave. A beam of infrared light is passed through the ATR crystal for example, a ZnSe prism, in such a way that it reflects off the internal surface in contact with the sample (Figure 1). This reflection forms the evanescent wave which extends into the sample. Therefore, this allows one to investigate the surface region of the electrode and discriminate against the bulk electrolyte signal. In the ATR-SEIRAS set-up, part of the evanescent wave passes through a ca. 15 nm thin polycrystalline Au metallic film working electrode. The penetration depth through the Au film and into the electrolyte is typically between 0.5 and 2  $\mu\text{m}$ , with the exact value being determined by the wavelength of light, the angle of incidence and the indices of refraction of the relevant media. We have been developing and optimising this technique, particularly with relation to the Au film deposition, and will report on the study of electrochemical processes in non-aqueous electrolytes in systems that are of interest to understanding film formation and intermediates relevant to both Li-ion and Li-air batteries.

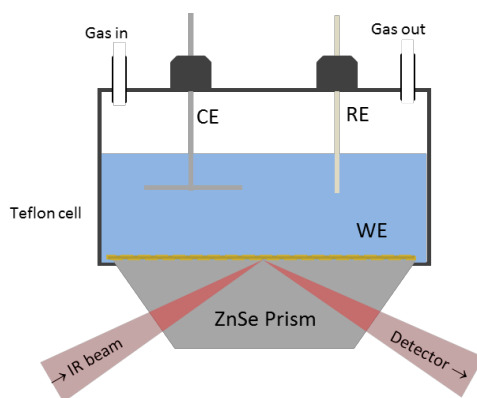


***Figure 1. ATR- SEIRAS Cell***

[1] M. Osawa, *Topics in Applied Physics*, **2001**, 81, 163-187

# High Voltage Cathode Material $\text{LiNi}_{0.5}\text{Mn}_{1.5}\text{O}_4$ for Li-ion Batteries

Xuejie Huang<sup>1</sup>, Mingxiang Lin<sup>1</sup>, Hao Wang<sup>1</sup>, Liubin Ben<sup>1</sup>, Yang Sun<sup>1</sup>, Yuyang Chen<sup>1</sup>, Lin Gu<sup>2</sup>, Zhenzhong Yang<sup>2</sup>, Xiqian Yu<sup>3</sup>, Xiaoqing Yang<sup>3</sup>, Haofei Zhao<sup>2</sup>, Richeng Yu<sup>2</sup>, Michel Armand<sup>4</sup>

<sup>1</sup>Key Laboratory for Renewable Energy, Beijing National Laboratory for Condensed Matter Physics, Institute of Physics, Chinese Academy of Sciences, Beijing 100190, China. <sup>2</sup>Laboratory for Advanced Materials & electron Microscopy, Beijing National Laboratory for Condensed Matter Physics, Institute of Physics, Chinese Academy of Sciences, Beijing 100190, China. <sup>3</sup>Brookhaven National Laboratory, Upton, NY 11973, USA. <sup>4</sup>CIC Energigune, Albert Einstein 48, 01510 Miñano, Álava, Spain.  
[xjhuang@iphy.ac.cn](mailto:xjhuang@iphy.ac.cn)

High-voltage spinel  $\text{LiNi}_{0.5}\text{Mn}_{1.5}\text{O}_4$  cathode material has specific energy (~640 mAh/g due to the high operation voltage of ~4.7 V. The relatively inexpensive Ni and Mn in  $\text{LiNi}_{0.5}\text{Mn}_{1.5}\text{O}_4$  make this cathode material particularly desirable for large-scale applications. However, the real application is hampered by long-standing issues such as capacity degradation and poor first cycle coulombic efficiency. Despite of extensive studies of the issues, their associated mechanisms are not fully understood.

A detailed investigations of its local atomic-level structure with lithium extraction /insertion is reported. We observed two types of local atomic-level migration of transition metals (TM) ions in  $\text{LiNi}_{0.5}\text{Mn}_{1.5}\text{O}_4$  particles during first charge via an aberration-corrected scanning transmission electron microscopy (STEM). The surface regions (~2nm) show an irreversible migration of TM ions into lithium tetrahedral sites to form a  $\text{Mn}_3\text{O}_4$ -like structure. The formation of these local structures and migration of TM ions are attributed to the destabilization of spinel  $\text{LiNi}_{0.5}\text{Mn}_{1.5}\text{O}_4$  cathode structure and evolution of a small amount of  $\text{O}_2$ . The surface  $\text{Mn}_3\text{O}_4$ -like structure contributes to the dissolution of TM ions. This structure as well as the rocksalt-like structures with heavy TM ions on the lithium pathways blocks the migration of lithium ions, resulting in building-up of charge transfer impedance and degradation of capacity. Since the  $\text{Mn}_3\text{O}_4$ -like and the rocksalt-like structures are formed as early as in the first charge to 4.9 V, they inevitably contribute to the poor first-cycle coulombic efficiency.

While a  $\text{LiNi}_{0.5}\text{Mn}_{1.5}\text{O}_4/\text{Li}$  half cell shows excellent cycling performances at 25 and 55°C, the  $\text{LiNi}_{0.5}\text{Mn}_{1.5}\text{O}_4/\text{MCMB}$  full cell has limited cycling life, especially at elevated temperatures. When the surface  $\text{LiNi}_{0.5}\text{Mn}_{1.5}\text{O}_4$  was modified by coating and superficial doping, the cycling performance of the full cell with MCMB anode has been much improved and the coulombic efficiency of discharge/charge is also obviously increased. Theoretical calculations analyses reveal that the stability of O at surface layer is enhanced by those surface modifications and detailed analyses will be reported.

# **Olivine with zero anti-site defect and three dimensional lithium diffusion paths**

Kyu-Young Park, Kisuk Kang

Department of Materials Science and Engineering and Research Institute of Advanced Materials (RIAM),

Seoul National University, 1 Gwanak-ro, Gwanak-gu, Seoul 151-742, Korea

Center for Nanoparticle Research at Institute for Basic Science (IBS), Seoul National University, 1

Gwanak-ro, Gwanak-gu, Seoul

*e-mail address: matlgen1@snu.ac.kr*

## **Abstract**

Lithium iron phosphate (LFP) has attracted tremendous attention as a next-generation electrode material in lithium rechargeable batteries for large scale energy storage systems due to the use of low-cost iron and chemical/electrochemical stability. While the lithium diffusion in LFP, the essential property in battery operation, is relatively fast due to the one-dimensional tunnel present in the olivine crystal, the tunnel is inherently susceptible to immobile anti-site defects which, if any, block the lithium diffusion and lead to the inferior performance. Herein, we demonstrate that the kinetic issue arising from the defects in LFP can be completely eliminated in a new olivine LFP, which we successfully synthesized for the first time. The doping in the olivine structure reduces the concentration of defects in the tunnel by 7 orders of magnitude. Moreover, it opens up a new lithium diffusion path along the [101] direction making the olivine LFP as a three-dimensional lithium diffuser. We also find that the intrinsic energy barrier for phase transition gets notably lower in the lithium excess olivine LFP. The fundamentally different nature of the new olivine than normal LFP additionally induces faster charging capability, lowering thermal solid-solution temperature and less memory effect.

# On the Influence of Mechanical Compression on the Impedance of Aged LiFePo<sub>4</sub> - Graphite Cells

Reinhold Koch<sup>1,2\*</sup>, Andreas Jossen<sup>1</sup>

<sup>1</sup> Institute for Electrical Energy Storage Technology, Technische Universität München, Karlstr. 45, 80333 Munich, Germany

<sup>2</sup> TUM CREATE, 1 CREATE Way, Singapore 138602, Singapore

\*reinhold.koch@tum.de

The impedance of a battery cell is influenced by a variety of parameters, like temperature and state of charge. The influence of mechanical force on a cell's impedance has not been reported so far as well as the interdependency of cooled and non-cooled cells during constrained operation.

We tested unconstrained cells, constrained cells which were liquid cooled during operation to 25 °C and cells which were intentionally insulated from the compression plates in order to eliminate the heat sink effect of cooling from large metal plates. After 1400 cycles we saw that the compression force had an immediate effect on the impedance of all three cells. Figure 1 shows an unconstrained cell which shows an almost immediate reduction in its impedance by around a factor of 4 with the maximum applied compression force of 7 bar. After releasing the cell the impedance “bounced back” again to its unconstrained values in an exponential way, i.e. the first change was very quickly, but it took several hours to reach the original impedance values.

The influence of cooled or insulated compression is most dominant when the cell is only constrained by a small compression force. Figure 2 shows that the capacity fade of an insulated cell which has been constrained with a small compression force of 0.5 bar has initially lower capacity as the unconstrained cell but overtakes it over of the lifetime. The biggest difference can be seen between the cooled and the non-cooled cell. Even if they have been constrained with the same compression force the cooled cell starts with a lower capacity and loses it much quicker than the insulated cell.

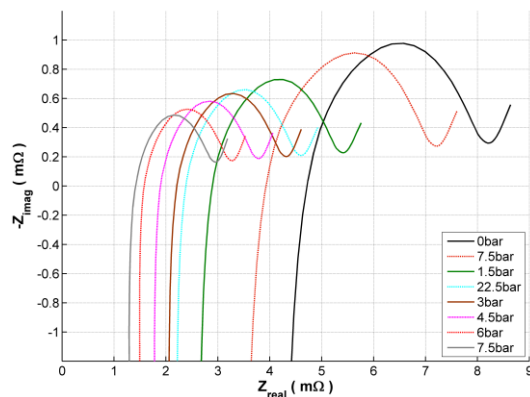


Figure 1: Influence of the compression force on the impedance of the LiFePo<sub>4</sub> pouch cell which was cycled under unconstrained conditions.

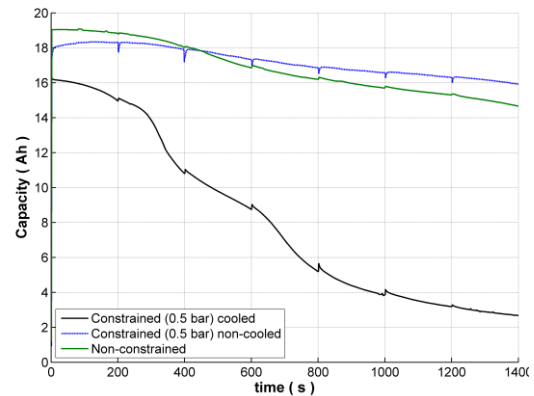


Figure 2: Capacity fade during constrained and non-constrained operation

The graphite electrode has a volume change of up to 7% during a charge discharge cycles, it is also the electrode most affected by aging.

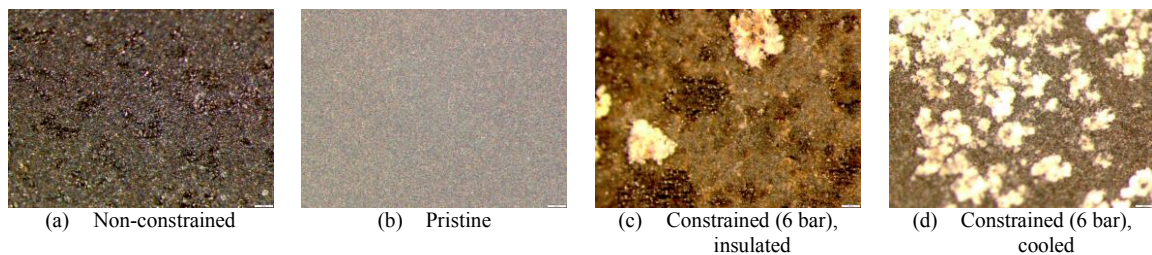


Figure 3: Microscopic pictures of the graphite electrode of the used cells..

Figure 3 shows, that the formation of crystalline structures is stronger in constrained cells, where also the impedance change by compression as shown in Figure 1 was stronger.



# Computational data mining to boost the next generation batteries R&D: the composite electrode architecture

Alejandro A. Franco<sup>1,2,3</sup>, Garima Shukla<sup>1,2,3</sup>, Matias A. Quiroga<sup>1,2,3</sup>, Kan-Hao Xue<sup>1,2,3</sup>, Trong-Khoa Nguyen<sup>1,2,3</sup>, Guillaume Blanquer<sup>1,2,3</sup> and Yinghui Yin<sup>1,2,3</sup>

<sup>1</sup>Laboratoire de Réactivité et Chimie des Solides (LRCS) - Université de Picardie Jules Verne & CNRS, UMR 7314 – 33 rue Saint Leu, 80039 Amiens Cedex, France

<sup>2</sup>Réseau sur le Stockage Electrochimique de l'Energie (RS2E), FR CNRS 3459, France

<sup>3</sup>ALISTORE-ERI European Research Institute, FR CNRS 3104, 80039 Amiens Cedex, France.

[alejandro.franco@u-picardie.fr](mailto:alejandro.franco@u-picardie.fr)

History teaches us that energy forms can be used to make practical things without knowing the nature or fully understanding the fundamentals of those energy forms. This affirmation is not unrealistic: Volta invented the first electric battery in 1800, almost 100 years before than electrons were discovered (credited to Thomson in 1897).<sup>1</sup> Therefore, the subsequent relatively fast penetration of rechargeable batteries in the market was mainly based on trial-error synthesis of materials and testing, and it is only since recent years supported by deep theoretical tools at the single material level.<sup>2</sup> But the automotive lithium ion battery (LIB) industry has reached a point where detailed optimization studies of the composite electrodes, made of complex mixtures of active material and additive particles with multiple sizes, binder and electrolyte, are vital to achieve high performance at low environmental and economic cost.<sup>3</sup> Then, the development of a theoretical framework helping on the design of efficient composite electrodes is urgently needed. Indeed, significant progress has been made in linking composite electrode structural properties to ionic transport and cell capacity response using computer-aided reconstruction of real electrode structure. However holistic approaches by combining electrode composition with fabrication parameters are crucial to produce results coherent with experiment.<sup>4,5</sup>

In this contribution we report an innovative multiscale computational modeling platform being developed in our laboratory, devoted to perform *in silico* data mining of composite electrodes architectures at multiple scales.<sup>6-11</sup> Such architectures are described in terms of particle and pore size distributions, three-dimensional binder spatial distributions and electrolyte solvent compositions. The platform combines multiple simulation paradigms: 1) stochastic discrete-particle methods devoted to describe the different steps along composite electrode fabrication and to predict the arising microstructure; 2) mesoscopic simulation approaches devoted to extract fundamental electrochemical and transport parameters; 3) continuum models devoted to gather these data in order to simulate cells and to detect electrodes architectures maximizing the cell capacity and energy density. The promising predictive capabilities of the platform will be illustrated, in comparison with experimental knowledge, within three concrete application contexts: all solid state LIBs with composite electrodes, lithium air batteries and lithium sulfur batteries.

1. A.A. Franco, Ed., Rechargeable Lithium Batteries: from fundamentals to applications, Woodhead/Elsevier publishing, Cambridge (2015).
2. C. C. Fischer, K.J. Tibbetts, D. Morgan, G. Ceder, *Nature materials*, **5**(8) (2006) 641.
3. M. Armand, J.-M. Tarascon, *Nature*, **451** (7179) (2008) 652.
4. S. E. Trask *et al.*, *J. Power Sources*, **259** (2014) 233.
5. A.A. Franco, C. Frayret, Modeling in the design of batteries for large and medium-scale energy storage, book chapter in: Advances in batteries for large- and medium-scale energy storage, C. Menictas, M. Skyllas-Kazacos, T.M. Lim, Eds., Woodhead/Elsevier publishing, Cambridge (2014).
6. A. A. Franco, *RSC Adv.*, **3** (2013) 13027.
7. H. Xue, T.-K. Nguyen, A. A. Franco, *J. Electrochem. Soc.*, **161** (2014) E3028.
8. K.H. Xue, E. McTurk, L. Johnson, P.G. Bruce, A.A. Franco, *J. Electrochem. Soc.*, **162**(4) (2015) A614.
9. M.A. Quiroga, A.A. Franco, *J. Electrochem. Soc.*, **162** (7) (2015) E73.
10. M. Quiroga, K.H. Xue, T.K. Nguyen, H. Huang, M. Tulodziecki, A.A. Franco, *J. Electrochem. Soc.*, **161** (8) (2014) E3302.
11. A.A. Franco, Multiscale modeling of electrochemical devices for energy conversion and storage, book chapter in: Encyclopedia of Applied Electrochemistry, edited by R. Savinell, K.I. Ota, G. Kreysa (publisher: Springer, UK) (2013).

# Study of ceramic-polymer/lithium interface for lithium air batteries

Louise Freneck<sup>acd</sup>, Renaud Bouchet<sup>d</sup>, Philippe Stevens<sup>c</sup>, Nitash Balsara<sup>ab</sup>

- a) *Environmental Energy Technologies Division, Lawrence Berkeley National Laboratory, Berkeley, California 94720 USA*
- b) *Joint Center for Energy Storage Research (JCESR), Lawrence Berkeley National Laboratory, Berkeley, California 94720, USA*
- c) *Electricité de France, R&D division, LME/M29, Avenue des Renardières F-77818 Moret sur Loing Cedex, France*
- d) *LEPMI UMR 5279 CNRS Grenoble INP Univ. de Savoie Univ. Joseph Fourier, 38402 St Martin d'Hères, France*  
*lfrenck@lbl.gov*

Two main advantages of Lithium-air batteries are their very high energy densities and low costs. There are two approaches to the development of these batteries: the anhydrous system which uses an organic electrolyte, and the aqueous system which uses an aqueous electrolyte [1]. An advantage of the aqueous system is its safety since toxic or inflammable solvents are not used. The negative lithium electrode is separated from the aqueous electrolyte by a thin ceramic water and gas tight membrane which enables the battery to have an extremely low self-discharge rate. The interface between the lithium metal and the ceramic membrane plays an important role in the cycling performance of the aqueous lithium air cell. However, the poor or non-chemical stability of most ceramic electrolytes in contact with lithium metal limits the performance. A possible strategy to improve the interface between ceramic electrolyte and lithium metal might be by the use of polymer membranes [2].

Here, we study the effect of a polymer membrane between a ceramic electrolyte and lithium metal. Block copolymer electrolytes, such as polystyrene-block-poly (ethylene oxide) copolymer electrolyte (SEO) mixed with lithium bis(trifluoromethanesulfonyl)imide (LiTFSI) salt, were used in this study. The ceramic electrolyte was a Lithium Ion Conducting Glass Ceramic (LICGC) purchased from Ohara Corporation (1 inch X 1 inch 150 $\mu$ m thick), and was used as the single ion conductor. In this work, lithium ion - lithium metal transfer from a lithium ion conducting polymer interface has been studied by impedance spectroscopy. Furthermore, in order to know if the sandwich polymer-ceramic cell showed an additional interfacial resistance, ionic conductivity experiments using electrochemical impedance spectroscopy were performed. Besides, polarization loss quantification at a lithium ion conducting polymer/single ion conductor interface was studied by DC current measurement by the Srinivasan et al method [3]. Finally, the interface between the ceramic and the polymer was studied by synchrotron hard X-Ray micro tomography experiments on symmetric lithium-sandwich polymer-ceramic cells, in order to confirm the intimacy of the ceramic and the polymer.

1. P.G. Bruce, S. A. Freunberger, L. J. Hardwick, J-M. Tarascon, *Nature Materials*, 11, 19-29 (2012)
2. G.M. Stone, S.A. Mullin, A.A. Teran, D.T. Hallinan, A.M. Minor, A. Hexemer, N.P. Balsara, *Journal of the Electrochemical Society* 159(3) A222-A227 (2012)
3. Mehrotra, P. N. Ross, V. Srinivasan, *Journal of the Electrochemical Society*, 161 (10) A1681-A1690 (2014)

# The Influence of Anomalous Diffusion on the Impedance Response of LiCoO<sub>2</sub>|C Batteries

Salim Erol and Mark E. Orazem  
Department of Chemical Engineering  
University of Florida, Gainesville, FL 32611 USA  
[meo@che.ufl.edu](mailto:meo@che.ufl.edu)

This paper provides the results of impedance measurements on commercially available LiCoO<sub>2</sub>|C coin-type cells. The impedance response was shown to be extremely sensitive to temperature, state-of-charge, overcharge, and over-discharge. Interestingly, the impedance showed a persistent change to the electrochemical characteristics of a coin cell subject to overcharge; whereas, the electrochemical characteristics returned to normal for a coin cell subject to over-discharge. In early work, a measurement model analysis was used to show the reversibility of the impedance behavior of an over-discharged cell and the irreversibility of the impedance response of an overcharged cell.<sup>1</sup>

The impedance response of LiCoO<sub>2</sub>|C batteries has distinguishing characteristics that should, in principle, be associated with the electrochemical characteristics of the battery. A key feature is the low-frequency impedance that appears in a Nyquist plot as a straight line with an angle with respect to the real axis greater than the 45 degrees expected for a diffusion impedance.<sup>2</sup>

A process model for impedance analysis was developed in the context of reactions and transport processes that were hypothesized to govern the performance of the Li-ion battery. At the carbon electrode, lithium ions and solvent were considered to react to form a solid-electrolyte interphase (SEI). In addition, lithium ions were assumed to diffuse through the SEI to intercalate into the graphene layers. As these two processes involve an addition of currents, the corresponding impedances were considered to be in parallel. Anomalous diffusion of lithium ions was invoked at the LiCoO<sub>2</sub> electrode to account for the low-frequency line that had a slope steeper than that predicted by ordinary diffusion. This model was fit to all impedance data collected. The model provided a good description for impedance of batteries under normal operating potentials and temperatures. The contribution of anomalous diffusion was diminished at elevated temperatures, suggesting that the free-energy well associated with anomalous or sticky diffusion was shallow.

This work provides an alternative explanation for the slope of the low-frequency impedance response for LiCoO<sub>2</sub>|C cathodes that is steeper than that associated with Fickian diffusion impedance. This effect is clearly associated with the unique properties of the LiCoO<sub>2</sub>|C cathode as the low-frequency impedance response of other Li-ion battery cathodes, e.g., LiFePO<sub>4</sub> and LiMn<sub>2</sub>O<sub>4</sub>, show different behaviors.<sup>3</sup> Osaka et al.<sup>2</sup> have attributed this behavior to the different time constants for diffusion to particles of different sizes. The present work shows that anomalous diffusion may provide an alternative explanation that is specific to the properties of LiCoO<sub>2</sub>.

## References

1. S. Erol, M. E. Orazem, and R. P. Muller, Influence of overcharge and over-discharge on the impedance response of LiCoO<sub>2</sub>|C batteries, *J. Power Sources* **270** (2014), 92-100.
2. T. Osaka, T. Momma, D. Mukoyama, and H. Nara, Proposal of novel equivalent circuit for electrochemical impedance analysis of commercially available Lithium ion battery, *J. Power Sources*, **205** (2012), 483-486.
3. M. Greenleaf, H. Li, and J. Zheng, Application of physical electric circuit modeling to characterize Li-ion battery electrochemical processes, *J. Power Sources*, **270** (2014), 113-20.

# How to make an ideal electrolyte based on bis(trifluorosulfonyl)imide-based ionic liquid for lithium-ion and lithium-sulfur batteries

Masaki Yamagata, Yukiko Matsui, Takuya Takahashi, Satoshi Uchida, and Masashi Ishikawa  
 Department of Chemistry and Materials Engineering,  
 Faculty of Chemistry, Materials and Bioengineering, Kansai University  
 3-3-35 Yamate-cho, Suita 564-8680, Japan  
 e-mail address: yamagata@kansai-u.ac.jp

Ionic liquids are still attractive candidates for use as electrolytes in electrochemical energy storage devices, because of their relatively low flammability and reactivity, and because of their electrochemical stability, wide liquidus temperature range, and acceptable ionic conductivity. We have reported a promising ionic liquid based on bis(fluorosulfonyl)imide (FSI<sup>−</sup>) for lithium-ion batteries since 2006. [1] This liquid with a lithium salt offers incredible charge-discharge performances; despite the relatively high viscosity of the electrolyte, it affords not only reversible and stable cycling but also rapid charge-discharge performance for both negative and positive electrodes. [2] Herein, we report the results from charge-discharge tests, focusing on the effect of the electrolyte component; LiFSI is used as the lithium source for the electrolyte and is compared to LiTFSI (TFSI<sup>−</sup> = bis(trifluoromethylsulfonyl)imide). In addition, we also investigate how the concentration of the lithium salts promotes the more stable and rapid charging-discharging of lithium-ion cell.

To clarify the effect of concentration of LiFSI on the dependencies of the discharge capacity retention of a graphite electrode in EMImFSI and EMImTFSI (EMIm<sup>+</sup> = 1-ethyl-3-methylimidazolium) on the charge-discharge C-rate, which were evaluated by determining the 5-cycle durability for each C-rate operation after primary charge-discharge cycling at the 0.1/0.1 C-rate, are summarized in Figure 1a. Here, the discharge capacity retention was calculated as  $C_x/C_2$ , where  $C_x$  and  $C_2$  are the specific discharge capacities for each cycle ( $x$ ) and for the second cycle (1.0 C-rate), respectively. The remarkable aspect in this figure is that the high concentration (1.46 mol dm<sup>−3</sup>) of LiFSI improves the output characteristics in comparison with 0.43 mol dm<sup>−3</sup> LiFSI/EMImFSI despite the electrolyte possessing a lower ionic conductivity, while 1.46 mol dm<sup>−3</sup> LiTFSI/EMImFSI decreases the rate capability of the graphite compared with 0.43 mol dm<sup>−3</sup> LiTFSI/EMImFSI. The high-concentration of LiFSI/EMImFSI also enables stable charge-discharge operation of the graphite electrode in low temperature. (Figure 1b)

In the present study, we also discuss such an advantages of the use of high-concentration LiFSI/EMImFSI for lithium-sulfur battery.

## Acknowledgment

This work is partly supported by Specially Promoted Research for Innovative Next Generation Batteries of Advanced Low Carbon Technology Research and Development Program (ALCA-SPRING) promoted by JST.

## References

- [1] M. Ishikawa *et al.*, *J. Power Sources*, 2006, 162, 658-662.
- [2] Y. Matsui *et al.*, *Electrochemistry*, 2012, 80, 808-811; M. Yamagata *et al.*, *J. Power Sources*, 2013, 227, 60-64; *Electrochim. Acta*, 2013, 110, 181-190; Y. Matsui *et al.*, *J. Power Sources*, 2015, 279, 766-773.

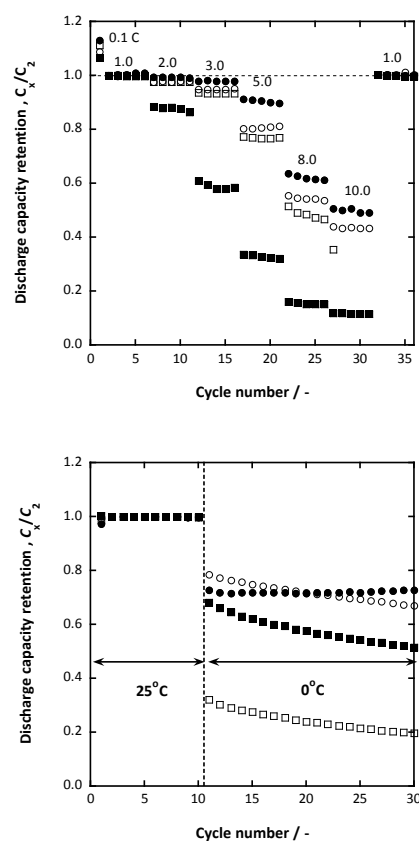


**Fig. 1.** (a) Discharge rate capability and (b) low temperature behavior of the graphite electrode in LiFSI/EMImFSI (1.46 mol dm<sup>−3</sup>: ●, 0.43 mol dm<sup>−3</sup>: ○) and LiTFSI/EMImFSI (1.46 mol dm<sup>−3</sup>: ■, 0.43 mol dm<sup>−3</sup>: □).

# RuO<sub>2</sub>-nanoparticles-coated $\delta$ -MnO<sub>2</sub> as efficient catalytic cathode for high-performance Li-O<sub>2</sub> batteries

Guoqing Wang,<sup>a</sup> Shuangyu Liu,<sup>a</sup> Jian Xie,<sup>\*ab</sup> Fangfang Tu,<sup>a</sup> Shichao Zhang,<sup>c</sup> Tiejun Zhu,<sup>a</sup> Gaoshao Cao,<sup>b</sup> Xinbing Zhao<sup>ab</sup>

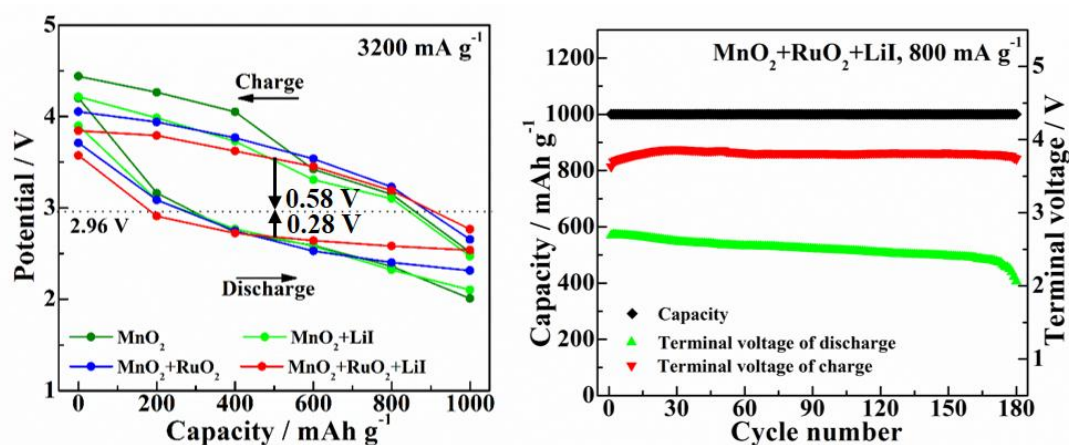
<sup>a</sup>State Key Laboratory of Silicon Materials, School of Materials Science and Engineering, Zhejiang University, Hangzhou 310027, China

<sup>b</sup>Key Laboratory of Advanced Materials and Applications for Batteries of Zhejiang Province, Hangzhou 310027, China

<sup>c</sup>School of Materials Science and Engineering, Beijing University of Aeronautics and Astronautics, Beijing 100191, China

[21126107@zju.edu.cn](mailto:21126107@zju.edu.cn), [xiejian1977@zju.edu.cn](mailto:xiejian1977@zju.edu.cn)

The Li-O<sub>2</sub> battery has almost tenfold practical energy density than the current Li-ion battery; however, the use of Li-O<sub>2</sub> battery is restricted by poor cycle capability and low energy efficiency. In this work, RuO<sub>2</sub> nanoparticles was coated on the surface of  $\delta$ -MnO<sub>2</sub> by a facile sol-gel method, and the resulting composite was used as a high-performance cathode catalyst in Li-O<sub>2</sub> battery. After coating, we found that the discharge product Li<sub>2</sub>O<sub>2</sub> turn to form a thin film at the surface of MnO<sub>2</sub>, which could be easily formed and decomposed in discharge and charge processes. And with a soluble catalyst (LiI) added in the electrolyte, the battery show a high round-trip efficiency, with a low discharge and charge overpotential of 0.28 V and 0.58V, respectively, even at a high current of 3200 mA g<sup>-1</sup>. Excellent cycling stability can also be achieved in a fixed capacity (1000 mAh g<sup>-1</sup>, 180 times at 800 mA g<sup>-1</sup>) mode.



## References:

- 1 S. Y. Liu, G. Q. Wang, J. Xie, F. F. Tu, H. Y. Yang, S. C. Zhang, T. J. Zhu, G. S. Cao, X. B. Zhao, *Nanoscale*, 2015, DOI: 10.1039/C5NR01344E
- 2 S. Y. Liu, Y. G. Zhu, J. Xie, Y. Huo, H. Y. Yang, T. J. Zhu, G. S. Cao, X. B. Zhao, S. C. Zhang, *Adv. Energy Mater.*, 2014, 4(9)
- 3 Z. L. Jian, P. Liu, F. J. Li, P. He, X. W. Guo, M. W. Chen, H. S. Zhou, *Angew. Chem. Int. Ed.* 2014, 53, 442-446

# Impact of Relative Humidity on Sulfate-based Cathode Materials

Leiting Zhang<sup>1,2</sup>, Jean-Marie Tarascon<sup>2,3\*</sup>, and Guohua Chen<sup>1\*</sup>

<sup>1</sup>Department of Chemical and Biomolecular Engineering, The Hong Kong University of Science and Technology, Clear Water Bay, Kowloon, Hong Kong, P.R. China

<sup>2</sup>FRE 3677 “Chimie du Solide et de l’Énergie”, Collège de France, 11 Place Marcelin Berthelot, 75231 Paris Cedex 05, France

<sup>3</sup>Institute for Advanced Study, Visiting Professor of the Department of Chemical and Biomolecular Engineering, The Hong Kong University of Science and Technology, Clear Water Bay, Kowloon, Hong Kong, P.R. China

[lzhangag@connect.ust.hk](mailto:lzhangag@connect.ust.hk); [jean-marie.tarascon@college-de-france.fr](mailto:jean-marie.tarascon@college-de-france.fr); [kechengh@ust.hk](mailto:kechengh@ust.hk)

Recently, sulfate-based compounds have been widely investigated as cathode materials for lithium-ion batteries, and various samples [LiFeSO<sub>4</sub>F, Li<sub>2</sub>Fe(SO<sub>4</sub>)<sub>2</sub>, LiFeSO<sub>4</sub>OH, Fe<sub>2</sub>O(SO<sub>4</sub>)<sub>2</sub>, Na<sub>2</sub>Fe<sub>2</sub>(SO<sub>4</sub>)<sub>3</sub>, *etc.*] have been explored.<sup>1</sup> Thanks to a greater electronegativity of sulfate [(SO<sub>4</sub>)<sup>2-</sup>] over phosphate group [(PO<sub>4</sub>)<sup>3-</sup>], the open-circuit voltage of these materials can be significantly increased. However, it should be noted that most sulfate-based compounds are soluble in water. This not only raises issues of proper material processing, but also challenges the stability of the material at highly humid environment.

In this study, tavorite-type LiFeSO<sub>4</sub>F was adopted to demonstrate the influence of relative humidity (RH) on its electrochemical performance. The compound was synthesized using an ionothermal method. The RH was manipulated over a range of 55–85% at 25 °C, and the corresponding structural change of the tavorite-type LiFeSO<sub>4</sub>F was monitored by X-ray diffraction (XRD). Surprisingly, nearly 80% of starting material was converted to FeSO<sub>4</sub>·H<sub>2</sub>O in less than 2 hours in 85% RH, and FeSO<sub>4</sub>·7H<sub>2</sub>O was identified as the main phase after 72 hours. Such degradation is of course less in the range of weeks in 55% RH. Aware of this issue, several sulfate-based compounds were tested under the same protocol, and it was found that the moisture sensitivity was inherent to most sulfate-based materials, whatever Li or Na-bearing, with a different degree of severity depending upon their structure and state of division. In contrast, we pleasantly found that Fe-based oxysulfate Fe<sub>2</sub>O(SO<sub>4</sub>)<sub>2</sub> are not moisture sensitive.

Therefore, to properly store and process sulfate-based materials, the relative humidity should be closely controlled. Means to mitigate the reactivity against water via surface coating with PEDOT/carbon, hierarchical nanostructuring, or others will be presented.

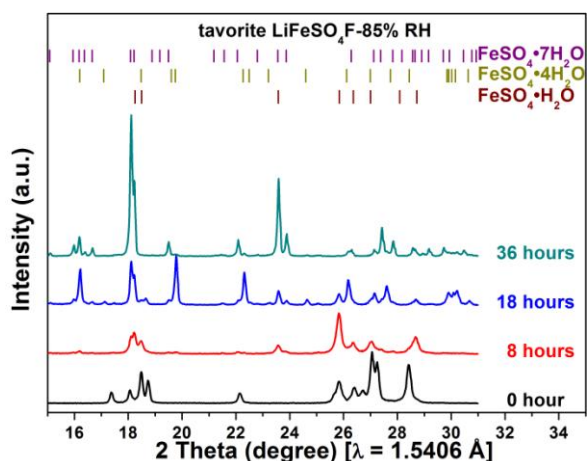


**Fig. 1.** Structural evolution of tavorite-type LiFeSO<sub>4</sub>F as a function of time in 85% RH at 25 °C

## Reference

- 1 G. Rousse and J. M. Tarascon, *Chem. Mater.*, 2014, **26**, 394–406.

# Design of Sulfur Based Electrolyte Additives for Advanced Lithium-ion Batteries

*Atetegeb Meazah Haregewoin<sup>1</sup>, Ermias Girma Legesse<sup>2</sup>, Liao Lee Wei<sup>1</sup>, Jyh-Chiang Jiang<sup>2</sup>, Shawn D. Lin<sup>3</sup>, Bing-Joe Hwang<sup>1,4</sup>*

*1NanoElectrochemistry Laboratory, Department of Chemical Engineering, National Taiwan University of Science and Technology, Taipei 106*

*2Computational and Theoretical Chemistry Laboratory, Department of Chemical Engineering, National Taiwan University of Science and Technology, Taipei 106*

*3Catalysis Laboratory, Department of Chemical Engineering, National Taiwan University of Science and Technology, Taipei 106*

*4National Synchrotron Radiation Research Center, Hsinchu 30076, Taiwan*

*[amharegewoin@mail.ntust.edu.tw](mailto:amharegewoin@mail.ntust.edu.tw)*

In recent years, lithium ion rechargeable batteries are commercialized as a preferable power source for portable consumer products. The performance of a lithium ion battery can be related to the solid electrolyte interface (SEI) layer formed on electrode surface and this film formation depends mainly on electrolyte composition<sup>1,2</sup>. Currently lithium-ion batteries mainly use either ethylene carbonate based (EC) electrolytes, which do not function at low temperature, or propylene carbonate (PC) based electrolytes which, due to their inability to form a solid electrolyte interface layer, are incompatible with graphite anodes. The use of additives, such as ethylene sulfite (ES)<sup>3</sup>, is an approach to addressing the PC electrode compatibility problem. In the current work, we report designing and screening of potential electrolyte additives derived from ES. To illustrate the potential of the selected additive and hence the screening technique, two representative electrolyte additive structures were selected, synthesized and experimentally tested. The mesocarbon microbead (MCMB) electrode showed an excellent electrochemical performance in a PC based electrolyte with 2% additives. The first cycle coulombic efficiency of the proposed additives was >84%, increasing to 99% after the second cycle. When compared with previously reported sulfur or halogen containing additives, the computationally designed additives resulted in better coulombic efficiency. CV, SEM, and XRD results confirmed the suppression of PC co-intercalation and electrode exfoliation. The results show that the method developed for screening potential additive structures works very well with PC-based electrolytes.

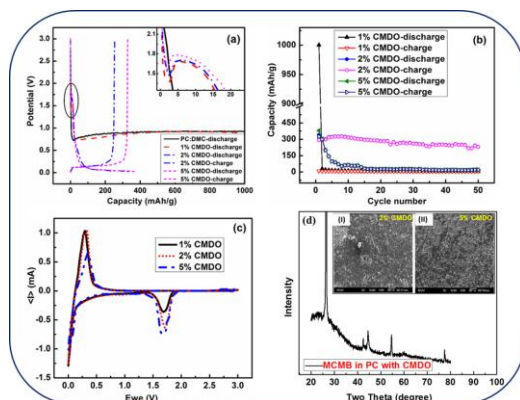


Figure 1. The first charge/discharge profile (a), cycling behaviors (b), cyclic voltammogram (c), and SEM images of MCMB in 1 M LiPF<sub>6</sub>/PC: DMC (1:1 v/v) with different concentrations of CMDO.

## References

- <sup>1</sup> J. T. Li, J. C. Fang, H. Su, S. G. Sun, *Prog Chem.*, 23 (2011) 349-356.
- <sup>2</sup> M. Q. Xu, L. D. Xing, W. S. Li, *Prog Chem.*, 21 (2009) 2017-2027.
- <sup>3</sup> G. H. Wrodnigg, J. O. Besenhard, M. Winter, *J Electrochem Soc.*, 146 (1999) 470-472.



# Self-Discharge and Cycling Stability in the Li-S System: Where Every Cell Component Plays a Role

Matthew J. Lacey<sup>a</sup>, Anurag Yalamanchili<sup>a,b</sup>, Viking Österlund<sup>a</sup>, Fabian Jeschull<sup>a</sup>, Julia Maibach<sup>a</sup>, Carl Tengstedt<sup>b</sup>, Kristina Edström<sup>a</sup> and Daniel Brandell<sup>a</sup>

<sup>a</sup> Department of Chemistry – Ångström Laboratory, Uppsala University  
Box 538, Lägerhyddsvägen 1, SE-751 21 Uppsala, SWEDEN

<sup>b</sup> Scania CV AB, SE-151 87 Södertälje, Sweden  
matthew.lacey@kemi.uu.se

The Li-S battery has been the subject of renewed and intense interest in recent years by virtue of the very high energy density of the Li-S couple: fully assembled cells with energy densities of 500-600 Wh/kg – two to three times higher than the state-of-the-art Li-ion batteries – are widely thought to be a realistic proposition[1]. The greatest advances have come in the development of the positive electrode, with a wide variety of conducting host structures proposed to enable high utilisation of active sulfur species, decent rate capability and maintain stable cycling over hundreds of cycles.

However, the negative electrode or indeed consideration of the system as a whole is relatively rare. For example: it is increasingly deemed important that high active material loading in the positive electrode can be demonstrated, but the thickness of the Li anode and the volume of electrolyte used – both of these enormously important for energy density and cycle life in a full cell - are often absent from experimental sections. The ability of cells to withstand self-discharge when not in operation, which is perhaps the toughest test of effective control of polysulfide intermediates, is also rarely investigated.

In this work, we will present an overview of the variety of factors influencing self-discharge and cycle stability, from basic electrochemical and surface analysis studies of the redox shuttle in LiNO<sub>3</sub>-containing electrolytes, to measurement of the rate and reversibility of self-discharge over moderately long idle periods and the cycle stability of high-loading and high-efficiency cells with low excesses of electrolyte and lithium metal. New results from the extension of our existing work on functional binders[2] will also be presented within this context.

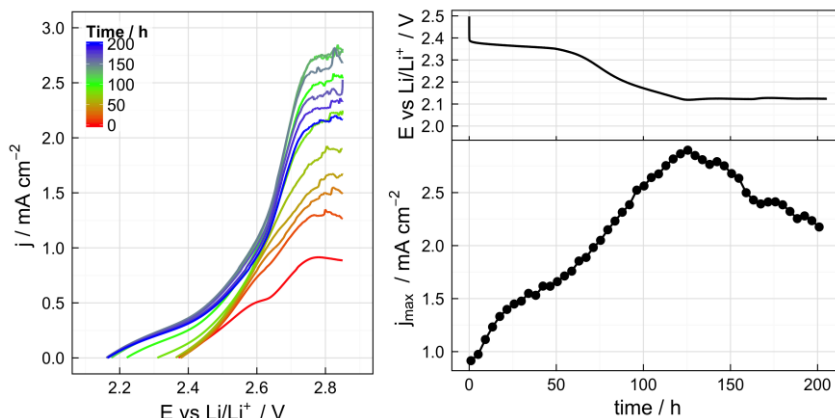


Figure: analysis of lithium polysulfide concentration changes during self-discharge with an *in situ* probe electrode[3] inserted between the electrodes of a Li-S cell. left) a series of LSVs at the probe electrode showing oxidation of lithium polysulfides, right) cell voltage and peak probe current (i.e., roughly corresponding to concentration) over 200 hours at cell OCV.

- [1] S. Urbonaitė, T. Poux, P. Novák, Progress Towards Commercially Viable Li-S Battery Cells, *Adv. Energy Mater.* (2015) 1500118.
- [2] M.J. Lacey, F. Jeschull, K. Edström, D. Brandell, Functional, water-soluble binders for improved capacity and stability of lithium–sulfur batteries, *J. Power Sources*. 264 (2014) 8–14.
- [3] M.J. Lacey, K. Edström, D. Brandell, Analysis of soluble intermediates in the lithium–sulfur battery by a simple *in situ* electrochemical probe, *Electrochem. Comm.* 46 (2014) 91–93.





# Does Size really Matter? New Insights into the Intercalation Behavior of Anions into a Graphite Based Positive Electrode

Kolja Beltrop<sup>\*</sup>, Paul Meister, Olga Fromm, Martin Winter, Tobias Placke

University of Münster, MEET Battery Research Center, Institute of Physical Chemistry Corrensstr. 46, 48149 Münster, Germany

<sup>\*</sup>[kolja.beltrop@uni-muenster.de](mailto:kolja.beltrop@uni-muenster.de)

The increasing demand for large scale energy storage capabilities causes a big field of research to make the battery systems safer and environmentally benign. A promising approach is the replacement of conventional volatile and highly flammable organic solvent-based electrolytes by ionic liquids (ILs) as the main component of the electrolyte. ILs exhibit excellent properties such as a broad electrochemical stability window, a high thermal stability, non-flammability and a high ionic conductivity.[1] A further prevention of pollution is the application of carbon-based, transition metal-free electrode materials. Recently, “dual-ion” and “dual-graphite” cells were introduced which are composed of a lithium-incorporating anode and an anion incorporating graphite-based cathode.[2][3] During charge the ions intercalate into the electrode active materials and are released back into the electrolyte during discharge (see Figure 1). Since the cathode potential reaches and may even exceed 5 V vs.  $\text{Li/Li}^+$ , electrolytes that exhibit a high stability vs. oxidation are necessary. For that reason, ILs with their versatile properties were introduced and investigated. The state of the art electrolyte for this system is composed of a solution of lithium bis(trifluoromethanesulfonyl) imide ( $\text{LiTFSI}$ ) in *N*-butyl-*N*-methylpyrrolidinium bis(trifluoromethanesulfonyl) imide ( $\text{Pyr}_{14}\text{TFSI}$ ). In order to increase the specific capacity of this system, one main strategy is to focus on the intercalation of smaller anions than TFSI into the graphite structure. In this context, the major challenge is the synthesis of ILs or mixtures of ILs with organic electrolytes consisting of small anions to provide an electrochemically stable electrolyte. Interestingly, not only the size and shape of the intercalated anions plays a major role in view of onset potential for anion uptake as well as discharge capacity. Instead, also more complex coherences such as ion association, self-aggregation of ions as well as solvent co-intercalation have to be taken into consideration. In this work, we investigate the electrochemical intercalation of anions with different shapes and sizes from either IL or organic based electrolytes into a graphite-based cathode. Against this background, the influence of side chain modifications within the anion structure on the intercalation behavior was studied using different electrochemical analysis techniques. Therefore, in this contribution we will give new insights to the question if the anion size is the main issue to tailor the reversible capacity for anion intercalation.

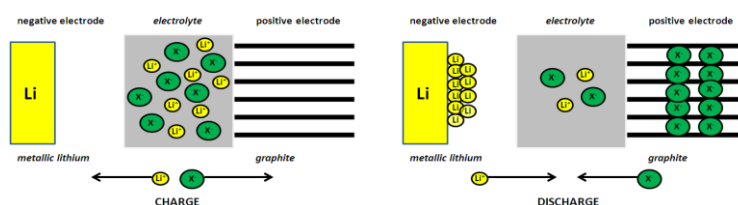


Figure 1: Schematic illustration of the operating principle of a "dual-ion cell".[2]

- [1] A. Lewandowski, A. Swiderska-Mocek, Journal of Power Sources, 194 (2009) 601-609.
- [2] T. Placke, P. Bieker, S.F. Lux, O. Fromm, H.W. Meyer, S. Passerini, M. Winter, Zeitschrift für Physikalische Chemie, 226 (2012) 391-407.
- [3] S. Rothermel, P. Meister, G. Schmuelling, O. Fromm, H.-W. Meyer, S. Nowak, M. Winter, T. Placke, Energy & Environmental Science, (2014).



# Novel Electrochemical-Thermal Modeling for Lithium-ion Battery Design based on a Fast Reduced P2D Electrochemical Model

Nan Lin, Georg Lenze, Urike Krewer

*Institute of Energy and Process Systems Engineering, TU Braunschweig*

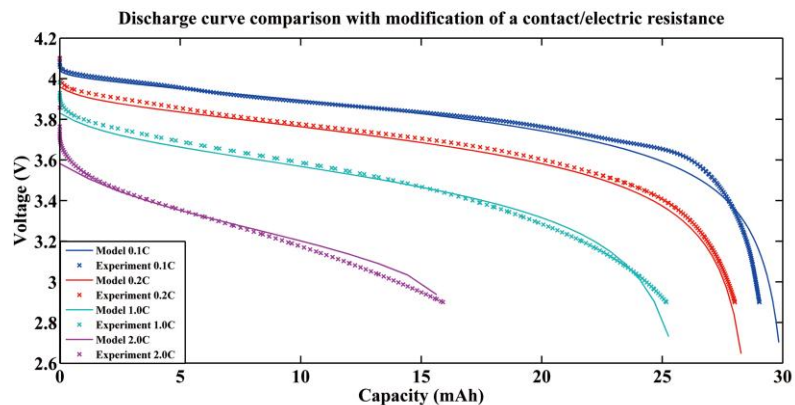
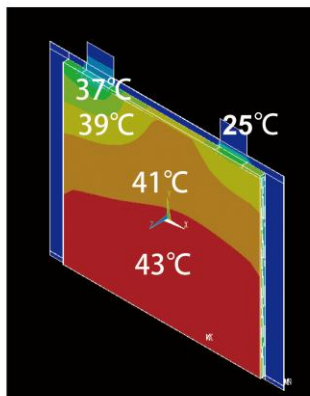
*Franz-Liszt-Strasse 35, 38106 Braunschweig, Germany*

[n.lin@tu-braunschweig.de](mailto:n.lin@tu-braunschweig.de) [g.lenze@tu-braunschweig.de](mailto:g.lenze@tu-braunschweig.de) [u.krewer@tu-braunschweig.de](mailto:u.krewer@tu-braunschweig.de)

Lithium ion batteries have been intensively investigated regarding novel electrode materials and the processes in the cell. They are getting more and more widely applied for powering electric vehicles and electronic devices. Practically, thermal management of lithium-ion batteries has become a major topic. Recently first coupling models which combine an electrochemical model with a 3-D thermal model have been developed to contribute to battery design and thermal management [1]. However, they cannot be applied into realistic case optimization with multiple parameters, because the calculation efficiency of these models cannot satisfy the present requirement in industries [2].

In this work, we combine a 3-D thermal model with a reduced P2D electrochemical model, with respect to an Al-doped LMO pouch cell. The cell was manufactured in the Battery LabFactory Braunschweig – enabling validation and to determine the full composition and geometric parameters of the cell. The classical P2D model was reduced to a 1-D model by using an analytical solution for solid diffusion and was coupled with a 3D-CFD thermal model. The model shows the temperature, potential and concentration distribution of the whole pouch cell under various discharge rates. Moreover, the thermal analysis with applied cooling strategy is shown to serve primary battery design. The simulation results assist to analyze the relationship between thermal behavior and electrochemical behavior in order for a further understanding and optimizing of internal parameters and geometry. The present model with its reduction is sufficiently fast and allows us to conduct real-time multi-parameter and multi-case optimization.

Figure 1 (left) shows the temperature distribution results for clamp cooling and 5C discharging of an Al-doping LMO pouch cell. Due to the clamp cooling path, obvious temperature differences from different cell positions are observed. As a consequence, a better thermal management is needed, since cell temperature affects the temperature-dependent electrochemical behavior of the cell. On the right hand side, we can see the validation of the electrochemical sub-model. The simulation results make a good agreement with the experimental data, as well as in a short calculation time. The introduced good coupling model can well assist with better understanding the temperature-dependent battery process and practical battery design for industrial satisfaction.



Reference:

- [1] T. Bandhauer, S. Garimella, T.F. Fuller, J. Electrochem. Soc. 162 (2014) A137–A148.
- [2] V. Ramadesigan, P.W.C. Northrop, S. De, S. Santhanagopalan, R.D. Braatz, V.R. Subramanian, J. Electrochem. Soc. 159 (2012) R31–R45.

# Functional Binders – SEI Formers, Dispersants and Local Electrolyte Components

Fabian Jeschull, Matthew. J. Lacey, Daniel Brandell  
Department of Chemistry – Ångström Laboratory, Uppsala University  
Box 538, 751 21 Uppsala, Sweden  
Fabian.Jeschull@kemi.uu.se

Electrode binders have long been considered as components which merely provide good adhesion to the current collector and maintain the physical integrity of the composite electrode in Li-ion batteries. In the pursuit of larger gravimetric energy densities, longer lifetime and lower cost – for instance for electrification of transport – new negative and positive electrode materials such as silicon and sulfur are explored. These novel cell chemistries pose new demands on the binder, challenging the conventional (and ecologically problematic) poly(vinylidene difluoride) (PVdF)[1,2,3].

For negative electrode materials, water-based alternatives, particularly carboxymethyl cellulose sodium salt (CMC-Na), poly(acrylic acid) (PAA) and its sodium salt (PAA-Na), form more favorable solid-electrolyte interface (SEI) layers and tolerate larger volume changes, thus extending the cycle life considerably in many Li-battery cell chemistries utilizing graphite or silicon. They have proven themselves beneficial beyond the conventional merits of an electrode binder and have therefore recently received significant interest in the battery research field.

In a previous investigation by our group [4], CMC-Na and PAA-Na are compared with PVdF-based polymers as binders in graphite electrodes in an aggressive, propylene carbonate-rich solvent. Appropriate surface coverage and low degrees of swelling were identified as key parameters for the stability of graphite in this environment, which could be provided by the alternative binder systems. We have very recently extended this concept to ether-based Li-S cells and silicon electrodes.

This work demonstrated that careful choice of the binder can enable reversible cycling of graphite anodes at high capacity and with high coulombic efficiency in purely ether-based electrolytes (*Fig. 1a*). This has strong implications for the Li-S battery system, where so far only a limited number of studies have addressed the negative electrode and where a vast excess of lithium is generally required in order to achieve acceptable cycle life [5].

For silicon electrodes, the effect of surface coverage on the cycling stability of silicon electrodes is strongly dependent on the amount and type of binder chosen, due to the large volume expansion during the alloying process and the resulting electrode disintegration. This highlights the implications of surface interactions between the binder and other composite electrode components (*Fig. 1b*) and sheds new light on the relation between electrode compositions and cell failure.

## References:

- [1] M. Lacey, F. Jeschull, K. Edström, D. Brandell, *J. Phys. Chem. C*, **118** (2014) 25890.
- [2] M. Lacey, F. Jeschull, K. Edström, and D. Brandell, *J. Power Sources* 264, 8 (2014)
- [3] Mazouzi et al. *Power Sources* **280**, 533 (2015).
- [4] F. Jeschull, M. Lacey, D. Brandell, *Electrochim. Acta* (2015), doi:10.1016/j.electacta.2015.03.072
- [5] Brückner et al., *Adv. Func. Mater.* **24**, 1284 (2014).

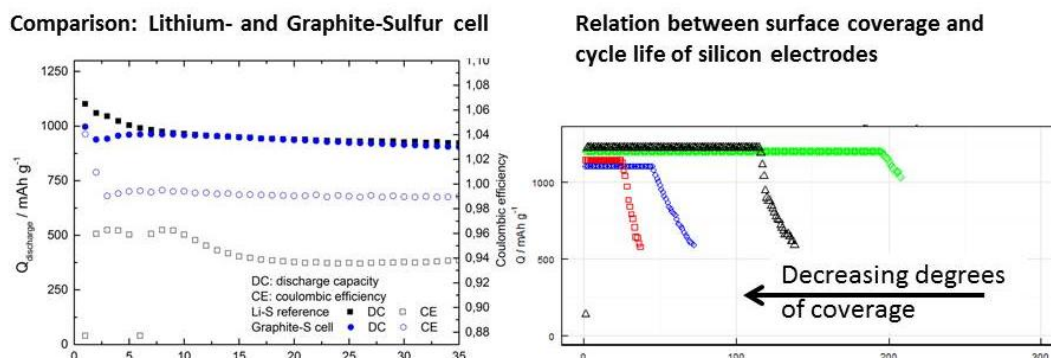


Figure 1: (a) capacity profile and coulombic efficiencies of a lithium- and graphite-sulfur cell respectively, (b) cycle life of various silicon electrodes as a function of binder coverage

# Ionic Liquids and Polymer electrolytes for Li-metal batteries

Elie Paillard<sup>1</sup>, Lorenzo Grande<sup>2</sup>, Marija Kirchhöfer<sup>3</sup>, Irene Osada<sup>2</sup>, S. Koch<sup>2</sup>, S. Passerini<sup>2</sup>

<sup>1</sup>Helmholtz Institute Münster (Forschungszentrum Jülich)

Corrensstrasse 46 (MEET) 48149 Münster, Germany

<sup>2</sup>Helmholtz Institute Ulm (Karlsruhe Institute of Technology)

Helmholtzstr. 11, 89081 Ulm, Germany

<sup>3</sup>Institute of Physical Chemistry, University of Münster

Corrensstr. 28-30, 48149 Münster, Germany

e.paillard@fz-juelich.de

If new ‘beyond Li-ion’ technologies are being proposed or developed using alternative cathodes (Li-O<sub>2</sub>, Li-S) which, by themselves, are challenging, a common point with all these technologies is the use of Li metal, a typical ‘pre Li-ion’ anode. Although it offers the highest theoretical capacity among all lithiated anodes, its implementation in commercial Li-metal batteries has been successful using polymer electrolytes only. A major drawback of these electrolytes being their room temperature performance and, in general, below 60-80°C, Shin *et al.* [1] proposed the use of ionic liquids (ILs) as non-volatile and non-flammable plasticizers, allowing the decrease of Li-metal polymer battery operation down to 40°C [2]. On the other hand, several reports pointed out the excellent lithium plating (and cycling) behavior, using liquid, ILs-based electrolytes [3, 4]. ILs constitute a wide family of chemicals with properties that differ significantly. Their chemistry influence their bulk properties, but also the interfacial properties with Li metal (formation of the so-called Solid Electrolyte Interphase (SEI) [5]). Finally, in case liquid electrolytes are used, hard contact points can result from the separator and alter the SEI evolution either favorably or detrimentally, depending on the ionic liquid. Beside low and room temperature operation, dendrite formation is a major concern when dealing with Li metal electrodes. If, at high charging currents, dendrites growth is rather well understood as resulting from ionic species transport [6,7], their formation, especially at lower current densities, is more debated as the SEI, cell assembly and any defect, all participate in triggering dendrites growth.

An overview of Li-metal electrode use in both solid and liquid IL-based electrolytes will be given with emphasis on the conditions allowing homogeneous Li metal deposition and long term cycling.

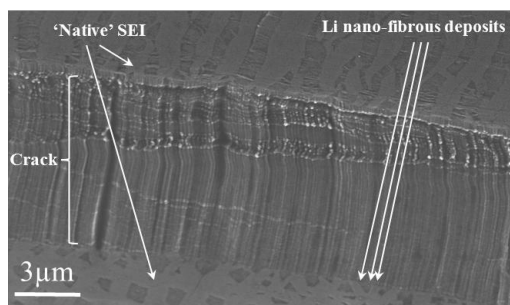


**Figure 1.** SEM image of a Li electrode, showing a crack and revealing the underlying Li structure after the plating of 10 mAh cm<sup>-2</sup> of Li (i.e. 50 μm) at 0.1 mAh cm<sup>-2</sup> in 0.1 LiTFSI – 0.9 PYR<sub>14</sub>TFSI

## References:

1. J. H. Shin, W. H. Henderson, S. Passerini, *Electrochem. Commun.* 5 (2003) 1016–1020
2. M. Wetjen, G.-T. Kim, M. Joost, G. B. Appetecchi, M. Winter, S. Passerini, *J. Power Sources* 246 (2014) 846–857
3. P. C. Howlett, D. R. MacFarlane, A. F. Hollenkamp, *Electrochem. S.-S. Lett.*, 7 (5) (2004) A97–A101
4. E. Paillard, Q. Zhou, W. A. Henderson, G. B. Appetecchi, M. Montanino, and S. Passerini, *J. Electrochem. Soc.*, 156 (11) (2009) A891–A895
5. E. Peled, *J. Electrochem. Soc.* 126 (1979) 2047–2051
6. J.-N. Chazalviel, *Phys. Rev. A* 42 (1990) 7355–7367
7. C. Monroe, J. Newman, *J. Electrochem. Soc.* 150 (2003) A1377–A1384

# Novel V-containing cathode materials for Li-ion Batteries

**M.V. Reddy<sup>1,2\*</sup>**, A. Shahul<sup>3</sup>, S. Adams<sup>1</sup>, J.J. Vittal<sup>3</sup>, B.V.R. Chowdari<sup>4</sup>

<sup>1</sup>Department of Materials Science & Engg, <sup>2</sup> Department of Physics, <sup>3</sup> Department of Physics, National University of Singapore, Singapore 117542

\*Presenting author e-mail adds. : msemvvr@nus.edu.sg; phymvvr@nus.edu.sg

<http://www.researcherid.com/rid/B-3524-2010>; Ph.:65162607; Fax.: 65-6777-6126

## Abstract

Recent commercial lithium ion batteries (LIBs) consists of layer-type lithium cobalt oxide, spinel  $\text{LiMn}_2\text{O}_4$  or  $\text{LiFePO}_4$  as the cathode and graphite as the anode material, and electrolyte consists of a non-aqueous Li- ion conducting solution or immobilized gel-polymer as an electrolyte. LIBs with an operating voltage of 3.6 V are extensively used in the present-day electronic mobile devices. However, for high-power applications like back-up power supplies and electric/hybrid electric vehicles, the LIBs need to satisfy several additional criteria, such as cathode must show high charge potential and electrode material must show mixed ion conduction. Finally cost-reduction, safety-in-operation at high current charge/discharge rates and low-temperature cycling are needed for practical applications.

In my talk, I will discuss our group recent electrochemical properties of selected V-based cathodes,  $\text{LiVPO}_4\text{F}$ ,  $\alpha_1\text{-LiVOPO}_4$  and novel,  $\text{MVO}(\text{HPO}_4)(\text{C}_2\text{O}_4)_{0.5}$ ,  $\text{M}_2[(\text{VO})_2(\text{HPO}_3)_2(\text{C}_2\text{O}_4)]$  ( $\text{M} = \text{Li, K, Na}$ ). They were prepared by carbothermal reduction method and solvo-hydrothermal method followed heat treatment. Materials were characterized by Rietveld refinement X-ray diffraction, X-ray photo electron spectroscopy, SEM, density and BET surface area methods. Electro analytical studies were carried out using cyclic voltammetry, galvanostatic cycling and electrochemical impedance spectroscopy techniques. The charge cycling profiles shows a flat potential of 4.2V vs. Li, which higher than  $\text{LiFePO}_4$  cathodes. Comparative cycling performance and advantages of matrix elements,  $\text{HPO}_4$  and  $\text{HPO}_3$  groups on electrochemical cycling are discussed in detail.

Key words: Cathodes; Lithium ion batteries; characterization techniques.

## References

1. M.V. Reddy, G.V. Subba Rao, B.V. R. Chowdari "Metal oxides and oxysalts as anode materials for lithium ion batteries" Chemical Reviews 113(2013)5364-5457
2. M. Nagarathinam, K. Saravanan, E. J. Han Phua, M. V. Reddy, B. V. R. Chowdari, J. J. Vittal Hybrid anion (phosphate/oxalate) open framework 4 V cathode materials Angewandte Chemie International 51(24)(2012)5866-5870
3. M. Shahul, M. Nagarathinam, M. V. Reddy, B. V. R. Chowdari, J. J. Vittal "Studies on tetragonal  $\alpha_1\text{-LiVOPO}_4$ " Journal of Materials Chemistry 22(2012)7206-7213
4. M. Shahul, M. Nagarathinam, M. V. Reddy, Schreyer, Martin, B. V. R. Chowdari, J. J. Vittal "LiVO(HPO<sub>4</sub>)(C<sub>2</sub>O<sub>4</sub>)<sub>0.5</sub>: A New Generation Cathode Material for Lithium Ion Batteries" Journal of Materials Chemistry A 1(2013) 5721-5726.
5. A. Shahul Hameed, M. V. Reddy, B. V. R. Chowdari and J. J. Vittal "Carbon coated  $\text{Li}_3\text{V}_2(\text{PO}_4)_3$  from the single-source precursor,  $\text{Li}_2(\text{VO})_2(\text{HPO}_4)_2(\text{C}_2\text{O}_4)\cdot 6\text{H}_2\text{O}$  as cathode and anode materials for Lithium ion batteries" Electrochimica Acta 128(2014)184-191
6. M. V. Reddy, G.V. Subba Rao and B. V. R. Chowdari (Studies on  $\text{LiVPO}_4\text{F}$ ) Journal of Power Sources 195 (2010)5768-5774.

# Unexpected Cycle Aging of a Commercial 18650 Cell

Po-Han Lee, She-huang Wu

Department of Materials Engineering, Tatung University  
No.40, Sec. 3, Zhongshan N. Rd., Taipei City 104, Taiwan (R.O.C)  
ud7878@hotmail.com

The aging mechanism of a lithium ion battery comprised of a  $\text{LiNi}_{1/3}\text{Mn}_{1/3}\text{Co}_{1/3}\text{O}_2/\text{LiMn}_2\text{O}_4$  composite positive electrode and graphite anode at 2C rate had been studied with an incremental capacity technique [1, 2]. The results indicate that capacity fade is mainly caused by loss of inventory (LLI) during the first stage then followed by loss of active material (LAM) in the second stage. However, the degradation mechanisms and their correlation with cell performance fade are not only dependent on the cell chemistry but also on the cell design and manufacture technique.

Commercial 18650 lithium ion cells containing a blend of  $\text{LiNi}_{0.5}\text{Mn}_{0.3}\text{Co}_{0.2}$  (NMC) and  $\text{LiMn}_2\text{O}_4$  (LMO) materials as cathode and graphite as anode with a nominal capacity of 2.15 Ah were used in this study. The capacity retention of the commercial cells was performed by charging at 0.5C followed by a constant voltage step until current was lower than 0.04C and discharging at 0.2, 0.5, 1.0, 2.0C rates, respectively. The results, shown in Fig. 1, manifests that a longer cycle life is achieved at the higher C-rate (2C), which is contrary to the generally accepted notion that high C-rate will accelerate cell aging. To reveal the reasons, cells were cycled at 0.04C for 1 cycle after every 100 cycles and the plots of the incremental capacity analysis of the 0.04C cycles of the cells discharged with 1 and 2C rates are shown in Fig. 1(b) and (c), respectively. The 3.5V peak which can be attributed to intercalation of  $\text{Li}^+$  ions into graphite to form  $\text{LiC}_x$  shifts to higher voltage and its intensity decreases with number of cycle. It suggests that the capacity loss is contributed by LLI and LAM of anode, whereas the significant decreasing at 3.6V peak indicates the degradation of NMC and LLI. The peaks at 3.95 and 4.05V are the characteristics of  $\text{LiMn}_2\text{O}_4$ . It can be observed that the peak at 3.95V decreases significantly while slight change in intensity of the 4.05V peak upon cycling. That can be caused by the loss of anode material and the reaction between  $\text{LiC}_{12}$  and  $\text{LiC}_6$  come up early. It also induces the appearance of the peak at voltage between 3.8 and 3.88V. The cell cycled with 1C discharging rate shows a prompt loss of anode material that can be manifested from the sudden decreasing of the 3.5V peak between 300<sup>th</sup> and 400<sup>th</sup> cycles (Fig. 1(b)). However, the lowering of the 3.5V peak is less significant for the cell cycled with discharging rate of 2.0C. That suggests the unexpected results can be attributed to the differences in rate of anode material loss upon cycling with various discharging rates. The reasons for the different rates of anode material loss may be caused by the different extent of  $\text{Li}^+$  ion extracted from intercalated graphite when cells were discharged at various rates. The suggestion is hoped to be supported by the post-mortem analysis of the cells cycled at various discharging rates.

## Reference

- [1] M. Dubarry, C. Truchot, M. Cugnet, B.Y. Liaw, K. Gering, S. Sazhin, D. Jamison, C. Michelbacher, Journal of Power Sources, 196 (2011) 10328-10335.
- [2] M. Dubarry, C. Truchot, B.Y. Liaw, K. Gering, S. Sazhin, D. Jamison, C. Michelbacher, Journal of Power Sources, 196 (2011) 10336-10343.

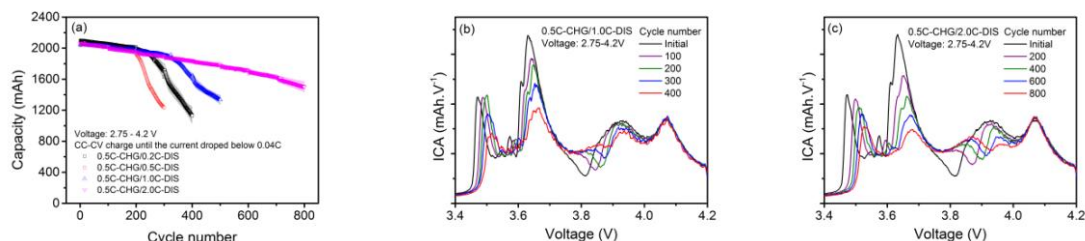


Fig. 1. (a) Results of capacity retention of the cells charged at 0.5C with CC-CV mode and discharged at various rates (0.2, 0.5, 1.0, 2.0C) and ICA plots of the charge curves of 0.04C cycle for every 100 cycles for cells cycled with discharging rate of (b) 1.0 and (c) 2.0C.



# Towards a rechargeable battery technology based on calcium

A. Ponrouch,<sup>1</sup> C. Frontera,<sup>1</sup> F. Bardé,<sup>2</sup> M.R. Palacín<sup>1</sup>

1. Institut de Ciència de Materials de Barcelona (ICMAB-CSIC)

Campus UAB, E-08193 Bellaterra, Catalonia (Spain).

2. Toyota Motor Europe, Research & Development 3, Advanced Technology 1, Technical Centre,  
Hoge Wei 33 B, B-1930 Zaventem, (Belgium).

aponrouch@icmab.es

The development of a rechargeable battery technology using light electropositive metal anodes would bring in a breakthrough in energy density.<sup>1</sup> For  $M^{n+}$  charge carriers, the number of ions that must react to achieve a certain electrochemical capacity is diminished by two ( $n=2$ ) or three ( $n=3$ ) when compared to  $Li^+$ .<sup>2</sup> Proof-of-concept has been achieved for highly polarizing  $Mg^{2+}$  with complex electrolyte compositions to enable electrodeposition (plating) and covalent host cathodes to diminish coulombic interactions.<sup>3,4,5</sup> An analogous technology based on  $Ca^{2+}$  would hold promise for faster reaction kinetics (and thus better power performance) due to its lower polarizing character, and be attractive on cost and environmental grounds, but the electrodeposition of calcium was thought to be impossible to date<sup>6</sup> and research mostly restricted to non rechargeable systems.<sup>7,8,9,10</sup> Here we demonstrate the feasibility of calcium plating using conventional organic electrolytes, such as those used for the Li-ion technology. The parameter affecting the reversibility of the plating/stripping process upon cycling will be discussed. These results constitute the first step towards the development of a new rechargeable battery technology using calcium anodes.<sup>11</sup>

---

<sup>1</sup> Muldoon, J., *Chem. Rev.* **114**, 11683-11720 (2014)

<sup>2</sup> Amatucci, G.G. *et al.*, *J. Electrochem. Soc.* **148**, A940-A950 (2001)

<sup>3</sup> Aurbach, D. *et al.*, *Nature*, **407**, 724-727 (2000)

<sup>4</sup> Yoo, H.D. *et al.*, *Energy Environ. Sci.* **6**, 2265-2279 (2013)

<sup>5</sup> Muldoon, J. *et al.*, *Energy Environ. Sci.* **5**, 5491-5950 (2012)

<sup>6</sup> Aurbach, D., Skaletsky, R., Gofer, Y., *J. Electrochem. Soc.* **138**, 3536-3545 (1991)

<sup>7</sup> Sammells, A.F., Schumacher, B., *J. Electrochem. Soc.* **133**, 235-236 (1986)

<sup>8</sup> Staniewicz, R.J., *J. Electrochem. Soc.* **127**, 782-789 (1980)

<sup>9</sup> Hayashi, M., Arai, H., Ohtsuka, H., Sakurai, Y., *J. Power Sources* **119-121**, 617-620 (2003)

<sup>10</sup> See, K.A. *et al.*, *Adv. Energy Mater.* **3**, 1056-1061 (2013)

<sup>11</sup> Ponrouch A., Frontera C., Bardé F., Palacín M.R., *Submitted for publication.*

## **Rate Determining Factors at Graphite Electrodes - from charge transfer resistances to ion transport resistances -**

Shohei Maruyama<sup>1,2</sup>, Kohei Miyazaki<sup>1</sup>, Tomokazu Fukutsuka<sup>1</sup>, Takeshi Abe<sup>1,2</sup>

<sup>1</sup>Graduate School of Engineering, Kyoto University, Nishikyo-ku, Kyoto 615-8510

<sup>2</sup>CREST, Japan Science and Technology Agency  
*abe@elech.kuic.kyoto-u.ac.jp*

Large-size lithium-ion batteries (LIBs) have been developed for the use of battery electric vehicles. For BEVs, the long cruising distance and short charging time are imperative. The former is determined by the energy density (the product of battery voltage and battery capacity) and the latter is determined by the power density (the product of voltage and current). Present LIBs for BEV-use possess large power densities by the sacrifice of energy densities. On the other hand, recent LIBs widely used for portable devices have large energy densities with small power densities. In the case of LIBs for BEV-use, shorter charging times are necessary since the time to put petrol in present gasoline car is within several minutes. In order to shorten the charging times, reduction of internal resistances in the LIBs for BEV-use must be required.

The internal resistances in LIBs are composed of various processes; (1) electron transfer between a current collector and active material, (2) electron transport in a composite electrode, (3) ion (lithium ion and counter anion) transport in a composite electrode, (4) lithium-ion transfer at interface between active material and electrolyte, (5) lithium-ion diffusion in active material, (6) ion (lithium ion and counter anion) transport in bulk electrolyte through separator. Among these six resistances, we have focused on (3) and (4).

Here we report the charge transfer and ion transport resistances at graphite electrodes. For the former issue, we will show the factors which determine the charge transfer resistances, and for the latter issue, we will show the ion transports are influenced by the pore sizes, in particular, meso- to macro-pores.

This research was supported by JST, CREST.

# Fundamental Analysis of Lithium-ion Battery Performance and Degradation in Context of Particle Size Distribution

Fridolin Röder, Ulrike Krewer

*Institute of Energy and Process Systems Engineering, TU Braunschweig  
Franz-Liszt-Strasse 35, 38106 Braunschweig, Germany  
[f.roeder@tu-braunschweig.de](mailto:f.roeder@tu-braunschweig.de), [u.krewer@tu-braunschweig.de](mailto:u.krewer@tu-braunschweig.de)*

Lithium-Ion battery electrodes consist of active material particles with varying size. This heterogeneity is quantified using particle size distribution (PSD). Even though it is reported that the distribution of the electrode material is precisely adjustable by modern production processes [1], the effect of the actual PSD on battery performance and degradation is often neglected in theoretical model based analysis.

In this work we present a fundamental model-based analysis of the effect of particle size distribution (PSD) on Lithium-Ion battery performance and degradation. We use a mathematical electrode model with distributed particle size to analyze the influence of shape and scale of the distribution. In figure 1 (left), distributions with different shape but almost equal mean radius are shown. Performance of electrodes with the respective distributions are analyzed using the electrochemical model. Figure 1 (right) shows the electrode potential vs. capacity and illustrates the significant impact of a distribution's shape. It can be seen that the electrode capacity significantly decreases with diversification of the distribution. Moreover, we identify different dynamical charging behavior of the particles in such a system. The results show how the interaction between the large and small sized particles in this composition can be explained and why this leads to uneven surface overpotentials and reaction rates. The observations open up novel approaches to investigate and understand also degradation of such particle based electrodes. We therefore investigate the degradation caused by the change of the PSD during battery usage, which is caused by particle cracking or agglomeration. This change of the distribution is modeled based on a distribution evolution equation [2].

The presented work indicates that the PSD and its change considerably impacts the performance and degradation of Lithium-Ion batteries. We suggest that the distributions and its evolution should be of particular interest for future studies of degradation of particle based electrodes.

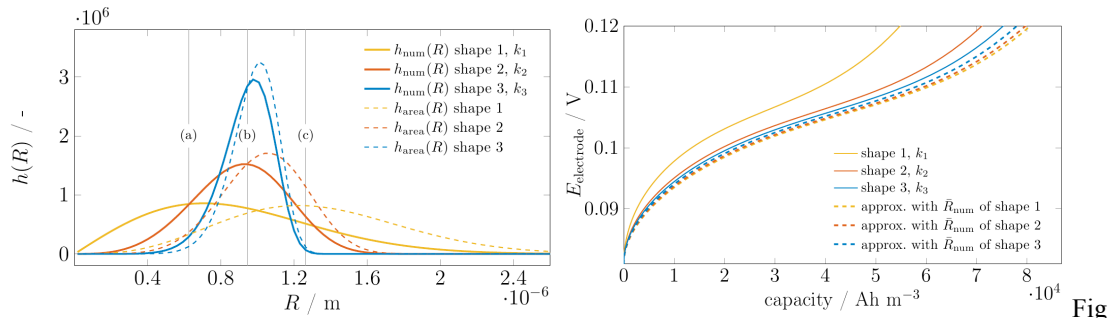


Fig 1: PSD shape variation (left) and simulation of electrode performance (right)

## References:

- [1] G. T.-K. Fey, Y. G. Chen, H.-M. Kao, Electrochemical properties of prepared via ballmilling, Journal of Power Sources 189 (2009) 169–178.
- [2] D. Ramkrishna, Population Balances: Theory and applications to particulate systems in engineering, Academic Press, 2000.

# Synthesis and electrochemistry performance of Na[FeTi]O<sub>4</sub> as anode material for sodium-ion batteries

Jun Wang, Xin He, Haidong Liu, Tim Risthaus, Jie Li

MEET Battery Research Center/Institute of Physical Chemistry, University of Muenster  
Corrensstrasse 46, 48149 Muenster, Germany  
[jie.li@uni-muenster.de](mailto:jie.li@uni-muenster.de)

In the past two decades, lithium-ion batteries (LIBs) have been successfully used in mobile electronic devices. However, material costs continuously increase as lithium reserves are limited both in amount and geographical location. The interest in sodium-ion batteries (NIBs) has been on the rise in recent ten years and NIBs currently constitute the most attractive alternative chemistry for rechargeable batteries. NIBs are also eligible for large-scale production, because sodium is much cheaper and more abundant in the earth's crust, and the potential of sodium metal is only 0.3 V higher than that of lithium metal.<sup>1, 2</sup> Therefore, supplementary to the progress in the field of advanced LIBs, it is also imperative to develop NIBs in order to provide sufficiently safe and low-cost energy storage devices.

Recent advances in the development of NIBs are mostly on positive electrode materials. Numerous cathode compounds capable of efficient Na<sup>+</sup>-ions (de)insertion have been reported so far.<sup>3</sup> However, much less studies have focused on the anode materials for NIBs.<sup>4</sup> Although hard carbonaceous materials could show the ability to reversibly (de)insert Na<sup>+</sup> ions, these materials display worse capacity retentions than their lithium counterparts.<sup>5</sup> Titanium (Ti)-based intercalation compounds have been proved to be another important class of anode materials for NIBs in terms of their safety properties and low potentials.

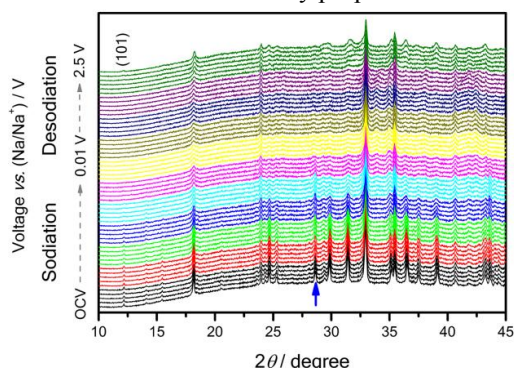


**Figure 1.** *In situ* XRD analysis of the (de-)sodiation mechanism of Na[FeTi]O<sub>4</sub> materials. XRD patterns obtained upon discharge and charge processes of the Na[FeTi]O<sub>4</sub> electrode.

We report a novel class of Fe and Ti-based Na[FeTi]O<sub>4</sub> anode materials for NIBs. The material exhibits an orthorhombic structure, which shows a reversible capacity of 181 mAh g<sup>-1</sup> under a current density of 17.7 mA g<sup>-1</sup> (0.1 C) and good cycling performance (more than 95% capacity retention after 500 cycles at 2 C). The novel class of orthorhombic Na[FeTi]O<sub>4</sub> could be promising anode materials for NIBs with low cost and long cycle life. *In situ* X-ray diffraction (XRD) results indicate that Na<sup>+</sup> ions behave in topotactic insertion and extraction manners inside this material (Figure 1). Meanwhile, gas evolutions during the initial redox process are analyzed by an *operando* mass spectrometry technique. The result suggests that the Na[FeTi]O<sub>4</sub> material exhibits an enhanced safety (Figure 2).

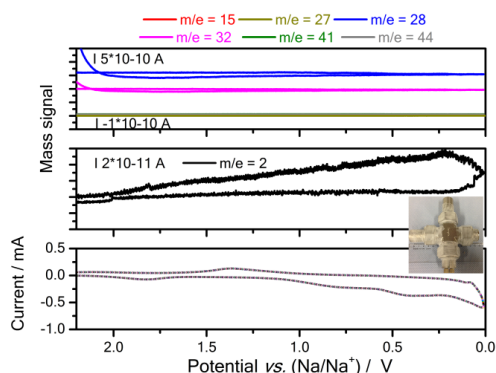


**Figure 2.** Cyclic voltammetric plot of the Na/Na[FeTi]O<sub>4</sub> cell for *operando* MS analysis (0.01-2.5 V; 0.1 mV s<sup>-1</sup>) and the evolving gas species with molecular weights of 2 (black), 15 (red), 27 (dark yellow), 28 (blue), 41 (magenta), 32 (olive) and 44 g mol<sup>-1</sup> (gray) formed upon the initial redox process. Inset: Optical image of the *in house* developed cross-shaped cell.

## References

- [1] Wagner R., Preschitschek N., Passerini S., Leker J., Winter M., *J. Appl. Electrochem.* 2013, 43, 481.
- [2] Yabuuchi N., Kubota K., Dahbi M., Komaba S., *Chem. Rev.* 2014, 114, 11636.
- [3] Kim H., Hong J., Park K. Y., Kim H., Kim S. W., Kang K., *Chem. Rev.* 2014, 114, 11788.
- [4] Senguttuvan P., Rousse G., Seznec V., Tarascon J. M., Palacin M. R., *Chem. Mater.* 2011, 23, 4109.
- [5] Oh S. M., Myung S. T., Yoon C. S., Lu J., Hassoun J., Scrosati B., Amine K., Sun Y. K., *Nano Lett.* 2014, 14,

# The impact of CO<sub>2</sub> evolved from the reduction of VC and FEC during the formation cycle of lithium-ion batteries

K. Uta Schwenke<sup>1</sup>, Sophie Solchenbach<sup>1</sup>, Benjamin Strehle<sup>1</sup>, Michael Metzger<sup>1</sup>, Stefano Meini<sup>2</sup>, Julien Demeaux<sup>3</sup>, Brett L. Lucht<sup>3</sup>, Hubert A. Gasteiger<sup>1</sup>

<sup>1</sup> Chair of Technical Electrochemistry, Technische Universität München, 85748 Garching, Germany

<sup>2</sup> BASF SE, GCN/EE – M311, 67056 Ludwigshafen, Germany

<sup>3</sup> Department of Chemistry, University of Rhode Island, Kingston, RI 02881, USA

uta.schwenke@tum.de

The solid electrolyte interphase (SEI), which is formed on the anode of a lithium-ion battery during the initial cycle(s), provides lithium ion conduction and electrical passivation, and thus allows stable lithium ion intercalation without further electrolyte reduction. To tailor this interphase for more efficient protection, additives such as vinylene carbonate (VC) or fluoroethylene carbonate (FEC) are added to the electrolyte which is usually composed of LiPF<sub>6</sub> in cyclic (e.g., EC) and linear alkyl carbonates (e.g., EMC).

In this study we use electrolytes of LiPF<sub>6</sub> in pure VC and FEC in order to understand their influence on the SEI, which is characterized with XPS and FTIR. While VC yields Poly-VC at coverages which strongly increase with the VC concentration, FEC yields next to large quantities of LiF also some polycarbonate, which, however, does not scale with the FEC concentration. Furthermore, we use on-line electrochemical mass spectrometry (OEMS), which was set-up for the analysis of Li-O<sub>2</sub> cells [1] and further modified to study the gassing behavior of Li-ion cells [2,3]. Figure 1a displays that both VC and FEC evolve mainly CO<sub>2</sub> at potentials of  $\approx 2$  and  $\approx 1.5$  V<sub>Li</sub>, respectively, i.e., substantially more positive than the C<sub>2</sub>H<sub>4</sub> gas evolution at  $\approx 0.9$  V<sub>Li</sub> from EC reduction [4]. Interestingly, CO<sub>2</sub> was one of the earliest SEI-additives studied in Li-ion batteries [5,6]. As shown in Figure 1b, continuous PC (propylene carbonate) intercalation and reduction is avoided by addition of 1 atm CO<sub>2</sub>, and stable cycling comparable to cells with 2% FEC is obtained. Thus, this study will focus on a comparison of the efficacy and the mechanistic working principles of currently employed additives with that of the direct addition of CO<sub>2</sub>.

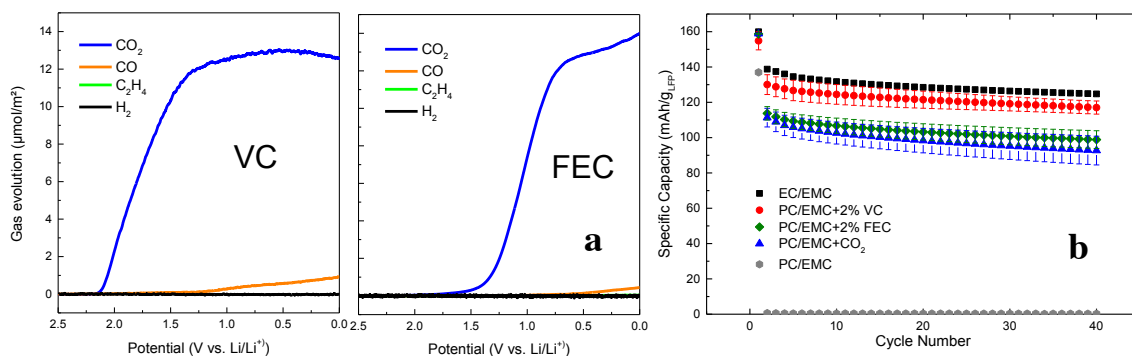


**Figure 1:** (a) Gas evolution rate per carbon electrode surface area as a function of reduction potential of a pure VC and FEC electrolyte (1M LiPF<sub>6</sub>). (b) Galvanostatic cycling performance at 25°C of LFP/graphite electrodes with 1M LiPF<sub>6</sub> in EC/EMC (3:7) or PC/EMC (3:7) without and with 2% of VC, 2% FEC, or under 1 atm CO<sub>2</sub>. The cells were cycled between 3.8 V and 2.7 V at rates of C/20 (1<sup>st</sup> cycle) and C/10 (2<sup>nd</sup> and 3<sup>rd</sup> cycle), followed by 37 cycles at C/5.

## References:

- [1] Tsiouvaras, Meini, Buchberger, Gasteiger, *J. Electrochem. Soc.*, **2013**, 160, A471
- [2] Metzger, Marino, Sicklinger, Haering, Gasteiger, *J. Electrochem. Soc.*, **2015**, 162, A1123
- [3] Zhang, Metzger, Solchenbach, Payne, Meini, Gasteiger, Garsuch, Lucht, *J. Phys. Chem. C*, submitted
- [4] Novak, Joho, Imhof, Panitz, Haas, *J. Power Sources*, **1999**, 81-82, 212
- [5] Besenhard, Wagner, Winter, Jannakoudakis, Jannakoudakis, Theodoridou, *J. Power Sources*, **1993**, 44, 413
- [6] Aurbach, Ein-Eli, Chusid, Carmeli, Babai, Yamin, *J. Electrochem. Soc.*, **1994**, 141, 603

**Acknowledgments:** Support of BASF SE in the framework of its scientific network on electrochemistry and batteries is acknowledged by TUM and URI.

# Homogeneous Catalysts for Li-Oxygen Cells

James T. Frith, Luyi Yang, Nuria Garcia-Araez, John R. Owen  
 University of Southampton  
 B29, Highfield campus, SO17 1BJ, UK  
 J.Frith@soton.ac.uk

Lithium-oxygen cells have a theoretical specific energy of around 5 times that of Li-ion cells, this makes them ideally suited for powering electric vehicles. However early lithium-oxygen cells, as proposed by Abraham and Jiang [1], have faced a series of problems. Primarily these problems were due to the instability of commonly used carbonate electrolytes with superoxide [2-3], a product of oxygen reduction. The introduction of electrolytes that are stable to superoxide attack [4-5] has led to great improvements in cell performance. However the insoluble and insulating nature of the primary discharge product, lithium peroxide, limits cell capacity and adversely affects the cycle life of cells [6].

This work examines the relationship between homogenous catalysts and the resulting enhancements seen in cell performance. In particular the increase in the practical cell capacity seen when employing ethyl viologen as a homogeneous catalyst for the discharge reaction was investigated [7-8]. The enhancement seen in the cell capacity is a direct result of the mediator action of the ethyl viologen which promotes the 2-electron reduction of oxygen while at the same time moving the site of oxygen reduction away from the electrode surface (Fig 1). Improvements to the round trip efficiency were also investigated using homogeneous catalysts for the charge reaction, in a similar manner to that demonstrated by Bruce *et al.* [9].

As well as looking into the enhancement of cell performance seen when using homogeneous catalysts the role of the electrolyte was also investigated. The electrolyte was found to play an important role in determining the action of homogeneous catalysts.

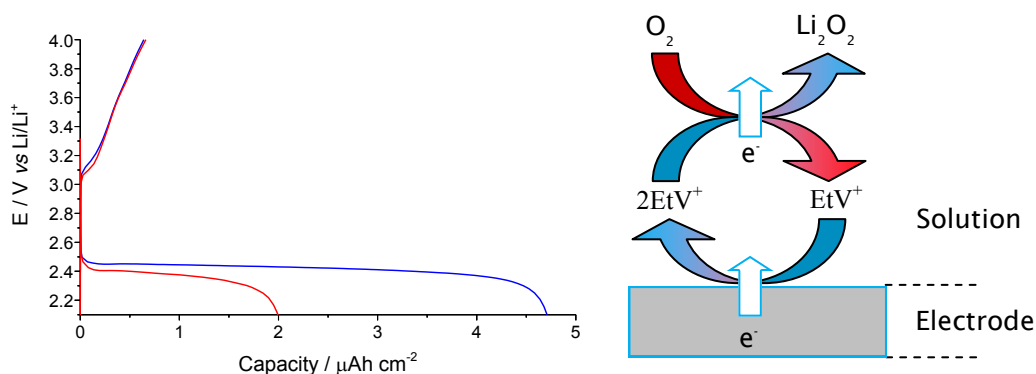


**Figure 1.** Galvanostatic discharge of a glassy carbon electrode in oxygen saturated 100 mM LiTFSI, Pyr<sub>14</sub>TFSI with (—) 0 mM EtV(OTf)<sub>2</sub>, (—) 0.5 mM EtV(OTf)<sub>2</sub>. Current: 20  $\mu A \cdot cm^{-2}$ . Diagram - Mode of action of ethyl viologen when catalysing the 2-electron reduction of oxygen in a Li-O<sub>2</sub> cell.

- [1] K. M. Abraham and Z. Jiang, *J. Electrochem. Soc.*, 143 (1996) 1.
- [2] F. Mizuno, S. Nakanishi, Y. Kotani, S. Yokoishi, and H. Iba, *Electrochemistry*, 78 (2010) 5.
- [3] S. a Freunberger, Y. Chen, Z. Peng, J. M. Griffin, L. J. Hardwick, F. Bardé, P. Novák, and P. G. Bruce, *J. Am. Chem. Soc.*, 133 (2011) 20.
- [4] K. U. Schwenke, S. Meini, X. Wu, and H. A. Gasteiger, *Phys. Chem. Chem. Phys.* ( 2013).
- [5] J. T. Frith, N. Garcia-Araez, A. E. Russell, and J. R. Owen, *Electrochem. Commun.* (2014).
- [6] V. Viswanathan, K. S. Thygesen, J. S. Hummelshøj, J. K. Nørskov, G. Girishkumar, B. D. McCloskey, and a C. Luntz, *J. Chem. Phys.*, 135 (2011) 21.
- [7] M. J. Lacey, J. T. Frith, and J. R. Owen, *Electrochem. Commun.*, 26 (2013).
- [8] L. Yang, J. T. Frith, N. Garcia-Araez, and J. R. Owen, *Chem. Commun.*, (2014).
- [9] Y. Chen, S. A. Freunberger, Z. Peng, O. Fontaine, and P. G. Bruce, *Nat. Chem.*, 5 (2013) 6.

# Understanding Na-O<sub>2</sub> Electrochemistry in Non-aqueous Na-O<sub>2</sub> Batteries

Nadège Bonnet-Mercier, Raymond A. Wong and Hye Ryung Byon  
Byon Initiative Research Unit (IRU) / RIKEN  
2-1 Hirosawa, Wakoshi, Saitama, 351-0198 Japan  
nadege.b@riken.jp and hrbyon@riken.jp

Metal-oxygen (or metal-air) batteries have been considered as one of promising energy storages to fulfill the increasing demand on high energy density system for applications from portable electronic devices to electric vehicles. The non-aqueous sodium-oxygen (Na-O<sub>2</sub>) battery is particularly attractive because of its expected low cost since Na is abundant element on earth and its reasonably high specific energy (~1.1 kWh/kg, which is almost twice of lithium-ion batteries). In addition, the first demonstration of Na-O<sub>2</sub> battery revealed moderate overpotential for both discharge and charge [1] unlike the Li-O<sub>2</sub> battery suffering from huge overpotential for charge [2]. However, there is little knowledge for Na-O<sub>2</sub> electrochemistry, which is associated with low Coulombic efficiency and poor cycle life in the Na-O<sub>2</sub> battery [1, 3-4].

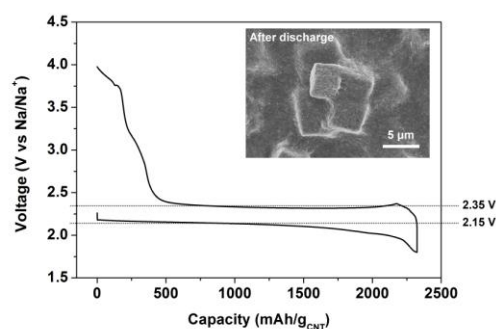
We studied Na-O<sub>2</sub> electrochemistry using carbon nanotubes (CNT) as positive electrode and diglyme/Na trifluoromethanesulfonate as electrolyte. The Na-O<sub>2</sub> cell delivers a capacity of around 2500 mAh/g<sub>CNT</sub> as shown in Figure 1. During discharge, cubic products with micrometer size are formed on the CNT (Figure 1 inset), which are completely decomposed during charge. The XRD pattern in Figure 2 demonstrates that the primary discharge product is sodium superoxide crystal (NaO<sub>2</sub>). The NaO<sub>2</sub> can be formed at a thermodynamic potential of 2.27 V (vs Na/Na<sup>+</sup>).



Figure 1 shows discharge and charge plateau at 2.15 V and 2.35 V, respectively. This demonstrates moderate discharge and charge overpotential in a range of 0.08~0.12 V. Online electrochemical mass spectroscopy (OEMS) analysis confirms the 1e<sup>-</sup> process for both discharge and charge (up to 80%), where the O<sub>2</sub> gas evolution is predominant. However, over 80% charge, the potential drastically increases up to 4.0 V and H<sub>2</sub> and CO<sub>2</sub> start evolving. The XRD in Figure 2 reveals no reflection of NaO<sub>2</sub> after 80% charge, indicating that the Na-O<sub>2</sub> electrochemical reaction terminates within 80% charge. The resultant low Coulombic efficiency arises from side reaction (e.g., instability of electrolyte and CNT) during discharge. In addition, formation of Na dendrites in the negative electrode is observed after charge. These unintended reactions eventually lead to poor cyclability. We discuss detailed analyses of side reactions and strategies to improve cycling performance in the presentation.

## References

- [1] P. Hartmann et al. *Nat. Mater.* 12 (2013) 228.
- [2] P. Bruce et al. *Nat. Mater.* 11 (2012) 19
- [3] N. Zhao et al. *Phys. Chem. Chem. Phys.* 16 (2014), 15646
- [4] X. Bi et al *Chem. Commun.* 51 (2015) 7665



**Figure 1:** Galvanostatic discharge-charge curves at room temperature and at a current rate of 60 mA/g. Inset: SEM image of discharge product.

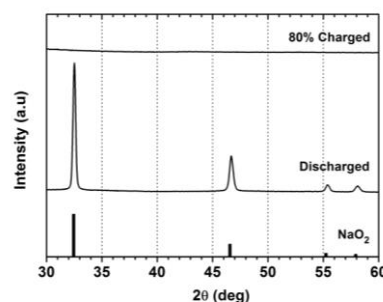


**Figure 2:** XRD patterns of CNT electrode after discharge and after 80% charge. The bottom is reference for NaO<sub>2</sub> (JCPDS reference card, 01-089-5949).



# A High Energy, Long-life Li-S Battery Enabled by Mille-Feuille Structure Electrode

Chia-Nan Lin, Chih-Ching Chang, Chun-Lung Li, Jason Fang

*Material and Chemical Research Laboratories, Industrial Technology Research Institute  
195, Sec. 4, Chung Hsing Rd., Chutung, Hsinchu, Taiwan 31040, R.O.C.  
cnlin0908@itri.org.tw*

In order to overcome the issues of sulfur insulation and polysulfides dissolve in electrolyte on lithium-sulfur (Li-S) battery, the research focus on a micro- and macroscopic structure design of activity materials and cathode electrode. First, the nano-sized sulfur particles were dispersed on the carbon black matrix using an in-situ redox reaction. The sulfur-carbon (S-C) nanocomposite morphology most likely the *hylocereus undatus* structure (Fig. 1). Because the smaller S particles have larger specific surface area, it may lead better S utilization and faster charge/discharge rate. The S-C nanocomposite has 78 wt % S loading. Second, we designed a mille-feuille structure with inserting S-C nanocomposite between carbon membranes with high porosity and high conductivity (Fig. 2). The mass loading of the S cathode was 2~3 mg/cm<sup>2</sup> and higher than the most sample reported in the literature. The designed electrodes not only provide the polysulfide migration in the electrolyte but also inhibit the Al foil corrosion at the high operating voltages. In addition, a dynamic battery management system was also used in this studying, and these complex designs and fabrication processes compromise the utilization efficiency of S and long cyclic life. The charging/discharging results show that the S-C electrode can deliver specific discharge capacity of 1250 mAh/g at 0.5C and also demonstrate a long cycle life exceeding 1000 cycles. To our knowledge, the extremely low capacity-decay rate (0.04% per cycle) may be the best performance in this field.

## Hylocereus undatus structure

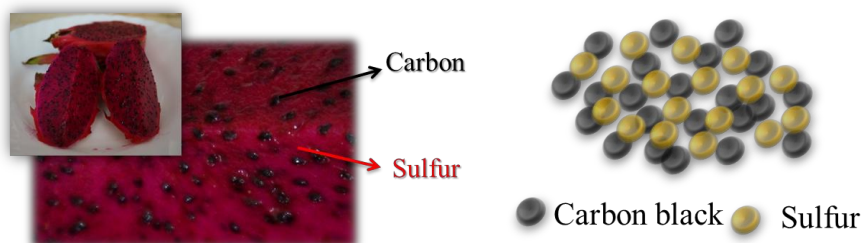


Figure 1. The morphology schema of S-C nanocomposites.

## Mille Feuille structure

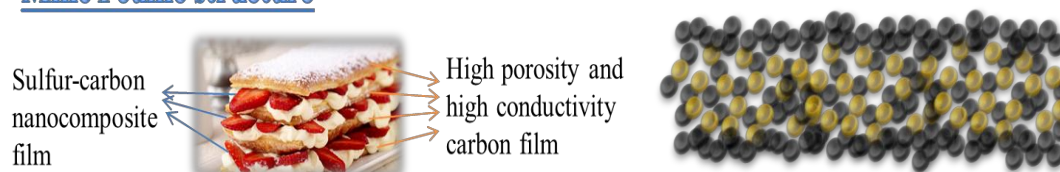


Figure 2. The morphology schema of S-C mille-feuille structure electrode.



# Development of a high energy density sulfide-based all-solid-state battery

Satoshi Fujiki, Yuichi Aihara, Takanobu Yamada, Seitaro Ito, Hajime Tsuchiya,  
Youngsin Park\*, and Seokgwang Doo\*

Samsung R&D Institute Japan, Minoh Semba Center Bldg. 13F, Semba Nishi 2-1-11, Minoh, Osaka,  
562-0036, Japan

\* Samsung Electronics Co., Ltd., 130 Samsung-ro, Yeongtong-gu, Suwon-si, Gyeonggi-do, 443-803,  
Republic of Korea  
s.fujiki@samsung.com

All-solid-state lithium-ion battery (SSB) with a non-flammable solid electrolyte is one of the promising candidates for next-generation high performance power source because of its low risk of safety concerns. Sulfide-based lithium ion-conductive solid electrolytes have attracted growing interests to be used in such SSBs, because of their non-flammability, high ionic conductivity and electrochemical stability.<sup>1, 2</sup> However, there are still some serious issues to overcome before the realization of SSB for practical applications. Since the ionic and electric conduction paths are given by the contacts of solid electrolyte particles, the cell impedance is typically higher than those of conventional liquid electrolyte lithium-ion batteries. Consequently, most of the SSBs need an external pressure during the charging and discharging processes.<sup>3</sup> Also, some literatures have suggested the necessity of a thin buffer layer on the cathode surface to prevent the mutual diffusion of atoms between the metal oxide and sulfide electrolyte.<sup>3,4</sup> Thus, in order to create a SSB of practical size, we adopted  $\text{Li}_2\text{O-ZrO}_2$  (LZO) thin layer coating on the cathode material for reducing the solid-solid interface resistance.<sup>5</sup> Although a number of basic scientific studies have already been reported, development of a practical size device is still premature.

We fabricated a large size SSB by a slurry coating method from the composite slurries containing polymer binders. The battery attained the capacity of 500 mAh in a single cell. Total capacity of a stacked cell was 2000mAh with the power density of 175Wh/kg. The single cell retained the capacities above 80% after 300 cycles without an artificial external pressure (Figure 2). In this work, we demonstrated the applicability of the sulfide based electrolyte for a practical size SSB. Although further development is still needed, SSBs hold a great promise as next generation energy storage.

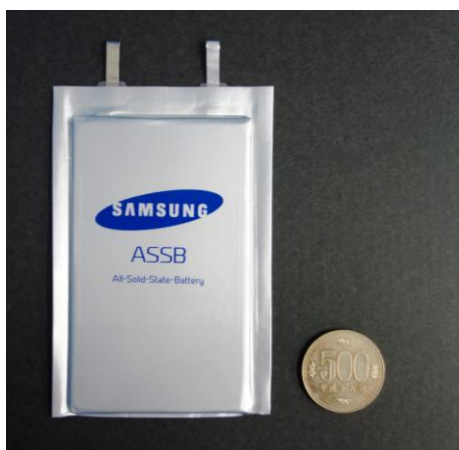


**Fig. 1.** The 2000mAh class cell with the power density of 175 Wh/kg .

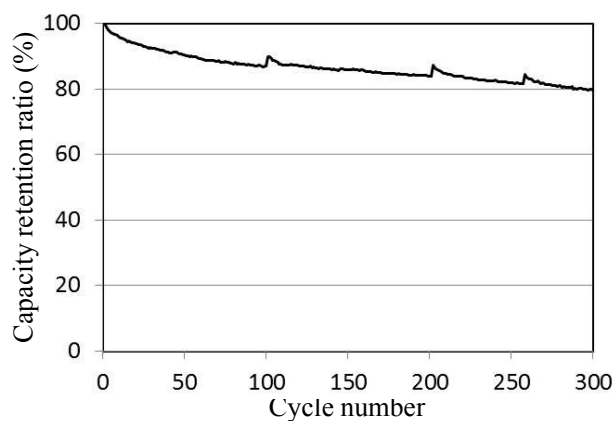


**Fig. 2.** Cycle performance of 300mAh-class single cell at 60 °C.

1. F. Mizuno, A. Hayashi, K. Tadanaga, and M. Tatsumisago, *Advanced Materials*, **17**, 918 (2005).
2. N. Kamaya, K. Homma, Y. Yamakawa, M. Hirayama, R. Kanno, M. Yonemura, T. Kamiyama, Y. Kato, S. Hama, K. Kawamoto, and A. Mitsui, *Nature Materials*, **10**, 682 (2011).
3. N. Machida, J. Kashiwagi, M. Naito, and T. Shigematsu, *Solid State Ionics*, **225**, 354 (2012).
4. N. Ohta, K. Takada, L.-Q. Zhang, R.-Z. Ma, M. Osada, and T. Sasaki, *Advanced Materials*, **18**, 2226 (2006).
5. S. Ito, S. Fujiki, T. Yamada, Y. Aihara, Y. Park, T.-Y. Kim, S.-W. Baek, J.-M. Lee, S. Doo, and N. Machida. *J. Power Sources*, **248**, 943 (2014).

# The role of defects and oxygen functionalities in carbon nanotube-based electrodes for the lithium-oxygen battery

Raymond A. Wong<sup>1,2</sup>, Hye Ryung Byon<sup>1,\*</sup>

<sup>1</sup>Byon Initiative Research Unit, RIKEN 2-1 Hirosawa, Wako, Saitama 351-0198, Japan

<sup>2</sup>Department of Energy Sciences, Tokyo Institute of Technology, 4259 Nagatsuta-cho, Midori-ku, Yokohama 226-8502, Japan

raymond.wong@riken.jp, hrbyon@riken.jp

Tremendous research interest has been directed towards the non-aqueous lithium-oxygen (Li-O<sub>2</sub>) battery due to its high theoretical energy density (~3.5 kWh kg<sup>-1</sup>) with the potential to fully satisfy electric vehicle and grid leveling applications. The Li-O<sub>2</sub> battery chemistry consists of metallic Li and gaseous O<sub>2</sub> on the negative and positive electrodes respectively, giving a reversible overall reaction  $2\text{Li}^+ + \text{O}_2 + 2e^- \rightleftharpoons \text{Li}_2\text{O}_2$ , where solid Li<sub>2</sub>O<sub>2</sub> is the desired discharge product. To maximize this high energy density, it is paramount that stable, lightweight materials be used for the positive electrode. To this note, very few materials can compete with carbon due to its attractive properties including cost, relative abundance, weight, conductivity and porosity, all which are ideal properties for the positive electrode. However, it has been recently established that the use carbon can potentially exasperate chemical and electrochemical parasitic reactions occurring during discharge/recharge leading to the formation of insulating Li carboxylates and carbonates, all of which compromise the cycleability of the system.[1, 2] Therefore, it is of great interest to examine the characteristics of carbonaceous materials which can vary significantly with respect to synthesis procedures, defects, edges, and surface functional groups, all of which can greatly affect battery performance. Herein, we reveal the individual effects of defects and oxygen functional groups by systematically investigating their individual effects on carbon nanotubes (CNT) by *in-situ* on-line electrochemical mass spectrometry (OEMS) and extracted discharge/recharged CNT electrodes by *ex-situ* chemical analyses.

In this study, 4 different carbonaceous materials derived from commercial as-prepared CNTs were examined: (1) pristine, (2) o-functionalized, (3) defective, and lastly (4) graphitized CNTs. CNTs were used due to its well-defined structure, ease of surface modification and for the ability to fabricate binder-free positive electrodes. Oxygen functional groups were introduced onto the outer walls *via* chemical oxidation process. Defective CNTs were obtained by annealing o-functionalized CNTs in Ar (900°C) which removes the majority of o-functionalities. Graphitized CNTs were obtained through very high temperature annealing (2800°C). With these materials, binder-free, self-standing CNT electrodes were fabricated through a simple vacuum filtration process. Typical cell parameters involved 0.5M LiClO<sub>4</sub> in tetraglyme as the electrolyte with current density of 50 mA g<sup>-1</sup> (60 uA).

OEMS oxygen consumption measurements show that all 4 electrodes exhibit ~2 e<sup>-</sup>/O<sub>2</sub> during discharge suggesting prominent Li<sub>2</sub>O<sub>2</sub> formation, which is a contrast to recharge which shows e<sup>-</sup>/O<sub>2</sub> values that are significantly >2 e<sup>-</sup>/O<sub>2</sub> suggesting irreversibility and significant electrochemical parasitic reactions occurring during recharge. Figure 1 shows the pristine CNT (a) galvanostatic discharge/recharge curves, (b) corresponding discharge O<sub>2</sub> consumption, and (c) gas evolution from a linear sweep voltammogram after galvanostatic discharge to 1000 mAh g<sup>-1</sup>. Further details, results and discussion will be provided in the presentation.

[1] McCloskey, B.D., Valery, A., Luntz, A.C., Gowda, S.R., Wallraff, G.M., Garcia, J.M., Mori, T., Krupp, L.E., 2013. Combining Accurate O<sub>2</sub> and Li<sub>2</sub>O<sub>2</sub> Assays to Separate Discharge and Charge Stability Limitations in Nonaqueous Li-O<sub>2</sub> Batteries. *J. Phys. Chem. Lett.* 4, 2989–2993.

[2] Ottakam Thotiyl, M.M., Freunberger, S.A., Peng, Z., Bruce, P.G., 2013. The Carbon Electrode in Nonaqueous Li-O<sub>2</sub> Cells. *J. Am. Chem. Soc.* 135, 494–500.

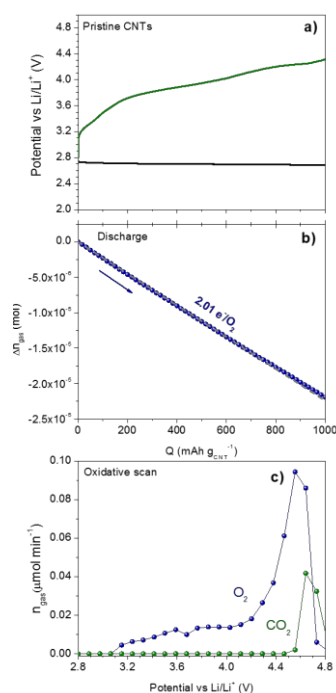


**Fig. 1** – (a) galvanostatic discharge/recharge of pristine CNTs at 60uA (b) O<sub>2</sub> consumption during discharge (c) gas evolution of linear sweep voltammogram (0.05 mV/s) after discharge to 1000 mAh g<sup>-1</sup>

# Improvements in the aqueous lithium-iodine battery

Georgios Nikiforidis, Hye Ryung Byon\*

Byon Initiative Research Unit (IRU), RIKEN, 2-1 Hirosawa, Wako, Saitama 351-0198, Japan  
georgios.nikiforidis@riken.jp, hrbyon@riken.jp

The novel aqueous lithium-iodine (Li-I<sub>2</sub>) battery has proven to be a cost-effective and high-performance energy storage technology that can be utilized in small (e.g. portable batteries) and large grid-scale (e.g. redox-flow battery, RFB) energy storage applications [1-2]. The significant advantage of this system is its energy storage capability of ~0.33 kWh kg<sup>-1</sup> attributed to the suitable operating potential (~3.5 V vs. Li/Li<sup>+</sup>) and high solubility of the I<sup>-</sup>/I<sub>3</sub><sup>-</sup> redox couple in the aqueous solution (~8.5 M in KI) as the catholyte. Besides, the operating potential of the I<sup>-</sup>/I<sub>3</sub><sup>-</sup> redox couple (0.536 V versus SHE) can avoid the electrolysis of water. The energy density can be further amplified by increasing the volume capacity of the aqueous catholyte since energy density is proportional to the concentration of I<sup>-</sup>/I<sub>3</sub><sup>-</sup> redox couple and the amount of solution. Previous studies on this system have reported current densities up to 12 mA cm<sup>-2</sup> could be applied with high storage capacity (~98% of the theoretical capacity), Coulombic efficiency (>99.5%) and cyclic performance (>99.5% capacity retention for 200 cycles) [1,3]. Yet, there is a lot of room for improvement. Subsequent studies have been focusing on two areas; 1) the improvement of the existing system through the enhancement of the electrochemical behavior of the I<sup>-</sup>/I<sub>3</sub><sup>-</sup> reaction (Fig. 1A) and 2) the development of a prototype Li-I<sub>2</sub> battery bearing solar cell. Regarding the first scope, catholyte without LiI yielded comparable performance to the cells containing LiI with regards to specific capacity and energy, voltaic and coulombic efficiencies as well as enhanced cycleability (>200 cycles) (Figs. 1B & C). Electrolytes containing only LiI/I<sub>2</sub> (without KI) showed enhanced specific capacity (by a factor of 3 but poor cycleability (due to the presence of Li)). Mixing of Pt with carbon replacing with (Pt-free) carbon current collectors produces slightly improved voltaic efficiencies (Fig. 1B) and more reversible behavior. Regarding, the new prototype system, it involves harvesting solar light by using hematite (α-Fe<sub>2</sub>O<sub>3</sub>) coated FTO photoanode for the I<sup>-</sup>/I<sub>3</sub><sup>-</sup> electrolyte. Preliminary results on the battery system under illumination show a great enhancement in the voltaic efficiency during charging (Fig. 1D).

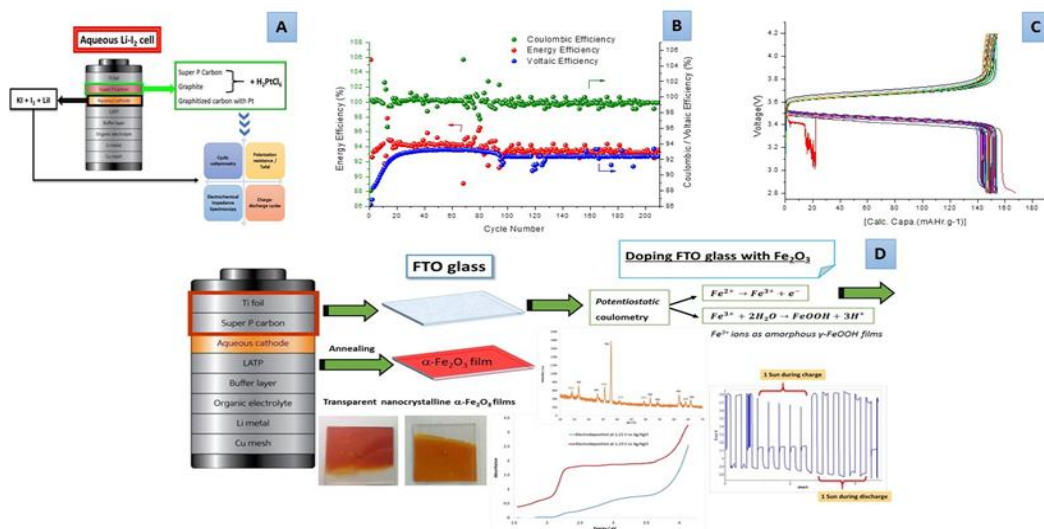


Figure 1: A) Schematic showing the investigation of the aqueous Li-I<sub>2</sub> cell. Electrochemical performance of Li-I<sub>2</sub> cell in 1.5 M KI and 0.3 M I<sub>2</sub> at a current rate of 1 mA cm<sup>-2</sup> B) Cyclic performance presenting Coulombic voltaic and energy efficiencies C) Two hundred cycled charge/discharge profile presenting specific capacity upon charge/discharge cycles D) Schematic showing process of doping FTO with α-Fe<sub>2</sub>O<sub>3</sub>, UV-Vis and XRD pattern of the α-Fe<sub>2</sub>O<sub>3</sub> FTO photoanode, charge/discharge behavior (t = 10 min) of the α-Fe<sub>2</sub>O<sub>3</sub> FTO photoanode based Li-I<sub>2</sub> cell under 1 SUN at a current rate of 1 mA cm<sup>-2</sup>. The catholyte is 1 M KI 0.03 M LiI 0.08 M I<sub>2</sub>.

[1] Y. Zhao, H.R. Byon, *Nature Commun.* **4**, 1896 (2013), doi: 10.1038/ncomms2907

[2] Y. Zhao, N. B. Mercier, H. R. Byon, *ChemPlusChem* **80** 344 (2015), doi: 10.1002/cplu.201402038

[3] Y. Zhao, M. Hong, G. Yu, H.C. Choi, N. B. Mercier, H. R. Byon, *Nano Lett.* **14** 1085 (2014), doi: 10.1021/nl404784d

# Electrochemical Behavior of Oxygen in Phosphonium Ionic Liquids as Electrolytes for Lithium Air Batteries

Katsuhiko Tsunashima,<sup>1</sup> Hayato Fujimoto,<sup>1</sup> Hsien Hau Wang,<sup>2</sup> Larry Curtiss,<sup>2</sup> Khalil Amine,<sup>2</sup> Youhei Mizuguchi<sup>3</sup>

<sup>1</sup> Department of Materials Science, National Institute of Technology, Wakayama College, 77 Noshima, Nada-cho, Gobo, Wakayama 644-0023, Japan

<sup>2</sup> Argonne National Laboratory, 9700 South Cass Avenue, Argonne, IL 60439, USA

<sup>3</sup> Nippon Chemical Industrial Co., Ltd., 9-11-1 Kameido, Koto-ku, Tokyo 136-8515, Japan  
E-mail: tsunashima@wakayama-nct.ac.jp (K. Tsunashima)

Lithium air batteries are one of the most promising next generation secondary batteries that have extremely high specific energy density when compared to the conventional lithium ion batteries. The electrochemical processes in lithium air batteries include an electroreduction of oxygen at the cathode, thereby generating the oxygen species such as a superoxide anion in the cathode interface. Such an oxygen species is highly reactive to decompose the electrolytes and/or solvents in the electrolytic media, giving unfavorable decrease in the cycling performance of the battery cells.

On the other hand, room-temperature ionic liquids (RTILs), i.e. organic molten salts with melting points below ambient temperature, have received a great deal of attention as electrolytic media for various electrochemical systems due to the fact that RTILs have high electrochemical stability. Particularly, RTILs have been regarded as potential electrolytic media for lithium secondary batteries because of their stability and safety performances. From this point of view, we have designed a new class of phosphonium cation-based RTILs based on bis(trifluoromethylsulfonyl)amide (TFSA) anion as lithium battery electrolytes [1]. However, the application of the phosphonium RTILs to the electrolytes used in lithium air battery has been rarely reported. In this work, we present the electrochemical investigation of the oxygen reduction in the phosphonium RTILs (Fig. 1) as potential candidates for the lithium air battery electrolytes.

The preparation of phosphonium RTILs was carried out by aqueous ion exchange reactions of precursor phosphonium halides with Li-TFSA. The cyclic voltammetry and chronoamperometry measurements were carried out using a typical three-electrode cell consisting of a glassy carbon electrode as a working electrode, a Pt counter electrode and an Ag/Ag<sup>+</sup> reference electrode under oxygen atmosphere.

All phosphonium RTILs employed in this work showed the cathodic voltammetric response for the electrochemical oxygen reduction. It was found that the unsubstituted phosphonium RTILs (e.g. P<sub>2225</sub>-TFSA and P<sub>4441</sub>-TFSA) gave reversible cyclic voltammograms, whereas the introduction of substituents into phosphonium cations (e.g. P<sub>222(101)</sub>-TFSA and P<sub>222(3CN)</sub>-TFSA) tended to result in a decrease in the peak currents and/or reversibility. As shown in Fig. 2, P<sub>4441</sub>-TFSA exhibited relatively high peak currents with high reversibility in the voltammogram when compared to the corresponding ammonium RTIL. These results suggest that the unsubstituted phosphonium RTILs can be regarded as candidates for the air battery electrolytes.

## Reference

[1] K. Tsunashima, M. Sugiya, *Electrochem. Commun.* 9 (2007) 2353.

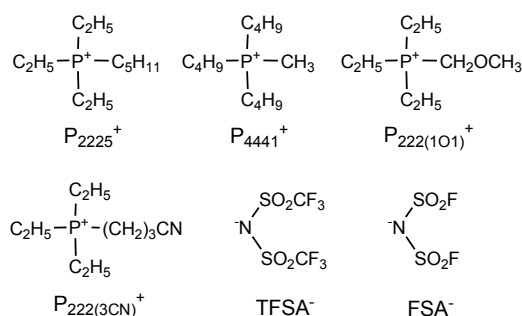


Fig. 1 Ionic components of ILs in this work.

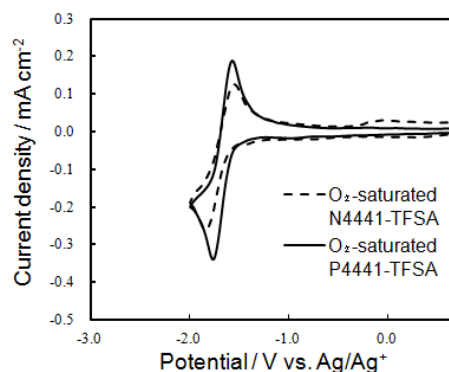


Fig. 2 Cyclic voltammograms measured in O<sub>2</sub>-saturated ILs with a 10 mVs<sup>-1</sup> potential sweep rate.

# Thermal Runaway Behavior of 18650 Li-ion Cells Before and After Storage Degradation at High Temperature

Omar Mendoza<sup>1</sup>, Shuichi Taniguchi<sup>1</sup>, Yuki Maruyama<sup>1</sup>, Hiroaki Ishikawa<sup>2</sup>,  
Yoshitsugu Sone<sup>3</sup>, Minoru Umeda<sup>1\*</sup>,  
Nagaoka Univ. of Technol.<sup>1</sup>, Indus. Technol. Insti. of Ibaraki Prefect.<sup>2</sup>,  
Japan Aero. Explo. Agency<sup>3</sup>  
1603-1, Kamitomioka, Nagaoka, Niigata 940-2188, Japan  
\*mumeda@vos.nagaokaut.ac.jp

Thermal analysis of Li-ion secondary cells is important for ensuring their safety and reliability. Recently, the use of Li-ion cells has been growing globally with a large number of cells powering a wide range of applications in variety of environments, and there have been several reported incidents raising safety concerns. Some of the cases have been related to overheating (thermal runaway) of Li-ion cells, leading to possible fire and explosion.<sup>1)</sup> In this work we analyze the thermal runaway behavior of 18650 Li-ion cells before and after storage and cycling degradation at high temperatures. The thermal behavior of the cells is analyzed using accelerating rate calorimetry. Non-self-heating, self-heating and thermal runaway regions of the cells as a function of state of charge and temperature are identified and compared among the cells.

Non-degraded and degraded commercial available 18650 Li-ion secondary cells were tested. The nominal capacity of the cells is 2550 mAh and the anode and cathode materials are graphite and LiCoO<sub>2</sub> + additives, respectively. In order to degrade the cells, these were stored at 80 °C and 100% SOC for one week. The cells were tested inside an accelerating rate calorimeter (ARC) 2000<sup>TM</sup> to record the thermal behavior and cell temperatures during the charge/discharge process. The cells were charged/discharged using a battery tester (KIKUSUI, PFX2011).

Figure 1 shows the self-heating rate before and after degradation of 18650 cells at 100% and 0% SOC. At 0% SOC, the cell after degradation (red) exhibits a higher self-heating rate than the cell before degradation (green), indicating that the cell becomes thermally unstable after degradation. On the other hand, at 100% SOC, the cell after degradation (blue) shows a lower self-heating rate than the cell before degradation (black), this is likely due to the reduce in capacity of the cell by the degradation. There is a difference of 380.9 mAh between the cells before and after degradation, it seems that this difference affects the thermal behavior of the cells when these are fully charged.

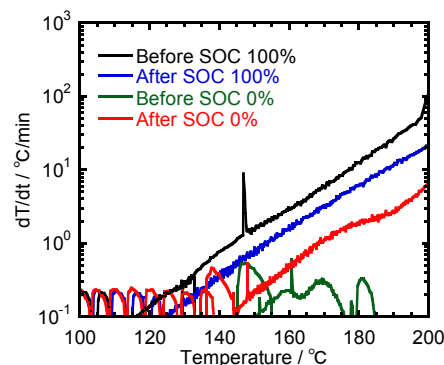


Fig. 1 Self-heating rate of 18650 Li-ion secondary cells before and after degradation at 0 and 100% SOC.

## References

- 1) W. Qingsong, P. Ping, Z. Xuejuan, C. Guanquan, S. Jihua, C. Chunhua, *Journal of Power Sources*, **208** (2012) 210.



# Enhancing cycling stability of tin dioxide anode for lithium-ion batteries with a stretchable polyimide matrix

Yingshun Li<sup>a,b</sup>, Jieqing He<sup>a</sup>, Hui Zhou<sup>a</sup>, Wenpei Kang<sup>b,c</sup>, Denis Y. W. Yu<sup>a,b,\*</sup>

<sup>a</sup> School of Energy and Environment, <sup>b</sup> Center of Super-Diamond and Advanced Films (COSDAF),

<sup>c</sup> Department of Physics and Materials Science, City University of Hong Kong, Hong Kong SAR, China

email: [yingsli@cityu.edu.hk](mailto:yingsli@cityu.edu.hk), [denisyu@cityu.edu.hk](mailto:denisyu@cityu.edu.hk)

Tin-based material is an attractive choice for next generation high energy density lithium-ion battery (LIB) because of a good balance between electrochemical and mechanical properties, such as specific capacity, reaction potential, amount of volume change with lithiation and material density. Discharge capacity of more than 700 mAh g<sup>-1</sup> can be achieved readily. Even though the capacity is less than that of silicon, the volume expansion of Sn-based materials are smaller than that of Si-based materials, and is therefore easier to manage in a coated electrode. Among the different Sn-based material, metallic tin, with a bulk density of more than 7 g cm<sup>-3</sup>, has a theoretical capacity of 994 mAh g<sup>-1</sup> with high volumetric energy density. However, it suffers from poor cycle performance, partly due to the large number of phases transitions that the material undergoes with lithiation.<sup>1</sup> In addition, melting point of tin is only about 230°C, limiting the processibility of the material and also increasing the chance of cold welding during charge-discharge. Tin oxides such as SnO and SnO<sub>2</sub> have also been highly researched as anode materials for LIB. The presence of oxygen suppresses the phase transitions of Sn-Li, raises the melting temperature of the material, reduces the amount of volume expansion during lithiation and increases the cycle stability of the material.<sup>2</sup> During initial discharging, the materials undergo a conversion reaction to form Li<sub>2</sub>O, followed by alloying of Sn and Li.<sup>2,3</sup> Most research papers limit the charge potential to about 1V (utilization of only the Sn-Li alloy reaction), but the first cycle efficiency is less than 40%, meaning that in a full cell configuration, excess cathode has to be used to overcome the lithium lost during the first cycle. First cycle efficiency and energy density can be improved further by raising the charge potential to utilize the Li-O reaction, but it often results in fast capacity drop.<sup>3-6</sup>

In this study, we stabilize both the conversion and alloy reactions of nano-SnO<sub>2</sub> in a stretchable polyimide (PI) matrix. The nanoparticles allow efficient lithium storage and the PI matrix keeps the integrity of the secondary particles by buffering the volume change and preventing material loss during charge and discharge. Even with sodium carboxymethyl cellulose as the binder in the electrode, a capacity of more than 700 mAh g<sup>-1</sup> remains after 50 cycles for the SnO<sub>2</sub>-PI matrix samples when cycled between 0.01 and 2.5 V. Capacity retention is 97% after 100 cycles, as opposed to 80% without PI matrix (as shown in Fig. 1). Detailed work to study the effect of the amount of PI and polymerization conditions on electrochemical performance is underway and the charge-discharge mechanism will be discussed at the meeting. By utilizing both the conversion and alloy reactions of SnO<sub>2</sub>, first cycle efficiency is improved to more than 60% and capacity is increased by 51.8% compared to just using the Sn-Li alloy reaction.

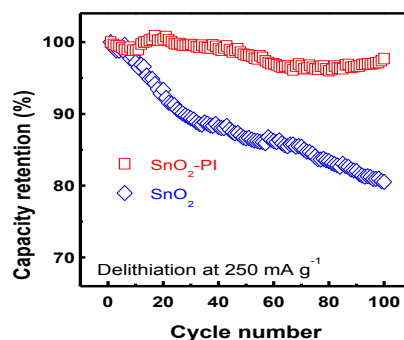


Figure 1. Cycling performance of SnO<sub>2</sub> (diamond) and SnO<sub>2</sub>-PI matrix (square) between 0.01 and 2.5V with a current of 250 mA g<sup>-1</sup>. Both samples were initiated for 5 cycles at 100 mA g<sup>-1</sup> before the cycling test.

## References:

1. J. Q. Wang, I. D. Raistrick & R. A. Huggins, *J. Electrochem. Soc.* **133**, 457 (1986).
2. T. Brousse, R. Retoux, U. Herterich & D. M. Schleich, *J. Electrochem. Soc.* **145**, 1 (1998).
3. I. A. Courtney & J. R. Dahn, *J. Electrochem. Soc.* **144**, 2943 (1997).
4. H-J. Ahn, H-C. Choi, K-W. Park, S-B. Kim & Y-E. Sung, *J. Phys. Chem. B* **108**, 9815 (2004).
5. X. W. Lou, Y. Wang, C. Yuan, J. Y. Lee & L. A. Archer, *Adv. Mater.* **18**, 2325 (2006).
6. X. Zhu, Y. Zhu, S. Murali, M. D. Stoller & R. S. Ruoff, *J. Power Sources* **196**, 6473 (2011).

# A comparison of the thermal stability of electrolytes for Li- and Na-ion batteries

Liwei Zhao<sup>a</sup>, Shigeto Okada<sup>b</sup>

<sup>a</sup> Elements Strategy Initiative for Catalysts and Batteries (ESICB), Kyoto University

<sup>b</sup> Institute for Materials Chemistry and Engineering, Kyushu University  
6-1 Kasuga-koen, Kasuga 816-8580, Japan  
s-okada@cm.kyushu-u.ac.jp

Electrolytes have essential effect on the electrochemical properties and thermal stability of batteries. For Li-ion batteries, organic solvent-based electrolytes have been widely applied in practical application. Many studies had been carried out on the electrolytes to investigate their characteristics and to improve battery performances. Recently ambient temperature sodium-ion batteries have drawn interest as a power source for large-scale grid energy storage due to the low cost and abundant resources of sodium. Na is located below Li in the periodic table and they share similar chemical properties in many aspects. The fundamental principles of the Na-ion batteries and Li-ion batteries are identical. Therefore, much of new components for Na-ion batteries could be developed according to their counterparts for Li-ion batteries and the electrolytes are no exception. Kinds of Na salt-containing organic solvent-based electrolyte have been successfully used in investigation of various Na-ion batteries. However, unlike that done for the electrolytes of Li-ion batteries, few studies have been performed on the electrolytes of Na-ion batteries [1-4], especially about their thermal characteristics. In the present work, kinds of NaClO<sub>4</sub> or NaPF<sub>6</sub>-containing organic solvent-based electrolytes were studied by a thermogravimetry-differential scanning calorimeter (TG-DSC). By comparing the Na-salt electrolytes to their Li-salt counterparts, the thermal stability of the electrolytes of Na-ion batteries were evaluated. At the same, the mechanisms of electrolyte thermal decomposition were also discussed.

The organic solvents and electrolytes in the present work were commercially available or self-prepared. The temperature profiles of 1-3  $\mu$ l test electrolyte in a hydraulic-sealed stainless steel pan were carried out by the TG-DSC system. During measurement, the TG signal was monitored simultaneously to confirm that there was no leakage.

Figure 1 shows the DSC curves of 1, 2 and 3  $\mu$ l 1 M NaClO<sub>4</sub>/PC and 1 M LiClO<sub>4</sub>/PC sole electrolytes. Both kinds of electrolytes gave exothermic heat at around 300°C due to the thermal decomposition of the electrolytes. However, the exothermic peaks were obviously different, including peak shape, peak position and peak intensity. This phenomenon indicated that these two kinds of electrolytes had completely different thermal decomposition mechanism only because of the different cations of the salts. Similar comparisons were also carried out on other kinds of electrolytes. Detailed discussion will be presented in the meeting.

## Reference

- [1] X. Xia, M.N. Obrovac, and J.R. Dahn, *Electrochem. Solid-State. Lett.*, **14** (2011) A130-A133.
- [2] S. Komaba, W. Murata, T. Ishikawa, N. Yabuuchi, T. Ozeki, T. Nakayama, A. Ogata, K. Gotoh, and K. Fujiwara, *Adv. Funct. Mater.*, **21** (2011) 3859-3867.
- [3] C. Vidal-Abarca, P. Lavela, J. L. Tirado, A. V. Chadwick, M. Alfredsson, and E. Kelder, *J. Power Sources*, **197** (2012) 314-318.
- [4] A. Ponrouch, E. Marchante, M. Courty, J.-M. Tarascon, and M.R. Palacin, *Energy Environ. Sci.*, **5** (2012) 8572-8583.

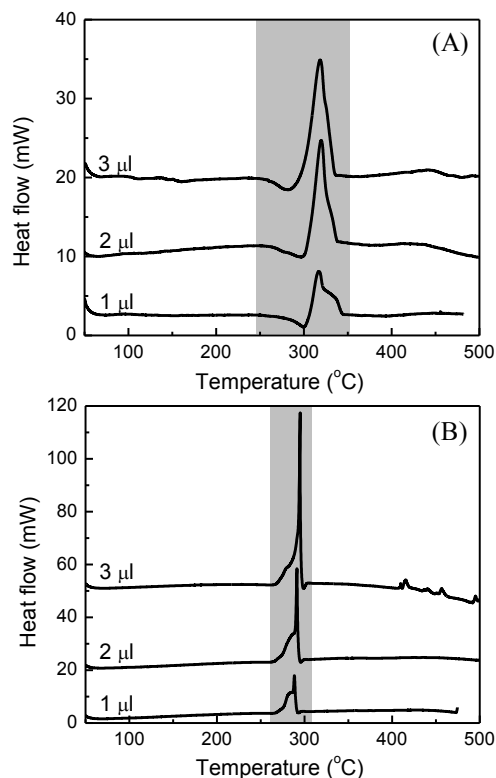


Fig. 1 DSC curves of (A) 1 M NaClO<sub>4</sub>/PC and (B) 1 M LiClO<sub>4</sub>/PC.

# Application of ionic liquid electrolytes to Si electrode as a Li-ion battery anode

Masahiro Shimizu, Hiroyuki Usui, and Hiroki Sakaguchi\*

Department of Chemistry and Biotechnology, Graduate School of Engineering, Tottori University  
4-101 Minami, Koyama-cho, Tottori 680-8552, Japan  
sakaguch@chem.tottori-u.ac.jp

Li-ion batteries are one of the most popular energy storage devices due to their high energy densities. In the light of application for large-scale systems such as power supply for electric vehicles and stationary battery, a further increase in its energy density has been required. Silicon is a promising anode material replacing the currently used graphite due to its high theoretical capacity of  $3580 \text{ mA h g}^{-1}$  ( $\text{Li}_{15}\text{Si}_4$ ). There is, however, the critical issue that Si undergoes severe volume expansion and contraction during alloying and dealloying reactions with Li. The volumetric changes ratio per Si atom from Si to  $\text{Li}_{15}\text{Si}_4$  correspond to 380%, which results in the generation of high stresses and large strains in the active material. The strains accumulated by repeated charge–discharge cycling cause disintegration of the Si electrode leading to a rapid capacity fading. On the other hand, an electrolyte is one of the key factors determining the battery performance. Room temperature ionic liquids have received much attentions as an alternative to a conventional organic electrolyte consisting of carbonate-based solvents because of their excellent physicochemical properties of high thermal stability, negligible vapor pressure, and wide electrochemical window. We demonstrated that the cycle stability of the Si electrode is remarkably improved by using the ionic liquid of 1-((2-methoxyethoxy)methyl)-1-methylpiperidinium bis(trifluoromethylsulfonyl) amide (PP1MEM-TFSA). An ether functional group in the PP1MEM cation reduces an interaction between Li ion and TFSA anion compared to the piperidinium-based ionic liquid with the cation having an alkyl side chain, which can promote Li-insertion into the Si electrode, and increase its reversible capacity. PP1MEM-TFSA delivered a comparatively high capacity of  $1050 \text{ mA h g}^{-1}$  even at the 100th cycle, whereas the capacity in an organic electrolyte of 1.0 M LiTFSA-dissolved in propylene carbonate (PC) drastically decreased to  $110 \text{ mA h g}^{-1}$  (Fig. 1). In this study, we investigated the origin of the improved cycling performance of Si electrodes in the ionic liquid electrolyte by analyzing the deterioration mechanisms for Si electrodes in organic and ionic-liquid electrolytes from the viewpoint of the Li-insertion distributions.

Raman spectroscopy is a powerful tool for identifying the crystallinity of an active material. Crystalline Si (c-Si) electrochemically reacts with Li to form c- $\text{Li}_{15}\text{Si}_4$  phase at room temperature. The c-Si then undergoes amorphization after the Li-extraction process to transform into amorphous Si (a-Si), when the band position of  $520 \text{ cm}^{-1}$  in a Raman spectrum showing c-Si typically shifts to  $490 \text{ cm}^{-1}$  indicating a-Si. By taking advantage of this nature obtained by the Raman scattering, Si that reacted with Li can be distinguished from unreacted Si. It was revealed that, in the case of using PC, crystalline Si locally remained in the electrode after cycling, and Li–Si alloying and dealloying reactions occurred in limited regions. This leads to the generation of intensive stress accumulation due to the extreme volume changes of Si in the regions inside the electrode, causing severe disintegration of the Si electrode. Consequently, the anode property of the Si electrode in PC resulted in the very poor performance. In contrast to the organic electrolyte, Li–Si reactions uniformly took place over the entire electrode in PP1MEM-TFSA, which relatively avoided any stress accumulation leading to its disintegration. This is considered to be the reason why the cycle performance of the Si electrode was significantly improved by using the ionic liquid instead of the conventional electrolytes [1].

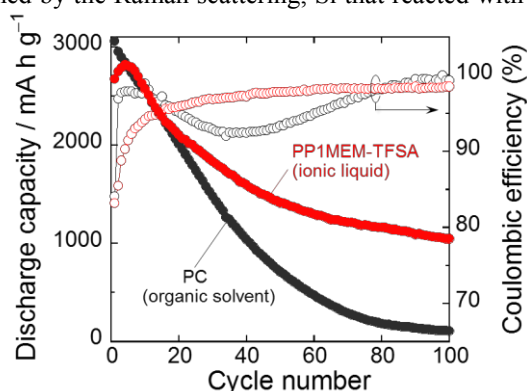


Fig. 1 Dependence of discharge (Li-extraction) capacities and coulombic efficiencies on cycle number for Si electrodes in the electrolytes using PC (organic solvent) and PP1MEM-TFSA (ionic liquid).

## Reference

[1] M. Shimizu, H. Usui, T. Suzumura, H. Sakaguchi, *J. Phys. Chem. C*, **119** (6) (2015) 2975–2982.



# Flexible MXene Nanosheets: Negative Electrode Materials for Lithium-Ion and Sodium-Ion Batteries

Masashi Okubo,<sup>1,2</sup> Satoshi Kajiyama,<sup>1</sup> Xianfen Wang,<sup>1</sup> Hiroki Iinuma,<sup>1</sup>  
Ryohei Morita,<sup>3</sup> Kazuma Gotoh,<sup>2,3</sup> Atsuo Yamada<sup>1,2</sup>

<sup>1</sup>Department of Chemical System Engineering, School of Engineering, The University of Tokyo, Hongo 7-3-1, Bunkyo-ku, Tokyo 113-8656, Japan

<sup>2</sup>Unit of Elements Strategy Initiative for Catalysts & Batteries (ESICB), Kyoto University, Japan

<sup>3</sup>Graduate School of Natural Science and Technology, Okayama University, Tsushima-naka 3-1-1, Okayama 700-8530, Japan  
m-okubo@chemsys.t.u-tokyo.ac.jp

Electrochemical energy storage is receiving much attention because of the strong industrial and social demands for their widespread use in the smart grid. However, high-energy batteries utilizing ion (de)intercalation electrodes are not satisfactory for high-power applications, while high-power electrochemical capacitors generally have low energy density. This trade-off between the power and energy densities intrinsically originates from the charge storage mechanism of the electrodes: ion (de)intercalation stores charge more slowly than a double layer, whereas a double layer stores less charge than ion (de)intercalation. Therefore, the pseudocapacitance (or redox capacitance) has become an increasingly important mechanism for charge storage, where the energy and power densities are partially liberated from the trade-off.

We have targeted a novel family of nanosheet compounds, MXenes, as potential pseudocapacitor electrodes for lithium-ion and sodium-ion batteries. MXenes are chemically derived from layered  $M_{n+1}AX_n$  or MAX phases (M: early transition metal, A: A-group element, and X: C and/or N) [1,2]. As the MXene has both a high electrical conductivity and large surface area, its application to pseudocapacitor electrodes holds great promise [3,4]. In this presentation, we report on  $Ti_{n+1}C_nT_x$  ( $n = 1, 2$ ) as negative electrode materials for lithium-ion and sodium-ion batteries.  $Ti_{n+1}C_nT_x$  consists of abundant and low-cost elements, enabling fabrication of sustainable energy sources. The pseudocapacitance of  $Ti_{n+1}C_nT_x$  allows batteries to be liberated from the trade-off between high energy and high power [5].

$Ti_2CT_x$  and  $Ti_3C_2T_x$  were synthesized by treating the MAX phases  $Ti_2AlC$  and  $Ti_3AlC_2$  with a HF aqueous solution. The charge-discharge experiments revealed that both MXenes deliver a large reversible capacity. For example, Figure 1 shows the charge-discharge curves of  $Ti_2CT_x$  measured between the cut-off voltages of 0.1–3.0 V versus  $Na/Na^+$  at 20 mA/g. After the initial few cycles,  $Ti_2CT_x$  exhibits stable and efficient electrode performance. The charge/discharge profiles exhibit a capacitor-type slope in the range of 0.1–2.3 V (an average operating potential of 1.3 V), delivering a reversible capacity of approximately 175 mAh/g with good cycle stability (12% and 19% losses of the second capacity after 50 and 100 cycles, respectively).

Detailed reaction mechanism of MXene nanosheets will be discussed on the basis of ex situ XRD, X-ray absorption spectroscopy, and solid state  $^{23}Na$  magic angle spinning NMR.

[1] M. R. Lukatskaya, *et al.*, *Science*, **2013**, 341, 1502-1505.

[2] M. Ghidui, *et al.*, *Nature*, **2014**, 516, 78-81.

[3] M. Naguib, *et al.*, *Electrochem. Commun.*, **2012**, 16, 61-64.

[4] O. Mashtalir, *et al.*, *Nat. Commun.*, **2013**, 4, 1716.

[5] X. Wang, *et al.*, M. Okubo, & A. Yamada, *Nat. Commun.*, **2015**, 6, 6544.

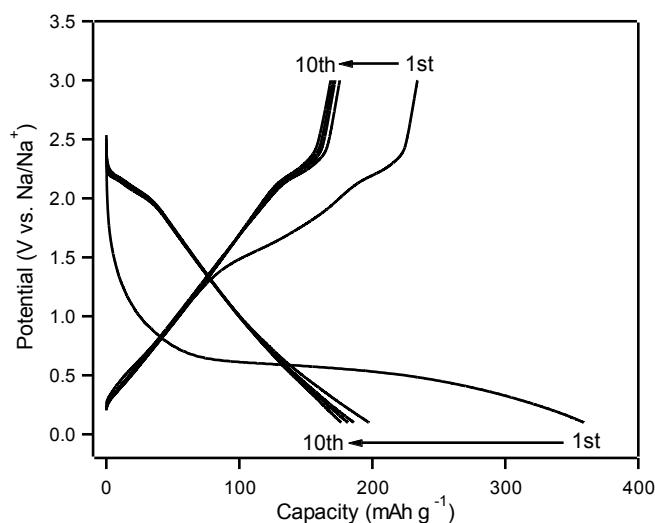


Figure 1. Charge-discharge curves for MXene  $Ti_2CT_x$  at 20 mA/g.

# ***In-situ* XRD of High Voltage Lithium Insertion Electrodes**

Michael G. Palmer, Andrew Hector, John Owen  
University Of Southampton  
School of Chemistry, University of Southampton, Hampshire, SO17 1BJ  
M.Palmer@soton.ac.uk

High voltage lithium-ion electrodes have recently been suggested for application in high energy density batteries for electric vehicles. Olivine structured lithium metal phosphates are a group of positive electrode materials, of which the best developed phase,  $\text{LiFePO}_4$ , is now commercially available and used in applications from power tools to electric vehicles.<sup>1</sup> The isostructural  $\text{LiCoPO}_4$ <sup>2</sup> can operate at higher potentials but is less used due to poor conductivity and cycling behavior.

This work looks at optimizing the  $\text{LiCoPO}_4$  electrode, in terms of carbon coated loading, particle shape and morphology. *In-Situ* XRD was carried out to examine changes in phase behavior during cycling using a cell designed in house<sup>3</sup>. The cell contained an aluminum foil current collector that also acted as the X-ray window. Domed lithium was used as the negative electrode to allow for an even pressure to be applied across the diameter of the stack, countering the effect of deformation of the aluminum window under pressure and allowing a similar electrochemical performance to be achieved to that observed in a standard Swagelok cell.

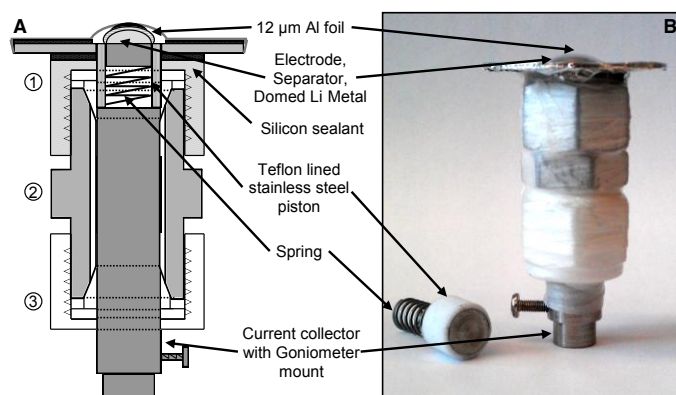


**Figure 1** (a) Schematic and (b) image of the electrochemical cell used in the *in situ* XRD studies.

*Ex-situ* XANES data were collected on cycled electrodes to observe the changes in oxidation state of cobalt across the bulk of the electrode and to investigate the origins of the strong dependence of cycling performance on the atmosphere and thermal conditions used in the material synthesis.

<sup>1</sup> C. Macilwain, *Nature*, 2006, **444**, 17; O.-K. Park, Y. Cho, S. Lee, H.-C. Yoo, H.-K. Song and J. Cho, *Energy Environ. Sci.*, 2011, **4**, 1621.

<sup>2</sup> J. Liu, T. E. Conry, X. Song, L. Yang, M. M. Doeff and T. J. Richardson, *J. Mater. Chem.*, 2011, **21**, 9984.

<sup>3</sup> M. R. Roberts, A. Madsen, C. Nicklin, J. Rawle, M. G. Palmer, J. R. Owen, and A. L. Hector, *J. Phys. Chem. C*, 2014, **118**, 6548.

# Improved Performance of Silicon Anode for Li-Ion Batteries: Understanding the Surface Modification Mechanism of Fluoroethylene Carbonate as an Effective Electrolyte Additive

Chao Xu<sup>1</sup>, Fredrik Lindgren<sup>1</sup>, Bertrand Philippe<sup>2</sup>, Mihaela Gorgoi<sup>3</sup>, Fredrik Björefors<sup>1</sup>, Kristina Edström<sup>1</sup> and Torbjörn Gustafsson<sup>1</sup>

<sup>1</sup>Department of Chemistry - Ångström Laboratory, Uppsala University, Box 538, SE-75121 Uppsala, Sweden;

<sup>2</sup>Department of Physics and Astronomy, Uppsala University, Box 516, SE-75121, Uppsala, Sweden;

<sup>3</sup>Helmholtz-Zentrum Berlin, 12489 Berlin, Germany

E-mail: chao.xu@kemi.uu.se

Silicon as a negative electrode material for lithium-ion batteries has substantially higher capacity than conventional graphite electrode, but suffers from problems such as low coulombic efficiency and poor capacity.<sup>1-4</sup> In this study, fluoroethylene carbonate (FEC) was used as electrolyte additive for commercialized LP40 (1 M LiPF<sub>6</sub>, ethylene carbonate (EC) : diethyl carbonate (DEC) = 1:1) electrolyte and significantly improved cyclability of silicon-based electrode. The solid electrolyte interphase (SEI) formed from the decomposition of ethylene carbonate (EC) and diethyl carbonate (DEC), without the FEC additive present, was observed to cover surface voids and lead to an increase in polarization. However, with the presence of FEC, which degrades at a higher reduction potential than EC and DEC, instantaneously a conformal SEI was formed on the silicon electrode as shown in figure 1. The decomposition of the FEC additive was investigated by synchrotron-based X-ray photoelectron spectroscopy (PES) giving a chemical composition depth-profile. The reduction products of FEC were found to mainly consist of LiF and -CHF-OCO<sub>2</sub>- type compounds. This stable SEI layer sufficiently limited the emergence of large cracks and preserved the original surface morphology as well as suppressed the additional SEI formation from the other solvent. Moreover, FEC influenced the lithium salt LiPF<sub>6</sub> decomposition reaction and may have suppressed further salt degradation. This study highlights the vital importance of how the chemical composition and morphology of the SEI influence battery performance.

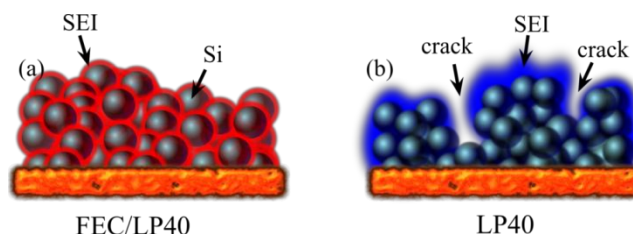


Figure 1. Schematic representation of the SEI formation on silicon anode which is long-time cycled with different electrolytes FEC/LP40 (a) and LP40 (b), respectively. The two SEI layers are different in compositions and highlighted with different colors.

## References

1. Obrovac, M. N.; Christensen, L. *Electrochem. Solid-State Lett.* **2004**, *7*, A93.
2. Etacheri, V.; Marom, R.; Elazari, R.; Salitra, G.; Aurbach, D. *Energy Environ. Sci.* **2011**, *4*, 3243.
3. Ryu, J. H.; Kim, J. W.; Sung, Y.-E.; Oh, S. M. *Electrochem. Solid-State Lett.* **2004**, *7*, A306.
4. Oumellal, Y.; Delpuech, N.; Mazouzi, D.; Dupré, N.; Gaubicher, J.; Moreau, P.; Soudan, P.; Lestriez, B.; Guyomard, D. *J. Mater. Chem.* **2011**, *21*, 6201.

# Semi-solid flow battery: an emerging electrochemical system

Edgar Ventosa,<sup>a</sup> Cristina Flox,<sup>b</sup> Joan Ramon Morante,<sup>b</sup> and Wolfgang Schuhmann<sup>a</sup>

<sup>a</sup> *Analytische Chemie – Center for Electrochemical Sciences (CES), Ruhr-Universität Bochum, Universitätstr. 150, D-44780 Bochum, Germany.*

<sup>b</sup> *Catalonia Institute for Energy Research, Jardins de les Dones de Negre, e1, 08930 Sant Adria de Besos, Barcelona, Spain.  
edgar.ventosa@rub.de*

Redox flow batteries (RFB) are promising technologies for energy storage due to the long life, low cost, high round-trip efficiency and independent scalability of energy and power capabilities. Semi-solid flow batteries (SSFBs) are a special class of RFB, in which anolyte and catholyte consist of flowable suspensions of solid active materials rather than dissolved redox species. Thus, the concentration of active redox centres in the anolyte and catholyte of the SSFB can be significantly increased.<sup>1</sup> Using intercalation type active materials such as those typically used in Li-ion batteries (LIBs), e.g.  $\text{Li}_4\text{Ti}_5\text{O}_{12}$ ,  $\text{LiCoO}_2$  or  $\text{LiNi}_{0.5}\text{Mn}_{1.5}\text{O}_4$ , the energy densities can reach up to  $300\text{--}500\text{ W h L}^{-1}$ , which is more than 10 times higher than that of all-vanadium RFBs ( $40\text{ W h L}^{-1}$ ). Compared to LIBs, SSFBs present several advantages: (I) power and energy can be scaled independently, (II) the amount of inactive materials such as current collectors or housing is decreased, and (III) the manufacturing processes become simpler and more cost-effective.

Since SSFBs deploy Li-ion or Na-ion host materials, SSFBs and classic solid electrode batteries share the same chemistry. However, the replacement of solid electrodes of classic ion batteries by the fluid electrodes employed in semi-solid flow batteries brings new electrochemical challenges. After revising the fundamentals of the operating principles of SSFBs, two particular new challenges are presented and discussed: i) the critical influence of the electrical conductivity of the active materials,<sup>2</sup> and ii) the new role of the solid electrolyte interphase (SEI).<sup>3,4</sup> In the first case, the weaker electrical conductivity of fluid electrodes allows ionic and electric phenomena to be easily differentiated, which is used to study the electric charge/discharge mechanisms of battery materials. In the second case, the SEI changes from ionic to electron barrier, for classic solid electrode batteries and SSFBs, respectively, and results in different limitations.

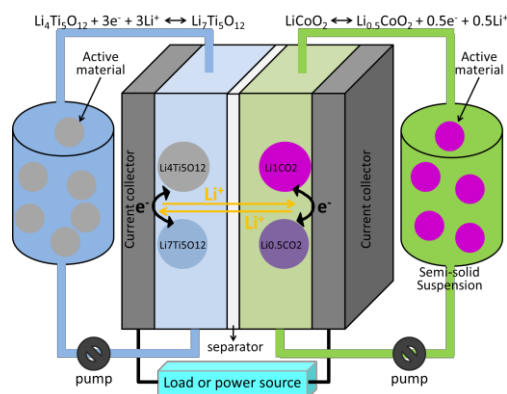


**Figure 1.** Scheme of a semi-solid flow battery based on  $\text{Li}_4\text{Ti}_5\text{O}_{12}$  and  $\text{LiCoO}_2$

1. M. Duduta, B. Y. Ho, V. C. Wood, P. Limthongkul, V. E. Brunini, W. C. Carter and Y.-M. Chiang, *Adv. Energy Mater.*, **2011**, 1, 511
2. E. Ventosa, M. Skoumal, F. J. Vazquez, C. Flox, J. Arbiol, J. R. Morante, *ChemSusChem*, **2015**, DOI: 10.1002/cssc.201500349
3. E. Ventosa, D. Buchholz, S. Klink, C. Flox, L. Gomes-Chagas, C. Vaalma, W. Schuhmann, S. Passerini and J. R. Morante, *Chem. Commun.*, **2015**, 51, 7298
4. E. Ventosa, G. Zampardi, C. Flox, F. La Mantia, W. Schuhmann, J. R. Morante, in preparation.

**Acknowledgement** The research leading to these results has received funding from the European Union Seventh Framework Programme (FP7/2007- 2013) under grant agreement n8 608621

# Insights into the Absorption Mechanism of Carbon Nanotube Paper-Titanium Dioxide as a Multifunctional Barrier for Lithium-Sulfur Batteries

Guiyin Xu, Bing Ding, Hui Dou, Ping Nie, Jin Pan, Xiaogang Zhang\*

Jiangsu Key Laboratory of Materials and Technology for Energy Conversion, College of Material Science and Engineering, Nanjing University of Aeronautics and Astronautics  
Nanjing, 210016, P. R. China

\*Email: azhangxg@163.com

Lithium-sulfur (Li-S) batteries are considered to be one of the most promising energy storage devices in next generation high energy power system, owing to their high specific capacity ( $1675 \text{ mAh g}^{-1}$ ) and energy density ( $2600 \text{ Wh kg}^{-1}$ ).<sup>1-3</sup> However, the insulation of sulfur and high solubility of lithium polysulfide in the organic electrolyte lead to the low utilization of active materials and the poor cycling performances, which seriously impede the rapid development of Li-S batteries.<sup>4-6</sup>

In this work, we discover that a multifunctional carbon nanotube paper/titanium dioxide barrier can effectively reduce the loss of active materials and suppress the diffusion of lithium polysulfide to the anode (**Figure 1**), thereby improving the cycling stability of lithium-sulfur batteries. Moreover, we investigate the special interactions between  $\text{TiO}_2$  and sulfur species with scanning transmission electronic microscope (STEM), X-ray photoelectron spectroscopy (XPS), Raman spectra, and the density functional theory (DFT) calculation. Results of these studies will be presented and discussed.

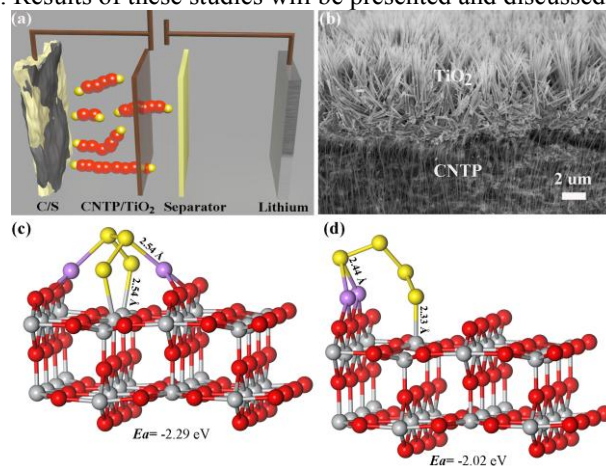


**Figure 1.** (a) Illustration for the special construction of Li-S batteries. (b) Scanning electron microscopy (SEM) image of CNTP/ $\text{TiO}_2$  cross-section. (c, d) The representative geometries of the  $\text{Li}_2\text{S}_4$  molecules on rutile  $\text{TiO}_2$  (110) surface.

## References

- (1) Ji, X. L.; Lee, K. T.; Nazar, L. F. *Nat. Mater.* **2009**, *8*, 500-506.
- (2) Bruce, P. G.; Freunberger, S. A.; Hardwick, L. J.; Tarascon, J. M. *Nat. Mater.* **2012**, *11*, 19-29.
- (3) Su, Y. S.; Manthiram, A. *Nat. Commun.* **2012**, *3*, 1166.
- (4) Yin, Y. X.; Xin, S.; Guo, Y. G.; Wan, L. J. *Angew. Chem. Int. Ed.* **2013**, *52*, 13186-13200.
- (5) Xu, G.; Ding, B.; Nie, P.; Shen, L.; Dou, H.; Zhang, X. *ACS Appl. Mater. Interfaces* **2013**, *6*, 194-199.
- (6) Wei Seh, Z.; Li, W.; Cha, J. J.; Zheng, G.; Yang, Y.; McDowell, M. T.; Hsu, P. C.; Cui, Y. *Nat. Commun.* **2013**, *4*, 1331.

# Electrochemical Performance of 0.5Li<sub>2</sub>MnO<sub>3</sub>–0.5Li(Mn<sub>0.375</sub>Ni<sub>0.375</sub>Co<sub>0.25</sub>)O<sub>2</sub> Composite Cathode Using Pyrrolidinium-based Ionic Liquid Electrolytes

Jagabandhu Patra<sup>1</sup>, Prem Prakash Dahiya<sup>2</sup>, Jason Fang<sup>3</sup>, Yu-Wei Lin<sup>3</sup>,  
Chung-Jen Tseng<sup>4</sup>, S. Basu<sup>5</sup>, S. B. Majumder<sup>2</sup>, Jeng-Kuei Chang<sup>1,\*</sup>

<sup>1</sup> Institute of Materials Science and Engineering, National Central University, Taiwan

<sup>2</sup> Materials Science Centre, Indian Institute of Technology, Kharagpur, West Bengal, India

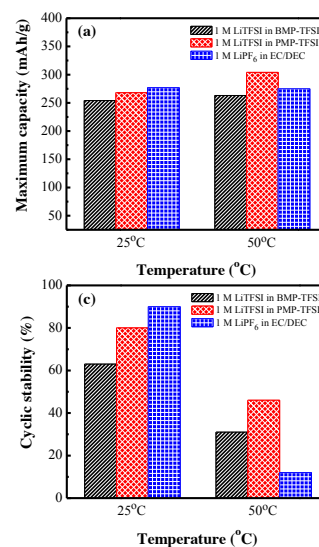
<sup>3</sup> Division of Energy Storage Materials & Tech, Industrial Technology Research Institute, Taiwan

<sup>4</sup> Department of Mechanical Engineering, National Central University, Taiwan

<sup>5</sup> Department of Physics and Meteorology, Indian Institute of Technology, Kharagpur, West Bengal, India

\*e-mail address-[jkchang@ncu.edu.tw](mailto:jkchang@ncu.edu.tw)

**Abstract:** High-energy-density 0.5Li<sub>2</sub>MnO<sub>3</sub>–0.5Li(Mn<sub>0.375</sub>Ni<sub>0.375</sub>Co<sub>0.25</sub>)O<sub>2</sub> composite cathodes for lithium rechargeable batteries are synthesized using an auto-combustion method. The electrode charge-discharge properties are studied at 25°C and 50°C in Li<sup>+</sup>-containing N-butyl-N-methylpyrrolidinium bis(trifluoromethanesulfonyl)imide (BMP-TFSI) and N-propyl-N-methylpyrrolidinium bis(trifluoromethanesulfonyl)imide (PMP-TFSI) ionic liquid (IL) electrolytes. The IL electrolytes possess high decomposition temperature (~400 °C) and thus they are ideal for high-safety applications. As compared to Li<sup>+</sup>/BMP-TFSI IL, Li<sup>+</sup>/PMP-TFSI IL exhibits higher ionic conductivity and lower viscosity. As a result, the composite cathode exhibits comparatively superior electrochemical performance in Li<sup>+</sup>/PMP-TFSI IL electrolyte. With an increase in cell temperature from 25 to 50 °C, the maximum capacities and rate capabilities of both IL cells are significantly improved. The discharge capacities of 304 mAhg<sup>-1</sup> (@10 mA g<sup>-1</sup>) and 223 mAhg<sup>-1</sup> (@100 mA g<sup>-1</sup>) are obtained at 50 °C for the Li<sup>+</sup>/PMP-TFSI cell, which are superior to those for a control cell with a conventional organic electrolyte. We have reported that at elevated temperature the cyclability of the composite cathode is markedly improved when the IL electrolytes (rather than a conventional organic electrolyte) are used. We also performed immersion tests to evaluate the electrode deterioration and post mortem characterizations by SEM and XRD to explain the improved performance of 0.5Li<sub>2</sub>MnO<sub>3</sub>–0.5Li(Mn<sub>0.375</sub>Ni<sub>0.375</sub>Co<sub>0.25</sub>)O<sub>2</sub> in IL electrolytes. The pyrrolidinium based IL electrolytes can be used as safe electrolytes for lithium-ion batteries with the Li-rich rich composite cathode.



# New Concept Aqueous Rechargeable Batteries with High Energy Densities

Yuping Wu<sup>1,2,\*</sup>, Zheng Chang<sup>2</sup>, Yanfang Wang<sup>2</sup>

*College of Energy, Nanjing Tech University, Nanjing 211816, Jiangsu Province, China  
New Energy and Materials Laboratory (NEML), Department of Chemistry & Shanghai Key Laboratory  
of Molecular Catalysis and Innovative Materials, Fudan University, Shanghai 200433, China  
e-mail: wuyp@njtech.edu.cn, wuyp@fudan.edu.cn*

Batteries is originally from aqueous solution. To further increase their energy densities, one revolutionary example of rechargeable batteries is the birth of lithium ion batteries in the early 1990s. However, the safety from the combustible organic electrolytes is a serious and challenging problem in the case of large-scale applications such as energy storage in smart grids. As a result, it comes back to aqueous electrolyte again to search for a solution. The aqueous solution should be neutral and green, and one example is aqueous rechargeable lithium batteries (ARLBs) and aqueous rechargeable sodium batteries (ARSBs) [1-3]. Recently, the energy density is markedly improved in comparison with that for lithium ion batteries due to the “cross-over” effect instead of the traditional overpotentials [4]. This effect will bring unpredicted promise for the new power sources since it can markedly increase the output voltage of aqueous batteries to above 3 V, much higher than the theoretical stable window of water, 1.23 V. The estimated practical energy density will be much higher than those for lithium ion batteries. For example, the estimated practical energy densities for 2nd and 3rd generations ARLBs will be 170-230 and > 400 Wh/kg [4-6]. This opens new choices for smart grids and electric vehicles as a chemistry of post lithium ion batteries.

**Acknowledgment:** Financial support from Distinguished Young Scientists Program of NSFC (51425301) is gratefully appreciated.

## References:

- [1] W. Tang, L.L. Liu, Y.S. Zhu, H. Sun, Y.P. Wu, K. Zhu, *Energy Environ. Sci.*, 5, 6909-6913 (2012).
- [2] W. Tang, Y.S. Zhu, Y.Y. Hou, L.L. Liu, Y.P. Wu, K.P. Loh, H.P. Zhang and Kai Zhu, *Energy Environ. Sci.*, 6, 2093-2104 (2013).
- [3] B.H. Zhang, Y. Liu, X.W. Wu, Y.Q. Yang, C.L. Hu, Z.B. Wen, Y.P. Wu, *Chem. Commun.*, 50, 1209 - 1211 (2014).
- [4] X.J. Wang, Y.Y. Hou, Y.S. Zhu, Y.P. Wu, R. Holze, *Sci. Rep.*, 3, 1401 (2013).
- [5] X.J. Wang, Q.T. Qu, Y.Y. Hou, F.X. Wang, Y.P. Wu, *Chem. Commun.*, 49, 6179 - 6181 (2013).
- [6] Z. Chang, X.J. Wang, Y.Q. Yang, J. Gao, L.L. Liu, M.X. Li, Y.P. Wu, *J. Mater. Chem. A.*, 2 (45), 19444 – 19450 (2014).



# Free standing sulfur-composite cathode for lithium-sulfur batteries

Almagul Mentbayeva<sup>1,2</sup>, Aishuak Konarov<sup>1,2</sup>, Ayaulym Belgibayeva<sup>1,3</sup>, Nurzhan Umirov<sup>1,2</sup>, Zagipa Bakenova<sup>1</sup>, Toru Hara<sup>1,2</sup>, Zhumabay Bakenov<sup>1,2\*</sup>

<sup>1</sup>*Institute of Batteries LLC, Nazarbayev University Research and Innovation System  
Kabanbay Batyr 53, Astana 010000, Kazakhstan*

<sup>2</sup>*Nazarbayev University, Kabanbay Batyr 53, Astana 010000, Kazakhstan*

<sup>3</sup>*Gumilev Eurasian National University, Mirzoyan 2, Astana 010008, Kazakhstan  
z.bakenov@nu.edu.kz*

Lithium sulfur (Li/S) battery is an attractive electrochemical energy storage system with a high theoretical specific capacity of 1672 mAh g<sup>-1</sup> and a theoretical energy density of 2600 Wh kg<sup>-1</sup> [1]. Sulphur is a promising active material also because of its abundance, low-cost and environmentally friendliness when compared with certain toxic transition-metal compounds.

However, practical application of Li/S batteries is hindered by several drawbacks as: the electrical-insulating nature of sulfur results in its low utilization; lithium polysulfides intermediate products of electrochemical process are easily soluble into the organic electrolytes, which leads to severe capacity fading and low coulombic efficiency.

Numerous attempts have been made to overcome these disadvantages by mixing sulfur with conducting agents such as conducting carbon materials and/or conductive polymers [2-3]. In result the utilization of sulfur and capacity per the unit mass of sulfur have been improved by these methods. Carbon nanotubes (CNTs) have been extensively studied as conductive matrix to load sulfur due to their large specific surface area and abundant active sites [4]. Though more open porous structures formed by CNTs greatly improved electrolyte infiltration. However, the addition of a large amount of conducting agent and binder results in the lower practical capacity per the unit mass of cathode composite. Furthermore, conventional electrodes for lithium-ion batteries need current collectors, such as metal foils, resulting in even lower available gravimetric capacity of electrode.

In current work a novel sulfur/polyacrylonitrile/multiwalled carbon nanotube ternary composite electrode (S/PAN/MWCNT) without binder and current collector was prepared by simple technique and examined as a cathode for Li/S battery (Fig. 1). The partially pyrolyzed and cyclized PAN can stabilize sulfur and suppress the sulfur dissolution into electrolyte solutions through the redistribution of electrons in the outermost electronic orbitals of sulfur or through forming chemical bonds between PAN and sulfur, because of polarized C-N chemical bonds.

Formation of a homogeneous hierarchical mesoporous structure was observed by SEM, EDS mapping and XRD techniques. The lithium cell with this ternary composite cathode delivered a discharge capacity of 489 mAh per gram of cathode (1450 mAh g<sup>-1</sup> S) in the second cycle at 0.2 C, and retained about 85% of this value over 200 cycles. Even up to 2 C rate, the lithium cell demonstrated an excellent rate capability, delivering a highly reversible discharge capacity of 950 mAh g<sup>-1</sup>.



Fig 1. Schematic of the S/PAN/MWCNT binder free cathode preparation and it's cycleability at 0.2 C.

## References

- [1] X. L. Ji, L. F. Nazar, J. Mater. Chem. 20 (2010) 9821–9826.
- [2] Y. Zhao, Z. Bakenova, Y. Zhang, Z. Bakenov, Ionics DOI: 10.1007/s11581-015-1376-4.
- [3] Y. Zhang, Y. Zhao, Z. Bakenov, Nanoscale Research Letters 9 (2014) 137-143.
- [4] W. Zheng, Y. W. Liu, X. G. Hu, C. F. Zhang, Electrochim. Acta 51 (2006) 1330-1335.

## Acknowledgements

This was supported by the Sub-project #157-2013 funded under the Technology Commercialization Project supported by the World Bank and the Government of the Republic of Kazakhstan.



# The Design and Preparation of Multi-dimensional Nanostructured Materials and electrochemical storage

Shujiang Ding

Department of Applied Chemistry, Xi'an Jiaotong University, Xi'an, China, 710049

Email: dingsj@mail.xjtu.edu.cn

Herein, we report some facile and general methods to directly grow metal oxide ( $\text{TiO}_2$ ,  $\text{SnO}_2$ ,  $\text{NiO}$ ,  $\text{Co}_3\text{O}_4$  and  $\text{NiCo}_2\text{O}_4$ ) or metal sulfide ( $\text{MoS}_2$ ) nanosheets on sulfonated polystyrene spheres, modified CNTs or graphene oxide. After calcinations in air or inert atmosphere, these materials were converted into metal oxides hollow spheres assembled from nanosheets and metal oxides nanosheets@carbon (amorphous, graphene and CNTs) materials. Due to the porous structure (derived from the pile of nanosheets) and internal voids, these metal oxide nanosheets can store more lithium ions, have more fast lithium ions transfer rate and thus exhibit improved lithium storage capability. The graphene and CNTs support serves as a highly conductive substrate that is beneficial to the better lithium ions storage performance.

Keywords: Nanosheets; Hollow; Graphene; Carbon Nanotubes; Lithium-ions Batteries; Supercapacitor

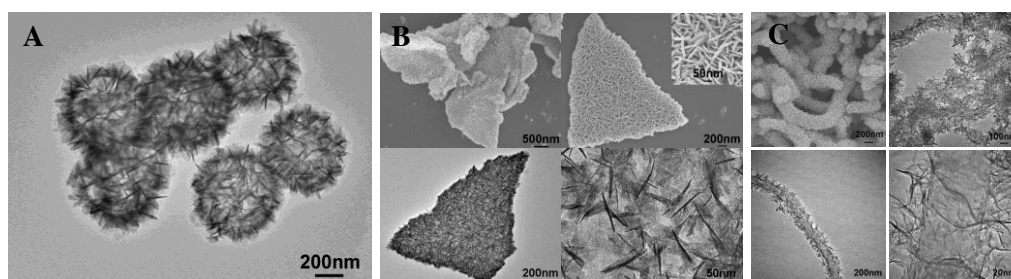


**Fig. 1** SEM and TEM images: A)  $\text{SnO}_2$  nanosheets hollow spheres; B)  $\text{SnO}_2$  nanosheets@graphene; C)  $\text{TiO}_2$  nanosheets@CNTs.

## References:

- [1] Ding, S., Chen, J.; Lou X. Adv. Funct. Mater., 2011, 21, 4120.
- [2] Ding, S.; Chen, J.; Wang Z.; Cheah Y.; Madhavi, S.; Lou X., J. Mater. Chem., 2011, 21, 1677.
- [3] Ding, S.; Chen, J.; Luan, D.; Boey, F.; Madhavi, S.; Lou X., Chem. Commun., 2011, 47, 5780.
- [4] Ding, S.; Lou X., Nanoscale, 2011, 3, 3566.

# **The role of the oxygen in the $\text{Li}_2\text{MnO}_3$ cathode material for the Li-ion batteries**

Eunseog Cho, Kihong Kim, Changhoon Jung, Hyo Sug Lee, Kyoungmin Min, Woo Sung Jeon,  
Gyeong-Su Park, and Jaikwang Shin

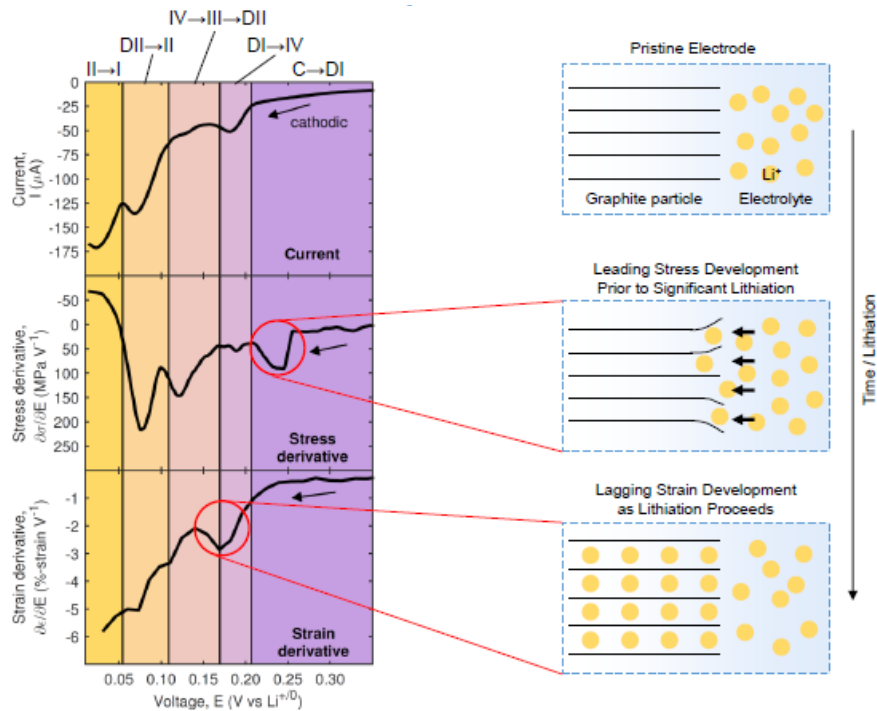
*Platform Technology Lab, Samsung Advanced Institute of Technology, Samsung Electronics*  
*130 Samsung-ro, Yeongtong-gu, Suwon-si, 443-803, Gyeonggi-do, Korea*  
*eunseog.cho@samsung.com*

In order to develop a battery with the large capacity and the long life cycle for the electric vehicles and the mobile devices, Li-rich layered oxides have been proposed and widely investigated.  $\text{Li}_2\text{MnO}_3$  was known to be electrochemically inactive in the past studies. However, the recent researches have proven that it could be electrochemically active under the higher cell voltage. In this perspective,  $\text{Li}_2\text{MnO}_3$  is being newly focused as the great potential candidate and it also contains a large number of lithium ions compared to other conventional cathode materials such as  $\text{LiCoO}_2$ . Recently, many experimental and theoretical studies reported that the oxygen atom rather than the manganese plays an important role in the operation of the battery. However, the fundamental role of oxygen during the charge-discharge cycle has not been fully understood. In this talk, we will present our recent findings using theoretical calculations based on the density functional theory as well as the experimental measurements of the characteristics of cell charge-discharge behavior and *in situ* XANES spectroscopy. More specifically, following understandings will be mainly discussed. (1) Oxygen atoms in the transition metal layer mainly participate in the charge compensation process for the electrochemical activity of  $\text{Li}_2\text{MnO}_3$ . (2) Oxygen atom can be released at the very early stage of the charge cycle and this leads to the cell voltage drop. (3) During delithiation process, the oxygen-loss is accelerated and the oxygen released structure becomes more energetically stable. (4) The reduced intensity and the shift of the XANES spectra are originated from the oxygen-loss phenomena.

# Electrochemical Stiffness in Lithium Ion Batteries

Andrew A. Gewirth, Hadi Tavassol, Elizabeth M. C. Jones, Nancy R. Sottos  
University of Illinois  
600 S. Mathews Avenue, Urbana, IL 61801 USA  
agewirth@illinois.edu

Higher power and charging rates are essential for large scale adoption of lithium-ion batteries in transportation applications. While lithium-ion batteries are ubiquitous in portable electronics, their performance and lifetime suffer during high rate charging and high power discharging. In such extreme electrochemical conditions, the mechanical response of electrode materials governs their degradation behavior. Here, we present a new technique to probe the electrochemically-induced mechanics of electrodes by calculating the electrochemical stiffness of electrodes via coordinated *in situ* stress and strain measurements. Through the electrochemical stiffness, we elucidate inherent and rate-dependent mechanical responses of graphitic battery electrodes. We find that stress and strain are asynchronous as shown in the figure. In particular, stress development is found to lead strain development as different graphite-lithium intercalation compounds are formed. Additionally, our analysis reveals inversely scaled rate-dependent behaviors for stress and strain responses. Stress scales as scan rate while strain scales with charge (or, equivalently, capacity). These measurements provide a new paradigm for understanding mechanical effects in intercalation systems, such as batteries. Stress arises as resistance to lithiation, while strain arises as a consequence of lithiation. Electrochemical stiffness measurements provide new insights into the origin of the rate-dependent chemo-mechanical degradations, and provide a probe to evaluate advanced battery electrodes.



# Forward and reverse differential-pulse applied in the formation of solid electrolyte interface with constant temperature addition in lithium ion battery

Jung-Chi Wang<sup>1</sup>, Fu-Ming Wang<sup>1,2\*</sup>

<sup>1</sup>*Graduate Institute of Applied Science and Technology, National Taiwan University of Science and Technology*

<sup>2</sup>*Sustainable Energy Center, National Taiwan University of Science and Technology*

*43 Keelung Road, Section 4, Taipei 10607, Taiwan*

*Correspondence: mccabe@mail.ntust.edu.tw*

The solid electrolyte interface (SEI) is a chemical-formed membrane, which has good ion conductivity and electron insulation as well as a protection layer that prevents the exfoliation of graphite in redox process. Normally, the first cycle in commercial protocol uses a constant current and constant voltage method (CC-CV), and this process creates a highly porous and polarized SEI, which degrades the performance of Li ions battery [1]. In our previous result, the forward and reverse differential-pulse method (FRDP) is studied to improve the characteristics of SEI [2]. In this study, the SEI formation adds a constant temperature in combined with FRDP.

The constant temperature-FRDP mechanism (CT-FRDP) is investigated in two kinds of electrolytes, EC/EMC and EC/PC/DEC at the temperatures of 25 and 40°C. All of the battery samples are charged and cycled at a high rate and a high temperature in order to examine the performance. In addition, the electrode's surface is also observed by scanning electron microscopy, electrochemical impedance spectroscopy, X-ray photoelectron spectroscopy, and Li ion kinetics analysis.

The results indicate that a unique species is found and furnishes a temporary redox behavior only during the CT-FRDP process. This unique species sensitively works on anode's surface and enhances the formation of SEI. We believe that temporary redox behavior creates a new reaction mechanism of SEI and this reaction pathway displays a crucial route for battery application.

## Reference

- [1] F. M. Wang, H. Y. Wang, M. H. Yu, Y. J. Hsiao and Y. Tsai, *J. Power Sources* 196 (2011) 10395.
- [2] F. M. Wang, J. C. Wang and J. Rick, *Electrochim. Acta* 147 (2014) 582.

# Advanced Anode Materials combining Conversion & Alloying Energy Storage Mechanism for Lithium-Ion Batteries

Franziska Mueller,<sup>1,2</sup> Dr. Dominic Bresser,<sup>1,4</sup> Ulderico Ulissi,<sup>1</sup> Prof. Dr. Stefano Passerini<sup>1</sup>

<sup>1</sup> Helmholtz Institute Ulm (HIU), Chemistry of the Battery<sup>3</sup>, Helmholtzstr. 11, 89081, Ulm, Germany

<sup>2</sup> Institute of Physical Chemistry, University of Muenster, Corrensstr. 28/30, 48149 Muenster, Germany

<sup>3</sup> Karlsruhe Institute of Technology (KIT), P.O. Box 3640, 76021 Karlsruhe, Germany

<sup>4</sup> INAC/SPRAM/PCI, CEA Grenoble, UMR-5819, CEA-CNRS-UJF, 17 Rue de Martyrs, 38054 Grenoble, Cedex 9, France

franziska.mueller@kit.edu

The steadily increasing demand for high-energy storage devices for portable consumer electronics as well as for large-scale applications as, for instance, electric vehicles, propels the battery research forward. Nowadays, lithium-ion batteries are the state-of-the-art energy storage device due to their high energy, power density and efficiency, as well as long durability [1]. However, especially for large-scale applications the energy density of commercial batteries is still insufficient. Thus, the utilization of new active materials with higher specific capacity than the currently used anode and cathode materials might enable an improved energy density [1]. Accordingly, instead of insertion or intercalation anode materials alternative higher specific capacity anode materials reversibly storing lithium by an alloying or conversion process are intensively investigated. Herein, we present our studies on anode materials based on mixed conversion/alloying lithium-ion storage mechanism, which are ideally characterized by low (de-)lithiation potential, high coulombic efficiency and long-term cycling stability. In order to gain deeper insights into the crystal structure of the synthesised samples and into the mixed conversion/alloying lithium storage mechanism of this rather new class of materials various characterisation method as, for instance, X-ray diffraction, X-ray photoelectron spectroscopy, X-ray absorption spectroscopy, scanning electron microscopy and electrochemical techniques were employed.

In Fig. 1 the galvanostatic cycling tests for two anode materials from the class of transition metal-doped metal oxides are presented. Both materials show a highly stable cycling behaviour with an extraordinary high specific capacity compared to the conventionally utilised anode material graphite ( $372 \text{ mAh g}^{-1}$ ). The specific capacity of Fe-doped ZnO is about  $1100 \text{ mAh g}^{-1}$  after 60 cycles. Fe-doped SnO<sub>2</sub> reaches a reversible specific capacity of more than  $1500 \text{ mAh g}^{-1}$  after 10 cycles.

By means of our studies, we were able to elucidate the crystal structure and to propose a lithium storage mechanism for Fe-doped oxides. The family of transition metal-doped metal oxides show a great potential as high capacity anode material for application in lithium-ion batteries. Moreover, our recent studies demonstrate the potential of utilizing mixed alloying/conversion lithium storage materials in practical applications.

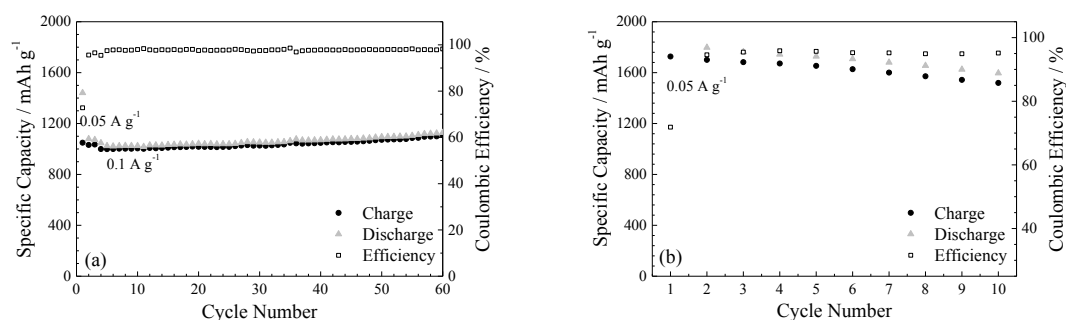


**Fig. 1.** Specific capacity vs. cycle number; cut-off potentials: 0.01 V and 3.0 V vs. Li/Li<sup>+</sup>. (a) Carbon coated iron-doped zinc oxide [2]; (b) carbon coated iron-doped tin oxide [3].

[1] B. Scrosati, J. Garche, Lithium batteries: Status, prospects and future, J. Power Sources 195 (9) (2010) 2419-2430.

[2] F. Mueller, D. Bresser, E. Paillard, M. Winter, S. Passerini, Influence of the carbonaceous conductive network on the electrochemical performance of ZnFe<sub>2</sub>O<sub>4</sub> nanoparticles, J. Power Sources: 236 (2013) 87-94.

[3] F. Mueller, D. Bresser, V.S.K. Chakravadhanula, S. Passerini, Fe-doped SnO<sub>2</sub> nanoparticles as new high capacity anode material for secondary lithium-ion batteries, manuscript submitted.

# In-situ Raman Spectroscopy and EQCM study of Lithium-Sulfur Batteries

Heng-Liang Wu, Laura A. Huff and Andrew A. Gewirth  
 Department of Chemistry, University of Illinois at Urbana-Champaign,  
 600 S. Mathews Avenue, Urbana, IL 61801 USA.  
 notcool@illinois.edu

In this talk, in-situ Raman spectroscopy and electrochemical quartz crystal microbalance (EQCM) measurements were used to investigate the mechanism of sulfur reduction in lithium-sulfur battery slurry cathodes. Raman spectroscopy shows that long chain polysulfides ( $S_8^{2-}$ ) were formed via  $S_8$  ring opening in the first reduction process at  $\sim 2.4$  V vs  $Li/Li^+$  and short chain polysulfides such as  $S_4^{2-}$ ,  $S_4^-$ ,  $S_3^{2-}$  and  $S_2O_4^{2-}$  were observed with continued discharge at  $\sim 2.3$  V vs  $Li/Li^+$  in the second reduction process. These polysulfides are all reversible during charge process. Elemental sulfur can be reformed in the end of the charge process. (1-4)

Rate constants obtained for the appearance and disappearance polysulfide species show that short chain polysulfides are directly formed from  $S_8$  decomposition. The rate constants for  $S_8$  reappearance and polysulfide disappearance on charge were likewise similar, suggesting that polysulfide oxidation and reduction is quasi-reversible. The formation rate of polysulfide species depends on the potential. The rate obtained at 1.5V is three times larger than 2.2 V, suggesting the larger driving force in the decomposition  $S_8$  and the formation of short chain polysulfides. The formation of polysulfide mixtures at partial discharge was quite stable for at least 2hr. We also examined the effect of  $CS_2$  addition on the sulfur reduction mechanism. Electrochemical and Raman results show that  $CS_2$  stabilizes the  $S_8^{2-}$  product and inhibits further discharge of the cell.

In-situ EQCM results show that the sulfur-carbon cathode gains Sauerbray-mass during the first discharge plateau. The crystal resistance ( $R_c$ ) was used to monitor the viscosity ( $\eta_L$ ) and density ( $\rho_L$ ) of the polysulfides in contact with electrode as well as the change of electrode surface. (5) The change in  $R_c$  after first discharge plateau suggests that the Sauerbray equation is no longer valid and that the porosity of sulfur-carbon cathode increases particularly in the lower potential region (e.g. 1.5 V). The battery performance results also show the more stable capacity in the cycling region between 3.2 V to 1.8 V relative to 3.2 V to 1.5 V. Finally, we also report that new additives in Li-S batteries both stabilize polysulfides and contribute to better cycling performance.

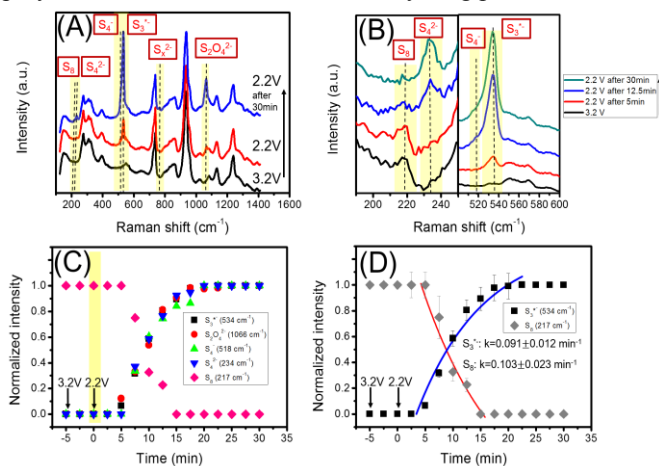


Figure 1(A-B) In-situ Raman spectra of the sulfur-carbon cathode obtained at partial discharge (C-D) The normalized intensity of sulfur species were plotted as a function of time and fit to extract a rate (k).

## References:

- (1) Barchasz, C. et al., Anal. Chem. 2012, 84, 3973.
- (2) Cuisinier, M. et al., J. Phys. Chem. Lett. 2013, 4, 3227.
- (3) Yeon, J.-T. et al., J. Electrochem. Soc. 2012, 159, A130.
- (4) Hagen, M. et al., J. Electrochem. Soc. 2013, 160, A1205.
- (5) Marx, K.A. et al., Biomacromolecules. 2003, 4, 1099.

# Explore the Failure Mechanism in Lithium-ion Batteries by Forensic Analysis Techniques

Alvin Wu, Dean Wu, Carl Wang; Ph. D.  
Underwriters Laboratories Taiwan Co., Ltd.  
1/F, 260, Da-Yeh Road, Peitou, Taipei City, Taiwan 112  
[Alvin.Wu@ul.com](mailto:Alvin.Wu@ul.com)

In the investigation of field incidents involve with lithium-ion batteries, it is always critical to understand the root cause so the safety issues can be identified and improved. However, in reality, finding the root cause and failure mechanism of failed lithium-ion batteries is a big challenge due to two reasons. First of all, the battery may be burned or destroyed so it is hard to find any significant evidence. Secondary, there are usually multiple contributing factors come together to result in catastrophic failure in a battery, so it is not easy to have a solid conclusion of the real cause of the incident.

In order to address this complicated situation, this study proposes a method with a series of forensic analysis techniques is to explore all potential root causes that could arise from issues in battery design, quality and aging effects [1] [2]. A typical process to identify the potential paths of a battery failure event is given in Figure 1 below. To analyze the possible root causes, all of the detailed background information, such as the environmental conditions, system operation status while failure occurs and all data recorded by the battery management system will need to be collected as the basis to logistically develop the basic hypothesis. To check the validity of the assumptions, a forensic analysis approach will be the best way to directly find out scientific evidences. Furthermore, the simulation of all conditions to repeat the field event will sometimes be helpful to achieve a more solid conclusion regarding the failure mechanisms behind the battery incident. A good example of investigation project using the forensic analysis techniques to study the battery field event is the Boeing 787 battery incident in January 2013 at Logan International Airport [3]. The cell design was investigated thoroughly by reverse engineering, analytical techniques, non-destructive and destructive analysis, and simulation of abuse conditions to correlate well between the root causes and safety behaviors under various operating conditions, hence the root cause to the field event can be successfully identified with specific evidences provided.

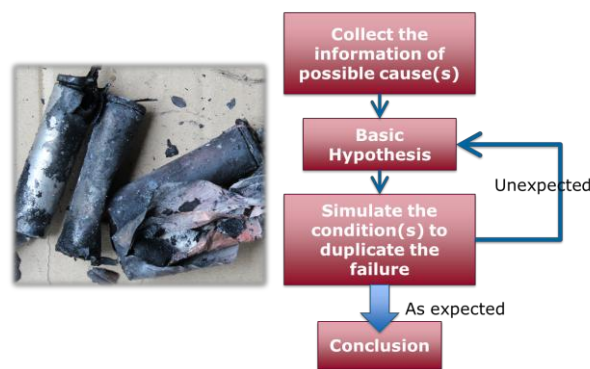


Figure 1. Typical Process to Identify the Root Causes behind Battery Failures

In this study, the key forensic analysis techniques will be introduced and the rationales to link between failure mechanism and battery failure modes will be presented. The forensic analysis method is a powerful tool to identify the root causes behind battery failures.

## Reference

1. [http://newscience.ul.com/wp-content/uploads/2014/04/NS\\_SE\\_Article\\_Forensic\\_Analysis\\_For\\_LIB.pdf](http://newscience.ul.com/wp-content/uploads/2014/04/NS_SE_Article_Forensic_Analysis_For_LIB.pdf)
2. Wu, Alvin, "Lesson Learned from Battery Failures - Best Practice of Forensic Analysis", UL presentation at IEEE ISPCE conference, USA/Chicago, 2015.
3. <http://www.dailymail.co.uk/wires/ap/article-2856441/NTSB-points-battery-defect-Boeing-787-fire.html>
4. Chapin, J. Thomas, et al., "Multi-Level Forensic and Functional Analysis of the 787 Main/APU Lithium Ion Battery", US Government Public Report from NTSB website, 2014

# Research on Polymeric Artificial Solid-Electrolyte-Interphase for Enhanced Performance of Li-ion Battery Anodes

Nae-Lih Wu<sup>a</sup>, Fu-Sheng Li<sup>a</sup>, Yu-Shiang Wu<sup>b</sup>, Jackey Chou<sup>c</sup>, Martin Winter<sup>d</sup>

<sup>a</sup>*Department of Chemical Engineering, National Taiwan University Taipei, Taiwan*

<sup>b</sup>*Department of Mechanical Engineering, China University of Science and Technology, Taiwan*

<sup>c</sup>*Long Time Technology Corp., New Taipei City, Taiwan*

<sup>d</sup>*MEET Battery Research Center, University of Münster, Germany*

*E-mail: nlw001@ntu.edu.tw*

The properties of the interface between electrode active materials and electrolyte are known to have profound effects on the performance of Li-ion batteries (LIBs). A large amount of research has so far been devoted to modifying the surfaces of active materials in order to enhance the overall performance of the electrodes. Majority of the research has resorted to inorganic oxide coatings, presumably due to their chemical stability, and different beneficial effects have been claimed for both cathode and anode materials. Relatively there have been fewer studies on polymeric coating. Compared with the inorganic ones, the polymeric coatings require much lower processing temperature, and when used water as solvent, can be considered as more environmentally-friendly alternative. In addition, the rich chemistry of the polymeric coating intrinsically possess a greater flexibility for dealing with wide varieties of active materials and electrolytes for maximum performance.

For LIB anodes, there are two important issues to deal with for achieving high-energy and high-power performance. First, decomposition of electrolyte at the anode surface takes place at sufficient low potential leading to the formation of a passivation film, known as solid electrolyte interphase (SEI). Formation of the SEI consumes Li ion inventory and hence reduces the overall capacity of the battery cell. Therefore, the amount of the stable SEI layer should theoretically kept at a minimum. Secondly, the power densities for the state-of-the-art graphite electrodes remain insufficient.

In this presentation, we report our studies on developing various polymeric coatings for LIB anodes, particularly for graphite and graphite/Si composite. It is demonstrated that the properties of the anodes in different aspects, such as chemical/electrochemical, mechanical, and wetting behaviors, can be substantially changed with various combinations of different polymer blends. It is shown that both the cycle life and the power performance of the anodes can be remarkably enhanced by simple polymer coating method.



# Manufacturing and Performance of solid-state thin-film batteries

S. Uhlenbruck<sup>1</sup>, H.-G. Gehrke<sup>1</sup>, S. Lobe<sup>1</sup>, C.L. Tsai<sup>1</sup>, C. Dellen<sup>1</sup>, A. Bunting<sup>1</sup>, M. Bitzer<sup>1</sup>, J. Dornseiffer<sup>1</sup>, T. van Gestel<sup>1</sup>, and O. Guillon<sup>1,2</sup>

<sup>1</sup>*Forschungszentrum Jülich GmbH, Institute of Energy and Climate Research,  
Materials Synthesis and Processing (IEK-1), 52425 Jülich, Germany*

<sup>2</sup>*Rheinisch-Westfälische Technische Hochschule (RWTH) Aachen, Institut für Gesteinshüttenkunde,  
Mauerstr. 5, 52064 Aachen, Germany*

*s.uhlenbruck@fz-juelich.de*

The combination of solid ceramic-like electrolytes with inorganic electrodes, thus creating an all solid-state battery, requires a sophisticated co-processing, taking into account the different chemical and thermal stabilities of the applied materials. *Thin-film* batteries allow – on the one hand – a detailed analysis of the compatibility of active storage material and the electrolyte because of dense layer morphology (ideal case) and well-defined planar interfaces. On the other hand, thin-film batteries also have the potential for energy storage solutions in applications with short-term or low power consumption. Optionally, a stacking of active thin layers can increase the energy content.

In general, the deposition and crystallization of a functional layer for solid-state battery cells requires a heat incidence that can lead to an undesired and detrimental diffusion of constituents into the substrate or into adjacent components, to mechanical stresses and resulting cracks due to different coefficients of thermal expansion, or even to a decomposition of parts of the battery. The purpose of this work is a comparison of different materials, Lithium-oxynitride (LiPON) based and Lithium-Lanthanum-Zirconium-oxide (LLZ) based electrolyte materials, and different thin-film deposition processes (for example physical vapor deposition, spin-coating, dip-coating, ink-jet-printing) that are applied to thin-film solid-state battery cells, and their impact on the microstructure, the inter diffusion and, as a result, on the performance of the cells. Analysis was done, among others, by high-resolution scanning electron microscopy, secondary ion mass spectrometry, nuclear reaction analysis, Rutherford backscattering, electrochemical impedance spectroscopy, galvanostatic charge-discharge measurements and cyclic voltammetry.

As an outlook, the economic feasibility of thin-film deposition technologies like physical vapor deposition is discussed.

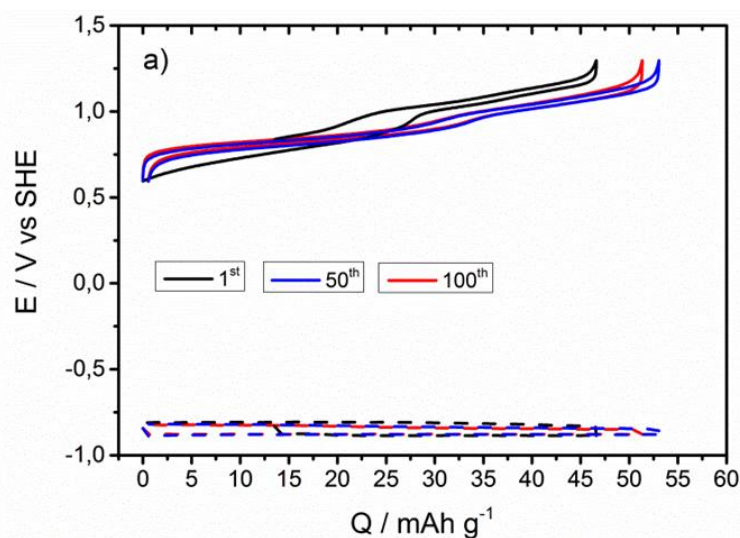
# Aqueous Zinc-Ion Batteries based on Prussian Blue Derivatives

Fabio La Mantia<sup>1,2</sup>

<sup>1</sup>Energiespeicher- und Energiewandlersysteme, Universität Bremen, Badgasteiner Str. 1, 28359 Bremen, Germany

<sup>2</sup>Fraunhofer Institut IFAM, Wiener Straße 12, 28359 Bremen, Germany  
fabio.lamantia@rub.de

Stationary battery systems have been proposed as plausible alternative for the storage of renewable energy sources in power grid. For this application, aqueous electrolytes are preferred, which offer several important advantages compared to organic electrolytes, i.e. non-flammability, cost effectiveness, as well as higher ionic conductivity, salt solubility and thermal capacity. However, most of the aqueous batteries have low voltage, short life cycle, and low stability, deriving from the potential stability window of the electrolyte. We have investigated a zinc-ion battery based on copper hexacyanoferrate (CuHCF) and



Potential profile of CuHCF (solid line) and Zn film (dashed line) at different cycles.

metallic Zn in different aqueous electrolytes. CuHCF works as host structure for the insertion of many different monovalent cations, such as Na<sup>+</sup>, K<sup>+</sup>, and NH<sub>4</sub><sup>+</sup>, and it works as well as hosting structure for different divalent cations. Among them, Zn<sup>2+</sup> can be intercalated at two potentials, equal to 0.8 V (NHE) and 1.1 V (NHE). The average operational voltage of this battery system is equal to 1.73 V at a current rate of 60 mA g<sup>-1</sup> (1 C). In a ZnSO<sub>4</sub> aqueous solution at pH value of 6, the system appears stable for more than 100 cycles, and delivers a specific power of 480 mW g<sup>-1</sup> at a current rate equal to 10 C, considering both mass of positive and negative electrodes. The performances of the battery are affected strongly by the intercalation of Zn<sup>2+</sup> in the CuHCF structure, and by the hydrogen evolution on the surface of the zinc electrode. In particular, it has been observed that H<sub>2</sub> evolution can cause a shift of pH near the surface of the zinc electrode, favoring the stabilization of ZnO, which hinders the performances of the battery. In fact, ZnO is blocking the reaction of dissolution of zinc, due to its insulating character. This detrimental mechanism is blocked when the surface of the zinc becomes rougher, thus enhancing the zinc deposition reaction, which results in a flower-like structure. Moreover, the effect of the anion of the zinc salt on the cycle life and stability of the battery has been analyzed.

# Symposium 3: Investigation of the growth of a SEI-like surface layer on $\text{LiNi}_{0.5}\text{Mn}_{1.5}\text{O}_4$ high voltage cathodes

Klaus Wedlich, Carsten Korte, Detlef Stolten  
Institute of Energy and Climate Research (IEK-3) Forschungszentrum Jülich GmbH  
D-52428 Jülich, Germany, e-mail: k.wedlich@fz-juelich.de

The utilization of high voltage cathode materials (HVC), which provide cell voltages of over 4.5 V, is a promising strategy to increase the specific energy and power density of Li-Ion-Batteries (LIB's). In contrast to commercial available 4 V-cathodes, the electric potential of HVC's exceed the stability window of conventional electrolytes, based on alkylcarbonate solvents [1]. This results in the formation of a surface layer on the cathode analogous to well-known anodic SEI [2-4]. Assuming a simple layer growth, we developed a geometrical model of anodic SEI growth. Such a model implies a linear dependence between the capacity-based state-of-health (SoH-Q) and the impedance-based (cell resistance) state-of-health (SoH-R). The change of the capacity ( $\Delta Q$ ) with time exhibits a square root time dependency which implies a diffusion controlled growth of the surface layer on the anodes.

Adapting this model to high-voltage  $\text{LiNi}_{0.5}\text{Mn}_{1.5}\text{O}_4$ -cathodes (LNMO) which were cycled 300 times and more, show a linear correlation between SoH-Q and SoH-R. A non-square root time dependency of  $\Delta Q$  exhibits a non-diffusion-controlled process. The incremental capacity (IC), which can be obtained from charge/ discharge curves, shows a steady capacity change for a broad potential range. When using carbon, LTO and metallic Li as anode materials we investigate strong differences in the degradation behaviour of these cells. As the capacity loss is caused by the consumption of active lithium in the cathodic and anodic surface layers, cells with Li-Anodes show only a moderate degradation in contrast to cells with carbon or LTO anodes, which are not able to compensate the loss of active material. Carbon anodes additionally seem to promote the degradation of the cells. By constructing LTO-limited cells we found that the degradation is mainly driven by the capacity loss of the cathode. We identified the growth of a surface layer as main ageing mechanism in HVC's.

A characterisation and comparison of the surface layers of the different electrodes is performed by SEM, XPS-analyses and ToF-SIMS measurements.

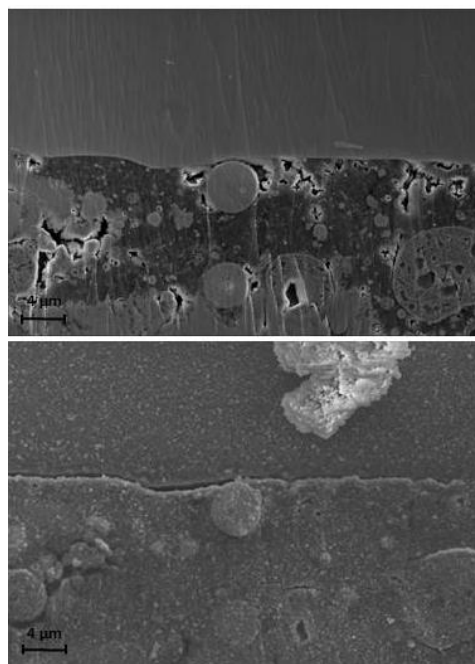


**Figure 1:** surface layer on a LNMO cathode before and after 83 cycles

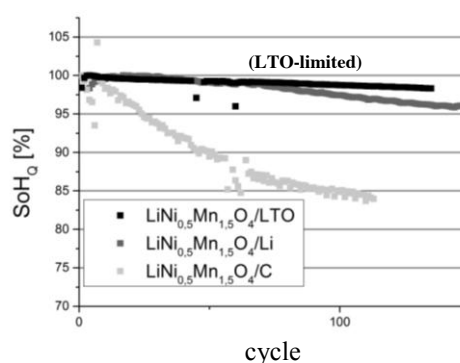


**Figure 2:** comparison of SoH-Q with cycles

- [1] K. Xu, Chem Rev, 104 (2004) 4303-4417.
- [2] J.B. Goodenough, Y. Kim, Chem Mater, 22 (2009) 587-603.
- [3] L. Yang, B. Ravdel, B.L. Lucht, Electrochem Solid St, 13 (2010) A95-A97.
- [4] S.K. Martha, E. Markevich, et al., J Power Sources, 189 (2009) 288-296.

# Electrode properties of the restacked MnO<sub>2</sub>-based nanosheets with vacancy defects

Shinya Suzuki, Masaru Miyayama

Department of Applied Chemistry, School of Engineering, The University of Tokyo  
7-3-1 Hongo, Bunkyo-ku, 113-8656 Tokyo, Japan  
sin@fmat.t.u-tokyo.ac.jp

## [Introduction]

The Li–Ni–Co–Mn oxide system is a promising alternative to LiCoO<sub>2</sub> or LiNi<sub>x</sub>Co<sub>1-x</sub>O<sub>2</sub> cathode materials, owing to the large capacity and low cost, and dependence of the electrode properties of Li–Ni–Co–Mn oxide on chemical composition have been extensively investigated. Ni–Co–Mn oxide nanosheets are the potential electrode materials for thin-film energy storage devices. But few studies have been conducted on the preparation of Ni–Co–Mn oxide nanosheets. We tried to prepare novel redoxable nanosheets of Ni–Mn oxide as the stage prior to the formation of Ni–Co–Mn oxide nanosheets. In the process, we obtained the novel nanosheets with vacancy defects. In this study, the restacked Ni–Mn oxide nanosheets with vacancy defects were prepared and its electrode properties for lithium-ion batteries were examined.

## [Experimental]

A layered Na<sub>0.55</sub>Ni<sub>0.25</sub>Mn<sub>0.75</sub>O<sub>2</sub> was prepared by solid state reaction. Nanosheets of Ni–Mn oxide with a chemical composition of H<sub>x</sub>Ni<sub>0.19</sub>Mn<sub>0.75</sub>O<sub>2</sub> (N19M75 nanosheets) were obtained by exfoliation of the proton-exchanged form of Na<sub>0.55</sub>Ni<sub>0.25</sub>Mn<sub>0.75</sub>O<sub>2</sub>. The reaction of N19M75 nanosheets with HNO<sub>3</sub> resulted in the formation of a restacked material with a chemical composition of H<sub>x</sub>Ni<sub>0.12</sub>Mn<sub>0.75</sub>O<sub>2</sub>. Then, H<sub>x</sub>Ni<sub>0.12</sub>Mn<sub>0.75</sub>O<sub>2</sub> (N12M75) nanosheets were obtained by exfoliation of H<sub>x</sub>Ni<sub>0.12</sub>Mn<sub>0.75</sub>O<sub>2</sub>. Restacked N12M75 nanosheets were prepared by the reaction with LiOH solution, and the electrode properties were examined for the prepared restacked materials.

## [Results and Discussion]

Lateral dimensions were 50–500 nm for N19M75 nanosheets, which were composed of 1–2 oxide layers. N12M75 was obtained by re-exfoliation of restacked H<sub>x</sub>Ni<sub>0.12</sub>Mn<sub>0.75</sub>O<sub>2</sub> nanosheets. **Figure 1** shows atomic force micrograph of N12M75 nanosheets (upper) and cross section of the region indicated by the line in the upper image (lower). The structure of N19M75 and N12M75 nanosheets was the same, and this indicates that dissolution of Ni occurs without any structural change, resulting in nanosheets with vacancy defects. Restacked N12M75 nanosheets were prepared by the reaction with LiOH solution, and the chemical composition of the restacked compound was determined by ICP-AES, yielding Li<sub>0.23</sub>Ni<sub>0.12</sub>Mn<sub>0.75</sub>O<sub>2</sub>·0.26H<sub>2</sub>O. **Figure 2** shows the discharge and charge curves of the restacked N12M75 nanosheets. At initial discharge and subsequent charge, restacked N12M75 nanosheets showed capacities of 160 and 180 mAh g<sup>-1</sup>, respectively. The restacked N12M75 nanosheets exhibited inferior cycling durability may be due to the low electronic conductivity. The vacancy defects generated by Ni dissolution may serve as ionic conducting paths for small cations such as H<sup>+</sup> and Li<sup>+</sup> penetrating through oxide layer. Lithium-ion diffusion behavior through nanosheets with vacancy defects is on investigation and will be reported.

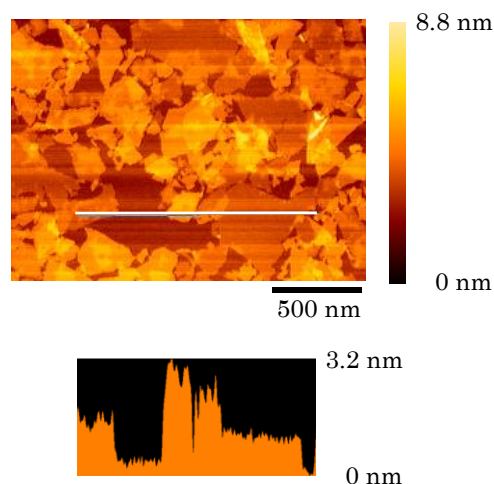


**Figure 1.** Atomic force micrograph of N12M75 nanosheets (upper), and cross sectional analysis by the line (lower).

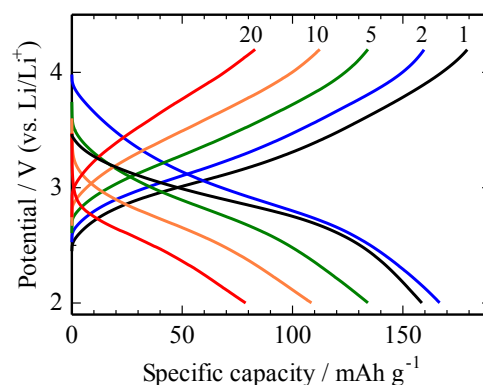


**Figure 2.** Discharge and charge curves of restacked N12M75 nanosheets. The current density was 100 mA g<sup>-1</sup>. The numbers in the figure indicate cycle number.

# Superior electrochemical performance of Li-rich $\text{Li}_{1.188}\text{Ni}_{0.198}\text{Co}_{0.087}\text{Mn}_{0.553}\text{O}_2$ cathode material by coating Li–La–Zr–O solid electrolyte

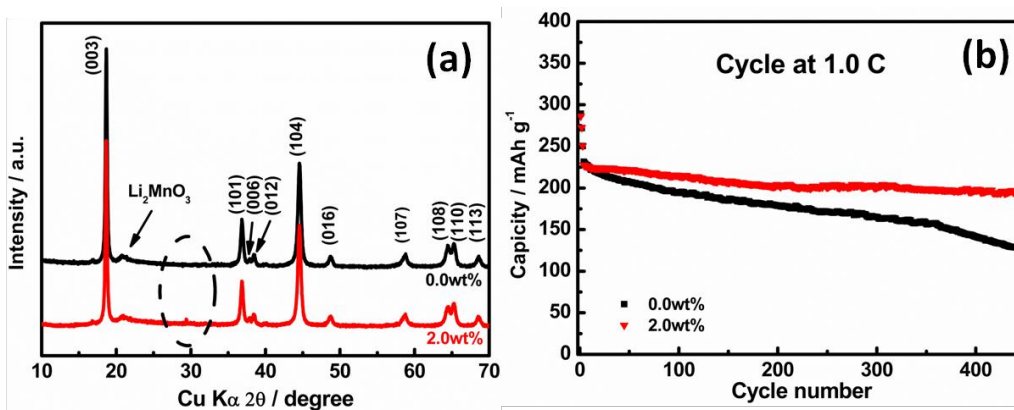
Shou-Yu Shen<sup>1</sup>, Ling Huang<sup>1\*</sup>, Jun-Tao Li<sup>2</sup>, Shi-Gang Sun<sup>1, 2\*</sup>

<sup>1</sup> College of Chemistry and Chemical Engineering, Xiamen University, Xiamen 361005, China

<sup>2</sup> College of Energy & School of Energy Research, Xiamen University, Xiamen 361005, China

E-mail: huangl@xmu.edu.cn; sgsun@xmu.edu.cn

**ABSTRACT:** Li-rich Mn-based layered oxide materials have been received great attention owing to the characteristic of high discharge capacity above 250 mAh/g between 2.0–4.8 V, relative low cost and high thermal stability, but this oxide material also has other drawbacks such as poor rate capacity, large irreversible capacity loss during the first cycle and voltage fade. Surface coating on the active material is considered as an effective strategy to suppress the side reaction in the surface of electrode and can apparently improve cell's electrochemical performance. In this report, Li-rich Mn-based layered oxide  $\text{Li}_{1.188}\text{Ni}_{0.198}\text{Co}_{0.087}\text{Mn}_{0.553}\text{O}_2$  (LMO) material is successfully coated with Li–La–Zr–O solid electrolyte (LLZO) by sol–gel process. Both LLZO-coated LMO and pristine materials are characterized by x-ray diffraction (XRD), scanning electron microscopy (SEM), transmission electron microscopy (TEM), inductively coupled plasma–atomic emission spectrometry (ICP–AES) and electrochemical impedance spectroscopy (EIS) to understand the effect of LLZO coating layer on the LMO materials. After 450 cycles at 1 C, the 2 wt% LLZO coated LMO material exhibits a significant cycle stability of 193 mAh/g capacity with a capacity retention of 84.8 % compared to the LMO material of 125.4 mAh/g with a capacity retention of 54.1 %, which could mainly own to the improvement of the surface stability and suppressing the side reactions by Li–La–Zr–O coating layer. In addition, 2 wt% LLZO coating layer could also improve the rate performance of the electrode by reducing interfacial charge–transfer resistance obviously.



**ACKNOWLEDGMENT:** This work was supported by the NSFC (Grant Nos. 21273184, 21321062 and 21373008), and the “973” program (Grant No. 2015CB251102),

## REFERENCES

- (1) Z-H Lua, and J. R. Dahn, Understanding the Anomalous Capacity of  $\text{Li}/\text{Li}[\text{Ni}_x\text{Li}_{(1/3-2x/3)}\text{Mn}_{(2/3-x/3)}]\text{O}_2$  Cells Using In Situ X-Ray Diffraction and Electrochemical Studies. *J. Electrochem. Soc.*, 2002, 149, A815-A822.
- (2) A. R. Armstrong, M. Holzapfel, P. Nova, C. S. Johnson, S-H Kang, M. M. Thackeray, and P. G. Bruce, Demonstrating Oxygen Loss and Associated Structural Reorganization in the Lithium Battery Cathode  $\text{Li}[\text{Ni}_{0.2}\text{Li}_{0.2}\text{Mn}_{0.6}]\text{O}_2$ , *J. Am. Chem. Soc.* 2006, 128, 8694-8698.

# Hierarchical Mn<sub>2</sub>O<sub>3</sub> Hollow Microspheres of high performance as Anode of LIBs and XANES studies of Conversion Reaction Mechanism

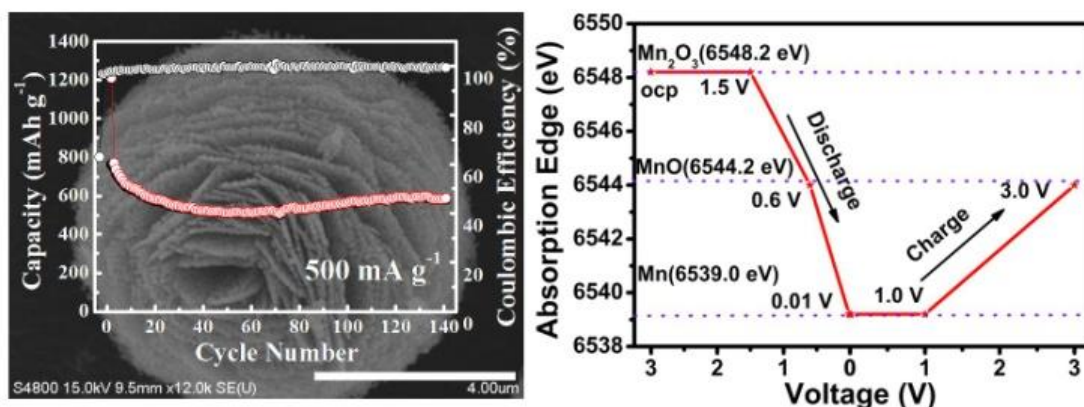
Hang su<sup>1</sup>, Jun-Tao Li<sup>1</sup>, Ling Huang<sup>2</sup>, Shi-Gang Sun<sup>1,2\*</sup>

<sup>1</sup> College of Energy & School of Energy Research, Xiamen University, Xiamen 361005, China

<sup>2</sup> College of Chemistry and Chemical Engineering, Xiamen University, Xiamen 361005, China

E-mail: sgsun@xmu.edu.cn

Hierarchical Mn<sub>2</sub>O<sub>3</sub> hollow microspheres of diameter about 6–10  $\mu\text{m}$  were synthesized by solvent-thermal method. When served as anode materials of LIBs, the hierarchical Mn<sub>2</sub>O<sub>3</sub> hollow microspheres could deliver a reversible capacity of 580 mAh g<sup>-1</sup> at 500 mA g<sup>-1</sup> after 140 cycles, and a specific capacity of 422 mAh g<sup>-1</sup> at a current density as high as 1600 mA g<sup>-1</sup>, demonstrating a good rate capability. Ex situ X-ray absorption near edge structure (XANES) spectra reveals that, for the first time, the pristine Mn<sub>2</sub>O<sub>3</sub> was reduced to metallic Mn when it discharged to 0.01 V, and oxidized to MnO as it charged to 3 V in the first cycle. Furthermore, the XANES data demonstrated also that the average valence of Mn in the sample at charged state has decreases slowly with cycling number, which signifies an incomplete lithiation process and interprets the capacity loss of the Mn<sub>2</sub>O<sub>3</sub> during cycling.



**ACKNOWLEDGMENT:** This work was financially supported by NSFC (Grant Nos. 21373008, 21321062, 21273184)

## REFERENCES:

- (1) Su, H.; Xu, Y.F.; Feng, S.C.; Wu, Z.G.; Sun, X.P.; Shen, C.H.; Wang, J.Q.; Li, J.T.; Huang, L.; Sun, S.G.; ACS Applied Materials & Interfaces, In press
- (2) Armand, M.; Tarascon, J. M., Nature 2008, 451, 652-657.
- (3) Tarascon, J. M.; Armand, M., Nature 2001, 414, 359-367.
- (4) Deng, Y. F.; Li, Z. N.; Shi, Z. C.; Xu, H.; Peng, F.; Chen, G. H., RSC Adv., 2012, 2, 4645-4647.
- (5) Lv, D. P.; Bai, J. Y.; Zhang, P.; Wu, S. Q.; Li, Y. X.; Wen, W.; Jiang, Z.; Mi, J. X.; Zhu, Z. Z.; Yang, Y., Chem. Mater., 2013, 25, 2014-2020.



# Gadolinium silicide/silicon composite anode for next-generation lithium-ion battery

Hiroyuki Usui<sup>a</sup>, Masahito Nomura<sup>a</sup>, Hiroki Nishino<sup>a</sup>, Masatoshi Kusatsu<sup>b</sup>, Tadatoshi Murota<sup>b</sup>, Hiroki Sakaguchi<sup>a,\*</sup>

<sup>a</sup> Department of Chemistry and Biotechnology, Graduate School of Engineering, Tottori University

<sup>b</sup> Intelligent Chemical Group, R&D Division, Santoku Corp.

4-101 Minami, Koyama-cho, Tottori 680-8552, Japan

4-14-34 Fukae-Kitamachi, Higashinada-ku, Kobe 658-0013, Japan

sakaguch@chem.tottori-u.ac.jp

Silicon (Si) has attracted much attention as anode material due to its huge theoretical capacity, while there are critical disadvantages of a low electronic conductivity and significant volume changes during Li-insertion/extraction. We have revealed that the performance of composite electrodes, consisting of transition metal silicides and Si, can be improved by the synergetic effects of their properties [1-4]. In particular, we found that lanthanum silicide (La-Si) is very effective [1-2]. In contrast, the effect of other rare-earth metal silicides on the performance has never explored yet. In this study, we chose samarium (Sm), gadolinium (Gd), and dysprosium (Dy) as rare-earth elements to be silicides, and investigated the anode performance of composite electrodes consisting of the silicides and Si.

Composite active materials of rare-earth metal silicides (*Ln*-Si) and elemental Si were synthesized by an arc melting method. Thick-film electrodes of the active material powder were prepared on current collectors of copper foils by a gas-deposition (GD) method [1-4]. An elastic deformation property of silicide electrodes was measured by an indentation test using a dynamic ultra-micro hardness tester. Electrode performances were evaluated in a beaker-type three-electrode cell using 1 M LiBF<sub>4</sub>/propylene carbonate as the electrolyte. Charge-discharge tests were carried out at 303 K with potential ranges of 0.005–2.000 V vs. Li/Li<sup>+</sup> under 3.0 A g<sup>-1</sup>. This current density corresponds to a current rate of 1.2 C.

Figure 1 shows the variation in the discharge capacities of these composite electrodes following the increase in the number of charge-discharge cycles. In contrast with the Si electrode showing a quick capacity decay caused by its pulverization, the all composite electrodes exhibited improved performances. In particular, the Gd-Si/Si electrode maintained a very large discharge capacity of 840 mA h g<sup>-1</sup> even after 1000 cycles, which clearly demonstrating its distinctly excellent performance [4]. The discharge capacity of Gd-Si/Si is much larger than the graphite's theoretical capacity of 372 mA h g<sup>-1</sup>. To evaluate the contribution of these silicides to the composite electrodes' capacities, we synthesized silicide electrodes composed of Sm-Si, Gd-Si, and Dy-Si. These silicide electrodes showed very small capacities of around several ten mA h g<sup>-1</sup> though the capacities stably maintained for a long cycle, as in the case of La-Si electrodes [1,2]. This indicates that the composite electrodes derive nearly all capacities not from silicides but from elemental Si. Electrical conductivities of *Ln*-Si powders were measured under a uniaxial press using a two probes method. The *Ln*-Si powders showed three orders of magnitude higher conductivity than a Si powder, and that there was no difference in the conductivity was observed among the *Ln*-Si powders. On the other hand, Gd-Si exhibited a more elastic property in comparison with other silicides (Table 1), indicating that it released effectively the stress from Si during Li-insertion/extraction and suppressed silicon's pulverization.

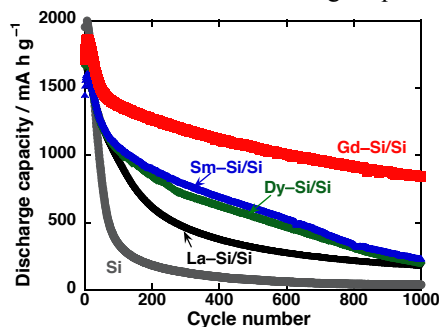


**Fig. 1** Cycling performances of *Ln*-Si/Si composite electrodes (*Ln*: La, Sm, Gd, and Dy).

**Table 1** Mechanical properties of various rare-earth metal silicides (*Ln*-Si): reference breaking strength for *Ln*-Si particles and indentation work rate ( $\eta_{it}$ ) for *Ln*-Si thick-film electrodes. Values in parentheses indicate the standard deviation of the measured values.

	Reference breaking strength / MPa	$\eta_{it}$ / %
Si	374 (±54.7)	13 (±2.0)
La-Si	237 (±37.5)	31 (±2.1)
Sm-Si	206 (±26.1)	28 (±2.1)
Gd-Si	155 (±37.2)	41 (±3.2)
Dy-Si	196 (±17.3)	26 (±2.2)

## References

- [1] H. Sakaguchi and H. Usui, *Electrochemistry*, **80** (2012) 45.
- [2] H. Usui, M. Shimizu, H. Sakaguchi, *J. Power Sources*, **235** (2013) 29.
- [3] H. Usui, K. Nouno, Y. Takemoto, H. Sakaguchi *et al.*, *J. Power Sources*, **268** (2014) 848.
- [4] H. Usui, M. Nomura, H. Nishino, M. Kusatsu, T. Murota, H. Sakaguchi, *Mater. Lett.*, **130** (2014) 61.

# One-pot synthesis of NaTi<sub>2</sub>(PO<sub>4</sub>)<sub>3</sub>/rGO nanocomposite for sodium-ion batteries

Ha-Kyung Roh<sup>a</sup>, Hyun-Kyung Kim<sup>a</sup>, Myeong-Seong Kim<sup>a</sup>, Kwang Chul Roh<sup>b</sup> and Kwang Bum Kim<sup>\*a</sup>

<sup>a</sup> Department of Material Science and Engineering, Yonsei University, Seoul, Republic of Korea.

<sup>b</sup> Energy Efficient Materials Team, Energy & Environmental Division, Korea Institute of Ceramic Engineering & Technology, Seoul, Republic of Korea.

[\\*kbkim@yonsei.ac.kr](mailto:*kbkim@yonsei.ac.kr)

## Abstract

NASICON-structured NaTi<sub>2</sub>(PO<sub>4</sub>)<sub>3</sub> has been considered as an outstanding potential cathode material for Na-ion batteries (NIBs) because of its good Na-ion intercalation reversibility and extremely small structural changes during charge/discharge cycling.<sup>1</sup> Despite these advantages, NaTi<sub>2</sub>(PO<sub>4</sub>)<sub>3</sub> suffers from intrinsically poor electronic conductivity, which leads to poor charging/discharging rate performance of NIBs. Up to now, several effective ways have been proposed to improve the electrochemical properties such as specific capacity and cycling stability, including reduction of the particle size to nanoscale, the addition of a surface coating and the synthesis of composite materials with conductive carbons.<sup>2</sup>

In particular, the composites of NASICON-structured materials with carbonaceous materials such as mesoporous carbon and graphene or reduced graphene oxide (rGO) has been recently proposed to enhance electronic conductivity of the electrode for improving the cycling performance.<sup>3</sup> Graphene acts as a template due to its high specific surface area not only to deposit nano-sized metal oxide but also to connect the nano particles along a 2-dimensional conduction path. Furthermore, graphene can provide a void space against the volume changes of the metal oxide particles during lithium ion insertion/extraction process, which can improve the cycling performance. However, previously reported methods to fabricate of these composites require multistep, time-consuming processes, and complicated.<sup>4</sup> Moreover, in this multistep method, the sodiation and heat treatment steps unfavorably affect the size, morphology and homogeneity of the resulting NaTi<sub>2</sub>(PO<sub>4</sub>)<sub>3</sub> particles. Accordingly, their electrochemical properties showed only a marginal improvement compared with the bare NaTi<sub>2</sub>(PO<sub>4</sub>)<sub>3</sub>.

In this study, we report a simple one-pot synthesis of NaTi<sub>2</sub>(PO<sub>4</sub>)<sub>3</sub>/rGO nanocomposites *via* a microwave-assisted solvothermal method that combines the advantages of simplicity and efficiency. Electrodes prepared from the nanocomposites provide excellent cycling performance and rate capability, indicating great potential for their use in NIBs. More details on the synthetic procedure, electrochemical and structural properties will be presented at the meeting.

## References

1. Il Park *et al*, *J Electrochem Soc* **2011**, *158*, A1067.
2. Pang, G. *et al*, *J Mater Chem A* **2014**, *2*, 20659.
3. Li *et al*, *J Electrochem Soc* **2014**, *161*, A1181.
4. Pang, G. *et al*, *Nanoscale* **2014**, *6*, 6328.



# Understanding the Improved Electrochemical Properties of $\text{Li}_2\text{O}-2\text{B}_2\text{O}_3$ Coated $\text{LiNi}_{0.5}\text{Mn}_{1.5}\text{O}_4$ for Lithium-ion Batteries

Ji Su Chae<sup>1,2</sup>, Sun-Min Park<sup>1</sup>, Won-Sub Yoon<sup>2</sup>, Kwang Chul Roh<sup>1,\*</sup>

<sup>1</sup>*Energy & Environmental Division, Korea Institute of Ceramic Engineering & Technology, 101, Soho-ro, Jinju-si, Gyeongsangnam-do, 660-031, Republic of Korea*

<sup>2</sup>*Department of Energy Science, Sungkyunkwan University, Suwon 440-746, Republic of Korea*

\* [rkc@kicet.re.kr](mailto:rkc@kicet.re.kr)

## Abstract

A  $\text{Li}_2\text{O}-2\text{B}_2\text{O}_3$  coated  $\text{LiNi}_{0.5}\text{Mn}_{1.5}\text{O}_4$  cathode active material was synthesised to enhance the thermal stability of  $\text{LiNi}_{0.5}\text{Mn}_{1.5}\text{O}_4$  electrodes used in lithium ion batteries. The  $\text{Li}_2\text{O}-2\text{B}_2\text{O}_3$  coating prevented the surface of the  $\text{LiNi}_{0.5}\text{Mn}_{1.5}\text{O}_4$  electrode from being directly exposed to the liquid electrolyte, thereby suppressing the dissolution of Mn from the electrode surface into the electrolyte and the undesirable formation of a solid-electrolyte-interphase layer. The surface-coated electrode showed 81% capacity retention during high-temperature (60 °C) cycling. The results of the electrochemical impedance spectroscopy (EIS) indicated that the improved performance of the surface-coated electrode slowed the increase in cell impedance during cycling. The  $\text{Li}_2\text{O}-2\text{B}_2\text{O}_3$  coating effectively slowed the surface of the  $\text{LiNi}_{0.5}\text{Mn}_{1.5}\text{O}_4$  electrode from being directly exposed to the liquid electrolyte, thereby suppressing the dissolution of  $\text{Mn}^{3+}$  ions from the surface of the spinel cathode active material into the electrolyte. The  $\text{Li}_2\text{O}-2\text{B}_2\text{O}_3$  coating will pave the way for improving the electrochemical cycling of various cathode active materials at elevated temperatures

## References

1. W. Soppe, F. Aldenkamp, H.W. den Hartog, J. Non-Cryst. Solids **1987**, 91, 351.
2. H.-W. Chan, J.-G. Duh, S.-R. Sheen, Surf. Coat. Technol. **2004**, 188–189, 116
3. H. Sahan, H. Goktepe, S. Patat, A. Lgen, Solid State Ionics **2008**, 178, 1837
4. J. Liu, A. Manthiram, J. Phys. Chem. C **2009**, 113, 15073

# In-Situ Observation of Solid Electrolyte Interphase (SEI) Formation in Electrochemical Surface Plasma Resonance (EC-SPR)

Sylvia Ayu Pradanawati<sup>1</sup>, Fu Ming Wang<sup>1,2\*</sup>

<sup>1</sup>Graduate Institute of Applied Science and Technology, National Taiwan University of Science and Technology

<sup>2</sup>Sustainable Energy Center, National Taiwan University of Science and Technology

43 Keelung Road, Section 4, Taipei 10607, Taiwan

Correspondence: mccabe@mail.ntust.edu.tw

Electrochemical surface plasma resonance (EC-SPR) is a powerful instrument for in-situ observation of SEI formation. Propagation constant of surface plasma is sensitive to variation in the refractive index (RI) at the surface of metal film of electrode [1]. SPR provides high sensitivity, real time monitoring, and label free detection [2]. Gold electrode is used to detect the real time SEI formation in accompanied with electrochemical reaction. The optical response of the SEI strongly affects the SPR angles due to the RI is changing.

In this study, EC-SPR is used to simulate the SEI formation in electrochemical reaction of lithium ion battery. 1M LiPF<sub>6</sub> in EC/EMC (sample A) and 1M LiPF<sub>6</sub> + 0.1 wt% Lithium benzimidazole (LIB) in EC/EMC (sample B) were used in this research. The experiment sets up in a scan rate of 0.5 mV/s in order to characterize the salt effect on SEI formation. Figure 1a and b show that sample B has a higher delta angle (Fig. 1a) and lower intensity (Fig. 1b) compare with sample A only show lower delta angle and higher delta intensity. Variation on delta degree is correlated to the different SEI formation [3].

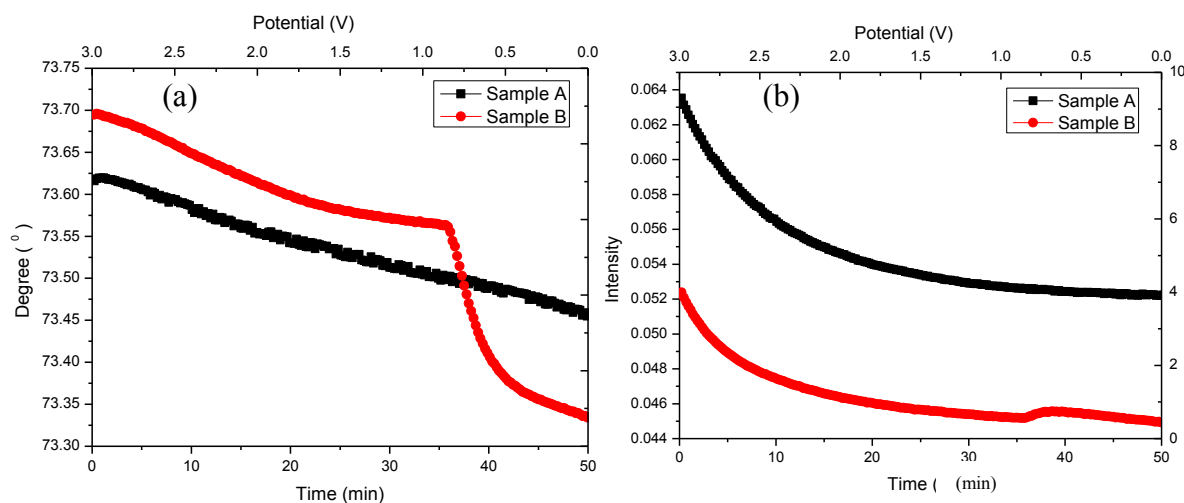


Fig. 1 a) Sensogram and b) Intensity detection of Sample A and Sample B

Sample	Delta Angle	Delta Intensity
Sample A	0.057	0.012
Sample B	0.429	0.008

## References

- (1) J. Homola, *et. al.*, Springer Ser Chem Sens Biosens 2006, 4, 45.
- (2) Huamin Liang, *et. al.*, Sensor and Actuators B: Chemical, 2010, 149, 212.
- (3) F. Kong *et. al.*, Journal of Power Sources, 2001, 97-98, 58-66

# Electrochemical-mechanical Coupled Phenomena in Silicon-based Li-ion Batteries Using X-ray Tomographic Characterization

Juan M. Paz-Garcia<sup>1</sup>, Oluwadamilola O. Taiwo<sup>2</sup>, Paul R. Shearing<sup>2</sup>, Donal Finegan<sup>2</sup>, Rajmund Mokso<sup>3</sup>, Erika Tudisco<sup>1</sup>, Matti Ristinmaa<sup>1</sup>, Stephen Hall<sup>1,4</sup>

<sup>1</sup> Division of Solid Mechanics, Lund University, Lund, Sweden

<sup>2</sup> Electrochemical Innovation Laboratory, Dept. Chemical Engineering, University College London, UK

<sup>3</sup> Swiss Light Source, Paul Scherrer Institut, Villigen, Switzerland

<sup>4</sup> European Spallation Source AB, Lund, Sweden

Juanma.paz@me.com

Lithium-ion batteries (LIBs) are common in portable electronics and they have also attracted significant interest in electric vehicles and large-scale storage applications. Electrochemical processes in LIBs produce microstructural evolution of the porous electrode material, altering the capacity, charging behaviour, durability and lifetime of the cells. Nowadays, intense research is devoted to develop new generations of advanced batteries with high energy density. For example, alloying Silicon anodes are promising electrodes with theoretical energy density up to  $\sim 4200$  mAh/g against the  $\sim 375$  mAh/g of graphite, which is still the most used anode material in commercial batteries. Silicon electrodes, however, have the drawback of exhibiting extreme volume changes during the lithiation process ( $\sim 300\%$  compared to  $\sim 10\%$  of graphite). Volume changes within a battery's constrained case involve mechanical strains on the fundamental components of the material, which eventually causes the battery to fail.

Non-destructive 3D X-ray imaging techniques are suitable for the study of these coupled electrochemical and mechanical phenomena, as they allow the visualization of the evolution of the microstructure properties of the LIBs during cycles of charge/discharge. Herein, we combine synchrotron radiation and lab-scale X-ray computed microtomography for the study of silicon-based LIBs.

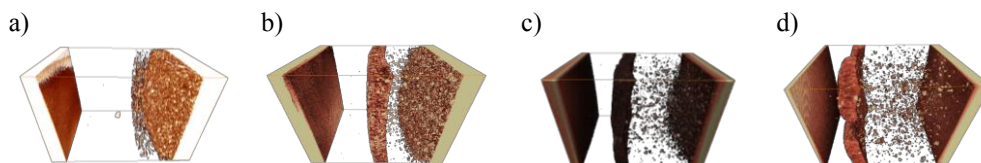


**Figure:** Evolution of a half-cell battery (Li foil as anode at the left side, Si powder as cathode at the right side) during the first lithiation step at different degree of lithiation: a) fresh b)  $\sim 25\%$ , c)  $\sim 50\%$ , d)  $\sim 75\%$ . Volume changes of the electrodes cause the displacement of the separator, which eventually collapses causing the battery fail. X-ray tomography allows quantitative identification of the different lithiated-silicon phases.

For these experiments, bespoke designed, X-ray transparent, functional Si – Li cells were assembled to make possible *in situ* and *in operando* tests (i.e., simultaneous tomographic imaging and electrochemical testing). The observed microstructural volume changes are quantified using well-known geometric parameters. Full 3D strain/deformation measurements are performed using a digital volume correlation (DVC) technique. Results presented here throw light upon the large capacity loss during the first lithiation in alloying LIBs, facilitating the development of electrochemo-mechanical models based on the micromechanical observations.

## References:

- [1] J. Gonzalez et al. X-ray microtomography characterization of Sn particle evolution during lithiation/delithiation in lithium ion batteries. *Journal of Power Sources* 285 (2015) 205-209.
- [2] K. Zhao et al. Concurrent reaction and plasticity during initial lithiation of crystalline silicon in Lithium-Ion batteries *Journal of Electrochemical Society*. 159 (2012) A238-A243.
- [3] W. Zhang. A review of the electrochemical performance of alloy nodes for lithium-ion batteries. *Journal of Power Sources* 196 (2011) 13-24.

## Acknowledgments:

Paz-Garcia acknowledges the support from the International Campus of Excellence - Andalucía Tech

# Carbonized Polydopamine/Sulfur Composite with One-Dimensional Structure for High Performance Lithium Sulfur Batteries

Yuebin YANG<sup>a,1</sup>, Hui XU<sup>b,1</sup>, Xusong QIN<sup>b</sup>, Yuanfu DENG<sup>b,c</sup>, Guohua CHEN<sup>a,b,\*</sup>

<sup>a</sup> Department of Chemical and Biomolecular Engineering, The Hong Kong University of Science and Technology, Clear Water Bay, Kowloon, Hong Kong SAR, China

<sup>b</sup> Centre for Green Products and Processing Technologies, Guangzhou HKUST Fok Ying Tung Research Institute, Guangzhou 511458, China

<sup>c</sup> The Key Laboratory of Fuel Cell Technology of Guangdong province, School of Chemistry and Chemical Engineering, South China University of Technology, Guangzhou, 510640, China;

<sup>1</sup> These authors contributed equally to this work.

[yyangar@connect.ust.hk](mailto:yyangar@connect.ust.hk); [kechengh@ust.hk](mailto:kechengh@ust.hk)

Lithium-ion batteries are the most commonly used devices for energy storage in the market. However, their prospects are seriously restricted due to limited energy density, which prevents them from applications in the market of electric vehicles for long-range travelling. With a theoretical energy density of 2600 Wh kg<sup>-1</sup>, lithium sulfur batteries have been proved to be a perfect alternative since 2009 when researchers reported a novel lithium sulfur battery with improved specific capacity and cycling performance [1]. Furthermore, the non-toxic nature of sulfur renders it environmentally friendly, making Li-S batteries attractive for storage of renewable energy. In this study, one-dimensional carbonized polydopamine (C-PDA) shell were subtly designed employing the polymerization and graphitization of coated polydopamine layer with controlled thickness on pre-synthesized iron oxide nanotubes, followed by the infiltration of sulfur. The properties and performance of the composite (S@C-PDA) as the cathode material in lithium sulfur (Li-S) batteries were examined and evaluated. It was demonstrated that the prepared one-dimensional C-PDA shells have a diameter ~80 nm and a length of 200-300 nm; the sulfur particles could diffuse through the pores (diameter: ~3 nm) and be well dispersed at the polydopamine inner layer with a thickness of 8-15 nm (**Fig. 1(a)**). The assembled battery exhibited a high capacity at 1C (~800 mAh/g) with stable cycling of 200 cycles (**Fig. 1(b)**). In addition, it was demonstrated that the battery could run to 800 cycles with fair capacity at a current density of 2C/4C (**Fig. 1(c)**). The good performance is attributed to the good conductivity of C-PDA layer and the strong interaction between Li<sub>x</sub>S and C-PDA, the carbonized product of polydopamine which helps modify the carbon surface and is capable of trapping the soluble polysulfide in the electrolyte. The one-dimensional structure of C-PDA shell and the smaller pore size on the wall can also prevent the agglomeration of sulfur particles, contributing to the improved specific capacity and cycling stability. While the Li-S battery developed following this route still suffers from slight capacity decay during cycling, its high performance in capacity and cycling ability suggest a promising cathode material for future lithium sulfur batteries.

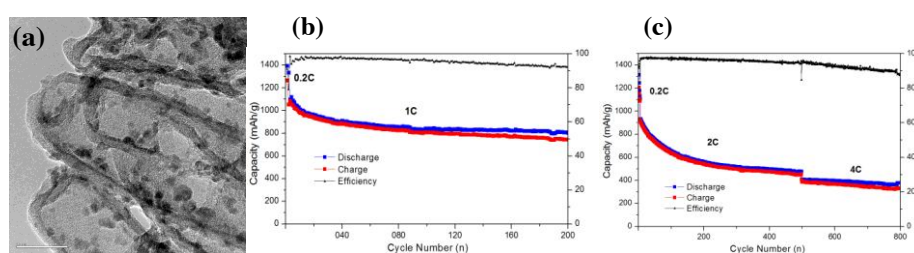


**Fig. 1.** TEM images (a) of single-walled C-PDA nanotubes impregnated with sulfur with a scale bar of 200 nm; Cycling performance of C-PDA@S nanotubes at a current density of 1C for 300 cycles (b) and 2C/4C for 800 cycles.

## Reference

[1] Ji X, Lee K T, Nazar L F. A highly ordered nanostructured carbon-sulphur cathode for lithium-sulphur batteries[J]. Nature materials, 2009, 8(6): 500-506.

# Highly Concentrated Electrolytes for 5-V Cathodes

Minoru Inaba, Rin Masuhara, Yusuke Shimizu, Michihiro Hasinokuchi, and Takayuki Doi  
Department of Molecular Chemistry and Biochemistry, Doshisha University  
1-3 Tatara-Miyakodani, Kyotanabe, Kyoto 610-0321, Japan  
minaba@mail.doshisha.ac.jp

Highly concentrated electrolytes have many unique properties,<sup>1-4</sup> such as  $\text{Li}^+$ -intercalation into graphite anode without EC,<sup>1,3</sup> suppression of  $\text{S}_8^{2-}$  ion dissolution in Li-S batteries, etc., and is attracting much attention of many researchers. In highly concentrated electrolytes, all solvent molecules are strongly coordinated with  $\text{Li}^+$  ions, and hence the stability of the electrolytes against oxidation is improved significantly. Yoshida et al. reported that  $\text{LiCoO}_2$ , which is a 4-V cathode, can be charged and discharged in a LiTFSI/triglyme (1:1) electrolyte with good cycleability,<sup>3</sup> though triglyme is an ether compound and usually cannot be used as solvent.

5-V cathodes, e.g.  $\text{LiNi}_{0.5}\text{Mn}_{1.5}\text{O}_4$  and  $\text{LiCoPO}_4$ , are promising for the next-generation LIBs with high energy densities. Unfortunately no electrolyte systems that tolerate the highly oxidative 5 V cathode have been reported so far. In the present study, we investigated the effect of concentration on the stability of highly concentrated electrolytes,  $\text{LiPF}_6/\text{PC}$  and  $\text{LiBF}_4/\text{PC}$ , against a 5-V cathode,  $\text{LiNi}_{0.5}\text{Mn}_{1.5}\text{O}_4$  to realize 5 V LIBs with high energy densities.

Figure 1 compares charge/discharge curves of a 5-V spinel  $\text{LiNi}_{0.5}\text{Mn}_{1.5}\text{O}_4$  in standard ( $0.83 \text{ mol kg}^{-1}$ , 1 M,  $\text{Li}/\text{PC} = 11.8$ ) and highly concentrated ( $4.9 \text{ mol kg}^{-1}$ ,  $\text{Li}/\text{PC} = 2$ )  $\text{LiBF}_4/\text{PC}$  at  $30^\circ\text{C}$ . The charge/discharge rate of C/10 was employed to exaggerate electrolyte decomposition. Though the  $\text{LiNi}_{0.5}\text{Mn}_{1.5}\text{O}_4$  can be charged and discharged in both electrolytes, the irreversible capacity ( $Q_{\text{irr}}$ ) in 1 M  $\text{LiBF}_4/\text{PC}$  was high ( $76 \text{ mAh g}^{-1}$ ) because of vigorous electrolyte decomposition. In contrast,  $Q_{\text{irr}}$  was significantly reduced in the concentrated electrolyte, which indicated that stability against oxidation was improved in the highly concentrated electrolyte. Similar tendency was also observed in highly concentrated  $\text{LiPF}_6/\text{PC}$  electrolytes, though polarization on charging and discharging were much higher.

The half-cell was fully charged to 5.0 V, and kept at  $60^\circ\text{C}$  for 3 days in  $\text{LiPF}_6/\text{PC}$  electrolytes. The amount of Mn deposited on lithium counter electrode was evaluated by ICP as a measure of dissolved Mn ions. Figure 2 shows the variation of the amount of Mn deposited on lithium counter electrode with  $\text{Li}/\text{PC}$  ratio. The amount of dissolved Mn ions decreased with increasing  $\text{Li}/\text{PC}$  ratio, which indicated that the use of highly concentrated electrolytes is also effective for suppressing Mn ion dissolution.

This work was supported by a Kyoto Area Super Cluster Program, Japan Science and Technology Agent (JST), Japan.

**References:** [1] S.-K. Jeong et al., *J. Power Sources*, **175**, 540 (2008).; [2] K. Dokko, et al., *J. Electrochem. Soc.*, **160**, A1304 (2013).; [3] K. Yoshida, et al., *J. Am. Chem. Soc.*, **133**, 13121 (2011).; [4] Y. Yamada, et al., *ACS Appl. Mater. Interfaces*, **6**, 10892 (2014).

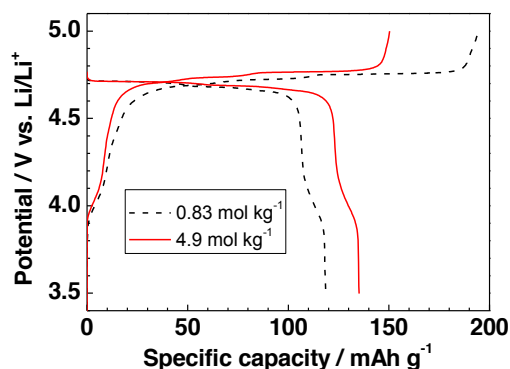


Fig. 1 Charge and discharge curves of  $\text{LiNi}_{0.5}\text{Mn}_{1.5}\text{O}_4$  in  $0.83 \text{ mol kg}^{-1}$  (1 M) and  $4.9 \text{ mol kg}^{-1}$   $\text{LiBF}_4/\text{PC}$  at  $30^\circ\text{C}$ . Charge and discharge rate: C/10.

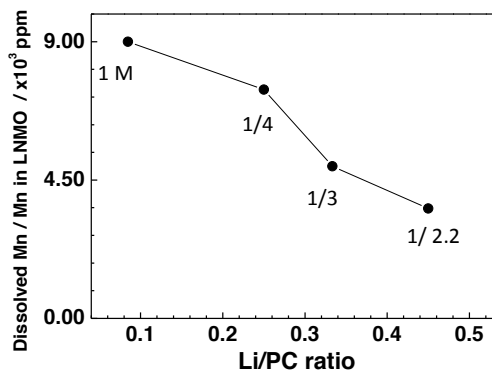


Fig. 2 Variation of the amount of dissolved Mn with  $\text{Li}/\text{PC}$  after kept at  $60^\circ\text{C}$  for 3 days at SOC 100% in  $\text{LiPF}_6/\text{PC}$  of different concentrations.

# Polyoxometalates for Non-aqueous Redox Flow Battery Applications

Jee-Jay James Chen<sup>1</sup>, Mark A. Barteau<sup>2</sup>

*Department of Chemical Engineering*

*University of Michigan, Ann Arbor, MI 48109-2136, USA*

*2301 Bonisteel Blvd, Ann Arbor, MI 48109*

*jjchenum@umich.edu*

## Abstract

Energy has been a key issue in this generation, with various energy resources, such as solar and wind power, being investigated. These renewable energy resources are attractive, but the method of storing the energy is one of the main problems. Redox Flow batteries designed to store energy in the electrolyte can address the energy storage problem[1]. Polyoxometalates (POMs), with versatile, tunable properties, undergo multielectrons redox reactions which may meet the requirements of high performance Redox Flow Batteries.

Research conducted to date has focused on the electrochemical characteristics of different combinations of Keggin polyoxometalates ( $\text{XM}_m\text{O}_{40}^{n-}$ ). The initial goal of the project is to select suitable polyoxometalate species that can be used for Redox Flow Batteries.

Various counter – cation exchanged POMs have been examined.  $\text{Li}_3$ ,  $\text{Na}_3$ ,  $\text{Mg}_{1.5}$  and  $\text{Ca}_{1.5}$  salts POMs have been synthesized and tested. Generally, spectra for 1A or 2A salts showed 3 redox couples, but the peak positions are slightly different. The effects of 1A or 2A cations on cell potentials are fairly minor.

Cation of phosphorous, arsenic and silicon were compared here by testing  $\text{XMo}_{12}\text{O}_{40}^{3-/4-}$  and  $\text{XW}_{12}\text{O}_{40}^{3-/4-}$  forms ( $\text{Li}_3\text{PMo}_{12}\text{O}_{40}$ ,  $\text{Li}_3\text{AsPMo}_{12}\text{O}_{40}$ ,  $\text{Li}_4\text{SiMo}_{12}\text{O}_{40}$ ,  $\text{Li}_3\text{PW}_{12}\text{O}_{40}$ ,  $\text{Li}_4\text{SiW}_{12}\text{O}_{40}$ .) The predicted behavior of P, As, and Si substituted Keggin ions is based on the negative charge density of the compound affecting its redox potential. The number of redox couples is not affected by the heteroatom charge..

$\text{Li}_4\text{PMo}_{11}\text{VO}_{40}$ ,  $\text{Li}_5\text{PMo}_{10}\text{V}_2\text{O}_{40}$ , and  $\text{Li}_6\text{PMo}_9\text{V}_3\text{O}_{40}$  mixed addenda POMs were also compared. Each compound exhibits multiple redox couples. Different reduction and oxidation peaks appear compared to pure  $\text{Li}_3\text{PMo}_{12}\text{O}_{40}$ . The mechanism of addenda element effects on POM redox properties is still unclear, but the mixed addenda elements play an important role in determining the redox properties. Investigation of the mix addenda POMs is the focus of current investigations.

Charge/discharge tests of  $\text{Li}_3\text{PMo}_{12}\text{O}_{40}$  show relatively high coulombic efficiency ( $\sim 90\%$ ), which suggests that the reaction is stable during the experiment. In other words, the POM can be reversibly reduced and oxidized with minimal degradation. which validates the possibility of using POMs in non-aqueous media for RFBs.

## References

- (1) Weber, A. Z., Mench, M. M., Meyers, J. P., Ross, P. N., Gostick, J. T., & Liu, Q. (2011). Redox flow batteries: a review. *Journal of Applied Electrochemistry*, 41(10), 1137-1164.

# Lithium Containing Polymeric Binder for Improved Performance of Li-Ion Batteries

Seung Sik Hwang, Jun-Hwan Ku, Jae-Man Choi

*Energy Lab, Samsung Advanced Institute of Technology, Samsung Electronics  
130 Samsung-ro, Yeongtong-gu, Suwon-si, Gyeonggi-do, Republic of Korea  
hwangssik@samsung.com*

Lithium-ion batteries occupy a large and increasing share of the energy storage device market as a result of their excellent performance in terms of long-life, energy density and high safety. Among the various electrode materials for LIBs, graphites which are representative of carbon materials have been the most commonly used negative electrode materials due to their low working potential close to lithium metal anode, and remarkable cycling performance. As lithium-ion cells typically operate beyond the thermodynamic stability of organic electrolytes, the reduction products arising from chemical reactions during the first few cycles form passivating films on the carbon anode surface, as we call it solid electrolyte interphase (SEI).[1] Such SEI, which is comprised of electrochemically insulating layer, plays important roles of preventing the further electrochemical reactions between electrode surface and electrolyte and enabling only lithium ions tunnel through the layer. It is well known that the formation of SEI layers is a determinant factor on the performance of LIBs, affecting cycle-life, life time, power capability and even safety.[2] While the SEI plays an essential part in delivering the best performance in cells, the development of SEI layers are caused by the irreversible reaction accompanying an electrolyte decomposition, which makes the coulombic efficiency to decrease during the first few cycles. When the stable SEI is not formed, any accidental misuse such as overcharge, high temperature exposure, and mechanic impact might damage the already formed SEI, resulting in more irreversible reaction during charging. The new anode surface, exposed to the electrolyte, immediately reacts with it to form a fresh thin protective film, which eventually leads to a poor cycleability and other undesirable properties in LIBs. Thus, to improve the performance of the cell, not only minimization of the electrolyte degradation but also thinner SEI film which provides an excellent passivating roll is required because thick and resistive SEI film is not favorable to battery operation.

Many research studies are thus focused on the improvement of the chemical nature and morphology of SEI. For the modification to SEI films having superior properties, several previous papers reported the polymer binder including the SEI ingredients and their electrochemical effects of LIBs.[3,4] The effects of the surface modification of the graphite electrode by the functional polymer binder, such as poly(acrylic acid), have been reported in several papers. Concretely, it has been demonstrated that the polyion complex layer, which have oxygen species as functional groups, could play the role like artificial SEI to assist the facile penetration of Li ions. Obviously, the stable and efficient operation of LIBs is closely connected with ingredients of surface films, morphology, and coverage feature.

Here we report that artificial pre-SEI, which is driven by Li ions containing polymeric binder with functional group (-COO-Li), can reduce the electrolyte decomposition and enhance the initial coulombic efficiency and cycleability. Furthermore, electrochemical performance is compared for SEI films that are produced from some different binders, in which different degree of lithium quantity is included in the polymer matrix. Li containing polymeric binder is a favorable candidate for the development of carbonaceous materials having high surface area and small particle size.

## Reference

- [1] E. Peled, *Journal of The Electrochemical Society*, 1979, 126, 2047.
- [2] J. P. Gabano, *Lithium Batteries*, AP, 1983, 43
- [3] K. Xu, *Chemical Reviews*. 2004, 104, 4303.
- [4] S. Komaba, N. Yabuuchi, T. Ozeki, K. Okushi, H. Yui, K. Konno, Y. Katayama, and T. Miura, *Journal of Power Sources*, 2010, 195, 6069.



# Characterizing Interfacial and Bulk Phase Processes in LIB Using EIS

Jianbo Zhang<sup>1,2\*</sup>, Jun Huang<sup>1</sup>

<sup>1</sup> State Key Laboratory of Automotive Safety and Energy, Tsinghua University, Beijing, China, 100084

<sup>2</sup> Beijing Co-innovation Center for Electric Vehicles, Beijing Institute of Technology, Beijing 100081, China

[jbzhang@mail.tsinghua.edu.cn](mailto:jbzhang@mail.tsinghua.edu.cn)

Electrochemical Impedance Spectroscopy (EIS) is a powerful electrochemical analysis technique known for its unique capability to differentiate between electrochemical processes of various natures. On the basis of widely different time-scales, EIS allows to reveal the limiting factors in reaction mechanisms, and mass-transport processes, thereby giving insight for the optimization of electrochemical devices.

The power of EIS to resolve electrochemical processes is often obscured by the complexity such as the frequency dispersion, time constants distribution, and spatial variation in real system under study. This talk gives a review of three major approaches to increase the resolution of EIS.

In the testing approaches, micro-sized single particles [1] and ultra-thin film [2] were employed as the test objects to greatly suppress the spatial distribution. Sharp and clear impedance spectroscopy amenable to regression analysis were obtained. Reference electrode [3] was introduced into the LIB to differentiate the impedance of the positive and negative electrodes. In the analysis approach, measurement model [4] was proposed to explore the error structures in the measured impedance and to generate weighting coefficients [5] to be used in the regression. Distribution of the relaxation times [6] was taken into consideration in regression with a general multiple RC circuits connected in series. In the modeling approach, building more structural information of the electrode into the model greatly enhanced the power of prediction. Transmission line model [7] improves over the lumped equivalent electric circuit for planar electrode by assuming a distributed constant along the pores of the electrode. Newman's model [8] further takes into account the diffusion inside the active particles in the porous electrode.

In our recent work [9][10], a three scale EIS model was developed to take into account the agglomerates that frequently exist in the electrodes of LIB. The model first mathematically describes the electrochemical reactions and species transport inside the micron-sized agglomerate consisting of submicron-sized primary particles, and then extends the agglomerate model to the whole porous electrode using the Newman's approach. Compared with the existing two-scale impedance models, the present model is featured with a refined description of the structure of the electrode/electrolyte interface at the primary active material particle, and an analytical formulation of electrochemical reactions and species transport inside the agglomerates. The model is validated using electrochemical impedance spectroscopy (EIS) data of an NMC positive electrode in a three-electrode lithium-ion cell over a wide range of SOC. The identified values of key model parameters are corroborated by results from other experiments or the literature. A parametric study reveals that the characteristic frequency of lithium ion diffusion in the electrolyte can be comparable or even smaller than that in the active material particle. As a result, EIS models capable of distinguishing between the solid phase diffusion and liquid phase diffusion should be used to extract the lithium ion diffusivities from impedance data.

## Reference:

- [1]. DOKKO, K., et al. Journal of the Electrochemical Society, 2001, 148.5: A422-A426.
- [2]. Mohamedi, M., et al Journal of The Electrochemical Society 149.1 (2002): A19-A25.
- [3]. Jansen A N, Dees D W, Abraham D P, et al. Journal of Power Sources, 2007, 174(2): 373-379.
- [4]. Agarwal, Pankaj, Mark E. Orazem, and Luis H. Garcia - Rubio. Journal of the Electrochemical Society 142.12 (1995): 4159-4168.
- [5]. Orazem, Mark E., et al. Electrochimica acta 38.14 (1993): 1903-1911.
- [6]. JP Schmidt, et al. Journal of Power Sources 196 (2011) 5342-5348
- [7]. Itagaki, Masayuki, et al. Electrochemistry 75.8 (2007): 649-655.
- [8]. J Meyers et al. Journal of The Electrochemical Society, 147 (8) 2930-2940 (2000)
- [9]. J Huang, H Ge, Z Li, J Zhang. An Agglomerate Model for the Impedance of Secondary Particle in Lithium-Ion Battery Electrode. Journal of The Electrochemical Society, 2014, 161(8): E3202-E3215.
- [10]. J Huang, Z Li, J Zhang, S Song, Z Lou, N Wu. An Analytical Three-Scale Impedance Model for Porous Electrode with Agglomerates in Lithium-Ion Batteries, Journal of The Electrochemical Society, 2015, 162(4): A585-A595.



# Consequences of Electrolyte Degradation for the Electrochemical Performance of NCM Battery Materials

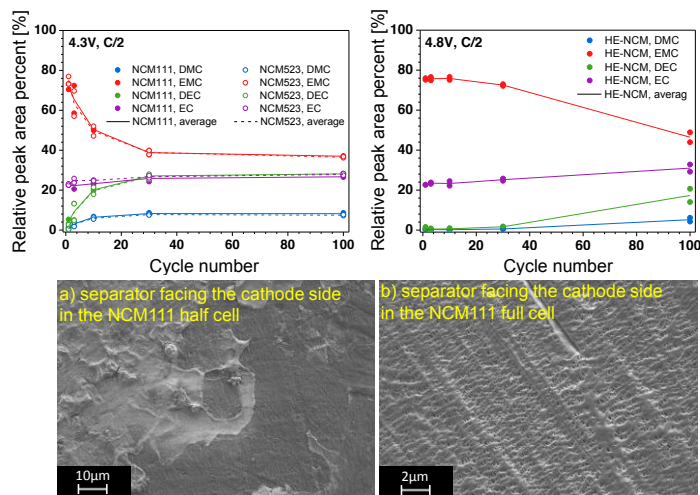
H.-J. Peng<sup>1,2</sup>, S. Urbonaitė<sup>1</sup>, C. Villevieille<sup>1</sup>, H. Wolf<sup>2</sup>, K. Leitner<sup>2</sup>, P. Novák<sup>1</sup>

<sup>1</sup>Electrochemistry Laboratory, Paul Scherrer Institute and <sup>2</sup>BASF SE

<sup>1</sup>CH-5232 Villigen PSI, Switzerland and <sup>2</sup>D-67056 Ludwigshafen, Germany  
hai-jung.peng@psi.ch

The stability of the electrolyte towards both the positive and the negative electrode is one of the key factors determining the long-term cycling performance of a lithium-ion battery. It is especially important when higher cycle rates are needed or when the electrode materials are operated at high potentials ( $>4.5$  V vs.  $\text{Li}^+/\text{Li}$ ) [1]. The latter includes lithium-rich nickel cobalt manganese oxide (called hereafter HE-NCM), which offers high energy density due to a higher operating potential but outside the electrolyte stability window. Alkoxide anion, which is a reduction product of linear carbonates, has been reported to play an important role in the multi-step electrolyte decomposition [2]. However, the consequences of this electrolyte degradation for the electrochemical performance of the cells are not yet well understood. In order to shed light on this issue, it is necessary to understand the parameters influencing the formation of the alkoxide anion.

In this work, the effects of current density and upper cut-off potential on the formation of the alkoxide anion were studied. Half cells based on conventional NCMs (NCM111 and NCM523) were compared to half cells including HE-NCM (with LP57 electrolyte, 1M  $\text{LiPF}_6$  in  $\text{EC}:\text{EMC} = 3:7$  wt %, in both cases). The occurrence of trans-esterification reaction, which provides an indication of the formation of the alkoxide anion, was detected by means of gas chromatography. Comparison of the results for cells cycled at  $C/2$  and  $C/10$  rates revealed the great impact of anode passivation on the extent of the trans-esterification reaction (and hence the production of alkoxide anion). In addition, the upper cut-off potential was also identified to be an important parameter, where higher potentials seem to mitigate the formation of the alkoxide anion. Further investigation of NCM111 full cells (based on electrochemical cycling, gas chromatography, and electron microscopy) suggested that electrolyte instability towards the anode (if not only the alkoxide anion formation) can eventually result in surface layer build-up on the cathode side. Therefore, stable anode passivation is not only essential for the anode performance but also for the state-of-health of the cathode and in turn the overall cell performance.



## References

- [1] J. B. Goodenough, Y. Kim, *Chem. Mater.*, 22, 587–603 (2010).
- [2] G. Gachot, P. Ribière, D. Mathiron, S. Grugeon, M. Armand, J.-B. Leriche, S. Pilard, and S. Laruelle, *Anal. Chem.*, 83, 478–485 (2011)

## Acknowledgments

The authors are grateful for financial support from BASF SE. Mr. R. Dietze, Mr. V. Schmitt, and Ms. M. Kimmel are acknowledged for the experimental support and Ms. V. Laschak for the gas chromatography measurements.

# Characterisation of Electrode Materials for Li-Ion Batteries Using *Operando* Neutron Powder Diffraction

Wei Kong Pang<sup>1,2</sup>, Vanessa K. Peterson

<sup>1</sup> Australian Nuclear Science and Technology Organisation, Locked Bag 2001, Kirrawee DC, NSW, 2232, Australia

<sup>2</sup> Institute for Superconducting and Electronic Materials, University of Wollongong, NSW, 2500, Australia

E-mail: weikong.pang@ansto.gov.au

Nowadays, Li-ion batteries (LIBs) are the primary choice of power source for portable electronic devices, including mobile phones, laptops, as well as electric vehicles. The working principle of a LIB is to store energy in chemical form by using charge-balancing Li ions that reversibly insert into the electrodes. The structure and chemistry of the electrodes determines their functional mechanism, and the removal and insertion of Li ions can significantly affect structure. Consequently, the structure and phase evolution of LIB electrodes during battery charge and discharge can be complex, with these processes underpinning function and electrochemical performance of the whole battery. Therefore, a mechanistic understanding of the reaction pathways, i.e. the atomistic and molecular-scale origin of battery performance<sup>1-5</sup>, will enable the rational improvement of electrode materials and pave the way for entirely new battery systems. The suitable elemental contrast, relatively-large penetration depth, and non-destructive interaction with matter that neutrons offer couples with the fast-detection ability of modern instrumentation to enable neutron powder diffraction to probe, in real time, the bulk crystallographic changes of electrodes in functioning batteries, with such experimental approaches known as *operando* studies. In this presentation, examples of *operando* neutron powder diffraction studies of electrode materials performed using WOMBAT<sup>6</sup>, the high-intensity neutron powder diffractometer at the Australian Nuclear Science and Technology Organisation, will be presented, demonstrating the importance of diffraction techniques in battery research.

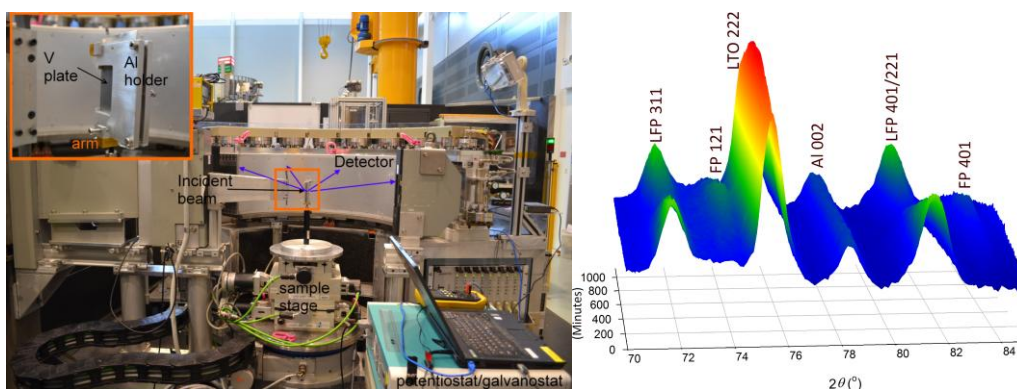


Figure 1. (Left) Experimental setup used for *operando* battery research with WOMBAT and (right) a contour plot of *operando* data from the  $\text{LiFePO}_4||\text{Li}_4\text{Ti}_5\text{O}_{12}$  pouch-type battery during charge-discharge.

LFP =  $\text{LiFePO}_4$ , FP =  $\text{FePO}_4$ , and LTO =  $\text{Li}_4\text{Ti}_5\text{O}_{12}$

## References:

- (1) Pang, W. K.; Sharma, N.; Peterson, V. K.; Shiu, J.-J.; Wu, S.-H. *J. Power Sources* **2014**, *246*, 464-472.
- (2) Pang, W. K.; Peterson, V. K.; Sharma, N.; Shiu, J.-J.; Wu, S.-h. *Chem. Mater.* **2014**, *26*, 2318-2326.
- (3) Pang, W. K.; Kalluri, S.; Peterson, V. K.; Dou, S. X.; Guo, Z. *Phys. Chem. Chem. Phys.* **2014**, *16*, 25377-25385.
- (4) Pang, W. K.; Peterson, V. K. *J. Appl. Cryst.* **2015**, *48*, 280-290.
- (5) Pang, W. K.; Alam, M.; Peterson, V. K.; Sharma, N. *J. Mater. Res.* **2014**, *30*, 373-380.
- (6) Studer, A. J.; Hagen, M. E.; Noakes, T. J. *Physica B* **2006**, *385-386, Part 2*, 1013-1015.

# Synthesis and Catalytic Activity of Ni Doped $\text{CoFe}_2\text{O}_4$ Hollow Nanospheres as Bi-functional Catalysts for Lithium Air Batteries

Jing-Hua Tian\*, Yujiao Xu, Yue Fu, Jin Wang, Ruizhi Yang\*

College of Physics, Optoelectronics and Energy & Collaborative Innovation Center of Suzhou Nano Science and Technology, Soochow University, Suzhou, 215006, China

E-mail: jhtian@suda.edu.cn, yangrz@suda.edu.cn

Many metal oxides have been reported as a promising substitute for the precious metal based catalysts in fuel cells and metal-air batteries, due to their relatively abundance, affordable, environmentally-friendly.<sup>[1]</sup> Nevertheless, the intrinsic electrical conductivity of most metal oxide is quite poor due to their chemical structure and non-stoichiometric composition.<sup>[2]</sup>

In this study, we present the synthesis and investigation of Ni doped  $\text{CoFe}_2\text{O}_4$  hollow nanospheres ( $\text{Ni}_x\text{Co}_{1-x}\text{Fe}_2\text{O}_4$ ,  $0 \leq x \leq 1$ ) with a simple hydrothermal approach, hoping to improve the conductivity and catalytic active sites for the metal oxide, and then enhancing its electrocatalytic activity. The preliminary results are shown in Fig. 1. Fig. 1a) shows the SEM image of the original  $\text{CoFe}_2\text{O}_4$  nanospheres, the inset shows clearly the hollow structure. The morphology and structure of the nanospheres have no change with doping. Fig. 1b) shows the oxygen reduction reaction (ORR) curves of the  $\text{Ni}_x\text{Co}_{1-x}\text{Fe}_2\text{O}_4$  ( $x = 0, 0.25, 0.5, 0.75$ ), the onset potential shifts positively with the doping. A significant change occurs when  $x$  reaches 0.5 ( $\text{Ni}_{0.5}\text{Co}_{0.5}\text{Fe}_2\text{O}_4$ ), it shows the best catalytic activity with the highest diffusion limiting current density and about 60 mV positive shift for the half-wave potential comparing with  $\text{CoFe}_2\text{O}_4$ . Fig. 1c) shows the oxygen evolution reaction (OER) comparison of the  $\text{Ni}_x\text{Co}_{1-x}\text{Fe}_2\text{O}_4$ . The  $\text{Ni}_{0.75}\text{Co}_{0.25}\text{Fe}_2\text{O}_4$  ( $x=0.75$ ) exhibits the best catalytic activity with more negative onset potential (0.3 V vs. Ag/AgCl) and maximum current density ( $36.0 \text{ mA/cm}^2$  at 1.0 V). Fig. 1d) gives the electrochemical impedance spectra (EIS) of the  $\text{Ni}_x\text{Co}_{1-x}\text{Fe}_2\text{O}_4$  in  $\text{N}_2$ -saturated 0.1 M KOH at 0.8 V at a rotating speed of 1600 rpm. It shows clearly that the charge transfer resistance decreases with the increasing of Ni doping content, which is perfect correlation with the OER activity. Besides, we believe that with the Ni doping, the new redox couple  $\text{Ni}^{2+}/\text{Ni}^{3+}$  has a synergistic effect with the Co and Fe redox couples for the OER process, which likely explain why the best catalytic activity of the doped  $\text{CoFe}_2\text{O}_4$  could be achieved under suitable doping content.

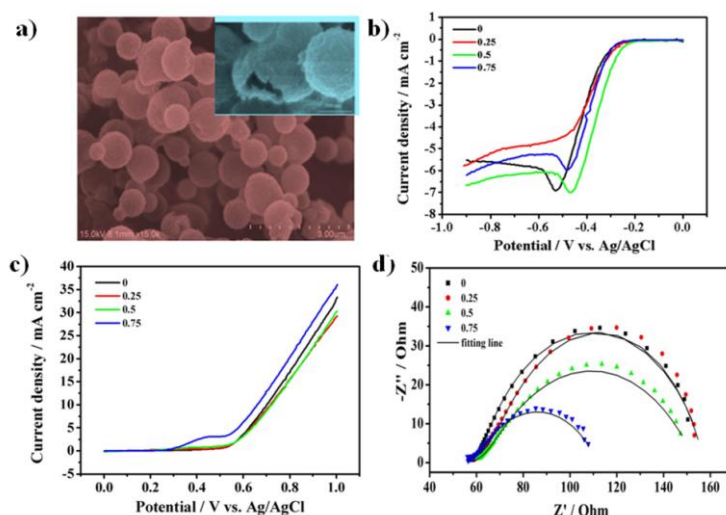


Fig. 1a) SEM image of the  $\text{CoFe}_2\text{O}_4$  hollow nanospheres, the inset is a typical broken nanosphere. b) ORR, c) OER and d) Nyquist plots of  $\text{Ni}_x\text{Co}_{1-x}\text{Fe}_2\text{O}_4$  ( $x = 0, 0.25, 0.5, 0.75$ ).

This work is supported by National Natural Science Foundation of China (No.51272167, 21206101 and 21303114).

## References:

- [1] Y. Shao, S. Park, J. Xiao et al., ACS Catalysis 2 (2012) 844-857.
- [2] R.A. Rincón, E. Ventosa, F. Tietz et al., ChemPhysChem., 15 (2014) 2810-2816.

# Advances on the Zinc-Cerium Redox Flow Battery for Energy Storage

L.F. Arenas, C. Ponce de León, F.C. Walsh.

*Electrochemical Engineering Laboratory, Energy Technology Research Group, Faculty of Engineering and the Environment, University of Southampton SO17 1BJ, UK*

+44 2380598384, [lfam1g13@soton.ac.uk](mailto:lfam1g13@soton.ac.uk)

The zinc-cerium redox flow battery (Zn-Ce RFB) is an emerging utility-scale energy storage technology addressing the requirements for assimilation of renewable sources into the power grid [1]. High cell potential is its main advantage. The equilibrium cell potential of 2.48 V is the highest among practical, aqueous RFBs. Additional advantages include its lack of halide emissions and the moderate cost of the electrolyte, in comparison to vanadium reagents.

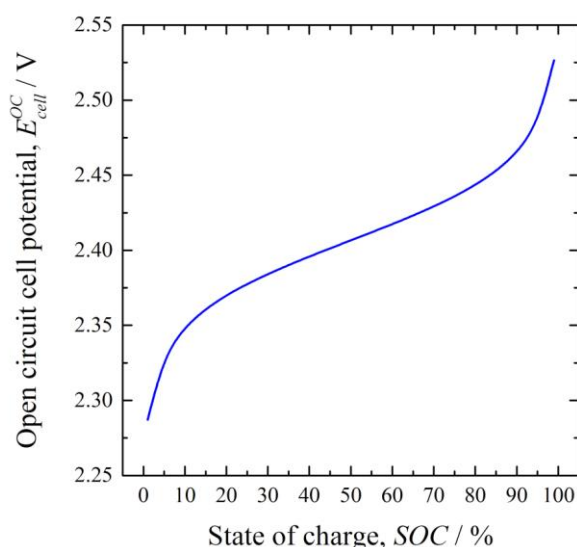


**Fig 1.** Open circuit cell potential vs. SOC of the Zn-Ce RFB.

In our recent work, the impact of cell potential components has been assessed, taking into consideration ohmic losses produced by electrolyte resistance, electrical connections and the resistivity of electrode materials. Activation overpotentials were also considered. This enabled cell potential vs. applied constant current density profiles for different operating conditions, identifying critical cell and cell stack design aspects and precise calculation of the resulting operating voltage. The resistivity of the main electrolyte compositions reported in the literature was measured at different operating temperatures and with varying acid content. The cell potential was also related to the state of charge (SOC) of the cell (Fig. 1), as established by the limiting cerium positive half-cell. Further research will focus on mass transport characterization using different positive electrode materials and cell monitoring.

The Zn-Ce RFB is based on the reduction of Ce(IV) to Ce(III) ions at the inert, positive electrode via the oxidation of metallic zinc at the negative electrodes, with the inverse reactions occurring during charge. Methanesulfonic acid is used as support electrolyte, enabling high concentrations of cerium and facilitating compact zinc deposits. Other works have focused on electrode materials, electrolyte composition and additives for performance enhancement [1]. This system is also been used as a develop platform for 3-D printing manufacture of flow cells.

**Keywords:** cell potential, cerium, energy storage, methanesulfonic acid, redox flow battery, zinc

**Reference:** [1]. Walsh F.C., Ponce de León C., Berlouis L., Nikiforidis G., Arenas-Martínez L.F., Hodgson D., Hall D. The development of Zn-Ce hybrid redox flow batteries for energy storage and their continuing challenges. *ChemPlusChem*. 80 (2014) 288.

# Enhancing electrochemical performance of layered oxide cathode materials for Li/Na ion batteries

Sihui Wang<sup>1</sup>, Xuehang Wu<sup>1</sup>, Shouding Li<sup>1</sup>, Jianghuai Guo<sup>1</sup>, Yixiao Li<sup>1</sup>, Yong Yang<sup>1,2</sup>

<sup>1</sup>State Key Lab of Physical Chemistry of Solid Surface & Department of Chemistry, <sup>2</sup>School of Energy Research, Xiamen University, Xiamen, 361005, China. e-mail: yyang@xmu.edu.cn

Li-ion battery systems have started to extend its roles from portable electronics, power tools to automobile applications such as hybrid and plug-in electric vehicles. However, it is necessary to enhance their electrochemical performance such as energy density and cycle life, for promoting their competition capability as vehicle power system. Obviously, electrode materials, especially positive electrode materials either working voltage or reversible capacity determine the energy density of the Li-ion batteries at mostly<sup>[1,2]</sup>.

In the presentation, some new research progress of the layered oxide cathode materials for Li/Na ion batteries will be reported. For example, we show that Ti modification could provide a promising way to realize this target with bifunctional role<sup>[3]</sup>. For example it is able to substitute Mn in the lattice framework and form a stable surface layer. It therefore results in a more stable energy density for the Ti-modified  $\text{Li}_{1.2}\text{Mn}_{0.54-x}\text{Ti}_x\text{Ni}_{0.13}\text{Co}_{0.13}\text{O}_2$  ( $x = 0.04, 0.08, \text{ and } 0.15$ ) materials during cycling. The evolution of dQ/dV curves show that the layered/spinel phase transformation is suppressed by the introduction of strong Ti-O bond in the framework. In addition, SEM, TEM, and EIS results confirm that more uniform and stable interface layer are formed on Ti-modified  $\text{Li}_{1.2}\text{Mn}_{0.54-x}\text{Ti}_x\text{Ni}_{0.13}\text{Co}_{0.13}\text{O}_2$  ( $x = 0.04, 0.08, \text{ and } 0.15$ ) materials compared with Ti-free  $\text{Li}_{1.2}\text{Mn}_{0.54}\text{Ni}_{0.13}\text{Co}_{0.13}\text{O}_2$ . The stable interface layer on the lithium-rich oxides is also beneficial to further reducing side reactions and resulting in stable surface layer resistance.

In addition, it is found that the introduction of  $\text{Zn}^{2+}$  in the Na-Ni-Mn-O system can effectively overcome the drawback of voltage decay when charged to a higher cutoff voltage ( $>4.0$  V), and significantly improve capacity retention compared to the unsubstituted material during cycling<sup>[4]</sup>. In addition, a smoother charge/discharge profile can be observed between 3.0 and 4.0 V for Zn-substituted samples, demonstrating that  $\text{Na}^+$ /vacancy ordering can be suppressed during sodium insertion/extraction.  $\text{Na}_{0.66}\text{Ni}_{0.26}\text{Zn}_{0.07}\text{Mn}_{0.67}\text{O}_2$  can deliver an initial capacity of  $132 \text{ mAh g}^{-1}$  at  $12 \text{ mA g}^{-1}$  with a high average voltage of 3.6 V and a capacity retention of 89% after 30 cycles.

## References

- 1) M. Armand, J.-M. Tarascon; Nature, 2008, 451, 682
- 2) Z. L. Gong, Y. Yang; Energy & Environmental Science; 2011, 4, 3223-3242
- 3) S.H.Wang, Y.X.Li, et al, Physical Chemistry & Chemical Physics, 2015, 17, 10151
- 4) X.H.Wu, J.H.Guo, et al, J Power Sources, 2015, 281, 18



# Block Copolymer-Templates for the Design of Three-Dimensional Interpenetrating Current Collectors for Submicrostructured Electrodes

Selina Tillmann<sup>a</sup>, Daniel Hermida Merino<sup>b</sup>, Martin Winter<sup>a</sup>, Isidora Cekic-Laskovic<sup>a</sup>, Katja Loos<sup>c</sup>

<sup>a</sup>MEET Battery Research Center, University of Muenster, Corrensstr. 46, 48149 Muenster, Germany

<sup>b</sup>Laboratory Dubble CRG c/oESRF 6, rue Jules Horowitz BP220, 38043 Grenoble Cedex, France

<sup>c</sup>University of Groningen, Department of Polymer Chemistry & Zernike Institute for Advanced Materials, Nijenborgh 4, NL-9747AG Groningen, The Netherlands

Selina.Tillmann@uni-muenster.de

Electrodes for lithium-ion batteries, having a large inner surface area combined with good lithium-ion transport properties and a high electronic conductivity, are considered promising candidates for overcoming the current limitations of electrochemical energy storage by improving the energy and power density. To realize electrodes with improved transport properties for lithium ions, block copolymers serve as a template for the generation of highly ordered three-dimensional, low density metal foams, acting as an interpenetrating conductive electrode matrix.[1]

In this study the versatile morphologies of the block copolymer system poly(styrene)-*b*-poly(4-vinylpyridine) (PS-*b*-P4VP) were utilized by the incorporation and variation of the amount of the amphiphile (3-pentadecylphenol). Various morphologies such as double gyroid and hexagonal packed cylinders were identified (Figure 1) by Scanning Electron Microscopy (SEM) and Small Angle X-ray Scattering (SAXS) experiments.

Through selective removal of the amphiphile void spaces within the polymer template are created which are then filled with nickel via electroless plating. Subsequently, the polymer template is removed by temperature controlled degradation and the metal framework is recovered.[2]

Electrodeposition was used for the incorporation of active material into the porous current collector and the chemical composition of the deposit was analyzed applying X-ray Photoelectron Spectroscopy (XPS) and Raman Spectroscopy. To investigate the electrochemical performance of the tailor-made submicrostructured electrodes, cycling and rate capability experiments were performed and compared to reference bulk electrodes.

Our initial studies show promising results making these kinds of microstructured electrodes interesting for the development of new generation high power/high energy batteries.

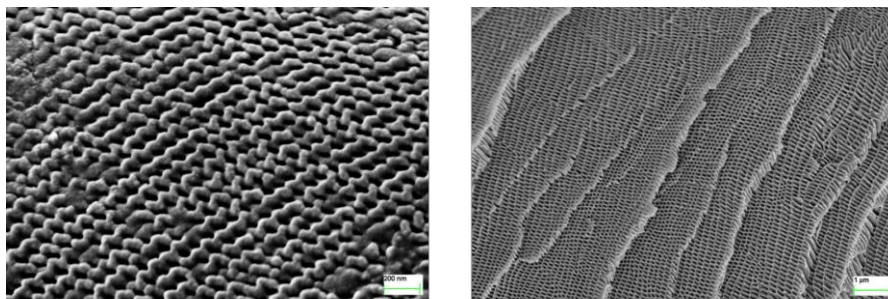


**Figure 1: SEM micrographs of two polymer morphologies as templates for three-dimensional, interpenetrating current collectors.**

## References:

- [1] M.K. Song, S. Park, F. M. Alamgir, J. Cho, M. Liu, Nanostructured electrodes for lithium-ion and lithium-air batteries: the latest developments, challenges, and perspectives, *Mater. Sci. Eng. R.* 72 (2011) 203.
- [2] I. Vukovic, G. t. Brinke, K. Loos, Block copolymer template-directed synthesis of well-ordered metallic nanostructures, *Polym.* 54 (2013) 2591.

# Aqueous Li (or Na)-ion Batteries for Grid-scale Energy Storage

Yonggang Wang\* and Yongyao Xia

*Department of Chemistry and Shanghai Key Laboratory of Molecular Catalysis and Innovative Materials, Institute of New Energy, iChEM(Collaborative Innovation Center of Chemistry for Energy Materials), Fudan University, Shanghai 200433, China.*

*Address: Handan Road 220, Fudan University, Shanghai, China.*

*e-mail address: ygwang@fudan.edu.cn*

In view of the limited oil storage and the global warming threats, it has been a worldwide topic to build a low carbon society supported by sustainable energy, such as wind and solar energy. Large-scale (i.e. grid-scale) energy storage is key to integrate intermittent the renewable energy resources like wind and solar into the power grid. Therefore, it is attracting extensive attention to develop large-scale energy storage devices with high efficiency, super-long cycle life, high safety, high power density, low cost and proper energy density.<sup>[1]</sup>

In this talk, I introduce the results of our academic investigation about aqueous Li (or Na) batteries and their application in grid-scale energy storage. In 2005, we invented a new type hybrid supercapacitor in which the activated carbon (AC) was used as an anode and the Li-ion intercalated compound  $\text{LiMn}_2\text{O}_4$  was used as a cathode in an aqueous electrolyte containing Li-ions.<sup>[2,3]</sup> Then, we investigated the capacity fading mechanism of aqueous Li-ion batteries (LIBs), and developed long-life aqueous LIBs based on carbon-coated  $\text{LiTi}_2(\text{PO}_4)_3$  anode.<sup>[4]</sup> Currently, aqueous hybrid energy storage devices based on  $\text{LiMn}_2\text{O}_4$  cathode and AC/  $\text{LiTi}_2(\text{PO}_4)_3$  composite anode are being commercialized for grid-scale energy storage or stationary energy storage. Recently, we are focusing on aqueous Li-ion batteries and Na-ion batteries with a  $\text{Li}^+$  (or  $\text{Na}^+$ ) exchange membrane to separate cathode and anode, such as rechargeable Zn-Cu battery<sup>[5]</sup> and I/polymer batteries. We hope these achieved results can light on the design of high safe and low cost batteries for grid-scale energy storage.

## References

1. B. Dunn, H. Kamath, J.-M. Tarascon, *Science* 2011(334)928.
2. Y. G. Wang, Y. Y. Xia, *Electrochem. Commun.* 2005(7)1138.
3. Y. G. Wang, Y. Y. Xia, *J. Electrochem. Soc.* 2006(153)A450.
4. J. Y. Luo, W. J. Cui, P. He, Y. Y. Xia, *Nat. Chem.* 2010(2)760.
5. X. L. Dong, Y. G. Wang, Y. Y. Xia, *Scientific Reports* 2014(4)6916.

# Surface phase transformation and $\text{CaF}_2$ coating for enhanced electrochemical performance of Li-rich Mn-based Cathodes

Xiaoyu Liu, Tao Huang, Aishui Yu\*

*Department of Chemistry, Fudan University  
220 Handan Road, Shanghai, 200433, China  
asyu@fudan.edu.cn*

To overcome the voltage decay upon cycling and increase the initial coulombic efficiency of the layered Li-rich Mn-based oxides, the double modification combining  $\text{Na}_2\text{S}_2\text{O}_8$  treatment with  $\text{CaF}_2$  coating has been first proposed in this study. The precondition  $\text{Na}_2\text{S}_2\text{O}_8$  treatment activates the  $\text{Li}_2\text{MnO}_3$  phase gently and generates a stabilized three-dimensional spinel structure on the surface of particles, leading to a suppression of surface reaction and structure conversion during the subsequent electrochemical process. The mitigation of phase transformation for  $\text{Na}_2\text{S}_2\text{O}_8$ -treated  $\text{Li}_{1.2}\text{Mn}_{0.54}\text{Ni}_{0.13}\text{Co}_{0.13}\text{O}_2$  alleviates the voltage decay and energy density degradation upon long-term charge-discharge cycling. In order to further restrain the capacity loss derived from the HF attack and manganese dissolution, 40 wt%  $\text{Na}_2\text{S}_2\text{O}_8$  treated-sample has been modified by an amorphous  $\text{CaF}_2$  layer with nano-scale thickness. The first-reported  $\text{CaF}_2$ -coated/40 wt%  $\text{Na}_2\text{S}_2\text{O}_8$  treated- $\text{Li}_{1.2}\text{Mn}_{0.54}\text{Ni}_{0.13}\text{Co}_{0.13}\text{O}_2$  presents excellent electrochemical properties with a high initial coulombic efficiency of 99.2 %, a capacity retention rate of 89.2% after 200 cycles and a high-rate capability of  $152.1 \text{ mAh g}^{-1}$  at 3C. Furthermore, A novel lithium-ion battery consisting of surface-treated  $\text{Li}_{1.2}\text{Mn}_{0.54}\text{Ni}_{0.13}\text{Co}_{0.13}\text{O}_2$  cathode and nano- $\text{Li}_4\text{Ti}_5\text{O}_{12}$  anode delivers a capacity of  $99.2 \text{ mAh g}^{-1}$  and a specific energy of  $202 \text{ Wh kg}^{-1}$  with an output voltage of 2.03 V based on the total weight of both active electrode materials. The cell also exhibits an excellent cycling stability and high-rate capability.



# Li-ion battery operation limits

Andrzej Lewandowski, Pawel Jakobczyk  
Faculty of Chemical Technology, Poznan University of Technology  
60-965 Poznan, Poland  
andrzej.lewandowski@put.poznan.pl

Operation of lithium ion-batteries, and therefore their efficiency, is limited both by thermodynamic and kinetic factors. Fact of such limits presence is usually compressed to a statement that the capacity  $q$  of the cell (or electrode material) depends on the operation rate (current). However, the capacity is a proportionality constant in the equation describing free enthalpy change,  $\Delta G$ , during cell charging/discharging:  $\Delta G = q \cdot \Delta E$  (where  $\Delta E$  is the potential change). Consequently, the postulated variation of the capacity is forbidden by the principle of maximum work:  $\Delta G = W_{\max}$ . This suggests that the  $q$  value, typically determined as the current and time product ( $q = I \cdot t$ ) must formally remain constant. Therefore, experimentally detected capacity variation as a function of operation rate (current density) reflects (i) heat generation and (ii) kinetic limits.

Heat release during Li-ion battery operation is one of the most fundamental property from the point of view of energy storage efficiency and fire safety. The irreversible heat, generated during charging and discharging,  $Q_{\text{irr}}$ , is always exothermic and is given by:  $Q_{\text{irr}} = I^2 R_s t$  (where  $I$ ,  $R_s$  and  $t$  indicate current, series resistance and time, respectively). Value of  $R_s$  can be estimated from impedance spectroscopy. Amount of energy dissipated in the form of heat increases with the operation rate which results in lowering the observed electric work – it is usually interpreted as the battery or electrode capacity decrease. If at low operating rates only 1% of energy is exchanged as a heat, increase of  $I$  value by a factor of 7 leads to  $Q_{\text{irr}}$  increase to ca. 50%. The reversible heat  $Q_{\text{rev}}$  is proportional to the entropy change,  $\Delta S$ , associated with the lithiation and delithiation of electrode materials:  $Q_{\text{rev}} = T \Delta S$ . The entropy change may be estimated from the dependence of open circuit electrode potential  $E$  on temperature  $T$ :  $\Delta S = F(dE/dT)$  in a non-isothermal cell (where  $F$  is the faraday constant).

The temperature of a cell, or a part of it, is determined by the heat balance between the amount of heat generated inside and that dissipated. When battery size increases, the ratio of heat cooling area to heat generating volume decreases, which is associated with increased fire risk. Process of temperature increase can be followed by the electrolyte decomposition reactions, with generation of gaseous products. The most commonly accepted mechanism for fire propagation proceeds via a radical generation mechanism. Exact description of processes leading to thermal runaway of Li-ion batteries is not known, but probably involves an endothermic pyrolysis of the electrolyte to form flammable gases, which then react with air and ignite. This leads to an exothermic process of flame propagation and release of additional heat amount which reinforces pyrolysis, producing free radicals at an increasing level.

The observed ‘capacity decrease’ with increasing battery operation rate may be due to kinetic reasons: (i) resistance of the SEI layer,  $R_{\text{SEI}}$  (ii) resistance of the charge transfer reaction,  $R_{\text{ct}}$  and (iii) diffusion impedance of lithium in the solid phase of the electrode material,  $Z_{\text{Li}}$  (usually expressed as the Warburg impedance). All these parameters can be determined from *ac* impedance spectroscopy curves deconvolution. Lithium diffusion impedance and low values of exchange current density seem to be the limiting processes. However, when a passivation layer is formed on the anode surface instead of the conducting SEI, it can significantly limit the battery operation rate. In the case of electrode materials which undergo drastic volume change during lithiation/delithiation (such as for example Si anode), breaking of electron conduction paths can reduce the active mass of electrode in electric contact with a current collector and strongly limit the device capacity.

# Ge@GeO<sub>2</sub> core@shell nanoparticles/multi-layer carbon composites as anode materials for lithium-ion batteries

Qi-Hui Wu<sup>1</sup>, Jinhang Hu<sup>1</sup>, Yang Yang<sup>2</sup>, Chengyuan Huang<sup>2</sup>, Hang Li<sup>1</sup>, Guoliang Chen<sup>2</sup>, Mingsen Zheng<sup>3</sup>, Qing-Biao Li<sup>1</sup>

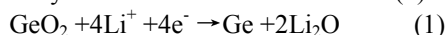
<sup>1</sup>School of Chemistry and Life Science, Quanzhou Normal University, Quanzhou 362000, Fujian, China

<sup>2</sup>Department of Chemistry and Environment Science, Minnan Normal University, Zhangzhou 36300, Fujian, China

<sup>3</sup>School of Chemistry and Chemical Engineering, Xiamen University, Xiamen 361005, Fujian, China  
qhwwu@qztc.edu.cn

Germanium (Ge) is one of the most promising alternative anode materials owing to its high theoretical capacity of 1600 mAh/g as formation Li<sub>22</sub>Ge<sub>5</sub> alloy [1], which is about 4 times of those of graphitic materials. Compared with silicon (Si), Ge is seldom studied because of concerns on its cost. But Ge has about 400 times higher lithium diffusivity at room temperature, 10<sup>4</sup> times higher electrical conductivity, and less significant specific volume change during lithiation/delithiation than Si [2]. These properties endue Ge to be an excellent anode material for fast charge/discharge lithium-ion batteries (LIBs). But the volume change during lithium insertion/extraction is still an impediment before Ge is commercially used in LIBs. The goal of this study is to synthesize Ge@GeO<sub>2</sub> core@shell nanoparticles/multi-layer carbon composites (Ge@GeO<sub>2</sub>/C) and then investigate their electrochemical properties as anode electrodes for LIBs. We expected that with wrap of GeO<sub>2</sub> around the Ge nanoparticles, they would show better electrochemical performance as the electrode integrity could be more easily maintained.

Fig. 1 shows the cycling performances of Ge@GeO<sub>2</sub>/C and Ge/C samples at a rate of 0.1 C (1 C = 1 A/g) for 50 cycles. The potential range is from 0.01 V to 1.5 V (vs Li/Li<sup>+</sup>). The first discharge capacities of the Ge@GeO<sub>2</sub>/C and Ge/C electrodes are very close, which are 2114.5 and 2116.7 mAh/g. The second discharge capacities for Ge@GeO<sub>2</sub>/C is 1207.0, and for Ge/C is 1311.12 mAh/g, giving the Coulombic efficiencies of 57.1% and 61.9%. The Ge/C electrode possesses the higher Coulombic efficiency at first cycle than Ge@GeO<sub>2</sub>/C probably due to the absence of reaction (1)



Compared to Ge@GeO<sub>2</sub>/C, the Ge/C electrode shows a higher capacity at the initially several cycles because of relatively high content of Ge. However, after 20 cycles, the Ge@GeO<sub>2</sub>/C electrode exhibits better capacity retentivity. At the 50<sup>th</sup> cycle, the capacities of the two electrodes are 1018.5 and 797.4 mAh/g, which indicates capacity retentions of 48.2% and 37.7% for Ge@GeO<sub>2</sub>/C and Ge/C electrodes, respectively. The GeO<sub>2</sub>@Ge/C sample presents much better cyclability than Ge/C. This may assign to its unique core@shell structure that could protect the integrity of the electrode during cycling.

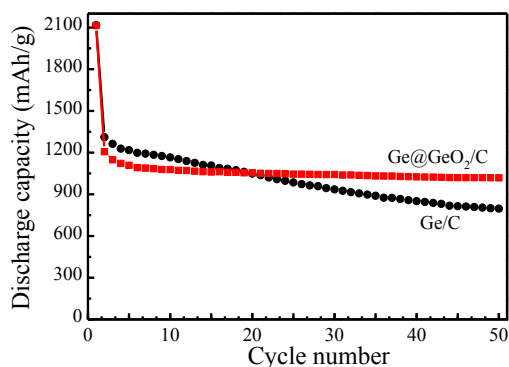


Fig. 1 The cycling capabilities of Ge@GeO<sub>2</sub> core@shell/C and Ge/C composites as anode electrodes for lithium-ion batteries

## References:

1. O.B. Chae, S. Park, J.H. Ku, J.H. Ryu, S.M. Oh, *Electrochim. Acta* 55 (2010) 2894-2900.
2. L.C. Yang, Q.S. Gao, L. Li, Y. Tang, Y.P. Wu, *Electrochem. Commun.* 12 (2010) 418-421.

# High performance mesoporous metallurgical silicon nanowire anode for lithium ion batteries

Xiaopeng Li,\* Ralf B. Wehrspohn

*Institute of Physics, Martin-Luther-Universität Halle-Wittenberg, Halle 06099, Germany*

*\*Current address: CAS Key Laboratory of Low-Carbon Conversion Science and Engineering, Shanghai Advanced Research Institute, Chinese Academy of Sciences, Shanghai 201210, China*

*Email: lixp@sari.ac.cn*

Silicon, ranked as the 2nd abundant element in the earth crust, is reshaping our daily life from personal electronics (e.g. laptop, smart phone) to solar modules. The purity level of Si as a direct measure of its electronic properties, directly determines its market price varying from \$2 to thousands of dollars per kg. Electronic grade Si (EG-Si) with the highest purity of >99.9999999% (9N) is widely used in the microelectronics industry, while the solar grade Si (SG-Si) with the purity of 99.9999% (6N) is currently applied in the solar cell industry. In the lithium ion battery (LIB) area, silicon is a very promising anode material. At room temperature, 1 mole Si can alloy 3.75 mole Li delivering a theoretical capacity of 3579 mAh/g, whereas, graphite only have a theoretical capacity of 372 mAh/g.

As a cheap Si source, metallurgical silicon (MG-Si) is readily available with production rate million tons per year, which is highly attractive for applying in LIBs. MG-Si can be easily modified to form large area of porous Si nanowires (SiNW) from MG-Si through metal assisted chemical etching (MaCE) at room temperature. The unique mesoporous feature in SiNWs is created by the dissolution of metal impurities inside MG-Si. Herein we demonstrate for the first time that nanowired MG-Si can be applied as a lithium ion battery anode without any post modification (e.g. carbon or conductive polymer coating). Since inner mesoporosity well accommodate the volume expansion during the lithiation/delithiation process, MG-SiNWs show a reversible capacity of about 2111 mAh/g at a current rate of 0.2 C, an excellent stability of over at least 50 cycles (see Figure 1), as well as a good rate capability.

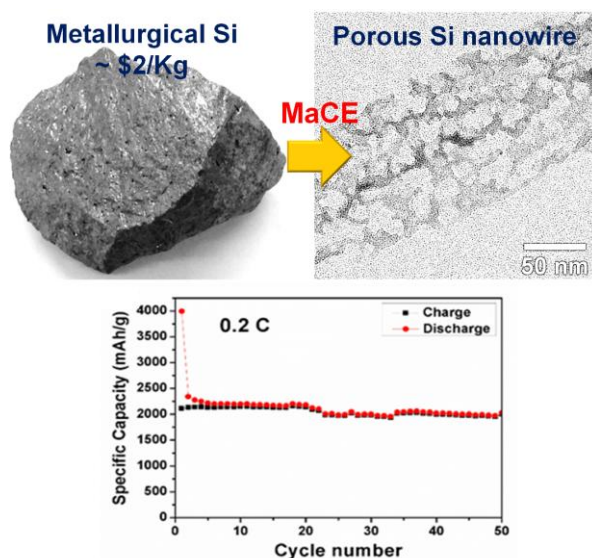


**Figure 1** Optical image of metallurgical silicon, TEM image of mesoporous MG-Si nanowire and the corresponding LIB performance.

## **Studies on ionic transport in liquid and polymeric electrolytes based on novel organic salts**

M. Dranka, J. Zachara, M. Marcinek, L. Niedzicki, M. Kalita, A. Bitner, G. P. Jankowski, Z. Żukowska  
and W. Wieczorek

*Faculty of Chemistry, Warsaw University of Technology, ul. Noakowskiego 3, 00-664 Warszawa, Poland  
e-mail: [wladek@ch.pw.edu.pl](mailto:wladek@ch.pw.edu.pl)*

In spite of over thirty years of intensive studies on various types of liquid and polymeric electrolytes still there is a need for the new systems which characterized by conductivities electrochemical stabilities and safety superior to currently commercially available electrolytes. Although most of the investigations are carried out on lithium electrolytes sodium analogues seems to be equally important. One of the ways to enhance properties of the studied electrolytes is to develop new salts having relatively large anions with delocalize charge which lead to the limitation in the formation of ionic associates and in turn to the improvement in the conductivity and cation transference numbers. In the present work examples of newly developed lithium and sodium salts and their use in liquid as well as polymeric electrolytes based on low as well as high molecular weight systems will be presented.

Complementary series of crystal structures of lithium and sodium salts will be presented.. Single-crystal X-ray analysis of the salts adducts with aprotic solvents: glymes – dimethyl ethers of poly(ethylene glycols) – and crown ethers have been performed to correlate their molecular structures and properties with spectroscopic and thermal data. Comprehensive structure analysis of crystalline materials reveals valuable information about coordination ability of the studied anions and provides the basis to develop the model of poly(ethylene oxide) electrolytes and liquid systems. Presented results reveal new aggregation modes at high concentrations of lithium salts involving releasing cations by self-assembly of anionic subnetwork and shed some light on electrochemical performance of the studied anions. X-ray data are supported by FT-IR and FT-Raman studies.

In addition exemplary data of the studies of these new type electrolytes in lithium and sodium ion batteries will be presented.

# **The Benefits of Hydrothermal Flow Reactors for High Power and High Energy Lithium-ion Battery Electrode Materials**

Mechthild Luebke<sup>1,2</sup>, Zhaolin Liu<sup>2</sup>, Ian Johnson<sup>1</sup>, Jawwad Darr<sup>1</sup>

<sup>1</sup>*University College London, United Kingdom*

<sup>2</sup>*Institute of Materials Research and Engineering, Agency for Science, Technology and Research (A\*STAR), 3 Research Link, Singapore 117602, Singapore  
(mechthild.lubke.13@ucl.ac.uk)*

The clean materials technology group at UCL has developed continuous hydrothermal flow synthesis (CHFS) processes for the continuous synthesis of a range of metal oxides, sulfides and other inorganic advanced functional materials, particularly, Li ion battery electrodes. The CHFS process involves the engineered mixing of a stream of superheated water (typically at 450 °C and >22MPa) with a metal salt containing aqueous solution in the presence of various additives for both control of oxygen stoichiometry, size and shape etc. Another recent innovation in CHFS is in the successful scale-up of the process to pilot plant using a newly patented confined jet mixer, which shows tremendous promise for large scale production of nanoparticles (>1 kg/h). The modulation of process design, process scale and reaction conditions enables overall specific material properties like high levels of dopants, variation in particle size and morphology and the synthesis of composite materials.

Recently, it has been shown that these properties can be used to make high power and high energy battery electrode materials especially just via high level of dopants. Doping high levels of oxide supercapacitor transition metals into a cheap lithium-ion insertion material can improve the electronic conductivity and also drastically increase the stored charge via additional pseudocapacitive effects from the surface. On the other hand doping an alloy anode metal ion into a cheap insertion host can improve the specific capacity and also widen the operational potential window.

Exemplified, both strategies will be presented for an anatase TiO<sub>2</sub> host with a particle size of less than 7 nm and a BET surface area higher than 230 m<sup>2</sup> g<sup>-1</sup>, which is also directly suitable for scaling up. For the high power application 25 at% of niobium have been used which resulted in a specific capacity of 50 mAh g<sup>-1</sup> at an applied current of 15 A g<sup>-1</sup>. For the high energy application up to 15 at% of Sn have been used which resulted in a specific capacity of 350 mAh g<sup>-1</sup> at an applied current of 100 mA g<sup>-1</sup>.

# **In situ polyol-assisted synthesis of Zn<sub>2</sub>SnO<sub>4</sub> nanocrystals/graphene nanohybrid as high-performance anode for Li-ion batteries**

Gang Wang, Jun Peng, Yongtao Zuo, Gang Li, Feng Yu, Bin Dai, Xuhong Guo

*School of Chemistry and Chemical Engineering, Key Laboratory for Green Processing of Chemical Engineering of Xinjiang Bingtuan, Shihezi University, Shihezi 832003, P.R. China*

*Email: gwangshzu@163.com*

Lithium-ion batteries (LIBs) are the power source of choice not only for popular consumer electronics but also for upcoming electric vehicles. Due to the limited capacity of graphite, many efforts have been focused on finding substitutes with larger capacity and slightly more positive intercalation voltage compared to Li/Li<sup>+</sup>, so as to reduce the possible safety problems of lithium plating. Metal oxides, typically providing a capacity more than two times larger than that of graphite with higher potential, have aroused wide interest. As an example, the theoretical capacity of SnO<sub>2</sub> can reach as high as 780 mAh g<sup>-1</sup> with the lithiation mechanism:  $\text{SnO}_2 + 4\text{Li} \rightarrow \text{Sn} + 2\text{Li}_2\text{O}$ ,  $\text{Sn} + x\text{Li} \rightarrow \text{Li}_x\text{Sn}$  ( $x \leq 4.4$ ). Recently, this strategy has been gradually expanded to ternary tin-based oxides (M<sub>2</sub>SnO<sub>4</sub>) owing largely to their unique properties emerging from electronic correlations and cooperative effects between different metal cation, which are less prominent in monometallic binary phases. However, their application in practical LIBs is still significantly hindered by the poor cyclic performance arising from poor conductivity and huge volume expansion during charge/discharge.

Graphene (GR) has a large specific surface area, excellent conductive, mechanical, and hydrophobic properties and is chemically stable, making it an ideal support. Fabrication of graphene/metal oxide composites is expected to be an effective and practical method to resolve these problems. From the viewpoint of structure, on one hand, metal oxides anchored or dispersed on GR not only suppress the agglomeration and restacking of GR but also increase the available surface area of the GR alone, leading to high electrochemical activity. On the other hand, GR as a support of metal oxides can induce the nucleation, growth and formation of fine metal oxide nano-/microstructures with uniform dispersion and controlled morphology on the surface of graphene with high chemical functionality. The final graphene-supported metal oxide can form a perfect integrated structure with a developed electron conductive network and shortened ion transport paths. Significant synergistic effects often occur in graphene/metal oxide composites because of size effects and interfacial interactions. However, in situ growth of metal oxide nanocrystals, especially multi-cationic metal oxides nanocrystals, on the surface of GR sheets still be difficult to achieve.

Zinc stannate (Zn<sub>2</sub>SnO<sub>4</sub>), a cubic inverse spinel structured A<sub>2II</sub>B<sub>IV</sub>O<sub>4</sub> compound (space group Fd3m), is well known for its high electron mobility, high electrical conductivity. Therefore, Zn<sub>2</sub>SnO<sub>4</sub> represents a promising material for application as an anode material in lithium ion batteries. Herein, we report a facile one-pot in situ polyol-assisted hydrothermal route to prepare Zn<sub>2</sub>SnO<sub>4</sub> nanocrystals/graphene (Zn<sub>2</sub>SnO<sub>4</sub>/GR) nanohybrid. The Zn<sub>2</sub>SnO<sub>4</sub> nanocrystals (5-10nm) are uniformly dispersed and immobilized by the graphene nanosheets reduced from GO. The electrochemical tests showed that the Zn<sub>2</sub>SnO<sub>4</sub>/GR hybrid exhibits an obviously improved electrochemical performance compared with bare Zn<sub>2</sub>SnO<sub>4</sub>, indicating its promising application as anode for Li-ion batteries.

## **References**

- [1] G. Wang, et al., Journal of Materials Chemistry A 2015, 3: 3659-3666
- [2] G. Wang, et al., Electrochimica Acta, 2011, 56: 9515–9519
- [3] F. Yu, et al., Nano Energy, 2014, 3, 64-79.

# Hybridization of graphene sheets and carbon-coated Fe<sub>3</sub>O<sub>4</sub> hollow nanoparticles as a high-performance anode material for lithium-ion batteries

Gang Wang, Yongtao Zuo, Jun Peng, Gang Li, Feng Yu, Bin Dai, Xuhong Guo

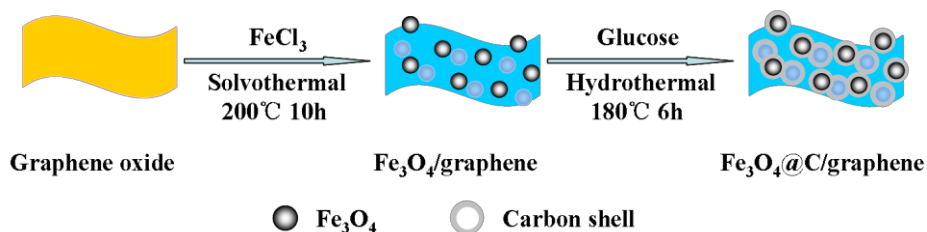
School of Chemistry and Chemical Engineering, Key Laboratory for Green Processing of Chemical Engineering of Xinjiang Bingtuan, Shihezi University, Shihezi 832003, P.R. China

Email: gwangshzu@163.com

In order to meet the increasing requirements for electric vehicles (EVs) and hybrid electronic vehicles (HEVs) applications, significant achievements have been gained in the research of anode materials with superior capacity for lithium-ion batteries (LIBs), such as Si, Sn and transition metal oxides. Among these potential anode materials, Fe<sub>3</sub>O<sub>4</sub> shows high theoretical capacity (928 mAh g<sup>-1</sup>), low cost, eco-friendliness, and natural abundance, thus has attracted considerable attention. However, its large volume expansion/contraction and severe particle aggregation associated with the Li<sup>+</sup> insertion and extraction process lead to electrode pulverization and loss of interparticle contact and, consequently, result in a large irreversible capacity loss and poor cycling stability.

A variety of appealing strategies have been utilized to solve these intractable problems, including the use of carbon-based nanocomposites and various Fe<sub>3</sub>O<sub>4</sub> nanostructures/microstructures. However, to keep large reversible capacity combined with high Coulombic efficiency, achieving long cycling life and good rate capability of Fe<sub>3</sub>O<sub>4</sub> electrode material still remains a great challenge. Recently, a new type of nanoarchitecture, a hollow structure together with carbon coating, was proposed and it manifests improved cycling performance and rate capability. To circumvent the challenges faced by inner-pore filling or exterior coating, a flexible confining structure is expected to provide enough buffer space for improving the cycling stability of anode materials by reducing the pulverization.

Graphene, a new two-dimensional carbon material, is recently expected to be an advanced anode material in LIBs due to its superior electrical conductivity, high surface-to-volume ratio, ultrathin thickness, structural flexibility, and chemical stability. More importantly, graphene can also be used in composites with metal oxide nanoparticles (NPs) to improve the electrochemical performance of these particles because the ultrathin flexible graphene layers not only can provide a support for anchoring well-dispersed NPs and work as a highly conductive matrix for enabling good contact between them but also can effectively prevent the volume expansion/contraction and aggregation of NPs during Li charge/discharge process. Therefore, we take the advantages of the characteristics of graphene to construct two-dimensional Fe<sub>3</sub>O<sub>4</sub>@C/graphene composites, uniting the two building blocks for reducing the pulverization of these materials and enhancing their cycling stability, as well as inhibiting the degree of restacking of graphene (Scheme 1). First, the Fe<sub>3</sub>O<sub>4</sub>/graphene hybrids were synthesized via a facile, one-step solvothermal approach by the in situ conversion of FeCl<sub>3</sub> to Fe<sub>3</sub>O<sub>4</sub> and simultaneous reduction of GO to graphene in ethylene glycol. Then, carbon shells were coated onto Fe<sub>3</sub>O<sub>4</sub> NPs by dispersing the Fe<sub>3</sub>O<sub>4</sub>/graphene hybrids in glucose aqueous solution for hydrothermal treatment. It is found that the Fe<sub>3</sub>O<sub>4</sub>@C/graphene composite has the advantages of the two building blocks and exhibits a large reversible capacity, enhanced cyclic stability, and excellent rate capability.



Scheme 1 Schematic representation of the fabrication process of Fe<sub>3</sub>O<sub>4</sub>@C/graphene composite

## References

- [1] G. Wang, et al., Journal of Materials Chemistry A 2015, **3**: 3659-3666
- [2] G. Wang, et al., Electrochimica Acta, 2011, **56**: 9515– 9519
- [3] F. Yu, et al., Nano Energy, 2014, **3**, 64-79.

# Enabling Catalytic Oxidation of $\text{Li}_2\text{O}_2$ at Liquid-Solid Interface: A Successful Evolution for an Aprotic Li-O<sub>2</sub> Battery

Ping He

College of Engineering and Applied Sciences, National Laboratory of Solid State Microstructures,  
Nanjing University, Nanjing, Jiangsu, 210093, PR China  
Pinghe@nju.edu.cn

As we know, rechargeable lithium-O<sub>2</sub> batteries, especially in organic aprotic electrolyte, have attracted much worldwide attention due to its high theoretical energy density of 3450 Wh kg<sup>-1</sup> (including lithium and oxygen). However, for the aprotic Li-O<sub>2</sub> battery, the insulating discharge product  $\text{Li}_2\text{O}_2$  is accumulated and blocked the porous cathode gradually, which results in the high charging voltage, leading to the low round-trip efficiency, poor cycle life and even detrimental electrolyte decomposition. As seen in **Figure 1**. A novel strategy based on redox mediators as the soluble oxidation catalyst has been proposed to reduce the charge overpotential.<sup>[1-3]</sup> TEMPO<sup>+</sup>/TEMPO redox couple has dramatically reduced the charge voltage of  $\text{Li}_2\text{O}_2$  oxidation and promote the round-trip efficiency of this battery system. The soluble catalyst transfer solid/solid interfacial electrochemical reaction to solution/solid interfacial chemical oxidation, which indeed provides significant evolution for aprotic Li-O<sub>2</sub> battery. In this report, we highlight the work concerning the soluble catalyst of TEMPO and summarized the fundamental criteria of the suitable redox mediators as mobile OER catalyst. Meanwhile, we develop another new redox couple, 10-methyl-10H-phenothiazine (MPT), as soluble catalyst in aprotic Li-O<sub>2</sub> battery.<sup>[4]</sup> Its formal redox potential of 3.67 V vs. Li<sup>+</sup>/Li makes it a promising redox candidate. The overpotential with MPT redox mediator is 800 mV, which far below that of without MPT in non-aqueous Li-O<sub>2</sub> battery. At the end of our report, we also propose some challenges and disadvantage of soluble catalyst using in aprotic Li-O<sub>2</sub> battery.

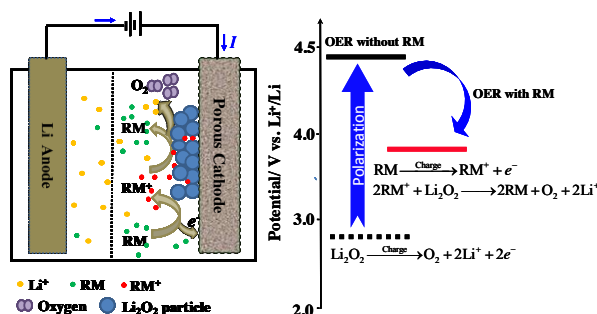


Figure 1. The proposed catalytic mechanism of the OER with a suitable redox mediator as the soluble catalyst in an aprotic Li-O<sub>2</sub> battery.

## Reference

- [1]. H.-D. Lim, H. Song, J. Kim, H. Gwon, Y. Bae, K.-Y. Park, J. Hong, H. Kim, T. Kim, Y. H. Kim, X. Lepró, R. Ovalle-Robles, R. H. Baughman, K. Kang, *Angew. Chem. Int. Ed.* **2014**, 53, 3926–3931;
- [2]. M. Z. Yu, X. D. Ren, L. Ma, Y. Y. Wu, *Nat. Commun.* **2014**, 5, 5111-5116;
- [3]. Y. H. Chen, S. A. Freunberger, Z. Q. Peng, O. Fontaine, P. G. Bruce, *Nat. Chem.* **2013**, 5, 489-494
- [4]. N. N. Feng, P. He, H. S. Zhou, *ChemSusChem*, **2014**, 8, 600.



# Studies of Non-metal Elements Doped Carbon Coated Electrode Materials of Lithium (Sodium) Ion Batteries

Haimei Liu, Cong Wang, Wei Shen

College of Environmental and Chemical Engineering, Shanghai University of Electric Power,  
Shanghai 200090, China

e-mail :liuhm@shiep.edu.cn

State Key Laboratory of Chemical Resource Engineering, Beijing University of Chemical Technology,  
Beijing 100029, China

Carbon coating is a low cost and high-efficiency modification approach which is widely used to modify various lithium ion batteries electrode materials<sup>[1]</sup>, such as  $\text{LiFePO}_4$ ,  $\text{Li}_3\text{V}_2(\text{PO}_4)_3$ ,  $\text{Li}_4\text{Ti}_5\text{O}_{12}$ , etc. Nowadays, non-metal elements doping, such as N or B doping<sup>[2,3]</sup>, are widely adopted on carbon-based materials and exhibited obvious modification effects. Based on the above analyses, a novel modification approach, non-metal elements doped carbon coating, has been proposed in this work. In this work, N- and B-doped carbon coating has been used to improve the electrochemical performances of  $\text{Li}_3\text{V}_2(\text{PO}_4)_3$ <sup>[4,5]</sup>, compared with pure carbon coating, these two non-metal elements doped carbon coating approaches exhibited more obvious modification effects on  $\text{Li}_3\text{V}_2(\text{PO}_4)_3$ .

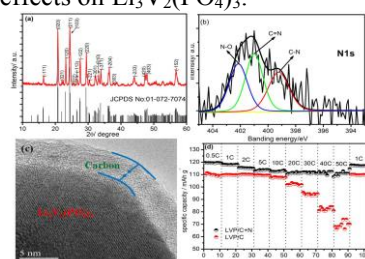


**Fig. 1** (a) XRD patterns, (b) XPS spectra, (c) HRTEM images and (d) rate stability for LVP/C+N.

XRD patterns of N-doped carbon coating  $\text{Li}_3\text{V}_2(\text{PO}_4)_3$  (LVP/C+N) indicate that N-doped carbon coating make no effects on the structure of  $\text{Li}_3\text{V}_2(\text{PO}_4)_3$ . As shown in Fig. 1b, N is successfully doped in carbon coating layer of  $\text{Li}_3\text{V}_2(\text{PO}_4)_3$ ; there is an uniform and complete carbon layer on the surface of LVP/C+N particles (Fig. 1c), therefore, compared with LVP/C, LVP/C+N shows much better rate stability.

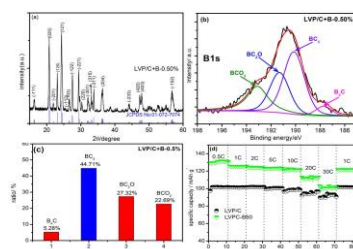


**Fig. 2** (a) XRD patterns, (b) XPS spectra, (c) distribution diagram and (d) rate stability for LVP/C+B.

Based on XRD patterns in Fig. 2, moderate B-doped carbon coating make no effects on the structure of  $\text{Li}_3\text{V}_2(\text{PO}_4)_3$ . As shown in Fig. 1b, B is successfully doped in carbon coating layer of  $\text{Li}_3\text{V}_2(\text{PO}_4)_3$ ; there are four doping types:  $\text{BC}_3$ ,  $\text{BC}_2\text{O}$ ,  $\text{BCO}_2$ ,  $\text{B}_4\text{C}$  existed in LVP/C+B. These four doping types has different distributions in LVP/C+B. Compared with LVP/C, LVP/C+B shows much better rate performance.

Moreover, the N-doped carbon coating modification approach are also used to improve the electrochemical properties of  $\text{Na}_3\text{V}_2(\text{PO}_4)_3$  sodium ion batteries electrode material. Based on the test results of XPS, N element is successfully doped in the carbon layer of  $\text{Na}_3\text{V}_2(\text{PO}_4)_3$ , which further improve the electronic conductivity and defect level of carbon coated layer.

## References

- [1] H. Li, H. S. Zhou, *Chem. Commun.* 2012, **48**:1201-1217.
- [2] Y. Zhao, L. Yang, S. Chen et al., *J. Am. Chem. Soc.* 2013, **135**: 1201-1204.
- [3] L. S. Panchakarla, K. S. Subrahmanyam, S. K. Saha et al., *Adv. Mater.* 2009, **21**: 4726-4730.
- [4] C. Wang, W. Shen, H. M. Liu, *New J. Chem.* 2014, **38**: 430-436.
- [5] C. Wang, Z. Guo, W. Shen, Q. J. Xu, H.M. Liu, Y.G. Wang, *Adv. Funct. Mater.* 2014, **24**: 5511-5521.
- [6] W. Shen, C. Wang, Q. J. Xu, H.M. Liu, Y.G. Wang, *Adv. Energy Mater.* 2014, **5**, 201400982.

# Temperature Effects on Porous $\text{ZnCo}_2\text{O}_4$ Anode for Lithium-ion Batteries

Ji-Xuan Fu, Wei-Ting Wong and Wei-Ren Liu\*

Department of Chemical Engineering, Chung Yuan Christian University, Chung Li District, Taoyuan City, Taiwan

Correspondence: WRLiu1203@gmail.com

Herein,  $\text{ZnCo}_2\text{O}_4$  is synthesized via hydrothermal method with different annealing temperature [1]. X-ray diffraction (XRD), Brunauer-Emmett-Teller (BET), scanning electron microscopy (SEM) are used to study the structure and characteristics of the obtained powders. Thermogravimetric analysis (TGA) of the precursors is also carried out in this study. The morphology of  $\text{ZnCo}_2\text{O}_4$  turns to sphere-like with porous structure when the annealing temperature as high as 600 °C (Figure 1). The as-prepared porous  $\text{ZnCo}_2\text{O}_4$  nanospheres synthesized at 600 °C have been applied as anode materials of Li-ion batteries, the initial discharge capacity is 1800.4 mAh/g. After 30 cycles, the capacity still retain 1242.2 mAh/g (Figure 2). The AC data shows that the  $\text{ZnCo}_2\text{O}_4$  nanospheres have lower surface layer resistance. The porous nanostructures and large surface area are responsible for superior performance. Moreover, it is indicated that porous  $\text{ZnCo}_2\text{O}_4$  nanospheres synthesized at 600 °C show larger capacity and better performance than 500 °C and 700 °C, because of their more complete structure.

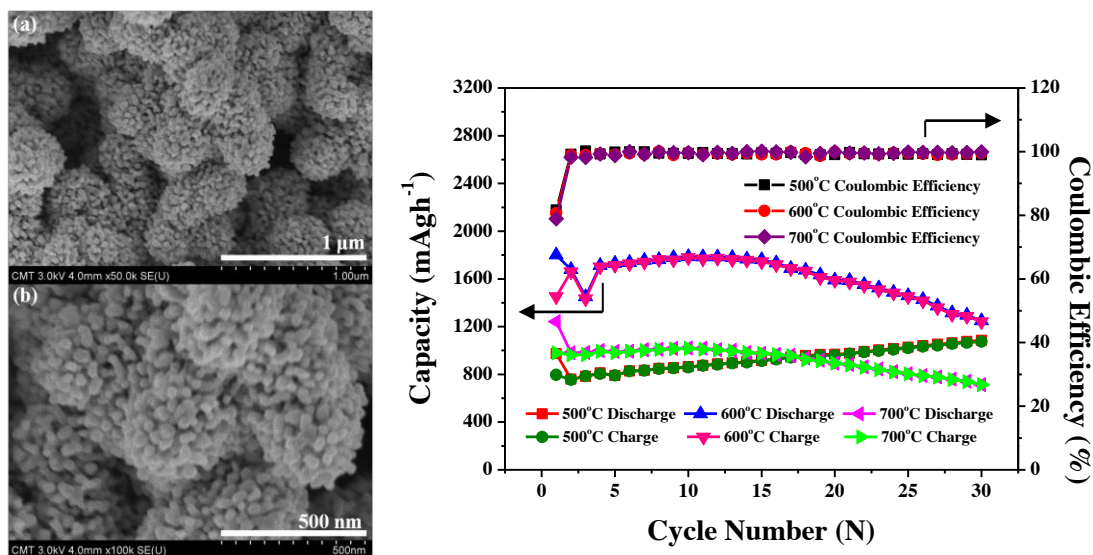


Figure 1 SEM images of  $\text{ZnCo}_2\text{O}_4$  synthesized at 600 °C: (a) low magnification; (b) high magnification.

Figure 2 Cycle performance of  $\text{ZnCo}_2\text{O}_4$  synthesized at 500 °C, 600 °C and 700 °C.

## Reference

[1] Haowen Liu, Jin Wang, *Electrochimica Acta* 92 (2013) 371-375.

# Effects of $\text{Al}^{3+}/\text{Cl}^-$ co-doping on the electrochemical properties of $\text{Li}_{1.2}\text{Ni}_{0.4}\text{Mn}_{0.6}\text{O}_{2.2}$ cathode materials for lithium ion batteries

Yu-Cheng Liu<sup>a</sup>, Nae-Lih Wu<sup>b</sup> and Wei-Ren Liu<sup>a,\*</sup>

<sup>a</sup>Department of Chemical Engineering, Chung Yuan Christian University, Chung Li, Taiwan

<sup>b</sup>Department of Chemical Engineering, National Taiwan University, Taipei, Taiwan

\*E-mail address: [WRLiu1203@gmail.com](mailto:WRLiu1203@gmail.com) (W. R. Liu)

Tel: +886-3-265-4140; fax: +886-3-265-4199

The Li-rich layered cathode materials,  $\text{Li}_{1.2}\text{Ni}_{0.4-x}\text{Al}_x\text{Mn}_{0.6}\text{O}_{2.2-y}\text{Cl}_y$  ( $0 \leq x \leq 0.03$  and  $0 \leq y \leq 0.03$ ), were successfully synthesized from a co-precipitation precursor at 900 °C in air. The influence of  $\text{Al}^{3+}$ - $\text{Cl}^-$  co-substitution on the morphology, structure and electrochemical performance was characterized by X-ray diffraction (XRD), scanning electron microscope (SEM), X-ray photoelectron spectroscopy (XPS), transmission electron microscopy (TEM) and electrochemical and charge–discharge cycling. Via doping Al/Cl ions in the cathode, the electrochemical performance could not only be enhanced in room temperature but also quite well in high working temperature of 55 °C. The as-synthesized optimal-composition of  $\text{Li}_{1.2}\text{Ni}_{0.37}\text{Al}_{0.03}\text{Mn}_{0.6}\text{O}_{2.17}\text{Cl}_{0.03}$  deliver reversible capacity of 176 mAh/g and coulombic efficiency was 84.31% at the 23th cycle. For 55 °C test, the discharge capacity demonstrates a very good capacity of as high as 206 mAh/g and capacity loss rate was only 0.95 mAh  $\text{g}^{-1}$  cycle<sup>-1</sup> at the 21th cycle. Figure 1 shows that the differential capacity vs. voltage plots derived from the cycling curves at 55 °C. We find that the  $\text{Al}^{3+}$ - $\text{Cl}^-$  co-doped materials reduction peaks change were smaller than those of undoped materials during 20th cycle, and lithium ions are extracted and inserted into the layered phase by one-step process. The  $\text{Al}^{3+}$ - $\text{Cl}^-$  co-substitution enhanced structural stability by formation of strong Mn–Cl and Ni–Cl bonds revealed by XPS analysis[1]. Moreover, the  $\text{Al}^{3+}$ - $\text{Cl}^-$  co-doped materials was increased by 33.32% and impedance was reduced by 52.17% compared to bare sample.

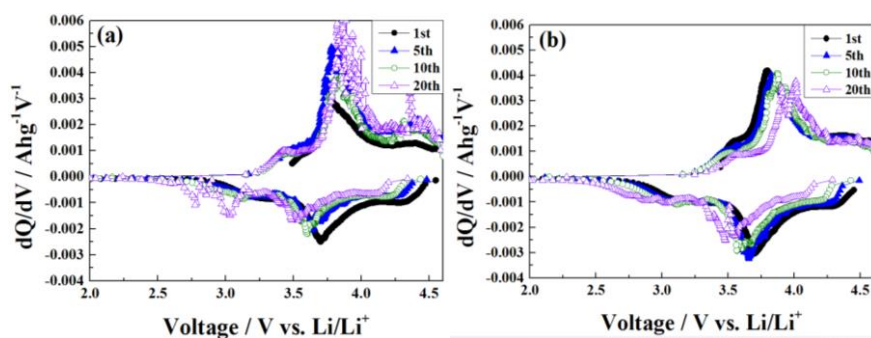


Figure 1 Differential capacity vs. voltage of  $\text{Li}_{1.2}\text{Ni}_{0.4-x}\text{Al}_x\text{Mn}_{0.6}\text{O}_{2.2-y}\text{Cl}_y$  cells cycled at 2.0–4.6 V. (a)  $\text{Li}_{1.2}\text{Ni}_{0.4}\text{Mn}_{0.6}\text{O}_{2.2}$ , (b)  $\text{Li}_{1.2}\text{Ni}_{0.37}\text{Al}_{0.03}\text{Mn}_{0.6}\text{O}_{2.17}\text{Cl}_{0.03}$ . (●) First cycle, (▲) 5th cycle, (○) 10th cycle and (Δ) 20th cycle.

## References

[1] Y. Chen, Qi. Jiao, L. Wang, Y. Hu, N. Sun, Y. Shen, Y. Wang, C. R. Chimie 16 (2013) 845–849.

# Binder Effects and Architecture Design of Si-based Composite Anode for Li-ion batteries

Yu-Chian Shie, Jeng-Shin Lu and Wei-Ren Liu \*

Department of Chemical Engineering, Chung Yuan Christian University, Chung Li, Taiwan

\*E-mail address: [WRLiu1203@gmail.com](mailto:WRLiu1203@gmail.com) (W. R. Liu)

Tel: +886-3-265-4140; fax: +886-3-265-4199

Si-based anodes in lithium ion batteries (LIBs) offer exceptionally high theoretical capacity, but it has dramatic volume change during lithiation/delithiation processes which typically leads to rapid anode degradation. Here we designed a facile and self-assembly strategy to construct three dimensional (3D) polymeric network as a promising binder for high-performance Si-SiC recovered the waste slurry from solar panels anodes through in-situ interconnecting alginate chains by additive divalent cations,  $\text{Sr}^{2+}$ ,  $\text{Ca}^{2+}$  and  $\text{Mg}^{2+}$ . The highly cross-linked alginate network allows superb mechanical property and strong interactions, which can restrain the dramatic volume. The affinity of alginate chains respect to divalent ions decreases in the following order:  $\text{Sr}^{2+} > \text{Ca}^{2+} > \text{Mg}^{2+}$  [1]. The structure and surface morphology of the composite were carried out by XRD, FE-SEM, viscometer and FTIR and electrochemical analysis were also performed to investigate the effect of the operating parameters. The viscosity became larger by additive divalent cations. (Figure 2) As a result, it has prolonged cycle life and less impedance by the highly cross-linked alginate network with  $\text{Sr}^{2+}$ . The retention still has 80% after 100 cycles.(Fig. 2)

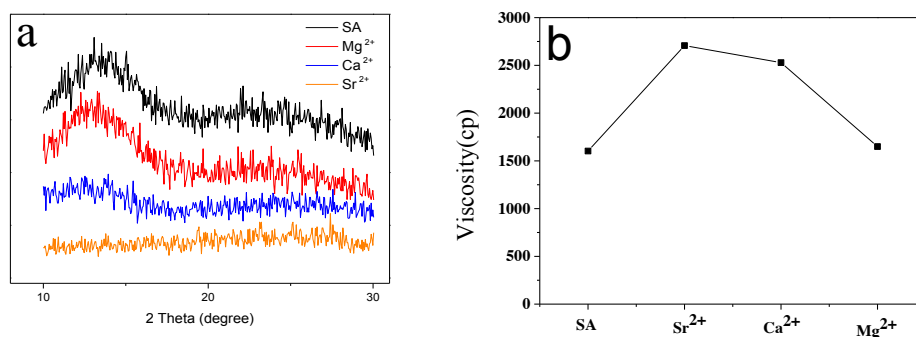


Figure 1 Preparation of binder added different divalent cations: (a) XRD patterns; (b) viscosity measurement.

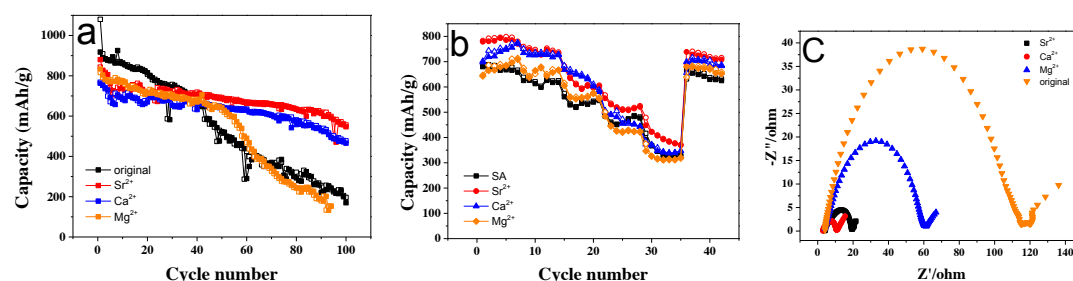


Figure 2 Electrochemical properties of SA,  $\text{Sr}^{2+}$ ,  $\text{Ca}^{2+}$  and  $\text{Mg}^{2+}$ : (a) cycling tests; (b) Rate capability; (c) EIS spectra.

## Reference

[1] R. Russo, M. Malinconico, and G. Santagata, "Effect of cross-linking with calcium ions on the physical properties of alginate films," *Biomacromolecules*, vol. 8, pp. 3193-3197, 2007.

# Highly Stable Sn-C Nanocomposite as an Anode Material for Lithium ion Batteries

Liang-Yin Kuo, Ju-Hsiang Cheng, Chun-Jern Pan, Ming-Yao Cheng, and Bing-Joe Hwang\*

*Department of Chemical Engineering, National Taiwan University of Science and Technology*

*No.43, Sec. 4, Keelung Rd., Taipei 106, Taiwan*

[liangshiny@hotmail.com](mailto:liangshiny@hotmail.com); [bjh@mail.ntust.edu.tw](mailto:bjh@mail.ntust.edu.tw)

An environmental-friendly and highly efficient Sn-based anode materials were synthesized via a green process for use in lithium-ion batteries and showed high energy densities, good cycle life performance and a decrease in cost and safety hazards.

This new material has been developed based on the nano-sized Cu seeds which act as the nuclei for well dispersion of the thermally reduced Sn and provide an internal anchoring function to depress growth of Sn particles resulting from its higher melting point compared to pure Sn during thermal reaction. Besides that, the purging gas during high temperature sintering which not only reduce tin metal but also prolong the cycle life of the composite material.

The results showed that the first discharge capacity was 1225 mAh/g as well as the first cycle columbic efficiency was 80%, and the capacity retention was 84% after 30 cycles. Under a 200 mA/g current density cycling, the first discharge capacity was 1131 mAh/g as well as first cycle columbic efficiency was 87%, and the capacity retention was 80% after 200 cycles.

# Development of Lithium Ion Batteries Using Fiber-Type Current Collectors

Yi-Hung Liu<sup>1,3</sup>, Tomoaki Takasaki<sup>2</sup>, Kazuya Nishimura<sup>2</sup>, Masahiro Yanagida<sup>1</sup>, Tetsuo Sakai<sup>1</sup>

<sup>1</sup>National Institute of Advanced Industrial Science and Technology

1-8-31Midorigaoka, Ikeda, Osaka 563-8577, Japan, yihung-ryuu@aist.go.jp

<sup>2</sup>Kawasaki Heavy Industries, Ltd.

1-18, 2-chome, Wadayama-dori, Hyogo-ku, Kobe, 652-0884, Japan, takasaki\_t@khi.co.jp

<sup>3</sup>Department of Greenery, National University of Tainan

No.67, Rong-Yu St. Tainan, 701 Taiwan, yhliu@mail.nutn.edu.tw

## 1. Introduction

With regard to the remarkably growing market for electric vehicles (EVs), hybrid electric vehicles (HEVs) and stationery energy storage applications in recent years, development of larger lithium ion battery (LIB) systems with high performance and low price is urgently required. To match the requirement, we have successfully developed fiber-type electrodes for LIBs without using any binders and conductive agents.<sup>1,2</sup> However, a predoping process is necessary to apply the battery using fiber-type electrodes, making it impractical. To extend the previous research works, this study therefore focuses on the development of LIBs using the fiber-type electrodes, which can be applied without any predoping process.

## 2. Experimental

To prepare the fiber-type cathode, a carbon fiber tow containing 12,000 single fibers was used as the current collector matrix. The fiber tow was electrodeposited a Mn-O layer in an  $\text{Mn}(\text{NO}_3)_2$  solution, followed by a hydrothermal treatment at 110°C for 20 h, in which LiOH solution was used as the reaction solution. The hydrothermally treated fibers were further rinsed by deionized water and dried in a vacuum atmosphere at 160 °C for 6 h, then the fiber-type Li-Mn-O cathode can be obtained. A coin-type test cell (R2032), containing the fiber-type cathode and carbon fiber anode, was used to carry out the galvanostatic charge/discharge experiments. The electrolyte used in the test cells was 1 M  $\text{LiPF}_6$  in a mixture of ethylene carbonate (EC) and diethyl carbonate (DEC) at the ratio of 1:1 (v/v).

## 3. Results and Discussion

Fig. 1 shows the morphologies of the original carbon fiber (a) and the typical as-prepared fiber-type cathode (b). The untreated carbon fiber retains its smooth surface without any contamination or defects, thus providing a favorable surface for the synthesis reaction. After the hydrothermal reaction, a layer consisted of nanoparticles was coated on the carbon fiber in a random and loose manner, bearing a number of void space. Fig. 2 shows the cycle performance and its coulomb efficiency of a full cell using the fiber-type cathode and carbon fiber anode. The capacity slightly decreased from 125 to 100 mAh/g at the 30th cycle; while its coulomb efficiency tends to be stable at a value of 95%, except for the first cycle. The high coulomb efficiency indicated that both the cathode and anode materials are favorable hosts for lithium ions to reversibly intercalate/deintercalate.

## References

- 1) J. Yao, K. Nishimura, T. Mukai, T. Takasaki, K. Tsutsumi, Kondo-Francois Aguey-Zinsou, and T. Sakai, *ECS Electrochem. Lett.*, **1**, A83-A86 (2012).
- 2) J. Yao, T. Takasaki, K. Nishimura, T. Mukai, and T. Sakai, *J. Electrochem. Soc.*, **160**, A980-A984 (2013).

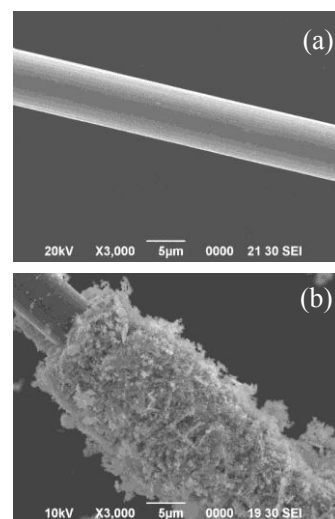


Fig. 1 Morphologies of the original carbon fiber (a) and typical fiber-type Li-Mn-O cathode (b).

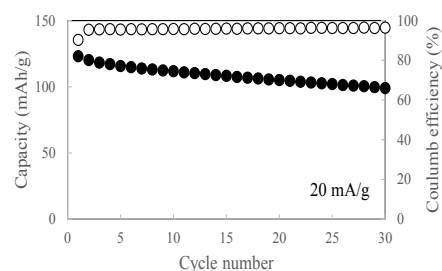


Fig. 2 Cycle performance and coulomb efficiency of the full cell using the fiber-type cathode and carbon fiber anode.

# Effect of nano sized tin composite on graphite as anode for lithium ion battery

Chia-Chin Chang<sup>\*a</sup>, Li-Chia Chen<sup>a</sup>, Yung-Der Juang<sup>b</sup>

<sup>a</sup>Department of Greenery, National University of Tainan, Tainan, Taiwan

<sup>b</sup>Department of Material Science, National University of Tainan, Tainan, Taiwan

e-mail address: [ccchang@mail.nutn.edu.tw](mailto:ccchang@mail.nutn.edu.tw) (C.-C. Chang)

In the past, the capacity enlargement by a lot of Sn composites modification has been widely attractive. However, less attention has been focused on the effect of Sn composites on the reaction between carbon substrate and electrolyte. This issue is noteworthy since the carbon matrix is the major anode substrate for lithium ion batteries (LIBs). Although the anode capacity of LIBs was greatly raised by nano-sized Sn modification on carbon substrate, it is difficult to find out the effect on the carbon matrix caused by the Sn composites [1]. So, in this study, we try to fabricate the carbon anode with relatively less Sn composites modification by chemical modified and pyrolysis methods to highlight the influence of the Sn composites on the carbon matrix.

Nano-tin composites on graphite materials can be obtained through a simple chemical reaction between  $\text{Sn}(\text{BF}_4)_2$  and  $\text{Na}_2\text{S}_2\text{O}_4$  in aqueous solution and converted to  $\text{SnO}_2$  after pyrolysis. The size of nano-tin composites is around 14.7 nm. The graphite anodes with Sn-based nanocomposites show a capacity retention over 97.3% after 50 cycles, as shown in Fig. 1. As can be observed in Fig. 2, the original IR peaks at 2826 and 2988  $\text{cm}^{-1}$  shift to 2855 and 2935  $\text{cm}^{-1}$ , which are attributed to the  $\nu(\text{CH}_2)$  in  $(\text{CH}_2\text{OCO}_2\text{Li})_2$  [2,3], after the modification with Sn-based composites. The spectral results provide the evidence that the presence of Sn-based composites on the graphite surface can inhibit the reaction of  $(\text{CH}_2\text{OCO}_2\text{Li})_2$  with HF to protect the carbon surface from electrolyte decomposition and improve the cycling performance in LIBs.

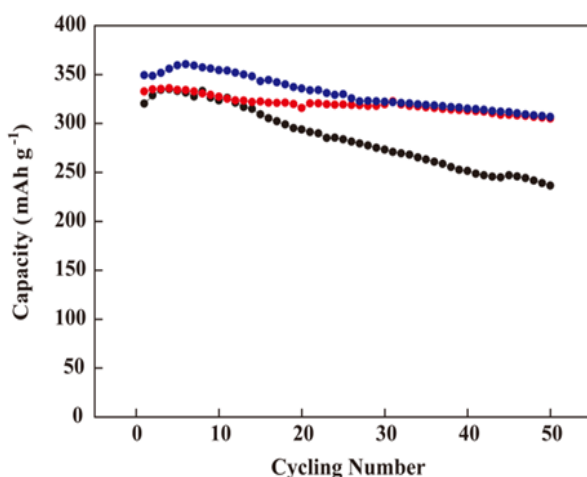


Fig. 1 Cycling performance of the pristine (black), the pre-modified (blue), and the annealed (red) graphite anodes.

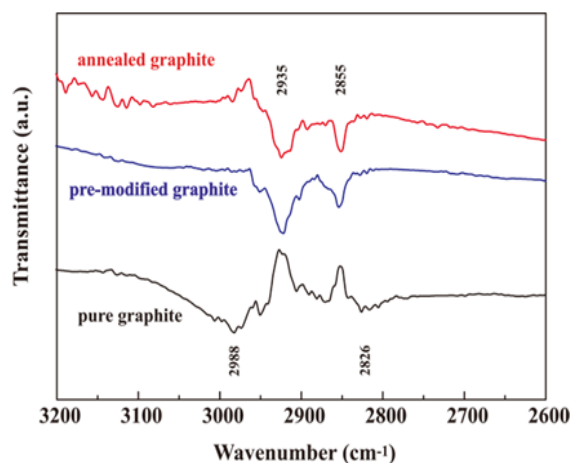


Fig. 2 IR spectra of the pristine (black), the pre-modified (blue), and the annealed (red) graphite anodes after cycling test.

## Reference

- [1] C.-C Chang, S.-J. Liu, J.-J. Wu, and C.-H. Yang, *J. Phys. Chem. C*, 111(2007) 16423.
- [2] D. Aurbach, Y. Gofer, M. Ben-Zion, and P. Aped, *J. Electroanal. Chem.*, 339 (1992) 451.
- [3] D. Aurbach, B. Markovsky, I. Weissman, E. Levi, and Y. Ein-Eli, *Electrochim. Acta*, 45 (1999) 67.



# A modified RAPET approach to $\text{Li}_4\text{Ti}_5\text{O}_{12}$ defect spinel nanoparticles as anode material for lithium ion batteries

Ralph Nicolai Nasara<sup>a</sup>, Kuan-Wei Lu<sup>a</sup>, Yen-Ting Pan<sup>a</sup>, Ping-Chun Tsai<sup>a</sup>, Wei-chih Lin<sup>a</sup>, Chung-Ta Ni<sup>a,c</sup>, Shih-kang Lin<sup>a,b,c,d\*</sup>, and Kuan-Zong Fung<sup>a,c</sup>

<sup>a</sup>Department of Materials Science and Engineering, National Cheng Kung University, Tainan 70101, Taiwan; <sup>b</sup>Promotion Center for Global Materials Research, National Cheng Kung University, Tainan 70101, Taiwan; <sup>c</sup>Research Center for Energy Technology and Strategy, National Cheng Kung University, Tainan 70101, Taiwan; <sup>d</sup>Center for Micro/Nano Science and Technology, National Cheng Kung University, Tainan 70101, Taiwan

\*Corresponding author: E-mail: linsk@mail.ncku.edu.tw; Tel: +886-6-2757575 ext. 62970

Lithium titanate defect spinel ( $\text{Li}_4\text{Ti}_5\text{O}_{12}$ ) is one of the most promising anode materials for lithium ion batteries (LIBs) because its negligible volume change and stable operating voltage during charging/discharging. However, the intrinsic insulating property of  $\text{Li}_4\text{Ti}_5\text{O}_{12}$  hinders its high power applications. Compositing and nanonization are two approaches to overcome this drawback. The former enhances the external electrical conductivity of  $\text{Li}_4\text{Ti}_5\text{O}_{12}$ , while the latter shortens the length of diffusion during charging/discharging. In this work,  $\text{Li}_4\text{Ti}_5\text{O}_{12}$  defect spinel anode nanoparticles were synthesized via a modified reaction under autogenic pressure at elevated temperature (RAPET) technique. Unlike the conventional white  $\text{Li}_4\text{Ti}_5\text{O}_{12}$  powders, blue  $\text{Li}_4\text{Ti}_5\text{O}_{12}$  nanoparticles were fabricated. The microstructures and electrochemical properties, namely cycle performance and rate capability of  $\text{Li}_4\text{Ti}_5\text{O}_{12}$  nanoparticles were examined. In addition, *ab initio* calculations based on density function theory (DFT) were performed to clarify the enhanced electrochemical properties of the  $\text{Li}_4\text{Ti}_5\text{O}_{12}$  defect spinel. The formation mechanism of the  $\text{Li}_4\text{Ti}_5\text{O}_{12}$  nanoparticles as well as the origin of superior electrochemical properties is elaborated in this paper.

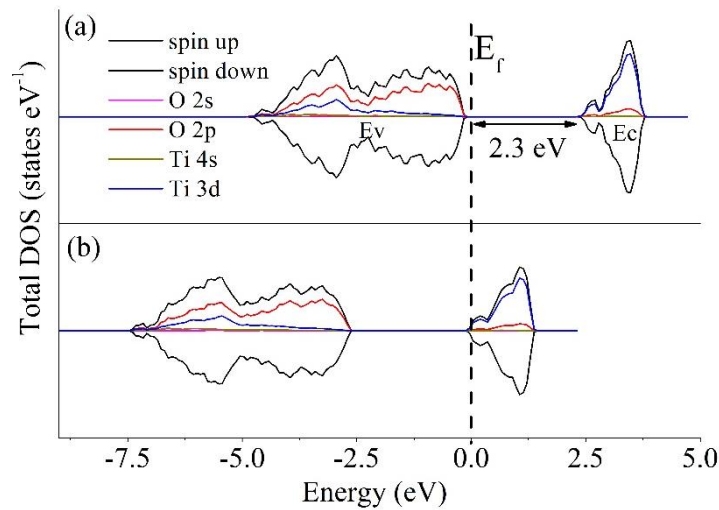


Figure 1. Total density of states (DOS) of (a) the pristine  $\text{Li}_4\text{Ti}_5\text{O}_{12}$  and (b) the reduced  $\text{Li}_4\text{Ti}_5\text{O}_{11.875}$ , where the Fermi energy was aligned to 0 eV in the energy scale.



# ***Ab initio*-aided $\text{Li}_4\text{Ti}_5\text{O}_{12}$ defect spinel electrode materials designs for durable lithium ion batteries**

Shih-kang Lin<sup>a,b,c,d</sup>, Ping-chun Tsai<sup>a</sup>, and Wen-Dung Hsu<sup>a,b,c</sup>

<sup>a</sup>Department of Materials Science and Engineering, National Cheng Kung University, Tainan 70101, Taiwan; <sup>b</sup>Promotion Center for Global Materials Research, National Cheng Kung University, Tainan 70101, Taiwan; <sup>c</sup>Research Center for Energy Technology and Strategy, National Cheng Kung University, Tainan 70101, Taiwan; <sup>d</sup>Center for Micro/Nano Science and Technology, National Cheng Kung University, Tainan 70101, Taiwan

\*Corresponding author: E-mail: linsk@mail.ncku.edu.tw; Tel: +886-6-2757575 ext. 62970

To meet the great demands of reliable and durable energy-storage systems for the “smart-grid society”, lithium ion batteries (LIBs) with better efficiency, stability, and safety are required. The  $\text{Li}_4\text{Ti}_5\text{O}_{12}$  (LTO) defect spinel is the most promising anode materials for long-life LIBs because of its merits of negligible volume changes ( $\sim 1\%$ ) and stable operating voltage during charging/discharging. The volume changes of LTO are more than ten times less than the conventional graphite materials (10%) and much less than various Si (400%) and alloy materials. However, the insulating property of LTO that results in poor rate capability limits its range of power-oriented applications. Doping transition metals is a commonly seen strategy to enhance electrical and electrochemical properties of LTO. However, the general trend for doping-induced effects on LTO is unclear. In this work, *ab initio* calculations are performed to study the phase stability, electronic structures, and electrochemical properties of the transition metal M-doped LTO ( $\text{Li}_4\text{M}_{0.125}\text{Ti}_{4.875}\text{O}_{12}$ ). In addition, an attempt was made to explore new 4-5-12 defect spinel other than the known  $\text{Li}_4\text{Ti}_5\text{O}_{12}$  and  $\text{Li}_4\text{Mn}_5\text{O}_{12}$  defect spinel. The class of the  $\text{Li}_4\text{Me}_5\text{O}_{12}$  defect spinel with the framework of  $[\text{Li}_{1/3}\text{Me}_{5/3}]_{16d}(\text{O}_4)_{32e}$  was investigated. With the aid of *ab initio* calculations, general trends of doping-induced physical property changes, such as the changes of lattice parameters, phase stabilities, average operating voltages, and electrical properties, were revealed. All M-doped LTO showed high structural stability during charging/discharging, indicating the excellent cyclability and high safety of LTO remains for the M-doped LTO. Nevertheless, doping significantly affects the electronic structure of LTO. The desired dopant for the M-doped LTO and potential “nature’s missing 4-5-12 defect spinel” as anode materials in LIBs is proposed.

Keywords: Li ion battery;  $\text{Li}_4\text{Me}_5\text{O}_{12}$ ; *ab initio* calculation; defect spinel

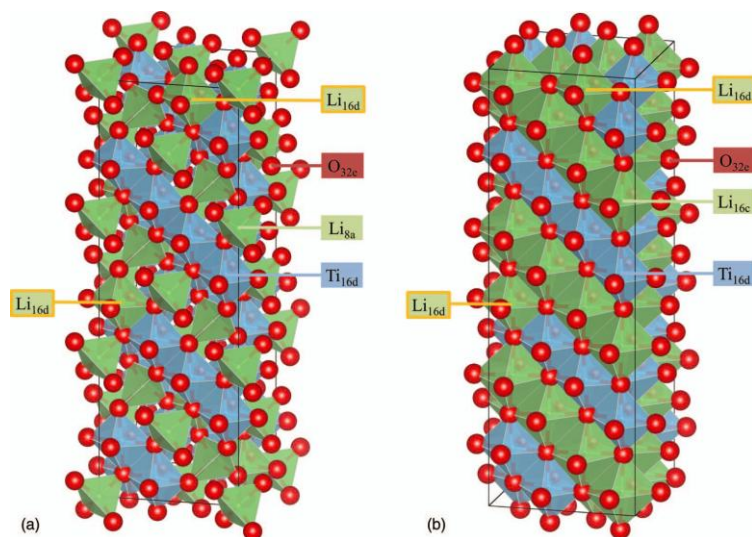


Figure 1. Full supercell models of (a)  $\text{Li}_{32}\text{Ti}_{40}\text{O}_{96}$  for the  $\text{Li}_4\text{Ti}_5\text{O}_{12}$  phase and (b)  $\text{Li}_{56}\text{Ti}_{40}\text{O}_{96}$  for the  $\text{Li}_7\text{Ti}_5\text{O}_{12}$  phase.

## Reference

(1) Ping-chun Tsai; Wen-Dung Hsu; Shih-kang Lin. Atomistic Structure and Ab Initio Electrochemical Properties of  $\text{Li}_4\text{Ti}_5\text{O}_{12}$  Defect Spinel for Li Ion Batteries. *J. Electrochem. Soc.* **2014**, 161, A439–A444.

# Characterizations and electrochemical properties of high energy mechanical milled Si as anode for Li-ion batteries

Shang-Chieh Hou<sup>a</sup>, Chia-Chin Chang<sup>b</sup>, Jow-Lay Huang<sup>a</sup>, Shun-Min Yang<sup>b</sup>

<sup>a</sup>Department of Materials Science and Engineering, National Cheng Kung University, Tainan 70101, Taiwan.

E-mail: Shang-Chieh Hou, n58001044@mail.ncku.edu.tw.

E-mail: Jow-Lay Huang, jlh888@mail.ncku.edu.tw

<sup>b</sup>Department of Greenery, National University of Tainan, Tainan 70101, Taiwan.

E-mail: Chia-Chin Chang, ccchang@mail.nutn.edu.tw

High energy mechanical milling (HEMM) is known as a cheap, facile and scale-up way to reduce powder size and induce amorphization and alloying under non-equilibrium. In this work, silicon powders  $\text{Si}_\text{H}$ ,  $\text{Si}_\text{W}$  and  $\text{Si}_{\text{H+W}}$  were prepared by HEMM, wet milling and combined HEMM and wet milling from pristine silicon,  $\text{Si}_\text{P}$ , (D50 ~10  $\mu\text{m}$ ). Tackled powders were investigated as anode materials for Li-ion batteries. Upon HEMM, pristine silicon powder processed repeatedly cold welding and fracturing and formed micrometric silicon aggregate (D50 ~5  $\mu\text{m}$ ) constructed by cold welded submicrometric particles after HEMM 9 hrs for  $\text{Si}_\text{H}$ .  $\text{Si}_\text{H}$  showed the nanocrystallite embedded in amorphous region confirmed by TEM. Randomly Nanocrystalline/amorphous interface assumed to provide additional path for Li ion diffusion. However, secondary hard agglomeration caused by cold welding hindered this benefit and speed up crumbling of the agglomerate reflecting on poor cyclic performance compared to reduced  $\text{Si}_\text{W}$  (D50 ~0.4  $\mu\text{m}$ ) of discrete primary particle. The agglomeration broke along interfaces of welded primary particles by further wet milling for  $\text{Si}_{\text{H+W}}$  and reduced the secondary particle size (D50 ~0.3  $\mu\text{m}$ ). It significantly improved the cyclic performance during discharge-charge process compared to  $\text{Si}_\text{H}$  and  $\text{Si}_\text{W}$ .

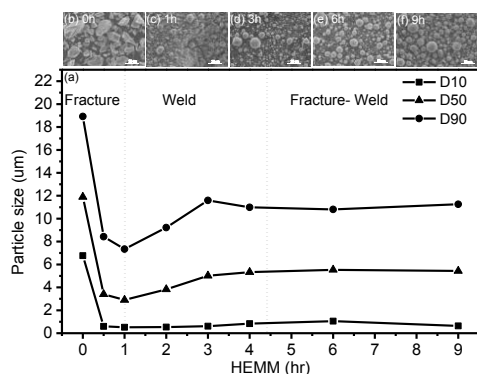


Fig. Particle size variation with time of HEMM (a). SEM images of silicon powder with varied time of HEMM for (b) 0h, (c) 1h, (d) 3h, (e) 6h and (f) 9h.

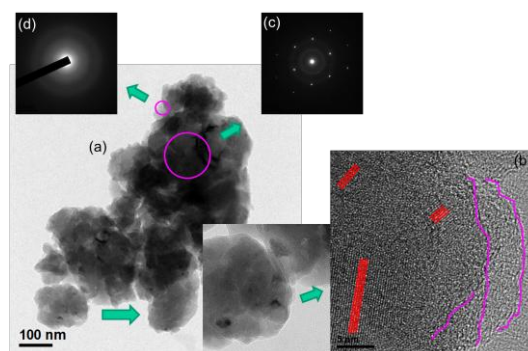


Fig. (a) TEM image of  $\text{Si}_\text{H}$  aggregate, (b) HRTEM image of cold welded joining, (c) SAED pattern of crystalline area, (d) SAED pattern of amorphous area.

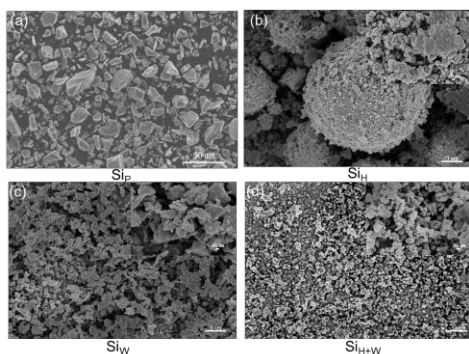


Fig. SEM micrographs of the (a)  $\text{Si}_\text{P}$ , (b)  $\text{Si}_\text{H}$ , (c)  $\text{Si}_\text{W}$  and (d)  $\text{Si}_{\text{H+W}}$

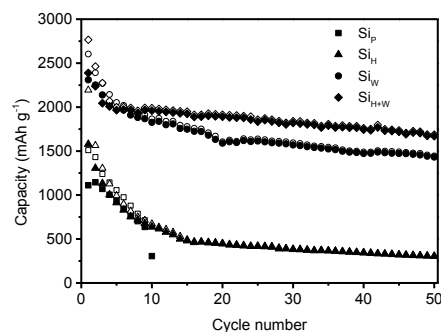


Fig. Cycling performance of  $\text{Si}_\text{P}$ ,  $\text{Si}_\text{H}$ ,  $\text{Si}_\text{W}$  and  $\text{Si}_{\text{H+W}}$  conducted at current density 200 mA/g between 0.02 V to 1.5 V.

# Near-Field Optical Spectroscopy and Imaging of the SEI Layer on Sn, Si and Graphite Li-ion Anodes

Robert Kostecki, Maurice Ayache, Simon Lux, Ivan Lucas  
Lawrence Berkeley National Laboratory,  
Berkeley, CA, 94720 United States  
r\_kostecki@lbl.gov

Most Li-ion battery systems operate beyond the thermodynamic stability limits of the electrolytes. Reactions between positive and negative electrodes and the electrolyte result in the formation of new phases and interphases, which hinder further electrolyte decomposition and assure battery operation over the lifespan of the application. Fundamental investigations of the electrode material properties of electrochemical systems are essential for improvements in electric energy storage technologies<sup>1</sup>. Among the most critical aspects of Li-ion battery operation is the solid electrolyte interphase (SEI) layer<sup>2</sup>, which forms at the negative electrode surface due to the electroreduction of the electrolyte during initial charge/discharge cycles<sup>3,4</sup>. This highly inhomogeneous, ionically conductive and electrically resistive film prevents further electrolyte decomposition at the electrode surface and assures long-term operation of Li-ion battery cells. The chemical composition and functional mechanism of the SEI are not well understood, due to the technical barriers associated with characterization methodologies across length and temporal scales that correspond to the SEI basic components and processes.<sup>5</sup>

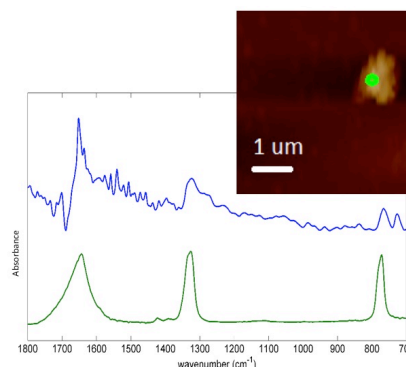
The requirements for long-term stability of Li-ion batteries are extremely stringent and necessitate control of the chemistry at a wide variety of temporal and structural length scales. This presentation provides an overview of infrared apertureless near-field scanning optical microscopy (IR aNSOM) as a valuable emerging tool in the chemical characterization of interfacial layers at the nanometer scale in electrochemical systems. This work demonstrates an IR aNSOM study of the SEI layer, on a model Sn, Si and graphite electrodes. IR aNSOM images recorded at several wavelengths reveal significant chemical contrast variations tied to specific topographic features and distribution of lithium carbonate and lithium ethylene dicarbonate on the sample surface.

## Acknowledgements

This work was supported by the Assistant Secretary for Energy Efficiency and Renewable Energy, Office of Vehicle Technologies of the U.S. Department of Energy, under contract no. DE-AC02-05CH11231. This work was also supported in part by the Chemical Science Division, Office of Basic Energy Sciences, Office of Nuclear Nonproliferation, and the U.S. Department of Energy under Contract No. DE-AC02-05CH11231.

## References

1. "Basic Research Needs for Electrical Energy Storage", Report of the Basic Energy Sciences Workshop on Electrical Energy Storage, April 2-4, 2007
2. Peled, E. *J. Electrochem. Soc.* **1979**, *126*, 2047–2051.
3. Aurbach, D.; Ein-Ely, Y.; Zaban, A. *J. Electrochem. Soc.* **1994**, *141*, 10–12.
4. Möller, K.-C.; Santner, H. J.; Kern, W.; Yamaguchi, S.; Besenhard, J. O.; Winter, M. *J. Power Sources* **2003**, *119-121*, 561–566.
5. Winter, M. *Zeitschrift für Phys. Chemie* **2009**, *223*, 1395–1406.



Synchrotron IR near-field spectroscopy of the SEI on Si(111) electrode at deeply subwavelength (~20 nm) resolution.

# Application of Amorphous Carbon-Coated Electrodes in Vanadium Redox Flow Battery

Chao-Yen Kuo<sup>a</sup>, Heng-Wei Chiang<sup>a</sup>, Chien-Hong Lin<sup>a</sup>, Hwa-Jou Wei<sup>a</sup>, Bing-Joe Hwang<sup>b\*</sup>

*a Division of Energy Storage, Department of Chemistry, Institute of Nuclear Energy Research  
No. 1000, Wenhua Rd., Jiaan Village, Longtan District, Taoyuan City 32546, Taiwan (R.O.C.)*

*b Department of Chemical Engineering, National Taiwan University of Science and Technology*

*No.43, Sec. 4, Keelung Rd., Da'an Dist., Taipei 106, Taiwan (R.O.C.)*

*waynelj0627@gmail.com*

Due to energy crisis and environmental pollution caused by limiting fossil fuels and their waste emissions, much effort has been put in on the topic of sustainable, renewable and clean energy alternatives such as solar and wind energy. However, due to the intermittent and uncontrollable nature of these resources, it might lead to the fluctuation of electricity distribution and causing damages to traditional grids. Therefore, energy storage systems are needed to store these energies and maintain the quality of the grids. Vanadium flow battery is one of the potential candidates since it's advantageous in decouplization of energy and power density, deep charge-discharge ability, long cycle life, etc. However, it suffers severe crossover, slow reaction kinetics and low reversibility of vanadium ions that prohibit its commercialization and general usage. In our study, we proposed a facile method to improve the disadvantages by forming amorphous carbon layers on the carbon felt electrodes. The functional groups and defects on the surface of electrodes might offer more active sites for vanadium ions and promote the kinetics and reversibility of the redox reaction. Surface analysis and electrochemical measurements were conducted to study the mechanisms and confirm the results we observed.

# Investigation of surface and bulk structural modifications in Li/Mn-rich cathode materials of Li-ion batteries using X-ray absorption spectroscopy

Richard Kloepsch,<sup>\*</sup> Jatinkumar Rana,<sup>#</sup> Gerhard Schumacher,<sup>#</sup> John Banhart,<sup>#</sup> Martin Winter<sup>\*</sup> and Jie Li<sup>\*</sup>  
<sup>\*</sup>MEET battery research center, University of Muenster,  
 Corrensstr. 46, D-48149 Muenster, Germany.  
<sup>#</sup>Helmholtz-Zentrum Berlin für Materialien und Energie,  
 Hahn-Meitner-Platz-1, D-14109 Berlin, Germany.  
 r.kloepsch@uni-muenster.de

Li/Mn-rich ‘layered-layered’ cathode materials (LMR) with the general formula  $x \text{Li}_2\text{MnO}_3 \cdot (1-x) \text{LiMO}_2$  (M=Mn, Co, Ni; typically:  $x=0.5$ ) provide very high, reversible discharge capacities above  $200 \text{ mAh g}^{-1}$  at a high average potential of around  $3.75 \text{ V vs. Li/Li}^+$ . For this reason, this material class is of major academic and commercial interest, as its commercialization would result in a boost in energy density for secondary lithium batteries.[1,2] Despite their highly promising electrochemical properties,[3] LMR-oxides to date still face numerous challenges, such as insufficient cycling stability and the decay of the operating voltage upon prolonged cycling in a wide voltage range (‘voltage decay’).[4] Most X-ray absorption spectroscopy (XAS) studies on cathode materials are carried out in transmission mode, which provides local structural information of the bulk material.[5] However, the material surface is also of great interest, as it stands in direct contact with the highly oxidizing electrolyte. For this purpose, Oxygen K-edge Near-Edge X-ray absorption fine structure (NEXAFS) measurements were carried out in the total electron yield mode (Fig.1). As it can be seen, the data of the pristine state resembles that of the discharged (re-lithiated) state at  $2.5 \text{ V}$ , while the charged (de-lithiated) states of the 1<sup>st</sup> and 2<sup>nd</sup> cycle resemble one another. These results indicate reversible structural changes taking place also at the material surface.

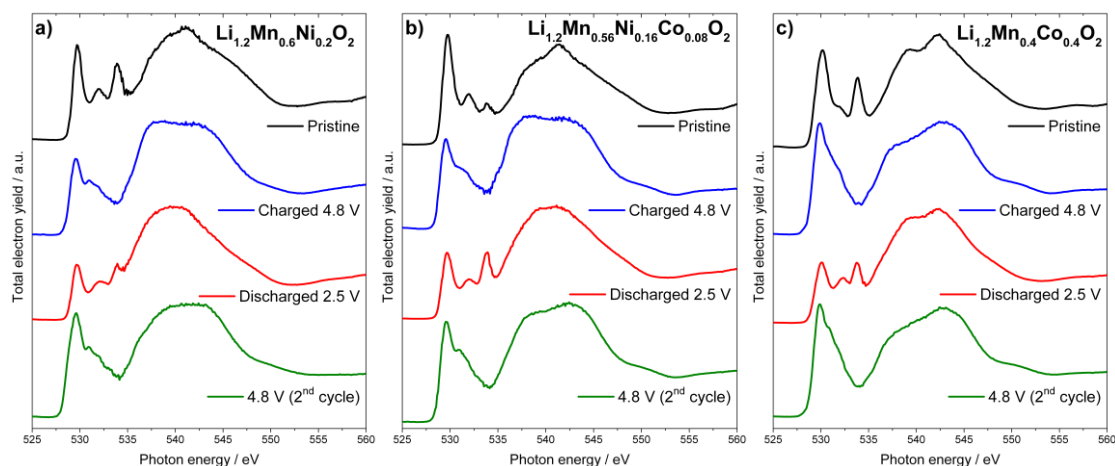


**Figure 1:** Normalized O K-edge NEXAFS data of LMR cathodes  
 a)  $\text{Li}_{1.2}\text{Mn}_{0.4}\text{Co}_{0.2}\text{O}_2$  b)  $\text{Li}_{1.2}\text{Mn}_{0.56}\text{Ni}_{0.16}\text{Co}_{0.08}\text{O}_2$  and c)  $\text{Li}_{1.2}\text{Mn}_{0.4}\text{Co}_{0.4}\text{O}_2$   
 in the indicated states of charge.

## References:

- [1] M.M. Thackeray, C. Wolverton, E.D. Isaacs, *Energy & Environmental Science* 5 (2012) 7854.
- [2] K.G. Gallagher, S. Goebel, T. Greszler, M. Mathias, W. Oelerich, D. Eroglu, V. Srinivasan, *Energy & Environmental Science* 7 (2014) 1555.
- [3] X. He, J. Wang, R. Kloepsch, S. Krueger, H. Jia, H. Liu, B. Vortmann, J. Li, *Nano Research* 7 (2014) 110.
- [4] J.R. Croy, D. Kim, M. Balasubramanian, K. Gallagher, S.-H. Kang, M.M. Thackeray, *J Electrochem Soc* 159 (2012) A781.
- [5] J. Rana, R. Kloepsch, J. Li, T. Scherb, G. Schumacher, M. Winter, J. Banhart, *J. Mater. Chem. A* 2 (2014) 9099.

# **Olivine with zero anti-site defect and three dimensional lithium diffusion paths**

Kyu-Young Park, Inchul Park<sup>a,b</sup>, Hyungsub Kim<sup>a,b</sup>, Gabin Yoon<sup>a</sup>, Hyeok-Jo Gwon<sup>c</sup>, Yongbeom Cho<sup>a</sup>,  
Young Soo Yun<sup>a</sup> Kisuk Kang\*

Department of Materials Science and Engineering and Research Institute of Advanced Materials (RIAM),  
Seoul National University, 1 Gwanak-ro, Gwanak-gu, Seoul 151-742, Korea

Center for Nanoparticle Research at Institute for Basic Science (IBS), Seoul National University, 1  
Gwanak-ro, Gwanak-gu, Seoul

*e-mail address: matlgen1@snu.ac.kr*

## **Abstract**

Lithium iron phosphate (LFP) has attracted tremendous attention as a next-generation electrode material in lithium rechargeable batteries for large scale energy storage systems due to the use of low-cost iron and chemical/electrochemical stability. While the lithium diffusion in LFP, the essential property in battery operation, is relatively fast due to the one-dimensional tunnel present in the olivine crystal, the tunnel is inherently susceptible to immobile anti-site defects which, if any, block the lithium diffusion and lead to the inferior performance. Herein, we demonstrate that the kinetic issue arising from the defects in LFP can be completely eliminated in a new olivine LFP, which we successfully synthesized for the first time. The doping in the olivine structure reduces the concentration of defects in the tunnel by 7 orders of magnitude. Moreover, it opens up a new lithium diffusion path along the [101] direction making the olivine LFP as a three-dimensional lithium diffuser. We also find that the intrinsic energy barrier for phase transition gets notably lower in the lithium excess olivine LFP. The fundamentally different nature of the new olivine than normal LFP additionally induces faster charging capability, lowering thermal solid-solution temperature and less memory effect.

# **Rice Husks Based Nanosilica as Anode Materials for Lithium-Ion Batteries**

Arenst Andreas Arie<sup>1\*</sup>, Susan Olivia Limarta<sup>1</sup>, Hans Kristianto<sup>1</sup>,  
Martin Halim<sup>2</sup> and Joong Kee Lee<sup>2</sup>

<sup>1</sup>*Department of Chemical Engineering, Parahyangan Catholic University,  
Ciumbuleuit 94, Bandung, Indonesia*

<sup>2</sup>*Center of energy Convergence, Korea Institute of Science and Technology,  
Hwarangno 5-o-gil Seongbukgu, Seoul ,Korea*

*\*e-mail address : arenst@unpar.ac.id*

Rice husks (RHs) are the natural sheaths that form on rice grains during their growth and are removed as waste during processing the grains. Husks have no commercial value and are normally combusted openly, thereby causing environmental pollution and disposal problems. After calcination, RHs produced of about 20% ash of which 90% was silica. Silica is the major inorganic constituent of the rice husk, and by carrying out an acid chemical treatment followed by the process of burning, it is possible to extract high-surface area amorphous silica. In this work, nanosilica was prepared from the rice husks derived amorphous silica by sol-gel method. The optimal preparation conditions for the preparation of silica nanoparticles were obtained and the as prepared silica nanoparticles were characterized by x-ray diffraction (XRD), scanning electron microscopy (SEM), transmission electron microscopy (TEM), Fourier Transform Infra Red (FTIR) Spectroscopy and x-ray photoelectron spectroscopy (XPS). The XRD analysis indicated the amorphous structure of the prepared silica nanoparticles while the SEM and TEM images exhibited mono dispersed nano sized silica particles. Nanosilica were then tested as anode materials for lithium ion batteries using cycle tests and cyclic voltammetry. Cycle tests showed that a stable cycling until the 50<sup>th</sup> cycle was demonstrated by rice husk based nano silica particles with a high initial coulombic efficiency.

# ***In-Situ* X-ray Diffraction on the Lithium-Ion Migrating in Micro-Porous Separator**

Pin-ChinWu<sup>1</sup>, Po-Wei Yang<sup>2</sup>, Yu-Fan Chen<sup>2</sup>, Chih-Wei Hu<sup>2</sup>, Yen-Fa Liao<sup>3</sup>, Tsan-Yao Chen<sup>2\*</sup>, Chia-Chin Chang<sup>2\*</sup>

<sup>1</sup>Department of Greenenergy, National University of Tainan

<sup>2</sup>Department of Engineering and System Science, National Tsing-Hua University

<sup>3</sup>National Synchrotron Research Radiation center

## **Abstract**

The structure change of commercial polypropylene/polyethylene/polypropylene (PP/PE/PP) trilayer micro-porous film, used as a separator of lithium ion batteries (LIBs), undergo different charging-discharging current densities was investigated by means of *in-situ* X-ray diffraction (XRD). The unpredictable nanoscale crystalline structure change of both PP and PE are discovered during charging process. The embedded lithium ions is supposed to be the main cause to the increasing of lattice space. Especially in the PP(040) phase, the maximum extended spacing ( $\Delta d/d_0$ ) of 1.54%, in contrast to it before charging, is found after the LIBs is fully charged; while other phases usually has  $\Delta d/d_0$  less than 0.5%. No other phases has the effect as evident as PP(040) phase. That means the behavior is selective. We also found that the structure cannot return to that before charging even the LIB is fully discharged, which indicates the process is irreversible. Moreover, the embedded of lithium also shows a charging current dependent behavior that slower charging rate has more significant effect on the lattice spacing increasing. The crystalline structure of the separator undergo different charging rate is firstly revealed by using *in-situ* XRD and the results can be used for improving and rationally designing separators which can broadly be applied in diverse conditions, such as low temperature.



# **Suppression of degradation of lithium ion batteries for $\text{LiFePO}_4\text{@C}$ batteries by nano Si surface modification**

Wenyu Yang, Xiang Chen, Mingzhong Zou, Guiying Zhao, Jiaxin Li, Yingbin Lin, Zhigao Huang\*

College of Physics and Energy, Fujian Normal University, Fujian Provincial Key Laboratory of Quantum Manipulation and New Energy Materials, Fuzhou, 350117, China

**Abstract:** Si nanoparticles are deposited uniformly on the  $\text{LiFePO}_4\text{@C}$  electrode by a spray technique. And the effect of Si incorporation on the electrochemical performances of  $\text{LiFePO}_4\text{@C}$  18650 cylindrical cells is investigated systematically by charge-discharge testing, cyclic voltammograms, AC impedance spectroscopy, respectively. At the same time, the aging and degradation of those cells have been studied. Non-destructive electrochemical methods were used to examine the capacity loss, voltage drop, resistance change, lithium loss, and active material loss during the life testing. The measuring results of the cycle life indicated that the capacity loss was strongly influenced by the rate, temperature, surface modification and discharge states (DOS). Especially, nano Si surface modification suppresses greatly the degradation of those cells. Moreover, the rate, temperature, time, and surface modification dependences of the cycle life were discussed.

# Processing and Characterization of $\text{Li}_4\text{Ti}_5\text{O}_{12}$ (LTO) Spinel Thin -Film for Li Battery Applications

Shu-Yi Tsai<sup>1</sup>, Chung-Ta Ni<sup>1</sup>, Kuan-Zong Fung<sup>1</sup>

<sup>1</sup>Research Center for Energy Technology and Strategy, Department of Materials Science and Engineering, National Cheng Kung University, No. 1, University Road, Tainan 70101, Taiwan, ROC  
*willxkimo@yahoo.com.tw*

Lithium titanium oxide spinel  $\text{Li}_4\text{Ti}_5\text{O}_{12}$  has been reported to be a zero-strain lithium insertion host material because it exhibits extremely small variations of the lattice parameters during the charge and discharge processes. In general, Poor adhesion between thin-film electrode and substrates is the common cause for performance degradation of thin-film electrode during repeated charge/discharge tests. Thus,  $\text{Li}_4\text{Ti}_5\text{O}_{12}$  spinel may be the ideal candidate for the anode of thin-film Li ion battery for long cycle applications.

However, unmodified  $\text{Li}_4\text{Ti}_5\text{O}_{12}$  usually exhibits poor rate performance, which mainly results from its low electronic conductivity (ca.  $10^{-13} \text{ S}\cdot\text{cm}^{-1}$ ) and moderate  $\text{Li}^+$  diffusion coefficient ( $10^{-8} \text{ cm}^2\cdot\text{s}^{-1}$ ). In addition, different electrochemical behaviors will be expected when  $\text{Li}_4\text{Ti}_5\text{O}_{12}$  spinel is prepared in thin-film compared to that in power forms. Therefore, the objective of this work is (1) to enhance the conductivity of  $\text{Li}_4\text{Ti}_5\text{O}_{12}$  spinel by substitution of aliovalent dopants for Ti ions, (2) to fabricate thin film of  $\text{Li}_4\text{Ti}_5\text{O}_{12}$  spinel by using RF-sputtering technique, (2) to investigate the effect of annealing temperature/atmospheres on the electrical/electrochemical properties of thin film  $\text{Li}_4\text{Ti}_5\text{O}_{12}$ , (3) to evaluate the feasibility of using thin film of  $\text{Li}_4\text{Ti}_5\text{O}_{12}$  as anode for Li microbattery applications. In this study, the  $\text{Li}_4\text{Ti}_5\text{O}_{12}$  thin film was deposited on either the Si substrate or glass substrate by sputtering technique. The crystallization of deposited  $\text{Li}_4\text{Ti}_5\text{O}_{12}$  thin film will be enhanced by annealing at various atmospheres and temperatures. The single phase  $\text{Li}_4\text{Ti}_5\text{O}_{12}$  was finally obtained after co- sputtering of Li-containing and Ti-containing targets. The crystal structure and crystallization will be examined by glancing XRD. The resistivity of  $\text{Li}_4\text{Ti}_5\text{O}_{12}$  thin film will be evaluated by four probe technique and our novel micrometre measurement system. The capacity of  $\text{Li}_4\text{Ti}_5\text{O}_{12}$  thin film will be evaluated from charge/discharge test

# Observation of Spinel Formation on Capacity Fading of Li-rich Layer-structured Cathode Materials

Chung-Ta Ni, Shu-Yi Tsai, Kuan-Zong Fung, Wei-Zhi Lin

*Department of Materials Science and Engineering, National Cheng Kung University*

*No.1 University Road, Tainan City, Taiwan 70101*

*chungtani@gmail.com*

Li rich layered composite cathode  $x\text{Li}_2\text{MnO}_3 \cdot (1-x)\text{LiMO}_2$  ( $M = \text{Mn, Ni, Co, etc.}$ ) materials have received much attention due to their high reversible capacity greater than 250mAh/g for Li-ion battery applications. There are few mechanisms have been proposed to explain their intercalation/deintercalation behavior based on the charge/discharge results. Although the initial capacity of Li-rich layer-structured cathode may reach as high as 250 mAh/g, a gradual capacity fading after cycling was observed. In Order to understand the causes for capacity fading of these  $x\text{Li}_2\text{MnO}_3 \cdot (1-x)\text{LiMO}_2$  materials, detailed structural analysis/characterization was performed.

In this work, the TEM structural analysis clearly shows that the formation of spinel phase after cycling. The layer structure to spinel phase transformation may be caused by the redox reaction of transition metal ions through charging/discharging tests. The reasons for capacity may be due to a large lattice distortion resulting in lattice breakdown accompanying repeated intercalation/deintercalation. Interestingly, the surface treatment of a spinel coating on the Li-rich layer-structured cathode tends to suppress the capacity fading compared to the uncoated ones.

Therefore, the effect of changing oxidation state of transition metal ions in the layered structures on the capacity fading was examined using XRD, SEM, TEM

# Island-like deposition of lithium manganese oxide spinel ( $\text{LiMn}_2\text{O}_4$ ) in all-solid-state thin film lithium ion battery

Tien-Hsiang Hsueh, Chi-Hung Su, Der-Jun Jan, Yuh-Jenq Yu, Yuan-Ruei Jheng  
*Physics Division, Institute of Nuclear Energy Research*  
*Address: No.1000, Wenhua Rd., Longtan Dist., Taoyuan City 325, Taiwan (R.O.C.)*  
*Email address: Tien-Hsiang Hsueh*

Thin-film lithium-ion batteries (LiBs) are the most competitive low-power sources for various kinds of micro-electro-mechanical systems and have been extensively researched. In this paper, the battery was composed of thin film lithium metal anode, lithium phosphorus oxynitride (LiPON) solid electrolyte, and island-like deposition of lithium manganese oxide spinel ( $\text{LiMn}_2\text{O}_4$ ) cathode. LiPON and  $\text{LiMn}_2\text{O}_4$  were deposited by a radio frequency magnetron sputtering system, and lithium metal was deposited by thermal evaporation coater. Electrochemical characterization of this flexible lithium-ion battery shows a discharge capacity of  $110 \mu\text{Ah}$  between 4.3V and 3V at a current density of  $10 \mu\text{A}/\text{cm}^2$  (0.5C). The capacity retention was achieved 90% after 50 charge-discharge cycles between 4.3V and 3V at a current density of  $20 \mu\text{A}/\text{cm}^2$  (1C). Obviously, island-like deposition of thin film increased the charge exchange rate; this lithium-ion battery also exhibited a high C-rate performance, with better capacity retention of 61% at  $200 \mu\text{A}/\text{cm}^2$  (10C).

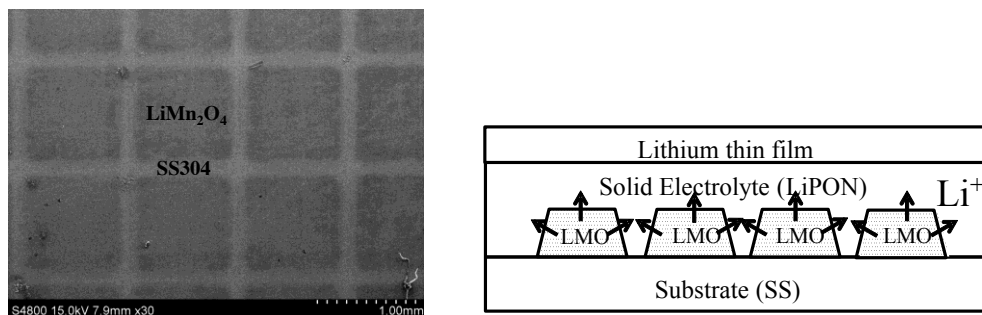


Figure L. SEM image of island-like deposition of  $\text{LiMn}_2\text{O}_4$  thin film.

Figure R. Scheme of the island-like deposition of  $\text{LiMn}_2\text{O}_4$  thin films in all-solid-state lithium ion battery.

## Reference:

1. C. F. Li, W. H. Ho, C. S. Jiang, M. J. Wang and S. K. Yen, J. Power Sources 196, 768 (2011).
2. R. Kali and A. Mukhopadhyay, J. Power Sources 247, 920 (2014).

# Synthesis of Si Nanoparticles by Atmospheric Microwave Plasma

Joon soo Kim\*, Bo yun Jang\*\*, Jin seok Lee, Jeong boon Koo, Jeong eum Lee

*Korea Institute of Energy Research*

*152, Gajeong-ro, Yuseong-gu, Daejeon, 305-343, Korea*

*\*jskim@kier.re.kr, \*\*byjang@kier.re.kr*

Si nanoparticles have been promising materials for electronic devices, photovoltaics, lithium ion battery anode, optical and biological applications. To use active material as lithium ion battery anode we were synthesized by atmospheric microwave plasma pyrolysis method using  $\text{SiCl}_4$  as starting materials.  $\text{H}_2$  was the main parameter during the synthesis of Si nanoparticles as shown in the following reaction,  $\text{SiCl}_4 + 2\text{H}_2 \leftrightarrow \text{Si} + 4\text{HCl}$ .  $\text{H}_2$  flow rate effects on Si nanoparticles were investigated by using SEM, TEM, XRD, and XPS. Atmospheric microwave plasma pyrolysis system for synthesis of Si nanoparticles consisted of a power generator, feeder, reactor, trap and scrubber.  $\text{H}_2$  was injected through two nozzles in atmospheric microwave plasma pyrolysis system and referred to as swirling and reactive gas. From SEM, TEM, XRD, and XPS analysis,  $\text{H}_2$  flow rate and  $\text{H}_2$  injection method in plasma and reaction zone were critical to synthesize crystalline Si nanoparticles. Much more amount of  $\text{H}_2$  than the amount of  $\text{H}_2$  expected was required to synthesize crystalline Si nanoparticles from  $\text{SiCl}_4$ . The  $\text{H}_2$  as swirling gas was more important than  $\text{H}_2$  as reactive gas because of  $\text{H}_2$  flow rate. The synthesized Si nanoparticles had core-shell structures covered with amorphous  $\text{SiO}_x$  shell.

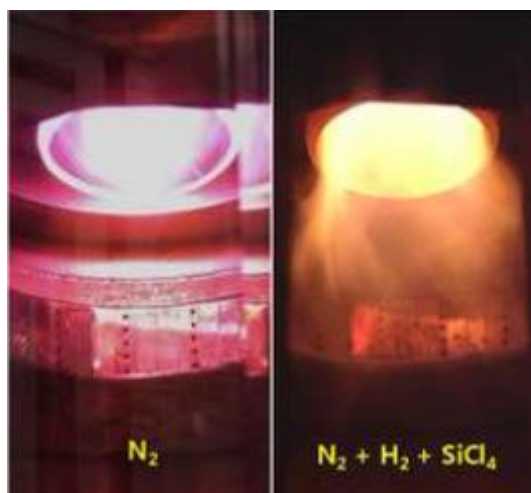


Photo images of microwave plasma in reactor



(a)

(b)

Synthesized Si nanoparticles (a) without and (b) with  $\text{H}_2$  as swirling gas

# Tuning the Electronic Structure of Layered Oxides Electrodes for Reversible Anionic Redox in Lithium Ion Batteries

Biao Li, Huijun Yan, Li An, Hang Wei, Jin Ma, Dingguo Xia\*

*Beijing Key Lab of Theory and Technology for Advanced Batteries Materials, College of Engineering, Peking University, Beijing 100871, P. R. China. Email: [dgxia@pku.edu.cn](mailto:dgxia@pku.edu.cn)*

Lithium ion batteries have been increasingly urged with high energy density and long cycle life to meet the increasing requirements for portable electronics, use of renewable energy and electric vehicles. The availability of the appropriate cathode material is crucial for the development of lithium ion batteries.  $\text{Li}_{1+x}\text{Ni}_y\text{Co}_z\text{Mn}_{1-x-y-z}\text{O}_2$  can deliver a high capacity of more than  $250 \text{ mA h g}^{-1}$ , provoking world wide attentions for lithium rich layered oxides, such as  $\text{Li}_2\text{Ru}_{1-y}\text{M}_y\text{O}_3$  ( $\text{M}=\text{Mn}$ ,  $\text{Sn}$ , and  $\text{Ti}$ ) and  $\text{Li}_{1.211}\text{Mo}_{0.467}\text{Cr}_{0.3}\text{O}_2$ . A common feature accounting for the high capacities of these lithium rich materials is supposed to be the two redox processes involving both of cation and anion<sup>[1]</sup>. However, the stability of these high capacity electrodes is limited for long cycle life due to its structural unstability, which is supposed to be caused by the excessive participation of the anionic redox<sup>[2]</sup>. Here, in this work, we expect to develop a strategy by tuning the electronic structure of the layered oxides to realize the reversibility of the anionic redox. It is shown by DFT calculation method that the reversible anionic redox can be obtained within a certain extent of participation in redox reaction of the anionic ions. We chose interstitial site doping in the layered oxides of  $\text{Li}_2\text{RuO}_3$  to tune its electronic structure. The resulted materials show decreased covalency and lowered O 2p band. The charge/discharge behavior has significant change for the first cycle and subsequent cycles.

This work was financially supported by the National High Technology Research and Development Program (2012AA052201, 2012AA110102), the National Natural Science Foundation of China (11179001).

## Reference

- [1] Sathiya, M. et al. Reversible anionic redox chemistry in high-capacity layered-oxide electrodes. *Nature Materials* 12, 827-835 (2013).
- [2] Goodenough, J. B. & Park, K. S. The Li-ion rechargeable battery: a perspective. *Journal of the American Chemical Society* 135, 1167-1176 (2013).

## Electrochemical Studies of binary oxides, $\text{MO}_2$ (M= Ti, Mn, Mo, Ru)

**M.V. Reddy**<sup>1,2\*</sup>, S. Adams<sup>1</sup>, B.V.R. Chowdari<sup>2</sup>

<sup>1</sup>Department of Materials Science & Engg, <sup>2</sup>Department of Physics, University of Singapore, Singapore 117542

\*Presenting author e-mail adds. : msemvvr@nus.edu.sg; phymvvr@nus.edu.sg

<http://www.researcherid.com/rid/B-3524-2010>; Ph.:65162607; Fax.: 65-6777-6126

### Abstract

The reaction mechanisms of Li-ion batteries materials are broadly classified in to intercalation/de-intercalation, alloying-de-alloying, conversion reaction and alloying and conversion reaction. Binary oxides like  $\text{MO}_2$  (M= Mn, Ru, Ti, Mo) undergoes intercalation reaction with Li. In order to understand the effect of matrix element and crystal structure, we studied the comparative electrochemical studies of  $\text{MO}_2$ . The discharge -charge profiles and capacity values of various binary metal oxides  $\text{MO}_2$  (M= Ti, Mn, Mo, Ru) are shown in Fig. 1. Samples were prepared by various chemical methods. Preliminary electrochemical studies show a reversible capacity (1<sup>st</sup> charge) are 150, 160, 140 and 280 mAh/g respectively for  $\text{TiO}_2$ ,  $\text{MoO}_2$ ,  $\text{MnO}_2$ , and  $\text{RuO}_2$  at a current rate of 33 mA/g at room temperature. The discharge-charge profiles show a differences in the discharge-charge voltage profiles was noted with different matrix elements. The charge voltage of the order of  $\text{MnO}_2 > \text{RuO}_2 > \text{TiO}_2 > \text{MoO}_2$ . Two stages of voltage plateaux was noted with  $\text{MoO}_2$  compounds. Ex-situ XRD studies on selected voltages were discussed in detail and also preliminary electrochemical studies with Li-air battery studies were presented on select materials.

Key words:  $\text{MoO}_2$  (M= Mo, Mn, Ru, Ti) ; Intercalation reaction ; Electroanalytical studies; Li-air batteries

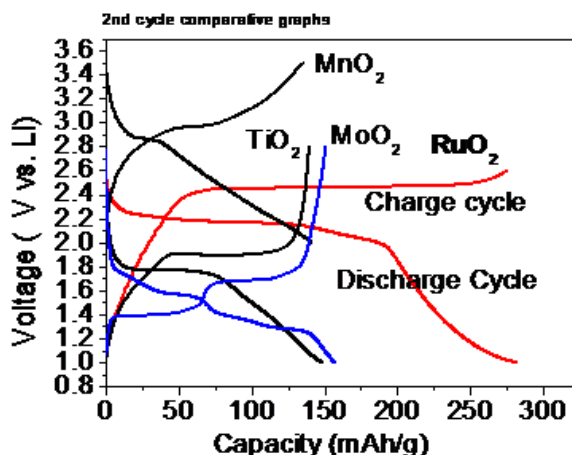


Fig.1: Comparative Voltage vs. Capacity discharge and charge cycles (2<sup>nd</sup>) of  $\text{MoO}_2$  samples

### References

1. M.V. Reddy, G.V. Subba Rao, B.V. R. Chowdari "Metal oxides and oxysalts as anode materials for lithium ion batteries" Chemical Reviews 113(2013)5364-5457
2. M.V. Reddy, Valerie Teoh Xiao Wie, Nguyen Thi Bao Nguyen, Michelle Lim Yi Ying, B.V.R. Chowdari "Effect of 0.5 M  $\text{NaNO}_3$ ; 0.5 M  $\text{KNO}_3$  and 0.88M  $\text{LiNO}_3$ :0.12M  $\text{LiCl}$  molten salts, and heat treatment on electrochemical properties of  $\text{TiO}_2$ " Journal of the Electrochemical Society 159(6) (2012)A762-A769.

# Composite positive electrode using sulfur/micro porous carbon for high-performance lithium-sulfur battery

Yukiko Matsui, Takuya Takahashi, Satoshi Uchida, Masaki Yamagata, and Masashi Ishikawa  
Department of Chemistry and Materials Engineering, Faculty of Chemistry, Materials and  
Bioengineering, Kansai University  
3-3-35 Yamate-cho, Suita 564-8680, Japan  
e-mail address: yamagata@kansai-u.ac.jp

Recent growth and demand for portable electronics and large-scale applications, such as electric vehicles and renewable energy storage devices, require advanced lithium-ion batteries that have high power and high storage capacity. These ideal characteristics can be achieved by improving charge-discharge performance of positive electrodes, and rightly, many efforts have been done to develop cathode active materials. Lithium sulphide ( $\text{Li}_2\text{S}$ ) is one of a promising cathode material for high-energy lithium batteries, because of its extremely high theoretical capacity of  $1672 \text{ mAh g}^{-1}$ . However, it is difficult to realize high-performance of lithium-sulfur battery due to some crucial problems, especially low electric conductivity of sulfur and dissolution of polysulfides formed during charge-discharge operation. Herein, we prepared and investigated a highly stable sulfur positive electrode using micro-porous carbon in several non-aqueous electrolytes including solvate ionic liquid electrolyte [1] to constructing high-performance lithium-sulfur battery.

Figure 1 shows charge-discharge cyclability of a composite electrode based on micro-porous carbon containing sulfur (a S/C electrode) in several non-aqueous electrolytes; solvate ionic liquid electrolyte composed of LiTFSI, tetraethylene glycol dimethyl ether (tetraglyme, G4) and hydro fluoro ether (HFE)[1],  $1.0 \text{ mol dm}^{-3}$  LiFSI/EMImFSI ( $\text{FSI}^- = \text{bis}(\text{fluorosulfonyl})\text{imide}$ ;  $\text{EMIm}^+ = 1\text{-ethyl-3-methylimidazolium}$ ), and a conventional organic-solvent-based electrolyte ( $1.0 \text{ mol dm}^{-3}$   $\text{LiPF}_6/\text{EC}+\text{DMC}$ ) at charge-discharge rate of 0.1/0.07 C-rate in a cell voltage range from 1.0 V (or 1.2 V for LiFSI/EMImFSI) to 3.0 V. Stable charge-discharge operations of the S/C electrode with ca.  $1100 \text{ mAh g}^{-1}$  at a  $100^{\text{th}}$  cycle are observed regardless of the kinds of the electrolytes, suggesting that using micro-porous carbon might provide high retainability of polysulfides. Figure 2 compares the discharge capacity of the S/C composite electrode in three solvate ionic liquid-based electrolyte; LiFSI/G4, LiFSI/G4+HFE, and LiTFSI/G4+HFE as well as  $\text{LiPF}_6/\text{EC}+\text{DMC}$  at a discharge C-rate from 0.1 to 2.0 C-rate. An apparent contrast in discharge capability is observed more than 1.0 C-rate. Among the cells with four electrolytes, the remarkably high rate capability is achieved for the cell with the LiFSI/G4+HFE system; its discharge capacity exhibits ca.  $1200 \text{ mAh g}^{-1}$  at 2.0 C-rate.

In the present study, we also constructed a Si/S cell to evaluate its practical usability. According to charge-discharge measurements, the Si/S cell shows highly stable cycling behavior with high discharge capacity over  $900 \text{ mAh g}^{-1}$  for 300 cycles

## Acknowledgment

This work is partly supported by Specially Promoted Research for Innovative Next Generation Batteries of Advanced Low Carbon Technology Research and Development Program (ALCA-SPRING) promoted by JST.

## References

- 1) K. Dokko *et al.*, *J. Electrochem. Soc.*, **160**, A1304 (2013).

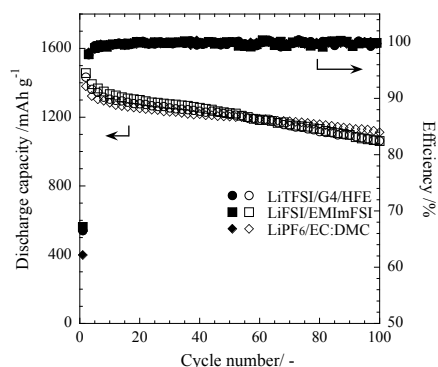


**Fig. 1.** Cycleability and charge-discharge efficiency of the S/C composite electrode at 0.1/0.07C-rate in LiTFSI/G4+HFE, LiFSI/EMImFSI, and  $\text{LiPF}_6/\text{EC}+\text{DMC}$ .

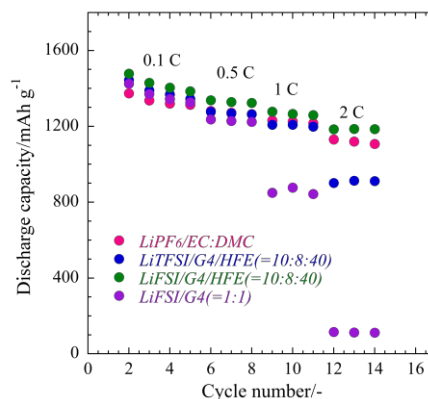


**Fig. 2.** Discharge rate capability of the S/C composite electrode in several electrolytes at a charge-discharge rate from 0.1/0.1 to 0.1/2.0 C-rate



# Thermal modeling of a lithium-ion battery module for hybrid electric vehicle applications

Boram Koo, Jaeshin Yi, and Chee Burm Shin\*

*Ajou University, Department of Energy Systems Research*

*Suwon 443-749, South Korea*

*\*cbshin@ajou.ac.kr*

The lithium-ion battery (LIB) is a preferred power source for hybrid electric vehicle (HEV) applications due to its outstanding characteristics such as high energy density, modular scalability, long cycle life, and low self-discharge rate among others. In a battery module for HEV applications, an uneven temperature distribution in the module can be created depending on the operating conditions and the types of thermal management. Uneven temperature distribution in a module could cause an electrical imbalance and thus lead to the lower performance and shorter life of battery. It is, therefore, important to calculate accurately the uneven temperature distribution in a battery module in order to achieve the optimum performance and long life of the battery module.

In this work, a modeling is performed to investigate the effect of the operating condition on the thermal behavior of an LIB module. The thermal conductivities of the various compartments of a battery cell are estimated based on the equivalent network of parallel/series thermal resistances of the battery components. The heat generation rate in an LIB cell is calculated by using the modeling results of the potential and current density distribution of a battery cell. The temperature distributions in the LIB module obtained from the modeling are in good agreement with the experimental measurement.

The battery module consisting of 8 prismatic pouch-type LIB cells modeled in this work is shown in Fig. 1. In Fig. 2, the temperature distributions of the LIB cells within the module at a few cross sections along the y direction are shown at the discharge time of 960 s with the discharge rate of 3C for natural convection cooling. The temperatures of the two cells located at the bottom and top of the module are lower than those of the other cells.

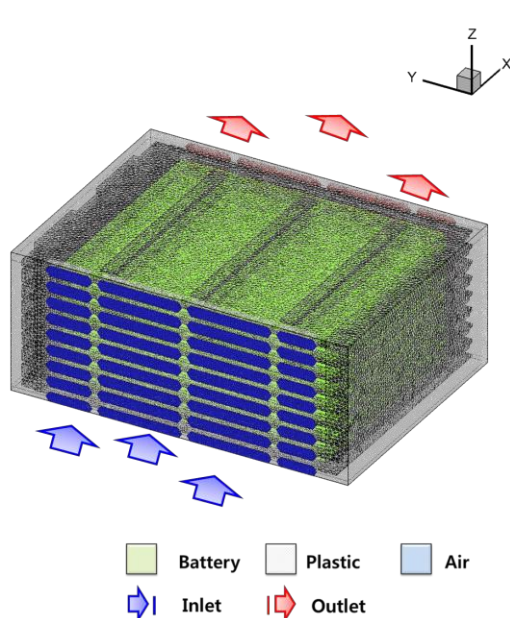


Fig. 1. Finite volume mesh used for CFD calculations and the direction of cooling air flow.

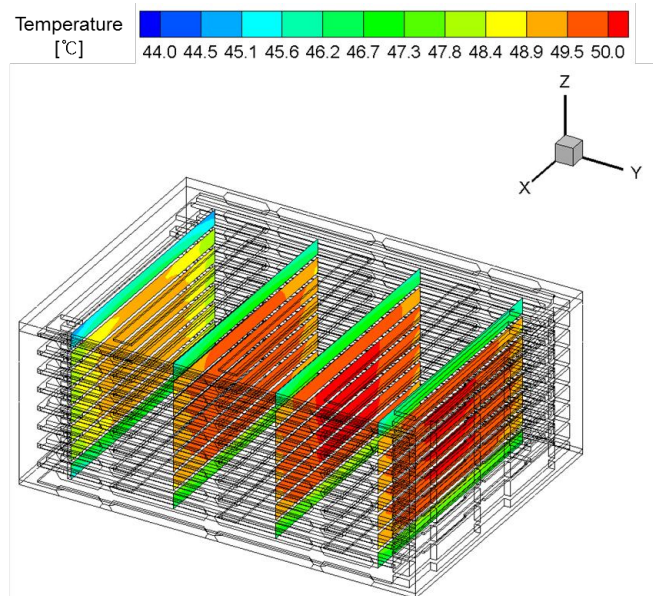


Fig. 2. Temperature distributions of the LIB cells within the module at a few cross sections along the y direction at the discharge time of 960 s with the discharge rate of 3C for natural convection cooling.

# Development of Charge Transport Model in Composite Polymer Electrolytes

Askarova G., Ablayeva K., Sivokhina Ye., Galeyeva A., Kurbatov A.  
*al-Farabi Kazakh National University*  
*71 al-Farabi Ave., 050040, Almaty, Kazakhstan*  
*gertie858@gmail.com*

Recent research and development advancements of lithium power sources has shown that composite polymer electrolytes have gained a significant attention. Composite polymer electrolytes are difficult organized heterogeneous materials, so it seems to be practically impossible to create a highly conductive electrolyte using random selection of raw materials and manufacturing method. Thereby, it is especially important to determine the mechanism of charge transport through the CPE.

The composite based on PVDF, with the incorporation of an inorganic filler -  $\text{TiO}_2$  and  $\text{LiClO}_4$ , as the dopant salt was selected in this study. The effect of changes in physical and chemical properties, shape, quantity and methods of the filler particles incorporation in the polymer membrane were observed.

Results of the experiment showed that small concentrations (1-5%) of the filler contribute to increase the ionic conductivity, but further additive (10-50%) triggers the opposite mechanism. The shape of the particles and their distribution influenced on the stability of electrode-electrolyte interface. Analysis of all the variations is optimal point correlation of mechanical properties and high ionic conductivity.

The mechanism of charge transfer based on the acid-base interaction between the filler particles and the lithium cation was proposed. This illustrates competitive character of introduced components leads to a change in the kinetics of the processes occurring at the electrode-electrolyte interface. It is believed that the introduction of neutral filler, facilitates the formation of polymer dative bands that leads to a decrease in its bonding strength between the cation of lithium and polymer chains, which increases the ion migration.

# **Influence of the Used Carbons and Binders to the Electrochemical Properties of Li-S Cathode**

Tomáš Kazda<sup>1</sup>, Jiří Vondrák<sup>1</sup>, Marie Sedlaříková<sup>1</sup>, Andrea Fedorková Straková<sup>1,2</sup>, Marek Slávik<sup>3</sup> and Pavel Čudek<sup>1</sup>

<sup>1</sup>*Brno University of Technology, Faculty of Electrical Engineering and communication, Department of Electrical and Electronic Technology, Technická 10, 602 00 Brno, Czech Republic*

<sup>2</sup>*Department of Physical Chemistry, Faculty of Sciences, P. J. Šafárik University in Košice, Moyzesova 11, SK-04154 Košice, Slovak Republic*

<sup>3</sup>*Graphene Batteries AS c/o Sintef, Forskningsveien 1, 0314 Oslo, Norway*

*e-mail: xkazda02@stud.feec.vutbr.cz*

Electromobility undergoes a rapid development in the world nowadays. The problem of current electric vehicles (EV) is the lack of battery capacity which limits their potential range. The solution of this problem could be Li-S batteries with their theoretical capacity of 1675 mAh/g and specific energy of ~ 3200 Wh/kg which greatly exceeds the possibilities of current commercial batteries. Before releasing these batteries into practice, it is necessary to solve a number of problems, such as a very complicated conversion of sulphur to Li<sub>2</sub>S and back again without settling soluble polysulfide at the anode during cycling, which leads to a decrease of capacity. Another problem is the expansion of sulphur during cycling, when, during the conversion of sulphur to Li<sub>2</sub>S, the volume expansion of about 80% occurs. This expansion leads to a big stress to the cathode and decreases its capacity. A possible solution of both these problems is the correct choice of carbon which encapsulates sulphur and a binder which can respond to the changes of volume without the loss of contact between particles of the electrode. This paper deals with the influence of used carbon and binder to the electrochemical properties of Li-S batteries. Standard Super P carbon and mesoporous carbon in combination with binders PVDF, PEO and PVP were used for testing. It was found that there was an increase of the capacity and stability of the electrode during cycling at various C-Rates. A stable and reversible capacity of about 600 mAh/g was achieved during cycling at 0.2 C and almost 400 mAh/g during cycling at 0.5 C.

## **Acknowledgement:**

This research has been carried out in the Centre for Research and Utilization of Renewable Energy (CVVOZE). Authors gratefully acknowledge the financial support from the Ministry of Education, Youth and Sports of the Czech Republic under NPU I programme (project No. LO1210), BUT specific research programme (project No. FEKT-S-14-2293), project VVGS-2014-166 and FEI Company.

# Interaction between Carbon Defects and Polysulfides in Lithium Sulfur Battery

Hui-Yu Hung<sup>a</sup>, Chao-Yen Kuo<sup>a,b</sup>, Jian-Ting Chin<sup>a</sup>, Chen-Jui Huang<sup>a</sup>, Men-Che Tsai<sup>a</sup>, Bing-Joe Hwang<sup>a\*</sup>

<sup>a</sup>*Department of chemical engineering, National Taiwan University of Science and Technology  
No.43, Sec. 4, Keelung Rd., Da'an Dist., Taipei 106, Taiwan (R.O.C.)*

<sup>b</sup>*Division of Energy Storage, Department of Chemistry, Institute of Nuclear Energy Research  
No. 1000, Wenhua Rd., Jiaan Village, Longtan District, Taoyuan City 32546, Taiwan(R.O.C.)  
bjh@mail.ntust.edu.tw*

The lithium-sulfur battery is a promising rechargeable lithium-ion battery system that has a high theoretical capacity of 1675 (mAh/g) and high theoretical energy density (2500 Wh/kg). However, it suffers several drawbacks such as poor conductivity and huge volume change of active materials, dissolution of intermediates, safety issue of lithium metals, etc. which prevent it to be commercialized. In this study, synthesized carbon materials with various defects and functional groups were introduced to prepare sulfur/carbon composites and investigate the interactions between carbon defects and sulfur or polysulfides. Further characterization and electrochemical measurements were conducted to establish the relationship between the interactions and electrochemical performance of sulfur/carbon composite materials.

# Electrochemical Intercalation of Anions into Graphite – The Role of Anion Structure and Solvent Properties

Kolja Beltrop<sup>\*</sup>, Paul Meister, Olga Fromm, Martin Winter, Tobias Placke

University of Münster, MEET Battery Research Center, Institute of Physical Chemistry Corrensstr. 46,  
48149 Münster, Germany

<sup>\*</sup>[kolja.beltrop@uni-muenster.de](mailto:kolja.beltrop@uni-muenster.de)

The increasing demand for large scale energy storage capabilities causes a big field of research to make the battery systems safer and environmentally benign. A promising approach is the replacement of conventional volatile and highly flammable organic solvent-based electrolytes by ionic liquids (ILs) as the main component of the electrolyte. ILs exhibit excellent properties such as a broad electrochemical stability window, a high thermal stability, non-flammability and a high ionic conductivity.[1] A further prevention of pollution is the application of carbon-based, transition metal-free electrode materials. Recently, “dual-ion” and “dual-graphite” cells were introduced which are composed of a lithium-incorporating anode and an anion incorporating graphite-based cathode.[2][3] During charge the ions intercalate into the electrode active materials and are released back into the electrolyte during discharge (see Figure 1). Since the cathode potential reaches and may even exceed 5 V vs.  $\text{Li}/\text{Li}^+$ , electrolytes that exhibit a high stability vs. oxidation are necessary. For that reason, ILs with their versatile properties were introduced and investigated. The state of the art electrolyte for this system is composed of a solution of lithium bis(trifluoromethanesulfonyl) imide ( $\text{LiTFSI}$ ) in *N*-butyl-*N*-methylpyrrolidinium bis(trifluoromethanesulfonyl) imide ( $\text{Pyr}_{14}\text{TFSI}$ ). In order to increase the specific capacity of this system, one main strategy is to focus on the intercalation of smaller anions than TFSI into the graphite structure. In this context, the major challenge is the synthesis of ILs or mixtures of ILs with organic electrolytes consisting of small anions to provide an electrochemically stable electrolyte. Interestingly, not only the size and shape of the intercalated anions plays a major role in view of onset potential for anion uptake as well as discharge capacity. Instead, also more complex coherences such as ion association, self-aggregation of ions as well as solvent co-intercalation have to be taken into consideration. In this work, we investigate the electrochemical intercalation of anions with different shapes and sizes from either IL or organic based electrolytes into a graphite-based cathode. Against this background, the influence of side chain modifications within the anion structure on the intercalation behavior was studied using different electrochemical analysis techniques. Therefore, in this contribution we will give new insights to the question if the anion size is the main issue to tailor the reversible capacity for anion intercalation.

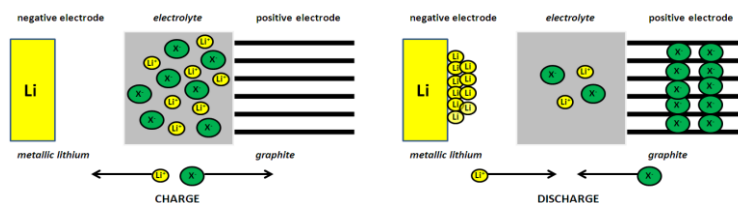


**Figure 1: Schematic illustration of the operating principle of a "dual-ion cell".[2]**

- [1] A. Lewandowski, A. Swiderska-Mocek, Journal of Power Sources, 194 (2009) 601-609.
- [2] T. Placke, P. Bieker, S.F. Lux, O. Fromm, H.W. Meyer, S. Passerini, M. Winter, Zeitschrift für Physikalische Chemie, 226 (2012) 391-407.
- [3] S. Rothermel, P. Meister, G. Schmuelling, O. Fromm, H.-W. Meyer, S. Nowak, M. Winter, T. Placke, Energy & Environmental Science, (2014).



# Investigation of the Degradation Mechanism of $\text{Li}_x\text{Ni}_y\text{Mn}_z\text{Co}_{1-y-z}\text{O}_2$ Cathode Materials for Lithium Ion Batteries

Wonyoung Chang<sup>1,\*</sup>, Sooyeon Hwang<sup>1</sup>, Woo-Sung Choi<sup>2</sup>, Seung Min Kim<sup>3</sup>, Young Sun Shin<sup>1</sup>, Byung-Won Cho<sup>1</sup>, Kyung Yoon Chung<sup>1</sup>, Eric A. Stach<sup>4</sup>, Heon-Cheol Shin<sup>2</sup>

<sup>1</sup>*Center for Energy Convergence, Korea Institute of Science and Technology, Seoul 136-791, Republic of Korea*

<sup>2</sup>*School of Materials Science and Engineering, Pusan National University, Busan 609-735, Republic of Korea*

<sup>3</sup>*Carbon Convergence Materials Research Center, Korea Institute of Science and Technology, Wanju-gun 565-905, Republic of Korea*

<sup>4</sup>*Center for Functional Nanomaterials, Brookhaven National Laboratory, Upton, New York 11973, United States*

\**cwy@kist.re.kr*

Ni-based layer structured cathode materials have been considered as one of the most promising candidates for next generation batteries due to their higher energy density, less toxicity, and lower cost compared with those of  $\text{LiCoO}_2$ . Each of transition metal inside layered lithium transition metal oxides acts to relieve the charge imbalance that occurs during either the insertion or removal of lithium from the structure during the reduction or oxidation process, and thus their incorporation strongly affects the overall electrochemical performance. For example, the incorporation of Ni increases the overall capacity of the cathode; however, Ni-rich cathodes have also been associated with significant safety issues. Here, we take advantage of electron microscopy to directly investigate the evolution of the surface structure of  $\text{Li}_x\text{Ni}_y\text{Mn}_z\text{Co}_{1-y-z}\text{O}_2$  cathode materials with y and z of 0.8 and 0.1, 0.6 and 0.2, 0.4 and 0.3 (referred to as NMC811, NMC622, NMC433, respectively) that have been cycled under various cutoff voltage conditions. Bright field (BF) images, selected area electron diffraction (SAED) patterns, and electron energy loss (EEL) spectra from the oxygen K-edge and transition metal (TM: nickel, manganese, cobalt) L-edges of charged NMC cathode materials are recorded from individual particles as a function of charge cut-off voltages. Statistical analysis for several particles is also performed in order to examine particle-to-particle variation, which becomes significant in NMC having a high Ni content. This study demonstrates that the transition metal content has a strong impact on both the electrochemical properties and the structural stability of charged NMC materials, and the structural degradation is critically affected by the cutoff voltage. For better understanding of degradation mechanism under high cut-off voltage operation, the relation between impedance change and the degree of cycle degradation will be also discussed. All the details will be available at the meeting.

# Detailed “Mapping” of Internal Resistance in Li-S Batteries

Matthew J. Lacey, Kristina Edström, Daniel Brandell  
Department of Chemistry – Ångström Laboratory, Uppsala University  
Box 538, Lägerhyddsvägen 1, SE-751 21 Uppsala, SWEDEN  
matthew.lacey@kemi.uu.se

Measurement of internal resistance is an important indicator of state-of-health and stability in batteries. This is frequently accomplished with the use of electrochemical impedance spectroscopy (EIS), which is a powerful technique enabling the probing of a range of processes across a wide timescale, but one which requires specialist equipment and can very often be difficult to interpret correctly. Furthermore, it can be a complex task to incorporate impedance measurements into standard battery testing procedures such as galvanostatic cycling.

In this work we describe a relatively simple experiment for visualising the change in internal resistance in a battery during galvanostatic cycling based on the current-interrupt method. Repeated short interruptions in the current, for example, every few minutes for a fraction of a second, can be easily analysed by a simple computer program and presented as a ‘heat map’ to visualise the changes in internal resistance over the full state-of-charge range and over many cycles.

This technique has been applied here to the study of the Li-S cell, which, due to its unique electrochemistry, shows significant changes in resistance during charge and discharge, asymmetry between the charge and discharge processes and often unpredictable changes over a large number of cycles, even if the capacity is relatively stable. The timescale of the measurement may also be varied allowing, in principle, the separation of ionic/electronic resistances from, for example, charge transfer. The use of this technique for the comparison of different electrode materials will also be presented.

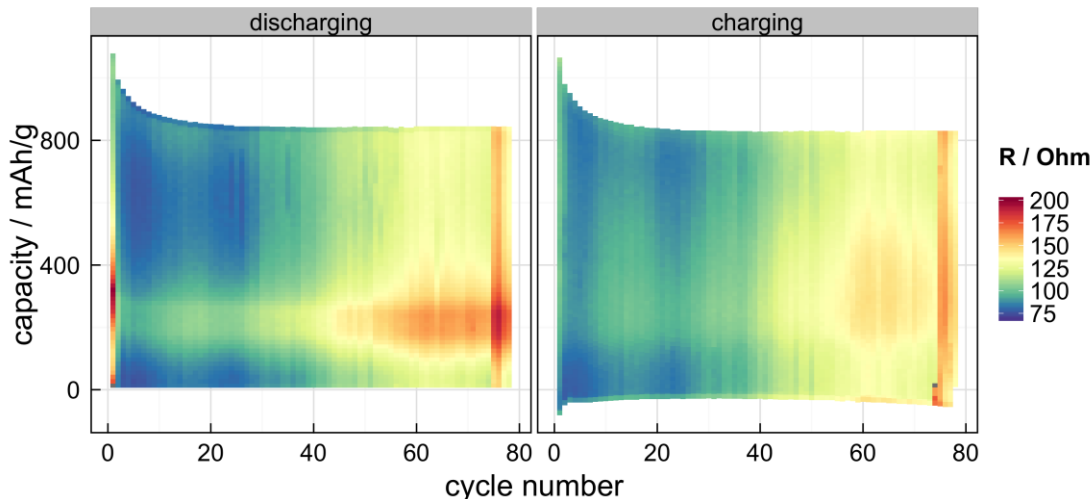


Figure: internal resistance “map” of a Li-S cell cycled galvanostatically at a constant rate of  $C/10$ . The plot above comprises 9,727 unique measurements. Resistance,  $R$  was determined by measuring  $dE/dI$  over a 0.5 s current interruption every five minutes.



# Nanostructured ZnFe<sub>2</sub>O<sub>4</sub>-based anodes for lithium-ion batteries – Novel synthesis route and analytical study on metal dissolution

Tobias Placke, Haiping Jia, Britta Vortmann, Martin Winter

*University of Münster, MEET Battery Research Center, Institute of Physical Chemistry, Corrensstr. 46,  
48149 Münster, Germany*

*\*tobiasplacke@uni-muenster.de*

The ever-growing demand for next-generation lithium-ion batteries (LIBs) with high specific energy/energy density as well as high power performance has prompted widespread research to develop novel electrode materials for both the anode and cathode.[1] There are mainly three types of anode materials for LIBs according to the different lithiation storage mechanisms: (1) intercalation materials such as graphite and insertion materials such as Li<sub>4</sub>Ti<sub>5</sub>O<sub>12</sub> spinel oxides or TiO<sub>2</sub> anatase; (2) lithium alloying materials, such as Si or Sn and (3) conversion materials, such as transition metal oxides like Fe<sub>3</sub>O<sub>4</sub> and MnO which store charge via a conversion reaction ( $\text{MO}_x + 2x\text{Li} \rightleftharpoons \text{M} + x\text{Li}_2\text{O}$ ). Among the latter ones, the nanostructured metal oxides, such as tin oxide and cobalt oxide have been extensively studied as alternative anode materials for use in LIBs over the past few years because of their large number of possibilities and their high specific capacity.[2, 3] Fe<sub>3</sub>O<sub>4</sub>, for example, gives a theoretical capacity of 926 mAh g<sup>-1</sup>, considering the completely reversible formation of four Li<sub>2</sub>O per formula unit.[3] The theoretical capacity of these transition metal oxides can be further increased by replacing one iron atom by an element which can reversibly form an alloy with lithium, such as zinc. This would result in an enhanced theoretical capacity of ca. 1000 mAh g<sup>-1</sup>, according to the reversible reaction involving nine lithium ions per formula unit of ZnFe<sub>2</sub>O<sub>4</sub>. [4] Considerable efforts have been devoted for the synthesis of ZnFe<sub>2</sub>O<sub>4</sub> with a variety of nanostructures, such as hollow spheres, octahedrons, nanofibers and nanorods.[5, 6] However, these morphologies were fabricated by synthetic or high temperature methods such as thermal decomposition, sol-gel or electrospinning technique. Among these methods, the sol-gel process has been considered to be a facile and effective way for designing novel nanomaterials with attractive properties. This is due to its simplicity, low cost of the raw material and equipment, possible large-scale production and most important advantage that the obtained material mostly present crystalline phase. In this work, we report a facile synthesis route, i.e. an ionic liquid-assisted sol-gel synthesis method, for the preparation of ZnFe<sub>2</sub>O<sub>4</sub>. The obtained material demonstrates a uniform morphology with fine particles which are composed of 50 nm-sized ZnFe<sub>2</sub>O<sub>4</sub> crystallites. Sucrose is employed as carbon source to coat the ZnFe<sub>2</sub>O<sub>4</sub> with a thin layer so as to enhance the surface electronic conductivity as well as the surface area for use as high-capacity and high-power anode material. Furthermore, analytical studies are carried out to identify the possibility of metal dissolution during electrochemical cycling at different operating conditions as well as the influence on the overall material stability.

- [1] R. Wagner, N. Preschitschek, S. Passerini, J. Leker, M. Winter, *Journal of Applied Electrochemistry*, 43 (2013) 481-496.
- [2] D. Bresser, F. Mueller, M. Fiedler, S. Krueger, R. Kloepsch, D. Baither, M. Winter, E. Paillard, S. Passerini, *Chemistry of Materials*, 25 (2013) 4977-4985.
- [3] A. Brandt, A. Balducci, *Journal of Power Sources*, 230 (2013) 44-49.
- [4] D. Bresser, E. Paillard, R. Kloepsch, S. Krueger, M. Fiedler, R. Schmitz, D. Baither, M. Winter, S. Passerini, *Adv. Energy Mater.*, 3 (2013) 513-523.
- [5] Y. Deng, Q. Zhang, S. Tang, L. Zhang, S. Deng, Z. Shi, G. Chen, *Chemical Communications*, 47 (2011) 6828-6830.
- [6] P. Lavela, J.L. Tirado, *Journal of Power Sources*, 172 (2007) 379-387.

# Buffer Effects of Electrolyte Additives on Lead-Acid Flow Batteries

Hsun-Yi Chen, Chih-Wei Chang, and Dong-Yi Chao

National Taiwan University, Dept. of Bio-Industrial Mechatronics Engineering

No. 1, Sec. 4, Roosevelt Rd., Taipei, 10617, Taiwan

hsunyichen@ntu.edu.tw

A single-flow, membrane-less lead acid redox flow battery (RFB), which is comprised of inexpensive components and materials, is promising for stationary energy storage. However, the lead-acid RFB currently has limited cycle life and low energy efficiency when operated at high C-rate, and is not ready for power grid applications.

One crucial factor that is identified to be responsible for degradation of lead-acid RFBs is the formation of passivation layers on electrodes when acidity of the electrolyte fluctuates appreciably. Although the growth mechanism is not fully understood, it is believed that a low conductive film of  $Pb_3O_4$  can form at the positive electrodes when the pH value of the electrolyte is relatively low. As shown in Fig. 1, deep charge/discharge cycles of a lead-acid RFB can induce significant electrolyte pH changes, and ultimately leads to a trend towards lower pH values. Accumulation of the passivation layer at electrodes during charge/discharge cycles then, in turn, leads to poor battery efficiency and higher proton concentration in the electrolyte in the long run.

In order to alleviate changes of proton concentration, pH buffering agents such as potassium acetate or sodium borate can be added to the electrolyte. This study focuses on investigating the buffer effects of various electrolyte additives on lead-acid RFBs. The quality of electroplated Pb and  $PbO_2$  with and without buffering additives is compared through impedance measurements and optical micrographs. Cyclic voltammetry will be performed for different electrolyte systems before conducting long term charge/discharge cycling experiments. We aim to identify the effective kind and the appropriate amount of additives for lead-acid RFBs to prolong their cycle life.

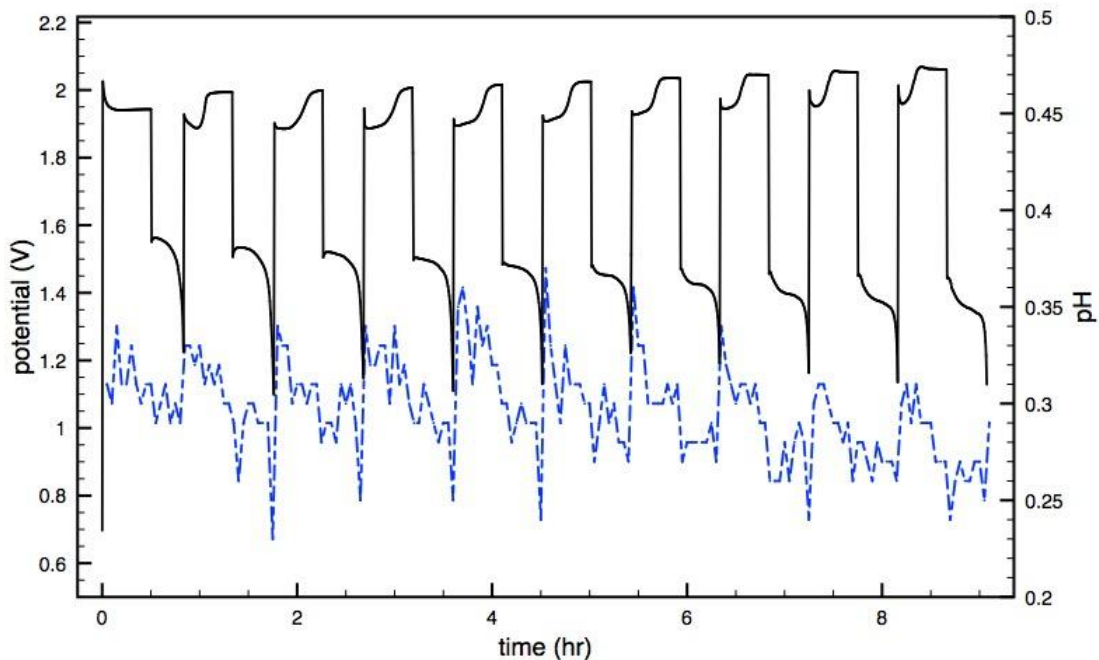


Fig. 1. Black line represents cell potential vs. time response for 10 charge/discharge cycle at current density of  $15 \text{ mAcm}^{-2}$ . Blue dashed line indicates pH values of the methanesulfonat based electrolyte.

# Probing the Oxygen Evolution Efficiency of Redox Mediator-Catalyzed Lithium-Oxygen Batteries using On-Line Electrochemical Mass Spectrometer

Zhuojian Liang, Yi-Chun Lu\*

Department of Mechanical and Automation Engineering, Shun Hing Institute of Advanced Engineering,  
The Chinese University of Hong Kong, Shatin, N.T., Hong Kong SAR, China

\*yichunlu@mae.cuhk.edu.hk

High charge overpotential is a major challenge in achieving efficient Li-O<sub>2</sub> batteries with long cycle life.<sup>1</sup> Redox mediators have been reported effective in reducing the overpotential during charge of Li-O<sub>2</sub> batteries.<sup>2-6</sup> However, limited evidence is available on how redox mediators influence the gas evolution efficiency upon charging.

In this study, we exploit quantitative on-line electrochemical mass spectrometer (OEMS)<sup>7,8</sup> to analyze the gas evolved during charge with and without redox mediator. Among many reported redox mediators, lithium iodide (LiI)<sup>2,3</sup> is one of the most effective and widely used redox mediators for rechargeable Li-O<sub>2</sub> batteries. Figure 1 shows the first galvanostatic charging voltage profile of a pre-discharged Vulcan carbon electrode and the corresponding evolution rate of O<sub>2</sub> and CO<sub>2</sub> measured during charge by the OEMS. The reduced overpotential for the cell with 10mM LiI agrees with a previous studies.<sup>2,3</sup> In both cells, a high evolution rate of O<sub>2</sub> was observed throughout the charge, indicating the domination of reversible Li<sub>2</sub>O<sub>2</sub> oxidation in the charge process with and without LiI. The OER/ORR ratio, which characterizes the degree of O<sub>2</sub> recovery efficiency and the rechargeability, is 0.860 and 0.868 for cells with and without LiI, respectively. The deviation of the ratio from 1.000 suggests that parasitic reactions still exists when the cell is charged with LiI. In addition, the similar ratios imply that the O<sub>2</sub> efficiency is not affected by LiI. In both cells, the oxygen evolution reaction (OER) is followed by CO<sub>2</sub> evolution, which is widely observed to be generated from decomposition of carbon cathode, electrolyte or parasitic products (e.g. carbonate)<sup>8</sup>. The charge voltage of the cell without LiI increases faster than the cell with LiI. The former exhibits a voltage peak during charge, which is accompanied by a dip in the O<sub>2</sub> gas evolution profile. Such features were not observed in the cell with 10mM LiI, suggesting different charging mechanisms with and without LiI, which leads to difference in gas evolution patterns. Our study provides direct quantitative evidence on the efficacy of catalytic effect and gas evolution of redox mediators for Li-O<sub>2</sub> batteries. Further investigation on the parasitic products and the long term catalytic effect of the reported redox mediators (e.g. LiI,<sup>2,3</sup> 2,2,6,6-Tetramethylpiperidin-1-yl)oxyl (TEMPO),<sup>4</sup> iron phthalocyanine (FePc)<sup>6</sup>) will be discussed.

**References:** (1) Lu et al., *Energy Environ. Sci.* 2013, 6, 750. (2) Chase et al., US patent US 20120028137 A1. 2012 (3) Lim et al. *Angew. Chem. Int. Ed.* 2014, 53, 3926. (4) Bergner et al. *J. Am. Chem. Soc.* 2014, 136, 15054. (5) Chen et al. *Nat. Chem.* 2013, 5(6), 489. (6) Sun et al. *J. Am. Chem. Soc.* 2014, 136, 8941. (7) Tsiouvaras et al., *J. Electrochem. Soc.* 2013 160, 3, A471. (8) McCloskey et al., *J. Phys. Chem. Lett.*, 2011, 2, 1161. **Acknowledgment:** This work is supported by Research Grants Council of the Hong Kong (Early Career Scheme CUHK24200414).

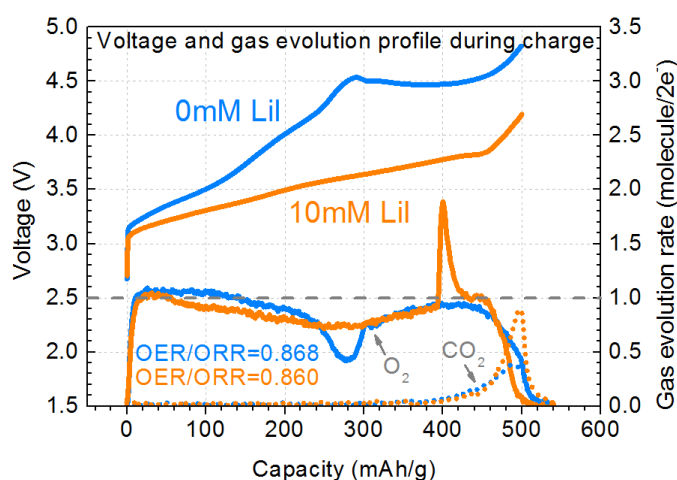


Fig. 1. First galvanostatic charging voltage and gas evolution profile of Li-O<sub>2</sub> cells with and without 10mM LiI in 1M LiTFSI diglyme. The cells were discharged at 500mA/g to 500mAh/g prior to charge. The spike in the 10mM LiI OER profile is caused by the accumulation and sudden release of a gas bubble in the cell, which do not affect the overall OER quantification.

## **Study of the kinetic of LiFePO<sub>4</sub> oxidation in aqueous solutions**

Malchik F., Kurbatov A.

*al-Farabi Kazakh National university*

*71 al- Farabi Ave., Almaty, Republic of Kazakhstan*

[Frodo-007@mail.ru](mailto:Frodo-007@mail.ru)

Based on the analysis of chemical oxidation of LiFePO<sub>4</sub> cathode material in aqueous solutions we attempted to identify the mechanism of lithium deintercalation in oxidation.

It was shown that the reaction rate depends on the concentration of the oxidant and the pH. At low concentrations of oxidizing agent in alkaline media limiting step is the delivery of oxidant to the surface of the particles. After reaching a certain concentration of oxidant, the reaction rate becomes constant, which may be due to a change in the limiting stage - the reaction on the surface. In the range of pH 7-10, the impact the basic solution to the oxidation rate is negligible. Although outside of this area, we can observe a significant increase in the rate of reaction in acidic media and the slowdown in alkaline media. In acidic media is possible to achieve complete oxidation of the material in a short time (300-600 s), allowing to quickly determine the degree of oxidation of Fe in the compound.

# Towards the mechanism of $\text{Mg}^{2+}$ -ions intercalation into $\text{V}_2\text{O}_5$ as the cathode material

Sladjana Martens<sup>1</sup>, Lukas Seidl<sup>1,2</sup>, Jiwei Ma<sup>1,3</sup>, Ehab Mostafa<sup>1</sup>, Huinan Si<sup>4</sup>, Xinping Qiu<sup>4</sup>, Ulrich Stimming<sup>2,5</sup> and Oliver Schneider<sup>1</sup>

<sup>1</sup>*Institut für Informatik VI, Joint Research Institute for Advanced Power Sources for Electric Vehicles, Technische Universität München, 85748 Garching, Germany*

<sup>2</sup>*Physik-Department, Technische Universität München, James-Franck Str. 1, 85748 Garching*

<sup>3</sup>*Department of Chemistry, Sorbonne Universités-UPM, Paris, France*

<sup>4</sup>*Department of Chemistry, Joint Research Institute for Advanced Power Sources for Electric Vehicles, Tsinghua University, Beijing 100084, China*

<sup>5</sup>*School of Chemistry, Newcastle University, Newcastle upon Tyne, NE1 7RU United Kingdom*

Rechargeable Li-ions batteries are still the frontrunners for powering portable electronic devices and for use in electric vehicles<sup>1</sup>. Improving the safety and energy density of the Li-ions batteries is the focus of current research. Besides improving the materials characteristics used in the Li-batteries and thus the overall battery performance, an alternative pathway consists in replacement of lithium by other elements, for example magnesium. Rechargeable Mg batteries have been already recognized as a promising technology for energy storage and conversion and lot of work has already been done on their development<sup>2</sup>. Furthermore,  $\text{V}_2\text{O}_5$  has been studied as a positive electrode material showing good performance not just for  $\text{Li}^+$  but also for  $\text{Mg}^{2+}$  ions insertion<sup>3</sup>. However, the energy and power density of current Mg ion batteries is much lower than for Li ion batteries.

In this study several synthetic routes such as sonochemical modification of commercial  $\text{V}_2\text{O}_5$  powder, anodization of V metal, electrochemical deposition and hydrothermal synthesis have been used to obtain  $\text{V}_2\text{O}_5$ . Scanning electron microscopy revealed different morphologies, varying from nanofibers obtained by the sonochemical treatment and electrochemical deposition, nanotubes obtained by the anodization method and hollow nanospheres of  $\text{V}_2\text{O}_5$  obtained by the hydrothermal synthesis (cf. Figure 1). The interaction of the prepared materials with the  $\text{Mg}^{2+}$  ions using different electrolytes has been studied via electrochemical techniques such as slow scan cyclic voltammetry (SSCV), potentiostatic intermittent titration technique (PITT) and electrochemical impedance spectroscopy (EIS), in order to understand the mechanism of the intercalation process and to analyze the influence of the morphology on the kinetics<sup>4</sup>.

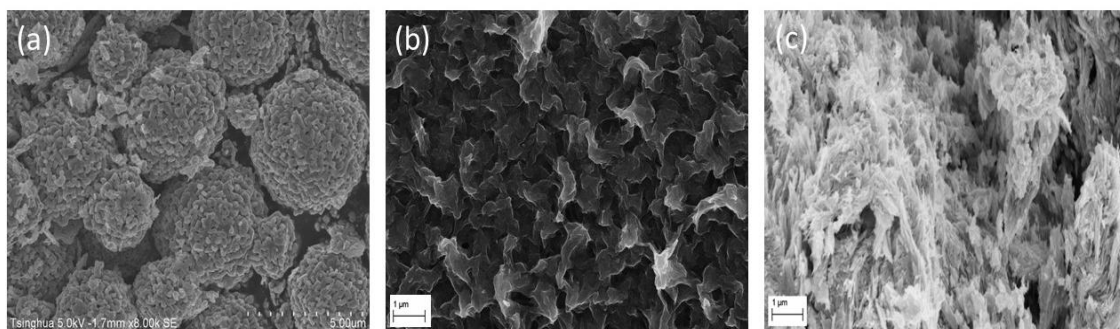


**Figure 1.** SEM images of (a) hollow  $\text{V}_2\text{O}_5$ -nanospheres, (b) electrodeposited  $\text{V}_2\text{O}_5$  and (c) ultrasonicated  $\text{V}_2\text{O}_5$

1. B. Dunn, H. Kamath, J-M. Tarascon, *Science* 334 (2011) 928
2. H. D Yoo, I. Shterenberg, Y. Gofer, G. Gershinsky, N. Pour, D. Aurbach, *Energy Environ. Sci.* 6 (2013) 2265
3. G. Gershinsky, H. D. Yoo, Y. Gofer, D. Aurbach, *Langmuir* 29 (2013) 10964
4. M. D. Levi, D. Aurbach, *Electrochim. Acta* 45 (1999) 167

# Electrochemical characteristics of a $\text{Li}_4\text{Ti}_5\text{O}_{12}$ /Marimo carbon composite

Kazuhiro Soutome<sup>1</sup>, Kenta Iwasawa<sup>1</sup>, Mika Shiraishi<sup>2</sup>, Risa Shiraishi<sup>2</sup>, Mikka Nishitani-Gamo<sup>2</sup>,

Toshihiro Ando<sup>3</sup>, Mika Eguchi<sup>1</sup>

<sup>1</sup> Ibaraki University, 4-12-1, Nakanarusawa, Hitachi, Ibaraki, 316-8511, Japan

<sup>2</sup> Toyo University, 2100 Kujirai, Kawagoe, Saitama 350-8585, Japan

<sup>3</sup> National Institute for Materials Science, 1-1 Namiki, Tsukuba, Ibaraki 305-0044, Japan

E-mail: eguchi@mx.ibaraki.ac.jp

## 1. INTRODUCTION

Lithium ion batteries have attracted attention as a possible methodology for solving current environmental and energy problems. However, a greater power density and cycle life are required to satisfy industrial needs.  $\text{Li}_4\text{Ti}_5\text{O}_{12}$  is as an alternative anode material to graphite due to its long cycle life and good high-rate performance. Unfortunately,  $\text{Li}_4\text{Ti}_5\text{O}_{12}$  has poor electronic conductivity (ca.  $10^{-13} \text{ S cm}^{-1}$ ) [1]. We have used a new carbon material called “Marimo carbon” as a conductivity assistant in order to improve the overall electric conductivity. Marimo carbon has a spherical structure that consists of an oxidized diamond as its core and radial carbon nanofilaments (CNFs) [2]. The electrolytes can easily sink into the vacant spaces of the CNFs, consequently, the improved electric conductivity is expected to obtain with the  $\text{Li}_4\text{Ti}_5\text{O}_{12}$ /Marimo carbon composite. Although acetylene black is widely used as a conductivity assistant, the material can easily aggregate to give a non-uniform distribution. Conversely, it is expected that Marimo carbon will provide a better accessibility by allowing the  $\text{Li}_4\text{Ti}_5\text{O}_{12}$  particles to fit in between the vacant spaces of the CNFs.

## 2. EXPERIMENTS

Ni/Oxidized diamond were used as a catalyst for the synthesis of the catalyst, Marimo carbon. Marimo carbon was grown by heating the catalyst at 550 °C for 3 h in methane gas as the reactant. Marimo carbon was then added to a 0.4 M LiOH solution and dispersed with an ultrasonic generator. (Marimo carbon was not added to a preparation of pure  $\text{Li}_4\text{Ti}_5\text{O}_{12}$ .) Hydrogen peroxide and titanium tetraisopropoxide were then added, and the solution was stirred for 1 h. The solution was transferred into a Teflon-lined stainless steel autoclave, which was then heated at 130 °C for 12 h. After cooling to room temperature, the solid product was obtained by centrifugation and washed with distilled water. The sample was then dried in vacuo and calcined at 400 °C for 6 h in argon. Electrochemical measurements for the composite were performed using CR2032 type cells. In the preparation of the working electrodes, a mixture of either a  $\text{Li}_4\text{Ti}_5\text{O}_{12}$ /Marimo carbon composite or pure  $\text{Li}_4\text{Ti}_5\text{O}_{12}$  was pasted on Cu foil with polyvinylidene fluoride (9:1 wt.%). Lithium foil was used as a counter electrode, and a solution of 1 M  $\text{LiPF}_6$  in ethylene carbonate and diethyl carbonate (EC + DEC = 1:1 vol.%) were used as an electrolyte.

## 3. RESULTS AND DISCUSSION

Figure 1 shows the rate performances of all samples with discharge rates ranging from 1 to 20 C. The discharge capacity decreases with an increasing discharge rate. In particular, pure  $\text{Li}_4\text{Ti}_5\text{O}_{12}$  shows the greatest amount of decay as a function of an increasing discharge rate. This indicates that pure  $\text{Li}_4\text{Ti}_5\text{O}_{12}$  has poor electrical conductivity because it lacks a conductive path. In comparison, the decay of  $\text{Li}_4\text{Ti}_5\text{O}_{12}$  with Marimo carbon composite is smaller. This is particularly observed in the discharge capacity of  $\text{Li}_4\text{Ti}_5\text{O}_{12}$ /50 wt.% Marimo carbon, which has a value of  $128.5 \text{ mAh g}^{-1}$  (Pure  $\text{Li}_4\text{Ti}_5\text{O}_{12}$  is only  $43.8 \text{ mAh g}^{-1}$ ) at 10 C. This is 73.4 % (Pure  $\text{Li}_4\text{Ti}_5\text{O}_{12}$  is only 25 %) of the theoretical capacity of  $\text{Li}_4\text{Ti}_5\text{O}_{12}$  ( $175 \text{ mAh g}^{-1}$ ), which suggests that the electrical conductivity was improved by the conductive path of Marimo carbon. These results show that Marimo carbon did indeed function as a conductivity assistant.

### References

- [1] Wei Fang et al., *Solid State Ionics*, **244**, 52-56, (2013)
- [2] K. Nakagawa et al., *J. Mater. Sci.*, **44** [1], 221-226, (200)

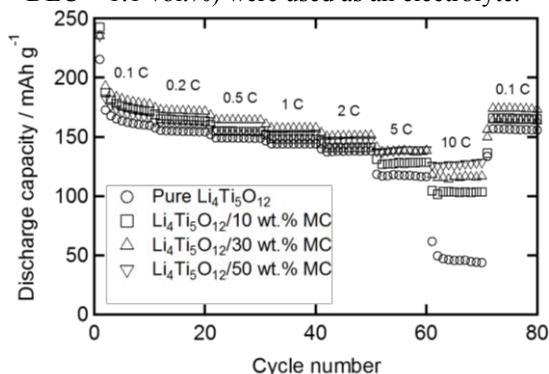


Fig.1 Discharge capacity versus cycle number at different discharge rates (0.1 C–10 C).



# In-Situ EC-STM, EQCM and EIS Studies of interfacial processes in Na ion battery electrolytes

Lukas Seidl<sup>1,2</sup>, Luis Flacke<sup>1</sup>, Sladjana Martens<sup>2</sup>, Ulrich Stimming<sup>1,3</sup>, Oliver Schneider<sup>2</sup>

<sup>1</sup>*Physik-Department, Technische Universität München  
James-Franck Str. 1, 85748 Garching  
lukas.seidl@tum.de*

<sup>2</sup>*Institute für Informatik 6, Technische Universität München  
Boltzmannstr. 3, 85748 Garching*

<sup>3</sup>*School of Chemistry, Newcastle University  
Queen Victoria Road, Newcastle Upon Tyne, NE1 7RU*

Li<sup>+</sup>-ion batteries (LIBs) are the state of the art energy storage technology in the transport sector and for portable electronic devices[1]. With respect to large scale applications, for instance as electricity buffer in combination with renewable energy sources, such as solar and wind power, LIBs suffer from high costs, mainly caused by the high Li-metal price, and limited resources[2]. While Li has a price of more than 4\$US per kg, the price of 1kg Na is much less 0.5\$US[3], and it is evenly distributed throughout the world, making it hence a promising Li-substitute.

Similar to the case of LIB anodes, it would be desirable to also use graphitic anodes for Na<sup>+</sup>-ion batteries, not only due to their ease in handling and their low costs, but also, because at least for Li ions the metal ion intercalation is highly reversible. For Na<sup>+</sup>-ions however, theoretical first-principal calculations predicted that no binary Na-graphite-intercalation-compounds (Na-GIC) can form due to an energetic instability[4]. Nevertheless, it was experimentally shown that Na<sup>+</sup>-ions can very well intercalate into graphite in the presence of an appropriate solvation shell, which leads to the formation of ternary Na-GICs[5].

In the present study, a range of electrolytes composed of sodium-salts, such as NaClO<sub>4</sub>, NaPF<sub>6</sub> and NaOTf, in combination with a variety of carbonate- (ethylene carbonate (EC), dimethyl carbonate (DMC), propylene carbonate (PC)) and ether-based solvents (mono-, di-, tri- and tetraglyme) is tested in view of their ability to form ternary Na-GICs. Electrochemical tests are the starting point, being complemented by application of in-situ methods, like Electrochemical Scanning Tunneling Microscopy (EC-STM) (Figure 1), the Electrochemical Quartz Crystal Microbalance technique (EQCM) and Electrochemical Impedance Spectroscopy (EIS).

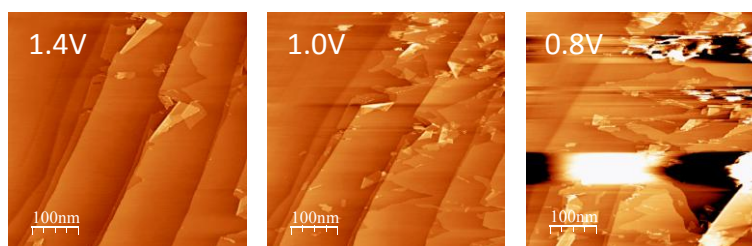


**Figure 1:** EC-STM images of a graphite electrode showing an exfoliation as a result of the cointercalation of Na<sup>+</sup>-ions and PC molecules, at different potentials with respect to Na/Na<sup>+</sup>

- [1] M. Armand, J.M. Tarascon, *Nature*. 451 (2008) 652–7.
- [2] J.B. Goodenough, *J. Solid State Electrochem.* 16 (2012) 2019–2029.
- [3] V. Palomares, P. Serras, I. Villaluenga, K.B. Hueso, J. Carretero-González, T. Rojo, *Energy Environ. Sci.* 5 (2012) 5884.
- [4] K. Nobuhara, H. Nakayama, M. Nose, S. Nakanishi, H. Iba, *J. Power Sources*. 243 (2013) 585–587.
- [5] B. Jache, P. Adelhelm, *Angew. Chem. Int. Ed. Engl.* 53 (2014) 10169–73.

# On the high and low temperature performances of Na-ion batteries: Hard carbon as a case study

A. Ponrouch,<sup>1</sup> C. Frontera,<sup>1</sup> F. Bardé,<sup>2</sup> M.R. Palacín<sup>1</sup>  
1. Institut de Ciència de Materials de Barcelona (ICMAB-CSIC)  
Campus UAB, E-08193 Bellaterra, Catalonia (Spain).  
aponrouch@icmab.es

Research on sodium-ion battery materials has recently boosted within the scientific community, as sodium resources are “unlimited”, low cost, and geographically distributed. [1,2] As graphite does unfortunately not significantly insert sodium ions [3], hard carbon (HC hereafter) is today the only practical negative electrode active material. Its main drawback is the high irreversible capacity upon the first cycle, well known also in Li-ion cells, which has important implications for cell balancing. This phenomenon is commonly related to surface reactivity and thus we have attempted to reduce it through coating. We developed a simple physical method, enabling conformal uniform particle coating [4,5] decreasing the surface area and allowing significant improvement in terms of the first cycle coulombic efficiency. [6]

After mitigation of the first cycle irreversible capacity loss, we became interested on the thermal dependence of HC electrochemical performance. The impressive thermal stability window of electrolytes based on a mixture of ethylene carbonate (EC) and propylene carbonate (PC) (vitreous transition for temperatures near -95°C and a single exothermic peak around 250°C in the DSC curves) [7] prompted us to undertake a systematic study on the electrochemical performances of HC electrodes tested at various temperatures ranging from -15°C up to 75°C. The performances of carbon coated HC cycled at 25°C and 75°C were evaluated at various C rates. A significantly higher reversible capacity is recorded upon cycling at 75°C (ca. 450 mAh/g at C/10) than at 25°C (ca. 325 mAh/g at C/10) with similar coulombic efficiencies (higher than 99% after 5 cycles). The reversible capacities recorded upon cycling at 0°C (ca. 260 mAh/g) and -15°C (ca. 265 mAh/g) at C/10 are very similar to the one achieved at 25°C and in all cases the coulombic efficiency was found to be higher than 99%. [6]

Electrochemical performances of HC at various temperatures pointed at the IR drop of the cell being determinant for achieving the highest reversible capacity (450 mAh/g at C/10, 75°C) and rate capability (340 mAh/g at 2C, 75°C) ever reported. Overall such results are encouraging in terms of high and low temperature Na-ion batteries operation which is highly important for application.

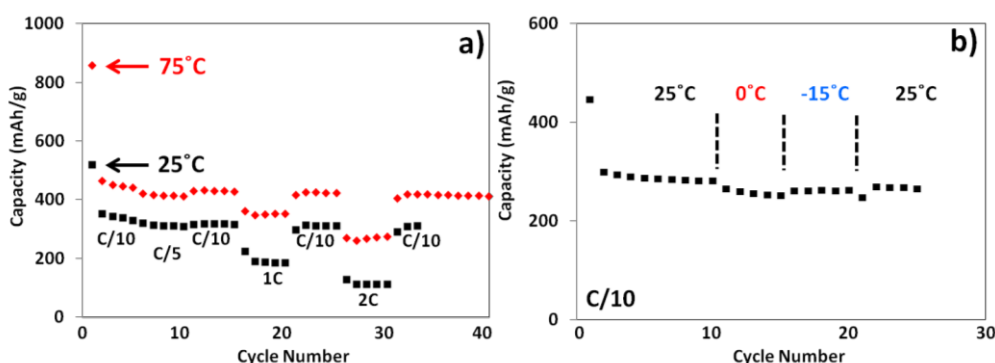


Fig. 1 Discharge capacity versus cycle number of carbon coated hard carbon cycled at temperatures ranging from -15°C to 75°C and at C rates ranging from C/10 up to 1C for both charge and discharge.

- [1]. N. Yabuuchi, K. Kubota, M. Dahbi, S. Komaba, *Chem. Rev.*, 114 (2014) 11636.
- [2]. A. Ponrouch, D. Monti, A. Boschini, B. Steen, P. Johansson, M. R. Palacín, *J. Mater. Chem. A*, 3 (2015) 22.
- [3]. A. Metrot, D. Gurerard, D. Billaud, A. Herold, *Synthetic Metals*, 1 (1979) 363.
- [4]. A. Ponrouch, A. R. Goñi, M. T. Sougrati, M. Ati, J.-M. Tarascon, J. Nava-Avendaño, M. R. Palacín, *Energy Environ. Sci.*, 6 (2013) 3363.
- [5]. A. Ponrouch, M. R. Palacín, *ECS Trans.*, 58 (2014) 27.
- [6]. A. Ponrouch, M.R. Palacín, *Electrochem. Commun.*, 54 (2015) 51.
- [7]. A. Ponrouch, E. Marchante, M. Courty, J.- M. Tarascon, M. R. Palacín, *Energy Environ. Sci.*, 5 (2012) 8572.



# Au-nanocrystals-decorated $\delta$ -MnO<sub>2</sub> as efficient catalytic cathode for high-performance Li-O<sub>2</sub> batteries

Guoqing Wang,<sup>a</sup> Shuangyu Liu,<sup>ab</sup> Jian Xie,<sup>\*ac</sup> Fangfang Tu,<sup>a</sup> Huiying Yang,<sup>b</sup> Shichao Zhang,<sup>d</sup> Tiejun Zhu,<sup>a</sup> Gaoshao Cao,<sup>c</sup> Xinbing Zhao<sup>ac</sup>

<sup>a</sup>State Key Laboratory of Silicon Materials, School of Materials Science and Engineering, Zhejiang University, Hangzhou 310027, China

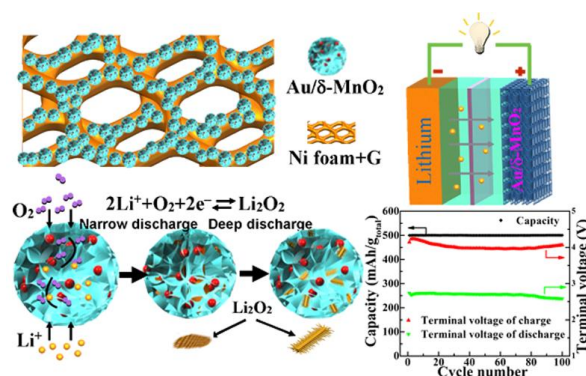
<sup>b</sup>Pillar of Engineering Product Development, Singapore University of Technology and Design, 20 Dover Drive, Singapore 138682, Singapore

<sup>c</sup>Key Laboratory of Advanced Materials and Applications for Batteries of Zhejiang Province, Hangzhou 310027, China

<sup>d</sup>School of Materials Science and Engineering, Beijing University of Aeronautics and Astronautics, Beijing 100191, China

[21126107@zju.edu.cn](mailto:21126107@zju.edu.cn), [xiejian1977@zju.edu.cn](mailto:xiejian1977@zju.edu.cn)

Li-O<sub>2</sub> battery works based on the reversible formation and decomposition of Li<sub>2</sub>O<sub>2</sub>, which is insulating and highly reactive. Designing catalytic cathode capable of controlling the Li<sub>2</sub>O<sub>2</sub> growth recently becomes a challenge to overcome this barrier. In this work, we gave a new design of catalytic cathode by growing porous honeycomb-like Au/ $\delta$ -MnO<sub>2</sub> electrocatalyst directly on conductive substrate. We found that Au/ $\delta$ -MnO<sub>2</sub> can catalyze the directed growth of Li<sub>2</sub>O<sub>2</sub> into thin/small form, only inside  $\delta$ -MnO<sub>2</sub> honeycombs, and along the surface of  $\delta$ -MnO<sub>2</sub> sheets. We proposed the catalytic mechanism of Au/ $\delta$ -MnO<sub>2</sub>, where Au plays a critical role in catalyzing the nucleation, crystallization and conformal growth of Li<sub>2</sub>O<sub>2</sub> on  $\delta$ -MnO<sub>2</sub> sheets. Li-O<sub>2</sub> batteries with Au/ $\delta$ -MnO<sub>2</sub> catalytic cathode show excellent electrochemical performance due to this favorable Li<sub>2</sub>O<sub>2</sub> growth habit. The battery yields a high capacity of 10600 mAh g<sup>-1</sup> with a low polarization of 0.91 V at 100 mA g<sup>-1</sup>. Superior cycling stability can be achieved in both capacity-limited (500 mAh g<sup>-1</sup>, 165 times at 400 mA g<sup>-1</sup>) and unlimited (ca. 3000 mAh g<sup>-1</sup>, 50 cycles at 800 mA g<sup>-1</sup>) modes.



## References:

- 1 S. Y. Liu, G. Q. Wang, J. Xie, F. F. Tu, H. Y. Yang, S. C. Zhang, T. J. Zhu, G. S. Cao, X. B. Zhao, *Nanoscale*, 2015, DOI: 10.1039/C5NR01344E
- 2 S. Y. Liu, Y. G. Zhu, J. Xie, Y. Huo, H. Y. Yang, T. J. Zhu, G. S. Cao, X. B. Zhao, S. C. Zhang, *Adv. Energy Mater.*, 2014, 4(9)

# In-situ STM characterization of ionic liquids on Au(111) and HOPG electrodes in the presence of lithium salt

Xiao-Yan Hu, Jia-Wei Yan, Bing-Wei Mao

*State Key Laboratory of Physical Chemistry of Solid Surfaces, College of Chemistry and Chemical Engineering, Xiamen University, Xiamen 361005, China*  
jwyan@xmu.edu.cn

Ionic liquids (ILs) as electrolytes for lithium batteries have attracted considerable attention due to their unique properties such as wide electrochemical window, non-flammability, and thermal stability and environment friendly, which can lead to a great improvement in system safety<sup>[1]</sup>. Understanding the interfacial property of electrode/IL interface is extremely important for successful applications of ionic liquids in electrochemical energy devices<sup>[2]</sup>. In this article, we employ in-situ STM combined with electrochemical measurements to investigate the surface processes of Au(111) and HOPG electrodes in TFSI and FSI based ionic liquids containing 0.5 mol·L<sup>-1</sup> LiTFSI. On Au(111), the presence of the lithium salt has a predominant influence on the structure and property of the Au(111)/IL interfaces. Tremendous morphological changes occur upon cathodic potential excursion: formation of lithium oxide film corresponding to the reduction of oxygen in stage I; formation of loose monolayer film to highly faceted morphology as a result of the reduction of trace amount of water in stage II; initial stage of SEI formation in stage III as a consequence of the decomposition of ionic liquid, the deposition of lithium as well as the formation Au–Li alloying<sup>[3]</sup>. We mention that the CVs of Au(111) in different ionic liquids show similar characteristics and therefore we would expect that the formation of SEI on Au(111) in ionic liquids may be a common feature in the presence of lithium salt. On HOPG, the addition of Li salt can promote the decomposition of FSI anion and the formation of SEI in Py<sub>13</sub>FSI, and thus further suppress the intercalation of the cations and decomposition of the ionic liquid solvent to a certain extent. However, the SEI formed in Py<sub>13</sub>TFSI containing Li salt cannot efficiently passivate the surface so that large scale exfoliation of HOPG is still observed. The results imply that the chemical compositions of the SEIs in Py<sub>13</sub>FSI and Py<sub>13</sub>TFSI are considerably different, which critically influence the compatibility of the ionic liquids with graphite electrodes. In addition, trace amounts of oxygen and water can cause the formation of a film-like structure on Au(111), but show no apparent influence on HOPG.

**Acknowledgments** This work was supported by the National Basic Research Program of China (2012CB932902) and the National Natural Science Foundation of China (21033007, 20973144, 21321062).

## Reference

- [1] M. Galinski, A. Lewandowski, I. Stepniak, *Electrochim. Acta*, 2006, 51, 5567–5580.
- [2] Y. Z. Su, Y. C. Fu, Y. M. Wei, J. W. Yan, B. W. Mao, *ChemPhysChem*, 2010, 11, 2764–2778.
- [3] X.Y. Hu, C.L. Chen, S. Tang, W.W. Wang, J.W. Yan, B.W. Mao, *Chinese. Sci. Bull.*, 2015, Ahead of Print.

# Effect of Electrode Composition on the Electrochemical Performance of the MnO Negative Electrode Materials for Li-ion Batteries

Duri Kim, Mina You, and Ji Heon Ryu\*

Graduate School of Knowledge-based Technology and Energy, Korea Polytechnic University  
Sangidaehak-ro, Siheung-si, Gyeonggi-do 429-793, Korea  
ryujh@kpu.ac.kr

Transition metal oxides ( $\text{MO}_x$ ,  $M = \text{Co}, \text{Fe}, \text{Mn} \dots$ ) are negative electrode active materials for high-capacity lithium-ion batteries because of their excellent lithium storage capability by conversion reaction. The  $\text{MO}_x$  has high theoretical specific capacity, however, it has very weak points of poor energy efficiency (both of the Coulombic and voltage efficiency) and low operating cell voltage due to the high reaction voltage of negative electrode.

$\text{MnO}$  is the promising transition metal oxide-based negative electrode material with high theoretical specific capacity of 740 mAh/g because of its low cost and relatively low reaction voltage, which is reversibly decomposed to metallic Mn and  $\text{Li}_2\text{O}$ .

In this study, we tried to investigate the electrochemical performance of MnO electrodes with the variation of particle size and electrode composition. The purchased MnO and ball-milled MnO (BM-MnO) were used as active materials for the variation of particle size. BM-MnO was prepared by planetary-mill with alumina ball and ethanol as dispersant for 1 hr with 350 rpm. The composite electrodes were prepared by coating the slurry of active material, PVdF (polyvinylidene fluoride) binder, and conducting aid (denka black) with 90:5:5, 80:10:10 and 70:15:15 compositions on a piece of Cu foil. The coin-type cell (CR2032) were assembled in a glove box with Li foil, 1 M  $\text{LiPF}_6$  in EC : EMC (3 : 7 in volume. ratio) as the electrolyte, and a PP separator. Electrochemical performances were evaluated by using battery cycler (WBCS3000).

Both the initial capacity and cycle performance of MnO were improved as the contents of carbon black increased regardless whether milling or not. Because the BM-MnO had smaller particle size and high surface area, it need more electronic pathways. Therefore, the BM-MnO showed under 300 mAh/g at both ambient and elevated temperature except the case of 15 % carbon black. The MnO materials went through the conversion reaction and converted to the nanosized Mn and  $\text{Li}_2\text{O}$ . The electrochemical performance might be strongly related at the electronic pathway as well as the particle size of metal oxide. And then, both the MnO and BM-MnO had very poor cycle performance at elevated temperature (60°C). The effect of electrode configuration on the high-temperature performance will be also presented.

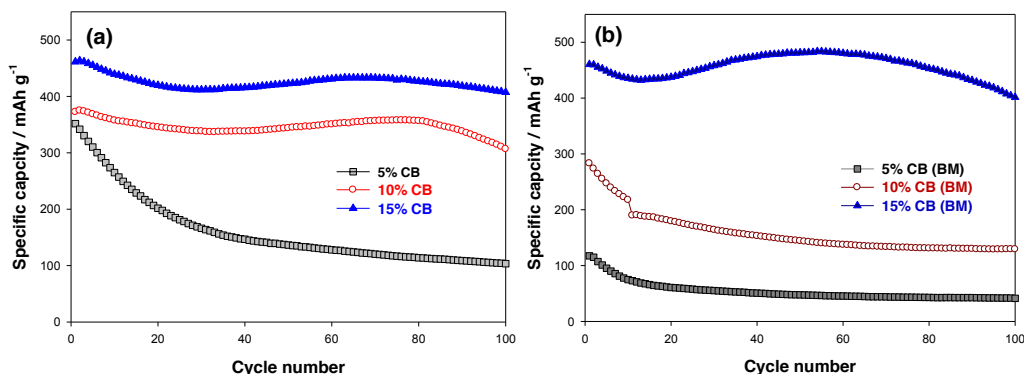


Figure 1. Cycle performance of (a) MnO and (b) BM-MnO at room temperature.

# Improvement of High-Temperature Performance of the $\text{LiMn}_2\text{O}_4$ Positive Electrode by the Addition of $\text{Li}_3\text{PO}_4$

Min Young Hong, Hyojin Jung, and Ji Heon Ryu\*

*Graduate School of Knowledge-based Technology and Energy, Korea Polytechnic University  
Sangidaehak-ro, Siheung-si, Gyeonggi-do 429-793, Korea  
ryujh@kpu.ac.kr*

$\text{LiMn}_2\text{O}_4$  (LMO) has been attracted attention as the positive material of large-scale Li-ion batteries for EVs or ESS because of the characteristic of low cost and superior safety. However, its wide commercial use has been restricted due to the poor electrochemical performance at high temperature. Potential failure modes are the degradation of graphite negative electrode by the attack of Mn(II) ion dissolved from the LMO positive electrode. Therefore, most of the previous researches are focused on the inhibition of Mn dissolution from the LMO or the prevention of the electro-reduction of Mn(II) ion at the surface of the negative electrode.

In this study, we tried to remove the dissolved Mn ions in the electrolyte by the precipitation method. Also, we found that the addition of  $\text{Li}_3\text{PO}_4$  in the electrolyte could sharply reduce the concentration of Mn(II) ion. The Mn ions were expected to be precipitated to the  $\text{Mn}_3(\text{PO}_4)_2$  by the reaction with  $\text{PO}_4$  anions.

The standard LMO electrode was prepared with the LMO (Aldrich), carbon black (Super P), and polymeric binder (KF1100) in a weight ratio of 8:1:1. The 1 and 5 weight % of the  $\text{Li}_3\text{PO}_4$  were also added respectively to the mixture during the electrode preparation process. The addition of the  $\text{Li}_3\text{PO}_4$  improved the electrochemical performance at 60°C and the use of 1 weight %  $\text{Li}_3\text{PO}_4$  was the best because of the loss of initial specific capacity at the use of 5 weight %.

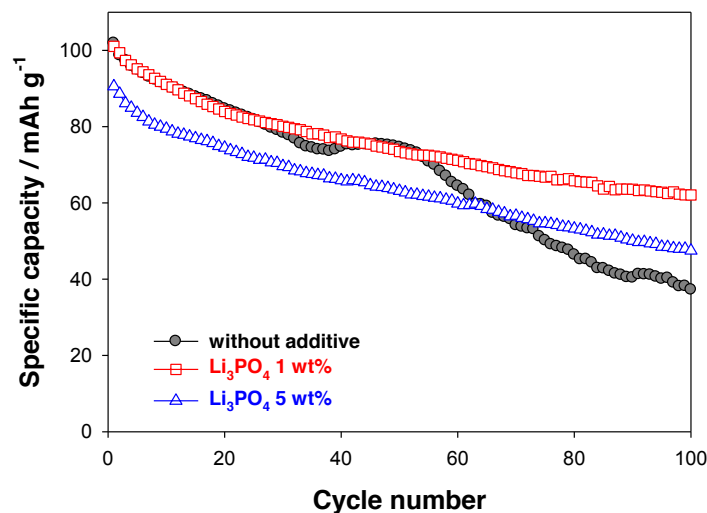


Figure 1. Cycle performance of  $\text{LiMn}_2\text{O}_4$  with  $\text{Li}_3\text{PO}_4$  additives at high temperature.

# **Silicon-carbon anode by plasma enhanced chemical vapor deposition for lithium-ion batteries**

Chen-Hsuan Lai, Ing-Song Yu\*, Fa-Hsing Yeh,

*Department of Materials Science and Engineering, National Dong-Hwa University*

*No. 1, Sec. 2, Da Hsueh Rd., Shoufeng, Hualien 97401, Taiwan, R.O.C.*

[benson40310@gmail.com](mailto:benson40310@gmail.com), [isyu@mail.ndhu.edu.tw](mailto:isyu@mail.ndhu.edu.tw)\*

The demand of high performance of Li-ion battery anode is increasing for the defense industry and livelihood. Recently, silicon-carbon composites were proposed to promote the electrochemical properties of Li-ion battery. Various technologies can be employed to fabricate Si-C composite for the anode of Li-ion battery. In this study, we tried to deposit Si films (from 240 nm to 960 nm) on the surface on carbon anode by plasma enhanced chemical vapor deposition (PECVD) at low temperature. We can find small amount of Si can improve the capacity of anode. As the thickness of Si thin film increase, we can get better charge-discharge performance of anode. First irreversible discharge capacity and second discharge capacity is very stable in compare with other Si-C anode materials. Besides, in repeatedly cycling test, the charge-discharge capacity did not drop quickly because of silicon. Our method does improve the volume expansion problem of Si-C composite anodes. The coulombic efficiency is higher than 85% for all samples. From the results of secondary electron microscopy (SEM) and Raman spectroscopy, the sample with Si thickness 960 nm has better electrical capacity and its surface has better protection for the carbon anode. From the electron probe microanalyzer (EPMA) analysis, we can find silicon deposited uniformly and the content increasing for longer deposition time. In conclusion, this research has proposed a creative method to prepare the anode of Li-ion battery. Our experiments have proved carbon anode with Si films by PECVD higher capacity and high coulombic efficiency for the anode of Li-ion battery.

# A Novel Air Electrode Comprising Core-Shell Particles for MH/Air Secondary Battery

Hideyuki Sano<sup>1</sup> and Masatsugu Morimitsu<sup>\*1,2</sup>

<sup>1</sup>Department of Science of Environment and Mathematical Modeling,

<sup>2</sup>Department of Environmental Systems Science,  
Doshisha University

1-3 Tatara-miyakodani, Kyotanabe, Kyoto 610-0394, Japan

\*E-mail: mmorimit@mail.doshisha.ac.jp

A metal hydride (MH)/air secondary battery consists of a gas diffusion electrode as the positive electrode, a hydrogen storage alloy as the negative electrode, and a KOH solution as the electrolyte. Oxygen in air reacts at the positive electrode during discharge, which means that the MH/air battery has no active mass stored in the positive electrode so that the weight and volume of the positive electrode are unnecessary to increase with increasing battery capacity. This is particular to this battery, since other air batteries have a limitation on the discharge capacity of the positive electrode because of the plugging by solid discharge product. From the reasons, we have been developing the MH/air secondary battery especially for high energy density applications such as electric vehicles. While in our previous studies, the conductive and catalyst-supporting material of the positive electrode was nickel powders, which have high durability in alkaline media and have shown a good cycleability for oxygen evolution and reduction [1], a further development is necessary for the positive electrode to reduce the weight and polarization for oxygen reactions. In this work, we tried to apply core-shell material to the positive electrode instead of nickel powders, which was nickel coated oxide particles and the oxide was smaller than nickel in density, in order to develop a novel positive electrode in combination with  $\text{Bi}_2\text{Ir}_2\text{O}_{7-z}$  and PTFE. The preparation procedure and performance of the novel positive electrode were examined, and the MH/Air secondary battery using the developed positive electrode was assembled and evaluated.

The core-shell material was nickel coated silica particles and  $\text{Bi}_2\text{Ir}_2\text{O}_{7-z}$  powders used as the bi-functional catalyst were prepared through co-precipitation in the solution dissolving  $\text{H}_2\text{IrCl}_6$  and  $\text{Bi}(\text{NO}_3)_3$  by addition of excess NaOH solutions, followed by calcination of the precipitates. These were mixed with PTFE and pressed onto a nickel mesh to form a sheet, and finally heated at 370 °C under nitrogen atmosphere to make the positive electrode. Cyclic voltammetry was performed to measure the polarization of the positive electrode with a three electrode cell in which one side of the positive electrode touched air and the other side faced 6 mol/L KOH solutions. The battery performance was further studied with using the MH negative electrode comprising  $\text{A}_2\text{B}_7$  type of hydrogen storage alloys. The negative electrode was produced by and supplied from FDK Co., Ltd.

The positive electrode comprising nickel coated silica particles was successfully developed, in which the oxide catalyst was loaded and dispersed on the core-shell particle well by the new method developed in this work. The oxygen reduction behaviors of the positive electrode were examined by cyclic voltammetry, and the result is shown with that obtained with the positive electrode using nickel powders [1], as shown in Fig. 1. The weight of the developed electrode was reduced by 48% compared to the previous nickel-based electrode, and the cathodic polarization was decreased in this study. The MH/Air secondary battery in this work also showed stable voltages for charge and discharge for more than 10 hours.

*This work was financially supported by “Advanced Low Carbon Technology Research and Development Program (ALCA)” of Japan Science and Technology Agency (JST). The authors acknowledge FDK Co., Ltd. for supplying the MH negative electrode.*

## Reference

[1] S. Terui, M. Morimitsu, The 226th ECS Meeting, #2182, Cancun (2014).

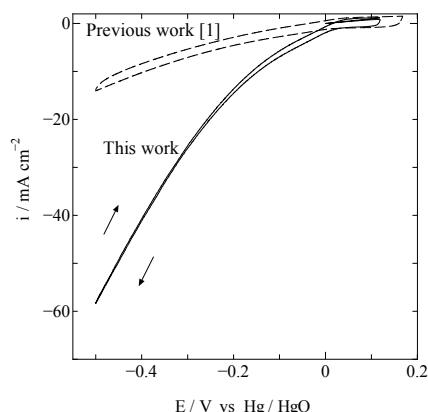


Fig.1 Cyclic voltammograms of the positive electrodes at 5 mV/s.

# High Capacity and High Energy Density of Air Secondary Battery Using Metal Hydride Negative Electrode

Tsukasa Gejo<sup>1</sup>, Shintaro Terui<sup>1</sup>, and Masatsugu Morimitsu<sup>\*1,2</sup>

<sup>1</sup>Department of Science of Environment and Mathematical Modeling,

<sup>2</sup>Department of Environmental Systems Science,  
Doshisha University

1-3 Tatara-miyakodani, Kyotanabe, Kyoto, 610-0394, Japan

\*E-mail: mmorimit@mail.doshisha.ac.jp

A metal hydride/air secondary battery is a new class of air battery, which consists of hydrogen storage alloy in the negative electrode in combination with alkaline aqueous solutions and the air electrode. This battery has a very unique property; no plugging by discharge product occurs on the positive electrode so that discharge capacity has no limitation on the positive electrode. This means that the battery capacity and energy density are significantly dependent of the capacity and capacity density of the negative electrode. In this study, the negative electrode with hydrogen storage alloys was modified in composition and activation process to improve the capacity and the capacity density, and then the MH/air secondary battery using the modified negative electrode was examined. We evaluated the capacity, capacity density, and MH utilization of the negative electrode and the cell voltage, capacity, and energy density of the battery to compare to our previous results [1].

MH negative electrodes were produced by and supplied from FDK Co., Ltd. and comprised a porous nickel matrix containing an  $A_2B_7$  type of hydrogen storage alloy and a binder, in which the electrode size (4.0 cm x 4.6 cm, 0.52 to 0.73 mm in thickness) are almost the same as the previous ones [1]. The capacity of the MH electrode was varied with the amount and weight ratio of hydrogen storage alloy. The activation process of the negative electrode was carried out with changing the charge-discharge rate, the overcharge ratio, and others. For this experiment, the MH electrode was placed and pressurized between two  $Ni(OH)_2$  electrodes with 6 mol/L KOH solutions. The MH/air battery was assembled in a PTFE container, in which from the bottom to the top, there were the negative electrode, the membrane separator with 6 mol/L KOH solutions, and the positive electrode. The positive electrode was the mixture of graphite as conductive material,  $Bi_2Ir_2O_{7-z}$  as bi-functional catalyst, and PTFE as binder, which was the same as the previous one [1].

Some parameters of the activation process of the MH negative electrode influenced on the practical discharge capacity, the MH utilization, and the polarization during charge and discharge. The optimization of such parameters was done and the activated negative electrodes achieved 1.8 Ah, 1,929 Ah/L, and 301 Ah/kg (labeled as NE-A) or 2.3 Ah, 1,707 Ah/L, and 279 Ah/kg (labeled as NE-B), which were improved in capacity or capacity density compared to the previous results [1]. Figure 1 shows the comparison of discharge curves of MH/air secondary batteries using the negative electrodes of NE-A and NE-B in this study and that of the previous study. While the discharge voltages of these three batteries are almost the same in Fig. 1, the discharge capacity is increased in the batteries developed in this study. The energy densities were 868 Wh/L and 126 Wh/kg (with NE-A) and 825 Wh/L and 130 Wh/kg (with NE-B), and the high capacity battery with NE-B discharged 2.19 Ah. The volumetric energy density of 800 Wh/L is beyond the theoretical one of lithium ion secondary battery (LIB), and the results obtained in this study has proven that the MH/air secondary battery has a higher potential in energy density than LIB.

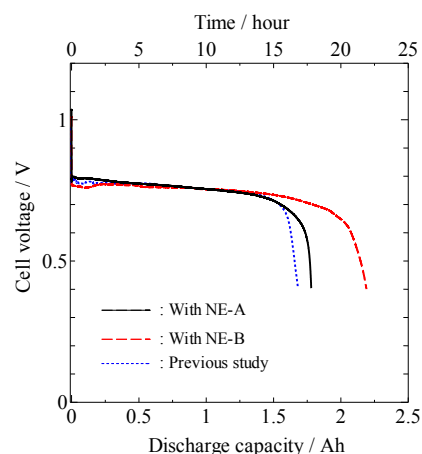


Fig. 1 Comparison of discharge curves of MH/Air secondary batteries at 0.1 C.

*This work was financially supported by “Advanced Low Carbon Technology Research and Development Program (ALCA)” of Japan Science and Technology Agency (JST). The authors acknowledge FDK Co., Ltd. for supplying the MH negative electrode.*

Reference: [1] S.Terui, M. Morimitsu, 226<sup>th</sup> ECS meeting, Abs#2182, Cancun, Mexico (2014).



# Durable Mesoporous Core-Shell Lithium Titanate-Carbon Composite as Anode in Lithium ion Batteries

Chi-Ying Vanessa Li\*, Ching-Kit Ho, Zhao-Feng Deng and Kwong-Yu Chan<sup>^</sup>

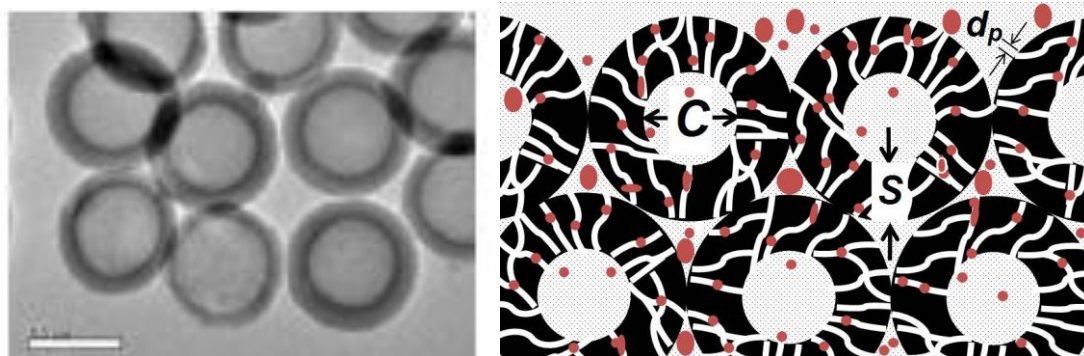
Department of Chemistry, The University of Hong Kong,

Pokfulam, Hong Kong

\* [cyvli@hku.hk](mailto:cyvli@hku.hk), <sup>^</sup> [hsccky@hku.hk](mailto:hsccky@hku.hk)

Lithium titanate, particularly  $\text{Li}_4\text{Ti}_5\text{O}_{12}$  has been applied as viable anode materials in Li-ion batteries due to its good structure stability. [1-3] Present material forms lack mesoporous structures and surface area for reactions, restricting the energy and power densities of Li-ion battery system. With the high discharge rate performance limited by the low electronic conductivity of the material ( $< 10^{-11} \text{ Sm}^{-1}$ ), addition of carbon is one of the effective way in enhancing the rate performance and operation temperature range. [1]

In this study,  $\text{Li}_4\text{Ti}_5\text{O}_{12}$ -carbon composites were synthesized by impregnation of  $\text{Li}_4\text{Ti}_5\text{O}_{12}$  into hollow core mesoporous shell hierarchical carbon of controlled dimensions. These  $\text{Li}_4\text{Ti}_5\text{O}_{12}$ -carbon composites benefit from higher electronic conductivity, increased surface area of the active material and possibly length scale effect. With controlled structure of HCMS in terms of hollow core diameter, thickness of the shell and diameter of the mesopores, the electrochemical behavior of mesoporous  $\text{Li}_4\text{Ti}_5\text{O}_{12}$ -carbon composite was optimized.



(left) TEM image of the starting precursor – hollow core mesoporous shell carbon; and (right) Schematic diagram of nanoparticles of  $\text{Li}_4\text{Ti}_5\text{O}_{12}$  embedded in the HCMS carbon with controllable structure (diameter of hollow core (C), thickness of the mesoporous shell (S), and pore diameter ( $d_p$ ); red dots are  $\text{Li}_4\text{Ti}_5\text{O}_{12}$  nanoparticles).

## Acknowledgement

This work was supported by The University of Hong Kong (HKU) Strategic Research Theme on Clean Energy, University Development Fund on Initiative on Clean Energy, and Innovation and Technology Fund of the Hong Kong SAR (ITS/076/11).

## References

1. C.Y.V. Li, C.K. Ho, Z.F. Deng, and K.Y. Chan, Electrochemical Study of Mesoporous Core-Shell Lithium Titanate Carbon Composite with Controlled Microstructure As Anode in Lithium Ion Batteries for Wide Temperature Range, *2014 AIChE Annual Meeting, November 2014, Atlanta, GA, U.S.A.*
2. S.W. Ting, C.Y.V. Li, H. Yung, C.K. Ho and K.Y. Chan, Structural and Electrochemical Studies of Mesoporous  $\text{Li}_4\text{Ti}_5\text{O}_{12}$ - $\text{TiO}_2$  Composite Spheres as Anode Material for Lithium ion Batteries, *222nd ECS Meeting, October 2012, Honolulu, Hawaii, U.S.A.*
3. C.Y.V. Li, S.W. Ting, Z. Yang, W. Zhuang, X. Lu, H. Yung and K.Y. Chan, Lithium Titanate Prepared from Mesoporous  $\text{TiO}_2$  Fiber as Anode Material for Lithium Ion Batteries, *222nd ECS Meeting, October 2012, Honolulu, Hawaii, U.S.A.*



# Output Performance of MH/Air Secondary Battery using $\text{Bi}_2\text{Ru}_2\text{O}_{7-z}$ Catalyst in Positive Electrode

Shohei Yamaguchi<sup>1</sup> and Masatsugu Morimitsu<sup>\*1,2</sup>

<sup>1</sup>Department of Science of Environment and Mathematical Modeling,

<sup>2</sup>Department of Environmental Systems Science,

Doshisha University

1-3 Tatara-miyakodani, Kyotanabe, Kyoto, 610-0394, Japan

\*E-mail: mmorimit@mail.doshisha.ac.jp

A metal/air battery is one of the promising candidates for next generation secondary battery, because of high theoretical energy density over a lithium ion secondary battery (LIB), although no metal/air secondary battery has achieved such high performance in operation so that the development of the air secondary batteries utilizing a variety of negative electrode's materials (Li, Na, Ca, or Mg) is in progress. A novel rechargeable air battery has been also investigating by our group, which uses hydrogen storage alloy in the negative electrode with concentrated KOH solutions and the discharge and charge reactions are water generation and decomposition [1]. The positive electrode's reactions are oxygen reduction and evolution during discharge and charge, and the polarization of the positive electrode significantly depends on the bi-functional oxygen catalyst, which was pyrochlore type of composite oxide,  $\text{Bi}_2\text{Ir}_2\text{O}_{7-z}$  in our previous work [1]. In this study, another pyrochlore oxide,  $\text{Bi}_2\text{Ru}_2\text{O}_{7-z}$ , was applied to the oxygen catalyst, and the preparation, characterization, and performance of the oxide catalyst were investigated. The positive electrode and MH/air battery using the catalyst were also developed to examine the output performance and compare to the previous one using  $\text{Bi}_2\text{Ir}_2\text{O}_{7-z}$ .

$\text{Bi}_2\text{Ru}_2\text{O}_{7-z}$  was prepared through co-precipitation in the solution containing  $\text{RuCl}_3$  and  $\text{Bi}(\text{NO}_3)_3$  by adding NaOH solutions, followed by calcination of the precipitates. In the procedure, the concentration of NaOH, calcination temperature and time, and others were changed, and the obtained oxide for each condition was characterized by XRD, SEM, and EDX. The positive electrode comprising the oxide catalyst, Ni powders, and PTFE was prepared and the polarization behaviors were examined. The MH/air secondary battery consisted of the MH negative electrode supplied by FDK, the positive electrode, and the separator with KOH solution. The battery was operated with constant current at ambient temperature without air or oxygen flow to the positive electrode.

The obtained oxides were  $\text{Bi}_2\text{Ru}_2\text{O}_{7-z}$  without byproduct when the examined firing temperature ranged from 500 °C to 800 °C, while the concentration of NaOH showed some effects on crystallographic structure and particle size of the oxide. The particle size of  $\text{Bi}_2\text{Ru}_2\text{O}_{7-z}$ , which was 20-50 nm, was smaller than that of  $\text{Bi}_2\text{Ir}_2\text{O}_{7-z}$  prepared at the same temperature and NaOH concentration in our previous study [1]. The positive electrode was fabricated using the oxide catalyst at different composition ratios from 10 wt% to 30 wt%, a fixed ratio (10wt.%) of PTFE, and nickel powders in balance, and the results on polarization for oxygen reduction and evolution during discharge and charge revealed that 25 wt.% of oxide was recommended, for which the positive electrode presented lower polarization for both  $\text{O}_2$  reactions than that with  $\text{Bi}_2\text{Ir}_2\text{O}_{7-z}$ . Furthermore, the possible discharge current of the MH/air secondary battery with  $\text{Bi}_2\text{Ru}_2\text{O}_{7-z}$  developed in this study was 900 mA in maximum and the output power density achieved 174 W/L, which was better than that with  $\text{Bi}_2\text{Ir}_2\text{O}_{7-z}$  [1], as shown in Fig. 1.

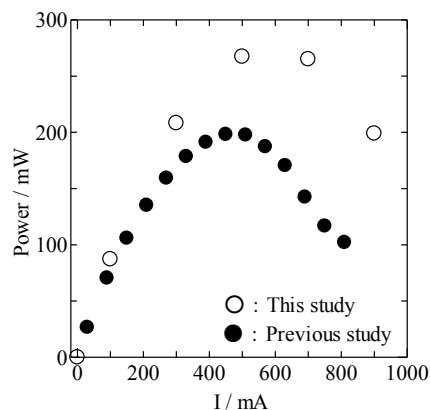


Fig. 1 Current-output power relationship of MH/air secondary batteries.

*This work was financially supported by “Advanced Low Carbon Technology Research and Development Program (ALCA)” of Japan Science and Technology Agency (JST). The authors acknowledge FDK Co., Ltd. for supplying the MH negative electrode.*

## Reference

- [1] H. Matsuda and M. Morimitsu, The 224<sup>th</sup> ECS meeting, Abs#26, San Francisco (2013).

# A High Energy Density of MH/Air Secondary Battery Using $A_2B_7$ Type of Hydrogen Storage Alloys

Chika Baba<sup>1</sup>, Kenji Kawaguchi<sup>2</sup>, and Masatsugu Morimitsu\*<sup>1,3</sup>

<sup>1</sup>Department of Science of Environment and Mathematical Modeling,

<sup>2</sup>Organization for Research Initiatives and Development,

<sup>3</sup>Department of Environmental Systems Science,

Doshisha University

1-3 Tatara-miyakodani, Kyotanabe, Kyoto 610-0394, Japan

\*E-mail: mmorimit@mail.doshisha.ac.jp

A metal/air secondary battery is expected as one of the next generation energy storage devices which could achieve a high energy density, since the positive electrode uses oxygen in air so that the discharge capacity theoretically depends only on the negative electrode. While many efforts have been done to realize this battery, it has been known that the discharge product of the air battery using less noble metals such as lithium and magnesium induces the plugging of the positive electrode, resulting in a small discharge capacity, a difficulty of a high current operation, and a poor cycleability. We have been also developing a different type of air battery from them, which comprises the negative electrode using hydrogen storage alloys in combination with an alkaline aqueous electrolyte, and our previous studies on the battery performance showed stable charge and discharge voltages and an improvement in power density [1]. However, a high capacity density of MH electrode is needed to further improve an energy density and a high rate performance. In this paper, we report an improvement in energy density of the MH/air secondary battery with using the negative electrode comprising  $A_2B_7$  type of hydrogen storage alloys with some modification in their composition and structure.

The negative electrode (MH electrode) used  $A_2B_7$  type of hydrogen storage alloys, Ni powders, and polyethylene powders, which were mixed and pressed to make a sheet of *ca.* 45 mm x 45 mm. Charge-discharge behaviors of the negative electrode were studied using a three-electrode cell equipped with the Hg/HgO reference electrode. The positive electrode (air electrode) was consisted of nickel powders as a conductive and catalyst-supporting material,  $Bi_2Ir_2O_{7-z}$  powders as a bi-functional catalyst, and a PTFE binder.  $Bi_2Ir_2O_{7-z}$  powders were prepared through the co-precipitation and calcination process; equimolar  $H_2IrCl_6 \cdot 6H_2O$  and  $Bi(NO_3)_3 \cdot 5H_2O$  were dissolved in water and then the precipitates obtained by adding excess NaOH solutions in the metal salt solution under oxygen bubbling, followed by washing, drying, and heating at 370 °C in  $N_2$  atmosphere. The MH/air secondary battery using these electrodes and 6 mol/L KOH solutions was operated at constant current at *ca.* 25 °C without air or oxygen flow to the positive electrode.

The discharge capacity of the improved negative electrode was about 1.8 Ah, which corresponded to the capacity density of 1789 Ah/L and 287 Ah/kg. The polarization behaviors of the negative electrode at different states of charge indicated that the negative electrode's resistance was *ca.* 0.2  $\Omega$ , irrespective of SOC. Figure 1 shows the charge-discharge curves of the MH/air secondary battery, in which the stable charge and discharge voltages are seen and the average voltages are *ca.* 1.56 V and *ca.* 0.79 V, respectively. The energy densities calculated from this result, which is based on the total volume or weight of the battery's components, are 779 Wh/L and 106 Wh/kg. The battery was able to operate at 1100 mA (83 mA/cm<sup>2</sup>) in maximum with no plugging, and the maximum power and power density were found to be 316 mW and 193 W/L.

This work was financially supported by "Advanced Low Carbon Technology Research and Development Program (ALCA)" of Japan Science and Technology Agency (JST). The authors also acknowledge FDK Co., Ltd. for supplying the MH negative electrode.

## References

[1] H. Matsuda and M. Morimitsu, The 224th ECS meeting, Abs#26, San Francisco (2013).

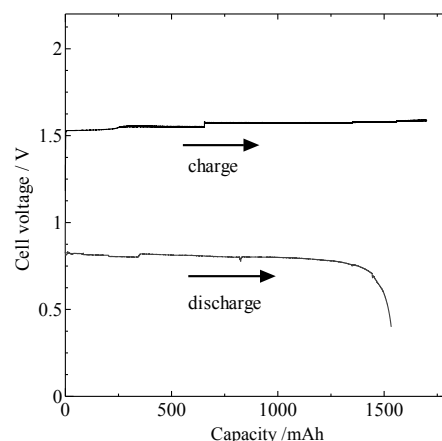


Fig. 1 Charge-discharge curves of the MH/air secondary battery at 100 mA.

# Synthesis of $\text{NaTi}_2(\text{PO}_4)_3$ thin-film and electrochemical behavior in aqueous solutions

Fumihiro Sagane

Department of Electronics and Materials Science, Graduate School of Engineering, Shizuoka University,  
3-5-1 Johoku, Naka-ku, Hamamatsu, Shizuoka, 432-8011, Japan  
e-mail sagane.fumihiro@shizuoka.ac.jp

$\text{Na}^+$ -ion secondary batteries have been paid much attention as the post  $\text{Li}^+$ -ion secondary batteries, due to their much abundant Na-resources. So far, we have found that the  $\text{Na}^+$ -ion transfer at the solid/organic solution interface was faster than that of  $\text{Li}^+$ -ion[1]. Therefore,  $\text{Na}^+$ -ion batteries are expected to exhibit high power by using highly ionic conductive aqueous solutions, although the energy densities is inferior to  $\text{Li}^+$ -ion batteries. In the present study,  $\text{NaTi}_2(\text{PO}_4)_3$  negative electrode reported by Okada, et.al. is focused[2]. In order to catch the electrochemical behavior clearly, the thin-film electrode without binders is synthesized and their electrochemical behavior in the aqueous solution is discussed.

$\text{NaTi}_2(\text{PO}_4)_3$  thin-film was synthesized by sol-gel method. The sol of  $\text{NaOC}_2\text{H}_5$ ,  $\text{Ti}(\text{OC}_3\text{H}_7)_4$ ,  $\text{P}_2\text{O}_5$  and ethanol was spin coated on the quartz substrate, and then the substrate was sintered at 1273 K under  $\text{O}_2$  flow condition.  $\text{NaTi}_2(\text{PO}_4)_3$  preparation was confirmed by X-ray diffraction and Raman spectroscopy, although a trace of  $\text{TiO}_2$  impurity was observed. From the scanning electron microscopy (SEM), the closely dispersed submicrometer-sized particles were observed, as shown in Fig 1. For the electrochemical measurements, carbon coat was conducted on the thin-film surface, which works as the conductive additives and current collectors. Cyclic voltammogram of the thin-film electrode in  $0.2 \text{ mol dm}^{-3} \text{ Na}_2\text{SO}_4(\text{aq})$  showed the sharp reduction and oxidation peak around at  $-0.8 \text{ V}$  (vs. $\text{Ag}/\text{AgCl}$ ), corresponding to the  $\text{Na}^+$ -ion insertion and extraction, respectively. Figure 2 shows the impedance spectrum of the thin-film electrode at  $-0.8 \text{ V}$ . One semi-circle was clearly observed and the semi-circle showed the electrode potential dependency. Therefore, we can conclude the semi-circle ascribes to the charge transfer resistance of  $\text{Na}^+$ -ion. From the temperature dependency of the interfacial resistance, the activation energy corresponding to the  $\text{Na}^+$ -ion insertion/extraction was calculated to be  $26 \text{ kJ mol}^{-1}$ . The result was much smaller than that of  $\text{Li}^+$ -ion transfer at the electrode/organic solution interface and which means the aqueous  $\text{Na}^+$ -ion batteries are expected to be high power. In the poster presentation, the  $\text{Na}^+$ -ion diffusion in the electrode materials will be also discussed.

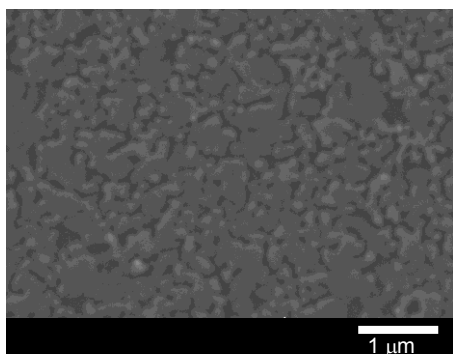


Fig.1 SEM image of the  $\text{NaTi}_2(\text{PO}_4)_3$  thin-film

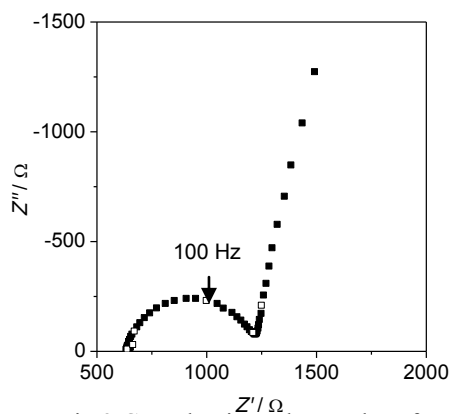


Fig.2 Complex impedance plot of  $\text{NaTi}_2(\text{PO}_4)_3$  thin-film in  $\text{Na}_2\text{SO}_4(\text{aq})$  at  $-0.8 \text{ V}$ .

## References :

- [1] F. Sagane, T. Abe, Y. Iriyama and Z. Ogumi, *J.Power Sources*, 146, 749-752 (2005).
- [2] S. Park, I. Gocheva, S. Okada and J. Yamaki, *J.Electrochem.Soc.*, 158 A1067-1070 (2011)

# Dynamics of the Phase Transition Behavior of the $\text{LiFePO}_4$ Investigated by Time-resolved X-ray Diffraction at Various Temperatures

Takuya Mori,<sup>1</sup> Kazufumi Otani,<sup>1</sup> Toshiyuki Munesada,<sup>1</sup> Kentaro Yamamoto,<sup>1</sup> Titus Masese,<sup>1</sup>  
Yuki Orikasa,<sup>1</sup> Koji Ohara,<sup>2</sup> Katsutoshi Fukuda,<sup>2</sup> Yukinori Koyama,<sup>2</sup> Toshiyuki Nohira,<sup>3</sup>  
Rika Hagiwara,<sup>4</sup> Zempachi Ogumi,<sup>2</sup> and Yoshiharu Uchimoto<sup>1</sup>

<sup>1</sup> Graduate School of Human and Environmental Studies, Kyoto University, Sakyo-ku, Kyoto, 606-8501, Japan

<sup>2</sup> Office of Society-Academia Collaboration for Innovation, Kyoto University, Uji, Gokashou, Kyoto, 611-0011, Japan

<sup>3</sup> Institute of Advanced Energy, Kyoto University, Uji, Gokashou, Kyoto, 611-0011, Japan

<sup>4</sup> Graduate School of Energy Sciences, Kyoto University, Sakyo-ku, Kyoto, 606-8501, Japan  
mori.takuya.83e@st.kyoto-u.ac.jp

$\text{LiFePO}_4$  is one of the promising cathode material for lithium-ion batteries as it exhibits high chemical stability and relatively high rate performance.<sup>[1]</sup> The origin of the high rate performance exemplified in  $\text{LiFePO}_4$  should provide design principles for further development of high rate cathode materials. The (dis)charge reaction of  $\text{LiFePO}_4$  proceeds through a two phase behavior between Li-rich  $\text{Li}_{1-x}\text{FePO}_4$  (LFP) and Li-poor  $\text{Li}_x\text{FePO}_4$  (FP). Under high rate cycling, we revealed the metastable phase formation of  $\text{Li}_{0.6}\text{FePO}_4$  ( $\text{L}_x\text{FP}$ ) which acts as a buffer layer between Li-rich phase (LFP) and Li-poor phase (FP).<sup>[2]</sup> However, the detailed reaction between LFP and FP during high rate cycling has not been fully understood due to short lifetime of metastable  $\text{L}_x\text{FP}$  phase. To investigate the phase transition mechanism, with respect to  $\text{L}_x\text{FP}$  phase, cycling was conducted at elevated temperatures because  $\text{L}_x\text{FP}$  is thermodynamically stable above 200°C.<sup>[3]</sup> The electrolyte used was a binary molten salt based on  $\text{MN}(\text{SO}_2\text{CF}_3)_2$  (M=Li, Cs). Herein, we demonstrate a two-step (dis)charge potential plateau in  $\text{LiFePO}_4$  upon cycling at 230°C. The phase transition behavior is investigated by using *operando* time-resolved X-ray Diffraction (TR-XRD) at various temperatures.

Charge tests were performed using three-electrode cells at 170°C and 230°C. The working electrode comprised a mixture of carbon-coated  $\text{LiFePO}_4$ , acetylene carbon black, and polyimide binder (90:5:5(wt%)) coated on Al foil current collectors. Li-Al alloy wires were used as the counter and reference electrodes.

Conventional single charge plateau curve is observed at 170°C, while the charge curve at 230°C shows two plateau regions. An initial low potential plateau indicates the phase transition of LFP to  $\text{L}_x\text{FP}$ , and the second higher potential plateau indicates the phase transition of  $\text{L}_x\text{FP}$  to FP. *operando* XRD measurements conducted at 230°C reveal the formation of  $\text{L}_x\text{FP}$  phase during the charge process.

We will also show the phase transition behavior of  $\text{LiFePO}_4$  at lower temperature regions, and discuss the origin of the high rate performances of  $\text{LiFePO}_4$ .

## Acknowledgement

This study was partially supported by JSPS Grants-in-Aid for Scientific Research Grant Numbers 13370272.

## References

- [1] N. Meethong, Y.-H. Kao, W. C. Carter, and Y. M. Chiang, *Chem. Mater.*, **2010**, 22, 1088.
- [2] Y. Orikasa, T. Maeda, Y. Koyama, H. Murayama, K. Fukuda, H. Arai, E. Matsubara, Y. Uchimoto, and Z. Ogumi, *J. Am. Chem. Soc.*, **2013**, 135, 5497.
- [3] J. L. Dodd, R. Yazami, and B. Fultz, *Electrochem. Solid-State Lett.*, **2006**, 9, A151.

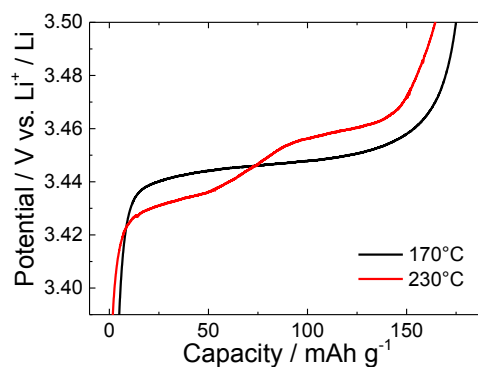


Fig.1. Charge potential curves of  $\text{LiFePO}_4$  at 170°C and 230°C, at a current density commensurate to 17.0 mA g<sup>-1</sup> (1C).

# Temperature Dependence of Effective Ionic Conductivity in Composite Electrode of Lithium Ion Battery

Kezheng Chen<sup>1</sup>, Yuki Orikasa<sup>1</sup>, Takuya Mori<sup>1</sup>, Zyun Siroma<sup>2</sup>, Shiro Kato<sup>3</sup>,  
Hajime Kinoshita<sup>3</sup>, Yoshiharu Uchimoto<sup>1</sup>

<sup>1</sup> Graduate School of Human and Environmental Studies, Kyoto University, Yoshidanihonmatsu-cho, Sakyo-ku, Kyoto, 606-8501, JAPAN

<sup>2</sup> Research Institute for Ubiquitous Energy Devices, National Institute of Advanced Industrial Science and Technology (AIST), Midorigaoka, Ikeda, Osaka 563-8577, JAPAN

<sup>3</sup> Energy conversion Reserch Laboratory, KRI, Inc., 134, Chudoji Minami-machi, Shimogyo-ku, Kyoto, 600-8813 JAPAN  
chen.kezheng.48s@st.kyoto-u.ac.jp

Lithium ion batteries are the leading candidate for energy storage devices in electric vehicles due to their high energy and power density. However, drawback of lithium ion batteries is reduced energy and power densities at low temperatures<sup>[1]</sup>. One of the major factors is considered to be the effective ionic conduction in composite electrode which might cause poor performance at low temperature. Unfortunately, it is difficult to distinguish the electronic conductivity and the ionic conductivity in composite electrodes. Therefore, the effect of ionic conductivity in composite electrode is not well understood. In this study we introduce the measurement method for simultaneous measurement of effective electronic and ionic conductivities in composite electrodes to clarify the temperature dependence of effective ionic conductivity in composite electrodes.

The electrochemical cell which contains 6 probes connecting with the LiFePO<sub>4</sub> composite electrode was used. For the electronic and the ionic conduction electrodes, Al foils and Li foils were used, respectively. Two potentiostats and bias voltage were connected to the cell. After open circuit voltage is measured, the two potentiostats were operated with this voltage as the set point. And then, a bias voltage was applied between the two working electrodes. The ionic and electronic current was measured by current meters. The measurement principle is explained in the literature.<sup>[2]</sup>

Figure 1 shows the reported ionic conductivity of LiPF<sub>6</sub> / EC : EMC (3:7 wt)<sup>[3]</sup> and the effective ionic conductivity in the composite electrodes (LiFePO<sub>4</sub> : Acetylene Black : PVDF = 80:5:15 wt) measured in this study. The temperature dependence of ionic conductivity obeys the Vogel-Tammann-Fulcher (VTF) equation<sup>[3]</sup>:

$$\sigma = AT^{-1/2} \exp[-B/(T-T_0)],$$

where  $A$ ,  $B$  and  $T_0$  are constant, apparent activation energy and the temperature at which the conductivity becomes zero. The apparent activation energy of bulk electrolyte is 3.12 kJ / mol and that in the composite electrode is 4.14 kJ / mol. One of possibility causing larger activation energy in composite electrodes is high viscosity in low temperature. The high activation energy in composite electrode results in poor rate performance at low temperature.

## Acknowledgement

This work was partly supported by the Exploratory Research Grant from KRI, Inc.

## References

- [1] G. Nagasubramanian, *J. Appl. Electrochem.*, **31**, 99-104 (2001).
- [2] Z. Siroma, J. Hagiwara, K. Yasuda, M. Inaba, A. Tasaka, *J. Electroanal. Chem.*, **648**, 92-97 (2010).
- [3] M.S. Ding, K. Xu, S. S. Zhang, K. Amine, G. L. Henriksen, T. R. Jow, *J. Electrochem. Soc.*, **148**, A1196-A1204 (2001).

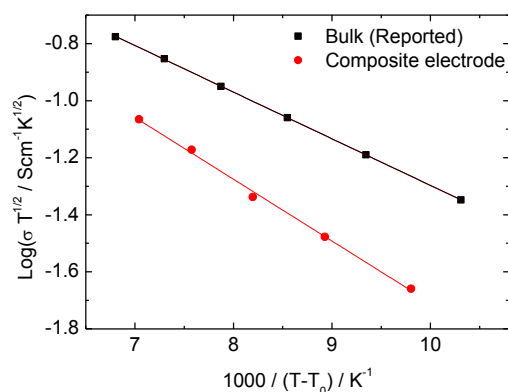


Fig. 1 Temperature dependence of ionic conductivity of bulk and in composite electrode.

# **Modified Carbon Felt via a Facile Oxidation Treatment as an Efficient Electrode for a Vanadium Redox Flow Battery**

Heng-Wei Chiang\*, Chao-Yen Kuo, Chien-Hong Lin, Hwa-Jou Wei\*

*Institute of Nuclear Energy Research*

*No. 1000, Wenhua Rd., Jiaan Village, Longtan District, Taoyuan City 32546, Taiwan (R.O.C.)*

*hengwei@iner.gov.tw*

Carbon felt is commonly used in vanadium redox flow batteries (VRFB) as electrode material. Through electron transfer, the active substances in the electrolyte solution undergo a redox reaction. This study investigated the process of carbon felt by using a facile oxidation method. FT-IR, contact angle and XPS were measured to confirm functional groups (-OH, -COOH) were on the surface of our material. In addition, hydrophilicity was improved, leading to the improvement of charge transfer. At a current density of 80 mA/cm<sup>2</sup>, energy efficiency of the VRFB was increased by 2%–3% comparing with that using untreated carbon felt. Therefore, oxidation of carbon felt is proved to be a simple, rapid, and effective way to enhance the performance of battery while excluding external influences on the environment.

# Adventures in Dioxygen Electrochemistry

Iain Aldous\*, Laurence Hardwick

Department of Chemistry, Stephenson Institute for Renewable Energy, University of Liverpool,  
Liverpool, L69 7ZF, UK

\*i.m.aldous@liv.ac.uk and hardwick@liverpool.ac.uk

The study of chemistry and electrochemistry of dioxygen in non-aqueous electrolyte is essential for unlocking the potential of alkali metal-oxygen batteries that have high theoretical specific energies ( $\text{Li-O}_2$  3505  $\text{Wh Kg}^{-1}$ ,  $\text{Na-O}_2$  1581  $\text{Wh Kg}^{-1}$  and  $\text{K-O}_2$  2820  $\text{Wh Kg}^{-1}$ ).<sup>1-3</sup> Recent attention on these systems have emphasised the chemical sensitivity of dioxygen in the presence of lithium, water and solvent donor number and potential dependent subtle changes within electrolyte configuration at the oxygen-cathode interface.<sup>4, 5</sup> The employment of spectroelectrochemistry that probe electrode interfacial regions is required to understand the role of each component of the dioxygen cathode interface and their effects on dioxygen reduction and oxygen evolution reactions (ORR/OER). This will ascertain the conditions necessary to produce a practically viable and electrochemically reversible oxygen cathode. Presently our comprehension of the effect of changing the alkali metal cation size on the ORR/OER mechanism and electrode interface effects remains incomplete. Recent work on the effects of changing the size of tetraalkylammonium supporting conductive salts has already displayed changes in kinetics of ORR on glassy carbon and gold electrodes.<sup>6</sup> Our presentation here will focus on our continued study into understanding the interfacial effects of changing alkali metal cation size on the oxygen cathode interface for alkali metal-oxygen batteries.

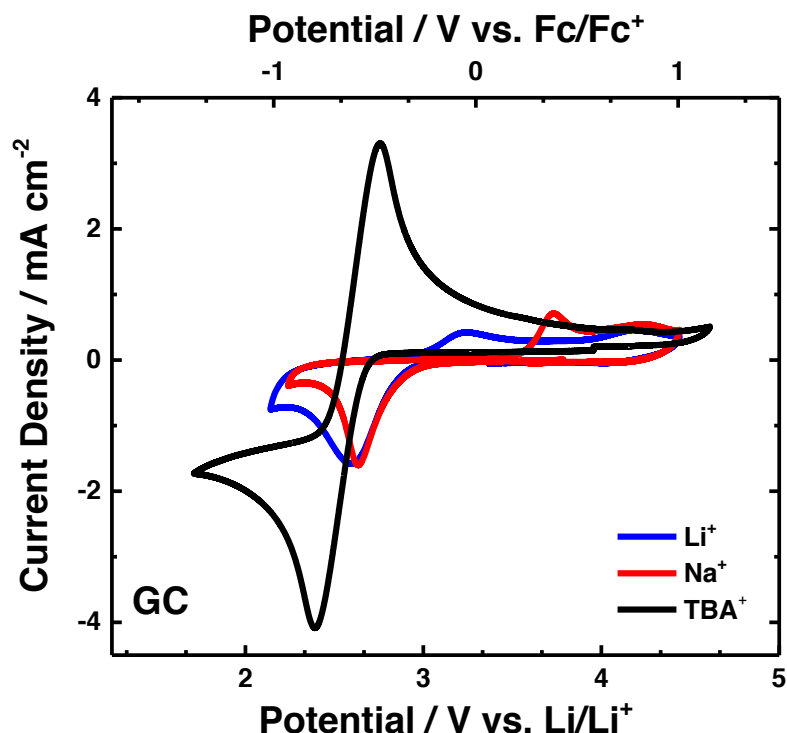


**Fig 1** Cyclic voltammetry of oxygen enriched 0.1M LiOTf, NaOTf, and TBAOTf in acetonitrile (MeCN) on a glassy carbon working disc electrode, 0.1mV s<sup>-1</sup>, 23°C

1. P. G. Bruce, S. A. Freunberger, L. J. Hardwick and J.-M. Tarascon, *Nat. Mater.*, 2012, **11**, 19-29.
2. P. Hartmann, C. L. Bender, M. Vračar, A. K. Dürr, A. Garsuch, J. Janek and P. Adelhelm, *Nat. Mater.*, 2013, **12**, 228-232.
3. X. Ren and Y. Wu, *J. Am. Chem. Soc.*, 2013, **135**, 2923-2926.
4. L. Johnson, C. Li, Z. Liu, Y. Chen, S. A. Freunberger, P. C. Ashok, B. B. Praveen, K. Dholakia, J.-M. Tarascon and P. G. Bruce, *Nat. Chem.*, 2014, **6**, 1091-1099.
5. N. B. Aetukuri, B. D. McCloskey, J. M. García, L. E. Krupp, V. Viswanathan and A. C. Luntz, *Nat. Chem.*, 2015, **7**, 50-56.
6. I. M. Aldous and L. J. Hardwick, *J. Phys. Chem. Lett.*, 2014, **5**, 3924-3930.

## High Energy Solid State Battery

Chih-Ching Chang, Chia-Nan Lin, Chun-Lung Li, Chia-Chen Fang  
*Industrial Technology Research Institute*  
195, Sec. 4, Chung Hsing Rd., Chutung, Hsinchu, Taiwan 31040, R.O.C.  
[changcc@itri.org.tw](mailto:changcc@itri.org.tw)

The development of electric vehicles (EVs) is an inevitable trend in the future. The core technology of the EVs is battery which directly affects the driving distance of EVs. According the roadmap of NEDO, the target for driving distance per charging is 200 km in 2020, 500 km in 2030. Thus the weight energy density of the battery, respectively, must reach the 250Wh / Kg in 2020 and 500Wh / Kg in 2030. It is 3-5 times higher than those batteries in used, and safety would be a critical issue when the development of electrode material focuses on increasing energy by utilizing cathodes and anodes with either high capacity or high voltage. But the common used liquid electrolyte can't meet the demand because of narrow electrochemical window, dissolution of active materials from the cathode, flammable problem, and so on. Although a lot of research efforts have been devoted to developing new electrolytes system to solve above problems, but it is still difficult to address the above problems simultaneously. The solid state electrolyte may be a good candidate among various solutions. However, the several problems of developing solid-state battery needed to overcome. For example, the ionic conductivity of solid electrolyte in room temperature is too low; high impedance interface affect charge-discharge efficiency; the energy density and stability of batteries is poor; the compatibility of lithium metal is poor leading to passivation and safety concerns after prolonged operation.

In this post, research focuses on highly conductive solid electrolyte membrane, high-energy composite cathode and active anode with multiple protection technologies. By this sophisticated technologies, we present a novel architectures of high energy solid-state batteries which would be ideal for use in EVs.



# SEI stabilizer agent epicyanohydrin for cathodes used in LIBs

Arailym Nurpeissova<sup>1</sup>, Da-In Park<sup>2</sup>, Sung-Soo Kim<sup>1</sup>

<sup>1</sup> *Graduate School of Energy Science and Technology, Chungnam National University, Daejeon 305-764, Republic of Korea*

<sup>2</sup> *SK Innovation Co., Daejeon 305-712, Republic of Korea*

*Araiko1987@gmail.com*

The use of epicyanohydrin as an additive to a LiPF<sub>6</sub> salt-based electrolyte in 1:1:1 EC:EMC:DMC was investigated as a potential candidate for high-power lithium-ion batteries operated at 60 °C. Epicyanohydrin polymerized to form a thermally stable, thin, conductive, and evenly distributed protective film on the cathode surface, preventing the dissolution of the cathode material LiNi<sub>0.6</sub>Co<sub>0.2</sub>Mn<sub>0.2</sub>O<sub>2</sub> and suppressing interfacial impedance, and thereby protecting the surface from further reaction with the electrolyte at 60 °C. It was demonstrated that the cycling performance of the cathode material with the additive was enhanced due to the formation of the epicyanohydrin-derived polymer SEI.

**Keywords:** LIB; electrolyte; additive; SEI; polymer;

# Simulation Analysis of Reaction Distribution in LiFePO<sub>4</sub> Composite Electrodes

Shoma Ida<sup>1</sup>, Yuki Orikasa<sup>1</sup>, Hideyuki Komatsu<sup>2</sup>, Koji Kitada<sup>2</sup>, Yukinori Koyama<sup>2</sup>, Zempachi Ogumi<sup>2</sup>, and Yoshiharu Uchimoto<sup>1</sup>

<sup>1</sup>Graduate School of Human and Environmental Studies, Kyoto University, Yoshida-Nihonmatsucho, Sakyo-ku, Kyoto, 606-8501, JAPAN

<sup>2</sup>Office of Society-Academia Collaboration for Innovation, Kyoto University, Uji, Gokashou, Kyoto, 611-0011, JAPAN  
shoma.ida.25n@st.kyoto-u.ac.jp

Morphological optimization of composite electrodes is one of the most crucial factors to the performance of lithium ion batteries, and therefore the guideline for the preparation of composite electrodes is important. One of the factors governing battery performance should be reaction distribution in composite electrodes. The reaction distribution, which arises in the depth direction of the electrode, decreases power density and causes degradation. In our previous work, the existence of reaction distribution in the LiFePO<sub>4</sub> composite electrodes was observed experimentally by using 2D imaging X-ray absorption spectroscopy. When the porosity of the composite electrode was low, the reaction distribution was observed clearly.<sup>[1]</sup> However, it is still difficult to directly observe the dynamics of reaction distribution in composite electrodes. The purpose of this study is to verify the reaction distribution based on the Newman model simulation.<sup>[2]</sup> In addition, we discuss a numerical estimation of the parameter that is difficult to determine experimentally, such as the effective diffusion coefficients of the electrolyte in the heterogeneous porous electrodes.

The simulation was performed for the discharge reaction of LiFePO<sub>4</sub> at a rate of 10 C until 0.45Li insertion. Insertion of Li into the active material was depicted as a shrinking-core model. The effective electronic and ionic conductivities of the composite electrodes were measured by simultaneous measurement<sup>[3]</sup> and used in the simulation. The diffusion coefficient of the electrolyte used in the simulation was compensated with Bruggeman's equation.<sup>[2]</sup>

The reaction distribution obtained from the simulation shows an agreement with the experimental results when the porosity parameter is set to be larger value than the measured value. This means that the effective diffusion coefficients of the electrolyte in the heterogeneous porous electrodes is larger than the compensated values with Bruggeman's equation in homogeneous media. Considering that the measured effective ionic conductivities are also larger than the compensated values with Bruggeman's equation as shown in Fig. 2, these discrepancies between ideal and actual values can originate from the heterogeneity of the pores in the electrodes.

## Acknowledgement

This study was partially supported by the Research and Development Initiative for Scientific Innovation of New Generation Batteries (RISING) project of the New Energy and Industrial Technology Department Organization (NEDO) in Japan.

## References

- [1] Y. Gogyo, H. Yamashige, M. Katayama, Y. Orikasa, Y. Inada, T. Ota, H. Arai, Y. Uchimoto, Z. Ogumi, *Meeting Abstracts of 222<sup>nd</sup> ECS Meeting*, **2012**, 2, 156
- [2] M. Doyle, T. Fuller, J. Newman, *J Electrochem Soc.* **1993**, 140(6)
- [3] Y. Orikasa, Y. Gogyo, H. Yamashige, K. Chen, T. Mori, K. Yamamoto, T. Masese, Z. Shiroma, S. Kato, H. Kinoshita, Y. Uchimoto, *Meeting Abstracts of 17<sup>th</sup> IMLB*, **2014**, 4, 726

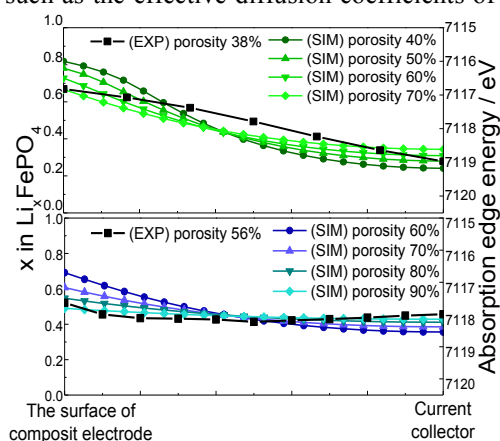


Fig.1. Experimental and numerical reaction distribution in composite electrode, discharged at a rate of 10 C

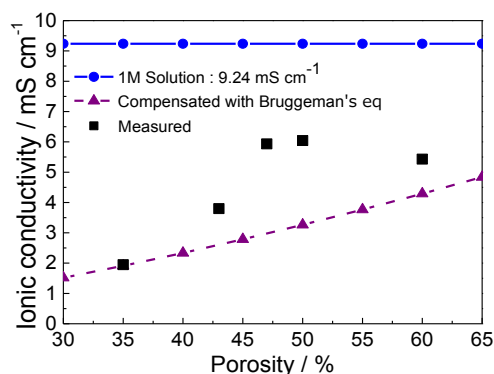


Fig.2. Ionic conductivity in composite electrodes that was measured by simultaneous measurement

A dimensional stability of SnO<sub>2</sub> nanoparticles during Li<sup>+</sup> insertion/de-insertion was improved by confining them within a highly crosslinked graphene framework. The composite was prepared by reacting an optimal amount of benzene-1,4-diboronic acid (BDBA) with SnO<sub>2</sub>-anchored graphene oxide (SG) having a high density of oxygen functionalities, which was introduced by irradiating ozone on as-synthesized SG. The resultant composite (SGF) possessed a high boron/carbon ratio and a low fraction of unreacted boronic acid groups, indicating a high crosslinking density of a framework. The highly crosslinked SGF showed an excellent stability at a high capacity level when cycled between 0.1 and 3.0 V vs. Li/Li<sup>+</sup>. Further decrease of a low-end potential limit induced the instability of boronic ester linkage. The SGF delivered capacities greater than 940 mAh·g<sup>-1</sup> after 150 cycles at 200 mA·g<sup>-1</sup>, exhibiting a fading rate of 1.3 mAh·g<sup>-1</sup>·cycle<sup>-1</sup> (from 2<sup>nd</sup> to 150<sup>th</sup> cycles). This was distinctly contrasted with 10.4 mAh·g<sup>-1</sup>·cycle<sup>-1</sup> for SGF prepared without ozone-treatment and cycled between 0.01 and 3.0 V vs. Li/Li<sup>+</sup>. The rate capabilities of SGF were also comparable to or better than those in previous reports for SnO<sub>2</sub>/graphene composites, implying that a highly crosslinked nature of SGF does not hamper the electroactivity of SnO<sub>2</sub>.

# ***In-Situ* SEM Observations of Li Plating/Stripping Reactions through Li-Pt Alloying on a LiPON Electrolyte**

Toshio Kimura<sup>1,2</sup>, Munekazu Motoyama<sup>1,2</sup>, and Yasutoshi Iriyama<sup>1,2</sup>

<sup>1</sup>*Department of Materials, Physics and Energy Engineering, Nagoya University  
Furo-cho, Chikusa-ku, Nagoya, Aichi 464-8603, Japan*

<sup>2</sup>*JST-ALCA*

*7 Gobancho, Chiyoda-ku, Tokyo 102-0076, Japan*

*munekazu@numse.nagoya-u.ac.jp*

## **Introduction**

The theoretical energy density of Li metal (2062 Ah L<sup>-1</sup>) is much greater than those of rechargeable anodes in the present lithium ion batteries (e.g. graphite, < 1000 Ah L<sup>-1</sup>). Controlling Li plating/stripping reactions is thus important for next-generation-battery technologies with Li metal anodes such as all-solid-state-lithium batteries (SSLB) and Li-air batteries. Inorganic solid-state electrolytes blocks Li dendrite growth, which is always a critical problem in organic liquid electrolytes. Particularly, amorphous electrolyte plays a key role in suppress the Li growth toward the cathode. Previous work studied the Li plating/stripping reactions with lithium phosphorous oxynitride (LiPON) coated with a Cu current collector (CC) [1]. This study focuses on Li nucleation and growth behaviors at Pt-CC/LiPON interfaces as compared to non-alloying CCs (e.g. Cu) using *in-situ* scanning electron microscopy (SEM).

## **Experimental**

The top and bottom of a Li<sub>1.3</sub>Al<sub>0.3</sub>Ti<sub>1.7</sub>(PO<sub>4</sub>)<sub>3</sub> (LATP) sheet (1.25 × 1.25 cm<sup>2</sup>, Ohara Co.) were coated with 2.5-μm-thick LiPON layers by magnetron sputtering. A CC film (Cu, Pt) was deposited on the top LiPON surface by pulsed laser deposition (PLD). The CC area was controlled to be 5.0 mm in diameter. A Li film with a diameter of 9.0 mm was deposited on the LiPON surface on the bottom by vacuum evaporation. An all-solid CC/LiPON/LATP /LiPON/Li cell was sandwiched with Cu and brass plates. The Cu plate has a viewport in the center. Li electrodeposition was performed under galvanostatic conditions. Current densities were estimated for the whole area of a CC with a diameter of 5.0 mm.

## **Results & Discussion**

Figure 1 shows a voltage transient during Li electrodeposition at 100 μA cm<sup>-2</sup> with a 30-nm-thick Pt CC. In the stage A (Li-Pt alloying), no Li particles appear on a Pt CC in contrast to the case with a Cu CC. However, numerous Li particles suddenly appear when the voltage decreases to the negative peak (stage B). Figure 2 shows surface SEM images after Li electrodeposition at 50–1000 μA cm<sup>-2</sup> with Pt CCs of 30 nm in thickness. The number density of Li particles increases with increasing current density. Li islands never coalesce with each other even at 1000 μA cm<sup>-2</sup>. We will discuss the difference in mechanism of Li metal nucleation and growth between Cu and Pt CCs.

## **Reference**

[1] M. Motoyama, M. Ejiri, and Y. Iriyama, *Electrochemistry*, **82**, 364 (2014).

## **Acknowledgments**

The authors gratefully acknowledge JST-ALCA and JSPS, 26870272 for the financial support.

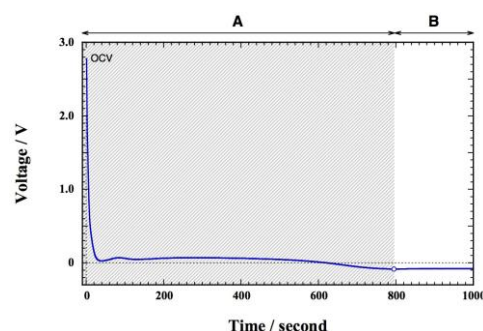


**Figure 1.** Voltage transient during Li electrodeposition with a Pt CC of 30 nm in thickness at 100 μA cm<sup>-2</sup>.

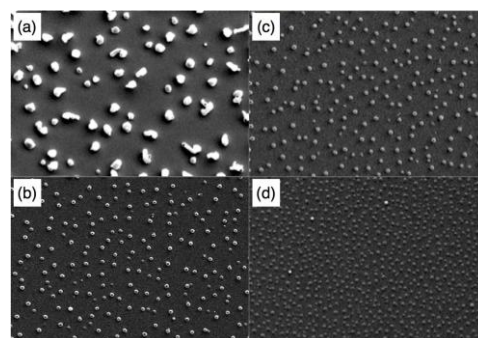


**Figure 2.** SEM images of Li particles electrodeposited with Pt CCs of 30 nm in thickness at (a) 50, (b) 100, (c) 300, and (d) 1000 μA cm<sup>-2</sup>. 180 C cm<sup>-2</sup>

# Correlation between Interfacial Reaction Behavior and Cycling Characteristics of Silicon-based Anodes in Li-ion Batteries

Hyuntak Jo,<sup>a</sup> Xuan-Minh Tran,<sup>b</sup> Dan-Thien Nguyen,<sup>b</sup>  
Hyo Ki Hwang,<sup>c</sup> Kil Ku Kang,<sup>c</sup> Seung-Wan Song<sup>a,b,\*</sup>

<sup>a</sup>*Dept. of Energy Science and Technology, <sup>b</sup>Dept. of Fine Chemical Engineering & Applied Chemistry,*  
*Chungnam National University, Republic of Korea*

<sup>c</sup>*R&D Institute, EG Corp., Republic of Korea*  
*swsong@cnu.ac.kr*

Silicon-based carbon composite is a potential alternative anode material for high-energy density Li-ion batteries due to higher theoretical specific capacity of silicon than commercialized graphite and appropriate operation voltage. However, the major drawback of the commercialization of silicon-based anode material is a short cycle life originated from volume change of silicon during lithiation/delithiation and electrical and mechanical disintegration of particles. A variety of challenges to acquire a good performance is on going in order to overcome those issues. One of the most promising approaches is the control of electrode-electrolyte interfacial reaction for the formation of a stable solid electrolyte interphase (SEI), on the basis of a fundamental understanding of interfacial reaction mechanisms. Utilization of electrolyte additives, modification of surface property of active material, etc. have been researched to improve the interfacial stability. In this presentation, we report the interfacial reaction behavior of silicon and its carbon-delivered anodes, and its correlation to their cycling characteristics.

## Acknowledgments

This research was supported by the Korean Ministry of Trade, Industry & Energy (10049609) and by Korean Ministry of Education and National Research Foundation (2012026203).

# Anion Conductivities of Positively-charged Hydroxides with One-dimensional Channel Framework

Rui Di, Kohei Miyazaki, Tomokazu Fukutsuka, Takeshi Abe  
Graduate School of Engineering, Kyoto University, Nishikyo-ku, Kyoto 615-8510  
[dirui@elech.kuic.kyoto-ac.u.jp](mailto:dirui@elech.kuic.kyoto-ac.u.jp)

In this work, a hydroxide  $\text{Yb}_3\text{O}(\text{OH})_6\text{Cl}_{1-x}\text{OH}_x \cdot 2\text{H}_2\text{O}$  with one-dimensional channel framework structure has been synthesized hydrothermally. In order to investigate the anion conductivity of this compound, we carried out anion exchange using KOH solution, and  $\text{Yb}_3\text{O}(\text{OH})_6\text{OH} \cdot 2\text{H}_2\text{O}$  was obtained. We measured the anion conductivities of these two compounds by A.C. impedance spectroscopy. We evaluated the influences of temperature and relative humidity on the anion conductivity of  $\text{Yb}_3\text{O}(\text{OH})_6\text{Cl}_{1-x}\text{OH}_x \cdot 2\text{H}_2\text{O}$ .

## 1. Introduction

Electrolyte is an important factor which can influence the performance of batteries or sensors. Generally, liquid electrolytes have relatively higher ion conductivities and are frequently used in almost all batteries. But, there are also some problems to be improved, such as electrolyte leakage and the limitation of operating temperature. To solve these problems, the development of solid electrolytes is required. In this work, we focused on an one-dimensional channel framework structure hydroxide  $\text{Yb}_3\text{O}(\text{OH})_6\text{Cl} \cdot 2\text{H}_2\text{O}$  which has a cationic framework and an ability for anion-exchange reactions with small ions. Therefore, it can be expected as an anion conductor. We investigated the conductivity of these compounds by A.C. impedance spectroscopy.

## 2. Experimental

$\text{Yb}_3\text{O}(\text{OH})_6\text{Cl} \cdot 2\text{H}_2\text{O}$  was synthesized by hydrothermal method [1] and anion exchange was successfully made by reacting  $\text{Yb}_3\text{O}(\text{OH})_6\text{Cl} \cdot 2\text{H}_2\text{O}$  with KOH aqueous solution. We added polytetrafluoroethylene (PTFE) as a binder in  $\text{Yb}_3\text{O}(\text{OH})_6\text{Cl}_{1-x}\text{OH}_x \cdot 2\text{H}_2\text{O}$  powder and pressed into a pellet. The pellets were used for the A.C. impedance measurement using amplitude of 20 mV and frequency range of  $1 \times 10^6$ –1 Hz. The conductivity of  $\text{Yb}_3\text{O}(\text{OH})_6\text{Cl} \cdot 2\text{H}_2\text{O}$  was also measured using an amplitude of 100 mV and a frequency range of  $1 \times 10^6$ –1 Hz.

## 3. Results and Discussion

From the Nyquist plots of  $\text{Yb}_3\text{O}(\text{OH})_6\text{Cl}_{1-x}\text{OH}_x \cdot 2\text{H}_2\text{O}$ , a semi-circle was observed and its size showed the dependence of temperature and relative humidity. Therefore, we ascribed the resistance component to ionic conductivity through positively-charged hydroxide. An activation energy derived from the Arrhenius plots of the ion conductivity of  $\text{Yb}_3\text{O}(\text{OH})_6\text{Cl}_{1-x}\text{OH}_x \cdot 2\text{H}_2\text{O}$  was calculated (shown in Fig.1). The value is  $25.1 \text{ kJ mol}^{-1}$  which was larger than the activation energy of alkaline electrolyte [2]. Therefore, there were higher energy barrier of ion transportation in solid electrolyte.

The result of electrochemical impedance measurement of  $\text{Yb}_3\text{O}(\text{OH})_6\text{Cl} \cdot 2\text{H}_2\text{O}$  also showed that the feasibility as a chloride ionic conductor, but it is necessary to be improved further in its conductivity.

## 4. Reference

- [1] H.V. Goulding, et al. *J. Am. Chem. Soc.*, 132.39 (2010).
- [2] N. Agmon, *Chem. Phys. Lett.*, 319.3 (2000).

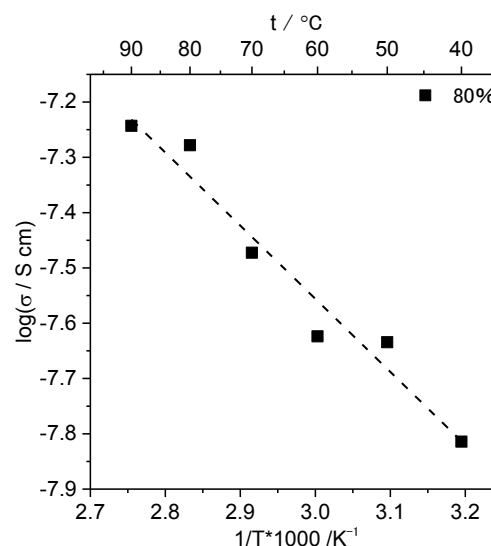


Fig. 1 Arrhenius plot of the conductivity of  $\text{Yb}_3\text{O}(\text{OH})_6\text{Cl}_{1-x}\text{OH}_x \cdot 2\text{H}_2\text{O}$ .

# Electrochemical Properties of Surface-treated Hard Carbon Electrode

Wen Ma, Kohei Miyazaki, Tomokazu Fukutsuka, and Takeshi Abe  
Graduate School of Engineering, Kyoto University,  
Nishikyo-ku, Kyoto 615-8510, Japan  
[abe@elech.kuic.kyoto-u.ac.jp](mailto:abe@elech.kuic.kyoto-u.ac.jp)

## Introduction

Lithium-ion batteries have been used in EVs due to their high energy densities. However, lithium-ion batteries possess some problems to be solved for the further improvement. One of them is the enhancement of rate capabilities. The rate of lithium-ion batteries is influenced by several factors such as ion diffusion in the composite electrodes, charge transfer resistances, diffusion in the active materials, etc. Among them, we have studied the charge transfer resistances. The charge transfer resistances are inverse proportion to the frequency factor and  $\exp(-E_a/RT)$ , where  $E_a$ ,  $R$ , and  $T$  denote to the activation energy, gas constant, and absolute temperature. Therefore, the decrease of the charge transfer resistances can be made by the increase of the frequency factors and the decrease of  $E_a$ . As for the negative electrodes of lithium-ion batteries, graphite electrodes have been mainly used. Hard carbon electrodes have been also used in HEVs since the rate performance is superior to that of graphite. This will be principally due to the large frequency factors. Then, we have focused on the surface treatment of hard carbon electrodes to decrease the activation energy of  $E_a$ . Here, we report the electrochemical properties of surface-treated hard carbon electrodes by  $\text{Li}_3\text{PO}_4$ .

## Experimental

Glassy carbon electrodes were used as model electrodes in this study. In advance, the glassy carbon electrodes have been heat-treated at 773 K in the air for 1 h. Surface treatment of the glassy carbon electrodes was made by the sputtering of  $\text{Li}_3\text{PO}_4$  by the several conditions. Three-electrode cell was fabricated by using surface-treated glassy carbon electrode as a working electrode and lithium metal for counter and reference electrodes. Electrolyte solution was  $1 \text{ mol dm}^{-3} \text{ LiClO}_4 / \text{EC} + \text{DEC} (1:1)$ . Cyclic voltammograms were conducted with a potential range of 0 – 3 V at a scan rate of 1 mV/s. Ac impedance spectra of the glass carbon electrodes were measured at given potentials and temperatures.

## Results and discussion

Cyclic voltammograms (Fig. 1) of the surface-treated glassy carbon showed the large reductive and oxidative currents which corresponded to the insertion and extraction of lithium-ion at the electrode, respectively. In addition, it was found that the surface-treatment enhanced the glassy carbon electrode properties by comparing the pristine one. Fig. 2 shows Nyquist plots at various potentials. As is observed in Fig. 2, various semi-circles were seen. Assignment of each semi-circle will be discussed in the conference.

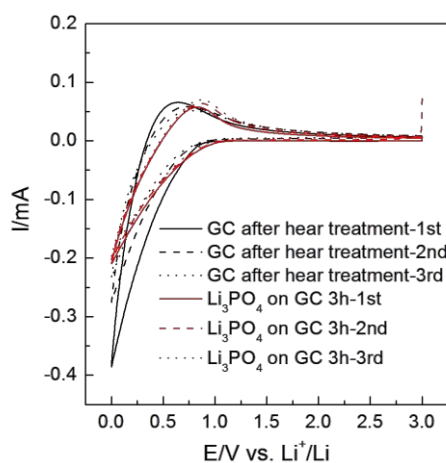


**Fig. 1** Cyclic voltammograms of surface-treated glassy carbon and pristine glassy carbon in  $1 \text{ mol dm}^{-3} \text{ LiClO}_4/\text{EC}+\text{DEC} (1:1)$ .

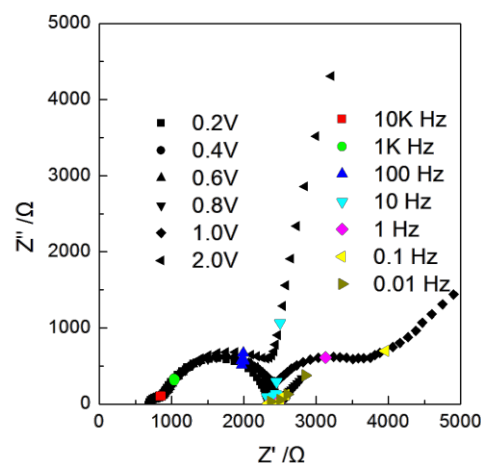


**Fig. 2** Impedance spectra of surface-treated glassy carbon in  $1 \text{ mol dm}^{-3} \text{ LiClO}_4/\text{EC}+\text{DEC} (1:1)$  at potential of 0.4 V.

# Operando X-ray absorption spectroscopic study on magnesium metal anode reaction for magnesium rechargeable battery

Masashi Hattori<sup>1</sup>, Kentaro Yamamoto<sup>1</sup>, Koji Nakanishi<sup>2</sup>, Takuya Mori<sup>1</sup>, Titus Masese<sup>1</sup>, Yuki Oriksa<sup>1</sup>, Yukinori Koyama<sup>2</sup>, Zempachi Ogumi<sup>2</sup>, and Yoshiharu Uchimoto<sup>1</sup>

<sup>1</sup> Graduate School of Human and Environmental Studies, Kyoto University, Sakyo-ku, Kyoto, 606-8501, Japan

<sup>2</sup> Office of Society-Academia Collaboration for Innovation, Kyoto University, Uji, Gokashou, Kyoto, 611-0011, Japan

hattori.masashi.27r@st.kyoto-u.ac.jp

Magnesium rechargeable batteries have paid attention for next generation batteries because of their high theoretical capacity, safety, and abundance. As the electrolytes for magnesium batteries, Grignard reagents have been mainly used<sup>[1]</sup>. However, the stability of the electrolytes in high potential and their corrosive nature are major problems. In recent years, magnesium deposition/dissolution in magnesium inorganic salts with ether-based solvents have been reported<sup>[2]</sup>. For the further development of electrolyte for magnesium batteries, reaction mechanism at electrolyte/magnesium metal interface should be elucidated. In this study, bulk structure of electrolyte is investigated by Raman spectroscopy, X-ray absorption spectroscopy (XAS) and the theoretical calculation. And then, we develop *operando* soft X-ray measurement system for magnesium battery and apply to the analysis of electronic and local structure of electrolyte during magnesium deposition.

Cyclic voltammetry(CV) was conducted in a three-electrode cells. Then different electrolytes are used; 1) 0.5 M magnesium bis(trifluoromethane sulfonyl) amide (Mg(TFSA)<sub>2</sub>)/triglyme, 2) 0.5 M Mg(TFSA)<sub>2</sub>/2-MeTHF, 3) 0.25 M Mg(AlCl<sub>2</sub>EtBu)<sub>2</sub>/THF. Platinum plate and magnesium rod were used as working electrode and counter electrode, respectively. The structures of bulk were analyzed by XAS measurements. *Operando* XAS measurements were performed at different potential during magnesium deposition. Mg K-edge XAS measurements were carried out at the beam line BL27SU at SPring-8 (Japan).

While magnesium deposition/dissolution is observed in (Mg(TFSA)<sub>2</sub>)/triglyme, magnesium is not deposited in Mg(TFSA)<sub>2</sub>/2-MeTHF. Fig. 1 shows local structural changes around magnesium in magnesium deposition process in 0.5 M Mg(TFSA)<sub>2</sub>/triglyme electrolyte. When the potential is lowered, decrease in the peak intensity and peak from magnesium metal were observed. The decrease of peak intensity reflects the desolvation process of triglyme.

## Acknowledgement

This study was partially supported by the Research and Development Initiative for Scientific Innovation of New Generation Battery (RISING) Project under the auspices of New Energy and Industrial Technology Development Organization (NEDO), Japan.

## References

- [1] D. Aurbach, Z. Lu, A. Schechter, Y. Gofer, H. Gizbar, R. Turgeman, Y. Cohen, M. Moshkovich and E. Levi, *Nature*, **2000**, 407, 724.
- [2] Y. Oriksa, T. Masese, Y. Koyama, T. Mori, M. Hattori, K. Yamamoto, T. Okado, Z.-D. Huang, T. Minato, C. Tassel, J. Kim, Y. Kobayashi, T. Abe, H. Kageyama and Y. Uchimoto, *Sci. Rep.*, **2014**, 4, 5622.

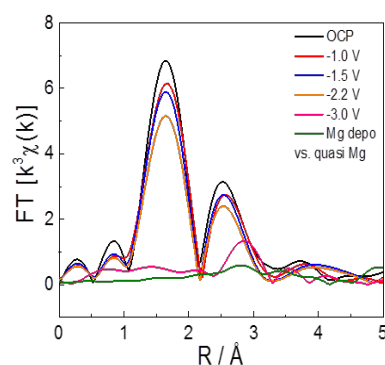


Fig. 1. Fourier Transform of EXAFS oscillation of 0.5 M Mg(TFSA)<sub>2</sub> / triglyme during Mg deposition.



# Interfacial Lithium-ion Transfer between Graphite Negative Electrode and Sulfide Solid Electrolyte

Meiqi Huang<sup>1</sup>, Tomokazu Fukutsuka<sup>1</sup>, Kohei Miyazaki<sup>1</sup>, Akitoshi Hayashi<sup>2</sup>, Masahiro Tatsumisago<sup>2</sup>  
and Takeshi Abe<sup>1</sup>

<sup>1</sup> Graduate School of Engineering, Kyoto University, Kyoto, Kyoto 615-8510, Japan

<sup>2</sup> Graduate School of Engineering, Osaka Prefectural University, Sakai, Osaka 599-8531, Japan  
fuku@elech.kuic.kyoto-u.ac.jp

## Introduction

All-solid-state lithium secondary batteries using inorganic solid electrolytes instead of liquid electrolytes have been expected as next-generation secondary batteries with high safety and high reliability. Among the inorganic solid electrolytes, sulfide-based solid electrolyte such as  $\text{Li}_2\text{S-P}_2\text{S}_5$  based glass solid electrolyte has received much attention due to the high lithium-ion conductivities and room temperature pressure sintering<sup>[1]</sup>. Graphite has been used as the negative electrode materials in lithium-ion batteries, but little work of graphite in sulfide solid electrolyte has been done<sup>[2]</sup>. We focused on the interfacial reaction between graphite and sulfide solid electrolyte, which will play a main role on the rate capability of all-solid-state batteries. Here we report lithium-ion transfer at the interface between graphite negative electrode and sulfide-based glass electrolyte.

## Experimental

A three-electrode cell was assembled by using graphite sheet (76  $\mu\text{m}$ ) as working electrode, lithium metal as counter and reference electrodes, and a layered electrolyte consists of 75 $\text{Li}_2\text{S}$ -25 $\text{P}_2\text{S}_5$  glass pellet and 1  $\text{mol dm}^{-3}$   $\text{LiClO}_4$ /propylene carbonate (PC). Cyclic voltammetry and electrochemical impedance spectroscopy were carried out.

## Results

Figure 1 shows the cyclic voltammogram of graphite sheet. An oxidation-reduction current was observed between 0 – 0.5 V (vs.  $\text{Li/Li}^+$ ). Since lithium ion cannot intercalate into graphite sheet in  $\text{LiClO}_4/\text{PC}$ , this oxidation-reduction peak indicates that lithium-ion intercalation/de-intercalation proceeded at the interfacial between graphite sheet and 75 $\text{Li}_2\text{S}$ -25 $\text{P}_2\text{S}_5$  glass pellet. In the Nyquist plot, one semi-circle was observed and assigned to interfacial lithium-ion transfer process. In the meeting, the activation energy for the interfacial lithium-ion transfer process will be discussed.

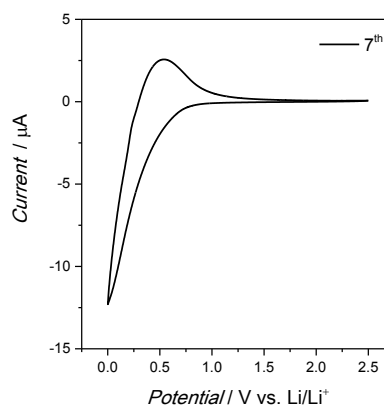


**Fig. 1** Cyclic voltammogram of graphite sheet at the 7th cycle.

## Reference

- [1] A. Sakuda *et al.*, *Sci. Rep.*, **3**, 2261 (2013).
- [2] Y. Seino *et al.*, *Solid State Ionics*, **176**, 2389 (2005).

## Acknowledgement

This work was financially supported by ALCA-SPRING of the Japan Science and Technology Agency.

# Low Temperature Performances of $\text{LiNi}_{0.6}\text{Co}_{0.2}\text{Mn}_{0.2}\text{O}_2$ /graphite Batteries

Chil Hoon Doh, You Jin Lee, Adnan Yaqub, Minji Hwang, Jeong Hee Choi,  
Hae Young Choi

*Korea Electrotechnology Research Institute*

*12, Bulmosan-ro 10beon-gil, Seongsan-gu, Changwon-si, Gyeongsangnam-do, 642-120, Korea*

*chdoh@keri.re.kr*

We report on low temperature behavior of electrodes based on their loading amount, thickness and packing density for Li ion batteries consisting of graphite/ $\text{LiNi}_{0.6}\text{Co}_{0.2}\text{Mn}_{0.2}\text{O}_2$  cells.

In order to investigate the main factors to limit low temperature operation of LIBs, three types of cells, coin-type half cells, coin-type full cells and pouch-type full cells were prepared. Also, discharge capacity and capacity retention, using coin type full cell were comparatively studied both at room temperature (25°C) and low temperature (-32°C).

Electrochemical impedance spectroscopy and galvanostatic technique were used for understanding the low temperature performance of the cells.

Samples having a lower loading exhibited better capacity retention than those in the case of a higher loading due to the limited Li-ion diffusion within the thicker electrodes.

The design of a LIB for using low temperature environment must be carried out on the basis of a comprehensive understanding of crucial structural & material parameters such as electrode thickness or active material loading.

# Ion Transport in Graphite Composite Electrode

XimengLi<sup>1</sup>, Shohei Maruyama<sup>1,2</sup>, Kohei Miyazaki<sup>1</sup>, Tomokazu Fukutsuka<sup>1</sup>, and Takeshi Abe<sup>1,2</sup>

<sup>1</sup>Graduate School of Engineering, Kyoto University, Nishikyo-ku, Kyoto 615-8510, JAPAN

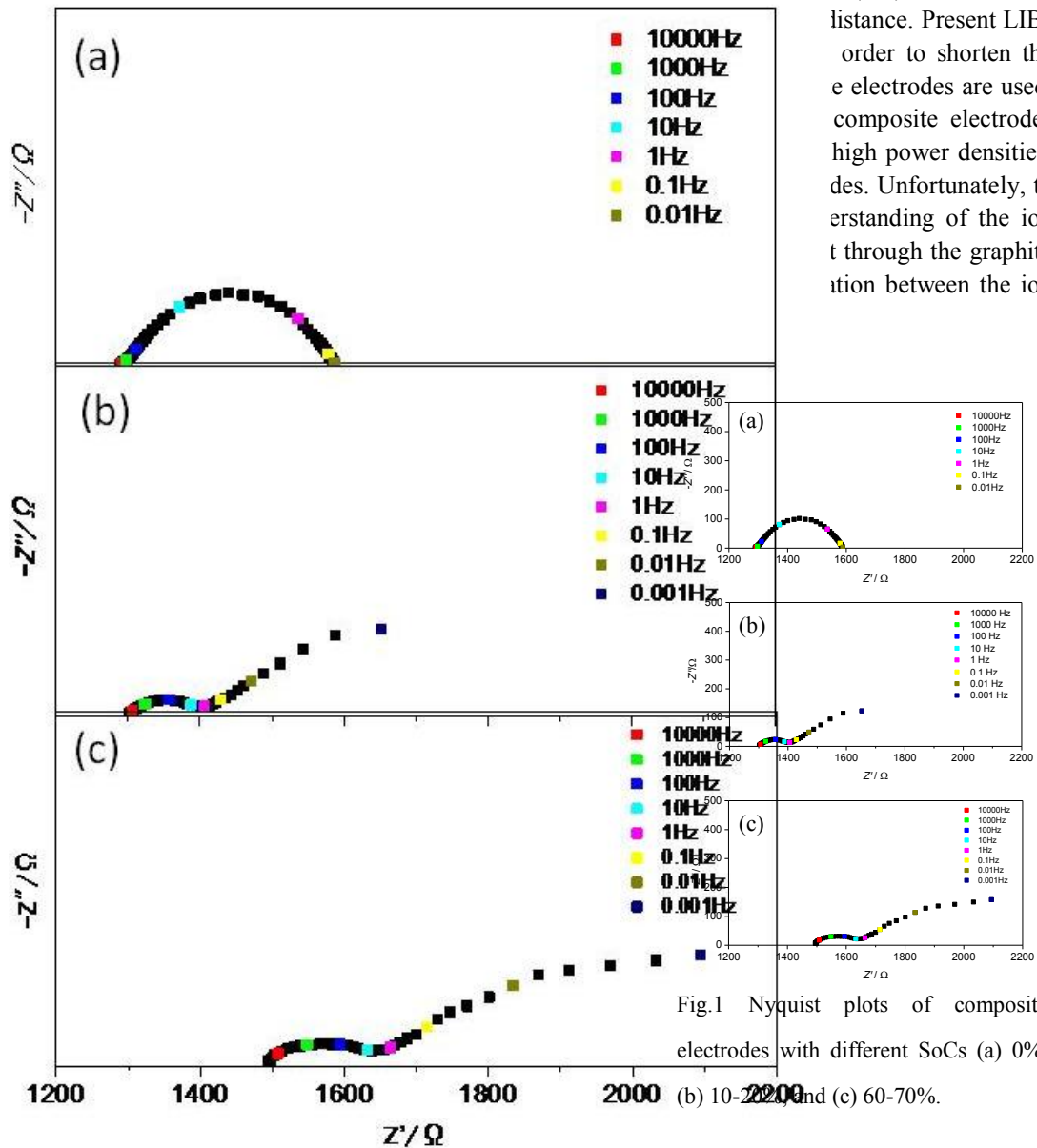
<sup>2</sup>CREST, JST, 4-1-8 Honcho, Kawaguchi, Saitama, 332-0012, JAPAN

abe@elech.kuic.kyoto-u.ac.jp

## Introduction

Increasing concerns about environmental and energy problems accelerate the demands for high-energy-density batteries. Lithium-ion batteries (LIB) have large energy densities and have been well

known for their long cycle life (EV). However, the short distance. Present LIBs are used in order to shorten the distance between the electrodes are used. Graphite composite electrodes with high power densities, designed. Unfortunately, to understand the ion transport through the graphite intercalation between the ion



## References

[1]T. Ohzuku, Y. Iwakoshi, and K. Sawai, *J. Electrochem.Soc.*, **140**, 2490(1993).

## Acknowledgement

This work was financially supported by CREST, JST.

# Rechargeability of Zinc Electrodes Evaluated by *In Situ* Analysis

Hajime Arai<sup>†</sup>, Akiyoshi Nakata, Masaki Ono, Tadashi Kakeya, Tomokazu Yamane, Katsutoshi Fukuda, Hajime Tanida, Miwa Murakami, Yoshiharu Uchimoto\* and Zempachi Ogumi

Office of Society-Academia Collaboration for Innovation, Kyoto University,  
Gokasho, Uji, Kyoto 611-0011 Japan

\* Graduate School of Human and Environmental Studies, Kyoto University  
Yoshida-nihonmatsu-cho, Sakyo, Kyoto 606-8501 Japan

<sup>†</sup> h-arai@saci.kyoto-u.ac.jp

## Introduction

Zinc is an ideal material for use as a negative electrode in batteries, showing high specific capacity and high reducing power. However, significant morphological changes of the zinc electrode during its oxidation-reduction cycles, such as dendrite growth and shape changes, have limited the development of zinc-based secondary batteries [1]. To observe the morphological changes associated with capacity degradation, application of *in situ* battery analytical methods is promising. In this study the zinc electrode behavior was examined by X-ray fluorescence (XRF) imaging [2] to capture the zinc distribution near the electrode and X-ray diffraction (XRD) mapping to visualize the shape changes during cycling. The dissolution of the zinc species affecting the rechargeability of the zinc electrode is demonstrated.

## Experimental

The distribution of zinc species near the electrode was evaluated by projection-type XRF imaging in reflection geometry. Zinc deposition on a copper working electrode (WE) followed by its dissolution was employed in ZnO containing 4 M KOH using a zinc plate as a counter electrode (CE). The XRF images near Zn-K absorption edge (9.8 keV) were recorded every 5 s using a two-dimensional detector. The shape change of the ZnO composite electrode were monitored by XRD mapping in a transmission mode with ca. 900 pixels per electrode. Both experiments were employed at BL28XU, SPring-8 (Hyogo, Japan).

## Results and Discussion

The XRF imaging shows dissolved zinc species in the electrolyte before the reduction (Fig. 1(a)), and then zinc-rich zone near the working electrode with hydrogen bubbles during the reduction (Fig. 1(b)). At the end of the reduction, many pillar-like deposits, namely dendrite, are visible (Fig. 1(c)). A concentrated zinc zone containing the bubbles is seen on oxidation (Fig. 1(d)), indicating the formation of soluble zinc species, presumably in supersaturation. The observation of the zinc species in supersaturated solutions by XAFS and NMR would provide useful information.

The XRD mapping indicates the loss of ZnO at the edge and the growth in the center of the electrode in the course of cycling, showing typical shape change phenomena. It is shown that the shape change causing the capacity loss is closely related to the zinc solubility in the electrolyte, implying the importance of fixation of zinc species at the electrode for better rechargeability.

## Acknowledgment

This work was supported by RISING of NEDO.

## Reference

- [1] X.G. Zhang, in *Encyclopedia of Electrochemical Power Source*, Vol. 5, pp. 454 (2009).
- [2] A. Nakata et al., *Electrochemistry*, submitted.

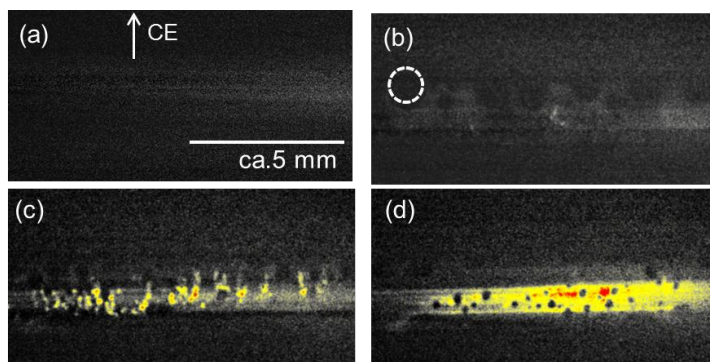


Fig. 1. XRF images of zinc species near WE (a) before the reduction, (b) during reduction with hydrogen bubbles (shown in dotted circle), (c) at the end of the reduction and (d) during oxidation. Color in brighter white corresponds to higher zinc density.

# Oxide-Based All-Solid-State Rechargeable Lithium Batteries with $\text{LiNi}_{1/3}\text{Mn}_{1/3}\text{Co}_{1/3}\text{O}_2$ -Glass Ceramic Solid Electrolyte Composite Prepared by Aerosol Deposition

Takehisa Kato<sup>1,2</sup>, Shinya Iwasaki<sup>1,2</sup>, Yuta Yamamoto<sup>3</sup>, Munekazu Motoyama<sup>1,2</sup>, and Yasutoshi Iriyama<sup>\*1,2</sup>

1. Department of Materials, Physics and Energy Engineering, Nagoya University, Furo-cho, Chikusa-ku, Nagoya, 464-8603, Japan, \*[iriyama@numse.nagoya-u.ac.jp](mailto:iriyama@numse.nagoya-u.ac.jp)

2. JST, ALCA, 5, Sanbancho, Chiyoda-ku, Tokyo, 102-0075, Japan

3. High Voltage Electron Microscope Laboratory, EcoTopia Science Institute, Nagoya University, Furo-cho, Nagoya, 464-8603, Japan

In order to develop bulk-type all-solid-state-lithium batteries (SSBs), fabrication techniques for composite films with dense electrodes and solid electrolytes are required. However, a highly resistive reaction layer forms at the electrode/solid electrolyte interface in some material systems when the electrode and solid electrolyte are sintered together at high temperature [1]. Here, we focus on aerosol deposition (AD) which is a ceramic film fabrication technique that operates at room temperature [2]. In this work, we prepared composite films composed of  $\text{LiNi}_{1/3}\text{Co}_{1/3}\text{Mn}_{1/3}\text{O}_2$  (NMC) and highly  $\text{Li}^+$  conductive solid electrolyte by AD and examined their charge-discharge properties as SSBs.

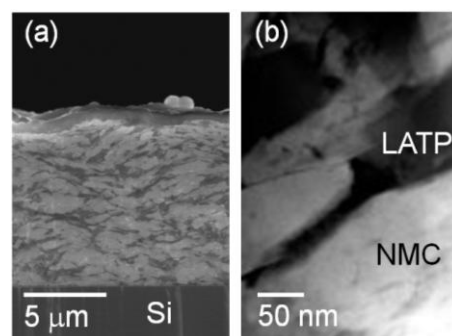
Mixed powders composed of NMC (D50 = 10  $\mu\text{m}$ ) and  $\text{Li}_{1+x}\text{Al}_y\text{Ti}_{2-y}\text{Si}_x\text{P}_{3-x}\text{O}_{12}$  (LATP) (D50 = 0.5  $\mu\text{m}$ ) at a predetermined weight ratio were used as starting materials for AD. These mixed powders were jetted to Si and  $\text{Li}_7\text{La}_3\text{Zr}_2\text{O}_{12}$  (LLZ) by AD [3]. AD films were characterized by XRD, FE-SEM, and TEM. Lithium films were deposited on the other side of LLZ from which the AD films are formed by vacuum evaporation. Charge-discharge measurements of resultant SSBs (Li/LLZ/NMC-LATP) were carried out in an Ar-filled glove box using a constant current then constant voltage (current taper).

Fig. 1a shows a cross-sectional SEM image of an AD film with a weight ratio of NMC:LATP=20:1 on Si. From EDX analysis, black and white regions in the SEM image correspond to LATP and NMC, respectively. Hence, NMC and LATP were uniformly dispersed in the AD film. Fig. 1b shows a TEM image of a NMC/LATP interfacial region of the film. Nano-size voids were densely filled with LATP. Only XRD peaks associated with Si, NMC, and LATP were observed in AD films, and no XRD peaks originating from a reaction layer of a sintered mixture of NMC and LATP were observed. Therefore, it is considered that AD films were fabricated without any heating.

Fig. 2 shows charge-discharge curves of a SSB at 100 °C. The charge current density was kept constant at 50  $\mu\text{A cm}^{-2}$  (i.e. 1/10C), and the discharge current density was varied from 50-1000  $\mu\text{A cm}^{-2}$ . The charge curves after 2 cycles show the same profile regardless of discharge current density. The discharge capacity at a 3-V cutoff with 50  $\mu\text{A cm}^{-2}$  was 135  $\text{mAh g}^{-1}$ , which corresponded to 90% of capacity in liquid electrolyte [4]. Finally, the discharge capacity was 17  $\text{mAh g}^{-1}$  at a 3-V cutoff with 1000  $\mu\text{A cm}^{-2}$ . Charge-discharge reactions were carried out over 90 cycles, and discharge capacity maintained 97% of the first cycle. It is expected that the highly  $\text{Li}^+$  conductive glass ceramic LATP serves to conduct  $\text{Li}^+$  and inhibit crack spreading associated with volume change of the active material, resulting in stable charge-discharge reactions.

**Acknowledgement** This work was supported by JST-ALCA.

**References** [1] K. H. Kim et al., J. Power Sources, 196 (2011) 764. [2] J. Akedo, J. Am. Ceram. Soc., 89 (2006) 1834. [3] R. Murugan et al., Angew. Chem. Int. Ed., 46 (2007) 7778. [4] T. Ohzuku and Y. Makimura, Chem. Lett., 7 (2001) 642.



**Fig. 1.** (a) Cross-sectional SEM image and (b) TEM image of NMC-LATP composite film.

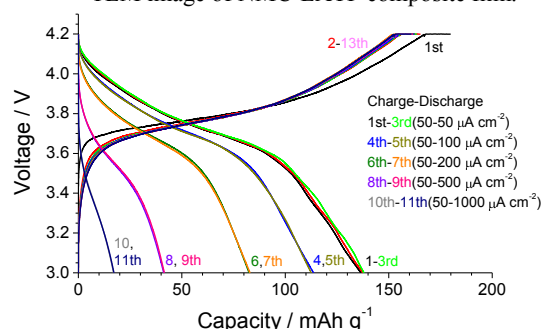


**Fig. 2.** Charge-discharge curves for a Li/LLZ/NMC-LATP cell at 100 °C. AD films thickness is 20  $\mu\text{m}$ .

# The performance of All Solid State Li ion Battery with Composite Sulfide Solid Electrolyte

Won jae Lee, Yong Hwan Gwon, Seong Ju Sim, You Jin Lee,  
Doo Hun Kim, Chil Hoon Doh

*Korea Electrotechnology Research Institute*

*12, Bulmosan-ro 10beon-gil, Seongsan-gu, Changwon-si, Gyeongsangnam-do, 642-120, Korea  
wjlee@keri.re.kr*

We report the performance of all solid state (ASS) Li ion battery with composite sulfide solid electrolyte. First, Li-P-S sulfide electrolyte by high energy ball milling was prepared. Then, 5 types of composite sulfide solid electrolytes were made using ball-milled Li-P-S sulfide and PEO (10. 20. 30. 40, 50 wt%). Here, LiClO<sub>4</sub> salt (ratio of 1/18) was used in order to enhance Li conductivity of PEO polymer.

In order to measure Li conductivity of Li-P-S or composite sulfide solid electrolytes, test cell was prepared with 2032 coin cell holder.

Li conductivity of high energy ball milling Li-P-S sulfide electrolyte was approximately  $1 \times 10^{-3}$  S/cm. With increasing amount of PEO, Li conductivity of composite sulfide solid electrolyte decreased upto approximately  $1 \times 10^{-5}$  S/cm.

The electrochemical performance of all solid state Li ion battery with Li-P-S or composite sulfide solid electrolytes will be discussed.

# Facile Synthesis of CuO Nanochains as Anode Materials for Lithium-Ion Batteries

Fei-Fei Cao<sup>1,2</sup>, Yi-Chi Zhang<sup>1</sup> and Yu-Guo Guo<sup>2</sup>

<sup>1</sup> College of Sciences, Huazhong Agricultural University,

<sup>2</sup> Institute of Chemistry, Chinese Academy of Sciences

<sup>1</sup> No.1 Shizishan Street Hongshan District, 430070 Wuhan, P. R. China

<sup>2</sup> Zhongguancun North First Street 2, 100190 Beijing, P.R. China

caofeifei@mail.hzau.edu.cn, ygguo@iccas.ac.cn

CuO, one of the transition-metal oxides, is considered a very appealing anode material for next generation advanced lithium-ion batteries. However, its practical application is hindered due to the rapid capacity decay resulting from the mechanical pulverization and large volume variations during Li<sup>+</sup> insertion and extraction.

The polycrystalline CuO nanochains were fabricated by a facile wet-chemical method. The BET specific surface area and BJH pore volume are 123.1 m<sup>2</sup> g<sup>-1</sup> and 0.82 cm<sup>3</sup> g<sup>-1</sup> respectively. SEM and TEM results suggest that the CuO nanochains are composed of nanoparticles with size of 8nm. The electrochemical result indicates that the one-dimensional structure may also contribute to the enhanced rate performance. The assembled nanochain structure endows it with high rate capacities of 710, 680, 600, 530 and 390 mAh g<sup>-1</sup> at charge/discharge rate of 0.1C, 0.2C, 0.5C, 1C and 2C, exhibiting a higher capacity and better rate performance as anode material.

## References:

- [1] J. Maier, *Nat. Mater.* **2005**, 4, 805 .
- [2] F.F. Cao, Y.G. Guo, L.J. Wan, *Energy Environ. Sci.* **2011**, 4, 1634 .
- [3] C. K. Chan, H. Peng, G. Liu, K. McIlwrath, X.F. Zhang, R. A. Huggins, Y. Cui, *Nat. Nanotechnol.* **2008**, 3, 31 .
- [4] F. F. Cao, J.W. Deng, S. Xin, H.X. Ji, O. G. Schmidt, L.J. Wan, Y.G. Guo, *Adv. Mater.* **2011**, 23, 4415.
- [5] X. Jiang, T. Herricks, Y. Xia, *Nano Lett.* **2002**, 2, 1333

# Reinforced composite gel-polymer electrolytes for lithium-sulfur batteries

Dauren Batyrbekuly<sup>1</sup>, Almagul Mentbayeva<sup>1,2</sup>, Yongguang Zhang<sup>3</sup>, Indira Kurmanbayeva<sup>1</sup>, Kuralay Korzhynbayeva<sup>1</sup>, Altynay Akhmedinova<sup>2</sup>, Zhumabay Bakenov<sup>1,2\*</sup>

<sup>1</sup>*Institute of Batteries LLC, Kabanbay Batyr 53, Astana 010000, Kazakhstan*

<sup>2</sup>*Nazarbayev University, Kabanbay Batyr 53, Astana 010000, Kazakhstan*

<sup>3</sup>*Tianjin Key Laboratory of Laminating Fabrication and Interface Control Technology for Advanced Materials, Hebei University of Technology, Tianjin, 300130, China*  
z.bakenov@nu.edu.kz

Due to its high theoretical capacity of 1672 mAh g<sup>-1</sup> and high energy density of 2600 Wh kg<sup>-1</sup> sulfur is a very attractive candidate as a cathode material for rechargeable lithium battery [1-2]. However, most works on both LIBs and Li/S batteries still rely on conventional liquid organic carbonate solution as the preferred electrolyte, which intrinsically has many drawbacks including volatility, flammability and potential leakage, which are triggering the safety issues [3]. Therefore, the search for safer and more reliable electrolyte systems is urgent and polymer electrolytes are promising candidate in this regard. Poly(ethylene oxide)-based solid polymer electrolytes are common examples of safe electrolyte. However, since they are limited by low ion conductivity at ambient temperature, the development of novel gel electrolytes which entraps large amount of liquid electrolyte attracts big interest.

In this work we develop novel composite gel polymer electrolytes (GPEs) with high conductivity, high organic solvent uptake and high thermodynamic and mechanical stability for lithium/sulfur batteries by addition of ceramic filler into polymer matrix. The composite GPEs are fabricated allowing for facile transport of Li<sup>+</sup> ions but preventing leakage of electrolyte solution contained within the polymer membrane structure. Such GPE electrolytes have three unique features: electrolyte solution immobilization during battery cycling and rapid lithium ion transport. Furthermore, addition of functionalized natural and synthetic clay nanoparticles as ceramic filler allows overcoming the main problem of GPE – the loss of their mechanical strength when they are plasticized. Polymer nanocomposites uniquely combine the properties of inorganic and organic components providing the opportunities to develop novel advanced materials.

We have combined polymers and co-polymers (e.g., PMMA, PAN, P(AN-co-MMA), PVDF-HFP) with typical and novel Li-ion containing salt solutions (e.g., LiPF<sub>6</sub>, LiClO<sub>4</sub>, LiCF<sub>3</sub>SO<sub>3</sub>, and Li<sub>2</sub>B<sub>12</sub>F<sub>12-x</sub>H<sub>x</sub> dissolved in organic solvents). Among the inorganic layered hosts, montmorillonite (MMT) offers high aspect ratio, high cation exchange capacity, large specific surface area, appropriate interlayer charge. We have used functionalized with amino- and carboxyl-groups MMT and hallosite clay nanoparticles. A Li/S polymer cell containing a composite GPE, consisting of a solution of LiPF<sub>6</sub> in EC/DMC/DEC dispersed in (PVDF-HFP)/(PMMA)/MMT matrix, has exhibited a good cycling performance. This system is under investigation with evaluation of polymer matrices, the modification of nanoclays and their ratio in the composite electrolyte.

## References

- [1] M. Armand, J.M. Tarascon, Nature 451(2008) 652-657.
- [2] Y. Zhao, Z. Bakenova, Y. Zhang, Z. Bakenov, Ionics DOI: 10.1007/s11581-015-1376-4.
- [3] R.D. Rogers, K.R. Seddon, ACS Symposium Series 818, Washington. DC. 2002.

## Acknowledgements

This research was supported by the Research Grants #5156/GF4 and #4649/GF4 from the Ministry of Education and Science of the Republic of Kazakhstan for 2015-2017 years.



# Carboxymethyl Chitosan/Poly(ethylene oxide) as a Water Soluble Blend Binder for 5 V $\text{LiNi}_{0.5}\text{Mn}_{1.5}\text{O}_4$ Cathodes with Improved Cycle Stability in Li-Ion Batteries

Haoxiang Zhong, Yong Li, Jiarong He, Lingzhi Zhang

Key Laboratory of Renewable Energy, Guangzhou Institute of Energy Conversion, Chinese Academy of Sciences, Guangzhou, Guangdong 510640, China

Guangzhou Institute of Energy Conversion, Chinese Academy of Sciences, No.2 Nengyuan Rd., Guangzhou Guangdong, China  
zhonghx@ms.giec.ac.cn

## Abstracts:

Compared with the commercial non-aqueous polyvinylidene difluoride (PVDF) binder, the water soluble binder featuring environmental-friendly, low cost, and high safety is highly desirable for adhesive industry in lithium-ion batteries (LIBs). Carboxymethyl chitosan (CCTS)-poly (ethylene oxide) (PEO) was firstly reported as a water-soluble binder for 5 V  $\text{LiNi}_{0.5}\text{Mn}_{1.5}\text{O}_4$  cathode in Li-ion batteries. CCTS/PEO blends at different mass ratios are characterized by Fourier transform infrared (FTIR) spectroscopy, X-ray diffraction (XRD), and Differential Scanning Calorimetry (DSC) analysis. The electrochemical performance of  $\text{LiNi}_{0.5}\text{Mn}_{1.5}\text{O}_4$  cathode with CCTS/PEO blend binder was investigated and compared with the commercial non-aqueous polyvinylidene difluoride (PVDF).  $\text{LiNi}_{0.5}\text{Mn}_{1.5}\text{O}_4$  cathode using CCTS/PEO blend binder with an optimized ratio of (0.85/0.15, by mass) exhibited better cycling stability and lower ohmic resistance than that of PVDF.

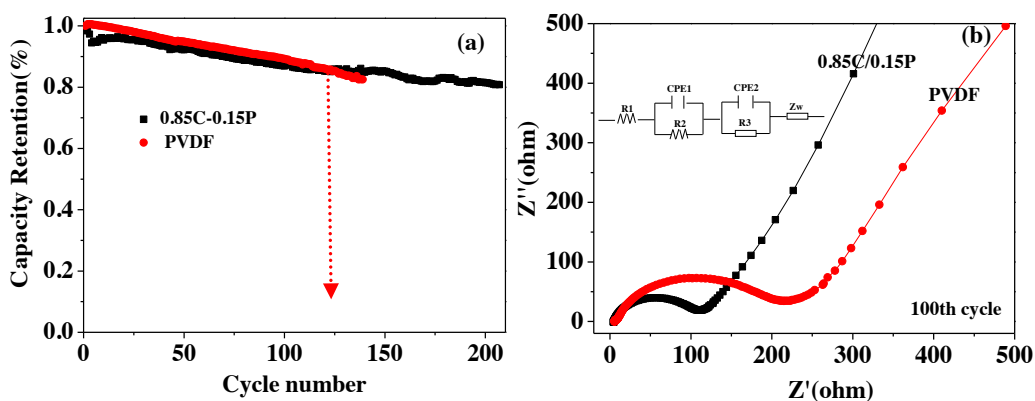


Fig. 1 Electrochemical performance of LNMO electrodes with different binders, (a) cycle stability, (b) EIS after 100 cycles

## References

- [1] L. Yue, L.Z. Zhang, H.X. Zhong, J. Power Sources 247 (2014) 327.
- [2] M.H. Sun, H.X. Zhong, S.R. Jiao, H.Q. Shao, L.Z. Zhang, Electrochimica Acta 127 (2014) 5.
- [3] H.X. Zhong, P. Zhou, L. Yue, D.P. Tang, L.Z. Zhang, J.App. Electrochem. 44 (2014) 45.
- [4] Z.L. Wang, N. Dupréa, A.C. Gaillot, B. Lestriez, J.F. Martin, S.P. Lise Daniel, D. Guyomard, Electrochimica Acta 62 (2012) 7.
- [5] K. Amine, H. Tukamoto, H. Yasuda, Y. Fujita, Journal of Power Sources 68 (1997) 5.

## Mechanisms of Activated Carbon in Lead-Carbon Battery

Wenli Zhang<sup>a</sup>, Jian Yin<sup>a</sup>, Zheqi Lin<sup>a</sup>, Haibo Lin<sup>a,b\*</sup>, Haiyan Lu<sup>a</sup>, Yue Wang<sup>a</sup>, Jinpeng Bao<sup>a</sup>, Tingting Liu<sup>a</sup>

*a. College of Chemistry, Jilin University, Changchun 130012, China*

*b. Key Laboratory of Physics and Technology for Advanced Batteries of Ministry of Education,  
Jilin University, Changchun, 130012, China*

\* E-mail address: [lhb910@jlu.edu.cn](mailto:lhb910@jlu.edu.cn)

Renewable energy has become an important terminology in our era. Electrochemical energy storage devices play an important role in utilizing renewable energy, which is efficient and economic. The most urgent issue is developing robust batteries with long lifespan in deep charge-discharge condition. Among all electrochemical power sources, lead-carbon battery is one of the most promising technologies to be used in large scale renewable energy storage [1]. Lead-carbon battery, a ramification of traditional lead acid battery, has got fast development in the past decade especially in the application of hybrid electrical vehicles [2]. Nevertheless, lead-carbon battery faces great challenges in the application in renewable energy storage. The elaboration of the mechanism of activated carbon in lead-carbon battery will help us design more effective Pb-C bi-material structures and battery composed thereof.

In this study, we demonstrate that activated carbon (AC) contributes little capacitive capacity via electrical double layer capacitor in the charge process. However, AC contributes hydrogen adsorption pseudo-capacitance and it is the electrodeposition of Pb on the surface of AC that dominates the charge process of AC lead-carbon electrode.

Besides, the hydrogen evolution reaction (HER) on AC is prohibited by the reversible hydrogen adsorption at high charge rates. While, at low charge rates, the current efficiency of lead-carbon electrode decreases due to HER on AC.

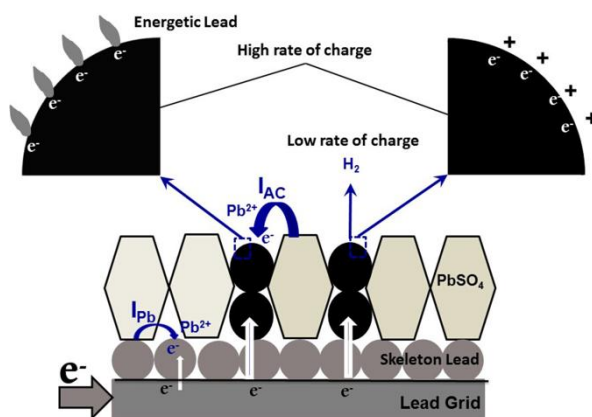


**Fig. 1** Schematic diagram of the mechanism of activated carbon in lead-carbon electrode.

## Acknowledgements

This work was supported by Graduate Innovation Fund of Jilin University, National Natural Science Foundation of China (No. 21273097) and the key project in Jilin Province (No. 20126010).

## References

- [1] W. Zhang, H. Lin, H. Lu, D. Liu, J. Yin, Z. Lin, J. of Mater. Chem. A, 3 (2015) 4399-4404.  
[2] D. Pavlov, T. Rogachev, P. Nikolov, G. Petkova, J. Power Sources, 191 (2009) 58-75.

# 3D Hierarchical Porous Carbon Derived from Lignin with Enhanced Lithium Storage Capability

Wenli Zhang<sup>a</sup>, Jian Yin<sup>a</sup>, Zheqi Lin<sup>a</sup>, Haibo Lin<sup>a,b\*</sup>, Haiyan Lu<sup>a</sup>, Yue Wang<sup>a</sup>, Jinpeng Bao<sup>a</sup>, Tingting Liu<sup>a</sup>

*a. College of Chemistry, Jilin University, Changchun 130012, China*

*b. Key Laboratory of Physics and Technology for Advanced Batteries of Ministry of Education, Jilin University, Changchun, 130012, China*

*\* E-mail address: lhb910@jlu.edu.cn*

Carbon materials with various morphologies and structures have been extensively investigated for the anode materials of lithium ion batteries (LIBs) [1]. Graphite is widely adopted due to its natural abundance and high stability. Nevertheless, graphite has a low theoretical capacity of  $372 \text{ mAh g}^{-1}$ , which is unsuitable for applications needing high power and energy. Hierarchical porous carbon (HPC) has been researched for lithium ion batteries, due to its high reversible lithium capacity and fast lithium storage kinetics [2]. HPC is usually prepared from template methods, which is complicated and expensive. Lignin is an abundant natural ingredient in the world. Lignin-based products can effectively reduce the demand of fossil fuel and is beneficial for a sustainable society. Recently, lignin based hierarchical porous carbons (LHPCs) have been prepared by various template methods, and are mainly investigated for electrode materials in supercapacitors. The preparation of LHPCs from a facile method is valuable, and the use of LHPCs as anode materials in lithium ion battery is attractive.

In this paper, hierarchical porous carbon derived from lignin (denoted as LHPC) was prepared via a facile method. The obtained LHPC was composed of unique 3D macroporous network with mesopores and micropores decorated on carbon walls. The LHPC displayed a stable, high capacity of  $386 \text{ mAh g}^{-1}$  after 560 galvanostatic charge-discharge cycles at a current density of  $500 \text{ mA g}^{-1}$ . Furthermore, LHPC displayed high cycling stability and perfect rate capability.

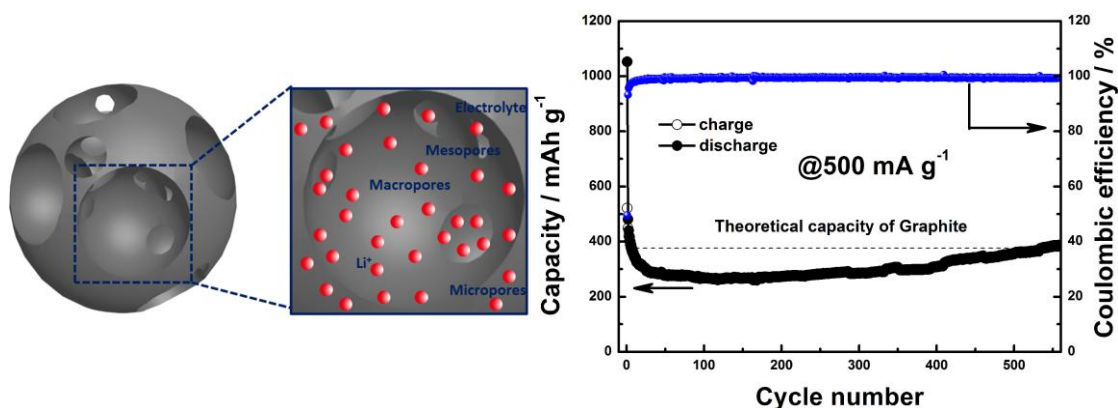


**Fig. 1** Schematic diagram of the lithium ion storage in LHPC, and the galvanostatic charge-discharge cycling performance of LHPC/Li half-cell at a high current density of  $500 \text{ mA g}^{-1}$ .

## Acknowledgements

This work was supported by Graduate Innovation Fund of Jilin University, National Natural Science Foundation of China (No. 21273097) and the key project in Jilin Province (No. 20126010).

## References

- [1] A.D. Roberts, X. Li and H. Zhang, *Chem. Soc. Rev.* 43 (2014) 4341–4356.
- [2] F. Zhang, K.-X. Wang, G.-D. Li and J.-S. Chen, *Electrochem. Commun.* 11 (2009) 130–133.

# A novel PVDF-HFP/PET/PVDF-HFP composite membrane by electrospinning and solution-casting techniques for LiFePO<sub>4</sub> lithium-ion batteries

Yi-Shiuan Wu<sup>1</sup>, Chun-Chen Yang<sup>1,2</sup>, Sin-Ping Luo<sup>1,2</sup>, Yi-Lin Chen<sup>1,2</sup>

<sup>1</sup>Battery Research Center of Green Energy, Ming Chi University of Technology

<sup>2</sup>Department of Chemical Engineering, Ming Chi University of Technology  
No.84, Gongzhuan Rd., Taishan Dist., New Taipei City 24301, Taiwan (R.O.C.)

yishiuan@mail.mcut.edu.tw

The novel composite polymer membrane was fabricated via electrospinning and solution-casting methods. The polymer composite membrane is consisted of three component layers, i.e., two PVDF-HFP layers plus a middle layer of PET nanofiber nonwoven, with a PVDF-HFP/PET/PVDF-HFP sandwich structure (Fig. 1). The characteristic properties of the composite polymer membranes were studied by SEM, XRD, TGA, micro-Raman spectroscopy, galvanostatic charge-discharge test, and impedance spectroscopy. The ionic conductivity and the electrolyte uptake of the conventional PE separator and the composite polymer membrane were also examined and compared (Table 1). It was found that the ionic conductivity can be achieved  $\sim 10^{-3}$  S cm<sup>-1</sup>; the electrolyte uptake was  $\sim 282$  wt.%. The LiFePO<sub>4</sub>/Li cells with the PE separator and the composite polymer membrane were assembled and examined. Fig. 2 shows that the overall cells with the composite polymer membrane exhibit higher discharge capacities than those with the PE separator at 0.2C~10C rates (e.g.,  $Q_{sp,ave}$ : 148.4 vs. 140.9 mAh g<sup>-1</sup> at 0.2C rate). In Fig. 3, we found that the capacity retention of the composite polymer membrane at 1C/1C rate for 200 cycles was  $\sim 80.1\%$ ; however, only 73.5% for the PE separator. We also found that the coulombic efficiencies of the cells with the composite polymer membrane and the PE separator were 99.7% and 96.7%, respectively. According to the results, it was discovered that the electrochemical performances of the composite polymer membrane are much better than those of the PE separator. It was demonstrated that the composite polymer membrane with a sandwich structure is a promising separator for lithium-ion batteries [1-3].

**Keywords:** composite polymer membrane, electrospinning, solution-casting, PVDF-HFP, PET, LiFePO<sub>4</sub>

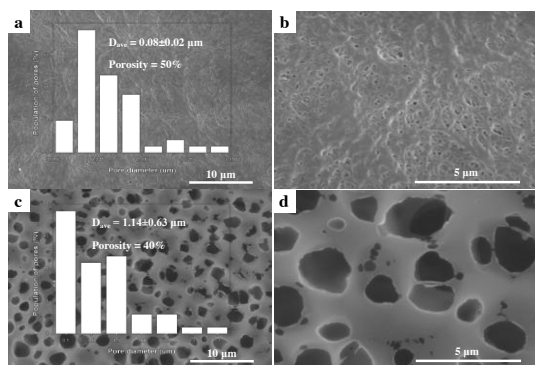


**Fig. 1.** SEM images of (a) the PE separator and (c) the composite polymer membrane; (b) and (d) are the corresponding enlarged images of (a) and (c), respectively. Insets show the pore size distribution of the separators.

**Table 1.** Comparison of the ionic conductivity and the electrolyte uptake of the separators.

Separators	Ionic conductivity (S cm <sup>-1</sup> @20°C)	Electrolyte uptake (wt.%)
Composite polymer membrane	$6.4 \times 10^{-3}$	282
PE	$1.8 \times 10^{-5}$	59

## References

- [1] J.L. Hao, J. Membr. Sci. 428 (2013) 11.
- [2] X.F. Li, J. Membr. Sci. 455 (2014) 368.
- [3] M. Xia, J. Power Sources 266 (2014) 29.

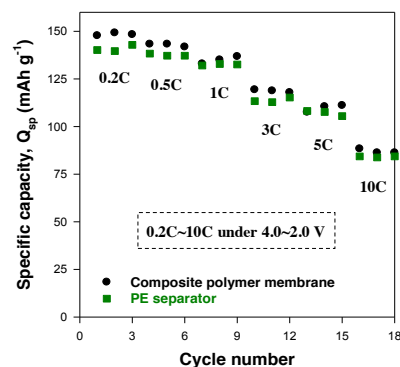


**Fig. 2.** Discharge C-rate capability of the LiFePO<sub>4</sub>/Li half cells assembled with the separators.

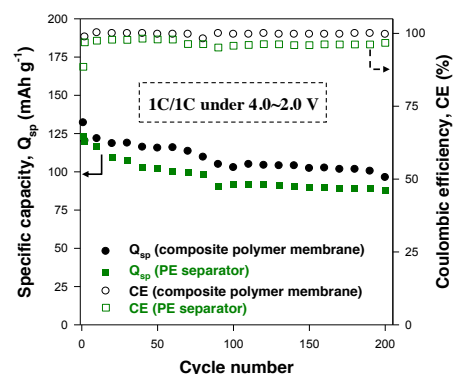


**Fig. 3.** Discharge capacity and coulombic efficiency of the LiFePO<sub>4</sub>/Li half cells assembled with the separators.

# **Na<sub>0.44</sub>MnO<sub>2</sub>–Hard Carbon Sodium-Ion Battery using N-propyl-N-methylpyrrolidinium Bis(fluorosulfonyl)imide Ionic Liquid Electrolyte**

Chueh-Han Wang, Xu-Feng Luo, Cheng-Hsien Yang, Jeng-Kuei Chang\*  
*Institute of Materials Science and engineering, National Central University*  
No. 300, Jhong-Da Rd., Taoyuan, 32001, Taiwan  
[jkchang@ncu.edu.tw](mailto:jkchang@ncu.edu.tw)

In this work, Na<sub>0.44</sub>MnO<sub>2</sub> and hard carbon are used as the cathode and the anode, respectively, in a sodium-ion battery. At first, the NaMnO<sub>2</sub>/Na half cell and the hard carbon/Na half cell are studied both in conventional ethylene carbonate/diethyl carbonate mixed electrolyte containing 1 M NaClO<sub>4</sub> and in N-propyl-N-methylpyrrolidinium bis(fluorosulfonyl)imide ionic liquid electrolyte with 1 M sodium bis(fluorosulfonyl)imide. In the ionic liquid electrolyte, the Na<sub>0.44</sub>MnO<sub>2</sub> and hard carbon electrodes can show reversible capacities of 115 mAh/g and 280 mAh/g, respectively. Based on the obtained electrochemical properties, a Na<sub>0.44</sub>MnO<sub>2</sub>/hard carbon full cell with the ionic liquid electrolyte is constructed. A satisfactory high-rate capability and excellent cyclic stability are recognized. Because the high thermal stability, low volatility, and low flammability of the ionic liquid electrolyte, high safety and good durability of the cell are warranted. The proposed cell could have great potential for practical applications.

# A quantitative analysis on the failure mechanism of nano-Si electrode and the effect of fluoroethylene carbonate

Jae Gil Lee, Jongjung Kim, Jeong Beom Lee, Hosang Park, Tae-jin Lee, Ji Heon Ryu<sup>a</sup>, and Seung M. Oh

*Department of Chemical and Biological Engineering, and Institute of Chemical Processes, Seoul National University, Seoul 151-744, Republic of Korea*  
*a Graduate School of Knowledge-based Technology and Energy, Korea Polytechnic University, Siheung-si, Republic of Korea*

seungoh@snu.ac.kr

Silicon has emerged as an alternative negative electrode material to conventional carbonaceous materials because of its high capacity and low working potential. However, its commercialization has been hindered by low Coulombic efficiency and poor cycle performance. The low Coulombic efficiency is because of irreversible consumption of  $\text{Li}^+$  ions and electrons during charge/discharge. Because  $\text{Li}^+$  ions are supplied from the positive electrode and their total amount is limited, the continuous irreversible reactions induce capacity degradation of cell.

On Si negative electrode, there are two major routes for the irreversible reactions; reductive electrolyte decomposition and Li trapping. These irreversible reactions are deeply associated with severe volume change during cycling. Repeated volume change causes crack formation within the Si particles. Then, the new Si surface is exposed to the electrolyte solution, and subsequently the electrolyte is reductively decomposed on the surface. The volume change also weakens contact between particles. Therefore inserted  $\text{Li}^+$  ions and electrons cannot be released from the Li-Si alloy phases due to the contact resistance. It is called Li trapping.

In this research, two irreversible reactions on nano-Si electrode are quantitatively divided by a novel calculation model. The lithiation/de-lithiation capacities and QOCV(quasi-open circuit voltage) after lithiation step are used for the calculation. The QOCV is converted to depth of charge with capacity unit by using GITT(galvanostatic intermittent titration technique) experiment for the calculation of the capacity only consumed for Li-Si alloy formation.

Then, the model is applied to the nano-Si electrode with two different electrolyte systems; EC/DEC solvent and with FEC(fluoroethylene carbonate). The irreversible reaction capacities are divided successfully by the model and the two electrolyte systems represent definitely different aspects. In EC/DEC solvent system, continuous electrolyte decomposition and large amount of Li trapping is observed. The accumulated electrolyte decomposition products constitute a thick layer and then, facilitate the contact loss between particles.

In FEC co-solvent system however, both of irreversible capacities are alleviated. The suppressed electrolyte decomposition induces very thin SEI layer and the electrically conductive network is well maintained after long cycles. Therefore the failure behavior in EC/DEC solvent system is prevented, which results in a better Coulombic efficiency and cycle performance.

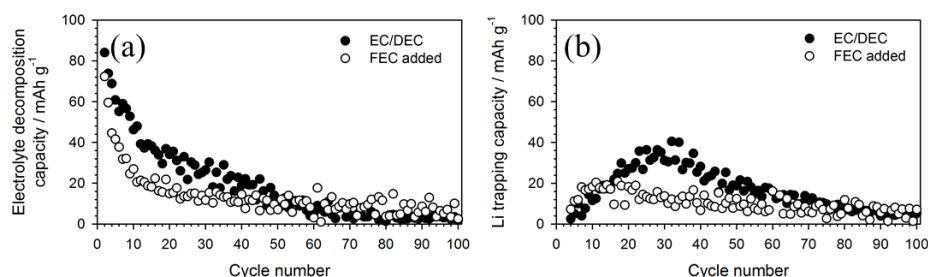


Figure 1. (a) Electrolyte decomposition capacity and (b) Li trapping capacity

# Identifying Solution Based Catalysts for the Lithium Oxygen Battery

William Richardson, Nuria Garcia-Araez  
University of Southampton  
Chemistry, University of Southampton, Southampton, SO17 1BJ, UK.  
w.richardson@soton.ac.uk  
07821118694

Increasing demand for lighter, more powerful batteries has driven research into alternative battery technologies. One system that has received significant attention is the Lithium-Oxygen battery. This system exploits the reduction of oxygen by lithium metal, forming lithium peroxide, to provide a theoretical specific energy of  $3500 \text{ Wh kg}^{-1}$ . One of the major problems facing the Lithium-Oxygen battery is the passivation of the air electrode caused by insoluble lithium oxides and lithium carbonate blocking access to the pores. These products are not completely oxidized on charging and therefore accumulate within the electrode causing the capacity to fade with each cycle.

This work focuses on identifying solution based catalysts in non-aqueous electrolytes to facilitate the oxidation of these insoluble products. The catalysts are oxidized at a higher potential than the lithium peroxide but undergo much faster electron transfer. Once oxidized the catalyst is able to oxidize any lithium peroxide/ lithium carbonate remaining, unblocking the pores and retaining the cells capacity over subsequent cycles. The figure below displays cyclic voltammetry of oxygen reduction and evolution with (black) and without (red) a catalyst. This demonstrates that that incorporation of such a catalyst can have a significant effect on reducing cell passivation dramatically improving the cycle life of the cell.

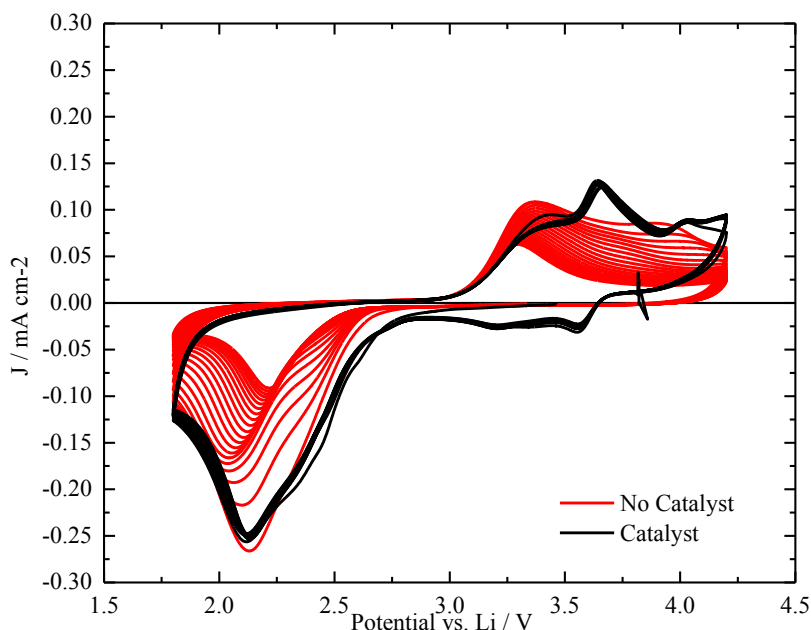


Figure 1: Cyclic voltammetry at  $50 \text{ mV s}^{-1}$  of a two electrode cell containing a glassy carbon working electrode (3mm) and Lithium foil counter/ reference electrode under an oxygen atmosphere. The electrolyte consisted of diglyme containing  $0.1 \text{ M LiTFSI}$  with (black) and without (red) a catalyst.



# **W<sup>6+</sup>&Br<sup>-</sup>-codoped Li<sub>4</sub>Ti<sub>5</sub>O<sub>12</sub> Anodes with Super Rate Performance**

Q. Y. Zhang<sup>a</sup>, C. Y. Ouyang<sup>b</sup> and L. Z. Zhang<sup>a</sup>

<sup>a</sup> *Key Laboratory of Renewable Energy, Guangzhou Institute of Energy Conversion, Chinese Academy of Sciences, Guangzhou 510640, China*

<sup>b</sup> *Department of Physics, Jiangxi Normal University, Nanchang 330022, PR China*

*Rm. 503, Renewable Energy Building, Guangzhou Institute of Energy Conversion, CAS, No.2 Nengyuan Rd., Guangzhou 510640, PR China*

*Q.Y. Zhang (qianyuzhang@ms.giec.ac.cn); C.Y. Ouyang (cyouyang@hotmail.com); L.Z. Zhang (lzzhang@ms.giec.ac.cn)*

**Abstract:** We report a novel Li<sub>4</sub>Ti<sub>5-x</sub>W<sub>x</sub>O<sub>12-x</sub>Br<sub>x</sub> (x=0.025, 0.050 and 0.100) anode material simultaneously doped with W<sup>6+</sup> and Br<sup>-</sup> ion prepared by a simple solid-state reaction in air, aiming to significantly improve its electrical conductivity of Li<sub>4</sub>Ti<sub>5</sub>O<sub>12</sub>. Our theoretical calculation predicts that codoping with W<sup>6+</sup> on the Ti<sup>4+</sup> site and Br<sup>-</sup> on the O<sup>2-</sup> site can remarkably narrow down the band gap, and thus facilitates the electron transport in the lattice of LTO. The comparative experiments prove that W&Br-codoped LTO exhibits higher electrical conductivity compared with undoped LTO as expected, thus improved rate capability and specific capacity. Particularly, Li<sub>4</sub>Ti<sub>5-x</sub>W<sub>x</sub>O<sub>12-x</sub>Br<sub>x</sub> (x=0.05) exhibits the best rate capability and cyclic stability with an outstanding capacity retention of 88.7% even at 10 C rate after 1000 cycles. This codoping strategy with high valance transition metal and halide ions holds promise to be applied to other insulating cathode materials suffering from inferior electrical conductivity.



# Synthesis and characteristics of hyper-branched oligomer directly coated on high voltage cathode material in lithium ion battery

Nadya Nissaulya<sup>1</sup>, Chorng-Shyan Chern<sup>1</sup>, Fu-Ming Wang<sup>2,3\*</sup>

<sup>1</sup>*Department of Chemical Engineering, National Taiwan University of Science and Technology*

<sup>2</sup>*Graduate Institute of Applied Science and Technology, National Taiwan University of Science and Technology*

<sup>3</sup>*Sustainable Energy Center, National Taiwan University of Science and Technology*

*43 Keelung Road, Section 4, Taipei 10607, Taiwan*

*Correspondence: mccabe@mail.ntust.edu.tw*

Recently, a hyper-branched bismaleimide oligomer (so called STOBA) was utilized as an electrode additive for lithium ion batteries [1]. It was reported that STOBA increases the battery safety and decreases the irreversibility of electrochemical reaction due to the coating of oligomer on electrode's surface. According to the literatures [2], N,N'-4,4'-diphenylmethane-bismaleimide (BMI) was attempt to enhance the high voltage performance for lithium-ion batteries. When 0.1 wt% of BMI added into the control electrolyte, the high voltage cycling performance of LiCoO<sub>2</sub> is improved evidently while charging up to 4.5 V rather than the conventional 4.2 V.

In this study, the epoxy acrylate (EA) is used to replace and compare with the BMI in order to precisely define and control the reaction mechanism of STOBA. Two kinds of STOBAs, the BMI and barbituric acid (BTA) and the EA and BTA, are chosen for directly reaction with Al doped LiCoO<sub>2</sub>. In this investigation, BTA is used to react with BMI and EA thermally. Hence, the reactions will be performed under typical temperature that permitted the BTA to generate free radicals. At the end of process, we will compare the formed oligomers by characterized them into fourier transform infrared spectroscopy (FT-IR), gel permeation chromatography (GPC), thermogravimetric analysis (GPA), differential scanning calorimetry (DSC) and electrochemical (EC) properties.

## **Reference**

[1] F. M. Wang, S. C. Lo, C. S. Cheng, J. H. Chen, B. J. Hwang, H. C. Wu, *J. Membrane Sci.* 368 (2011) 165.

[2] C. C. Lin, H. C. Wu, J. P. Pan, C. Y. Su, T. H. Wang, H. S. Sheu, N. L. Wu, *Electrochim. Acta* 101 (2013) 11.

# Failure mechanism of SiO negative electrode during high temperature storage

Jongjung Kim, Hosang Park, Jae Gil Lee, Ji Heon Ryu<sup>a</sup>, and Seung M. Oh<sup>\*,z</sup>

Department of Chemical and Biological Engineering, and Institute of Chemical Processes, Seoul National University, Seoul 151-744, Republic of Korea

<sup>a</sup> Graduate School of Knowledge-based Technology and Energy, Korea Polytechnic University, Siheung-si, Republic of Korea  
seungoh@snu.ac.kr

## ■ Introduction

As the market of electric vehicle (EV) is expanded gradually, the characteristics of lithium ion batteries (LIB) such as high energy density, high power, and safety are considerably emphasized. Silicon is promising anode due to higher theoretical capacity ( $\text{Li}_{15}\text{Si}_4$ ,  $3579 \text{ mA h g}^{-1}$ ) compared to that of graphite ( $\text{LiC}_6$ ,  $372 \text{ mA h g}^{-1}$ ). Because of poor cycle performance, many studies related to silicon have focused on improvement of capacity by reducing volume expansion, whereas there have barely been studied about thermal behavior of silicon-based anode. Herein we report failure mechanism of SiO negative electrode by storage at  $85^\circ\text{C}$

## ■ Experimental

SiO (325mesh, Sigma Aldrich) was mixed with super-P and PVdF (70:20:10 wt. ratio) and a slurry was coated on copper foil. The 2032-typed coin cell was assembled in an Ar-filled dry box with Li counter electrode and  $1.3 \text{ M LiPF}_6$  dissolved in a mixture of ethylene carbonate (EC) and diethyl carbonate (DEC)=3:7 (vol. ratio). The galvanostatic discharge/charge cycling was made at  $320 \text{ mA g}^{-1}$  in the potential range of  $0.040\sim 1.5 \text{ V}$  (vs.  $\text{Li/Li}^+$ ). After 5 cycles, cell was stored at  $85^\circ\text{C}$  for 24 h with de-lithiated state. And then cell is moved to room temperature and recycled. EIS, FE-SEM, XPS were examined to understand electrochemical phenomenon.

## ■ Results and discussion

Capacity of SiO negative electrode rapidly decreases after  $85^\circ\text{C}$  storage. Compared with non-thermal storage, unknown failure mechanism occurs during thermal storage. OCV of SiO negative electrode during thermal storage continuously increase. This means that SEI of SiO negative electrode induced by EC decomposition is damaged during thermal storage [1]. In order to repair SEI, additional electrolyte decomposition occurs permanently during thermal storage. SEI is getting thicker and thicker due to repetitive damage and repair process during thermal storage. As a result, Li ion undergoes kinetic barriers by large resistance caused by thick SEI after thermal storage.

The detailed electrochemical results will be reported in the meeting.

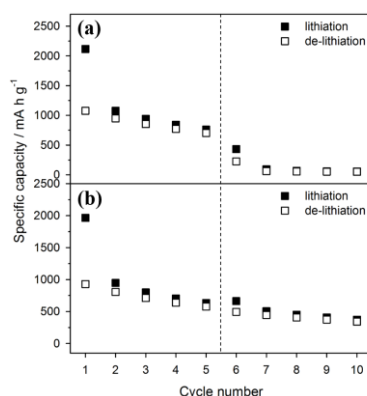


**Figure 1.** Cycle performance of SiO negative electrode (a) with  $85^\circ\text{C}$  storage for 24 h, (b) without storage.

## ■ Reference

1. H. Park, T. Yoon, Y. Kim, J. G. Lee, J. Kim, H.-s. Kim, J. H. Ryu, J. J. Kim, and S. M. Oh, *Journal of The Electrochemical Society*, **162** (6), A892-A896 (2015).

# Environmentally friendly binders for lithium ion batteries

Nicholas Löffler<sup>1,2</sup>, Guk-Tae Kim<sup>1,2</sup>, Diogo Vieira Carvalho<sup>1,2</sup>, Stefano Passerini<sup>1,2</sup>

<sup>1</sup>Karlsruhe Institute of Technology (KIT), P.O. Box 3640, 76021 Karlsruhe, <sup>2</sup>Helmholtz Institute Ulm (HIU), Helmholtzstraße 11, 89081 Ulm

[Nicholas.loeffler@kit.edu](mailto:Nicholas.loeffler@kit.edu)

In view of limited crude oil resources and climate endangering emissions (e.g. CO<sub>2</sub>) deriving from the consumption of fossil fuels, lithium ion battery technology is currently facing a new great challenge: its implementation in large-scale devices like (hybrid) electric vehicles and stationary energy storage to balance the intermittent supply of renewable energy sources such as wind, solar and tidal [1-3].

In contrast to the sustainable and “green” character of the energy to be stored, today’s commercially available rechargeable lithium ion batteries cannot be considered as particular “green” energy storage systems. Therefore, continuously growing research efforts are focusing on the utilization of environmentally benign battery components (e.g. active materials, binders, separators) to manufacture “greener” and more sustainable lithium ion batteries [4-6].

In this sense, we focus in our work on the replacement of today’s most widely used binder – solvent system: polyvinylidenedifluoride (PVdF), which is dissolved in N-methyl pyrrolidone (NMP). Although PVdF exhibits excellent physical and electrochemical properties as binder for electrodes, it suffers of a few clearly recognizable drawbacks, among which toxicity of the solvent, end-of-life disposal (no easy recycling) of the polymer and high costs of materials and processing, are of major importance [4]. Therefore, it is desired to substitute the PVdF/NMP system with water-based binder systems, which are environmentally friendly and less costly [5].

A major drawback of aqueous processing (e.g. with carboxymethyl cellulose (CMC) as binder) of metal oxides as active materials is the corrosion (due to increasing pH) of the aluminium current collector and consequently inferior electrochemical performances [7]. We report on several approaches to simultaneously avoid corrosion issues and guarantee mechanical properties which allow the processing of water-based electrode formulations. In this regard we focus on the investigation of additives, enabling the aqueous processing of electrodes with electrochemical performances comparable to the conventional PVdF/NMP system. Moreover, we are researching a new group of water soluble polymers as binder for lithium ion batteries. We concentrate on a basic understanding of the interaction between the active material and the binder polymers as well as the influence of the above mentioned additive.

The electrodes containing different polymeric binders are studied concerning electrochemical properties and cycling performance in half- and full- cells. The influences of different additives/polymers are investigated with SEM, XPS and IR techniques.

The electrochemical performances of aqueous based-electrodes using an acidic solution as additive in the manufacturing process are in a comparable range with organic solvent based cathode and anode electrodes.

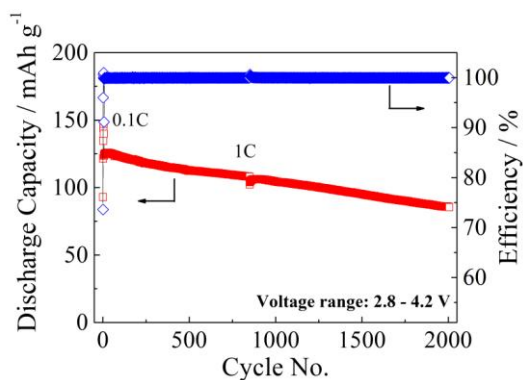


**Figure: Specific capacity and efficiency of a full Li-ion cell comprising a water processed NMC cathode and graphite anode.**

- [1] B. Scrosati and J. Garche, *J. Power Sources*, 2010, **195**, 2419
- [2] R. Marom, S. F. Amalraj, N. Leifer, D. Jacob and D. Aurbach, *J. Mater. Chem.*, 2011, **21**, 9938
- [3] K. Zaghib, A. Mauger, H. Groult, J. B. Goodenough and C. M. Julien, *Materials*, 2013, **6**, 1028
- [4] F.M. Courtel, S. Niketic, D. Duguay, Y. Abu-Lebdeh and I.J. Davidson, *J. Power Sources*, 2011, **196**, 2128
- [5] I. Kovalenko, B.Zdyrko, A. Magasinski, B. Hertzberg, Z. Milicev, R. Burtovyy, I. Luzinov and G. Yushin, *Science*, 2011, **334**, 75
- [6] L. Jabbour, R. Bongiovanni, D. Chaussy, C. Gerbaldi and D. Beneventi, *Cellulose*, 2013, **20**, 1523
- [7] N. Loeffler, J. v. Zamory, N. Laszczynski, I. Doberdo, G.-T. Kim, S. Passerini, *J. Power Sources*, 2014, **248**, 915

# Enhanced Li-air batteries using redox mediator

Seon Hye Yoon, Chan Kyu Lee and Yong Joon Park

*Department of Advanced Materials Engineering, Kyonggi University,  
San 94-6, Iui-dong, Yeongtong-gu, Suwon-si, Gyeonggi, 443-760, Korea  
yjpark2006@kyonggi.ac.kr*

Development of next generation energy-storage system is one of the greatest challenges of the modern society because the commercial batteries cannot meet the requirement for large scale applications such as electric vehicles. Li/air batteries have attracted enormous research attention as promising next generation energy-storage system due to their high theoretical energy density. However, they are still facing several bottlenecks to overcome before practical applications.

Basic reaction of the non-aqueous Li/air batteries is formation of  $\text{Li}_2\text{O}_2$  on discharging and dissociation of that on charging ( $\text{Li}^+ + \text{O}_2 \rightleftharpoons \text{Li}_2\text{O}_2$ ) on the surface of air electrode [1-3]. One of the major issues is that the dissociation of solid and insulating  $\text{Li}_2\text{O}_2$  is not so fast and efficient because of kinetic limitation attributed to the poor electron transport between the  $\text{Li}_2\text{O}_2$  particles and the electrode surface. This feature of non-aqueous Li/air batteries results in undesirable electrochemical properties such as large over-potential, low rate-capability, and limited cyclic performance. An interesting approach to alleviate these problems is introduction of redox mediator as an electron-hole transfer agent to facilitate the dissociation of  $\text{Li}_2\text{O}_2$  [4-5]. The redox mediator can replace the slow reaction between insulating  $\text{Li}_2\text{O}_2$  particles and the solid electrode surface with the fast reaction between redox mediator ( $\text{M}/\text{M}^+$ ) and  $\text{Li}_2\text{O}_2$  particles, which leads to efficient dissociation of reaction products and reduced over-potential. In this study, we proposed multi-functional redox mediator as a new strategy to enhanced Li/air batteries. The cell using multi-functional redox mediator presented enhanced electrochemical performance, which indicated that it could be an effective new approach for superior Li-air batteries.

[1] R. Black, B. Adams and L. F. Nazar, *Adv. Energy Mater.*, 2012, 2, 801

[2] F. Li, T. Zhang and H. Zhou, *Energy Environ. Sci.*, 2013, 6, 1125

[3] J. Christensen, P. Albertus, R. S. Sanchez-Carrera, T. Lohmann, B. Kozinsky, R. Liedtke, J. Ahmed and A. Kojic, *J. Electrochem. Soc.*, 2012, 159, R1

[4] Y. Chen, S. A. Freunberger, Z. Peng, O. Fontaine and P. G. Bruce, *Nature Chemistry* 5, 489 (2013)

[5] Y. Wang and Y. Xia, *Nature chemistry* 5, 445 (2013)

# Physiochemical characteristics of graphene nanosheets affecting their electrochemical Na<sup>+</sup> storage properties

Xu-Feng Luo, Chueh-Han Wang, Cheng-Hsien Yang, and Jeng-Kuei Chang\*  
*Institute of Materials Science and Engineering, National Central University*  
No. 300, Jhong-da Rd., Taoyuan, 32001, Taiwan  
[jkchang@ncu.edu.tw](mailto:jkchang@ncu.edu.tw)

Pores and surface functional groups are endowed on graphene nanosheets (GNSs) to improve their electrochemical Na<sup>+</sup> storage properties. An optimal capacity of 220 mA/g is obtained (at charge–discharge rate of 30 mA g<sup>-1</sup>) in ethylene carbonate/diethyl carbonate mixed electrolyte containing 1 M NaClO<sub>4</sub>. *Ex situ* X-ray photoelectron spectroscopy and synchrotron X-ray diffraction techniques are employed to study the electrode charge storage mechanism. The results indicate that reversible surface redox reactions at electrode surface are predominant for the charge storage in a potential range of 0.5–2.0 V (vs. Na/Na<sup>+</sup>), while Na<sup>+</sup> intercalation/deintercalation between carbon layers occurs at lower potentials. It is found that with increasing the charge–discharge rate by >300-fold (to 10 A g<sup>-1</sup>), a capacity of as high as 85 mAh g<sup>-1</sup> can be retained, reflecting excellent rate capability of our electrode. The physiochemical characteristics that affect the Na<sup>+</sup> storage performance are explored. A highly promising GNS anode for sodium-ion batteries is proposed.

# High Energy Density Electrode Materials Prepared with Metal-Organic Coordination-Polymers for the Applications in LIBs

Jian Chen, Shifeng Yang, Jiao Zhao, Panpan Su, Qihua Yang, Can Li

Dalian National Laboratory of Clean Energy, iChEM, Dalian Institute of Chemical Physics, Chinese Academy of Sciences  
No.457, Zhongshan Road, Dalian 116023, China  
chenjian@dicp.ac.cn

Nanostructured electrode materials can greatly improve the electrochemical performance in LIBs.<sup>1-3</sup> In this work, we developed the metal-organic coordination-polymers as the soft template, and synthesized a series of nanostructured oxides which exhibit outstanding performance in LIBs.

The metal-organic coordination-polymers were synthesized by the soft chemical assembly of metal-ion precursors and organic coordination ligands in the solution. The metal oxides obtained from the metal-organic coordination-polymers usually display almost the same morphology as their precursors. Even the crystal plane orientation could also be inherited from the metal-organic coordination-polymers due to the self-templated nature. Owing to the strong coordination effect, the preparation of metal oxides with the metal-organic coordination-polymer precursors plays a vital role when fabricating metal oxides with multiply metal elements, perfect crystalline and nanostructures.

3,4,9,10-Perylenetetracarboxylic dianhydride (PTCDA) has a rigid and planar molecular structure, which guides its derivatives to inherit a similar lamellar structure. By employing PTCDA as the ligand, we prepared  $\text{LiNi}_{0.5}\text{Mn}_{1.5}\text{O}_4$  and  $\text{ZnMn}_2\text{O}_4$  nanoplate assemblies inheriting the morphology from the precursors. The nanoplate-stacked  $\text{LiNi}_{0.5}\text{Mn}_{1.5}\text{O}_4$  cathode material as shown in Fig. 1 exhibits excellent rate capability and cycling stability, delivering  $120.9 \text{ mAh g}^{-1}$  at a high discharge rate of 40 C and maintaining 84.7% over 500 cycles (Fig. 2). The energy and power density of the material is  $500 \text{ Wh kg}^{-1}$  and  $24 \text{ kW kg}^{-1}$ , respectively, exhibiting a great prospective in application for the power batteries of electric vehicles. The spinel mixed-metal oxides  $\text{MMn}_2\text{O}_4$  ( $\text{M}=\text{Co}, \text{Ni}, \text{Zn}$ ) nanoplate assemblies were prepared by using the similar synthesis route. The prepared  $\text{ZnMn}_2\text{O}_4$  shows the high specific capacity of  $1277 \text{ mAh g}^{-1}$  and good cycling ability when served as the anode materials in LIBs.

By employing the ligand of 1,4,5,8-naphthalenetetracarboxylic dianhydride (NTCDA), the hexagonal nanorings, nanoplates, and nanoparticles of  $\text{Co}_3\text{O}_4$  were derived from the Co-NTCDA coordination-polymers, respectively. When the  $\text{Co}_3\text{O}_4$  hexagonal nanorings (shown in Fig. 3) were served as the anode materials in LIB, they display higher reversible capacity and the improved cycling stability compared with the commercial  $\text{Co}_3\text{O}_4$  nanoparticles. The materials maintain a specific capacity of  $1370 \text{ mAh g}^{-1}$  at the end of the 30<sup>th</sup> charging-discharging cycle (Fig. 4).

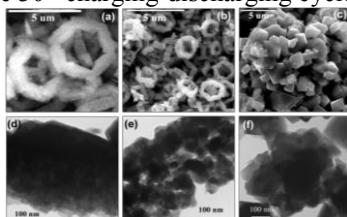


Fig.1 SEM images (a)  $\text{NiMn}_3\text{-ptcda}$ ; (b)  $\text{NiMnO}$ ; (c)  $\text{LiNi}_{0.5}\text{Mn}_{1.5}\text{O}_4$ ; (d-e) the corresponding TEM images of (a-c).

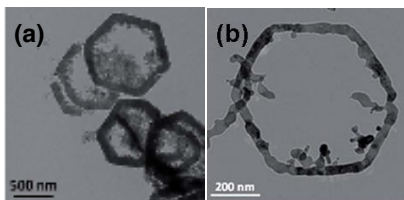


Fig.3 TEM images (a) Hydrolysis products of Co-NTCDA; (b)  $\text{Co}_3\text{O}_4$ .

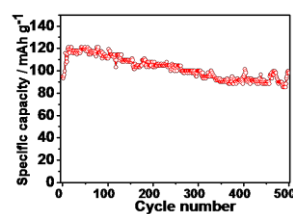


Fig.2 Cycling performance of  $\text{LiNi}_{0.5}\text{Mn}_{1.5}\text{O}_4$  nanoplates at a discharge rate of 40 C.

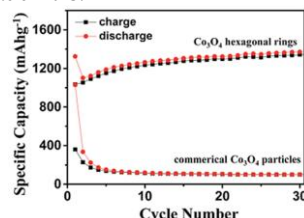


Fig.4 Cycling performance of the  $\text{Co}_3\text{O}_4$  hexagonal rings and commercial  $\text{Co}_3\text{O}_4$  particles at 100 mA/g.

## Reference

1. Kuthanapillil M. Shaju and Peter G. Bruce /Dalton Trans., 2008, 5471–5475
2. Jingang Yang, Fangyi Cheng, Xiaolong Zhang, et al./J. Mater. Chem. A, 2014, 2, 1636–1640
3. Yu Chen, Hui Xia, Li Lu, et al./J. Mater. Chem., 2012,22, 5006-5012

# Development of Air Electrode with $\text{Bi}_2\text{Ir}_2\text{O}_{7-z}$ Nano-catalyst for MH/Air Secondary Battery

Shintaro Terui<sup>1</sup> and Masatsugu Morimitsu<sup>\*1,2</sup>

<sup>1</sup>Department of Science of Environment and Mathematical Modeling,

<sup>2</sup>Department of Environmental Systems Science

Doshisha University

1-3 Tatara-miyakodani, Kyotanabe, Kyoto 610-0394, Japan

\*E-mail: mmorimit@mail.doshisha.ac.jp

Metal/air batteries use oxygen in air as the active mass of the positive electrode (*i.e.*, air electrode) which has theoretically no limitation of the possible discharge capacity, while currently commercialized air batteries are still limited to a primary one and an air secondary battery has not been realized in commercial applications. We have been developing a novel rechargeable air battery consisting of an air electrode, an alkaline electrolyte, and an MH negative electrode, *i.e.*, MH/air secondary battery, which has demonstrated a good cycleability more than 300 charge-discharge cycles and a high energy density over 845 Wh/L [1, 2]. For a further improvement in cell performance, one of the important points is a low polarization air electrode for oxygen reactions during charge and discharge. Especially, a major challenge is to lower the polarization during discharge at a high current density, for which the air electrode is needed to increase the reaction surface area and enhance the gas permeability. The aim of this study is to modify and control the dispersibility of the nano-catalyst on carbon, the conductive supporting material, and to improve the gas diffusion behaviors of the air electrode. We also investigated the performance of the air electrode and the MH/air secondary battery.

The air electrode used graphite powders as a conductive material,  $\text{Bi}_2\text{Ir}_2\text{O}_{7-z}$  as a bi-functional catalyst, and PTFE as a binder. Graphite powders and oxide catalysts were mixed in two ways; the one is directly mixing them (solid phase mixing) and the other is that they were mixed in ethanol with Triton-X as a dispersing agent (liquid phase mixing). Then, the catalyst loaded graphite powders were mixed with PTFE and paraffin. The PTFE weight ratio was changed up to 30 wt.%. The mixture was rolled and pressed on a nickel mesh, and then the dispersing agent was removed using acetone, followed by heating at 370 °C under nitrogen atmosphere to obtain the air electrode. The polarization behaviors of the air electrode were examined by cyclic voltammetry using a three-electrode cell, in which one side of the air electrode was exposed to air and the other side to 6 mol/L KOH solution.

The results with some modification on the preparation procedure of the air electrode indicated that liquid phase mixing is effective to improve the dispersibility of oxide catalysts on graphite powders compared to solid phase mixing from SEM observation, and the polarization of the air electrode during discharge was small compared to that of our previous study [2]. Especially, the oxygen reduction showed a low polarization at a high current density, while no significant change in the onset potential for oxygen reduction was seen, implying that the overpotential for electron transfer at a low current density is unchanged. In the modification of the preparation procedure, the PTFE ratio was also important on the cathodic polarization of the air electrode; for example, a low weight ratio of PTFE induced a low polarization, which would be due to the enhancement in oxygen permeability in the air electrode. In this paper, we will also present a new method to make the air electrode in which the nano-oxide catalyst is loaded more uniformly and held on graphite powders and the results of the performance of MH/air secondary cells using the graphite-based electrode with nano  $\text{Bi}_2\text{Ir}_2\text{O}_{7-z}$ .

*This work was financially supported by “Advanced Low Carbon Technology Research and Development Program (ALCA)” of Japan Science and Technology Agency (JST). The authors also acknowledge FDK Co., Ltd. for supplying the MH negative electrode.*

## References

- 1) M. Morimitsu, T. Kondo, N. Osada, and K. Takano, *Electrochemistry*, Vol. 78, No. 5, pp. 493-496 (2010).
- 2) S. Terui, M. Morimitsu, The 226th ECS meeting, Abs#2182, Cancun (2014).

# Guar Gum as the Binder for Si Anode of Lithium-Ion Battery

Jun-Tao Li<sup>1\*</sup>, Jie Liu<sup>2</sup>, Zhan-Yu Wu<sup>1</sup>, Tao Zhang<sup>1</sup>, Ling Huang<sup>2</sup>, Shi-Gang Sun<sup>2</sup>

<sup>1</sup> College of Energy, Xiamen University, Xiamen 361005, China

<sup>2</sup> College of Chemistry and Chemical Engineering, Xiamen University, Xiamen 361005, China

e-mail: jtli@xmu.edu.cn

Si is a promising anode material with a high theoretical specific capacity and a low electrochemical potential of lithiation/delithiation. However, the commercial use of Si-based anodes is still hindered mainly due to the huge volume change in the cycling process, resulting in degradation of the electrode and rapid loss of capacity. The binders are critical to maintain the electrode structure and thereby to achieve repeatable lithium ion battery operation. Different candidates of new binders for Si-based anodes developed up to now include carboxymethyl cellulose (CMC), poly(acrylic acid) (PAA), polyamide imide (PAI), Na alginate (SA).<sup>1,2</sup> In this abstract, a biopolymer, guar gum (GG), has been applied as the new binder for Si anode. Due to the large amounts of polar hydroxyl groups in guar gum molecule (Fig 1a), the robust interaction between guar gum binder and Si nanoparticles is achieved, resulting in a stable Si anode during cycling. More specially, the guar gum binder can effectively transfer lithium ions to the Si surface, which is similar to polyethylene oxide solid electrolyte. The GG binder shows more robust mechanical property with 3.7 times higher viscosity and 1.6 times higher hardness than that of SA binder. At the current density of 2100 mA g<sup>-1</sup>, the Si nanoparticles anode (100 nm) with GG binder delivers a capacity of 2222 mAh g<sup>-1</sup> after 100 charge-discharge cycles, which is much higher than that with SA binder (1377 mAh g<sup>-1</sup>). Our studies for GG binder open a new binder design perspective for Si anodes.

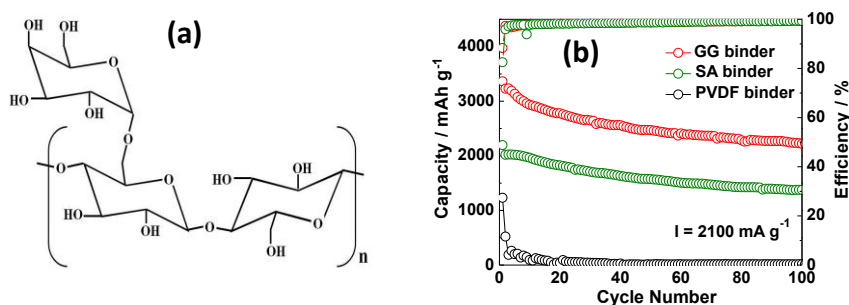


Fig 1 (a) Chemical structures of guar gum, (b) Comparison of electrochemical performance of Si nanoparticles anodes with different binders at 2100 mA g<sup>-1</sup> between 0.01 and 1.2 V, in 1 M LiPF<sub>6</sub>/EC+DMC+DEC (1:1:1, v: v: v) with 2 wt% VC and 10 wt% FEC.

**Acknowledgment:** This work was supported by NSFC (21373008, 21321062, 21273184), and the Natural Science Foundation of Fujian Province of China (2015J01063)

## References

1. Kovalenko I, Zdyrko B, Magasinski A, Hertzberg B, et al, *Science* 2011, **334**, 75.
2. Liu J, Zhang Q, Wu ZY, Wu JH, Li JT, Huang L, Sun SG, *Chem Commun*, **2014**, 50, 6386
3. Liu J, Zhang Q, Wu ZY, Li JT, Huang L, Sun SG, *ChenElectroChem*, **2015**, 2, 611



# **In-Situ Electrochemical Analysis for Electrolyte in Vanadium Redox Flow Battery**

Jung Hoon Yang, Jong-Ho Park, Joonmok Shim, Jae-Deok Jeon, Chang-Soo Jin  
*Energy Storage Department, Korea Institute of Energy Research,  
Daejeon 305-343, Republic of Korea  
enviroma@kier.re.kr*

Surge in demand for electrical energy has been a common phenomenon around world. In addition, greenhouse gas emission is another challenge. As a solution to these problems, large-capacity energy storage system have been proposed. Vanadium redox flow battery(VRB) is one of the most viable alternatives. It has two representative advantages:(1) independent design of battery power and capacity and (2) indefinite life of the vanadium electrolytes. However, VRB operation is accompanied by a lot of side reactions including air oxidation of the V(II) ions, hydrogen evolution at the negative electrode, differential transfer of vanadium ions from one half-cell to the other and volumetric transfer of electrolyte from one half-cell to the other. Those side reactions cause the imbalance of capacity in the negative and the positive parts, consequently the loss of operational capacity.

Transfer of the vanadium ions through the membrane can be readily overcome simply by remixing the positive and negative electrolyte because it do not cause the oxidation state imbalance between the positive and negative electrolyte. However, side reactions such as air oxidation and hydrogen evolution can be only corrected by adjusting the oxidation state of the individual half-cell.

Therefore, it is very important to monitor the oxidation state of the individual half-cell and choose the appropriate correction procedures. The open-circuit cell voltage (OCV) is traditionally introduced to indicate the overall cell state of charge(SOC) during the battery operation. This technique employs the Nernst equation to determine the SOC under the assumption that the electrolyte oxidation states are balanced. It cannot give the accurate SOC for the individual half-cell, especially when the oxidation state is imbalanced.

In this study, we suggest a SOC monitoring technique by adapting the in-situ electrochemical analysis cell. By using this cell, we can measure the electrochemical properties of each electrolytes applying cyclic voltammetry, polarization and electrochemical impedance spectroscopy.

# Tuning structure and in situ XRD characterization of Li-rich layered cathode Materials for lithium ion batteries

Chong-Heng Shen<sup>1</sup>, Ling Huang<sup>1\*</sup>, Jun-Tao Li<sup>2</sup>, Shi-Gang Sun<sup>1, 2\*</sup>

<sup>1</sup> College of Chemistry and Chemical Engineering, Xiamen University, Xiamen 361005, China

<sup>2</sup> College of Energy & School of Energy Research, Xiamen University, Xiamen 361005, China

E-mail: [huangl@xmu.edu.cn](mailto:huangl@xmu.edu.cn); [sgsun@xmu.edu.cn](mailto:sgsun@xmu.edu.cn)

**ABSTRACT:** The Li-rich layered oxide materials are one of the most promising cathode materials for the next generation of high energy lithium ion batteries due to their high specific capacities, low cost and high safety. Nevertheless, this material has a low coulombic efficiency at the 1<sup>st</sup> cycle, poor rate capability and voltage fade during discharge process. The voltage fade has become a serious problem to keep the Li-rich layered oxide materials from practical use. In order to improve the electrochemical performance of the Li-rich layered oxide materials, in recent years, extensive efforts such as surface coating and preparation of nanoparticles have been devoted to improve the electrochemical performance. However, all those efforts could merely improve the performance to a certain extent. It is well known that the structures of the electrode materials, especially the surface structures are a crucial factor that determines the rate for Li<sup>+</sup> intercalation/de-intercalation. So we have developed Surface structure tuning and solvothermal method of layered metal oxide to prepare this materials, the electrochemical experiment results indicated the as-prepared Li –rich layered oxide materials have excellent rate capacities. In-situ X-ray diffraction (XRD) is a useful technique to monitor the structural changes by real time. With aid of in situ XRD, we captured the information on appearing of the  $\beta$ -MnO<sub>2</sub> phase for the first time, and traced the process of its transformation into layered Li<sub>0.9</sub>MnO<sub>2</sub> in situation through in-situ XRD carefully. It is confirmed that the layered Li<sub>0.9</sub>MnO<sub>2</sub> will transform into spinel phase in subsequent cycles by further TEM results. Our research revealed the key step and mechanism to the “Voltage fade” in Li-rich layered material, which could be instructive and meaningful to inhibit the “Voltage fade” of layered Li-rich materials and improve cycle performances.

## References:

1. M. M. Thackeray, S. H. Kang, C. S. Johnson, J. T. Vaughey, R. Benedek, S. A. Hackney, *Journal of Materials Chemistry*., 2007, **17**(30), 3112.
2. M. N. Richard, I. Koetschau, J. R. Dahn, *Journal of the Electrochemical Society*., 1997, **144**(2), 554-557
3. X. Q. Yang, X. Sun, J. McBreen, *Electrochemistry Communications*., 2000, **2**(10), 733-737

**ACKNOWLEDGMENT:** This work was supported by the NSFC (Grant Nos. 21273184, 21321062 and 21373008), and the “973” program (Grant No. 2015CB251102),

# A batwing-like SiO<sub>2</sub>/PVdF-g-PMMA membrane for high-performance lithium-ion batteries

Zhaohui Li\*, Wenjun Li, Chenlu Yang, Xiaozhen Xiao, Gangtie Lei

Key Laboratory of Environmentally Friendly Chemistry and Applications of Ministry of Education,  
College of Chemistry, Xiangtan University,  
Xiangtan City, Hunan Province, 411105, PR China  
e-mail address: lzh69@xtu.edu.cn

Electrospinning technology has been widely utilized to fabricate fibrous gelled polymer electrolyte (FGPE) because it could facilely prepare porous polymer membrane with high porosity and well inter-connective micrometer pores [1, 2]. However, it is because the FGPE has many inter-connective pores in micrometer scale, the absorbed electrolyte might leak out the porous PVdF matrix during cycling resulting in deterioration of battery performances. To retain electrolyte within the fibrous poly(vinylidene fluoride) (PVdF) membranes, poly(methyl methacrylate) (PMMA) was grafted to the electrospun SiO<sub>2</sub>/PVdF nanocomposite fibers via atom transfer radical polymerization (ATRP).

The as-prepared polymer membrane was subsequently activated with the electrolyte 1.0 M LiPF<sub>6</sub> in a mixture of ethylene carbonate/diethylene carbonate (EC/DEC) to form a fibrous gelled polymer electrolyte (FGPE). Effect of grafting degree of PMMA on the morphology, mechanical and electrochemical properties of the fibrous membranes was investigated.

The SiO<sub>2</sub>/PVdF fibrous membrane grafted with 20 wt% PMMA looks like a bat wing (Fig. 1a), the PMMA component surrounds the nanocomposite fibers. It possesses a high ionic conductivity of  $2.31 \times 10^{-3} \text{ S cm}^{-1}$  at room temperature, and a high tensile strength of 8.2 MPa due to integration of the fibers into a coherent whole by the grafted PMMA. The assembled Li/LiFePO<sub>4</sub> cells using this FGPE as separator could deliver 156 and 130 mAh g<sup>-1</sup> at the rates of 0.1 and 2C (Fig. 1b), respectively, and maintain 97% of the initial capacity at 0.1C rate after 90 cycles. The results indicate the FGPE possesses good electrochemical performances and thus is suitable for high-performance lithium-ion batteries.

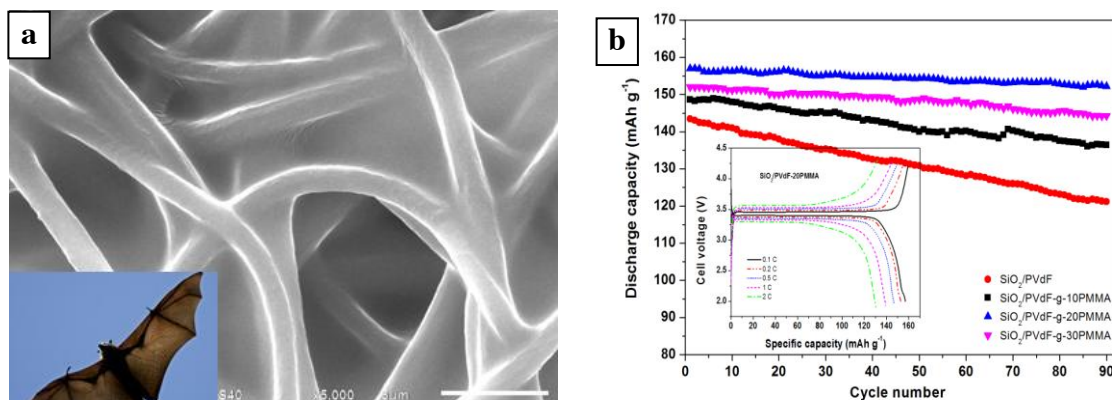


Fig. 1. SEM image (a) of the fibrous SiO<sub>2</sub>/PVdF-g-PMMA membranes (Scale bar: 5 μm. Inset is the digital photo of a bat.), and its electrochemical properties (b).

## Acknowledgements

The authors greatly appreciate the financial support from the Natural Science Foundation of China (No. 21174119 & 51002128).

## References

1. Z. Cui, E. Drioli, Y.M. Lee, Recent progress in fluoropolymers for membranes, Prog. Polym. Sci. 39 (2014) 164-198.
2. C. L. Yang, H. Y. Liu, Q. L. Xia, Z. H. Li, Q. Z. Xiao, G. T. Lei, Effects of SiO<sub>2</sub> Nanoparticles and Diethyl Carbonate on the Electrochemical Properties of a Fibrous Nanocomposite Polymer Electrolyte for Rechargeable Lithium Batteries, Arab. J. Sci. Eng., 39 (2014) 6711-6720.

# Hybrid $V_2O_5/C$ coated Li- rich manganese-based solid solution and its improved electrochemical properties

Zhaohui Li\*, Kailing Sun, Can Peng, Xiaozhen Xiao, Gangtie Lei

Key Laboratory of Environmentally Friendly Chemistry and Applications of Ministry of Education,  
College of Chemistry, Xiangtan University,  
Xiangtan City, Hunan Province, 411105, PR China  
e-mail address: lzh69@xtu.edu.cn

Low coulombic efficiency in the first cycle and poor rate capability limit the practical application of Li-rich manganese-based solid solution (LMSS) in high-power lithium-ion batteries [1, 2]. To resolve these problems, a core-shell type of  $Li_{1.2}Mn_{0.54}Co_{0.13}Ni_{0.13}O_2@V_2O_5/C$  (LMSSVC) material was prepared through sol-gel process by using sucrose as carbon source. SEM and TEM images were taken to observe its morphology while XRD pattern was used to determine its crystal structure. Effect of the  $V_2O_5/C$  hybrid shell on the electrochemical properties of the LMSS material was investigated by cyclic voltammetry, electrochemical impedance spectroscopy and galvanostatic charge-discharge measurement.

It can be found that from Fig. 1 (a, b) some  $V_2O_5$  nanoparticles embed evenly in the amorphous carbon matrix was coated on the surface of the LMSS, forming the core-shell morphology.  $V_2O_5$  and carbon components were confirmed to exist in the coating layer by the EDX pattern of the selected area in Fig.1b. The LMSSVC has a porous structure (Fig. 1c), which would not only facilitate good penetration of electrolyte into the interior of bulk particles but also accommodate the volume change of crystals during cycling.

Owing to the Li-host nature of  $V_2O_5$  material and electronic conductivity of carbon, the LMSSVC displays 96% of columbic efficiency in the first cycle at 0.1C rate while the pristine LMSS is 73%. Compared with the LMSS and LMSSV [3], the LMSSVC could deliver the specific capacities of 269, 258, 245, 229, 207 and 176  $\text{mAh g}^{-1}$  at the rates of 0.1C, 0.2C, 0.5C, 1C, 2C and 5C (Fig. 2), respectively, exhibiting a good rate capability. Furthermore, the LMSSVC maintains 92% of the initial capacity at 0.1C rate after 50 cycles, indicating a suitable cycling performance. The results indicate that surface-coating of hybrid  $V_2O_5/C$  layer is an effective method to improve not only the initial columbic efficiency but also the rate capability of the LMSS material.

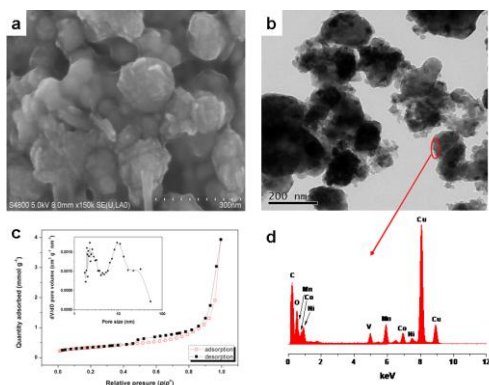


Fig.1. SEM (a) and TEM (b) images of the LMSSVC and its nitrogen adsorption isotherms and pore size distribution (c) and EDX pattern of the selected area in the TEM image (d).

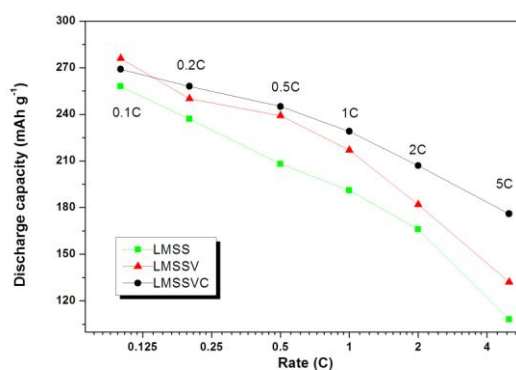


Fig.2. Rate capabilities of the LMSS, LMSSV and LMSSVC samples in the voltage range of 2.0-4.8V at room temperature.

## Acknowledgements

The authors greatly appreciate the financial support from the Natural Science Foundation of China (No. 21174119 & 51002128).

## References

1. H.J. Yu, H.S. Zhou, High-energy cathode materials ( $Li_2MnO_3$ - $LiMO_2$ ) for lithium-ion batteries, *Journal of Physical Chemistry Letters*, 4(8) (2013) 1268-1280.
2. Q.C. Xiao, K.L. Sun, H.L. Zhang, et al, High performance  $Li_{1.2}(Mn_{0.54}Co_{0.13}Ni_{0.13})O_2$  with  $AlF_3$ /carbon hybrid shell for lithium ion batteries, *Materials Technology*, 29(A2) (2014) A70-A76.
3. W.B. Nie, Q.C. Xiao, J.L. Wang, et al, Preparation of  $Li_{1.2}Mn_{0.54}Co_{0.13}Ni_{0.13}O_2@V_2O_5$  Core-shell Composite and Its Electrochemical Properties, *Journal of Inorganic Materials*, 29(3) (2014) 257-263.

# Effects of electrolyte additive on the electrochemical properties of lithium-ion batteries based on $\text{Li}_4\text{Ti}_5\text{O}_{12}$ anode materials

Cheng-Yao Lee, Hao-Ting Peng, She-huang Wu, Jeng-Yu Lin\*

*Department of Chemical Engineering, Tatung University*

*No.40, Sec 3, Zhongshan N. Rd., Taipei City 104, Taiwan (R.O.C)*

[jylin@ttu.edu.tw](mailto:jylin@ttu.edu.tw)

## Abstract

In recent years,  $\text{Li}_4\text{Ti}_5\text{O}_{12}$  (LTO) has being extensively developed as a promising alternative anode material for Li-ion batteries because of its excellent Li-ion intercalation/extraction reversibility and negligible volume change. Moreover, it exhibits a flat discharge platform at 1.55 V (vs. Li) which is higher than the reduction potential of the most organic electrolytes [1], thus avoiding solid electrolyte interphase (SEI) film formation on the surface of LTO particles and ensuring a longer cycling life and better safety of the battery. However, the SEI formation on the LTO surface was found when discharge to 0.01 V [2].

In this study, the electrochemical properties and the SEI formation of electrolyte with different concentrations of butadiene sulfone (BS) on LTO electrodes were studied. According to the results of galvanostatic charge/discharge tests, the LTO electrode charged/discharged in the electrolyte containing 0.5 wt% BS showed the superior electrochemical performance to that in the absence of BS. It was found that the use of BS as an additive can stabilize the SEI film on the LTO surface, and therefore improve the rate capability and electrochemical stability of LTO electrodes. Therefore, the introduction of BS as an additive has promising potential application for improved the electrochemical properties of LTO electrodes especially when discharged to low voltage.

## Reference

- [1] T. Ohzuku, A. Ueda, N. Yamamoto, J. Electrochem. Soc. 142 (1995) 1431.
- [2] T. F. Yi, J. Shu, Y. R. Zhua, X. D. Zhu, C. B. Yue, A. N. Zhou, and R. S. Zhu, Electrochim. Acta. 54 (2009) 7464–7470.

# High-performance lithium-ion batteries based on C/ $\text{Li}_4\text{Ti}_4.95\text{Al}_{0.05}\text{O}_{12}$ anode materials

Pei-Sin Yin, Hao-Ting Peng, Jeng-Yu Lin\*

*Department of Chemical Engineering, Tatung University, Taipei 104, Taiwan*

[jylin@ttu.edu.tw](mailto:jylin@ttu.edu.tw)

## Abstract

Currently, graphite has been considered as the commonly-used anode material in commercial lithium-ion batteries (LIBs). The low operating voltage of graphite in nature leads to the reduction of lithium metal on its surface ( $\sim 0.2\text{V}$  vs.  $\text{Li}^+/\text{Li}$ ) during discharging, thus possibly affecting the safety of LIBs [1].

In recent years,  $\text{Li}_4\text{Ti}_5\text{O}_{12}$  has been considered as a promising material to replace the graphite as anode material. Since  $\text{Li}_4\text{Ti}_5\text{O}_{12}$  has high operating potential plateau (at  $1.55\text{V}$  vs.  $\text{Li}^+/\text{Li}$ ), the deposition of lithium metal is therefore suppressed. Nevertheless, the electronic conductivity of  $\text{Li}_4\text{Ti}_5\text{O}_{12}$  is very poor ( $10^{-13}\text{S cm}^{-1}$ ) and the diffusivity of lithium ion in  $\text{Li}_4\text{Ti}_5\text{O}_{12}$  is also small ( $10^{-8}\text{cm}^2\text{ s}^{-1}$ ), which would limit the electrochemical performance of  $\text{Li}_4\text{Ti}_5\text{O}_{12}$  at high rates [2].

In this study,  $\text{Li}_4\text{Ti}_5\text{Al}_{0.05}\text{O}_{12}/\text{C}$  composite was synthesized via sol-gel method, in which citric acid was used as carbon source and chelating agent. The  $\text{Li}_4\text{Ti}_5\text{Al}_{0.05}\text{O}_{12}/\text{C}$  composite electrode demonstrated superior rate capability to pristine  $\text{Li}_4\text{Ti}_5\text{O}_{12}$ . For instance, its reversible discharge capacity can achieve up to 165, 158, 157, 140 and 118  $\text{mA}\cdot\text{h/g}$  at current density of 1C, 5C, 10C, 20C and 25C, respectively. Moreover, the  $\text{Li}_4\text{Ti}_5\text{Al}_{0.05}\text{O}_{12}/\text{C}$  composite electrode can retain 96% of its initial capacity even after 50 charge/discharge cycles. These results signified that the  $\text{Li}_4\text{Ti}_5\text{Al}_{0.05}\text{O}_{12}/\text{C}$  composite electrode can be considered as one of the promising anode materials for high-performance LIBs.

## References

1. P.G. Balakrishnan, R. Ramesh, T. Prem Kumar, Journal of Power Sources 155 (2006) 401.
2. C. H. Chen, J. T. Vaughey, A. N. Jansen, D. W. Dees, A. J. Kahaian, T. Goacher and M. M. Thackeray, J. Electrochem. Soc. 148 (2001) A102.
3. C. Jiang, M. Ichihara, I. Honma, and H. Zhou, Electrochem. 52 (2007) 6470.
4. T.F. Yi, Y. Xie, L.J. Jiang, J. Shu, C.B. Yue, A.N. Zhoua, and M.F. Ye, RSC Advances 2 (2012) 3541.
5. X. Li, M. Qu, Y. Huai, and Z. Yu, Electrochim. Acta 55 (2010) 2978.

# Next generation of Self Terminated Oligomer Branched Architecture (STOBA) in Li-rich ( $\text{Li}_{1.2}\text{Ni}_{0.2}\text{Mn}_{0.6}\text{O}_2$ ) high capacity cathode material of lithium ion battery

Lyu-Ye Yang<sup>1</sup>, Nan-Hung Yeh<sup>1</sup>, Fu-Ming Wang<sup>1,2\*</sup>

<sup>1</sup>Graduate Institute of Applied Science and Technology, National Taiwan University of Science and Technology

<sup>2</sup>Sustainable Energy Center, National Taiwan University of Science and Technology

43 Keelung Road, Section 4, Taipei 10607, Taiwan

Correspondence: mccabe@mail.ntust.edu.tw

Lithium-Ion battery has several great performances such as high energy density, no memory effect, low self-discharge and high charge-discharge rate. It is widely used in portable electronics and the storage of alternative energy program. Recently, the development of electric vehicle (EV) is growing; it is necessary to reinforce the safety of battery.

Our research is studying to increase the safety and give maintenance to the electrochemistry properties by using two kinds of STOBAs (Self-Terminated Oligomers Branched Architecture, STOBA). The STOBA is used to add into cathode slurry and prepares an electrode. The cathode particle covers a high ionic conductive oligomer; however, the oligomer will be further polymerized while the battery temperature rises. The battery performance such as safety and electrochemistry properties is observed in high temperature (60 °C). The LLNNO ( $\text{Li}_{1.2}\text{Ni}_{0.2}\text{Mn}_{0.6}\text{O}_2$ ) [1] is a potentially high voltage cathode material and is used in our research. Figure 1 shows the LLNMO half-cells are not affected by the STOBA addition. We believe that the STOBA technology will provide a promising performance in the next generation of lithium ion battery.

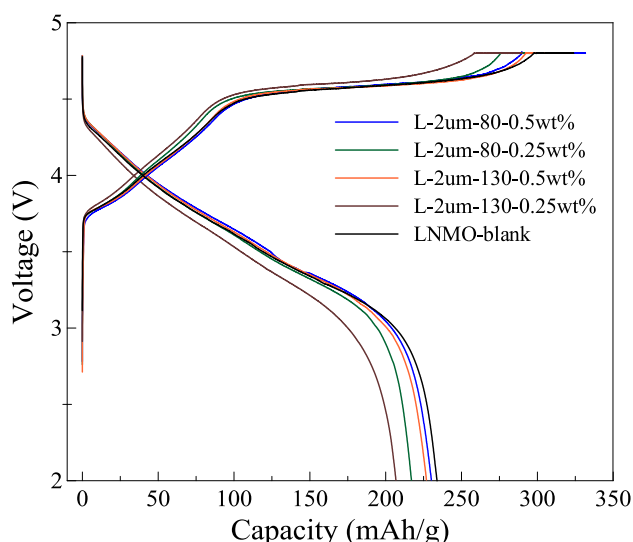


Figure 1 The 1<sup>st</sup> cycle charge-discharge result of Lithium-Ion battery which add STOBA in anode or not (blank).

## References

[1] Sunny Hy *et al.*, J. Am. Chem. Soc. 136 (2014) 999.



# Combined theoretical ab-initio and experimental study on $\text{LiVO}_3$ , a novel conversion-type negative electrode for lithium-ion batteries

Jeong Beom Lee<sup>a</sup>, Janghyuk Moon<sup>b</sup>, Oh B. Chae<sup>a</sup>, Ji Heon Ryu<sup>c</sup>, Maenghyo Cho<sup>b</sup>, Kyeongjae Cho<sup>b,d</sup>, and Seung M. Oh<sup>a,†</sup>

<sup>a</sup> Department of Chemical and Biological Engineering, Seoul National University, Seoul 151-744, South Korea

<sup>b</sup> WCU Multiscale Mechanical Design Division, Department of Mechanical and Aerospace Engineering, Seoul National University, Seoul 151-742, South Korea

<sup>c</sup> Graduate School of Knowledge-based Technology and Energy, Korea Polytechnic University, Gyeonggi, 429-793, South Korea

<sup>d</sup> Department of Materials Science and Engineering and Department of Physics, The University of Texas at Dallas, Richardson, TX 75080, USA

†Correspond to [seungoh@snu.ac.kr](mailto:seungoh@snu.ac.kr)

Lithium-ion batteries (LIBs) have become indispensable parts of modern society due to their high applicability on mobile devices. Carbon-based materials played a significant role in the commercialization of LIBs owing to their long-term stability and cheap prices. However, as applications of power sources increase, the demand for LIBs with higher energy density increases as well. Hence it became necessary to develop alternative electrode materials to overcome the limited capacity of carbonaceous materials. One of the promising candidates is the metal oxide which stores lithium-ion with a conversion reaction. In the conversion reaction, there is no limitation on lithium storage sites since the original framework of oxides is broken along with lithiation. Thus the specific capacity of the material is extremely high compared to graphite or other insertion-type electrode materials. The only factor to limit its capacity is the oxidation states of the transition metal which works as redox center. As shown in Figure 1, there exists a correlation between atomic number of transition metals and the potential of the conversion reaction. This trend is a result of the difference in energy levels of 3d and 4s orbitals which are affected by the number of protons in the nucleus. Since it is hard to reduce titanium and vanadium to their elemental states, there have been no reports on conversion-type lithium storage in those metals. However, it can be inferred from the regression curve that there could be vanadium oxides which show conversion-type lithium storage around 0 V (vs.  $\text{Li/Li}^+$ ).

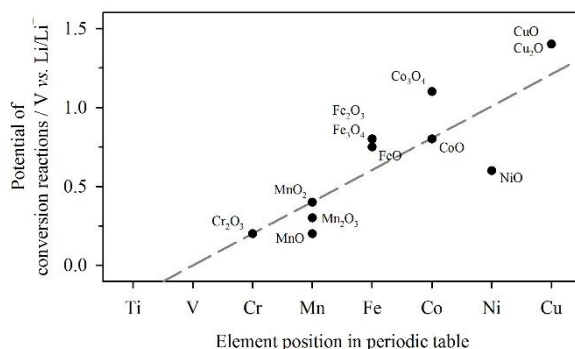


**Figure 1. The empirical values and their regression curve of conversion plateau of 3d transition metal oxides[1].**

In this work, we propose lithium metavanadate ( $\text{LiVO}_3$ ) as a novel conversion-type negative electrode.  $\text{LiVO}_3$  provides reversible capacity over  $1,000 \text{ mAh g}^{-1}$ , which is much higher than other vanadium oxides, with long plateau around 0 V (vs.  $\text{Li/Li}^+$ ). Electrochemical techniques such as PITT and GITT were mainly used to elucidate the lithium storage mechanism of the material. Moreover, various tools including synchrotron X-ray spectroscopy and ab-initio quantum calculation were also employed to obtain more detailed information on the structure change during lithiation.

## Reference

- [1] J. Cabana, L. Monconduit, D. Larcher, M.R. Palacin, Beyond intercalation-based Li-ion batteries: the state of the art and challenges of electrode materials reacting through conversion reactions., Adv. Mater. 22 (2010) E170–192. doi:10.1002/adma.201000717.



# Structural Effects of Spinel $\text{LiMn}_{1.5}\text{Ni}_{0.5}\text{O}_4$ on Their Electrochemical Properties

Josh Y. Z. Chiou, Shou-Huang Su, She-huang Wu\*  
Department of Materials Engineering, Tatung University  
40 Chungshan N. Rd., Sec. 3, Taipei 104, Taiwan  
e-mail: [shwu@ttu.edu.tw](mailto:shwu@ttu.edu.tw)

$\text{LiMn}_{1.5}\text{Ni}_{0.5}\text{O}_4$  (LNMO) samples were synthesized via a spray combustion method followed by heat treatment at temperature of 900°C for 12 hours (LNMO900) and post annealing at 700°C under air for various durations (0 to 96 hours), shown as LNMO700- $X$ , where  $X = 0 \sim 96$  ). Moreover, sample heated at 900°C for 12 hours followed by quenching in liquid nitrogen (LNMO900Q) and sample calcined under oxygen atmosphere instead of air (LNMO900O) were also prepared. The crystalline structures and amounts of secondary phases were studied by X-ray powder diffraction (XRD). Slight shifting of the (111) reflection peak of spinel to lower angle and lowering the intensity of the rock-salt phase ( $\text{Ni}_x\text{O}$  or  $\text{Li}_x\text{Ni}_{1-x}\text{O}$  or  $\text{Li}_x\text{Ni}_y\text{Mn}_z\text{O}$ ) upon increasing the annealing time were observed as reported previously [1]. The appearance of the peaks in addition to those of the LNMO900 sample in the 700°C annealed samples, that manifests the existence of order ( $P4_332$ ) phase in the annealed LNMO samples. Neutron powder diffraction (NPD) with Reitveld refinement was employed to investigate the phase fractions of the ordered, disordered  $Fd\bar{3}m$ , and rock-salt  $\text{Li}_x\text{Ni}_{1-x}\text{O}$  the prepared samples. The morphology and particle size of samples were analyzed by Scanning Electron Microscopy (SEM). It was found that similar particle size of 1-1.5  $\mu\text{m}$  is determined independent of annealing process. From the results of the capacity retention study for the prepared samples, LNMO900 shows the best cycling performance among the prepared samples. The reasons of these results will be revealed from the studies of cyclic voltammetry at various scan rates and electrochemical impedance spectroscopy of the coin-cells prepared with the prepared samples in company with the dissolution test of transition  $\text{Mn}^{2+}$  and  $\text{Ni}^{2+}$  into electrolyte with/without cycling. The relationship between the crystalline structure and the cycling performance of LNMO will be understood in the near future.

## References

- [1] L. Cai, Z. Liu, K. An, C. Liang, J. Mater. Chem. A 1 (2013) 6908.
- [2] S.-h. Wu, S.-H. Su, J.-J. Shiu, "Effects of heat-treatment on the crystalline structure and cycling performance of  $\text{LiNi}_{0.5}\text{Mn}_{1.5}\text{O}_4$  cathode materials", in preparation.

# **Preparation and Electrochemical Performance of Turpentine Oil Derived Carbon Nanohorns as Anode Materials for Lithium-Ion Batteries**

Arenst Andreas Arie<sup>1\*</sup>, Inez Devina<sup>1</sup>, Ratna Frida Susanti<sup>1</sup>,  
Hary Devianto<sup>2</sup>, Martin Halim<sup>3</sup> and Joong Kee Lee<sup>3</sup>

<sup>1</sup>*Department of Chemical Engineering, Parahyangan Catholic University,  
Ciumbuleuit 94, Bandung, Indonesia*

<sup>2</sup>*Department of Chemical Engineering, Bandung Institute of Technology,  
Ganesha 10 Bandung, Indonesia*

<sup>3</sup>*Center of energy Convergence, Korea Institute of Science and Technology,  
Hwarangno 5-o-gil Seongbukgu, Seoul ,Korea*

*\*e-mail address : arenst@unpar.ac.id*

Carbon nanohorns (CNHs) consist of horn-like tubes approx. 3–25 nm in diameter and 20–150 nm in length, which are closed at one end with a cone. The single-wall CNHs generally occur as an aggregate with a particle size ranging from 100 nm to several  $\mu\text{m}$ . Similar to graphenes and carbon nanotubes, CNHs also demonstrate good electrical and thermal conductivity, as well as high mechanical stability and high specific surface area. They are generally produced by laser ablation of pure graphite with high production rate and high yield, and typically form radial aggregates. In this paper, we prepared turpentine oil derived CNHs using nebulized spray pyrolysis technique and report on the electrochemical performances of such nano carbon structures. The structure and morphology of the resulting nano carbons were investigated with X-ray powder diffraction (XRD), Raman spectroscopy, Scanning Electron Microscope (SEM) and Transmission Electron Microscope (TEM). Cyclic voltammetry (CV) and cyclic test of the CNHs as an anode material for lithium ion batteries were also studied. The CNHs show a high specific capacity in the first cycle and high capacity retention until the 50<sup>th</sup> cycle at a constant current density of 100 mA/g, showing its potential use as an anode material in lithium-ion batteries. Those electrochemical characteristics were a result of the unique nanostructure and high conductivity of CNHs.

# Low-Temperature Operation Performance of LiFSI-Based Low EC Content Electrolyte with Specific Solvation State

Satoshi Uchida, Masaki Yamagata and Masashi Ishikawa

Department of Chemistry and Materials Engineering, Faculty of Chemistry, Materials and Bioengineering, Kansai University, 3-3-35 Yamate-cho, Suita 564-8680, Japan  
masaishi@kansai-u.ac.jp

The conventional electrolytes for Li-ion batteries are composed of  $\text{LiPF}_6$  or  $\text{LiBF}_4$  salts and mixed solvents of ethylene carbonate (EC) with a high dielectric constant and linear carbonates with low viscosity. The conventional electrolytes contain 30 – 50 vol.% EC to obtain high ionic conductivity by sufficient dissociation of Li salts. However, since EC has high melting point ( $38^\circ\text{C}$ ), the conventional electrolytes are not suitable for low-temperature ( $\leq -20^\circ\text{C}$ ) operation of Li-ion batteries. To achieve excellent low-temperature operation performance, the EC content should be reduced. On the other hand, reduction of EC content leads to decrease of ionic conductivity of electrolytes and generally degrade room-temperature rate performance of Li-ion batteries.

Previously, we found that lithium bis(fluorosulfonyl)imide (LiFSI) shows good ionic conductivity in a low EC content mixed solvent by very weak interaction between  $\text{Li}^+$  and FSI $^-$ . In addition, we also reported that the LiFSI-based low EC content (10 vol.%) electrolyte has specific dissolution process and shows outstanding room temperature rate performance than the conventional electrolytes.<sup>1)</sup> This result indicates that our electrolyte has possibility of achieving both excellent low-temperature operation performance and room-temperature rate performance. Therefore, we optimize the solvents composition of our electrolyte for above objective and evaluate its low-temperature operation performance in this work.

1.0 or 2.0  $\text{mol dm}^{-3}$  LiFSI dissolved in mixed solvents of EC, dimethyl carbonate (DMC) and ethylmethyl carbonate (EMC) (1:4.5:4.5 v/v/v) was used as the electrolyte with low EC content (denoted by 1.0 or 2.0  $\text{mol dm}^{-3}$  LiFSI/EC:DMC:EMC = 1:4.5:4.5 v/v/v), while 1.0  $\text{mol dm}^{-3}$   $\text{LiPF}_6$ /EC:EMC = 1:1 v/v were used as reference conventional electrolyte. Graphite or  $\text{LiNi}_{1/3}\text{Mn}_{1/3}\text{Co}_{1/3}\text{O}_2$  (NMC) composites containing conductive additive and binder were used as negative and positive electrodes, respectively. The respective mass of active materials in the negative and positive electrodes were ca. 4.5 and 9.5  $\text{mg cm}^{-2}$ . We assembled graphite/NMC cells with each electrolyte and evaluated their battery performances.

Fig. 1 shows room-temperature charge-discharge rate performances of graphite/NMC cells containing each electrolyte ( $1\text{C} = 160 \text{ mA g}^{-1}$ ). Our low EC content electrolytes shows better rate performance than reference conventional electrolyte. It should be noted that 2.0  $\text{mol dm}^{-3}$  LiFSI system shows superior rate performance even though the ionic conductivity of low EC content system decreases with increasing concentration of LiFSI. This result indicate that the room-temperature rate performance of our low EC content system is dominated specific dissolution process that was previously reported<sup>1)</sup> rather than bulk ionic conductivity. Fig. 2 shows charge-discharge curves ( $1\text{C}$ ) measured at  $-20^\circ\text{C}$  of graphite/NMC cells containing each electrolyte. In low-temperature operation, 1.0  $\text{mol dm}^{-3}$  LiFSI system shows best performance. Although low-temperature operation performance was sensitive to increase in bulk viscosity, 2.0  $\text{mol dm}^{-3}$  LiFSI system shows far superior low-temperature operation performance than reference conventional electrolyte.

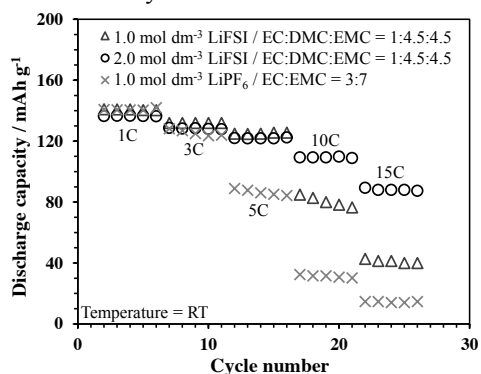


**Fig. 1** Charge-discharge rate performance of Graphite/NMC cells with various electrolytes.

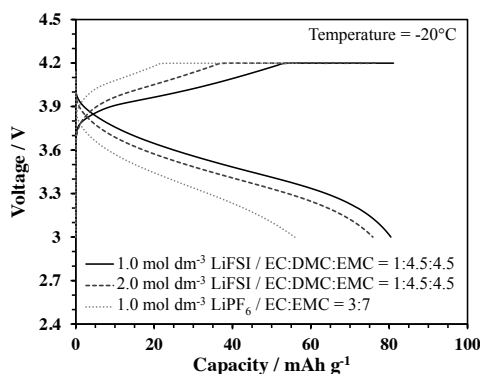


**Fig. 2** Charge-discharge curves of Graphite/NMC cells with various electrolytes at  $-20^\circ\text{C}$ .

1) S. Uchida et al., 226<sup>th</sup> Meeting of The Electrochemical Society, A5-0301 (2014)

# All-Solid-State Li Battery Using Garnet Structure Ta-substituted $\text{Li}_7\text{La}_3\text{Zr}_2\text{O}_{12}$ as Solid Electrolyte

Chih-Long Tsai<sup>1,2</sup>, Christian Dellen<sup>1,2</sup>, Hans-Gregor Gehrke<sup>1,2</sup>, Sandra Lobe<sup>1,2</sup>, Sven Uhlenbruck<sup>1,2</sup>, and Olivier Guillon<sup>1,2</sup>

1. Forschungszentrum Jülich GmbH, Institute of Energy and Climate Research, Materials Synthesis and Processing (IEK-1), 52425 Jülich, Germany
2. Jülich Aachen Research Alliance: JARA-Energy

All-solid-state Li battery containing oxide-class solid electrolyte is considered to be out stand from their high safety and higher energy density. Compared to the other class the solid Li ionic conductors, oxide-class Li ion conductors have additional advantages of easier material handling during synthesis, higher chemical stability and wider electrochemical window. The use of LLZ as solid electrolyte for solid-state battery had been reported in several papers. However, the reported solid-state batteries were all constructed with a thin film cathode which was made either by physical vapor or sol-gel deposition[1-2]. The thin film cathodes were usually under or around 1  $\mu\text{m}$  in thickness which made the energy density of these batteries not practical.

In order to realize the using of oxide-class Li ion conductor as solid electrolyte for a Li battery, Ta-substituted  $\text{Li}_7\text{La}_3\text{Zr}_2\text{O}_{12}$  (LLZ:Ta) powder had been synthesized via solid state reaction. LLZ:Ta with an optimized sintering parameter exhibits a high Li ion conductivity of  $7.8 \times 10^{-4} \text{ S cm}^{-1}$  at 30 °C with a relative density of ~94%. The material was further implanted as a solid electrolyte by using screen printing to put on thick  $\text{LiCoO}_2$  (> 50  $\mu\text{m}$ ) as cathode. A proper sintering process was invested for well bonding the thick cathode layer to the supporting electrolyte. The constructed all-solid-state Li batteries exhibited good charge-discharge utilization of active material of more than 80% which is equal to a capacity density of  $\sim 0.9 \text{ mAh cm}^{-2}$  at 100 °C. It also exhibited good cycle ability that one hundred of cycles were achieved at temperature of 50 °C. Thus, LLZ:Ta shows as a promising candidate for all-solid-state Li battery. However, the reduction of high internal resistance of the cell is still the major challenge for further improvement of the battery performance, especially if the application of this all solid state Li battery is toward room temperature. During this presentation, results from material chemical stability, cell morphology, electrochemical performance and the challenges of building up Li battery by using LLZ:Ta will be discussed.

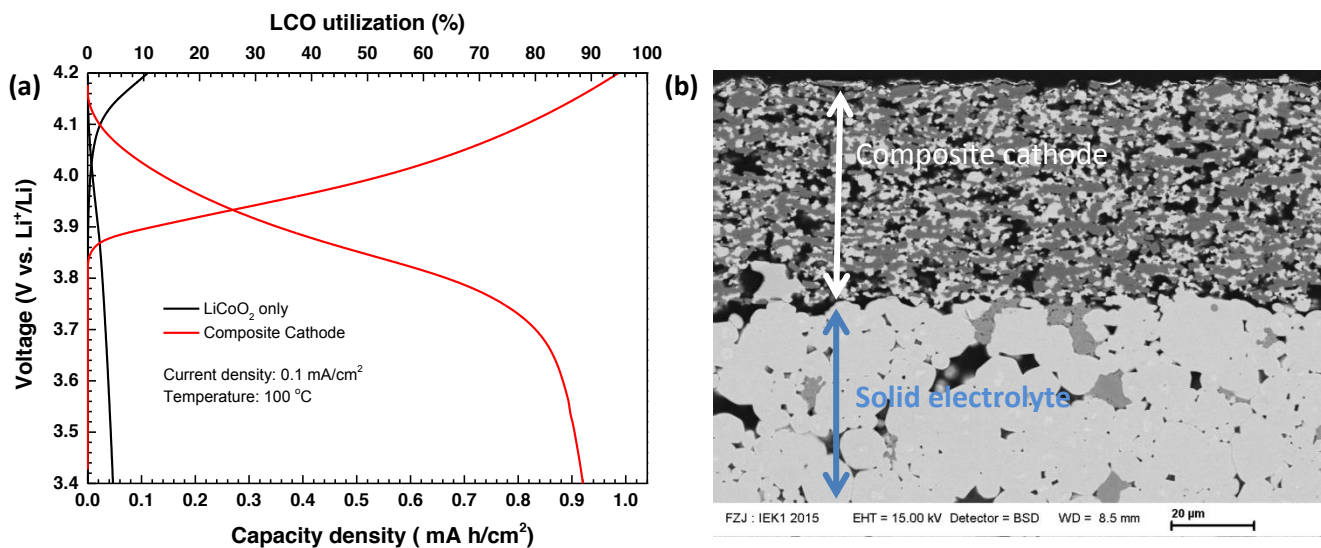


Figure (a) galvanostatic charge-discharge profile for using different cathodes and (b) microstructure of composite cathode.

[1] M. Kotobuki et al, *Ceramics International* 39 (2013) 6481

[2] Y. Jin et al, *J. Power Sources* 239 (2013) 326

# Three Dimensional Cu/C/Ge Heterostructured Electrodes for High-performance Li ion Batteries

Dong-Wan Kim<sup>1</sup>, Gwang-Hee Lee<sup>1</sup>, Joosun Kim<sup>2</sup>

<sup>1</sup>*School of Civil, Environmental and Architectural Engineering, Korea University, Seoul 136-713, Korea*

<sup>2</sup>*High-Temperature Energy Materials Research Center, Korea Institute of Science and Technology, Seoul 136-791, Korea*  
*dwkim1@korea.ac.kr*

It is of great significance to improve the power density of Li ion batteries in pursuit of high-end products and technologies. Various nanoscale structures including nanoparticles, nanowires, nanosheets, and nanotubes have been designed for high-efficiency energy applications. In particular, electrodes for Li-ion batteries with a long cycle life, high energy, and high power rate capability can be associated with three-dimensional (3-D) nanoarchitectures. There are two types of 3-D nanoarchitectures: self-supported nanoelectrode materials and nanoarchitected current collectors. Self-supported nanoelectrode materials have direct electronic pathways, allowing for efficient charge transport and the accommodation of the volume expansion during  $\text{Li}^+$  insertion/removal cycling. Herein, we fabricated two types of 3-D nanoarchitected current collectors consisting of 1-D Cu/C core/sheath nanowires and 2-D Cu/C core/sheath nanonets. High-capacity Ge nanoarrays were deposited onto the as-prepared Cu/C nanowires or Cu/C nanonets via thermal evaporation and a  $\text{GeO}_2$  removal process. The obtained samples have advantages over Li-ion battery anodes because of the highly porous ordered and aligned nanostructures. The Cu/C nanonet-based Ge anodes exhibited a large reversible capacity of  $933 \text{ mA h g}^{-1}$  at a rate of 1 C over 1000 cycles and an excellent rate capability of  $1017 \text{ mA h g}^{-1}$  at a rate of 10 C over 200 cycles. More importantly, as the Ge nanoarrays mass loading increased, the areal capacity can be successfully enhanced to  $2.4 \text{ mA h cm}^{-2}$ . Our strategy on the 3-D nanoarchitected electrodes has significant advantages such as a long cycle life and high-rate capabilities for the anode design of Li-ion batteries and also allows for their potential application to other applications, such as supercapacitors, solar cells, and so on.

# **The Effects of Substrates on the Phase Formation Behavior and the Electrochemical Properties of $\text{Li}_2\text{MnSiO}_4$ Cathode Thin Films Deposited by RF Sputtering for Thin Film Batteries**

Suman Chae<sup>1</sup>, Joongpyo Shim<sup>2</sup>, Gyungse Park<sup>3</sup> and Ho-Jung Sun<sup>1\*</sup>

<sup>1</sup>*Department of Materials Science & Engineering,*

<sup>2</sup>*Department of Nano & Chemical Engineering,*

<sup>3</sup>*Department of Chemistry,*

*Kunsan National University, Jeonbuk, 573-701, Korea*

*\*hjsun@kunsan.ac.kr*

Lithium ion batteries have been widely used in mobile electronics applications by virtue of their high energy density. Recently, the solid-state thin film batteries have received growing attention because of their on-board capability with microelectronic circuits such as microelectromechanical systems and smart cards [1]. They consist of a cathode, electrolyte, and an anode. Among them, the thin film cathode plays a key role in the aspect of providing high capacity, thus the selection of the material and its properties in thin film form are important. Various kinds of cathode materials have been developed in bulk form [2]. Among them,  $\text{Li}_2\text{MnSiO}_4$  has been considered as an attractive cathode material due to its potential high capacity, being expected to use more than one Li ion per formula unit because of its two redox couples,  $\text{Mn}^{2+}/\text{Mn}^{3+}$  and  $\text{Mn}^{3+}/\text{Mn}^{4+}$  [3]. Its theoretical capacity is 333 mAh/g.

In this research,  $\text{Li}_2\text{MnSiO}_4$  thin films were deposited on various substrates by rf sputtering method. The substrates were Al foil, SUS and Ni ones which were electrically conductive for being used as current collectors. Powder-type  $\text{Li}_2\text{MnSiO}_4$  sputtering targets with and without carbon were prepared by solid-state reaction using planetary ball-mill. As-deposited thin films were amorphous, thus for some samples, post-annealing was applied in order to crystallize the films. Oxygen should be prevented during both the deposition and annealing processes in order to suppress the oxidation of  $\text{Mn}^{2+}$  of the  $\text{Li}_2\text{MnSiO}_4$  phase. It was revealed that the formation of  $\text{Li}_2\text{MnSiO}_4$  phase was favorable on the SUS substrates. The electrochemical performances of both crystallized and amorphous  $\text{Li}_2\text{MnSiO}_4$  thin films were evaluated with liquid electrolyte in coin cells. The capacities of  $\text{Li}_2\text{MnSiO}_4$  cathode thin films with carbon were higher than those without carbon. Improved cycling properties of the  $\text{Li}_2\text{MnSiO}_4$  cathode thin films were appeared.

## **References**

- [1] Y.-N. Zhou, M.-Z. Xue, and Z.-W. Fu, J. Power Sources 234, 310 (2013).
- [2] B. Xu, D. Qian, Z. Wang, and Y. S. Meng, Mater. Sci. Engin. R 73, 51 (2012).
- [3] R. J. Gummow and Y. He, J. Power Sources 253, 315 (2014).

# Synthesis and Characterization of LiFePO<sub>4</sub> Composite Cathode Material Modified with in-situ Graphene and Solid-State Electrolyte

\*<sup>2</sup>Chun-Chen Yang, <sup>1,2</sup>Jer-Huan Jang, <sup>1,2</sup>Jia-Rong Jiang

\*Department of Chemical Engineering, Ming Chi University of Technology, New Taipei City 243, Taiwan, R.O.C.

<sup>1</sup>Department of Mechanical Engineering, Ming Chi University of Technology, New Taipei City 243, Taiwan, R.O.C.

<sup>2</sup>Battery Research Center of Green Energy, Ming Chi University of Technology, New Taipei City 243, Taiwan, R.O.C.

(\*Corresponding author, E-mail: [ccyang@mail.mcut.edu.tw](mailto:ccyang@mail.mcut.edu.tw))

## Abstract

The LiFePO<sub>4</sub>/C (LFP/C) was synthesized by a solid-state ball-milled method; LATP solid electrolyte was prepared by a sol-gel method. The surface-modified LiFePO<sub>4</sub>/C composite cathode materials was co-coated with both in-situ graphene and Li<sub>1.4</sub>Al<sub>0.4</sub>Ti<sub>1.6</sub>(PO<sub>4</sub>)<sub>3</sub> (LATP) solid-state electrolyte via a one-pot sol-gel process. The surface-modified LiFePO<sub>4</sub>/C cathode materials were examined by XRD, SEM/EDX, TEM, micro-Raman spectroscopy, EA, and XRF. The 2032 coin half-cell was assembled to examine the electrochemical performance of the surface-modified LiFePO<sub>4</sub>/C cathode materials. The galvanostatic charge-discharge test was conducted in the potential range of 2 - 4.0 V using LiPF<sub>6</sub> + EC: DEC (1:1, v/v) electrolyte at various C-rates (0.1C-10C) at 25°C, 55°C and -20°C. It was revealed that the capacities retention of the bare LFP/C and the surface-modified LFP/C cathode materials at 1C/1C for 200 cycles are 89.53% and 91.28%, respectively, at 25°C. Moreover, we also found that the capacities retention of the bare LFP/C and the surface-modified LFP/C cathode materials at 1C/1C for 200 cycles are 58.7% and 86.2%, respectively, at 55°C. At -20°C, the discharge capacity of the surface-modified LFP/C cathode materials is around 100 mA g<sup>-1</sup>; in comparison, only 60-70 mAh g<sup>-1</sup> for bare LFP/C material. According to the results, we found that the as-prepared GNS+LATP co-coated LFP/C materials exhibit excellent electrochemical performance. It can be a promising candidate cathode material for the rechargeable lithium ion battery.

**Keywords:** Li<sub>1.4</sub>Al<sub>0.4</sub>Ti<sub>1.6</sub>(PO<sub>4</sub>)<sub>3</sub> (LATP), in-situ Graphene, Sol-gel method, LiFePO<sub>4</sub>, Li-ion battery

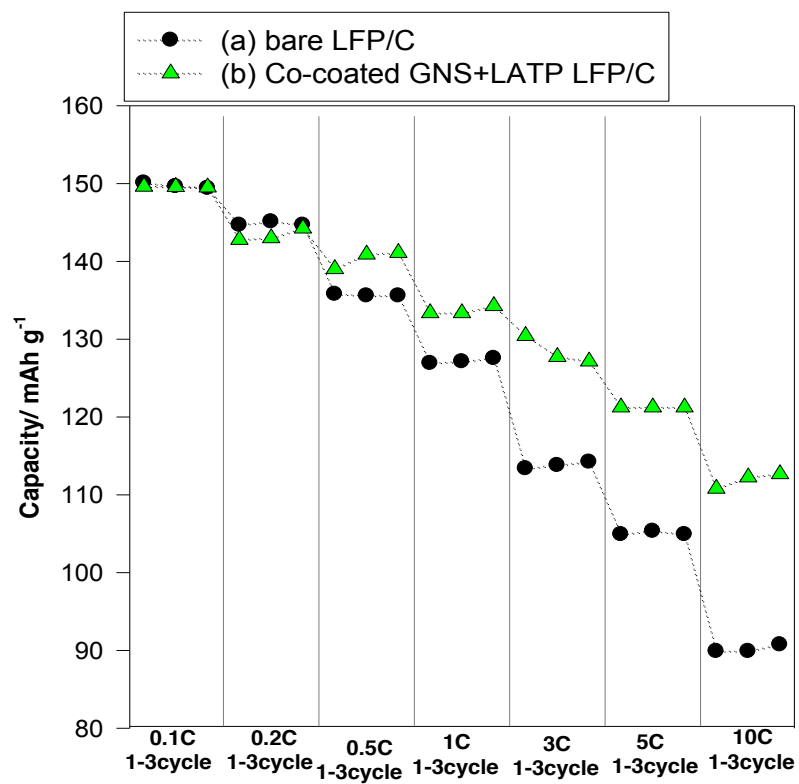


Fig. 1



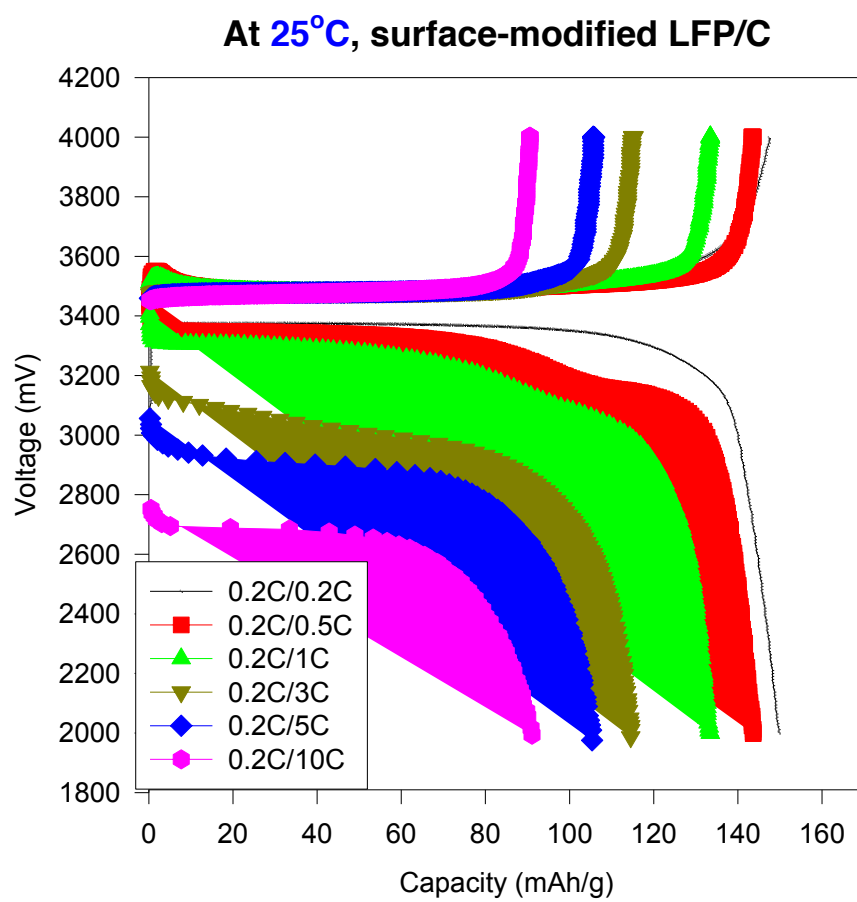


Fig. 2

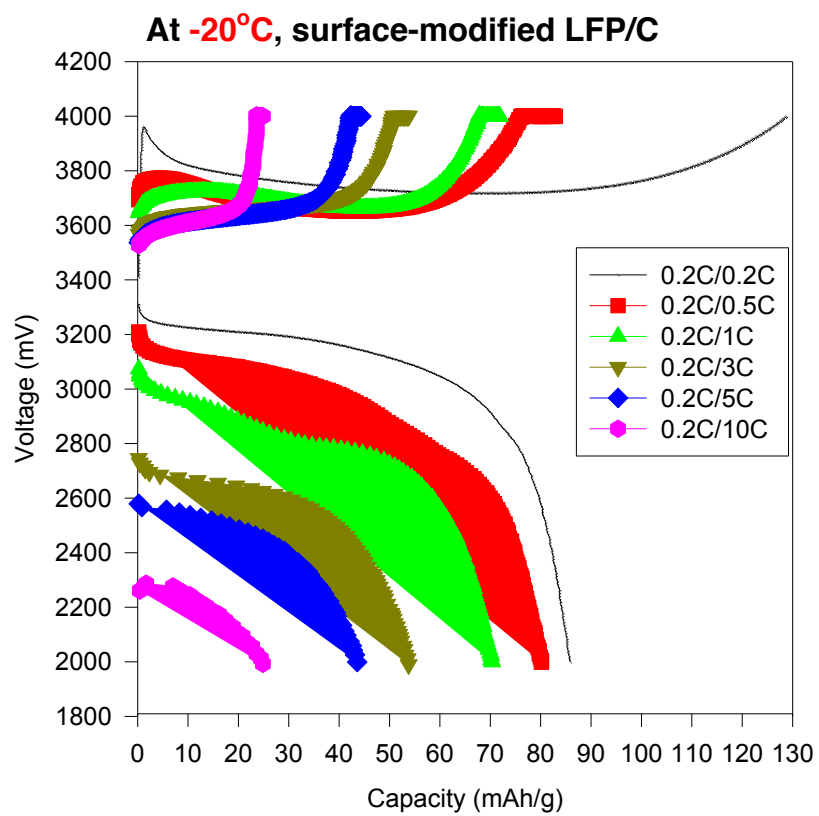


Fig. 3

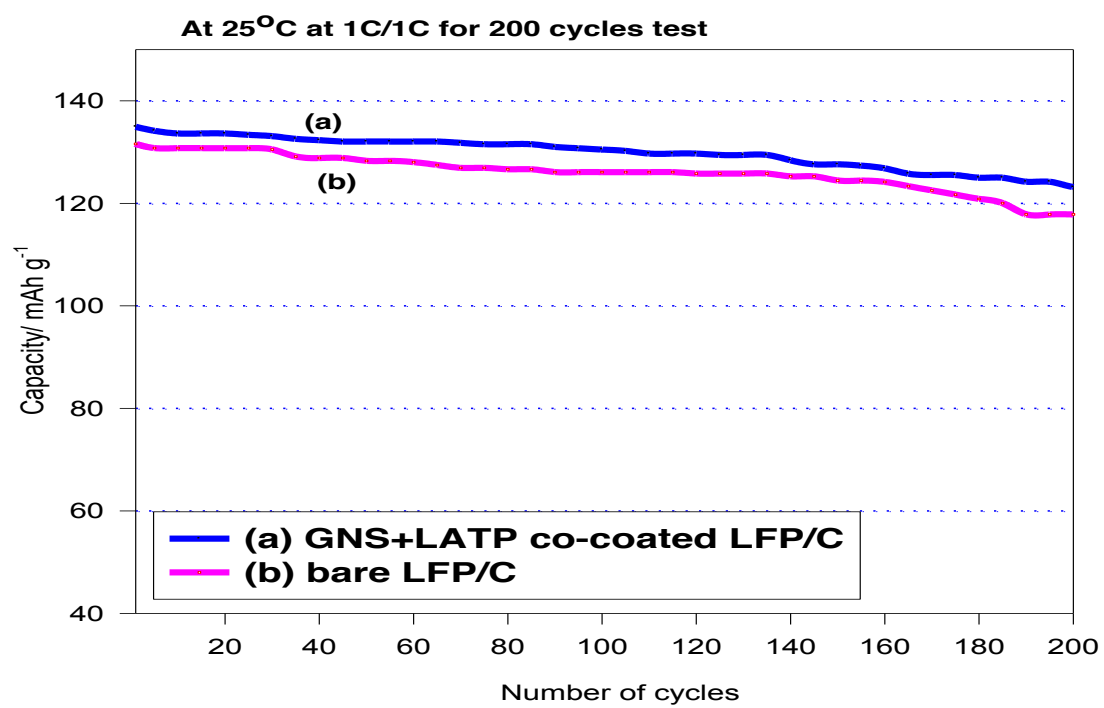


Fig. 4

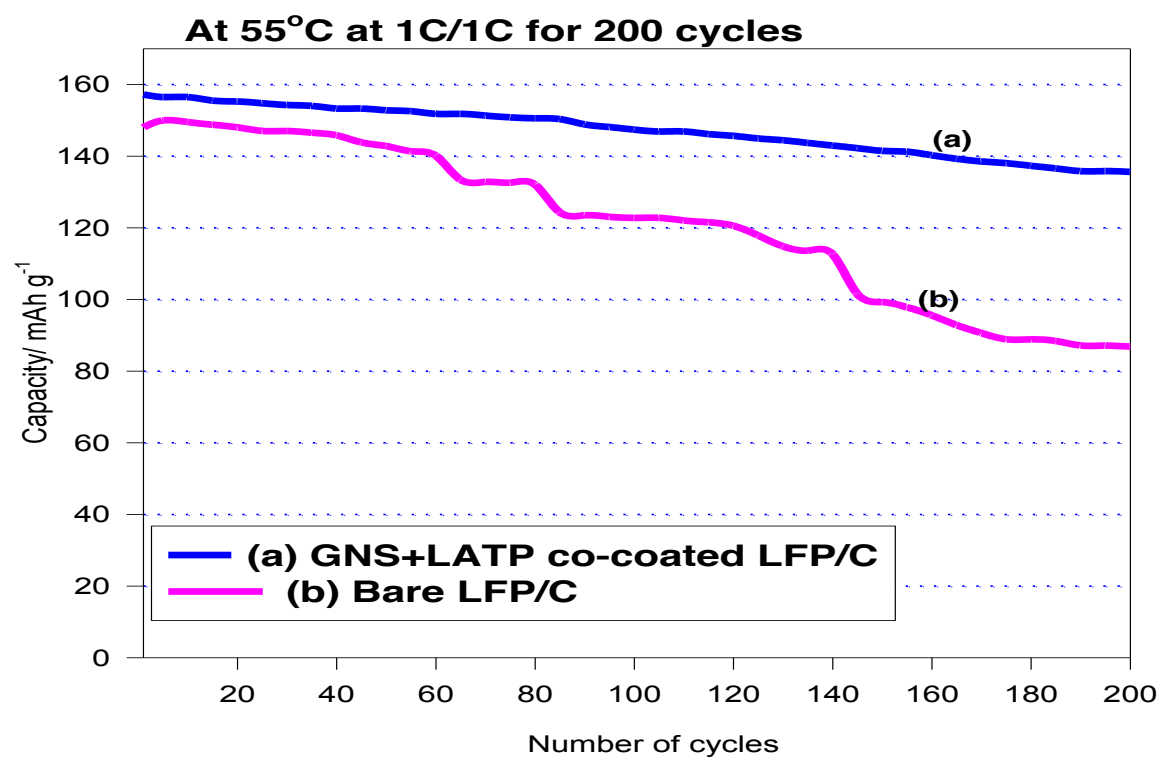


Fig. 5

**Table 1**

The discharge capacities of GNS+LATP co-coated LFP/C at various rates, 0.2-10C at -20°C

<b>-20°C</b>	<b>Charge (mAh)</b>	<b>Discharge (mAh)</b>	<b>CE/ %</b>	<b>Active material (g)</b>	<b>Discharge capacity (mAh/g)</b>
<b>0.2C/0.2C</b>	0.606	0.404	66.67	0.004704	85.88
<b>0.2C/0.2C</b>	0.606	0.404	66.67	0.004704	85.88
<b>0.2C/0.2C</b>	0.412	0.398	96.60	0.004704	84.61
<b>0.2C/0.5C</b>	0.455	0.378	83.08	0.004704	80.36
<b>0.2C/0.5C</b>	0.39	0.377	96.67	0.004704	80.14
<b>0.2C/0.5C</b>	0.385	0.375	97.40	0.004704	79.72
<b>0.2C/1C</b>	0.382	0.333	87.17	0.004704	<b>70.79</b>
<b>0.2C/1C</b>	0.338	0.331	97.93	0.004704	<b>70.37</b>
<b>0.2C/1C</b>	0.336	0.33	98.21	0.004704	<b>70.15</b>
<b>0.2C/3C</b>	0.335	0.249	74.33	0.004704	52.93
<b>0.2C/3C</b>	0.253	0.253	100.00	0.004704	53.78
<b>0.2C/3C</b>	0.256	0.251	98.05	0.004704	53.36
<b>0.2C/5C</b>	0.256	0.204	79.69	0.004704	43.37
<b>0.2C/5C</b>	0.209	0.205	98.09	0.004704	43.58
<b>0.2C/5C</b>	0.21	0.207	98.57	0.004704	44.01
<b>0.2C/10C</b>	0.211	0.113	53.55	0.004704	24.02
<b>0.2C/10C</b>	0.117	0.117	100.00	0.004704	24.87
<b>0.2C/10C</b>	0.121	0.127	104.96	0.004704	27.00

**Table 2**

The discharge capacities of GNS+LATP co-coated LFP/C at various rates, 0.2-10C at 25°C

<b>25°C</b>	<b>Charge (mAh)</b>	<b>Discharge (mAh)</b>	<b>CE/ %</b>	<b>Active material (g)</b>	<b>Discharge capacity (mAh/g)</b>
<b>0.2C/0.2C</b>	0.632	0.56	88.61	0.00392	142.86
<b>0.2C/0.2C</b>	0.578	0.587	101.56	0.00392	149.74
<b>0.2C/0.2C</b>	0.598	0.596	99.67	0.00392	152.04
<b>0.2C/0.5C</b>	0.605	0.558	92.23	0.00392	142.35
<b>0.2C/0.5C</b>	0.563	0.563	100.00	0.00392	143.62
<b>0.2C/0.5C</b>	0.574	0.568	98.95	0.00392	144.90
<b>0.2C/1C</b>	<b>0.571</b>	<b>0.522</b>	<b>91.42</b>	<b>0.00392</b>	<b>133.16</b>
<b>0.2C/1C</b>	<b>0.523</b>	<b>0.523</b>	<b>100.00</b>	<b>0.00392</b>	<b>133.42</b>
<b>0.2C/1C</b>	<b>0.527</b>	<b>0.523</b>	<b>99.24</b>	<b>0.00392</b>	<b>133.42</b>
<b>0.2C/3C</b>	0.529	0.448	84.69	0.00392	114.29
<b>0.2C/3C</b>	0.452	0.449	99.34	0.00392	114.54
<b>0.2C/3C</b>	0.452	0.45	99.56	0.00392	114.80
<b>0.2C/5C</b>	0.453	0.411	90.73	0.00392	104.85
<b>0.2C/5C</b>	0.415	0.413	99.52	0.00392	105.36
<b>0.2C/5C</b>	0.417	0.414	99.28	0.00392	105.61
<b>0.2C/10C</b>	<b>0.417</b>	<b>0.353</b>	<b>84.65</b>	<b>0.00392</b>	<b>90.05</b>
<b>0.2C/10C</b>	<b>0.355</b>	<b>0.357</b>	<b>100.56</b>	<b>0.00392</b>	<b>91.07</b>
<b>0.2C/10C</b>	<b>0.361</b>	<b>0.361</b>	<b>100.00</b>	<b>0.00392</b>	<b>92.09</b>

**Table 3**

The cycle-life performances of the bare and GNS+LATP co-coated LFP/C composites at various cycles at 1C/1C for 200 cycles at 25°C

Sample	Data			Capacit	Fading
	$Q_{1st}/$ mAh $g^{-1}$	$Q_{100th}/$ mAh $g^{-1}$	$Q_{200th}/$ mAh $g^{-1}$	ty loss at 200 <sup>th</sup> cycle/ %	rate at 200 <sup>th</sup> / mAh $g^{-1}$ cycle <sup>-1</sup>
Bare LFP/C	131.60	126.09	117.83	10.46 %	0.069
GNS+LATP co-coated LFP/C	134.93	130.49	123.17	8.72%	0.059

**Table 3**

The cycle-life performances of the bare and GNS+LATP co-coated LFP/C composites at various cycles at 1C/1C for 200 cycles at 55°C

Sample	Data			Capacit	Fading
	$Q_{1st}/$ mAh $g^{-1}$	$Q_{100th}/$ mAh $g^{-1}$	$Q_{200th}/$ mAh $g^{-1}$	y loss at 200 <sup>th</sup> cycle/ %	rate at 200 <sup>th</sup> / mAh $g^{-1}$ cycle <sup>-1</sup>
Bare LFP/C	148.02	122.77	86.88	62.19%	0.307
GNS+LATP co-coated LFP/C	157.23	147.39	135.58	13.77%	0.108

## References

- [1] J. Li, L. Zhang, L. Zhang, W. Hao, H. Wang, Q. Qu, H. Zheng, “In-situ growth of graphene decorations for high-performance  $\text{LiFePO}_4$  cathode through solid-state reaction”, *Journal of Power Sources* 249 (2014) 311-319.
- [2] H. Wu, Q. Liu, S. Guo, “Composites of Graphene and  $\text{LiFePO}_4$  as Cathode Materials for Lithium-Ion Battery: A Mini-review”, *Nano-Micro Letters* 6 (2014) 316-326.
- [3] B. Yao, Z. Ding, J. Zhang, X. Feng, L. Yin, “Encapsulation of  $\text{LiFePO}_4$  by in-situ graphitized carbon cage towards enhanced low temperature performance as cathode materials for lithium ion batteries, *Journal of Solid State Chemistry* 216 (2014) 9-12.
- [4] Y. Liang, Z. Lin, Y. Qiu, X. Zhang, “Fabrication and characterization of LATP/PAN composite fiber-based lithium-ion battery separators” *Electrochimica Acta* 56 (2011) 6474-6480.
- [5] H. Morimoto, H. Awano, J. Terashima, Y. Shindo, S. Nakanishi, N. Ito, K. Ishikawa, S. Tobishima, “Preparation of lithium ion conducting solid electrolyte of NASICON-type  $\text{Li}_{1+x}\text{Al}_x\text{Ti}_2-x(\text{PO}_4)_3$  ( $x = 0.3$ ) obtained by using the mechanochemical method and its application as surface modification materials of  $\text{LiCoO}_2$  cathode for lithium cell” *Journal of Power Sources* 240 (2013) 636-643.



# Characterization of sodium based ternary polymer electrolytes

Andrea Boschin and Patrik Johansson  
Chalmers University of Technology,  
SE - 412 96 Göteborg, SWEDEN  
andrea.boschin@chalmers.se

At present sodium ion batteries (SIBs) represent a possibly cheaper and more sustainable alternative to lithium ion batteries [1]. Indeed, while sodium shows similar chemical and electrochemical properties to lithium, paving the way for fast development, the resources of sodium are in principle unlimited. The SIB electrolyte research is diverse; organic solvents, polymers, and ionic liquids are all being used as matrices [1-3]. Ion conducting solid polymer electrolytes (SPEs) avoid the usage of organic solvents and can thereby enable fabrication of flexible, safe and compact solid-state structures. The ionic conductivities of sodium and lithium SPEs, based on poly (ethylene oxide) (PEO) are comparable [4-6], however, both having rather low conductivity values: ( $10^{-7}$ - $10^{-5}$ )  $\text{Scm}^{-1}$  at room temperature.

The main part of the research performed so far on  $\text{Na}^+$  conducting SPEs was carried out during the 1990's [5-6]. Recently [7], we have characterized the binary SPE systems NaTFSI-PEO and NaFSI-PEO, where basically the TFSI anion acts inhibiting on crystallization, as previously shown for the corresponding Li-based SPEs [8], while the FSI anion, despite being chemically very similar, seems to favor it – in these often semi-crystalline systems. The highest ionic conductivity at 20°C was obtained for NaTFSI(PEO)<sub>9</sub>.

In order to further improve the ionic conductivity without compromising safety [9], different amounts of N-propyl-N-methyl-pyrrolidinium (PYR<sub>13</sub>) based ionic liquids (ILs) with the very same anions (FSI, TFSI) have here been added; creating ternary polymer electrolytes NaX-PEO-PYR<sub>13</sub>X. The resulting ternary systems are compared with the analogous binary systems in terms of basic physico-chemical properties obtained by dielectric spectroscopy, differential scanning calorimetry, and Raman spectroscopy. Overall, the addition of ILs to the binary systems increases their conductivity and the PEO chain mobility. These effects are most likely due to the presence of the PYR<sub>13</sub> cation, which does not interact strongly with the PEO chains, and the contribution of the different ions is crucial in view of application of ternary systems in SIBs.

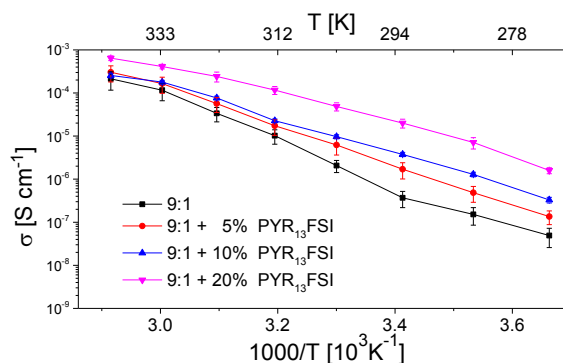


**Figure 1:** Ionic conductivities of the NaFSI(PEO)<sub>9</sub>-PYR<sub>13</sub>FSI system.

## References

1. A. Ponrouch *et al.*, Journal of Material Chemistry A 3 (2015) 22
2. V. Palomares *et al.*, Energy & Environmental Science 5 (2012) 5884
3. M. H. Slater *et al.*, Advanced Functional Materials 23 (2013) 947
4. J. W. Fergus, Solid State Ionics 227 (2012) 102
5. A. Ferry *et al.*, Electrochimica Acta 43 (1998) 1387
6. M. Perrier *et al.*, Electrochimica Acta 40 (1995) 2123
7. A. Boschin and P. Johansson, Electrochimica Acta, (2015) accepted
8. L. Edman *et al.*, Journal of Materials Research 15 (2000) 1950
9. J. H. Shin *et al.*, Electrochemistry Communications 5 (2003) 1016

# Synthesis of Ternary Spinel Iron-Cobalt-Nickel Oxide/Carbon Black Composites as a High-Performance Bifunctional Electrocatalyst for Rechargeable Zinc-Air Batteries

Yu-Ju Chien, Chi-Chang Hu\*

Department of Chemical Engineering, National Tsing Hua University  
101, Sec. 2, Kuang-Fu Rd., Hsin-Chu city, 30013 Taiwan  
annq2465@yahoo.com.tw

\*corresponding author : cchu@che.nthu.edu.tw

Among various metal-air batteries, the rechargeable zinc-air battery has been considered to be an attractive choice because of its unique benefits, such as low cost, safety, and environment friendliness [1]. However, there are still many challenges to overcome, such as inherent sluggish kinetics of the oxygen reduction reaction (ORR) and oxygen evolution reaction (OER) and high overpotential [2]. It has been reported that transition metal oxides are the most promising bifunctional electrocatalysts in alkaline solution [3]. The substitution of nickel by iron in spinel  $\text{NiCo}_2\text{O}_4$  was found to enhance oxygen evolution in the alkaline media [4]. Here, we employ an iron-doped  $\text{NiCo}_2\text{O}_4$  spinel structure supported on carbon black as an efficient bifunctional electrocatalyst for both the ORR and OER. The hybrid electrocatalyst is facilely synthesized via hydroxide precipitation and thermal treatment. The carbon black induced into the iron-doped  $\text{NiCo}_2\text{O}_4$  reduces the overpotential and markedly promotes the currents of the ORR and OER in alkaline electrolytes. The activity of  $\text{Fe}_x\text{Ni}_{1-x}\text{Co}_2\text{O}_4$ /carbon black composites is much higher than that of their corresponding oxides for both the ORR and OER. Furthermore, the rechargeable zinc-air battery with the optimized  $\text{Fe}_x\text{Ni}_{1-x}\text{Co}_2\text{O}_4$ /carbon black composite as a bifunctional electrocatalyst displays a high activity and good stability during a full cell charge-discharge process.

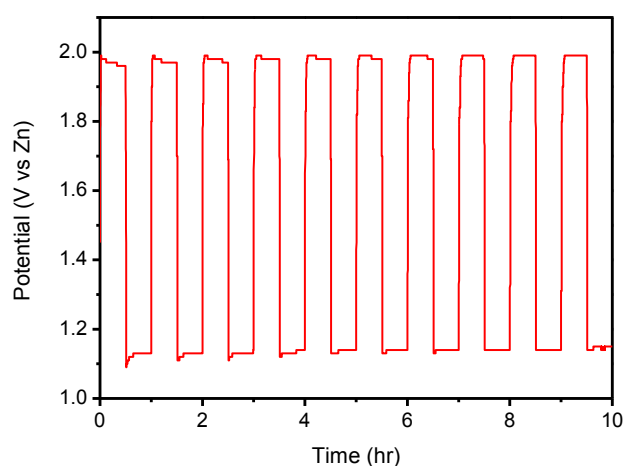


Fig. 1. The repeated charge-discharge curves of a Zn-air battery with a  $\text{Fe}_x\text{Ni}_{1-x}\text{Co}_2\text{O}_4$ /carbon black composite working as the air cathode during discharging and the oxygen evolution anode during charging.

## References

1. M. Prabu, P. Ramakrishnan, H. Nara, T. Momma, T. Osaka and S. Shanmugam, *ACS Appl. Mater. Interfaces*, 2014, 6, 16545-16555.
2. M. Armand and J. M. Tarascon, *Nature*, 2008, 451, 652-657.
3. Y. Liang, Y. Li, H. Wang, J. Zhou, J. Wang, T. Regier and H. Dai, *Nat. Mater.*, 2011, 10, 780-786.

4. D. Chanda, J. Hnát, M. Paidar and K. Bouzek, *Hydrogen Energy Publications*, 2014, 39, 5713-5722.

# A comparative study on $\text{Li}^+$ ion migration characteristics in the interphases of positive and negative electrodes

Tae-jin Lee, Taeho Yoon, Jiwon Jung, Jiyong Soon, Jae Gil Lee, Ji Heon Ryu<sup>1</sup>, and Seung M. Oh\*

Department of Chemical and Biological Engineering, Seoul National University, 1 Gwanak-ro, Gwanak-gu, Seoul 151-742, South Korea

<sup>1</sup> Graduate School of Knowledge-based Technology and Energy, Korea Polytechnic University, Gyeonggi, 429-793, South Korea\*Correspond to [seungoh@snu.ac.kr](mailto:seungoh@snu.ac.kr)

Lithium-ion batteries, beyond the traditional IT mobile devices, has attracted to be applied to EV and ESS. It is required higher energy density to meet these expectations. It would be one method for 5V class positive electrodes to be applied, they have not been commercialized due to their operation voltage beyond the stable electrochemical stability windows of electrolytes[1]. The commonly used electrolytes are decomposed and surface film deposit on these high voltage positive electrodes[2].

Film is the interphase between electrolytes and positive electrodes. Because it is  $\text{Li}^+$  migration path in solid, more sluggish than liquid electrolytes, it determines the kinetics and the reversibility of positive electrodes[3]. Studies on these phenomena have been mainly performed for SEI on negative electrodes[4, 5]. But, it has not been paid attention about the characteristics of  $\text{Li}^+$  migration in the film deposited on positive electrodes. So, this study is necessary more than anything else to improve properties of interphase on positive electrodes.

In this study, the  $\text{Li}^+$  ion conductivity of film is analyzed by some comparative studies with SEI on negative electrodes, which has been mainly studied. At first, it needs to be calibrated about the quantities of the decomposed electrolytes or thickness of interphase between them prior to the analysis of their ion conductivity. In cyclic voltammetry of only electrolyte system, anodic current is much lower than cathodic current.(Fig. 1. (a), (b)) This means indirectly film is much thinner than the SEI. Nevertheless, EIS shows that film resistance is much larger than SEI(Fig. 2.(a), (b)), it means that ion conductivity of film is inferior compared to SEI. This implies that components of these two interphases are different from each other. So, the ultimate goal of this study is to find out the different mechanism of  $\text{Li}^+$  migration in film on positive electrodes compared to SEI on negative electrodes.

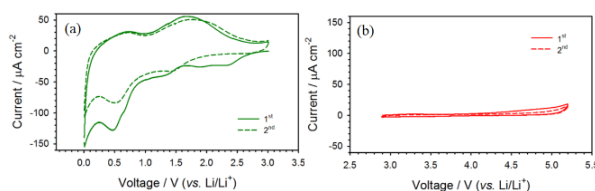


**Fig. 1.** Cyclic voltammetry of the commonly used electrolytes. 1.3 M  $\text{LiPF}_6$  in EC : EMC : DEC = 3 : 2 : 5 (v/v/v). Pt /  $\text{Li}^0$  /  $\text{Li}^0$  (W/C/R) 3 electrode cell. (a) Cathodic current (b) Anodic current

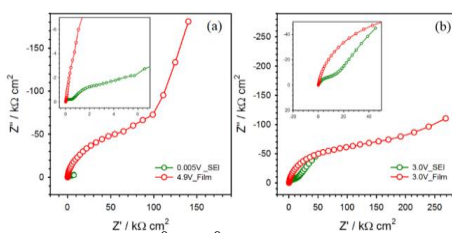


**Fig. 2.** A.C impedance spectroscopy of Pt /  $\text{Li}^0$  /  $\text{Li}^0$  (W/C/R) 3 electrode cell after voltage sweep. (a) Charged state; 0.005V and 4.9V (vs.  $\text{Li/Li}^+$ ) (b) Discharged state; both 3.0V (vs.  $\text{Li/Li}^+$ )

- [1] J.B. Goodenough, Y. Kim, Journal of Power Sources, 196 (2011) 6688-6694.
- [2] T. Yoon, D. Kim, K.H. Park, H. Park, S. Jurng, J. Jang, J.H. Ryu, J.J. Kim, S.M. Oh, Journal of The Electrochemical Society, 161 (2014) A519-A523.
- [3] K. Xu, A. von Cresce, Journal of Materials Chemistry, 21 (2011) 9849-9864.
- [4] E. Peled, Journal of The Electrochemical Society, 126 (1979) 2047-2051.
- [5] S. Shi, P. Lu, Z. Liu, Y. Qi, L.G. Hector, H. Li, S.J. Harris, Journal of the American Chemical Society, 134 (2012) 15476-15487.

# Size-regulated Precursor-Based Synthesis of Lithium-Rich Layered Cathode Material Deriving High Rate Capability

Shingo Kaneko<sup>1,2,5,\*</sup>, Yuichi Sato<sup>1,2</sup>, Futoshi Matsumoto<sup>2,3</sup>, Junwei Zheng<sup>4,5</sup> and Decheng Li<sup>4,5,\*</sup>

<sup>1</sup>Research Institute for Engineering, <sup>2</sup>Lithium Battery Open-laboratory, and <sup>3</sup>Department of Material and Life Chemistry, Kanagawa University, 3-27-1, Rokkakubashi, Kanagawa-ku, Yokohama 221-8686, Japan, <sup>4</sup>College of Physics, Optoelectronics and Energy & Collaborative Innovation Center of Suzhou Nano Science and Technology, and <sup>5</sup>Key Laboratory of Lithium Ion Battery Materials of Jiangsu Province, Institute of Chemical Power Sources, Soochow University, Suzhou 215006, China  
\*Corresponding Author: (S.K.) fs111747wx@kanagawa-u.ac.jp, (D.L.) lidecheng@suda.edu.cn

Lithium-rich layered cathode material is now considered as a promising cathode material candidate due to its high energy density. This type of cathode material, however, has severe drawbacks of a rapid capacity fading arising from charge/discharge cycle repetitions and a low electron conductivity leading to capacity decrease at high current density. To overcome such problems, additional modifications (e.g., those where cathode materials are coated with other stable one to protect from undesired side-reaction) [1, 2] and additional treatments (e.g., those where they are adopted to maximally promote the potential properties of the material) have been majorly proposed [3, 4], but there is still a room for innovation to arrange structural and morphological feature of the material itself. Our group have recently reported the good cycle stability and the high rate capability of a  $\text{Li}_{1.2}\text{Ni}_{0.18}\text{Mn}_{0.59}\text{Co}_{0.03}\text{O}_2$  cathode material modified with  $\text{LiCoPO}_4$  nanoparticles [5]. We herein present a unique strategy to obtain size-regulated precursor fine particles, whose morphology was also controlled to have a microscopic homogeneity based on a reverse microemulsion technique (Fig. 1A). The cathode material with the same composition of  $\text{Li}_{1.2}\text{Ni}_{0.18}\text{Mn}_{0.59}\text{Co}_{0.03}\text{O}_2$  was synthesized from such precursor particles in order to look at the impact of such a precursor synthesis on the eventual cell performances of the material (Fig. 1B). The resulting material demonstrated a good cycle stability (50th cycle discharge capacity: 281 mAh/g at 20 mA/g) without any additional modifications or treatments and a high capacity retention (52%) even at 640 mA/g (Fig. 2A). According to the impedance spectra of an electrode made from the cathode material, the overall features of the small semicircle observed in the high frequency after charging (Fig. 2B, inset) are almost identical regardless of the cycle number. This is a good indicator demonstrating that for the particles of the cathode material, a coherent smart solid-electrolyte-interface (SEI) layer may be formed on the surface of the particles whereby they are protected from any undesirable side-reactions during the following cycles after the 1st cycling. In addition, this experimental fact strongly supports the result shown in Fig. 2A exhibiting that the cathode material has the potential ability to yield a long-term smooth  $\text{Li}^+$  diffusion even under high-rate conditions.

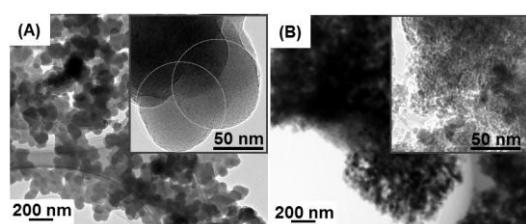


Fig. 1 TEM images of the particles for (A) as-obtained precursor and (B) cathode material. The insets show magnified images of each specimen.

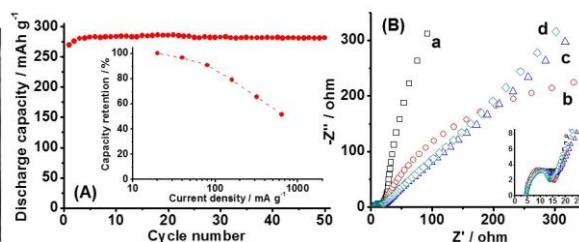


Fig. 2 Electrochemical measurements of  $\text{Li}_{1.2}\text{Ni}_{0.18}\text{Mn}_{0.59}\text{Co}_{0.03}\text{O}_2$ . (A) Cyclic performance of the cell operated at a current density of  $20 \text{ mA g}^{-1}$  between 2.0 and 4.8 V. The inset displays the capacity retention after 50 cycles at each current density from 20 to  $640 \text{ mA g}^{-1}$  vs. the current densities. (B) Electrochemical impedance spectra represented as Nyquist plots of the electrode before cycling (a) and after 1st (b), 15th (c) and 30th (d) chargings to 4.8 V.

## References

- [1] D. Li et al., J. Power Sources, 160, 1342 (2006).
- [2] H. Wu et al., J. Power Sources, 195, 2909 (2010).
- [3] J.-S. Kim et al., J. Power Sources, 153, 258 (2006).
- [4] A. Ito et al., J. Power Sources, 183, 344 (2008).
- [5] B. Liu et al., Electrochim. Acta, 56, 6748 (2011).

## Acknowledgement

This study was financially supported by the National Nature Science Foundation of China (contract number: 21073130).

# Low Temperature Characteristics of Surface Film Derived from Elemental Sulfur Additive on Graphite Negative Electrode

Sunhyung Jurng<sup>a</sup>, Hyun-seung Kim<sup>a</sup>, Jae Gil Lee<sup>a</sup>, Ji Heon Ryu<sup>b</sup>, Seung M. Oh<sup>a,\*</sup>

<sup>a</sup> Department of Chemical and Biological Engineering, Seoul National University, 1 Gwanak-ro, Gwanak-gu, Seoul 151-744, South Korea

<sup>b</sup> Graduate School of Knowledge-based Technology and Energy, Korea Polytechnic University, Gyeonggi, 429-793, South Korea

\* Correspond to [seungoh@snu.ac.kr](mailto:seungoh@snu.ac.kr)

It is well known that graphite negative electrode, which represents the preferred anode material in LIBs, delivers poor electrochemical performance in low temperature condition. The reduced ability of graphite at low temperature has been attributed to several factors; ion mobility in the electrolyte, transport properties of passivation films, increased charge transfer resistance and reduced solid state ion diffusivity within graphene sheets. In the past decades, several approaches have been pursued to overcome these limitations.

In this work, our prime concern is to access the low temperature characteristic of surface film derived from elemental sulfur additive, and further understand the how chemical composition of SEI has an effect on the low temperature performance of graphite. To this purpose, a comparative study is made on the surface films derived from the sulfur-added and sulfur-free electrode, from which the performance at low temperature, the resistances and chemical composition of sulfur-derived surface film are addressed. Electrochemical impedance spectroscopy (EIS) is utilized to study the resistance of electrodes and to evaluate its dependence on temperature, whereas X-ray photoelectron spectroscopy (XPS) is used to analyze the film composition of surface films.

Compared to the sulfur-free electrode, adding 0.5% sulfur showed good performance at low temperature condition. SEI film with sulfur compounds is less resistive at low temperature, especially in the charge transfer step. The elemental sulfur is reduced at the 1st lithiation step, producing long chain polysulfide which readily reacts with carbonate electrolytes (EC, EMC, and DEC) [1]. As a result, generated thiocarbonates make sulfur-containing SEI composed of  $\text{Li}_2\text{S}$ , C-S-C, and  $-\text{CO}_2\text{S}-$  on the graphite electrode. Finally, we propose the mechanism of SEI formation with elemental sulfur additive through a reaction between carbonate electrolyte and long chain polysulfide, and the relation between SEI composition and charge transfer barrier.

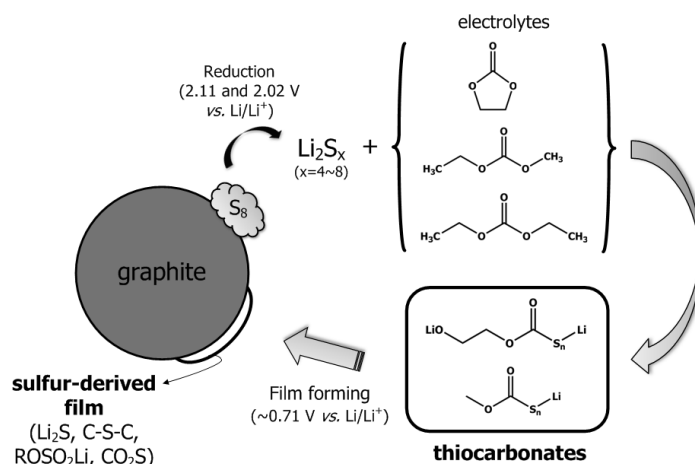


**Fig. 1. Proposed mechanism of the film forming process with elemental sulfur additive in graphite negative electrode.**

## Reference

[1] T. Yim, M.-S. Park, J.-S. Yu, K.J. Kim, K.Y. Im, J.-H. Kim, G. Jeong, Y.N. Jo, S.-G. Woo, K.S. Kang, I. Lee, Y.-J. Kim, Effect of chemical reactivity of polysulfide toward carbonate-based electrolyte on the electrochemical performance of Li-S batteries, *Electrochim. Acta*, 107 (2013) 454.

# A Renaissance for Solid Polymer Electrolyte through Alternative Host Materials: Polycarbonates

Daniel Brandell, Bing Sun, Jonas Mindemark  
Department of Chemistry – Ångström Laboratory, Uppsala University  
Box 538, 751 21 Uppsala, Sweden  
Daniel.Brandell@kemi.uu.se

Solid polymer electrolytes (SPEs) have since their discovery in the 1970s been considered a promising class of materials for different electrochemical applications due to their mechanical flexibility, chemical and electrochemical stability, non-toxicity and the safety of the resulting devices – not least for rechargeable Li-batteries. SPEs have, however, not yet been realized to any great extent due to several shortcomings, primarily their inherent low ionic conductivity. This is likely associated to the rather limited number of polymer host materials which have been explored by the research community: the overwhelming majority of relevant publications and patents have been on poly(ethylene oxide) (PEO) materials. PEO displays some appealing properties such as low  $T_g$  and a good dissolution of many Li-salts, but are also associated with problems: semi-crystallinity, low cation transference numbers, and temperature sensitivity. Despite intense research on this category of materials during several decades, where the inclusion of inorganic nanoparticles have constituted the perhaps most promising strategy for achieving higher ionic conductivities, the conductivity values have not yet reached the levels which are considered necessary for most commercial applications ( $10^{-2}$ - $10^{-3}$  S/cm) without the inclusion of a significant part of liquid components.

The rapidly expanding market for electric vehicles (EVs) demand batteries with higher energy density, improved safety, and prolonged lifetime. These criteria are largely met by SPEs, and the research field could therefore experience a true renaissance if some of the inherent problems for this class of materials are properly solved. Alternative polymer materials to PEO could then provide a route forward and bring SPEs further towards implementation in commercial devices.

In this context, we have been targeting polycarbonates – specifically, poly(trimethylene carbonate) (PTMC) – for Li- and Li-ion batteries. PTMC has a somewhat higher  $T_g$  than PEO, but is amorphous and display better mechanical integrity, not least at higher temperatures. The  $\text{Li}^+$  transference numbers are also much higher than for PEO. We have recently shown that functional Li-batteries can be constructed using PTMC as an electrolyte host material for LiTFSI salt [1]. We have also shown that the ion transport and/or mechanical properties can be improved by lowering the  $T_g$  through monomer functionalization, cross-linking [2] or through co-polymerization with polyesters [3]. Moreover, we have been able to significantly improve the device performance by tailoring the battery fabrication procedure using oligomer components [4] and utilized X-ray Photoelectron Spectroscopy (XPS) to better understand the interfacial chemistry between the SPE and common Li-battery electrode materials [5].

In this current presentation, we will discuss in-depth studies of the ionic transport properties in the PTMC-materials investigated by an interplay of computational (Molecular Dynamics) and experimental techniques (NMR, impedance spectroscopy, FTIR), and highlight some key characteristics in comparison with PEO-based SPE counterparts. The differences regarding polymer-ion interactions present novel insights for strategies to improve the transport properties of SPEs. We will also discuss PTMC-based SPEs which are operational in Li-battery cells at ambient temperatures, without any addition of liquid components.

## References:

- [1] B. Sun, J. Mindemark, K. Edström, D. Brandell, *Solid State Ionics*, **262** (2014) 738.
- [2] J. Mindemark, L. Imholt, D. Brandell, *Electrochim. Acta* (2015)
- [3] J. Mindemark, E. Törmä, B. Sun, D. Brandell, *Polymer*, **63** (2015) 91.
- [4] B. Sun, J. Mindemark, K. Edström, D. Brandell, *Electrochem. Commun.*, **52** (2015) 71.
- [5] C. Xu, B. Sun, T. Gustafsson, K. Edström, D. Brandell, M. Hahlin, *J. Mater. Chem. A*, **2** (2014) 7256.

# Electrochemical behaviour of tin(IV) oxide electrodes in lithium-ion batteries at high potentials

Solveig Böhme, Kristina Edström, Leif Nyholm  
Department of Chemistry – Ångström Laboratory  
Uppsala University  
Box 538, 751 21 Uppsala, SWEDEN  
solveig.bohme@kemi.uu.se

In commercial lithium-ion batteries graphite is currently the most common anode material. However, graphite has a rather limited volumetric and gravimetric capacity which is a drawback when higher energy densities are required, for instance, in cars. Here, other materials with higher capacities and energy densities like the alloying materials tin and silicon are, hence, required. Even bigger capacities could be obtained using tin oxide based compounds due to a combination of the tin oxide conversion reaction converting lithium to tin and lithium oxide and the alloying reaction between tin and lithium. However, tin oxides usually suffer a great capacity loss after the first cycle due to the irreversibility of the tin oxide reduction.<sup>[1,2]</sup> Nevertheless, there have been some reports suggesting a limited reversibility of the tin(IV) oxide conversion.<sup>[3-6]</sup>

In this work we have investigated the voltammetric behaviour of tin(IV) oxide electrodes within different potential windows in order to study the influence of the alloying reaction on the conversion reaction (excluding the alloying reaction by cycling to 0.9 V vs.  $\text{Li}^+/\text{Li}$ ). In addition, rather high voltages (up to 3.7 V vs.  $\text{Li}^+/\text{Li}$ ) were applied to check the tin(IV) oxide conversion reversibility as well as electrode and electrolyte stability under these conditions. The results were also compared with those presented in an earlier model study carried with our group.<sup>[6]</sup> Cycling experiments were likewise carried out at 60°C and these results will be compared to those obtained for cycling at room temperature. The products formed at different potentials and temperatures were investigated using XPS and SEM. The results confirmed the presence of a partial reversibility of the tin(IV) oxide conversion reaction which was enhanced at 60°C. It will be demonstrated that cycling at a higher temperature lead to larger capacities of tin(IV) oxide electrodes. In addition, the influence of different cycling rates on the capacity will be discussed.

1. Courtney, I.A. and Dahn, J.R., *J. Electrochem. Soc.*, **1997**, *144*, 2045-2052.
2. Courtney, I.A.; McKinnon, W.R. and Dahn, J.R., *J. Electrochem. Soc.*, **1999**, *146*, 59-68.
3. Chouvin, J.; Branci, C.; Sarradin, J.; Olivier-Fourcade, J.; Jumas, J.C.; Simon, B. and Biensan, P., *J. Power Sources*, **1999**, *81-82*, 277-281.
4. Chouvin, J.; Olivier-Fourcade, J.; Jumas, J.C.; Simon, B.; Biensan, P.; Fernández Madrigal, F.J.; Tirado, J.L. and Pérez Vicente, C., *J. Electroanal. Chem.*, **2000**, *494*, 136-146.
5. Sun, X.; Liu, J. and Li, Y., *Chem. Mater.*, **2006**, *18*, 3486-3494
6. Böhme, S.; Edström, K. and Nyholm, L., On the electrochemistry of tin oxide coated tin electrodes in lithium-ion batteries, *Electrochim. Acta*, **2015** (in press).



# Capacity enhancement of semi-solid flow capacitor using quinonic compounds

H. Saito, D. Komatsu, T. Tomai, I. Honma

*Institute of Multidisciplinary Research for Advanced Materials, Tohoku University, Japan*

*2-1-1, katahira, Aoba-ku, Sendai, Miyagi, Japan*

*hayate@mail.tagen.tohoku.ac.jp*

For grid-scale energy storage, the semi-solid flow cell, consisting of an electrochemical charge-discharge cell connected to an external circulatory system of pumps and reservoirs, has been developed. Among the flow cells, semi-solid flow capacitor (SFC) stores electrical charge in an electrical double layer at the carbon-electrolyte interface in a flowable carbon-electrolyte suspension (slurry), so the SFC exhibits higher power density than semi-solid flow battery<sup>[1]</sup>. However, compared to the battery system, SFC slurry has limited energy density.

Our previous study revealed that the fixed capacitor using the nanoporous carbon holding organic compounds exhibited high energy density ( $>20 \text{ Wh kg}^{-1}$ ) and high power density ( $>5 \text{ A g}^{-1}$ ) without the degradation after 10000 charge/discharge cycles<sup>[2]</sup>. To address the limitation of the energy density (capacity) of SFC slurry, in this study, we enhanced the capacity of the slurry by using redox-active organic compounds (Fig. 1). We applied the nanoporous carbon holding quinonic/hydroquinonic compounds to carbon-electrolyte suspension (quinonic/hydroquinonic slurry) for flowable electrodes in the SFC.

The flowable quinonic/hydroquinonic slurry electrode was prepared by dispersing the organic compound-carbon composite in 0.5 M  $\text{H}_2\text{SO}_4$  aqueous solution. We employed tetrachlorohydroquinone (TCHQ) as cathode active material and anthraquinone (AQ) as anode active material in positive and negative slurry electrodes, respectively. The weight ratio of the organic compound-carbon composite to 0.5 M  $\text{H}_2\text{SO}_4$  aqueous solution was fixed at 13 : 87. The flowability of the slurry was maintained in the range less than this weight ratio. Fig. 2 shows the potential profiles of the positive and negative slurry electrodes. By using the redox reactions of quinonic/hydroquinonic compounds in positive and negative slurry electrodes, we achieved the enhancement of the capacity of the slurry for SFC.

**References:** [1] V. Presser, *et al.*, *Adv. Energy Mater.*, **2**, 895 (2012).

[2] T. Tomai, S. Mitani, D. Komatsu, Y. Kawaguchi, I. Honma., *Sci. Rep.*, **4**, 3591, (2014).

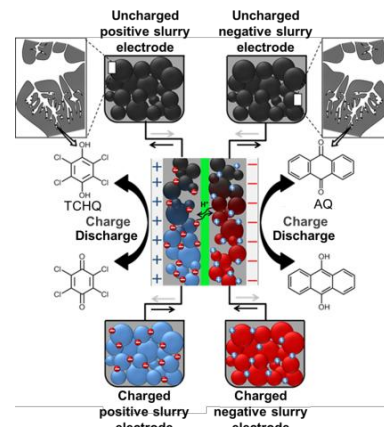


Fig. 1. Schematic of semi-solid flow capacitor using quinonic and hydroquinonic compounds as redox active materials.

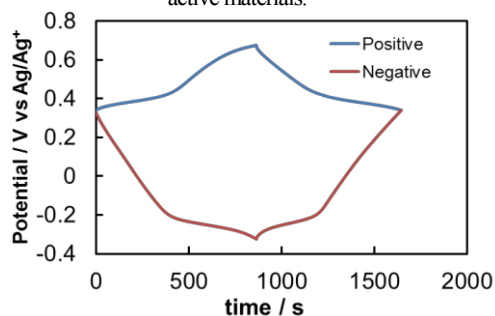


Fig. 2. Potential profiles of the positive (TCHQ) and negative (AQ) quinonic/hydroquinonic slurry electrodes.

# Combination effects of graphene oxide as carbon black and maleimide as electrolyte additive in lithium ion batteries

Ahmad Fauzan<sup>1</sup>, Fu Ming Wang<sup>1,2\*</sup>

<sup>1</sup>Graduate Institute of Applied Science and Technology, National Taiwan University of Science and Technology

<sup>2</sup>Sustainable Energy Center, National Taiwan University of Science and Technology

43 Keelung Road, Section 4, Taipei 10607, Taiwan

Correspondence: mccabe@mail.ntust.edu.tw

Recently, reduced graphene oxide (rGO) have been considered as an attractive material due to its intrinsic characteristics such as physical, mechanical and electrical properties since the discovery of its freestanding form in 2004 [1]. Due to its superior electrical conductivity and high theoretical surface area, rGO has been considered favorably as a promising material for secondary batteries such lithium-ion battery anodes [2].

In this study, rGO is used to a carbon black into Si/C anode electrode in order to enhance the capacity and electrochemical reversibility. According to the research [3], the carbon-oxygen functional groups on rGO are able to fabricate ionic host SEI, which improves the performance of lithium-ion battery including reversible capacity and cycle ability.  $\text{Li}^+$ , MI, and  $\text{H}_2\text{O}$  are fabricated to form a unique ionic host SEI on the rGO's surface duo to the higher reduction potential of the combined reaction.

Figure 1 shows three kinds of electrolyte additives (MI,  $\text{H}_2\text{O}$ , MI/ $\text{H}_2\text{O}$ ) has been added compares with the blank electrolyte. The electrolyte contains MI/ $\text{H}_2\text{O}$  demonstrates better performance via others. This result demonstrates that the ionic host SEI is able to fully functionalize in battery system in which promotes application of lithium-ion rechargeable batteries.

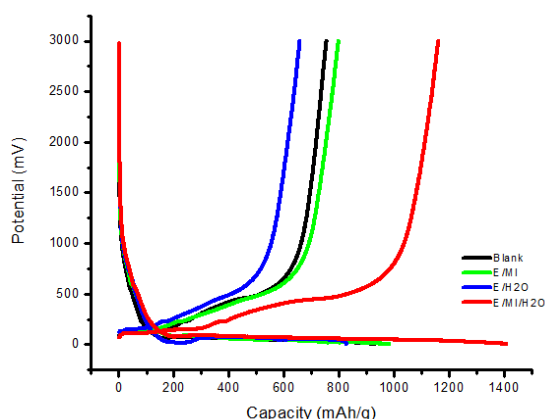


Figure 1 Charge and discharge curves of batteries.

## References

- (1) K. S. Novoselov, *et al.*, Science 306 (2004) 666.
- (2) R. Mukherjee, *et al.*, ACS Nano 6 (2012) 7867.
- (3) C. S. Cheng, *et. al.*, Electrochimica Acta 6 (2013) 425.

# Physical Model Simulation for Degradation of Li-ion Battery

Juichi Arai<sup>a</sup>, Ryo Saito<sup>a</sup>, Yusuke Ando<sup>a</sup> and Fumitaka Goto<sup>b</sup>

<sup>a</sup> Technology Center, Yamaha Motor Co., Ltd., Shizuoka 438-8501, Japan

<sup>b</sup> CD-adapco Japan, Kanagawa 222-0033, Japan  
araij@yamaha-motor.co.jp

Lithium ion batteries (LIBs) are widely used as power sources in electric vehicles, which include such as power-assisted bicycles (e-bikes), electric assisted wheel-chairs, and electric scooters, as a power source. In commercial products, there is a need for a stable power supply; it is of important in commercial products, however, LIBs lose their energy and power during charge-discharge cycles and during storage. To design and develop reliable products, it is necessary to understand and control the lifespan of LIBs's life. There have been many attempts to extensive efforts focused on the development of battery-life models to analysis analyze the degradation of LIBs's degradation. [1] Among them, the differential voltage analysis method is a useful technique to investigate the reason for the capacity loss in LIBs. [2] The in one study, it was shown showed that the reduction in battery capacity fade was due to the loss of positive/negative capacity balance caused by resulting from the side reactions at the negative electrode. However, this method cannot provide the information regarding the interior inside of the cell. In this study, we investigate the reduction in the capacity of studied LIBs's capacity fade by using a physical model-based simulation for charge-discharge cycles and storage.

The physical-model simulation program provides the charge-discharge voltage profiles by using the experimental potential property of negative and positive electrodes, as well a large number and huge sets of physical and cell design parameters. [3] The electrode potential profiles were obtained by performing a half-cell experiment using with the electrodes taken from the commercial LIB (2.2Ah, composed of  $\text{LiNi}_{0.5}\text{Co}_{0.3}\text{Mn}_{0.2}\text{O}_2$  (NMC) positive and graphite negative electrode). The cell design parameters were measured, and other physical parameters were collected from references and tuned for the discharge voltage profiles of a virgin cell. The charge-discharge test was conducted under the condition of 0.5 C constant current (CC) and 4.2 V constant voltage (CV) mode charge, and a 1.0 C CC mode discharge to 3 V at 45°C. The storage test was carried out at 60°C with a 100% state-of-charge (SOC). The cell capacity was also measured every 100 cycles or 2–4 weeks with a 0.2 C CC-4.2 V CV charge and a 0.2 C CC discharge to 3 V at 25°C. We performed the numerical simulations for these measured discharge voltage profiles was used to determine explore the effect of the cell resistance ( $R_{\text{cell}}$ ) and the usable range of both positive ( $\delta_{p-\text{max}}$ ,  $\delta_{p-\text{min}}$ ) and negative ( $\delta_{n-\text{max}}$ ,  $\delta_{n-\text{min}}$ ) electrodes. The numerical fitting for the cycle test and storage test was successfully realized using the done with those five parameters. The cell resistance  $R_{\text{cell}}$  increased non-linearly with the number of cycles number and storage time. These changes were reproduced by adjusting the cell's positive temperature coefficient (PTC) resistance, (which is a kind-type of safety device possessed by equipped in commercial LIBs having a specific certain resistance). The  $\delta_{n-\text{min}}$  increased with the number of cycles and storage time, while the  $\delta_{p-\text{min}}$  remained stayed almost constant, indicating that the capacity fading in LIBs is due was mainly caused by to the reduction in of the usable range of the negative electrode, as previously studies reported. [4,5] The small change of  $\delta_{p-\text{min}}$  indicated supported that the upper potential point of the positive electrode remained stayed constant in order to sustain the electrochemical stability. The change in the physical properties of LIBs after several cycles and other storage times are being under investigated using physical model simulations.

[1] J. Wang, J. Purewal, P. Liu, J. H-Garner, S. Soukazian, E. Sherman, A. Sorenson, L. Vu, H. Tataria, and M. W. Verbrugge, *J. Power Sources*, **269**, 937–948 (2014).

[2] I. Bloom, A. N. Jansen, D. P. Abraham, J. Knuth, S. A. Jones, V. S. Battaglia, and G. L. Henriksen, *J. Power Sources*, **139**, 295–303 (2005).

[3] A. Sakti, J. J. Michalek, S. Chun, and J. F. Whitacre, *Int. J. Energy Res.*, **37**, 1562–1568 (2013).

[4] A. Smith, and J. R. Dahn, *J. Electrochem. Soc.*, **159**, A290 (2012)

[5] A. J. Smith, H. M. Dahn, J. C. Burns, and J. R. Dahn, *J. Electrochem. Soc.*, **159**, A705 (2012).

**Commentaire [A1]:** Tip: Although this is a compound word, the rule states that for words that end with "-ly", the hyphen is not used.

**Commentaire [A2]:** Tip: Note that the endash is used to denote a range, and not the hyphen.

**Commentaire [A3]:** If this is a variable, please use italics.

**Mis en forme :** Police :Times New Roman, 10 pt, Italique

**Commentaire [A4]:** I have edited the References. In American English, an "and" is used after the series comma that follows the penultimate item in a list so it was inserted before the final author name in each list of authors.

# The electronegativity effects of maleimide based electrolyte additives in SEI formation of lithium ion battery

Giyanto<sup>1</sup>, Fu-Ming Wang<sup>1,2\*</sup>

<sup>1</sup>Graduate Institute of Applied Science and Technology, National Taiwan University of Science and Technology

<sup>2</sup>Sustainable Energy Center, National Taiwan University of Science and Technology

43 Keelung Road, Section 4, Taipei 10607, Taiwan

Correspondence: mccabe@mail.ntust.edu.tw

Rechargeable lithium-ion batteries are among the most promising technologies for various applications such as portable electronics, electric vehicles and power storage system for power grids. The performance of Li-ion batteries is greatly affected by the effectiveness of the solid electrolyte interface (SEI) layer, which is formed on the surface of graphite anode at the first cycle. Use of electrolyte additives is one of the most economic and effective methods for determining, modifying, and improving the formation of an effective SEI layer. Maleimide-based additive is one of the commercial additives that have been shown to improve the capability and cycle-ability due to its high reductive potential compared with carbonates [1-2].

This study evaluates the effects of the fluoro (F-MI) and cyanide (CN-MI) functional groups in maleimide to the SEI formation and the battery performance. Figure 1 shows that 1M LiPF<sub>6</sub> in EC:PC:DEC (3:2:5 in volume) containing 0.1 wt % of CN-MI additives is the most appropriate additives to improvement battery performance. From the charge-discharge curve, it shows that the electrolyte containing O-MI (without functional group), F-MI, and CN-MI additives increase the first discharge capacity by 3%, 3.5%, 4.8% compared with the electrolyte without any additives. Figure 2 shows the discharge capacity is 2.1% (O-MI), 7.1% (F-MI), and 11.7% (CN-MI) greater than the electrolyte without additives after 10 cycles. It indicates that the CN-MI additive is able to form a stable SEI layer and enhances the battery performance.

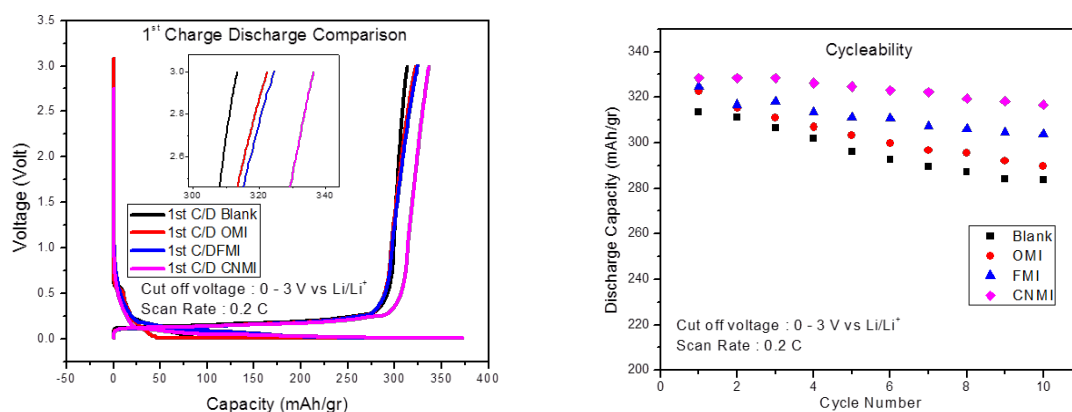


Figure 1 (a) The first charge discharge curves, (b) Cycle-ability results.

## References

- (1) S. S. Zhang, J. Power Sources 162 (2006) 1379-1394.
- (2) F. M. Wang, Electrochimica Acta 54 (2009) 3344-3355.
- (3) Victor A. Agubra, Jeffrey W. Fergus, J. Power Sources 268 (2014) 153-162.

# **The High Performance Silicon Anodes Including New Water Based Binder in Lithium Ion Batteries**

Nam Seon Kim, Soo Jung Kim, Dae Won Park, Gwang Sik Choi  
*Aekyung Chemical Co. R&D Center*  
217-2 Shinseong-dong, Yuseong-Gu, Daejeon 305-805, Republic of Korea

*sunsa@aekyung.kr*

Silicon based negative active material has very high charge capacity and is widely applied to a high capacity battery. However, the silicon based negative active material may expand by about 300% to about 400% during charge and discharge.

Recently much attention has been devoted developing functional binders that can improve adhesion on silicon particle and accommodate substantial volume change during the charge/discharge process to maintain the electrode structure.

The binders for silicon electrodes hold stiff polymeric backbones as like carboxymethyl cellulose (CMC), poly(acrylic acid), and alginate show better electrochemical performance than commercial binders. Despite promising progress, the current research on polymer binders for silicon is still far from the practical application where high mass loading is necessary for the high areal capacity.

Here we report high performance silicon anodes using new water based binder including inorganic binder. This polymer matrix is compatible with lithium ion slurry manufacturing process, and can maintain both electric conductivity and mechanical integrity during the battery operation which results in good stability, rate capability, and cycle-life characteristics at high mass loading ( $>4.5 \text{ mg/cm}^2$ ).

# Development of short-termed and highly effective graphite felt surface treatment process for all-vanadium redox flow battery applications

Donghyun Kil, Hansung Kim\*

Dept. of Chemical and Biomolecular Engineering, Yonsei University  
50 Yonsei-ro, Seodaemun-gu, 120-749 Seoul, Korea

\*e-mail: [elchem@yonsei.ac.kr](mailto:elchem@yonsei.ac.kr)

Vanadium redox flow battery (VRFB) is one of the most promising candidates for the large-scale energy storage system [1]. It stores the electrical energy by utilizing different vanadium redox reactions and provides sufficient energy efficiency at lower current density operations. However, at higher current density operations, its energy efficiency drops significantly due to the poor electrochemical activity of pristine graphite felt electrodes. Although several surface modification to enhance electrochemical activity of the graphite felt were proposed [2, 3], many required long treatment time and high energy which is not favorable as it increased overall operating price for VRFBs [4].

In light of this, we devised a novel surface treatment method based on combined use of oxidizing gases and mild heat, which is both fast and low energy consuming [5]. The electrochemical activity of treated graphite felt, and its application as an electrode material for vanadium redox flow battery (VRFB) was investigated. X-ray Photoelectron spectroscopy study revealed that a high concentration of the oxygen functional groups was successfully introduced to the surface of the treated felt which enhanced the wettability and charge transfer property of the electrode. Moreover, the surface roughness of the treated graphite felt increased significantly, which should be advantageous as it can provide abundant surface active site for the vanadium redox reactions to take place. The electrochemical properties of the treated graphite felt were evaluated with cyclic voltammetry and electrochemical impedance spectroscopy, and it was found that the graphite felt treated with just 6 minutes at 180 °C showed best electrochemical activity. When the as-prepared electrode was used as the positive and negative electrode of the VRFB, it was able to retain high energy efficiency even at high current density operation. At 150 mA/cm<sup>2</sup>, VRFB with treated graphite felt maintained energy efficiency of 75.7% which is significantly higher than that of pristine graphite felt (62.0%).

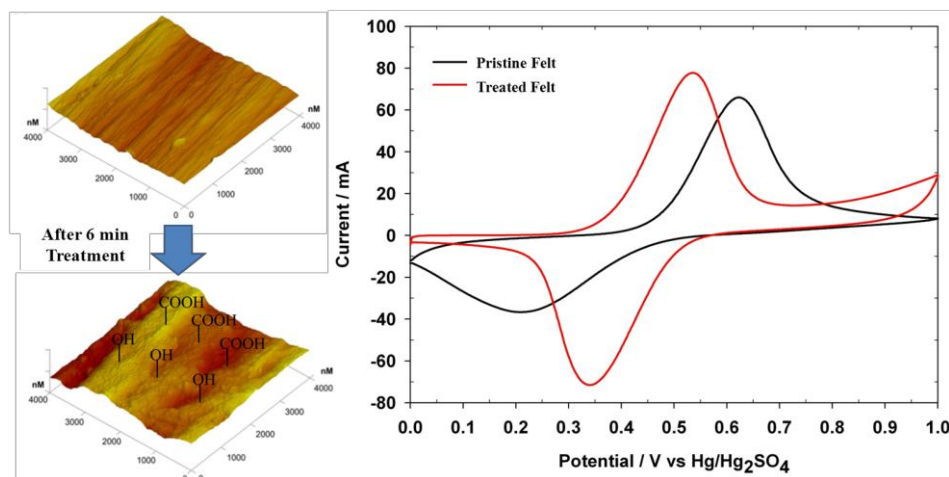


Fig. 1 AFM and cyclic voltammetry image of pristine and treated graphite felt.

## Reference

1. Skyllas-Kazacos, M., et al., International Journal of Energy Research, 2010. **34**(2): p. 182-189.
2. Wu, X.X., et al., Journal of Power Sources, 2014. **263**: p. 104-109.
3. Gao, C., et al., Electrochimica Acta, 2013. **88**: p. 193-202.
4. Sun, B. and M. Skyllas-Kazacos, Electrochimica Acta, 1992. **37**(7): p. 1253-1260.
5. Kim, K.J., et al., Materials Chemistry and Physics, 2011. **131**(1-2): p. 547-553

# Electrochemical performance of lithium-rich ( $\text{Li}_{1.2}\text{Ni}_{0.2}\text{Mn}_{0.6}\text{O}_2$ ) high-capacity cathode of lithium battery modified with fluorine-benzimidazole-based Li salt addition in electrolyte

Jian-Hua Wu<sup>1</sup>, Fu-Ming Wang<sup>1,2\*</sup>

<sup>1</sup>Graduate Institute of Applied Science and Technology, National Taiwan University of Science and Technology

<sup>2</sup>Sustainable Energy Center, National Taiwan University of Science and Technology

43 Keelung Road, Section 4, Taipei 10607, Taiwan

Correspondence: mccabe@mail.ntust.edu.tw

$\text{LiPF}_6$  is widely used lithium salt, which plays a critical role in initiating electrochemical reaction in lithium ion batteries [1]. However,  $\text{LiPF}_6$  suffers from its  $\text{PF}_5$  side reaction, which degrade the solid electrolyte interface (SEI), and lead to formation of  $\text{LiF}$  and  $\text{HF}$  [2]. Due to the Lewis acid basic reaction, benzimidazole-base lithium salt (BZ) which is electrolyte additive can form pentafluorophosphate benzimidazole between the benzimidazole ion and  $\text{PF}_5$ . The pentafluorophosphate benzimidazole anion can inhibit the decomposition of  $\text{LiPF}_6$  by inhibiting  $\text{PF}_5$  side reaction [3].

In order to improve a high ionic conductivity and high voltage application, benzimidazole salt is combined fluoro-functional group. This two kind of new fluorine based benzimidazole salt (1F-BZ & 2F-BZ) are used as electrolyte additives for high voltage lithium-rich ( $\text{Li}_{1.2}\text{Ni}_{0.2}\text{Mn}_{0.6}\text{O}_2$ ) high-capacity cathode [4] of lithium batteries.

In this study, 1M  $\text{LiPF}_6$  in EC/EMC(Blank), 1M  $\text{LiPF}_6$ +0.1 wt% lithium benzimidazole in EC/EMC(BZ), +0.1 wt% lithium fluorobenzimidazole in EC/EMC(1F-BZ) and +0.1 wt% lithium difluorobenzimidazole in EC/EMC(2F-BZ) were used for electrolyte in this research. According to the discharge cyclic performance (Figure 1) of  $\text{Li}_{1.2}\text{Ni}_{0.2}\text{Mn}_{0.6}\text{O}_2$  cathode half cells, which charge/discharge voltage were between 3V and 4.9V, fluorine-benzimidazole salt can improve the cyclic stability of  $\text{Li}_{1.2}\text{Ni}_{0.2}\text{Mn}_{0.6}\text{O}_2$  cathode half cell, and extend the life of battery in operation at high voltage. In addition, Cyclic voltammetry, electrochemical impedance spectroscopy and Scanning electron microscope measurement have been used to characterize the materials in this study.

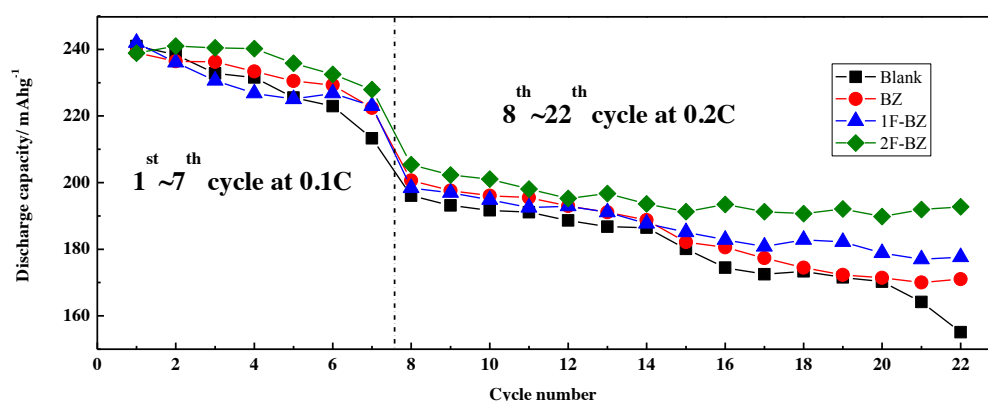


**Fig. 1.** The discharge cyclic performance of  $\text{Li}_{1.2}\text{Ni}_{0.2}\text{Mn}_{0.6}\text{O}_2$  cathode half cells for Blank, BZ, 1F-BZ and 2F-BZ electrolyte at room temperature. (The 1<sup>st</sup>~7<sup>th</sup> cycle at 0.1C-rate and the 8<sup>th</sup>~22<sup>th</sup> cycle at 0.2C.)

## References

- [1] S.S Zhang, T.R Jow, K Amine, G.L Henriksen<sup>b</sup>, Journal of Power Sources 107 (2002) 18-23.
- [2] Sheng Shui Zhang, Journal of Power Sources 162 (2006) 1379–1394.
- [3] Sylvia Ayu Pradanawati, Fu-Ming Wang, John Rick, Electrochimica Acta 135 (2014) 388–395.
- [4] Sunny Hy, Felix Felix, John Rick, Wei-Nien Su, and Bing Joe Hwang, J. Am. Chem. Soc. 2014, 136, 999-1007.



# Polypyrrole as the Coating Agent and Nitrogen Precursor for the Fabrication of Nitrogen-Doped Graphite Felts as Positive Electrode for a Vanadium Redox Flow Battery

Sangki Park, Hansung Kim\*

Dept. of Chemical and Biomolecular Engineering, Yonsei University  
50 Yonsei-ro, Seodaemun-gu, 120-749 Seoul, Korea

\*e-mail: [elchem@yonsei.ac.kr](mailto:elchem@yonsei.ac.kr)

Redox flow batteries operating via the oxidation and reduction of active electrolyte materials have recently received significant attention as electrochemical energy storage systems for renewable energy due to their long life, flexible design, and high energy efficiency [1,2]. Of the various redox flow batteries, vanadium redox flow batteries (VRFBs) are considered to be promising candidates because the same element is used in both half-cells, which avoids crossover contamination of the electrolyte [3,4]. The energy efficiency of VRFB primarily depends on the electrochemical activity of electrode because the redox reaction of vanadium ion occurs on the electrodes surface during charge-discharge process [5,6]. Therefore, it is important to select the suitable electrode materials for VRFB. Carbon-based materials, particularly graphite felt, are widely used as VRFB electrodes because of their high resistance to corrosion in the acidic electrolyte. However, the poor electrochemical activity of graphite felt electrodes remains a technological hurdle for VRFB systems [7]. For this reason, various post treatments of graphite felt including thermal treatment in air, acid treatment, electrochemical oxidation and modification with metal have been applied to enhance the electrocatalytic activity and reversibility of carbon felt electrodes for VRFB. In this study, the graphite felts doped with nitrogen in the presence of transition metal were prepared and studied as positive electrodes in VRFBs. These materials were synthesized by a direct coating of thin layer of polypyrrole (Ppy) on the surface of graphite felt, followed by subsequent carbonization in the presence of transition metal. Impregnation of transition metal to the nitrogen doped graphite felt increased the nitrogen content in the carbon structure during the Ppy pyrolysis, which could improve the catalytic activity towards  $\text{VO}^{2+} / \text{VO}_2^+$  redox reactions. The enhanced performance is attributed to the abundant active nitrogen functional groups created on the graphite felt which are beneficial to the fast electrochemical kinetics of vanadium redox reaction.

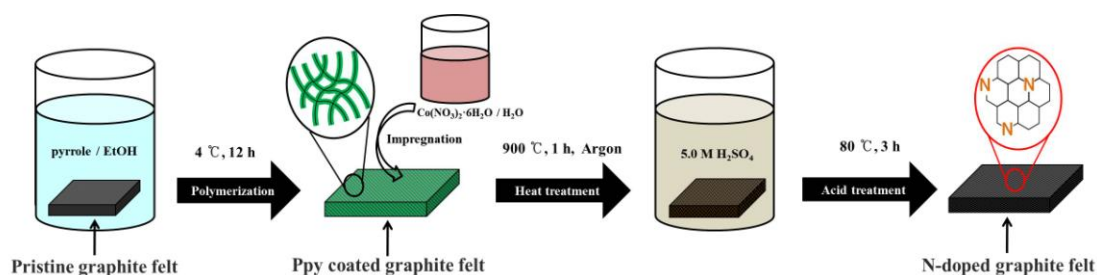


Fig 1. Schematic diagrams of the N-doped graphite felt fabrication process.

## Reference

1. E. Sum and M. Skyllas-Kazacos, *J. Power Sources*, 1985, **15**, 179-190.
2. F. Cheng, J. Liang, Z. Tao and J. Chen, *Adv. Mater.*, 2011, **23**, 1695-1715.
3. W. Wang, S. Kim, B. Chen, Z. Nie, J. Zhang, G.-G. Xia, L. Li and Z. Yang, *Energy Environ. Sci*, 2011, **4**, 4068.
4. P. Qian, H. Zhang, J. Chen, Y. Wen, Q. Luo, Z. Liu, D. You and B. Yi, *J. Power Sources*, 2008, **175**, 613-620.
5. K. J. Kim, Y.-J. Kim, J.-H. Kim and M.-S. Park, *Mater. Chem. Phys.*, 2011, **131**, 547-553.
6. Z. González, C. Botas, P. Alvarez, S. Roldán, C. Blanco, R. Santamaría, M. Granda and R. Menéndez, *Carbon*, 2012, **50**, 828-834.
7. W. Zhang, J. Xi, Z. Li, H. Zhou, L. Liu, Z. Wu and X. Qiu, *Electrochim. Acta*, 2013, **89**, 429-435.



# Electrochemical Studies of Tin Film Model Electrode for Magnesium-ion Batteries

Xuan Minh Tran, Dan Thien Nguyen, Seung-Wan Song\*

*Dept. of Fine Chemical Engineering & Applied Chemistry, Chungnam National University  
Daejeon 305-764, Republic of Korea  
swsong@cnu.ac.kr*

Magnesium-ion battery has recently gained a considerable attention as a potential candidate for a next generation beyond-lithium energy storage system, because of its outstanding merit in regard to higher volumetric capacity ( $3833 \text{ mAhcm}^{-3}$ ) than  $2061 \text{ mAhcm}^{-3}$  of lithium [1]), earth abundance, low cost and safety. Nonetheless, due to the formation of magnesium oxide film that blocks the transportation of  $\text{Mg}^{2+}$  ions and restrains a reversible dissolution of  $\text{Mg}^{2+}$  ion and deposition of Mg, the use of Mg metal as an anode has been limited. Extensive research effort has been devoted to find appropriate electrolyte components that permit the reaction reversibility and to improve cycling ability of the anode. The utilization of a new anode material is an alternative choice. Tin had been suggested as one of the alternative anode materials for magnesium-ion batteries [2] but not only a satisfied cycling ability but also a consensus regarding the electrochemical/interfacial reaction behavior have not been achieved. In this presentation, we report the electrochemical studies of tin film model electrode, which is prepared by pulse laser deposition, in magnesium cells.

## Acknowledgement

This work was supported by the Korean Ministry of Education and National Research Foundation (20122026203).

## References

- [1] P. Novak, R. Imhof, O. Haas, *Electrochim. Acta* 45 (1999) 351.
- [2] N. Singh, T. S. Arthur, C. Ling, M. Matsui, F. Mizuno, *Chem. Comm.* 49 (2013) 149.

# Transport properties of $\text{Li}^+$ Mixtures in Two Phosphonium Containing Ionic Liquids

Vitor L. Martins, Nédher Sanchez-Ramirez, Mauro C. C. Ribeiro and Roberto M. Torresi  
*Instituto de Química, Universidade de São Paulo. C.P. 26077, 005513-970 São Paulo (SP), Brazil.*  
*rtorresi@iq.usp.br*

Ionic liquids (ILs) are salt that present melting point below 100 °C and are compound only by ions. This means that they present intrinsic ionic conductivity, which make them interesting alternative to be used as electrolytes. In addition, they present high chemical and thermal stability and extremely low vapour pressure. Among the cations that the IL can be composed, imidazolium is one of the most common and investigated by research groups in different areas, mainly energy storage devices. The anion bis(trifluoromethanesulfonyl) imide ( $\text{Tf}_2\text{N}^-$ ) is also broadly investigated since the ILs composed by this anion present low viscosity and high ionic conductivity, in addition they are hydrophobic. With the aim to apply these ILs as Li-ion battery electrolyte, one must consider the mixture of these liquids with  $\text{Li}^+$  salt, and understand the effect of this addition in the physicochemical properties of the mixture. Many research groups investigated this effect in ILs containing imidazolium and  $\text{Tf}_2\text{N}^-$ . They reported an undesirable effect in the transport properties when the  $\text{Li}^+$  salt is added to the IL. As  $\text{Li}^+$  is added, the viscosity increases resulting in a decrease of the ionic conductivity, comparing to the neat ILs. As the obtained results for imidazolium composed ILs containing the anion  $\text{Tf}_2\text{N}^-$  are not suitable to be used as Li-ion battery electrolyte due to the high viscosity and low ionic conductivity at room temperature, the search for others ILs is still open.

Normally, large phosphonium cations are found in the literature, which have high viscosity, but some small phosphonium were also reported. ILs containing small phosphonium cations present lower viscosity and they are promising for electrolytes application. Phosphonium ILs have lower viscosity and higher ionic conductivity than the ammonium analogues. Also, they have a high electrochemical stability for the neat IL at room temperature and high lithium deposition-dissolution efficiency at 100 °C.

This work presents the physicochemical characterization of two ionic liquids (ILs) with small phosphonium cations, the triethylpentylphosphonium bis(trifluoromethanesulfonyl)imide ( $[\text{P}_{2225}][\text{Tf}_2\text{N}]$ ) and the (2-methoxyethyl)trimethylphosphonium bis(trifluoromethanesulfonyl)imide ( $[\text{P}_{222(201)}][\text{Tf}_2\text{N}]$ ) and their mixtures with  $\text{Li}^+$ . Properties as electrochemical window, density, viscosity and ionic conductivity are presented. The diffusion coefficient was obtained by two different techniques, PGSE-NMR and Li electrodeposition with microelectrodes. In addition, the  $\text{Li}^+$  transport number was also calculated by the PGSE-NMR technique and by an electrochemical approach. The use of these three techniques showed that the PGSE-NMR technique underestimate the diffusion coefficient of charge species. The  $\text{Li}^+$  transport number found is as high as 0.54. Raman spectroscopy and molecular dynamics simulations were used to evaluate the short-range structure of the liquids, they suggested that the interaction between  $\text{Li}^+$  and the  $\text{Tf}_2\text{N}^-$  anion is similar to other ILs containing the same anion. However, the MD simulations also showed that the  $\text{Li}^+$  interact differently with the cation containing an alkyl ether chain.

In summary, the ILs containing phosphonium cations present interesting properties to be considered as electrolytes for Li ion batteries. They present wide electrochemical window, ionic conductivity and even with the  $\text{Li}^+$  addition, the mixtures still present relatively high ionicity compared with ILs containing others cations. The  $\text{Li}^+$  mixture of the IL containing the cation with an alkyl ether chain presents higher ionicity than its analogue with an alkyl chain, as showed by PGSE-NMR,  $\text{Li}^+$  diffusion coefficient and transport number calculation. The Raman spectroscopy suggested that the aggregates formed between  $\text{Li}^+$  and the anion are similar to the aggregates formed in ILs containing others cations. Even the ILs containing an alkyl ether chain and an alkyl chain seems to present similar aggregates. On the other hand, MD simulations showed that despite the number of neighbours of  $\text{Li}^+$  is similar in both ILs, the  $\text{Li}^+$  can be found near the alkyl ether chain with higher probability than near the alkyl chain. The alkyl ether chain presence changes the way that  $\text{Li}^+$  interacts with the IL cation.

# The structural evolution of cathode materials in the current generation of commercial lithium-ion batteries

Neeraj Sharma

*School of Chemistry, UNSW Australia, Sydney NSW 2052 Australia*

[Neeraj.sharma@unsw.edu.au](mailto:Neeraj.sharma@unsw.edu.au)

Li-ion batteries are widely used in portable electronic devices and are considered as promising candidates for higher energy applications. Many challenges, such as energy density and battery lifetimes, need to be overcome before this particular battery technology can be implemented in such applications. To overcome these challenges we need to understand what is happening inside batteries at an atomic level while they function. *In situ* neutron diffraction is performed to probe the crystal-structure of two commercial Li-ion battery cathodes  $\text{Li}(\text{Ni}_{1/3}\text{Mn}_{1/3}\text{Co}_{1/3})\text{O}_2$  and  $\text{Li}(\text{Co}_x\text{Ni}_y\text{Al}_z)\text{O}_2$  while they are undergoing electrochemical cycling (charge/discharge) in a battery (see Figure 1). We depict the experimental approach and necessary requirements for the collection of *in situ* neutron diffraction of sufficient standard for thorough and detailed structural analyses of the electrode components of interest within the batteries. *In situ* structural characterisation of the cathode is undertaken under different electrochemical conditions, including varying applied currents and at elevated temperature ( $45^\circ\text{C}$ ). Additionally, the structural consequences for overcharging these cathodes above the limits set by the manufacturer are determined.

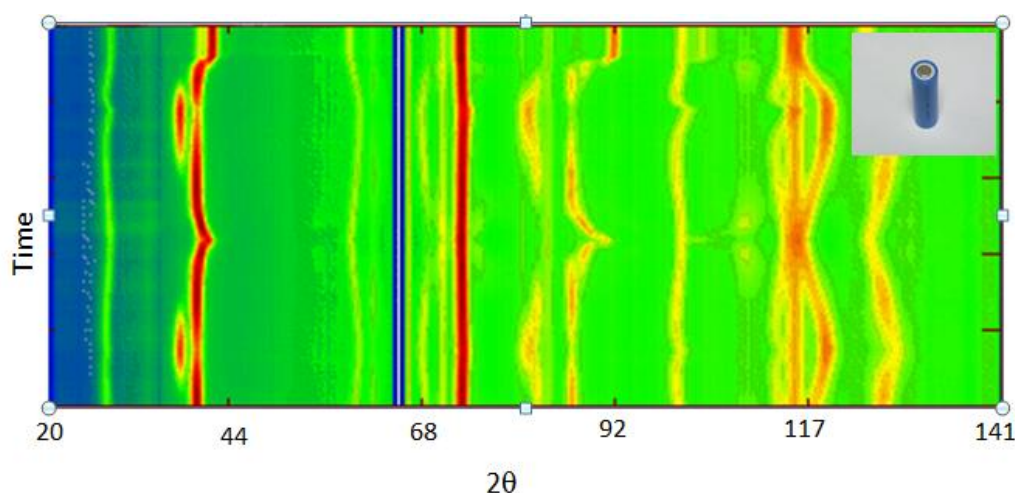


Figure 1: Collated *in situ* neutron diffraction data of a commercial lithium ion battery

# **Application of modified rosin-derivatives as promising adhesives for lithium titanium oxide electrodes in lithium ion batteries**

Hwa Jin Lee, Seul Lee, Eun-Suok Oh\*

*School of Chemical Engineering*

*University of Ulsan, 93 Daehak-ro, Nam-Gu, Ulsan 680-749, Korea.*

*esoh1@ulsan.ac.kr*

These days, the interest of lithium ion batteries (LIBs) has been gradually shifted to electric vehicles (EV) and energy storage system (ESS) for small mobile devices. It indicates that high-powered LIBs become more and more important as well as high-capacity LIBs. Lithium transition metal oxide is an attractive active material because it is structurally very stable during repeated cycles. Among them, lithium titanium oxide (LTO) has high operating voltage at 1.55 V (vs.  $\text{Li/Li}^+$ ) and no volume expansion, leading to high rate capability and long cycle life.

For this anode active material, we demonstrated the advantages of using rosin, bio-derivative, as a binder additive in our previous study. As a result, when increasing the amount of the rosin additive to the polyvinylidene fluoride (PVdF) binder, the crystallinity of PVdF decreases and ultimately contributes to the increase in the rate capability and capacity of the LTO electrode [1].

In this study, several modified rosin-derivatives are used for the additives of the PVdF binders to improve the cell performance of LTO electrodes. A variety of physical and electrochemical characterization techniques are applied to explain the effect of the rosin-derivative additives.

## Reference

- [1] S.-J. Kim, B.-R. Lee, E.-S. Oh, *Journal of Power Sources* 273, 608 (2015).

# Improving the Cycling Performance of the Layered Ni-Rich Oxide Cathode by Introducing the Low-Content $\text{Li}_2\text{MnO}_3$

Jun Yang, Mengyan Hou and Yongyao Xia\*

Department of Chemistry, Shanghai Key Laboratory of Molecular Catalysis and Innovative Materials, Institute of New Energy, Fudan University, Shanghai 200433, People's Republic of China. Fax: +86-21-51630318. E-mail: [yyxia@fudan.edu.cn](mailto:yyxia@fudan.edu.cn)

Recently, Ni-rich layered oxide  $\text{LiNi}_{0.8}\text{Co}_{0.1}\text{Mn}_{0.1}\text{O}_2$  is considered as one of most potential cathode materials for high energy density LIBs due to its larger reversible capacity ( $\sim 200 \text{ mAh g}^{-1}$ ), lower cost and toxicity compared to the commercial  $\text{LiCoO}_2$  cathode<sup>1</sup>. Despite these advantages, Ni-rich layered oxide still presents some intrinsic problems such as the poor cycle property and structure instability upon long-term cycling. So far, numerous efforts have been devoted to further improve electrochemical performance of Ni-based layered oxide cathode material. One strategy is the surface coating of the cathode materials with metal oxides, fluoride, phosphate<sup>2-3</sup>. The coated layer can be served as isolated layer to avoid the side reaction of the cathode surface with electrolyte. In addition, the ion doping and substitution were also considered as an alternative method to improve the electrochemical performance of the cathode materials<sup>5</sup>. Though these modifications have reached a certain effect, one urgent problem still needs to be addressed that the rapid fading of capacity induced by the structure change upon long-term cycling.

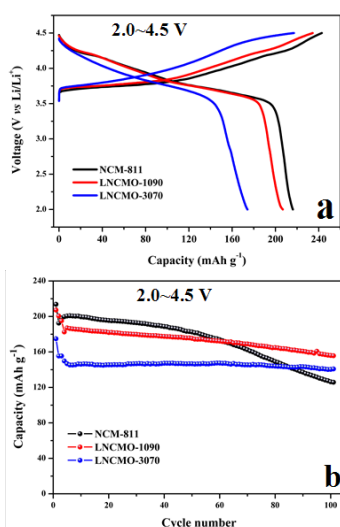


**Figure 1.** (a) The first charge-discharge curves and (b) the cycling performance of the as-prepared cathodes between 2~4.5V at a current density of  $20 \text{ mA g}^{-1}$ .

In this paper, introducing the low-content  $\text{Li}_2\text{MnO}_3$  to layered Ni-rich oxide cathode is utilized to improve their cycling performance. The existence of  $\text{Li}_2\text{MnO}_3$  component in the solid solution  $x\text{Li}_2\text{MnO}_3 \cdot (1-x)\text{LiNi}_{0.8}\text{Co}_{0.1}\text{Mn}_{0.1}\text{O}_2$  ( $0 \leq x \leq 0.3$ ) has been testified by XRD, electron diffraction. The  $\text{Li}_2\text{MnO}_3$  component can be served as stabilized species existed in the solid solution when charging to 4.5 V. As a result,  $0.1\text{Li}_2\text{MnO}_3 \cdot 0.9\text{LiNi}_{0.8}\text{Co}_{0.1}\text{Mn}_{0.1}\text{O}_2$  can exhibit more capacity retention of 75% after 100 cycles at  $0.1 \text{ C}$  ( $20 \text{ mA g}^{-1}$ ) between 2~4.5V compared with  $\text{LiNi}_{0.8}\text{Co}_{0.1}\text{Mn}_{0.1}\text{O}_2$  (59 %), which may be ascribed to the stabilized effect of  $\text{Li}_2\text{MnO}_3$  component on the layered structure of Ni-rich oxide cathode.

## Reference

1. Whittingham, MS, *Chem. Rev.*, 2004, 104, 4271-4301.
2. X.H. Xiong, Z.X. Wang, H.J. Guo, Q. Zhang, X.H. Li, *J. Mater. Chem. A*, 2013, 1, 1284-1288.
3. J. Eom, K.S. Ryu, J. Cho, *J. Electrochem. Soc.*, 2008, 155, A228-A233.
4. Weihua Chen, Juanjuan Zhao, Yanyang Li, Shao Li, Chuanchuan Jin, Changchun Yang, Xiangming Feng, Jianmin Zhang, and Liwei Mi, *ChemElectroChem*, 2014, 1, 601-610.
5. S.-W. Wooa, S.-T. Myungb, H. Banga, D.-W. Kima, Y.-K. Sun, *Electrochim. Acta*, 2009, 54, 3851-3856.

# Template-free synthesis of porous $\text{Co}_3\text{O}_4@\text{C}$ hierarchical structure for high performance lithium-ion batteries

Lingbin Kong<sup>a,b,\*</sup>, Yang Li<sup>a</sup>, Maocheng Liu<sup>a</sup>, Xixin Wang<sup>a</sup>, Ming Shi<sup>a</sup>, Jinbei Liu<sup>b</sup>, Long Kang<sup>b</sup>

<sup>a</sup> State Key Laboratory of Advanced Processing and Recycling of Non-ferrous Metals, Lanzhou University of Technology, Lanzhou 730050, China. E-mail: konglb@lut.cn

<sup>b</sup> School of Materials Science and Engineering, Lanzhou University of Technology, Lanzhou 730050, China

Lithium-ion batteries (LIBs) have been commercialized for mobile phones and laptop computers. Recently, LIBs widely expected to drive electric vehicles and hybrid electric vehicles due to their high energy density and power densities, which are in great demand as energy sources and clean energy storage. Transition-metal oxides ( $\text{M}_x\text{O}_y$ , where M is Co, Ni, Fe, Cu, etc.) have emerged as potential anode materials for LIBs because they deliver a theoretical specific capacity far larger than that of commercial graphite material ( $372 \text{ mAh g}^{-1}$ )<sup>[1-2]</sup>. Among these metal oxides,  $\text{Co}_3\text{O}_4$  has attracted great attention due to its high reversible capacities at a relatively low potential, which greatly spurs the rapid development in this field. Unfortunately, the practical application of  $\text{Co}_3\text{O}_4$  in LIBs is still hindered with problems of rapid capacity fading and poor rate capability. In an attempt to overcome these significant drawbacks, it is considered an efficient strategy to design porous/hollow microstructures of  $\text{Co}_3\text{O}_4$  with high surface area and permeability, or coat a thin carbon layer onto the surface of  $\text{Co}_3\text{O}_4$  materials<sup>[3-4]</sup>.

In this work, hierarchical porous  $\text{Co}_3\text{O}_4@\text{C}$  microspheres were successfully synthesized via a template-free method. Firstly,  $\text{Co}_3\text{O}_4$ -based microspheres have been synthesized by a facile ultrasonic spray pyrolysis method. Subsequently, the  $\text{Co}_3\text{O}_4@\text{C}$  composite microspheres have been obtained via a hydrothermal method. As the anodic materials for LIBs, these hierarchical porous  $\text{Co}_3\text{O}_4@\text{C}$  microspheres exhibited enhanced cycling performance ( $986 \text{ mAh g}^{-1}$  at a current density of  $500 \text{ mA g}^{-1}$  after 50 cycles) and high rate capabilities ( $760 \text{ mAh g}^{-1}$  at current densities of  $1000 \text{ mA g}^{-1}$ , respectively) compared with bare  $\text{Co}_3\text{O}_4$  microspheres. This outstanding electrochemical behavior was ascribed to the porosity and carbon coating layers of the  $\text{Co}_3\text{O}_4@\text{C}$  microspheres, which could allow better penetration of electrolyte, achieve a higher reactive area, promote the mobility of ions/electrons and protect the structural integrity of the  $\text{Co}_3\text{O}_4@\text{C}$  microspheres.

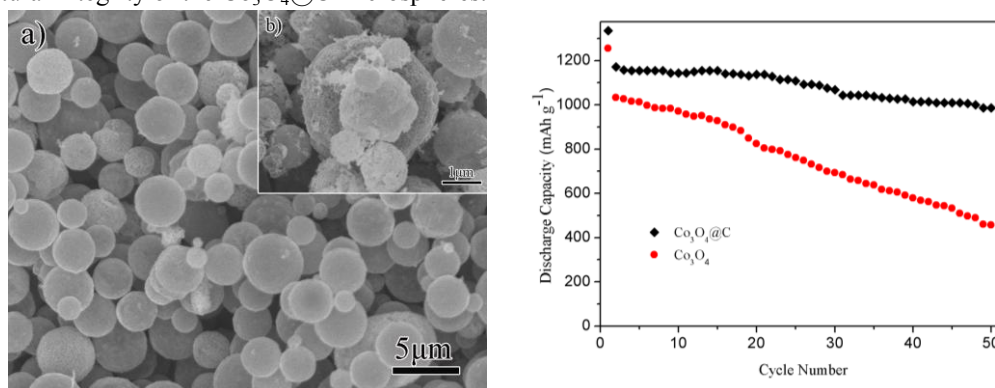


Fig. 1 a) SEM image of porous  $\text{Co}_3\text{O}_4$  microspheres. b) SEM image of porous  $\text{Co}_3\text{O}_4@\text{C}$  microspheres (Left) and discharge cycling performance of porous  $\text{Co}_3\text{O}_4$  and  $\text{Co}_3\text{O}_4@\text{C}$  microspheres electrodes at  $500 \text{ mA g}^{-1}$  (Right)

## Acknowledgements:

This work is supported by the National Natural Science Foundation of China (51362018, 21403099).

## References:

- [1] P. Poizot, S. Laruelle, S. Grugeon, L. Dupont, J. M. Tarascon, *Nature*, 407 (2000) 496.
- [2] M. Y. Son, J.H. Kim, Y.C. Kang, *Electrochim. Acta*, 116 (2014) 44.
- [3] J Chen, X.H Xia, J.P Tu, Q.Q Xiong, Y.X Yu, X.L Wang, C.D Gu, *J. Mater. Chem.*, 22 (2012) 15056.
- [4] Y.P Gan, H.Q Gu, H Xiao, Y Xia, X.Y Tao, H Huang, J Du, L.S Xu, W.K Zhang, *New J. Chem.*, 38 (2014) 2428.

# Self-healing Sn composite lithium-ion battery electrode with high capacity and good cycling stability

Jing Ma, Chaofan Yun, Wang Wang, Xue-Qian Wang, Chun-Ling Liu, Wen-Sheng Dong  
Key Laboratory of Applied Surface and Colloid Chemistry (SNNU), MOE, School of Chemistry and  
Chemical Engineering, Shaanxi Normal University, Xi'an, 710062, China  
ccliutt@snnu.edu.cn

Sn-based materials have been intensively studied as negative electrode candidates for LIB because of their much higher specific capacity (theoretical capacity is  $993 \text{ mAh g}^{-1}$ ). However, these materials suffer from volume expansion/shrinkage during lithium ion alloying/de-alloying. Such morphological changes cause loose contacts between the anode material and the current collector, resulting in poor charge/discharge cycling characteristics.

The biological systems in nature have the ability to self-heal when damaged, we called itself-healing, which is an important survival feature in nature because it increases the life time of living creatures. We can imagine if the volumetric changes of the tin electrode can be cured by itself just like biological systems, the lithium ion batteries will have a high capacity and along cycle life. In order to prepare a self-healing tin electrode, Firstly, we prepared the material that could be self-healing by the interaction of the intermolecular hydrogen bonds. The preparation of repeated destruction and self-healing material included two steps. First, dimer acid reacted with divinyl three amine to obtain the amine oligomer by amidation reaction. Then the product further reacted with urea to form polyamidoamine supramolecular polymer through a series of programmed reaction. Highly branched dendritic structure and a large amount of oriented hydrogen bonds between the molecules made it possible to achieve the self-healing material. Then tin nanoparticles were embedded in this self-healing material, thus successfully preventing the aggregation of tin nanoparticles and buffering the occurring volume strain, which accompanied the reversible (de-)alloying process. Such material presented higher specific capacity and more stable cycling performance, especially when charged at large current density.

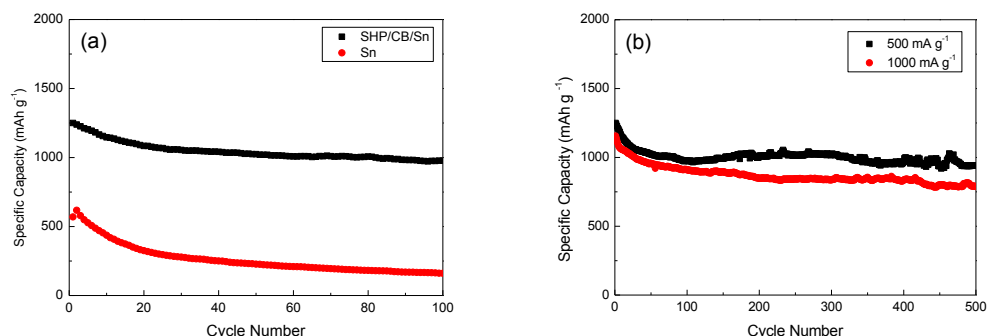


**Figure 1.** The cycling performance for SHP/Sn and pure Sn at current density of  $500 \text{ mA g}^{-1}$  (a) and SHP/Sn material at different current densities (b).

The electrochemical characterization of the composites confirmed that SHP/Sn showed excellent electrochemical performance when used as an anode for rechargeable lithium ion batteries. The initial reversible capacity is  $1250 \text{ mAh g}^{-1}$  at a constant current density of  $500 \text{ mA g}^{-1}$ , after 100 cycles it still remained a capacity of  $986 \text{ mAh g}^{-1}$ , which was 78.9% of the first charge capacity.

## References

- [1] D. Montarnal, P. Cordier, C. Soulie-Ziakovic, F. Tournilhac, L. Leibler, J. Poly. Sci.: Part A 46 (2008) 7925–7936.
- [2] C. Wang, H. Wu, Z. Chen, M.T. McDowell, Y. Cui, Z. Bao, Nat. Chem. 5 (2013) 1042–1048.

# Re-building Daniell Cell with a Li-ion exchange Film

Xiaoli Dong, Yonggang Wang\* & Yongyao Xia

Department of Chemistry and Shanghai Key Laboratory of Molecular Catalysis and Innovative Materials, Institute of New Energy, iChEM (Collaborative Innovation Center of Chemistry for Energy Materials), Fudan University, Shanghai 200433, China.

Address: Handan Road 220, Fudan University, Shanghai, China.

\*E-mail address: ygwang@fudan.edu.cn

Daniell cell (i.e. Zn-Cu battery) is widely used in chemistry curricula to illustrate how batteries work, although it has been supplanted in the late 19th century by more modern battery designs because of  $\text{Cu}^{2+}$ -crossover-induced self-discharge and un-rechargeable characteristic. Herein, it is re-built by using a ceramic Li-ion exchange film to separate Cu and Zn electrodes for preventing  $\text{Cu}^{2+}$ -crossover between two electrodes. The re-built Zn-Cu battery can be cycled for 150 times without capacity attenuation and self-discharge, and displays a theoretical energy density of  $68.3 \text{ Wh kg}^{-1}$ . It is more important that both electrodes of the battery are renewable, reusable, low toxicity and environmentally friendly. Owing to these advantages mentioned above, the re-built Daniell cell can be considered as a promising and green stationary power source for large-scale energy storage.

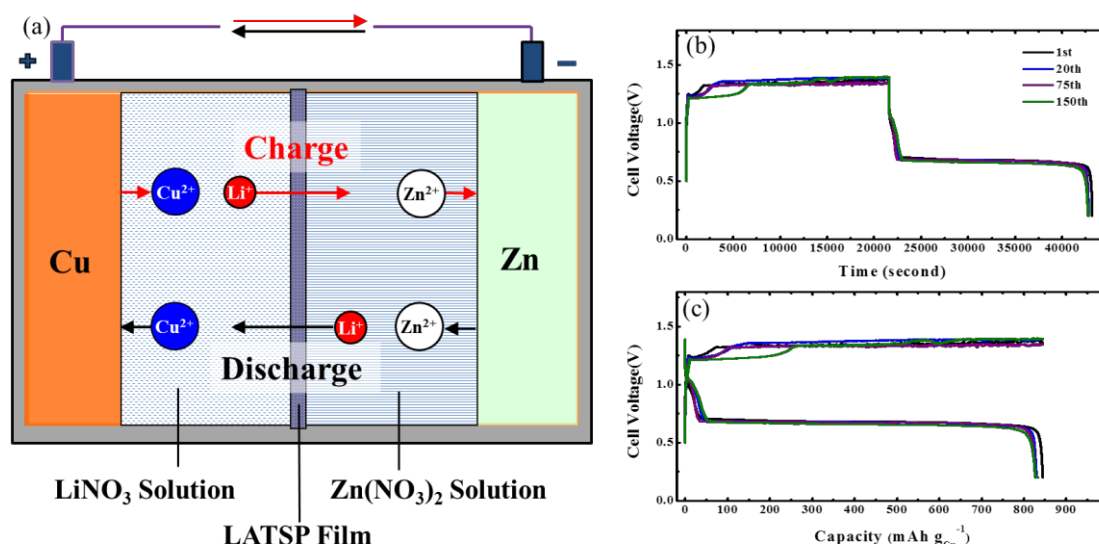


Figure. Fabrication and electrochemical investigation of the rechargeable Zn-Cu battery with a Li-ion exchange membrane.

- (a) Schematic illustration and operating mechanism of the rechargeable Zn-Cu battery.  
(b) Electrochemical investigation of the rechargeable Zn-Cu battery based on cell voltage vs. time.  
(c) Cyclic profile of the rechargeable Zn-Cu battery based on cell voltage vs. capacity.

## References

1. Armand, M. & Tarascon, J. M. Building better batteries. *Nature* **451**, 652–657 (2008).
2. Lu, Y. H., Goodenough, J. B. & Kim, Y. Aqueous cathode for next-generation alkali-ion batteries. *J. Am. Chem. Soc.* **133**, 5756–5759 (2011).
3. Dunn, B., Kamath, H. & Tarascon, J. M. Electrical energy storage for the grid: a battery of choices. *Science* **334**, 928–935 (2011).
4. Dong, X. L., Wang, Y. G. & Xia, Y. Y. Re-building Daniell Cell with a Li-ion exchange Film. *Sci. Rep.* **4**, 6916 (2014).



# A high performance lithium-ion sulfur battery based on a $\text{Li}_2\text{S}$ cathode using dual-phase electrolyte

Lina Wang, Yonggang Wang\* and Yongyao Xia\*

Department of Chemistry, Shanghai Key Laboratory of Molecular Catalysis and Innovative Materials, Institute of New Energy, and Collaborative Innovation Center of Chemistry for Energy Materials, Fudan University, Shanghai 200433, China

E-mail: ygwang@fudan.edu.cn; yyxia@fudan.edu.cn.

Fully-lithiated lithium sulfide ( $\text{Li}_2\text{S}$ ) is more desirable than sulfur as a high capacity cathode material because it allows use of a variety of lithium-free anode materials, such as graphite, Si, Al, etc., to form Li-ion sulfur batteries. Unfortunately,  $\text{Li}_2\text{S}$  cathode still suffers from the polysulfides shuttling over discharge-charge cycles. It is worse that  $\text{Li}_2\text{S}$  was considered electrochemically inactive for a long time.<sup>1,2</sup> Lately, Yang et al. demonstrated firstly that  $\text{Li}_2\text{S}$  can be activated after overcoming a huge potential barrier ( $\sim 1$  V) at the beginning of initial charge process.<sup>3</sup> Figure 1a schematically illustrates the activation of  $\text{Li}_2\text{S}$  over initial charge process. The  $\text{Li}_2\text{S}$  cathode must overcome a huge potential barrier at the beginning of delithiation (i.e.  $\text{Li}_2\text{S} \rightarrow \text{Li}_{2-y}\text{S} + y\text{Li}^+ + ye^-$ ). The huge potential barrier then disappears after the outer surface layer of solid  $\text{Li}_2\text{S}$  is electrochemically oxidized into liquid and soluble lithium polysulfides ( $\text{Li}_2\text{S}_x$ ,  $4 \leq x \leq 8$ ). The phenomenon should be attributed to that the lithium bonding environment in  $\text{Li}_2\text{S}$  is more like that in lithium polysulfides than in pure electrolyte, which may facilitate the charge transfer process between  $\text{Li}_2\text{S}$  and the polysulfides.<sup>3</sup> Furthermore, it can be assumed that the further charging after formation of lithium polysulfides includes both electrochemical and chemical reactions. The surface polysulfides ( $\text{Li}_2\text{S}_x$ ,  $4 \leq x < 8$ ) can be further electrochemically oxidized into the longer-chain polysulfides. Simultaneously, the liquid charge product (e.g. longer-chain polysulfides) can also oxidize the solid  $\text{Li}_2\text{S}$  through direct chemical reaction. As mentioned above, the liquid and soluble polysulfides not only improve the charge transfer for solid  $\text{Li}_2\text{S}$ , but also play the role of redox mediators.

Here, we report a new approach to utilize  $\text{Li}_2\text{S}$  efficiently based on a rechargeable Li-S battery with dual-phase-nonaqueous electrolyte, as illustrate in Figure 1b, in which the electrolyte for  $\text{Li}_2\text{S}$  cathode and the electrolyte for anode is separated by a protective lithium super ionic conductor glass film (LISICON) of  $\text{Li}_{1+x+y}\text{Al}_x\text{Ti}_{2-x}\text{Si}_y\text{P}_{3-y}\text{O}_{12}$  (LTAP). The LTAP is permeable to Li-ions while impermeable to polysulfide-anions. As a result, parasitic reactions associated with the polysulfides shuttle effect is totally eliminated in this cell architecture, and the chemistry of the cell can be therefore stabilized. The polysulfides intermediates can be constrained in the cathode apartment to efficiently facilitate oxidation of  $\text{Li}_2\text{S}$ , thus commercially available micro-sized  $\text{Li}_2\text{S}$  without further processing is able to be used as cathode active material directly. The realization of a Li-ion sulfur battery by successfully replacing metallic lithium with aluminum or graphite anode is demonstrated in our initial study.

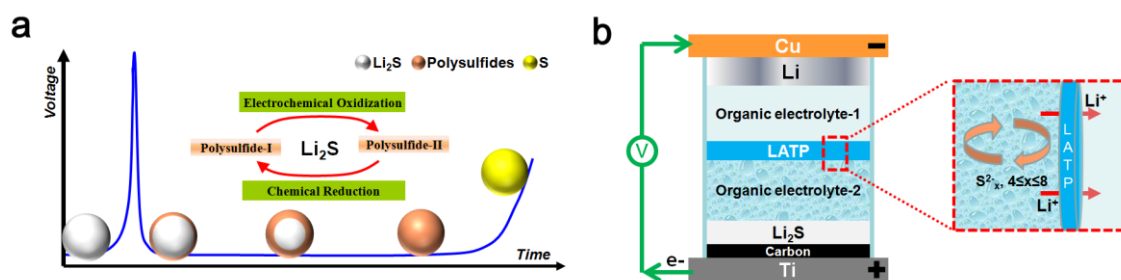


**Figure 1.** Schematic illustrations. (a) Schematic illustration of activation process of  $\text{Li}_2\text{S}$  cathode over initial charge. (b) Schematic of the architecture for Li-S battery composed of (–) Cu foil/Li metal/organic electrolyte-1/ceramic separator (LTAP)/organic electrolyte-2/ $\text{Li}_2\text{S}$  cathode/Super P carbon/Ti foil (+) from top to bottom.

## Reference

1. M. N. Obrovac and J. R. Dahn, *Electrochem. Solid-State Lett.*, 2002, **5**, A70–A73.
2. B. H. Jeon, J. H. Yeon, K. M. Kim and I. J. Chung, *J. Power Sources*, 2002, **109**, 89–97.
3. Y. Yang, G. Zheng, S. Misra, J. Nelson, M. F. Toney and Y. Cui, *J. Am. Chem. Soc.*, 2012, **134**, 15387–15394.

# Aqueous Lithium-Ion Batteries Using O<sub>2</sub> Self-elimination Polyimides Electrodes

Long Chen, Wangyu Li, Zhaowei Guo, Yonggang Wang, Congxiao Wang and Yongyao Xia\*  
Department of Chemistry, Shanghai Key Laboratory of Molecular Catalysis and Innovative Materials,  
Institute of New Energy, Collaborative Innovation Center of Chemistry for Energy Materials, Fudan  
University  
Shanghai 200433, China,  
\*e-mail: [yyxia@fudan.edu.cn](mailto:yyxia@fudan.edu.cn)

Lithium-ion (and sodium-ion) battery (LIB and SIB) using aqueous electrolyte may solve the safety problem of LIB using highly toxic and flammable organic solvents. It is also expected to exhibit much longer cycling life than these commercialized aqueous secondary batteries, e.g., lead-acid and nickel-metal hydrogen. Aqueous LIB was first reported by Dahn's group in 1994, the cell could operate at an average voltage near 1.5 V with a specific energy density of 75 Wh/kg based on the total weight of both electrode materials<sup>[1]</sup>. Recently, many efforts have been devoted to develop aqueous lithium-ion batteries, but all have poor cycling stability: the capacity retention is typically less than 50% after 100 cycles. Very recently, we have demonstrated that, the discharged state lithium-ion intercalated compounds (LIC) of any negative electrode candidates for the aqueous lithium-ion batteries would react with water and O<sub>2</sub>, which is the primary cause of the capacity fading upon cycling<sup>[2]</sup>. In principle, the O<sub>2</sub> evolution can be avoided by controlling the cut-off charge voltage and using sealed system. However, it is impossible to absolutely avoid the O<sub>2</sub> evolution using the aqueous electrolyte, especially when the cell was overcharged. On the other hand, taking view of these commercialized aqueous secondary batteries, they could be designed as the sealed system. This is because that the anode electrode material can eliminate O<sub>2</sub> itself if the O<sub>2</sub> evolution occur in the cathode during charge process. Unfortunately, most Li-ion intercalated compounds do not behave the same performance. Very recently, many organic electrode materials have been examined as cathode or anode for non-aqueous LIB or SIB, especially polymers and these multiple carbonyl groups conjugated Quinone and its derivatives with a controlling voltage varying from 1.5 V to 3.0 V vs. Li<sup>+</sup>/Li. In the present work, we interestingly reported that these organic materials, for example polyimide, can not only show excellent Li-ion storage profile in aqueous electrolyte, but also behave the O<sub>2</sub> self-elimination performance (**Fig. 1**): Polyimide electrode can adopt two Li<sup>+</sup> becoming lithiated compound (discharged state). When the cell was overcharged, the O<sub>2</sub> evolution will occur on the cathode, and diffusion into anode, the lithiated polyimide (discharged state) can react with O<sub>2</sub> and be reversibly oxidized into polyimide itself.

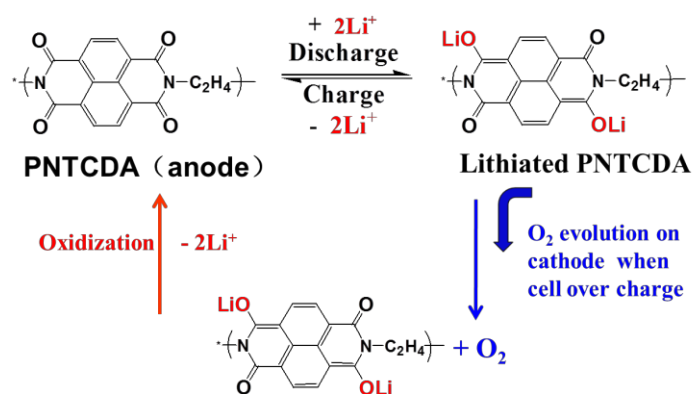


**Fig.1** O<sub>2</sub> self-elimination performance and redox mechanism of PNTCDA.

A sealed polyimide-AC/LiNO<sub>3</sub>/LiMn<sub>2</sub>O<sub>4</sub> aqueous LIB exhibited excellent stability with capacity retention over 95% after 1000 cycles at 2C condition, even when the cell was once overcharged.

## Reference

1. Li, W., Dahn, J. R. & Wainwright, D. Science **264**, 1115–1118 (1994).
2. Luo, J.Y., Cui, W.J., He, P., Xia, Y.Y. Nat. Chem. **2**, 760-765 (2010).

# Facile Formation of 3D Nanoporous Anodic TiO<sub>2</sub>-TiN Composite Films as Anode Materials for Lithium Rechargeable Batteries

Haruki Sakuyama<sup>a</sup>, **Song-Zhu Kure-Chu**,<sup>\*,a</sup> Hitoshi Yashiro<sup>a</sup>, Kuniaki Sasaki<sup>a</sup>  
Hiroyo Segawa<sup>b</sup>, Kenji Wada<sup>b</sup>, and Satoru Inoue<sup>b</sup>

<sup>a</sup> Faculty of Engineering, Iwate University, 4-3-5, Ueta, Morioka, 020-8551, Japan

<sup>b</sup> National Institute for Materials Science (NIMS), Namiki 1-1, Tsukuba, Ibaraki, 305-0044, Japan

\*E-mail address: [chusongz@iwate-u.ac.jp](mailto:chusongz@iwate-u.ac.jp)

Recently, TiO<sub>2</sub> nanotubes formed by anodization on Ti foils have attracted great attention as a potential anode material for Li-ion batteries (LIB). This is because the TiO<sub>2</sub> nanotubes provide a high specific surface that benefits the intercalation of Li ions, and Li insertion in TiO<sub>2</sub> occurs at a higher potential (~1.5–1.7 V vs Li/Li<sup>+</sup>) that avoids reduction of Li, thus improving the safety of the LIBs. However, some conducting additive phase have to be mixed into TiO<sub>2</sub> as anode materials for LIBs due to their poor conductive nature. The present study is aimed at fabricating nanoporous TiO<sub>2</sub>-TiN composite films from Ti foils by a tailored anodization in aqueous electrolytes.

Figure 1 shows a representative 3D nanoporous titania film formed by anodizing a Ti foil in a NO<sub>3</sub><sup>-</sup> containing aqueous electrolyte. The anodic titania film composed of multi-tiered nanoporous layers with close-packed cylindrical pores in  $\phi$ 30–60 nm. The tier thickness of porous titania films varied dramatically with the composition of electrolytes, anodizing voltage, and current density. Figure 2 gives the XPS spectra of N1s for the anodized specimen in Fig.1. The spectrum for the film surface showed two peaks corresponding to absorbed ions of NO<sub>3</sub><sup>-</sup> and NH<sup>+</sup>, whereas the spectra after Ar<sup>+</sup> sputtering revealed a new peak close to the binding energy of titanium nitride in TiN, thus confirming the formation of TiN in the anodic titania film. Details on experimental results including FE-SEM, XRD, and electrochemical evaluation as binder-free anode materials for Li rechargeable batteries will be reported on the meeting.

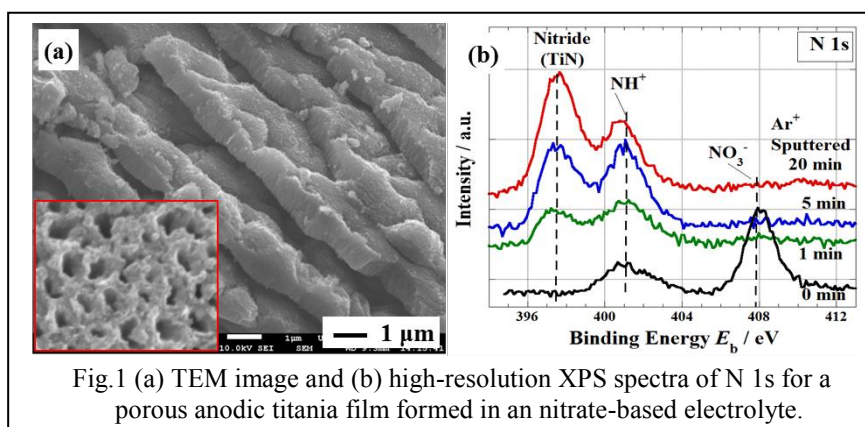


Fig.1 (a) TEM image and (b) high-resolution XPS spectra of N 1s for a porous anodic titania film formed in an nitrate-based electrolyte.

# Electrodeposition of Silicon for the Preparation of Submicrostructured Electrodes

Selina Tillmann, Martin Winter, Isidora Cekic-Laskovic

*MEET Battery Research Center, University of Muenster, Corrensstr. 46, 48149 Muenster, Germany*

*Selina.Tillmann@uni-muenster.de*

In order to advance the replacement of fossil fuel by renewable energy sources, current limitations in energy and power density of lithium-ion batteries need to be overcome. Electrodes offering a large inner surface area combined with good lithium-ion transport properties are promising candidates to improve energy and power density of lithium-ion batteries.[1]

Our approach in this respect is the fabrication of 3-D submicrostructured electrodes based on silicon as active material which is well known for its high theoretical capacity but pronounced volume change during cycling.[2]

In this study we report on the electrodeposition of silicon from an organic solvent suitable for the preparation of nano-/microstructured electrodes and the chemical and electrochemical characteristics of the deposits. Silicon was electrochemically deposited on a nickel current collector by applying a constant potential. Depending on the total current, deposits ranging from several nanometers to a few microns of thickness were obtained. The chemical composition of the obtained silicon films was analysed using X-ray Photoelectron Spectroscopy (XPS), X-ray Diffraction (XRD) and Raman spectroscopy.

To validate the electrochemical performance of the active material, cyclic voltammograms were recorded. Additionally, cycling experiments and the C-rate capability of the electrodes was investigated in half cells using 1M LiPF<sub>6</sub> in EC:DEC 3:7 + 2wt% VC as electrolyte.

Additionally, the effect of the volume expansions during (de)insertion of lithium ions into the deposited silicon was investigated as a function of the thickness of the deposit using Scanning Electron Microscopy (SEM) and XRD.

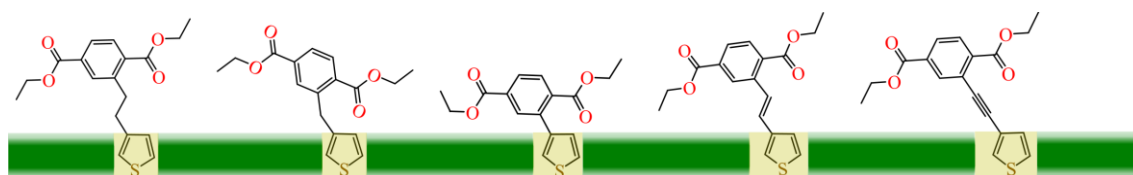
## References:

- [1] M.K. Song, S. Park, F. M. Alamgir, J. Cho, M. Liu, Nanostructured electrodes for lithium-ion and lithium-air batteries: the latest developments, challenges, and perspectives, Mater. Sci. Eng. R. 72 (2011) 203.
- [2] W.J. Zhang, A review of the electrochemical performance of alloy anodes for lithium-ion batteries, J. Pow. Sour. 196 (2011) 13.

# Synthesis and Redox Properties of Thiophene-Terephthalate Building Blocks for Low Potential Conducting Redox Polymers

Xiao Huang,<sup>[a]</sup> Li Yang,<sup>[b]</sup> Jonas Bergquist,<sup>[a]</sup> Maria Strømme,<sup>[b]</sup> Adolf Gogoll,<sup>\*[a]</sup> Martin Sjödin<sup>\*[b]</sup>  
<sup>[a]</sup> Uppsala University, Synthetic Organic Chemistry, Department of Chemistry - BMC, Box 576, 751 23 Uppsala, Sweden  
<sup>[b]</sup> Uppsala University, Nanotechnology and Functional Materials, Department of Engineering Sciences, Box 534, 751 21 Uppsala, Sweden  
xiao.huang@kemi.uu.se

Conducting polymers nowadays find widespread use in a range of application areas including organic energy storage, organic light emitting diodes, solar cells, actuators, and bioelectronics.<sup>[1-3]</sup> By introducing functional groups to a conducting polymer backbone, the functionality of conducting polymers can be expanded even further, and the specificity can be increased. In the case of energy storage, the functional groups can *e.g.* yield greatly enhanced specific energies. Herein, we report on the synthesis of a series of building blocks for a new type of low potential conducting redox polymer and their characterization by electrochemical redox property studies including both experimental and computational approaches. These building blocks are composed of thiophene and terephthalate pendant groups connected by various linkers. We observe that the recyclability and reduction potentials are crucially related to the functional linkage between the thiophene and terephthalate subunits. This shows that removing the conjugation between the pendant group and the thiophene backbone could both favor the polymerization and lower the reduction potential of the material. These results constitute the starting point for further studies on a new type of thiophene based low potential redox polymer targeting anode electrode applications.



- [1] F. Rosciano, M.M. Salamone, Riccardo Ruffo, M. Sassi, L. Beverina, *J. Electrochem. Soc.* 160 (2013) A1094-A1098.  
[2] T.F. Otero, J. Arias-Pardilla, H. Herrera, J.L. Segura, C. Seoane, *Phys. Chem. Chem. Phys.* 13 (2011) 16513–16515.  
[3] C.Y. Wang, A.M. Ballantyne, S.B. Hall, C.O. Too, D.L. Officer, G.G. Wallace, *J. Power Sources* 156 (2006) 610–614.

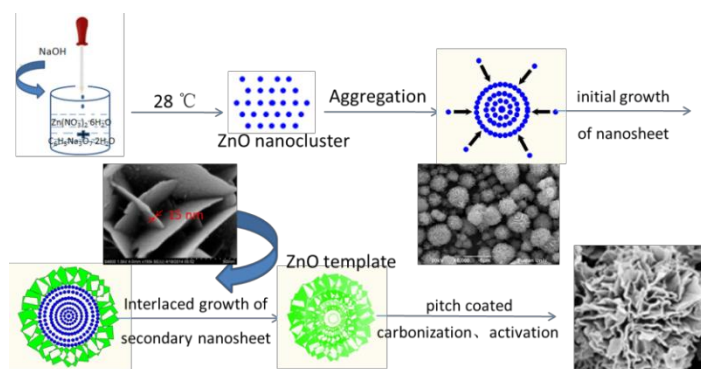
# Three-Dimensional Activated Porous Carbon /Sulfur Composites as Cathode Materials for Lithium-Sulfur Batteries

Lan Zhou, Tao Huang\*, [Aishui Yu\\*](#)

*Department of Chemistry, Shanghai Key Laboratory of Molecular Catalysis and Innovative Materials,  
Institute of New Energy, Fudan University, Shanghai 200433, China  
[asyu@fudan.edu.cn](mailto:asyu@fudan.edu.cn)*

Lithium sulfur battery, which use sulfur as a cathode and Li as an anode, have taken more and more attention for its high theoretical specific capacity of 1675 mAh g<sup>-1</sup> and high theoretical specific energy of 2600 Wh kg<sup>-1</sup>. Despite these particular advantages, several troublesome issues associated with the sulfur cathode severely limits the practical use of sulfur in an electrode, such as, the highly electrical insulating nature of sulfur, the redox shuttle of dissolved polysulfide ions and the volume expansion of sulfur cathode materials.

In this work, sulfur (S) encapsulated into nitrogen-doped porous carbon nanofiber webs (CNFWs) was obtained by a modified oxidative template route, carbonization-activation and thermal treatment. The sulfur was dispersed and immobilized homogeneously into the micropores of nitrogen-doped porous carbon nanofiber webs (CNFWs) with high electrical conductivity, extremely high surface area and large pore volume, which alleviated the polysulfide shuttle phenomenon and made a contribution to the good electrochemical performance. To further increase the contact area with the electrolyte, three-dimensional flower-shaped activated porous carbon/sulfur composites (FA-PC/S) are also fabricated for the first time via a simple method utilizing flower-shaped ZnO as a template and pitch as the carbon precursor, followed by carbonization-activation and thermal treatment. A typical flower-shaped FA-PC spherical structure is composed of many nanopetals intersecting with one another. Because of the unique three-dimensional flower-shaped porous spherical structure, FA-PC has high reactivity, high electrical conductivity and a short transport length for the Li ion. Furthermore, the rich micropores of the FA-PC offer enough space to accommodate the volume expansion that occurs during the discharge process of the encapsulated sulfur as well as confine the electrochemical reaction products of the sulfur cathode within the micropores. The electrochemical tests show that both three-dimensional activated porous carbon /sulfur composites have a high initial discharge capacity, a good cycling stability and excellent rate capability.



# Carbon-coated $\text{Na}_3\text{V}_2(\text{PO}_4)_3$ Nanocomposite as a Novel High Rate Cathode Material for Aqueous Sodium Ion Batteries

Ludan Zhang, Tao Huang, Aishui Yu\*

*Department of Chemistry, Shanghai Key Laboratory of Molecular Catalysis and Innovative Materials,  
Institute of New Energy, Fudan University, Shanghai 200433, China  
asyu@fudan.edu.cn*

Aqueous rechargeable sodium ion batteries has attracted a lot of interests because of its low cost, huge abundance of sodium resources and promising application for large-scale electric energy storage. Herein, we proposed the carbon-coated  $\text{Na}_3\text{V}_2(\text{PO}_4)_3$  nanocomposite ( $\text{Na}_3\text{V}_2(\text{PO}_4)_3/\text{C}$ ) as a cathode material, which was prepared using a simple sol-gel method. The structure and morphology analyses showed that the highly crystalline  $\text{Na}_3\text{V}_2(\text{PO}_4)_3$  nanoparticle with an average size of 350 nm is well coated by a carbon layer with a thickness of 3 nm. Electrochemical tests showed that at high current rates, the  $\text{Na}_3\text{V}_2(\text{PO}_4)_3/\text{C}$  cathode exhibited excellent electrochemical performance. Impressively, it delivered a discharge specific capacity of 94.5 mAh/g at 10C (1176 mA/g), 90.5 mAh/g at 15C (1764 mA/g) and 71.7 mAh/g at 20C (2352 mA/g). To the best of our knowledge, the notable rate capability has never been reported before for aqueous sodium ion batteries. The enhanced electrochemical behavior could be attributed to the combined advantages of  $\text{Na}_3\text{V}_2(\text{PO}_4)_3$  nanoparticles and carbon layer in the unique core-shell structure, which improved the intrinsic poor electronic conductivity of  $\text{Na}_3\text{V}_2(\text{PO}_4)_3$  greatly. Our results confirmed the prepared  $\text{Na}_3\text{V}_2(\text{PO}_4)_3/\text{C}$  nanocomposite should be a promising cathode candidate for aqueous sodium ion batteries.



# Redox Active Polymers: Pursuing a Size-Selective Strategy for High Performance Non-Aqueous Redox Flow Batteries

E.C. Montoto Blanco; J. Hui; N. Gavvalapalli, E. Chenard; K. Cheng, T. Lichtenstein; J. S. Moore and J. Rodríguez-López

*Department of Chemistry, University of Illinois at Urbana-Champaign  
600 S Mathews Avenue, Urbana, IL, 61801, P: +1(217) 300 7354, F: 217-265-6290  
joaquinr@illinois.edu*

Symposium 3: Batteries for Tomorrow's World

Non-aqueous redox flow batteries (NRFBs) are a potentially viable alternative to their aqueous counterparts as they offer a wider range of redox active species and electrolytes available for their design.[1] However, the low ionic conductivity observed when non-dedicated ion-exchange membranes are used in organic solvents has slowed down their wide-scale implementation. Separating the redox active species in the electrolyte compartments by size-exclusion while allowing free flow of the supporting electrolyte presents a potentially powerful alternative to the use of poorly-performing ion-exchange membranes. In our case, this approach is made possible by the careful design and evaluation of Redox Active Polymers (RAPs), together with porous commercial off-the-shelf separators, as shown in **Figure 1**. RAPs consist of a polymeric unconjugated backbone that is decorated with high energy density and highly stable redox active pendants that display facile electron transfer.

We will present our advances towards implementing such strategy using viologen-, N-oxide-, alkoxybenzene- and nitrobenzene- based redox active polymers (RAPs) with the aim of creating an “ALL RAP” non-aqueous redox flow battery with an open circuit voltage in excess of 2.0 V. Our first studied system, based on viologen RAPs with molecular weight between 21 and 318 kDa exhibited size-dependent transport across the porous separator.[2] This was achieved with RAPs that displayed a high solubility of up to 2.7 M, reversible electron transfer, and 94-99% charge/discharge efficiency. Microelectrode voltammetry allowed to prove facile electron transfer even in highly concentrated solutions (+1.0 M). Preliminary testing using a stirred cell showed the possibility of integrating RAPs and porous separators into a working device that achieved stable charge/discharge and only 2% crossover over several hours. We are working towards the development of guidelines that aid our understanding of RAP electrochemistry. The application of new electrochemical and ionic imaging methods based on scanning electrochemical microscopy using micro- and nano- electrodes developed in our group [3] has allowed us to better understand the careful balance between RAP size and ion and electron mobility. We will discuss how these guidelines have significantly aided our molecular design and how they impact the performance of this new type of flow batteries.

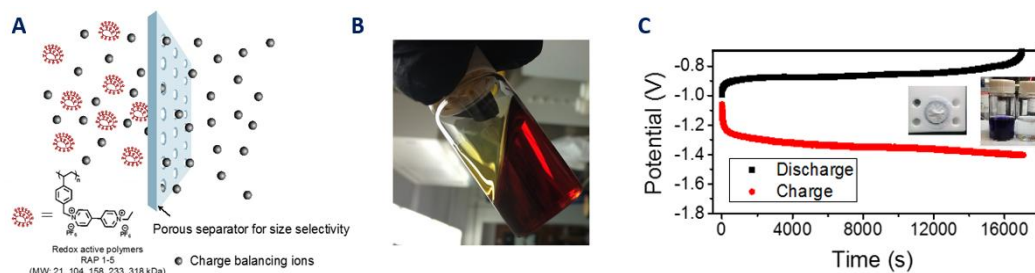


**Figure 1.** Redox Active Polymers. A) Size selectivity across a porous separator, B) Solubility in the M range and C) Stable charge and discharge with low crossover using a commercial porous separator.

- [1] R.M. Darling, K.G. Gallagher, J.A. Kowalski, S. Ha, F.R. Brushett. Pathways to Low-Cost Electrochemical Energy Storage: a Comparison of Aqueous and Nonaqueous Flow Batteries. *Energy Environ. Sci.* 7 (2014) 3459.
- [2] N. Gavvalapalli, J. Hui, K. Cheng, T. Lichtenstein, M. Shen, J.S. Moore and J. Rodríguez-López. J. Impact of Redox Active Polymer Molecular Weight on the Electrochemical Properties and Transport Across Porous Separators in Non-Aqueous Solvents. *J. Am. Chem. Soc.* 136 (2014) 16309.
- [3] Z. J. Barton, and J. Rodríguez-López. Lithium Ion Quantification Using Mercury Amalgams as In Situ Electrochemical Probes in Nonaqueous Media. *Anal. Chem.* 86 (2014) 10660.



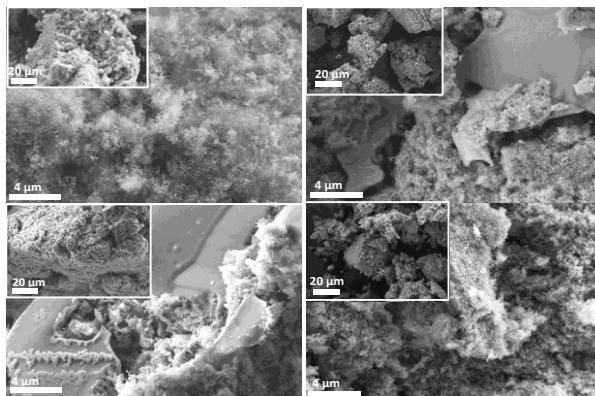
# Search for Perfect Carbonaceous Sulphur Hosts for Li–S Batteries

Sigita Urbonaite, Petr Novák

*Electrochemical Energy Storage Section, Electrochemistry Laboratory, Paul Scherrer Institute,  
5232 Villigen PSI, Switzerland  
sigita.urbonaite@psi.ch*

Lithium–sulphur batteries have been studied for several decades, motivated by predictions of a high specific charge of 1672 mAh/g and a high specific energy of 2,500 Wh/kg [1]. They are among the most promising systems for the next generation of rechargeable lithium batteries. However, the development of Li–S batteries faces a number of challenging problems on the way to reaching maximum performance and commercialization. One of them is the insulating nature of sulphur, necessitating the addition of conductive additives to the electrode material. Whereas a wide range of factors contribute to the overall performance of the Li–S system [2], reported optimization procedures typically focus on the development of novel structured cathodes, in which the conductive environment of sulphur is optimized. The most widely used conductive additive for electrodes is carbon, many different forms of which are being employed for positive electrodes in Li–S batteries [3–6]. The perfect carbon host for accommodating sulphur would, of course, have to provide electronic conductivity, but it should also help in maintaining a high specific charge and high coulombic efficiency by containing polysulfides, as to suppress the polysulfide shuttle and loss of active material.

Here we present a systematic study of various commercially available carbons used as hosts for S in positive Li–S battery electrodes. The influence of pore volume, pore-size distribution and surface area on the performance of Li–S cells was investigated in combination with several S impregnation/infiltration methods (morphologies of C–S composites and sulphur distribution after its impregnation/infiltration using the different methods are shown in the figure below). Correlations between cycling performance of Li–S cells and properties of carbons on the one hand and impregnation methods on the other hand are shown. It was found that predominantly mesoporous materials with their open structure lead to the best specific charge and capacity retention during cycling. In contrast, highly microporous carbons displayed poor specific-charge values and fast specific-charge fading over the cycling duration.



## References

- [1] X. Ji, K.T. Lee, L.F. Nazar, *Nat. Mat.* 8, 500–506 (2009).
- [2] S. Urbonaite, P. Novák, *J. Power Sources* 249, 497–502 (2014).
- [3] H. Wang, Y. Yang, Y. Liang, J.T. Robinson, Y. Li, A. Jackson, Y. Cui, H. Dai, *Nano Lett.* 11, 2644–2647 (2011).
- [4] Y. Yang, G. Yu, J.J. Cha, H. Wu, M. Vosgueritchian, Y. Yao, Z. Bao, Y. Cui, *Nano Lett.* 5, 9187–9193 (2011).
- [5] S. Evers, L.F. Nazar, *Acc. Chem. Res.* 46, 1135–1143 (2013).
- [6] Y. Yang, G. Zheng, Y. Cui, *Chem. Soc. Rev.* 42, 3018–3032 (2013).

## Acknowledgements

BASF SE is acknowledged for financial support within the ‘BASF Scientific Network on Electrochemistry and Batteries’.

Experimental work of J. Boland, as a part of his senior sophister Nanoscience course, is gratefully acknowledged.

# Lithium iron methylene diphosphonate, a new organic-inorganic hybrid material for Li-ion batteries.

Sébastien Sallard <sup>\*,1</sup>, Sebastian Schmidt <sup>1</sup>, Denis Sheptyakov <sup>2</sup>, Petr Novák <sup>1</sup>, Claire Villevieille <sup>1</sup>

<sup>1</sup> Electrochemistry Laboratory, Paul Scherrer Institut, 5232 Villigen PSI, Switzerland

<sup>2</sup> Laboratory for Neutron Scattering and Imaging, Paul Scherrer Institut, 5232 Villigen PSI, Switzerland  
sebastien.sallard@psi.ch

The research on positive electrode materials for Li-ion batteries has generally been focused on inorganic compounds such as transition metal oxides, phosphates or silicates. The variety of different purely inorganic compounds is however limited. Introducing an organic component into the inorganic framework would give rise to various new synthetic possibilities and might therefore in the future allow adjustments of the electrochemical properties of the metal ions by the influence of neighboring organic groups. Only few examples of such organic-inorganic hybrid materials are known in the literature. The most promising already reported example of a positive electrode material for Li-ion batteries where a rigid organic group was implemented to define the structure is  $[\text{Fe(III)(OH)}_{0.8}\text{F}_{0.2}(\text{bdc})]\cdot\text{H}_2\text{O}$  developed by G. Férey et al.<sup>1</sup>

To introduce a new class of organic-inorganic hybrid materials for Li-ion batteries with versatile organic parts, we chose to investigate transition metal diphosphonates. The material lithium iron methylene diphosphonate was selected as reference material as proof of concept for hybrid materials for positive electrode in Li-ion batteries.

Lithium iron methylene diphosphonate was synthesized by a simple hydrothermal route, yielding a material with a new crystalline phase. In a half-cell configuration, it exhibits a specific charge of 90 mAh/g upon lithiation (reduction), which remains stable for more than 100 cycles (Figure 1). The specific charge even continuously increases after 60 cycles to reach a value of 118 mAh/g after 160 cycles. The large irreversibility of the first and the second cycle with a different potential profile is assumed to originate from the removal of residual  $\text{H}^+$  in the structure upon delithiation, leading to enhanced electrolyte decomposition. The consecutive delithiation steps do not any longer show this feature, thereby increasing the coulombic efficiency drastically from very low in the first cycle ( $\sim 40\%$ ) to a more reasonable value ( $> 90\%$ ) after 10 cycles, reaching a stable value of 97% after 50 cycles. *Operando* XANES confirmed the oxidation and reduction of iron during the cycling.

The results obtained provide a basis for investigations on the influence of different heteroatoms or organic entities substituted to the diphosphonate on the electrochemistry of the hybrid material, which is the focus of our future research.

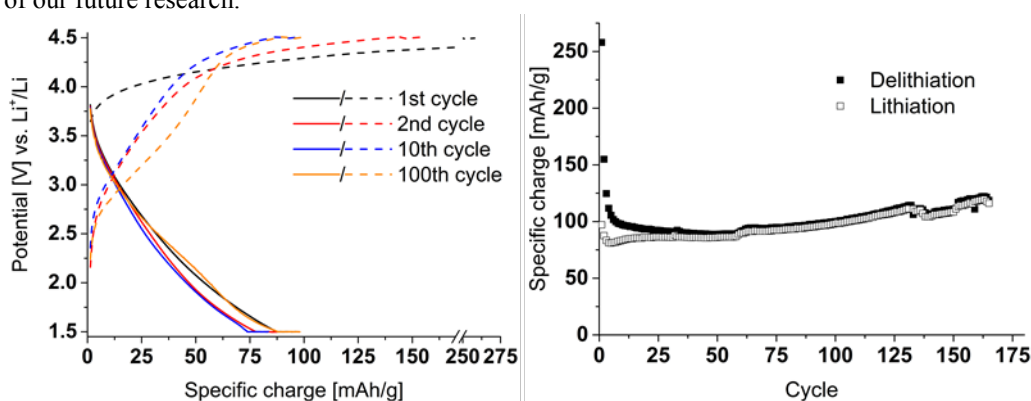


**Figure 1 left:** Galvanostatic profile of lithium iron methylene diphosphonate cycled in a half-cell configuration. After each half-cycle, a 1 h potentiostatic step was implemented. **Right:** The corresponding evolution of the specific charge during cycling of lithium iron methylene diphosphonate.

1. Férey, et al. *Angewandte Chemie International Edition* **2007**, 46 (18), 3259-3263.

# Polymer Binders Evaluation for Improved Lithium-ion Batteries Positive Electrodes via Water-based Processing Route

A. Robba, D. Sotta, S. Chazelle, M. Chami, S. Jouanneau Si Larbi  
CEA, Department for Electrical and Hydrogen Transportation (LITEN/DEHT/SRGE),  
17 rue des Martyrs, F-38054 Grenoble Cedex 9, France  
e-mail address: [dane.sotta@cea.fr](mailto:dane.sotta@cea.fr)  
*Symposium 3: Batteries for Tomorrow's World*

Lithium-ion batteries have now spread as the leading energy storage technology for a wide variety of applications such as portable electronics, electrified transportation and stationary systems. Research efforts attempt to decrease their overall cost and environmental impact by considering eco-friendly design and process from material synthesis to batteries recycling [1,2]. Water-based process for electrode manufacturing is now used at industrial scale for anodes but it is far less developed for cathodes due to several issues such as material sensitivity towards water and aluminum current collector corrosion during coating process [3,4].

Here we report electrode formulations evaluations using lithium nickel-manganese-cobalt lamellar oxide ( $\text{LiNi}_{1/3}\text{Mn}_{1/3}\text{Co}_{1/3}\text{O}_2$ , NMC) as active material and several polymer binders for water-based suspensions. Slurry manufacturing was improved by adding acidification step aimed at decreasing suspension pH and thus avoiding aluminum pitting when coating. NMC analysis with XRD and ICP-MS didn't show any impact of slurry acidification on material structure. The addition of latex binder at the end of slurry manufacturing was privileged as a well-established means to improve electrode mechanical properties (adhesion on current collector, flexibility). Styrene-butadiene rubber emulsion (SBR) was tested as the reference latex for water-based formulations, but it exhibited poor electrochemical stability at cathode high voltages. This degradation due to polymer oxidation led to poor cycling performances in coin cells. On the contrary a non-SBR latex such as "latex 2" exhibited satisfying performances when compared to reference electrodes using PVdF as a binder (Figure 1). The combination of slurry acidification and proper latex selection is thus thought as an effective way to improve aqueous formulations for cathodes.

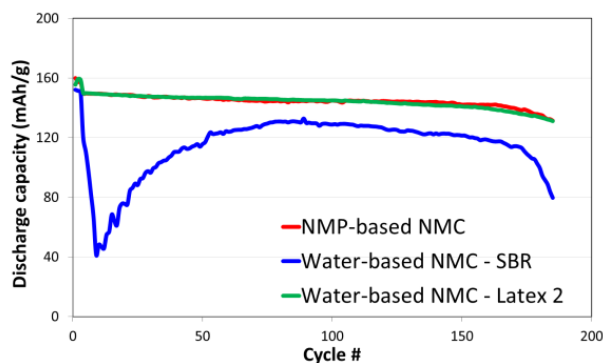


Figure 1 : C/2 discharge capacity upon cycling in half coin-cells NMC/Li (1.3 mAh/cm<sup>2</sup> NMC loading, [3-4.35 V vs.  $\text{Li}^+/\text{Li}$ ] voltage range, room temperature)

## References:

- [1] J. Li, R.B. Lewis, J.R. Dahn, Sodium Carboxymethyl Cellulose - A Potential Binder for Si Negative Electrodes for Li-Ion Batteries, *Electrochem. Solid-State Lett.*, 10 (2007) A17.
- [2] D.A. Notter, M. Gauch, R. Widmer, P. Wäger, A. Stamp, R. Zah, H.-J. Althaus, Contribution of Li-ion batteries to the environmental impact of electric vehicles, *Environ. Sci. Technol.*, 44 (2010) 6550.
- [3] N. Loeffler, J. von Zamory, N. Laszczynski, I. Doberdo, G.-T. Kim, S. Passerini, Performance of  $\text{LiNi}_{1/3}\text{Mn}_{1/3}\text{Co}_{1/3}\text{O}_2$ /Graphite batteries based on aqueous binder, *J. Power Sources*, 248 (2014) 915.
- [4] Q. Wu, S. Ha, J. Prakash, D.W. Dees, W. Lu, Investigations on High Energy Lithium-Ion Batteries with Aqueous Binder, *Electrochim. Acta*, 114 (2013) 1.

# **BaZr<sub>x</sub>Ce<sub>0.8-x</sub>Y<sub>0.2</sub>O<sub>3-δ</sub> (x = 0.5, 0.6, 0.7) Proton Conductors Prepared by Spark Plasma Sintering**

Junfu Bu, Pär Göran Jönsson, Zhe Zhao

*Department of Materials Science and Engineering, KTH Royal Institute of Technology, SE-100 44*

*Stockholm, Sweden*

[junfu@kth.se](mailto:junfu@kth.se)

Dense BaZr<sub>x</sub>Ce<sub>0.8-x</sub>Y<sub>0.2</sub>O<sub>3-δ</sub> (x = 0.5, 0.6, 0.7) proton conductors, which can be used for intermediate temperature solid oxide fuel cells (ITSOFCs), were successfully prepared by Spark Plasma Sintering (SPS) at 1350 °C without sintering aids addition. Though SPS had been used for various ceramic preparation, there is no success case for preparation of dense Ce-containing BaZr<sub>0.8-x</sub>Ce<sub>x</sub>Y<sub>0.2</sub>O<sub>3</sub> (0 < x ≤ 0.8) or BaZr<sub>0.9-x</sub>Ce<sub>x</sub>Y<sub>0.1</sub>O<sub>3</sub> (0 < x ≤ 0.9) based proton conductors as far as we know. This is due to the Ce<sup>4+</sup> reduction in a reducing atmosphere. Therefore, it is really a meaningful and tough work to realize a preparation of high-quality Ce-containing BaZrO<sub>3</sub>-BaCeO<sub>3</sub> based proton conductors by using the SPS technique.

In this work, the prepared dense BaZr<sub>x</sub>Ce<sub>0.8-x</sub>Y<sub>0.2</sub>O<sub>3-δ</sub> (x = 0.5, 0.6, 0.7) proton conductors were characterized by XRD, SEM and EDS, in order to determine phase purity, morphology and element composition of prepared pellets, respectively. In addition, the conductivities of these samples were determined at different atmospheres: dry air, wet N<sub>2</sub> and wet H<sub>2</sub>. Moreover, the potential electronic conduction contribution to the total conductivity was also identified by using different oxygen partial pressures (1 - 10<sup>-24</sup> atm) in combination with an XPS analysis. Several important achievements were obtained in this work and these achievements should have positive promotion for present ITSOFCs, such as:

- (1) The sintering temperature was lowered by 300 °C without sintering aids addition compared to conventional sintering.
- (2) This lowered sintering temperature can significantly improve the electrode and electrolyte co-fired preparation, and this will maintain the porous properties of electrode as well as the dense properties of electrolyte.
- (3) The obtained conductivity data shows that the materials can be used as proton conductors for ITSOFC applications. Moreover, it was found that the electronic contribution to the total conductivity can be neglected after the analysis of the total conductivities at different oxygen partial pressures combined with an XPS analysis.
- (4) Furthermore, the relative density of the prepared BZCY532 pellet is 0.995 and the grain size has a narrow distribution (400 - 500 nm). The pore-free microstructure promised a serious study on the proton conductivity without the potential influence of pores. And the fine grain size of 400 - 500 nm promised the better mechanical strength for thin electrolyte SOFC cell structure. In our opinion, this work should be an important improvement in preparation of BaZrO<sub>3</sub>-BaCeO<sub>3</sub> based proton conductors.

# Towards Control of Major Degradation Processes in Solid Oxide Electrolysis Cells

Sergey N. Rashkeev,<sup>1,\*</sup> Michael V. Glazoff,<sup>2</sup> Stephen J. Herring<sup>2</sup>

<sup>1</sup>*Qatar Environment & Energy Research Institute, P.O. 5825 Doha, Qatar*

<sup>2</sup>*Idaho National Laboratory, Idaho Falls, ID 83415, USA*

\*e-mail: [srashkeev@qf.org.qa](mailto:srashkeev@qf.org.qa)

Materials used for different components (electrodes, electrolyte, steel interconnects, etc.) of solid oxide electrolyzer cell (SOEC) devices for hydrogen production have to function in aggressive, corrosive environments and in the presence of electric fields. This results in a number of degradation processes at interfaces between components. In this study, we used a combination of first-principles, density-functional-theory (DFT) calculations, and thermodynamic modeling to elucidate the main processes that contribute into the two major degradation mechanisms in SOECs: (i) delamination of oxygen electrode in typical SOEC device consisting of yttria-stabilized zirconia (YSZ) electrolyte and Sr-doped LaMnO<sub>3</sub> (LSM) oxygen electrode, and; (ii) vaporization of Cr-rich volatile species from interconnect materials.

We found that high temperature inter-diffusion of different atomic species across the LSM/YSZ interface significantly affects structural stability of the materials and their interface. In particular, we found that La and Sr substitutional defects positioned in ZrO<sub>2</sub> oxide and near LSM/YSZ interface significantly change oxygen transport which may develop pressure buildup in the interfacial region and eventually develop delamination process. Simple models for estimating these effects are proposed, and different possibilities for inhibiting and/or mitigating undesirable delamination processes are discussed. In particular, we discuss possible modifications of operational regimes for SOEC devices. It is shown that applying alternating current (AC) voltage pulses with specific shapes and at a certain frequency range to SOECs could significantly reduce oxygen delamination in these devices and increase their lifetime. This operational scheme provides wide possibilities to increase longevity of SOEC devices required for their use in commercial hydrogen production processes, without any significant modification of used materials and/or cell design. Developed simulation method possesses a broad generality and be employed in a number of other industrial processes.

Vaporization of Cr-rich volatile species from interconnect materials is another major source of degradation that limits the lifetime of planar solid oxide devices systems with metallic interconnects such as Solid Oxide Fuel Cells (SOFC) and Solid Oxide Electrolysis Cells (SOEC). Some metallic coatings (Ni, Co, and Cu) may significantly reduce the Cr release from interconnects and slow down the oxide scale growth on the steel substrate. To shed additional light upon the mechanisms of such protection and find a suitable coating material for ferritic stainless steel materials widely used for interconnects, we used a combination of first-principles calculations, thermodynamics, and diffusion modeling to investigate which factors determine the quality of the Ni metallic coatings. We found that Cr migration in Ni coatings is determined by a delicate combination of the nickel oxidation, Cr diffusion, and phase transformation processes. Although the formation of Cr<sub>2</sub>O<sub>3</sub> oxide is more exothermic than that of NiO, the kinetic rate of the chromia formation in the coating layer and its surface is significantly reduced by the low mobility of Cr in nickel oxide and in NiCr<sub>2</sub>O<sub>4</sub> spinel. These results are in a good agreement with diffusion modeling for Cr diffusion through the Ni coating layer on the ferritic 441 steel substrate.

## References:

1. Michael V. Glazoff, Sergey N. Rashkeev, and J. Stephen Herring. Reduction of Chromium Vaporization from Interconnects with Nickel Coatings in Solid Oxide Devices. *International Journal of Hydrogen Energy* 39, 15031-15038 (2014).
2. Sergey N. Rashkeev and Michael V. Glazoff. Control of Oxygen Delamination in Solid Oxide Electrolyzer Cells via Modifying Operational Regime. *Applied Physics Letters* 99, N 17, 173506 (2011).
3. Sergey N. Rashkeev and Michael V. Glazoff. Atomic-Scale Mechanisms of Oxygen Electrode Delamination in Solid Oxide Electrolyzer Cells. *International Journal of Hydrogen Energy* 37, Issue 2, 1280-1291 (2012).

# **Design and Development of a Fuel Cell Power Module for High Altitude and Long Endurance Unmanned Aerial Vehicles**

Tae-Hyun Yang, Young-Jun Sohn, Minjin Kim, Seung-Gon Kim  
*Fuel Cell Research Center, Korea Institute of Energy Research*  
*152 Gajeong-ro, Yuseong-go, Daejeon 305-343, Rep. of Korea*  
[thyang@kier.re.kr](mailto:thyang@kier.re.kr)

As increasing power density and performance of polymer electrolyte membrane fuel cell (PEMFC), this system has been applied to the Unmanned Aerial Vehicle (UAV) as a power source. Especially, HALE (high altitude and long endurance) UAVs have various applications which are not only military missions like surveillance but also commercial needs such as meteorological observation, aerial photograph, and internet network build. To realize these great potentials of HALE UAV, high energy density and specific energy power generator should be needed. The fuel cell power module has gained recognition as one of the most possible candidate. However, many technological huddles lie ahead, for example, thermal and water management in the extreme atmospheric environment of stratosphere, ultra-light manufacturing technology for fuel cell stack and BOPs, and high energy density fuel containing method. In this work, the fuel cell system design for the UAV was discussed in terms of operating conditions under conditions of extreme low temperature and pressure, lightening method of stack, and enhancing performance of membrane and electrode assembly and stack.

# Modeling of Structure Formation and Fracturing in Polymer Electrolyte Membranes

Michael Eikerling, Mahdi Ghelichi and Alix Melchy

Department of Chemistry, Simon Fraser University  
8888 University Drive, Burnaby, BC, V5A1S6, Canada  
meikerl@sfu.ca

Polymer electrolyte membranes (PEMs) play a key role as separator and proton transport media in electrochemical energy technologies, most prominently in polymer electrolyte fuel cells (PEFCs). Current membranes require sufficient hydration for efficient proton conduction. The self-organized structure of the membrane, formed from comb-shaped ionomers with acid-terminated sidechains, dictates its water sorption behavior, transport properties, durability and lifetime. In spite of decades of research, this structure has remained controversial. The first part of this contribution focuses on ionomer bundle formation in water. We will present results of a recently developed theory [1] and of molecular dynamics simulations. The strengths of hydrophobic and electrostatic interactions are varied to explore their effect on the aggregation process, as illustrated in Figure 1. The bundle network morphology is the basis for a model of fracture formation in PEMs, discussed in the second part. The fracturing process is mapped onto a lattice percolation problem. Bundle breaking in the lattice is the elementary breaking step. At the lattice level, various regimes fracture formation exist, depending on the strength of correlations between elementary breaking events. The limit with weak correlations is the random percolation regime. Strong correlations lead to a nucleation regime, with a clear-cut fracture line, through an avalanche regime, characterized by sudden bursts of elementary breakages. An important aspect of this modeling work is to relate these regimes to physical parameters describing the material. In the random percolation regime, the time to formation of a sample-spanning fracture is analytically derived as a function of bundle properties and the local stress distribution.

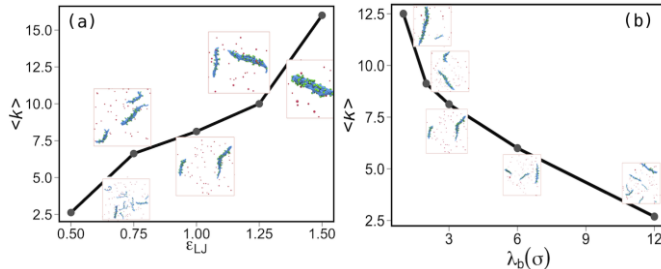


**Figure 1.** Changes of the average aggregate size,  $\langle k \rangle$ , as a function of variation in strengths of hydrophobic interactions (a) and electrostatic interactions (b).

[1] P.-É. A. Melchy and M. H. Eikerling, *Phys. Rev. E* 89, 032603 (2014).

# Shorting in Proton Exchange Membrane Fuel Cells

Yeh-Hung Lai\* and Corey Schaffer

*General Motors Company*

*895 Joslyn Ave*

*Pontiac, MI 48340*

*U.S.A.*

*\*yeh-hung.lai@gm.com*

Ohmic shorting through the membrane has been identified as one of the major failure modes in Proton-Exchange-Membrane fuel cells (PEMFC) [1]. Shorting occurs when electrons flow directly from the anode to the cathode instead of through the device being powered. Ohmic shorting not only can reduce the PEMFC performance, but also can lead to local heat generation in the vicinity of the short, causing membrane damage that can ultimately result in gas crossover failure. Two types of membrane shorts have been observed during the fuel cell testing: soft shorts and hard shorts. A soft short is a sub-critical short that results from the conductive carbon fibers or debris penetrating through the membrane. The soft shorts do not immediately lead to fuel cell failure; however, significant accumulation of soft shorts can reduce the overall cell resistance and compromise fuel cell durability through cell voltage degradation. A hard short is a critical short that is the result of significant heat release from an existing soft short. A hard short can directly lead to membrane crossover and cell failure. Hard shorts occur suddenly in an operating fuel cell stack where one cell develops a cell voltage reversal well below -1 V [2].

The present study is composed of two major parts. The first is to investigate the fuel cell operating conditions that lead to cell reversal and hard shorts. The second is on the development of a test method to determine the number and severity of soft shorts that may result in hard shorts when these adverse fuel cell conditions are met. The ultimate objective of the study is to prevent the PEM fuel cell shorting failure through better material designs and fuel cell operation controls.

In the first part of the study, we stepwise dried out a single large-active-area fuel cell by decreasing the inlet gas dew points while under galvanostatic control. At a critical dew point, the cell potential dropped rapidly to reach a negative voltage that we limited to -1 V. No electronic short or any observable damage to the cell was detected in this experiment. Tests were conducted at various cell current densities and inlet temperatures, which showed that the corresponding cell resistance at the onset of rapid cell voltage drop decreases as the current density increases or as the temperature decreases. Good correlation is found between the cell resistance and the onset of cell reversal at various current densities. When the cell reversal limit of -1V was removed, we found that hard shorts can develop at a cell voltage around -3V, confirming the importance of operating the fuel cell within the operating window developed in this study.

In the second part of this study, we have proposed the use of a current distribution circuit board [3] in a fixture that induces uniform compression over a 32 cm<sup>2</sup> area of a sample that consists of a piece of proton exchange membrane or a membrane electrode assembly sandwiched between two layers of gas diffusion layers. By incrementally increasing the compressive pressure and subjecting the sample to a voltage of 0.6 V, we can measure increasing shorting currents in some of the 0.5 cm<sup>2</sup> current distribution segments. By de-convoluting the current density distribution measured in this experiment, the number and severity of each short can be identified and the robustness of various material sets against soft shorts can be compared.

1. A.B. LaConti, M. Hamdan, R.C. McDonald, Mechanism of Membrane Degradation for PEMFCs, in Mechanisms of Membrane Degradation for PEMFCs, in: W. Vielstich, A. Lamm, H.A. Gasteiger (Eds), *Handbook of Fuel Cells: Fundamentals, Technology and Applications*, Vol. 3, John Wiley & Sons, New York, 2003, pp. 647–662.
2. Gittleman, C. S., Coms, F. D., and Lai, Y. H., "Chapter 2: Membrane Durability: Physical and Chemical Degradation", *Polymer Electrolyte Fuel Cell Degradation*, Editors: Matthew M. Mench, E. Caglan Kumbur, T. Nejat Veziroglu, Elsevier (2012).
3. J.J. Gagliardo, J.P. Owejan, T.A.Trabold, and T.W.Tighe, *Nucl. Instrum. Meth. A*, 605 (2009) 115-118.



# High Activity Pyrolyzed Iron-FA as Potential Pt-Substitute for Oxygen Reduction Reaction

Hsin-Chih Huang<sup>1</sup>, Sun-Tang Chang<sup>2</sup>, Chen-Hao Wang<sup>1\*</sup>, Li-Chyong Chen<sup>3</sup>, Kuei-Hsien Chen<sup>3,4</sup>

<sup>1</sup>*Department of Materials Science and Engineering, National Taiwan University of Science and Technology, Taipei, 10607, Taiwan*

<sup>2</sup>*National Synchrotron Radiation Research Center, Hsinchu 30076, Taiwan*

<sup>3</sup>*Center for Condensed Matter Sciences, National Taiwan University, Taipei, 10617, Taiwan*

<sup>4</sup>*Institute of Atomic and Molecular Science, Academia Sinica, Taipei, 10617, Taiwan*

E-mail: [chwang@mail.ntust.edu.tw](mailto:chwang@mail.ntust.edu.tw)

The operation of proton exchange membrane fuel cell (PEMFC) is limited by the slow reaction of oxygen reduction reaction (ORR) at cathode side,<sup>[1]</sup> which is traditionally solved by using platinum catalysts. However, platinum utilization is limited by its natural abundance and high cost. Therefore, the replacement of platinum with an efficient, durable, and inexpensive material is currently one of major research efforts in fuel cell development.

Non-precious metal catalyst is one of potential materials for cathode applications. Transition metal macrocyclic compounds, such as porphyrin, phthalocyanine, tetraazannulene and polypyrrole have been reported to be good cathode materials.<sup>[2-4]</sup> Among these compounds, Fe- and Co-based macrocyclic compounds have been reported to have the high catalytic activity for ORR.<sup>[5, 6]</sup> This work demonstrates the non-precious metal catalyst by using folic acid as a new nitrogen precursor mixed with iron and carbon black for fuel cell application. The ORR measurements reveal that the optimized condition of catalyst shows an excellent ORR activity, and the electron transfer number and %H<sub>2</sub>O<sub>2</sub> is 3.99 and 0.5%, respectively. The ORR mechanisms have to be investigated furthermore.

Keywords: Fuel Cells, Oxygen Reduction Reaction, Non-Precious Metal Catalysts

[1] A.J. Appleby, O.A. Velev, J.G. LeHellico, A. Parthasarthy, S. Srinivasan, D.D. DesMarteau, M.S. Gillette, J.K. Ghosh, Polymeric perfluoro bis-sulfonimides as possible fuel cell electrolytes, *Journal of the Electrochemical Society*, 140 (1993) 109-111.

[2] N.A. Savastenko, V. Brüser, M. Brüser, K. Anklam, S. Kutschera, H. Steffen, A. Schmuhl, Enhanced electrocatalytic activity of CoTMPP-based catalysts for PEMFCs by plasma treatment, *Journal of Power Sources*, 165 (2007) 24-33.

[3] I.H. P. Bogdanoff, M. Hilgendorff, I. Dorbandt, S. Fiechter and H. Tributsch, Probing Structural Effects of Pyrolysed CoTMPP-based Electrocatalysts for Oxygen Reduction via New Preparation Strategies, *Journal of New Materials for Electrochemical Systems*, 7 (2004) 85-92.

[4] Y. Lu, R.G. Reddy, The electrochemical behavior of cobalt phthalocyanine/platinum as methanol-resistant oxygen-reduction electrocatalysts for DMFC, *Electrochimica Acta*, 52 (2007) 2562-2569.

[5] X.-Y. Xie, Z.-F. Ma, X. Wu, Q.-Z. Ren, X. Yuan, Q.-Z. Jiang, L. Hu, Preparation and electrochemical characteristics of CoTMPP-TiO<sub>2</sub>NT/BP composite electrocatalyst for oxygen reduction reaction, *Electrochimica Acta*, 52 (2007) 2091-2096.

[6] H. Liu, C. Song, Y. Tang, J. Zhang, J. Zhang, High-surface-area CoTMPP/C synthesized by ultrasonic spray pyrolysis for PEM fuel cell electrocatalysts, *Electrochimica Acta*, 52 (2007) 4532-4538.

# **The Oxygen Electoreduction Reaction Performance of Pt Catalysts Supported on Commercial Blacks and Nanostructured Carbons: Multiwall Nanotubes and Nanofibers**

E.N. Gribov<sup>\*1,2</sup>, A.N. Kuznetsov<sup>1</sup>, V.A. Golovin<sup>1,2</sup>, D.V. Krasnikov<sup>1,2</sup>, V.L. Kuznetsov<sup>1,2</sup>, A.G. Okunev<sup>1,2</sup>

<sup>1</sup> *Boriskov Institute of Catalysis, Lavrentieva str. 5, Novosibirsk, 630090, Russia*

<sup>2</sup> *Novosibirsk State University, Pirogova str. 2, Novosibirsk, 630090, Russia*

(\*) corresponding author: [gribov@catalysis.ru](mailto:gribov@catalysis.ru)

One of the promising approaches to reduce the content of platinum in the Pt/C catalysts for the oxygen electroreduction reaction (ORR) in polymer electrolyte fuel cells (PEMFC) is to increase the activity and Pt utilization by optimizing the morphological properties and the structure of the porous carbon supports. In recent decades, nanostructured carbon supports - carbon nanotubes and nanofibers received much attention because of the higher electrical conductivity and the effective mass transport properties.

In this work we synthesized a series of 20 and 40 mass % Pt/C electrocatalysts based on commercial carbon blacks and nanostructured carbon supports: the original and the modified multiwall carbon nanotubes (CNTs), catalytic filamentous carbon (CFC) and commercial carbon blacks. The Pt particle sizes were found in the 2.8 – 12 nm range, as obtained from the TEM studies and gas-phase CO chemisorption measurements. The electrochemically active surface of Pt in the Pt/C catalysts was calculated using the electrooxidation of chemisorbed CO. The mass and surface activities as well as the activation energies in the ORR were obtained by rotating disc electrode in the 10-35 °C temperature range in 0.1 M HClO<sub>4</sub> solution.

It was found that the mass and surface activities depend strongly on the porous and morphological carbon properties. The ORR activity of 40 mass. % Pt/CNT was greatly improved as compared to the commercial sample (20 mass. % Pt/Vulcan XC-72).

CNT support was modifying by carbon deposition in order to increase Pt dispersion. 20 mass. % Pt/C catalysts prepared on modified carbon support showed the higher ORR activity as compared to the unmodified carbon.

The effect of the Pt particle size and morphology and texture of carbon supports on the ORR activities of Pt/C catalysts is discussed in the paper.

Authors thank Dr. Kazakova M. and Dr. Voropaev I. for the provided carbon materials. This work was supported by the RFBR grant № 13-03-01023. The work is also supported by the Ministry of Education and Science of the Russian Federation”.

# Novel Pd-Fe-Co Core-Core-Shell Anode Nanocatalyst in Alkaline Anion-Exchange Membrane Alcohol Fuel Cells

**Kenneth I. Ozoemena**<sup>\*,1,2</sup>

<sup>1</sup>*Energy Materials, CSIR Materials Science and Manufacturing, Pretoria 0001, South Africa*

<sup>2</sup>*School of Chemistry, University of the Witwatersrand, Johannesburg 2050, South Africa*

*Tel. + 27-12-841-3664, Fax. + 27-12-841-2135*

*E-mail: [kozoemena@csir.co.za](mailto:kozoemena@csir.co.za)*

Nanostructured electrocatalysts are extremely important for the development of high-performance alcohol direct alkaline fuel cells (ADAFCs). The use of microwave irradiation to tune the physico-chemical properties of inorganic materials has been known for some decades. However, there is a limited literature on the use of microwave irradiation to control the structure, size and electrochemistry of nanocatalysts for fuel cells. To close this knowledge gap, we have been investigating novel synthetic technique involving microwave irradiation which we termed “microwave-induced top-down nanostructuring and decoration” (MITNAD) for making Pd-based ternary core-shell nanoparticles (FeCo@Fe@Pd/C) with sub-10 nm diameter size for the development of ADAFCs [1-3].

In our most recent study [3], we investigated the performance of FeCo@Fe@Pd core-core-shell nanocatalyst, supported on carboxylate-functionalized multi-walled carbon nanotubes (MWCNT-COOH), as anode catalyst for passive and active anion-exchange membrane direct polyhydric alcohol fuel cell (AEM-DPhAFC). The two polyhydric alcohols investigated were glycerol (Gly) and ethylene glycol (EG). Using nuclear magnetic resonance (NMR), we analyzed the exhaust products of the AEM-DGFC operated at low temperatures and proved that the FeCo@Fe@Pd/MWCNT as anode exhibits high selectivity towards the complete and exhaustive oxidation of polyhydric alcohols. This presentation will discuss all our recent findings on the electrocatalytic properties of FeCo@Fe@Pd/MWCNT for application in AEM-DPhAFC.

## References

- (1) O.O. Fashedemi, B. Jules, K.I. Ozoemena, *Chem. Commun.*, **2013**, 49, 2034-2036.
- (2) O.O. Fashedemi, K.I. Ozoemena, *Phys. Chem. Chem. Phys.* **2013**, 15, 20982-20991
- (3) O.O. Fashedemi, H.A. Miller, A. Marchionni, F. Vizza and K.I. Ozoemena, *J. Mater. Chem. A*, **2015**, 3, 7145–7156

# Is the Tafel approximation sufficient to predict electrocatalyst performance in polymer electrolyte fuel cells?

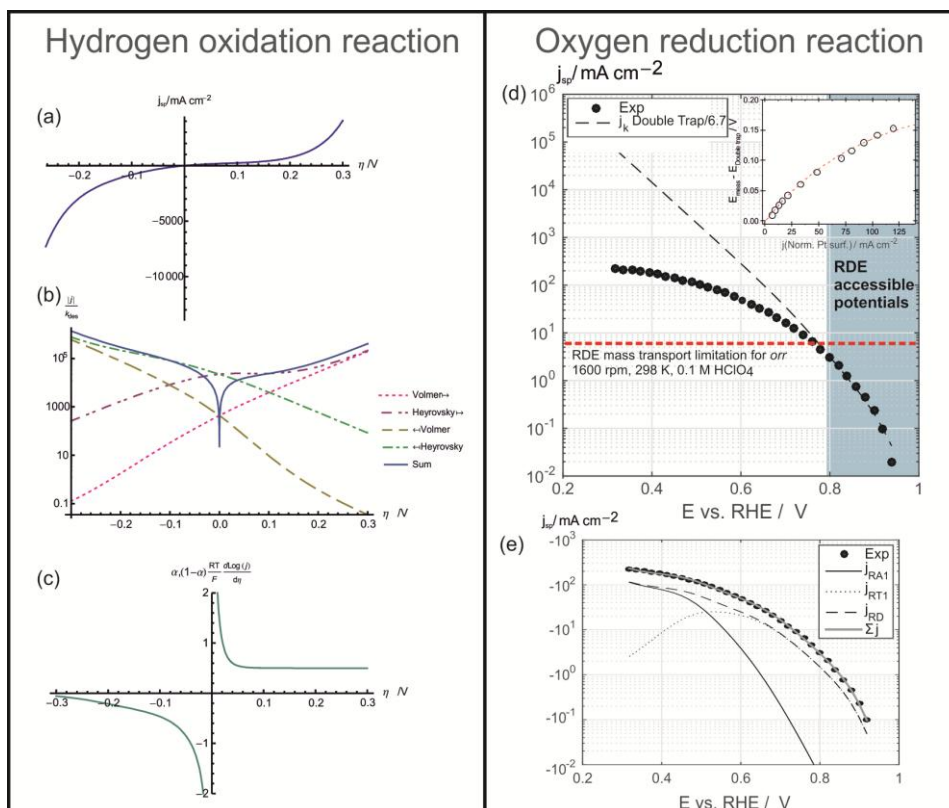
Anthony Kucernak, Matthew Markiewicz, Christopher Zalitis

Imperial College London

Imperial College Rd, London, SW7 2AZ, United Kingdom

a.kucernak@imperial.ac.uk

Description of fuel cell electrocatalysis typically involves approximations to the underlying governing formulae. For instance, it is often assumed that at large overpotentials we may use the Tafel approximation – that is that the reaction under study is controlled by one electron transfer step across a relatively large range of potentials, and that the surface remains relatively invariant across that potential regime. Such an approach is typically used to describe oxygen reduction reaction (*orr*). Alternatively, a Butler-Volmer type dependence close to the reversible potential is often assumed e.g. for the hydrogen oxidation reaction (*hor*). Parameters for these models are often obtained by extrapolating the performance achievable at a rotating disk electrode (RDE) under severe mass transport limitation. However, mathematical tools have moved on considerably since the advent of electrochemical kinetics, and it is now possible to analytically solve many important surface limited reactions. Recently we have developed a new method of measuring electrocatalyst performance under conditions of high mass transport [1, 2]. We have used this approach and electrochemical modelling to understand important aspects of the *hor* and *orr* [3, 4]. Examples are given in Figure 1 (a)-(c) in which analytical solutions for the *hor* may be used to follow the different components of the reaction at different overpotentials and understand the regions in which limiting Tafel slopes may occur. Similarly for the oxygen reduction reaction modelling of the electrochemical reaction is possible only when a blocking species is present on the electrode at high overpotentials Figure 1 (d)-(e). This paper will discuss the relevance of these results to modelling of the *hor* and *her* in fuel cells.



## References

- [1] C.M. Zalitis, D. Kramer, A.R. Kucernak, Physical Chemistry Chemical Physics, 15 (2013) 4329-4340.
- [2] C.M. Zalitis, D. Kramer, J. Sharman, E. Wright, A.R. Kucernak, ECS Trans., 58 (2013) 39-47.
- [3] M. Markiewicz, C.M. Zalitis, A.R. Kucernak, Electrochim. Acta, (2015) In press.
- [4] C.M. Zalitis, J. Sharman, E. Wright, A.R. Kucernak, Electrochim. Acta, (2015) Accepted.

# Performance and Stability of New Oxide Catalyst Supports under PEFC Operating Conditions

Alexandra Pătru<sup>1</sup>, Johannes Biesdorf<sup>1</sup>, Antoni Forner Cuenca<sup>1</sup>, Emiliana Fabbri<sup>1</sup>, Pierre Boillat<sup>1,2</sup>,  
Thomas Justus Schmidt<sup>1,3</sup>

<sup>1</sup>*Electrochemistry Laboratory, Paul Scherrer Institut, 5232 Villigen PSI, Switzerland*

<sup>2</sup>*Neutron Imaging and Activation Group, Paul Scherrer Institut, 5232 Villigen PSI, Switzerland*

<sup>3</sup>*Laboratory of Physical Chemistry, ETH Zurich, 8093 Zurich, Switzerland*  
*alexandra.patru@psi.ch*

Up to date, the literature reports stability studies for new oxide catalyst supports for Polymer Electrolyte Fuel Cell (PEFC) cathodes where the degradation protocols are generally realised at the laboratory, liquid electrolyte cell level (room temperature, non-optimised catalytic layer) [1]. Only few data are available regarding the processing of this new alternative supports for Pt in a PEFC and the stability under real operating conditions of the derived Membrane Electrode Assemblies (MEAs).

In this context, this work addresses the long-term stability issues of PEFCs based on a new cathode catalyst generation. Commercial Pt/IrTiO<sub>2</sub> (Umicore®) and home-made Pt/Sb-doped SnO<sub>2</sub> (SbSnO<sub>2</sub>) were used as new cathode catalysts and referenced to the properties of standard Pt/C (TKK) on the single cell MEA level.

The fuel cell performances and stabilities of the various MEAs are examined in differential cells (small-size single cells operated at high stoichiometry) [2]. Accelerated stress test protocols, e.g., potential or start-stop cycling were applied to the different home-made MEAs. The different contributions to the overall cathode overpotentials i.e., kinetic and mass transport losses inside the catalyst and the gas diffusion layers, respectively, are separated with the help of pulsed oxygen and helox operation, a method recently developed in our group [3], throughout the accelerated stress tests. Structural changes of the electrodes are furthermore monitored by electron microscopy. Thus study demonstrates the benefits and drawbacks of oxide support materials for PEFC cathodes.

## Acknowledgement

The authors thank Umicore AG&Co. KG and the Competence Center for Electricity and Mobility (CCEM) of Switzerland for their financial support within the project DuraCat.

## References

- [1] Y. Takabatake, Z. Noda, S.M. Hayashi, K. Sasaki, International Journal of Hydrogen Energy 39, 5074-5082 (2014).
- [2] P. Oberholzer, P. Boillat, R. Siegrist, A. Kastner, E.H. Lehmann, G.G. Scherer, A. Wokaun, Electrochemistry Communications 20, 67-70 (2012).
- [3] P. Boillat, P. Oberholzer, A. Kastner, R. Siegrist, E.H. Lehmann, G.G. Scherer, A. Wokaun, Journal of Electrochemical Society 159(7), F210-F218 (2012).

# Shaped Pt Bimetallic Nanoparticles: Linking the Anisotropic Growth to the Electrocatalytic Properties

Lin Gan<sup>1,2</sup>, Chunhua Cui<sup>2</sup>, Fabio Dionigi<sup>2</sup>, Peter Strasser<sup>2</sup>

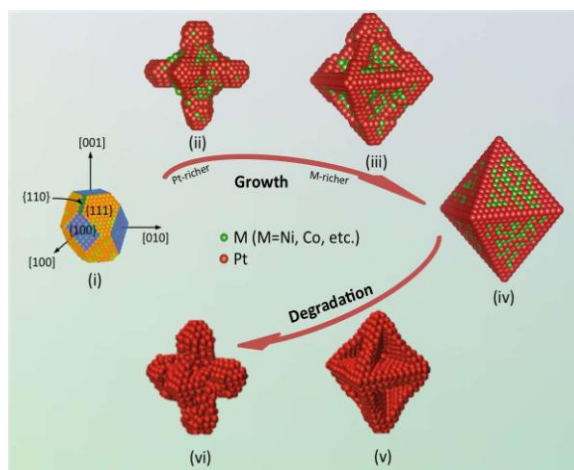
<sup>1</sup> Division of Energy and Environment, Graduate School at Shenzhen, Tsinghua University, Shenzhen 518055, PR China

<sup>2</sup> The electrochemical Catalysis, Energy and Materials Science Laboratory, Department of Chemistry, Technical University Berlin, 10623 Berlin, Germany

Email: lgan@sz.tsinghua.edu.cn

Shaped platinum (Pt) alloy nanoparticles (e.g. Pt alloy nanooctahedra) represent a class of highly active oxygen reduction electrocatalysts for fuel cells.<sup>1,2</sup> While different methods have been developed for preparing Pt alloy nanooctahedra, they showed vastly different electrocatalytic properties.<sup>3,4</sup> Understanding the nanoparticle growth mechanism is essential for rational syntheses of shaped Pt bimetallic nanoparticles with desired electrocatalytic properties.

In this talk, we present some of our recent works on understanding and possible controlling ways of the anisotropic growth mechanism and the associated electrocatalytic properties of Pt-Ni octahedral electrocatalysts by using state-of-the-art aberration-corrected scanning transmission electron microscopy (STEM) and electron energy loss spectroscopy (EELS). Our results reveal a novel element-specific anisotropic growth mechanism of Pt bimetallic nano-octahedra where compositional anisotropy couples to geometric anisotropy.<sup>5</sup> A Pt-rich phase evolves into precursor nano-hexapods followed by a slower step-induced deposition of a M-rich (M=Ni, Co, etc.) phase at the concave hexapod surface forming the octahedral facets. The element-specific anisotropic growth provides the origin of previously reported compositional segregation (Ni-rich facets and Pt-rich corners/edges) and chemical degradation pathway of the Pt-Ni octahedra, which underwent a selective etching of the Ni-rich {111} facets and thus activity instability during the ORR electrocatalysis in acidic electrolyte. Furthermore, we explored possible ways for tailoring the element-specific anisotropic growth trajectories to improve the electrocatalytic activities and stabilities of the Pt alloy nanooctahedra. Our results provide a comprehensive understanding on the atomic-scale “life-cycle” model of the Pt bimetallic nanooctahedra electrocatalysts and provide useful insight into rational catalyst designs with desired phase segregations and electrocatalytic properties.



## References

1. Gasteiger, H. A.; Markovic, N. M. *Science* 2009, 324, 48.
2. Stamenkovic, V. R.; Fowler, B.; Mun, B. S.; Wang, G. F.; Ross, P. N.; Lucas, C. A.; Markovic, N. M. *Science* 2007, 315, 493.
3. Wu, J.B.; Gross, A.; Yang, H. *Nano Lett* 2011, 11, 798
4. Cui, C.; Gan, L.; Heggen, M.; Rudi, S.; Strasser, P. *Nature Mater* 2013, 12, 765.
5. Gan, L.; Cui, C.; Heggen, M.; Dionigi, F.; Rudi, S.; Strasser, P. *Science* 2014, 346, 1502.

# Study of LSCM-CGO-Ni Anode Characteristics by Electrochemical Impedance Spectroscopy

Samir Boulfrad<sup>a</sup>, Aziz Nechache<sup>a</sup>, Mark Cassidy<sup>b</sup>, Enrico Traversa<sup>a</sup>, John T.S. Irvine<sup>b</sup>

<sup>a</sup> *Division of Physical Sciences and Engineering, King Abdullah University of Science and Technology-KAUST, Thuwal 4700, KSA*

<sup>b</sup> *School of Chemistry, University of St. Andrews, Scotland, UK*  
*aziz.nechache@kaust.edu.sa*

Anode compositions made of  $(\text{La}_{0.75}\text{Sr}_{0.25})_{0.97}\text{Cr}_{0.5}\text{Mn}_{0.5}\text{O}_3$  (LSCM) and gadolinia doped ceria (CGO) with and without additional submicron Ni, or exsolved Ni nanoparticles were characterized by electrochemical impedance spectroscopy. Thus, increasing the content of the ionic conductor results in a decrease of the impedance in the frequency range [100 Hz - 10 Hz]. The effect of the catalyst component was studied while maintaining the same electronic conductivity in the tested materials. Enhanced catalytic activity was shown to greatly decrease the impedance, especially in the frequency range [100 Hz - 1 Hz]. Moreover, the effects of the working temperature and the anode gas flow rate were studied. It appears that increasing the gas flow rate results mainly in an important decrease of the impedance from 1 Hz to 0.01 Hz. Besides, increasing the temperature leads to a very important decrease of the whole impedance, meaning that all the main electrochemical mechanisms related to the cell functioning are thermally activated.

# Advanced EIS Study of the Ionic Conduction in Nanocrystalline Yttrium-Doped Ceria

L. Fernandez Macia<sup>1</sup>, D. Van Laethem<sup>1</sup>, S. Van Steenberge<sup>2</sup>, D. Depla<sup>2</sup>, J. Deconinck<sup>1</sup>, A. Hubin<sup>1</sup>

<sup>1</sup> Research group Electrochemical and Surface Engineering, Vrije Universiteit Brussel, Pleinlaan 2, 1050 Brussel, Belgium

<sup>2</sup> Research group DRAFT, Department of Solid State Sciences, Ghent University, Krijgslaan 281/S1, 9000 Ghent, Belgium

email: lucferna@vub.ac.be

Solid electrolytes exhibit electrical conductivity due to the presence of mobile ions which act as charge carriers through the crystalline structure. For their use in solid oxide fuel cells (SOFCs), a sufficient electrical conductivity is achieved by operating at high temperatures. To reduce the application temperature, research is dedicated to increase the electrical conductivity of the ceramic material otherwise. One way is reducing the grain size. At present it is not clear how the microstructure of solid state electrolytes affects the electrical conduction. In literature, the experiments on nanocrystalline solid oxides yield contradictory observations. A good understanding of the relationship between microstructure and ion conductivity would open the possibility to engineer advanced thin materials for SOFCs.

We propose an experimental and modeling approach that aims at unraveling the electrical behavior of thin film electrolytes, by considering the crystalline nature of the material. Through careful comparison of simulations and measurements we want to explain the observed electrical properties of these materials to predict how their conductivity can be enhanced.

The complex electrical properties at different temperatures of yttrium-doped ceria, with different grain sizes and doping concentrations, are determined by electrochemical impedance spectroscopy (EIS). The solid oxide is deposited by reactive magnetron sputtering, which allows modifying the morphology and composition in a controlled way [1]. Improved electrode geometry is also studied. The geometry of an interdigitated electrode structure is designed by 2D simulations for the solid oxide film in contact with the substrate. The spectra recorded with this structure are compared with those measured with two coplanar stripe electrodes.

The impedance modeling with equivalent circuits are performed using a fitting algorithm that provides a quantitative, statistically founded description of the electrochemical system [2-3]. However, our investigation goes beyond the classical EIS analysis. A finite element model (FEM) of the electrical conductivity has been recently developed to simulate impedance spectra and electrical conductivities as a function of grain size and temperature [4]. It is based on the application of the linear phenomenological relations to a crystal lattice. The comparison of the performance of both modeling alternatives will demonstrate the strength of the FEM to adequately explain ion conductivity in nanocrystalline solid oxides.

The presented analysis aims to elucidate the experimental evidence that is not explained by the available physical models. The unique combination of advanced modeling and complete experimental approaches represents a valuable contribution to understand the electrical properties and ion conduction of solid electrolytes.

[1] S. Van Steenberge, W.P. Leroy, D. Depla, *Thin Solid Films* 553 (2014) 2-6.

[2] Y. Van Ingelgem, E. Tourwé, O. Blajiev, R. Pintelon, A. Hubin, *Electroanalysis* 21 (6) (2009) 730-739.

[3] L. Fernández Macía, M. Petrova, A. Hubin, *Journal of Electroanalytical Chemistry* 737 (2015) 46-53.

[4] D. Van Laethem, J. Deconinck, D. Depla, A. Hubin (2015) Submitted.

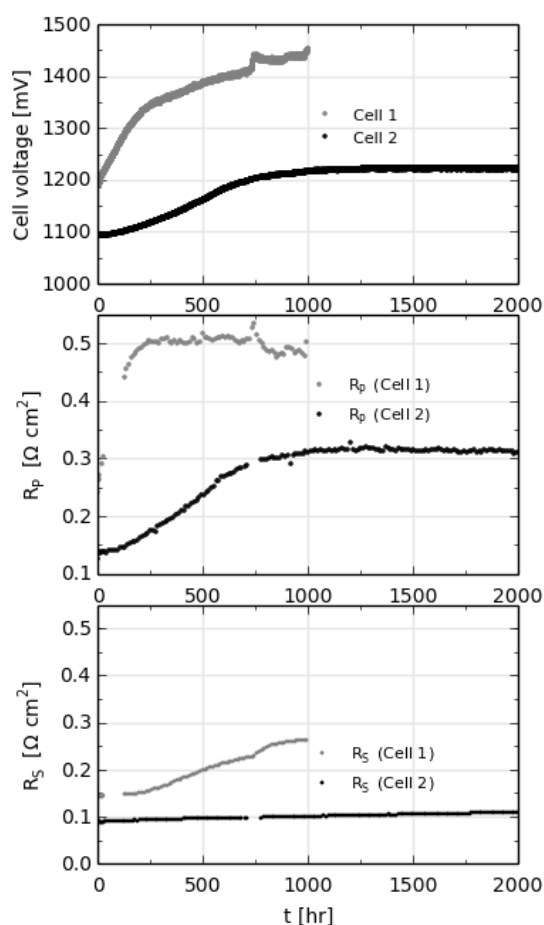


# Ni/YSZ Electrodes Optimized for Stability at High Electrolysis Current Density

Anne Hauch, Karen Brodersen, Peter S. Jørgensen and Ming Chen  
 Department of Energy Conversion and Storage, Technical University of Denmark  
 DTU Risø Campus, Frederiksborgvej 399, DK-4000 Roskilde, Denmark  
[hauc@dtu.dk](mailto:hauc@dtu.dk)

Cermet Ni/YSZ electrodes are by far the most often applied fuel electrode for solid oxide electrolysis cells (SOEC) and promising results have been shown as reviewed recently[1]. Tietz and co-workers showed promising long-term stability for such SOEC with a degradation rate of  $\sim 3\%$ /kh at high current density ( $-1\text{ A/cm}^2$ ) and high  $p(\text{H}_2\text{O})$ ; however it has been suggested that the long-term degradation rate has to be decreased to a few tens of a percent/kh for the SOEC technology to reach commercial breakthrough [2]. Previous work has shown that the Ni-network is not stable during long-term steam electrolysis at high currents e.g. due to Ni coarsening [2] and Ni migration away from the innermost few microns of the electrode [3][4].

In this work we focus on optimization of the Ni/YSZ electrode structure to ensure long-term stability at high current density ( $-1\text{ A/cm}^2$ ), high steam conversion rate and inlet  $p(\text{H}_2\text{O}) = 0.9\text{ atm}$ . After the initial degradation within the first 1 kh a linear long-term degradation rate of only  $0.3\text{--}0.4\%$ /kh was obtained at  $-1\text{ A/cm}^2$  and  $800\text{ }^\circ\text{C}$ . The increased long-term stability is shown in the figure where long-term test at  $-1\text{ A/cm}^2$  and  $800\text{ }^\circ\text{C}$  for a S-o-A SOEC (Cell 1) is compared with a cell (Cell 2) in which the optimized Ni/YSZ micro-structured electrode was applied. The figure shows cell voltages, polarization resistances ( $R_p$ ) and ohmic resistances ( $R_s$ ) over time during SOEC test at identical test conditions for the two cells. The increased performance and durability originates from a Ni/YSZ structure that has been optimized with respect to porosity, particle sizes, matching of particle sizes including pore sizes and phase percolation. The microstructural characteristics of the optimized Ni/YSZ electrodes have been investigated and quantified using SEM imaging, image analysis and 3D reconstructions; and the microstructural characteristics of Cell 1 and Cell 2 are compared and discussed in view of the electrochemical performance and durability obtained for the two cells.



- [1] S.D. Ebbesen, S.H. Jensen, A. Hauch, M.B. Mogensen, Chem. Rev. 114 (2014) 10697–734.
- [2] E. Lay-Grindler, J. Laurencin, J. Villanova, P. Cloetens, P. Bleuet, A. Mansuy, et al., J. Power Sources. 269 (2014) 927–936.
- [3] M. Chen, Y.-L. Liu, J.J. Bentzen, W. Zhang, X. Sun, A. Hauch, et al., J. Electrochem. Soc. 160 (2013) F883–F891.
- [4] A. Hauch, F. Karas, K. Brodersen, M. Chen, Proc. 11th Eur. SOFC and SOE Forum, 2014: p. 88.

# Development of Composite Electrolyte Membranes for Polymer Electrolyte Fuel cells Operating at Low Humidity

Sangaraju Shanmugam\* and Kriangsak Ketpang

*Department of Energy Systems Engineering, Daegu Gyeongbuk Institute of Science & Technology, 50-1, Sang-Ri, Hyeonpung-Myeon, Dalseong-Gun, Daegu, Republic of Korea, 711-873; sangarajus@dgist.ac.kr*

Polymer electrolyte fuel cells (PEFC) operated at elevated temperature and low relative humidity (RH) have been attracted considerable attention due to improving electrode kinetics, enhancing anode resistance to CO poisoning, and simplifying thermal management of the system [1]. However, the current PEFC technology, utilizes perfluorosulfonic acid (PFSA) polymer membranes, e.g., Nafion, as electrolyte, exhibits poor performance at elevated temperature and low RH. The deterioration of PEMFC performance at elevated temperature and low RH is mainly attributed to the loss of proton conductivity [2]. Operating PEFC at elevated temperature and low RH lead to membrane dehydration which dramatically reduces the proton conductivity. Thus, it is highly desirable to enhance proton conductivity Nafion membrane at elevated temperature and low RH in order to achieve high PEFC performance at elevated temperature and low RH.

In this presentation, I will discuss the PEFC operated at elevated temperature and low relative humidity by creating additional proton transport channels in a perfluorosulfonic acid membrane using metal oxide nanotubes, graphene inorganic clusters. The performance of composite membranes was evaluated by making MEA and subsequently the composite membranes were investigated the  $H_2/O_2$  fuel cell at 100 °C under 100 %RH and at 80 °C under 18 %RH.  $ZrO_2$  composite membrane operated at 100 °C has 1.6 times higher than commercial membrane (NRE-212) and recast Nafion membrane. On the other hand, the Nafion- $ZrO_2$  composite membrane delivered maximum power density of  $440 \text{ mW cm}^{-2}$ , which is 3 times higher than that of the performance obtained from NRE-212 and recast Nafion membranes [3]. The higher PEFC performance at 100 °C and low RH was due to the hygroscopic property of metal oxide, which can retain water at 100 °C and due to the tubular morphology which facilitates the proton transport channel through membrane.

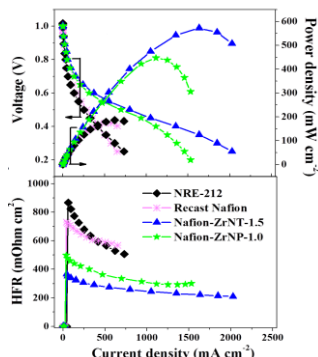


**Fig. 1.** Polarization curves of various composites membrane operated at 80 °C under 18% RH.

## References:

- [1]. K. A. Mauritz and R. B. Moore, *Chem. Rev.* 104 (2004) 4535.
- [2]. K. Ketpang, K. Lee, S. Shanmugam, *ACS Appl. Mater. & Interfaces* 6 (2014) 16734.
- [3]. K. Ketpang, B. Son, D. H. Lee, S. Shanmugam, *J. Mem.Sci.*, (2015)[10.1016/j.memsci.2015.03.096](https://doi.org/10.1016/j.memsci.2015.03.096).

# Fabrication of platinum electrodes with high roughness factor using a 3D-support

M. Frei<sup>1</sup>, J. Erben<sup>1</sup> and S. Kerzenmacher<sup>1</sup>

<sup>1</sup>Laboratory for MEMS Applications,

IMTEK – Department of Microsystems Engineering, University of Freiburg,  
Georges-Koehler-Allee 103, 79110 Freiburg, Germany  
kerzenma@imtek.de

Implantable glucose fuel cells are promising for the sustainable power supply of medical implants. Theoretically, they can generate sufficient electricity to power medical implants such as cardiac pacemakers [1] from electrochemical oxidation of the body's own glucose. However, endogenous substances such as, for instance amino acids, dramatically diminish the performance of the anodes by blocking the catalytic sites [1]. Hence, to enhance the long-time performance high specific surface areas have to be achieved. Our aim is to show that by increasing the roughness factor of the anode (RF; ratio of surface area to geometrical area) and, thus, obtaining more catalytically active sites, higher current densities can be sustained. The state-of-the-art electrodes are fabricated by electro deposition in a Pt-Cu-electrolyte using a flat layer of evaporated platinum as substrate, resulting in electrode RFs of  $6500 \pm 700$  [2]. By using an electro spun carbon as substrate, that in our case already offers a RF of 173 by itself for the platinum deposition, significantly higher RFs should be achievable. In theory, a 173 times higher RF may be achieved if the platinum deposition process can be transferred to the 3-dimensional substrate.

The new electrodes were deposited onto electro spun carbon fiber mats [3] using the established pulsed electro deposition process [2]. So far, 20, 40, 80, 120 and 240 pulses have been applied with 1000 s of waiting time in open circuit potential (OCP) in between the pulses to ensure that fresh electrolyte is available throughout all parts of the porous substrate. To date, this results in electrodes with RFs of about 3900, 5800, 9400, 12600 and 17300 respectively.

To compare the structure of the deposited platinum on the electro spun substrate to the state-of-the-art electrodes, pictures have been taken with a scanning electron microscope (Fig.1, C and D). A and B of figure 1 show the cauliflower-like structure of the porous platinum deposited on the flat substrate [2] for comparison. In figure 1C, the transition from platinum-deposited (right) and non-platinum-deposited (left) electro spun substrate is shown. The deposited platinum already exhibits the same cauliflower-like structure (Fig. 1C) as state-of-the-art electrodes, even though only 20 pulses have been applied to the system compared to the 1200 pulses of the state-of-the-art process [2]. The approximate mean distance of the deposited fibers is  $(610 \pm 260)$  nm, whereas their diameter only reaches  $(240 \pm 74)$  nm leaving a pore size of about 400 nm. Therefore, the pores of the electro spun substrate are wide enough to make more platinum deposition feasible without clogging becoming a problem.

In conclusion, electrodeposition of platinum on electro spun carbon fiber mats is a promising strategy to increase the roughness factor of the anodes for the implantable glucose fuel cell. In future experiments, we will further increase the RF and test the performance of the electrodes in simulated tissue fluids.

## References

- [1] Köhler et al., ChemElectroChem, 1 (2014) 1895 – 1900
- [2] Köhler et al., J. Power Sources, 242 (2013) 255 – 263
- [3] Erben et al., 2nd EU-ISMET (2014), Book of Abstracts, 169

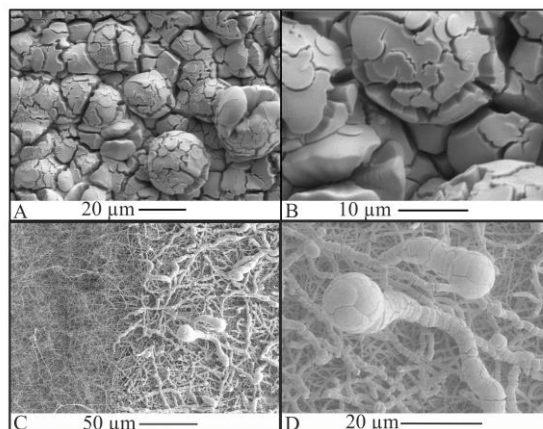


**Fig. 1:** SEM pictures of a state-of-the-art porous platinum electrode (A,B) [2] and platinum deposited onto electro spun carbon (C,D). Electrodes were fabricated by a pulsed electro deposition process [2] with 1200 (A,B) or 20 (C,D) pulses, respectively.

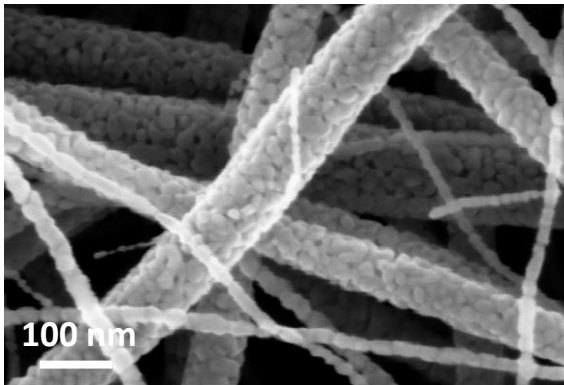
# Electrospun Nanofiber Catalysts for Green Technology

Wenjing (Angela) Zhang, Debora Marani, Rafael Hubert Silva, Rebecka Maria Larsen Wercheister, Kent Kammer Hansen, Vincenzo Esposito, Severine Ramousse  
*Department of Energy Conversion and Storage, Technical University of Denmark*  
*Roskilde, Denmark*  
*wenz@dtu.dk*

The greatest advantages of electrospinning is the possibility of generating composite networks from a rich variety of materials with the ability to control composition, morphology and secondary structure which allows design of optimum material characteristics for variable applications. We used this simple and versatile method to design 3D polymer nanofiber membranes and ceramic metal oxide nanofiber catalysts for green technology with significant improvement in electrochemical performance.

In this talk, we will present several projects that address the sizable challenges in electrochemical devices by electrospinning: 1) electrolyte/catalysts composite electrodes for proton exchange membrane fuel cells; 2) Ceramic nanofiber cathode for solid oxide fuel cells, and 3)  $\text{TiO}_2$  nanofibers catalysts doped with  $\text{WO}_3$  and  $\text{V}_2\text{O}_5$  for deNO<sub>x</sub> in flue gas purification system. The morphology, crystalline structures and composition of nanofibers are intensively studied by SEM, TEM, XRD, BET and elemental analysis. The outcomes of these unique nanofibrous structures are significant improvements in catalytical performance and durability. This brings fuel cell technology and deNO<sub>x</sub> system one step forward toward green technology in real life.

**a.**



**b.**

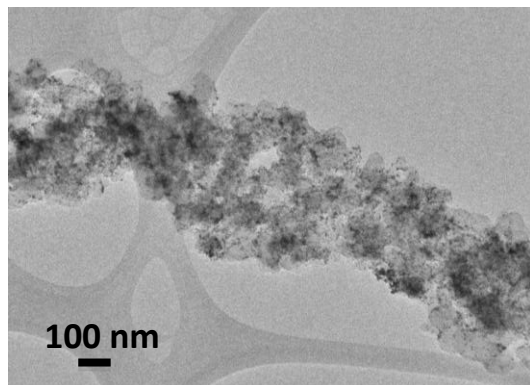


Figure 1. (a) SEM image of  $\text{TiO}_2$  nanofibers doped with  $\text{WO}_3$  and  $\text{V}_2\text{O}_5$ ; (b) TEM image of Pt-C/Nafion nanofiber electrode.

# Pt-Ru/C Anode Performance of Polymer Electrolyte Fuel Cell under Carbon Dioxide Atmosphere

Sayoko Shironita<sup>1</sup>, Kazutaka Sato<sup>1</sup>, Kazuma Yoshitake<sup>1</sup>, and Minoru Umeda<sup>1,2,\*</sup>

<sup>1</sup>Nagaoka University of Technology, 1603-1, Nagaoka, Niigata 940-2188, Japan

<sup>2</sup>JST ACT-C, 4-1-8 Honcho, Kawaguchi, Saitama 332-0012, Japan

\*mumeda@vos.nagaokaut.ac.jp

For the power generation of polymer electrolyte fuel cells (PEFCs), hydrogen gas including reformed gas is fueled to the fuel cell anode. The reformed hydrogen gas contains a small amount of carbon oxide and 10-30% carbon dioxide [1]. The carbon dioxide is reported to be reduced at Pt electrode [1]. And, a Pt-Ru/C-based membrane electrode assembly (MEA) can reduce it at 0.06-0.3 V vs. DHE [2,3]. However, the reactivity of the carbon dioxide and the reductant adsorption, which both influence the hydrogen oxidation reaction, are not adequately understood. In this study, the reactivity of carbon dioxide and adsorption state of the reductant were investigated using the PEFC containing the Pt-Ru/C-based MEA.

Nafion 117 and Nafion 112 membranes were used as a polymer electrolyte membrane. Electrocatalysts of Pt/C (Pt: 45.7 wt.%), Pt-Ru/C (Pt:Ru=32.6:16.9 wt.% (molar ratio: Pt:Ru=1:1), and Pt:Ru=29.5:22.9 wt.% (molar ratio: Pt:Ru=2:3)) were sprayed on gas diffusion layers. The electrolyte membrane was sandwiched by two pieces of the gas diffusion layers which were coated electrocatalysts layers (metal amount: 1.0 mg cm<sup>-2</sup>), and then hot-pressed. Thus, the desired MEA was obtained. Geometric electrode area of the MEA was 3 × 3 cm<sup>2</sup>. The MEA has a Pt-Ru/C as a working electrode and a Pt/C as a counter electrode. The prepared MEA was installed in a single cell having a dynamic hydrogen electrode (DHE) as a reference electrode. The temperature of the single cell was controlled at 40, 60, 80, 90, and 95°C. Humidified carbon dioxide gas (purity: 99.995%) and humidified hydrogen gas (purity: 99.999%) were supplied to the working and counter electrode, respectively, at the flow rate of 50 cm<sup>3</sup> min<sup>-1</sup> by a PEFC power generation unit. Cyclic voltammograms were measured at a potential scan rate of 10 mV s<sup>-1</sup> and the potential scan range was settled to be 0.06–0.70 V vs. DHE. For comparison, Pt/C electrocatalyst was also used as the working electrode.

To investigate the anode performance of the Pt-Ru/C-based MEA in a single cell equipped with a reference electrode (DHE) under carbon dioxide atmosphere. Figure 1 shows the cyclic voltammograms of Pt/C and Pt-Ru/C (Pt:Ru=1:1 or 2:3) MEAs at 95°C cell temperature under nitrogen and carbon dioxide atmospheres. When it was swept toward the positive direction, the current density peaks are observed at around 0.2-0.6 V vs. DHE in all graphs in Fig. 1. These peaks are known to be re-oxidation peaks of the carbon dioxide reductant. The arrows show onset potentials at each electrocatalysts. The onset potential of re-oxidation peak at Pt/C is much positive than that at Pt-Ru/C electrocatalysts. The Pt-Ru/C (Pt:Ru=2:3) shifts toward negative direction in the electrocatalysts. It is considered that the Pt to Ru ratio in Pt-Ru/C affects the re-oxidation of carbon dioxide reductant and its desorption process.

[1] K. Kortsdottir, C. F. Fernández, and R. W. Lindström, *ECS Electrochem. Lett.*, **2**, F41-F44, (2013).

[2] S. Shironita, K. Karasuda, M. Sato, and M. Umeda, *J. Power Sources*, **228**, 68-74 (2013).

[3] S. Shironita, K. Karasuda, K. Sato, and M. Umeda, *J. Power Sources*, **240**, 404-410 (2013).

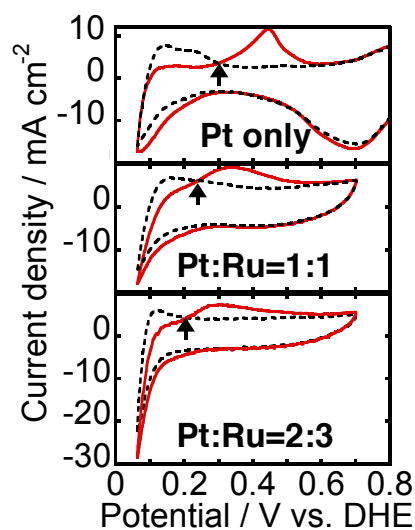


Fig. 1 Successive cyclic voltammograms at Pt/C and Pt-Ru/C (Pt:Ru=1:1 and 2:3) of MEA under nitrogen (dotted line) and carbon dioxide (solid line) atmospheres. Cell temperature: 95°C. Sweep rate: 10 mV s<sup>-1</sup>.



# A DEMS Study on the Influence of Ag Add-Atoms on Pd-based Catalysts for Methanol Oxidation in Alkaline Environment

Tilman Jurzinsky, Carsten Cremers, Karsten Pinkwart, Jens Tübke  
Fraunhofer Institute for Chemical Technology ICT  
Joseph-von-Fraunhofer-Str. 7, 76327 Pfaffzettel, Germany  
tilman.jurzinsky@ict.fraunhofer.de

In the last decades, the enhancement of anion-exchange membranes (AEMs) took big steps regarding the stability in alkaline environment while having proper ion exchange capacities and ionic conductivities. Due to this development, it is possible to use AEMs in direct alcohol fuel cells (DAFCs) making them anion-exchange membrane direct alcohol fuel cells (AEM-DAFCs). By changing the pH conditions of the fuel cell from acidic to alkaline, electrode reaction kinetics are positively influenced and platinum-free catalysts are feasible for alcohol oxidation reaction (AOR) and oxygen reduction reaction (ORR). While for ORR metals and oxides like Ag and  $\text{MnO}_2$  are promising catalysts, for AOR promising catalysts are Pd-based catalysts like PdAg/C and PdNi/C.

Complete oxidation of methanol into  $\text{CO}_2$  is essential for an efficient energy production. From the literature it is known that besides  $\text{CO}_2$  there are two more side products occurring during methanol oxidation in alkaline media: formaldehyde and formic acid. As there are fewer electrons exchanged during formation of these side products, the production of formaldehyde and formic acid during methanol oxidation reaction (MOR) is equivalent to a loss of faradaic current compared to a complete oxidation of methanol to  $\text{CO}_2$ . That is why it is crucial to investigate on catalysts which are able to reach high  $\text{CO}_2$  current efficiencies (CCE).

To further understand the influence of add-metals on Pd and the resulting gain in electrolytic activity, this study aims for a deeper understanding of the methanol electro-oxidation mechanism on Pd-based bimetallic catalysts. Differential electrochemical mass spectrometry (DEMS) is a powerful tool to investigate the product distribution during methanol electro-oxidation and  $\text{CO}_2$  current efficiency. Besides this, it is possible to identify poisoning species on the catalysts during MOR by methanol stripping experiments in DEMS setup giving a hint on the stability of the catalysts in fuel cell operation.

In a former study, we reported on the catalytic activity of PdAg/C catalysts for MOR in alkaline media.[1] Based on these findings, we

further investigated on the poisoning behavior, CCE and product distribution of Pd/C, Ag/C and PdAg/C via cyclic voltammetry, CO stripping and methanol stripping experiments in a DEMS flow cell setup.

Figure 1 shows the patterns derived from cyclic voltammetry for different catalysts in a 0.1M  $\text{CH}_3\text{OH}$  + 0.5M KOH solution in the DEMS flow cell with a Pt-electrode and a reversible hydrogen electrode (RHE) as counter- and reference-electrode, respectively. For comparison a Pt/C (Hi-SPEC3000) catalyst was also investigated as a reference material. Besides a higher CCE value for bimetallic Pd-based catalysts it could also be shown by methanol stripping experiments that catalyst poisoning is less for Ag containing Pd-based catalysts than for plain Pd/C or Pt/C.

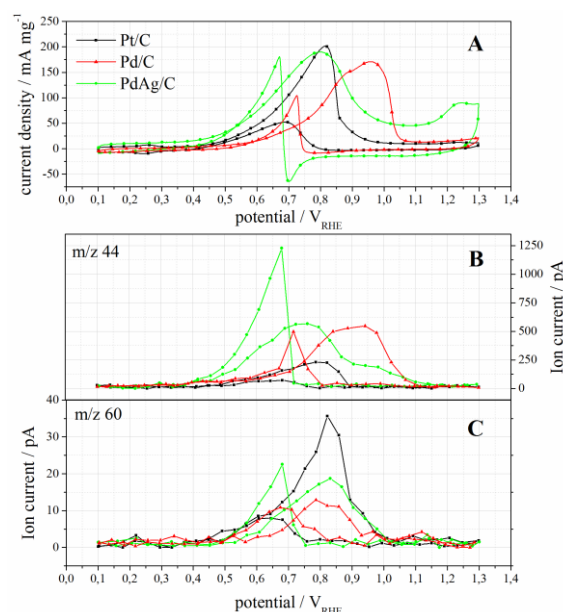


Figure 1: CV plots (A) of Pt/C, Pd/C and PdAg/C in 0.1M  $\text{CH}_3\text{OH}$  + 0.5M KOH in a DEMS flow cell and corresponding MS signals for  $\text{CO}_2$  (B) and methyl ester of formic acid (C).

## References

- [1] T. Jurzinsky, C. Cremers, F. Jung, K. Pinkwart, J. Tübke, International Journal of Hydrogen Energy (2015).

# Proposal of Oxide-Based Compounds as Non-Platinum Group Metals and Carbon-Free Cathodes for Polymer Electrolyte Fuel Cells

Akimitsu ISHIIHARA<sup>a</sup>, Makoto HAMAZAKI<sup>b</sup>, Tomoaki HAYASHI<sup>b</sup>, Yuko TAMURA<sup>b</sup>, Yuji KOHNO<sup>b</sup>, Koichi MATSUZAWA<sup>b</sup>, Shigenori MITSUSHIMA<sup>a, b</sup>, Hideto IMAI<sup>c</sup>, and Ken-ichiro OTA<sup>b</sup>

<sup>a</sup> Institute of Advanced Sciences, Yokohama National University

<sup>b</sup> Green Hydrogen Research Center, Yokohama National University  
79-5, Tokiwadai, Hodogaya-ku, Yokohama 240-8501, JAPAN

<sup>c</sup> Device Functional Analysis Group, NISSAN ARC, Ltd.

1 Natsushima-cho, Yokosuka, 237-0061, Japan

a-ishi@ynu.ac.jp

## Background

Development of non-platinum group metals cathodes is required for practical application of polymer electrolyte fuel cells. We focused on group 4 and 5 metal oxide-based compounds because their high chemical stabilities in acidic media. We attempted to enhance the activity of the oxygen reduction reaction (ORR) to prepare nano-sized oxide-particles by use of metal organic complexes such as oxy-metal phthalocyanines as precursors with multi-walled carbon nanotubes as supports<sup>1</sup>. Although the ORR activities drastically increased, the stabilities of these catalysts were low because the deposited carbon derived from phthalocyanines degraded under cathode conditions. Therefore, in order to achieve both high ORR activity and high durability, we need to develop the oxide-based cathodes without carbon materials.

## Catalyst design of non-platinum group metals and carbon-free cathodes

To prepare the non-precious metal and carbon-free cathodes, the basic idea is a combination of electro-conductive oxides and oxides with active sites for the ORR. We focused on titanium oxide, Ti<sub>4</sub>O<sub>7</sub>, known as magneli phase, as electrical conductive. On the other hand, titanium-niobium complex oxides (Nb-doped TiO<sub>2</sub>) were applied to create the active sites. The strategy of the preparation of the Ti-Nb complex oxides and Ti<sub>4</sub>O<sub>7</sub> was a dry ball-milling and a reductive heat-treatment in this study. We performed start-stop cycle test (triangular wave, 1.0 - 1.5 V vs. reversible hydrogen electrode (RHE), N<sub>2</sub>, a scan rate: 0.5 V s<sup>-1</sup>) and load cycle test (rectangular wave, 0.6 - 1.0 V vs. RHE, O<sub>2</sub>, holding time: 3 s) were performed as degradation tests using a 3-electrode cell in 0.1 M H<sub>2</sub>SO<sub>4</sub> at 30 °C.

## Demonstration of high durability

Figures 1 (a) and (b) show the dependence of the ratio of the ORR current obtained by chronoamperometry at 0.7 V at the beginning and during the start-stop cycle test,  $N_{iCA@0.7V}$ , and Dependence of  $N_{iCA@0.65V}$  at the beginning and during the load cycle test. Surprisingly, in both cases the  $N_{iCA@0.7V}$  and  $N_{iCA@0.65V}$  increased until 5000 cycles, and they became nearly constant over 5000 until 20000 cycles. These results demonstrated that the all oxide-based (carbon-free) cathodes had high durability in both high and low potential regions.

## Acknowledgement

The authors thank for the New Energy and Industrial Technology Development Organization (NEDO) for financial support.

## References

- 1) A. Ishihara, M. Chisaka, Y. Ohgi, K. Matsuzawa, S. Mitsuhashi and K. Ota, *Phys. Chem. Chem. Phys.*, 17, 7643-7647 (2015).
- 2) Fuel Cell Commercialization Conference of Japan (FCCJ), Proposals of the development targets, research and development challenges and evaluation methods concerning PEFCs, [http://www.fccj.jp/pdf/23\\_01\\_kt.pdf](http://www.fccj.jp/pdf/23_01_kt.pdf)

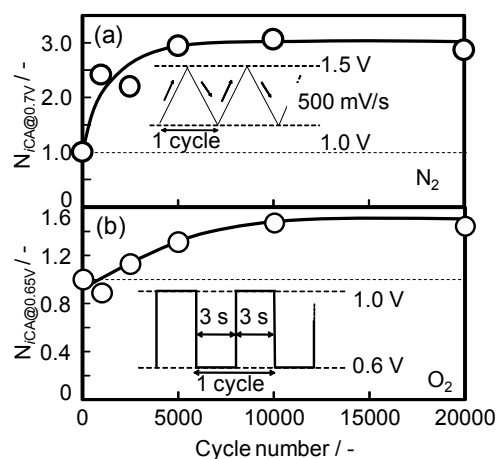


Fig.1 (a) Dependence of  $N_{iCA@0.7V}$  at the beginning and during the start-stop cycle test, (b) Dependence of  $N_{iCA@0.65V}$  at the beginning and during the load cycle test.

# Corrosion Characteristics of Ni-free Nitriding Stainless Steel as Bipolar Plate Material for PEFC

Yang Yu<sup>1</sup>, Sayoko Shironita<sup>1</sup>, Kunio Nakatsuyama<sup>2</sup>, Kenichi Souma<sup>1,3</sup>, Minoru Umeda<sup>1\*</sup>

<sup>1</sup> Department of Materials Science and Technology, Nagaoka University of Technology,  
1603-1, Kamitomioka, Nagaoka, Niigata 940-2188, Japan

<sup>2</sup> Nakatsuyama Heat Treatment Co., Ltd., 1-1089-10 Nanyou, Nagaoka, Niigata 940-1164, Japan

<sup>3</sup> Hitachi Industrial Equipment Systems Co., Ltd., 3 Kanda Neribe, Chiyoda, Tokyo 101-0022, Japan

\*mumeda@vos.nagaokaut.ac.jp

In recent years, due to high electrical conductivity, formability, manufacturability, gas impermeability and superior mechanical properties, metallic bipolar plates such as stainless steel are used to connect the polymer electrolyte fuel cell (PEFC) in series. However, one big problem of the bipolar plate is the corrosion in the actual cell environment [1]. The purpose of the present study is to evaluate the corrosion behaviors of Ni-free nitriding SUS445N stainless steels with different treatment conditions of temperature and time by a linear sweep voltammetry measurement. The nitriding stainless steel has been reported to have high resistance and good electrical conductivity [2]. Non-treatment stainless steel SUS445 was used for comparison.

The Ni-free nitriding stainless steels used in this study were the SUS445N stainless steels heat treated under the nitrogen gas atmosphere at 1150 and 1200° C for 2 h. In order to analyze the corrosion characteristics of the SUS445N stainless steel, a corrosion test was conducted in a schale electrochemical cell with a platinum coil counter electrode, an Ag/Ag<sub>2</sub>SO<sub>4</sub> reference electrode, and the SUS445N stainless steel as the working electrode. The electrolyte was 0.5 mol dm<sup>-3</sup> H<sub>2</sub>SO<sub>4</sub> solution. Before the liner sweep voltammetry (LSV) measurement, the stainless steels were washed with distilled water and acetone for 5 min in sonication and then 30 min Ar gas bubbling was conducted. Subsequently, the cathodic treatment was carried out under the potential of -0.47 V vs. SHE for 1 min and then kept the cell under the rest potential for 5 min. During this step, the invisible H<sub>2</sub> gas generated on the surface of the sample was removed by Ar bubble. For the electrochemical test, the potential was scanned from the rest potential to 1.1 V vs. SHE at a scan rate of 0.33 mV s<sup>-1</sup>.

Figure 1 shows liner sweep voltammograms of SUS445 and SUS445N stainless steel in Ar-saturated 0.5 mol dm<sup>-3</sup> H<sub>2</sub>SO<sub>4</sub> solution at room temperature. The SUS445N stainless steels were heat treated at 1150°C and 1200°C for 2 hours, respectively. The anodic current densities in passive region of SUS445N (1200°C) sample are about one order of magnitude lower than those for the SUS445N (1150°C) specimen. And the passive region current densities of SUS445N (1150°C) sample are almost the same as non-treatment stainless steel. That means the SUS445N stainless steel heat treated at 1200° C has a higher resistance to corrosion than that heat treated at 1150°C. The polarization curve of SUS445N (1150°C) sample has the current peak that forms passive layer at about -0.2 V vs. SHE. However, there is no current peak for SUS445N (1200°C) sample. It is found that the treat temperature plays an important role of improving the corrosion resistant of nitriding SUS445N stainless steel. From the results of GD-OES, the improvement of the corrosion resistance can be explained by the N, Al and Cr components on the surface of the nitriding stainless steel.

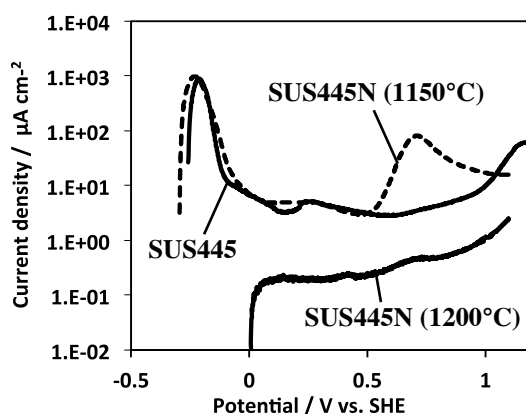


Fig. 1 Polarization curves of SUS445, SUS445N (1150°C) and SUS445N (1200°C) stainless steels in Ar-saturated 0.5 mol dm<sup>-3</sup> H<sub>2</sub>SO<sub>4</sub> solution at room temperature. Scan rate: 0.33 mV s<sup>-1</sup>.

[1] X. Z. Yuan, H. Wang, J. Zhang, D. P. Wilkinson, *J. New. Mat. Electrochem, Systems*, **8**(2005)257.

[2] K. Miura, K. Nakatsuyama, M. Umeda, *Electrochemistry*, **80** (2012)1012.





# Liquid fuel cells with polymer fiber membrane and non-precious metal catalysts

Xiaodong Yang<sup>1</sup>, Chi Chen<sup>2</sup>, Zhiyou Zhou<sup>1</sup>, Shigang Sun<sup>1</sup>

1. Collaborative Innovation Center of Chemistry for Energy Materials, College of Chemistry and Chemical Engineering, Xiamen University, Xiamen, Fujian 361005, PR China
2. College of Chemical Engineering, East China University of Science and Technology

Presenting author: [xiaodong\\_yang@xmu.edu.cn](mailto:xiaodong_yang@xmu.edu.cn)

Corresponding author: [zhouzy@xmu.edu.cn](mailto:zhouzy@xmu.edu.cn), [sgsun@xmu.edu.cn](mailto:sgsun@xmu.edu.cn)

Liquid fuel cells are a kind of electrochemical energy convertor with borohydride aqueous solution or light hydrocarbons as fuel. They are with merits of high efficiency, low environmental impact as well as circumventing the problem of hydrogen storage in  $H_2/O_2$  fuel cells. The main challenges of the liquid fuel cells are the fuel crossover and sluggish kinetics of oxygen reduction reaction (ORR). Ion exchange membrane (IEM) is a very important component in traditional liquid fuel cells. It is used to screen ion transport and limit the fuel crossover. However, IEMs have poor performance in limiting fuel crossover in the actual working conditions. The fuel crossover through the IEM and then poisoning the cathodic catalysts greatly decrease the performance of liquid fuel cells. In addition, the high cost of both IEM and noble metal catalysts limits the commercialization of the liquid fuel cells.

In this work, we presented a high active and durable Fe/N/C catalyst for ORR by employing 2-aminothiazole (2-AT) as precursor that contains both N and S elements. Excellent activity and fuel-tolerance has been observed. The excellent fuel-tolerance helps to circumvent the fuel crossover problem in liquid fuel cells. By employing the Fe/N/C catalyst, a polymer fiber membrane (PFM) was introduced in liquid fuel cells to replace IEM<sup>[1]</sup>. The PFM is in a non-woven structure and acts as a thin liquid electrolyte layer in liquid fuel cells. All ions can transport freely in the PFM. As a consequence, the resistance between electrodes was greatly reduced. At the same time, the price of PFM is much lower compared with IEM. The performances of liquid fuel cells were improved greatly when PFM was used in direct borohydride fuel cell (DBFC)<sup>[1]</sup> and direct methanol fuel cell (DMFC)<sup>[2]</sup>.

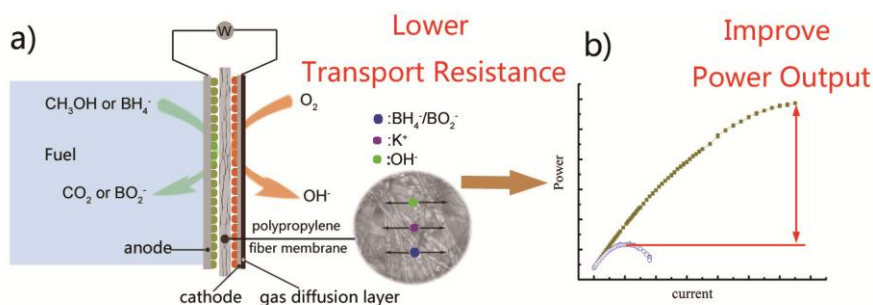


Figure. a) Illustration of liquid fuel cells using porous polypropylene fiber separator as membrane. Fuel (borohydride or methanol) can cross over freely through this permeable membrane, so cathode catalyst should be resistant to methanol. b) The power output was improved because of the low resistance with porous porous polypropylene fiber membrane.

## Reference:

- [1] X.D. Yang, Y.N. Liu, S. Li, X.Z. Wei, L. Wang, Y.Z. Chen, Scientific reports 2 567
- [2] X.D. Yang, Y.N. Liu, Y. Fang, L. Wang, S. Li, X.Z. Wei. J. Power Sources, 234, 272-276

# Designing Efficient Nanocatalysts for Oxygen Reduction Reaction

Jin-Song Hu,<sup>1,\*</sup> Zi-Dong Wei,<sup>2</sup> Li-Jun Wan<sup>1</sup>

<sup>1</sup>*Institute of Chemistry, Chinese Academy of Science, Beijing 100190, China;*

<sup>2</sup>*College of Chemistry and Chemical Engineering, Chongqing University, Chongqing 400044, China*

*E-mail: [hujis@iccas.ac.cn](mailto:hujis@iccas.ac.cn)*

The rapidly increasing energy demand for human activities stimulates the lasting research interests to develop renewable energy alternatives worldwide. Fuel cell, as a clean and efficient energy conversion device, is one of promising techniques in tackling future global energy crisis. The big challenges for the practical application of this technique are to minimize the use and maximize the catalytic activity of scarce, expensive but still best platinum-based catalysts, and tackle the issue of the sluggish cathode oxygen reduction reaction (ORR).<sup>1,2</sup>

In this presentation, several reasonable ways for designing new nanocatalysts with high electrocatalytic activities and superior stability for ORR will be discussed. For example, 1) By improving the structures of Pt-based catalysts and harnessing the synergetic catalytic effect from support, a series of nanocatalysts with efficient usage of Pt component and enhanced electrocatalytic performance were developed, including Pt nanocrystal assembled hollow Pt nanostructures hanged onto graphene layer,<sup>3</sup> well-dispersed Pt nanocrystals on Mn<sub>3</sub>O<sub>4</sub> coated CNTs prepared via an in-situ self-deposition process,<sup>4</sup> and CNx/CNTs embedded with Pt nanocrystals for improving stability,<sup>5</sup> etc. 2) For further minimizing the catalyst cost, a variety of non-PGM (platinum group metal) catalysts with comparable/superior electrochemical performance and durability were developed, such as in-situ nitrogen-doped nanoporous carbon nanocables,<sup>6</sup> improved graphene/carbon nanotube composites,<sup>7</sup> and selectively-nitrogen-doped graphene via space confinement etc.<sup>8</sup> 3) The further improvement of the performance can be achieved by introducing transition metal or nanostructures into these nanocatalysts.<sup>9,10</sup> 4) A molten salt-assisted strategy was also developed to synthesize a new type of nanoporous nitrogen-doped carbon materials, which exhibited superior electrocatalytic activity for ORR even better than commercial Pt/C.<sup>11</sup> 5) Lastly, A simple, reproducible and cost-effective protocol to produce a nanocomposite from graphene supported layered double hydroxide will be also discussed, which will be interesting for cost-effective mass production of electrocatalysts for industrial applications.<sup>12</sup>

- [1] M. K. Debe, *Nature*, **2012**, 486, 43.
- [2] A. Rabis, P. Rodriguez and T. J. Schmidt, *ACS Catal.*, **2012**, 2, 864.
- [3] Y.P. Xiao, S. Wan, X. Zhang, J.S. Hu, Z.D. Wei, and L.J. Wan, *Chem. Commun.* **2012**, 48, 10331.
- [4] Y.P. Xiao, W.J. Jiang, S. Wan, X. Zhang, J.S. Hu, Z.D. Wei, and L.J. Wan, *J. Mater. Chem. A* **2013**, 1, 7463.
- [5] L. Guo, W.J. Jiang, Y. Zhang, J.S. Hu, Z.D. Wei, and L.J. Wan, *ACS Catalysis*, **2015**, 5, 2903.
- [6] W.J. Jiang, J.S. Hu, X. Zhang, Y. Jiang, B.B. Yu, Z.D. Wei, and L.J. Wan, *J. Mater. Chem. A* **2014**, 2, 10154-10160.
- [7] Y. Zhang, W.J. Jiang, X. Zhang, L. Guo, J.S. Hu, Z.D. Wei, and L.J. Wan, *Phys. Chem. Chem. Phys.*, **16**, 13605-13609.
- [8] W. Ding, Z.D. Wei, S.G. Chen, X.Q., T. Yang, J.S. Hu, D. Wang, L.J. Wan, S.F. Alvi, and L. Li, *Angew. Chem. Int. Ed.*, **2013**, 52, 11755.
- [9] W.J. Jiang, Y. Zhang, L. Guo, Y. Jiang, B.B. Yu, J.S. Hu, Z.D. Wei, and L.J. Wan, *submitted*.
- [10] Y. Zhang, W.J. Jiang, X. Zhang, L. Guo, J.S. Hu, Z.D. Wei, and L.J. Wan, *ACS Appl. Mater. Interfaces*, in revision.
- [11] Y. Zhang, W.J. Jiang, X. Zhang, L. Guo, J.S. Hu, Z.D. Wei, and L.J. Wan, *to be submitted*.
- [12] R.J. Huo, W.J. Jiang, S.L. Xu, F.Z. Zhang, and J.S. Hu, *Nanoscale*, **2014**, 6, 203.

# **Review of the Latest Advances and Current Challenges of Anion Exchange Membrane Fuel Cell Technology**

Dario R. Dekel

*Technion – Israel Institute of Technology  
Technion City, Haifa, 32000 Israel  
dario@technion.ac.il*

The alkaline Anion Exchange Membrane Fuel Cell (AEM-FC) is a new and blooming technology. It keeps the advantages of the solid polymer electrolyte membrane based fuel cell, and due to its alkaline polymer medium it provides a real opportunity to replace the Pt electrocatalysts and therefore to solve the major cost barriers of the mainstream proton exchange membrane fuel cell (PEM-FC) technology. AEM-FCs have been rapidly developed for the past five years, and for the first time there are tens of research groups developing unique AEMs with outstanding properties as well as first groups developing non-Pt electrocatalysts for oxidation reduction reaction (ORR) replacing finally the expensive Pt based electrodes used in PEM-FC cathodes.

In spite of this impressive and rapid development, AEM-FCs are still far from reaching a practical use, and still major advances are required. Among present challenges that should be now overcome are: development of highly active non-Pt electrocatalysts for hydrogen oxidation reaction (HOR), AEMs with higher immunity to CO<sub>2</sub>, and stable anion conductive functional groups able to withstand higher temperatures at low relative humidity. To recognize AEM-FC as a real future technology, all those development challenges must be addressed without exception. Advances in developments in those three specific fields will facilitate rapid acceptance of AEM-FC technology and allow development of first affordable fuel cell products.

In this talk, the latest advances in the technology and critical insights of current challenges will be presented.

# Well-ordered Ru@Pt Core-shell Nanocatalysts with Tunable Composition and Enhanced Electrocatalytic Properties

Jianguo Liu\*, Jin Xie, Zhigang Zou

College of Engineering and Applied Sciences, Nanjing University, Nanjing 210093, China, Email :  
jianguoliu@nju.edu.cn

Among various kinds of fuel cells, direct methanol fuel cells (DMFCs) have been attracting significant interest and research efforts for its great potential to be commercialized as the major power source for portable electric devices, due to the facile storage and refilling characteristics of methanol fuel. However, two critical issues have to be confronted when designing an effective methanol oxidation electrocatalysts: catalysts poisoning and dissolution. Alloying Pt with other metals, such as Ru, Pd, Au and so forth, has been extensively investigated to improve CO tolerance and catalytic activity of the MOR catalysts. Among them, Pt-Ru alloy was shown to have the best overall performance, which was traditionally attributed to a bi-functional mechanism or ligand effect. However, ruthenium dissolution remains the major reason for the invalidation of fuel cells, especially at high potentials experienced during startup and shutdown [1-3]. Compared to PtRu alloy nanocatalysts, Ru (core)-Pt (shell) catalysts are highly promising for DMFCs.

Ru@Pt NPs synthesized by polyalcohol method were reported to have enhanced methanol oxidation activity. However, in these studies, Ru cores often existed in a disordered state. And Pt atoms tend to diffuse into the disordered Ru cores through defects. Therefore, alloying was often obtained instead of uniform Pt shell formation. Hsieh and co-workers reported a green synthesis route to well-ordered Ru@Pt NPs that showed superior durability and excellent CO tolerance for hydrogen oxidation reaction [4]. We developed a microwave reaction technique that allowed the use of ethanol as an eco-friendly reductant and solvent under relatively mild conditions. The as-produced Ru@Pt catalysts show a higher methanol oxidation activity and CO-deactivation resistance than the commercial Pt-Ru catalysts. Meanwhile, they also exhibit substantial durability upon long term potential cycling. Fig. 1 shows the cyclic voltammetry, fuel cell tests, XRD, and TEM images of JM-PtRu/C and Ru@Pt0.5/C.

Our results indicate that ordered thin-layer core-shell Ru@Pt can not only enhance the catalytic properties, but also efficiently protect ruthenium from dissolution. This type of core-shell catalysts will be potential for solving the dilemma of long term durability in DMFCs anodes.

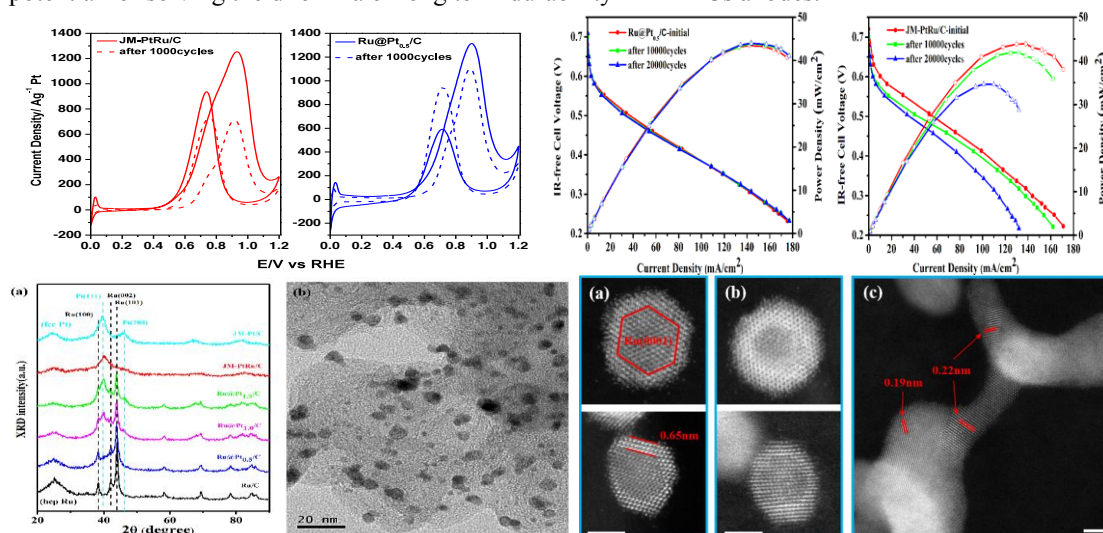


Figure 1. Catalytic activity, stability, XRD, and TEM images of JM-PtRu/C and Ru@Pt0.5/C. Cyclic voltammograms of JM-PtRu/C, Ru@Pt0.5/C in 1M CH<sub>3</sub>OH (up), IV Curves and Power density of JM-PtRu/C, Ru@Pt0.5/C in Fuel Cell.

## References

- [1] M.K. Debe, A.K. Schmoekel, G.D. Vernstrom, et al. J. Power Sources, 161 (2006) 1002-1011.
- [2] E. Antolini, J. Solid State Electrochem., 15 (2011) 455-472.
- [3] P. Piela, C. Eickes, E. Brosha, F. Garzon, P. Zelenay, J. Electrochem. Soc., 151 (2004) A2053-A2059.
- [4] Y.C. Hsieh, Y. Zhang, D. Su, et al. Nat. Commun., 4 (2013) 9.

# Oxygen Reduction Activity and Durability of Pt Electrocatalysts Supported on Platelet Carbon Nanofibers

Etsushi Tsuji<sup>1</sup>, Takenori Yamasaki<sup>2</sup>, Yoshitaka Aoki<sup>1</sup>, Ken-ichi Shimizu<sup>3</sup>, Soo-Gil Park<sup>4</sup>,  
Hiroki Habazaki<sup>1</sup>

<sup>1</sup>*Division of Materials Chemistry, Faculty of Engineering, Hokkaido University,  
Sapporo, Hokkaido 060-8628, Japan*

<sup>2</sup>*Graduate School of Chemical Sciences and Engineering, Hokkaido University,  
Sapporo, Hokkaido 060-8628, Japan*

<sup>3</sup>*i-SEM Laboratory, Sagamihara Incubation Center, 1880-2, Kamimizo, Chuo-ku, Sagamihara 252-0243,  
Japan*

<sup>4</sup>*Department of Engineering Chemistry, Chungbuk National University,  
Cheong-ju 361-763, Republic of Korea*

habazaki@eng.hokudai.ac.jp

Nanocarbon materials are of great importance in electrochemical energy storage and conversion systems, including lithium ion batteries, electrochemical capacitors and polymer electrolyte fuel cells. Our research group has reported the template-assisted synthesis of carbon nanofibers by liquid phase carbonization of polymers (1-3). The resultant carbon nanofibers have unique orientation of carbon layers, and platelet-type carbon nanofibers (p-CNFs) with hexagonal carbon layers stacked to the fiber axis are developed. Since the edge planes of hexagonal carbon layers are exposed at the most of p-CNFs surface. Here, we report the uniform deposition of Pt nanoparticles on the p-CNFs and the high activity and durability of the Pt/p-CNFs electrodes for oxygen reduction reaction (ORR).

Porous anodic alumina films with cylindrical pores of ~50 nm pore diameter were used as template. The p-CNFs were prepared by heating a mixture of the template and polyvinyl chloride powders in high purity argon atmosphere to 600°C. p-CNFs were further heat-treated at higher temperatures up to 1400°C to control the graphitization degree. Pt deposition was carried out using dinitro-diamine platinum(II) and ethanol as a reductant. Pt nanoparticles were also deposited on commercial Ketjen black (KB) for comparison. Electrochemical measurements were carried out by using rotating disk electrode with normal three electrode system. Pt wire and Ag/AgCl was used as a counter electrode and reference electrode, respectively. The electrolyte used was 0.05 M sulphuric acid.

The Pt nanoparticles of approximately 3 nm were homogeneously deposited on the p-CNFs, rather than on KB. The homogeneity was improved on the p-CNFs heat-treated at higher temperatures, probably since more reactive edges of hexagonal carbon layers were exposed after heat treatment at higher temperatures. The electrochemical activity per Pt surface area became higher on the Pt/p-CNFs that heat treatment of p-CNFs was conducted at higher temperatures. Remarkable durability enhancement was also found when we used the p-CNFs heat-treated at 1400°C. After potential cycles of 200 between 0.5 V and 1.5 V, Pt/p-CNF (1500°C) shows only less than 10% reduction of the ORR activity, whereas the activity reduction was as high as ~90% for the Pt/KB. The p-CNFs are promising carbon support for ORR electrocatalysts with high activity and durability.

## References

1. H. Habazaki, M. Kiri, M. Hayashi and H. Konno, *Mater. Chem. Phys.*, **105**, 367 (2007).
2. H. Habazaki, M. Hayashi, H. Konno and M. Inagaki, *J. Surf. Finish. Soc. Jpn.*, **56**, 352 (2005).
3. H. Konno, S. Sato, H. Habazaki and M. Inagaki, *Carbon*, **42**, 2756 (2004).

# **Solid Oxide Fuel Cells - A Clean and Efficient Energy Technology for the Future**

Nguyen Q. Minh  
*Center for Energy Research*  
*University of California, San Diego*  
*9500 Gilman Drive, La Jolla, CA 92093-0417, USA*  
*nminh@ucsd.edu*

Solid oxide fuel cell (SOFC) technology has received attention in the past 20 years as a clean and efficient energy conversion technology for a variety of practical fuels. The attractive features of the technology include cell and stack design flexibility, multiple cell fabrication options, multifuel and multifunctional capacity and operating temperature choices. The SOFC has been under development for a broad spectrum of power generation applications. Many of the applications have progressed to hardware demonstration and prototype/precommercial stages, especially those with power outputs of 200 kW or less. Significant advancements have been made in several technological areas critical to the development and commercialization of the fuel cell: performance, fabrication scaleup and miniaturization, fuel utilization and performance degradation and durability. The SOFC can also operate in reverse (electrolysis) mode (referred to as solid oxide electrolysis cell or SOEC) and has been considered for hydrogen/oxygen production from steam and syngas from mixtures of steam and carbon dioxide. This paper summarizes and discusses the development status and recent progresses in the development of the SOFC for power generation and hydrogen/chemical production.

# Ion Exchange Polymer Threaded in MOF as a Potential Electrolyte with Fast Exchange and High Selectivity

Kwong-Yu Chan, Liang Gao, Chi-Ying Vanessa Li  
Department of Chemistry, The University of Hong Kong  
Pokfulam Road, Hong Kong  
hrsccy@hku.hk

The high porosity, high surface area and uniform ordered structure of metal organic frameworks (MOFs) have been explored in board applications. Inspired by Kitigawa and co-workers [1], we extend the concept of “*in situ* polymerization in MOF” to include polymers functionalized to provide ion-exchangeable sites. We report a porous metal-organic framework composite with flexible anion-exchange polymers threaded within the host cavity. [2] Polyvinyl benzyl trimethylammonium hydroxide (PVBTAH) threaded in ZIF-8 (PVBTAH~ZIF-8) (Fig. 1) is synthesized in steps of chloro-monomer impregnation, *in situ* polymerization, amination, and alkaline ion exchange. The synthesized non-cross-linked PVBTAH~ZIF-8 material exhibits superior ion-exchange kinetics compared to conventional ion-exchange resins (Fig. 2). The open porous structure of MOF allows the physically trapped polymers to contact solvent freely and exchange ions efficiently, as oppose to the conventional ion-exchange resins in which the binding sites are hidden within the polymeric beads, preventing full utilization of ion exchange sites. It has good potential to be applied as a hybrid polymeric electrolyte in advanced fuel cells and flow batteries which demands high ionic selectivity.

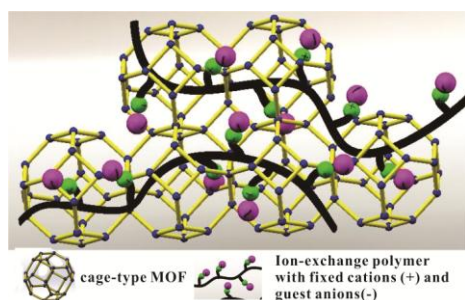


**Fig. 1** Schematic illustration of the PVBTAH anion exchange polymer in MOF ZIF-8.

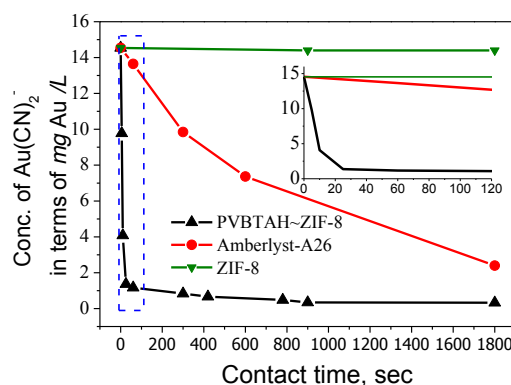


**Figure 2.**  $\text{Au}(\text{CN})_2^-$  concentration after immersing equal masses of PVBTAH~ZIF-8 and Amberlyst-A26 in  $\text{KAu}(\text{CN})_2$  solution. Inset shows enlarged profiles of the first 120 seconds.

- [1] T.Uemura, K.Kitagawa, S. Horike, T. Kawamura, S. Kitagawa, M. Mizuno, and K. Endo, “Radical polymerisation of styrene in porous coordination polymers”, *Chem. Commun.*, 48 (2005) 5968-70.  
[2] L. Gao, C.Y. V. Li, K.Y. Chan, and Z.N. Chen, "Metal-Organic Framework Threaded with Aminated Polymer Formed in Situ for Fast and Reversible Ion Exchange", *J. Am. Chem. Soc.*, 136 (2014) 7209-7212.



# RDE system for ORR measurements at elevated (>100 C) temperature and pressure conditions

Michael Fleige, Gustav K.H. Wiberg, and Matthias Arenz  
*Department of Chemistry and Nano-Science Center, University of Copenhagen  
Universitetsparken 5, 2100 Ø Copenhagen, Denmark*

*m.fleige@chem.ku.dk*

**Abstract.** Rotating disk electrodes (RDE) are widely used for mimicking conditions in polymer electrolyte fuel cells (PEMFCs), for example for ex situ measurements of the catalytic activity of fuel cell catalysts. However, using RDE current densities are much lower compared to fuel cells, as in liquid electrolyte mass transport of dissolved reactant gases is limited by orders of magnitude lower concentrations and diffusion coefficients compared to gas phase. Furthermore, owing greatly reduced gas solubility by increasing vapor pressure of water at elevated temperatures, RDE studies in open systems have been limited to about 60 C.<sup>1</sup> Employing RDE at elevated pressure would allow increasing reactant gas solubility and raising the boiling point of water. In addition, conc. phosphoric acid (PA), which is typically not considered in RDE studies due its even lower gas solubility, could be used for RDE measurements at sufficient gas concentration.

This presentation will discuss a developed RDE system that was integrated in an elevated pressure and temperature electrochemical cell setup reported earlier.<sup>2,3</sup> The RDE system is based on a magnet coupled drive, avoiding use of a rotary seal autoclave feed-through as proposed previously.<sup>4</sup>

We tested the magnet coupled RDE up to 100 bar pressure by studying the ORR on polycrystalline Pt as a test reaction in 0.5 M H<sub>2</sub>SO<sub>4</sub> as well as conc. PA electrolyte. By increasing the pressure of oxygen in the closed cell, the diffusion limited current densities can be increased by almost two orders of magnitude in dilute electrolyte and RDE measurements in conc. PA are enabled. The RDE system also was successfully tested at elevated temperatures up to 140 C. Kinetic measurements of the ORR under elevated pressure conditions are currently in preparation.

<sup>1</sup> U. Paulus, T.J. Schmidt, H. Gasteiger, and R.J. Behm, J. Electroanal. Chem. **495**, 134 (2001).

<sup>2</sup> G.K.H. Wiberg, M.J. Fleige, and M. Arenz, Rev. Sci. Instrum. **85**, 085105 (2014).

<sup>3</sup> M.J. Fleige, G.K.H. Wiberg, and M. Arenz, under Review.

<sup>4</sup> J. McBreen, W.E. O'Grady, and R. Richter, J. Electrochem. Soc. **131**, 1215 (1984).

# Durable MEAs for PEM electrolyser systems operating at high current densities

P. Lettenmeier<sup>a</sup>, R. Wang<sup>b</sup>, R. Abouatallah<sup>b</sup>, A. S. Gago<sup>a</sup>, K. A. Friedrich<sup>a</sup>

<sup>a</sup>*Institute of Engineering Thermodynamics, German Aerospace Center  
Pfaffenwaldring 38-40, 70569 Stuttgart, Germany*

<sup>b</sup>*Hydogenics Corporation, 220 Admiral Boulevard, Mississauga, ON L5T 2N6, Canada*

philipp.lettenmeier@dlr.de

Hydrogen can be used as an energy vector for renewable energies such as solar or wind by using water electrolysis systems [1]. Commercially, it can be electrochemically produced by alkaline and proton exchange membrane (PEM) electrolysis, at which the investment cost of the later is presently almost three times higher than the alkaline technology [2]. However, the main advantage of PEM electrolyzers is the possibility to operate at much higher current densities with a significant potential for cost reduction owing to the compact design [3]. An open question is still the life time of the membrane electrode assembly (MEA) of the PEM electrolyser operating at high performance. In this work rainbow stacks with MEAs from different suppliers are tested in a 20 kW PEM electrolyser ( $2.5 \text{ N m}^3 \text{ H}_2 \text{ h}^{-1}$ ) operating constantly and dynamically up to  $5 \text{ A cm}^{-2}$ . The  $120 \text{ cm}^2$  active area MEAs have membranes with the same thickness but different Ir-based catalyst loadings. The cell voltage ( $E_{\text{cell}}$ ) increases ca. 50 mV at  $1.25 \text{ A cm}^{-2}$  when reducing the anode loading by 30% (Figure 1a), although this parameter does not influence the degradation rate. It is possible to reduce the cell voltage by 150 mV at  $3.3 \text{ A cm}^{-2}$  by increasing the temperature from  $28^\circ$  to  $48^\circ \text{ C}$ . At the maximum current density the stack temperature and  $E_{\text{cell}}$  reach almost  $65^\circ \text{ C}$  and 2.5 V, respectively. Operating the electrolyser at low current densities has an impact in the  $\text{H}_2$  crossover. The most durable MEAs do not experience any lost in performance after more than 3000 h of operation under stationary and dynamic regimes. Post-mortem characterisation and water analysis are carried out to determine the degradation mechanism of the rest of the MEAs.

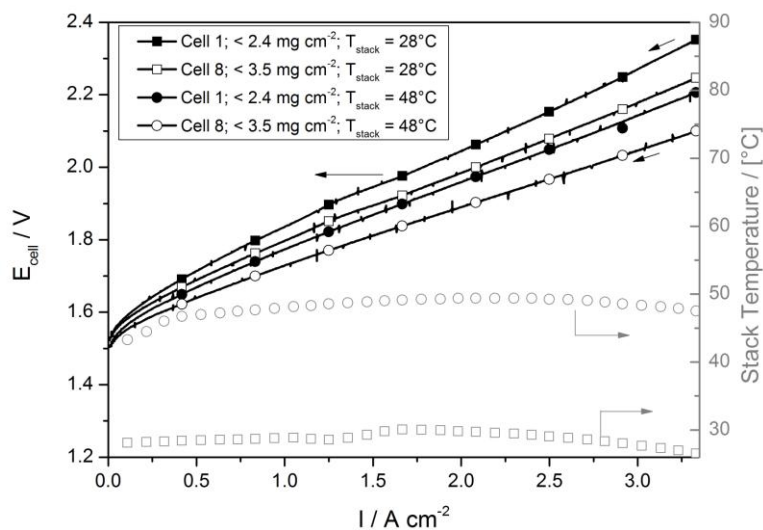


Fig. 1. Cell voltage and current density characteristics of a  $120 \text{ cm}^2$  stack with half of the cells having anode catalyst loadings of  $2.4 \text{ g cm}^{-2}$  and the other half with  $3.5 \text{ g cm}^{-2}$ . The measurements are performed at 7 bar and two different stack temperatures. The step rate of the rectifier is  $4.2 \text{ mA cm}^{-2} \text{ s}^{-1}$ .

## References

- [1] A. Sternberg, A. Bardow, Energy Environ. Sci. (2015) 389.
- [2] Fuel Cells and Hydrogen Joint Undertaking, Report: Commercialisation of Energy Storage in Europe, 2015.
- [3] M. Carmo, D.L. Fritz, J. Mergel, D. Stolten, Int. J. Hydrogen Energy 38 (2013) 4901.

# Amperometric Study of the Oxygen Reduction Reaction on Oxide Free Metals: Evidence for the Reduction of Pre-adsorbed Dioxygen and its Dependence on the Metal Substrate

Guy Denuault, Samuel C. Perry  
University of Southampton  
University Road, Southampton SO17 1BJ, UK  
gd@soton.ac.uk

We present experimental results which provide new insight on the electrochemical reduction of oxygen on oxide free metals. Using chronoamperometry at microdisc electrodes in aqueous media, we investigated the oxygen reduction reaction (ORR) on the millisecond timescale and found an unexpected chronoamperometric response. At long times, the amperometric response follows the theoretical diffusion controlled chronoamperogram at microdiscs<sup>1,2</sup> thereby indicating that the ORR rate is solely controlled by the diffusion of dissolved oxygen towards the microelectrode. However, at short times, typically below 50 ms, the reduction of oxygen produces a large extra current whose magnitude was found to depend on the electrode metal, deliberate electrode poisoning, the oxygen concentration in solution, and the rest time prior to a potential step being performed. Remarkably the extra charge recorded at short times was found to systematically vary with reported theoretical calculations of the binding energy of oxygen with respect to the electrode material,<sup>3</sup> figure 1.

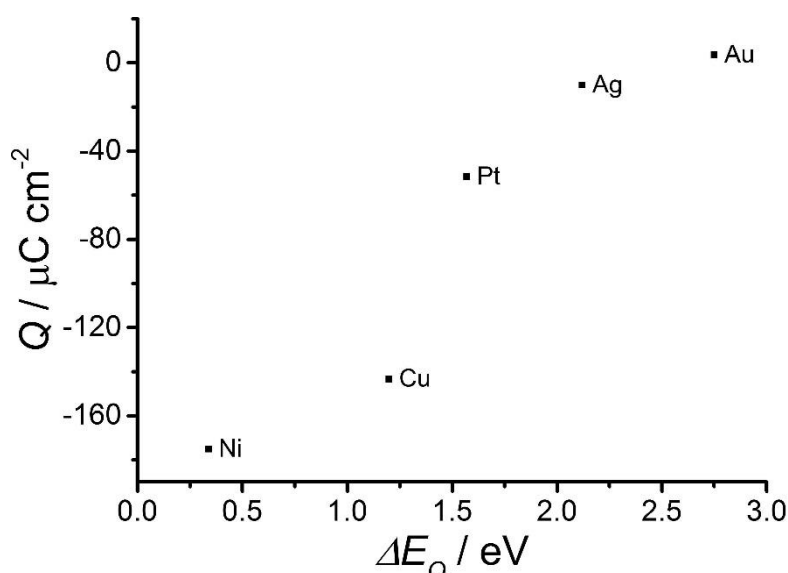


Figure 1: Extra charge calculated from the difference between experimental and theoretical current transients for the oxygen reduction reaction at Ni, Cu, Pt, Ag and Au against the binding energy reported by Norskov et al.<sup>3</sup> for those metals toward oxygen.

Overall the results provide clear experimental evidence for the reduction of oxygen pre-adsorbed on oxide free metals. By taking steps to manipulate the amount of pre-adsorbed oxygen we also show that the extra current can be systematically altered. These results provide not only a new insight into the ORR mechanism but also a new strategy to investigate the properties of ORR catalysts and a clear link between experimental and theoretical data.

- (1) Shoup, D.; Szabo, A. *J. Electroanal. Chem.* **1982**, 140, 237-245.
- (2) Mahon, P. J.; Oldham, K. B. *Anal. Chem.* **2005**, 77, 6100-6101.
- (3) Norskov, J. K.; Rossmeisl, J.; Logadottir, A.; Lindqvist, L.; Kitchin, J. R.; Bligaard, T.; Jonsson, H. *J. Phys. Chem. B* **2004**, 108, 17886-17892.

# Pt-free Catalyst for Oxygen Reduction Reaction in Fuel Cells

Ding Wei, Li Li, Siguo Chen, Xueqiang Qi, Zidong Wei\*

School of Chemistry and Chemical Engineering, Chongqing University, Shazhengjie 174, Chongqing, 400044, China  
zdwei@cqu.edu.cn

Developing catalytic materials for oxygen reduction reactions (ORR) with high performance and low cost has been one of the major challenges for large-scale applications of fuel cells. The involved scientific issues include theoretical understanding of the catalysis mechanisms, catalyst material design and synthesis, and integration of catalysts into fuel cell operations. Among various catalytic materials,  $sp^2$  carbon materials having abundant free-flowing  $\pi$ -electrons are potential catalysts for the ORR. Breaking the electroneutrality of graphitic materials by doping with heteroatoms to create charged sites favorable for  $O_2$  adsorption is the key factor in enhancing ORR activity, regardless of whether the dopant is electron-rich (e.g. N) or electron-deficient (e.g. P, B).<sup>[1]</sup> As for nitrogen doped carbon catalyst, the molecular structure of nitrogen is a critical role in affecting its catalytic properties. Recently, we presented a strategy for the selective synthesis of pyridinic- and pyrrolic-nitrogen-doped graphene (NG) by the use of layered montmorillonite (MMT) as a quasi-closed flat nanoreactor.<sup>[2]</sup> The confinement effect of MMT extensively constrains the formation of quaternary N because of its tetrahedral  $sp^3$  configuration but facilitates the formation of planar N, i.e. pyridinic and pyrrolic N which have planar  $sp^2$  configuration (fig. 1a). The content of planar N sites was inversely proportional to the interspace width ( $\delta$ ) of the

MMT, and it reached a maximum of 90.27% with the MMT interspace width at 0.46 nm. The planar N doped graphene exhibited a low electrical resistance and high electrocatalytic activity with a half-wave potential of the ORR that lags behind the state-of-the-art carbon-supported platinum by only 60 mV in an acidic electrolyte. As for integration of catalysts into fuel cell operations, the exposure of the active sites to the interface, where electrons, protons, oxygen and product water can flow in or exit out, is particularly important. It would be better if the catalysts are porous enough to accommodate the linkage of various species-transport channels to their active sites: voids for  $O_2$  and water, a polymer chain for protons, and a carbon framework for electrons. At this point, we developed a “shape fixing via salt recrystallization” method to efficiently synthesize nitrogen-doped carbon material with a large number of active sites exposed to the three-phase zones.<sup>[3]</sup> The active sites (activated by planar pyridinic and pyrrolic N atoms with  $sp^2$  hybrid orbitals, which only appear at the outside fringe of a graphene sheet) appear in large quantities on the edges of numerous pores. A three dimensional network catalyst structure with a high density of ORR active sites, which is conducive to mass transport and high utilization of active sites, was constructed (fig. 1b). The cathode catalyst in a proton exchange membrane fuel cell produces a peak power of  $600 \text{ mWcm}^{-2}$ , making this among the best non-precious metal catalysts for the ORR reported so far.

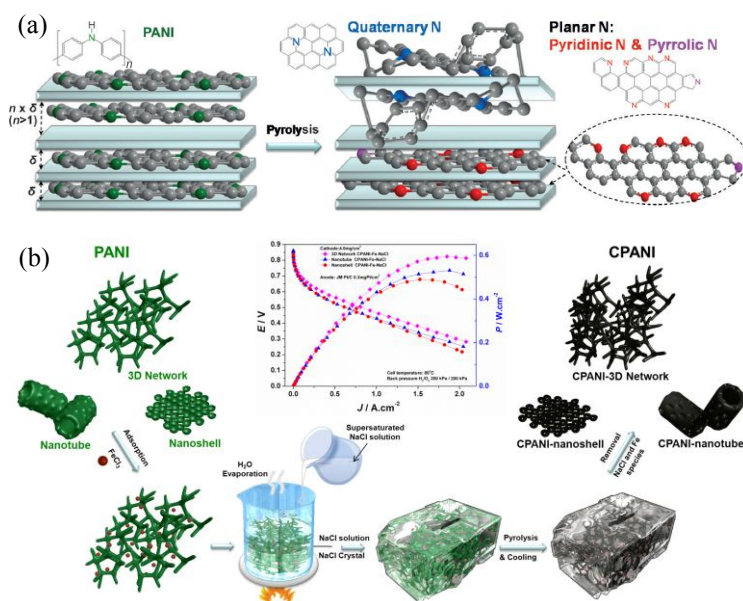


Figure 1. (a) the selective synthesis inside and outside MMT, (b) shape Fixing via Salt Recrystallization Method.

## References

- [1] Y. Zhao, L. -J. Yang, S. Chen, X. -Z. Wang, Y. -W. Ma, Q. Wu, Y.-F. Jiang, W. -J. Qian, Z. Hu. *J. Am. Chem. Soc.* **2013**, 135, 1201
- [2] W. Ding, Z. D. Wei, S. G. Chen, X. Q. Qi, T. Yang, J. S. Hu, D. Wang, L.-J. Wan, S. F. Alvi, L. Li. *Angew. Chem. Int. Ed.* **2013**, 52, 11755.
- [3] W. Ding, L. Li, K. Xiong, Y. Wang, W. Li, Y. Nie, S. G. Chen, X. Q. Qi, Z. D. Wei. *J. Am. Chem. Soc.*, **2015**, DOI: 10.1021/jacs.5b002

# Preparation of Ni-Co Nanowire Arrays Anode Electrocatalyst and the Performance of Direct Urea-Hydrogen Peroxide Fuel Cell

Fen Guo, Dianxue Cao<sup>\*</sup>, Ke Ye, Kui Cheng, Mengmeng Du, Dongming Zhang

Key Laboratory of Superlight Materials and Surface Technology, Ministry of Education, College of Materials Science and Chemical Engineering, Harbin Engineering University, Harbin, 150001, P.R. China.

E-mail address: caodianxue@hrbeu.edu.cn

Waste water containing Urea is discharged every day in the form of urine or chemical fertilizer factory sewage. Direct urea fuel cell (DUFC) is composed of urea electro-oxidation in the anode and oxygen or hydrogen peroxide electro-reduction in the cathode[1]. The fuel cell can play a dual role by generating electricity and alleviating urea-rich pollutant in one step. Nickel proves to be an effective catalyst for urea electro-oxidation[2]. Studies show that the composition of catalyst would be rather influential on the performance of urea electro-oxidation. In this work, polycarbonate (PC) membrane was used as the template to prepare Ni-Co nanowire arrays (NWAs) electrode. Without ion sputtering or thermal evaporation of metals on the template as conductive film, PC membrane is attached on low melting point alloy, which is re-usable and easy for handling. The electrodeposition keeps running until a layer of Ni-Co substrate is formed even after the pores are completely filled with nickel and cobalt. When the mass ratio of nickel and cobalt salts in the electrodeposition solution was 9:1, the as-prepared Ni-Co NWAs electrode demonstrated best performance for urea electro-oxidation, i.e., a maximum oxidation current density of  $380 \text{ mA cm}^{-2}$  and an onset oxidation potential of  $0.188 \text{ V}$  vs.  $\text{Ag}/\text{AgCl}$  in  $5 \text{ mol L}^{-1}$   $\text{KOH}$  and  $0.33 \text{ mol L}^{-1}$  urea. Importantly, the onset oxidation potential hardly exhibited negative shifts with the increase of cobalt salt content.

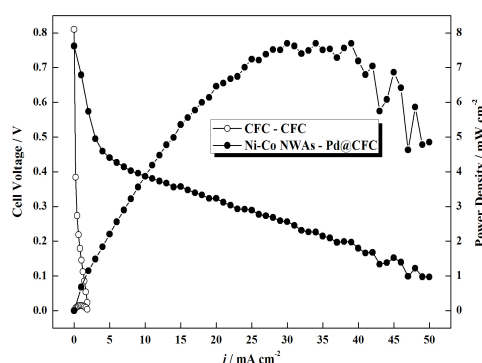


Fig.1. The digital photograph and the SEM image of Ni-Co NWAs electrode (inset); Fig.2. The performance of direct urea-hydrogen peroxide fuel cell. Open dots: CFC at both sides, solid dots: Ni-Co NWAs and Pd@CFC respectively.

Fig.1 shows the digital photograph of Ni-Co NWAs electrode. The black side is PC membrane filled with nanowires. The back side is a layer of Ni-Co substrate. The inset is the SEM image of NWAs electrode after dissolving the PC membrane in dichloromethane. The nanowires stand on the Ni-Co substrate and array in line like ears of wheat. Fig.2 displays the performance of direct urea-hydrogen peroxide fuel cell. At the cathode side,  $\text{H}_2\text{O}_2$  is used as the oxidant and Pd@carbon fiber cloth (CFC) acts as cathode catalyst. The anode fuel, urea, is electro-catalyzed by Ni-Co NWAs electrode. The whole cell achieves an open circuit voltage of  $0.76 \text{ V}$  and a maximum power density of  $7.7 \text{ mW cm}^{-2}$ . For comparison, the fuel cell is operated with carbon fiber cloth as electrocatalysts at both sides. The maximum power density is negligible with that of Ni-Co NWAs and Pd@CFC electrodes.

## Acknowledgements

This paper is funded by the International Exchange Program of Harbin Engineering University for Innovation-oriented Talents Cultivation

## Reference

- [1] R. Lan, S. Tao, J.T. Irvine, A direct urea fuel cell – power from fertiliser and waste, *Energy & Environmental Science* 3 (2010) 438-441.
- [2] R.L. King, G.G. Botte, Hydrogen production via urea electrolysis using a gel electrolyte, *Journal of Power Sources* 196 (2011) 2773-2778.

# Nature of Active Sites and Origin of Large Overpotential of the Oxygen Reduction Reaction on Pt(111) Surface

Junxiang Chen, Yuwen Liu, Shengli Chen  
*Department of Chemistry, Wuhan University, Wuhan, China*  
*slchen@whu.edu.cn*

The large overpotential of the oxygen reduction reaction (ORR) even on the best metal electrocatalyst, Pt, is one of the major barrier for the commercialization of fuel cells. Moreover, its origin has been a standing problem that challenges both the theoretical and experimental electrochemists. In this study, the problem is tackled by distinguishing the active sites from the surface spectator phases of oxygenated adsorbates through systematic density functional theory (DFT) calculations. By rationalizing the cyclic voltammetric (CV) features with the DFT-calculated adsorption isotherms for the oxygenation and reduction processes on Pt(111) surface, we conclude that there are mainly two types of oxygenated surface phases at potentials of ORR relevance (below ca. 1.07 V), namely, the  $(\sqrt{3}\times\sqrt{3})R30^\circ$ -patterned co-adsorption network of OH\*s and H<sub>2</sub>O\*s and the  $\sqrt{3}\times\sqrt{3}$ -structured O\*s. In a potential region below ca. 0.85 V, the electrode surface should be covered by a globally ordered OH\*s/H<sub>2</sub>O\*s network, while a pure phase of O\*s should form at potential above ca. 1.07 V. In between these potentials, the locally ordered OH\*s/H<sub>2</sub>O\*s networks and the clusters of O\*s coexist on the surface.

The correlation between the DFT-derived isotherms and that implied by the CV responses also suggests that the OH\*s and O\*s both prefer to form locally ordered phases during the oxygenation and reduction processes on Pt(111) surface, rather than distribute themselves randomly; the butterfly-shaped CV responses in the low potential region can be attributed to the competition between the energetically favoured Pt-OH\* bond formation and the energetically disfavoured decrease of the average distance of H<sub>2</sub>O\*s to the surface accompanying the dissociation of H<sub>2</sub>O\* to OH\* in the co-adsorption network; the highly unsymmetrical oxidative/reductive responses in the high potential region of CV is associated with the nucleation and growth type of formation of O\* clusters.

Various possible reaction channels for the ORR are investigated on Pt(111) surfaces covered by the two types of spectator phases. The results indicate that the surface phase of the  $\sqrt{3}\times\sqrt{3}$ -structured O\*s has much stronger blocking effect on the starting step in the ORR, namely, the adsorption reaction of O<sub>2</sub>, than the OH\*s/H<sub>2</sub>O\*s network phase. This suggests that the latter provides the main active sites for the ORR below ca. 1.07 V. The large onset overpotential and the potential-dependent Tafel slopes of the ORR are thus well explained in terms of the evolution of the strong spectator phase of O\*s with potential. A new type of proton/electron-transfer (PET) coupled O<sub>2</sub> adsorption step, in which the O<sub>2</sub> adsorption is accompanied by a PET to an OH\* in the OH\*s/H<sub>2</sub>O\*s network, rather than to the O<sub>2</sub> itself as generally believed, is identified to be the initial and also the activity-determining step in the ORR.

The present results show very distinct roles of various oxygenated adsorbates. The adsorbed oxygen atoms, O\*s, act mainly as surface spectators for the ORR. By forming hexagonal networks, OH\*s and H<sub>2</sub>O\*s also act as spectators to block the surface sites for the ORR. On the other hand, the formed networks provide reaction sites and environments for the ORR, with some OH\*s and H<sub>2</sub>O\*s participating into the reaction as intermediates and/or PET mediators. Therefore, the earlier proposition that OH\*s produced from water dissociation act solely as spectators, and that they are different in nature from OH\*s involved in the ORR, seems not correct. It is also implied that the binding strength of O\* impacts the ORR activity of Pt predominantly by modulating the numbers of the available O<sub>2</sub> adsorption sites, rather than the activation barriers or the natures of the rate-determining steps as proposed previously.



# Electron Transfer over Non-precious Metal Catalysts for Oxygen Reduction Reactions

Chang Hyuck Choi and Karl J. J. Mayrhofer

Department of Interface Chemistry and Surface Engineering, Max-Planck-Institut für Eisenforschung  
Max-Planck-Straße 1, 40237 Düsseldorf, Germany  
c.h.choi@mpie.de

In parallel with increasing global energy demands, polymer electrolyte membrane fuel cells (PEMFCs) have attracted great attentions as clean and efficient electrochemical energy conversion devices. As the nub of technology for high performing PEMFCs, catalysts are key components especially for overcoming sluggish kinetics of oxygen reduction reactions (ORRs). While Pt (or its alloys) has been widely used for the efficient ORRs, great recent efforts have been made to find non-precious metal catalysts for reducing high cost of the PEMFCs. Among the many candidates, FeNC catalysts, a class of catalysts consisting of Fe and N species doped on carbonaceous supports, demonstrate considerable ORR activity in an acidic environment [1, 2]. However, further developments have been still challenging because of less competent activity and stability.

For the maximizing catalytic performance, it is critical to understand the underlying electrochemical ORR mechanisms of the FeNC catalysts. Numerous experimental and theoretical studies have been substantially performed to figure out the ORR catalysis on the FeNC catalysts [3, 4]. Despite the ambitious efforts, however, the rational design of high-performing catalysts is still limited due to insufficient understanding on ORR catalysis of the FeNC, which is generally on the basis of an inner-sphere electron transfer (IS-ET) model that assumes  $O_2$  adsorption prior to the first electron transfer step [4].

Herein, we prepared the FeNC catalyst free from the inactive Fe species to address the importance of an outer-sphere electron transfer (OS-ET) mechanism during its ORRs. The prepared catalyst consisted dominantly with Fe- $N_4$  coordination sites with N-functionalities doped on the carbonaceous supports, thereby enabling to be considered as an ideal catalyst without interferences from the inactive Fe species. The FeNC showed irrational ORR behaviors in an acidic electrolyte such as no enhancement in  $H_2O_2$  selectivity in the presence of  $CN^-$  ions, low relationship between ORR activity and  $Fe^{2+/3+}$  redox potential, and activity loss without deformations of Fe-/N-species, which were not fully understood by the conventional belief that  $O_2$  adsorption precedes the ET step (IS-ET). To elucidate the electrocatalytic trends, we introduced a contribution of OS-ET mechanism in the first electron transfer step during the ORRs, and found that ORR activity of the FeNC was determined by the ionic strength in the electrolyte and by the electrode potential of the electrode. In accordance with the OS-ET mechanism, a linear relationship was established between work functions of the FeNC and their ORR activities after the degradation by  $H_2O_2$  treatment without any considerable deformations of  $O_2$  adsorption sites. The results therefore suggest an insight that contributions of the OS-ET and correlated tuning parameters as well as the traditional IS-ET should be also considered for the design of advanced FeNC catalysts in the future.

## References

- [1] M. Lefèvre, E. Proietti, F. Jaouen and J. P. Dodelet, *Science*, 324 (2009) 71–74.
- [2] G. Wu, K. L. More, C. M. Johnston and P. Zelenay, *Science*, 332 (2011) 443–447.
- [3] C. H. Choi, H. Lim, M. W. Chung, J. C. Park, H. Shin, H. Kim, and S. I. Woo, *J. Am. Chem. Soc.* 136 (2014) 9070–9077.
- [4] U. Tylus, Q. Jia, K. Strickland, N. Ramaswamy, A. Serov, P. Atanasov, and S. Mukerjee, *J. Phys. Chem. C*, 118 (2014), 8999–9008.

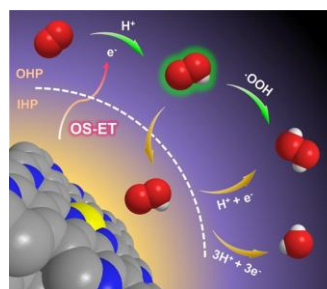


**Figure 1.** Schematic description of the OS-ET model in ORRs of the FeNC catalysts

# Development of Sulfonated Poly(Arylene Ether Sulfone) Multi-Block Membranes for PEMFC Application

Byungchan Bae

Fuel Cell Laboratory, Korea Institute of Energy Research (KIER), 152, Gajeong, Yuseong, Daejeon, 305-343, Korea

E-mail: bcbae@kier.re.kr

Perfluorosulfonic acid (PFSA) polymers are the most promising state-of-the-art materials as proton exchange membranes (PEM) for fuel cells, however, there are some drawbacks such as high production cost and hydrothermal stability. Aromatic membranes based on hydrocarbon polymers have been studied as alternatives. Among them, multi-block copolymers seem to be promising to compete with PFSA resulting high proton conductivity even under low RH conditions.[1, 2]

In this report, novel sulfonated poly(arylene ether sulfone)s multi-block copolymer membranes containing highly sulfonated hydrophilic blocks were synthesized as shown in Figure 1.[3] Different local concentration of sulfonic acid in their hydrophilic blocks affected chemical and physical properties of the SPAES. To investigate the effects of chemical composition on their membrane properties, different hydrophilic oligomers sharing same hydrophobic blocks gave us exact comparison of effect of hydrophilic blocks. The higher concentration of sulfonic acid groups resulted in higher proton conductivity under certain relative humidity conditions than that of the state-of-the-art perfluorinated sulfonic acid membrane and showed that the well-developed phase separation of SPAES. Moreover, physical properties of these SPAES including water behavior, humidity dependence of proton conductivity were investigated along with morphology characterizations by transmission electron microscopy (TEM) for PEMFC application.

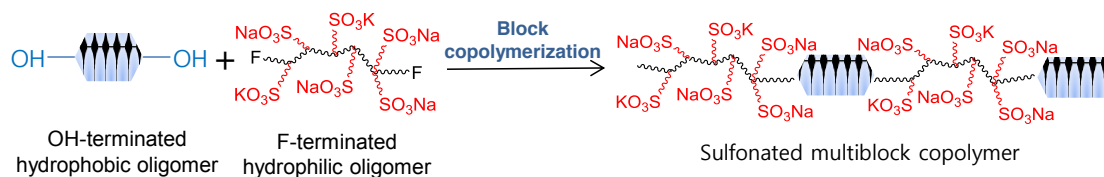


Figure 1. Concept for synthesis of the multi-block copolymer.

Two types of oligomers, F-terminated and OH-terminated telechelic oligomers, were synthesized by controlling the feed ratio of dihydroxyl- and difluoro-monomers. Their number of repeating unit (X and Y) was analyzed by GPC and  $^1\text{H}$  NMR. Copolymerization with F-terminated and OH-terminated telechelic oligomers via nucleophilic aromatic substitution, gave high-molecular-weight multi-block PESs. Each block length was controlled to have different values with X5Y10, X10Y10, X20Y10 and X20Y20.

The SPAES X10Y10 membrane showed highest proton conductivity than that of our previous random and block copolymers at wide range of humidity. The best balanced membrane was SPAES X10Y5 membrane with high proton conductivity and lower water uptake. Consequently, the SPAES X10Y5 membrane showed high cell performance under various conditions (510 mA/cm<sup>2</sup>, 290 mA/cm<sup>2</sup> @ 0.6V under 80% and 50 % RH conditions at 80°C, respectively). Systematic approaches for developing alternative block SPES membrane for low RH condition will be discussed.

## References

- [1] H.-S. Lee, A. Roy, O. Lane, J.E. McGrath, *Polymer*, 49 (2008) 5387-5396.
- [2] B. Bae, T. Yoda, K. Miyatake, H. Uchida, M. Watanabe, *Angew. Chem. Int. Ed.*, 49 (2010) 317-320.
- [3] S. Lee, J. Ann, H. Lee, J.-H. Kim, C.-S. Kim, T.-H. Yang, B. Bae, *J. Mater. Chem. A*, 3 (2015) 1833-1836.



# Challenges of NPGM Oxide Cathode for PEFCs

Ken-ichiro Ota<sup>a</sup>, Koichi Matsuzawa<sup>a</sup>, Shigenori Mitsushima<sup>a,b</sup>, Akimitsu Ishihara<sup>b</sup>

Yokohama National University,

<sup>a</sup>Green Hydrogen Research Center, <sup>b</sup>the Institute of Advanced Sciences

79-5 Tokiwadai, Hodogaya-ku, Yokohama, 240-8501 JAPAN

e-mail address: ken-ota@ynu.ac.jp

Polymer electrolyte fuel cells (PEFCs) are commercially available in Japan. Total number of installed Ene-Farm, the home cogeneration systems using PEFC, is over 12,000 and the thermal efficiency of over 90 % has been achieved. The commercialization of fuel cell vehicles has been started in Japan at the end of last year as the ultimate clean car due to their cleanness, high power density and low operating temperature. However, a cost reduction is needed and the cost of Pt is a key for the reduction. And the estimated amount of Pt reserve is too small to supply for the huge number of fuel cell systems. Pt is used for both anode and cathode catalysts. As a cathode catalyst, Pt has a large oxygen over potential compared to an anode. Pt has some instability in acid and oxygen containing atmosphere in nature. Pt is oxidized in oxygen containing atmosphere and PtO<sub>2</sub> is thermochemically stable at room temperature. Once Pt oxide is formed, the oxide could dissolve chemically. Pt oxide dissolves chemically and the solubility is around 1 ppm at room temperature in sulfuric acid. The dissolution followed the acid dissolution mechanisms. These things are chemical nature of Pt. In order to commercialize the fuel cell systems widely, the development of a non-precious metal cathode is strongly required.

We believe that high stability in cathodic condition is essentially required for the cathode catalyst. We started this study by searching stable materials in acid and in oxygen containing atmosphere by measuring the solubility in sulfuric acid. The solubilities of group 4 and 5 metal oxides are smaller than that of Pt in acidic and oxidative atmosphere. This means that these oxides are more stable than Pt at the cathodic condition of PEFC. However, these oxides are generally insulator. In order to get some electrical conductivity, these oxides should be modified by the formation of oxygen vacancy and/or the substitution of foreign atoms. We have reported that partially oxidized group 4 and 5 metal carbonitrides and metal complexes which contain nitrogen were stable in an acid solution and had a definite catalytic activity for the oxygen reduction reaction (ORR) (1-4). In this paper we will report the reasons why we need a non platinum group metal (NPGM) oxide cathode and our recent results of the oxide cathode for PEFCs.

Powders of metal (Metal: Ta, Zr, Nb, Ti) compounds (carbonitride or metal complexes that contain nitrogen) were heat-treated at 800-1200°C. After heat treatment, the compounds changed to oxides that contained small amount of carbon and nitrogen. Heat treated powder was mixed with alcohol, carbon and Nafion. The mixture was dipped on a glassy carbon rod (5 mm diameter) and the working electrode was made. All electrochemical measurements were examined in 0.1 M H<sub>2</sub>SO<sub>4</sub> at 30°C under atmospheric pressure using a conventional 3-electrode cell. The RHE was used for the reference in the same solution. Slow scan voltammetry (scan rate: 5 mVs<sup>-1</sup>) was performed under O<sub>2</sub> and N<sub>2</sub> atmosphere to obtain the current for the oxygen reduction reaction (ORR).

An appropriate oxidation is essential to have a definite catalytic activity for the ORR. In order to improve the current density especially at high potentials we have tried to use metal complexes that have nitrogen as starting materials. More than 1000 times improvements in catalytic activity have been obtained using these materials. By the single cell test we have obtained more than 300 mA/g at 0.85 V vs. RHE for ORR at room temperature. We also have obtained more than 1 A/cm<sup>2</sup> using a 5 x 5 cm fuel cell at 80°C. These materials have great potential for PEFC cathode,.

Acknowledgement : The authors wish to thank to the New Energy and Industrial Technology Development Organization (NEDO) for their financial support.

## References

- 1) A.Ishihara, Y.Shibata, S.Mitsushima, K.Ota, J.Electrochem. Soc., 155, B400.(2008)
- 2) A.Ishihara, M.Tamura, Y.Ohgi, M.Matsumoto, K.Matsuzawa, S.Mitsushima, H.Imai, K.Ota, J.Phys.Chem. C, 117, 18837-18844 (2013)
- 3) A. Ishihara, M. Chisaka, Y. Ohgi, K. Matsuzawa, S. Mitsushima and K. Ota, Phys. Chem. Chem. Phys., 17, 7643-7647 (2015).
- 4) N Uehara, A. Ishihara, M Matsumoto, H. Imai, Y. Kohno, K. Matsuzawa, S. Mitsushima, K. Ota, Accepted for publication, Electrochim. Acta,

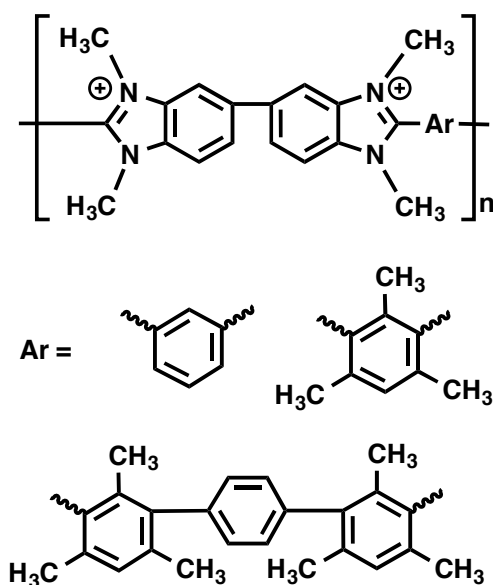
# Membranes with Potential AAEMFC Applications: Structure-Property Relationships of Methylated Poly(benzimidazole)s

T. J. Peckham, A. G. Wright, O. D. Thomas, M. P. Kulkarni, K. J. W. Y. Soo and S. Holdcroft\*

Department of Chemistry, Simon Fraser University  
8888 University Drive, Burnaby, British Columbia, Canada V5A 1S6  
tpeckham@sfu.ca

There has been considerable interest in alkaline anion exchange membranes (AAEMs) fuel cells as high efficiency, low emission, energy converters.<sup>1</sup> In contrast to the platinum used in proton exchange membrane fuel cells, AAEMFC use cheaper, non-noble metal catalysts, thereby potentially giving them a considerable advantage.<sup>2</sup> However, development of AAEMs has been hindered by the instability of commonly-used cationic groups (e.g., ammonium, phosphonium) under conditions of high pH and elevated temperature. While progress has recently been made in this area, virtually all AAEMs studies have focused on the issue of degradation rather than attempts to obtain a phenomenological understanding of how polymer structure and ionic content relate to observed membrane properties (e.g., anionic conductivity).

At Simon Fraser University, we have been developing benzimidazolium-based anion exchange membranes (AEMs) for a variety of applications, including AAEMFCs.<sup>3</sup> Very recently, we have developed a synthetic method that allows us to control the ionic content of these polymers.<sup>3c</sup> Using this technique, we have now been able to compare the properties not only between polymers with different backbone structures (examples shown below) but also within each series wherein ionic content is varied in a controlled fashion. This presentation will detail the results of our exploratory work on structure-property relationships for these methylated poly(benzimidazoles).



1. J. R. Varcoe, R. C. T. Slade *Fuel Cells* **2005**, 5, 187 – 200.
2. J. Pan, C. Chen, L. Zhuang, J. Lu *Acc. Chem. Res.* **2012**, 45, 473 – 481.
3. a) O. D. Thomas, K. J. W. Y. Soo, T. J. Peckham, M. P. Kulkarni, S. Holdcroft *Polym. Chem.* **2011**, 2(8), 1641 – 1643; b) O. D. Thomas, K. J. W. Y. Soo, T. J. Peckham, M. P. Kulkarni, S. Holdcroft *JACS* **2012**, 134(26), 10753 – 10756; c) A. G. Wright, S. Holdcroft *ACS Macro Letters* **2014**, 3(5), 444 – 447.

# The Performance and Stability of the Oxygen Reduction Reaction on Pt-based Nanorods: An Experimental and Computational Study

Kuan-Wen Wang<sup>a</sup>, Jeng-Han Wang<sup>b</sup>, Yu-Ting Liang<sup>a</sup>

<sup>a</sup> Institute of Materials Science and Engineering, National Central University, Taoyuan 320, Taiwan

<sup>b</sup> Department of Chemistry, National Taiwan Normal University, Taipei 116, Taiwan

E-mail: kuanwen.wang@gmail.com

The development of Pt-based catalysts towards the oxygen reduction reaction (ORR) for polymer electrolyte membrane fuel cells (PEMFCs), through control of the morphology, alloying components, structures, and supports has attracted much attention. When compared with Pt nanoparticles (NPs), graphene or carbon-supported Pt nanomaterials with different aspect ratios, alloying components or morphologies especially nanorods (NRs) have shown enhanced ORR performance owing to the electronic modification effect.<sup>1-5</sup> In this study, we have investigated the ORR activity and stability of Pt<sub>3</sub>M (M = Au, Ag, and Pd) NRs, which have potentially good activity and stability, both experimentally and computationally. Pt<sub>3</sub>M NRs with an aspect ratio of 4.0 have been prepared to study their ORR activity and stability by electrochemical measurement and Density functional theory (DFT) calculations. The ORR activity of Pt<sub>3</sub>M NRs is related to the degree of modification of the oxophilicity ( $\Delta E_{ads}$ ), which is the difference between  $E_{ads}(\text{O}^*$  or  $\text{OH}^*)$  for Pt and its alloys. DFT results suggest that since  $\Delta E_{ads}$  of PtPd NRs is -0.11 eV, the modification effect of alloying with Pd is insignificant. On the other hand, Au can noticeably modify the Pt surface so that the  $\Delta E_{ads}$  is 0.47 eV. However, due to the oxygen containing species (OCS\*) induced Pt surface segregation, the structure of PtAu becomes unstable during accelerated durability test (ADT). As a result, although the  $\Delta E_{ads}$  of PtAg is not as high as that of PtAu, the structure is relatively stable with or without OCS\*, thus promoting the ORR stability with a decay of 9 % during ADT.<sup>6</sup>

## References

1. Y. T. Liang, C. W. Liu, H. S. Chen, T. J. Lin, C. Y. Yang, T. L. Chen, C. H. Lin, M. C. Tu, K. W. Wang, RSC Adv. 2015, DOI: 10.1039/C5RA01130B.
2. C. W. Liu, Y. C. Wei, C. C. Liu, K. W. Wang, J. Mater. Chem. 22 (2012) 4641-4644.
3. T. H. Yeh, C. W. Liu, H. S. Chen, K. W. Wang, Electrochem. Commun. 31 (2013) 125-128.
4. Y. C. Tseng, H. S. Chen, C. W. Liu, T. H. Yeh, K. W. Wang, J. Mater. Chem. A 2 (2014) 4270-4275.
5. H. S. Chen, Y. T. Liang, T. Y. Chen, Y. C. Tseng, C. W. Liu, S. R. Chung, C. T. Hsieh, C. E. Lee, K. W. Wang, Chem. Commun. 50 (2014) 11165-11168.
6. Y. T. Liang, S. P. Lin, C. W. Liu, S. R. Chung, T. Y. Chen, J. H. Wang, K. W. Wang, Chem. Commun. 51 (2015) 6605-6608.

# The Steady State coverage of oxygenated species on Platinum and its influence on the Oxygen Reduction and Hydrogen Oxidation Reaction in acid electrolyte

Yu-Jia Deng, Gustav K.H. Wiberg, Matthias Arenz

Nano-Science Center, Department of Chemistry, University of Copenhagen, Universitetsparken 5, DK-2100 Copenhagen Ø, Denmark

[dengyujia@chem.ku.dk](mailto:dengyujia@chem.ku.dk)

In this work, we employ a recently developed stripping technique to investigate the equilibrium coverage of oxygenated species such as  $\text{OH}_{\text{ad}}$  and  $\text{O}_{\text{ad}}$  and how they influence the oxygen reduction reaction (ORR) and the hydrogen oxidation reaction (HOR) [1]. The main aim is to distinguish between dynamic and steady state conditions and find out whether the different respective oxygenated species  $\text{OH}_{\text{ad}}$ ,  $\text{O}_{\text{ad}}$  and Pt-oxide dominate distinctive potential regions. As is shown in Fig. 1, at steady state in Ar saturated 0.1 M  $\text{HClO}_4$  electrolyte only insignificant amounts of oxygenated species are observed  $< 0.60 \text{ V}_{\text{RHE}}$  and no influence on the HOR or ORR is seen. The first adsorbed species is  $\text{OH}_{\text{ad}}$  and at  $0.95 \text{ V}_{\text{RHE}}$  the adlayer is completed. With increasing potential  $\text{OH}_{\text{ad}}$  can be oxidized further to  $\text{O}_{\text{ad}}$  and at  $1.1 \text{ V}_{\text{RHE}}$ , only  $\text{O}_{\text{ad}}$  is on the surface. An oxide is formed at even more positive potentials. We also conduct the experiment by changing Ar to  $\text{O}_2$  or  $\text{H}_2$  saturated solution, we find that the inhibition of ORR correlates with the completion of the  $\text{OH}_{\text{ad}}$ -layer and only at more negative potentials than  $0.95 \text{ V}_{\text{RHE}}$ , the ORR can proceed. HOR is however active up to about  $1.1 \text{ V}_{\text{RHE}}$ , as it can alter the  $\text{OH}_{\text{ad}}$  coverage [2].

In the next step, we compare the different behaviour towards the ORR on polycrystalline Pt in three different acids with varying anion adsorption strength, i.e.  $\text{HClO}_4$ ,  $\text{H}_2\text{SO}_4$  and  $\text{H}_3\text{PO}_4$ . We will present unexpected results, leading to a new model for explaining the influence of anions for the inhibition of the ORR in  $\text{H}_3\text{PO}_4$  as compared to  $\text{H}_2\text{SO}_4$  or  $\text{HClO}_4$ .

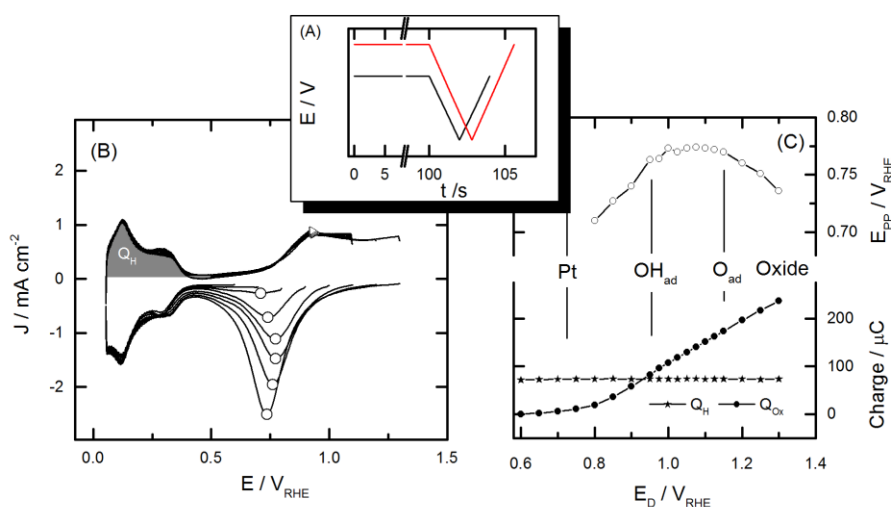


Fig. 1. (A) Examples of applied voltage profiles: the potential hold at ( $E_D$ ) is followed by a negative and positive sweep at a sweep rate of  $0.5 \text{ V s}^{-1}$ . (B) Polarization curves of PC Pt in argon saturated in 0.1 M  $\text{HClO}_4$  for different hold potentials. Key features have been highlighted: charge integration of the oxide peak ( $Q_{ox}$ ) and  $H_{upd}$  features ( $Q_H$ ) as well as the oxide reduction peak position ( $E_{pp}$ ). (C)  $E_{pp}$ ,  $Q_{ox}$  and  $Q_H$  versus hold potentials [2].

## References

- [1] Gustav K.H. Wiberg, Matthias Arenz, J. Power Sources 217 (2012) 262–267.
- [2] Yu-Jia Deng, Matthias Arenz, Gustav K.H. Wiberg, Electrochem. Commun. 53 (2015) 41–44.

## **Evolution of “ENE-FARM” and the Activities for the Market Expansion in Panasonic**

Eiichi Yasumoto, Masataka Ozeki  
*Corporate Engineering Division, Appliances Company*  
*Panasonic Corporation*  
*3-1-1 Yagumo-naka-machi, Moriguchi City, Osaka 570-8501, Japan*  
*yasumoto.eiichi@jp.panasonic.com*

ENE-FARM is a residential fuel cell cogeneration system which simultaneously produces electricity and hot water as a distributed power source. The heat produced during power generation can be used for water heating, so it contributes to primary energy saving by its high efficiency and also boosts energy security.

The cumulative sales of ENE-FARM, which became the world's first residential fuel cell when it was released in Japan in May 2009, reached 100,000 units in September 2014. As mentioned above, the market is expanding with strong support from the government. But in order to be a self-sustained business, big cost-reduction is required from fuel cell manufacturers and we need to continue our challenge to create and enlarge the fuel cell market.

To achieve this goal, Panasonic has updated the model every 2 years. We have recently released a new model (4<sup>th</sup> generation) fuel cell in April 2015. We achieved in driving down the end user price to 1.6 million JPY.

Also, compared to the previous model, the number of components has been reduced by 15% and also the weight of the total system is reduced by 15% (from 90kg to 77kg).

And we have improved stack performance it has been optimized the MEA, so there is a 20% reduction in the rare-metal Platinum used for the stack. In addition to the cost reduction, we increased product durability from 60,000 hours to 70,000 hours and adopted the continuous power generation mode into the unit.

Additionally, Panasonic started a new challenge from April 2014. We launched a new model with the German heating appliance manufacturer, Viessmann, for the German market. Based on the bigger heat demand and cost difference between electricity and gas price, we believe that it has a big market potential in European countries.

Panasonic believes that ENE-FARM has a big role with regard to energy management with high efficiency, supporting renewable energy, and the focus on local energy management using decentralized power systems. Fuel cell is the core technology to establish the hydrogen society of the future. Panasonic will continue to contribute to make a better life, a sustainable and safe society and the solution to environment issues in co-operation with global partners.

In this presentation, introduction of the latest model ENE-FARM in Panasonic and its elemental technology will be reported.

### **Acknowledgements**

Some parts of this work were carried out under contract with New Energy and Industrial Technology Development Organization (NEDO) in Japan.

# Preparation and Properties of PTFE Reinforced Novel Anion Exchange Membranes Based on Silane Crosslinked Imidazolium Containing Poly(2,6-dimethyl-1,4-phenylene oxide)

Jingshuai Yang, Chao Liu, Liping Gao, Yixin Xu, Niya Ye, Ronghuan He\*  
 Department of Chemistry, College of Sciences, Northeastern University,  
 Shenyang, 110819, China  
 E-mail address: herh@mail.neu.edu.cn

Recently, alkaline anion exchange membrane fuel cells (AEMFCs) have attracted extensive attention due to several advantages, such as non-use of noble metals as catalyst, much more facility of electrochemical reactions<sup>[1]</sup>. The anion exchange membrane (AEM) is the core of an AEMFC, which should meet with high conductivity, low swelling, enough mechanical strength and good stability under strong basic environment and elevated temperatures<sup>[1,2]</sup>.

Through bromination of alkyl side chains, bromomethylated poly(2,6-dimethyl-1,4-phenylene oxide) (BPPO) polymers were synthesized with bromination degrees from 20% to 71%. In order to achieve high conductivity, the polymer with high bromination degree of 71% was used to fabricate cross-linked membranes. The imidazolium functionalization of the membranes were performed by reacting BPPO with methylimidazole and imidazolium-functionalized silane simultaneously. The crosslinked network was then formed by hydrolysis in an acid medium. The chemical structure of the crosslinked membranes is shown in Fig.1. Moreover, the polytetrafluoroethylene (PTFE) was used as a matrix polymer to reinforce the mechanical stability<sup>[3]</sup> to obtain uniform composite membranes. Results illustrated that the conductivity of membranes increased as the increase of methylimidazolium groups in the membranes. For example, the conductivity of the membrane with an molar ratio of 7:3 for methylimidazolium and imidazolium-modified silane was higher than 30 mS cm<sup>-1</sup> in water at temperatures of 80 °C, which also possessed enough mechanical strength. The results indicated that the PTFE reinforced imidazolium-modified silane cross-linked membranes can be used as membrane electrolytes for AEMFCs.

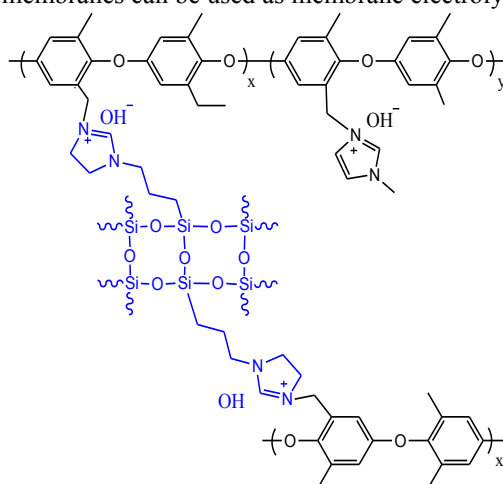


Fig. 1 Chemical structure of imidazolium-functionalized silane crosslinked poly(2,6-dimethyl-1,4-phenylene oxide) anion exchange membranes

Funding of this work is acknowledged from the Natural Science Foundation of China (51172039), the Fundamental Research Funds for the Central Universities of China (N130305001) and Scientific Research Fund of Liaoning Provincial Education Department (L2014103).

## References

- [1] Varcoe J R, Atanassov P, Dekel D R, et al. Energy Environ. Sci. 2014, 7, 3135
- [2] Katzfuß A, Gogel V, Jörisen L, et al. J. Membr. Sci. 2013, 425-426, 131.
- [3] Qu C, Zhang H, Zhang F, et al. J. Mater. Chem. 2012, 22, 8203.

# Effective Pd-based electrode nanomaterials for H<sub>2</sub>/O<sub>2</sub> Solid Polymer Electrolyte fuel cells

Roberta Alvarenga Isidoro<sup>1</sup>, Elisabete Inácio Santiago<sup>1</sup>, Nihat Ege Sahin<sup>2</sup>, Teko W. Napporn<sup>2</sup>, K. Boniface Kokoh<sup>2</sup>,

<sup>1</sup> Instituto de Pesquisas Energéticas e Nucleares, Av. Professor Lineu Prestes, 2242, Cidade Universitária, São Paulo-SP, Brasil

<sup>2</sup> Université de Poitiers, IC2MP UMR-CNRS 7285, 4, rue Michel Brunet, B27, TSA 51106 – 86073 Poitiers cedex 09 - France

boniface.kokoh@univ-poitiers.fr

Platinum is widely used as electrode catalyst in Solid Polymer Electrolyte Fuel Cells (SPE-FCs) but it is an expensive material and not abundantly available. For these reasons lots of works have concentrated to develop and search for alternative electrode materials. As platinum group metals (PGM) must be, step by step, replaced by less costly and available transition metals (TM) for a widespread application of these sustainable energy sources, efforts are being made either to decrease the noble scarce metals or to “dilute” their content with TM co-catalysts addition [1]. For this concern, palladium, that is more abundant on earth than Pt and known to have excellent ability toward the oxygen reduction reaction (ORR), is herein used as cathode material in a H<sub>2</sub>/O<sub>2</sub> SPE-FC. Understanding the material structure provides relevant information on its catalytic properties. On this objective, carbon supported PdM (M = Cu, Ni and Ag) nanomaterials were synthesized from the microwave-assisted heating method [2]. The crystal structure and crystallite size, the chemical composition and morphology of the homemade catalysts were performed with various physicochemical techniques prior to their electrochemical characterization with O<sub>2</sub>-saturated diary electrolytes.

The presentation will look at the electrical performances a 5 cm<sup>2</sup> single SPE-FC at 80 °C using low catalysts loadings (0.4 mg cm<sup>-2</sup>) in the membrane electrode assembling. As finding, the microwave heating method has been successfully used for preparing Pd-based cathode materials with small particle size, which deliver 480 mW cm<sup>-2</sup> at 1.4 A cm<sup>-2</sup>.

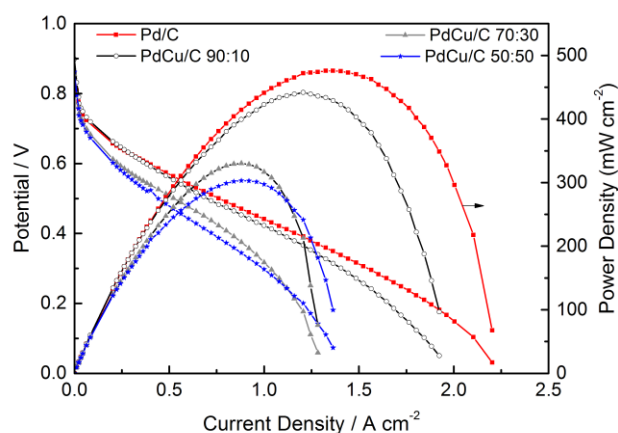


Figure 1. Cell voltage and power density obtained in a 5 cm<sup>2</sup> single H<sub>2</sub>/O<sub>2</sub> SPE-FC with Nafion<sup>®</sup> 115 membrane at 80 °C: (-) Pt (0.4 mg cm<sup>-2</sup>) / H<sub>2</sub> (3 atm) // O<sub>2</sub> (3 atm) / PdM (0.4 mg cm<sup>-2</sup>) (+).

**Acknowledgments:** The authors gratefully acknowledge financial support from the French National Research Agency ChemBio-Energy and CAPES foundation for providing a Travel scholarship to R.A. Isidoro

[1] J. Wu, H. Yang, Platinum-Based Oxygen Reduction Electrocatalysts, *Acc. Chem. Res.*, 46 (2013) 1848-1857.

[2] T.S. Almeida, L.M. Palma, P.H. Leonello, C. Morais, K.B. Kokoh, A.R. De Andrade, An optimization study of PtSn/C catalysts applied to direct ethanol fuel cell: Effect of the preparation method on the electrocatalytic activity of the catalysts, *J. Power Sources*, 215 (2012) 53-62.

# A Novel Approach to Develop MIEC material: CeO<sub>2</sub>-ZrO<sub>2</sub> composite

Aditya Maheshwari and Hans-Dieter Wiemhöfer

*Institute of Inorganic and Analytical Chemistry, University of Muenster, Germany.*

*Corrensstrasse 28/30, 48149 Muenster*

*e-mail address: [a.maheshwari@uni-muenster.de](mailto:a.maheshwari@uni-muenster.de) (A. Maheshwari)*

*[hdw@uni-muenster.de](mailto:hdw@uni-muenster.de) (H.-D. Wiemhöfer)*

Mixed ionic electronic conductors (MIECs) such as doped ceria as well as zirconia have been studied for their applications in a wide range as anode additives, electro catalysis, gas separators etc. [1-5]. Although with the acceptor doping, ceria shows a good MIEC behavior but only at very low oxygen partial pressures, where Ce<sup>4</sup> reduces to Ce<sup>3+</sup> generating electrons. In this case electronic conductivity becomes nearly equal to the ionic conductivity in the range of 10<sup>-10</sup>-10<sup>-15</sup> bar *p*(O<sub>2</sub>). However, at normal *p*(O<sub>2</sub>), acceptor doped ceria has a negligible electronic conductivity. On the contrary, in donor doped ceria, ionic conductivity is negligible at normal *p*(O<sub>2</sub>). Mixing the two effects by doping with donor+acceptor dopants does not enhance the MIEC behavior but decreases the effective conductivity due to the cancellation of the opposite effects from donor and acceptor dopants [6].

In the present work, an approach to produce MIEC CeO<sub>2</sub>-ZrO<sub>2</sub> composite materials is developed. In past, these ceria-zirconia composites drew a great deal of attention as additive layers between the electrolyte and electrode. However, the most emphasis has been given to the ionic conductivity [7-9] and not a substantial research has been done on developing these CeO<sub>2</sub>-ZrO<sub>2</sub> composites as MIEC materials. The present work addresses this approach and for this purpose, Ta<sup>5+</sup> doped ceria (TDC) and YSZ, well-known electronic and ionic conductors, respectively, have been taken as base oxide materials. The samples are prepared *via* classical mixed-oxide route using Acetone as medium. The powders were dried/calcined at 400 °C and subsequently pressed in the form of circular pellets. Pressed pellets were sintered and then used for impedance and Hebb-Wagner measurements.

The samples with TDC to YSZ weight ratio of 1:1 and 2:1 were investigated, as a first step. The samples showed conductivities lower than that of each of the two separate constituents, TDC and YSZ. This can be attributed to a highly resistive interface between the ceria and zirconia particles. In order to decrease this interface resistivity, in a first attempt the electronic resistance was reduced by doping 1 mol% Co. A further reduction in the grain boundary resistivity was achieved by adding 20 wt% Na<sub>2</sub>CO<sub>3</sub>. We attribute this to an additional improvement of the ionic part of the grain boundary conductivity. The results overall showed a nearly 10 times higher conductivity with Co<sup>2+</sup> and a nearly 10 000 times higher conductivity after Na<sub>2</sub>CO<sub>3</sub> addition in the final TDC-YSZ composite. Furthermore, to combine the separate effects of Co and Na<sub>2</sub>CO<sub>3</sub>, the composites with 1 mol% Co + Na<sub>2</sub>CO<sub>3</sub> addition were prepared and investigated for their total and electronic conductivities, separately. The amounts of both the additives were optimized afterwards and final doped TDC-YSZ sample showed a good ionic as well as electronic conductivities. Hence, the use of both CoO and Na<sub>2</sub>CO<sub>3</sub> as additives leads to a greatly optimized mixed conducting ceramic composite with a remarkably increased net conductivity for ions and electrons in the intermediate temperature range. A detailed overview will be provided in the presentation during the meeting.

## References:

- [1] H. Inaba, H. Tagawa, Solid State Ionics, 83 (1996) 1-16.
- [2] S.R. Bishop, T.S. Stefanik, H.L. Tuller, Journal of Materials Research, 27 (2012) 2009-2016.
- [3] J. Sunarso, S. Baumann, J.M. Serra, W.A. Meulenbergh, S. Liu, Y.S. Lin, J.C. Diniz da Costa, Journal of Membrane Science, 320 (2008) 13-41.
- [4] J.-P. Eufinger, M. Daniels, K. Schmale, S. Berendts, G. Ulbrich, M. Lerch, H.-D. Wiemhofer, J. Janek, Physical Chemistry Chemical Physics, 16 (2014) 25583-25600.
- [5] M. Mogensen, N.M. Sammes, G.A. Tompsett, Solid State Ionics, 129 (2000) 63-94.
- [6] A. Maheshwari, M. Daniels, K. Schmale, H.-D. Wiemhöfer, International Proceedings of Computer Science & Information Technology, 56 (2012).
- [7] T. Kawada, H. Yokokawa, M. Dokiya, N. Sakai, T. Horita, J. Van Herle, K. Sasaki, J. Electroceram., 1 (1997) 155-164.
- [8] Y. Mishima, H. Mitsuyasu, M. Ohtaki, K. Eguchi, J. Electrochem. Soc., 145 (1998) 1004-1007.
- [9] A. Tsoga, A. Gupta, A. Naoumidis, P. Nikolopoulos, Acta Materialia, 48 (2000) 4709-4714.



# **The Effect of NiO on the Conductivities of $\text{BaZr}_x\text{Ce}_{0.8-x}\text{Y}_{0.2}\text{O}_{3-\delta}$ ( $x = 0.5, 0.6, 0.7, 0.8$ ) Proton Conductors**

Junfu Bu, Pär Göran Jönsson, Zhe Zhao

*Department of Materials Science and Engineering, KTH Royal Institute of Technology, SE-100 44*

*Stockholm, Sweden*

[junfu@kth.se](mailto:junfu@kth.se)

The effects of NiO on the sintering behaviors, morphologies and conductivities of  $\text{BaZr}_x\text{Ce}_{0.8-x}\text{Y}_{0.2}\text{O}_{3-\delta}$  ( $x = 0.5, 0.6, 0.7, 0.8$ ) proton conductors were systematically investigated. 1 wt.% NiO powder was added by different methods during the sample preparations: (i) added during ball-milling before powder mixture calcination, (ii) no NiO addition in the whole preparation procedure and (iii) added after powder mixture calcination. The conductivities of these dense  $\text{BaZr}_{0.5}\text{Ce}_{0.3}\text{Y}_{0.2}\text{O}_{3-\delta}$  (BZCY532),  $\text{BaZr}_{0.6}\text{Ce}_{0.2}\text{Y}_{0.2}\text{O}_{3-\delta}$  (BZCY622),  $\text{BaZr}_{0.7}\text{Ce}_{0.1}\text{Y}_{0.2}\text{O}_{3-\delta}$  (BZCY712) and  $\text{BaZr}_{0.8}\text{Y}_{0.2}\text{O}_{3-\delta}$  (BZCY802) ceramics were investigated in dry air, wet  $\text{N}_2$  and wet  $\text{H}_2$  atmospheres, respectively. Furthermore, their electronic conduction were also identified in a broad oxygen partial pressure range from 1 atm to  $10^{-24}$  atm. According to current achieved results, it can be concluded that it is preferable to add the NiO during powder preparation, which can lower the sintering temperature and also increase the conductivity of BZCY532-based electrolytes.

# Effects of H<sub>3</sub>PO<sub>4</sub> leaching on the performance and degradation of high temperature-proton exchange membrane fuel cells

**Lung-Yu Sung, Kan-Lin Hsueh, Shu-Mei He, Wen-Sheng Chang**

*Green Energy and Environment Research Labs, Industrial Technology Research Institute  
Bldg.64, No.195, Sec.4, Chung Hsing Rd., Chutung, Hsinchu, 31040, Taiwan  
[richardsung@itri.org.tw](mailto:richardsung@itri.org.tw)*

## Abstract

The impact of H<sub>3</sub>PO<sub>4</sub> electrolyte leaching on the performance and degradation of polybenzimidazole fuel cells were investigated in the temperature range of 120~190 °C without gas humidified. From test results of cell performance indicated that the best cell's assembly pressure and operating temperature are at 60 kgf-cm and 180 °C, while the cell has a minimum internal impedance (~4 mΩ). The cell was operated over 600 hrs continuously at high current loading (500 mA/cm<sup>2</sup>), the cell's average voltage decay rate was 1.58 mV h<sup>-1</sup>. The H<sub>3</sub>PO<sub>4</sub> content in water discharged from the cell outlet was measured by using acid-base titration method. The amount of H<sub>3</sub>PO<sub>4</sub> on the cathode side is 3.5 times on the anode side, and the total amount of H<sub>3</sub>PO<sub>4</sub> leaching was about 30 mg. Further from the electrochemical impedance spectroscopy (EIS) analysis, we found that the cell's internal resistance and charge transfer resistance are increased significantly with the H<sub>3</sub>PO<sub>4</sub> leaching. However, there is no mass transfer limiting behavior observed on Nyquist plots at low frequencies region. These results are quite in consistent to the cell's IV polarization curve.

## References

- [1] Q. Li, J.O. Jensen, R.F. Savinell, N.J. Bjerrum, "High temperature proton exchange membranes based on polybenzimidazoles for fuel cells," *Progress in Polymer Science*, 34, pp. 449-477 (2009).
- [2] C. Yang, P. Costamagna, S. Srinivasan, J. Benziger, A.B. Bocarsly, "Approaches and technical challenges to high temperature operation of proton exchange membrane fuel cells," *J. Power Sources*, 103, pp. 1-9 (2001).
- [3] W.L. Harrison, M.A. Hickner, Y.S. Kim, J.E. McGrath, "Poly(arylene ether sulphone) copolymers and related systems from disulphonated monomer building blocks: synthesis, characterization, and performance-a topical review," *Fuel Cells*, 5, pp. 201-212 (2005).
- [4] T. Ogoshi, Y. Chujo, "Organic-inorganic polymer hybrids prepared by the sol-gel method," *Compos. Interf.*, 11, pp. 539-66 (2005).
- [5] Q. Li, R. He, J.O. Jensen, N.J. Bjerrum, "PBI-based polymer membranes for high temperature fuel cells-preparation, characterization and fuel cell demonstration," *Fuel Cells*, 4, pp. 147-159 (2004).
- [6] S. Aharoni and M. Litt, "Synthesis and some properties of poly-(2,5-trimethylene benzimidazole) and poly-(2,5-trimerhylene benzimidazole hydrochloride)," *J. Polymer Science Part A: Polymer Chemistry*, 12, pp. 639-650 (1974).
- [7] J. S. Wainright, J. T. Wang, D. Weng, and R. F. Savinell, "Acid-doped polybenzimidazoles: a new polymer electrolyte," *J. The Electrochemical Society*, 142, pp. L121 (1995).
- [8] B. Xing and O. Savadogo, "Hydrogen/oxygen polymer electrolyte membrane fuel cells (PEMFCs) based on alkaline-doped polybenzimidazole (PBI)," *Electrochemistry Communications*, 2, pp. 697-702 (2000).
- [9] S. R. Samms, "Thermal Stability of Proton Conducting Acid Doped Polybenzimidazole in Simulated Fuel Cell Environments," *Journal of The Electrochemical Society*, 143, pp. 1225 (1996).

# Effect of Thermal Effect on Phase Transformation of Plasma Sprayed Protective Oxides on SOFC Metallic Interconnects

Chung-Ta Ni<sup>1,2</sup>, Shu-Yi Tsai<sup>1,2</sup>, Kuan-Zong Fung<sup>1,2</sup>, Hsin-Chia Ho<sup>2</sup>

<sup>1</sup>Research Center for Energy Technology and Strategy,

<sup>2</sup>Department of Materials Science and Engineering,

National Cheng Kung University, No. 1, University Road, Tainan 70101, Taiwan, ROC

z8702009@email.ncku.edu.tw

In order to reduce the cost of solid oxide fuel cells (SOFCs), less expensive and more conductive metallic interconnects have been recently used to replace ceramic interconnects for intermediate temperature applications<sup>1-3</sup>. Metallic interconnects commonly use chromium-containing alloy that form chromia scales at high temperatures. However, chromium oxide easily reacts with perovskite cathode causing ion diffusion and degradation in electrical conduction.

To suppress the growth of chromium oxide, a protective oxide layer with adequate electronic conductivity may be thermally sprayed on the surface of metallic interconnect. Conducting oxides with either perovskite or spinel structure were deposited on metallic interconnect using thermal spray technique in this study. Due to the high deposition temperature during thermal spray coating, the structural and conduction properties of the protective oxides are strongly affected by the thermal spray process. For example, the dramatic change in temperature during thermal spray may change the crystal structure and then conductivity of protective oxide.

Thus, the objective of this work is to investigate the effect of thermal reduction/oxidation on the structural properties of protective oxides. The crystal structure, morphology and electrical conduction of oxide films and metallic substrate were examined by using XRD, FESEM and resistance measurement.

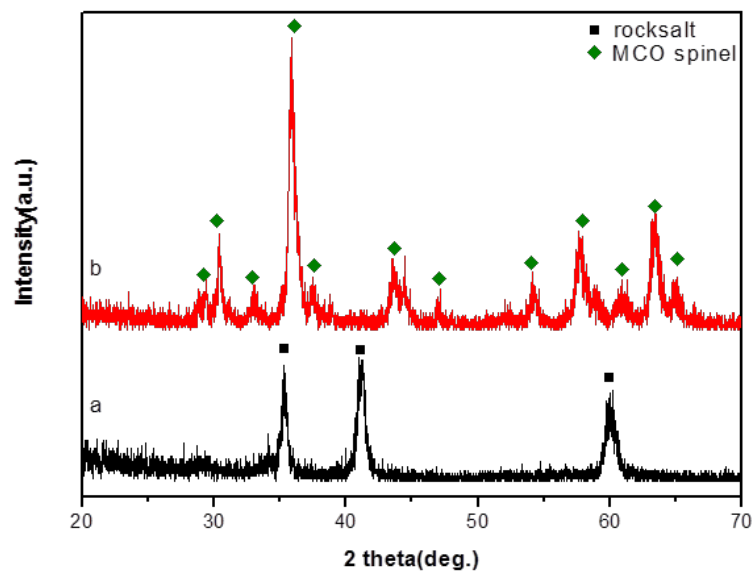


Figure 1. XRD trace of MCO spinel powder prepared from oxides.

## References

1. T. Horita, Y. Xiong, K. Yamaji, N. Sakai, and H. Yokokawa, *J. Electrochem. Soc.*, **150**, A243-8 (2003).
2. T. Brylewski, M. Nanko, T. Maruyama, and K. Przybylski, *Solid State Ion.*, **143** 131-50 (2001)
3. S. Linderorth, P. V. Hendriksen, M. Mogensen, and N. Langvad, *J. Mater. Sci.*, **31**, 5077-82 (1996).

# Effect of Composite Cathode on Polarization Reduction for Solid Oxide Fuel Cells based on Microstructure and Ion-Conduction Consideration

Shu-Yi Tsai<sup>1,2</sup>, Chung-Ta Ni<sup>1,2</sup>, Kuan-Zong Fung<sup>1,2</sup>, Yu-Fan Chang<sup>2</sup>

<sup>1</sup>Research Center for Energy Technology and Strategy,

<sup>2</sup>Department of Materials Science and Engineering,

National Cheng Kung University, No. 1, University Road, Tainan 70101, Taiwan, ROC

*z8702009@email.ncku.edu.tw*

Solid oxide fuel cells(SOFCs) have been known as the desired conversion devices for electricity generation by an electrochemical reaction of a fuel with an oxidant. In SOFC, oxygen ion conductors are commonly used as the electrolytes. Among several oxygen ion conductors such as CeO<sub>2</sub>, stabilized Bi<sub>2</sub>O<sub>3</sub> and ZrO<sub>2</sub>, Bi<sub>2</sub>O<sub>3</sub>-based systems show the highest oxygen ion conductivity. The resistance of Bi<sub>2</sub>O<sub>3</sub> against reduction may be enhanced by the addition of proper dopants. However, the OCV of SOFC using Bi<sub>2</sub>O<sub>3</sub>-based electrolyte is still too low to be practical. On the contrary, Bi<sub>2</sub>O<sub>3</sub>-based system may become a good ionic component for a composite cathode.

In this study, Y<sub>2</sub>O<sub>3</sub>-stabilized Bi<sub>2</sub>O<sub>3</sub> (YSB) is mixed with Sr-doped LaMnO<sub>3</sub> (LSM) to form a composite cathode. The volume fraction and size effect of LSM on the polarization resistance were investigated at various temperatures ranging from 500°C to 650°C using a symmetric cell consisting of LSM-YSB composite electrodes on both side of the electrolyte.

The reduced polarization measured from composite cathode was observed from the samples that mixed YSB with very fine LSM powder. Compared to submicron-sized LSM, the polarization resistance measured from nano-sized LSM-YSB composite electrodes is 50% lower at 650°C. It is believed that the composite cathode with desired nanostructure is able to extend triple phase boundary and provide numerous reaction sites for electrochemical reaction to occur. In additions, the composite electrodes using LSM-YSB combination also shows lower polarizations than LSM-SDC and LSM-YSZ combinations

# Conductive oxide supported Co<sub>3</sub>O<sub>4</sub> nanocomposite as robust catalysts for oxygen reduction and evolution reaction

Hsiao-Chun Huang<sup>†</sup>, Chun-Jern Pan<sup>†</sup>, Wei-Nien Su<sup>§</sup> and Bing-Joe Hwang<sup>\*†</sup>

<sup>†</sup>*Department of Chemical Engineering, National Taiwan University of Science and Technology, Taipei 106, Taiwan, R. O. C.*

<sup>§</sup>*Graduate Institute of Applied Science and Technology, National Taiwan University of Science and Technology, Taipei 106, Taiwan*

[bjh@mail.ntust.edu.tw](mailto:bjh@mail.ntust.edu.tw)

Oxygen reduction reaction (ORR) and oxygen evolution reaction (OER) are the heart of several renewable energy technologies such as water electrolysis, metal-air batteries, and fuel cells. Recently, carbon supported Ru based catalysts have been reported as high performance catalyst for oxygen evolution reaction. However, Ru based catalysts suffers from high cost and severe degradation in electrocatalytic activity after long term operation.

In this study, we synthesized transition metal doped TiO<sub>2</sub> via solvothermal synthesis as electrocatalyst support in alkaline media. The metal-doped TiO<sub>2</sub> (M-TiO<sub>2</sub>) is expected to exhibit high stability at operational conditions and can be used as a bifunctional support for both ORR and OER reaction. Then, cobalt oxide will be deposited on transition metal doped TiO<sub>2</sub> as co-catalyst via hydrothermal processes. The cobalt oxide M-TiO<sub>2</sub> nanocomposite shows high activity and stability for both OER and ORR reaction compared to bare cobalt oxide and M-TiO<sub>2</sub> support. The catalytic enhancement might be resulted from the synergic effect between cobalt oxide and M-TiO<sub>2</sub> support. The developed nanocomposite would be a promising system to replace Pt and can be adapted as bifunctional catalysts for both oxygen reactions.

# Preparation of Highly Conductive TiO<sub>2</sub> Supported Pt Catalyst and Its Electrochemical Performance

Chen-Yu Tsai<sup>a</sup>, Yi-Chen Wu<sup>a</sup>, Men-Che Tsai<sup>a</sup>, Chun-Jern Pan<sup>a</sup>, Bing-Joe Hwang<sup>a\*</sup>

<sup>a</sup>*Department of chemical engineering, National Taiwan University of Science and Technology  
No.43, Sec. 4, Keelung Rd., Da'an Dist., Taipei 106, Taiwan (R.O.C.)  
bjh@mail.ntust.edu.tw*

The long-term performance of polymer electrolyte membrane fuel cells (PEMFCs) that depend on the stability of support can be improved by using highly stable metal oxides to replace carbon which occurs electrochemically corrode during cell operation. In this work, highly-conductive TiO<sub>2</sub> supported Pt catalysts were synthesized and electrochemical performance was investigated for use in fuel cell application. First, TiO<sub>2</sub> nanoparticles were synthesized using a solvothermal method. SiO<sub>2</sub> coating was then applied to the TiO<sub>2</sub> nanoparticle surface by using the Hexamethyldisilazane method (HMDS) in order to inhibit the particle growth during heat treatment under H<sub>2</sub> environment. The phase of TiO<sub>2</sub> nanoparticles changed from anatase phase to rutile phase and eventually transformed to Magnéli phase when the temperature rises to 1000°C. It was found that the electrical conductivity of TiO<sub>2</sub> increases with increasing reduction temperature but at the cost of decrease in the surface area. The electrochemical performance shows that Pt catalyst, loaded on the TiO<sub>2</sub> support which is treated by the HMDS method and H<sub>2</sub> reduction, exhibits the good reactivity for methanol oxidation reaction (MOR) and oxygen reduction reaction (ORR). Such performance is attributed to a higher surface area and improved electrical conductivity. Durability test show that TiO<sub>2</sub> supported Pt catalyst has better stability and anti-corrosive abilities when compared to the commercial catalyst (JM20).

# Structural Stability of Mixed Conducting $\text{La}_{0.8}\text{Ca}_{0.2}\text{Fe}_{1-x}\text{Co}_x\text{O}_3$ ( $x=0\sim 0.4$ ) Perovskite in Different Atmospheres

Chung-Ta Ni, Shu-Yi Tsai, Kuan-Zong Fung, Yu-Cheng Su, Han-Lung Liu  
*Department of Materials Science and Engineering, National Cheng Kung University*  
*No.1 University Road, Tainan City, Taiwan 70101*  
*chungtani@gmail.com*

Perovskite type  $\text{LaFeO}_3$  is a mixed ionic/electronic conductor exhibits good stability at various oxygen partial pressure, however  $\text{LaFeO}_3$  showed low conductivity which also limited its applications. The addition of aliovalent dopants is known to be an effective way to enhance the conductivity of many perovskite oxides. The objective of this work is to enhance the conductivity of  $\text{LaFeO}_3$  by using the method of double doping in perovskite's cation sublattices. For instance, Ca ions was added into A-site cation sublattice for substitution of La ions. On the other hand, Co ions were added into B-site cation sublattices for substitution of Fe ions. The samples were prepared using solid state reaction method based on the formula of  $\text{La}_{0.8}\text{Ca}_{0.2}\text{Fe}_{1-x}\text{Co}_x\text{O}_3$  ( $x=0\sim 0.4$ ). After sintering at  $1300^\circ\text{C}$ , the powder compacts with various compositions were densified. All the  $\text{La}_{0.8}\text{Ca}_{0.2}\text{Fe}_{1-x}\text{Co}_x\text{O}_3$  samples showed typical p-type semiconducting behavior with increasing conductivities at higher temperatures. The addition of Co tends to enhance the conductivity of  $\text{La}_{0.8}\text{Ca}_{0.2}\text{FeO}_3$ . When 40% of B-site cation sublattice was replaced by Co ions, the conductivity of  $\text{La}_{0.8}\text{Ca}_{0.2}\text{Fe}_{1-x}\text{Co}_x\text{O}_3$  was enhanced from 90 S/cm to 255 S/cm. However, the stability of  $\text{La}_{0.8}\text{Ca}_{0.2}\text{Fe}_{1-x}\text{Co}_x\text{O}_3$  tends to decrease with increasing amount of Co addition. For instance, 40% Co-doped  $\text{La}_{0.8}\text{Ca}_{0.2}\text{Fe}_{1-x}\text{Co}_x\text{O}_3$  was found to decompose into  $\text{La}_2\text{O}_3$  and metallic Co, Fe when the sample was heat-treated with 10% $\text{H}_2$  at  $800^\circ\text{C}$ . The enhancement in conductivity and instability in reducing atmosphere will be rationalized in light of defect chemistry and bond strength between the transition metal and oxygen ions.

## References

1. D. Bayraktar, F. Clemens, S. Diethelm, T. Graule, Jan Van herle, P. Holtappels, J. of the European Ceram. Soc., 27, [6], (2007), 2455
2. S. Diethelm, J. Van herle, P.H. Middleton, D. Favrat, J of Power Sources, 118, [1–2], (2003), 270

# Rotating Disk Electrode Studies on the Effect of Nafion on the Oxygen Reduction Reaction for Pt/C and Pt Alloy/C

Kazuma Shinozaki<sup>a, b, c</sup> and Shyam S. Kocha<sup>a</sup>

<sup>a</sup> National Renewable Energy Laboratory, Golden, CO 80401, USA.

<sup>b</sup> Colorado School of Mines-Department of Chemistry, Golden, CO 80401, USA.

<sup>c</sup> Toyota Central R&D Labs., Inc., Nagakute, Aichi, 480-1192, Japan.

kshinoza@mines.edu, shyam.kocha@nrel.gov

The effect of Nafion on oxygen reduction reaction (ORR) activity of proton exchange membrane fuel cell catalysts has recently been studied by using rotating disk electrode (RDE) methods on single crystalline, polycrystalline Pt surfaces and nanostructured thin film (3M NSTF) in 0.1 M HClO<sub>4</sub> [1-5]. In these studies, thin ionomer films (nm to 10's of nm) were applied to the electrode surfaces by capping with ionomer. A positive shift on the onset potential for OH and other oxide species formation and a suppression of the ORR activity is typically observed after capping. Subbaraman et al. [1] attributed the features observed on cyclic voltammograms under inert atmosphere to sulfonate anion adsorption on Pt surfaces using a CO displacement method. In addition, based on the parallel activity trend on Pt (111), (110) and (100) surfaces with that obtained in sulfuric acid solution, they concluded that sulfonate anion adsorption was the main cause for lowered ORR activity. In contrast to these detailed kinetics studies on well-defined Pt surfaces, little work has been reported on Pt/C catalysts [6]. The lack of studies can be considered as a consequence of following aspects: (i) ionomer inclusion in a catalyst ink tends to increase ink dispersion in sonication (ii) elimination of ionomer from the ink can result in poor catalyst film quality (iii) ionomer is often used to glue catalysts on substrate surfaces such as glassy carbon [7]. However, we have recently discovered that ionomer is not necessary to obtain well-dispersed stable thin catalyst films [8]. Moreover, the use of extremely thin and uniform films is indispensable to the kinetics study of ORR catalysts without hindrance from O<sub>2</sub> diffusion limitations within the catalyst layer.

In this work, we have investigated the effect of Nafion ionomer on the ORR activity as well as CVs under inert atmosphere for several commercial Pt/C and Pt Alloy/C catalysts by employing thin-uniform catalyst films obtained by advanced film fabrication techniques [8]. Nafion capped catalyst films were obtained by applying a diluted Nafion solution on Nafion-free films followed by drying in air at 23°C. Figure 1 depicts ionomer to carbon (I/C) ratio dependence of the specific activity of various catalysts at 0.9 V vs. RHE in 0.1 M HClO<sub>4</sub>.

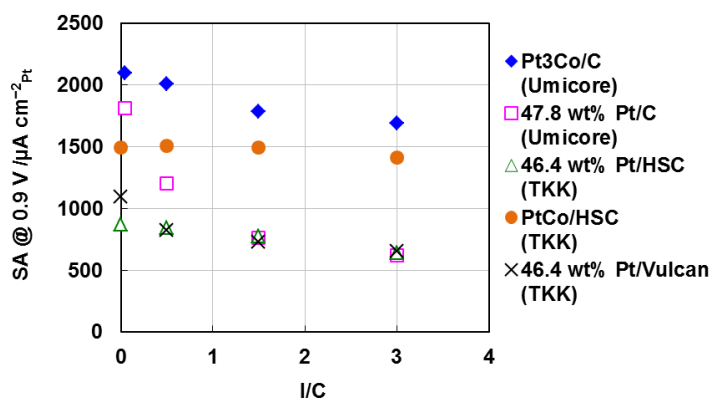


**Figure 1.** I/C dependence of SA for Pt/C and PtCo/C catalysts (0.1 M HClO<sub>4</sub>, 20 mVs<sup>-1</sup>, -0.01 to 1.0 V, 100kPa O<sub>2</sub>, 23°C).

## References

- [1] R. Subbaraman, D. Strmcnik, V. Stamenkovic, and N. M. Markovic, *J. Phys. Chem. C*, 114 (2010) 8414.
- [2] R. Subbaraman, D. Strmcnik, A. P. Paulikas, V. R. Stamenkovic, and N. M. Markovic, *ChemPhysChem*, 11 (2010) 2825.
- [3] A. M. Gómez-Marín, A. Berná, and J. M. Feliu, *J. Phys. Chem. C*, 114 (2010) 20130.
- [4] M. Ahmed, D. Morgan, G. A. Attard, E. Wright, D. Thompsett, and J. Sharman, *J. Phys. Chem. C*, 115 (2011) 17020.
- [5] K. Kodama, A. Shinohara, N. Hasegawa, K. Shinozaki, R. Jinnouchi, T. Suzuki, T. Hatanaka, and Y. Morimoto, *J. Electrochem. Soc.*, 161 (2014) F649.
- [6] S. S. Kocha, J. W. Zack, S. M. Alia, K. C. Neyerlin, B. S. Pivovar, *ECS Trans.*, 50 (2) (2012) 1475.
- [7] T. J. Schmidt, H. A. Gasteiger, O. D. Staeb, P. M. Urban, D. M. Kolb, R. J. Behm, *J. Electrochem. Soc.*, 145 (1998) 2354.
- [8] K. Shinozaki, B. S. Pivovar, S. S. Kocha, *ECS Trans.*, 58 (1) (2013) 15.



# Simulated Design of High-altitude Long-endurance Unmanned Aerial Vehicles using Regenerative Fuel Cell Systems

Minjin Kim, Young-Jun Sohn, and Tae-Hyun Yang  
Korea Institute of Energy Research, Fuel Cell Research Center  
152 Gajeong-ro, Yuseong-gu, Daejeon, 305-343, Republic of Korea  
minjin@kier.re.kr

Recently, unmanned aerial vehicles (UAVs) have been tried to apply to commercial missions such as meteorological observation, communication, and internet network as well as traditional military missions. Research works about high-altitude long-endurance (HALE) UAVs are especially focused on those applications. A regenerative fuel cell (RFC) system is one of solutions to achieve HALE of UAVs. RFC consist of a fuel cell, gas tanks, and water electrolysis. The RFC-solar cell hybrid system can operate without additional fuel supplement for a long time. However there are actually some limitations for the HALE UAVs based on RFC systems. Performance factors in terms of the weight and efficiency of RFC components should be more improved. In this study, feasibilities of HALE for RFC based UAVs have been checked on the current technology basis. In detail, flight stability of the RFC hybrid UAV according to the architecture and component's specifications has been known. Furthermore some solutions for substantial and stable HALE of the target UAV are considered.

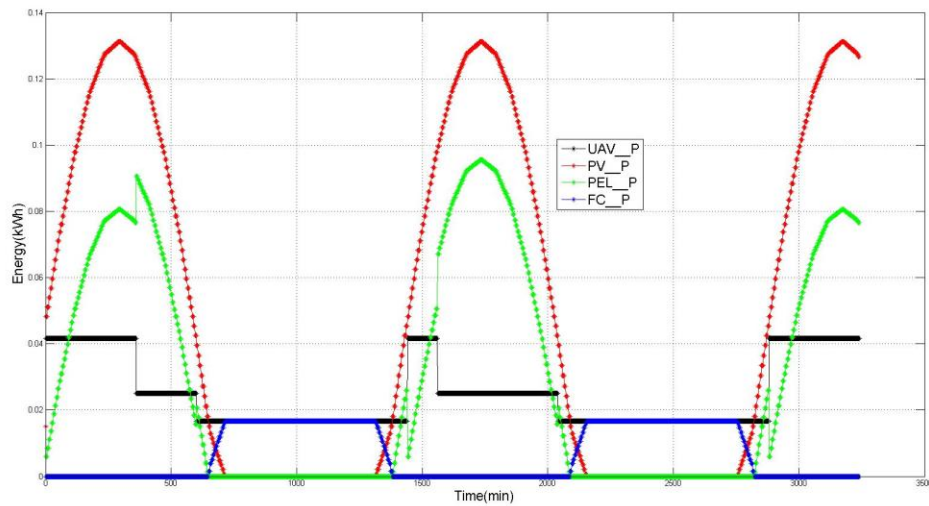


Fig. 1. The stability of flying for unmanned aerial vehicles using regenerative fuel cell.

# Synthesis and characterization of electrocatalysts PtSnEu/C for anode in direct alcohol fuel cell

Patricia Gon Corradini<sup>a\*</sup>, Nathalia Abe Santos<sup>a</sup>, Valdecir Paganin<sup>a</sup>, Ermete Antolini<sup>b</sup> and Joelma Perez<sup>a</sup>

<sup>a</sup>Instituto de Química de São Carlos, USP, C.P.780, São Carlos, SP 13560-970, Brazil

<sup>b</sup>Scuola di Scienza dei Materiali, Via 25 aprile 22, 16016, Cogeletto, Genova, Italy

\*patcorradini@gmail.com

The demand for power sources for portable and stationary applications is increasing significantly. Fuel cell (FC) systems with higher energy density are seen as a potential candidate to fill the growing gap between energy demand and supply for mobile applications. [1] The direct ethanol fuel cell (DEFC) has attracted much attention from researchers and manufacturers, and several efforts were implemented to improve its performance of catalysts electro-activity for ethanol oxidation. Several studies based on bimetallic catalysts reported that the best catalyst is PtSn, since it has higher current densities and ethanol oxidation reaction (EOR) has lower onset potential than on platinum. The modified PtSn/C electrodes with rare earths gradually have been reported to improve the EOR kinetics. [2] This paper evaluated the effect of Eu addition on the catalytic activity and stability of PtSn/C catalysts. The PtSnEu/C catalysts were obtained by a modification of polyol procedure propose by Sun *et al.*[3] All materials are 20 wt% of metal (Pt+Sn+Eu) on carbon, and different metal atomic proportions were evaluated. All catalysts were characterized by EDX, XDR, TEM and XPS. The XRD patterns of commercial Pt/C and PtSn/C; and different PtSnEu/C catalysts are shown in Fig.1a. For all catalysts, the first peak is the diffraction of the (002) plane of the hexagonal structure of carbon. The diffraction peaks at around 39, 46, 68 and 81° are corresponding to Pt (111), (200), (220) and (311) planes, respectively, which indicates that the Pt exists in the face centered cubic (fcc) phase. The diffraction peak of the (220) plane on PtSn/C and different PtSnEu/C catalysts slightly shifts to lower  $2\theta$  values with respect to the corresponding peak on Pt/C, indicated the incorporation of Sn atom into the lattice of Pt. Although the diffraction peaks associated with metallic Sn and Eu or their oxides do not appear in the patterns, their presence cannot be discarded since Sn and Eu may appear in the form of PtSn alloy or their oxides with amorphous structure. DEFC polarization and power density curves at 90 °C using Pt/C, PtSn/C and PtSnEu/C as anode catalysts are shown in Fig. 1b. The DEFC with PtSnEu/C as anode catalysts showed the best performance for all current densities. The PtSnEu (70:15:15) showed the power density around 13 mW cm<sup>-2</sup> at 35 mA cm<sup>-2</sup>. The experimental results revealed that the addition of Eu to PtSn/C catalyst can significantly enhance the catalytic activity for ethanol oxidation. Probably, the europium oxides can promote the formation of OH species, which facilitate the removal of adsorbed intermediates, and to improve the PtSn/C catalytic. [4]

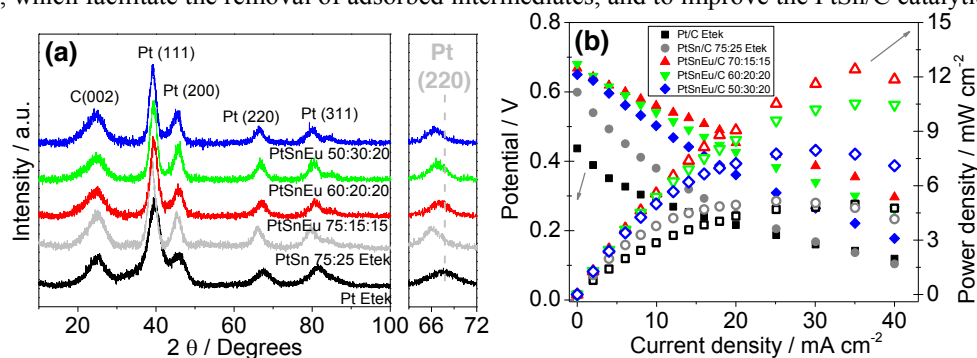


Figure 1. (a) X-ray diffraction patterns for PtSnEu/C electrocatalysts. (b) Polarization and power density curves obtained in a single DEFC with Pt/C, PtSn/C and PtSnEu/C as anode electrocatalysts for ethanol oxidation at 90 °C and 3 atm O<sub>2</sub> pressure, using a 1 mol L<sup>-1</sup> ethanol solution. Cathode: 30 wt% Pt/C. Metal loading for anode and cathode: 1 mg<sub>Pt</sub> cm<sup>-2</sup>.

Acknowledgments: Fapesp (Process: 2012/12189-8; 2013/17549-5 and 2013/16930-7), CNPq and Capes

## References

- [1] S. Abdullah, S.K. Kamarudin, U.A. Hasran, M.S. Masdar, W.R.W. Daud, J Power Sources, 262 (2014) 401-406.
- [2] J.M. Jacob, P.G. Corradini, E. Antolini, N.A. Santos, J. Perez, Appl Catal B-Environ, 165 (2015) 176-184.
- [3] S. Sun, C.B. Murray, D. Weller, L. Folks, A. Moser, Science, 287 (2000) 1989-1992.
- [4] F. Wang, Y. Zheng, Y. Guo, Fuel Cells, 10 (2010) 1100-1107.

# Development of a cathode material for durable PEFC through the encapsulation of Pt into carbon mesopores

Akari Hayashi<sup>a,b,c,d</sup>, Yasuto Minamida,<sup>b</sup> Zhiyun Noda,<sup>a,b</sup> and Kazunari Sasaki<sup>a,b,c,d</sup>  
Kyushu University <sup>a</sup>International Research Center for Hydrogen Energy, <sup>b</sup>Faculty of Engineering,  
<sup>c</sup>WPI-I2CNER, <sup>d</sup>NEXT-FC  
744 Motooka Nishi-ku Fukuoka 819-0395, Japan  
hayashi.akari.500@m.kyushu-u.ac.jp

Reduction of Pt active sites over time is a serious issue for practical use of PEFC. A few nanometer Pt particles on carbon supports have tendency to agglomerate, or dissolve and re-precipitate to under the potential change, resulting in formation of larger particles. In this study, suppressing such Pt particle growth and then increasing durability of electrocatalysts are targeted by reducing the mobility of Pt particles on the carbon support. Principally, Pt particles are introduced into nanochannels of mesoporous carbon (MC), whose diameter is ca. 10 nm. The idea comes from increased stability on the curved surface comparing to flat surface. This idea is also supported by theoretical study.<sup>1</sup>

Electrocatalysts were synthesized from platinum(II) acetylacetonate as a precursor by supporting ca. 30 wt% Pt on our original MC, which was made from the self-organization formaldehyde/resorcinol and Pluronic F127.<sup>2</sup> The resulting electrocatalyst was named as Pt/MC and used as a cathode catalyst. For the anode, a commercially available Pt/Ketjen black catalysts (TEC10E50E, TKK Corp.) was in use. Membrane electrode assemblies (MEAs) were prepared by spraying the dispersion containing catalyst and Nafion ionomer on both sides of Nafion membrane. For the comparison, Pt deposited on commercial available Vulcan XC72 carbon black (Pt/VC) was also made and used as a cathode catalyst.

Current-voltage (IV) characteristics of MEAs were measured in this study. Initial IV characteristic of Pt/MC-MEA resulted in same as that of Pt/VC-MEA after optimizing the MEA preparation condition. In order to evaluate durability of MEAs, accelerating degradation tests were performed using potential cycles between 0.6 and 1.0 V vs RHE, where dissolution and re-precipitation of Pt particles occur.<sup>3</sup> During the durability evaluation, IV performance of Pt/MC-MEA momentarily went down probably owing to the flooding problem. Therefore, ohmic loss, concentration loss, and overvoltage were analyzed separately after ohmic resistance was found by impedance measurements. As expected, increase in concentration loss, most likely derived from the flooding, was observed when IV performance went down momentarily. When the change in overvoltage was compared, the overvoltage was lower for Pt/MC-MEA than Pt/VC-MEA in all the cases after 5000, 20000, and 40000 cycles. Therefore, encapsulation of Pt nanoparticles into carbon nanochannels was successfully increased durability.

Change in size of Pt particles before and after 40000 potential cycles was evaluated by TEM images. As seen Figure 1, the size of Pt particles in Pt/MC increased after the potential cycle, but some of them increased more and others did less. Then, surface and transmitted images were obtained at the same position in order to evaluate Pt size change inside the nanochannels, and so the growth of Pt particles was found much suppressed within the nanochannels, which is most likely due to reduced Pt mobility inside the nanochannels.

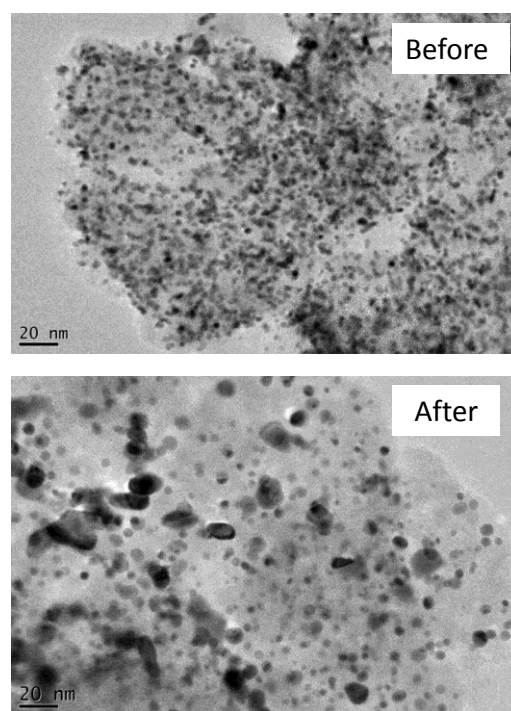


Figure 1. TEM images of Pt/MC cathode before and after the potential cycle test.

- [1] A. Staykov et al., *J. Phys. Chem. C*, 118, 8907 (2014)
- [2] A. Hayashi et al., *Electrochim. Acta*, 53(21) 6117 (2008)
- [3] A. Ohma et al., *ECS Trans.*, 41, 755 (2011)

# Role of Interfaces of Au@Pt Nanoparticles in the Electrocatalysis of Alcohol Oxidation

Lingyi Peng, Hao Yang, Jia Li, Hongda Du, Lin Gan\*

*Division of Energy and Environment, Graduate school at Shenzhen, Tsinghua University, Shenzhen 518055, PR China*

*Email: lgan@sz.tsinghua.edu.cn*

Pt monolayers deposited on gold substrate (denoted as Au@Pt<sub>ML</sub>) have shown promising electrocatalytic activities on alcohol electro-oxidation due to the previously established lattice strain effect.<sup>1</sup> While Au@Pt<sub>ML</sub> have been constructed by under potential deposition of a Cu monolayer on Au{111} single crystal and subsequent galvanic displacement by Pt, the Pt overlayers deposited on Au nanoparticles in a similar way formed three-dimensional nanoclusters (denoted as Au@Pt<sub>cluster</sub>) instead of a monolayer. Such Au@Pt<sub>cluster</sub> may exhibit different electrocatalytic properties from the previously well-studied Au@Pt<sub>ML</sub> counterpart. Here, we showed that the Au/Pt interface formed by the supported Pt nanoclusters and the underling Au nanoparticles could play a previously overlooked important role during the electrocatalysis of alcohol oxidation. By increasing the coverage of the supported Pt nanoclusters on the Au nanoparticles, the specific activities for methanol oxidation and ethanol oxidation increased first and then decreased. This trend cannot be fully accounted by the previously established strain effect, but instead is in a good consistency with the trend of the Au/Pt interface density. Density functional theory calculations prove that the toxic CO<sub>ad</sub> intermediate formed during alcohol oxidation shows a higher binding energy on the Au/Pt interface than that adsorbed on the nearby Pt surface. These results suggest that the toxic CO<sub>ad</sub> intermediate could transfer from the catalytic Pt sites to the Au/Pt interface site, leading to increased available Pt sites for efficient alcohol oxidation electrocatalysis and thus increased catalytic activity.

## References

- (1) Li, M.; Liu, P.; Adzic, R. R. *The Journal of Physical Chemistry Letters* **2012**, 3, 3480.
- (2) Loukrakpam, R.; Yuan, Q.; Petkov, V.; Gan, L.; Rudi, S.; Yang, R.; Huang, Y.; Brankovic, S. R.; Strasser, P. *Phys Chem Chem Phys* **2014**, 16, 18866.
- (3) Brankovic, S. R.; Wang, J. X.; Adzic, R. R. *Surface Science* **2001**, 474, L173.

# Enhanced proton conductivity of polybenzimidazole membranes synthesized via direct-casting process for high temperature fuel cells

He-yun Du<sup>a</sup>, Shaiu-Wu Lai<sup>a</sup>, Ming-Chih Tsai<sup>b</sup>, Jyh-Chien Chen<sup>b</sup>, Chen-Hao Wang<sup>b</sup>, Li-Chyong Chen<sup>a</sup>  
and Kuei-Hsien Chen<sup>a, c</sup>

<sup>a</sup> Center for Condensed Matter Sciences, National Taiwan University, 106 Taipei, Taiwan

<sup>b</sup> Department of Materials Science and Engineering, National Taiwan University of Science and Technology, 106 Taipei, Taiwan

<sup>c</sup> Institute of Atomic and Molecular Science, Academia Sinica, 106 Taipei, Taiwan

I, Roosevelt Road, Section 4, Taipei, Taiwan 10617, R. O. C  
elle7164@gmail.com

Poly[2,2'-(p-phenylene)-5,5'-bibenzimidazole] (p-PBI) has superior tensile strength because of its para-oriented structure and has attracted much interest in recent years. However, p-PBI polymer which shows low solubility in organic solvent only can dissolved in strong acids, such as methanesulfonic acid. Consequently, a direct-casting method (also called sol-gel method) was proposed to prepare the PA doped p-PBI membrane from the high temperature polymerization solutions in polyphosphoric acid. In this study, we compared the properties of p-PBI and meta-PBI membranes that were fabricated by direct-casting method. Moreover, we investigated the performance of these membranes in high temperature proton electrolyte membrane fuel cell. The acid doping levels and proton conductivity of p-PBI membrane by direct-casting are around 30 mol PA/PRU and its proton conductivity is around  $0.2 \text{ S cm}^{-1}$  at around  $160^\circ\text{C}$ . The effects of casting process variables on membrane properties were also investigated by atomic force microscopy measurement. The enhanced single cell performance of p-PBI membrane is attributed to the high proton conductivity of p-PBI by direct-casting method.

# Synthesis and Characterization of Carbon-Based Non-Precious-Metal Cathode Catalysts from Polyimide Fine Particles

Yuta Nabae<sup>1</sup>, Teruaki Hayakawa<sup>1</sup>, Hideharu Niwa<sup>2,3</sup>, Yoshihisa Harada<sup>2,3</sup>, Masaharu Oshima<sup>3</sup>, Atsushi Matsunaga<sup>4</sup>, Aayano Isoda<sup>4</sup>, Kazuhisa Tanaka<sup>4</sup>

<sup>1</sup> Department of Organic and Polymeric Materials, Tokyo Institute of Technology, 2-12-1 S8-26 Ookayama, Meguro-ku, Tokyo 152-8552, Japan.

<sup>2</sup> Institute for Solid State Physics, The University of Tokyo, 5-1-5 Kashiwanoha, Kashiwa, Chiba 277-8581, Japan.

<sup>3</sup> Synchrotron Radiation Research Organization, The University of Tokyo, SPring-8, 1-1-1, Koto, Sayo-cho, Sayo-gun, Hyogo 679-5198, Japan.

<sup>4</sup> Toshiba Fuel Cell Power Systems Corporation, 4-1, Ukishima-cho, Kawasaki-ku, Kawasaki-shi, Kanagawa 210-0862 Japan.  
nabae.y.aa@m.titech.ac.jp

One major problem for polymer electrolyte membrane fuel cells in commercial applications is the cost and scarcity of platinum, which is used as the cathode catalyst, and the development of precious-metal-free cathode catalysts is strongly desired. We have explored the synthesis of a carbon-based catalyst from polyimide fine particles. Polyimide is a thermo resistive polymer and the morphology of precursor can be retained even after the carbonization; therefore, finer morphology can be expected.

Polyimide fine particle was prepared as shown in Figure 1. Fine nano-particles around 100-150 nm were successfully prepared. Thus obtained precursor was converted into a carbon-based catalyst by the multi-step pyrolysis<sup>1)</sup>.

Figure 2 shows the performance of a fuel cell with the developed cathode catalyst. The cell exhibits good fuel cell performance ( $1.0 \text{ A cm}^{-2}$  at 0.6 V and 80 °C) along with promising durability<sup>2)</sup>.

Thus obtained materials have been fully characterized by spectroscopy such as XPS and X-ray adsorption, and the detailed data will be discussed in the presentation.

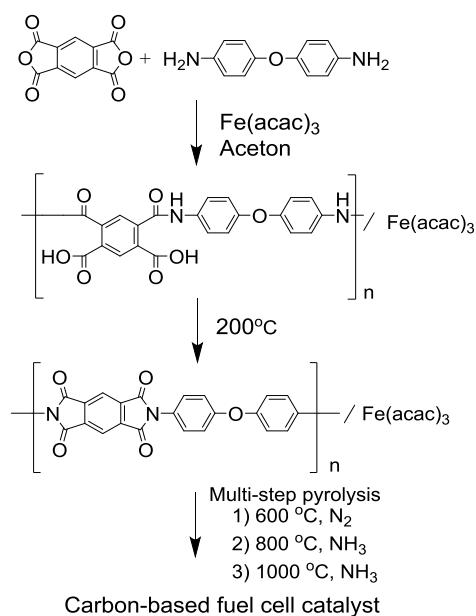


Figure 1. Schematic of material synthesis.

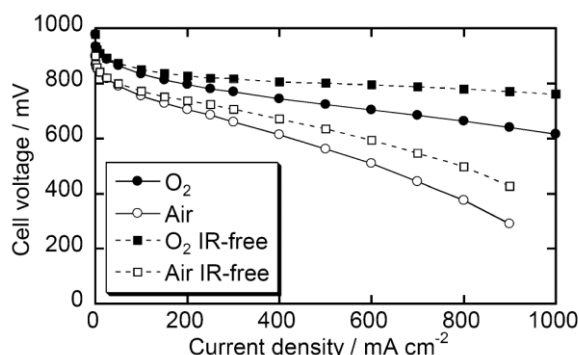


Figure 2. I-V polarization curve of the fuel cell. Cathode: the developed catalyst  $4 \text{ mg cm}^{-2}$ ;  $\text{O}_2$  or air 0.2 MPa. Anode: PtRu/C catalyst  $0.4 \text{ mg-PtRu cm}^{-2}$ ;  $\text{H}_2$  0.2 MPa. Electrolyte: Nafion NR211.  $T$ : 80 °C.

## Acknowledgements

This study was financially supported by NEDO.

## References

- 1) Nabae, Y. et al. *Catal. Sci. Technol.* **2014**, 4, 1400.
- 2) Nabae, Y. et al. *J. Mater. Chem. A* **2014**, 2, 11561.

# Fundamental Studies on Oxygen Reduction Reaction and Hydrogen Peroxide Reduction Reaction with RRDE technique

Nozomi Kawakami<sup>1</sup>, Hirohisa Yamada<sup>1</sup>, Takanori Kobayashi<sup>1</sup>, Zyun Siroma<sup>3</sup>, Katsumi Katakura<sup>1</sup> and Minoru Inaba<sup>2</sup>

<sup>1</sup>Department of Chemical Engineering, National Institute of Technology, Nara College, 22 Yata-cho, Yamatokoriyama, Nara 639-1080, Japan  
yamada@chem.nara-k.ac.jp

<sup>2</sup>Department of Molecular Chemistry and Biochemistry, Doshisha University, Miyako-dani, Tadara, Kyotanabe, Kyoto 610-0321, Japan

<sup>3</sup>National Institute of Advanced Industrial Science and Technology (AIST), Osaka 563-0026 Japan

## 1. Introduction

Polymer electrolyte fuel cells (PEFCs) are expected as one of the clean, highly effective energy conversion systems, and are developed intensively. However many problems remain to be solved before commercialization of PEFCs. Hydrogen peroxide formation at anode and cathode in PEFCs is one of the most important issues for the durability of the MEA in PEFC. We reported that larger amount of hydrogen peroxide formed as an intermediate in oxygen reduction reaction (ORR) on the electrode with lower catalyst loadings<sup>1, 2)</sup>. In present study, we evaluated the ORR activity on prepared electrodes with different Pt/C loadings by RRDE technique, and examined H<sub>2</sub>O<sub>2</sub> formation path in ORR.

## 2. Experimental

Commercially available 50 wt% Pt/C (TKK Inc, TEC-10E50E) catalyst was used in RRDE measurement. The RRDE consist of a glassy carbon (GC) disk electrode and a Pt ring electrode. An aliquot of the ultra-sonicated catalyst ink was carefully dropped on the GC disk electrode to adjust each Pt/C loading densities. Linear sweep voltammetry was performed from 0.05 to 1.0 V at 10 mV s<sup>-1</sup> in O<sub>2</sub> saturated 0.1 M HClO<sub>4</sub> to investigate ORR and hydrogen peroxide formation on Pt/C catalyst with different loadings by RRDE technique, and then a ring electrode potential was hold at 1.2V. Similar voltammetric measurement from 0.05 to 1.4 V at 10 mVs<sup>-1</sup> was carried out to evaluate hydrogen peroxide reduction reaction (HPRR) in deaerated 0.1M HClO<sub>4</sub> solution with H<sub>2</sub>O<sub>2</sub> additive by RDE technique.

## 3. Results and Discussion

Fig. 1 shows CVs per mass of Pt on prepared electrode with different catalyst loadings. A characteristic behavior such as hydrogen adsorption/desorption, Pt oxide formation and its reduction were observed on each samples, and then the current of CV per mass of Pt was almost equal to each catalyst loadings. Therefore, each electrode at different catalyst loadings was successfully modified on GC disk electrode. Fig. 2 shows H<sub>2</sub>O<sub>2</sub> formation rate measured by RRDE technique. An amount of H<sub>2</sub>O<sub>2</sub> formation was larger with lowering disk potential and decreasing catalyst loading on GC substrate. Fig. 3 shows LSV measurement results in HPRR. Hydrogen peroxide reduction current at catalyst loading of 1.41 μg<sub>Pt</sub> cm<sup>-2</sup> was lower than diffusion limiting current calculated value from Levich equation. Therefore, the HPRR was drastically affected by catalyst loadings compared with the ORR.

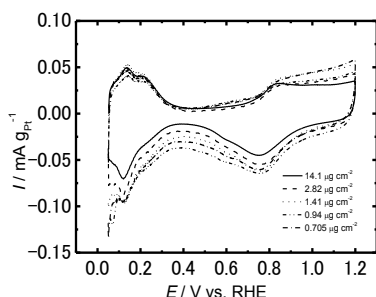


Fig. 1 CVs on 46 wt% Pt/C catalysts with different catalyst loadings on GC in Ar saturated 0.1 M HClO<sub>4</sub>. Scan rate : 50 mV s<sup>-1</sup>.

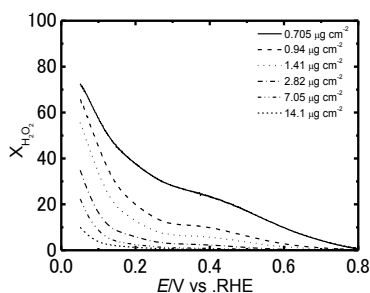


Fig. 2 The ratio of H<sub>2</sub>O<sub>2</sub> formation during ORR on 46wt% Pt/C with different catalyst loadings on GC in O<sub>2</sub> saterated 0.1 M HClO<sub>4</sub>. Rotating rate : 1600 rpm.

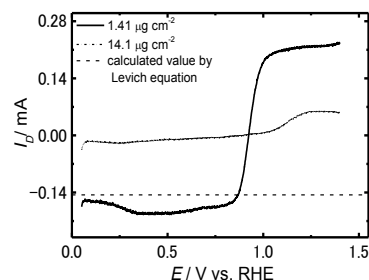


Fig. 3 Hydrogen peroxide reduction current on 46wt% Pt/C catalyst loaded at 1.41 and 14.1 μg cm<sup>-2</sup>. Rotating rate:1600 rpm.

## 4. References

- 1) M. Inaba, H. Yamada, J. Tokunaga and A. Tasaka, *Electrochemical and Solid-State Letters*, **7** (12), A474-A476 (2004).
- 2) M. Inaba, H. Yamada, R. Umebayashi, M. Sugishita and A. Tasaka, *Electrochemistry*, **75** (2), 207-212 (2007).

# Study on Ion conductivity of Mg-Al Layered Double Hydroxides prepared by electrochemical co-precipitation method.

Yuya KITAGUCHI, Hirohisa YAMADA, and Katsumi katakura

Department of chemical Engineering, National Institute of Technology, Nara College

22 Yata-cho, Yamatokoriyama, Nara 639-1080, Japan

yamada@chem.nara-k.ac.jp

## Introduction

Layered Double Hydroxides (LDHs) have been studied by many researchers for their interesting properties such as ion exchangers, adsorbents, polymer stabilizer, catalyst, and so on. LDHs are well known as anionic clays include anion species and water molecules in the interlayer which consist of positively charged metal hydroxide layers. It was reported that some types of LDHs prepared by co-precipitated method have high OH<sup>-</sup> conductivity and high performance as electrolyte for Alkaline Fuel Cells (AFCs) by Tatsumisago *et. al.*. Co-precipitation method is generally used for LDH synthesis, while we reported Electrochemical co-precipitated method which enable to form LDH thin film on an electrode surface<sup>2)</sup>. Therefore, we prepared Mg-Al LDHs by electrochemical co-precipitation method and evaluated their OH<sup>-</sup> conductivity.

## Experiments

The LDH was synthesized by co-precipitation and electrochemical co-precipitation method. In co-precipitation method, 0.075 mol dm<sup>-3</sup> Mg(NO<sub>3</sub>)<sub>2</sub> + 0.025 mol dm<sup>-3</sup> Al(NO<sub>3</sub>)<sub>3</sub> solution was stirred under Ar atmosphere. After deaeration, NaOH aq. was added and held the pH ca. 10 and aged the solution at 80 °C for 18h to synthesized the LDH. Electrochemical co-precipitation method is as following, Pt sheet was used as a working electrode and immersed in a 0.10 mol dm<sup>-3</sup> aqueous solution containing Mg(NO<sub>3</sub>)<sub>2</sub> and Al(NO<sub>3</sub>)<sub>3</sub> under Ar atmosphere. Galvanostatic electrolysis was carried out at -16 mA cm<sup>-2</sup> for 10 min. The crystalline structure and surface morphologies on the prepared samples were evaluated by XRD and SEM, respectively. The conductivity of prepared samples were measured by the AC impedance method at the 60 °C under the RH = 80%.

## Results and discussion

Fig. 1 shows XRD patterns of the electrochemical co-precipitated thin film on the Pt surface and co-precipitated sample. Characteristic peaks 11° (003) and 22° (006) in LDH is observed on both samples, therefore Mg-Al LDH is successfully synthesized by electrochemically and chemically method. Fig. 2 shows SEM image on (a) electrochemical co-precipitated LDH and (b) co-precipitated Mg-Al LDH. A plate-like shape was observed on both samples. Ion conductivity of Mg-Al LDH at 60°C under RH = 80% are shown in Fig. 3. Electrochemically co-precipitated LDHs have a little smaller conductivity than co-precipitated samples, while LDHs which prepared at x = 0.25 of Mg<sub>1-x</sub> - Al<sub>x</sub> LDH composition have a highest conductivity on each sample.

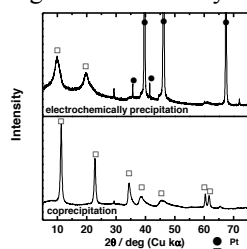


Fig. 1 XRD patterns of electrochemical co-precipitated sample and co-precipitated sample.

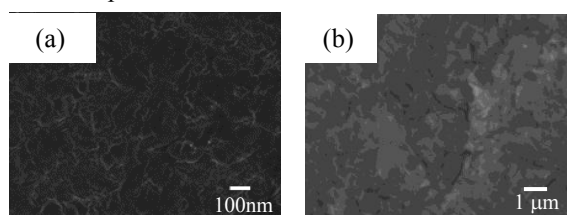


Fig. 2 SEM images on (a) Electrochemical co-precipitated sample and (b) co-precipitated sample.

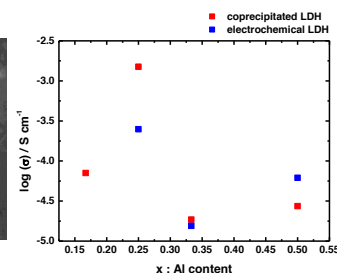


Fig. 3 Ion conductivity on co-precipitated LDH and electrochemical co-precipitated LDH at 60°C under 80%RH.

## Reference

- 1) Yoshihiro Furukawa, Kiyoharu Tadanaga, Akitoshi Hayashi, and Masahiro Tatsumisago, *Solid State Ionics* **192**, 185 (2011).
- 2) Federica Prinetto, Giovanna Ghiotti, Patrick Graffin, Didier Tichit, *Microporous and Mesoporous Materials* **39**, 229 (2000).
- 3) Chihiro OBAYASHI, Mituru ISHIZAKA, Takayoshi KONISHI, Hirohisa YAMADA, and Katsumi KATAKURA, *electrochemistry*, **80**, 1 (2012).



# **$\text{La}_{0.2}\text{Sr}_{0.25}\text{Ca}_{0.45}\text{Ti}_{1-x-y}\text{Nb}_x\text{Ni}_y\text{O}_3$ as Potential Anode Material for IT-SOFCs**

Aziz Nechache, Samir Boulfrad, Shahid P. Shafi, Enrico Traversa  
*Division of Physical Sciences and Engineering, King Abdullah University of Science and Technology-KAUST, Thuwal 4700, KSA*  
*aziz.nechache@kaust.edu.sa*

Strontium titanate perovskite oxides have attracted a lot of interest as serious candidates to overcome the limitations of the state-of-the-art Ni-YSZ cermet, especially at intermediate temperatures. Co-doping the A site of strontium titanate with La and Ca resulted in an electronic conductivity of  $37 \text{ S.cm}^{-1}$  at  $600^\circ\text{C}$  [1].

In this paper, we aim to further increase the anodic performance of this material by additionally co-doping the B site with Ni and Nb. The expected exsolution of Ni nanoparticles is believed to boost the catalytic activity, while the Nb doping would increase the electronic conductivity. Therefore,  $\text{La}_{0.2}\text{Sr}_{0.25}\text{Ca}_{0.45}\text{Ti}_{1-x-y}\text{Nb}_x\text{Ni}_y\text{O}_3$  powders were synthesized using the solid-state reaction route. Structural, electrical, thermo-mechanical and electrochemical characterizations are performed to evaluate the potentiality of this material as anode component for intermediate temperature solid oxide fuel cells.

## References:

- 1- A. D. Aljaberi and J. T. S. Irvine, *J. Mater. Chem. A*, 2013, **1**, 5868–5874.

# Effects of Solvents for Dispersion Solutions on Membrane-Electrode Assembly for Proton Exchange Membrane Fuel Cells – Overvoltage and Durability

Gyu-Hyeon Oh, Mun-Sik Shin, Moon-Sung Kang, Jin-Soo Park\*

*Department of Environmental Engineering, College of Engineering, Sangmyung University, 31 Sangmyungdae-gil, Dongnam-gu, Cheonan, Chungnam Province 330-720, Republic of Korea*

*\*energy@smu.ac.kr*

Proton exchange membrane fuel cells (PEMFCs) is currently considered as a potential next-generation alternative energy technology because of the high energy density and high abundance of hydrogen in nature. One of the most important parts in PEMFCs is membrane-electrode assembly (MEA) which provides the electrochemical reactions at electrode, the permeation of fuel and/or oxidant gas and the drainage of water product. The structure of electrode in MEA significantly determines the performance of PEMFCs. In MEA, Nafion dispersion is the most widely used as the ionomer binder for catalyst inks. A high performance MEA requires the combination of performance and durability. The former could be achieved by reducing overvoltages, and the latter by reducing electrode cracking. The structure of electrodes in MEA significantly determines the performance and durability of PEMFCs. Electrode structure of MEA, including the pt-ionomer interface, could be determined when electrodes are solidified from catalyst inks during a drying step. Thus, the properties of the solvent system in catalyst inks play an important role in determining the electrode structure in MEA. The solvent system is mainly influenced by the solvents in polymer dispersions. The various solvents for catalyst inks were used and investigated the performance and durability of electrolyte membranes prepared by the casting of Nafion polymer solutions using the various solvents. The properties of membranes were investigated in terms of proton conductivity, mechanical stability, chemical stability, ect.

## ACKNOWLEDGMENTS

This research is supported by Basic Science Research Program through the National Research Foundation of Korea (NRF) funded by the Ministry of Science, ICT and Future Planning (NRF-2014R1A1A1006067).

## REFERENCES

- [1] Q. Wang, D. Song, T. Navessin, S. Holdcroft, Z. Liu, A mathematical model and optimization of the cathode catalyst layer structure in PEM fuel cells, *Electrochimica Acta*, 50 (2004) 725.
- [2] S. Wei, B. A. Peppley, K. Kunal, An improved two-dimensional agglomerate cathode model to study the influence of catalyst layer structural parameters, *Electrochimica Acta*, 50 (2005) 3359.
- [3] D. Song, Q. Wang, Z. Liu, M. Eikerling, Z. Xie, T. Navessin, S. Holdcroft, A method for optimizing distributions of Nafion and Pt in cathode catalyst layers of PEM fuel cells, *Electrochimica Acta*, 50 (2005) 3347.
- [4] M. Srinivasarao, D. Bhattacharyya, R. Rengaswamy, S. Narasimhan, Multivariable optimization studies of cathode catalyst layer of a polymer electrolyte membrane fuel cell, *International journal of hydrogen energy*, 35 (2010) 6356.
- [5] J. Marquis, M. O. Coppens, Achieving ultra-high platinum utilization via optimization of PEM fuel cell cathode catalyst layer microstructure, *Chemical engineering science*, 102 (2013) 151.
- [6] Y.S. Kim, C. F. Mack, N. H. Hjelm, R. P. Rengaswamy, S. Narasimhan, Highly durable fuel cell electrodes based on ionomers dispersed in glycerol, *Physical Chemistry Chemical Physics*, 16 (2014) 5927-5932.
- [7] C. Welch, A. Labouriau, A. Hjelm, R. Orler, B. Johnston, C. Kim, Nafion in Dilute Solvent Systems: Dispersion or Solution?, *ACS Macro Letters*, 12 (2012) 1403-1407.

# Preparation and Characterization of Anion Conducting Ionomer Binder based on Quaternized Polybenzimidazole for Solid Alkaline Fuel Cells

Mun-Sik Shin, Moon-Sung Kang, Jin-Soo Park\*

*Department of Environmental Engineering, College of Engineering, Sangmyung University, 31 Sangmyungdae-gil, Dongnam-gu, Cheonan, Chungnam Province 330-720, Republic of Korea*

*\*energy@smu.ac.kr*

Much efforts are recently devoted to alkaline fuel cells using anionic polymeric membranes. Solid alkaline fuel cells (SAFCs) are operated in the same principle of alkaline fuel cells, but use solid type electrolytes. SAFCs have the advantages that are easier to handle systems at low operating temperatures (roughly room temperature  $\sim 70^\circ\text{C}$ ), to have higher reaction kinetics at the electrodes than proton exchange membrane fuel cells (PEMFCs) and to use non-noble metal catalysts. In addition, SAFCs are recently being highlighted to overcome the disadvantages of carbonate precipitates, leakage of liquid KOH electrolyte, and system complexity by using solid electrolytes. This solid electrolytes were prepared by quaternized polymers having a function to exchange anions. According to the recent works, alkaline doped PBI membranes exhibited good ionic conductivity, acceptable mechanical strength, high thermal stability, and low methanol permeability.

For fuel cell applications, membrane-electrode assemblies should be prepared for solid alkaline fuel cells. However, few researches on ionomer binder solutions for preparation of electrodes of MEAs were carried out.

In this study, new anion conducting polymer were synthesized using quaternized polymers as ionomer binder. A quaternized polybenzimidazoles (PBIs) having quaternized intermediate 4-methyl-4-glycidylmorpholin-4-ium chloride (MGMC) in the main-chain and/or in the side group were synthesized for use as anion conducting ionomer binder for SAFCs. The quaternized polymers were investigated in terms of ionic conductivity, IEC, FT-IR, NMR etc. The thermal stability, mechanical properties, hydroxide conductivity and membrane stability were also investigated.

## ACKNOWLEDGMENTS

This work was supported in part by the KIST Institutional Program (Project No. 2E24841).

## REFERENCES

- [1] J.S. Yang, L.N. Cleemann, T. Steenberg, C. Terkelsen, Q.F. Li, J.O. Jensen, H.A. Hjuler, N.J. Bjerrum, R.H. He, High Molecular Weight Polybenzimidazole Membranes for High Temperature PEMFC, Fuel Cells, 14 (2014) 7-15.
- [2] L.C. Jheng, S.L.C. Hsu, B.Y. Lin, Y.L. Hsu, Quaternized polybenzimidazoles with imidazolium cation moieties for anion exchange membrane fuel cells, Journal of Membrane Science, 460 (2014) 160-170.
- [3] H.Y. Hou, S.L. Wang, Q.A. Jiang, W. Jin, L.H. Jiang, G.Q. Sun, Durability study of KOH doped polybenzimidazole membrane for air-breathing alkaline direct ethanol fuel cell, Journal of Power Sources, 196 (2011) 3244-3248.
- [4] K.J.W.Y. Soo, An Investigation into Polybenzimidazoles as Anion Exchange Membranes, Science: Department of Chemistry, 2013.
- [5] Z. Xia, S. Yuan, G. Jiang, X. Guo, J. Fang, L. Liu, J. Qiao, J. Yin, Polybenzimidazoles with pendant quaternary ammonium groups as potential anion exchange membranes for fuel cells, Journal of Membrane Science, 390-391 (2012) 152-159.

# Copper-Incorporated Carbon Catalysts for Oxygen Reduction Reaction

Marika Muto, Masaru Kato, Ichizo Yagi

Graduate School of Environmental Science, Hokkaido University

N10W5 Sapporo 060-0810 Japan

m-Muto@ees.hokudai.ac.jp

Platinum metal group (PMG) catalysts are used for oxygen reduction reaction (ORR) at cathodes in state-of-the-art polymer electrolyte fuel cells (PEFCs). Since the PMG catalysts contain expensive rare metals, they should be replaced with rare-metal-free catalysts for widespread PEFCs. Recently, electrocatalysts synthesized from carbon and transition metal complexes have been studied [1,2]. It is known that ORR catalysts with multi-nuclear-active sites have high ORR activity [3]. It is also known that natural ORR catalysts such as laccases have a multinuclear copper complex as an active center and show high ORR activity [4], suggesting that laccase-inspired artificial ORR catalysts prepared from carbon and a multi-nuclear copper complex would show high ORR activity.

In this work, we incorporated a trinuclear copper complex ( $[\text{Cu}_3(\text{trz})_3(\mu_3\text{-OH})]\text{Cl}_2 \cdot 6\text{H}_2\text{O}$ , Fig. 1) [5] into graphene nanosheets to synthesize laccase-inspired electrocatalysts for ORR, where graphene nanosheets worked as an electrical conductive material and the trinuclear copper complex with a triangle core imitated the active center of laccases.

The trinuclear copper complex was prepared from copper chloride and 1,2,4-triazole according to the literature [5]. This copper complex and graphene oxide (GO) were mixed and then reduced in two methods. The first method is heat treatment at high temperature (1173 K) for a short time (45 s). The second method is electrochemical reduction on a glassy carbon (GC) electrode (-1.1 V vs.  $\text{Ag}|\text{AgCl}$ , 300 s). We carried out powdery X-ray diffraction (XRD) analysis, X-ray photoelectron spectroscopy (XPS) and inductively coupled plasma atomic emission spectroscopy (ICP-AES) to characterize the catalysts. For electrochemical measurements of the catalysts, the powdery catalyst was suspended in an ethanol-Nafion mixture to make ink containing the catalyst. The catalyst ink was put on a GC electrode and dried under the air at room temperature. Linear Sweep Voltammetry (LSV) was carried out under a saturated  $\text{O}_2$  atmosphere using a rotary disk electrode to obtain current-potential curves. Britton-Robinson buffered solutions were used as electrolyte solutions.

The heat or electrochemical reduction improved ORR activity. The catalyst obtained after the heat treatment showed higher ORR activity than that obtained after the electrochemical reduction. This result indicated that the two reduction methods might give different structures of ORR active sites. XPS spectra of the catalyst before and after the heat treatment were recorded to obtain information on structural changes. A peak originating from C-O was observed before the heat treatment. It disappeared after the heat treatment. This result indicated that GO was reduced to rGO by the heat treatment. The  $\text{Cu}2\text{p}$  spectra showed that  $\text{Cu}^{\text{II}}$  was also reduced to  $\text{Cu}^{\text{I}}$ . A new peak was observed in N1s spectra after the heat treatment. This peak might be attributed to new configuration that triazole rings were incorporated into graphene nanosheets.

We measured LSV of the heat-treated catalyst in a wide range of pHs (pH 1 to pH 13) to understand pH-dependence of the ORR activity. The highest ORR activity was observed at pH 13.

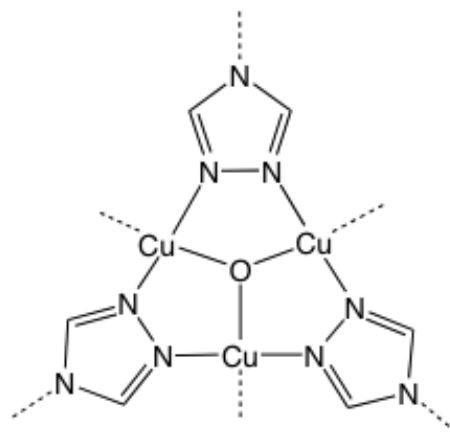


Fig. 1 Coordination structure of  $[\text{Cu}_3(\text{trz})_3(\mu_3\text{-OH})]\text{Cl}_2 \cdot 6\text{H}_2\text{O}$

**References.** [1] K. Kamiya, K. Hashimoto, S. Nakanishi, *Chem. Commun.*, 2012, **48**, 10213–10215. [2] T. Taniguchi, et al., *Part. Part. Syst. Charact.*, 2013, **30**, 1063–1070. [3] M. Thorum, J. Yadav, A. Gewirth, *Angew. Chem. Int. Ed.*, 2009, **48**, 165–167. [4] N. Mano, V. Soukharev, A. Heller, *J. Phys. Chem. B*, 2006, **110**, 11180–11187. [5] T. Yamada, G. Maruta, S. Takeda, *Chem. Commun.*, 2011, **47**, 653–655

# Oxygen reduction reaction on Au@Pt nanoparticles and Au(100) electrode

Yong Li Zheng, Yao Yao, Dong Mei and Yan-Xia Chen\*

*Hefei National Laboratory for Physical Science at Microscale and Department of Chemical Physics, University of Science and Technology of China, Hefei, 230026, China*

[yachen@ustc.edu.cn](mailto:yachen@ustc.edu.cn)

Oxygen reduction reaction (ORR) at Au@Pt nanoparticles (NPs) and the redox reaction of hydrogen peroxide ( $\text{O}_2 + 2\text{H}^+ + 2\text{e}^- \rightleftharpoons \text{H}_2\text{O}_2$ ) at Au(100) electrode/0.1 M  $\text{HClO}_4$  interface have been investigated. On Au@Pt NPs, we found that the Au@1 ML Pt NPs in the series of Au@0.7-4 ML Pt NPs has the best ORR activity and its half wave potential for ORR is found to be ca. 30 mV more positive than that for pc-Pt and 20% Pt/C. XPS and SERS study revealed that the enhancement of ORR activity at Au@Pt nanoparticle originate from the charge transfer from Au core to Pt shell.

On Au(100) electrode, we found that i) the kinetics for electrochemical oxidation of  $\text{H}_2\text{O}_2$  to  $\text{O}_2$  is very fast, which occurs at potential very close to its equilibrium potential ( $E_{\text{O}_2/\text{H}_2\text{O}_2}^{\text{eq}}$ ); ii) the kinetics for  $\text{O}_2$  reduction to  $\text{H}_2\text{O}_2$  is much slower than that for  $\text{H}_2\text{O}_2$  oxidation with H-D kinetic isotope effect of above two; iii) the onset overpotential of  $\text{H}_2\text{O}_2 + 2\text{H}^+ + 2\text{e}^- \longrightarrow 2\text{H}_2\text{O}$  is ca. 1.4 V. The origin for the high overpotential at the onset for  $\text{O}_2$  reduction at Au(100) is limited by the thermodynamic equilibrium potential for  $\text{O}_2 + 2\text{H}^+ + 2\text{e}^- \rightleftharpoons \text{H}_2\text{O}_2$  due to the fast kinetics of  $\text{H}_2\text{O}_2$  oxidation.

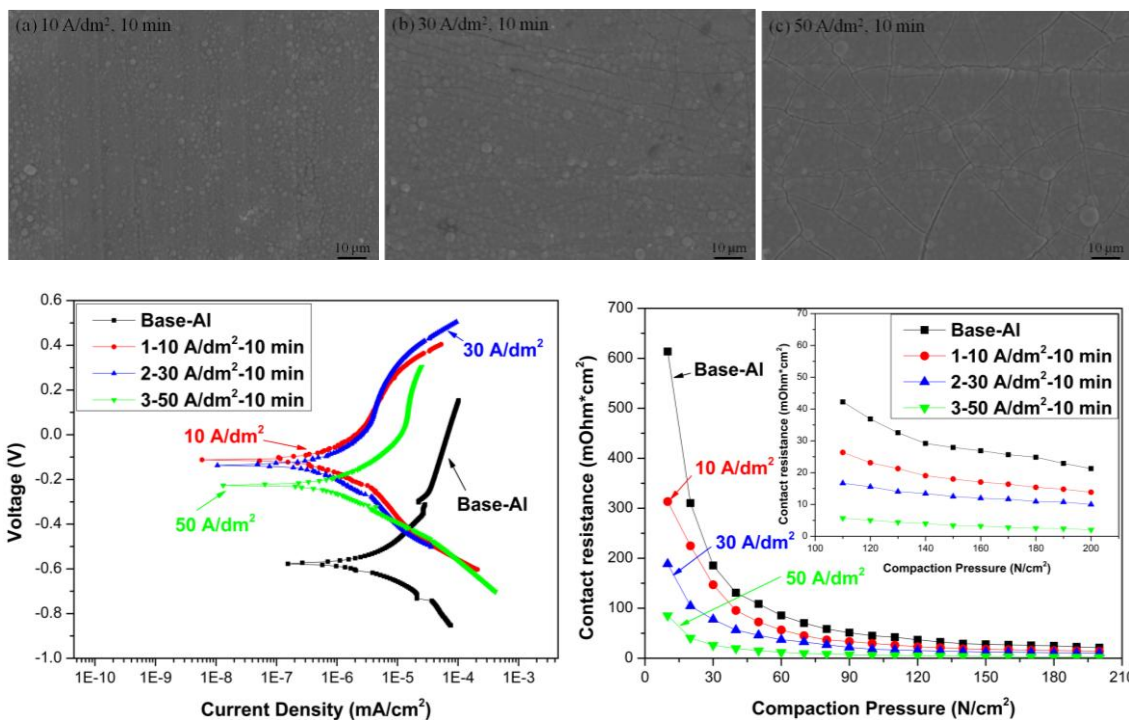
**Keywords:** hydrogen peroxide oxidation, hydrogen peroxide reduction, oxygen reduction, core-shell nanoparticles, Au(100) electrode, overpotential, kinetics, ligand effect

# Improvement on corrosion resistance and conductivity by electroplated coatings on aluminum 5052 bipolar plate of proton exchange membrane fuel cell

Kung-Hsu Hou, Hsiang-Cheng Wang, Ming-Der Ger, Chen-En Lu  
*Chung-Cheng Institute of Technology, National Defense University*  
*No.75, Shihyuan Rd., Dasi Dist., Taoyuan City 33551, Taiwan (R.O.C.)*  
*khou@ndu.edu.tw*

In this study, the trivalent Cr-C coatings were electroplated on aluminum 5052 substrate for an application of BPPs because of their excellent electric conductivity and corrosion resistance. The corrosion behavior of the BPPs with and without Cr-C coatings was measured by liner polarization and potentiodynamic measurements. The SEM images of surface morphology showed that the thickness of the coating was about 1.1 to 3.5  $\mu\text{m}$  and increased with raising coating current density. The surface morphology at 10  $\text{A}/\text{dm}^2$  is without cracks and pinholes happened than those at 30  $\text{A}/\text{dm}^2$  and 50  $\text{A}/\text{dm}^2$ . Moreover, the polarization curve with different current density (10, 30, 50  $\text{A}/\text{dm}^2$ ) represented the coating prepared at 10  $\text{A}/\text{dm}^2$  and 10 minutes possessing the lowest corrosion current density ( $I_{\text{corr}}=3.67 \times 10^{-7} \text{ A}/\text{cm}^2$ ). Interfacial contact resistance (ICR) of the bipolar plate coated with Cr-C coating at 10  $\text{A}/\text{dm}^2$  is improved obviously, presenting an ICR of 19.48  $\text{m}\Omega\text{cm}^2$  under 138  $\text{N}/\text{cm}^2$  which is superior to the others and less than the standard of DOE (10  $\text{m}\Omega\text{cm}^2$ ). The results of scanning electron microscope (SEM) and ICR before and after corrosion tests indicate that the aluminum 5052 bipolar plate with Cr-C coating is considerably stable electrochemically.

Keywords: Electroplating, Cr-C coating, Corrosion resistance, Bipolar plates, PEMFC.



## References

- [1] Y. Hung, K.M. El-Khatib, H. Tawfik, Testing and evaluation of aluminum coated bipolar plates of pem fuel cells operating at 70  $^{\circ}\text{C}$ , J. Power Sources 163(2006) 509-513.
- [2] Z. Li, K. Feng, Z. Wang, X. Cai, C. Yao, Y. Wu, Investigation of single-layer and multilayer coatings for aluminum bipolar plate in polymer electrolyte membrane fuel cell, Int. J. Hydrog. Energy 39(2014) 8421-8430.
- [3] H.C. Wang, K.H. Hou, C.E. Lu, M.D. Ger, The study of electroplating trivalent CrC alloy coatings with different current densities on stainless steel 304 as bipolar plate of proton exchange membrane fuel cells, Thin Solid Films 570(2014) 209-214.

# Titanium-niobium oxides as non-platinum cathodes for polymer electrolyte fuel cells

Tamura Yuko<sup>1</sup>, Akimitsu Ishihara<sup>2</sup>, Yuji Kohno<sup>1</sup>, Koichi Matsuzawa<sup>1</sup>, Shigenori Mitsushima<sup>1,2</sup>, and Ken-ichiro Ota<sup>1</sup>

<sup>1</sup>Green Hydrogen Research Center, Yokohama National University

<sup>2</sup>Institute of Advanced Sciences, Yokohama National University

79-5 Tokiwadai, Hodogaya-ku, Yokohama 240-8501, Japan

E-mail: a-ishi@ynu.ac.jp

## Introduction

Development of non-platinum electrocatalysts for oxygen reduction reaction (ORR) is required for real commercialization of polymer electrolyte fuel cells. We have focused on group 4 and 5 metal oxide-based compounds<sup>1)</sup>, because they have high chemical stabilities in acidic media and are less costly than platinum. In order to obtain high durable catalysts, we proposed oxide-based cathodes without carbon<sup>2)</sup>. Although both creation of active sites and formation of electro-conductive paths are necessary to act as actual cathodes, it is difficult to optimize them simultaneously. In this study, we focused on the formation of the active sites for the ORR to investigate the conditions at which the ORR generates by preparing titanium-niobium oxides.

## Experimental

30 cm<sup>3</sup> of Titanium(IV) Isopropoxide (99.99%, Aldrich) and 4 cm<sup>3</sup> of Niobium(V) pentaethoxide (99.99%, Aldrich) were mixed in 30 cm<sup>3</sup> of 2-Methoxyethanol to be TiO<sub>2</sub>:Nb<sub>2</sub>O<sub>5</sub> = 8:2 as a precursor solution. 2-Methoxyethanol solution dispersed with Ti-Nb oxide particles was prepared according to the sol-gel method<sup>3)</sup> as a catalyst ink. The ink was dropped on a glassy carbon rod. After drying the ink, it was heat-treated at 1050, 800, 600 °C in air and at 1050, 800, 700, 600 °C in 4%H<sub>2</sub>/Ar to obtain working electrodes. All electrochemical measurements were performed in 0.1 mol dm<sup>-3</sup> H<sub>2</sub>SO<sub>4</sub> at 30 °C with a 3-electrode cell. A reversible hydrogen electrode (RHE) and a glassy carbon plate were used as the reference and the counter electrodes, respectively. Slow scan voltammetry (SSV) was performed with a scan rate of 5 mV s<sup>-1</sup> from 0.2 to 1.2 V vs. RHE under O<sub>2</sub> and N<sub>2</sub> atmosphere to obtain ORR current. The ORR current density (*i*<sub>ORR</sub>) was based on the electric charge of the double layer capacitance of the oxides.

## Results and discussion

Figure 1 shows the potential-*i*<sub>ORR</sub> curves of Ti-Nb oxides heat-treated at 1050, 800, 600 °C in air (air) and at 1050, 800, 700, 600 °C in 4%H<sub>2</sub>/Ar (red). The Ti-Nb oxides heat-treated in air showed no ORR current below 0.6 V. On the other hand, the ORR current was observed over 0.8 V by the heat-treatment in 4%H<sub>2</sub>/Ar, and the ORR activities changed by the temperature. Therefore, we found that the heat-treatment under reductive atmosphere produced the ORR activity, and the heat-treatment temperature of 700 °C was suitable for achieving high ORR activity. These results suggest that the emergence of the ORR activity is related to the appropriate reduction of Ti and/or Nb nearby surface.

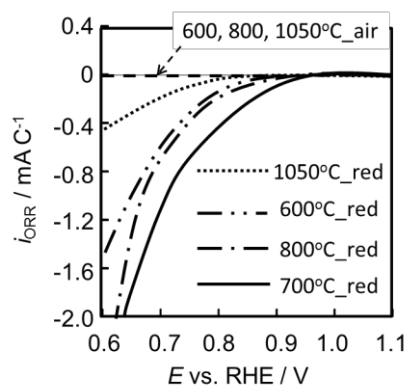


Fig.1 Potential-*i*<sub>ORR</sub> curves of specimens prepared at 1050, 800, 700, 600 °C in 4%H<sub>2</sub>/Ar and at 1050, 800, 600 °C in air.

## Acknowledgements

The authors thank the New Energy and Industrial Technology Development Organization (NEDO) for financial support.

## Reference

- 1) A. Ishihara, M. Tamura, Y. Ohgi, M. Matsumoto, K. Matsuzawa, S. Mitsushima, H. Imai, and K. Ota, *J. Phys. Chem. C*, 117, 18837 (2013).
- 2) M. Hamazaki, A. Ishihara, M. Arao, M. Matsumoto, Y. Kohno, K. Matsuzawa, S. Mitsushima and K. Ota, *ECS Trans.*, 64(3), 239 (2014).
- 3) H. Matsuda, T. Mizushima, and M. Kuwabara, *J. Ceram. Soc. Japan*, 107(3), 290 (1999).

# Evaluation of durability of titanium-niobium oxides mixed with $\text{Ti}_4\text{O}_7$ as non-precious metals and carbon-free cathodes for PEFC in sulfuric acid at 80 °C

Makoto HAMAZAKI<sup>a</sup>, Akimitsu ISHIHARA<sup>b</sup>, Yuji KOHNO<sup>a</sup>, Koichi MATSUZAWA<sup>a</sup>,  
Shigenori MITSUSHIMA<sup>a, b</sup>, and Ken-ichiro OTA<sup>a</sup>

<sup>a</sup> Green Hydrogen Research Center, Yokohama National University,

<sup>b</sup> Institute of Advanced Sciences, Yokohama National University

79-5, Tokiwadai, Hodogaya-ku, Yokohama 240-8501, JAPAN

a-ishi@ynu.ac.jp

## Introduction

Development of non-precious metals and carbon free cathodes as alternative materials of platinum supported carbon catalysts is required for practical application of polymer electrolyte fuel cells (PEFCs). Thus, we prepared the oxide based catalysts which were composed of niobium-titanium oxides with active sites and titanium oxides with magneli phase of  $\text{Ti}_4\text{O}_7$  as electric conductive<sup>1</sup> ( $\text{Ti}_x\text{Nb}_y\text{O}_z + \text{Ti}_4\text{O}_7$ ).

We revealed that the  $\text{Ti}_x\text{Nb}_y\text{O}_z + \text{Ti}_4\text{O}_7$  catalysts exhibited high durabilities in 0.1 mol dm<sup>-3</sup>  $\text{H}_2\text{SO}_4$  at 30 °C.<sup>2</sup> However, we have not evaluated yet the durabilities of these catalysts at higher temperature, 80 °C, which is a close to real PEFC conditions. In addition, a glassy carbon (GC) rod commonly used as a substrate was severely oxidized at 80 °C. We therefore used a  $\text{Ti}_4\text{O}_7$  rod as a substrate because of its high stability and conductivity<sup>1</sup>. In this study, we evaluated the durability of the  $\text{Ti}_x\text{Nb}_y\text{O}_z + \text{Ti}_4\text{O}_7$  in 0.1 mol dm<sup>-3</sup>  $\text{H}_2\text{SO}_4$  at 80 °C using the  $\text{Ti}_4\text{O}_7$  rod as the substrate.

## Experimental

$\text{Ti}_x\text{Nb}_y\text{O}_z + \text{Ti}_4\text{O}_7$  catalysts were prepared by dry ball-milling with  $\text{TiO}_2$  and  $\text{Nb}_2\text{O}_5$  powder mixture and reductive heat-treatment in 4%  $\text{H}_2/\text{Ar}$  at 1050 °C for 50 h.<sup>2</sup> The powder catalysts were supported about 0.1 mg on the top of the  $\text{Ti}_4\text{O}_7$  rod. In order to evaluate the electrochemical stabilities of the catalysts in 0.1 mol dm<sup>-3</sup>  $\text{H}_2\text{SO}_4$  at 80 °C, a start-stop cycle test<sup>3</sup> (triangular wave, 1.0 - 1.5 V vs. reversible hydrogen electrode (RHE),  $\text{N}_2$ , a scan rate: 0.5 V s<sup>-1</sup>) and a load cycle test<sup>3</sup> (rectangular wave, 0.6 - 1.0 V vs. RHE,  $\text{O}_2$ , holding time: 3 s) were performed as degradation tests using a 3-electrode cell. An RHE and a GC plate were used as the reference and the counter electrodes, respectively. During the degradation tests, chronoamperometry at 0.7 V under  $\text{O}_2$  atmosphere was performed to evaluate the catalytic activity of oxygen reduction reaction (ORR). The durability was evaluated by a ratio of  $i_{\text{ORR}} @ 0.7 \text{ V}$  during degradation test to that at initial,  $N_{i_{\text{ORR}} @ 0.7 \text{ V}}$ .

## Results and discussion

Fig. 1 shows the variation of  $N_{i_{\text{ORR}} @ 0.7 \text{ V}}$  of the  $\text{Ti}_x\text{Nb}_y\text{O}_z + \text{Ti}_4\text{O}_7$  during start-stop and load cycle tests. In both tests, the values of the  $N_{i_{\text{ORR}} @ 0.7 \text{ V}}$  slightly changed during the initial potential cycling up to 2500 cycle. However, these values kept 1 above 5000 up to 20000 cycle, indicating that the  $\text{Ti}_x\text{Nb}_y\text{O}_z + \text{Ti}_4\text{O}_7$  had superior stability for both start-stop and load cycle tests in 0.1 mol dm<sup>-3</sup>  $\text{H}_2\text{SO}_4$  at 80 °C. Therefore, we successfully demonstrated that the active sites on the titanium-niobium oxides are highly stable both low and high potential regions at 80 °C. In other words, non-precious metals and carbon-free cathodes based on Group 4 and 5 metal oxides have essentially high durability as we expected.

## Acknowledgement

The authors thank for the New Energy and Industrial Technology Development Organization (NEDO) for financial support.

## References

1. F. C. Walsh, R. G. A. Wills, *Electrochim. Acta*, 55, 6342 (2010).
2. A. Ishihara, M. Hamazaki, Y. Kohno, K. Matsuzawa, S. Mitsushima, and K. Ota, in preparation.
3. Fuel Cell Commercialization Conference of Japan (FCCJ), Proposals of the development targets, research and development challenges and evaluation methods concerning PEFCs, [http://www.fccj.jp/pdf/23\\_01\\_kt.pdf](http://www.fccj.jp/pdf/23_01_kt.pdf)

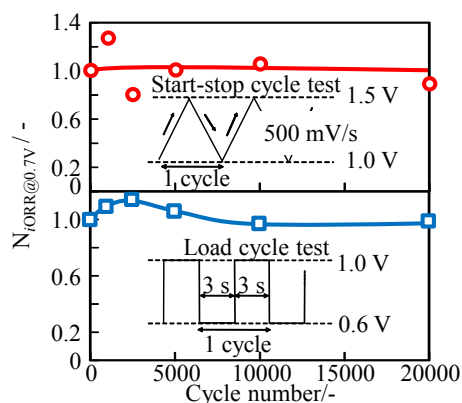


Fig. 1 Variation of  $N_{i_{\text{ORR}} @ 0.7 \text{ V}}$  of  $\text{Ti}_x\text{Nb}_y\text{O}_z + \text{Ti}_4\text{O}_7$  during start-stop cycle test.



# Kinetics of oxygen reduction reaction on titanium oxide-based catalysts prepared from oxy-titanium tetra-pyrazino-porphyrazine in acidic media

T. HAYASHI<sup>1</sup>, A. ISHIHARA<sup>2</sup>, Y. KOHNO<sup>1</sup>, K. MATSUZAWA<sup>1</sup>, M. MITSUSHIMA<sup>1,2</sup> and K. OTA<sup>1</sup>

<sup>1</sup>Green Hydrogen Research Center, Yokohama National University

<sup>2</sup>Institute of Advanced Sciences, Yokohama National University

79-5 Tokiwadai, Hodogaya-ku, Yokohama 240-8501, Japan,

a-ishi@ynu.ac.jp

## Introduction

Development of non-noble metal cathodes as alternative materials of platinum is required for practical application of polymer electrolyte fuel cells. We found that the titanium oxide-based compounds with multi-walled carbon nanotubes ( $\text{TiC}_x\text{N}_y\text{O}_z/\text{MWCNTs}$ ) prepared from oxy-titanium tetra-pyrazino-porphyrazine (TiOTPPz) with heat treatment under low oxygen partial pressure showed high oxygen reduction reaction (ORR) activity [1, 2]. However, the ORR mechanism on the titanium oxide-based catalysts has not yet analyzed in detail. In this study, we tried to investigate the ORR mechanism on the  $\text{TiC}_x\text{N}_y\text{O}_z/\text{MWCNTs}$  by using rotating ring disk electrode (RRDE) method.

## Experimental

TiOTPPz and multi-walled carbon nanotube (MWCNT) were mixed and conducted dry-ball-milling. The mixture was heated to 900 °C under Ar and then kept under Ar containing 0.05% $\text{O}_2$  and 2% $\text{H}_2$  for several hours. All electrochemical measurements were performed using an RRDE cell contained 0.1 mol  $\text{dm}^{-3}$   $\text{H}_2\text{SO}_4$  at 30 °C. Cyclic voltammetry was performed in  $\text{O}_2$  or  $\text{N}_2$  from 0.2 to 1.2 V vs. RHE (reversible hydrogen electrode) at a scan rate of 5  $\text{mV}\cdot\text{s}^{-1}$ . These measurements were performed in the same manner as previously described [3].

## Results and discussion

Fig.1 shows disc and ring currents as a function of disc potentials for oxygen reduction on  $\text{TiC}_x\text{N}_y\text{O}_z/\text{MWCNT}$  prepared with 3 h oxidation. We calculated the hydrogen peroxide formation rate,  $x_{\text{H}_2\text{O}_2}$ , from the disk and ring current in Fig. 1. Then, the  $x_{\text{H}_2\text{O}_2}$  @0.6V was approximately 10% at 1600 rpm. In addition, we estimated the individual rate constants of ORR ( $k_1$ ,  $k_2$ , and  $k_3$ ) based on the Damjanovic model [3, 4, 5]. These constants correspond to four electron reduction of oxygen, two electron reduction of oxygen, and reduction of hydrogen peroxide, respectively. The value of  $k_1/k_2$  means the selectivity of four electron reduction of oxygen. The value of  $k_1/k_2$  on the  $\text{TiC}_x\text{N}_y\text{O}_z/\text{MWCNT}$  was approximately 7 and almost similar to that of the platinum catalyst [4]. Consequently, we revealed that the  $\text{TiC}_x\text{N}_y\text{O}_z/\text{MWCNTs}$  have high selectivity of four electron reduction.

## Acknowledgment

The authors thank for ORIENT CHEMICAL INDUSTRIES CO., LTD for supply of oxy-titanium tetra-pyrazino-porphyrazine (TiOTPPz) and the New Energy and Industrial Technology Development Organization (NEDO) for financial support.

## References

- [1] A. Ishihara et al., *J. Phys. Chem. C*, **117**, 18837 (2013).
- [2] T. Hayashi et al., *ECS Trans.*, **64**, 247 (2014).
- [3] N. Uehara et al. *Electrochim. Acta.*, to be submitted.
- [4] A. Damjanovic et al., *J. Chem. Phys.*, **45**, 4057 (1966).
- [5] K. L. Hsueh et al., *J. Electroanal. Chem. Interfacial Electrochem.*, **153**, 79 (1983).

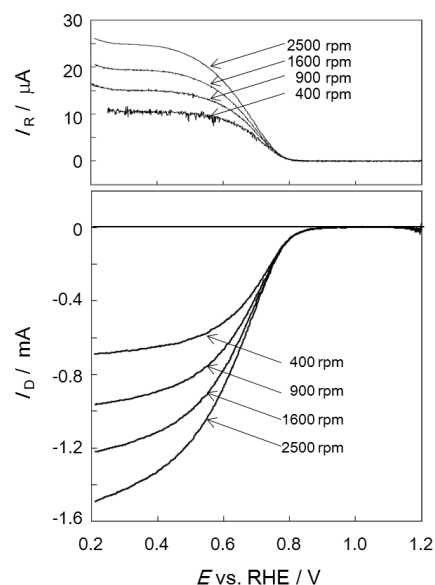


Fig.1 Disc and ring currents as a function of disc potential for  $\text{O}_2$  reduction on  $\text{TiC}_x\text{N}_y\text{O}_z/\text{MWCNT}$  prepared with 3 h oxidation. Ring potential: 1.2 V vs. RHE.

# Synthesis of sulfonated block copolymer for polymer electrolyte fuel cells operating at intermediate temperature.

Kwangjin Oh, Sangaraju Shanmugam

*Department of Energy Systems Engineering*

*Daegu Gyeongbuk Institute of Science and Technology (DGIST), Daegu 711-817, Republic of Korea*  
*sangarajus@dgist.ac.kr*

Polymer electrolyte membrane fuel cell (PEMFC) is one of the promising energy conversion systems due to high efficiency and environmental compatibility [1]. However, the current PEMFC uses commercialized perfluorosulfonic acid (PFSA) polymers as a proton exchange membrane, which has the issues of high production cost, poor recyclability, and limited operational temperature [2]. And also the fuel cell performance under elevated temperature condition is poor because of low water management and low T<sub>g</sub> [3]. Thus, in order to achieve high PEMFC performance, the proton conductivity under low relative humidity should be improved. We can solve this problem using non-fluorinated hydrocarbon membrane. Because it has a good thermal stability, low cost, and good durability at intermediate temperature. Although it has good properties, but its fuel cell performance is lower than PFSA based membranes due to its low proton conductivity. To solve this problem, non-fluorinated membrane containing partially asymmetric chemical structure and sulfonated block copolymer was prepared and characterized using <sup>1</sup>H-NMR; eventually studied for PEMFC at intermediate temperature. Sulfonated block copolymer exhibits an excellent proton conductivity under 70-100% RH as well as good power density when FC operating under 75-100% RH. Other parameters such as water uptake, ion exchange capacity (IEC) and morphology will be discussed in this presentation.

[1] D.P. Wilkinson, J. Zhang, Y.J. Wang, *Chem. Rev.*, **111** (2011) 7625.

[2] M.S. Jung, T.H. Kim, Y.J. Yoon, C.G. Kang, D.M. Yu, J.Y. Lee, H.J. Kim, Y.T. Hong, *J. Membr. Sci.*, **459** (2014) 72.

[3] S. Latorrata, P.G. Stampino, C. Cristiani, G. Dotelli, *J. Hydro. Ener.*, **39** (2014) 5350.

# Synthesis of membrane electrode assemblies for proton-exchange membrane fuel cells.

Nick Daems<sup>a</sup>, Sam Milis<sup>a</sup>, Paolo P. Pescarmona<sup>a,b</sup> and Ivo F.J. Vankelecom<sup>a</sup>

<sup>a</sup> Centre for Surface Chemistry and Catalysis, KU Leuven, Kasteelpark Arenberg 23, post box 2461, 3001 Heverlee, Belgium.

<sup>b</sup> Department of Chemical Engineering, University of Groningen, Nijenborgh 4, 9747 AG Groningen, The Netherlands.

[nick.daems@biw.kuleuven.be](mailto:nick.daems@biw.kuleuven.be)

Proton-exchange membrane fuel cells (PEMFC) have attracted substantial attention in the last decades as a green and non-polluting power source, especially for application in vehicles [1]. A membrane is an essential component of a PEMFC, as it allows protons to pass from the anode half-cell to the cathode half-cell while avoiding reagents to interact directly with each other. Besides having a good proton conductivity, the membrane also needs to be chemically, mechanically and thermally stable. Nafion is generally the material of choice for manufacturing proton-exchange membranes (PEM) in fuel cells. However, due to its high cost, the development of cheaper membranes with comparable or better properties than those made of Nafion is highly important for the commercialization of fuel cells.

Here, we present sulfonated polyvinylidene fluoride (PVDF) membranes as a promising alternative for Nafion membranes in PEMFCs. The membranes were synthesized by means of the following steps: 1) synthesis of PVDF membrane by means of phase inversion; 2) PVDF activation with KOH and reaction with styrene and 3) sulfonation with chlorosulfonic acid to ultimately obtain a stable, proton-conducting membrane [1]. These materials display important assets: (1) the presence of a fixed PVDF matrix, which will limit membrane swelling; (2) PVDF is a rather cheap bulk product; (3) sulfonation throughout the whole membrane cross-section, which allows direct catalyst-proton conductor contact and could thus provide easy transfer of protons.

In the fuel cell setup, a membrane forms part of the membrane electrode assembly (MEA). The standard procedure to prepare MEAs is via hot or cold pressing of membrane, electrocatalyst and gas diffusion layer (GDL). This is a labour-intensive procedure that is hard to automate, leaving processing complicated. Moreover, all separate layers have to be mechanically stable, so membranes are intrinsically thick (typically more than 50  $\mu\text{m}$ ), hence showing poor mass transfer. Therefore, two novel, alternative techniques were tested to produce the MEAs: (1) dipcoating, in which the membrane is brought into contact with a dispersion containing a solvent, the electrocatalysts and poly(sodium 4-styrenesulfonate) and (2) binderless deposition, where a suspension containing the electrocatalyst and a solvent/swelling agent for PVDF is spread across the membrane surface.

SEM images of the sulfonated membranes (Fig. 1A) revealed that asymmetric membranes with a dense top layer and a porous supporting layer were successfully obtained in all cases. A first evaluation of the proton conductivity as a function of temperature of these new membranes compared to the state-of-the-art Nafion membranes (Fig. 1B), revealed that the PVDF membranes achieve similar or better conductivities than Nafion, especially at higher temperatures. These higher conductivities can be explained based on the higher number of acid sites in the sulfonated PVDF membranes, as proven by their higher ion exchange capacities (1.8 mmol/g) compared to Nafion (1.3 mmol/g). In the near future, the performance of these PEMs will be evaluated in a  $\text{H}_2/\text{O}_2$  fuel cell setup, as part of the MEA. Even if the evaluation of these cheaper membranes is still in its initial phase, their conductivity values already reveal that this type of membranes can be a very promising alternative to Nafion membranes.

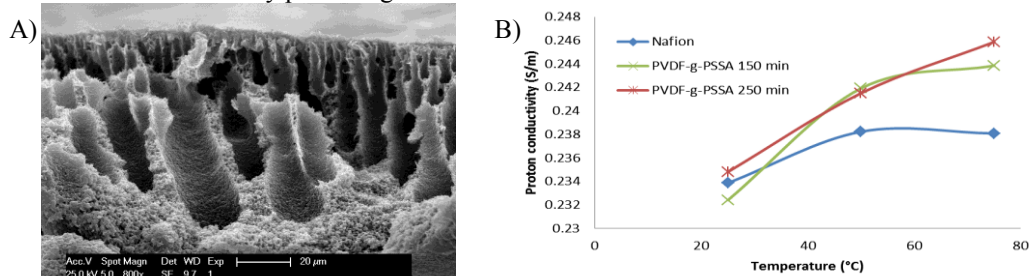


Figure 1: (A) SEM picture of PVDF-g-PSSA membrane and (B) comparison of conductivity as a function of temperature for Nafion and sulfonated PVDF membranes.

[1] T. Lehtinen, G. Sundholm, S. Holmberg, F. Sundholm, P. Björnbom and M. Bursell, *Electrochimica Acta*, 43 (1998) 1881-1890.

# Metalloporphyrin-Modified Perovskite-Type Oxide for Cathode Catalyst in Alkaline Fuel Cell

Tsukasa Nagai, Shin-ichi Yamazaki, Naoko Fujiwara, Masafumi Asahi, Zyun Siroma, and Tsutomu Ioroi  
*Research Institute of Electrochemical Energy, Department of Energy and Environment  
National Institute of Advanced Industrial Science and Technology (AIST)  
1-8-31, Midorigaoka, Ikeda, Osaka 563-8577, Japan  
tsukasa-nagai@aist.go.jp*

Alkaline fuel cell (AFC) has attracted attention due to the potential use of non-Pt-based catalyst. Perovskite-type oxides are considered one of the promising candidates for alkaline-resistant electrocatalyst with high oxygen reduction reaction (ORR) activity<sup>1</sup>. Recent researches on perovskite catalyst reported that the La-Mn based perovskite and La-Co based perovskite in carbon supported catalyst contributes to reduction and/or disproportionation of H<sub>2</sub>O<sub>2</sub><sup>2</sup>. Therefore, it may be possible to promote the overall reaction on a carbon-supported perovskite catalyst by adding a co-catalyst with high two-electron O<sub>2</sub> reduction activity. In this study, perovskite/carbon was modified by a cobalt octaethylporphyrin (Co-OEP) showing two electron O<sub>2</sub> reduction activity. ORR activity of the catalyst was investigated in alkaline media by a rotating ring disk electrode (RRDE) method.

The precursors of perovskite-type oxide (La<sub>0.6</sub>Sr<sub>0.4</sub>Mn<sub>0.6</sub>Fe<sub>0.4</sub>O<sub>3</sub>) were obtained by evaporating an aqueous solution of a mixture of La(NO<sub>3</sub>)<sub>3</sub>·6H<sub>2</sub>O, Sr(NO<sub>3</sub>)<sub>2</sub>, Mn(NO<sub>3</sub>)<sub>2</sub>·6H<sub>2</sub>O, Fe(NO<sub>3</sub>)<sub>3</sub>·9H<sub>2</sub>O, and polyvinyl pyrrolidone (PVP). The mixtures were heated in air at 600°C. The BET surface area of La<sub>0.6</sub>Sr<sub>0.4</sub>Mn<sub>0.6</sub>Fe<sub>0.4</sub>O<sub>3</sub> was measured to be 31 m<sup>2</sup> g<sup>-1</sup>. The perovskite/carbon (La<sub>0.6</sub>Sr<sub>0.4</sub>Mn<sub>0.6</sub>Fe<sub>0.4</sub>O<sub>3</sub>/C) was prepared by mixing La<sub>0.6</sub>Sr<sub>0.4</sub>Mn<sub>0.6</sub>Fe<sub>0.4</sub>O<sub>3</sub> and carbon black (Vulcan XC 72) in an agate pot at a rotation speed of 400 rpm for 30 min. Cobalt octaethylporphyrin (Co-OEP) was adsorbed on La<sub>0.6</sub>Sr<sub>0.4</sub>Mn<sub>0.6</sub>Fe<sub>0.4</sub>O<sub>3</sub>/C by an evaporation-to-dryness method. A glassy carbon electrode was used as a working electrode. A reversible hydrogen electrode (RHE) and a platinum electrode were used as a reference and counter electrodes, respectively.

The hydrodynamic voltammograms for the prepared catalysts show the onset potential of the Co-OEP/La<sub>0.6</sub>Sr<sub>0.4</sub>Mn<sub>0.6</sub>Fe<sub>0.4</sub>O<sub>3</sub>/C catalyst is shifted to positive direction and the ORR current was drastically increased, compared to the perovskite/C and Co-OEP/C catalyst. Decreased ring current was clearly confirmed relative to that for Co-OEP/C.

The fraction of HO<sub>2</sub><sup>-</sup> production during oxygen reduction as estimated from RRDE voltammograms ( $X_{\text{H}_2\text{O}_2}$ )<sup>3</sup> for the Co-OEP/La<sub>0.6</sub>Sr<sub>0.4</sub>Mn<sub>0.6</sub>Fe<sub>0.4</sub>O<sub>3</sub>/C was much lower (ca. 0.15) than those for Co-OEP/C (ca. 0.7), indicating enhancement of quasi-four-electron reduction of O<sub>2</sub> by combining Co-OEP and La<sub>0.6</sub>Sr<sub>0.4</sub>Mn<sub>0.6</sub>Fe<sub>0.4</sub>O<sub>3</sub>. The reason for high ORR activity of the Co-OEP/La<sub>0.6</sub>Sr<sub>0.4</sub>Mn<sub>0.6</sub>Fe<sub>0.4</sub>O<sub>3</sub>/C catalyst is that HO<sub>2</sub><sup>-</sup> which produced by Co-OEP is reduced to OH<sup>-</sup> by perovskite-type La<sub>0.6</sub>Sr<sub>0.4</sub>Mn<sub>0.6</sub>Fe<sub>0.4</sub>O<sub>3</sub>.

To compare the ORR performances of porphyrin/perovskite/carbon with different compositions of perovskite oxide or structures of porphyrin complex, we prepared catalysts with several types of perovskite and porphyrin complex. ORR activity was also enhanced by Co-OEP-modification of other types of La-based perovskite-type oxide. Porphyrin complex with two different structures (cobalt tetraphenylporphyrin (Co-TPP), iron octaethylporphyrin (Fe-OEP)) were added to the La<sub>0.6</sub>Sr<sub>0.4</sub>Mn<sub>0.6</sub>Fe<sub>0.4</sub>O<sub>3</sub>/C. The onset potential of the Co-TPP-modified catalyst and Fe-OEP-modified catalyst did not shift to the positive direction, because of the lower activity compared to Co-OEP.

## Acknowledgement

The authors are grateful to Tokuyama Corporation for providing the anion exchange resin (AS-4).

## References

- 1) D.B. Meadowcroft, *Nature*, **226**, 847 (1970).
- 2) T. Poux et al., *Catal. Today*, **189**, 83 (2012).
- 3) U.A. Paulus et al., *J. Electroanal.Chem.*, **134**, 495 (2001).

# The Degradation of Oxygen Reduction Activity at Stepped Platinum Surfaces in Acidic Media

Yan-Xia Chen,\* YongLi Zheng, Zhengda He and Jie Wei

*Hefei National Laboratory for Physical Sciences at Microscale, Department of Chemical Physics,  
University of Science and Technology of China, Hefei, 230026, China  
yachen@ustc.edu.cn*

Understanding the structure-activity relationship of Pt group metals toward oxygen reduction reaction (ORR) is one of the most extensively investigated topics in the past 60 years, because of its great significance in both fundamental studies and in guiding the rational design of improved ORR catalysts for low temperature fuel cells. From Systematic studies by Feliu's group, it is found that in acid media the ORR activity at Pt[n(111)×(111)] stepped surfaces decreases with the increase in the terrace width, i.e., Pt(331)>Pt(332)>Pt(221)>Pt(111). They found that the ORR is a complex process affected by many different factors and neither surface charge nor oxygen-containing species coverage alone are a determining factor of the electrode activity. Instead, adlayer structures and the relation between adsorbed water, H<sub>2</sub>O<sub>ads</sub>, water dissociation products, OH<sub>ads</sub> or O<sub>ads</sub>, and PtO oxide species coverage affect the whole energetics of the adsorption processes and may determine the surface reactivity.<sup>1</sup> Beside the information on the structure activity relationship, long term stability is also a very important factor to guide the design of practical ORR catalysts.

In order to have a deeper understanding of structure-activity relationship and checking the long term stability of Pt[n(111)×(111)] vicinal faces toward ORR, conventional electrochemical studies using hanging meniscus rotating disk electrode configuration and DFT calculation have been carried out. We find that i) in the first positive-going potential scan in 0.1 M HClO<sub>4</sub>, ORR activity decreases with the order of Pt(331)>Pt(332)>Pt(111), confirming well the data reported by Feliu's group; ii) there is a decrease of ORR activity with decrease in potential scan rate when keeping upper potential limit (E<sub>h</sub>) at 1.0 V<sub>RHE</sub> and electrode rotation speed constant, or with increase in electrode rotation speed while keeping constant scan rate or with time in chronoamperometric transients at constant potentials; iii) Under otherwise identical condition, the decay of ORR current increases in the order of Pt(111)<Pt(331)>Pt(332). All these phenomena suggest poisoning of Pt[n(111)×(111)] during ORR, and the extent for the poisoning decrease in the order of Pt(332)>Pt(331)>Pt(111). The trends in ORR activity and extent of degradation can be well explained by the difference in the binding strength of O-atoms at step and terrace sites at Pt(hkl) surfaces, as supported by DFT calculation. Present study indicate that the activity trends derived from the polarization curves recorded in the first positive-going potential scan, as usually used to evaluate the catalysts' ORR activity, cannot be simply taken as guideline for rational design of improved catalysts for ORR, since the active sites may be poisoned soon during ORR.

## Reference

(1) Gomez-Marin, A. M.; Rizo, R.; Feliu, J. M. *Catalysis Science & Technology* **2014**, *4*, 1685.

# Novel Poly(ether sulfone)s with Clustered Sulfonic Groups for PEMFC Applications at Various Relative Humidity

Shih-Wei Lee,<sup>a</sup> Jyh-Chien Chen,<sup>a</sup> Jin-An Wu,<sup>a</sup> Kuei-Hsien Chen<sup>b,c</sup>

<sup>a</sup>Department of materials science and engineering, National Taiwan University of Science and Technology, No. 43, Sec 4, Keelung road, Taipei 106, Taiwan

<sup>b</sup>Institute of Atomic and Molecular Science, Academia Sinica, Taipei, 10617, Taiwan.

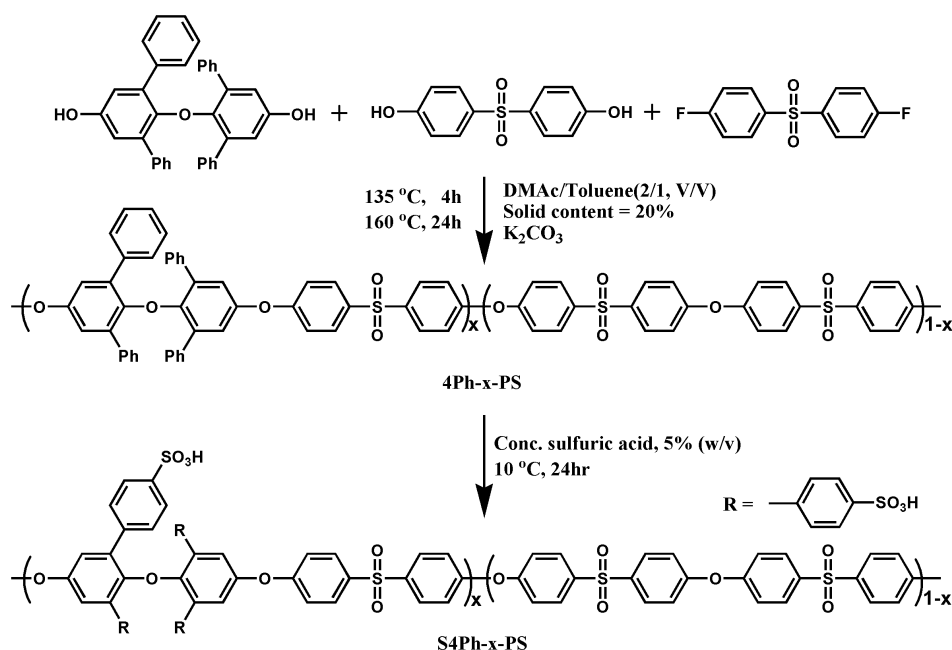
<sup>c</sup>Center for Condensed Matter Sciences, National Taiwan University, No. 1 Sec. 4 Roosevelt Road, Taipei, 10617, Taiwan.

Presenting author. Tel.: +886 227376526. E-mail address: D10304015@mail.ntust.edu.tw (S. H. Lee)

Corresponding author. Tel.: +886 227376526. E-mail address: jcchen@mail.ntust.edu.tw (J. H. Chen)

Symposium 4: Advances in Fuel Cells from Materials to Systems

Novel sulfonated co-poly (ether sulfone)s (S4Ph-x-PS) based on a new aromatic diol containing four phenyl groups were synthesized and characterized by NMR analysis and titration. The sulfonated co-poly (ether sulfone)s had good proton conductivity in the range of 0.004 to 0.110 S/cm. Single H<sub>2</sub>/O<sub>2</sub> fuel cells based on S4Ph-40-PS loaded with 0.25 mg/cm<sup>2</sup> catalyst (Pt) exhibited the maximum power density of 466.9 mW/cm<sup>2</sup>, which was closed to that of Nafion 212 (533.5 mW/cm<sup>2</sup>) at 80 °C with humidity at 80% RH. While in low relative humidity (53%), fuel cells based on S4Ph-35-PS showed higher peak power density (234.9 mW/cm<sup>2</sup>) than that of Nafion.



Scheme 1. Synthesis route of S4Ph-x-PS copolymers.

Table 1. Peak power density of S4Ph-35-PS and Nafion 212 at 80 °C with various relative humidity.

Relative humidity (%)	S4Ph-35-PS (mW/cm <sup>2</sup> )	Nafion 212 (mW/cm <sup>2</sup> )
53%	234.9	214.0
66%	289.1	344.7
80%	445.1	533.5
100%	372.9	847.4

# IL-FE-SEM Study for Ambience Dependence of Degradation of Pt/C Catalyst

Misako Ikeyama, Taro Kinumoto, Sawaka Kitayama, Miki Matsuoka,  
Tomoki Tsumura and Masahiro Toyoda

Dept. of Appl. Chem., Graduate School of Eng., Oita Univ., 700 Dannoharu, Oita, 870-1192, JAPAN  
kinumoto@oita-u.ac.jp

The carbon black-supported Pt nanoparticle catalyst (Pt/C) is generally employed as the cathode catalyst of proton exchange membrane fuel cells (PEMFCs); unfortunately, it deteriorates with loss of the electrochemical surface area (ECSA). There are several degradation processes that have been qualitatively considered to be responsible for the loss of ECSA [1]. And hence, technology that can be used to continuously monitor the degradation of specific Pt particles in Pt/C is important to further quantitatively understand the degradation process. We have carried out the identical location field emission scanning electron microscopy (IL-FE-SEM) for semi-quantitatively analysis for the degradation mechanism during accelerated degradation test (ADT) according to FCCJ [2]. In this presentation, the effect of atmosphere on the degradation of Pt nanoparticles is reported.

Pt/C catalyst (TEC10E50E, Tanaka Kikinzoku Kogyo, Pt weight = 46.7 wt%) was dispersed on a glassy carbon disk, and then Nafion thin film was formed on the catalyst (calculated thickness = 80 nm), which was employed as the test electrode. FE-SEM observation of Pt/C catalyst was carried out and the observation point was defined for IL-FE-SEM. After that, the test electrode was transferred to a glass half-electrochemical cell filled with 0.1 mol dm<sup>-3</sup> HClO<sub>4</sub> aqueous solution. The potential pulse test (0.6 V - 1.0 V, pulse time = 3 s) was carried out as ADT under N<sub>2</sub> and O<sub>2</sub> atmosphere. IL-FE-SEM observation and cyclic voltammetry measurements were carried out after an arbitrary test period.

Figure 1 shows typical IL-FE-SEM images under O<sub>2</sub> atmosphere. The typical morphological changes were observed for Pt particles such as shrinkage and growth of the particles, disappearance, migration, coalescence, transformation, precipitation on carbon support. Those phenomena were also observed under N<sub>2</sub> atmosphere.

Figure 2 shows the frequencies for degradation processes of Pt particles based on IL-FE-SEM results. Closed and open plots are the results under N<sub>2</sub> and O<sub>2</sub> atmosphere, respectively. The frequency for summation of shrinkage and disappearance are shown as square plots and reached the maximum of ca. 20% for both atmospheres. Growth of the particle was also observed and the frequency (circle plots) under O<sub>2</sub> atmosphere was slightly higher than that under N<sub>2</sub> atmosphere after the 10,000 pulses. The frequency of coalescence (triangular plots) under O<sub>2</sub> atmosphere was clearly higher than that under N<sub>2</sub> atmosphere during the durability test. On the other hand, the frequencies of precipitation (inverted triangle plots) were slightly higher for N<sub>2</sub> atmosphere. Thus, degradation of Pt/C depends on the atmosphere and more details will be mentioned in the presentation.

- [1] Y. Shao-Horn, et al., *Top. Catal.*, **46**, 285 (2007).
- [2] T. Kinumoto, et al., *Electrochemistry*, **83**, 12 (2015).

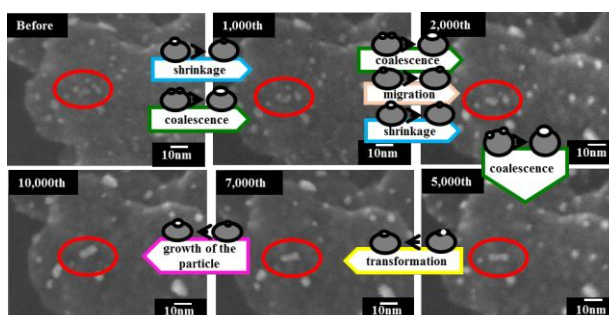


Fig. 1 Typical IL-FE-SEM images of Pt/C during the durability test under O<sub>2</sub>

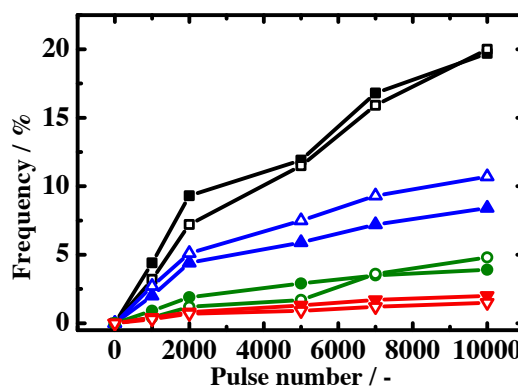


Fig. 2 Frequency for degradation of Pt particles during the durability tests.

# **Fabrication of Anode Microporous Layer with Carbon Nanotubes and its Effect on Proton Exchange Membrane Fuel Cell Performance**

Sheng-Wei Huang, Min-Hsing Chang

*Department of Mechanical Engineering, Tatung University*

*Taipei, 104, Taiwan*

*mhchang@ttu.edu.tw*

Proton exchange membrane fuel cells (PEMFC) have received much attention in the past decades as a clean power source for many potential applications like automotive or stationary power plants. However, its performance still needs improvement in order to meet the requirement of fast response in the power delivery system. One of the major problems restricting the cell performance is the water management within the membrane electrode assembly (MEA). The amount of liquid water flux from anode to cathode induced by the electroosmosis phenomenon and the effect of back-diffusion due to the condensation of water vapor at cathode catalyst layer (CL) are both typically important factors which may affect the water balance within the MEA profoundly. The water management performance depends heavily on the gas diffusion layer (GDL) which is a critical component of MEA. In general, the GDL is sandwiched between the CL and the gas flow channel and a dual-layer structure which consists of a macroporous substrate made by carbon paper or carbon cloth and a thin carbon layer coated on its surface. The thin carbon layer is named microporous layer (MPL) which is adjacent to the CL on both sides of MEA and generally contains carbon black powder and hydrophobic agent like polytetrafluoroethylene (PTFE) for the management of two-phase water flow. Accordingly, the GDL properties are quite important in water management and it becomes a challenge to achieve maximum cell performance by improving the GDL properties. Numerous studies have been published in the literature to investigate the effects of GDL and MPL on PEMFC performance. Most of them focused on the effects of cathode GDL or MPL. The study for the influence of anode MPL is relatively limited and it still needs to be explored further. The purpose of this research is to measure the variation of cell performance for a PEMFC using multiwall carbon nanotubes (CNTs) as the composition of MPL material in the anode GDL. The CNT loading and the PTFE content in the anode MPL are adjusted and their effects on the cell performance are explored. Accordingly, the optimal composition of anode MPL including CNT loading and PTFE content could be determined. The techniques of electrochemical impedance spectroscopy and cyclic voltammetry have been used in the experiments. The results show that the employment of multiwall CNT as anode MPL material indeed may improve the cell performance. The optimal composition of anode MPL is found to be 1.0 mg/cm<sup>2</sup> of CNT loading with 20 wt% of PTFE content. Results provide a full understanding for the role of CNT in the fabrication of MPL for a PEMFC system.



# Synthesis of Pt Nanoparticles using Microbubble-assisted Low-Voltage Low Frequency Solution Plasma Processing

Genki Horiguchi<sup>1</sup>, Hidenobu Shiroishi<sup>1\*</sup>, Yu Chikaoka<sup>1</sup>, Masato Uehara<sup>2</sup> and Naoki Matsuda<sup>2</sup>

<sup>1</sup>Tokyo National College of Technology, <sup>2</sup>National Institute of Advanced Industrial Science and Technology

<sup>1</sup>Kunugida 1220-2, Hachioji, Tokyo, JAPAN, <sup>2</sup>807-1, Shukumachi, Tosu, Saga 841-0052, Japan  
\*h-shiroishi@tokyo-ct.ac.jp

## 1. Introduction

A solution plasma processing method at a low voltage and a low frequency, abbreviated as SPP-LVLF, is promising for the synthesis of Pt nanoparticles for polymer electrolyte fuel cells because of a simple and easy method and low environmental load. However, one of major problems with the method is that the size of Pt particles is too large (5 - 20 nm) to use as catalysts. In this report, we show the synthesis of 3.3 nm Pt particles by a microbubble-assisted SPP-LVLF (abbreviated as MBSP).

## 2. Experimental

Microbubbles were generated in a 0.86 – 2.58 mM KNO<sub>3</sub> aqueous solution heated to 45°C using a microbubble generator (OKE-MATRIX-MB01, OK engineering Ltd.). The solution was fed to a flow cell at a 24 mL min<sup>-1</sup>, where a tungsten wire (1.0 mmφ, Nilaco Corp.) and one or two Pt wire(0.5 mmφ, Nilaco Corp.) were inserted with 0.2 mm gap. Pt nanoparticles were produced by applying half-wave rectified waves (440 V) with a power transformer (SD41-02KB, Toyozumi Dengenkiki Corp.) between the two electrodes for 4 to 10 min. The solution was filtered with a membrane filter (Millipore 0.1 μm), then Vulcan XC-72R (Cabot) was suspended to the solution with stirring for 24 h. After the suspension was concentrated by a rotary evaporator, the Pt nanoparticles mixed with XC-72R (Pt/XC72) were washed by decantation with Milli-Q water, and were allowed to dry under vacuum. The Pt/XC72 were characterized by XRD, FE-SEM, and TG.

A 2.0 mg of the Pt/XC72 catalysts was suspended by shaking with zirconia balls in 1 mL of 0.1 wt% Nafion-MeOH by ultrasonication. A 10 μL of the suspension was cast onto a glassy-carbon disk (6 mm φ, 0.283 cm<sup>2</sup>) – Pt ring electrode (Nikko Keisoku) and dried for 1 h under N<sub>2</sub> atmosphere. Electrochemical properties were investigated by the rotating ring-disk electrode (RRDE) method with the modified electrode as a working, a RHE as a reference, and a gold wire as a counter electrodes in 0.1 M HClO<sub>4</sub>. Finally, an accelerated durability test (ADT) was performed by the FCCJ cycle test method with a triangular wave (1.0 to 1.5 V).

## 3. Results and Discussion

Table 1 shows the number of light emissions and the particle sizes of Pt prepared by the MBSP method at various KNO<sub>3</sub> concentrations. The number of plasma emission tended to increase with the concentration of KNO<sub>3</sub>, which is due to the increase in the ionic conductivity. The size of Pt nanoparticles was severely affected by the concentration of KNO<sub>3</sub>, and the Pt nanoparticles synthesized in 2.06 mM KNO<sub>3</sub> was the smallest in the condition.

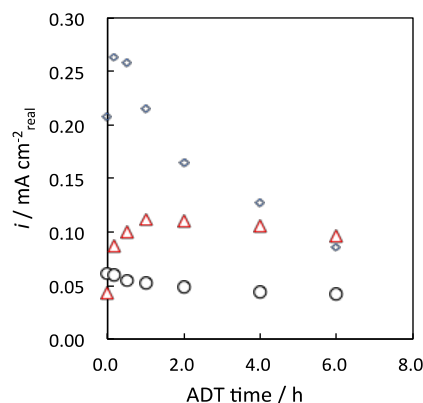
Fig. 1 shows the dependence of oxygen reduction current normalized by initial electrochemical surface area at 0.95 V on ADT time. The ORR current of the catalysts prepared by the MBSP was higher than that of Pt/XC72 (E-TEK).

Table 1 Result of Pt nanoparticle synthesis by the microbubble-assisted LVLF-SP method at various KNO<sub>3</sub> concentrations.

Sample No.	[KNO <sub>3</sub> ] / mM	Number of light emissions / min <sup>-1</sup>	Particle size of Pt / nm <sup>1)</sup>
1	0.86	60.0	8.50 ± 1.11
2	1.72	442.8	7.63 ± 0.36
3	1.89	95.2	3.93 ± 0.23
4	2.06	318.9	3.25 ± 0.12
5*	2.06	493.8	3.93 ± 0.09
6	2.58	498.1	7.31 ± 0.88

1) Analyzed by XRD measurements with Scherrer equation.

\*Using two Pt wires.



**Fig. 1.** Dependence of ORR current density normalized by initial ECSA at 0.95 V on ADT time in 0.1 mol/L HClO<sub>4</sub> under N<sub>2</sub> at 298K. ○: 20% Pt/XC72(E-TEK), △: Pt/XC72 (MBSP)-3.25±0.12 nm, ◇: Pt/XC72(MBSP)-3.93±0.09 nm.

# Novel Polybenzimidazoles Containing Bulky Side Groups for High-temperature Polymer Electrolyte Membranes Fuel Cell Applications

Jyh-Chien Chen,<sup>a</sup> Ping-Yen Chen,<sup>a</sup> Kuei-Hsien Chen,<sup>b,c</sup>

<sup>a</sup>Department of Materials Science and Engineering, National Taiwan University of Science and Technology, 43 Sec. 4, Keelung Road, Taipei 10607, Taiwan

<sup>b</sup>Institute of Atomic and Molecular Science, Academia Sinica, Taipei, 10617, Taiwan.

<sup>c</sup>Center for Condensed Matter Sciences, National Taiwan University, No. 1 Sec. 4 Roosevelt Road, Taipei, 10617, Taiwan.

Presenting author. Tel.: +886 227376526. E-mail address: D10304001@mail.ntust.edu.tw (P. Y. Chen)

Corresponding author. Tel.: +886 227376526. E-mail address: jcchen@mail.ntust.edu.tw (J. C. Chen)

Symposium 4: Advances in Fuel Cells from Materials to Systems

The most widely used PBI for HT-PEMFC applications is poly-2,2'-(*m*-phenylene)-5,5'-bibenzimidazole (*m*-PBI), which possesses several excellent qualities such as thermal stability, mechanical strength, acid-attracting ability and proton conductivity. Numerous PBIs have been synthesized and investigated for such applications. However, PBIs based on new tetraamines are relatively rare. In this study, we report three polybenzimidazoles, **P1~P3**, derived from new tetraamines. **P1~P3** exhibited good thermal stability, oxidative stability, mechanical properties as well as solubility in common aprotic polar solvents. In addition, the phosphoric acid-doped **P1~P3** membranes exhibited high proton conductivity in the range of  $3.99 \times 10^{-2} \sim 5.34 \times 10^{-2} \text{ S cm}^{-1}$ . They also demonstrated high performance on single cell test, with peak power density of 478~636  $\text{mW/cm}^2$  at 160 °C with acid uptakes of 199~241 %.

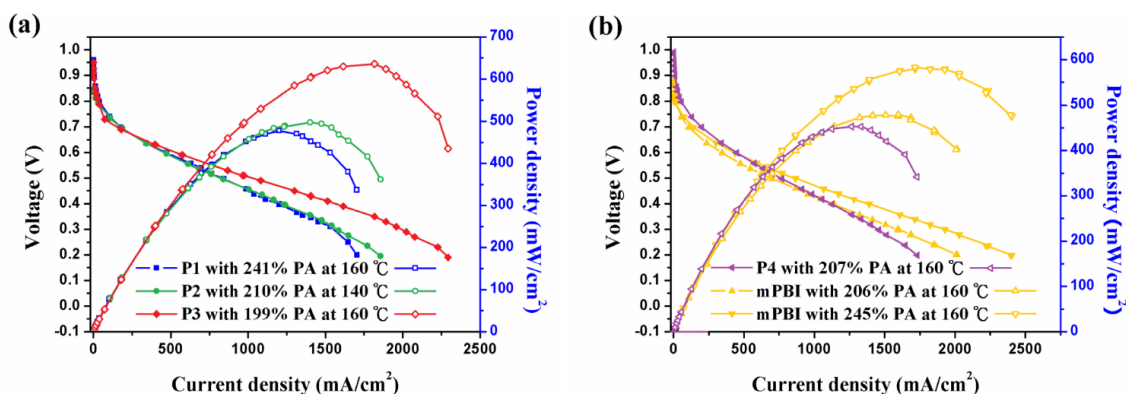
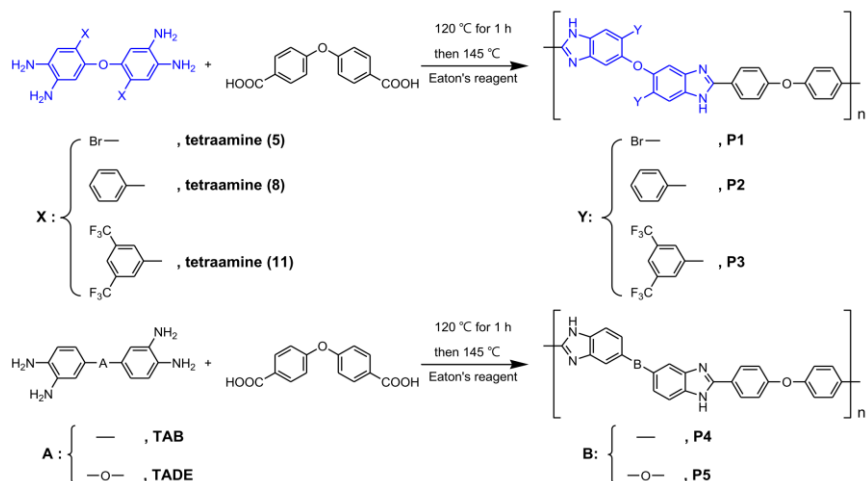


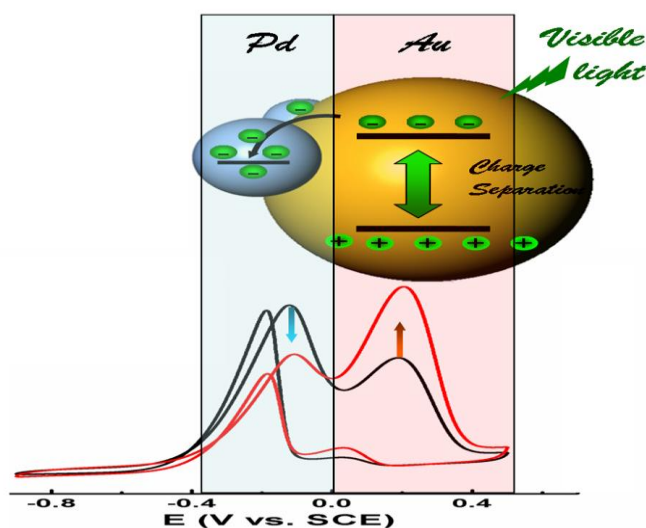
**Figure 1.** Polarization curves of PBIs.

# Plasmonic Induced Inhibition and Enhancement of the Electrocatalytic Activity for Ethanol Oxidation on Pd/Au Hetero-Nanoraspberries

Xiaoqiang Cui

*Department of Materials Science, Key Laboratory of Automobile Materials of MOE and State Key Laboratory of Superhard Materials, Jilin University, Changchun, 130012, People's Republic of China  
xqcui@jlu.edu.cn*

Plasmonic modulating the catalytic performances of metallic nanostructures shows great potential in developing novel materials for catalysis. Besides the challenges of devising new catalysts with high activity while keeping controllable plasmonic property, the mechanisms beneath the enhancement of the activity by surface plasmon resonance (SPR) is still under exploring. We designed and implemented a Pd-Au bimetallic heterostructure that carry the well-defined surface plasmonic resonance property of Au NPs that used as the core to tune the electrocatalytic performance on the hetero-nanostructures' surface. With excellent morphology control, we provide chances of tuning their catalytic properties with respect to the Pd antenniform nanoislands and the incorporated Au cores. We also demonstrate that, with visible-light irradiation, the electron resonated with the photons could transfer to the Pd nanopetals from Au, resulting in the enhancement of electrocatalytic performance on Au and inhibition on Pd. Besides, the anti-poisoning property and stability of as-prepared samples can also be enhanced by the visible-light-irradiation.



# Effect of dispersion methods on oxygen reduction and ammonia oxidation activity for a MWCNT supported Pt catalyst

Ryo Shirasaka<sup>1</sup>, Sakumi Aoyagi<sup>1</sup>, Hidenobu Shiroishi<sup>1\*</sup>, Keiji Nagai<sup>2</sup>, Hiraku Ota<sup>3</sup>, and Mika N.- Gamo<sup>3</sup>  
(Tokyo National College of Technology<sup>1</sup>, Tokyo Institute of Technology<sup>2</sup>, Toyo University<sup>3</sup>)  
1220-2 Kunugida, Hachioji, Tokyo, 193-0997 Japan<sup>1</sup>  
h-shiroishi@tokyo-ct.ac.jp

## 1. Introduction

In the case of evaluating the activity of a catalyst with the rotating ring disk electrode (RRDE) method, casting an aliquot of the catalyst suspension, which is mostly prepared with ultrasonic wave or planetary ball mill, on a glassy carbon (GC) electrode is the general method. However the dispersing quality of the catalyst on the GC electrode depends on kinds of catalysts and solvent in the suspension<sup>1, 2)</sup>. In this research, we have investigated the dispersiveness of the multiwall carbon nanotube-supported Pt catalyst (Pt/MWCNT) on the GC electrode prepared with four devices: an ultrasonic bath, a planetary ball mill, a stirrer, and a shaker. The evaluation of the dispersiveness has been performed by microscope observation and electrocatalytic measurements for oxygen reduction and ammonia oxidation reaction.

## 2. Experimental

3.6 wt% Pt/MWCNT ( $5.57 \pm 0.11$  nm) was synthesized with a microwave-polyol method. 2 mg of Pt/MWCNT was suspended in 1 mL of 0.1 wt% Nafion-MeOH by four dispersion methods: 1) ultrasonic method (sample name: US-ultrasonic exposure time), 2) stirring method (sample name: ST-rotating speed-stirring time), 3) planetary ball mill method (sample name: PB-rotating speed-rotating time-the number of zirconia balls) and 4) shaking method with adding zirconia balls (SH-rotating speed-shaking time-number of zirconia balls). 10  $\mu$ L of each suspension was cast on a GC electrode and dried in air for 1 h. The dispersiveness of each electrode was observed with digital microscope (MSP-3080, PANRICO). In electrochemical measurements, ECSA was estimated with conducting CO-stripping in 0.1 M HClO<sub>4</sub> using RHE as a reference electrode and Au wire as a counter electrode. The activity of ammonia oxidation was evaluated in 0.1 M NH<sub>3</sub>-0.1 M KOH under N<sub>2</sub> atmosphere after the activity of oxygen reduction reaction was performed in 0.1 M KOH under N<sub>2</sub> or O<sub>2</sub> atmosphere by the RRDE method.

## 3. Results and Discussion

Fig. 1 shows the microscopic images of the GC electrode surface prepared by various dispersion methods. The dark area of the images is GC electrode surface, whereas the catalyst particles exist in the bright diffuse area. The catalyst particles prepared by ultrasonic (Fig. 1(a)) or planetary ball mill (Fig. 1(d)) methods was uniformly dispersed on the GC electrode surface compared to those by stirring (Fig. 1(b)) or shaking (Fig. 1(c)) method by which the catalyst particles often aggregated at the center not to reach the circumference of the GC electrode surface. The amount of H<sub>2</sub>O<sub>2</sub> generated by electrochemical oxygen reduction reaction with the electrode prepared by ultrasonic or planetary ball mill method tended to be larger than those by stirring or shaking method, indicating that the quantity of H<sub>2</sub>O<sub>2</sub> cannot be precisely determined without uniform dispersion of the catalyst on the GC electrode. The electrode prepared by stirring or shaking is not good at ammonia oxidation. The aggregated catalyst would affect the adsorption of NH<sub>3</sub> on the catalyst surface by generating N<sub>2</sub> gas. From these results, the difference in the condition of the catalyst cast on the GC electrode is suggested to depend on the dispersion method, consequently, the optimization of the dispersion method is indispensable for the precise evaluation of the catalyst activity.

- (1) T. Okajima, *Electrochemistry*, **81**, 717 (2013).
- (2) T. Kinumoto, *Electrochemistry*, **79**, 116 (2011).
- (3) Z. Liu et al., *J. Power Sources*, **139**, 73 (2005).

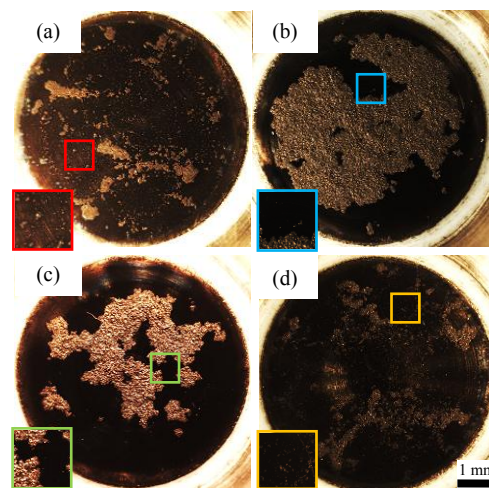


Fig. 1 Microscope images of GC|0.1  $\mu$ m Nafion [33.6 wt% Pt/MWCNT] electrodes prepared by various dispersion methods, (a) US-30 min, (b) ST-500 rpm-24 h, (c) SH-1000 rpm-1 h-3 and (d) PB-250 rpm-30 min-12.

# Mass Transfer Analysis of Anode-Supported Honeycomb Solid Oxide Fuel Cells

Sou IKEDA<sup>1</sup>, Shota KOTAKE<sup>1</sup>, Hironori NAKAJIMA<sup>1,2,3</sup>, and Tatsumi KITAHARA<sup>1,2,3</sup>

<sup>1</sup>Department of Hydrogen Energy Systems, Graduate School of Engineering, Kyushu University,

<sup>2</sup>Department of Mechanical Engineering, Faculty of Engineering, Kyushu University,

<sup>3</sup>International Institute for Carbon-Neutral Energy Research (I<sup>2</sup>CNER), Kyushu University,  
744 Motoooka, Nishi-ku, Fukuoka 819-0395, Japan

Email: sou.ikeda.fcsl@gmail.com, nakajima@mech.kyushu-u.ac.jp

An anode-supported honeycomb solid oxide fuel cell can achieve high volumetric power density and improve thermo-mechanical durability at high temperatures. We have so far fabricated the honeycomb cell with a cathode layer of LSM and an electrolyte layer of 8YSZ on a porous anode honeycomb substrate of Ni/8YSZ. The anode-supported honeycomb cell exhibited promising volumetric power densities[1]. Effect of flow channel configurations on the cell performance was investigated in terms of the hydrogen partial pressure distributions in the cell under operation as well[1]. In this study, we compare the differences of measured current-voltage and current-power density curves between the honeycomb cells having porous substrate thicknesses of 0.5 mm and 1.0 mm shown in Fig. 1 under different hydrogen flow rates. Thinner substrate gives better performance for smaller fuel flow rates. The effect of hydrogen partial pressure distributions associated with the anode-substrate thickness on the cell performance is numerically clarified with finite element modeling.

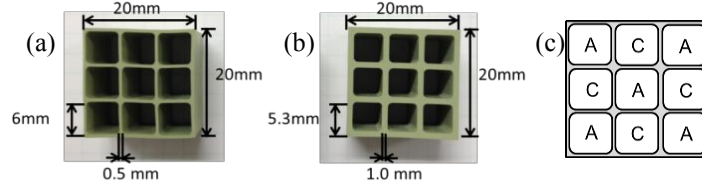


Fig. 1 Cross-sectional pictures of the honeycomb cells with anode substrate thicknesses of (a) 0.5 mm and (b) 1.0 mm. (c) A and C represent anode and cathode flow channels, respectively.

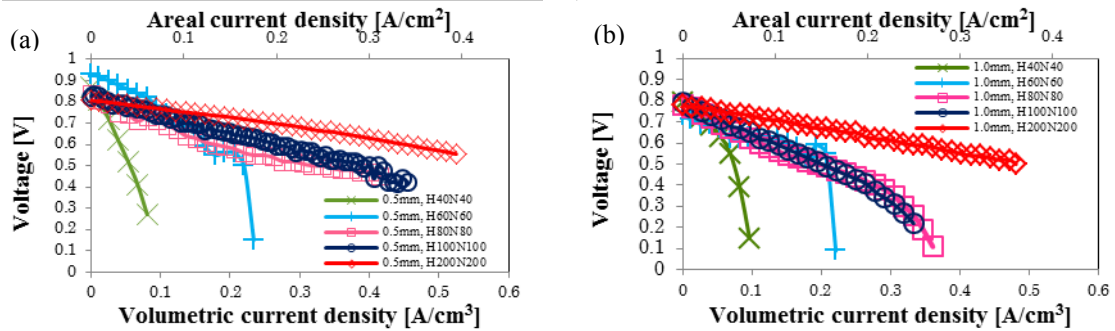


Fig. 2 Current-voltage characteristics for the honeycomb cell with anode thicknesses of (a) 0.5 mm and (b) 1.0 mm at 850 °C, H<sub>2</sub>/N<sub>2</sub>: 40/40, 60/60, 80/80, 100/100, and 200/200 cm<sup>3</sup>/min, air: 400 cm<sup>3</sup>/min in total.

Reference:

[1] S. Kotake, H. Nakajima, and T. Kitahara, "Flow Channel Configurations of an Anode-Supported Honeycomb Solid Oxide Fuel Cell" *ECS Trans.*, **57**(1), B815 (2013).

# ***Synthesis and Characterization of High Temperature Proton Conductor Sr(Ce<sub>0.6</sub>Zr<sub>0.4</sub>)O<sub>3-δ</sub> co-doped with Indium and Yttrium***

**I-Ming Hung<sup>a,\*</sup>**, Hao-Ying Cheng<sup>a</sup>, Sheng-Wei Lee<sup>b,c</sup>, Jeng-Kuei Chang<sup>b,c</sup>, Jing-Chie Lin<sup>b,c</sup>, Jason Shian-Ching Jang<sup>b,c</sup>, Chuan Li<sup>d</sup> and Chi-Shiung Hsi<sup>e</sup>

<sup>a</sup> *Department of Chemical Engineering and Materials Science, Yuan Ze University, No. 135, Yuan-Tung Rd., Chungli, Taoyuan 320, Taiwan.*

<sup>b</sup> *Institute of Materials Science and Engineering, National Central University  
No.300, Zhongda Rd., Chungli City, Taoyuan 320, Taiwan.*

<sup>c</sup> *Department of Mechanical Engineering, National Central University,  
No.300, Zhongda Rd., Chungli City, Taoyuan 320, Taiwan.*

<sup>d</sup> *Department of Biomedical Engineering, National Yang-Ming University  
No.155, Sec.2, Linong Street, Taipei 112, Taiwan*

<sup>e</sup> *Department of Materials Science and Engineering, National United University,  
No.1, Lienda Rd., Miaoli 360, Taiwan.*

Solid oxide fuel cells (SOFCs) are electrochemical power-generation systems characterized by high conversion efficiency, low environmental impact, excellent fuel flexibility, and ability to use non-precious-metal catalysts. Typical SOFCs, which operate at a temperature of approximately 1000 °C, are based on oxygen-ion-conducting electrolytes. Recently, SOFCs based on proton-conducting electrolytes (H<sup>+</sup>-SOFC) have attracted considerable attention due to their relatively low operation temperature (400-800 °C) that facilitates the selection of the sealing and interconnection materials, control of the interactions between the electrode/electrolyte, and lowering of the thermal expansion mismatch between the cell components. Moreover, lowering the operation temperature also reduces the capital costs and prolongs cell lifetime. The key issue for H<sup>+</sup>-SOFC development is finding a suitable proton-conducting electrolyte material.

In this study, Sr(Ce<sub>0.6</sub>Zr<sub>0.4</sub>)<sub>0.85</sub>In<sub>0.15-x</sub>Y<sub>x</sub>O<sub>3-δ</sub> proton-conducting oxides are prepared by citrate-EDTA complexing method. The basic properties and electrochemical properties of Sr(Ce<sub>0.6</sub>Zr<sub>0.4</sub>)O<sub>3-δ</sub> co-doped with indium and yttrium are investigated. Its micro-structure patterns and sintered behavior are characterized by X-ray diffraction (XRD), field-emission scanning electron microscope (FE-SEM) and thermal mechanical analyzer (TMA). The XRD patterns and SEM images shows that the Sr(Ce<sub>0.6</sub>Zr<sub>0.4</sub>)<sub>0.85</sub>In<sub>0.15-x</sub>Y<sub>x</sub>O<sub>3-δ</sub> powder was synthesized with Zr<sub>0.5</sub>Ce<sub>0.5</sub>O<sub>2</sub> impurity phase. The relative sintering density of all Sr(Ce<sub>0.6</sub>Zr<sub>0.4</sub>)<sub>0.85</sub>In<sub>0.15-x</sub>Y<sub>x</sub>O<sub>3-δ</sub> is higher than 99%. The conductivity of the sintered Sr(Ce<sub>0.6</sub>Zr<sub>0.4</sub>)<sub>1-x</sub>Y<sub>x</sub>O<sub>3-δ</sub> disk measured at various temperatures in air using the 2-probe DC method. The conductivity of Sr(Ce<sub>0.6</sub>Zr<sub>0.4</sub>)<sub>0.85</sub>Y<sub>0.15</sub>O<sub>3-δ</sub> apparently increased as the temperature above 600 °C. The conductivity of Sr(Ce<sub>0.6</sub>Zr<sub>0.4</sub>)<sub>0.85</sub>Y<sub>0.15</sub>O<sub>3-δ</sub> is 0.000984 S/cm and 0.01467 S/cm at 600°C and 900°C, respectively. The phase stability of Sr(Ce<sub>0.6</sub>Zr<sub>0.4</sub>)<sub>0.85</sub>In<sub>0.15-x</sub>Y<sub>x</sub>O<sub>3-δ</sub> was investigated in 80 °C water for 60h, no second phase was observed.



# Crosslink-free highly sulfonated multi-block poly(arylene ether sulfone) multi-block membranes for PEMFC

Sojeong Lee and Byungchan Bae\*

Fuel Cell Laboratory, Korea Institute of Energy Research (KIER), 152, Gajeong, Yuseong, Daejeon, 305-343, Korea

E-mail: bcbae@kier.re.kr

Perfluorinated sulfonic acid (PFSA) membranes for fuel cell, such as Nafion (DuPont) and Aquivion (Solvay), are commonly used because of their high ionic conductivities and excellent mechanical properties; however, their high manufacturing cost and low thermal stability are major drawbacks. Heat-resistant and inexpensive aromatic hydrocarbon-based membranes seem to be successful potential alternatives to PFSA membranes.[1,2] More recently, the introduction of highly sulfonated hydrophilic blocks (almost one sulfonic acid per benzene ring) resulted in comparable proton conductivity to those of PFSA membranes. However, most of these compounds contained crosslinks because decafluorobiphenyl or hexa-fluorobenzene chain-extenders were used. Crosslinking during polymerization resulted in undesirable low solubility and defects.

In this study, we succeeded in synthesizing high-molecular weight SPAES multi-block polymers free from perfluorinated end-groups and crosslinking defects.[3] A block sulfonated poly (arylene ether sulfone) copolymer (SPAES) was synthesized through nucleophilic aromatic substitution between hydrophilic and hydrophobic oligomeric precursors. By increasing the purity of the oligomers and determining the optimum solvent for each segment, polymerization successfully generated high-molecular weight polymers. Highly sulfonated hydrophilic block polymers were designed and the resultant block membrane showed very high proton conductivity even under low RH as shown in Figure 1. (0.48 and 0.035 S cm<sup>-1</sup> at 90% and 40% RH, respectively, at 80°C) These values were higher than that of a commercial PFSA membrane. The presence of well-formed proton pathways from the hydrophilic clusters was confirmed by TEM; these explain the very high proton conductivity even under low RH conditions. The fuel-cell performance reached 250 mA cm<sup>-2</sup> at 0.7 V at 120°C, 40% RH, and atmospheric conditions.

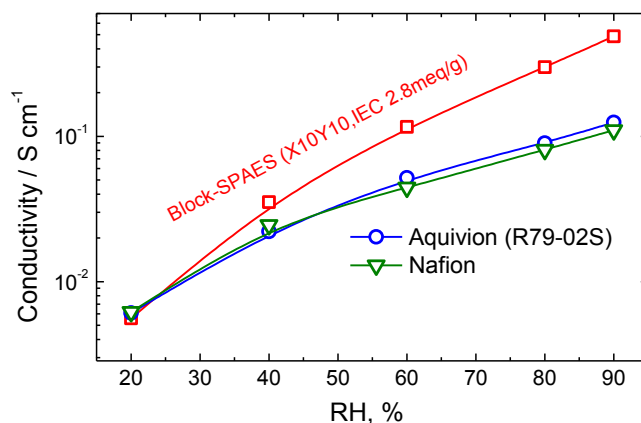


Figure 1. RH dependence of Proton conductivity of block SPAES, Aquivion, and Nafion membranes at 80°C.

## References

- [1] M. A. Hickner, H. Ghassemi, Y. S. Kim, B. R. Einsla and J. E. McGrath, Chem. Rev., 2004, 104, 4587.
- [2] B. Bae, K. Miyatake and M. Watanabe, in Polymer Science: A Comprehensive Reference, ed.-in-chief, M. Krzysztow and M. Martin, Elsevier, Amsterdam, 2012, pp. 621.
- [3] S. Lee, J. Ann, H. Lee, J.-H. Kim, C.-S. Kim, T.-H. Yang, B. Bae, J. Mater. Chem. A, 2015, 3, 1833.

# Proton Conducting ~~Polymer Electrolyte~~ Composite Membranes with Improved Oxidative Stability for PEMFC

Hyejin Lee and Byungchan Bae\*

Fuel Cell Laboratory, Korea Institute of Energy Research (KIER), 152, Gajeong, Yuseong, Daejeon, 305-343, Korea

E-mail: [lhyejin0130@kier.re.kr](mailto:lhyejin0130@kier.re.kr)

Mis en forme : Soulignement□

Alternative hydrocarbon-based (HC) membranes for proton exchange membrane fuel cell (PEMFC) application have been developed to overcome high cost of perfluorosulfonic acid membrane (Nafion). However, commercialization of HC membranes has been impeded due to its poor chemical (oxidative) stability during fuel cell operation. In this study, we prepared HC composite membranes with cerium ions and its investigated possibility as radical quencher was investigated for suppressing oxidative decomposition of HC membranes.

Composite polymer electrolytes were prepared by immersion and mixing method using sulfonated poly(arylene ether sulfone) (SPES, 50% DS) along with different content of cerium ion.<sup>[1]</sup> FE-SEM mapping imaging, ICP-AES and <sup>1</sup>H-NMR confirmed successful exchange of sulfonic acid group with metal ions. Also, influence of the additives on water uptake, IEC and proton conductivity was examined.

The effects of cerium ion on HC membrane oxidative stability were investigated through hydrogen peroxide exposure experiment (ex-situ) and accelerated OCV durability test (in-situ). According to the results durability test as shown in Figure 1, the oxidative degradation of HC-membranes was suppressed by quenching effect of found to be decreased with cerium ions. Long-term stability of more than 2000 h was achieved with the composite membrane whereas corresponding pristine SPES membrane showed attained only 700 h (Fig. 1). We will also compare two different methods, mixing and impregnation, for the preparation of composite membranes. The obtained results indicate that the cerium ions functioned as radical quencher to suppress oxidative degradation in the membranes. Especially, the composite membrane made by immersion method was more stable than that made by mixing method.

This study has suggested the important alternative to improve the electrolyte membrane durability for fuel cells.<sup>[1]</sup>

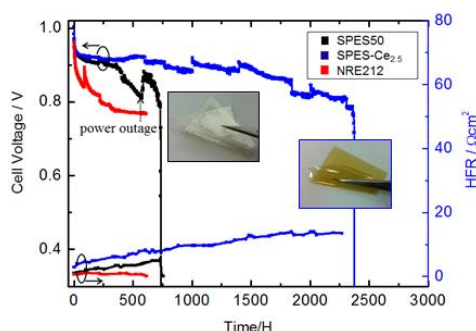


Figure 1. Time-dependent OCV and HFR values during long-term of the fuel cells-cell test at DOE conditions.

## References



[1] H. Lee, Y.-W. Choi, T.-H. Yang, B. Bae, J. ~~Korean~~Kor-ean Electrochem. Soc., 17 (2014) 44-48.

(저널명 확인바람)

Mis en forme : Surlignage

# Improving the Electrocatalytic Activity of Binary Alloy $\text{Cu}_x\text{Pd}_y$ for Methanol Oxidation Reaction by Tailoring Chemical Composition

Xuan Zhang\*, Jia-Wei Zhang, Bei Zhang

College of Chemistry, Chemical Engineering & Biotechnology, Donghua University  
Shanghai 201620, China.

e-mail address: xzhang@dhu.edu.cn

The promising potential in providing future sustainable and clean power source has inspired enormous interest on fuel cells during decades, especially on direct methanol fuel cells (DMFC). Pt- and Pd-based materials are the most popular anode electrocatalysts in DMFC for methanol oxidation reaction (MOR) [1]. However, the commercial mass production of noble Pt- and Pd-based catalysts for DMFC are strongly limited by their high cost, poor durability and low resistance to CO poisoning. Therefore, reducing the cost and improving the performance of electrocatalysts, are two crucial problems blocking a practical application. Alloying noble metal with less expensive metals (Cu, Fe, etc.) has been recognized to be an efficient approach, and it is also known that the composition ratio of alloy is very important in tailoring the catalytic activity [2]. As our continuous study on Pt-based electrocatalysts for both MOR and biosensor [3-6], here we will present research results on improving the activity of binary alloy  $\text{Cu}_x\text{Pd}_y$  electrocatalyst for MOR by tailoring its chemical composition. It has been found that the activity is strongly dependent on chemical composition of alloy (Fig. 1). The preparation, characterization, performance, and enhancement mechanism will be discussed in detail.

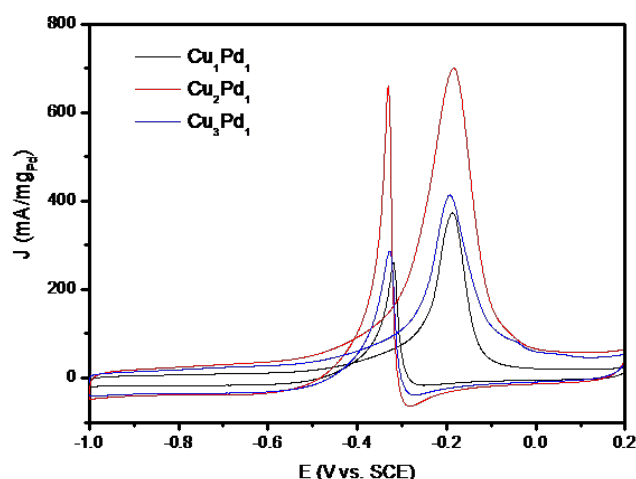


**Fig. 1** Cyclic voltammograms for the methanol oxidation reaction in 1M NaOH + 1M MeOH solution.

## References:

1. Huang H. J., Wang X., *J Mater. Chem. A* **2014**, 2, 6266–6291.
2. Scofield M. E., Koenigsmann C., Wang L., Liu H., Wong S. S., *Energy Environ. Sci.* **2015**, 8, 350–363.
3. Zhang X., Ma L.-X., *J. Power Sources* **2015**, 286, 400–405.
4. Zhang X., Zhang B., Li X.-D., Ma L.-X., Zhang J.-W., *Int. J. Hydrogen Energy* **2015**, in press.
5. Zhang X., Zhang B., Liu D.-Y., Qiao J.-L., *Electrochim. Acta* **2015**, in press.
6. Zhang X., Ma L.-X., Zhang Y.-C., *Electrochim. Acta* **2015**, in press.

# Preparation and structural and electrical properties of calcium-doped and nickel-doped yttrium chromate(III)

M. Stygar<sup>\*1)</sup>, W. Tejchman<sup>\*\*2)</sup>, J. Dąbrowa<sup>\*3)</sup>, T. Brylewski<sup>\*4)</sup>

<sup>\*</sup>AGH University of Science and Technology, Faculty of Materials Science and Ceramics  
al. Mickiewicza 30, 30-059 Kraków, Poland

stygar@agh.edu.pl<sup>1)</sup>; dabrowa@agh.edu.pl<sup>3)</sup>; brylew@agh.edu.pl<sup>4)</sup>

<sup>\*\*</sup> Pedagogical University of Cracow, Faculty of Geography and Biology  
ul. Podchorążych 2, 30-084 Kraków, Poland  
watejch@up.krakow.pl<sup>2)</sup>

Calcium-doped and nickel-doped yttrium chromate (YCCN) are very promising materials with regard to application as conductive coatings for ferritic stainless steels in interconnects – structural elements in intermediate-temperature solid oxide fuel cells (IT-SOFCs). They are characterized by high physicochemical stability and adequate electrical conductivity in the operating temperatures of IT-SOFCs. The synthesis of  $Y_{0.8}Ca_{0.2}Cr_{1-x}Ni_xO_3$  powders with  $x=0, 0.15$ , and  $0.3$  was carried out using the sol-gel method, with EDTA and glycine as chelating agents. Based on the results of thermal analysis (TG/DTA) – Fig.1, phase composition (XRD) – Fig. 2, and morphological observations (SEM) of the gel precursors heated over the range of 800-1200°C, the optimal calcination parameters were found, allowing powders with the desired phase constitution and fine-grain structure to be obtained.

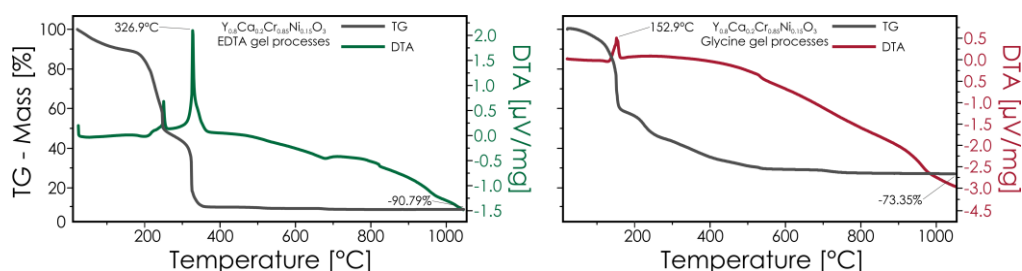


**Fig. 1.** DTA/TG thermal curves recorded for  $Y_{0.8}Ca_{0.2}Cr_{0.85}Ni_{0.15}O_3$  precursor gels.

The XRD analysis indicated that a pure orthorhombic perovskite phase was obtained only for the glycine nitrate method. Perovskites obtained using the EDTA chelating agent were characterized by multi-phase structure, with the predominant phase exhibiting a similar structure to that of  $YCrO_3$ .

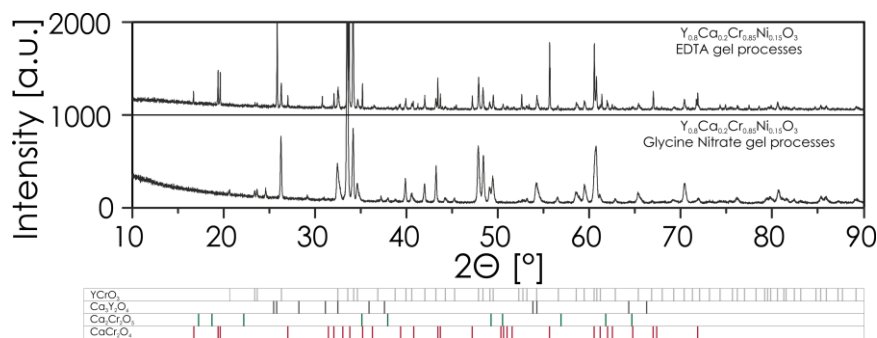


**Fig. 2.** XRD patterns obtained for  $Y_{0.8}Ca_{0.2}Cr_{0.85}Ni_{0.15}O_3$  powders.

After calcination, milling and compacting, the powders were sintered in the range of 1400-1700°C, and a number of dense, polycrystalline sinters were obtained. The sample with the best properties and an average relative density of 96.6% was obtained for the samples sintered for 1 hr in air at 1600°C. The influence of the composition of  $Y_{0.8}Ca_{0.2}Cr_{1-x}Ni_xO_3$  sinters on their physicochemical properties is analyzed based on the results of XRD, SEM-EDS and electrical conductivity measurements, with possible applications as conductive coatings considered to be the main criteria.

Financial support from the National Science Centre for PRELUDIUM 6, project no. 2013/11/N/ST5/01391 (reg. number), is gratefully acknowledged.

# Oxidation kinetics and microstructure of oxide products formed on the Crofer 22APU ferritic stainless steel in a dual atmosphere

M. Stygar<sup>\*1)</sup>, J. Dąbrowa<sup>\*2)</sup>, T. Brylewski<sup>\*3)</sup>

*\*AGH University of Science and Technology, Faculty of Materials Science and Ceramics  
al. Mickiewicza 30, 30-059 Kraków, Poland  
stygar@agh.edu.pl<sup>1)</sup>; dabrowa@agh.edu.p<sup>2)</sup>; brylew@agh.edu.p<sup>3)</sup>*

Solid oxide fuel cells (SOFCs) are highly promising devices that might become efficient sources of electrical energy and heat in the future. The construction of planar-type SOFC requires bipolar interconnects which separate air and fuel flows and provide both electrical contact and mechanical support for the cells in a stack. The reduction of SOFC operating temperatures to the 923–1073 K range made it possible to employ cost-effective metallic interconnects such as ferritic stainless steel (FSS).

In real SOFC operating conditions, exposure to air (cathode side) and the Ar-H<sub>2</sub>-H<sub>2</sub>O mixture (anode side) occurs at the opposite sides of the interconnect (dual atmospheres). This means that the distribution of the chemical potential of oxygen and hydrogen inside the interconnect is different than in the case of separate oxygen and hydrogen atmospheres (single atmosphere).

In this work, the oxidation behavior of the Crofer 22 APU FSS in a dual atmosphere is investigated. The results obtained for various oxidation times are compared with those obtained under corresponding conditions in single atmospheres. In each case, the oxidation of the examined steel follows the parabolic rate law. The analysis of the morphology, phase, and chemical composition indicates that the presence of gradients of chemical potentials of oxygen and hydrogen to a great extent determines the products of oxidation. The theoretical explanation of oxidation mechanisms is presented.

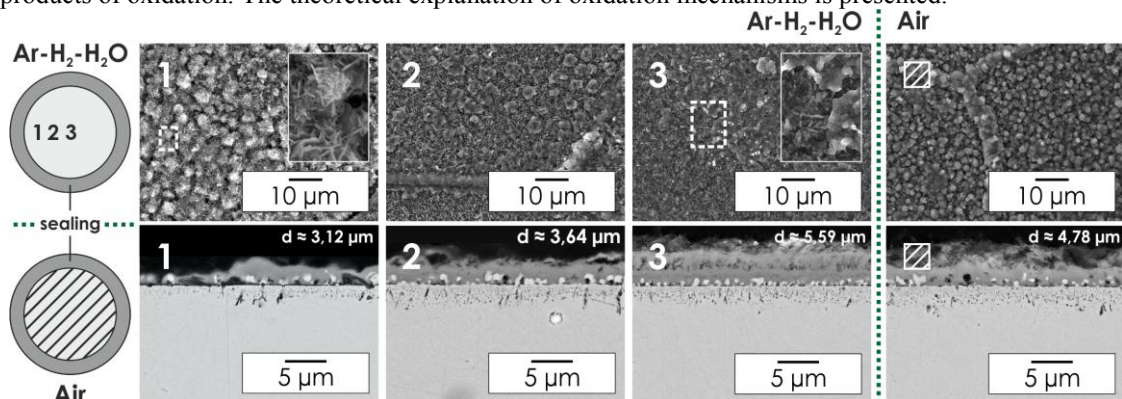


**Fig. 1.** SEM results obtained after 1000 hrs at 1073K for different areas of the oxidized samples from both air and fuel sides.

Additionally, a non-uniformity of scale thickness is observed on the fuel side. This phenomenon is explained via numerical modeling of gas flow in an experimental setup.

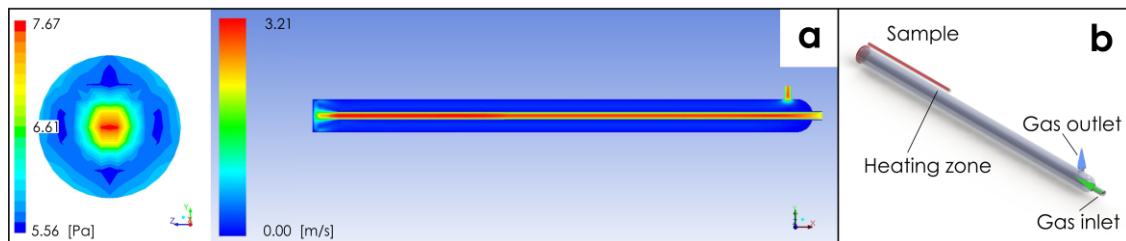


**Fig. 2.** Model of gas flow in an experimental setup. The distribution of static gas pressure on the sample's surface is presented.

Financial support from the National Science Centre for PRELUDIUM 6, project no. 2013/11/N/ST5/01391 (reg. number), is gratefully acknowledged.

# Electrochemical performance of double perovskite $\text{Pr}_2\text{NiMnO}_6$ as cathode for intermediate temperature solid oxide fuel cells

ZHAO Hui, SUN Liping, LI Huan, HUO Lihua

Key Laboratory of Functional Inorganic Material Chemistry, Ministry of Education, School of Chemistry and Materials Science, Heilongjiang University, Harbin 150080 P. R. China Address

e-mail: zhaohui98@yahoo.com

In order to explore the feasibility of non-cobalt cathode materials for IT-SOFCs, we intend to investigate the high-temperature electrochemical properties of B-site ordered double perovskite materials  $\text{A}_2\text{BB}'\text{O}_6$  with Ni and Mn located alternatively in B and B' site. The specific alternating arrangement of B and B' cations in  $\text{A}_2\text{BB}'\text{O}_6$  structure can be of great interest from the catalytic point of view, since the electrocatalytic properties are generally determined by the nature, oxidation states and the relative arrangement of B-site cation. In this sense, double perovskite oxide  $\text{Pr}_2\text{NiMnO}_6$  was studied as the cathode material for IT-SOFCs. The reactivity test indicated that no reaction occurred between  $\text{Pr}_2\text{NiMnO}_6$  and CGO at temperatures up to 1200 °C in air. The thermal expansion coefficient (TEC) of  $\text{Pr}_2\text{NiMnO}_6$  is  $10.6 \times 10^{-6} \text{ K}^{-1}$  in air and  $11.5 \times 10^{-6} \text{ K}^{-1}$  in nitrogen atmosphere within a temperature range of 100-800 °C. The electrochemical properties of  $\text{Pr}_2\text{NiMnO}_6$  cathode was characterized by ac impedance and dc polarization methods, respectively. The lowest area specific resistance (ARS) of  $\text{Pr}_2\text{NiMnO}_6$  cathode is  $0.38 \Omega \text{ cm}^2$  at 700 °C in air. The dependence of ASR with oxygen partial pressure indicates that the charge transfer process is the rate-limiting step for oxygen reduction reaction on  $\text{Pr}_2\text{NiMnO}_6$  cathode.

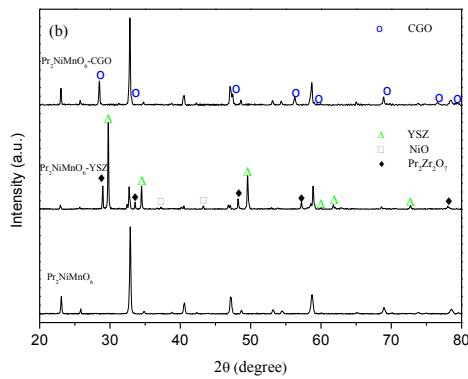


Fig. 1 The XRD patterns of  $\text{Pr}_2\text{NiMnO}_6$  with YSZ and CGO after calcined at 1200°C for 12h in air

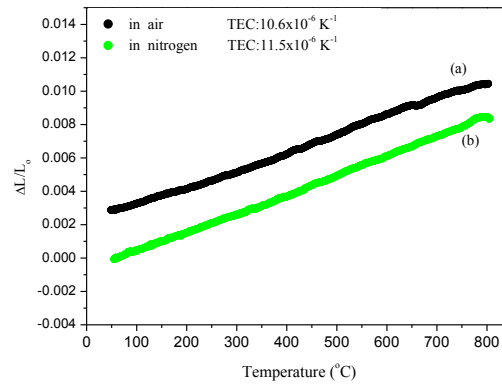


Fig.2 The thermal expansion curves of  $\text{Pr}_2\text{NiMnO}_6$  in (a) air and (b) nitrogen atmosphere

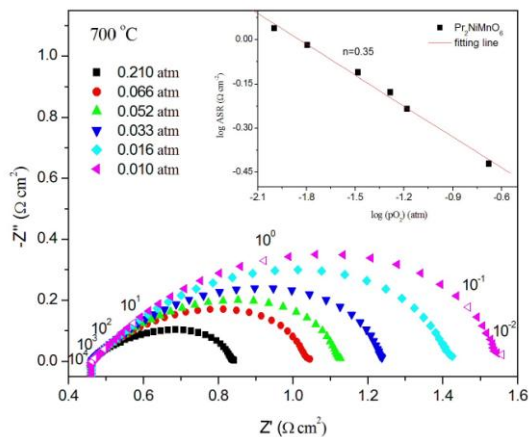


Fig.3 Nyquist plot of  $\text{Pr}_2\text{NiMnO}_6$  cathode under various oxygen partial pressures measured at 700°C. Inset shows the dependence of polarization resistance on oxygen partial pressure at 700°C.

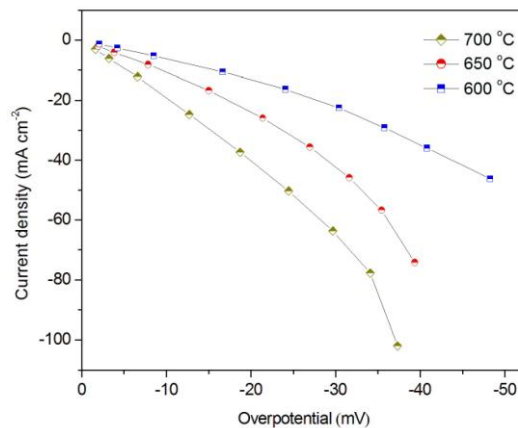


Fig.4 The overpotential-current density curves of  $\text{Pr}_2\text{NiMnO}_6$  cathode measured at different temperatures in air.

# The Porous Polyimide Membranes Derived from Diamine Monomer Containing Benzimidazole Unit for High Temperature Fuel Cells

Mun-Sik Shin, Jin-Soo Park\*

*Department of Environmental Engineering, College of Engineering, Sangmyung University, 31 Sangmyungdaegil, Dongnam-gu, Cheonan, Chungnam Province 330-720, Republic of Korea*

*\* energy@smu.ac.kr\**

The development of high-temperature polymer electrolyte membrane fuel cell (HT-PEMFCs, working at 150-200 °C) has been done worldwide in order to solve some of the problems of current cells based on Nafion® (CO tolerance, kinetics, water management, etc.). These problems can be overcome by HT-PEMFC, which has been shown to provide several benefits compared to low temperature operation, such as increased kinetics of the oxygen reduction reaction, greater tolerance of the platinum catalyst to CO and better heat management so that the cooling and hydration system can be simplified.

For HT-PEMFCs, the main issue is to develop a proton-exchange membrane with high proton conductivity, high chemical stability, and high mechanical strength at high temperatures and low humidification. Development of thermally stable polymer electrolyte membranes with higher proton conductivity as well as mechanical stability is a key challenge in commercializing PEM fuel cells operating above 100 °C. So far, polybenzimidazole (PBI) membranes have been satisfying good characteristics at temperatures up to 200 °C.

The proton conductivity of phosphoric acid (PA) doped PBI membranes highly depends on the acid doping level (ADL) of the membranes, defined as the mole number of PA per molar repeating unit of the polymer. However, high doping levels often cause excess swelling or even complete loss of the mechanical strength of the membranes due to the strong plasticizing effect of the dopant. The aromatic polyimides (PIs) is another family of engineering plastics well known for their excellent thermal stability, high mechanical strength and modulus, superior electrical properties and good chemical resistance. Polyimide (PI) units are expected to be able to improve the mechanical strength due to their relatively weak interactions with the doped acid molecules in comparison with benzimidazole units.

In this study, the porous polyimide membranes containing benzimidazole were prepared in order to increase the mechanical strength and proton conductivity for HT-PEMFC. The poly(imide benzimidazole)s was synthesized, and the porous membranes was fabricated by porogen. The porous polyimides membranes containing benzimidazole were investigated in terms of ionic conductivity, ADL, FT-IR, mechanical strength, etc.

## ACKNOWLEDGMENTS

This work was supported in part by Basic Science Research Program through the National Research Foundation of Korea (NRF) funded by the Ministry of Science, ICT and Future Planning (NRF-2014R1A1A1006067) and by the Danish Agency for Science, Technology and Innovation in the frame of the 4M Centre.

## REFERENCES

- [1] Q. Li, J.O. Jensen, R.F. Savinell, N.J. Bjerrum, High temperature proton exchange membranes based on polybenzimidazoles for fuel cells, *Progress in Polymer Science*, 34 (2009) 449-477.
- [2] J. Li, X. Li, S. Yu, J. Hao, W. Lu, Z. Shao, B. Yi, Porous polybenzimidazole membranes doped with phosphoric acid: Preparation and application in high-temperature proton-exchange-membrane fuel cells, *Energy Conversion and Management*, 85 (2014) 323-327.
- [3] S. Yuan, X. Guo, D. Aili, C. Pan, Q. Li, J. Fang, Poly(imide benzimidazole)s for high temperature polymer electrolyte membrane fuel cells, *Journal of Membrane Science*, 454 (2014) 351-358.
- [4] H. Pan, S. Chen, Y. Zhang, M. Jin, Z. Chang, H. Pu, Preparation and properties of the cross-linked sulfonated polyimide containing benzimidazole as electrolyte membranes in fuel cells, *Journal of Membrane Science*, 476 (2015) 87-94.

# Comparison of fuel cells based on different cathode and anode enzymes

Valentina Grippo<sup>a</sup>, Roland Ludwig<sup>b</sup>, Renata Bilewicz<sup>a</sup>

<sup>a</sup>Faculty of Chemistry, University of Warsaw, Pasteura 1, 02-093 Warsaw, Poland

<sup>b</sup>Department of Food Sciences and Technology, Food Biotechnology Laboratory, BOKU – University of Natural Resources and Life Sciences, Muthgasse 18, 1190 Vienna, Austria

v.grippo@chem.edu.uw.pl

Electron exchange between conducting surfaces and immobilized redox enzymes can be accomplished either by direct electron transfer (DET), or by a pathway involving redox-active mediating compounds (MET). In our recent papers we reported the liquid-crystalline lipid cubic phase [Fig 1] as a convenient matrix for incorporating enzymes and holding them on the electrode surface in a fully active form. Biofuel cells based on cubic phase do not need additional separating membranes and can be easily miniaturized. The lipidic membrane is biocompatible and stable in the presence of water. <sup>[1, 2]</sup>

We report on the fabrication and characterization of sugar/oxygen based biofuel cells (BFC) operating in neutral sugar containing buffer. Two enzymes have been related as anode and two as cathode materials for the biofuel cell.

*Corynascus thermophilus* CDH (CtCDH)<sup>[3]</sup> and *D-fructose dehydrogenase* (FDH) are catalyzing oxidation of carbohydrates. Their efficiencies were compared to that of Zinc in the hybrid fuel cell. *Myrothecium verrucaria* bilirubin oxidase (MvBOx) and *Cerrena Unicolor* Laccase (Lc) were used as the cathodic bioelements.

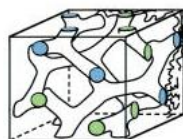


[Fig 1] Structure of Monoolein liquid-crystalline cubic phase

- [1] Ewa Nazaruk, Ehud M. Landau, Renata Bilewicz, *Electrochimica Acta* 2014, 140, 96-100;
- [2] Ewa Nazaruk, Ewa Górecka, Renata Bilewicz, *Journal of Colloid and Interface Science*, 2012, 385, 130-136;
- [3] Roland Ludwig, Roberto Ortiz, Christopher Schulz, Wolfgang Harreither, Christoph Sygmund, Lo Gorton, *Anal Bioanal Chem*, 2013, 405, 3637-3658



# Triode Operation for Enhancing the Performance of H<sub>2</sub>S-Poisoned SOFCs for CH<sub>4</sub> Steam Reforming

Antoinette Boreave, Foteini M. Sapountzi<sup>a</sup>, Michail N. Tsampas<sup>a</sup>, Chunhua Zhao<sup>a</sup>, Laurence Retailleau<sup>a</sup>, Dario Montinaro<sup>b</sup> and Philippe Vernoux<sup>\*a</sup>

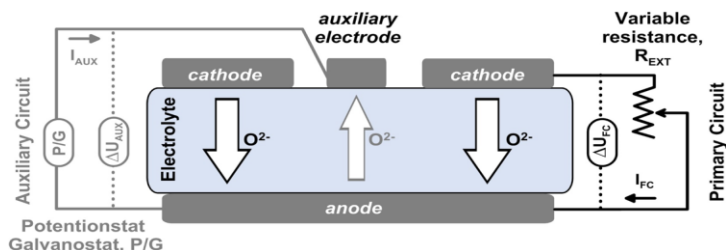
<sup>a</sup>*Institut de Recherches sur la Catalyse et l'Environnement de Lyon, UMR 5256, CNRS, Université Claude Bernard Lyon 1, 69626 Villeurbanne, France*

<sup>b</sup>*SOFCpower S.p.A., I-38017, Mezzolombardo, Italy*

[\\*philippe.vernoux@ircelyon.univ-lyon1.fr](mailto:philippe.vernoux@ircelyon.univ-lyon1.fr)

Performances of Solid Oxide Fuel Cells (SOFCs) were investigated in triode operation mode under methane steam reforming in presence of H<sub>2</sub>S. Both the catalytic performances for methane steam reforming and the electrochemical properties of the anode are drastically dropped by the presence of H<sub>2</sub>S impurities introduced through the use of fuels such as natural gas. Indeed, typically 1-30 ppm H<sub>2</sub>S content can be observed in natural gas. Conventional Ni-based cermet anode exhibit strong deactivation when exposed to few ppm H<sub>2</sub>S. This loss is generally attributed to sulfur adsorption on Ni active sites.

Triode operation is a novel approach for enhancing the performances of fuel cells and electrolyzers. This concept is based on the introduction of a third electrode (auxiliary electrode) in addition to the conventional anode and cathode. This auxiliary electrode is located at the cathode side, as shown in the following figure:



Electrodes were deposited by screen printing of commercial powders (Marion Technologies) on YSZ discs (Dynamic Ceramic, 8% mol Y<sub>2</sub>O<sub>3</sub>-ZrO<sub>2</sub>) with diameter of 20 mm and 1.6 mm thickness. The anode electrode was a Ni/GDC film of 40 μm thickness and a surface area of 1.76 cm<sup>2</sup> and was sintered at 1250°C for 2 hours. The cathode and the auxiliary electrodes were composed of LSM oxides (La<sub>0.65</sub>Sr<sub>0.35</sub>MnO<sub>3</sub> - fuel Cell Materials, LSM35) mixed with YSZ (Tosoh). The cathode was a ring shaped electrode at the periphery of 0.93 cm<sup>2</sup> surface area, and the auxiliary was a circular dot electrode of 0.31 cm<sup>2</sup> surface area at the center of the cathode but separated from the cathode. They were sintered at 1150°C for 2 hours.

To study the performances of the bottom cells, we have used a test rig (ProboStat, NorECs, Netherland). The sealing between the anodic and cathodic compartments was ensured by a gold ring which was annealed at 1040°C for 4 days under air. For current collection, Pt meshes were used for cathode and auxiliary while Ti mesh, catalytically inactive, was used for anode. Prior to the experiments, the catalysts were reduced under pure H<sub>2</sub> at 900°C for 2 hours. The effect of the addition of H<sub>2</sub>S in the reaction mixture has been investigated (1 ppm of H<sub>2</sub>S/He, 2%CH<sub>4</sub>/He – Air Liquide, 5% H<sub>2</sub>O added with a thermostated water saturator regulated at 33 °C) under 200cc/min flow while cathode and auxiliary were exposed under synthetic air (Linde 99,995%). The products of the reaction were analyzed by using a Hiden Analytical HPR20 quadripole mass spectrometer.

H<sub>2</sub>S poisoning was followed in open circuit mode, in fuel cell mode and in triode operation mode at 900°C. Triode operation cannot avoid or limit the catalytic degradation of the SOFC cell exposed to 1 ppm H<sub>2</sub>S but can maintain higher anodic electrochemical performances. This confirms that active sites for catalytic conversion (methane steam reforming) and those for electrochemical oxidation of hydrogen are not the same. The cell performances loss is mainly attributed to the degradation of the catalytic activity, then decreasing the concentration of electroactive species, i.e. hydrogen. Triode operation can slightly compensate the deactivation of the catalytic sites most probably with a local production of H<sub>2</sub>, from H<sub>2</sub>O electrolysis. Some specific triode operations can be found to achieve a thermodynamic efficiency close to the unity to avoid any energy overconsumption.

Acknowledgements: this work was financed by the EU 7<sup>th</sup> Framework Program, Fuel Cells and Hydrogen Joint Technology Initiative, under the frame of the T-CELL project (grant agreement 298300).



# Electrochemical characterization of Marimo carbon supported Pt–Pd

Kazuma Furuhashi<sup>1</sup>, Mika Shiraishi<sup>2</sup>, Risa Shiraishi<sup>2</sup>, Mikka Nishitani-Gamo<sup>2</sup>, Toshihiro Ando<sup>3</sup>,  
Mika Eguchi<sup>1</sup>

<sup>1</sup> Ibaraki University, 4-12-1 Nakanarusawa, Hitachi, Ibaraki, 316-8511, Japan

<sup>2</sup> Toyo University, 2100 Kujirai, Kawagoe, Saitama, 350-8585, Japan

<sup>3</sup> National Institute for Material Science, 1-1 Namiki, Tsukuba, Ibaraki, 305-0044, Japan

E-mail:eguchi@mx.ibaraki.ac.jp

## 1. INTRODUCTION

Pt is utilized as a catalyst for polymer electrolyte fuel cells (PEFCs). However, because Pt is a novel metal, a method must be devised to reduce its required amount in PEFCs. A widely-studied solution for reducing the amount of Pt is to employ a binary catalyst composed of both Pt and Pd. The addition of Pd is suggested to reduce the amount of required Pt without lowering the activity of the catalyst. This catalyst is generally used in the form of nanoparticles that are dispersed uniformly on a carbon black support in order to increase a surface area of the catalyst. However, the surface area of the dispersed Pt on a carbon black support is smaller due to its tendency to aggregate. We have used Marimo carbon as an alternative for a catalyst support [1]. Marimo carbon is a spherical carbon that is composed of carbon nanofilaments (CNFs). Catalysts can therefore be supported in a highly dispersed form on the CNFs. Consequently, there is an expected increase in the surface area of the Pt, which can also increase its likelihood in contributing positively towards the reaction. In this study, we evaluated the efficacy of a Pt-Pd binary catalyst supported on Marimo carbon.

## 2. EXPERIMENTS

The Marimo carbon was synthesized by thermal chemical vapor deposition (CVD) method. The oxidized diamond supported Ni catalyst were heated at 550 °C for 3 hours in a quartz reactor with methane gas flow. Preparation of the catalyst was accomplished with a modified, nanocolloidal solution method. Marimo carbon was first dispersed in an aqueous solution of sodium hydroxide. After the addition of citric acid to disperse the metal ions and a mixed solution of Pd chloride and chloroplatinic acid were then added. Finally, a solution of sodium borohydride was added to the mixed suspension as a reducing agent, and the Marimo carbon supported Pt-Pd catalyst (Pt-Pd/MC) was obtained[2].

## 3. RESULTS AND DISCUSSION

The scanning electron microscope (SEM) image of the Pt-Pd/MC is shown in Figure 1. The structure of the Marimo carbon was preserved even after the preparation of the catalyst. The binary metal nanoparticles appeared as multiple white spots on the surface of the CNFs. Figure 2 displays the TEM images of the prepared catalyst. The nanoparticles of the catalyst were observed on the CNFs of the Marimo carbon. In particular, nanoparticles ranging from 2~6 nm exhibited a high dispersion on the support. The approximate feed ratio of Pt to Pd was calculated based on spectral peaks obtained from energy dispersive X-ray spectroscopy. On the basis of these results, the utilization of a modified, nanocolloidal solution methodology to form Marimo carbon supported Pt-Pd nanoparticles proved to be a suitable methodology for catalysis.

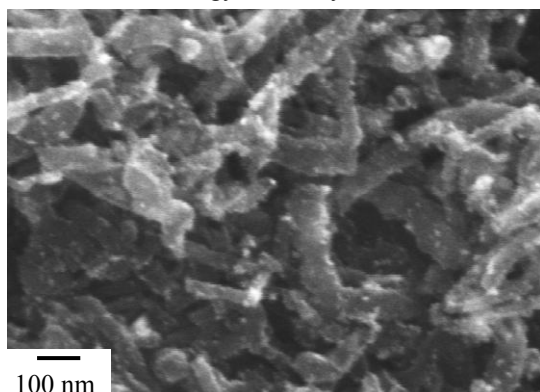


Fig. 1 SEM image of the Pt-Pd / Marimo carbon

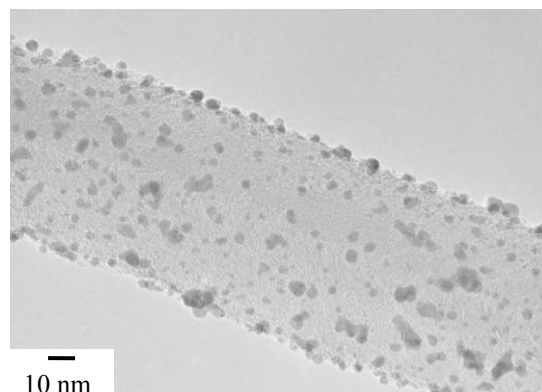


Fig. 2 TEM image of the Pt-Pd / Marimo carbon

## References

- [1] K. Nakagawa et al., *J Mater Sci*, **44**, 221-226, (2009)
- [2] M. Eguchi et al., *Trans. Mat. Res. Soc. Japan*, **38**[4], 549-553, (2013)

# Enhancement of polymer electrolyte fuel cell performance using a Marimo carbon

Koki Baba<sup>1</sup>, Risa Shiraishi<sup>2</sup>, Mika Shiraishi<sup>2</sup>, Mikka Nishitani-Gamo<sup>2</sup>, Toshihiro Ando<sup>3</sup>, Mika Eguchi<sup>1</sup>

<sup>1</sup> Ibaraki University, 4-12-1 Nakanarusawa, Hitachi, Ibaraki, 316-8511, Japan

<sup>2</sup> Toyo University, 2100 Kujirai, Kawagoe, Saitama, 350-8585, Japan

<sup>3</sup> National Institute for Material Science, 1-1 Namiki, Tsukuba, Ibaraki, 305-0044, Japan

E-mail: eguchi@mx.ibaraki.ac.jp

## 1. INTRODUCTION

Polymer electrolyte fuel cells (PEFCs) can function with a high efficiency for fast start-up time. Platinum nanoparticles supported on the high surface area of nanoporous carbon materials (Pt/CB) are primarily used as a catalyst in PEFCs. However, there are two key technical challenges, (i) the ORR activity needs to be enhanced in order to reduce the overall expense from the high platinum loading amounts, and (ii) the long term durability of the catalysts must be improved in order to extend the operational lifetimes of the catalyst [1]. We have applied Marimo carbon as a catalyst support for the PEFCs. The Marimo carbon is composed of many carbon nanofilaments (CNFs), and the CNFs are interwoven to form a spherical secondary shape. This structure should be favorable toward its utilization in PEFCs. In this study, we prepared MEAs using a Pt catalyst supported on the Marimo carbon (Pt/MC) and/or conventional carbon black (Pt/CB) and investigated the performance of the PEFC.

## 2. EXPERIMENTS

The Pt/MC was prepared by a modified nanocolloidal solution method [2]. MEAs with an active area of 25 cm<sup>2</sup> were prepared using the Pt/MC and/or commercial Pt/CB. Catalyst inks were prepared by mixing a carbon support catalyst with a 5% Nafion solution in deionized water. The weight ratio of carbon to Nafion (I/C) was 0.14 (in the case of Pt/MC) and 0.74 (in the case of Pt/C). These inks were painted with a brush onto the decal surface of the Teflon sheets. Spraying was controlled to result in a catalyst layer with a Pt loading of 0.2 mg<sub>Pt</sub> cm<sup>-2</sup>. Anode and cathode catalyst decals were then hot-pressed onto the opposite sides of a Nafion 212 membrane at 11.5 kN and 428 K for 10 min. The combination of the anode and cathode decals were (A) Pt/CB in anode and Pt/CB in cathode, (B) Pt/CB in anode and Pt/MC in cathode and (C) Pt/MC in anode and Pt/MC in cathode. I-V performance curves of single cell MEAs was carried out at 353 K under a controlled atmosphere. Reactant gas flows were fixed at 200 SCCM for both the H<sub>2</sub> and air.

## 3. RESULTS AND DISCUSSION

Figure 1 shows I-V performance curves for each of the MEAs. The Pt/MC (B and C) gave a higher maximum current density in comparison to the Pt/CB (A). This property can be attributed to the weave structure of the CNFs. If Marimo carbon is used, the reactant gases and the produced water can easily diffuse into the unique structure of the catalyst layer. This characteristic decreases the diffusion polarization, and also increases the maximum current density. The activation polarization (the slope of the lower current density region in the I-V curve) was calculated for each of the anode/cathode combinations, and it was determined that Pt/MC (C) < Pt/CB (A and B). The activation polarization depends on the Pt catalytic activity on the carbon surface. In the case of the carbon black support, some of the Pt catalysts were supported on the surface of the inner pores. The porous structure of carbon black suppressed contact between the Pt catalyst and reactant gases, which thus caused a decrease in the catalytic activity of the Pt particles on the inner pore surface. In the case of Pt/MC, the structure of the Marimo carbon didn't suppress the activity of the Pt particles on the CNF surface. This unique structure of Marimo carbon imparts a superior single cell performance in comparison to carbon black.

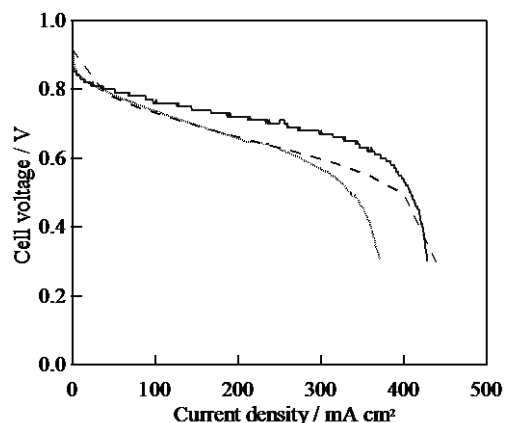


Fig. 1 I-V curves using (A) Pt/CB and Pt/CB (solid line), (B) Pt/CB and Pt/MC (dashed line), and (C) Pt/MC and Pt/MC (dotted line).

## References

- [1] B. Li et al., *Journal of Power Sources*, **262**, 488-493, (2014)
- [2] K. Baba et al., *Japanese Journal of Applied Physics*, **52**, 06GD06, (2013)

# The Effect of Heat-Treatment on the Oxygen Reduction Reaction Activity of Carbon-Supported PtCoAg Electrocatalysts

Zi-Jun Lin, Hong-Shou Chen, Yu-Ting Liang, Kuan-Wen Wang\*

*Institute of Materials Science and Engineering, National Central University, No.300, Zhongda Road, 32001, Taoyuan, Taiwan  
e-mail: kuanwen.wang@gmail.com*

Carbon-supported PtCoAg nanoparticles (NPs) were synthesized and applied as electrocatalysts for oxygen reduction reaction (ORR). In order to improve the activity and stability, the catalysts were heat-treated in  $H_2$  in the temperature range between 420 and 570 K (named as H-420, H-470, H-520 or H-570). The catalysts were characterized by X-ray diffraction (XRD), X-ray absorption spectroscopy (XAS), Transmission Electron Microscopy (TEM) and electrochemical measurements. The numbers of unoccupied d-states ( $h_{Ts}$ ) values of PtCoAg NPs obtained from XAS show that the catalysts with lower  $h_{Ts}$ , have lower unfilled d-states, weaker Pt-O bonds, and less Pt oxide formation, leading to the promotion of ORR kinetics. The optimal heat-treatment temperature was found to be 470 K, where the highest ORR catalytic activity and lowest  $h_{Ts}$  were obtained. H-470 has superior ORR activity to as-prepared and other heat-treated PtCoAg NPs as displayed in Figure 1, and its mass activity (MA) at 0.9 V is 50 times higher than that of as-prepared PtCoAg NPs. After 1000 cycles of accelerated durability test (ADT) under  $O_2$ , the ORR activity of H-470 is higher than that of as-prepared one with a decay of 50.6 vs. 99.9 %. The enhancement of ORR stability may be due to the effect of heat-treatment on the structure and electronic states of Pt for H-470 catalysts.

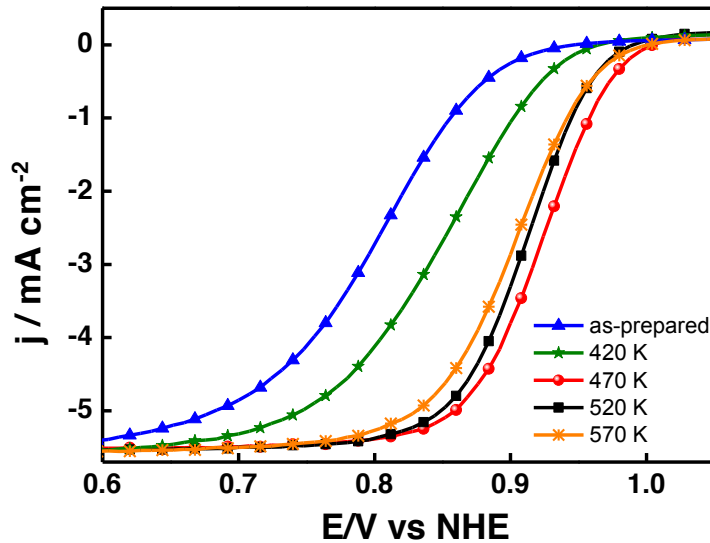


Figure 1 The linear sweep voltammetry(LSV) results of as-prepared and heat-treated PtCoAg catalysts.

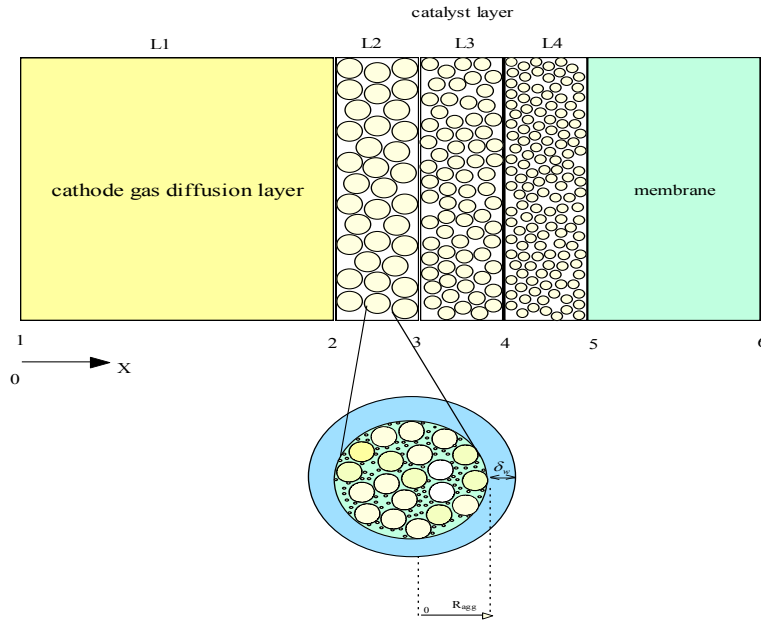
# Mathematical Model of Non-Uniform Cathode Catalyst Layer on the Performance of PEMFC

Kuo-Wei Chiang<sup>1</sup>, Bo-Syun Cheng<sup>1</sup>, and Ken-Ming Yin<sup>1\*</sup>

<sup>1</sup> Department of Chemical Engineering and Materials Science,  
Yuan Ze University, Chung Li, Taoyuan 32003, Taiwan

\* Corresponding author, cekenyin@yzu.edu.tw

The distribution of materials property in the catalyst layer is studied. The cathode catalyst layer is divided into three equal spaced layers with uniform property in each layer. The tri-layer is sandwiched between the gas diffusion layer and the membrane for the evaluation of cathode electrode performance at various degrees of humidification (please see the Figure). Each catalyst layer is characterized by the agglomerate size, gas porosity, and void fraction of electrolyte within the agglomerate. The agglomerate is composed of carbon supported platinum (Pt/C) dispersed in the solid electrolyte. In the model, oxygen gas dissolves in the outer liquid film of the agglomerate, diffuses across the film, diffuses into the electrolyte in the void of the agglomerate, and reacts on the surface of Pt/C. For the tri-layer catalyst layer studied, better cell performance is obtained if smaller gas porosity, lower electrolyte fraction within the agglomerate, and larger agglomerate size are concentrated to the face of membrane.



# Anion-conductive areas on anion exchange membranes analyzed by current-sensing atomic force microscopy under controlled conditions

Taro Kimura,<sup>1</sup> Masanori Hara,<sup>1</sup> Junji Inukai,<sup>1</sup> Makoto Uchida,<sup>1,3</sup> Manai Shimada,<sup>1,2,3</sup> Hideaki Ono,<sup>1,3</sup> Shigefumi Shimada,<sup>1</sup> Kenji Miyatake,<sup>1,3</sup> Masahiro Watanabe<sup>1</sup>

<sup>1</sup>University of Yamanashi,

<sup>2</sup>TAKAHATA PRECISION JAPAN Co. Ltd

<sup>3</sup>JST-CREST

<sup>1,4</sup>Takeda, Kofu, Yamanashi, 400-8510, Japan

<sup>2,3,90</sup>Maemada, Sakaigawa-cho, Fuefuki, Yamanashi, 406-0843, Japan

<sup>3,4-1-4</sup>Hon-cho, Kawaguchi, Saitama, 332-0012, Japan

jinukai@yamanashi.ac.jp, miyatake@yamanashi.ac.jp

Anion exchange membrane fuel cells (AEMFCs), potentially operated with non-precious metal catalysts, are actively studied. To achieve higher performances of AEMFCs, understanding the ion transport mechanism and the structures of ion conductive paths is important. Current-sensing atomic force microscopy (CS-AFM) has attracted attentions for its capability of observing the surface morphology and ion conductive regions on ion-conductive electrolyte membranes on the nanometer scale. At present, most of these studies have been carried out on proton exchange membranes; few results were reported on AEMs, and the surface anion conductivities are still unclear.<sup>1)</sup> In this study, by using CS-AFM under a temperature/humidity controlled CO<sub>2</sub>-free air, the surface morphology and the current distribution were simultaneously observed on the AEM surfaces.

Two membranes, QPE-bl-3 (IEC=1.80 meq g<sup>-1</sup>) and QPAF-1 (IEC=1.18 meq g<sup>-1</sup>), (Fig. 1) were synthesized in our laboratory, where QPE-bl-3 is a block copolymer whereas QPAF-1 a random copolymer. The membrane was pressed on a gas-diffusion electrode (GDE) with a catalyst layer composed of Pt/C and a commercial binder (AS-4, Tokuyama Corp.). The membrane on the GDE was installed in a homemade environment-control chamber.<sup>2)</sup> CS-AFM measurements were carried out in ultrapure air at temperature of 40 °C and humidities of 50% and 70% RH. Topographies and current images were obtained by using a Pt-coated cantilever at the contact mode with the contact force of 10 nN.

Fig. 2 shows topographies and current images obtained on the two AEMs at 40 °C and 70% RH. The surface of QPE-bl-3 (Fig. 2a) was very flat with the maximum height difference of only 20 nm in the scanned area of 1 μm x 1 μm. The surface of QPAF-1 (Fig. 2b) was also flat, but small, nanometer corrugations were observed over the surface. Fig. 2c shows the current image on QPE-bl-3. Large anion conductive regions and non-conductive regions of tens of nanometers were separately observed. In the current image on QPAF-1 (Fig. 2d), highly-dispersed small anion conductive spots were observed. Profiles of the membranes, such as the ratio of anion conductive areas, the pseudo average current densities, and the cross sectional current distributions, were systematically and statistically studied on the two membranes. The difference in the performances of the power generation using the two AEMs was correlated with the difference in those surface properties of the membranes.

## References

1) Q. He and X. Ren, J. Power Sources, 220, 373, (2012).

2) M. Hara et al., J. Phys. Chem. B, 117, 3892 (2013).

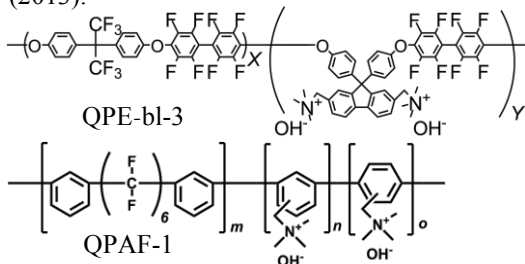


Fig. 1. Chemical structures of QPE-bl-3 and QPAF-1.

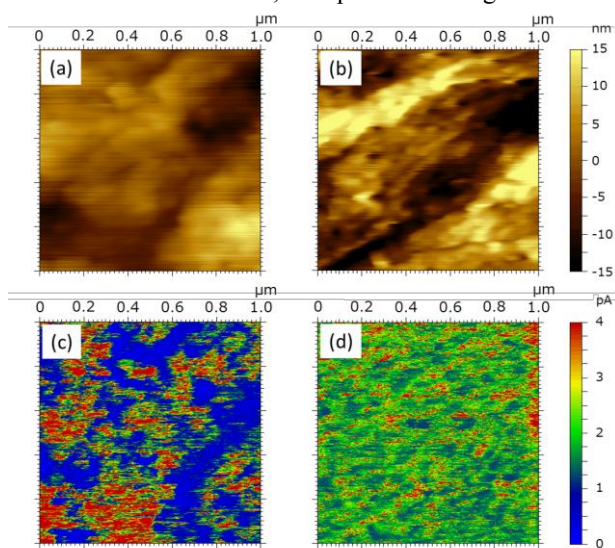


Fig. 2. Topographies and current images of QPE-bl-3(a), (c) and QPAF-1(b), (d), respectively, at 40 °C and 70% RH.

# Structural and Electrical properties of Ru-doped $\text{BaCe}_{0.90}\text{Y}_{0.10}\text{O}_{3-\delta}$ Thin Film

Masanori Ochi<sup>1</sup>, Shohei Yamaguchi<sup>1</sup>, Takaaki Suetsugu<sup>1</sup>, Naoya Suzuki<sup>1</sup>, Kinya Kawamura<sup>1</sup>,  
Takashi Tsuchiya<sup>1</sup>, Masaki Kobayashi<sup>2</sup>, Hiroshi Kumigashira<sup>2</sup> and Tohru Higuchi<sup>1</sup>

<sup>1</sup>Department of Applied Physics, Tokyo University of Science, Tokyo 125-8585, Japan

<sup>2</sup>Photon Factory, KEK, Tsukuba, Ibaraki 305-0801, Japan

[1515701@ed.tus.ac.jp](mailto:1515701@ed.tus.ac.jp)

Acceptor-doped perovskite-type oxide  $\text{Y}^{3+}$ -doped  $\text{BaCeO}_3$  (BCY) bulk crystal exhibits high proton conduction at intermediate temperature (IMT) region under water vapor atmosphere. This proton conduction is expected for electrochemical application of electrolyte of solid oxide fuel cell (SOFC). Furthermore, Matsumoto and co-workers have reported that Ru-doped BCY (BCRY) ceramics exhibit the electron-proton mixed conduction in IMT region [1]. Although the mixed conducting of BCRY can be used as an electrode material of SOFC, the structural and electrical properties of BCRY electrode film have not been clarified thus far. In this study, we have prepared the BCRY thin films with various film thickness on  $\text{Al}_2\text{O}_3$  substrates by RF magnetron sputtering and characterized their structural and electrical properties.

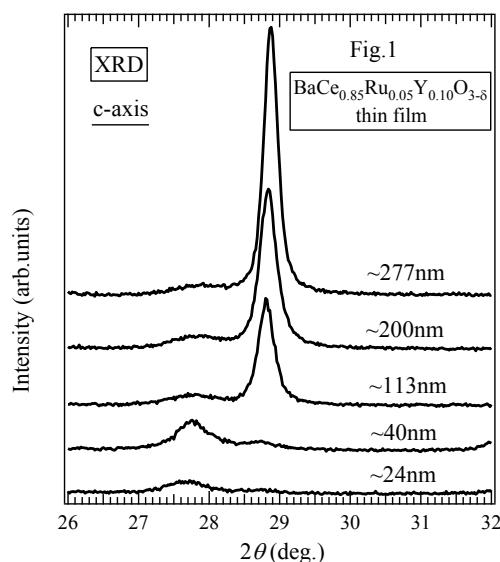
The BCRY thin films were deposited on  $\text{Al}_2\text{O}_3$  substrates by RF magnetron sputtering using ceramics target. The chemical composition of BCRY was  $\text{BaCe}_{0.85}\text{Ru}_{0.05}\text{Y}_{0.10}\text{O}_{3-\delta}$ . The RF power, deposition pressure and substrate temperature were fixed at 80 W,  $4.0 \times 10^{-3}$  Torr, and 600 °C, respectively. The Ar gas flow rate was 20 sccm. The thickness was changed from 20 nm to 300 nm. The structural properties were characterized using X-ray diffraction (XRD). The electronic structures were characterized using photoemission spectroscopy (PES). The electrical conductivity of in-plane direction was measured using AC or DC impedance spectroscopy through the Pt interdigital electrode.

Fig.1 exhibits the XRD patterns of BCRY thin films with various film thickness. These films crystallized without post annealing. The thicker films above ~100 nm exhibit (002) peak of Orthorhombic (*Incn*) structure of  $\text{BaCeO}_3$ . The thinner films below ~50 nm exhibit (002) peak of Orthorhombic (*Pmcn*) structure of  $\text{BaCeO}_3$ .  $\text{BaCeO}_3$  was reported to exhibit structural phase transition from *Pmcn* to *Incn* structures at 563 K [2]. The thin films in this study have *Incn* and *Pmcn* structure by changing film thickness. This indicates that the lattice constant of *c*-axis changes largely by film thickness due to the lattice mismatch between BCRY film and  $\text{Al}_2\text{O}_3$  substrate. Therefore, the proton and electron conductivities of BCRY thin films are indicated to be effected by the film thickness.

In this presentation, the author will show details of electrical conductivity, electronic structure of BCRY thin films and discuss about the electron-proton conduction of BCRY thin films.

## References

- [1] H. Matsumoto *et al.*, J. Electrochem. Soc. **152** (2005) A488~A492.
- [2] T. Higuchi *et al.* Solid State Ionics **270** (2015) 1~5.



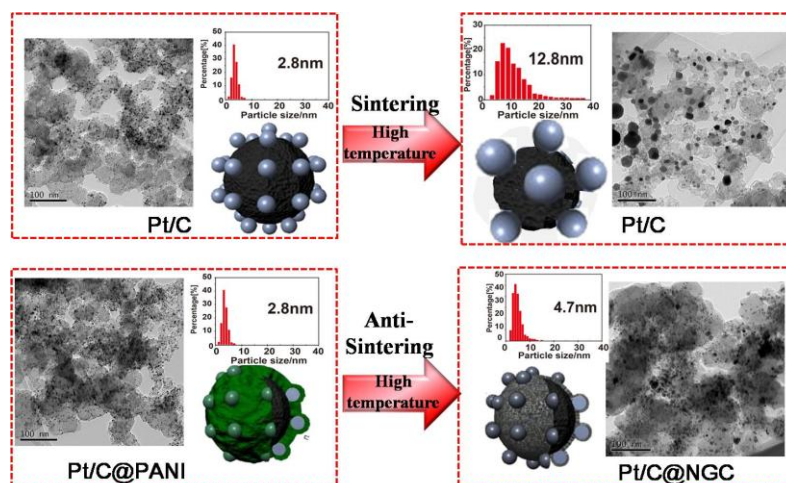


# Pt/C Trapped in Activated Graphitic Carbon Layers as a Highly Durable Electrocatalyst for Oxygen Reduction Reaction

Yao Nie, Siguo Chen, Wei Ding, Xiaohong Xie, Yun Zhang, Zidong Wei\*

Chongqing Key Laboratory of Chemical Process for Clean Energy and Resource Utilization, School of Chemistry and Chemical Engineering, Chongqing University, Chongqing, 400044; China  
zdwei@cqu.edu.cn

Proton exchange membrane fuel cells (PEMFCs) have drawn significant attention as a novel alternative to traditional power sources due to their high energy conversion efficiency and low environmental impact<sup>[1]</sup>. At present, the most commonly used cathode catalysts are highly dispersed 2-5 nm Pt nanoparticles (NPs) supported on carbon. However, the insufficient electrocatalytic activity and durability of Pt cathode catalysts still remains a major obstacle for PEMFCs applications<sup>[2]</sup>. Seldom reports have focused on enhancing the structural integrity and the corrosion resistance of Pt-based catalysts by covering Pt nanoparticles surface with an active sites-containing layer to realize both superior durability and high activity. In this work, we designed a novel strategy to address both durability and activity issues via coating a nitrogen-containing graphitic carbon (NGC) layer onto the surface of Pt/C catalyst (Pt/C@NGC). The NGC, which is usually employed as an ameliorative carbon support or a promising Pt-free ORR catalyst<sup>[3,4]</sup>, is elaborately introduced to the Pt/C surface to not only inhibit migration and dissolution of Pt nanoparticles, but also act as the secondary active site supplier that imparting activity to the integral catalyst without blocking the inner Pt catalytic active sites. Corrosion of carbon support also can be alleviated due to the protection of the outer graphitic cover. Moreover, the NGC precursor, polyaniline, was ingeniously used to inhibit Pt NPs from serious sintering, thus guaranteeing the feasibility of the design concept of the Pt/C@NGC. This new nanoarchitecture, incorporating simultaneously above desirable design rationales, exhibits much improved durability and activity over commercial Pt/C for ORR.



- [1] H. A. Gasteiger, S. S. Kocha, B. ompalli, F. T. Wagner, *Appl. Catal. B* 2005, **56**, 9.
- [2] P. J. Ferreira, G. J. la O', Y. S. Horn, D. Morgan, R. Makharia, S. Kocha, H. A. Gasteiger, *J. Electrochem. Soc.* 2005, **152**, A2256.
- [3] W. Ding, Z. D. Wei, S. G. Chen, X. Q. Qi, T. Yang, J. S. Hu, D. Wang, L. J. Wan, S. F. Alvi, L. Li, *Angew. Chem. Int. Ed.*, 2013, **52**, 1
- [4] J. Sanetuntikul, T. Hang, S. Shanmugam, *Chem Commun.*, 2014, **50**, 9473

# Shape Fixing via Salt Recrystallization: A Morphology-Controlled Approach to Convert Nanostructured Polymer to Carbon Nanomaterial as a High Active Catalyst for Oxygen Reduction Reaction

Wei Ding,\* Wei Li, Guangping Wu, Li Li, Siguo Chen, Xueqiang Qi, Zidong Wei\*

School of Chemistry and Chemical Engineering, Chongqing University, Shazhengjie 174, Chongqing, 400044, China

zdw@cqu.edu.cn; dingwei128@cqu.edu.cn

The ability to control mesoscale architectures of carbon materials is essential to possess unique functionality that yields faster, cheaper, higher performing, and longer lasting carbon materials for energy conversion and storage, as well as for the development of catalytic materials for the oxygen reduction reaction (ORR). In the past decade, numbers of methods had been developed to control compose, morphology, porosity of macromolecular compounds which can be used as precursor of carbon materials. We aim to build a connection that could accurately transfer macromolecular compounds to carbon materials by simply pyrolysis without destroying the original architectures. This will provide a powerful and facile method to control mesoscale architectures of carbon materials, and will derive many interesting carbon materials. We report a “shape fixing via salt recrystallization” method to accurately transfer self-assembled polyaniline to the final N-doped carbon materials by fixed and fully sealed inside NaCl crystal via recrystallization of NaCl solution. We demonstrated that the N-doped carbon materials with 3D network, nanotube, and nanoshell morphology are realized by the invented method. The NaCl crystal provides a fully closed nanoreactor, which changes the behavior of transition from precursor to carbon materials, and facilitates N incorporation and graphitization during pyrolysis. Use of the invented N-doped carbon material as cathode catalyst in a proton exchange membrane fuel cell produces a peak power of  $600 \text{ mWcm}^{-2}$ , making this among the best non-precious metal catalysts for the oxygen reduction reaction reported so far. This greatly improved performance can be attributed to the unique advantages of this method, which achieves a high microporosity, with a high density of ORR active-sites located along the efficient mass transport pathway (composed of meso- and macropores), resulting in a high utilization of active-sites. This developed method provides a simple but efficient and versatile approach to the construction of carbon nanomaterials with controlled porous structures and morphologies, for industrial purposes ranging from catalysis and sensors to supercapacitors and lithium-ion batteries.

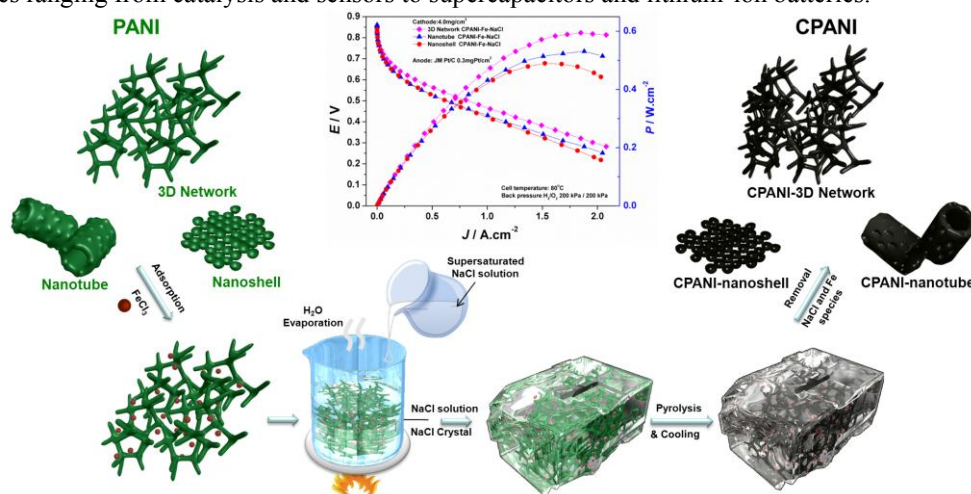


Figure 1. Shape Fixing via Salt Recrystallization Method.

## References

- [1] W. Ding, L. Li, K. Xiong, Y. Wang, W. Li, Y. Nie, S. G. Chen, X. Q. Qi, Z. D. Wei. *J. Am. Chem. Soc.*, **2015**, DOI: 10.1021/jacs.5b002



# The Effect of Nafion Ionomer on Electroactivity of Palladium-Polypyrrole Catalysts for Oxygen Reduction Reaction

M. Góral-Kurbiel<sup>1</sup>, A. Drelinkiewicz<sup>1</sup>, R. Kosydar<sup>1</sup>, J. Gurgul<sup>1</sup>, B. Dembińska<sup>2</sup>, P. J. Kulesza<sup>2</sup>,  
E. Bielańska<sup>1</sup>, M. Ruggiero<sup>1</sup>

<sup>1</sup>*Jerzy Haber Institute of Catalysis and Surface Chemistry Polish Academy of Sciences,  
Niezapominajek 8, 30-239 Krakow, Poland;*

<sup>2</sup>*Department of Chemistry, University of Warsaw, Pasteura 1, 02-093 Warsaw, Poland*

Nowadays a variety of aspects concerning the polymer electrolyte membrane fuel cells is extensively studied. The structure of electrocatalyst layer (architecture) is crucial as it determines the mass-transport processes encountered during the electrochemical processes [1]. In the preparation of the catalysts tested in oxygen reduction reaction (ORR) a commonly used method is based on the preparation of an ink composed of the catalyst powder and Nafion ionomer (perfluorosulfonic acid). The role of acid/alkaline functionalities of supports in modification of noble metal particles reactivity has been well documented in various types of reactions carried out on heterogeneous catalysts [2]. Thus, it may be expected that the presence of the Nafion acid functionalities in a close proximity to the Pt, Pd-nanoparticles, as in the ink, would affect their chemisorption properties via electron modification. However, to the best of our knowledge the Nafion – Pt, Pd interaction effect has not been taken yet into consideration in discussing the results of ORR on Pt, Pd-electrocatalysts.

Present studies concentrated on the preparation, characterization and electroactivity of palladium – polypyrrole (Pd/PPY) catalysts for ORR. In particular, the effect of Nafion ionomer on their electroactivity was evaluated. The results were reported in our work [3, 4]. In all catalysts prepared by the “water-in-oil” microemulsion method, the Pd nanoparticles of ca. 7 nm in size appeared regardless of the Pd content (ranging from 2 to 20 wt.%). For comparison, carbon black (Vulcan XC-72) supported catalyst (20 wt.% Pd) was also synthesized. Mixing of the Pd/PPY samples with Nafion ionomer reduced their surface area and porosity. The microporous structure was preferentially blocked whereas some changes in the mesoporous structure resulted in decreased average pore diameter. Chemical interaction due to Nafion acid functionalities affected the N-state of pyrrole as well as electron state of Pd in the Pd/PPY catalysts. These interactions played an essential role in the electroactivity of Pd/PPY catalyst for ORR. The increased amount of Nafion relative to that of PPY reduced limiting current density whereas the half-wave potential shifted to more positive value (Fig. 1) and the fraction of hydrogen peroxide remarkably decreased. The observed enhanced ability of the Pd/PPY catalyst towards oxygen reduction via 4-electron pathway might arise from modification of Pd-sites reactivity induced by the presence of Nafion.

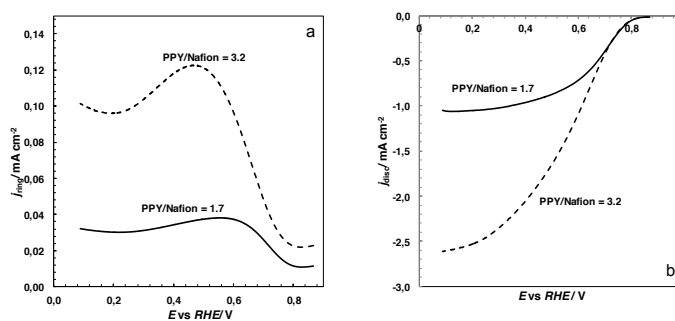


Fig. 1. Normalized (background subtracted) rotating **a** ring and **b** disc voltammograms for ORR on 20 % Pd/PPY catalyst mixed with Nafion, with PPY/Nafion weight ratio of 3.2 (dashed lines) and 1.7 (solid lines). Electrolyte: 0.5 M H<sub>2</sub>SO<sub>4</sub>. Rotation rate: 1,600 rpm. Scan rate: 5 mV s<sup>-1</sup>

## References

- [1] R. Antolini, Appl. Catal. B 100 (2010) 413
- [2] J.M. Thomas, W.J. Thimas Principles and practice of heterogeneous catalysis. VCH Verlagsgesellschaft mbH, Weinheim (1997) Federal Republic of Germany
- [3] M. Góral-Kurbiel, A. Drelinkiewicz, R. Kosydar, B. Dembińska, P.J. Kulesza, J. Gurgul, Electroanalysis 5 (2014) 23
- [4] M. Góral-Kurbiel, A. Drelinkiewicz, R. Kosydar, J. Gurgul, B. Dembińska, P.J. Kulesza, J. Solid State Electrochem. 18 (2014) 639

*Acknowledgments:* Financial support from National Science Centre, grant no. 2011/01/D/ST5/04917

# Graphene-Carbon Nanofibers Composite Film As a Highly Active Catalyst Support for Formic Acid Electrooxidation

Xuan Jian, Xian Liu, Yang huimin, Zhenhai Liang\*

College of Chemistry and Chemical Engineering, Taiyuan University of Technology

No.79 west Yingze street, Taiyuan, Shanxi, China, 030024

e-mail: [liangzhenh@sina.com](mailto:liangzhenh@sina.com); [liangzhenhai@tyut.edu.cn](mailto:liangzhenhai@tyut.edu.cn)

**Abstract:** Direct formic acid fuel cells (DFAFCs) was superior in fuel cells and had aroused more concerns<sup>[1-2]</sup>. It was generally known that the performance of a catalyst layer in a fuel cell was influenced by dispersivity and stability of nanoparticles on the surface of support materials. So, seeking novel catalyst support materials for DFAFCs had became one of the research hot topics in DFAFCs fields<sup>[3]</sup>.

In this study we had demonstrated the preparation of a novel composite film using the excellent electric properties of graphene (GR) and the unique advantages of carbon nanofibers (CNFs). The CNFs was fabricated through the template-directed by using ultrathin Te nanowires as templates and glucose as carbon source<sup>[4]</sup>. Graphene oxide was dropped on the glass carbon electrode (GCE) and reduced by direct electrochemistry in N<sub>2</sub>-saturation 0.1 M KCl solution. Pt-Pd bimetallic catalysts had been deposited on the graphene-CNFs composite film modified GCE by cyclic voltammetry (CVs).

The electrocatalytic properties of different modified electrodes were measured shown in Figure 1. Both the hydrogen adsorption/desorption region and PtPd bimetallic catalysts oxide reduction region can be observed in the Figure 1A. The peak current in the Figure 1B for the PtPd/GR/CNFs was 3.38 mA, which was approximately twice of the PtPd bimetallic catalysts directly deposited on the naked GCE (1.64 mA). The results indicated that the addition of GR/CNFs composite film as catalyst support greatly improved not only Pt-Pd nanoparticles deposition (Figure 1A), but also the catalytic activity for formic acid electrooxidation (Figure 1B).

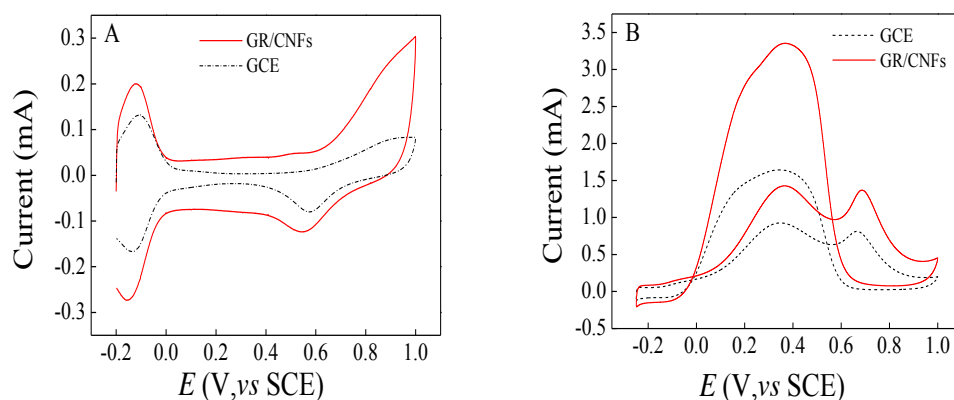


**Figure 1: A.** CVs of Pt-Pd bimetallic catalysts modified different substrate electrodes in 0.5 M H<sub>2</sub>SO<sub>4</sub> solution at 50mV·s<sup>-1</sup>.

**B.** CVs of Pt-Pd bimetallic catalysts modified different substrate electrodes in 0.5 M H<sub>2</sub>SO<sub>4</sub> and 0.5 M HCOOH solution at 50mV·s<sup>-1</sup>.

## Reference:

- [1] J. F. Chang, L. G. Feng, C. P. Liu, et al. An Effective Pd-Ni<sub>2</sub>P/C anode catalyst for direct formic acid fuel cells[J]. *Angew. Chem. Int. Ed.*, 2014, 53, 122-126.
- [2] W. Gao, J. E. Mueller, Q. Jiang, et al. The role of co-adsorbed CO and OH in the electrooxidation of formic acid on Pt (111)[J]. *Angew. Chem. Int. Ed.*, 2012, 51, 9584 – 9589
- [3] S. D. Yang, C. M. Shen, Y. Y. Liang, et al. Graphene nanosheets-polypyrrole hybrid material as a highly active catalyst support for formic acid electro-oxidation[J]. *Nanoscale*, 2011, 3, 3277-3284
- [4] H. W. Liang, L. Wang, S. H. Yu, et al. Carbonaceous nanofiber membranes for selective filtration and separation of nanoparticles[J]. *Adv. Mater.*, 2010, 22, 4691-4695.

# **Development of Nanofiber Reinforced PEM Impregnated with Hydrocarbon Polymer Electrolytes**

Eun-Su Lee, Nayoung Kim, Dong-Hoon Lee and Moo-Seok Lee

*Green Materials Research Group, Kolon Central Research Park, Kolon Industries, Inc., 207-2, Mabuk-Dong,*

*Giheung-Gu, Yongin-Si, Gyeonggi-Do, Korea*

*(E-mail: leems@kolon.com)*

Stability of polymer electrolyte membrane stands out always important issue as well as proton conductivity. The reinforced membrane can be a good solution to enhance the mechanical and dimensional stability for not only perfluorosulfonic acid polymer but also hydrocarbon based polymer. In this study, we have prepared nanofiber reinforced polymer electrolyte membranes for proton exchange membrane fuel cells. The nanofiber reinforced PEMs was impregnated by introducing hydrocarbon polymer electrolytes into nanoweb substrate. Due to high porosity and the intrinsic structure of reinforced PEMs, mechanical and dimensional stability are improved without sacrificing membrane performance. Consequently, reinforced PEMs exhibited higher physical properties than neat PEMs. The results suggested that the nanofiber reinforced PEMs could be utilized as an alternative proton exchange membrane for fuel cell applications.

## **Acknowledgement:**

This work was supported by the World Premier Materials (WPM) Program (10037748, Development of Reinforced Composite Membrane for Fuel Cell Using Hydrocarbon based Polymers) funded by the Ministry of Trade, Industry and Energy (MOTIE, Korea)

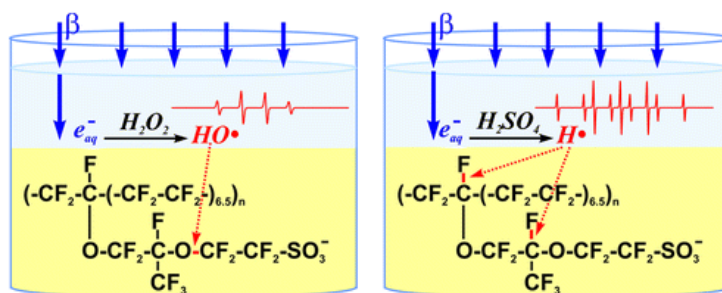
# Structure and Property Changes of PFSA Ionomer Upon Exclusive Reaction with HO• and H• Radicals

L. Ghassemzadeh, T. J. Peckham, T. Weissbach, X. Luo and S. Holdcroft\*

*Department of Chemistry, Simon Fraser University  
8888 University Drive, Burnaby, British Columbia, Canada V5A 1S6  
tpeckham@sfu.ca*

In a polymer electrolyte membrane fuel cell, the membrane is subjected to a chemically oxidizing environment at the cathode and a chemically reducing environment at the anode. Formation of hydrogen peroxide and gas crossover reactions can lead to radical formation in the fuel cell. The formation of H•, HO• and HOO• radicals has been proven by ESR. Detection of these radicals, together with the carbon center radical, showed the possibility of radical attack as the source for the chemical degradation of the polymer. A variety of in-situ and ex-situ analyses were used for studying the chemical degradation of the membrane. Ex-situ Fenton's reagent tests provide a mixture of oxidative radicals, HO• and HOO•, while in-situ fuel cell operation yields both oxidative radicals, HO• and HOO•, and the reductive H• radical.

In this work,<sup>1</sup> electron beam (e-beam) irradiation is used to selectively generate H• and HO• radicals. ESR analyses of irradiated solutions containing spin traps confirm the selective formation of individual radicals. Nafion® membrane, exposed to each radical separately, was characterized by solid state <sup>19</sup>F NMR. Changes in molecular structure were detected for different portions of the polymer chain. The changes in ion exchange capacity and proton conductivity were monitored before and after irradiation. It was shown that the chemical structure of the polymer is sensitive to both oxidative and reductive radicals. The position of attack for the oxidative HO• radical is the C-O bond closer to the end of the side chain. The position of attack for the reductive H• radical is the tertiary carbon in the main chain and the side chain. While the possibility for the formation of oxidative radicals in the fuel cell is higher, the H• radical appears to cause more damage.



1. L. Ghassemzadeh, T. J. Peckham, T. Weissbach, X. Luo, S. Holdcroft *JACS* **2013**, *135*(42), 15923 – 15932.

# Bi-imidazolium Cation Crosslinked Poly(2,6-dimethyl-1,4-phenylene oxide) Anion Exchange Membranes for Fuel Cell Application

Xiangnan He, Yanan Hao, Fuheng Zhai, Ronghuan He\*  
Department of Chemistry, College of Sciences, Northeastern University,  
Shenyang, 110819, China  
E-mail address: herh@mail.neu.edu.cn

The anion exchange membrane fuel cells (AEMFCs) provide the possibility to use non precious metals as the electrode catalysts in the cells. Due to this main advantage, AEMFCs and correlative materials have attracted extensive attentions<sup>[1-2]</sup>. The anion exchange membrane (AEM) is one of the most key components, whose properties determine the performance of the AEMFCs. AEMs which possess more quaternary ammonium groups could exhibit high conductivity. However, significant swellings and decreased mechanical strength may also connect with the high content of the quaternary ammonium and thus deteriorate the durability of the membranes<sup>[3,4]</sup>.

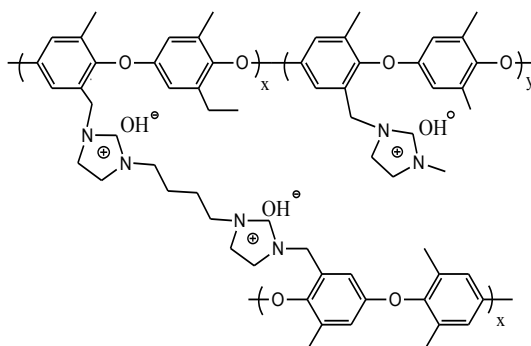


Fig. 1 Chemical structure of di-imidazolium cation crosslinked poly(2,6-dimethyl-1,4-phenylene oxide)

In the present work, novel AEMs based on cross-linked poly(2,6-dimethyl-1,4-phenylene oxide) (PPO) were fabricated and investigated. Bromomethylated PPO (BPPO) polymers with a bromination degree of 71% were first synthesized by bromination of the alkyl side chains. The crosslinked membranes were then prepared from BPPO, methylimidazole and 1,4-bis(imidazolyl)butane. The membranes with various degree of cross-linking could be obtained by adjusting the molar ratio of methylimidazole and 1,4-bis(imidazolyl)butane. FTIR and TGA measurements confirmed the occurrence of the crosslinking reaction. The experimental results indicated that the conductivity, water uptake and swellings of the membranes increased as the increased content of methylimidazole in the membranes. The high hydrophilicity of the PPO with a methylimidazolium grafting degree of 100% resulted in high solubility of the membrane in water, especially at elevated temperatures. However, crosslinked membranes with crosslinking degrees from 10% to 100% were rather stable and could be used as AEMs. The membrane with a crosslinking degree of 10% exhibited the highest conductivity of 39 to 55 mS cm<sup>-1</sup> in water over a temperature range 60 - 80 °C. The results indicated that the bi-imidazolium cation crosslinked membranes have the potential to be used as membrane electrolytes for AEMFCs.

Funding of this work is acknowledged from Natural Science Foundation of China (51172039).

## References

- [1] Lin B, Dong H, Li Y, Si Z, Gu F, Yan F. Chem. Mater. 2013, 25, 1858.
- [2] Varcoe J R, Atanassov P, Dekel D R, Herring A M, Hickner M A, Kohl P A, Kucernak A R, Mustain E W, Nijmeijer K, Scott K, Xu T, Zhuang Z. Energy Environ. Sci. 2014, 7, 3135
- [3] Hu J, Wan D, Zhu W, Huang L, Tan S, Cai X, Zhang X. ACS Appl. Mater. Interfaces 2014, 6, 4720.
- [4] Zhang F, Zhang H, Qu C. ChemSusChem 2013, 6, 2290.

# Comparison of the Degradation process during the bus application loading cycling in PEMFC

D.G. Sanchez<sup>1</sup>, Indro Biswas<sup>1</sup>, Denis Tremblay<sup>2</sup>, P.A. Jacques<sup>2</sup>, K.A. Friedrich<sup>1</sup>.

*1 Deutsches Zentrum für Luft und Raumfahrt (DLR), Institut für Technische Thermodynamik, Pfaffenwaldring 38-40, 70569 Stuttgart, Germany*

*2 Commissariat à l'énergie atomique et aux énergies alternatives (CEA) Grenoble Liten, Rue des martyrs, 38054 Grenoble cedex 9, France*

## ABSTRACT

Fuel cells, power generation devices, have been recognized as one essential solution to diminishing supplies of fossil fuel, environmental pollution, and global warming. Fuel cell technology has enjoyed great advancement in the last few years being in our days a reality for automation application.

In this work, particular attention is paid to the local analysis of performance and degradation of cells operated under a synthetic cycle for bus application. This cycle it seems to be very aggressive with fast and high changes in current load between 0.2A/cm<sup>2</sup> and 1.4 A/cm<sup>2</sup> the cell was run approximately for 300h under. In order to study locally the degradation influence of inlet gas humidification on cell performance all the experiments were performed with the DLR- PCB segmented cell current density measurements, other global effect were studied using in-situ diagnostic tools, such as cyclic voltammetry. The changes observed locally in the current densities distributions were investigated locally by post-mortem ex-situ investigations by XPS to determine changes in the chemical composition of the different layers during the experiment

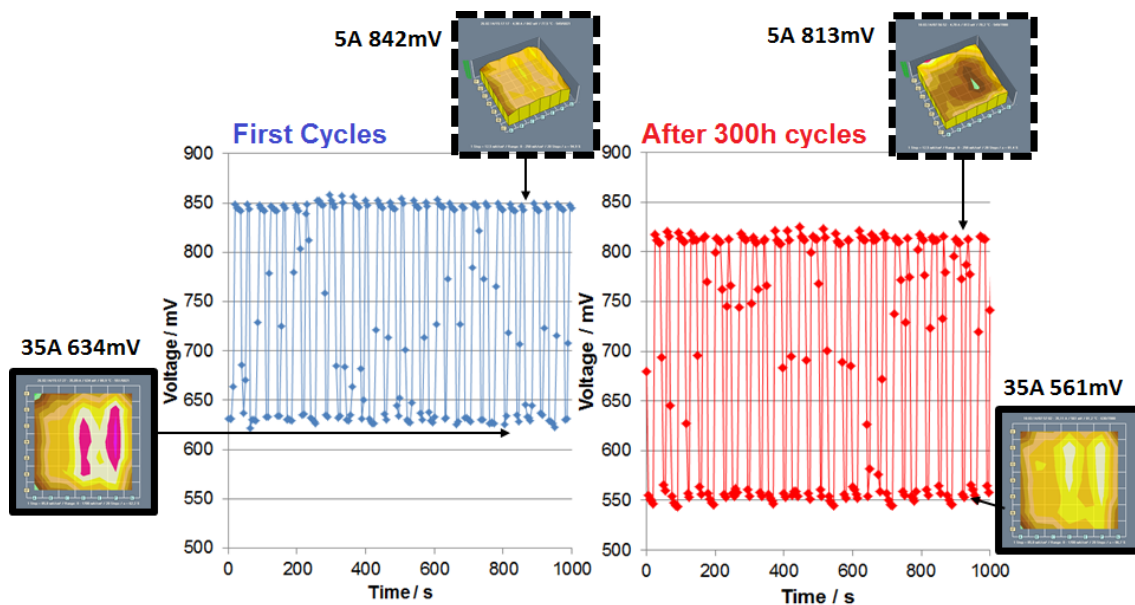


Figure 1 Comparison of the voltage responses and current density distributions at the beginning and after 300h of the bus application cycle.

# Characterization of ultra-low loading MEAs fabricated by electrospray deposition

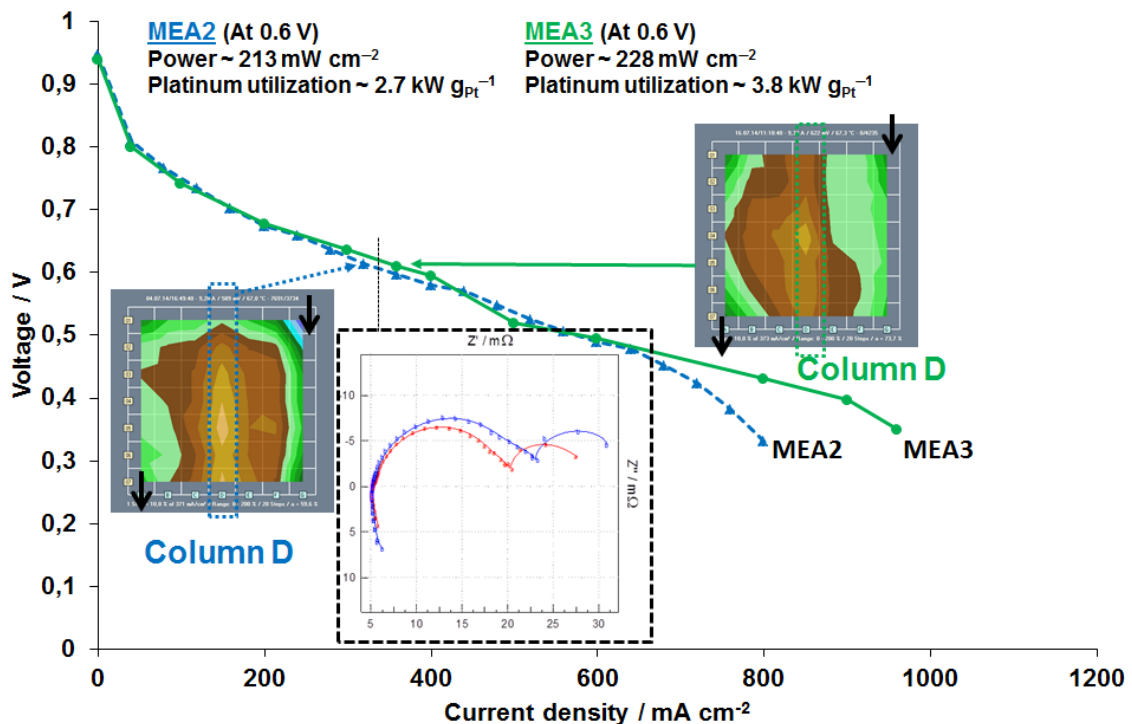
B. Martinez-Vazquez<sup>1</sup>, D.G. Sanchez<sup>2</sup>, J.L. Castillo<sup>1</sup>, K.A. Friedrich<sup>2</sup>, P.L. Garcia-Ybarra<sup>1</sup>

<sup>1</sup>*Dpt. Física Matemática y de Fluidos, Facultad de Ciencias, UNED,  
Senda del Rey 9, 28040 Madrid, Spain*

<sup>2</sup>*Deutsches Zentrum für Luft und Raumfahrt (DLR), Institut für Technische Thermodynamik,  
Pfaffenwaldring 38-40, 70569 Stuttgart, Germany*

## ABSTRACT

Ultralow Pt-loading electrodes can be manufactured by electro-hydrodynamic atomization of a catalytic ink[1]. MEAs of 25 cm<sup>2</sup> with different catalytic loadings were produced using this technique. Electrodes with 0.02 mgPt cm<sup>-2</sup>, 0.04 mgPt cm<sup>-2</sup> and different Nafion® concentrations were tested in a fuel cell test station fed with hydrogen & air. The best mass-related performance was obtained for an asymmetric MEA with a global load of 0.06 mgPt cm<sup>-2</sup> with a platinum utilization of 3.8 kW grPt<sup>-1</sup> at 0.6 V, 70 °C and 1.5 bar. Analysis under different pressures, relative humidity and gas flow rates were performed using a segmented cell to measure local current distribution and electrochemical impedance spectroscopy (EIS). In addition, long-term operation for 100 hours were also carried out to test the electrode durability. The potential of these MEAs for reduction of noble metal loading is discussed.



Comparison between the MEA2 (blue triangles) and MEA3 (green circles) polarizations curves at Tc: 70°C, Pressure:1.5 bar, Stoichiometry: H2:1.5 Air:2 and RH:100%. Current distributions and EIS plots correspond to a constant current density of 360 mA cm<sup>-2</sup>

[1] S. Martin, B. Martinez-Vazquez, P. L. Garcia-Ybarra, J. L. Castillo, J. Power Sources 229 (2013) 179–184.

# Cross-Linked Imidazolium-Based Anion Exchange Membranes

Yixin Xu, Jingshuai Yang, Ronghuan He\*

*Department of Chemistry, College of Sciences, Northeastern University,  
Shenyang, 110819, China*

*E-mail address: herh@mail.neu.edu.cn*

The alkaline fuel cells based on the anion exchange membranes (AEMs) have recently attracted much attention mainly due to the possibility for using non-noble metals as the electrode catalyst. As the core component of the fuel cell, the AEMs should satisfy the requirements of high ionic conductivity, sufficient mechanical strength, and superior stability and durability towards strong bases. The most commonly used AEMs are quaternary-ammonium-based polymer membranes<sup>[1,2]</sup>. The AEMs containing quaternary phosphonium<sup>[3]</sup>, imidazolium<sup>[4]</sup> and guanidinium<sup>[5]</sup> groups are also reported. However, There are some challenges to AEMs such as the degradation of the polymer in alkaline medium and slow mobility of the hydroxide ions than that of protons. Therefore development of the AEMs with superior properties is needed.

We synthesized the imidazolium-functionalized cross-linked poly(aryl ether ketone)s (CL-ImPAEKs) to prepare the AEMs. The homemade PAEK polymer was first brominated with a bromination of about 50% (containing four methyl bromides per repeat unit of the PAEK). The brominated-PAEKs were secondly quaternized by conversion of all the methyl bromides into methyl imidazoles. Two imidazoles, i.e., 1-methylimidazole and 2-undecylimidazole with a mole ratio of 4:1 were used to perform the conversion. The employed C2-substituted imidazoles are expected to bring about the AEMs high tolerance towards strong bases. Crosslinking of the polymer via -N= sites of the imidazole rings with different structure of the crosslinkers were performed to obtain the CL-ImPAEKs. The hydroxide form CL-ImPAEK membranes showed conductivities of 0.01 to 0.05 S cm<sup>-1</sup> in water at a temperature range of 25 to 80 °C. The conductivity of the obtained CL-ImPAEK membranes could maintain at least 120 h at 60 °C. The results indicated that the CL-ImPAEK-based membranes have the potential to be used as membrane electrolyte for anion exchange membrane fuel cells.

Funding of this work is acknowledged from Natural Science Foundation of China (51172039).

## References

- [1] Wu L, Li CR, Tao Z, Wang H, Ran J, Bakangura E, Zhang ZH, Xu TW. *Int. J. Hydrogen. Energ.* 2014, 39, 9387.
- [2] Han JJ, Peng HQ, Pan J, Wei L, Li GW, Chen C, Xiao L, Lu JT, Zhuang L. *ACS Appl. Mater. Interfaces.* 2013, 5, 13405.
- [3] Noonan KJT, Hugar KM, Kostalik HA, Lobkovsky EB, Abruna HD, Coates GW. *J. Am. Chem. Soc.* 2012, 134, 18161.
- [4] Lin BC, Dong HL, Li YY, Si ZH, Gu FL, Yan F. *Chem. Mater.* 2013, 25, 1858.
- [5] Liu L, Li Q, Dai JW, Wang H, Jin BK, Bai RK. *J. Memb. Sci.* 2014, 453, 52.



C

# Spatially Confined MnO<sub>2</sub> Nanostructure Enabling Long-Term Reversible Two-Electron Transfer in Mixed Pseudocapacitor-Battery Electrode

Y. T. Weng<sup>a\*</sup>, H. A. Pan<sup>a</sup>, R. C. Lee<sup>a</sup>, T. Y. Huang<sup>a</sup>, Y. Chu<sup>a</sup>, J. F. Lee<sup>b</sup>, H. S. Sheu<sup>b</sup>, N. L. Wu<sup>a</sup>

<sup>a</sup>Department of Chemical Engineering, National Taiwan University, Taipei 106, Taiwan

<sup>b</sup>National Synchrotron Radiation Research Center, Hsinchu 30076, Taiwan

\* Corresponding author email address: [d96524013@ntu.edu.tw](mailto:d96524013@ntu.edu.tw)

Long-term reversible charge-transfer for MnO<sub>2</sub>-based pseudocapacitor electrode has up to now been limited to one-electron transfer between Mn(IV) and Mn(III) ion over an operating potential (OPW) not greater than 1 V. A novel material design strategy is demonstrated to substantially widen (up to 2 V) the OPW of MnO<sub>2</sub>-based aqueous pseudocapacitive electrode and to enable two-electron transfer between Mn(IV) and Mn(II) ions sustainable over thousands of cycles. The material design involves, via a facile solution chemistry method, forming spatially confined MnO<sub>2</sub> nanodomains (approximately 4 nm in size) of which the surfaces are surrounded by electrochemically inactive SiO<sub>2</sub> with extensive interfacial Mn • O • Si bonding. The MnO<sub>2</sub> • SiO<sub>2</sub> (MSO) composite electrode exhibits mixed pseudocapacitor • battery behavior with two-electron transfer in an aqueous Li<sub>2</sub>SO<sub>4</sub> electrolyte between • 1 V and 1 V versus Ag/AgCl/saturated KCl and no Mn ion dissolution or phase transformation into more compact lattice structure, which otherwise occur in the conventional bulk MnO<sub>2</sub> electrode and lead to fast charge-storage capacity deterioration, during long-term cycling. In operando synchrotron X-ray absorption analyses reveal a two-step charge-transfer process, consisting of a solid-solution mechanism between Mn(IV) and Mn(III) and a two-phase reaction mechanism between Mn(III) and Mn(II). The presented MSO nanostructure holds great promise for high-capacity, high-energy supercapacitor applications.

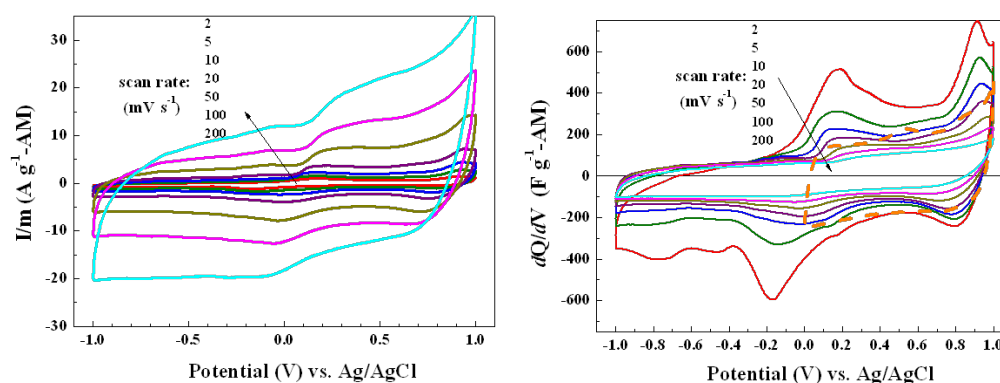


Figure 1: Electrochemical characterization: voltammograms of the MSO electrode.

# Electrochemical Characteristics of Composite Materials as Carbon & Metal Oxide for Hybrid Capacitor

Soo-Gil Park<sup>a,\*</sup>, Joeng-Jin Yang<sup>a</sup>, Han-Joo Kim<sup>b</sup> and Young-Jae Yuk<sup>b</sup>

<sup>a</sup>Chungbuk National University, 1 Chungdae-Ro, Seowon-Gu, 362-763, Cheongju, Republic of Korea

<sup>b</sup>Purechem Co., Ltd, 151 Namseok-Ro, Nami-Myeon, Seowon-Gu, 362-813, Cheongju, Republic of Korea

\*sgpark@cbnu.ac.kr

Electrochemical capacitors (ECs), also called super-capacitors or ultra-capacitors, are charge storage device with capacities intermediate between those of electrolytic capacitors and rechargeable batteries. ECs store charge at the electrode/electrolyte interface either through conventional non-Faradic means, by forming an electric double layer or by a limited Faradic reaction. The development of high performance capacitors requires improvements in all components such as activate material, electrolyte, binder and cell configuration. Recently, researchers have begun to explore the combination of both Faradic and non-Faradic processes in the same hybrid device to overcome the limits of conventional EDLCs [1-3].

Activated carbons as spheres having high specific surface areas have been used in many applications such as adsorbents and electrode materials of ECs. Activated carbon spheres were prepared by three-step process. First, glucose was carbonized by hydrothermal method using autoclave. Next, obtained carbon spheres were activated with potassium carbonate by chemical activation. Finally, through the heating treatment, activated carbon spheres were obtained. When the heating treatment increases, the capacities increase until 80Fg<sup>-1</sup>. Also, we prepared Li<sub>4</sub>Ti<sub>5</sub>O<sub>12</sub>-CNT composite materials synthesized to enhance of power density of Li<sub>4</sub>Ti<sub>5</sub>O<sub>12</sub>, which is used as a negative active material that has a zero-strain behavior and high charge-discharge performance [4]. The spherical Li<sub>4</sub>Ti<sub>5</sub>O<sub>12</sub> and Li<sub>4</sub>Ti<sub>5</sub>O<sub>12</sub> carbon nanotube (CNT) composites were synthesized using a colloid system. The electrochemical properties of the composites were thoroughly examined to determine their applicability as hybrid capacitor anodes. The spherical Li<sub>4</sub>Ti<sub>5</sub>O<sub>12</sub>-CNT composite electrical conductivity was improved over that of the spherical Li<sub>4</sub>Ti<sub>5</sub>O<sub>12</sub> composite. The synthesized composites were utilized as the anode of a hybrid capacitor, which was assembled with an activated carbon (AC) positive electrode. The CNTs attached on spherical Li<sub>4</sub>Ti<sub>5</sub>O<sub>12</sub> contributed to a 51% reduction of the equivalent series resistance of the Li<sub>4</sub>Ti<sub>5</sub>O<sub>12</sub>-CNTs/AC hybrid capacitor compared to the Li<sub>4</sub>Ti<sub>5</sub>O<sub>12</sub>/AC hybrid capacitor. When applied in a hybrid capacitor, we confirmed the decreasing ESR of the hybrid capacitor. Thus, the LTO-CNT 1wt.% and LTO-CNT 2 wt.% hybrid capacitors had capacities that were 31.6% and 62.7% larger than that of the LTO-AC hybrid capacitor, respectively, in a current density of 10 mA cm<sup>-2</sup> at cycles. The addition of CNTs improved the hybrid capacitor because of the electron path formation in LTO materials. The synthesized composite electrode shows a promising candidate for electrode materials used in high power hybrid capacitors.

[1] B. E. Conway, *Kluwer Academic, New York*, (1999)

[2] R. Kötzt, M. Carlen, *Electrochim. Acta* **45**, 2483 (2000).

[3] E. Frackowiak, F. Béguin, *Carbon* **39**, 937 (2001).

[4] T.F. Yi, L.J. Jiang, J. Shu, C.B. Yue, R.S. Zhu, H.B. Qiao, *J. Phys. Chem. Solids*, **71**, 1236 (2010).

# Advanced Auxiliary Materials in EDLC for Enhancing Power and Energy

Masashi Ishikawa and Masaki Yamagata

*Department of Chemistry and Materials Engineering,  
Faculty of Chemistry, Materials and Bioengineering, Kansai University  
3-3-35 Yamate-cho, Suita 564-8680, Japan  
e-mail address: masaishi@kansai-u.ac.jp*

Electric double layer capacitors (EDLCs) have attracted great attention as an electric power source because they have a high power density and long cycle life when compared to other power devices, e.g., lithium-ion batteries. We have to, however, improve their performances more for various advanced applications such as a hybrid electric vehicle (HEV) and electric vehicle (EV). We reported that specific power density of EDLC can be improved by applying various natural polymers, e.g., alginate acid (Alg) and chitosan, as a matrix of gel electrolytes [1]. This effect is ascribed to decreased resistances at an interface between an electrode and electrolyte, which is originated from high affinity between the natural polymer materials and carbon materials such as activated carbon.

To enhance and utilize this characteristics we attempted to apply various natural polymers to EDLC as a binder for activated carbon electrodes, and improved their performances [2]. The cell with Alg binder shows high discharge capacitance and excellent rate capability when compared to the other cells with CMC and PVdF binders. This result suggests that the electrode with Alg has a lower internal resistance due to higher affinity between activated carbon and the natural polymer, which reduces a reaction resistance at the electrode/electrolyte interface. This property is consistent well with our previous affinity test [1]. The present merit of Alg binder is also confirmed from the results of AC impedance measurements as follows. Regarding Nyquist plots of each test cell with Alg, CMC, and PVdF binder, in a middle frequency range related to ionic diffusion inside an activated carbon electrode, the cell with Alg binder exhibits desirable characteristics, which should contribute to lower internal resistance. Thus the present natural polymer material is an attractive component in EDLC application to improve its power density, keeping its desirable specific energy.

Recently, we also applied gelatin material to binder in EDLCs. Our gelatin derivatives can keep electrode materials such as activated carbon and conductive materials steady as a important function of electrode binder. Resulting electrode films with gelatin are very strong enough to protect themselves against a manual scratching. An internal electric resistance in the gelatin-applied electrode sheets is somewhat higher than that in CMC-SBR-based electrode sheets. However, not only their mechanical strength but also their resistivity against oxidation, which we found in cell-cycling and cell-floating tests, are quite attractive. The applied electrode can be prepared in aqueous media including gelatin, conductive auxiliaries, and activated carbons. Thus the gelatin-based preparing process can provide us with environmentally friendly, safe and low-cost production for EDLC electrode sheets.

## Acknowledgements

The authors are indebted to Prof. H. Tamura (Kansai University) for many helpful discussions on the preparation of polysaccharide-based materials. The present work was supported by Grant-in-Aid for Scientific Research and “Strategic Project to Support the Formation of Research Bases at Private Universities”: Matching Fund Subsidy from MEXT, Japan.

## References

- [1] M. Yamagata, K. Soeda, S. Yamazaki, M. Ishikawa, *Electrochem. Solid-State Lett.*, 2011, 14, A165.
- [2] M. Yamagata, S. Ikebe, K. Soeda, M. Ishikawa, *RSC Advances*, 2013, 2013, 103.

# Pseudocapacitance of ruthenium oxide in buffered solutions

Wataru Sugimoto, Sho Makino

Shinshu University, Center for Energy and Environmental Science  
3-15-1 Tokida Ueda, Nagano, 386-85657 Japan  
wsugi@shinshu-u.ac.jp

Various metal oxides have been proposed as promising electrode materials for aqueous pseudocapacitors. Electrolytes near neutral pH are often used owing to its environmental friendliness and its low corrosiveness. We have recently started to explore buffered solutions as electrolytes for pseudocapacitors. Despite  $\text{RuO}_2$  being the model pseudocapacitive material, the electrochemical capacitor properties of  $\text{RuO}_2$  in neutral electrolytes are less known compared to the behavior in acidic or basic electrolytes. Here we explore the pseudocapacitive behavior of ruthenium oxide nanoparticles and nanosheets in buffered solutions as an environmentally benign electrolyte.

The pseudocapacitive charge storage in poorly-crystalline hydrous  $\text{RuO}_2$  nanoparticles and highly-crystalline  $\text{RuO}_2$  nanosheets derived from layered  $\text{Na}_{0.2}\text{RuO}_{2.1}$  were investigated. Capacitance comparable to or higher than  $\text{H}_2\text{SO}_4$  were obtained in acetic acid-lithium acetate ( $\text{AcOH-AcOLi}$ ) buffered solutions, depending on the ionic strength and pH. At constant pH,  $\text{AcOH-AcOLi}$  with higher ionic strength (molarity) lead to higher capacitance, owing to the presence of higher concentration of the adsorbent in the electrolyte. Figure 1 shows voltammograms of  $\text{RuO}_2 \cdot n\text{H}_2\text{O}$  in various  $\text{AcOH-AcOLi}$  solutions. The cyclic voltammograms for 2.0 M  $\text{AcOH-AcOLi}$  (pH = 5.36) completely overlaps with that in  $\text{H}_2\text{SO}_4$ , implying an analogous charge storage mechanism. On the other hand, the electrochemical behavior in 2.0 M  $\text{AcOH-AcOLi}$  with pH = 4.44 and 3.42 are quite different. For pH = 3.42, the electrical double layer capacitance is completely lost. This peculiarity is attributed to adsorption of molecular  $\text{AcOH}$  (not  $\text{AcO}^-$ ) on the surface of  $\text{RuO}_2$ , blocking the electrical double layer formation.

$\text{RuO}_2$  nanosheets afforded 20 to 50% higher capacitance than  $\text{RuO}_2 \cdot n\text{H}_2\text{O}$ . The highest capacitance is obtained with 5 M  $\text{AcOH-AcOLi}$  (pH=5.4)  $1,038 \text{ F g}^{-1}$  at  $2 \text{ mV s}^{-1}$ , which is almost 1.5 times higher than the benchmark  $\text{RuO}_2 \cdot n\text{H}_2\text{O}$  in  $\text{H}_2\text{SO}_4$  electrolyte ( $720 \text{ F g}^{-1}$ ).  $\text{RuO}_2$  nanosheet electrodes also perform well in bio-electrolytes such as phosphate buffered saline ( $837 \text{ F g}^{-1}$ ) and fetal bovine serum ( $772 \text{ F g}^{-1}$ ).

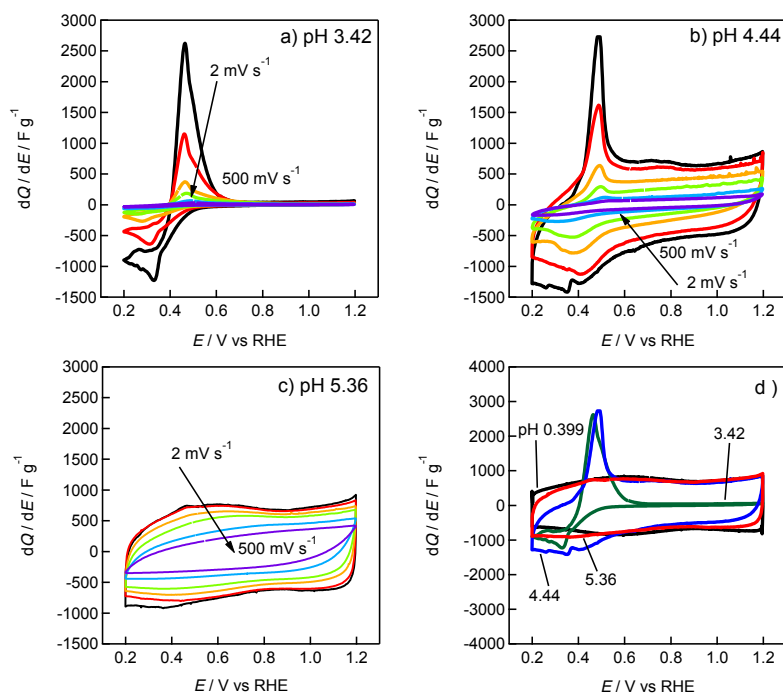


Figure 1. Cyclic voltammograms of  $\text{RuO}_2 \cdot n\text{H}_2\text{O}$  at 2, 5, 20, 50, 200,  $500 \text{ mV s}^{-1}$  in 2.0 M  $\text{AcOH-AcOLi}$  at pH of a) 3.42, b) 4.44, and c) 5.36. d) Cyclic voltammograms of  $\text{RuO}_2 \cdot n\text{H}_2\text{O}$  at  $2 \text{ mV s}^{-1}$  in 2.0 M  $\text{AcOH-AcOLi}$  with various pH and 0.5 M  $\text{H}_2\text{SO}_4$ .

# Facile Simulation of Electric Double-Layer Capacitance Based on Helmholtz Models

Hsisheng Teng, Wei Hsieh, Hsin-Chieh Huang,

*Department of Chemical Engineering and Research Center for Energy Technology and Strategy, National Cheng Kung University, Tainan 70101, Taiwan*  
*hteng@mail.ncku.edu.tw*

Promoting the charge storage performance of electric double-layer capacitors requires a simulation model for the double-layer formation mechanism as well as the characterization of the electrode-electrolyte interface. Unfortunately, previous models are applicable only to electrodes with a specific pore size. We propose a universal model, based on the Helmholtz theory, to outline the double-layer formation mechanism in carbons with a wide pore size distribution.

In this study, we determine that surface-based capacitance ( $C/S$ ) value of cylinder-like mesopores decreases with a decrease in pore size due to an increase in the influence of wall curvature on ion layering while slit-shaped micropores exhibit constant  $C/S$  values irrespective of pore size. The pore structures and pore size distribution of the carbon are analyzed using a method based on non-local density functional theory (NLDFT). The simulated capacitance values of three distinct forms of carbons present excellent agreement with the experiment data, thereby verifying the reliability and feasibility of the proposed model.

We also present a strategy for the determination of constant  $C/S$  values in micropores. Our findings demonstrate that the number of solvent molecules in such confined spaces decreases with a decrease in slit width, which weakens polarizability at the interface. This model reveals the molecule-sieving effect of micropores, which is critical to the precision of capacitance prediction.

# Oxygen Functional Groups of Incompletely Reduced Graphene Oxides for a Thin-film Electrode of Supercapacitor

Jong-Huy Kim\*, Young-Joon Oh, Jung-Joon Yoo, Yong-Il Kim, and Jae-Kook Yoon  
Korea Institute of Energy Research  
#152 Gajeong-ro, Yuseong-gu, Daejeon, 305-343, KOREA(South)  
kjhy@kier.re.kr

For incompletely reduced graphene oxides (RGOs), an effect of oxygen functional groups such as carboxyl, phenol, carbonyl, and quinone on electrochemical capacitive behavior was studied. To prepare RGO thin-film electrodes, a simple fabrication process by (i) dropping and evaporating the graphene oxide (GO) solution, (ii) irradiating pulsed light, and (iii) heat-treating at 200–360 °C was applied. It was notable that the pulsed light irradiation was effective to prevent the disfiguring of deposited GO thin-film during the thermal reduction.

As increasing the thermal reduction temperature from 200 to 360 °C, interlayer distances of the RGOs obtained from XRD analyses were gradually decreased from 0.379 to 0.354 nm. XPS O 1s spectra analyses showed that the atomic percentages of carboxyl and phenol of the RGOs were sustained as  $5.40 \pm 0.36$  and  $4.77 \pm 0.41$  at% respectively. Meanwhile, those of carbonyl and quinone of the RGOs were gradually declined from 3.10 to 1.81 and from 1.32 to 0.65 at% respectively.

For all RGO thin-film electrodes with different thermal reduction temperature, the specific capacitances at the scan of  $5 \text{ mV s}^{-1}$  were sustained as ca.  $220 \text{ F g}^{-1}$  in 6 M KOH and  $93 \text{ F g}^{-1}$  in 0.5 M  $\text{Na}_2\text{SO}_4$ . However, in 1 M  $\text{H}_2\text{SO}_4$ , the specific capacitance was gradually decreased from 171 to  $136 \text{ F g}^{-1}$  as increasing the reduction temperature. After 100,000 cycles under the scan rate of  $500 \text{ mV s}^{-1}$  but in different electrolytes of 6 M KOH, 1 M  $\text{H}_2\text{SO}_4$ , and 0.5 M  $\text{Na}_2\text{SO}_4$ , the RGO thin-film electrodes reduced at 200 °C exhibited ca. 92, 54, and 104 % of the initial capacitances respectively. The atomic percentages of the oxygen functional groups involved in the pseudocapacitive Faradaic reaction were decreased after the cycle test. Especially in 1 M  $\text{H}_2\text{SO}_4$ , quinone group was decreased to ca. 48 % of initial atomic percentage, which seems to be a main reason for the drastic reduction of capacitance.

At the scan of  $5 \text{ mV s}^{-1}$  the specific pseudocapacitance per unit atomic percentage for either carboxyl or phenol group in 6 M KOH was obtained as  $12.59 \text{ F g}^{-1} \text{ at}\%^{-1}$ . For carbonyl group in 1 M  $\text{H}_2\text{SO}_4$ , it was a slightly deviated value as  $13.55 \text{ F g}^{-1} \text{ at}\%^{-1}$ . For quinone group in 1 M  $\text{H}_2\text{SO}_4$ , it was  $27.09 \text{ F g}^{-1} \text{ at}\%^{-1}$ . For all RGO thin-film electrodes tested at the scan rate from 5 to  $500 \text{ mV s}^{-1}$ , averaged values of the specific pseudocapacitance per unit atomic percentage for carboxyl or phenol, carbonyl, and quinone groups were obtained as  $12.2 \pm 2.8$ ,  $12.8 \pm 2.5$ , and  $25.6 \pm 5 \text{ F g}^{-1} \text{ at}\%^{-1}$  respectively.

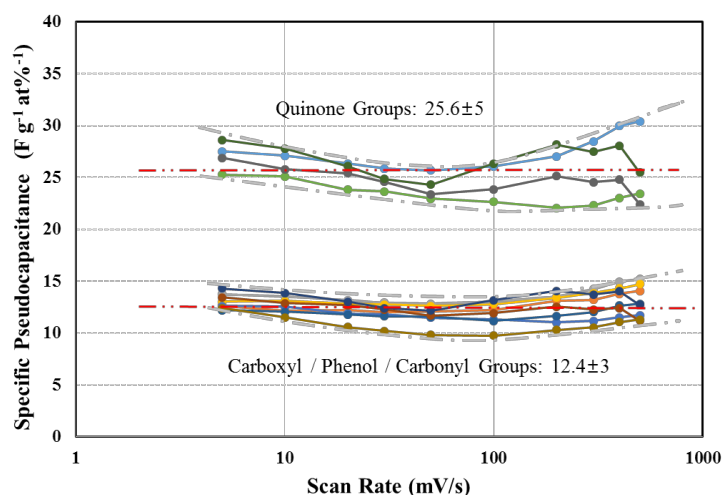


Figure. Specific pseudocapacitance per atomic percent of oxygen functional groups.

# Graphite-Fluoride Lithium Hybrid Capacitor

Soshi Shiraishi, Yasuyoshi Shiraishi,

Graduate School of Science and Technology, Gunma University

Kiryu, Gunma 376-8515, Japan

soshishiraishi3@gunma-u.ac.jp

Hiroyuki Fujimoto

Osaka Gas Co., Ltd., Osaka 554-0051, Japan

## 1. Introduction

Graphite fluoride is one of graphite intercalation compounds and used as lubricate and cathode material of primary battery. The graphite fluoride-lithium primary ((CF)<sub>n</sub>/Li) battery has been commercially used because of its high energy density, excellent discharge performance, and low self-discharge property. The battery reaction is shown as follows.



The cathode of the discharged (CF)<sub>n</sub>/Li battery is known to be the nano-composite of carbon and LiF<sup>1)</sup>. Several years ago, the author (S.S) found that the carbon product derived from the de-fluorination of graphite fluoride by charge-transfer complex such as lithium naphthalene has highly electrochemical capacitance regardless of its low microporosity<sup>2)</sup>. This suggests that the cathode discharge-product of (CF)<sub>n</sub>/Li battery can also work as active material of electrochemical capacitor. Thus, the authors revealed that the discharged (CF)<sub>n</sub>/Li battery can be re-charged as new hybrid electrochemical capacitor. In this paper, the authors announce the basic performance of the hybrid electrochemical capacitor using the discharged (CF)<sub>n</sub>/Li battery.

## 2. Experimental

Commercial graphite fluoride powder (Central Glass Co., Ltd., Japan) or Li foil (Honjo Metal Co., Ltd., Japan) was used as cathode or anode active material for (CF)<sub>n</sub>/Li battery, respectively. The sealed two-electrode cell for (CF)<sub>n</sub>/Li battery was constructed using these electrode materials, poly-propylene porous separator, and 1M LiPF<sub>6</sub>/ethylene carbonate and ethyl methyl carbonate electrolyte. The cell was discharged to lower cut-off voltage of 1V under galvanostatic condition (40 mA g<sup>-1</sup>) as the battery and then was re-charged/discharged between 2V and 4V as the capacitor.

## 3. Results and Discussion

The discharge-charge curves were shown in Fig.1. The first discharge-curve is the plateau around 2.5V, which is characteristic for the battery. The successive charge-discharge curves show the triangle shape, which means capacitive performance. This suggests that the carbon/LiF nano-composite as discharge-product of the cathode operates as the positive electrode of the capacitor and that the Li metal is electrochemically deposited / dissolved at the negative electrode. The authors term this new hybrid capacitor system as “Graphite-Fluoride Lithium Capacitor (GFLC)”. The GFLC indicates the higher energy density and power density than the EDLC and the performance is comparable to that of the Li-ion capacitor as shown in Fig.2.

## References

- 1) H. Touhara, H. Fujimoto, N. Watanabe, and A. Tressaud, *Solid State Ionics*, **14**, 163-170 (1984).
- 2) S. Shiraishi, et al., Carbon 2010 extended abstracts, No.349 (2010).

**Acknowledgment** A part of this research is supported by JSPS KAKENHI Grant No. 26410250.

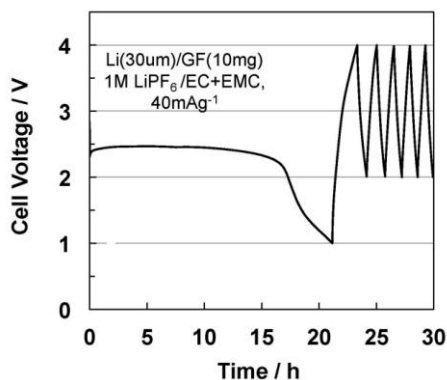


Fig. 1 Discharge-charge curve of (CF)<sub>n</sub>-Li battery.

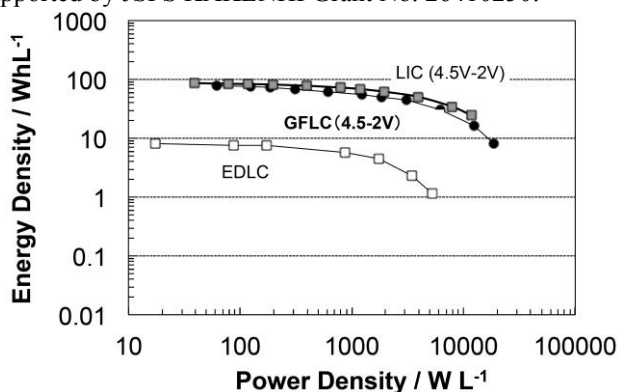


Fig. 2 Ragone plot of the GFLC, Li ion capacitor (LIC), and EDLC.



# Towards Green Aqueous Capacitors with Chitin as Binder

Elzbieta Frackowiak, Adam Kolodziej, Krzysztof Fic

*Institute of Chemistry and Technical Electrochemistry, Poznan University of Technology,*

*Berdychowo 4, 60-965 Poznan, Poland*

[elzbieta.frackowiak@put.poznan.pl](mailto:elzbieta.frackowiak@put.poznan.pl)

Electrochemical capacitors are a subject of significant interest in the scientific community over the last few decades due to their outstanding features and perspective of use. They can be charged and discharged within seconds and operate up to million cycles. They may be also considered as environmentally-friendly devices when operating in neutral aqueous electrolyte, e.g.  $\text{Na}_2\text{SO}_4$ ,  $\text{Li}_2\text{SO}_4$ ,  $\text{KI}$ . However, carbon electrodes are conventionally bounded by fluorine-based polymers as polytetrafluoroethylene (PTFE) and polyvinylidenedifluoride (PVdF) which are highly hydrophobic, hence, limiting wettability of electrodes in aqueous electrolytes. Many efforts have been devoted to overcome this disadvantage and apply more sustainable materials as carbon electrodes binders. Use of cellulose has been recently reported and shown a great opportunity to consider biopolymers as useful substances in terms of carbon binding.<sup>1</sup> This work presents the application of another widely abundant biopolymer, chitin, as binder for carbon electrodes operating in aforementioned electrolytes.

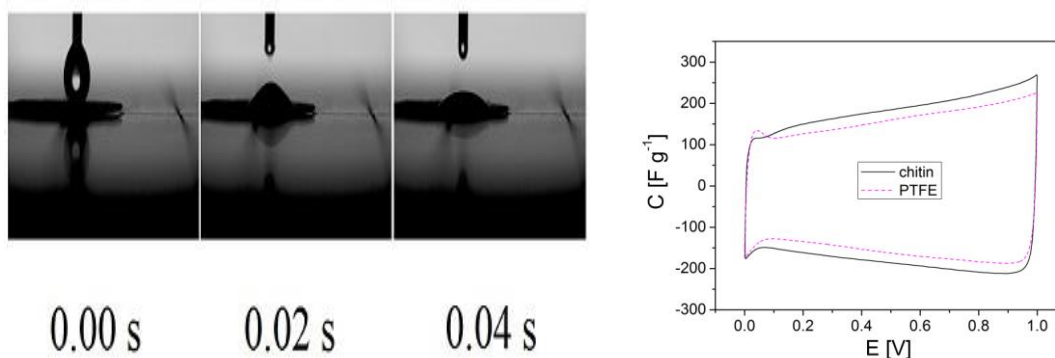


Figure 1. Contact angle measurements of chitin-bounded electrode (left), and cyclic voltammograms ( $10 \text{ mV s}^{-1}$ ) for chitin- and PTFE- bounded electrodes (NORIT Supra 30) operating in 1M KI (right).

Chitin-bounded electrodes have shown promising performance, comparable to those bounded by PTFE. Cyclic voltammetry method confirmed good charge propagation across the electrode/electrolyte interface, presumably originating from improved electrode wettability. Moreover, galvanostatic charging/discharging measurements have indicated good capacitance retention while increasing current density. Application of chitin as a binder also results in limitation of activity of electrochemically generated iodine via trapping in biopolymer structure. Thus, chitin appears to be a cheap, environmentally sustainable alternative for fluoropolymers reflecting promising results and is being worth more-in-depth study.

## References

- [1] N. Bockenfeld, S. S. Jeong, M. Winter, S. Passerini, A. Balducci, *Journal of Power Sources*, 2013, 221, 14-20

## Acknowledgements

This article was financially supported by Swiss Contribution within the Polish-Swiss Research Programme, Project No. PSPB 107/2010.

# Ion Exchange Optimization of Polyaniline Films in Deep Eutectic Solvents for Supercapacitor Application

A. Robert Hillman, Karl S. Ryder, Abdulcabbar Yavuz  
Department of Chemistry, University of Leicester  
Leicester, LE1 7RH, UK  
ay54@le.ac.uk

Charge transfer and mass transport in energy storage devices can be improved by using nano-materials, which have greater surface area leading to an increase in power.<sup>1</sup> One suggestion is to design three-dimensional multifunctional nanoscale electrodes.<sup>2</sup> Polymer modified electrodes are intrinsically porous in nature and offer a large reactive surface area. This 3D reaction zone has the prospect of high species flux entering into the bulk of the polymer modified film, leading to an increase in the capacitance, which makes them suitable candidates for battery/supercapacitor devices. Most of the studies on supercapacitors focus on the deposition and cycling of the electrode material. However, the study of the electrolyte for supercapacitor applications has not received as much attention to date.

Here, the combination of novel Deep Eutectic Solvent (DES) electrolyte with polyaniline (PANI) modified electrodes, having conjugated backbones allowing for extensive delocalisation of electrons, is presented for supercapacitor application. In this study, significant attention is given to characterization of the fundamental electrochemical process during faradaic reaction of pseudocapacitance, complementing empirical study of the performance, stability and processability of supercapacitors.

There is abundant literature relating to conducting polymers in conventional liquid media where solvent transport is a very important part of film dynamics. In DES media, which are entirely composed of ions (consisting of a hydrogen bond donor (HBD) and a quaternary ammonium salt (QAS)), questions of solvent transfer do not occur. However, there is a much more complicated situation in terms of anion vs cation transfer. In particular, the anion used here is a complex anion ( $\text{Cl}^-$  with HBD). As the moving species is large, it may move too slowly in the context of supercapacitor. Therefore, cation movement may be preferred. Electrochemical (cyclic voltammetry) and acoustic wave (QCM) measurements were combined as an in-situ technique (EQCM) to study the motion of mobile species populations between DESs and PANI films. Since the ionic liquids are very viscous media that may affect film rigidity significantly, acoustic admittance measurement were used to obtain film ion population change data rigidly as a function of potential range, scan rate and scan numbers of deposition of PANI films, temperature and composition of DESs, and scan rate of redox switching of PANI in DESs.

Generally, thin PANI films ( $< 40 \text{ nmol cm}^{-2}$ ) have more cation dominated redox switching reaction. However, thick films have two significant characteristics depending on timescale. Normally, thinner films are more likely to have a surface control mechanism which is desirable for energy storage devices. However, the results showed that the rate limiting process does not just depend on film coverage but also depends on the growth conditions of the films; in particular the scan rate and potential window during polymerization could lead to different switching responses and performance of the resulting films. The HBD of the DES and temperature also affect the ion dynamics of PANI. A specific capacitance value of  $803 \text{ F g}^{-1}$  which is only 61% of the theoretical one was obtained from PANI cycling in Ethaline (a mixture of  $\text{Ch}^+\text{Cl}^-$  and ethylene glycol). The decreasing of specific capacitance of PANI is small with increasing scan rate indicating high power density of the materials. Excellent stability (more than 30 000 cycles) of PANI films in DESs was also demonstrated.

1 P. V. Braun and R. G. Nuzzo, *Nature Nanotechnology*, 2014, **9**, 962-963.

2 D. R. Rolison, J. W. Long, J. C. Lytle, A. E. Fischer, C. P. Rhodes, T. M. McEvoy, M. E. Bourg and A. M. Lubers, *Chem. Soc. Rev.*, 2009, **38**, 226-252.

# **Lithium manganese phosphate-gold nanoparticles composite as an efficient lithium ion electrochemical capacitor**

**Chinwe O. Ikpo<sup>a\*</sup>, Ntuthuko W. Hlongwa<sup>a</sup>, Kenneth I. Ozoemena<sup>b, c</sup>, Emmanuel I. Iwuoha<sup>a</sup>,  
Natasha Ross<sup>a</sup>, Miranda Ndipingwi<sup>a</sup>, Myra Nzaba<sup>a</sup>, Milua Masikini<sup>a</sup>, Nolubabalo Matinise<sup>a</sup>,  
Nomxolisi Dywili<sup>a</sup>, Priscilla Baker<sup>a</sup>**

*<sup>a</sup>SensorLab, Department of Chemistry, University of the Western Cape  
Private Bag X17 Bellville, Cape Town 7535, South Africa.*

*<sup>b</sup>Energy Materials, Materials Science and Manufacturing, Council for  
Scientific and Industrial Research (CSIR), Pretoria 0001, South Africa.*

*<sup>c</sup>School of Chemistry, University of the Witwatersrand, Johannesburg 2050, South Africa.*

E-mail: cikpo@uwc.ac.za

The next generation of electrical energy devices requires the combination of electrochemical storage systems with high power density and energy density. Electrochemical capacitors are known to have high power density and can be charged and discharged in seconds, up to millions of times [1]. However, they are characterised by low energy density. This drawback can be compensated for in a hybrid electrochemical system with a complementary electrode material that offers high energy density. Lithium manganese phosphate (LMP) is an inexpensive material that is capable of delivering a maximum energy density of  $\sim 700 \text{ Wh kg}^{-1}$ . Although it has low electrical conductivity, the lithium redox chemistry allows an operating voltage that is higher than electrochemical capacitors [1, 2]. In this research, we present for the first time, lithium manganese phosphate modified with gold nanoparticles (LMP/Au) as an electrode material for applications in lithium ion electrochemical capacitors. LMP was synthesized through a sol-gel synthetic route with subsequent calcination and coating with gold nanoparticles. The lithium ion electrochemical capacitor was prepared on a nickel foam substrate with carbon black to enhance the conductivity. All electrochemical measurements were carried out in 1 M  $\text{Li}_2\text{SO}_4$  electrolytic solution. The incorporation of gold nanoparticles to enhance the LMP is novel and preliminary findings show that the electrochemical performance of the LMP/Au nanocomposite is better than the unmodified LMP and this will be fully described during the conference.

## References

1. H. Abruña, Y. Kiya, J. Henderson, Batteries and electrochemical capacitors, *Physics Today* Online 61 (2008) 43.
2. J. Kim, R. Vijaya, L. Zhu, Y. Kim, Improving electrochemical properties of porous iron substituted lithium manganese phosphate in additive addition electrolyte, *Journal of Power Sources* 275 (2015) 106.



# Physico-Chemical Features of Carbons and their Behavior in Electrochemical Capacitors

Teresa A. Centeno<sup>a</sup>, Belén Lobato<sup>a</sup>, Gelines Moreno-Fernández<sup>b</sup>, Andrea Balducci<sup>c</sup>

<sup>a</sup> Instituto Nacional del Carbón (INCAR-CSIC). Apartado 73.33080 Oviedo (Spain)

<sup>b</sup> Instituto de Ciencia de Materiales de Madrid (ICMM-CSIC). Sor Juana Ines de la Cruz, 3, Cantoblanco, 28049 Madrid (Spain)

<sup>c</sup> Helmholtz Institute Ulm. Karlsruhe Institute of Technolog. Helmholtzstrasse 11, 89081 Ulm (Germany)  
teresa@incar.csic.es

Research on the more relevant factors governing the performance of carbons in electrochemical capacitors has been intensive over the past few years. Unfortunately, contradictory information has been obtained and there is still great controversy.

The study of a large variety of materials, including activated carbons, templated mesoporous carbons, carbon nanotubes, carbon fibers, carbon gels, carbide-derived carbons and graphene-type materials, shows that a systematic characterization is highly required to gain reliable insights into the different role of their properties in the electrochemical behaviour.

This approach illustrates that the total surface determined by standard adsorption of N<sub>2</sub> at 77 K may be misleading due to different reasons: i) it may be no longer available for the electrolyte ions. The existence of a distribution of pore sizes and/or constrictions at the entrance of the pores may hinder the access of the electrolyte to the overall porosity, ii) the filling of narrow cavities is a very slow process at 77 K and the equilibrium may not be achieved under the standard operation times. In such a case, the specific surface area determined by adsorption does not match the electrochemically active surface of the carbon and iii) some carbon materials suffer from a drop in their specific surface area upon fabrication of electrodes with features of the existing commercial devices. Therefore, the popular approach based on the specific surface area and the pore size of carbons to assess their suitability in electrochemical capacitors cannot be used in a straightforward manner.

It was found that carbons follow general patterns. Although the extent of the double layer has been identified as a key factor, other features, such as surface chemistry, electric conductivity, etc. also play a role. The corresponding impact is highly dependent on the electrolyte.

New correlations between structural and chemical characteristics of carbons and their performance allow evaluating the current challenges of nanocarbons in electrochemical capacitors.

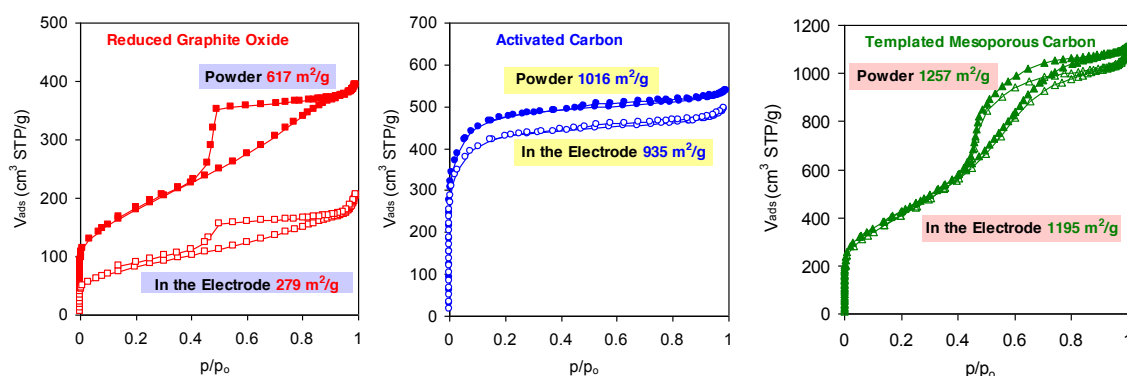


**Fig. 1.** N<sub>2</sub> adsorption isotherms for different carbon materials and their corresponding electrodes. The values are referred to carbon mass.

- [1] F. Stoeckli, T.A. Centeno. J. Mater. Chem. A 1 (2013) 6865.
- [2] J. Sánchez-González, F. Stoeckli, T.A. Centeno. J. Electroanal. Chem. 657 (2011) 176.
- [3] S. Pohlmann, B. Lobato, T.A. Centeno, A. Balducci. Phys. Chem. Chem. Phys. 15 (2013) 17287.
- [4] B. Lobato, R. Wendelbo, V. Barranco, T. A. Centeno. Electrochim. Acta 149 (2014) 245.
- [5] B. Lobato, V. Vretenar, P. Kotrusz, M. Hulman, T.A. Centeno. J. Colloid Interface Sci. 446 (2015) 203.

# The Electric Double Layer has a Life of its Own

M. Salanne,<sup>a,b,c,\*</sup> C. Pean,<sup>a,b,d</sup> C. Merlet,<sup>a,b</sup> B. Rotenberg,<sup>a,b</sup> P.A. Madden,<sup>e</sup> P.-L. Taberna,<sup>a,d</sup> B. Daffos,<sup>a,d</sup> P. Simon,<sup>a,d</sup> Y. Gogotsi,<sup>f</sup> M. Haeffele,<sup>c</sup> D. Limmer,<sup>g</sup> D. Chandler<sup>h</sup>

<sup>a</sup> Réseau sur le Stockage Electrochimique de l'Energie (RS2E), FR CNRS 3459, France

<sup>b</sup> Sorbonne Universités, UPMC Univ Paris 06, UMR 8234, PHENIX, F-75005, Paris, France

<sup>c</sup> Maison de la Simulation, CNRS/CEA/INRIA/Univ. Orsay/Univ. Versailles, France

<sup>d</sup> CIRIMAT, UMR CNRS 5085, Univ Paul Sabatier, 31062 Toulouse Cedex 9, France

<sup>e</sup> Department of Materials, University of Oxford, Parks Road, Oxford OX1 3PH, UK

<sup>f</sup> Department of Materials Science & Engineering, Drexel University, Philadelphia, USA

<sup>g</sup> Princeton Center for Theoretical Science, Princeton, New Jersey, USA

<sup>h</sup> Department of Chemistry, University of California, Berkeley, Berkeley, California, USA

\* Corresponding author email address: mathieu.salanne@upmc.fr

The electric double layer is generally viewed as simply the boundary that interpolates between an electrolyte solution and a metal surface. Contrary to that view, molecular simulations show that the interface between ionic liquids and carbon electrode can exhibit structures and fluctuations that are not simple reflections of surrounding bulk materials. This rich behavior is absent from a mean-field picture that averages over intraplanar structure. The charge of the electrode is screened by the interfacial fluid and induces subtle changes in its structure, which cannot be captured by the conventional Gouy-Chapman theory. [1]

In recent years, we have performed molecular dynamics simulations on a variety of systems made of the 1-butyl-3-methylimidazolium hexafluorophosphate ionic liquid (either pure or mixed with acetonitrile) and a variety of carbon electrodes: planar graphite, carbide-derived carbons and nanoporous graphene. A key aspect of our simulations is to use a realistic model for the electrodes, by allowing the local charges on the carbon atoms to vary dynamically in response to the electrical potential caused by the ions and molecules in the electrolyte. [2]

These simulations have allowed us to gain strong insight on the structure and dynamics of ionic liquids at electrified interfaces. Even in the simpler case of planar surfaces, surprising ordering effects have been observed on a range of applied potentials [3]. Then, from the comparison between graphite and porous CDC electrodes, we have elucidated the molecular mechanism at the origin of the increase of the capacitance enhancement in nanoporous carbons [4,5]. The simulations also provide us the diffusion coefficients of the ions and the charging times for the full supercapacitor device. [6]

## References

- [1] S. Perkin, M. Salanne, P.A. Madden, R. Lynden-Bell, *PNAS*, 2013, 110, E4121.
- [2] C. Merlet, C. Pean, B. Rotenberg, P.A. Madden, P. Simon, M. Salanne, *J. Phys. Chem. Lett.*, 2013, 4, 264.
- [3] C. Merlet, D.T. Limmer, M. Salanne, R. van Roij, P. Madden, D. Chandler, B. Rotenberg, *J. Phys. Chem. C*, 2014, 118, 18291.
- [4] C. Merlet, B. Rotenberg, P.A. Madden, P.L. Taberna, P. Simon, Y. Gogotsi, M. Salanne, *Nature Materials*, 2012, 11, 306.
- [5] C. Merlet, C. Pean, B. Rotenberg, P.A. Madden, B. Daffos, P.L. Taberna, P. Simon, M. Salanne, *Nature Communications*, 2013, 4, 2701.
- [6] C. Pean, C. Merlet, B. Rotenberg, P.A. Madden, P.L. Taberna, B. Daffos, M. Salanne, P. Simon, *ACS Nano*, 2014, 8, 1576.

# On-chip Carbide Derived Carbon Thin Films for Microsupercapacitors

Peihua Huang,<sup>a,b</sup> K. Brousse,<sup>a,b</sup> C. Lethien,<sup>c</sup> M. Respaud,<sup>d</sup> Y. Gogotsi,<sup>c</sup> P.-L. Taberna,<sup>a,b</sup> and P. Simon,<sup>a,b</sup>

<sup>a</sup> *Université Paul Sabatier, CIRIMAT UMR CNRS 5085, 118 route de Narbonne, 31062 Toulouse, France.*

<sup>b</sup> *Réseau sur le Stockage Electrochimique de l'Energie (RS2E), FR CNRS 3459, France. Université Paul Sabatier, CIRIMAT UMR CNRS 5085, 118 route de Narbonne, 31062 Toulouse, France.*

<sup>c</sup> *Institut d'Electronique, de Microélectronique et de Nanotechnologie (IEMN), CNRS UMR 8520 and Institut de Recherche sur les Composants logiciels et matériels pour l'Information et la Communication Avancée (IRCICA), CNRS USR 3380, Université Lille 1 Sciences et Technologies, Avenue Poincaré, 59652 Villeneuve d'Ascq CEDEX, France.*

<sup>d</sup> *Université de Toulouse; INSA; UPS; LPCNO, 135 avenue de Rangueil, F-31077 Toulouse, France and CNRS; UMR 5215 ; LPCNO, F-31077 Toulouse, France*

<sup>e</sup> *A. J. Drexel Nanomaterials Institute & Department of Materials Science and Engineering, Drexel University, Philadelphia, PA 19104, USA.  
Email: huang@chimie.ups-tlse.fr*

With evolution of functions, micro-electronic components demand more and more power. While the main battery of the whole device might fail to power everything, on-chip microsize power sources are required. Microbatteries suffer from low power performance owing to kinetic limit of intrinsic redox reactions [1]. Carbon based microsupercapacitors could be a solution for high power application thanks to energy storage by adsorption of electrolyte ions inside carbon porous network without kinetic limit [2]. Among all porous carbon materials, carbide derived carbons (CDCs) could be fabricated from chlorination of carbide, which is ceramic, enabling on-chip microfabrication process. Moreover, CDCs could offer high capacitance thanks to its tunable nanoporous network [3], making it perfect candidate for microsupercapacitors.

In this present work, we have successfully fabricated on-chip titanium carbide derived carbon (TiC-CDC) thin films by chlorination of PVD deposited TiC ceramic thin films on silicon wafer.

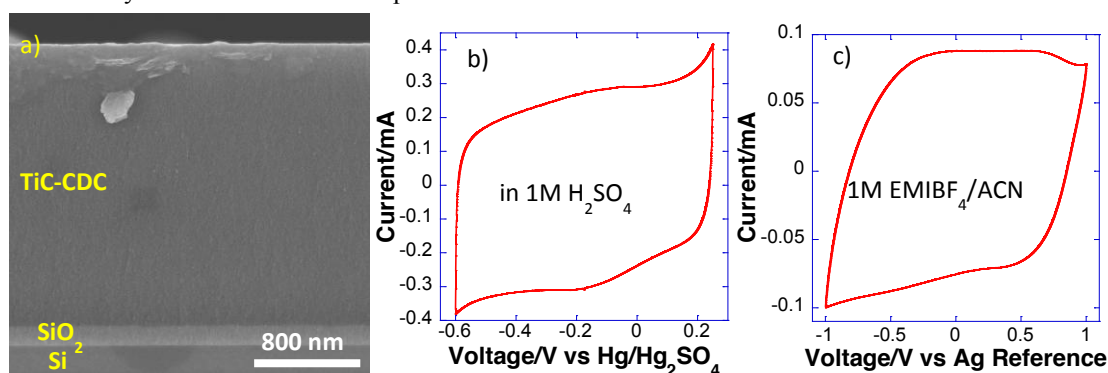


Figure 1 a) SEM photo of on-chip TiC-CDC thin film after chlorination (cross section); Voltammogram recorded at 20 mV/s in b) 1M H<sub>2</sub>SO<sub>4</sub> and c) 1M EMIBF<sub>4</sub> in acetonitrile (ACN).

The TiC-CDC thin film is uniform in thickness according to Figure 1a. Voltammograms of the material in both aqueous and organic electrolytes at 20 mV/s indicate capacitive behavior of chlorinated TiC-CDC thin film. 135 mF/cm<sup>2</sup> and 51.8 mF/cm<sup>2</sup> were achieved in 1M H<sub>2</sub>SO<sub>4</sub> aqueous electrolyte and 1M EMIBF<sub>4</sub> in ACN, respectively. Thus, nanoporous TiC-CDC thin films could be potentially applied as microsupercapacitors electrodes after patterning into interdigitated configuration.

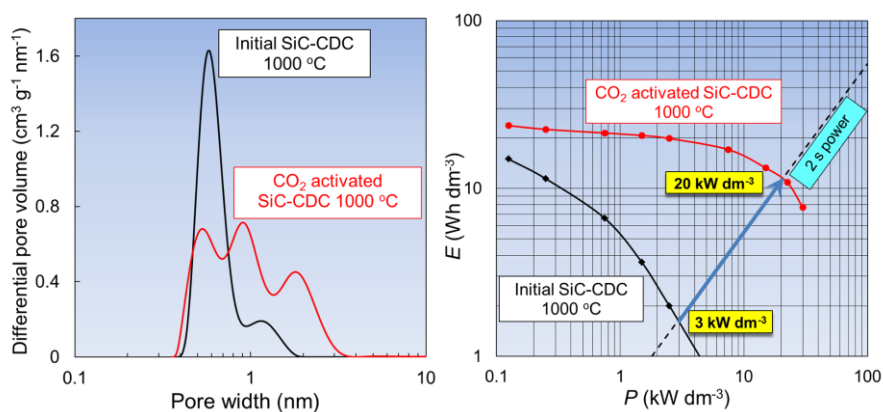
## Reference

- [1] J.W. Long, B. Dunn, D.R. Rolison, H.S. White, Chemical Reviews, 2004, 104, 4463-4492.
- [2] P. Simon, Y. Gogotsi, Nature Materials, 2008, 7, 845-854.
- [3] J. Chmiola, C. Largeot, P.L. Taberna, P. Simon, Y. Gogotsi, Science, 2010, 328, 480-483.

# Surprisingly Large Improvements in SiC-CDC Based EDLC via Simple CO<sub>2</sub> Activation Method

Indrek Tallo, Ester Tee, Enn Lust, Thomas Thomberg, Heisi Kurig, Alar Jänes  
*Institute of Chemistry, University of Tartu*  
*14A Ravila Street, 50411 Tartu, Estonia*  
*indrek.tallo@ut.ee*

Silicon carbide derived carbon (SiC-CDC) is the cheapest and easiest to synthesize of all carbide derived carbon (CDC) materials. However, without using a prior templating method or additional modification, the intrinsic electrochemical properties of SiC-CDC are well below those of other CDC materials, such as TiC-CDC, WC-CDC or Mo<sub>2</sub>C-CDC. This can be attributed to the too narrow average pore sizes, which limit the mass transport inside the carbon particles. Although there are many activation methods for porous carbons available, which can increase the pore diameters, the CO<sub>2</sub> oxidation is one of the easiest. In this work nanoporous CDC were synthesized from SiC powders via gas phase chlorination within the temperature range from 1000 °C to 1100 °C. Thereafter the CDCs were additionally activated by CO<sub>2</sub> treatment method, resulting in nearly two-fold increase in specific surface area. The results of X-ray diffraction, high-resolution transmission electron microscopy and Raman spectroscopy showed that the synthesized CDC materials are mainly amorphous, however containing small graphitic crystallites, exposed mainly on surface regions of carbon powders. The low-temperature N<sub>2</sub> sorption experiments were performed and the specific surface areas, calculated according to Brunauer-Emmett-Teller theory, from 1100 m<sup>2</sup> g<sup>-1</sup> up to 2270 m<sup>2</sup> g<sup>-1</sup> were obtained, depending on the extent of CO<sub>2</sub> activation. The energy and power density characteristics of the supercapacitors based on 1 M (C<sub>2</sub>H<sub>5</sub>)<sub>3</sub>CH<sub>3</sub>NBF<sub>4</sub> solution in acetonitrile and SiC-CDC as an electrode material were investigated using the cyclic voltammetry, electrochemical impedance spectroscopy, galvanostatic charge/discharge and constant power discharge methods. The electrochemical data indicated huge increase in specific capacitance and thus, in energy density. Most importantly, the activation of SiC-CDC with CO<sub>2</sub> significantly improves (more than 40%) the performance (energy density, power density, etc.) of the supercapacitors especially at higher potential scan rates and at higher power loads [1].



## Acknowledgements:

The present study was supported by the Estonian Center of Excellence in Science project 3.2.0101.11-0030, Estonian Energy Technology Program project 3.2.0501.10-0015, Material Technology Program project 3.2.1101.12-0019, Project of European Structure Funds 3.2.0601.11-0001, Estonian target research project IUT20-13, Ministry of Education and Research Personal Research Grant PUT55 and project 3.2.0302.10-0169.

## Reference:

[1] E. Tee, I. Tallo, H. Kurig, T. Thomberg, A. Jänes, E. Lust, Huge enhancement of energy storage capacity and power density of supercapacitors based on the carbon dioxide activated microporous SiC-CDC, *Electrochimica Acta*, 161 (2015) 364-370.



# New materials for in-situ pre-lithiation of the graphite anode in lithium ion capacitor

Paweł Jeżowski<sup>a</sup>, Olivier Crosnier<sup>b</sup>, Thierry Brousse<sup>b</sup>, François Béguin<sup>a</sup>

<sup>a</sup>Poznan University of Technology, Institute of Chemistry and Technical Electrochemistry, ul. Berdychowo 4, 60-965 Poznan, Poland

<sup>b</sup>IMN (Université Nantes-CNRS), 2 rue de la Houssinière, 44322 Nantes, France

[pawel.jezowski@put.poznan.pl](mailto:pawel.jezowski@put.poznan.pl)

The lithium ion capacitor (LIC) is a high energy hybrid system which combines an electrical double-layer (EDL) positive electrode made from nanoporous carbon with a negative graphite lithium intercalation electrode [1]. The electrolyte is a lithium salt which is generally dissolved in ethylene carbonate : dimethyl carbonate (EC:DMC) mixture. In the first concept of LIC, an auxiliary metallic lithium electrode has been used for graphite pre-lithiation. Latter, pre-lithiation has been proposed directly from the electrolyte [2] to circumvent the possible safety issues related with metallic lithium implementation, and also to simplify the device design. This leads to a decrease of electrolyte concentration and conductivity, which might have a negative impact on LIC power. Therefore, the most recent idea consists in irreversibly de-intercalating lithium from lithium metal oxide (lithium molybdenum oxide -  $\text{Li}_2\text{MoO}_3$  or lithium iron oxide -  $\text{Li}_5\text{FeO}_6$ ) incorporated in the positive activated carbon electrode [3]. However, in case of these oxides, the extraction potential of lithium ions exceeds 4.5 V vs. ref.  $\text{Li}/\text{Li}^+$ , which causes detrimental electrochemical oxidation of the electrolyte.

In this presentation, we investigated new materials (lithiated oxides and lithiated organic molecules) from which high amount of lithium can be irreversibly de-intercalated at potential lower than 4.5 V vs. ref.  $\text{Li}/\text{Li}^+$ . Figure 1a shows the evolution of electrodes and cell potentials during graphite lithiation at C/20. The reached capacity of  $360 \text{ mAh g}^{-1}$  indicates that the composition of the intercalation compound is close to the first stage  $\text{LiC}_6$ . The LIC cell demonstrated an excellent cycle life at different current loads from  $250 \text{ mA g}^{-1}$  to  $650 \text{ mA g}^{-1}$  in the potential range from 2.2 ~ 4.0 V (Figure 1b). The specific energy and power are close to  $50 \text{ Wh kg}^{-1}$ , and  $500 \text{ W kg}^{-1}$ , respectively (for comparison, the energy density of EDLC is  $3\text{-}10 \text{ Wh kg}^{-1}$  for EDLC, and the power density of lithium ion batteries is around  $300 \text{ W kg}^{-1}$  [4]).

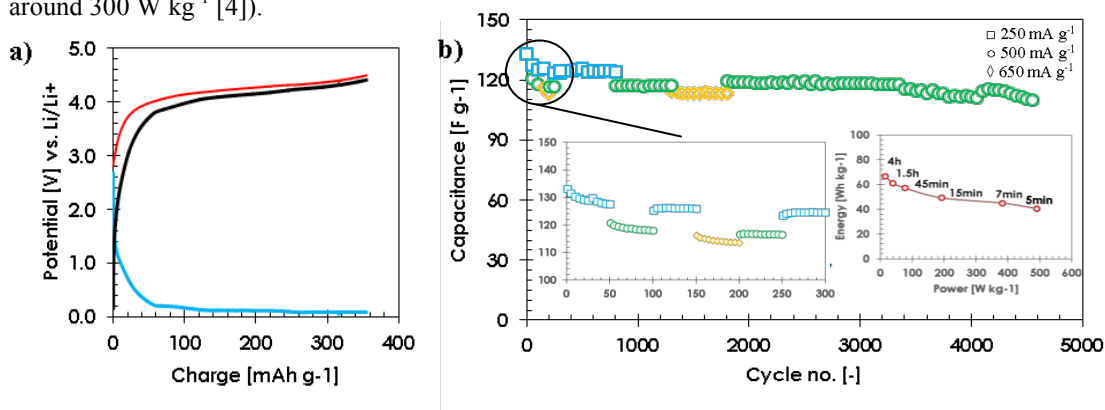


Fig 1. a) Evolution of electrodes and cell potentials during graphite pre-lithiation at C/20; b) Cycle life of the cell in the potential range 2.2 - 4.1 V with Ragone plot as inset. The electrolyte was  $1 \text{ mol L}^{-1}$   $\text{LiPF}_6$  in EC:DMC (vol. 1:1)

[1] T. Aida, K. Yamada and M. Morita, *Electrochem. Solid-State Lett.* 9 (2006) A534.

[2] V. Khomenko, E. Raymundo-Piñero, F. Béguin, *J. Power Sources* 177 (2008) 643.

[3] M.-S. Park, Y.-G. Lim, J.-H. Kim, Y.-J. Kim, J. Cho and J.-S. Kim, *Adv. Energy Mater.* 1 (2011) 1002.

[4] F. Béguin, E. Frackowiak, *Supercapacitors: Materials, Systems and Applications*, Wiley-VCH, Weinheim, 2013

# "Recent advances on the understanding of ion adsorption/transfer in nanoporous carbon electrodes; application to supercapacitors"

**Patrice Simon<sup>1,2</sup>, B. Daffos<sup>1,2</sup>, P.L. Taberna<sup>1,2</sup>, W.-Y. Tsai<sup>1,2</sup>, P. Huang<sup>1,2</sup>, K. Brousse<sup>1,2</sup>**

<sup>1</sup> *Université Paul Sabatier, CIRIMAT UMR CNRS 5085, F-31062 Toulouse, France*

<sup>2</sup> *RS2E, FR CNRS 3459, F-31062 Toulouse, France*

In the past decade, lot of attention has been put on electrochemical double layer capacitors (EDLCs), also known as supercapacitors, since they are one of the most promising electrochemical energy storage devices for high power delivery or energy harvesting applications. The charge storage mechanism in supercapacitor electrodes relies on electrostatic attraction between the electrolyte ions and the charges at the electrode surface, leading to a charge separation at the electrolyte/electrode interface.

During this presentation, we will show how the careful design of the carbon/electrolyte interface can help in designing high energy density carbons for supercapacitor applications. In a first step, by using Carbide-Derived Carbons (CDCs), we will show the control of the carbon porous structure impacts the capacitance of nanostructured carbons that sharply increases for pore sizes less than 1 nm. The combination of several techniques like in-situ NMR spectroscopy, EQCM and Molecular Dynamics simulations has then been used for studying the ion confinement effect in carbon nanopores and helped in developing our basic understanding of the electrolyte/carbon interactions in confined pores.

A last part of the presentation will be focused on some recent results on the development of micro-supercapacitors using bulk microporous carbon films. These micro-systems were prepared from the chlorination of sputtered bulk TiC films deposited onto Si wafer. Extremely high volumetric ( $500 \text{ F.cm}^{-3}$ ) and areal capacitance ( $> 150 \text{ mF.cm}^{-2}$ ) could be obtained, paving the way for the design of high energy micro-supercapacitors.

## References:

1. "Materials for Electrochemical Capacitors: Building a Battery of the Future"  
P. Simon and Y. Gogotsi, *Nature Materials*, 7 (2008) 845-854.
2. "Anomalous increase in carbon capacitance at pore size below 1 nm"  
J. Chmiola, G. Yushin, Y. Gogotsi, C. Portet, P. Simon and P.L. Taberna, *Science*, 313 (2006) 1760-1763.
3. "On the molecular origin of supercapacitance in nanoporous carbon electrodes"  
C. Merlet, B. Rotenberg, P.A. Madden, P.-L. Taberna, P. Simon, Y. Gogotsi, and M. Salanne, *Nature Materials* 11 (2012) 306-310.
4. "Electrochemical Quartz Microbalance (EQCM) study of ion dynamics in nanoporous carbons"  
W.-Y. Tsai, P.L. Taberna, P. Simon, *JACS*, 136 (2014) 8722-8728

# Faradaic and Non-faradaic Interactions at the Electrode/Electrolyte Interface in Electrochemical Capacitors

Krzysztof Fic, Jakub Menzel, Elzbieta Frackowiak

*Poznan University of Technology, Institute of Chemistry and Technical Electrochemistry*

*Berdychowo 4, 60-965 Poznan*

*elzbieta.frackowiak@put.poznan.pl*

The mechanism of energy storage in electrochemical capacitors is quite well understood, however, there are still some issues related especially with carbon electrode ageing which need more in depth studies. It is widely accepted that ion transport within the carbon electrode bulk strongly depends on the porosity structure and interconnection of ions; presumably, there are some more specific criteria for effective ion transportation. It seems that some ions approach the interface easily and can be reversibly transported from/to electrolyte bulk, dependently on polarization applied. On the other hand, some ions – once interface is reached - tend to remain at the interface and cannot be reversibly desorbed. Such ‘memory effect’ of the electrode has rather negative influence on the supercapacitor cyclability and charging/discharging efficiency.

Our investigations performed for negative electrode have demonstrated that the voltage range of this electrode might be shifted towards hydrogen evolution potential and even easily exceeding this value. It is noteworthy that the interactions between the electrode and electroadsorbed hydrogen are the strongest in case of 6 mol/L KOH solution. Hydrogen stored *in statu nascendi* in the ultramicropores of the activated carbon keeps the potential of the electrode in deep cathodic region and allows reaching a higher voltage of the total system. More detailed investigations were focused on the influence of carbon microstructure on self-discharge of the electrode.

Typical oxidative working conditions of positive electrode resulted in a fast aggravation of the electrode material and significant capacitance fade in alkaline, neutral and acidic electrolyte, whatever type, especially for electrode with relatively high oxygen and micropore content. In order to avoid electrolyte decomposition and to improve electrode potential window, the electrolytes with redox activity (e.g. based on iodides, bromides) have been investigated. Results obtained suggest that redox activity of aforementioned species shifts the oxygen evolution potential towards higher value and prevents capacitance fade during cycling. The most recent studies suggest that electrolyte for positive electrode should retain the pH value during operation; in this case, the electrochemical response is sensitive for oxygen functionalities which might influence the pH value directly on the electrode/electrolyte interface.

This paper will report on electrochemical performance of various anions such as Cl, I, Br, SO<sub>4</sub>, NO<sub>3</sub> as well as cations of such metals as Li, Na, K, Cs, Mg, and Cu at electrode/electrolyte interface studied by various frequency-dependent methods such as electrochemical impedance spectroscopy and electrochemical quartz crystal microbalance (EQCM). Activated carbons with various type of porosity have been investigated in order to correlate porosity-related features with electrochemical parameters such as capacitance value, various type of resistance (ESR, EDR) and frequency response (mass change). Finally, aforementioned considerations will be discussed in direct regard of cyclability issues of carbon electrodes.

# Electrochemical Characterization of an Aqueous Hybrid Capacitor with Zinc and Activated Carbon Electrodes

Hiroshi Inoue, Kentaro Konishi, Eiji Higuchi and Masanobu Chiku

Department of Applied Chemistry, Graduate School of Engineering, Osaka Prefecture University  
Sakai, Osaka 599-8531, Japan  
inoue-h@chem.osakafu-u.ac.jp

## Introduction

Electric double layer capacitors (EDLCs) have attracted attention because of their high power density, long cycle life, etc. Aqueous electrolytes have advantages such as high ionic conductivity, low cost, incombustibility, low environmental load and so on, compared to organic electrolytes. However, the operating voltages of aqueous EDLCs are actually lower than the theoretical decomposition voltage of water, 1.23 V, leading to low energy and power densities. This is a serious issue of the aqueous EDLCs. Asymmetric capacitors or hybrid capacitors (HCs) composed of various faradaic electrodes and a non-faradaic activated carbon (AC) electrode have been investigated in order to increase the energy and power densities of EDLCs. It has been reported that HCs composed of an AC negative electrode and various oxide positive electrodes, realized the operating voltages over 1.23 V, leading to higher energy and power densities. On the other hand, there seems to be not so much researches about faradaic negative electrodes for aqueous HCs. We have assembled a new aqueous HC using Zn with large hydrogen overpotential as a negative electrode material and evaluated its electrochemical properties [1]. In the present study, we improved operating voltage of the aqueous HC with Zn and AC electrodes to realize higher energy and power densities.

## Experimental

An AC fiber cloth (GCI) was used as a positive electrode material of the present aqueous HC cell. The AC cloth was stuck on a glassy carbon plate with the carbon paste and heated at 100°C for 1 h to prepare an AC electrode. The AC electrode was impregnated with a (1 M  $\text{ZnCl}_2$  + 0.048 M HCl) solution as an electrolyte under a vacuum. An experimental HC cell was assembled using the AC and Zn sheet electrodes based on our previous paper [1]. The sulfonated-polypropylene separator was impregnated with the (1 M  $\text{ZnCl}_2$  + 0.048 M HCl) aqueous solution under a vacuum and stacked between the two electrodes. For comparison, an EDLC cell with two AC electrodes was also assembled. All charge-discharge cycling tests for the HC and EDLC cells were galvanostatically carried out at 2 mA. In all measurements temperature was kept at 30 °C.

## Results and Discussion

Figure 1 shows charge-discharge curves of positive and negative electrodes for the EDLC and HC cell as their operating voltage was changed between 0 and 2.0 V. With the present electrolyte, the EDLC cell could work well until the maximum operating voltage of 2 V. Fig. 1 shows the HC cell also worked well until the maximum operating voltage of 2 V, which was much higher than the previous aqueous HC with Zn negative electrode and alkaline electrolyte (1.4 V). In the HC cell, the potential of the Zn negative electrode was nearly constant because the following faradaic reaction reversibly occurred;  $\text{Zn} = \text{Zn}^{2+} + 2\text{e}^-$ . On the other hand, the potential of the AC positive electrode greatly changed during charge-discharge cycling. Specific capacitance was calculated from an average slope of the discharge curve for each cell, and the specific capacitance of the HC cell was much higher than that of the EDLC cell, so the increase in power and energy densities of the cell can be expected.

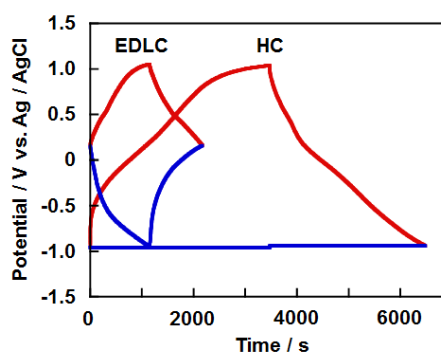


Fig. 1 Charge-discharge curves of both electrodes for EDLC and HC.

## Reference

[1] H. Inoue, T. Morimoto, S. Nohara, *Electrochem. Solid-State Lett.*, 10 (2007) A261.

# Hybrid capacitors for moderate energy storage and high power applications: double layer formation and soluble redox couples

J. Lee,<sup>a,b</sup> D. Weingarth,<sup>a</sup> and V. Presser<sup>a,b,\*</sup>

<sup>a</sup> INM - Leibniz Institute for New Materials, 66123 Saarbrücken, Germany

<sup>b</sup> Saarland University, 66123 Saarbrücken, Germany

\* Corresponding author's email address: volker.presser@inm-gmbh.de

Supercapacitors are electrochemical energy storage devices ideally suited for high power applications; yet, their relatively low energy density is a limiting factor for many energy applications. Therefore, many current studies on supercapacitors are dedicated to explore strategies to increase the energy density while keeping the power density as high as possible. A highly promising approach employs aqueous electrolytes which enable the use of redox reactions either of the electrode material (e.g., surface functional groups or redox active metal oxides), or capitalize Faradaic reactions of the electrolyte itself. [1] The latter, or can be called as redox electrolyte hybrid capacitor, is a rather new approach which synergistically combines electrolyte systems related to redox batteries and electrodes known from supercapacitors. In contrast to conventional supercapacitors, this novel concept needs to ensure the physical separation of two different electrolyte reservoirs. This can be accomplished with ion exchange membranes (IEMs) which prevent redox active ions from crossing the membrane.

Up to the present, IEMs have been broadly investigated for redox flow batteries as the molecular dynamics in the presence of IEMs plays determining role in the performance of the redox flow battery system. On the contrary, only a few investigations have been carried out using IEMs in supercapacitor systems despite its growing importance on designing hybrid capacitors with redox active electrolytes. As a different behavior in the molecular dynamics is expected in the presence of IEMs for electric double layer (EDL) formation and redox reaction, a separate investigation of IEMs is required excluding redox reactive species. Here, we study the influence of IEMs in aqueous double layer capacitors in order to study separate effects of IEMs on the molecular dynamics in regards to double layer formation; and as a second part of the study, a redox electrolyte/double layer hybrid capacitor will be explored.

For the double layer capacitors, we investigated the electrochemical performance of an aqueous system (1 M Na<sub>2</sub>SO<sub>4</sub>) utilizing thin cation and anion exchange membranes (15-60 µm) and compare the results to a conventional porous polymer separator (namely, hydrophilic polytetrafluoroethylene). While the best rate performance was obtained from the porous separator retaining capacitances of about 88 % at a current density of 5 A/g, the thinnest IEM showed comparable capacitance retention of about 82 %.

In addition, we also present comparative first results applying a new type of redox electrolyte. We can show (Figure 1) that the use of thin IEMs allows not only increased capacitance gained from redox-active electrolyte but also high power performance as the ion diffusion for double layer formation is enhanced through shorter crossing-over distance for non-redox active ions.

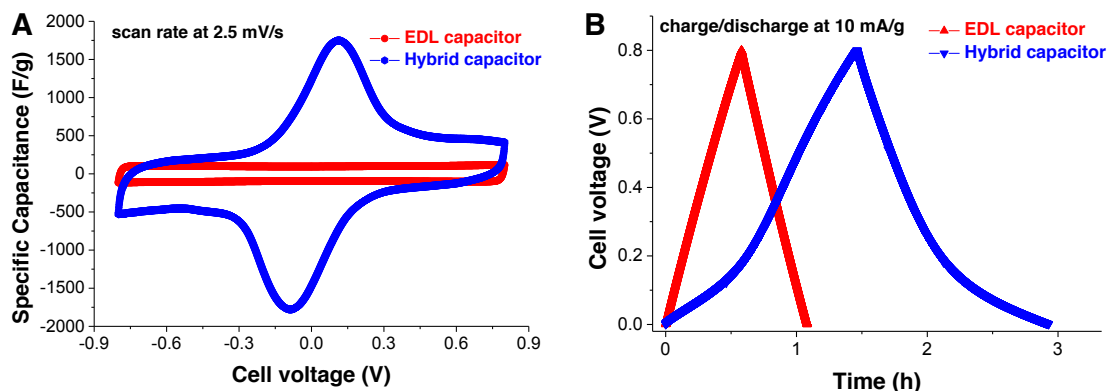


**Figure 1** Electrochemical performance of an EDL capacitor and a hybrid capacitor; cyclic voltammograms (A) and charge/discharge curves at constant current density (B).

[1] E. Frackowiak, K. Fic, M. Meller, G. Lota, *Electrochemistry Serving People and Nature: High-Energy Ecocapacitors based on Redox-Active Electrolytes*, *Chemsuschem*, 5 (2012) 1181-1185.

# Ultrafast Electrochemical Characteristics of nc-TiO<sub>2</sub> (B)/Nanocarbon Composites for Hybrid Capacitor System

Etsuro Iwama,<sup>1)</sup> Takumi Furuhashi,<sup>1)</sup> Yuta Abe,<sup>1)</sup> Keita Okazaki,<sup>1)</sup> Shintaro Aoyagi,<sup>1)</sup> Junichi Miyamoto,<sup>1)</sup> Wako Naoi,<sup>2),3)</sup> and Katsuhiko Naoi<sup>1), 2), 3)\*</sup>

<sup>1)</sup>Department of Applied Chemistry, Tokyo Univ. of Agriculture & Technology, 2-24-16 Naka-cho, Koganei, Tokyo 184-8588, Japan

<sup>2)</sup>Division of Arts & Sciences, K & W Inc., 1-3-16-901 Higashi, Kunitachi, Tokyo 186-0002, Japan

<sup>3)</sup>Advanced Capacitor Research Center, Tokyo Univ. of Agriculture & Technology, 2-24-16 Naka-cho, Koganei, Tokyo 184-8588, Japan

\*E-mail: k-naoi@cc.tuat.ac.jp

We have been applying our original in-situ material processing technology called ‘Ultra-Centrifuging (UC) treatment’ to prepare a novel ultrafast nano-crystalline Li<sub>4</sub>Ti<sub>5</sub>O<sub>12</sub> (nc-LTO) /carbon nanofiber (CNF) composite electrode for the generation-II capacitive energy storage device of ‘Nanohybrid Capacitor (NHC)’ producing more than triple energy density of a conventional electrochemical capacitor [1]. Establishment of the LTO-NHC mass production technology is scheduled to 2017-2018 [2]. To further improve the energy density of the LTO-NHC, we have been pursuing LTO alternatives. Among different candidates, TiO<sub>2</sub> (B) possesses several advantages such as its 2-folds theoretical capacity (335 mAh g<sup>-1</sup>) of LTO (175 mAh g<sup>-1</sup>) and the comparable redox potential (1.6 V vs. Li/Li<sup>+</sup>). In addition, TiO<sub>2</sub>(B) is an industrially attractive material because of its inexpensive raw materials and its environmentally benign synthesis using only aqueous solution (e.g., water-soluble complexes) without any Li-sources [3]. Using the combination of UC treatment and hydrothermal treatment, nano-rectangular TiO<sub>2</sub>(B) (4-7 nm) has been successfully synthesized with the existence of nanocarbons (e.g., single-walled carbon nanotubes (SWCNT), multi-walled CNTs (MWCNT), and Ketjen Black (KB)). The use of four-nuclear Ti-complex [3] and the co-existence of nanocarbons during the synthesis simultaneously realized the minimized *b*-axis growth (4-5 nm, see Fig.1), the hyper dispersion of TiO<sub>2</sub>(B) nanoparticles, and the least contamination of TiO<sub>2</sub> impurities (anatase and rutile etc...). The integration of all these advantageous features endows the smooth and ultrafast Li<sup>+</sup> intercalation of TiO<sub>2</sub>(B) (236 mAh g<sup>-1</sup> at 300C in case of MWCNT, 1C = 335 mAh g<sup>-1</sup>) into A1 and A2 sites eliminating the plateau at undesirably high potential of 1.8-2.0 V vs. Li/Li<sup>+</sup>, which is often referred as TiO<sub>2</sub> anatase or TiO<sub>2</sub>(B) C1 site peaks [3]. The co-relation between the electrochemical performance and the quantified “dispersibility of TiO<sub>2</sub>(B) within TiO<sub>2</sub>(B)/nanocarbon composite” indicates that the UC-treated TiO<sub>2</sub>(B) composites possess ideal nano-entanglements of *b*-axis controlled TiO<sub>2</sub>(B) and nanocarbons, which can reconcile both of high loading of TiO<sub>2</sub>(B) (70-80 in weight) and the ultrafast electrochemical responses.

## References

- [1] K. Naoi *et al.*, *Energy & Environ. Sci.*, 2012, **5**, 9363.
- [2] Nippon Chemi-Con announces: The advanced new technology Nano-hybrid Capacitor (<http://www.chemi-con.co.jp/e/company/pdf/20100326-1.pdf>)
- [3] a) M. Kobayashi *et al.*, *Chem. Mater.*, 2007, **19**, 5373.; b) A. R. Armstrong *et al.*, *Chem. Mater.*, 2010, **22**, 6426.; c) Y. Ren *et al.*, *Angewandte. Chem. Int. Ed.*, 2012, **51**, 2164.

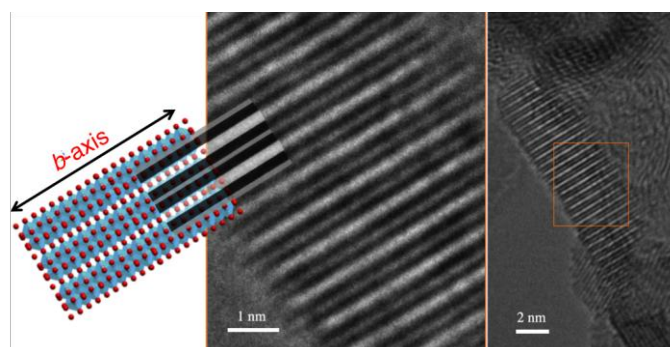


Fig.1 A magnified view of the ultrafine lattice patterns of TiO<sub>2</sub>(B) and the corresponding crystal unit drawn by CrystalMaker™.

# Nitrogen-doped Mesoporous Carbon for Supercapacitor Application

Yong-Yao Xia, Yan-Fang Song and Dan-Dan Zhou

*Department of Chemistry, Institute of New Energy, Collaborative Innovation Centre of Chemistry for Energy Materials, Fudan University, Shanghai 200433, China. E-mail address: yyxia@fudan.edu.cn*

Compared with a wide pore distribution ranging from micropores (<2 nm) to macroporous and a random pore connection of activated carbon (AC), the highly ordered mesoporous carbons (OMCs) possess a quite narrow distribution in mesopore range and uniform pore connection, it shows much better electrochemical performances than conventional high-surface activated carbon at high current densities both in aqueous and nonaqueous electrolyte. Introducing nitrogen atom into the carbon framework plays an important role in the capacitance enhancement of OMCs due to the faradaic redox reactions by increasing of electron donor capability and improvement of electrode wettability. As for porous electrode, the surface area, pore size, pore distribution, pore structure, and morphology play important roles in the capacitive behaviors. In the present work, we will introduce several kinds of N-doped OMCs.

- (1) **Nitrogen-doped ordered mesoporous carbon (N-doped OMC) with a high surface area**[1]: A N-doped OMC was synthesized by using an organic–inorganic co-assembly method, in which resorcinol was used as the carbon precursor, dicyandiamide as the nitrogen precursor, silicate oligomers as the inorganic precursors, and F127 as the soft template. The N-doped OMC possesses a surface area as high as 1374 m<sup>2</sup>/g and a large pore size of 7.4 nm. It delivers a reversible specific capacitance as high as 308 F/g in 1 M H<sub>2</sub>SO<sub>4</sub> aqueous electrolyte, of which 58% of the capacity is due to pseudo-capacitance.
- (2) **Nitrogen-doped hierarchical mesoporous/microporous carbon (NMMC) derived from ordered carbide** [2]: NMMC was prepared by synthesizing nitrogen-doped mesoporous titanium-carbide/carbon composite, followed by in situ chlorination of carbides. The NMMC possesses a high surface area (1344 m<sup>2</sup>/g), large pore volumes (0.902 cm<sup>3</sup>/g), narrowed mesopore-size distributions (centered at 4.6 nm) and micropores drilled on the mesopore walls. The obtained carbon exhibits excellent performance with a reversible specific capacitance as high as 325 F/g in 1.0M H<sub>2</sub>SO<sub>4</sub> aqueous electrolytes contributed by the double-layer capacitance and pseudo-capacitance.
- (3) **Nitrogen-doped ordered mesoporous carbon nanofiber array (NOMCNFA)** [3]: A NOMCNFA was prepared by a combination of a hardtemplating and a soft-templating method. The obtained N-enriched carbon material has a high surface area (1030 m<sup>2</sup>/g) and a large pore volume (2.35 cm<sup>3</sup>/g), with uniform mesopores located at 15.0 nm. The material with a nitrogen content of 6.7 wt% shows a high capacitance of 264 F/g in 1.0M H<sub>2</sub>SO<sub>4</sub> electrolyte and a good rate capability with a capacitance retention of 86% at 10 A/g vs. 0.5 A/g. It also delivers an excellent cycling stability without capacitance fading over 10000 cycles.

## References:

- 1) Y. F. Song, L. Li, Y. G. Wang, C. X. Wang, Z. P. Guo and Y. Y. Xia, *ChemPhysChem*, 15, 2084-2093 (2014).
- 2) Y. F. Song, S. Hu, X. L. Dong, Y. G. Wang, C. X. Wang and Y. Y. Xia, *Electrochim. Acta.*, 146, 485-494 (2014).
- 3) D. D. Zhou, W. Y. Li, X. L. Dong, Y. G. Wang, C. X. Wang and Y. Y. Xia, *J. Mater. Chem. A*, 1, 8488-8496 (2013).

# Innovative conducting salts and solvents for advanced electrochemical double layer capacitors

Andrea Balducci<sup>a</sup>, Christoph Schütter<sup>a</sup>, Sebastian Pohlmann<sup>b</sup>, Claudia Ramirez-Castro<sup>b</sup>, Tamara Husch<sup>c</sup>, Martin Korth<sup>c</sup>

<sup>a</sup> *Helmholtz Institute Ulm, Helmholtzstraße 11, 89081 Ulm, Germany*

<sup>b</sup> *MEET-Institute of Physical Chemistry/University of Münster Corrensstraße 28/30, 48149 Münster*

<sup>c</sup> *Ulm University, Institute for Theoretical Chemistry, Albert-Einstein-Allee 11, 89081 Ulm, Germany*

*andrea.balducci@kit.edu*

In state of the art electrochemical double layer capacitors (EDLCs), activated carbons (AC) are used as electrode active materials, while solutions of tetraethylammonium tetrafluoroborate (Et<sub>4</sub>NBF<sub>4</sub>) in propylene carbonate (PC) or acetonitrile (AN) are used as electrolytes. These combinations of materials enable the realization of EDLCs with operative voltages of 2.7 to 2.8 V, extraordinary cycle life (>500.000 cycles), high power (up to 10 kW kg<sup>-1</sup>) and energy in the order of 5Whkg<sup>-1</sup>[1].

Many works indicated that an increase of the EDLCs energy would allow the introduction of these high power devices in a larger number of applications and, consequently, it would increase the market size of EDLCs [1-2]. Therefore, in the last years many efforts have been made to increase the energy of EDLCs.

The energy  $E$  stored in an EDLC system is described by the equation  $E=1/2 CV^2$ , where  $C$  is the capacitance and  $V$  the operative voltage of the device. Considering this equation, it is evident that to increase the operative voltage in the most convenient strategy to increase the energy of these devices. Consequently, the development of innovative electrolytes is a key aspect for the realization of high energy EDLCs: in the future new solvents, new conducting salts as well as new ionic liquids need to be considered.

In this work we report about the development of innovative conducting salts and about the use of computational screening for the identification of innovative solvents for EDLCs.

In the past only a relatively low number of studies focused on the development of new conducting salts for high voltage EDLCs. Nevertheless, the conducting salt play a key role on the double layer formation and, thus, on the energy and power of EDLCs. Recently we investigated the influence of conductive salts on the physical-chemical as well as electrochemical properties of PC based [2]. We showed that the operative voltage of EDLCs containing PC-based electrolytes can be increased by a mere change in conductive salt. However, anions and cations forming the conductive salt have to be carefully selected, as the choice of salt influences both electrochemical properties as well as ion transport properties of EDLC electrolytes, leading to an impact on energy and power storage in EDLC devices.

As mentioned above, the introduction of electrolyte materials that withstand higher operative voltages than state of the art systems can be considered a key-point for the realization of high energy, high cycle life EDLCs. To avoid time consuming “trial and error” experiments, it is desirable to “rationalize” this search for new materials. An important step in this direction is the systematic application of computational screening approaches. Taking this point into account, we tried to correlate results obtained via an innovative computational screening with the experimental results, in order to check, if the latter results are validating the prediction of the computation and therefore, if computation is a feasible tool for the determination of new electrolytes [3].

## References

- [1] F. Béguin, V. Presser, A. Balducci, E. Frackowiak, , *Advanced Materials*, 26 (2014) 2219-2251
- [2] C. Ramirez-Castro, A. Balducci, *Journal of the Electrochemical Society* 162 (5) A5020-A5030 (2015)
- [3] C. Schütter, T. Husch, M. Korth, A. Balducci, submitted for publication



# On chip 3D pseudocapacitive and carbon based electrochemical microsupercapacitors at the wafer level

K. Brousse<sup>1,3,4</sup>, E. Eustache<sup>1,2,4</sup>, P. Huang<sup>3,4</sup>, C. Douard<sup>2</sup>, B. Daffos<sup>3,4</sup>, P.L. Taberna<sup>3,4</sup>, J. Le Bideau<sup>2</sup>, T. Brousse<sup>2,4</sup>, P. Simon<sup>3,4</sup> and C. Lethien<sup>1,4</sup>

<sup>1</sup>IEMN CNRS UMR8520 – Université Lille 1 (Fr) / <sup>2</sup>IMN JR CNRS UMR6502 – Université de Nantes (Fr) / <sup>3</sup>CIRIMAT CNRS UMR5085 – Université Paul Sabatier Toulouse III (Fr) / <sup>4</sup>RS2E FR 3459 CNRS (Fr)

[Thierry.brousse@univ-nantes.fr](mailto:Thierry.brousse@univ-nantes.fr) / [simon@chimie.ups-tlse.fr](mailto:simon@chimie.ups-tlse.fr) / [Christophe.lethien@iemn.univ-lille1.fr](mailto:Christophe.lethien@iemn.univ-lille1.fr)

**Submitted to:** Novel Insights to Electrochemical Capacitors – 5<sup>th</sup> symposium

Electrochemical microsupercapacitors ( $\mu$ SC) is a key device to get autonomous smart microsystems [1, 2]. The performances of  $\mu$ SC are limited by the footprint area available for the micropower sources. To enhance the surface capacitance of a  $\mu$ SC, two strategies has been developed depending on electrodes material. For pseudocapacitive materials such as manganese dioxide ( $\text{MnO}_2$ ) or ruthenium dioxide ( $\text{RuO}_2$ ), the areal capacitance of the electrodes is improved by achieving a step-conformal deposition of thin film on high aspect ratio 3D scaffold. By combining electrodeposition and atomic layer deposition technologies, the surface capacitance of a pseudocapacitive thin film is significantly improved by the Area Enlargement Factor (AEF) of the 3D topology [3]. The capacitance of a 250 nm thick  $\text{MnO}_2$  thin film moves from 11  $\text{mF}/\text{cm}^2$  (2D topology) up to 700  $\text{mF}/\text{cm}^2$  when the deposition is achieved on 3D silicon micropillars (75  $\mu\text{m}$  depth). Interesting results obtained on 3D interdigitated symmetrical full device will be presented in aqueous (0.5M  $\text{Na}_2\text{SO}_4$ ) and ionic liquid electrolytes. Collective fabrication on a 3 inch silicon wafer will be reported. For carbon based  $\mu$ SC, carbon derived carbide (CDC) material is a suitable candidate to fabricate on chip  $\mu$ SC at the wafer level [4, 5]. Titanium carbide has been sputtered on a 3 inch silicon wafer. The surface capacitance of the  $\mu$ SC directly depends on the film thickness. The sputtering parameters has been tuned to reach a low stress and highly conductive metal carbide material (up to 12.5  $\mu\text{m}$  thick). Inductively Coupled Plasma / Reactive Ion Etching technology is used to fabricate on chip interdigitated planar TiC electrodes. The resulting interdigitated electrodes are chlorinated at 450  $^\circ\text{C}$  under  $\text{Cl}_2$  to fabricate CDC based  $\mu$ SC at the wafer level.  $\mu$ SC performances will also be presented in aqueous (1M  $\text{H}_2\text{SO}_4$ ) and organic electrolyte (1M EMIBF<sub>4</sub>/AN).

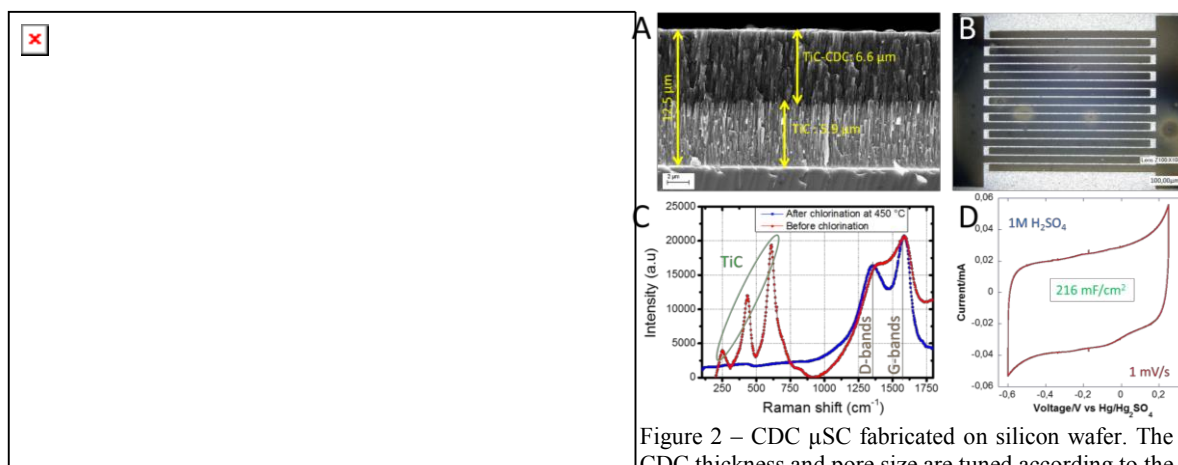


Figure 2 – CDC  $\mu$ SC fabricated on silicon wafer. The CDC thickness and pore size are tuned according to the chlorination parameters. The capacitance of CDC single electrode reaches 216  $\text{mF}/\text{cm}^2$  (6.6  $\mu\text{m}$  thick).

[1] M.F. El-Kady, R.B. Kaner, Nature communications, 4 (2013) 1475.

[2] D. Pech, M. Brunet, H. Durou, P. Huang, V. Mochalin, Y. Gogotsi, P.-L. Taberna, P. Simon, Nature Nanotechnology, 5 (2010) 651-654.

[3] E. Eustache, P. Tilmant, L. Morgenroth, P. Roussel, G. Patriarche, D. Troadec, N. Rolland, T. Brousse, C. Lethien, Advanced Energy Materials, 4 (2014) 1301612.

[4] P. Huang, M. Heon, D. Pech, M. Brunet, P.-L. Taberna, Y. Gogotsi, S. Lofland, J.D. Hettinger, P. Simon, Journal of Power Sources, 225 (2013) 240-244.

[5] J. Chmiola, C. Largeot, P.L. Taberna, P. Simon, Y. Gogotsi, Science, 328 (2010) 480-483.

# Combination of Li-salt-based electrolytes with activated carbon electrodes for the development of hybrid battery-supercapacitors

S. Dsoke, T. Zhang, B. Fuchs, M. Secchiaroli, S. Kaymaksiz and M. Wohlfahrt-Mehrens  
Zentrum für Sonnenenergie- und Wasserstoff-Forschung Baden-Württemberg  
Helmholtzstrasse 8, D-89081 Ulm, Germany  
sonia.dsoke@zsw-bw.de

Hybrid battery-supercapacitors are high energy/high power devices obtained through the combination of high energy materials, normally employed in Li-ion Batteries (LIBs), and high power carbonaceous materials, used in Electrochemical Double Layer Capacitors (EDLCs) [1]. Various hybridization approaches can be used in order to realize such devices. In one of these hybridizations anode and cathode are composite electrodes containing both Li-insertion and carbonaceous materials internally [1]. A broad variety of Li-salt-based organic electrolytes have been used in these devices [1-3]. However, these electrolytes are developed for pure Li-batteries materials but not for capacitor materials. This work investigates the interactions among several Li-salt-based organic electrolytes and pure activated carbon (AC) electrodes. Important condition is that the system is stable at the working potential of the Li-insertion materials. Fig. 1 reports the electrochemical stability window (ESW) of one of the most used commercial electrolyte (1M LiPF<sub>6</sub> in EC:DMC) and of other electrolyte formulations developed by our group. Unfortunately, the commercial electrolyte starts to decompose at the voltage where Li<sub>4</sub>Ti<sub>5</sub>O<sub>12</sub> (LTO) works. It was found that the cathodic stability window can be improved by properly modulating solvent and salt compositions in the electrolyte. This study contributes to develop high performance and stables hybrid-battery supercapacitors.

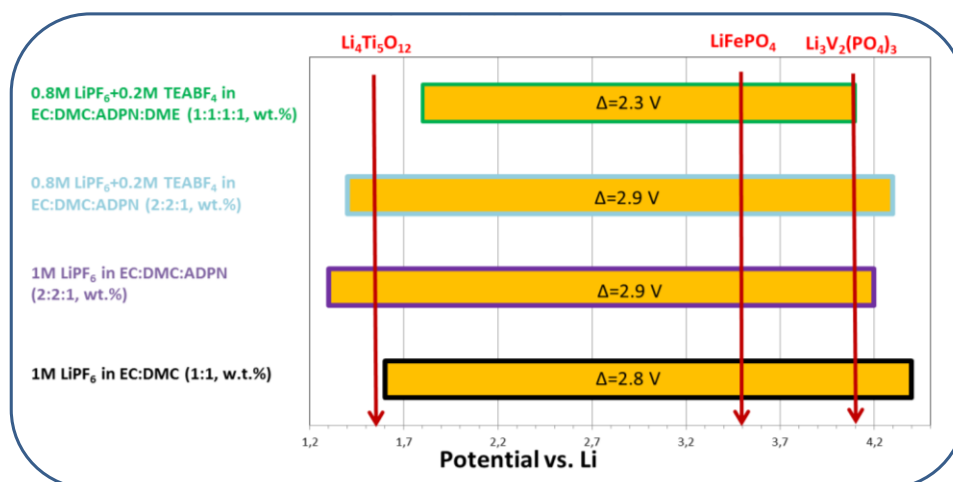


**Fig.1** – Electrochemical stability window of a commercial electrolyte (1M LiPF<sub>6</sub> in EC:DMC) and of three new electrolyte formulations with AC-based electrodes. The red arrows indicate the working voltage of some of the Li-insertion materials normally employed in hybrid battery-supercapacitors.

## Acknowledgements

Financial support from the German Federal Ministry of Education and Research (BMBF) under the Grant FKZ 03EK3021 (project Novacap) is gratefully acknowledged.

## References

- [1] D. Cericola, P. Novák, A. Wokaun, R. Kötz, J. Power Sources 196 (2011) 10305– 10313
- [2] C.M. Ionica-Bousquet, D. Munoz-Rojas, W.J. Casteel, R.M. Pearlstein, G.G. Kumar, G.P. Pez, M.R. Palacin, J Power Sources 196 (2011) 1626-1631
- [3] S. Liu, S Liu, K. Huang, J. Liu, Y. Li, D. Fang, H. Wang, Y. Xia, J Solid State Electrochem 16 (2012) 1631-1634

# On Combined Capacitive and Nernstian Mechanisms for Improved Electrochemical Energy Storage

George Z. Chen

<sup>a</sup> *Department of Chemical and Environmental Engineering, and Energy and Sustainability Research Division, Faculty of Engineering, The University of Nottingham, Nottingham NG7 2RD, UK ;*

<sup>b</sup> *Department of Chemical and Environmental Engineering, and Centre for Sustainable Energy Technologies, Faculty of Science and Engineering, The University of Nottingham Ningbo China, Ningbo, Zhejiang 315100, P. R. China. E-mail: [george.chen@nottingham.ac.uk](mailto:george.chen@nottingham.ac.uk)*

As a classic topic in research and development, electrochemical energy storage (EES) is gaining unprecedented fast growing academic and industrial interests in recent years, thanks at least partly to the great success in material and device innovations and commercialization of lithium ion batteries and carbon based supercapacitors. In terms of storage and discharge performance, lithium ion and other rechargeable batteries are commonly perceived to be the champion in terms of high energy density or specific energy, whilst supercapacitors are known for their fast charging-discharging capability and long cycle life. However, there has always been the technological and commercial desires to make batteries as fast as supercapacitors, or supercapacitors with the high capacity of batteries. To achieve this goal, various new concepts have been coined and demonstrated in laboratory, such as lithium ion capacitor, sodium ion capacitor, redox electrolyte supercapacitor, supercabattery and supercapattery [1-4].

In terms of electrochemistry, a charging or discharging process (CDP) at the electrode level could be physical or chemical, or both. The physical electrode CDP is well understood to be associated with the electrical double layer and it is **capacitive** in nature, i.e. the current-potential relation is the same as that of a capacitor. For a chemical electrode CDP, reactions take place involving electron transfer (ET) at the interface between the electrode and the electrolyte, or between the current collector and the active material on the electrode. Many reversible or quasi-reversible ET reactions at the electrode | electrolyte interface can be described by the Nernst Equation, and this **Nernstian mechanism** is the basis of the redox electrolyte supercapacitor [2,3]. The Nernstian behaviour can also be seen in some ET reactions at the “current collector” | “active material” interface such as those in batteries. However, in many other cases, ET reactions occurring at the “current collector” | “active material” interface involve electrons in the delocalized bands of the active material. Such processes would follow the **capacitive mechanism** and are well represented by pseudo-capacitance [4]. Combining the Nernstian and capacitive mechanisms into one device for charge storage is the common strategy in all the new concepts mentioned above, but such a combination requires theoretical and technological reconsideration. For example, the four cyclic voltammograms (CVs) in **Fig. 1** are all evidence of reversible or quasi-reversible CDP on electrode, but only the rectangular CV in (c) can be used for derivation of capacitance. This presentation will offer more explanations and discussions with several examples from the literature and the author’s own laboratory.

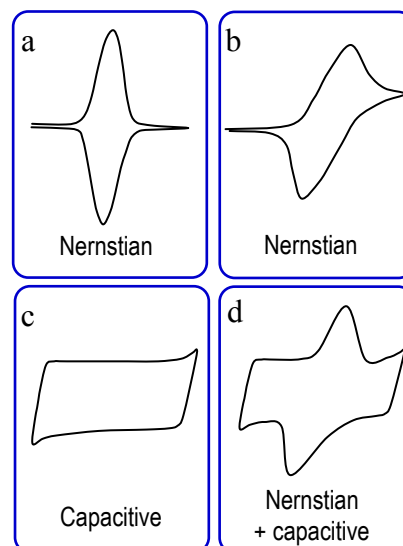


**Fig. 1.** Schematic illustration of cyclic voltammograms of (a) reversible, and (b) quasi-reversible Nernstian CDPs, (c) capacitive CDP, and (d) combined Nernstian and capacitive CDP.

**Acknowledgement:** This research was funded by E.ON AG (International Research Initiative—Energy Storage 2007) and Ningbo Municipal Government (3315 Plan and the IAMET Special Fund, 2014A35001-1). Responsibility for the content of this report lies with the author.

## References

- [1] J. Ding et al, *Energy Environ. Sci.* 8 (2015) 941.
- [2] B. Akinwolemiwa, C. Peng, G.Z. Chen, *J. Electrochem. Soc.* 162 (2015) A5054.
- [3] K. Fic, M. Meller, E. Frackowiak, *J. Electrochem. Soc.* 162 (2015) A5140.
- [4] G.Z. Chen, *Prog. Nat. Sci.-Mater. Int.* 23 (2013) 245.

# Design and Modification of Inorganic/Organic Polyoxometalates-Carbon Pseudocapacitive Electrodes

Keryn Lian, Matthew Genovese and Yeewei Foong  
Department of Materials Science and Engineering  
University of Toronto, Toronto Ont. Canada  
Keryn.lian@utoronto.ca

Multi-walled carbon nanotube (MWCNT) electrodes modified with mixtures of polyoxometalates (POMs) were investigated for electrochemical capacitor (EC) applications. Although different POMs, e.g.  $\text{PMo}_{12}\text{O}_{40}^{3-}$  ( $\text{PMo}_{12}$ ) and  $\text{PW}_{12}\text{O}_{40}^{3-}$  ( $\text{PW}_{12}$ ), have their own characteristic electrochemical activity windows, they showed very unique electrochemical behavior when these POM ions are combined in solution. The resulting electrochemical behavior as reflected in cyclic voltammograms are very different from the individual POM ions. Further analyses revealed that the POM ions do not just mix physically, but instead react to form  $\text{PMo}_{12-x}\text{W}_x$  mixed addenda chemistries. By simply mixing  $\text{PMo}_{12}$  and  $\text{PW}_{12}$  in different ratios, a variety of mixed addenda ions, each with unique electrochemical properties, can be readily synthesized.

Leveraging this novel mixed addenda synthesis, unique POM redox behavior can be captured using layer-by-layer (LbL) deposition on CNT to design molecular coatings that demonstrate desired pseudocapacitive characteristics. The best performance was achieved with a coating that superimposed a 3:1  $\text{PMo}_{12}\text{O}_{40}^{3-}$ - $\text{PW}_{12}\text{O}_{40}^{3-}$  mixed layer on a 1:1  $\text{GeMo}_{12}\text{O}_{40}^{4-}$ - $\text{SiMo}_{12}\text{O}_{40}^{4-}$  mixed layer (Fig.1), which resulted in an 11X capacitance enhancement over bare CNT. This dual layer electrode also demonstrated a close to rectangular CV profile attributed to the overlapping redox features of the POM combination. The design of custom POM coatings to engineer the electrode surface represents a promising strategy for the development of high performance pseudocapacitive electrodes. In this talk, we will discuss several different POM mixtures, their electrochemical behavior, the mechanisms of mixed addenda POM formation, and the effects of their multilayer superimposed combination on MWCNT.

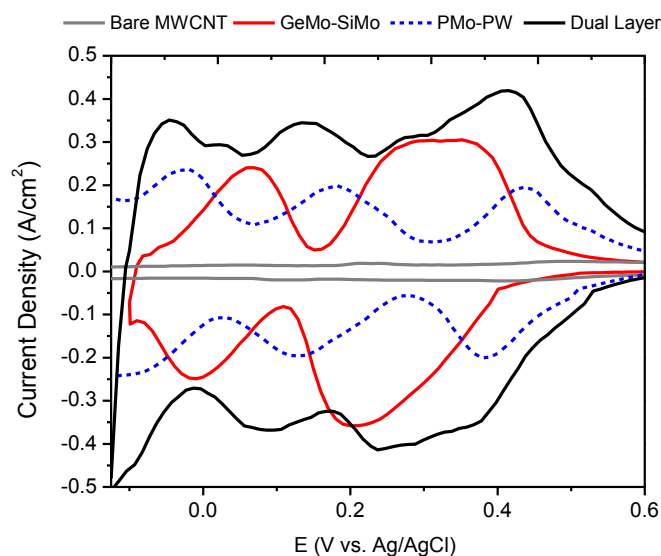


Fig. 1 Cyclic Voltammograms of the bare CNT (gray), the 3:1  $\text{PMo}_{12}\text{O}_{40}^{3-}$ - $\text{PW}_{12}\text{O}_{40}^{3-}$  mixed layer on CNT (blue dashed line), the 1:1  $\text{GeMo}_{12}\text{O}_{40}^{4-}$ - $\text{SiMo}_{12}\text{O}_{40}^{4-}$  mixed layer on CNT (red) and the combined 3:1  $\text{PMo}_{12}\text{O}_{40}^{3-}$ - $\text{PW}_{12}\text{O}_{40}^{3-}$  / 1:1  $\text{GeMo}_{12}\text{O}_{40}^{4-}$ - $\text{SiMo}_{12}\text{O}_{40}^{4-}$  dual layer on CNT (black).

# Valuing Electrochemical Capacitor Technology

John R. Miller<sup>a,b</sup> and Sue M. Butler<sup>a</sup>

<sup>a</sup>*JME, Inc.*  
23500 Mercantile Road, Suite L  
Beachwood, Ohio USA 44122  
<JMEcapacitor@att.net>

<sup>b</sup>*Case Western Reserve University*  
*Electrical Engineering and Computer Science*  
Cleveland, Ohio USA 44106

The value of energy storage, when added to a power system, depends strongly on operating details. Moreover, value can be realized in a variety of ways, for instance by reducing the initial system cost, its operating cost, or its life-cycle costs; enhancing system power performance; increasing system operating efficiency; lowering maintenance requirements; or improving overall system reliability (1). A priori quantification of this value is often possible for systems having known (or at least correctly assumed) operating modes, which then permits comparisons to be made between systems without and with energy storage of various types and amounts.

Electrochemical capacitor (EC) technology (sometimes referred to by the product names Supercapacitor or Ultracapacitor) has several unique characteristics compared with the many different types of reversible energy storage. In general, ECs have a characteristic response time of about one second (time for a full discharge or a full charge), can cycle more than one-million times with minimal performance fade, and will operate with extraordinarily high reliability. On the negative side, ECs generally have more than 100-times higher initial cost than other popular energy storage technologies. Even at such costs, ECs are overwhelming selected as the storage technology of choice in certain applications because of the value they bestow.

This presentation focuses on the value that can be provided by adding energy storage to a power system. Several important applications are examined to quantify the value offered by EC technology compared with a no-storage system and with systems using other storage technologies. A goal is to convincingly demonstrate that characteristics other than energy/mass are important and in fact largely responsible for the rapid annual world-wide growth rate of electrochemical capacitor energy storage technology.

(1) John R. Miller, *Science* **335**, p1312 (2012).

# On the Performance and Self-Discharge of a Redox-Active Electrolyte Supercapacitor Based on an Ionic Liquid Modified with Ferrocene

Dominic Rochefort, Han Jin Xie, Bruno Gelinas  
Chemistry Department, Université de Montréal  
CP6128 Succ. Centre-Ville, Montréal, Qc CANADA H3C3J7  
dominic.rochefort@umontreal.ca

Energy storage in carbon-based electrochemical capacitors is mainly achieved via the formation of the electric double-layer at the electrode-electrolyte interface. Non-faradaic charge storage allows reaching high power levels for prolonged cycling but the energy density remains limited to the extent of active surface area accessible to the ions composing the electrolyte. Increasing the energy of carbon-based electrodes can be achieved by modifying their surface with grafted electroactive centers to add a faradaic contribution to the charge storage. Another strategy to increase energy via faradaic reactions and which has been the subject of an increased interest over the last 2 or 3 years, is to dissolve an electroactive molecule in the electrolyte. The electroactive species can either be added to the solvent in the presence of the supporting electrolyte (redox additive electrolyte) or the supporting electrolyte may also be the electroactive species in redox-active electrolyte supercapacitors (RESCs).[1, 2] While these systems may be appealing due to their simplicity and the potentially higher energy densities offered, it is still difficult to predict if they will make it into real devices or remain within the walls of academic labs. Indeed, more developments and studies will be necessary to clearly define the metrics of charge storage, to increase cell voltage and to prevent self-discharge in RESCs.[3, 4] to name only a few of the issues they are facing currently. This research will focus on these two last issues.

This contribution discusses on the use of an electroactive ionic liquid as the electrolyte in a RESC based on activated carbon electrodes. The electroactive ionic, presented in Figure 1, uses an alkyylimidazolium cation with a new type of anion obtained from the modification of the bis(trifluoromethylsulfonyl)imide (Tf<sub>2</sub>N) anion with ferrocene.[5]

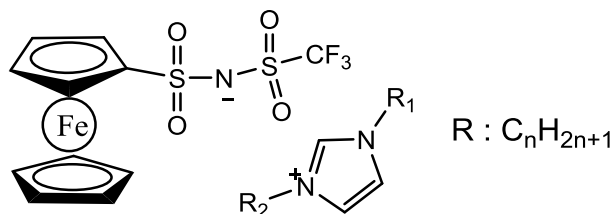


Figure 1. Structure of the alkyylimidazolium ferrocenylsulfonyle(trifluoro-methylsulfonyl)imide (FcTfN) electroactive ionic liquid.

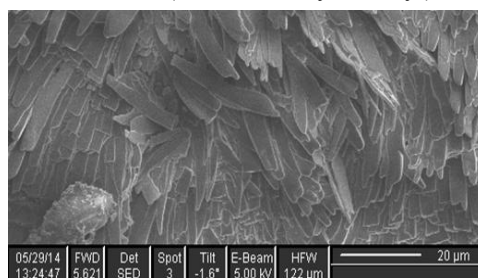


Figure 2. SEM image of the film formed at the positive electrode from the deposition of the oxidized FcTfN anion.

The electrochemistry of these alkyylimidazolium-FcTfN ionic liquids, either pure or diluted with acetonitrile in symmetrical cells made of Black Pearls 2000 activated carbon electrodes was investigated by cyclic voltammetry and galvanostatic charge-discharge experiments. The RESC could be operated at a maximum voltage of 2.5 V and provided a 126 % increase in capacitance compared to the same device with a non-electroactive ionic liquid (EMIm Tf<sub>2</sub>N). The evaluation of increase in energy storage will be discussed in terms of capacitance and energy density. We found that at high concentrations in electroactive ionic liquid, the self-discharge was significantly hindered due to the deposition of the oxidized anion on the electrode surface (Figure 2). This film was dissolved into the electrolyte following the reduction of the ferrocenium-TfN zwitterion back to the ferrocene-TfN anion. This way of suppressing self-discharge without semi-permeable membranes is advantageous to avoid increasing complexity, cost, volume and weight of the device.

- [1] S. Roldan, C. Blanco, M. Granda, R. Menendez, R. Santamaria, *Angew. Chem. Int. Ed.*, 50 (2011) 1699-1701. [2] E. Frackowiak, M. Meller, J. Menzel, D. Gastol, K. Fic, *Faraday Discussions*, 172 (2014) 179-198. [3] L.B. Chen, H. Bai, Z.F. Huang, L. Li, *Energy Environ. Sci.*, 7 (2014) 1750-1759. [4] B. Akinwolemiwa, C. Peng, G.Z. Chen, *J. Electrochem. Soc.*, 162 (2015) A5054-A5059. [5] B. Gélinas, D. Rochefort, *Electrochim. Acta*, 162 (2015) 36-44.



# Graphene-based Electrochemical Capacitors

Peng-Cheng Gao,<sup>1,2</sup> Laura Coustan,<sup>1,2</sup> Wan-Yu Tsai,<sup>2,3</sup> Carlos.R. Pérez,<sup>4</sup> Patricia A. Russo,<sup>5</sup> Yury Gogotsi,<sup>4</sup> Nicola Pinna,<sup>5</sup> Patrice Simon,<sup>2,3</sup> Frédéric Favier<sup>1,2</sup>

1. Institut Charles Gerhardt Montpellier, UMR 5253 CNRS, Université de Montpellier, 34095 Montpellier cedex, France

2. Réseau sur le Stockage Electrochimique de l'Energie (RS2E), FR CNRS 3459, France

3. CIRIMAT, UMR 5085 CNRS Université Paul Sabatier 118 route de Narbonne, 31062 Toulouse, France

4. Department of Materials Science and Engineering & A.J. Drexel Nanotechnology Institute Drexel University 3141 Chestnut St., Philadelphia, PA 19104, United States

5. Institut für Chemie, Humboldt-Universität zu Berlin, Brook-Taylor -Straße 2, 12489 Berlin  
fredf@um2.fr

Thanks to its remarkable physical and morphological properties, graphene has been considered as potential electrode material for supercapacitors. Attractive performances were expected, especially because of its high electronic conductivity and large theoretical developed surface area. Beside a few exceptions, most of the studies in the field report on specific capacitances in the same range as for electrode materials based on activated carbon, typically about 100 to 150 F/g. These limitations have been assigned to material restacking, structural defects, and complex surface chemistry controlling both active surface area and electrode conductivity. To address these performance limitations, we have explored two different approaches. The first one is on the synthesis of graphene-like carbide derived carbons produced by chlorination of SiC nanosheets obtained by the magnesio-thermal reduction of a silica/graphene oxide nanocomposite. The resulting microporosity in the graphene sheets is shown to strongly improve the rate capability of the electrode material [1]. The second approach is on the decoration of the open surface of graphene layers by pseudocapacitive materials, including  $\text{Fe}_3\text{O}_4$  and  $\text{MnO}_2$  [2,3]. The resulting nanocomposite materials show attractive power capability thanks to the electronic conductivity of graphene while the pseudocapacitive metal oxides strongly contribute to the energy density.

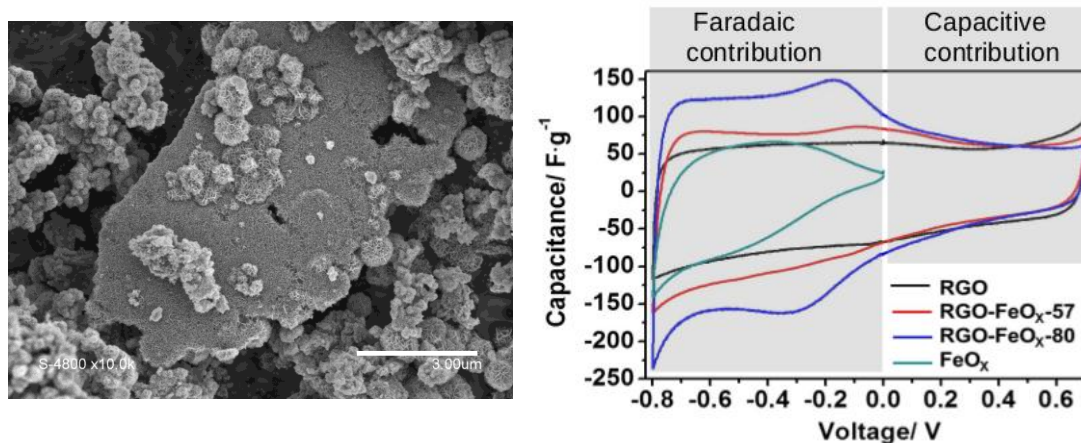


**Fig. 1.** SEM image of GO decorated by  $\text{MnO}_2$  as produced by microwave-assisted reaction (left), and cyclic voltammograms of  $\text{FeO}_x$ , rGO, and rGO- $\text{FeO}_x$  composites at different  $\text{FeO}_x$  loadings at a scan rate of  $5 \text{ mV} \cdot \text{s}^{-1}$  in 1 M  $\text{Na}_2\text{SO}_4$  aqueous electrolyte (right).

## References

- [1] Graphene-like carbide derived carbon for high-power supercapacitors, P.-C. Gao, W.-Y. Tsai, B. Daffos, P.-L. Taberna, C.R. Pérez, Y. Gogotsi, P. Simon, F. Favier, *Nano Energy*, 2015, 12, 197-206
- [2] Impact of the morphological characteristics on the supercapacitive electrochemical performances of  $\text{FeO}_x$ /Reduced Graphene Oxide nanocomposites, P.-C. Gao, P.A. Russo, D.E. Conte, S. Baek, F. Moser, N. Pinna, T. Brousse, F. Favier, *ChemElectroChem*, 2014, 1, 4, 747-754
- [3] Microwave-Assisted Decoration of Carbon Substrates for Manganese Dioxide-Based Supercapacitors, L. Coustan, F. Favier, *Journal of The Electrochemical Society*, 2015 162(5): A5133-A5139

# Metal Organic Frameworks as precursors of porous carbon materials for supercapacitor applications

L. Coustan<sup>a,b</sup>, V. Armel<sup>a</sup>, F. Jaouen<sup>a</sup>, F. Favier<sup>a,b</sup>

<sup>a</sup>Institut Charles Gerhardt Montpellier UMR 5235 CNRS, Université Montpellier 2

<sup>b</sup>Réseau sur le Stockage Electrochimique de l'Energie (RS2E), FR CNRS 3459, France

2 Place Eugène Bataillon - 34095 Montpellier CEDEX 5

*laura.coustan@etud.univ-montp2.fr*

Research efforts in electrochemical double layer capacitors (EDLCs) are currently focused on the enhancement of the energy density which relies on the electrode active material and electrolyte nature. As a matter of fact, a large number of publications is dedicated to the development of carbon based materials with optimized characteristics, including enhanced electronic conductivity, high surface area and optimized porous structure. The pore size distribution, inherited from the carbon precursor structure as well as synthetic conditions, appears to be critical, especially in the micro/meso pore range. Alternatively, the effect of doping with metals and/or hetero-elements is also thoroughly investigated.

In the present work, we have studied the electrochemical behavior of novel electrode materials based on porous carbons derived from the pyrolysis of so-called sacrificial metal-organic frameworks (MOFs) pyrolysis. The richness of the MOF chemistry suggests some attractive opportunities for the control of the pore size distribution as well as metal and nitrogen doping levels in the resulting carbons.

In a first step, an imidazolate Zn-based MOF, ZIF 8 (Fig.1, left), was selected. Such a ZIF 8 material has recently been used as a precursor to synthesize a Fe-N-C catalyst with unprecedented activity and power performance in fuel cell applications owing to the high microporous area and pore accessibility of its carbon substrate [1]. In the present study, this MOF precursor led to a series of carbon materials with large surface areas and tailored pore size distributions thanks to controlled synthetic conditions. Here, we report on the supercapacitive behavior of these MOF-derived carbons with various Cr doping levels.

In a second step, the MOF precursor was changed to ZIF 61 (Fig.1, right) and the impact of the resulting pore structure on the capacitive behavior of the corresponding electrode material was investigated.

The storage performances and mechanisms of these various electrode materials are discussed. This investigation opens the way for the use of tailored MOF-derived carbons as innovative electrode materials for supercapacitors.

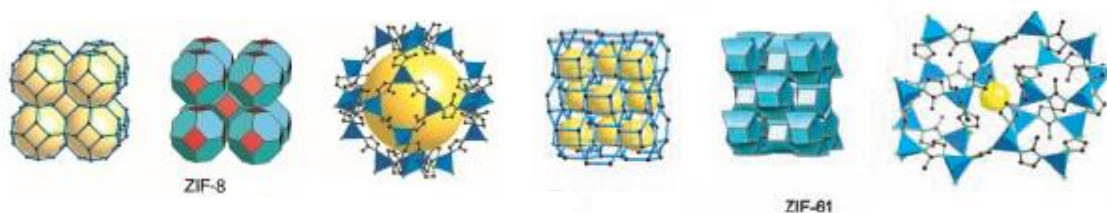


Fig. 1. The single crystal x-ray structures of ZIF-8 (left) [2] and ZIF-61 (right) [3]. For each, the network is shown as a stick diagram (left) and as a tiling (center). (Right) The largest cage in each ZIF is shown with ZnN<sub>4</sub> tetrahedra in blue H atoms are omitted for clarity.

[1] Juan Tian, Adina Morozan, Moulay Taher Sougrati, Michel Lefevre, Regis Chenitz, Jean Paul Dodelet, Deborah Jones, Frederic Jaouen, *Angew. Chem. Int. Ed.* 52 (2013), 6867–6870

[2] JKyo Sung Park, Zheng Ni, Adrien P. Cote, Jae Yong Choi, Rudan Huang, Fernando J. Uribe-Romo, Hee K. Chae, Michael O’Keeffe, and Omar M. Yaghi, *PNAS*, 103 (2006) 27, 10186-10191

[3] Rahul Banerjee, Anh Phan, Bo Wang, Carolyn Knobler, Hiroyasu Furukawa, Michael O’Keeffe, Omar M. Yaghi, *Science* 319, (2008) 939



# FeWO<sub>4</sub> as a new high volumetric capacitance material for aqueous electrochemical supercapacitors

N. Goubard,<sup>a,b,c</sup> O. Crosnier,<sup>a,c</sup> F. Favier,<sup>b,c</sup> C. Payen,<sup>a</sup> P. Leone<sup>a</sup> and T. Brousse<sup>a,c</sup>

<sup>a</sup> Institut des Matériaux Jean Rouxel (IMN), 2 rue de la Houssinière, 44322 Nantes Cedex 3, France

<sup>b</sup> Institut Charles Gerhardt Montpellier, Place Eugène Bataillon, 34095 Montpellier, France

<sup>c</sup> Réseau sur le Stockage Electrochimique de l'Énergie (RS2E), FR CNRS 3459, 80039 Amiens Cedex, France

olivier.crosnier@univ-nantes.fr

The volumetric capacitance of supercapacitors is one of the limiting factors of today's stationary applications. New materials with improved storage properties are necessary to meet the requirements concerning high-performance energy storage devices while considering a reasonable manufacturing cost and a low environmental impact<sup>1,2</sup>. Moreover, not only the specific capacitance, but also the volumetric properties play a key role, especially for stationary applications. In order to meet those requirements, our interest has focused on high-density oxides operating in aqueous electrolytes.

Metal tungstates (M<sup>2+</sup>WO<sub>4</sub>) represent an important group of inorganic high-density oxides with excellent functional and electronic properties<sup>3</sup>. Iron tungstate (FeWO<sub>4</sub>), crystallizes in the wolframite-type structure, characterized by distorted [MO<sub>6</sub>] and [WO<sub>6</sub>] octahedra, and has recently been studied in lithium-ion batteries<sup>4</sup>. FeWO<sub>4</sub> has been synthesized *via* various low-temperature methods (polyol-mediated<sup>5</sup>, hydrothermal<sup>6</sup> synthesis...) in order to obtain high specific surface area nanoparticles which have been characterized by XRD, TEM (Figure 1) and electrochemically tested as supercapacitor electrode materials in a 5M LiNO<sub>3</sub> aqueous electrolyte at 20 mV/s (Figure 2). The material exhibits very promising properties and *in operando* Mössbauer spectroscopy experiments, performed in a specially designed cell, have revealed that the Fe<sup>2+</sup>/Fe<sup>3+</sup> surface redox reactions are clearly involved in the storage mechanism. The synthesis conditions, materials characterizations and electrochemical performance will be detailed in the presentation.

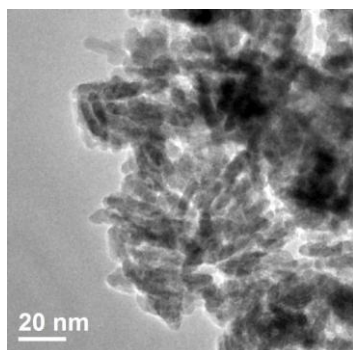


**Figure 1 :** TEM image of FeWO<sub>4</sub> obtained via polyol-mediated synthesis

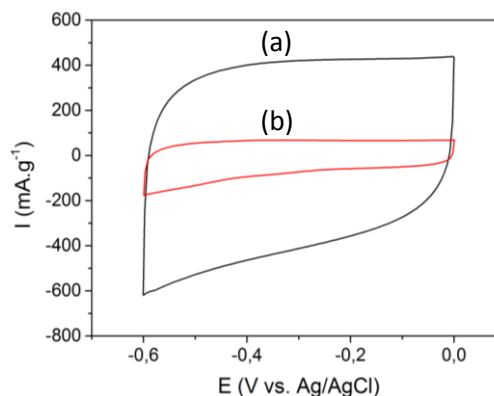


**Figure 2 :** Cyclic voltammograms of FeWO<sub>4</sub> obtained via (a) polyol-mediated and (b) hydrothermal synthesis

## References

- [1] Simon, P.; Gogotsi, Y. *Nat. Mater.* 2008, 7, 845.
- [2] Long, J. W.; Bélanger, D.; Brousse, T.; Sugimoto, W.; Sassin, M. B.; Crosnier, O. *MRS Bull.* 2011, 36, 513.
- [3] Kim, D. W.; Cho, I.-S.; Shin, S. S.; Lee, S.; Noh, T. H.; Kim, D. H.; Jung, H. S.; Hong, K. S., *J. Solid State Chem.*, 2011, 184, 2103.
- [4] Wang, W.; Hu, L.; Ge, J.; Hu, Z.; Sun, H.; Sun, H.; Zhang, H.; Zhu, H.; Jiao, S. *Chem. Mater.*, 2014.
- [5] Ungelenk, J.; Speldrich, M.; Dronskowski, R.; Feldmann, C. *Solid State Sci.*, 2014, 31, 62.
- [6] Yu, S. H.; Liu, B.; Mo, M. S.; Huang, J. H.; Liu, X. M.; Qian, Y. T. *Adv. Funct. Mater.*, 2003, 13, 639.

# Micro-Supercapacitors Based on Carbon Hybrid Fibers

Yuan Chen

*School of Chemical and Biomedical Engineering, Nanyang Technological University, Singapore  
N1.2-B1-16, 62 Nanyang Drive, Singapore 637459  
chenyuan@ntu.edu.sg*

Micro-supercapacitors are promising energy storage devices for miniaturized portable electronics. Their main limitation, however, is the low volumetric energy density. We produced hybrid carbon fibers using the capillary chromatography column as a one-dimensional hydrothermal micro-reactor, in which reduced graphene oxide (rGO) and single-walled carbon nanotubes (SWCNTs) self-assembled into an interconnected SWCNT network with rGO sheets interposed along the microfiber axis to create a mesoporous microstructure of a large surface area ( $396 \text{ m}^2/\text{g}$ ) and a high electrical conductivity ( $102 \text{ S/cm}$ ). The resultant fiber showed capacity of  $300 \text{ F/cm}^3$ . The fiber micro-supercapacitors exhibited a high volumetric energy density of  $\sim 6.3 \text{ mWh/cm}^3$ .<sup>1</sup>

Furthermore, the all-carbon hybrid fibers can be controllably functionalized to yield versatile composite fibers with either capacitive or Faradic characteristics. By matching the specific capacitances of one  $\text{MnO}_2$ -coated rGO/SWCNT fiber as battery-type (positive) electrode and the other N-doped rGO/SWCNT fiber as capacitor-type (negative) electrode, we constructed fiber-based asymmetric micro-supercapacitors with a voltage window of  $1.8 \text{ V}$  and excellent cycling stability.<sup>2</sup>

These results demonstrate the great potentials of graphene and carbon nanotubes in building fiber supercapacitors as miniaturized energy storage devices.<sup>3</sup>

## References:

1. Nature Nanotechnology, 2014, 9, 555–562
2. Advanced Materials, 2014, 26, 6790–6797
3. Chemical Society Reviews, 2015, 44, 647–662

# Preparation and characterization of Mn oxide-based composites for high-performance asymmetric supercapacitors

Chi-Chang Hu, Arturas Adomkevicius, Shin-Ming Li, Tzu-Man Ou  
Department of Chemical Engineering, National Tsing Hua University  
101, Sec. 2, Kuang-Fu Rd., Hsin-Chu city, 30013 Taiwan  
cchu@che.nthu.edu.tw

Recently, a lot of investigations focus on extending the cell voltage in order to enlarge the specific energy of asymmetric supercapacitors (ASCs). Here, we proposed two routes for preparing Mn oxide-based composites with ideal pseudocapacitive characteristics to demonstrate the material design concept for ASCs [1,2].

A 3D reduced graphene oxide/carbon nanotube (rGO/CNT) structure with a good wetting property, high porosity, and large surface area is homogeneously deposited with amorphous manganese oxide (a-MnO<sub>x</sub>) by CV deposition. The flowery a-MnO<sub>x</sub> structure with slender petals (ca. 5-8 nm) on the framework of hierarchically porous rGO/CNT matrix not only enables full utilization of a-MnO<sub>x</sub> but also retains sufficient conductivity and porosity for the high-rate charge-discharge application. The use of a-MnO<sub>x</sub> on the 3D rGO/CNT material produces high specific capacitance of MnO<sub>x</sub> (ca. 1200 F/g) which is much higher than that of a-MnO<sub>x</sub> ( $C_{S,Mn} = 233$  F/g). The specific energy and specific power of a-MnO<sub>x</sub>/rGO/CNT (single electrode) are respectively as high as 46.2 Wh/kg and 33.2 kW/kg.

Sodium pre-doped manganese oxide is prepared via a simple synthesis method for the ASC application. The pre-doping quantity of sodium significantly affects the crystallite size and morphology of resultant oxide nanoparticles, leading to the variation in capacitive performances. An aqueous ASC with a cell voltage of 2.4 V is demonstrated using activated carbon as the negative electrode and Na-doped Mn oxide/carbon as the positive electrode. The specific energy and power of this ASC (based on total mass of active materials) measured at 20 A g<sup>-1</sup> are equal to 22.72 Wh/kg and 24.41 kW/kg, respectively.

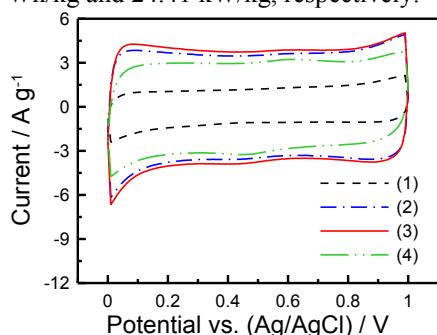


Fig. 1 Cyclic voltammograms of (1) MnO<sub>2</sub>, (2) Na-doped MnO<sub>2</sub>-10, (3) Na-doped MnO<sub>2</sub>-15, and (4) Na-doped MnO<sub>2</sub>-20 in 0.5 M Na<sub>2</sub>SO<sub>4</sub> at 25 mV s<sup>-1</sup>.

## References

- [1] S.M. Li, et. al, J. Power Sources 225 (2013) 347.
- [2] T.M. Ou, et. al, J. Electrochem. Soc. 162 (2015) A5001.

# Structure and Capacity of a Tin-Copper-CNT Composite Anode and its Lithium Ion Hybrid Capacitor Performance

Dah-Shyang Tsai, Wei-Wen Chiang, Chung-Lun Hsieh

Department of Chemical Engineering, National Taiwan University of Science and Technology

43, Keelung Road, Section 4, Taipei, Taiwan 10607

e-mail address: dstsai@mail.ntust.edu.tw

We have fabricated the lithium ion capacitor with tin-copper-CNT composite anode and activated carbon cathode, and found attributes worthy of further investigation. This report aims to study preparation and structure details of the tin-copper-CNT composite anode, which is critical to the capacitor performance.

The anode composite has been prepared with electrodeless deposition of tin and copper on the slightly oxidized CNT bundle and lithiation down to 0.08 V (vs.  $\text{Li/Li}^+$ ). The prelithiation step makes tin and copper sufficient alloyed with lithium and builds a proper layer of solid electrolyte interface (SEI), so that the anode may exhibit large and sufficiently steady capacity.

Figure 1(a) shows the outside diameter of the multi-walled CNT raw material is  $\sim 10\text{-}30$  nm. After coating of tin and copper, the CNT diameter grows and roughens because of the attached metal layer, as illustrated in Figure 1(b). Figure 1(c) indicates that prelithiation in a half cell increases the tube diameter further, also cut the tube short. The charge and discharge curves of Sn/Cu/CNT electrode at  $0.1\text{ A g}^{-1}$  are plotted in Figure 2(a), when the electrode was prelithiated between 2.0 and 0.08 V (vs.  $\text{Li/Li}^+$ ). The first cycle displays a large capacity of significant irreversibility,  $\sim 1600\text{ mAh g}^{-1}$ , because of SEI buildup. The capacity of the second and third cycle is much less,  $\sim 600\text{ mAh g}^{-1}$ , which is the cycle capacity. When the lithiated Sn/Cu/CNT anode is assembled with an activated carbon electrode with a mass ratio 1:1.5, the hybrid capacitor demonstrates a large amount of energy capacity, as illustrated in Figure 2(c). At low current, the energy density can reach  $90\text{ Wh kg}^{-1}$  when the voltage window is set 3.8 V. Figure 2(b) presents the electrode potential variations during charge and discharge at low current  $0.1\text{ A g}^{-1}$  and window 3.8 V. The charge/discharge curves are near triangular shape.

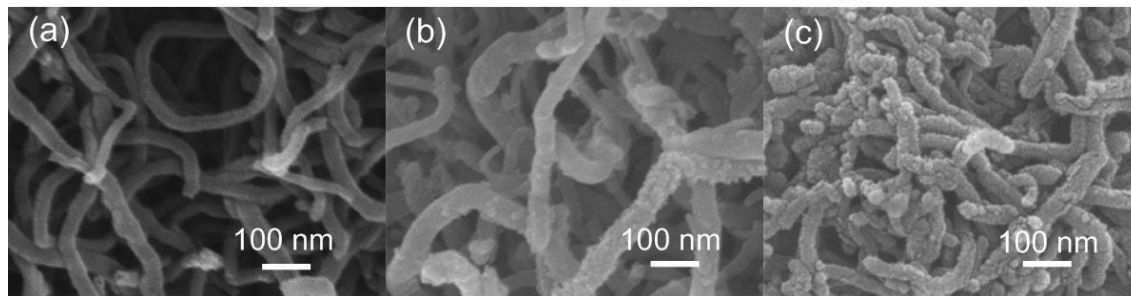


Figure 1 Microstructure of CNT anode (a) before tin coating and lithiation, (b) after tin electrodeless deposition and before lithiation, (c) after lithiation.

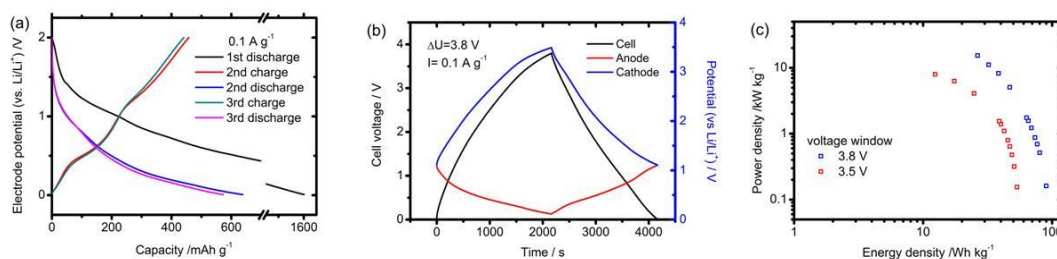


Figure 2 Prelithiation of anode and the performance of lithium ion capacitor. (a) Anode lithiation between 2.0 and 0.08 V (vs.  $\text{Li/Li}^+$ ); (b) cell voltage and anode/cathode potential variations during galvanostatic charge/discharge in  $\Delta U=3.8\text{ V}$  and  $I=0.1\text{ A g}^{-1}$ ; (c) ragone plot of lithium ion capacitor in  $\Delta U=3.8\text{ V}$  and  $3.5\text{ V}$ .

# Fabrication of Graphene Microspheres for High Performance Supercapacitor Applications

JunHui Jeong, Hyun-Kyung Kim, SukWoo Lee, Kwang-Bum Kim\*  
*Laboratory of Energy Conversion and Storage Materials,  
Department of Material Science and Engineering, Yonsei University,  
134 Shinchon-dong, Seodaemoon-gu, Seoul, 120-749, Republic of Korea*  
\*kbkim@yonsei.ac.kr

Supercapacitors are attracting much attention for use in high power energy storage devices. Electrode materials for supercapacitors are carbon-based materials such as activated carbon, carbon nanotubes, graphene and their composite. Among them, activated carbon is the most widely used electrode materials in commercial supercapacitors due to their reasonable cost and scalable production.<sup>1</sup>

Recently, graphene, a one-atom thick two-dimensional honeycomb carbon nanostructure, has been investigated as an electrode material for supercapacitors, owing to its high surface area ( $2630 \text{ m}^2\text{g}^{-1}$ ), sufficient porosity, superior conductivity ( $10^4 \text{ Scm}^{-1}$ ), and excellent mechanical stability.<sup>2</sup> However, one particular issue with graphene is its tendency to aggregate due to strong intersheet adhesion by van der Waals attraction. Restacking of sheets not only reduces its specific surface area, but also compromises their electrochemical properties. Therefore, strategies for preventing graphene aggregation have been studied, which typically include introducing spacer in-between graphene layers, such as carbon black,<sup>3</sup> carbon nanotubes,<sup>4</sup> metal oxide,<sup>5</sup> and conducting polymer<sup>6</sup>, functionalizing graphene sheets to develop wrinkle on graphene surface,<sup>7</sup> and developing three-dimensional architectures by hard template method or graphene self-assembly.<sup>8</sup>

Unlike two-dimensional graphene sheets, the three-dimensional graphene structure assembled with two-dimensional graphene sheets have high free volume and excellent compressive properties, and can tightly pack without significantly reducing the accessible surface area.<sup>9</sup>

In this study, we report a novel strategy for fabrication of graphene micro-sphere by spray-drying method using ionic liquid as a nanospacer between graphene sheets. More details on the fabrication procedure, electrochemical and structural properties will be presented at the meeting.

## References

1. Simon,P., *et al.*, *Nat. Mater.*, **2008**, 7, 845
2. Zhu,Y.W., *et al.*, *Adv. Mater.*, **2010**, 22, 3906
3. J.Yan, *et al.*, *Carbon*, **2010**, 48, 1731
4. M.-Q.Zhao, *et al.*, *ACS nano*, **2012**, 6, 10759
5. R.B.Rakhi, *et al.*, *Adv. Energy Mater.*, **2012**, 2, 381
6. X.-C.Chen, *et al.*, *Chem. Commun.*, **2012**, 48, 5904
7. Yang, X., *et al.*, *Adv. Mater.*, **2011**, 23, 2833
8. Choi,B.G., *et al.*, *ACS nano*, **2012**, 6, 4020
9. Luo, J.Y., *et al.*, *ACS nano* **2011**, 5, 8943

# In-situ Electrochemical Quartz Crystal Microbalance (EQCM) Study of Ion Dynamics and Charge Storage Mechanism for Supercapacitors

W.-Y. Tsai,<sup>a</sup> J. M. Griffin,<sup>b</sup> A. C. Forse,<sup>b</sup> C. P. Grey,<sup>b</sup> P.-L. Taberna,<sup>a</sup> P. Simon<sup>a</sup>

<sup>a</sup> Université Paul Sabatier, CIRIMAT UMR CNRS 5085, 118 Route de Narbonne, 31062 Toulouse, France and Réseau sur le Stockage Electrochimique de l'Energie (RS2E), FR CNRS 3459, France

<sup>b</sup> Department of Chemistry, University of Cambridge, Lensfield Road, Cambridge, CB2 1EW, UK.  
tsai@chimie.ups-tlse.fr

Electrical double layer capacitors (EDLCs), or supercapacitors hold an important position among all the energy storage systems owing to their high power capabilities. Nowadays, the main challenge for supercapacitors is to increase their energy density without sacrificing their high power nature. Aside from the development of novel constituent materials (electrode, electrolytes, etc.), obtaining a fundamental understanding of the charge storage mechanism at molecular scale also holds the key for future design of supercapacitors.[1] Recently, it has been reported that Electrochemical Quartz Crystal Microbalance (EQCM) technique can serve as a gravimetric probe to study the concentration and compositional changes in porous carbon.[2] Therefore, it can be a powerful tool for studying the in-situ ion transport and the solvation effect during charging in the confined carbon micropores.

In the first part of this work, carbide-derived carbon (CDC) with two different average pore sizes (1 and 0.65 nm) were tested in neat and acetonitrile (AN)-solvated ionic liquid (EMI-TFSI). Ion adsorption during charging in these systems was characterized by in-situ EQCM and cyclic voltammetry (CV) measurements. Results have shown that different charge storage mechanisms are involved for positive and negative polarization. Experimental acetonitrile solvation numbers were estimated for EMI<sup>+</sup> cation, and partial desolvation was observed when decreasing the carbon pore size from 1 down to 0.65 nm. In the second part, in-situ NMR [3] was coupled with in-situ EQCM for investigating the same electrode/electrolyte system (YP-50F in  $\text{P}(\text{Tf}_2\text{B})_4/\text{AN}$ ) by potentiostatic measurements. Thanks to the quantitative nature of NMR, the amount of cation and anion at different charge states could be determined, and different charging mechanisms have been found for different electrode polarizations. In-situ EQCM results agree well with NMR results, and offer important information on ion solvation inside the micropores. The combination of these two in-situ techniques brings important insights on the charge storage mechanisms and the EDL structure upon charging.

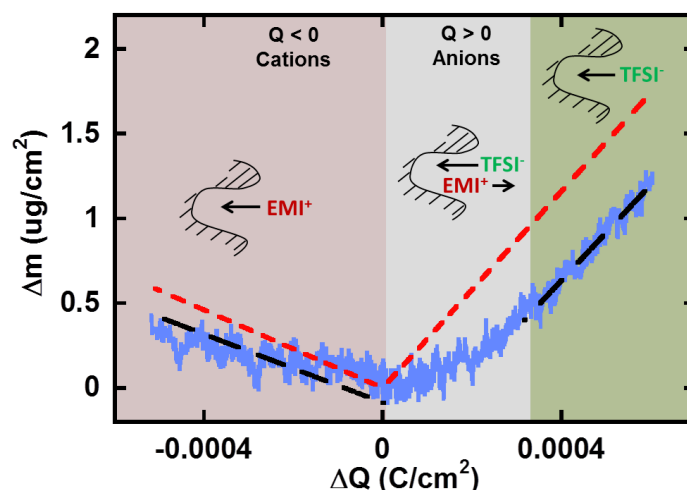


**Figure 1:** Scheme of ion transport in 1-nm pores during different charging states (taking neat EMI-TFSI as example)

## References

- [1] P. Simon and Y. Gogotsi, *Nat. Mater.*, **7**, 11, 845–854 (2008)
- [2] M. D. Levi, G. Salitra, N. Levy, D. Aurbach, and J. Maier, *Nat. Mater.*, **8**, 11, 872–875 (2009)
- [3] H. Wang, A. C. Forse, J. M. Griffin, N. M. Trease, L. Trognko, P.-L. Taberna, P. Simon, and C. P. Grey, *J. Am. Chem. Soc.*, **135**, 50, 18968–18980 (2013)

# Influences of Residual Water in Porous Carbon Electrodes on Their Cycling Behavior in Organic Electrolyte Solutions

Masayuki Morita, Takuma Izumi, Yuya Noguchi, Masahiro Tokita, Kenta Fujii, and Nobuko Yoshimoto  
Graduate School of Science and Engineering, Yamaguchi University,  
2-16-1 Tokiwadai, Ube 755-8611, Japan  
morita@yamaguchi-u.ac.jp

Carbon materials having high specific surface area, such as activated carbon (AC), have been used as the electrodes of electric double-layer capacitors (EDLCs). In EDLCs using organic nonaqueous electrolytes, water contents in the solution phases significantly influence the capacitor performances [1]. Those carbon materials usually contain small amounts of water in their pore structures. However, their influences on the capacitor performances are still unclear because it is rather difficult to determine quantitatively the water content in AC after proper thermal treatments. We have proposed a simple method that can estimate the water contents in high surface area carbon materials [2]. In this paper, the effects of the residual water in the electrode on the capacitor performances are investigated.

Commercially available AC was used as the electrode material. For the estimation of water in AC, acetonitrile (AN) and propylene carbonate (PC) of battery grade (water content < 5 ppm) were used as the organic solvents. Carbon materials properly treated were immersed in the solvents or in the solutions dissolving supporting electrolyte. Changes in the water content in the solution phase after the carbon immersion were monitored by a Karl-Fisher titration method. Capacitor performances of the carbon electrodes containing different amounts water were examined by constant-current cycling of a symmetric two-electrode cell.

The water content in AC was found to be kept almost equilibrium after vacuum-drying at 100 °C or above. The amounts of water released (desorbed) from AC after the vacuum-drying was generally higher in AN solvent than in PC solvent. This result would be caused by differences in the affinity of the solvent molecule with the pore-wall surface of AC. The Langmuir adsorption isotherms were obtained for AC in AN and PC solvents, after the assumption that the water adsorbed inside AC keeps adsorption equilibrium with the water dissolved in the organic solvent [2]. The amount of water released from the pore structure of AC depended on the electrolytic salt in the solution phase.

AC samples with different water contents were obtained by changing the vacuum-drying conditions. Figure 1 shows the influences of the residual water in AC electrode on the variations in the capacitance and internal resistance during the constant-current cycling with high-voltage (3.5 V) loading. The residual water affects much on the variations in the capacitance and internal resistance of the cell with repeated cycles.

## References

- [1] P. W. Ruch, D. Cericola, A. Foelske, R. Kötzt, and A. Wokaun, *Electrochim. Acta*, **55**, 2352 (2010).
- [2], T. Izumi, M. Egashira, N. Yoshimoto, and M. Morita, *Extended Abst. 80th Annual Meeting of ECSJ* (1E08), p. 135 (2013); *Extended Abst. 7th Asian Conference on Electrochemical Power Sources (ACEPS-7)*(2B13), p. 38 (2013).

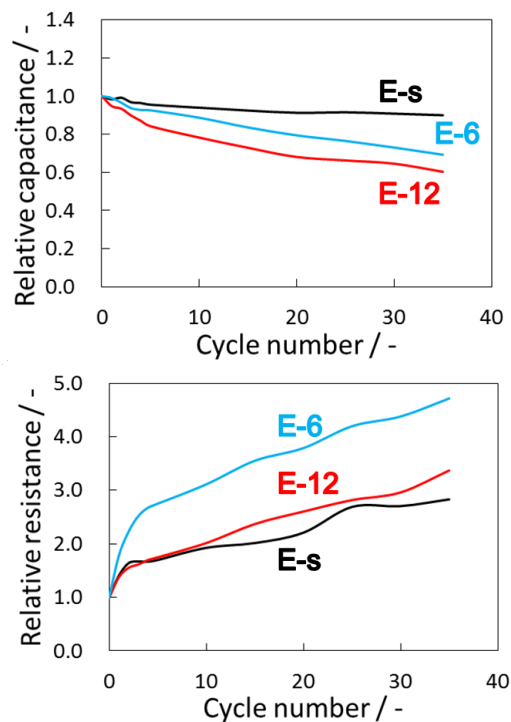


Fig. 1 Variations in the relative capacitance and internal resistance for the cell with AC electrodes containing different amounts of residual water (E-6 > E-12 > E-s).



# High Voltage Graphene Capacitor Technology

Tavo Romann, Erik Anderson, Ove Oll, Piret Pikma, Enn Lust  
*Institute of Chemistry, University of Tartu,*  
*Ravila 14A, 50411 Tartu, Estonia*  
*tavo.romann@ut.ee*

Supercapacitor cell voltages are too low and time constant too high for a typical capacitor's application – smoothing ac ripple in dc voltage converters. Modern electronic devices, such as computers, USB chargers, or mobile phones, have a typical rail voltage of 3.3 or 5 V and use capacitors within range of 4–10 V. Unfortunately, suitable electrolytic capacitors have very low energy density.

We have demonstrated [1] that in 1-butyl-1-methylpyrrolidinium dicyanamide (BMPDCA) ionic liquid a graphene electrode passivates at 10 V and at the same time the conductivity of the single-layer graphene sheet increases more than 5 times. The protective self-healing nanolayer formed is a new carbon-nitrogen material polydicyanamide (PDCA, identified by *in situ* infrared spectroscopy [2]) with dielectric constant value up to 9.8. In Figs. 1b and 2a it is shown that a large surface area reduced graphene oxide (RGO) electrode can be completely passivated – i.e. coated with a thin protective dielectric layer and have low leaking current density even at 10 V.

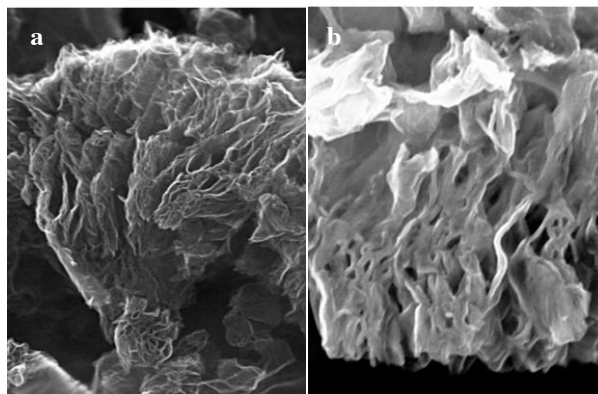


**Fig 1.** Electron microscopy images of an unmodified (a) and a passivated (b) RGO electrode (scale bar is 1  $\mu\text{m}$ ).

It is proposed that a hybrid capacitor can be constructed using a thinner RGO negative electrode and a passivated RGO positive electrode. Good stability (>10000 cycles), high efficiency (>99.8% coulombic) and time constants within 0.01 and 0.2 ms have been demonstrated for the passivated RGO electrodes. In the cell voltage range from 4 to 10 V, capacitors with RGO electrodes outperform any commercial capacitor technology by better energy density (Fig. 2b). Thus, the new technology proposes that graphene-based materials can dominate in the future capacitor market, currently worth US\$ 18 billion.

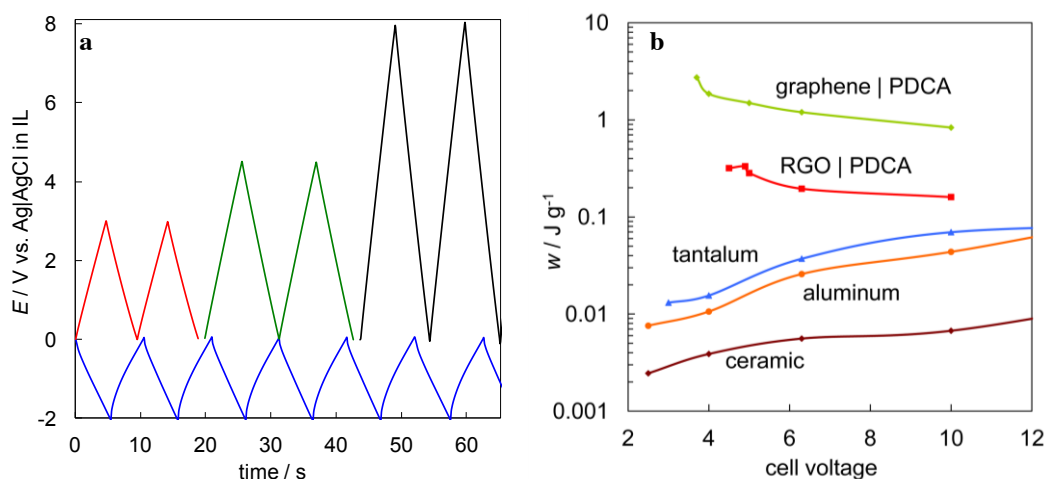


**Fig. 2.** a) Constant current charge-discharge curves [1] for the passivated and unmodified (blue line) RGO electrodes in BMPDCA. b) Energy density of PDCA and commercial capacitor technologies.

- [1] T. Romann, O. Oll, P. Pikma, K. Kirsimäe, E. Lust, 4–10 volt capacitors with graphene-based electrodes and ionic liquid electrolyte, *J. Power Sources* 280 (2015) 606–611.  
 [2] T. Romann, O. Oll, P. Pikma, H. Tamme, E. Lust, *Electrochim. Acta* 125 (2014) 183–190.



# **The influence of Pore Size Distribution and surface area both are analyzed by QSDFT on capacitance and ESR of EDLC consists of activated carbon form coal tar pitch**

Jing-Mei LI, Chung-Ting Tsai, Chi-Shyan Mai, Sen-Tsan Shen, Ming-Da Fang  
China Steel Chemical Corporation (Taiwan)  
No.42 Chung-Lin Road, Hsiao Kang, Kaohsiung, 81233, Taiwan  
02772@e-cscc.com.tw

Activated carbon considered a mature material for many applications has introduced as electrochemical double layer capacitor (EDLC) active material for decades. For supercapacitor, tremendous efforts are devoted to understanding the correlation between specific surface area (SSA) of activated carbon and specific capacitance. Rare works are done with the pore size distribution (PSD) effect on electrochemical performance, not to mention inaccurate way to gain SSA or partial PSD through classical, macroscopic thermodynamic method which is not the most proper model for activated carbon [1] or material with micropores. With not only incorrect model but also much more complicated and broad PSD, how PSD affects the capacitance and equivalent series resistance (ESR) is still vague, even though ca. 0.7 nm was regarded as the most efficient pore size of carbide-derived carbon (CDC) which has quite narrow PSD for creating capacitance with TEABF<sub>4</sub>/ACN electrolyte [2].

DFT are powerful technique that describes sorption and behavior of inhomogeneous fluids confined in nanoporous materials [1] and QSDFT is recently developed approach and quantitatively accounts for surface heterogeneity effects to provide a more reliable pore size assessment and specific surface area [3]. In this work, the activated carbons developed by China Steel Chemical Corporation from coal tar pitch are analyzed by QSDFT and coin cell format EDLC are assembled with acetonitrile (ACN) and propylene carbonate (PC), respectively. The correlation of PSD and capacitor performance is found out through 4 different SSA activated carbons both in ACN and PC system and empirical equations are developed to unveil the most efficient pore offers highest specific capacitance per SSA and the most efficient pore improves ESR more significantly. With above information, electrochemical properties of activated carbon can be predicted by simple gas adsorption/desorption approach and it will be easier to tailor activated carbon by needs or demands.

## **Reference**

- [1] Juan Tascón, Novel Carbon Adsorbents, Elsevier, 2012
- [2] J. Chmiola, C. Largeot, P.L. Taberna, P. Simon, and Y. Gogotsi, *Angew. Chem. Int. Ed.* 2008, 47, 3392–3395
- [3] J. Silvestre-Albero, A. Silvestre-Albero, F. Rodríguez-Reinoso, M. Thommes, *Carbon* 2012, 50, 3128–3133

## **New materials for electrochemical capacitors**

Galyna Shul and Daniel Bélanger\*

*Département de Chimie, Université du Québec à Montréal, CP 8888, succ. Centre-Ville  
Montréal (Québec), Canada, H3C 3P8*

\* belanger.daniel@uqam.ca

Electrochemical double layer capacitors are currently being investigated by academic, governmental and industrial laboratories. The interest for these energy storage systems stems from their potential applications in portable electronic devices, energy recovery and transportation.

Carbon is currently the electrode material of choice for most practical devices due to its good capacitive behavior and performance and excellent chemical stability upon cycling. However, advances are needed to improve the energy density of carbon-based electrochemical capacitors. Approaches currently under investigation involve the use of quinone molecules, either dissolved in the electrolyte (so called redox active electrolyte), adsorbed or covalently grafted to a porous carbon material. In this presentation, we will present results for these systems by focusing on the charge/discharge behavior of full cells and their self-discharge. The advantages and limitations of these systems will be discussed.

# Effect of ZnO on Capacitive Properties of Core / Hybrid Shell Arrays

A. Pruna<sup>a,b,c,\*</sup>, Q. Shao<sup>a</sup>, J.A. Zapien<sup>a,d</sup>, A. Ruotolo<sup>a</sup>

<sup>a</sup>*Department of Physics and Materials Science, City University of Hong Kong, Kowloon, Hong Kong SAR, China*

<sup>b</sup>*Faculty of Physics, University of Bucharest, 405 Atomistilor Str., 077125 Bucharest-Magurele, Romania*

<sup>c</sup>*Universidad Politecnica de Valencia, Camino de Vera s/n, 46022 Valencia, Spain*

<sup>d</sup>*Center of Super-Diamond and Advanced Films (COSDAF), City University of Hong Kong, Kowloon, Hong Kong SAR, China*

\*corresponding author: [ai.pruna@gmail.com](mailto:ai.pruna@gmail.com)

Complex core-shell nano-architectures were synthesized and investigated for electrochemical energy storage application by employing ZnO nanorods as core array and polypyrrole (PPy) –graphene oxide (GO) hybrids as shells. The structure, morphology and electrochemical properties of core-shell arrays were investigated by XRD, FTIR and RAMAN spectroscopy. Cyclic voltammetry was performed in order to analyze the electrochemical properties and evolution of inner and outer shell charge. The results indicated a synergetic effect of ZnO nanorods and PPy-GO hybrids towards improved capacitance while a strong dependence of the capacitive performance of ZnO/PPy-GO core-shell arrays on deposition potential and deposition charge for ZnO arrays was revealed. These instructions are an example of what a properly prepared meeting abstract should look like. Proper column and margin measurements are indicated.

**Keywords:** ZnO, polypyrrole, graphene oxide, core-shell, supercapacitor

# **A General Strategy for the Fabrication of High Performance Microsupercapacitors**

Qiu Jiang, Narendra Kurra and H.N. Alshareef

*Mr. Qiu Jiang, Dr. Narendra Kurra, and Prof. H. N. Alshareef*

*Materials Science and Engineering, King Abdullah University of Science and Technology (KAUST)*

*Thuwal 23955-6900, Saudi Arabia*

*qiu.jiang@kaust.edu.sa*

We propose a generic strategy for microsupercapacitor fabrication that integrates layers of reduced graphene oxide (rGO) and pseudocapacitive materials to create electrode heterostructures with significantly improving cycling stability and performance. Our approach involves a combination of photolithography and a simple transfer method of free-standing reduced graphene oxide film onto an Au/patterned photoresist bilayer. The resulting stack (rGO/Au/patterned resist/substrate) is then used for the electrochemical deposition of various pseudocapacitive materials before the final step of lift-off. To prove the viability of this method, we have successfully fabricated microsupercapacitors (MSCs) with the following interdigitated electrode heterostructures: MnO<sub>2</sub>/rGO, Co(OH)<sub>2</sub>/rGO and PANI/rGO. These MSCs show better performance and cycling stability compared to the single layer, (i.e., rGO-free) counterparts. The interdigitated electrode heterostructures result in MSCs with energy densities in the range of 3-12 mWh/cm<sup>3</sup> and power densities in the range of 400-1200 mW/cm<sup>3</sup>, which is superior to the Li thin film batteries (E = 10 mWh/cm<sup>3</sup>), carbon, and metal oxide based MSCs (E = 1-6 mWh/cm<sup>3</sup>). These results can be explained by a facilitated nucleation model, where surface topology of the rGO film creates a favourable environment for the nucleation and growth of pseudocapacitive materials with strong interfacial contacts and enhanced surface area. This approach opens up a new avenue in fabricating MSCs involving a variety of heterostructures combining electrical double layer carbon type with Faradaic pseudocapacitive materials for enhanced electrochemical performance.

# **Polyaniline-RuO<sub>2</sub> Core-Shell Nanostructured Arrays for Very Stable and High Performance Pseudocapacitors**

Chuan Xia, Wei Chen, Xianbin Wang, Mohamed N. Hedhili, Nini Wei, Husam N. Alshareef\*

*Mr. C. Xia, Dr. W. Chen, Dr. X. B. Wang, Dr. M. H. Hedhili, Ms. N. N. Wei, Prof. H. N. Alshareef  
Material Science and Engineering, King Abdullah University of Science and Technology (KAUST),  
Thuwal, 23955-6900, Kingdom of Saudi Arabia  
chuan.xia@kaust.edu.sa*

Conducting polymers such as polyaniline (PAni) show great potential as pseudocapacitor materials for electrochemical energy storage applications. Yet, the cycling instability of PAni resulting from structural alteration is a major hurdle to its commercial application. Here we report the development of nanostructured PAni-RuO<sub>2</sub> core-shell arrays as electrodes for highly stable pseudocapacitors with excellent energy storage performance. A thin layer of RuO<sub>2</sub> grown by atomic layer deposition (ALD) on PAni nanofibers plays a crucial role in stabilizing the PAni pseudocapacitors and improving their energy density. The pseudocapacitors, which are based on optimized PAni-RuO<sub>2</sub> core-shell nanostructured electrodes, exhibit very high specific capacitance (710 F g<sup>-1</sup> at 5 mV s<sup>-1</sup>) and power density (42.2 kW kg<sup>-1</sup>) at an energy density of 10 Wh kg<sup>-1</sup>. Furthermore, they exhibit remarkable capacitance retention of ~88% after 10,000 cycles at very high current density of 20 A g<sup>-1</sup>, superior to that of pristine PAni based pseudocapacitors. This prominently enhanced electrochemical stability successfully demonstrates the buffering effect of ALD coating on PAni, which provides a new approach for the preparation of metal-oxide/conducting polymer hybrid electrodes with excellent electrochemical performance.

# Facile Fabrication of High-Performance All-Solid-State Micro-supercapacitors through Laser Micromachining

Hsin-Chieh Huang, Hsisheng Teng

*Department of Chemical Engineering and Research Center for Energy Technology and Strategy, National Cheng Kung University, Tainan 70101, Taiwan  
hteng@mail.ncku.edu.tw*

Micro-supercapacitors (MSCs) are designed and fabricated to serve as power sources or energy storage units in microelectronic devices [1]. We employed a novel approach to fabricate MSCs based on activated mesophase pitch (aMP) carbon as the active material in conjunction with laser micromachining on a substrate deposited with aMP. The aMP carbon, which contains hierarchically connected micropores and mesopores, was effective for storing charge at high rates and high voltages [2]. The in-plane interdigitated architecture of the microelectrodes obtained from laser patterning was clearly defined and the design effectively facilitated transport of electrolyte ions into carbon micropores. Electrochemical measurements indicated that the specific capacitance of the all-solid-state aMP-based MSC was  $10 \text{ F cm}^{-3}$  at  $1 \text{ V s}^{-1}$ . At a high scan rate of  $100 \text{ V s}^{-1}$ , a specific capacitance of  $2.7 \text{ F cm}^{-3}$  was recorded, which is an unprecedented performance for supercapacitors. The combination of the highly accessible area of aMP and the interdigitated in-plane design resulted in a high-frequency response of the MSCs, showing a resistive-capacitive time constant of 7 ms. These impressive performances of the MSCs indicate that the developed fabrication methods are compatible with current fabrication processes for microelectronic devices and could provide a favorable opportunity for developing various micro- and nano-sized energy devices to satisfy the requirements of portable, miniaturized electronic equipment.

## References

- [1] M. Beidaghi, Y. Gogotsi, *Energy Environ. Sci.* 7 (2014) 867.
- [2] H.C. Huang, C.W. Huang, C.T. Hsieh, H. Teng, *J. Mater. Chem. A* 2 (2014), 14963.

Acknowledgement: This research was supported by the Ministry of Science and Technology, Taiwan (MOST 103-3113-E-006-009, MOST 104-3113-E-006-005) and by the Ministry of Education, Taiwan (The Aim for the Top University Project to the National Cheng Kung University).

# Improving energy performance of electrochemical capacitors by combining redox reaction with hydrogen storage phenomena

Jakub Menzel, Krzysztof Fic, Elzbieta Frackowiak

*Institute of Chemistry and Technical Electrochemistry, Poznan University of Technology,  
Berdychowo 4, 60-965 Poznan, Poland  
[elzbieta.frackowiak@put.poznan.pl](mailto:elzbieta.frackowiak@put.poznan.pl)*

The major disadvantage of modern C/C supercapacitors is a limited energy output of 10Wh/kg for the device and a high cost of 1Wh. In order to reach the demand of market, the goal for new supercapacitors is energy density at the level of 30 Wh/kg with a cost of 1Wh lower than 1\$. The energy value of these devices is strictly related to two parameters, i.e. capacitance value and operating voltage range ( $E=0.5C \cdot V^2$ ). The capacitance of supercapacitors depends on the active surface area of electrode material, electrolyte accessibility to this surface and distance between electrodes. On the other hand, the voltage limit of these devices is strictly related to electrochemical stability window of electrolyte used. Keeping in mind only these two parameters the most preferable systems are organic ones due to a significant capacitance value ( $\sim 100$  F/g for active electrode material) and high voltage limit ( $\sim 2.7$ V for acetonitrile based electrolytes). The disadvantage of these systems is high cost of Wh/kg and usage of harmful organic solvents. The alternative for these systems might be capacitors with cheap neutral aqueous electrolytes. The advantage of such solutions are low cost, environmental friendliness and possibility of capacitance improvement by utilization of redox active species as source of pseudocapacitance. But still even with capacitance reaching  $\sim 300$  F/g such systems are characterized by relatively low energy performance due to narrow electrochemical voltage window of water; theoretically, water based electrolytes are limited to maximum 1.23V, but due to high hydrogen evolution overpotential in several electrolyte solutions it is possible to extend the maximum voltage window to 1.5V. In such condition when negative electrode reaches very low potential value one can expect hydrogen electrosorption on carbon material and increased capacitance.

This work reports on the influence of different cations attracted on the negative electrode and iodine/iodide redox shuttle operating on the positive side. It has been found that the proper separation of electrolytes for positive and negative electrode allows extension of the voltage window above 1.2V and enhancement of capacitance of negative electrode by hydrogen electrosorption/desorption reaction. Such combination of electrolytes can severely increase the energy and power performance of aqueous based capacitors.

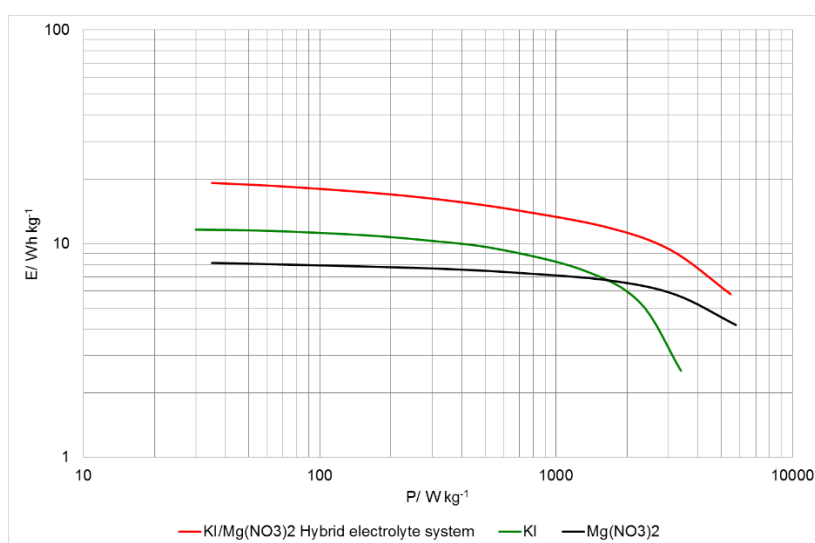


Figure1. Ragone plot for systems in different electrolytes compared to hybrid electrolyte capacitor. Energy and power values calculated only for mass of active material.

# Thermal modeling of an ultracapacitor module for automotive applications

Sung June Park<sup>1</sup>, Jaeshin Yi<sup>1</sup>, and Chee Burm Shin<sup>1\*</sup>, Kyung-Seok Min<sup>2</sup>, Jongrak Choi<sup>2</sup> and Ha-Young Lee<sup>3</sup>

<sup>1</sup>Ajou University, Department of Energy Systems Research

<sup>2</sup>Manufacturing Technology Center, LS Mtron Ltd.

<sup>3</sup>UC Team/ R&D, LS Mtron Ltd.

<sup>1</sup>Suwon 443-749, South Korea, <sup>2</sup>Gunpo 431-831 South Korea, <sup>3</sup>Anyang 431-831 South Korea  
\*cbshin@ajou.ac.kr

Ultracapacitors, also known as supercapacitors, have the potential to meet the increasing power requirements of energy-storage systems for automotive applications. As compared to batteries, ultracapacitors offer a higher power density, higher efficiency, and longer shelf and cycle life. Because the performance of an ultracapacitor depends on temperature, it is important to calculate accurately the thermal behavior of a single ultracapacitor cell and the module composed of multiple ultracapacitor cells for the efficient and reliable systems integration of an ultracapacitor in automotive applications.

In this work, modeling is performed to study the thermal behavior of an ultracapacitor module. The ultracapacitor module is subject to the charge/discharge cycling with constant-current between 1.35V and 2.7V. The validation of the modeling approach is provided through the comparison of the modeling results with the experimental measurements.

Fig. 1 shows the schematic diagram of the ultracapacitor module composed of the 18 ultracapacitor cells (3.7V/3000F) from LS Mtron Ltd. In Fig. 2, the variation of surface temperature with time from the experiment is compared with that from modeling during the charge-discharge cycles with the constant current of 200 A.

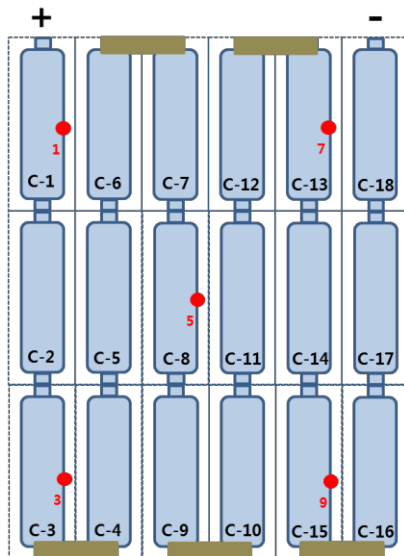


Fig.1. Schematic diagram of an ultracapacitor module.

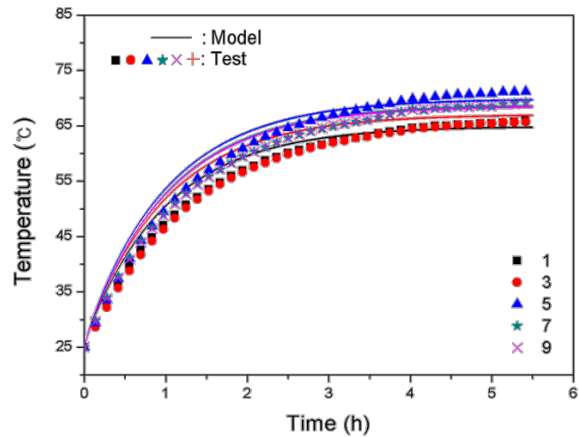


Fig. 2. Comparison between the modeling results and experimental data of the variations of surface temperature at the five different indicated in Fig. 1.



# Performance improvement of AC/AC capacitors in aqueous medium through selection of current collectors

Paula Ratajczak, Adam Ślesięński, Elżbieta Frąckowiak, François Béguin  
ICTE, Poznan University of Technology  
Berdychowo 4, 60-965, Poznan, Poland  
paula.ratajczak@doctorate.put.poznan.pl

Lately, aqueous electrolytes based on neutral alkali sulfates revealed the possibility of increasing the value of maximum cell potential, owing to a high over-potential for di-hydrogen evolution at the negative activated carbon (AC) electrode. We demonstrated that AC/AC capacitors with stainless steel current collectors in aqueous  $\text{Li}_2\text{SO}_4$  exhibit long time performance under floating up to 1.5 V [1]. Notwithstanding, for further development of these capacitors, there is still a need to explore low cost, safe and environment friendly components, while keeping optimal performance of the system.

In this study, we show that easily available and relatively cheap nickel is an alternative material to corrodible stainless steel. Another objective of the presentation is to combine the two kinds of current collectors, in their most advantageous operation conditions, in order to extend the lifetime of an AC/AC capacitor in  $\text{Li}_2\text{SO}_4$ . Cyclic voltammetry, galvanostatic cycling, electrochemical impedance spectroscopy and floating up to high cell potential have been used to detect the onset of reactions involving the electrolyte and current collectors, and thereof the performance limits of the supercapacitors. The time constants of 0.46 s and 0.57 s for the cells with nickel (-)/nickel (+) and nickel (-)/steel (+) configurations, respectively, reveal a favourable impact of nickel on the dynamics of charge exchange in the cell, when compared to 0.80 s with steel (-)/steel (+) configuration. Moreover, the size of the high-frequency semi-circle in Figure 1a reveals that the supercapacitor with combined collectors presents the lowest charge transfer resistance value (0.94  $\Omega$ ), when compared to 1.1  $\Omega$  and 1.24  $\Omega$  for nickel (-)/nickel (+) and stainless steel (-)/stainless steel (+) cell, respectively. Finally, the most stable resistance values (with no corrosion of the positive current collector) during floating at 1.6 V were revealed by the cell with nickel (-)/stainless steel (+) combination of collectors, owing to -105 mV shift of the operating electrode potentials. As in the case of symmetric nickel (-)/nickel (+) cell, the performance of the asymmetric one is not much disturbed by the appearance of nickel oxidation compounds on the edges of the negative current collector, and the resistance remains stable till the end of the test (Figure 1b) [2]. The presentation will also consider the parameters which are responsible for changes of electrochemical performance when using current collectors of different thickness and diverse origin.

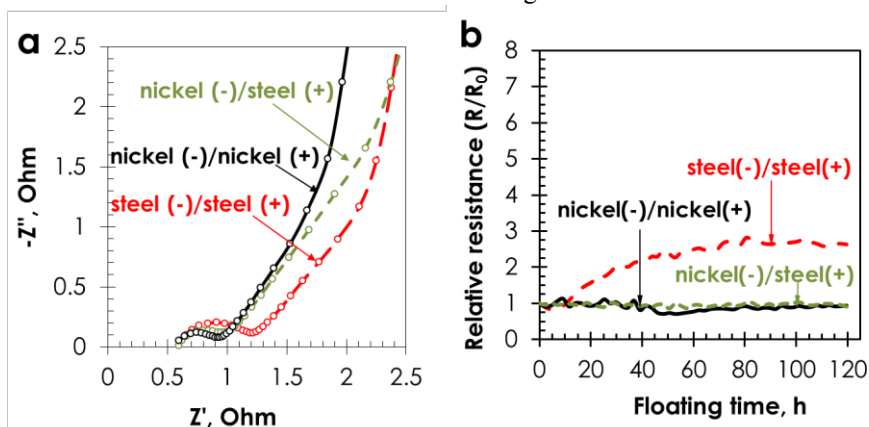


**Figure 1.** Performance of AC/AC capacitors with different couples of current collectors in 1 mol L<sup>-1</sup>  $\text{Li}_2\text{SO}_4$ : (a) Nyquist impedance plot; (b) resistance evolution during floating at 1.6 V.

## Acknowledgments

The Foundation for Polish Science (FNP) is acknowledged for funding the ECOLCAP Project realized within the WELCOME Program, co-financed from European Union Regional Development Fund.

## References

- [1] P. Ratajczak, K. Jurewicz, P. Skowron, Q. Abbas, F. Béguin, *Electrochim. Acta*, 2014, **130**, 344-350
- [2] Q. Abbas, P. Ratajczak, P. Babuchowska, A. Le Comte, D. Bélanger, T. Brousse, F. Béguin, *J. Electrochem. Soc.*, 2015, **162**, A5148-A5157.

# Optimizing the high cell potential performance of AC/AC supercapacitors based on two aqueous electrolytes

Paula Ratajczak, Piotr Gajewski, François Béguin

ICTE, Poznan University of Technology

Berdychowo 4, 60-965, Poznan, Poland

paula.ratajczak@doctorate.put.poznan.pl

In recent years, neutral aqueous electrolytes have been more and more often implemented in AC/AC electrochemical capacitors. They offer several important advantages as compared to solutions in organic solvents, such as high ionic conductivity allowing high power operation, environmental friendliness and possibility of manipulation in ambient conditions. Furthermore, as we already demonstrated, neutral 1 mol L<sup>-1</sup> Li<sub>2</sub>SO<sub>4</sub> displays good performance with stainless steel collectors under floating up to 1.5 V [1], which is more than the thermodynamic stability window of only 1.23 V in water medium. Therefore, it is interesting to search for solutions which would allow the operating cell potential to be further increased while using aqueous electrolytes.

In this context, we present a concept of AC/AC supercapacitor using two aqueous solutions of potassium hydroxide (0.5 mol L<sup>-1</sup> KOH) and sodium sulfate (1.0 mol L<sup>-1</sup> Na<sub>2</sub>SO<sub>4</sub>) as catholyte and anolyte, respectively, a cation exchange membrane as separator, and stainless steel collectors [2]. According to thermodynamic considerations, due to the pH difference between the two electrolytes (pH<sub>KOH</sub> = 13.2; pH<sub>Na2SO4</sub> = 6.6), the system is theoretically able to operate up to 1.62 V. We experimentally proved it by CVs in Figure 1a, where the curves are not featured by a current leap due to electrolyte reduction at the negative electrode and/or electrochemical oxidation of the positive carbon electrodes at the highest cell potential (1.6 V). Nevertheless, as verified by two-electrode cell experiment with reference electrode at cell potential of 1.6 V, the potential of the positive electrode exceeds the thermodynamic limit of electrolyte oxidation, while there is still some margin at the negative electrode before reaching dihydrogen evolution. An adjustment of positive and negative electrodes mass ratio (m<sub>+</sub>/m<sub>-</sub>=2.25) enables to extend the operating cell potential to 1.6 V, with E<sub>-</sub> = -0.748 V and E<sub>+</sub> = 0.852 vs NHE (Figure 1b).

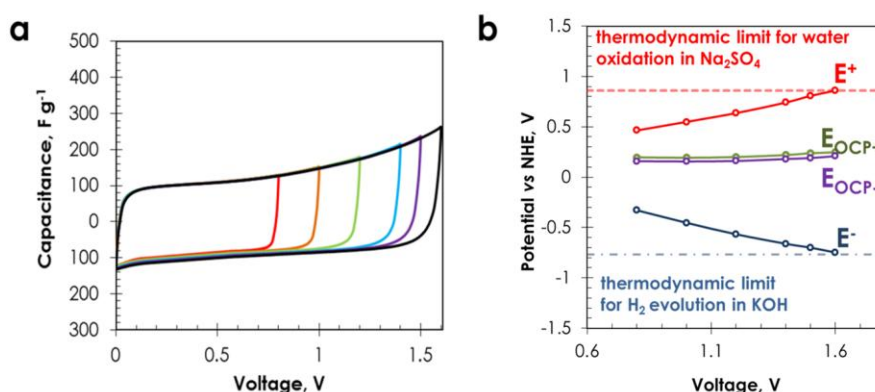


**Figure 1.** (a) CVs (0.4 mV s<sup>-1</sup>) of AC/AC supercapacitor in (-) 0.5 mol L<sup>-1</sup> KOH / 1.0 mol L<sup>-1</sup> Na<sub>2</sub>SO<sub>4</sub> (+) recorded up to 0.8, 1.0, 1.2, 1.4, 1.5 and 1.6 V; (b) electrodes potential range vs. cell potential measured during galvanostatic cycling at 40 mA g<sup>-1</sup> on a cell with unequal electrode masses (m<sub>+</sub>/m<sub>-</sub>=2.25). E<sub>OCP</sub> - open circuit potential.

Strategies to enhance the operating cell potential by optimizing the AC electrodes, the current collectors and the design of the cation exchange membrane will be presented. Electrochemical techniques will be used to detect the onset of reactions involving the electrolyte and to critically discuss the possible performance optimization of this new electrochemical capacitor generation.

## Acknowledgements

The Foundation for Polish Science (FNP) is acknowledged for funding the ECOLCAP Project realized within the WELCOME Program, co-financed from European Union Regional Development Fund.

## References

- [1] P. Ratajczak, K. Jurewicz, P. Skowron, Q. Abbas, F. Béguin, *Electrochim. Acta*, 2014, **130**, 344-350
- [2] P. Ratajczak, F. Béguin, *J. Am. Chem. Soc.*, 2015, submitted

# Activated carbon electrode expansion during EDL charging in various salt aqueous electrolytes

Paweł Jeżowski, François Béguin

Poznan University of Technology, Institute of Chemistry and Technical Electrochemistry, Berdychowo 4, 60-965 Poznan, Poland

[pawel.jezowski@put.poznan.pl](mailto:pawel.jezowski@put.poznan.pl)

In recent years, the performance of electrical double-layer capacitors (EDLCs) has been investigated in a wide range of electrolytes. Especially, it has been demonstrated that high values of working cell potential up to 1.5 - 2.0 V can be reached with AC/AC (AC = activated carbon) capacitors in aqueous alkali sulphates [1-3]. Due to the low cost and environment friendly character of these media, and the high values of energy density which could be reached after further improvements, it is of interest to understand the mechanisms of ions storage using in-situ techniques.

In-situ dilatometry has been developed lately to investigate EDL capacitors. This technique was introduced in 1982 by Biberacher et al [4] to study the expansion of electrodes during electrointercalation in layered materials using organic electrolytes. In 2006, Hahn et al were the first to apply dilatometry during charging/discharging of EDLCs in organic electrolyte, and they showed a relatively unexpected expansion of electrodes [5].

In this work, in-situ dilatometry is applied to study the expansion of activated carbon electrodes in aqueous alkali ( $\text{Li}^+$ ,  $\text{Na}^+$  and  $\text{Cs}^+$ ) sulfates. At -0.4 V vs AC reference electrode, the value of expansion reaches around 0.200  $\mu\text{m}$  for  $\text{Cs}^+$ , while for  $\text{Li}^+$  and  $\text{Na}^+$  the expansion is close to 0.150  $\mu\text{m}$ . The dramatic increase of expansion at -1.030 V vs AC reference, e.g., 1.150  $\mu\text{m}$  and 1.650  $\mu\text{m}$  for  $\text{Li}^+$  and  $\text{Cs}^+$ , respectively, might be attributed to hydrogen chemisorption in the working AC electrode, which should theoretically start to take place at ca -0.59 V vs AC reference at pH=6.5. The higher expansion in 1 mol  $\text{L}^{-1}$   $\text{Cs}_2\text{SO}_4$  as compared to 1 mol  $\text{L}^{-1}$   $\text{Li}_2\text{SO}_4$  suggests that alkali ions are stored desolvated in the porosity of AC. This interpretation will be discussed in light of complementary experiments in order to better elucidate the state of adsorbed ions.

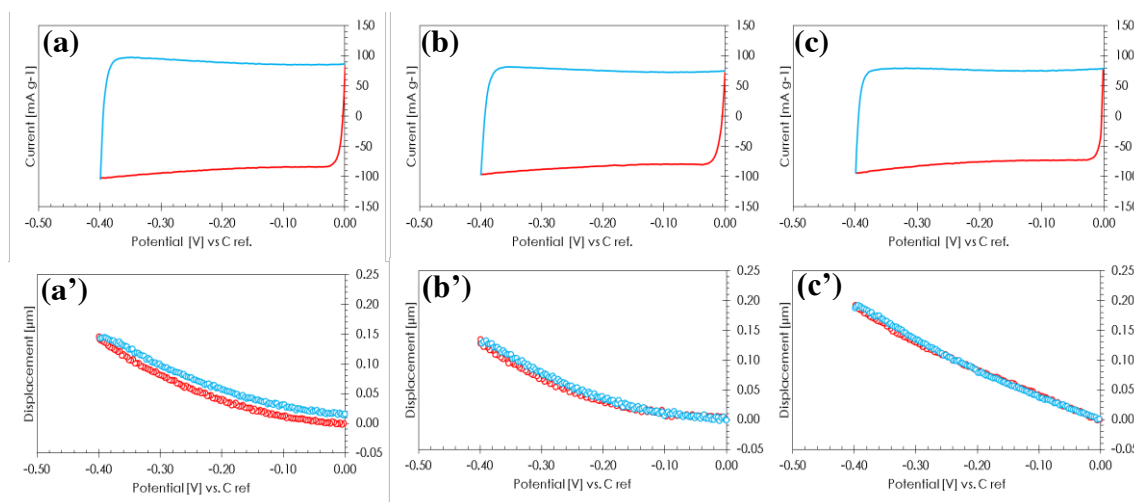


Fig. 1 Cyclic voltammograms (1  $\text{mV s}^{-1}$ ) and expansion of AC electrodes (charging – red; discharging – blue) during negative polarization scanning: (a – a') in 1 mol  $\text{L}^{-1}$   $\text{Li}_2\text{SO}_4$ , (b – b') in 1 mol  $\text{L}^{-1}$   $\text{Na}_2\text{SO}_4$ , (c – c') in 1 mol  $\text{L}^{-1}$   $\text{Cs}_2\text{SO}_4$ .

- [1] L. Demarconnay, E. Raymundo, F. Béguin, *Electrochem. Comm.* 12 (2010) 1275.
- [2] K. Fic, G. Lota, M. Meller, E. Frackowiak, *Energy Environ. Sci.* 5 (2012) 5842.
- [3] P. Ratajczak, K. Jurewicz, F. Béguin, *J. Appl. Electrochem.* 44 (2014) 475.
- [4] W. Biberacher, A. Lerf, J.O. Besenhard, H. Möhwald, T. Butz, *Mater Res Bull* 17 (1982) 1385
- [5] M.Hahn, O.Barbieri, R.Gallay, R. Kötz, *Carbon* 44 (2006) 252

# Porous Carbon Nanofiber with Phosphorus and Nitrogen Dual-Doping for High Performance Supercapacitors

Guiyin Xu, Qi Sheng, Bing Ding, Aixiu Wang, Zhi Chang and Hui Dou\*

Jiangsu Key Laboratory of Materials and Technology for Energy Conversion, College of Material Science and Engineering, Nanjing University of Aeronautics and Astronautics

Nanjing, 210016, P. R. China

\*Email: dh\_msc@nuaa.edu.cn

Supercapacitors have high power density, long cycle life, fast charge/discharge rates, and low manufacturing costs, which have been extensively used in civilian and military areas.<sup>1</sup> Carbon materials as promising electrode materials for supercapacitors show excellent electrochemical performance due to their high surface area and good electrical conductivity.<sup>2,3</sup> However, carbon-based electrode materials in supercapacitor applications offer lower specific capacitance and energy density, when compared with pseudocapacitor electrode materials such as metal oxides and conductive polymers.

In this work, phytic acid was selected as protonic acid dopant to synthesize 3D network polyaniline (PANI) nanofibers (**Figure 1**). Then, PANI nanofibers were transformed to nitrogen and phosphorus co-doped carbon nanofiber (NPCNFs) by pyrolysis and porous nitrogen and phosphorus co-doped carbon nanofibers (PNPCNFs) by chemical activation. NPCNFs have a high specific surface area, large pore volume and heteroatom doping, which could enhance the electrochemical performance for supercapacitors. Therefore, NPCNFs have a high specific capacitance of 280 F g<sup>-1</sup> measured in three-electrode system (1 A g<sup>-1</sup>) and a high energy density of 16.3 Wh kg<sup>-1</sup> measured in two-electrode system.

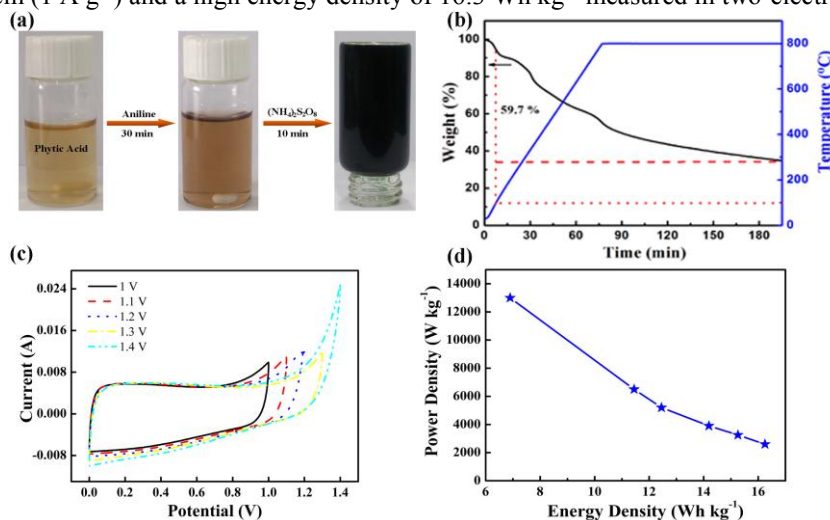


**Figure 1.** (a) Digital photographs of (left) phytic acid, (middle) aniline/phytic acid, and (right) polyaniline (PANI) nanofibers in a glass bottle. (b) TG curve of NPCNFs from the pyrolysis of PANI nanofibers under an inert atmosphere. (c, d) Cyclic voltammetry curves at 10 mV s<sup>-1</sup> and Ragone plot of symmetric capacitor based on PNPCNFs.

## References

- (1) Zhao, Y.; Hu, C.; Hu, Y.; Cheng, H.; Shi, G.; Qu, L. *Angew. Chem. Int. Ed.* **2012**, *124*, 11533-11537.
- (2) Qie, L.; Chen, W. M.; Wang, Z. H.; Shao, Q. G.; Li, X.; Yuan, L. X.; Hu, X. L.; Zhang, W. X.; Huang, Y. H. *Adv. Mater.* **2012**, *24*, 2047-2050.
- (3) Xu, G. Y.; Han, J. P.; Ding, B.; Nie, P.; Pan, J.; Dou, H.; Li, H. S.; Zhang, X. G. *Green Chem.* **2015**, *17*, 1668-1674.

# **Influence of 1,2-Dimethoxyethane Additive on the Electrochemical Characteristics of EMImTFSI Based Electrolytes for Supercapacitors**

Jaanus Eskusson, Alar Jänes, Enn Lust  
*Institute of Chemistry, University of Tartu, Estonia*  
*14a Ravila Str.*  
*Jaanus.Eskusson@ut.ee*

The electrochemical characteristics of the electrical double layer capacitors (so-called supercapacitors) consisting of the microporous titanium carbide derived carbon (TiC-CDC) electrodes and 1M  $(\text{C}_2\text{H}_5)_3\text{CH}_3\text{NBF}_4$  solutions in pure 1-Ethyl-3-methylimidazolium bis(trifluoromethylsulfonyl)imide (EMImTFSI) and mixtures with 1,2-Dimethoxyethane (by different volume ratios) based electrolytes have been studied using cyclic voltammetry and electrochemical impedance spectroscopy methods.

These systems have been selected because mentioned solvents have different relative macroscopic dielectrical permittivity ( $\epsilon$ ), different viscosities and melting temperatures as well as different dipole moment values (vertical component). The specific capacitance, phase angle and series resistance values dependent on the solvent system used have been established. It was shown that the electrolyte solution chemical composition has noticeable effect on the electrochemical characteristics calculated.

Specific conductivity and viscosity values have been obtained and compared with electrochemistry data. The region of ideal polarisability  $\Delta E \geq 3.5$  V has been achieved in all mixed electrolytes investigated. The limiting capacitance, characteristic time constant and complex power values depend noticeably on the electrolyte studied, i.e. on the viscosity and specific conductivity of electrolyte solution used.

## **Acknowledgements**

The present study was supported by the Estonian Center of Excellence in Science project 3.2.0101.11-0030, Estonian Energy Technology Program project 3.2.0501.10-0015, Material Technology Program project 3.2.1101.12-0019, Project of European Structure Funds 3.2.0601.11-0001, Estonian target research project IUT20-13, Grant ETF9184 and project 3.2.0302.10-0169.

# Holey Graphene Nanosheets with Surface Oxygen-containing Groups for High Supercapacitor Performance in Ionic Liquid Electrolyte

Cheng-Hsien Yang,<sup>1</sup> Po-Ling Huang,<sup>1</sup> Xu-Feng Luo,<sup>1</sup>

Chueh-Han Wang,<sup>1</sup> Chi Li,<sup>1</sup> Yi-Hsuan Wu,<sup>1</sup> Jeng-Kuei Chang<sup>\*,1,2,3</sup>

<sup>1</sup> Institute of Materials Science and Engineering, National Central University, Taiwan

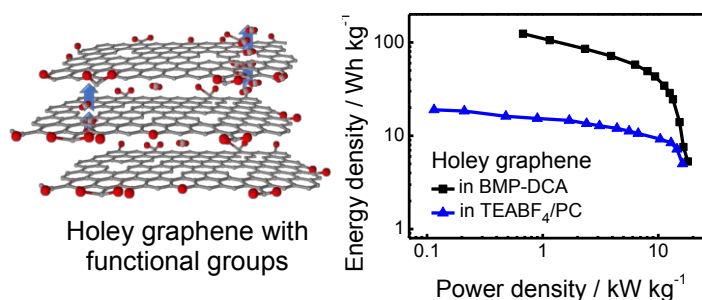
<sup>2</sup> Department of Chemical and Materials Engineering, National Central University, Taiwan

<sup>3</sup> Department of Mechanical Engineering, National Central University, Taiwan

\*300, Zhongda Rd., Zhongli District, Taoyuan City 32001, Taiwan (R.O.C.)

\*e-mail address-[jkchang@ncu.edu.tw](mailto:jkchang@ncu.edu.tw)

**Abstract:** Pores and surface functional groups are created on graphene nanosheets (GNSs) to improve supercapacitor properties in a butylmethylpyrrolidinium-dicyanamide (BMP-DCA) ionic liquid (IL) electrolyte. The GNS electrode exhibits an optimal capacitance of 330 F g<sup>-1</sup> and a satisfactory rate capability within a wide potential range of 3.3 V at 25 °C. Pseudocapacitive effects are confirmed using X-ray photoelectron spectroscopy. Under the same conditions, carbon nanotube and activated carbon electrodes show capacitances of 80 and 81 F g<sup>-1</sup>, respectively. Increasing the operation temperature increases the conductivity and decreases the viscosity of the IL electrolyte, further improving cell performance. At 60 °C, a symmetric-electrode GNS supercapacitor with the IL electrolyte is able to deliver maximum energy and power densities of 140 Wh kg<sup>-1</sup> and 52.5 kW kg<sup>-1</sup> (based on the active material on both electrodes), respectively, which are much higher than the 20 Wh kg<sup>-1</sup> and 17.8 kW kg<sup>-1</sup> obtained for a control cell with a conventional organic electrolyte.



# Electrochemical Performance of Nitrogen Doped Nano-channel Carbon Structures in Redox Electrolyte Supported Supercapacitor.

Prakash Ramakrishnan, Sangaraju shanmugam\*

*Department of Energy Systems Engineering,  
Daegu Gyeongbuk Institute of Science & Technology (DGIST),  
Daegu, 711-873, Republic of Korea*

*\*sangarajus@dgist.ac.kr*

Over the past few decades, great interest has been devoted on porous carbon materials in energy storage and conversion devices, and gas sorbent applications owing to their cost-effectiveness, tunable microstructure, at ease of availability and surface functionalization [1]. Particularly in supercapacitor (SCs) energy storage system, as it stores energy by electrostatic interaction between electrode-electrolyte interfaces based on the Electrical double layer phenomenon, so the amount of charge stored directly dependent on the surface area of any electrode material [2]. Thus, Porous carbon material being considered as the potential electrode material for SC owing to large surface area, chemical stability and low cost [3]. A large variety of porous carbons of different dimensions have been studied as SC electrode materials. However, many of them showed disadvantages such as the high ionic resistance, low electrical conductivity and low compatibility of conductive pathways to store charge, which unfavorable for high energy storage and high power devices criteria. So the performance of SCs not only depends on the physical, but also intimately on the chemical properties of the electrode material. Alternately, the polarization of surface functional groups on carbon materials would indeed enhance the wettability in aqueous medium and decrease the necessity of high surface area or high porosity of electrode materials. However, instabilities of these surface functionalities matters the prolong life time of SCs [4]. Recently, several research groups have focused on adding electrochemically active species or mediators such as phenylenediamine, quinones, halides, transition metal sulfate in aqueous medium, so called redox active electrolytes (RAE), to enhance the energy storage in SCs. However, the irreversibility of RAE for long time and high self-discharge rate in the aqueous electrolyte are of major concerns for commercial realization. The above mentioned issues are addressed in our present study. We developed novel nano-channel carbon structures and utilized in optimized RAE, hydroquinone, mediated electrolyte system. The electrochemical performance in two electrode system showed excellent supercapacitor performance in terms of energy storage ( $22 \text{ Wh kg}^{-1}$ ), pro-long cycle life (15000 cycles), and self-discharge (10 hours).

## References:

- (1). A. S. Arico, B. Scrosati, J. M. Tarascon, W. Van Schalkwijk, Nat. Mater. 4 (2005) 366-377.
- (2). R. Kotz, M. Carlen, Electrochim. Acta., 45, 2483 (2000).
- (3). E. Frackowiak, F. Be'guin, Carbon 39 (2001) 937-950.
- (4). D. Hulicova, M. Kodama, H. Hatori, Chem. Mater. 18 (2006) 2318-2326.



# Hydrothermally Prepared Reduced Graphene Oxide and Manganese Oxide Nano Rod Composite Materials for Supercapacitor Applications

A.K.Satpati\* and M. K. Dey

Analytical Chemistry Division,

Bhabha Atomic Research Centre

Trombay, Mumbai-400085, India

\*Corresponding author: [asatpati@barc.gov.in](mailto:asatpati@barc.gov.in)

## Abstract

Supercapacitors are the energy storage devices having superior power density than battery and recently developed materials have improved the energy density to compete with battery. In addition to that supercapacitors have high cycle life and very high dynamic charge propagation [1]. Metal oxides are the recent materials of interest due to their high capacitance and fast redox response. Among the metal oxides, manganese oxides ( $\text{MnO}_2$ ) are highly favored due to its high energy density, natural friendliness and high natural abundances.

In the present investigation nano composite materials of reduced graphene oxide and  $\text{MnO}_2$  nano rods were synthesized using hydrothermal method. Graphene oxide was prepared using modified Hummers's method [2]. The as prepared graphene oxide was mixed with potassium permanganate and placed inside the Teflon lined autoclave. The mixture was treated at  $170^\circ\text{C}$  for 24 hrs, and the nano composite material was formed. X-ray diffraction analysis has revealed the formation of  $\text{MnO}_2$ . Atomic Force microscopy (AFM) measurements as shown in Fig. 1 A have detected the formation of graphene sheets, the thickness of the grapheme sheets were obtained around 1.1 nm. Scanning electron microscopy (SEM) of the nano composite material has shown that the graphene sheets were well embedded with  $\text{MnO}_2$  nano rods, as shown in Fig.1 B.

Electrochemical measurements were carried out by recording the cyclic voltammetry, electrochemical impedance and the charge discharge measurements in 0.5 M  $\text{Na}_2\text{SO}_4$  solution. The materials remained stable in continuous cyclic voltammetry measurements. Strong contribution of the Warburg parameter in Nyquist plot of the electrochemical impedance measurement has revealed diffusion of charged species inside the porous structure of the composite material. The charge discharge property of the materials is shown in Fig. 1 C. Stable charge discharge characteristics were obtained for the experiments carried out up to 400 cycles. The redox property was reversible with no signature of material degradation due to the redox reaction was observed. The discharge specific capacitance of  $650\text{ Fg}^{-1}$  was observed at the discharge current density of  $2\text{ Ag}^{-1}$ . Manganese oxide nano composite material exhibits the supercapacitor property by insertion/deinsertion of proton and alkali metal ions in acidic and alkaline solution respectively during the charge-discharge cycle [2]. Current mapping of the substrate using scanning electrochemical microscopy (SECM) has detected the high capacitance of the substrate. SECM approach curves have shifted from negative feedback to positive feedback response at different levels of charging of the capacitor.

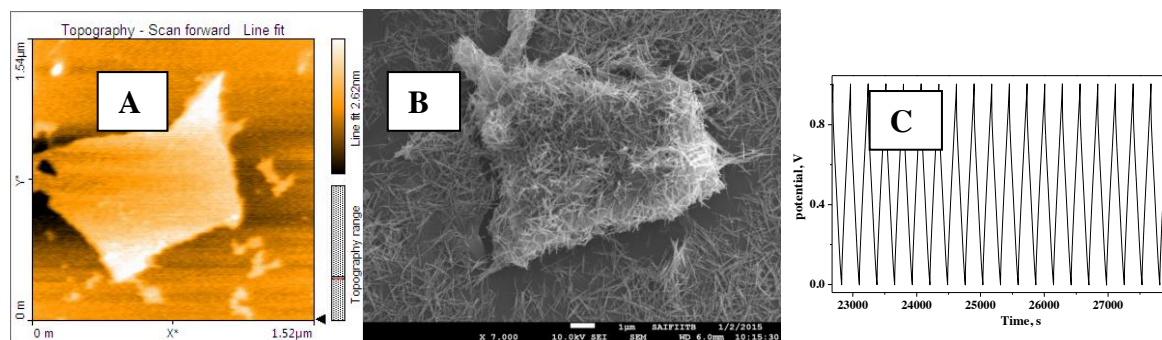


Figure 1 (A) AFM topograph of the  $\text{MnO}_2$  deposits (B) SEM micrograph (C) Charge discharge cycle of the  $\text{MnO}_2$ /graphene oxide nano composite material.

A comprehensive report about the characterization of the deposits, their supercapacitor behavior, electrochemical mapping and the transport of charge through the deposits will be presented in the conference

## References

1. J.R. Miller, P. Simon, Science 321 (2008) 651.
2. W. S. Hummers, R. E. Offeman, Preparation of graphitic oxide. J. Am. Chem. Soc. 80 (1958) 1339-1339
3. S. Sopcic, R. Peter, M. Petravic, Z. Mandi, Journal of Power Sources 240 (2013) 252.



# Nondestructive production of magnetic graphene towards energy applications

Mahmoud Mohamed Mahmoud Ahmed,<sup>1</sup> Masaki Ujihara<sup>1</sup> and Toyoko Imae<sup>1,2</sup>

<sup>1</sup> Graduate Institute of Applied Science and Technology, National Taiwan University of Science and Technology, 43 Section 4, Keelung Road, Taipei 10607, Taiwan

<sup>2</sup> Department of Chemical Engineering, National Taiwan University of Science and Technology, 43 Section 4, Keelung Road, Taipei 10607, Taiwan.

E-mail: D10222802@mail.ntust.edu.tw, web site: <http://imaelab.jpn.org/>

Graphene can be prepared from a graphite intercalation compound (GIC)<sup>1</sup> with acceptor-type intercalator, FeCl<sub>3</sub>.<sup>2</sup> When the FeCl<sub>3</sub>-GIC is treated with primary amines at 90 °C for 6 h, the GIC expands to a few layers.<sup>3</sup> The expansion is further facilitated, as the alkyl chain of primary amines becomes longer, while tertiary amines cannot penetrate inside the GIC because of their structural steric hindrance. The primary amine adsorbed in the GIC is oriented to form a bilayer by an indirect reactions among FeCl<sub>3</sub>-graphene-amine, and this process plays an important role in the expansion of the GIC, in contrast to the reaction of primary amines with donor-type GICs.<sup>4</sup> Then the expanded-GIC is sonicated to exfoliate the graphene sheets. The obtained material exhibited a superparamagnetic property due to the remaining iron compounds. This approach using FeCl<sub>3</sub>-GIC and primary amine is preferable for the mass production of graphene because of the mild reaction conditions and the short treatment time for exfoliation from the chemically stable FeCl<sub>3</sub>-GIC. Moreover, the magnetization of graphene nano-composites could be useful for magnetic-recovery processes, electromagnetic heating, and the other electrochemical applications.

## References:

1. Zhao, W.; Tan, P. H.; Liu, J.; Ferrari, A. C., Intercalation of few-layer graphite flakes with FeCl<sub>3</sub>: Raman determination of Fermi level, layer by layer decoupling, and stability. *Journal of the American Chemical Society* 2011, 133 (15), 5941-5946.
2. Zhan, D.; Sun, L.; Ni, Z. H.; Liu, L.; Fan, X. F.; Wang, Y.; Yu, T.; Lam, Y. M.; Huang, W.; Shen, Z. X., FeCl<sub>3</sub> - Based Few - Layer Graphene Intercalation Compounds: Single Linear Dispersion Electronic Band Structure and Strong Charge Transfer Doping. *Advanced Functional Materials* 2010, 20 (20), 3504-3509.
3. M. Ujihara, M. M. M. Ahmed, T. Imae and Y. Yamauchi, Massive-exfoliation of magnetic graphene from acceptor-type GIC by long-chain alkyl amine. *J. Mater. Chem. A*, 2014, (2), 4244 - 4250.
4. Maluangnont, T.; Bui, G. T.; Huntington, B. A.; Lerner, M. M., Preparation of a homologous series of graphite alkylamine intercalation compounds including an unusual parallel bilayer intercalate arrangement. *Chemistry of Materials* 2011, 23 (5), 1091-1095.

# **Improved Electrochemical Performance of Hybrid supercapacitor using highly dispersed Carbon-AlPO<sub>4</sub> binary coated H<sub>2</sub>Ti<sub>12</sub>O<sub>25</sub> as anode**

Seung-Hwan Lee, Hyeong Jong Choi , Jin Hyeon Kim, Young-Hie Lee\*  
*Department of Electronics Materials Engineering, Kwangwoon University*  
*Kwangwoon University, Wolgye 1-dong, Nowon-gu, Seoul, Korea*  
*e-mail: [inyoungezz@nate.com](mailto:inyoungezz@nate.com)*

Lithium ion secondary batteries and supercapacitors are currently being used electric vehicles and energy storage devices [1]. Lithium ion secondary batteries and supercapacitors have high energy density and power density, respectively. Hybrid supercapacitors are energy storage devices which combine respective advantages of lithium ion secondary batteries and supercapacitors. The H<sub>2</sub>Ti<sub>12</sub>O<sub>25</sub> is expected to have better electrochemical performance than Li<sub>4</sub>Ti<sub>5</sub>O<sub>12</sub> as an anode material in hybrid supercapacitors. In this paper, we designed using activated carbon (AC) as a cathode and H<sub>2</sub>Ti<sub>12</sub>O<sub>25</sub> with carbon-AlPO<sub>4</sub> binary coating as an anode. We also investigated the effects of the carbon-AlPO<sub>4</sub> binary coating on the electrical conductivity and the electrochemical performance. [2,3].

[1] K. Karthikeyana, V. Aravindanb, S.B. Leea, I.C. Janga, H.H. Lima, G.J. Parkc, M. Yoshioc, and Y.S. Leea, Journal of Alloys and Compounds, volume 504, pp. 224-227 (2010)

[2] Qiang Wang, Zhenhai Wen, and Jinghong Li, Advanced Materials Functional, volume 16, pp. 2141-2146 (2006)

[3] J. Akimoto, K. Chiba, N. Kijima, H. Hayakawa, S. Hayashi, Y. Gotoh, and Y. Idemotob, Journal of The Electrochemical Society, volume 158(5), pp. A546-A549 (2011)

# **Superior Power and Energy density based on hybrid electrodes of Activated carbon- $\text{H}_2\text{Ti}_{12}\text{O}_{25}$ anode for hybrid supercapacitor**

Esther Baek, Jeong Hyun Lee, Hong-Ki Kim, Young-Hie Lee<sup>\*</sup>  
*Department of Electronics Materials Engineering, Kwangwoon University*  
*Kwangwoon University, Wolgye 1-dong, Nowon-gu, Seoul, Korea*  
*e-mail: [best910@kw.ac.kr](mailto:best910@kw.ac.kr)*

Recently, the new energy storage device called hybrid supercapacitor has been studied to implement higher power density (than lithium secondary batteries) and energy density (supercapacitor) for EVs. The hybrid supercapacitor combining the advantage of both supercapacitors and lithium secondary batteries has been studied by many researchers. We proposed the combination of activated carbon as cathode,  $\text{H}_2\text{Ti}_{12}\text{O}_{25}$  (HTO) as anode by previous study [1, 2]. The HTO has flat potential plateau at approximately 1.55V and capacity of 236mAh/g [3]. In this study, to improve power and energy density [4], we fabricated hybrid supercapacitor using hybrid anode of Activated carbon- $\text{H}_2\text{Ti}_{12}\text{O}_{25}$  materials and activated carbon as a cathode.

- [1] S. H. Lee, H. K. Kim, J. H. Lee, S. G. Lee, Y. H. Lee, *Mater. Lett.* 143, pp. 101-104 (2015)
- [2] S. H. Lee, S. G. Lee, J. R. Yoon, H. K. Kim, *J. Power Sources* 279, pp. 839-843 (2015)
- [3] J. Akimoto, K. Chiba, N. Kijima, H. Hayakawa, S. Hayashi, Y. Gotoh, and Y. Idemoto, *Journal of The Electrochemical Society*, volume 158(5), pp. A546-A549 (2011)
- [4] H. S. Choi, J. H. Im, T. H. Kim, J. H. Park, C. R. Park, *J. Mater. Chem.*, 22, pp. 16986-16993 (2012)

# Pulse Electropolymerization Synthesis of Polypyrrole Layers on Multiwalled Carbon Nanotubes coated Cotton Fabrics

Caihong Liu, Yaping Zhao, Hangyue Zhu, Hong Zhao, Zaisheng Cai  
*College of Chemistry, Chemical Engineering & Biotechnology, Donghua University, Shanghai, China*  
E-mail address: [zhaoyaping@dhu.edu.cn](mailto:zhaoyaping@dhu.edu.cn)

With the development of portable wearable electronics, flexible energy materials are being paid more and more attention. Cotton fabric, one of the most common materials in the textile industry, with a hierarchical structure and hydrophilic functional groups such as hydroxyl groups, has been employed as a substrate in flexible electrodes in order to reduce the weight of the substrate and boost the specific surface of the active material<sup>[1-3]</sup>. In this work, a new in-situ preparation method of flexible electrode materials is exploited, using a pulse electropolymerization technique is used to fabricate micrometre particles of polypyrrole (PPy) on conductive cotton fabrics, which is pre-coated with multiwalled carbon nanotubes (MWNT) by a 'dip and dry' method, from an aqueous solution containing cetyltrimethyl ammonium bromide (CTAB) and potassium chloride (KCl) without using any chemical additives. The conductivity of PPy@MWNT/Cotton is controlled by changing the applied voltage, pulse duration and pulse cycle. The obtained fabrics are characterized by fourier transform infrared spectroscopy (FTIR), X-ray powder diffraction (XRD) and scanning electron microscopy (SEM), and the electrochemical properties are examined by cyclic voltammetry, charge/discharge analysis. The cyclic voltammetry test further reveals that the fabric electrodes showed a specific capacitance of  $180 \text{ F} \cdot \text{g}^{-1}$  and good cycling performance (exceeding 90 % capacitance retention after 1000 cycles) in aqueous electrolyte. The developed method is simple and can be directly applied in natural fiber, which has good prospects for developing flexible electrode materials.

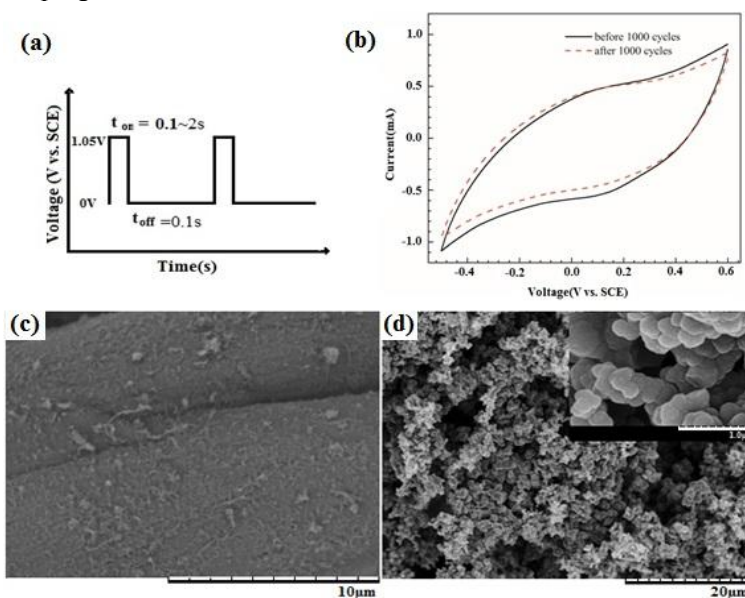


**Fig.1** (a) a description of the employed pulse voltages for the electrochemical polymerization of pyrrole; (b) CVs of PPy@MWNT/Cotton obtained by pulse electropolymerization before and after 1000 cycles in 1 M NaCl aqueous solution. Scan rate:  $5 \text{ mV s}^{-1}$ ; SEM images of (c) MWNT/Cotton and (d) PPy@MWNT/Cotton fabrics (higher magnification on the right)

This work was financially supported by the National Natural Science Foundation of China (51303022) and the Fundamental Research Funds for the Central Universities (2232015D3-17).

## References

- [1] K. Jos, Carlos R. Perez, John K. McDonough, *Energy & Environmental Science* 12 (2011) 5060.
- [2] S. P. Bharath, J. Manjanna, A. Javeed, *Bulletin of Materials Science* 1 (2015) 169.
- [3] J. Xu, D. Wang, Y. Yuan, *Cellulose* 2 (2015) 1355.

# Li<sub>4</sub>Ti<sub>5</sub>O<sub>12</sub> / Activated Carbon Hybrid Capacitor for High Voltage Operation

Tsukasa Ueda,<sup>1</sup> Kenji Oshima,<sup>1</sup> Natsuki Miyashita,<sup>1</sup> Shinichi Seto,<sup>1</sup> Etsuro Iwama,<sup>1</sup>  
Wako Naoi,<sup>2,3</sup> and Katsuhiko Naoi,<sup>1,2,3,\*</sup>

<sup>1</sup> Department of Applied Chemistry, Tokyo Univ. of Agriculture & Technology,  
2-24-16 Naka-cho, Koganei, Tokyo 184-8588, Japan

<sup>2</sup> Division of Arts & Sciences, K & W Inc., 1-3-16-901 Higashi, Kunitachi, Tokyo 186-0002, Japan

<sup>3</sup> Advanced Capacitor Research Center, Tokyo Univ. of Agriculture & Technology,  
2-24-16 Naka-cho, Koganei, Tokyo 184-8588, Japan

\* E-mail: k-naoi@cc.tuat.ac.jp

Hybrid-capacitor systems have been enthusiastically developed in order to augment the energy density of conventional electric double layer capacitor systems [1-2]. One of the representative cases is the combination of a negative electrode with faradic Li-intercalation (e.g., Li<sub>4</sub>Ti<sub>5</sub>O<sub>12</sub> (LTO)) and a positive electrode with non-faradic anion adsorption (e.g., activated carbon (AC)), used in lithium-based electrolytes (e.g., lithium tetrafluoroborate (LiBF<sub>4</sub>) dissolved in propylene carbonate (PC)). So far, the operating voltage of LTO/AC hybrid capacitors using PC-based electrolyte systems has been limited to 3.0 V, although the energy density of the hybrid capacitor can be easily increased with an increment of its operating voltage [3]. Previously, the degradation mechanism for LTO/AC system over 3.0 V was investigated; especially focusing on the electrochemical behaviour at the LTO / electrolyte interface [4]. Summarized results suggest that the degradation over 3.0 V is mainly due to the H<sub>2</sub>-based gas evolution resulted from the reduced decomposition of PC on LTO surface.

In this report, based on the elucidated degradation mechanism, linear sulfones were tested as high-withstand-voltage solvents and the potential replacement of PC. The LTO / AC cells were assembled as various forms (coin cell, H-type cell, laminate cell and also three electrode cells using a lithium metal reference) depending on a purpose, in 1 M LiBF<sub>4</sub> / PC or 1 M LiBF<sub>4</sub> / ethyl isopropyl sulfone (EiPS [5], Fig.1). Float durability tests were performed on the cells at 3.5 V. After aging tests, we analyzed the gaseous products of the cells by gas chromatography. Among tested samples, the system using EiPS showed the most promising performances. The EiPS system showed the stable electrochemical performance even at the high cell voltage of 3.5 V with significant suppression of the evolved gas volume (Fig.1). The EiPS system is indicated the excellent cycleability, maintaining 95 % of the initial capacity over 1000 cycles (Fig.2).

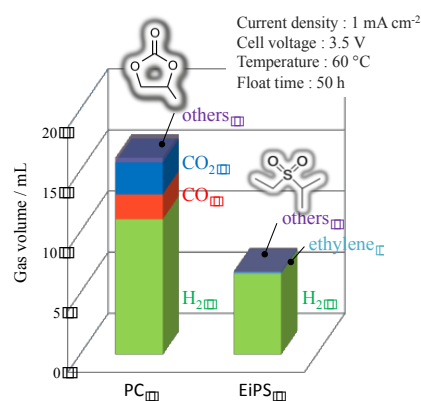


Fig.1 The amount of generated gas after float durability tests at 3.5V.

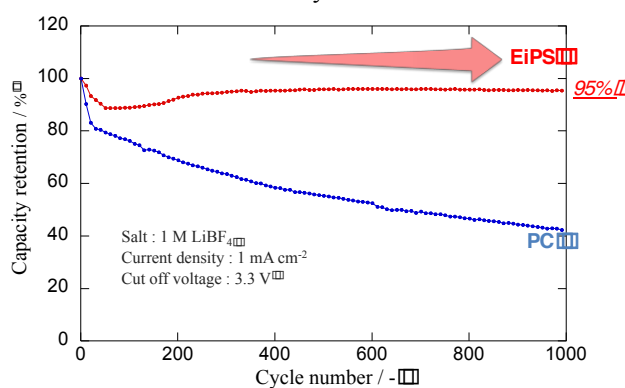


Fig.2 Results of Charge-Discharge cycle tests for LTO / AC cells using PC system and EiPS system

## References

- [1] G. G. Amatucci et al., J. Electrochem. Soc., 2001, 148, A930.
- [2] K. Chiba et al., J. Electrochem. Soc., 2011, 158, A1320.
- [3] J. J. Yang et al., Electrochim. Acta, 2012, 86, 277.
- [4] K. Oshima et al., the 7th Asian Conference on Electrochemical Power Sources (ACEPS), Osaka, 2013, 2P-33.
- [5] K. Chiba et al., J. Electrochem. Soc., 2011, 158, A872.

# Detailed Analysis on Carbon-Nested Ultrafast nano-LiFePO<sub>4</sub> Prepared by Means of Ultracentrifugation for Hybrid EES

Kazuaki Kisu<sup>1</sup>, Shota Nakashima<sup>1</sup>, Yuki Sakai<sup>1</sup>, Etsuro Iwama<sup>1</sup>, Yuki Orikasa<sup>2</sup>, Patrick Rozier<sup>3</sup>,  
Wako Naoi<sup>4</sup>, Patrice Simon,<sup>3</sup> and Katsuhiko Naoi<sup>1,4,5</sup>

<sup>1</sup> Department of Applied Chemistry, Tokyo University of Agriculture & Technology, 2-24-16 Naka-cho,  
Koganei, 184-8588, Tokyo Japan

<sup>2</sup> Graduate School of Human and Environment Studies, Kyoto University, Yoshida-nihonmatsu-cho,  
Sakyo-ku, Kyoto 606-8501, Japan

<sup>3</sup> University of Toulouse III Paul Sabatier, CIRIMAT-CNRS UMR 5085, 118 route de Narbonne, F-31602  
Toulouse Cedex 9, France

<sup>4</sup> Division of Arts and Sciences, K & W Inc., 1-3-16-901 Higashi, Kunitachi, Tokyo 186-0002, Japan

<sup>5</sup> Advanced Capacitor Research Center, Tokyo University of Agriculture & Technology,  
2-24-16 Naka-cho, Koganei, Tokyo 184-8588, Japan

\*E-mail: k-naoi@cc.tuat.ac.jp

Phosphate cathode materials such as LiFePO<sub>4</sub> (LFP), LiMnPO<sub>4</sub> (LMP), and Li<sub>3</sub>V<sub>2</sub>(PO<sub>4</sub>)<sub>3</sub> (LVP) have been regarded as attractive active materials for hybrid electrical energy storage (EES) system, because of their high thermal stability and superior safety properties provided by the stable (PO<sub>4</sub>)<sup>3-</sup> unit. In particular, phospho-olivine LFP has attracted much attention for its excellent cyclability with its decent theoretical capacity of 170 mAh g<sup>-1</sup> at reaction potential of 3.4 V vs. Li/Li<sup>+</sup> [1]. However, its lithium storage performances are limited by its poor rate capability, meaning fast decay of specific capacity at high charge-discharge rate, owing to its intrinsic low electrical conductivity (10<sup>-9</sup> - 10<sup>-10</sup> Ω<sup>-1</sup> cm<sup>-1</sup>) and slow diffusion of Li<sup>+</sup> (10<sup>-14</sup> - 10<sup>-15</sup> cm<sup>2</sup> s<sup>-1</sup>) [2]. To overcome these limitations, we have proposed new concept of three - phase structure (Fig.2) containing crystalline LFP (= Core), amorphous LFP (= Shell 1), and hollow structured carbon; Ketjen Black (KB) (= Shell 2) synthesized using our original *in-situ* ultracentrifugation materials processing technology (UC process) [3]. The encapsulated crystalline and amorphous LFP nanoparticle within the KB prepared by UC-process improves the electronic conductivity and Li<sup>+</sup> diffusivity in the whole LFP/KB composites, simultaneously producing a amorphous phase of LFP in the exterior particles that acts as excellent rate performance owing to high Li-ion diffusion coefficient of LFP. Additionally, the three-layer structure induces peculiar electrochemical behavior such as the slope like charge discharge profile, indicating the existence of the solid solution dominates. This LFP/KB composite enabled a 100C rate (36 seconds) discharge with 160 mAh g<sup>-1</sup>, and 82% of capacity retention at the slowest discharge rate of 1C (Fig.2). Such an ultrafast charge-discharge performance opens the possibility of using LFP as a cathode material for ultrafast lithium ion batteries with a stable cycle performance over 2,000 cycles at a 10C rate, maintaining 90% of the initial capacity.

## Reference

- [1] A. K. Padhi, *et al.*, J. Electrochem. Soc., 1997, 144, 1188-1194.
- [2] G. Kobayashi, *et al.*, Adv. Funct. Mater., 2009, 19, 395-403.
- [3] K. Naoi, *et al.*, J. Electrochem. Soc., 2015, 162 (6), A1-A7.

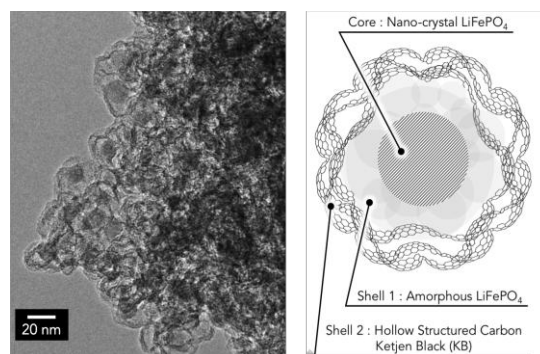


Fig.1 HRTEM image of the LFP/KB composites to observe all over the composite structure, and schematic illustration.

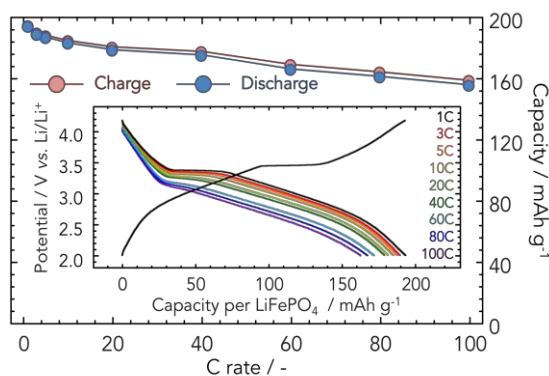


Fig.2 Plots of discharge capacity vs. C-rates for charge and discharge side. Charge-discharge profiles of the LFP/KB composite at different discharge C-rates from 1 to 100 C as an inset.

# 4V-rated “Nanohybrid Supercapacitor” utilizing Ultrafast b-axis-controlled TiO<sub>2</sub> (B) Nanocrystals

Shintaro Aoyagi,<sup>1)</sup> Takumi Furuhashi,<sup>1)</sup> Yuta Abe,<sup>1)</sup> Keita Okazaki,<sup>1)</sup> Junichi Miyamoto,<sup>1)</sup> Etsuro Iwama,<sup>1)</sup> Wako Naoi,<sup>2),3)</sup> and Katsuhiko Naoi<sup>1), 2), 3)\*</sup>

<sup>1)</sup>Department of Applied Chemistry, Tokyo Univ. of Agriculture & Technology, 2-24-16 Naka-cho, Koganei, Tokyo 184-8588, Japan

<sup>2)</sup>Division of Arts & Sciences, K & W Inc., 1-3-16-901 Higashi, Kunitachi, Tokyo 186-0002, Japan

<sup>3)</sup>Advanced Capacitor Research Center, Tokyo Univ. of Agriculture & Technology, 2-24-16 Naka-cho, Koganei, Tokyo 184-8588, Japan

\*E-mail: k-naoi@cc.tuat.ac.jp

The commercial pursuit of hybrid (asymmetric) capacitor systems has been gradually increasing for the applications such as a system stabilizer of microgrid system, uninterruptible power supply (UPS), and energy storage of compact electric vehicles. A next-generation capacitor; Nano-hybrid capacitor (NHC), comprising nanocrystalline lithium titanate (LTO) grafted on carbon nanofiber for negative and activate carbon (AC) for positive electrodes, has achieved 3 times higher energy density than that of conventional EDLC, while maintaining the power density of EDLC [1]. Establishment of LTO-NHC mass production technology is scheduled to 2017-2018 [2]. Next step is to increase the energy density of the LTO-NHC system without sacrificing its high performance and reliability. One approach is to replace LTO anode by alternative materials with higher theoretical capacity (LTO = 175 mAh g<sup>-1</sup>). Bronze-typed TiO<sub>2</sub> (TiO<sub>2</sub>(B)) has attracted much attention for such an application because of its high theoretical capacity (335 mAh g<sup>-1</sup>) and the safe redox potential of 1.6 V vs. Li/Li<sup>+</sup>. Using the combination of our original ultracentrifugation (UC) treatment and hydrothermal treatment, nano-rectangular TiO<sub>2</sub>(B) (4-7 nm) has been successfully synthesized with the existence of nano carbons (e.g., single-walled carbon nanotubes (SWCNT), multi-walled CNTs (MWCNT), and Ketjen Black (KB)). The UC-treated TiO<sub>2</sub>(B) has the minimized *b*-axis length (4 nm) as small as previous reports [3], while our nanocrystalline(nc)-TiO<sub>2</sub>(B) is highly dispersed and directly attached on the surface of nanocarbons owing to our *in-situ* synthesis method. The UC-HT TiO<sub>2</sub>(B)/nanocarbon composite electrodes showed an excellent electrochemical performance; the high capacity of 236 mAh g<sup>-1</sup> per TiO<sub>2</sub>(B) at an ultra high rate of 300C (in case of MWCNT). Electrochemical performances of new-class hybrid capacitors based on the UC-treated TiO<sub>2</sub>(B) will be also presented. TiO<sub>2</sub>(B)-NHC, comprising a negative electrode of ultrafast nc-TiO<sub>2</sub>(B)/nanocarbon and a positive electrode of Super-Growth (single-walled) Carbon Nanotube (SGCNT) may enlarge the operation voltage of the NHC from 2.75 V (LTO-NHC) to 3.5-4.0 V (TiO<sub>2</sub>(B)-NHC), increasing the energy density of the device to 1.3-1.7 times of LTO-NHC.

## References

- [1] K. Naoi *et al.*, *Energy & Environ. Sci.*, 2012, **5**, 9363.
- [2] Nippon Chemi-Con announces: The advanced new technology Nano-hybrid Capacitor (<http://www.chemi-con.co.jp/e/company/pdf/20100326-1.pdf>)
- [3] a) M. Kobayashi *et al.*, *Chem. Mater.*, 2007, **19**, 5373.; b) A. R. Armstrong *et al.*, *Chem. Mater.*, 2010, **22**, 6426.; c) Y. Ren *et al.*, *Angewandte. Chem. Int. Ed.*, 2012, **51**, 2164.

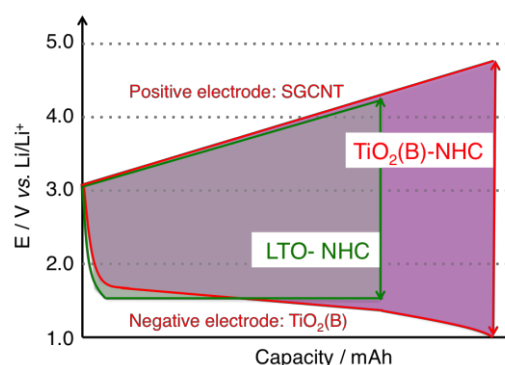


**Figure 1:** Comparison of potential-capacity curves between TiO<sub>2</sub>(B)-NHC (red) and LTO-NHC (green) systems.



# Criteria of Activated Carbon Electrical Double- Layer Capacitors in Propylene Carbonate- Based Electrolyte

Hsiao Hsuan Shen, Chi Chang Hu\*

*Department of Chemical Engineering, Tsing Hua University, Hsin Chu, TAIWAN*

*Address : No. 101, Section 2, Kuang-Fu Road, Hsinchu, Taiwan 30013, R.O.C.*

*Email: realseadog71@hotmail.com*

*\*Corresponding author, Email: cchu@che.nthu.edu.tw*

This study demonstrates the criteria for the operated potential window in activated carbon based electrical double-layer capacitors (EDLCs) in organic electrolyte. In this work, we utilize the floating test for 3000s to define the operated potential window at the beginning. The results from floating test simply show the potential window from - 2.1 V to 0.3 V against Ag / AgNO<sub>3</sub> is the proper potential window. Moreover, a negative activated carbon electrode (- 2.1 V) and a positive activated carbon electrode (0.3 V) are assembled in a 2.4 V symmetric cell. A symmetric cell charge- discharge 1152 cycles and the times of cycles are equal to have floating test 9hr. After charge- discharging, the specific capacitance decay 27 % and the electrochemical impedance spectroscopic (EIS) analyses show the crucial reason in the cell. From EIS results, the resistance increase as cycle increasing. Consequently, the floating test with EIS is a suitable method to efficiently define the operated potential window. The operated potential window from - 1.9 V to 0.2 V against Ag / AgNO<sub>3</sub> is stable for charge- discharge test on critical potential ranging from 1.9 V to 2.1 V for 10000 cycles and only 8 % of specific capacitance decay. Besides, the EIS results before and after charge- discharge 10000 cycles still an ideal performance of EDLCs.

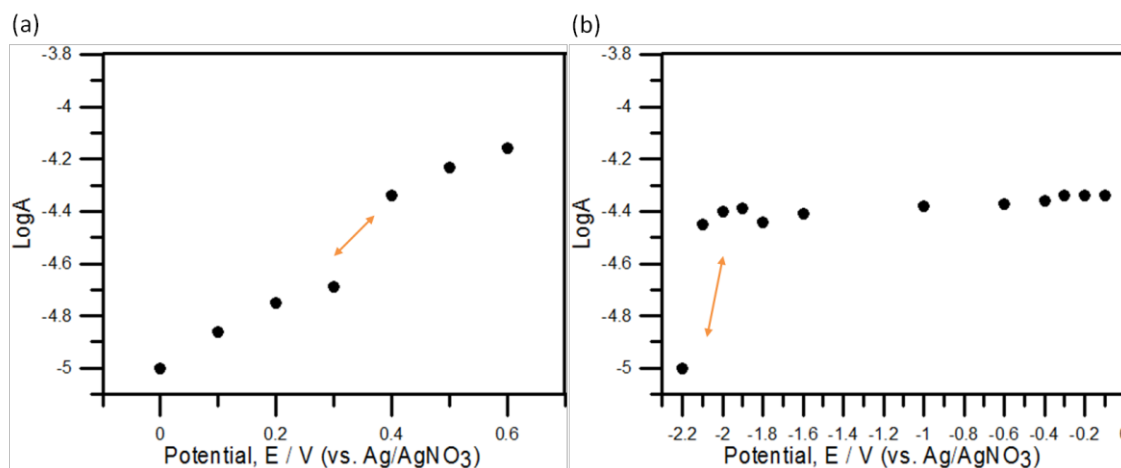


Figure 1 Log A from floating test 3000s against potential from (a) 0 V to 0.6 V and (b) - 0.1 V to - 2.2 V.



# Design and development of direct-growth in-situ doped Polypyrrole on carbon cloth as a high performance flexible supercapacitor

I. Shown<sup>1</sup>, A. Ganguly<sup>1</sup>, L. C. Chen<sup>2</sup>, K. H. Chen<sup>1,2</sup>

<sup>1</sup>*Institute of Atomic and Molecular Sciences, Academia Sinica, Taipei 10617, Taiwan.*

<sup>2</sup>*Center for Condensed Matter Sciences, National Taiwan University, Taipei 10617, Taiwan  
E-mail: [indrajit25@gmail.com](mailto:indrajit25@gmail.com)*

In the 21st century, the growing demand of the smart portable electronic gadgets, such as roll-up display, electric paper and wearable systems for smart electronics need to develop the flexible super capacitor with both high-power density and large energy density. Conducting polymers (CPs) are one of the most potential pseudo-capacitor materials for foundation of flexible-supercapacitors [1], motivating the existing energy storage devices towards the future advanced flexible electronic applications due to their high redox active specific capacitance and inherent elastic polymeric nature [2,3]. To the best of our knowledge, among conducting polymers, polypyrrole have shows better elasticity and conductivity than the polyaniline. To solve the flexibility of the stretchable supercapacitor, in this work, polypyrrole directly grown on the carbon cloth (CC) as electrodes for flexible supercapacitor. The electro deposition allowed well uniform deposition of polypyrrole coating on the carbon cloth current collector, thus offering a lower internal resistance for the novel direct growth binder free flexible electrode for supercapacitor application. The chemical composition and structural morphology of the electropolymerized polypyrrole with various inorganic dopants are characterized by Raman spectroscopy and scanning electron microscopy (SEM). The electrochemical performance of the fabricated electrodes was evaluated by cyclic voltammetry (CV), galvanostatic charge-discharge and electrochemical impedance spectroscopy (EIS). The high gravimetric capacitance of around 1100 F g<sup>-1</sup> per active mass of the polypyrrole has been achieved. These results clearly present a cost-effective and simple fabrication method of the polymers with enormous potential in flexible energy storage device applications. The detail electropolymerisation process and in-situ doping with various dopants and their electrochemical pseudo-capacitance performance with porosity and diffusion length study will be presented.

[1] I. Shown, A. Ganguly, L.C. Chen, K.H. Chen, Conducting polymer-based flexible supercapacitor, *Energy Science and Engineering*, 3 (2015) 2.

[2] Y.Y. Horng, Y.C. Lu, Y.K. Hsu, C.C. Chen, L.C. Chen, K.H. Chen, Flexible supercapacitor based on polyaniline nanowires/carbon cloth with both high gravimetric and area-normalized capacitance, *Journal of Power Sources*. 195 (2010) 4418.

[3] Y.K. Hsu, Y.C. Chen, Y.G. Lin, L.C. Chen, K.H. Chen, Direct-growth of poly (3,4-ethylenedioxythiophene) nanowires/carbon cloth as hierarchical supercapacitor electrode in neutral aqueous solution, *Journal of Power Sources*, 242 (2013) 718.

# An Energy Enhanced, Long-Life Supercabattery Based on High Discharge Efficiency Hybrid Electrodes

Yu-Wei Lin, Jun-Long Li, Chung-Hsiang Chao, Li-Duan Tsai, Jason Fang\*

Material and Chemical Research Laboratories, Industrial Technology Research Institute, Hsinchu, TAIWAN

No. 195, Sec. 4, Chung Hsing Rd., Chutung, Hsinchu 31040, TAIWAN

jasonfang0429@itri.org.tw

A supercabattery usually consists of asymmetric electrodes (i.e., internal series or parallel hybrid) with two different types of materials: one with supercapacitor feature and the other with battery characteristics. In this work, both types of materials were utilized in one electrode, forming the hybrid with voltage compensation to further improve the energy and the discharge efficiency of the energy storage device simultaneously. The electrochemical performances of the supercabattery were characterized by cyclic voltammetry, electrochemical impedance spectra, rate charge-discharge curves, and the cycle life tests. Such energy storage device shows the maximum energy density of  $20 \text{ Wh kg}^{-1}$  and the maximum power density of  $2500 \text{ W kg}^{-1}$ , respectively. Most importantly, the specific capacitance remains more than 80 % after 10,000 cycles, indicating good cycle life due to the enhanced stability of the hybrid electrodes.

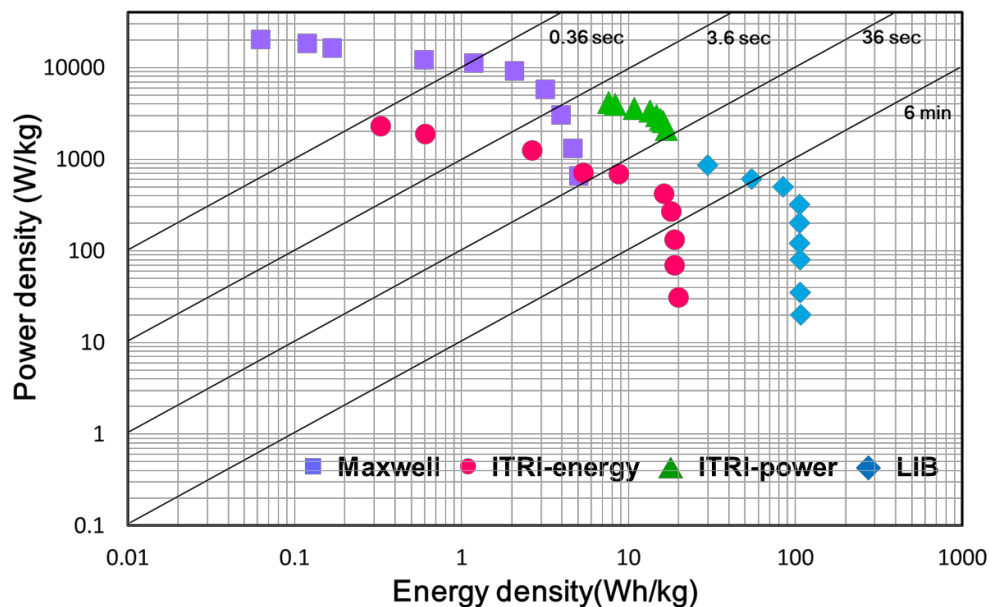


Fig. 1 . Comparison of various energy storage devices in Ragone plots

# Hydrothermal prepared Al-doped $\alpha$ -MnO<sub>2</sub> nanotube and its electrochemical performances for supercapacitors

Yang Li, Jing Li, Huaqing Xie

School of Environmental and Materials Science Engineering, College of Engineering, Shanghai Second Polytechnic University, Shanghai 201209, P. R. China  
liyang@sspu.edu.cn

$\alpha$ -MnO<sub>2</sub> and Al-doped  $\alpha$ -MnO<sub>2</sub> were synthesized via hydrothermal method. The morphologies, structures and electrochemical performances of as-synthesized un-doped and doped  $\alpha$ -MnO<sub>2</sub> were studied. As-prepared  $\alpha$ -MnO<sub>2</sub> present nanotube shape under scanning electron microscopy (SEM) and high resolution transmission electron microscopy (HRTEM). The band gaps of  $\alpha$ -MnO<sub>2</sub> are investigated by ultraviolet-visible absorption spectroscopy, which indicates that the band gap of  $\alpha$ -MnO<sub>2</sub> decreases with Al doping. The electrochemical performances of un-doped and doped  $\alpha$ -MnO<sub>2</sub> as electrode materials for supercapacitor were conducted by cyclic voltammetry and galvanostatical charge/discharge tests. The specific capacitances of un-doped and Al-doped  $\alpha$ -MnO<sub>2</sub> respectively reach 204.8 F·g<sup>-1</sup> and 228.8 F·g<sup>-1</sup> under 50 mA·g<sup>-1</sup> current density. It was discovered that the electrochemical impedance of Al-doped  $\alpha$ -MnO<sub>2</sub> was decreased via Al doping in electrochemical impedance spectra, which was beneficial to increase its electrochemical specific capacitance. Enhanced specific capacitance and preferable cycling stability up to 1000 cycles of Al-doped  $\alpha$ -MnO<sub>2</sub> present favorable prospect to be applied in supercapacitors.

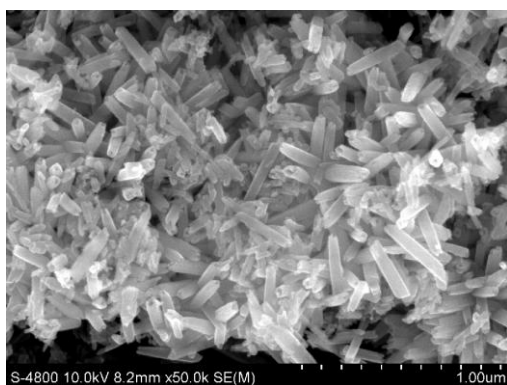


Fig.1 SEM image of as-synthesized  $\alpha$ -MnO<sub>2</sub>

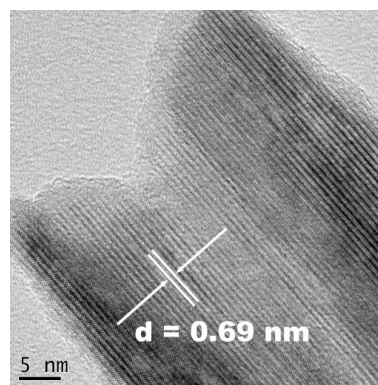


Fig.2 HRTEM image of as-synthesized  $\alpha$ -MnO<sub>2</sub>

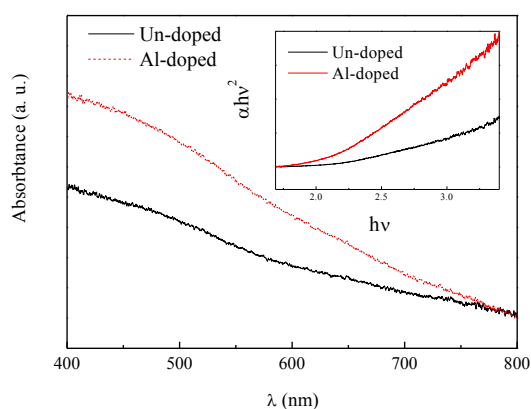


Fig.3 UV-visible spectra of as-prepared samples

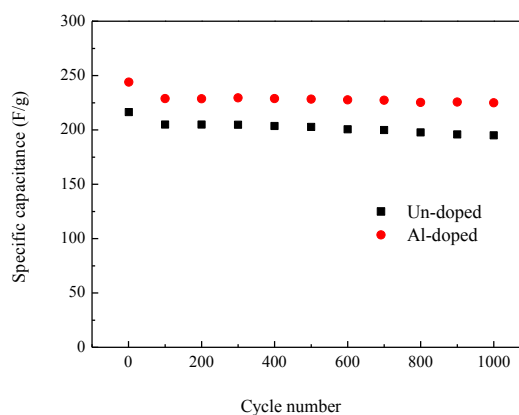


Fig.4 Cycling performances of un-doped and Al-doped  $\alpha$ -MnO<sub>2</sub>

# Enhancing Ultrahigh Loading with High Areal Specific Capacitance in Nickel–Cobalt Double Hydroxides/CNT composites for Supercapacitor Device.

Muniyandi Rajkumar, Yu-Hsuan Chou, Chi. Chang. Hu\*

*Department of Chemical Engineering, Tsing Hua University, Hsin Chu, TAIWAN*

*Address: No. 101, Section 2, Kuang-Fu Road, Hsinchu, Taiwan 30013, R.O.C.*

*Email: realeadog71@hotmail.com*

*\*Corresponding author, Email: cchu@che.nthu.edu.tw*

In this work, we have successfully synthesize  $(\text{Ni-Co})(\text{OH})_2/\text{CNT}$  electrode for high energy density supercapacitors by a facile two-step fabrication method. The contact between the double hydroxides and CNT determines the determines the specific capacitance, high-rate performance, and stability of  $(\text{Ni-Co})(\text{OH})_2/\text{CNT}$  composites when they were used as capacitive materials with high/ultrahigh material loading. To improve the contact, galvanostatic method and pulse-rest method were used to deposit the double hydroxides on the CNT and their morphologies were characterized by SEM analysis. From the SEM it clearly states that the pulse-rest method can make the hydroxides deposit more easily into the pores of CNT, which would be good for increasing the surface area of active materials rather than by galvanostatic method. Moreover, the thickness of samples made by pulse-rest method was much thinner than that made by chronopotentiometry (3  $\mu\text{m}$  for pulse-rest; 9.5  $\mu\text{m}$  for CP). In charge/discharge tests, the electrode material containing four layers of hydroxides exhibited  $3.68 \text{ F cm}^{-2}$  at  $2 \text{ A g}^{-1}$ . On the other hand, by combining with activated carbon, the asymmetric supercapacitor exhibits a cell voltage of 1.70 V, energy density of  $19.8 \text{ W h kg}^{-1}$  and power density of  $25.5 \text{ kW kg}^{-1}$  at high current density of  $30 \text{ A g}^{-1}$  respectively. Furthermore, the areal capacitance was increased by fabricating more layers of composites.

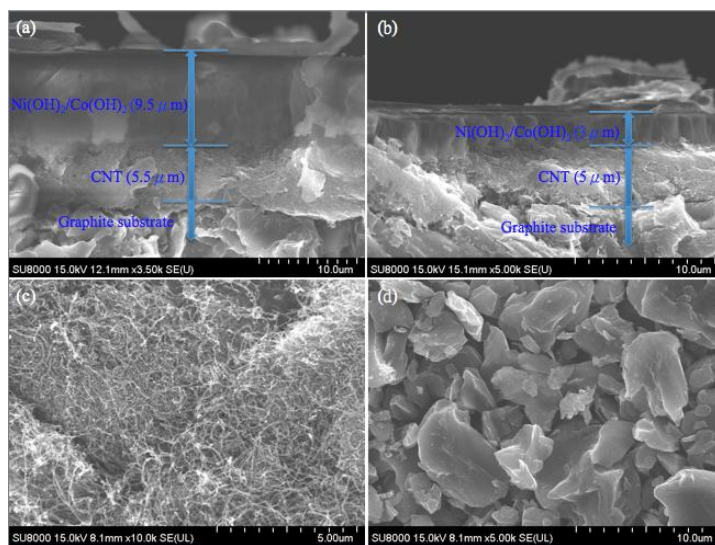


Fig.1. The SEM images of side-view of the  $(\text{Ni-Co})(\text{OH})_2/\text{CNT}$  composites deposited at (a) constant current and (b) pulse current. (c) and (d) are the SEM images of CNT and graphite substrate.

# Asymmetric Capacitors to Improve the Charge Efficiency of the Capacitive Deionization

Jianyun Liu<sup>1</sup>, Miao Lu<sup>1</sup>, Jianmao Yang<sup>2</sup>, Wenshu Cai<sup>1</sup>, Jian Cheng<sup>1</sup>, Zhubiao Xiong<sup>1</sup>

<sup>1</sup>College of Environmental Science and Engineering, State Environmental Protection Engineering Center for Pollution Treatment and Control in Textile Industry, Donghua University, 2999 North Renmin Road, Shanghai 201620, China. <sup>2</sup>Research Center for Analysis & Measurement, Donghua University, Shanghai 201620, China

E-mail address: jianyun.liu@dhu.edu.cn

Desalination is currently a very topical area of research. Capacitive deionization (CDI), as a new desalination technology, is developing very fast in recent year for developing new electrode materials and optimization of setup and operation parameters[1], because of its merits such as low energy consumption, high water recovery rate, the renewability of the electrode and easy operation with no secondary pollution due to low applied voltage [2, 3]. Activated carbon (AC), as the most commonly used commercially available and cost efficient carbon material, is still attractive as the typical CDI electrode material because of its high specific surface area, low cost, easy manufacturing on a large scale [2, 4, 5]. Charge efficiency (CE), defined as the ratio of the equivalent charge of adsorbed salt to the total charge input during charging process, is one of the most important parameters in CDI cell. The charge efficiency can be increased by membrane-based CDI cell [6, 7] or by chemical modification of electrode surface [8, 9] to diminish co-ions migration/repulsion. During the development of new electrode materials, there are still many basic concepts, such as the difference between positive electrode and negative electrode, stability of the electrode material, effect of polarization, necessary to be understood.

In this presentation, several asymmetric activated carbon composite electrode capacitors such as negatively charged sulfonated graphene(GP-SO<sub>3</sub>H), positively charged aminated graphene (GP-NH<sub>2</sub>) were reported in order to well understand the effect of the properties of positive and negative electrode materials on charge efficiency. It demonstrates that the non-membrane chemical modification on the carbon electrode materials is feasible to arrive at the high charge efficiency. Meanwhile, effect of the amphoteric metal oxides on charge efficiency was also discussed. With zinc oxide/activated carbon composite electrode (ZnO/AC) as a candidate, we explored the different function of ZnO/AC positive and negative electrode on charge efficiency by assembling the asymmetric capacitor. The mechanism was analysed based on pH variation of electrode surface and the zeta potential of ZnO. This research provides a particularly important base and guidance for the selection of electrode materials in capacitive desalination in order to realize the long term stability.

## References

- [1] Y. Oren, Capacitive deionization (CDI) for desalination and water treatment - past, present and future (a review), *Desalination*, 228 (2008) 10-29.
- [2] S. Porada, R. Zhao, A. van der Wal, V. Presser, P.M. Biesheuvel, Review on the science and technology of water desalination by capacitive deionization, *Prog. Mater. Sci.*, 58 (2013) 1388-1442.
- [3] M.A. Anderson, A.L. Cudero, J. Palma, Capacitive deionization as an electrochemical means of saving energy and delivering clean water. Comparison to present desalination practices: Will it compete?, *Electrochim Acta*, 55 (2010) 3845-3856.
- [4] L. Zou, G. Morris, D. Qi, Using activated carbon electrode in electrosorptive deionisation of brackish water, *Desalination*, 225 (2008) 329-340.
- [5] G. Wang, B. Qian, Q. Dong, J. Yang, Z. Zhao, J. Qiu, Highly mesoporous activated carbon electrode for capacitive deionization, *Separation and Purification Technology*, 103 (2013) 216-221.
- [6] R. Zhao, P.M. Biesheuvel, A. van der Wal, Energy consumption and constant current operation in membrane capacitive deionization, *Energy Environ. Sci.*, 5 (2012) 9520.
- [7] Y.J. Kim, J.H. Choi, Improvement of desalination efficiency in capacitive deionization using a carbon electrode coated with an ion-exchange polymer, *Water research*, 44 (2010) 990-996.
- [8] M. Andelman, Flow Through Capacitor basics, *Separation and Purification Technology*, 80 (2011) 262-269.
- [9] M. Lu, J.Y. Liu, J. Cheng, S.P. Wang, J.M. Yang, Functionalized Graphene/Activated Carbon Composite Electrodes for Asymmetric Capacitive Deionization, *Acta Phys-Chim Sin*, 30 (2014) 2263-2271.

# **Effects of joule-heating on the activated carbon for improved electric double layer capacitor**

Ick-Jun Kim, Sunhye Yang, Eun-Ji Oh, and Seong-Do Yun  
*Korea Electrotechnology Research Institute*  
*Changwon, 641-120, Korea*  
*ijkim@keri.re.kr*

These instructions are an example of what a properly prepared meeting abstract should look like. Proper column and margin measurements are indicated. Activated carbons have been widely used as electrode material because of their high surface area and low cost. However, EDLCs using activated carbons have been applied to the limited applications because they have lower energy density than that of battery. One of the best approaches to achieve both higher energy and higher power is to increase the acceptable working voltage of conventional EDLCs. The maximum voltage of EDLCs is limited to 2.5-2.7V due to the degradation caused by the adsorbed water and the acidic functional groups present in the pore with the electrolytes. In order to increase the working voltage, the heat treatment of the activated carbon at a temperature over 700 °C generally have been used to remove the absorbed water and the acid functional groups. However, heat treatment at higher temperature and a long time heat treatment cause a structural modification of the activated carbon, consequently resulting in a decrease in capacitance. In this study, in order to suppress the structure modification, Joule-heating method was applied to the commercial activated carbons.

# Reduced Graphene Oxide Decorated on MnO<sub>2</sub> Nanoflakes Grew on C/TiO<sub>2</sub> Nanowire Arrays for Supercapacitor

Sainan Yang, Yiju Li, Dianxue Cao, Guiling Wang\*

Key Laboratory of Superlight Materials and Surface Technology of Ministry of Education, College of Materials Science and Chemical Engineering, Harbin Engineering University, Harbin, 150001, P.R.China, E-mail: wangguiling@hrbeu.edu.cn

In recent years, supercapacitors draw a great deal of attention due to their high power density, long cycle life, rapid charging-discharging rates, wide range of operating temperatures and environmental friendliness<sup>[1]</sup>. As one type of transition metal oxides, MnO<sub>2</sub> is thought to be the most promising pseudo-capacitive material for its high-energy density, low cost, environmental compatibility, and natural abundance<sup>[2]</sup>. Unfortunately, the intrinsically poor electrical conductivity of MnO<sub>2</sub> is a hindrance to obtain high electrochemical performance. In order to overcome this issue, tremendous efforts have been focused on combining highly conductive materials such as graphene, carbon nanotube and activated carbon<sup>[3]</sup>. In this work, RGO decorated on MnO<sub>2</sub> nanoflakes, which are electrochemically deposited on preformed C/TiO<sub>2</sub> shell/core nanowire arrays to form a RGO/MnO<sub>2</sub>/C/TiO<sub>2</sub> shell/core arrays electrode. The electrochemical performance was investigated by cyclic voltammetric measurements, constant current charge/discharge measurements and electrochemical impedance spectroscopic measurements. The RGO/MnO<sub>2</sub>/C/TiO<sub>2</sub> exhibits high specific capacitance of 822.3 F g<sup>-1</sup> at a charge/discharge current density of 1 A g<sup>-1</sup> and 89.3% specific capacitance retained after 1000 cycles. The superior capacitive properties may due to the unique shell/core structure, which can enlarge the electrode/electrolyte contact area and provide more ion adsorption sites for charge-transfer reactions. And the C and RGO layer can provide electron transfer channels, which can provide fast electron transfer for faradic reactions.

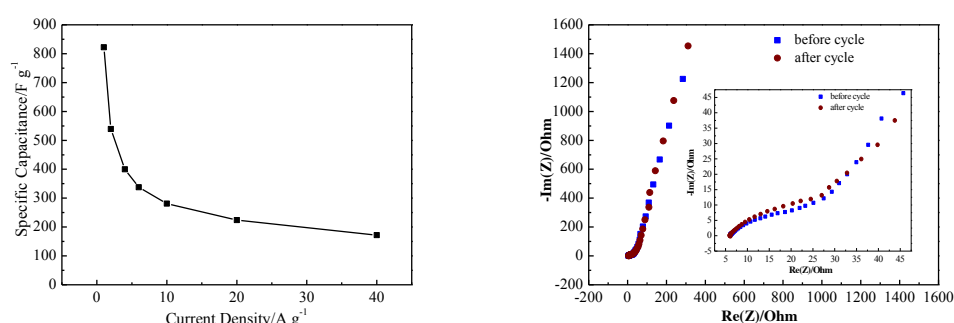


Fig. 1 corresponding specific capacitance of RGO/MnO<sub>2</sub>/C/TiO<sub>2</sub> electrode at current density from 1 to 40 A g<sup>-1</sup>(Left) and Impedance Nyquist plots of RGO/MnO<sub>2</sub>/C/TiO<sub>2</sub> electrode(Right).

## Acknowledgments

This paper is funded by the International Exchange Program of Harbin Engineering University for Innovation-oriented Talents Cultivation.

## References

- [1] G. Wang, L. Zhang, J. Zhang, Chemical Society reviews, 2012, 41 (2): 797-828.
- [2] W. Wei, X. Cui, W. Chen, D.G. Ivey, Chemical Society reviews 2011, 40 (3): 1697-1721.
- [3] J. Zhu, J. He, ACS Appl Mater Interfaces, 2012, 4 (3): 1770-1776.

# Synthesis and Characterisation of Sodium ion Pre-intercalated Manganese Oxide for High Performance Asymmetric Supercapacitors

A. Adomkevicius,<sup>a,b</sup> C. C. Hu,<sup>b\*</sup> and L. J. Hardwick<sup>a\*</sup>

<sup>a</sup> Department of Chemistry, Stephenson Institute for Renewable Energy, University of Liverpool, Liverpool L69 7ZF, United Kingdom

<sup>b</sup> Department of Chemical Engineering, National Tsing Hua University, 101, Sec. 2, Kuang-Fu Rd., Hsin-Chu 300, Taiwan

\* Corresponding author email address: cchu@che.nthu.edu.tw, hardwick@liverpool.ac.uk

Electrochemical supercapacitors have been widely investigated over the past few decades because of their increasing use within hybrid electric vehicles, starting assistance of fuel cells, and power sources of electronics. The main challenge in developing advanced supercapacitors for wider applications is to increase the specific energy density, without sacrificing power or life time while keeping low fabrication costs.

Manganese oxide-based materials have been under intense investigation as a pseudocapacitor electrode materials<sup>1</sup>. In this work, sodium doped MnO<sub>2</sub> (denoted as Na<sub>0.33</sub>MnO<sub>2</sub>) was synthesised under aqueous conditions at 75 °C. The microstructure and surface morphologies of Na<sub>0.33</sub>MnO<sub>2</sub> were analysed by powder X-ray diffraction, scanning electron microscopy, Raman spectroscopy, and electrochemical analysis. Cyclic voltammetry (CV) and galvanostatic charge/discharge measurements in a 0.5 M Na<sub>2</sub>SO<sub>4</sub> aqueous electrolyte demonstrated that Na<sub>0.33</sub>MnO<sub>2</sub> exhibits superior rate capability, outstanding capacitance retention, and a high total specific capacitance of 192 F·g<sup>-1</sup> at a current density of 200 A·g<sup>-1</sup>. The excellent rate capability of Na<sub>0.33</sub>MnO<sub>2</sub> is demonstrated by the variation in scan rate of CV from 5 to 1000 mV·s<sup>-1</sup> with 95% capacitance retention when the mass loading of Na<sub>0.33</sub>MnO<sub>2</sub> was increased from 0.5 to 1.0 mg·cm<sup>-2</sup>. Moreover, by increasing the mass loading of Na<sub>0.33</sub>MnO<sub>2</sub> up to 2.0 mg·cm<sup>-2</sup>, the electroactive material possesses a fairly high specific capacitance of 136 F·g<sup>-1</sup> and excellent capacitance retention (81%) as the scan rate is varied from 5 to 500 mV·s<sup>-1</sup>. From these results, Na<sub>0.33</sub>MnO<sub>2</sub> (i.e., Mn oxide pre-intercalated with electrolytic cations) contributes to faster mobility and exchange of cations in the electrolyte. This enables the surface and internal mass of active material to involve the redox transitions in order to provide high pseudocapacitance and outstanding rate capability.

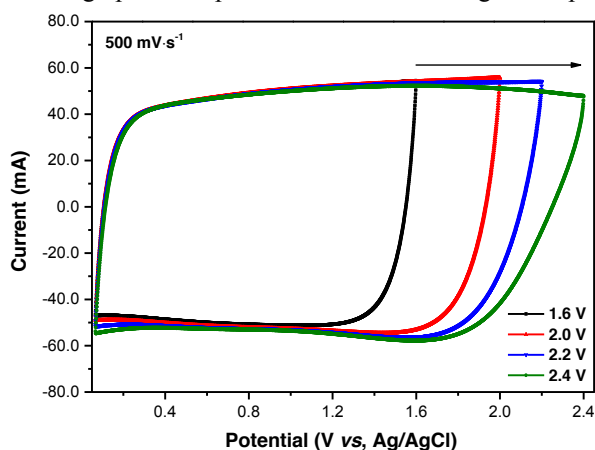


**Fig.** Represents CV's curves in the different potential window from 1.6 to 2.4 V of asymmetric Na<sub>0.33</sub>MnO<sub>2</sub>/activated carbon cell at scan rate of 500 mV·s<sup>-1</sup>.

An aqueous asymmetric supercapacitor with a cell voltage of 2.4 V is demonstrated using activated carbon as the negative electrode and 2.56 mg Na<sub>0.33</sub>MnO<sub>2</sub>/conductive carbon composite as the positive electrode. The specific energy and power of this device (based on total mass of the whole device) measured at 20 A·g<sup>-1</sup> are equal to 5.3 Wh·kg<sup>-1</sup> and 5265 W·kg<sup>-1</sup>, respectively.

## References

1. C.-C. Hu and T.-W. Tsou, *Electrochem. Commun.*, 2002, **4**, 105



# Nickel sulfide/carbon nanotube nanocomposites as cathode materials for hybrid supercapacitors

Chao-Shuan Dai,<sup>1</sup> Pei-Yi Chien,<sup>1</sup> Shu-Wei Chou,<sup>2</sup> Tsung-Wu Lin,<sup>2</sup> Jeng-Yu Lin<sup>1,\*</sup>

<sup>1</sup>*Department of Chemistry, Tunghai University*

*No. 181, Sec. 3, Taichung Port Rd., Taichung City 40704, Taiwan*

<sup>2</sup>*Department of Chemical Engineering, Tatung University*

*No. 40 ChungShan North Road, 3rd Section, Taipei 104, R.O.C.*

*e-mail: [jylin@ttu.edu.tw](mailto:jylin@ttu.edu.tw)*

Supercapacitors (SCs) have been widely recognized in a wide range of energy storage applications over the past decade, such as hybrid electric vehicles, mobile electronic devices, large industrial equipments, memory backup systems, and military devices. In this current work, a hybrid supercapacitor based on Ni<sub>3</sub>S<sub>2</sub>/multi-walled carbon tube (MWCNT) composite cathode and activated carbon (AC) anode was assembled. The hierarchically structured Ni<sub>3</sub>S<sub>2</sub>/MWCNT composites were synthesized via a facile glucose-assisted hydrothermal method, and the Ni<sub>3</sub>S<sub>2</sub> nanoparticles were homogeneously dispersed on the MWCNT surface. Additionally, the Ni<sub>3</sub>S<sub>2</sub>/MWCNT//AC hybrid supercapacitor can be operated reversibly between 0 and 1.6 V, and obtain a high specific capacitance of 55.8 F/g at 1 A/g, which delivers a maximum energy density of 19.8 Wh/kg at a power density of 798 W/kg. Moreover, 90% retention of specific capacitance was achieved after consecutive 1000 cycles with current density of 4A/g which shows excellent stability. The Ni<sub>3</sub>S<sub>2</sub>/MWCNT//AC hybrid supercapacitor can be viewed as an inexpensive energy storage system.

# Buffer Effect on Electrolytes towards Supercapacitors Application

Hsiu-Chuan Chien, Chi-Chang Hu\*

Department of Chemical Engineering, National Tsing Hua University

101, Sec. 2, Kuang-Fu Rd., Hsin-Chu city, 30013 Taiwan

elaine55667788@gmail.com

\*corresponding author: cchu@che.nthu.edu.tw

In this work, we report the effect of addition of buffer on different electrolytes to see the performance of the supercapacitors. The addition of buffer into the electrolyte decrease the difference on the localized pH value around the electrode. The results shows that without addition of buffer solution, the potential window in neutral solution is larger than in acidic or basic solution which contradicts with from thermodynamics prediction. This may due to the localized pH value around the electrode. According to Nernst equation, the potential of hydrogen adsorption and desorption would change along with pH value. So on adding buffer solution into the electrolyte will stabilize the localized pH value around the electrode. In conclusions, adding buffer solution could stabilize the localized pH value around the electrode and the adsorption may shifted towards the earlier potential which correspond to the thermodynamics prediction.

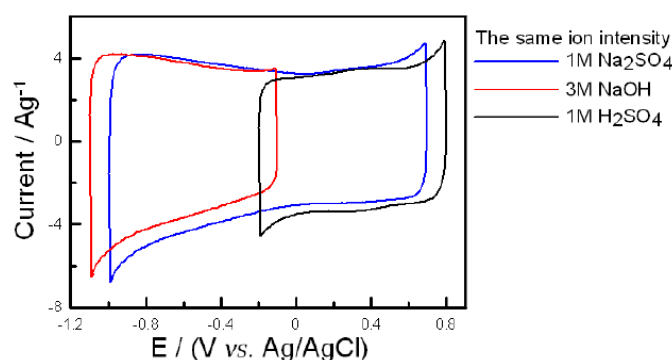


Fig.1 CV curves of activated carbon electrode measured in (a) 1M  $\text{Na}_2\text{SO}_4$  (b) 3M  $\text{NaOH}$  (c) 1M  $\text{H}_2\text{SO}_4$  at 25mV/s.

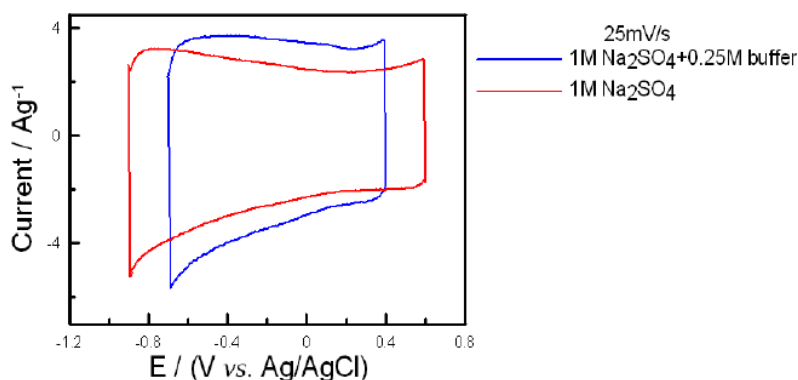


Fig.2 CV curves of activated carbon electrode measured in (a) 1M  $\text{Na}_2\text{SO}_4 + 0.25\text{M}$  buffer solution (b) 1M  $\text{Na}_2\text{SO}_4$  at 25mV/s.

# Effect of Nickel Oxide Type on the Electrochemical Behavior of Nickel-Graphene Oxide Hybrid – Towards Electrochemical Capacitor

Mohammad BinSabt, Ahmed Abdel Nazeer, Ahmed Galal  
Department of Chemistry, Faculty of Science, Kuwait University  
P.O. Box 5969 Safat 13060, Kuwait  
[Mohammad.Alsabt@ku.edu.kw](mailto:Mohammad.Alsabt@ku.edu.kw), Tel: (+965)24985587, Fax: (+965)24816482

Nickel oxide was formed by electrochemical polarization in 0.5 M KOH using cyclic voltammetry. The upper potential limits of the voltammetric scan controlled the type of oxide namely  $\beta$ -nickel hydroxide ( $\text{Ni}(\text{OH})_2$ ) and  $\gamma$ -nickel oxyhydroxide ( $\text{NiOOH}$ ). The two oxides were formed over a nickel electrode as previously mentioned [1]. Film of graphene oxide was then coated over the surface of the oxide using a microwave technique. The electrochemical behavior of the resulting hybrid film was then studied in different electrolytes. Cyclic voltammetry showed that the anodic current increases with a maximum with four layers of graphene-oxide films are reached with a quasi-reversible behavior in 0.5 M KOH solutions. The electrochemical impedance spectroscopy data proved that the capacitive component of the current increases in the same order.

Surface morphologies of the film formed were studied using atomic force microscopy (AFM) and field emission scanning electron microscopy (FE-SEM). The structure of the film was investigated using surface enhanced Raman spectroscopy (SERS). The data showed that the film is homogeneously distributed over the nickel oxide substrate. The cyclic charge/discharge of the hybrid film was also evaluated. A typical cyclic charging/discharging capacitance diagram is given in the figure. The effect of different types of oxides, number of graphene oxide layers and using different charging current on the charge/discharge behavior was studied.

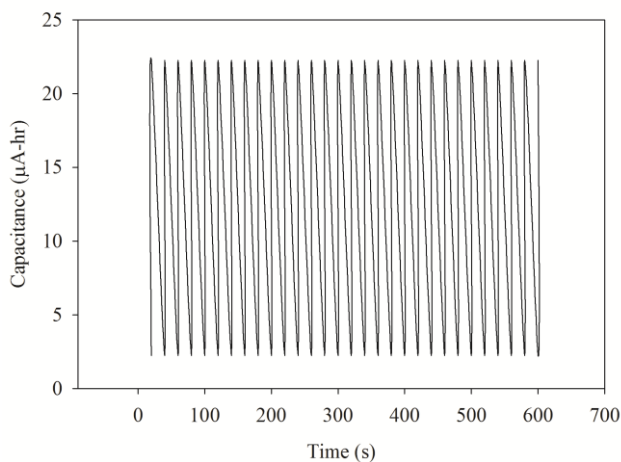


Figure. Galvanostatic charge/discharge curves of Graphen oxide/ $\text{Ni}(\text{OH})_2$  electrode at a current density of  $2 \text{ mA cm}^{-2}$ . (Capacitance values are not normalized to the mass of the film).

1] M. Alsabet, M. Grden, G. Jerkiewicz, (2011), Electrochemical growth of surface oxides on nickel. Part 1: Formation of  $\alpha$ - $\text{Ni}(\text{OH})_2$  in relation to the polarization potential, polarization time, and temperature, *Electrocatalysis*, 2, 317.

Acknowledgement: The Support of Kuwait University is highly appreciated. Research facilities were provided through Research Sectors Projects GS01/01 and SC09/13 of Kuwait University.

# In-situ Polymerization of Pyrrole in MoS<sub>2</sub> Nanosheets as Highly Conductive Materials with Large Surface Area for Supercapacitors

Chao-Chi Tu, Sheng-Sian Yang, Jun-Ming Chiu, Lu-Yin Lin\*

Department of Chemical Engineering and Biotechnology, National Taipei University of Technology, 1 Sec. 3, Zhongxiao E. Rd., Taipei 10608, Taiwan, R.O.C., E-mail (L. Y. Lin\*): [lylin@ntut.edu.tw](mailto:lylin@ntut.edu.tw)

Supercapacitors (SCs) have attracted much interest due to the potential integration of lithium ion batteries (high energy density) and capacitors (high power density). Molybdenum disulfide (MoS<sub>2</sub>) has been extensively studied as the material for SCs which potentially store charge by intersheet and intrasheet double-layers over individual atomic layers and by faradaic charge transfer processes on the Mo center due to its several oxidation states.<sup>1</sup> Conducting polymers based SCs have received specific attention due to the low cost, broad voltage window, and remarkable storage capacity/reversibility properties. However, direct utilization of bulk conducting polymers as the electrode materials leads to uncontrollable and insufficient exposure of conducting polymers to the electrolytes. By combining the layered transition metal sulfide with conducting polymers, the transition metal centers of metal dichalcogenides can provide strong coordination with nitrogen atoms in conducting polymers, which benefits controllable growth of conducting polymers onto the nanosheet surfaces and offer a uniform and large surface area to immobilize conducting polymers for the charge storage.<sup>2</sup> In this study, two-dimensional MoS<sub>2</sub> nanosheets were synthesized via a simple hydrothermal method, and in turn the conducting polymer, polypyrrole (Ppy), was oxidative polymerized in the solution containing MoS<sub>2</sub> nanosheet in an ice bath to prepare the composites with different ratios of MoS<sub>2</sub> and Ppy. The SEM and TEM images of MoS<sub>2</sub>, Ppy, and the composites with the ratios of 1:0.1, 1:0.5, 1:1, and 1:2 (MoS<sub>2</sub>:Ppy) were shown in **Figure 1**. The layered structure can be obviously observed for the MoS<sub>2</sub>, while the aggregations as well as the outstanding internetworks were found for the Ppy, and for the composites the layered structure can only be clearly obtained for the cases of 1:0.1 and 1:0.5, and for the higher amount of Ppy in the composites (the ratio of 1:1 and 1:2), the nanosheets were hard to be observed. The highest capacitance (182.28 F/g) was obtained for the SC electrode with the composite (ratio of 1:0.5 for MoS<sub>2</sub>:Ppy) as the material, which is higher than those of the SC electrode with MoS<sub>2</sub> (40.58 F/g) and Ppy (116.95 F/g) as the materials as examined using the CV plots (**Figure 2**), due to large charge accumulation surface area provided by the layered structure and the enhanced interconnecting networks given by Ppy for the composite case. The combination of two different classes of the SC material with complementary advantages to achieve the synthetic properties and realized enhanced capacitance is an attractive way to prepared SC with high performance and good cycling life in the future.

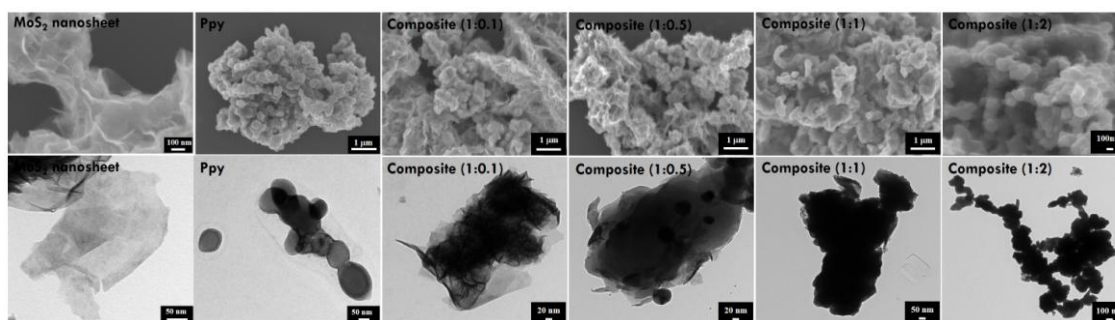


**Figure 1** The SEM and TEM images for MoS<sub>2</sub>, Ppy, and composites.

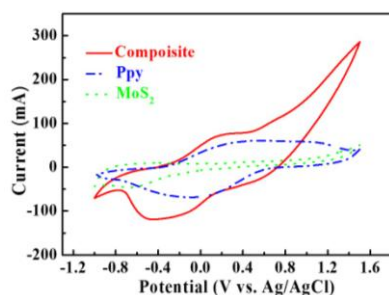


**Figure 2** The CV plots for the SC electrode with MoS<sub>2</sub>, Ppy, and composites as the materials.

## References

1. da Silveira Firmiano *et al.*, *Advanced Energy Materials* **2014**, *4*, 6, 1301380
2. Tang, H. *et al.*, *Adv Mater* **2014**, *1*

# Synthesis of Cobalt Sulfide Hydrangea Macrophylla Nanostructures with High Charge-Accumulation Surface Area for Supercapacitors

Jun-Ming Chiu, Chao-Chi Tu, Sheng-Sian Yang, Cheng-Feng Yu, Lu-Yin Lin\*

Department of Chemical Engineering and Biotechnology, National Taipei University of Technology, 1 Sec. 3, Zhongxiao E. Rd., Taipei 10608, Taiwan, R.O.C., E-mail (L. Y. Lin\*): [lylin@ntut.edu.tw](mailto:lylin@ntut.edu.tw)

Supercapacitors have attracted intense attention due to their features of high specific power density, fast charge and discharge rates, long durability, and environmental friendliness.<sup>1, 2</sup> Transition metal sulfides, *e.g.*, molybdenum sulfides,<sup>3</sup> tungsten sulfides,<sup>4</sup> and cobalt sulfides,<sup>5-7</sup> have been considered as one of the most promising pseudocapacitor electrode materials due to their potential properties of the high specific capacitance and cost effectiveness.<sup>3, 4</sup> In this study, a novel three-dimensional (3D) cobalt sulfide hydrangea macrophylla nanostructure was synthesized by using a simple one-pot method with a post-annealing treatment under the Ar atmosphere. The cobalt sulfide hydrangea macrophylla architectures are constructed by two-dimensional petals intertwined with each other with a thin carbon layer surrounded outside (**Figure 1a** and **1b**). The pseudo-capacitive properties of the cobalt sulfide material are evaluated by cyclic voltammetry (**Figure 2a**) and galvanostatic charge-discharge tests (**Figure 2b**) in a 6 M KOH solution. An extremely high specific capacitance of 1502.09 F g<sup>-1</sup> was obtained for the supercapacitor with the cobalt sulfide hydrangea macrophylla architectures at a charge-discharge current density of 0.5 A g<sup>-1</sup> after optimizing the loading amount (12.5 mg on 1 cm<sup>2</sup>) on the flexible substrate, *i.e.*, Ni foam, due to the large surface area for the charge accumulation and the high conductivity for the charge transfer provided by the 3D hydrangea macrophylla structure and the carbon layer attached outside the petals, respectively. The outstanding supercapacitor performance achieved with this promising hydrangea macrophylla cobalt sulfide therefore opens a window to the establishment of the structure-control techniques for improving the capacitance of the supercapacitors.

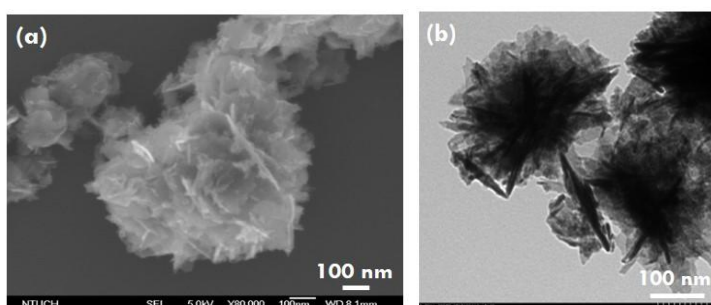


**Figure 1** (a) SEM image and (b) TEM image of the hydrangea macrophylla cobalt sulfide.

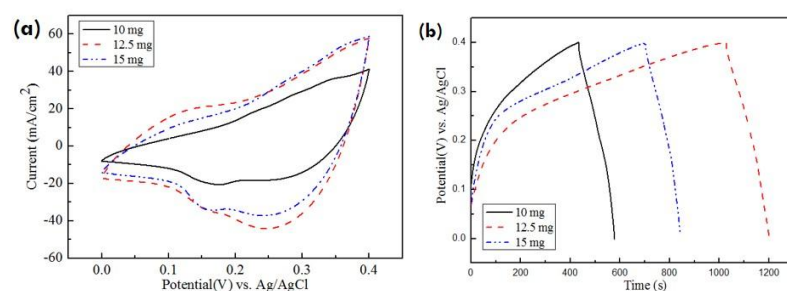


**Figure 2** (a) The cyclic voltammetry and (b) galvanostatic charge-discharge plot for the hydrangea macrophylla cobalt sulfide electrode with different loading amounts on the Ni foams.

## References

1. G. Wang *et al.*, *Chem. Soc. Rev.*, 2012, **41**, 797.
2. S. Xiong *et al.* Y. Qian, *Chem. Eur. J.*, 2009, **15**, 5320.
3. J. Wang *et al.*, *Nano Energ.*, 2014, **7**, 151.
4. S. Ratha and C. S. Rout, *ACS Appl. Mater. Interfaces*, 2013, **5**, 11427.
5. Q. Wang *et al.*, *CrystEngComm*, 2011, **13**, 6960.
6. F. Luo *et al.*, *Electrochim. Acta*, 2014, **123**, 183.
7. H. Wan *et al.*, *J. Power Sources*, 2013, **243**, 396.

# A Simple Method for Synthesizing Nickel Foam-supported Graphene with High Surface Area for Supercapacitors

Sheng-Sian Yang, Jun-Ming Chiu, Chao-Chi Tu, Lu-Yin Lin\*

Department of Chemical Engineering and Biotechnology, National Taipei University of Technology, 1 Sec. 3, Zhongxiao E. Rd., Taipei 10608, Taiwan, R.O.C., E-mail (L. Y. Lin\*): [lylin@ntut.edu.tw](mailto:lylin@ntut.edu.tw)

Carbon is a kind of novel materials that exists in various structural forms which have been investigated intensively. There is no doubt that hybrid structures composed of different carbon materials can extend the diversity of carbon-based structures, with integrated properties inherited from the constituent structures. However, insufficient surface area of the hybrid films makes them being unable to achieve high loading of electroactive materials and good contact with the electrolyte.<sup>1</sup> The nickel foam-supported graphene has a high surface area and three-dimensional porous architecture, making it have the potential to load more electroactive materials and improving the connection of the carbon and carbon structure to achieve a high electrical conductivity. These advantages make the nickel foam-supported graphene to be suitable for applying on the supercapacitors. Methane is usually used as the carbon precursor to fabricate nickel foam-supported graphene, but its toxic property makes it too dangerous to exhaust.<sup>2, 3</sup> Therefore, in this study, a simple, low cost and environment-friendly method was used to synthesize the nickel foam-supported graphene by a chemical vapor deposition method with the citric acid as the carbon precursor<sup>4</sup> to replace the toxic methane. The SEM images of the pure nickel foam and the nickel foam-supported graphene are shown in **Figure 1a** and **Figure 1b**, respectively. The pure nickel foam is a three-dimensional and porous structure, while few-layer graphene are found to cover on the nickel foam-supported graphene sample, whose surface is much rougher than that of the pure nickel foam.

On the other hand, manganese dioxide has been widely applied as the materials of supercapacitors because of its remarkable theoretical specific capacitance. Unfortunately, its poor conductivity limits its application on the energy storage devices. Therefore, the incorporation of 3D graphene foam as a 3D scaffold and MnO<sub>2</sub> with high theoretical specific capacitance is expected to achieve higher capacitance.<sup>1, 5</sup>

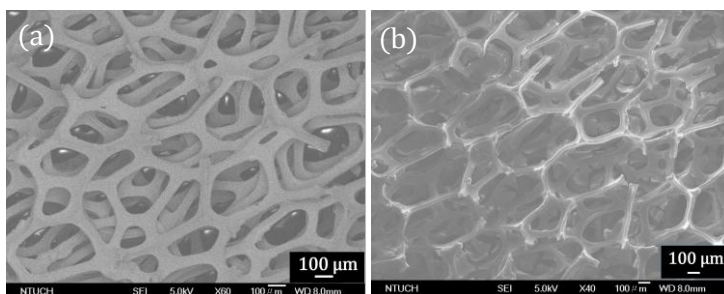


**Figure 1** SEM image of (a) the pure nickel foam and (b) the nickel foam-supported graphene.

## References

1. J. Liu *et al.*, *Energy Environ. Sci.*, 2014, **7**, 3709.
2. Y. Xue *et al.*, *Phys. Chem. Chem. Phys.*, 2013, **15**, 12220.
3. Z. Chen *et al.*, *Nat. Mater.*, 2011, **10**, 424.
4. D. Qu *et al.*, *Nanoscale.*, 2013, **5**, 12272.
5. Y. Li *et al.*, *J. Power Sources.*, 2014, **271**, 582.



# Design and fabrication of supercapacitor electrodes with good rate performance from hole graphene nanosheets

Zong-Huai Liu, Yunlong Bai, Gaini Zhang, Liping Kang, Zhibin Lei

Key Laboratory of Applied Surface and Colloid Chemistry (Shaanxi Normal University), Ministry of Education; School of Materials Science and Engineering, Shaanxi Normal University  
Chang'an Campus: No. 620, West Chang'an Avenue, Chang'an District, Xi'an 710119

Zhliu@snnu.edu.cn

Electrochemical capacitors can bridge the critical performance gap between the energy density of battery and high power density of conventional dielectric capacitor, they make the rapid storage and release of energy become possible [1]. In order to increase the energy density of electrochemical capacitors while retaining their intrinsic high power density, many researchers have focused attention on the development of the new electrode materials with novel structure and morphology. Transition metal nanosheets or graphene nanosheets are new classes of nanoscale materials, they have not only distinctive physicochemical properties, associated with dimensions in the nanometre range, but also large surface area and good electrical conductivity in comparison with their bulk materials [2], and the heterogeneous nanostructured hybrid electrodes having the advantages of transition metal nanosheets with high pseudocapacitance and graphene nanosheets with stable double-layer capacitance can be prepared by a nanosheet reassembling technology. In order to improve the electrolyte transport resistance in the vertical direction, the well-dispersed hole graphene nanosheets are prepared by hydrothermally treating graphene oxide in  $\text{H}_2\text{O}_2$  solution at  $100\text{ }^\circ\text{C}$  for 10 h and followed by refluxing it in  $\text{N}_2\text{H}_4\cdot\text{H}_2\text{O}$  at  $95\text{ }^\circ\text{C}$  for 1 h. The obtained hole graphene nanosheet electrode not only shows superior film-forming property, but also enhances the rate performance. Moreover, the mesoporous-assembled  $\text{MnO}_2$  is prepared by mixing the delaminated  $\text{MnO}_2$  nanosheet slurry and  $\text{NH}_4\text{HSO}_4$  and followed by heating the mixture at  $175\text{ }^\circ\text{C}$ . The optimized electrode shows a specific surface area of  $456\text{ m}^2/\text{g}$ , which gives a specific capacitance of  $281\text{ F/g}$  at a current density of  $0.25\text{ A/g}$ .

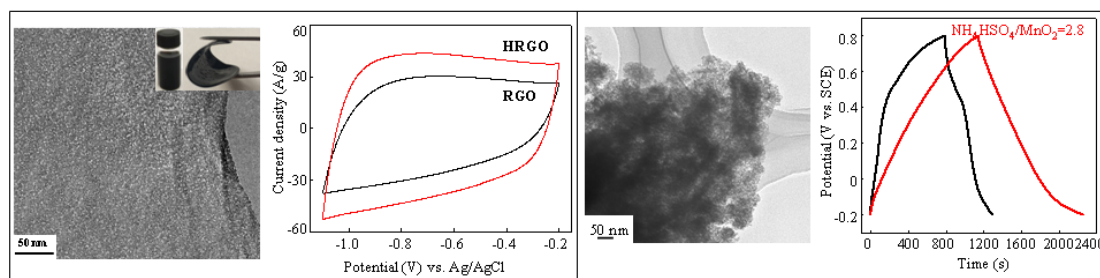


**Figure 1.** TEM image of the obtained hole graphene electrode and CV curves at  $200\text{ mV s}^{-1}$  (left) and TEM image of mesoporous-assembled  $\text{MnO}_2$  and the galvanostatic charge-discharge curves at a current density of  $0.25\text{ A g}^{-1}$  (right).

## References:

- [1] G.P. Wang, L. Zhang, J.J. Zhang, A review of electrode materials for electrochemical supercapacitors, *Chem. Soc. Rev.* 41 (2012) 797.
- [2] L.J. Deng, Z.P. Hao, J.F. Wang, G. Zhu, L.P. Kang, Z.-H. Liu, Z.P. Yang, Z.L. Wang, Preparation and capacitance of graphene/multiwall carbon nanotubes/ $\text{MnO}_2$  hybrid material for high-performance asymmetrical electrochemical capacitor, *Electrochim. Acta* 89 (2013) 191.

# Nanocrystalline vanadium trioxide as negative electrodes for asymmetric supercapacitors

Lingbin Kong<sup>a,b,\*</sup>, Xuejing Ma<sup>a</sup>, Weibin Zhang<sup>a</sup>, Yongchun Luo<sup>b</sup>, and Long Kang<sup>b</sup>

<sup>a</sup> State Key Laboratory of Advanced Processing and Recycling of Non-ferrous Metals, Lanzhou University of Technology, Lanzhou 730050, China. E-mail: konglb@lut.cn

<sup>b</sup> School of Materials Science and Engineering, Lanzhou University of Technology, Lanzhou 730050, China

Among storage devices, supercapacitors are promising due to their combined merits of power density and energy density compared to conventional capacitors and batteries. There are numerous reports on the positive electrode materials with high capacitances working in a wide potential window<sup>[1]</sup>. However, identification of suitable negative electrode is also an imperative one to counter balance the charges and to obtain the superior supercapacitive performance. Among the few negative electrode materials of supercapacitors, vanadium oxides have received significant attention because of their low cost, multiple variable oxidation states and wide potential windows.

Here, a high performance vanadium trioxide negative electrode material was synthesized via a facile strategy of heat treatment and its capacitive behaviour was successfully investigated in a neutral electrolyte. The pseudo capacitive behaviour of the vanadium trioxide was widely researched in 1 mol dm<sup>-3</sup> sodium sulfate aqueous electrolyte using cyclic voltammetry (CV), galvanostatic charge-discharge (GCD) test, and electrochemical impedance spectroscopy. As shown in Fig. 1a, the peaks of vanadium trioxide are in accordance with the reported data (JCPDF card No. 34-0187), revealing the existence of vanadium trioxide phase. Fig. 1b shows the typical CV curves of vanadium trioxide within a potential range of -1.0 V-1.0 V at scan rates of 5 mV s<sup>-1</sup>-100 mV s<sup>-1</sup>. The peak current increases linearly with the increment of the scan rate, which indicated that the kinetics of interfacial Faradic redox reactions and the rates of electronic and ionic transport are rapid enough in present scan rates<sup>[2]</sup>. The CV curves keep the original shape with the increasing scan rates, which indicate the nice ionic and electron conduction of this material. The high specific capacitance (SC) of 118 F g<sup>-1</sup> is achieved at a current density of 0.5 A g<sup>-1</sup> (Fig. 1c). The high SC in the wide potential window and the low diffusion and electron-transfer resistances in the neutral electrolyte of the vanadium trioxide show promise for its application in supercapacitor.

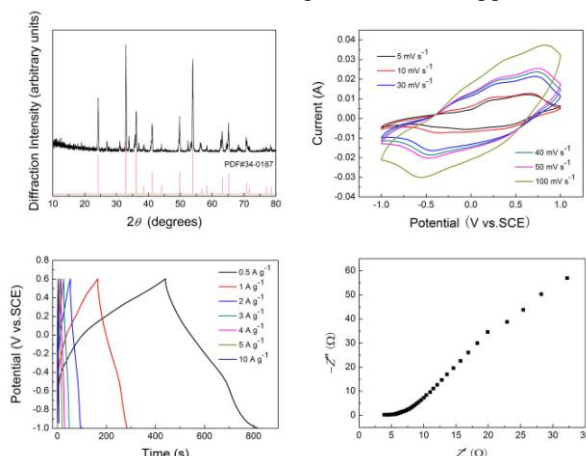


**Fig 1:** a, XRD pattern. b, CV curves. c, GCD curves. d, Nyquist plots of impedance spectra.

For vanadium trioxide, which possesses a 3D V-V framework, its V 3d electrons can itinerate along the V-V chains, leading to metallic behavior. In addition, tunneled structures exist in vanadium trioxide, which facilitates ion intercalation/deintercalation. Therefore, vanadium trioxide is particularly suitable as an electrode material, especially as the negative electrode material in supercapacitors.

Acknowledgements:

This work is supported by the National Natural Science Foundation of China (51362018, 21163010).

References:

- [1] H.Y. Li, K. Jiao, L. Wang, C. Wei, X.L. Li, B. Xie, J. Mater. Chem. A, 2 (2014) 18806.
- [2] X.J. Ma, L.B. Kong, W.B. Zhang, M.C. Liu, Y.C. Luo, L. Kang, Electrochim. Acta, 130 (2014) 660.



# Ordered mesoporous carbon nitride as an electrode material for high performance electrochemical capacitors

Yana Li, Li Wang, Fa-Jun Xia, Tong Yang, Chun-Ling Liu, Wen-Sheng Dong  
Key Laboratory of Applied Surface and Colloid Chemistry (SNNU), MOE, School of Chemistry and  
Chemical Engineering, Shaanxi Normal University, Xi'an, 710062, China  
clliutt@snnu.edu.cn

Although porous carbon materials exhibit large capacitances, the electrical conductivity suffers from a decrease with increasing porosity due to noncompatibility of conductive pathways or oxygen-containing functional groups, which largely limits the power capacity. Besides that, the ionic motion may be hindered in narrow nanopores, which reduces the rate of energy delivery. Thus, the development of carbon materials with high surface area, energy density, specific conductivity properties to improve the power density, and the long cycle life is highly desired.

In this work, the ordered mesoporous carbon nitride (OMCN) with uniform mesopores and a high surface area was synthesized with a nanocasting strategy using hexagonally ordered mesoporous silica SBA-15 as a template. Then, the as-obtained OMCN sample was applied as an electrode for high-performance supercapacitors.

Elemental analysis showed that the as-prepared material contained 16.3% N. Low-angle XRD pattern of the material showed a sharp diffraction peak at  $2\theta \sim 0.9^\circ$  and a weak peak at  $2\theta \sim 1.59^\circ$ , which can be indexed to the (100) and (110) reflections of the two-dimensional (2D) hexagonal (P6mm) structure, respectively. The pattern is similar to the XRD pattern of the parent mesoporous silica template SBA-15, which consists of a hexagonal arrangement of cylindrical pores interlinked by the micropores present in the walls. In the wide-angle region, the OMCN material showed a broad diffraction peak located at  $2\theta$  around  $25^\circ$ , corresponding to the (0 0 2) diffraction of amorphous carbon. The sample featured a type IV isotherm with a H1-shaped hysteresis loop over the  $P/P_0$  range of 0.4–0.8, and narrow pore size distributions, characteristics of highly ordered mesoporous materials. The BET surface area of the material was  $483 \text{ m}^2 \text{ g}^{-1}$ , and the average pore diameter was 4.4 nm.

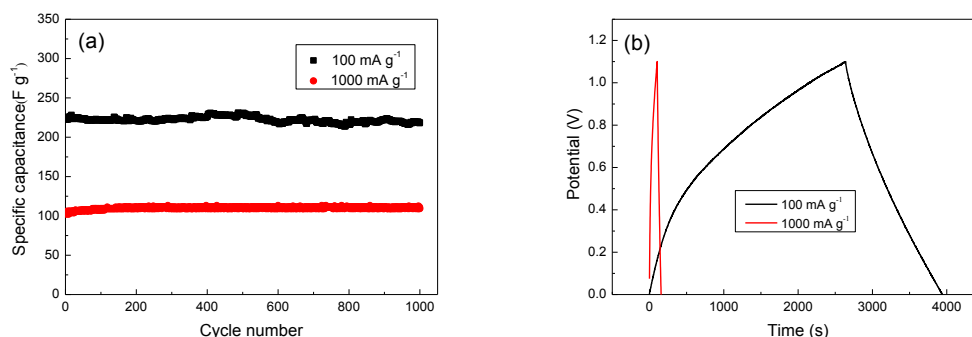


**Figure 1.** The cycling performance (a) and discharge-charge curves (b) for the OMCN material at different current densities.

The electrochemical measurements of the symmetric supercapacitor were carried out in a two-electrode coin cells at room temperature using 1 M KOH aqueous solution as the electrolyte. The OMCN electrode material showed a specific capacitance of  $223 \text{ F g}^{-1}$  at  $100 \text{ mA g}^{-1}$ , and after 1000 cycles it still remained a specific capacitance of  $218 \text{ F g}^{-1}$ , with a high capacity retention of 97%. At  $1000 \text{ mA g}^{-1}$  the OMCN electrode showed a initial specific capacitance of  $112 \text{ F g}^{-1}$  with a capacity retention of 108%. This electrode material exhibited a specific energy of  $9.6 \text{ Wh kg}^{-1}$  with the maximum specific power of  $28.6 \text{ kW kg}^{-1}$ , which is higher than that of the commercial aqueous capacitors (the power density value is 7~8  $\text{kW kg}^{-1}$ ). The good electrochemical performance of the OMCN material could be attributed to the combined effects of a high nitrogen doping level that changed the electron donor/acceptor characteristics of carbon, improved the wettability of the material in the electrolyte, and the large BET surface area that increased the surface area accessibility for electrolyte ion and enhanced the kinetics of ion and electron transport in electrodes and at the electrode/electrolyte interface.

# **Ni(OH)<sub>2</sub> Nanowires with High Performance as Supercapacitor Electrode via Cathodic Electrodeposition**

Zifan Zeng, Jiliang Zhu, Xiaohong Zhu, Xi Liu, Chuang Kou and Fangyuan Xie

*Department of Materials Science, Sichuan University*

*Chengdu 610064, China*

*Corresponding author e-mail address: jlzhu167@scu.edu.cn*

*Tel.: +86 28 85432078; fax: +86 28 85432078*

Cross-linked Ni(OH)<sub>2</sub> nanowires was prepared for the electrode materials of supercapacitor via cathodic electrodeposition. The deposition experiments were galvanostatically performed at the current density of 0.5 mA cm<sup>-2</sup> on Ni foam substrate without any surfactant and template. Scanning electron microscopy images indicated that the cross-linked Ni(OH)<sub>2</sub> nanowires were homogeneously distributed on Ni foam with length of 200 nm. The as-prepared Ni(OH)<sub>2</sub> nanowires exhibited ultrahigh specific capacitance of as high as 3637 F g<sup>-1</sup> at the current density of 0.5A g<sup>-1</sup> in the potential window of 0-0.4 V (vs. Ag/AgCl). This result indicates that the Ni(OH)<sub>2</sub> nanowires electrode grown on Ni foam can be considered as a promising candidate for the supercapacitor electrode materials.

# Synthesis and Electrochemical Analysis of Electrodeposited MnO<sub>2</sub>/C Composite Electrode for Supercapacitors

Nobuko Yoshimoto, In-Tae Kim, Nobuo Kouda, and Masayuki Morita  
Graduate School of Science and Engineering, Yamaguchi University,  
2-16-1 Tokiwadai, Ube 755-8611, Japan  
nobuko@yamaguchi-u.ac.jp

Composite materials based on metal oxides and carbon materials have widely been developed as a new route for achieving highly efficient Super capacitors<sup>1)</sup>. A manganese oxide family, typically MnO<sub>2</sub>, is a promising electrode material for electrochemical capacitors due to its low cost, natural abundance, environmental safety and its high theoretical capacitance. However, its low electrical conductivity is a major limiting factor in its electrochemical capacitor application. Such a poor electronic property is usually balanced by the addition of large amounts of conducting carbons like graphite, carbon black, carbon nanotubes, etc. Recently, Nakayama *et al.* have proposed an electrochemical method for preparing thin films of layered manganese oxide by anodic or cathodic synthesis<sup>2, 3)</sup>. They have proposed that the thin films of layered manganese oxide synthesized by the cathodic process exhibited an excellent pseudocapacitive behavior compared with the manganese oxide film grown anodically<sup>3)</sup>. In the present work, we have developed a composite electrode by cathodic deposition of manganese oxide on carbon electrodes with interconnected pores, and have examined its capacitive properties in an aqueous electrolyte solution.

The substrate electrode was prepared by mixing the carbon powder having interconnected pores (CNovel 10 nm, Toyo Tanso), acetylene black, and poly(tetrafluoroethylene). The mass ratio of these materials was 8:1:1. Manganese oxide were deposited on the carbon substrate by applying a constant potential of -0.2 V (vs. Ag/AgCl) in an aqueous solution containing 10 mM KMnO<sub>4</sub> and 250 mM KCl for 30 or 60 min. The deposit was characterized by means of XRD and FE-SEM. Electrochemical behavior of the composite electrode was measured by cyclic voltammetry (CV).

Cyclic voltammograms of the composite electrodes, MnO<sub>2</sub>/carbon, prepared for different polarization times are shown in Fig. 1, compared with carbon substrate electrode, where the measurements were conducted in 0.5 M Na<sub>2</sub>SO<sub>4</sub> solution with the scan rate of 2 mV s<sup>-1</sup>. All electrodes exhibit rectangular-shape voltammograms. The composite electrode prepared for 60 min. (MnO<sub>2</sub>/CNovel (60)) showed the highest current response. The specific capacitances calculated from the current-potential relations were 230 F g<sup>-1</sup> (MnO<sub>2</sub>/CNovel (60)), 172.4 F g<sup>-1</sup> (MnO<sub>2</sub>/CNovel (30)) and 83.5 F g<sup>-1</sup> (CNovel), respectively.

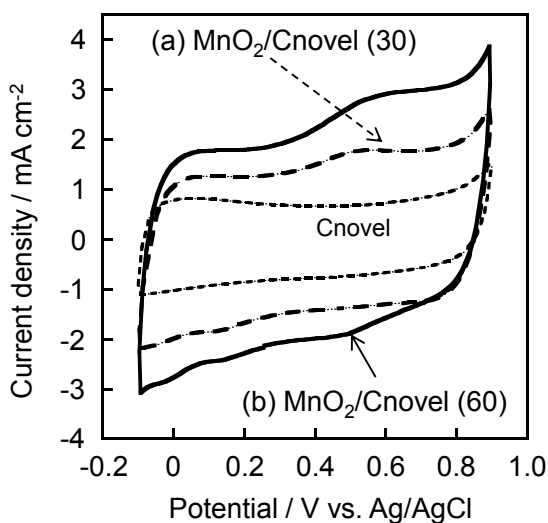


Fig. 1 Cyclic voltammograms of composite electrodes, MnO<sub>2</sub>/carbon, prepared for 30 minutes (a) and 60 minutes (b) in 0.5 M Na<sub>2</sub>SO<sub>4</sub> at the scan rate of 2 mV s<sup>-1</sup>.

## References

- 1) T. Bordjiba and D. Belanger, *Electrochim. Acta*, **55**, 3428 (2010).
- 2) M. Nakayama, T. Kanaya, and R. Inoue, *Electrochem. Commun.*, **9**, 1155 (2007).
- 3) M. Nakayama, M. Nishiyama, M. Shamoto, T. Tanimoto, K. Tomono, and R. Inoue, *J. Electrochem. Soc.*, **159**, A1176 (2012).

# **Low-cost and high performance supercapacitors based on up-cycled industrial mill scale**

Chaopeng Fu\* and Patrick S. Grant

*Department of Materials, University of Oxford  
Parks Road, Oxford OX1 3PH  
Tel: +44-1865-283713*

*\*chaopeng.fu@materials.ox.ac.uk*

Large scale electrical energy storage is receiving increasing world-wide attention because of its potentially important role in enabling a greater fraction of renewable electricity generation and use, and so reducing environmental pollution and climate change. Supercapacitors with high power density and long cycle life are of interest to complement batteries in various applications including transportation and stand-alone or grid-connected renewable power plants. Carbon-based electrodes with organic electrolytes dominate the commercial supercapacitor market. However, they cannot always meet the performance and cost targets for large scale energy storage applications. Therefore research efforts have continued to be focused on improving the performance of supercapacitors, and high capacitances and long cycle life have been achieved in laboratories by many research groups. However, complex synthesis methods and/or expensive raw materials, and non-scalable processing are often used to obtain this performance, which may not only restrict large-scale production, but also have unattractive cost implications.

Mill scale is a waste product from the steel industry and is composed of various iron oxides/hydroxides. This paper studies the supercapacitive behavior of mill scale received directly from a large steel plant, and after various cheap and scalable physical and chemical treatments. Techniques of cyclic voltammetry, charge/discharge and electrochemical impedance spectroscopy are used. The paper describes how, starting from intriguing but insufficient storage capacity, the mill scale can be readily manipulated and processed to produce a range of chemistries and morphologies. Ball milled mill scale with a specific capacitance of 92 F/g at a scan rate of 5 mV/s in Na<sub>2</sub>SO<sub>3</sub> electrolyte was transformed to different oxides using simple heat treatments, reaching 137 F/g, again at 5 mV/s in the same electrolyte. Then following further simple treatments, a capacitance of 240 F/g at a scan rate of 5 mV/s or 236 F/g at a discharge current density of 2 A/g was maintained at over 90% for 1,000 cycles. At each stage the chemical changes in the materials are described in detail, and the mechanisms for the progressive increases in performance discussed. Finally the future prospects for supercapacitors based on the scalable and low-cost processing of plentiful mill scale waste is presented.

# Electrochemical Co-deposition of Polyaniline with Inorganic Oxides for Pseudocapacitive Application

Xiao-Xia Liu, Li-Jie Sun, Ming-Hua Bai  
 Department of Chemistry, Northeastern University  
 3-11 Wenhua Road, Shenyang, 110819, China  
 xxliu@mail.neu.edu.cn

Pseudocapacitor is emerging as a new class of charge storage device with higher energy density compared to electrical double-layer capacitor. Conducting polymers and inorganic oxides have promising applications in pseudocapacitor due to their high specific capacitance compare to carbon materials. Their composites, especially nanocomposites, have special advantages due to the combined merits and synergistic effects of organic and inorganic components.

Polyaniline (PANI) has promising applications in pseudocapacitor. One-dimensional (1D) growth control of PANI has aroused great interest because an ordered arrangement of the polymer chains favours higher conductivity and better performance in applications. Although 1D growth is known to be intrinsic to PANI, heterogeneous nucleation on the initially-formed 1D PANI would result in irregularly-shaped PANI particles. 1D growth control of PANI through electrochemical co-deposition with inorganic oxides is a good way to fabricate 1D organic-inorganic composite through the suppression of this overgrowth on the surface active sites of initially-formed 1D PANI.

In this work, we will present the 1D growth control of PANI through electrochemical composition with inorganic oxides. Incorporation of oxide nanoparticles on the polymer chains was first conducted through electro-co-polymerization of aniline and *N*-substituted aniline grafted on surfaces of oxide nanoparticles to avoid the chain entanglement by electrostatic repulsion between positive charged oxide nanoparticles (Fig. 1).

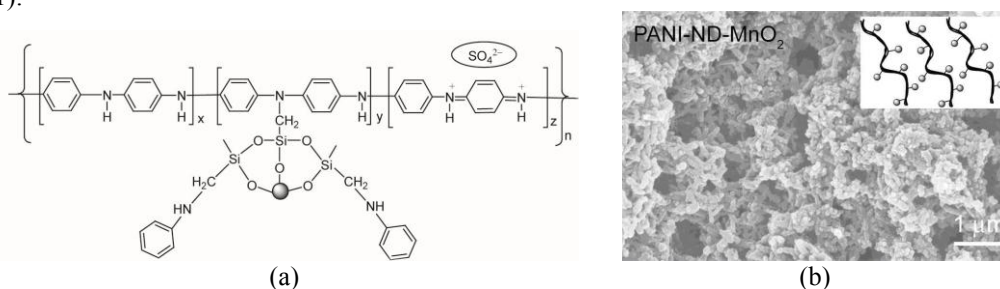


Fig. 1 (a) Schematic of incorporation of oxide nanoparticle onto PANI chain via triethoxysilylmethyl *N*-substituted aniline (ND); (b) SEM images of the obtained composite of PANI-ND-MnO<sub>2</sub>.

The local environment at the electrode surface for aniline polymerization was also tried to be controlled by the electrodeposition of inorganic oxides from their precursors like VO<sup>2+</sup> and Mn<sup>2+</sup>, in which process proton may be released and some of the anodic charges may be consumed to control the amount of the charge for aniline polymerization. 1D growth of PANI was successfully conducted to afford PANI based nanocomposites with improved pseudocapacitive properties (Fig. 2).

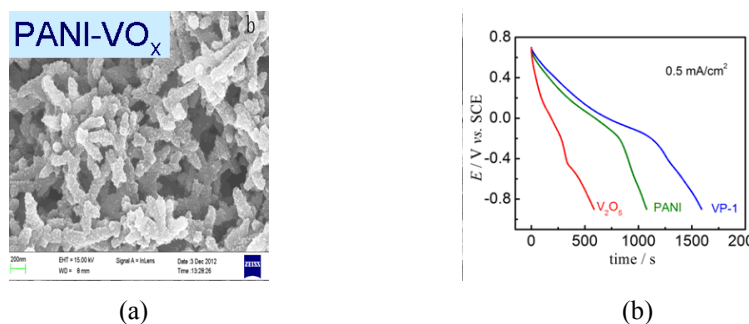


Fig. 2 (a) SEM images of PANI-VO<sub>x</sub> composite; (b) discharge profiles of PANI, VO<sub>x</sub> and PANI-VO<sub>x</sub>.

## Acknowledgments

We gratefully acknowledge financial supports from National Natural Science Foundation of China (project number: 21273029).

# Earth-Abundant Materials for Photocatalytic Water splitting

Yan-Gu Lin, Hong-Jhe Lin, Yu-Chang Lin

*National Synchrotron Radiation Research Center*

*101 Hsin-Ann Road, Hsinchu Science Park, Hsinchu 30076, Taiwan*

*lin.yg@nsrrc.org.tw*

Global climate warming and environment pollution have spurred scientists to develop new high-efficient and environmental-friendly energy technologies. Hydrogen is an ideal fuel for fuel cell applications. Hydrogen has to be produced from renewable and carbon-free resources using nature energies such as sunlight if one thinks of clean energy and environmental issues. In this regard, a photoelectrochemical (PEC) cell consisting of semiconductor photoelectrodes that can harvest light and use this energy directly for splitting water is a more promising way for hydrogen generation. Abundant and inexpensive oxide semiconductor such as ZnO has been recognized as a promising photoelectrode, but the photoconversion efficiency is substantially limited by its large band gap and rapid charge recombination. Recently, doping with 4d transition metal, such as Mo, has been carried out to remarkably enhance the PEC performance of many photoanodes including TiO<sub>2</sub>, BiVO<sub>4</sub>, and Fe<sub>2</sub>O<sub>3</sub>. Nevertheless, 1-D Mo-doped ZnO nanostructures have not been reported for PEC water splitting. We report the first demonstration of cobalt phosphate (Co-Pi) assisted Zn<sub>1-x</sub>Mo<sub>x</sub>O nanorods (NRs) as visible-light-sensitive photofunctional electrodes to fundamentally improve the performance of ZnO NRs for PEC water splitting. The maximum photoconversion efficiency could be successfully achieved as high as 1.05%, with the significant photocurrent density of 1.4 mA cm<sup>-2</sup>. More importantly, in addition to achieve the maximum incident photon to current conversion efficiency (IPCE) value of 86%, it could be noted that the IPCE of Zn<sub>1-x</sub>Mo<sub>x</sub>O photoanodes at the monochromatic wavelength of 450 nm is up to 12%. Our PEC performances are comparable to those of many oxide-based photoanodes in recent reports. The improvement in photoactivity of PEC water splitting may be attributed to the enhanced visible-light absorption, increased charge-carrier densities, and improved interfacial charge-transfer kinetics due to the synergistic effects of Mo incorporation and Co-Pi modification, thus contributing to photocatalysis. The new design of constructing highly photoactive Co-Pi assisted Zn<sub>1-x</sub>Mo<sub>x</sub>O photoanodes enriches the doping community and sheds light on developing high efficiency photoelectrodes for solar-hydrogen field.

## Reference:

- [1] Y.G. Lin, Y.K. Hsu, Y.C. Chen, S.B. Wang, J.T. Miller, L.C. Chen, and K.H. Chen, *Energy Environ. Sci.*, **5**, 8917 (2012).
- [2] Y.G. Lin, Y.K. Hsu, Y.C. Chen, L.C. Chen, S.Y. Chen, and K.H. Chen, *Nanoscale*, **4**, 6515 (2012).
- [3] Y.K. Hsu, Y.C. Chen, Y.G. Lin, L.C. Chen, and K.H. Chen, *J. Mater. Chem.*, **22**, 2733 (2012).
- [4] Y.G. Lin, Y.K. Hsu, A.M. Basilio, Y.T. Chen, K.H. Chen, and L.C. Chen, *Optics Express*, **22**, A21 (2014).
- [5] Y.K. Hsu, S.Y. Fu, M.H. Chen, Y.C. Chen, and Y.G. Lin, *Electrochimica Acta*, **120**, 1 (2014).
- [6] Y.G. Lin, Y.C. Chen, J.T. Miller, L.C. Chen, K.H. Chen, and Y.K. Hsu, *ChemCatChem*, **6**, 1684 (2014).
- [7] Y.G. Lin, Y.K. Hsu, Y.C. Chen, B.W. Lee, J.S. Hwang, L.C. Chen, and K.H. Chen, *ChemSusChem*, **7**, 2748 (2014).

# A Low-Cost Counter Electrode with a MoSe<sub>2</sub>/PEDOT:PSS Composite Catalytic Film for Dye-Sensitized Solar Cells

Yi-June Huang<sup>1</sup>, Miao-Syuan Fan<sup>1</sup>, Chun-Ting Li<sup>1</sup>, Chuan-Pei Lee<sup>1</sup>, R. Vittal<sup>1</sup>, Kuo-Chuan Ho<sup>1,2\*</sup>

<sup>1</sup>Department of Chemical Engineering, National Taiwan University, Taipei 10617, Taiwan

<sup>2</sup>Institute of Polymer Science and Engineering, National Taiwan University, Taipei 10617, Taiwan

\*E-mail: kcho@ntu.edu.tw

In dye-sensitized solar cells (DSSCs), platinum (Pt) is the most used catalyst as the counter electrode (CE) because of its high conductivity, stability and electrocatalytic activity toward I<sub>3</sub><sup>-</sup>/I<sup>-</sup> redox reaction. However, the high cost and energy-consuming fabrication process of the Pt CE limits its applicability. Two-dimensional (2D) molybdenum diselenide nanosheets, an earth-abundant compound, have been recently demonstrated as a promising material for the application in photovoltaic devices and electrocatalytic systems. With the incorporation of water-dispersible conducting polymer, poly(3,4-ethylene dioxithiophene): poly(4-styrene sulfonate) (PEDOT:PSS), we successfully synthesized MoSe<sub>2</sub>/PEDOT:PSS composite CEs via a facile fabricating route for use in Pt-free DSSCs.

In this study, a composite film containing MoSe<sub>2</sub> and PEDOT:PSS was deposited on fluorine-doped tin oxide (FTO) substrate by a drop-coating method. Three kinds of catalytic films of PEDOT:PSS, MoSe<sub>2</sub>, and MoSe<sub>2</sub>/PEDOT:PSS composite were investigated as the CEs for DSSCs. After the optimization of composition and thickness of the MoSe<sub>2</sub>/PEDOT:PSS composite film, a light-to-electricity conversion efficiency ( $\eta$ ) of 7.58% was achieved for the pertinent DSSC, which was found to be higher than those of cells with bare PEDOT:PSS (2.90%) and bare MoSe<sub>2</sub> (2.29%), and this efficiency (7.58%) is also comparable to that of the cell with a sputtered-Pt CE (7.81%, in Fig. 1). The catalytic ability and electrochemical properties of the CEs were quantified by cyclic voltammetry (CV) (Fig. 2), electrochemical impedance spectroscopy (EIS) (Fig. 3), and Tafel plots (Fig. 4). These measurements suggest that the superior performance of the DSSC with a MoSe<sub>2</sub>/PEDOT:PSS CE, as compared to those with either bare PEDOT:PSS or bare MoSe<sub>2</sub> CEs, is mainly attributed to its better electrocatalytic activity and lower charge transfer resistance toward the I<sub>3</sub><sup>-</sup> reduction reaction.

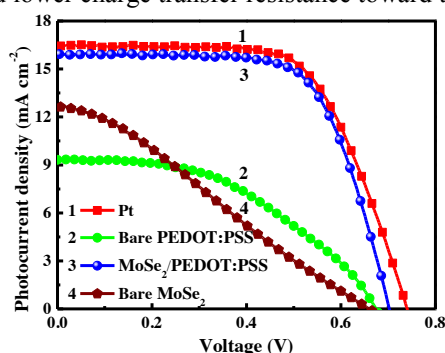


Fig. 1 Photocurrent density-voltage curves of the DSSCs with various CEs measured under 100 mW cm<sup>-2</sup> (AM 1.5G).

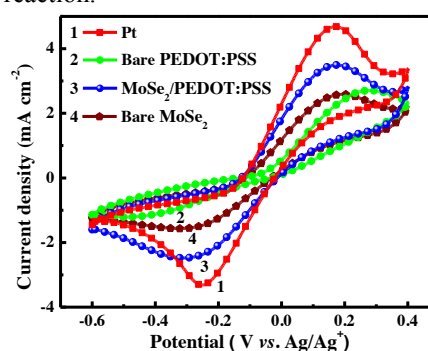


Fig. 2 Cyclic voltammograms of various CEs in an electrolyte of 10.0 mM LiI, 1.0 mM I<sub>2</sub>, and 0.1 M LiClO<sub>4</sub> in ACN.

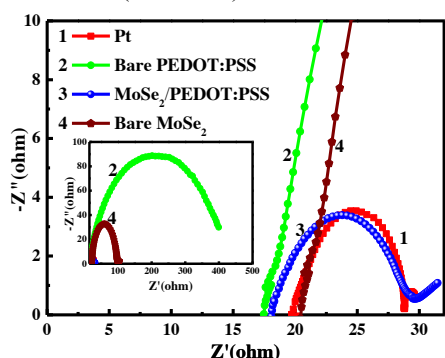


Fig. 3 EIS data of the symmetrical cell with various CEs.

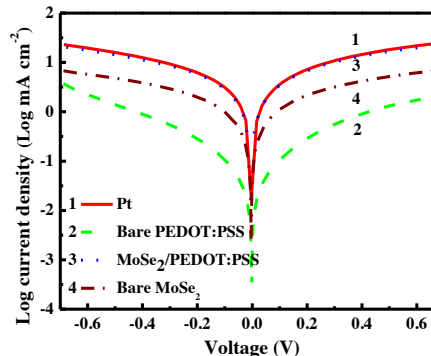


Fig. 4 Tafel polarization curves of the symmetrical cell with various CEs.

# **Resolving the Controversy about the Band Alignment between Rutile and Anatase: the Role of OH<sup>-</sup>/H<sup>+</sup> Adsorption.**

Peter Deák, Jolla Kullgren<sup>1)</sup> Bálint Aradi,<sup>1)</sup> Thomas Frauenheim,<sup>1)</sup> Ladislav Kavan<sup>2)</sup>

1) *Bremen Center for Computational Materials Science, University of Bremen, P.o.B. 330440, D-28334 Bremen, Germany*

2) *J. Heyrovský Institute of Physical Chemistry, Academy of Sciences of the Czech Republic, Dolejškova 3, CZ-18223 Prague 8, Czech Republic*

*University of Bremen, BCCMS, Am Fallturm 1, 28359 Bremen  
deak@bccms.uni-bremen.de*

The synergic effect of mixing rutile (R) and anatase (A) crystals in photocatalysis is often attributed to a staggered alignment of the band structures, but it is widely disputed whether the conduction band edge of rutile or that of anatase is higher. Photoelectron spectroscopy (PES) supports the former, flat-band potential (FBP) measurements the latter. Theoretical alignment of the bulk band structures, as well as calculated offsets across actual interfaces support the PES data. The theoretical study presented here shows that the FBP data can be explained by taking into account the adsorption of free OH<sup>-</sup> and H<sup>+</sup> ions in the electrolyte. We conclude that in case of sintered nano-powders, applied in actual photocatalysis, the dipole layer created by surface adsorption and the one at the R/A interface both have an influence on the alignment, and the end result may change from experiment to experiment.



# **Solution-Processed Nanostructured p-type Photocathodes for Solar Hydrogen Production**

Florian Le Formal, Mathieu S. Prévot, Xiaoyun Yu, Wiktor S. Bourée, Néstor Guijarro, and Kevin Sivula

*Laboratory for Molecular Engineering of Optoelectronic Nanomaterials,  
Institute of Chemical Science and Engineering, École Polytechnique Fédérale de Lausanne,  
CH-1015 Lausanne, Switzerland  
Florian.leformal@epfl.ch, kevin.sivula@epfl.ch*

High-efficiency solar-to-fuel energy conversion can be achieved using a photoelectrochemical (PEC) device consisting of an n-type photoanode in tandem with a p-type photocathode. However, the development of stable and inexpensive p-type photocathodes are needed to make PEC devices economically viable. In this presentation our group's progress in the development of economically-prepared, high performance photoelectrodes will be discussed along with the application toward overall PEC water splitting tandem cells. Specifically, how the use of scalable solution-processing techniques (e.g. colloidal processing of nanoparticles or sol-gels) leads to limitations in charge transport and charge transfer in the resulting thin-film photoelectrode will be examined. Strategies to overcome these limitations such as using charge extraction buffer layers, catalysts, annealing/doping and nanoparticle self-assembly will be additionally presented. Materials of interest are delafossite  $\text{CuFeO}_2$ , CZTS, CIGS, CdS and 2D-layered  $\text{MoS}_2$  and  $\text{WSe}_2$ .

# Graphene Oxides Based Photocatalyst for Solar Fuels

Kuei-Hsien Chen<sup>1,3</sup>, Indrajit Shown<sup>1</sup>, Hsin-Cheng Hsu<sup>2</sup>, Yo-Chong Chang<sup>2</sup>, Ming-Chih Tsai<sup>2</sup>,  
Chen-Hao Wang<sup>2</sup>, Tsu-chin Chou<sup>3</sup>, and Li-Chyong Chen<sup>3</sup>

<sup>1</sup> *Institute of Atomic and Molecular Science, Academia Sinica, Taipei, Taiwan;*

<sup>2</sup> *Department of Materials Science and Engineering, National Taiwan University of Science and Technology, Taipei, Taiwan;*

<sup>3</sup> *Center for Condensed Matter Sciences, National Taiwan University, Taipei 10617, Taiwan  
e-mail address: chenkh@pub.iams.sinica.edu.tw*

It's widely accepted that carbon dioxide accounts for the largest share of the anthropogenic greenhouse-gas emission. Not only the reduction of fossil-fuel consumption, but also CO<sub>2</sub> capturing and sequestration are needed to counter the inevitable threat. Unfortunately, most of the thermochemical processes for CO<sub>2</sub> valorization require extraneous energy input, which may result in the net growth of CO<sub>2</sub> emission. In this regard, photocatalytic conversion of CO<sub>2</sub> to hydrocarbons under solar excitation becomes a viable approach, to solve the energy and environmental crisis by recycling CO<sub>2</sub> to fuels. Bio-mimetic processes based on photosynthesis allowing simultaneous solar energy harvesting and CO<sub>2</sub> reductions thus become highly desirable. In this work, systematic investigation of GO for photocatalytic CO<sub>2</sub> reduction process has been performed based on various GOs synthesized in different conditions. Quantitative and qualitative determinations of the methanol formation have performed by Gas chromatography (GC) and Gas chromatography–mass spectrometry (GC-MS). Photocatalytic conversion of carbon dioxide (CO<sub>2</sub>) to hydrocarbons such as methanol makes possible simultaneous solar energy harvesting and CO<sub>2</sub> reduction, two birds with one stone for the energy and environmental issues. This work describes a high photocatalytic conversion of CO<sub>2</sub> to methanol using graphene oxides (GOs) as a promising photocatalyst. Modified Hummer's method has been applied to synthesize the GO based photocatalyst for the enhanced catalytic activity. Further, Cu and MoS<sub>2</sub> nanoparticles and were deposited on GO as co-catalysts to enhanced the photocatalysis reaction. Not only methanol, but also acetaldehyde were detected. Total solar to fuel yield of 6.8 mole g-cat-1 h-1 have been achieved, which is 240 times enhancement relative to the commercial P-25 photocatalyst. Detailed preparation and characterization of the catalysts will be addressed.

## References:

- [1] J.S. Hwang et al., Nanotechnology 24, 015702 (2013).
- [2] C.K. Chang et al., ACS Nano 7, 1333-1341 (2013).
- [3] H.C. Hsu et al., Nanoscale 5, 262-268 (2013).
- [4] I.Shown et al., Nano Letters 14, 6097-6103 (2014).

# Solar Water Splitting With Nanoimprinted Model Photoelectrodes

M. Schieda<sup>a\*</sup>, H. Krieger<sup>a</sup>, I. Herrmann-Geppert<sup>a,b</sup>, A. C. Bronneberg<sup>c</sup>, D. L. Olynick<sup>d</sup>, T. Klassen<sup>a,b</sup>

<sup>a</sup>*Helmholtz-Zentrum Geesthacht, Institute of Materials Research, Max-Planck-Str. 1, 21502 Geesthacht, Germany*

<sup>b</sup>*Helmut-Schmidt-Universität, Holstenhofweg 85, 22043 Hamburg, Germany*

<sup>c</sup>*Helmholtz-Zentrum Berlin, Institute Solar Fuels, Hahn-Meitner-Platz 1, 14109 Berlin, Germany*

<sup>d</sup>*Molecular Foundry, Lawrence Berkeley National Laboratory, One Cyclotron Road, Berkeley, CA 94720, USA*

*\*Presenting author: mauricio.schieda@hzg.de*

Photoelectrochemical water splitting has gathered significant attention in recent years as a very promising process for the sustainable generation of hydrogen. In a common photoelectrochemical cell design, either one or both electrodes contain semiconducting materials that, when exposed to light, generate charge carriers that can catalyze the water splitting reaction. While surface-structured photoelectrodes have consistently shown better performance, in most studies the structuring geometry is a byproduct of the material synthesis process. As a result, there is very limited control of the final surface structuring, and it is difficult to explore structure-property relationships.

We are employing nanoimprint lithography for the systematic fabrication of structured photoelectrodes with precisely defined surface structuring geometry. The resulting model systems are being used to investigate the influence of surface geometry on photoelectrochemical performance. For our initial model systems we have selected highly doped silicon as a substrate material. The choice of nanoimprint mold determines the dimension of the surface structuring features, while the final geometry and aspect ratio can be controlled by the etching parameters. The substrates are finally coated with TiO<sub>2</sub> and WO<sub>3</sub> by atomic layer deposition. The structured electrodes are extensively characterized in order to correlate structure to physicochemical properties and electrocatalytic performance in the water splitting reaction.

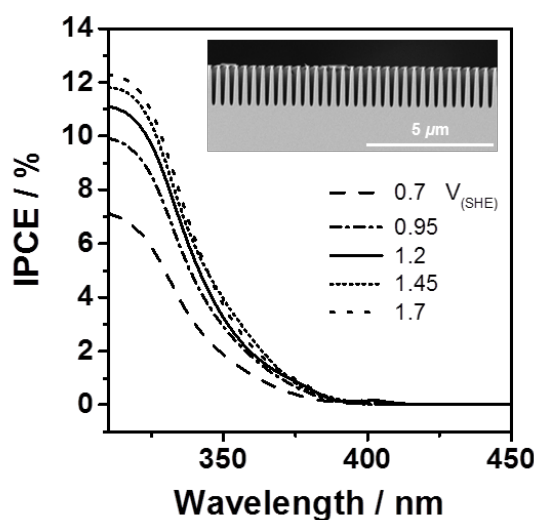


Figure 1. Incident photon-to-current efficiency (IPCE) of a photoanode prepared by ALD deposition of TiO<sub>2</sub> on n-Si (AM1.5G, H<sub>2</sub>SO<sub>4</sub> 0.5 M). Inset: SEM cross-section of structured n-Si substrate.

# The Challenge of Interfacing Catalysts, Protection layers, and Semiconductors in a Tandem Device

B. Seger<sup>1</sup>, M. Malizia<sup>1</sup>, D. Bae<sup>1</sup>, B. Mei<sup>1</sup>, T. Pedersen<sup>2</sup>, P. C. K. Vesborg<sup>1</sup>, R. Frydendal<sup>1</sup>, E. Paoli<sup>1</sup>, C. Slaup<sup>1</sup>, S. Horch<sup>1</sup>, O. Hansen<sup>2</sup>, I. Chorkendorff<sup>1</sup>

<sup>1</sup> CINF, Department of Physics, <sup>2</sup> Nanotech,  
Department of Physics, The Technical University of Denmark.  
E-mail: [ibchork@fysik.dtu.dk](mailto:ibchork@fysik.dtu.dk)

Hydrogen is the simplest solar fuel to produce and in this presentation we shall give a short overview of the pros and cons of various tandem devices [1,2]. The large band gap semiconductor needs to be in front, but apart from that we can choose to have either the anode in front or back using either acid or alkaline conditions. Since most relevant semiconductors are very prone to corrosion the advantage of using buried junctions and using protection layers offering shall be discussed [3-5]. In particular we shall show how doped TiO<sub>2</sub> is a very generic protection layer for both the anode and the cathode [6]. Next we shall discuss the availability of various catalysts for being coupled to these protection layers and how their stability and amount needed may be evaluated [7, 8, 9]. Examples of half-cell reaction using protection layers for both cathode and anode will be discussed though some of recent examples both under both alkaline and acidic conditions. Notably NiO<sub>x</sub> promoted by iron is a material that is transparent, providing protection, and is a good catalyst for O<sub>2</sub> evolution [10]. Si is a very good low band gap semiconductor and the optimal thickness of this in a tandem device will be discussed [11]. We have also recently started searching for large band gap semiconductors like III-V based or perovskite materials and follow the same strategy by using protection layers and catalysts [12]. Finally if time allows we shall also discuss the possibility of making high energy density fuels by hydrogenation of CO<sub>2</sub> instead of hydrogen evolution [13].

## References

- [1] A. B. Laursen et al., Energy & Environ. Science **5** 5577 (2012)
- [2] B. Seger et al. Energy & Environ. Science **7** 2397 (2014)
- [3] B. Seger, et al. Angew. Chem. Int. Ed., **51** 9128 (2012)
- [4] B. Seger, et al., JACS **135** 1057 (2013)
- [5] B. Seger, et al., J. Mater. Chem. A, **1** (47) 15089 (2013)
- [6] B. Mai et al. Submitted (2015).
- [7] R. Frydendal, et al. Chem.Elec.Chem **1** 2075 (2014).
- [8] E. A. Paoli, et al. Chemical Science, Chemical Science, **6** 190 (2015)
- [9] E. Kemppainen et al. In Preparation (2015)
- [10] B. Mei, et al. J. Phys. Chem. Lett. **5** 1948 (2014)
- [11] B. Dowon et al. Energy & Environ. Sci. **8** 650 (2015)
- [12] M. Malizia, et al. J. Mater. Chem. A DOI: 10.1039/C4TA00752B (2014)
- [13] A. Verdaguer-Casadevall et al. In Preparation (2015)

# Novel polymer counter electrode of dye-sensitized solar cells

Hyunwoong Seo<sup>1</sup>, Min-Kyu Son<sup>2</sup>, Shinji Hashimoto<sup>1</sup>, Naho Itagaki<sup>1</sup>, Kazunori Koga<sup>1</sup>, and Masaharu Shiratani<sup>1</sup>

<sup>1</sup>*Graduate School of Information Science and Electrical Engineering, Kyushu University  
744 Motoooka, Nishi-ku, Fukuoka 819-0395, Japan*

<sup>2</sup>*Department of Chemical Sciences and Engineering, École polytechnique fédérale de Lausanne  
Route Cantonale, 1015 Lausanne, Switzerland  
hw.seo@plasma.ed.kyushu-u.ac.jp*

In the research field of electrochemical solar cells, dye-sensitized solar cells (DSCs) have a hard time because perovskite solar cells have made new record of photochemical solar cells. Its efficiency increase is very precipitous. The efficiency which started from 3.8% in 2009 already exceeded 20%. However, perovskite solar cells have hysteresis problem and poor stability despite high performance. On the other hand, DSC is chemically and physically more stable and it is still attractive and competitive. Low manufacturing cost is one of its strong points. However, expensive materials such as Pt and transparent conductive electrode are still used in DSCs. Especially, Pt is a still dominant counter electrode material from initial stage in 1991 although various materials such as carbon, graphene, and polymer have been studied as counter electrode so far. Here, we studied on low cost polymer counter electrode for replacing Pt. Polymer counter electrode was based on poly(3,4-ethylenedioxythiophene):poly(4-styrenesulfonate) (PEDOT:PSS). Its insufficient catalytic reaction significantly decreased fill factor, resulting in low initial performance of DSC. In order to improve catalytic characteristics of polymer counter electrode, PEDOT:PSS layer was surface-modified by nano-particle addition. PEDOT:PSS was deposited on the counter electrode by spin-coating. Flat PEDOT:PSS layer with RMS of 10nm had small surface area and its catalytic reaction was limited. On the other hand, surface-modified PEDOT:PSS layer had enhanced catalytic characteristics with increased surface area. This catalytic activation supplied more electrons into electrolyte than Pt counter electrode and fill factor was much increased. Consequently, overall performance was also enhanced. We tried to investigate various nano-particle materials such as TiO<sub>2</sub>, ZnO, SiO<sub>2</sub>, ZrO<sub>2</sub> and so on. We arranged the effect of various nano-particles in this work and a DSC with improved PEDOT:PSS counter electrode had finally higher performance than a standard DSC with Pt counter electrode.

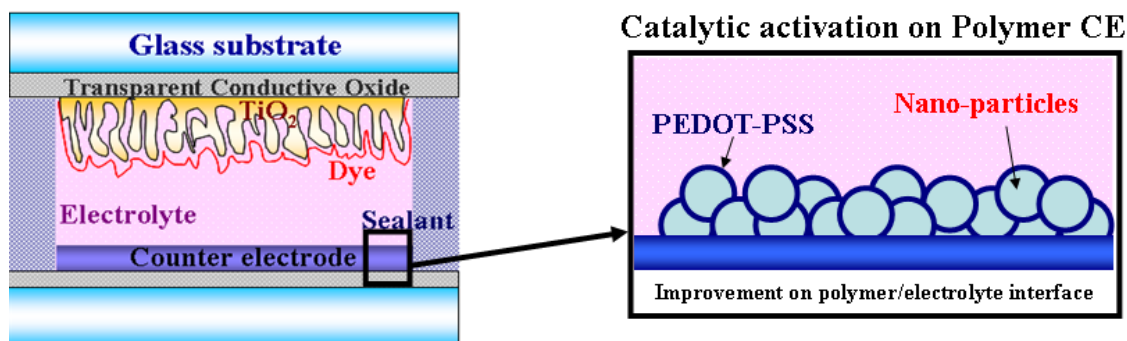


Fig. Catalytic activation of surface-modified polymer counter electrode

# Efficient sunlight-driven reduction of CO<sub>2</sub> to fuels based on Cu<sub>2</sub>O and perovskite absorbers

Marcel Schreier, A. Kari, L. Curvat, T. Moehl, F. Giordano, A. Abate, J. Luo, M.T. Mayer, M. Grätzel  
*Institut des Sciences et Ingénierie Chimiques, Ecole Polytechnique Fédérale de Lausanne*  
*EPFL ISIC LPI, Station 6, CH-1015 Lausanne, Switzerland*  
*marcel.schreier@epfl.ch*

CO<sub>2</sub>-derived fuels present an attractive way towards a sustainable energy system. Mimicking natural photosynthesis by synthesizing carbon based energy carriers using power from the sun allows for closing the anthropogenic carbon cycle and therefore represents an attractive way to store solar energy, a challenge which has not yet found a satisfying solution.

Our group pursues this goal from two angles. In one approach, we demonstrate the photoelectrochemical conversion of solar energy to CO, based on concepts which integrate light absorption and catalysis in a single device. In the second angle, we are exploiting the high open circuit voltage supplied by perovskite solar cells to achieve the unassisted conversion of CO<sub>2</sub> to CO with record efficiency.

Solar irradiation is the only source of energy of sufficient magnitude to replace fossil fuels. Its widespread use will, however, require very large surfaces of absorbers, which should therefore be fabricated from abundant and low cost materials. Here, we show the application of low-cost and scalable Cu<sub>2</sub>O photocathodes in combination with molecular rhenium catalysts, both in solution [1] and, as an extension of this work, molecularly grafted to the photoelectrode surface (Figure 1). From both approaches we observe large photocurrents and photovoltages, demonstrating protected Cu<sub>2</sub>O photocathodes as viable candidates for solar-driven CO<sub>2</sub> reduction processes. Investigating the charge transfer behaviour on these systems allows us to observe unexpected effects which provide new insight into the mechanism of Re-based CO<sub>2</sub> reduction catalysts.

Another type of low-cost solar absorber having attracted significant interest in recent years are CH<sub>3</sub>NH<sub>3</sub>PbI<sub>3</sub>-based solar cells. [2] In addition to achieving very high power conversion efficiencies, these devices exhibit large open circuit photovoltages, making them particularly suitable for water splitting and CO<sub>2</sub> conversion processes. Using these devices, our group has recently demonstrated the highly efficient conversion of solar energy to hydrogen with 12.3% efficiency. [3] Here, by combining series-connected perovskite solar cells with highly efficient electrocatalysts, we take this approach further to demonstrate the efficient splitting of CO<sub>2</sub> to CO and O<sub>2</sub> with record efficiencies exceeding 6.5%, using sunlight as the sole source of energy (Figure 2). [4] This approach is further being pursued towards the use of novel and low-cost nanostructured catalyst fabrication processes, which will also be presented.

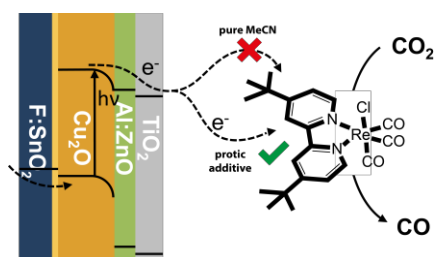


Figure 1: Schematic of the photoelectrochemical conversion of CO<sub>2</sub> on the surface of protected Cu<sub>2</sub>O photocathodes.

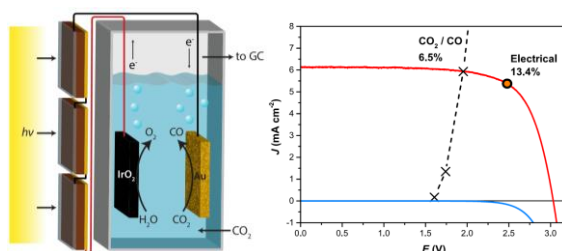


Figure 2: Schematic (left) and J-V curves (right) for the perovskite-driven photolysis of CO<sub>2</sub>.

- [1] M. Schreier, P. Gao, M.T. Mayer, J. Luo, T. Moehl, M.K. Nazeeruddin, et al., Efficient and selective carbon dioxide reduction on low cost protected Cu<sub>2</sub>O photocathodes using a molecular catalyst, *Energy Environ. Sci.* 8 (2014) 855-861.
- [2] M. Grätzel, The light and shade of perovskite solar cells, *Nat. Mater.* 13 (2014) 838-842.
- [3] J. Luo, J.-H. Im, M.T. Mayer, M. Schreier, et al., Water photolysis at 12.3% efficiency via perovskite photovoltaics and Earth-abundant catalysts, *Science*. 345 (2014) 1593-1596.
- [4] M. Schreier, L. Curvat, F. Giordano, L. Steier, A. Abate, et al., Efficient photosynthesis of carbon monoxide from CO<sub>2</sub> using perovskite photovoltaics, *Nat. Commun.* accepted.

# Some Chemical Routes to Form Compact Films of Dye-sensitized Solar Cells

Qinghong Zhang, Jie Zhang, Richuan Rui, Yaogang Li and Hongzhi Wang

*State Key Laboratory for Modification of Chemical Fibers and Polymer Materials, College of Materials Science and Engineering, Donghua University  
2999 North Renmin Rd., Songjiang District, Shanghai 201620, P. R. China.  
zhangqh@dhu.edu.cn*

Compact film of dye-sensitized solar cells (DSSCs) also as known as passivation layer or blocking layer, is formed over the conductive layer of glass prior to the oxide paste printing or coating, and is crucial to inhibit the electron back reaction. There are some physical routes to form perfect compact film such as the magnetron sputtering and atomic layer deposition. However, for a low-cost process as well as the flexible ploymeric substrates consideration, low-temperature process has some advantages over those physical ways. The conductive glass treated with dilute  $\text{TiCl}_4$  solution is widely used a wet chemical route to form compact film of DSSCs, but it is not stable enough and releases  $\text{HCl}$  during drying and subsequently annealing process. We presented some less reactive precursors such as aqueous anatase  $\text{TiO}_2$  sols [1], soluble and neutral titanium (IV) bis (ammonium lactato) dihydroxide [2], to form compact film via spinning coating, dip coating, spray coating as well as self-assembly [3]. In this paper, the less reactive precursor  $(\text{NH}_4)_2\text{TiF}_6$  solution [4] was used to fabrication compact film via liquid phase deposition, and very dense anatase  $\text{TiO}_2$  film where the crystallite size was less than 9 nm were deposited over FTO glass at temperature above 60 °C. Some novel technique such as all-semiconductor self-assembly (ASSA) was also presented to form compact film using various oxide colloids and compared with each other. The energy conversion efficiency ( $\eta$ ), fill factor, electrochemical impedance spectroscopy (EIS) were characterized to evaluate the DSSCs performance in the presence of compact film and in some cases an 20% increment of  $\eta$  was observed. The charge recombination resistance at  $\text{TiO}_2/\text{dye}/\text{electrolyte}$  interface was significant reduced in the presence of chemical route derived compact film, as verified with EIS.

## References:

1. Difeng Qian, Yaogang Li, Qinghong Zhang, Guoying Shi, Hongzhi Wang, *J. Alloy. Compd.*, 2011, 509(41), 10121-10126.
2. Yanmin Hao, Yichuan Rui, Yaogang Li, Qinghong Zhang, Hongzhi Wang, *Electrochim. Acta*, 2014, 117, 268-275.
3. Sujun Yuan, Yaogang Li, Qinghong Zhang, Hongzhi Wang, *Electrochim. Acta*, 2012, 79, 182-188.
4. Hailun Zong, Jie Zhang, Guoying Shi, Yaogang Li, Qinghong Zhang, Hongzhi Wang, *Electrochim. Acta*, 2015, in press, doi:10.1016/j.electacta.2015.03.128

# Photoelectrochemical Zero Bias Hydrogen Generation with a Novel Three Compartment Cell for Decreasing Theoretical and Total Water Electrolysis Voltage (10)

Kenji Sakamaki, Ryoko Kato, Haruka Endo, Masataka Sato, Yoichi Kamo  
Department of Chemistry, Fukushima College, National Institute of Technology (FC-NIT)  
Iwaki, Fukushima 970-8034, Japan  
sakenji@fukushima-nct.ac.jp

The first successful electrochemical photolysis of water reported by Fujishima and Honda in 1972 is a milestone in the history of advanced hydrogen generation [1, 2]. We have developed a novel three compartment cell with a combination of cation (basic) and anion (acidic) exchange membranes (electrolytes) bridging a neutral electrolyte. The three compartment cell generates internal bias induced by a proton concentration gradient, chemical bias, leading to a decrease of theoretical and total water electrolysis voltage for hydrogen generation [3-5].

The onset potential for hydrogen generation is only 1 V with two Pt electrode system in three compartment cell [3]. To extend the above concept, electrochemical water splitting voltage would be significantly decreased with much lower oxygen overpotential alternatives than Pt. Using dimensionally stable anode Ti or Pt/RuO<sub>2</sub>-IrO<sub>2</sub> (Permelec electrode, DeNorra), Ni or Fe in basic compartment cell and Pt in acidic compartment cell, we have accomplished the onset potential of 0.7-0.8 V for hydrogen evolution.

Photoelectrochemical (PEC) zero bias hydrogen generation has already been achieved with self-assembled nanoarchitecture anatase TiO<sub>2</sub> anode in three compartment cell [3-5]. We call this system fuel type (acid-base) PEC zero bias hydrogen generation or water splitting. The net charges are zero in all three solutions in compensation for photoinduced charge separation, leading to an efficient hydrogen generation. Tandem-cell designed to combine a visible light responsive photoelectrode with the chemical bias is performed with Fe(III) oxygen evolving catalyst crafted on Fe<sub>2</sub>O<sub>3</sub> hematite anode being stable in basic solution [6, 7]. We have succeeded in measuring a visible light zero bias photocurrent for hydrogen generation. Our finding is beneficial to the crucial prerequisite for hydrogen economy, environmentally benign large-scale low cost hydrogen production.

## References

1. A. Fujishima and K. Honda, *Nature*, **238**, 37 (1972).
2. A. Fujishima, K. Kohayakawa and K. Honda, *J. Electrochem. Soc.*, **122**, 1487 (1975).
3. K. Sakamaki and Y. Kamo, *65th ISE*, Lausanne, Switzerland, 141164 (2014).
4. M. Sato, Y. Kamo and K. Sakamaki, *MRS Symp. Proc.* Vol. **6544**, p. 1-6 (2013).
5. H. Endo, M. Sato, Y. Kamo and K. Sakamaki, *2<sup>nd</sup> AST 2014*, O-36, p.132, Japan, June 4-6 (2014).
6. T. Lindgren, H. Wang, N. Beermann, L. Vayssieres, A. Hagfeldt, S.-L. Lindquist, *Solar Energy Mater. Sol. Cells*, **71**, 231 (2002).
7. N.D. Carbonare, V. Cristino, S. Berardi, S. Carli, R. Argazzi, S. Caramori, L. Meda, A. Taca, C.A. Bignozzi, *ChemPhysChem*, **15**, 1164 (2014).



# Sol-gel TiO<sub>2</sub> blocking layers for dye-sensitized and perovskite solar cells: Electrochemical properties and electrochemical doping

Marketa Zukalova<sup>1</sup>, Ladislav Kavan<sup>1</sup>, Milan Bousa<sup>1</sup>, Zdenek Bastl<sup>1</sup> and David Havlicek<sup>2</sup>

<sup>1</sup>*J. Heyrovský Institute of Physical Chemistry, AS CR, Dolejškova 3, CZ-182 23 Prague 8, CR*

<sup>2</sup>*Dept. of Inorg. Chem., Faculty of Science, Charles University, Albertov 2030, Prague 2, CR*  
marketa.zukalova@jh-inst.cas.cz

Compact TiO<sub>2</sub> thin films are used as blocking layers in solid state dye sensitized solar cells (DSCs), and in the perovskite solar cells. Here, the TiO<sub>2</sub> film serves as an electron collector and simultaneously as a buffer layer, preventing recombination of photoexcited electrons from the substrate, typically F-doped SnO<sub>2</sub> conducting glass (FTO) with the hole conductor[1]. The compact TiO<sub>2</sub> film is grown on top of FTO, usually by spray pyrolysis, DC-magnetron sputtering, electrochemical deposition, atomic layer deposition and spin coating. Recently, we developed facile sol-gel dip coating technique producing dense and extremely mechanically stable TiO<sub>2</sub> thin films on various substrates from precursor solutions containing poly(hexafluorobutylmethacrylate) or hexafluorobutyl methacrylate as the structure-directing agents[2]. The films are quasi-amorphous, but crystallize to TiO<sub>2</sub> (anatase) upon heat treatment at 500°C. Blocking properties of the films were tested by cyclic voltammetry using Fe(CN)<sub>6</sub><sup>3-/4-</sup> in aqueous electrolyte solution as the model redox probe[3]. The same test was repeated by spiro-OMeTAD in dichloromethane electrolyte solution. The as-grown films can produce an excellent rectifying interface with almost no pinholes, however, defects are created upon heat treatment at 500°C in air, when anatase crystallization occurs. The overall area of thermally induced pinholes is comparable to that in spray-pyrolyzed titania films. The flat-band potentials,  $\phi_{FB}$  of the as-grown films are upshifted by about 0.2–0.4 V against the values predicted for a perfect anatase single-crystal surface, but they still follow the Nernstian pH dependence. Proton insertion into titania takes place during electrochemical n-doping in aqueous acidic electrolyte solution at sufficiently negative potential[4]. The good-quality films are ideally compact, mimicking the properties of a macroscopic single crystal electrode. In contrast to porous polycrystalline electrodes, the doping of our dense films persists for at least weeks, if the electrode is stored in air at room temperature. Doping manifests itself by permanent color changes and by characteristic morphological differences on the surface. The doped films still accommodate Li<sup>+</sup> by electrochemical insertion, but competition between Li<sup>+</sup> and H<sup>+</sup> ions in the lattice is detected by cyclic voltammograms.

Acknowledgement: This research was supported by the Grant Agency of the Czech Republic (contract No. 13- 07724S), European Union FP7 Programme (No. 604391 Graphene Flagship/PERHENE) and COST Action CM1104

[1] Grätzel, M. *Nat. Mater.* **2014**, *13*, 838-842.

[1] Lee, M. M.; Teuscher, J.; Miyasaka, T.; Murakami, T. N.; Snaith, H. J. *Science*, **338**, (2012), 643-647.

[2] Prochazka, J.; Kavan, L.; Zukalova, M.; Janda, P.; Jirkovsky, J.; Zivcova, Z. V.; Poruba, A.; Bedu, M.; Dobbelin, M.; Tena-Zaera, R. *Journal of Materials Research*, **28**, (2013), 385-393.

[3] Kavan, L.; Zukalova, M.; Vik, O.; Havlicek, D. *ChemPhysChem*, **15**, (2014), 1056-61.

[4] Zukalova, M. B., M.; Jirka, I.; Bastl, Z.; Kavan, L. *J. Phys. Chem. C* (2014), **118**, 25970–25977

# An Organic Semiconductor as a Photoanode for Solar Water Splitting

Pauline Borno, Mathieu Prévot, Xavier Jeanbourquin and Kevin Sivula

*Institute of Chemistry and Chemical Engineering, École Polytechnique Fédérale de Lausanne, Station 6  
1015 Lausanne Switzerland  
pauline.borno@epfl.ch*

For the past 30 years, photoelectrochemical cells (PEC) have held promise as an inexpensive route to convert renewable solar energy into chemically stored energy (solar fuels) on a scale suitable for the world energy demand. Indeed the use of solar fuel offers a decentralized and constant energy flux insensitive to daily or seasonal variation. A solar-to-hydrogen (STH) efficiency of over 20% has been shown to be theoretically feasible when using a PEC tandem cell for water-splitting and cells with high efficiency have been demonstrated, however the materials and fabrication are too expensive to compete with hydrogen production via standard photovoltaic devices in combination with electrolyzes. This has motivated a search for new materials that can offer high performance, but also low device cost. In the last decade, an emerging field of organic semiconductor materials has attracted much attention for solar photovoltaic devices due to their optoelectronic versatility and ability to be processed by solution based roll-to-roll techniques. Despite their popularity only a few reports have investigated these materials for solar water splitting due to their low stability in the harsh operating conditions.

In this work we demonstrate the successful use of a bare conjugated organic material as a photoanode for solar water splitting. Poly(benzimidazobenzophenanthroline) (BBL) n-type material was selected due to its rigid ladder-type backbone offering high stability in an aqueous environment and high thermal stability. A dispersion-assisted spray deposition technique was designed to overcome processing difficulties with this rigid, poorly-soluble material and the preparation of large-area of homogeneous films with controllable thickness is demonstrated. Optical and morphological characterization of the films performed by UV-vis measurement and scanning electron microscopy show very good absorption characteristics covering a broad range of the visible spectrum and a microporous morphology. Determination of the band gap at 1.86 eV and position of LUMO/HOMO level shows adequate energy position for its use as a photoanode in a tandem cell. The film was further characterized by electrochemical measurements (J-V curve under chopped light, cyclic voltammetry and impedance spectroscopy) and a photocurrent of 0.2 mAcm<sup>-2</sup> at 1.23 V vs. RHE was observed under standard illumination conditions in aqueous electrolyte with a sacrificial electron donor. Possible use for water oxidation is subsequently demonstrated in aqueous electrolyte with the direct observation of OH radical product. Mott-Schottky analysis reveals the independence of the flat band potential with respect to pH of electrolyte. Different surface treatments were finally investigated to reduce kinetics limitations for water oxidation and the direct production of molecular O<sub>2</sub> from water oxidation was observed.

# Novel Cathode and Photocathode Materials for Dye-Sensitized Solar Cells

L. Kavan<sup>1</sup>, Z. Vlckova-Zivcova<sup>1</sup>, H. Krysova<sup>1</sup>, P. Cigler<sup>2</sup>, P. Liska<sup>3</sup>, S. M. Zakeeruddin<sup>3</sup> and M. Grätzel<sup>3</sup>

<sup>1</sup>*J. Heyrovský Institute of Physical Chemistry, v.v.i., Academy of Sciences of the Czech Republic, Dolejškova 3, CZ-18223 Prague 8, Czech Republic.*

<sup>2</sup>*Institute of Organic Chemistry and Biochemistry, v.v.i. Academy of Sciences of the Czech Republic, Flemingovo nám. 2, 166 10 Prague 6, Czech Republic.*

<sup>3</sup>*Laboratory of Photonics and Interfaces, Institute of Chemical Sciences and Engineering, Swiss Federal Institute of Technology, CH-1015 Lausanne, Switzerland*

*Ladislav.Kavan@jh-inst.cas.cz*

Cathode in classical dye-sensitized solar cell (DSC) is usually a platinized F-doped SnO<sub>2</sub> (FTO) which, however, contributes by about >20-60% to the cost of the DSC-module. The search for cheaper cathode materials points at nanocarbons and graphene-based materials, particularly for Co-mediated DSCs.[1,2] Another alternative, which also works well with the I<sub>3</sub><sup>-</sup>/I<sup>-</sup> redox mediator, is the woven fabric consisting of transparent PEN fibers in warp and electrochemically platinized tungsten wires in weft.[3] (Patented by Sefar AG: Peter Chabreck et al., European Patent Specification EP 2 347 449 B1, published 25.03.2015.) This electrode outperforms the platinized FTO in serial ohmic resistance,  $R_s$  (1.5 vs. 8.2  $\Omega\text{cm}^2$ ), charge-transfer resistance for triiodide reduction (0.59  $\Omega\text{cm}^2$  vs. 0.76  $\Omega\text{cm}^2$ ) and offers comparable or better optical transparency in the visible and particularly in the near-IR spectral region ( $\approx 80\%$ ). The Pt-W/PEN cathode exhibits good stability during electrochemical load with the maximum (diffusion-limited) current both in cathodic and anodic directions, and during long term ( $\approx$ months) storage at open circuit. The practical dye-sensitized solar cells with either Pt-W/PEN or Pt-FTO cathodes show similar performance, confirming that the former is a promising alternative for replacement of conductive glass in the DSC cathodes. In the field of p-DSCs (with sensitized photocathode) the generic semiconductor material is p-NiO. An alternative p-semiconductor is B-doped nanodiamond which offers excellent chemical and electrochemically stability, optical transparency and favorable electrical properties. The electrochemical inertness of BDD is beneficial in view of the corrosive nature of certain electrolyte solutions used in DSCs. Spectral sensitization of nanodiamond was carried out by anchoring of dyes like 4-(bis-{4-[5-(2,2-dicyano-vinyl)-thiophene-2-yl]-phenyl}-amino)-benzoic acid (P1 from Dyenamo AB) with polyethyleneimine as a linker. The sensitized diamond exhibits stable cathodic photocurrents under visible light illumination in aqueous electrolyte solution with dimethylviologen serving as electron mediator.[4] In spite of the simplicity of the surface sensitization protocol, the photoelectrochemical performance is similar or better compared to that of other sensitized diamond electrodes which were reported in previous studies.[5]

Acknowledgement: This work was supported by the Czech National Foundation, contract No. 13-07724S.

## References

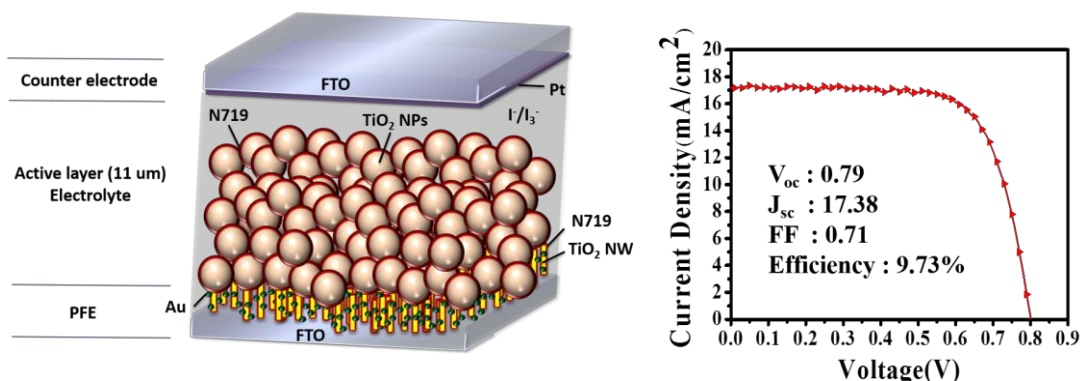
- [1] L. Kavan, J.-H. Yum, M. Grätzel, *Electrochim. Acta*, 128 (2014) 349.
- [2] L. Kavan, *Top. Curr. Chem.*, 348 (2014) 53.
- [3] L. Kavan, P. Liska, S. M. Zakeeruddin, M. Grätzel, *ACS Appl. Mater. Interfaces*, 6 (2014) 22343.
- [4] H. Krysova, Z. Vlckova-Zivcova, J. Barton, V. Petrak, M. Nesladek, M. Cigler, L. Kavan, *Phys. Chem. Chem. Phys.*, 17 (2015) 1165.
- [5] S. W. Yeap, D. Bevk, X. Liu, H. Krysova, A. Pasquarelli, D. Vanderzande, L. Lutsen, L. Kavan, M. Fahlman, W. Maes, K. Haenen, *RCS Adv.*, 4 (2014) 42044.

# Plasmon-Induced Efficiency Enhancement on Dye-Sensitized Solar Cell by a 3D TNW-AuNP Layer

Kuan-Jiuh Lin, Yin-Cheng Yen

Department of Chemistry, National Chung Hsing University  
250, Kuo Kuang Road, Taichung 402, Taiwan, R.O.C.  
kjlin@dragon.nchu.edu.tw

It is well known that the narrow absorption wavelength and low absorption coefficient of N719 dye is a major problem which limits the development of DSSCs. In order to overcome this problem, we propose a new type of plasmonic functionalized electrodes (PFEs) which can be used in different dye-absorbed DSSCs to enhance light harvest and cell efficiency by either antireflective (AR) properties of TNWs or/and plasmonic effect of Au nanoparticles (NPs). A remarkable plasmonic red-shift from 520 nm to 575 nm was observed in Au (11 nm). It was attributed that Au NPs have a specific bonding interaction with TNWs and plasmonic electrode exhibit a strong localized electric field. We demonstrated a 55.68% improvement in the case of  $\text{TiCl}_4$  treated Au (11 nm). The aforementioned superior PV performance achieved herein is mainly attributed to localized electric field improvement by plasmonic collective coupling effect within this favorable TNW-AuNP hybrid nanostructures. Moreover, the fabrication technique of PFEs is inexpensive, simple, and can easily be scaled up which is suitable for mass production. We believe new type of PFEs will beyond the current record of efficiency after optimization. Also, PFEs may open up numerous possibilities for the use of organic solar cells, electric photocatalysts and water splitting components.



Reference:

1. Yin-Cheng Yen, Po-Hung Chen, Jing-Zhi Chen, Jau-An Chen, and Kuan-Jiuh Lin\*, "Plasmon-Induced Efficiency Enhancement on Dye-Sensitized Solar Cell by a 3D TNW-AuNP Layer" ACS Appl. Mater. Interfaces, (2015), 7 (3), 1892–1898.
2. Jing-Zhi Chen, Wen-Yin Ko, Yin-Cheng Yen, and Kuan-Jiuh Lin\*, "Anti-reflection  $\text{TiO}_2$  Nanowire Electrode and Its Electrochromic Properties", ACS Nano (2012), 6, 6633 – 6639.

## In-situ photoelectrochemical polymerization approach for efficient solid-state dye sensitized solar cells

Jinbao Zhang,<sup>1</sup> Nick Vlachopoulos,<sup>2</sup> Erik Johansson,<sup>1</sup> Mohamed Jouini,<sup>3</sup> Gerrit Boschloo,<sup>1</sup> Anders Hagfeldt<sup>2</sup>

<sup>1</sup>Department of Chemistry-Ångström Laboratory, Uppsala University  
Lägerhyddsvägen 1, 75120 Uppsala, Sweden

<sup>2</sup>Laboratory of Photomolecular Science, Institute of Chemical Sciences and Engineering, École Polytechnique Fédérale de Lausanne (EPFL)

EPFL-FSB-ISIC-LSPM, Station 6, CH-1015 Lausanne, Switzerland

<sup>3</sup>Institution Université Paris Diderot Paris 7, Sorbonne Paris Cité,  
ITODYS UMR 7086 CNRS, 15 rue Jean-Antoine de Baïf, 75205 Paris Cedex 13, France  
Jinbao.zhang@kemi.uu.se

Conducting polymer-based hole conductors (HCs), directly deposited into the mesoporous structure of dye-coated TiO<sub>2</sub> electrodes by *in-situ* photoelectrochemical polymerization (PEP) method, have the advantage of easy penetration and uniform pore infiltration compared to small molecular HCs used in solid-state dye-sensitized solar cells (sDSCs). The aforementioned advantages of conducting polymer-based HCs generated by PEP would lead to an efficient charge separation at the TiO<sub>2</sub>/dye/HC interface. Besides, instead of the additional chemical doping for small-molecule HCs, the remarkably high hole conductivity of conducting polymer HCs resulting from *in-situ* electrochemical doping in PEP could provide a high charge collection yield in devices, making it a competitor to the usual alternatives, redox mediator-containing liquid electrolytes or small-molecule HCs, as dye solar cell charge-transport media.<sup>[1]</sup>

The present work is directed toward the study on how the parameters in PEP affect the physicochemical properties of the formed conducting polymer and, consequently, the corresponding solar cell performance. At first, an aqueous micellar electrolyte, instead of the usual organic solution, was demonstrated for the first time to be possible to use as PEP medium to generate PEDOT HC from *bis*-EDOT precursor.<sup>[2]</sup> The advantage of aqueous PEP over organic PEP is not only the fact that the process is inexpensive and environment-friendly character of the process, but also that the oxidation potentials of the precursor in aqueous solution is less positive, resulting to an increased driving force for PEP. The sDSCs based on PEDOT generated from aqueous PEP show a solar-to-electrical power conversion efficiency (PCE) of 5.2% with an organic sensitizer, as compared to 5.6% for similar devices based on organic PEP.<sup>[3]</sup> By comparison of the PEDOT properties for layers generated from the two approaches, a PEDOT variety with shorter polymer chains was obtained in aqueous PEP, as corroborated by matrix-assisted laser desorption mass spectrometry, resulting to better dye regeneration, but also to faster charge recombination in the devices.<sup>[4]</sup> A second direction of work is to use the less expensive precursor (monomer) EDOT as precursor to replace *bis*-EDOT. The PEP of EDOT was first time achieved in aqueous electrolyte due to the much lower oxidation potential than that in organic solution, where PEP is difficult; the corresponding sDSCs exhibit 3.0% efficiency.<sup>[5]</sup> Thirdly, an alternative monomer, 3,4-ethylenedioxythiophene (EDOT), was efficiently used in PEP by combining with organic metal-free charge-transfer (Donor- $\pi$ -Acceptor) dyes. The devices based on the PEDOT hole conductor have a PCE of 4.5%; this level of performance, achieved for the first time for PEDOT-based sDSCs, is attributed to the high hole conductivity of PEDOT and the good blocking effect from organic dyes;<sup>[6]</sup> At last, the importance of the dyes' chemical structure and energy levels on the PEP has been systematically investigated. It is shown that, on one hand, the dyes' blocking effect variations, due to the different chemical structure, play a significant role on the interfacial charge recombination; on the other hand, the redox potentials of the dyes could affect the kinetics of the PEP process and the final polymer properties. By effectively combination of an organic D- $\pi$ -A dye LEG4 and the formed PEDOT HC, a PCE of 7.1% with a record current (13.4 mAcm<sup>-2</sup>) has been recently achieved for sDSCs. This impressive photovoltaic performance was attributed to the high hole conductivity of PEDOT (2.0 Scm<sup>-1</sup>) generated from PEP, as well as the effective dye blocking effect, leading to a high yield of charge collection.

[1] Vlachopoulos, N., Zhang, J., Hagfeldt, A., *Chimia*, 2015, 69, 41-51

[2] Yang, L., Zhang, J., Shen, Y., et al., *J. Phys. Chem. Lett.* 2013, 4, 4026-4031

[3] Zhang, J., Yang, L., Shen, Y., et al., *J. Phys. Chem. C* 2014, 118, 16591-16601

[4] Zhang, J., Ellis, H., Yang, L., et al., *Anal. Chem.*, DOI:10.1021/ac504851f

[5] Zhang, J., Jarboui, A., Vlachopoulos, N., et al., *Electrochimica Acta*, doi:10.1016/j.electacta.2015.01.077.

[6] Zhang, J., Häggman, L., Jouini, M., et al. *ChemPhysChem*, 2014, 15, 1043-1047

|

Mis en forme : Gauche

# Microemulsion-assisted Zinc Oxide Synthesis: Morphology Control and its Applications in Photoanodes of Dye-Sensitized Solar Cells

Chuan-Pei Lee<sup>1</sup>; Chun-Ting Li<sup>1</sup>; Miao-Syuan Fan<sup>1</sup>; Yi-June Huang<sup>1</sup>; Ling-Yu Chang<sup>2</sup>; Jiang-Jen Lin<sup>2</sup>; Kuo-Chuan Ho<sup>1,2\*</sup>

<sup>1</sup>Department of Chemical Engineering, National Taiwan University, Taipei 10617, Taiwan

<sup>2</sup>Institute of Polymer Science and Engineering, National Taiwan University, Taipei 10617, Taiwan

\*E-mail: kcho@ntu.edu.tw

Zinc oxide (ZnO) has been reported as an alternative for dye-sensitized solar cells (DSSCs) due to it offers a large direct band gap of 3.37 eV, which is similar to TiO<sub>2</sub> and high electron mobility as well as provide surface area for dye-loading. Furthermore, ZnO also can be tailored to various nanostructures as compared to TiO<sub>2</sub> that provides a promising means for improving the performance of the photoanode in DSSCs.

In this study, we synthesize ZnO crystals with structures of hexagonal club (HC), intergrowth nanoparticles (INP), and hexagonal plate (HP) by microemulsion technique using the surfactants of cationic cetyltrimethylammonium bromide (CTAB), nonionic Triton<sup>®</sup> X-100, and anionic docusate sodium (AOT), respectively. From the X-ray diffraction (XRD) analysis, all the synthesized ZnO crystals show obvious peaks corresponding to (100), (002), (101) planes of ZnO, namely the wurtzite crystal phase. The scanning electron microscopy (SEM) and high-resolution transmission electron microscopy (HR-TEM) images (Fig. 1) reveal that each HC ZnO has two opposite hexagonal faces (parts), and it has average diameter of 350 nm and average length of 500 nm for each part; the INP ZnO has average diameter of 20~50 nm and inter-grown with each particle; the HP ZnO has average width of 650 nm and thickness of 120 nm. We believe that both the sub-micro sized HC and HP ZnO crystals will be meritorious in the present work as large particles are effective for light scattering; the nano-sized INP ZnO crystal will be meritorious in the present work as intergrowth structures are effective for electron transport in the photoanode of DSSCs. As expected, we obtained higher cell efficiency of 7.72% by using INP/HC/HP composite photoanode, as compared with commercial ZnO nanoparticles (3.53%).

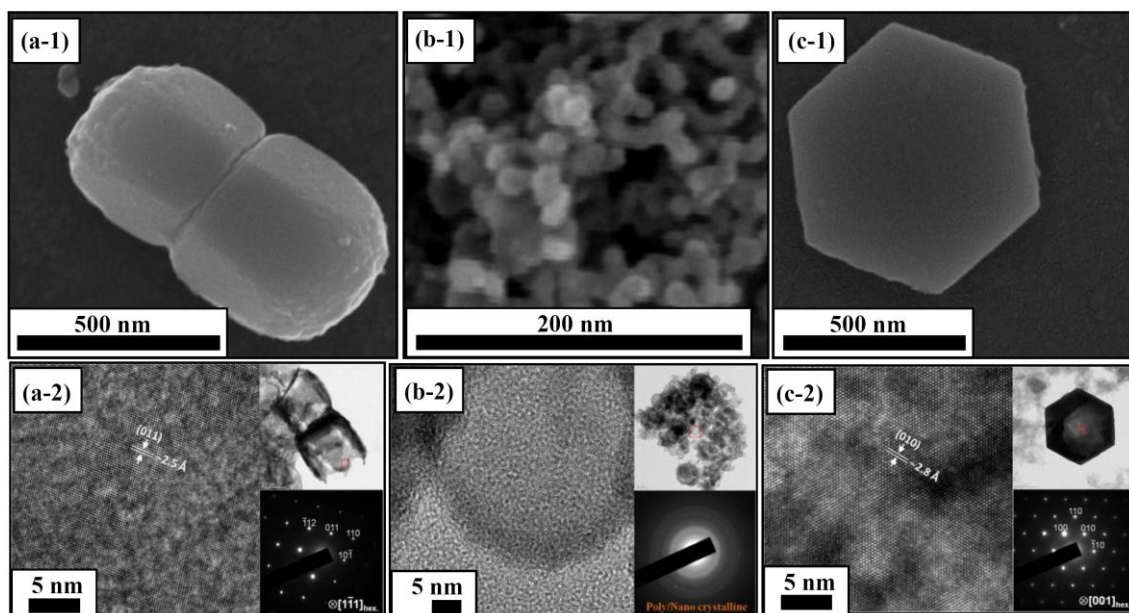


Fig. 1 (a) SEM and (b) HR TEM images for INP, HC and HP ZnO crystals.



# Highly Efficient Cobalt Selenide Hierarchical Nano-Wall for the Electro-Catalytic Counter Electrodes in Dye-Sensitized Solar Cells

I-Ting Chiu<sup>1</sup>, Chun-Ting Li<sup>1</sup>, Chuan-Pei Lee<sup>1</sup>, Pei-Yu Chen<sup>1</sup> and Kuo-Chuan Ho<sup>1,2,\*</sup>

<sup>1</sup> Department of Chemical Engineering, National Taiwan University, Taipei 10617, Taiwan

<sup>2</sup> Institute of Polymer Science and Engineering, National Taiwan University, Taipei 10617, Taiwan

\*E-mail: kcho@ntu.edu.tw

Recently, dye-sensitized solar cells have attracted more and more attention because the advantages of their high conversion efficiencies, low costs and simple preparation processes. In addition, they can work under low-light intensity and be applied onto flexible substrates. However, the development of DSSCs is limited by the usage of the expensive Pt counter electrode. Thus, the aim nowadays for developing a substitute material is not only to reach high cell efficiency ( $\eta$ ) but to maintain a low cost. Among all the potential substitutes, researchers have paid an intensive attention to cobalt selenide due to its earth abundance, high conductivity, and good electro-catalytic ability. Cobalt selenide counter electrode (CE) often possesses a structure of bulk or particles, thus the lack of dimensional electron transfer pathways and low active surface areas confine the pertinent DSSCs' performance.

In this work, we aim to prepare a low dimensional CoSe<sub>2</sub> with a structure of hierarchical nano-wall via a simple electro-deposition process. First, the cleaned fluorine-doped tin oxide glasses (1 cm<sup>2</sup>) were separately used as the working electrodes for a three-electrode system in three different aqueous bathes containing 5.0 mM cobalt chloride and 0.75 mM selenourea with pH values of 4.0, 6.0, and 8.0; the obtained CoSe<sub>2</sub> films were denoted as CoSe<sub>2</sub>-4, CoSe<sub>2</sub>-6, and CoSe<sub>2</sub>-8, respectively. A Pt foil and a Ag/Ag<sup>+</sup> electrode were used as the counter and reference electrodes, respectively. A pulse-potential voltage procedure was applied for 100 cycles for each bath; one cycle contained -0.9 V for 6 s and 0 V for 4 s. The obtained CoSe<sub>2</sub> films were treated via a post annealing process at 500 °C for 30 min in vacuum to obtain a good crystallinity. From the field-emission scanning electron microscopy (FE-SEM) images shown in Fig. 1, the CoSe<sub>2</sub>-4, CoSe<sub>2</sub>-6, and CoSe<sub>2</sub>-8 show the lump-like, ball-like and hierarchical nano-walled-like surface morphologies, respectively. Among them, CoSe<sub>2</sub>-8 simultaneously possesses the two-dimensional (2D) structures and a porous surfaces, which imply an outstanding electron transfer capability and a great electro-catalytic ability, respectively. From the cyclic voltammetry (CV) analysis, the cathodic peak current densities of CoSe<sub>2</sub>-4, CoSe<sub>2</sub>-6, and CoSe<sub>2</sub>-8 are 1.49, 1.36, 1.70 mA cm<sup>-2</sup>, respectively; indicating the electro-catalytic ability of those CoSe<sub>2</sub> films shows a tendency of CoSe<sub>2</sub>-8 > CoSe<sub>2</sub>-6 > CoSe<sub>2</sub>-4. In Fig. 1(e), the DSSCs with CoSe<sub>2</sub>-4, CoSe<sub>2</sub>-6, and CoSe<sub>2</sub>-8 CEs give the  $\eta$ 's of 8.41%, 7.83%, and 8.92%, respectively. It is notable that the hierarchical nano-wall CoSe<sub>2</sub>-8 renders the best  $\eta$ , which is even higher than that of Pt (8.25%); therefore, the earth abundant CoSe<sub>2</sub>-8 is a very promising material to replace Pt.

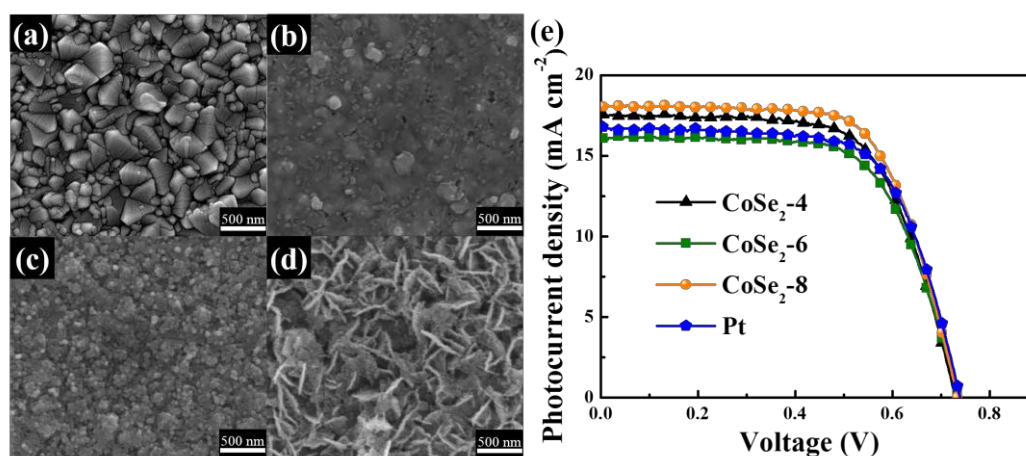


Fig. 1 FE-SEM images of (a) Pt film (b) CoSe<sub>2</sub>-4, (c) CoSe<sub>2</sub>-6, and (d) CoSe<sub>2</sub>-8. (e) Photocurrent density-voltage curves of the DSSCs with Pt and CoSe<sub>2</sub> CEs, obtained at 100 mW cm<sup>-2</sup>.



# Efficient Quasi-Solid-State Dye-Sensitized Solar Cells with Novel Polymeric Ionic Liquids

Yu-Hao Tseng<sup>1</sup>, Miao-Syuan Fan<sup>1</sup>, Chuan-Pei Lee<sup>1</sup>, Chun-Ting Li<sup>1</sup>, Ming-Chou Chen<sup>2</sup>, and Kuo-Chuan Ho<sup>1,3,\*</sup>

<sup>1</sup> Department of Chemical Engineering, National Taiwan University, Taipei 10617, Taiwan

<sup>2</sup> Department of Chemistry, National Central University, Taoyuan City 32001, Taiwan

<sup>3</sup> Institute of Polymer Science and Engineering, National Taiwan University, Taipei 10617, Taiwan

\* Corresponding author: kcho@ntu.edu.tw

Polymeric ionic liquids (PILs) have stirred great interest in the fields of polymer chemistry and materials science, not only because of the combination of the unique properties of ILs with the macromolecular architecture, but also a matter of creating new properties and functions. The major advantages of using a PIL instead of a traditional IL are the enhanced mechanical stability, improved processability, durability, and spatial controllability over the traditional IL species. Recently, PILs have been demonstrated as promising quasi-solid-state (QSS) electrolytes in dye-sensitized solar cells (DSSCs) for improving the cell efficiency or durability.

In this study, we synthesized two kinds of polymeric ionic liquids, named as RAFT-A and RAFT-B (Fig. 1), for the use of quasi-solid-state electrolyte in DSSC. The QSS-DSSC with RAFT-A achieved 7.15% cell efficiency ( $\eta$ ) having open-circuit voltage ( $V_{OC}$ ) of 0.75 V, short-circuit current density ( $J_{SC}$ ) of 14.69 mA cm<sup>-2</sup>, and fill factor ( $FF$ ) of 0.65. Meanwhile, the QSS-DSSC with RAFT-B exhibited an  $\eta$  of 7.71%, with  $V_{OC}$  of 0.79 V,  $J_{SC}$  of 14.86 mA cm<sup>-2</sup>, and  $FF$  of 0.60. In order to realize the difference of the cell efficiencies, the electrochemical impedance spectroscopy (EIS) technique was employed to analyze the interfacial resistance in pertinent DSSCs. It was found that the charge-transfer resistance at the TiO<sub>2</sub>/dye/electrolyte interface ( $R_{CT}$ ) of the QSS-DSSC with RAFT-B is lower than that of the cell with RAFT-A. Moreover, from the Bode plot of the above EIS data, we found that the QSS-DSSC with RAFT-B shows longer electron life-time (8.69 ms) than the cell with RAFT-A (7.39 ms). These EIS results are in consistency with their photovoltaic performances. These properly designed PILs pave a promising way for developing highly efficient QSS-DSSCs.

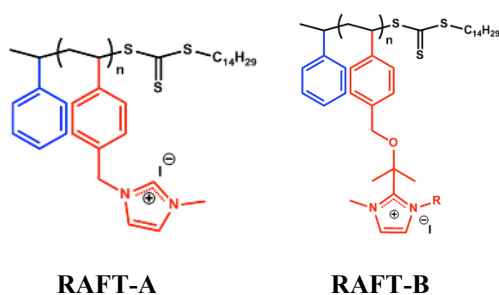


Fig. 1: The chemical structures of RAFT-A and RAFT-B.

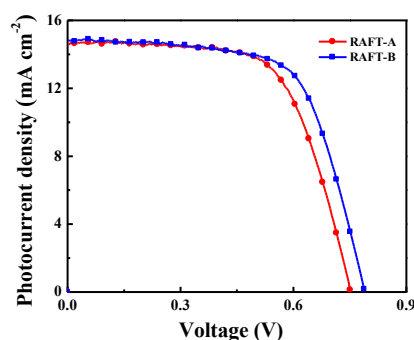


Fig. 2: Photovoltaic performance of the QSS-DSSCs with PILs, measured under 100 mW cm<sup>-2</sup>

# Thin film metallic glass as a diffusion barrier for flexible CIGS solar cell on stainless steel substrate: A feasibility study

Lingjun Xue, Jinn P. Chu\*, [Wahyu Diyatmika](#)

*Department of Materials Science and Engineering, National Taiwan University of Science and Technology*

*No. 43, Sec. 4, Keelung Rd., Da'an Dist., Taipei 10607, Taiwan (R.O.C.)*

*\*e-mail address: [jpchu@mail.ntust.edu.tw](mailto:jpchu@mail.ntust.edu.tw)*

Due to its high efficiency, long-term stable performance and potential for low-cost production, Copper indium gallium selenide (CIGS) solar cells have attracted considerable interests for the last decades. One of the trends is to fabricate them on flexible stainless steel substrates. However, during the high temperature processes, the detrimental elements from the substrates (mainly iron) may diffuse into the absorber layers, causing serious degradation in efficiency. In this study, we examine the feasibility of applying thin film metallic glasses (TFMGs) as diffusion barriers. In our preliminary works, the multilayer structures of steel/TFMG/Mo and steel/Mo were annealed and investigated. X-Ray diffraction results showed clear evidence of diffusion of Fe in the absence of TFMG barrier. According to this promising result, the CIGS solar cell devices were then processed and studied. The TEM-EDS results indicated that TFMG barrier efficiently blocked the substrate elements. The current-voltage (I/V) curve measurements results showed improved efficiency by depositing TFMG barrier. Between the two barriers, Zr-based TFMG barrier had better performance.

**Keywords:** CIGS thin film solar cell, stainless steel, thin film metallic glass, diffusion barrier

# A Novel Preparation Method for Titanium Dioxide in the Rutile Phase for Electrochemical Photocatalytic Applications

Yen-Chun Chuan Sun, Chi-Chang Hu\*

Department of Chemical Engineering, National Tsing Hua University

101, Sec. 2, Kuang-Fu Rd., Hsin-Chu city, 30013 Taiwan

\* Corresponding author: cchu@che.nthu.edu.tw

Solar water splitting on semiconductors (*e.g.*,  $\text{TiO}_2$ ) has been proposed to be a potential process for hydrogen generation. Since the bandgap of n-type  $\text{TiO}_2$  in the anatase phase is known to be 3.2 eV, it is a challenge for effective separation of electron/hole pairs under the visible light irradiation. This work aims to develop a  $\text{TiO}_2$  photo-anode with a high photocurrent density under the solar light illumination although most studies focused on the solar performance under the ultra violet (UV) light. This study tries to modify the Ti foil, including thermal growth of  $\text{TiO}_2$  in the rutile phase (R- $\text{TiO}_2$ ) and warm-water growth of R- $\text{TiO}_2$  nanoparticles with calcinations. These  $\text{TiO}_2$ -coated Ti photo-anodes possess outstanding photocatalytic abilities, which are considered to be promising electrochemical photocatalysts for solar energy applications. For example, R- $\text{TiO}_2$  with different compositions was successfully formed on titanium foils via thermal sintering between 300 and 900°C. This material is used as the photo-anode under simulated solar (visible) light illumination for water splitting and methylene blue degradation. The  $\text{TiO}_2$  photocurrent density performance is shown in **Fig. 1**. The photocurrent density of this photo-anode reaching  $337 \mu\text{A cm}^{-2}$  is obtained at an applied voltage of 3 V, which shows excellent stability over 1 V. Moreover, scanning electron spectroscopy (SEM), X-ray diffraction (XRD), UV-Vis diffuse reflectance spectra (DRS) are employed to characterize the films. The data of photocurrent-electrode potential curves, open-circuit potential, and cyclic voltammetry were employed to substantiate the explanations.

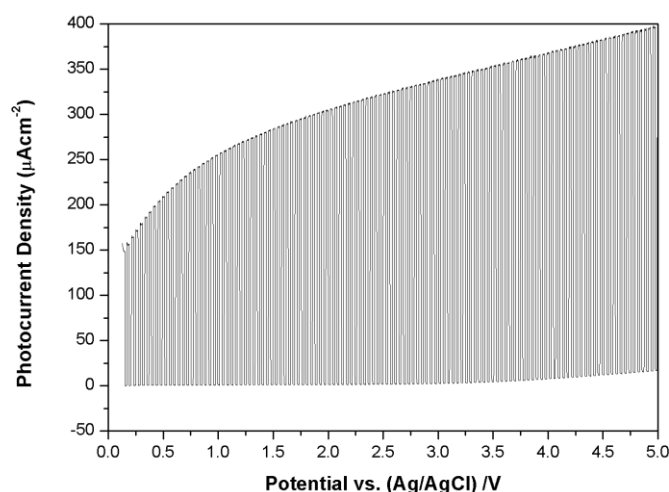


**Fig. 1** The photocurrent density against potential (*i-E*) curves for an R- $\text{TiO}_2$ /Ti photo-anode in 0.5 M  $\text{Na}_2\text{SO}_4$  under the simulated sunlight irradiation.

# Infrared transparent $\text{NiCo}_2\text{O}_4$ thin film as a Front Electrode for Solar Cells

Shu-Yi Tsai<sup>1</sup>, Chung-Ta Ni<sup>1</sup>, Kuan-Zong Fung<sup>1</sup>

<sup>1</sup>Research Center for Energy Technology and Strategy, Department of Materials Science and Engineering, National Cheng Kung University, No. 1, University Road, Tainan 70101, Taiwan, ROC  
willxkimo@yahoo.com.tw

Although most n-type TCOs have been used for applications such as passive components including transparent electrodes and IR reflecting coatings etc. TCOs with unique infrared transparency and adequate electrical conductivity are very useful in certain important applications. TCO like  $\text{NiCo}_2\text{O}_4$  is generally regarded as a mixed valence oxide that adopts an inverse spinel structure in which nickel occupies the octahedral sites and cobalt is distributed over both octahedral and tetrahedral sites<sup>1-3</sup>. Recently,  $\text{NiCo}_2\text{O}_4$  spinel thin film was found to be an infrared transparent conducting material with potential for optoelectronic applications. However, nickel-cobalt oxide spinel tends to become  $(\text{Ni},\text{Co})\text{O}$  with rock salt structure at higher temperatures. Thus, the functional properties of nickel-cobalt oxide are highly dependent upon its processing conditions such as precursors, temperatures, annealing atmospheres.

In this study, nickel-cobalt oxide with spinel structure was obtained from nitrates precursors after calcinations at 300°C for 24 h. With the proper selection of the annealing temperature,  $\text{NiO}$  and  $\text{CoO}$  may form conducting spinel structure or nearly perfect solid solution with rock salt structure. The sputtering deposited  $\text{Ni-Co-O}$  films also showed more than 70% transmittance in the infrared range. The electrical property of spinel film is measured using 4-probe technique. A resistivity as low as  $10^{-2} \sim 10^{-1}$  ohm/cm is obtained. The optical property of this spinel is also measured as a function of thickness/deposition time in the infrared wavelength range.

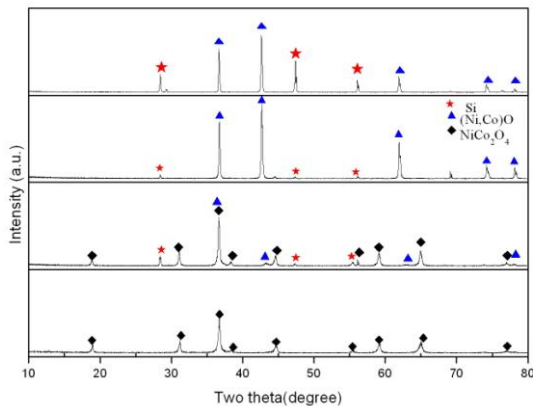


Fig. 1. XRD patterns of  $\text{Ni-Co}$  Oxide heated at various temperatures at 300°C, 500°C, 1000°C, 1500°C (from bottom to top)

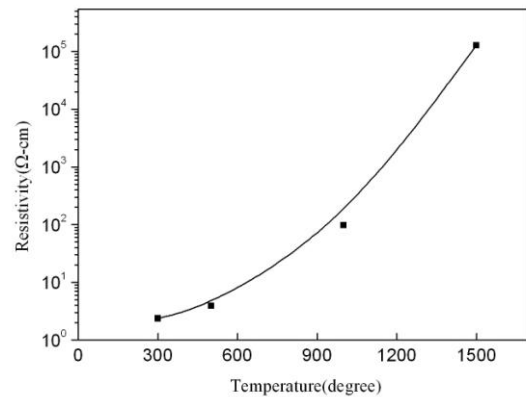


Fig. 2. Resistivity of  $\text{Ni-Co}$  Oxide plotted as a function of calcination temperatures at 300°C, 500 °C, 1000°C, and 1500°C.

1. M. Hamdani, J. F. Koenig and P. Chartier, *J Appl Electrochem*, 1988, **18**, 561-567.
2. J. Haenen, W. Visscher and E. Barendrecht, *J Electroanal Chem*, 1986, **208**, 297-321.
3. J. Haenen, W. Visscher and E. Barendrecht, *J Electroanal Chem*, 1986, **208**, 323-341.

# Laser Induced Degradation Study of $\text{CH}_3\text{NH}_3\text{PbI}_3$ Light Harvesting Oih-Perovskite Semiconductor

Taame Abraha Berhe<sup>1</sup>, Ching-Hsiang Chen<sup>1</sup>, Wei-Nien Su<sup>1,\*</sup>, Liang-Yih Chen<sup>2</sup>, Bing-Joe Hwang<sup>2,3,\*</sup>

<sup>1</sup>NanoElectrochemistry Laboratory, Graduate Institute of Applied Science and Technology, National Taiwan University of Science and Technology, Taipei 106, Taiwan

<sup>2</sup>NanoElectrochemistry Laboratory, Department of Chemical Engineering, National Taiwan University of Science and Technology, Taipei 106, Taiwan

<sup>3</sup>National Synchrotron Radiation Research Center, Hsin-Chu, 30076, Taiwan

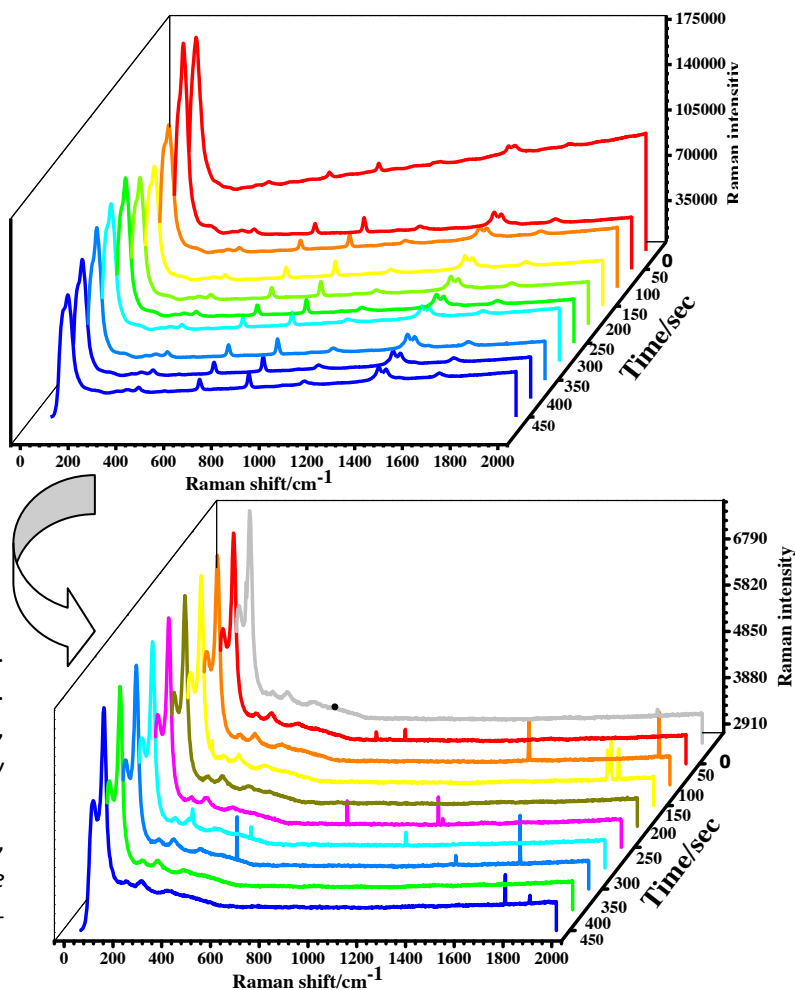
Corresponding Authors: E-mail: [bjh@mail.ntust.edu.tw](mailto:bjh@mail.ntust.edu.tw) (B.J. Hwang) and [wsu@mail.ntust.edu.tw](mailto:wsu@mail.ntust.edu.tw) (W.N. Su)

## Abstract:

Oih-PSCs have rapidly grown to the vanguard of solution-processable photovoltaic devices, however, the  $\text{CH}_3\text{NH}_3\text{PbI}_3$  light harvesting material degrades rapidly in ambient air, hindering their practical applications. In this work, we report a systematic investigation of laser induced degradation of Oih-perovskite. By using Raman spectroscopy and Photoluminescence spectroscopy to monitor structure and phase transformation in Oih-perovskite degradation process, we show the formation of a lead iodide,  $\text{PbI}_2$ , as the final step of the degradation mechanism and degradation product.

## Reference :

1. Quarti, G. Grancini, E. Mosconi, P. Bruno, J. M. Ball, M. M. Lee, H. J. Snaith, A. Petrozza and F. D. Angelis, *The Journal of Physical Chemistry Letters*, 2014, **5**, 279-284.
2. Maalej, Y. Abid, A. Kallel, A. Daoud, A. Lautié and F. Romain, *Solid State Communications*, 1997, **103**, 279-284.



# Hybrid Photoelectrochemical Systems Based on Self-Organized TiO<sub>2</sub> Nanotubes and Novel Chromophores

J.M. Macak<sup>\*,a</sup>, M. Krbal<sup>a</sup>, F. Bures<sup>b</sup>

<sup>a</sup> Center of Materials and Nanotechnologies, Faculty of Chemical Technology, University of Pardubice  
Nam. Cs. Legii 565, 530 02 Pardubice, Czech Republic

<sup>b</sup> Inst. of Organic Chemistry and Technology, Faculty of Chemical Technology, University of Pardubice  
Studentska 573, 532 10 Pardubice, Czech Republic

\*jan.macak@upce.cz

Development of advanced types of solar cells has tremendously accelerated in recent years all activities in the photovoltaics (PVs) driven by the needs to produce solar panels with as high efficiency as possible at lowest cost possible [1]. Realizing that classical silicon solar cells have their limits, such as poor function at low light intensities, lots of research has been carried out past two decades towards alternative technologies based on thin film solar cells (amorphous Si-H, CIGS, CdTe) [2], perovskite cells [3], dye-sensitized cells [4], and organic cells [5]. Even though, the overall efficiencies of advanced photovoltaic devices have grown up significantly (and this goes hand in hand with the development of production technologies), there is so far no solar cell that would have reliable stability and performance over many years of the cell service, that would be cheap, environmentally reasonable and potentially flexible. One of most competing technologies to silicon solar cells, when considering the efficiency, low-cost production and stability is based on thin films of semiconducting chalcogenides, such as Cu(In,Ga)Se<sub>2</sub> (CIGS) [6,7]. CIGS became recently materials of the choice as they represent in thin film solar cells chromophores of adjustable band gaps, good radiation stability and high optical absorption coefficient.

For solution processed CIGS thin film PVs cells, however, the limiting factors for further enhancement of the conversion efficiency involve the shape, size and grain boundaries of the chromophore films. The film morphology, defects and character of the grain boundaries predetermine the mobility (the loss) of free carriers in the chromophore film resulting in conversion efficiency maximum ~10 % for CIGS materials and multilayer solar cell design [8].

It is the grain size that is believed as crucial factor limiting the efficiency of photon-to-current conversion in current CIGS-based photovoltaic cells, especially solution processed [8]. It is very clear that in case of micrometer-thick chromophore layers in current multilayer cell design, the morphology of the chromophore layer is a function of deposition conditions and post-annealing treatment. Therefore, the variation of the grain size is limited resulting in lower efficiencies than are theoretically possible [8].

Among several more or less feasible approaches, there seems to be one straight-forward solution to improve the carrier mobility of semiconducting chalcogenides to the highest possible level with the projection to significantly increase the solar-to-electricity conversion efficiency of the CIGS solar cell. It stems from the use of high aspect ratio semiconducting TiO<sub>2</sub> nanotube arrays [9].

The presentation will show initial photo-electrochemical results for anodic TiO<sub>2</sub> nanotubes employed as highly ordered electron-conductive supports for host materials - chromophores with a suitable light absorbing capabilities, stability and great anchorage to TiO<sub>2</sub> nanotubes. We will focus on chromophores based on inorganic chalcogenides [10] and organic push-pull molecules [11].

## References

1. A. Jäger-Waldau, *PV Status Report 2013*, Joint Research Center, European Commission.
2. M.Konagai, *Jap. J. App. Phys.* 50 (2011) 030001.
3. P.P.Boix, K.Nonomura, N.Mathews, S.G.Mhaisalkar, *Materials Today* 17 (2014) 16.
4. B.O'Regan and M.Grätzel, *Nature* 353 (1991) 737.
5. C.J. Brabec, N.S. Sariciftci, J.C. Hummelen, *Adv. Funct. Mater.* 11 (2001) 15.
6. K. Ramanathan, et al., *Progress in Photovoltaics: Research and Applications* 11 (2003) 225.
7. I. Repins, et al., *Progress in Photovoltaics: Research and Applications* 16 (2008) 235.
8. D.B. Mitzi et al., *Thin Solid Films*, 517 (2009) 2158.
9. J.M. Macak et al., *Curr. Opin. Solid State Mater. Sci.* 1-2 (2007) 3.
10. J.M.Macak, T.Kohoutek, L. Wang, R. Beranek, *Nanoscale* 5 (2013) 9541.
11. J.M. Macak et al., *Ms in preparation*.

# Performance Enhancement of Perovskite-based Solar Cells with TiO<sub>2</sub> Scaffold by Optimizing Electron-Hole Transport

Hye-Rin Kim, Moon-Sung Kang

*Department of Environmental Engineering, Sangmyung University  
300 Anseo-dong, Dongnam-gu, Cheonan-si, Chungnam 330-720, Republic of Korea  
solar@smu.ac.kr*

In recent years there has been increased attention to perovskite solar cells due to their attractive features such as high energy conversion efficiency and low energy production cost. Due to its ambipolar and high light absorbing properties, perovskite can be used as efficient light absorber as well as electron (e<sup>-</sup>) or hole (h<sup>+</sup>) transport materials. During the past several years, the energy conversion efficiencies of the perovskite solar cells have been dramatically increased. The enhancement in the perovskite solar cell performances is mostly attributed to the development of efficient perovskite materials and structural configuration. However, many aspects of the photovoltaic properties are needed to investigate for further improvement of the solar cell efficiency. In this work, we have systematically studied the effects of photoelectrode and hole transport material (HTM) additives (*e.g.* *t*-BP and Li salt) on the photovoltaic characteristics. The perovskite solar cells were prepared by using conventional organometal halides (*e.g.* CH<sub>3</sub>NH<sub>3</sub>PbI<sub>3</sub>) and HTMs (*e.g.* Spiro-MeOTAD) as the base materials. A uniform and pinhole-free hole-blocking layer is necessary for high-performance perovskite-based solar cells. Several metal oxides were investigated to form thin blocking layers. We utilized the spin coating or screen printing method to coat the thin metal oxide layer on transparent conductive oxide substrate. Highly ordered nanoporous TiO<sub>2</sub> scaffold layer was also prepared via a surfactant-templating method for efficient charge transport. The effects of various additives on the photovoltaic properties were studied in terms of the electron-hole transports. The charge transport characteristics in the photoelectrode were systematically investigated through IMVS/IMPS and SLIM-PCV measurements.

## Acknowledgements

This work was supported in part by the Basic Science Research Program through the National Research Foundation of Korea (NRF) funded by the Korea government (MSIP) (No. 2012013811) and by the New & Renewable Energy R&D Program of the Korea Institute of Energy Technology Evaluation and Planning (KETEP) grant funded by the Korea government Ministry of Trade, Industry & Energy (MOITE) (No. 20123010010070).

# **Pt-free counter electrode of $\text{NiCo}_2\text{S}_4$ by two step dip-coating as dye-sensitized solar cells**

An-Lin Su, Zheng-Chang Huang, Jeng-Yu Lin,\*

*Department of Chemical Engineering, Tatung University,*

*No. 40, Sec. 3, ChungShan North Road, Taipei City 104, Taiwan, ROC*

*\*J.-Y. Lin. E-mail: jylin@ttu.edu.tw.*

Since the petrochemical energy resource causes the serious environment pollution, the development of the renewable energies becomes urgent and important. Dye-sensitized solar cells converting solar energy into electricity have attracted extensive attention since it was reported by Grätzel in 1991. A typical DSSC contains photoanode, counter electrode (CE), and  $\text{I}^-/\text{I}_3^-$  based redox electrolyte. However, noble platinum (Pt) is usually used as a CE material in DSSCs, thus resulting in the increase in the manufacturing cost of DSSCs.

Up to now, several low-cost alternatives have demonstrated Pt-like properties as CEs, such as carbon-based materials, conducting polymers and inorganic compounds. Among them, metal sulfides including CoS, NiS,  $\text{MoS}_2$  and  $\text{WS}_2$  have been considered as potential alternatives due to their excellent electrocatalytic activity. In this study,  $\text{NiCo}_2\text{S}_4$  (NCS) CE was prepared using a facile dip-coating method. First, NCS particles were synthesized via a hydrothermal method, and then dispersed in aqueous solution. Afterwards, bare fluorine-doped tin oxide (FTO) glass substrates were dipped in the surface-conditioner solution for 1 min, and subsequently dipped in the as-prepared NSC suspension solution for 10 min. It should be noted that the dip-coating approach has lots advantages including low cost, simply, without complicated equipment, and suitable for mass production. The DSSC assembled with the as-fabricated NCS CE exhibited a superior photovoltaic conversion efficiency of up to 6.95% than that of the device with Pt CE (6.36%), signifying its promising potential as a low-cost Pt-free CE in DSSCs.



# Surface Textured Silicon Photocathode for H<sub>2</sub> Production improves Photoelectrochemical Water Splitting efficiency

Kai-Chieh Tsai<sup>†</sup>, Hsin-Fu Teng<sup>§</sup>, Wei-Nien Su<sup>§</sup>, Bing-Joe Hwang<sup>†</sup>

<sup>†</sup>*Department of Chemical Engineering, National Taiwan University of Science and Technology, Taipei 106, Taiwan, R. O. C.*

<sup>§</sup>*Graduate Institute of Applied Science and Technology, National Taiwan University of Science and Technology, Taipei 106, Taiwan*  
[bjh@mail.ntust.edu.tw](mailto:bjh@mail.ntust.edu.tw)

The generation of hydrogen by solar-driven water-splitting is the focus of much current research, because it has the potential to be a clean and sustainable abundant energy source. Silicon is the most widely used semiconductor material in photovoltaic devices, due to its relatively low-cost and small band gap. Silicon surfaces with extremely high roughnesses not only exhibit enhanced light-trapping effects but also have a lower overpotential for photoelectrochemical hydrogen half-reactions. These qualities have resulted in photovoltaic device improvements with respect to optical, electrical, and chemical activity. A lot of methods, focused on silicon surface texturing, have been reported in the literature, e.g. surface etching. In this study silicon wafers with specific crystal planes were etched to form pyramid structures by using alkaline etching techniques. We combined alkaline etching and metal-assisted chemical etching to fabricate structures that included pyramids supporting nanowires. Both Si pyramids and nanowires were shown to significantly decrease light reflection. Based on this dual structure, light absorption, surface reaction areas and the resulting overall efficiency of photoelectrochemical H<sub>2</sub> production can be improved when compared to untreated silicon.

# **The Study of Carrier Transport/Transfer Mechanism inside CZTS/MS(M=Zn, Cd, Cu)/TiO<sub>2</sub> Nanorods for Solar Water Splitting**

Tsung-Yeh Ho, Liang-Yih Chen\*

*Department of Chemical Engineering, National Taiwan University of Science and Technology  
43, Section 4, Keelung Road, Taipei, 106, Taiwan.*

*sampras@mail.ntust.edu.tw*

Copper zinc tin sulfide (Cu<sub>2</sub>ZnSnS<sub>4</sub>, CZTS) is a kind of light-harvesting candidate material for solar energy conversion through photovoltaics or photoelectrochemical, owing to its suitable band gap (~1.5eV), non-toxic and high absorption coefficient (~10<sup>4</sup> cm<sup>-1</sup>). In this study, CZTS nanocrystals were coated on TiO<sub>2</sub> nanorods (NRs) with different kinds of chalcogenides as buffer layer, such as zinc sulfide (ZnS), cadmium sulfide (CdS) and copper sulfide (CuS). According to band alignment analysis, this a suitable heterogeneous structure could efficiently separate photogenerated electrons and holes. From performance analysis we found that the conversion efficiency of photoelectrode with CuS buffer layer could achieve 2.25% at 0.5V vs. RHE under illumination of one sun AM 1.5G. In the stability test, the CZTS/CuS/TiO<sub>2</sub> NRs could maintain 30 min without seriously decay at 1.23 V vs. RHE. UV-visible spectroscopy and Cyclic voltammetry (CV) were used for ~~the-determining~~ the bandgap and band edge positions of CZTS under different synthesis conditions. Finally, the carrier transport/transfer mechanism inside CZTS/MS (M=Zn, Cd, Cu)/TiO<sub>2</sub> NRs was characterized by electrochemical impedance spectroscopy (EIS) under one sun AM 1.5 G.

# Fabrication of Ti doping Hematite Nanotubes Arrays Photoanode via Anodic Electrodeposition for Solar Water Splitting

Yen-Jhih Chen and Liang-Yih Chen\*

*Dep. of Chemical Engineering, National Taiwan University of Science and Technology*

*No.43, Sec. 4, Keelung Rd., Da'an Dist., Taipei 106, Taiwan*

*sampras@mail.ntust.edu.tw*

Due to the suitable band gap ( $E_g = 2.1$  eV), hematite ( $\alpha\text{-Fe}_2\text{O}_3$ ) can allow light to be absorbed in visible region. Besides In addition, hematite is nontoxic and stable in water, so it is a suitable semiconductor material for solar water splitting. Herein, an anodic electrodeposition was developed to fabricate hematite nanotubes for harvesting the light and increasing the light scattering. In the syntheses, ZnO nanorods (NRs) prepared by hydrothermal method were immersed in  $\text{FeCl}_2$  aqueous solution as work electrode and were biased at 1 V vs. Ag/AgCl. During the process, ZnO NRs were reduced as  $\text{Zn}^{2+}$  ions to dissolve in aqueous solution and  $\text{Fe}^{2+}$  ions were oxidized as  $\text{Fe}^{3+}$  ions to form  $\gamma\text{-FeOOH}$  shell layers on the surfaces of ZnO NRs. Until all ZnO NRs were dissolved completely in aqueous solution,  $\gamma\text{-FeOOH}$  nanotubes were formed. To transform  $\gamma\text{-FeOOH}$  nanotubes as  $\alpha\text{-Fe}_2\text{O}_3$  nanotubes, a post-annealing process was employed at  $500^\circ\text{C}$ . However, the poor conductivity and slow oxygen evolution kinetic rate limited the performance of hematite photoanodes solar water splitting system. In order to enhance the conductivity, doping Ti ions into hematite nanotubes and promoting the crystalline at  $650^\circ\text{C}$  annealing temperature were conducted. Ti doping hematite nanotubes photoanode was decorated by  $\text{ZnFe}_2\text{O}_4$  layer and Co-Pi oxygen evolution catalysts furthermore to increase the band bending and to improve the carrier transfer rate in the interfaces of photoanode and electrolyte for optimizing water oxidation.

# Rutile TiO<sub>2</sub> Nanosheet Arrays on Thermally Oxidized TiO<sub>2</sub> Blocking Layer for Enhancing Efficiency of Perovskite Solar Cells

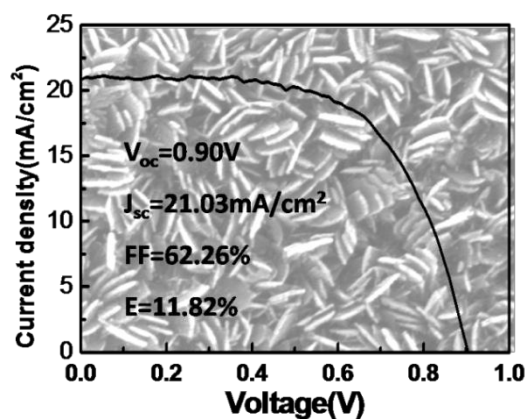
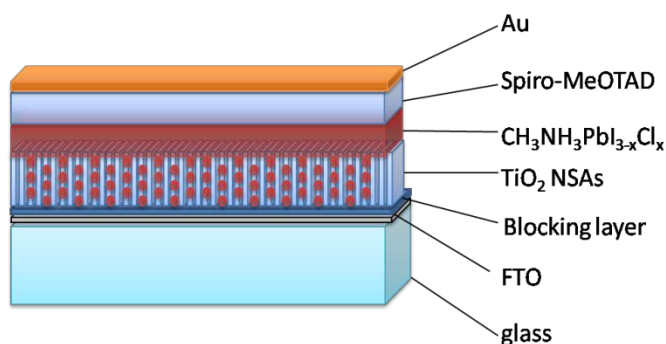
Nan Zhang, Miaoqiang Lv, Meidan Ye, Dajiang Zheng, Changjian Lin\*

*State Key Laboratory of Physical Chemistry of Solid Surfaces, Department of Chemistry, College of Chemistry and Chemical Engineering, Xiamen University*

*Xiamen 361005, China*

*E-mail: [cjlin@xmu.edu.cn](mailto:cjlin@xmu.edu.cn)*

**ABSTRACT:** Here we report a highly efficient perovskite solar cell based on a thermal oxidation TiO<sub>2</sub> compact layer and mesoporous TiO<sub>2</sub> nanosheet arrays(NSAs). The highly oriented two-dimensional(2-D) single-crystalline rutile TiO<sub>2</sub> were grown hydrothermally on the sputtered Ti film following one-step sintering process. This two-dimensional TiO<sub>2</sub> nanomaterial has advantages of enhancing charge collection and efficient incorporation of perovskite particles. Through the facial one-step sintering process, we have obtained a perovskite solar cell with photocurrent density of 21.03 mA/cm<sup>2</sup>, voltage of 0.90V, filling factor of 62.26% and power conversion efficiency (PCE) of 11.82% under the simulated AM 1.5G one sun illumination.



# Electrochemical Analysis of Dye Sensitized Solar Cell Employing Indoline-based and Ruthenium-based Dye Combined with Volatile and Non-Volatile Solution-based Electrolyte

Gerald Ensang Timuda, Runbang Tao, Keiko Waki

Tokyo Institute of Technology

4259 Nagatsuta-cho, Midori-ku, Yokohama-shi 226-8502, Japan

waki.k.aa@m.titech.ac.jp

Dye Sensitized Solar Cell (DSSC) was prepared using different combination of dyes and electrolytes. The dyes used are Ruthenium based, N719 dye, and Indoline-based, D205 dye. Both of the dyes was used in combination with electrolytes using volatile Acetonitrile based solvent and non-volatile 3-Methoxypropionitrile based solvent namely AN-50 and Z-50, respectively.

Under AM 1.5 simulated light source, the solar cells using AN-50 electrolyte show better performance than the Z-50. The N719 and D205 dyes show similar comparison of performance when they combined with AN-50 electrolyte, which shows the potential of this Indoline-type dye in competing with the well-known Ru-based, N719 dye. Interestingly, the D205 dye show apparent better performance than the N719 when Z-50 is used as electrolyte. Electrochemical Impedance Spectroscopy (EIS) at open circuit condition under AM 1.5 illumination was carried out to study intrinsic properties of the solar cells that responsible for the performance obtained. It was found that in this study, the electron diffusion length,  $L_n$ , of the solar cells employing AN-50 as the electrolyte is longer than the thickness of the  $\text{TiO}_2$  photo-anode film, which is the requirement of the efficient solar cell. Employing the same Z-50 electrolyte, the cell using D205 dye have  $L_n$  shorter than the  $\text{TiO}_2$  thickness, but still longer than the one using N719 dye, which explaining bigger performance obtained.

To scrutinize the mechanism involved in the power generation and study the effect of the carrier concentration on the impedance parameters, EIS measurement was carried out under different light intensity. The result will be presented and further discussed.

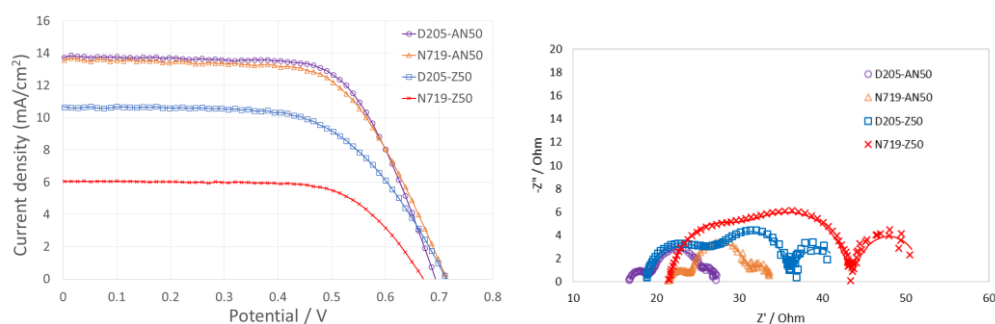


Figure 1. (Left) I-V characteristic and (Right) Nyquist plot of EIS under AM 1.5 Illumination

# Improvement of the photoelectrocatalytic performance of BiVO<sub>4</sub> by metal doping and co-catalyst decoration using an optical scanning droplet cell

Ramona Gutkowski, Kirill Sliozberg, Wolfgang Schuhmann

Analytical Chemistry - Center of Electrochemical Science (CES), Ruhr-Universität Bochum,  
Universitätsstr. 150, 44780 Bochum, Germany  
e-mail gutkowski.ramona@rub.de

Searching for efficient semiconductor materials for light induced water splitting with low band gaps absorbing in the visible part of the solar spectrum is of high interest. It is anticipated that the search for suitable materials is more successful investigating ternary or quaternary semiconductors instead of single metal oxides such as TiO<sub>2</sub> or ZnO. BiVO<sub>4</sub> is a promising and well-studied n-type semiconductor with a band gap of around 2.4 eV. Nevertheless, BiVO<sub>4</sub> itself is a bad electron conductor with additionally low hole transfer kinetics resulting, independently of the preparation method, in high recombination rates of photogenerated electron-hole pairs, thus limiting the efficiency.

In our work we searched for a way to further improve the photoelectrocatalytic efficiency of anodic deposited BiVO<sub>4</sub> films on FTO. Doping with different metals is a well-known method to increase the incident photon-to-current efficiency (IPCE), but strongly depends on the preparation method. For example, single doping with molybdenum<sup>1</sup> led to an increase of the IPCE for spin-coated films obtained by the metal-organic-decomposition method, while inject-printed BiVO<sub>4</sub> doped with molybdenum showed no increase in the IPCE. Furthermore, just by doping with tungsten a significant increase of the IPCE was observed<sup>2</sup>. Doping of BiVO<sub>4</sub> with Mo/W using a dispensing robotic system increased the IPCE up to 12 % at wavelengths below 400 nm<sup>3</sup>.

We employed anodic deposition of BiVO<sub>4</sub> and added different metal salts to the precursor solution. For doping with Fe, Mo and W we observed 10 times higher IPCE values (up to 20 % at 480 nm) as compared with the un-doped BiVO<sub>4</sub>. A further increase of the IPCE was achieved by doping BiVO<sub>4</sub> with W/B, W/Zn and especially with Mo/Zn and Mo/B, assuming improved electron conductivity leading to lower recombination of photogenerated electron-hole pairs finally resulting in higher photoelectrocatalytic efficiency.

A second method to improve the photoelectrocatalytic performance is the decoration of BiVO<sub>4</sub> or metal doped BiVO<sub>4</sub> with co-catalysts. Commonly Co-Pi<sup>2,4</sup>, FeOOH<sup>5</sup>, Co-borate<sup>6</sup>, Ni-borate<sup>7</sup> were used as co-catalysts for increasing the photocurrent of BiVO<sub>4</sub> modified electrodes. We focused on electrochemical deposition of Ni-based co-catalysts, like Ni-Co-oxide or Ni-Fe-oxide compared to Ni-oxide, Co-oxide and Fe-oxide. The layer thickness of the co-catalyst plays an important role and is proportional to the deposition time. A high co-catalyst loading blocks the incident light and consequently less photocurrents are observed. Beside the deposition time and concentration of the co-catalyst precursor the deposition technique, e.g. photodeposition, electrodeposition and photo-assisted electrodeposition are key parameters for the decoration of BiVO<sub>4</sub> with co-catalysts to enhance the oxygen evolution reaction. To have a fast deposition and characterization of these different co-catalysts a specifically designed optical scanning droplet cell with an automated electrolyte exchanging system was used. In this way we were able to create co-catalyst libraries and to directly characterize those avoiding time consuming conventional electrode preparation and deposition. Hence, we were able to compare photocurrents of different co-catalyst loadings, deposition techniques and deposition times on Mo-doped BiVO<sub>4</sub> in dependence on the applied bias potential.

<sup>1</sup> S. K. Pilli, T. E. Furtak, L. D. Brown, T. G. Deutsch, J. A. Turner, A. M. Herring, *Energy Environ. Sci.* **2011**, *4*, 5028.

<sup>2</sup> C. Jiang, R. Wang, B. A. Parkinson, *ACS Comb. Sci.* **2013**, *15*, 639–645

<sup>3</sup> H. S. Park, K. E. Kweon, H. Ye, E. Paek, G. S. Hwang, A. J. Bard, *J. Phys. Chem. C* **2011**, *115*, 17870.

<sup>4</sup> D. K. Zhong, S. Choi, D. R. Gamelin, *J. Am. Chem. Soc.* **2011**, *133*, 18370.

<sup>5</sup> J. A. Seabold, K.-S. Choi, *J. Am. Chem. Soc.* **2012**, *134*, 2186

<sup>6</sup> C. Ding, J. Shi, D. Wang, Z. Wang, N. Wang, G. Liu, F. Xiong, C. Li, *Phys. Chem. Chem. Phys.* **2013**, *15*, 4589

<sup>7</sup> S. K. Choi, W. Choi, H. Park, *Phys Chem Chem Phys* **2013**, *15*, 6499–6507

# Bi<sub>2</sub>S<sub>3</sub> Nanoparticle Modified TiO<sub>2</sub> Nanotube Arrays for High Efficiency of Photoelectrochemical Hydrogen Production

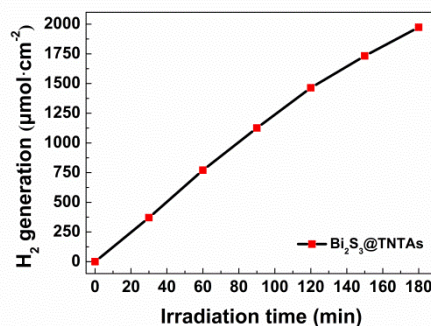
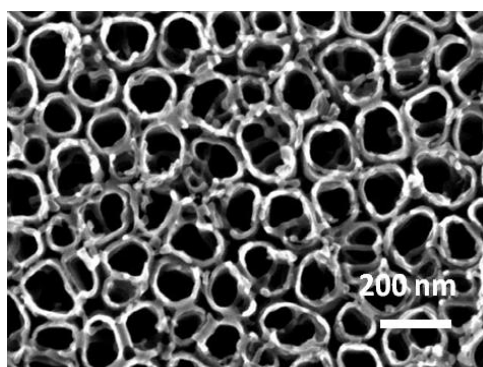
Zhi Wu, Yufeng Su, Jiangdong Yu, Lan Sun, Changjian Lin

State Key Laboratory for Physical Chemistry of Solid Surfaces, Department of Chemistry, College of Chemistry and Chemical Engineering, Xiamen University, Xiamen 361005, China

H<sub>2</sub> generation from photoelectrocatalytic water splitting utilizing solar light has attracted much interest ever since Fujishima and Honda firstly reported in 1972.<sup>1</sup> However, photoelectrochemical methods of conversion of solar energy to electrical or chemical power have suffered from low efficiency.<sup>2</sup> A way to enhance the photoactivity is to construct heterosystems which consist of a wide band gap n-type semiconductor combined with a narrow band gap semiconductor. Bismuth sulfide Bi<sub>2</sub>S<sub>3</sub> seems to be an appropriate material with a direct band gap of 1.28 eV and captures a large part of the solar spectrum, which is close to the ideal value required for photoelectrochemical applications.<sup>3-4</sup> In this work, the Bi<sub>2</sub>S<sub>3</sub> nanoparticles modified TiO<sub>2</sub> nanotube arrays (Bi<sub>2</sub>S<sub>3</sub>@TNTAs) were constructed by sequential chemical bath deposition (CBD) method. This unique heterostructure exhibited improved photoelectrochemical activity as compared to pure TiO<sub>2</sub> TNTAs. When adopted as photoanode, a more than 12-fold enhancement in photocurrent response was achieved, especially, the maximum hydrogen production rate reached 657  $\mu\text{mol}/(\text{h}\cdot\text{cm}^2)$  under 0.5 bias potential.

## References

1. Fujishima, A.; Honda, K. *Nature* **1972**, 238 (5385), 37-38.
2. Leung, D. Y.; Fu, X.; Wang, C.; Ni, M.; Leung, M. K.; Wang, X.; Fu, X. *ChemSusChem* **2010**, 3 (6), 681-694.
3. Bessekhoud, Y.; Robert, D.; Weber, J. *J. Photoch. Photobio A* **2004**, 163 (3), 569-580.
4. Cai, F. G.; Yang, F.; Jia, Y. F.; Ke, C.; Cheng, C. H.; Zhao, Y. *J. Mater. Sci.* **2013**, 48 (17), 6001-6007.



# **A Novel Titanium Electrowinning Process Using Specialized Segmented Diaphragms**

Rohan Akolkar, Chang-Jung Hsueh, Dai Shen, Mirko Antloga, Craig Virnelson, Uziel Landau, Mark DeGuire

*Case Western Reserve University  
10900 Euclid Avenue, Cleveland OH 44106  
Presenter e-mail address: [rna3@case.edu](mailto:rna3@case.edu)*

Titanium metal possesses high strength-to-weight ratio and excellent corrosion resistance. Due to these properties, titanium and its alloys find applications as structural materials in the aerospace and defense industry. However, titanium extraction from its ore via the conventional, non-electrolytic Kroll process is complex, energy-intensive and thus costly. Electrolytic extraction has been attempted previously albeit without success. A critical hurdle in electrolytic titanium extraction is the presence of multivalent titanium ions in the electrolytic cell, which trigger undesired processes of redox-shuttling and bipolar reactions. These processes destabilize the cell operation and drastically lower the cell efficiency.

At Case Western Reserve University, we are developing a revolutionary electrolytic titanium extraction process that addresses the aforementioned technical hurdles. Our process is based on the electrolysis of titanium tetrachloride from high-temperature (400-500°C) molten salts. The key innovation in our electrowinning process is a specialized diaphragm stack, which separates the catholyte and anolyte compartments of the cell. The diaphragm stack is designed to eliminate extraneous bipolar reactions while retarding the redox shuttling of multivalent titanium ions in the cell. This enables stable and energy-efficient electrolytic extraction of titanium sponge. In this talk, we will outline the fundamental electrochemical principles governing the operation of our electrolytic cell. The construction and operation of a prototype electrowinning reactor, and reactor performance in terms of the electrowinning efficiency and titanium sponge purity, will be discussed. Broader impacts of our electrowinning approach to other multivalent metal systems will be outlined.



# SLRR of UPD Monolayers – Fundamental Aspects and Interplay of UPD, Reaction Kinetics, and Nucleation

Stanko R. Brankovic<sup>1</sup>, Ela Bulut<sup>1</sup>, Dongjun Wu<sup>1</sup>, Hasan Kilic<sup>2</sup>,

<sup>1</sup>ECE Department, University of Houston, Houston, Texas, 77204-4005, USA

<sup>2</sup>Marmara University, Istanbul, Turkey

SRBrankovic@uh.edu

The deposition protocol based on *Surface Limited Redox Replacement* (SLRR) reaction of UPD monolayers [1] has gained a lot of attention in recent years [2-9]. The monolayers as well as thin films of arbitrary thickness can be deposited with great fidelity using this approach [9,10]. Their nucleation and morphology is found to be a direct function reaction kinetics of SLRR [11]. Understanding of the interplay between the experimental conditions during SLRR on one side and resulting SLRR reaction kinetics on the other is necessary if the true control of the deposit morphology is to be assumed using this deposition protocol.

Our work explores a fundamental relation between kinetics of Au deposition via SLRR of Pb UPD ML and experimental parameters of the SLRR process such as concentration of the UPD metal and depositing metal ions in the solution, effect of complexing agents and ions such as citrate, effect of temperature and effect of supporting electrolyte. The reaction solution in our kinetics studies contained both  $Pb^{2+}$  and  $Au^{3+}$  ions in 0.1 M  $HClO_4$  as a supporting electrolyte. The Pb coverage as a function of time during SLRR is calculated from the temporal change of the surface reflectivity. The typical results for Pb UPD ML coverage change during Au deposition via SLRR of Pb UPD ML obtained from reflectivity data are shown in Figure 1. Data such as one in Figure 1 are fitted with the model-rate equation of first order in terms of Pb UPD coverage which also takes into account the contribution of parallel SLRR of Pb UPD due to oxygen reduction reaction (ORR). This allowed a more realistic and more reproducible values of the rate constant,  $k'$ , for Au deposition process to be obtained. Our results

suggest a linear relation between the rate constant  $k'$  and  $Au^{3+}$  concentration. The increase in  $Pb^{2+}$  ion concentration for one order of magnitude increases the value of the fundamental rate constant for Au deposition via SLRR of Pb UPD ML for almost 100%. The presence of citrate ions in the solution lowers the value of rate constant but not significantly. The presented data show that effective manipulation of deposition kinetics can be achieved by proper choice of UPD and depositing metal ions concentration. This should have a strong implication when deposit morphology control is considered.

The authors acknowledge the support from NSF Chemistry division under the contract # 0955922.

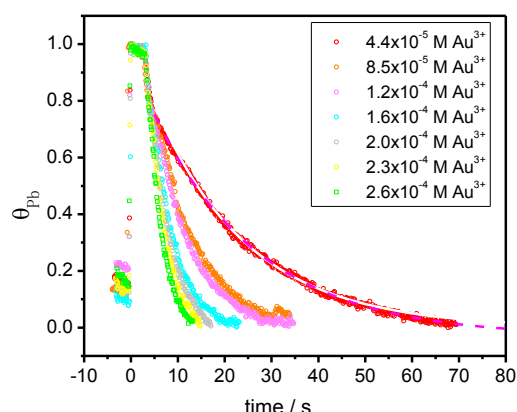


**Figure 1.** Pb UPD layer coverage transient during SLRR reaction:  $Pb_{UPD} + Au^{3+} = Pb^{2+} + Au$ .

## References:

- <sup>1</sup> S. R. Brankovic, J. X. Wang and R.R. Adzic, *Surface Science*, **474**, L173 (2001).
- <sup>2</sup> V. M. Brussel, G. Kokkinidis, A. Hubin, C. Buess-Herman, *Electrochim. Acta* **48**, 3909 (2003).
- <sup>3</sup> J. L. Znahm, M.B. Vukmirovic, Y. Xu, M. Marvikakis, R. R. Adzic, *Angewandte Chemie-International Edition*, **44**, 2132 (2005).
- <sup>4</sup> J. L. Znahm, M.B. Vukmirovic, K. Sasaki, A. U. Nilekar, M. Marvikakis, R. R. Adzic, *J. Am. Chem. Soc.*, **127**, 12480 (2005).
- <sup>5</sup> A. Kongkanand, and S. Kuwabata, *J. Phys. Chem. B*, **109**, 2319 (2005).
- <sup>6</sup> Y. D. Jin, Y. Shen, and S. J. Dong, *J. Phys. Chem. B*, **108**, 8142, (2004).
- <sup>7</sup> K. Sasaki, Y. Mo, J. X. Wang, M. Balasubramanian, F. Uribe, J. McBreen, R.R. Adzic, *Electrochim. Acta*, **48**, 3841, (2003).
- <sup>8</sup> R. Vasilic, L.T. Viyannalage and N. Dimitrov *J. Electrochem. Soc.*, **153**, C648, (2006).
- <sup>9</sup> Y.G. Kim, J.Y. Kim, D. Vairavapandian, J.L. Stickney, *J. Phys. Chem. B* **110**, 17998 (2006)
- <sup>10</sup> J. Nutariya, M. Fayette, N. Dimitrov, and N. Vasiljevic, *Electrochimica Acta*, **112**, 813 (2013).
- <sup>11</sup> D. Gokcen, Q. Yuan, S.R. Brankovic, *J. Electrochem. Soc.*, **161**, D3051 (2014).

# Electrodeposition of Electrocatalytic Nanostructures from Aqueous Solutions and Deep Eutectic Solvents: Aggregative Growth

Jon Ustarroz<sup>1</sup>, El Amine Mernissi Cherigui<sup>1</sup>, Bart Geboes<sup>2</sup>, Kadir Sentosun<sup>3</sup>, Pieter Bouckennooge<sup>1</sup>, Herman Terryn<sup>1</sup>, Sara Bals<sup>3</sup>, Tom Breugelmans<sup>2</sup>, Annick Hubin<sup>1</sup>

<sup>1</sup>*Research Group Electrochemical and Surface Engineering (SURF), Vrije Universiteit Brussel  
Pleinlaan 2, 1050, Brussels, Belgium*

<sup>2</sup>*Research Group Advanced Reactor Technology (ART), University of Antwerp  
Salesianenlaan 90, 2660 Hoboken, Belgium*

<sup>3</sup>*Research Group Electron Microscopy for Materials Science (EMAT), University of Antwerp  
Groenenborgerlaan 171, 2020 Antwerp, Belgium  
justarro@vub.ac.be*

Supported nanostructured electroactive materials are known to boost the efficiency of electrocatalytic processes. Although they can be fabricated by multiple methods, electrodeposition offers several advantages, since the nanostructures are grown on the final support. However, to produce highly electroactive nanostructures in a reproducible way, it is mandatory to optimize the electrodeposition processes. This requires a full understanding of the electrochemical nucleation and growth mechanisms on the nanoscale. During the last years, we have developed an approach based on using carbon coated TEM grids as electrodes. This way, by combining atomic-scale TEM characterization with electron tomography and electrochemical measurements, we have found evidence that has led us to suggest an electrochemical aggregative growth mechanism [1]. It includes nanocluster self-limiting growth, surface diffusion, aggregation and coalescence as important electrochemical growth mechanisms [2].

Besides, Deep Eutectic Solvents (DESs) have generated enthusiasm as a new generation of non-aqueous electrolytes [3]. Nanoscale electrodeposition from DESs is relatively new but has already been proven effective to deposit metallic nanostructures. Moreover, DESs are especially interesting because of their ability to stabilize nanoclusters [4] and to facilitate nanoparticle self-assembly. Hence, nanostructures that cannot be deposited from aqueous electrolytes could potentially be generated.

In this presentation, we first present a summary of the latest findings on the electrochemical nucleation and growth mechanisms involved in the generation of electroactive nanostructures, with special focus on phenomena such as nanocluster self-limiting growth and aggregation. Second, we discuss their electrocatalytic properties and stability. In this case, the evaluation of their structural and morphological features in 3D by electron tomography provides new insights into the processes leading to catalyst degradation [5]. Finally, we present the most recent findings on the electrodeposition of electroactive nanostructures from DESs. TEM characterization linked with electrochemical characterization allows studying the specific interactions of the solvent with the growing metallic phase [6]. These processes are of great interest to highlight possible benefits of the use of DESs as alternative electrolytes for nanoscale electrodeposition.

- [1] J. Ustarroz, J.A. Hammons, T. Altantzis, A. Hubin, S. Bals, H. Terryn, A generalized electrochemical aggregative growth mechanism, *Journal of the American Chemical Society*. 135 (2013) 11550–11561.
- [2] J. Ustarroz, T. Altantzis, J. a. Hammons, A. Hubin, S. Bals, H. Terryn, The Role of Nanocluster Aggregation, Coalescence, and Recrystallization in the Electrochemical Deposition of Platinum Nanostructures, *Chemistry of Materials*. 26 (2014) 2396–2406.
- [3] E.L. Smith, A.P. Abbott, K.S. Ryder, Deep eutectic solvents (DESs) and their applications., *Chemical Reviews*. 114 (2014) 11060–82.
- [4] J.A. Hammons, T. Muselle, J. Ustarroz, M. Tzedaki, M. Raes, A. Hubin, et al., Stability, Assembly, and Particle/Solvent Interactions of Pd Nanoparticles Electrodeposited from a Deep Eutectic Solvent, *The Journal of Physical Chemistry C*. 117 (2013) 14381–14389.
- [5] J. Ustarroz, B. Geboes, L. Stevaert, K. Sentosun, S. Bals, A. Hubin, et al., Tuning the electrochemical growth of platinum nanostructures towards larger surface areas for electrocatalysis, *Manuscript in Preparation*. (2015).
- [6] E.A. Mernissi Cherigui, P. Bouckennooge, K. Sentosun, J. Ustarroz, A. Hubin, S. Bals, et al., Electrodeposition of Nickel Nanostructures from Deep Eutectic Solvents: New Insights into Nucleation and Growth Mechanisms, *Manuscript in Preparation*. (2015).

# The Synthesis and Characterisation of Mesoporous Silica Films for use in Supercritical Fluid Electrodeposition

Andrew Lodge, Calum Robertson, Andrew Hector  
Department of Chemistry, University of Southampton  
University Road, Highfield, Southampton SO17 1BJ, United Kingdom  
a1c10@soton.ac.uk

Supercritical fluids have several unique properties that make them potential solvents for use in electrodeposition. The most important of these properties is the negligible surface tension of supercritical fluids, which enables them to penetrate fully to the bottom of pores. Supercritical fluids are also able to dissolve electrolyte salts. These properties allow supercritical fluids to be used as solvents in the supercritical fluid electrodeposition (SCFED) of metals such as copper or germanium. This has the potential to be used in applications such as microelectronics.

The formation of silica mesopores has been undertaken using the Electrochemically Assisted Surfactant Assembly (EASA) method pioneered by Walcarius.<sup>[2]</sup> This system uses cationic surfactants such as cetyltrimethylammonium bromide to form a porous template, around which the silica is electrodeposited to form a film of vertically aligned mesopores with a constant diameter. These mesoporous structures have been successfully deposited on titanium nitride and indium-doped tin oxide substrates and have a pore diameter of approximately 1.6 nm.<sup>[3]</sup> The size of the pores has also been tuned through the use of additives such as mesitylene, giving a mesoporous film with an increased pore size of 2.4 nm. The pore size can also be further tuned by varying the cationic surfactant used for the EASA deposition. The surface chemistry of the pores can also be fine-tuned by the grafting of functional groups onto the surface of the pores.

The synthesis of mesoporous silica films by the EASA technique and their surface modification and characterisation will be shown. Also shown will be the results of initial SCFED results indicating that the growing of nanometre scale wires inside the pores is possible.

[1] P. Bartlett *et al.*, PCCP, **2014**, 16, 9202.

[2] A. Walcarius *et al.*, Nature Mater., **2007**, 6, 602.

[3] C. Robertson *et al.*, PCCP, **2015**, 17, 4763.

# The Spontaneous Potential Oscillations in a Galvanostatic Copper Electrodeposition

Po-Fan Chan and Wei-Ping Dow\*

*Department of Chemical Engineering, National Chung Hsing University  
No.250, Kuo-Kuang Road, South District, Taichung City 40227, Taiwan, R.O.C.*

\*[dowwp@dragon.nchu.edu.tw](mailto:dowwp@dragon.nchu.edu.tw)

The spontaneous potential oscillations are observed in a galvanostatic copper electrodeposition using specific organic additives. Electrochemical studies reveal that the appearance of the spontaneous potential oscillations during copper electrodeposition is strongly dependent on the electrode rotating speed and the current density. The potential only spontaneously oscillated in the range of  $-0.44\text{V} \sim -0.49\text{V}$  with respect to saturated mercury-mercurous sulfate electrode (SMSE). This result implies that the electrochemical reduction of copper ions at the metal/solution interface is affected by those organic additives, and the electrochemical oscillation reaction depends on a specific potential range, which may relate with the adsorbed chemical species. In addition, the waveform of the potential oscillation is adjustable by the electrode rotating speed and the current density, and it affects the crystal structure and the surface microstructure of the deposited copper. The plated copper layers were characterized by FIB, FE-SEM, and HR-TEM. The spontaneous potential oscillations observed in the copper deposition are explained according to the electrochemical studies and the corresponding microstructure analyses.

# **Electrodeposition of Zn-Mn-Mo layers from citrate solutions**

Honorata Kazimierzak, Agnieszka Hara, Piotr Ozga

*Polish Academy of Sciences, Institute of Metallurgy and Material Science,  
30-059 Krakow, 25 Reymonta st., Poland*

*h.kazimierzak@imim.pl*

Zinc-manganese-molybdenum layers are proposed as environmentally friendly material for corrosion protection of steel. The combination of zinc and manganese in the alloy exhibits a synergistic effect and can result in significantly higher corrosion resistance of Zn-Mn alloy than the resistance of zinc and manganese separately. Further increase of the corrosion resistance of such alloy layers may be obtained by the addition of a next component showing passivating properties. Hexavalent molybdenum have passivating properties, and further does not exhibit carcinogenic effect, associated with the use of hexavalent chromium. Hence, Zn-Mn-Mo can be considered as a substitute for zinc based layers with carcinogenic Cr(VI)-based conversion film.

The preparation of ternary Zn-Mn-Mo alloys is difficult by conventional thermal methods because there are great differences in the melting and boiling temperatures of alloys components. Also, the very limited solubility of molybdenum in zinc is a significant problem. Hence electrodeposition can be considered as a way to obtain such alloys, and moreover it is a relatively simple and low-cost method of producing coatings. Citrates form complexes with Zn(II), Mn(II) and Mo(VI) and are non toxic, furthermore they provide pH stabilisation of electrolyte solutions, hence citrate baths were proposed for the electrodeposition of Zn-Mn-Mo alloys

The main purpose of this work was to analyze the kinetics of co-reduction of zinc, manganese and molybdenum from citrate electrolytes and to study the complexes formation and their stability in Zn-Mn-Mo-citrate system. Next aim was to determine the optimal conditions for electrodeposition of Zn-Mn-Mo coatings.

The thermodynamic model was built to indicate the range of bath parameters in which were homogeneous and stable electroactive species of zinc, manganese and molybdenum. The electrodeposits were obtained from stable, homogeneous Zn(II)-Mn(II)-Mo(VI) citrate with different concentrations of metals and citrate ions. The electrodeposition of alloy was conducted on the rotating disc electrode in the potentiostatic conditions. The kinetics and mechanism of electrodeposition was studied by cyclic voltammetry and by the determination of partial polarization curves of metals deposition and hydrogen evolution, in selected solutions of electrolytes with various concentrations of the individual components and various pH. The surface composition was determined by chemical analysis (WDXRF). The morphology of the resulted coatings was studied by SEM technique.

# Room Temperature Electrodeposition of Elemental Magnesium and Aluminum from Glyme-Based Electrolytes

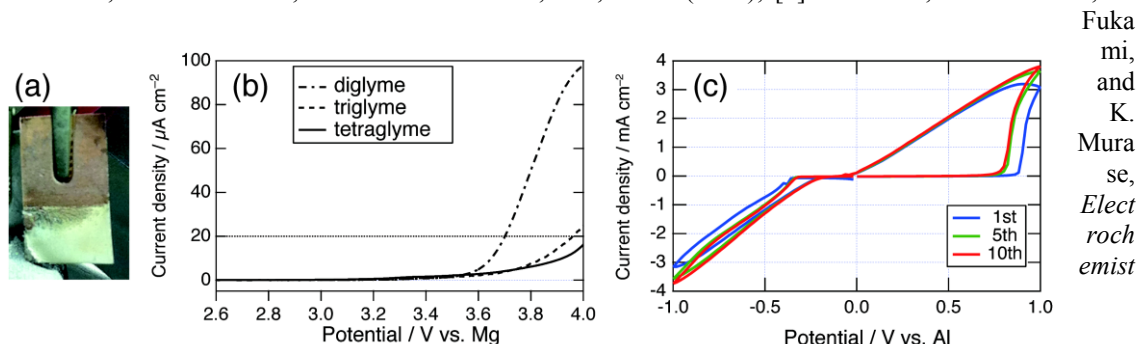
Atsushi Kitada, Yuu Kang, Kai Nakamura, Kazuhiro Fukami, Kuniaki Murase  
 Department of Materials Science and Engineering, Kyoto University  
 Yoshida-honmachi 36-1, Sakyo, Kyoto 606-8501, Japan  
 kitada.atsushi.3r@kyoto-u.ac.jp

Elemental magnesium (Mg) and aluminum (Al) have come to be viewed as interesting negative electrode materials for next generation secondary batteries because of their high energy densities (3839 mA h cm<sup>-3</sup> for Mg and 8042 mA h cm<sup>-3</sup> for Al), negative electrode potentials (−2.356 V vs. SHE for Mg and −1.68 V vs. SHE for Al) and natural abundance. Al is used for many industrial applications such as erosion-resistant plating. Because of their low electrode potentials aqueous solutions cannot be used, and thus efforts have been made to investigate aprotic solvents including ionic liquids (ILs) [1, 2]. However, problems including high volatilities even at room temperature (RT) and high moisture sensitivities of these reported electrolytes have prevented practical uses. Very recently Abe and Fukutsuka *et al.* reported that polyethyleneglycol dimethyl ethers (glymes) with boiling and flash points above 100 °C enable deposition and dissolution of Mg at RT [3]. Their approaches are quite reasonable to suppress volatilities with maintaining low cost. Our approach is based on (i) improvement of Mg electrolytes in terms of safety and (ii) investigation of novel electrolytes for Al electrodeposition using glymes. Here we introduce our recent studies on the several electrolyte solutions in which Mg or Al deposition and dissolution can take place at RT.

Elemental Mg was electrodeposited from a magnesium amide Mg(Tf<sub>2</sub>N)<sub>2</sub> and mixed solvents of glymes and an amide-based IL PP13-Tf<sub>2</sub>N [4]. Here PP13-Tf<sub>2</sub>N served as a supporting electrolyte, which increased conductivities from 0.50 to 2.6 mS cm<sup>-1</sup> at the Mg concentration of 0.1 mol dm<sup>-3</sup>, of which molar ratio was Mg(Tf<sub>2</sub>N)<sub>2</sub>:diglyme:PP13-Tf<sub>2</sub>N = 1:56:7. Flat deposition of Mg with metallic luster was successful on a Cu substrate at −1.0 V vs. Mg QRE using this solution (see Fig. 1a). It was also indicated that above −1.0 V dense deposition was difficult due to its large overpotential for Mg nucleation. Since the 1:56:7 mixed electrolyte was still volatile due to the presence of free or uncoordinated glyme molecules, we decreased the fraction of glymes to place more importance on safety of electrolytes. We prepared 1:8:7 mixtures, where almost all glymes coordinate to Mg<sup>2+</sup> and/or PP13<sup>+</sup> cations. In spite of the sizable decrease in glyme amount their conductivities were comparable (2.6–3.8 mS cm<sup>-1</sup>), and deposition and dissolution of Mg was observed as well. Moreover, their anodic stabilities became ca. +4 V vs. Mg as shown in Fig. 1b, much higher than the IL-free triglyme solution in ref. [3] (+3.4 V vs. Mg). Since anodic stabilities depend on degree of oxidative decomposition of glymes, the improvement should come from decrease in the amount of free glymes. However, sizable anodic overpotentials of about +0.6 V were observed for Mg dissolution [3,4]. How to reduce the anodic overpotentials is an open question in these amide-containing electrolytes.

Elemental Al was successfully deposited and dissolved at RT using AlCl<sub>3</sub>-dissolved diglyme as displayed in Fig. 1c [5]. The coulombic efficiency was 95% at the 10th cycle. We suggested that in this solution some neutral species of AlCl<sub>3</sub> changed into ionic ones of [AlCl<sub>2</sub>•(diglyme)<sub>2</sub>]<sup>+</sup> and AlCl<sub>4</sub><sup>−</sup>, giving good conductivity (4.06 mS cm<sup>-1</sup>). Since the molar ratio of AlCl<sub>3</sub>:diglyme was 1:5, sizable amount of free glymes should be present. Efforts are being made to reduce the amount of free glymes.

[1] R. Mohtadi, and F. Mizuno, *Beilstein J. Nanotechnol.*, **5**, 1291 (2014); [2] Y. Zhao and T. J. VanderNoot, *Electrochim. Acta*, **42**, 3 (1997); [3] T. Fukutsuka, K. Asaka, A. Inoo, R. Yasui, K. Miyazaki, T. Abe, K. Nishio, and Y. Uchimoto, *Chem. Lett.*, **43**, 1788, (2014); [4] A. Kitada, Y. Kang, Y. Uchimoto, and K. Murase, *J. Electrochem. Soc.*, **161**, D102 (2014); [5] A. Kitada, K. Nakamura, K.



Fuka  
mi,  
and  
K.  
Mura  
se,  
*Elect  
roch  
emist*

ry, **82**, 946 (2014).

**Figure 1.** (a) Photograph of Mg deposits on a Cu electrode using the 1:56:7 electrolytes, (b) LSVs of the 1:8:7 electrolytes with  $1 \text{ mV s}^{-1}$ , and (c) CVs of the  $\text{AlCl}_3$ -diglyme bath with  $20 \text{ mV s}^{-1}$ .

# Microvia filling in an Acidic Copper Plating Bath with Insoluble Anodes

Chu-Chi Liu, and Wei-Ping Dow\*

*Department of Chemical Engineering, National Chung Hsing University*

*250 Kuo Kuang Rd., Taichung 40227, Taiwan R.O.C.*

*\*dowwp@dragon.nchu.edu.tw*

Microvia filling of a printed circuit board (PCB) by acidic copper electroplating has been widely used in electronic industry. The filling mode of copper electrodeposition in microvia must be bottom-up form. Moreover, bottom-up filling phenomenon is believed to be related to the properties and interaction of plating additives.<sup>1</sup> Especially, the interaction of three (accelerator, suppressor, leveler) components have significantly effect on copper filling performance.

It was confirmed that soluble anodes (i.e., P-doped Cu anode) have disadvantage when they were used in the acidic copper plating bath. For instance, the shape of the soluble anodes are changeable with operating time, which may causes non-uniform current distribution to form unequal copper thickness on substrate. Therefore, a special functional insoluble anode was used to replace the soluble anode and conventional dimensionally stable anode (DSA) to maintain better bath stability.<sup>2</sup> The disadvantage of soluble anode can be improved by using the novel DSA.

In this work, a plating formula which was composed of chloride ions, suppressor (polyethylene glycol), leveler (quaternary ammonium species) and a novel accelerator instead of bis(3-sulfopropyl) disulfide (SPS). SPS is not appropriate for DSA system because of easy breakdown; therefore, we develop a novel accelerator, ACC, which has a longer lifetime and better performance for acceleration on copper deposition than SPS. Using DSA instead of P-doped Cu anode has another important contribution, that is, SPS reacts with the copper anode to produce Cu(I)-thiolate. The Cu(I)-thiolate is a strong accelerator in the presence of chloride ion. Cu(I)-thiolate will be accumulated in the copper plating bath to destroy the synergy between the suppressor and accelerator. DSA has no this issue because DSA has no copper. Herein, we will show that ACC combining with DSA can perform excellent copper fill in microvia.

## References

1. W. P. Dow, M. Y. Yen, S. Z. Liao, Y. D. Chiu, and H. C. Huang, *Electrochim. Acta*, **53**, 8228 (2008).
2. Y. T. Lin, M. L. Wang, C. F. Hsu, W. P. Dow, S. M. Lin, and J. J. Yang, *J. Electrochem. Soc.*, **160** (12), D3149 (2013).



# Using Graphene as a Conducting Layer and Barrier Layer for high aspect ratio Through Silicon Via Filling

Wei-Yang Zeng, and Wei-Ping Dow\*

*Department of Chemical Engineering, National Chung Hsing University  
250 Kuo Kuang Rd., Taichung 40227, Taiwan R.O.C.*

[dowwp@dragon.nchu.edu.tw](mailto:dowwp@dragon.nchu.edu.tw)

Traditional process for TSV fabrication is a dry process that includes the following step: (1) formation of vias by reactive ion etching; (2) formation of a SiO<sub>2</sub> isolation liner; (3) deposition of a TiN barrier layer and a copper seed layer; (4) via fill with copper electrodepositing. Herein, we attempt to use graphene to substitute the TiN barrier layer and the copper seed layer for reducing the traditional process procedure.

Graphene materials, including single layer and multi-layer graphene platelet, have recently drawn extensive attention due to their outstanding electrical and thermal properties. Reduction of graphene oxide (GO) is a method to prepare the graphene film. Since GO has a large amount of oxygen functional groups, it can be well dispersed in several solvents and enable it to be coated on a substrate by a chemical grafting method using a wet process.

In TSV technology, the thermo-mechanical fatigue may lead to failure in the TSV interconnects because the coefficient of thermal expansion (CTE) of copper is much higher than that of silicon. The packaging materials with different CTEs will induce large stresses at interfaces. To overcome this problem, we choose graphene sheets to substitute the copper seed layer since the CTE of graphene is closer to silicon than copper. In our research, we reduce the procedure of TSV fabrication using a wet process to simultaneously substitute barrier and seed layer with graphene, and to replace filled copper with filled nickel-tungsten alloy in high aspect ratio TSV. This replacement can result in lower fabrication cost compared with the traditional TSV process.

## References

1. P. Songfeng, and C. Hui-Ming, "The Reduction of Graphene oxide ", Carbon., 2012, 50, 3210-3228.
2. S. H. Choa, C. G. Song, and H. S. Lee, "Investigation of Durability of TSV Interconnect by Numerical Thermal Fatigue Analysis", Int. J. Pricis. Eng. Man., 2011, 12, 589-596.

# Surface Limited Redox Replacement Deposition of Pt Bimetallic Nanostructures

Natasa Vasiljevic, Benjamin Rawlings, Michael Mercer and Zakiya Al Amri  
*H.H. Wills Physics Laboratory, University of Bristol*  
*Tyndall Avenue, Bristol*  
[n.vasiljevic@bristol.ac.uk](mailto:n.vasiljevic@bristol.ac.uk)

Design of highly active Pt bimetallic nanostructures has been of great interest for development of commercially viable catalysts for fuel cells applications [1]. Design of Pt nanostructures with the atomic scale control such as the strained monolayers, Pt- alloys and Pt-clusters has been pursued by variety of methods and on different types of metal systems. The confinement and reduction of the dimensions to few atomic layers coupled with the neighbourhood of Pt to another metal, causes electronic and geometrical effects that can substantially alter the catalytic performance.

One of the most successful approaches that has been shown to produce Pt monolayers with high control of atomic structure is Surface Limited Redox Replacement (SLRR) [2, 3]. This method is based on the replacement of an underpotentially deposited (UPD) layer of a less noble metal by a more noble Pt through irreversible surface-controlled limited redox reaction.

Here in this talk we will describe SLRR based design of different types of Pt-nanostructures on Au and Pd/Au substrates: epitaxial films, alloys and clusters (different size and distribution). The advantages of using SLRR method to design high quality 2D model Pt bimetallic systems will be demonstrated by studies of their electrochemical and catalytic behavior as a function of structure (i.e. film thickness, alloy composition and clusters size i.e. surface coverage). The epitaxial Pt thin films (up to 10 ML thickness) have been grown in one cell configuration using Pb UPD with high efficiency and no surface roughness evolution compared to those grown by SLRR of Cu UPD [4]. The incorporation of Pb UPD sacrificial layer was exploited in the SLRR approach by interrupting replacement reaction at partial coverages to design range of Pt rich 2D  $Pt_x Pb_{1-x}$  alloys. The method has been used to examine alloys adsorption properties (H-UPD, CO) and catalytic behavior during formic acid oxidation changes as a function of composition [5]. Besides the metal UPD (such as Pb and Cu), we have introduced H-UPD as a new deposition sacrificial layer that can be used to design Pt-Pd bimetallic structures with superior activity compared to the pure Pt [6]. Presence of Pt on Pd films showed significant effect on the H-absorption which does not diminish even after several layers of Pt deposition. The same effect has been observed for partial coverage of Pt on the surface suggesting the important role of the Pt-Pd interface. The SLRR approach via Pb UPD and H-UPD have been used to design Pt clusters on Au and Pd/Au with the controlled areal coverage and distribution. The role of UPD layer in the clusters distribution as well as the structure will be presented and discussed.

## References:

1. M. K. Debe. Electrocatalyst approaches and challenges for automotive fuel cells, *Nature* 486, (2012), 43.
2. S. R. Brankovic, J. X. Wang, R. R. Adzic. Metal monolayer deposition by replacement of metal adlayers on electrode surfaces, *Surface Science* 474, (2001), L173.
3. R. R. Adzic, J. Zhang, K. Sasaki, M. B. Vukmirovic, M. Shao, J. X. Wang, A. U. Nilekar, M. Mavrikakis, J. A. Valerio, F. Uribe. Platinum monolayer fuel cell electrocatalysts, *Topics in Catalysis* 46, (2007), 249.
4. M. Fayette, Y. Liu, D. Bertrand, J. Nutariya, N. Vasiljevic, N. Dimitrov. From Au to Pt via Surface Limited Redox Replacement of Pb UPD in One-Cell Configuration, *Langmuir* 27, (2011), 5650.
5. M. P. Mercer, D. Plana, D. Fermin, N. Vasiljevic. Growth of epitaxial  $Pt_{1-x}Pb_x$  electrocatalysts by Surface Limited Redox Replacement and Study of their Adsorption Properties, (2015), In preparation.
6. J. Nutariya, M. Fayette, N. Dimitrov, N. Vasiljevic. Growth of Pt by surface limited redox replacement of underpotentially deposited hydrogen, *Electrochimica Acta* 112, (2013), 813.

## Journal Detail

**Credit Saferpay eCommerce****USD -200.00**

Transaction details	
Reference number	402190
Reason for payment	refund
Account	Saferpay eCommerce 40058-17762328
Application	Saferpay Backoffice
Card number	xxxx xxxx xxxx 2400
Expiration Date MM/YY	09/19
Card origin	TW (Taiwan)
Liability shift	No (MasterCard SecureCode)
Transaction ID	1xt4QMbM08l6vAfMnMpAbpUMn42b

Authorisation	
Authorisation date	22.09.2015 08:27:55
Authorisation Type	Normal (Final) Authorisation
Authorized Amount	USD -200.00

Payment Info	
Booking Date	22.09.2015 08:27:55

Payment details	
Provider	MasterCard SIX Payment Services E-Link
Owner name	JHENG YU LIN
Authorizations code	000000
Contract number	171334184
Terminal number	17762328
System Trace Audit Number	8589
Authorisation Identifier (GICC)	220875

## Cancellation

This transaction was not processed (closure) and can be therefore cancelled.

[Cancel now](#)

## Sales-Description

66th Annual Meeting of the International Society of Electrochemistry

# Chemical Deposition and Galvanic Replacement of Morphologically Controlled Cu<sub>2</sub>O Nanoparticle Films

Alexander Vaskevich, Mariano Susman, Israel Rubinstein  
*Department of Materials and Interfaces, Weizmann Institute of Science*  
*Rehovot 7610001, Israel*  
*alexander.vaskevich@weizmann.ac.il*

Nanostructured cuprous oxide (Cu<sub>2</sub>O) is an intriguing direct bandgap semiconductor material with potential applications as a UV-Vis light absorber in solar cells, a photocatalyst for the degradation of organic pollutants, a negative electrode in Li-ion batteries, and others.

It is known that the morphology and size of Cu<sub>2</sub>O nanoparticles (NPs) may affect their photocatalytic and light-absorption properties. However, the preparation of Cu<sub>2</sub>O NPs with morphological control has been largely restricted to colloidal syntheses and electrodeposition on conductive substrates.

We have developed an electroless (chemical) deposition (ELD) approach to direct preparation of Cu<sub>2</sub>O nanocrystal (NC) films on substrates, using CuSO<sub>4</sub>-HCHO-Citrate-NaOH solutions.<sup>1</sup> Our method shows a high degree of morphology control (see Figure 1). The average NC size can be varied by controlling the deposition time, while the crystallographic structure is determined by the solution composition (Figure 1). The NC films were studied by SEM, TEM, GIXRD and UV-Vis spectroscopy.

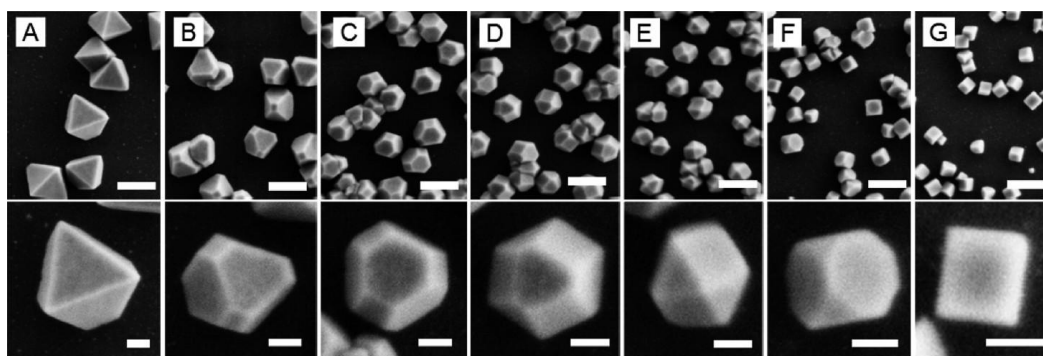


Figure 1. HRSEM images of ELD Cu<sub>2</sub>O NCs on glass substrates, Crystal morphology: (A) complete octahedra, (B) tip-truncated octahedra, (C) truncated octahedra, (D) truncated octahedra, (E) cuboctahedra, (F) tip-truncated cubes, and (G) complete cubes. Scale bars: 200 nm (top), 50 nm (bottom).

The supported Cu<sub>2</sub>O NCs were subjected to galvanic replacement (GR) reactions with metal salts at different pHs.<sup>2</sup> The solution pH in GRRs has been commonly considered an irrelevant parameter; yet, the solution pH plays a major role in GRRs involving metal oxide NPs. We studied Cu<sub>2</sub>O NCs as galvanic replacement (GR) precursors, undergoing replacement by gold and palladium, with the evolving nanostructures showing a strong dependence on the pH of the replacing metal salt solution. The resulting structures strongly depend on the solution pH, showing formation of Cu<sub>2</sub>O NCs decorated with smaller isolated metal (Me) NPs at higher pHs, and uniformly coated Cu<sub>2</sub>O@Me nanoarchitectures at lower pHs. Control of the pH enabled production of different nanostructures, from metal-decorated Cu<sub>2</sub>O NCs to uniformly-coated Cu<sub>2</sub>O-in-metal (Cu<sub>2</sub>O@Me) core-shell nanoarchitectures. The observed improved metal nucleation efficiencies at low pHs are attributed to changes in the Cu<sub>2</sub>O surface charge resulting from protonation of the oxide surface. GR followed by etching of the Cu<sub>2</sub>O cores provided metal nanocages, that collapsed upon drying; the latter was prevented using a sol-gel silica overlayer stabilizing the metal nanocages. Metal-replaced Cu<sub>2</sub>O NCs and their corresponding stabilized nanostructures may be useful as photocatalysts, electrocatalysts and nanosensors.

## References

- [1] Susman, M. D.; Feldman, Y.; Vaskevich, A.; Rubinstein, I. "Chemical Deposition of Cu<sub>2</sub>O Nanocrystals with Precise Morphology Control", *ACS Nano* 8 (2014) 162–174.
- [2] Susman, M. D.; Popovitz-Biro, R.; Vaskevich, A.; Rubinstein, I. "pH Dependent Galvanic Replacement of Colloidal and Supported Cu<sub>2</sub>O Nanocrystals with Gold and Palladium", *Small* DOI:10.1002/sml.201500044.

# TiO<sub>2</sub> nanotubes with wide spacing – a platform for electrodeposited nanostructures

Damian Kowalski<sup>1,2</sup>

<sup>1</sup> University of Reims Champagne-Ardenne  
Campus Moulin de la Housse, BP 1039 51687 REIMS Cedex 2, France

<sup>2</sup> University of Warsaw  
Faculty of Chemistry, Pasteura 1, 02-093 Warsaw, Poland  
damian.kowalski@univ-reims.fr

The anodizing is a high-voltage electrochemical conversion process that forms barrier-type oxide layers or nanoporous/nanotubular structures on valve metals and alloys mainly depending on the composition of electrolyte used.[1] The key to achieve the ordered nanoporous/nanotubular structures is a displacement of the film material above the original surface position due to synergistic effect of pits generation (field assisted oxide dissolution), stress generated at the metal-oxide interface including electrostriction and plastic oxide flow switching the growth of the barrier-film to nanotube/nanopore. Typically, the TiO<sub>2</sub> nanotube array formed in organic electrolytes such as glycerol, dimethyl sulfoxide, ethylene-glycol is obtained in the form of close packed structure in which the nanotubes nearly stick together with the tube walls. A fundamentally different nanostructure from that is obtained in diethylene-glycol electrolyte. The nanostructure is characterized by free standing nanotubes separated by an interconnecting space larger than the diameter of nanotubes (Fig. 1).

Herein we report on how to control the synthesis of TiO<sub>2</sub> nanotubes to achieve wide spacing between nanotubes. [2,3] We discuss functional properties of titania nanostructures and report the application of titania as a template material for electrodeposited nanostructures. We compare the template to anodic alumina oxide (AAO) which is one of the most widely used hard template materials; the secondary material is typically deposited in the pores of AAO forming nanowires of desired length and diameter. With TiO<sub>2</sub> nanotubes as a template it is possible to control deposition inside the nanotubes and/or space in between them. The resulting electrodeposited nanostructures are in the form of: nanopore array, inverse nanotube array and nanowires. A general scheme for electrodeposition in TiO<sub>2</sub> nanotubes with synthetic metals be presented. [4]

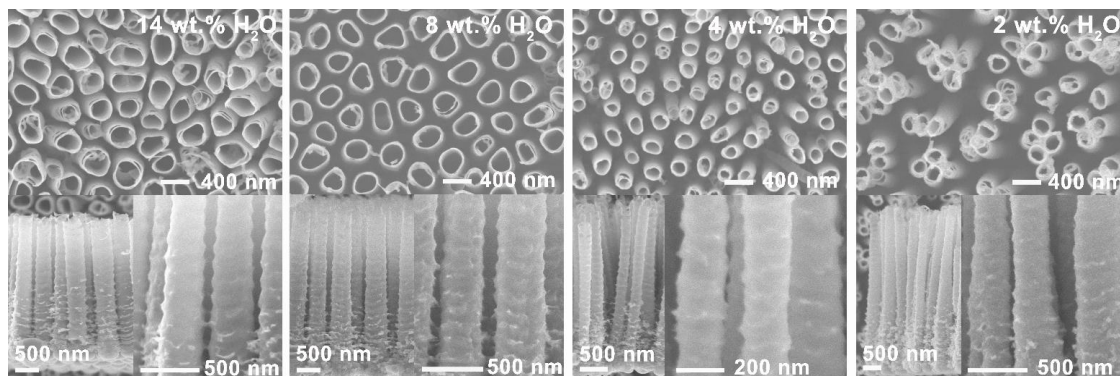


Fig. 1 SEM top and cross-section views for TiO<sub>2</sub> nanotubes formed at 60V for 16h in diethylene glycol electrolyte containing water content from 2-14 wt. %

## References:

- [1] D. Kowalski, D. Kim and P. Schmuki, *Nano Today*, **8** (2013) 235.
- [2] D. Kowalski, J. Malett, J. Michel, and M. Molinari, *J.Mater.Chem.A* **3** (2015) 6655.
- [3] D. Kowalski, J. Malett, and M. Molinari, *Submitted* (2015).
- [4] D. Kowalski, and P. Schmuki, *Chem. Comm.*, **46** (2010) 8585.

# Electrodeposition Process of Ni-Ga Bimetallic Catalyst in BMIm-OTF Ionic Liquid Electrolyte

Jinqiu Zhang, Xing Gu, Peixia Yang, Maozhong An

School of Chemical Engineering and Technology, Harbin Institute of Technology

P.O. Box 1247, No. 92 Xidazhi St., Harbin 150001, China

zhangjinqiu@hit.edu.cn

Ni-Ga bimetallic catalysts could catalyse the synthesis of methanol from CO<sub>2</sub> and H<sub>2</sub>, which was proposed by a computational screening study at first and then has been experimentally confirmed. Ni<sub>5</sub>Ga<sub>3</sub> was thought as the most active composition to take place of conventional Cu/ZnO/Al<sub>2</sub>O<sub>3</sub> catalyst [1, 2]. Compared with chemical synthesis method, electrochemical method is in-situ, convenient, chemical residue-free and easily controllable for catalyst preparation. In a traditional aqueous solutions, Ga is hardly to be electrodeposited because the standard potential of Ga<sup>3+</sup>/Ga is -0.549V is more negative than H<sup>+</sup>/H<sub>2</sub>. However, ionic liquid electrolytes offer a better thermal stability, a wider temperature range and wider electrochemical windows for the deposition of Ga. Cu-In-Ga-Sn thin film was successfully deposited in BMIm-OTF (1-Butyl-3-methylimidazolium trifluoromethanesulfonate) ionic liquid [3].

In this paper, Ni-Ga catalyst was electrodeposited in BMIm-OTF ionic liquid containing nickel chloride and gallium chloride. The electrodeposition and electrochemical measurements were performed using a CHI750D electrochemical workstation. A nickel sheet and a silver wire were used as the reference and the counter electrodes, respectively. The cathodic peak of gallium is at -1.75V (Fig.1a), but its cathodic current is smaller than that of nickel whose cathodic peak at -1.23V (Fig.1b). The co-deposition peak of Ni-Ga is at -1.35V. Micromorphologies, compositions, crystal structures and catalytic properties of Ni-Ga catalysts electrodeposited at different potential are studied. It can be seen from Fig.2 that the particle sizes are around 100nm.

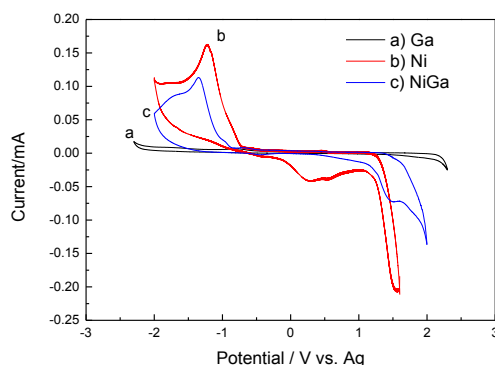


Fig.1 The 5<sup>th</sup> cyclic voltammetry curves of electrolytes containing (a) 20mmol/L gallium chloride, (b) 50mmol/L nickel chloride and (c) 50mmol/L nickel chloride and 20mmol/L gallium chloride.

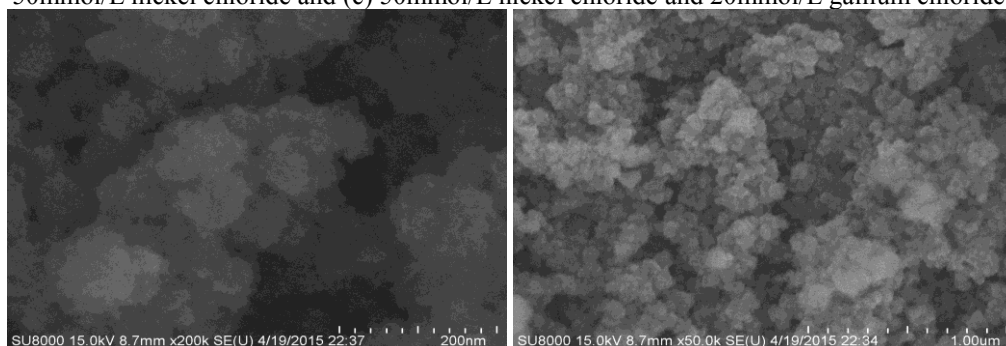


Fig.2 SEM images of Ni-Ga catalysts electrodeposited at -1.5V (vs. Ag) for 60min at 70°C.

## References

- [1] F. Studt, I. Sharafutdinov, F. Abild-Pedersen, et al. Nat. Chem. 6 (2014) 320–324.
- [2] I. Sharafutdinov, C. F. Elkjær, H. W. P. Carvalho, et al. J. Catal. 320 (2014) 77–88.
- [3] S. Ji, P. Yang, J. Zhang, et al. Mater. Lett. 133 (2014) 14–16.

# Using Cu Nanoparticles as Catalysts of Electroless Copper Deposition for Metallization of a Printed Circuit Board

Yao-Lin Tsai and Wei-Ping Dow\*

Department of Chemical Engineering, National Chung Hsing University

250 Kuo Kuang Rd., Taichung 40227, Taiwan, R.O.C.

\*dowwp@dragon.nchu.edu.tw

In recent years, electroless deposition process is commonly used for the metallization of through holes of printed circuit boards (PCBs). Up to now, Sn/Pd colloid process is used to initiate the Cu electroless deposition on the glass fiber and epoxy resin of PCB. However, Pd is very expensive and the residual Pd need to be removed from the epoxy resin after copper electroplating and patterning to prevent shortage between two copper lines. This step will largely increase the process cost. Based on this reason, we introduce a wet process to replace the Sn/Pd colloid process. We made use of a flexible substrate to synthesize copper nanoparticles (CuNPs). The mean particle size of the CuNP is smaller than 10 nm and their size distribution varies from 4 to 6 nm. Therefore, they perform a highly catalytic activity on Cu electroless deposition. Two critical technologies of the CuNP synthesis need to overcome. One is anti-oxidation of CuNPs, the other is the cost issue of the flexible substrate. We proposed solutions to overcome the two issues. The CuNPs were characterized by UV-Vis, FE-SEM, HR-TEM and XRD. The results show that CuNP can replace Sn/Pd colloid to act as the catalyst for copper electroless deposition on both glass fiber and resin materials. The back light and thermal reliability tests of the through hole of a PCB can pass the industrial specification.



# Combining Superfill and Leveling Capabilities: New Hybrid Polymers for Advanced Damascene Applications

N.T.M. Hai<sup>1</sup>, V. Grimaudo<sup>1</sup>, P. Moreno-García<sup>1,2</sup>, D. Lechner<sup>1</sup>, F. Stricker<sup>1</sup>, A. Riedo<sup>2</sup>, P. Wurz<sup>2</sup>, and P. Broekmann<sup>1</sup>

<sup>1</sup>*Department of Chemistry and Biochemistry, Interfacial Electrochemistry Group, University of Bern, Freiestrasse 3, 3012 Bern, Switzerland*

<sup>2</sup>*Physics Institute, Space Research and Planetary Sciences, University of Bern, Sidlerstrasse 5, 3012 Bern, Switzerland*

[peter.broekmann@dcb.unibe.ch](mailto:peter.broekmann@dcb.unibe.ch)

The on-chip metallization of vias and trenches for state-of-the-art microprocessor fabrication relies on an additive-controlled Cu deposition process (Damascene electroplating). The classical direct current (DC) approach of Damascene plating is based on the use of a three-component additive package commonly consisting of a suppressor polymer (e.g. polyalkylene glycols, PAGs), its specific anti-suppressor (bis-(sodium-sulfopropyl)-disulfide, SPS) and a so-called leveler.

In this contribution we demonstrate a successful bottom-up fill of single Damascene test features by using a two-component additive package consisting of SPS (bis-(sodium-sulfopropyl)-disulfide) and Imep polymers (polymerizates of imidazole and epichlorohydrin). Besides the successful feature fill a remarkable leveling effect is observed. Obviously, the Imep additive combines bottom-up fill capabilities with leveling characteristics in one single polymer component. These unique hybrid properties of the Imep are rationalized on the basis of an extended N-NDR (N-shaped negative differential resistance) being present in the linear sweep voltammogram of the SPS/Imep additive system during Cu electrodeposition (Figure 1).<sup>[1]</sup>

A serious drawback of classical Damascene leveler concepts is the high and non-uniform additive incorporation into the copper deposit that limits its post self-annealing (recrystallization). We will demonstrate that copper films deposited in the presence of Imep/SPS additive package are largely contamination-free thus allowing a fast post-deposition recrystallization. For the quantification of (trace) contaminants in the electroplated copper films we make use of a newly developed Laser Ionization/Ablation Mass Spectrometry (LIMS) depth profiling approach. With this technique even a sub-nm depth resolution can be achieved which is a crucial prerequisite for the identification of contaminations localized at Cu grain boundaries.

[1] N.T.M Hai and P. Broekmann, ChemElectroChem (accepted for publication)

[2] V. Grimaudo, P. Moreno-García, A. Riedo, M.B. Neuland, M. Tulej, P. Broekmann, and P. Wurz, Anal. Chem. 87(4), 2015, 2037-2041

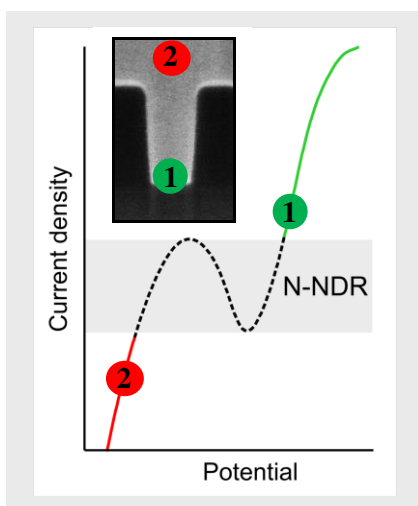


Figure 1: Characteristic N-NDR in the cyclic voltammogram of Cu electrodeposition in the presence of the SPS/Imep additive package. The appearance of the N-NDR is due to the time-delayed activation of the Imep-Cu(I)-MPS suppressor ensemble.

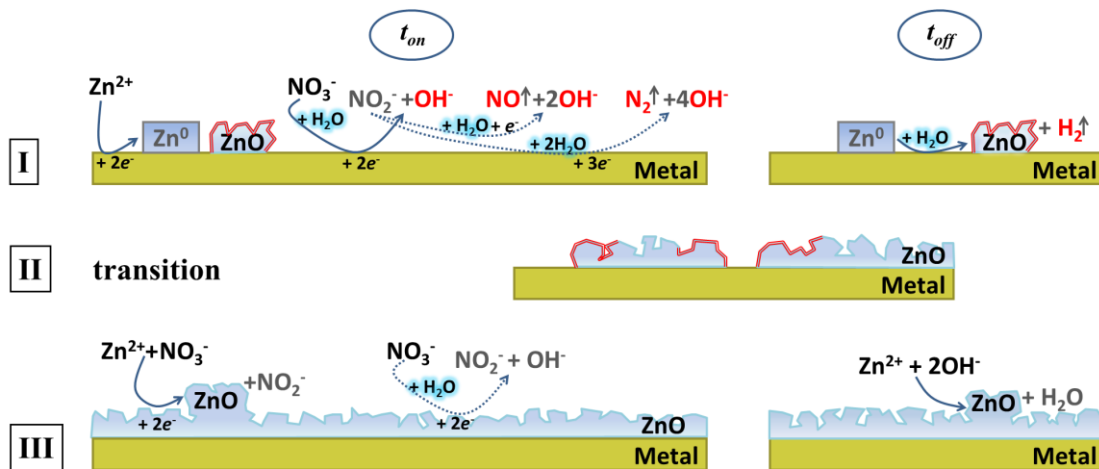
The ins-set show a successfully filled 130nm wide Damascene test feature.

# Interplay of Different Reaction Pathways in the Pulsed Galvanostatic Deposition of ZnO

M. Stumpp, T. H. Q. Nguyen, C. Lupo, D. Schlettwein  
*Justus-Liebig-Universität Gießen, Institut für Angewandte Physik*  
*Heinrich-Buff-Ring 16, 35392 Gießen, Germany*  
*schlettwein@uni-giessen.de*

Zinc oxide ZnO is a promising electrode material for the application in dye-sensitized solar cells (DSCs) and in devices for transparent electronics. Electrochemical deposition is an environmentally-friendly and energy-efficient technique for the deposition of crystalline ZnO and as no subsequent annealing is required, films can be prepared on temperature-sensitive substrates.

In the present work, aqueous solutions of  $\text{Zn}(\text{NO}_3)_2$  were used for electrodeposition of ZnO on gold substrates in micrometer dimensions under pulses of controlled current. Potential-time curves were acquired dependent on current density and pulse times  $t_{\text{on}}$  (current) and  $t_{\text{off}}$  (rest potential). Three significant stages (see scheme) were observed. Scanning electron and confocal laser microscopy analysis revealed a correlation between a successively completed coverage of the Au electrode by ZnO in stage I and an abrupt transition (stage II) of the deposition and rest potential to less negative values in stage III in which the characteristic growth mode of ZnO was observed. The deposition time at which such a transition was detected depended not only on the amount of deposited ZnO but also on the current density during electrodeposition and on the electrode geometry. An influence of different diffusion profiles of the reacting ions was thereby indicated. In order to elucidate the role of different redox reactions in the course of electrodepositions of ZnO, measurements were also carried out in various reference electrolytes. The three stages in the potential were only seen for pauses which were equal or longer than the current pulse. The significance of each stage and the corresponding reaction is discussed for the preparation of ZnO films completely covering an electrode surface to optimize the deposition for future applications in electronic devices or in DSCs.



Scheme 1: Dominating reactions (continuous arrows) and side reactions (dotted arrows) during a pulse ( $t_{\text{on}}$ ) and pause ( $t_{\text{off}}$ ) at the three stages (I-III) of deposition. Poisoning of the ZnO surface for subsequent crystallization of ZnO (double red line) by reaction products (also red) formed on the exposed metal surface was concluded from the observed changes in deposition potential.

If depositions from nitrate-based deposition solutions are aimed at to attain thin compact and pinhole-free semiconductor films as needed, e.g., in some electronic device applications, depositions in short pulses with sufficiently long pauses promise to be most successful and reliable. Use of a galvanostatic deposition mode to provide a fixed growth rate and a substrate even with a rather high overpotential for the reactions underlying the deposition can be of great use in this context because the established potential and its abrupt, easily detected transition can serve as a safe indicator for a successful coating of the substrate.

# A Ni - 4,4'-bipyridine - Ni single-molecule electrochemical transistor

R. J. Brooke<sup>1</sup> Chengjun Jin<sup>2</sup>, D. S. Szumski<sup>1</sup>, R. J. Nichols<sup>3</sup>, Bing-Wei Mao<sup>4</sup>, K. S. Thygesen<sup>2</sup>  
and W. Schwarzacher<sup>1\*</sup>,

1) *H. H. Wills Physics Laboratory, Tyndall Avenue, Bristol BS8 1TL, United Kingdom*

2) *Department of Physics, Technical University of Denmark, DK2800 Kongens Lyngby, Denmark*

3) *Department of Chemistry, University of Liverpool, Liverpool L69 7ZD, United Kingdom*

4) *Chemistry Department, Xiamen University, Xiamen 361005, China*

\*) *Email: w.schwarzacher@bristol.ac.uk*

Nanoscale electrochemistry not only enables the preparation of 4,4'-bipyridine (44BP) single-molecule junctions with oxide-free Ni electrodes, but also allows for control of their electrical transport by non-redox electrochemical gating<sup>1</sup>. The single-molecule junctions are prepared by the scanning tunneling microscope break junction (STM-BJ) technique<sup>2</sup>, which involves bringing a Ni STM tip into contact with an electrodeposited Ni film, then withdrawing the former to create first a nano-constriction exhibiting conductance quantization and subsequently a nano-gap, across which the 44BP can adsorb. The 44BP is dissolved in a pH 3, 0.05 M Na<sub>2</sub>SO<sub>4</sub> aqueous solution and the potentials of tip and substrate are controlled relative to a polypyrrole (PPy) quasireference electrode ( $\sim +0.31$  V with respect to saturated calomel).

In this presentation, we compare the conductances of Ni - 44BP - Ni and Au - 44BP - Au single-molecule junctions measured at a constant tip-substrate bias potential of 0.1 V, while varying the potential of the substrate. For both Ni and Au, the conductance increases as the substrate is made more negative and the metal Fermi level is raised relative to the 44BP frontier orbitals (**Figure 1**). This is the behaviour expected for transport via the 44BP lowest unoccupied molecular orbital (LUMO).

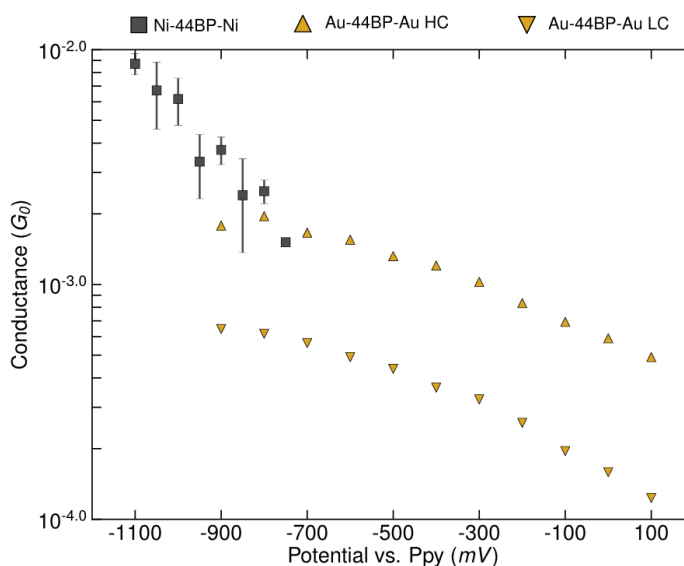


**Figure 1:** Conductance as a function of substrate potential for 4,4'-bipyridine (44BP) single-molecule junctions with different electrodes. HC and LC stand for High Conductance and Low Conductance respectively.

Note that not only is the measured conductance greater for single-molecule junctions with Ni electrodes, but so is the rate of change of conductance with substrate potential. As the substrate potential controls the electrochemical gating, this means that Ni-44BP-Ni is a more effective single-molecule electrochemical transistor than Au-44BP-Au. A further difference between Ni and Au lies in the fact that only one conductance value is measured for Ni-44BP-Ni, whereas two (HC and LC) are measured for Au-44BP-Ni.

Density functional theory calculations throw an interesting light on these results. They not only provide an explanation for the higher conductance of Ni-44BP-Ni single-molecule junctions, but also for the existence of only a single conductance peak. Of particular interest is the fact that they provide strong evidence that the current through the Ni-44BP-Ni device is highly spin-polarized.

## References:

- 1.) R. J. Brooke *et al.* Nano Lett. **15**, 275 (2015).
- 2.) B. Q. Xu and N. J. J. Tao, Science **301**, 1221 (2003).

# Oxygen Bubble Templated Anodic Deposition of Porous PbO<sub>2</sub>

M. Musiani, S. Cattarin, N. Comisso, P. Guerriero, L. Mattarozzi, E. Verlato

*IENI CNR*

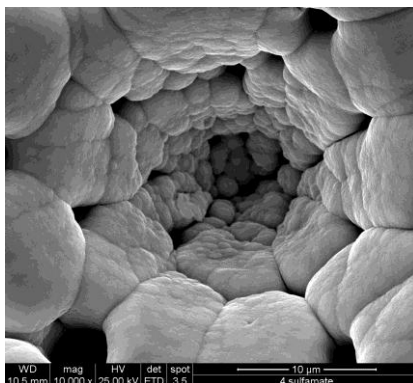
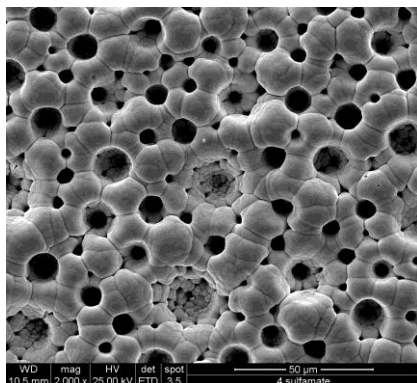
*Corso Stati Uniti 4, 35127 Padova*

*m.musiani@ieni.cnr.it*

The hydrogen bubble templated electrodeposition of porous metals and alloys has been extensively investigated, in recent years [1]. In this process, electrolyses performed at high current density cause simultaneous metal ions reduction and hydrogen evolution, leading to the formation on the cathode of deposits with a bimodal porosity. The deposits exhibit interconnected pores with quasi-circular mouths and typical diameters of tens of microns, due to the metal growth around the hydrogen bubbles, and nano-scale, irregular pores separating the assemblies of metal dendrites that constitute the metal layer.

In the present communication, we report on a preliminary investigation aimed at realizing an analogous process at the anode: the oxygen bubble templated anodic deposition of porous PbO<sub>2</sub>. Owing to possible uses of PbO<sub>2</sub> in energy storage and as inexpensive anode material, obtaining layers with a high surface roughness factor may be interesting [2, 3].

In typical experiments, high current densities (up to 4 A cm<sup>-2</sup>) were imposed to rotating disc anodes (usually Ni) in various deposition baths containing Pb(II) salts dissolved either in concentrated NaOH or in mildly acid solutions. Oxidation of Pb(II) ions to PbO<sub>2</sub> and oxygen evolution occurred simultaneously. Porous structures were obtained in most cases, but the void volume fraction was lower and the connections between neighbouring pores were less numerous in PbO<sub>2</sub> layers than in most metal layers described in the literature. None of the porous PbO<sub>2</sub> layers prepared so far exhibited a nano-scale porosity comparable to that of metal deposits. This result is ascribed to different electrocrystallization kinetics of PbO<sub>2</sub>, as compared to metals, and to its very low tendency to undergo dendritic growth. Work is in progress to optimize the deposit morphology and accurately measure their surface roughness factor.



Porous PbO<sub>2</sub> deposits obtained at 2 A cm<sup>-2</sup> from a lead sulfamate bath

[1] B.J. Plowman, L.A. Jones, S.K. Bhargava, Chemical Communications 51 (2015) 4331-4346.

[2] X Li, D. Pletcher, F.C. Walsh, Chemical Society Reviews 40 (2011) 3879-3894.

[3] U. Casellato, S. Cattarin, M. Musiani, Electrochim. Acta, 48 (2003) 3991-3998.

# Electrodeposition of Nanowires and Nanostructures from Supercritical Fluids

P. N. Bartlett

*University of Southampton*

*Chemistry, Highfield, Southampton, SO17 1BJ, UK*

*pnb@soton.ac.uk*

Supercritical fluids are potentially highly attractive media for the electrodeposition of metals and semiconductors into complex nanostructures [1]. Supercritical fluids readily penetrate porous and nanoporous structures because they have essentially zero surface tension. They also have low viscosities and hence show enhanced mass transport rates. Depending on the choice of electrolyte and solvent they can also have a wide electrochemical window. However these advantages do not come without several disadvantages; their generally low dielectric constants, and the necessity to work in sealed systems at elevated temperature and pressure. For these reasons the field of electrodeposition from supercritical fluids is still relatively unexplored with very little published work on electrodeposition from single phase supercritical systems.

In order to explore the possibilities of using electrodeposition from supercritical fluids to make sub 20 nm nanostructures and nanostructured devices we have focused on the electrodeposition of a range of p-block elements (Ga, In, Ge, Sn, Pb, Sb, Bi, Se and Te) from supercritical difluoromethane [2]. In this lecture I will present results of our latest results on electrodeposition of these elements from supercritical difluoromethane, the characterization of the electrodeposited materials, and work on the electrodeposition of sub-20 nm nanowires.

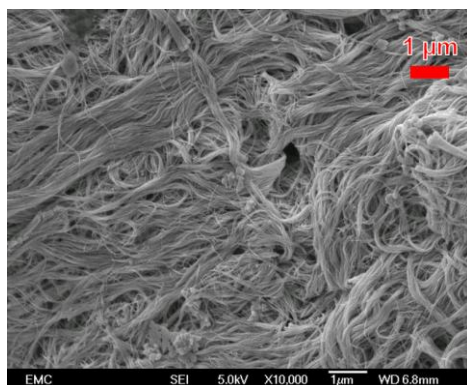


**Figure.** SEM image of 13 nm Te nanowires produced by electrodeposition through an anodic alumina template using supercritical difluoromethane.

**Acknowledgements:** This is a contribution from the SCFED Project ([www.scfed.net](http://www.scfed.net)), a multidisciplinary collaboration between the Universities of Southampton, Nottingham and Warwick and is funded by a Program Grant from EPSRC (EP/I033394/1).

## References

1. P. N. Bartlett, D. A. Cook, A. L. Hector, W. Levason, G. Reid, W. Zhang, M. W. George, J. Ke and D. C. Smith, "Electrodeposition from supercritical fluids", *Phys. Chem. Chem. Phys.*, **16**(2014)9202-9219.
2. P. N. Bartlett, D. C. Cook, M. W. George, J. Ke, W. Levason, G. Reid, W. Su and W. Zhang, "Phase behaviour and conductivity study of electrolytes in supercritical hydrofluorocarbons", *Phys. Chem. Chem. Phys.*, **13**(2011)190-198.

# In situ Scanning Tunneling Microscopy Imaging Self-Assembled Monolayers of Mercaptoacetic Acid and Cupric Ion on Au(111) Electrode

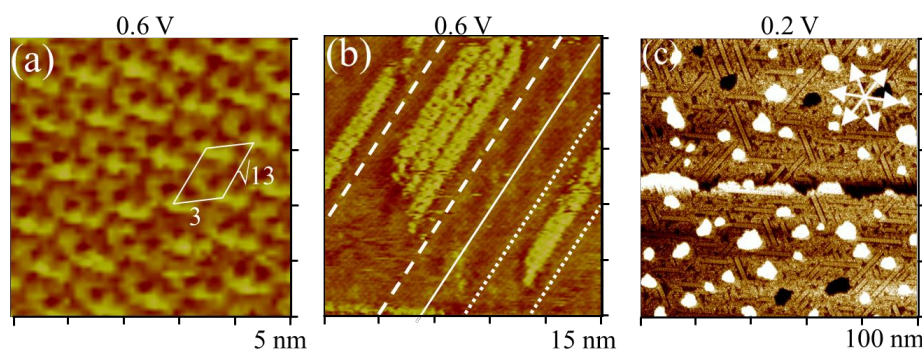
Shuehlin Yau\*

*Department of Chemistry, National Central University, Jhongli, Taiwan 320, ROC*

Voltammetry and scanning tunneling microscopy (STM) were used to study the coadsorption of mercaptoacetic acid (MAA) and cupric ions ( $\text{Cu}^{2+}$ ) on Au(111) electrode from 0.5 M sulfuric acid + 0.8 M  $\text{CuSO}_4$  + 0.03 mM MAA. Irreversibly adsorbed  $\text{Cu}^{2+}$  ions were reduced at 0.27 V first then at -0.2 V (vs. Ag/AgCl), ascribed to the underpotential and overpotential deposition processes, respectively. Counting the amount of charge involved in the stripping peak of the Cu deposit rendered quantification of  $\text{Cu}^{2+}$  ions codeposited with MAA on the Au(111) electrode, which yielded roughly  $7.7 \times 10^{14}$   $\text{Cu}^{2+}$  ions/ $\text{cm}^2$ .

MAA alone and MAA +  $\text{Cu}^{2+}$  were adsorbed in Au(111) -  $(3 \times \sqrt{13})$  and  $(p \times \sqrt{3})$  structures respectively, as shown below. It is likely that  $\text{Cu}^{2+}$  ions were coadsorbed with MAA, although the detailed structure of MAA +  $\text{Cu}^{2+}$  thin film was not clear. Adsorbed  $\text{Cu}^{2+}$  could be imaged by the STM, as seen as protruded linear segments seen in panel (b). They possibly interacted with  $-\text{CCO}^-$  groups of MAA molecules tethered to Au(111) electrode via their  $-\text{S}$  ends. But  $\text{Cu}^{2+}$  ions seemed to move on the electrode surface, which evaded high - quality STM imaging needed to quantify the amount of adsorbed  $\text{Cu}^{2+}$ .

Lowering the potential resulted in marked changes in the surface film, as shown in panel (c). At 0.2 V, Cu UPD commenced, which resulted in restructuring of the thin film. MAA molecules adsorbed on gold electrode now segregated onto the Cu deposit. The electrode surface was mostly disordered but local linear segments were imaged. Lowering potential to more negative values further caused changes of the thin film, resulting from the charged state of Cu adatoms and interaction between MAA molecules. They returned to the Au(111) electrode once the Cu deposit was oxidized at  $E > 0.4$  V. However, the film likely consisted of MAA +  $\text{Cu}^{2+}$  was organized differently from those seen at the pristine sample.



Three STM images collected with Au(111) electrode dosed with 30  $\mu\text{M}$  MAA (a), 30  $\mu\text{M}$  MAA + 0.88 M  $\text{Cu}^{2+}$  (b), and UPD of Cu at 0.2 V in 0.1 M  $\text{H}_2\text{SO}_4$  (c).

## Reference:

1. C.-S. Lai, Y.-Y. Chen, S. Yau, W.P. Dow, Y.-L. Lee, J. Electrochem. Soc. 161 (2014) D742.
2. Y. Fu, S. Chen, S. Yau, W.P. Dow, Y.-L. Lee, J. Electrochem. Soc. 160 (2014) D3295.
3. Y. Fu, T. Pao, S. Chen, S. Yau, W.P. Dow, Y.-L. Lee, Langmuir 28 (2012) 10120.



# Room Temperature Electrodeposition of Metallic Magnesium from Ethylmagnesiumbromide/Tetrahydrofuran and Ionic Liquid Mixtures

Lu Chen, Mike. Horne, Alan M. Bond, Jie Zhang  
School of Chemistry, Monash University  
Wellington Road, Clayton, Vic 3800, Australia  
Lu.chen@monash.edu

The deposition process, nucleation-growth mechanisms and magnesium speciation in deposition of metallic magnesium on an aluminium electrode at room temperature are reported using mixed deposition medium composed of 0.095 M ethylmagnesiumbromide/tetrahydrofuran (EtMgBr/THF) and 0.54 M ionic liquids such as:

1-Butyl-1-methylpyrrolidinium tris(pentafluoroethyl)trifluorophosphate (Py<sub>14</sub>FAP),  
1-Butyl-1-methylpyrrolidinium bis(trifluoromethylsulfonyl)imide (Py<sub>14</sub>TFSI),  
1-Butyl-1-methylpyrrolidinium bis(fluorosulfonyl)imide (Py<sub>14</sub>FSI),  
1-Butyl-1-methylpyrrolidinium tetrafluoroborate (Py<sub>14</sub>BF<sub>4</sub>),  
1-Butyl-1-methylpiperidinium bis(trifluoromethylsulfonyl)imide (PipTFSI),  
Ethyltrimethylpropylammonium bis(trifluoromethylsulfonyl)imide (N<sub>1123</sub>TFSI),  
Diethylmethyl(2-methoxyethyl)ammonium bis(trifluoromethylsulfonyl)imide (DEMETFSI).

Cyclic voltammetric results showed an electrochemically reversible Mg/Mg<sup>2+</sup> process in the case of [FAP]<sup>-</sup> and [TFSI]<sup>-</sup> based ionic liquids, but not for the [FSI]<sup>-</sup> and [BF<sub>4</sub>]<sup>-</sup> based ones. The difference is ascribed to IL dependent magnesium speciation. Analysis of chronoamperometric data revealed that in the presence of Py<sub>14</sub>FAP and PipTFSI, magnesium nucleation occurred via a 3D instantaneous nucleation and diffusion controlled semi-spherical growth model.<sup>[1]</sup> However, in the presence of Py<sub>14</sub>TFSI, DEMETFSI and N<sub>1123</sub>TFSI, deviations from this model are evident. Practical applications used a deposition media based on 90% of 1 M EtMgBr/THF mixed with 10% (v/v ratio) of ionic liquids. Deposition parameters such as current density and charge density influenced deposit appearance, crystallite size and preferred orientation. Py<sub>14</sub>FAP was found to be the most favourable IL for practical applications.

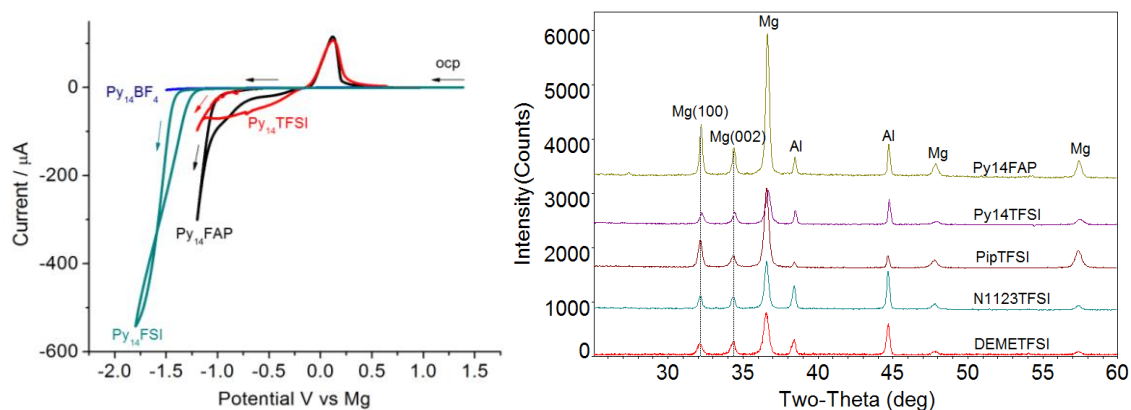


Figure 1: Cyclic voltammograms measurements on an aluminium electrode (0.0254 cm<sup>2</sup>) at a scan rate of 100 mV s<sup>-1</sup> from deposition medium containing 0.095 M EtMgBr/THF and 0.54 M Py<sub>14</sub>BF<sub>4</sub>, Py<sub>14</sub>FSI, Py<sub>14</sub>TFSI and Py<sub>14</sub>FAP. (Left) Figure 2: XRD characterization of magnesium electrodeposits from an aluminium substrate (0.24 cm<sup>2</sup>) in deposition medium containing 90% of 1M EtMgBr/THF and 10% (v/v ratio) of Py<sub>14</sub>FAP, Py<sub>14</sub>TFSI, PipTFSI, N<sub>1123</sub>TFSI and DEMETFSI, at constant deposition current density (11.7 mA/cm<sup>2</sup>) and charge density (42.24 C/cm<sup>2</sup>) (Right).

## References

[1] B. Scharifker, G. Hills, *Electrochim. Acta*, 28, (1983), 879

# Chloride Effect on Chiral Catalytic Activity in Magnetoelectrodeposition

R. Aogaki<sup>1,8</sup>, R. Morimoto<sup>2</sup>, M. Asanuma<sup>3</sup>, I. Mogi<sup>4</sup>,  
A. Sugiyama<sup>5</sup>, M. Miura<sup>6</sup>, Y. Oshikiri<sup>7</sup>, Y. Yamauchi<sup>8</sup>

<sup>1</sup> Polytechnic University, 2-20-12-1304, Ryogoku, Sumida, Tokyo 130-0026, Japan. <sup>2</sup> Saitama Pref. Showa Water Filtration Plant, Kasukabe, Saitama 344-0113, Japan. <sup>3</sup> Yokohama Harbour Polytechnic College, Yokohama 231-0811, Japan. <sup>4</sup> IMR, Tohoku University, Katahira, Sendai 980-8577, Japan. <sup>5</sup> Research Organization for Nano and Life Innovation, Waseda University, Shinjuku, Tokyo 169-0855, Japan. <sup>6</sup> Hokkaido Polytechnic College, Otaru, Hokkaido 047-0292, Japan. <sup>7</sup> Yamagata College of Industry and Technology, Yamagata 990-2473, Japan. <sup>8</sup> National Institute for Materials Science, Tsukuba, Ibaraki 305-0044, Japan.

e-mail: AOGAKI.Ryoichi@nims.go.jp

Chirality is a fundamental problem in chemistry and life science, and chiral catalysts play the most important scientific and technological roles in modern industry. In this sense, how to fabricate chiral catalysts is still an open question with important fundamental and technical interest.

Mogi has first found the appearance of the enantiomorphic activity of the electrodes deposited in vertical magnetic fields [1]. Then, the following studies clarified that the chiral activities of magnetoelectrochemically deposited surfaces are attributed to numerous chiral screw dislocations corresponding to 2D and 3D nuclei, which are created by minute vortexes termed micro- and nano-MHD flows, respectively, activated by magnetic field and macroscopic rotation [2].

**Electrochemical instability:** In electrodeposition, crystal nuclei are classified into two types, i.e., 2D nucleus with a 100  $\mu\text{m}$  scale of length and 3D nucleus with a 0.1  $\mu\text{m}$  scale of length. The former is activated in electric double layer, and the latter in diffusion layer. Then, 2D nuclei unstably develop under non-specific adsorption of ions at Helmholtz layer, but stably repeat birth and death under specific adsorption of ions such as chloride ion. On the other hand, 3D nuclei always develop in an unstable mode. As a result, in the absence of specific adsorption, chiral micro-MHD vortexes from 2D nuclei are dominant over the electrode surface, yielding L-active and D-active catalysts dependent on the direction of magnetic field. However, after adding chloride ions, the vortexes with 2D nucleation are suppressed, and only chiral nano-MHD vortexes from 3D nuclei survive, so that the situation is drastically changed.

**Effect of vertical MHD flow:** In electrodeposition under a vertical magnetic field  $B_0$ , as shown in Fig. 1, a macroscopic tornado-like vortex termed vertical MHD flow with an angular velocity  $\Omega$  emerges. On the electrode surface, iso-entropic particles, i.e., ionic vacancies are stoichiometrically produced, forming a non-viscous layer without friction. Due to disappearance of micro-MHD vortexes by adding chloride ions, this layer rotates with the vertical MHD flow, and the nano-MHD vortexes on the 3D nuclei receive precessions, so that other vortexes except for a specific rotational direction are prohibited. Since the direction is determined by the sign of the product  $B_0\Omega$ , irrelevantly to the direction of magnetic field, only chiral vortexes with anticlockwise (ACW) rotation arise, yielding clockwise (CW) screw dislocations. In view of the mirror-image relationship between enantiomorphic catalyst and its reagent, the electrode surface will always acquire L-activity.

Figure 2 shows the chloride effect, i. e., a chiral CW dislocation under ACW vortex, whereas as shown in Fig. 3, in the absence of the vortex, achiral surface with ACW and CW dislocations emerges.

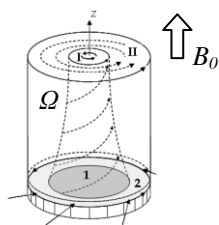


Fig. 1 Vertical MHD flow.

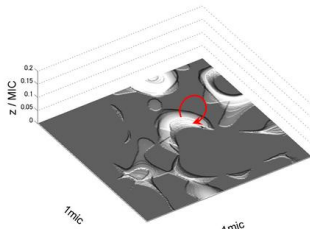


Fig. 2 CW chiral screw dislocation.

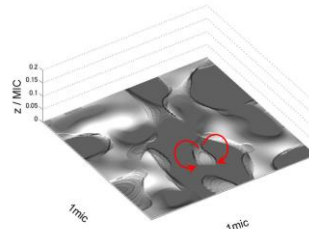


Fig. 3 ACW and CW screw dislocations.

[1] I. Mogi, K. Watanabe, *Int. J. Electrochem.*, 2011, ID: 239637 (2011). doi:10.4061/2011/23937.

[2] R. Aogaki and R. Morimoto, *Heat and Mass Transfer - Modeling and Simulation*, ed. M. Hossain, p.189, InTech, Croatia (2011). doi: 10.5772/21230.



# Characterization of the microstructure of reservoirs using electrodeposition method

Jianming Li, Xu Jin, Xiaoqi Wang, Liang Sun, Songtao Wu

*Petroleum Geology Research and Laboratory Center, PetroChina Research Institute of Petroleum Exploration & Development (RIPED)  
No. 20 Xueyuan Road, Haidian District, Beijing, 100083, P.R. China  
lijm02@petrochina.com.cn*

Reservoir microscopic pore structure (Figure 1) refers to the size and geometry of the reservoir rock pores and throats, and their distribution and interconnected relationships. Reservoir microscopic pore structure directly affects the reservoir porosity, storage, and permeability, the research on reservoir microscopic pore structure can help to evaluate the reservoir, find out reservoir distribution law, and even improve the productivity and recovery ratio of oil and gas. Therefore, how to accurately characterize the reservoir microscopic pore structure received more and more attention.

The Computed Tomography (CT) scanning technologies, including nano-CT, micro-CT, and industrial-CT, are widely used in the reservoir microscopic pore structure characterization. However, the micro-CT can only characterize micron pore structure with the maximum resolution of 0.7 micron; the resolution of nano-CT is higher than micro-CT, with the maximum resolution of 50 nm. In addition, the observing area of nano-CT is small, about 60 microns, which results higher cost of instrument operation and sample preparation. With the progress of oil and gas exploration and development, it has been found that there were abundant nanoscale pores and throats remained in the shale, tight sandstone, and other unconventional reservoirs. Due to the maximum resolution of CT scanning is 50 nm, the CT scanning technology is difficult to meet the needs of characterization of unconventional reservoirs.

In this presentation, we first combined the electrochemical deposition and SEM methods to characterize reservoir microscopic pore structure. As a result, we could directly observe the 3D microstructure of reservoirs smaller than 50 nm with large observing area (Figure 2). In addition, the connected pores and throats of reservoirs could be calculated.

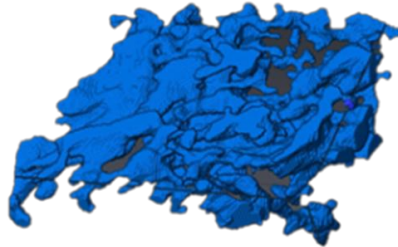


Figure 1. The typical microscopic pore structure of reservoir.

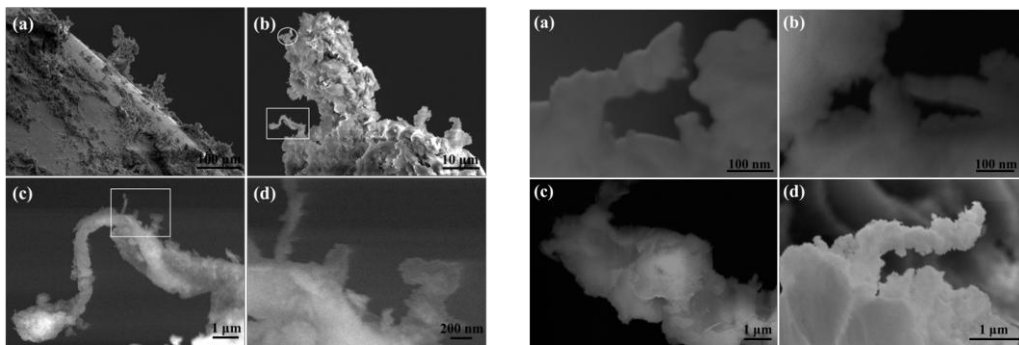


Figure 2. The typical observed 3D microstructure of reservoir.

# Conducting Electrochemical Deposition Reactions in Supercritical Carbon Dioxide Emulsified Electrolyte

Tso-Fu Mark Chang<sup>1,2,\*</sup>, Wei-Hao Lin<sup>3</sup>, Chun-Yi Chen<sup>1,2</sup>, Yung-Jung Hsu<sup>3</sup>, Chi-Chang Hu<sup>4</sup>, Tatsuo Sato<sup>1</sup>, Masato Sone<sup>1,2</sup>

<sup>1</sup>*Precision and Intelligence Laboratory, Tokyo Institute of Technology  
4259-R2-35 Nagatsuta-cho Midori-ku Yokohama 226-8503 Japan*

<sup>2</sup>*CREST, Japan Science and Technology Agency  
4259 Nagatsuta-cho Midori-ku Yokohama 226-8503 Japan*

<sup>3</sup>*Department of Materials Science and Engineering, National Chiao Tung University 1001 University  
Road Hsinchu Taiwan 30010 Republic of China*

<sup>4</sup>*Department of Chemical Engineering, National Tsing Hua University, 101, Section 2, Kuang-Fu Road,  
Hsinchu Taiwan 30013 Republic of China*

\*chang.m.aa@m.titech.ac.jp

Supercritical fluid is any substance at a temperature and pressure above its critical point. Surface tension of supercritical fluid is extremely low and the physical properties can be easily adjusted by controlling pressure and temperature. Therefore, supercritical CO<sub>2</sub> (sc-CO<sub>2</sub>) is applied in electrodeposition of materials to overcome problems encountered in continuous miniaturization of the electronic components. However, CO<sub>2</sub> is non-polar and has very low electrical conductivity. Thus, a surfactant is used to form emulsions composed of an aqueous electrolyte, sc-CO<sub>2</sub>, and the surfactant [1].

Materials electrodeposited with sc-CO<sub>2</sub> emulsified electrolyte (SCE) are reported to have properties very different from that electrodeposited under conventional conditions. Grain refinement and surface smoothening are reported for Ni and Cu films electrodeposited with the SCE [1-3]. Grain size of the Ni electrodeposited with the SCE could be less than 10 nm [2]. Most interestingly, single crystal or twin crystal structure of Cu are observed when the SCE is applied in filling of Cu into the nano-holes [3].

When the SCE is applied in cathodic deposition of TiO<sub>2</sub> films, deposited TiO<sub>2</sub> films are porous, and the films are composed of nano-scale primary particles and aggregates of the primary particles [4]. Grain coarsening and increase in size of the primary particles are observed for TiO<sub>2</sub> electrodeposited with the SCE when compared with the conventional case. ZnO mesocrystals are obtained when the SCE is applied in cathodic deposition of ZnO, [5].

TiO<sub>2</sub> obtained from cathodic deposition is usually amorphous. An additional heat treatment process, such as 400°C for 1 hr, is required to have crystalline TiO<sub>2</sub>. This heat treatment process would increase the process time and affect properties of the substrate and morphology of the TiO<sub>2</sub> films. In a recently study on cathodic deposition of TiO<sub>2</sub> films with the SCE, crystallinity of the TiO<sub>2</sub> was found to be significantly improved with increase of pressure from atmospheric pressure to 35 MPa. Anatase TiO<sub>2</sub> was obtained at a pressure higher than 25 MPa without any additional heat treatment process. The effect of pressure on crystallinity of TiO<sub>2</sub> deposited is named hydrobaric effect, because the deposition only takes place in the aqueous phase in the emulsions, and the effect is similar to the hydrothermal effect in some degree. This is the first report on hydrobaric effect, which is the effect of pressure on chemical reaction conducted in an aqueous solution. We believe the hydrobaric effect can be applied to remove or reduce high-temperature needed in some chemical processes.

A reference electrode is required to identify the electrochemical reactions take place and precisely control the electrochemical reactions in the SCE. However, there is no reference electrode for the SCE because of the high pressure and the complex conditions in the emulsions. In order to solve this problem, the idea of pseudo reference electrode is used. A palladium-hydride based material is found to be stable to provide potential readings close to a hydrogen reference electrode in the SCE [6]. With the newly developed reference electrode, more fundamental studies can be conducted to clarify effects of the SCE, and design of new functional materials with improved properties can be realized.

## Reference:

- [1] T.F.M. Chang, M. Sone, A. Shibata, C. Ishiyama and Y. Higo, *Electrochim. Acta*, **55** (2010) 6469.
- [2] T. Nagoshi, T.F.M. Chang, S. Tatuo, M. Sone, *Microelectron. Eng.*, **110** (2013) 270.
- [3] N. Shinoda, T. Shimizu, T.F.M. Chang, A. Shibata, M. Sone, *Thin Solid Films*, **529** (2013) 29.
- [4] T.F.M. Chang, W.H. Lin, Y.J. Hsu, C.Y. Chen, T.Sato, M. Sone, *Electrochem. Commun.*, **33** (2013) 68.
- [5] W.H. Lin, T.F.M. Chang, Y.H. Lu, T. Sato, M. Sone, K.H. Wei, Y.J. Hsu *J. Phys. Chem. C*, **117** (2013) 25596.
- [6] W.W. Wu, C.T. Hsu, T.F.M. Chang, M. Sone, C.C. Hu, *Electrochim. Acta*, **155** (2015) 209.

# Extremely Fast Filling by V-shape TSV and Cu(I)thiolate accumulation

Kazuo Kondo, Van Ha, Masayuki Yokoi

Osaka Prefecture University

1-1, Gakuen-cho, Naka-ku, Sakai, 599-8531, Japan

kkondo@chemeng.osakafu-u.ac.jp

Conventional Through Silicon Via(TSV) filling requires about 30 minutes(1-3) and have columnar TSV shape. A new conical(V-shape) TSV realize the extremely fast TSV filling of 5 minutes. A  $90\text{mA}/\text{cm}^2$  ultra high current density is applied, if compared to the less than  $10\text{mA}/\text{cm}^2$  conventional columnar TSV. The accelerator of Cu(I)thiolate cuprous complex form preferentially at the V-shape TSV bottom and realize this extremely fast 5 minutes.

## Results

1. Figure 1(a) shows the cross section of V-shape TSV. The TSV diameter is  $6\mu\text{m}$  and the depth is  $25\mu\text{m}$ . This TSV is filled with 5 minutes with  $90\text{mA}/\text{cm}^2$  of on-time of pulse reverse current(b).

2. The ring current of the rotating ring disk electrode for the cathodic region has been measured by T.Hayashi(4). With additives of SPS and Chloride, ten times more ring current is obtained if compared to without additive which J.White(5) have reported. T.Hayashi's ring current indicates that enough amount of cuprous is formed with the cathode.

3. The reaction rate from cupric to cuprous( $k_1$ ) is  $2 \times 10^{-4}$  and that from cuprous to copper( $k_2$ ) is 130(6). The huge reaction rate of  $k_2$  indicates once the cuprous forms it very quickly reduces to copper. The  $k_1$  is the rate determining step.

4. Figure 2 shows the role of cuprous and chloride and SPS additives. The chlorides adsorbs on the copper. These chlorides form electron bridges and reduce cupric to the cuprous, which fasten the rate determining step of  $k_1$ . These electron bridges occur everywhere on the copper. At the same time the chloride reduces the SPS to thiolate(monomer of SPS) and forms accelerating complex of Cu(I)thiolate. This Cu(I)thiolate releases the cuprous. If the Cu(I)thiolate is accumulated at the TSV bottom, the Cu(I)thiolate preferentially release the cuprous at the TSV bottom. Since the reaction rate from cuprous to copper,  $k_2$ , is huge the cuprous accelerates the TSV bottom.

5. Figure 3 shows the flow patterns by the numerical fluid dynamics computations with the columnar and V-shape TSV.

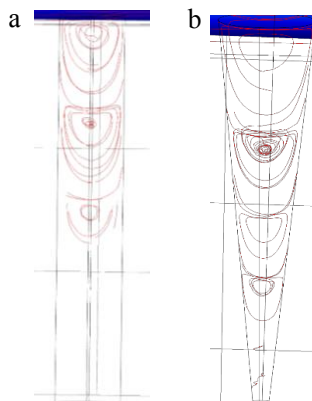


Fig.3 Flow patterns by numerical fluid dynamics computations with columnar(a) and V-shape(b) TSVs.

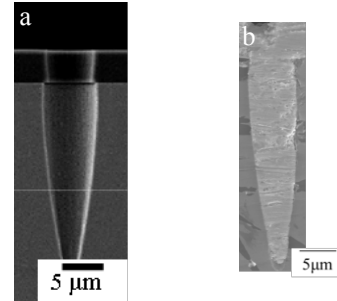


Fig1 Cross sections of V-shape TSVs. a; without filling, b; with filling

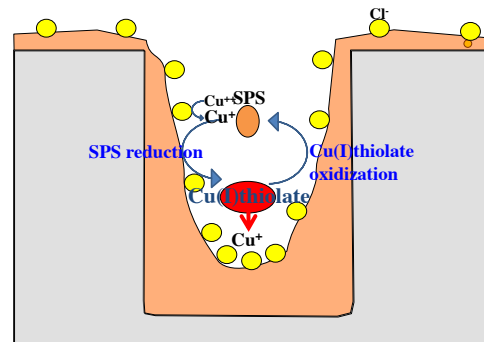


Fig.2 Role of Cu(I)thiolate on via bottom acceleration.

V-shape TSV. The upper end is the TSV mouth and lower end is the bottom. In Fig3a, a large vortex form at the TSV mouth for the columnar TSV. Two vortexes exist under this large vortex, however, the vortex deceases at the middle of the TSV. For the V-shape TSV of Fig.3b, a large vortex form at the TSV mouth and this vortex is larger than a. Three vortexes connects under this large vortex and the vortex continue to exist at 1/5 of TSV from the bottom. The vortex rotate the electrolyte within the vortex and the vortex accumulates the Cu(I)thiolate. Hence the vortex preferentially releases the cuprous at the V-shape TSV bottom. Since the reaction rate from cuprous to copper,  $k_2$ , is huge, the V-shape TSV TSV preferentially accelerates the TSV bottom. This is the reason why the ultra high current density of  $90\text{mA}/\text{cm}^2$  is applied without forming voids.

1.Radisic, Luhn O et al, Microelec. Eng. 88,701(2011) 2.Kadota H et al,JIEP13(3),213(2010) 3.Moffat T.P. and Josell D.J.ECS,159,D208(2012) 4. T. Hayashi,J.ECS, 162 (6) D199 (2015). 5. J. White, J. Appl. Electrochem., 17, 977 (1987) 6.N. Tantavichet , J.ECS, 150, C665(2003)

# Investigation Nitrogen Heterocyclic Compounds as Levelers for Electroplating Cu Filling by Electrochemical Method and Quantum Chemical Calculation

Zenglin Wang\*, Shaojun Ren, and Zhanwu Lei

School of Chemistry and Chemical Engineering, Shaanxi Normal University,  
Xi'an 710062, China,  
E-mail: wangzl@snnu.edu.cn

Leveler, as an indispensable role, improves the distribution of the current density and enhances the bottom-up filling performance. However, only some quaternary ammoniums cations as the levelers have been studied<sup>1</sup>. In this work, six nitrogen heterocyclic compounds (NHCs) bearing different functional groups were investigated as potential levelers for bottom-up filling.

From Fig.1, it was found that the cathodic potential shifted positive rapidly ( $\Delta\phi = 51.4$  mV) or changed little with an addition of 2-MPD or MPC, which indicated that 2-MPD and MPC had no inhibition for the Cu deposition. By contrast, the cathodic potential shifted negative rapidly with an addition of AHMP, HMMP, DPT, or 2-MP, which indicated that these NHCs had inhibition for the Cu deposition, and the inhibitive strength of 2-MP was the strongest ( $\Delta\phi = 106.0$  mV).

The potential difference ( $\Delta\eta$ ) can be used as an indicator to judge the bottom-up filling of electroplating copper solution<sup>2</sup>, but the bottom-up filling capability of the solution was not evaluated quantitatively by electrochemical measurement, and had to be determined by cross-sectional images after the electroplating filling. However, the deposition rates of electroplated Cu on the surface and at the bottom could be simulated by a Cu rotating disk electrode with different rotating speeds, and were direct relative to the coulomb value of Cu stripping peaks (Q) in the CV measurements. So, we proposed a relationship between the supper filling capability (SFC) and Cu stripping quantity,  $C = Q_{100\text{rpm}} / Q_{1000\text{rpm}}$ , where  $Q_{100\text{rpm}}$  and  $Q_{1000\text{rpm}}$  were corresponding coulomb value of Cu stripping peaks measured at 100 rpm and 1000rpm, respectively. The SFC was positively associated with the filling performance of the microvias, and the high SFC value was conducive to improve the filling performance and to reduce surface thickness of plated Cu film.

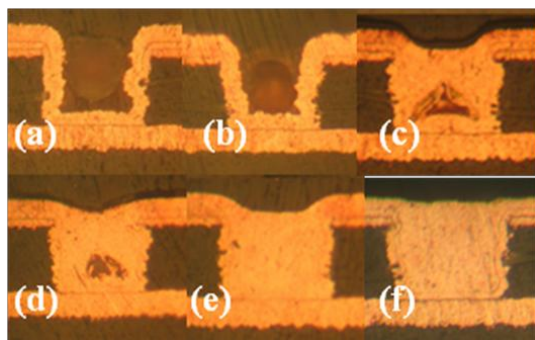


Fig. 1 Cross-sectional OM images of microvias with 1 ppm NHCs: (a) 2-MPD, (b) MPC, (c) AHMP, (d) HMMP, (e) DPT, (f) 2-MP

Furthermore, the absorption ability and active functional groups of NHCs were analyzed by quantum chemical calculations. The absorption ability of NHCs was negative correlation with energy gap ( $\Delta E$ ), and the  $-SH$  and  $=S$  groups in the NHCs were the most active reaction sites for surface absorption on Cu surface, which **was** differ from conventional nitrogen active site in quaternary ammoniums. In addition, the scanning electron microscope and X-ray diffraction results indicated that the uniformity and brightness of the electroplated Cu film were improved by an addition of AHMP, HMMP, DPT, and 2-MP the duo to a significant change of the Cu crystalline orientation in plating deposition.

The authors would like to thank Research Fund for the National Natural Science Foundation of China (No.21273144) and Doctoral Program of Higher Education of China (No.20110202110004, the Fundamental Research Funds for the Central Universities (No. GK201301004)

## References

1. C. Wang, M. An, P. Yang, and J. Zhang, *Electrochem. Commun.*, **18**, 104, (2012).
2. S. M. Huang, C. W. Liu, and W. P. Dow, *J. Electrochem. Soc.*, **159**, D135, (2012).

# Chirality Induction by Galvanostatic Magneto-electrodeposition

Iwao Mogi<sup>1</sup>, Ryoichi Aogaki<sup>2</sup>, Kazuo Watanabe<sup>1</sup>

<sup>1</sup>Institute for Materials Research, Tohoku University, Katahira, Sendai 980-8577, Japan.

<sup>2</sup>Polytechnic University, Sagami-hara, Kanagawa 252-5196, Japan.

e-mail: mogi@imr.tohoku.ac.jp

Studies of chiral surface formation in deposition and crystal growth processes are significant not only in pharmaceutical catalysis but also in the homochiral molecular evolution on early earth. Electrodeposition in magnetic field (magneto-electrodeposition; MED) was found to produce enantioselective metal surfaces for amino acids [1-4]. However, the previous MED experiments were conducted with potentiostatic modes, and the exploration of MED condition has not been sufficient for the understanding of chiral formation mechanism. Here we show the chiral behaviors of Cu film surfaces prepared by galvanostatic MED.

The Cu films were electrodeposited on a Pt disc electrode at constant currents of  $-4$  -  $-22$  mA cm<sup>-2</sup> in a 50 mM CuSO<sub>4</sub> aqueous solution containing 0.5 M H<sub>2</sub>SO<sub>4</sub>. The total passing charge was 0.4 C cm<sup>-2</sup> in all the MED experiments, and the film thickness was approximately 150 nm. The electrochemical cell was placed in the bore center of a cryocooled superconducting magnet, and the magnetic field of 5 T was applied parallel (+5T) or antiparallel (-5T) to the faradaic currents.

The MED films were used as electrodes, and their chiral behaviors were examined using voltammetric measurements of alanine. Fig. 1 shows voltammograms of alanine enantiomers on the Cu +5T-film electrode, which is prepared at a deposition current of  $-11$  mA cm<sup>-2</sup>. The chiral behavior is observed in the oxidation current difference between the enantiomers: The peak current of D-alanine is greater than that of L-alanine. Such chiral behavior is termed D-activity.

We examined the chiral behavior of the +5T-film and -5T-film electrodes prepared at various deposition currents. To evaluate the chirality in voltammograms, an enantiomeric excess (*ee*) ratio can be defined as  $ee = (i_p^L - i_p^D) / (i_p^L + i_p^D)$ , where  $i_p^L$  and  $i_p^D$  represent the peak currents of L- and D-alanines, respectively. The positive sign of the *ee* ratio represents L-activity, and the negative one represents D-activity. Fig. 2 shows the *ee* ratios versus the deposition currents for the +5T-film and -5T-film electrodes and that the chiral sign depends on both the electrodeposition current and the polarity of magnetic field. Furthermore, we found that the specific adsorption of chloride ions on the surfaces causes drastic influence on the chiral formation and that such influence depends on the chloride concentration. At the certain concentrations chiral symmetry breaking was observed for the polarity of magnetic field. These new findings are discussed on the basis of magnetohydrodynamic vortices and the rate-determining steps in electrodeposition.

[1] I. Mogi, K. Watanabe, *Int. J. Electrochem.*, (2011) ID: 239637.

[2] I. Mogi, K. Watanabe, *Magnetohydrodynamics*, 48 (2) (2012) 251-259.

[3] I. Mogi, K. Watanabe, *Chem. Lett.* 41 (11) (2012) 1439-1441.

[4] I. Mogi, R. Morimoto, R. Aogaki, K. Watanabe, *Sci. Rep.*, 3 (2013) 2574.

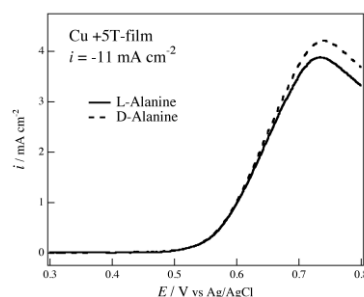


Fig. 1. Voltammograms of alanine enantiomers on the +5T-film electrodes, which were prepared at a deposition currents of 11 mA cm<sup>-2</sup>.

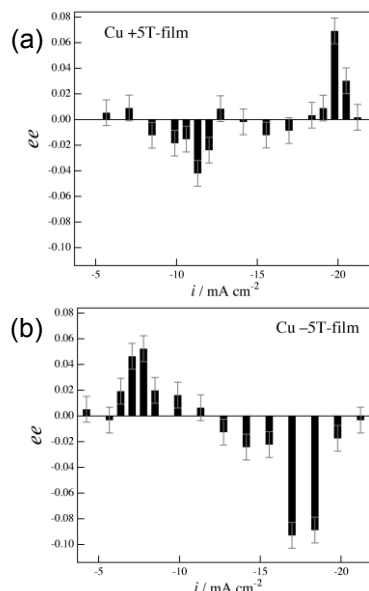


Fig. 2 Enantiomeric excess (*ee*) ratios in the voltammograms of alanine enantiomers vs the deposition currents for (a) +5T-film and (b) -5T-film.

# Effect of Plating Additives on Microstructure and Properties of Electrodeposited Ni-Fe Alloy

Mao-Chun Hung<sup>a</sup>, Po-Fan Chan<sup>a</sup>, Wei-Ping Dow<sup>a,\*</sup>, Hsiao-Yen Lee<sup>b</sup>, Yi-Sheng Lin<sup>b</sup>  
and Ping-Feng Yang<sup>b</sup>

<sup>a</sup> *Department of Chemical Engineering, National Chung Hsing University,*

<sup>b</sup> *Group R&D/Material Lab, Advanced Semiconductor Engineering Group*

<sup>a</sup> *250 Kuo Kuang Rd., Taichung 40227, Taiwan, R.O.C.*

<sup>b</sup> *26 Chin 3rd Rd., Nantze Export Processing Zone, Kaohsiung 81103, Taiwan, R.O.C*

*\* dowwp@dragon.nchu.edu.tw*

With the evolving technology, the frame mounted design of electronic components has increasingly become high-density, which leads to the electronic elements that are inevitably vulnerable to electromagnetic interference and then affect other electronic products' functions. The solution is to use well conductive material that operates the shielding process. The material includes metals and conductive polymers which are common sources of the protective materials in dealing with the main conductive surface. Although this masking method has been widely recognized, several problems are still observed in practice, including the vulnerability to scaling, abrasion, corrosion and process load.

In this study, we adopt Ni-Fe alloy film as the shielding material and manufacture it by electroplating. We intend to explore the effects of plating solution composition, plating parameter and plating additives on structural strength and magnetic properties of the Ni-Fe alloy film. In electroplating, plating additives play important roles. The results suggest that various additives lead to different crystalline orientations, grain sizes, and surface roughness. A correlation between the plated structure and the magnetic properties is studied. Additionally, anti-corrosion is improved by doping a few boron in the film. The ultimate goal of the study is to meet the requirements of electronic industry in manufacturing Ni-Fe alloy with high permeability and good corrosion resistance.

# Amperometric Detection of Bilirubin via A Room-Temperature Ionic Liquid Imprinted Polymer Composite Electrode

Mei-Jywan Syu\*, Yan-Di Tseng

Department of Chemical Engineering, National Cheng Kung University

No. 1, University Rd., Tainan, Taiwan 701

syumj@mail.ncku.edu.tw syumei2014@gmail.com

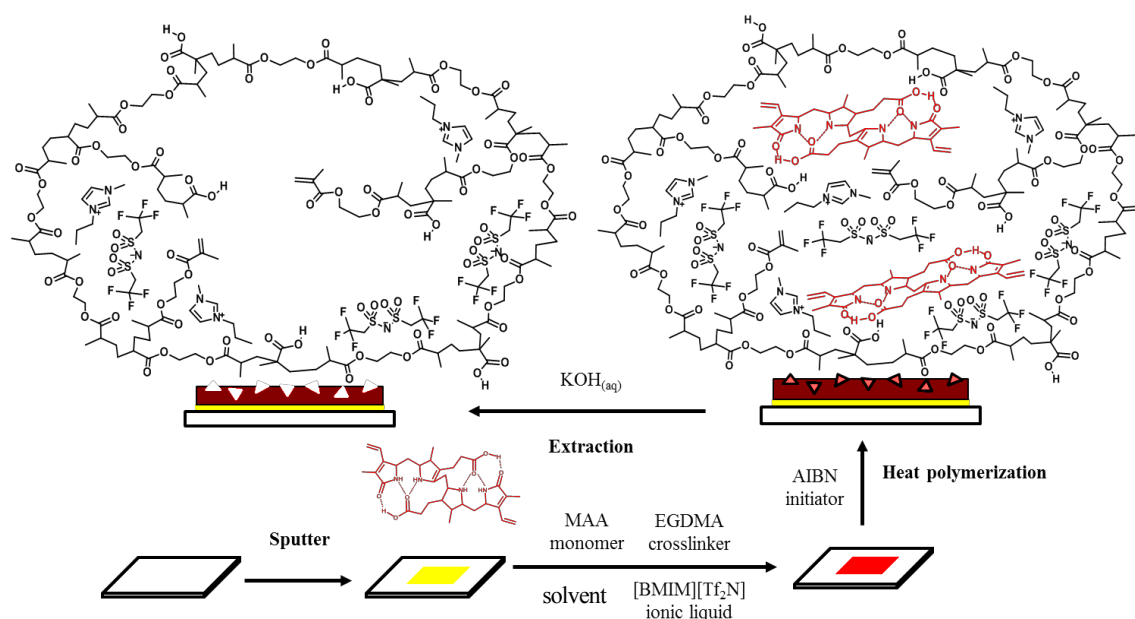
Bilirubin is a metabolite of hemoglobin. The concentration of bilirubin in serum is always regarded as an important physiological index for the liver-related disease. In this work, the molecularly imprinted polymer (MIP) with the room-temperature ionic liquid (RTIL) and bilirubin template molecule was fabricated onto the surface of the Au electrode. Both methacrylic acid (MAA) and ethylene glycol dimethyl acrylate (EGDMA) were used as the functional monomers. EGDMA was also used as the crosslinker. 1-Butyl-3-methylimidazolium bis(trifluoromethylsulfonyl)imide ([BMIM][TF<sub>2</sub>N]) was the chosen RTIL. Together with bilirubin, the bilirubin-imprinted [BMIM][TF<sub>2</sub>N]-poly(MAA-co-EGDMA) ([BMIM][TF<sub>2</sub>N]-poly(MAA-co-EGDMA) composite) was synthesized onto the Au surface. The SEM images showed that the average thickness of the RTIL-imprinted polymeric film was approximately 1.98  $\mu\text{m}$ . Most of the imprinted bilirubin template molecule could be removed from the imprinted [BMIM][TF<sub>2</sub>N]-poly(MAA-co-EGDMA) film after being extracted properly. Consequently, the specific binding cavity for bilirubin molecules was created after the extraction was applied to the polymer film.

RTIL could enhance the amperometric signal of the MIP electrode. The imprinting factor of  $5.52 \pm 0.09$  and the detection sensitivity of  $0.367 \pm 0.019 \mu\text{A}/\text{cm}^2/\text{mg}/\text{dL}$  were achieved, respectively, from the imprinted [BMIM][TF<sub>2</sub>N]-poly(MAA-co-EGDMA) fabricated Au electrode. The RTIL-MIP electrode is able to detect bilirubin in the low concentration ranging from 0.2~1.0 mg/dL. The selectivity of bilirubin versus biliverdin was 2.13. Additionally, the RTIL-MIP electrode could distinguish bilirubin in the presence of serum. Therefore, the results confirm the feasibility of the RTIL-MIP electrode for the detection of bilirubin in serum.

Keywords: bilirubin, molecularly imprinted polymer (MIP), room-temperature ionic liquid (RTIL)

## References

1. MJ Whitcombe. J Mol Recognit 19, 106–180 (2006)
2. M Opallp. A Lesniewski, J Electro Chem 656, 2–16 (2011)
3. AH Wu, MJ Syu. Biosens Bioelectron 21(12), 2345–2353 (2006)





# Properties of electroless Ni–P/BN(h) composite coatings at elevated temperatures

Chih-I Hsu<sup>a</sup>, Gao-Liang Wang<sup>b</sup>, Ming-Der Ger<sup>c</sup>, Kung-Hsu Hou<sup>d,\*</sup>

<sup>a</sup> School of Defense Science, Chung Cheng Institute of Technology, National Defense University, Taoyuan, Taiwan

<sup>b</sup> Department of Marketing Management, Takming University of Science and Technology, Taipei, Taiwan

<sup>c</sup> Department of Chemistry and Material Engineering, Chung Cheng Institute of Technology, National Defense University, Taoyuan, Taiwan

<sup>d</sup> Department of Power Vehicle and Systems Engineering, Chung Cheng Institute of Technology, National Defense University, Taoyuan, Taiwan

\*Corresponding author. Tel.: +886-3-3809257; fax: +886-3-3906385

<sup>a</sup> E-mail address: [s1322509@gmail.com](mailto:s1322509@gmail.com)

## Abstract

Boron nitride (BN(h)) with a hexagonal close-packed structure has excellent electrical insulation and thermal conductivity. Due to the fact that the plane between the layers is only bounded by Van der Waals forces, it can slide against each other easily as it sustained a resistant force, thus it was often used as a solid lubricant in anti-wear areas. In this study, the submicron BN(h) particles were co-deposited with Ni–P matrix onto iron substrates that by electroless technology. After plating, the Ni–P/BN(h) composite coatings were heat-treated for 1 h at 200°C, 300°C, 400°C, 500°C, and 600°C, respectively. The wear and corrosion resistance of the heat-treated composite coatings were measured. Moreover, X-ray diffraction (XRD) analysis and scanning electron microscopy (SEM) were used to characterize the coatings. The corrosion behavior of the Ni–P and Ni–P/BN(h) coated specimen were evaluated through polarization curves and electrochemical impedance spectroscopy (EIS) in 3.5 wt.% NaCl aqueous solution at the room temperature. Results show that Ni–P/BN(h) composite coatings heat-treated at about 400°C had the maximum hardness, good wear resistance, and corrosion resistance had been improved after heat-treated.[1-3]

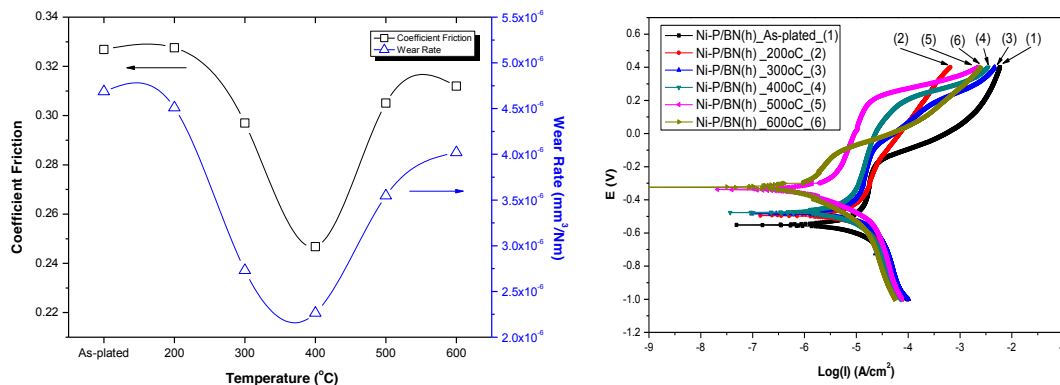


Fig. 1. Variation of friction coefficient and wear rate of composite coatings with heat treatment temperature.

Fig. 2. Polarization curves of specimens prepared at different conditions.

## References

- [1] I.R. Mafi, C. Dehghanian, Studying the effects of the addition of TiN nanoparticles to Ni–P electroless coatings, *Applied Surface Science*, 258 (2011) 1876–1880.
- [2] D. Dong, X.H. Chen, W.T. Xiao, G.B. Yang, P.Y. Zhang, Preparation and properties of electroless Ni–P–SiO<sub>2</sub> composite coatings, *Applied Surface Science*, 255 (2009) 7051–7055.
- [3] Z. Li, J. Wang, J. Lu, J. Meng, Tribological characteristics of electroless Ni–P–MoS<sub>2</sub> composite coatings at elevated temperatures, *Applied Surface Science*, 264 (2013) 516–521.



# Characterization of the Cr-C-Si<sub>3</sub>N<sub>4</sub> Composite Coatings Electroplated from a Trivalent Chromium Bath

Chia Wen Liao, Kung Hsu Hou, Ming Der Ger  
*Chung-Cheng Institute of Technology, National Defense University*  
33551 Taoyuan County, Taiwan  
celinek8888@gmail.com

Electroplated chromium coatings have been widely used in the automotive and manufacture industries. Due to it with high hardness, shiny appearances, excellent wear resistance and corrosion resistance. The chromium alloys can be obtained from trivalent or hexavalent chromium baths by an electroplating process. However, a conventional Cr(VI) manufacturing process is considered to be a significant problem due to the serious health and environmental hazards. Compared with Cr(VI) plating process, the manufacturing process of Cr(III) has numerous environmental, health and technical advantages. Thus, Cr(III) plating is worth studying, because they are considered to be suitable technology to replace conventional Cr(VI) plating while maintaining the excellent characteristics of chromium plating for certain applications. However, the brittleness of Cr(III) materials limit its scope of application. Many investigations have revealed that the second phase particles are commonly introduced into the materials to enhance its physical, chemical or mechanical properties, such as WC, Al<sub>2</sub>O<sub>3</sub>, CeO<sub>2</sub>, SiO<sub>2</sub>, TiO<sub>2</sub>, SiC and Si<sub>3</sub>N<sub>4</sub>. Therefore, in this study, we suggest using of Si<sub>3</sub>N<sub>4</sub> particles because Si<sub>3</sub>N<sub>4</sub> exhibits excellent friction reducing and wear resisting capability and there are no reports about Cr-C-Si<sub>3</sub>N<sub>4</sub> composite coatings produced by the electrodeposition in a trivalent chromium plating bath.

In the present work, Cr-C-Si<sub>3</sub>N<sub>4</sub> composite coatings were obtained by electroplating under DC conditions from a trivalent chromium bath containing suspended Si<sub>3</sub>N<sub>4</sub> particles. The plating parameters are including Si<sub>3</sub>N<sub>4</sub> concentration in the plating bath and current density. The results of the coating's properties such as that the microstructure, the corrosion resistance, the micro-hardness and the wear resistance were investigated. The surface and cross-sectional micrograph (as shown in Fig. 1) indicates that Si<sub>3</sub>N<sub>4</sub> particles (dark points) are dispersed uniformly within the coatings. The volume percentage content of Si<sub>3</sub>N<sub>4</sub> particles within Cr-C-Si<sub>3</sub>N<sub>4</sub> coatings is about 17.4 vol.%. The surface of Cr-C coatings has a granular morphology and a fine granular morphology exists in Cr-C-Si<sub>3</sub>N<sub>4</sub> composite coatings. It is found that Si<sub>3</sub>N<sub>4</sub> particles can refine grains. Owing to the introduction of Si<sub>3</sub>N<sub>4</sub> particles, the corrosion resistance of the coatings is improved. The hardness of Cr-C-Si<sub>3</sub>N<sub>4</sub> coatings enhances up to 950 Hv, it's higher than 820 Hv of the Cr-C coating's hardness. Wear test results show that Cr-C-Si<sub>3</sub>N<sub>4</sub> coatings have the better wear resistance than Cr-C coatings. This is attributed to the dispersive strengthen effects of Si<sub>3</sub>N<sub>4</sub> result in promoting the composite coatings material strength.

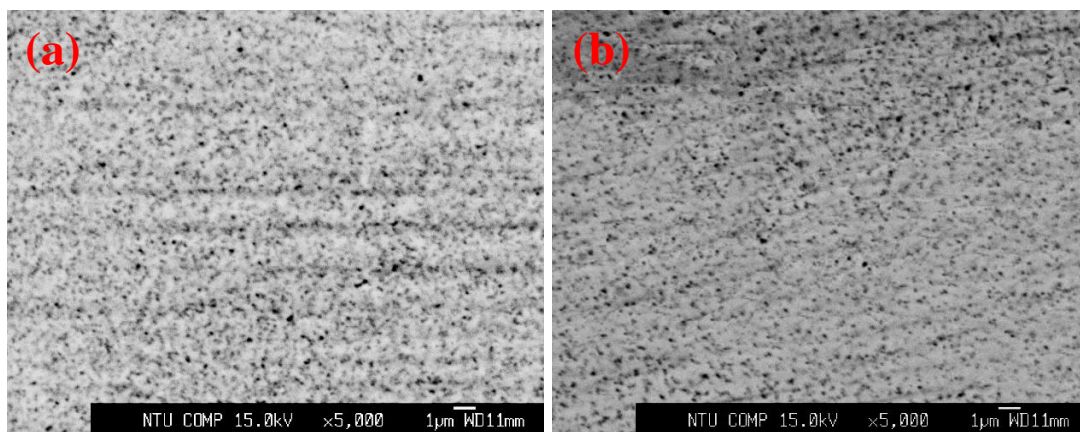


Fig. 1. The microstructure surface morphologies (back scattering model) show that of (a) plane view, and (b) cross-sectional view of the Cr-C-17.4 vol.% Si<sub>3</sub>N<sub>4</sub> composite coating.

# Electrostatic Field-Assisted Direct Potentiostatic and Pulse-Potential Electrodeposition of Prussian Blue Films

Cheng-Lan Lin, Kuen-Yi Ding

*Department of Chemical and Materials Engineering, Tamkang University  
No. 151, Yingzhuan Rd., Tamshui Dist., New Taipei City 25137, Taiwan  
cclin@mail.tku.edu.tw*

Micropatterned functional material thin films have been extensively used in many applications such as energy conversion and storages, fuel cells, photocatalysis, micro-electronics and sensors. Methods of photolithography, micro-contact printing or inkjet printing have been employed to prepare these micropatterned thin films. These procedures usually consist of multiple surface treatment steps. It is envisaged that a micropattern fabrication procedure with fewer surface modification steps would increase its efficiency and reduce cost. In this study, a new method that directly creates a micropatterned thin film on an ITO/PET conducting plastic substrate by electrostatic-assisted electrodeposition is proposed and demonstrated. A micropatterned electrostatic film (mESF), which composed of patterned polyacrylate bumps array on a polyethylene substrate, is firstly attached onto the conductive side of an ITO/PET substrate. Upon the removal of the mESF, a patterned electrostatic field is exhibited on the ITO surface by contact electrification. Micropatterned Prussian blue (PB) thin film then can be directly formed on the surface by potentiostatic or pulse potential electrodeposition under the influence of the electrostatic field. Effects of the electrodeposition parameters on the morphology of the resulted micropatterned PB films are investigated. Possible mechanism of the electrostatic-assisted electrodeposition method is proposed. This method might find its potential applications in preparing micropatterned function material films on conducting substrates.

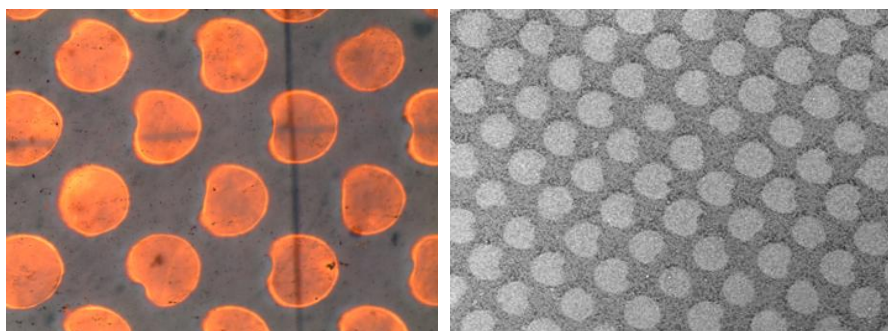


Figure 1 Optical microscope and scanning electron microscope images of a typical micropatterned PB film prepared by electrostatic field-assisted electrodeposition.

# Copper Coatings for Used Nuclear Fuel Containers: Corrosion Testing

Peter Keech<sup>1</sup>, Sridhar Ramamurthy<sup>2</sup>, Rachel Partovi-Nia<sup>2</sup>, Jian Chen<sup>2</sup>, Becky Jacklin<sup>2</sup>, David Shoesmith<sup>2</sup>

<sup>1</sup>Nuclear Waste Management Organization, 22 St. Clair Ave, Toronto, ON, M4T 2S3

<sup>2</sup>Surface Science Western, Western University, 999 Collip Cir. London, ON, N6G 0J3

pkeech@nwmo.ca

The use of copper as a barrier against corrosion in deep geological repositories (DGRs) for used fuel containers (UFCs) has been explored in Europe, Asia and Canada for many decades, as metallic copper provides thermodynamic stability against anoxic corrosion. Extensive review of corrosion data reveals that damage will be limited to nanometres per year or less, or fewer than 1.3 mm in one million years<sup>1</sup>. In recent years, Canada's Nuclear Waste Management Organization (NWMO) has been developing methods for depositing thin copper coatings directly onto steel-based UFC materials that provide suitable strength to withstand geological processes for many years. The result is the NWMO Mark II UFC, shown in Figure 1, both as a schematic and as a fabricated prototype. This container offers many potential manufacturing and handling advantages, owing to its modest size and low weight; the container depicted is just over 2 m long and < 5 t fully loaded, and compares favourably to a loaded KBS-3 container (> 4 m long and > 25 t)<sup>2</sup>.

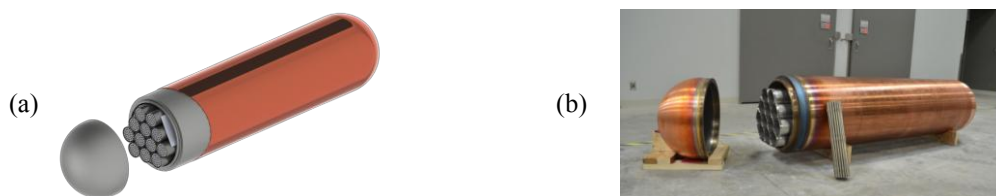
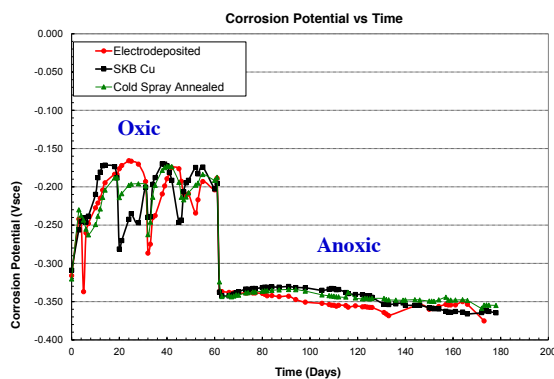


**Figure 1: NWMO Mark II Used Fuel Container (a) Schematic and (b) Prototype**

Electrodeposition and cold spray have been explored for coatings, with the former proving to be superior for pre-fabrication (i.e. empty containers/lids), while the latter offers advantages for completing the coating over the closure zone, following weld sealing of a loaded container. As the corrosion barrier, it is necessary for the copper coatings to perform as well (or better) than wrought copper materials, for which a large copper corrosion database exists. Corrosion testing of the coating materials has been extensive, consisting of long term exposures to oxic and anoxic conditions as well as accelerated electrochemical measurements. Coating materials have demonstrated corrosion performance that is similar to that of the wrought copper reference materials, with the exception of the accelerated testing in which there are subtle differences among the materials with respect to surface texturing, observed via post-experiment surface analysis. However, throughout the experiments, there is consistency among corrosion potential measurements for the coating and wrought materials, as these fall within a few mV of each other under different conditions such as oxic and anoxic exposures and in accelerated electrochemical measurements. An example is presented in Figure 2, for an experiment that was initially oxic and then anoxic. Results from all of these experiments and the supporting surface analysis, will be described in this paper.

**Figure 2: Corrosion Potential versus time plot for the samples exposed initially under O<sub>2</sub> purging, then followed by Ar-purging**



<sup>1</sup> Scully, J.R., Edwards, M., 2013. Review of NWMO Copper Corrosion Allowance, NWMO Technical Report, NWMO-TR-2013-04, Nuclear Waste Management Organization, Toronto, Canada.

<sup>2</sup> H. Raiko, R. Sandström, H. Rydén, M. Johansson, 2010, Design analysis report for the canister, SKB-TR-10-28, Svensk Kärnbränslehantering AB, Stockholm, Sweden.

# Electrodeposition of Nickel Nanostructures from Deep Eutectic Solvents: New Insights into Nucleation and Growth Mechanisms

El Amine Mernissi Cherigui<sup>1</sup>, Pieter Bouckennooge<sup>1</sup>, Kadir Sentosun<sup>2</sup>, Jon Ustarroz<sup>1</sup>, Herman Terryn<sup>1</sup>, Sara Bals<sup>2</sup>, Annick Hubin<sup>1</sup>

<sup>1</sup>*Research Group Electrochemical and Surface Engineering (SURF), Vrije Universiteit Brussel  
Pleinlaan 2, 1050, Brussels, Belgium*

<sup>2</sup>*Research Group Electron Microscopy for Materials Science (EMAT), University of Antwerp  
Groenenborgerlaan 171, 2020 Antwerp, Belgium  
justarro@vub.ac.be*

Supported nanostructured electroactive materials can be fabricated by multiple methods. However, electrodeposition offers several advantages since the nanostructures are grown on the final support. To produce highly electroactive nanostructures, the electrochemical nucleation and growth mechanisms on the nanoscale need to be understood. In this context, Deep Eutectic Solvents (DESs) have generated great enthusiasm as a new generation of non-aqueous electrolytes [1]. They offer several advantages, such as high stability at high temperatures and broad electrochemical windows. Likewise, DESs are easier to prepare, less toxic and much cheaper than room temperature ionic liquids (RTILs) [1]. Nanoscale electrodeposition from DESs is relatively new but has already been proven effective to deposit metallic nanostructures. Moreover, DESs are especially interesting because of their ability to stabilize nanoclusters [2] and to facilitate nanoparticle self-assembly. Hence, nanostructures that would not be attainable with traditional aqueous electrolytes could potentially be generated.

During the last years we have developed an approach based on using carbon coated TEM grids as electrodes. This way, by combining atomic-scale TEM characterization with electron tomography and electrochemical measurements, we have found evidence that has led us to suggest an electrochemical aggregative growth mechanism [3]. It includes nanocluster self-limiting growth, surface diffusion, aggregation and coalescence as important electrochemical growth mechanisms [4].

In this presentation, we use this approach to evaluate the electrodeposition of nickel nanostructures from a 1:2 choline chloride – urea DES. Electrochemical techniques, such as cyclic voltammetry and chronoamperometry, are employed to understand the electrochemical reactions occurring during nickel deposition. Special attention is given to the interaction between the solvent and the electrodeposited nickel phase. The influence of temperature, electrolyte composition and applied potential waveforms on the early stages of nucleation and growth was evaluated. FESEM, XPS and TEM characterization is combined with electrochemical data to gain understanding on these phenomena and to highlight possible benefits of the use of DESs as alternative electrolytes.

The outcome of this investigation shows that, within a wide range of deposition parameters, a large population of small nickel nanostructures (< 20-30 nm) can be obtained. Interestingly, these nanostructures are formed by aggregated nanoclusters of few nanometers in diameter [5]. This indicates a self-limiting growth mechanism, which may be caused by the interaction of the DES with the growing nickel phase. These results show that metal electrodeposition from DESs can be of great interest to produce nanostructures with electrocatalytic properties.

- [1] E.L. Smith, A.P. Abbott, K.S. Ryder, Deep eutectic solvents (DESs) and their applications., *Chemical Reviews*. 114 (2014) 11060–82.
- [2] J.A. Hammons, T. Muselle, J. Ustarroz, M. Tzedaki, M. Raes, A. Hubin, et al., Stability, Assembly, and Particle/Solvent Interactions of Pd Nanoparticles Electrodeposited from a Deep Eutectic Solvent, *The Journal of Physical Chemistry C*. 117 (2013) 14381–14389.
- [3] J. Ustarroz, J.A. Hammons, T. Altantzis, A. Hubin, S. Bals, H. Terryn, A generalized electrochemical aggregative growth mechanism, *Journal of the American Chemical Society*. 135 (2013) 11550–11561.
- [4] J. Ustarroz, T. Altantzis, J. a. Hammons, A. Hubin, S. Bals, H. Terryn, The Role of Nanocluster Aggregation, Coalescence, and Recrystallization in the Electrochemical Deposition of Platinum Nanostructures, *Chemistry of Materials*. 26 (2014) 2396–2406.
- [5] E.A. Mernissi Cherigui, P. Bouckennooge, K. Sentosun, J. Ustarroz, A. Hubin, S. Bals, et al., Electrodeposition of Nickel Nanostructures from Deep Eutectic Solvents: New Insights into Nucleation and Growth Mechanisms, *Manuscript in Preparation*. (2015).

# Electrodeposition of CuMn thin film from a nonaqueous electrolyte

Pu-Wei Wu<sup>1,\*</sup>, Po-Chun Chen<sup>2</sup>, Chia-Yun Hsu<sup>1</sup>, Shih-Cheng Chou<sup>1</sup>  
Aniruddha Joi<sup>3</sup>, Yezdi Dordi<sup>3</sup>, Jyh-Fu Lee<sup>4</sup>

<sup>1</sup>*Department of Materials Science and Engineering, National Chiao Tung University  
Hsinchu 300, Taiwan, R.O.C.*

<sup>2</sup>*Biomedical Electronics Translational Research Center, National Chiao Tung University  
Hsinchu 300, Taiwan, R.O.C.*

<sup>3</sup>*LAM Research Inc., 4650 Cushing Parkway, Fremont, CA 94538 U.S.A.*

<sup>4</sup>*National Synchrotron Radiation Research Center, Hsin-chu 300, Taiwan, R.O.C.*

\* [ppwu@mail.nctu.edu.tw](mailto:ppwu@mail.nctu.edu.tw)

CuMn alloyed film is of particular interest for surface corrosion protection and diffusion barrier in semiconductor Cu damascene processing. In this work, we carry out the electrodeposition of CuMn thin film using a nonaqueous electrolyte. Precursors including  $C_{10}H_{14}CuO_4$  and  $Mn(C_5H_7O_2)_2$  are dissolved in solvents of  $C_2H_4(OH)_2$  and  $CH_3COOH$ , followed by galvanostatic deposition onto Pt-coated ITO substrates. Parameters including precursor concentrations (their molar ratios), plating temperature, plating time, and electrode distance are deliberately varied to identify the optimized processing conditions for uniform CuMn deposit. Material characterization including scanning electron microscope, energy dispersive X-ray spectroscopy, X-ray diffraction spectrometer, and X-ray photoelectron spectroscopy are employed to investigate the composition, surface uniformity, phase, and crystallinity of the CuMn film. In addition, X-ray absorption spectroscopy is involved to understand the reduction process of Cu and Mn cations in the plating bath and the atomic distribution of the Cu and Mn in the deposit. Electrochemical parameters are carefully explored to explain the deposition mechanism and its effect on the resulting compositional inhomogeneity and overall makeup of the CuMn film.

## Synthesis and characterization of metal sulfides for solar devices

Serena Cinotti<sup>1</sup>, Francesco Di Benedetto<sup>2</sup>, Andrea Giaccherini<sup>1</sup>, Claudio Zafferoni<sup>1</sup>, Giordano Montegrossi<sup>3</sup>, Annalisa Guerri<sup>1</sup>, Francesco Carlà<sup>4</sup>, Roberto Felici<sup>4</sup>, Massimo Innocenti<sup>1</sup>

<sup>1</sup>*Department of Chemistry, University of Florence, Via della Lastruccia 3-13, 50019 Sesto Fiorentino (Florence), Italy*

<sup>2</sup>*Dept. Earth Sciences, Univ. Florence (Italy), Via La Pira 4, 50121 Firenze, Italy*

<sup>3</sup>*IGG, Istituto di Geoscienze e Georisorse, CNR, via G. La Pira 4, 50121, Firenze, Italy*

<sup>4</sup>*ESRF, 6, Rue Horowitz, F-BP 220, 38043, Grenoble, Cedex, France*

*claudio.zafferoni@unifi.it*

Semiconductors of interest in the solar energy conversion field were prepared by electrodeposition. In particular, we used the E-ALD (Electrochemical Atomic Layer Deposition) [1] method to build a p-n junction. The obtained ultra-thin films were characterized through SXRD (Surface X-Ray Diffraction), with the aim of performing a structural characterization of the grown films.

E-ALD is a layer-by-layer electrodeposition based on the alternate Under Potential Deposition (UPD) of atomic layers of the elements constituting a compound. The starting point was the deposition of the p layer, (Cu-Zn-S), prepared alternating the UPD of the binary sulfides, CuS and ZnS. After the optimization of the deposition condition of the p film [2-4], the electrochemistry behavior of the Cd solution on the substrate covered by the p films has been studied, in order to optimize the deposition of the n film (CdS). To determine the UPD of Cd, voltammetric studies of the Cd solution on the Ag electrode covered by the p films have been done. In these condition the window of electroinactivity of the new substrate is small, thus it is possible to observe the UPD and the bulk reduction peak of Cd, but it is impossible determine the amount of Cd deposited by linear stripping voltammetric studies, because the redissolution potentials of Cd and Cu-Zn are overlapped. In order to verify the effective deposition of Cd and the UPD nature of the deposition, some different samples have been prepared and then characterized by X-Ray Photoelectron Spectroscopy (XPS) and SEM microscopy and microanalysis. The samples have been growth layer-by-layer, or by EC-ALD, or checking the amount of Cd deposited integrating the charge deposited during time with an appropriate software, in a way to assure the deposition of a single monolayer.

XPS results show the presence of cadmium as sulfides in all the samples and in comparable amount, thus verifying the UPD nature of the cathodic peak at less negative potential.

In situ SXRD measurements performed at ESRF (Grenoble), allowed to investigate the growth mechanism of Cu-Zn-S thin films (the p layer). The growth of the film was monitored by following the evolution of the Bragg peaks. Analysis of these data are still in progress but the samples show crystallinity, proposing E-ALD as method to grow structurally ordered thin films.

- [1] B.W. Gregory and J.L. Stickney, Electrochemical atomic layer epitaxy (ECALE), J. Electroanal. Chem., (1991) 300 543-561.
- [2] M. Innocenti, I. Bencistà, S. Bellandi, C. Bianchini, F. Di Benedetto, A. Lavacchi, F. Vizza, M.L. Foresti, ., Electrochemical layer by layer growth and characterization of copper sulfur thin films on Ag(1 1 1), Electrochim. Acta, (2011) 58 599-605.
- [3] M. Innocenti, L. Becucci, I. Bencistà, e. Carretti, S. Cinotti, L. Dei, F. Di Benedetto, A. Lavacchi, F. Marinelli, E. Salvietti, F. Vizza and M.L. Foresti, Ternary cadmium and zinc sulfides and selenides: electrodeposition by ECALE and electrochemical characterization, J. Electroanal. Chem., (2013) 710 17-21.
- [4] M. Innocenti, S. Cinotti, I. Bencistà, E. Carretti, L. Becucci, F. Di Benedetto, A. Lavacchi and M.L. Foresti, Electrochemical Growth of Cu-Zn Sulfides of Various Stoichiometries, J. Electrochem. Soc., (2014) 161 (1) D14-D17

# Using Copolymers as Suppressors in a Copper Plating Bath for Through-Hole Filling

Shih-I Wen, and Wei-Ping Dow\*

*Department of Chemical Engineering, National Chung Hsing University  
205 Kou-Kuang Rd., Taichung, 40227 Taiwan, R.O.C.  
dowwp@dragon.nchu.edu.tw*

Recently, a copper electroplating technique, namely butterfly technique (BFT) <sup>[1]</sup>, was developed to achieve a void-free filling of a through hole (TH) of a printed circuit board (PCB). However, the BFT for TH filling caused an issue of thick copper layer on the PCB surface, which increases the process cost due to a requirement of post copper etching process. Literature has mentioned that copolymers have strong suppression on copper electroplating than poly(ethylene glycol) (PEG). The strong suppressor can minimize surface copper thickness to achieve excellent filling performance. In this work, we employ a copper filling formula to perform the TH filling. Several copolymers were employed as suppressors to replace PEG. The result shows that the surface copper thickness is decreased by using the copolymer. It can not only enhance the copper filling performance but also increase plating efficiency.

## Reference

1. W. P. Dow, H. H. Chen, M. Y. Yen, W. H. Chen, K. H. Hsu, P. Y. Chuang, H. Ishizuka, N. Sakagawa, R. Kimizuka, "Through-Hole Filling by Copper Electroplating", *Journal of The Electrochemical Society*, 2008, 155, D750-D757.

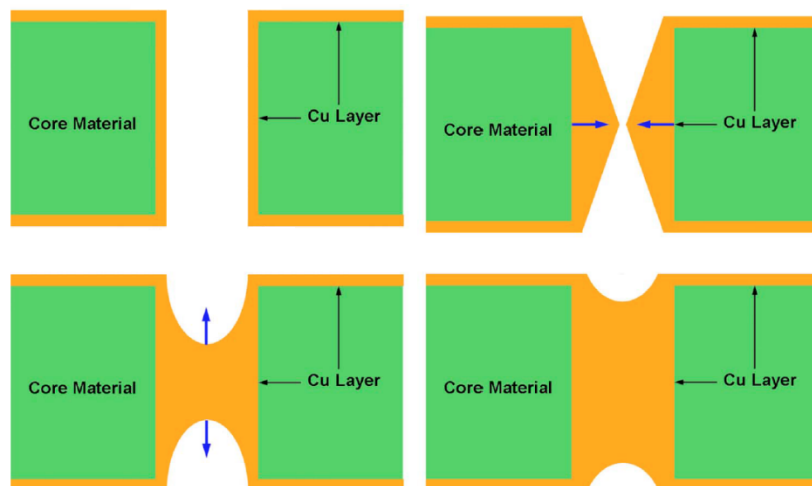


**Figure 1.** Illustrations of TH filling by butterfly technique. <sup>[1]</sup>



# Electromagnetic Shielding Polyamide Fabrics prepared by Electroless Ni Plating with Chitosan-Nickel Complexes Activation

Yaping Zhao, Hong Zhao, Caihong Liu, Bingzheng Song, Zaisheng Cai  
College of Chemistry, Chemical Engineering & Biotechnology, Donghua University, Shanghai, China  
E-mail address: [zhaoyaping@dhu.edu.cn](mailto:zhaoyaping@dhu.edu.cn)

Electroless plating has been used for modifying the surface of textiles and imparting potential for textile products with functional and decorative applications [1]. Electroless nickel plating has been widely applied due to its deposit properties, such as good electrical and magnetic properties, excellent corrosion and wear resistance as well as deposit uniformity, etc [2]. Noble metal palladium is usually employed as the catalyst sites in the conventional activation processes to initiate the electroless plating, in which the cost of Pd and its compounds are very expensive. It is important to develop a cost effective activation method to replace Pd activating solution [3]. In this work, electromagnetic shielding polyamide fabrics are prepared using chitosan-nickel (CS-Ni) complexes as activators and sodium borohydride as reductant during the pretreatment process, followed by electroless nickel plating. CS-Ni complexes are prepared by the complexing adsorption between  $\text{Ni}^{2+}$  and CS which pre-coated on fabrics. A hydrazine reduction chemical plating nickel reaction system with ammonia as complexing agent is utilized to obtain a pure Ni coating on textiles. The surface morphology, microstructure and composition of the nickel-plated fabrics are analyzed by using emission scanning electron microscopy (FESEM) and energy dispersive spectroscopy (EDS), X-ray diffraction (XRD) and thermogravimetric analysis (TG). The prepared polyamide fabrics has a saturation magnetization of 330 emu/g and a excellent electromagnetic shielding effectiveness (SE) of 50-80 dB during 300kHz~3000MHz. This approach reveals a promising potential to fabricate electromagnetic shielding materials, in which nickel salt is as activator instead of metallic palladium to realize the palladium-free activation.

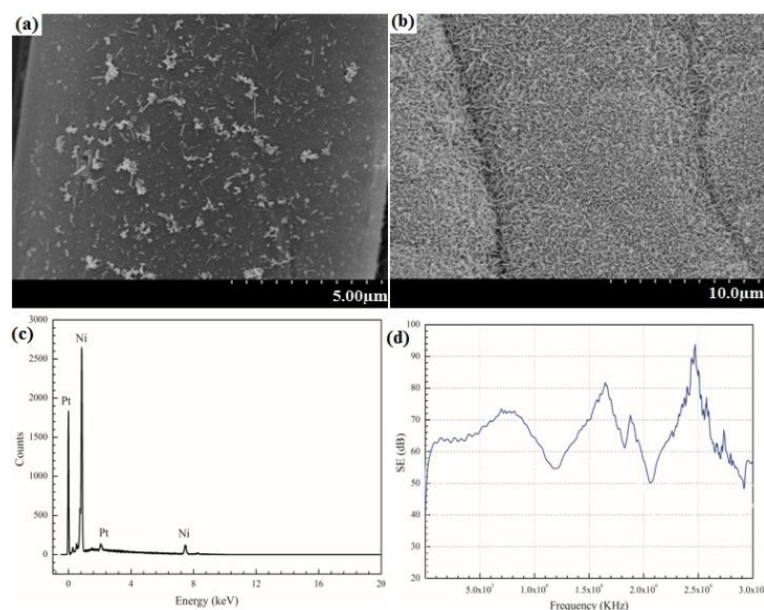


**Fig.1 FESEM images of the obtained fabrics (a) after activation and (b) after electroless plating; (c) EDS picture and (d) SE curve of the nickel-plated polyamide fabric**

This work was financially supported by the Shanghai Municipal Natural Science Foundation (12ZR1400400) and the Fundamental Research Funds for the Central Universities (2232015D3-17)

## References

- [1] Y. Yu, C. Yan, Zi, Zheng. *Advanced Materials* 26(2014)5508.
- [2] Z. Song, Z. Xie, G. Yu, et al. *Journal of Alloys & Compounds* 623 (2015) 274.
- [3] G. Sh, W. Li, Y. Lu. *Surface & Coatings Technology* 253 (2014) 221.



# **Electrodeposition of Copper, Indium, Gallium and Selenium on Molybdenum Investigated by Voltammetry, X-Ray Diffraction, and Scanning Electron Microscopy/Energy Dispersive Spectroscopy**

Viswanathan S. Saji, Yu-Beom Yeon, Chi-Woo Lee  
*Department of Advanced Materials Chemistry, Korea University*  
*2511 Sejongro, Sejong Special Self-Governing City 339-700, Korea*  
*cwlee@korea.ac.kr*

As the climate change continues, harvesting solar energy and solar energy conversion by means of photovoltaic materials in particular are receiving significant scientific interest. In this work, a systematic investigation was performed to study the variation of voltammetric peaks during electrodeposition of copper, indium, gallium, and selenium on molybdenum electrode. The objective of the work was to methodically understand the variation of different oxidation-reduction peaks from unary to quaternary composition so that the comprehensive understanding on their peaks can be arrived. The electrodeposits were then characterized by X-ray diffraction, scanning electron microscopy/energy-dispersive spectroscopy. The results are expected to be helpful to get new insight, for example, on the variation of different voltammetric peaks originating from molybdenum as well as indium.

## **References**

1. Y.-P. Fu, R.-W. You, and K.-K. Lew, J. Electrochem. Soc., 156, E133 (2009).
2. V.S. Saji, I.-H. Choi, and C.-W Lee, Sol. Energy, 85, 2666 (2011).
3. V.S. Saji and C.-W. Lee, Electrochim. Acta, 137, 647 (2014).

# Contact Resistance of Thin Gold Overlay on Cu-Sn Alloy Electrodeposits with Various Compositions

Toshihiro Nakamura, Takayo Yamamoto, Tomio Nagayama  
Kyoto Municipal Institute of Industrial Technology and Culture  
91Chudoji Awata-cho, Shimogyo-ku, Kyoto 600-8815, Japan  
86nakat@tc-kyoto.or.jp

Electrodeposition is a key technology for thin-layer process in the fields of surface finishing for electronic materials. High connector reliability can be achieved by using a gold plating on the electrical contacts. Gold, when applied to the contact interface, has the capability of providing a stable and low contact resistance over the operating life of most applications, because gold is a noble metal and does not form corrosion product films. Thin gold coatings can establish a stable and low contact resistance but decreasing the thickness of a gold plating tends to increase the porosity which enlarges the contacts' vulnerability to pore corrosion. Pore corrosion can occur at the under layer plate and exposed base metal locations where pores in the gold coincide with pores in the under layer plate. Accordingly, the durability of the thin gold plated products depends on quality of under layer greatly. Typically, nickel plating is widely used under layer for gold. However, nickel is classified as a skin sensitizer and as a material suspected as being able to cause cancer via inhalation. The Control of Substances Hazardous to Health (CoSHH, U.K.) Regulations 2002 require that skin exposure to nickel and nickel salts is prevented or adequately controlled at work. In contrast, we recently demonstrated that silver white Cu-Sn alloy electrodeposits(40-55mass%Sn), called "speculum alloy," which has been investigated as an promising alternative to an allergenic nickel coating, can be obtained from environmentally-friendly cyanide-free Sulfosuccinate Bath[1]. In this study, the contact resistance of the thin gold(Au0.1 $\mu$ m) overlay on Cu-Sn alloy electrodeposits containing 40 to 71mass% Sn were examined by the aging test (salt spray test) compared with bright nickel coating.

The contact resistance of thin gold overlay on the bright nickel coating began to increase, after only eight hours, much more quickly than that of Cu-Sn alloy deposits. On the other hand, Cu-Sn alloy deposits as an under layer restrained degradation of contact resistance, in particular, thin gold overlay on the Cu-Sn alloy deposits containing 40 to 55 mass% Sn, called "speculum alloy," maintained a lower contact resistance during the salt spray test for prolonged periods (Fig. 1). Contact resistance durability of the specimens using Sn rich Cu-Sn alloy deposits with Sn contents of 61 mass% or above tended to reduce with increasing Sn content. Gold thickness can be reduced by using the Cu-Sn alloy deposits as an undercoat.

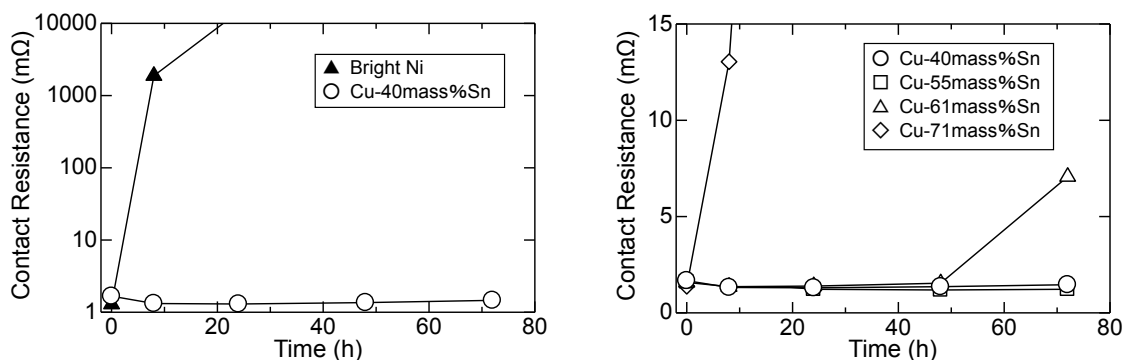


Fig.1. Effect of salt spray test on contact resistance of thin gold(Au0.1 $\mu$ m) overlay on Cu-Sn alloy electrodeposits with various compositions or Bright Ni

- [1] T. Nakamura, T. Nagayama, T. Yamamoto, Y. Mizutani, H.Nawafune, Mater. Sci. Forum., **654-656**, 1912(2010).

# Electrochemical preparation of novel metal-like lustrous films

Takuya Tokuda, Dan Takamura, Katsuyoshi Hoshino\*

Department of Image and Materials Science, Graduate School of Advanced Integrated Science,  
Chiba University, 1-33 Yayoi-cho, Inage-ku, Chiba, 263-8522, Japan

\*E-mail: k\_hoshino@faculty.chiba-u.jp

## 1. Introduction

Metallic lusters exhibited by gold, silver, and copper have designability and functionality for many applications such as automotive coatings, roof coatings, printing inks, cosmetics, and plastic materials for protective and decorative purposes. For such applications, metal effect pigments or flakes of metals have been used and produced by grinding metal granules in a ball mill. After filtration, the pigment flakes are supplied in the form of a paste with organic compounds. By applying the paste, the metal flakes cause a lustrous properties in the films since they are oriented parallel to the substrate plate after drying. However, these metal flakes in the paint have some drawbacks such as sedimentation, corrosion, and heavy weight. In order to overcome these drawbacks, the organic materials for use in the gold-like coatings have been investigated. Recently, our group reported the first chemical synthesis of organic materials capable of forming air-stable gold-like coatings.<sup>1, 2)</sup> Following this chemical approaches, we also successfully produced lustrous metal-like films using an electrochemical technique. In this study, we report the preliminary study on their electrochemical preparation method and their spectroscopic characterization.

## 2. Experimental

3-Methoxythiophene (MeOT), lithium perchlorate (anhydrous) ( $\text{LiClO}_4$ ), sodium dodecyl sulfate (SDS), and distilled water were purchased from Wako Pure Chemical Industries, Ltd and used as supplied. 1-butanol (>99%) was purchased from Kanto Chemical Co., Inc. and used as supplied. Films were obtained by electro-oxidation of 0.1 M MeOT dissolved in mixed solution ( $\text{H}_2\text{O}$ :1-butanol = 96:4 vol%) containing 0.1 M  $\text{LiClO}_4$  and 0.1 M SDS at room temperature using cyclic voltammetry. The working ITO electrode and the counter Pt plate were immersed in the main compartment of the two-compartment type electrolysis cell. The auxiliary compartment, which is separated from the main one by a sintered glass frit, had an immersed KCl agar bridge connected to the reference saturated calomel electrode (SCE). The produced films were characterized by UV-vis reflection spectra using a spectrophotometer (U-3000, Hitachi) with an integrating sphere, observation using an optical microscope (VHX-2000, Keyence), and wide-angle X-ray diffraction measurements (XRD) using a diffractometer (Rigaku SmartLab) equipped with a  $\text{CuK}\alpha$  ( $\lambda = 1.54 \text{ \AA}$ ) source.

## 3. Results and Discussion

Fig. 1 shows the photograph of a lustrous metal-like film produced by cyclic voltammetry at a sweep rate of 10 mV/s in the potential range between -0.5 V and 1.3 V (the number of sweep: 11). Fig. 2 shows the reflection spectra of the film (solid line) and a vacuum-evaporated gold film (dashed line). The former spectrum is nearly the same as the latter in shape and a rising wavelength of reflectance, indicating that the recognized color of the film is gold. The XRD measurement of the film exhibited reflections at  $2\theta = 7.96$  and  $26.04^\circ$ . Based on previous reports on the structural analyses of the poly(3-alkylthiophenes), its reflections indicate a well-defined lamellar structure. The peak at  $2\theta = 7.96^\circ$  correspond to first-order and higher order reflections from the lamellar interlayer spacing, and the peak at  $2\theta = 26.04^\circ$  correspond to the stacking distance of the thiophene rings between two molecular chains. This highly ordered structure most likely exhibits the lustrous feature of the film.

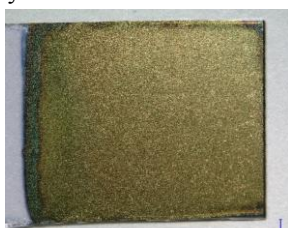


Fig. 1 Photograph of the metal-like lustrous film.

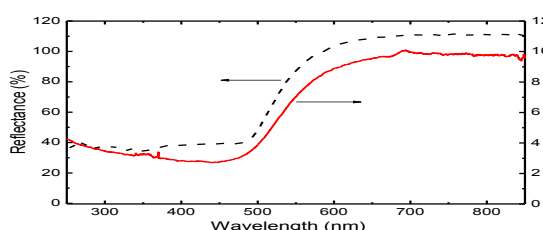


Fig. 2 Reflection spectra of the metal-like lustrous film (solid line) and vacuum-evaporated gold film (dashed line)

- 1) R. Tagawa, H. Masu, T. Itoh and K. Hoshino, *RSC Adv.*, **4**, 24053 (2014).
- 2) K. Hoshino, *J. Jpn. Soc. Colour Mater.*, **88**, 101 (2015)

# Intelligent Self-lubricant Composite Nickel Coating based on Phase Transition of Polystyrene and Polymethyl Methacrylate Particles

Satoru WATANABE<sup>a</sup>, Isao SHITANDA<sup>a,b</sup>, Yoshinao HOSHI<sup>a</sup>, Tatsuo AIKAWA<sup>a</sup>,  
Masayuki ITAGAKI<sup>a,b</sup>

<sup>a</sup>Department of Pure and Applied Chemistry, Faculty of Science and Technology,  
Tokyo University of Science, Noda, Chiba 278-8510, Japan.

<sup>b</sup>Research Institute for Science and Technology,  
Tokyo University of Science, 2641, Yamazaki, Noda, Chiba 278-8510, Japan.  
E-mail address: shitanda@rs.noda.tus.ac.jp(I.Shitanda)

## 1. Introduction

In the present study, we demonstrated a polystyrene (PS) and polymethyl methacrylate (PMMA) particles composite nickel coatings for new intelligent self-lubricant film. Phase transition is the transformation of thermodynamic system from one phase to another one by heat transfer. PS and PMMA particles are known to show a glass-liquid phase transition at 100°C and 105°C, respectively. The PS and PMMA particles composite coating films are expected to increase its lubricity drastically by transformed to liquid phase over the glass-liquid phase transition temperature. Certainly, the particles may show good lubricant property in a low temperature. In this study, we investigated the lubricant properties in detail.

## 2. Experimental

PS and PMMA particles were prepared by soap-free emulsion polymerization [1,2]. The PS and PMMA particles of 0.2, 0.6 and 1.0  $\mu\text{m}$  diameter were used throughout. A Watts bath is used as the plating bath. The particles were injected in the Watts bath containing a cationic surfactant, hexadecyl trimethyl ammonium bromide (CTAB). The electroplating under constant current condition was carried out by two electrode system. Copper and nickel sheets were used as the working electrode and counter electrode, respectively. Friction coefficient of the plating film was evaluated by Bowden-Leben type reciprocating friction tester under following measurement conditions; friction load: 10 N, sliding distance: 6 mm, sliding count: 250 times, test temperature: 40, 70 and 100 °C.

## 3. Results and Discussion

SEM images of 0.2  $\mu\text{m}$  polystyrene particle composite nickel coating was shown in Fig. 1. It was confirmed that polystyrene particles are incorporated into the nickel plating film uniformly. The relationship between the friction coefficient and temperature of the plating film was shown in Fig. 2. The friction coefficient of the composite coating films at 100 °C became smaller than that at 40°C and 70°C. In the case of 100 °C, the friction coefficient of 0.2  $\mu\text{m}$  PS particles composite plating film was estimated about 0.11, which was 2.9 times lower than that of a bare nickel plating film.

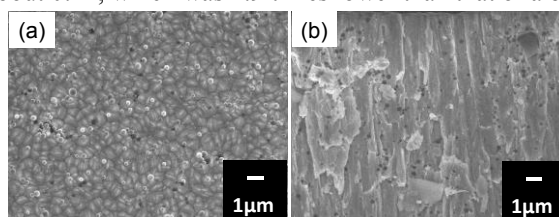


Fig. 1 SEM images of 0.2  $\mu\text{m}$  polystyrene particle composite nickel coating. (a): surface image, and (b) : cross-section image. The nickel film was electrodeposited at  $-30 \text{ mA cm}^{-2}$  for min.

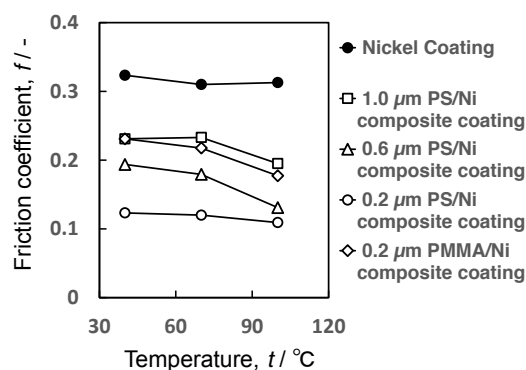


Fig. 2 Changes in the coefficient of friction by changing temperature of the plating film

## Acknowledgements

We would like to thank Sasaki laboratory members (Tokyo University of Science) for helping the lubricant tests.

## Reference

- [1] Xin Du, Junhui He, *J. Appl. Polym. Sci.*, **108**, 1755 (2008).
- [2] Kai Kang, Cheng You Kan, Yi Du, De Shan Liu, *J. Appl. Polym. Sci.*, **99**, 1934 (2006).

# Effect of Supercritical Carbon Dioxide on Crystal Structure of Electrodeposited Cobalt Films

Xun Luo<sup>1</sup>, Chun-Yi Chen<sup>1,2,\*</sup>, Tso-Fu Mark Chang<sup>1,2</sup>, Masato Sone<sup>1,2</sup>

<sup>1</sup>*Precision and Intelligence Laboratory, Tokyo Institute of Technology*

*4259-R2-35 Nagatsuta-cho Midori-ku Yokohama 226-8503 Japan*

<sup>2</sup>*CREST, Japan Science and Technology Agency*

*4259 Nagatsuta-cho, Midori-ku, Yokohama 226-8503, Japan*

*\* chen.c.ac@m.titech.ac.jp*

Electrodeposition is a commonly used method to fabricate components used in electronic devices [1]. However, formations of defects in the electrodeposited materials are crucial problems when applied in electronic devices, especially when the devices are miniaturized. Co is a commonly used material in electronic devices, such as random-access memory. Eliminating defects in the electrodeposited Co is more critical when demand of higher memory density is needed.

Evolution of H<sub>2</sub> gas and adsorption of the H<sub>2</sub> gas bubbles on surface of the cathode are believed to be one of the major causes of defects formed in the electrodeposited materials [2]. In previous studies, an electrodeposition method with supercritical CO<sub>2</sub> emulsions (SCE) is found to be effective in removing defects formed in the electrodeposited materials [3-5]. H<sub>2</sub> and CO<sub>2</sub> are both non-polar, therefore, desorption of the H<sub>2</sub> gas bubbles can be significantly improved after usage of the CO<sub>2</sub>. However, because of the non-polar property, electrical conductivity and metal salts solubility are both very low in CO<sub>2</sub>. Therefore, surfactants are needed to form an emulsified electrolyte composed of the supercritical CO<sub>2</sub> and the aqueous electrolyte to allow conduction of an electrochemical reaction [3]. In addition, effects of surface smoothening and grain refinement are observed in the electrodeposited Ni [4] and Cu [5] films. However, Co materials fabricated by electrodeposition with SCE (EP-SCE) have not been well studied. In this study, the SCE is applied in electrodeposition of Co. Effects of the SCE in removal of defects, morphology, and crystal structures of the Co films are evaluated.

A two-electrode system and high pressure apparatus for formation of the SCE were used in this study [4]. Co films with a theoretical thickness of about 70 μm when 100% current efficiency is achieved were electrodeposited on pure Cu (99.99%) plates, which is the cathode electrode. Pure Pt (99.99%) plate was used as the anode electrode. Both electrodes have dimensions of 10mm\*20mm\*0.5mm. The Co electrolyte was composed of CoSO<sub>4</sub> · 6H<sub>2</sub>O 300 g/L, CoCl<sub>2</sub> · 6H<sub>2</sub>O 45 g/L and H<sub>3</sub>BO<sub>3</sub> 40 g/L. The deposition temperature was varied from 25 to 40 °C. For formation of the SCE, non-ionic surfactants, polyoxyethylene lauryl ether (C<sub>12</sub>H<sub>25</sub>(OCH<sub>2</sub>)<sub>15</sub>OH)<sub>2</sub>, were used. The pressure for EP-SCE was 15 MPa. Current density was varied from 5.0 to 15.0 A/dm<sup>2</sup>. A scanning electron microscope (SEM) was used to observed surface of the films. X-ray diffraction (XRD) method was used to conduct crystal structural analysis of the Co films.

For the Co films obtained from the electrodeposition at ambient pressure and without the surfactant, hemi-spherical shaped particles were observed by SEM. After adding the surfactants into the bath, morphology of the particles were still hemi-spherical with uniform size, but average diameter of the particles sharply decreased from roughly 12 μm to 6 μm. We suggested the effect is caused by adsorption of the surfactant on surface of the cathode. When EP-SCE at 15 MPa was used, shape of the particles changed. Ridge-like morphology was observed, and growing orientation of the particles was perpendicular to surface of the electrode. In addition, the XRD results showed crystal structure of the Co films was mainly hexagonal close-packed (hcp) structure, and the crystal structure was mainly face-centered cubic structure after application of the EP-SCE.

[1] M. Gad-el-Hak, *The MEMS Handbook* (CRC, Taylor & Francis, Boca Raton, Florida., 2006).

[2] W.L. Tsai, P.C. Hsu, Y. Hwu, C.H. Chen, L.W. Chang, J.H. Je, M.H. Lin, A. Groso, G. Margaritondo, *Nature*, **417** (2002) 139.

[3] H. Yoshida, M. Sone, A. Mizushima, K. Abe, X.T. Tao, S. Ichihara, S. Miyata, *Chem. Lett.*, (2002) 1086.

[4] T.F.M. Chang, M. Sone, A. Shibata, C. Ishiyama, Y. Higo, *Electrochim. Acta*, **55** (2010) 6469.

[5] T.F.M. Chang, T. Shimizu, C. Ishiyama, M. Sone, *Thin Solid Films*, **529** (2013) 25.

# Control of Crystal Orientation of Electrodeposited Aluminum Films from Bath Using DMSO<sub>2</sub> as a Solvent

Yuya Ito\*, Nobuaki Watanabe, Ichiro Koiwa

College of Science and Engineering, Kanto Gakuin University

1-50-1, Mutsuurahigashi, Kanazawa-ku, Yokohama-shi, Kanagawa 236-8501, Japan

koiwa@kanto-gakuin.ac.jp

The control of the crystallographic orientation is one of the most important techniques for a semiconductor device process, corrosion process and crystal growth process. Especially for aluminum, the crystallographic orientation has some influence on the initiation and propagation of localized corrosion and oxidation. In this study, we have investigated the effect of deposition potential on the crystal orientation using aluminum chloride and dimethyl sulfone (DMSO<sub>2</sub>) for an organic solvent.

We used two different composition baths, that the mol ratio between dimethyl sulfone and aluminum chloride is 10:3 and 10:5. The electrodeposition performed under nitrogen atmosphere after dehydration process at 150 °C for 30 minutes. The aluminum films have been electroplated for electric potential region from -0.5 V to -3.0 V by using Al/Al<sup>3+</sup> reference electrode. Bath temperature is 150 °C, and substrate is a copper sheet (10 x 10 mm).

Figures 1 and 2 shows scanning electron microscope (SEM) images of the samples. The bright and smooth surface was observed in the samples from the 10:3 bath. In contrast, matt surface and granular crystals were observed in those from those from the 10:5 bath. Figure 3 shows X-ray diffraction patterns of the films. It is found that the crystallographic orientations of the samples were changed accompanied by deposition potential. The intensity of the (200) peak is stronger than that of (111) for the films from 10:3 bath. The peak intensity ratio between (111) and (200) is 2:1 for the bulk materials. These results show that the films are strongly oriented along the (200) plane. On the other hand, the films from 10:5 bath are slightly oriented along the (200) plane.

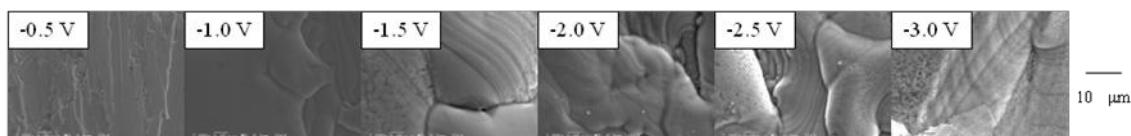


Fig.1 SEM images of the samples from 10 : 3 bath.

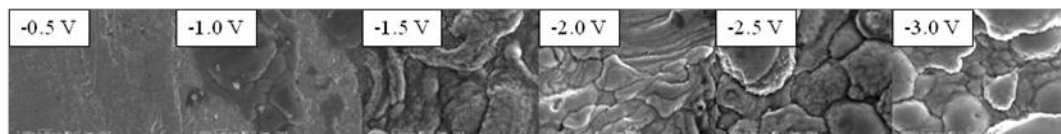


Fig.2 SEM images of the samples from 10 : 5 bath.

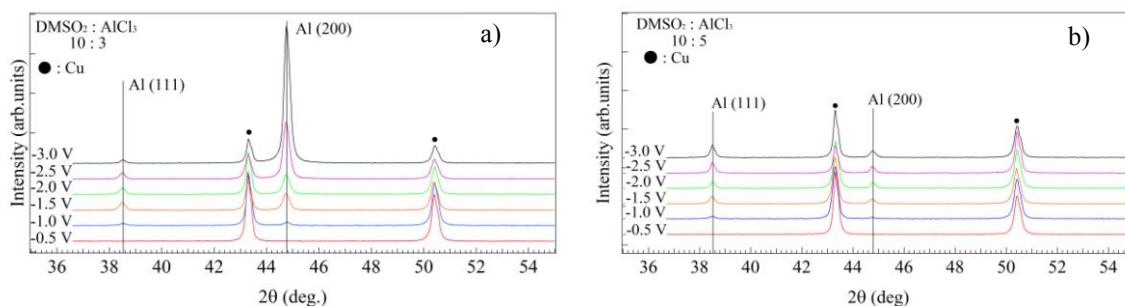


Fig.3 X-ray diffraction patterns of the films; a) plated from 10 : 3 bath, b) plated from 10 : 5 bath.

## Acknowledgements

This work was partially aided by the MEXT supported Program for the Strategic Research Foundation at Private Universities.

# Pulse Electroplating of Cu-Mo Alloy Film Using Disodium Molybdate

Sho Kawamura, Nobuaki Watanabe, Ichiro Koiwa

Kanto Gakuin University, Kanazawa-ku, Yokohama-shi, Kanagawa 236-8501, Japan  
m15J6002@kanto-gakuin.ac.jp

Electronic devices are desired to be larger integration, smaller size, higher speed and higher power, resulting in larger thermal generation, recently. Thermal generation from electronic devices such as a light emitting diode (LED) deteriorates reliability and shortens lifetime, also it causes thermomechanical stress, leading to distorting and breaking chips or packages. A substrate for heat radiation is necessary for LED and thermal coefficient value of substrate is desired to be near that about LEDs. There are some previous studies of Mo alloy films, however there is few study of Cu-Mo alloy films. In this paper, we propose a Cu-Mo alloy films, formed by electrochemical technique, as the heat radiation substrate for the LEDs.

Bath composition is following, copper ( $\text{CuSO}_4 \cdot 5\text{H}_2\text{O}$ ) whose concentration is  $0.13 \text{ mol/dm}^3$ , disodium molybdate ( $\text{Na}_2\text{MoO}_4 \cdot 2\text{H}_2\text{O}$ ) whose concentration is  $0.53 \text{ mol/dm}^3$ , and trisodium citrate whose concentration is  $0.91 \text{ mol/dm}^3$ . In addition, pulse plating conditions are as follows, a current density is controlled from 1 to  $100 \text{ mA/cm}^2$ . A duty cycle and frequency are fixed at 0.1 and 1Hz, respectively, and a bath temperature is controlled from 2 to  $60^\circ\text{C}$ . Surface was observed by scanning electron microscope (SEM). The composition of plated film was analyzed by energy dispersive X-ray spectrometry (EDS). An adhesion strength of electroplated Cu-Mo alloy film to a nickel substrate was evaluated by using a universal mechanical strength tester (Romulus, Quad Group Inc, shipped by Phototecnica co.Ltd.)

Figure 1 shows effect of current density on the Mo content in the plated films. The molybdenum content of electroplated Cu-Mo films abruptly increased with increasing current density for the region of current density less than  $10 \text{ mA/cm}^2$ , then the Mo content gradually decreased with increasing current density for the region less than  $50 \text{ mA/cm}^2$ , and it somewhat increased for the higher current density region. Maximum Mo content is 18.3 at % at  $10 \text{ mA/cm}^2$ .

Figure 1 shows three typical scanning electron micrographs of Cu-Mo alloy films plated at  $5.0 \text{ mA/cm}^2$  (a),  $10 \text{ mA/cm}^2$  (b),  $100 \text{ mA/cm}^2$  (c), respectively. Surface morphology of the plated film at  $5.0 \text{ mA/cm}^2$  shows closely packed grain structure and the grain boundaries were clearly observed. On the other hand, that at 10 and  $100 \text{ mA/cm}^2$  show flat surface and finer particles are observed. The differences between two films are mainly caused by Mo content, 6.8 at% and 18.3 at%, 14.3 at %.

Table 1 shows effect of current density on adhesion strength between electroplated Cu-Mo alloy and Ni substrate. The adhesion strength decreased with increasing current density for the region of current density less than  $50 \text{ mA/cm}^2$  and the minimum value of  $7.0 \text{ kg/cm}^2$  was obtained at  $50 \text{ mA/cm}^2$ . However, the maximum adhesion strength,  $106 \text{ kg/cm}^2$ , was obtained at  $100 \text{ mA/cm}^2$ .

This work was partially aided by MEXT-supported Program for the Strategic Research Foundation at Private Universities.

[1] T.Watanabe, T.Naoe, A.Mitsuo, S.Katsumata, Preparation of Fe-Mo, Co-Mo, Ni-Mo Amorphous Alloys by Electroplating Method, *J. Finish. Soc. Jpn.*, 40, 105(1989)

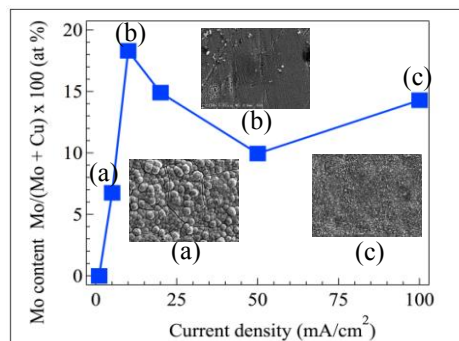


Fig.1 Effect of current density on Mo content of the Cu-Mo alloy films under the condition of duty cycle (0.1), frequency (1Hz), stirring speed (500 rpm), and bath temperature ( $30^\circ\text{C}$ ).

Table.1 Effect of current density on adhesion strength.

Current density ( $\text{mA/cm}^2$ )	Adhesion strength ( $\text{kg/cm}^2$ )
10	25.0
20	22.0
50	7.0
100	106.0

# Zn-AlO<sub>x</sub>(OH)<sub>y</sub> Composite Films Prepared from Non-Suspended Solution by Electrochemical Technique

Ichiro Koiwa\*, Nobuaki Watanabe\*, Akihiro Yamamoto\*, Kenta Chokki\* and Kazuhiro Yabe\*\*

\*Department Applied Chemistry, College of Science and Engineering Kanto Gakuin University

1-50-1 Mutsurahigasi, Kanazawa-ku, Yokohama-shi, Kanazawa 236-8501, JAPAN

koiwa@kanto-gakuin.ac.jp

\*\* Oki Engineering Co., Ltd., 3-20-16 Hikawadai, Nerima-ku, Tokyo 179-0084, Japan

The coexistence of nonmetal particles in metallic matrix improve the mechanical and chemical properties such as wear resistance, self-lubrication, corrosion resistance and metal-polymer adhesion. Dr. S.Oue and his co-workers have reported that Zn-Al<sub>2</sub>O<sub>3</sub> composite films were plated from non-suspended solution by using quaternary ammonium salt<sup>1)</sup>. The zinc matrix with aluminum oxide particles composite films from non-suspended solution containing quaternary ammonium salts were also investigated. The solution contains 520 mol/m<sup>3</sup> ZnSO<sub>4</sub>·7H<sub>2</sub>O and 79 mol/m<sup>3</sup> Al<sub>2</sub>(SO<sub>4</sub>)<sub>3</sub>·14-18H<sub>2</sub>O as metal source. A quaternary ammonium salts of Benzyltrimethyltetradecylammonium chloride dehydrate (BDTAC, Wako Co.,Ltd.) was used in this study.

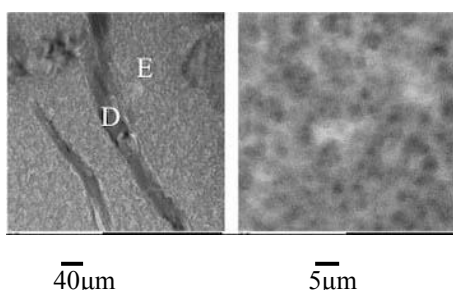


Fig.1 Transmission electron micrographs of the samples with maximum Al content.

Table 1 Composition of area D in Fig.1.

Element	Weight %	Atomic %
O	4.4	15.7
Al	0.8	17.0
Zn	94.8	82.6

Table 2 Composition of area E in Fig.1

Element	Weight %	Atomic %
O	7.8	20.6
Al	18.6	29.2
S	3.4	4.5
Zn	70.2	45.6

Figure 1 shows micrographs observed by transmission electron microscopy (TEM). Two different deposits were observed, one is needle-shaped deposit and the other is closely packed fine particle area. Magnified photograph shows closely packed fine particle area and fine particles are clearly observed. Table 1 shows result of composition analysis of D area, needle-shaped deposit, in Fig.1. The area is composed of 82.6 at% zinc, 17.0 at% aluminum and 15.7at% oxygen. Table 2 shows result of composition analysis of E area, closely packed fine particle area, in Fig.1. The area is composed of 45.6 at% zinc, 29.2 at% aluminum, 20.6 at% oxygen and 4.5 at% sulfur. The zinc content of area D, needle-shaped deposit, is much higher than that of area E, closely paced fine particle area. On the other hand, the aluminum content of area E is much higher than that of area D. It is concluded based on above results that the needle-shaped deposit is mainly composed of Zn or ZnO, and the fine particle is mainly composed of Al(OH)<sub>3</sub> or Al<sub>2</sub>O<sub>3</sub>. The origin of sulfur is not clear, because there is no sulfur in this plating bath except for sulfur of sulfate. Since the oxygen content in area E is higher than that in area D, it is suggested that the codeposited aluminum increases oxygen content in the films.

According to above results, the aluminum have been deposited from aqueous solution by using the quaternary ammonium salts of Benzyltrimethyltetradecylammonium chloride dehydrate and aluminum is deposited with oxygen and formed the fine particles. Therefore, this method is effective to codeposit aluminum from aqueous solution and to form the composite film from non-suspended solution. The co-deposited particles is too fine to detected X-ray diffraction and crystallinity is too low to detected by electron beam diffraction.

## Acknowledgement

This work was partially aided by MEXT-supported Program for the Strategic Research Foundation at Private Universities

## References

- 1) S. Oue, H. Nakano, S. Kobayashi, T. Akiyama, and K. Okumura, *J. Surface Finishing Soc. Jpn.*,53 920 (2002) .



# Electrodeposition of mono-layer graphene from carboxylic acid under hydrothermal condition

Y. Okamura, T. Tomai, I. Honma

*Institute of Multidisciplinary Research for Advanced Materials, Tohoku University, Japan*

*2-1-1 Katahira, Aoba-ku, Sendai 980-8577, Japan*

*okamura@mail.tagen.tohoku.ac.jp, tomai@tagen.tohoku.ac.jp*

Graphene is two-dimensional carbon sheet with honeycomb structure, and has attracted attention for its excellent properties. Thus, it is expected that graphene is promising material in a wide range of applications, including electronics, spintronics, optoelectronics, sensors, batteries and supercapacitors. For applications of graphene, various techniques for synthesis of graphene have been developed, such as the graphitization of silicon carbide surfaces and catalytic chemical vapor deposition (CVD) on metals. Most of the synthesis methods require high-temperature condition above 1000 °C.

Recently, the method for synthesis of single-walled carbon nanotubes (SWCNTs) by the electrochemical reaction was reported<sup>2</sup>. In this method, SWCNTs are deposited by the electrochemical decomposition of acetic acid at room temperature. This reaction produces a carboxylate anion, an aldehyde, an alcohol, and a hydrocarbon. During cathodic reaction, the reduction process from acetic acid to ethane will produce  $C_2H_5$  radicals, and the carbon material is synthesized by partial dehydrogenation and recombination of each radicals. This method has an advantage in synthesis of carbon materials under mild temperature condition by the assistance of electrochemical reaction. However, the method of synthesis graphene by electrochemical reaction has never been reported before.

In this study, we report the novel synthesis route for mono-layer graphene using hydrothermal electrolysis. Hydrothermal electrolysis is the electrolysis method combined with hydrothermal reaction. Graphene sheet was produced over the surface of Pt substrate as a working electrode by applying a small negative potential (-3.5 V) against Pt counter electrode in an aqueous solution of carboxylic acid (formic acid, acetic acid, propionic acid) as a carbon source under sub-critical condition (300 °C, 10 MPa).

Figure 1 shows a scanning electron microscope (SEM) image of the Pt substrate after hydrothermal electrolysis in an aqueous solution of acetic acid. From SEM image as shown in Figure 1, we observed the wrinkles in the carbon sheet, which were independent of location of grain boundary. It is confirmed that the carbon sheet material is deposited by electrochemical reaction under sub-critical condition. Figure 2 shows Raman spectra of the carbon sheet material on the Pt substrate. G ( $1580\text{ cm}^{-1}$ ) and 2D ( $2690\text{ cm}^{-1}$ ) bands due to graphene formation were observed. It is known that intensity of G band ( $I_G$ ) is weaker than that of 2D band ( $I_{2D}$ ) in the Raman spectra of mono-layer graphene. From Raman spectra as shown in Figure 2, we concluded that carbon sheet material on the Pt substrate contains mono-layer graphene. In contrast, only amorphous carbon is deposited by the electrochemical decomposition of acetic acid at room temperature. It is supposed that the growth of high crystalline graphene under hydrothermal condition will result from etching of amorphous carbon due to the oxidation effect of sub-critical water.

Besides, graphene was synthesized by hydrothermal electrolysis using formic or acetic acid as a carbon source, whereas small amount of amorphous carbon was deposited using propionic acid. It is generally known that  $CH_3$  and  $C_2H_5$  radicals are more stable than  $C_3H_7$  radical. Therefore, it is supposed that the growth of graphene using formic or acetic acid is caused by stability of each hydrocarbon radicals.

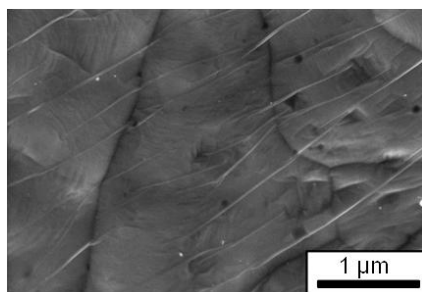


Figure 1. SEM image of graphene on Pt substrate after hydrothermal electrolysis

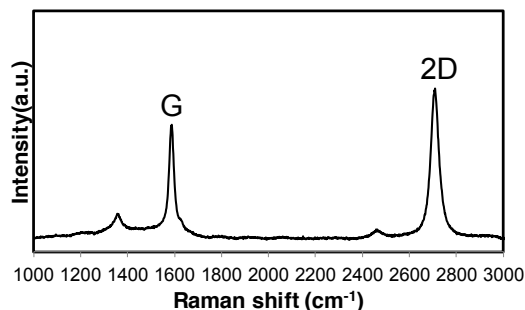


Figure 2. Raman spectra of graphene on Pt substrate after hydrothermal electrolysis

## References:

- (1) A. K. Geim, K. S. Novoselov, *Nat. Mater.* **2007**, 6, 183-199.
- (2) A. Shawky, *et al.*, *Carbon*, **2012**, 50, 4184-4191.

# Electrodeposition of Cu<sub>2</sub>O from Aqueous Lactate Solutions – Studies on Copper(II) Complexes in Alkaline Deposition Baths

Kuniaki Murase,<sup>1,\*</sup> Yusuke Seki,<sup>1</sup> Tsutomu Shinagawa,<sup>2</sup> Atsushi Kitada,<sup>1</sup> and Kazuhiro Fukami<sup>1</sup>

<sup>1</sup>Department of Materials Science and Engineering, Kyoto University

36-1 Yoshida-hommachi, Sakyo-ku, Kyoto 606-8501, Japan

<sup>2</sup>Electronic Materials Research Division, Osaka Municipal Technical Research Institute

1-6-50 Morinomiya, Joto-ku, Osaka 536-8553, Japan

\*murase.kuniaki.2n@kyoto-u.ac.jp

Cuprous oxide (Cu<sub>2</sub>O) is known as an intrinsic p-type semiconductor with 2.1 eV bandgap, and has attracted increasing attention as a solar cell material. The electrodeposition of Cu<sub>2</sub>O from basic (*i.e.* alkaline) aqueous baths containing copper(II) salt and lactate ( $L = C_3H_5O_3^-$ ) as complex former was first reported by Rakhshani and co-workers [1] and further developed by the groups of Switzer [2], Izaki and Shinagawa [3]. Copper complex(es) dissolved in the basic lactate baths, however, still remains undetermined. A pH speciation diagram for the Cu(II)-lactate system calculated using formation constants of  $CuL^+$ ,  $CuL_2$ , and  $CuL_3^-$ , tabulated in ref. [4], indicates that the baths lead to the formation of  $Cu(OH)_2$  precipitate at pH > 8, whereas the baths in the basic region retain their clearness, while their color changes to dark blue (Fig. 1a). Figure 1c shows a set of UV-vis absorption spectra for 0.4 M  $Cu(CH_3COO)_2 - 3.0$  M lactic acid (HL) baths with various pH values adjusted by NaOH. Beyond pH 6, a blue shift and concomitant decrease in absorbance were observed, implying the formation of chelate complex(es) to increase the splitting of *d*-orbital of copper. Given that the lactate ion(s) chelates  $Cu^{2+}$  ion, the maximum ligand-to-metal ratio should be 2 like  $CuL_2$ , since a Jahn-Teller  $d^9$   $Cu^{2+}$  ion has a tendency to form a square-planar complex. If this is the case, the presence of  $CuL_3^-$  is questionable. In more basic pH region, Panzer *et al.* tentatively supposed a basic dimer complex [5], while Herranen *et al.* claimed the formation of  $H_2L^{2-}$  ions ( $= C_3H_4O_3^{2-}$ ) with the deprotonated  $\alpha$ -hydroxyl-group, yielding  $Cu(H_2L)_2^{2-}$  and  $Cu(H_2L)_2(OH)^{3-}$  [6]. Figure 1b shows a titration curve acquired by titrating 50 mL of 0.4 M  $Cu(ClO_4)_2 - 3.0$  M lactic acid solution with 9.27 M NaOH; here, a curve calculated assuming the above three complexes  $CuL^+$ ,  $CuL_2$ , and  $CuL_3^-$  [4] is also shown. The most notable point is that the final equivalence point (C) for the experimental curve is found about halfway between calculated equivalence points for (A)  $HL + OH^- \rightarrow L^- + H_2O$  and (B)  $Cu(II) + 2OH^- \rightarrow Cu(OH)_2$ , suggesting the final Cu(II)-lactate complex has a formula  $Cu_xL_y(OH)_x^{(y-x)-}$  without  $H_2L^{2-}$  species; the most likely candidate is  $CuL_2(OH)^-$ .

[1] A. E. Rakhshani *et al.*, *Thin Solid Films*, **148**, 191 (1987); [2] T. D. Golden *et al.*, *Chem. Mater.*, **8**, 2499 (1999); [3] T. Shinagawa *et al.*, *Cryst. Growth Des.*, **13**, 52 (2013); [4] E. Martell and R. M. Smith, *Critical Stability Constants*, Vol. 5, Plenum Press, NY, 1982, p.291; [5] A. Osherov *et al.*, *Chem. Mater.*, **25**, 692 (2013); [6] S. Leopold *et al.*, *J. Electroanal. Chem.*, **547**, 45 (2003).

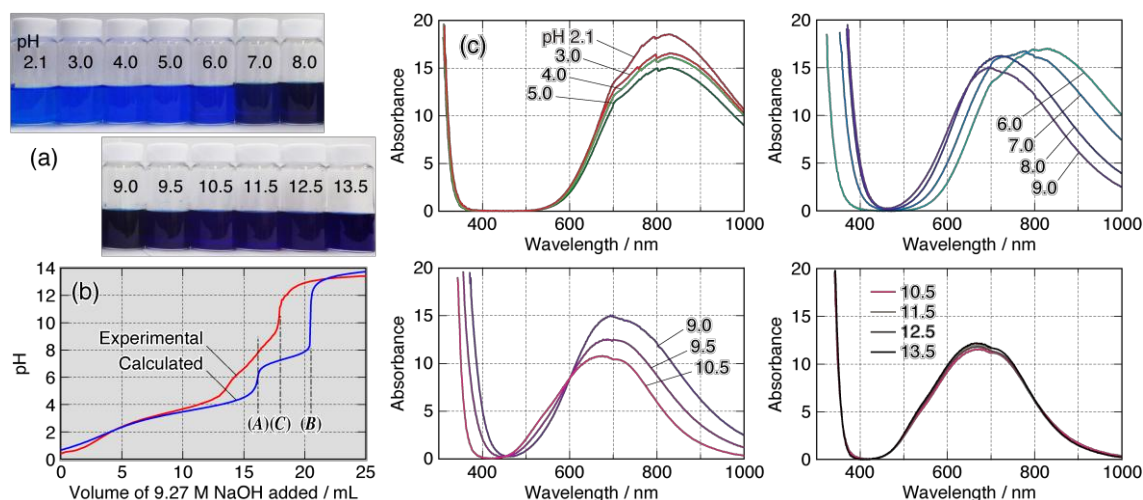


**Figure 1.** (a) Photograph, (b) titration curves, and (c) a set of visible absorption spectra for Cu(II)-lactate solutions in the pH range 2.1–13.5. The spectra were collected using a quartz cell with 1 mm path and

converted to the absorbance values for standard 1 cm path.

# Mechanical properties of electrodeposited Fe-Ni alloys in the Invar composition range

Tomio Nagayama, Takayo Yamamoto, Toshihiro Nakamura  
Kyoto municipal institute of industrial technology and culture  
91 Chudoji Awata-cho, Shimogyo-ku, Kyoto-city, Kyoto, 600-8815, Japan  
nagayama@tc-kyoto.or.jp

Invar Fe-Ni alloys with Ni contents around 36 mass% have lower coefficients of thermal expansion (CTEs) near room temperature than those of pure Fe and Ni. Thus, MEMS devices required to have dimensional thermal stability are expected to be provided by Invar Fe-Ni alloy electrodeposition, which can allow shape refinement and strengthening of those devices. We have already produced electrodeposited Fe-Ni alloys with Ni contents in the Invar composition range (36 to 40 mass% Ni) as free-standing films from a plating bath containing saccharin as a strength reducer [1, 2]. It was also reported that as-deposited Invar Fe-Ni alloys had larger CTEs than those of as-cast Invar alloys, moreover, heat treatment at 400 °C or above was necessary to stabilize CTEs of the electrodeposited Invar alloys to those of as-cast Invar alloys [1, 2]. Therefore, it is possible to anticipate strength degradation due to grain coarsening. Additionally, it is also concerned that embrittlement [3] occurs by grain boundary segregation of sulfur originated from saccharin after the heat treatment. In this study, the influences of heat treatment on mechanical properties of the electrodeposited Invar Fe-Ni alloys were examined by tensile testing.

The Invar Fe-Ni alloy electrodeposition carried out on a stainless steel substrate using sulfate / chloride electrolytes with additives at 40 mA / cm<sup>2</sup>. Bath compositions [1] were as follows: FeSO<sub>4</sub> (0.3 to 0.35 mol / L), NiSO<sub>4</sub> (0.95 mol / L), NiCl<sub>2</sub> (0.17 mol / L), boric acid (0.49 mol / L), sodium saccharin (0.008 mol / L) and malonic acid (0.05 mol / L). The bath temperature was maintained at 50 °C and the bath pH was adjusted to pH 2.3. Pure Fe and Ni sheets were used as anodes. Electrodeposited Fe-Ni alloys with Ni contents of 36, 38 and 40 mass% as free-standing films were obtained by varying Fe ion concentration in the plating baths. Dumbbell type specimens with thickness of about 100µm for tensile testing were prepared by an etching method. Figure 1 shows the effects of heat treatment temperature on CTE (30 to 100 °C), ultimate tensile strength (UTS), elongation (δ) and hardness of the Fe-Ni alloy specimens. The CTEs of the as-deposited Invar Fe-Ni alloy films were 8 to 10 ppm / °C which were larger than those of as-cast Invar Fe-Ni alloys. After 400 °C heat treatment, the CTEs drastically dropped to 4 to 5 ppm / °C, and the CTEs reached comparable values to those of as-cast Invar Fe-Ni alloys by annealing at 500 °C or above. Plastic deformation was observed for all specimens on tensile testing. UTS and hardness of the as-deposited Invar alloy films exhibited around 700 MPa and 250HV, respectively, which were higher than those of conventional Invar alloys having UTS and hardness of about 500 MPa and 150HV, respectively. The higher UTS and hardness values were maintained up to 500 °C. By annealing at 600 °C, UTS and the hardness sharply decreased and exhibited comparable values to those of as-cast Invar alloys. Elongation was almost inverse proportional to strength without drastic δ devaluation (i.e. δ < 1 %) which was reported for electrodeposited Ni and Fe-Ni alloys with Ni contents of 60 mass% or above containing sulfur with heat treatment at 400 °C or above [3]. The electrodeposited Invar alloys contained sulfur of about 0.02 mass%; nevertheless, there was no severe embrittlement after 300 to 600 °C heat treatment. Sulfur in the electrodeposits with heat treatment existed as not a filmy sulfide at grain boundary which causes grain boundary embrittlement, but a granular Fe-Ni-S compound in the Fe-Ni alloy matrix.

[1] T. Yamamoto *et al.*, *J. Surf. Sci. Soc. Jpn.*, **62**, 702 (2011) (in Japanese). [2] T. Yamamoto *et al.*, Abst. 63rd Ann. Meet. of ISE, s10-061 (2012). [3] W. H. Safranek, *The Properties of Electrodeposited Metals and Alloy* 2nd edition, p.340, AESF (1986).

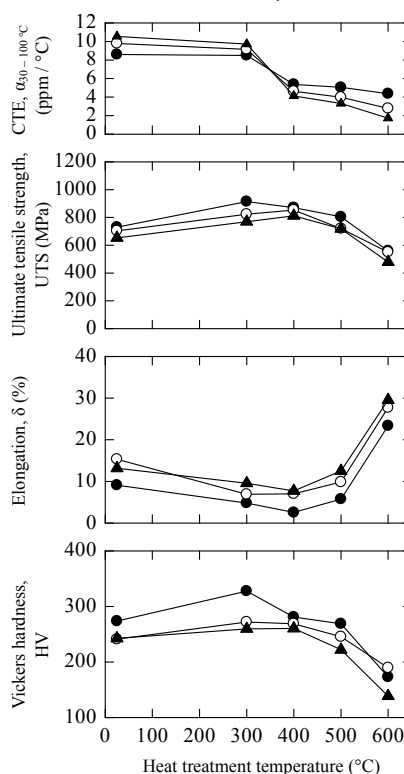


Figure 1 Effects of heat treatment temperature on CTE, ultimate tensile strength (UTS), elongation (δ) and hardness of electrodeposited Invar Fe-Ni alloys with Ni contents of 36 (solid triangle: ▲), 38 (open circle: ○) and 40 mass% (solid circle: ●).

# One-step Synthesis of Porous BiOBr Film From Bi Plate Via Electrochemical Method

Caimei Fan\*, Yingyuan Hu, Rui Li, Xiaoming Mao

College of Chemistry and Chemical Engineering, Taiyuan University of Technology, Taiyuan, Shanxi, PR China

[fancm@163.com](mailto:fancm@163.com)

With the industrialization and urbanization increasing, the environmental problem and the energy crisis have become a subject of great interest to researchers worldwide. Semiconductor photocatalysis shows great promise in the solution of environmental and energy problems. Owing to the superior electrical, optical, and mechanical properties, photocatalysis has been widely used in many aspects such as air/water purification, solar cell, biological field, gas sensors, and electrochromic devices. Recently, BiOBr has promising practical applications due to its layered tetragonal matlockite structure, indirect transition band gap, and stronger oxidation abilities<sup>[1]</sup>. Most of investigations have focused on the synthesis and characterization of BiOBr nanopowder catalysts. However, limitations associated with separation and recycling difficulties, high aggregation tendency and potential risks for humans hamper their practical application<sup>[2]</sup>. Therefore, to counter these impediments, it is extremely necessary to develop an immobilized BiOBr thin film to achieve excellent photocatalytic activity and extend industrial applications. Moreover, from an environment-friendly perspective, electrophoretic deposition and anodic oxidation should be a desirable strategy to develop BiOBr film and had attracted great research interests<sup>[3-4]</sup>.

In this study, a novel electrochemical approach had been developed to prepare porous BiOBr thin film with bulk Bi plate as anode and Ti sheet as cathode. The experiments were conducted at 4 V for 1 h (25°C) in 100 mL aqueous solution containing 0.5 mol/L KBr and 0.06 mol/L ethylenediamine tetraacetic acid (EDTA). The pH value was adjusted to 8 with 5 mol/L NaOH solution. The schematic preparation process was depicted in **Figure 1A**.

Furthermore, the BiOBr film has also been used in the photodegradation of methyl orange (MO) under ultraviolet light irradiation, and the results indicated that the BiOBr film expressed excellent photocatalytic activities and good chemical stability (**Figure 1B**), facilitating its practical application.

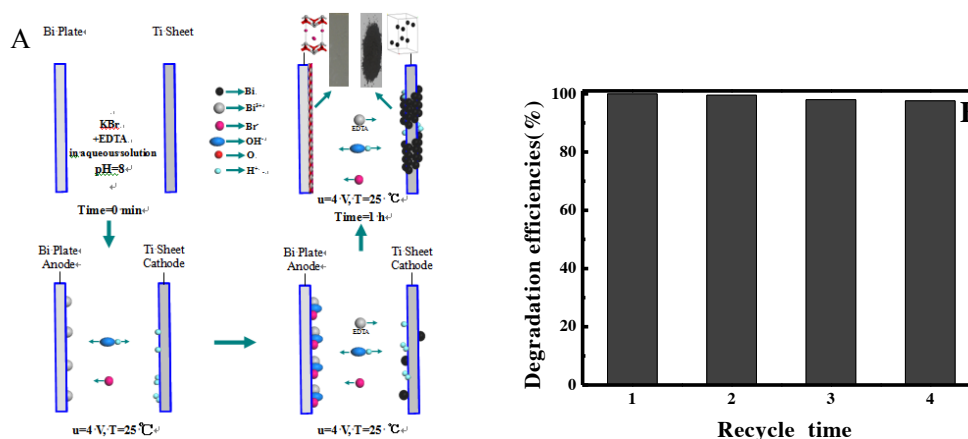


**Figure 1A.** The schematic preparation process for BiOBr films.

**Figure 1B.** Four cycles of photocatalytic process were repeated on one BiOBr film in degrading 50 mL 10 mg/L MO under UV light irradiation.

## Reference:

- [1] R. Li, C. M. Fan, X. C. Zhang, et al. Preparation of BiOBr thin films with micro-nano-structure and their photocatalytic applications[J]. *Thin Solid Films*, 2014, 562: 506-512.
- [2] M. R. Hoffmann, S. T. Martin, W. Y. Choi, et al. Environmental applications of semiconductor photocatalysis[J]. *Chem. Rev.* 1995, 95: 69-96.
- [3] A. Fernandez, G. Lassaletta, V.M. Jimenez, et al. Preparation and characterization of TiO<sub>2</sub> photocatalysts supported on various rigid supports (glass, quartz and stainless steel). Comparative studies of photocatalytic activity in water purification[J]. *Appl. Catal. B: Environ.* 1995, 7: 49-63.
- [4] Y. J. Chang, J. W. Lee, H. P. Chen, et al. Photocatalytic characteristics of TiO<sub>2</sub> nanotubes with different microstructures prepared under different pulse anodizations[J]. *Thin Solid Films*, 2011, 519: 3334-3339.

# Application of Amorphous Alloy Plating to Various Industrial Fields.

Sachio Yoshihara\*, Wataru Oikawa\*\*, Yoshifusa Ishikawa\*\*, Kazuyoshi Suzuki\*\*\*, Daisuke Suzuki\*\*\*

*\*Graduate School of Engineering, Utsunomiya University*

*7-1-2 Yoto, Utsunomiya, Tochigi 321-8585, Japan*

*\*\*Nippon Platec*

*7-334 Nishimishima Nasushiobara, Tochigi 329-2756, Japan*

*\*\*\*Vantec Co., Ltd.*

*321 Niku-cho Nasushiobara, Tochigi 329-2733, Japan*

[sachioy@cc.utsunomiya-u.ac.jp](mailto:sachioy@cc.utsunomiya-u.ac.jp)

## Introduction

1. One of the surface hardening treatment of aluminum alloy is iron alloy plating on the surface. It was reported that thin enough iron alloy film deposition would not inhibit its high thermal conductivity of base material-aluminum alloy and would improve the wear resistance of the surface. Especially, Fe-Cr alloy plated coating shows quite high surface hardness and high wear resistance. From this reason such finishing has been adopted as the surface coating for aluminum alloy brake disc of the racing motorcycle for world championship. However, thus plated Fe-Cr alloy coating do not show enough corrosion resistance, so more high corrosion resistance will be desirable for iron alloy plating. In this report newly developed iron based amorphous alloy plating technology has been proposed.
2. Recently especially after Fukushima accident of nuclear power plant caused by Tsunami, from the point of view of environmental aspects and depletion of fossil fuel, hydrogen as a clean energy will be the most attracting secondary energy. Hydrogen production by water electrolysis is beneficial because of the resources are almost inexhaustible and do not emit any harmful substances. Hydrogen has been already widely used as a household fuel cell (Trade name "Ene-Farm") in Japan. Hereinafter the demand for hydrogen storage and supply will spread according to the spread of fuel-cell vehicles. However, for further spread of the hydrogen energy, the cost reduction of hydrogen manufacturing unit will be indispensable. The development of high-performance cathode electrode of water electrolyzer will reduce the cost of hydrogen production equipment and running costs.[1] This research will focus on the application of the Ni, W and P (relatively inexpensive material) amorphous alloy electrode fabricated by use of electrodeposition (relatively inexpensive method) as the electrode for water electrolyzer. For the industrial use of water electrolyzer, sustainable energy e.g. solar energy, wind power and water power will be indispensable, because of the input electric energy cost. Such electric energy produced by sustainable energy will fluctuate. So connecting water electrolyzer must have enough endurance for such a fluctuating electric power. So we have also evaluated the anti-corrosion behavior of thus plated electrode material at open circuit conditions in alkaline aqueous solution.

## Results and Discussions

1. From the experiment Fe-Ni-W amorphous alloy plated film showed higher corrosion resistance comparing to Fe-Cr alloy plated film in 3 % NaCl aqueous solution. It was confirmed the improvement of corrosion resistance according to the increase of W content in the film. The contents of W in the film could be controlled by increasing the concentration of W in the plating bath.
2. The LSV measurement in 30 % KOH aqueous solution (typical alkaline water) implied that amorphous Ni-P coated electrode by use of electrodeposition showed larger exchange current density for hydrogen evolution reaction, and also showed the lower hydrogen overvoltage. On the other hand amorphous Ni-W-P coated electrode showed lower corrosion current density. So amorphous plated alloy will be a desirable candidate for practical use of the electrode for water electrolyzer for sustainable energy.

## Reference

[1] Sachio Yoshihara, Daisuke Suzuki, Kouji Someya, Takanori Kikuchi, Yoshifusa Ishikawa, Electrode Performance of Newly Developed Ni-W-S Deposited Alloy for Alkaline Water Electrolysis, *ECST Transactions*, Volume 53, Issue 19 Green Electrodeposition 3, 15-25 (2013)

# Characterization of $\text{AlCl}_3$ /Diglyme Solution for Aluminum Electrodeposition

Kai Nakamura, Atsushi Kitada, Kazuhiro Fukami, Kuniaki Murase  
Department of Materials Science and Engineering, Kyoto University  
Yoshidahonnmachi, Sakyo, Kyoto 606-8501, Japan  
nakamura.kai.54u@st.kyoto-u.ac.jp

Aluminum (Al) has industrial importance because of its lightweight property, natural abundance and corrosion resistance. It is well known that Al metal cannot be electrodeposited from aqueous solutions due to its low redox potential ( $-1.68$  V vs. SHE), while it can be obtained from high temperature molten salts, organic solvents and ionic liquids [1]. However, these electrolytes are highly volatile, highly viscous, and/or expensive for practical use. Glymes have boiling points and flash points over  $100$  °C which give low volatilities at room temperature. Recently we found that Al can be electrodeposited from  $\text{AlCl}_3$ /diglyme solution at room temperature [2]. However, at room temperature the cathodic current density was about  $3 \text{ mA cm}^{-2}$  and more than  $10 \text{ mA cm}^{-2}$  is needed for paractical Al electroplating. Here, we investigated suitable condition for fast electrodeposition in  $\text{AlCl}_3$ /diglyme solution.

All electrochemical experiments were performed at room temperature in an Ar-filled glove box. Al sheets were used as counter and reference electrodes. A Cu sheet was used as working electrode (WE) after being washed with acetone.  $\text{AlCl}_3$  and diglymes were mixed with molar ratio of  $\text{AlCl}_3$ :diglyme = 1:5 ( $1.4 \text{ mol dm}^{-3}$ ) and used as electrolytes. Molar conductivities and viscosities were measured at  $35$ – $70$  °C in an Open Dry Chamber (Daikin) with  $\text{H}_2\text{O} < 40\text{ppm}$ .

Figure 1 shows the cyclic voltammogram (CV) measured for the Cu electrode in the  $\text{AlCl}_3$ /diglyme solution at  $30$ – $70$  °C. The maximum value of current density was observed at  $60$  °C and current density decreased at  $70$  °C. At  $60$  °C cycling efficiency was about 70%. At  $70$  °C it was observed that the electrolyte became gradually brown, or thermally decomposed. It indicates that  $60$  °C is the temperature suitable for fast electrodeposition of Al in  $\text{AlCl}_3$ /diglyme solution. Table 1 shows physical properties of  $\text{AlCl}_3$ /diglyme solution at each temperature. Conductivities increased and viscosities decreased as the temperature is raised. The diglyme solution showed the conductivity of  $3.97$ – $6.48 \text{ mS cm}^{-1}$ . A previous spectroscopic study showed that molecular species ( $\text{AlCl}_3 \cdot \text{diglyme}$ ) and ionic ones of four-Cl coordinated  $\text{AlCl}_4^-$  and six-O/Cl-coordinated  $[\text{AlCl}_2(\text{diglyme})_2]^+$  exist in  $1.7 \text{ mol dm}^{-3}$   $\text{AlCl}_3$ /diglyme solution [3]. Therefore, sufficient conductivity should result from these ionic species. Since  $\text{AlCl}_4^-$  is known to be electrochemically inactive, it is assumed that Al can be electrodeposited by desolvating  $[\text{AlCl}_2(\text{diglyme})_2]^+$ .

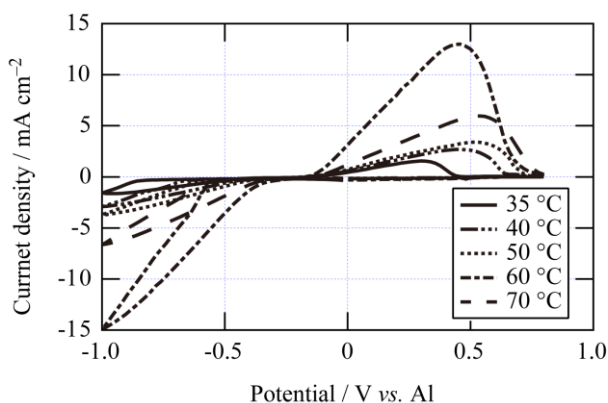


Figure 1. CVs measured for  $\text{AlCl}_3$ /diglyme (1:5 by mol) at each temperature. Sweep rate:  $20 \text{ mV s}^{-1}$ .

Table 1. Conductivities and viscosities of  $\text{AlCl}_3$ /diglyme solution measured at  $35$ – $70$  °C.

Temperature	Conductivity ( $\text{mS cm}^{-1}$ )	Viscosity ( $\text{mPa s}$ )
$35$ °C	3.97	2.92
$40$ °C	4.48	2.67
$50$ °C	5.53	2.35
$60$ °C	6.48	2.03

[1] Y. Zhao and T. J. VanderNoot, *Electrochim. Acta*, **42**(1), 3 (1997).

[2] A. Kitada, K. Nakamura, K. Fukami, and K. Murase, *Electrochemistry*, **82**(11), 946 (2014).

[3] H. Nöth, R. Rurländer, and P. Wolfgardt, *Z. Naturforsch., B: Chem. Sci.*, **37B**, 29 (1982).



# Numerical Simulation of Current Density Distribution between Vertical Cu Electrodes

A. Iwanaga<sup>a\*</sup>, H. Matsushima<sup>b</sup>, S. Miyazawa<sup>c</sup>, S. Nagano<sup>c</sup>

<sup>a</sup>Y-labo, Furukawa, Osaki, Miyagi 989-6131, Japan.

<sup>b</sup>Faculty of Engineering, Hokkaido University, Sapporo 060-8628, Japan.

<sup>c</sup>Alps Electric. Co. Ltd, Furukawa, Osaki, Miyagi 989-6181, Japan.

\*E-mail: atsushi.iwanaga@gmail.com

## I. Introduction

Electrodeposition in a magnetic field (B) is different from the deposition mechanism in the absence of B. The reason might be caused by the flow of magnetic convection (Magnetohydrodynamics, MHD). Lorentz force induced by a magnetic field directly influences on the ion species near the electrode surface, while the mechanical stirring does not work there due to the viscosity. Although numerical simulations of MHD have been studied by many researchers [1,2], the relation between Cu electrodeposition and MHD convection is not sufficiently clear. We believe that the understanding of the natural convection and current distribution during the electrodeposition should be important for simulating MHD convection precisely.

We focus the electrical neutrality equation that gives the relation between electric field and concentration in electrolyte and simulate the current density and electric field during Cu electrodeposition [3]. In the present work, two current components by diffusion and electric migration could be separately calculated in the consideration of the diffusion coefficient and mobility of  $\text{Cu}^{2+}$  and  $\text{SO}_4^{2-}$  ions. We will apply the present results of current density distribution for simulating MHD convection.

## II. Results and discussion

Schematic diagram of electrolytic cell is shown in Fig. 1. The current density distributions across L1 and L2 line are calculated under galvanostatic mode ( $20 \text{ A m}^{-2}$ ) for 500 sec. Figure 2 shows Y-direction components of current density at 36 sec (solid line) and 500 sec (dotted line), respectively. Although the value of current density was almost about  $20 \text{ A m}^{-2}$  through whole area, ones at top and bottom area were slightly shifted from the set value (Fig. 2 (a)). This is explained by the gradient of the diffusion layer normal to the electrode. The concentration at the top part is lower than center area, while it is opposite at bottom one. The shift was increased with increasing in the deposition time.

## REFERENCES

- [1] S. Muehlenhoff, et al., *Electrochim. Acta*, 69 (2012) 209.
- [2] G. Mutschke, A. Hess, A. Bund, J. Froehlich, *Electrochim. Acta*, 55 (2009) 1543.
- [3] S.Kawai, K.Nishikawa, Y.Fukunishi, S.Kida, *Electrochim. Acta*, 53 (2007) 257.

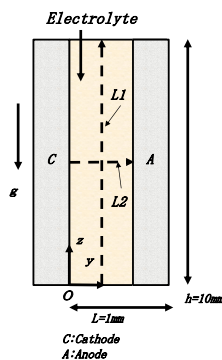


Fig.1 Schematic diagram of electrolytic cell

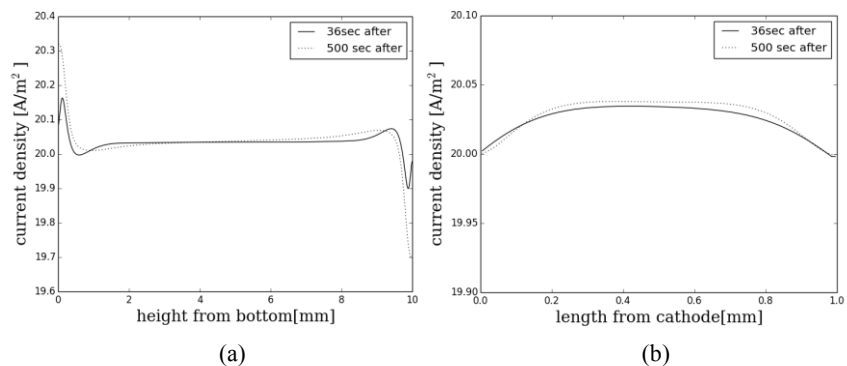


Fig.2 Numerical analysis of current density distribution across (a) L1 and (b) L2 direction during Cu electrodeposition for 36 sec and 500 sec. (0.6 M  $\text{CuSO}_4$ )



# Voltammetric Study and Electrodeposition of Zinc in *N*-butyl-*N*-methylpyrrolidinium Bis(trifluoromethanesulfonyl)imide Room Temperature Ionic Liquid

Yu-Sheng Wang<sup>a</sup>, Po-Yu Chen<sup>a,b,\*</sup>

<sup>a</sup>Department of Medicinal and Applied Chemistry, Kaohsiung Medical University, Kaohsiung City 80708, Taiwan

<sup>b</sup>Department of Chemistry, National Sun Yat-sen University, Kaohsiung City 80424, Taiwan

\*Corresponding author. Tel.: +886 7 3121101x2587; fax: +886 7 3125339.

E-mail address: [pyc@kmu.edu.tw](mailto:pyc@kmu.edu.tw) (P.-Y. Chen).

## Abstract:

In this study, the electrochemical behaviors of Zn(II) from different precursors were investigated by various electrochemical techniques using platinum and glassy carbon as the working electrodes in *N*-butyl-*N*-methylpyrrolidinium bis(trifluoromethanesulfonyl)imide room temperature ionic liquid (BMP-TFSI)<sup>1</sup>. The Zn(II) species were introduced into BMP-TFSI by adding ZnCl<sub>2</sub>, (Zn(TFSI)<sub>2</sub>)<sup>2</sup> or directly electrolyzing Zn metal. In the cyclic voltammetric experiments, we found that the reduction of Zn(II) from (Zn(TFSI)<sub>2</sub>) showed a larger over-potential than that from ZnCl<sub>2</sub>. We suppose that the chloride ion (Cl<sup>-</sup>) may compete with the TFSI<sup>-</sup> anion and affect the coordination environment of zinc, leading to a more positive reduction potential of ZnCl<sub>2</sub>. For the Zn(II) species from anodic dissolution of Zn metal, a kinetically stable but thermodynamically unstable Zn(II) species was produced, which gradually transformed to the thermodynamically stable Zn(II) species and finally showed the same electrochemical behavior as that of Zn(II) species from (Zn(TFSI)<sub>2</sub>).

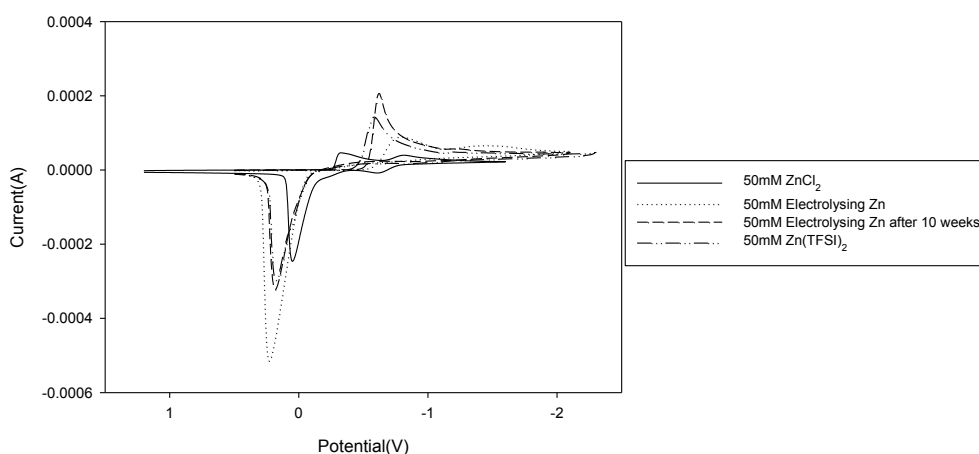


Fig.1. Cyclic voltammetric experiments of different Zn(II) precursors in BMP-TFSI ionic liquid

## Reference:

1. MacFarlane, D. R.; Forsyth, S. A.; Golding, J.; Deacon, G. B., Ionic liquids based on imidazolium, ammonium and pyrrolidinium salts of the dicyanamide anion. *Green Chem.* **2002**, 4 (5), 444-448.
2. Yamagata, M.; Tachikawa, N.; Katayama, Y.; Miura, T., Electrochemical behavior of iron(II) species in a hydrophobic room-temperature molten salt. *Electrochemistry (Tokyo, Jpn.)* **2005**, 73 (8), 564-566.

# Recovery of Nanosilver from Si-Wafer Manufacturing Wastes

Tzu-Hsuan Tsai, Yu-Pei Shih

*Department of Materials and Mineral Resources Engineering,  
National Taipei University of Technology, Taipei 10608, Taiwan  
tzhtsai@ntut.edu.tw*

Nanosilver is one of the fastest growing products in the nanotechnology industry, and it is already used in catalysis [1], surface enhanced Raman scattering [2] and many medical applications due to its strong anti-microbial ability [3]. This study successfully used Si-wafer manufacturing wastes to produce nanosilver. Various wastes are formed during Si-wafer manufacturing. Silver ions could be found in the HF etching solutions for forming porous Si. We produced nanosilver using the etching solutions by adding the recovered Si powder from silicon sawing waste. After silver ions reduced to nanosilver and parts of Si oxidized to  $\text{SiO}_2$  in the etching solution, the solid was collected and observed via a scanning electron microscope (Fig. 1), indicating nanosilver is formed on Si powder. In order to purify silver,  $\text{NaOH(aq)}$  was added to dissolve Si or  $\text{SiO}_2$ . As a result, a solution with nanosilver was obtained in the filtrate and observed via a transmission electron microscopy (Fig. 2). The recovery yield of silver from the etching solutions was higher than 99.5%. In addition, most HF could be converted to low toxic  $\text{Na}_2\text{SiF}_6\text{(s)}$ .

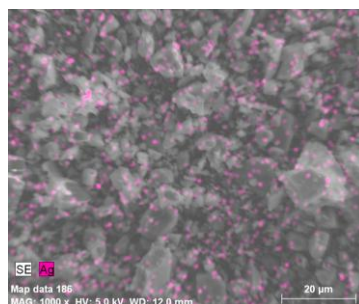


Fig. 1 A SEM image of the collected solid after redox reactions of  $\text{Ag}^+$  and Si in etching solutions.

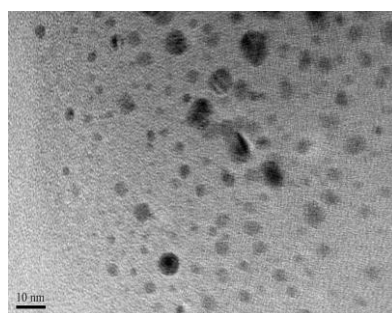


Fig. 2 A TEM image of the obtained solution with nanosilver.

## References

1. V.V. Volkov, T.A. Kravchenko, V.I. Roldughin, *Russ. Chem. Rev.* 82 (2013) 465–482.
2. A.L. Filgueiras, D. Paschoal, H.F.D. Santos, A.C. Sant’Ana, *Spectrochimica Acta Part A: Molecular and Biomolecular Spectroscopy*, 136 (2015) 979–985.
3. X. Chen, H.J. Schluesener, *Toxicology Letters* 176 (2008) 1–12.

# Fabrication of the three-dimensional micro structure by Fe-Ni alloy electroforming process -Effect of saccharin concentration-

Takayo Yamamoto, Tomio Nagayama, Toshihiro Nakamura  
Kyoto Municipal Institute of Industrial Technology and Culture  
91 Chudoji Awata-cho, Shimogyo-ku, Kyoto-city, Kyoto, 600-8815, Japan  
yamamoto@tc-kyoto.or.jp

Fe-Ni alloys in the content range from 36 to 42 mass% Ni have lower coefficients of thermal expansion (CTEs) near room temperature than those of pure Fe and Ni. Thus, it can be expected to fabricate the next-generation MEMS (Microelectromechanical systems) devices required to have high dimensional stability by a low CTE Fe-Ni alloy electroforming process, which can allow shape refinement and thermal stability in dimension of those devices. However, a strict control in the characteristic composition of the Fe-Ni alloy electrodeposits is difficult because of the anomalous codeposition phenomenon. In addition, a three-dimensional processing with a precious control is required for a fabrication of the MEMS micro structures. Therefore, it is necessary to investigate the effects of the deposition conditions to produce micro structures with uniform composition and shape. In this study, optimum deposition conditions for fabricate a uniform Fe-42 mass% Ni alloy micro structure which can be expected to have a low CTE comparable to that of Si mainly used in MEMS devices by the electroforming process were examined.

The Fe-Ni alloy electroforming was carried out by electrodeposition through negative UV photoresists with 100  $\mu\text{m}$  x 100  $\mu\text{m}$  square dot patterns of 30  $\mu\text{m}$  in height on a stainless steel (SUS 304, 10 mm x 10 mm in area) substrate. The Fe-Ni alloy electrodeposition was operated at 20 mA/cm<sup>2</sup> using sulfate/chloride electrolytes with additives. Bath compositions [1] were as follows: FeSO<sub>4</sub> (0.35 mol/L), NiSO<sub>4</sub> (0.95 mol/L), NiCl<sub>2</sub> (0.17 mol/L), H<sub>3</sub>BO<sub>4</sub> (0.49 mol/L), sodium saccharin (0.008 mol/L) and malonic acid (0.05 mol/L). The bath temperature was 323 K and the bath pH was adjusted to pH 2.0. After the electrodeposition, the resists were removed by sodium hydroxide solution.

Fig. 1a shows a typical 45° tilt view FE-SEM image of the obtained Fe-Ni alloy micro structure. The micro structure having 100  $\mu\text{m}$  x 100  $\mu\text{m}$  square open areas with a structure height of 14.8 $\pm$ 2.4  $\mu\text{m}$  was obtained. The Fe contents at points indicated by cross marks in Fig. 1a were from 56.0 to 59.1 mass% as a result of EPMA analysis. The values of Fe content and height of the Fe-Ni alloy micro structure with Ni content around 42 mass% were widely ranged under this electrolytic condition. From FE-SEM observation of the surface morphology, the micro structure had two different morphologies: spherical and angular grain, as shown Fig. 1b. Subsequently, in order to modify the deposit morphology of the Fe-42 mass% Ni alloy structure, Fe-Ni alloy electrodeposition was operated in the bath with high saccharin concentration of 0.04 mol/L. Fig. 1c shows a typical FE-SEM image of the obtained Fe-Ni alloy micro structure at saccharin concentration of 0.04 mol/L. The Fe contents and the height of the Fe-Ni alloy micro structure were 57.0 $\pm$ 0.1 mass% and 15.8 $\pm$ 1.1  $\mu\text{m}$ , respectively, the variation of the values of Fe content and height was reduced by increasing saccharin concentration. As shown Fig. 1d, the uniform spherical grains were observed on the surface of the micro structure.

From these results, it is found that it is possible to fabricate the uniform Fe-42 mass% Ni micro structure having square open areas which was precisely transcribed from the shapes of the photoresists from the bath with high saccharin concentration.

[1] T. Yamamoto, T. Nagayama, T. Nakamura, Y. Mizutani, *J. Surf. Finish. Soc. Jpn.*, **62**, 702 (2011) (in Japanese).

Acknowledgement: This work was supported by Adaptable & Seamless Technology Transfer Program through Target-driven R&D, JST.

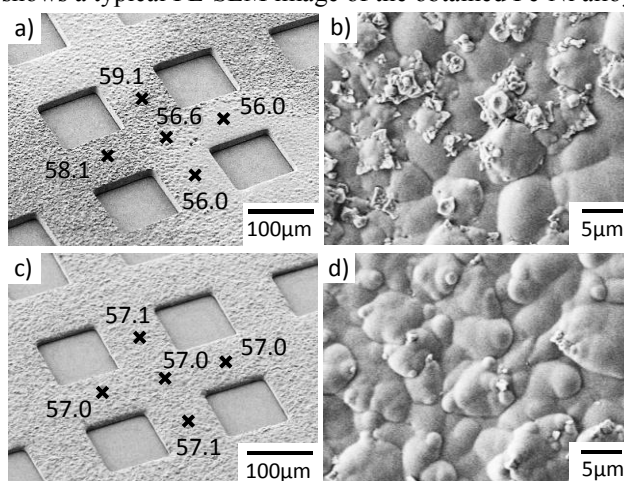


Fig.1 The low and high magnification FE-SEM images of surface morphology of the electrodeposited Fe-Ni alloy three-dimensional micro structure obtained from the baths containing saccharin of 0.008 mol/L (a, b) and 0.04 mol/L (c, d). Numbers and Cross marks indicate Fe contents and positions for Fe content evaluation, respectively.

# Thermal Stability and Sulfidizing Resistance of High Reflective Sn/Ag<sub>3</sub>Sn-based Films Electrodeposited on Cu

Toru Ogasawara, Song-Zhu Kure-Chu\*, Hitoshi Yashiro, and Kuniaki Sasaki

*Department of Chemical and Bioengineering, Iwate University*

*Ueta 4-3-5, Morioka, Iwate, 020-8551, Japan*

*\*E-mail address: [chusongz@iwate-u.ac.jp](mailto:chusongz@iwate-u.ac.jp)*

Light emitting diode (LED) light sources have been widely used in various fields like television display, room lighting, and automotive headlight, due to their high energy-saving capacity, low voltage requirement, small size, long life, etc. Generally, LED electroluminescence components in the package are set on Ag-coated Cu alloy plates as LED lead frame, which is required to provide stable light reflective performance and excellent electrical and thermal conductivity. Since Ag is a noble metal with increasing price of Ag nowadays, it is highly desirable to search a low-cost coating material with high reflectivity and durability to replace the costly Ag film on the lead frame.

This investigation reported various multilayered Sn/Ag-based films on Cu alloys toward high reliable reflective films for LED lead frame. The multilayered Sn/Ag<sub>3</sub>Sn-based films consisted of an Ag-Sn alloy of 20–500 nm thickness covered on a reflowed Sn (denoted as Sn-RF) layer on Cu alloy plates, which can be roughly divided into two categories, i.e., Sn/Ag<sub>3</sub>Sn and Sn/Ag<sub>3</sub>Sn/Ag films, corresponding to the thickness of electrodeposited Ag layer. Fig.1 gives the representative reflective spectra of multilayered Sn/Ag<sub>3</sub>Sn and Sn/Ag<sub>3</sub>Sn/Ag films before (solid lines) and after heating at 373 K for 120 h (dotted lines), comparing to commercial Ag, Sn-RF, and Au films on Cu alloys. The initial reflectivity of as-deposited Sn/Ag<sub>3</sub>Sn films were around 70% (450 nm), which was lower than an Ag film (~90%) but much higher than an Au film (~24%). The multilayered Sn/Ag<sub>3</sub>Sn/Ag films, on the other hand, exhibited a high reflectivity equivalent to a commercial bright Ag film, which can be attributed to the smoother surface inherited from the underlying Sn-RF film on Cu alloys. Noticeably, the reflectivity of multilayered Sn/Ag<sub>3</sub>Sn-based films was stable even after heating at 373 K for 120 h, indicating a good thermal stability.

Moreover, sulfidizing resistance of multilayered Sn/Ag<sub>3</sub>Sn-based films before and after heating was also investigated by accelerated sulfidizing tests with a 2 ml/L (NH<sub>4</sub>)<sub>2</sub>S<sub>x</sub> solution. The microstructures and various characteristics of the Sn/Ag<sub>3</sub>Sn-based films were investigated by means of FE-SEM, XRD, XPS, and TEM (FIB), etc.

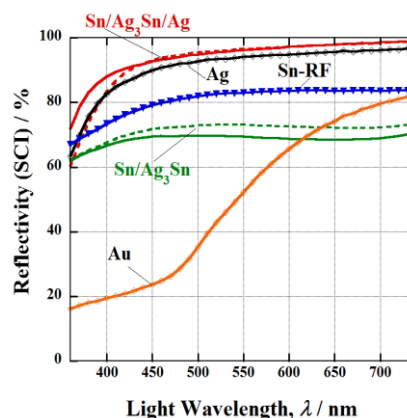


Fig.1 Reflective spectra of multi-layered Sn/Ag<sub>3</sub>Sn and Sn/Ag<sub>3</sub>Sn/Ag films before and after heating at 373 K for 120 h.

# Synthesis of ZIF-8 metal organic framework thin film on ZnO nanorods

Liza Rassaei,<sup>a</sup> Alla Dikhtiarenko,<sup>b</sup> Hamid Reza Zafarani,<sup>a</sup> Ernst J. R. Sudhölter,<sup>a</sup> Jorge Gascon,<sup>b</sup> \*Hanan Al-Kutubi,<sup>a</sup>

<sup>a</sup> *Laboratory of Organic Materials and Interfaces, Department of Chemical Engineering, Delft University of Technology, Julianalaan 136, 2628 BL Delft, The Netherlands.*

<sup>b</sup> *Catalysis Engineering Section, Department of Chemical Engineering  
Delft University of Technology, Julianalaan 136, 2628 BL Delft, The Netherlands  
E-mail: [Lrassaei@tudelft.nl](mailto:Lrassaei@tudelft.nl)*

Metal-organic frameworks (MOFs) are porous solid materials formed by coordination bonds between metal ions or clusters and organic linkers. Although they have already wide applications, their combination with other functional materials results in the formation of new multi-functional hybrid materials with combined or synergistic properties of the individual components. These new nanohybrid materials with novel properties expand the applications of metal organic frame works.

Here, we present a new method to synthesize thin films of the well-known metal organic framework ZIF-8 on zinc oxide nanorods. 2-methyl imidazole solution was casted on electrochemically grown zinc oxide nanorods on fluorine-doped tin oxide glass. Casting a thin film of the linker solution on the zinc oxide nanorods allows the underlying morphology to be preserved, leading to the facile and precise formation of nanostructured hybrid materials under short reactions times and conventional heating. This method allows for the fast and facile formation of nanostructured metal organic framework-semiconductor nanohybrid thin films with minimum use of both solvents and linker. We also present the effect of various synthesis parameters on the morphology of the resulting thin film, and the role of solvent.

# Electroless Deposition of Amorphous Nickel–Tungsten–Phosphorus Alloys with Superior Resistance to Crystallization

Xinyu Liu<sup>1</sup>, Xun Zhan, Frank Ernst, Rohan Akolkar\*

*Case Western Reserve University*

*10900 Euclid Avenue, Cleveland, Ohio, USA*

(<sup>1</sup>Presenting Author: [xxl438@case.edu](mailto:xxl438@case.edu); \*Corresponding Author: [rna3@case.edu](mailto:rna3@case.edu))

Werner Richtering

*Atotech Deutschland GmbH*

*Erasmusstraße 20, 10553 Berlin, Germany*

Amorphous nickel (Ni) alloys such as nickel-phosphorus (Ni–P), deposited using electroless plating, are applied as non-magnetic under-layers in heat-assisted magnetic recording (HAMR) devices. However, during subsequent processing and end use, the amorphous Ni layers are exposed to high temperature, which causes crystallization and undesired ferromagnetism. In this study, we fabricate and characterize *ternary* Ni alloys, such as nickel–tungsten–phosphorus (Ni–W–P), with improved resistance to crystallization.

First, we developed an alkaline electroless deposition process for fabricating Ni–W–P thin-films with tungsten content in the 1–3 atomic % range. During electroless Ni–W–P deposition, the electrochemical kinetics of the oxidation and reduction half-reactions and their interdependencies were characterized using polarization measurements on a rotating disc electrode. Using differential scanning calorimetry, we characterized the crystallization temperature of Ni–W–P films. We found that increasing the tungsten fraction increases the crystallization resistance. Potential physical origins of this phenomenon will be discussed.

# Metallic Glass Coatings for Aluminum Current Collectors – Corrosion Inhibition

Pei-Yu Lai<sup>1</sup>, Jinn P. Chu<sup>2\*</sup>, Bing-Joe Hwang<sup>3</sup>

<sup>1,2</sup> Dept. of Materials Science and Engineering, National Taiwan University of Science and Technology

<sup>3</sup> Dept. of Chemical Engineering, National Taiwan University of Science and Technology

<sup>1,2,3</sup> No. 43, Sec. 4, Keelung Rd., Da'an Dist., Taipei 10607, Taiwan (R.O.C.)

\*e-mail address: [jpchu@mail.ntust.edu.tw](mailto:jpchu@mail.ntust.edu.tw)

Has known to the public, corrosion of current collectors would lead to a gradual increase in internal resistance of cells and, in consequence, cause the fading of capacity and shorten the battery life. Aluminum has been the material of choice as cathode current collectors for lithium batteries since its native oxide layer could help resist corrosion. However, the oxide film still suffers from corrosion problem especially under high operating voltages. Metallic glasses (MGs) are expected to be promising materials for corrosion inhibition due to the absence of grain boundaries. So, to circumvent this corrosion issue, we use MGs as inhibitors to prevent Al current collectors from degrading in lithium ion batteries.

In this presentation, MGs are deposited on Al foils by magnetron sputtering. The MGs systems chosen include Zr- and W-based. We compare the outcomes of corrosion phenomena on Al foils with different MGs systems from proceeding electrochemical tests and surface analyses. The thickness effect is also discussed in the study.

**Keywords:** Metallic glass coating, lithium battery, Al current collector, corrosion

# Local Measurement of Hydrogen Diffusion in Steel Sheet

Yudai Yamamoto<sup>1</sup>, Misako Jin<sup>1</sup>,

Yuichi Kitagawa<sup>2</sup>, Takayuki Nakanishi<sup>2</sup>, Yasuchika Hasegawa<sup>2</sup>, Koji Fushimi<sup>2</sup>

<sup>1</sup>*Graduate School of Chemical Sciences and Engineering, Hokkaido University,  
Kita-ku, Sapporo 060-8628, Japan*

<sup>2</sup>*Faculty of Engineering, Hokkaido University, Kita-ku, Sapporo 060-8628, Japan  
kfushimi@eng.hokudai.ac.jp*

During the atmospheric corrosion of the steels, hydrogen atoms are absorbed into the steel and often initiate the deterioration of mechanical properties of the steels, inducing hydrogen embrittlement. For inhibiting hydrogen embrittlement, it is necessary to elucidate mechanism and kinetics of not only absorption but also diffusion of hydrogen atoms in steel. Conventionally, diffusion coefficient of hydrogen atoms in steel sheet samples was estimated using Devanathan-Stachurski (DS) double electrochemical cell [1]. The DS cell method enables only to measure currents of hydrogen entry and exit side cells, the difference of which corresponds to hydrogen atoms permeated into the sample. Compared with the entry current, however, the exit current was very small and then it was difficult to use DS cell in the case of local measurement.

The authors have modified the DS cell with a flow channel in the entry side cell and discovered that the perturbation in the flow-rate causes the changes in the hydrogen exit current  $i_{\text{exit}}$  as well as hydrogen entry current  $i_{\text{entry}}$  [2]. When a sine wave was used for the perturbation,  $i_{\text{entry}}$  and  $i_{\text{exit}}$  showed similar waveforms with phase shifts depending on the perturbation frequency. The phase shift was arisen from diffusional delay in  $i_{\text{exit}}$  and was expected to be a new parameter to discuss the diffusivity of hydrogen atoms in the samples. In this study, a micro-capillary cell technique was also applied to the modified DS cell to realize local measurements. Furthermore, a series of finite element method (FEM) numerical calculations were conducted for the simulation and the estimation of the diffusion of hydrogen in the steel sheet, assuming that both hydrogen entry and exit reactions were in mass-transport limitation and the phase shift was only arisen from the diffusion.

The DS cell with a micro-capillary cell of an inner diameter of 250  $\mu\text{m}$  was successfully applied to measure the local hydrogen permeation into a single grain or two grains of a mild steel sheet with a thickness of 100  $\mu\text{m}$ . During the sinusoidal perturbation in the entry side cell, the phase shift on a single grain was two times larger than that on the grain boundary. It was indicated that the hydrogen permeation was accelerated due to existence of the grain boundary. From the comparison with theoretical diffusion equation of hydrogen in the steel sheet sample [3], it was revealed that the diffusion coefficient on the grain boundary was at least two-times larger than that in the single grain. These results suggested that the metallurgical structure of steel substrate strongly influenced to the hydrogen permeation. The FEM calculation of two- and three-dimensional diffusion problems also revealed that the fluctuation in the flow-rate of the electrolyte solution gave rise to the phase shift of current waves depending on the diffusivity in the substrate. The difference in phase shift due to local diffusivity was simulated as well as the size effect of local substrates where hydrogen atoms were permeated.

## References

- [1] M.A.V. Devanathan, Z. Stachurski, *Proc. R. Soc. Lond. A* **270** (1962) 90.
- [2] K. Fushimi, M. Jin, T. Nakanishi, Y. Hasegawa, T. Kawano, M. Kimura, *ECS Electrochem. Lett.* **3** (2014) C21.
- [3] K. Sekine, *Chem. Lett.* **4** (1975) 841.



# **Alloy Anodization in Fluoride-Containing Electrolytes**

Hiroaki Tsuchiya, Min-Su Kim, Toshiaki Erami, Yuki Otani, Shinji Fujimoto  
*Division of Materials and Manufacturing Science, Graduate School of Engineering, Osaka University*  
*2-1 Yamada-oka, Suita, Osaka 565-0871 Japan*  
*tsuchiya@mat.eng.osaka-u.ac.jp*

Properties and structures of oxide layers, including passive films, on metals and alloys can be tuned by tailoring electrochemical conditions. It is well-known that the morphology of oxide layers can be also controlled by electrochemical approaches. Among the approaches reported, anodization is one of the most established examples, where self-organized nanoporous oxide layers are formed on aluminum substrate by electrochemical anodization in acidic electrolytes. In the decades it has been reported that self-organization takes place – the formation of self-organized nanoporous and nanotubular oxide layers – on the other metals such as titanium, zirconium, tantalum etc. by anodization. The key to achieve such self-organization is to treat in a small amount of fluorides under optimized conditions and the morphology (diameter and thickness) of oxide layers are varied depending not only on anodization condition but also on substrate. Therefore, anodization to form the self-organized nanostructures has been applied for a variety of substrates. The present work reports alloy anodization in fluoride-containing electrolytes, focusing on how microstructure and chemical composition of alloy affect the growth and morphology of oxide layers.

# Corrosion studies using non radioactive isotopes of H, Zn and Fe

Achim Walter Hassel<sup>1,2</sup>, Martina Hafner<sup>1</sup>, Bernhard Gallistl<sup>2</sup>

*1 Christian Doppler Laboratory for Combinatorial Oxide Chemistry at the*

*2 Institute for Chemical Technology of Inorganic Materials,*

*Johannes Kepler University Linz, 4040 Linz, Austria*

*achimwalter.hassel@jku.at*

Investigations with isotope enriched materials are amongst the most intriguing ones in chemistry. Typically such materials are rather expensive due to the tedious enrichment process. The price can easily reach 1000 € per gram for a material with an isotopic enrichment of 98 % or more. This is for example the case when highly enriched <sup>57</sup>Fe is used. One example will illustrate how this non radioactive isotope can be used in designing experiments for studying complex corrosion processes in which more than one source exists for the element of interest.

Hydrogen exists in three isotopes and is the only element that has different names and symbols for these named protium H, deuterium D and tritium T. While the latter is radioactive the first two are not. The reason for these different names is probably due to relatively easy way for high enrichment at an affordable price at least for H and D. Besides this the isotopic effect is much stronger than for any other element due to the large relative mass change of 100 % from H to D. In an attempt to better understand the different oxide products that form on press hardened galvanized steel [1] artificial corrosion product were synthesized from both light and heavy water solutions H<sub>2</sub>O and D<sub>2</sub>O to yield deuterised corrosion products such as simonkolleite, hydrozincite and akaganeite. IR transmission spectroscopy was used to characterize these products and to quantify the shift in wavenumbers of bonds with modified reduced mass. Standard addition NMR spectroscopy was used to quantify the unavoidable H/D exchange during preparation.

Zn being one of the most important elements in corrosion science is also of high interest for such studies. As one example the structure of a passive film forming under alkaline conditions on the amphoteric zinc depends on the pH of the solution. Not only zinc oxide and hydroxides play a role but also more complex zinc corrosion products such as hydrozincite, simonkolleite or akaganeite may be formed if the other elements are present. Even in trace amounts zinc can influence the following processes due to its ability for underpotential deposition, which are not only of academic interest but also of technical relevance e.g. for the crystallography of technical coatings. Also corrosion inhibitors may contain Zn as constituent. In cases in which processes are combined it may be unclear but of interest how much zinc originates from the one or the other source. Thus it might be necessary to distinguish zinc from zinc, something that is chemically not possible. Inductively coupled plasma mass spectrometry (ICP-MS) is a modern way for distinguishing various isotopes. For experiments with Zn a pure Zn isotope may be used but there is a much smarter way. Natural zinc consists of 48.6 % <sup>64</sup>Zn, 27.9 % <sup>66</sup>Zn, 4.1 % <sup>67</sup>Zn, 18.8 % <sup>68</sup>Zn, 0.6 % <sup>70</sup>Zn isotopes (in at.%). Since zinc is used in dissolved form as corrosion inhibitor in cooling water circuits, also nuclear power plants. However, neutron capture converts <sup>64</sup>Zn into <sup>65</sup>Zn which decays over <sup>65</sup>Cu by a hard  $\gamma$ -ray radiation. Therefore Zinc which is used in nuclear power plants is intentionally depleted in <sup>64</sup>Zn (< 1%) before use and is called DZO (depleted zinc oxide). The approach described here does not make use of pure monoisotopic zinc; it rather simply uses zinc with a strongly deviating isotope pattern. When combined with flow type scanning droplet cell microscopy FT-SDCM electrochemical depth profiling becomes possible that distinguishes zinc from zinc [2].

[1] R. Autengruber, G. Luckeneder, A. W. Hassel, **63** (2012) 12–19

[2] M. Hafner, A. W. Hassel, Corros. Sci. *submitted*

# Analysis of Corrosion Behavior of ASTM A416 Steel by Electrochemical Impedance Spectroscopy

Yu-Min Chen and Mark E. Orazem  
*Department of Chemical Engineering*  
*University of Florida, Gainesville, FL 32611 USA*  
[meo@che.ufl.edu](mailto:meo@che.ufl.edu)

During the past few decades, segmental bridges incorporating post-tensioned tendons have been widely adopted for bridge construction because they can withstand heavier loads and allow for longer spans. However, corrosion of the steel tendons has become a significant problem, leading, in some cases, to structural failure.

The corrosion behavior of ASTM A416 steel was studied in a simulated pore solution<sup>1</sup> containing 2 g/L  $\text{Ca(OH)}_2$ , 8.33 g/L NaOH and 23.3 g/L KOH with a pH of 13.8. Experiments were conducted using a traditional three-electrode setup. The ASTM A416 steel working electrode was polished sequentially with #120, 320 and 600 grit silicon carbide papers. The working electrode was subsequently degreased with ethanol and washed with water before each experiment. The counterelectrode consisted of a 5 mm  $\times$  50 mm platinum sheet, and an Mg/MgO reference electrode was used to avoid possible chloride contamination. The electrolyte temperature was maintained at 298 K by a temperature controller. The dissolved oxygen content was maintained at 8ppm by sparging ultra-high-purity-grade air.

The time required to reach steady-state was found to depend on potential. Generally, a steady open-circuit potential was reached after 200ks (56 h). For -0.1V (OCP), 50ks (14 h) was required to reach steady state; whereas, at +0.3V (OCP), 250ks (69 h) was required. Electrochemical impedance spectroscopy (EIS) was measured at different elapsed times with a frequency range 500Hz – 0.05Hz. Once a steady-state was reached, EIS measurement were performed at different potentials ranging from -0.3V to +0.3V (OCP). The low-frequency EIS results show a straight line between 22.5° to 45°, suggesting the influence of a porous electrode behavior. The process model included an ohmic resistance ( $R_e$ ) in series with a parallel combination of an anodic reaction impedance ( $Z_a$ ), a cathodic reaction impedance ( $Z_c$ ), and a constant phase element. Measurements at  $\pm 50\text{mV}$  were used to confirm that both the anodic and cathodic impedances played a role in the model.

The process model allowed estimation of oxide film thickness and corrosion rate. The oxide film thickness was estimated from CPE parameters using the power-law model developed by Hirschorn et al.<sup>2</sup> The oxide film thickness was estimated to be 15 nm for potentials from -0.3V to 0.2V (OCP). At more anodic potentials, +0.3V (OCP), the oxide film thickness was found to be 25 nm. The corrosion rate was estimated from the anodic charge-transfer resistance extracted from the process model. The corrosion rate at the open-circuit potential after an elapsed time of 2 hours (7.2 ks) was estimated to be 64  $\mu\text{m}/\text{year}$ . A statistically significant value for the anodic charge-transfer resistance could not be obtained after steady-state was reached, thus the corrosion rate could not be calculated. Similarly, the steady-state corrosion rate could not be estimated for potentials smaller than +0.3V (OCP). The steady-state corrosion rate at +0.3V (OCP) was estimated to be 50  $\mu\text{m}/\text{year}$ .

1. L. Li and A. A. Sagüés, "Effect of chloride concentration on the pitting and repassivation potentials of reinforcing steel in alkaline solutions." Paper 99-567, Proceedings of Corrosion/99, National Association of Corrosion Engineer, Houston, TX, 1999.
2. B. Hirschorn, M. E. Orazem, B. Tribollet, V. Vivier, I. Frateur, and M. Musiani, "Constant-phase element behavior caused by resistivity distributions in films: I. theory," J. Electrochem. Soc., **157** (2010), C452-C457.

# Copper Coatings for Used Nuclear Fuel Containers: Corrosion Testing

Peter Keech<sup>1</sup>, Sridhar Ramamurthy<sup>2</sup>, Rachel Partovi-Nia<sup>2</sup>, Jian Chen<sup>2</sup>, Becky Jacklin<sup>2</sup>, David Shoesmith<sup>2</sup>

<sup>1</sup>Nuclear Waste Management Organization, 22 St. Clair Ave, Toronto, ON, M4T 2S3

<sup>2</sup>Surface Science Western, Western University, 999 Collip Cir. London, ON, N6G 0J3

pkeech@nwmo.ca

The use of copper as a barrier against corrosion in deep geological repositories (DGRs) for used fuel containers (UFCs) has been explored in Europe, Asia and Canada for many decades, as metallic copper provides thermodynamic stability against anoxic corrosion. Extensive review of corrosion data reveals that damage will be limited to nanometres per year or less, or fewer than 1.3 mm in one million years<sup>1</sup>. In recent years, Canada's Nuclear Waste Management Organization (NWMO) has been developing methods for depositing thin copper coatings of copper directly onto steel-based UFC materials that provide suitable strength to withstand geological processes for many years. The result is the NWMO Mark II UFC, shown in Figure 1, both as a schematic and as a fabricated prototype. This container offers many potential manufacturing and handling advantages, owing to its modest size and low weight; the container depicted is just over 2 m long and < 5 t fully loaded, and compares favourably to a loaded KBS-3 container (> 4 m long and > 25 t)<sup>2</sup>.

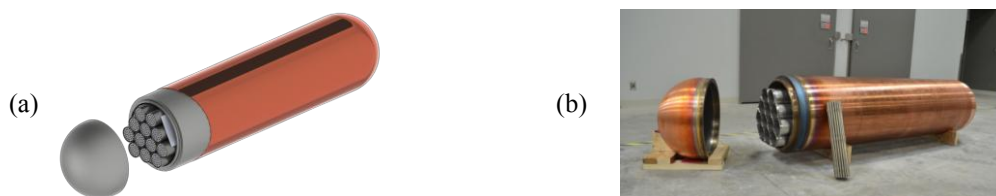
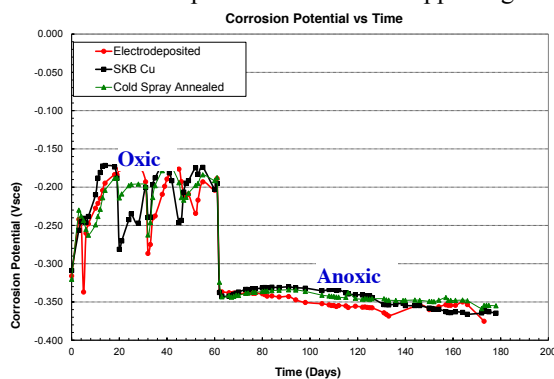


**Figure 1: NWMO Mark II Used Fuel Container (a) Schematic and (b) Prototype**

Electrodeposition and cold spray have been explored for container production, with the former proving to be superior for pre-fabrication (i.e. empty containers/lids), while the latter offers advantages for completing the coating over the closure zone, following weld sealing of a loaded container. As the corrosion barrier, it is necessary for the copper coatings to perform as well (or better) than wrought copper materials, for which a large copper corrosion database exists. Corrosion testing of the coating materials has been extensive, consisting of long term exposures to oxic and anoxic conditions as well as accelerated electrochemical measurements. Coating materials have demonstrated corrosion performance that is similar to that of the wrought copper reference materials, with the exception of the accelerated testing in which there are subtle differences among the materials with respect to surface texturing, observed via post-experiment surface analysis. However, throughout the experiments, there is consistency among corrosion potential measurements for the coating and wrought materials, as these fall within a few mV of each other under different conditions such as oxic and anoxic exposures and in accelerated electrochemical measurements. An example is presented in Figure 2, for an experiment that was initially oxic and then anoxic. Results from all of these experiments and the supporting surface analysis, will be described in this paper.

**Figure 2: Corrosion Potential versus time plot for the samples exposed initially under O<sub>2</sub> purging, then followed by Ar-purging**



<sup>1</sup> Scully, J.R., Edwards, M., 2013. Review of NWMO Copper Corrosion Allowance, NWMO Technical Report, NWMO-TR-2013-04, Nuclear Waste Management Organization, Toronto, Canada.

<sup>2</sup> H. Raiko, R. Sandström, H. Rydén, M. Johansson, 2010, Design analysis report for the canister, SKB-TR-10-28, Svensk Kärnbränslehantering AB, Stockholm, Sweden.

# Electrochemical behavior of electrodeposited Ni-W nanostructured alloys

N. Shakibi Nia, M. Lagarde, J. Creus, X. Feaugas, C. Savall

*LaSIE UMR 7356 CNRS, Université de La Rochelle, Av. Michel Crépeau, 17042 La Rochelle, France.*

*Email address: [niusha.shakibi\\_nia@univ-lr.fr](mailto:niusha.shakibi_nia@univ-lr.fr), [xavier.feaugas@univ-lr.fr](mailto:xavier.feaugas@univ-lr.fr)*

Nanocrystalline electrodeposited coatings have been the subject of numerous studies due to their supposed resistance against corrosion and their particular mechanical, electrical and magnetic properties. However, the superior corrosion resistance of lower grain size metals, particularly at the nanometer scale, has not been yet clearly established [1]. Actually, as grain size decreases, other parameters like surface roughness, crystallographic orientation, chemical contamination, vacancies concentration, internal stresses at different scales ..., which can affect the corrosion resistance, are also modified. The aim of our approach is to better understand the influence of the microstructural parameters, mainly grain size and tungsten content, on the corrosion resistance.

Additive free citrate-ammonium bath is used to obtain Ni-W alloys, by applying direct and pulse currents. In order to extend the grain size range conserving the alloy element content constant, some of these coatings were annealed under vacuum conditions at various temperatures during one hour. A multi-scale characterization of the metallurgical states of electrodeposited nanocrystalline coatings using a combination of several microstructural techniques (DSC, XRD, SEM, EBSD, TEM and AFM) has permitted the characterization of the morphology, the grain size, the crystallographic texture and the nature of grain boundaries. These complementary techniques permit to define transition scales that are necessary to discuss the physical meaning of the different microstructural features [2]. The influence of deposition parameters on chemical contamination by light elements is evaluated by Secondary Ion Mass Spectrometry (SIMS) analysis and the amounts of these elements are quantified systematically by hot extraction measurements [3]. At last, polarization curves were used to study the anodic behavior and the kinetics of the Hydrogen Evolution Reaction in acidic ( $\text{H}_2\text{SO}_4$  1M, pH 3) and alkaline (NaCl 0,6M, pH 10) deaerated solutions.

According to our results, the grain size refinement strongly depends on the elaboration parameters (current density, temperature, electrodeposition bath composition ...) which also influence the light elements contamination (O, H, N, C) and/or the alloying addition. The analyses of the polarization curves in acidic media revealed that the tungsten addition promotes the dissolution of the protective passive film and favors the localized corrosion in alkaline media. It is suggested that the tungsten addition plays an important role on the electrochemical reactivity in both anodic and cathodic domains and that the other metallurgical parameters such as grain size intervene only at second order.

[1] K.D. Ralston, N. Birbilis and C.H.J. Davies, *Scripta Materialia* 63 (2010) 1201-1204.

[2] C. Savall, A. Godon, J. Creus, X. Feaugas, *Surface and Coatings Technology* 206 (2012) 4394-4402.

[3] N. Shakibi Nia, J. Creus, X. Feaugas, C. Savall, *Journal of Alloys and Compounds* 609 (2014) 296-301.

# Corrosion inhibition of steel by flavonoid model molecules: naringin, neohesperidin, rutin

D. Veys-Renaux<sup>1,\*</sup>, E. Rocca<sup>1</sup>, N. M'hiri<sup>2,3</sup>, S. Reguer<sup>4</sup>, I. Ioannou<sup>2</sup>, M. Ghoul<sup>2</sup>

<sup>1</sup>Institut Jean Lamour – UMR CNRS 7198, Université de Lorraine, BP70239 Vandoeuvre les Nancy, 54506, France.

<sup>2</sup>Université de Lorraine, ENSAIA – Laboratoire d'Ingénierie des biomolécules (LIBio), TSA 40602 Vandoeuvre les Nancy, 54518, France.

<sup>3</sup>Université de la Manouba, Institut Supérieur de Biotechnologie de Sidi Thabet, Ecophysiologie et Procédés Agroalimentaires – UR11ES44, BP 66 Ariana-Tunis, 2020, Tunisia.

<sup>4</sup>DiffAbs beamline, Synchrotron Soleil, L'Orme des Merisiers, Saint-Aubin, BP48 Gif sur Yvette, 91192, France.

\*delphine.veys-renaux@univ-lorraine.fr

In the framework of new ecological challenges, many plant extracts appear as promising green corrosion inhibitors. Their efficiency is generally attributed to the antioxidant properties of secondary metabolites, as flavonoid molecules, which are produced by plants in order to fight against environment attacks. However, due to the large number of molecules contained in plant extracts, the corrosion inhibition mechanisms remain largely unknown.

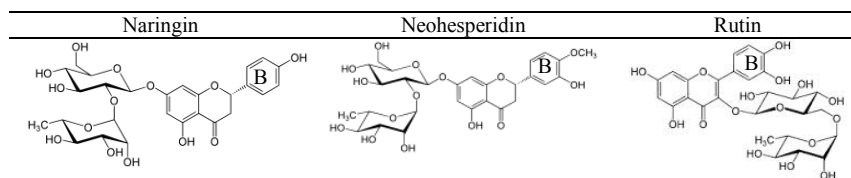


Table 1: Chemical formulae of the model flavonoid molecules

In acidic medium, the electrochemical impedance spectroscopy (EIS) measurements performed in HCl at pH 1 in water/ethanol medium show that the inhibiting properties through an adsorption mechanism are directly linked to the antioxidant activity of molecules which was determined by the ABTS test. Actually, the best inhibition efficiency is obtained with rutin characterized by two adjacent OH groups on the B-ring (catechol group), which also explains the radical scavenging activity and the chelation of metallic cations (especially  $\text{Fe}^{2+}$ ).

In more alkaline medium, at pH 4, the corrosion behavior is governed by the formation of a tri-dimensional conversion film made of iron and flavonoid, as revealed by SEM observations.

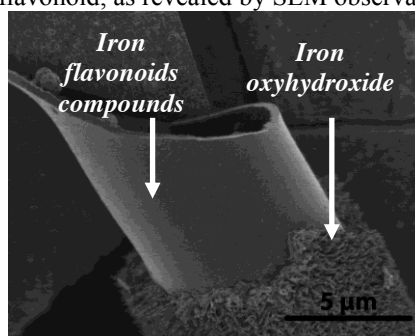


Fig 2: Passive films formed at pH4 in presence of rutin on steel (peeled off part)

This paper focuses on the inhibiting effect on steel corrosion of three model flavonoids with various antioxidant properties: naringin, neohesperidin and rutin.

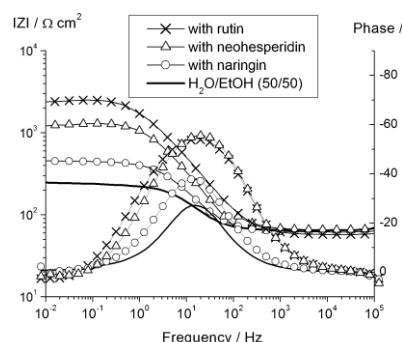


Fig. 1: EIS measurements (Bode plot) of steel immersed in HCl (pH1, water/EtOH medium)

For a deeper understanding, compounds were synthesized from precipitation at pH 4 of iron salt in presence of flavonoid molecules and investigated by Raman spectroscopy and X-ray Absorption Spectroscopy measurements (XAS). Results show that the formation of conversion products requires the coordination of  $\text{Fe}^{3+}$  by the two O atoms attached to the B ring. From an electrochemical point of view, a cathodic inhibition attributed to the oxygen scavenger role of the antioxidant molecules was observed. Nevertheless, the anodic protection depends on the covering properties of the conversion film (when it is formed), related to the molecule structure.

# Towards high-throughput Corrosion Screening using Bipolar Electrochemistry

Sara Munktell, Leif Nyholm, Fredrik Björefors

*Department of Chemistry - Ångström Laboratory, Uppsala University,  
Box 538, SE-75121 Uppsala Sweden  
e-mail: sara.munktell@kemi.uu.se*

In this work the concept of using arrays of bipolar electrodes for a fast and simple way to screen corrosion properties is presented.

When an isolated conducting object is exposed to an external electric field the resulting potential difference across its surface can cause part of the total current to pass through said object. The result of this is that the object will act as an anode and a cathode simultaneously and that there will be a gradient in electrochemical potential ranging between the two end poles. The effect has proved useful in various industries and research fields with applications ranging from large scale chemical reactors to the modification of nano-objects<sup>1</sup>.

We have previously demonstrated that bipolar electrochemistry can be used to generate gradients in corrosion damage on steel samples to evaluate their corrosion properties<sup>2</sup>. When a number of steel samples are placed together in an array configuration and subjected to an external field they all act as individual bipolar electrodes, and in this way many samples can be compared in the same experiment at the same time. The shape of the gradient that forms on the anodic end of the samples will depend on the steels corrosion resistance.

When all steel samples placed together are of the same type the BPE-induced gradients are all alike. If steels of different corrosion properties are placed together the least resistant steel will pass more of the current and therefore corrode further<sup>3</sup>. This effect can be used to enhance differences between samples. An example of this is shown in Figure 2.

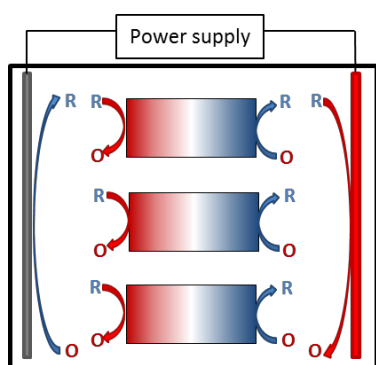


Figure 1: Schematic of the BPE-array setup.

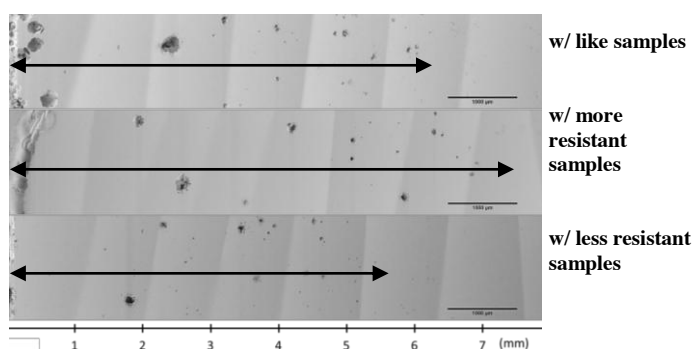


Figure 2: Gradients on the same type of steel from different setups, arrows roughly indicates the length of the gradient.

## References

- [1] G. Loget, D. Zigah, L. Bouffier, N. Sojic, A. Kuhn, *Accounts of Chemical Research* 2013, **46**, 2513-2523.
- [2] S. Munktell, M. Tydén, J. Höglström, L. Nyholm, F. Björefors, *Electrochemistry Communications* 2013, **35**, 274-277.
- [3] S. Munktell, L. Nyholm, F. Björefors, *Journal of Electroanalytical Chemistry* 2015, **747**, 77-82.

# Photo-electrochemical degradation of anodized titanium surface observed using EIS and ellipso-microscopy

Koji Fushimi, Haruya Ikeyama, Yuichi Kitagawa, Takayuki Nakanishi, Yasuchika Hasegawa,  
Mikito Ueda, Toshiaki Ohtsuka  
*Faculty of Engineering, Hokkaido University*  
*Kita 13-Jo, Nishi 8-Chome, Kita-ku, Sapporo 060-8628, Japan*  
*kfushimi@eng.hokudai.ac.jp*

Titanium alloys are known well as highly corrosion resistive materials and are used in chemical plants and seashore. It is mainly due to the formation of passive oxide film that is chemically stable in corrosive environment for general materials. However, the oxide of titanium alloy has an n-type semiconductive property and structure of anatase, which is frequently used as a photo-catalyst in various fields. Therefore, it is important to consider the degradation behavior due to photo-assisted corrosion of titanium alloy used in the sunshine.

Electrochemical impedance spectroscopy (EIS) and ellipso-microscopy of titanium electrode anodized in sulfuric acid solution were carried out during the irradiation of ultra-violet (UV) light with a wavelength of 325 nm. EIS revealed that the UV-light irradiation of the anodized surface induced a photo-electrochemical reaction of the titanium oxide film on the surface as well as oxygen evolution. A charge transfer resistance increased in the initial stage and then decreased, while a film capacitance increased continuously. The change of the film was dependent on the applied potential during the irradiation. Furthermore, ellipso-microscopy gave a series of heterogeneous images of the oxide film, depending on a crystallographic texture of the titanium substrate. The basal plane of 0001 tended to be covered with a relatively thin oxide film, which was changed dramatically by the irradiation.

A localized UV-light irradiation of anodized titanium surface with a photo-mask allowed the selective change of the oxide film as shown in Figure 1. It is suggested that the local irradiation is effective not only to fabricate a pattern on the surface but also to modify the surface homogeneously. The later might be beneficial to improve a corrosion resistance of the titanium.

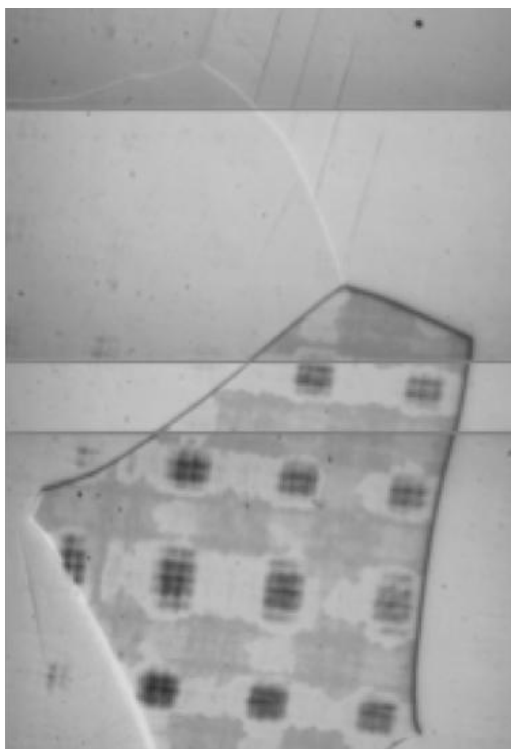


Figure 1. Locally damaged titanium surface by irradiation of UV-light with a mesh.



# Passivation Behavior of Type-316L Stainless Steel in the Presence of Hydrogen Sulfide Ions Generated from Liquid-Phase Ion Gun

Jun-Seob Lee\*, Yuichi Kitagawa\*\*, Takayuki Nakanishi\*\*, Yasuchika Hasegawa\*\*, Koji Fushimi\*\*

\*Graduate School of Chemical Sciences and Engineering, Hokkaido University,

Kita-13, Nishi-8, Kita-ku, Sapporo 060-8628, Japan

\*\*Faculty of Engineering, Hokkaido University, Kita-13, Nishi-8, Kita-ku, Sapporo 060-8628, Japan

Junseobl@cse.hokudai.ac.jp

Passivation and depassivation of stainless steels in sulfide-containing environment such as crude oil and gas wells have become of particular interests for practical applications [1]. Hydrogen sulfide ion ( $\text{HS}^-$ ) is an aggressive anion and forms a sulfide layer on the stainless steel surface. The sulfide layer shows protective or non-protective properties depending on the corrosion reaction [2, 3]. It is important to understand passivation and depassivation in a presence of  $\text{HS}^-$ . Recently, the authors have developed a liquid-phase ion gun (LPIG) to release an infinitesimal amount (ppm-order) of  $\text{HS}^-$  by reducing a silver/silver sulfide microelectrode and applied to induce the local sulfidation on a silver surface [4]. The application of LPIG enables to elucidate the passivation and/or depassivation of stainless steels induced by hydrogen sulfide ions. In this study, effects of  $\text{HS}^-$  on passivity of type-316L stainless steel were examined by using LPIG for the first time.

The fabrication procedure of a silver/silver sulfide LPIG microelectrode was basically identical with that reported previously [4]. A diameter of the microelectrode was 500  $\mu\text{m}$ . A three-electrode electrochemical cell with a platinum counter electrode and an Ag/AgCl/sat. KCl reference electrode (SSE) was used for electrochemical measurements of a substrate electrode of the stainless steel. The surface of the stainless steel was passivated by a potentiostatic polarization at 0.9  $V_{\text{SSE}}$  for 100 s. When a distance between microelectrode and substrate electrode was sustained with 125  $\mu\text{m}$ , the microelectrode was connected with the substrate electrode and galvanostatically reduced to generate  $\text{HS}^-$  by using a battery-driving DC signal source in pH 8.4 boric acid-borate buffer solution, while the substrate stainless steel electrode was continuously polarized at 0.9  $V_{\text{SSE}}$ . Electrochemical impedance was measured at a constant frequency of 15 Hz and in a frequency range of  $10^{-2}$  to  $10^4$  Hz with an amplitude voltage of 10 mV. Moreover, silver wire and tungsten wire electrodes were used to estimate concentration of  $\text{HS}^-$  and pH value, respectively, in the narrow space between microelectrode and substrate electrode before and after the galvanostatic polarization of LPIG microelectrode. Auger electron spectroscopy (AES) was also used to analyze the passive film on the stainless steel when it was formed with or without presence of  $\text{HS}^-$  generation by LPIG.

From the open circuit potential measurement of the silver and tungsten wire electrodes during the LPIG polarization for generation of  $\text{HS}^-$ , concentration of  $\text{HS}^-$  and pH values in the narrow space were estimated with less than 10 ppm and ca. pH 9.5, respectively. During potentiostatic polarization of the stainless steel and LPIG microelectrode, current density increased with increase in concentration of  $\text{HS}^-$ . It is considered that further reactions could be induced by  $\text{HS}^-$  during the passivation of the steel surface. The impedance at 15 Hz increased during the polarization in the presence of  $\text{HS}^-$  by LPIG, while that continuously decreased after stopping the generation of  $\text{HS}^-$  and removing the microelectrode to the solution bulk because of [a](#)-dilution of  $\text{HS}^-$ . Moreover, a charge transfer resistance of passive film formed in the presence of  $\text{HS}^-$  increased with increase in  $\text{HS}^-$  concentration. AES revealed that the S-containing layer formed with  $\text{HS}^-$  was thicker than that formed without  $\text{HS}^-$ . It was demonstrated that the passive layer formed on type-316L stainless steel at 0.9  $V_{\text{SSE}}$  in pH 8.4 buffer solution was stabilized by the presence of  $\text{HS}^-$ .

## References

1. T. A. Ramanarayanan, S. N. Smith, *Corrosion*, 46 (1990) 66.
2. A. Davoodi, M. Pakshir, M. Babalee, G. R. Ebrahimi, *Corros. Sci.*, 53 (2011) 399.
3. H. H. Huang, J. T. Lee, W. T. Tsai, *Mater. Chem. Phys.*, 58 (1999) 177.
4. J.-S. Lee, K. Fushimi, Y. Kitagawa, T. Nakanishi, Y. Hasegawa, *J. Electrochem. Soc.*, 162 (2015) C115.

# Corrosion Inhibition of Pure Aluminium by 8-Hydroxyquinoline: Combined Electrochemical and DFT Studies

Fatah Chiter<sup>a,b</sup>, Corinne Lacaze-Dufaure<sup>a</sup>, Sabrina Marcelin<sup>a</sup>, Nadine Pébère<sup>a</sup>, Hao Tang<sup>b</sup>

<sup>a</sup> Université de Toulouse, CIRIMAT, UPS/INPT/CNRS

ENSIACET, 4 Allée Emile Monso – CS 44362, 31030 Toulouse, France

<sup>b</sup> CEMES, UPR CNRS 8011, 29 rue Jeanne Marvig, BP 94347, 31055 Toulouse, France

Nadine.Peber@ensiacet.fr

Since the beginning of the 1990s, the high toxicity associated with chromates has imposed restrictions on their use in industrial applications. As a consequence, intense research efforts are being undertaken to find new environmentally friendly compounds as corrosion inhibitors of aluminium and aluminium alloys. It was shown that 8-HQ acts as an effective corrosion inhibitor for different metals and alloys, such as magnesium [1], copper [2] and aluminium [3-5]. Fig. 1 shows the chemical structure of 8-HQ. The molecule contains nitrogen, oxygen heteroatoms and aromatics rings which are the basic requirements for inhibitive action.

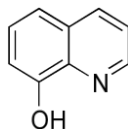


Fig. 1: Molecular structure of the 8-HQ (C<sub>9</sub>H<sub>7</sub>NO)

The aim of the present work is to investigate, at atomic scale, the corrosion inhibition mechanisms of 8-HQ on pure aluminium surfaces by using *ab initio* calculation. The final goal of the study was to correlate theoretical approach to experimental ones (electrochemical data and surface analysis) in order to extract the factors which are favourable to the inhibition processes. A better understanding of the corrosion inhibition mechanisms will help to rationalize the search of new species that could provide corrosion protection close to that afforded by chromates.

Density functional theory (DFT)-based concepts were used to investigate the adsorption of the 8-HQ and its derivatives that could be present in acidic, alkaline or neutral media, *i.e.* the 8-HQ tautomer and dehydrogenated species. The Al(111) surface was modelled by a periodic slab and dispersed corrected computations were performed and discussed, in term of adsorption sites and adsorption topology. A detailed electronic structure analysis of the molecule (charge transfer, density of states, partial charges) led to the determination of the nature of the bonding (physisorption or chemisorption) and to the characterization of the molecule/metal interface that is really meaningful because the surface properties of the system depends on the bonding. In parallel, electrochemical measurements were performed on pure aluminium in an aqueous solution for different pH (from 3 to 10). It was shown that in acidic or alkaline solutions, 8-HQ decreased the uniform corrosion rate of the aluminium indicating an adsorption mechanism on the bare surface whereas in neutral solution the dissolution mechanism was modified showing that the inhibitor interacts with the aluminium oxide and the passive layer was strengthened.

## References

- [1] H. Gao, Q. Li, Y. Dai, F. Luo, H.X. Zhang, Corrosion Science 52 (2010) 1603-1609.
- [2] G.P. Cicileo, B.M. Rosales, F.E. Varela, J.R. Vilche, Corrosion Science 40 (1998) 1915-1926.
- [3] C. Casenave, N. Pébère, F. Dabosi, Materials Science Forum 192-194 (1995) 599-610.
- [4] L. Garrigues, N. Pébère, F. Dabosi, Electrochimica Acta 41 (1996) 1209-1215.
- [5] S.V. Lamaka, M.L. Zheludkevich, K.A. Yasakau, M.F. Montemor, M.G.S. Ferreira, Electrochimica Acta 52 (2007) 7231-7247.

## Acknowledgments

This work was carried out in the framework of the "ICAADE" project with the financial support of the Agence Nationale de la Recherche (ANR-2011 JS08015 01(2012-2015)). This work was performed using HPC resources from CINES under allocations made by GENCI (Grand Équipement National de Calcul Intensif) and using HCP resources of CALMIP (Calcul Midi-Pyrénées).

# Influence of water concentration on growth efficiency of barrier-type anodic film on magnesium

Khurram Shahzad<sup>a</sup>, Etsushi Tsuji<sup>a,b</sup>, Yoshitaka Aoki<sup>a,b</sup>, Shinji Nagata<sup>c</sup>, Hiroki Habazaki<sup>a,b</sup>

<sup>a</sup>Graduate School of Chemical Sciences and Engineering, <sup>b</sup>Faculty of Engineering, Hokkaido University, Kita-13, Nishi-8, Kita-ku, Sapporo 060-8628, Japan

<sup>c</sup>Institute for Materials Research, Tohoku University, 2-1-1 Katahira, Sendai 980-8577, Japan  
Khurram5433@outlook.com

Magnesium and its alloys have growing interest as structural materials for aerospace, electronics and automotive industries, owing to their low density and high strength/weight ratios, and therefore are considered as alternatives to aluminum alloys. However, poor corrosion resistance of magnesium limits their applications. Surface treatments, including anodizing, are needed for their practical applications, and in contrast to many anodizing metals such as aluminum, titanium, niobium etc, the studies on growth behaviour of the magnesium in aqueous electrolytes are limited because of difficulty of uniform film formation in these electrolytes. Recent studies on magnesium disclose that the corrosion of magnesium in ethylene glycol (EG) solution can be improved by fluoride addition as a consequence of the formation of a protective film [1]. Habazaki *et al.* and Hernandez *et al.* reported recently the formation of fluoride-based barrier-type anodic film on magnesium at high efficiency in organic electrolytes containing water [2, 3]. Despite these recent advances, no report on the formation of barrier type film on magnesium at high efficiency in aqueous electrolyte is present. Therefore, in the present study the influence of water concentration on film growth efficiency is examined in EG-water electrolytes containing phosphate and fluoride.

Magnesium films of 220-230 nm thickness were prepared by DC magnetron sputtering on flat anodized aluminum and glass substrate. Sputtered films were anodized at a constant current density of 10 A m<sup>-2</sup> to the selected voltages in EG-water electrolytes containing phosphate and fluoride with various concentrations of H<sub>2</sub>O at 293 K. Anodizing was also performed in phosphate free and phosphate containing aqueous electrolytes. Electron microscopies (SEM and TEM) were used for the investigation of surface and cross section of anodic films, while X-ray diffraction and Rutherford backscattering spectroscopy were employed for film structure and composition respectively.

Figure 1 shows an example of the surface and cross section of the anodic film formed in phosphate containing aqueous electrolyte. It is obvious that anodic film shows smooth surface with flat and parallel metal/film and film/electrolyte interfaces even in EG-free aqueous electrolyte. The thickness of anodic film estimated from TEM is 113 nm, which corresponds to the formation ratio of 1.13 nm V<sup>-1</sup>, whereas this formation ratio was 1.8 nm V<sup>-1</sup> in EG-0.18 vol. % water, indicating large influence of water concentration on formation ratio. XRD and selected area diffraction pattern disclosed that structure of anodic film was amorphous in EG-0.18 vol% water and transform to crystalline phase at water concentration  $\geq 10$  vol. %. RBS analysis revealed that film efficiency was reduced from 100 % in EG-0.18 vol% water to approximately 50% in aqueous electrolyte, while film composition is not largely affected with increasing water concentration.

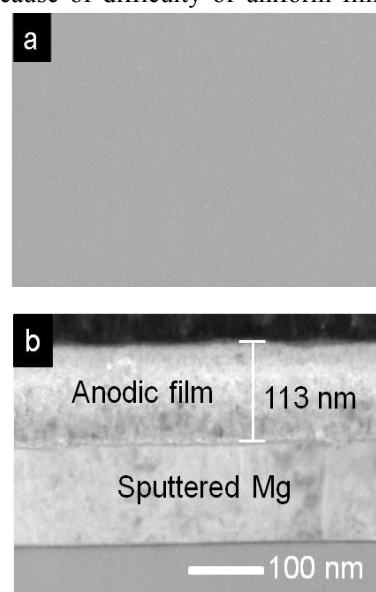


Fig. 1 (a) Surface SEM and (b) cross-sectional TEM images of an anodic film formed on the sputtered magnesium film to 100V in aqueous electrolyte containing 0.1 mol dm<sup>-3</sup> NH<sub>4</sub>F and 0.1 mol dm<sup>-3</sup> K<sub>2</sub>HPO<sub>4</sub> at 293 K.

## References

- [1] G. Song, D. StJohn, *Corros. Sci.* 46 (2004) 1381–1399
- [2] H. Habazaki, F. Kataoka, E. Tsuji, Y. Aoki, S. Nagata, P. Skeldon, G.E. Thompson, *Electrochem. Comm.*, 46 (2014) 30–32.
- [3] J. M. Hernandez, A. Nemcova, X. L. Zhong, H. Liu, M. A. Arenas, S. J. Haigh, M. G. Burke, P. Skeldon, G.E. Thompson, *Electrochim. Acta* 138 (2014) 124–131.

# Assessing Uniform Corrosion of Aluminum Alloys 2024-T3, 6061-T6, and 7075-T6 in Aqueous Immersion Conditions

I-Wen Huang, Rudolph G. Buchheit  
*Fontana Corrosion Center, The Ohio State University*  
2041 N. College Rd. Columbus, OH 43210  
[huang.697@osu.edu](mailto:huang.697@osu.edu)

High strength aluminum alloys are known to be particularly susceptible to localized corrosion induced by heterogeneous intermetallics, but the ability to quantitatively assess uniform corrosion along with pitting has become a major challenge for pit growth prediction. [1] The pit depth measurement is shown to be affected by reference surface changing due to uniform corrosion as well as pit agglomeration. Therefore, the ability to measure pit depths and uniform corrosion simultaneously by profilometric methods to compensate for the reference surface recession has become a critical correction needed in aqueous conditions.

In this work, pitting corrosion and uniform dissolution of aluminum alloys 2024-T3, 7075-T6 and 6061-T6 were characterized quantitatively using optical profilometry (OP) after free immersion in 0.01 to 1.0 M NaCl solutions as a function of pH (3, 5, 8, 10), temperature (20, 40, 60, 80°C) and exposure time (1 day, 1 week, and 1 month). Samples were cut into 1 cm<sup>2</sup> coupons and then partially painted by lacquer to keep intact surface free from corrosion. Uniform dissolution was estimated by carefully measuring the step height between the masked surface and the exposed surface along with pitting information including pit depth, diameter, area, and volume. The influence of pH, chloride ion concentration, and temperature will be discussed in detail.

This investigation of uniform corrosion is supported by electrochemical experiment where cathodic limiting current was slowed by the reduced oxygen solubility at elevated temperature. Electrochemical impedance spectroscopy (EIS) results also show elevated polarization resistance at high temperature from 10<sup>4</sup> to 10<sup>9</sup> (ohm·cm<sup>2</sup>) and potentiostatic tests show that pit initiation frequency was much lower at high temperature. It was also found that a passive film formation creates a surface inert to oxygen reduction reaction during a long term immersion, which was not seen in short term electrochemical tests, protecting the surface at high temperature conditions. Corrosion product and passive film analysis were performed by energy-dispersive X-ray spectroscopy (EDS) and electron diffraction. Samples prepared by focused ion beam (FIB) were examined to identify the composition and microstructure of corrosion product in both low and high temperatures.

In addition, to validate the proposed pit morphology influenced by uniform corrosion, long term sample immersion and B117 salt spray chamber tests were also employed. Maximum pit depth was carefully found and a detailed profile scan was conducted by OP. This pit profile obtained unveils the altering pit geometry with uniform corrosion. In this presentation, details of the experimental method and the results will be presented and the implication of these results on corrosion damage accumulation will be addressed.

## References

[1] M. K. Cavanaugh, R. Buchheit, N. Birbilis, *Corr. Sci.* 52 (2010) 3070-3077.

# Micro-pattern Corrosion Screening on Bimetallic Corrosion for Microelectronic Application

Arindom Goswami, Po-Fu Lin and Oliver Chyan,  
*Interfacial Electrochemistry and Materials Research Lab*  
*University of North Texas*  
*Denton, Texas TX 76203*  
*Chyan@unt.edu*

As the miniaturization trend on integrated circuit continues, the minute dimensions ( $< 20$  nm) involved in advanced microelectronic device architecture can greatly accelerate the progression of on-chip corrosion into a severe reliability threat. In particular, various interfaces formed between multilayer film stacks can generate dissimilar contacts with significant galvanic potential differences to active on-chip corrosion under favorable semiconductor processing conditions. Currently, 10-13 layers of Cu interconnects provide digital communication framework within a modern 14 nm IC chip set. The Cu interconnects are fabricated by dual damascene patterning technique that utilizes chemical-mechanical planarization (CMP) process to remove excess Cu deposit. Furthermore, the increased noble character of new diffusion barriers like Ru can further intensify the Cu galvanic corrosion especially in CMP corrosive chemical environments. In electronic packaging area, heavy corrosion on Al bond pad in a Cu wire bonded assembly was identified as a critical failure mode. In some cases, corroded Al pad is subjected to positive bias and/or Cl contamination. Even though there can be one or more of factors such as chemical environments, bimetallic contacts and positive bias to activate the observed bimetallic corrosion, the exact corrosion activation mechanism(s) remain unclear; as such the effective corrosion prevention can't be achieved. In this paper, we report the research efforts to establish bimetallic corrosion mechanism(s) and explore effective prevention strategy using micro-pattern corrosion screening metrology combined with electrochemical and x-ray photoelectron spectroscopy (XPS) techniques. As illustrated in Fig. 1, patterns of Cu micro-dots were deposited, through a micro-dot mask, on selected barrier metal substrates including Ta, Ru, and Ta/Ru alloy. The Cu corrosion on the testing pattern was observed in real time under digital optical microscope to evaluate Cu corrosion rate in different chemical environments and record surface transformations of Cu corrosion. The corrosion screening reveals that Cu contacts with Ru leads to enhanced galvanic corrosion of Cu as compared to Cu/Ta. The corrosion mechanisms of Cu/Ru and Cu/Ta were established (Fig. 2) in various CMP related chemical environments. Our corrosion screening data showed pyrazole could inhibit Cu corrosion more effectively than benzotriazole in highly alkaline tetramethyl ammonium hydroxide solution [1]. In device packaging area, SEM/EDX and optical microscopy reveal the early state of Al/Cu bimetallic corrosion mostly follows the grain boundaries on an Al bonding pad. As such, better understanding where the corrosion starts and how erosion progresses under specific chemical environments will aid in the development of effective corrosion inhibition strategies for microfabrication application.

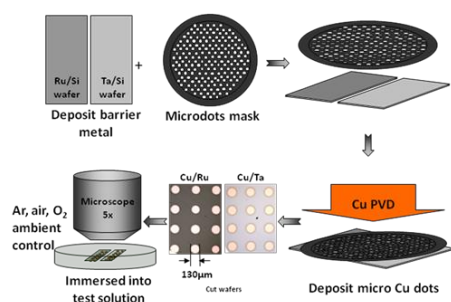


Fig. 1: Micro-pattern Corrosion Screening Metrology.

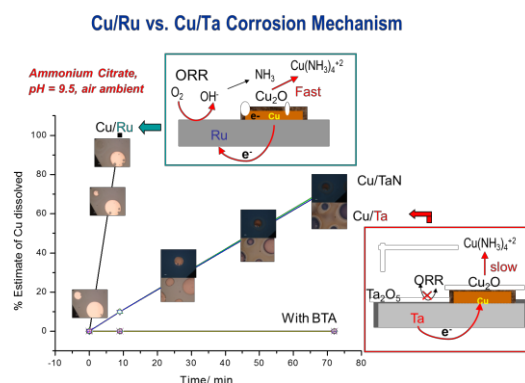


Fig. 2: Proposed corrosion mechanism for Cu/Ru vs. Cu/Ta in ammonium citrate.

[1]: "Study of Pyrazole as Copper Corrosion Inhibitor in Alkaline Post Chemical Mechanical Polishing Cleaning Solution" Goswami, A.; Koskey, S.; Mukherjee, T.; Chyan, O., *ECS J. Solid State Sci. Technol.* 2014, 3(10), P293-P297.

# Electrochemical corrosion behavior of permanganate conversion coating on AZ31B magnesium alloys — Long term evaluation by EIS

Shun-Yi Jian, Yueh-Lien Lee, and Chao-Sung Lin\*

Department of Materials Science and Engineering, National Taiwan University  
1, Roosevelt Road, Section 4, Taipei 106, Taiwan

\*Correspondent: csclin@ntu.edu.tw

The permanganate conversion coating on magnesium generally contains defects such as cracks, which deteriorate the coating adhesion and corrosion resistance.<sup>1-6</sup> As a result, in our previous study, we reported a new route to form a thin, nearly crack-free  $\text{MnO}_2$ -rich conversion coating on magnesium alloys.<sup>7</sup> The excellent properties of the permanganate conversion coating (PCC) treatment was performed in the solution composed of 0.1 M potassium permanganate ( $\text{KMnO}_4$ ), 0.025 M manganese nitrate ( $\text{Mn}(\text{NO}_3)_2$ ), and 0.02M potassium dihydrogen phosphate ( $\text{KH}_2\text{PO}_4$ ) at room temperature for 90 s. To further understand its electrochemical corrosion behaviors, the electrochemical impedance spectroscopy (EIS) technique is performed for coated magnesium alloys in this study, including permanganate conversion coating and commercial chromate conversion coating (Dow 1). The EIS measurement was conducted after immersion in 0.05 M NaCl and 0.1 M  $\text{Na}_2\text{SO}_4$  solution for different time periods up to 48 h. The EIS data in Fig. 1(a) as a function of immersion time reflected the evolution process of the permanganate coated AZ31B, including stages of the growth (0.5-24 h immersion) and the deterioration (30-48 h immersion) of the film. Similarly, the chromate coated AZ31B, including stages of the growth (0.5-18 h immersion) and the deterioration (24-48 h immersion) of the film. Thereby, the different electrochemical behavior of the conversion coated AZ31B is mainly due to their different properties and structure. Based on the EIS measurement, microstructure and composition analysis of the conversion coated AZ31B by SEM and TEM was also proposed for understanding the corrosion process of passive film. With the form of the impedance spectrum could be determined the mechanism of the corrosion process.

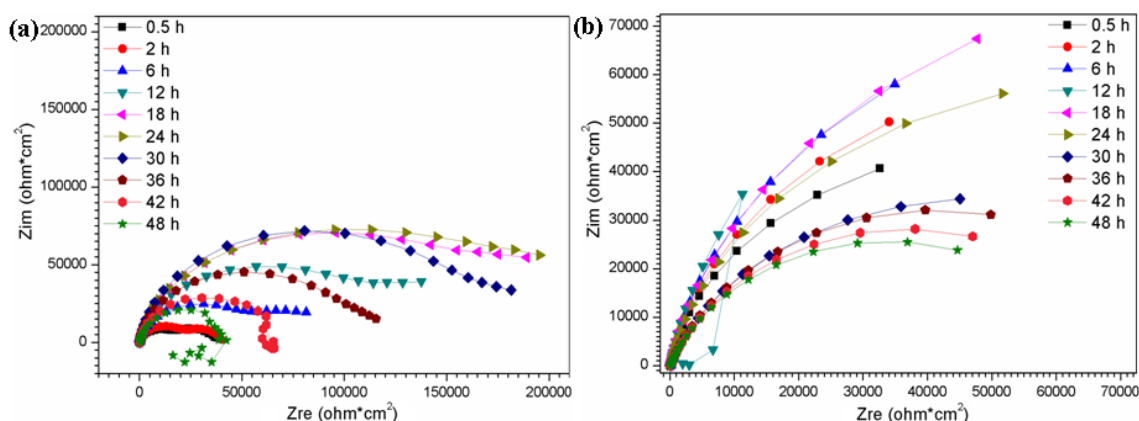


Fig. 1. Nyquist plots recorded on (a) permanganate and (b) chromate conversion coated AZ31B in 0.05 M NaCl and 0.1 M  $\text{Na}_2\text{SO}_4$  solution at various immersion times.

## References

1. K. Z. Chong, T. S. Shih, *Mater. Chem. Phys.*, **80**, 191 (2003).
2. M. Zhao, S. Wu, J. Luo, Y. Fukuda, H. Nakae, *Surf. Coat. Technol.*, **200**, 5407 (2006).
3. H. Zhang, G. C. Yao, S. L. Wang, Y. H. Liu, H. J. Luo, *Surf. Coat. Technol.*, **202**, 1825 (2008).
4. W. Zhou, D. Shan, E. H. Han, W. Ke, *Corros. Sci.*, **50**, 329 (2008).
5. C. S. Lin, C. Y. Lee, W. C. Li, Y. S. Chen, G. N. Fang, *J. Electrochem. Soc.*, **153**, B90 (2006).
6. Y.L. Lee, Y.R. Chu, W.C. Li, C.S. Lin, *Corros. Sci.*, **70**, 74 (2013).
7. S.Y. Jian, Y.R. Chu, C.S. Lin, *Corros. Sci.*, **93**, 301 (2015).

# Evaluation of the corrosion behaviour of epoxy coated carbon steel at the damaged zone in saturated $\text{Ca(OH)}_2$ with varying concentration of chloride ions by localized electrochemical impedance spectroscopy

T. Balusamy and T. Nishimura\*

*Materials Recycling Design Group, Research Center for Strategic Materials,  
National Institute for Materials Science, Ibaraki, Tsukuba, Japan*

e-mail:- [THANGARAJ.Balusamy@nims.go.jp](mailto:THANGARAJ.Balusamy@nims.go.jp)

## Abstract

Local electrochemical impedance spectroscopy (LEIS) provides a rapid and *in-situ* imaging of surface of corroding systems with high spatial resolution, which provide the relevant information pertaining to the corrosion mechanism of metals in a variety of environments. Recent years, micro-electrochemical systems were developed to probe the localized corrosion behavior of metals/alloys, which could enable real time assessment, and provide corroborative evidences to understand the local corrosion process [1]. The present study focuses on the localized corrosion process at the damaged zone of epoxy coated steel in saturated  $\text{Ca(OH)}_2$  with varying concentrations of chloride ions. The LEIS measurements were performed over the defect ( $\sim 500 \mu\text{m}$ ) on epoxy coated steel using 50 mV amplitude potential. The microprobe with a  $10 \mu\text{m}$  tip was set directly above the damaged zone to measure its typical impedance response. The distance between the tip of the microprobe and the sample surface is  $\sim 50\text{--}100 \mu\text{m}$ . For 3D scanning, the microprobe was stepped over a designated area (X-Y axis) of the electrode surface. The excitation frequency for impedance measurements was fixed at 10 Hz for the line scan and 3D mapping. The degradation of the damaged zone of the epoxy coated steel in saturated  $\text{Ca(OH)}_2$  with varying concentration of chloride ions is monitored by measuring the change in localized  $|Z|$  (Figs. 1 (a, b, c and d)). The typical 3D mapping of the damaged zone in saturated  $\text{Ca(OH)}_2$  with 0.05 % NaCl is shown in Fig. 1(d). The line profiles and 3D mapping clearly indicate the decrease in  $|Z|$  with an increase in concentration of chloride ions while broadening of the line profile near the damaged zone indicates the increase in the extent of degradation of the damaged zone of the coated steel with an increase of concentration of chloride ions.

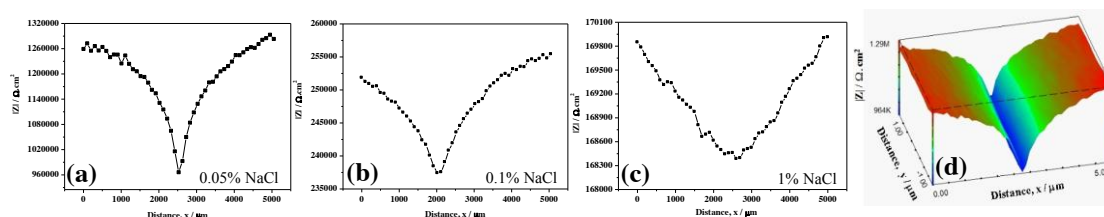


*Fig.1 LEIS line (a, b and c) and 3D profile (d) of the damaged zone of epoxy coated steel in Saturated  $\text{Ca(OH)}_2$  with varying concentration of chloride ions*

## Acknowledgement

The funding provided by NIMS in the form of postdoctoral fellowship can be gratefully acknowledged

## Reference

[1] V. M. W. Huang et al., *Electrochimica Acta*, 56 (2011) 8048.



## **Au Immersion on mid NiP Substrates – Balance between NiP Dissolution and Au -Adhesion properties**

Presenting author, B. Schafsteller,

Co Authors: M. Wuensche\*; S. Weissbrod, G. Vazhenin, C. Donner

*Atotech Germany GmbH; Berlin, Erasmusstrasse 20, 10553 Berlin  
constanze.donner@atotech.com*

The immersion Au deposition on NiP – layers is a key process for PCB manufacturing. It is mandatory that parallel to the Au deposition a Ni- dissolution occurs to ensure an electron balance. Concurrent cathodic side reactions inducing moreover Ni dissolution should be suppressed just as the copper dissolution of exposed copper areas in case of insufficient Nickel plating at through hole and interconnect PCB structures.

The Nickel dissolution itself is preferable an inhomogeneous process with a sufficient number of active grain size to ensure at one hand good adhesion of the Au layer but avoid on the other hand a deep crevice corrosion. This balance depends via complex forming agents onto the dissolution rate of Nickel. Hereby it must be thoroughly distinguished between the effect of quasistationary complex concentration within the electrolyte and temporarily available increase of complex concentration at the surface due to its release from the Au complexes. Electrochemical quartz micro balance measurements combined with XRF and FIB investigations reveal the importance of concentration gradients onto the PCB substrates in the different stages of the Au immersion process starting from the induction period, via the Au deposition onto NiP to the Au deposition onto Au. The role of copper as galvanic coupling element and its control is discussed in this context..



# Zinc anodizing at high voltage in alkaline media

D. Veys-Renaux<sup>1,\*</sup>, E. Rocca<sup>1</sup>, K. Guessoum<sup>2</sup>

<sup>1</sup> Institut Jean Lamour, Université de Lorraine – CNRS, Faculté des Sciences et Techniques, 54500 Vandoeuvre les Nancy, France.

<sup>2</sup> Université de Béjaia, Faculté de Technologie, 06000 Béjaia, Algeria.

\*delphine.veys-renaux@univ-lorraine.fr

Micro-arc oxidation constitutes an interesting “green” alternative process in the field of surface treatments of aluminum, magnesium and titanium for about twenty years. It consists in a high-voltage oxidation beyond the dielectric breakdown occurring at the interface metal/oxide/electrolyte. Due to the high temperature reached in the resulting plasma, the grown coatings are dry ceramic layers, exhibiting interesting corrosion and wear resistance. This process is generally performed in alkaline media containing additives favoring both the growth rate and the corrosion resistance of the coated materials such as aluminates and silicates. This original paper focuses on the study of micro-arc treatments performed on zinc [1], which could lengthen the service life of sacrificial anodes.

An electrochemical study during zinc anodizing process revealed that the formation of the first stable insulating layer necessary to reach the dielectric breakdown (and therefore to initiate the sparks) is in competition with the dissolution of zinc. Therefore, beyond a maximum value of pH, starting with the micro-arc regime is no more possible. On the other hand, the addition of silicates or aluminates to the reference electrolytic bath (KOH 0.05 M) facilitates the occurrence of the sparking initiation: around 200 V in KOH 0.05 M, around 150 V with aluminates additives (0.05 M), around 100 V with silicates additives (0.05 M).

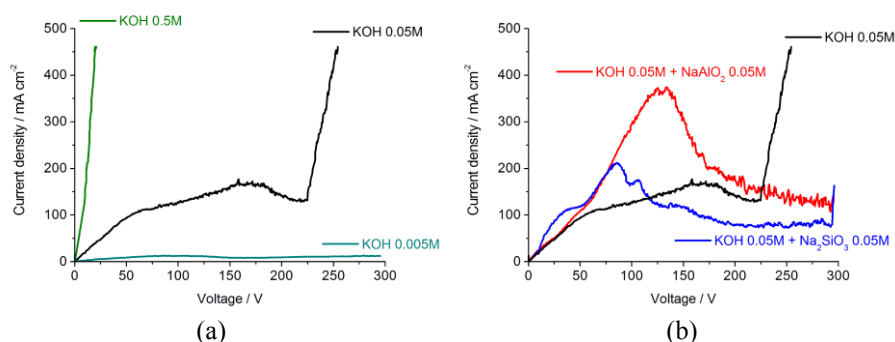


Fig.1: Potentiodynamic scans ( $15 \text{ V min}^{-1}$ ) performed on Zn in various alkaline media: effect of pH (a), effect of the presence of additives (b).

Post-treatment characterizations of the treated materials performed by FEG-SEM observations coupled with EDX analyses showed that the thickness, the morphology and the composition of the coatings highly depend on the anodizing voltage and the electrolytic bath composition.

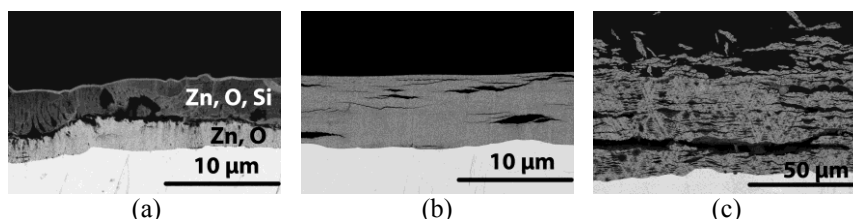


Fig.2: Cross-sections observed after 15 min of potentiostatic anodizing: at 50 V in KOH 0.05 M +  $\text{Na}_2\text{SiO}_3$  0.05 M (a); at 50 V in KOH 0.05 M (b); at 150 V in KOH 0.05 M (c).

In terms of corrosion resistance, open-circuit potential measurements, potentiodynamic polarizations and electrochemical impedance spectroscopy measurements were performed in NaCl 0.1 M and showed a very slight improvement of the performances of the treated materials regarding an untreated one since the obtained coatings are cracked and dusty.

# Fabrication of super-liquid-repellent aluminum mesh with chemical etching/anodizing

Katsutoshi Nakayama,<sup>a</sup> Etsushi Tsuji,<sup>a,b</sup> Yoshitaka Aoki,<sup>a,b</sup> and Hiroki Habazaki<sup>a,b</sup>

<sup>a</sup>Graduate School of Chemical Sciences and Engineering, Hokkaido University

<sup>b</sup>Division of Materials Chemistry & Frontier Chemistry Center, Faculty of Engineering, Hokkaido University

North 13, West 8, Kita-ku, Sapporo 060-8628, Japan

e-mail: k.nakayama@cse.hokudai.ac.jp

Controlling the wettability of solid surfaces is of considerable importance in daily life and in industries. In particular, superoleophobic surfaces, on which oil droplets, as well as water, can keep spherical shape and roll off easily, have attracted much attention because of their superior properties, including icephobicity, corrosion resistance and so on. The authors have been fabricated superoleophobic surfaces that repel even octane droplets (surface tension: 22 mN m<sup>-1</sup>) on aluminum plate with micro/nano-dual pore structure, which has been introduced by chemical etching, anodizing, pore widening and fluoroalkyl coating [1]. In this study, we have introduced additional roughness of the order of 100  $\mu$ m by using Al mesh instead of Al plate. We observed further improved superoleophobicity for low surface tension liquids. In addition, we also examined liquid separation property of the hierarchical aluminum mesh with different coating layers to control the wettability.

Commercial aluminum mesh was chemically etched in aqueous solutions containing 0.2 mol dm<sup>-3</sup> CuCl<sub>2</sub> and 1 mol dm<sup>-3</sup> HCl to form micrometer-size half-cubic pits uniformly. Then, the etched specimen was anodized in 0.3 mol dm<sup>-3</sup> H<sub>2</sub>SO<sub>4</sub> at a constant voltage of 25 V for 180 s at 15°C to form a nanoporous oxide film and immersed in 5 wt% H<sub>3</sub>PO<sub>4</sub> for 900 s at 30°C to expand the size of nanopores. Finally, the specimen surface was coated with mono-[2-(perfluorooctyl)methyl]phosphate (FAP) or tetradecyl phosphate (TDP) layers simply by immersing in 1 mmol dm<sup>-3</sup> FAP or TDP/ethanol solution for 2 days.

Figs.1a-d show SEM images of aluminum mesh surface chemically etched, anodized and pore-widened. The hierarchical triple-pore structure including large pores of mesh, half-cubic etch pits and nanopores can be observed. The respective pore sizes are about 150  $\mu$ m, 1-2  $\mu$ m and 40 nm. After FAP coating, the hierarchical surface showed superoleophobicity as shown in Fig. 2. The surface revealed super-liquid-repellency even for hexane droplet (surface tension: 18 mN m<sup>-1</sup>) with advancing contact angle of 158° and the contact angle hysteresis of 3°. Although the FAP-coated surface was oleophilic with a contact angle of hexane on the flat surface was only 30°, superoleophobicity was successfully obtained by the introduction of such hierarchical surface morphology.

After TDP alkyl phosphate coating instead of FAP fluoroalkyl phosphate coating, the hierarchical aluminum mesh was superhydrophobic/superoleophilic. This mesh used successfully as a membrane to separate cyclohexane/water or rapeseed oil/water mixtures almost completely with only the organic liquids penetrating through the mesh. This separation is that water was perfectly repelled and oil passed through the mesh. In addition, the hierarchical aluminum mesh without organic coating separated also these oil/water mixtures if the surface was pre-wetted with water. In this case, water passed through the mesh and oil was almost-totally repelled. The separation efficiencies of both surfaces were approximately 95%.

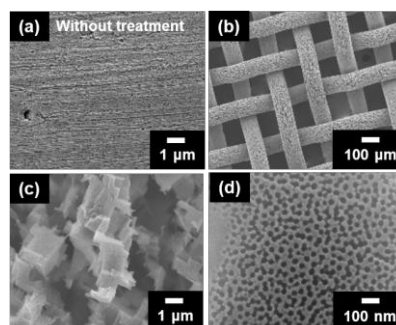


Fig. 1 SEM images of the aluminum mesh (a) without treatment and (b-d) chemically etched, anodized and pore-widened.



Fig. 2 Liquid droplets on the superoleophobic aluminum mesh surface: 1. rapeseed oil, 2. hexadecane, 3. dodecane, 4. acetone, 5. ethanol, 6. octane, 7. 2-propenol, 8. hexane.

## Reference

[1] K. Nakayama, E. Tsuji, Y. Aoki, and H. Habazaki, *RSC Adv.* 4(2014) 30927-30933.

# Corrosion of Indium Tin Oxide Films in SiO<sub>2</sub> Solutions

Leo Chau-Kuang Liao\* and Jia-Lin Jhan

Department of Chemical Engineering and Materials Science, Yuan Ze University, Chung-Li  
32003, Taoyang city, Taiwan

\*e-mail: lckliu@saturn.yzu.edu.tw

Indium tin oxide (ITO) films show transparent and conducting properties and have been widely used as substrates for optoelectronic devices. The stability of the ITO films, such as corrosion in solution environments, was studied to understand corrosion mechanisms. In this work, we investigated the corrosion of ITO films in SiO<sub>2</sub> solutions when voltage was applied to the ITO electrodes in different time treatments at room temperature. The ITO films were put in both the anode (positive) and cathode (negative) electrodes in 1wt% SiO<sub>2</sub> solutions with setting 15V to the electrochemical system. Results showed that SiO<sub>2</sub> particles moved to and deposited on the anode electrode, whereas, the color of the cathode electrode changed from transparent to black. The black area on the ITO demonstrated non-conductive film by the current-voltage test. The properties of the treated cathode electrodes were further analyzed using analytical instruments to study the phenomena. The XRD spectra shows that strong ITO peaks were demonstrated for the electrochemical treatment for 0 and 1 minutes as shown in Figure 1. However, the XRD spectrum reveals the prominent peaks of metal In appear significantly after the sample treatment for 30 minutes as shown in Figure 1. The disappearance of ITO and formation of In XRD peaks as functions of time were also observed according to the XRD data. The surface morphologies of the cathode samples were demonstrated using the SEM images as shown in Figure 2. Small amount of the particles on the ITO surface were formed for 1 minute treatment as shown in Figure 2(a). Moreover, the In particles grew from the reductive reaction of ITO were displayed in Figure 2(b). The reductive corrosion mechanism of ITO was revealed and discussed in this study.

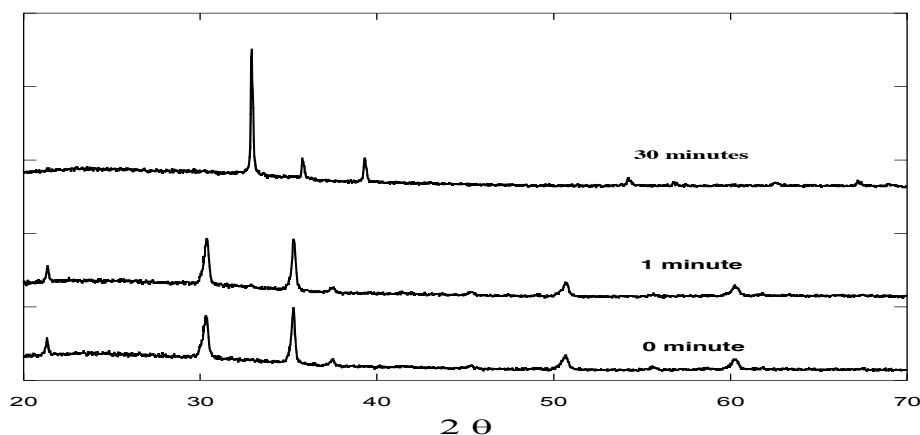


Figure 1. XRD spectra of the ITO corrosion samples for different time treatments.

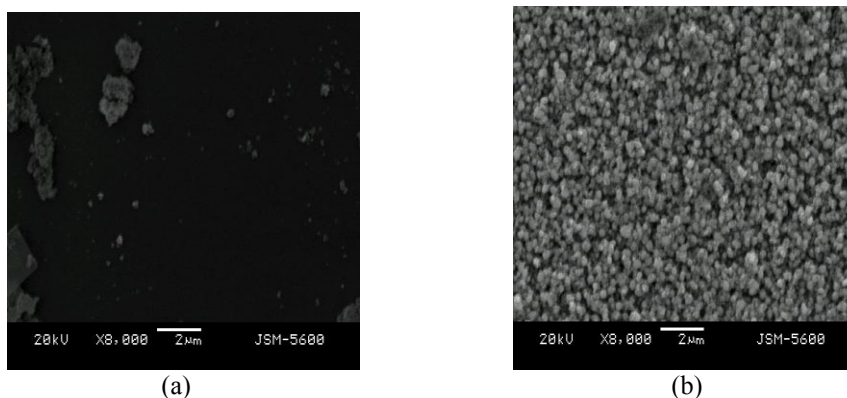


Figure 2. SEM images of the corrosion ITO films for (a) 1 minute and (2) 30 minutes

# Electrochemical Investigation on Passivation Characteristic of P110 Steel in Alkaline Solution

Chengqiang Ren, Ye Peng, Jiameng Li, Jingsi Hu, Bo Liu, Li Liu

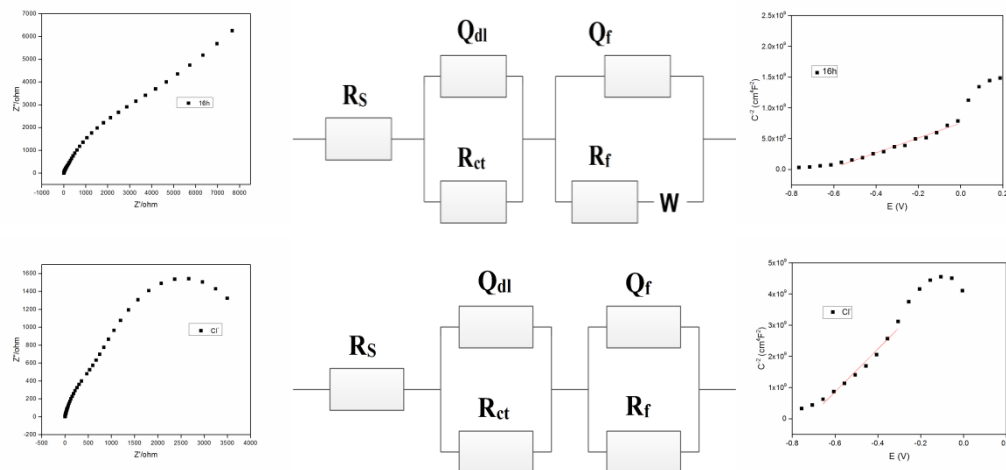
School of Materials Science and Engineering, Southwest Petroleum University

Chengdu, 610500, P. R. China

chengqiangren@163.com

In order to understand the formation and damage of passive film on the surface of casing steel caused by alkaline solution at hydration stage and aggressive ion at corrosion stage respectively in the oil well, experiments were operated in the simulated concrete pore solution. Electrochemical behaviors, including electrochemical impedance spectroscopy, potentiodynamic polarization and Mott-Schottky curve, were measured.

The stability passivation occurred after 16h immersion in the simulated concrete pore solution. The electrochemical impedance spectroscopy presented high frequency capacitive loop and low frequency Warburg impedance, and n-type semiconductor property was found. However,  $\text{Cl}^-$  destroyed passive film. As a result, passivation curve disappeared, and two capacitive loops were observed. The donor concentration in the film increased significantly.



## Acknowledgements

Financial supports by National Natural Science Foundation of China (51374180) and open fund (PLN1306) of State Key Laboratory of Oil and Gas Reservoir Geology and Exploitation (Southwest Petroleum University) are acknowledged.

## References

- [1] Sánchez M, Gregori J, Alonso C, Electrochemical impedance spectroscopy for studying passive layers on steel rebars immersed in alkaline solutions simulating concrete pores, *Electrochim. Acta* 52 (2007) 7634.
- [2] Fattah-Alhosseini A, Soltani F, Shirsalimi F, The semiconducting properties of passive films formed on AISI 316 L and AISI 321 stainless steels: A test of the point defect model (PDM), *Corros. Sci.* 53 (2011) 3186.
- [3] Feng X, Zuo Y, Tang Y, The degradation of passive film on carbon steel in concrete pore solution under compressive and tensile stresses, *Electrochim. Acta* 58 (2011) 258.

# Protection of Al93Mg7 Alloy against Corrosion in NaCl Containing Solutions Using Silane and Silane-Graphene Films

Mohammad BinSabt, Kamal Shalabi, Faizah M. Al-Kharafi, Ahmed Galal

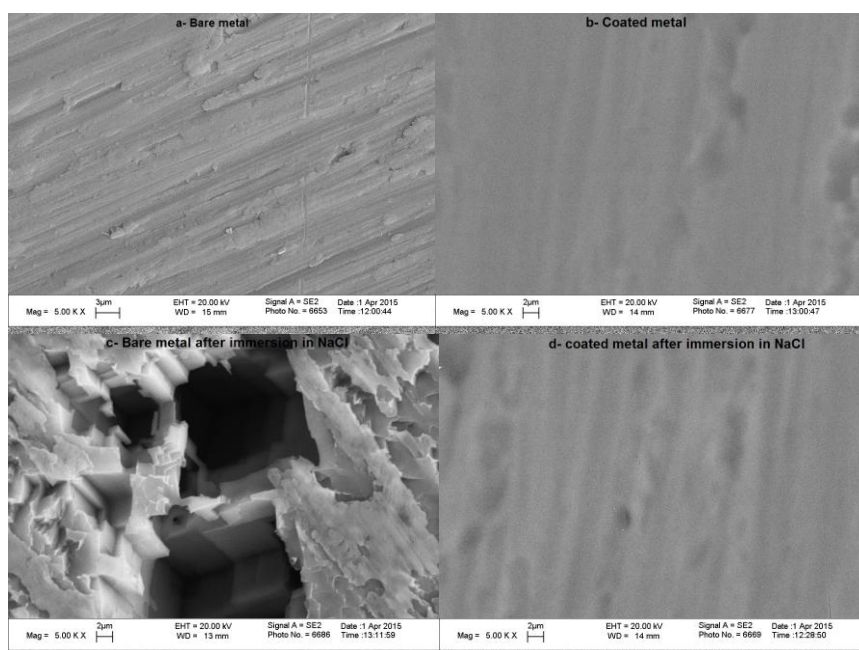
*Department of Chemistry, Faculty of Science, Kuwait University*

*P.O. Box 5969 Safat 13060, Kuwait*

[galal@sci.cu.edu.eg](mailto:galal@sci.cu.edu.eg), Tel: (+965)97580341, Fax: (+965)24816482

The corrosion protection of surface treated Al93Mg7 alloy in 3.5% NaCl containing aqueous electrolytes using films of 1,2-bis(triethoxysilyl)ethane and silane-graphene hybrids is studied. The electrochemical behavior of the alloy was studied using potentiodynamic polarization, electrochemical impedance spectroscopy (EIS) and the surface structure was investigated using scanning electron microscopy and energy-dispersive X-ray spectroscopy and X-ray photoelectron spectroscopy techniques. The surface coating was administered to the alloy by immersion of the chemically pretreated surface. A highly cross-linked film was developed of the silane film and the hydrated aluminium oxide layer.

Effect of immersion time in silane showed that optimum protection efficiency was achieved after 30 minutes. The silane film showed a high protection namely against pitting development. SEM images proved that pits develop only over unprotected surfaces. EIS data showed high protection efficiencies up to 168 hours of immersion in the chloride-containing solution. Graphene oxide was mixed with the silane solution with different ratios. The efficiency of protection increased in presence of graphene structures as the hydrophobicity of the surface increases. The surface was characterized using surface enhanced Raman spectroscopy (SERS).



SEM micrographs of Al93Mg7 surface (a, b) bare and silane coated Al93Mg7 before immersion in 3.5% NaCl, (c) bare Al93Mg7 after 24 h of immersion in 3.5% NaCl, (d) unscratched silane-coated Al93Mg7 after 24 h of immersion in 3.5% NaCl at 25°C.

Acknowledgement: The Support of Kuwait University is highly appreciated. Research facilities were provided through Research Sectors Projects GS01/01 and SC 02/13 of Kuwait University.

## Corrosion resistance of zinc diffusion layers on aluminium

M. Stepanova<sup>1,\*</sup>, O. Lunder<sup>1,2</sup>, J.H. Nordlien<sup>1,3</sup>, K. Nisancioglu<sup>1</sup>

<sup>1</sup> *Department of Materials Science and Engineering, Norwegian University of Science and Technology, NO-7491 Trondheim, Norway*

<sup>2</sup> *SINTEF Materials and Chemistry, NO-7465 Trondheim, Norway*

<sup>3</sup> *Sapa Precision Tubing, Precision Tubing Technology Centre, NO-4265 Håvik, Norway*

\* +47 73593970, mariia.stepanova@ntnu.no

Thin walled aluminium extruded tubes for heat exchangers are widely used by the automotive industry. More stringent lifetime requirements for the HVAC&R (Heat, Ventilation, Air Conditioning and Refrigeration) market necessitate improved corrosion resistance to pitting. This work investigates cathodic protection of aluminium surface modified by diffused zinc surface layer. 3000 type Al-Mn alloy multi-port extruded tubes were coated with zinc by thermal-arc spraying. The samples were afterwards heat treated at various temperatures and durations to obtain solid-state AlZn alloy diffusion layer at the surface. The Zn depth profiles obtained were characterized by glow discharge optical emission spectroscopy (GD-OES). Corrosion of the diffusion layers was subsequently determined by immersion in acidified artificial sea water solution at 25 °C, during which the open circuit potential change was recorded with respect to time. The samples were taken out at various times and their weight loss was measured. The surface microstructure and chemistry before and after corrosion were examined by scanning electron microscopy and energy-dispersive X-ray spectroscopy. Samples were also etched by argon sputtering to selected depths and subsequently characterized electrochemically. The Zn-rich layer is effective in cathodic protection against pitting. However, the layer is also susceptible to uniform self-corrosion. The well-known relationship between the corrosion potential of AlZn alloys and Zn concentration [1] was extended over a wider concentration range and related further to the corrosion rate in acidified synthetic seawater. The database thus developed is useful for optimizing the diffusion layer thickness and Zn concentration profile in the layer to minimize uniform corrosion, and therefore maximize service lifetime, without reducing the protection against pitting.

1. Stephen D. Cramer and Bernard S. Covino, Jr., ASM Handbook, Volume 13B - Corrosion: Materials, p. 96, ASM International, USA (2005).



# Electrochemical properties of $\eta$ -MgZn<sub>2</sub> phase in sulfuric acid : anodizing behavior at high potential

J. Tardelli, E. Rocca\*

*Institut Jean Lamour, Université de Lorraine – CNRS, Faculté des Sciences et Techniques, 54500  
Vandoeuvre les Nancy, France.*

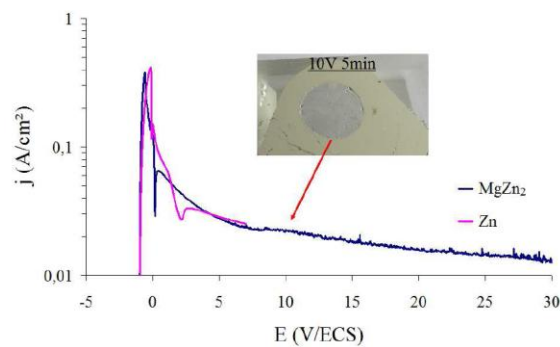
*\*emmanuel.rocce@univ-lorraine.fr*

The  $\eta$ -MgZn<sub>2</sub> phase is an important intermetallic phase present in some galvanized coatings on steel, but also is present as strengthening phase in many aluminum alloys belonging to the 7XXX series.

The objective of this work is to characterize the electrochemical behavior of MgZn<sub>2</sub> phase in the classical electrolyte of aluminum anodizing, H<sub>2</sub>SO<sub>4</sub> 2 M.

Firstly, bulk phase was synthesized by melting pure zinc and magnesium at 700 °C during 1 hour in a furnace under argon flux, then the sample was annealed at 400 °C during 12 hours.

As expected by the E-pH diagram of zinc and magnesium, the MgZn<sub>2</sub> phase undergoes a rapid dissolution in sulfuric acid medium at open-circuit potential. The surface analysis show a classical morphology of metallic dissolution.



Nevertheless, at the voltage of aluminium anodizing process, MgZn<sub>2</sub> phase reveal a passivation plateau, as shown in Fig. 1. The passive current density remains relatively high, around 20 mA cm<sup>-2</sup> at 10 V, but the dissolution rate of the phase is drastically reduced and we observe the formation of a thin layer of oxide on the surface.

SEM analysis and X-ray photoelectron spectroscopy allowed us to determine the overall composition of the oxide, Mg<sub>x</sub>Zn<sub>1-x</sub>O. The growth kinetic of oxide was characterized in function of voltage and anodizing time by in-situ electrochemical impedance spectroscopy measurements at high voltage. Moreover, these impedance measurements revealed the blocking behavior of the oxide layer at certain voltage and time.

# Passive Film Characterization on New Ternary Ti-Ta-Zr Alloy Surface

C. Vasilescu, S. I. Drob, S. Preda, J. M. Calderon Moreno, P. Osiceanu  
Institute of Physical Chemistry "Ilie Murgulescu" of Romanian Academy  
Spl. Independentei 202, 060031, Bucharest, Romania  
cora\_vasilescu@yahoo.com

The new Ti-15Ta-5Zr alloy was elaborated with the aim to be use as implant material; indeed, this alloy accomplishes the most necessary requirements: non-toxic elements, biphasic  $\alpha + \beta$ , stable, homogeneous microstructure (by optical, SEM and XRD techniques), a good hardness, proper mechanical properties and low Young's modulus of 42.2 GPa (from stress-strain curve)

The composition and thickness of the alloy passive film were determined by XPS from survey spectrum, high resolution spectra, respectively by sputter depth profile (Fig. 1). The alloy passive film contains  $\text{TiO}_2$  and  $\text{Ti}_2\text{O}_3$  oxides and very resistant  $\text{Ta}_2\text{O}_5$  and  $\text{ZrO}_2$  oxides with a thickness of  $8.5 \pm 1$  nm, being thicker than that of Ti and other implant alloys. By its content and thickness, this passive film confers a higher resistance to corrosion for the new Ti-15Ta-5Zr alloy.

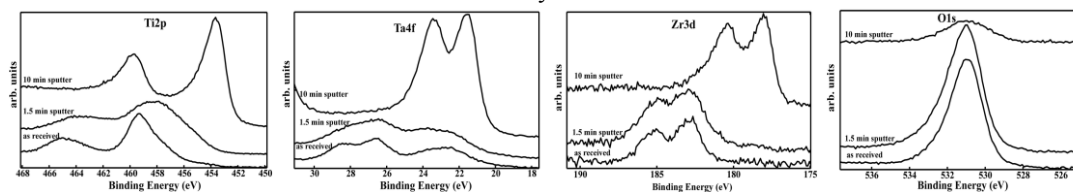


Fig. 1 High resolution spectra for the native passive film on Ti-15Ta-5Zr alloy surface

The interactions of the new alloy with Ringer solution of different pH values (3.54; 7.49; 8.98) simulating the severe functional conditions of an implant were studied by the potentiodynamic cyclic and linear polarization and electrochemical impedance spectroscopy (EIS) methods. Also, the open circuit potentials and corresponding potential gradients were monitored for 500 immersion hours in Ringer solution.

The electrochemical measurements (Fig. 2a) attested a noble behavior of Ti-15Ta-5Zr alloy in comparison with Ti: the shift of the corrosion and passivation potentials to more electropositive values, the decrease of the passive and corrosion current densities, a better tendency to passivation, a higher polarization resistance (about 10 times higher) and lower corrosion rate (about 50 times smaller). All these facts are due to the alloying elements Ta and Zr which stabilize and reinforce the alloy passive film.

The impedance Nyquist spectra (Fig. 2b) as open arches had bigger diameters and impedance values for the alloy than for Ti, describing a more insulating, thicker passive film. Bode impedance spectra (Fig. 2c) showed linear slopes and high impedance values which confirm the superior capacitive response of the alloy. Bode phase angle spectra (Fig. 2d) displayed two phase angle which suggest a passive film with two layers: the higher phase angle corresponds to the barrier, compact, inner layer and the lower phase angle indicates the porous, outer layer. An electric equivalent circuit with two time constants was fitted.

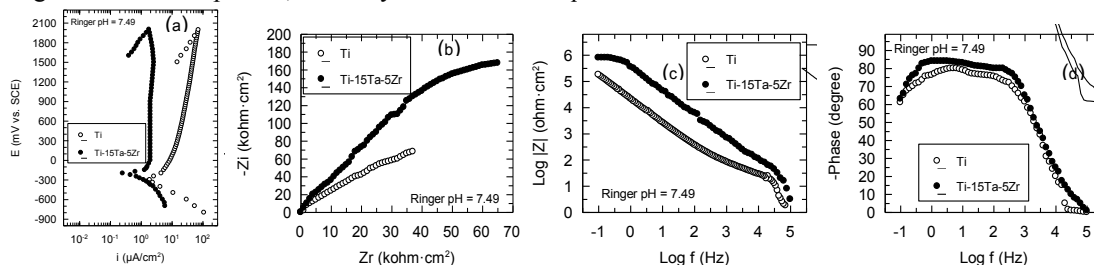


Fig. 2 Cyclic polarization curve (a), Nyquist (b), Bode impedance (c) and Bode phase angle (d) spectra for Ti-15Ta-5Zr alloy in Ringer solution of pH = 7.49

The alloy open circuit potentials increased in time, namely, the alloy passive film thickened over time, enhancing its resistance. Because the alloy open circuit potential gradients had very low values, it is not possible to appear galvanic or local corrosion on its surface, even for long term (500 h).



# A New Dental Alloy with Improved Properties: Its Corrosion Resistance in Various Conditions Simulating Oral Cavity Environment

S. I. Drob, C. Vasilescu, J. M. Calderon Moreno, P. Osiceanu  
Institute of Physical Chemistry "Ilie Murgulescu" of Romanian Academy  
Spl. Independentei 202, 060031, Bucharest, Romania  
sidrob@chimfiz.icf.ro

A new alloy with Co-Cr base containing resistant Nb and Zr elements (Co-Cr-Nb-Mo-Zr) was synthesized; this alloy has a homogeneous microstructure (by scanning electron microscopy, SEM), favorable mechanical properties and better corrosion resistance comparing with commercial Co-Cr base alloys. X-ray diffraction (XRD) method determined the constituent phases and energy dispersive X-ray spectrum (EDX) identified the quantity of the alloying elements.

X-ray photoelectron spectroscopy (XPS) analyzed the composition of the native passive film existing on the alloy surface; this comprises protective chromium and cobalt oxides and, in addition, very resistant niobium and zirconium oxides. It is expected that this passive layer to be more compact, more insulating, and more resistant than those on the surface of the similar alloys.

The corrosion resistance of Co-Cr-Nb-Mo-Zr alloy was studied in artificial Carter-Brugirard saliva of various pH values (2.54; 7.84; 9.11) and in saliva doped with 0.05M NaF (pH = 8.21) which reproduce the real conditions from the oral cavity. The normal pH is about 7.4; after a meal, the pH can reach 3 - 4 value and in the case of infections or inflammations, a value of about 8 - 9.

Three electrochemical methods were used: cyclic potentiodynamic polarization to estimate the main electrochemical parameters (corrosion -  $E_{\text{corr}}$  and passivation -  $E_p$  potentials, tendency to passivation -  $|E_{\text{corr}} - E_p|$ , and passive current density -  $i_p$ ); linear polarization method, by Tafel representations supplied the main corrosion parameters (corrosion current density -  $i_{\text{corr}}$ , corrosion rate -  $V_{\text{corr}}$ , polarization resistance -  $R_p$  and ion release rate); electrochemical impedance spectroscopy (EIS) that furnished Nyquist and Bode spectra and electrical parameters of the electric equivalent circuit describing the physical phenomena at the interface between alloy and artificial Carter-Brugirard saliva. The cyclic potentiodynamic curves evinced the alloy self-passivation characterized by the more favorable, more electropositive corrosion and passivation potentials, better tendency to passivation and lower passive current densities referring to the commercial Co-Cr alloy (Table 1). Corrosion current densities, corrosion rates and ion release rates had low values placed under the permitted limits ( $V_{\text{corr}}$  - limit of 0.25  $\mu\text{m/Y}$ ). Corrosion resistance had very high values, fact that denotes a very resistant passive film (Table 1).

Table 1. Main electrochemical and corrosion parameters for Co-Cr-Nb-Mo-Zr alloy in Carter-Brugirard saliva

Parameter	Saliva pH = 2.54		Saliva pH = 7.84		Saliva pH = 9.11		Saliva + 0.05M NaF pH = 8.21	
	Commercial alloy	New alloy	Commercial alloy	New alloy	Commercial alloy	New alloy	Commercial alloy	New alloy
$E_{\text{corr}}$ (mV)	-410	-380	-353	-270	-413	-370	-438	-406
$E_p$ (mV)	-200	-300	-250	-220	-200	-300	-200	-300
$ E_{\text{corr}} - E_p $ (mV)	212	80	153	50	213	70	238	106
$i_p$ ( $\mu\text{A}/\text{cm}^2$ )	3.9	3.5	1.8	1.6	3.7	3.5	4.5	4.2
$i_{\text{corr}}$ ( $\mu\text{A}/\text{cm}^2$ )	0.022	0.018	0.013	0.011	0.015	0.014	0.038	0.031
$V_{\text{corr}}$ ( $\mu\text{m/Y}$ )	0.249	0.14	0.148	0.0858	0.167	0.109	0.431	0.242
$R_p$ ( $\text{k}\Omega \cdot \text{cm}^2$ )	0.589	251.9	1.25	751.4	1.23	264.3	0.546	216.5
Ion release rate ( $\text{nm}/\text{cm}^2$ )	25.29	14.20	15.04	8.70	16.96	11.95	43.79	24.56

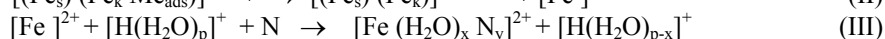
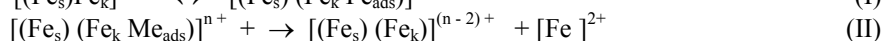
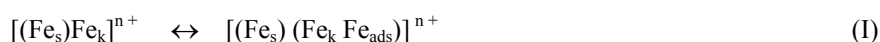
Electrochemical impedance spectroscopy indicated an insulating film depicted by high impedance and phase angle values, proving a more capacitive, resistant passive film on the alloy surface, comparing with the commercial Co-Cr alloys.

# Comparative analysis of the Anodic Dissolution of Iron at low and high over potentials

M.A. Pletnev

*Kalashnikov Izhevsk State Technical University, 7 Studencheskaya street  
426069 Izhevsk, Russia  
[pletnev@list.ru](mailto:pletnev@list.ru)*

Reaction of anodic dissolution of hydrophilic metals in the low-voltage surge follows:



When N – nucleophilic species dissolved in the electrolyte solution (anions or water molecules).

Crystal of iron is anodically polarized and has the charge ( $n^+$ ). The preceding stage represents the partial destruction of the crystal lattice with the formation of semi-crystalline state of  $\text{Fe}_k$ . The next stage is getting out of the metal atom from the kink and the transition into the adsorbed state  $\text{Fe}_{\text{ads}}(\text{I})$ . Speed limiting stage (an act of anodic depolarization of the iron as a cooperative electronic system with a force too low polarization of the Fermi level) is entering into the surface layer of electrolyte (interaction with water and other nucleophilic components of the electrolyte N) leaves the surface of the metal ion (II - III). The overvoltage of this process can be identified with the surge stage of the discharge-ionization.

In the acid solutions the binding energies are much larger and the O...O distances are shorter compared to pure water. Consequently, with increasing pH the activation energy of the iron ions hydration (III) to be reduced, while the dissolution rate to be increased. Such data were obtained in most articles.

Bandwidth limiting anodic current does not depend on pH, nature of the anion, but depends on the concentration of anions. To interpret the experimental data on the limiting currents of anodic dissolution a phenomenological approach is proposed based on the concept of soliton. Bandwidth limiting anodic current does not depend on pH, nature of the anion, but depends on the concentration of anions. To interpret the experimental data on the limiting currents of anodic dissolution proposed a phenomenological approach based on the concept of solitons as the dissolution of the concentration waves moving parallel to the flat surface of low index faces.

Comparative analysis of the anodic dissolution of iron at low and high potentials has showed that these processes have different mechanisms. Models anodic dissolution of iron interpreted in the light of the notion of co-operative nature of the electron subsystem of the metal. Assumed that the mechanism of anodic ionization of iron at low overvoltages is ions desorption from the surface, which requires "embed" it in the electrolyte layer near the electrode. To interpret the experimental data on the limiting currents of anodic dissolution a phenomenological approach is proposed based on the concept of solitons.

# Local Electrochemical Study on the Effect of Residual Stresses on Localized Corrosion Susceptibility of Type 316 Stainless Steels

Lin Niu, Xiaoping Han, Yu Liu, Weiwei Zhang, Rui Ma, Shuai Li, Tong Li  
*School of Chemistry and Chemical Engineering, Shandong University*  
*27 Shanda Nanlu, Jinan 250100, P.R. China.*  
*E-mail: lniu@sdu.edu.cn*

One of the major obstacles for accurately determining the corrosion resistance of metallic alloys is the lack of knowledges concerning the effect of correlative parameters (especially mechanical ones) on the initiation and propagation processes of localized corrosion [1]. Therefore, it is of great significance to pursue a deeper understanding of corrosion mechanisms of metals with the development of a multidisciplinary approach involving material, chemical, physical and mechanical sciences. To study the kinetics of heterogeneous electrochemical processes in localized corrosion, the local electrochemical probes with advantages of in-situ measurement and high spatial resolution have attracted apparent attentions [2].

In this work, the combinations of conventional electrochemical methods (e.g. potentiodynamic polarization curves) and local probe approaches based on local electrochemical measurements such as scanning electrochemical microscope (SECM) and scanning vibrating electrode technique (SVET) have been devoted to study at the micro-scale the correlation between surface residual stresses (especially the local stress gradients inside the tested area) and the electrochemical behavior and localized corrosion susceptibility of type 316 stainless steels in chloride-containing solution. The objective of the present study is to further clarify the “mechano-chemical interaction” in relevant ‘materials, mechanics and environments’ system, and to investigate the spatial distribution of the electrochemical reactions and finally determine the corrosion rate of the metal.

## References

- [1] V. Vignal, N. Mary, R. Oltra, J. Peultier, A mechanical-electrochemical approach for the determination of precursor sites for pitting corrosion at the microscale, *J. Electrochem. Soc.* 153(2006) B352-B357.
- [2] R. Oltra, Local electrochemical methods in corrosion research, in: R. Oltra, V. Maurice, R. Akid, P. Marcus (Eds.), *Local probe techniques for corrosion research*, CRC Press, New York, 2007, pp.1-11.

## Acknowledgements

This work is supported by the National Natural Science Foundation of China (No.51171094).

# Assessing and Predicting Concurrent Uniform Corrosion of Aluminum Alloys as a Function of pH, Temperature, Time, and [Cl<sup>-</sup>]

I-Wen Huang, Rudolph G. Buchheit  
*Fontana Corrosion Center, The Ohio State University*  
*2041 N. College Rd. Columbus, OH 43210*  
*huang.697@osu.edu*

High strength aluminum alloys are known to be particularly susceptible to localized corrosion induced by heterogeneous intermetallics, but the ability to quantitatively assess uniform corrosion along with pitting has become a major challenge for pit growth prediction. The pit depth measurement is shown to be affected by reference surface changing due to uniform corrosion as well as pit agglomeration. Therefore, the ability to measure pit depths and uniform corrosion simultaneously by profilometric methods to compensate for the reference surface recession has become a critical correction needed in aqueous conditions.

In this work, pitting corrosion and uniform dissolution of aluminum alloys 2024-T3, 7075-T6 and 6061-T6 were characterized quantitatively using optical profilometry (OP) after free corrosion exposures in 0.01 to 1.0 M NaCl solutions as a function of pH, temperature and exposure time. Uniform dissolution was estimated by carefully measuring the step height between the masked surface and the exposed surface along with pitting information. Results showing that a temperature and pH has a complex impact on Al alloy corrosion behavior. Under neutral and alkaline conditions, the corrosion rate of all three alloys at 80°C had the lowest corrosion rate, appearing to be related to the fact that slowed oxygen reduction reaction. This result is supported by the electrochemical experiment where cathodic limiting current was slowed by the reduced oxygen solubility at elevated temperature. Electrochemical impedance spectroscopy (EIS) result also showed elevated polarization resistance at high temperature from  $10^4$  to  $10^9$  (ohm·cm<sup>2</sup>). It was also found that a passive film formation and breakdown intermittently during a long term immersion, which was not observable in short term electrochemical tests, protecting the surface in high temperature conditions. Corrosion product and passive film analysis was performed by energy-dispersive X-ray spectroscopy (EDS) and electron diffraction. Samples prepared by focused ion beam (FIB) were examined to identify the composition and microstructure of corrosion product in both low and high temperatures. Moreover, a statistical corrosion model was established according to all measurement acquired through immersion tests. In general, Al alloy 6061 has slower uniform corrosion rate than 2024 and 7075. In order to validate the proposed pit morphology influenced by uniform corrosion, long term sample immersion and B117 salt spray chamber tests were also employed. Maximum pit depth was carefully found and a detailed profile scan was conducted by OP. This pit profile obtained unveils the altering pit geometry with uniform corrosion.

In addition, artificial neural network (ANN) modeling was utilized as a powerful statistic tool to recognize corrosion pattern in different environment and being able to generate predictions based on the input data. A successful prediction of uniform corrosion was given with linear regression value approximately 0.94 for AA2024 and AA7075 alloys. Aforementioned uniform corrosion modification to pit depth was found to be phenomenal in certain environmental conditions. In this poster, details of the experimental method and the results will be presented and the implication of these results on corrosion damage accumulation modeling will be addressed.

# Influence of Crevice Thickness to Corrosion Behavior of API X80 Steel under Disbonded Coating in Acid Soil Environment

Bo Zhao, Zhiyong Liu, Cuiwei Du, Xiaogang Li, Binan Shou, Tong Xu  
China Special Equipment Inspection And Research Institute  
2 Building, Xiyuan, Hepingjie, Chaoyang District Beijing, P.R. China  
Zhaobo19840626@163.com

In this work, an experimental device of disbonded coating model in yingtian soil simulation was prepared, and the corrosion behavior of X80 steel in it was studied by anodic polarization curves, electrochemical impedance spectroscopy (EIS) and scanning electron microscope (SEM). As the results showed, anode region of X80 steel would appear “passivation” behavior when the crevice thickness was about 35  $\mu\text{m}$ , but the anodic current density increased and anode active dissolution tendency enhanced with the crevice thickness becoming larger.

According to the result of EIS, the inductive loop appeared in low frequency area, which indicated that adsorption reaction appeared on electrode surface. The fitting equivalent circuit showed that the solution resistance ( $R_s$ ) of electrode reaction decreased monotonously with crevice thickness becoming larger, and the charge transfer resistance ( $R_{ct}$ ) achieved the minimum and maximum values at the thickness were 150  $\mu\text{m}$  and 400  $\mu\text{m}$  after its early decreasing rapidly.

The microstructure showed that, the corrosion product present the structure of regular sheets on X80 steel surface, but it disappeared and due to porosity with the thickness becoming larger. After removal corrosion product, it could be found that the corrosion of the sample surface was the most serious in the crevice thickness of 100 $\mu\text{m}$ , and the pitting appeared at this situation.

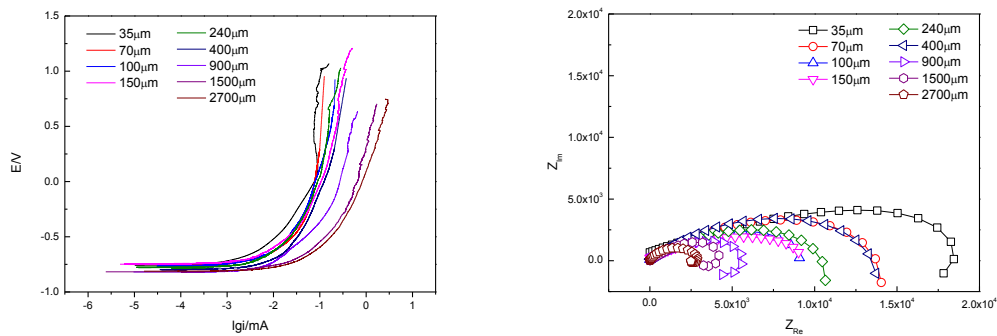


Fig1. X80 steel with different disbonded crevice thickness of (a)potentiodynamic polarization, (b)EIS .

# Electrochemical Performance of Oxygen Evolving Anodes in Sulphate Electrolyte for Copper Electrowinning

Wenting Xu<sup>1</sup>, Geir Martin Haarberg<sup>1</sup>, Svein Sunde<sup>1</sup>

<sup>1</sup>Department of Materials Science and Engineering, Norwegian University of Science and Technology  
NO-7491 Trondheim, Norway  
wenting.xu@ntnu.no

In industrial copper electrowinning, the oxygen evolution reaction (OER) is the main anode reaction. Compared with conventional lead-based anodes, dimensionally stable anodes (DSA) can decrease the OER overpotential and increase the energy efficiency during electrolysis since DSA have high catalytic activity and stability against corrosion. Application of DSA offers a commercially viable and environmentally friendly alternative in copper electrowinning [1].

Many researchers have studied the characteristics of DSA in order to find the most suitable DSA for oxygen evolution in copper sulphate electrolyte [2]. In addition, electrochemical stability in sulphate electrolytes, mechanical stability and structural integrity are also essentially required for those anodes in copper electrowinning. In this paper, industrial DSAs consisting of mixed metal oxide coatings on titanium including tantalum oxide ( $\text{Ta}_2\text{O}_5$ ), iridium oxide ( $\text{IrO}_2$ ), and ruthenium oxide ( $\text{RuO}_2$ ) were investigated in sulphate electrolyte at 60 °C in the context of copper electrowinning. X-ray diffraction (XRD) and scanning electron microscopy (SEM) were employed to examine the crystal structure, composition of the catalytic layer and its surface morphology. The electrochemical properties of the different catalytic layer were studied by cyclic voltammetry (CV), as shown in Fig.1. The behaviour of surface charges for these different coatings have been evaluated by CV tests under varying scan rates. Overvoltage of oxygen evolution for each DSA has been determined by steady state polarization analysis, as shown in Fig.2. The paper will relate the influence of composition on performance and durability of these DSA electrodes under industrially relevant operating conditions.

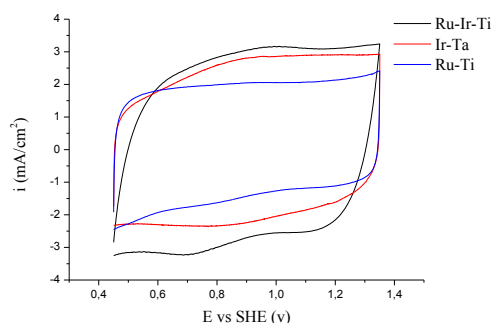


Fig.1. Cyclic voltammetry of three anodes scanned at 50 mV/s at 60 °C in copper sulphate electrolyte (1.2 mol/L  $\text{Cu}^{2+}$  and 1.8 mol/L  $\text{H}^+$ )

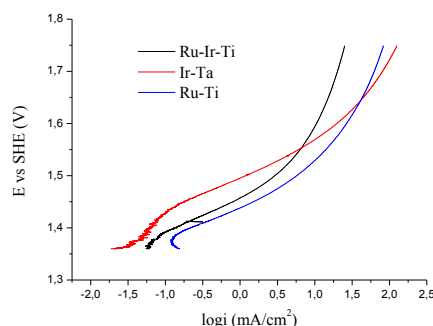


Fig.2. Polarization curves for oxygen evolution reaction on three anodes

## Reference

- [1] S. Trasatti, Electrocatalysis: understanding the success of DSA, *Electrochimica Acta*, 2000, **45**, 2377-2385.
- [2] F. Moradi and C. Dehghanian, Addition of  $\text{IrO}_2$  to  $\text{RuO}_2+\text{TiO}_2$  coated anodes and its effect on electrochemical performance of anodes in acid media, *Progress in Natural Science: Materials International*, 2014, **24**, 134-141.

# Earth Abundant Iron Diselenide Nanorod Arrays as the Flexible Electro-Catalytic Counter Electrode for Dye-Sensitized Solar Cells

Chun-Ting Li<sup>1</sup>; Chuan-Pei Lee<sup>1</sup>; I-Ting Chiu<sup>1</sup>; Kuo-Chuan Ho<sup>1,2\*</sup>

<sup>1</sup>Department of Chemical Engineering, National Taiwan University, Taipei 10617, Taiwan

<sup>2</sup>Institute of Polymer Science and Engineering, National Taiwan University, Taipei 10617, Taiwan

\*E-mail: [kcho@ntu.edu.tw](mailto:kcho@ntu.edu.tw)

Recently, transition metal compounds have been successfully reported as the electro-catalytic counter electrodes (CE) in dye-sensitized solar cells (DSSCs). Generally, transition metal compounds provide good electro-catalytic ability, high conductivity, large effective surface area, and good stability for the regeneration of the redox species (*e.g.*,  $\text{I}^-/\text{I}_3^-$ ); therefore, they show a great potential to replace the traditional noble metal, platinum (Pt). Among those transition metal compounds,  $\text{FeSe}_2$  film was reported as an earth abundant, a highly electro-catalytic, and a thermodynamically stable material toward the reduction of  $\text{I}^-/\text{I}_3^-$ . However, the reported  $\text{FeSe}_2$  film often lacks of low-dimensional structures, and thus the fill factor (*FF*) of pertinent DSSC was limited.

In this study, we aim to synthesize a  $\text{FeSe}_2$  nanorod array on a flexible Fe foil via a simple anodization method followed by a post-selenization thermal treatment. From the X-ray diffraction pattern (XRD) analysis, the  $\text{FeSe}_2$  nanorod array shows a ferroselite  $\text{FeSe}_2$  crystalline with the orthorhombic structure (JCPDS No. 65-2570). From field-emission scanning electron microscopy (FE-SEM) image shown in Fig. 1(a), it is observed that the  $\text{FeSe}_2$  nanorod array was growth perpendicularly onto the Fe foil, and they possessed a one-dimensional (1D) structure with an average diameter about 100 nm and an average length about 1  $\mu\text{m}$ . This 1D  $\text{FeSe}_2$  nanorod array was believed to benefit the electron transport capability of a CE, resulting better electro-catalytic ability and the cell efficiency. From the cyclic voltammetry (CV) analysis, the cathodic peak current density of  $\text{FeSe}_2$  nanorod array shows a value of  $1.12 \text{ mA cm}^{-2}$ , which is very close to that of the Pt film ( $1.43 \text{ mA cm}^{-2}$ ); therefore, the  $\text{FeSe}_2$  nanorod array was considered to have the comparable electro-catalytic ability to that of Pt. In Fig. 1(b), the photocurrent density–voltage curves of the DSSCs with Pt and  $\text{FeSe}_2$  nanorod array films as the CEs gave cell efficiencies ( $\eta$ ) of 7.80% and 7.59%, respectively. It can be said that the obtained  $\text{FeSe}_2$  nanorod array is a highly potential electro-catalytic material to replace Pt.

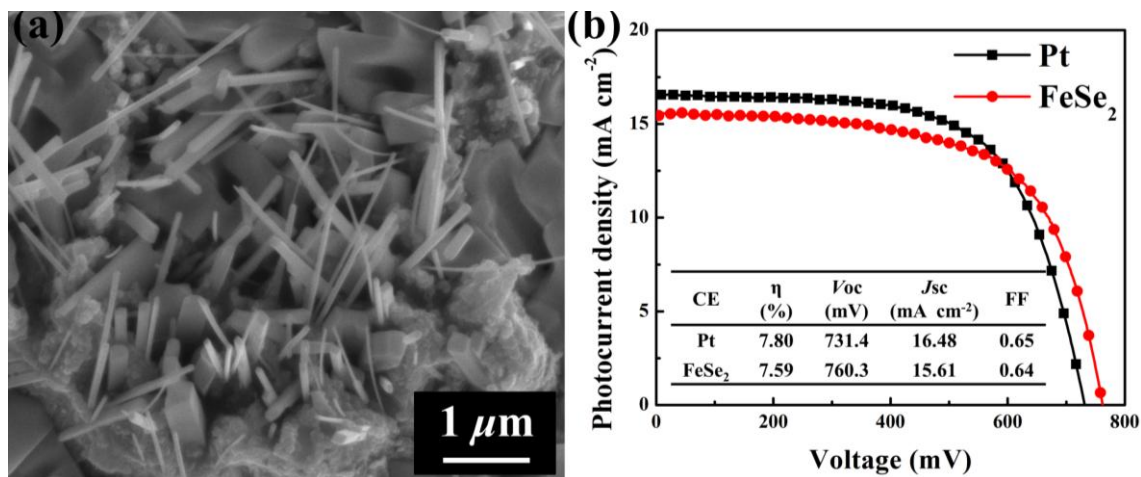


Fig. 1 (a) FE-SEM image of  $\text{FeSe}_2$  nanorods and (b) photocurrent density–voltage curves of the DSSCs with Pt and  $\text{FeSe}_2$  films as the CEs.

# Investigation of the Structure of Fe–N–C Complexes for Oxygen Reduction Reactions

Dangsheng Su

*Shenyang National Laboratory for Materials Science, Institute of Metal Research,  
Chinese Academy of Science,  
Wenhua Road 72, Shenyang 110016, China  
dssu@imr.ac.cn*

Searching for non-precious metal-based catalyst is an important research topic for a realistic application of fuel cell technology. Transition metal-based compounds or even metal-free catalysts have been reported to be active in oxygen reduction reactions (ORR). The performance of such non-precious metal catalysts still needs further optimization for replacing Pt-based catalysts.

In acidic medium, Fe/N co-modified carbon electrocatalysts have attracted great attention due to their high activity and stability in oxygen reduction reaction (ORR). Compared to iron-free N-doped carbon electrocatalysts, Fe/N-modified electrocatalysts show four-electron selectivity with better activity. This is believed relevant to the unique Fe–N complexes. However, the Fe–N structure remains an issue of discussion. We used *o,m,p*-phenylenediamine as nitrogen precursors to tailor the Fe–N structures in heterogeneous electrocatalysts which contain FeS and Fe<sub>3</sub>C phases. The electro- catalysts have been operated for 5000 cycles with a small 39 mV shift in half-wave potential. By combining advanced electron microscopy and Mossbauer spectroscopy, we have identified the electrocatalytically active Fe–N<sub>6</sub> complexes (FeN<sub>6</sub>, [Fe<sup>III</sup> (porphyrin)(pyridine)<sub>2</sub>]). The identification of the FeN<sub>6</sub> structure as a possible active site for ORR will pave the way towards new advanced Fe–N based electrocatalysts.

In alkaline medium, it is reported that both metal-free (for instance, N-doped carbon) and non-precious metal-based catalysts (for instance transition metals) are active in ORR. We are making a systematic study on what really catalyzes ORR in nitrogen-doped nanocarbon and Fe/N/C electrocatalysts. The new findings will be presented in this talk.

## References:

- Yansong Zhu, Bingsen Zhang, Xin Liu, Da-Wei Wang, and Dangsheng Su, *Angew. Chem. Int. Ed.* 2014, 53, 10673  
Yansong Zhu, Bingsen Zhang, Zhenbao Feng, and Dangsheng Su, *Catalysis Today*, accepted  
Yansong Zhu, Bingsen Zhang, Dangsheng Su, submitted



# Nitride-Stabilized Tungsten Carbide Electrocatalysts for Hydrogen Evolution Reaction

Wei-Fu Chen, Kotaro Sasaki, Jonathan M. Schneider, Chiu-Hui Wang, James T. Muckerman, Etsuko Fujita

Chemistry Department, Brookhaven National Laboratory  
PO Box 5000 Upton, NY 11973-5000 USA  
wfchen@bnl.gov

Alternative materials to platinum-based catalysts are required to sustainably produce hydrogen from water at low overpotentials. Progress has been made in utilizing tungsten carbide-based catalysts, however, their performance is currently limited by the density and reactivity of active sites, and insufficient stability in acidic electrolytes. Inspiration for designing such a material can be found in hydrotreating catalysts.<sup>[1]</sup> Molybdenum carbides and tungsten carbides have been investigated most extensively as catalysts or catalyst supports for the HER.<sup>[2]</sup> To make carbides better HER catalysts, nanostructuring the surface to increase the number of reactive facets is an effective approach. The catalytic activity of metal carbides can be further modified by the incorporation of nitrogen. We have reported that the incorporation of nitrogen in a NiMo alloy enhances its corrosion resistance.<sup>[3]</sup> Interestingly, pyrolysis of nitrogen-rich polydiaminopyridine and  $\text{H}_2\text{WO}_4$  in the presence of Fe can produce the nitride-rich WC-WN nanocomposite,<sup>[4]</sup> however its HER activity was limited by the nitride-rich surface.

In this study, attempts to synthesize graphene-supported tungsten carbide and nitride nanocomposites by using aniline as the reactive nitrogen source lead to the formation of an active, durable electrocatalyst (Fig. 1) for the HER in acidic environments.<sup>[5]</sup> By using in situ solid-state approach, we have successfully prepared  $\text{W}_2\text{C}$ -WN nanocomposites on graphene nanoplatelets without using gaseous carbon or nitrogen sources. Incorporation of the  $\text{W}_2\text{C}$ -WN nanoparticles on GnP brings about a significant enhancement in the HER kinetics (Fig. 2), and faster electron transport due to the remarkable reduction in charge transfer resistance. The optimum carbonitriding and unique  $\text{W}_2\text{C}$ /WN nanostructures evidenced by HRTEM, XRD, X-ray absorption spectroscopy as well as electrochemical behavior will be discussed at the meeting.

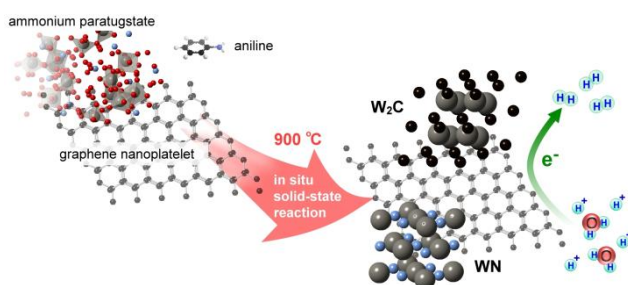


**Fig. 1** The synthesis of graphene nanoplatelet-supported  $\text{W}_2\text{C}$  and WN nanoparticles from ammonium paratungstate, aniline and graphene nanoplatelets. Dark grey balls: W, blue balls: N, black balls: C, and red balls: oxygen.

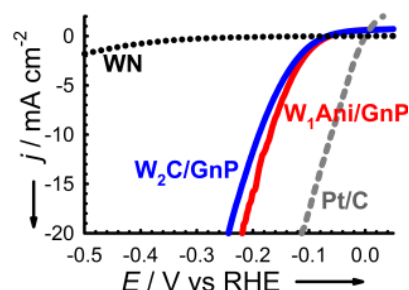


**Fig. 2** The polarization curves of  $\text{W}_2\text{C}$ /GnP ( $2.2 \text{ mg cm}^{-2}$  of  $\text{W}_2\text{C}$ ),  $\text{W}_1\text{Ani/GnP}$ , commercial WN ( $2.2 \text{ mg cm}^{-2}$  of WN) and Pt/C ( $2 \text{ mg Pt cm}^{-2}$ ) catalysts. blue balls: N, black balls: C, and red balls: oxygen.

## Reference:

- [1] W.-F. Chen, J. T. Muckerman, E. Fujita, *Chem. Commun.* **2013**, 49, 8896-8909
- [2] (a) Y. Liu, T. G. Kelly, J. G. Chen, W. E. Mustain, *ACS Catal.* **2013**, 3, 1184-1194. (b) R. Michalsky, Y.-J. Zhang, A. A. Peterson, *ACS Catal.* **2014**, 4, 1274-1278
- [3] W.-F. Chen, K. Sasaki, C. Ma, A. I. Frenkel, N. Marinkovic, J. T. Muckerman, Y. Zhu, R. R. Adzic, *Angew. Chem. Int. Ed.* **2012**, 51, 6131-6135.
- [4] Y. Zhao, K. Kamiya, K. Hashimoto, S. Nakanishi, *Angew. Chem. Int. Ed.* **2013**, 52, 13638-13641.
- [5] W.F. Chen, J. M. Schneider, K. Sasaki, C.-H. Wang, J. Schneider, S. Iyer, S. Iyer, Y. Chu, J. T. Muckerman, E. Fujita, *ChemSusChem*, **2014**, 7, 2414-2418.

# Gold-promoted structurally ordered intermetallic palladium cobalt nanoparticles for the oxygen reduction reaction

Kotaro Sasaki<sup>1</sup>, Kurian A. Kuttiyiel<sup>1</sup>, Dong Su<sup>2</sup>, Lijun Wu<sup>3</sup>, Yimei Zhu<sup>3</sup>, Radoslav R. Adzic<sup>1</sup>  
<sup>1</sup>Chemistry Department, <sup>2</sup>Center for Functional Nanomaterials, <sup>3</sup>Department of Condensed Matter  
Physics and Materials Science, Brookhaven National Laboratory, Upton, New York 11973, USA.  
ksasaki@bnl.gov

The search for new materials for the oxygen reduction reaction (ORR) has been challenging since the ORR is a sluggish reaction and requires high Pt content; this drawback still hampers the large scale applications of electrochemical conversion and storage devices, such as fuel cells, Li-air batteries, and electrolyzers. Key strategies to reduce Pt contents involve alloying Pt with other transition metals<sup>1</sup>, de-alloying non-precious metals to obtain a Pt rich shell<sup>2</sup> and core-shell-structured nanoparticles<sup>3</sup>. These approaches, to some degree, increase Pt utilization, but cannot fully solve the problem of Pt dependence. On the other hand, the study of ORR on Pd-based catalysts has received less attention than on Pt due to the lower activity and stability of the former<sup>4</sup>. Previous studies have mainly been pursued on the Pd alloy catalysts with various shapes and structures, and little experimental studies have been focused on structurally ordered intermetallic Pd-based nanocatalysts. However, using certain material composition and structure, ordered intermetallic phases can be obtained at nanometre ranges.

In the present paper, we address this challenge by demonstrating a simple method to synthesize core-shell-structured PdCo nanoparticles that can be further transformed into ordered intermetallic phases by addition of Au atoms and subsequent annealing<sup>5</sup>. The discovery of unusual ordering of PdCo atoms ( $3\times$  (times) and  $2\times$ ) along the [111] direction in the AuPdCo nanoparticles with twin boundaries and with stable {111}, {110} and {100} facets is revealed using high-resolution transmission electron microscope (HRTEM) and scanning transmission electron microscope (STEM) coupled with electron energy-loss spectroscopy (EELS) and electron diffraction patterns (EDPs). To our knowledge, no prior evidence of such intermetallic phases in nanoparticles of PdCo alloy has been reported. These structurally ordered intermetallic AuPdCo nanoparticles tend to behave similar to Pt catalyst for ORR, but more interestingly have much better stability than Pt in alkaline media. Furthermore, microscopic analyses of the catalyst show that atomic ordering of the nanoparticles can significantly affect the catalytic activity. The increased activity and durability of the catalyst is accredited to multiple facets and the structural ordering observed in the nanoparticles. We have established a simple and cost effective methodology to synthesize structurally ordered intermetallic PdCo nanoparticles, and it is believed that this approach may offer numerous possibilities in tailoring other transition metal intermetallics for various energy conversion and storage applications.

## Acknowledgements:

This research was performed at Brookhaven National laboratory under contract DE-AC02-98CH10886 with the US Department of Energy, Office of Basic Energy Science, Material Science and Engineering Division, Division of Chemical Sciences, Geosciences and Biosciences Division. Beamlines X18A at the NSLS are supported in part by the Synchrotron Catalysis Consortium, US Department of Energy Grant No DE-FG02-05ER15688.

## References:

1. V.R. Stamenkovic, M. Arenz K. J. J. Mayrhofer, C. A. Lucas, G. Wang, P. N. Ross, N. M. Markovic, *Nat. Mater.* 6, 241–247 (2007).
2. M. Oezaslan, M. Heggen, P. Strasser, *J. Am. Chem. Soc.* 134, 514–524 (2012).
3. K. Sasaki, H. Naohara, Y. Cai, Y. Choi, P. Liu, M.B. Vukmirovic, J.X. Wang, R.R. Adzic, *Angew. Chem. Int. Ed.* 49, 8602–8607(2010).
4. M. Shao, *J. Power Sources* 196, 2433–2444 (2011).
5. K. A. Kuttiyiel, K. Sasaki, D. Su, L. Wu, Y. Zhu, R.R. Adzic, *Nat. Commun.*, 5 (2014) 5185, DOI: 10.1038/ncomms6185.

# O<sub>2</sub> Reduction at Graphite Electrodes Modified with MN4 Macrocyclic Complexes and Pyridine Grafted Carbon Nanotubes

Federico Tasca<sup>a,\*</sup>, Javier Recio<sup>b,c</sup>, José H. Zagal<sup>a</sup>, Nataly Silva<sup>a</sup>, Carmen Castro<sup>a</sup>, Cesar Zúñiga<sup>a</sup>, María Paz Oyarzun<sup>a</sup>

<sup>a</sup>*Department of Chemistry of Materials, Faculty of Chemistry and Biology, University of Santiago of Chile, Santiago, Chile.*

<sup>b</sup>*Department of Inorganic Chemistry, Faculty of Chemistry, Catholic University of Chile, Santiago, Chile.*

<sup>c</sup>*Center of nanotechnology and advanced materials, CIEN-UC, Catholic University of Chile, Santiago, Chile.*

\**Federico.tasca@usach.cl.*

Metallophthalocyanines and metalloporphyrins are well known electrocatalysts for the reduction of O<sub>2</sub> (ORR) and have been extensively investigated with the aim of a better understanding of the ORR at modified electrodes and with the final scope of replacing Pt in fuel cells. Inorganic catalysts mimicking the structure of active redox centers of redox enzymes are taking place. For example Cho et al. reported higher electrocatalytic activity than Pt/C catalyst for a Fe-phthalocyanine with an axial ligand anchored on single walled carbon nanotubes that mimics the active site of *cytochrome c* oxidase [1]. Fundamental studies of MN macrocyclic complexes adsorbed on carbon nanotubes (CNTs) and on pyridine modified CNTs as catalysts for the ORR are missing. Preliminary studies in basic media show that when MN macrocyclic complexes are adsorbed at CNTs (single walled and double walled) modified electrodes an increment of almost two orders of magnitude of catalytic activity expressed as log *i* at constant potential is observed [2,3]. The reaction mechanism deduced from Tafel slopes analysis appears to be the same among the MN4 complexes adsorbed and non-adsorbed on CNT, suggesting that the CNTs support does not interfere with the reaction mechanism. An increased electroactive area and therefore an increased amount of active sites and an increment of the formal potential of the catalyst seem to be the cause of this increment. The results show the same volcano trend reported before where the activity increases as the formal potential of the metal catalyst redox center is shifted to more positive values [4]. When CNTs are modified with 4-aminopyridine aryl diazonium salts and then with axially ligated phthalocyanines even higher activities are observed but volcano correlations are distorted by the effect of the axial ligand.

## Acknowledgements.

This work was funded by Fondecyt Projects 11130167, 1140199, 3130538 and 3150271. M.P.O is grateful to a Conicyt doctoral fellowship.

## References

- [1] R. Cao, R. Thapa, H. Kim, X. Xu, M.G. Kim, Q. Li, N. Park, M. Liu, J. Cho, *Nat. Commun.*, 4 (2013) 33071.
- [2] C.A. Gutiérrez, J.F. Silva, F.J. Recio, S. Griveau, F. Bedioui, C. Caro, J.H. Zagal. *Electrocatalysis* 5 (2014) 3
- [3] J. H. Zagal, S. Griveau, J. Silva, T. Nyokong, F. Bedioui, *Coord.Chem. Revs* 254 (2010) 2755.
- [4] J.H. Zagal, F.J. Recio, C.A. Gutiérrez, C. Zúñiga, M.A. Páez, C. Caro. *Electrochemistry Communications*. 41 (2014) 24.

# On The Effects of Bromide Adsorption on the Rates of Redox Reactions

Adriel J.J. Jebaraj, Nicholas Georgescu and Daniel A. Scherson  
Department of Chemistry, Case Western Reserve University  
Cleveland, OH 44106-7078  
[dxs16@case.edu](mailto:dxs16@case.edu)

A method has been developed and implemented that allows correlations to be established between the rates of a redox reaction on the disk of a Pt rotating ring-disk electrode, the coverage of bromide,  $\theta_{\text{Br}^-}$  and the applied potential,  $E$ . Illustrations are provided for the effects of adsorbed bromide on Pt electrodes which enhances in one case the reduction of iron(III) hexaaquo,  $[\text{Fe}(\text{H}_2\text{O})_6]^{3+}$ , and depresses the reduction of hydrogen peroxide in 0.1 M  $\text{HClO}_4$  solutions. These experiments were performed in  $\text{Br}^-$ -containing solutions at concentrations in the  $\mu\text{M}$  range. The experimental strategy involves application of a potential step from a value at which there is no  $\text{Br}^-$  adsorption,  $E_0$ , to a more positive potential at which  $\text{Br}^-$  undergoes adsorption under strict diffusion control,  $E_{\text{ads}}$ , over periods on the order of seconds. Evidence that the redox reactions do not interfere with  $\text{Br}^-$  adsorption process was obtained from in situ differential reflectance measurements performed in the absence and in the presence of the redox active species yielded virtually identical results. Correlations between  $\theta_{\text{Br}^-}$  and time for various  $E_{\text{ads}}$  were obtained from the analysis of chronoamperometric curves recorded in solutions devoid of the redox reactant from the temporal response of the Pt ring shielding currents for  $\text{Br}^-$  oxidation.<sup>1</sup> The information derived from these measurements was then used to establish the dependence of the disk current due to the redox reaction and the amount of solution phase  $\text{H}_2\text{O}_2$  produced, as measured by the ring, on both  $E_{\text{ads}}$  and  $\theta_{\text{Br}^-}$ . Shown in Panel A, Fig. 1, are plots of the peroxide reduction currents,  $i_{\text{disk}}$ , as a function of  $E_{\text{ads}}$  recorded in a 1 mM  $\text{H}_2\text{O}_2$  solution containing 10  $\mu\text{M}$  KBr in 0.1 M  $\text{HClO}_4$  for the Pt disk of a Pt|Pt RRDE at  $\omega = 200$  rpm, based on chronoamperometric data acquired following a potential step from  $E_0 = 0.03$  V to various values of  $E_{\text{ads}}$ . Corresponding plots of  $i_{\text{disk}}$  vs  $\theta_{\text{Br}^-}$  for various values of  $E_{\text{ads}}$  as indicated in the legend are given in Panel B in the same figure. These data are currently under analysis to extract kinetic parameters as a function of both coverage and potential.

**Acknowledgements.** This work was supported by a grant from the National Science Foundation.

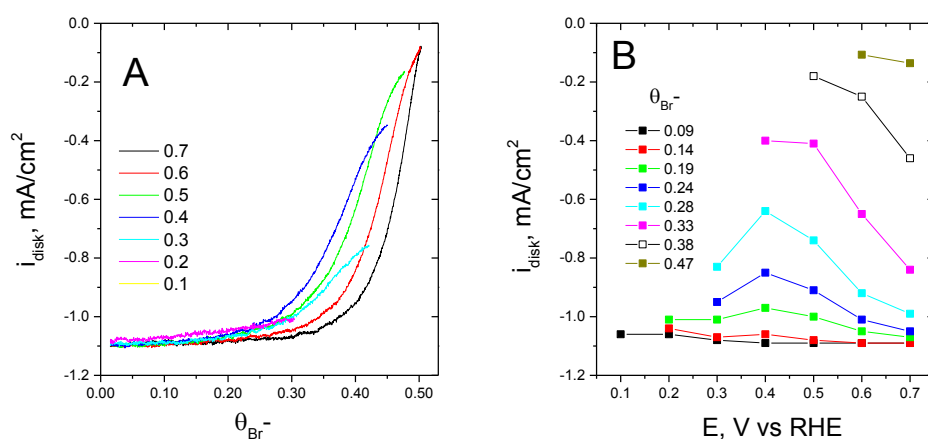


**Figure 1.** Panel A. Peroxide reduction currents as a function of  $E_{\text{ads}}$  recorded in a 1 mM  $\text{H}_2\text{O}_2$  solution containing 10  $\mu\text{M}$  KBr in 0.1 M  $\text{HClO}_4$  for the Pt disk of a Pt|Pt RRDE at  $\omega = 200$  rpm, based on chronoamperometric data acquired following a potential step from  $E_0 = 0.03$  V to various values of  $E_{\text{ads}}$ . Panel B. Plot of  $i_{\text{disk}}$  vs  $\theta_{\text{Br}^-}$  for various values of  $E_{\text{ads}}$  as indicated in the legend.

## References

1. N. M. Markovic, H. A. Gasteiger, B. N. Grgur, and P. N. Ross, *J. Electroanal.Chem.*, 467, 157, 1999.

# Activity and stability of electrodeposited nanoporous Pt based catalysts towards oxygen reduction

B. Geboes<sup>1,2</sup>, J. Ustarroz<sup>2</sup>, K. Sentosun<sup>3</sup>, S. Bals<sup>3</sup>, A. Hubin<sup>2</sup>, T. Breugelmans<sup>1,2</sup>

<sup>1</sup> Research Group Advanced Reactor Technology (ART), University of Antwerp, Salesianenlaan 90, 2660 Hoboken, Belgium

<sup>2</sup> Research Group Electrochemical and Surface Engineering (SURF), Vrije Universiteit Brussel, Pleinlaan 2, 1050 Brussels, Belgium

<sup>3</sup> Research Group Electron Microscopy for Materials Science (EMAT), University of Antwerp Groenenborgerlaan 171, 2020 Antwerp, Belgium  
bart.geboes@uantwerpen.be

Polymer electrolyte membrane fuel cells (PEMFC) provide a promising link in the future sustainable energy cycle. However, the major disadvantages today are the high capital cost [1] and insufficient stability [2] of the applied Pt nanoparticle electrocatalysts.

In this work, highly porous transition metal nanoparticles (Pt, Ni) were electrochemically deposited on a glassy carbon substrate using a dual pulse technique. These NP's could be synthesized with high selectivity and the morphology of the nanoclusters was tuned by changing electrolyte composition and deposition parameters. Both morphological properties (particle size, porosity, surface roughness, high index planes, etc.) and ORR reduction activity were elucidated using a combination of surface analysis techniques (HAADF-STEM and Electron tomography) and electrochemical techniques (linear and cyclic voltammetry).

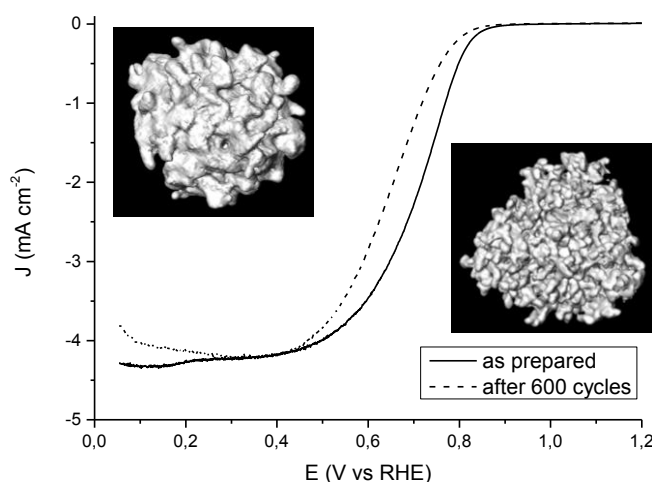


**Figure 1: Activity decrease related to the porosity relapse after subsequent potential cycling.**

The as prepared Pt nanoparticles with diameter ranging between 40-60 nm revealed nanometer scale artifacts and an increased activity towards ORR. A contraction of the Pt-Pt bond distance and the consequential changes in electronic properties could explain the elevated activity. However, upon subsequent potential cycling (600 cycles between 0,05 V and 1,4 V vs RHE) the porosity of the particles appeared to decrease from 12% to only 2%. In accordance with this relapse in porosity also the ORR activity appeared to decrease as indicated by a 100 mV shift in the linear sweep voltammograms.

The application of this described methodology as a first step in the synthesis of core-shell nanoparticles through galvanic displacement appeared a valid strategy in this work with respect to their ORR activity and stability. We have previously shown the potential catalytic enhancement of comparable core-shell NP's prepared by galvanic displacement towards ORR [3].

[1] T. E. Lipman, et. al., *Energy Policy* 32 (2004) 101-125

[2] Singh R.K. et.al., *Phys. Chem. Chem. Phys.*, 15 (2013) 13044

[3] Geboes B. et. al., *Journal of Applied Catalysis B: Environmental*, 150-151 (2014) 249

# Dynamics of Pt/Ru Based Alloy Catalysts in Formate Oxidation Process – a DFT and In-Situ XAS Approach

Petr Krtil<sup>a</sup>, Tatsuya Hiratoko<sup>a</sup>, Hana Hoffmannová<sup>a</sup>, Jonathan E. Mueller<sup>b</sup> and Timo Jacob<sup>b</sup>

<sup>a</sup> J. Heyrovsky Institute of Physical Chemistry, Academy of Sciences of the Czech Republic

Dolejskova 3, 18223 Prague, Czech Republic

<sup>b</sup> Institute of Electrochemistry, University of Ulm

Albert-Einstein-Allee 47, D-89081 Ulm, Germany

Petr.Krtil@jh-inst.cas.cz

Alloy-based electrocatalysts are currently being intensively studied as electrode catalysts for fuel cells. The alloys are believed to operate either via a ligand effect or via a bifunctional mechanism, which may apply either separately or simultaneously. The ligand effect is connected with capability of tuning the electronic structure of an alloy by controlling its composition; the bifunctional mechanism implies a work-sharing between different surface atoms which host different adsorbed reactants or reaction intermediates. The traditional approach in the optimization of alloy catalysts considers the surface structure to be static, *i.e.*

the active sites are created during the catalyst synthesis and do not change over the course of the electrocatalytic reaction. This assumption has been challenged by both theoretical<sup>1</sup> and experimental studies,<sup>2, 3</sup> describing selective, reaction-triggered surface segregation of the alloy.

The presented work probes the dynamic evolution of the catalyst surface structure of a model bifunctional catalyst based on Pt and Ru. *In-situ* X-ray absorption spectroscopy (XAS) both in XANES and EXAFS modes is used to monitor the time-evolution of the Pt<sub>2</sub>Ru surface structure during formate oxidation. The formate oxidation process proceeds via an adsorbed CO intermediate affects the local environment of both alloy components. Ru, which is originally present at the surface in a form of surface oxide is apparently partially reduced when CO replaces the oxygen-containing species on Ru (see Fig. 1). CO for oxygen replacement conforms to first order kinetics and matches the exponential decay of the observed formate oxidation current (see Fig. 1b). The apparent reduction of surface-confined Ru results in a more homogeneous distribution of Ru in the catalyst particles; the local chemical composition starts to approach the average chemical composition obtained in chemical analyses. The observed experimental trends are analysed with the help of density functional theory (DFT) calculations and the most likely surface structures and active sites are identified.

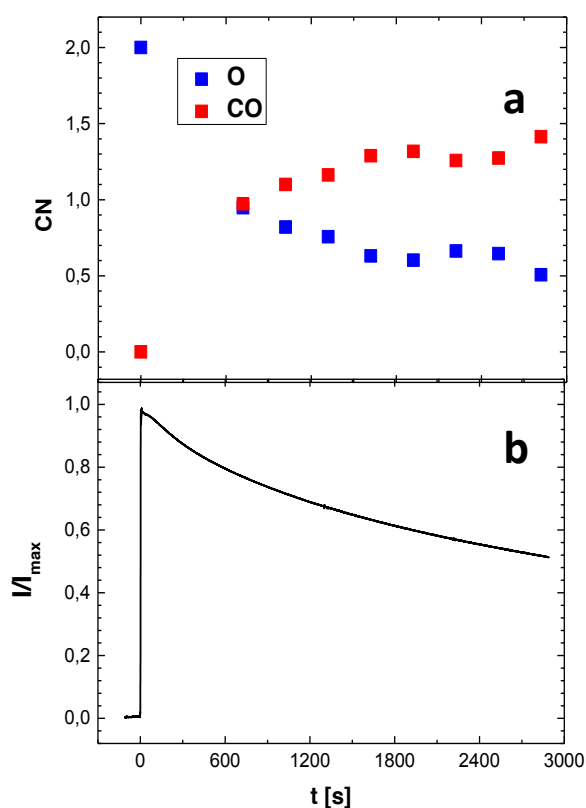


**Figure 1** Time dependence of the number of oxygen atoms and CO groups coordinating an average Ru atom in a nano-particulate Pt<sub>2</sub>Ru catalyst (a) during potentiostatic oxidation of 0.2M formate in 0.1M perchloric acid at 0.4 V vs. RHE. The corresponding chronoamperometric signal is shown in panel (b).

<sup>1</sup> S. Venkatchalam, T. Jacob, *Phys. Chem. Chem. Phys.*, **11**, 326 (2009).

<sup>2</sup> H. Hoffmannová, M. Okube, V. Petrykin, P. Krtil, J.E. Mueller, T. Jacob, *Langmuir*, **29**, 9046 (2013).

<sup>3</sup> J.E. Mueller, L.A. Kibler, T. Jacob, P. Krtil, *Phys. Chem. Chem. Phys.*, **16**, 15029 (2014).

# Performance of PEMFC Half Cells Prepared Using Hierarchical Microporous-Macroporous Carbon Supported Pt-Catalyst

Silver Sepp, Jaak Nerut, Kersti Vaarmets, Indrek Tallo, Enn Lust  
*Institute of Chemistry, University of Tartu*  
*14a Ravila Str. 50411, Tartu, Estonia*  
*e-mail silver.sepp@ut.ee*

Hierarchical Microporous-Macroporous Carbons (HMMPC) with different physical and electrochemical properties have been synthesized. Their pore size distribution and well defined hierarchical porous structure makes them interesting object to be used as a catalyst support in polymer electrolyte membrane fuel cells (PEMFC) [1, 2]. It has been shown, that HMMPCs are suitable materials to be used as catalyst support [3]. Studies have proven that electrodes prepared using HMMPCs are much more active towards oxygen electroreduction than commercially used carbon materials [2, 3]. Pt-nanoparticles were deposited onto studied carbon materials using  $\text{NaBH}_4$  reduction method. Fuel cell half-cells have been prepared with Pt-activated HMMPCs using catalyst coated membrane method. The structure of studied materials has been characterized using XRD, SEM and gas adsorption/desorption measurements. The electrochemical active surface area was estimated from  $\text{H}_2$  adsorption method in the form of cyclic voltammograms and the half-cell resistances were investigated using electrochemical impedance spectroscopy. Polarization curves have been measured for materials prepared applying various synthesis conditions and compared with data for commercial Vulcan XC72-based catalyst materials. It was found that synthesized carbon supports are suitable for PEMFC half-cell application due to their high catalytic activity and stability.

## Acknowledgements

This work was supported by Estonian Centre of Excellence in Research Project TK117T "High-technology Materials for Sustainable Development", Material Technology Program project No. 3.2.1101.12-0014, Material Technology Program project No. 3.2.1101.12-0019, Estonian Energy Technology Programme project No. SLOKT 10209T, Estonian target research project IUT20–13 and ESF Grant ETF8865.

## References

1. E. Härk, J. Nerut, K. Vaarmets, I. Tallo, H. Kurig, J. Eskusson, K. Kontturi, E. Lust, J. Electroanal. Chem. 2013, 689, 176-184.
2. S. Sepp, E. Härk, P. Valk, K. Vaarmets, J. Nerut, R. Jäger, E. Lust, J. Solid State Electrochem. 2014, 18(5), 1223 – 1229.
3. K. Vaarmets, J. Nerut, E. Härk, E. Lust, Electrochim. Acta. 2013, 104, 216 - 227.

# Electrochemical CO<sub>2</sub> Reduction at Platinum Surface Structured Electrodes in Room Temperature Ionic Liquids

Carlos M. Sánchez-Sánchez<sup>a,b</sup>, Florin A. Hanc-Scherer<sup>c</sup> and Enrique Herrero<sup>d</sup>

<sup>a</sup> Sorbonne Universités, UPMC Univ Paris 06, UMR 8235, Laboratoire Interfaces et Systèmes Electrochimiques, F-75005, Paris, France.

<sup>b</sup> CNRS, UMR 8235, LISE, F-75005, Paris, France.

<sup>c</sup> Babes-Bolyai University, Faculty of Chemistry and Chemical Engineering, 11 Arany Janos Street, RO-400028 Cluj-Napoca, Romania.

<sup>d</sup> Instituto Universitario de Electroquímica, Universidad de Alicante, Ap. 99, 03080, Alicante, Spain.  
carlos.sanchez@upmc.fr

The interface between metallic electrodes and the ionic pairs present in room temperature ionic liquids (RTILs) is still far from being well understood [1,2]. Single crystal electrodes represent the most convenient type of surface structured electrodes for studying the impact of RTIL ions adsorption in relevant electrocatalytic reactions, such as surface sensitive electrochemical CO<sub>2</sub> reduction. We propose here, for the first time, the formation of a stable complex formed between CO<sub>2</sub> and the imidazolium based cation [C<sub>2</sub>mim<sup>+</sup>] as a result of a radical-radical coupling reaction, in which both reactants have been previously electrochemically reduced. The formation of such a stable complex (C<sub>2</sub>mim-CO<sub>2</sub><sup>-</sup>) blocks CO<sub>2</sub> reduction after a single electron transfer and inhibits CO<sub>2</sub> and imidazolium dimerization reactions. However, the electrochemical reduction of CO<sub>2</sub> under those conditions provokes the electrochemical cathodic degradation of the imidazolium based RTIL. This important limitation in CO<sub>2</sub> recycling by direct electrochemical reduction is overcome by adding a strong acid, [H<sup>+</sup>][NTf<sub>2</sub><sup>-</sup>], in solution. Then, protons become preferentially adsorbed on the electrode surface by displacing the imidazolium cations and inhibiting their electrochemical reduction. As it is shown in Figure 1, this fact allows the surface sensitive electro-synthesis of HCOOH from CO<sub>2</sub> reduction in [C<sub>2</sub>mim<sup>+</sup>][NTf<sub>2</sub><sup>-</sup>] [3], being Pt(110) identified here as the most active among the basal plane electrodes studied.

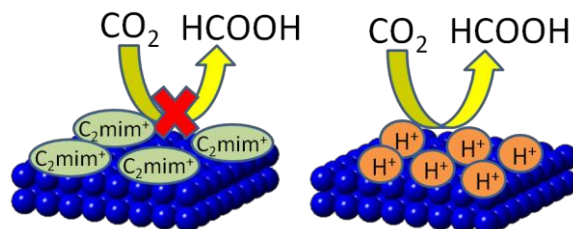


Figure 1. Electrochemical CO<sub>2</sub> reduction in two different Pt-RTIL interfaces.

## References

- [1] F.A. Hanc-Scherer, C.M. Sánchez-Sánchez, P. Ilea, E. Herrero, ACS Catal., 3 (2013) 2935-2938.
- [2] B.A. Rosen, A. Salehi-Khojin, M.R. Thorson, W. Zhu, D.T. Whipple, P.J.A. Kenis, R.I. Masel, Science 334 (2011) 643-644.
- [3] B.C.M. Martindale, R.G. Compton, Chem. Commun., 48, (2012) 6487-6489.



# Effects from modifying carbon nanofiber supports on metal nanoparticle catalyzed CO<sub>2</sub> reduction

Ida Hjorth, Navaneethan Muthuswamy, De Chen  
Norwegian University of Technology and Science  
Trondheim, Norway  
ida.hjorth@ntnu.no

Solar energy can be harnessed indirectly to convert CO<sub>2</sub> in an artificial photosynthesis process. The electricity produced by photo-voltaic systems, wind turbines or hydro-power stations, can be used to run electrolyzers, where CO<sub>2</sub> is electrochemically reduced into carbon monoxide, methane or alcohols. There are currently no stable, efficient and selective catalysts for the process, and therefore new catalytic materials must be designed such that these problems can be solved.

A promising strategy is to include catalyst nanoparticles in the design, since a larger fraction of the surface atoms will be at an edge or a corner, which may increase the reactivity. In addition, they provide a larger surface area which will increase the activity of the catalyst. These catalyst particles can be dispersed on electrically conductive carbon nanofibers. It is shown that modification of the carbon surface by removal of oxygen or doping, can improve the dispersion of metal nanoparticles[1]. In addition, support effects can be tuned to accept or donate electrons to the particle[2]. While these materials are interesting materials for catalysis, they have not received much attention for the CO<sub>2</sub> reduction. Due to their high potential, carbon nanofiber supported metal nanoparticles should be studied also for this reaction.

Cu is a natural starting point, as it is the most active metal for hydrocarbon production[3]. In this project, different types of carbon nanofibers are doped or oxidized, and oxygen groups are removed from the surface. Cu nanoparticles are deposited on the fibers, by colloid deposition, impregnation and the Pechini method. The copper is also alloyed with zinc. The final catalyst powers are tested for electrochemical CO<sub>2</sub> reduction in a CO<sub>2</sub> saturated aqueous KHCO<sub>3</sub> solution, where the selectivity, activity and stability of the catalyst is studied.

Preliminary results show that copper colloids deposited on carbon nanotubes where the oxygen groups are removed are more active and selective towards methane formation, compared to colloids deposited on tubes that are oxidized and decorated with a comparable copper loading and particle size distribution.

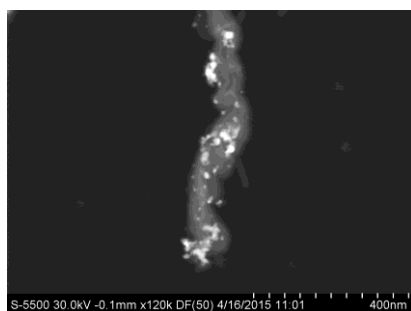


Figure: STEM micrograph of a Copper-Zinc decorated CNT.

## References:

- (1) N. Muthuswamy et al., Phys. Chem. Chem. Phys., 2013, 15
- (2) W. Chen et al., Chem. Commun., 2014, 50
- (3) K. Kuhl et al., Energy Environ. Sci., 2012, 5

# Electrochemical Water Reduction in Highly Concentrated Electrolytes: Theory and Experiments

Adriano S. O. Gomes<sup>1,2</sup>, Zareen Abbas<sup>1</sup>, Nina Simic<sup>2</sup>, Mats Wildlock<sup>2</sup> and Elisabet Ahlberg<sup>1</sup>

<sup>1</sup>*Department of Chemistry and Molecular Biology, University of Gothenburg  
SE 41296 Gothenburg, Sweden*

<sup>2</sup>*AkzoNobel Pulp and Performance Chemicals, SE-44580, Sweden  
adriano.gomes@chem.gu.se*

The electrosynthesis of sodium chlorate is one of the most important industrial practices. In the process the main cathodic reaction is water reduction. The electrolyte is composed of sodium chlorate and sodium chloride with a total salt concentration of about 8.0 moles L<sup>-1</sup>. The process optimum temperature is 80 °C and improving the cathodic current efficiency for hydrogen evolution under such conditions is a challenge. The reaction occurs at mild steel electrodes, which are not selective for hydrogen evolution and sodium dichromate is added to the electrolyte to avoid side reactions [1, 2]. However, the overpotential for water reduction is still considered high, which leaves room for improvements [3].

One question to be answered is: how does the salt concentration affects the electrochemical water reduction kinetics? Monte-Carlo simulations have shown that the water activity decreases at increasing salt concentration and the extent of such decrease is salt specific (Figure 1a). Experiments have also demonstrated that the water reduction kinetics are salt concentration dependent (Figure 1b). The aim of this study is to investigate to what extent these effects are connected to each other, including also the temperature dependence. Discussions will be based on reaction kinetics, mechanisms and the structure of the electrode-electrolyte interface.

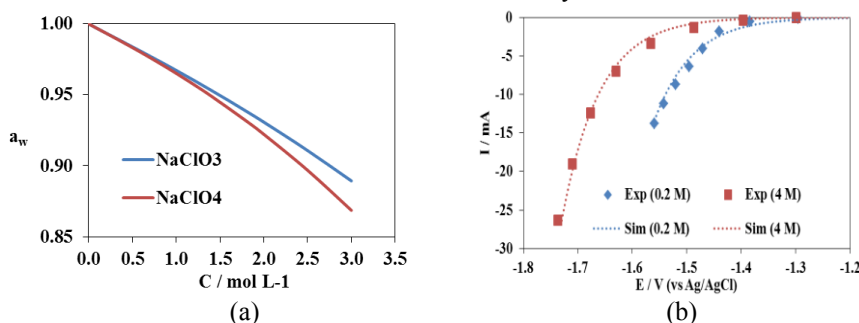


**Figure 1** – (a) Water activity as a function of salt concentration for NaClO<sub>4</sub> and NaClO<sub>3</sub>. (b) Experimental (symbols) and simulated kinetic currents (dotted lines) for water reduction in electrolytes containing NaClO<sub>4</sub> at 0.2 and 4.0 mol L<sup>-1</sup>.

[1] G. Lindbergh, D. Simonsson, *Journal of Electroanalytical Society*, 137 (1990) 3094-3099.

[2] C. Wagner, *Journal of the Electrochemical Society*, 101 (1954) 181-184.

[3] A. Cornell, D. Simonsson, *Journal of the Electrochemical Society*, 140 (1993) 3123-3129.

# Tuning the activity and stability of Pt for oxygen reduction by means of the lanthanide contraction

M. Escudero-Escribano, P. Malacrida, U. Grønbjerg, V. Tripkovic, J. Schiøtz, J. Rossmeisl, I. Chorkendorff, I.E.L. Stephens

Department of Physics, Technical University of Denmark  
Fysikvej, Building 307, 2800 Kgs. Lyngby, Denmark  
ifan@fysik.dtu.dk

In order to reduce the Pt loading at the cathode of proton exchange membrane fuel cells (PEMFCs), more active and stable catalysts are needed to drive the oxygen reduction reaction. Most research has focussed on achieving this by alloying Pt with Fe, Co, Ni or Cu [1,2]. However, these compounds typically degrade under PEMFC conditions, due to dealloying. Alloys of Pt and rare earths may be inherently less prone to dealloying under reactions conditions, due to their negative enthalpy of formation.[2,3]

Herein, we present a systematic study on the trends in activity of nine novel Pt-lanthanide and Pt-alkaline earth electrodes ( $\text{Pt}_5\text{Ca}$ ,  $\text{Pt}_5\text{Sr}$ ,  $\text{Pt}_5\text{La}$ ,  $\text{Pt}_5\text{Ce}$ ,  $\text{Pt}_5\text{Sm}$ ,  $\text{Pt}_5\text{Gd}$ ,  $\text{Pt}_5\text{Tb}$ ,  $\text{Pt}_5\text{Dy}$  and  $\text{Pt}_5\text{Tm}$ ). These compounds are amongst the most active polycrystalline extended surfaces of Pt-based ever reported. Moreover, our recent study showed that  $\text{Pt}_x\text{Gd}$  is highly active in the nanoparticulate form.[4] On the bulk alloys, a Pt overlayer with a thickness of few Pt layers is formed under reaction conditions (Fig. 1A) [5]. It turns out that the lattice parameter is the descriptor for both the activity *and* stability of these materials (Fig 1B). We rationalise this finding using a density functional theory based model. We show that the lanthanide contraction can be used as tool to tune the catalyst performance.

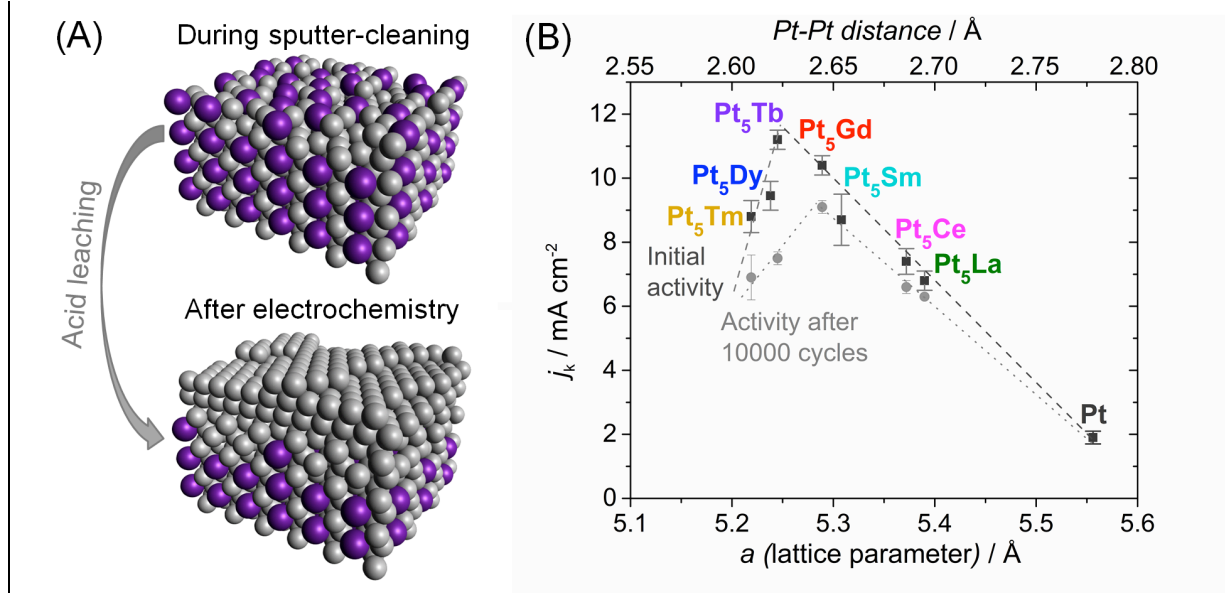


Fig 1. (A) Schematic three-dimensional views of the  $\text{Pt}_5\text{M}$  ( $\text{M}$  = lanthanide or alkaline earth metal) structure during sputter-cleaning and after electrochemistry. (B) Experimental 'activity-lattice parameter' volcano plot: ORR kinetic current density measured at 0.9 V vs. RHE as a function of the lattice parameter and the Pt-Pt distance for polycrystalline  $\text{Pt}_5\text{M}$  electrocatalysts after initial ORR activity (dark grey squares) and after 10 000 cycles between 0.6 and 1.0 V vs. RHE (grey circles).

- [1] H. A. Gasteiger, S.S. Kocha, B. Sompalli, F.T. Wagner, *Appl. Catal. B*, 9 (2005) 56.
- [2] I.E.L. Stephens, A.S. Bondarenko, U. Grønbjerg, J. Rossmeisl, I. Chorkendorff, *Energy Environ. Sci.*, 5 (2012) 6744-6762.
- [3] P. Hernandez-Fernandez, F. Masini, D.N. McCarthy, C.E. Streb, D. Friebe, D. Deiana, P. Malacrida, A. Nierhoff, A. Bodin, A.M. Wise, J.H. Nielsen, T.W. Hansen, A. Nilsson, I.E.L. Stephens, I. Chorkendorff, *Nature Chemistry*, 6 (2014) 732-738.
- [4] A. Velázquez-Palenzuela, F. Masini, A.F. Pedersen, M. Escudero-Escribano, D. Deiana, P. Malacrida, T.W. Hansen, D. Friebe, A. Nilsson, I.E.L. Stephens, I. Chorkendorff, *J. Catal.*, in press (2015).
- [5] M. Escudero-Escribano, A. Verdager-Casadevall, P. Malacrida, U. Grønbjerg, B.P. Knudsen, A.K. Jepsen, J. Rossmeisl, I.E.L. Stephens, I. Chorkendorff, *J. Am. Chem. Soc.*, 134 (2012) 16476-16479.

# Electroreduction of CO on mesoporous Cu and oxide-derived mesoporous Cu electrodes

D. Guay,<sup>1</sup> C. Roy,<sup>1</sup> S. Garbarino,<sup>1</sup> I. E. L. Stephens<sup>2</sup> and I. Chorkendorff<sup>2</sup>

<sup>1</sup> INRS-Énergie, Matériaux, Télécommunications, P.O. 1020, Varennes,  
Quebec, Canada J3X 1S2  
guay@emt.inrs.ca

<sup>2</sup> Center for Individual Nanoparticle Functionality, Department of  
Physics, Building 312, Technical University of Denmark,  
DK-2800 Lyngby, Denmark.

Climate change is considered one of the greatest environmental threats of our times. The atmospheric concentration of greenhouse gases has increased steadily over the past century. Human activities produce an annual excess of 3.9% CO<sub>2</sub> to the natural carbon cycle. This raise in CO<sub>2</sub> emission has resulted in an increase of atmospheric CO<sub>2</sub> during the last 200 years from approximately 270 ppm to 385 ppm. This is thought to cause atmospheric warming, which is associated with a global climate change and a planetary temperature increase.

Strategies for reducing CO<sub>2</sub> buildup in the atmosphere includes: 1) reduction of the amount of CO<sub>2</sub> produced by increasing the energy efficiency or changing the primary energy source; 2) development of technologies for capture, sequestration and storage of CO<sub>2</sub>; and 3) use of CO<sub>2</sub> as raw material to generate high value-added chemical products. Moreover, the transformation of CO<sub>2</sub> into a value-added product represents a means to store energy in the form of chemical bond, allowing that energy to be readily transported and used elsewhere. This can be achieved by supplying physical energy in the form of electricity. Under that scheme, CO<sub>2</sub> conversion makes sense if the input energy is from a renewable source such as sunlight (photochemical process) or wind, solar and hydroelectricity (electrochemical process).

The ERC can proceed through two-, four-, six-, and eight-electron reduction pathways in gaseous, aqueous, and non-aqueous phases at both low and high temperatures. The major reduction products are carbon monoxide, formate/formic acid, oxalate/oxalic acid, formaldehyde, methanol, methane, ethylene, ethanol, amongst others. According to the reaction thermodynamics, the conversion of CO<sub>2</sub> into various organic compounds by electroreduction is not very demanding. However, challenges remain, such as the slow kinetics, even when electrocatalysts and high electrode reduction potential are applied.

Hori et al. conducted extensive studies on the electroreduction of CO<sub>2</sub>, emphasizing the important of defects (steps and vacancies) on the process [1]. More recently, Tang *et al* have discussed the importance of uncoordinated sites in the electrosynthesis of hydrocarbon [2]. Recent studies from Kanan's group have shown the high activity of oxide-derived copper foils for CO<sub>2</sub> and CO reduction [3,4].

In the present work, we have prepared a series of mesoporous Cu electrodes using the so-called dynamic hydrogen bubble tempting method. These electrodes were either used in their as-deposited state or oxidized in air and electrochemically reduced prior to being used for the electroreduction of CO. The electrodes thus formed were characterized by XRD, SEM and cyclic voltammetry. Following that, they were used as electrodes for the reduction of CO. In all cases, the products formed were H<sub>2</sub>, C<sub>2</sub>H<sub>4</sub>, C<sub>2</sub>H<sub>6</sub> acetate and ethanol. To the best of our knowledge, this is the first time ethanol production is reported from CO reduction on Cu. Under optimized conditions, the as-deposited mesoporous Cu electrode can achieve up to 42% current efficiency at potentials as low as -0.25 V RHE. In comparison, after oxide formation and reduction, the best mesoporous Cu electrode yields a current efficiency of only 35% at the same potential. However, the overall current on that last electrode is more than one order of magnitude higher than on as-deposited mesoporous Cu, which translates into a factor of two larger partial current for the production of value-added compounds.

- 
- 1 Y. Hori, I. Takahashi, O. Koga, N. Hoshi, J. Phys. Chem. B 106 (2002) 15.
  - 2 W. Tang *et al* Phys. Chem. Chem. Phys. 14 (2012) 76.
  - 3 C.W. Li, M.W. Kanan, J. Am. Chem. Soc. 134 (2012) 7231.
  - 4 C.W. Li, J. Ciston, M.W. Kanan, Nature, 508 (2014) 504.

# Investigations of Triple Phase Boundary Regions in Bifunctional Air Electrodes Using Partially Immersed Platinum Electrodes

Atsunori Ikezawa, Kohei Miyazaki, Tomokaszu Fukutsuka, Takeshi Abe  
Graduate School of Engineering, Kyoto University  
Nishikyo-ku, Kyoto 615-8510  
myzkohei@elech.kuic.kyoto-u.ac.jp

## Introduction

There has been increasing interest in metal-air secondary batteries such as zinc-air secondary batteries. However, the large overpotential of air electrodes hinders the widely use of metal-air secondary batteries. In air electrodes, the electrochemical reactions occur only at the regions where three different species (electron, electrolyte, and oxygen gas) were transported, so-called triple-phase boundary (TPB) regions. Therefore, TPB regions in air electrodes have significant influences on the overpotential and the power density of metal-air batteries. Since practical porous gas diffusion electrodes are too complicated to be analyzed in detail, partially immersed electrode systems had been applied for the investigation of the properties of TPB regions as a model electrode. In our previous work using partially immersed electrode systems, it was found that thin liquid film effectively serves to expand TPB regions for ORR, but the liquid film hardly increases OER currents [1].

In practical air electrodes, influences of CO<sub>2</sub> should be considered. It was reported that some carbonate salts, such as K<sub>2</sub>CO<sub>3</sub>, precipitate in air electrodes and degrade their performance. In order to solve this problem, air electrodes using anion exchange membrane (AEM) were proposed [2]. In this case, TPB regions are formed on anion exchange ionomer. For the investigation of the property of the TPB regions formed on ionomers, partially immersed ionomer-coated electrode systems have been applied [3].

In this study, we investigate partially immersed anion exchange ionomer-coated Pt segmented electrodes as a model of the TPB region in AEM-typed air electrodes and compared with partially immersed Pt segmented electrodes, a model of the TPB region in conventional air electrodes. As an anion exchange ionomer, we use Tokuyama AS-4, which is one of the most widely used ones.

## Experimental

AS-4-coated Pt segmented electrodes (AS-4/Pt) were prepared by dropping of diluted AS-4 solutions on Pt segmented electrodes with a micro syringe. Schematic illustration of Pt segmented electrode was presented in elsewhere [1]. The thicknesses of AS-4 films were measured by a contact type surface roughness meter. A three-electrode electrochemical cell was used for electrochemical measurements. Partially immersed Pt segmented electrodes and partially immersed AS-4/Pt were used as working electrodes. A Hg/HgO electrode and Pt wire were used as a reference electrode and a counter electrode respectively. Aqueous solutions of KOH were used as electrolytes (saturated with mixed gases of O<sub>2</sub> and Ar at given ratio). Potentiostatic measurements were carried out under the mixed gases at the same ratios for KOH solution and steady-state oxygen reduction currents were measured. Segmental currents on Pt segments were also measured simultaneously with I-V converter.

## Result and discussion

Fig. 1 shows the segmental currents for cathodic oxygen reductions on partially immersed AS-4/Pt with 600 nm thickness of AS-4 film in an aqueous solution of 0.1 mol dm<sup>-3</sup> KOH (saturated with O<sub>2</sub>). Relatively high oxygen reduction currents were observed above 2.0 mm and the liquid levels on the electrodes were observed at 2.0 ~ 2.9 mm. Therefore, it was suggested that AS-4 film having contact with air served as an effective TPB region as with liquid thin films. However, total oxygen reduction currents were lower on AS-4/Pts than on Pt segmented electrodes. This is because oxygen transport properties and ion conductivities of AS-4 are still lower than those of KOH solutions.

## Reference

- [1] A. Ikezawa et al., ECS meeting abstracts, MA2014-02 (2014) abstract 32.
- [2] N. Fujiwara et al., J. Power Sources, 196 (2011) 808.

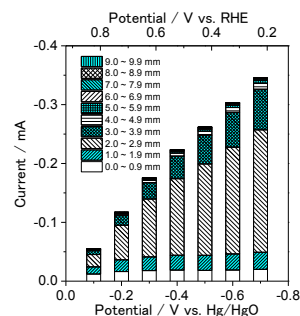


Fig. 1. Segmental currents for cathodic oxygen reduction of AS-4/Pt in 0.1 mol dm<sup>-3</sup> KOH aq. Film thicknesses was 600 nm. Oxygen partial pressures were 1 atm.

[3] M. Inaba et al., J. Electroanal. Chem., 417 (1996) 105.

# Catalytic Activities of Perovskite-type Oxide Thin Films and Single Crystals as Oxygen Electrodes in Alkaline Media

Yuto Miyahara, Kohei Miyazaki, Tomokazu Fukutsuka, and Takeshi Abe  
Graduate School of Engineering, Kyoto University  
Kyoto daigaku-katsura, Nishikyo-ku, Kyoto 615-8510, Japan  
myzkohei@elech.kuic.kyoto-u.ac.jp

There has been increasing interest in alkaline rechargeable zinc-air batteries because the battery offers a high theoretical energy density compared to current rechargeable batteries [1]. One of the advantageous features of this battery is that it has a wide range of selectivity for oxygen electrode catalysts because of the use of alkaline electrolytes. Since one of the biggest challenges of this battery is a high overpotential at an oxygen electrode, many researchers have tried to find oxygen electrode catalysts especially from cost-effective transition metal oxides. Most metal oxides have inadequate electronic conductivity as an electrode catalyst. Therefore, almost all the experiments in the literature employed so-called composite electrodes consisting of the oxides, conductive additives (such as carbon powders) and binders. This is also the case for perovskite type oxides, which are known as good oxygen electrode catalysts [2, 3]. In order to study the intrinsic electrochemical properties of the above oxides as an oxygen electrode, the use of model electrodes without any binders and conductive additives is desirable. In this research, therefore, electrochemical behaviors of perovskite oxides were evaluated using the thin films grown by pulsed laser deposition (PLD) method or the single crystals fabricated by floating zone (FZ) method.

Perovskite-oxide thin films were prepared by PLD method using Pt tip for a substrate [4]. As for the single crystals, FZ-grown perovskite rod was cut and polished to obtain desired lattice planes. Rotating disk electrodes (RDEs) were assembled using above thin films or single crystals and a RDE rod. For comparison, composite electrodes consisting of  $250 \mu\text{g cm}^{-2}$  perovskite particles,  $50 \mu\text{g cm}^{-2}$  Vulcan XC-72, and  $50 \mu\text{g cm}^{-2}$  anion conductive ionomer (AS-4, Tokuyama) were prepared on a glassy-carbon RDE. A three-electrode electrochemical cell was used as electrochemical measurements. RDEs, Pt wire, and reversible hydrogen electrode (RHE) were used as working, counter, and reference electrodes, respectively. For activity tests toward oxygen reduction reaction (ORR) and oxygen evolution reaction (OER), a solution of  $1.0 \text{ mol dm}^{-3}$  KOH (saturated by  $\text{O}_2$ ) was used as an electrolyte. For qualitative electronic conductivity measurements, a solution of  $1.0 \text{ mol dm}^{-3}$  KOH +  $20 \text{ mmol dm}^{-3}$   $\text{K}_3[\text{Fe}(\text{CN})_6]$  solution (saturated by Ar) was used as an electrolyte.

XRD measurement confirmed that phase-pure perovskite thin films were obtained by PLD. With respect to the result of electron conductivity measurements using ferricyanide/ferrocyanide, both perovskite thin films and perovskite single crystals showed good electronic conductivities. ORR polarization curves of  $\text{La}_{0.8}\text{Sr}_{0.2}\text{CoO}_3$  (LSCO) crystal and a composite electrode consisting of LSCO powder, Vulcan XC-72, and AS-4 were shown in Figure. This result suggested that ORR activity of LSCO crystal was quite low compared with that of composite electrode. Similar result was obtained when using perovskite thin films. As for OER, the activity difference between model electrodes and composite electrodes was smaller compared with the result of ORR. Detail will be discussed in the conference.

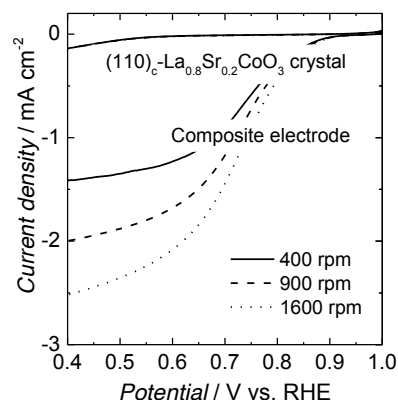


Figure. ORR polarization curves of pseudocubic  $\text{La}_{0.8}\text{Sr}_{0.2}\text{CoO}_3$ (110) crystal and composite electrode consisting of  $\text{La}_{0.8}\text{Sr}_{0.2}\text{CoO}_3$  powder, Vulcan XC-72, and AS-4.

## References

- [1] F. Cheng and J. Chen, Chem. Soc. Rev., 41 (2012) 2172.
- [2] J. Suntivich, H. A. Gasteiger, N. Yabuuchi, H. Nakanishi, J. B. Goodenough, and Y. Shao-Horn, Nat. Chem., 3 (2011) 546.
- [3] J. Suntivich, K. J. May, H. A. Gasteiger, J. B. Goodenough, and Y. Shao-Horn, Science, 334 (2012) 1383.
- [4] Y. Miyahara, K. Miyazaki, T. Fukutsuka, and T. Abe, J. Electrochem. Soc., 161(6) (2014) F694.

# CO<sub>2</sub> Electroreduction on Heteroatom-doped Carbon Catalyst

Ana Sofia Varela, Wen Ju, Peter Strasser  
Technische Universität Berlin.  
Straße des 17. Juni 124 10623 Berlin, Germany  
ana.s.varelagasque@mailbox.tu-berlin.de

Direct electrocatalytic conversion of CO<sub>2</sub> to synthesis gas (H<sub>2</sub>/CO) and hydrocarbons is a promising alternative for the production carbon based chemicals. Ideally, the driving force for this process would be the surplus electricity from renewable sources allowing storing the excess of electricity as chemical energy [1].

Most of the studies on CO<sub>2</sub> electro-reduction (CO<sub>2</sub>RR) have focus on metallic catalyst, mostly Cu, which has a unique capability of producing considerable amounts of hydrocarbons. Nevertheless, on Cu the CO<sub>2</sub>RR poor selectivity and its place at high overpotentials, which implies important energy losses [2, 3]. Alternatively gold and silver have been studied for the reduction of CO<sub>2</sub> to form CO/H<sub>2</sub> mixtures which can be used in the production of synthetic fuels via the Fischer-Tropsch process [4]. To make this process technologically viable, however, it is crucial to find affordable and earth abundant catalyst.

For this contribution we will discuss our latest results on CO<sub>2</sub> electroreduction. In particular, we will focus on heteroatom-doped carbon catalyst. We show that these materials are highly active and selective towards the reduction of CO<sub>2</sub> to CO/H<sub>2</sub> mixtures outperforming gold catalysts. Furthermore we prove that sufficiently strong interaction between CO and the metal enables the protonation of CO and the formation of hydrocarbons. Our results highlight a promising new class of low-cost, abundant electrocatalysts for synthetic fuel production from CO<sub>2</sub>.

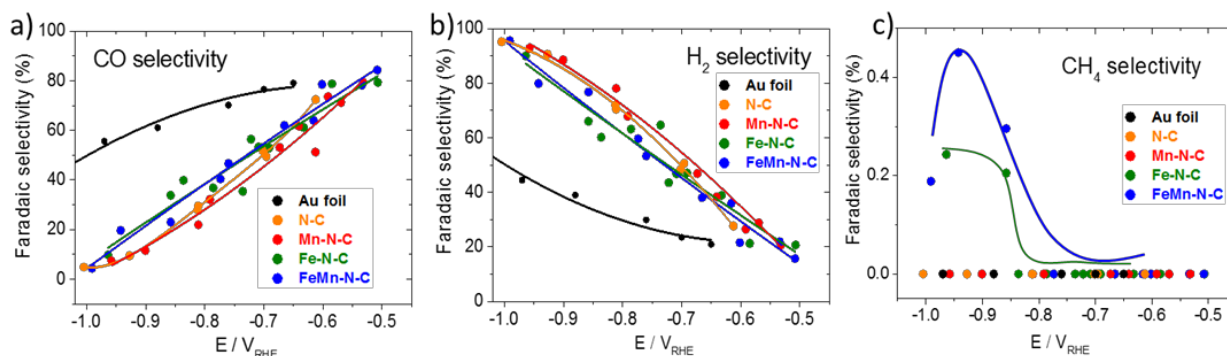


**Figure 1:** Faradaic selectivities of CO (a) and H<sub>2</sub> (b) and CH<sub>4</sub> (c) on gold (black), N-C (orange), Mn-N-C (red), Fe-N-C (green) and FeMn-N-C (blue); conditions: 10 minutes at constant electrode potential in CO<sub>2</sub> saturated 0.1M KHCO<sub>3</sub> at 0.785 mg/cm<sup>2</sup> catalyst loading. Lines to guide the eye.

## References

- [1] J. Qiao, Y. Liu, F. Hong, J. Zhang, A review of catalysts for the electroreduction of carbon dioxide to produce low-carbon fuels, *Chemical Society Reviews*, 43 (2014) 631-675.
- [2] K.P. Kuhl, E.R. Cave, D.N. Abram, T.F. Jaramillo, New insights into the electrochemical reduction of carbon dioxide on metallic copper surfaces, *Energy & Environmental Science*, 5 (2012) 7050-7059.
- [3] Y. Hori, A. Murata, R. Takahashi, Formation of hydrocarbons in the electrochemical reduction of carbon dioxide at a copper electrode in aqueous solution, *Journal of the Chemical Society, Faraday Transactions 1: Physical Chemistry in Condensed Phases*, 85 (1989) 2309-2326.
- [4] Y. Hori, A. Murata, K. Kikuchi, S. Suzuki, Electrochemical reduction of carbon dioxides to carbon monoxide at a gold electrode in aqueous potassium hydrogen carbonate, *Journal of the Chemical Society, Chemical Communications*, (1987) 728-729.



# Activity and Selectivity of NiFe Layered Double Hydroxide Electrocatalyst for Seawater Electrolysis

Fabio Dionigi, Tobias Reier, Zarina Pawolek, Manuel Gliech and Peter Strasser  
*Technische Universität Berlin, Institut für Chemie,  
Straße des 17. Juni 124, 10623 Berlin, Germany.  
fabio.dionigi@tu-berlin.de*

Generation of hydrogen and oxygen from seawater electrolysis is an attractive process for fuel production since the majority of liquid water available to mankind at the Earth's surface is salty water.[1]

Chlorine evolution reaction (CER) is a competing reaction to oxygen evolution reaction (OER) when seawater is used as electrolyte. Although OER is thermodynamically favored over CER, the poor kinetics of the OER makes CER the dominant reaction in many catalytic systems.

NiFe layered double hydroxide (LDH) has been reported to catalyze the OER reaction in alkaline media at low overpotentials comparable with the performance of noble metals catalysts.[2] In our study, its activity and stability for seawater oxidation have been investigated with a rotating disk electrode in chloride containing electrolytes with basic and slightly basic pH. The electrochemical experiments are combined with products analysis (Figure 1) in order to estimate the selectivity for oxygen evolution. In particular, CER and hypochlorite formation are investigated by an in-line quadrupole mass spectrometer (QMS) and iodometric titration respectively.

NiFe LDH shows a high selectivity for OER in alkaline electrolytes (pH 13) containing 0.5 M NaCl, a chloride ions concentration typical of seawater. In 0.3 M borate buffer (pH 9.2) with 0.5 M NaCl the electrochemical experiments show degradation in performance at current densities approaching 10 mA/cm<sup>2</sup>, despite the high selectivity at lower current densities. This degradation of the anodic current is not observed in pH 13 (0.1 M KOH) in the presence of the same concentration of NaCl.

Despite the effect of the other ions present in seawater has not been tested yet, NiFe LDH shows promising results for its application as anode in a seawater electrolyzer operating under alkaline pH.

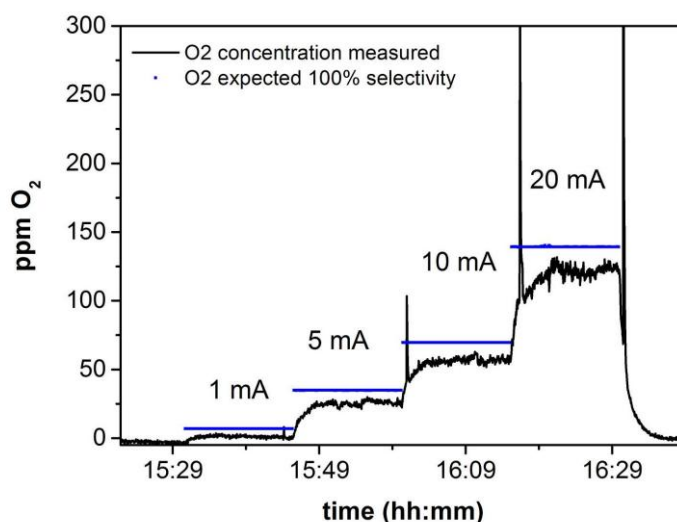


**Figure 1.** Oxygen evolution measured with a QMS during chronopotentiometry experiments at 1 mA, 5 mA, 10 mA and 20 mA for 15 min each. The blue lines are the expected O<sub>2</sub> level if selectivity were 100%. Catalyst: NiFe LDH on carbon Vulcan in 0.1 M KOH (pH 13) electrolytes containing 0.5 M NaCl.

## References

- [1] H.K. Abdel-Aal, K.M. Zohdy, M. Abdel Kareem, Hydrogen Production Using Sea Water Electrolysis, *The Open Fuel Cells Journal*, 3 (2010) 1-7.
- [2] M. Gong, Y.G. Li, H.L. Wang, Y.Y. Liang, J.Z. Wu, J.G. Zhou, J. Wang, T. Regier, F. Wei, H.J. Dai, An Advanced Ni-Fe Layered Double Hydroxide Electrocatalyst for Water Oxidation, *J Am Chem Soc*, 135 (2013) 8452-8455.

# Self-Supported Co<sub>4</sub>FeP Nanosheet Arrays Supported on Carbon Cloth: An Efficient Catalyst for Electrochemical Hydrogen Evolution

Yan Shen\*, Man Li

Wuhan National Laboratory for Optoelectronics, HuaZhong University of Science and Technology, Wuhan 430074, China

\*Corresponding author. Tel: +8613307198723. E-mail: ciac\_sheny@mail.hust.edu.cn

## Abstract

Searching for inexpensive hydrogen evolution reaction (HER) electrocatalysts with high activity has attracted considerable research interest in the past years. Reported herein is the fabrication of self-supported Co<sub>4</sub>FeP nanosheets arrays on commercial carbon cloth (Co<sub>4</sub>FeP/CC) from its Co<sub>4</sub>FeLDH/CC precursor by a low-temperature phosphidation reaction. Remarkably, as an integrated three dimensional hydrogen-evolving electrocatalyst, Co<sub>4</sub>FeP/CC maintains its activity for at least 20 hours and exhibits a Tafel slope of 50.72 mVdec<sup>-1</sup> in acidic solution. Catalytic current density can approach 10 mAcm<sup>-2</sup> at an overpotential of 49 mV. Synergistic effect of Co and Fe has been shown to significantly improve the acid stability and show almost the same HER activity as noble metals such as Pt.

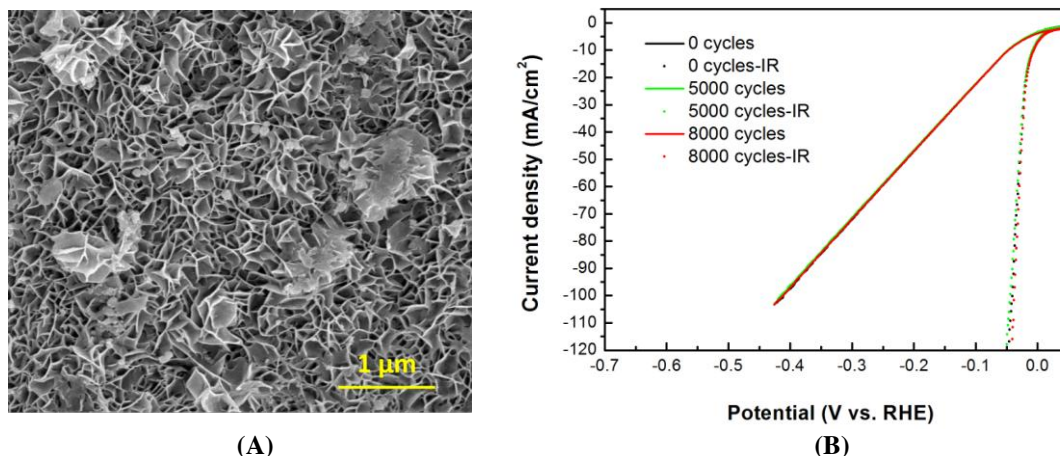


**Figure 1.** (A) Representative SEM images of Co<sub>4</sub>FeP on carbon cloth and (B) Polarization curves of Co<sub>4</sub>FeP/CC initially and after after 5000,8000cycles at a scan rate of 100 mV/s between 0 and -0.15 V vs RHE (0.5M H<sub>2</sub>SO<sub>4</sub>)

## Acknowledgements

This work was supported by the Wuhan National Lab for Optophonics, Huazhong University of Science and Technology.

## References (see example below)

1. Walter, M. G.; Warren, E. L.; McKone, J. R.; Boettcher, S. W.; Mi, Q.; Santori, E. A.; Lewis, N. S. *Chem. Rev.* 2010, 110, 6446.
2. Lukowski, M. A.; Daniel, A. S.; Meng, F.; Forticaux, A.; Li, L.; Jin, S. J. *Am. Chem. Soc.* 2013, 135, 10274.
3. Popczun, E. J.; McKone, J. R.; Read, C. G.; Biacchi, A. J.; Wiltrout, A. M.; Lewis, N. S.; Schaak, R. E. *J. Am. Chem. Soc.* 2013, 135, 9267.

## Bimetallic catalysts and metal-free catalysts for ORR

Claudio Zafferoni<sup>1</sup>, Giulia Tuci<sup>2</sup>, Giuliano Giambastiani<sup>2</sup>, Massimo Innocenti<sup>1</sup>

<sup>1</sup>*Department of Chemistry, University of Florence, Via della Lastruccia 3-13, 50019 Sesto Fiorentino (Florence), Italy*

<sup>2</sup>*Institute of Chemistry of OrganoMetallic Compounds, ICCOM-CNR, Via Madonna del Piano 10, 50019 Sesto Fiorentino, (Florence),  
claudio.zafferoni@unifi.it*

Actually platinum is still the most common metal catalyst in both anode and cathode fuel cell. In spite of the many attempts made in the last decade to develop non-Pt based catalysts for low temperature air cathodes, Pt remains the catalyst of choice, at least for acid based fuel cells. The situation in alkaline electrolytes is rather different; due to the stability of non-noble metals in this environment, many more opportunities are available for the development of non-Pt catalysts for the Oxygen Reduction Reaction (ORR) and for the Ethanol Oxidation Reaction (EOR). To completely remove Pt and to replace it with less expensive materials, bimetallic electrocatalysts have been proposed to exploit a synergic mechanism with one metal able to break the O-O bond of the molecular oxygen at the cathode side and the second metal effective in reducing the adsorbed oxygen so formed [1]. An alternative approach to the design of promising electrocatalysts for the fuel cell application is represented by light-heteroelement doped carbon nanomaterials (CNMs), and in particular nitrogen-doped CNMs (N-CNMs) [2]. In this contest we report the contribution of two different and parallel way to synthetize and test new electrocatalysts for the ORR:

- 1) Trying to combine by electrodeposition low-cost and Pt-free metal catalysts in order to match and directly act on the rate determinate step of the ORR.
- 2) Experimentally testing and designing of N-Decorated Nanomaterials in order to univocally identify the active site of reaction.

For point one, Silver and cobalt, whose catalytic activity against the ORR have been reported long ago [3-4] were combined together by electrodeposition on a glassy carbon electrode. The activity of the small amount of the binary Ag-Co catalyst ( $17 \mu\text{g cm}^{-2}$ ) were compared with the catalytic activity of the only-silver deposits that had given the best catalytic effect in Ref 5 and the rotating ring electrode (RDE) measurements were performed to estimate the average number of exchanged electron during the reaction. On the other hand a starting new method of surface modification of carbon nanotubes by N-Decoration via Aryldiazonium Salt (Tour) protocol [6] was used to study the contribution of pyridine groups on the ORR. Following our preliminary studies on acridine- and pyridine-functionalized carbon nanotubes the catalytic activities of new samples were estimated by rotating ring disk electrode (RRDE) measurements in order to clarify the main contribution of the substituted pyridine groups.

[1]F. Loglio, E. Lastraioli, C.Bianchini, C. Fontanesi, M.Innocenti, A. Lavacchi, F.Vizza and M.L.Foresti, Cobalt monolayer islands on Ag(111) for ORR catalysis, *ChemSusChem*, (2011) 4(8) 1112-1117.

[2]Wang, D.-W.; Su, D. Heterogeneous nanocarbon materials for oxygen reduction reaction, *Energy Environ. Sci.* (2014) 7 576–591

[3]C. Coutenceau, L. Demarconnay, C. Lamy, J. -M Léger, Development of electrocatalyst for solid alkaline fuel cell *J. Power Sources*, (2006) 156 14.

[4]A. Zwetanova, K. Juttner, The electrocatalytical influence of underpotential lead and thallium adsorbates on the cathodic reduction of oxygen on (111), (100) and (110) silver single-crystal surfaces, *J. Electroanal. Chem.*, (1981) 119 149-164.

[5]M. Innocenti, C. Zafferoni, A. Lavacchi, L. Becucci, F. Di Benedetto, E. Carretti, F. Vizza, M.L. Foresti, Electroactivation of Microparticles of Silver on Glassy Carbon for Oxygen Reduction and Oxidation Reactions, *J. Electrochem. Soc.* (2014) 161 (7) D1-D7

[6]G. Tuci, C. Zafferoni, S. Caporali, P. D'ambrosio, M. Ceppatelli, A. Rossin, T. Tsoufis, M. Innocenti, G. Giambastiani, Tailoring Carbon Nanotube N-Dopants While Designing Metal-Free Electrocatalysts for the Oxygen Reduction Reaction, *ACS Catalysis*, 2013 3 2108–2111

# Porphyrin-Polyoxometalates@Pt Modified Electrodes for Electrocatalytic Hydrogen Evolution Reaction

Dejin ZANG, A. Bonnefont, L. Ruhlmann\*

Laboratoire d'Electrochimie et de Chimie Physique du Corps Solide, Université de Strasbourg, 4 rue Blaise Pascal, 67000, Strasbourg, France

[dejin.zang@etu.unistra.fr](mailto:dejin.zang@etu.unistra.fr), [lruhlmann@unistra.fr](mailto:lruhlmann@unistra.fr)

Polyoxometalates (POMs) are anionic, nanometer-sized clusters of highly oxidized early transition metals and oxygen with a wide span of physical and chemical properties (redox, electronic, charge, bioactivity, etc.)<sup>[1]</sup>. They can also be used for the stabilisation of metallic nanoparticles due to their negative charge and their interaction with metals. In the recent years, the combination of POM with metallic nanoparticle catalysts was found to exhibit interesting activity and selectivity for some catalytic reactions in water and organic solvent.<sup>[2]</sup>

Various types of electrostatic porphyrin-POM@Pt films were synthesized and their activities of the electrocatalytic hydrogen evolution reaction were tested (cf. Figs. 1,2 and 3).

For instance, the multilayer films  $[\text{H}_2\text{PhMe}_3\text{P}^{4+} \cdot 4\text{TsO}^- / \text{Zn}_4(\text{H}_2\text{O})_2(\text{P}_2\text{W}_{15}\text{O}_{56})_2^{16-} 16\text{Na}^+ @\text{Pt}]_n$  were uniformly assembled in a sequential layer-by-layer way (LBL) onto ITO electrode (Fig. 2)<sup>[3]</sup> with varied numbers of cycle of deposition  $n$  ( $n = 0.5, 1, 2, 5, 10, 15, 20$ ). The first step is the formation of one monolayer of cationic porphyrin ( $n = 0.5$ ), then the modified electrode is dipped in the solution containing POM@Pt nanoparticles ( $n = 1$ ). The process is repeated several times in order to increase the thickness of the films and  $n$ . The growth of the hybrid inorganic/organic film could be followed by UV-visible spectroscopy and in-situ electrochemical quartz microbalance.

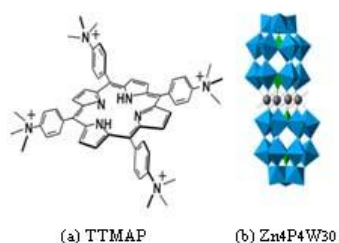


Fig 1. Molecular structures of porphyrin and POM.

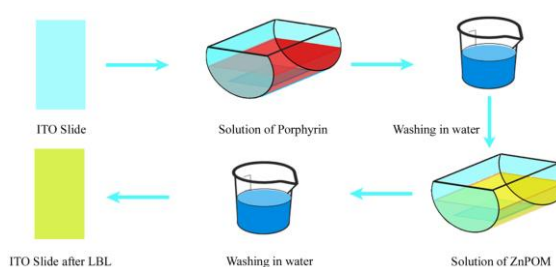


Fig 2. The procedure of layer by layer

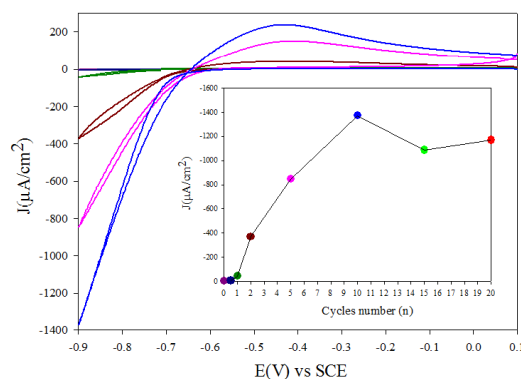


Fig 3. Electrocatalytic hydrogen evolution reaction using  $[\text{TTMAP}/\text{Zn}_4\text{P}_4\text{W}_{30}@\text{Pt}]_n$  in aqueous solution,  $v = 10 \text{ mV s}^{-1}$ ,  $\text{pH}=6.5$ ,  $0.5 \text{ M H}_2\text{PO}_4^- / \text{HPO}_4^{2-}$  aqueous solution.

The multilayer films of  $[\text{TTMAP}/\text{Zn}_4\text{P}_4\text{W}_{30}@\text{Pt}]_n$  exhibit high catalytic activity for the hydrogen evolution reaction (Fig. 3).

## Acknowledgements

We thank China scholarship council (CSC), and Fudan University (Shanghai, China) for funding this work.

## References

- [1] C. L. Hill in Comprehensive Coordination Chemistry II, Vol. 4 (Ed.: A. G. Wedd), Elsevier, Oxford, 2004, pp. 679 – 759; b) M. T. Pope in Comprehensive Coordination Chemistry II, Vol. 4 (Ed.: A. G. Wedd), Elsevier, Oxford, 2004, pp. 635 – 678.
- [2] Y. Wang, I. A. Weinstock, Chem. Soc. Rev., 2012, 41, 7479-7496
- [3] a) L. Ruhlmann, G. Genet, J. Electroanal. Chem. 2004, 568, 315-321; b) L. Ruhlmann, L. Nadjo, J. Canny, R. Thouvenot, Eur. J. Inorg. Chem. 2002, 975-986; c) I. Ahmed, R. Farha, M. Goldmann, L. Ruhlmann, Chem. Commun., 2013, 49, 496.

# A Study of the Catalytic Activity of a Schiff Base Ligand on Electrochemical Reduction of Carbon Dioxide: Indirect Electrocatalytic Synthesis of Isonicotinic Acid

Kobra Ghobadi, Hamid R. Zare, Hossein Khoshro, Alireza Gorji, Abbas A. Jafari

*Department of Chemistry, Yazd University, Yazd, 89195-741, Iran*

*Fax No.: +98 3538210991 Tel. No.: +98 35 38122669*

*E-mail address: Ghobadi\_74@yahoo.com*

## Abstract

In the recent years, the increasing of carbon dioxide in the atmosphere has been a problem in the world due to it might lead to global climate warming. Hence, using of CO<sub>2</sub> in synthesis of organic and inorganic compounds to decrease the CO<sub>2</sub> content of atmosphere has received considerable attention [1]. The large overpotential for reduction of CO<sub>2</sub> causes to low recycling efficiency of this molecule to useful products [2]. Hence, finding catalysts to decrease high overpotential and to increase the selectivity of the reduction processes has become an important concern.

In this work, N,N-bis(3-hydroxy-2-naphthaldehyde)-m-phenylenediamine (NMPD) was used as an excellent electrocatalyst for reduction of the carbon dioxide in an acetonitrile solution at room temperature. The CO<sub>2</sub> electrocatalytic reduction mechanism was investigated by cyclic voltammetry. Voltammetric results indicate that the produced CO<sub>2</sub><sup>•-</sup>, in the presence of NMPD, acts as an intermediate to reduce pyridine [3]. The coulometry results and FTIR, <sup>1</sup>H, <sup>13</sup>C NMR characterization proved the isonicotinic acid formation. In constant potential coulometry, constant potential of -2.0 V was applied to the working electrode. The results showed that the pyridine conversions were about 100% after passing 2.9 F mol<sup>-1</sup> of the starting compound (pyridine) at room temperature. The determined yield of isonicotinic acid was about 75%. Finally, it was suggested the electrocatalytic activated CO<sub>2</sub> has a dual activity toward pyridine and an ECC'C mechanism was proposed for isonicotinic acid production.

## References:

- [1] H.D. Gibson, Chem.Rev. 96 (1996) 2063-2096.
- [2] E. Lamy, L. Nadjo, J. Saveant, J. Electroanal. Chem. 78 (1977) 403-407.
- [3] H. Khoshro, H.R. Zare, A.A. Jafari, A. Gorji, Electrochem. Commun. 51 (2015) 69-71.

# Oxygen evolution reaction: correlation between electronic property and OER activity for $\text{La}_{1-x}\text{Sr}_x\text{CoO}_3$ ( $x=0, 0.2, 0.4, 0.6, 0.8, 1$ ) perovskite oxides

Xi Cheng<sup>[a]</sup>, Emiliana Fabbri<sup>[a]</sup>, Maarten Nachtegaal<sup>[b]</sup>, Raphael Haumont<sup>[c]</sup> and Thomas J. Schmidt<sup>[a,d]</sup>

[a] Electrochemistry Laboratory, Paul Scherrer Institute, 5232 Villigen, Switzerland

[b] Paul Scherrer Institute, 5232 Villigen, Switzerland

[c] SP2M, ICMMO, Université de Paris-Sud XI, 91405 Orsay, France

[d] Laboratory of Physical Chemistry, ETH Zurich, 8093 Zurich, Switzerland

xi.cheng@psi.ch

Perovskite Oxides ( $\text{ABO}_3$ ) with alkaline or rare-earth cations in the A-site and first row transition metal cations in the B-site have shown the potentials of being viable oxygen electrode catalysts in alkaline solution<sup>1</sup>. Furthermore, it was demonstrated that their physical-chemical properties as well as their catalytic activity can be significantly influenced by substitution or partial substitution of the A and/or B-site by other elements giving  $(\text{A}_x\text{A}'_{1-x})(\text{B}_y\text{B}'_{1-y})\text{O}_3$  compositions. A particular interesting case is the series of  $\text{La}_{1-x}\text{Sr}_x\text{CoO}_3$  oxides. It was reported that this series of oxides possessed interesting evolutions of physical-chemical properties as a function of Sr fraction, in terms of conductivity<sup>2</sup>, bulk structure<sup>3</sup> and amount of oxygen vacancies<sup>4</sup> in the lattice. Hence, in the present work, we report a thorough bulk structure, surface and electrochemical study of the series of  $\text{La}_{1-x}\text{Sr}_x\text{CoO}_3$  oxides ( $x=0, 0.2, 0.4, 0.6, 0.8, 1$ ) which allows us to draw important conclusions of the influence of bulk and surface properties of perovskite materials on the electrochemical activity towards the OER.

While some reports showed that the oxidation state of the Co cations in the  $\text{La}_{1-x}\text{Sr}_x\text{CoO}_3$  might be changed from  $3^+$  to  $4^+$  varying the Sr content in the oxide series<sup>3</sup>, other authors reported that no significant Co oxidation state change occurred with the Sr substitution<sup>5</sup>. To clarify the effect of Sr substitution on the Co oxidation state of  $\text{La}_{1-x}\text{Sr}_x\text{CoO}_3$  series, X-ray absorption measurements were carried on some of as prepared  $\text{La}_{1-x}\text{Sr}_x\text{CoO}_3$  oxides. Moreover, the surface segregation of Sr among the  $\text{La}_{1-x}\text{Sr}_x\text{CoO}_3$  oxides is well known<sup>6</sup>. This effect may block the active site at the oxide surface and, thus, need to be carefully investigated. Furthermore, discrepancy between theoretical and experimental studies could be easily understood only if the actual catalyst surface is accurately investigated. Herein, we also report the surface characterization by X-ray photoelectron spectroscopy (XPS). The bulk structure of the oxides was characterized by X-ray diffraction (XRD), combined with ex-situ conductivity, scanning electron microscope and specific surface area (BET) analyses. The oxygen evolution reaction (OER) was investigated by cyclic voltammetry and chronoamperometric measurements.

Our result shows that when the La is replaced by Sr gradually, a phase transition from Rhombohedral ( $\text{LaCoO}_3$ ) to cubic structure ( $\text{La}_{0.8}\text{Sr}_{0.2}\text{CoO}_3$ ) occurs combined with the aligning of Co-O-Co angle. The latter enhances the overlap between the occupied O-2p valence band and the unoccupied Co-3d conduction bands, which is considered as one of the main parameter that describes the increase of ex-situ electronic conductivity of  $\text{La}_{1-x}\text{Sr}_x\text{CoO}_3$  oxides as a function of Sr fraction. Moreover, the trend of the OER activity vs. conductivity suggests a correlation between the ex-situ electronic conductivity and the OER activity of  $\text{La}_{1-x}\text{Sr}_x\text{CoO}_3$  oxides. Therefore, we propose that OER activity of  $\text{La}_{1-x}\text{Sr}_x\text{CoO}_3$  oxides is related to the electronic structure of the oxides, that is, the OER activity could be improved by enhancing the overlap between the occupied O-2p valence band and the unoccupied Co-3d conduction bands.

1. Fabbri, E.; Haberer, A.; Waltar, K.; Kotz, R.; Schmidt, T. J., Developments and perspectives of oxide-based catalysts for the oxygen evolution reaction. *Catal Sci Technol* **2014**, 4 (11), 3800-3821.
2. Mineshige, A.; Inaba, M.; Yao, T. S.; Ogumi, Z.; Kikuchi, K.; Kawase, M., Crystal structure and metal-insulator transition of  $\text{La}_{1-x}\text{Sr}_x\text{CoO}_3$ . *J Solid State Chem* **1996**, 121 (2), 423-429.
3. Efimova, E.; Efimov, V.; Karpinsky, D.; Kuzmin, A.; Purans, J.; Sikolenko, V.; Tiutiunnikov, S.; Troyanchuk, I.; Welter, E.; Zajac, D.; Simkin, V.; Sazonov, A., Short- and long-range order in  $\text{La}_{1-x}\text{Sr}_x\text{CoO}_3$  and  $\text{La}_{1-x}\text{Ba}_x\text{CoO}_3$ . *Journal of Physics and Chemistry of Solids* **2008**, 69 (9), 2187-2190.
4. Mizusaki, J.; Mima, Y.; Yamauchi, S.; Fueki, K.; Tagawa, H., Nonstoichiometry of the Perovskite-Type Oxides  $\text{La}_{1-x}\text{Sr}_x\text{CoO}_3$ -Omega. *J Solid State Chem* **1989**, 80 (1), 102-111.
5. Hueso, J. L.; Holgado, J. P.; Pereniguez, R.; Mun, S.; Salmeron, M.; Caballero, A., Chemical and electronic characterization of cobalt in a lanthanum perovskite. Effects of strontium substitution. *J Solid State Chem* **2010**, 183 (1), 27-32.
6. Jung, W. and H.L. Tuller, Investigation of surface Sr segregation in model thin film solid oxide fuel cell perovskite electrodes. *Energy & Environmental Science*, **2010**, 5 (3), 6081-6088

# Electrocatalytic oxidation of urea on Ni(II)cyclam-modified nanoparticulate TiO<sub>2</sub> anodes for promoting the H<sub>2</sub> evolution on Pt counterelectrodes

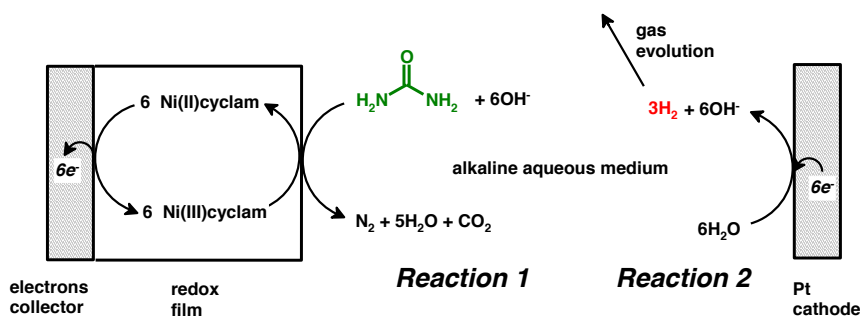
J. Manríquez,<sup>1</sup> S. Murcio-Hernández,<sup>1</sup> J.J. Pérez-Bueno,<sup>1</sup> S. Sepúlveda<sup>2</sup>

<sup>1</sup> Centro de Investigación y Desarrollo Tecnológico en Electroquímica S.C., Parque Tecnológico Querétaro s/n, Sanfandila, 76703, Pedro Escobedo, Querétaro, México.

<sup>2</sup> Centro de Innovación, Investigación y Desarrollo en Ingeniería y Tecnología, Universidad Autónoma de Nuevo León, Nuevo León, México.

\*e-mail: [jmanriquez@cideteq.mx](mailto:jmanriquez@cideteq.mx)

In this investigation we studied the electrochemical oxidation of urea (Reaction 1, Scheme 1) on Ni(II)cyclam-modified nanoparticulate TiO<sub>2</sub> anodes (**OTE/npTiO<sub>2</sub>/Ni(II)cyclam**), where optically transparent electrodes (OTEs) were utilized as electrons collectors. Thereafter, this anodic reaction was coupled with polycrystalline Pt cathodes, where the H<sub>2</sub> evolution (Reaction 2, Scheme 1) was promoted in alkaline aqueous medium. For comparison purposes, the Reaction 2 was also promoted on Pt cathodes when Ni(II)cyclam-modified OTEs (**OTE/Ni(II)cyclam**) were utilized for carrying out the Reaction 1.



Scheme 1

Our results showed that the standard potential for the H<sub>2</sub> evolution ( $E^0_{\text{H}_2\text{O}|\text{H}_2} = -0.83\text{V vs. NHE}$ ) was measured on the Pt cathode when a potential of 1.0V vs. NHE was applied to the **OTE/npTiO<sub>2</sub>/Ni(II)cyclam**/electrolyte interface (where the urea oxidation was taking place) with the aid of a potentiostat. On the contrary, the standard potential for the H<sub>2</sub> evolution was achieved on the Pt electrode when a potential of 1.2V vs NHE was applied to the **OTE/Ni(II)cyclam**/electrolyte interface (in order to promote the urea oxidation). These interesting results demonstrated that the applied potential for promoting the urea oxidation on Ni(II)cyclam-modified electrodes was 0.2V-shifted in cathodic sense in the presence of nanoparticulate TiO<sub>2</sub> films, thus revealing a remarkable electrocatalytic phenomena which can be attributed to the surface composition of the TiO<sub>2</sub> nanoparticles.



# Property of Oxide Film and Activity of $\text{Li}_x\text{Ni}_{2-x}\text{O}_2/\text{Ni}$ Anode for Alkaline Water Electrolysis

Sho Fujita<sup>a</sup>, Koichi Matsuzawa<sup>a</sup>, Yuji Kohno<sup>a</sup>, Ikuo Nagashima<sup>c</sup>, Yoshio Sunada<sup>d</sup>, Akiyoshi Manabe<sup>e</sup>,  
Yoshinori Nishiki<sup>e</sup>, Shigenori Mitsushima<sup>a,b</sup>

<sup>a</sup>Green Hyd. Res. Cntr., YNU, <sup>b</sup>IAS.YNU, <sup>c</sup>Kawasaki Heavy Industries, Ltd., <sup>d</sup>ThyssenKrupp Uhde  
Chlorine Engineers (Japan), Ltd., <sup>e</sup>Permelec Electrode Ltd.,  
<sup>a,b</sup>79-5 Tokiwadai, Hodogaya-ku, Yokohama 24-8501, Japan

<sup>c</sup>1-1 Kawasaki-cho, Akashi 673-8666, Japan

<sup>d</sup>7F Sukura Nihonbashi Buildings, 1-13-12 Nihonbashi Kayaba-cho, Chuo-ku, Tokyo 103-0025, Japan

<sup>e</sup>2023-15 Endo Fujisawa 252-0816, Japan

fujita-sho-nx@ynu.jp

## Introduction

Anode of alkaline water electrolysis (AWE) is usually Ni based material which is stable under steady electrolysis<sup>1)</sup>. However, durability of Ni based anode should be improved to connect with unstable renewable energies, because it deteriorates under potential cycling. In order to improve durability and activity against fluctuating electricity, the lithium doped NiO coated Ni anode ( $\text{Li}_x\text{Ni}_{2-x}\text{O}_2/\text{Ni}$ ) has been proposed<sup>2)</sup>. The  $\text{Li}_x\text{Ni}_{2-x}\text{O}_2/\text{Ni}$  had high stability and conductivity, but the relationship between the conductivity and lithium amount has been unclear. In this study, we have investigated the effect of increasing  $x$  of  $\text{Li}_x\text{Ni}_{2-x}\text{O}_2$  on the electronic conductivity and the catalytic activity for oxygen evolution reaction (OER) in alkaline medium.

## Experimental

A LiOH coated Ni plate (The Nilaco corp., 99.4%) was oxidized at 1000 °C for 1 h in air to prepare a  $\text{Li}_x\text{Ni}_{2-x}\text{O}_2/\text{Ni}$  working electrode. The  $x$  in  $\text{Li}_x\text{Ni}_{2-x}\text{O}_2$  was varied from 0 to 0.36. A Ni coil and reversible hydrogen electrode (RHE) were used as a counter electrode and reference electrode, respectively. All measurements were performed with three-electrodes electrochemical cell at  $30 \pm 1^\circ\text{C}$ . The electrolytes were 7.0 M (=mol dm<sup>-3</sup>) of KOH.

Resistance of the surface oxide layer was measured by electrochemical impedance spectroscopy with frequency range from 0.1 to 10<sup>5</sup> Hz. The catalytic activity for the OER was evaluated by slow scan voltammogram (SSV) between 0.7 and 1.8 V vs. RHE with scan rate of 5 mVs<sup>-1</sup>.

## Results and discussion

Surface resistances of  $\text{Li}_{0.10}\text{Ni}_{1.90}\text{O}_2$ ,  $\text{Li}_{0.14}\text{Ni}_{1.86}\text{O}_2$  and  $\text{Li}_{0.36}\text{Ni}_{1.64}\text{O}_2$  were 8.2, 7.5 and 4.9  $\Omega\text{cm}^2$ , respectively. It decreased with the increase of  $x$  in  $\text{Li}_x\text{Ni}_{2-x}\text{O}_2$  in all experimental conditions of this study.

Figure 1 shows polarization curves of the  $\text{Li}_x\text{Ni}_{2-x}\text{O}_2/\text{Ni}$  in 7 M KOH at 30°C. The  $\text{Li}_x\text{Ni}_{2-x}\text{O}_2/\text{Ni}$  whose  $x$  was from 0.10 to 0.29 had significantly higher catalytic activity than others for the OER. Their Tafel region of these electrodes, all slopes were showed around 50 mVdec<sup>-1</sup>, which was almost same as that of Ni. On the other hand, the catalytic activity for the OER on  $\text{Li}_x\text{Ni}_{2-x}\text{O}_2/\text{Ni}$  whose  $x$  was 0.36 was much lower than that whose  $x$  was below 0.29. Therefore, the conductivity of surface oxide was increased with  $x$ , but excess lithium doping decreased the activity for the OER.

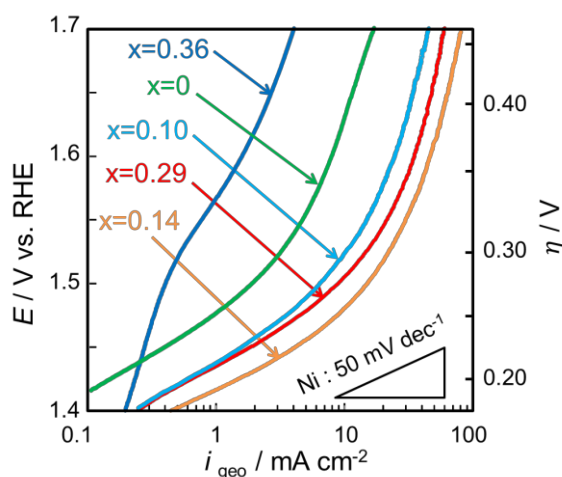


Fig. 1 Polarization curves of the  $\text{Li}_x\text{Ni}_{2-x}\text{O}_2/\text{Ni}$  at  $30 \pm 1^\circ\text{C}$  in 7M KOH.

## Reference

- 1) S. Mitsushima, K. Matsuzawa, *J. Hydr. Ener. Syst. Soc. Jpn.*, **36**, 11 (2011)(in Japanese).
- 2) H. Ichikawa, K. Matsuzawa, Y. Kohno, I. Nagashima, Y. Sunada, Y. Nishiki, A. Manabe, and S. Mitsushima, *ECS Trans*, **58**(33), 9 (2014).



# **Electrocatalytic Effect of IrO<sub>2</sub>-Ta<sub>2</sub>O<sub>5</sub> | Ti in the Electrochemical Degradation of Phenanthrene, Naphthalene and Fluoranthene in Wastewater from the Electrokinetic Treatment of Polluted Soil by Hydrocarbons**

R. A. Herrada,<sup>1</sup> O. Cuevas,<sup>1</sup> F. Manríquez,<sup>1</sup> A. Medel,<sup>1</sup> I. Sirés,<sup>2</sup> and E. Bustos<sup>1</sup>

<sup>1</sup>*Department of Science, Centro de Investigación y Desarrollo Tecnológico en Electroquímica, S. C. Parque Tecnológico Querétaro s/n, Sanfandila, Pedro Escobedo, 76703, Querétaro, Qro. Mexico.*

<sup>2</sup>*Laboratori de Ciència i Tecnologia Electroquímica de Materials, Departament de Química Física, Facultat de Química, Universitat de Barcelona, Martí i Franqués 1-11, 08028, Barcelona, Spain.*

[ebustos@cideteq.mx](mailto:ebustos@cideteq.mx)

Nowadays the problem of water pollution has become more relevant for three main reasons: the first one is the increment in the generation of pollutants, the second one is that has increased awareness of the risk posed to the environment and the third one has arisen by the high cost of remediation. For the previous reason, remediation technologies that help to restore contaminated areas are very important.

Within remediation technologies highlights the electro-remediation due to many factors, such as its efficiency, its short operation time and a great ability to work with a wide range of contaminants. Currently there are factors that can be study and tested to improve this technology. A key factor is the coating of the electrodes employed for the treatment of contaminated waters, which plays a key role in the efficiency of the remediation process. The ability to modify electrodes provides a path of great importance to improve the performance thereof in the process of electro-remediation.

This research identifies the synthesis technique as painting and electrophoresis as the best for coating the electrodes with iridium oxide and tantalum oxide for the removal of hydrocarbons in contaminated water as Phenanthrene, Naphthalene and Fluoranthene with efficiencies major than 80 % in menus of 180 min. This degradation of hydrocarbons was by the presence of radical hydroxyls and active chlorine in interface produced during the electrokinetic treatment of polluted soil by hydrocarbons.

# A study of the Formation of $\text{Co}_{1-x}\text{Fe}_x\text{S}_2$ in Microwave Synthesis and its Electrocatalytic Properties towards Oxygen Reduction and Hydrogen Evolution

Gert Göransson, Alexander Björling and Elisabet Ahlberg  
Department of Chemistry and Molecular Biology, University of Gothenburg  
Box 100, 405 30 Gothenburg, Sweden  
gert.goransson@chem.gu.se

Pyrite ( $\text{FeS}_2$ ), the most abundant sulphur mineral in the Earth surface environment well known and studied since several centuries back, has received growing attention in the research community in the last years. All the transition metals from Mn to Zn can form disulphide pyrite type structures, all with different electronic and magnetic properties [1].  $\text{FeS}_2$  is classified as a van Vleck paramagnetic semiconductor and  $\text{CoS}_2$  as a ferromagnetic metal, a mixture of the two in complete solid solution is expected to be a compound with half-metal properties. The increased interest for tuning the band gap by doping e.g.  $\text{FeS}_2$  structure with other elements has its origin in the need of this kind of control in the construction of future spintronic and photovoltaic devices. Another field with great needs for compounds with tuneable conduction bands is electrocatalysis and in this work two of the most important reduction reactions in the aspect of green chemistry, oxygen reduction and hydrogen evolution, are studied.

$\text{Co}_{1-x}\text{Fe}_x\text{S}_2$  was chosen as a tuneable compound on the basis that Co is known to reduce  $\text{O}_2$  to either  $\text{H}_2\text{O}$  or  $\text{H}_2\text{O}_2$  depending on its environment, where a less electron “rich” environment gives mainly  $\text{H}_2\text{O}_2$  [2, 3]. Introduction of Fe into a  $\text{CoS}_2$  structure may slow the electron “availability” down and possibly favour reduction to  $\text{H}_2\text{O}_2$ , but still be conductive enough to provide fast total kinetics.

Various compositions of  $\text{Co}_{1-x}\text{Fe}_x\text{S}_2$  have been made using high temperature synthesis [4] or by hydrothermal synthesis [5], the latter method was chosen in this study and both conventional oven and microwaves (MW) were used and compared as heating sources. A simple aqueous solution with di-valent metal ions and thiosulphate as the sulphur source was used. However, the only phase pure compound that was readily formed without additives was  $\text{Co}_{2/3}\text{Fe}_{1/3}\text{S}_2$ . Certain mechanistic insights were given by comparing oven and MW synthesis, as the time frame of the heating ramp is different. XRD and SEM was used to characterise the products.

The  $\text{MS}_2$  materials were attached to a gold electrode by the ability of sulphur to form bonds with gold. The kinetics for oxygen reduction and hydrogen evolution will be presented.

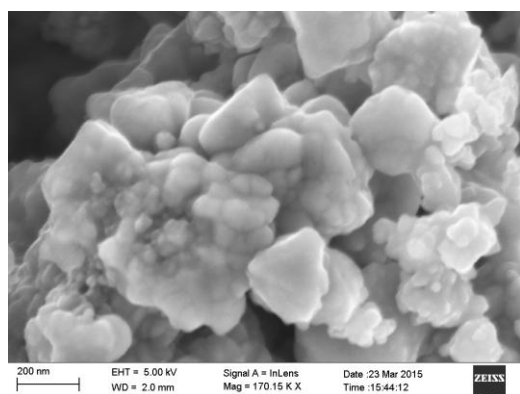


Figure 1. MW synthesised  $\text{Co}_{2/3}\text{Fe}_{1/3}\text{S}_2$ .

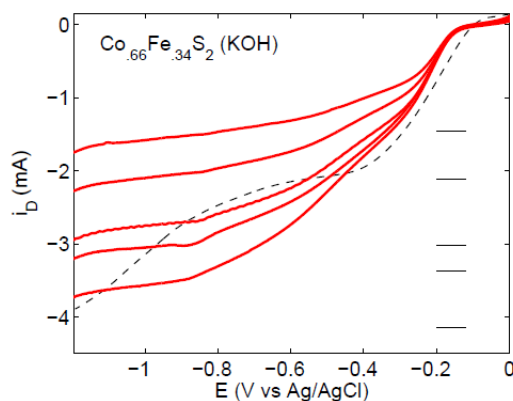


Figure 2.  $\text{O}_2$  reduction on a rotating  $\text{Co}_{2/3}\text{Fe}_{1/3}\text{S}_2$  covered Au electrode.

- [1] W.M. Temmerman, P.J. Durham, D.J. Vaughan, *Phys. Chem. Minerals* 20 (1993) 248-254
- [2] J.R.T. Johnsson Wass, I. Panas, J. Asbjörnsson, E. Ahlberg, *J. Electroanal. Chem.* 599 (2007) 295-312
- [3] J.S. Jirkovský, A. Björling, E. Ahlberg, *J. Phys. Chem. C* 116 (46) (2012) 24436-24444
- [4] S.R. Butler, R.J. Bouchard, *J. Cryst. Growth* 10 (1971) 163-169
- [5] J-T. Han, Y-H. Huang, W. Huang, *Matt. Letters* 60 (2006) 1805-1808

# Preparation and Characterization of Platinum Nanoparticles Supported on Silica-Carbon Black Nanocomposites for Methanol Oxidation Reaction

Cheng-Lan Lin, Ju-Yu Yeh

Department of Chemical and Materials Engineering, Tamkang University  
No. 151, Yingzhuan Rd., Tamshui Dist., New Taipei City 25137, Taiwan  
cclin@mail.tku.edu.tw

Electrocatalysts composed of platinum nanoparticles supported on silica-carbon black nanocomposites (Pt/SiO<sub>2</sub>-C) for methanol oxidation reaction (MOR) are prepared and characterized in this study. Silica nanoparticles are firstly synthesized by sol-gel method on Vulcan XC-72 carbon black surface to form SiO<sub>2</sub>/C composites, and Pt nanoparticles are then decorated onto the composites using polyol method to obtain Pt-SiO<sub>2</sub>/C electrocatalysts. Electrocatalysts with SiO<sub>2</sub>/C weight ratio of 2/98 to 12/88 are prepared and the Pt loading of the electrocatalysts is measured using inductively coupled plasma-optical emission spectroscopy to be ~20 wt%. The average diameter of the Pt nanoparticles is about 3 nm as estimated from transmittance electron microscope images. Electrochemical properties and MOR performances of the electrocatalysts are investigated using cyclic voltammetry, chronoamperometry and CO-stripping voltammetry. The results indicated that Pt/SiO<sub>2</sub>-C electrocatalysts have superior MOR catalytic activity, more negative surface-absorbed CO oxidation onset potential, averagely larger electrochemical active surface area and better stability than a commercial E-TEK Pt/C electrocatalyst. Electrochemical impedance spectroscopy analysis showed that the Pt/SiO<sub>2</sub>-C electrocatalyst with the SiO<sub>2</sub>/C weight ratio of 8/92 has comparable charge transfer resistance as the commercial E-TEK PtRu/C electrocatalyst, and suggested that the bi-functional mechanism might be responsible for the enhanced MOR performance. It is envisioned that the Pt/SiO<sub>2</sub>-C might served as new potential candidate of the MOR electrocatalyst for direct methanol fuel cell.

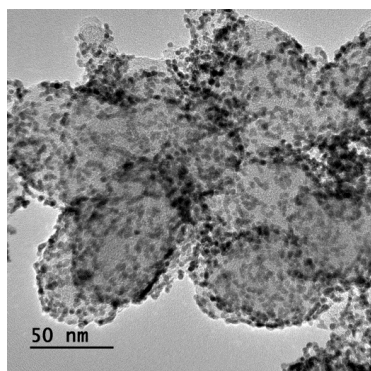


Figure 1 TEM image of a Pt/SiO<sub>2</sub>-C electrocatalyst.

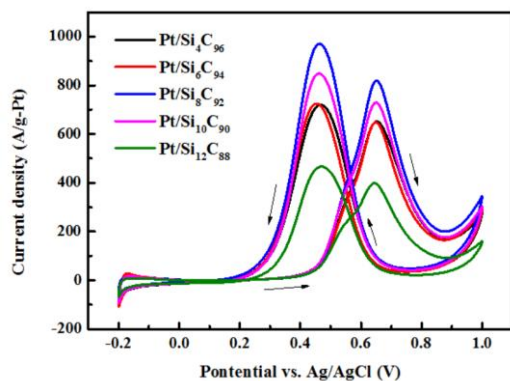


Figure 2 Cyclic voltammograms of the Pt/SiO<sub>2</sub>-C electrocatalysts in 0.5 M H<sub>2</sub>SO<sub>4</sub> solution containing 1.0 M methanol.

# Multi-Components Amorphous Metal-Oxides Catalysts for Oxygen Evolution Reaction

Chia-Ying Chiang, Po-Tso Ting

*Department of Chemical Engineering, National Taiwan University of Science and Technology  
Taipei, Taiwan (106)  
cychiang@mail.ntust.edu.tw*

With the rapid development of economy and industry, global energy demand increases enormously. People use petroleum as energy source for a long time, while the stock of this finite source decreases rapidly. Moreover, in order to protect environment, clean and renewable energy sources are considered to replace petroleum, which is a finite source and causes air pollution. Hydrogen energy source producing from water splitting is one of the best ways to solve energy source insufficient, protecting environment. Recently, photovoltaic system combines with dc-dc converter and electrolyzer is a common way to produce hydrogen and oxygen by water electrolysis. However, the conversion efficiency of this system is only 8%, and the potential of producing hydrogen is around 1.9 V, which is largely higher than the minimum potential of hydrogen production by water splitting (1.23 V). The main restriction of photovoltaic system is on the performance of electrodes. Efficiency of producing hydrogen and oxygen depends on the catalytic efficiency of electrode. Furthermore, the reaction of water splitting is primary controlled by the extremely low rate of oxygen production process. Until now, the most efficient catalysts of producing oxygen in water splitting are noble metal, which is rare and the cost is high. These two characteristics of noble metal are not suitable for mass production. Therefore, the object of this research is to find a material which is cheap, abundant on earth's upper crust, stable over a long period of time, and has high current density ( $>0.5 \text{ mA/cm}^2$ ) at low overpotential ( $< 0.3 \text{ V}$ ).

Metal oxides are considered as the stable catalysts which have high catalytic activity for oxygen evolution reaction (OER), such as  $\text{IrO}_2$ , spinel solids and amorphous metal oxides. In addition, amorphous metal oxides have been proved that they have potential to replace noble metal as OER materials. Niobium is abundant on earth's upper crust, and its oxide has been proved to have photochemical ability to produce oxygen in water splitting. Therefore, this research will focus on the series of niobium oxides for OER. Photochemical metal-organic deposition (PMOD) is one of the best ways to make amorphous thin films, due to the cost of this process is cheap, operating temperature and pressure are low, equipment is simple and it is suitable for multicomponent amorphous oxides preparation. In order to check the kinetic performance of catalysts, cyclic voltammetry curve (CV) is plotted. From the CV curve, cobalt oxide is a relatively high catalytic activity catalyst for OER, when the current density reaches  $0.5 \text{ mA/cm}^2$  while the potential only required 1.45 V. In addition, Iron oxide and niobium oxide require potential 1.63 V and 2.5 V, respectively, to reach the same current density. However, when cobalt doped with niobium and iron by the ratio of 1 : 2 : 2, the Tafel slope of  $\text{Nb}_{20}\text{Co}_{40}\text{Fe}_{40}$  is smaller than cobalt oxide. This indicates a more efficient catalyst is prepared. More detailed analysis and mechanism will be given in this talk.

# Development and Characterization of Nanostructured Multifunctional Materials for Photoelectrochemical and Electrocatalytic Reduction of Carbon Dioxide and Water Splitting

Pawel J. Kulesza

*Faculty of Chemistry, University of Warsaw, Pasteura 1, PL-02-093 Warsaw, Poland.  
pkulesza@chem.uw.edu.pl*

Through intentional and controlled combination of metal oxide semiconductors, we have been able to drive effectively photoelectrochemical reduction of carbon dioxide. The combination of titanium (IV) oxide ( $\text{TiO}_2$ ) and copper (I) oxide ( $\text{Cu}_2\text{O}$ ) has been explored toward the reduction of carbon (IV) oxide ( $\text{CO}_2$ ) before and after sunlight illumination. Application of the hybrid system composed of both above-mentioned oxides resulted in high current densities originating from photoelectrochemical reduction of carbon dioxide mostly to methanol ( $\text{CH}_3\text{OH}$ ) as demonstrated upon identification of final products. The role of  $\text{TiO}_2$  is not only stabilizing: the oxide is also expected to prevent the recombination of charge carriers.

When it comes to the development of electrocatalytic systems for reduction of carbon dioxide, instead of conventional Pd (or Pt) nanoparticles, nanosized Pd (or Pt) immobilized within tridentate Schiff-base ligands of the supramolecular complex of the type,  $[\text{Pd}(\text{C}_{14}\text{H}_{12}\text{N}_2\text{O}_3)\text{Cl}_2]_2 \cdot \text{MeOH}$ , have been considered. Reduction of carbon dioxide begins now at less negative potentials and is accompanied by significant enhancement of the  $\text{CO}_2$ -reduction current densities. Among important issues are specific interactions between nitrogen coordinating centers and metallic palladium sites at the electrocatalytic interface.

There has been growing interest in the development of photoanode materials for sunlight-driven oxygen generation (photoelectrochemical water splitting to oxygen and hydrogen). Among important issues is that the semiconducting oxide should be characterized by indirect optical transition in the visible part of the solar spectrum. We demonstrate here utility of gold and hematite nanoparticles (modified or stabilized with simple and derivatized Keggin-type molybdate and tungstate polyoxometallates) to enhance photocurrents generated by mesoporous tungsten trioxide,  $\text{WO}_3$ , photoanodes irradiated with visible light in aqueous solutions. The possibility of the plasmonic effect and interactions between the gold plasmons will be addressed. Independent diagnostic experiments, voltammetric with Pt microdisk electrode and amperometric type with Clark oxygen sensor, have confirmed the appearance of oxygen during photooxidation of water. In a case of the enhancement effect at  $\text{WO}_3$  films doped with borotungstic acid-stabilized hematite, the observed phenomena could be rationalized either in terms of the presence of new conduction band structures in doped  $\text{WO}_3$  films or a marked increase in the degree of hydration of the doped oxide structures.

# Unexpected Good Deed of a Traditional Poison: Sulfur-Adsorption Enhanced Activity and Stability of Pt for Oxygen Reduction Reaction

Yanyan Wang, YuYe J. Tong  
 Department of Chemistry, Georgetown University  
 37<sup>th</sup> and O Streets NW, Washington DC 20057  
 yyt@georgetown.edu

Sulfur is a well-known poison in both heterogeneous catalysis and electrocatalysis<sup>[1]</sup>. But recently, we have observed that it can also do good deeds: enhancing oxygen reaction (ORR)<sup>[2]</sup>, CO<sup>[3]</sup> as well as methanol oxidation reaction<sup>[4]</sup> on Pt. The adsorbed sulfur coverage dependence of ORR on commercial Pt black (Johnson-Matthey) obtained in a more detailed recent study is shown in Figure 1, confirming the previously observed activity enhancement effect. Moreover, we have observed recently that sulfur adsorption can also enhanced the stability of Pt black when the latter was subjected to accelerated stability test: after 40k potential cycles between 0.6V to 1.1V (vs. RHE) under saturated O<sub>2</sub> at room temperature, the electrochemical surface area (ECSA) of the S-adsorbed (~16%) Pt black was reduced by ~25% as compared to ~52% for pure Pt black, well above the DOE's 2017 target.

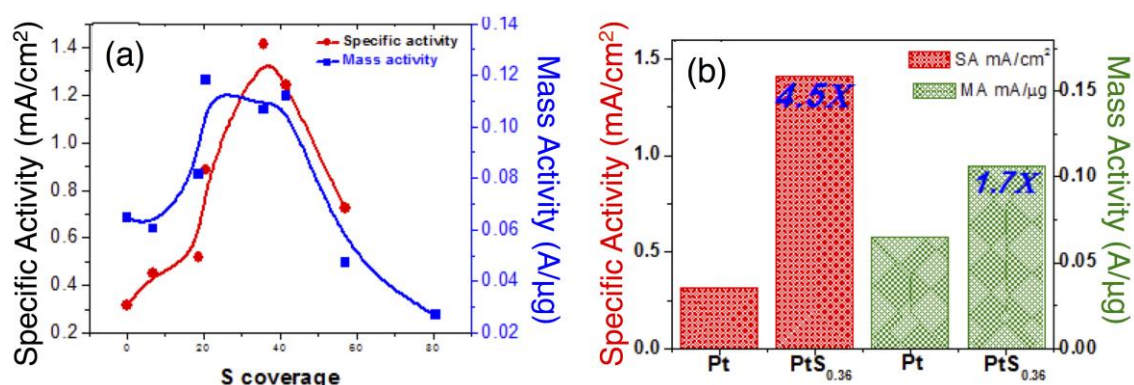


**Figure 1.** (a) The S-coverage dependent specific activity (left) and mass activity (right) of ORR on Pt black. (b) Comparison of the activities for the sample with 36% S-coverage with pure Pt black. 4.5 times and 1.7 times enhancement in specific activity and mass activity respectively were observed.

In this presentation, in addition to electrochemical data, we will discuss mechanistic insights afforded by in situ surface enhanced IR absorption and Raman spectroscopic studies on why sulfur adsorption can enhance ORR and stability of Pt black. The spectroscopic results obtained strongly suggest that S-adsorption induced enhanced O<sub>2</sub> adsorption and delayed Pt oxidation may well be the reasons for observed enhanced activity and stability.

- [1] Y. Y. J. Tong, *Chem. Soc. Rev.* **2012**, *41*, 8195-8209.
- [2] I.-S. Park, Y. Y. J. Tong, *Electrocatal.* **2013**, *3*, 117-122.
- [3] I.-S. Park, D.-J. Chen, D. O. Atienza, Y. Y. J. Tong, *Catalysis Today* **2013**, *202*, 175-182.
- [4] I.-S. Park, D. O. Atienza, A. M. Hofstead-Duffy, D. J. Chen, Y. Y. J. Tong, *ACS Catal.* **2012**, *2*, 168-174.

# Synthesis of CoFe<sub>2</sub>O<sub>4</sub>/Nitrogen-doped Graphene and Its Catalytic Performance for ORR

Qingli Hao, Wu Lei, Lei Lu, Xifeng Xia

*Key Laboratory for Soft Chemistry and Functional Materials, School of Chemical Engineering, Nanjing University of Science and Technology  
Nanjing 210094, China*

*E-mail: qinglihao@njust.edu.cn; haoqingli@yahoo.com*

Due to the sluggish kinetics of oxygen reduction reaction (ORR), the development of efficient electrocatalysts for ORR becomes the key task and main challenge in the renewable energy technologies. Platinum (Pt) and Pt-based alloys are the best known and most active ORR catalysts, but the high cost, their low durability and poor susceptibility to poisoning definitely limit the commercialization of Pt-based catalysts<sup>[1-4]</sup>. Herein, we report a nanostructured hybrid CoFe<sub>2</sub>O<sub>4</sub> loaded on N-doped reduced graphene oxide (CoFe<sub>2</sub>O<sub>4</sub>/NG) as an efficient synergistic ORR catalyst. The hybrid was prepared through a facile one-step solvothermal method followed by calcination. It exhibited a comparable catalytic activity as commercial Pt/C with a preferential four-electron pathway in the ORR, while it outperformed Pt/C in terms of stability and resistance to CO poisoning and methanol crossover. It was able to fully combine the advantages of both CoFe<sub>2</sub>O<sub>4</sub> nanoparticles and N-doped reduced graphene oxide, achieving a more positive ORR onset potential than CoFe<sub>2</sub>O<sub>4</sub> loading on non-doped reduced graphene oxide in the previous literature. Moreover, the multi-metal oxide shows better catalytic activity to ORR than the single metal oxide does. Interestingly, we found high crystalline degree of spinel CoFe<sub>2</sub>O<sub>4</sub> can contribute to its excellent onset potential in ORR activity of CoFe<sub>2</sub>O<sub>4</sub>/NG, apart from the active nature of CoFe<sub>2</sub>O<sub>4</sub>/NG. Therefore, its simple preparation method, low-cost, efficient catalytic activity, excellent stability and great resistance to CO poisoning and methanol crossover can make CoFe<sub>2</sub>O<sub>4</sub>/NG a promising ORR catalyst to replace the high costly commercial Pt/C.

The work was supported by the National Natural Science Foundation of China (No. 21103092), Program for NCET-12-0629, the Ph.D. Programs Foundation of Ministry of Education of China (No.20133219110018), Qing Lan Project and Six Major Talent Summit (XNY-011), the Science and Technology Support Plan (No. BE2013126), and PAPD of Jiangsu Province, China.

## References:

- [1] G Wu, K L More, C M Johnston, *et al.* Science, 2011, 332(6028): 443-447.
- [2] S Wang, L Zhang, Z Xia, *et al.* Angewandte Chemie International Edition, 2012, 51(17): 4209-4212.
- [3] J Wu, L Qi, H You, *et al.* Journal of the American Chemical Society, 2012, 134(29): 11880-11883.
- [4] Guo S, Sun S. Journal of the American Chemical Society, 2012, 134(5): 2492-2495.



# Electrocatalytic and Photocatalytic Hydrogen Production

Mehmet AYDEMİR, Duygu AKYÜZ, Burag AGOPCAN, Cevat SARIOĞLU, M.Kasım ŞENER, Fatma Karaca ALBAYRAK, Atif KOCA\*

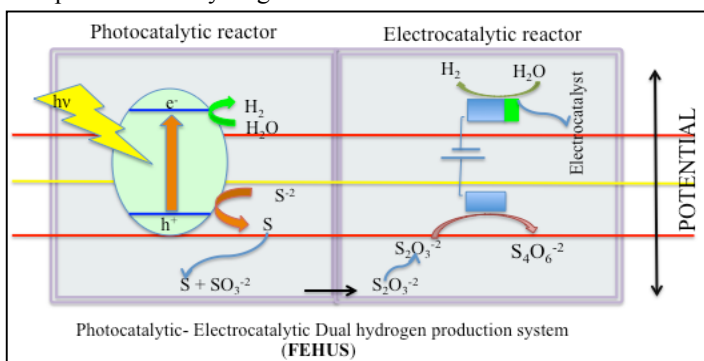
Engineering Faculty, Marmara University, 34722 Göztepe, Istanbul- Turkey  
Tel:902163480292; Fax:902163480293; E-mail: akoca@marmara.edu.tr

## Electrocatalytic Materials

In order to solve the global warming and carbon dioxide emission problems caused by the fossil fuels, new technologies for solar energy conversion and storage into chemical energy, hydrogen, are now attracting attention. Now a day's hydrogen is generally produced from fossil fuels and from water electrolysis by using electricity. Hydrogen could take its merit position in the global energy sector, if hydrogen could be efficiently produced with low cost and simple ways by using alternative energy resources. Sustainable, renewable, and clean hydrogen can be produced if solar energy is used as energy source and water is used as hydrogen source in hydrogen production system. In these type systems, solar energy converted into electricity with proper methods is used indirectly in water electrolysis or directly used to convert water to chemical energy as hydrogen energy [1,2]. Presently, the solar-to-hydrogen energy conversion efficiency is too low for the technology to be economically sound. Consequently, a high-performance system therefore needs to be developed for a sustainable hydrogen energy system. In the scope of this study, to produce efficient and low cost hydrogen by using alternative energies with simple ways; **we designed and optimized a “photocatalytic-electrocatalytic dual hydrogen production system (FEHUS)” which combined discontinuous photocatalytic and electrocatalytic systems in one continuous dual system.**

In the electrolysis chamber of FEHUS, which was design in study, an “electrocatalytic electrolysis system” (use solar energy indirectly) and in the photocatalytic chamber, a “photocatalytic hydrogen production system” (use solar energy directly) was used. In the photocatalytic chamber of FEHUS, photocatalysts, which are active in both of the UV and visible part of the light spectrum. As a result of the light absorption of photocatalysts, while water-hydrogen reduction reaction took place at the conduction band (CB) of the photocatalysts, sacrificial  $S^{2-}$  electrolyte oxidized to  $S_2O_3^{2-}$  with the help of  $SO_3^{2-}$  at the valance band (VB) of the photocatalysts.  $S_2O_3^{2-}$  produced in the photocatalytic chamber of FEHUS was used as redox species in the electrolysis chamber. Usage of  $S_2O_3^{2-}$  in the electrolysis chamber, the cell potential of water electrolysis considerably decreased. Moreover usage of electrocatalysts on the cathode decreased the over-potential of the cathode for the hydrogen reduction reaction.

$CuInS_2$ ,  $AgInS_2$ ,  $ZnS$ ,  $CdS$  and mixture of these ( $Cd_{(1-x)}Zn_xS$ ) and  $ZnS$ ,  $CdS$  and ( $Cd_{(1-x)}Zn_xS$ ) doped with  $TiO_2$  and  $WO_3$  were used as photocatalysts in the photocatalytic chamber of FEHUS. Phthalocyanines, azido functionalized graphene oxide ( $GO-N_3$ ) and azido functionalized reduced graphene oxides ( $RGO-N_3$ ), phthalocyanines decorated and azido functionalized reduced graphene oxides ( $RGO-N_3-MPCs$ ), and cobaloximes were used as electrocatalyst on the cathode of the electrolysis system of FEHUS. Overpotential of hydrogen evolution reaction on GCE decreased 0.50 V with electrocatalysts on the



cathode. Moreover water electrolysis potential decreased about 0.80 V, when electrolyte of photocatalytic reaction was used as the electrolyte of the electrolysis cell. Consequently, more efficient, cheap, simple, pure and oxygen-free hydrogen was produced with this newly developed FEHUS. With this study, solar energy was successfully stored as hydrogen with a more efficient manner in a FEHUS.

**Acknowledgement:** This work is supported by the research fund of TÜBİTAK (Project no: 113M991) and Marmara University (Project no: FEN-C-YLP-080415-0118).

## References

1. Akihiko Kudo, Photocatalysis and solar hydrogen production, Pure Appl. Chem., Vol. 79, No. 11, pp. 1917–1927, 2007.
2. Koca, Atif, Hydrogen evolution reaction on glassy carbon electrode modified with titanyl phthalocyanines, International Journal Of Hydrogen Energy 34, 2009, 2107-2112.



# Investigation of ORR activity of strained thin film Pt electrocatalyst produced by pulsed laser deposition

S.E.Temmel<sup>1</sup>, E.Fabbri<sup>1</sup>, D.Pergolesi<sup>2</sup>, T.Lippert<sup>2</sup>, T.J.Schmidt<sup>1,3</sup>

*1) Electrochemistry Laboratory, Paul Scherrer Institut, 5232 Villigen PSI, Switzerland*

*2) Materials Group, Paul Scherrer Institut, 5232 Villigen PSI, Switzerland*

*3) Laboratory of Physical Chemistry, ETH Zürich, 8093 Zürich, Switzerland*

*Corresponding author: [sandra.temmel@psi.ch](mailto:sandra.temmel@psi.ch)*

Polymer electrolyte fuel cells (PEFCs) play a key role in the development of sustainable automotive technology due to their low operating temperature, high energy densities and emission-free operation mode. Nevertheless, the large-scale production of these environmentally friendly devices is still constrained by the large overpotential arising from the oxygen reduction reaction (ORR) at the cathode, limiting their overall performance. Since state-of-the-art PEFC electrocatalysts all contain Pt, many efforts are being devoted to improve its electrocatalytic activity[1].

Varying the inter-atomic distance of Pt atoms to modify the adsorption properties of oxygen species on its surface represents a promising strategy [2]. In this context, we present a novel approach for producing a model Pt electrocatalyst with different inter-atomic spacing. Pulsed laser deposition was applied to prepare ultra-thin and differently strained Pt films on single crystalline strontium titanate substrates with (100) and (111) orientation. X-ray diffraction measurements confirmed their epitaxial orientation and high crystalline quality. *In situ* reflection high energy electron diffraction (RHEED) measurements revealed that the Pt films grow preferentially in a three dimensional Volmer-Weber mode. A distinct thickness-dependent morphology is observed by scanning electron microscopy..

The electrochemical surface properties of the as-produced Pt films were examined by cyclic voltammetry and CO stripping. The influence of varying inter-atomic Pt distances on the ORR activity was determined using a specifically designed flow cell.

Here we present the first results on the structural and the electrochemical analyses of the Pt films. It will be demonstrated that strained Pt films exhibit a superior activity towards ORR as compared to the single crystalline fully relaxed bulk structure.

[1] [A.Rabis, P.Rodriguez and T.J.Schmidt, ACS Catal. 2012, 2, 864–890](#)

[2+] [P. Strasser, Nature chemistry, 2010, 2, 454-460](#)

# Determination of Oxygen Binding Energy from Simple Amperometric Experiments and its Application Towards the Evaluation of Novel Materials for the Oxygen Reduction Reaction

Samuel C. Perry, Guy Denuault  
University of Southampton  
University Road, Southampton SO17 1BJ, UK  
scp2g08@soton.ac.uk

Electrocatalytic activity of pure metals towards the oxygen reduction reaction (ORR) has been shown to be dependent on the binding energy of oxygen towards said metal ( $\Delta E_O$ )<sup>1</sup>, with platinum being regarded as the optimum noble metal for the ORR. Previously, the assessment of  $\Delta E_O$  for novel materials, metals and alloys required independent DFT studies for comparison with pure metal values in the literature. We present experimental results which offer an alternative means to evaluate the magnitude of  $\Delta E_O$  for ready comparison of materials using chronoamperometry at microdisc electrodes in aqueous media. When investigating the ORR on the millisecond timescale we found an unexpected additional chronoamperometric response for sampling times of less than around 50 ms, indicating that the ORR rate is not solely controlled by the diffusion of dissolved oxygen towards the microelectrode<sup>2,3</sup>. Careful analysis of this extra current under varying conditions with strict controls on electrode and solution conditions showed the extra current to be due to the reduction of pre-adsorbed dioxygen from the solution. When plotted against the binding energies reported to dioxygen, the associated charge ( $Q$ ) produces a calibration curve, Figure 1.

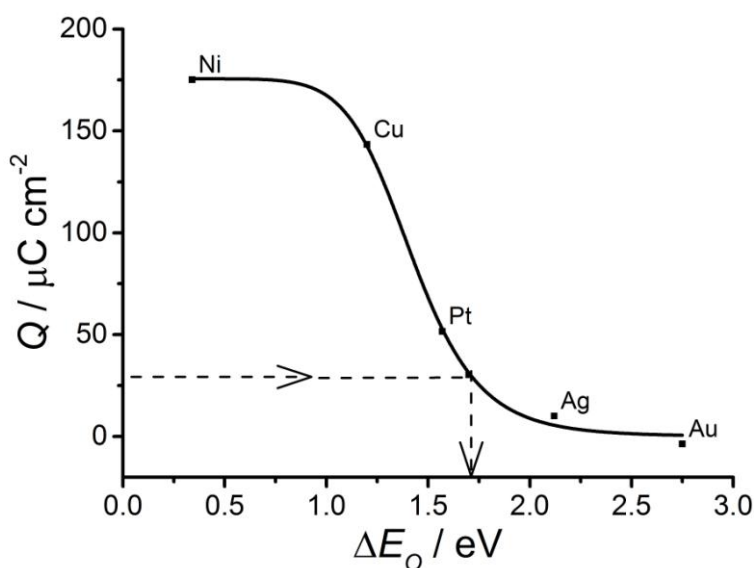


Figure 1: Extra charge calculated from the difference between experimental and theoretical current transients for the oxygen reduction reaction against the binding energy ( $\Delta E_O$ ) reported by Norskov et al.<sup>3</sup> for those metals toward oxygen. The connected sigmoid is intended as a guide for use as a calibration curve for the calculation of  $\Delta E_O$  from chronoamperometric data.

The constructed curve offers a simple means for the determination of  $\Delta E_O$  without the need for complex DFT or other computational analysis, thereby offering a method for a rapid interrogation of the ORR behaviour of a novel material. This is illustrated in Figure 1 with the determination of  $\Delta E_O$  for a mixed metal alloy from experimental data.

- (1) Norskov, J. K.; Rossmeisl, J.; Logadottir, A.; Lindqvist, L.; Kitchin, J. R.; Bligaard, T.; Jonsson, H. *J. Phys. Chem. B* **2004**, *108*, 17886-17892.
- (2) Shoup, D.; Szabo, A. *J. Electroanal. Chem.* **1982**, *140*, 237-245.
- (3) Mahon, P. J.; Oldham, K. B. *Anal. Chem.* **2005**, *77*, 6100-6101.

# Electrochemical CO<sub>2</sub> Reduction on Pd-based Bimetallic Catalysts

Ruud Kortlever<sup>1</sup>, Ines Peters<sup>1</sup>, Collin Balemans<sup>1</sup>, Meital Shviro<sup>2</sup>,

Youngkook Kwon<sup>1</sup>, David Zitoun<sup>2</sup>, Marc T.M. Koper<sup>1</sup>

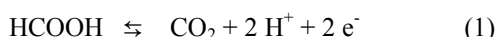
<sup>1</sup>Catalysis and Surface Science, Leiden Institute of Chemistry, Leiden University

<sup>2</sup>Nanomaterials on Surfaces Lab, Bar-Ilan University

e-mail address: ruud.kortlever@gmail.com

The electrocatalytic reduction of carbon dioxide has attracted the interest of electrochemists and inorganic chemists for decades as a key reaction in facilitating a sustainable low-temperature redox cycle for energy storage and conversion.<sup>1</sup> However, major issues still need to be resolved before the reduction of CO<sub>2</sub> to fuels becomes practically feasible.<sup>2</sup> The main problems holding back electrocatalytic CO<sub>2</sub> reduction are the high overpotentials needed and the poor product selectivity and faradaic efficiency, since the hydrogen evolution reaction (HER) is a competing reaction in the potential window in which CO<sub>2</sub> reduction takes place. To overcome these problems new catalyst systems need to be developed that increase the product selectivity and efficiency of electrocatalytic CO<sub>2</sub> reduction, while simultaneously lowering the overpotentials.

In biological systems, formate dehydrogenase enzymes show efficient reduction of CO<sub>2</sub> to formic acid at low overpotentials. Armstrong and Hirst have recently discussed how these redox enzymes can reversibly catalyze reaction 1:<sup>3</sup>



but there is no fundamental reason why inorganic metallic catalysts could not do the same, since “reversible electrocatalysts” are expected to exist for two-electron transfer reactions.<sup>4</sup> Metallic catalysts that are very active for formic acid oxidation are mostly palladium- or platinum-based catalysts.

We have combined palladium and platinum; both by depositing (mono-)layers of palladium on a platinum substrate<sup>5</sup> and by synthesizing Pd<sub>x</sub>Pt<sub>(100-x)</sub>/C alloy nanoparticles and tested these materials for the reduction of CO<sub>2</sub>. These catalysts show a very low onset potential of 0.0 V vs. RHE for the reduction of CO<sub>2</sub> to formic acid in a pH 6.7 electrolyte. While the deposited layers of palladium on platinum show a very fast deactivation due to CO poisoning, the Pd<sub>x</sub>Pt<sub>(100-x)</sub> nanoparticles can be optimized to avoid such a fast deactivation and show a maximum faradaic efficiency of ~88% after 1 hour of electrolysis at -0.4 V vs. RHE for Pd<sub>70</sub>Pt<sub>30</sub>/C. Furthermore, since the Pd-Pt catalysts are also active for the oxidation of formic acid, we demonstrated that these catalysts can reversibly reduce CO<sub>2</sub> to formic acid and oxidize formic acid to CO<sub>2</sub> (See Fig. 1).

When Pd (mono)layers were deposited on an Au substrate the reduction of CO<sub>2</sub> yielded C<sub>1</sub> to C<sub>4</sub> hydrocarbons. The same products were observed for the reduction of CO<sub>2</sub> on PdNi alloy nanoparticles. This is an unique result, since until now only copper is known to produce C<sub>1</sub> and C<sub>2</sub> hydrocarbons. The formation of hydrocarbon products was studied by varying the Pd-layer thickness on bulk Au and on Au nanoparticles and as a function of PdNi alloy nanoparticles composition.

## References

- [1] M. Gattrell, N. Gupta, A. Co, *Energy Convers. Manage.* **2007**, 48, 1255.
- [2] N.S. Spinner, J.A. Vega, W.E. Mustain, *Catal. Sci. Tech.* **2012**, 2, 19.
- [3] Armstrong, F. A.; Hirst, J. *PNAS* **2011**, 108, 14049.
- [4] Koper, M. T. M. *J. Electroanal. Chem.* **2011**, 660, 254.
- [5] R. Kortlever, C. Balemans, Y. Kwon, M.T.M. Koper, *Catal. Today* **2015**, 244, 58.

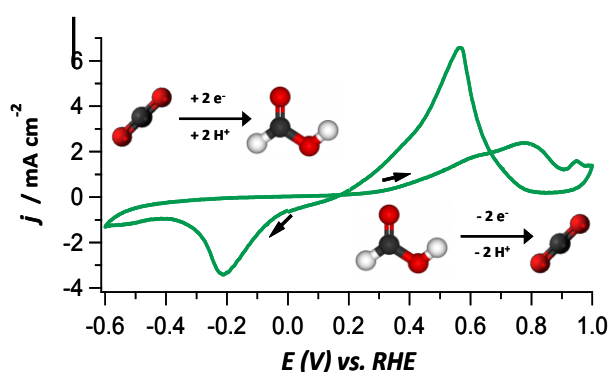


**Fig. 1:** Cyclic voltammogram of reversible CO<sub>2</sub> reduction and formic acid oxidation on a Pd-Pt electrode in a pH 6.7 electrolyte in the presence of CO<sub>2</sub> and formic acid.

# ORR activities of Au-Modified Stepped Pt Single Crystal Electrodes

Kensaku Kodama, Ryosuke Jinnouchi, Naoko Takahashi, Hajime Murata, Yu Morimoto  
 Toyota Central R&D Labs., Inc.  
 41-1 Yokomichi, Nagakute, Aichi 480-1192, Japan  
 kkodama@mosk.tytlabs.co.jp

Pt nanoparticles are one of the most promising electrocatalysts for polymer electrolyte fuel cells (PEFCs), because of moderate oxophilicity of Pt metal surface for oxygen reduction reaction (ORR) and high specific surface areas with their morphologies. The activity and durability of Pt nanoparticles, however, still need to be improved for automobile applications. Among the various crystallographic sites on the particle, low-coordinated Pt atoms at the edge parts have been shown to have negligible contributions for the ORR activity and become the starting site of consecutive dissolutions of Pt because of their high oxophilicities [1, 2]. These observations suggest that replacing Pt atoms in the edge parts of a Pt nanoparticle by nobler Au atoms can improve the durability without reducing the ORR activity. Recently, Jinnouchi et al., using a first principles theory, showed that the Pt-Au replacements at the edge parts even improve the ORR activity by changing the oxophilicity of the Pt nanoparticle [2]. This prediction is experimentally tested using a model Pt surface in the present study.

Figure 1 shows the CVs for Pt (111), Pt (322), the structure of which is shown in Fig.2a, and the Au-modified Pt (322) (denoted Au/Pt (322)). By the Au-modification, the Pt (100)-step peaks at 0.29 V disappeared while the Pt (111)-terrace contribution between 0.05 – 0.4 V remained unaffected. This data suggests that the step Pt atoms have been selectively masked by Au atoms. (The selective masking was also supported by X-ray photoelectron spectroscopy; the number density of Au atoms on the Pt surface was consistent with that of (100) step sites.) Fig. 2b shows a possible structure, where the Au atoms occupy 4-fold hollow sites on the (100) step. The Au-modified structure, where the additional Au atoms form new steps and the original step Pt rows are regarded as the second rows from the edges of the new terraces, is an ideal model catalyst where the low-coordinated Pt atoms have been replaced by Au atoms.

Figure 3 shows the ORR polarization curves and Tafel plots of the ORR kinetic currents for Pt (111), Pt (322) and Au/Pt (322). The ORR-improving factors at 0.9 V are 2.8 from Pt (111) to Pt (322), and 1.4 from Pt (322) to Au/Pt (322), showing the definite improving effect of the Au modification, which agrees with the theoretical prediction [2]. The origin of the Au-effect as well as the step-induced ORR improvement will be discussed in the meeting.

**References** [1] M.H. Shao et al., *Nano Lett.*, **11** (2011) 3714 [2] R. Jinnouchi et al., *to be submitted*  
**Acknowledgement** This work was financially supported by NEDO.

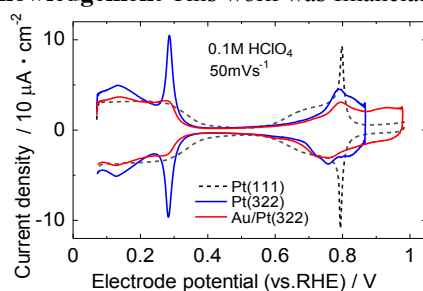


Fig.1 CVs.

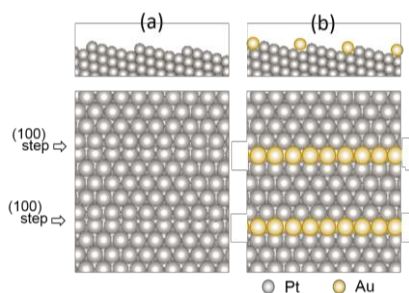


Fig. 2 Side and top views of (a) a bare Pt (322) and (b) a possible structure of the Au-modified Pt (322).

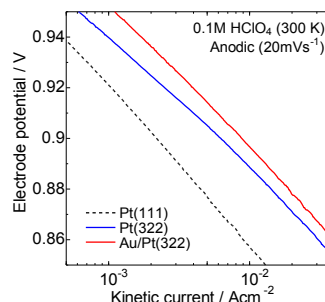
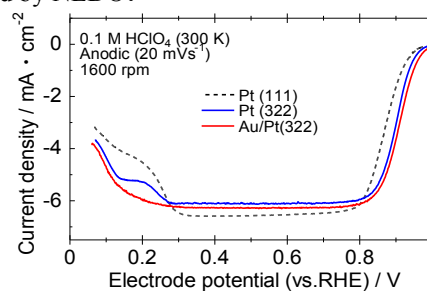


Fig.3 ORR polarization curves (upper part) and Tafel plots for the kinetic currents (lower parts).

# Investigation of Hydrazine Oxidation at Co Fiber Structure Decorated with Pt Nanoparticles

L. Tamašauskaitė-Tamašiūnaitė, A. Zabielaite, S. Lichušina, A. Matusevičiūtė, D. Šimkūnaitė, A. Selskis, E. Norkus

*Center for Physical Sciences and Technology  
A. Gostauto 9, LT-01108 Vilnius, Lithuania  
loreta.tamasauskaite@ftmc.lt*

In the present study the activity of the Co with a fiber structure decorated by Pt nanoparticles (denoted as Pt/Co<sub>fiber</sub>) was investigated towards the oxidation of hydrazine. The platinum-cobalt catalysts were deposited on the Cu surface using simple and cost-effective electrochemical and chemical methods. At first, Co coating with a fiber structure and the thickness of ~3 μm was electroplated onto the Cu surface. Then, the Pt nanoparticles were deposited on the prepared Co<sub>fiber</sub>/Cu by its immersion into the 1 mM H<sub>2</sub>PtCl<sub>6</sub> + 0.1 M HCl solution at the temperature of 25 °C for 10, 20 and 60 s, respectively. The morphology, structure and composition of the prepared catalysts were characterized by means of Field Emission Scanning Electron Microscopy, Energy Dispersive X-ray Spectroscopy and Inductively Coupled Plasma Optical Emission Spectroscopy. The electrocatalytic properties of catalysts were evaluated with respect to the oxidation of hydrazine in an alkaline medium by means of cyclic voltammetry and chrono-techniques.

It was found that the Pt loadings were 5.4, 15.4 and 28.7 μg cm<sup>-2</sup> in the prepared Pt(Co<sub>fiber</sub>)/Cu catalysts after the immersion of Co<sub>fiber</sub>/Cu into the platinum-containing solution for 10, 30 and 60 s, respectively. It was found that the cobalt with a fiber structure decorated with the platinum nanoparticles show enhanced electrocatalytic activity towards the oxidation of hydrazine in an alkaline medium as compared to that of bare Pt and Co deposited on the Cu surface.

# Pt (Pd) Monolayer on Au Formed by One-Pot Chemical Process with Enhanced Electrocatalytic Performance on Ethanol Oxidation

Han Wang, Wen-Bin Cai\*

*Collaborative Innovation Center of Chemistry for Energy Materials and Department of Chemistry, Fudan University, Shanghai 200433, China*  
wbcai@fudan.edu.cn

Low-abundance precious metals Pt and Pd are generally required in the anode catalysts of fuel cells to drive the electrocatalytic oxidations of small alcohol molecules. In order to maximize their utilization in practical catalysts, an effective way is to synthesize by design the Pt (Pd) monolayer (ML) shell-suitable core nanostructures in which the shell atoms can be fully utilized and the catalytic activity of Pt (Pd) shell may be enhanced by its interaction with the core. Besides other applications, Au@Pt and Au@Pd core-shell structured catalysts were reportedly favorable for the electro-oxidations of alcohol and formic acid, respectively<sup>[1]</sup>. So far, the widely recognized synthesis of Au@Pt(Pd)-ML is based on a two-step process involving an initial UPD of Cu on Au followed by galvanic redox replacement of Cu with Pt(Pd). That process requires external potential control, which is unfavorable for a scale-up fabrication<sup>[2,3]</sup>. Herein, with the delicate control over the concentration of Pt or Pd-precursor in a CO-containing solution, a ML of Pt, Pd or Pd+Pt can be deposited either on Au/C or on Au nanofilm at room temperature in one-pot chemical synthesis without any external potential control<sup>[4]</sup>. The ML formation was characterized on Au@Pt-ML/C with XRD and TEM-EDS measurement (Fig.1A) or on Au/Pt-ML film with ATR-IR measurement using CO as the surface probe. The as-synthesized Au@Pt-ML/C showed a remarkable enhancement in ethanol oxidation in terms of activity and durability (Fig.1B). The Au@M-ML/C also showed a pH sensitive activity toward ethanol electro-oxidation.



**Fig. 1** (A). XRD patterns of Au@Pt-ML/C, Au/C and Pt/C; (B). Chronoamperometric plots recorded at 0.75 V (RHE) in 1 M NaOH + 1 M ethanol.

**Acknowledgements:** Financial supports from NSFC (grant No. 21273046 and 21473039) and SMCS (grant NO.11JC140200) are highly appreciated

## References:

- [1] M. Li, P. Liu, R.R. Adzic, *J Phys. Chem. Lett.*, 3 (2012) 3480-3485.
- [2] B. Peng, J.Y. Wang, H.X. Zhang, Y.H. Lin, W.B. Cai, *Electrochem. Commun.* 11 (2009) 831-833.
- [3] S. H. Wang, H.X. Zhang, W.B. Cai, *J. Power Sources*, 212 (2012) 100-104.
- [4] S. Brimaud, R.J. Behm, *J. Am. Chem. Soc.*, 135 (2013) 11716-11719.

# Bridging across Electrocatalytic Performances of Nanomaterials & Interfacial Species Evolution with Realtime ATR-IR Spectroscopy

Wen-Bin Cai\*, Kun Jiang, Ye Wang

Collaborative Innovation Center of Chemistry for Energy Materials and Department of Chemistry, Fudan University, Shanghai 200433, China  
wbcai@fudan.edu.cn

Over the past four decades, infrared spectroscopy with either external or internal reflection mode has played an important part in probing the electrode/electrolyte interface because of its capability to detect submonolayer change. With increasing application of electrocatalytic nanomaterials such as carbon supported or unsupported nanoparticles as well as nanofilms to hydrogen energy utilization including low-temperature hydrogen production and fuel cells<sup>[1,2]</sup>, a great deal of work has been aimed at the synthesis, characterization and performance of various electrocatalysts. In contrast, fewer investigations have been directed to the understanding of the electrocatalytic performances in terms of the corresponding interfacial chemistry at molecular level. To address the issue, we recently applied real time ATR-IR spectroscopy to investigate the interfacial molecular evolution during room-temperature hydrogen production from formic acid decomposition at Pd/C and Pd-B/C at OCP<sup>[1,2]</sup> as well as the electro-oxidation of formic acid on Pd black at constant and scanned potentials<sup>[2]</sup>. Also, *in situ* ATR-IR was extended for the first time to investigate the dealloying effect on ethanol oxidation reaction (EOR) at Pd-Ni-P nanofilm electrode in alkaline media<sup>[3,4]</sup>.

We monitored spectroscopically the accumulation of CO poisoning species and the simultaneous production of CO<sub>2</sub> at the solution side of the interface<sup>[1,2]</sup>. It is revealed that anti-CO poisoning nature of boron-doped Pd nanocatalyst at least partly contributes to its much higher turnover frequency (TOF) rate in hydrogen production. The CO accumulation at OCP significantly decreases the activity of Pd black toward formic acid oxidation, which can be resumed after a short positive potential pulse to activate CO oxidation (Fig.1). *In situ* ATR-IR spectroscopy enables to correlate the electrocatalytic performances of pristine and dealloyed Pd-Ni-P nanofilms toward EOR<sup>[4]</sup>. In response to the significantly enhanced oxidation current over time on the dealloyed nanofilm is the increased spectral intensities of interfacial species (such as CO and acetate that are respectively involved in the C1 and C2 pathways of EOR, not shown). In addition, the spectral results indicate that relative contribution of the C1 pathway to the C2 pathway increases on the dealloyed nanofilm as compared to that on the pristine one.

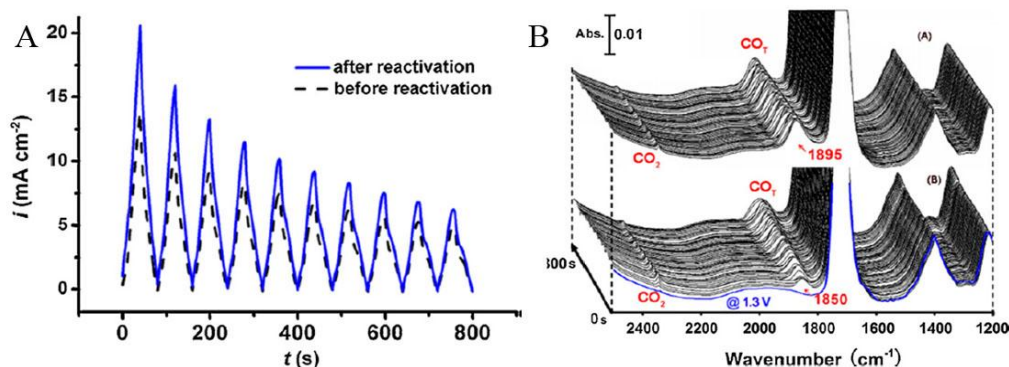


**Fig. 1** (A) Chronoamperometric curves for the Pd black/Au electrode in 5 M FA + 0.1 M HClO<sub>4</sub> solution for two potentiodynamic measurements between 0.1 and 0.5 V at 10 mV s<sup>-1</sup> before and after reactivation at 1.3 V (RHE). (B) Corresponding time-evolved IR spectra in the two runs of potentiodynamic measurements.

**Acknowledgements:** Financial supports from NSFC (grant No. 21273046 and 21473039) and SMCS (grant NO.11JC140200) are highly appreciated.

## References:

- [1] K. Jiang, K. Xu, S.Z. Zou, W.B. Cai, *J. Am. Chem. Soc.*, 136 (2014) 4861-4864.
- [2] H. X. Zhang, S. H. Wang, K. Jiang, W.B. Cai, *J. Power Sources*, 199 (2012) 165-169.
- [3] Y.Y. Yang, J. Ren, Q. X. Li; S.G. Sun, Z.Y. Zhou, W.B. Cai, *ACS Catal.*, 4(2014), 798-803.
- [4] Y. Wang, K. Jiang, W.B. Cai, *Electrochim. Acta*, 162(2015) 100-107.



# Three Dimensional Precious Metal Free Electrocatalysts for Water Splitting

Chuan Zhao, Xunyu Lu, Changlong Xiao  
School of Chemistry, The University of New South Wales  
Kensington Campus, Sydney, New South Wales, 2052  
chuan.zhao@unsw.edu.au

In an electrolytic water splitting cell, the production of H<sub>2</sub> at the cathode is severely constrained by the sluggish kinetics of the oxygen evolution reaction (OER) on the anode. As a consequence, highly efficient OER catalysts are required to lower the energy barrier to improve the overall energy efficiency. So far, IrO<sub>2</sub> and RuO<sub>2</sub> are the benchmark OER catalysts, owing to their high catalytic activity. Nevertheless, these precious metals are costly and their supply is not sustainable, therefore are not suitable for large-scale applications. Hence, enormous research efforts have been devoted to the development of low cost OER electrocatalysts based on first-row transition metals and their oxides, which exhibit good OER activity with significantly lowered fabrication costs.<sup>1,2</sup> Among these catalysts, nickel and cobalt based composites have shown promise as active catalyst materials for OER, which usually require overpotentials around 350 ~ 450 mV to deliver a current density (*j*) of 10 mA cm<sup>-2</sup>. Nevertheless, effective strategies are desired to further enhance the OER activity of the transition metal based catalysts to a level that is comparable to the benchmark IrO<sub>2</sub> and RuO<sub>2</sub>. Furthermore, to be used for industrial applications, OER catalysts also need to meet more strict criteria such as delivery of very high current densities ( $\geq 500$  mA cm<sup>-2</sup>) at low overpotentials ( $\leq 300$  mV), and mechanical robustness and prolonged durability during strong gas evolution.

The presentation concerns our strategies and progress in enhancing the OER activity of non-precious metal based OER catalysts, including downscaling, and/or making mesoporous structures Co<sub>3</sub>O<sub>4</sub> based OER catalysts,<sup>3,4</sup> using carbon nanomaterials as substrates to immobilize nanoparticle catalysts,<sup>5,6</sup> and making multi-metallic catalysts by taking advantage of synergistic metal-metal interactions.<sup>3,4</sup> Finally, we show a hierarchically structured three-dimensional nickel-iron electrodes fabricated by electrodeposition,<sup>7</sup> which only requires an overpotential of 200 mV to initiate the reaction, and is capable of delivering current densities of 500 and 1000 mA cm<sup>-2</sup> at overpotentials of 240 and 270 mV, respectively. To the best of our knowledge, this is the most efficient oxygen evolution electrode in alkaline electrolytes reported so far.

- (1) Smith, R. D. L.; Prevot, M. S.; Fagan, R. D.; Zhang, Z. P.; Sedach, P. A.; Siu, M. K. J.; Trudel, S.; Berlinguette, C. P. *Science* **2013**, 340, 60.
- (2) Gong, M.; Li, Y. G.; Wang, H. L.; Liang, Y. Y.; Wu, J. Z.; Zhou, J. G.; Wang, J.; Regier, T.; Wei, F.; Dai, H. J. *J. Am. Chem. Soc.* **2013**, 135, 8452.
- (3) Lu, X.; Ng, Y. H.; Zhao, C. *ChemSusChem* **2014**, 7, 82
- (4) Xiao, C. Lu, X.; Zhao, C. *Chem. Comm.*, **2014**, 50, 10122
- (5) Lu, X.; Zhao, C. *J. Mater. Chem. A*, **2013**, 1, 12053
- (6) Lu, X.; Yim, W.; Bryan, B.H.R.; Zhao, C. *J. Am. Chem. Soc.*, **2015**, 137, 2901
- (7) Lu, X.; Zhao, C. *Nat. Commun.*, **2015**, 6, 6616



# Highly Active and Stable Iron-nitrogen-doped Carbon with Hollow-core-mesoporous-shell (HCMS) Structure for Oxygen Reduction Reaction

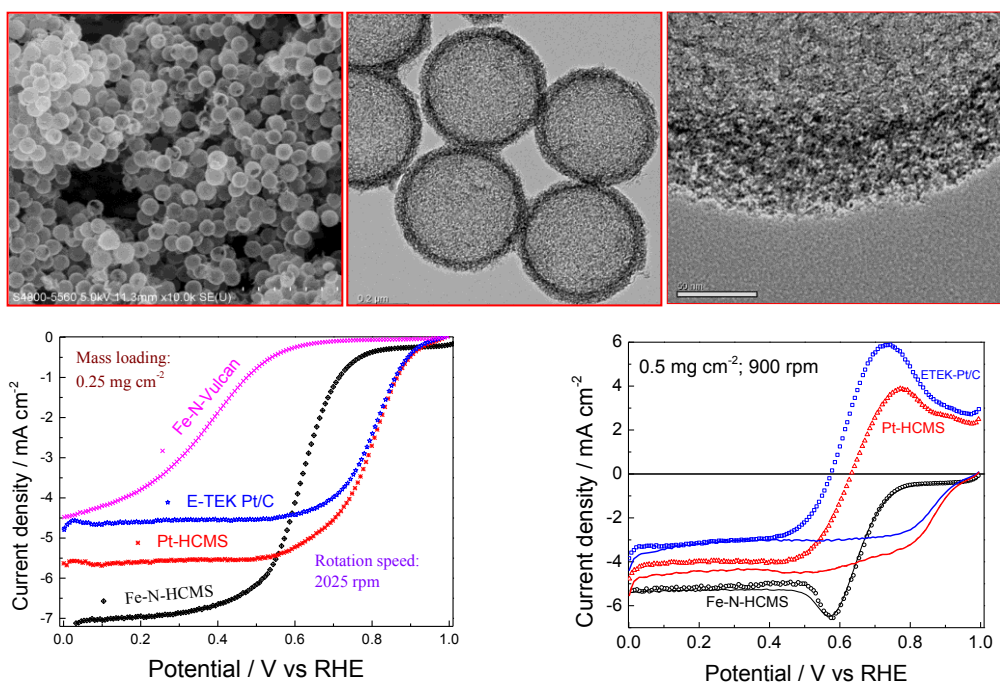
Ming Zhou, Kwong-Yu Chan\*

The University of Hong Kong

Department of Chemistry, HKU, Pokfulam Road, Hong Kong

\*Email: [hrcscky@hku.hk](mailto:hrcscky@hku.hk)

The electrochemical oxygen reduction reaction (ORR) has been studied for decades in the development of fuel cells and lately for growing interests in rechargeable metal-air batteries and microbial fuel cells. The ORR is actively investigated to overcome the unresolved issues of mass-transport limitation, high costs and degradability of electrocatalysts. Non-precious metal and nitrogen doped carbons have attracted much attention for their low costs, good electrochemical activity, and durability in ORR. With a lattice structure similar to that of graphite, nitrogen doped carbon has high crystallinity and intrinsically limited in microporosity and high surface area. It is desirable to use a hierarchical hollow core-mesoporous shell (HCMS) geometry to create multi-scale porosity and enhance mass transfer of ORR.



1. M. Zhou, C. Z. Yang, K. Y. Chan, *Adv. Energy Mater.* **2014**, *4*, 1400840;
2. F. Li, M. Morris, K. Y. Chan, *J. Mater. Chem.*, 2011, *21*, 8880;

## Electrocatalysis of oxygen reduction and water oxidation using metal oxides embedded in nitrogen-doped carbon

Justus Masa<sup>1</sup>, Wei Xia<sup>2</sup>, Anqi Zhao<sup>2</sup>, Martin Muhler<sup>2</sup> and Wolfgang Schuhmann<sup>1</sup>  
*Ruhr-Universität Bochum*

<sup>1</sup>Analytical Chemistry and Center for Electrochemical Sciences-CES  
Ruhr-Universität Bochum, NC04/788, D-44780 Bochum (Germany)

Fax: (+)49 234 3214683

<sup>2</sup>Laboratory of Industrial Chemistry, Ruhr-University Bochum, NBCF 04/690, D-44801  
Bochum (Germany)

[Justus.masa@rub.de](mailto:Justus.masa@rub.de)

Achieving economic and environmental viability of hydrogen production through water splitting using energy derived from sustainable sources is the hallmark of the hydrogen economy. Electrocatalysis of water is possibly the most advanced green means of H<sub>2</sub> production. When coupled to a fuel cell, the produced H<sub>2</sub> can directly be used to generate power at the site of generation thus eliminating geographical constraints to power provision. The state-of-the art catalysts for electrocatalytic water splitting are derived from platinum group metal oxides, typically RuO<sub>2</sub> and IrO<sub>2</sub>, while for fuel cells; it is mainly platinum or its alloys. Although non-precious metal catalysts for both O<sub>2</sub> reduction and water oxidation exists, their notorious instability is by far the single unresolved impediment hampering practical applications. In this presentation, exceptionally active bifunctional catalysts for oxygen electrodes obtained by selective pyrolysis and subsequent mild calcination of cobalt, manganese and nickel N<sub>4</sub>-macrocyclic complexes to form the respective oxides of the metals M<sub>x</sub>O<sub>y</sub> embedded in a porous nitrogen-rich shell will be discussed.<sup>[1]</sup> A second part of the presentation will discuss the design of highly stable and active bifunctional catalysts for reversible oxygen electrodes by oxidative thermal scission, where we concurrently rupture nitrogen-doped carbon nanotubes and oxidize Co and Mn nanoparticles buried inside them to form spinel Mn–Co oxide nanoparticles partially embedded in the nanotubes.<sup>[2]</sup> High dual activity for O<sub>2</sub> reduction and evolution surpassing those of Pt/C, RuO<sub>2</sub>, and IrO<sub>2</sub> is achieved using these catalysts. This raises the prospect of functional low-cost, non-precious-metal bifunctional catalysts in metal–air batteries and reversible fuel cells, among others, for a sustainable and green energy future. The presentation will also cover detailed discussion of the long term stability of the catalysts.

### References

- [1] J. Masa, W. Xia, I. Sinev, A. Zhao, Z. Sun, S. Grützke, P. Weide, M. Muhler, W. Schuhmann. Mn<sub>x</sub>O<sub>y</sub>/NC and Co<sub>x</sub>O<sub>y</sub>/NC Nanoparticles Embedded in a Nitrogen-Doped Carbon Matrix for High-Performance Bifunctional Oxygen Electrodes. *Angew. Chem. Int. Ed.*, 53: (2014) 8508–8512.
- [2] A. Zhao, J. Masa, W. Xia, A. Maljusch, M. Willinger, G. Clavel, K. Xie, R. Schlögl, W. Schuhmann, W. Schuhmann. Spinel Mn–Co Oxide in N-Doped Carbon Nanotubes as a Bifunctional Electrocatalyst Synthesized by Oxidative Cutting. *J. Am. Chem. Soc.*, 136 (2014) 7551–7554.

# Theoretical Thoughts on Electronic Interactions between Metallic Electrocatalysts and Oxide Supports

T. Binninger<sup>1)</sup>, E. Fabbri<sup>1)</sup>, T.J. Schmidt<sup>1,2)</sup>, D. Kramer<sup>3)</sup>

<sup>1)</sup>*Paul Scherrer Institut, Electrochemistry Laboratory, 5232 Villigen PSI, Switzerland*

<sup>2)</sup>*Laboratory of Physical Chemistry, ETH Zurich, 8093 Zurich, Switzerland*

<sup>3)</sup>*Engineering Materials, University of Southampton, SO17 1BJ Southampton, UK*

*d.kramer@soton.ac.uk*

In spite of decades of research, no commercially viable alternative to supported Pt nanoparticles as oxygen reduction reaction (ORR) catalyst at the cathode side of low-temperature polymer electrolyte fuel cells (PEFC) has emerged. Supporting nano-particulate Platinum electrocatalysts on high surface area carbons made the use of Platinum-Group-Metals (PGMs) viable from a cost perspective. It has, however, become clear that the stability of carbon supports is compromised under common PEFC operating conditions, making carbon corrosion one of the lifetime determining degradation processes. Using a small number of thermodynamically stable oxides, improved stability towards cycling could be demonstrated in recent years [1].

The impact of radically changing the physical nature of the support from carbon to oxide on electrocatalytic properties of the supported electrocatalyst remains a topic of great interest. Strong Metal-Support Interactions (SMSI), influencing the catalytic activity of Pt nanoparticles, are well known in heterogeneous catalysis [2]. The topic has also gained traction in electrocatalysis in recent years due to an increased research focus on non-carbon supports. Experiments have revealed an influence of the metal oxide type and the metal oxide surface stoichiometry on the stability and the activity of the supported Pt particles [3,4]. So far, however, the precise theoretical understanding of the origin of these metal-support interactions remained deficient.

We present results from a theoretical study of metal-support interactions, focusing on electronic effects. Using Density-Functional-Theory (DFT), we investigated Pt<sub>55</sub> clusters supported on various SnO<sub>2</sub>-type supports: Undoped SnO<sub>2</sub> slabs as well as Sb-doped and In-doped ones with both stoichiometric and reduced (110) surfaces were used in the study. We followed an approach to identify purely electronic interactions between the Pt clusters and the support oxide by excluding lattice relaxation effects in the calculation of the combined system of Pt cluster and support. We relate our results to a more fundamental understanding of electronic metal-support interactions in terms of thermodynamic equilibration of the electron systems in the support oxide and the Pt nanoparticles. The possible influence of the observed interactions on the catalytic activity towards ORR was quantified by calculating the changes in the binding energy of an oxygen adatom on the outer surface of the Pt nanoparticle. The resultant order of magnitude of the influence of electronic metal-support interactions on the catalytic ORR activity is in agreement with recent experimental findings for Pt nanoparticles supported on oxidized and on reduced SnO<sub>2</sub> thin-film surfaces [4].

## Acknowledgements

T.B. gratefully acknowledges funding through the STFC Futures Early Career Award from the STFC Batteries and Electrochemical Energy Devices Network. This work was furthermore supported by CCEM Switzerland and Umicore AG & Co KG within the project DuraCat. The authors acknowledge the use of the IRIDIS High Performance Computing Facility, and associated support services at the University of Southampton, in the completion of this work. Furthermore, this work used the ARCHER UK National Supercomputing Service (<http://www.archer.ac.uk>).

## References

- [1] A. Rabis, P. Rodriguez, T.J. Schmidt, *ACS Catalysis* **2**, 864-890
- [2] S.J. Tauster and S.C. Fung, *Journal of Catalysis* **55**, 29-35 (1978).
- [3] K. Kakinuma, M. Uchida, T. Kamino, H. Uchida, M. Watanabe, *Electrochimica Acta* **56**, 2881-2887 (2011).
- [4] A. Rabis, D. Kramer, E. Fabbri, M. Worsdale, R. Kötz, and T.J. Schmidt, *The Journal of Physical Chemistry C* **118**, 11292-11302 (2014).

# Microscopic and Electrochemical Signatures of Copper-poly(propyleneimine) Metallodendrimer System

Candice Rassie, Lindsay Wilson, Prof. Priscilla Baker, Prof. Emmanuel Iwuoha  
Sensorlab, Department of Chemistry, University of the Western Cape  
Robert Sobukwe Road, Bellville, 7535, Cape Town, South Africa  
[2734778@myuwc.ac.za](mailto:2734778@myuwc.ac.za) and [eiwuoha@uwc.ac.za](mailto:eiwuoha@uwc.ac.za)

Metallodendrimers are synthetic, highly branched macromolecules which incorporate a metallic center, thereby improving the molecules catalytic behaviour[1]. These macromolecules have been proven to have many applications, one of which is its electrocatalytic behavior as a platform for electrochemical biosensors [2]. The objective of this work is to study the electrochemical characteristics as well as the morphology of a first generation poly(propyleneimine) based copper functionalized metallodendrimer (CuPPI), for its application in electrochemical biosensing. The CuPPI metallodendrimer was physically adsorbed onto the surface of a gold (Au) electrode to form an Au|CuPPI electrode system, which was then electrochemically characterized by cyclic and square wave voltammetric techniques. The electrochemical characterization reveals primary anodic and cathodic peaks at  $E_{pa} = 220\text{mV}$  and  $E_{pc} = 180\text{mV}$  respectively, along with secondary peaks which represent a cascade reaction occurring within the dendritic structure. These primary peaks are attributed to the oxidation of the reduced form of Cu(I) to Cu(II) and its subsequent reduction back to Cu(I). The CuPPI metallodendrimer was found to be electroactive on Au electrode and has diffusion coefficient (D) values of  $4.124 \times 10^{-5} \text{ cm}^2 \text{ s}^{-1}$  (in the absence) and  $3.29 \times 10^{-5} \text{ cm}^2 \text{ s}^{-1}$  (in the presence) of oxygen in the cell solution. The surface morphology of the poly(propyleneimine) dendrimer (PPI) and its copper-functionalized derivative, i.e. CuPPI, were compared using atomic force microscopy (AFM). High resolution transmission electron microscopy (HR-TEM) and high resolution scanning electron microscopy (HR-SEM), as shown in **figure 1** below reveals that CuPPI has a layered crystalline structure. The metallodendrimer would be a suitable platform for electrochemical biosensing applications since the diffusion coefficient is only very slightly affected by the presence of oxygen. The layered structure afforded a suitable enhancement in surface area for the immobilization of biological molecules such as enzymes. The metallodendrimer was used as an electrocatalytic platform for the determination of a TB patient's metabolic profile towards various TB drugs such as isoniazid and ethambutol.

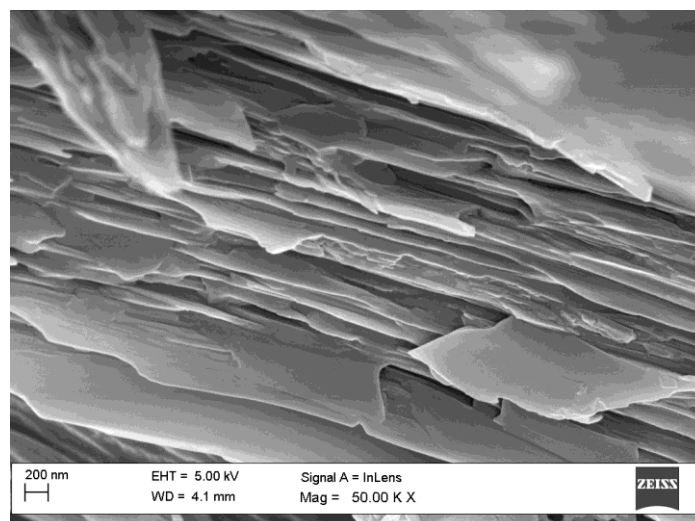


**Figure 1: HR-SEM image of copper poly(propyleneimine) metallodendrimer at 50KX magnification**

## References

1. Smith, G., R. Chen, and S. Mapolie, Journal of Organometallic Chemistry, 2003. **673**(1–2): p. 111-115.
2. Arotiba, O.A., et al., Electrochimica Acta, 2007. **53**(4): p. 1689-1696.

# Heat-treated 3,5-diamino-1,2,4-triazole/graphene Hybrid Functions as an Oxygen Reduction Electrocatalyst with High Activity and Stability

Hiroyuki Koshikawa, Kazuhide Kamiya, Shuji Nakanishi, Kazuhito Hashimoto  
 Department of Applied Chemistry, The University of Tokyo  
 7-3-1 Hongo, Bunkyo-ku, Tokyo 113-8656, Japan  
 kamiya@light.t.u-tokyo.ac.jp

Electrochemical oxygen reduction reaction (ORR) is important as a cathode reaction of various types of fuel cells. Thus, development of electrocatalysts composed only of abundant elements is strongly required. In natural systems, multi-copper (Cu) oxidases, such as laccase and bilirubin oxidase, catalyze the four-electron ORR for respiration with lower over-potential than Pt in neutral pH conditions.<sup>1)</sup> In these enzymes, modulation of the electronic state and molecular structures of the atomic Cu centers through coordination with amino acid residues is believed to be essential for their high catalytic activities.<sup>2)</sup> For this reason, numerous studies have been conducted to synthesize Cu-N complexes by mimicking the coordination structure of those enzymes. For example, a copper complex of 3,5-diamino-1,2,4-triazole (Cu-DAT) supported on carbon black exhibited an onset potential of 0.73 V (vs. RHE) at pH 7 for the ORR, which is the highest value among Cu-based catalysts reported to date.<sup>3)</sup> However, the weakness of molecular catalysts caused by decomposition of organic ligands is the major obstacle for their application. We recently reported that stable graphene materials with iron (Fe)-N coordination bonds can be synthesized by the short-duration heat treatment (< 60 s) of graphene oxides (GO) in the presence of an Fe-N complex, and the resulting catalyst exhibited both the high activity and stability of the ORR.<sup>4)</sup> Therefore, it is worth investigating whether this synthesis method can be applied to Cu-DAT to enhance its robustness.

The heat-treated catalyst (HT/Cu-DAT) was synthesized by heating Cu-DAT in the presence of GO at 900 °C for 45 s. The Cu-DAT complex supported on a carbon black (non-HT/Cu-DAT) was prepared as described in the previous paper.<sup>3)</sup> ORR activities were evaluated using a rotating ring-disk electrode (RRDE) in a 0.1 M phosphate-buffer solution (pH 7.0). Elemental and structural analysis were performed by X-ray photoelectron spectrometry (XPS) and extended X-ray absorption fine structure (EXAFS) analyses.

Fig. 1 shows the  $j$  vs.  $U$  curves for HT/Cu-DAT and non-HT/Cu-DAT in the presence of oxygen. HT/Cu-DAT generated a cathodic current with an onset potential of 0.79 V (vs. RHE) and exhibited the ORR catalytic activity comparable to that of non-HT/Cu-DAT. To our knowledge, the onset potential of HT/Cu-DAT is the highest value reported to date among Cu-based ORR catalysts in neutral solution.<sup>5)</sup> To evaluate the stability, 1000 cycles of CV were conducted for both catalysts. Although the absolute current density value at 0.6 V (vs. RHE) after the CV cycling decreased by 77% for non-HT/Cu-DAT, it decreased only by 22% for HT/Cu-DAT. These results indicated that the stability of HT/Cu-DAT was enhanced by the heat treatment. The XPS and EXAFS results suggested that N atoms coordinated to Cu atoms were doped into the graphene network during the heat treatment for HT/Cu-DAT (Fig. 2(a)), leading to the improved stability of the catalyst. In contrast, Cu-DAT was only physically adsorbed onto the carbon black particles in non-HT/Cu-DAT (Fig. 2(b)).

**References:** 1) N. Mano, *et al.*, *J. Phys. Chem. B* 110 (2006) 11180-11187.

2) E. I. Solomon *et al.*, *Chem Rev.* 114 (2014) 3659-3853.

3) M. S. Thorum *et al.*, *Angew. Chem. Int. Ed.* 48 (2009) 165-167.

4) K. Kamiya *et al.*, *Chem. Commun.* 48 (2012) 10213-10215.

K. Kamiya, H. Koshikawa *et al.*, *ChemElectroChem* 1 (2014) 877-884.

5) H. Koshikawa *et al.*, *submitted*.

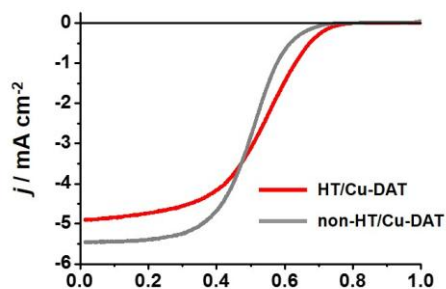


**Fig. 1.**  $j$  vs.  $U$  curves for HT/Cu-DAT (red) and non-HT/Cu-DAT (blue).

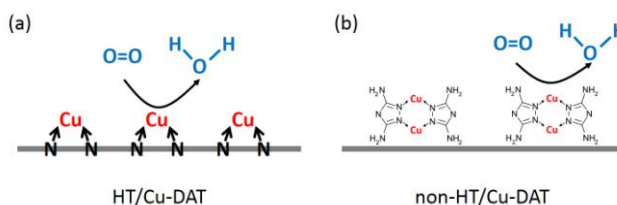


**Fig. 2.** Schematic illustrations of the reactive center for ORR in (a) HT/Cu-DAT and (b) non-HT/Cu-DAT.

# Electrochemical Responses of Transglutaminase Immunosensor Developed on a Polypyrrole-Cobalt (II) Salicyladiimine Dendritic Composite Material

Lindsay Wilson, Candice Rassie, Prof. P. Baker, Prof. E. Iwuoha  
SensorLab, Department of Chemistry, University of the Western Cape,  
Robert Sobukwe Road, Bellville, 7535, Cape Town, Republic of South Africa  
[2724554@myuwc.ac.za](mailto:2724554@myuwc.ac.za) and [eiwuoha@uwc.ac.za](mailto:eiwuoha@uwc.ac.za)

Transglutaminase (tTG), a calcium dependent enzyme catalysis protein cross linkages such as glutamine to the lysine on proteins. Transglutaminase exhibits high specificity towards glutamine substrates and forms an enzyme complex with gliadin that produces an immune response against this complex [1-2]. This immune response resulted in the identification of transglutaminase as the auto antigen of celiac disease. Since transglutaminase is predominantly involved in the activation and progression of celiac disease, it results in the production of antibodies against it. This then results in the harmful damage to the small intestine which reduces food digestion diffusion into the blood vessels [3]. The standard diagnosis of celiac disease is tedious and expensive. The diagnosis of coeliac disease can be done by the measurement of antibodies against transglutaminase [4]. In this work, an electrochemical impedimetric immunosensor was developed for the detection of anti-transglutaminase antibodies. The immunosensor consisted of a polypyrrole-cobalt (II) salicyladiimine metallodendrimer composite on a platinum electrode with transglutaminase as the recognition element. Atomic force microscopy was used to determine surface roughness of the modified platinum electrode with values of 879.24 nm, 76.55 nm and 364.27 nm for polypyrrole, cobalt (II) salicyladiimine and their respective composite. The composite provided a suitable micro-environment for monitoring antibody-antigen interactions in conjunction with their cyclic voltammetry. Electrochemical impedance spectroscopy parameters such as exchange current and heterogeneous rate constant are used to evaluate immunosensor where the rate constants were  $2.7 \times 10^{-6} \text{ cm}^2 \text{ s}^{-1}$ ,  $4.6 \times 10^{-6} \text{ cm}^2 \text{ s}^{-1}$  and  $4.16 \times 10^{-6} \text{ cm}^2 \text{ s}^{-1}$  for cobalt (II) salicyladiimine metallodendrimer, polypyrrole and their composite. Impedimetric detection of anti-transglutaminase antibody gave a limit of detection of 201 ng/mL and linear range of  $10^{-5}$  -  $10^{-4}$  mg/mL with correlation coefficient of 0.948.

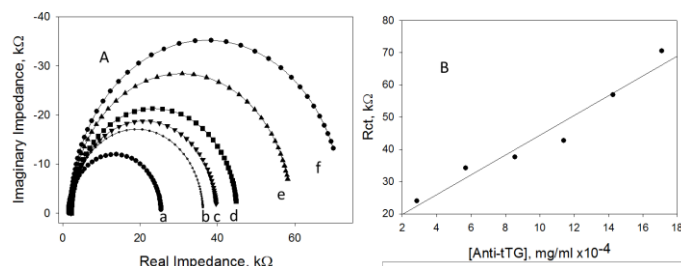


Figure 1. Nyquist plot for anti-tTG antibody incubation at, (a)  $2.85 \times 10^{-4}$  mg/mL, (b)  $5.7 \times 10^{-4}$  mg/mL, (c)  $8.55 \times 10^{-4}$  mg/mL, (d)  $11.4 \times 10^{-4}$  mg/mL, (e)  $14.25 \times 10^{-4}$  mg/mL, (f)  $17.1 \times 10^{-4}$  mg/mL and calibration graph for immunosensor  $R_{ct}$  versus anti-tTG antibody concentration in 0.1 M phosphate buffer. B) Calibration plot for the detection of anti-tTG antibody in 0.1 phosphate buffer.

## Ref.

1. A. Sabatino, A. Vanoli, P. Giuffrida, O. Luinetti, E. Solica, G. Corazza, *Autoimmunity Reviews*, 11 (2012) 746
2. S. Reif, A Lerner, *Autoimmunity Reviews*, 3 (2004) 45
3. W. Dieterich, T. Ehnis, M. Bauer, P. Donner, U. Volta, E. Riecken, D. Schuppan. *Nature Medicine*, 3 (1997) 7
4. L. Rivera, J. Sanchez, P. Sanchez, I. Katakis, C. O'Sullivan. *Biosensors and Bioelectronics*, 26 (2011) 4471



# Novel Structured Pt-Based Intermetallic Electrocatalysts for ORR

Deli Wang, Jing Zhu, Sufen Liu, Jie Wang, Zexing Wu

*School of Chemistry & Chemical Engineering, Huazhong University of Science & Technology  
1037 Luoyu Road, Wuhan, China  
wangdl81125@hust.edu.cn*

The rational synthesis of active, durable, and low-cost catalysts is of particular interest to fuel cell applications. Pt is a key element in both anode and cathode of fuel cells. However, Pt is currently costly and scarce, it poses a question of how to lower the Pt loading and increase the efficiency. Most of previous studies focused on Pt alloyed with some 3d-transition metals, such as Fe, Co, Ni, etc. The activity and stability need to be further improved for fuel cell applications. To enhance and optimize the performance and durability of Pt for the oxygen reduction reaction, we look beyond Pt-metal disordered alloys and describe a new class of Pt-based ordered structured intermetallic nanoparticles for the oxygen reduction reaction. In our studies, we found that carbon supported Pt<sub>3</sub>Co and PtCu<sub>3</sub> ordered intermetallic nanoparticles can be easily formed using a simple impregnation-reduction method followed by high temperature pretreatment. Ordered Pt<sub>3</sub>Co intermetallic cores with a 2-3 atomic-layer thick platinum-rich shell showed over 200% increase in mass activity and over 300% increase in the specific activity compared with the disordered Pt<sub>3</sub>Co alloy nanoparticles for the ORR. Electrochemical and chemical dealloying methods were implemented on Cu<sub>3</sub>Pt/C nanoparticles to control the atomic-level morphology and activating the performance for oxygen reduction reaction (ORR). It is found that by controlling electrochemical dealloying parameters resulted in different morphology, while the chemical leaching gave rise to a spongy structure. Both dealloying methods yielded enhanced specific and mass activity for ORR and higher stability relative to Pt/C. These findings are important to build next-generation fuel cell catalysts.

## Reference

- [1] D. Wang, Y. Yu, J. Zhu, S. Liu, D. A. Muller, H.D. Abruña, Nano Letters, 15 (2015) 1343-1348.
- [2] D. Wang, H. L. Xin, R. Hovden, H. Wang, Y. Yu, D. A. Muller, F. J. DiSalvo, H. D. Abruña, Nat. Mater., 12(2013), 81-87.
- [3] D. Wang, Y. Yu, H. L. Xin, R. Hovden, P. Ercius, J. A. Mundy, H. Chen, J. H. Richard, D. A. Muller, F.J. DiSalvo, H. D. Abruña, Nano Letters, 12 (2012) 5230-5238.

# Facile synthesis of starch-scaffolded bimetallic Au-Pt nanostructure and electrocatalysis

Christian Engelbrekt, Nedjeljko Seselj, Jens Ulstrup, Jingdong Zhang\*

Department of Chemistry, Technical University of Denmark, 2800 Kgs. Lyngby, Denmark.

[cheng@kemi.dtu.dk](mailto:cheng@kemi.dtu.dk), [jz@kemi.dtu.dk](mailto:jz@kemi.dtu.dk)\*

A facile, one-pot synthesis procedure has been developed for the preparation of two types of bimetallic Au-Pt nanostructures. By controlling the timing and conditions of the syntheses, gold nanoparticle (AuNP) cores (1) with an atomically thin platinum shell nanoparticles, and (2) encapsulated in a porous network of 2-3 nm platinum nanoparticles (PtNPs) can be prepared, denoted Au@Pt NPs and nanoflowers (NFs), respectively.

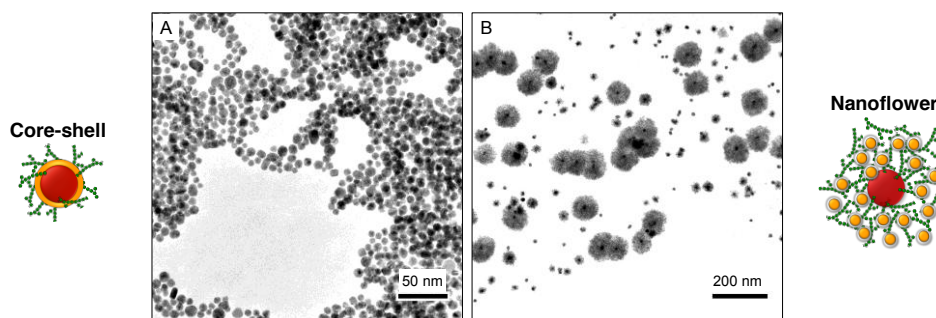


**Figure 1.** Transmission electron micrographs of (A) Au-Pt core-shell NPs, Au@Pt NPs and (B) Au cores encapsulated by a porous network of 2-3 nm PtNPs.

The exact concentration of Pt precursor and the dynamics of its reduction are critical for core-shell formation as rapid precursor reduction leads to unwanted nucleation of PtNPs. Formation of an atomically thin Pt shell leads to a drastic change in optical properties. The localized surface plasmon resonance (LSPR) of the Au core is almost completely dampened and the colloid changes color from red to brown. Meanwhile, no significant change in particle size is detectable by transmission electron microscopy (TEM). Electrochemical characterization of the Au@Pt NPs reveals a large Pt response confirming the formation of a core-shell structure.

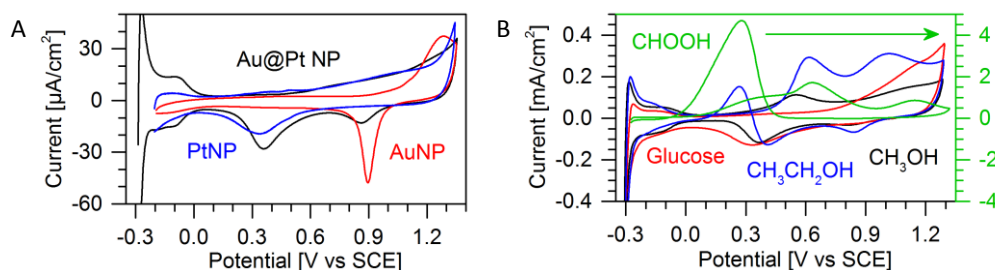


**Figure 2.** (A) Cyclic voltammograms of Au@Pt NPs, AuNPs and PtNPs on glassy carbon electrode (GCE) in 0.1 M  $\text{H}_2\text{SO}_4$ . (B) Cyclic voltammograms of Au@Pt NPs on GCE in 0.1 M  $\text{H}_2\text{SO}_4$  with 0.1 M methanol, glucose, ethanol or formic acid. Scan rate is 50 mW/s in all cases.

The as-synthesized Au@Pt NPs were tested as catalysts for electrocatalytic oxidation of small organic fuel molecules, i.e. methanol, ethanol and formic acid. Especially promising results were obtained for formic acid oxidation during which the Au@Pt NPs showed good resistance towards poisoning.

The AuNP core size can be controlled through a seeded growth approach from 8 to 80 nm. Varying the reaction conditions during shell synthesis enabled the formation of a porous network of individual 2-3 nm PtNPs surrounding a single AuNP core rather than the thin shell deposited directly on the AuNP. Nanoflowers with PtNP network shells from a few nm to more than 100 nm were prepared.



## Effect of Iron Precursor on Oxygen Reduction Reaction of Fe-N-C Catalyst in PEMFC

Vuri Ayu Setyowati, Hsin-Chih Huang, Chen-Hao Wang\*

*Department of Materials Science and Engineering, National Taiwan University of Science and Technology, 10607, Taipei, Taiwan.*

\*chwang@mail.ntust.edu.tw

The non-precious metal catalyst by using transition metal with nitrogen-doped carbon material shows the good activity of oxygen reduction reaction (ORR), which has the opportunity to replace the high-cost platinum catalyst in the proton exchange membrane fuel cell (PEMFC) in the recent studies [1-3]. In this study, various iron precursors were chose to mix with polyaniline and carbon black (XC-72), and subsequently the mixture was introduced to the furnace for the pyrolysis. For the preparation of Fe-N-C catalyst, the ratio of polyaniline and XC72 was 1:1, the Fe content was fixed to 7 wt.% for the preparation of Fe-N-C catalyst. The electrochemical analysis shows that  $\text{FeCl}_3 \cdot 6\text{H}_2\text{O}$  mixed with polyaniline are the preferred iron precursor ( $\text{FeCl}_3\text{-PANI-C}$ ) to get higher ORR activity than the others, which its electron-transfer number is around 3.99. The Raman spectrum of  $\text{FeCl}_3\text{-PANI-C}$  shows the ratio of G-band and D band ( $I_G/I_D$ ) corresponding to the degree of graphitization. The higher activity of catalyst has the lower  $I_G/I_D$  on Raman spectra due to high nitrogen functionalities content [4]. The ratio between C/N/O is determined by XPS spectra, showing the high ratio of N element of  $\text{FeCl}_3\text{-PANI-C}$ . The N composition is consisted of pyrrolic N, cyanide, and quaternary N. The major N composition of  $\text{FeCl}_3\text{-PANI-C}$  is quaternary N about 57.73%. XANES spectra of  $\text{FeCl}_3\text{-PANI-C}$  shows that the oxidation state of central Fe is 3+ and the changing of coordination structure occurs after pyrolysis. The stability tests of  $\text{FeCl}_3\text{-PANI-C}$  shows only 50mV decay after 30000 cycle times.

1. Du, H.-Y., et al., *A high performance polybenzimidazole-CNT hybrid electrode for high-temperature proton exchange membrane fuel cells*. Journal of Materials Chemistry A, 2014. **2**(19): p. 7015-7019.
2. Huang, H.-C., et al., *Pyrolyzed Cobalt Corrole as a Potential Non-Precious Catalyst for Fuel Cells*. Advanced Functional Materials, 2012. **22**(16): p. 3500-3508.
3. Chang, S.-T., et al., *Vitalizing fuel cells with vitamins: pyrolyzed vitamin B12 as a non-precious catalyst for enhanced oxygen reduction reaction of polymer electrolyte fuel cells*. Energy & Environmental Science, 2012. **5**(1): p. 5305-5314.
4. Liu, S., et al., *The key role of metal dopants in nitrogen-doped carbon xerogel for oxygen reduction reaction*. Journal of Power Sources, 2014. **269**(0): p. 225-235.

# Size, Shape and Morphology Effects on Catalytic Activity of Oxygen Reduction Reaction

Minhua Shao

*Department of Chemical and Biomolecular Engineering, Hong Kong University of Science and Technology, Kowloon, Hong Kong  
kemshao@ust.hk*

Low temperature fuel cells are electrochemical devices that convert chemical energy directly to electricity. They have great potential for both stationary and transportation applications and are expected to help address the energy and environmental problems that have become prevalent in our society. Despite their great promise, commercialization has been hindered by lower than predicted efficiencies and the high cost of Pt-based electrocatalysts in the electrodes. For more than five decades, the predominant work has been focused on the development of novel catalysts for the cathodic reaction (oxygen reduction reaction), which has sluggish kinetics and is responsible for the high overpotential. Recent intensive research efforts have led to the development of less expensive and more abundant materials for fuel cells, such as non-precious metal catalysts, metal oxides/carbides, and precious metal alloys.

In this talk, I will present recent progress in developing advanced catalysts for oxygen reduction reaction in my group, with an emphasis on core-shell and shape controlled Pt- and Pd-based nanocrystals. The composition, morphology and size effects on the catalytic activities will be explored. The mechanisms for activity enhancement will also be discussed based on the results of density functional theory (DFT) calculations.

1. S.-I. Choi, M.H. Shao, N. Lu, A. Ruditskiy, H.-C. Peng, J. Park, S. Guerrero, J. Wang, M. J. Kim, Y.N. Xia, *ACS Nano* 2014, 8: 10363–10371
2. M.H. Shao, A. Peles, J.H. Odell, *Journal of Physical Chemistry C* 2014, 118: 18505-18509.
3. S.-I. Choi, S. Xie, M.H. Shao, N. Lu, S. Guerrero, J. Odell, J. Park, J. Wang, M. King, Y.N. Xia, *ChemSusChem* 2014, 7: 1476-1483.
4. M.H. Shao, J.H. Odell, A. Peles, D. Su, *Chemical Communications* 2014, 50: 2173-2176.
5. M.H. Shao, G. He, A. Peles, J.H. Odell, J. Zeng, D. Su, J. Tao, T.K. Yu, Y.M. Zhu, Y.N. Xia, *Chemical Communications* 2013, 49: 9030-9032.
6. M.H. Shao, B.H. Smith, S. Guerrero, L. Protsailo, D. Su, K. Kaneko, J. H. Odell, M.P. Humbert, K. Sasaki, J. Marzullo, R.M. Darling, *Physical Chemistry Chemical Physics* 2013, 15: 15078-15090.
7. S.-I. Choi, S. Xie, M.H. Shao, J.H. Odell, H.-C. Peng, J. Park, X. Xia, N. Lu, J. Wang, M. J. Kim, Y.N. Xia, *Nano Letters* 2013, 13: 3420-3425.
8. M.H. Shao, J.H. Odell, M. Humbert, T.K. Yu, Y.N. Xia, *Journal of Physical Chemistry C* 2013, 117: 4172-4180.
9. M.H. Shao, A. Peles, K. Shoemaker, *Nano Letters* 2011, 11: 3714-3719.
10. M.H. Shao, T.K. Yu, J.H. Odell, Y.N. Xia, *Chemical Communications* 2011, 47: 6566-6568.
11. M.H. Shao, A. Peles, K. Shoemaker, M. Gummalla, P. Njoki, J. Luo, C.J. Zhong, "Enhanced oxygen reduction activity of platinum monolayer on gold nanoparticles", *Journal of Physical Chemistry Letters* 2011, 2: 67-72.
12. M.H. Shao, K. Shoemaker, A. Peles, K. Kaneko, L. Protsailo, *Journal of the American Chemical Society* 2010, 132 (27): 9253-9255.

# High-Performance Electrocatalyst for Oxygen Reduction Derived from Riboflavin and Iron

Shuihua Tang, Haixin Huangfu, Yuxiao Deng, Leping Sui, Zhen Dai, Zhentao Zhu, Xiaolong Qin, Jiawei Yuan

State Key Lab of Oil and Gas Reservoir Geology & Exploitation  
8 Xindu Avenue, Xindu District, Chengdu 610500, P R China

[spraytang@hotmail.com](mailto:spraytang@hotmail.com)

Pt-based materials are widely used as electrocatalysts for oxygen reduction reaction (ORR). However, the high cost will hinder the development of fuel cells. Consequently, great efforts on non-precious metal catalysts (NPMCs) have been investigated extensively, and nitrogen-containing catalyst is considered as the most promising candidate due to its high activity, remarkable performance stability [1-2].

In this work, Fe-N-C electrocatalyst with excellent performances was prepared via one-step heat-treatment method using riboflavin as nitrogen and carbon source, and ferric chloride as transition metal precursor. This approach has the advantages of cheap and nontoxic precursors, simple process, and easy scale-up. The ORR activity and stability of catalyst were characterized by linear sweep voltammetry (LSV) and chronoamperometry in 0.5 M H<sub>2</sub>SO<sub>4</sub> solution. Effects of heat-treatment temperature and Fe contents were investigated. The catalyst prepared with Fe content of 7 wt% and heat-treated at 800 °C exhibits the highest ORR activity. The LSV curves before and after 1000 cycles are shown in **Fig. 1** (Middle), the performance decay is negligible above 0.3 V; the chronoamperometric response at 0.3 V (vs Ag/AgCl) is shown in **Fig. 1** (Right), the catalyst activity keeps more than 93% of the initial activity after 10800s. All of these indicate the stability of catalyst is excellent.

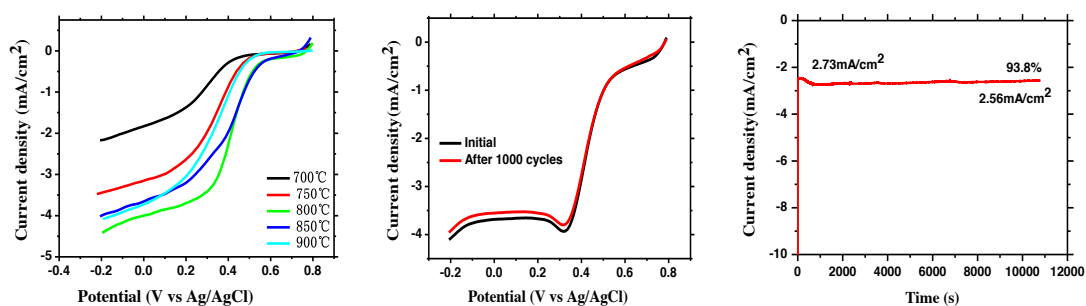


**Fig.1** LSV curves of Fe-N-C catalysts prepared at various heat-treatment temperatures (Left), before and after 1000 cycles (Middle) and Chronoamperometric response at 0.30 V (vs Ag/AgCl) (Right) in O<sub>2</sub> saturated 0.5 M H<sub>2</sub>SO<sub>4</sub> solution at room temperature.

## References

- [1] M. Lefèvre, E. Proietti, F. Jaouen, J. Dodelet. *Science*, **2009**, 324, 71
- [2] K. P. Gong, F. Du. *Science*, **2009**, 323, 760
- [3] K. L. Wang, H. Wang, S. Ji. *Rsc Adv*, **2013**, 3, 12309
- [4] H. W. Liang, W. Wei, Z. S. Wu. *J Am Chem Soc*, **2013**, 135, 16002

# Pt<sub>3</sub>Ni intermetallic with Pt-rich surface supported on porous carbon as a high efficient electrocatalyst for oxygen reduction reaction

Bin-Wei Zhang, Yan-Xia Jiang, Shi-Gang Sun

State Key Laboratory of Physical Chemistry of Solid Surfaces, Department of Chemistry, College of Chemistry and Chemical Engineering, Xiamen University  
Xiamen 361005, (P. R. China)  
yxjiang@xmu.edu.cn

The slow rate of the oxygen reduction reaction (ORR) at the cathode is one of the main challenges for the development of polymer electrolyte membrane fuel cells (PEMFCs). Commercial ORR catalysts is generally Pt-based catalysts, however, the high cost and scarcity of Pt are the key obstacles for its broad deployment in fuel cells. Recently, it is of great interest to explore more active catalysts, with superior performance and durability, than the traditionally employed carbon-supported Pt (Pt/C) nanoparticles. To achieve this target, the Pt-base bi- and tri-metallic electrocatalysts, such as alloying Pt with the 3d-transition metals (Fe, Co, Ni), have been rationally synthesized and shown with greatly enhanced activities for the ORR. Vojislav et al [1] found that the Pt<sub>3</sub>Ni(111) with its outermost is Pt-rich, is more active for ORR than the Pt(111) and more active than Pt/C. In this work, we developed a simple and novel method to synthesis the Pt<sub>3</sub>Ni with Pt-rich surface in the porous graphitic carbon (Pt<sub>3</sub>Ni/PC), in which controlled thermal treatment of the precursor of Pt and Ni formed the desired Pt-rich surface. The method can be readily scaled up to produce high-performance electrocatalysts with the Pt-rich structure, and importantly it can be generalized toward the design of other multimetallic systems.

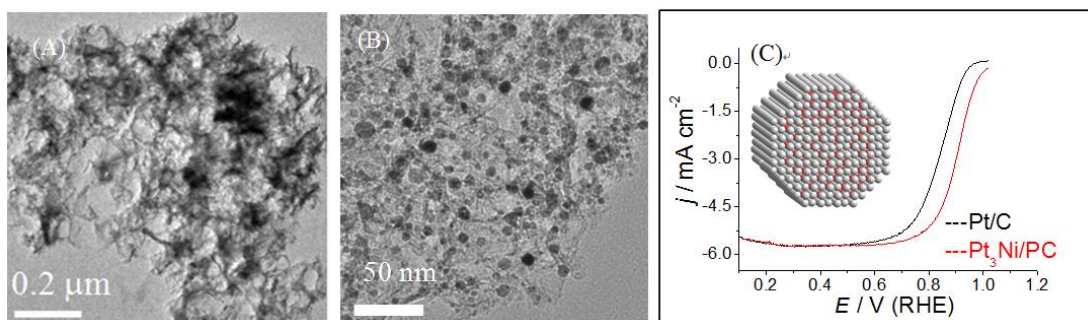


Figure 1 The TEM images of PC (A) and Pt<sub>3</sub>Ni/PC (B), and (C) ORR polarization curves for Pt/C and Pt<sub>3</sub>Ni/PC in O<sub>2</sub>-saturated 0.1 M HClO<sub>4</sub> at room temperature; 1,600 rpm and 10 mV s<sup>-1</sup> of sweep rate. The insert in (C) shows the model of Pt<sub>3</sub>Ni/PC.

TEM image of porous graphitic carbon is shown in Figure 1A, which shows the morphology of PC and confirms that PC is porous graphitic carbon. TEM image of Pt<sub>3</sub>Ni/PC is shown in Figure 1B, clearly demonstrated that the Pt<sub>3</sub>Ni nanoparticles with well dispersed and high loaded in the PC. The size of the Pt<sub>3</sub>Ni nanoparticles was measured from 200 nanoparticles in the TEM images of Pt<sub>3</sub>Ni/PC, and it was determined to be  $3.87 \pm 1.24$  nm for Pt<sub>3</sub>Ni/PC. The polarization curves for the ORR on Pt/C and Pt<sub>3</sub>Ni/PC in an O<sub>2</sub>-saturated 0.1 M HClO<sub>4</sub> solution are shown in Figure 1C. For two catalysts, the diffusion-limiting currents were obtained to be  $\sim 5.6$  mA cm<sup>-2</sup>. And the mixed kinetic-diffusion control region occurs between 0.6 V and 1.0 V, in this region, the half-wave potential of an ORR polarization curve,  $E_{1/2}$ , is often used to evaluate the electrocatalytic activity of a catalyst. The  $E_{1/2}$  was respectively 0.841 and 0.905 V in Pt/C and Pt<sub>3</sub>Ni/PC, and it showed a marked positive shift of 64 mV on Pt<sub>3</sub>Ni/PC related to Pt/C. The Pt<sub>3</sub>Ni/PC exhibited a mass activity of 0.69 mA/μgPt on the basis of the total mass of Pt at 0.9 V versus a reversible hydrogen electrode (RHE), which was 3.8 times greater than that of the Pt/C catalyst (0.18 mA/μgPt).

This work was supported by National Science Foundation of China (Grant No. 21273180).

## References:

1. Vojislav R S, Ben F, Bongjin S M, Wang G F, Philip N R, Christopher A L, Nenad M M. Sci. 1 (2007) 315.

# Supersaturation Dependent Evolution of Nanocrystal Surfaces and its Application in the Synthesis of Noble Metal Nanocatalysts with Enhanced Electrocatalytic Properties

Zhaoxiong Xie, Qiaoli Chen, Haixin Lin, Yanyan Jia, Zhenming Cao, Yaqi Jiang, Lansun Zheng  
*State Key Laboratory of Physical Chemistry of Solid Surfaces, Collaborative Innovation Center of Chemistry for Energy Materials, College of Chemistry and Chemical Engineering, Xiamen University, Xiamen, Fujian, China*  
*e-mail: zxxie@xmu.edu.cn*

Many physical and chemical properties of crystals depend on the surface structures because of the anisotropic properties of crystal. In past several decades, surface chemists have acquired great achievements on the studies of surface structure dependent properties by applying bulk single crystals. However, in many applied fields, such as catalysis, nanocrystals are concerned. It is therefore very important to achieve nanocrystals with different crystal surface. In recent years, numerous efforts have been paid to the control of surface structure, it is still extremely difficult to predict or design the surface structure of micro-/nano- crystals. General methods for the control of the exposed crystal face are still lack.

Based on thermodynamics, we reason that the surface energy of the exposed facets is direct proportional to the supersaturation of the growth units in the growth medium during the crystal growth (Thomson-Gibbs equation):

$$\Delta G = \mu_l dn_l + \mu_c dn_c + \sigma dS = 0$$

$$\Delta\mu = \mu_l - \mu_c = \frac{2\sigma v}{h}$$

According to this theory, we successfully designed and achieved surface structure evolution of some ionic crystals, molecular crystals by controlling the supersaturation during the crystal growth process. It has been found the surface energies of nanocrystals increase with the increase of supersaturation of crystal growth unit.

As has been known, nanocrystals with exposed high-energy crystal facets usually show better electrocatalytic activities, due to abundant unsaturated coordination atoms and atomic steps and ledges. However, in order to minimize the surface energy of the crystals, the high-energy facets quickly disappeared in the crystal growth process. By understanding the crystal growth habit under the nonequilibrium (supersaturated) condition, it is easy to control the nanocrystal crystal surfaces with high surface energy. For example, we synthesized Au nanocrystals exposed by different surface (such as (111), (100), (221), and (110)) by simply regulating reduction rate of metal precursor, by which the supersaturation of metal crystal growth unit were tuned. In addition, Pd, Pd-Au alloy nanocrystals with enhanced electrocatalytic properties have also been successfully synthesized.

\* This work was supported by the National Basic Research Program of China (Grants 2011CBA00508 and 2015CB932301) and the National Natural Science Foundation of China (Grants 21131005, 21333008)

## References:

- [1] Q. Kuang, X. Wang, Z.Y. Jiang, Z.X. Xie, L.S. Zheng, *Acc. Chem. Res.*, 2014, 47: 308.
- [2] H. X. Lin, Z. C. Lei, Z. Y. Jiang, C. P. Hou, D. Y. Liu, M. M. Xu, Z. Q. Tian, Z. X. Xie, *J. Am. Chem. Soc.*, 2013, 135: 9311.

# Exploration of efficient low-platinum and non-platinum catalysts for oxygen reduction reaction

## Symposium 9: Electrocatalytic Materials

Meiling Xiao, Jianbing Zhu, Junjie Ge, Changpeng Liu and Wei Xing\*  
Changchun Institute of Applied Chemistry, Chinese Academic of Sciences  
Renmin Street 5625, Changchun, Jilin  
xingwei@ciac.ac.cn

Electrochemical oxygen reduction is a critical process for many energy storage and conversion devices. Although Pt and Pt-based alloys have proven to be the most efficient catalysts for ORR, the high cost and limited reserve of Pt significantly hinder their large-scale applications. Additionally, the Pt and Pt-based catalysts undergo degradation during long-term electrochemical operation. Great efforts have been devoted to search for effective and stable catalysts with decreased Pt loading and even non-platinum catalysts. Our recent work is associated with the advance in this research field. For the design of low-platinum catalysts, strongly coupled platinum nanotubes and nitrogen-doped graphene was synthesized by in-situ galvanic replacement reaction. This novel-structured catalysts exhibited higher activity and durability than the commercial Pt/C catalyst, with a mass activity of 0.35 A mg<sup>-1</sup><sub>Pt</sub> at 0.9 V, 1.69 times higher than commercial Pt/C (0.13 A mg<sup>-1</sup><sub>Pt</sub> at 0.9 V). For the exploration of non-platinum catalysts, meso/macroporous nitrogen-doped carbon architectures with iron carbide encapsulated in graphitic layers were fabricated by pyrolysing of polymers and iron sources. Electrochemical analysis revealed that this carbon-based material with well-designed pore structure can be promising alternatives to platinum for oxygen reduction reaction in both acidic and alkaline solutions.

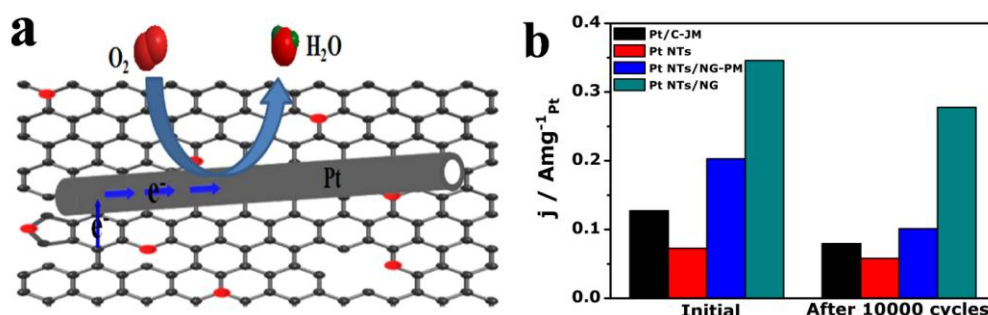


Figure 1. a) Schematic view of oxygen reduction process on Pt NTs/NG catalyst; b) Mass activity for Pt/C-JM, Pt NTs, Pt NTs/NG catalysts before and after durability test.

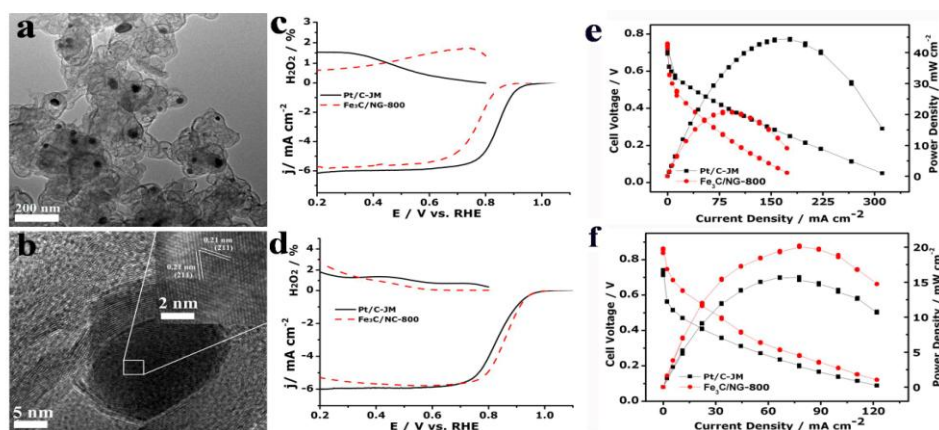


Figure 2. a,b) TEM and HRTEM images of Fe<sub>3</sub>C-NG; ORR performance in c) 0.1 M HClO<sub>4</sub> solution, d) 0.1 M KOH solution; Methanol fuel cell performance with e) proton exchange membrane and f) alkaline membrane.

# Reduction induced surface amorphization enhances oxygen evolution reaction activity in Co<sub>3</sub>O<sub>4</sub>

Xue Leng,<sup>a</sup> Qingcong Zeng,<sup>a</sup> Kuang-Hsu Wu,<sup>a</sup> Ian R. Gentle,<sup>a</sup> Dawei Wang<sup>b</sup>  
<sup>a</sup>*School of Chemistry and Molecular Biosciences, the University of Queensland,  
Brisbane, QLD 4072, Australia*  
<sup>b</sup>*School of Chemical Engineering, the University of New South Wales  
Sydney, New South Wales 2052, Australia*  
Email: [i.gentle@uq.edu.au](mailto:i.gentle@uq.edu.au)  
[da-wei.wang@unsw.edu.au](mailto:da-wei.wang@unsw.edu.au)

Oxygen evolution reaction (OER) is one of the paramount steps in sustainable energy conversion and storage technologies.<sup>1-3</sup> Spinel oxide Co<sub>3</sub>O<sub>4</sub> has long been recognized as a promising alternative non-precious OER electrocatalyst for its good activity and low cost. Numerous nanostructured Co<sub>3</sub>O<sub>4</sub> materials have been developed in order to acquire better OER performance.<sup>4-6</sup> Herein, we have adopted thermal H<sub>2</sub> annealing and air exposure to modify the surfaces of crystalline Co<sub>3</sub>O<sub>4</sub>. Our results demonstrate the remarkably enhanced OER activity of the surface modified Co<sub>3</sub>O<sub>4</sub> electrocatalyst despite its increased crystal size and reduced surface area. The improved OER performance is believed to be relevant to the surface amorphous layer consisting of hydrated cobalt (oxy)hydroxide species on the reduced Co<sub>3</sub>O<sub>4</sub>.

## REFERENCES

1. H. B. Gray, *Nat. Chem.*, **1**, 112 (2009).
2. M. G. Walter, E. L. Warren, J. R. McKone, S. W. Boettcher, Q. Mi, E. A. Santori, N. S. Lewis, *Chem. Rev.*, **110**, 6446-6473 (2010).
3. H. Wang, H. Dai, *Chem. Soc. Rev.* **42**, 3088-3113 (2013).
4. M. Hamdani, R. N. Singh, P. Chartier, *Int. J. of Electrochem. Sc.*, **5**, 556-577 (2010).
5. H. Tüysüz, Y. Hwang, S. Khan, A. Asiri, P. Yang, *Nano Res.*, **6**, 47-54 (2013).
6. B. S. Yeo, A. T. Bell, *J. Am. Chem. Soc.*, **133**, 5587-5593 (2011).



# Catalyst Layer Structures for Enhancement of Redox Reactions of Oxovanadium Ions

Jun Maruyama<sup>a</sup>, Tsutomu Shinagawa<sup>b</sup>

<sup>a</sup>Environmental Technology Research Division, <sup>b</sup>Electronic Material Research Division, Osaka Municipal Technical Research Institute, 1-6-50, Morinomiya, Joto-ku, Osaka 536-8553, Japan  
maruyama@omtri.or.jp

Vanadium redox flow batteries (VRFBs) have attracted much interest as a promising electrical energy storage system due to their suitability for large-scale energy storage and capability to withstand fluctuating power supplies. The slow reaction rate of the electrode reactions is a serious problem in VRFB technology, which has to be overcome to improve the efficiency of the VRFB. Recently, the high catalytic activity was found at a carbonaceous thin film with Fe and four nitrogens (Fe-N<sub>4</sub> site) combined in a carbon matrix in the square-planar configuration and exposed to the surface [1]. The carbonaceous thin film was supported on cup-stack carbon nanotube (CSCNT). In this study, the structure modification of the catalyst layer formed from the thin-film coated CSCNT was attempted for the enhancement of the VRFB positive electrode reactions

The 1:10 weight ratio mixture of iron phthalocyanine (FePc) powder and CSCNT was put in a crucible with a cap and heat-treated at 800 °C after raising the temperature at 1 °C min<sup>-1</sup> in an argon atmosphere. A treatment with an acid solution was carried out to remove any soluble metallic species from the surface. The obtained sample was then labeled CFePc01-800. An aliquot of 5 mg of CFePc01-800 was added to the mixture of 0.5×*x* (*x* = 0.1, 0.2, 0.5, 1) cm<sup>3</sup> of 5 wt % Nafion solution and 0.5×(1−*x*) cm<sup>3</sup> of high-purity water, which was then ultrasonically dispersed to produce a catalyst paste, pipetted on a glassy carbon rotating disk electrode (GC RDE), and dried overnight to form the catalyst layers, CFePc01-800-Naf*x*. The catalyst layer was similarly formed using CSCNT at *x* = 1. Aliquots of 5 mm<sup>3</sup> of 4 M NaOH and *y* (*y* = 5, 10, 15) mg of MgO nanoparticles was added to the catalyst paste of *x* = 0.5. After similarly pipetting and drying it, MgO was removed by an HCl treatment to form the catalyst layer, CFePc01-800-Naf*x*-MgO*y*.

Figure 1 shows the relationships between the electrode potential and the current for the VO<sub>2</sub><sup>+</sup> reduction and VO<sup>2+</sup> oxidation. A small current was observed for GC without any catalyst loading (bare GC). The CSCNT loading increased the current, in particular, for the VO<sup>2+</sup> oxidation. The higher VO<sub>2</sub><sup>+</sup> reduction current was observed for CFePc01-800 than that for CSCNT, which was due to the catalysis of the Fe-N<sub>4</sub> structure. The reduction current was dependent on *x* and the substantial increase was attained at *x* = 0.5. This dependency was attributed to two conflicting factors: the decreases in the diffusion resistance by the Nafion phase and the extent of dispersion of CFePc01-800 in the catalyst paste with a decrease in *x*. The addition of MgO nanoparticles to the catalyst paste was efficient to further enhance both VO<sub>2</sub><sup>+</sup> reduction and VO<sup>2+</sup> oxidation currents. The diffusion of the ions was enhanced through the pores formed by the MgO nanoparticles functioning as the template.

[1] J. Maruyama, T. Hasegawa, S. Iwasaki, T. Fukuhara, Y. Orikasa, Y. Uchimoto, Extended Abstract, ES49, Carbon 2015, Dresden, Germany, July 15 (2015).

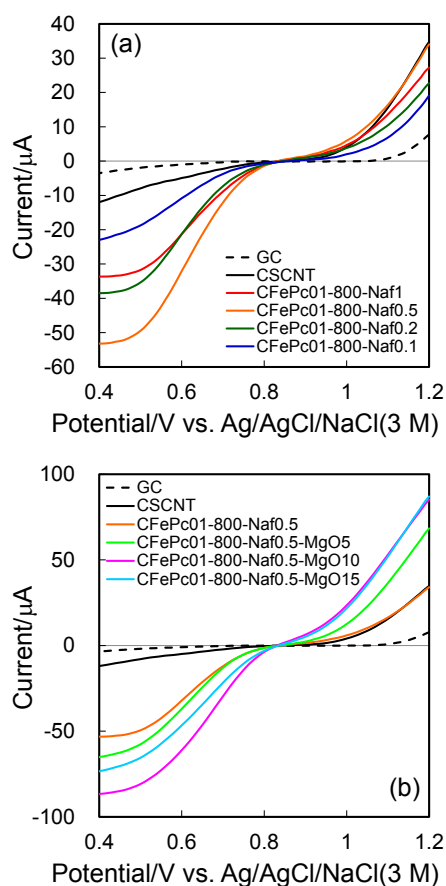


Fig. 1. Relationships between electrode potential and current measured in Ar-saturated VO<sub>2</sub><sup>+</sup>(5 mM)–VO<sup>2+</sup>(5 mM)–H<sub>2</sub>SO<sub>4</sub>(1 M) at 25 °C for bare GC and catalyst layers formed from CSCNT, and CFePc01-800 with various amount of (a) Nafion, (b) Nafion and MgO. The MgO particles were removed after the catalyst layer formation. The amount of the sample fixed on the electrode was 20 μg. The geometric electrode surface area was 0.071 cm<sup>2</sup>. The potential scan rate was 10 mVs<sup>-1</sup>. The rotation rate of the electrode was 2000 rpm. The sign of the oxidation (anodic) current was taken as positive.



# Electroreduction of Oxygen with Brominated Metallo-Corroles

Lior Elbaz\*, Naomi Levi

Bar-Ilan University, 1 Max and Ana Webb St.  
Ramat-Gan 52900, Israel  
\*lior.elbaz@hotmail.com

Zeev Gross, Atif Mahammed  
Technion, Haifa 32000, Israel

Fuel cell technology raised new interest over the past two decades due to the increasing oil prices, non-sustainability of fossil fuel and the consequences of combustion on air pollution and climate changes. Two aspects limit the practicality and energy conversion efficiency in polymer electrolyte membrane fuel cells: the rate-limiting oxygen reduction reaction at the cathode and the low abundance and high cost of platinum, which still remains the most efficient catalyst.

Significant effort has been made to develop alternative non-precious metal catalysts (NPMCs) for oxygen reduction. Many of those catalysts have been inspired by biological processes in that their active centers consist of transition metal complexes such as metallo-porphyrins. So far, studies conducted with such catalysts show that their activity and stability is lower than that of the state-of-the-art platinum based catalysts. In most recent years a new class of NPMCs has shown great promise; the metallo-corroles.

A series of first row transition metal  $\beta$ -pyrrole-brominated 5,10,15-tris(penta-fluoro phenyl) - Corroles [M(tpfc)Br<sub>3</sub>, M=Mn, Fe, Co, Ni and Cu] were synthesized and tested as catalysts for oxygen reduction in acidic aqueous solutions. Both the reduced form and the oxidized forms of these corroles were characterized by means of NMR, EPR and UV-vis measurements. Rotating Ring-Disk electrode (RRDE) was used to test the kinetic performance of these corroles in the catalytic reaction of oxygen reduction (ORR). The corroles were adsorbed on a high surface area carbon powder (BP2000) prior to electrochemical measurements, to create a unique composite material. The comparison between the corroles with different metal centers showed a favorable

catalytic performance of the ORR in the case of the Co-Corrole, which showed an onset potential of only 0.8V vs. RHE (Figure 1).

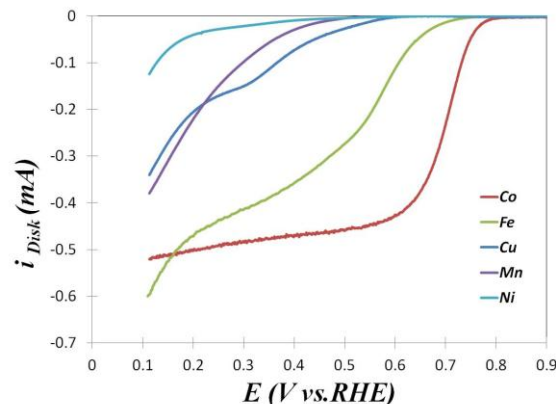


Figure 1: RDE measurements of metallo-corroles at 900 rpm and 5 mV/s in 0.5M H<sub>2</sub>SO<sub>4</sub>

# Platinum-modified Covalent Triazine Frameworks as Methanol-tolerant Oxygen Reduction Electrocatalysts

Kazuhide Kamiya<sup>1</sup>, Ryo Kamai<sup>2</sup>, Kazuhito Hashimoto<sup>1</sup> and Shuji Nakanishi<sup>1</sup>

<sup>1</sup>Department of Applied Chemistry, School of Engineering, The University of Tokyo, 7-3-1 Hongo, Bunkyo-ku, Tokyo 113-8656, Japan, <sup>2</sup>Research Center for Advanced Science and Technology, The University of Tokyo, 4-6-1 Komaba, Meguro-ku, Tokyo 153-8904, Japan, kamiya@light.t.u-tokyo.ac.jp

Covalent organic frameworks (COFs) are cross-linked porous polymers, which have great potential in catalysis area because of their unique porous structure (i.e. high surface area), mechanical robustness and high design flexibility. Especially, covalent triazine frameworks (CTFs), which have 1,3,5-triazine structure as units, possess the high density of nitrogen (N) atoms in their organic pore, which can strongly immobilize metal centers. Recently, Palkovits *et al.* reported that platinum-modified CTF (Pt-CTF) functioned as a solid catalyst for the selective low-temperature oxidation of methane to methanol [1]. In general, the oxidation of methanol can easily proceed compared to methane oxidation because the C-H bond energy of methanol is much smaller than that of methane. Thus, the catalytic activity for methane partial oxidation to methanol let us assume that Pt-CTF has no activity to oxidize methanol (i.e. methanol tolerance). The methanol tolerance is the essential property for the cathode catalyst of direct methanol fuel cells (DMFC) as the methanol-cross-over effect is one of the issues to be addressed. However, the application of the frameworks as electrocatalysts has not been achieved to date because of their poor electrical conductivity.

In the present work, we have successfully applied CTF-based materials to electrocatalysts by hybridizing non-conductive CTFs with conductive carbon particles (CPs). Specifically, the hybridized material was obtained by the polymerization of CTFs on CPs in molten  $\text{ZnCl}_2$ . Then, Pt atoms were grafted in the pore of CTFs by the impregnated with platinum chloride (Pt-CTF/CP, Figure 1). The resulting catalyst showed apparent electrocatalytic activity for oxygen reduction reaction (ORR). In case of a commercial 20 wt% Pt/C, after the addition of 1 M  $\text{CH}_3\text{OH}$ , the onset potential of the cathodic current shifted approximately 200 mV in the negative direction in the presence of oxygen (Figure 2 inset). In contrast, surprisingly, the overlap of the  $\text{CH}_3\text{OH}$  oxidation current with that of the ORR was almost negligible for Pt-CTF/CP even in the presence of 1 M  $\text{CH}_3\text{OH}$  as shown in Figure 2. These results clearly showed that Pt-CTF/CP exhibited a high methanol tolerance during the ORR, as we expected. This is the first demonstration of the potential for CTF-based materials to serve as electrocatalysts [2].

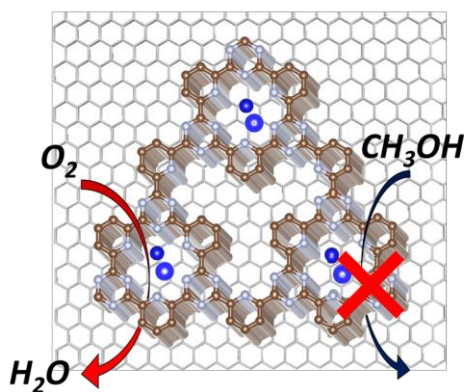


Figure 1 Schematic illustration of Pt-CTF/CP (gray: N, blue: Pt and brown: C).

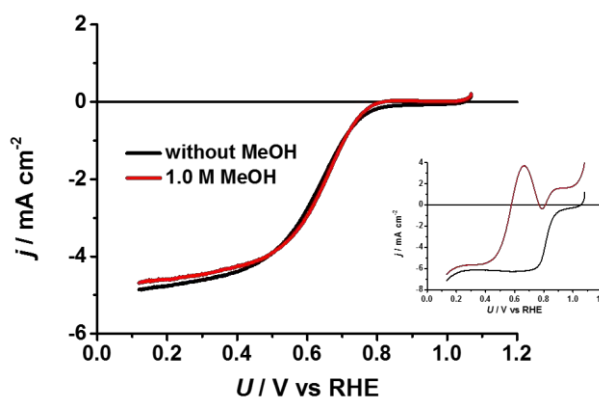


Figure 2  $j$  vs.  $U$  curves for Pt-CTF/CP and (inset) 20 wt% Pt/C in 0.5 M  $\text{H}_2\text{SO}_4$  saturated with dissolved oxygen. Methanol concentration: (black) 0 M and (red) 1.0 M.

[1] Palkovits *et al.* *Angew. Chem. Int. Ed.* **48**, 6909, (2009)

[2] **K. Kamiya** *et al.* *Nat. Commun.* **5**, 5040, (2014)

# Metal-doped Pyrochlore as Novel Anode Material for Intermediate Solid Oxide Fuel Cell

Chien-Yeh Pan, Chia-Kan Hao and Chi-Shen Lee\*

Department of Applied Chemistry, National Chiao Tung University, No. 1001, University Road Hsinchu, Taiwan

Tel: +886-3-5712121#56520; E-mail: chishen@mail.nctu.edu.tw, neilgodiva2008@hotmail.com

## Abstract

In this study, pyrochlore phase  $\text{La}_2(\text{Ce}_{1-x}\text{V}_x)_2\text{O}_{7+\delta}$  ( $x=0.05, 0.1, 0.15, 0.2$ ) and perovskite phase  $\text{La}_{0.8}\text{Sr}_{0.2}\text{Ga}_{0.8}\text{Mg}_{0.2}\text{O}_{3-\delta}$  (LSGM) were synthesized by sol-gel method and used as anode and electrolyte materials for intermediate temperature solid oxide fuel cell (IT-SOFC). These materials were characterized by X-ray diffraction, ICP-AES, SEM-EDS, TPR and EIS. The  $\text{La}_2(\text{Ce}_{0.8}\text{V}_{0.2})_2\text{O}_{7+\delta}$  showed good ionic conductivity and a bottom cell made up of  $\text{La}_2(\text{Ce}_{0.8}\text{V}_{0.2})_2\text{O}_{7+\delta}$  / LSGM/LSCF-GDC (anode/electrolyte/cathode) was fabricated for fuel cell characterization. The as fabricated cell exhibited the optimized power density of  $0.141 \text{ W/cm}^2$  at  $700^\circ\text{C}$ . These results suggested that  $\text{La}_2(\text{Ce}_{0.8}\text{V}_{0.2})_2\text{O}_{7+\delta}$  is a potential anode material for application in IT-SOFC.

# Molybdenum Disulfide/Nitrogen-Doped Graphene Composite as an Electrocatalytic Material for Dye-Sensitized Solar Cells

Miao-Syuan Fan<sup>1</sup>, Chuan-Pei Lee<sup>1</sup>, Chun-Ting Li<sup>1</sup>, Yi-June Huang<sup>1</sup>, R. Vittal<sup>1</sup>, and Kuo-Chuan Ho<sup>1,2\*</sup>

<sup>1</sup> Department of Chemical Engineering, National Taiwan University, Taipei 10617, Taiwan

<sup>2</sup> Institute of Polymer Science and Engineering, National Taiwan University, Taipei 10617, Taiwan

\* E-mail: kcho@ntu.edu.tw

Recently, molybdenum disulfide ( $\text{MoS}_2$ ) and graphene (Gr) have been considered as attractive 2-dimensional (2D) materials due to their good catalytic activity and conductivity, and they have many potential applications in electronic devices, including lithium storage, photoresponsive memory devices and dye-sensitized solar cells (DSSCs). Compared with pristine Gr, the nitrogen-doped graphene (NGr) could compensate the deficiency of active sites without decrease the conductivity, which enhanced the performance of electrochemical reaction. On the other hand, molybdenum sulfide ( $\text{MoS}_2$ ) with its remarkable properties such as catalytic ability and mechanical strength, which can be used over a wide electrochemical system and electronic device. However, the weak point of  $\text{MoS}_2$  is that the active site is limiting to its edge. Thus, the approach to expose the edge of  $\text{MoS}_2$  is a critical segment to improve the performance of this material.

In this study, we prepared various NGr/ $\text{MoS}_2$  composite films via simple drop-coating method as the counter electrode (CE) for DSSCs. As shown in Fig. 1, when the  $\text{MoS}_2$  sheet was used as the CE in a DSSC, it showed a low cell efficiency ( $\eta$ ) of 6.20% ( $V_{OC}$  of 0.79 V,  $J_{SC}$  of  $13.46 \text{ mA cm}^{-2}$ , and  $FF$  of 0.58), while that of the cell showed an  $\eta$  of 6.20% ( $V_{OC}$  of 0.68 V,  $J_{SC}$  of  $12.72 \text{ mA cm}^{-2}$ , and  $FF$  of 0.64) when the bare NGr was used as a CE. We fabricate various NGr/ $\text{MoS}_2$  composite CEs by varying the weight ratio of NGr from 0 to 12wt%. The optimized  $\eta$  of 7.82% ( $V_{OC}$  of 0.77 V;  $J_{SC}$  of  $15.36 \text{ mA cm}^{-2}$ , and  $FF$  of 0.66) was achieved for the DSSC with an NGr/ $\text{MoS}_2$  composite film (8wt% NGr), which is comparable to that of the cell with a platinum (Pt) CE (8.25%). Due to the presence of NGr support, the  $\text{MoS}_2$  exposes more edges for the electrochemical reduction of  $\text{I}^-/\text{I}_3^-$  (Fig. 2). The cyclic voltammetry (CV), electrochemical impedance spectra (EIS), and Tafel curve show that the NGr/ $\text{MoS}_2$  composite film exhibits the superior electrocatalytic ability for the reduction of  $\text{I}_3^-/\text{I}^-$ . Moreover, the rotating disc electrode (RDE) was used to calculate the effective electrocatalytic surface area ( $A_e$ ) of NGr/ $\text{MoS}_2$  composite film ( $0.73 \text{ cm}^2$ ), which is much larger than that of Pt ( $0.196 \text{ cm}^2$ ). The analysis confirmed that the NGr/ $\text{MoS}_2$  composite CE is a noteworthy Pt substitution for the CE in DSSCs.

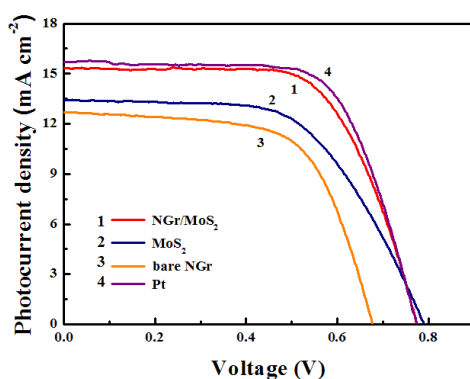


Fig. 1 Photocurrent density–voltage curves of the DSSCs with  $\text{MoS}_2$ , bare NGr, Pt, and NGr/ $\text{MoS}_2$  (8wt% NGr) CEs, obtained at  $100 \text{ mW cm}^{-2}$ .

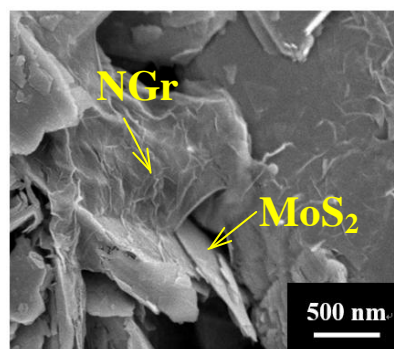


Fig. 2 SEM for the NGr/ $\text{MoS}_2$  composite film (8wt% NGr).

# A Pt-Free Counter Electrode based on Novel Cobalt Diselenide Architectures for Dye-Sensitized Solar Cells

Yi-June Huang<sup>1</sup>, Chuan-Pei Lee<sup>1</sup>, Miao-Syuan Fan<sup>1</sup>, Chun-Ting Li<sup>1</sup>, R. Vittal<sup>1</sup>, Kuo-Chuan Ho<sup>1,2\*</sup>

<sup>1</sup>Department of Chemical Engineering, National Taiwan University, Taipei 10617, Taiwan

<sup>2</sup>Institute of Polymer Science and Engineering, National Taiwan University, Taipei 10617, Taiwan

\*E-mail: kcho@ntu.edu.tw

Platinum (Pt) is one of the preferred electrocatalytic materials for electrochemical devices, including fuels cells, water electrolyzers, and dye-sensitized solar cell (DSSCs). However, the overuse of Pt limits its future usage. Therefore tremendous efforts have focused on the development of Pt-free counter electrode (CE) for DSSCs. Recently earth-abundant inorganic electrocatalysts have been widely investigated as promising CE materials for DSSCs. Here we report the synthesis of novel cobalt diselenide (CoSe<sub>2</sub>) architecture for use as the CE in DSSCs.

In this study, we synthesize CoSe<sub>2</sub> crystals with structures of atomic shell (Fig. 1a) by surfactant-assisted hydrothermal technique using the nonionic surfactant Triton<sup>®</sup> X-100. From the X-ray diffraction (XRD) analysis, the synthesized CoSe<sub>2</sub> crystals show obvious peaks corresponding to (200), (210), (211), (220), (311), (023), (311), (023) planes of CoSe<sub>2</sub> (JCPDS card no. 89-2002). As shown in Fig. 1b, the scanning electron microscopy (SEM) images reveal that the atomic shell-like CoSe<sub>2</sub> crystal has extremely rough surface for each shell, and it has an outer diameter of 40  $\mu\text{m}$  and a shell thickness of 250 nm. We inferred from the SEM images that the rough and two-sided surfaces of each shell of the atomic shell-like CoSe<sub>2</sub> crystal would be meritorious in the present work as high surface area is effective for the reduction reaction of triiodide (I<sub>3</sub><sup>-</sup>). Subsequently, the atomic shell-like CoSe<sub>2</sub> crystals was coated on fluorine-doped tin oxide (FTO) substrate as the CE for a DSSC, which was consisted of a TiO<sub>2</sub> film adsorbed with N719 dye as the photoanode. A power conversion efficiency ( $\eta$ ) of 6.08% with an open-circuit voltage ( $V_{\text{OC}}$ ) of 0.70 V, a fill factor ( $FF$ ) of 0.62, and a short-circuit current density ( $J_{\text{SC}}$ ) of 14.06  $\text{mA cm}^{-2}$  was achieved under the illumination of simulated solar light (AM 1.5G) with intensity of 100  $\text{mW cm}^{-2}$ , which is significantly higher than that of a cell using a CE with the commercial CoSe<sub>2</sub> crystals ( $\eta$ : 4.27%,  $V_{\text{OC}}$ : 0.71 V,  $FF$ : 0.61,  $J_{\text{SC}}$ : 9.91  $\text{mA cm}^{-2}$ ).

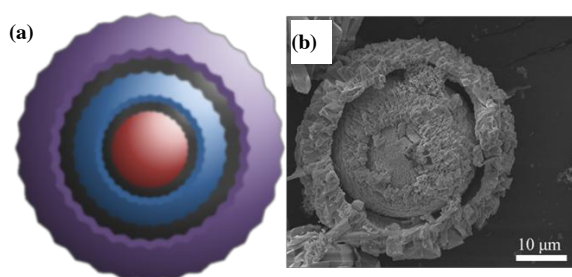


Fig. 1 (a) Schematic representation of atomic shell structure. (b) The SEM image of the atomic shell-like CoSe<sub>2</sub> crystal.

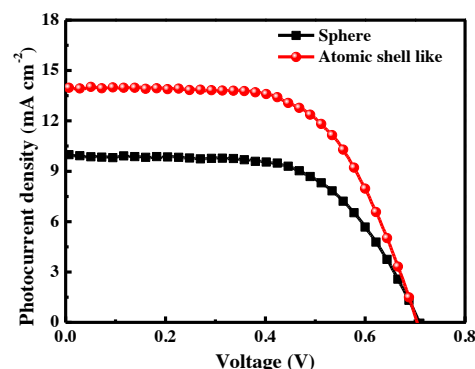


Fig. 2 Photocurrent density-voltage curves of the DSSCs with the commercial CoSe<sub>2</sub> crystals and the atomic shell-like CoSe<sub>2</sub> crystals on their CEs, measured under 100  $\text{mW cm}^{-2}$  (AM 1.5G).

# Synergistic Electrocatalytic Effects on Oxides + Ag - Electrodes for Oxygen Reduction and Evolution

Hatem M. A. Amin, Lingxing Zan, Mohammed Soltani, Sevda Ayata, Christoph Bondü, Helmut Baltruschat  
*University of Bonn*  
*Roemerstrasse 164, 53117 Bonn*  
*baltruschat@uni-bonn.de*

For metal air batteries, a highly reversible electrocatalyst is needed, i. e. a catalyst for both OER and ORR. In alkaline solution, Ag is known to be the best electrocatalyst for oxygen reduction. However, Ag is not catalyzing oxygen evolution. Spinel oxides such as  $\text{Co}_3\text{O}_4$  and various Perovskites have been shown to be good catalysts for oxygen evolution but are not very good for oxygen reduction. We have recently shown that a particular mixture of a Ag catalyst with  $\text{Co}_3\text{O}_4$  nanoparticles leads to a catalyst which not only combines the good performance of Ag for the ORR with that of  $\text{Co}_3\text{O}_4$  for the OER, but shows a better activity than its components.<sup>1, 2</sup>

Here, we will present further insights and demonstrate that this effect is also observed for various perovskites. The effect is also observed when  $\text{Co}_3\text{O}_4$  or the perovskites are deposited on smooth Ag electrodes. We determined the free Ag surface area by underpotential deposition of Pb and thus showed that the specific synergistic effect per free Ag surface area is even larger.

Using differential electrochemical mass spectrometry (DEMS) and  $^{18}\text{O}$  - isotope exchange has been shown in the past that during oxygen evolution at oxides the oxygen of the lattice is participating in the oxygen evolution reaction.<sup>3-6</sup> This method will be applied to the above catalysts as well.

Acknowledgement: Funding of this project by the BMBF (LuLi - project 03X4624A) is gratefully acknowledged.

- 1 H. M. A. Amin, H. Baltruschat, D. Wittmaier and K. A. Friedrich, *Electrochimica Acta*, 2015, **151**, 332-339.
- 2 D. Wittmaier, N. Wagner, K. A. Friedrich, H. M. A. Amin and H. Baltruschat, *J. Power Sources*, 2014, **265**, 299-308.
- 3 M. Wohlfahrt-Mehrens and J. Heitbaum, *J. Electroanalytical Chemistry*, 1987, **237**, 251-260.
- 4 K. Macounova, M. Makarova and P. Krtil, *Electrochemistry Communications*, 2009, **11**, 1865-1868.
- 5 S. Fierro, T. Nagel, H. Baltruschat and C. Comninellis, *Electrochemical and Solid State Letters*, 2008, **11**, E20-E23.
- 6 S. Fierro, T. Nagel, H. Baltruschat and C. Comninellis, *Electrochemistry Communications*, 2007, **9**, 1969-1974.

## A Shortcut: Core (Rutile) – Shell (Anatase) Nanorods for Highly Efficient Solar Water-Splitter

Hogiartha Sutiono, Ching-Hsiang Chen, Wei-Nien Su, Liang-Yih Chen\*, Bing-Joe Hwang\*  
*Department of Chemical Engineering, National Taiwan University of Science and Technology*  
43, Section 4, Keelung Road, Taipei 106, Taiwan  
[sampras@mail.ntust.edu.tw](mailto:sampras@mail.ntust.edu.tw) (Liang-Yih Chen) & [bjh@mail.ntust.edu.tw](mailto:bjh@mail.ntust.edu.tw) (Bing-Joe Hwang)

In this study, the crystal growth behavior of TiO<sub>2</sub> nanorods (NRs) array, which was directly grown on the FTO substrate, could be controlled through a simple procedure. It was found that the position of FTO substrate inside the Teflon-liner during hydrothermal synthesis was strikingly important to control the preferred crystal growth direction. By simply changing the position of FTO substrate, TiO<sub>2</sub> NRs array with unusual crystallographic properties could be obtained. Interestingly, it could produce a remarkable saturation photocurrent of 2.32 mA cm<sup>-2</sup> at 1.23 V<sub>RHE</sub> which outclassed any published reports for pristine TiO<sub>2</sub> photoanode water-splitter. Initially, the finding of unusual crystallographic properties ((110) and (101) facets) was believed severely enhanced the photoelectrochemical (PEC) water-splitting performance. But, after the anatase phase was found in the NRs system, the exact role of (110) and (101) facets towards this superior PEC water-splitting performance became obscured. The existence of anatase phase, which was revealed by Raman spectroscopy technique, was considered to be the main factor in improving charge separation and PEC water-splitting performance simultaneously. The strategy of adding saturated aqueous solution of a particular salt additive into the crystal growth solution not only could modulate the interaction between NRs, but also could control the portion of anatase phase in the NRs system. It was understandable that the wider distance between NRs could enlarge the accessible surface area of the NRs which could facilitate a better charge transfer in the electrode/electrolyte interface. Regarding the arrangement between rutile and anatase phases in the NRs, it was predicted that the anatase phase was naturally formed on the surface of NRs (anatase phase acted as the shell part). This prediction got confirmed by the Transmission Electron Microscopy (TEM) and Tip Enhanced Raman Spectroscopy (TERS) results which were taken from the edge of the nanorod. In addition, annealing temperature variation was selected to investigate the phase transformation and its effect on PEC water-splitting performance. Lastly, it is noteworthy that the existence of anatase phase was not the only factor that could enhance the PEC water-splitting performance. The unusual crystallographic properties of the rutile core part as the result of FTO substrate position modification during hydrothermal synthesis, was believed also responsible in this superior performance.



# The effect of surface functional groups of carbon nanofiber on oxygen reduction reaction

Xinsheng Zhang, Rensheng Zhong, Dongfang Niu, Wei-Kang Yuan

State Key Laboratory of Chemical Engineering, East China University of Science and Technology

130 Meilong Road, Shanghai 200237, China

[xs.zhang@ecust.edu.cn](mailto:xs.zhang@ecust.edu.cn)

In our previous studies, we have studied the effect of CNFs surface microstructures and functional groups on oxygen reduction reaction (ORR) by using CNFs as catalyst or catalyst support to load metal nanoparticles. The P-CNFs exhibit the highest ORR activity because they have higher ratio of edge atoms to basal atoms, and the T-CNFs have the most negative ORR onset potential and the least ORR peak current for their lowest ratio of edge atoms to basal atoms<sup>[1-2]</sup>. By using CNFs as support, the electrocatalyst supported on P-CNFs shows higher electrochemical surface area and more positive ORR onset reduction potential than electrocatalyst supported on other CNFs and activated carbon<sup>[3-4]</sup>.

Surface functional groups are showed to have a positive influence on the ORR activity of CNFs. As shown in Table 1, CNFs with nitrogen-containing groups exhibit the highest ORR activity, followed by carboxyl groups, carbonyl groups and hydroxyl groups. The oxygen reduction of CNFs with nitrogen-containing groups proceed almost entirely through the four-electron reduction pathway, while the electrodes of CNFs with carboxyl groups, carbonyl groups and hydroxyl groups proceed a two-electron reduction at low potentials followed by a gradually four-electron reduction at more negative potentials.

We also have found CNFs with hydroxyl groups (CNF-OH) are more conducive to support Pt catalyst than carboxyl groups (CNF-OX), so Pt/CNF-OH presents a better activity towards ORR than Pt/CNF-OX.

Table 1 Electrochemical data for five modified CNF/GC electrodes.

Sample	$E_{OP}$ (V)	$E_p$ (V)	$j_p$ ( $\text{mA}\cdot\text{cm}^{-2}$ )	$n$ @0.6V K-L plot
CNF-P	-0.222	-0.344	-0.339	2.11
CNF-OX	-0.144	-0.254	-0.384	2.43
CNF-OH	-0.166	-0.281	-0.350	2.19
CNF-CO	-0.144	-0.264	-0.363	2.35
CNF-ON	-0.134	-0.286	-0.788	3.25

## References

- [1] Jun-Sheng Zheng, Xin-Sheng Zhang, Ping Li, Xing-Gui Zhou, Wei-Kang Yuan. Microstructure effect of carbon nanofiber on electrocatalytic oxygen reduction reaction. *Catalysis Today*, 2008,131:270–277.
- [2] Yuan-Hang Qin, Hou-Hua Yang, Xin-Sheng Zhang, Ping Li, Chun-An Ma. Effect of carbon nanofibers microstructure on electrocatalytic activities of Pd electrocatalysts for ethanol oxidation in alkaline medium, *International Journal of Hydrogen Energy*, 2010, 35:7667-7674.
- [3] Jun-Sheng Zheng, Xin-Sheng Zhang, Ping Li, Jun Zhu, Xing-Gui Zhou, Wei-Kang Yuan. Effect of carbon nanofiber microstructure on oxygen reduction activity of supported palladium electrocatalyst, *Electrochem. Commun.*, 2007, 9 : 895–900.
- [4] Yuan-Hang Qin, Yue-Jiang, Hou-Hua Yang, Xin-Sheng Zhang\*, Xing-Gui Zhou, Li Niu and Wei-Kang Yuan, Synthesis of highly dispersed and active palladium/carbon nanofiber catalyst for formic acid electrooxidation, *Journal of Power Sources*, 2011,196: 4609-4612

## Acknowledgments

The present study was supported by the Nature Science Foundation of China (21073061), the State Key Laboratory of Physical Chemistry of Solid surfaces (Xiamen University). State Key Laboratory Breeding Base of Green Chemistry Synthesis Technology (Zhejiang University of Technology), and the 111 Project (B08021).



## **Ni-based bimetallic nanoparticles as active and durable catalysts towards hydrogen oxidation reaction**

Yu-Xiang Mao<sup>†</sup>, Chun-Jern Pan<sup>†</sup>, Men-Che Tsai<sup>†</sup>, Wei-Nien Su<sup>§</sup>, Bing-Joe Hwang<sup>†\*</sup>

*<sup>†</sup>Department of Chemical Engineering, National Taiwan University of Science and Technology, Taipei 106, Taiwan, R. O. C.*

*<sup>§</sup>Graduate Institute of Applied Science and Technology, National Taiwan University of Science and Technology, Taipei 106, Taiwan*

*\*[bjh@mail.ntust.edu.tw](mailto:bjh@mail.ntust.edu.tw)*

Fuel cells have been considered as potential candidate for alternative energy generation system. Unfortunately, the use of precious Pt catalyst limits its wide spread application. In order to reduce the cost, the research focus was suggested to shift from proton exchange membrane fuel cell to alkaline anion exchange membrane system. The hydrogen oxidation reaction (HOR) on anode side is fast in acidic environment, whereas in alkaline environment the reaction rate is two ordered magnitude lower than that in acidic. Therefore, enhancement of reaction kinetic for HOR in alkaline media is the key for improving the performance of entire fuel cell system.

In this study, the non Pt-based catalyst was developed for applied in hydrogen oxidation reaction. The non-precious Ni-based catalyst, alloying with Pd and Ru as the second metals, has been developed. In the catalyst preparation, the modified watanabe method has been adapted to prepare bimetallic NiM(M=Pd, Ru) catalyst. The synthesized bimetallic catalysts is well alloyed and the size in between 3-5 nm. The hydrogen oxidation activity was evaluated by cyclic voltammograms (CV) and linear sweep voltammograms (LSV) on the rotating disk electrode in 0.1 M KOH alkaline media. The catalysts exhibit comparable catalytic activity for HOR as compared to commercial Pt/C catalyst. In addition, the synthesized bimetallic catalyst shows superior activity than Pt/C towards hydrogen evolution reaction. The developed bimetallic NiM(M=Pd, Ru) catalyst is promising candidate to replacing Pt as HOR catalyst and has potential to be bifunctional catalyst for catalyzing both hydrogen oxidation and evolution reaction.

# **Physioelectrochemical properties and catalytic activity of green synthesized metal oxide nanoparticles and conductive polymer composite film**

A. Ehsani,

*Department of Chemistry, Faculty of science, Qom university, Qom, Iran*

E-mail address: ehsani46847@yahoo.com

NiO nanostructures (NiONPs ) have been extensively investigated because of their promising applications in various fields. NiO nanostructures are potential catalysts for oxidation reactions of CO and for substituting noble metal catalysts due to their high catalytic activity, low-cost, and availability. Ni-based and its oxide-based nanomaterials were of great interest for their extensive applications in catalysis, gas sensor, Li ion battery and biosensors for a long time. The study of conducting polymer modified electrodes is motivated primarily from the anticipation of a synergistic electrocatalytic benefit from the very good conducting and mechanical properties and their good adhesion to the electrode substrate [1, 2]. Herein, we describe a simple strategy dispersing of NiONPs within the conducting polymer matrix by in situ electropolymerization using an ionic surfactant as the supporting electrolyte.

In this work, NiONPs was prepared by a simple and green method using Rosmarinus officinalis extract containing phenolic constituents as both the chelating and the stabilizing agents. NiO nanoparticles/poly ortho amino phenol composite as electro-active electrodes for electro catalytic oxidation of methanol with good uniformity are prepared by electropolymerization. Composite of NiONps/POAP was synthesized by cyclic voltammetry (CV) methods and electrochemical properties of film were investigated by using electrochemical techniques. New composite modified electrode shows a significantly higher response for methanol oxidation.

## **References**

- [1] A. Ehsani, M. G. Mahjani, M. Jafarian, A. Naeemy, *Electrochim. Acta* 71 (2012) 128-133.
- [2] A. Ehsani, M.G. Mahjani, M. Bordbar, S. Adeli, *J. Electroanal. Chem.* 710 (2013) 29-35.

# Orange II mineralization on C-modified nanoparticulate TiO<sub>2</sub> cathodes able for producing OH<sup>•</sup> radicals through the O<sub>2</sub> reduction which is simultaneously generated on a grade 2 Ti anode via the H<sub>2</sub>O oxidation

J. Manríquez,<sup>1\*</sup> A.I. Pérez-Jiménez,<sup>1</sup> S. Murcio-Hernández,<sup>1</sup> L.N. Méndez-Alvarado,<sup>1,2</sup> R. Fuentes-Ramírez,<sup>2</sup> G. Carreño-Aguilera,<sup>3</sup> L.A. Godínez, R.A. Herrada-García,<sup>1</sup> E. Bustos<sup>1</sup>

<sup>1</sup> Centro de Investigación y Desarrollo Tecnológico en Electroquímica S.C., Parque Tecnológico Querétaro s/n, Sanfandila, 76703, Pedro Escobedo, Querétaro, México.

<sup>2</sup> División de Ciencias Naturales y Exactas, Departamento de Ingeniería Química, Universidad de Guanajuato, Noria Alta s/n, 36050, Guanajuato, Guanajuato, México.

<sup>3</sup> División de Ingenierías, Departamento de Geomántica e Hidráulica, Universidad de Guanajuato, Juárez 77, Centro, 36000, Guanajuato, Guanajuato, México.

\*e-mail: [jmanriquez@cideteq.mx](mailto:jmanriquez@cideteq.mx)

In this investigation we study the orange II dye mineralization on C-modified nanoparticulate TiO<sub>2</sub> cathodes (**OTE/npTiO<sub>2</sub>/C**, where an optically transparent electrode (OTE) and carbon vulcan powder (C) were utilized as conductive substrate and carbon material, respectively) that can produce OH<sup>•</sup> radicals through the O<sub>2</sub> reduction. In this way, the O<sub>2</sub> consumed by the **OTE/npTiO<sub>2</sub>/C** cathodes is simultaneously produced on a grade 2 Ti anode where the H<sub>2</sub>O oxidation is carried out. On the other hand, the orange II mineralization was also carried out on bare nanoparticulate TiO<sub>2</sub> electrodes (**OTE/npTiO<sub>2</sub>**) for comparison purposes.

Our results showed a color removal of 99% (estimated by absorbance reduction at 480nm) when a potential of -0.1V vs. Ag|AgCl (3M NaCl) is applied to the system **OTE/npTiO<sub>2</sub>/C** which remains immersed for 7 h in an O<sub>2</sub>-saturated electrolyte. This electrolyte condition was achieved with the aid of the Ti counter-electrode that simultaneously oxidizes H<sub>2</sub>O at a potential of +1.4V vs. Ag|AgCl (3M NaCl), which is promoted after the anode polarization is activated. On the contrary, the color removal efficiency for the system **OTE/npTiO<sub>2</sub>** achieves only 16% for the same experimental setup, thus revealing that the O<sub>2</sub> reduction on the **OTE/npTiO<sub>2</sub>/C** electrodes was enhanced by the presence of the C materials. Complementarily, the remnant total organic carbon (TOC) that were measured for the electrochemical treatments carried out with **OTE/npTiO<sub>2</sub>/C** and **OTE/npTiO<sub>2</sub>** electrodes showed values of 55 and 85%, respectively, in good accordance with the color removal tendencies.

To better understand the last results, the production of OH<sup>•</sup> radicals on **OTE/npTiO<sub>2</sub>/C** and **OTE/npTiO<sub>2</sub>** electrodes was followed during the first 1 h of the electrochemical treatments. Interestingly, it was found that the OH<sup>•</sup> generation from both TiO<sub>2</sub> surfaces has the same tendency in the absence or in the presence of C materials, thus indicating that the OH<sup>•</sup> radicals generation do not depend from the applied potential to the anodes because these species should be chemically produced after the O<sub>2</sub> reduction is taking place. On the contrary, the measured charge transfer resistances ( $R_{ct}$ ) for the O<sub>2</sub> reduction on polarized **OTE/npTiO<sub>2</sub>/C** (10.17k $\Omega$ ) and **OTE/npTiO<sub>2</sub>** (45.47k $\Omega$ ) electrodes clearly revealed that the O<sub>2</sub> reduction rate on the **OTE/npTiO<sub>2</sub>/C** electrodes was 4.5 times faster than for the **OTE/npTiO<sub>2</sub>** electrodes. This result strongly suggest that the color removal on **OTE/npTiO<sub>2</sub>/C** electrodes it was predominantly promoted by the products of the O<sub>2</sub> reduction (O<sub>2</sub><sup>•-</sup>, HO<sub>2</sub><sup>•-</sup>), which are thermodynamically able for activate the reduction of the azo groups (N=N) localized in the molecules of orange II. Finally, the mineralization process of the previously reduced orange II molecules was enhanced with the aid of the chemically generated OH<sup>•</sup> radicals.

# Study of ethanol electro-oxidation on PtNd/C and PtSnNd/C: stability test and FTIR.

Nathalia Abe Santos\*, Patricia Gon Corradini and Joelma Perez  
Instituto de Química de São Carlos, Universidade de São Paulo (USP),  
Avenida Trabalhador São-carlense 400, 13560-970, São Carlos, Brazil  
\*abe.nathalia@yahoo.com.br

The development of efficient catalysts for direct ethanol fuel cells (DEFC) requires to understand the influence of physical and chemical properties of materials in catalytic activity. Therefore, this abstract describes the preparation of carbon-supported catalysts with a metal load of 20% wt, (metal = Pt, Sn and/or Nd) by formic acid method<sup>1</sup> and the study of their catalytic activities for ethanol oxidation reaction. The catalysts were characterized by physical and electrochemistry techniques. X-ray diffraction analysis showed diffraction patterns with typical peaks of face-centered cubic structure of Pt. Average particle sizes of 4 and 5 nm were respectively observed for PtSn/C and Nd-based catalysts by transmission electron microscopy. EDX data indicated the catalysts composition: PtSn (90:10), PtNd (76:24) e PtSnNd (71:12:17). XPS analysis was performed for all catalysts. The catalytic activity for ethanol oxidation was evaluated for potential sweeps and chronoamperometry. Performing analysis at activity for ethanol oxidation after and before stability evidenced that Nd-based catalysts (PtNd/C and PtSnNd/C) have the largest activity for ethanol oxidation reaction after test. CO stripping measurements also showed a significant change in the form of linear sweep voltammetry curves of CO oxidation after and before stability for catalysts PtSn/C and PtSnNd/C. This change was not observed for PtNd/C catalyst. It is known that CO electro-oxidation reaction on Pt is structure-sensitive<sup>2</sup>, the results can indicate changes in the surface structure of Sn-based catalysts, whereas no changes are observed on surface structure of PtNd/C. The evaluation of products and intermediaries of the ethanol oxidation reaction by Fourier transform infrared spectroscopy indicated the formation acetaldehyde and acetic as the main products and CO<sub>2</sub> traces. In conclusion, these findings clearly demonstrate that, despite the low reaction yielding, all catalysts are able to break C-C bonds and generated CO<sub>2</sub>. In addition, compared to PtSn/C catalyst, Nd-based catalysts present enhanced catalytic activity for ethanol oxidation after stability test and such improvement can be influenced by the presence Nd on the surface structure of catalyst.

## Acknowledgments

N. A. S. thanks FAPESP (2013/17549-5) and P. G. C. thanks FAPESP (2012/12189-8). Thanks are also due to the FAPESP (2013/16930-7) and the Brazilian Synchrotron Light National Laboratory (LNLS) for assisting the XPS measurements.

## References

1. Gonzalez, E. R. T., E. A.; Pinheiro, A.; L. N.; Perez, J., Patente Brasileira. *Processo de obtenção de catalisador de platina dispersa ancorada em substrato através da redução por ácido fórmico* **1997**, INPI-SP (n° 00321).
2. Beden, B.; Bilmes, S.; Lamy, C.; Leger, J. M., Electrosorption of Carbon-Monoxide on Platinum Single-Crystals in Perchloric-Acid Medium. *Journal of Electroanalytical Chemistry* **1983**, 149 (1-2), 295-302.

# Catalytic Performance and Characterization of Iron Oxide-Based Composite Catalyst for Reduction of CO<sub>2</sub>

Joosun Kim<sup>a,\*</sup>, Donghyun Bae<sup>a,b</sup>, Miyoung Yoon<sup>a</sup>, Eunseok Kwon<sup>a,c</sup>, Seunghwan Lee<sup>a,d</sup>, Jooho Moon<sup>c</sup>,  
Hyunjung Shin<sup>d</sup>

<sup>a</sup>*High-Temperature Energy Materials Research Center, Korea Institute of Science and Technology, 5  
Hwarang-ro 14-gil, Seongbuk-gu, Seoul 136-791, Korea*

<sup>b</sup>*Department of Materials Science and Engineering, Andong National University, 1375 Gyeongdong-ro,  
Andong-si, Gyeongsangbuk-do 760-749, Korea*

<sup>c</sup>*Department of Materials Science and Engineering, Yonsei University, 50 Yonsei-ro, Seodaemun-gu,  
Seoul 120-749, Korea*

<sup>d</sup>*Department of Energy Science, Sungkyunkwan University, 2066 Seobu-ro, Suwon-si, Gyeonggi-do 440-  
746, Korea*

\*joosun@kist.re.kr

CO<sub>2</sub> is one of the most widely known greenhouse gases which cause the global warming, therefore CO<sub>2</sub> capture and sequestration have attracted much attention. Water gas shift (WGS) is a reaction for producing CO<sub>2</sub> and H<sub>2</sub> from CO and water vapor. Conversely, it is possible to remove CO<sub>2</sub> from the air via reverse water gas shift (RWGS) reaction which is an endothermic reaction above 600°C.[1-2] Also, coupling the RWGS reaction with the co-electrolysis can produce synthesis gas (i.e. syngas) consisting of H<sub>2</sub> and CO, a Fischer-Tropsch (FT) process converts the syngas into hydrocarbons which is useful fuels such as gasoline, diesel, ethanol and methanol. However, catalyst materials for RWGS reaction are limited to noble metals such as Pt, Rh, Pd and Au, because RWGS reaction requires high operating temperature. Although the noble metals show highly catalytic activity and stability at elevated temperature, they have significant barriers to commercialization due to high cost and limited natural abundance. Therefore, it is necessary to develop cost-effective and highly active catalyst for low-temperature RWGS reaction. In this study, composite catalyst, which includes iron oxide as catalyst and gadolinia-doped ceria (GDC) as oxygen storage, was fabricated for the reduction of CO<sub>2</sub> in RWGS reaction. Catalytic tests were carried out in a fixed-bed quartz reactor with a different gas mixture ratio of CO<sub>2</sub> and H<sub>2</sub> as reactants in the temperature range of 450 to 700°C. The gases which passed through the composite catalyst were injected to gas chromatograph (GC), and then the CO<sub>2</sub> conversion rate and CO selectivity were analyzed. From the experimental results, it was confirmed that the obtained composite catalyst for the reduction of CO<sub>2</sub> shows highly catalytic activity corresponding noble metals such as Pt, Rh, Pd and Au.

## References

- [1] D. Kim, S. Han, H. Yoon, Y. Kim, Reverse water gas shift reaction catalyzed by Fe nanoparticles with high catalytic activity and stability, *J. Ind. Eng. Chem.* 23 (2015) 67.
- [2] W. Luhui, L. Hui, L. Yuan, C. Ying, Y. Shuqing, Influence of preparation method on performance of Ni-CeO<sub>2</sub> catalysts for reverse water-gas shift reaction, *J. Rare Earth.* 31 (2013) 559.

# Electrochemical Oxidation of Dibenzothiophene and Dibenzothiophene Sulphone

M. M. Dávila-Jiménez<sup>(1)</sup>, M. González-Perea<sup>(1)</sup>, M. P. Elizalde-González<sup>(2)</sup>, P. Ruíz-Gutiérrez<sup>(1,2)</sup>  
<sup>(1)</sup>Facultad de Ciencias Químicas, <sup>(2)</sup>Centro de Química. Universidad Autónoma de Puebla.  
Facultad de Ciencias Químicas. Edificio 105 H. Ciudad universitaria, Col. San Manuel, Avenida San Claudio y 18 Sur, C.P 72570, Puebla, Puebla

mdavila.uap.mx@gmail.com

Sulfur containing compounds as the methyl-substituted dibenzothiophene, are very recalcitrant substances and are associated with environmental problems in soils, water and atmosphere. In this work the model molecules dibenzothiophene (DBT) and dibenzothiophene sulfone (DBTO<sub>2</sub>) were electrochemically degraded in an acetonitrile-aqueous system on platinum electrodes at 32 mA cm<sup>-2</sup>. As result of the oxidation-reduction process of 920 ppm of DBT or DBTO<sub>2</sub> in a not divided cell, two liquid immiscible phases were formed: a) a high dense phase (HDP), and b) a lower density phase (LDP). These two phases were separated and analyzed by GC-FID, GC-MS, HPLC-DAD, UV-Vis and FTIR techniques. The LDP analysis of the electrolyzed solution of DBT by GC-FID using a polar column showed that the DBT was completely degraded (Fig. 1a and b) and only one product was detected. In the HDP a greater number of products (\*) were detected (Fig.1c). These compounds are substantially more polar than those that remain in the LDP. The last was demonstrated by the values of the conductivity, pH and by chromatography. GC-MS analysis using a non-polar column of the LDP after electrolysis showed that the products P1 and P2 are the same for DBT and DBTO<sub>2</sub> (Fig. 2a and 2b). The analysis of the electrolysis products and the percentage of DBTO<sub>2</sub> removed from the reaction mixture ACN-H<sub>2</sub>O during 6 hours of electrolysis was studied by HPLC-DAD (Fig. 3).

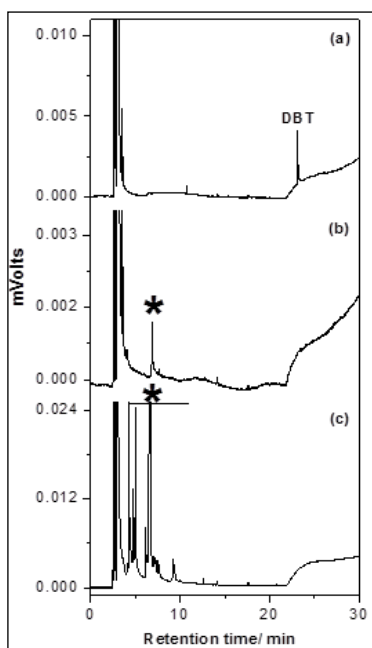


Figure 1

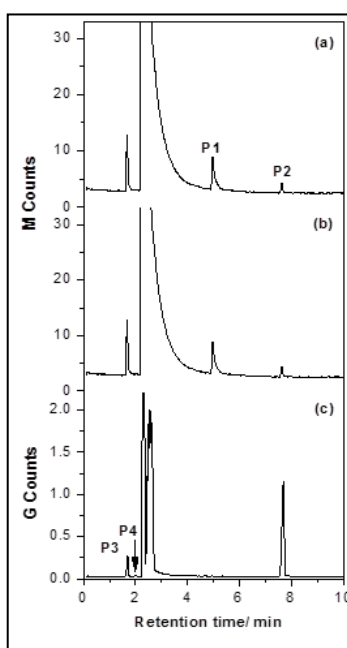


Figure 2

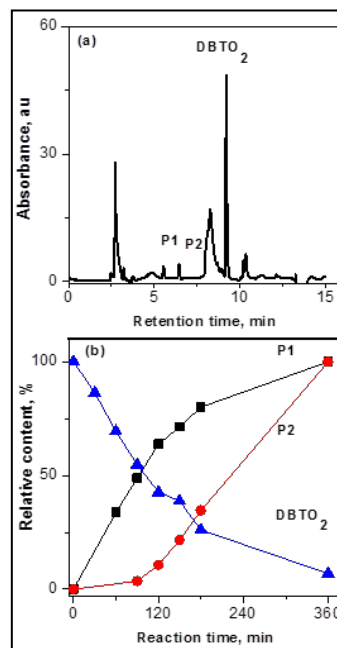


Figure 3

GC-FID (**Figure 1**) and GC-MS (**Figure 2**) chromatograms of DBT of the LDP before (a) and after electrochemical oxidation (b). HDP after electrolysis (c). DBT (a) and DBTO<sub>2</sub> (b) of the LDP and of DBT (c) of the HDP in Figure 2. HPLC-DAD of electrolysis products of DBTO<sub>2</sub> (**Figure 3**).

## ACKNOWLEDGMENTS

The authors thank for the financial support of the project 56-VIEP-BUAP. We also acknowledge J.A. Zárate and E. Rubio (CUVYT-BUAP) for the GC-FID-MS analysis of the samples.

# Electrochemical Investigation of Water Reduction on Goethite, Lepidocrocite and Mild Steel in Slightly Alkaline Electrolyte

Kristoffer Hedenstedt<sup>1,2</sup>, Nina Simic<sup>1</sup>, Mats Wildlock<sup>1</sup> and Elisabet Ahlberg<sup>2</sup>

<sup>1</sup>AkzoNobel Pulp and Performance Chemicals, SE-445 80 Bohus, Sweden

<sup>2</sup>Department of Chemistry and Molecular Biology, University of Gothenburg,

Kemigården 4, SE-412 96 Gothenburg, Sweden

kristoffer.hedenstedt@chem.gu.se

Cathodes made out of mild steel were taken from two different sodium chlorate plants presenting completely different characteristics. Surface characterisation with SEM, EDX and XRD showed that goethite was present on one of them while lepidocrocite was the corrosion product present on the second. It was also established that the electrode with lepidocrocite had longer starting period, i.e. before reaching sufficient current efficiency.

The kinetics of the hydrogen evolution reaction was studied on the two different iron-oxy-hydroxides as well as on fresh mild steel under slightly alkaline conditions. Tafel slopes of 200-250 mV/decade showed that the first electron transfer is rate limiting but the transfer coefficient is small, ranging from 0.24 to 0.3, Figure 1. It is concluded that the hydrogen evolution reaction on all three electrodes takes place on  $\text{Fe}(\text{OH})_2$ , which must first be formed on the surface [1, 2]. Since the transfer coefficient is low, the transition state is closer to the adsorbed hydrogen than to the water in solution. Hence the active site for water reduction is proposed to be the protonated  $\equiv \text{Fe}(\text{II})-\text{OH}_2^+$  surface group independent if the starting material is  $\alpha$ -FeOOH,  $\gamma$ -FeOOH or mild steel. The mechanism for hydrogen evolution is discussed in the

context of the general Volmer-Tafel-Heyrovsky scheme valid for metal surfaces. The kinetic results indicate that the thickness and conductivity of the layers are more important for the performance than the crystallographic structure of the oxide

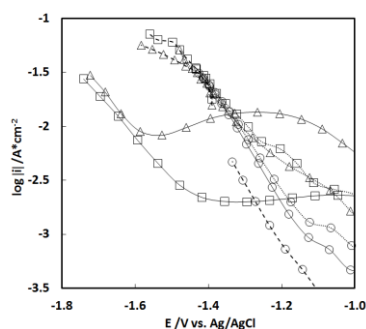


**Figure 1.** Linear sweeps of the mild steel (○),  $\alpha$ -FeOOH (□) and  $\gamma$ -FeOOH (△) electrodes before (—), during (---) and after (····) steady state current measurements.

1. M. Cohen, K. Hashimoto, The cathodic reduction of  $\gamma$ -FeOOH,  $\gamma$ -Fe<sub>2</sub>O<sub>3</sub>, and oxide films on iron, J. Electrochem. Soc., 121 (1974) 42-45
2. B. Beverskog, I. Puigdomenech, Revised pourbaix diagrams for iron at 25-300°C, Corrosion Science, 38, 12, (1996) 2121-2135

# A Reliable and Quantitative Characterization of Electrocatalysts Towards the Oxygen Reduction Reaction from LSV/RDE Experiments

L. Fernandez Macia<sup>1</sup>, B. Geboes<sup>1,2</sup>, J. Ustarroz<sup>1</sup>, L. Stevaert<sup>1</sup>, T. Breugelmans<sup>1,2</sup>, A. Hubin<sup>1</sup>

<sup>1</sup> Research group Electrochemical and Surface Engineering (SURF), Vrije Universiteit Brussel, Pleinlaan 2, 1050 Brussel, Belgium

<sup>2</sup> Research Group Advanced Reactor Technology (ART), University of Antwerp, Salesianenlaan 30, 2660 Hoboken, Belgium

email: [lucferna@vub.ac.be](mailto:lucferna@vub.ac.be)

The large development of the polymer electrolyte membrane fuel cells in the last decades has made the oxygen reduction a widely investigated reaction. Due to its sluggish kinetics, extensive research is devoted to find optimal electrocatalysts for the oxygen reduction reaction (ORR). As a consequence, the study of the ORR has become one of the standard electrochemical analyses for the characterization of electrocatalysts.

The catalytic activity towards the ORR can be studied by linear sweep voltammetry in combination with a rotating disc electrode (LSV/RDE) [1]. Besides the kinetic characterization, the technique allows identifying the reaction mechanism with the quantification of the number of electrons transferred. The kinetic study of the electrocatalysts often involves the use of the Koutecky-Levich analysis to calculate the number of transferred electrons and the kinetic current. At the diffusion limited current region, the number of electrons is estimated; whereas the catalytic activity (i.e. the kinetic current) is estimated at low overpotentials for the ORR, where the fuel cell would perform. Therefore, the determination of the characteristic electrochemical parameters of the catalyst is obtained by means of the analysis at two potentials of separated regions of the current-potential experiment. This is done at the risk of neglecting irregularities on the current-potential response of the material, which might be present at the selected potentials, altering the shape of the LSV/RDE curve and making the Koutecky-Levich analysis difficult.

In this work, the electrochemical parameters of catalysts are determined from LSV/RDE experiments by means of a statistically-founded fitting procedure [2-3]. This method offers the advantage of using one integrated current-potential relation that accounts for mass and charge transfer steps. Hence, the whole polarization curve is considered, rather than just the part in which only mass or charge transfer is supposed to be rate determining. In this sense, it brings an enormous advantage to the analysis of electrocatalytic processes. The procedure is designed for the reliable determination of characteristic parameters (i.e. number of electrons, kinetic current and charge transfer coefficient) from only one LSV/RDE experiment. Provided that the experimental reproducibility is ensured, this methodology eliminates the need of multiple experiments to characterize quantitatively the electrochemical system. This aspect is also a benefit for assessing the catalytic activity, reducing the problematic related to the ageing of the electrocatalyst. Recently, this method has been proven to represent a strong tool to detect deviations of actual LSV/RDE measurements from the theoretical curve [3], which is of great interest to understand the mechanism of the electrochemical process.

Nanostructured Pt catalysts are chosen for this study due to their high activity towards the ORR and high surface to volume ratios. Pt dendritic nanostructures are electrodeposited on glassy carbon RDEs by a potentiostatic double pulse, optimized to enhance the electrochemically active surface area [4-5]. To characterize the catalysts electrochemically, LSV/RDE experiments with different rotation speeds are performed. The experimental data are used to investigate the interesting advantages of the fitting methodology for the reliable estimation of the characteristic parameters of the electrocatalytic process.

- [1] B. Geboes, I. Mintsouli, B. Wouters, J. Georgieva, A. Kakaroglou, S. Sotiropoulos, E. Valova, S. Aramyanov, A. Hubin, T. Breugelmans, *Applied Catalysis B: Environment* 150-151 (2014) 249-256.
- [2] L. Fernández Macía, E. Tourwé, R. Pintelon, A. Hubin, *Journal of Electroanalytical Chemistry* 690 (2013) 127-135.
- [3] L. Fernández Macía, R. Pintelon, A. Hubin, *Journal of Electroanalytical Chemistry* 720-721 (2014) 147-155.
- [4] J. Ustarroz, T. Altantzis, J.A. Hammons, A. Hubin, S. Bals, H. Terryn, *Chemistry of Materials* 26 (2014) 2396-2406.
- [5] J. Ustarroz, B. Geboes, L. Stevaert, K. Sentosun, S. Bals, A. Hubin, T. Breugelmans, H. Terryn (2015), Manuscript in preparation.



# Synthesis of MnO<sub>2</sub>/Carbon Composites as Electrode Materials for Supercapacitors

Chien-Te Hsieh, Dong-Ying Tzou, Hsiu-Hui Hsu, Yu-Ming Chiang  
Department of Chemical Engineering and Materials Science, Yuan Ze University  
135 Yuan-Tung Road, Chung-Li 32003, Taiwan  
[cthsieh@saturn.yzu.edu.tw](mailto:cthsieh@saturn.yzu.edu.tw)

## Abstract

Carbon nanotubes (CNTs) and graphene nanosheets (GNs) supported by MnO<sub>2</sub> nanoneedles have been synthesized through a chemical-wet route without any thermal treatment. The electrochemical capacitive performances of MnO<sub>2</sub>/carbon composite electrodes are characterized by cyclic voltammetry, galvanostatic charge-discharge cycling, and *ac* impedance spectroscopy.

The electrochemical performance of MnO<sub>2</sub>-based capacitors is enhanced by the synergistic effect that combines the MnO<sub>2</sub> and the carbon supports, promoting more active sites available for charge transfer and electric double-layer in the hybrid architecture. The enhanced performance of MnO<sub>2</sub>-based capacitors can be ascribed to the fact that the design of hybrid structure is capable of (i) maximizing the utilization of MnO<sub>2</sub> nanoneedles and (ii) leading to fast chemical reaction kinetics including ionic electro-sorption and charge transfer. This method provides a simple and fast way to deposit MnO<sub>2</sub> onto carbon supports as electrode materials for energy-storage devices.

**Keyword:** Electrochemical capacitors; Manganese dioxide; Graphene nanosheets; Carbon nanotubes; Specific capacitance

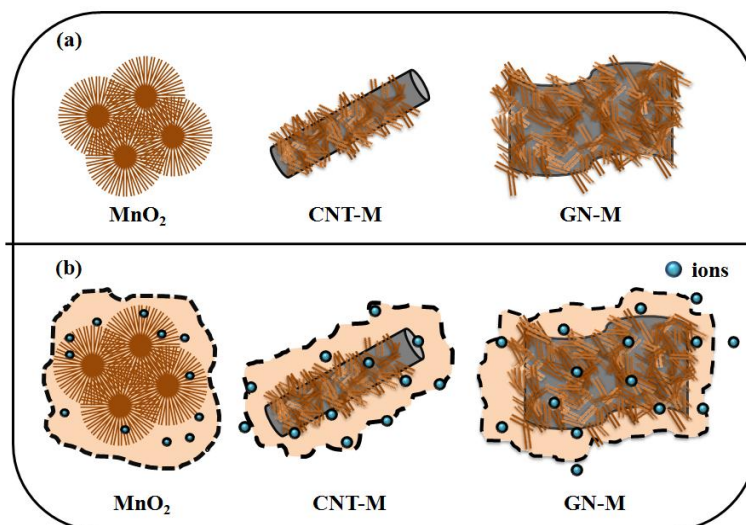


Figure 1. Schematic illustrating (a) the morphologies of MnO<sub>2</sub>, CNT-M, and GN-M composites through the chemical-wet way, and (b) the diffusion of Li ions through different MnO<sub>2</sub> nanostructures from Li<sub>2</sub>SO<sub>4</sub> electrolyte.

## Reference

- [1] Y. Cheng, L. Songtao, H. Zhang, C.V. Varanasi, J Liu, Nano lett. 12 (2012) 4206-4211.
- [2] S. Chen, J. Zhu, X. Wu, Q. Han, X. Wang, ACS Nano 4 (2010) 2822-2830.
- [3] H. Jiang, Y. Dai, Y. Hu, W. Chen, C. Li. ACS Sustable Chem. Eng. 2 (2014) 70-74.

# New palladium phosphide catalysts for fuel cell relevant reactions

A. Kucernak, K. F. Fahy, B. Kakati, V. N. Naranammalpuram Sundaram

Department of Chemistry, Imperial College London  
South Kensington, London SW7 2AZ, United Kingdom  
anthony@imperial.ac.uk

A number of recent publications have demonstrated the interesting corrosion and catalytic properties of transition metal phosphides in acidic media[1-3]. These phosphides may have interesting applications as durable electrocatalysts in polymer electrolyte membrane fuel cells (PEMFCs) direct methanol fuel cells (DMFCs), and electrolyzers.

Although Palladium is often touted as a potential alternative to platinum as an electrocatalyst, it suffers from lower stability, due to the higher solubility and lower thermodynamic stability of palladium in acidic media. One method of improving stability is by alloying the palladium with phosphorus, which is known in the literature to produce corrosion resistant compounds[4], which can be important in achieving good electrochemical stability[3].

In this study we demonstrate an easily scalable method for producing carbon-supported transition metal phosphides and use this method to produce palladium phosphides containing 28 at.% and 33 at.% phosphorus. XRD and TEM demonstrated that the palladium phosphides showed the same particle size (~5 nm) and morphology as the Pd/C precursor, making them easy to incorporate into a fuel cell, without the need for an additional support.

The palladium phosphides show increased activity towards the HOR compared to the Pd/C and also promising HER activity in 0.1 M perchloric acid. The ORR activity of the phosphides was also promising, with good stability of potential cycling compared to Pd/C and Pt/C.

Thermogravimetric analysis shows that the phosphides also have increased stability compared to Pd/C and the electrochemical durability of the phosphides is also good compared to the Pd/C.

The catalysts were tested as both anode and cathode catalysts in a polymer electrolyte fuel cell.

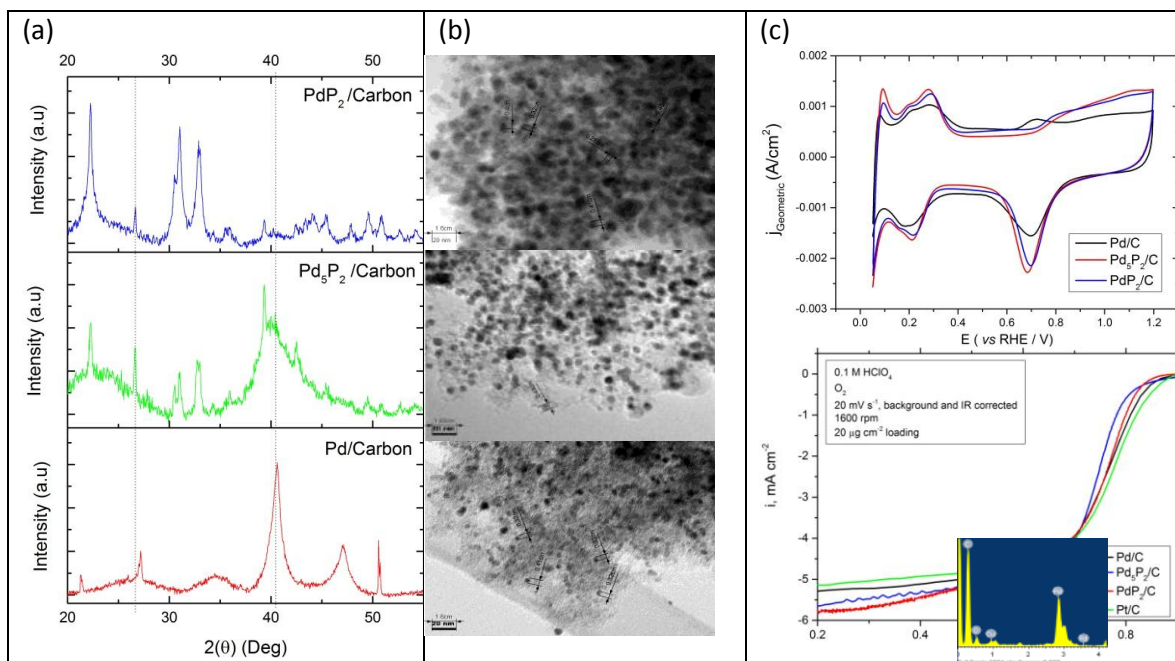


**Figure 1** (a) XRD traces of the Pd/C precursor and the palladium phosphide materials. (b) TEM images of the Pd/C and palladium phosphide materials. (c) CV and HER activity of the Pd/C and palladium phosphides performed in 0.1 M perchloric acid.

## References

- [1] E.J. Popczun, C.G. Read, C.W. Roske, N.S. Lewis, R.E. Schaak, *Angew. Chem.-Int. Edit.*, 53 (2014) 5427-5430.
- [2] P. Xiao, M.A. Sk, L. Thia, X. Ge, R.J. Lim, J.-Y. Wang, K.H. Lim, X. Wang, *Energy Environ. Sci.*, 7 (2014) 2624-2629.
- [3] A.R.J. Kucernak, V.N. Naranammalpuram Sundaram, *Journal of Materials Chemistry A*, 2 (2014) 17435-17445.
- [4] J.L. Carbajal, R.E. White, *Journal of The Electrochemical Society*, 135 (1988) 2952-2957.

# Electrodeposition of Novel Materials as ORR Catalysts for MEAs

Ludwig Asen<sup>a,b,\*</sup>, Ehab Mostafa<sup>a</sup>, Wenbo Ju<sup>a,c</sup>, Sladjana Martens<sup>a</sup>, Ulrich Heiz<sup>b</sup>, Ulrich Stimming<sup>c,d</sup> and Oliver Schneider<sup>a</sup>

<sup>a</sup> *Institut für Informatik VI, Technische Universität München, Schleißheimer Str. 90a, 85748 Garching, Germany*

<sup>b</sup> *Chemistry Department, Technische Universität München, Lichtenbergstr. 4, 85748 Garching, Germany*

<sup>c</sup> *Physics Department, Technische Universität München, James-Franck-Str. 1, 85748 Garching, Germany*

<sup>d</sup> *School of Chemistry, Bedson Building, Newcastle University, Newcastle upon Tyne, NE1 7RU United Kingdom*

\*ludwig.asen@tum.de

Hydrogen fuel cell driven electric vehicles represent a promising technology on the verge of market introduction, but the efficiency of fuel cells is still far below the thermodynamic limit. The high amount of Pt catalyst therefore required to deliver the power needed leads to costs too high for widespread market introduction, especially in the automotive sector. Especially overpotentials of several hundred mV at the cathode side due to the sluggish kinetics of the oxygen reduction reaction (ORR) is responsible for these drawbacks.

Catalytic materials with higher activity for the ORR and enhanced durability as well as reduced Pt loading can both bring down the costs and enhance the efficiency and therefore the competitiveness of fuel cell driven vehicles. Recently it has been shown that polycrystalline Platinum - rare-earth metal (RE) alloys show very promising catalytic properties for ORR, e.g. an increase in the kinetic current density by a factor of 3-5 compared to pure Pt [1,2]. They were reported to show a good stability due to their high heat of formation and the formation of a dense Pt overlayer during the initial de-alloying steps [2]. The overlayer is under compressive strain, causing the high activity [2]. Also for Pt-RE nanoparticles prepared in a cluster source, an enhanced mass activity was found [3].

For applying these alloys in actual fuel cells, the major challenge is to synthesize such nanoparticles with a method, which can be up-scaled to provide enough material for MEA fabrication and subsequently for widespread production for practical applications. This is challenging due to the very low standard potentials of the rare earth elements.

In this study electrochemical deposition was selected as a scalable method. However, due to the low deposition potential of rare-earth metals, aqueous electrolytes could not be used for these experiments. Therefore ionic liquids were chosen as electrolyte, because they offer a wide electrochemical window and in literature a successful deposition of selected pure rare-earth metals had been claimed [4], but there are also reports showing fundamental obstacles for deposition of RE metals from some ionic liquids [5]. Therefore in a second approach organic solvents with an added supporting electrolyte were evaluated, which have also a wide potential window and where high amounts of precursors can be dissolved.

For both electrolyte systems, the electrochemical processes in solutions containing Pt precursors, rare earth metal ions and mixtures of both for alloy deposition were discussed by the use of electrochemical techniques, partially in combination with the electrochemical quartz crystal microbalance (EQCM) technique, and ex-situ and in-situ scanning probe microscopy techniques as well as electrocatalytic measurements for the ORR. Aside from the gold electrode of the EQCM, Boron-doped Diamond (BDD) was used as working electrode, as it is a very inert electrode and allows even wider potential windows in non-aqueous media [6]. Deposited layers were characterized by EDS and surface science methods.

## References:

- [1] I.E.L. Stephens, A.S. Bondarenko, U. Gronbjerg, J. Rossmeisl, I. Chorkendorff, *Energ. Environ. Sci.*, 5 (2012) 6744-6762.
- [2] P. Malacrida, M. Escudero-Escribano, A. Verdager-Casadevall, I.E.L. Stephens, I. Chorkendorff, *J. Mater. Chem. A*, 2 (2014) 4234-4243.
- [3] P. Hernandez-Fernandez, F. Masini, D.N. McCarthy, C.E. Strebel, D. Friebe, D. Deiana, P. Malacrida, A. Nierhoff, A. Bodin, A.M. Wise, J.H. Nielsen, T.W. Hansen, A. Nilsson, E.L. Stephens, I. Chorkendorff, *Nat Chem*, 6 (2014) 732-738.
- [4] S. Legeai, S. Diliberto, N. Stein, C. Boulanger, J. Estager, N. Papaiconomou, M. Draye, *Electrochem. Commun.*, 10 (2008) 1661-1664.
- [5] L.-H. Chou, C.L. Hussey, *Inorg. Chem.*, 53 (2014) 5750-5758.
- [6] S. Ayata, A. Stefanova, S. Ernst, H. Baltruschat, *J. Electroanal. Chem.*, 701 (2013) 1-6.

# **Ru/M Bi-layered Oxide Catalysts for Oxygen Evolution Reaction (OER) in Acidic Water Splitting**

Jin Yeong Kim, Jihui Choi, Sung Hoon Hong, Hoyoung Kim, Eunkyong Hwang and Soo-Kil Kim  
*School of Integrative Engineering, Chung-Ang University,  
Heukseokno 84, Dongjak-gu, Seoul 156-756, Republic of Korea  
sookilkim@cau.ac.kr*

Due to the sluggishness of the oxygen evolution reaction (OER) and its harsh conditions of low pH and high overpotential, development of a highly active and stable catalysts<sup>(1,2)</sup> have been a long huddle for the commercialization of acidic water electrolysis. Besides the well-known Pt-based catalysts, PGM oxides such as RuO<sub>x</sub> and IrO<sub>x</sub> have been largely investigated<sup>(4,5,6)</sup>, still the necessity to lower the cost and enhance their activity and stability remains.

In this work, Ru/M (M=transition metal) bi-layered catalysts were fabricated using electrodeposition on Ti substrates. The oxides were further fabricated by annealing process in air condition at various temperatures. OER activity and stability of the various Ru/M bi-layered oxides were investigated by cyclic voltammetry. The enhanced catalytic properties were correlated with the material characteristics investigated through various characterization tools including FESEM, XPS, EDS, XRD, etc.

The results indicated that surface morphologies, roughness, and modification of electronic structure evolved by M as well as the annealing conditions were responsible for the enhanced catalytic properties of Ru/M bi-layered oxide catalysts over conventional thermal RuO<sub>x</sub> catalysts.

## **REFERENCES**

- (1) ChemCatChem, 2011, 3, 1159-1165.
- (2) Int. J. Hydrogen Energy 2013, 38, 4901-4934.
- (3) J. Power Sources 2007, 171, 558-566
- (4) ChemElectroChem 2014, 1, 2075-2081
- (5) Electrochem. Solid-State Lett. 2010, 13, B36-B39
- (6) J. Electrochem. Soc, 1984, 131, 72-77

# Electrocatalysts for CO<sub>2</sub>-C1 Fuel Inter-conversion

Eunkyoung Hwang, Sung Hoon Hong, Jihui Choi, Jin Yeung Kim, Hoyoung Kim, Soo-Kil Kim\*

School of Integrative Engineering, Chung-Ang University

84 Heukseok-ro, Dongjak-gu, Seoul, 156-756, Korea

\*E-mail address : sookilkim@cau.ac.kr

Electrochemical reduction of CO<sub>2</sub> to C1 fuel has recently been intensively studied as a method to reduce and utilize CO<sub>2</sub>. Under proper reduction conditions including types of catalysts, electrolytes, and reduction potential, CO<sub>2</sub> can be converted into various types of useful fuels such as formic acid, carbon monoxide, methane, and longer hydrocarbons [1, 2, 3].

Among the converted fuels, formic acid is highly desired due to its various applications as a feedstock chemical and the fuel of direct formic acid fuel cell. Some transition metal catalysts such as Hg, Pb, Cd and Tl have been known as efficient catalysts for the production of formic acid with high faradaic efficiency close to 90%, still the environmental concerns for those toxic metals remain as a problem [4]. Therefore, the development of environmental friendly catalyst with high efficiency and selectivity is necessary. Moreover, if a certain catalyst can be used both in the reduction of CO<sub>2</sub> to formic acid and its oxidation to CO<sub>2</sub>, a unitized regenerative fuel cell based on the inter-conversion between CO<sub>2</sub>-C1 fuel (formic acid in this work) can be realized.

Therefore, this study aims to develop the catalyst materials that can be commonly used both in the reduction of CO<sub>2</sub> to formic acid and its revers reaction. We developed Sn-based alloy catalyst by electrodeposition and tested their activities toward the inter-conversion. All the electrolysis was conducted in the home-made H-type cell separated by a proton exchange membrane. The conversion products were analyzed using high performance liquid chromatography and electrochemical analysis including cyclic voltammetry. We have found that Sn-based alloy nano catalysts with certain composition were highly effective for the inter-conversion reactions and can be a potential candidate for the common electrode in the CO<sub>2</sub> based unitized regenerative fuel cell. Details will be given at the conference.

1. M. Gattrell, N. Gupta and A. Co, Energy Convers. Manage. 48 (2007), 1255–1265.
2. B. Hu, C. Guild, S.L. Suib, J. CO<sub>2</sub> Util. 1 (2013) 18-27.
3. A. Taheri Najafabadi, Int. J. Energy Res. 37 (2013) 485-499.
4. Masashi Azuma, Kazuhito Hashimoto, Masahiro Hiramoto, Masahiro Watanabe and Tadayoshi Sakata, J. Electrochem. Soc. 137, issue 6 (1990), 1772-1778

# Synthesis of Pt-CuO Composite via Electrodeposition Followed by Galvanic Replacement-Heat Treatment and Its Application to Non-Enzymatic Glucose Sensor

Seulki Kim, Changhyun Lee, Noseung Myung  
Department of Applied Chemistry, Konkuk University  
Chungju, Chungbuk 380-701, South Korea  
kelly2313@naver.com

Nanocomposite films of metal (Pt or Au) decorated CuO were synthesized via electrodeposition followed by a galvanic replacement reaction combined with heat treatment. First, Cu/Cu<sub>2</sub>O nanocomposite was electrodeposited under galvanostatic conditions using a 0.4 M CuSO<sub>4</sub> and 3 M lactate solution. pH of the electrolyte was adjusted to 9 using 5 M NaOH. Potential oscillations were observed during the galvanostatic deposition of the film, which indicated deposition of Cu/Cu<sub>2</sub>O layers. Cu/Cu<sub>2</sub>O films were subjected to a galvanic replacement reaction in solutions containing PtCl<sub>4</sub> or HAuCl<sub>4</sub> to produce Pt or Au modified Cu<sub>2</sub>O. Annealing of the Pt-or Au-Cu<sub>2</sub>O electrodes at 375°C for 10 hours in air resulted in Pt-or Au-CuO nanocomposite electrodes. The structure and morphology of the electrodes were characterized with EDX, XRD and SEM. The resulting electrode exhibited electrocatalytic activity for glucose. Effects of interferences were also studied in detail.

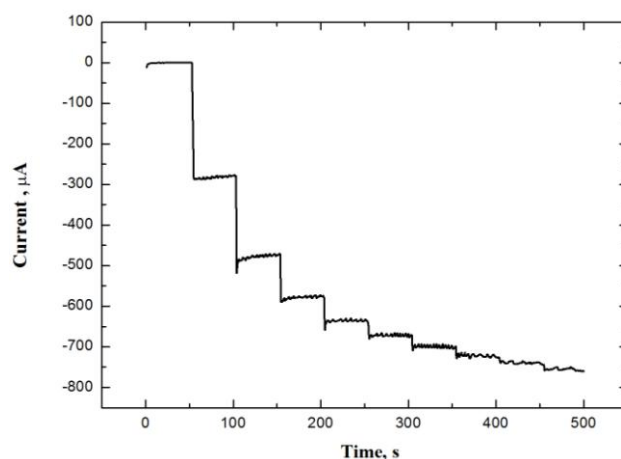


**Figure 1. Amperometric response to successive additions of 2 M glucose at a constant potential of 0.6V (vs. Ag/AgCl/3 M NaCl).**

# Anisotropic gold nanoplates – characterization and application in catalysis

Lidia Jagoda Opuchlik, Renata Bilewicz  
University of Warsaw, Faculty of Chemistry  
1 Louis Pasteur Street, 02093 Warsaw, Poland  
lgoralska@chem.uw.edu.pl

In recent years, Au nanoparticles have been center of attention of researchers. The progress in synthetic methods allowed to obtain not only spherical but also non-spherical nanoparticles e.g. plates, prisms, rods, wires and shells [1]. Anisotropic nanoparticles rise special interest due to their unique optical properties that result from possession of nonequivalent axes. The variety of shapes that can be obtained during the process of synthesis allow to improve the working efficiency of sensors due to the enhanced effective surface area and mass transport. Gold nanoparticles are interesting from the viewpoint of catalysis [2] but also as drug delivery systems and in thermal therapy of cancer [3].

We synthesized anisotropic gold nanoplates capped with thiosulfate via reaction of  $\text{HAuCl}_4$  with  $\text{Na}_2\text{S}_2\text{O}_3$  [4] and use them for the preparation of catalytic surfaces. UV – Vis Spectroscopy, DLS (size and zeta potential), and SEM were employed to characterize the NPs. GCE electrode was decorated with anisotropic gold nanoplates by drop casting and used in the oxygen reduction reaction (ORR). The reduction process includes two electrons and two protons and hydrogen peroxide is the final product. The measurements were held in three different supporting electrolytes: McIlvaine buffer of pH 5.5, 0.5M sulfuric acid and 0.1M KOH and the results were compared.

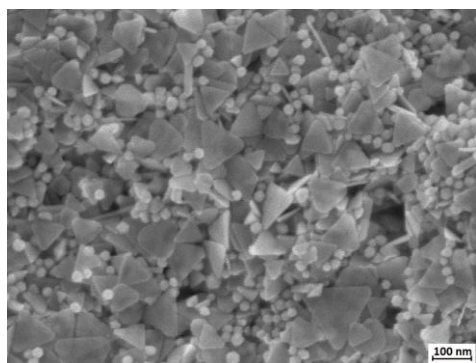


Fig.1 SEM image of GCE electrode modified with anisotropic gold nanoplates.

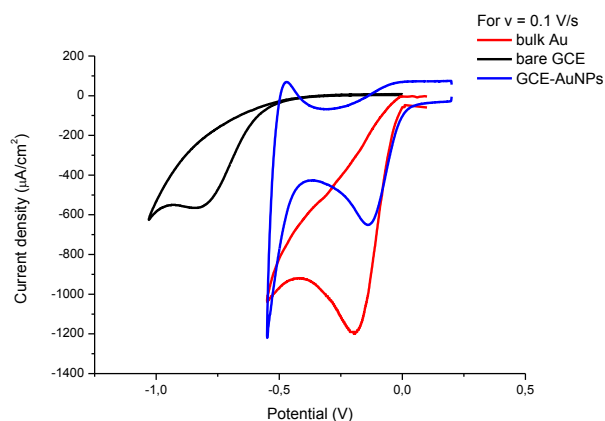


Fig.2 Cyclic voltammograms, registered in McIlvaine buffer of pH 5.5, depicting the differences in the ORR for bulk AuE, bare GCE and GCE decorated with Au nanoplates .

- [1] R. G. Chaudhuri, P. Santanu, Core/shell nanoparticles: classes, properties, synthesis mechanisms, characterization, and applications, *Chemical Reviews* 112 (2012) 2373 - 2433
- [2] Y. Wang, E. Laborda, K. R. Ward, K. Tschulik, R. G. Compton, A kinetic study of oxygen reduction reaction and characterization on electrodeposited gold nanoparticles of diameter between 17 nm and 40 nm in 0.5 M sulfuric acid, *Nanoscale* 5 (2013) 9699 - 9708
- [3] J. Gautier, E. Allard-Vannier, K. Herve-Aubert, M. Souce, I. Chourpa, Design strategies of hybrid metallic nanoparticles for theragnostic applications, *Nanotechnology* 24 (2013) 432002 - 432015
- [4] G. Zhang, J. Jasiński, J. L. Howell, D. Patel, D. P. Stephens, A. M. Gobin, Tunability and stability of gold nanoparticles obtained from chloroauric acid and sodium thiosulfate reaction, *Nanoscale Research Letters* 7 (2012) 337 - 345

# Composition, Structure, and Kinetics of RuO<sub>2</sub>-Ta<sub>2</sub>O<sub>5</sub>/Ti Anode for Oxygen Evolution in H<sub>2</sub>SO<sub>4</sub> Solutions

Takahiro Hirai<sup>1</sup>, Tian Zhang<sup>1</sup>, and Masatsugu Morimitsu<sup>\*1,2</sup>

<sup>1</sup>Department of Science of Environment and Mathematical Modeling,

<sup>2</sup>Department of Environmental Systems Science,

Doshisha University

1-3 Tatara-miyakodani, Kyotanabe, Kyoto 610-0394, Japan

\*E-mail: mmorimit@mail.doshisha.ac.jp

RuO<sub>2</sub>-Ta<sub>2</sub>O<sub>5</sub> coated Ti anodes obtained by thermal decomposition are possible to significantly reduce the cell voltage up to 700 mV in metal electrowinning compared to traditional Pb alloy anodes and this voltage reduction is achieved by amorphization of the mixed oxide coating by low temperature thermal decomposition, resulting in high catalytic activity for oxygen evolution in acidic media [1]. Our recent studies on the kinetics of the amorphous RuO<sub>2</sub>-Ta<sub>2</sub>O<sub>5</sub> coating have revealed that the high catalytic activity is caused by the increase in active surface area of the amorphous coating, which consists of RuO<sub>2</sub> nano particles uniformly dispersed in amorphous Ta<sub>2</sub>O<sub>5</sub> matrix. This hybrid structure is self-assembled and is produced during thermal decomposition process. The active surface area influences on polarization of the mass transfer process for oxygen evolution, while there is little information on the electron transfer and overpotential of the amorphous coating. In this paper, we investigated the surface morphology, polarization, and Tafel slope of RuO<sub>2</sub> and RuO<sub>2</sub>-Ta<sub>2</sub>O<sub>5</sub> coatings obtained at different temperatures and Ru:Ta ratios for oxygen evolution in H<sub>2</sub>SO<sub>4</sub> solutions.

The anodes were prepared by thermal decomposition of precursor solutions containing Ru (III) and Ta (V). Ru:Ta mole ratios were 30:70, 50:50, or 100:0 (*i.e.*, RuO<sub>2</sub> only), and thermal decomposition was carried out at a temperature of 280 °C, 300 °C, 360 °C, or 500 °C. The characterization of the coatings was done with XRD, SEM, and EDX. Electrochemical measurements by cyclic voltammetry and linear sweep voltammetry were performed with a conventional three-electrode cell with KCl-saturated Ag/AgCl reference electrode and 2.0 mol/L H<sub>2</sub>SO<sub>4</sub> solutions.

Figure 1 shows Tafel slopes at different thermal decomposition temperatures and Ru mole ratios. Tafel slope was 65 mV in maximum in this study and was obtained with the RuO<sub>2</sub>-Ta<sub>2</sub>O<sub>5</sub> coating (Ru=30 mol%) prepared at 500 °C. In this case, well-grown RuO<sub>2</sub> particles were observed on the coating surface, while Tafel slope was down to 47 mV with the RuO<sub>2</sub> coating even at the same temperature. This seems to be reasonable, because RuO<sub>2</sub> is active for oxygen evolution, but Ta<sub>2</sub>O<sub>5</sub> is inactive. However, the difference in Tafel slope was also related to the surface morphology; both RuO<sub>2</sub> and RuO<sub>2</sub>-Ta<sub>2</sub>O<sub>5</sub> coatings showed a lot of large crystalline RuO<sub>2</sub> particles (200 nm or more), while the particle of about 20 nm co-existed only on the RuO<sub>2</sub> coating. The similar effect of Ru ratio on Tafel slope was also observed at other thermal decomposition temperatures. On the other hand, Tafel slope decreased with lowering thermal decomposition temperature at a fixed Ru ratio, and it was suggested that thermal decomposition temperature is important to the kinetics for oxygen evolution; the RuO<sub>2</sub> particle size strongly depends on the temperature, and Tafel slope is varied with the particle size and dispersibility of RuO<sub>2</sub>. The results obtained in this study further implied a possibility that the rate-determining step was changed by the particle size of RuO<sub>2</sub>.

*This work was financially supported by "Kyoto Area Super Cluster Program" of Japan Science and Technology Agency (JST).*

## Reference

[1] T. Zhang, M. Morimitsu, *Proceedings of Electrometallurgy 2012*, TMS, pp. 29-34 (2012).

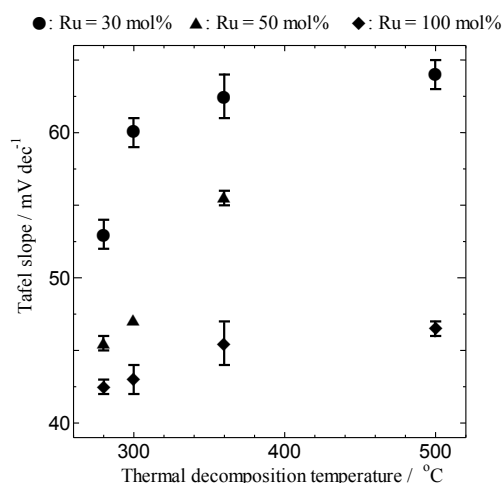


Fig. 1 Tafel slopes for oxygen evolution on RuO<sub>2</sub> or RuO<sub>2</sub>-Ta<sub>2</sub>O<sub>5</sub> coatings.



# Effects of Precursor Solution on Morphology and Catalytic Activity of RuO<sub>2</sub>-based Ti anode for Oxygen Evolution

Shuhei Kimura<sup>1</sup>, Kenji Kawaguchi<sup>2</sup>, and Masatsugu Morimitsu<sup>\*1,3</sup>

<sup>1</sup>Department of Science of Environment and Mathematical Modeling,

<sup>2</sup>Organization for Research Initiatives and Development,

<sup>3</sup>Department of Environmental Systems Science,  
Doshisha University

1-3 Tatara-miyakodani, Kyotanabe, Kyoto 610-0394, Japan

\*E-mail: mmorimit@mail.doshisha.ac.jp

A titanium electrode coated with RuO<sub>2</sub>-Ta<sub>2</sub>O<sub>5</sub> mixture is obtained by thermal decomposition of a precursor solution containing Ru and Ta salts, and it has been revealed by our group that decreasing thermal decomposition temperature makes RuO<sub>2</sub> amorphous in the coating in which nano RuO<sub>2</sub> particles appears and has a high catalytic activity for oxygen evolution in acidic media [1]. In production of such metal oxides by thermal decomposition, the procedure and condition to prepare the precursor solution, *e.g.*, metal salt, solvent, mixing method, and temperature, affect the crystallographic and morphological property and electrochemical activity of the mixed oxide coating; *e.g.*, the literature has reported that the electrocatalytic property of crystalline RuO<sub>2</sub> coated Ti electrodes depends on ruthenium salts used in the precursor solution [2]. However, there has been little information on the effects of precursor solution on electrocatalysis of amorphous RuO<sub>2</sub>-based coatings for oxygen evolution in acidic aqueous solutions. This paper reports such effects on amorphous RuO<sub>2</sub>/Ti or RuO<sub>2</sub>-Ta<sub>2</sub>O<sub>5</sub>/Ti electrodes.

RuO<sub>2</sub>-Ta<sub>2</sub>O<sub>5</sub>/Ti and RuO<sub>2</sub>/Ti electrodes examined in this study were prepared by thermal decomposition at 280°C. RuO<sub>2</sub>-Ta<sub>2</sub>O<sub>5</sub> coatings used precursor solutions containing (a) RuCl<sub>3</sub> · nH<sub>2</sub>O and TaCl<sub>5</sub> or (b) Ru(NO<sub>3</sub>)<sub>3</sub> and TaBr<sub>5</sub> in 1-butanol or ethanol where the Ru ratio was 80 mol%. RuO<sub>2</sub> coatings were created with precursor solutions comprising Ru(NO<sub>3</sub>)<sub>3</sub> in distilled water or ethanol. XRD, SEM, and EDX were used for surface analysis of the coatings, and electrochemical measurements were conducted with 2.0 mol/L H<sub>2</sub>SO<sub>4</sub> solutions in a conventional three-electrode cell.

Figure 1 shows the cyclic voltammograms of RuO<sub>2</sub>-Ta<sub>2</sub>O<sub>5</sub>/Ti electrodes prepared with the precursor solutions (a) and (b). The precursor solution (a) is the typical one that has been used in our group, while the solution (b) is modified with non-chloride source for Ru. XRD patterns of these two electrodes showed no clear diffraction peaks, indicating that the oxide coatings are amorphous. However, SEM observation revealed that both the coatings comprised flat areas and cracks and some RuO<sub>2</sub> particles were seen on the flat areas where the particle size of the electrode (a) was a few nm, while that was about 20 nm for the electrode (b). This suggests that the precursor solution affects the growth of RuO<sub>2</sub> during thermal decomposition. Because the active component for oxygen evolution is only RuO<sub>2</sub> and Ta<sub>2</sub>O<sub>5</sub> is inactive, the decrease in particle size of RuO<sub>2</sub> induces higher active surface area, resulting in lower polarization for oxygen evolution. On the other hand, RuO<sub>2</sub>/Ti electrodes produced with distilled water or ethanol in the precursor solutions showed no significant change in surface morphology and RuO<sub>2</sub> particle size, and the polarization curves were overlapped for them, indicating no difference in catalytic activity for oxygen evolution. More detailed results on the effects of metal salt and solvent on surface morphology and polarization will be given in this paper.

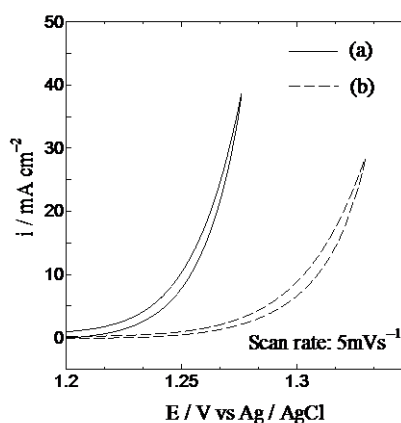


Fig.1 Cyclic voltammograms of RuO<sub>2</sub>-Ta<sub>2</sub>O<sub>5</sub>/Ti anodes

*This work was financially supported by “Kyoto Area Super Cluster Program” of Japan Science and Technology Agency (JST).*

## References

- [1] T. Zhang, M. Morimitsu, *Proc. of Electrometallurgy 2012*, TMS, pp. 29-34 (2012).
- [2] S. Ardizzone, M. Falcicola, S. Trasatti, *J. Electrochem. Soc.*, Vol. 136, pp. 1545-1550 (1989).

# Formation and Electrochemical Behaviors of RuO<sub>2</sub>-Ta<sub>2</sub>O<sub>5</sub> Coating on Pb Substrate for Oxygen Evolution

Yusuke Ujino<sup>1</sup>, Kenji Kawaguchi<sup>2</sup>, and Masatsugu Morimitsu<sup>\*1,3</sup>

<sup>1</sup>Department of Science of Environment and Mathematical Modeling,

<sup>2</sup>Organization for Research Initiatives and Development,

<sup>3</sup>Department of Environmental Systems Science,

Doshisha University

1-3 Tatara-miyakodani, Kyotanabe, Kyoto, 610-0394, Japan

\*E-mail: mmorimit@mail.doshisha.ac.jp

Copper or zinc electrowinning use acidic aqueous solutions, and the anodic reaction is oxygen evolution for which lead alloy electrodes have been utilized for a long time. Recently an amorphous oxide coated titanium anode, MSA<sup>®</sup> [1], has been increasingly applied, in which titanium is appropriate to the substrate for such metal oxide coatings, because of its high corrosion resistance in strong acidic media by formation of non-conductive titanium oxide film. On the other hand, lead or lead alloy are cost-efficient compared to titanium and there has been no challenge to apply lead or lead alloy to the substrate of oxide coated anodes, especially with amorphous RuO<sub>2</sub>-Ta<sub>2</sub>O<sub>5</sub>. In this paper, we report the preparation of RuO<sub>2</sub>-Ta<sub>2</sub>O<sub>5</sub> coatings on lead or lead alloy substrates and the results on surface analysis and electrochemical behaviors for oxygen evolution of the amorphous coatings.

RuO<sub>2</sub>-Ta<sub>2</sub>O<sub>5</sub> coatings were formed on lead or lead alloy substrates by thermal decomposition method as previously reported [1]; the precursor solution containing Ru(III) and Ta(V) was painted and heated at 280 °C, and the painting to heating process was repeated. A titanium substrate was also used for comparison. The characterization of the oxide coatings was done with XRD, SEM, and EDX. Cyclic voltammetry and constant current electrolysis were performed in 2.0 mol/L H<sub>2</sub>SO<sub>4</sub> solutions at 40 °C to evaluate polarization and stability of the amorphous oxide coating for oxygen evolution.

The oxide coatings were successfully created on lead or lead alloy substrates, in which the pretreatment of the substrate affected the obtained coating condition. EDX results presented Ru and Ta which were distributed on the whole of the coating surface, while XRD results presented the diffraction pattern of PbO, suggesting that the substrate was partly oxidized at 280°C and PbO was formed between the substrate and the coating like as the insulator because of its low conductivity. This was supported by the fact that cyclic voltammograms of RuO<sub>2</sub>-Ta<sub>2</sub>O<sub>5</sub>/Pb or Pb alloy electrodes initially showed a quite low current even at the potential range in which oxygen evolution occurs on RuO<sub>2</sub>-Ta<sub>2</sub>O<sub>5</sub>/Ti electrodes. Then the current density increased with the number of cycles, implying that PbO is oxidized to conductive PbO<sub>2</sub> during anodic potential scans. The stability of the oxide coating formed on Pb or Pb alloy was examined by constant current electrolysis, and the results were compared to that obtained with RuO<sub>2</sub>-Ta<sub>2</sub>O<sub>5</sub>/Ti (Fig. 1). The analysis of the coating surface on Pb or Pb alloy after the electrolysis gave information on the reason for the voltage change shown in Fig. 1 and the degradation mechanism; the oxide coating works for oxygen evolution only within several hours for the coated Pb alloy electrode (a) and in about 40 hours for the coated Pb electrode (b), then the stable voltage seen at 2 to 2.2 V corresponds to oxygen evolution on PbO<sub>2</sub> after the RuO<sub>2</sub>-Ta<sub>2</sub>O<sub>5</sub> coatings are consumed and disappeared. The results suggest that the amorphous oxide coating formed on Pb or Pb alloy by thermal decomposition is unstable for oxygen evolution due to the oxidation of Pb.

This work was partly done with financial support by “Kyoto Area Super Cluster Program” of Japan Science and Technology Agency (JST).

## References

- [1] M. Morimitsu, *Proceedings of Electrometallurgy 2012*, TMS, pp. 49-54 (2012).
- [2] T. Zhang, M. Morimitsu, *Proceedings of Electrometallurgy 2012*, TMS, pp. 29-34 (2012).

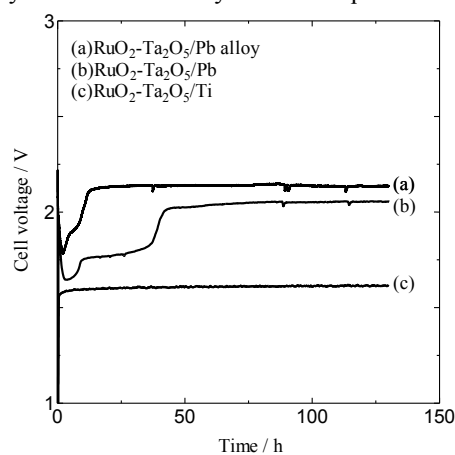


Fig. 1 Cell voltage during electrolysis at 50 mA in 2.0 mol/L H<sub>2</sub>SO<sub>4</sub> at 40 °C.

# Effects of Composition of Amorphous IrO<sub>2</sub>-Ta<sub>2</sub>O<sub>5</sub> Coatings on Oxygen Evolution in Alkaline Solutions

Kousuke Kumamoto<sup>1</sup>, Tian Zhang<sup>1</sup>, and Masatsugu Morimitsu\*<sup>1,2</sup>

<sup>1</sup>*Department of Science of Environment and Mathematical Modeling,*

<sup>2</sup>*Department of Environmental Systems Science,*

*Doshisha University*

*1-3 Tatara-miyakodani, Kyotanabe, Kyoto 610-0394, Japan*

\*E-mail: mmorimit@mail.doshisha.ac.jp

Oxygen evolution in alkaline solutions is known as the anodic reaction of alkaline water electrolysis or the charge reaction at the positive electrode of air secondary batteries, while the material possible to use for this gas evolution is limited; *e.g.*, nickel alloys are only commercialized for alkaline water electrolysis, but the positive electrode of the air secondary battery is still requiring a novel material for oxygen evolution and reduction. The difficulty to find an appropriate material is caused from highly corrosive environment of alkaline solutions to metals, alloys, oxides, and other conductive compounds. Under the situation, one of the authors of this paper has revealed that crystalline IrO<sub>2</sub>-Ta<sub>2</sub>O<sub>5</sub> coatings obtained by thermal decomposition have a high durability for electrolysis at 1 A/cm<sup>2</sup> in 4 mol/L NaOH solutions [1] and has also demonstrated that amorphous IrO<sub>2</sub>-Ta<sub>2</sub>O<sub>5</sub> coatings prepared at low thermal decomposition temperature has lower oxygen overpotential than crystalline ones [2]. Therefore, this work focused on the effects of Ir:Ta composition of amorphous IrO<sub>2</sub>-Ta<sub>2</sub>O<sub>5</sub> coatings on oxygen evolution in alkaline solutions. Amorphous IrO<sub>2</sub>-Ta<sub>2</sub>O<sub>5</sub> coatings at different mole ratio were prepared on titanium substrates and analyzed by SEM observation, and the oxygen evolution behaviors in KOH solutions were investigated by cyclic voltammetry and constant electrolysis.

A titanium plate was used as a substrate to create the amorphous IrO<sub>2</sub>-Ta<sub>2</sub>O<sub>5</sub> coatings by thermal decomposition of precursor solutions containing Ir(IV) and Ta(V) in 1-butanol. The Ir mole ratio in the precursor solution was 40 mol%, 60 mol%, or 80 mol%, and thermal decomposition was carried out at 360 °C. The crystallographic structure, surface morphology, and Ir:Ta ratio were analyzed by XRD, SEM, and EDX. Electrochemical measurements were conducted using a three-electrode cell or a two-electrode cell with 5.0 or 6.0 mol/L KOH solutions at 40 °C. The reference electrode was an Hg/HgO electrode, and the counter electrode was a platinum plate.

All coatings prepared on titanium in this work were amorphous, because no diffraction peak was found that was independent of Ir mole ratio. The surface morphology of such amorphous coatings was basically smooth areas and cracks, while the electrochemical behaviors were influenced on the Ir mole ratio. The double layer charge measured by cyclic voltammetry increased with increasing Ir mole ratio, and the voltammograms for oxygen evolution revealed that the catalytic activity was enhanced with more Ir in the coating. This is reasonable, since IrO<sub>2</sub> is catalytic, but Ta<sub>2</sub>O<sub>5</sub> is non-catalytic to O<sub>2</sub> evolution. The constant current electrolysis was also performed to examine the stability of the amorphous IrO<sub>2</sub>-Ta<sub>2</sub>O<sub>5</sub> coatings. The results obtained at 50 mA/cm<sup>2</sup> revealed that the amorphous coatings of Ir=80 mol% kept stable voltage over 100 hours, although the voltage increased earlier with the coatings of Ir=40 mol% and 60 mol%. EDX analysis of the coatings before and after the electrolysis indicated that the degradation of the coating occurred with tantalum consumption, which is faster than iridium on the coatings of Ir=40 mol% or 60 mol%, suggesting that Ta<sub>2</sub>O<sub>5</sub> was predominantly consumed for oxygen evolution in alkaline solutions which is quite different from the results obtained in acidic aqueous solutions.

*This work was financially supported by "Advanced Low Carbon Technology Research and Development Program (ALCA)" of Japan Science and Technology Agency (JST).*

## References

- [1] M. Morimitsu, C. Murakami, K. Kawaguchi, R. Otagawa, and M. Matsunaga, *Journal of New Materials for Electrochemical Systems*, Vol. 7, pp. 323-327 (2004).
- [2] S. Unoki, T. Zhang, and M. Morimitsu, The 224th ECS meeting, Abs#27, San Francisco (2013).

# Oxygen Evolution Reaction Behavior of Vapor Grown Carbon Fiber and The Loading Effect of LaMnO<sub>3</sub> in KOH Aqueous Solution

Makoto Eto, Taro Kinumoto, Kohei Ono, Tomoki Tsumura, Masahiro Toyoda

Dept. of Appl. Chem., Graduate School of Eng., Oita Univ., 700 Dannoharu, Oita, 870-1192, JAPAN

[kinumoto@oita-u.ac.jp](mailto:kinumoto@oita-u.ac.jp)

Oxygen evolution reaction (OER) in aqueous solutions is the discharge reaction for air batteries such as metal|air and metal hydride|air (MH|air) batteries. If the carbonaceous material is used as the cathode materials, the corrosion of carbonaceous materials would be serious because the standard potential of carbon oxidation reaction (COR at 0.27 V) is less negative than that of OER (1.23 V). Ross and Sokol studied the OER in alkaline solution at 50 °C using acetylene black, which is commercially available carbonaceous material, and they reported that the current efficiency of OER ( $\varepsilon_{\text{OER}}$ ) is lower than that for COR below 550 mV vs. Hg|HgO. [1] On the other hand, vapor grown carbon fiber (VGCF, SHOWA DENKO K.K.) is one of the high crystalline carbonaceous materials; thereby,  $\varepsilon_{\text{OER}}$  is expected to be high for application to air batteries. Then, we have investigated  $\varepsilon_{\text{OER}}$  of VGCF by *in-situ* measurement using a dissolved oxygen sensor [2]. In this presentation, the effects of the concentration of KOH and the loading of LaMnO<sub>3</sub> (typical OER catalyst) on  $\varepsilon_{\text{OER}}$  are reported.

The loading of LaMnO<sub>3</sub> on VGCF (LaMnO<sub>3</sub>/VGCF) was carried out by a co-precipitation method [2]. VGCF or LaMnO<sub>3</sub>/VGCF was dispersed on Ti substrate and fixed with a thin film of anion-exchange-membrane (ionomer solution: AS-4, TOKUYAMA K.K.) Then, those were employed as the working electrode. OER study was carried out by chronoamperometry every 0.05 V between 1.40 ~ 1.70 V. Holding time is set at 10 hours. Hg / HgO electrode and a Ni mesh were employed as the reference electrode and as the counter electrode, respectively. The electrolyte solution was 0.1 or 1.0 mol dm<sup>-3</sup> KOH aqueous solution to simulate the condition of MH|air battery. A dissolved oxygen sensor (DO meter, InLab<sup>®</sup> OptiOx, METTLER TOLEDO) was placed near the working electrode to measure the amount of oxygen production in the electrolyte [2].

Figure 1 shows the steady – state polarization curves and amounts of oxygen produced in the electrolyte upon application of potential for VGCF. In the case of 0.1 mol dm<sup>-3</sup> KOH used, both of dissolved oxygen and current were increased above 1.65 V; on the other hand, those were increased above 1.60 V in 1.0 mol dm<sup>-3</sup> KOH used. These results show that the onset potential for OER becomes to be low by increasing in KOH concentration.

Figure 2 shows  $\varepsilon_{\text{OER}}$  of VGCF and LaMnO<sub>3</sub>/VGCF. Here,  $\varepsilon_{\text{OER}}$  was estimated from the ratio between the electric quantity ( $Q_{\text{CA}}$ ) used during the chronoamperometry measurements and the quantity ( $Q_{\text{O}_2}$ ) that was responsible for the oxygen production ( $N$ ).  $\varepsilon_{\text{OER}}$  of VGCF is depended on KOH concentration; unfortunately, it reaches even at *ca.* 17.5% in 1.0 mol dm<sup>-3</sup> KOH solution. The onset potential for OER of LaMnO<sub>3</sub>/VGCF is lower than for VGCF and  $\varepsilon_{\text{OER}}$  is increased by loading with LaMnO<sub>3</sub>. However,  $\varepsilon_{\text{OER}}$  tends to decrease at higher potential region as similar to the result of VGCF.

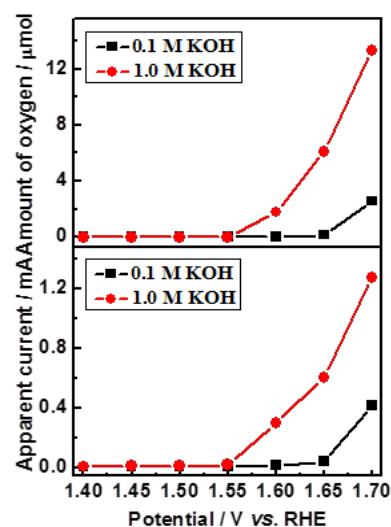


Fig. 1 Steady – state polarization curves and amounts of oxygen for VGCF in 0.1 M and 1.0 M KOH aq.

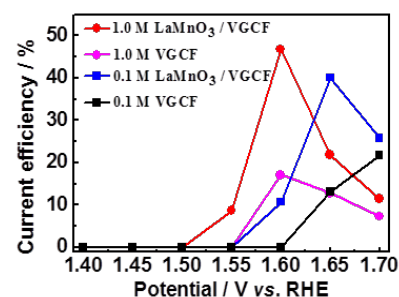


Fig. 2 Current efficiencies for OER of VGCF and LaMnO<sub>3</sub> / VGCF.

This work supported by “Advanced Low Carbon Technology Research and Development Program (ALCA)” of Japan Science and Technology Agency (JST).

[1] P. N. Ross and H. Sokol, *J. Electrochem. Soc.*, **133**, 1079-1084 (1986).

[2] K. Ono, T. Kinumoto et al., *ECS Trans.*, Accepted for publication in ECS Transaction.

# Oxygen Reduction on RuO<sub>2</sub>-Ta<sub>2</sub>O<sub>5</sub> Mixed Oxide Catalyst in Alkaline Solution

Yukiko Ishimura<sup>1</sup>, Kenji Kawaguchi<sup>2</sup>, and Masatsugu Morimitsu<sup>\*1,3</sup>

<sup>1</sup>*Department of Science of Environment and Mathematical Modeling,*

<sup>2</sup>*Organization for Research Initiatives and Development,*

<sup>3</sup>*Department of Environmental Systems Science,*

*Doshisha University*

*1-3 Tatara-miyakodani, Kyotanabe, Kyoto 610-0394, Japan*

*\*E-mail: mmorimit@mail.doshisha.ac.jp*

A metal/air secondary battery has a high theoretical energy density, and the positive electrode reaction is changed with the negative electrode and the electrolyte. In case of metal hydride/air secondary battery utilizing the negative electrode comprising hydrogen storage alloys and alkaline aqueous solutions as the electrolyte, the positive electrode should work for oxygen reduction during discharge and oxygen evolution during charge [1]. The positive electrode is a gas-diffusion electrode and a bi-functional catalyst, with which oxygen reactions should occur at three-phase interfaces of catalyst/air/alkaline solution and at a low polarization, is needed. However, oxygen reduction has a high overpotential over 300 mV and makes the loss of discharge voltage; thereby the voltage efficiency and the practical energy density are still low. Polarization for oxygen evolution should be also minimized, and our group has recently revealed that RuO<sub>2</sub>-Ta<sub>2</sub>O<sub>5</sub> mixed oxide obtained by thermal decomposition, especially the amorphous mixed oxide prepared at low temperature, has a high catalytic activity for oxygen evolution from alkaline solutions [2]. This novel catalyst would be one of the candidates for the bi-functional catalyst of the metal/air secondary battery, although no information has been reported on the electrochemical behaviors for oxygen reduction in alkaline solutions. In this work, thin RuO<sub>2</sub>-Ta<sub>2</sub>O<sub>5</sub> films were prepared on disk and the polarization behaviors for oxygen reduction were investigated with rotating disk electrode (RDE) and compared to the results obtained with platinum.

RuO<sub>2</sub>-Ta<sub>2</sub>O<sub>5</sub> mixed oxides were prepared by thermal decomposition of precursor solutions which comprised 1-butanol solution containing Ru (III) and Ta (V) ions. One side of a titanium disk was painted with the precursor solution and heated at a temperature of 300 °C or 500 °C to make a thin oxide film, which was analyzed by XRD and SEM. Electrochemical measurements were carried out using a three-electrode cell with RDE and 6 mol/L KOH solutions. The polarization behaviors were measured in the solution after treating with N<sub>2</sub> and then with O<sub>2</sub>. Oxygen reduction current was obtained by subtracting the polarization curves obtained under N<sub>2</sub> and O<sub>2</sub> conditions. A platinum disk of the same size as the titanium one was also used as the working electrode for comparison of the catalytic activity to RuO<sub>2</sub>-Ta<sub>2</sub>O<sub>5</sub> mixed oxides at different rotation rates.

XRD and SEM results showed that the crystallinity of RuO<sub>2</sub> reduced with decreasing thermal decomposition temperature and large aggregated RuO<sub>2</sub> particles seen in the oxide film prepared at 500 °C changed to uniformly dispersed nano-particles at 300 °C. Polarization measurements with those films presented oxygen reduction current starting at about 0 V vs. Hg/HgO reference electrode in 6 mol/L KOH. The diffusion-limited current for oxygen evolution was also observed with RuO<sub>2</sub>-Ta<sub>2</sub>O<sub>5</sub> films prepared at 300 °C and 500 °C and increased with increasing rotating rate. The catalytic activity for oxygen reduction for the mixed oxide of 300 °C was higher than that of 500 °C, which is reasonable because the former has nano RuO<sub>2</sub> particles which provide more active surface areas. Compared to platinum, RuO<sub>2</sub>-Ta<sub>2</sub>O<sub>5</sub> (300 °C) still showed a higher catalytic activity for oxygen reduction.

*This work was financially supported by “Advanced Low Carbon Technology Research and Development Program (ALCA)” of Japan Science and Technology Agency (JST).*

## Reference

- [1] M. Morimitsu, T. Kondo, N. Osada, K. Takano, *Electrochemistry*, Vol. 78, No. 5, pp. 493-496 (2010).
- [2] H. Shobayashi, T. Zhang, M. Morimitsu, *Proceeding of The 37th Symposium on Electrolysis Technology*, pp. 52-55, Osaka (2013).

# Graphene and Carbon nanotube Composites as Electrode Materials for Electrochemical Capacitors in Organic Electrolyte

Chien-Te Hsieh, Dong-Ying Tzou, Yu-Fu Chen, Jen-Hao Hsueh  
Department of Chemical Engineering and Materials Science, Yuan Ze University  
135 Yuan-Tung Road, Chung-Li 32003, Taiwan  
[cthsieh@saturn.yzu.edu.tw](mailto:cthsieh@saturn.yzu.edu.tw)

## Abstract

Electrochemical capacitors have been fabricated using graphene nanosheets (GNs) modified with carbon nanotubes (CNTs) as electrode materials and LiClO<sub>4</sub>/propylene carbonate as organic electrolyte. A homogenizing method is used to insert CNTs into the GNs, forming three-dimensional carbon framework. The electrochemical properties of three-dimensional carbon composites are characterized by cyclic voltammetry, galvanostatic charge-discharge cycling, and *ac* impedance spectroscopy in the LiClO<sub>4</sub> electrolyte.

This improved performance can be assigned to that the presence of CNTs assists not only more electro-active sites on the GNs surface but also better for Li ions diffusion and electrolyte wetting in the carbon framework. The energy density of CNT/GN-based electrochemical capacitor can reach as high as 15 Wh kg<sup>-1</sup> at a power density of 2,500 W kg<sup>-1</sup>, analyzed by the Ragone plot. Accordingly, the CNT/GN hybrid composite can be considered as a promising electrode material for Li-ion electrochemical capacitors due to its low cost, high performance, and easy fabrication.

**Keywords:** Electrochemical capacitors, Graphene nanosheets, Carbon nanotubes, organic electrolyte, Three-dimensional carbon composites

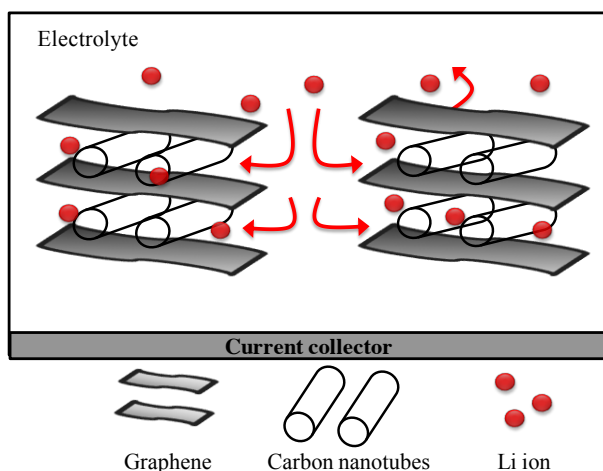


Figure 1. Schematic illustrating the diffusion of Li ions in the CNT/GN framework.

## Reference

- [1] X. Sun, M. Xie, G. Wang, H. Sun, A.S. Cavanagh, J.J. Travis, S.M. George, J. Lian, J. Electrochem. Soc. 159 (2012) 364-369.
- [2] J.J. Yoo, K. Balakrishnan, J. Huang, V. Meunier, B.G. Sumpter, A. Srivastava, M. Conway, A.L.M. Reddy, J. Yu, R. Vajtai, P.M. Ajayan, Nano Lett. 11 (2011) 1423-1427.
- [3] S. Chen, J. Zhu, X. Wu, Q. Han, X. Wang, ACS Nano 4 (2010) 2822-2830.

# Porous $\text{Co}_3\text{V}_2\text{O}_8$ Nanostructures as Promising Electrocatalyst for Oxygen Evolution Reaction in Alkaline Medium

Suyeon Hyun, Vignesh Ahilan and Sangaraju Shanmugam\*

*Department of Energy Systems Engineering,  
Daegu Gyeongbuk Institute of Science & Technology (DGIST),  
50-1, Sang-Ri, Hyeonpung-Myeon, Dalseong-Gun, Daegu,  
Republic of Korea, 711-873  
E-mail: sangarajus@dgist.ac.kr*

Increased energy demands provide opportunities for the development of new technologies for energy conversion and storage device. Water splitting technology, a promising approach, has been investigated for many years to the storage of electrical energy. However in large scale production of the oxygen evolution reaction (OER) for water splitting occurs with large overpotential due to the sluggish kinetics and complex four electron transfer process. So to accelerate the reaction rate and lower the overpotential, an active OER catalyst is necessary [1]. So far, the noble metal catalysts such as Pt, Ru and Ir have shown excellent OER activity and durability. Despite of their good catalytic activity, high cost and scarcity limit their application. Thus, a material with high performance, inexpensive and eco-friendly design is required.

In this study, we have synthesized an inexpensive and highly active OER electrocatalyst,  $\text{Co}_3\text{V}_2\text{O}_8$  with different morphologies using the electrospinning technique and followed by pyrolysis [2]. The OER potential of 1.52 and 1.56V Vs RHE in 1M aqueous KOH electrolyte was observed for  $\text{Co}_3\text{V}_2\text{O}_8$  with nanotube and nanoparticle, respectively morphology. The synthesis and electrocatalytic properties of these materials will be discussed in this presentation.

## Reference

- [1] M. Prabu, K. Ketpang, S. Shanmugam, *Nanoscale* 6 (2014), 3173-3181
- [2] Xing, M., Kong, L.-B., Liu, M.-C., (...), Y.-C. *J. Mater. Chem. A* 2 (2014), 18435-18443

# Functionalization of Carbon Felt as Catalytic Material for Vanadium Redox Flow Battery

Chen-Hao Wang<sup>1\*</sup>, Yu-Chen Shih<sup>1</sup>, Yu-Chung Chang<sup>1</sup>, Ning-Yih Hsu<sup>2</sup>, Yi-Sin Chou<sup>2</sup>

<sup>1</sup>Department of Materials Science and Engineering, National Taiwan University of Science and Technology, 10607, Taipei, Taiwan.

<sup>2</sup>Chemistry Division, Institute of Nuclear Energy Research, Atomic Energy Council, 32546, Taoyuan, Taiwan.

E-mail: [chwang@mail.ntust.edu.tw](mailto:chwang@mail.ntust.edu.tw)

Carbon-based materials as electrode materials are widely used for the energy storage application of vanadium redox flow batteries (VRFBs). However, the electrochemical activity of the carbon-based material was poor, which limits the electrochemical performance of VRFB. Some methods can improve the electrodes activity of carbon-based materials. For example, the functionalization method enhances the functional groups on the surface of electrode [1, 2], and nanostructure control method tunes the surface morphology of electrode [3].

In this work, we try to enhance the electrochemical activity of carbon felt by using the functionalization method, making the high performance and high efficiency of carbon felt electrode for VRFBs. The functionalized carbon felt electrode performs a good electrochemical activity of  $\text{VO}^{2+}/\text{VO}_2^+$  redox reaction in a three-electrode method test. By employing the functionalized carbon felt electrodes in the both electrodes of VRFB, it shows good coulombic efficiency, voltage efficiency, and energy efficiency which are around 93.8%, 81.1% and 76.1%, respectively.

Keywords: Functionalization, Vanadium Redox Flow Battery, Carbon Felt

[1] L. Yue, W. Li, F. Sun, L. Zhao, L. Xing, Carbon, 48 (2010) 3079-3090.

[2] S. Wang, X. Zhao, T. Cochell, A. Manthiram, The Journal of Physical Chemistry Letters, 3 (2012) 2164-2167.

[3] W.Y. Li, J.G. Liu, C.W. Yan, J. Solid State Electrochem., 17 (2013) 1369-1376.



# Catalytic Activity and Durability for Oxygen Evolution on LaNiO<sub>3</sub>/Ni for Alkaline Water Electrolysis under Potential Cycling

Jiajin Bi<sup>a</sup>, Koichi Matsuzawa<sup>a</sup>, Yuji Kohno<sup>a</sup>, Shigenori Mitsushima<sup>a,b</sup>  
<sup>a</sup>Green. Hyd. Res. Cntr. Yokohama Nat. Univ., <sup>b</sup>IAS, Yokohama Nat. Univ.  
79-5, Tokiwadai, Hodogaya-ku, Yokohama 240-8501, Japan,  
cel@ml.ynu.ac.jp

## Introduce

For the hydrogen society without CO<sub>2</sub> emission, it is necessary to produce hydrogen using fluctuating power supply from renewable energy. In order to obtain the active and durable anode for alkaline water electrolysis (AWE) against fluctuating power, we have already reported that a nickel with lithiated NiO coating showed high activity and durability under potential cycling<sup>1</sup>. Because of good electric conductivity and activity, nickel containing perovskite-type oxides which sintered at high temperature are regarded as candidate materials, but the examination of the durability is not accomplished<sup>2</sup>. Therefore, in this study, we have investigated the oxygen evolution reaction (OER) activity and durability of a LaNiO<sub>3</sub>/Ni as an AWE anode using fluctuating supply.

## Experimental

The LaNiO<sub>3</sub> powder was prepared by the thermal decomposition of precursor containing lanthanum nitrate hexahydrate and nickel acetate tetrahydrate at 1073 K for 12 h in air<sup>3</sup>. Then, a Ni electrode which was coated by LaNiO<sub>3</sub> with polyvinyl alcohol (PVA) was sintered at 773-973 K. A process of dipping of the electrode into the precursor, drying, and sintering at 773 K was repeated for six times. Finally, the electrodes were heat-treated for 1 h at 1073 K in air to obtain a LaNiO<sub>3</sub>/Ni (LNO\_773, 873, or 973 of sintering temperature) as a working electrode. The LNO was analyzed by XRD before and after electrochemical measurements.

The electrochemical measurements were carried out at 30±1 °C, using with RHE and Ni coil as a reference electrode and counter electrode, respectively. Potential cycle was carried out for 25,000 cycles between 1.0 and 1.8 V with scan rate of 100 mVs<sup>-1</sup>. The catalytic activity for the OER was evaluated by slow scan voltammetry between 0.5 and 2.0 V with scan rate of 5.0 mVs<sup>-1</sup> during the potential cycling.

## Results and discussions

Figure 1 shows the OER currents at 1.6 V vs. RHE on the LNOs with various sintering temperature during potential cycling. The OER currents on the LNOs were stable during potential cycling. In contrast, the OER current on Ni decreased dramatically with the increase of cycle, even the initial current of OER on Ni was much larger than that on the LNOs in this study<sup>1</sup>.

OER currents at 1.0 mA cm<sup>-2</sup>, as an index of the OER activity, of the LNOs were slightly higher than that of Ni, and Ni with lithiated NiO coating before potential cycling, but they were lower than that of Ni after potential cycling. Therefore, the OER activity of the LNOs should be almost the same to Ni.

According to XRD analysis, Ni(OH)<sub>2</sub> formed on the Ni electrode after potential cycling. This is attributed the degradation of the OER currents on Ni. In the case of the LNOs after potential cycling, LaNiO<sub>3</sub> and Ni were detected as same as that before electrochemical measurements.

From above results, LaNiO<sub>3</sub>/Ni would be an alternative anode electrode for alkaline water electrolysis using with electric power which is produced from renewable energy.

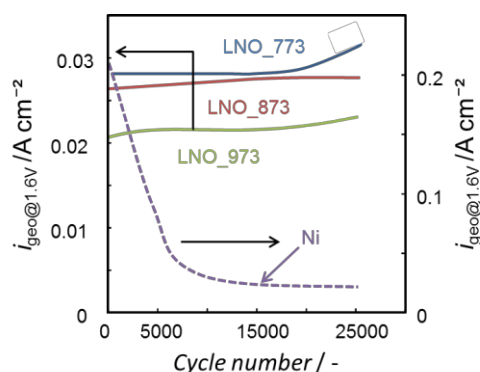


Fig. 1 OER current on LaNiO<sub>3</sub>/Ni and Ni at 1.6 V vs. RHE during potential cycling at 30 °C.

## Reference

- (1) H. Ichikawa, K. Matsuzawa, Y. Kohno, I. Nagashima, Y. Sunada, Y. Nishiki, A. Manabe, and S. Mitsushima, *ECS Trans.*, **58**(33), 9 (2014).
- (2) R. N. Singh, L. Bahadur, J. P. Pander, and S. P. Singh, *Journal of Applied Electrochemistry*, **24**, 149(1994).
- (3) T. Noda, K. Komaki, and T. Kawasaki, *Panasonic Tech. J.*, **55**, 108 (2009) (In Japanese).

# Screening of Ru-based Electrocatalysts for Oxygen Reduction by Scanning Electrochemical Microscopy

Yu-Ching Weng, Wei-Fen Xiong  
*Department of Chemical Engineering*  
*Feng Chia University, Taichung, Taiwan, 40724*  
*ycweng@fcu.edu.tw*

Oxygen reduction reaction (ORR) electrocatalyst is one of the most hot issues in the academia and industries due to its application in polymer electrolyte membrane fuel cells (PEMFCs). In this report, a high-throughput screening technique based on scanning electrochemical microscopy (SECM) with a tip-generation–substrate-collection (TG–SC) mode was applied to identify potential electrocatalysts for ORR. Bimetallic ruthenium (Ru-M, M = V, Cr, Mn, Fe, Co, Ni, Cu and Zn) based chalcogenide (S, Se, Te) arrays were fabricated and screened for activity as ORR electrocatalysts. The potential electrocatalysts were then characterized by SEM, EDX, XRD and XPS. The catalytic activity of potential electrocatalysts were further examined during cyclic voltammetric scans of the substrate with a tip close to the substrate. The quantitative rate of ORR on the candidate substrates was determined for different substrate potentials from SECM approach curves by fitting to a theoretical model. The ruthenium based electrocatalysts that showed high activity for ORR were identified in this work.

# Fundamental Studies on Electrochemical Oxidative Properties of a Gold Nanoparticle-Attached Palladium Electrode

Hiromu Yoshida, Munetaka Oyama

*Department of Material Chemistry, Graduate School of Engineering, Kyoto University  
Nishikyo-ku, Kyoto 615-8520, Japan  
oyama.munetaka.4m@kyoto-u.ac.jp*

Metal nanoparticles (NPs) have been attracting active attention as functional units for electrode modifications because they can change the electronic communications on the conductive materials. If we would like to attach gold NPs (AuNPs) on the ITO surfaces, the functional bridging reagents such as (3-mercaptopropyl)-trimethoxy-silane or charged polymers have been adopted.

While many successful results have been obtained using the bridging reagents, our group is proposing a simple methodology to attach AuNPs on the ITO surfaces [1]. Namely, by applying a seed-mediated growth method, which was originally developed for synthesizing metal nanorods in aqueous solution [2], to the surface modification, the crystal growth of AuNPs on the ITO surfaces could be performed from the Au nano-seed particles adsorbed on the ITO with keeping adhesion contacts. As the results, some successful electroanalysis could be performed using thus prepared AuNP-attached ITO electrodes [3].

While we have been utilizing Au nano-seed particles followed by the nanostructural growth in growth solutions, only the attachment of Au nano-seed might change the electrochemical characteristics of the base conducting materials. Although the effects of Au nano-seed on ITO electrodes were relatively scarce, we explored the combinations of Au nano-seed particles with bulk metal electrodes, such as Au, Pt, Ni and Pd electrodes.

Consequently, in the cases of Au and Pt electrodes, no remarkable changes in electrochemical responses were observed. However, interesting changes in electrochemical responses were observed for an AuNP-modified Ni electrode [4]. Furthermore, as an unusual phenomenon, we could observe the electrocatalytic oxidation of water in alkaline solutions with an AuNP-modified Pd electrode [5].

In the latter case of the AuNP-modified Pd electrode, it is characteristic that the oxidation peak is observed with an enhanced current magnitude, implying the electrocatalytic oxidation. However, the reproducibility of the electrochemical responses was not very good. Therefore, we explored some factors to affect the oxidative responses. As the result, it was found that the polish of a base Pd electrode was quite important to observe oxidative peaks. As well, the polish should be carried out just before immersing the base electrode into a solution of Au nano-seeds.

Also, we studied the effects of NaBH<sub>4</sub>, which is used to form Au nano-seed particles as a reducing reagent, on the redox properties of a Pd base electrode. As the result, formed hydrogen in the reaction of NaBH<sub>4</sub> was found to make appearance of the oxidative responses, which are similar to those observed with an AuNP-modified Pd electrode. This result implies complex aspects of surface redox reactions on Pd in alkali solutions.

Some trials to make clear the mechanisms of the appearance of the oxidative currents will be presented at the meeting.

[1] M. Kambayashi, J. Zhang, M. Oyama, *Cryst. Growth Des.*, **5**, 81–84 (2005).

[2] N. R. Jana, L. Gearheart, C. J. Murphy, *J. Phys. Chem. B*, **105**, 4065–4067 (2001).

[3] M. Oyama, *Anal. Sci.*, **26**, 1–12 (2010).

[4] T. Uemoto, Y. Nakayama, X. Chen, G. Chang, M. Oyama, *Electroanalysis*, **27**, in press (2015).

[5] Y. Nakayama, M. Oyama, *Chem. Commun.*, **49**, 5228–5230 (2013).

# Polarization for a toluene hydrogenation electrolyzer with various concentration of toluene feed

Yuki sawaguchi<sup>1)</sup>, Yasutomo Takakuwa<sup>1)</sup>, Kensaku Nagasawa<sup>1)</sup>, Yuji Kohno<sup>1)</sup>,  
Koichi Matsuzawa<sup>1)</sup> and Shigenori Mitsushima<sup>1, 2)</sup>

<sup>1)</sup> Green Hydrogen Research Center, <sup>2)</sup> IAS, Yokohama National University, 79-5 Tokiwadai, Hodogaya-ku, Yokohama 240-8501, Japan,

## Introduction

Usage of renewable energy get a lot of attention for a way to sustainable society. To supply of renewable energy on demand, large-scale of energy for storage and transportation is needed. We pay attention the organic hydride especially toluene-methylcyclohexane system as a carrier for energy storage and transportation. Direct electrohydrogenation electrolyzer for toluene using renewable energy has been under development applying PEFC and industrial electrolysis technology as a high energy conversion efficiency technology [1]. To improve efficiency of the electrolyzer, factorial analysis for polarization is needed.

In this study, a method of factorial analysis with reversible hydrogen electrode (RHE) has been developed to evaluate the polarization of electrolyzer for direct hydrogenation of toluene.

## Experimental

An anode was DSE<sup>®</sup> (Permelec Electrode Ltd.) electrode for oxygen evolution. A cathode was 0.5 mg cm<sup>-2</sup> of PtRu/C catalyst (Tanaka Kikinzoku Kogyo) coated on a carbon paper (SGL Carbon) electrode that was assembled on a Nafion<sup>®</sup> (DuPont) membrane that was hydrophilized for anode side. Nominal electrode area was 11.3 cm<sup>2</sup>. To guard breaking membrane, 25  $\mu$ m of a spacer was put between anode and electrolyte membrane, and back pressure of anode side was 500 mmAq higher than cathode side. 10 ml min<sup>-1</sup> of sulfuric acid and 5 ml min<sup>-1</sup> of toluene (TL)/methylcyclohexane (MCH) were fed to anode and cathode compartment, respectively. Concentration of TL was in the range from 5 to 100 %. A Luggin capillary for a RHE was placed near the anode. Polarization was evaluated with constant cell voltage measurement at 1.3~2.5 applied cell voltage, 60 °C. Resistance of electrolyte evaluated by AC impedance at 10<sup>5</sup>~10<sup>-1</sup> Hz.

## Results and discussion

Figure 1 shows the IR corrected potential-current curves of constant cell voltage measurement with various concentration of TL feed. Dashed dotted line shows the theoretical potential of 0.15 V vs RHE for anode and 1.23 V vs RHE for cathode. The polarization curves for anode and cathode were almost the same even lower TL concentration up to 100 mA cm<sup>-2</sup>. The anode and cathode overpotentials were 0.32-0.35 and 0.19-0.24 V at 10 mA cm<sup>-2</sup>, respectively. At 100 mA cm<sup>-2</sup>, they were 0.46-0.53 and 0.28-0.41 V, respectively. Therefore, the anode overpotential was significantly larger than that of the cathode, but the difference between anode and cathode decreased with the increase of current density. The anode overpotential was hardly affected by TL concentration. On the other hand, the cathode overpotentials increased with decrease of TL concentration and they significantly increased in the higher current density. Simultaneously, hydrogen evolution reaction was observed, which should correspond to lack of TL mass transfer to the catalyst.

## Acknowledgment

This work was supported by Cross-ministerial Strategic Innovation Promotion Program (SIP), “energy carrier” (Funding agency: JST). The anode was supplied by Permelec Electrode Ltd. We appreciate the person concerned them.

## References

[1] S. Mitsushima, Y. Takakuwa, K. Nagai, K. Matsuzawa, Proceedings of the Grand Renewable Energy 2014, O-Hf-5-1(Aug., 2014, Tokyo).

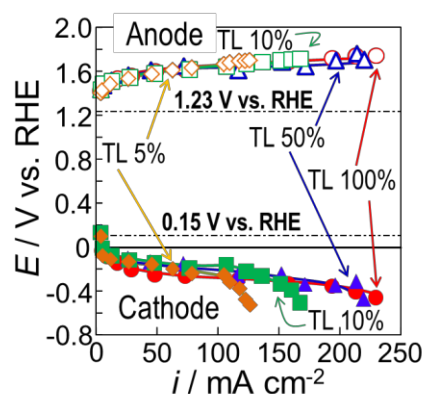


Fig.1 IR corrected electrode potential as a function of current density for various concentration of toluene feed at 60°C.



# Electrocatalytic Synthesis of Cinnamic Acid by Reaction of Electrocatalytic Activated CO<sub>2</sub> with Phenylacetylene

Kobra Ghobadi, Hamid R. Zare, Hossein Khoshro, Alireza Gorji, Abbas A. Jafari

*Department of Chemistry, Yazd University, Yazd, 89195-741, Iran*

*Fax No.: +98 3538210991 Tel. No.: +98 35 38122669*

*E-mail address: Ghobadi\_74@yahoo.com*

## Abstract

Carbon dioxide has received considerable attention as an available and abundant source in synthesis of organic compounds. But the large overpotential is required to convert of this inert molecule to a reactive particle for participating in a chemical reaction [1]. In order to more convenient convert of unreactive CO<sub>2</sub> molecule to desired products in electrochemical synthesis, different molecular and a number of transition metal complexes have been used as electron transfer mediators [2]. Complex of [Ni<sup>II</sup>(Me<sub>4</sub>-NO<sub>2</sub>Bzo)<sub>2</sub>[14]tetraeneN<sub>4</sub>)] has an excellent electrocatalytic activity for CO<sub>2</sub> reduction [3]. In our previous work, application of [Ni<sup>II</sup>(Me<sub>4</sub>-NO<sub>2</sub>Bzo)<sub>2</sub>[14]tetraeneN<sub>4</sub>)] complex for cyclic carbonates electrosynthesis was reported [4].

Cinnamic acid is used in certain pharmaceuticals and also in the manufacturing of different esters [5]. In this work, the [Ni<sup>II</sup>(Me<sub>4</sub>-NO<sub>2</sub>Bzo)<sub>2</sub>[14]tetraeneN<sub>4</sub>)] complex was used for electrocatalytic reduction of CO<sub>2</sub>. Then, cinnamic acid was electrosynthesised by reaction of the reduction product of CO<sub>2</sub>, (CO<sub>2</sub><sup>•-</sup>), with phenylacetylene. The results indicate that the cathodic current of the complex was increased in the presence of CO<sub>2</sub> and the anodic peak current was disappeared. Also, a rise in the electrocatalytic current of CO<sub>2</sub> reduction was observed after addition of phenylacetylene. Controlled potential coulometry was carried out in an undivided glass cell equipped with a gas inlet and outlet with a graphite rod as the cathode, a platinum plate as the anode and Ag/Ag<sup>+</sup> (0.01 M AgNO<sub>3</sub> in 0.1 M TBAP acetonitrile solution) as the reference electrode. After separation of products by liquid-liquid extraction and preparative TLC, the spectral characterization, FTIR, <sup>1</sup>H and <sup>13</sup>C NMR, demonstrated cinnamic acid is the main product of electrolysis.

## References:

- [1] H. D. Gibson, Chem.Rev. 96 (1996) 2063-2096.
- [2] C. Amatore, A. Jutand, J. Am. Chem. Soc. 113 (1991) 2819.
- [3] H. Khoshro, H. R. Zare, A. Gorji, M. Namazian, Electrochim. Acta. 113 (2014) 62.
- [4] H. Khoshro, H. R. Zare, M. Namazian, A. A. Jafari, A. Gorji, Electrochim. Acta. 113 (2013) 263-268.
- [5] G. S. SureshKumar, P. G. Seethalakshmi, N. Bhuvanesh, S. Kumaresan, J. Mol. Struc. 1050 (2013) 88-96.

# Preparation of Graphene Supported PtCoMo by Electroless Deposition

L. Tamašauskaitė-Tamašiūnaitė, G. Kisielius, T. Kilmonis, A. Balčiūnaitė, I. Stankevičienė, A. Jagminienė, A. Matusevičiūtė, E. Norkus  
*Center for Physical Sciences and Technology*  
*A. Gostauto 9, LT-01108 Vilnius, Lithuania*  
*loreta.tamasauskaite@ftmc.lt*

In the present work the graphene supported PtCoMo catalysts were prepared by a simple and cost-effective galvanic displacement technique. At first, the Co or CoMo was deposited on the surface of graphene powder via electroless deposition. Then, the Pt crystallites were deposited on the prepared Co/graphene or CoMo/graphene catalysts by their immersion into platinum-containing solution for various time periods. The electrocatalytic properties of the Co/graphene, CoMo/graphene and PtCoMo/graphene catalysts towards the oxidation of borohydride and methanol in an alkaline medium were investigated by means of cyclic voltammetry and chrono-techniques.

The electrocatalytic activity values of the PtCoMo/graphene catalysts prepared under various conditions are compared and discussed on the basis of electrochemical data.

# Ruthenium Nanocomposites for Electrochemical Detection: Design and Modification of Graphene Electrodes for Biosensors

Ausra Baradoke<sup>1</sup>, Isabel Pastoriza-Santos<sup>2</sup>, Elisa Gonzalez-Romero<sup>3</sup>

<sup>1</sup>Department of Nanoengineering, Center for Physical Sciences and Technology, Savanoriu ave. 231, Vilnius, Lithuania, LT-0200

<sup>2</sup>Colloid Chemistry Group, Department of Physical Chemistry, University of Vigo, University Campus, Vigo, Spain, ES-36310 Vigo, Spain

<sup>3</sup>Electroanalysis and Biosensors Group, Department of Analytical and Food Chemistry, University of Vigo, University Campus, Vigo, Spain, ES-36310  
ausra.baradoke@ftmc.lt

Electrochemical detection is a promising approach for the next generation of diagnostic methods [1]. We used innovative Screen-Printed Graphene Electrodes (SPGPHEs), because of its high thermal and electric conductivity [2] and nanoparticles, because of catalytic properties, which can be used for increasing sensitivity and selectivity of detection.

For investigation, graphene electrodes were modified with ruthenium nanoparticles synthesized in autoclave. Triangular ruthenium nanoparticles prepared using hydrothermal synthesis method [3]. Formed ruthenium nanoparticles were analyzed using transmission electron microscope and the modified surface was analyzed using scanning electron microscope (SEM) (Fig. 1). Cyclic voltammograms of  $\beta$ -Nicotinamide (NADH) on bare SPGPHE and SPGPH/PoPD/RuNPs modified electrode showed that the electrocatalytic current increased significantly (40%) in case that the RuNPs were present onto the electrode surface.

A remarkable catalytic oxidation current at the modified electrode occurred at ca. 0V, which negatively shifted higher than 400 mV, compared with that at bare electrode (Fig. 2). A study of the electrocatalytic behavior of NADH oxidation on the SPCE/GPH with RuNPs in phosphate buffer (PBS) was carried out in this work. We found that the current of NADH oxidation increases (Fig. 2) and peak potential shifts to lower potential, when we use Ru nanoparticles. This system can be used for biosensors, because ruthenium nanoparticles increase the active surface area and provide electron transfer with strong catalytic properties.

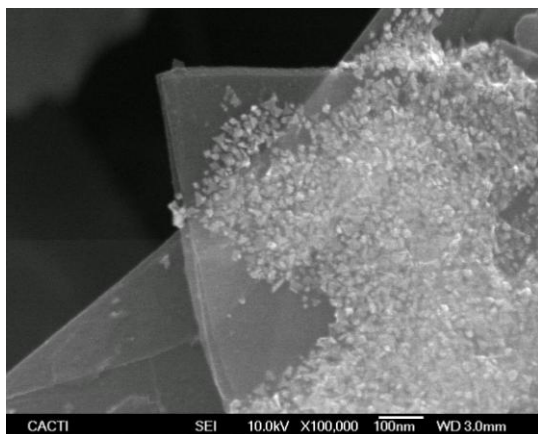


Fig. 1. SEM image of graphene (SPGPH) surface modified by ruthenium nanoparticles.

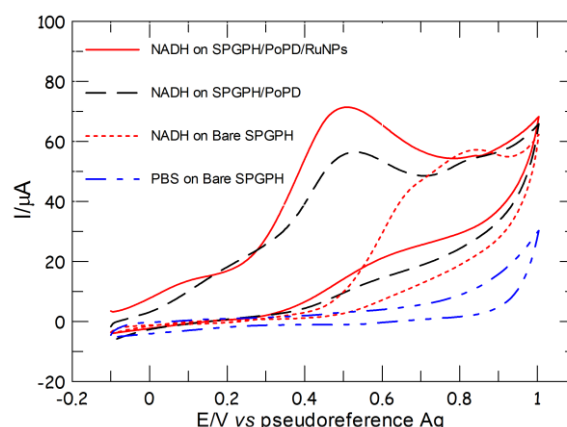


Fig. 2. Cyclic voltammograms of SPGPH electrodes with and without RuNPs in the presence of 5 mM NADH in 0.1 M PBS (pH 6.8), scan rate: 50 mVs<sup>-1</sup>.

## References:

- [1] J. Wang, Biosen. Bioelectron., 21, 1887 (2006).
- [2] Li Li, et al., Talant., 113, 1 (2013).
- [3] An-Xiang Yin, et al., Am. Chem. Soc., 134, 20479 (2012).



# REDOX PROPERTIES AND ELECTROCATALYTIC OXYGEN REDUCING PERFORMANCES OF VARIOUS NOVEL METAL PHTHALOCYANINES

Zuhal Yazar,<sup>a</sup> Mehmet Pişkin,<sup>b</sup> Zafer Odabaş,<sup>a</sup> Ali Rıza Özkaya<sup>a</sup>

<sup>a</sup>Marmara University, Department of Chemistry, Istanbul, Turkey

<sup>b</sup>Çanakkale 18 Mart University, Çanakkale Vocational School of Technical Sciences, Çanakkale, Turkey  
aliozkaya@marmara.edu.tr

Phthalocyanine (Pc) derivatives have been receiving increasing interest due to their applicability in various advanced technological areas such as energy conversion and/or storage devices, photodynamic therapy, photovoltaic cells, sensors, electrochromic materials and catalysis. The applicability of these compounds in the mentioned areas strongly depends on their electronic and electrochemical properties. Thus, the determination of the electron transfer properties of novel Pc derivatives is highly important in term of the identification of possibility of the usage in these areas.

The electrocatalytic activity of compounds for dioxygen reduction has vital importance since this reaction, occurring at one of the electrodes of both fuel cells and metal-air batteries, has slow electrode kinetics. The studies in literature showed some type of Pc complexes display high catalytic activity for dioxygen reduction.<sup>1</sup> This work involves the identification of redox properties of various novel mononuclear tetra-alpha substituted metal Pcs by voltammetric and *in situ* spectroelectrochemical measurements. It also includes the investigation of their electrocatalytic performances for dioxygen reduction by dynamic voltammetry measurements, with the aim of determining their suitability for usage as oxygen reduction catalyst in energy conversion and/or storage devices.

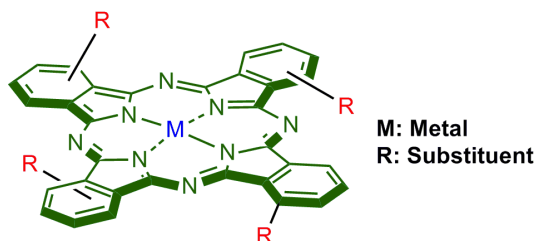


**Fig.1.** Molecular structure of mononuclear tetra-alpha substituted metal Pc template.

## REFERENCES

- [1]. İ. Koç, M. Özer, A.R. Özkaya, Ö. Bekaroğlu, *Dalton Trans.*, **32**, 6368–6376 (2009).

**Acknowledgement:** This work was supported by Marmara University, Scientific Research Projects Committee.

# On the role of $\text{Cl}^-$ : Synergistic effects with $\text{Cu}_2\text{O}$ for the electroreduction of $\text{CO}_2$ to multi-carbon fuels

Seunghwa Lee<sup>a</sup>, Jaeyoung Lee<sup>a,b</sup>

<sup>a</sup>Electrochemical Reaction and Technology Laboratory, School of Environmental Science and Engineering, Gwangju Institute of Science and Technology (GIST), Gwangju, 500-712, South Korea.

<sup>b</sup>Ertl Center for Electrochemistry and Catalysis, Research Institute for Solar and Sustainable Energies, GIST, Gwangju, 500-712, South Korea.

Gwangju Institute of Science and Technology (GIST), Gwangju, 500-712, South Korea.  
jaeyoung@gist.ac.kr

In recent years, reducing anthropogenic  $\text{CO}_2$  is of great interest because of its detrimental effect on environmental ecosystem. As one of possible solutions for the  $\text{CO}_2$  problem, electrochemical reduction of  $\text{CO}_2$  using metal oxide catalyst draws a considerable attention [1-3]. Specifically adsorbed anions have a crucial role in electrochemical reaction, often affecting directly the structure of electrode material and heterogeneous reaction environment near the electrode surface [4]. Such various known features can be also utilized in the electrochemical reduction of  $\text{CO}_2$ . We report the superior  $\text{CO}_2$  electrolysis on the oxygen-evacuated  $\text{Cu}_2\text{O}$  with aid of  $\text{Cl}^-$ . Under the electrolytic system, high multi-carbon fuels (e.g.,  $\text{C}_2\text{H}_5\text{OH}$ ,  $\text{C}_3\text{H}_7\text{OH}$ , and even  $\text{C}_4\text{H}_{10}$ ) are generated with obviously high total faradaic efficiency and stably for long time period. One would attribute the remarkable electrocatalysis to synergism between the  $\text{Cu}_2\text{O}$  and  $\text{Cl}^-$  such as suppression of proton adsorption on the surface of electrode leading to low hydrogen evolution reaction and enhanced  $\text{Cu}_2\text{O}$  preservation. From our studies, we provide that preferential production of high carbon number molecules can be achieved on the use of Cu-based catalysts and the interesting results opens up further opportunities of  $\text{CO}_2$ -fed chemical plants.

## References

- [1] J. Lee, Y. Kwon, R. L. Machunda, H. J. Lee, Electrocatalytic Recycling of  $\text{CO}_2$  and Small Organic Molecules, *Chem. Asian J.*, **4** (2009) 1516.
- [2] D. Kim, S. Lee, J. D. Ocon, B. Jeong, J. K. Lee, J. Lee, Insights into autonomously formed oxygen-evacuated  $\text{Cu}_2\text{O}$  electrode for the selective production of  $\text{C}_2\text{H}_4$  from  $\text{CO}_2$ , *Phys. Chem. Chem. Phys.*, **17** (2015) 824.
- [3] S. Lee, J. D. Ocon, Y. Son, J. Lee, Alkaline  $\text{CO}_2$  Electrolysis toward Selective and Continuous  $\text{HCOO}^-$  Production over  $\text{SnO}_2$  Nanocatalysts, *J. Phys. Chem. C*, **119** (2015) 4884.
- [4] Y. Hori, A. Murata, R. Takahashi, Formation of Hydrocarbons in the Electrochemical Reduction of Carbon Dioxide at a Copper Electrode in Aqueous Solution, *J. Chem. Soc., Faraday Trans. 1*, **85** (1989) 2309.

# New Air Electrode Catalysts Based on Mn Oxide Nanosheet/ Nanocarbon Composite Materials for Li Air Batteries

Morihiro Saito<sup>1\*</sup>, Shinpei Kosaka<sup>1</sup>, Chiaki Tsukada<sup>1</sup>, Hiroshi Suzuki<sup>1</sup>, Hidenobu Shiroishi<sup>2</sup>,  
Yumi Tanaka<sup>3</sup>, and Shiro Seki<sup>4</sup>

<sup>1</sup>Department of Applied Chemistry, Tokyo University of Agriculture and Technology, Tokyo 184-8588

<sup>2</sup>Department of Chemical Science and Engineering, Tokyo National College of Technology, Tokyo 193-0997

<sup>3</sup>Department of Industrial Chemistry, Tokyo University of Science, Tokyo 162-0826

<sup>4</sup>Central Research Institute of Electric Power Industry, Tokyo, 201-8511

\*e-mail: mosaito@cc.tuat.ac.jp

In recent years, Li air secondary batteries (LABs) have been attracted much attention as next-generation energy storage because of the possibility of greatly higher energy density ( $> 500 \text{ Wh kg}^{-1}$ ) than that of Li-ion batteries (LIBs). However, the LAB systems have some serious problems to be solved before the commercialization; e.g. suppression of Li metal dendrite at the anode, improvement of durability of electrolyte solutions against electrochemical oxidation, preparation of high performance air electrode catalysts at the cathode, etc. Especially for the air electrode catalysts, both catalytic activities for  $\text{O}_2$  reduction reaction (ORR) and  $\text{O}_2$  evolution reaction (OER), and also durability for electrochemical oxidation are demanded. In this study, we prepared two kinds of Mn oxide nanosheet (MnNS)/nanocarbon (carbon nanotube (CNT) or Ketjen black (KB)) composite materials, i.e. MnNS/CNT and MnNS/KB, and evaluated the electrochemical properties of ORR and OER activities along with the durability.

The MnNS was synthesized by single-step solution method [1] by adding the mixture of 30wt%  $\text{H}_2\text{O}_2$  (2 g) and 0.6 M TMAOH (24 mL) to 0.3 M  $\text{MnCl}_2$  (20 mL), and then stir during one night at 500 rpm to obtain ca.  $8.7 \text{ g L}^{-1}$  MnNS colloidal dispersion. 20 mL of the MnNS colloidal dispersion was mixed with proper amount of nanocarbon (CNT or KB) dispersed in ethanol (50 mL) under ultrasonic vibration for 90 min, and then 0.1 M LiCl (40 mL) was gradually dropped to the colloidal dispersion to form the composite materials. After being filtered, the composites were heat-treated at  $400^\circ\text{C}$  for 5 h in Ar atmosphere. Characterization of the samples was conducted by X-ray diffraction (XRD) analysis and transmission electron microscope (TEM) observation. The ORR and OER activities were examined by hydrodynamic voltammetry (HV) using a rotating ring-disk electrode (RRDE) in 0.1 M KOH at  $50^\circ\text{C}$  [2].

Fig. 1(a) and (b) show the TEM images of MnNS/CNT and MnNS/KB composites, respectively. In both samples, the each component of MnNS, CNT and KB were homogeneously mixed and seemed to have good contact between MnNS and nanocarbons. From the result of HV curves for the composites (Fig. 2(a)), the MnNS/KB exhibited a higher ORR activity than the MnNS/CNT and only MnNS. This indicates that the ORR activity of MnNS was effectively enhanced by compositing with KB. From a very large ORR current for the MnNS/KB, it is considered that the KB was successfully inserted between MnNSs and constructed suitable electron paths for the MnNS. On the other hand, for the OER, (Fig. 2(b)), a higher OER current was also attained for the MnNS/KB compared to that for the MnNS/CNT. However, the onset potentials of MnNS/KB and KB were too negative below 1.23 V, implying the OER current included oxidation current of KB. The further discussion will be presented at the meeting.

We gratefully thank to Tokuyama Co. for providing alkaline ionomer binder. This work was supported by JST "A Tenure-track Program" and JSPS "KAKENHI" (25870899) from MEXT, Japan.

[1] K. Kai et.al., *J. Am. Chem. Soc.*, **130**, 15938 (2008). [2] N. Ohno et.al., *Top. Catal.*, **52**, 903 (2009).

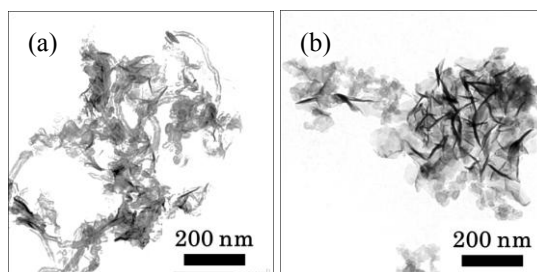


**Fig. 1.** TEM images of (a) MnNS/CNT and (b) MnNS/KB composites heat-treated at  $400^\circ\text{C}$  in Ar.

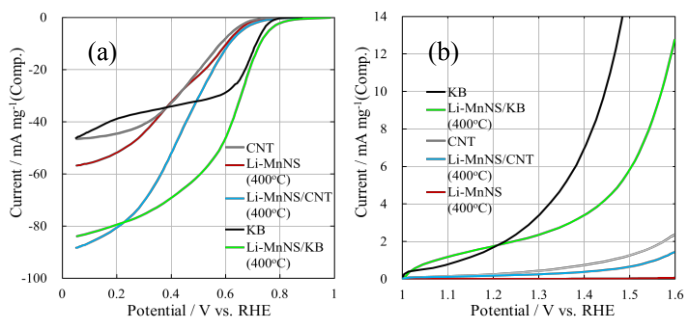


**Fig. 2.** HV curves of (a) ORR and (b) OER for the MnNS/nanocarbon composites heat-treated at  $400^\circ\text{C}$  in Ar, MnNS, KB and CNT in  $\text{O}_2$  saturated 0.1 KOH at  $50^\circ\text{C}$ .

# Motion control of TiO<sub>2</sub>/Pt/Au nanomotor by UV light irradiation

Takuma SUZUKI<sup>a</sup>, Yoshinao HOSHI<sup>a</sup>, Isao SHITANDA<sup>a,\*</sup>, Masayuki ITAGAKI<sup>b</sup>

<sup>a</sup>*Department of Pure and Applied Chemistry, Faculty of Science and Technology,  
Tokyo University of Science, Noda, Chiba 278-8510, Japan.*

<sup>b</sup>*Research Institute for Science and Technology,  
Tokyo University of Science, 2641, Yamazaki, Noda, Chiba 278-8510, Japan.*

\*E-mail address: [shitanda@rs.noda.tus.ac.jp](mailto:shitanda@rs.noda.tus.ac.jp) (I.Shitanda)

Nanomotors are nanoscale devices propelled by the electrocatalytic decomposition of a chemical fuel [1]. Motion control of nanomachines are currently the subject of intense interest due to their potential applications in nanomachinery, nanomedicine, nanoscale transport [2]. In this study, we prepared a TiO<sub>2</sub>/Pt/Au nanomotor, and tried to control its driving speed by switching ON/OFF of the ultraviolet light irradiation.

The TiO<sub>2</sub>/Pt/Au nanomotor was prepared by a sequential electrodeposition of the gold, platinum, titanium dioxide segments into a porous alumina membrane template (Catalog no. 6809–6022; Whatman, Maidstone, U.K.). The titanium dioxide segment was prepared according to a procedure reported by S. Karuppuchamy et al [3]. A solution containing 0.06 mol dm<sup>-3</sup> TiOSO<sub>4</sub>, 0.09 mol dm<sup>-3</sup> hydrogen peroxide and 0.3 mol dm<sup>-3</sup> potassium nitrate was used as plating solution. The electrode potential was set at -1.1 V vs. Ag/AgCl for 5 min. Then, the aluminum membrane was sintered at 500 °C for 1 h. The sputtered silver layer and sacrificial silver layer was dissolved using a 2 mol dm<sup>-3</sup> nitric acid. The membrane was then dissolved in a 3 mol dm<sup>-3</sup> NaOH solution for 1 h to completely release the nanowires. Movement of TiO<sub>2</sub>/Pt/Au nanomotor was observed in 5 % H<sub>2</sub>O<sub>2</sub> solution with and without ultraviolet (UV) light irradiation.

Figure 1 shows a field emission scanning electron microscopy (FE-SEM) image of a TiO<sub>2</sub>/Pt/Au nanomotor. This nanomotor's length and diameter were about 4.2 μm and 200 nm, respectively. Figure 2 shows the average speeds of the TiO<sub>2</sub>/Pt/Au nanomotor with and without UV light irradiation. In the case of the without UV irradiation, the average speed of the nanomotor was 33 μm s<sup>-1</sup>. On the other hand, under UV irradiation, the speed of the nanomotor was 45 μm s<sup>-1</sup>, indicating that the speed of the nanomotor became faster by UV light irradiation. Light acceleration mechanism is suggested that decomposition of the hydrogen peroxide fuel on the TiO<sub>2</sub> surface. If no UV light was irradiated, hydrogen peroxide is oxidized only on the Pt surface, and the hydrated protons (H<sub>3</sub>O<sup>+</sup>) generated by hydrogen peroxide oxidation. The H<sub>3</sub>O<sup>+</sup> is moved toward to the Au side, and reduced on the Au surface. Thus, this nanomotor is driven by the water flow near nanomotor surface by self-electrophoresis [4]. If UV is irradiated, hydrogen peroxide is also oxidized on the TiO<sub>2</sub> surface by the photocatalytic reaction. Therefore, oxidation of H<sub>2</sub>O<sub>2</sub> is promoted, and then driving speed was found to increase.

## Acknowledgement

This work was partially supported by Inamori foundation (I. Shitanda).

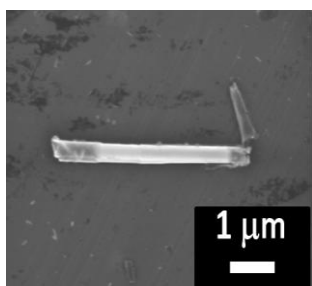


Fig.1 FE-SEM image of TiO<sub>2</sub>/Pt/Au nanomotor

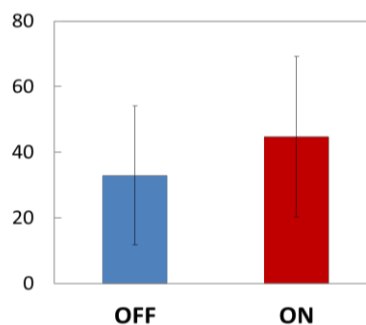


Fig.2 Driving speed of TiO<sub>2</sub>/Pt/Au nanomotor with and without UV light irradiation in 5 % H<sub>2</sub>O<sub>2</sub> solution.

## References

- [1] W. F. Paxton, et al., Journal of the American Chemical Society, 126 (2004) 13424.
- [2] J. Burdick, et al., Journal of the American Chemical Society, 130 (2008) 8164.
- [3] S.Karuppuchamy, et al., Solid State Ionics, 151 (2002) 19.
- [4] J. Wang, ACS Nano, 3 (2009) 4.

# Gold Nanoparticles Modified Cobalt-Boron-Copper and Cobalt-Boron-Tungsten-Copper as Electrocatalysts for Borohydride Oxidation

E. Norkus, L. Tamašauskaitė-Tamašiūnaitė, Z. Sukackienė, A. Balčiūnaitė, A. Selskis  
*Center for Physical Sciences and Technology*  
*A. Gostauto 9, LT-01108 Vilnius, Lithuania*  
*eugenijus.norkus@ftmc.lt*

The direct borohydride fuel cell is based on borohydride oxidation and oxygen electrochemical reduction, so the main attention is paid to the search of new nanostructured substances, which will be able to increase the efficiency of fuel cells as well as to use simple and cheap catalysts formation technologies.

In the present study investigation of sodium borohydride oxidation on cobalt-boron-copper and cobalt-boron-tungsten-copper modified with Au nanoparticles (denoted as Au/CoB/Cu and Au/CoBW/Cu) is presented. A series of the Au/CoB/Cu and Au/CoBW/Cu catalysts with low Au loadings were prepared by a simple way which involves electroless CoB and CoBW deposition followed by a spontaneous Au displacement from the gold-containing solution. The morphology and composition of the prepared catalysts were characterized using Field - Emission Scanning Electron Microscopy and Energy Dispersive X-ray Spectroscopy. The electrochemical behavior of the fabricated catalysts was examined towards the oxidation of  $\text{BH}_4^-$  ions in an alkaline medium by means of cyclic voltammetry and chrono-techniques.

It has been determined that the average size of Au crystallites deposited by galvanic displacement of CoB and CoBW adlayers varies from 6 up to 50 nm depending on the immersion time of CoB and CoBW/Cu electrodes into the gold-containing solution. The prepared Au/CoBW/Cu catalysts with the Au loadings in the range from 5.8 to 23.2  $\mu\text{g cm}^{-2}$  and Au/CoB/Cu with the Au loadings in the range from 8.0 to 44.2  $\mu\text{g cm}^{-2}$  demonstrated a significantly higher electrocatalytic activity towards the oxidation of  $\text{H}_2$  generated by catalytic hydrolysis of  $\text{BH}_4^-$  and the oxidation of  $\text{BH}_4^-$  ions as compared to those of bare Au, CoB/Cu or CoBW/Cu.

The prepared Au/CoB/Cu and Au/CoBW/Cu catalysts with low Au loadings seem to be a promising anodic material for direct borohydride fuel cells.

# Synthesis of Metal Nanoparticle/Graphene Nanocomposites using Atmospheric-Pressure-Microplasma-Assisted Electrochemistry

Huin-Ning Huang<sup>1</sup>, Wei-Hung Chiang<sup>1</sup>

<sup>1</sup>Department of Chemical Engineering, National Taiwan University of Science and Technology, Taipei 10607, Taiwan

No.43, Sec. 4, Keelung Rd., Da'an Dist., E2-510 room, Taipei 106, Taiwan (R.O.C.)

[z22765820@gmail.com](mailto:z22765820@gmail.com)

Graphene represents a new type of carbon materials and have attracted lot of attention is due to its exceptional physical and chemical properties. Recently experimental and theoretical studies have been shown that the composites of metal nanoparticles (NPs)/graphene can process superior electrocatalytic property, making them promising candidates for fuel cell electrodes. However, conventional approach to synthesis metal NPs/graphene composites usually involve time-consuming and laborious wet-chemistry-based methods.

Here we present an facile synthesis metal NPs/graphene composites using a novel atmospheric-pressure microplasma-assisted electrochemistry. Microplasmas are defined as gaseous discharges formed in electrode geometries where at least one dimension is less than 1mm. Additionally, microplasmas can be operated with an aqueous solution as an electrode. Energetic species formed in the microplasma are capable of initiating electrochemical reactions and nucleating particles in solution without the need for a chemical reducing agent. In our experiments result, we found metal NPs can be synthesis in a minute time scale using atmospheric-pressure-microplasma-assisted electrochemistry, and we further extend this technology to synthesis metal NPs/graphene composites. As-produced samples were characterized by SEM , XRD , Raman and UV-Vis spectroscopy.

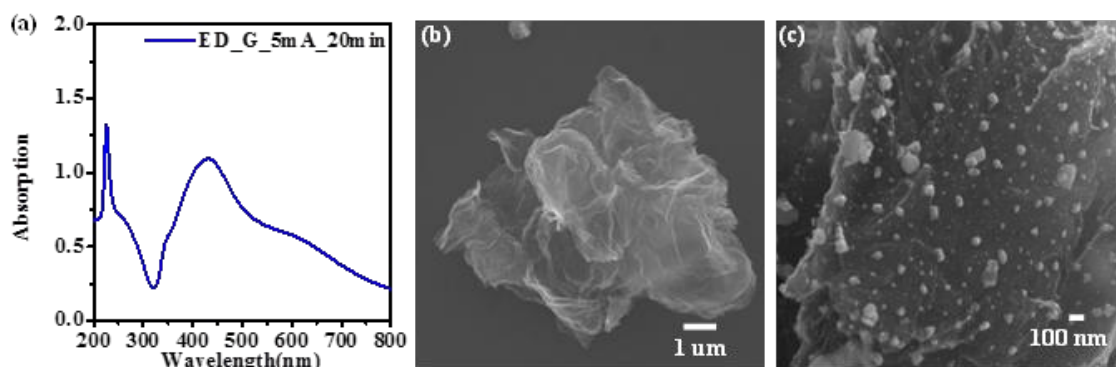


Figure. 1 (a) UV-Vis absorbance spectra of Ag NPs/graphene hybrid synthesized by microplasma. (b) FESEM picture of graphene raw material (c) FESEM picture of sample which processed by microplasma.

# The Use of Environmentally-Friendly Natural Polyols as Cu(II) Ligands in Electroless Copper Plating Processes

Eugenijus Norkus<sup>1</sup>, Janė Jačiauskienė<sup>1</sup>, Kęstutis Prušinskas<sup>1</sup>, Irena Stalnionienė<sup>1</sup>, Loreta Tamašauskaitė-Tamašiūnaitė<sup>1</sup>, Dordi Yezdi<sup>2</sup>, Aniruddha Joi<sup>2</sup>

<sup>1</sup>*Center for Physical Sciences and Technology, A. Goštauto 9, LT-01108 Vilnius, Lithuania*

<sup>2</sup>*Lam Research Corporation, 4650 Cushing Parkway, CA 94538 Fremont, U.S.A.*

*eugenijus.norkus@ftmc.lt*

The aim of the study presented herein was comparison of the parameters of process of electroless copper plating – mainly plating rate and nanoscale surface roughness of the copper deposits obtained, – using different polyols as copper(II) ligands under the similar conditions.

The ligands considered were glycerol, xylitol, *D*-mannitol, *D*-sorbitol and saccharose.

Cu(II) ligands are important components of common formaldehyde-containing alkaline electroless copper plating baths:



From one hand, the ligands used should form Cu(II) complexes stable enough to prevent Cu(OH)<sub>2</sub> formation, since the solubility product of Cu(OH)<sub>2</sub> is of the order 10<sup>-18</sup> and the concentration of “free” (uncomplexed) Cu(II) ions in the pH range 11–14 cannot exceed 10<sup>-12</sup>–10<sup>-18</sup> M, respectively. On the other hand, it is worth to note that kinetics of copper deposition as well as the properties of copper deposits (compactness, exterior, morphology and crystal structure) in high extent depend on the nature of ligands used for Cu(II) binding into complexes in electroless copper plating solutions.

The data on composition and stability of Cu(II) complexes with mentioned ligands also are presented and discussed.

## Different-sized truncated Pd nanocubes for glucose electrooxidization

Nan-Kuang Chou, Meng-Shan Hsieh, Chien-Liang Lee\*

*Department of Chemical and Materials Engineering, National Kaohsiung University of Applied Sciences*

*No. 415, Chien Kung Rd., Kaohsiung 807, Taiwan*

*e-mail address: [cl\\_lee@kuas.edu.tw](mailto:cl_lee@kuas.edu.tw); [cl\\_lee@url.com.tw](mailto:cl_lee@url.com.tw)*

Regular Pd nanocubes enclosed by (100) planes is of interesting for being as high-performance catalyst in non-enzymatic glucose sensor [1]. In this study, we symmetrically synthesized 22.8 nm and 34 nm truncated Pd nanocubes with eight (111) facets on corners and six (100) facets on planes and successfully used them as catalysts for glucose electrooxidation in 0.1 M NaOH solution. On the basis of the same Pd weight, the 22.8 nm Pd nanocubes showed  $0.044 \text{ cm}^2$  in electrochemical surface area (ESA), higher than  $0.037 \text{ cm}^2$  for the ESA of the 34 nm Pd nanocubes. The smaller Pd catalysts also have high anodic current in a reaction, in which glucose was oxidized to gluconolactone upon the promotion of Pd-OH. Additionally, the appearance of (111) planes induced two-ranged sensitivities when these two truncated Pd nanocubes were used in a non-enzymatic glucose sensor. Compared to larger Pd nanocubes, the smaller truncated Pd nanocubes had higher sensitivity, which were  $0.0618 \text{ mA mM}^{-1} \text{ cm}^{-2}$  within a linear range from 0.01 mM to 0.5 mM and  $0.0203 \text{ mA mM}^{-1} \text{ cm}^{-2}$  within a linear range from 1 mM to 15 mM for sensing glucose.

### References:

- [1] J.-S. Ye, C.-W. Chen, C.-L. Lee, Pd nanocubes as non-enzymatic glucose sensor, *Sensors and Actuators B: Chemical* 208 (2015) 569-574.



# Electrophoretic deposition of graphene sheets on porous nickel foam as effective catalysts for oxygen evolution reaction and hydrogen peroxide sensor

Yi-Shan Wu, Chien-Liang Lee\*

*Department of Chemical and Materials Engineering, National Kaohsiung University of Applied Sciences*

*No. 415, Chien Kung Rd., Kaohsiung 807, Taiwan*

*e-mail address: [cl\\_lee@kuas.edu.tw](mailto:cl_lee@kuas.edu.tw); [cl\\_lee@url.com.tw](mailto:cl_lee@url.com.tw)*

A method for the electrophoretic deposition of defective graphene sheets (DGSs) on porous Ni foams (DGS/Ni foam) is demonstrated. The comparative raman spectra showed that significant D band and G band on the DGS/Ni foam as compared to bare Ni foam, confirming the successful deposition of DGSs on the Ni foam. Additionally, the X-ray photoelectron spectra depicted the domination of C-OH and C=O on the surface of DGS/Ni foam. Additionally, the prepared DGS/Ni foam was successfully as high-performance catalysts for oxygen evolution reaction (OER) and hydrogen peroxide sensor. Compared to 1.67 V (vs. RHE) by conventional Pt/C catalyst, the DGS/Ni foam showed early onset potential started from 1.5 V (vs. RHE) and higher anodic current toward OER in a 0.1 M KOH electrolyte. In the application on hydrogen peroxide sensor, the DGS/Ni foam as compared with bare Ni foam showed larger current for reducing H<sub>2</sub>O<sub>2</sub> in the phosphate buffered saline solution. There were two linear current-responses relationships for the sensitivities on the DGS/Ni foam, which has 12.3  $\mu\text{A}\cdot\text{mM}^{-1}\cdot\text{cm}^{-2}$  from 1.6 mM to 7.6 mM and 4.7  $\mu\text{A}\cdot\text{mM}^{-1}\cdot\text{cm}^{-2}$  from 9.6 mM to 27.6 mM. The data in the selective tests depicted that DGS/Ni foam showed remarkable tolerance to foreign ascorbic acid and uric acid, confirming the potential of DGS/Ni foam as a H<sub>2</sub>O<sub>2</sub> sensor.

# Bacteria Derived Carbon as High-Performance Electrocatalysts

Yuan Chen

*School of Chemical and Biomedical Engineering, Nanyang Technological University, Singapore  
N1.2-B1-16, 62 Nanyang Drive, Singapore 637459  
chenyuan@ntu.edu.sg*

Nitrogen and phosphorus dual doped carbon materials have shown competing catalytic activity as metal-free catalysts for oxygen reduction reaction (ORR) and hydrogen-evolution reaction (HER). Prevailing methods to synthesize such carbon catalysts require high purity chemicals and gases, excessive amount of strong acids and bases, or costly organic precursors. Here, we show that bacteria can be used as a novel precursor to synthesize heterogeneous carbon materials with nitrogen and phosphorus dual functionalities by carbonization.

In the first case, *E. coli* cells were directly carbonized by heat treatment in Ar. The resulting carbon material has a large surface area up to 636 m<sup>2</sup>/g, and is comprised of up to 7.64 at% nitrogen and 8.53 at% phosphorus. The carbon material obtained at an optimum carbonization condition of 1000 °C for 2 h shows excellent catalytic performances, comparable to that of a 20 wt% Pt-C catalyst, with ~50% higher limiting current density, for ORR in near four-electron transfer processes and excellent durability. The outstanding electrocatalytic performances are credited to the fine tuning of nitrogen species by carbonization conditions and the synergy between nitrogen and phosphorus dual functionalities.<sup>1</sup>

In the second case, *S. aureus* cells were carbonized, resulting carbon material with a large surface area of 341 m<sup>2</sup>/g with nitrogen and phosphorus dual functionalities of 4.88 at% nitrogen and 4.23 at% phosphorus. Mesopores were further introduced by carbonization together with ZnCl<sub>2</sub> to increase the surface area to 816 m<sup>2</sup>/g. After cathodic treatment, the *S. aureus* derived carbon catalyst exhibits highly efficient electrocatalytic activity for the HER in acidic electrolytes. It demonstrates low onset overpotential of 76 mV, a Tafel slope of 58.4 mV/dec and a large normalized exchange current density of 1.72 × 10<sup>-2</sup> mA/cm<sup>2</sup>, which is comparable to or even better than that of existing metal-free and well-fabricated metallic catalysts. The excellent activity can be attributed to the synergistic effects of nitrogen and phosphorus, abundant mesopores, and structural and surface chemistry changes induced by the cathodic treatment.<sup>2</sup>

These two cases demonstrate the great potential of using bacteria to obtain carbon materials with a tailored structure and composition as electrocatalysts for sustainable chemical processes.

## References:

1. Catalysis Today, 2015, 249, 228–235
2. Journal of Materials Chemistry A, 2015, 3, 7210–7214

# RuO<sub>2</sub> nanoparticles loaded well-defined iron-nitrogen doped mesoporous core-shell carbon spheres as an effective cathode for rechargeable lithium-oxygen battery

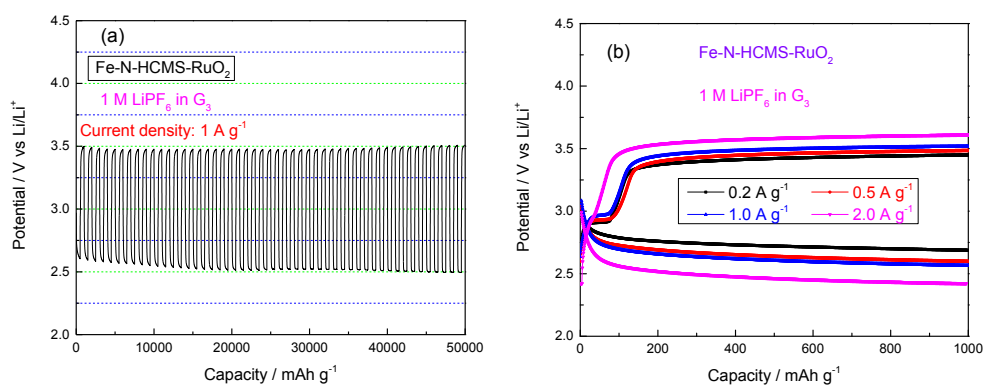
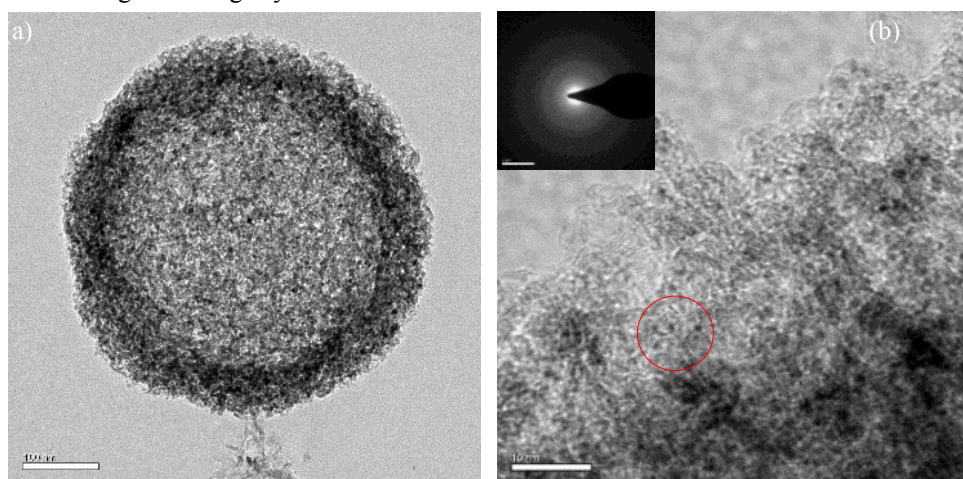
Ming Zhou, Kwong-Yu Chan\*

The University of Hong Kong

Department of Chemistry, HKU, Pokfulam Road, Hong Kong

\*Email: [hrcscky@hku.hk](mailto:hrcscky@hku.hk)

Fine RuO<sub>2</sub> nanoparticles are successfully deposited onto the iron-nitrogen doped core-shell carbon spheres via a thermal oxidation method. This composite demonstrates low over-potential during both charge and discharge process and presents excellent durability with less than 3% voltage efficiency loss after 50 charge-discharge cycles.



1. M. Zhou, C. Z. Yang, K. Y. Chan, *Adv. Energy Mater.* **2014**, *4*, 1400840;
2. F. Li, M. Morris, K. Y. Chan, *J. Mater. Chem.*, 2011, *21*, 8880;

# Controllable Synthesis of Metal Nanoparticle/Graphene Nanoribbon Composites

Shan-Yu Wang, Yan-Sheng Li, and Wei-Hung Chiang\*

Department of Chemical Engineering, National Taiwan University of Science and Technology  
No.43, Sec. 4, Keelung Rd., Da'an Dist., E2-510, Taipei 106, Taiwan (R.O.C.)  
michael810212@gmail.com

## Abstract

Here we report a controllable synthesis of Ag/GNRs composites using a two-step reaction route. First, we synthesized and functionalized GNRs from low to high by a facile carbon nanotube chemical unzipping. The functionalization of GNRs could be tuned by controlling reaction conditions (temperature, time, and oxidant concentration), confirming by scanning electron microscopy (SEM) and X-ray photoelectron spectroscopy (XPS) characterizations. (Fig. 1 and Fig. 2) Second, Ag NPs can be decorated onto the GNRs surface through a wet-chemical-based redox reaction. In our present experiment, we found that the loading of Ag NPs can be further controlled by controlling the reaction conditions. Detailed materials characterizations including SEM and UV-Vis spectroscopy (Fig. 2 and Fig. 3) show that Ag/GNRs composites were successfully synthesized in our experiment. And we also obtained Ag/GNRs substrate is extremely suitable for surface-enhanced Raman spectroscopy (SERS).

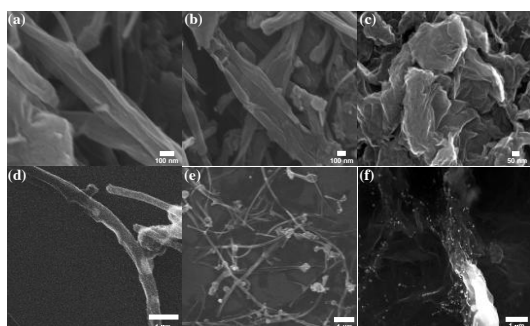


Figure1. SEM images of as-produced GNRs and Ag/GNRs with different (a, d) low surface functionality (L-GNRs and L-Ag/GNRs), (b, e) medium surface functionality (M-GNRs and M-Ag/GNRs) and (c, f) high surface functionality (H-GNRs and H-Ag/GNRs).

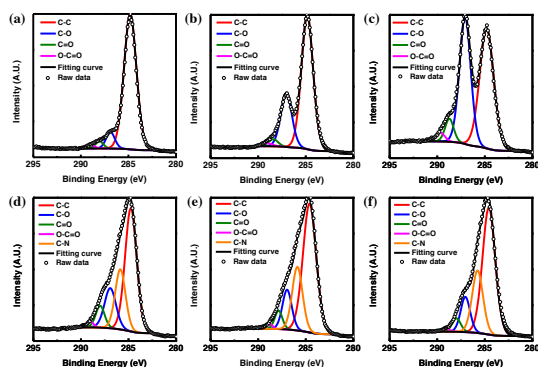


Figure2. XPS C1s spectra of as-produced GNRs

and Ag/GNRs with different (a, d) low surface functionality (L-GNRs and L-Ag/GNRs), (b, e) medium surface functionality (M-GNRs and M-Ag/GNRs) and (c, f) high surface functionality (H-GNRs and H-Ag/GNRs).

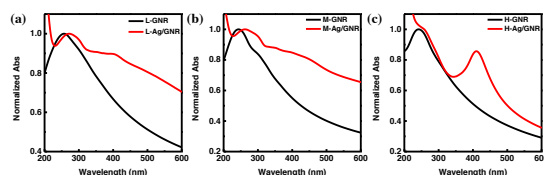


Figure3. UV-vis spectra of as-produced GNRs and Ag/GNRs with different (a) low surface functionality (L-GNRs and L-Ag/GNRs), (b) medium surface functionality (M-GNRs and M-Ag/GNRs) and (c) high surface functionality (H-GNRs and H-Ag/GNRs).

# Synthesis and Characterization of Highly Active Ir Nanoparticles for Oxygen Evolution Reaction in Acid Media

P. Lettenmeier, S. Hosseiny, L. Wang, A. S. Gago, K. A. Friedrich

*Institute of Engineering Thermodynamics, German Aerospace Center  
Pfaffenwaldring 38-40, 70569 Stuttgart, Germany*

*Philipp.lettenmeier@dlr.de*

Proton exchange membrane (PEM) water electrolysis is one of the most promising technologies for a sustainable and emission-free hydrogen production due to its high power density and high efficiency [1]. High amounts of expensive noble metals, such as platinum and iridium for cathode and anode side respectively, contribute significantly to the high investment cost of the stack [2]. Therefore, lower loadings of platinum group metals can reduce significantly the overall cost of PEM electrolysis. In this work we synthesise nano-sized iridium particles by reducing  $\text{IrCl}_3$  in anhydrous  $\text{C}_2\text{H}_6\text{O}$  at room temperature. Transmission electron microscopy (TEM) images show Ir clusters with a uniform particle size distribution (Figure 1a). X-ray diffraction (XRD) analysis reveals a cubic face centred structure of the Ir nanoparticles with a crystallite size of approx. 1.8 nm. X-ray photoelectron spectroscopy (XPS) confirms the metallic properties of the Ir particles covered with a very thin oxide layer. Atomic force microscopy (AFM) measurements show that a catalyst layer containing the Ir nanoparticles and Nafion ionomer has a non-uniform surface electrical conductivity. Rotating disc electrode (RDE) investigations such as cyclic and linear voltammetry are performed and the results compared with commercial Ir black. The synthesized catalyst shows a nine-fold higher activity towards oxygen evolution reaction (OER) than Ir black at 0.25 V overpotential and 25°C. This result is in good agreement with the CO-stripping measurements (Figure 1b) from which  $6.9 \times 10^{-4}$  and  $4.4 \times 10^{-4} \text{ mol}_{\text{CO}} \text{ gr}_{\text{Ir}}^{-1}$  active sites are determined for Ir nanoparticles and Ir black, respectively. The effect of thermal treatment and electrochemical performance of the catalysts in the PEM electrolyser are discussed as well.

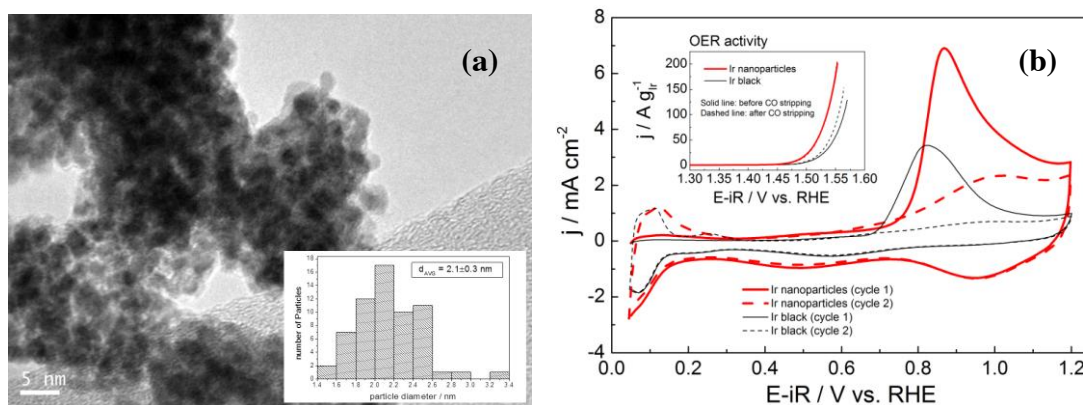


Fig. 1. (a) TEM image with particle size distribution of Ir nanoparticles and (b) CO-stripping in comparison with commercial Ir black. The measurements were carried out at a scan rate of  $50 \text{ mV s}^{-1}$ , in Ar-saturated 0.5 M  $\text{H}_2\text{SO}_4$  electrolyte. The inset of (b) shows the corresponding mass activity characteristics for OER measured at  $5 \text{ mV s}^{-1}$ . The rotation speed of the electrode is 2500 rpm.

## References

- [1] M. Carmo, D.L. Fritz, J. Mergel, D. Stolten, *Int. J. Hydrogen Energy* 38 (2013) 4901.
- [2] K.E. Ayers, E.B. Anderson, C. Capuano, B. Carter, L. Dalton, G. Hanlon, J. Manco, M. Niedzwiecki, *ECS Trans.* 33 (2010) 3.

# Assembly of hybrids based on Keggin POMs and Co-tris(imidazolyl) complexes with bifunctional electrocatalytic activities

Wanli Zhou,<sup>ab</sup> Jun Peng,<sup>\*a</sup>

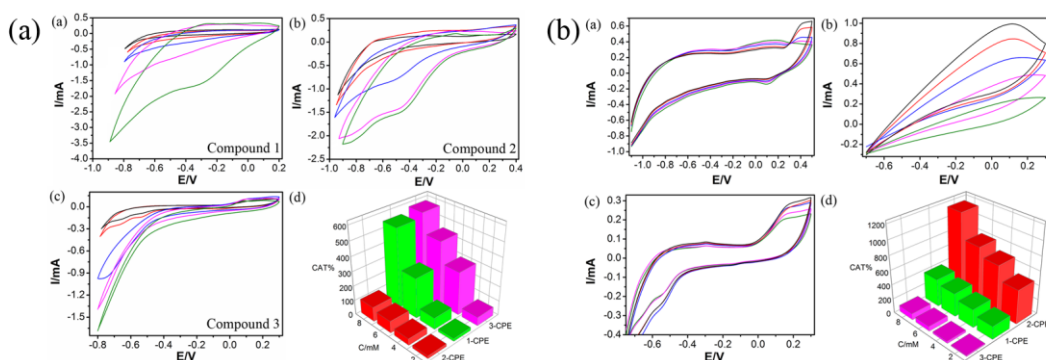
<sup>a</sup> Key Laboratory of Polyoxometalate Science of Ministry of Education, Faculty of Chemistry, Northeast Normal University

Changchun, Jilin, 130024, PR China

<sup>b</sup> Faculty of Chemistry, Tonghua Normal University

Tonghua, Jilin, 134002, PR China

E-mail: jpeng@nenu.edu.cn



Three new organic-inorganic hybrid compounds based on the Keggin POMs and Co-tib motifs were hydrothermally synthesized by utilizing a pH-dependent approach in the same POM/Co/tib reaction systems. The electrocatalytic properties of compounds **1-3** were studied by cyclic voltammetry, and compounds **1-3** displayed bifunctional electrocatalytic activities toward reduction of nitrite and oxidation of ascorbic acid (AA). The electrocatalytic efficiencies of n-CPE are in an order of **3-CPE** > **1-CPE** > **2-CPE** for nitrite reduction, and **2-CPE** > **1-CPE** > **3-CPE** for AA oxidation. These results indicate that Keggin  $\alpha$ -BW<sub>12</sub> hybrids exhibit better performances than that for Keggin  $\alpha$ -SiW<sub>12</sub> hybrid towards electrocatalytic reduction of NO<sub>2</sub><sup>-</sup>, and conversely, Keggin  $\alpha$ -SiW<sub>12</sub> hybrid exhibits a better performance towards electrocatalytic oxidations of AA than those for Keggin  $\alpha$ -BW<sub>12</sub> hybrids. The differences of electrocatalytic performances between the two series of Keggin POM hybrids and among  $\alpha$ -BW<sub>12</sub> hybrids are perhaps due to the differences in their structures and electrochemical properties.

We thank the National Natural Science Foundation of China (Grant 21373044) for financial supports.

## References

- [1] B. X. Dong, J. Peng, A. X. Tian, J. Q. Sha, L. Li, H. S. Liu, *Electrochim. Acta.*, 2007, 52, 3084.
- [2] W. L. Zhou, J. Peng, Z. Y. Zhang, Z. Y. Shi, S. U. Khan, H. S. Liu, *RSC Adv.*, 2015, 5, 35753.

# SUCCESSFUL STRATEGIES TO OVERCOME THE CARBON ELECTRODE SURFACES FOULING OF PHENOLS

Abdel-Nasser Kawde  
*Chemistry Department, King Fahd University of Petroleum and Minerals,  
Dhahran, 31261, Saudi Arabia  
akawde@kfupm.edu.sa*

The first strategy to overcome the well-known carbon electrodes surface fouling of phenols is about a simple and rapid method for the preparation of a disposable porous Cu-modified graphite pencil electrode (Cu-GPE) for sensing 4-nitrophenol (4-NP). The bare and Cu-modified graphite pencil electrodes were characterized by cyclic voltammetry and SEM. The two electrodes displayed distinct electrocatalytic activities in response to the electrochemical redox reaction of 4-NP. A difference of three orders of magnitude is obtained in the amperometric detection limits of 1.9 mM on porous Cu-modified vs. 1.0 mM on bare-graphite pencil electrode at 3s. The Cu-GPEs are fabricated utilizing a simple single method, and at an extremely low cost with high stability, selectivity, and sensitivity, offering a promising tool for sensing 4-NP.

The second strategy was developed for phenol and chlorophenols, and conducted on the surface of glassy carbon by cyclic and square-wave stripping voltammetry, and by Fourier-transform infrared spectroscopy. The surface fouling is accompanied by the appearance of reversible peaks at lower potential range (+0.1 to +0.4 V), which grew up with CV cycling and attributed to the electro-redox reactions of formed polymer film via electropolymerization. The electroanalytical monitoring of formed polymer oxidation peaks improved both sensitivity and detection limit by thirty-five and ten times, respectively. The FT-IR supported semiempirical prediction attributed the electropolymerization to the formation of ortho-para and/or ortho-meta C-C coupled-system.

## Acknowledgments

The author acknowledges the support provided by King Fahd University of Petroleum & Minerals (KFUPM) for funding this work through project no. SB141010.

## References

1. A. Kawde and Md. Aziz, Porous Copper-Modified Graphite Pencil Electrode for the Amperometric Detection of 4-Nitrophenol, *Electroanalysis*, 26 (2014) 2484.
2. A. Kawde, M. Morsy and N. Odewunmi, Electroanalytical Determination of Phenols, US Patent, USPTO (2014) 14/242,844.
3. A. Kawde, M. Morsy, N. Odewunmi, W. Mahfouz, From Electrode Surface Fouling to Sensitive Electroanalytical Determination of Phenols, *Electroanalysis*, 25 (2013) 1547.

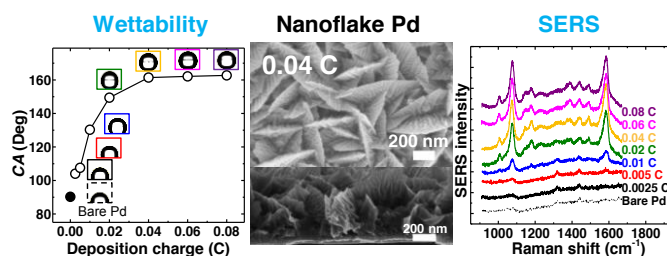


# Electrodeposition of Nanoflake Pd Structures: Structure-Dependent Wettability and SERS Activity

Hwakyeung Jeong, Jongwon Kim\*

Department of Chemistry, Chungbuk National University  
Cheongju, Chungbuk 361-763, Korea  
hkborn@naver.com

The nanostructured metal surfaces have unique physical and chemical properties different from bulk state, and then such metal surfaces provide various applications. Specific properties of nanostructured metal surfaces can be controlled by their shape and size. Therefore, the fabrication of well-defined nanostructured metal surfaces has been the subject of intensive research. The electrodeposition methods with simplicity in fabrication route provide clean nanostructured metal surfaces. In this work, a one-step electrodeposition of nanoflake Pd structures onto clean Au surfaces without the use of additives was reported. The fine structure of the nanoflake Pd surfaces was regulated by controlling the deposition charge. The wetting property and surface-enhanced Raman scattering (SERS) activity among the characteristic properties of nanostructured metal surfaces have been received great attention. The wettability of solid surfaces is important in many technological fields, such as fabrication of self-cleaning materials, manipulation of biomaterials, and microfluidics. And the SERS techniques provide useful applications, such as biological sensing and trace analysis. In present work, the effect of the structural variations on the wettability and SERS activity was examined. The wettability of nanoflake Pd structures was closely related to the fine structures of Pd deposits and their surface roughness. The SERS activity of the nanoflake Pd surfaces was dependent on the sharp edge sites on the Pd structures. Nanoflake Pd structures with deposition charge of 0.04 C exhibited superhydrophobic natures and reproducible SERS activity. The effect of the metal surface structures on the wettability and the SERS activity provides insight into the fabrication of functional metal nanostructures.



## Reference

- (1) Lafuma, A.; Quere, D. *Nat. Mater* **2003**, 2, 457-460
- (2) Yang, C.; Tartaglino, U.; Persson, B. N. J. *Phys. Rev. Lett.* **2006**, 97, 116103
- (3) Choi, S.; Jeong, H.; Choi, K.-h.; Song, J.Y.; Kim, J. *ACS Appl. Mater. Interfaces* **2014**, 6, 3002-3007
- (4) Xu, D.; Yan, X.; Diao, P. *J. Phys. Chem. C* **2014**, 118, 9758-9768

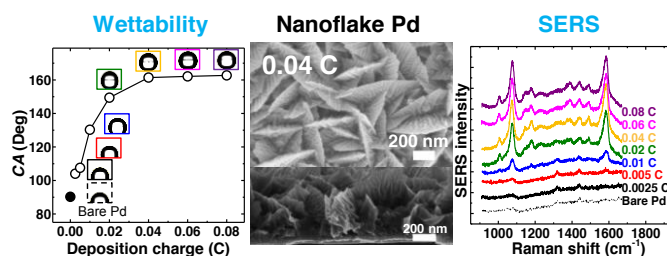


# Electrodeposition of Nanoflake Pd Structures: Structure-Dependent Wettability and SERS Activity

Hwakyeung Jeong, Jongwon Kim\*

Department of Chemistry, Chungbuk National University  
Cheongju, Chungbuk 361-763, Korea  
hkborn@naver.com

The nanostructured metal surfaces have unique physical and chemical properties different from bulk state, and then such metal surfaces provide various applications. Specific properties of nanostructured metal surfaces can be controlled by their shape and size. Therefore, the fabrication of well-defined nanostructured metal surfaces has been the subject of intensive research. The electrodeposition methods with simplicity in fabrication route provide clean nanostructured metal surfaces. In this work, a one-step electrodeposition of nanoflake Pd structures onto clean Au surfaces without the use of additives was reported. The fine structure of the nanoflake Pd surfaces was regulated by controlling the deposition charge. The wetting property and surface-enhanced Raman scattering (SERS) activity among the characteristic properties of nanostructured metal surfaces have been received great attention. The wettability of solid surfaces is important in many technological fields, such as fabrication of self-cleaning materials, manipulation of biomaterials, and microfluidics. And the SERS techniques provide useful applications, such as biological sensing and trace analysis. In present work, the effect of the structural variations on the wettability and SERS activity was examined. The wettability of nanoflake Pd structures was closely related to the fine structures of Pd deposits and their surface roughness. The SERS activity of the nanoflake Pd surfaces was dependent on the sharp edge sites on the Pd structures. Nanoflake Pd structures with deposition charge of 0.04 C exhibited superhydrophobic natures and reproducible SERS activity. The effect of the metal surface structures on the wettability and the SERS activity provides insight into the fabrication of functional metal nanostructures.



## Reference

- (1) Lafuma, A.; Quere, D. *Nat. Mater* **2003**, 2, 457-460
- (2) Yang, C.; Tartaglino, U.; Persson, B. N. J. *Phys. Rev. Lett.* **2006**, 97, 116103
- (3) Choi, S.; Jeong, H.; Choi, K.-h.; Song, J.Y.; Kim, J. *ACS Appl. Mater. Interfaces* **2014**, 6, 3002-3007
- (4) Xu, D.; Yan, X.; Diao, P. *J. Phys. Chem. C* **2014**, 118, 9758-9768

# Electrochemical Formation of Cu Nanoparticles in Tributyl-Methylammonium bis((trifluoromethyl)sulfonyl)imide Room-Temperature Ionic Liquid

Nai-Chang Lo<sup>a</sup>, Po-Yu Chen<sup>b\*</sup>

<sup>a</sup>Department of Chemistry, National Cheng Kung University, Tainan 701, Taiwan

<sup>b</sup>Department of Medical and applied Chemistry, Kaohsiung Medical University Kaohsiung City 80708, Taiwan  
pyc@kmu.edu.tw

In this study, Cu nanoparticles (Cu NPs) were prepared by controlled-potential bulk electrolysis at -2.0 V and dispersed in tributylmethylammonium bis((trifluoromethyl)sulfonyl)imide room-temperature ionic liquid (Bu<sub>3</sub>MeN-TFSI RTIL)<sup>1</sup>; the chemical structure of RTIL are shown in Fig 1. The Cu(I) species were introduced into the RTIL by anodic dissolution of a Cu metal wire. The Cu NPs shown in Fig 2 were characterized with transmission electron microscope (TEM) and scanning electron microscope (SEM). Then Cu NPs-IL were mixed with the graphite powder and spread onto the screen-printed carbon electrode (SPCE) to form the IL-graphite-CuNPs composite electrode (IL-GP-Cu NPs). The electrochemical behavior of IL-GP-Cu NPs were investigated in 1 M NaOH by cyclic voltammetry (CV), however, the stability of IL-GP-Cu NPs was not good enough and further experiments are still needed.

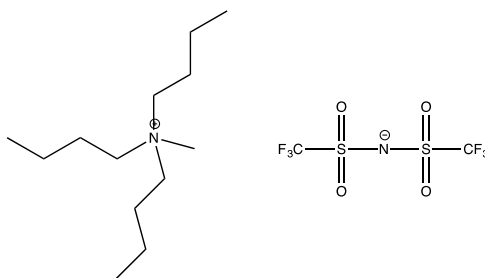


Fig 1. Chemical structure of Bu<sub>3</sub>MeN-TFSI

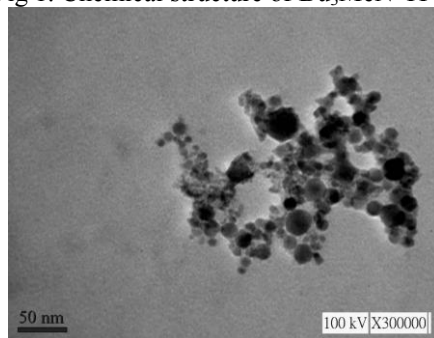


Fig 2. TEM image of Cu NPs

## Reference:

1. Matsumoto, H.; Yanagida, M.; Tanimoto, K.; Nomura, M.; Kitagawa, Y.; Miyazaki, Y., Highly conductive room temperature molten salts based on small trimethylalkylammonium cations and bis(trifluoromethylsulfonyl)imide. *Chem. Lett.* **2000**, (8), 922-923.

# Synthesis of Excavated Trioctahedral Au–Pd Alloy Nanocrystals with Tunable Composition for Electro-Oxidation of Ethanol

Qiaoli Chen, Zhaoxiong Xie\*

State Key Laboratory of Physical Chemistry of Solid Surfaces, Collaborative Innovation Center of Chemistry for Energy Materials, and Department of Chemistry, College of Chemistry and Chemical Engineering

Xiamen University, Xiamen 361005 (China)

E-mail: zxxie@xmu.edu.cn

Direct ethanol fuel cells (DEFCs) have received a great interest and attention due to its high energy density and easy storage and transport. Besides, ethanol is clean energy that can be produced from a wide range of sources.[1] But the mechanism of the electro-oxidation of ethanol is much complicated because it should cleave C–C bonds and refers to the transfer of 12 electrons.[2] What's more,  $\text{CH}_3\text{COOH}$  and  $\text{CH}_3\text{CHO}$  are always dominant in the final products. Ethanol is difficult to be oxidized on Pt-based electrocatalysts. In order to replace for platinum and pursue for fast kinetic and high stability, Pd-based nanocrystals are emerging as an attractive electrocatalysts in DEFCs, which are more active towards electro-oxidation of ethanol in alkaline media than in acidic media.[3] On the other hand, the catalytic activity is highly depended on the surface structure and composition of catalysts.[4] The excavated structures gather the features of high specific area and well-defined facets, which would lead to absolutely improvement on electrocatalytic performances. [5]

Herein, we report the synthesis of excavated trioctahedral Au–Pd alloy nanocrystals with tunable composition. It is also demonstrated that the as-prepared Au–Pd alloy nanocrystals exhibit higher electrocatalytic activity towards ethanol oxidation than Pd black. Figure 1 shows the characterization of the as-prepared Au–Pd alloys nanocrystals.

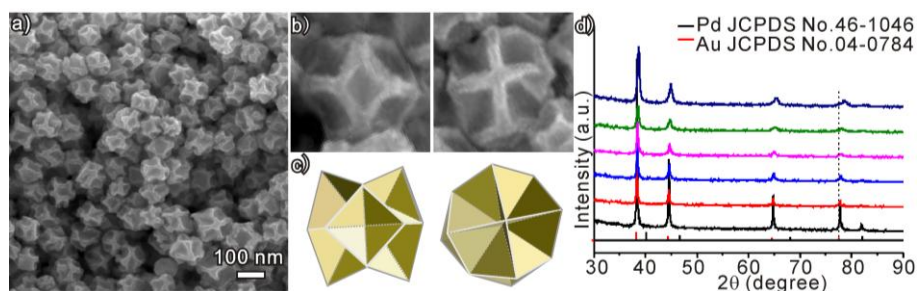


Figure 1. a) SEM image of Excavated Trioctahedral Au–Pd alloy nanocrystals; b-c) SEM image of magnified single Au–Pd nanocrystal and corresponding model; d) XRD pattern of Au–Pd alloy nanocrystals with different compositions.

This work was supported by the National Basic Research Program of China (2011CBA00508 and 2015CB932301), the National Natural Science Foundation of China (21131005, 21333008, and 21401155, J1310024)

## References

- [1] D. Y. Zhang, Z. F. Ma, X. X. Yuan, Chemical industry and engineering process, 24 (2005) 126-131.
- [2] G. A. Camara, T. Iwasita, J. Electroanal. Chem. 578 (2005) 315-321.
- [3] C. Bianchini, P. K. Shen, Chem. Rev. 109 (2009) 4183–4206.
- [4] N. Tian, Z. Y. Zhou, S. G. Sun, Y. Ding, Z. L. Wang, Science 316 (2007) 732-735.
- [5] Y. Jia, Y. Jiang, J. Zhang, L. Zhang, Q. Chen, Z. Xie, L. Zheng, J. Am. Chem. Soc. 136 (2014) 3748-3751.

# Electrochemical Responses of Transglutaminase Immunosensor Developed on a Polypyrrole-Cobalt (II) Salicyladiimine Dendritic Composite Material

Lindsay Wilson, Candice Rassie, Prof. P. Baker, Prof. E. Iwuoha  
SensorLab, Department of Chemistry, University of the Western Cape,  
Robert Sobukwe Road, Bellville, 7535, Cape Town, Republic of South Africa  
[2724554@myuwc.ac.za](mailto:2724554@myuwc.ac.za) and [eiwuoha@uwc.ac.za](mailto:eiwuoha@uwc.ac.za)

Transglutaminase (tTG), a calcium dependent enzyme catalysis protein cross linkages such as glutamine to the lysine on proteins. Transglutaminase exhibits high specificity towards glutamine substrates and forms an enzyme complex with gliadin that produces an immune response against this complex [1-2]. This immune response resulted in the identification of transglutaminase as the auto antigen of celiac disease. Since transglutaminase is predominantly involved in the activation and progression of celiac disease, it results in the production of antibodies against it. This then results in the harmful damage to the small intestine which reduces food digestion diffusion into the blood vessels [3]. The standard diagnosis of celiac disease is tedious and expensive. The diagnosis of coeliac disease can be done by the measurement of antibodies against transglutaminase [4]. In this work, an electrochemical impedimetric immunosensor was developed for the detection of anti-transglutaminase antibodies. The immunosensor consisted of a polypyrrole-cobalt (II) salicyladiimine metallodendrimer composite on a platinum electrode with transglutaminase as the recognition element. Atomic force microscopy was used to determine surface roughness of the modified platinum electrode with values of 879.24 nm, 76.55 nm and 364.27 nm for polypyrrole, cobalt (II) salicyladiimine and their respective composite. The composite provided a suitable micro-environment for monitoring antibody-antigen interactions in conjunction with their cyclic voltammetry. Electrochemical impedance spectroscopy parameters such as exchange current and heterogeneous rate constant are used to evaluate immunosensor where the rate constants were  $2.7 \times 10^{-6} \text{ cm}^2 \text{ s}^{-1}$ ,  $4.6 \times 10^{-6} \text{ cm}^2 \text{ s}^{-1}$  and  $4.16 \times 10^{-6} \text{ cm}^2 \text{ s}^{-1}$  for cobalt (II) salicyladiimine metallodendrimer, polypyrrole and their composite. Impedimetric detection of anti-transglutaminase antibody gave a limit of detection of 201 ng/mL and linear range of  $10^{-5}$  -  $10^{-4}$  mg/mL with correlation coefficient of 0.948.

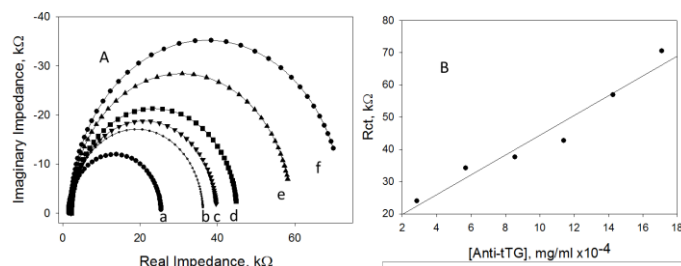


Figure 1. Nyquist plot for anti-tTG antibody incubation at, (a)  $2.85 \times 10^{-4}$  mg/mL, (b)  $5.7 \times 10^{-4}$  mg/mL, (c)  $8.55 \times 10^{-4}$  mg/mL, (d)  $11.4 \times 10^{-4}$  mg/mL, (e)  $14.25 \times 10^{-4}$  mg/mL, (f)  $17.1 \times 10^{-4}$  mg/mL and calibration graph for immunosensor  $R_{ct}$  versus anti-tTG antibody concentration in 0.1 M phosphate buffer. B) Calibration plot for the detection of anti-tTG antibody in 0.1 phosphate buffer.

## Ref.

1. A. Sabatino, A. Vanoli, P. Giuffrida, O. Luinetti, E. Solica, G. Corazza, *Autoimmunity Reviews*, 11 (2012) 746
2. S. Reif, A Lerner, *Autoimmunity Reviews*, 3 (2004) 45
3. W. Dieterich, T. Ehnis, M. Bauer, P. Donner, U. Volta, E. Riecken, D. Schuppan. *Nature Medicine*, 3 (1997) 7
4. L. Rivera, J. Sanchez, P. Sanchez, I. Katakis, C. O'Sullivan. *Biosensors and Bioelectronics*, 26 (2011) 4471

# Enhancement on ORR activity of N-doped carbon catalysts derived from melamine based polymer

Dong Wook Lee, Woong Hee Lee, Hansung Kim\*

Dept. of Chemical and Biomolecular Engineering, Yonsei University  
50 Yonsei-ro, Seodaemun-gu, 120-479, Seoul, Korea

\*e-mail: [elchem@yonsei.ac.kr](mailto:elchem@yonsei.ac.kr)

The study of the oxygen reduction reaction (ORR) is an important issue in fuel cell. Generally, Pt-based catalysts are used as the electrical catalyst for the ORR [1]. However, because of the high cost and limited supply of Pt, substantial research efforts have been devoted recently to develop a highly active non-noble catalyst for the ORR to replace Pt. Alternative materials such as metal oxides [2], transition metal chalcogenides [3], nitrogen-doped carbons [4] have been reported as non-precious ORR catalysts. Among them, nitrogen-doped carbons are highly favoured as non-precious metal catalysts for the ORR because of their relatively high activity and stability. Recently, melamine ( $C_3H_6N_6$ ), which is an industrial material with three triazine heterocyclic organic compound, has been extensively examined as a nitrogen precursor in the preparation of nitrogen-doped carbon catalysts because of its low-cost and high nitrogen content [5]. Various works using melamine were conducted previously. However, they were mostly used in the form of monomer.

In this study, we investigated the ORR activity of nitrogen-doped carbon catalysts that were prepared by pyrolyzing melamine-based polymer-coated carbon black and compared it with that prepared using melamine monomer as a nitrogen precursor. Additionally, we also examined the synergic effect of presence of cobalt. The linear sweep voltammogram that was conducted in an alkaline solution shows that the ORR activity of the nitrogen-doped carbon catalysts increases significantly close to that of Pt/C when a polymerized melamine is used as a nitrogen precursor instead of a melamine monomer. From the XPS-N 1s analysis, the introduction of the melamine-based polymer positively contributes to the nitrogen doping content and formation of a graphitic-N and pyridinic-N, which is known to be an active site for the ORR. Therefore, based on the quantitative analysis of the experimental results, melamine-based polymer is a promising precursor of nitrogen-doped carbon catalysts for ORR catalysts.

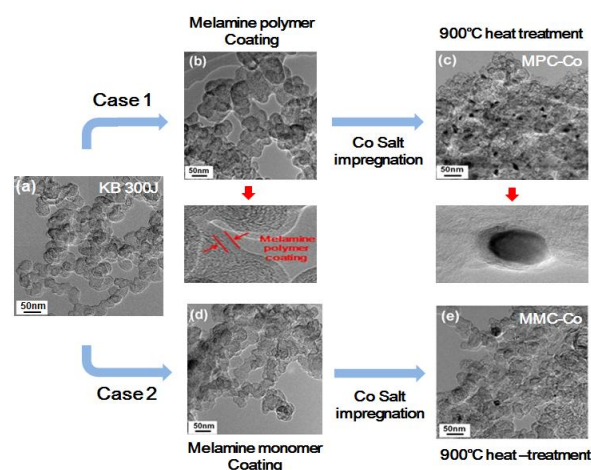


**Fig.1** HR-TEM images that correspond to each to prepare MPC-Co (case 1) and MMC-Co (case 2)

## References

1. C. Wang, H. Daimon, T. Onodera, T. Koda and S. Sun, *Angew Chem Int Ed Engl*, **47**, 3588 (2008).
2. F. Cheng, Y. Su, J. Liang, Z. Tao and J. Chen, *Chemistry of Materials*, **22**, 898 (2010).
3. M. R. Gao, J. Jiang and S. H. Yu, *Small*, **8**, 13 (2012).
4. H.-S. Oh, J.-G. Oh, W. H. Lee, H.-J. Kim and H. Kim, *International Journal of Hydrogen Energy*, **36**, 8181 (2011).
5. J. S. Lee, G. S. Park, S. T. Kim, M. Liu and J. Cho, *Angewandte Chemie*, **125**, 1060 (2013).

# Structure vs. Properties Relation in Novel RuPt Core-Edge Catalyst Nanoclusters

S. R. Brankovic<sup>1,2</sup>, Q. Yuan<sup>1</sup>, H. A. Doan<sup>2</sup> and Lars Grabow<sup>2</sup>

1) Electrical and Computer Engineering Department

2) Chemical and Biomolecular Engineering Department

University of Houston, Houston TX 77204-4005

SRBrankovic@uh.edu

Using a two-step process consisting of underpotential deposition techniques and surface limited red-ox replacement a novel so called “2D core-edge” monolayer catalyst morphology was synthesized. The core-edge nanoclusters are deposited on Au(111) and are composed of a Ru core surrounded by a Pt edge, RuPt<sub>ML-CE</sub>/Au(111). STM analysis confirms that the synthesized 2D core-edge nanoclusters are of monoatomic height and CV experiments confirm their superior CO electro-oxidation activity that exceeds the activity of Ru<sub>ML</sub>/Au(111) and Pt<sub>ML</sub>/Au(111) by nearly an order of magnitude. The unique catalytic activity of the RuPt<sub>ML-CE</sub>/Au(111) catalyst is explained in terms of its rich adsorption energy landscape, which is a direct result of the surface reconstruction of the Ru core to form concentric ripples, Figure 1 [1]. The characteristics of the adsorption energy landscape of the rippled core-edge structure were determined by a combination of DFT calculations and SNFTIRS experiments and point towards thermodynamically favorable radial transport from the Ru core to the active Ru-Pt interface. The diffusion of OH in the radial direction is slow, while CO is relatively mobile. Based on the experimental and computational data we propose a mechanism in which immobile OH species prevent CO diffusion and cause a transport controlled current plateau in the CV graph at low potentials. At higher potentials the Ru core region becomes active for CO oxidation leading to temporary removal of OH. This allows rapid diffusion of CO in the Ru core region to the Ru-Pt interface, where it can rapidly react. We postulate that the investigated RuPt<sub>ML-CE</sub>/Au(111) catalyst has

(electrochemical) applications beyond CO oxidation, e.g. methanol oxidation, and that analogous core-edge structures with different metal components can be synthesized. Our synthesis technique for the preparation of this novel 2D morphology opens up a new and entirely unexplored design space for monolayer catalysts, specifically if a reaction can benefit from bi-functional catalytic behavior.

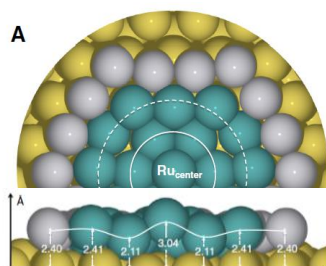


**Figure 1.** Half-cut of the RuPt core-edge nanocluster with cross-section showing the rippled morphology and displacement of the atoms with respect to underlying Au substrate.

<sup>1</sup> L. Grabow, Q. Yuan, H. A. Doan, and S.R. Brankovic, Surf. Sci. doi.org/10.1016/j.susc.2015.03.021



# Improved Visible-light Photoelectrochemical Water Oxidation using Titanium Dioxide /Antimony Trisulfide Heterojunction Structure

Yung-Tao Sung, Jun-Ming Chiu, Chao-Chi Tu, Lu-Yin Lin

Department of Chemical Engineering and Biotechnology, National Taipei University of Technology, 1 Sec. 3, Zhongxiao E. Rd., Taipei 10608, Taiwan, R.O.C., E-mail (L. Y. Lin\*): [lylin@ntut.edu.tw](mailto:lylin@ntut.edu.tw)

Since Fujishima and Honda have reported on the photoelectrolysis of water into hydrogen and oxygen on a  $\text{TiO}_2$  photoelectrode,<sup>1</sup> the semiconductor-based device for water splitting by solar energy has become one of the most important ways for oxygen generation.<sup>2</sup> Generally,  $\text{TiO}_2$  is one of the ideal candidates for its low cost, good photocatalytic activity, and chemical stability.<sup>3</sup> However, due to the large band gap ( $\sim 3.2$  eV),  $\text{TiO}_2$  can only harvest the ultraviolet (UV) light which takes only 5% of sunlight, resulting in low energy conversion efficiency.<sup>4</sup> Nonetheless, antimony trisulfide ( $\text{Sb}_2\text{S}_3$ ) has a smaller band gap ( $\sim 1.65$  eV) and band positions of  $-3.75$  and  $-5.4$  eV respectively for the conduction band and the valence band,<sup>5</sup> which is a suitable coating material for  $\text{TiO}_2$  nanorod array to perform oxygen generation. In this study,  $\text{Sb}_2\text{S}_3$  has been successfully synthesized by a chemical bath deposition method and coated onto the  $\text{TiO}_2$  nanorod arrays to form a heterojunction structure for obtaining higher photocurrent density. **Figure 1** is the scanning electron microscope (SEM) image of  $\text{TiO}_2$  nanorod array. The diameter and length of the nanorods are estimated to be  $0.1\ \mu\text{m}$  and  $2\ \mu\text{m}$ , respectively. The UV-visible spectroscopic measurement was carried out to the absorption of the samples as shown in **Figure 2**. It is observed that the  $\text{TiO}_2$  nanorod array hardly harvests light above  $400\ \text{nm}$ . On the contrary, the heterojunction structure shows an enhanced absorbance for the wavelength in the range of  $400$  to  $550\ \text{nm}$ . Finally, the photoelectrochemical performances of the electrode with  $\text{TiO}_2$  and  $\text{TiO}_2/\text{Sb}_2\text{S}_3$  heterojunction structures were measured by using a linear sweep voltammetry (LSV) plots as presented in **Figure 3**. An enhanced photocurrent density of  $0.32\ \text{mA}/\text{cm}^2$  at  $1.23\ \text{V}$  vs. RHE was obtained, which is higher than that of the electrode with bare  $\text{TiO}_2$  nanorod array. The better performance for the case with  $\text{TiO}_2/\text{Sb}_2\text{S}_3$  heterojunction structures is due to the enhanced visible light absorption and better electron migration resulting from the heterojunction property.

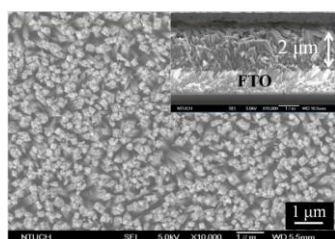


**Fig. 1** The SEM image of the top-view for  $\text{TiO}_2$  nanorod array, and the side-view image is also inserted in this figure.

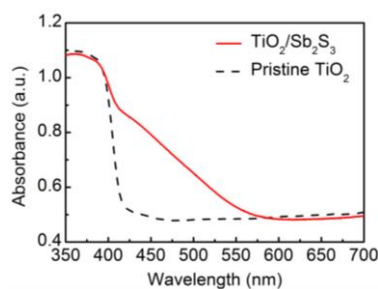


**Fig. 2** Absorption spectra of pristine  $\text{TiO}_2$  nanorod and  $\text{TiO}_2/\text{Sb}_2\text{S}_3$ .

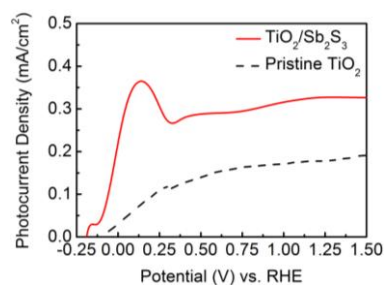


**Fig. 3** LSV plots of pristine  $\text{TiO}_2$  nanorod and  $\text{TiO}_2/\text{Sb}_2\text{S}_3$ .

## References

1. A. Fujishima *et al.*, *Nature*, 1972, 238, 37
2. M. Gratzel *et al.*, *Nature*, 2001, 414, 338
3. X. Chen *et al.*, *Chem. Rev.*, 2010, 110, 6503
4. J. Luo *et al.*, *J. Phys. Chem. C*, 2012, 113, 11956
5. Boxi *et al.*, *J. Phys. Chem. C*, 2012, 116, 1579

# Kinetic Isotope Effect on Hydrogen Evolution and Oxidation Reaction

Hisayoshi Matsushima, Shota Shibuya, Ryota Ogawa, Mikito Ueda  
Faculty of Engineering, Hokkaido University,  
Kita 13 Nishi 8, Sapporo, Hokkaido 060-8628, Japan  
matsushima@eng.hokudai.ac.jp

Water electrolysis has been studied for deuterium separation for long time. The advantage is the high separation factor. The effective separation mechanism is attributed to the kinetic factors for hydrogen evolution reaction (HER). Nowadays, many researchers have actively investigated the Tafel slope and the exchange current of a polycrystalline platinum electrode, while the kinetic studies of deuterium evolution reaction (DER) are hardly measured experimentally [1]. Concerning on hydrogen oxidation reaction (HOR) which is the reverse reaction of HER, the comprehensive investigation is still under discussion [2]. Moreover, the fundamental kinetic data of deuterium oxidation reaction (DOR) have not been measured at all. We have proposed the new separation system combined with PEM fuel cell [3] and investigated the electrochemical kinetic factors of the hydrogen electrode reactions in both acid and alkaline aqueous solutions.

The working electrode was a  $0.785 \text{ cm}^2$  polycrystalline Pt disk and the counter one was coiled Pt wire. The reference electrode was Hg/Hg<sub>2</sub>SO<sub>4</sub> saturated with K<sub>2</sub>SO<sub>4</sub>. The rotating disc electrode with the rotation rate of 900, 1600, 2500 and 3600 rpm was used. The polarization curves were recorded by linear sweep voltammetry at the scan rate of  $\pm 0.01 \text{ V s}^{-1}$ .

Figure 1 shows the polarization curves for (a) HER/HOR in 0.05 M H<sub>2</sub>SO<sub>4</sub> and (b) DER/DOR in 0.05 M D<sub>2</sub>SO<sub>4</sub> electrolyte. Before the electrochemical measurements, open circuit potentials (OCP) were -0.725 V in H<sub>2</sub>SO<sub>4</sub> and -0.730 V in D<sub>2</sub>SO<sub>4</sub> electrolyte, respectively. The evolution reaction currents were independent of the rotation rate in both electrolytes, while the oxidation ones were significantly influenced by the forced convection at more than (a) -0.65 V and (b) -0.70 V, respectively. The limiting current densities, which were induced by the diffusional limitation of the dissolved hydrogen gas, appeared at high electrode potential ( $E > -0.5 \text{ V}$ ). The separation factors during hydrogen evolution and oxidation reaction will be reported.

## REFERENCES

- [1] M. M. Jaksic, B. Johansen, R. Tunold, *Int. J. Hydrogen Energy*, **18**, 817 (1993).
- [2] B. E. Conway, B. V. Tilak, *Electrochim. Acta*, **47**, 3571 (2002).
- [3] H. Matsushima, T. Nohira, T. Kitabata, Y. Ito, *Energy*, **30**, 2413 (2005).

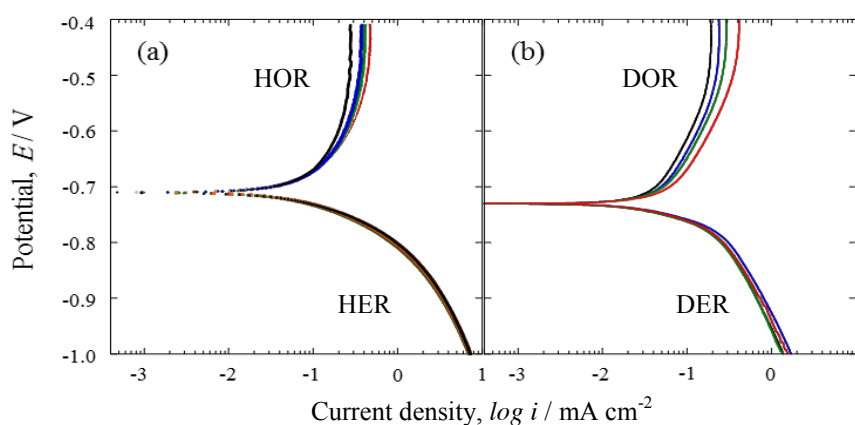


Figure 1 Polarization curves for (a) HER/HOR in 0.05 M H<sub>2</sub>SO<sub>4</sub> and (b) DER/DOR in 0.05 M D<sub>2</sub>SO<sub>4</sub> on Pt with several rotation rates, 900 rpm (black line), 1600 rpm (blue line), 2500 rpm (green line) and 3600 rpm (red line). (Sweep rate,  $0.01 \text{ V s}^{-1}$ ).



# Fabrication of nanostructured copper phosphate electrodes for the detection of $\alpha$ -amino acids

Ching-Chou Wu, Ming-Yuan Lee

Department of Bio-industrial Mechatronics Engineering, National Chung Hsing University

No. 250 Kuo-Kuang Rd. Taichung, Taiwan 402

ccwu@dragon.nchu.edu.tw

Increased attention has recently focused on the fabrication of different nanostructured copper compounds due to their unique surface-enhanced photocatalytic and electrocatalytic [1] characteristics.  $\text{Cu}_3(\text{PO}_4)_2$ -deposited electrodes capable of detecting nonelectroactive  $\alpha$ -amino acids (AAs) are developed by the dissolution-precipitation method. The  $\text{Cu}_3(\text{PO}_4)_2$ -dominated compounds of flake-shaped nanostructures, as shown in Fig. 1(a), can be quickly and uniformly deposited on the surface of acicula-nanostructured  $\text{Cu}(\text{OH})_2$ -electrodeposited electrodes in a 100 mM  $\text{Na}_2\text{HPO}_4$  solution (pH 5.0) within 2 h. Analysis of X-ray photoelectron spectroscopy and electrochemical kinetics shows an oxidative reaction at +0.11 V can increase the ratio of  $\text{H}_2\text{PO}_4^{1-}$  on the electrode surface and produce the  $\text{Cu}^{\text{II}}(\text{H}_2\text{PO}_4)_2$  complex. Moreover, the  $\text{Cu}^{\text{II}}$  compounds and the AAs can form complexes to accompany the chemical oxidation of AAs and the formation of the  $\text{Cu}^{\text{I}}$  complex, increasing the amount of oxidative current detected via the chemical-electrochemical mechanism. Figure 1(b) takes cysteine (Cys) as an example to show the electrocatalytic property of the  $\text{Cu}_3(\text{PO}_4)_2$  electrodes, presenting a diffusion-controlled behavior. The amperometric response presented good linearity and sensitivity in the range of 143–600  $\mu\text{M}$  for electroactive and nonelectroactive  $\alpha$ -AAs. The  $\text{Cu}_3(\text{PO}_4)_2$ -deposited electrode has potential as an AA sensor for integration into separation systems such as high performance liquid chromatography for use in biomedical diagnostics and food industry applications [2].

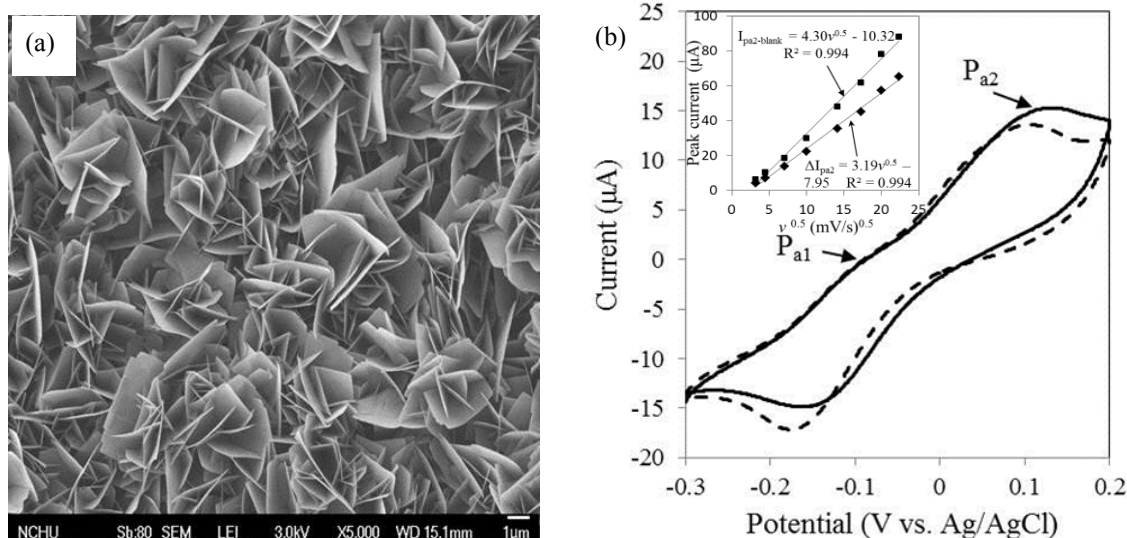


**Fig. 1** (a) SEM morphological images of the  $\text{Cu}(\text{OH})_2$ -deposited electrodes after being dipped for 2 h in 100 mM  $\text{Na}_2\text{HPO}_4$  solutions of 5.0 for 2 h. (b) The cyclic voltammograms (CVs) measured in blank (dashed line) and 1mM Cys-containing (solid line) 20 mM  $\text{Na}_2\text{HPO}_4$  (pH 5.0) with a 20 mV/s scanning rate. Inset shows the  $I_{Pa2-blank}$  and  $\Delta I_{Pa2}$  versus the square root of scan rate ( $v$ ).

[1] M.Y. Lee, J. Peng, C.C. Wu, Geometric effect of copper nanoparticles electrodeposited on screen-printed carbon electrodes on the detection of  $\alpha$ -,  $\beta$ - and  $\gamma$ -amino acids, *Sens. Actuators, B* 186 (2013) 270–277.

[2] M.-Y. Lee, S.-J. Ding, C.-C. Wu, J. Peng, C.-T. Jiang, C.-C. Chou, Fabrication of nanostructured copper phosphate electrodes for the detection of  $\alpha$ -amino acids, *Sens. Actuators, B* 206 (2015) 584–591.

# A poly(benzoxazine) as binder matrix for OER catalysts derived from Prussian blue analogue precursors

Stefan Barwe, Stefan Klink, Wolfgang Schuhmann

Analytical Chemistry – Center for Electrochemical Science (CES), Ruhr-Universität Bochum,  
Universitätsstr. 150, 44780 Bochum, Germany  
stefan.barwe@rub.de

Electrocatalysis is facing two major issues next to the development of low-cost and non-precious metal catalysts; catalysts have to be immobilized on an electrode surface in a stable manner and non-conductive catalysts necessitate the addition of conducting additives. In our work we introduce poly(benzoxazine) (pBO) resins as a new class of binder material into the field of electrocatalysis. pBOs consist of highly crosslinked networks of benzoxazine monomers or oligomers, whereas benzoxazines (BO) are heterocyclic compounds comprising an oxazine ring connected to a benzene ring. They arise from Mannich type reactions of primary amines, aldehydes and phenol derivatives. The complexity due to the large variety of starting materials leads to a nearly endless diversity in possible new benzoxazine resins with properties such as (i) near-zero shrinkage during polymerization, (ii) little water absorption, (iii)  $T_g$  higher than other thermosets, (iv) no need of strong acids and bases as catalysts, (v) economical and commercial available starting materials and (vi) no side-products after polymerization.<sup>1</sup>

Thermal polymerization of a mixed film of a bisphenol A and aniline based BO monomer and a Prussian blue analogue (PBA) drop-casted on an electrode surface led to a polymer layer with incorporated PBA particles (Figure 1). Pyrolysis transformed the deposited pBO/PBA film into a conducting carbon matrix doped with metal oxides (Figure 1). The metal oxide composition is determined by the PBA precursor used for drop-casting, various stoichiometries of Ni, Co, Mn and Fe are possible. Scanning electron microscopy (SEM) and energy dispersive X-ray spectroscopy (EDX) verify the composition and appearance of the resulting metal oxide particles. Moreover, the cubic structure of a manganese hexacyanocobaltate precursor is not affected by the pyrolysis and inclusion into the carbon matrix. The produced C/PBA composites show a significant activity towards the OER (while a pure pBO based carbon matrix shows no activity), furthermore is it exceeding the activity of the pyrolysis product of the same PBA immobilized in a Nafion layer. Consecutive cyclic voltammograms exhibit a rising catalytic activity with each cycle. This increase in activity is evoked by the detachment of carbon matrix, releasing more and more active sites of the catalyst. Galvanostatic measurements promote the catalyst activation and reveal a stability of at least 14 h. Hence, we were able to generate OER active catalysts, based on transition metal oxides, embedded into a conducting carbon matrix with a good stability via pyrolysis of a two-component system directly on an electrode surface, obviating the need of additional binder or conducting additives.

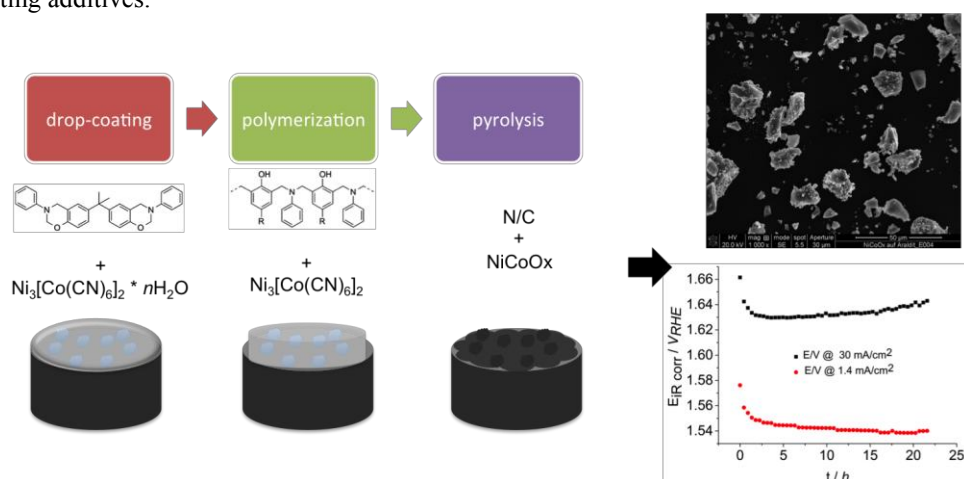


Figure 1: Schematic representation of the electrode preparation; SEM picture of  $\text{NiCoOx}$  particles; measured potential change at two different current densities (black squares: potential at 30  $\text{mA}/\text{cm}^2$ ; red circles: potential at 1.4  $\text{mA}/\text{cm}^2$ ).

<sup>1</sup> N. N. Ghosh, B. Kiskan, Y. Yagci, *Progr. Polym. Sci.* **2007**, 32, 1344

# Three-dimensional Nickel Film Electrodeposited on Porous Carbon Sponge: High Catalytic Performance and Low-cost Anode for Urea Electro-oxidation in Alkaline Medium

Ke Ye<sup>\*</sup>, Dianxue Cao, Hongyu Zhang, Long Yang, Xin Wang, Kui Cheng

Key Laboratory of Superlight Materials and Surface Technology, Ministry of Education, College of Materials Science and Chemical Engineering, Harbin Engineering University, Harbin, 150001, P.R. China.

e-mail address: yeke@hrbeu.edu.cn

In order to satisfy the increasing global demands for energy, alternative clean energy sources independent of fossil fuels, must be developed. Urine is the most abundant waste on the earth. The largest constituent of human or animal urine is urea ( $\text{CO}(\text{NH}_2)_2$ ), which is a significant organic source of H, C, O, and N. In addition, a large amount of wastewater with different concentrations of urea is produced during the industrial synthesis of urea, suggesting the availability of a considerable amount of urea in municipal wastewater. Thus, urea rich wastewater has been identified as a source for sewage disposal, hydrogen production and fuel cells [1]. Direct urea fuel cell (DUFC) is composed of urea in alkaline electrolyte as the fuel and humidified oxygen as the oxidant. The theoretical open circuit voltage of DUFC is 1.147 V, which is comparable with that of  $\text{H}_2\text{--O}_2$  fuel cell (1.23 V). Highly efficient electrocatalysts play key roles for improvements of the DUFC performance [2]. Nickel is an ideal non-noble metal anode catalyst for DUFC due to its high activity with low cost, but the planar and flat nickel electrode had a defect that the onset oxidation potential of urea reached higher than 0.35 V (vs. Ag/AgCl), which would reduce the open circuit voltage of DUFC. Therefore, facile and reasonable design and fabrication of three-dimensional (3D) structures is imperative for high electrocatalytic activity towards urea electro-oxidation in alkaline medium. Highly porous 3D structures are one of the optimal candidates due to the superior porosity and high specific surface area which can afford easy transport pathways for both electrons and ions.

Herein, we report the Ni electrocatalysts directly deposited on the porous carbon sponge with high electrocatalytic performance for urea electro-oxidation in alkaline medium. Highly porous nickel@carbon sponge electrode with low cost is synthesized via a facile sponge carbonization method coupled with a direct potentiostatic electrodeposition of Ni on the surface of carbon sponge at a constant potential of  $-1.0$  V (vs. Ag/AgCl) for 4200 s (Fig. 1). The obtained electrodes are characterized by X-ray diffraction (XRD), scanning electron microscopy (SEM) and energy dispersive X-ray spectroscopy (EDX). The catalytic performances of urea electro-oxidation in alkaline medium are investigated by cyclic voltammetry (CV) and chronoamperometry (CA). The Ni@carbon sponge electrode exhibits three-dimensional open network structures with a large surface area. Remarkably, the Ni@carbon sponge electrode shows much higher electrocatalytic activity and lower onset oxidation potential towards urea electro-oxidation compared to a Ni/Ti flat electrode synthesized by the same procedure. The Ni@carbon sponge electrode achieves an onset oxidation potential of 0.24 V (vs. Ag/AgCl) and a peak current density of  $290 \text{ mA cm}^{-2}$  in  $5 \text{ mol L}^{-1}$  NaOH and  $0.10 \text{ mol L}^{-1}$  urea solutions accompanied with a desirable stability. The impressive electrocatalytic activity is largely attributed to the high intrinsic electronic conductivity, superior porous network structures and rich surface Ni active species, which can largely boost the interfacial electroactive sites and charge transfer rates for urea electro-oxidation in alkaline medium, indicating promising applications in fuel cells.

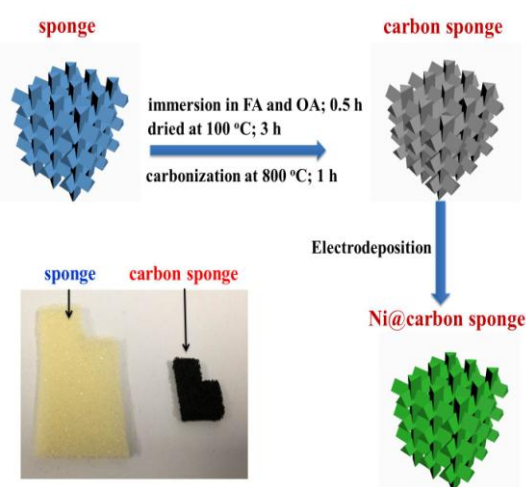


**Fig. 1.** Schematic diagram of the preparation process of Ni@carbon sponge electrode

[1] W. Yan, D. Wang, L.A. Diaz, G.G. Botte, *Electrochim. Acta* 134 (2014) 266–271.

[2] K. Ye, D. Zhang, F. Guo, K. Cheng, G. Wang, D. Cao, *J. Power Sources* 283 (2015) 408–415.

# Degradation of IrO<sub>2</sub>-Ta<sub>2</sub>O<sub>5</sub> / Ti anode with toluene contamination

Kenji Matsumae<sup>1)</sup>, Kohei Nagai<sup>1)</sup>, Yuji Kohno<sup>1)</sup>, Koichi Matsuzawa<sup>1)</sup>, Shigenori Mitsushima<sup>1, 2)</sup>

1) Green Hydrogen Research Center, Yokohama National University,

2) IAS, Yokohama National University.

79-5, Tokiwadai, Hodogaya-ku, Yokohama 240-8501, Japan

cel@ml.ynu.ac.jp

## Introduction

Organic chemical hydride system, especially toluene (TL) / methylcyclohexane (MCH) system, is one of the most efficient systems for hydrogen storage and transportation. We have focused on a direct hydrogenation electrolyzer to improve energy conversion efficiency of the TL / MCH system. In the electrolyzer, cathode and anode reactions are hydrogenation of TL and oxygen evolution reaction (OER), respectively. TL that crosses over from cathode to through electrolyte membrane would adsorb onto the anode surface. It causes the overpotential increase and the degradation acceleration [1]. IrO<sub>2</sub> based electrocatalyst-coated electrode often used for OER in acidic medium, and adding tantalum to IrO<sub>2</sub> based catalyst inhibits the overpotential increase by organic contamination [1]. However, degradation of IrO<sub>2</sub>-Ta<sub>2</sub>O<sub>5</sub> / Ti electrode with TL contamination had never reported enough.

In this study, we have studied the relationship between annealing temperature for IrO<sub>2</sub>-Ta<sub>2</sub>O<sub>5</sub> / Ti electrode and degradation of the anodes to improve high durability.

## Experimental

A working electrode was a Ti plate coated IrO<sub>2</sub>-Ta<sub>2</sub>O<sub>5</sub> by thermal decomposition at 500 or 700°C. The degradation was investigated under constant current electrolysis at 400 mA cm<sup>-2</sup> in 1 M (= mol dm<sup>-3</sup>) H<sub>2</sub>SO<sub>4</sub> with saturated TL and benzyl alcohol at 60°C in a 2-electrode electrochemical cell. During electrolysis, polarization and catalyst loading were determined by a 3-electrode electrochemical cell in 1 M H<sub>2</sub>SO<sub>4</sub> with or without saturated TL and X-ray fluorescence thickness meter.

## Result and discussion

Fig. 1 shows Ir loading and cell voltage as a function of time. The vertical arrows on the cell voltages show determination of electrochemical properties with 3-electrode electrochemical cell. After the determination, electrolysis continued. The change of cell voltages between before and after the determination might be affected by the change of behavior of the toluene adsorbed on the electrode. The Ir loading decreased with time, and the consumption rate of electrode for 700°C of the thermal decomposition temperature was lower than that for 500°C. The lifetimes, which were the time at 4 V of the cell voltage, tested electrode for 500°C and 700°C of thermal decomposition temperature were 250 h and 350 h, respectively. Therefore, high temperature thermal decomposition would decrease Ir consumption rate and extended lifetime of electrode.

Fig. 2 shows polarization curves of electrode for 700°C of thermal decomposition temperature before and after electrolysis in 1 M H<sub>2</sub>SO<sub>4</sub> with and without saturated TL. Before electrolysis, the decrease of current density by TL contamination was hardly observed. However, the current density decreased by TL contamination after electrolysis. Therefore, affinity of TL on the electrocatalyst might increase with consumption of the electrocatalyst during electrolysis and the difference of the current density with and without TL increased during electrolysis.

## Acknowledgment

This research has been supported by Cross-ministerial Strategic Innovation Promotion Program (SIP)-“energy carrier” (Funding agency: JST). We appreciated person concerned.

## Reference

[1] M. Takahashi, *Soda to Enso*, **39**, 531(1988)[ in Japanese].

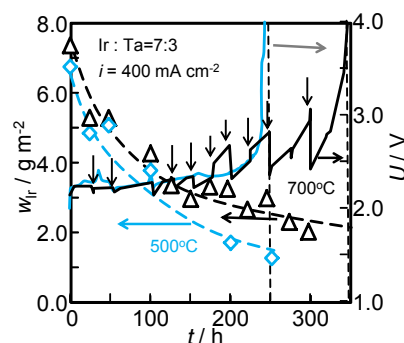


Fig. 1 Ir loading and cell voltage as a function of time for IrO<sub>2</sub>-Ta<sub>2</sub>O<sub>5</sub> / Ti at 500 and 700°C of the thermal decomposition, during electrolysis at 400 mA cm<sup>-2</sup> and 60°C in 1M H<sub>2</sub>SO<sub>4</sub> with saturated toluene and benzyl alcohol.

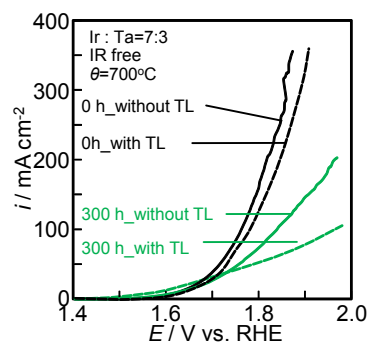


Fig. 2 Polarization curves for IrO<sub>2</sub>-Ta<sub>2</sub>O<sub>5</sub> / Ti at 700°C of the thermal decomposition before and after 300h of electrolysis at 400 mA cm<sup>-2</sup> and 60°C in 1M H<sub>2</sub>SO<sub>4</sub> with and without saturated toluene.

# Design and fabrication Co<sub>3</sub>O<sub>4</sub>-based electrode and its application for H<sub>2</sub>O<sub>2</sub> electroreduction

Kui Cheng\*, Shuying Kong, Tian Ouyang, Dianxue Cao

Key Laboratory of Superlight Material and Surface Technology of Ministry of Education, College of Material Science and Chemical Engineering, Harbin Engineering University, Harbin 150001, China  
e-mail address [chengkui@hrbeu.edu.cn](mailto:chengkui@hrbeu.edu.cn)

As one type efficient and clean energy converters, fuel cell has attracted much attention in recent years [1]. However at the current stage of technology, the cost is one of the big obstacles hindering the commercialization of fuel cells. Especially, the high noble metal loading required for the oxygen reduction reaction (ORR) occurred at the cathode region (0.4 mg cm<sup>-2</sup> Pt for ORR, 0.05 mg cm<sup>-2</sup> Pt for the anode reaction [2]). In order for the fuel cell to replace the internal combustion engines currently used, significant decrease in the cost is urgently required. Very recently, H<sub>2</sub>O<sub>2</sub> replaced O<sub>2</sub> as oxidant has been investigated in several low-temperature fuel cells, particularly in air-free environments (space or underwater) [3, 4]. That is due to its easy handling, storage, faster reduction kinetics than oxygen and higher standard reduction potential than oxygen [5, 6]. Recent study has also shown that H<sub>2</sub>O<sub>2</sub> as a powerful oxidant could significantly increase the power density of a fuel cell. Among several types of electrocatalysts for H<sub>2</sub>O<sub>2</sub> reduction, Co<sub>3</sub>O<sub>4</sub> have been conceived as a promising cost-effective and scalable alternative, in place of precious metals, for H<sub>2</sub>O<sub>2</sub> electroreduction.

A facile synthesis of morphology-controlled Co<sub>3</sub>O<sub>4</sub> nanostructures through the solvothermal synthesis was successfully demonstrated (Figure 1). With the control of the solvent composition, we have obtained five different nanostructures (nanosheet, nanowire, ultrafine nanowire net, nanobelts, and nano-honeycombs). The ethanol introduced in the synthesis processes plays an important role on the crystal size, morphology, as well as their catalytic performance for H<sub>2</sub>O<sub>2</sub> electroreduction. The sample prepared in the 2:1 C<sub>2</sub>H<sub>5</sub>OH/H<sub>2</sub>O solvent displays an ultra-fine nanowire net morphology, which possesses an open, porous nanostructure with a large surface area. These characteristics of Co<sub>3</sub>O<sub>4</sub> nanostructures make it facilitate electrons/ions transferring and enhance the catalytic efficiency when used as an electrode. The resulting electrode shows better performance for H<sub>2</sub>O<sub>2</sub> electroreduction in an alkaline medium in terms of the catalytic activity than Co<sub>3</sub>O<sub>4</sub> nanowire array electrode prepared in the pure water solvent. In the solution of 3.0 mol L<sup>-1</sup> KOH+0.5 mol L<sup>-1</sup> H<sub>2</sub>O<sub>2</sub>, the current density at -0.4 V could maintained at 0.214 A cm<sup>-2</sup> during the test period. This simple solvothermal method has a great potential for the preparation of morphology-controlled Co<sub>3</sub>O<sub>4</sub> nanostructures due to its facile synthesis, low cost, especially high performance for H<sub>2</sub>O<sub>2</sub> reduction.

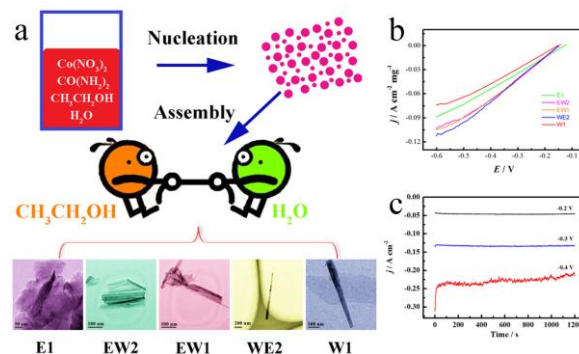


Figure 1 (a) Schematic diagram showing the mechanism for the formation of different nanostructures Co<sub>3</sub>O<sub>4</sub>. (b) The comparison of the as-prepared Co<sub>3</sub>O<sub>4</sub> nanostructures in the growth solution with different C<sub>2</sub>H<sub>5</sub>OH/H<sub>2</sub>O volume ratios. Chronoamperometric curves for H<sub>2</sub>O<sub>2</sub> reduction on the as-prepared Co<sub>3</sub>O<sub>4</sub> using C<sub>2</sub>H<sub>5</sub>OH/H<sub>2</sub>O volume ratio 1:2 (WE2) at different potentials.

- [1] K.-D. Kreuer, S. J. Paddison, E. Spohr, M. Schuster, *Chem. Rev.* **2004**, *104*, 4637-4678.
- [2] I. E. L. Stephens, A. S. Bondarenko, U. Gronbjerg, J. Rossmeisl, I. Chorkendorff, *Energy Environ. Sci.* **2012**, *5*, 6744-6762.
- [3] D. J. Brodrecht, J. J. Rusek, *Appl. Energy* **2003**, *74*, 113-124.
- [4] C. P. de León, F. C. Walsh, A. Rose, J. B. Lakeman, D. J. Browning, R. W. Reeve, *J. Power Sources* **2007**, *164*, 441-448.
- [5] D. Cao, J. Chao, L. Sun, G. Wang, *J. Power Sources* **2008**, *179*, 87-91.
- [6] J. Ma, Y. Sahai, R. G. Buchheit, *J. Power Sources* **2010**, *195*, 4709-4713.



# Carbonaceous Thin Film Coating with Fe–N<sub>4</sub> Site for Enhancement of Dioxovanadium Ion Reduction

Jun Maruyama<sup>a</sup>, Takahiro Hasegawa<sup>a</sup>, Satoshi Iwasaki<sup>a</sup>, Tomoko Fukuhara<sup>a</sup>, Yuki Orikasa<sup>b</sup>, Yoshiharu Uchimoto<sup>b</sup>

<sup>a</sup>Osaka Municipal Technical Research Institute, 1-6-50, Morinomiya, Joto-ku, Osaka 536-8553, Japan

<sup>b</sup>Kyoto University, Yoshida-nihonmatsu-cho, Sakyo-ku, Kyoto 606-8501, Japan  
maruyama@omtri.or.jp

Vanadium redox flow batteries (VRFBs) have attracted much interest as a promising electrical energy storage system due to their suitability for large-scale energy storage and capability to withstand fluctuating power supplies. The slow reaction rate of the electrode reactions is a serious problem in VRFB technology, which has to be overcome to improve the efficiency of the VRFB. Recently, the high catalytic activity was found at a carbonaceous thin film with Fe and four nitrogens (Fe–N<sub>4</sub> site) combined in a carbon matrix in the square-planar configuration and exposed to the surface [1]. The carbonaceous thin film was supported on cup-stack carbon nanotube (CSCNT). In this study, we investigated the influence of the amount of loading on the enhancement of the VRFB positive electrode reactions.

The *m*:1 (*m* = 0.1, 0.2, 0.5, 1) weight ratio mixture of iron phthalocyanine (FePc) powder and CSCNT was put in a crucible with a cap and heat-treated at 800 °C after raising the temperature at 1 °C min<sup>−1</sup> in an argon atmosphere. A treatment with an acid solution was carried out to remove any soluble metallic species from the surface. The obtained sample was then labeled CFePc*m*-800. The sample was characterized by a transmission electron microscope (TEM), X-ray photoelectron spectroscopy (XPS). The pore structure was examined by the nitrogen adsorption isotherm and the X-ray absorption fine structure (XAFS) at the Fe-*K* edge was measured to investigate the local structure around Fe.

Figure 1 shows the TEM images of CSCNT and CFePc1-800. The carbonaceous thin film derived from FePc was observed as well as aggregates of Fe. Figure 2 shows the relationships between the electrode potential and the current for the VO<sub>2</sub><sup>+</sup> reduction and VO<sub>2</sub><sup>2+</sup> oxidation. The VO<sub>2</sub><sup>2+</sup> oxidation current was increased by the coating between 0.8 and 1.0 V, but decreased above 1.0 V to be nearly half with an increase in *m* up to 1. In contrast, the VO<sub>2</sub><sup>+</sup> reduction current was significantly increased and reached the maximum at *m* = 0.2. The dependency on the amount of loading will be discussed based on the results on the specific surface area, the electrochemically active area measured by the cyclic voltammogram, the surface Fe concentration measured by XPS, the local structure around Fe.

[1] J. Maruyama, T. Hasegawa, S. Iwasaki, T. Fukuhara, Y. Orikasa, Y. Uchimoto, Extended Abstract, ES49, Carbon 2015, Dresden, Germany, July 15 (2015).

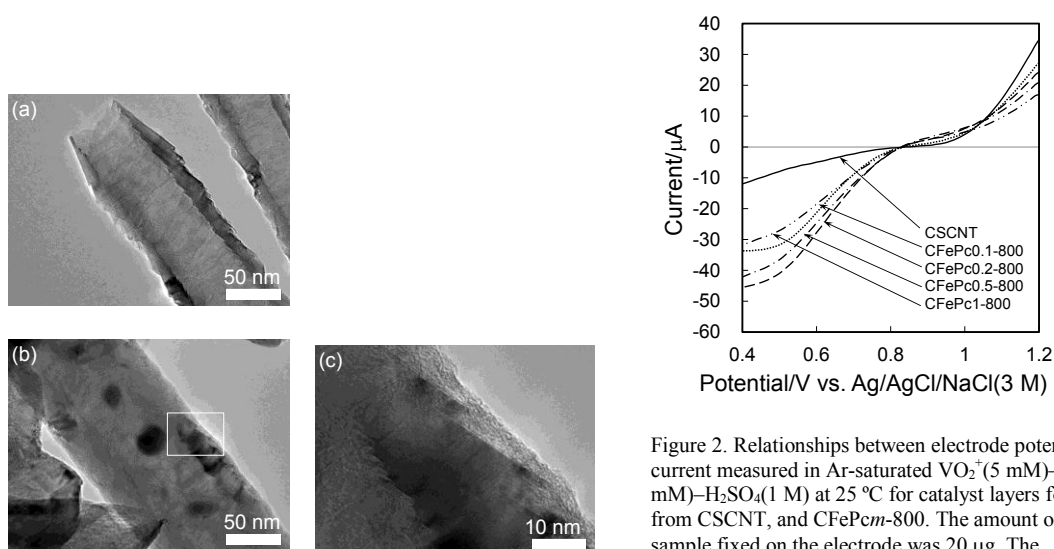


Figure 1. TEM images of (a) CSCNT and (b) CFePc1-800. Figure 1(c) shows an expanded image of the enclosed area in Figure 1(b).

Figure 2. Relationships between electrode potential and current measured in Ar-saturated VO<sub>2</sub><sup>+</sup> (5 mM)–VO<sub>2</sub><sup>2+</sup> (5 mM)–H<sub>2</sub>SO<sub>4</sub> (1 M) at 25 °C for catalyst layers formed from CSCNT, and CFePc*m*-800. The amount of the sample fixed on the electrode was 20 μg. The geometric electrode surface area was 0.071 cm<sup>2</sup>. The potential scan rate was 10 mV s<sup>−1</sup>. The rotation rate of the electrode was 2000 rpm.

# Preparing electrocatalysts for energy conversion by inkjet printing and photonic curing in one fabrication process

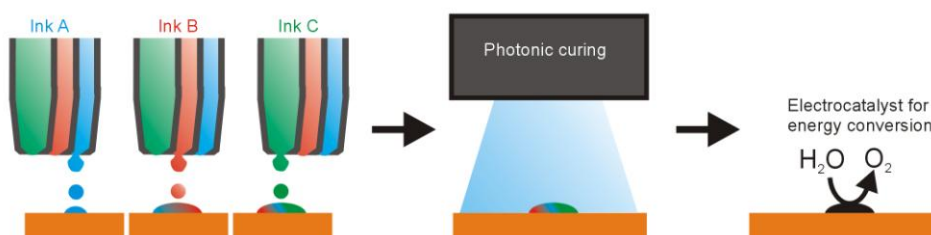
Andreas Lesch, Victor Costa Bassetto, Hubert H. Girault  
École Polytechnique Fédérale de Lausanne, Switzerland  
andreas.lesch@epfl.ch

Searching for new electrocatalysts gains in importance due to upcoming changes in the power grid, in particular with the integration of several electrochemical energy conversion and storage systems including fuel cells, electrolyzers and redox flow batteries. The underlying electrochemical reactions, for instance the oxygen reduction reaction (ORR) or the oxygen evolution reaction (OER), take place in catalyst layers in which electrocatalysts represent the active sites. Currently, precious metals (e.g. Pt) and precious metal oxides (e.g. IrO<sub>2</sub> and RuO<sub>2</sub>) supported on carbon black are the most commonly used electrocatalysts for the ORR and OER, respectively.

However, the use of such compounds is usually connected with high material cost, partially limited reserves and in case of ORR catalysts even low catalytic activity. Therefore, many efforts are made to either reduce the amount of required precious metals and to increase at the same time the catalyst utilization or to modify or replace the noble catalysts by alternative non-precious, low cost materials. Binary or ternary systems have found much attraction, but catalytic activity of such complex systems is difficult to predict. One approach is to prepare combinatorial catalyst libraries that can be screened for instance by optical methods or scanning electrochemical microscopy to identify the most active compositions.

One approach to prepare such libraries is made by dispensing metallic nanoparticle solutions or inks containing metal precursors by using inkjet printing.<sup>[1-3]</sup> Inkjet printing is a digital, mask-less material deposition technique where picoliter droplets decorate with micrometer resolution those substrate areas where a specific functionality is targeted. After the printing process, the ink is converted into a solid composition by thermal and/or chemical means to evaporate ink additives and to cure nanoparticles but also to favor the chemical reduction of metal cations. The applied temperatures for the latter can easily reach several hundred degrees Celsius requiring specific substrates and the temporary placement of the printed patterns inside a furnace. Recently, photonic curing has been introduced as a powerful non-equilibrium thermal post-processing tool for printing applications.<sup>[4]</sup> Thanks to light pulses in the millisecond range, generated from a Xenon flash lamp, the heat transferred during catalyst formation is mainly located in the ink and just on the substrate surface allowing the utilization of even low temperature substrate materials.

In this contribution, new approaches for employing an inkjet printer with three printheads and integrated photonic curing station for the inkjet printing and in-line photonic curing of various nanoparticulate and metal precursor inks (e.g. Pt, IrO<sub>2</sub>, Co<sub>3</sub>O<sub>4</sub> and Cu) will be introduced to obtain electrocatalysts, combinatorial libraries and catalyst layers.



## References:

- [1] E. Reddington, A. Sapienza, B. Gurau, R. Viswanathan, S. Sarangapani, E. S. Smotkin, T. E. Mallouk, *Science* **1998**, 280, 1735-1737.
- [2] X. Liu, Y. Shen, R. Yang, S. Zou, X. Ji, L. Shi, Y. Zhang, D. Liu, L. Xiao, X. Zheng, S. Li, J. Fan, G. D. Stucky, *Nano Letters* **2012**, 12, 5733-5739.
- [3] J. A. Haber, Y. Cai, S. Jung, C. Xiang, S. Mitrovic, J. Jin, A. T. Bell, J. M. Gregoire, *Energy Environ. Sci.* **2014**, 7, 682-688.
- [4] N. Marjanovic, J. Hammerschmidt, J. Perelaer, S. Farnsworth, I. Rawson, M. Kus, E. Yenel, S. Tilki, U. S. Schubert, R. R. Baumann, *J. Mater. Chem.* **2011**, 21, 13634-13639.

# Pd-based bimetallic nanocatalysts for alkaline glucose electrooxidation and fuel cells application

Cheng-Chuan Chen, and Lin-Chi Chen\*

Department of Bio-Industrial Mechatronics Engineering, National Taiwan University

No. 1, Sec. 4, Roosevelt Road, Taipei 10617, Taiwan

[chenlinchi@ntu.edu.tw](mailto:chenlinchi@ntu.edu.tw)

Direct glucose fuel cell (DGFC) is one of the potential green energy sources in the future because glucose, a six carbon sugar, is renewable, abundant and non-toxic in nature. One molecule of glucose can theoretically release 24 electrons and provide  $2870 \text{ kJ mol}^{-1}$  through a complete glucose oxidation reaction. Recently, several noble metal catalysts have been developed to improve the catalytic activity of DGFC [1,2]. However, only partial oxidation of glucose occurs practically and two electrons are released per molecule. This indicates that there is still plenty of room to improve the glucose catalytic performance. For this reason, the extensive investigation of electrocatalysts catalyze GOR has been made to generate a higher electricity. Very recently, there are many studies focus on finding an idea catalyst to improve the GOR efficiency. In this respect, the approach to find out a new electrocatalyst with the high catalytic activity and stability is a potential research direction in DGFC. Catalyst material often plays a determining role in fuel cell performance, and platinum (Pt) has long been a main and indispensable component for most anode catalysts, including the ones used for DGFC study. However, Pt is a costly noble metal and is easy to be self-poisoned by adsorbed intermediates. By this reason, palladium (Pd) based catalysts have been studied for electrocatalytic GOR in DGFC. It also has been known that the catalytic activity of Pd monometallic catalyst is still not sufficient to reach the notably higher GOR current density. Hence Pd-based bimetallic catalysts are used in alkaline glucose electrooxidation to reach a higher GOR current density through a synergistic effect [2]. This presentation focuses on studying the effects of carbon supported bimetallic Pd-based catalysts (Pd-Bi/C and Pd-Ni/C) prepared by an alkaline polyol synthesis and their application in DGFC. Physicochemical properties (e.g., XRD, XPS, and HR-TEM) and electrochemical behaviors (e.g., CV and CA) are studied to understand how catalysts affect the GOR performance. We also discuss the influence of surfaces properties of carbon supports on Pd catalyzed glucose in this work [3]. Compared to the Pd/C, the prepared catalysts provide the higher electrochemical surface area, improved catalytic activities, and better stability.

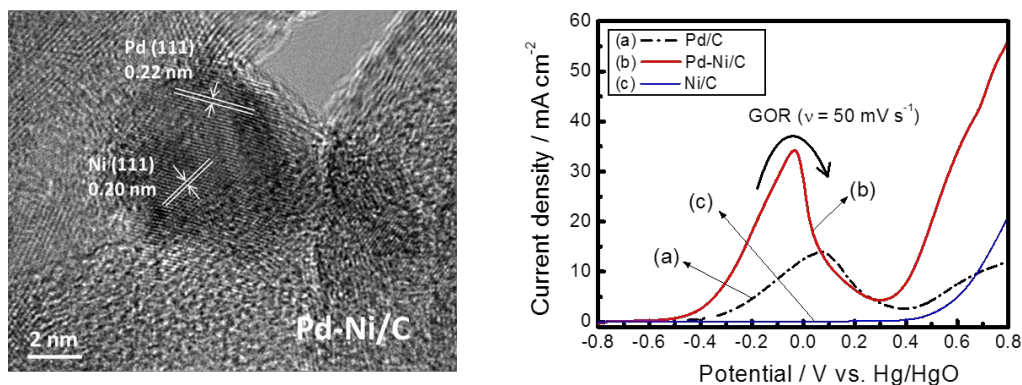


Fig. 1 Alkaline GOR performance of carbon supported Pd<sub>shell</sub>-Ni<sub>core</sub> electrocatalysts (Pd-Ni/C).

## References

- [1] L.L. Yan, A. Brouzgou, Y.Z. Meng, M. Xiao, P. Tsiakaras, S.Q. Song, Appl. Catal. B: Environ. 150 (2014) 268-274.
- [2] D. Basu, S. Sood, S. Basu, Chem. Eng. J. 228 (2013) 867-870.
- [3] C.C. Chen, C.L. Lin, L.C. Chen, Electrochim. Acta 152 (2015) 408-416.



# Carbon Cladded TiO<sub>2</sub> Nanotubes Enabling Highly Defined RuO<sub>2</sub> Decoration for Efficient Supercapacitor Performance

Yanyan Song,<sup>a</sup> Zhida Gao,<sup>a</sup> Patrik Schmuki<sup>b</sup>

<sup>a</sup> Research Center for Analytical Sciences, College of Sciences, Northeastern University  
Wenhua Road 3-11, Shenyang 110004, China  
yysong@mail.neu.edu.cn

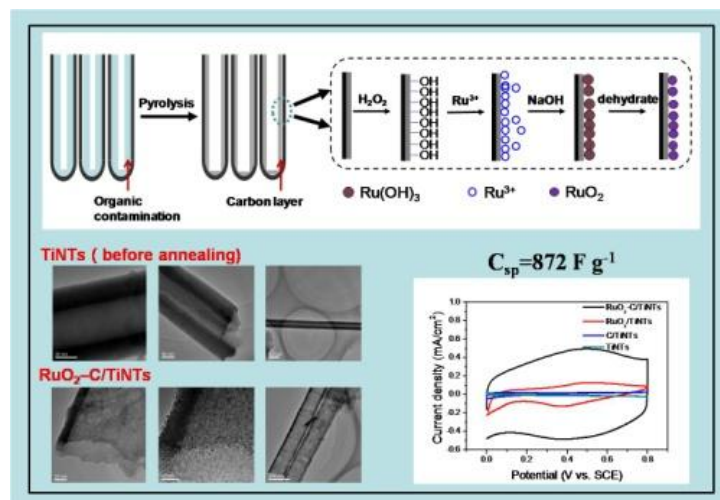
<sup>b</sup> Department of Materials Science, WW4-LKO, University of Erlangen-Nuremberg  
Martensstrasse 7, D-91058 Erlangen, Germany  
schmuki@ww.uni-erlangen.de

As a supercapacitor material, the gold standard is RuO<sub>2</sub> as it provides intrinsically fast, high and reversible intercalation properties and a comparatively high electron conductivity. For example, hydrous ruthenium oxide (HRO) has been reported to show a high mass specific capacitance of 600 to 750 F g<sup>-1</sup>. Nevertheless, the theoretical specific capacitance of 1400 to 2200 F g<sup>-1</sup>, is even higher. In order to more efficiently exploit the expensive HRO it should be ideally dispersed as a nanoparticle of only a few nm diameters on a suitable electron-conductive scaffold. In order to provide an ideal scaffold electrode geometries that provide an optimized ion diffusion path into the solid and through the electrolyte are desired. To address these requirements recently self-ordered TiO<sub>2</sub> nanotubular arrays have been explored directly for their super capacitive performance. Previous findings however show a limited success which is due to the comparably small and sluggish red-ox switching properties of TiO<sub>2</sub> (in all crystal polymorphs) and even more problematic is the limited electrical conductivity of the TiO<sub>2</sub> nanotubes

In this work we demonstrate a procedure that allows a highly conformal coating of self-organized TiO<sub>2</sub> nanotubes with a graphite-like thin carbon layer. This well conducting coating then can be further modified using established carbon chemistry to anchor an active RuO<sub>2</sub> nanoparticle layer on the tube walls. Used as 3D pseudocapacitor electrodes capacitance value of up to 87 times higher than plain TiO<sub>2</sub> nanotube arrays and a very high yield of utilization of RuO<sub>2</sub> can be reached. Additionally this configuration shows an excellent long-term cycling stability with only 4.4% decrease of initial capacitance after 1000 cycles. A key to this improvement is that here introduced treatment reduces the electrical conductivity of an anatase tube drastically. This opens up a platform to novel applications and enhanced functionality of TiO<sub>2</sub> nanotubes.

## Acknowledgements

This work was supported by the National Natural Science Foundation of China (No. 21322504, 11174046, 21275026), the Fundamental Research Funds for the Central Universities (N140505001, N140504006).



# One-step hydrothermal route to fabricate novel $\text{ZnIn}_2\text{S}_4/\text{g-C}_3\text{N}_4$ heterojunction photocatalysts with highly-efficient visible light response

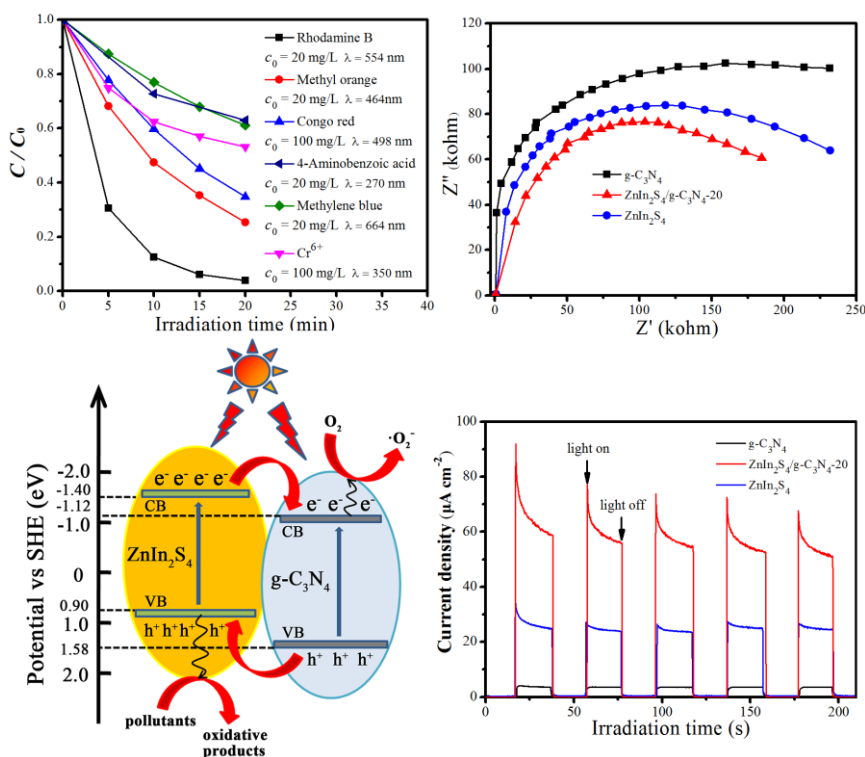
Xiaoheng Liu\*, Wei Chen

Key Laboratory of Education Ministry for Soft Chemistry and Functional Materials, Nanjing University of Science and Technology, Nanjing 210094, China

No. 200 Xiaolingwei street, Nanjing, Jiangsu province, China

xhliu@mail.njust.edu.cn

Heterogeneous  $\text{ZnIn}_2\text{S}_4/\text{g-C}_3\text{N}_4$  hybrid composites, as highly-efficient visible-light-driven photocatalysts, were firstly fabricated by a simple one-step hydrothermal route; wherein the porous  $\text{g-C}_3\text{N}_4$  ultrathin nanosheets (NSs) serve as platform supporting to in-situ immobilize the cubic  $\text{ZnIn}_2\text{S}_4$  nanoparticles (NPs). The resultant  $\text{ZnIn}_2\text{S}_4/\text{g-C}_3\text{N}_4$ -20 composite with 20 mg  $\text{g-C}_3\text{N}_4$  exhibits efficient photocatalytic activities, excellent photo-stability and versatile photocatalytic abilities towards organic dye degradation and Cr (VI) reduction. The significant enhancement of photocatalytic activity is attributed to the effective separation of photo-generated charge carrier pairs based on the construction of close heterogeneous interface, which can obviously lengthen the life span of holes and electrons pairs. The effective charge transfer from cubic  $\text{ZnIn}_2\text{S}_4$  to porous  $\text{g-C}_3\text{N}_4$  ultrathin NSs was confirmed by photoluminescence quenching, transient photocurrent-time (I-t) curves and electrochemical impedance spectroscopy (EIS) Nyquist plots.



# A method for the simultaneous cleansing of H<sub>2</sub>S and SO<sub>2</sub>

K. Petrov<sup>a</sup>, D. Uzun<sup>a</sup>, E. Razkazova-Velkova<sup>b</sup>, V. Beschkov<sup>b</sup>,

<sup>a</sup>*Institute of Electrochemistry and Energy Systems „Acad. Evgeni Budevski”, Bulgarian Academy of Sciences, Acad. G. Bonchev Str., Bl.10, 1113 Sofia, Bulgaria*

<sup>b</sup>*Institute of Chemical Engineering, Bulgarian Academy of Sciences, Acad. G. Bonchev Str., Bl. 103, 1113 Sofia, Bulgaria*

A method for the simultaneous electrochemical purification of hydrogen sulfide and sulfur dioxide from Black Sea waters or industrial wastes is proposed. Fundamentally the method is based on the electrochemical affinity of the pair H<sub>2</sub>S and SO<sub>2</sub>. The reactions (oxidation of H<sub>2</sub>S and reduction of SO<sub>2</sub>) proceed on proper catalyst in a flow reactor, without an external power by electrochemical means. The partial curves of oxidation of H<sub>2</sub>S and reduction of SO<sub>2</sub> have been studied electrochemically on different catalysts (CoPc/C; La<sub>1.3</sub>Sr<sub>0.7</sub>NiO<sub>4</sub>; Bulk Graphite; and 6% Pt/C). Following the additive principle the rate of the process has been found by intersection of the curves, shown in Fig.1.

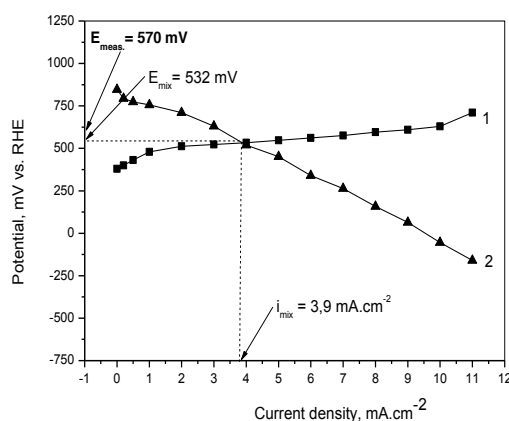


Fig. 1. Polarization curves for the oxidation of H<sub>2</sub>S (1) and the reduction of SO<sub>2</sub> (2).

The overall process rate has been studied in a flow type reactor. Similar values of the process rate have been found. This is a proof of the electrochemical mechanism of the reactions. As a result the electrochemical method at adequate conditions is developed. The process is able to completely convert the initial reagents (concentrations C<sub>H<sub>2</sub>S</sub>, C<sub>SO<sub>2</sub></sub> = 0), which is difficult given the chemical kinetics. Finally we should state, that the best application in our view, is the cleansing of H<sub>2</sub>S in Black Sea waters together with SO<sub>2</sub> containing gases from coal power plants located on the shore. The preliminary calculations show that 1 m<sup>3</sup> Black Sea water (C<sub>H<sub>2</sub>S</sub>=8 mg.l<sup>-1</sup>) converts SO<sub>2</sub> from 3 m<sup>3</sup> waste gas C<sub>SO<sub>2</sub></sub>=1000ppm).

## References:

- Spiro, M., Freund, P., 1983. *Journal of Electroanalytical Chemistry*, 144, p. 293.
- Wagner, C., Traud, W. Z., 1938. *Elektrochem*, 44, p. 391.
- Petrov, K., Srinivasan, S., 1996. *International Journal of Hydrogen Energy*, 21 pp. 163-169.
- Petrov, K., Baykara, S. Z., Ebrasu, D., Gulin, M., Veziroglu, A., 2011. *International Journal of Hydrogen Energy*, 36 pp. 8936-8942.



# Simultaneous scaling-free electrochemical production of caustic and oxygen from domestic wastewater for sulfide control in sewers

Hui-Wen Lin<sup>1</sup>, Korneel Rabaey<sup>1,2</sup>, Jurg Keller<sup>1</sup>, Zhiguo Yuan<sup>1</sup> and Ilje Pikaar<sup>1\*</sup>

<sup>1</sup>The University of Queensland, Advanced Water Management Centre (AWMC), QLD 4072, Australia

<sup>2</sup>Laboratory of Microbial Ecology and Technology (LabMET), Ghent University, Coupure Links 653, 9000 Ghent, Belgium

Email: [h.lin@awmc.uq.edu.au](mailto:h.lin@awmc.uq.edu.au)

\*Email: [i.pikaar@uq.edu.au](mailto:i.pikaar@uq.edu.au)

Hydrogen sulfide induced sewer corrosion is a notorious problem that costs wastewater utilities billions of dollars each year globally [1]. Two of the most commonly used chemical abatement strategies by the water industry are oxygen injection and periodic caustic shock-loading for killing/removal of the sewer biofilm responsible for hydrogen sulfide generation [2]. Although these two strategies are implemented successfully at full-scale, the frequent transport, handling, and storage of pure oxygen and caustic soda often come with serious safety concerns as well as with negative public image. Hence, on-site production approaches can alleviate many of these concerns.

Here we present a novel three-compartment electrochemical cell which simultaneously produces caustic and oxygen from sewage (Figure 1). The middle compartment is fed with a concentrated NaCl solution and is separated from the anode by an anion exchange membrane and from the cathode by a cation exchange membrane, creating a chloride flux from middle compartment to anode, and a sodium flux from middle compartment to cathode. Sewage was continuously fed to the anode and oxygen was continuously generated in the anode compartment. Cathode was operated in a batch mode where water was reduced to H<sub>2</sub> and OH<sup>-</sup> which recombines with the Na<sup>+</sup> to form NaOH.

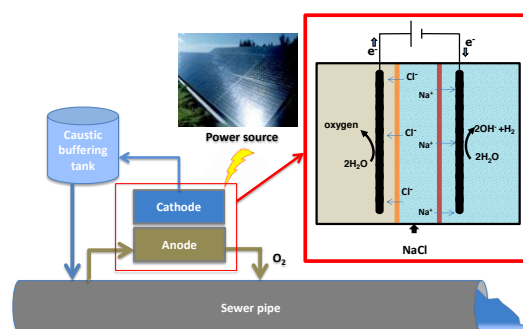


Fig. 1. Simplified schematic overview of the concept

Caustic was efficiently produced from sewage over a period of 12 weeks with an average Coulombic efficiency (CE) of 84.1±1.1% at practically relevant caustic strengths. Equally important, dissolved oxygen (DO), was continuously produced in the sewage at a CE of ~50%, a significantly higher efficiency than conventional oxygen injection (i.e. <30%) [3]. This continuous aeration of the sewage benefits sewer pipes downstream by maintaining aerobic conditions and oxidizing residual sulfide. The obtained DO levels in sewage ranged between 3.8-12.6 mg/L O<sub>2</sub>, depending on the current-to-flow ratio. The two produced chemicals can be applied to sewer pipes alternatively with caustic shock-loading to remove sewer biofilms and oxygen suppressing biofilm development between caustic shocks leading to prolonged biofilm recovery and thus reducing the required frequency for caustic addition. The only inputs to this system are electricity and sodium chloride. In a practical situation, the process can be driven by a solar panel, making it a very sustainable solution. It also eliminates the safety issues related to the transport and storage of concentrated chemicals. To the author's best knowledge, this is the first time that a sustainable solution is proposed to alleviate the notorious and costly problem for water utilities globally.

## References

- [1] I. Pikaar, K. R. Sharma, S. Hu, W. Gernjak, J. Keller, Z. Yuan, Reducing sewer corrosion through integrated urban water management, *Science*. 345(2014) 812-814.
- [2] R. Ganigue, O. Gutierrez, R. Rootsey, Z. Yuan, Chemical dosing for sulfide control in Australia: An industry survey, *Water Res.* 45 (2011) 6564-6574.
- [3] D. W. De Haas, K. Sharma, S. Corrie, K. O'Halloran, J. Keller, Z. Yuan, Odour control by chemical dosing: A case study, *Water Journal*. 35 (2008) 138-143.

# Validation of Polymeric artificial muscles with a Proportional- Integral control system

Valero, Laura L.<sup>1,2-a</sup>, Otero, Toribio F.<sup>2-b</sup>, Estévez, Angel<sup>1</sup> Rodríguez, Eduardo<sup>1</sup>

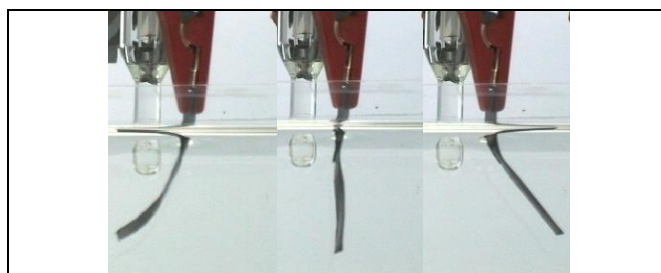
<sup>1</sup> Universidad Autónoma del Estado de México, Engineering school, Toluca 50000 México.

<sup>2</sup> Universidad Politécnica de Cartagena, Physical Chemistry, Center for Electrochemistry and Intelligent Materials (CEMI), 30203, Cartagena, Spain  
email: <sup>a</sup> [lvalero01@hotmail.com](mailto:lvalero01@hotmail.com), <sup>b</sup> [toribio.fotero@upct.es](mailto:toribio.fotero@upct.es).

**Keywords:** Artificial muscles, polymeric faradaic motors, movement control, position control system.

## Abstract:

Looking for engineers, physicists and robot applications use to consider polymeric bilayer actuators (or artificial muscles) as low reliable devices for soft tools or soft robotic developments. Here we present the electronic-mechanical (movement rate and position) characterization of a polypyrrole/tape bilayer bending actuator and how it was validated with a electronic proportional-integral (PI) control system. The angular rate of the movement results a linear function of the applied current and the described angle is a linear function of the consumed charge. The polypyrrole film was synthesized in presence of dodecylbenzene-sulphonate (DBS<sup>-</sup>) and ClO<sub>4</sub><sup>-</sup> anions: it exchanges cations during subsequent oxidation/reduction reactions. The correlation coefficients overcame 0.99: electro-chemo-mechanical polymeric motors are full reliable for technological applications. The electrochemical model explaining the relationships between charge, film volume variation, mechanical work, force and displacement. The applied engineering design requires new materials giving multifunctional devices: the best design is the one involving the lower number of components.



## Acknowledgments:

Authors acknowledge financial support from the Spanish Government (MCI) Project MAT2011-24973, the UAEM (Universidad Autónoma del Estado de México) – CONACYT Consejo Nacional de Ciencia y Tecnología (México) and COMECYT (Consejo Mexiquense de Ciencia y Tecnología). Jose G. Martinez acknowledges to the Spanish Education Ministry for a FPU grant (AP2010-3460).

## References

- [1] S. J. Ebbens, J. R. Howse, *Soft Matter*, 6 (2010) 726.
- [2] A. Agarwal, H. Hess, *Progress in Polymer Science*, 35 (2010) 252.
- [3] T. F. Otero, *Journal of Materials Chemistry*, 19 (2009) 681.
- [4] [Itik, M.](#), . IEEE Digital Library 2013

# Influence of the morphology of electrodeposited nanoparticles on their activity for the cyclisation reaction of allyl 2-bromobenzyl

T. Breugelmans<sup>1,2</sup>, B. Vanrenterghem<sup>1</sup>, B. Geboes<sup>1,2</sup>, J. Ustarroz<sup>2</sup>, S. Bals<sup>3</sup>, A. Hubin<sup>2</sup>

<sup>1</sup> Research Group Advanced Reactor Technology (ART), University of Antwerp, Salesianenlaan 90, 2660 Hoboken, Belgium

<sup>2</sup> Research Group Electrochemical and Surface Engineering (SURF), Vrije Universiteit Brussel, Pleinlaan 2, 1050 Brussels, Belgium

<sup>3</sup> Research Group Electron Microscopy for Materials Science (EMAT), University of Antwerp, Groenenborgerlaan 171, 2020 Antwerp, Belgium  
tom.breugelmans@uantwerpen.be

In recent years there has been a growing search for clean, catalytic and environmentally friendly methodologies in organic synthesis. To tackle these issues, an electrosynthetic methodology can be applied. Electrochemical syntheses mostly need fewer steps, produce less waste, provide a cheaper reagent and require less auxiliaries [1]. However, a major drawback is that those electrosynthetic processes require very negative electrode potentials that are inadequate for use in industrial production processes due to exuberant energy costs. Attempts to reduce the large overpotentials are directed towards improving catalytic activity of the electrode materials.

In this work, the link between the morphology of the catalyst material and the electrosynthetic pathway was investigated. In a first step, nanoparticles of transition metals (Ag, Cu, Pd, Ni, Pt and Au) were electrochemically deposited and the effect of their morphological properties (particle size, porosity, ...) on the electrochemical syntheses were studied. The nature of the nanoclusters were tuned by changing the electrolyte composition and the deposition parameters. In a second step, core-shell electrocatalysts were constructed with Ag (the most active electrode material) as a shell metal and Cu as a core metal. We have previously shown the potential catalytic enhancement of comparable core-shell NP's prepared by galvanic displacement towards ORR [2].

The described strategy was evaluated for the intermolecular cyclisation of allyl 2-bromobenzyl ether until benzopyran, an important building block in pharmaceutical industry. The classical organic approach currently used in industry is characterized by a low conversion and poor environmental conditions due to the use of harmful solvents such as tributyltin hydride [3].

- [1] H.J. Schäfer, *Contributions of organic electrosynthesis to green chemistry*, Comptes Rendu Chimie, 14 (2011) 745.
- [2] B. Geboes, I. Mintsouli, B. Wouters, J. Georgieva, A. Kakaroglou, S. Sotiropoulos, E. Valova, S. Armyanov, A. Hubin, T. Breugelmans, *Surface and electrochemical characterisation of a Pt-Cu/C nanostructured electrocatalyst, prepared by galvanic displacement*, Journal of Applied Catalysis B: Environmental, 150-151 (2014) 249.
- [3] M.J. Medeiros, C.S.S. Neves, A.R. Pereira, E. Duñach, *Electroreductive intramolecular cyclisation of bromoalkoxylated derivatives catalysed by nickel(II) tetramethylcyclam in "green" media*, Electrochimica Acta 56 (2011) 4498-4503.

# Motion-driven Electrochromic Reactions for Self-powered Smart Window System

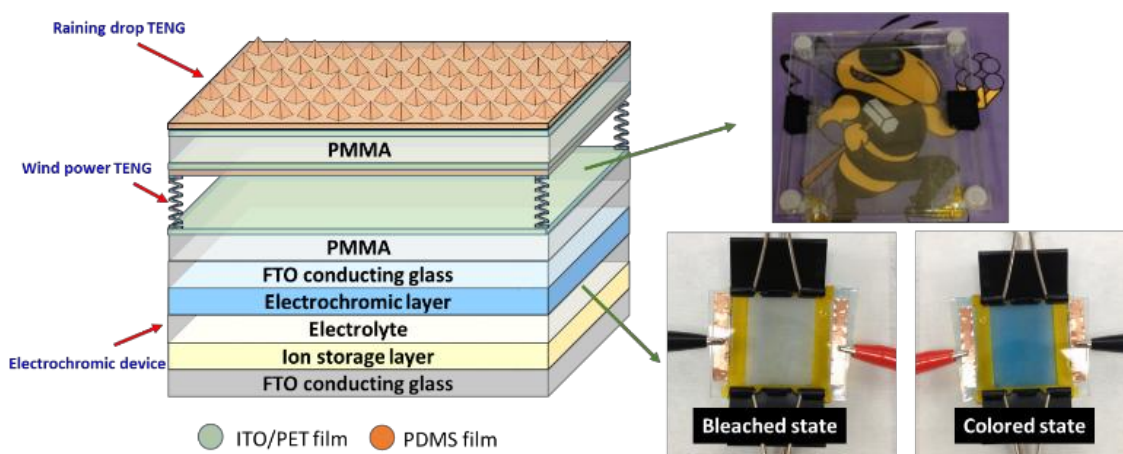
Min-Hsin Yeh<sup>a</sup>, Long Lin<sup>a</sup>, Zhong Lin Wang<sup>a,b\*</sup>

<sup>a</sup>*School of Material Science and Engineering, Georgia Institute of Technology, Atlanta, GA, USA*

<sup>b</sup>*Beijing Institute of Nanoenergy and Nanosystems, Chinese Academy of Sciences, Beijing, China  
500 10<sup>th</sup> St. NW, Atlanta, GA 30318, USA*

\*zhong.wang@mse.gatech.edu

Self-powered systems have been developed to integrate variable devices into a standalone system with multiple functions, including sensing, communication, computation, *etc.* The wireless, miniaturized and the large number of components in the system require a renewable, sustainable and clean power supply, and energy harvesting from the ambient environment will be a perfect solution for this problem. In this regard, the triboelectric nanogenerator (TENG) was recently invented to convert the mechanical energy into electricity, based on the coupling effect of contact electrification and electrostatic induction. Here in this work, we established a fully-integrated self-powered smart window composed of a dual-mode TENG and an ECD. The entire device was a transparent, multi-layered structure, which was compatible with the smart window structure. The ECD was composed of Prussian blue (PB) nanoparticles and zinc hexacyanoferrate (ZnHCF) nanocubes as the electrochromic material and the ion storage layer, respectively. By operating with conventional electrochemical workstation, the maximum reversible change in transmittance ( $\Delta T$ ) of 32.6% could be achieved with respect to an external DC voltage. The TENG consisted of a multi-layered structure with micro-patterned polydimethylsiloxane (PDMS) thin films and transparent electrodes, which could be employed for harvesting the kinetic energy from wind impact and water droplet, with an optimized output power of 130 mW/m<sup>2</sup>. By assembling the two devices on the same substrate, the self-powered smart window system was successfully realized with a transmittance change of up to 32.4% with visualized color variations as well, which could compete with the results demonstrated by the electrochemical workstation. This work sheds light on motion-driven electrochemical reactions and paves the way for a promising applications of the TENGs, which will push forward the development of self-powered systems. This research is a substantial advancement towards the practical application of nanogenerators and self-powered systems, and it paves the way for the development of fully independent smart windows or high-performance displays.



## Key Reference:

- [1] Z. L. Wang, Self-powered nanotech., *Sci. Am.* 298 (2008) 82.
- [2] Z. L. Wang, Triboelectric nanogenerators as new energy technology for self-powered systems and as active mechanical and chemical sensors, *ACS Nano* 7 (2013) 9533.
- [3] M. H. Yeh, L. Lin, P. K. Yang, and Z. L. Wang, Motion-driven electrochromic reactions for self-powered smart window system, *ACS Nano* (2015) (In press, DOI: acsnano.5b00706)



# Electrochemical Sequential Flow Reactors for removing Textile Dyes Using Different Anodes

Ana S. dos Santos Fajardo<sup>1</sup>, Maiara Barbosa Ferreira<sup>2</sup>, Rui C. Martins<sup>1</sup>,  
Djalma Ribeiro da Silva<sup>2</sup>, Rosa M. Quinta-Ferreira<sup>1</sup>, Carlos A. Martinez-Huitle<sup>2</sup>

<sup>1</sup> CIEPQPF - Centro de Investigação em Engenharia dos Processos Químicos e Produtos da Floresta, GERST - Group on Environment, Reaction, Separation and Thermodynamic, University of Coimbra, Coimbra, Portugal

<sup>2</sup> Laboratório de Eletroquímica Ambiental e Aplicada, Institute of Chemistry, Federal University of Rio Grande do Norte, Lagoa Nova - CEP 59.072-970, RN, Brazil.

E-mail: [carlosmh@quimica.ufrn.br](mailto:carlosmh@quimica.ufrn.br)

## Symposium 10

The textile industry produces large amounts of waste water during washing and dyeing containing large amounts of dyes which are not fixed on the surface of fibers, and as a result are eliminated along with the coloration of textile effluents (water courses, affecting its transparency, gas solubility and may have carcinogenic and mutagenic properties) [1]. As an innovative alternative, the electrochemical processes for treating wastewater containing organic matter have been proposed. The application of electrochemical technologies for wastewater treatment is benefiting from advantages such as versatility, environmental compatibility and potential cost effectiveness [2,3]. This technique has been recently used for decolorizing and degrading dyes from aqueous solutions by several scientific groups [1,3]. A large variety of electrochemical systems have been tested for the treatment of dyeing wastewaters by EO: conventional three-electrode cells with two-compartment or one-compartment and divided or undivided two electrode cells or tank reactors have been widely utilized. Other authors have employed flow cells with parallel electrodes and flow plants with a three-phase three-dimensional electrode reactor or a bipolar trickle tower reactor Fig. 10 in Ref. [1] illustrates some electrochemical plants and cells designed for this technique operating in batch mode to attain the maximum solution decontamination. The cells are divided or undivided and contain monopolar and sometimes bipolar electrodes.

The hydrodynamics of the cell plays a fundamental role in the mass transport towards the electrodes to efficiently oxidize organics pollutants. However, few attempts have been published until now [4], using flow cells with planar electrodes in a serial configuration increasing oxidation rate of pollutants. In this frame, we propose the use of electrochemical technology as an alternative for removing synthetic dyes (Remazol Red RB (RRB), Novacron Yellow (NY) from aqueous solutions by employing two kinds of flow cell systems (single flow cell (SFC) and dual flow cell (DFC) investigating the influence of operating parameters using as electrocatalytic materials: Ti/Pt, Ti/Pt-SbSn, Ti/IrO<sub>2</sub>-Ta<sub>2</sub>O<sub>5</sub> and boron doped diamond (BDD) electrodes. The results obtained in SFC system allow to identify the best experimental conditions for applying in DFC, that result in high current efficiency and low energy-cost, demonstrating that the use of plants with different stacks favors the complete elimination of organic pollutants in the effluents when electrochemical reactors with non-active and active electrodes are combined.

[1] C. A. Martinez-Huitle, E. Brillas, Appl. Catal. B: Environ. 87 (2009) 105.

[2] J. H. Bezerra-Rocha, A. M. S. Solano, N. S. Fernandes, D. R. da Silva, J. M. Peralta-Hernandez, C. A. Martinez-Huitle, Electrocatal. 3 (2012) 1.

[3] E. Brillas, C.A. Martínez-Huitle, Appl. Catal. B: Environ. 166-167 (2015) 603-643.

[4] M.B. Ferreira, J.H.B. Rocha, J.V. de Melo, C.A. Martinez-Huitle, M.A.Q. Alfaro, Electrocatalysis 4 (2013) 274-282.

# In situ Analysis of Electrochemical Fabrication Processes Using Raman Spectroscopy with Plasmonic Sensors

T. Homma<sup>1,2</sup>, Y. Sun<sup>1</sup>, M. Kunimoto<sup>2</sup>, M. Saito<sup>2</sup>, M. Yanagisawa<sup>2</sup>

<sup>1</sup> Department of Applied Chemistry, Waseda University, Shinjuku, Tokyo 169-8555, Japan

<sup>2</sup> Nanotechnology Research Center, Waseda University, Shinjuku, Tokyo 162-0041, Japan  
t.homma@waseda.jp

Electrochemical processes play a key role for fabricating various micro and nano devices and systems. While they have been widely used featuring their controllability and capability to form uniform deposits onto wide, non-flat surfaces, further precise control is required for achieving higher performances as well as improving the fabrication processes. These processes are quite complicated since numbers of factors simultaneously affect the deposition reactions taking place at solid-liquid interface where analytical tools are limited. For this, we focused on surface enhanced Raman spectroscopy (SERS) and proposed “plasmonic sensors” which have designed nanostructures at surface to achieve very high enhancement effect, and applied them to analyze various processes [1,2]. In addition, we also applied theoretical approaches such as density functional theory (DFT) calculations to investigate the processes in combination with the Raman spectroscopy [3]. In this paper, results of these approaches to analyze electrochemical fabrication processes will be introduced.

We have developed two types of the plasmonic sensors as shown in Fig. 1. The “reflection” type sensor consists of metal which is active for plasmonic enhancement, such as Ag, Au, and Cu, with centrifuge-grooved nanostructure. The pitch of the grooves was designed according to the wave length of the incident laser to maximize the enhancement, and the sensors can be directly used as substrates (working electrode) for the electrochemical processes (Fig.1(a)). On the other hand, “transmission” type sensor (Fig. 1(b)) can be applied to various processes and materials regardless of the variation in substrates. By using these sensors, we analyzed electrodeposition and electroless deposition processes to form various nanostructures, focusing upon the behaviors of the species, such as additives and reductants, at the deposition sites. In addition, we have also developed a system to analyze the behavior of additives in the pores of through silicon via (TSV). A model-pore was fabricated using a Si substrate modified with metal nanoparticles, which was covered with a trench-shaped structure consisting of poly(dimethylsiloxane) (PDMS). The incident laser for the SERS measurement was focused at the substrate surface through the PDMS structure, and it was confirmed that the signal of additives could be detected in situ in high sensitivity, without interference of the signals originated from PDMS, and their behavior was investigated in detail.

This work was financially supported in part by "Development of Systems and Technology for Advanced Measurement and Analysis," Japan Science and Technology Agency, and Grant-in-Aid for Scientific Research (A), MEXT, Japan.

[1] B. Jiang, T. Ouchi, N. Shimano, A. Otomo, M. Kunimoto, M. Yanagisawa, T. Homma, *Electrochim. Acta*, **100**, 317 (2013).

[2] B. Jiang, S. Wodarz, M. Kunimoto, M. Yanagisawa, T. Homma, *Electrochemistry*, **81**, 674 (2013).

[3] B. Jiang, M. Kunimoto, M. Yanagisawa, T. Homma, *J. Electrochem. Soc.*, **160**, D366 (2013).

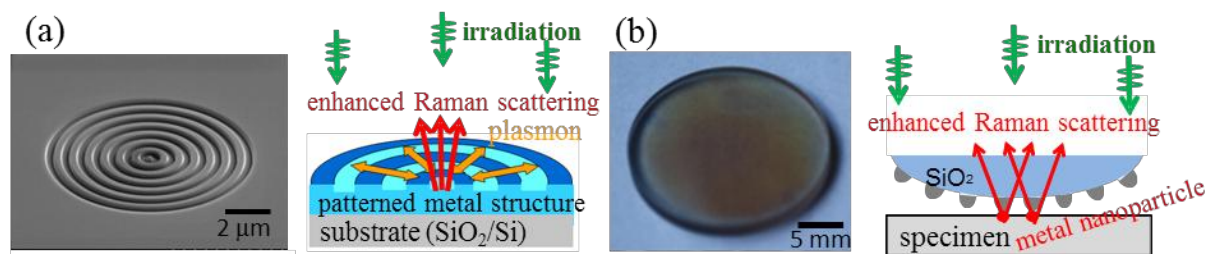


Fig. 1 Images and schematic diagrams of "reflection-type," (a), and "transmission-type," (b) plasmonic sensors.

# Influence of electrode material on microbial fuel cell treating a synthetic and a winery wastewater

Yeray Asensio<sup>1</sup>, Eduardo D. Penteado<sup>2</sup>, Iciar B. Montes<sup>1</sup>, Carmen M. Fernandez-Marchante<sup>1</sup>, Marcelo Zaiat<sup>2</sup>, Justo Lobato<sup>1</sup>, Pablo Cañizares<sup>1</sup>, Ernesto R. Gonzalez<sup>3</sup>, Manuel A. Rodrigo<sup>1</sup>

<sup>1</sup> Department of Chemical Engineering, University of Castilla-La Mancha, Enrique Costa Building, Campus Universitario s/n, 13071 Ciudad Real, Spain

<sup>2</sup> Laboratório de Processos Biológicos (LPB), Centro de Pesquisa, Desenvolvimento e Inovação em Engenharia Ambiental, Escola de Engenharia de São Carlos (EESC), Universidade de São Paulo (USP), Engenharia Ambiental - Bloco 4-F, Av. João Dagnone, 1100, Santa Angelina, 13.563-120 São Carlos, SP, Brazil

<sup>3</sup> Departamento de Física Química, Instituto de Química de São Carlos (IQSC), Universidade de São Paulo (USP), Avenida Trabalhador São-carlense, 400 - CEP 13566-590 São Carlos, SP 13560-970, Brazil  
manuel.rodrigo@uclm.es

Microbial fuel cell (MFC) is an emerging technology that has gained researchers' attention because they can simultaneously treat wastewater and recover energy. The MFC converts the chemical energy contained in organic matter into electricity using microorganisms that oxidize the soluble organics, transferring electrons to the anode. Several factors influence on the performance and the application of MFC technology, such as operating conditions, reactor configuration, membrane type and external resistance. However, the performance and the costs of electrodes are one of the key points for the application of MFC technology and information is needed on their long-term stability. Therefore, in this work the aim is to determine the performance of different types of carbon electrodes using a synthetic and winery wastewater as substrates in a dual chamber MFC. Carbon felt, carbon cloth, carbon foam and carbon paper were used as electrodes in anode and cathodes.

Results demonstrate that electricity can be efficiently produced with both types of wastewater producing 100 mV of average voltage with the best electrode. Biological treatment was efficient in terms of COD removal with daily removals around 2220 mg L<sup>-1</sup> d<sup>-1</sup> (55%) for the synthetic wastewater and around 700 mg L<sup>-1</sup> d<sup>-1</sup> (10%) for the winery waste. The lower efficiency observed in MFC fed with winery wastewater can be explained taking into account that the winery wastewater contains important concentrations of recalcitrant species which are difficult to be biodegraded.

In this study, the MFC operated with carbon felt produced significantly more power than other carbon electrodes. The morphology, surface area of electrodes influenced in microbial adhesion consequently in biological treatment and power generation. Therefore, the choice of electrode material may have significant consequences for biofilm-electrode formation and current production in MFC technology pure cultures.

## Acknowledgments

The authors are grateful to FAPESP (Fundação de Amparo à Pesquisa do Estado de São Paulo) for supporting this research (Process 2014/07904-5, 2011/23026-0 and 2009/15984-0) and to CNPq and CAPES for additional financial support. Financial support from the Spanish government through contract CTQ2013-49748-EXP is also gratefully acknowledged.

## References

- (1) Rodriguez, L.; Villasenor, J.; Buendia, I. M.; Fernandez, F. J. *Water Science and Technology* **2007**, *56*, 95.
- (2) Rabaey, K.; Verstraete, W. *Trends in Biotechnology* **2005**, *23*, 291.
- (3) Logan, B. E.; Hamelers, B.; Rozendal, R. A.; Schrorder, U.; Keller, J.; Freguia, S.; Aelterman, P.; Verstraete, W.; Rabaey, K. *Environmental Science & Technology* **2006**, *40*, 5181.
- (4) Rodrigo, M. A.; Canizares, P.; Lobato, J.; Paz, R.; Saez, C.; Linares, J. J. *Journal of Power Sources* **2007**, *169*, 198.
- (5) Sciarria, T. P.; Tenca, A.; D'Epifanio, A.; Mecheri, B.; Merlino, G.; Barbato, M.; Bonin, S.; Licoccia, S.; Garavaglia, V.; Adani, F. *Bioresource Technology* **2013**, *147*, 246.

# Remediation of bovine slurry wastewater using electrochemical advances oxidation process.

Ricardo Salazar<sup>a</sup>, Jorge Vidal<sup>a</sup>, Lidia Espinoza<sup>a</sup>, César Huiliñir<sup>b</sup>, Lorena Cornejo<sup>c</sup>

<sup>a</sup> Laboratorio de Electroquímica Medioambiental, LEQMA. Departamento de Química de los Materiales,

<sup>b</sup> Departamento de Ingeniería Química. Universidad de Santiago de Chile, USACH, Casilla 40, Correo 33, Santiago, Chile. <sup>c</sup> Laboratorio de Investigaciones Medioambientales de Zonas Áridas, LIMZA.

Universidad de Tarapacá, UTA. Arica, Chile

E-mail: [ricardo.salazar@usach.cl](mailto:ricardo.salazar@usach.cl)

In this work we studied the remediation of wastewater containing bovine slurry from a Chilean meat producer company, using electrochemical advances oxidation process (EAOPs).

On the one hand, we studied the degradation of organics from wastewater with a BDD/stainless steel system by electrochemical-oxidation. A rapid decolorization and mineralization was reached at short time of electrolysis without adding supporting electrolyte and in the presence of sodium chloride or sodium sulphate.

On the other hand a combination of anaerobic biological treatment followed by solar photoelectro-Fenton (SPEF) treatment was performed. Bio Assays were performed in an anaerobic bioreactor for 30 days, thermostated at 35 °C. On the other hand, the electrolysis was performed in an open electrochemical cell of 400 mL, with temperature control of the solution at 35 °C using a current density of 50 mA cm<sup>-2</sup>, initial pH of 3.0, with a concentration of catalyst Fe<sup>2+</sup> 1.0 mM and 0.05 M Na<sub>2</sub>SO<sub>4</sub> as supporting electrolyte, exposed to direct sunlight. An air diffusion cathode of carbon-PTFE and an anode of boron doped diamond (BDD) were used, both electrodes with an area of 2.5 cm<sup>2</sup> and gap 1 cm. The slurry samples were treated separately, by anaerobic digestion and SPEF. By anaerobic digestion, a 90% of COD removal was reached, after 30 incubation days with a production of methane gas of >100 mL. By SPEF, almost a complete mineralization was achieved after 4 hours of electrolysis. Considering the good results obtained by each treatment separately, wastewaters were treated by combining both methods. First, 83% COD decay was reached by anaerobic treatment producing >100 mL de methane. Then, by SPEF, a complete remotion of organic compounds was obtained.

By the use of EAOPs, water without color and organic compounds was produced by electrochemical processes or the combination with biological process.

## References

- [1] S. Garcia-Segura, R. Salazar, E. Brillas, Mineralization of phthalic acid by solar photoelectro-Fenton with a stirred boron-doped diamond/air-diffusion tank reactor: Influence of Fe<sup>3+</sup> and Cu<sup>2+</sup> catalysts and identification of oxidation products, *Electrochimica Acta* 113 (2013) 609–619.
- [2] Salazar, S. Garcia-Segura, M.S. Ureta-Zañartu, E. Brillas, Degradation of disperse azo dyes from waters by solar photoelectro-Fenton, *Electrochimica Acta* 56 (2011) 6371– 6379.
- [3] J. Urzúa, C. González-Vargas, F. Sepúlveda, M.S. Ureta-Zañartu, R. Salazar, Degradation of conazole fungicides in water by electrochemical oxidation, *Chemosphere* 93 (2013) 2774–2781.

## Acknowledgments

The authors thank the financial support of FONDECYT GRANT 1130391 and projects FONDEQUIP EQM120065, MECESUP USACH 1298 and FONDAP CONICYT SERC Chile 15110019. The authors are also grateful to Frigorífico Cordillera S.A. and DICYT-USACH for their support in carrying out this work.

# Flow-through Electrochemical Cells for Efficient Dye Removal

Minghua Zhou\*, Liang Ma, Weilu Yang, Gengbo Ren, Fangke Yu

Key Laboratory of Pollution Processes and Environmental Criteria of Ministry of Education,  
College of Environmental Science and Engineering, Nankai University,  
94 Weijin Road, Tianjin 300071, P. R. China  
E-mail: zhousmh@nankai.edu.cn

Many environmental electrochemical methods have showed promising applications in the area of biorefractory and toxic pollutants abatement due to their high efficiency and environmental viability, especially electrochemical advanced oxidation processes (EAOPs) that generate powerful hydroxyl radicals [1, 2]. Among which, electro-Fenton process is a promising alternative, which is based on the in-situ electrogeneration of  $\text{H}_2\text{O}_2$  by the oxygen reduction reaction, and has been reported to be effective for the degradation of phenols, dyes, pesticides, pharmaceuticals, and personal care products (PPCPs).

In most of the EAOPs studies, flat plate electrodes are used in flow-by mode. However, this flow cells would prevent rapid reaction rates of contaminants due to diffusional limitations, and would require numerous flat plate electrodes configured in parallel to obtain an adequate specific surface area for contaminant removal. Besides the reactors explorations using three-dimensional electrodes [3], the research on the development of novel electrochemical cells operated in a flow-through mode has being attracted considerable interests due to the significant enhancement in mass-transport rates of contaminants.

In this work, some novel flow-through electrochemical cells were developed for efficient dye removal. A simple modification method was used to modify graphite felts cathode to improve degradation performance. The cathode was characterized by various tests including scanning electron microscope and linear sweep voltammetry, and the electro-generation of hydrogen peroxide on this electrode was optimized as a function of pH, current density and oxygen sparge rate. Afterwards, the generation characteristics of hydrogen peroxide in the flow-through electrochemical cells were evaluated and compared. The degradation of organic pollutants in these reactors was studied, using methylene blue and methyl orange as model pollutants. The effects of some key parameters for the treatment performance were investigated, such as  $\text{Fe}^{2+}$  concentration, pH, flow rate and initial dye concentration. And the possible mechanisms for cathode adsorption, oxidation, regeneration, as well as cathode lifetime were studied. Compared with the treatment in conventional electrochemical cells, this reactor demonstrated much lower energy consumption and instant clean effect, providing a new approach to enhance the decontamination efficiency.

**Keywords:** EAOPs; Electro-Fenton, Dye wastewater treatment; Flow-through reactor

## References

- [1] Brillas E., Sirés I., Oturan M.A. Electro-Fenton process and related electrochemical technologies based on Fenton's reaction chemistry. *Chem. Rev.* **2009**, 109: 6570-6631.
- [2] Sirés I., Brillas E. Remediation of water pollution caused by pharmaceutical residues based on electrochemical separation and degradation technologies: A review. *Environ. Int.* **2012**, 40: 212-229.
- [3] Zhang C., Jiang Y.H., Li Y.L., Hu Z.X., Zhou L., Zhou M.H. Three-dimensional electrochemical process for wastewater treatment: A general review. *Chem. Eng. J.* **2013**, 228: 455-467.

# Electrochemical activation of environmental catalysis

Philippe Vernoux<sup>\*a</sup>

<sup>a</sup>Institut de Recherches sur la Catalyse et l'Environnement de Lyon, UMR 5256, CNRS,  
Université Claude Bernard Lyon 1, 69626 Villeurbanne, France

\*philippe.vernoux@ircelyon.univ-lyon1.fr

Electrochemical Promotion of Catalysis (EPOC), also called Non-Faradaic Electrochemical Modification of Catalytic Activity (NEMCA), is a promising concept for boosting catalytic processes and advancing the frontiers of catalysis [1]. This innovative field aims to modify *in-operando* both the activity and the selectivity of catalysts, in a reversible and controlled manner. EPOC utilizes solid electrolyte materials (ionically conducting ceramics) as catalytic carriers. Ions contained in these electrolytes are electrochemically supplied to the catalyst surface and act as promoting agents to modify the catalyst electronic properties in order to achieve optimal catalytic performance. It thus provides a unique means of varying promoter levels at the metal surface under reaction conditions by simply changing the potential of the catalyst film. The main advantage of EPOC is that the electrochemical activation magnitude is much higher than that predicted by Faraday's law. Therefore, EPOC requires low currents or potentials. Moreover, promoting species such as  $O^{2-}$  cannot be formed via gaseous adsorption and cannot be easily dosed by chemical ways. The EPOC technology consists in the implementation of catalysis in an electrochemical cell by using electrochemical catalysts which consist of a catalytic layer interfaced on an ionically conducting ceramic support. The latter serves as an electrically controlled source or sink of ionic promoter species that activate and modulate the behavior of the catalytic surface. Figure 1a displays a typical EPOC reactor. The catalytic layer, typically 40 nm to 10  $\mu m$  thick, is deposited on a dense solid electrolyte membrane (Figure 1a). This catalytic layer must be electronic conductor to allow the polarization. Therefore, the catalyst is also an electrode and is then named catalyst-electrode. A counter-electrode and a reference electrode, both catalytically inert, are deposited on the other side of the membrane (Figure 1a). An electrical current density (1-500  $\mu A/cm^2$ ) or potential ( $\pm 2$  V) is applied between the catalyst and the counter electrode. The reactants are co-fed over the porous electrochemical catalytic layer. Figure 1b displays a typical example of an EPOC experiment for the propane deep oxidation. The electrochemical catalyst was composed of a Pt thin film deposited by Physical Vapor Deposition (PVD) on a dense membrane of Yttria-Stabilized Zirconia (YSZ), an  $O^{2-}$  ionic conductor. A positive current (from +10 up to +500  $\mu A$ ) can strongly increase the propane conversion with a non-Faradaic manner, since the activation is up to 300 times higher than that predicted by the Faraday's law through the electrochemical oxidation of propane. This lecture will give an overview of recent advances of EPOC for environmental applications, such as hydrocarbon oxidation, soot combustion and NOx abatement.

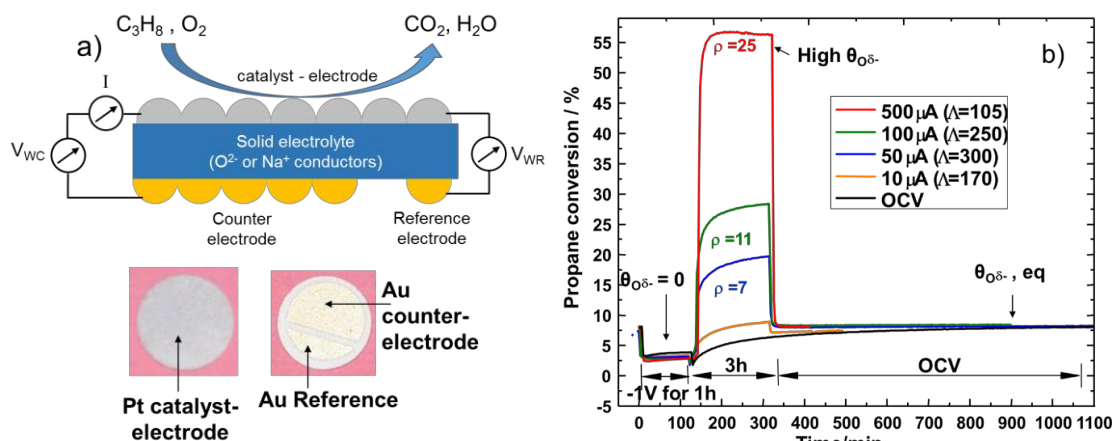


**Figure 1:** a) Schematic of an EPOC reactor and photos of an electrochemical catalyst: thin Pt catalyst-electrode / dense membrane of Yttria-Stabilized Zirconia (YSZ)/ Au counter and reference electrodes and b) Typical example of an EPOC experiment. Electrochemical catalyst: Pt (0.1  $mg/cm^2$ )/YSZ/Au,  $T=390^\circ C$ ,  $C_3H_8/O_2 = 2000$  ppm/1%.

[1] P. Vernoux, L. Lizarraga, M.N. Tsampas, F.M. Sapountzi, A. De Lucas-Consuegra, J.L. Valverde, S. Souentie, C.G. Vayenas, D. Tsiplakides, S. Balomenou, E.A. Baranova, Chem. Rev. 113 (2013) 8192.

# Reaction Selectivity of IrO<sub>2</sub>-Ta<sub>2</sub>O<sub>5</sub> Nano-Amorphous Hybrid Catalysts for Oxygen Evolution and Metal Oxide Deposition

Kenji Kawaguchi<sup>1\*</sup> and Masatsugu Morimitsu<sup>2\*\*</sup>

<sup>1</sup>Organization for Research Initiatives and Development,

<sup>2</sup>Department of Environmental Systems Science,  
Doshisha University

1-3 Tatara-miyakodani, Kyo-tanabe, Kyoto 610-0394, Japan

\*kkawaguc@mail.doshisha.ac.jp, \*\*mmorimit@mail.doshisha.ac.jp

The anodic reaction in industrial electrolysis using acidic electrolytes such as electrowinning, electroplating, and electrolytic production of thin metal film is mainly oxygen evolution, in which there are some cases where the oxygen evolution potential happens to increase with the deposition of metal oxide or oxyhydroxide when the anode is the coated titanium anode with IrO<sub>2</sub>-Ta<sub>2</sub>O<sub>5</sub> catalysts prepared at a high temperature more than 450 °C. This is caused by the unwanted side reaction of metal ions existing in the electrolyte; *e.g.*, Pb(II) ions are oxidized to form PbO<sub>2</sub> on the anode in electrowinning of copper, and the deposited PbO<sub>2</sub> film is partially reduced to non-conductive PbSO<sub>4</sub> during open-circuit condition.

This paper presents a novel and unique structure consisting of nano catalytic oxide particles in combination with an amorphous non-active oxide matrix, which is able to apply to an oxygen evolution anode in industrial electrolysis and suppress such unwanted side reactions. This catalyst can be prepared by a simple procedure; a precursor solution containing active and non-active metals in the form of complex ions is painted on a metal substrate followed by thermal decomposition. These metal oxides are immiscible and have a large difference in the oxide formation temperature so that the active metal oxide is formed as nano-size particles which are dispersed in the non-active metal oxide matrix.

The active metal oxide is IrO<sub>2</sub> and the non-active oxide is Ta<sub>2</sub>O<sub>5</sub> in this paper. Thermal decomposition of a precursor solution containing Ir(IV) with Ta(V) at a temperature below 650 °C results in the amorphous Ta<sub>2</sub>O<sub>5</sub> matrix, while IrO<sub>2</sub> in the matrix is generated in the crystalline or amorphous (nano-size particles) form depending on the thermal decomposition temperature. Low temperature calcination at 380 °C or less produces the hybrid structure with nano IrO<sub>2</sub> particles in the Ta<sub>2</sub>O<sub>5</sub> phase as shown in Fig. 1a, although the crystalline IrO<sub>2</sub>-contained oxide, *i.e.*, with aggregated IrO<sub>2</sub> particles, can be seen by thermal decomposition at a high temperature of 470 °C (Fig. 1b). The IrO<sub>2</sub>-Ta<sub>2</sub>O<sub>5</sub> nano-amorphous hybrid catalyst induces excellent catalytic activity for oxygen evolution and a high overpotential for crystallization of PbO<sub>2</sub> in acidic aqueous solutions, demonstrating that the nano-amorphous hybrid catalyst has high reaction selectivity for wanted and unwanted reactions.

*This work was financially supported by “Kyoto Area Super Cluster Program” of Japan Science and Technology Agency (JST).*

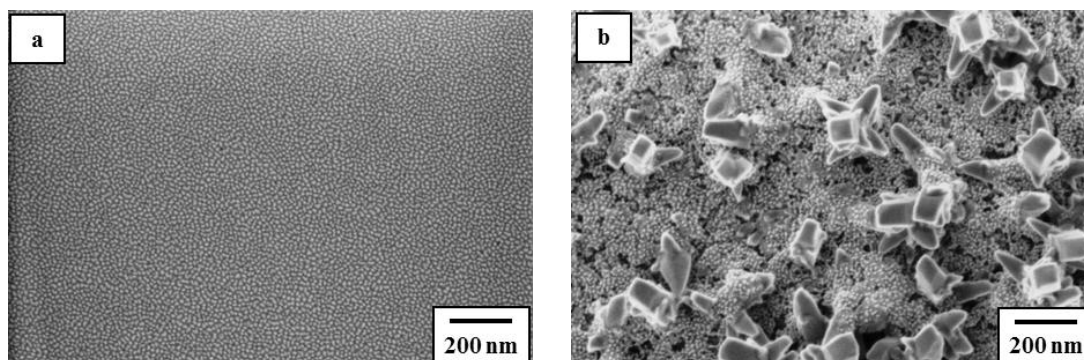


Fig. 1 Surface morphologies of nano-amorphous hybrid IrO<sub>2</sub>-Ta<sub>2</sub>O<sub>5</sub> (a) and crystalline IrO<sub>2</sub>-Ta<sub>2</sub>O<sub>5</sub> (b).



# Removal of emerging pollutants and biodegradable organic matter from wastewater by combined electrochemical -biological processes

O. Rodríguez-Nava<sup>a,b</sup>, M. A. Arellano-González<sup>c</sup>, A.-C Texier<sup>b</sup>, Ignacio González<sup>c</sup>

<sup>a</sup> *Escuela Nacional de Ciencias Biológicas, Instituto Politécnico Nacional, Departamento de Ingeniería en Sistemas Ambientales. Av. Wilfrido Massieu s/n, Unidad Profesional Adolfo López Mateos, Gustavo A. Madero, D.F. 07738, México*

*Universidad Autónoma Metropolitana-Iztapalapa, <sup>b</sup> Departamento de Biotecnología, <sup>c</sup> Departamento de Química, Av. San Rafael Atlixco 186, Col. Vicentina, Iztapalapa C. P. 09340, D. F., Mexico*

Nowadays emerging pollutants are present in natural waters, drinking water supplies and municipal wastewater, representing a serious problem in natural ecosystems due to their toxicity and causing DNA damage and oxidative stress in living organisms. Despite that, their concentrations in wastewater range from nanograms to milligrams, they are also persistent in Wastewater Treatment Plants (WWTP). The WWTP are designed for removing Biodegradable Organic Matter (BOM) through metabolic abilities of different microorganism constituting the biological consortium; these microorganisms are sensitive to the presence of these pollutants. Therefore, it is necessary to propose a pre-treatment prior to biologic reactor treatment, with the aim of eliminating selectively these pollutants and prepare an adequate feeder for the biological reactor. In this work, two kind of recalcitrant pollutants are considered: pharmaceuticals and chlorinated organic compounds and two different electrochemical pretreatment are proposed.

This work shows the feasibility of coupling an electrooxidation and biological system for removal of recalcitrant drugs (Bezafibrate, Gemfibrozil, Indomethacin and Sulfamethoxazole, BGIS) and BOM from wastewater, attaining high removal efficiencies without affecting the performance of activated sludge [1]. BGIS degradation was performed by advanced electrochemical oxidation using Boron Doped Diamond (BDD) as electrode and activated sludge process to BOM degradation in continuous reactor. The electrochemical parameters ( $1.2 \text{ L s}^{-1}$  and  $1.56 \text{ mA cm}^{-2}$ ) were chosen to operate filter press laboratory reactor, FM01-LC throughout microelectrolysis test, in order to remove drugs without decreasing BOM and chlorine concentration control to avoid bulking formation in a biological process. The wastewater previously treated by FM01-LC was fed to activated sludge to remove 100% of BGIS and 83% of BOM respectively, whereas the BGIS contained in wastewater without electrochemical pretreatment were persistent in biological process and promote bulking formation.

In the case for chlorinated organic compound degradation, the electrochemical oxidation is discarded due to the production of a polymer film at the electrode surface causes electrode deactivation. In order to avoid the problems caused by oxidation, electrochemical reductive dechlorination (electrocatalytic hydrogenolysis, ECH) has been suggested as an alternative and promising pretreatment method. The efficient dechlorination of 2-chlorophenol to phenol was achieved under electrochemical conditions where proton reduction and atomic hydrogen adsorption took place. The Pd-Ni alloy/Ti electrode (previously prepared by electrodeposition) showed the highest dechlorination efficiency (100% removal) and phenol formation (100% formation) at a potential of  $-0.40 \text{ V}$  vs  $\text{Ag/AgCl(s)/KCl(sat)}$ . The electrolysis was performed in a plate electrodes reactor (ECO-CELL). The chemical composition of the electrochemical reactor effluent was adjusted to feed a biological reactor (denitrifying process) for its complete mineralization.

1. O. Rodríguez-Nava, H. Ramírez-Saad, O. Loera, I. González, *J. Hazard. Mater.*, submitted
2. M. A. Arellano-González, A.-C Texier, L. Lartundo-Rojas, I. González, *J. Appl. Catal. B. Environ.*, submitted.



# A Bifunctional Air Electrode Catalyzed by Transition Metal Ferricyanide Derivatives for an Iron-air battery

R.D., H.A. Figueredo Rodriguez, C. Ponce de León, F.C. Walsh  
*University of Southampton*  
*University Road, Southampton, SO17 1BJ*

Perovskites have been gaining importance in rechargeable metal air batteries as bifunctional air electrodes and have been gradually been considered as substitutes for noble metals such as Pt, Pd, Ir or Ru typically used as a catalyst for the air electrode [1]. The activity of the transition metal compounds found in perovskites towards the reduction and evolution of oxygen has been demonstrated at low overpotentials however, the synthesis of these materials requires elevated temperature [2].

Transition metal complexes with ferricyanide (Prussian blue derivatives) are low-cost and can be produced in the form of insoluble nanoparticles by a single room-temperature step. They are already promising bifunctional oxygen catalysts, and when combined with a very small loading of palladium ( $0.5 \text{ mg cm}^{-2}$ ), they form an air electrode with exceptional bifunctionality and durability.

The co-precipitation of  $\text{Ni}^{2+}$  with  $[\text{Fe}(\text{CN})_6]^{3-}$  was used to produce  $\text{Ni}_3[\text{Fe}(\text{CN})_6]_2$  complex as a convenient route to synthesize low cost catalyst. The resulting catalyst was mixed with Nafion® and carbon black to form a paste that was spread onto a carbon powder/paper gas diffusion layer in order to manufacture bifunctional air electrodes. The electrodes were prepared in the absence and in the presence of palladium catalyst and tested in a 3-electrode cell at 20-60 °C. The results show that  $\text{Ni}_3[\text{Fe}(\text{CN})_6]_2$  with and without Pd had high bifunctional activity towards oxygen. It is believed that the original compound decomposes into mixed Ni/Fe hydroxides in the alkaline electrolyte which may co-catalyze each other in a similar way to the mixed Ni/Fe oxides [3].

The presentation also includes some preliminary results of the bifunctional electrode when coupled with an iron electrode and the design characteristics of the iron-air battery used.

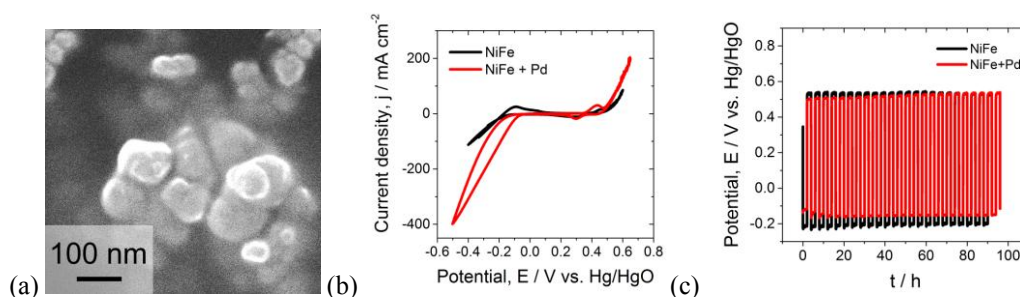


Figure 1

(a) Electron micrographs of  $\text{Ni}_3[\text{Fe}(\text{CN})_6]_2$  nanoparticles from suspension, (b) cyclic voltammetry of the nanoparticles on the surface of a carbon-based gas diffusion electrode, with and without a  $0.5 \text{ mg cm}^{-2}$  loading of Pd ( $v = 1 \text{ mVs}^{-1}$ ), and (c) charge-discharge stability of both air electrodes over 4 days at  $20 \text{ mA cm}^{-2}$  current density.

[1] F. Cheng, J. Chen, Chem. Soc. Rev., 41 (2012), pp. 2172-92.

[2] T. Takeguchi, T. Yamanaka, H. Takahashi, et al., J. Am. Chem. Soc., 135 (2013), pp. 11125-30.

[3] X. Li, F.C. Walsh, D. Pletcher, Phys. Chem. Chem. Phys., 13 (2011), pp. 1162-67.

## Acknowledgments

This work was enabled by an EU grant FP7 (NECOBAUT Grant agreement no. 314159).

# Electrochemical Processes Based on Fenton's Reaction for Wastewater Treatment. An Eco-Friendly, Efficient and Affordable Technology: Then, Now and Tomorrow

Sergi Garcia-Segura\*<sup>1,2</sup>, Enric Brillas<sup>1</sup>

<sup>1</sup>*Laboratori d'Electroquímica dels Materials i del Medi Ambient, Universitat de Barcelona (Spain)*

<sup>2</sup>*Laboratório de Eletroquímica Ambiental Aplicada, Universidade Federal do Rio Grande do Norte (Brazil)*

\*E-mail address: [sergigarcia@ub.edu](mailto:sergigarcia@ub.edu)

Electrochemical Advanced Oxidation Processes (EAOPs) are promising technologies for the decontamination of wastewaters polluted with persistent organic products (POPs). The principal environmental problems of POPs involve the visual contamination, carcinogenic effects, toxicity, and other noxious effects even at low concentration. Indirect electrochemical processes based on Fenton's reaction have proved a fast and efficient removal of several pollutants from lab-scale up to pre-pilot plant scale (see Fig. 1 and 2).

In this work, we present an overview of electrochemical processes based on Fenton's reaction and their potentialities and weaknesses as environmental friendly technologies to depollute industrial wastewaters containing POPs. The basis and principles of these technologies will be described making a special emphasis on the advances in the last decade. Starting from the conventional electro-Fenton and finishing with the systems involving photocatalytic and photochemical reactions to enhance the mineralization efficiency. The new challenges on the field will be raised, highlighting topics such as the costs and the use of renewable sources of energy.



Fig. 1- Solar photoelectro-Fenton pre-pilot flow plant.

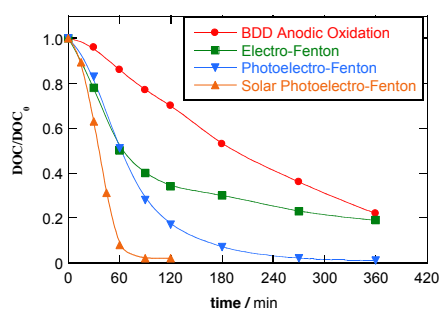


Fig. 2- Normalized DOC abatement with electrolysis time for different EAOPs.

**Aknowdledgements.** Financial support from Ministerio de Ciencia e Innovación (Spain) under project CTQ2010-16164 (co-financed with Feder funds), and the PNPD/CAPES postdoctoral fellowship awarded to S.G.S. are acknowledged.

# Development of Lithium Recovery Technique from Seawater by using Innovative Electrodialysis with Lithium Ionic Superconductor

Tsuyoshi Hoshino

*Breeding Functional Materials Development Group, Department of Blanket Systems Research, Rokkasho Fusion Institute, Sector of Fusion Research and Development,  
Japan Atomic Energy Agency  
2-166 Obuch, Omotedate, Rokkasho-mura, Kamikita-gun, Aomori, 039-3212, Japan  
hoshino.tsuyoshi@jaea.go.jp, hoshino.tsuyoshi@jaea.jp*

Lithium (Li) is rapidly becoming a valuable commodity. As a means of addressing global warming, the world is increasingly turning to the use of Li-ion batteries in electric vehicles and as storage batteries in the home; therefore, there is a growing need for Li. Furthermore, as a fuel for fusion reactors, tritium is produced by the reaction of lithium with neutrons in a tritium-breeding material.

I have proposed a new method for Li recovery from seawater by electrodialysis using an organic membrane impregnated with the ionic liquid PP13-TFSI [1]. Only Li ions can significantly permeate this membrane and thus pass from the anode side to the cathode side. Because the other ions (Na, etc.) in seawater are much less capable of permeating the membranes, Li becomes selectively concentrated on the cathode side (Fig. 1). In the measurements of the ion concentration on the cathode side as a function of the duration of the applied dialysis voltage (2V), the Li concentration increased with time, reaching 5.94% after 2 h. The other ions in seawater did not permeate the membrane. With both ends of the impregnated membrane covered with a Nafion 324 overcoat to prevent outflow of the ionic liquid, the Li concentration increased to 22.2%.

Furthermore, I propose a method for recovering Li from seawater by using world-first dialysis, wherein Li only permeates from the negative electrode side to the positive electrode side through a Li ionic superconductor functioning as a Li separation membrane (LISM). Measurements of the Li ion concentration at the positive electrode side as a function of dialysis duration showed that the Li recovery ratio increased to approximately 7% after 72 h with no applied electric voltage, and an electrical power of 0.04 V and 0.1 mA was generated (Fig. 2). Moreover, other ions in the seawater did not permeate the LISM. With both ends of the LISM bound with a negative and positive electrode, hydrated Li ion was transformed to Li ion only because Li ion can permeate through the LISM [2].

This new recovery method shows good energy efficiency and is easily scalable and is thus suitable for the industrialized mass production of Li in South American countries, which have briny water containing Li.

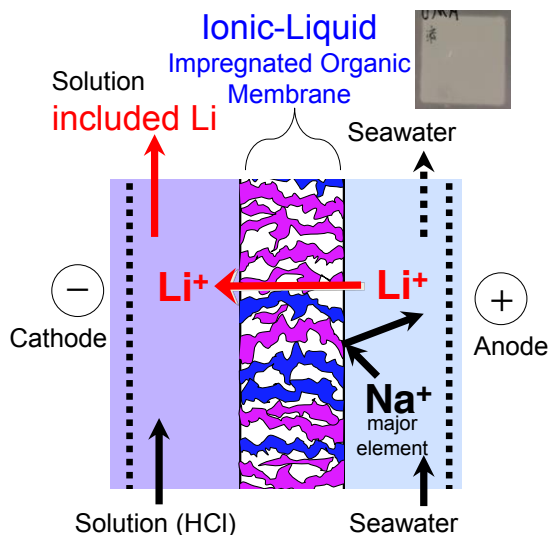


Fig1. Schematic of Li recovery method using an ionic-liquid-impregnated organic membrane.

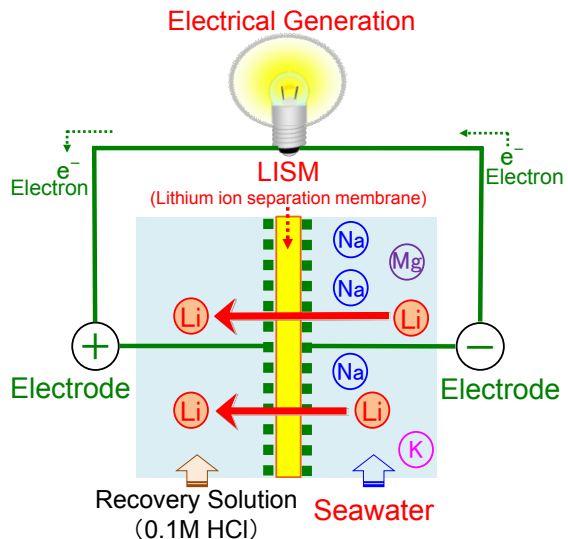


Fig2. Schematic of Li ion recovery from seawater by using innovative dialysis with LISM.

[1] T. Hoshino, Desalination, 317, 11-16 (2013).

[2] T. Hoshino, Desalination, 359, 59-63 (2015).

# Comparative Degradation of *trans*-Cinnamic and *trans*-Ferulic Acids by Electrochemical Advanced Oxidation Processes

Nelly Flores, Pere L. Cabot, Francesc Centellas, José Antonio Garrido, Rosa M. Rodríguez, Enric Brillas, Ignasi Sirés

Laboratori d'Electroquímica dels Materials i del Medi Ambient, Departament de Química Física, Facultat de Química, Universitat de Barcelona, Martí I Franquès 1-11, 08028 Barcelona, Spain  
e-mail address: nellyflorestapia@gmail.com

*Trans*-cinnamic acid ((E)-3-phenylprop-2-enoic acid) and *trans*-ferulic acid ((E)-3-(4-hydroxy-3-methoxyphenyl)prop-2-enoic acid) are main components in olive oil mill wastewaters [1]. In the last decades, electrochemical advanced oxidation processes (EAOPs) based on the electrogeneration of strongly oxidizing  $\bullet\text{OH}$  radicals have shown promising results for the remediation of wastewaters [2]. This communication presents a comparative study on the degradation of *trans*-cinnamic and *trans*-ferulic acids in acidic media by different EAOPs such as electrochemical oxidation with electrogenerated hydrogen peroxide (EO- $\text{H}_2\text{O}_2$ ), electro-Fenton (EF) and photoelectro-Fenton (PEF).

Electrolyses were carried out with a stirred tank reactor of 100 cm<sup>3</sup> equipped with a 3 cm<sup>2</sup> boron-doped diamond (BDD) anode and a 3 cm<sup>2</sup> carbon-polytetrafluoroethylene air-diffusion cathode for continuous  $\text{H}_2\text{O}_2$  generation. Synthetic aqueous solutions with 100 mg dm<sup>-3</sup> of total organic carbon (TOC) of *trans*-cinnamic or *trans*-ferulic acid in 0.05 mol dm<sup>-3</sup>  $\text{Na}_2\text{SO}_4$  at pH 3.0 were degraded by applying a current density between 16.7 and 100 mA cm<sup>-2</sup> for 360 min. In the EF and PEF experiments, 0.50 mmol dm<sup>-3</sup>  $\text{Fe}^{2+}$  was added as catalyst of Fenton's reaction, whereas in PEF, the solution was irradiated with a 6 W UVA lamp of  $\lambda_{\text{max}} = 360$  nm.

It was found that the solutions of both acids were mineralized at analogous rate for each procedure at given current density. The oxidation ability of EAOPs tested increased in the sequence  $\text{EO-H}_2\text{O}_2 < \text{EF} < \text{PEF}$ . At the end of the treatments at 33.3 mA cm<sup>-2</sup>, for example, TOC reductions of 68%, 78% and 98% for *trans*-cinnamic acid and of 61%, 79% and 96% for *trans*-ferulic acid, respectively, were obtained. An almost total mineralization was only reached by PEF, the most powerful EAOP in both cases. The increase in current density enhanced the mineralization rate for all the treatments due to the larger production of  $\bullet\text{OH}$  radicals from the acceleration of water oxidation at the BDD surface and in EF and PEF, of Fenton's reaction as a consequence of the greater generation of  $\text{H}_2\text{O}_2$  at the air-diffusion cathode. Thus, after 120 min of PEF process, TOC was reduced by 64% at 16.7 mA cm<sup>-2</sup> and much more rapidly up to 82% at 100 mA cm<sup>-2</sup> for *trans*-cinnamic acid, whereas it was removed from 74% to 81% when the current density varied from 33.3 to 100 mA cm<sup>-2</sup> for *trans*-ferulic acid. The decay of both acids obeyed a pseudo-first-order reaction, as determined by reversed-phase HPLC. They disappeared after about 360 min of EO- $\text{H}_2\text{O}_2$ , only needing between 10 and 35 min for EF and PEF. The much rapid decay in the two latter processes indicates that  $\bullet\text{OH}$  radicals formed from Fenton's reaction can destroy much more quickly both acids than those produced at the BDD anode. Short-linear aliphatic carboxylic acids were quantified by ion-exclusion HPLC. Oxalic acid was always the final product more largely generated. It was slowly and continuously accumulated in EO- $\text{H}_2\text{O}_2$  because of the slow destruction of precedent products by  $\bullet\text{OH}$  radicals formed at the BDD surface. The Fe(III)-oxalate complexes produced in EF and PEF were slowly removed under the action of  $\bullet\text{OH}$ , but completely photodecarboxylated to  $\text{CO}_2$  upon UVA irradiation. The quicker disappearance of oxalic acid by PEF then explains that this procedure is the most powerful EAOP for the remediation of acidic solutions of *trans*-cinnamic and *trans*-ferulic acids.

**Acknowledgements:** Financial support from MINECO (Spain) under project CTQ2013-48897-C2-1-R, co-financed with FEDER funds, and the PhD grant awarded to N. Flores by Senescyt (Ecuador) are acknowledged.

## References

- [1] D. Bickers, P. Calow, H. Greim, J.M. Hanifin, A.E. Rogers, J.H. Saurat, I.G. Sipes, R.L. Smith, H. Tagami, A toxicologic and dermatologic assessment of cinnamyl alcohol, cinnamaldehyde and cinnamic acid when used as fragrance ingredients, *Food Chem. Toxicol.* 43 (2005) 799-836.
- [2] I. Sirés, E. Brillas, M.A. Oturan, M.A. Rodrigo, M. Panizza, Electrochemical advanced oxidation processes: today and tomorrow. A review, *Environ. Sci. Pollut. Res.* 21 (2014) 8336-8367.

# Towards a More Competitive Advanced Electrochemical Technology: New Carbon-Based Electrodes Combination for Wastewater Treatment

Emmanuel Mousset, Zuxin Wang, Olivier P. Lefebvre

Centre for Water Research, Department of Civil and Environmental Engineering, National University of Singapore,

1 Engineering Dr. 2, Singapore 117576, Singapore

*ceeem@nus.edu.sg*

The release of hazardous persistent organic pollutants (POPs) into the environment is a common concern since they can be detected in low amounts in rivers, lakes, oceans, and even drinking water all over the world. Since these pollutants cannot be significantly removed in conventional wastewater treatment plants current interest is focusing on the development of simple, safe, effective, and economical physico-chemical technologies for the total removal of POPs. Electrochemical advanced oxidation processes (EAOPs) producing electrochemically high oxidizing species like  $\cdot\text{OH}$  are particularly promising [1]. Among them electro-Fenton has emerged because of its many advantages including  $\text{H}_2\text{O}_2$  electro-generation and  $\text{Fe}^{2+}$  electro-regeneration at the cathode avoiding the addition of chemicals and the production of sludge. It can also achieve very high degradation and mineralization rates of numerous organic pollutants [2]. To increase the cost-effectiveness of the process, it is important to develop novel and more cost-effective electrode materials.

In this context, new cathode materials consisting of carbon cloth and carbon fibers shaped as a brush or as a wire have been tested in the electro-Fenton (EF) process and compared to more conventional electrode materials (graphite, carbon felt and boron-doped diamond (BDD) and Platinum (Pt)). To select the best cathode, the performance of these electrodes was evaluated with a number of parameters, including maximal  $\text{H}_2\text{O}_2$  concentration, specific surface area, current efficiency, applied charge, energy consumption and material cost. The multi-criteria approach concluded that the carbon fiber brush outcompeted all other cathodes, especially in terms of  $\text{H}_2\text{O}_2$  production (Fig. 1a). This performance was attributed to the high specific surface area of the brush and was successfully explained by a modeling approach. This cathode was then used for studies performed with different anode materials. The influence of the different electrode combination on the degradation and mineralization kinetics (phenol) was carried out. A major finding was that carbon cloth material performed comparably to a more expensive Pt anode (Fig. 1b). In conclusion, the combination of carbon fiber brush cathode and carbon cloth anode gave promising performance, especially in consideration of process upscaling issues.

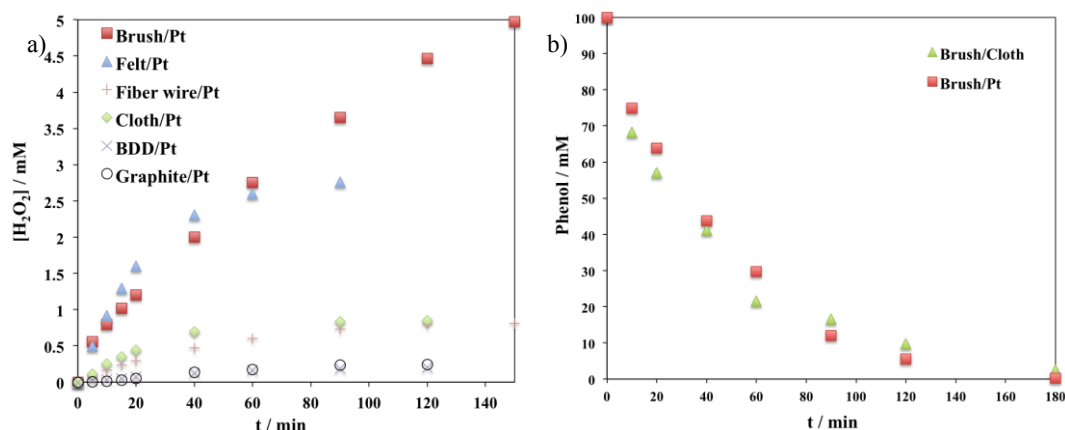


Figure 1a) Performance of carbon fiber brush cathode vs. other materials; b) performance of carbon fiber brush cathode combined with carbon cloth anode vs. Platinum.

## References

- [1] I. Sirés, E. Brillas, M.A. Oturan, M.A. Rodrigo, M. Panizza. Environ. Sci. Pollut. Res. Int. 21 (2014) 8336–8367.
- [2] E. Mousset, N. Oturan, E.D. van Hullebusch, G. Guibaud, G. Esposito, M.A. Oturan. Appl. Catal. B Environ. 160-161 (2014) 666–675.

# **Abatement of pollutants in water by different electrochemical approaches**

Onofrio Scialdone, Adriana D'Angelo, Simona Sabatino, Alessandro Galia  
*Università degli Studi di Palermo*  
*Viale delle Scienze, 90100 Palermo*  
*onofrio.scialdone@unipa.it*

Electrochemical based technologies are very promising methods for treating wastewaters containing organic and inorganic pollutants resistant to biological processes or toxic for microorganisms. These methods present numerous advantages including the utilization of a green reagent such as the electron, very high removal of numerous recalcitrant pollutants, efficient disinfection, high flexibility and no necessity to transport or stock chemical oxidants or reductants. On the other hand, a wide utilization of such methods is likely to be limited by: (i) the cost of electric energy necessary to drive electrode reactions; (ii) the cost of the supporting electrolyte for waste waters with no adequate conductivity and (iii), for some applications, by the cost of electrodic materials.

To avoid the supply of electric energy to the system, various solutions were proposed including the utilization of microbial fuel cells, reverse electrodialysis or microbial reverse electrodialysis processes, while the utilization of microfluidic apparatuses can allow to work with wastewater with low conductivity.

The potential utilization of these kinds of apparatuses (microbial fuel cells, reverse electrodialysis, microbial reverse electrodialysis, microfluidic cells) for the treatment of wastewater will be discussed.

# On the necessity of field studies for direct electrochemical drinking water disinfection

M.E.H. Bergmann<sup>1</sup>, W. Schmidt<sup>2</sup>, J. Hartmann<sup>1</sup>

Anhalt University, Köthen, Bernburger Str. 55, D-06366 Köthen/Anh., Germany

<sup>2</sup>TZW Dresden, Wasserwerkstraße 2, 01326 Dresden

[h.bergmann@emw.hs-anhalt.de](mailto:h.bergmann@emw.hs-anhalt.de)

Direct electrochemical drinking water disinfection in flow-through cells, the so-called *Inline Electrolysis* (IL), is a well-known but poorly understood process for water hygienization. This is the reason, why the method is to this day not allowed for legal application in Germany, albeit it is used in many other countries. To close the knowledge gap, water authorities, research centers and companies producing electrochemical disinfection cells have completed a joint project on IL. The main goal was to identify conditions of safe cell exploitation, i.e. conditions of satisfying disinfectant production on the one hand, and minimized by-product formation on the other hand. Several electrode materials (mixed oxide coatings and boron doped diamond) and different technical cells were studied with respect to their chlorine production and by-product formation. Amongst others, chlorate, perchlorate, bromate, THM [1] and AOX were the by-products of increased interest. Current density was varied between 10 and 571 A m<sup>-2</sup> mostly at temperatures between 15 °C and 30 °C over all experiments. Natural waters with and without chloride addition, and artificial waters were tested.

Results revealed significant differences in chlorine production due to different activities of anode materials used by cell producers. Electrolysis at chloride concentration between 20 and 250 mg dm<sup>-3</sup> conducted in laboratory cells with mixed metal oxide anodes was safe with respect to chlorate and perchlorate formation when the mode of applied current according to own rules of cell producers was respected. Chlorate was only found in studies with one electrode material. Usually, bromide concentration should not be higher than 1 mg dm<sup>-3</sup> to avoid bromate formation. Doped diamond electrodes showed still unacceptable chlorate and perchlorate formation. In contrast to lab-scale experiments, field studies at technical scale showed chlorate formation for all mixed oxide anode materials. Non-optimized cell constructions are responsible for this behavior. Perchlorate was only detected in technical cells using diamond doped electrodes.

The formation of organic by-products in waters free of bromide was comparable to chemical chlorination of drinking waters, when for example THM concentration is not allowed to be higher than 50 µg dm<sup>-3</sup>.

Results can be interpreted as a step toward legal application of IL. New criterions were defined for better discussion of results from laboratory-scale experiments [2]. Results are currently used to discuss new limiting concentration that is not yet clearly defined for chlorate and perchlorate in drinking water. It seems to be necessary to define test routines for technical electrolyzers. Model water systems were defined for this purpose.

## Acknowledgment

The authors wish to thank T. Iourtchouk and D. Gerngross (AU), G. Nüsse and M. Fischer (TZW), A. Grunert (UBA) for participation and German DVGW, DBU and the companies Ecotron, Hydrosys, Newtec and RWO for project support (FKZ W 10/02/08-B and FKZ 25386-23).

## References

- [1] Bergmann, M.E.H., Iourtchouk, T., Hartmann, J., On the THM formation during Inline Electrolysis - first systematic laboratory-scale studies, Chemical Engineering Transactions, 41 (2014) 127-132
- [2] Bergmann, M.E.H., Iourtchouk, T., Schmidt, W., Hartmann, J., Fischer, M., Nüsse, G., Gerngroß, H., Laboratory- and technical-scale comparison of chlorate and perchlorate formation during water electrolysis-a field study; Journal of Applied Electrochemistry, <http://link.springer.com/article/10.1007/s10800-015-0826-z> (13<sup>th</sup> April 2015)

# **Sustainable Electrolysis for Electrowinning and Electrorefining of Metals in Molten Salts and Aqueous Electrolytes**

Geir Martin Haarberg and Junli Xu

*Department of Materials Science and Engineering, Norwegian University of Science and Technology,*

*NO-7491 Trondheim Norway*

[geir.martin.haarberg@ntnu.no](mailto:geir.martin.haarberg@ntnu.no)

Fundamental laboratory studies can provide possibilities for developing sustainable electrolysis processes for metal deposition in terms of energy and environment. Laboratory experiments were carried out to study electrodeposition of iron from molten salts and aqueous solutions using an inert oxygen evolving anode to eliminate the emissions of CO<sub>2</sub>. The possibilities of molten salt electrorefining of metallurgical grade silicon to produce solar grade silicon were also investigated. Electrochemical techniques were used to study the electrochemical behaviour of dissolved iron, silicon, and titanium species. Bulk electrolysis was carried out to deposit pure iron, silicon, and titanium. The deposits were characterized by SEM/EDS and XRD analyses. Calculations based on laboratory studies indicate that great improvements in terms of reduced energy consumption and CO<sub>2</sub> emissions can be achieved by successful implementation of new technologies. Electrolysis may also play an important part in recycling of waste to recover the metal value. Electrodeposition of lead, indium and tin was studied in molten chloride electrolytes.



# Electrocatalytic properties of Cu-/Ni-loaded nanoporous carbons for the electrooxidation of alcohols

Leticia García-Cruz<sup>1</sup>, Vicente Montiel<sup>1</sup>, Conchi O. Ania<sup>2</sup>, Jesús Iniesta<sup>1\*</sup>

<sup>1</sup> Dept. Química Física e Instituto de Electroquímica, Universidad de Alicante, E-03080 Alicante, Spain.

<sup>2</sup> Instituto Nacional del Carbón (INCAR, CSIC), 33011 Oviedo, Spain,  
jesus.iniesta@ua.es

Nanoparticulated systems incorporating non-precious metals are gaining much interest as a replacement of low performing and high cost noble metals in different research fields such as electroanalysis, electrocatalysis, fuel cells and electrosynthesis, among others. Copper has a rich redox chemistry, with many oxidative reactions being catalyzed by different copper complexes and oxides. However, copper species easily undergo corrosion under certain electrolytes for which an important issue to improve the performance of copper-based materials is to control the size, shape, composition, structure and dispersion of the metallic nanoparticles. Similarly, the electrocatalytic properties of nickel hydroxide/oxyhydroxide -Ni(OH)<sub>2</sub>/NiOOH- electrodes for the electro-oxidation of unsaturated alcohols (i.e., alken-1-ols or alkyn-1-ols) in alkaline medium have also been explored. Despite the excellent results concerning stereoselectivity and conversion yields, there are still important limitations related to the deactivation of nickel electrode surface and the formation of inactive species during long cycling electrooxidative runs [1,2].

To this end, a series of nickel and copper-doped nanoporous carbons were prepared using various precursors (coal, lignocellulose and organic polymers) and synthetic routes [3,4]. Initially, the electrochemical response of the prepared materials towards the electrooxidation of alcohols was investigated, correlating the electrocatalytic activity with the characteristics of the electrode materials (porosity, surface chemistry of the nanoporous carbon, copper and nickel loading and dispersion), and the type and concentration of the alcohol molecule. The best performing metal-doped nanoporous carbon electrodes were selected for the preparation of copper/carbon and nickel/carbon films. To do that, several catalytic inks were prepared and deposited onto carbon cloth (Toray Paper) by using airbrushing technique. The different doped carbon electrodes with nickel and copper were characterized by SEM, TEM, XPS and electrochemical techniques such as cyclic voltammetry. The electrooxidation of small organic alcohols, e.g. propargyl alcohol PGA was performed to look into nickel and copper catalytic properties in addition to study how the carbon matrix influences on the final product of alcohol electrooxidation.

Preparative electrolyses in alkaline conditions at either controlled potential or current intensity were carried out to assess the electrocatalytic activity of copper nanoparticles and carbon matrix affects on the final oxidation products. Furthermore, the feasibility of the scale up of the process was also evaluated using a polymer electrolyte membrane electrochemical reactor (PEMER), as well as the feasibility of the Cu and Ni-doped nanoporous carbons as electrodes in direct alcohol fuel cells under alkaline conditions.

## References

- [1] L. García-Cruz, J. Iniesta, T. Thiemann, V. Montiel, Surprising electrooxidation of propargyl alcohol to (Z)-3-(2-propynoxy)-2-propenoic acid at a NiOOH electrode in alkaline medium, *Electrochemistry Communications* 22 (2012) 200.
- [2] L. García-Cruz, A. Sáez, CO. Ania, J. Solla-Gullón, T. Thiemann, J. Iniesta, V. Montiel, Electrocatalytic activity of Ni-doped nanoporous carbons in the electrooxidation of propargyl alcohol, *Carbon* 2014;73:291-302.
- [3] M. Haro, B. Ruiz, M. Andrade, A.S. Mestre, J.B. Parra, A.P. Carvalho, CO. Ania, Dual role of copper on the reactivity of activated carbons from coal and lignocellulosic precursors, *Microporous and Mesoporous Materials* 2012; 154; 68–73.
- [4] CO. Ania, T.J. Bandoz. Metal-loaded polystyrene-based activated carbons as dibenzothiophene removal media via reactive adsorption. *Carbon* 2006;44:2404-12.

# Direct Electrochemical Hydrogenation of Aromatic Molecules at Pt Electrode in Microemulsion Electrolyte Solution

Mitsuru Wakisaka<sup>1,2</sup> and Masashi Kunitake<sup>3</sup>

<sup>1</sup>Fuel Cell Nanomaterials Center, University of Yamanashi, 6-43 Miyamae, Kofu 400-0021, Japan

<sup>2</sup>JST, PRESTO, 4-1-8 Honcho, Kawaguchi, Saitama 332-0012, Japan

<sup>3</sup>Graduate School of Science and Technology, Kumamoto University,

2-39-1 Kurokami, Kumamoto 860-8555, Japan

wakisaka@yamanashi.ac.jp

To build a hydrogen-based society, it is imperative to establish a large-scale hydrogen supply system. Organic chemical hydrides have been drawing attention as hydrogen carriers because they are liquid at ambient temperature and pressure. Recently, Chiyoda Corporation has verified a large-scale hydrogen storage and transportation system by using an organic chemical hydride technology, involving catalytic hydrogenation of toluene forming methylcyclohexane (MCH) and dehydrogenation of MCH [1].

From viewpoints of effective use of electricity from renewable sources and energy conversion efficiency, direct electrochemical hydrogenation (DEH) of toluene is preferable to fix hydrogen. So far, there have been several studies of the DHE of toluene by applying a membrane electrode assembly (MEA) consisting on a polymer electrolyte and Pt-based nanoparticle electrodes [2]. However, it is open to question whether the MEA technique is best suited to the DEH of liquid aromatic organics since MEAs have originally been developed for fuel cells in which reactants are gaseous.

In a bicontinuous microemulsion (BME), electrochemical contact with micro aqueous and organic solution phases can be simultaneously achieved by controlling hydrophilicity and lipophilicity on an electrode surface [3]. In the present study, we have, for the first time, applied a BME technique, instead of MEA, to the DEH of toluene, and successfully obtained a significant reduction current at a Pt electrode in a BME solution.

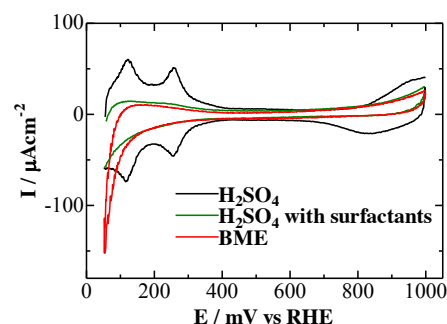
The BME solution was prepared from toluene, a  $\text{H}_2\text{SO}_4$  solution and surfactants (sodium 1-dodecanesulfonate and a co-surfactant). A mirror-finished polycrystalline Pt electrode and a reversible hydrogen electrode (RHE) were employed as working electrode and reference electrode, respectively.

Fig. 1 shows cyclic voltammograms (CVs) of the Pt electrode in  $\text{H}_2\text{SO}_4$  with / without the surfactants and in the BME solution. In the  $\text{H}_2\text{SO}_4$  solution, the Pt electrode exhibited a characteristic reversible hydrogen adsorption wave below 400 mV. However, it was found that the surfactants hindered the hydrogen adsorption due to an adsorption of surfactants on the Pt surface. In the BME solution, it should be pointed out that a large reduction current was raised at a more positive potential than the hydrogen evolution reaction (HER). Fig. 2 shows steady-state polarization curves in these solutions. It is clearly seen that the reduction currents in the BME solution are significantly larger than those in the other solutions in the whole potential region between 0 and 100 mV.

This preliminary result indicates that the BME technique, much simpler and cheaper than the MEA technique, has a great potential for the DEH of liquid aromatic organics.

## References

- [1] Y. Okada, E. Sasaki, E. Watanabe, S. Hyodo, H. Nishijima, *Int. J. Hydrog. Energy* 31 (2006) 1348.
- [2] K. Miyoshi, Y. Sato, S. Mitsushima, 224<sup>th</sup> ECS meeting abstracts (2013) 759: V. Kalousek, P. Wang, T. Minegishi, T. Hisatomi, K. Nakagawa, S. Oshima, Y. Kobori, J. Kubota, K. Domen, *ChemSusChem* 7 (2014) 2690.
- [3] E. Kuray, S. Nagatomo, K. Sakata, D. Kato, O. Niwa, T. Nishimi, M. Kunitake, *Anal. Chem.* 87 (2015) 1489; S. Yoshitake, A. Ohira, M. Tominaga, T. Nishimi, M. Sakata, C. Hirayama, M. Kunitake, *Chem. Lett.* 3 (2002) 360.



**Fig. 1** CVs of a Pt electrode in  $\text{H}_2\text{SO}_4$  with / without surfactants and BME solution.

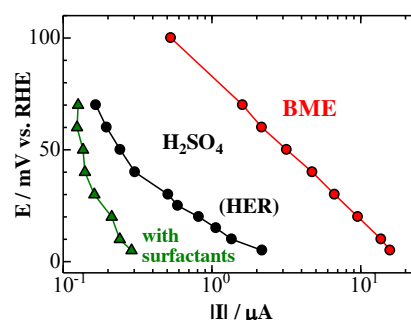


**Fig. 2** Steady-state polarization curves at the Pt electrode in the  $\text{H}_2\text{SO}_4$  with / without surfactants and BME solution.

# Hydrogen production and storage by coupling of catalysis and electrochemistry

J. González-Cobos<sup>1</sup>, V.J. Rico<sup>2</sup>, A.R. González-Elipé<sup>2</sup>, J.L. Valverde<sup>1</sup>, A. de Lucas-Consuegra<sup>1</sup>

<sup>1</sup>Department of Chemical Engineering, School of Chemical Sciences and Technology, University of Castilla-La Mancha, Av. Camilo José Cela 12, 13005 Ciudad Real, Spain

<sup>2</sup>Laboratory of Nanotechnology on Surface, Institute of Materials Science of Sevilla (CSIC-Uni. Sevilla), Av. Américo Vespucio 49, 41092 Sevilla, Spain  
Antonio.Lconsuegra@uclm.es

One of the most interesting processes for hydrogen production is the steam reforming of alcohols by using catalysts such as Cu, Pt, Pd or Ni supported on metal oxides such as ZnO or CeO<sub>2</sub>. On the other hand, many efforts are devoted to finding safe and efficient systems for H<sub>2</sub> transport and storage [1]. The use of ionically conducting materials (e.g., K-βAl<sub>2</sub>O<sub>3</sub>) as electroactive catalyst supports has shown to be an useful tool for in-situ activating Pt-based catalysts in the methanol steam reforming reaction by the electrochemical migration of promoter ions (e.g., K<sup>+</sup> ions) [2]. In the present work, the controlled production, storage and release of H<sub>2</sub> have been studied on novel Ni catalysts with very high porosity (Figure 1a), prepared by the oblique-angle deposition method. As can be observed in Figure 1b, under steam reforming conditions, the application of a negative electric current or potential and the consequent migration of K<sup>+</sup> ions from the K-βAl<sub>2</sub>O<sub>3</sub> to the Ni surface favored the dissociative adsorption of methanol and the formation of carbon surface compounds. Subsequently, in inert atmosphere, a positive polarization led to the decomposition of these compounds and the release of H<sub>2</sub>, CO<sub>2</sub> and CO. Hence, this electrocatalytic system showed a great practical interest for the simultaneous production and storage of hydrogen (up to more than 15 g H<sub>2</sub>/100 g Ni) and its in-situ release in a controlled and reversible way.

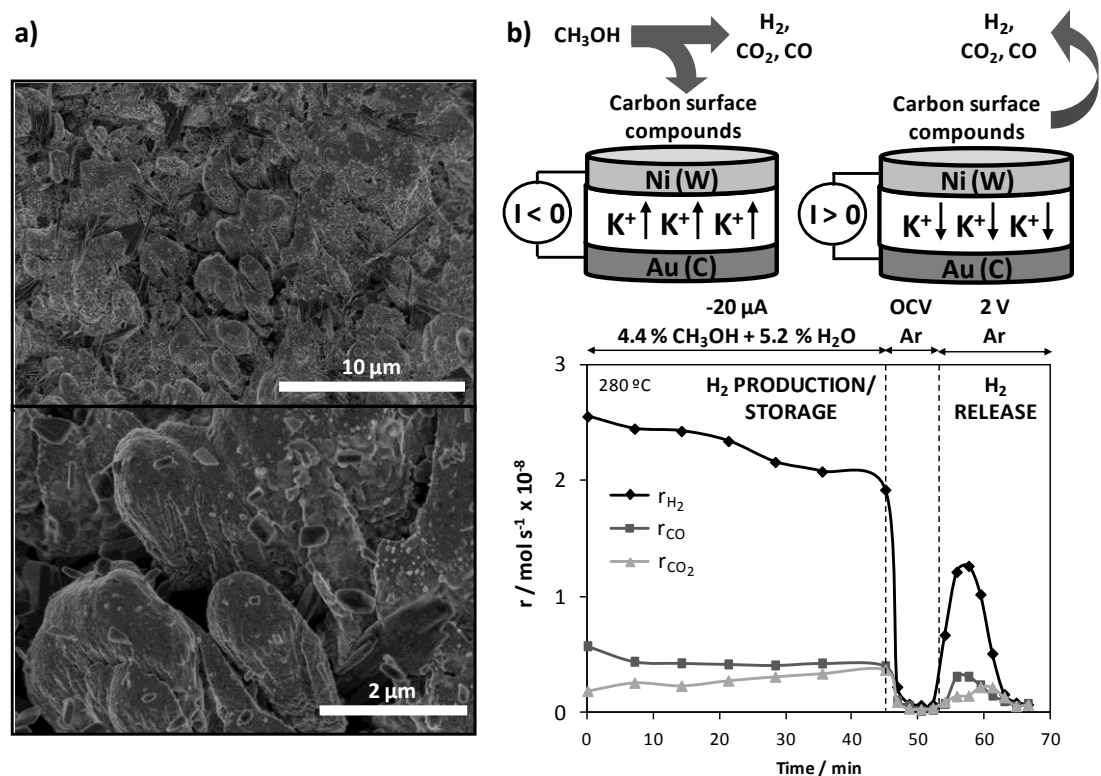


**Figure 1.** SEM images of a highly porous Ni catalyst film prepared by oblique-angle deposition (a). Controlled production and release of H<sub>2</sub>, CO and CO<sub>2</sub> by application of an electric current or potential (b).

## References

- [1] A.F. Dalebrook, W. Gan, M. Grasemann, S. Moret, G. Laurenczy, Chem. Commun. 49 (2013) 8735.
- [2] A. de Lucas-Consuegra, J. González-Cobos, V. Carcelén, C. Magén, J.L. Endrino, J.L. Valverde, J. Catal. 307 (2013) 18.

# Graphene-based electrodes: a new promising material for a more competitive electro-Fenton technology

Emmanuel Mousset, Muhammad Syafiq Bin Ahmad, Zuxin Wang, Olivier Lefebvre  
Centre for Water Research, Department of Civil and Environmental Engineering, National University of Singapore,  
1 Engineering Dr. 2, Singapore 117576, Singapore  
*ceelop@nus.edu.sg*

Electrochemical advanced oxidation processes (EAOPs) are being developed in order to treat the hazardous persistent organic pollutants (POP) that are being released into the environment, especially in water. These methods are based on the electrochemical generation of a very powerful oxidizing agent, in the form of the hydroxyl radical ( $\cdot\text{OH}$ ), which can mineralize and therefore destroy organics. Among these processes, electro-Fenton, based on the Fenton's reagent ( $\text{H}_2\text{O}_2$  and  $\text{Fe}^{2+}$ ) electro-(re)generation, has emerged for its many advantages, including no chemical addition, no sludge production and very high organic pollutant mineralization rates [1].

The electrode material is the key parameter that determines the effectiveness of the process and therefore effort have been directed towards the development of novel cost-effective materials, such as carbon-based electrodes. Among them, graphene material is becoming very popular. Its exceptional properties, including electronic and thermal conductivities have triggered a graphene gold rush; however the potential of graphene as an electrode material for environmental applications is only starting to be considered [2].

In this context, this study discusses first the production of a graphene electrode through a cost-effective method and second its performance evaluation in the electro-Fenton process. In order to make graphene-based electrodes, graphene was first synthesized through two distinct pathways: chemical method and electrochemical exfoliation. The latter gave better performance not only regarding the quality of the graphene obtained as determined by transmission electron microscopy (Fig. 1a) but also in terms of chemical requirement, equipment requirement and reproducibility. Therefore, this method was selected to elaborate a graphene-based electrode by using the ink-coating technique on carbon cloth. The electrode was characterized by cyclic voltammetry and then used as cathode for electro-Fenton.  $\text{H}_2\text{O}_2$  production was monitored over time to evaluate the performance of the graphene-based electrode. The graphene-coated cloth was able to produce twice as much  $\text{H}_2\text{O}_2$  as the uncoated one (Fig. 1b), demonstrating the role of graphene to enhance process efficiency. The presentation will include data on degradation of several micro-pollutants and a technico-economical discussion of the potential environmental applications for the technology.

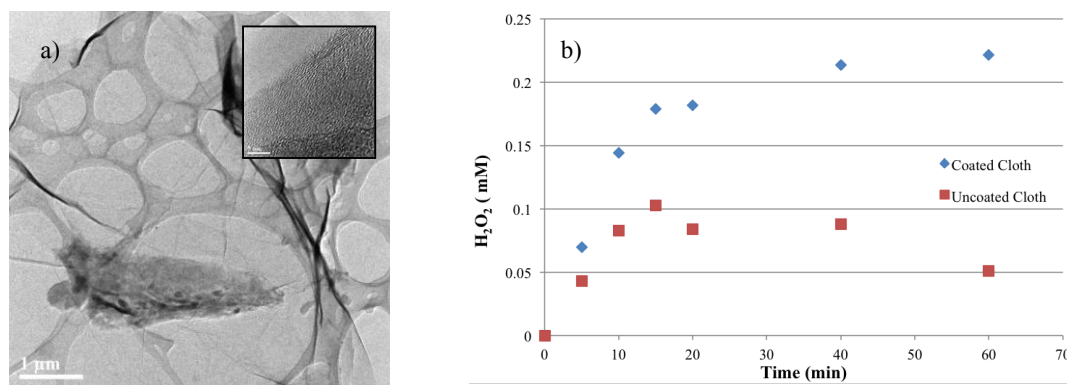


Figure 1a. TEM pictures of graphene sheet produced with electrochemical exfoliation (insert: lattice on the edge of the sheet); b) Comparison between graphene-coated cloth vs. uncoated cloth for  $\text{H}_2\text{O}_2$  electro-generation performance.

## References

- [1] E. Brillas, I. Sirès, M.A. Oturan, Electro-Fenton process and related electrochemical technologies based on Fenton's reaction chemistry, *Chem. Rev.* 109 (2009) 6570–6631.
- [2] F. Zhao, L. Liu, F. Yang, N. Ren, E-Fenton degradation of MB during filtration with Gr/PPy modified membrane cathode, *Chem. Eng. J.* 230 (2013) 491–498.

# Non-noble metal-containing doped graphitic carbons as electrocatalysts for the cogeneration of electricity and aniline

Nick Daems<sup>a</sup>, Jonatan Wouters<sup>a</sup>, Ivo F.J. Vankelecom<sup>a</sup> and Paolo P. Pescarmona<sup>a,b</sup>

<sup>a</sup> Centre for Surface Chemistry and Catalysis, K.U. Leuven, Kasteelpark Arenberg 23, post box 2461, 3001 Heverlee, Belgium.

<sup>b</sup> Department of Chemical Engineering, University of Groningen, Nijenborgh 4, 9747 AG Groningen, The Netherlands.

[nick.daems@biw.kuleuven.be](mailto:nick.daems@biw.kuleuven.be)

The cogeneration of electricity and valuable chemicals in a fuel cell is an emerging field of research in the context of sustainability [1]. An interesting example thereof is the cogeneration of electricity and aniline in a  $\text{H}_2/\text{PhNO}_2$  fuel cell [1,2]. This process allows the conversion of nitrobenzene into aniline, which is an important reagent used in industry for the synthesis of methylene diphenyl diisocyanate, a precursor in the production of polyurethane. The development of a suitable electrocatalyst is of crucial relevance for achieving high current and selectivity towards hydroxylamine in a  $\text{H}_2/\text{PhNO}_2$  fuel cell.

Here, we present novel electrocatalysts for the conversion of nitrobenzene to aniline, based on N-doped graphitic carbon materials prepared by controlled pyrolysis of polyaniline containing non-noble metal centers [3]. These materials display important assets: (1) metals with at least two accessible oxidation states to successfully adsorb aniline and initiate its reduction; (2) the extended delocalized  $\pi$ -system of the N-doped carbon granting good electrical conductivity.

The polyaniline-based electrocatalysts were synthesized by varying the type and loading of metal species (Fe, Cu and Co) and the pyrolysis temperature, and by studying the effect of the extent of acid leaching to remove inactive metal species. The performance of these electrocatalysts in the reduction of nitrobenzene was evaluated by means of linear sweep voltammetry (LSV) in a half cell containing 5 mM nitrobenzene in 0.3 M  $\text{HClO}_4$  in ethanol.

The nature of the metal center, its final content and the pyrolysis temperature proved to strongly affect the electrocatalyst performance in terms of onset potential and current densities. The performance of the electrocatalysts in the nitrobenzene reduction enhanced from Fe to Cu to Co (see Fig. 1 A). In general, the performance improved by increasing the metal loadings. The optimal activity in the reduction of nitrobenzene was reached with the materials pyrolysed at 900°C (see Fig. 1 B). By means of the Koutecký-Levich equations, it was determined that the amount of exchanged electrons ( $n$ ) was close to 6 at -0.75 V for the Co- and Cu-based electrocatalysts, indicating a selective production of the desired aniline. This represents a relevant improvement compared to the most promising electrocatalysts reported in the literature for this reaction (Cu/MWCNTs ( $n = 4$  at -0.75V) [1,2]. These results highlight the potential of our novel noble-metal-free electrocatalysts for the reduction of nitrobenzene to aniline in a fuel cell setup with the cogeneration of electricity.

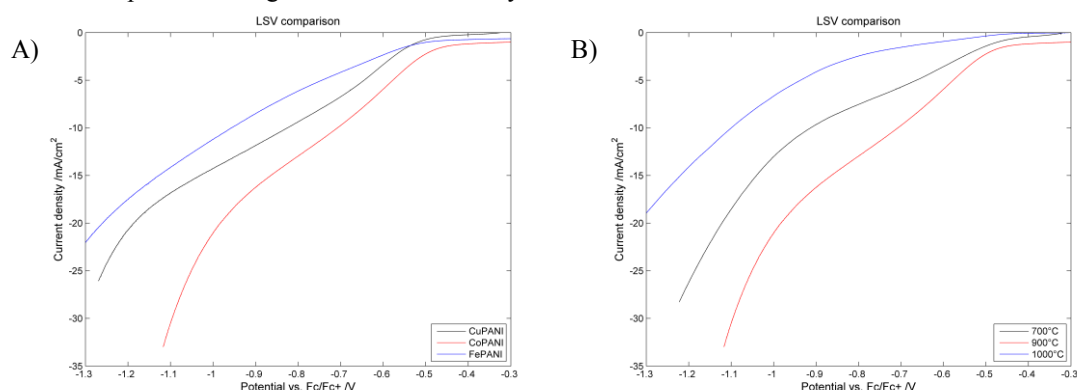


Figure 1: (A) LSV plots of electrocatalysts with different metal species and (B) LSV plots of the cobalt-containing electrocatalyst at different temperatures.

- [1] X. Sheng, B. Wouters, T. Breugelmans, A. Hubin, I.F.J. Vankelecom, P.P. Pescarmona, *Appl. Catal. B Environ.* 147 (2014) 330–339.
- [2] B. Wouters, X. Sheng, A. Bosch, T. Breugelman, E. Ahlberg, I.F.J. Vankelecom, P.P. Pescarmona, A. Hubin, *Electrochim. Acta.* 111 (2013) 405–410.
- [3] G. Wu, K.L. More, C.M. Johnston, P. Zelenay, *Science.* 332 (2011) 443–447.

# Development of Reactive Ion Exchange Membranes for Electro-Disinfection

Javier Llanos<sup>\*1</sup>, Sabri Kalkan<sup>2</sup>, Alexandra Raschitor<sup>1</sup>, Bahadır K. Körbahti<sup>2</sup>, Pablo Cañizares<sup>1</sup>, Manuel A. Rodrigo<sup>1</sup>

<sup>1</sup>Department of Chemical Engineering, University of Castilla-La Mancha, Avenida Camilo José Cela 12, 13005 Ciudad Real, Spain

<sup>2</sup>Faculty of Engineering, Chemical Engineering Department, University of Mersin, Çiftlikköy 33343 Mersin, Turkey

<sup>\*</sup>Corresponding author: Javier.Llanos@uclm.es

Electro-disinfection processes are gaining increasing attention because of their simple control, easiness of operation and effectiveness, being widely used in applications such as the disinfection of swimming pools and becoming a very promising alternative in the reclaiming of treated wastewater. Combination of disinfection with electrodialysis could be of interest in these processes, in particular when reclaimed wastewater is to be used in irrigation, because of the high standards required to the outcoming low-salinity stream in order to prevent diseases.

In the present work, novel anionic and cationic composite membranes are developed and tested for this purpose. These membranes contain microparticles of different materials, added with the purpose of behaving as bipolar electrodes and hence of promoting the production of disinfection reagents in the different compartments of the electrochemical cell.

Results obtained depends largely on the type of microparticles added ( $\text{TiO}_2$  and  $\text{RuO}_2$ ) and they demonstrate that hypochlorite can be effectively produced in the compartments placed in both sides of the membranes, demonstrating that microparticles behave as effective bipolar electrodes (Figure 1). Disinfection tests are used as proof of concept and they confirm the feasibility of these processes. Characterization of the new membranes is also assessed in this work.

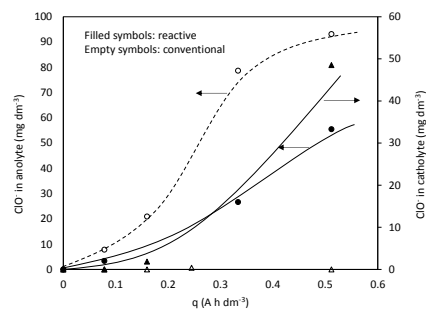


**Fig. 1.** Hypochlorite synthesis in a divided cell. Comparison of conventional and reactive Nafion membranes. Filled symbols: reactive; Empty symbols: conventional.  $\Delta$  Catholyte;  $\circ$  Anolyte

## Acknowledgements

This work has been supported by JCCM (Junta de Comunidades de Castilla-La Mancha, Spain) through the Project PEII-2014-039-P and by the Spanish government and EU through FEDER 2007-2013 PP201010

# Flexible Pinpoint Electrolysis Unit by Using of Boron-doped Diamond Powder (BDDP) Based Polymer Composites for Dental Treatments

Tsuyoshi Ochiai,<sup>1,2</sup> Mio Hayashi,<sup>1</sup> Shoko Tago,<sup>1</sup> Kazuo Hirota,<sup>3</sup> Takeshi Kondo,<sup>2</sup>  
Kazuhito Satomura,<sup>4</sup> Akira Fujishima<sup>1,2</sup>

<sup>1</sup>Photocatalyst Group, Kanagawa Academy of Science and Technology, KSP Bldg. East 407, 3-2-1 Sakado, Takatsu-ku, Kawasaki City, Kanagawa 213-0012, Japan, <sup>2</sup>Photocatalysis International Research Center, Tokyo University of Science, Japan, <sup>3</sup>Research Laboratory of Materials & Equipment for Oral Health Care, Inc., THINK Keihin Bldg. 2F-G03, 1-1 Minamiwatarida-cho, Kawasaki-ku, Kawasaki City, Kanagawa 210-0855, Japan, <sup>4</sup>Department of Oral Medicine, School of Dental Medicine, Tsurumi University, 2-1-3 Tsurumi, Tsurumi-ku, Yokohama 230-8501, Japan

[pg-ochiai@newkast.or.jp](mailto:pg-ochiai@newkast.or.jp)

You might have experienced... when the cavity has reached the pulp, we have to ask for a dentist to remove dead and infected material away from a root canal of the tooth with dental instruments, and then sterilize the root canal by NaClO. This is conventional “root-canal therapy”. However, sometime remaining bacteria can lead to not only periapical periodontitis but also serious health issues. Recently, we have reported a pinpoint electrolysis unit with BDD microelectrode and its great potential for dental treatments such as sterilization of root-canal [1]. However, inflexible polycrystalline BDD film peeled off from the substrates easily. In this study, we devise flexible pinpoint electrolysis unit by using of BDDP-based polymer composite for dental treatment.

The unit was prepared as shown in Figure 1. A metal wire surface was coated by BDDP-based polymer composite consist of BDDP [2] and 20% Nafion<sup>®</sup> dispersion solution at a specified mixing ratio as an anode. A Pt-ribbon with ion-exchange membrane was spirally wound around the metal wire's surface as a cathode. When DC voltage is applied between the anode and the cathode in the water, ozone and oxidative intermediates are generated. The unit showed almost the same sterilization ability as 1 wt% of aqueous NaClO treatment in *in vitro* assessment in the root-canal of human teeth. Moreover, the BDDP-based polymer composite has excellent durability which hardly causes cracks and peeling off even by repeated bending during the electrolysis. The superiority of BDDP-based polymer composite over simple and easy-to-handle pinpoint electrolysis unit, in terms of the flexibility, durability, and disinfection activity was demonstrated with the conventional methods and conditions. This research is attractive to develop a practical unit for dental treatment.

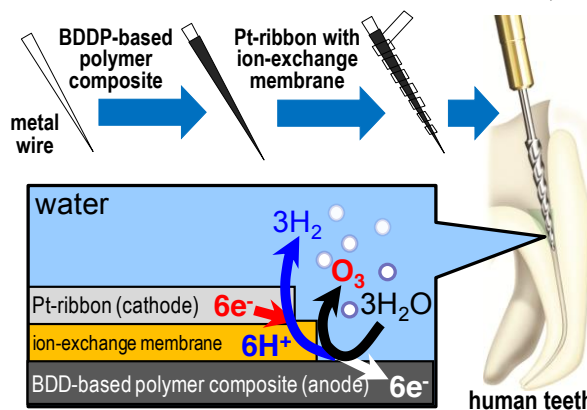


**Figure 1.** Schematic image of the flexible pinpoint electrolysis unit with BDDP-based polymer composites and its preparation.

## Acknowledgements

This work was partially supported by the JSPS KAKENHI Grant Number 25871218. We are grateful to Mr. I. Udagawa (Tokyo University of Science) for preparing the BDDP.

## References

- [1] Ochiai, T.; Ishii, Y.; Tago, S.; Hara, M.; Sato, T.; Hirota, K.; Nakata, K.; Murakami, T.; Einaga, Y.; Fujishima, A. *ChemPhysChem* **2013**, *14*, 2094-2096.
- [2] Kondo, T.; Sakamoto, H.; Kato, T.; Horitani, M.; Shitanda, I.; Itagaki, M.; Yuasa, M. *Electrochem. Commun.* **2011**, *13*, 1546-1549.



# **Electrochemical protocols for measurement of polycyclic aromatic hydrocarbons in environmental samples**

Priscilla G L Baker, Meryck Ward, Christopher Sunday, Milua Masikini, Stephen Mailu, Euodia Hess  
and Emmanuel Iwuoha

*SensorLab, Department of Chemistry, University of the Western Cape, PB X17, Bellville 7535, South  
Africa; [pbaker@uwc.ac.za](mailto:pbaker@uwc.ac.za)*

PAHs are widely distributed in the atmosphere, soils, sediments and ground water as well as marine sediments. Emissions of PAHs into the air can be transported over long distances before deposition into soils, vegetation, sea or inland waters occur via atmospheric precipitation. Due to the low solubility of PAHs in aqueous media as well as their strong hydrophobic nature, these PAHs contaminants associate with particulate material in the aquatic environment with underlying sediments as their ultimate sink. High performance liquid chromatography (HPLC) is the standard method employed for the determination of the 16 priority PAHs identified by World Health Organisation (WHO). Various electrochemical methods have been used for the screening and detection of these PAHs contaminants. However, HPLC methods have a number of disadvantages associated with the method i.e. isomeric PAH peaks which partially overlap, preparation of the samples is time consuming due and matrix interferences complicate efficient measurement and quantification.

SensorLab researcher have developed many viable sensor systems for screening and quantification of the WHO priority PAHs including anthracene, naphthalene, fluoranthene, chrysene, acenaphthylene, benzo[b]fluoranthene and triphenylene. The electrochemical methods employed for the detection of these PAHs include electrochemical quartz crystal microbalance for naphthalene and fluoranthene, based on luciferase inhibition(1), voltammetric evaluation of anthracene oxidation at Ag-Au Alloy nanoparticles/overoxidized-polypyrrole composite(2) and square wave voltammetry analysis of chrysene, acenaphthylene, benzo[b]fluoranthene and triphenylene at poly(phenazine-2,3-diimino(pyrrole-2-yl) electroactive actuator. This paper will concentrate on the selectivity and specificity criteria for detection of PAHs in samples of mixed composition, towards development of a multi-array sensor ensemble for reliable and cost effective electrochemical screening method for priority polycyclic aromatic hydrocarbons.

## References:

- (1) Constitution of novel polyamic acid/polypyrrole composite films by in-situ electropolymerization. EH Hess, T Waryo, OA Sadik, EI Iwuoha, PGL Baker *Electrochimica Acta* 128, p439–447 (2014).
- (2) Stephen N. Mailu, Tesfaye Waryo, PM. Ndangili, FR. Ngece, AA. Baleg, PGL Baker, EI Iwuoha. Determination of Anthracene on Ag-Au Alloy Nanoparticles/Overoxidized-Polypyrrole composite modified glassy carbon electrodes. *Sensors* 10 (2010) 9449-9465.



# Electrochemical Processes for Green Environment: the emerging technology in wastewater treatment

Bahadır K. Körbahti

Mersin University

Faculty of Engineering, Chemical Engineering Dept., Çiftlikköy 33343 Mersin, Turkey

korkbahti@mersin.edu.tr, korkbahti@gmail.com

Electrochemical processes for wastewater treatment have been attracted great attention in recent years. The oxidation of organic pollutants in wastewater could be accomplished by direct and indirect electrochemical mechanisms (Figure 1). In direct oxidation, organic pollutants are oxidized after adsorption on the anode surface with the involvement of the electron, which depends on the electrocatalytic activity of anode material. Although direct anodic oxidation is capable of removing organic pollutants from wastewater, direct oxidation reactions of organics on inert anodes are very slow due to reaction kinetics and limiting reactions. Therefore, most electrochemical methods are based on indirect electrolysis in which the organic pollutant is removed in the solution by active species produced in a reversible or an irreversible process, and the redox reagent can be electrogenerated by either anodic or cathodic process.

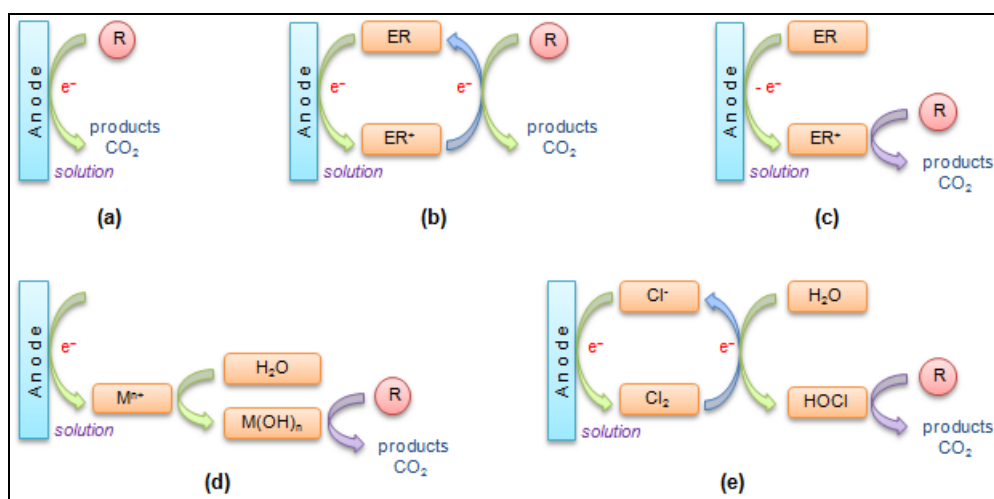


Figure 1. Mechanisms for the electrochemical oxidation of organic pollutants: (a) direct oxidation, (b)-(c) indirect oxidation by electrogenerated oxidizing reagent (ER), (d) indirect oxidation by metal hydroxides, (e) indirect oxidation by active chlorine.

In our research group, electrooxidation, electroreduction, electrodeposition, electrocoagulation, and electroflotation processes by direct and indirect mechanisms (Figure 1) have been investigated for the electrochemical abatement of phenols, pharmaceuticals, textile dyes, bilge water, paint industry wastewater, domestic wastewater, and removal of heavy metal ions using boron-doped diamond (BDD), platinum/iridium, platinum, stainless steel, iron, and graphite electrodes in electrochemical reactors of batch and continuous operating modes. It is possible to obtain complete oxidation of organic pollutants to  $\text{CO}_2$  or partial oxidation to intermediate compounds according to the process conditions. In our studies, we aimed to identify possible underlying phenomena of chemical reaction kinetics and mass transfer in electrochemical processes. It has been found that reaction order, activation energy, mass transfer coefficient, and energy consumption depend on the nature of the anode, hydrodynamic conditions, electrolyte type, applied current density, and pollutant concentration.

**Acknowledgements:** Prof. B.K.Körbahti would like to express his sincere appreciation to The Scientific and Technological Research Council of Turkey (TUBITAK), and Ministry of Development of Republic of Turkey (DPT) for their financial supports. The research projects of our group were supported by TUBITAK with Grant No's. MISAG-171, CAYDAG-106Y087, MAG-106M365, MAG-111M341; and DPT with Grant No. 02.K.120.290-15.

# Role of Sulfate and Persulfate Ions in Electrochemical Oxidation of Persistent Organics at a Boron-doped Diamond Anode

Ali Farhat<sup>a</sup>, Stephan Tait<sup>a</sup>, Jurg Keller<sup>a</sup>, Jelena Radjenovic<sup>a,b</sup>

<sup>a</sup> Advanced Water Management Centre, The University of Queensland, Queensland 4072, Australia

<sup>b</sup> Catalan Institute for Water Research (ICRA), Scientific and Technological Park of the University of Girona, 17003 Girona, Spain  
e-mail: a.farhat@awmc.uq.edu.au

The incomplete removal of persistent organic compounds such as pharmaceuticals and pesticides in conventional water and wastewater treatment plants have raised the interest for novel technologies capable of effectively degrading such organic contaminants. Electrochemical advanced oxidation processes (EAOPs) employing boron doped diamond (BDD) anodes have been previously reported to accomplish significant degradation of such trace organic contaminants. Previous studies have shown that BDD anodes are characterized with high overpotential for oxygen evolution where such anodes enhance the degradation rates of organics via direct oxidation and production of weakly adsorbed hydroxyl radicals (HO<sup>•</sup>). Besides HO<sup>•</sup> and other radical species, BDD anodes can also produce peroxy-species that may also contribute to bulk oxidation of contaminants. For example, previous research has reported BDD anodes are capable of oxidizing sulfate ions to peroxydisulfate (S<sub>2</sub>O<sub>8</sub><sup>2-</sup>), via sulfate radicals (SO<sub>4</sub><sup>•-</sup>) as intermediate products.

To further explore the role of sulfate in EAOPs, the present study quantified the rates of electrooxidation of several persistent organic contaminants (e.g., diatrizoate, carbamazepine, N,N-diethyl-meta-toluamide (DEET), iopromide, tribromophenol, triclosan and triclopyr) at BDD anode. Experiments were performed in sulfate anolyte at different operating conditions (concentrations/conductivities and current densities) and compared with inert nitrate and perchlorate anolytes. The observed electrooxidation rates of the persistent organic contaminants in sulfate anolyte were in the range of 12 – 66 h<sup>-1</sup>, significantly higher than the values obtained for nitrate anolyte (0.83 – 5.4 h<sup>-1</sup>).

Given that in the absence of trace metals or other activators (e.g., UV light), persulfate was shown to exhibit slow oxidation kinetics with these persistent organic contaminants (k < 0.1 h<sup>-1</sup>), higher electrooxidation rates in the presence of sulfate were assigned to the electrochemical activation of sulfate ions to sulfate-based oxidizing species such as sulfate radicals (SO<sub>4</sub><sup>•-</sup>) and/or non-radically activated persulfate. In an attempt to segregate the effects of HO<sup>•</sup> radicals and SO<sub>4</sub><sup>•-</sup> radicals, the study also examined the electrooxidation of nitrobenzene at a BDD anode, as a typical HO<sup>•</sup> radical probe compound, and provided further evidence for the presence of SO<sub>4</sub><sup>•-</sup> radicals.

Sulfate-based solutions have been widely used as supporting electrolytes for electrochemical degradation of contaminants using BDD anode. Electrooxidation pathways have been largely explained by the role of HO<sup>•</sup> radicals and other reactive oxygen species. Our results imply electrochemical activation of sulfate ions, even at sulfate concentrations as low as 150 mg L<sup>-1</sup>. Thus, this study has implications in applications of BDD anodes in wastewater treatment, as the presence of sulfate may significantly affect the electrooxidation pathways and kinetics of persistent organic contaminants.

# Fluoride Removal from Drinking Water by Electrocoagulation in a Continuous Filter Press Reactor coupled to a Flocculator and Clarifier

M. A. Sandoval<sup>1\*</sup>, J. L. Nava<sup>2</sup>, R. Fuentes<sup>1</sup>, I. Rodríguez<sup>3</sup>

<sup>1</sup> Departamento de Ingeniería Química, Universidad de Guanajuato, Norial Alta S/N, Guanajuato, Guanajuato, 36050, México.

<sup>2</sup> Departamento de Ingeniería Geomática e Hidráulica, Universidad de Guanajuato, Av. Juárez 77, Zona Centro, Guanajuato, Guanajuato, 36000, México.

<sup>3</sup> Facultad de Ingeniería-Instituto de Metalurgia, Universidad Autónoma de San Luis Potosí, Av. Sierra Leona 550, San Luis Potosí, San Luis Potosí, 78210, México.

\*ma.sandovallopez@ugto.mx

The problems related to water scarcity in Mexico and many regions in the world are due to geographical location, low rainfall and uncontrolled consumption. They have forced communities to use groundwater which contains fluoride concentrations above the maximum level recommended by the World Health Organization ( $1.5 \text{ mg L}^{-1}$ ). Fluoride pollution in the environment occurs through two different ways: natural sources and anthropogenic sources [1]. Recent studies performed in Mexico have demonstrated the presence of fluoride in Central and Northwestern regions with concentrations up to  $9.5 \text{ mg L}^{-1}$ . The level of fluoride in drinking water is an important factor in human health. It has both beneficial and harmful effects. It helps prevent teeth deterioration and dental caries but long-term consumption of water containing excess of fluoride ( $>4 \text{ mg L}^{-1}$ ) can lead to fluorosis of the teeth and bones [2]. The electrocoagulation (EC) has been considered as an alternative to remove fluoride in drinking water treatment because it lowers the amount of sludge and also provides some significant advantages such as, quite compact and easy operation, no chemical additives needed, and high flow rates [3].

Testing water for EC treatment was prepared from analytic reagents to obtain  $10 \text{ mg L}^{-1} \text{ F}^{-}$  in  $0.5 \text{ g L}^{-1} \text{ Na}_2\text{SO}_4$  and  $1.5 \text{ mg L}^{-1} \text{ NaClO}$  at  $\text{pH} = 7.7$ , giving an electrical conductivity of  $410 \mu\text{S cm}^{-1}$ . This solution resembles water from deep wells in Central region in Mexico. The system consists of a continuous filter press cell in which the coagulant is produced. The resulting solution (mixture of water and coagulant) is passed to a flocculator to induce flocculation of aluminum-fluoride flocs. Then, the solution is introduced to a clarifier, which is a sludge settler, to separate the sludge from the clarified water. The connection of current intensity supplied to the electrodes was in monopole configuration. Aluminum electrodes with 99.7% purity were used as anodes and cathodes. This reactor, coupled to a flocculation and clarification units, was developed in our laboratory. EC tests were performed with current densities of  $4\text{--}8 \text{ mA cm}^{-2}$  under different hydrodynamic conditions imposed by volumetric flow rates, comprised between  $0.1$  and  $0.4 \text{ L min}^{-1}$ . Fluoride was analyzed in the resulting clarified solution. After dissolution of the floc, aluminum was also analyzed. SEM, EDA-X and FTIR analyzes were performed.

Fig. 1 shows residual fluoride concentration as a function of mean linear flow rates in the EC reactor at a current density of  $6 \text{ mA cm}^{-2}$ . The experimental and theoretical aluminum doses are also shown. At  $0.91$  and  $1.82 \text{ cm s}^{-1}$ , we obtained the desired residual fluoride concentration ( $<1.5 \text{ mg L}^{-1}$ ).

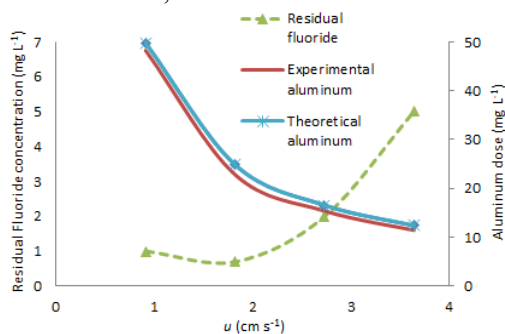


Fig. 1. Influence of the mean linear flow rate on the residual fluoride concentration and aluminum dose for synthetic water at a current density of  $6 \text{ mA cm}^{-2}$ .

SEM experiments showed a  $69 \mu\text{m}$  amorphous floc. EDA-X ratified that the aluminum flocs entrap the fluoride. FTIR analysis suggested a  $\text{Al(OH)}_3\text{-F}_x$  reaction.

## References.

- [1] M. Mohammad, S. Muttucumaru, J. Hazard. Mater. 131 (2006) 118.
- [2] M. A. Sandoval, J. L. Nava, R. Fuentes, I. Rodríguez, Sep. Pur. Technol. 134 (2014) 163.
- [3] Q. Zuo, X. Chen, W. Li, G. Chen, J. Hazard. Mater. 159 (2008) 452.

# Synthesis of a Novel Polymeric Ionic Liquid for Electrochromic Device Application

Miao-Syuan Fan<sup>1</sup>, Ling-Yu Chang<sup>2</sup>, Chuan-Pei Lee<sup>1</sup>, R. Vittal<sup>1</sup>, Jiang-Jen Lin<sup>2</sup>, Kuo-Chuan Ho<sup>1,2,\*</sup>

<sup>1</sup> Department of Chemical Engineering, National Taiwan University, Taipei 10617, Taiwan

<sup>2</sup> Institute of Polymer Science and Engineering, National Taiwan University, Taipei 10617, Taiwan

\* E-mail: kcho@ntu.edu.tw

Ionic liquids (ILs) are one of the most promising quasi-solid-state (QSS) electrolytes for many electrochemical devices. However, traditional room temperature IL electrolytes exist in the liquid state. The fluidity and potential leakage of traditional IL electrolytes is still unavoidable, which limits their practical applications. Recently, the polymeric ILs have received growing attention as alternatives to the organic liquid electrolytes and traditional IL electrolytes since the unique properties of ILs are incorporated with the polymer. In this study, we synthesized a novel polymeric IL electrolyte for use in complementary electrochromic devices (ECDs).

With the evolution of nanotechnology, the nano-sized particles of Prussian blue analogues (PBA) have received wide attention in electrochromic devices (ECDs). Since the electrochemical growth of PBA thin film on a transparent conducting substrate has been a challenging task due to poor stability of the deposition bath which consisted of a metal salt and ferric cyanide, there is a tendency for the rapid co-precipitation after mixing. We first synthesized zinc hexacyanoferrate (ZnHCF) nanoparticles through surface modification using sodium ferrocyanide decahydrate, which benefits its uniformity and the dispersity. Furthermore, a uniform nano-structural ZnHCF thin film can be prepared by the spin-coating method, which is suitable for the large-scale production.

Subsequently, a new polymeric IL electrolyte (Fig. 1), namely poly(oxyethylene)-imide imidazolium perchlorate (POEI-ClO<sub>4</sub>), was prepared and investigated for QSS-ECDs. Herein, POEI-ClO<sub>4</sub> acts simultaneously as a charge-transfer mediator in the electrolyte and a polymer for the gelation of an organic solvent-based electrolyte; the complementary QSS-ECD is composited of a poly(3,3-diethyl-3,4-dihydro-2H-thieno-[3,4-b][1,4]dioxepine) (PProDOT-Et<sub>2</sub>) thin film, a ZnHCF thin film and the POEI-ClO<sub>4</sub> gel electrolyte. The thermal stability of the novel polymeric IL electrolyte, POEI-ClO<sub>4</sub>, was characterized by a thermogravimetric analyzer (TGA). The 5% weight loss temperature (Td<sub>5%</sub>) of the POEI-ClO<sub>4</sub> was 272 °C. The ECD using POEI-ClO<sub>4</sub> gel electrolyte was operated at the applied potentials of 1.5 V for bleaching and -1.8 V for coloring. As shown in Fig. 2, the pertinent QSS-ECDs exhibited a superior transmittance change ( $\Delta T$ ) of 56% at 590 nm. This newly designed polymeric IL, POEI-ClO<sub>4</sub>, provides a new material and great potential for realizing highly efficient QSS-ECDs.

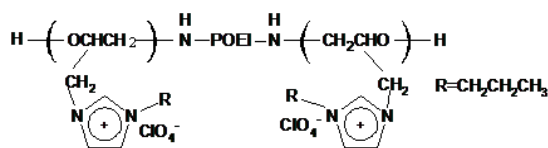


Fig. 1 The chemical structure of POEI-ClO<sub>4</sub>.

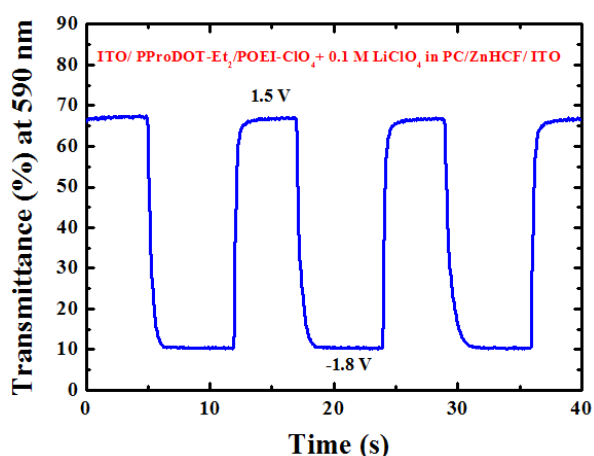


Fig. 2 The transmittance response at 590 nm for the complementary ECD in response to the applied potentials of 1.5 and -1.8 V (ZnHCF vs. PProDOT-Et<sub>2</sub>).

# A High Contrast Complementary Electrochromic Device with Sub-second Response Time

Hsin-Fu Yu<sup>1</sup>, Jen-Yuan Wang<sup>2</sup>, Min-Chuan Wang<sup>2</sup>, Der-Jun Jan<sup>2</sup>, You-Shiang Lin<sup>3</sup>, Man-kit Leung<sup>3</sup>, Kuo-Chuan Ho<sup>1\*</sup>

<sup>1</sup>*Department of Chemical Engineering, National Taiwan University, Taipei 10617, Taiwan*

<sup>2</sup>*Physics Division, Institute of Nuclear Energy Research, Taoyuan 32546, Taiwan*

<sup>3</sup>*Department of Chemistry, National Taiwan University, Taipei 10617, Taiwan*

\*E-mail: kcho@ntu.edu.tw

A complementary electrochromic device (ECD), composed of anodically coloring poly(N',N'',N'''-tris[N,N-bis-(4'-diphenylamino-biphenyl-4-yl)phenyl]-1,3,5-benzene-tricarboxamide) (PG1) thin film and cathodically coloring poly(3,3-diethyl-3,4-dihydro-2H-thieno-[3,4-b][1,4]dioxepine) (PProDOT-Et<sub>2</sub>) thin film, has been fabricated. The proposed ECD exhibits sub-second scale switching time of less than 0.2 s and significant transmittance change of 53% at 590 nm. In addition, this ECD shows negligible decay in transmittance change after continuous 5,000 cycles at room temperature. In order to understand the mechanism behinds its fast-switching feature, an electrochemical quartz crystal microbalance (EQCM) is coupled with cyclic voltammetry (CV) to explore the ionic transport processes occur in both thin films.

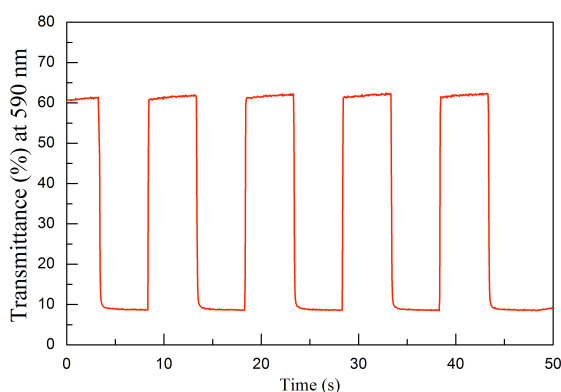


Fig 1. Dynamic transmittance curves for the PProDOT-Et<sub>2</sub>/PG1 ECD switched with an interval of 5 s.

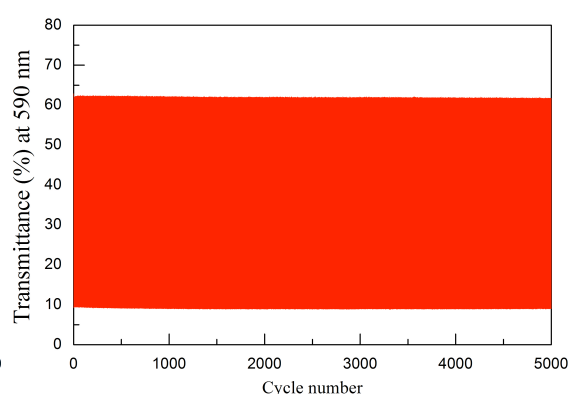


Fig 2. Cycling stability data for the PProDOT-Et<sub>2</sub>/PG1 ECD with a switching interval of 2 s.

**Solar cell surface reflectivity optimized by controlled metal etching**  
**Metal ion additive effect on the morphology of silicon etching**

**Conductive  $\text{Ti}_x\text{Mo}_x\text{O}_2$  Oxide Supported Pt nano-crystals**  
**Used as High-Performance Catalyst for Oxygen Reduction Reaction**

Po-Chih Tsai<sup>†</sup>, Hsin-Fu Deng; Wei-Nien Su<sup>§</sup>; Bing-Joe Hwang<sup>\*†‡</sup>

<sup>†</sup>Nano- Electrochemistry Laboratory, Department of Applied Science and Technology,  
National Taiwan University of Science and Technology, Taipei 106, Taiwan

<sup>§</sup>Graduate Institute of Applied Science and Technology, National Taiwan University of  
Science and Technology, Taipei 106, Taiwan

<sup>‡</sup> National Synchrotron Radiation Research Center, Hsinchu 30076, Taiwan  
National Taiwan University of Science and Technology, Taipei 106, Taiwan  
[bjh@mail.ntust.edu.tw](mailto:bjh@mail.ntust.edu.tw)

Solar cell conversion efficiency can be improved by optimizing many key factors, including surface reflectivity. In this work we used an anisotropic wet chemical etching method combined with metal additive assisted chemical etching to form various silicon structures on the wafer's surface to evaluate their reflectivity. We investigated the effect of various additive metal compounds ( $\text{FeCl}_3$ ,  $\text{CoCl}_2$ ,  $\text{NiCl}_2$ ,  $\text{SnCl}_4$ ,  $\text{AgNO}_3$ ,  $\text{CuSO}_4$ ), together with variations in their concentrations, the reaction times allowed and the reaction temperature. This work, by relating solar energy conversion efficiency to the cell's surface morphology, shows the crucial importance of surface design optimization to the resulting final cell's performance. Metal-assisted wet chemical etching is an efficient method to fabricate, we investigated several kinds of metal ion compound and we found there are two compound react interesting. Hence, we decide to go deep into this two compound  $\text{CuSO}_4$  and  $\text{FeCl}_4$ . In our research, we consider the reaction times, reaction temperature and concentration of metal ion compound in order to observe the morphology of silicon wafer, electrochemical reaction and reflectivity, confirm it with SEM, potential state and UV-vis, respectively.

Mis en forme : Indice

Mis en forme : Indice

Mis en forme : Indice

Here the approach of synthesis involves anchoring of Pt nanoparticles on the  $\text{Ti}_{1-x}\text{Mo}_x\text{O}_2$  nanosupports. While the structural defects of  $\text{Ti}_{1-x}\text{Mo}_x\text{O}_2$  are made by doping Mo into anatase  $\text{TiO}_2$  structure and hydrogen treatment at high temperature ( $300^\circ\text{C}$ ). The structural of this material were studied by the experimental Raman, electronic conductivity measurements.

Rotating disk electrode (RDE) measurements showed that 20wt% Pt/ $\text{Ti}_{0.9}\text{Mo}_{0.1}\text{O}_2$  catalyst had 1.5 times and 9.1 times higher Pt mass activity for ORR than those of 10 wt% Pt/ $\text{Ti}_{0.9}\text{Mo}_{0.1}\text{O}_2$  and commercial Pt/C catalysts, respectively. The observed high activity of metal oxide supported Pt catalyst could be attributed to the role of the advanced oxide support with electron donation from support to Pt catalyst surface, oxygen vacancies on nanosupport surface and high conductivity. Pt nanocatalysts on the advanced robust non carbon  $\text{Ti}_{0.9}\text{Mo}_{0.1}\text{O}_2$  nanosupports also exhibits improved stability against Pt sintering under a potential cycling regime (3000 cycles from 0.4 V to 1.0 V vs. RHE) due to strong metal support interaction (SMSI) between Pt catalyst and support materials. This approach can be extended to the different catalysis reactions such as CO oxidation, hydrogenation, etc.

# Electrochemical synthesis of hydrogen peroxide coupled with UV-C for the oxidation of endocrine disruptor compounds

R.J.M. Bisselink, L.Feenstra  
TNO dept. of Water Treatment  
Utrechtseweg 48, 3704 HE Zeist, the Netherlands  
Roel.Bisselink@tno.nl

Hydrogen peroxide ( $\text{H}_2\text{O}_2$ ) can be applied in various markets (e.g. disinfection, waste water treatment and the pulp & paper industry). The current application of hydrogen peroxide however still requires shipment, handling and storage and therefore sufficient safety precautions. On-site or in-situ production of hydrogen peroxide therefore has clear advantages. Another attractive benefit is that only oxygen (or air) and electricity is needed for the electrochemical production of hydrogen peroxide. Within our laboratory we achieved concentrations up 10% hydrogen peroxide using a plate-and-frame electrolyser. This setup showed with previous research that efficient indirect oxidation of various reactive dyes could be achieved [1]. The same setup was used in this research in which we investigated the indirect oxidation of endocrine disruptor compounds (EDCs) originating from hospital waste waters. Eight compounds being caffeine, diclofenac, ifosfamide, ( $\pm$ )-metoprolol, naproxene, pentoxifylline, ( $\pm$ )-sotalol and trimethoprim were selected due to their presence in the hospital waste water. Hydrogen peroxide was produced under constant current and two types of UV-C lamps were employed to assess its effect on the oxidation. Characterisation of the system indicated that hydrogen peroxide was produced with near to 100% current efficiency.

## References

[1] Jerič et al., *Acta Chim. Slov.* **60** (2013), 666-672.



# Indium recovery from secondary sources by electrowinning

R.J.M. Bisselink, M.A.C. Panjer  
TNO dept. of Water Treatment  
Utrechtseweg 48, 3704 HE Zeist, the Netherlands  
Roel.Bisselink@tno.nl

The increasing amount of electronics, such as consumer products and green technologies (e.g. solar PV cells) increases demand of metals such as indium. The European Commission has placed indium amongst a list of materials classified as critical [1]. The increasing demand of these critical metals together with the dependency on import drives research to investigate the recovery of valuable metals from secondary sources, so called urban mining. Flat panel displays (FPD) and CIGS type PV cells were selected as source material for the recovery of indium. A hydrometallurgical process is under development within the RECLAIM project of which electrowinning is the final step. Solvent extraction is used prior to electrowinning to purify indium and uses hydrochloric acid as stripping acid, as it enables selective stripping of indium [2]. In this research, we investigated the electrodeposition of indium using cyclic voltammetry and chronoamperometry. Cyclic voltammetry at graphite shows that the potential for indium electrodeposition is separated from the hydrogen evolution potential with approx. -0.4 V. Chronoamperometry will be used to investigate the influence of electrode potential, indium concentration and impurities on the current efficiency and product purity amongst others.

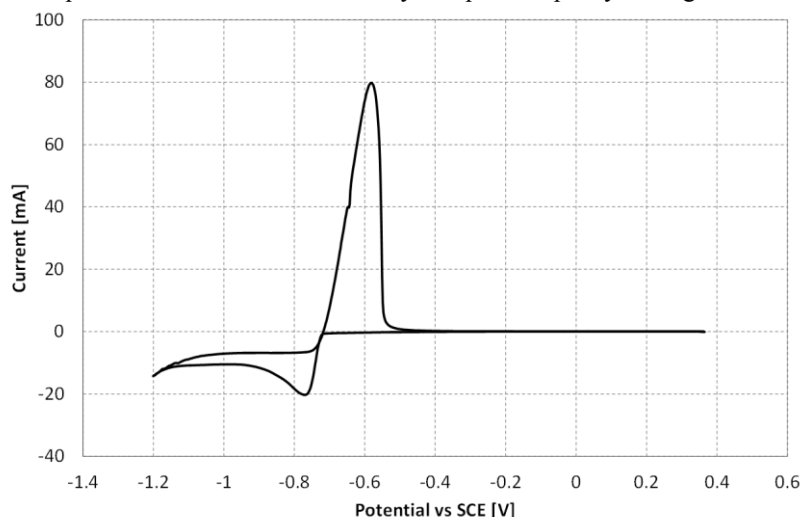


**Figure 1** Cyclic voltammogram of 10 g/l indium(III) in 1 M HCl at graphite.

## Acknowledgements

This research project (RECLAIM) has been financially supported by the European Commission under the 7th Framework Programme through the Nanosciences, nanotechnologies, materials & new production technologies (NMP) research theme, grant number 309620. The project website [www.re-claim.eu](http://www.re-claim.eu) gives more inside information on project objectives and partners.

## References

- [1] European Commission, report on critical raw materials for the EU, report of the Ad hoc Working Group defining critical raw materials, May 2014
- [2] S. Virolainen et al., *Hydrometallurgy* **107** (2011), 56-61.

# Electrochemical oxidation of Disperse Yellow 3 dye using BDD electrodes

Cláudio Márcio de Castro, Paulo Olivi

*Departamento de Química, Faculdade de Filosofia, Ciências e Letras de Ribeirão Preto*

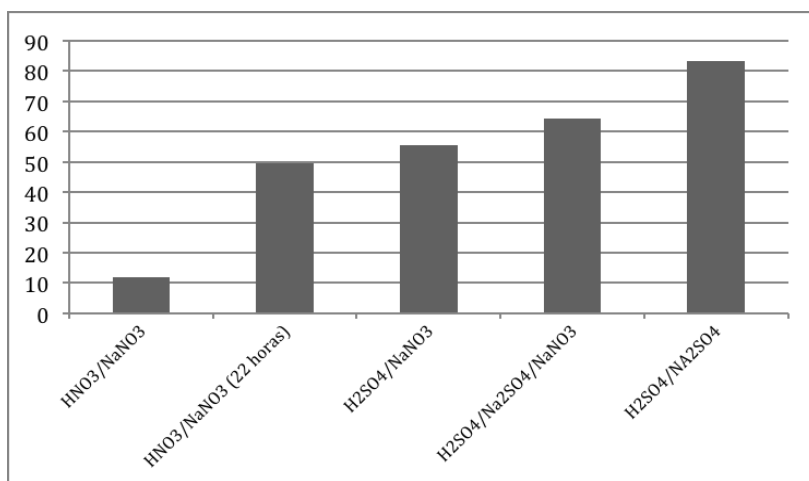
*Universidade de São Paulo, CEP 14040-901, Ribeirão Preto, SP, Brazil*

The increase of industrial activities and the production of dyes resulted in environmental problems due to the generated effluents<sup>1</sup>. Among the various types of azo dyes, Disperse Yellow 3 (DY3) presents carcinogenic potential<sup>2</sup> and needs to be removed from wastewaters.

In this work the electrochemical oxidation of DY3 on boron-doped diamond anode (BDD) was investigated in different conditions as an alternative to degrade it and to produce less toxic effluents.

Electrolyzes performed in sulfuric acid medium indicate that it was possible to decrease the solution absorbance and to mineralize DY3 dye using BDD anodes. Cyclic voltammetry results showed that the dye does not present oxidation or reduction peaks, which suggest that the DY3 degradation does not occur directly and may occur indirectly due to the formation of oxidant agents.

The increment of sulfuric acid concentration or the increasing of the concentration of sulfate ions, results in a higher efficiency of the dye degradation. The result suggests that the DY3 degradation occurs mainly due to the sulfate radical formation from the interaction of hydroxyl radicals generated on the surface of BDD and sulfate ions. Electrolyzes carried out in nitric acid/sodium nitrate solutions confirms that the presence of sulfate is an important factor in order to obtain high degradation degree.



Percentage removal of TOC in different electrolytes in solution of pH 0,5 and ionic strength of 1,95 mol L<sup>-1</sup> after 2 hours of electrolysis.

<sup>1</sup> Ghaly, A. E.; Ananthashankar, R.; Alhattab, M.; Ramakrishnan, V.V.; Production, Characterization and Treatment of Textile Effluents: A Critical Review, *J. Chem. Eng. Process Technol.*, 5, 1-18 (2014).

<sup>2</sup> Li, K.; Beaumont, J., Evidence on the carcinogenicity of C.I. disperse yellow 3, *ed. Oehha*, (2012).

# Coupling Wind Turbines and PV Panels to Electrochemical Processes: Treatment of Wastewater and Soil Polluted with Herbicides

Souza, F.L.<sup>1</sup>; Sáez, C.<sup>2</sup>; Llanos, J.<sup>2</sup>; Lanza, M.V.<sup>1</sup>; Cañizares, P.<sup>2</sup>; Rodrigo, M.A.<sup>2</sup>.

<sup>1</sup>*Chemical and Molecular Physical Department. Institute of Chemistry of Sao Carlos, University of Sao Paulo. Av. Trabalhador Sao Carlense 760 Sao Carlos. SP. Brazil.*

<sup>2</sup>*Chemical Engineering Department. Faculty of Chemical Sciences and Technologies, University of Castilla-La Mancha. Av. Camilo José Cela 12.13005 Ciudad Real. Spain*

\* [javier.llanos@uclm.es](mailto:javier.llanos@uclm.es)

Electrochemical technologies are an efficient alternative for the removal of pesticides from wastewater and soil [1]. Their main operational cost and environmental impact is associated with the use of electricity. A way to minimise this impact is to use a renewable source of energy, which also allows the use of this technology in remote applications, where no grid electricity is available [2]. This work aims at coupling wind turbine and photovoltaic panels to Conductive-Diamond Electrochemical-Oxidation (CDEO) and to Electrokinetic Soil Flushing (EKSF), comparing the results obtained in the green remediation with those obtained when the systems are fed with a power supply. Pesticide 2,4 dichlorophenoxyacetic acid was used as model pollutant for all studies.

For EKSF remediation tests a horizontal methacrylate column (20 cm) with different compartments was used in order to compare the differences obtained with the different energy supplies. Reference experiments were carried out powering the systems potentiostatically using an electric field of  $1.0 \text{ V cm}^{-1}$ . The setup included two electrolyte compartments and reservoirs, using graphite as anode and cathode ( $10 \times 10 \text{ cm}^2$  each). Kaolinite was selected as a model low-permeability soil. The duration of the experiments was two weeks. Significant differences were obtained in the main parameters after this long period. Relevant amounts of the herbicide contained in the soil were removed in the three experimental setups. Main fluxes (electroosmosis and evaporation), changes in the most relevant parameters (pesticide concentration, total organic carbon, moisture conductivity and pH) during treatment and a complete post-mortem analysis are compared in order to give a comprehensive description of the most relevant processes occurring in the soil and to compare the performance of the remediation technology as a function of the electrical powering device used.

The CDEO of the wastewater polluted with pesticide were also studied using the PV array and the wind turbine and results were compared to those obtained powering the system galvanostatically with a power supply (reference experiment was carried out applying 3.0 A of the external current). In this case the experiments were shorter (two-days length). The electrolyses were applied to  $4 \text{ dm}^3$  of a solution containing  $100 \text{ mg dm}^{-3}$  2,4-D at natural pH (3.5) and  $3.0 \text{ g L}^{-1}$  NaCl as a supporting electrolyte. The mineralisation of wastewater was completely accomplished regardless of the way of powering the electrolytic cell, although differences in performance are clearly observed in the total organic carbon (TOC) and 2,4-D decays. These changes are explained in terms of the changing profile of the current intensity, which influences the concentrations of the oxidants produced and thereby the mediated electrolytic process.

## References

1. M.A. Rodrigo, N. Oturan, M.A. Oturan, Electrochemically Assisted Remediation of Pesticides in Soils and Water: A Review, *Chemical Reviews*, 114 (2014) 8720-8745.
2. J.A. Carta, J. González, V. Subiela, Operational analysis of an innovative wind powered reverse osmosis system installed in the Canary Islands, *Solar Energy*, 75 (2003) 153-168.
3. E. Mena, J. Villasenor, P. Canizares, M.A. Rodrigo, Effect of a direct electric current on the activity of a hydrocarbon-degrading microorganism culture used as the flushing liquid in soil remediation processes, *Sep. Purif. Technol.* 124 (2014) 217-223.

## Acknowledgements

The authors acknowledge funding support from the EU and Spanish Government through the MINECO Project CTM2013-45612-R, FEDER 2007-2013 PP201010 (Planta Piloto de Estación de Estación de Regeneración de Aguas Depuradas) and INNOCAMPUS. Brazil government by grant 2014/02580-7, Foundation for Research Support of the State of São Paulo (FAPESP) is gratefully acknowledged.

# Electrokinetic Remediation of Lead-contaminated Carbonate-rich Soil

Maria Villen-Guzman<sup>1</sup>, Jose M. Rodriguez-Maroto<sup>1</sup>, Cesar Gomez-Lahoz<sup>1</sup>,  
Matti Ristinmaa<sup>2</sup>, Stephen Hall<sup>2</sup>, Juan M. Paz-Garcia<sup>2</sup>

<sup>1</sup> Department of Chemical Engineering, University of Malaga, Malaga, Spain

<sup>2</sup> Division of Solid Mechanics, Lund University, Lund, Sweden

Juanma.paz@me.com

Soil contamination is a well-recognized environmental problem. Electrokinetic remediation (EKR) is, probably, the only feasible alternative among the different *in-situ* techniques for the remediation of low-permeability soils. EKR consists of the electrochemically-induced mobilization of contaminants by establishing an electric potential difference between two electrodes inserted in the soil. During the EKR process, the transport of ionic contaminants (as e.g. heavy metals) is mainly due to electromigration, while non-ionic contaminants (as e.g. organic compounds) migrate mainly by electroosmosis.

EKR requires some kind of enhancement in order to make the technique selective (in the target contaminant) and efficient (in terms of remediation and energy consumption). For example, in the case of a Pb-contaminated calcareous soil or soils with high content of carbonates, it is necessary to prompt the dissolution of the Pb-containing minerals (normally carbonates) using acid, or to extract the Pb from those minerals into aqueous complexes using chelating agents.

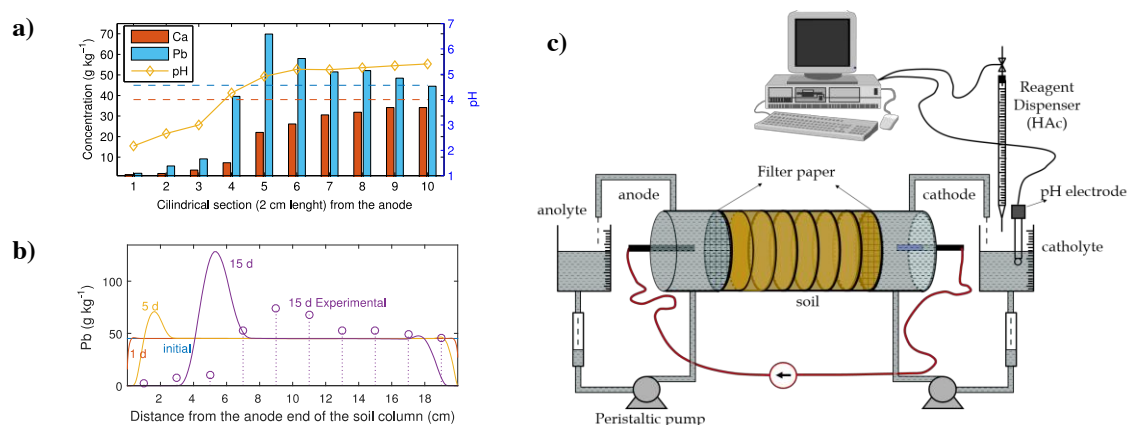


**Figure:** a) Experimental results for EKR remediation in a 20 cm length horizontal column 2 mA cm<sup>-2</sup> using acid enhancement. b) Simulation results for Pb transport. c) Scheme of the experimental setup.

In this work, we present a theoretical and numerical model to describe the coupled electrochemically-induced reactive-transport phenomena taking place in EKR processes in Pb-contaminated calcareous soils. We present here experimental and simulation results for EKR treatments in horizontal column at different lab scales. Numerically and experimentally obtained removal and energy efficiencies are presented and compared, for different enhanced treatments; using acids (acetic acid, nitric acid), extracting agents (acetate ion, citrate ion, EDTA) and ion exchange membranes and at different scales.

## Acknowledgments:

Villen-Guzman acknowledges the FPU grant obtained from the Spanish Ministry of Education. Paz-Garcia acknowledges the financial support from the International Campus of Excellence (ICE) Andalusia Tech.

## References:

- [1] Villen-Guzman et al. Scaling-up the acid-enhanced electrokinetic remediation of a real contaminated soil. *Electrochim. Acta* (2015). doi:10.1016/j.electacta.2015.02.067
- [2] Villen-Guzman et al. Acid Enhanced Electrokinetic Remediation of a Contaminated Soil using Constant Current Density: Strong vs. Weak Acid. *Sep. Sci. Technol.* 49 (2014) 1461–1468.
- [3] Villen-Guzman et al. Effects of the buffering capacity of the soil on the mobilization of heavy metals. Equilibrium and kinetics. *Chemosphere* 131 (2015) 78–84

# Development of Air Electrode Material Comprising Nano-oxide on Ni for MH/Air Secondary Battery

Masafumi Yasuno<sup>1</sup>, Kenji Kawaguchi<sup>2</sup>, and Masatsugu Morimitsu\*<sup>1,3</sup>

<sup>1</sup>Department of Science of Environment and Mathematical Modeling,

<sup>2</sup>Organization for Research Initiatives and Development,

<sup>3</sup>Department of Environmental Systems Science,

Doshisha University

1-3 Tatara-miyakodani, Kyotanabe, Kyoto 610-0394, Japan

\*E-mail: mmorimit@mail.doshisha.ac.jp

An MH/air secondary battery is one of the promising candidates for next generation energy storage devices, which has some distinctive features; for example, the discharge at the positive electrode uses oxygen in air, so that theoretically, there is no limitation on the active mass of the positive electrode and on the discharge capacity, leading a high theoretical energy density. We have been developing this battery to achieve such a high energy density, for which low polarization and high durability is important for the positive electrode. In our previous studies [1], nickel has been used as the conductive and catalyst-supporting material of the positive electrode, because of its high stability in strong alkaline solutions, while it is needed to improve the dispersibility of oxide catalysts on nickel powders to reduce the polarization of oxygen reactions during charge and discharge. In this study, we aimed to develop a new method to prepare oxide loaded nickel powders as the positive electrode's material, in which  $\text{Bi}_2\text{Ir}_2\text{O}_{7-z}$  was used as the catalyst and was tried to uniformly disperse on nickel powders by modified co-precipitation and calcination method.

$\text{Bi}_2\text{Ir}_2\text{O}_{7-z}$  was produced through co-precipitation and calcination process, which was calcination at 600 °C of the precipitates obtained from the metal salt solution containing Bi(III) and Ir(IV) by adding excess NaOH solutions. Nickel powders were added to the precursor solution before or after co-precipitation. The obtained oxide loaded nickel was characterized by XRD, SEM, and EDX and then used to prepare the positive electrode by mixing with PTFE, followed by pressing and heating at 370 °C. The polarization behaviors of the positive electrode were measured with a three-electrode cell, in which one side of the positive electrode faced 6 mol/L KOH solutions, and the other side to air.

XRD results of the product obtained by the addition of nickel powders after co-precipitation showed some diffraction peaks of  $\text{Bi}_2\text{Ir}_2\text{O}_{7-z}$ , Ni, and NiO, for which NiO seems to be formed during heating of the precipitates at 600 °C. SEM images of the product showed  $\text{Bi}_2\text{Ir}_2\text{O}_{7-z}$  particles on nickel powders, and the presence of the oxide was also supported by element distribution from EDX. Figure 1 shows the polarization curves of the positive electrode (a) prepared by using the  $\text{Bi}_2\text{Ir}_2\text{O}_{7-z}$  loaded Ni powders. The polarization is higher than that obtained with another positive electrode (b) consisting of nickel,  $\text{Bi}_2\text{Ir}_2\text{O}_{7-z}$ , and PTFE, in which nickel powders were mixed with the oxide particles separately prepared by co-precipitation and calcination process at the same conditions. The results suggest that a further modification of the process to form  $\text{Bi}_2\text{Ir}_2\text{O}_{7-z}$  on nickel powders is needed to suppress NiO and reduce the oxide size in order to enhance the dispersibility of the oxide catalyst.

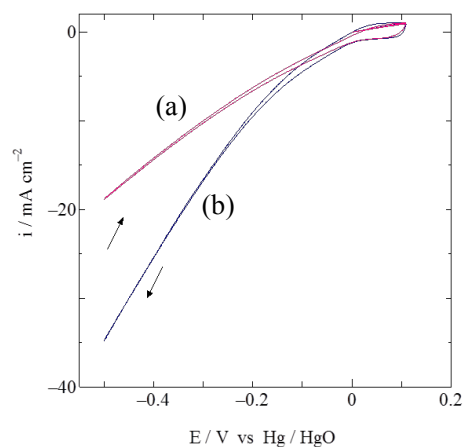


Fig. 1 Cyclic voltammograms of the positive electrodes at 5 mV/s.

*This work was financially supported by “Advanced Low Carbon Technology Research and Development Program (ALCA)” of Japan Science and Technology Agency (JST).*

## Reference

- [1] M. Morimitsu, T. Kondo, N. Osada, and K. Takano, *Electrochemistry*, Vol. 78, No. 5, pp. 493-496 (2010)

# A Challenge to Synthesize $\text{Bi}_2\text{Ir}_2\text{O}_{7-z}$ -based Hybrid Oxide for Oxygen Reduction

Kazuya Takeuchi<sup>1</sup>, Kenji Kawaguchi<sup>2</sup>, and Masatsugu Morimitsu<sup>\*1,3</sup>

<sup>1</sup>Department of Science of Environment and Mathematical Modeling,

<sup>2</sup>Organization for Research Initiatives and Development,

<sup>3</sup>Department of Environmental Systems Science,

Doshisha University

1-3 Tatara-miyakodani, Kyotanabe, Kyoto 610-0394, Japan

\*E-mail: mmorimit@mail.doshisha.ac.jp

Oxygen reduction reaction (ORR) is known as the cathodic reaction in fuel cell or metal/air battery and needs a high overpotential over 300 mV, which is still an issue in such applications. While the typical catalyst in practical uses is only platinum nanoparticles as in PEFC, it has been reported that  $\text{SnO}_2$  coexisting platinum on carbon materials has an effect to decrease the overpotential [1], although  $\text{SnO}_2$  itself has lower activity for ORR than platinum. A similar situation has been found in  $\text{IrO}_2$ - $\text{Ta}_2\text{O}_5$  mixed oxide catalyst for oxygen evolution, where  $\text{IrO}_2$  is highly active and  $\text{Ta}_2\text{O}_5$  is inactive, but the mixed oxide can possess a higher catalytic activity for oxygen evolution than  $\text{IrO}_2$  [2]. Such  $\text{Ta}_2\text{O}_5$  effects are in acidic solutions and for oxygen evolution, and there has been no investigation for oxygen reduction and in alkaline media. From these backgrounds, this work tried to produce a hybrid oxide comprising  $\text{Ta}_2\text{O}_5$  existing on  $\text{Bi}_2\text{Ir}_2\text{O}_{7-z}$  particles which are now being used as the bi-functional oxygen catalyst for metal hydride/air secondary battery by our group. This paper reports a possibility of hybridization of such pyrochlore type oxide with  $\text{Ta}_2\text{O}_5$  and the results on polarization for ORR in alkaline solutions.

$\text{Bi}_2\text{Ir}_2\text{O}_{7-z}$  powders were prepared by co-precipitation and calcination of the precipitates obtained by adding excess NaOH solutions into the metal salt solution containing Bi(III) and Ir(IV). The obtained powders were coated with a Ta precursor solution, which was  $\text{TaCl}_5$  dissolved in ethanol, and then heated to obtain  $\text{Ta}_2\text{O}_5$  coated  $\text{Bi}_2\text{Ir}_2\text{O}_{7-z}$ . Some conditions on the coating process and the heating temperature were examined, and the products were analyzed by XRD, SEM, and EDX. The polarization for oxygen reduction on the obtained hybrid oxide was measured with rotating disk electrode (RDE) and 0.1 mol/L KOH solutions and was compared to that on  $\text{Bi}_2\text{Ir}_2\text{O}_{7-z}$ .

The preliminary results on the condition of  $\text{Ta}_2\text{O}_5$  production by direct thermal decomposition of  $\text{TaCl}_5$  showed that  $\text{Ta}_2\text{O}_5$  was produced by heating at 650 °C for a few minutes, so that the similar condition was applied to the Ta precursor solution to make  $\text{Ta}_2\text{O}_5$  on  $\text{Bi}_2\text{Ir}_2\text{O}_{7-z}$ . Figure 1 shows the SEM image of the obtained product, which are almost the same as pure  $\text{Bi}_2\text{Ir}_2\text{O}_{7-z}$  in size and form. However, EDX analysis indicated that tantalum existed on the particles uniformly and the Ta content was 13.2 at.% in maximum in total of Bi, Ir, and Ta. The surface morphology of  $\text{Bi}_2\text{Ir}_2\text{O}_{7-z}$  particles was unchanged by Ta treatment, and it seems that  $\text{Ta}_2\text{O}_5$  growth is suppressed and nano  $\text{Ta}_2\text{O}_5$  is presented on  $\text{Bi}_2\text{Ir}_2\text{O}_{7-z}$  surface, because no diffraction peak of  $\text{Ta}_2\text{O}_5$  was observed for the hybrid oxide. The obtained hybrid oxide and pure  $\text{Bi}_2\text{Ir}_2\text{O}_{7-z}$  were separately loaded on a titanium disk with support by ionomers. For each case, the oxygen reduction current on RDE was recorded and showed a diffusion-limited current, although the onset potential of oxygen reduction was much lower than that measured with the air electrode using  $\text{Bi}_2\text{Ir}_2\text{O}_{7-z}$  as the catalyst in another experiment by our group. Therefore, the detailed comparison of the hybrid oxide to pure  $\text{Bi}_2\text{Ir}_2\text{O}_{7-z}$  for oxygen reduction activity is still under progress, and such results will be also shown in this paper.

This work was financially supported by “Advanced Low Carbon Technology Research and Development Program (ALCA)” of Japan Science and Technology Agency (JST).

## References

[1] T. Kinumoto, *Tanso*, Vol. 2014, No. 263, pp. 114-122 (2014).

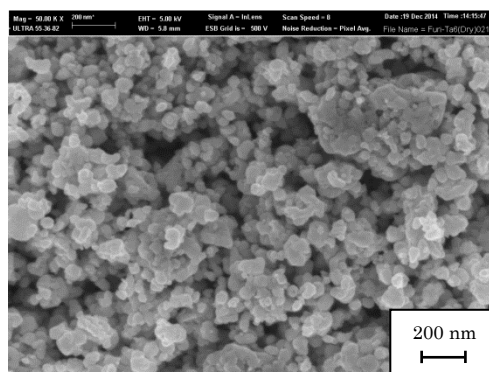


Fig. 1 SEM image of hybrid oxide.

[2] M. Morimitsu, *Journal of MMIJ*, Vol. 130, pp. 415-420 (2014).

# Electrokinetic remediation of natural soil polluted with the herbicide 2,4-D

M.A. Rodrigo, C. Risco, C. Sáez, R. López-Vizcaino, C.M. Fernandez-Marchante, P. Cañizares, V. Navarro

*Department of Chemical Engineering, Faculty of Chemical Sciences and Technologies, Universidad de Castilla-La Mancha, Campus Universitario s/n. 13005 Ciudad Real, Spain. Phone: +34926 29 53 00*

*Fax: +34926 29 52 56*

*manuel.rodrigo@uclm.es*

In the recent years, there is an increasing concern of agencies and scientific community about the use of pesticides because of their high risks to human health and the environment. In this context, the 2,4-dichlorophenoxyacetic acid (2,4-D) is a chlorinated phenoxy herbicide, widely used to control many types of broadleaf weeds. This systemic herbicide is considered moderately toxic by World Health Organization and it is known to affect the nervous system of humans and animals. Since this compound exhibit high water-solubility, lifetime and mobility, its continuous use may cause soil percolation and groundwater contamination.

Electrokinetic remediation (ER) of soil has become a leading technology in the treatment of low permeability contaminated soils due to the wide range of contaminants that can be eliminated (salts, metals and organic compounds) and to its operational flexibility. ER is based on the different processes that occur into the soil when a low DC electric potential is applied through a group of electrodes sited into the same soil: electromigration (movement of ions), electrophoresis (movement of charge particles) and electro-osmosis (movement of groundwater contained in the soil or water added to enhanced the operation conditions) (Lopez-Vizcaino et al., 2011; Lopez-Vizcaino et al., 2014).

In this context, the goal of this research has been to develop flushing electrokinetic technologies for the remediation of soil polluted with 2,4-D. To do this, experiments around 40 days of duration have been carried out in bench-scale set-ups (175 dm<sup>3</sup>), completely automatized. Electrical current, temperature, pH, humidity and pollutant concentration in electrolyte wells were daily monitored, and at the end of the experiments an in-depth post-mortem analysis of the complete soil sections was carried out.

Results show that during the electro-remediation process many processes controlled by electrochemical and non-electrochemical mechanisms take place simultaneously. Even in the case of low-permeability soil, gravity and evaporation fluxes are comparable to electrokinetic fluxes. Likewise, it was observed that 2,4-D is mobilized to the anode wells mainly by electromigration, and that it is also moved towards the cathode by electroosmotic drag. Results are discussed at the light of the present knowledge of the transport process and sound conclusions about the scale up of the process are drawn.

## Acknowledgements

This work has been supported by MINECO through the project CTM2013-45612-R.

Lopez-Vizcaino, R., Alonso, J., Canizares, P., Leon, M.J., Navarro, V., Rodrigo, M.A., Saez, C., 2014. Electroremediation of a natural soil polluted with phenanthrene in a pilot plant. *Journal of Hazardous Materials* 265, 142-150.

Lopez-Vizcaino, R., Saez, C., Mena, E., Villasenor, J., Canizares, P., Rodrigo, M.A., 2011. Electro-osmotic fluxes in multi-well electro-remediation processes. *Journal of Environmental Science and Health Part a-Toxic/hazardous Substances & Environmental Engineering* 46, 1549-1557.



# Degradation of Industrial Textile Dye Disperse Red BG by electro-oxidation: Role of Anode, pH and supporting electrolyte

*Ricardo Salazar<sup>1</sup>, Christian Candia-Onfray<sup>1</sup>, Carlos Alberto Martinez-Huitle<sup>2</sup>*

*<sup>1</sup>Laboratorio de Electroquímica Medioambiental, LEQMA. Departamento de Química de los Materiales, Universidad de Santiago de Chile, USACH, Casilla 40, Correo 33, Santiago, Chile. <sup>2</sup>Federal University of Rio Grande do Norte, Institute of Chemistry Lagoa Nova - CEP 59.072-970, RN, Brazil.*

*E-mail: [ricardo.salazar@usach.cl](mailto:ricardo.salazar@usach.cl)*

## Symposium 10

This study aimed to verify the efficiency of the electrochemical oxidation process for removal Disperse Red BG (DRBG) dye in aqueous solutions using different electrocatalytic materials: BDD, Ti/PbO<sub>2</sub>, Ti/Pt, and Ti/Ru<sub>0.3</sub>Ti<sub>0.7</sub>O<sub>2</sub> anodes. The results were obtained by applying different current densities (20 and 50 mAcm<sup>-2</sup>) at 25°C using different supporting electrolytes (Na<sub>2</sub>SO<sub>4</sub> 1.0 g L<sup>-1</sup> and NaCl 1.0 and 3.0 g L<sup>-1</sup>) under values of pH 3 and 7. The conditions were selected in order to mimic the real textile effluent discharge. The anodic oxidation of DRBG dye was monitored by COD, HPLC and spectrophotometry.

The results obtained showed that the solution remain colored after 180 min applying 20 mAcm<sup>-2</sup> all electrocatalytic materials, using Na<sub>2</sub>SO<sub>4</sub> as electrolyte, being more efficient for BDD follow by Ti/PbO<sub>2</sub> and Ti/Pt; while Ti/Ru<sub>0.3</sub>Ti<sub>0.7</sub>O<sub>2</sub> showed a poorly decolorization and DOC removal. At 20 mAcm<sup>-2</sup> only BDD electrode produces a total mineralization of the solution after 180 min of electrolysis.

Conversely, at NaCl medium, more efficient color removal was achieved using all electrodes. Decolorization and mineralization are depending of the applied density current and supporting electrolyte concentration. Ti/Ru<sub>0.3</sub>Ti<sub>0.7</sub>O<sub>2</sub>, BDD and Ti/PbO<sub>2</sub> reached >90% of COD and color removal in NaCl medium. By HPLC analysis, the behavior of DRBG during anodic oxidation using each anode was studied too. The corresponding kinetic analysis confirms the results mentioned before. Carboxylic acids formed during the mineralization of DRBG using each electrode were detected and quantified. The profiles of each acid depend of the anodic material, of the applied density current and supporting electrolyte.

## References

- [1] J. M. Poyatos, M. M. Muño, M. C. Almecija, J. C. Torres, E. Hontoria, F. Osorio. Advanced Oxidation Processes for Wastewater Treatment: State of the Art. *Water Air Soil Pollut* (2010) 205: 187-205
- [2] C. Comninellis. Electrocatalysis in the electrochemical conversión/combustión of organic pollutants for waste water treatment. *Electrochimica Acta*, Vol 39 (1994), 1857-1864.

We are grateful to DICYT-USACH and FONDECYT Grant 1130391.

# Development of Intermediate Temperature Fuel Cells using Methylcyclohexane Organic Hydride Fuel

Yosuke Imanishi, Tatsuma Yahara, Tatsuro Haruki, Yuki Orikasa, and Yoshiharu Uchimoto

Graduate school of Human and Environmental Studies, Kyoto University, Sakyo-ku, Kyoto 606-8501  
Japan

imanishi.yosuke.38z@st.kyoto-u.ac.jp

Recently, renewable energy has received a lot of attention because of its comparative safety and cleanness. However, the areas where renewable energy can be supplied substantially are often far from energy demand areas. It is essential to develop the technology of transportation for renewable energy. One of the attractive solutions for this problem is using methylcyclohexane (MCH) - Toluene (TL) organic hydride as fuel. The MCH - TL organic hydride system is a valuable system for hydrogen storage and transportation using hydrogenation and dehydrogenation chemical reactions. In the energy supply areas, TL and  $H_2$  produced by renewable energy react to form MCH. In the energy demand areas, MCH reacts to form TL and  $H_2$ , and TL is transported back to the energy supply areas. In this way, MCH - TL organic hydride is reusable compound. However, the fuel cell using MCH directly as fuel has not been studied widely. In this study, we developed two types of organic hydride fuel cells. One is the direct type fuel cell, where MCH is directly supplied to anode. The other is the internal reforming type fuel cell, in which internal reforming catalyst which reforms MCH to  $H_2$  and TL is placed in front of the electrode.

We used the proton conducting electrolyte based on  $CsH_2PO_4/SiP_2O_7$  composite<sup>[1]</sup>, and Pt/C (Chemix,  $1.0 \text{ mg cm}^{-2}$ ) as electrodes. A gaseous mixture of MCH (4%),  $H_2O$  (30%) and  $N_2$  (humidified MCH gas) was supplied to the anode electrode, and a gaseous mixture of  $H_2O$  (30%),  $O_2$  and  $N_2$  (humidified Air gas) was supplied to the cathode electrode. These measurements were conducted at  $260^\circ\text{C}$  under these gases.

Fig. 1 shows the cell voltage and power density as a function of current density of MCH fuel cell operating at  $260^\circ\text{C}$ . In the direct type cell, the open circuit voltage is 0.71 V, and the maximum current density and power density are  $10.9 \text{ mA cm}^{-2}$  and  $2.4 \text{ mW cm}^{-2}$  at  $5.8 \text{ mA cm}^{-2}$  respectively. This result represents electric power generation using MCH directly as fuel. On the other hand, in the internal reforming type, the open circuit voltage is 0.74 V. Compared with the direct type cell, higher power density,  $3.4 \text{ mW cm}^{-2}$  at  $9.2 \text{ mA cm}^{-2}$  is observed. These results imply MCH is dehydrogenated to form TL and  $H_2$  through internal reforming catalyst, and  $H_2$  is supplied to anode. However, the observed power density is less than that using humidified  $H_2$  gas as fuels. Residual MCH or TL might impede the electrochemical reaction in the anode.

## Acknowledgement

This study was partially supported by Cross-ministerial Strategic Innovation Promotion Program (SIP).

## References

- [1] T. Matsui, T. Kukino, R. Kikuchi, and K. Eguchi, *Electrochem. Solid-State Lett.*, **2005**, 8, A256-A258

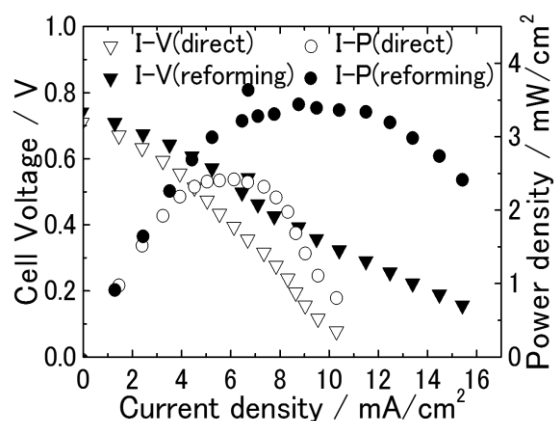


**Figure 1.** I-V and I-P characteristics in the direct type or the inner reforming type at  $260^\circ\text{C}$  under humidified MCH gas and humidified air gas.

# Toward Cost Effectiveness of Alkaline Water Electrolysis for Hydrogen Economy

Jong-Hoon Kim<sup>1,2,3</sup>, Jung-Nam Lee<sup>3</sup>, Chung-Yul Yoo<sup>4</sup>, Woong-Moo Lee<sup>3</sup>

1. Power Electronics Lab, Ajou University

Woncheon Hall #435, Ajou University 206, World cup-ro, Yeongtong-gu, Suwon 443-749, Korea,

2. LightBridge Inc.

GSBC #609, Lui-dong, Yeongtong-gu, Suwon 443-766, Republic of Korea

3. PAHPS Inc.

Hyomyung Bldg #402, 1029-7 Hogue-dong, Dongan-gu, Anyang, Republic of Korea

4. Korea Institute of Energy Research

152 Gajeong-ro, Yuseong-gu, Daejeon 305-343, Republic of Korea

jegallhun@gmail.com

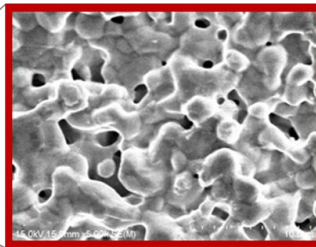
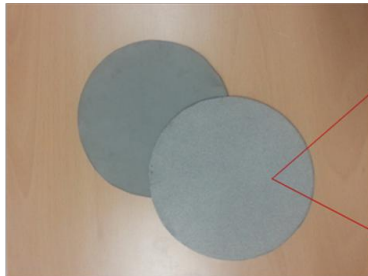
The light is being refocused on the value of the electrolysis market due to the renewable energy (especially in the increasing trend of the wind power and solar cell generation), the necessity of the energy storage system, and the applicability of electrolysis in the hydrogen station, and our research came to the conclusion that there is a solution for such a direction.

In order for the electrolysis to be actively applied in the industry, it not only has to have an advantage with regard to the efficiency but also in term of the cost. With such significance, the alkaline water electrolyzer which does not use expensive noble metal catalyst will be the most ideal electrolyzer.

In our lab, we used porous asymmetric high surface area nickel electrodes and manufactured stacks using such highly efficient electrodes.

In regard to the structural characteristic of electrodes, the obtained current density of the unit cell is close to  $600\text{mA}/\text{cm}^2$  at the voltage of  $1.8\text{V}$ , while also acquiring enough competence for commercialization in manufacturing cost and processing aspects.

Additionally in our lab, we have developed the miniaturized alkaline water electrolysis system through application the stack technique that we have, and now reviewing the applicability to the hydrogen station and HESS (Hydrogen Energy Storage System).

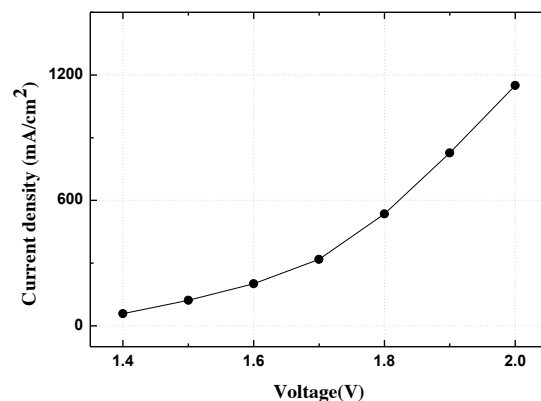


(a) Porous nickel electrode

- Size:  $16\Phi$
- Material: Nickel
- Active cell area:  $200\text{ cm}^2$
- Current density:  
 $>0.4\text{A cm}^{-2}$  at  $1.8\text{V}$
- Pore size:  $3\sim7\mu\text{m}$



(b) Stack with 10 cells



(c) Voltage-current curve

# Integrated Bundle Structure of Rolling Free Standing Triboelectric Nanogenerators and its Applications in Self-powered Copper Collecting Electrochemical system *via* Harvesting Hydropower

Min-Hsin Yeh<sup>a</sup>, Hengyu Guo<sup>a,b</sup>, Long Lin<sup>a</sup>, Zhen Wen<sup>a</sup>, Zhaoling Li<sup>a</sup>,  
Chenguo Hu<sup>b</sup>, and Zhong Lin Wang<sup>a,c\*</sup>

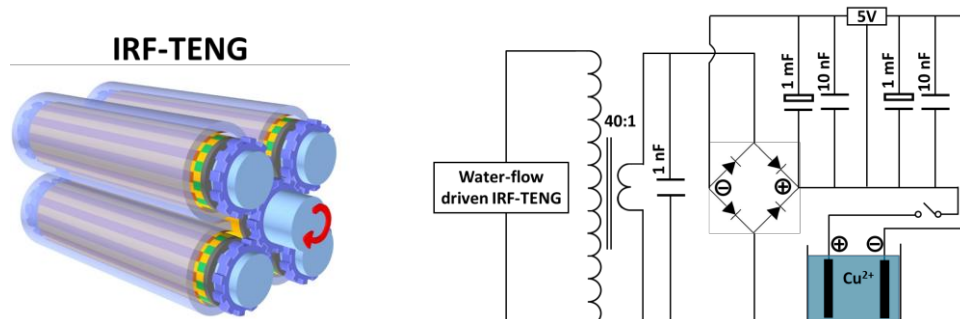
<sup>a</sup>*School of Material Science and Engineering, Georgia Institute of Technology, Atlanta, GA, USA*

<sup>b</sup>*Department of Applied Physics, Chongqing University, Chongqing 400044, People's Republic of China*

<sup>c</sup>*Beijing Institute of Nanoenergy and Nanosystems, Chinese Academy of Sciences, Beijing, China*  
500 10<sup>th</sup> St. NW, Atlanta, GA 30318, USA

\*zhong.wang@mse.gatech.edu

Plating wastewater contains various kinds of toxic chemical substances (*e.g.* acid cyanide, alkaline cleaning agent, and degreasing solvents) and heavy metals (*e.g.* copper, nickel, and chromium). Most of the heavy metals in wastewater are extremely harmful when they are discharged directly to the environment. Hence, providing an efficient treatment for removing or collecting these heavy metals before discharging becomes important and necessary. Copper (Cu) is one of most common heavy metal ion in the wastewater of printed circuit board (PCB) process. One of the most effective ways for collecting Cu ions is electrochemical process. Cu ions were removed with high efficiency from a dilute industrial effluent in an electrochemical reactor with plate electrode. However, additional direct current based power supplies are unavoidable part to drive it. Recently, self-powered systems have been developed to integrate variable devices into a standalone system with multiple functions, including sensing, communication, computation, *etc.* [1]. The wireless, miniaturized and the large number of components in the system require a renewable, sustainable and clean power supply, and energy harvesting from the ambient environment will be a perfect solution for this problem. In this regard, the triboelectric nanogenerator (TENG) was recently invented to convert the mechanical energy into electricity, based on the coupling effect of contact electrification and electrostatic induction. Here in this work, integrated bundle structure of rolling free standing triboelectric nanogenerator (IRF-TENG) with outstanding output performance and ultrahigh longterm stability was proposed for harvesting hydropower and further applied in self-powered electrochemical system for collecting Cu ions. With the above design, the IRF-TENG delivers an open-circuit voltage ( $V_{OC}$ ) up to  $\sim 450$  V and a short-circuit current of 0.2 mA under a rotation speed of 1000 rpm. Ultra robust characteristic can be fully realized by introducing the frictionless free standing TENG structure with rolling bearing for refilling its superficial charge. Moreover, several unit of rolling free standing TENG [2] can be integrated by means of incorporating with common mechanical gears to bring about the integrated bundle structure of rolling free standing TENG. By integrating with a power management circuit, stable DC output (5V, 4 mA) performance can be achieved by hydropower driven IRF-TENG to practically realize the concept of self-powered electrochemical system for collecting Cu ions. This work provides a significant progress of TENG and exhibits huge potential of the IRF-TENG as a high efficiency energy harvester for practical applications.



## Key Reference:

- [1] Z. L. Wang, Triboelectric nanogenerators as new energy technology for self-powered systems and as active mechanical and chemical sensors, *ACS Nano* 7 (2013) 9533.
- [2] H. Guo, J. Chen, M. H. Yeh, X. Fan, Z. Wen, Z. Li, C. Hu, and Z. L. Wang, An ultra-robust high-performance triboelectric nanogenerator based on charge replenishment, *ACS Nano* (2015) (Revised).

# **The Cone Penetration Test and 2D Imaging Resistivity as Tools to Simulate the Distribution of Hydrocarbon in Soil**

M. Pérez-Corona,<sup>1,2</sup> J. A. García,<sup>1,2</sup> G. Taller,<sup>2</sup> D. Polgár,<sup>2</sup> Z. Plank,<sup>2</sup> and E. Bustos<sup>1</sup>

<sup>1</sup>*Department of Science, Centro de Investigación y Desarrollo Tecnológico en Electroquímica, S. C. Parque Tecnológico Querétaro s/n, Sanfandila, Pedro Escobedo, 76703, Querétaro, Qro. Mexico.*

<sup>2</sup>*Geological and Geophysical Institute of Hungary. H-1143, Budapest, Hungary.*

[ebustos@cideteq.mx](mailto:ebustos@cideteq.mx)

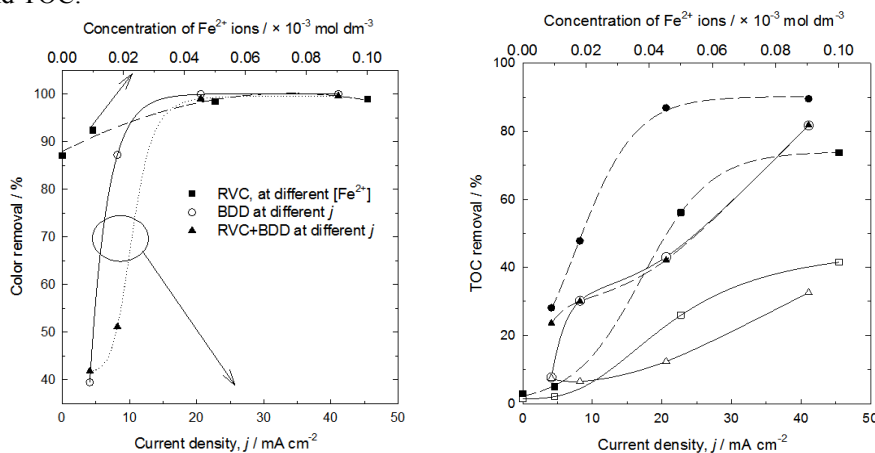
The purpose of geophysical electrical surveys is to determine the subsurface resistivity distribution by making measurements on the ground surface. From these measurements, the true resistivity of the subsurface can be estimated. The ground resistivity is related to various geological parameters, such as the mineral and fluid content, porosity and degree of water saturation in the rock.

Electrical resistivity surveys have been used for many decades in hydrogeological, mining and geotechnical investigations. More recently, they have been used for environmental surveys. To obtain a more accurate subsurface model than is possible with a simple 1-D model, a more complex model must be used. In a 2-D model, the resistivity values are allowed to vary in one horizontal direction (usually referred to as the  $x$  direction) but are assumed to be constant in the other horizontal (the  $y$ ) direction. A more realistic model would be a fully 3-D model where the resistivity values are allowed to change in all three directions. In this research, a simulation of the cone penetration test and 2D imaging resistivity are used as tools to simulate the distribution of hydrocarbons in soil.

# Electrochemical degradation of RB-5 dye by anodic oxidation, electro-Fenton and by combining anodic oxidation-electro-Fenton in a filter-press flow cell

I. Ishita, V.M. Vasconcelos, C. Ponce-de-León, M.R.V. Lanza, J.L. Nava  
Faculty of Engineering and the Environment, University of Southampton  
University Road, Southampton, SO17 1BJ

The removal of Reactive Black 5 (RB-5) was carried out by three methods; 1) anodic oxidation (AO) on Boron-Doped Diamond (BDD), 2) by electro-Fenton (EF) process where hydrogen peroxide was produced by  $O_2$  reduction on reticulated vitreous carbon (RVC) electrodes and 3) by the combination of AO-EF. The BDD and RVC electrodes were fitted in a filter-press flow cell in recycle batch mode of operation. The experimental set up for the AO and EF processes consisted on two electrolyte compartments separated by a Nafion membrane with the dye contained in the anolyte and the catholyte, respectively. The combined AO-EF process used only one electrolyte compartment. The color and total organic carbon (TOC) removal were more efficient when the AO and EF processes were used separately than the combined process, AO-EF. The influence of current density and initial concentration of ferrous ions were examined. The lowest energy efficiency ( $208 \text{ kWh kg}^{-1}$ ) with the EF process was found when  $-0.4 \text{ V vs Ag/AgCl}$  was applied to a RVC electrode and the concentration of  $Fe^{2+}$  was  $1.0 \times 10^{-4} \text{ mol dm}^{-3}$  achieving total color and 74% TOC removal in less than 90 min electrolysis. All the processes oxidize RB-5 dye completely and promote high percentages of TOC removal following a pseudo first order kinetic oxidation. The BDD electrode was the most effective material to remove RB-5 dye within 7.5 min and presented the highest apparent rate constant ( $0.835 \text{ min}^{-1}$ ) with 82% TOC removal within 30 min at an energy consumption of  $291 \text{ kWh kg}^{-1}$  and  $41.1 \text{ mA cm}^{-2}$  current density. In addition the results of using a mesh BDD electrode will be presented and compared with the electro-Fenton process in terms of energy consumption and TOC.



Color removal after 90 minutes of electrolysis (left) and TOC removal (right) at 30 minutes and 90 minutes of electrolysis: □) RVC at  $-0.4 \text{ V vs Ag/AgCl}$  varying  $Fe^{2+}$  ions, ○) BDD and △) RVC + BDD varying the current density. TOC removal at 90 minutes: ■) RVC at  $-0.4 \text{ V vs Ag/AgCl}$  varying  $Fe^{2+}$  ions, ●) BDD and ▲) RVC + BDD varying the current density. Supporting electrolyte  $0.5 \text{ mol dm}^{-3}$  of  $Na_2SO_4$  at  $23^\circ \text{C}$ , flow rate  $100 \text{ dm}^3 \text{ h}^{-1}$ . Initial concentration of RB-5 dye  $20 \text{ mg dm}^{-3}$ .

## References

- [1] J.A. Ramsay, T. Nguyen, "Decoloration of textile dyes by *Trametes versicolor* and its effect on dye toxicity", *Biotechnology Letters* 24 (2002) 1756-60.
- [2] C. Ponce de Leon, D. Pletcher, "Removal of formaldehyde from aqueous solutions via oxygen reduction using a reticulated vitreous carbon cathode cell", *Journal of Applied Electrochemistry* (1995) 307-14.
- [3] J. Lv, Y. Feng, J. Liu, Y. Qu, and F. Cui, "Comparison of electrocatalytic characterization of boron-doped diamond and  $SnO_2$  electrodes," *Applied Surface Science*, 283 (2013) 900-905.

## Combined soil washing and CDEO for the removal of oxyfluorfen from soils

Santos, E.V.<sup>1</sup>, C. Sáez<sup>2</sup>, Martínez-Huítile, C. A.<sup>1</sup>, Cañizares, P.<sup>2</sup>, M.A. Rodrigo<sup>2</sup>

<sup>1</sup>Federal University of Rio Grande do Norte, Natal, Brazil

<sup>2</sup>Universidad de Castilla-La Mancha, Ciudad Real, Spain

e-mail: elisama\_quimica@yahoo.com.br

Oxyfluorfen is a diphenyl-ether herbicide used for broad spectrum pre- and post-emergent control of annual broadleaf and grassy weeds in a variety of tree fruit, nut, vine, and field crops. The largest agricultural markets in terms of total pounds active ingredient are wine grapes and almonds. There are also non-agricultural ornamental and forestry uses. For this reason, it is very important the rapid actuation against accidental discharges of hazardous species with efficient technologies that remediate the soil rapidly and avoids diffuse pollution. The objective of this study was to investigate under laboratory conditions the behavior of oxyfluorfen in soils consisting of the soil washing with a sodium dodecyl sulphate solution followed by the electrolysis with BDD anodes of the resulting wastewater. Effect of the ratio surfactant /soil is going to be assessed trying to determine its influence in the soil washing efficiency and in the characteristics of the washing waste. Samples of polluted soil (kaolinite) were polluted with a solution prepared by dissolving oxyfluorfen in acetonitrile. The surfactant-aided soil-remediation was carried out in a stirred batch tank. The tank volume was 800 cm<sup>3</sup>. Low-permeability soil (1000 g) was used and polluted with 100 mg oxyfluorfen, adding 800 cm<sup>3</sup> of solubilizing agent (containing deionized water with different amounts of 100, 500, 2500 and 5000 mg dm<sup>-3</sup> of surfactant and 500 mg dm<sup>-3</sup> of NaHCO<sub>3</sub>). Degradation was monitored by total organic carbon (TOC), chemical oxygen demand (COD) reduction and concentration of SO<sub>4</sub><sup>2-</sup>, Cl<sup>-</sup>, ClO<sup>-</sup>, ClO<sub>3</sub><sup>-</sup> and ClO<sub>4</sub><sup>-</sup>, as function of electric charge passed (Q), during galvanostatic electrolysis of simulated effluent solution (700 dm<sup>-3</sup>) using BDD anodes by applying 30 mA cm<sup>-2</sup> at 25 °C. The particle size decreases during the electrochemical process because the electrolysis helps to break the emulsion, especially when dispersed particles are present in the solution Fig. 1. Surfactant aided soil washing with SDS solutions is an efficient technology from the removal of oxyfluorfen from spiked soils. Characteristics of the effluents obtained in the SASW process depends largely on the SDS/soil dosage. In spite of having the same chemical compounds, effluents are and behave in a completely different way, in particular because of the very different type of microdrops. Opposite to other AOP production, production of intermediates is almost negligible in this process. Only 4-(trifluoromethyl)-phenol and ortho-nitrophenol, coming from the oxidation of oxyfluorfen, were detected by HPLC. No intermediates coming from SDS were detected in spite of the high concentrations of SDS in various of the effluents. This indicates that intermediates formed during the process are very rapidly oxidized and that most important processes occurs on the micelles surfaces.

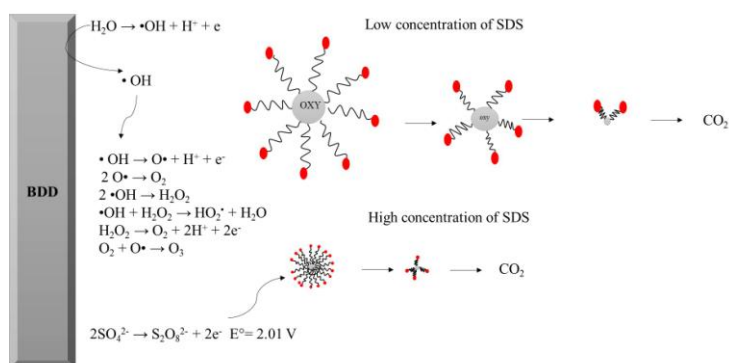


Fig. 1. Scheme of the electrochemical reactions and size particle

### Acknowledgements

E. V. Santos, acknowledges CAPES for her PhD fellowship and CNPq for the scholarship given for “doutorado sanduiche” under “Ciências sem Fronteiras” program to develop the experimental research at the UCLM-Spain. . Financial support of the Spanish Government through the MINECO Project CTM2013-45612-R.



# Extraction Agents for Removing Petroleum from Soil and Application of Electrolysis to Treat Washing Fluid

E.V Santos<sup>1</sup>, C. Sáez<sup>2</sup>, P. Cañizares<sup>2</sup>, M.A. Rodrigo<sup>2</sup>, C.A. Martínez-Huitle<sup>1</sup>

<sup>1</sup>*Federal University of Rio Grande do Norte, Natal, Brazil*

<sup>2</sup>*Universidad de Castilla-La Mancha, Ciudad Real, Spain*

*e-mail: [elisama\\_quimica@yahoo.com.br](mailto:elisama_quimica@yahoo.com.br)*

Petroleum in soil has been recognized as a serious health and environmental issue due to their carcinogenic, mutagenic and teratogenic properties. One of the commonly employed soil remediation techniques to clean up such contamination is soil washing or solvent extraction. It consists on the extraction of pollutants contained in the soil with a solution that helps to obtain an efficient transfer of the pollution from the soil to a liquid phase. In fact, it can be considered as a soil-liquid extraction operation unit, in which the pollutant is transferred from the solid soil to the liquid washing fluid. In the case of organics, the use of surfactant solutions is the most extended application. In order to treat this waste, efficient technologies have to be used as electrolysis with diamond electrodes because of its great robustness and efficiency. It may attain the total removal of pollution by mineralization. This work aims to evaluate the effectiveness of a treatment of a soil spiked with petroleum, consisting of the soil washing with a sodium dodecyl sulphate solution followed by the electrolysis with BDD anodes of the resulting wastewater. Effect of the ratio surfactant/soil is going to be assessed trying to determine its influence in the soil washing efficiency and in the characteristics of the washing waste. Samples of soil (kaolinite) were polluted with a solution prepared by dissolving petroleum in hexane. The surfactant-aided soil-remediation was carried out in a stirred batch tank. The tank volume was 800 cm<sup>3</sup>. Low-permeability soil (1000 g) was used and polluted with 5000 mg petroleum, adding 800 cm<sup>3</sup> of solubilizing agent (containing deionized water with different amounts of 100 at 5000 mg dm<sup>-3</sup> of surfactant and 500 mg dm<sup>-3</sup> of NaHCO<sub>3</sub>). Degradation was monitored by total organic carbon (TOC), chemical oxygen demand (COD) reduction and concentration of SO<sub>4</sub><sup>2-</sup>, Cl<sup>-</sup>, ClO<sup>-</sup>, ClO<sub>3</sub><sup>-</sup> and ClO<sub>4</sub><sup>-</sup>, zeta potential and mean size particle as function of electric charge passed (Q), during galvanostatic electrolysis of simulated effluent solution (700 dm<sup>-3</sup>) using BDD anodes by applying 30 mA cm<sup>-2</sup> at 25 °C. This process transfers the pollution from the soil to a soil washing solution, which becomes wastewater. Comparing the two effluents, it can be observed that the effluent of treatment 2 (with a higher concentration of surfactant in the washing fluid) has a much higher COD and TOC but mean size of particles is much smaller and superficial charge is much more negative. Conversely, in effluent of treatment 1 both petroleum and surfactant are contained in the same mass concentration. This means that very different results are expected when both effluents are treated by electrochemical technologies.

## Acknowledgements

E. V. Santos acknowledges CAPES for her PhD fellowship and CNPq for the scholarship given for “doutorado sanduiche” under “Ciências sem Fronteiras” program to develop the experimental research at the UCLM-Spain. Financial support of the Spanish Government through the MINECO Project CTM2013-45612-R is also acknowledged.



# Electrochemical Oxidation of 2-Naphthol on BDD Anodes: Dissolved Oxygen Participation, Mechanism and Theoretical Calculations

Amison Rick Lopes da Silva, Gustavo Rodrigues de Oliveira, Sergi Garcia-Segura\*,  
Carlos A. Martinez-Huitle\*

*Federal University of Rio Grande do Norte, Institute of Chemistry, Lagoa Nova - CEP  
59.072-970, RN, Brazil. Phone/Fax: +55 (84) 3215-3228.*

*\*E-mail adress: [sergigarcia@ub.edu](mailto:sergigarcia@ub.edu), [carlosmh@quimica.ufrrn.br](mailto:carlosmh@quimica.ufrrn.br)*

The electrochemical oxidation (EO) is presented as an alternative clean, efficient and economical for treating wastewater containing organic compounds [1]. However, it still needs some amendments concerning their mechanisms and kinetics followed. Comninellis and his research a group [2] have elucidated a theoretical model that permits us to predict the chemical oxygen demand (COD) and instantaneous current efficiency (ICE), during the EO of organic pollutants on synthetic boron-doped diamond electrodes (BDD) in a batch recirculation system under galvanostatic conditions. Several studies highlight the good correlation between theoretical predictions and empirical data, but it was noted that some data, from some experiments, were not in agreement with the theoretical model, since it achieved efficiencies above 100% [1,2,3]. Few studies [1,3] have reported phenomena that occur in electrocatalytic systems which were not deducted in the first models. Thus, we emphasize that the mineralization of organic compounds on BDD electrodes involves not only hydroxyl radicals but also the molecular oxygen present in air, in saturated aqueous solutions or strong oxidants generated from simultaneous reactions, as already showed by Comninellis [2]. Also, the identification of intermediates during EO of 2-naphthol were performed as well as theoretical chemistry calculations that confirms our assertions. With this information, this research attempts to show related phenomena anomalies from electrochemical oxidation of 2-naphthol using BDD anodes and varying the current density. The possibility of a correction to the Comninellis' model could be an important advance in the understanding of this process for its scale-up. Currently the performance of the electrocatalytic process is established by a complex interaction between different parameters that can be optimized, so it is necessary to the implementation of theoretical models to considered new phenomena.

[1] M. Panizza, P.A. Michaud, G. Gerisola, Ch. Comninellis, J. Electroanal. Chem. 507 (2001) 206.

[2] A. Kapalka, B. Lanova, H. Baltruschat, G. Fóti, Ch. Comninellis, J. Electrochem. Commun. 10 (2008) 1215.

[3] J. Young Choi, Y-J. Lee, J. Shin, J-W. Yang, J. Hazard. Mater. 179 (2010) 762–768.

*Aknowdledgements.* Financial support from CNPq (Brazil) under project 401519/2014-7, and the PNPd/CAPES postdoctoral fellowship awarded to S.G.S. are acknowledged.

# Electrochemical reduction of carbon dioxide to formic acid at tin cathode in divided and undivided cells: effect of operating parameters

Onofrio Scialdone, Simona Sabatino, Alessandro Galia

*Università degli Studi di Palermo*

*Viale delle Scienze, 90100 Palermo*

*onofrio.scialdone@unipa.it*

The electrochemical reduction of carbon dioxide is considered a relevant topic for both the synthesis of chemicals and the decrease of global warming. Indeed, the utilization of CO<sub>2</sub> as a feedstock for producing chemicals may contribute to alleviate global climate changes caused by the increasing CO<sub>2</sub> emissions and provide a relevant challenge in exploring new opportunities for catalytic and industrial development. Electrochemical processes could utilize excess energy from intermittent renewable sources to convert carbon dioxide in various products such as CO, formate and formic acid, methane and ethylene in water and oxalic acid, formic acid, CO as well as carboxylic acids (by reaction with suitable reagents such as aromatic ketones or benzylic halides) in aprotic solvents [1-3]. It has been shown that the selectivity of the process dramatically depends on the nature of the cathode. Four distinct classes of metal catalysts have been identified on the bases of the main products obtained by the cathodic reduction in water: (i) metals that mainly form formic acid (Pb, Hg, In, Sn, Cd, Ti); (ii) metals that mainly form carbon monoxide (Au, Ag, Zn, Pd, Ga); (iii) metals that mainly form H<sub>2</sub> (Pt, Ni, Fe, Ti); (iv) metals that form significant amounts of hydrocarbons such as methane and ethylene (Cu) [2]. In the last years, an increasing attention has been devoted to the conversion of carbon dioxide to formic acid in water. In particular, it has been shown that the utilization of cheap tin cathodes allow the production of formic acid with good Faradic Efficiencies (FE) [4-14], even higher under suitable operating conditions than that obtained at lead cathode [8].

Here, a study on the effect of some operating parameters on the electrochemical reduction of carbon dioxide to formic acid at tin cathode in divided and undivided cells will be presented.

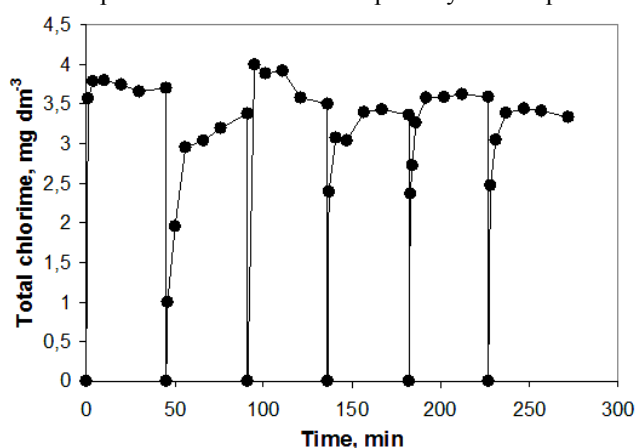
- [1] G. Centi and S. Perathoner, *Stud. Surf. Sci. Catal.*, 2004, 153, 1–8.
- [2] a) H. M. Jhong, S. Ma, P. J. Kenis, *Current Opinion in Chemical Engineering* 2 (2013) 191-199; b) Hori, Y., Kikuchi, K., Suzuki, S. (1985) *Chem. Lett.*, p. 1695; c) Azuma, Masashi, Hashimoto, Kazuhito, Hiramoto, Masahiro, Watanabe, Masahiro, Sakata, Tadayoshi (1990) *Journal of the Electrochemical Society*, 137 (6), pp. 1772-1778.
- [3] a) Ikeda, S., Takagi, T., Ito, K. (1987) *Bull. Chem. Soc. Jpn.*, 60, p. 2517; b) Un nostro articolo sull'elettrocarbossilazione con chetoni; b) Un nostro articolo sull'elettrocarbossilazione con alogenuri.
- [4] P. Bumroongsakulsawat, G. H. Kelsall, *Electrochim. Acta*, 141 (2014) 216 – 225.
- [5] F. Koleli et al. *Journal of Applied Electrochemistry*, Volume 33, Issue 5, May 2003, Pages 447-450
- [6] Wu, J., Risalvato, F., Zhou, X.-D. 2012 *ECS Transactions* 41 (33), pp. 49-60; J. Wu, F. G. Risalvato, F. S. Ke, P. J. Pellecchia, X.D. Zhou, *J. Electrochem. Soc.*, 159 (2012) F353-F359.
- [7] W. Lv, R. Zhang, P. Gao, L. Lei, *J. Power Sources*, 253 (2014) 276-281.
- [8] M. Alavarez-Guerra, A. Del Castillo, A. Irabien, *Chem. Eng. Resear. Des.*, 92 (2014) 692-701.
- [9] S. Kapusta, N. Hackerman, *J. Electrochem Soc.*, 3 (1983) 607.
- [10] Arun S. Agarwal, Yumei Zhai, Davion Hill, and Narasi Sridhar, *ChemSusChem* 2011, 4, 1301 – 1310.
- [11] J. Wu, P. Sharma. B. H. Harris, X.D. Zhou, *J. Power Sor.* 258 (2014) 189-1984.
- [12] A. Del Castillo, M. Alavarez-Guerra, A. Irabien, *AIChE J.*, 60 (2014) 3557.
- [13] Q. Wang, H. Dong, H. Yu, *J. Power Sources* 271 (2014) 278 – 284.
- [14] R. L. Machunda, H. K. Ju, J. Lee, *Current Applied Physics* 11 (2011) 986 – 988.

# On the continuity of chlorine production during electrochemical water disinfection

M.E.H. Bergmann  
Anhalt University, Köthen  
Bernburger Str. 55, D-06366 Köthen/Anh., Germany  
h.bergmann@emw.hs-anhalt.de

Direct electrochemical water disinfection is known for many decades of years but not yet legal for drinking water treatment in Germany. The method is known under several brand names such as *Inline Electrolysis*, *Anodic Oxidation*, *Tube Electrolysis*, and others [1]. The simplicity of forming chlorine species from dissolved chloride inside a divided or mostly undivided electrochemical cell is contrasted by blocking effects at the cathode – due to calcareous deposits (problem of water hardness). On-site chlorine production from artificial electrolytes is a way-out but seldom used. As a consequence, electrolysis must be interrupted. During a more or less shorter time, cathodes have to be cleaned by mechanical or chemical means. Another solution is the periodic change of electrode polarity to dissolve deposits anodically. Sophisticated cell constructions separate removed deposit particles using a special trapping zone.

Unfortunately, there is no method to make prognosis on the right time for electrode cleaning. Several methods such as potential monitoring and switching routines were tested in natural and artificial waters using lab-scale and technical cells mostly at room temperature. Only quartz microbalance measurement showed sufficient results. Unfortunately, this technology is not practicable under technical conditions. Change of electrode polarity may be responsible for 2 main effects: In periods of changing the polarity chlorine production is often temporarily interrupted and/or disturbed over a few minutes (Fig.1).



Furthermore, if calcareous deposits cannot be completely removed, a long-term reduction of free active chlorine production can be observed – lowering disinfection efficiency. The first effect should not be a general problem because minimization of chlorine addition is part of legislation for drinking water (dictate of minimization). Surprisingly, water authorities demand continuous chlorine production in places of possible application. Currently, the use of 2 alternately working cells is the most promising method to solve the problem.

**Fig. 1** Total chlorine concentration under normal conditions (technical bipolar cell, no separator, tap water, 14-17 °C) and during periods of changing electrode polarity.

In addition, technical cell must be equipped with means of chlorine concentration measurement to guarantee sufficient chlorine concentration level.

## Acknowledgment

The author wish to thank Dr. Andreas Rittel (Anhalt University) for technical and Dr. Karin Thudt (formerly MAN) for financial support.

## References

- [1] Bergmann, M.E.H.: Electrochemical water disinfection (EWD), Encyclopedia of Applied Electrochemistry, Springer, 335-342, ISBN 978-1-4419-6995-8

# Effect of Simulated Foulants on Membrane Fouling in Reverse Electrodialysis

Ye-Jin Jeong<sup>1</sup>, Chan-Soo Kim<sup>2</sup>, Nam-Jo Jeong<sup>2</sup>, Jin-Soo Park<sup>1,\*</sup>

<sup>1</sup>*Department of Environmental Engineering, College of Engineering, Sangmyung University, 31 Sangmyungdae-gil, Dongnam-gu, Cheonan, Chungnam Province 330-720, Republic of Korea*

<sup>2</sup>*Jeju Global Research Center, Korea Institute of Energy Research (KIER), 200 Haemajihae-ro, Gujwa-eup, Jeju-si, Jeju-do Province 361-290, Republic of Korea*

*\*e-mail: energy@smu.ac.kr*

Reverse electrodialysis is sustainable technology for generating energy from the mixing of concentrated salt solutions (e.g., sea water) and diluted salt solutions (e.g., river water) with different salinity. In RED a stack is alternating series of cation-exchange membranes (CEMs) and anion-exchange membranes (AEMs) between two electrodes that selectively transfer anions and cations. The main drawback to use ion-selective membranes is fouling to cause the difficulty in maintaining continuous operation and maintenance cost. In this study, the simulated foulants that might cause the membranes fouling existing in the sea and/or river water were proposed. This simulated foulants influenced membrane surface due to the electrostatic characteristics between the ion exchange membranes and the foulants. The influence of membrane fouling on the operating parameters in RED was investigated experimentally using various simulated foulants (i.e., natural organic matters and divalent ions), and open circuit voltage, stack resistance, and power density were measured and compared at different operation conditions.

## ACKNOWLEDGMENT

This research was financially supported in part by the New and Renewable Energy of Korea Institute of Energy Technology Evaluation and Planning (KETEP) grant funded by the Korean government's Ministry of Trade, Industry and Energy (No. 20143030071240).

## REFERENCES

- [1] D. A. Vermaas, D. Kunteng, M. Saakes, K. Nijmeijer, Fouling in reverse electrodialysis under natural Conditions, *Water Research* 47 (2013) 1289-1298.
- [2] D. A. Vermaas, J. Veerman, M. Saakes, K. Nijmeijer, Influence of multivalent ions on renewable energy generation in reverse electrodialysis, *Energy & Environmental Science* 7 (2014) 1434-1445.

# Supplying of Methane through Porous Carbon Anodes during Aluminium Electrolysis

Babak Khalaghi<sup>1</sup>, Henrik Gudbrandsen<sup>2</sup>, Ole Sigmund Kjos<sup>2</sup>, Karen Sende Osen<sup>2</sup>, Tommy Mokkelbost<sup>2</sup> and Geir Martin Haarberg<sup>1</sup>

<sup>1</sup>Department of Materials Science and Engineering, Norwegian University of Science and Technology, NO-7491 Trondheim Norway

<sup>2</sup>SINTEF Materials and Chemistry, NO-7465 Trondheim, Norway  
[babak.khalaghi@ntnu.no](mailto:babak.khalaghi@ntnu.no)

Currently consumable carbon anodes are utilized in the aluminium production process in molten salts. One of the major drawbacks of this type of anodes is the high amount of CO<sub>2</sub> emissions. Introduction of natural gas through the anode can decrease CO<sub>2</sub> emissions significantly and reduce consumption of the anode. This concept has been tried before [1-2] and promising results were found in some studies. The use of inert porous anodes is interesting since the energy demand would be reduced due to natural gas participating in the anode reaction. However, due to unavailability of a sufficiently inert anode for aluminium electrolysis until now, carbon anodes remain more attractive. On the other hand, using CH<sub>4</sub>/H<sub>2</sub> can lead to the formation and evolution of additional hydrogen fluoride. In this study, laboratory experiments were performed and carbon anodes with different graphite grades and porosities were tried. Also, the effects of other experimental parameters such as current density and gas flow rate were studied. Off-gas analysis was also performed and off-gas composition is discussed. Our preliminary results show that the methane participates in the anodic reaction. This leads to decreased carbon consumption.

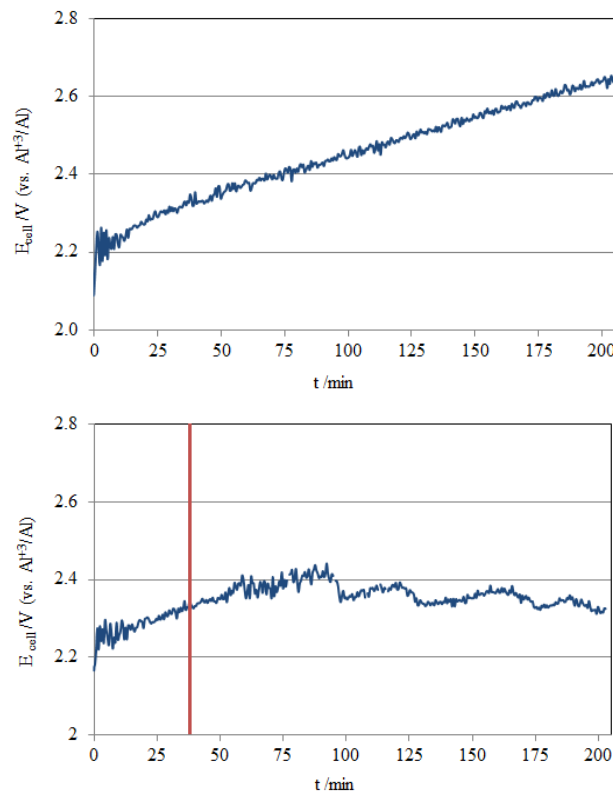


Figure 1: Variation of potential during the electrolysis of aluminium. Top: N<sub>2</sub> as inert gas. Bottom: Methane as reducing gas. The vertical line indicates the time when methane was introduced into the cell.

1. M. L. Kronenberg, "Gas Depolarized Graphite Anodes for Aluminium Electrowinning" *J. Electrochem. Soc.*, 116, (1969) 1160.
2. S. Xiao, et al., "SnO<sub>2</sub>-Based Gas (Methane) Anodes for Electrowinning of Aluminum" *Metallurgical and Materials Transactions B: Process Metallurgy and Materials Processing Science*, (2013) 1.

# Electrochemical modification of Ni catalyst with alkali ionic conductors for CO<sub>2</sub> hydrogenation

N.Gutiérrez-Guerra<sup>a</sup>, J. González-Cobos<sup>a</sup>, J.C. Serrano-Ruiz<sup>b</sup>, J.L. Valverde<sup>a</sup>, A. de Lucas-Consuegra<sup>a</sup>

*a) Departamento de Ingeniería Química, Facultad de Ciencias y Tecnologías Químicas, Universidad de Castilla-La Mancha, 13071 Ciudad Real, Spain.*

*b) Abengoa Research, C/Energía Solar 1, Palmas Altas, 41014, Sevilla, Spain*

*Antonio.Lconsuegra@uclm.es*

Different strategies are being developed to mitigate the global warming and climate change, which are mainly focused on the separation, storage and utilization of CO<sub>2</sub>. In this sense, hydrogenation of CO<sub>2</sub> can be considered as one of the most important chemical conversion reaction not only for the effective decrease of the overall CO<sub>2</sub> emissions but also for the production of many possible renewable fuels (hydrocarbons or alcohols). In this regard, different Ni catalysts films were prepared on K-βAl<sub>2</sub>O<sub>3</sub> by combining the organometallic paste deposition and the addition of a α-Al<sub>2</sub>O<sub>3</sub> powder, and tested in the CO<sub>2</sub> hydrogenation reaction. The complete characterization and its electrocatalytic performance were investigated in this work.

Figure 1 shows the influence of the applied potential on the steady-state variation of the selectivity toward CO and CH<sub>4</sub> at different temperatures (T = 240, 270 and 300 °C) with different feed composition (H<sub>2</sub>/CO<sub>2</sub> = 2-20 %). CO and CH<sub>4</sub> were already produced by means of the reverse water gas-shift: CO<sub>2</sub> + H<sub>2</sub> → CO + H<sub>2</sub>O and CO<sub>2</sub> methanation: CO<sub>2</sub> + 4H<sub>2</sub> → CH<sub>4</sub> + 2H<sub>2</sub>O. At all temperatures, the decrease in the applied potential led to a strong increase in the CO selectivity (electrophilic behavior) and a decrease of the CH<sub>4</sub> selectivity (electrophobic behavior). For instance, with a H<sub>2</sub>/CO<sub>2</sub> ratio of 20, the selectivity of the Nickel catalyst toward CO production was enhanced up to more than 95 %, depending on the reaction temperature. In the present work, under unpromoted conditions, a value of 50 % was obtained. Moreover, CH<sub>4</sub> production rate was increased against CO production at higher H<sub>2</sub> concentrations. The decrease in temperature also enhanced the methanation selectivity. Depending on both the applied potential and the reactions conditions, one can control the Ni activity and the selectivity toward CO and CH<sub>4</sub> by means of the controlled migration of K<sup>+</sup> ions from a solid electrolyte. Hence, one could in-situ control the preference formation of syngas or CH<sub>4</sub> production rate via CO<sub>2</sub> hydrogenation, which may be of significant practical importance.

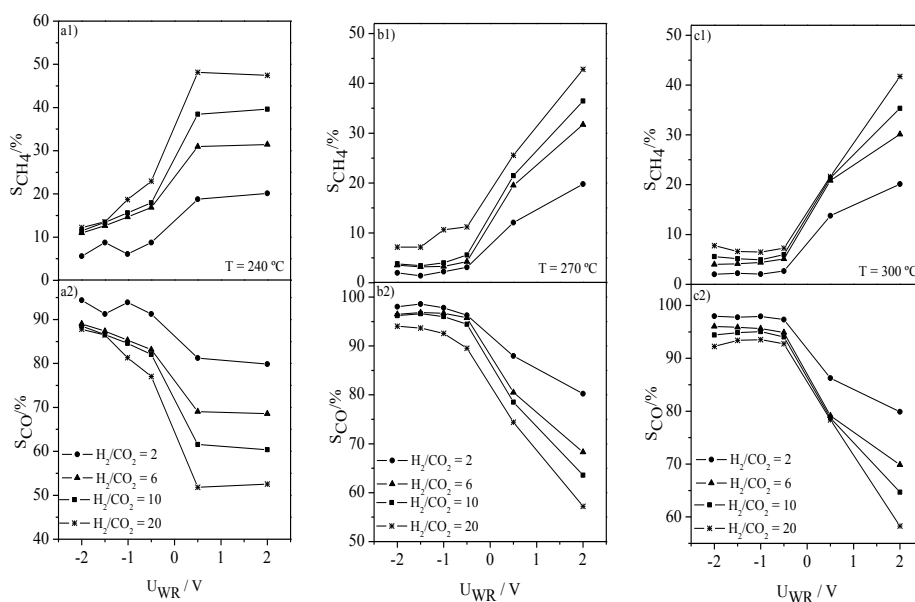


**Figure 1.** Effect of the applied potential ( $U_{WR}$ ) and the H<sub>2</sub> feed concentration on the selectivity of CH<sub>4</sub> and CO, at (a) 240 °C, (b) 270 °C and (c) 300 °C. Reactions conditions:  $F_T = 6 \text{ NL} \cdot \text{h}^{-1}$ .

# A Novel Processing Method and Simulation Based on Confined Etching Layer Technique

Lianhuan Han, Jie Zhang, Pei Huang, Dongping Zhan\*, Zhong-Qun Tian

Department of Chemistry, College of Chemistry and Chemical Engineering, and State Key Laboratory of Physical Chemistry of Solid Surfaces, Xiamen University, Xiamen 361005, China.

E-mail: dpzhan@xmu.edu.cn

Confined etchant layer technique (CELT) is a chemical etching technique induced by in-situ photo/electrochemistry and has been successfully applied to fabricate 3D microstructures for many kinds of materials, such as metals, metal alloys and semiconductors,[1] which is a replication technique with high-precision. Combined the relative motion between tool and substrate, a quasi-1D tool with large length-width ratio is designed and manufactured to perform large-scale machining with micro- or nano-precision. In this way, the mass transfer efficiency could be enhanced and the mass balance could be maintained easily. The etching reaction of substrate is supposed a simple reaction (K1) with a following reaction which could reach the absorption equilibrium (K2). The diffusion model coupled with deformed geometry model and laminar flow model in commercial finite element package Comsol Multiphysics is used to simulate the whole etching process. The profiles simulated fits well with experiment in different etching time and tool-substrate distances when K1 is  $3.2 \times 10^{-4} \text{ m s}^{-1}$  [2] and K2 is 0.01. In rotary motion model, an irregular GaAs surface is obtained after etching process. The simulation result has the similar profile also.

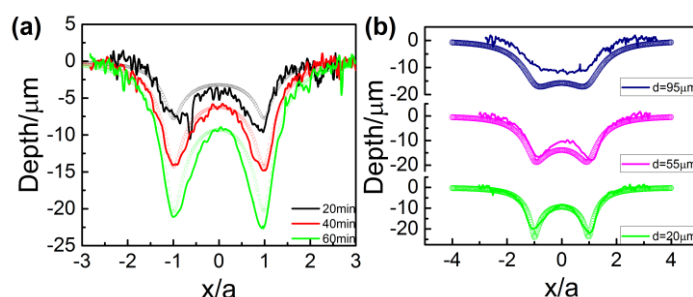


Fig. 1 The cross-sectional profile (solid line) of GaAs substrate etched in different time (a) and different tool-substrate distance (b); the corresponding cross-section simulated by deformed geometry model (symbols). The solution is 0.1 M NaBr and 1 M  $\text{H}_2\text{SO}_4$  with 50mM L-Cystine.

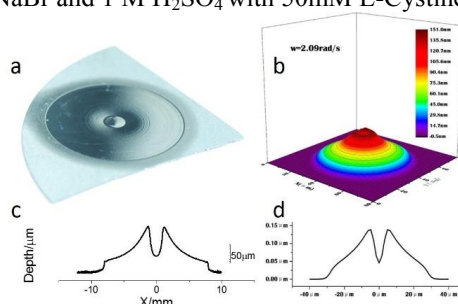


Fig. 2 (a) Optical image of an irregular surface obtained on a GaAs workpiece through the coupling effect of the CELT etching system and the mechanical motion; the rotating speed is 2.09 rad /s and the tool-substrate (GaAs) distance is 10  $\mu\text{m}$ ; (b) profilometric results of the irregular surface; (c) a preliminary 3D simulation image of the obtained irregular surface; (d) simulation result of the lateral profile of the irregular surface.

## References

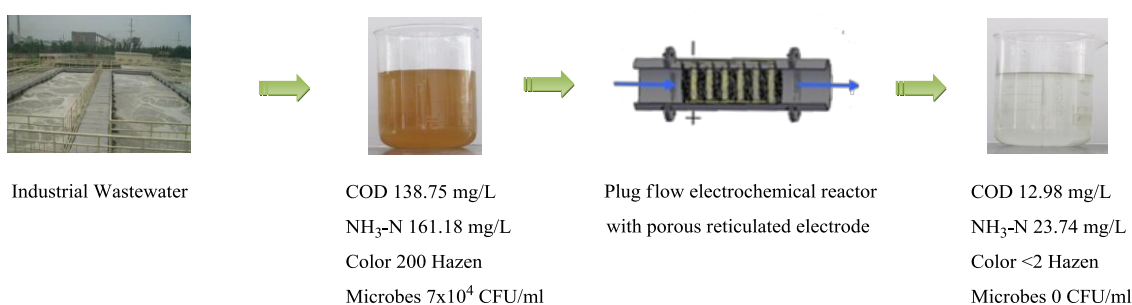
- [1] L. Zhang, X.Z. Ma, J.L. Zhuang, C.K. Qiu, C.L. Du, J. Tang, Z.W. Tian, Microfabrication of a Diffractive Microlens Array on n - GaAs by an Efficient Electrochemical Method, *Adv. Mater.*, 19 (2007) 3912-3918.
- [2] J. Zhang, J.C. Jia, L.H. Han, Y. Yuan, Z.Q. Tian, Z.W. Tian, D.P. Zhan, Kinetic Investigation on the Confined Etching System of n-Type Gallium Arsenide by Scanning Electrochemical Microscopy, *J. Phys. Chem. C*, 118 (2014) 18604-18611.

# Simultaneous Removal of COD and Ammonia Nitrogen using a Novel Electro-oxidation Reactor

Jiade Wang, Mingming Zhou, Guolong Huang, Yongping Gan

*College of Biological & Environmental Engineering, Zhejiang University of Technology, Hangzhou 310032, China, jdwang@zjut.edu.cn*

Electro-oxidation, one kind of advanced oxidation processes, has been gradually used to treat industrial wastewaters containing biorefractory compounds. A novel plug flow electrochemical reactor with porous reticulated electrodes was used to removal COD and ammonia nitrogen from pharmaceutical wastewater.



The results showed that COD and ammonia nitrogen were removed simultaneously. Under the optimal operating conditions with the initial pH of 8.3, the current density of 15 mA/cm<sup>2</sup> and the electrolysis time of 40min, concentrations of COD, ammonia nitrogen and color were decreased to 12.98 mg/L, 23.74 mg/L and 2 Hazen, respectively. Meanwhile, the amount of microbes in wastewater reduced from 7×10<sup>4</sup> CFU/ml to 0 CFU/ml.



In the actual engineering project with daily treatment capacity of 500 m<sup>3</sup>, the energy consumptions were 30.81 kW·h·kg<sup>-1</sup> COD and 28.39 kW·h·kg<sup>-1</sup> NH<sub>3</sub>-N. The average current efficiencies for COD and ammonia nitrogen reduction were 33.71% and 63.15%, respectively. The operating cost was \$ 0.8 per ton according to the local electricity price of \$ 0.14·kWh<sup>-1</sup> for industries. There were many advantages, such as strong adaptability, no adding chemicals, little or no secondary pollution, mild reaction conditions and simple equipment, etc. So, the electro-oxidation method had the strong prospect for the industrial wastewater treatment.

## References:

- [1] M. Panizza, A. G.Cerisola, Environ. Sci. Technol. 38 (2004) 5470.
- [2] A. Anglada, A. Urtiaga, A. I. Ortiz, Environ. Sci. Technol. 43 (2009) 2035.
- [3] V. Díaz, R. Ibáñez, P. Gómez, A.M. Urtiaga, I. Ortiz, Water Res. 45 (2011) 125.
- [4] R. Y. Zhu, C. Y. Yang, M. M. Zhou, J. D. Wang, Chem. Eng. J. 260 (2015) 427.



# Solid State Ammonia Synthesis – Present State and Perspective

Chung-Yul Yoo, Dae Sik Yun, Jong Hoon Joo, Ji Haeng Yu, Jong-Nam Kim, Hyung-Chul Yoon  
Korea Institute of Energy Research  
152 Gajeong-ro, Yuseong-gu, Daejeon 305-343, Republic of Korea  
cyoo@kier.re.kr

Ammonia has a potential as a carbon-free energy carrier since it contains 17.6wt% of hydrogen and can be easily stored and transported safely and efficiently [1]. The state-of-the-art industrial process for ammonia production is the Harbor-Bosch process. Although high temperature (450–500 °C) and pressure (150–300 bar) are used to dissociate triple-bonded nitrogen and to maximize the ammonia formation, the efficiency of the Haber–Bosch process is limited to 10–15%. Moreover, the process accompanies high greenhouse gases emission since hydrogen is produced from natural gas. In order to overcome the drawbacks of the Haber-Bosch process, the electrochemical ammonia synthesis has been developed as an alternative process [2, 3].

In this work, we have conducted systematic experiments on the electrochemical ammonia synthesis from nitrogen and steam using various solid state ion conductors. Perovskite- and fluorite-type oxides, solid acid phosphate, and Nafion have been employed to investigate the effects of temperature, applied current, and electrocatalyst on the ammonia formation rate [4-6]. The obtained ammonia formation rates and Faraday efficiencies are summarized in Table 1. Some of remaining challenges are outlined for further research.

Table 1 Summary of ammonia formation rate and Faraday efficiency.

Electrolyte (Mobile ion)	N <sub>2</sub> dissociation electrocatalyst	°C	NH <sub>3</sub> rate (mol·cm <sup>-2</sup> ·s <sup>-1</sup> )	Faraday efficiency (%)
Gd <sub>0.1</sub> Ce <sub>0.9</sub> O <sub>2-δ</sub> (O <sup>2-</sup> )	Pt	600	$3.6 \times 10^{-11}$	0.1
BaZr <sub>0.8</sub> Y <sub>0.2</sub> O <sub>3-δ</sub> (H <sup>+</sup> )	Ag	550	$4.9 \times 10^{-11}$	0.46
KH <sub>2</sub> PO <sub>4</sub> -KH <sub>5</sub> (PO <sub>4</sub> ) <sub>2</sub> (H <sup>+</sup> )	Fe <sub>3</sub> Mo <sub>3</sub> N-Ag	145	$2.2 \times 10^{-10}$	12
Nafion (H <sup>+</sup> )	Pt/C	60	$2.2 \times 10^{-9}$	0.1

- [1] K. Aika, Ammonia as an Energy Carrier for Renewable Energy, 2013 NH<sub>3</sub> FUEL CONFERENCE.
- [2] Giddy *et al.*, Review of electrochemical ammonia production technologies and materials, Int. J. Hydrogen Energy, 38, 14576 (2013).
- [3] Amar *et al.*, Solid-state electrochemical synthesis of ammonia: a Review, J. Solid State Electrochem., 15, 1845 (2011).
- [4] Jeong *et al.*, Electrochemical synthesis of ammonia from water and nitrogen using a Pt/GDC/Pt cell, Korean Chemical Engineering Research, 52, 58 (2014).
- [5] Yoo *et al.*, Electrochemical ammonia synthesis from water and nitrogen using solid state proton conductors, 13th International Conference on Inorganic Membranes (2014).
- [6] Yun *et al.*, Electrochemical ammonia synthesis from steam and nitrogen using proton conducting yttrium doped barium zirconate electrolyte with silver, platinum, and lanthanum strontium cobalt ferrite electrocatalyst, J. Power Sources, 284, 245 (2015).

# Removal of Persistent Organic Contaminants by Electrochemically Activated Sulfate

Ali Farhat<sup>a</sup>, Stephan Tait<sup>a</sup>, Jurg Keller<sup>a</sup>, Jelena Radjenovic<sup>a,b</sup>

<sup>a</sup> Advanced Water Management Centre, The University of Queensland, Queensland 4072, Australia

<sup>b</sup> Catalan Institute for Water Research (ICRA), Scientific and Technological Park of the University of Girona, 17003 Girona, Spain  
e-mail: a.farhat@awmc.uq.edu.au

The incomplete removal of persistent organic compounds such as pharmaceuticals and pesticides in conventional water and wastewater treatment plants have raised the interest for novel technologies capable of effectively degrading such organic contaminants. Electrochemical advanced oxidation processes (EAOPs) employing boron doped diamond (BDD) anodes have been previously reported to accomplish significant degradation of such trace organic contaminants. Previous studies have shown that BDD anodes are characterized with high overpotential for oxygen evolution where such anodes enhance the degradation rates of organics via direct oxidation and production of weakly adsorbed hydroxyl radicals (HO<sup>•</sup>). Besides HO<sup>•</sup> and other radical species, BDD anodes can also produce peroxy-species that may also contribute to bulk oxidation of contaminants. For example, previous research has reported BDD anodes are capable of oxidizing sulfate ions to peroxydisulfate (S<sub>2</sub>O<sub>8</sub><sup>2-</sup>), via sulfate radicals (SO<sub>4</sub><sup>•-</sup>) as intermediate products.

To further explore the role of sulfate in EAOPs, the present study quantified the rates of electrooxidation of several persistent organic contaminants (e.g., diatrizoate, carbamazepine, N,N-diethyl-meta-toluamide (DEET), iopromide, tribromophenol, triclosan and triclopyr) at BDD anode. Experiments were performed in sulfate anolyte at different operating conditions (concentrations/conductivities and current densities) and compared with inert nitrate and perchlorate anolytes. The observed electrooxidation rates of the persistent organic contaminants in sulfate anolyte were in the range of 12 – 66 h<sup>-1</sup>, significantly higher than the values obtained for nitrate anolyte (0.83 – 5.4 h<sup>-1</sup>).

Given that in the absence of trace metals or other activators (e.g., UV light), persulfate was shown to exhibit slow oxidation kinetics with these persistent organic contaminants (k < 0.1 h<sup>-1</sup>), higher electrooxidation rates in the presence of sulfate were assigned to the electrochemical activation of sulfate ions to sulfate-based oxidizing species such as sulfate radicals (SO<sub>4</sub><sup>•-</sup>) and/or non-radically activated persulfate. In an attempt to segregate the effects of HO<sup>•</sup> radicals and SO<sub>4</sub><sup>•-</sup> radicals, the study also examined the electrooxidation of nitrobenzene at a BDD anode, as a typical HO<sup>•</sup> radical probe compound, and provided further evidence for the presence of SO<sub>4</sub><sup>•-</sup> radicals.

Sulfate-based solutions have been widely used as supporting electrolytes for electrochemical degradation of contaminants using BDD anode. Electrooxidation pathways have been largely explained by the role of HO<sup>•</sup> radicals and other reactive oxygen species. Our results imply electrochemical activation of sulfate ions, even at sulfate concentrations as low as 150 mg L<sup>-1</sup>. Thus, this study has implications in applications of BDD anodes in wastewater treatment, as the presence of sulfate may significantly affect the electrooxidation pathways and kinetics of persistent organic contaminants.

# Intact Recovery of Carbon Nanotubes from their Conducting Polymer Composites via Selective Fenton-Oxidation

Li Guan<sup>a</sup> and George Z. Chen<sup>\*a,b</sup>

<sup>a</sup> Energy and Sustainability Research Division, Faculty of Engineering, The University of Nottingham, Nottingham NG7 2RD, UK; <sup>b</sup> International Academy of Marine Economy and Technology, The University of Nottingham Ningbo China, Ningbo, Zhejiang 315100, P. R. China.  
E-mail: [george.chen@nottingham.ac.uk](mailto:george.chen@nottingham.ac.uk)

Carbon nanotubes (CNTs) are one of the most studied and promising nano-fillers to enable the formation of polymeric composites with enhanced and improved functionalities. For example, composites of CNTs and electronically conducting polymers (ECPs, such as polypyrrole, PPy, and polyaniline, PAN) can offer superior performances in supercapacitors [1,2]. Perhaps the biggest challenge for ECP-CNT composite based supercapacitors to penetrate the energy markets is the fairly high cost/performance ratio that results from the current high market price of CNTs as raw materials. Therefore, it would be financially necessary to consider recovering the CNTs from their ECP composites in spent supercapacitors. Moreover, for implementing responsible innovation [3], the ECP-CNT composites in the spent supercapacitors should not be released to nature with respect to their potential health and environmental impacts.

It is demonstrated in this work that clean recovering of CNTs from ECP-CNT composites can be achieved by selective oxidation using Fenton's reagent ( $\text{H}_2\text{O}_2 + \text{Fe}^{2+}$ , pH=3) that completely mineralizes the ECP, but leaves the nanotubes intact (**Fig.1b**). In our tests of the Fenton oxidation, ECP-CNT composites progressively lost their redox activity (**Fig.1c**) and showed a drastic increase in charge transfer resistance.  $\text{CO}_2$  and  $\text{N}_2$  as degradation products of ECPs were also detected by gas chromatography. Importantly, it was found through characterization via various analytical techniques that the Fenton recovered CNTs (FRCNTs) were the major constituent in the solid residuals observed after the oxidation. Furthermore, in the cyclic voltammetric investigation on the electro-activity, the FRCNTs exhibited similar redox activity and comparable specific capacitance to the original CNTs, permitting the reuse for preparing a composite with PPy (**Fig.1d**).

In general, the selective Fenton oxidation to the ECPs coated on individual CNTs is a new and interesting concept, which is believed to be the first example of the CNT recovery from their polymer composites. This work may significantly improve the sustainability and competitiveness of supercapacitors for boosting commercialization.

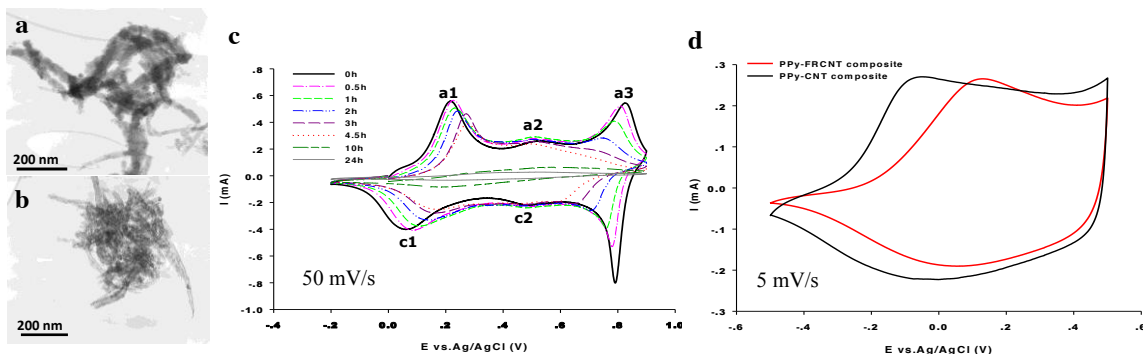


**Fig.1.** (a,b) TEM images of (a) as-prepared PAN-CNT and (b) its Fenton oxidation product. (c,d) CVs of (c) PAN-CNT in 1.0 mol/L HCl recorded at the indicated time for immersion in the Fenton's reagent ( $[\text{H}_2\text{O}_2]/[\text{Fe}^{2+}]=100$ ,  $[\text{Fe}^{2+}]=1.0$  mmol/L), and (d) PPy-FRCNT and PPy-CNT in 0.5 mol/L KCl.

**Acknowledgement:** This research was funded by E.ON AG (International Research Initiative—Energy Storage 2007) and Ningbo Municipal Government (3315 Plan and the IAMET Special Fund, 2014A35001-1). Responsibility for the content of this report lies with the authors.

## References

- [1] C. Peng, Jin, J. and G.Z. Chen, *Electrochim. Acta* 53 (2007) 525-537.
- [2] J.H. Chae, X.H. Zhou and G.Z. Chen, *Green*, 2 (2012) 41-54.
- [3] R. Owen, J. Bessant and M. Heintz (Eds.), *Responsible innovation: Managing the responsible emergence of science and innovation in society*, Wiley-Blackwell, 2013.

# Action Mechanism of Quaternary Ammonium Compound in the Electroreduction of Oxalic Acid to Glyoxylic Acid

Xinsheng Zhang, Ling Jin, Dongfang Niu, Wei-Kang Yuan

State Key Laboratory of Chemical Engineering, East China University of Science and Technology  
130 Meilong Road, Shanghai 200237, P.R. China  
[xszhang@ecust.edu.cn](mailto:xszhang@ecust.edu.cn)

Glyoxylic acid is an important intermediate in the perfumery, pharmaceutical and fine chemical industries. Production of glyoxalic acid by electroreduction of oxalic acid solutions has been investigated by many researchers<sup>[1-2]</sup>. Good yields of glyoxylic acid were reported with lead as the cathode material. But the key problem for commercializing the process is the cathode deactivation, the current efficiency and the reaction selectivity decrease dramatically throughout the operation. The cathode deactivation is not uncommon in electroreduction, such as dimerization of acetone to pinacol and electrohydrodimerization of acrylonitrile to adiponitrile<sup>[3]</sup>. There have been a few methods suggested for this problem<sup>[4]</sup>, e.g., washing the cathode with a dilute nitric acid, producing new apparent surface with electroplate, and mechanically cleaning the cathode surface. Unfortunately, all these are not considered as well acceptable by the industry. The adding additive (quaternary ammonium compound) into the catholyte was found to be the best way to keep the cathode from deactivation.

There are two major factors to decrease the current efficiency: increasing concentration of glyoxylic acid and decreasing activation of electrode, not single factor of cathode deactivation. It was also found that the electrode deactivation are affected by two reasons which being the higher concentration of glyoxylic acid and electrodeposition of a few metals of lower hydrogen overpotential on cathode.

When additives were added into electrolyte, the deactivation of cathode had not occurred in commercial model process. We found that the quaternary ammonium compounds can inhibit electrodeposition of metals ion on lead cathode to prevent from electrode deactivation, but also they inhibit evolution of hydrogen and inhibit electroreduction of oxalic acid. In another words, all reactions on cathode were depressed while electrolyte contained additives.

How do these additives act on electrode to increase current efficiency of glyoxalic acid? In fact, the additives could not only increase the mass transfer rate of oxalic acid from solution to electrode surface, but also accelerate desorption of glyoxylic acid from electrode surface, owing to tetraalkylammonium cations being formed ion pair with anions of glyoxalic acid or oxalic acid. So, we was put forward that the mechanism of phase transfer electrocatalysis of quaternary ammonium compound acted on cathode (see Fig. 1).

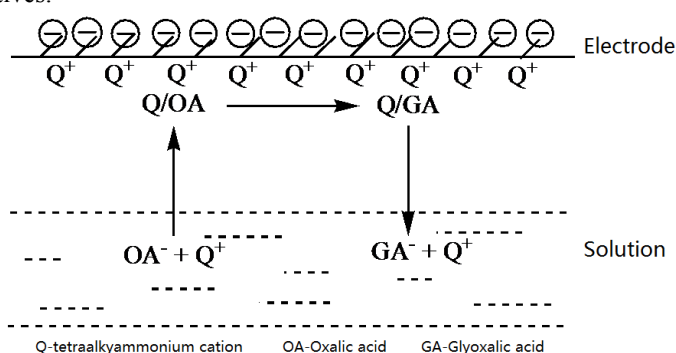


Fig. 1 Mechanism of Phase Transfer Electrocatalysis of Quaternary Ammonium Compound on Cathode

## References

- [1] Goodridge, F., Lister, K., Plimley, R. E., & Scott, K. Scale-up studies of the electrolytic reduction of oxalic to glyoxylic acid. *Journal of Applied Electrochemistry*, 1980,10, 55 – 60.
- [2] Tilak, E. V., & Weinberg, N. L. *Technique of electroorganic synthesis*, Part III. 1982, New York: Wiley.
- [3] Danly, D. E. (1981). Adiponitrile via improved EHD. *Hydrocarbon Processing*, 1981,60(4), 161 – 164.
- [4] Yang-Liu Zhou, Xin-Sheng Zhang, Ying-Chun Dai, Wei-Kang Yuan, Studies on chemical activators for electrode I: Electrochemical activation of deactivating cathode for oxalic acid reduction, *Chemical Engineering Science*, 2003, 58, 1021-1027.

## Acknowledgments

The present study was supported by the Nature Science Foundation of China (20376020), the State Key Laboratory of Physical Chemistry of Solid surfaces (Xiamen University). State Key Laboratory Breeding Base of Green Chemistry Synthesis Technology (Zhejiang University of Technology), and the 111 Project (B08021).

# Electrochemistry of Atomically Precise Metal Nanoclusters

Dongil Lee

*Department of Chemistry*

*Yonsei University*

*Seoul 120-749, Korea*

*dongil@yonsei.ac.kr*

Atomically precise metal nanoclusters containing a few to a few hundreds of atoms have been the focus of recent investigations because of their novel electronic, optical, and catalytic properties. They appear to represent the bulk-to-molecule transition region where electronic band energetics yield to quantum confinement effects and discrete electronic states emerge. I will firstly present recent advances in the synthesis of atomically precise gold nanoclusters and their size-dependent electrochemical and optical properties. Secondly, syntheses and characterizations of Au<sub>25</sub> nanoclusters doped with Pt and Pd will be presented. Electrochemical investigations of the doped nanoclusters showed that redox potentials of gold nanoclusters are significantly altered by doping with foreign metal atoms. Dramatic catalytic effect was observed for the reduction of azobenzene with gold nanoclusters doped with Pt and Pd. This effect can be ascribed to the doping-induced tuning of the redox potentials and enhanced electrocatalytic activity of the doped gold nanoclusters.

# Influence of Cations on the Control of the Multiple Redox States of Fullerene at the Ionic Liquid Electrochemical Interface

Hiroyuki Ueda<sup>a</sup>, Katsuhiko Nishiyama<sup>a,b</sup>, Soichiro Yoshimoto<sup>b,c</sup>

<sup>a</sup> Graduate School of Science and Technology, Kumamoto University

2-39-1 Kurokami, Chuo-ku, Kumamoto 860-8555, Japan

<sup>b</sup> Kumamoto Institute for Photo-Electro Organics (Phoenix)

3-11-38, Higashi-machi, Higashi-ku, Kumamoto 862-0901, Japan

<sup>c</sup> Priority Organization for Innovation and Excellence, Kumamoto University

2-39-1 Kurokami, Chuo-ku, Kumamoto 860-8555, Japan

so-yoshi@kumamoto-u.ac.jp

Precise control of the multiple redox states of organic molecules is one of the key technologies to realize high-efficient single-molecular electronic devices and organic rechargeable batteries. Fullerene has been expected to be a promising material due to its excellent electron accepting ability. Electrochemistry of fullerene films was investigated in several organic solvents. However, the control of the six redox states of fullerene was difficult because of the high solubility of fullerene anions in organic solvents. Recently, we succeeded in controlling the six redox reactions of fullerene at room temperature by using ionic liquids (ILs) [1]. In this study, we report the effect of the cations of ILs on the redox potentials of fullerene.

Tributylmethylammonium bis(trifluoromethylsulfonyl)imide ([N<sub>1,4,4,4</sub>][TFSI]), 1-butyl-1-methylpyrrolidinium bis(trifluoromethylsulfonyl)imide ([C<sub>4</sub>mpyr][TFSI]), 1-butyl-3-methylimidazolium bis(trifluoromethylsulfonyl)imide ([C<sub>4</sub>mim][TFSI]), triethylsulfonium bis(trifluoromethylsulfonyl)imide ([S<sub>2,2,2</sub>][TFSI]) were used. Prior to each experiment, Au(111) electrodes were annealed in a hydrogen flame, and then cooled down. The fullerene thin films were prepared by casting 50  $\mu$ M either C<sub>60</sub> or C<sub>70</sub> benzene solution onto a freshly-annealed Au(111) electrode. The electrochemical behavior of fullerene-modified Au(111) electrodes were investigated by cyclic voltammetry (CV) and differential pulse voltammetry (DPV).

Fig. 1 shows typical cyclic voltammograms of the fullerene-modified Au(111) electrodes in [C<sub>4</sub>mpyr][TFSI]. A clear difference could be observed between the first cathodic scan and subsequent scans, suggesting that overpotential is required to generate fullerene anions during the first cathodic scan. Each redox current gradually decreased with continuous scans, indicating the dissolution of fullerene anions into [C<sub>4</sub>mpyr][TFSI]. Table 1 shows the redox potential of C<sub>x</sub><sup>n-</sup>/C<sub>x</sub><sup>(n-1)-</sup> (C<sub>x</sub> = C<sub>60</sub>, C<sub>70</sub>, n = 1-6) ( $E_{n-(n-1)}$ ) in the ILs evaluated by DPV. The redox potentials were dependent on IL cations. Three or four redox couples of fullerene could be found in both [C<sub>4</sub>mim][TFSI] and [S<sub>2,2,2</sub>][TFSI] due to the low cathodic stability of [C<sub>4</sub>mim]<sup>+</sup> and [S<sub>2,2,2</sub>]<sup>+</sup>. For [C<sub>4</sub>mpyr][TFSI] and [N<sub>1,4,4,4</sub>][TFSI], the six redox couples of fullerene were observed. The average peak separation between any two successive redox potentials ( $\Delta E_{\text{ave}}$ ) increased in the order of [C<sub>4</sub>mpyr][TFSI] ( $\Delta E_{\text{ave}}$  = 380  $\pm$  10 mV) < [N<sub>1,4,4,4</sub>][TFSI] ( $\Delta E_{\text{ave}}$  = 450  $\pm$  20 mV).  $E_{6-5}$ ,  $E_{5-4}$ ,  $E_{4-3}$ , and  $E_{1-0}$  for C<sub>70</sub> in the ILs shifted to more positive potential than those for C<sub>60</sub>. These results indicate that the multiple redox states of fullerenes are controlled by not only the wide electrochemical potential window of ILs but also the strength of the interaction between fullerene and IL cations.

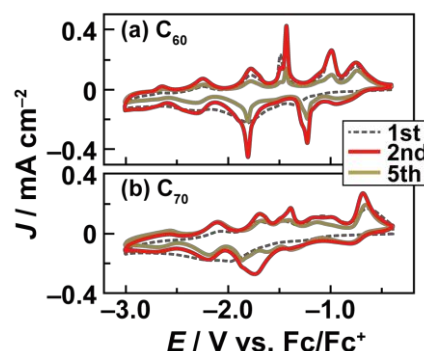


Fig. 1. CV profiles of (a) C<sub>60</sub>- and (b) C<sub>70</sub>-modified Au(111) electrodes in [C<sub>4</sub>mpyr][TFSI]. Scan rate: 100 mV s<sup>-1</sup>.

Table 1. Redox potentials of fullerene on Au(111) electrodes in the ILs.

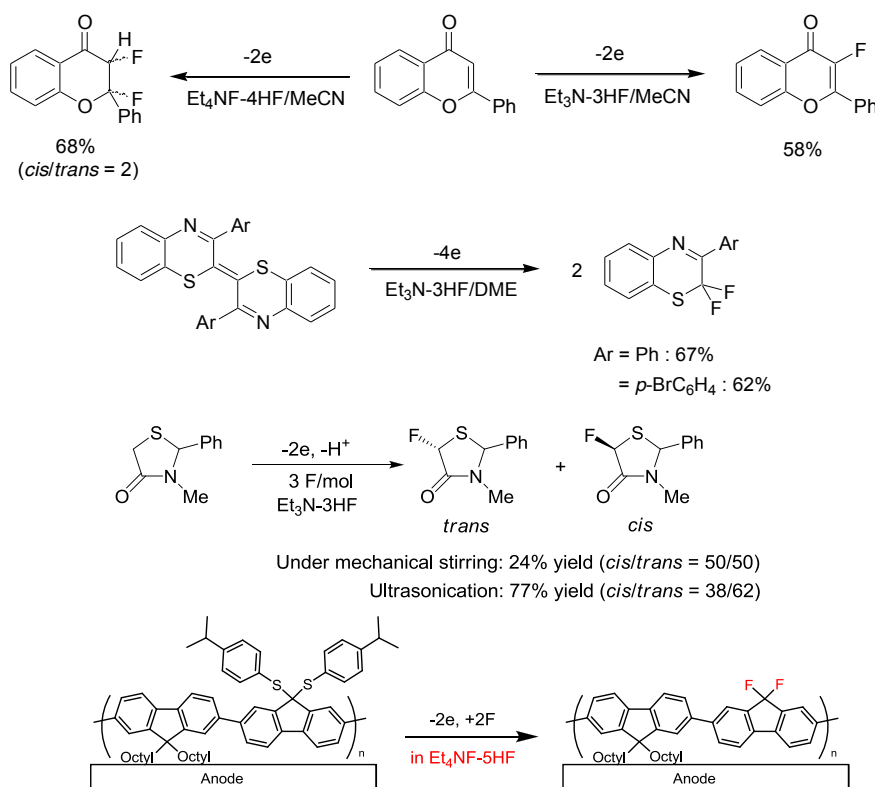
IL	C <sub>x</sub>	$E_{6-5}$ [V]	$E_{5-4}$ [V]	$E_{4-3}$ [V]	$E_{3-2}$ [V]	$E_{2-1}$ [V]	$E_{1-0}$ [V]
[N <sub>1,4,4,4</sub> ][TFSI]	C <sub>60</sub>	-3.55	-3.13	-2.60	-2.16	-1.69	-1.22
[N <sub>1,4,4,4</sub> ][TFSI]	C <sub>70</sub>	-3.37	-2.94	-2.46	-2.05	-1.72	-1.18
[C <sub>4</sub> mpyr][TFSI]	C <sub>60</sub>	-2.75	-2.28	-1.79	-1.48	-1.11	-0.85
[C <sub>4</sub> mpyr][TFSI]	C <sub>70</sub>	-2.65	-2.15	-1.78	-1.51	-1.27	-0.76
[C <sub>4</sub> mim][TFSI]	C <sub>60</sub>			-2.01	-1.62	-1.33	-1.01
[C <sub>4</sub> mim][TFSI]	C <sub>70</sub>				-1.55	-1.29	-0.74
[S <sub>2,2,2</sub> ][TFSI]	C <sub>60</sub>				-2.20	-2.00	-1.52
[S <sub>2,2,2</sub> ][TFSI]	C <sub>70</sub>				-2.25	-1.98	-1.41

# Selective Electrochemical Fluorination of Organic Molecules and Macromolecules Using Poly(HF) Salt Ionic Liquids

Toshio Fuchigami and Shinsuke Inagi

Department of Electronic Chemistry, Tokyo Institute of Technology,  
Nagatsuta, Midori-ku, Yokohama 226-8502, Japan  
fuchi@echem.titech.ac.jp

Organofluorine compounds are highly useful for our daily life. Fluorinated organic molecules and macromolecules are of much importance as new types of pharmaceuticals, agrochemicals, and functional materials. In order to prepare organofluorine compounds, fluorinated building blocks and chemical fluorination have been mainly employed, however, the former is limited and the latter requires hazardous and/or explosive fluorination reagents. Therefore, we have developed selective electrochemical fluorination using poly(HF) salt ionic liquids [1-4] and metal fluorides [5,6]. Our fluorination method is promising from a viewpoint of green chemistry because any hazardous reagents are not required and fluorination can be achieved in one step without leaving groups. In this talk, we focus on selective electrochemical fluorination of various heterocyclic compounds as well as conducting polymers [1,7,8].



## References

- 1) Fuchigami, T.; Inagi, S. *Chem. Commun (Feature Article)*. **2011**, 47, 10211.
- 2) Fuchigami, T.; Inagi, S. "Fluorinations", in "Organic Electrochemistry. 5th ed." Eds. O. Hamerich, B. Speiser, Taylor & Francis, **2015**, Chapter 14.
- 3) Fuchigami, T.; Inagi, S.; Atobe, M. "Fundamentals and Applications of Organic Electrochemistry", Wiley, **2014**, 104-15, 156-161.
- 4) Yin, B.; Inagi, S.; Fuchigami, T. *Beilstein J. Org. Chem.* **2015**, 11, 85.
- 5) Tajima, T.; Nakajima, A.; Fuchigami, T. *Angew. Chem. Int. Ed.* **2007**, 46, 3550.
- 6) Sawamura, T.; Inagi, S.; Fuchigami, T. *Angew. Chem. Int. Ed.* **2012**, 51, 4413.
- 7) Inagi, S.; Hayashi, S.; Fuchigami, T. *Chem. Commun.* **2009**, 1718.
- 8) S. Hayashi, S. Inagi, T. Fuchigami, *Macromolecules*, **2009**, 42, 3755; *Electrochemistry*, **2010**, 78, 114.

# Transition Metal $\alpha$ -Diimine Carbonyl Complexes for Electrocatalytic CO<sub>2</sub> Reduction

Joanne Tory, František Hartl

University of Reading

Department of Chemistry, University of Reading, Whiteknights Reading RG6 6AD, UK

j.tory@reading.ac.uk

There is substantial interest in the catalytic reduction of CO<sub>2</sub> to form products that are useful for energy storage and organic synthesis. In order to design more efficient catalysts, it is important to understand how the experimental conditions and molecular structure affect the catalytic activity of the system. We have studied a range of complexes related to the well-known [Re(CO)<sub>3</sub>(bpy)X] (bpy = 2,2'-bipyridine) [1] catalyst precursors using IR and UV-Vis spectroelectrochemical techniques. Reaction mechanisms and catalytic activity have been investigated for systems including the osmium complexes *trans*-(Cl)-[Os<sup>II</sup>(CO)(bpy)(PrCN)Cl<sub>2</sub>] (PrCN = butyronitrile) and *mer*-[Os<sup>III</sup>(CO)(bpy)Cl<sub>3</sub>] [2], the Group 6 dicarbonyl allyl complex [Mo<sup>II</sup>(CO)<sub>2</sub>(allyl)(bpy)(NCS)] [3], and [Mn(CO)<sub>3</sub>(iPr-DAB)Br] (iPr-DAB = *N,N'*-diisopropyl-1,4-diazabuta-1,3-diene) [4] which contains a non-aromatic  $\alpha$ -diimine ligand. We have also shown that the choice of solvent and working electrode can have a significant impact on the efficiency of electrocatalysis for the Group 6 complexes [M(CO)<sub>4</sub>(bpy)] (M = Cr, Mo, W). [5]

Here we will present a range of Group 7 complexes of the type [M(CO)<sub>3</sub>( $\alpha$ -diimine)X] (M = Mn, Re) with  $\alpha$ -diimine ligands such as 4,4'-bis(hydroxymethyl)-2,2'-bipyridine, 3,3'-dihydroxy-2,2'-bipyridine and *N,N'*-dimethylglyoxime that feature labile protons which may enhance the catalytic activity of the complexes and promote proton-coupled electron transfer. Combined chemical deprotonation and spectroelectrochemical experiments show that the reduction mechanisms of these complexes may be affected by reductive deprotonation of the  $\alpha$ -diimine ligands. Electrocatalysis is observed in the presence of CO<sub>2</sub> for both the rhenium and manganese complexes without addition of Brønsted acid.

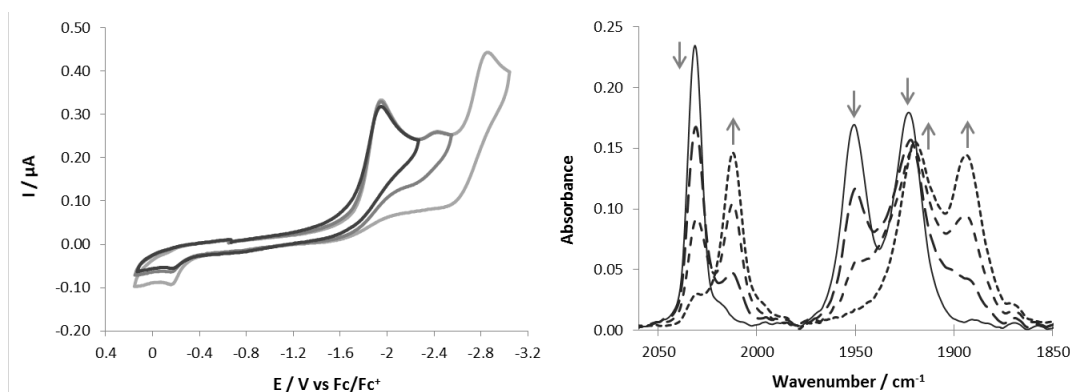


Figure 1. [Mn(CO)<sub>3</sub>(dgmH<sub>2</sub>)Br] in THF/Bu<sub>4</sub>NPF<sub>6</sub>: Cyclic voltammetry (left), and IR spectroelectrochemistry showing reduction to [Mn(CO)<sub>3</sub>(dgmH)Br]<sup>-</sup> (↑) within an OTTE cell (right).

1. F.P.A. Johnson, M.W. George, F. Hartl, J.J. Turner, *Organometallics* 1996, **15**, 3374-3387.
2. J. Tory, L. King, A. Maroulis, M. Haukka, M.J. Calhorda, F. Hartl, *Inorg. Chem.* 2014, **53**, 1382-1396.
3. J. Tory, G. Gobaille-Shaw, A.M. Chippindale, F. Hartl, *J. Organomet. Chem.* 2014, **53**, 1382-1396.
4. Q. Zeng, J. Tory, F. Hartl, *Organometallics* 2014, **33**, 5002-5008.
5. J. Tory, B. Setterfield-Price, R.A.W. Dryfe, F. Hartl, *ChemElectroChem* 2015, **2**, 213-217.



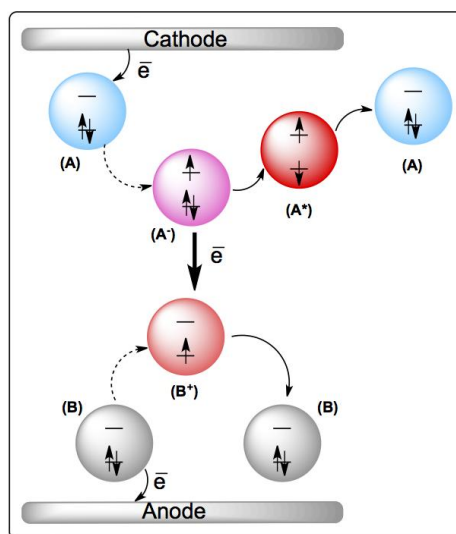
# Electrochemiluminescence of Quantum Dots and Clusters

Zhifeng Ding

*Department of Chemistry, The University of Western Ontario, London, ON N6A 5B7*

*zfding@uwo.ca*

Electrochemistry studies relations between electric work and chemical reactions, while photoelectrochemistry investigates the conversion between electrons and photons in chemical processes. Our lab at Western focuses on 4 research themes: scanning electrochemical microscopy of live cells, ionic liquids as novel electrolytes, electrochemiluminescence (ECL) and solar cells. Herein, we demonstrate our progresses on ECL of some nanocrystals.



ECL is the process in which electrogenerated radicals form excited species that emit light without the need for an external light source. ECL is a powerful analytical technique that is fast, highly sensitive and selective, requires low quantity and is cost effective. Herein, we illustrate our investigation on ECL of Au clusters and PbS nanocrystals in the near-infrared (NIR) region by combining conventional ECL detection with spectroscopic techniques to gain insights into thermodynamic and kinetic origins. Generating ECL light in the NIR is especially important for bioimaging applications.

# Electron-transfer Induced Reactions in Ru and Sn Complexes with Biological Activity

M. Fátima C. Guedes da Silva

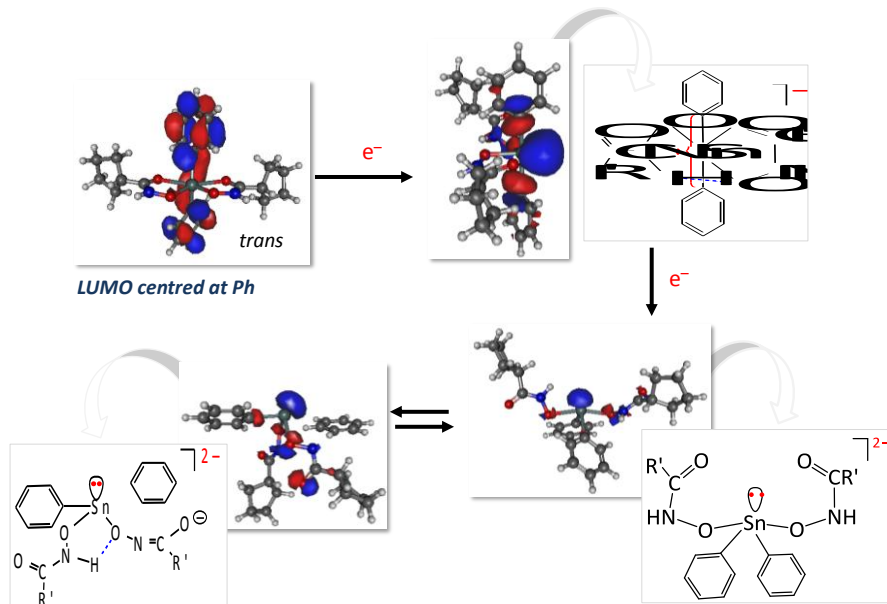
*Centro de Química Estrutural, Instituto Superior Técnico, Universidade de Lisboa, Av. Rovisco Pais, 1049-001, Lisboa, Portugal*  
[fatima.guedes@tecnico.ulisboa.pt](mailto:fatima.guedes@tecnico.ulisboa.pt)

Bond cleavage and/or formation often constitute fundamental steps in chemical reactions, and electrochemical methods can be conveniently applied to induce them by electron-transfer. Electrochemistry can not only induce chemical reactivity but also investigate the kinetics and mechanisms involved. Theoretical studies combined with experimental electrochemical results can provide an interpretation and rationalization by disclosing possible products, intermediates and pathways towards the establishment of the mechanisms.

Metal-based drugs 'activated by reduction' have become popular with platinum and ruthenium compounds since various metal-complexes can exist in rather inert high oxidation states in aqueous solution but are more labile and active in reduced oxidation states. Quantitative kinetic analysis by digital simulation of the cyclic voltammograms in Ru(III) compounds allowed the establishment of the mechanism of the processes involved and enabled a correlation between the redox potential, the rate constant for solvolysis and cytotoxicity.

Moreover, electrochemical/theoretical studies on organotin(IV) complexes with hydroxamate (Figure) and carboxylate type ligands disclosed the involvement, in the reduction process, of structural rearrangements, specifically (i) the cleavage of Sn-O(ligand) bonds (generating coordinative unsaturation) and (ii) a geometrical *trans*-to-*cis* isomerization.

Discussion of biological significance of these results will be presented.



## Acknowledgements

This work has been supported by the Fundação para a Ciência e a Tecnologia (FCT), Portugal (project UID/QUI/00100/2013). The author is grateful to Dr M. Kuznetsov for the theoretical studies.

# An electrochemical overview of the oxidative chemistry of ferrocenophanic and ruthenocene antiproliferative drugs

Eric Labbé<sup>a</sup>, Olivier Buriez<sup>a</sup>, Jose de Jesus Cazares-Marinero<sup>b</sup>, Hui Zhi Shirley Lee<sup>b,c</sup>, Pascal Pigeon<sup>b</sup>, Siden Top<sup>b</sup>, Gérard Jaouen<sup>b</sup>, Weng Kee Leong<sup>c</sup> and Christian Amatore<sup>a</sup>

<sup>a</sup> Ecole Normale Supérieure – PSL Research University, Département de Chimie, Sorbonne Universités-UPMC Univ. Paris 06, CNRS UMR 8640 PASTEUR, 24 rue Lhomond 75005 Paris, France

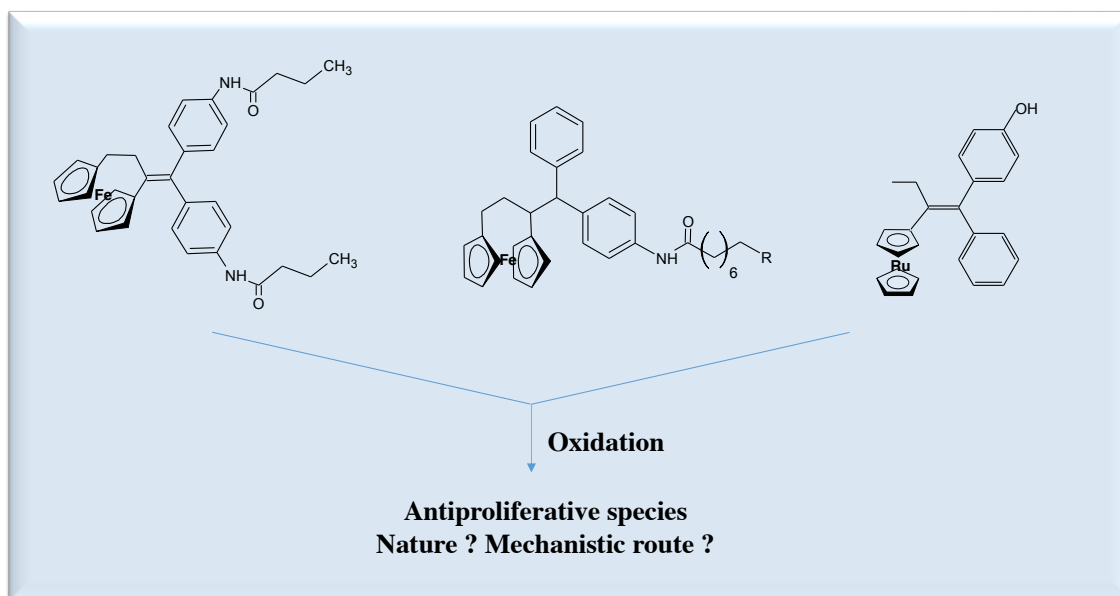
<sup>b</sup> Chimie ParisTech, Ecole Nationale Supérieure de Chimie de Paris, 11 rue Pierre et Marie Curie 75005 Paris, France

<sup>c</sup> Division of Chemistry and Biological Chemistry, Nanyang Technological University, 21 Nanyang Link, Singapore 637371

eric.labbe@ens.fr

The antiproliferative properties of ferrocene, combined to the anti-estrogenic effect of the tamoxifen skeleton, have inspired the preparation of “ferrocifen” anticancer drug candidates in G. Jaouen’s group. The oxidation mechanism of compounds in the phenol series has been thoroughly investigated [1,2], allowing the identification of quinone methides as the metabolites responsible for the antiproliferative activity.

Here we present the electrochemical behavior of new ferrocenophanic compounds [3,4] and a ruthenocifen [5]. These molecules undergo distinct oxidative sequences which are discussed with respect to the mechanistic features established for ferrocifens.



- [1] E. Hillard, A. Vessieres, L. Thouin, G. Jaouen, C. Amatore, *Angew. Chem.* 45 (2006) 285–290
- [2] P. Messina, E. Labbé, O. Buriez, E. Hillard, A. Vessieres, D. Hamels, S. Top, G. Jaouen, Y-M Frapart, D. Mansuy, C. Amatore, *Chem. Eur. J.* 18 (2012) 6581–6587.
- [3] J. Cazares-Marinero, E. Labbé, S. Top, O. Buriez, C. Amatore, G. Jaouen *J. Organomet. Chem.* 744 (2013) 92–100.
- [4] J. Cazares-Marinero, O. Buriez, E. Labbé, S. Top, C. Amatore, G. Jaouen *Organometallics* 32 (2013) 5926–5934.
- [5] H. Z. S. Lee, O. Buriez, E. Labbé, S. Top, P. Pigeon, G. Jaouen, C. Amatore, W. K. Leong *Organometallics* 33 (2014) 4940–4946.

# Break Junction under Electrochemical Gating: Fermi-level Tuning and Redox Manipulation

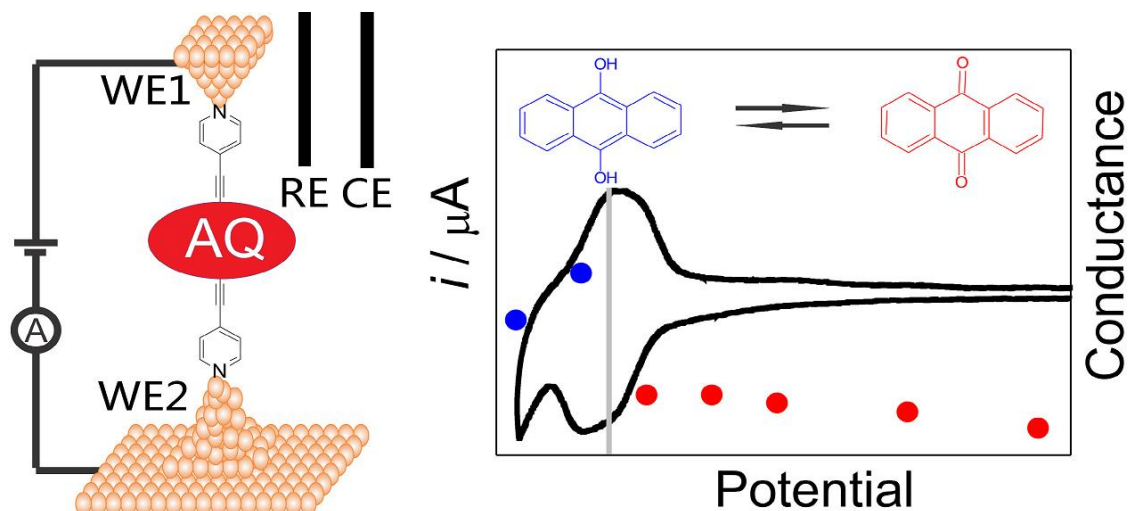
Wenjing Hong, Masoud Baghernejad, Cancan Huang, Thomas Wandlowski  
Department of Chemistry and Biochemistry, University of Bern, Bern, Switzerland  
Freiestrasse 3, CH-3012 Bern, Switzerland  
hong@dcb.unibe.ch / wenjinghong@gmail.com  
wa.dcb.unibe.ch/hong

Controlling charge transport through a single molecule connected to metallic electrodes remains one of the most fundamental challenges of single-molecule electronics. Break junction techniques are considered as ideal testbeds to investigate the charge transport on a single-molecule scale. An additional applied electrochemical gating in break junction experiments will provide a unique opportunity to manipulate the energy alignment and molecular redox processes on single-molecule scale. [1]

Using electrochemical STM based break junction technique, we systematically studied single-molecule electrochemical switches with different redox units, including ferrocene, naphthalenediimide, and tetrathiafulvalene. These studies indicate that the applied electrode potential can manipulate the redox states of single-molecule junctions, and the ON/OFF ratio of these switches between different redox states of the molecular junctions can reach up to four orders of magnitudes varying from different redox units.

On the other hand, the single-molecule conductance studies of 4,4-bipyridine, a redox-inactive molecule, demonstrate that the applied potential also aligns molecular frontier orbitals relative to the electrode Fermi-level, switching the molecule from an off resonance state to “partial” resonance. [2] A recent study of AQ-based molecules with the pyridine anchors showed that the single-molecule conductance could be controlled via both redox switching and Fermi level tuning by varying electrode potential. [3]

As a perspective, we will present our recent effort towards quantum interference effect single-molecule transistor under electrochemical gating.



Schematic to show the conductance tuning of an anthraquinone based single-molecule junction via energy alignment and redox manipulation

## References

- [1] C. Huang, W. Hong,\* *et al.*, *Chem. Soc. Rev.*, **2015**, 44, 889
- [2] M. Baghernejad, W. Hong,\* *et al.*, *Chem. Commun.*, **2014**, 50, 15975
- [3] M. Baghernejad, W. Hong,\* *et al.*, *J. Am. Chem. Soc.*, **2014**, 136, 17922

# The Effect of Ring-Size on the Anodic Oxidation of Cyclic Amides

James Y. Becker and Tatiana Golub

*Department of Chemistry, Ben-Gurion University of the Negev, Beer Sheva 84105,  
Israel*

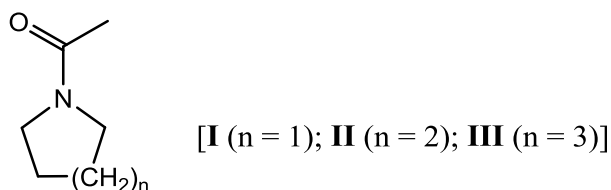
*Email: becker@bgu.ac.il*

Anodic oxidation of N-alkylamides has been investigated extensively in the presence of various nucleophiles such as water, alcohols or carboxylic acids, to afford the respective  $\alpha$ -hydroxy, -alkoxy or -carboxy derivatives as final products, with **no** C-N or N-CO bond-breaking:



Interestingly, the anodic oxidation of N-arylamides [**lacking** 'H' atom(s) at  $\alpha$  position to 'N'] led to three types of bond cleavages, depending on the substituent attached to the aryl group [1].

The present work describes the electrochemical properties of three cyclic amides, N-acylazacycloalkanes (**I** - **III**) by both cyclic voltammetry and preparative electrolysis in methanol, at C anodes [2]. The outcome under various experimental



conditions (current density, electricity consumption, nature of supporting electrolyte) led to the formation of four major type of products:  $\alpha$ -methoxy- and  $\alpha,\alpha'$ -dimethoxy cyclic amides, and two cyclic **ene**amide derivatives. Their relative ratio was found to be highly dependent on the nature of the electrolyte and current density.

## References

- [1] Tatiana Golub and James Y. Becker, *Org. Biomol. Chem. (OBC)*, **2012**, 10, 3906-3912.
- [2] T. Golub and J. Y. Becker, *J. Electrochem. Soc.*, **2013**, 160 (7), G1-G5.

# Oxazaborine and Triazaborine Chromophores, Electrochemical and Theoretical Study

Jiří Ludvík<sup>1</sup>, Tomáš Mikysek<sup>2</sup>, Hana Kvapilová<sup>1</sup>, František Josefík<sup>2</sup>

<sup>1</sup>J. Heyrovský Institute of Physical Chemistry, ASCR, v.v.i., Dept. of Molecular electrochemistry;  
Dolejškova 3, 182 23 Prague 8, Czech Republic [jiri.ludvik@jh-inst.cas.cz](mailto:jiri.ludvik@jh-inst.cas.cz)

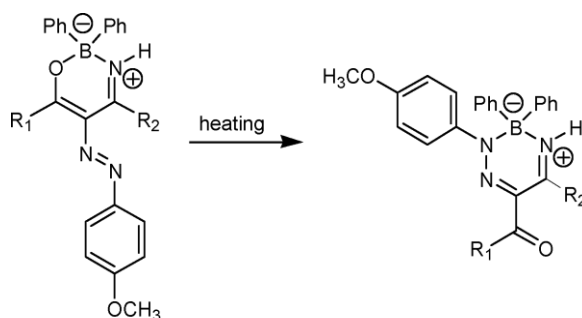
<sup>2</sup>University of Pardubice, Faculty of Chemical Technology, Studentská 573, Pardubice, CZ 532 10,  
Czech Republic

Unsaturated heterocyclic compounds containing a boron atom exhibit miscellaneous types of biological activity: antibacterial, antitumor, fungicidal, insecticidal, and herbicidal. Introduction of the boron atom into an organic molecule substantially changes its electronic – and redox – characteristics, which opens the way to the construction of optoelectronic materials for molecular electronics based on organic molecules. Borine-based materials could be thus used for organic light-emitting diodes (OLEDs).

The present contribution describes electrochemical properties of a series of newly synthesized compounds based on triazaborine core [1]. Their formation is based on a rearrangement of the oxazaborine [2] heterocycles as stable precursors. The studied molecules are bearing different donor and acceptor substituents changing and "tuning" their properties. Their reducibility and oxidizability were electrochemically investigated and the experimental data were correlated with quantum chemical calculations. The main attention has been paid to the investigation of the first oxidation and first reduction process of such compounds using cyclic voltammetry, rotating disk voltammetry and polarography.

In the homologous series of triazaborines the first reduction proceeds as a one-electron reversible process localized at the  $-N=C=N-$  part of the central heterocycle being in conjugation with the attached carbonyl. The first oxidation of triazaborines proceeds as a two-electron irreversible process, most probably of the ECE type, localized at the negatively charged boron atom and surrounding unsaturated structures including the substituted phenyl ring.

For better understanding of the relationship between the structure and redox properties, the Linear Free Energy relationship (LFER) approach using sigma (para) constants of Hammett type was applied, the oxidation and reduction centers were localized, the difference between  $E(\text{ox})$  and  $E(\text{red})$  was correlated with the HOMO-LUMO gap and with the longest-wavelength absorption bands taken from UV-vis spectra. The experimentally determined oxidation and reduction centers were compared with the calculated optimized structures and position of the frontier orbitals. The above presented interpretations were confirmed and the anomalous cases were elucidated.



## References:

- [1] František Josefík, Tomáš Mikysek, Markéta Svobodová, Petr Šimůnek, Hana Kvapilová and Jiří Ludvík; New Triazaborine Chromophores, their Synthesis via Oxazaborines, Electrochemical and DFT Study of their Fundamental Properties; *Organometallics* 33 (2014) 4931-4939.
- [2] Tomáš Mikysek, Hana Kvapilová, František Josefík, Jiří Ludvík; Electrochemical and theoretical study of a new series of bicyclic oxazaborines. *Anal. Lett.* (2015) – accepted, in print

# Electrochemically Induced Friedel-Crafts Arylation of Chalcone Epoxides and Enamides by Organic Redox Mediators

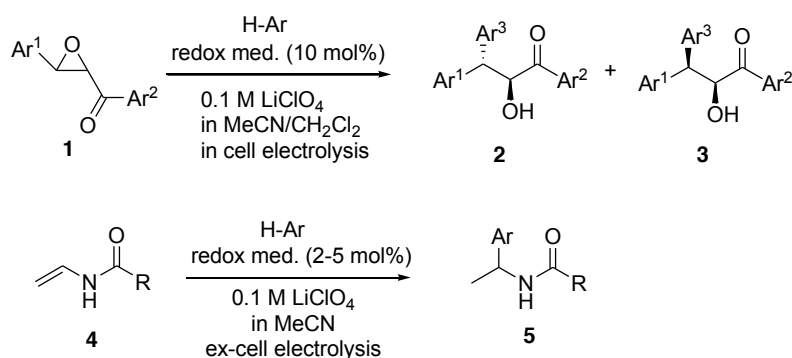
Chengchu Zeng, Nanling Lu, Longji Li

College of Life science & Bioengineering, Beijing University of Technology

Beijing 100124, China

zengcc@bjut.edu.cn

**Abstract:** Cation radical or anion radical, generated from electron transfer of a neutral organic molecule with an in-situ formed active species of a redox catalyst, is very active and readily undergo various chemical transformation, including cleavage, coupling and substitution reaction.<sup>1</sup> Herein, we will report two examples: 1) the indirect anodic oxidation of chalcone epoxides in the presence of electron-rich heteroarenes mediated by a triarylimidazole as a redox mediator,<sup>2</sup> and 2) Friedel-Crafts arylation of enamides induced by electrochemically generated triphenylamine cation radical via ex-cell electrolysis.<sup>3</sup> Cyclic voltammetry (CV) and controlled potential electrolysis was employed to explore their possible reaction mechanisms. Noteworthy, only catalytic amount of charge was required for the two types of reaction, which suggests that a chain reaction occurs upon initiation of a redox catalyst.



Scheme 1. Electrochemically Induced Friedel-Crafts Arylation of Chalcone Epoxides and Enamides.

## References

1. a) R. Francke, R. D. Little, *Chem. Soc. Rev.* **2014**, 43, 2492; b) Y. N. Ogibin, M. N. Elinson, G. I. Nikishin, *Russ. Chem. Rev.*, **2009**, 78, 89-140.
2. N.-N. Lu, N.-T. Zhang, C.-C. Zeng, L.-M. Hu, S. J. Yoo, R. D. Little *J. Org. Chem.*, **2015**, 80, 781-789.
3. L.-J. Li, C.-C. Zeng, R. D. Little, unpublished results.

# Real-time Electrochemical Monitoring Covalent Bond Formation in Solution via Nanoparticle-Electrode Collisions

Da Li<sup>a</sup>, Jingquan Liu<sup>b</sup>, Colin J. Barrow<sup>a</sup> and Wenrong Yang<sup>a\*</sup>

<sup>a</sup> School of Life and Environmental Sciences, Deakin University, Victoria-3217, Australia

<sup>b</sup> College of Chemical Science and Engineering; Laboratory of Fiber Materials and Modern Textile, the Growing Base for State Key Laboratory, Qingdao University, Qingdao 266071, China.

e-mail address: [wenrong.yang@deakin.edu.au](mailto:wenrong.yang@deakin.edu.au)

We describe an alternative electrochemical technique to monitor single covalent bond formation in real-time using nanoparticle-electrode collisions. The method is based on recognising the redox current when MP-11 functionalised graphene nanosheets collide with Lomant's reagent modified gold microelectrode. The amplified redox current reflects directly single-molecule attachments in the presence of MP-11 functionalised graphene nanosheets, attached covalently through the amino functionalities of the polypeptide chain, prepared by depositing Lomant's reagent, 3,3'-dithiodipropionic acid di(N-succinimidyl ester) on the electrode surface for self-assembled monolayers (SAMs) on gold electrodes. The average number of covalent bonds is in the range of  $155 \pm 30$  on a single nanosheet. This facile and highly sensitive monitoring method can be useful for investigating the fundamental of single-molecule reactions.

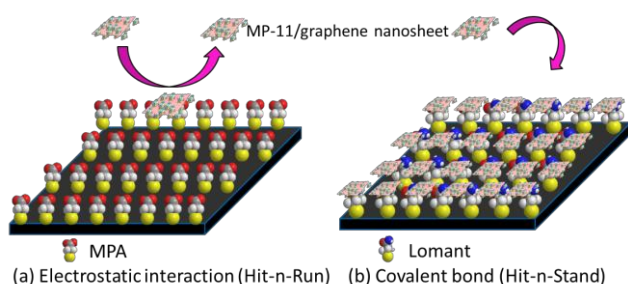


Figure 1. Schematic of monitoring covalent bond formation. (a) Non covalent bond (Electrostatic interaction), (b) Covalent bond. The amplified redox current from MP-11 can be monitored. An amino covalent bond forms when MP-11 functionalised graphene nanosheets reach Lomant's reagent (SAMs) modified gold electrode and stick on the SAMs. The amplified redox current from MP-11 was detected.

## References

- (1) Kim, J.; Kim, B.-K.; Cho, S. K.; Bard, A. J. *J. Am. Chem. Soc.* 2014, 136, 8173.
- (2) Li, D.; Liu, J.; Barrow, C. J.; Yang, W. *Chem. Commun.* **2014**, 50, 8197.
- (3) Wang, W.; Tao, N. *Anal. Chem.* 2013, 86, 2.
- (4) Xiao, X.; Pan, S.; Jang, J. S.; Fan, F.-R. F.; Bard, A. J. *J. Phys. Chem. C* 2009, 113, 14978.
- (5) Goldsmith, B. R.; Coroneus, J. G.; Khalap, V. R.; Kane, A. A.; Weiss, G. A.; Collins, P. G. *Science* 2007, 315, 77.
- (6) Goldsmith, B. R.; Coroneus, J. G.; Kane, A. A.; Weiss, G. A.; Collins, P. G. *Nano Lett.* 2008, 8, 189.



# Tunable Peptide-Based Molecular Wires: Experimental Evidence and Theoretical Insights

Jingxian Yu, John R. Horsley, and Andrew D. Abell

ARC Centre of Excellence for Nanoscale BioPhotonics (CNBP), School of Physical Sciences, The University of Adelaide, Adelaide, SA 5005, Australia  
Email: jingxian.yu@adelaide.edu.au

Electrochemical studies are reported on a series of peptides constrained into either a  $3_{10}$ -helix (**1-6**) or  $\beta$ -strand (**7-9**) conformation, with variable numbers of electron rich alkene containing side chains. Peptides (**1** and **2**) and (**7** and **8**) are further constrained into these geometries with a suitable side chain tether introduced by ring closing metathesis (RCM). Peptides **1**, **4** and **5**, each containing a single alkene side chain reveal a direct link between backbone rigidity and electron transfer, in isolation from any effects due to the electronic properties of the electron rich side-chains. Further studies on the linear peptides **3-6**, confirm the ability of the alkene to facilitate electron transfer through the peptide. A comparison of the electrochemical data for the unsaturated tethered peptides (**1** and **7**) and saturated tethered peptides (**2** and **8**) reveals an interplay between backbone rigidity and effects arising from the electron rich alkene side-chains on electron transfer. Theoretical calculations on  $\beta$ -strand models analogous to **7**, **8** and **9** provide further insights into the relative roles of backbone rigidity and electron rich side-chains on intramolecular electron transfer. Furthermore, electron population analysis confirms the role of the alkene as a ‘stepping stone’ for electron transfer. These findings provide a new approach for fine tuning the electronic properties of peptides by controlling backbone rigidity, and through the inclusion of electron rich side-chains. This allows for manipulation of energy barriers and hence conductance in peptides, a crucial step in the design and fabrication of molecular-based electronic devices.

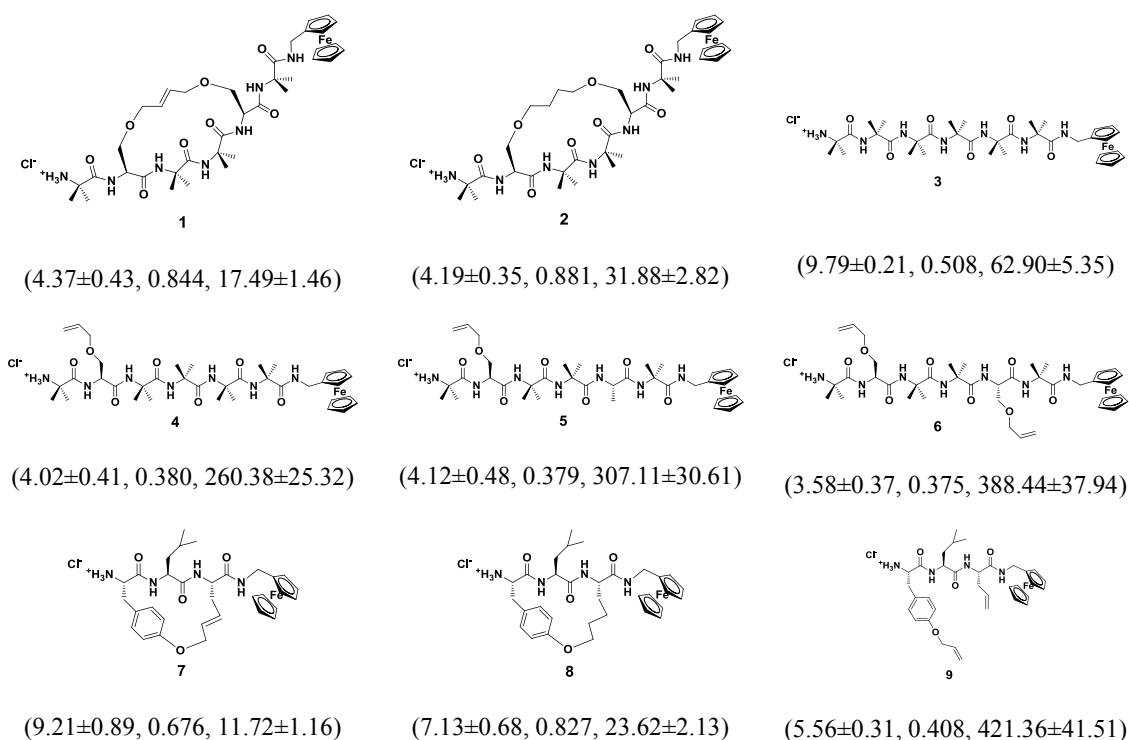


**Figure 1.** Molecular structures of  $3_{10}$ -helical (**1-6**) and  $\beta$ -strand peptides (**7-9**), and their electron transfer parameters. The three numbers listed in each bracket denote the surface concentration ( $\times 10^{-10} \text{ mole.cm}^{-2}$ ), formal potential (V vs AgCl/Ag) and electron transfer rate constant ( $k_{app}$ ) of the peptide shown above.

# **Electronic Structure Effects on Electron Transfer Controlled Hydrogen Bonding in Substituted Dinitrobenzene Electrogenenerated Anions As Receptors for 1,3-Diethylurea**

Carlos Frontana, Eduardo Martínez-González,  
*Centro de Investigación y Desarrollo Tecnológico en Electroquímica, SC  
Parque Tecnológico Querétaro S/N, Sanfandila, Pedro Escobedo, Querétaro,  
76703, Querétaro, México  
cfrontana@cideteq.mx*

In Electron Transfer Controlled Hydrogen Bonding (ETCHB), switching molecules experiment changes in their reduction potential values as hydrogen bond donor species are added to the solution, and is the basis of operation of many molecular switches [1-3]. Therefore, a comprehensive understanding of the mechanistic routes that govern electron transfer in these systems would allow the design of devices with specific applications. In the case of complexes formed via ETCHB with electrogenerated anions from dinitrobenzene isomers [3-6], proton transfer reactions were also observed, diminishing the stability of these intermediates. In this work, a similar electrochemical analysis was performed using 1,3-diethylurea to avoid protonation; showing two sequential reversible voltammetric signals, from which  $K_b$  (binding constant) values were calculated. The experimental behavior suggest that the mechanistic routes for ETCHB depend on the relative position of the nitro groups within the molecule: For o- and p-dinitrobenzenes radicals, a reduction involving an  $E_{rev} E_{rev} C$  mechanism occurs while for with m-dinitrobenzene radicals, the reaction evolves by an  $E_{rev} C$   $E_{rev}$  route, leading also to changes by inductive effect caused by substituents present.

## **Acknowledgments**

E. M.-G. thanks CONACYT for support his M. Sc. Studies (scholarship no. 270926). C. F. thanks CONACYT for support through project 107037.

References: [1]. E. Martínez-González, C. Frontana. *J. Org. Chem.* 2014, 79, 1131-1137; [2]. J. Bu, N. D. Lilienthal, J. E. Woods, C. E. Nohrden, K. T. Hoang, D. Truong, D. K. Smith. *J. Am. Chem. Soc.* 2005, 127, 6423-6429; [3]. C. Chan-Leonor, S. L. Martin, D. K. Smith. *J. Org. Chem.* 2005, 70, 10817-10822; [4]. M. A. Syroeshkin, A. S. Mendkovick, L. V. Mikhalechenko, A. Rusakov, V. P. Gulyai. *Russ. Chem. Bull., Int. Ed.* 2009, 58, 468-472.; [5]. A. S. Mendkovich, M. A. Syroeshkin, L. V. Mikhalechenko, A. I. Rusakov, V. P. Gulyai. *Russ. Chem. Bull., Int. Ed.* 2008, 57, 1492-1495; [6]. M. F. Nielsen, V. D. Parker. *Acta Chemica Scandinavica B.* 1988, 42, 93-100

# The Influence of Alkyl Chain Length of Viologens on the Performance of Their Electrochromic Devices

Hsin-Che Lu<sup>1</sup>, Ting-Hsiang Chang<sup>1</sup>, Chung-Wei Kung<sup>1</sup>, Sheng-Yuan Kao<sup>1</sup>, Kuo-Chuan Ho<sup>1,2\*</sup>

<sup>1</sup>Department of Chemical Engineering, National Taiwan University, Taipei 10617, Taiwan

<sup>2</sup>Institute of Polymer Science and Engineering, National Taiwan University, Taipei 10617, Taiwan

\*E-mail: kcho@ntu.edu.tw

Electrochromism refers to the phenomenon that materials alter their optical characteristics reversibly through the manipulation of different potential biases. Among all electrochromic materials, the N, N-substituted bipyridiniums (also named as viologens (RVs)) receive much attention for their attracting optical characteristics change between their dication state ( $RV^{2+}$ , bleached) and cation-radical state ( $RV^{\bullet+}$ , colored). The working principle of a typical viologens based electrochromic device (ECD) coupled with a redox active material, such as ferrocene (Fc), is shown in Fig. 1. The long-term stability of viologens based ECD is suffered from the poor solubility of  $RV^{\bullet+}$ , which leads to the recrystallization of viologens, as well as the agglomeration of  $RV^{\bullet+}$  onto the electrode. Either the above two phenomena would result in an irreversible coloring/bleaching process, and decrease the stability of the ECD. Therefore, the retardation of the diffusion rate of the viologens via immobilization or size control through tuning the alkyl chain lengths on the pyridine, has been regarded as a feasible approach to prevent the decay of the ECD caused by the agglomeration. In this study, the relation between the alkyl chain length of viologens and their electrochromic performance were investigated by measuring the diffusion coefficients, optical transmittance responses, and cycling stabilities of the viologens based ECDs. In Fig. 2, the apparent diffusion coefficients ( $D_{app}$ ) of 0.02 M methyl viologen (MV), ethyl viologen (EV), heptyl viologen (HV), and octadecyl viologen (OV) in pertinent ECDs coupled with 0.02 M redox couple Fc, were obtained by chronoamperometry and calculated by Cottrell equation. The apparent diffusion coefficients of these ECDs decrease with longer length of alkyl chain of viologens would elucidate the relation between alkyl chain length of viologens and their electrochromic performance. The agglomeration of viologens during operation was also investigated by an electrochemical quartz crystal microbalance (EQCM).

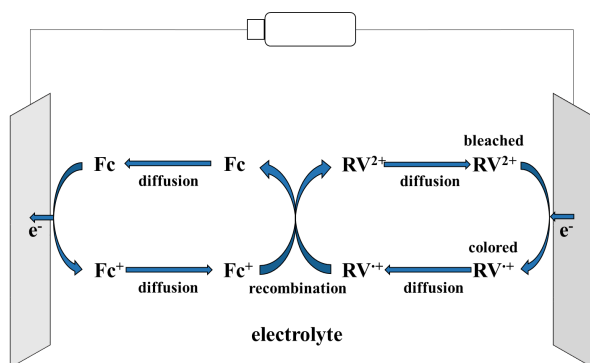


Fig. 1 Working principle of viologens based ECD.

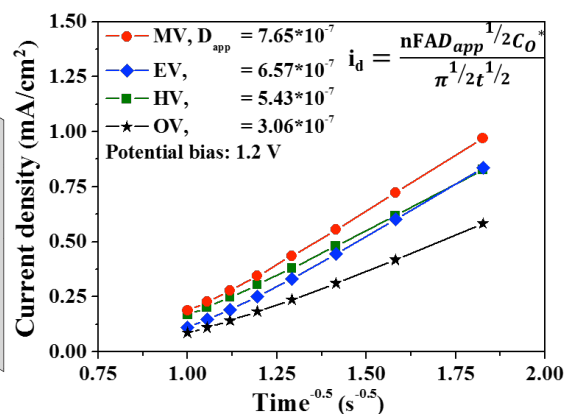


Fig. 2 Apparent diffusivities of viologens with variation of alkyl chain length.

# Substituent Effects on Electrochemical Properties and Oxygen Reduction Reaction Activity of Copper Complexes

Masafumi Asahi<sup>1</sup>, Shin-ichi Yamazaki<sup>1</sup>, Zyun Siroma<sup>1</sup>, Naoko Fujiwara<sup>1</sup>, Tsukasa Nagai<sup>1</sup>, Shinobu Itoh<sup>2</sup>, and Tsutomu Ioroi<sup>1</sup>

<sup>1</sup>Research Institute of Electrochemical Energy, Department of Energy and Environment  
National Institute of Advanced Industrial Science and Technology (AIST)  
1-8-31, Midorigaoka, Ikeda, Osaka 563-8577, Japan

<sup>2</sup>Department of Material and Life Science, Division of Advanced Science and Biotechnology  
Graduate School of Engineering, Osaka University  
2-1 Yamada-oka, Suita, Osaka 565-0871, Japan

[m.asahi@aist.go.jp](mailto:m.asahi@aist.go.jp)

## Introduction

Non-Pt-based cathode catalysts have been extensively investigated over the past several decades for the significance of cost reduction of polymer electrolyte fuel cells. Metallocomplex-type catalysts are considered as one prospective candidate of the cathode catalysts. Generally, the metallocomplex-type catalysts offer an isolated active metal center, which enables economical utilization of the metal. Besides this benefit, the fine tuning of the ligands would drastically effect on the electrochemical properties of the complexes.

We have focused on several bio-inspired copper complexes using pyridylalkylamine ligands as the models of copper containing enzymes. The electrochemical O<sub>2</sub> reduction reaction catalyzed by the complexes proceeded conjugated with the Cu<sup>II</sup>/Cu<sup>I</sup> redox pair by 4-electron manner in a neutral aqueous solution<sup>1</sup>. Although the copper complexes were found to show O<sub>2</sub> reduction activity in an aqueous solution, there is room to improve the activity. In this study, the copper complexes including a series of ligands substituted by carboxyl group were synthesized, and the substituent effects on their electrochemical properties and O<sub>2</sub> reduction activity were investigated at various pH.

## Experiments

The Cu<sup>II</sup> complexes supported by bmpa (bis(2-pyridylmethyl)amine, [1]) and their carboxyl derivatives (*o*-derivative [1-*o*], *m*-derivative [1-*m*], and *p*-derivative [1-*p*]) were synthesized according to the reported procedures with a slight modification<sup>2</sup> (Fig. 1).

Voltammograms under quiescent conditions were taken in 10 mM Britton-Robinson buffer solution (CH<sub>3</sub>COOH, H<sub>3</sub>PO<sub>4</sub>, H<sub>3</sub>BO<sub>3</sub>, supporting electrolyte: 10 mM Na<sub>2</sub>SO<sub>4</sub>) containing 0.3 mM of the copper complex. All measurements in this study were performed using glassy carbon as a working electrode, Pt coil as a counter electrode, and Ag|AgCl|KCl(sat.) as a reference electrode.

## Results and discussion

Cyclic voltammograms of the copper complex with each of the ligand (Cu-[1], Cu-[1-*o*], Cu-[1-*m*], and Cu-[1-*p*]) under Ar atmosphere at pH 7.0 show reversible voltammograms derived from Cu<sup>II</sup>/Cu<sup>I</sup> redox pair. This result indicates that the redox reaction is less inhibited by the substitution of the carboxyl groups. It also be founded that *o*-substitution causes the negative shift of the redox potential (*E*<sup>o</sup>) though *m*-, or *p*-substitution causes the positive shift of *E*<sup>o</sup>. The negative charge of *o*-carboxy group would give special electronic effect on the copper center due to adjacency.

The *E*<sup>o</sup>-pH diagram of Cu-[1], Cu-[1-*m*], and Cu-[1-*p*] observed substantially negative shift of the redox potential with the increase in pH. Contrary to that, that of Cu-[1-*o*] was less sensitive to the change of pH, which indicates hydroxide ions can be less likely to coordinate to Cu-[1-*o*]. It was thought to be advantageous for the O<sub>2</sub> reduction reaction.

The onset potential of electrochemical O<sub>2</sub> reduction activity of Cu-[1-*o*] tended to be slight higher than the other complexes. It would be attributed to higher reducing activity of Cu<sup>I</sup>-[1-*o*].

## References

1. M. Asahi et al., *Dalton Trans.*, **43**, 10705 (2014)
2. Ying-Ji Sun et al., *Inorg. Chem.* **52**, 10936 (2013)

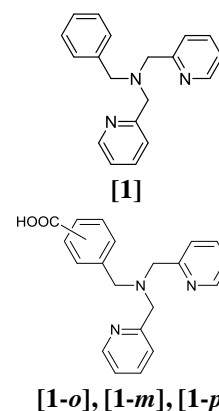


**Fig. 1** Structure of [1], [1-*o*], [1-*m*], and [1-*p*].

# Investigation of Electrode Reaction at Well-Defined Electrochemical Interfaces in Ionic Liquids

Miangang Li, Li Chen, Yunxin Zhong, Jiawei Yan, Bingwei Mao\*

*State Key Laboratory for Physical Chemistry of Solid Surfaces, College of Chemistry and Chemical Engineering, Xiamen University, Xiamen, 361005*  
*bwmao@xmu.edu.cn*

Room-temperature ionic liquids are a class of new solvents with low vapor pressure, wide electrochemical window, good ionic conductivity and thermal stability, and thus find a wide range of applications in various fields. However, owing to the high concentration, large size and asymmetric structure of the ions, the structure and kinetics at the electrochemical interfaces in ionic liquid are very different from those of conventional solvents. Substantial theoretical and experimental progresses have been achieved, which reveals that electric double layers in ionic liquids have unique layered structures<sup>[1,2]</sup>. However, investigations of the electrode reactions taking place in the double layer region in ionic liquid are very limited. Experiments and molecular dynamics simulations of redox reactions at the interface have been conducted, and kinetic behaviors have been analyzed using Butler-Volmer or Marcus-Hush model to estimate the charge transfer factor  $\alpha$  and reorganization energy  $\lambda$ <sup>[3]</sup>. But almost all of the works used microelectrodes as the working electrodes, and the influences of the detailed double layer structures on the reaction kinetics are far from clear.

In this work, we present an investigation of electrode reaction at well-defined electrochemical interfaces formed by Ag single-crystal electrodes with ionic liquids. Ag(111) single crystal electrode is chosen as the working electrode, whose double layer structure and adsorption of EMITFSI ionic liquids can be determined independently by AFM and STM, respectively. Fast voltammetry, double potential step chronoamperometry and electrochemical impedance spectroscopy are employed to study the kinetics of the electrode reaction. Together with the temperature-dependent measurements, kinetic parameters are obtained, and the influence of the double layer structure is discussed. The present work demonstrates the correlation of kinetics and structure at structurally well-defined electrochemical interface in ionic liquids.

This work was supported by the National Basic Research Program of China (2012CB932902, 2015CB251102) and the National Natural Science Foundation of China (21033007).

## References

- [1] Y.Z. Su, Y.C. Fu, Y.M. Wei, J.W. Yan, B.W. Mao, The Electrode/Ionic Liquid Interface: Electric Double Layer and Metal Electrodeposition, *Chemphyschem*, 11 (2010) 2764-2778.
- [2] M.V. Fedorov, N. Georgi, A.A. Kornyshev, Double layer in ionic liquids: The nature of the camel shape of capacitance, *Electrochem. Commun.*, 12 (2010) 296-299.
- [3] E.E.L. Tanner, L. Xiong, E.O. Barnes, R.G. Compton, One electron oxygen reduction in room temperature ionic liquids: A comparative study of Butler-Volmer and Symmetric Marcus-Hush theories using microdisc electrodes, *J. Electroanal. Chem.*, 727 (2014) 59-68.

# Original Porphyrin – Polyoxometalate Copolymers: Application for the Photocurrent Generation

Zhaohui HUO, I. Azcarate, E. Lacôte, B. Hassenknopf, C. Bucher, L. Ruhlmann

Laboratoire d'Electrochimie et de Chimie Physique du Corps Solide, Université de Strasbourg, 4 rue Blaise Pascal, 67000, Strasbourg, France

zhaohui.huo@etu.unistra.fr, lruhlmann@unistra.fr

Polyoxometalates (POMs) are metal-oxygen cluster anions constituted of metal elements in their highest oxidation state which can undergo reversible and multi-electron photoredox processes. Unfortunately, POMs can be excited (POM\*) only under UV irradiation. Chromophore-POMs could offer a way to overcome part of this problem. Various type of electrostatic or covalent POM-porphyrin copolymeric films were synthesized. First, poly-zinc octaethylporphyrin/viologen/POM films were obtained through incorporating various type of POM<sup>n-</sup> (Preyssler, Keggin, etc...) onto the copolymer poly-zinc octaethylporphyrin/viologen (poly-ZnOEP-V<sup>2+</sup>) obtained by electro-oxidation of the macrocycle in the presence of 4,4'-bipyridine [1]. Then, by metathesis reaction, the (partial) exchange of the initial counter ion PF<sub>6</sub><sup>-</sup> by the POM<sup>n-</sup> ([SiW<sub>12</sub>O<sub>40</sub>]<sup>4-</sup> or [NaP<sub>5</sub>W<sub>30</sub>O<sub>110</sub>]<sup>14-</sup>) gave the target copolymer poly-ZnOEP-V<sup>2+</sup>-POM<sup>n-</sup> (Fig. 1) [2]. Their formation was also studied by AFM and EQCM.

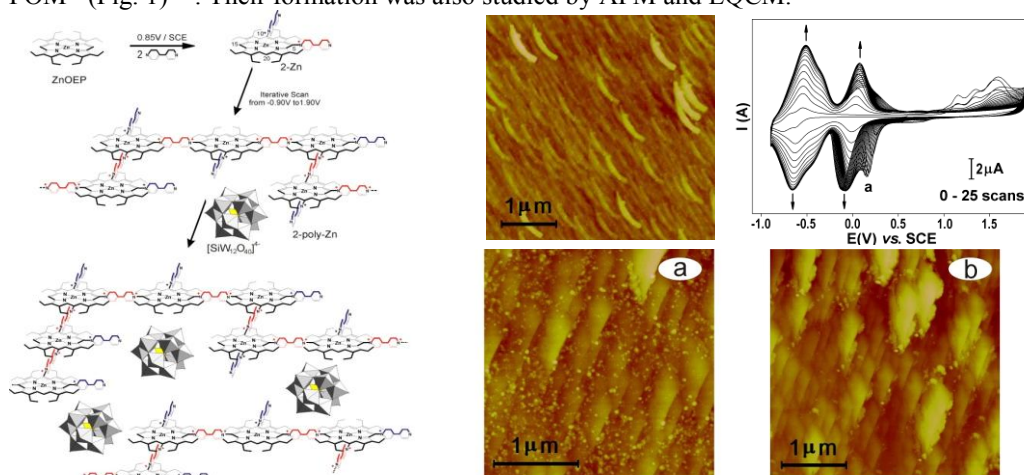


Fig 1. Left: formation of the copolymer poly-ZnOEP-Viologen (Poly-ZnOEP-V<sup>2+</sup>). Middle: AFM picture of poly-ZnOEP-V<sup>2+</sup> obtained after 25 iterative scans. Right: Cyclic voltammograms recorded during electropolymerization. The modified ITO electrode after soaking (a) 1 min and (b) 10 min in aqueous solution containing Keggin type POM ([SiW<sub>12</sub>O<sub>40</sub>]<sup>4-</sup>).

Second, hybrid POM-porphyrin copolymeric films were directly obtained by the electro-oxidation of ZnOEP in the presence of different type POMs (Lindqvist, Keggin and Dawson) bearing two pyridyl groups (POM(py)<sub>2</sub>) [3]. Fig. 2 shows one example of electropolymerization of conjugated Dawson-type POM-porphyrin copolymers. Their photovoltaic performances have been investigated by photocurrent transient measurements [4] (Fig. 3). The impedance measurement under visible illumination will be also presented and compared with the efficiency for the photocurrent generation.

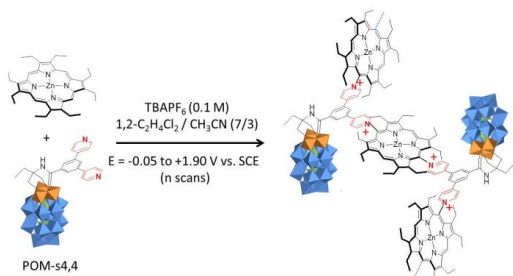


Fig 2. Copolymer **poly-POM-s4,4-ZnOEP**.

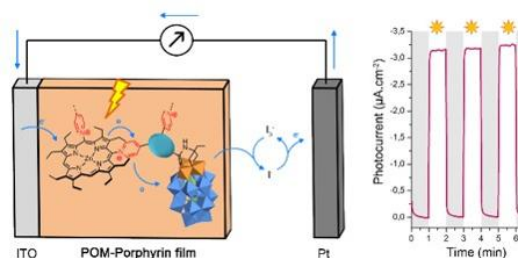


Fig 3. Photoelectrochemical response in aqueous solution.

## References

- [1] a) Ruhlmann, L. Schulz, A.; Giraudeau, A.; Messerschmidt, C.; Fuhrhop, J.-H. J. Am. Chem. Soc. 1999, 121, 6664. b) Ruhlmann, L.; Hao, J.; Ping, Z.; Giraudeau, A. J. Electroanal. Chem. 2008, 621, 22.
- [2] Schaming, D.; Allain, C.; Farha, R.; Goldmann, M.; Lobstein, S.; Giraudeau, A.; Hasenknopf, B.; Ruhlmann, L. Langmuir, 2010, 26, 5101-5109.
- [3] I. Azcarate, I. Ahmed, R. Farha, M. Goldmann, X. Wang, H. Xu, B. Hasenknopf, E. Lacôte, L. Ruhlmann, Dalton Trans., 2013, 42, 12688.
- [4] I. Azcarate, Z Huo, R. Farha, M. Goldmann, H. Xu, B. Hasenknopf, E. Lacôte, L. Ruhlmann, Chemistry - A European Journal chem., in press, DOI:10.1002/chem.201406178.

# Electrosynthesis Processes Based on Oxidative Couplings of Porphyrins for the Formation of Supramolecular Assemblies

L. Ruhlmann

Laboratoire d'Electrochimie et de Chimie Physique du Corps Solide, Université de Strasbourg, 4 rue  
Blaise Pascal, 67000, Strasbourg, France  
lruhlmann@unistra.fr

Porphyrins and porphyrin-containing materials have attracted considerable attention in recent last decades. For instance, in the photosynthesis process, chlorophyll possesses functions are able to convert sunlight energy into chemical energy. A number of researchers have attempted to construct artificial light-harvesting systems that provide important contributions not only to understand the natural systems but also to mimic nature in creating new efficient light-harvesting systems for energy conversion.

In this context, the presentation will be devoted to multiporphyrin systems obtained by electrosynthesis from oxidation of porphyrin macrocycle. Oxidation of the  $\pi$ -ring of a porphyrin macrocycle proceeds *via* two one-electron steps generating the  $\pi$ -radical cation and the dication, species known to be very reactive. Indeed, these cationic species have an electrophilic character, leading as first type of reactivity to reactions with nucleophilic compounds (Nu = pyridinyl or phosphine group). Thus, nucleophilic substitutions can be performed onto free carbons (carbons with one H in *meso* or  $\beta$  positions) of porphyrin macrocycles, allowing not only an easy grafting of substituents onto porphyrins, but also the synthesis of oligomers of porphyrins by using compounds having two nucleophilic sites (4,4'-bipyridine, diphosphine, etc.) as spacers between macrocycles (Fig. 1).<sup>[1]</sup> The second type of reactivity based on

oxidized porphyrins relies on couplings of oxidized porphyrins with each other, leading again to oligomers of porphyrins, but with direct links, *i.e.*, without spacers between macrocycles in this case. Even if classical oxidants can be used to perform such reactions, the advantage of these synthetic methods is that it is possible to perform them by an electrochemical pathway, since oxidized porphyrins can also be electrochemically obtained. Thus, the reactivity of porphyrin  $\pi$ -radical cations and dications, easily obtained by an electrochemical pathway, offers a new and facile synthesis method for obtaining multiporphyrin systems.<sup>[2]</sup>

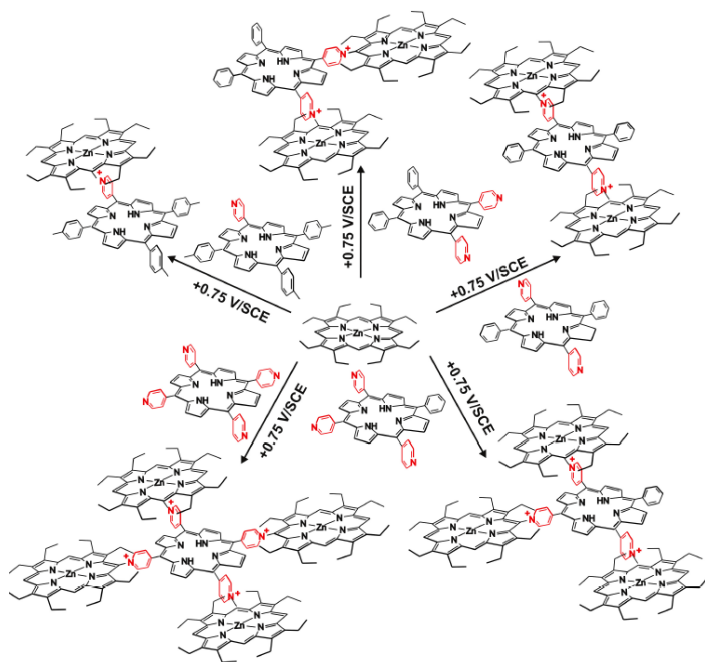


Fig 1. Electrosynthesis scheme of the oligomers with pyridinium spacers (see Ref. 1h).

## References

- [1] a) Giraudeau, A.; Ruhlmann, L.; El-Kahef, L.; Gross, M. *J. Am. Chem. Soc.* **1996**, *118*, 2969–2979. b) Ruhlmann, L.; Giraudeau, A. *Chem. Commun.* **1996**, 2007–2008. c) Giraudeau, A.; Lobstein, S.; Ruhlmann, L.; Melamed, D.; Barkigia, K. M.; Fajer, J. *J. Porphyrins Phthalocyanines* **2001**, *5*, 793–797. d) Ruhlmann, L.; Lobstein, S.; Gross, M.; Giraudeau, A. *J. Org. Chem.* **1999**, *64*, 1352–1355. e) Schaming, D.; Marggi-Poullain, S.; Ahmed, I.; Farha, R.; Goldmann, M.; Gisselbrecht, J.-P.; Ruhlmann, L. *New J. Chem.* **2011**, *35*, 2534–2543. f) Ruhlmann, L.; Giraudeau, A. *Eur. J. Inorg. Chem.* **2001**, 659–668. g) Ruhlmann, L.; Gross, M.; Giraudeau, A. *Chem. Eur. J.* **2003**, *9*, 5085–5096. h) Schaming, D.; Xia, Y.; Thouvenot, R.; Ruhlmann, L. *Chem. Eur. J.* **2013**, *19*, 1712–1719.
- [2] D. Schaming, L. Ruhlmann\*, Set 7, Handbook of Porphyrin Science, Karl Kadish, Roger Guilard, Kevin Smith, Eds., Published by World Scientific, 5 Toh Tuck Link, Singapore 596224. USA office: 27 Warren Street, Suite 401-402, Hackensack, NJ 07601. Chapter 167, Volume 32, Materials, "Electrosynthesis Processes Based on Oxidative Couplings of Porphyrins for the Formation of Eletrosynthesis Supramolecular Assemblies", **2014**, pp 127-171.



# The Correlation of Electrochemical Measurements and Molecular Junction Conductance Simulations in $\beta$ -Strand Peptides

J.R. Horsley, Dr. J. Yu, Prof. A.D. Abell  
ARC Centre of Excellence for Nanoscale BioPhotonics (CNBP),  
School of Chemistry and Physics,  
The University of Adelaide,  
Adelaide, SA 5005, Australia.  
john.horsley@adelaide.edu.au

## Abstract:

Understanding the electronic properties of single peptides is not only of fundamental importance, but it is also paramount to the realization of peptide-based molecular electronic components. Electrochemical and theoretical studies are reported on two  $\beta$ -strand-based peptides, one with its backbone constrained with a triazole-containing tether introduced by Huisgen cycloaddition (**1**) and the other a direct linear analogue (**2**). Density functional theory (DFT) and non-equilibrium Green's function were used to investigate conductance in molecular junctions containing peptides **3** and **4** (analogues of **1** and **2**). While the peptides share a common  $\beta$ -strand conformation, they display vastly different electronic transport properties due to the presence (or absence) of the side-bridge constraint and the associated effect on backbone rigidity. These studies reveal that the electron transfer rate constants of **1** and **2**, and the conductance calculated for **3** and **4**, differ by approximately one order of magnitude, thus providing two distinctly different conductance states and what is essentially a molecular switch. A definitive correlation of electrochemical measurements and molecular junction conductance simulations is demonstrated using two different charge transfer techniques. This study furthers our understanding of the electronic properties of peptides at the molecular level, which provides an opportunity to fine-tune their molecular orbital energies through suitable structural manipulation.

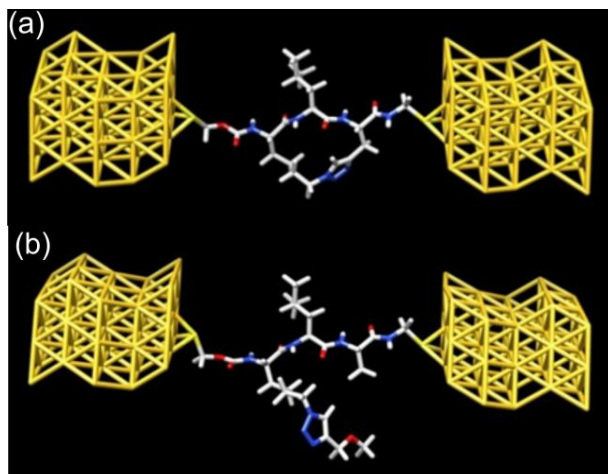


**Figure:** Vast differences in the electronic transport properties of the two novel peptides (a) constrained and (b) linear, measured by electrochemical techniques as well as molecular junction conductance simulations, provide two distinctly different conductance states, in what is essentially a molecular switch.



# Synthesis of a $\pi$ -conjugated porphyrin polymer film on electrode by electrooxidation of 5,15-di(4-aminophenyl)-10,20-diphenylporphyrinatozinc(II)

Suzaliza Mustafar, Kuo-Hui Wu, Kenji Takada, Ryojun Toyoda, Ryota Sakamoto, Hiroshi Nishihara

Department of Chemistry, Graduate School of Science, The University of Tokyo  
7-3-1, Hongo, Bunkyo-ku, Tokyo, 113-0033, Japan

Email: sakamoto@chem.s.u-tokyo.ac.jp, nishihara@chem.s.u-tokyo.ac.jp

Porphyrins have been a well-known family exhibiting interesting photochemical and electrochemical properties, that can be fine-tuned by introducing substituents on the porphyrin ring or simply introducing various kinds of metals at the center [1]. Porphyrin polymer films on electrode have been prepared by both electrooxidation and electroreduction methods [2], and the electropolymerized porphyrin films have been utilized as photosensitizer, electrochromic sensor, and sensitizer in dye-sensitized solar cells. In this research, we investigated the synthesis of a new  $\pi$ -conjugated porphyrin polymer film on glassy carbon (GC) and indium-tin oxide (ITO) by electropolymerization of 5,15-di(4-aminophenyl)-10,20-diphenylporphyrinatozinc(II) (**ZnP-1**). A plausible mechanism of the polymerization reaction is shown in Figure 1. When a consecutive potential scan between -0.7 V and 0.8 V vs.  $\text{Ag}^+/\text{Ag}$  was carried out in a 2 mM solution of **ZnP-1** in 0.1 M  $\text{Bu}_4\text{NClO}_4$ -dichloromethane at GC, an anodic wave at 0.546 V and a cathodic wave at 0.428 V increased, indicating formation of a redox active film on the electrode (Figure 2). The modified electrode thus formed showed a reversible redox reaction of surface-confined species, which were characterized using UV-Vis spectroelectrochemical measurements.

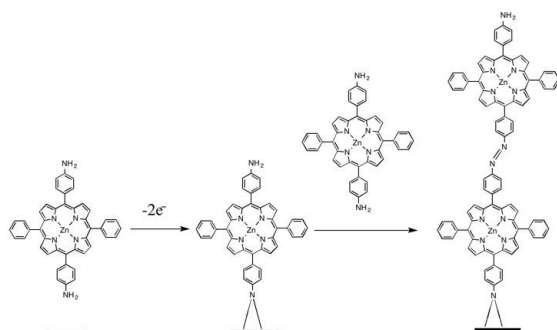


**Figure 1.** Schematic illustration of a proposed mechanism of the electrooxidative polymerization of **ZnP-1** on substrates.

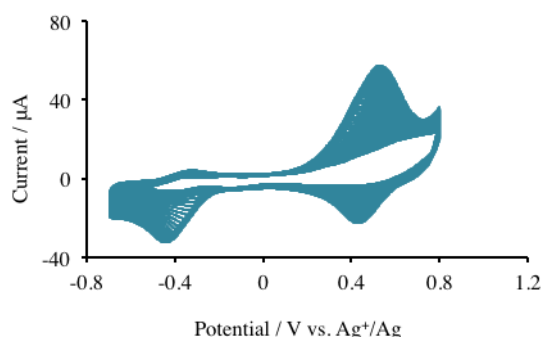


**Figure 2.** Cyclic voltammogram for electropolymerization of **ZnP-1** (2 mM) by consecutive potential scans (from 1st to 50th cycles) in 0.1 M  $\text{Bu}_4\text{NClO}_4$ -dichloromethane at GC.

- [1] W. Auwärter, D. Écija, F. Klappenberger, J.V. Barth, Porphyrins at interfaces, *Nature Chem.* 7 (2015) 105-120.
- [2] S-C. Huang, C-Y Lin, Reductive electropolymerization of N-methyl-3-pyridylethynyl-porphyrins, *Chem. Commun.* 51 (2015) 519-521.

# Catalytic reduction of O<sub>2</sub> by ferrous hemin over formation of ferrous hemin-O<sub>2</sub> adduct

Jingyuan Chen, Wenwen Li, Koichi Aoki,  
*Department of Applied Physics, University of Fukui,*  
3-9-1 Bunkyo, Fukui, 910-8507 Japan  
jchen@u-fukui.ac.jp

Hemin, an iron porphyrin, functions as a carriage of dioxygen in mammalian respiration in the ferrous form. It works also as an electrochemical catalyst of the reduction of dioxygen by reproducing the ferrous form from the ferric one. Since the carriage requires stabilization of the dioxygen adduct, the catalytic reduction of dioxygen with the ferric form might hinder the stabilization. This work aims at finding the discrimination between the functions of the carriage and of the catalysis. A hint of the finding lies in the difference between the remarkable catalytic currents in high concentrations of hemin and negligibly small ones in very low concentrations. The catalytic current (Fig.1 (b)) at the hemin-coated electrode is confirmed to occur at the stoichiometry of two hemin molecules and one dioxygen molecule. When this stoichiometry is applied to the dioxygen adduct of hemin as an intermediate species of the catalysis, high concentrations of dissolved hemin should provide the catalytic current. Spectro-electrochemistry (Fig.2) demonstrates that ferrous hemin is not oxidized simply to the ferric form but is converted to other species, e.g. the dioxygen adduct.

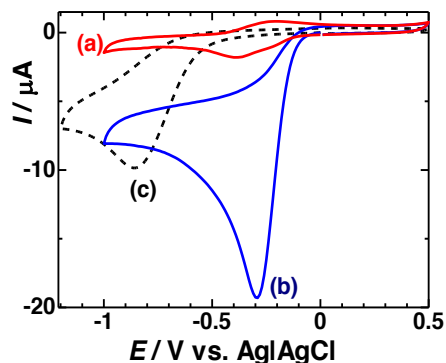


**Fig.1** Voltammograms at the hemin-coated GC electrode in (a) deaerated and (b) aerated phosphate buffer solution, pH 7.4 for  $\nu = 0.1 \text{ V s}^{-1}$ . (c) is at the bare GC electrode in the aerated solution.

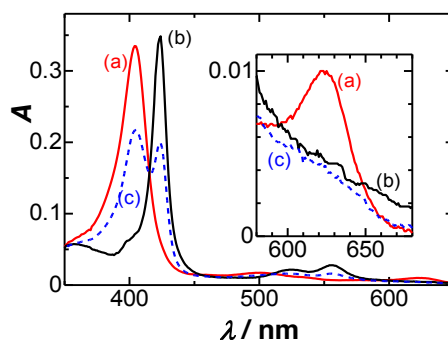


**Fig.2** UV-vis spectra of (a) hem( $\text{Fe}^{3+}$ ), (b) hem( $\text{Fe}^{2+}$ ) and (c) dioxygen-added hem( $\text{Fe}^{2+}$ ) for 30 s in the UV thin layer cell including 0.032 mM hemin + DMSO. The reduction was made at -0.6 V vs. Ag|AgCl for 10 min.

## Acknowledgements

This work was financially supported by Grants-in-Aid for Scientific Research (Grants 22550072) from the Ministry of Education in Japan.

# Influence of Decreased Intermolecular Coupling on the Electrochromic Switching-Rate of Substituted Phthalocyanine Thin Films

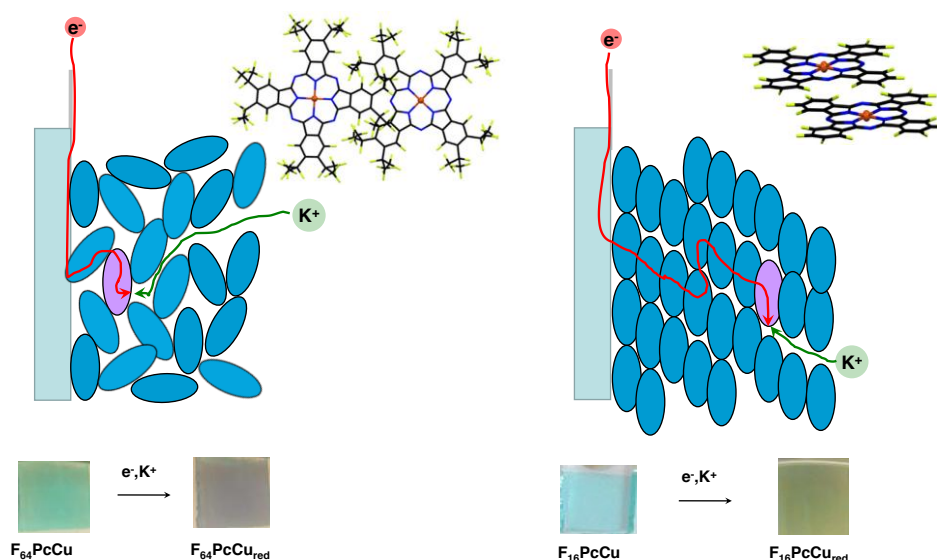
J. Weissbecker<sup>a</sup>, A. Loas<sup>b</sup>, S.M. Gorun<sup>b</sup>, D. Schlettwein<sup>a,\*</sup>

<sup>a</sup> Justus-Liebig-University Giessen, Institute of Applied Physics, and Laboratory of Materials Research, Heinrich-Buff-Ring 16, D-35392 Giessen, Germany.

<sup>b</sup> Seton Hall University, Department of Chemistry and Biochemistry, and Center for Functional Materials, 400 South Orange Avenue, South Orange, New Jersey 07079, USA.

\*schlettwein@uni-giessen.de (ISE member)

Electronic redox changes of thin films coupled with changes in absorption wavelengths or molar extinction coefficients are of interest, e.g., as smart windows, smart mirrors or smart curtains. Direct electrochromic devices are most promising. As an alternative to classical inorganic electrochromic layers like tungsten oxide, thin films of organic pigments and dyes like phthalocyanines are of interest as electrochromic layers because of their high molar extinction coefficients and a large change of color upon redox reactions allowing to use considerably thinner films and, hence, promising considerably faster switching within seconds rather than minutes [1].



In this work, thin homogeneous films (5-120 nm) of the electron deficient perfluorinated phthalocyanine F<sub>16</sub>PcCu and the perfluoroalkyl-substituted perfluorophthalocyanine F<sub>64</sub>PcCu have been prepared by physical vapor deposition onto ITO-glass and their redox characteristics in contact to aqueous solutions were studied. The films were readily reduced and re-oxidized at potentials slightly negative of the Ag/AgCl reference electrode confirming a significant stabilization of the produced anions by the electron-withdrawing fluorinated substituents. A significant color change accompanied the change of the molecular redox states. Electroneutrality of the films was ensured by (de-)intercalation of K<sup>+</sup>-counter ions upon reduction (re-oxidation). F<sub>64</sub>PcCu was reduced by one electron, F<sub>16</sub>PcCu by up to two, for thin films and slow charging rates. Steric hindrance of the fluorinated ligands influence the extent of intermolecular coupling. The perfluoroalkyl groups in F<sub>64</sub>PcCu thereby led to widely decoupled electronic states of the molecules in the thin films leading to facile diffusion of K<sup>+</sup>-counter ions in the films at, however, significantly reduced electrical conductivity of F<sub>64</sub>PcCu relative to F<sub>16</sub>PcCu. Time-resolved measurements served to analyze the interplay of the two mandatory transport processes. The difference in steric hindrance resulted in a change of the rate-limiting step. Thus, for films of F<sub>64</sub>PcCu the transport of electrons in the molecular films is rate-limiting, as opposed to counter ion diffusion in the case of F<sub>16</sub>PcCu. This switch underlines the importance of molecular structural parameters for the optimization of reaction rates in organic electrochromic thin films via intermolecular interactions.

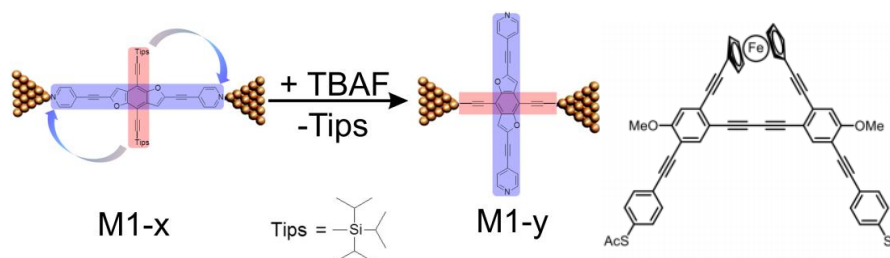
- [1] R. J. Mortimer, A.L. Dyer, J. R. Reynolds, Electrochromic organic and polymeric materials for display applications, *Displays* **27** (2006) 2-18.

## Tuning of charge transport in single molecule with the chemical and electrochemical methods

Cancan Huang, Wenjing Hong, Thomas Wandlowski  
Department of Chemistry and biochemistry, University of Bern  
Freiestrasse 3, CH-3012, Bern, Switzerland  
huangcancan1989@gmail.com

Molecular electronics targets the application of functionalized molecules as novel building blocks in electronics circuits. To reach this goal, understanding and tuning of charge transport in the single molecule comprise an essential prerequisite. We present the mechanical controllable break junction (MCBJ) and scanning tunneling microscopy break junction (STM-BJ) techniques to collect the charge transport information of the single molecules. To tune the charge transport effectively, we introduce the in situ chemical reaction and electrochemical gating methods.

1), The (benzodifuran) BDF - (oligo-(phenyleneethynylene)) OPE cruciform molecule are verified by single-molecule conductance measurement using MCBJ techniques with the conductance difference of more than one order of magnitude. Upon in-situ cleaving of the TIPS groups, the complete conversion from the M1-x junctions to M1-y junctions could be achieved. More importantly, the conductance pathway control via chemical tuning provides a unique flexibility in the modulation design, hence selective anchoring to electrodes.



2), We introduced the redox active unit ferrocene into A-shape molecule (shown above right). The electrochemical gating method based on the STM-BJ technique is used to control the state of iron ions to tune the charge transport properties of the single-molecule junctions.

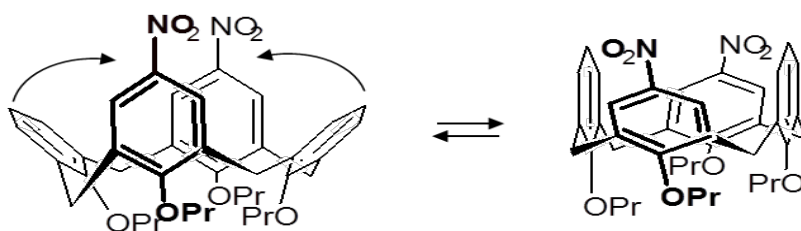
# Structure-controlled Electrochemical Reduction of mono- and di-, nitro or nitroso Calix[4]arenes

Alan Liška<sup>a,b</sup>, Jiří Ludvík<sup>a</sup>

<sup>a</sup> Department of Molecular Electrochemistry, J. Heyrovský Institute of Physical Chemistry AS CR, Dolejškova 2155/3, 182 23, Prague 8, Czech Republic;

<sup>b</sup> Department of Inorganic Chemistry, Charles University in Prague, Faculty of Science, Albertov 6, 128 43, Prague 2, Czech Republic  
[jiri.ludvik@jh-inst.cas.cz](mailto:jiri.ludvik@jh-inst.cas.cz)

The newly synthesized series of mono- and di-, nitro or nitroso calix[4]arenes has been investigated electrochemically. It was shown that besides the fundamental redox characterization, the electrochemical data contain also information about the space arrangement of the molecule as well as about dynamic 3D changes [1]. The interpretation is based on the comparison of observed electrochemical behaviour of homologous couples or triads taken from the studied series of compounds. Using the nitro- and nitroso group as a redox probes it was found that unsubstituted or *para*-nitro substituted *cone*-calixarenes are flexible, exhibiting in solution a periodic *pinched cone-pinched cone* interconversion, whereas the *1,3-alt*-conformation or any *meta*- substitution causes rigidity of the whole skeleton. All aromatic nitro- and nitroso groups in calixarenes appeared to be reducible at the same potential showing their electronic independency on the rest of the molecule [2].



## Acknowledgement:

This work was supported by the GACR grant No. 13-21704S, institutional support RVO: 61388955 and GAUK project No. 798214. The authors thank Prof. P. Lhoták and K. Flídrová for granting the compounds.

## References:

- [1] Alan Liška, Karolína Flídrová, Pavel Lhoták, Jiří Ludvík; *Monatsh Chem.* 146 (2015)857–862; DOI 10.1007/s00706-015-1441-8
- [2] Alan Liška, Pavel Vojtíšek, Albert J. Fry, Jiří Ludvík: *J.Org.Chem* 78 (2013) 10651 – 10656.

# Potential-Dependent Electrochemical Spectroscopy of Multiferrocenylthiophenes in a Nanogap Sensor

Klaus Mathwig,<sup>1,2</sup> Hamid R. Zafarani,<sup>3</sup> J. Matthäus Speck,<sup>4</sup> Sahana Sarkar,<sup>5</sup>  
Heinrich Lang,<sup>4</sup> Serge G. Lemay,<sup>5</sup> Oliver G. Schmidt<sup>1</sup>

<sup>1</sup>*Institute for Integrative Nanosciences, IFW Dresden, Germany*

<sup>2</sup>*Pharmaceutical Analysis, University of Groningen, The Netherlands*

<sup>3</sup>*Department of Chemical Engineering, Delft University of Technology, The Netherlands*

<sup>4</sup>*Anorganische Chemie, Technische Universität Chemnitz, Germany*

<sup>5</sup>*MESA+ Institute for Nanotechnology, University of Twente, Enschede, The Netherlands*  
k.h.mathwig@rug.nl

In nanofluidic electrochemical sensors, zeptomole quantities of analyte molecules can be detected: redox-active molecules travel diffusively between two electrodes separated by a nanoscale gap. They are repeatedly oxidized and reduced, thus generating a highly amplified current per molecule. In these sensors, Brownian motion of minuscule analyte molecule numbers leads to considerable fluctuations in the Faradaic currents. These fluctuations can be explored by electrochemical correlation spectroscopy [1] and stochastic amperometry [2] to extract molecular properties, namely diffusivity and reversible adsorptivity, the latter being highly pronounced at the high surface-to-volume ratio of a nanochannel [3].

Nanofluidic sensors so far have mostly been used to detect prototypical ferrocenes. Here, we employ them to study 2,3,4-triferrocenylthiophene (2,3,4-Fc<sub>3</sub>-C<sub>4</sub>HS) [4] by stochastic amperometry and correlation analysis. This compound displays three well-resolved electrochemically reversible one-electron-transfer processes using [N<sup>n</sup>Bu<sub>4</sub>][B(C<sub>6</sub>F<sub>5</sub>)<sub>4</sub>] (0.1 M) as electrolyte in dichloromethane – also when undergoing redox cycling in a nanochannel. By setting both electrodes to different fixed potentials corresponding to the different waves, we can perform redox cycling between arbitrary redox potentials. Thus, for the first time, we use electrochemical nanogap sensors to study the effective diffusion coefficient *as a function of the redox state* of a molecule.

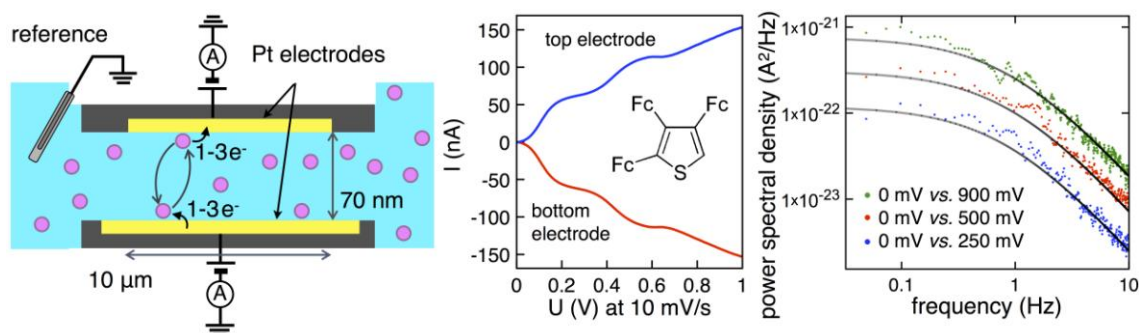


**Fig.** (a) Schematic cross-section of a nanogap sensor. (b) Cyclic voltammogram of 0.5 mM 2,3,4-Fc<sub>3</sub>-C<sub>4</sub>HS in the nanogap sensor (in 0.1 M [N<sup>n</sup>Bu<sub>4</sub>][B(C<sub>6</sub>F<sub>5</sub>)<sub>4</sub>] in dichloromethane). (c) Power spectral densities of 2,3,4-Fc<sub>3</sub>-C<sub>4</sub>HS undergoing redox cycling at different oxidation potentials.

## References:

- [1] M. A. G. Zevenbergen, P. S. Singh, E. D. Goluch, B. L. Wolfrum, S. G. Lemay, Electrochemical correlation spectroscopy in nanofluidic cavities, *Analytical Chemistry* 81 (2009) 8203.
- [2] P. S. Singh, H.-S. M. Chan, S. Kang, S. G. Lemay, Stochastic amperometric fluctuations as a probe for dynamic adsorption in nanofluidic electrochemical systems, *Journal of the American Chemical Society* 133 (2011) 18289.
- [3] D. Mampallil, K. Mathwig, S. Kang, S. G. Lemay, Reversible adsorption of outer-sphere redox molecules on Pt Electrodes, *The Journal of Physical Chemistry Letters*, *J. Phys. Chem. Lett.* 5 (2014) 636.
- [4] J. M. Speck, R. Claus, A. Hildebrandt, T. Rüffer, E. Erasmus, L. van As, J. C. Swarts, H. Lang, Electron Transfer Studies on Ferrocenylthiophenes: Synthesis, Properties, and Electrochemistry, *Organometallics* 31 (2012) 6373.

# **Terephthalate Functionalized Conducting Redox Polymers: Organic Anode Materials for Energy Storage**

Li Yang<sup>1</sup>, Xiao Huang<sup>2</sup>, Adolf Gogoll<sup>2</sup>, Maria Strømme<sup>1</sup>, Martin Sjödin\*<sup>1</sup>

<sup>1</sup>*Nanotechnology and Functional Materials, Department of Engineering Sciences, The Ångström Laboratory, Uppsala University, Box 534, SE-751 21 Uppsala, Sweden*

<sup>2</sup>*Department of Chemistry - BMC, Biomedical Centre, Uppsala University, Box 576, SE-751 23 Uppsala, Sweden*  
*li.yang@angstrom.uu.se*

Organic electrode materials with high charge capacity, conductivity and cycling stability are appealing for electric energy storage application due to the limited mining resources of inorganic alternatives and their energy consuming production and recycling processes. Carboxyl compounds, e.g. diethyl terephthalate (DeT), show high charge capacity and have been used in lithium and sodium batteries. DeT and its analogues can be prepared from biomass and recycled easily by combustion. However, poor conductivity and cycling stability of this compound hinders its applications in energy storage systems. These problems can be solved by attaching the redox compound onto a conducting polymer (CP) backbone with good stability in organic solvents. Such combination could improve the stability of the material during cycling. More importantly, the CP backbone becomes electronically conducting upon n- or p-doping which could improve the electron transfer within the material and avoid the need for carbon additives in batteries.

Based on our previous matching studies between DeT and thiophene-based CPs, we have prepared a conducting redox polymer (CRP) with terephthalate as the pendant group and polythiophene as the backbone. Both n- and p-doping of the CP backbone could be distinguished in cyclic voltammograms and redox peaks of DeT were found to be located in the n-doping region of the CP. This is the first report, to our knowledge, that successfully achieves redox activity of pendant groups in an electronically conducting region of a CP backbone. Kinetic studies of the CRP showed high rate constants for both reduction and oxidation of terephthalate moieties. Diffusion limitation was not observed for a CRP polymer film with a thickness of tens of micrometers. Given their p-doping capabilities, terephthalate-substituted CRPs may be used as both anode and cathode materials for energy storage applications.

## **References**

- [1] M. Armand, S. Grugeon, H. Vezin, S. Laruelle, P. Ribière, P. Poizot and J.-M. Tarascon. Conjugated Dicarboxylate Anodes for Li-ion Batteries, *Nature Materials* 2009, 8, 120-125.
- [2] Y.L. Liang, Z.L. Tao, J. Chen, Organic Electrode Materials for Rechargeable Lithium Batteries, *Adv. Energy Mater.* 2012, 2, 742-769.



# Extending Shell-isolated Nanoparticle-enhanced Raman Spectroscopy to Study Ordered/Disordered Adsorption of (Bi)sulfate on Au Single Crystal Electrodes

Meng Zhang<sup>1</sup>, William C. Valenzuela<sup>2</sup>, Run-Wen Yan<sup>1</sup>, Song-Yuan Ding<sup>1</sup>, Juan M. Pérez<sup>2</sup>, De-Yin Wu<sup>1</sup>, Bing-Wei Mao<sup>1\*</sup>, Juan M. Feliu<sup>2\*</sup>, Zhong-Qun Tian<sup>1\*</sup>

<sup>1</sup> State Key Laboratory of Physical Chemistry of Solid Surfaces and Department of Chemistry, College of Chemistry and Chemical Engineering; iChEM, Xiamen University, Xiamen 361005, China

<sup>2</sup> Instituto de Electroquímica, Universidad de Alicante, Apdo. 99, E-03080, Alicante, Spain  
E-mails: bwmao@xmu.edu.cn; juan.feliu@ua.es; zqtian@xmu.edu.cn

Surface-enhanced Raman spectroscopy (SERS) with high surface sensitivity and selectivity requires nanostructured substrates to promote localized or propagating surface plasmon (SP) mode, and therefore it had not been applied to study the processes taking place at atomically flat single crystalline surfaces of various electrodes. Since 2010, the invention of shell-isolated nanoparticle-enhanced Raman spectroscopy (SHINERS) has enabled SERS to study electrified single-crystal /electrolyte interfaces, but these studies have been limited into strong adsorption systems<sup>[1, 2]</sup>.

Very recently we utilized SHINERS to study the ordered and disordered adsorption of (bi)sulfate anions on Au single crystal electrode surfaces, aiming to reveal the interactions of the adsorbed molecules of different structure with surfaces. The potential-dependent SHINERS spectra on Au(111), Au(100) and Au(110) (Fig. 1) elucidate different adsorption behaviors on these surfaces with a distinct surface Raman feature from the adsorption of (bi)sulfate. The peaks in the low frequency region reveal the facet-dependent Au-O ( $\text{SO}_4^{2-}$ ) interaction, which is very difficult to be studied using other vibrational spectroscopies. The relevant DFT calculation is also performed to assign the spectral bands and explain the potential-dependency of the Raman features.

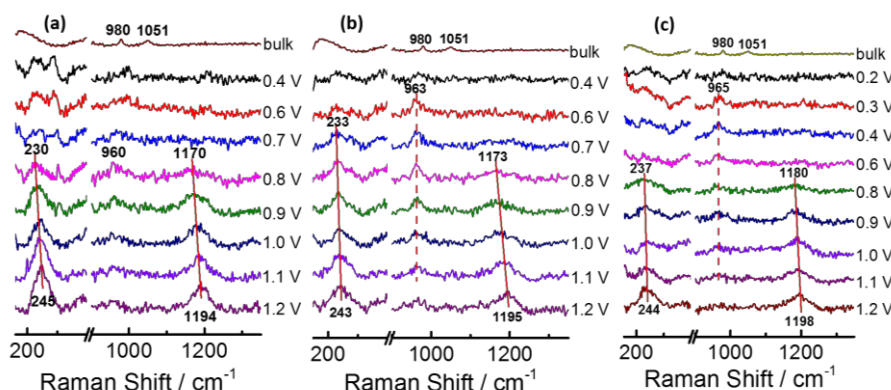


**Fig. 1.** SHINERS spectra of (bi)sulfate adsorption on (a) Au(111), (b) Au(100) and (c) Au(110) in 0.1 M  $\text{H}_2\text{SO}_4$ , laser power: 5 mW, collecting time: 100 s.

The present work further demonstrates that SHINERS could become a powerful tool to study fundamental issues of surface electrochemistry, not only strong but also weak interaction systems.

This work is supported by Natural Science Foundation of China (NSFC No. 21033007, 20973141).

## References

- [1] J. F. Li, Y. F. Huang, Y. Ding, Z. L. Yang, S. B. Li, X. S. Zhou, F. R. Fan, W. Zhang, Z. Y. Zhou, D. Y. Wu, B. Ren, Z. L. Wang, Z. Q. Tian, Shell-isolated nanoparticle-enhanced Raman spectroscopy, *Nature* 464 (2010) 392–395.
- [2] J. F. Li, Y. J. Zhang, A. V. Rudnev, J. R. Anema, S. B. Li, W. J. Hong, P. Rajapandian, J. Lipkowski, T. Wandlowski, Z. Q. Tian, *J. Am. Chem. Soc.* 137 (2015) 2400–2408.



# DFT Study of Surface Charging Effects on Oxygen Covered Pt(111)

Ali Malek, Mohammad J. Eslamibidgoli and Michael H. Eikerling

*Department of Chemistry, Simon Fraser University,  
8888 University Drive, Burnaby, BC, Canada V5A1S6  
e-mail: meikerl@sfu.ca*

Platinum plays an important role in catalysis and electrochemistry, and it is known that interaction of oxygen with Pt surfaces leads to the formation of platinum oxides and buckling of Pt surface atoms, which can affect the electrocatalytic reactivity[1]. Distribution of oxygen atoms and electronic charge density at the Pt-solution interface vary with the applied electrode potential. We use calculations based on density functional theory to investigate the various stages of oxidation of a Pt(111) surface. The system is modeled with a 5 layer slab within a  $3 \times 3$ ,  $4 \times 4$  and  $2\sqrt{3} \times 2\sqrt{3}$ -R30° supercell with atomic oxygen adsorbed on the Pt surface. Optimized configurations of the model system, are analyzed in view of oxygen adsorption energies, work function, average Pt atom displacement, surface charge density and dipole moment. It is found that below 50% coverage the favored surface configuration of adsorbed oxygen resides in *fcc* hollow sites. Additionally, the electronic density of states in *d*-orbitals of Pt atoms projected to the surface and sub-surface layer of Pt, and *d*-band center energies,  $\epsilon_d$ , will be analyzed as a function of the oxygen surface coverage. Effects of explicit water layers on oxide formation at the Pt surface will be discussed.

## References

- [1] G. Jerkiewicz, G. Vatankhah, J. Lessard, M. P. Soriaga, Y. S. Park, *Electrochim. Acta* 2004, 49, 1451–1459.

# Dynamic In Situ Neutron Reflectivity Studies of Metal Electrodeposition and Alloy Formation in Ionic Liquid Media

A. Robert Hillman,<sup>1</sup> Rachel M. Sapstead<sup>1</sup>, Virginia Ferreira<sup>1</sup>, Karen Smith,<sup>1</sup> Karl S. Ryder<sup>1</sup>, Emma Smith,<sup>2</sup> Nina-Juliane Steinke<sup>3</sup> and Robert M. Dalglish<sup>3</sup>

<sup>1</sup>University of Leicester, Leicester LE1 7RH, UK; <sup>2</sup>Nottingham Trent University, Nottingham NG11 8NS, UK; <sup>3</sup>Rutherford Appleton Laboratory, Didcot, Oxfordshire, OX11 0QX, UK  
e-mail: arh7@le.ac.uk

Rational design of interfacial structures for diverse applications – electrocatalysis, sensors, energy storage / conversion, optical devices and surface protection - has attracted huge research interest and synthetic methodologies have been developed for surface attachment of the relevant functionalities. Efficacy of the surface synthetic processes is generally established *via* structural and compositional probes. In the case of spectroscopic probes (e.g. FTIR, Raman, UV/visible), some *lateral* resolution is possible but the data are *vertically* integrated, so one does not know whether the functionality lies at the film/solution interface, within the film interior or at the electrode/film interface. In the case of imaging methods (e.g. SEM, STM, AFM), information is restricted to the external surface.

This motivates development of techniques that probe the interior of the film and do so with vertical spatial resolution. A technique that accomplishes this is neutron reflectivity (NR). The penetrating nature of neutrons permits *in situ* compositional and structural analysis of buried interfaces. Additionally, since the interaction of the neutrons is with the nuclei in the sample, the response is isotopically sensitive. This so-called "contrast variation" approach, most commonly implemented by H/D substitution (e.g. of the solvent), can provide unequivocal evidence of the spatial locations of film components, both the "fixed" species chemically bound to the electrode and the "mobile" species from solution that permeate the film.

While giving access to buried interfaces, the weak interaction of neutrons with the sample means that data acquisition times are long. Until recently, acquisition of a typical neutron reflectivity profile required several hours. While the spatial information was detailed and unique [1], observations were restricted to static conditions. As a first attempt to mimic *in operando* conditions, we used a boxcar averaging method to accumulate reflectivity profiles during repetitive potential cycles [2]. This reveals interesting departures from static conditions, but still requires long data acquisition times, is restricted to redox-stable materials and cannot be applied to single shot experiments, such as film deposition or dissolution.

A recent instrumental development, "event mode" data capture, involves recording of every neutron interaction with the surface. This permits setting of the averaging period (data "slices") post-experiment. When coupled with improvements in detector performance it decreases data acquisition times by approximately two orders of magnitude. This is consistent with dynamic electrochemical conditions that might be encountered in the operation of an electrochemical device or process. We now demonstrate this powerful new capability in the context of metal electrodeposition, dissolution and alloying involving single and multi-component films of Cu, Ag and Sn on Au electrodes exposed to choline chloride / hydrogen bond donor (ethylene glycol, urea) ionic liquid media.

NR measurements have been made for metal deposition and dissolution using different electrochemical control functions (potentiostatic, potentiodynamic and galvanostatic). We compare the NR responses for deposition of two metals simultaneously and sequentially; simplistically, these might be expected to generate a composite or alloy and a bilayer. In the latter instance, we compare the outcomes of deposition in either order. Indications of surface processes are given by surface imaging, by QCM nanogravimetric responses and by the electrochemical responses for film stripping. For example, the chronopotentiometric responses for galvanostatic stripping of Au/Ag/Cu and Au/Cu/Ag indicate access of Cu to the electrolyte in both cases. In the case of Au/Cu,Sn (in both combinations), alloy formation is indicated. NR data acquired under dynamic conditions (with event mode data capture) provide novel spatial insights into the dynamics of these deposition, alloying and dissolution processes.

[1] A. Glidle et al, Langmuir, 2003, **19**, 7746-7753.

[2] A. Glidle et al, Langmuir, 2009, **25**, 4093-4103.

# Mapping Oxygen Reduction at Individual Nanostructures Using High-Resolution Electrochemical-Topographical Imaging

Andrew J. Wain, Josh Lewis, and Mike A. O'Connell

*National Physical Laboratory  
Hampton Road, Teddington, United Kingdom, TW11 0LW  
andy.wain@npl.co.uk*

Electrochemical methods are essential for the development of new electroactive and electrocatalytic materials for emerging technologies such as sensors and energy conversion devices. Whilst macroscopic approaches such as cyclic voltammetry can provide detailed insights into electrokinetics and mechanism at the bulk or ensemble level, the information gleaned is spatially averaged and often fails to reveal how activity is distributed across the electrode surface. This information is vital in establishing structure-activity relationships, particularly for novel nanostructured materials that exhibit intrinsic heterogeneity at the smallest of scales.

Scanning electrochemical microscopy (SECM) provides a valuable approach to spatially resolved electrochemical characterization, and advanced hybrid techniques enable not only high-resolution electrochemical mapping, but simultaneous topographical imaging. Such dual function imaging allows one to pinpoint regions of high and low activity on the sample and correlate them with specific particles, structures or surface features.

This presentation will highlight recent developments in the high-resolution electrochemical and topographical imaging of nanostructured electrode surfaces. Focus will be on the combination of SECM with scanning ion conductance microscopy (SECM-SICM) through the development of double-barreled pipette probes comprising an open SICM barrel and a solid carbon SECM electrode. Unmodified probes allow electrochemical imaging of 150 nm diameter gold nanodisks using a simple reversible redox mediator whilst platinization of the carbon electrode adds greater functionality enabling oxygen reduction activity to be measured. This is demonstrated by mapping (i) competitive oxygen reduction and (ii) hydrogen peroxide generation at carbon electrodes decorated with platinum nanospheres and gold nanoaggregates. Individual particles are clearly resolved electrochemically and topographically, highlighting the potential of this technique to enable measurement of intrinsic electrokinetics at the single nanoparticle level.

# In-situ Study of Oxygen Reduction in DMSO Solution

Yu QIAO and Shen YE\*

Catalysis Research Center, Hokkaido University, Sapporo 001-0021, Japan

E-mail address: ye@cat.hokukai.ac.jp

Rechargeable Li-O<sub>2</sub> battery is regarded as one of the promising candidates for the next generation power sources of electrical vehicles because of its high theoretical energy density [1]. However, many fundamental issues about the reaction mechanism in the Li-O<sub>2</sub> battery, which are extremely important to understand and develop the novel battery system, are still unclear [2-4]. In the present work, mechanisms for the oxygen reduction reaction (ORR) and oxygen evolution reaction (OER) on a flat gold electrode in the aprotic polar solvent of dimethyl sulfoxide (DMSO) has been systematically investigated by electrochemistry in combination with *in-situ* UV-Vis absorption spectroscopy, surface-enhanced Raman vibrational spectroscopy (SERS) and *ex-situ* infrared spectroscopy [5].

In the Li-free DMSO solution, O<sub>2</sub> is efficiently reduced to the superoxide, which forms an ion-pair with the tetrabutylammonium (TBA) cation and shows an excellent stability in DMSO. The adsorption of the superoxide on the gold electrode surface has been observed by an *in-situ* SERS measurement. When the Li-ion is included in the DMSO, O<sub>2</sub> can be further electrochemically reduced to lithium peroxide (Li<sub>2</sub>O<sub>2</sub>) and deposited on the electrode surface. Figure 1 shows *in-situ* SERS measurement for the ORR/OER processes in O<sub>2</sub>-saturated 0.1M LiClO<sub>4</sub>-DMSO solution. In addition to the peaks from solvent and supporting electrolyte, a Raman peak was clearly observed 788 cm<sup>-1</sup> with the ORR current. This Raman band can be attributed to O-O stretching mode of Li<sub>2</sub>O<sub>2</sub> on the Au surface, indicating that Li<sub>2</sub>O<sub>2</sub> is formed on the electrode surface. Detailed analyses on the potential dependence of the Raman peak intensity, it was found that the Li<sub>2</sub>O<sub>2</sub> formation is a kinetically-controlled process and terminated at a certain film thickness on the electrode surface. At the same time, a large amount of superoxide is still produced in the solution which shows a UV-Vis absorption spectrum similar to that polarized in the Li-free DMSO solution, implying that Li-ions solvated by DMSO make ion-pairs with superoxide (denoted as LiO<sub>2</sub>) in solution. On the other hand, no evidence for the disproportionation reaction of LiO<sub>2</sub> to Li<sub>2</sub>O<sub>2</sub>, one of known reaction mechanisms proposed before [2], has been obtained in the bulk solution and on the electrode surface in the present study.

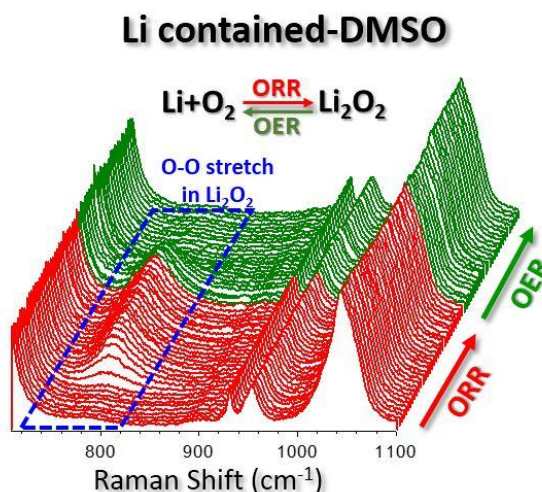


Fig. 1 *in-situ* Raman spectra on sputter gold surface in O<sub>2</sub> saturated Li-DMSO electrolyte.

Based on the quantitative analyses of the *in-situ* spectroscopic observations, the partial yields for LiO<sub>2</sub> and Li<sub>2</sub>O<sub>2</sub> have been estimated to elucidate the mechanism for the ORR/OER processes [5]. The present results are discussed in comparison to previous observations on porous carbon cathodes regarding the surface area, morphology as well as three-phase interface on the electrode and solution interface.

Detailed results and discussion will be given in the presentation.

## References:

1. Abraham, K. M.; Jing, Z. *J. Electrochem. Soc.* **1996**, *1*, 143.
2. Peng, Z.; Freunberger, S. A.; Tarascon, J.-M.; Bruce, P. G. *Angew. Chem., Int. Ed.* **2011**, *123*, 6475.
3. McCloskey, B. D.; Scheffler, R.; Speidel, A.; Luntz, A. C. *J. Phys. Chem. C* **2012**, *116*, 23897.
4. Luntz, A. C.; McCloskey, B. D., *Chem. Rev.* **2014**, *114*, 11721.
5. Qiao, Y.; Ye, S. *submitted to J. Phys. Chem. C*

# Potential-Dependent Behavior of Ionic Liquid [BMIM][TFSA] with Additives on a Gold Electrode Studied by Surface-Enhanced Infrared Absorption Spectroscopy

K. Motobayashi<sup>1</sup>, K. Minami<sup>2</sup>, K. Uchida<sup>1</sup>, N. Nishi<sup>2</sup>, T. Sakka<sup>2</sup>, and M. Osawa<sup>1</sup>

<sup>1</sup>Catalysis Research Center, Hokkaido University  
Sapporo 001-0021, Japan

<sup>2</sup>Graduate School of Engineering, Kyoto University  
Kyoto 615-8510, Japan  
kmotobayashi@cat.hokudai.ac.jp

Room temperature ionic liquids (RTILs) are promising electrolyte materials owing to their fascinating properties such as high thermal and electrochemical stabilities. However, the structure and dynamics of RTILs at the vicinity of electrodes are still under debate. Recently we reported hysteretic potential-dependence of ion density and orientation of [BMIM][TFSA] (Fig.), one of the RTILs with relatively high diffusivity and conductivity, on an Au electrode.<sup>1</sup> Spectroscopic studies of RTIL/electrode interfaces including ours have been performed with pure ionic liquids in vacuum or dry atmosphere to eliminate the effect of dissolved impurities. To understand what happens at the real interfaces such as those in batteries and capacitors, it is necessary to study potential-dependent behaviour of RTILs with additives such as water and Li<sup>+</sup> ions. Surface enhanced infrared absorption spectroscopy (SEIRAS) that can selectively probe solid/liquid interfaces is suited for this purpose. In the present work, we investigated how the additives affect the potential-dependent behaviour of [BMIM][TFSA] at the vicinity of an Au electrode by SEIRAS.

SEIRAS experiments have been performed on an Au thin film electrode chemically deposited on a Si prism in a vacuum-compatible glass cell. The electrode potential was controlled by a potentiostat against a Pt quasi-reference electrode and corrected by the redox potential of Fc/Fc<sup>+</sup> couple. Concentrations of water and Li<sup>+</sup> ion in RTILs were controlled by exposure to water-saturated Ar gas and addition of Li[TFSA], respectively.

Potential-dependent SEIRA spectra of [BMIM][TFSA]/Au electrode showed the threshold potentials for steep increasing/decreasing in the intensities of the vibrational bands, which indicated the existence of the energy barrier for anion-cation exchange at the first ionic layer on the electrode [1]. Addition of water to [BMIM][TFSA] did not affect the threshold potential for the anion-cation exchange, but resulted in higher slope of the increase in band intensities as a function of the potential. This indicates that the energy barrier for ion exchange at the first ionic layer remains even in the presence of water but the ion exchange becomes faster due to reduced Coulombic interaction between ions. On the other hand, addition of the Li salt results in more positive threshold potential for the exchange of cations to anions at the first layer. We concluded that the anionic complex (probably [Li(TFSA)<sub>2</sub>]<sup>-</sup>) have higher potential barrier to replace cations at the first layer than TFSA<sup>-</sup> owing to its bulky structure. The formation of anionic Li complex is supported by the decrease of the band intensity of the solvated TFSA<sup>-</sup> at potentials negative of pztc (potential of zero total charge). Anionic Li complex moves further away from the electrode at the negative potential. The different environment of water and Li ion in the vicinity of the electrode surface relative to that in the bulk liquid will be also reported in the presentation.

Reference: <sup>1</sup>K. Motobayashi et al., *J. Phys. Chem. Lett.* 4, 3110 (2013).

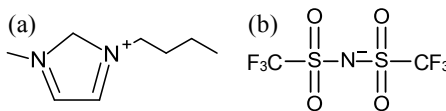


**Figure.** The Chemical structures of (a) BMIM<sup>+</sup>, and (b) TFSA<sup>-</sup>.

# An Infrared Study of the Few-Layer Graphene | Ionic Liquid Interface: Correlation between Electronic and Ionic Surface Structure

Ove Oll, Tavo Romann, Enn Lust  
Institute of Chemistry, University of Tartu  
Ravila 14a, Tartu, 50411 Estonia  
ove.oll@ut.ee

Detailed understanding of the interface between graphitic carbon materials and concentrated electrolytes is of great importance for the rational design of novel high energy and power density supercapacitors. It is of particular interest to describe how the limitation of quantum capacitance of semimetal electrodes influences the electrolyte part of the electrical double layer (EDL).

A novel technique of *in situ* infrared absorption (IRA) spectroscopy for the study of few-layer graphene (FLG) electrodes has been developed[1] and is applied for the study of the FLG|1-ethyl-3-methylimidazolium tetrafluoroborate (EMImBF<sub>4</sub>) ionic liquid interface. The surface specificity of the technique, as well as the plasmonic enhancement properties of the electrode is demonstrated. The IRA results show that, unlike previous theoretical considerations of the EDL between semimetals and electrolytes, the strong interaction between the electronic and ionic part of the EDL is of fundamental importance for the description of semimetal interfaces. Together with the data provided by *in situ* electroreflectance[1] technique of the electronic and energetic structure of the FLG electrode and differential capacitance potential dependence of the FLG|EMImBF<sub>4</sub> system, it is demonstrated that the screening of excess surface charge by the ionic liquid is strongly correlated with the potential dependent electronic properties of the electrode. This result is in agreement with our previous studies of semimetal interfaces, such as porous carbon[2] and thin-layer bismuth electrodes[3] in ionic liquid electrolyte.

## Acknowledgements

This work was supported by the Estonian Ministry of Education and Research Project IUT20-13, Estonian Science Foundation grant No. 9184 and Estonian Centres of Excellence in Research Project TK117T “High-technology Materials for Sustainable Development”.

## References

- [1] O. Oll, T. Romann, E. Lust, An infrared study of the few-layer graphene | ionic liquid interface: Reintroduction of *in situ* electroreflectance spectroscopy, *Electrochem. Commun.* 46 (2014) 22–25.
- [2] T. Romann, O. Oll, P. Pikma, H. Tamme, E. Lust, Surface chemistry of carbon electrodes in 1-ethyl-3-methylimidazolium tetrafluoroborate ionic liquid – an *in situ* infrared study, *Electrochimica Acta*. 125 (2014) 183–190.
- [3] T. Romann, O. Oll, P. Pikma, E. Lust, Abnormal infrared effects on bismuth thin film–EMImBF<sub>4</sub> ionic liquid interface, *Electrochem. Commun.* 23 (2012) 118–121.

# Influence of Electrolyte on Sulfur Redox Reactions: Combined RRDE and *in situ* UV-VIS Studies

Qingli Zou and Yi-Chun Lu\*

Department of Mechanical and Automation Engineering, The Chinese University of Hong Kong  
Shatin, N.T., Hong Kong SAR, China

\*yichunlu@mae.cuhk.edu.hk

Fundamental understanding of lithium–sulfur(Li-S) redox reactions is critical for realizing efficient and long-lasting rechargeable Li-S batteries.<sup>1-2</sup> Recently, we exploited rotating ring-disk electrode (RRDE) technique and specially-designed Li-S catholyte cell to examine sulfur reduction and oxidation behaviors in 1,3-dioxolane:1,2-dimethoxyethane (DOL:DME) and dimethyl sulfoxide (DMSO).<sup>3</sup> We showed that only part of the sulfur reduction capacity is obtained through direct electrochemical steps, and that the rest of the capacity is achieved via various subsequent chain-growth and disproportionation reactions that generate reducible species.<sup>3</sup> In addition, the reaction rates of electrochemical and chemical reactions of sulfur redox reactions directly influence the performance of metal sulfur batteries.<sup>3</sup>

In this study, we investigate the influence of both solvent and salt on the metal–S redox and disproportionation behaviors combining RRDE and *in situ* UV-Vis spectroscopic techniques. Figure 1 shows the *in situ* UV-VIS spectra of elemental sulfur ( $S_8$ ) reduction in lithium-containing salt in DMSO (blue series) and DOL:DME (red series) during *in situ* scan of cyclic voltammetry on a gold electrode. Reported reference UV-VIS spectra for various polysulfides are labeled.<sup>4,5</sup> Generally, longer polysulfide shows absorption at longer wavelength where shorter polysulfide shows absorption at shorter wavelength (except the  $S_3^{\cdot-}$  radical).<sup>4,5</sup> Upon reduction in DMSO (from dark blue to light blue),  $S_8^{2-}$  firstly formed as the predominant reduction product, which then dissociate to the  $S_3^{\cdot-}$  radical or further reduced to low-chain polysulfide between  $S_3^{2-} / S_4^{2-}$  and  $S_3^{2-} / S_2^{2-}$ . This is consistent with various reported studies<sup>6</sup> in high-dielectric solvents such as DMSO ( $\epsilon_{\text{DMSO}} = 46.5$ ).<sup>7</sup> Interestingly, neither high-chain polysulfides nor  $S_3^{\cdot-}$  radical can be identified during the *in situ* CV scanning in DOL:DME. This suggests that the long-chain polysulfides ( $S_8^{2-}$  and  $S_6^{2-}$ ) and the  $S_3^{\cdot-}$  radical are not stable in low-dielectric solvent ( $\epsilon_{\text{DOL}} = 7.13$ ;  $\epsilon_{\text{DME}} = 7.075$ )<sup>7</sup> and quickly disproportionate to shorter chain such as  $S_4^{2-}$ ,  $S_3^{2-}$  and  $S_2^{2-}$ . This result shows that such chemical disproportionation process is relative fast since the *in situ* UV-VIS scan cannot detect the appearance of long-chain polysulfides even with sub-second interval of UV-VIS collection. This is consistent with our hypothesis that the rates of the chemical chain-growth/disproportionation reactions are higher in low-dielectric solvents such as DOL:DME compared to high-dielectric solvents such as DMSO due to its poor stabilization of polysulfides. In-house reference samples of various polysulfide species in both DMSO and DOL:DME will be examined under the same UV-VIS configuration for accurate comparison. Detailed UV-VIS and RRDE investigation on the influence of both solvent and salt on the electrochemical and chemical processes of S-reduction and oxidation reactions will be discussed. **References:** (1) Bruce et al. *Nat. Mater.* 2012, 11 (1), 19. (2) Ellis et al., *Chem. Mater.* 2010, 22 (3), 691. (3) Lu et al., *J. Phys. Chem. C* 2014, 118 (11), 5733. (4) Barchasz et al., *Anal. Chem.* 2012, 84, 3973. (5) Kawase et al., *Phys. Chem. Chem. Phys.*, 2014, 16, 93446. (6) Merritt et al., *Inorg. Chem.*, 1970, 9 (2), 211. (7) Aurbach, D.; Weissman, Nonaqueous Electrochemistry, Aurbach, D., Ed. CRC Press: 1999. **Acknowledgment:** This work is supported by Research Grants Council of the Hong Kong (Theme-based Research Scheme T23-407/13-N and ECS CUHK24200414).

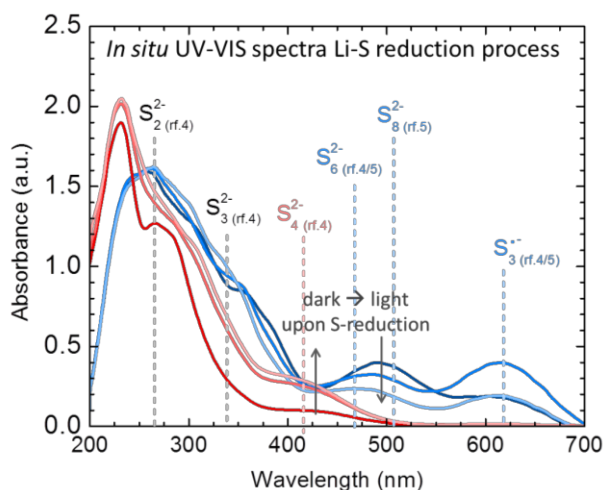


Fig. 1. *In situ* UV-VIS spectra of sulfur reduction on a gold working electrode during cyclic voltammetry scan in 2 mM  $S_8$  in 0.25 M  $LiClO_4$  in DMSO (blue lines) and 2 mM  $S_8$  in 1.0 M  $LiTFSI$  in DOL:DME (1:1 v/v). The reference electrode is  $Ag/Ag^+$  and the counter electrode is Pt.

# Surface enhanced Raman observation of molecular adsorbates on atomic local surface sites

Katsuyoshi Ikeda

<sup>a</sup>*Nagoya Institute of Technology, Gokiso, Showa, Nagoya 466-8555 Japan*

<sup>b</sup>*Japan Science and Technology Agency, PRESTO, Japan*

<sup>c</sup>*Global Research Center for Environment and Energy based on Nanomaterials Science, NIMS, Japan*

*Email: kiked@nitech.ac.jp*

Surface enhanced Raman scattering (SERS) has been usually conducted at rough surfaces of coinage metals because the nanometric surface features are needed for plasmonic enhancement of Raman signal intensity. Recently, we have reported on SERS observations on single crystalline Au surfaces of various orientations using sphere-plane type nanogap structures.<sup>1-4</sup> This technique has been also applied for observing well-defined surfaces of weak-SERS-active metals such as platinum group metals (PGMs).<sup>5-7</sup> The SERS study on atomically defined and ideally uniform surfaces indeed improve our understanding of metal-molecule interactions. However, it is also known that atomic local surface sites often exhibit unique activity in the fields of heterocatalysis or electrocatalysis. Therefore, selective observation of atomic local sites is needed for deeper understanding of metal-molecule interactions.

In the present work, we fabricated atomic Pd islands on defect sites of Au(111) such as step lines using the underpotential deposition technique. We then observed SERS spectra of molecular adsorbates on the Pd islands selectively by forming SERS active nanogap structures only on Pd atomic sites. When the Pd coverage was at the order of a few percent, the observed spectra varied with increasing the two-dimensional size of Pd islands, suggesting that the adsorption geometry of the molecules was sensitive to the local surface structures on the atomic scale.

## References :

- (1) K. Ikeda, N. Fujimoto, H. Uehara, K. Uosaki, *Chem. Phys. Lett.* 460, 205 (2008)
- (2) K. Ikeda, S. Suzuki, K. Uosaki, *Nano Lett.* 11, 1716 (2011)
- (3) K. Ikeda, S. Suzuki, K. Uosaki, *J. Am. Chem. Soc.* 135, 17387 (2013)
- (4) K. Ikeda, N. Fujimoto, K. Uosaki, *J. Phys. Chem. C* 118, 21550 (2014)
- (5) K. Ikeda, J. Sato, K. Uosaki, et al., *J. Phys. Chem. C* 113, 11816 (2009)
- (6) K. Ikeda, J. Sato, K. Uosaki, *J. Photochem. Photobiol. A* 221, 175 (2011)
- (7) J. Hu, K. Uosaki, K. Ikeda, *J. Am. Chem. Soc.* 136, 10299 (2014)



# Theoretical Simulation of Solid Electrolyte Interphases

Sara Panahian Jand, Payam Kaghazchi

*Physikalische und Theoretische Chemie, Freie Universität Berlin*

*Takustr. 3, 14195 Berlin, Germany*

*sara.jand@fu-berlin.de*

The solid electrolyte interphase (SEI) is a heterogeneous layer that is formed on the surface of electrodes in Li-ion batteries during the first charging cycles (due to the reduction of electrolyte species). The SEI layer plays a key role in the stability and operating parameters of Li-ion batteries. Therefore, a fundamental understanding of the structure of SEI layer is a prerequisite to develop high-performance Li-ion batteries.

In this work, we will present our theoretical studies on the structure of SEI layers. We will first discuss our density functional theory (DFT) calculations for LiF and Li<sub>2</sub>O nanoclusters on graphene, which have been observed in a recent experimental study [1]. We will show that, independent of being in contact or not with a graphene surface, crystalline-LiF nanoclusters with {100} facets grow in a three dimensional mode, but Li<sub>2</sub>O nanoclusters are amorphous [2]. These results are in agreement with the TEM images [1]. Furthermore, we will introduce a method to construct transferable force fields (FF) for inorganic components of the SEI layer (e.g. LiF and Li<sub>2</sub>O). The FF parameters are obtained by comparing physical quantities calculated with DFT and those calculated with classical potentials. We will show that the constructed FF gives similar atomic structures and stabilities (for nanoclusters and surfaces) to those obtained using DFT calculations [3].

Finally, we will present our recently developed quantum mechanics/molecular mechanics (QM/MM) approach, which can be used to study the electronic structure and ionic conductivity in the interfaces of SEI components [3].

[1] S. Chattopadhyay et al., Chem. Mater., **24**, 3038 (2012)

[2] S. Panahian Jand and P. Kaghazchi, J. Phys.: Condens. Matter, **26**, 262001 (2014)

[3] S. Panahian Jand and P. Kaghazchi, in preparation

# **Peculiar Excitation Waves during CO Electrooxidation on Pt Electrodes in an Electrochemical Flow Cell**

Katharina Krischer<sup>1</sup>, Philipp Bauer<sup>1</sup>, Munir M. Salman<sup>1</sup>, Antoine Bonnefont<sup>2</sup>

<sup>1</sup>*Physik-Department, Technische Universität München,*

*85748 Garching bei München, Germany*

<sup>2</sup>*Institut de Chimie de Strasbourg UMR 7177, Université Louis Pasteur, Strasbourg, France*

*Krischer@tum.de*

The electrochemical oxidation of CO on platinum electrodes exhibits a variety of nonlinear phenomena, such as bistability in the current-potential curve and current oscillations under potentiostatic conditions, or the formation of stable spatial domains with different CO coverages, and thus different reactivities, under galvanostatic conditions. In the talk, I will discuss recent results on self-organized reactivity patterns which form during the oxidation of CO in the presence of an electrolyte flow parallel to the electrode. Patterns in the CO coverage are recorded by means of spatially resolved ATR-FTIR spectroscopy. Typical patterns observed are tongue-shaped structures that align parallel to the flow and move in the direction perpendicular to the flow (Fig. 1). These wave fragments possess several peculiar properties: They may split, sending out a second wave in the backward direction; Two colliding waves penetrate each other forming a soliton-type collision state; Open ends do not grow into a spiral wave but propagate with a stable shape. Basic features of the dynamics can be understood on the basis of a model taking into account the reaction kinetics of CO oxidation, diffusion of CO parallel to the electrode and advection of CO, i.e. the transport of CO by the flow. Especially, the role of advection for pattern formation will be elaborated.

# Designing Better Electrocatalysts by Simply Counting Surface nearest Neighbors

Federico Calle-Vallejo<sup>1</sup>, Jakub Tymoczko, Viktor Colic, Quang Huy Vu, Marcus D. Pohl, Karina Morgenstern, David Loffreda, Philippe Sautet, Wolfgang Schuhmann, Aliaksandr S. Bandarenka

<sup>1</sup>*Université de Lyon, CNRS, Laboratoire de Chimie, ENS Lyon  
46 Allée d'Italie, 69364 Lyon Cedex 07, France  
federico.calle-vallejo@ens-lyon.fr*

The surface of a heterogeneous catalyst is normally composed of a variety of terraces and defects. Close-packed surfaces coexist with more open facets, steps and kinks. Among all those, it is often observed that only one specific type of sites is catalytically active, which gives rise to the concept of structure sensitivity [1, 2]. In order to achieve maximal catalytic activities, materials design techniques should identify those sites and suitable synthesis procedures must be used to increase their surface abundance.

Well-known computational methodologies such as Sabatier-type activity plots are able to determine the adsorption features of optimal electrocatalysts [3]. However, countless materials can possess such adsorption features, so additional material screenings are performed over large databases created from DFT calculations [4], which is rather time consuming. Therefore, more descriptive guidelines are needed to enable the rapid design of new catalysts and avoid exhaustive computational and experimental searches.

In this talk we will present a methodology to predict not only the adsorption features of optimal catalysts but also the geometric structure of their active sites. The methodology can take into account all types of sites on nanoparticles of different sizes [5]. We will illustrate the method on the particular case of the electrochemical oxygen reduction reaction catalyzed by platinum, where our technique provides a morphology rationale used to engineer highly active sites, without resorting to alloying and using three different affordable experimental methods.

## References

- [1] G.A. Somorjai, J. Carrazza, *Industrial & Engineering Chemistry Fundamentals*, 25 (1986) 63-69.
- [2] T. Zambelli, J. Wintterlin, J. Trost, G. Ertl, *Science*, 273 (1996) 1688-1690.
- [3] I.E.L. Stephens, A.S. Bondarenko, U. Gronbjerg, J. Rossmeisl, I. Chorkendorff, *Energy & Environmental Science*, 5 (2012) 6744-6762.
- [4] J. Greeley, I.E.L. Stephens, A.S. Bondarenko, T.P. Johansson, H.A. Hansen, T.F. Jaramillo, Rossmeisl, Chorkendorff, J.K. Nørskov, *Nat Chem*, 1 (2009) 552-556.
- [5] F. Calle-Vallejo, J.I. Martínez, J.M. García-Lastra, P. Sautet, D. Loffreda, *Angewandte Chemie International Edition*, 53 (2014) 8316-8319.

# Electrochemical Oxidation of Ammonia on Pt(100) in Alkaline Solutions

Ioannis Katsounaros,<sup>[a],[b],[c]</sup> Pietro P. Lopes,<sup>[b]</sup> Dusan Strmcnik,<sup>[b]</sup> Andrew A. Gewirth,<sup>[a]</sup>  
Marc T.M. Koper,<sup>[c]</sup> Nenad M. Markovic<sup>[b]</sup>

<sup>a</sup> *University of Illinois at Urbana-Champaign, Department of Chemistry, Urbana, IL, USA*

<sup>b</sup> *Argonne National Laboratory, Materials Science Division, Lemont, IL, USA*

<sup>c</sup> *Leiden Universiteit, Leiden Institute of Chemistry, Leiden, The Netherlands*

[i.katsounaros@umail.leidenuniv.nl](mailto:i.katsounaros@umail.leidenuniv.nl)

Ammonia is an essential component of the nitrogen cycle, as it is involved in a variety of natural or industrial processes of paramount importance, such as the biological nitrification in soil or the ammonia synthesis (nitrogen fixation). The oxidation of ammonia by electrochemical means may find applications in (i) energy conversion (ammonia fuel cells or “ammonia electrolysis”), (ii) ammonia sensors, (iii) environmental protection (removal of ammonia from waste streams), or (iv) electrosynthesis (e.g. production of hydroxylamine or nitric acid).

Nitrogen gas is the most favorable product of ammonia oxidation in terms of thermodynamics; however, its selective formation is in fact difficult. Platinum is the most active for the electrochemical oxidation of ammonia to nitrogen compared to other noble and transition metal polycrystalline surfaces. According to the two early mechanisms that have been proposed to describe the conversion of  $\text{NH}_3$  to  $\text{N}_2$ , nitrogen can be formed either by the  $\text{N}_{\text{ad}}$  dimerization or by recombination of two  $\text{NH}_x$  adsorbed species ( $x = 1, 2$ ). From experimental and computational studies there is not yet a consensus on the dominant mechanism of nitrogen formation during ammonia oxidation.

The activity of platinum for the conversion of ammonia to nitrogen relies on the presence of Pt(100) terraces, which are unique for this reaction. In particular, ammonia oxidation is a very structure-sensitive process, as Pt(100) is the only one of the three Pt basal planes which can convert  $\text{NH}_3$  to  $\text{N}_2$  selectively, while Pt(111) and (110) are practically inactive.

This presentation deals with the ammonia oxidation on the Pt(100) single-crystal electrode in alkaline solutions, using standard electrochemical methods in combination with electrochemical fourier transform infrared reflectance-absorption spectroscopy and differential electrochemical mass spectrometry. Our particular focus is on the nature of the adsorbed intermediate species and thereby on their potential role in the N-N coupling and the observed deactivation.

## *Acknowledgments*

This research was supported by a Marie Curie International Outgoing Fellowship within the 7th European Community Framework Programme to Ioannis Katsounaros under Award IOF-327650, and by the U.S. Department of Energy, Office of Science, Materials Sciences and Engineering Division.

# Oxygen Electroreduction at Non-uniform Pt Surfaces: From Model Electrodes to Nanostructured Catalysts

Aliaksandr Bandarenka

*Technische Universität München*

*Department of Physics, James-Frank-Str. 1, D-85748 Garching, Germany*

*bandarenka@ph.tum.de*

Electrocatalysis of the oxygen reduction reaction (ORR) is significant for both fundamental and applied electrochemistry, as it can be the key reaction for the future sustainable provision of renewable energy. Additionally, the ORR has become an important model process, which is critical for the better understanding of reactions at electrified solid / liquid interfaces.

It is now relatively well understood that an ideal catalyst for the ORR should bind the OH-reaction intermediates approximately 0.1 eV weaker than the model Pt(111) surface [1]. However, application of this knowledge to design “real-world”, often nanostructured electrocatalysts is not always straightforward. For instance, surface defects should normally bind the reaction intermediates stronger; therefore, defect surfaces are expected to have lower activity than Pt(111). This is indeed the case for the polycrystalline platinum electrodes. However, introduction of specific surface defects, for instance steps, can also substantially increase the catalytic activity. This is typical for e.g. Pt[n(111)x(111)] and Pt[n(111)x(100)] surfaces [2,3,4]. On the other hand, “normal-shape” Pt nanoparticles, which have large amount of under-coordinated sites (similar to those present at the high-index single crystal surfaces), do not demonstrate such non-trivial increase in the activity. Another surprising phenomenon is the dependence of the ORR specific activity of nanoparticles on both loading [5] and long-range order [6].

While the common way of improving the activity of metal electrodes is a modification of the electronic properties of the surface through alloying it with other metals, it turned out that in case of bulk alloys, the solute metal often dissolves from the surface layers. This leads to structures in which several strained Pt-enriched layers cover the bulk alloy and protect it from further dissolution. Namely strains in the resulting layers influence the ORR activity [1,7]. However, these systems are difficult to model, as the resulting structures are complex and highly dependent on preparation methods.

In the presentation, examples will be given of how to explain or even predict the non-trivial activity phenomena for high-index single crystal surfaces, polycrystalline electrodes and nanostructured materials using affordable experimental and theoretical approaches.

## References

1. I.E.L. Stephens et al, *Energy & Environ. Sci.* 5 (2012) 6744-6762.
2. V.R. Stamenkovic, B. Fowler, B.S. Mun, G.F. Wang, P.N. Ross, C.A. Lucas, N.M. Markovic, *Science*, 315 (2007) 493-497.
3. A. Hitotsuyanagi, M. Nakamura and N. Hoshi, *Electrochimica Acta*, 82 (2012) 512-516.
4. A. Kuzume, E. Herrero and J. M. Feliu, *J. Electroanal. Chem.*, 599 (2007) 333-343.
5. M. Nesselberger, et al, *Nature Materials*, 12 (2013) 919-924.
6. Y. Kang, X. Ye, J. Chen, Y. Cai, R.E. Diaz, R.R. Adzic, E.A. Stach, C.B. Murray. *J. Am. Chem. Soc.*, 135 (2013) 42-45.
7. P. Strasser et al, *Nature Chem.*, 2 (2010) 454-460.

# Effect of Acetonitrile Adsorption on the ORR on Platinum Single Crystal Electrodes. A Combined Electrochemical, Spectroscopic and DFT Study.

Enrique Herrero<sup>1</sup>, Adolfo Ferre-Vilaplana<sup>2</sup>, Valentín Briega-Martos<sup>1</sup>

<sup>1</sup>*Instituto de Electroquímica, Universidad de Alicante, Apdo. 99, E-03080 Alicante, Spain.*

<sup>2</sup>*Instituto Tecnológico de Informática, E-46022 Valencia, Spain, and Departamento de Sistemas Informáticos y Computación, EPS de Alcoy, Universidad Politécnica de Valencia, E-03801 Alcoy, Spain*

*\*e-mail address: herrero@ua.es*

The oxygen reduction reaction (ORR) is probably the most studied electrochemical reaction because its practical application on fuel cells and batteries. It has been mainly studied on aqueous solution but in recent years the research on of metal-air batteries using non-aqueous solvents has triggered the studies on those solvents. When water is replaced by other solvents, the interactions between the solvent and the electrode surface alter the reactivity of the electrode. These interactions of the solvent with the surface have to be perfectly understood if better electrocatalysts are to be designed. In order to study those effects, the ORR has been studied on platinum single crystal electrodes in hanging meniscus rotating disk configuration using aqueous solutions with different concentrations of acetonitrile. Acetonitrile, a small organic molecule, can be used as a paradigm of the possible interactions that can be found in a non-aqueous solution. For understanding the differences with water, low and high concentrations of acetonitrile have been used. On Pt(111) electrode, increasing amounts on acetonitrile leads to a higher onset for the ORR and lower limiting currents, a clear indication that the adsorption of acetonitrile is giving rise to the formation of some hydrogen peroxide as final product. For high acetonitrile concentrations, the limiting current is half of that obtained in the absence of acetonitrile, and thus the efficiency for hydrogen peroxide formation is approaching 100%. The half wave potential for the reaction almost coincide with the thermodynamic potential for the reduction of oxygen to hydrogen peroxide (=0.68 V) and thus suggesting that this reaction is taking place with a very low overpotential. For the Pt(100), lower currents and higher overpotentials are always obtained.

To understand those differences with the surface structure, the FTIR spectra of the process in deaerated solutions has been recorded. For the Pt(111) electrode, adsorbed acetonitrile is observed at high potentials, as previously reported [1]. Around 0.6 V, a reductive process in the adsorbed acetonitrile species takes place, which leads to changes in the adsorbed configuration. On Pt(100) electrode, this process takes place at much higher potentials. DFT calculations indicate that the presence of this reduced species is a key parameter in the formation of hydrogen peroxide. It can effectively transfer hydrogen atoms to adsorbed O-O species on Pt, leading to the formation of hydrogen peroxide.

## REFERENCES

[1] S. Morin, B.E. Conway, G.J. Edens, M.J. Weaver, J. Electroanal. Chem. 421 (1997) 213.

# Interface control in a chemically modified electrode for overpotential reduction

Shino Sato<sup>1,2</sup>, Kohei Uosaki<sup>1,2</sup>, Kei Murakoshi<sup>1</sup>, Katsuyoshi Ikeda<sup>2,3\*</sup>

<sup>1</sup>Department of Chemistry, Faculty of Science, Hokkaido University, Sapporo 060-0810 JAPAN,

<sup>2</sup>National Institute for Materials Science (NIMS), Tsukuba 305-0044 JAPAN,

<sup>3</sup>Nagoya Institute of Technology, Nagoya 466-8555 JAPAN

[s.shino@mail.sci.hokudai.ac.jp](mailto:s.shino@mail.sci.hokudai.ac.jp), [kikeda@nitech.ac.jp](mailto:kikeda@nitech.ac.jp)\*

## [Introduction]

A well-organized molecular monolayer can be self-assembly constructed on a metal surface. Such chemical modification is recognized as one of key issues to functionalize metal electrode surfaces. For example, metalloporphyrin-modified electrodes are known to act as electrocatalysts for oxygen reduction reaction (ORR). However, the reaction rate on such electrodes is significantly affected by electronic coupling between the metal substrate and catalyst molecules. In this work, we constructed Cobalt porphyrin(CoTPP)-modified electrodes with various metal-molecule interface structures using the layer-by-layer technique. The contribution of the interface structures to the overall reaction rate was examined by analyzing the polarization curves of ORR.

## [Experimental]

CoTPP-catalyst layers were immobilized on an Au electrode through various molecular wires such as alkanethiols or phenyldiisocyanides. To tune the interface structure between the wire molecules and the metal substrate, Pd monoatomic layers (Pd<sub>ML</sub>) were formed by the underpotential deposition technique. ORR was measured using the rotating disk electrode (RDE) method in oxygen-saturated 0.5 M H<sub>2</sub>SO<sub>4</sub> electrolyte solution.

## [Results and Discussion]

The upper panel of the figure illustrates the interface structures between the electrode and wire molecules with and without Pd<sub>ML</sub>. The adsorption geometry of the isocyanide anchor group (-CN) was confirmed using the infrared reflection absorption spectroscopy. In the presence of Pd<sub>ML</sub>, the anchor geometry changed from the on-top to the bridge configuration, indicating the stronger adsorption on Pd than on Au. In the case of thiols (-S), on the other hand, the presence of Pd<sub>ML</sub> is expected to weaken the adsorption.

The lower panel of the figure shows the polarization curves for ORR on the CoTPP-modified electrodes with the four different interface structures: Au-S, Au/Pd<sub>ML</sub>-S, Au-CN, and Au/Pd<sub>ML</sub>-CN. The difference of the ORR overpotential between Au-S and Au-CN was rather small. In the presence of Pd<sub>ML</sub>, however, the two anchor groups exhibited opposite tendency; Au/Pd<sub>ML</sub>-S showed larger ORR overpotential whereas Au/Pd<sub>ML</sub>-CN presented much smaller overpotential. This result clearly shows that the overall electrochemical reaction rate is strongly affected by the interface connection between the catalytic active sites and the conducting electrode even in rather slow ORR.

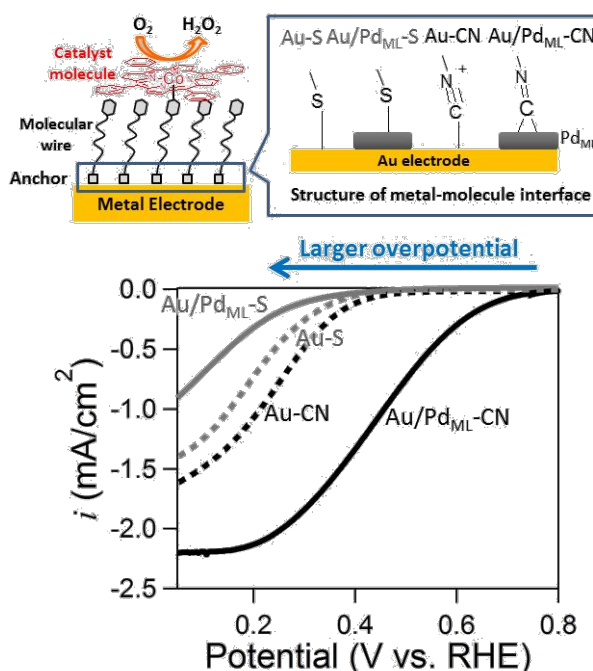


Figure. ORR polarization curves on Co-TPP catalyst layers formed on the molecular wire monolayer of Imidazole-terminated alkanethiols and isocyanides with and without Pd<sub>ML</sub>, measured by RDE method with rotation rate of 1000 rpm.

This result clearly shows that the overall electrochemical reaction rate is strongly affected by the interface connection between the catalytic active sites and the conducting electrode even in rather slow ORR.

# Designing In Situ Solid Electrolyte Interphase Studies using Surface-enhanced Raman Spectroscopy

Sunny Hy<sup>a,b</sup>, Felix<sup>b</sup>, Bing-Joe Hwang<sup>b</sup>

<sup>a</sup>Department of NanoEngineering, University of California San Diego, La Jolla CA USA

<sup>b</sup>Department of Chemical Engineering, National Taiwan University of Science and Technology, Taipei Taiwan  
SIhy@ucsd.edu

The mechanical and chemical properties of the solid electrolyte interphase (SEI) on the electrode surface dictates the overall battery properties that include rate performance, capacity retention and durability. Although extensive work has been done to try and elucidate its growth mechanism, transport properties, and chemical make-up, it still remains highly elusive due to its nano-scale thickness and complex heterogeneous structure<sup>1</sup>. To understand its chemical evolution during cycling, we developed an in situ surface-enhanced Raman Spectroscopy technique utilizing nano-sized Au particles coated with a chemically-inert SiO<sub>2</sub> coating that is applied directly to the electrode being studied. The use of the nano-sized Au particles allows for the exploration of different electrode systems that often determine the chemistry and growth mechanism of SEI. Here we demonstrate the feasibility of the technique looking at silicon electrode with two different electrolytes<sup>2</sup>, its use to elucidate the reaction mechanisms occurring on both cathode and anode surface within a lithium-excess cathode and graphite cell configuration<sup>3</sup>, and finally possible strategies for improving this novel technique such as applying Ag nanoparticles to explore surface ALD-coated cathode materials during in situ cycling.

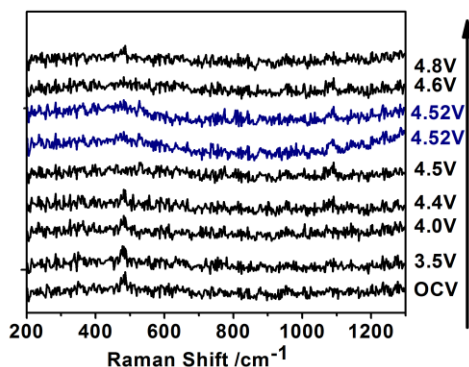


Figure 1 in situ SERS spectra during charging up to 4.8 V of the Al<sub>2</sub>O<sub>3</sub> ALD coated Li-excess cathode material

1. Shi, S.; Lu, P.; Liu, Z.; Qi, Y.; Hector, L. G.; Li, H.; Harris, S. J., Direct Calculation of Li-Ion Transport in the Solid Electrolyte Interphase. *Journal of the American Chemical Society* **2012**, 120905083455007.
2. Hy, S.; Felix, Chen, Y.-H.; Liu, J.-y.; Rick, J.; Hwang, B.-J., In situ surface enhanced Raman spectroscopic studies of solid electrolyte interphase formation in lithium ion battery electrodes. *Journal of Power Sources* **2014**, 256 (0), 324-328.
3. Hy, S.; Felix, F.; Rick, J.; Su, W. N.; Hwang, B. J., Direct In situ Observation of LiO Evolution on Li-Rich High-Capacity Cathode Material, Li[NiLiMn]O (0 ≤ x ≤ 0.5). *J Am Chem Soc* **2014**, 157 (3), 999-1007.



# Laser induced temperature jump investigation of the interface between Pt single crystals in contact with ionic liquids

Juan M. Feliu<sup>1</sup>, P. Sebastián<sup>1</sup>, R. Martínez-Hincapié<sup>1</sup>, A. Sandoval<sup>1,2</sup>, V. Climent<sup>1</sup>,

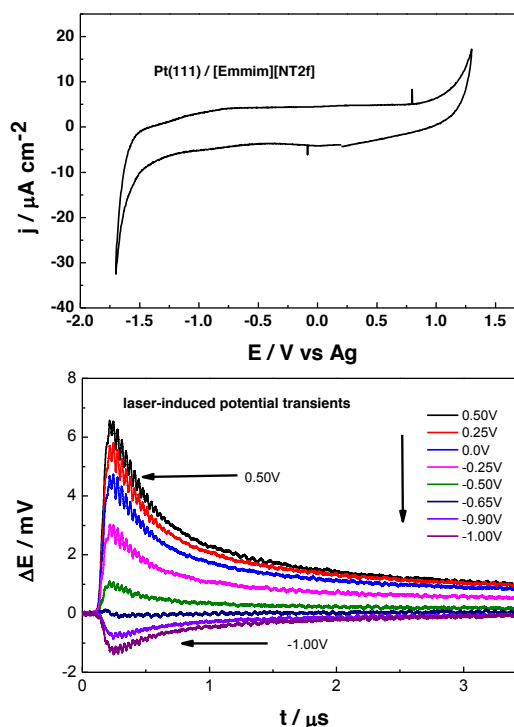
<sup>1</sup> Departamento de Química Física e Instituto Universitario de Electroquímica, Universidad de Alicante, Apartado 99, E-03080 Alicante, Spain

<sup>2</sup> Departamento de Química, Facultad de Ciencias, Universidad Nacional de Colombia, Cra. 30# 45-03, Edificio 451, Bogotá, Colombia  
*juan.feliu@ua.es*

Room temperature ionic liquids are a novel kind of solvents potentially suitable for many electrochemical applications. A deeper knowledge of the properties that characterize the metal /ionic liquid interphase is desirable for understanding its reactivity. However, in the case of platinum group metals, the number of available studies is very limited, especially on single crystal electrodes [1, 2]. The high electrocatalytic activity of platinum complicates the study of its interfacial properties. One of the main difficulties lies on the determination of the potential of zero charge, pzc, a very important interfacial parameter, whose calculation is not straightforward, even in aqueous solution.

Laser-induced temperature jump experiments provide information on the entropy changes of the double layer from which the potential of maximum entropy, pme, is available. The experimental response is dominated by the organization of the ionic network at the interface and is closely related to the pzc. From an electrostatic point of view, at potential values more negative than the pzc, the ionic network at the interphase should contain higher number of cations than anions and the response obtained from the laser perturbation should be negative. This response should decrease in magnitude by increasing the applied potential, as a consequence of the composition change. If the amount of cations equals that of anions, the response would be zero. In the absence of specific interactions, the pme should approach the pzc. The same, but opposite trends, should take place at potentials positive to the pzc.

The interface Pt(111)/[Emmim][NT2f] is investigated by laser-induced temperature method [3]. Comparison with similar analysis in aqueous solution, in a very wide pH range, show the differences between this novel interface and classical Pt/aqueous interfaces. Although the experimental response is potential dependent, thus revealing the different distribution of ions in the network as a function of the applied potential, the interchange between cation and anion is not as simple and depends on many parameters. All these considerations will be discussed.



- [1]Motobayashi, K., et al., Journal of Physical Chemistry Letters, 2013. 4(18): p. 3110-3114.  
[2]Sandoval, A.P, et al., Electrochemistry Communications, 2014. 46: p. 84-86.  
[3]Sebastián, P., et al., Electrochemistry Communications, 2015. 55: p. 39-42.

# C1 Molecule Adsorption-Dissociation on Pt and Cu-modified Pt Electrode Surfaces

Kun Jiang,<sup>1,2</sup> Sylvain Brimaud,<sup>2</sup> Wen-Bin Cai<sup>1</sup> and R. Jürgen Behm<sup>2</sup>

<sup>1</sup> Collaborative Innovation Center of Chemistry for Energy Materials and Department of Chemistry, Fudan University, Shanghai 200433, P.R. China

<sup>2</sup> Institute of Surface Chemistry and Catalysis, Ulm University, D-89069 Ulm, Germany  
e-mail: [wbc@fudan.edu.cn](mailto:wbc@fudan.edu.cn); [juergen.behm@uni-ulm.de](mailto:juergen.behm@uni-ulm.de)

The adsorption and oxidation behavior of C1 organic molecules like CH<sub>3</sub>OH, HCHO and HCOOH is of general importance not only from fundamental reasons, as model reactions in electrochemistry, but also because of their potential applications as fuel for green power sources like direct alcohol fuel cells. However, compared with the hydrogen oxidation reaction, the reaction mechanisms and intermediates formed during their reactive dissociation and oxidation on platinum group metal surfaces are far more complicated with several potential-dependent adsorbed intermediates [1].

Here we report results of a comparative investigation on the adsorption and dissociation behavior of methanol, formaldehyde and formic acid on Pt and Cu-modified Pt surfaces, employing a flow cell setup combined with *in situ* Attenuated Total Reflection Fourier Transform Infrared Spectroscopy (ATR-FTIRS) and online Differential Electrochemical Mass Spectrometry (DEMS), which allows for the simultaneous detection of adsorbed species and volatile products [2]. Negligible DEMS signals for volatile CO<sub>2</sub>, CO or HCOOCH<sub>3</sub> were recorded at fixed potential within the H<sub>upd</sub> region on both electrodes upon C1-molecules adsorption. However, differences were observed for the partially dissociated intermediates and for the CO<sub>ad</sub> coverages for Pt surface and the Pt surface modified by Cu-adlayer. Further measurements employing deuterated C1 compounds were also carried out for a better identification of the adsorbed intermediates. The overall implications of these findings on the reactive adsorption and dissociation processes will be discussed in this presentation.

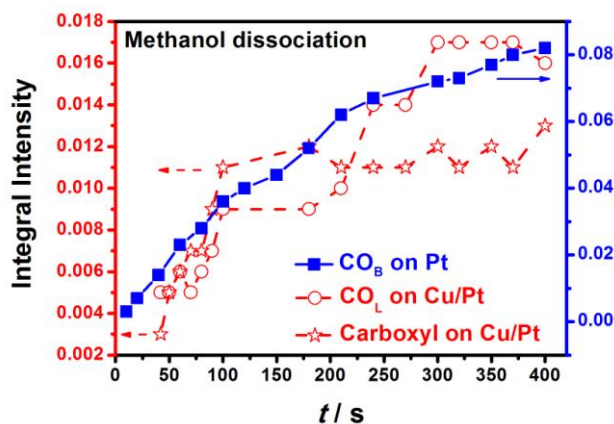


**Figure 1.** Time-resolved band intensity for intermediates during CH<sub>3</sub>OH adsorption-dissociation on either Pt or a Cu-modified Pt surface as monitored by *in situ* electrochemical ATR-IR

**Acknowledgements:** We gratefully acknowledge the support from the fellowship program of the Ministry of Science, Research and the Arts of Baden-Württemberg (AZ 6221.-CHN-2/310/1), as well as the support from NSFC (21273046 and 21473039) and STCSM (11JC140200).

## Reference

- [1] T. Iwasita, *Electrochim. Acta* 47 (2002) 3663-3674.
- [2] Y.X. Chen, M. Heinen, Z. Jusys, R.J. Behm, *Angew. Chem. Int. Ed.* 45 (2006) 981-985.

# Direct observation of electrochemical processes at single atomic layer: an advanced optical microscopy study

M.Azhagurajan<sup>1</sup>, Takashi Itoh<sup>1</sup>, and K. Itaya<sup>1</sup>.

<sup>1</sup>Frontier Institute for Interdisciplinary Sciences, Tohoku University, 6-3 Aramaki Aoba, Sendai  
980-8578, JAPAN

The evaluation of dynamic processes of electrochemical reactions of metals is an extremely important subject for both fundamental and practical points of view.[1,2] Although in situ SPM techniques can reveal those processes with atomic levels, observable scan areas are usually small electrochemical reactions taking place in the entire area of electrode surface. However due to slow scan speed and small observation area (usually in nanometer scale), the overall electrochemical process has not been understood completely.

In this study, we employed an optical microscopy technique called laser confocal microscopy-differential interference contrast microscopy (LCM-DIM) to understand the electrochemical dissolution/deposition process. The LCM-DIM has many capabilities of resolving mono-molecular steps and single atomic steps on Au, Pt, Pd and Si single crystal surfaces. We have also succeeded to see mono-molecular steps on many organic single crystal surfaces. The monatomic steps with a height of 0.23 nm on ultra-flat Pd (111) and 0.25 nm on ultra-flat Au (111) were clearly discerned in electrolyte solutions by this advanced optical microscopy, LCM-DIM. Figure 1(A) shows a LCM-DIM image obtained on the entire area of an ultra-flat Au (111) facet formed on a small single crystal bead [3].

Large (111) facets are usually formed on a relatively large crystal. Figure 1(B) shows an illustration of the deposition of Au in the atomic scale. Direct observation of electrochemical deposition and dissolution process at single atomic layer on ultra-flat Au (111) was shown in this study. It is indicated that the electrochemical processes of Au (111) can be followed with atomic step resolution. Detailed results will be discussed. Thus, it is evident that the combination of electrochemistry along with LCM-DIM is a potential technique for observing interfacial phenomena which can then be applied directly for an industrial scale application.

## References

1. Wen, R.; Lahiri, A.; Azhagurajan, M.; Kuzume, A.; Kobayashi, S.; Itaya, K. *J. Electroanal. Chem.* **2010**.
2. Wen R, Lahiri A, Azhagurajan M, Kobayashi S, Itaya K., *J. Amer. Chem. Soc.*, 2010, 132, 39, 13657.
3. M. Azhagurajan, R. Wen, A. Lahiri, Y. G. Kim, T. Itoh, and K. Itaya. *J Electrochem Soc.*, 160 (9) (2013) D361.

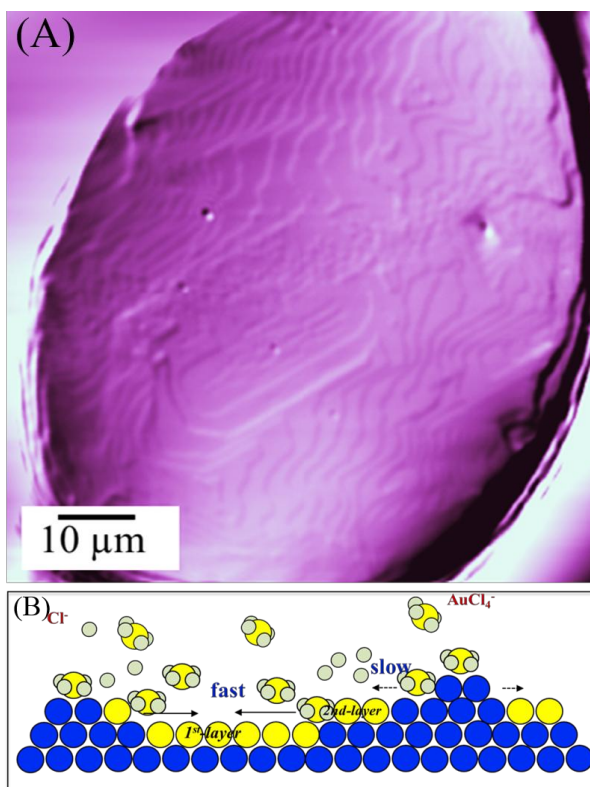


Figure 1(A) LCM-DIM image of a typical ultra-flat Au(111) surface was observed in air with a scan area of 140 x 140 μm, (B) Illustration of the Various Processes taking place during the deposition of gold

# Enhanced Electrocatalysis of Ethanol on Dealloyed Pd-Ni-P Film in Alkaline Media: an Infrared Spectroelectrochemical Investigation

Ye Wang, Wen-Bin Cai\*

Collaborative Innovation Center of Chemistry for Energy Materials and Department of Chemistry,  
Fudan University, Shanghai 200433, China  
wbcai@fudan.edu.cn

Dealloying treatment is an effective way to restructure bi- and tri- metallic catalytic materials, with an expectation to enhance a desired electrocatalytic reaction<sup>[1]</sup>. In order to further extend the application of dealloyed catalysts in electrocatalytic applications, fundamental understanding of the interfacial reactions occurring at corresponding electrode/electrolyte is essential. As a case study, electrocatalysis of ethanol in alkaline media on dealloyed Pd-Ni-P film has been recently investigated in our group<sup>[2,3]</sup>. A Pd-Ni-P film was electro-deposited on Au substrate, and the dealloying process was carried out by repetitive potential cycling in acidic media to leach out most Ni and P components. Surface structural and electronic properties of the pristine film and the dealloyed film were characterized and compared. Surface roughening, Pd-segregation and electronic property variation upon dealloying were confirmed. Cyclic voltammetry and chronoamperometry on the two films in ethanol-containing alkaline media were used to assess their electrocatalytic performances, demonstrating significantly enhanced and durable ethanol oxidation on the dealloyed film. More importantly, in situ attenuated total reflection surface enhanced infrared spectroscopy was initially extended to probe the interfacial molecular variations associated with the electrocatalytic reactions on these two films, to provide an insight into the enhanced electrocatalysis on the dealloyed film. It was revealed that the enhanced electrocatalysis correlates well with enhanced formation of both CO<sub>ad</sub> and acetate.

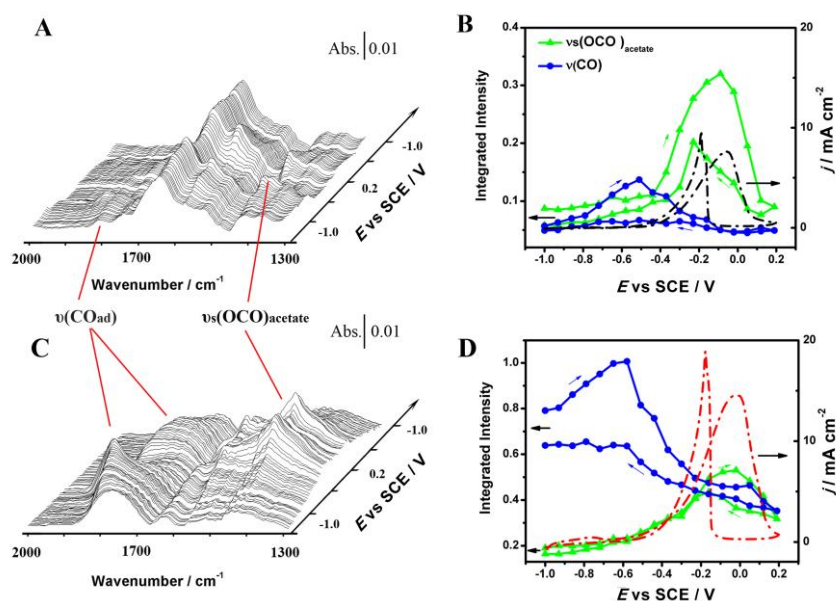


**Figure 1.** Potentiodynamic ATR-SEIRA spectra on the as-deposited Pd-Ni-P film (A) and the dealloyed film (C) in 0.1 M NaOH + 0.5 M CH<sub>3</sub>CH<sub>2</sub>OH; Potential-dependent band intensities for  $\nu(\text{CO}_{\text{ad}})$  (blue) and  $\nu_{\text{s}}(\text{OCO})$  of adsorbed acetate (green) with corresponding cyclic voltammograms recorded at 5 mV s<sup>-1</sup> on the as-deposited Pd-Ni-P film (B) and the dealloyed film (D) in 0.1 M NaOH + 0.5 M CH<sub>3</sub>CH<sub>2</sub>OH. Reference spectrum was taken at OCP in 0.1 M NaOH.

**Acknowledgements:** Financial supports from NSFC (grant No. 21273046 and 21473039) and SMCS (grant No.11JC140200) are highly appreciated.

## References:

- [1] R. Srivastava, P. Mani, P. Strasser, J Power Sources, 190 (2009) 40-47.
- [2] Y.Y. Yang, J. Ren, Q.X. Li, Z.Y. Zhou, S.G. Sun, W.B. Cai, ACS Catal, 4 (2014) 798-803.
- [3] Y. Wang, K. Jiang, W.-B. Cai, Electrochim. Acta, 162 (2015) 100-107.

# Raman Spectroscopic Detection of Electrochemical Oxidative Reaction of Single-Walled Carbon Nanotubes

Masato Tominaga,<sup>\*†‡</sup> Yudai Nagahama,<sup>†</sup> and Yuto Yatsugi<sup>†</sup>

<sup>†</sup>Graduate School of Science and Technology, Kumamoto University, Kumamoto 860-8555, Japan

<sup>‡</sup>Kumamoto Institute for Photo-Electro Organics (Phoenix), Kumamoto 862-0901, Japan

<sup>\*</sup>masato@gpo.kumamoto-u.ac.jp

The oxidative corrosion of carbon is an urgent problem because carbon is widely used as a platform electrode to immobilize catalysts. One of the factors in the gradual decrease of output power in fuel cells such as a polymer electrolyte fuel cell is the oxidative corrosion of the carbon supports. The oxidative corrosion of carbon is a complicated process that includes parallel oxidation pathways. Furthermore, the following electrochemical oxidation reaction ( $\text{C} + 2\text{H}_2\text{O} = \text{CO}_2 + 4\text{H}^+ + 4\text{e}^-$  0.207 V vs. NHE) of carbon by water molecules occurs at a much more negative potential than that thermodynamically expected, although the rate of this reaction is very slow. Understanding the mechanism of nucleation and growth in oxidative corrosion at the surface of  $\text{sp}^2$ -carbon is important for advancing its application. A considerable amount of electrochemical research has been directed towards elucidating the mechanism of the oxidation of the hexagonal plane  $\text{sp}^2$  carbon family, such as highly oriented pyrolytic graphite (HOPG), carbon nanotubes and graphene as model reaction systems. Recently, a number of studies using *ab initio* molecular orbital calculations have focused on the oxidation steps of hexagonal plane  $\text{sp}^2$  carbons. However, the detailed oxidation mechanism of such  $\text{sp}^2$  carbons is still unclear.

We recently reported the oxidative corrosion potential vs. pH diagram for single-walled carbon nanotubes (SWCNTs), as shown in Figure 1.<sup>1,2</sup> The Raman spectroscopy studies based on the encapsulation of  $\beta$ -carotene into SWCNTs revealed that there are three types of oxidative corrosion of SWCNTs: non-oxidized, end-cap oxidized (end-cap eliminated), and side-wall oxidized SWCNTs. SWCNTs are good models for experimentally analyzing the oxidative corrosion of  $\text{sp}^2$ -carbon. Furthermore, the effect of adsorbed molecular oxygen on the oxidative corrosion of SWCNTs in aqueous solution has been investigated using Raman spectroscopy.<sup>2</sup> We found that nucleation and growth of the oxidative corrosion began at defect sites in the presence of adsorbed oxygen, but occurred randomly in the absence of adsorbed oxygen. Similar behavior was observed for metallic-type SWCNTs (m-SWCNTs) and semiconductor-type SWCNTs (s-SWCNTs).

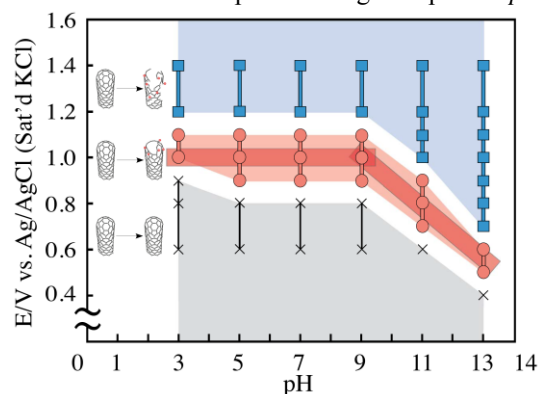


Figure 1. Diagram of potential vs. pH for the oxidative corrosion of SWCNTs (crosses: non-oxidized SWCNTs, circles: end-cap eliminated SWCNTs, squares: sidewall and end-cap oxidized SWCNTs).

## References

- Masato Tominaga, Yuto Yatsugi, Noriaki Watanabe, RSC Advances, **4** (2014) 27224-27227.
- Masato Tominaga, Yuto Yatsugi, Makoto Togami, RSC Advances, **4** (2014) 53833-53836.



# Electrochemistry of Two-Dimensional Materials

Matěj Velický<sup>a,\*</sup>, P.S. Toth<sup>a</sup>, M.A. Bissett<sup>a</sup>, I.A. Kinloch<sup>b</sup>, K.S. Novoselov<sup>c</sup>, Robert A.W. Dryfe<sup>a</sup>

<sup>a</sup>School of Chemistry, <sup>b</sup>School of Materials, <sup>c</sup>School of Physics and Astronomy, University of Manchester, Oxford Rd, Manchester, M13 9PL, UK

\*matej.velicky@manchester.ac.uk

Two-dimensional (2D) materials have generated enormous interest in electrochemistry-related applications, such as sensing and energy storage/conversion or corrosion protection [1]. Electrochemical performance of these materials is critical for their successful implementation in the abovementioned applications. Despite significant advances in the last five years, the electrochemistry of graphene remains far from being fully understood and there is currently a lack of consensus on some of its basic electrochemical properties. Furthermore, the recent surge in exploration of other 2D materials, such as MoS<sub>2</sub>, WSe<sub>2</sub> or h-BN, which have been studied far less than graphene, has opened a much wider landscape of possibilities in optoelectronics, electrochemical switching and photocatalysis, due to their complex electronic structure.

We address the key aspects of 2D materials' electrochemistry using a unique electrochemical probe, capable of measuring electrochemical response on a micrometer scale, and a range of microscopic and spectroscopic techniques. The key properties discussed here are: *charge transfer kinetics*, *capacitance*, and their dependence on the number of graphene layers and the role of defects/edges. Contrary to previous views, the basal plane of graphene is electrochemically active and there is slight decrease in electron transfer kinetics on graphene monolayer when compared to bulk graphite, as expressed by the heterogeneous electron transfer rate ( $k^0$ ) measurement of known redox mediators [2]. Another very important issue is degradation/contamination of the crystalline surface upon exposure to the atmosphere. Our recently published data show large differences between the atmosphere-aged and *in situ* cleaved surfaces for both materials are observed, which explains the vast variation of  $k^0$  values in literature [3]. These differences are attributed to oxidation and adsorption of airborne contaminants at the surface exposed to an ambient environment, as determined by X-ray photoelectron spectroscopy. Most importantly, the electrochemical response of semiconducting MoS<sub>2</sub> with an optical band gap of *ca.* 1.2 – 1.8 eV is shown to be strongly dependent on applied potential and incident illumination, promising a wealth of new applications based on vertical heterostructures of graphene and band-gapped 2D materials, as demonstrated by the schematic in Fig.1.

These findings have a direct implication for use of MoS<sub>2</sub> and graphene as electrodes materials and underline the need for an in-depth understanding of electrochemical properties of two-dimensional (2D) materials, which will maximize their potential in electrochemistry-related applications.

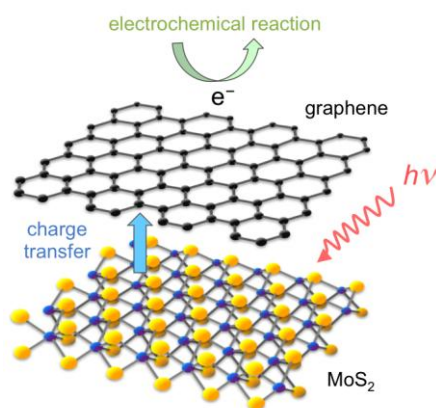


Fig. 1. Schematic of a vertical heterostructure of graphene and MoS<sub>2</sub>, designed for illumination-controlled charge extraction.

- [1] K.S. Novoselov, V.I. Fal'ko, L. Colombo, P.R. Gellert, M.G. Schwab, K. Kim, A roadmap for graphene, *Nature*, 490 (2012) 192-200.
- [2] P.S. Toth, A. Valota, M. Velický, I. Kinloch, K. Novoselov, E.W. Hill, R.A.W. Dryfe, Electrochemistry in a drop: a study of the electrochemical behaviour of mechanically exfoliated graphene on photoresist coated silicon substrate, *Chem. Sci.*, 5 (2014) 582-589.
- [3] M. Velický, D.F. Bradley, A.J. Cooper, E.W. Hill, I.A. Kinloch, A. Mishchenko, K.S. Novoselov, H.V. Patten, P.S. Toth, A.T. Valota, S.D. Worrall, R.A.W. Dryfe, Electron Transfer Kinetics on Mono- and Multilayer Graphene, *ACS Nano*, 8 (2014) 10089-10100.

# Atomistic Simulations for Designing High-Performance Electrode Materials for Polymer Electrolyte Fuel Cells

Ryosuke Jinnouchi, Kensaku Kodama, Eishiro Toyoda, Kenji Kudo, Naoki Kitano, Naoki Hasegawa and Yu Morimoto

Toyota Central Research & Development Laboratories, Inc.  
41-1 Yokomichi Nagakute, Aichi 480-1192, Japan  
e1262@mosk.tytlabs.co.jp

This presentation shows our recent research activities using atomistic simulations on electrode materials for polymer electrolyte fuel cells (PEFCs). Two topics are presented: DFT calculations on Pt electrocatalysts and molecular dynamics (MD) simulations using force fields on Nafion/Pt interfaces.

In the first topic, after a brief introduction of preliminary applications of DFT to single crystal surfaces [1–4], results on Pt nano-particles are presented [5]. Oxide formations are shown to be initiated by OH and O adsorbates formations at edges and corners of nano-particles as indicated by Fig. 1. Although some meta-stable structures of subsurface  $\text{PtO}_x$  are obtained by the calculations, they are formed only at potentials higher than usual operation potentials of PEFCs, e.g., 0.6–1.0 V (RHE). DFT results on Pt dissolutions indicate that dissolutions are also initiated at edges and corners of nano-particles [6]. To prevent oxidations and dissolutions, which are considered to lower the catalytic activity and durability, respectively, selective substitutions of Pt atoms at edges and corners by Au atoms are suggested to be promising.

In the second topic, MD simulation results are shown on  $\text{O}_2$  transport through Nafion to Pt surface [7]. Simulated results agree well with experimental results on  $\text{O}_2$  diffusivity,  $\text{O}_2$  solvability and limiting current density of ORR and indicate that the Nafion forms a high-density layer near the Nafion/Pt interface causing high interfacial resistivity for  $\text{O}_2$ -transport as shown in Fig. 2.

In summary, atomistic simulations, combined with well-focused experiments, are a powerful and essential approach for designing advanced electrode materials with desired properties for PEFCs.

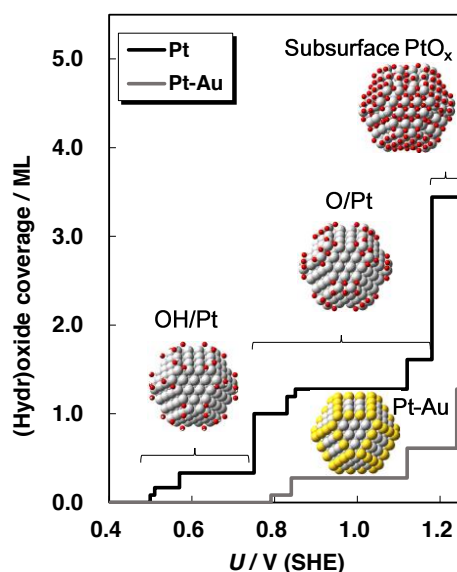


**Fig. 1** DFT results on oxide formations on Pt and Pt-Au nano-particles.

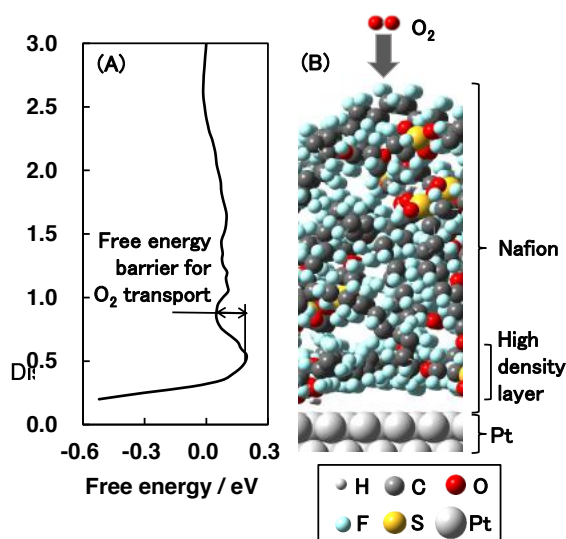


**Fig. 2** Free energy profile for  $\text{O}_2$  transport in the Nafion ionomer (B) and ionomer structure (B).

- [1] R. Jinnouchi and A. B. Anderson, *Phys. Rev. B*, **77**, 245417 (2008).
- [2] R. Jinnouchi, K. Kodama, T. Hatanaka and Y. Morimoto, *Phys. Chem. Chem. Phys.*, **13**, 21070 (2013).
- [3] R. Jinnouchi, T. Hatanaka, Y. Morimoto and M. Osawa, *Phys. Chem. Chem. Phys.*, **14**, 3208 (2012).
- [4] R. Jinnouchi, K. Kodama and Y. Morimoto, *J. Electroanal. Chem.*, **716**, 31 (2014).
- [5] R. Jinnouchi, K. Kodama and Y. Morimoto, to be prepared.
- [6] R. Jinnouchi, E. Toyoda, T. Hatanaka and Y. Morimoto, *J. Phys. Chem. C*, **114**, 17557 (2010).
- [7] R. Jinnouchi, K. Kudo, N. Kitano, N. Hasegawa and Y. Morimoto, to be prepared.

# Electrochemical Shell-Isolated Nanoparticle-Enhanced Raman Spectroscopy (EC-SHINERS)

Chao-Yu Li, Jin-Chao Dong, Xi Jin, Jian-Feng Li\*

*State Key Laboratory of Physical Chemistry of Solid Surfaces, College of Chemistry and Chemical Engineering, Xiamen University, Xiamen 361005, China*  
*E-mail: Li@xmu.edu.cn*

Surface-enhanced Raman spectroscopy (SERS) is a powerful technique that yields fingerprint vibrational information with ultra-high sensitivity. However, only roughened Ag, Au and Cu surfaces can generate strong SERS effect, and it also in principle excludes to directly study atomically flat single crystal surfaces that cannot effectively support the strong surface plasmon resonance (SPR). The lack of materials and morphology generality has severely limited the breadth of SERS practical applications on surface science, catalysis and electrochemistry.

Shell-isolated nanoparticle-enhanced Raman spectroscopy (SHINERS) was therefore invented to break the long-standing limitation of SERS. In SHINERS, Au@SiO<sub>2</sub> core-shell nanoparticles were rationally designed. The gold core acts as plasmonic antenna and encapsulated by an ultra-thin, uniform and pinhole-free silica shell, can provide high electromagnetic field to enhance the Raman signals of probed molecules. The inert silica shell acts as tunneling barrier prevents the core from interacting with the environment, eg. to avoid contaminated specials or disturbing signals.

Combined with electrochemical methods, SHINERS has already been applied to a number of challenging electrochemical systems, such as hydrogen and CO on Pt(hkl) and Rh(hkl), pyridine and SCN<sup>-</sup> adsorption on Au(hkl). Surface electro-oxidation and-reduction processes at Au(hkl) and Pt(hkl) single crystal electrode surfaces were also been in-situ monitored by electrochemical SHINERS technique. These pioneering studies demonstrate convincingly the ability of EC-SHINERS in exploring correlations between structure and reactivity as well as in monitoring intermediates at the interfaces. The concept of shell-isolated nanoparticle-enhancement is being applied to other spectroscopies such as infrared absorption, sum frequency generation and fluorescence.

## References:

1. Jian-Feng Li et al. *Nature* **464** (2010) 392.
2. Jian-Feng Li et al. *Nature Protoc.* **8** (2013) 52.
3. Jian-Feng Li et al. *J. Am. Chem. Soc.* **137** (2015) 2400.



# Molecular Insight into Wetted Oxide Surfaces and Oxygen Electrocatalysis

Kelsey A. Stoerzinger<sup>1</sup>, Wesley T. Hong<sup>1</sup>, Yueh-Lin Lee<sup>2</sup>, Livia Giordano<sup>2</sup>, Yang Shao-Horn<sup>1,2</sup>

<sup>1</sup>*Department of Materials Science & Engineering*, <sup>2</sup>*Mechanical Engineering Department*  
*Massachusetts Institute of Technology, 77 Massachusetts Ave. Cambridge, MA 02139 USA*  
*kstoerz@mit.edu*

Oxide materials are critical components in electrochemical applications such as gas sensing and catalysis of the oxygen reduction and evolution reactions (ORR and OER) in fuel cells and electrolyzers.[1] In each of these applications, the surface chemistry of the oxide is directly influenced by the presence of water molecules—in the atmosphere or an aqueous solution—that govern the hydroxylation and charge of surface.[2] The binding of hydroxyl groups and other oxygenated species on oxides surfaces has been proposed to govern oxygen electrocatalysis[3] and explain the hydrophilic/hydrophobic nature of oxide surfaces.[4] Unfortunately, directly measuring hydroxylation and surface adsorbates in water and correlating these species to wetting and catalytic activity is challenging. Utilizing recent advances in X-ray photoelectron spectroscopy (XPS) at near-ambient pressure (NAP-XPS), we quantitatively assess surface hydroxylation and adsorption of water on  $\text{LaMO}_3$  epitaxial thin films ( $M = \text{Cr, Mn, Fe, Co, Ni}$ ).[5] The affinity toward hydroxylation, coincident with strong adsorption energies calculated for dissociated water and hydroxyl groups by density functional theory (DFT), leads to strong H-bonding in wetting and can inhibit catalysis of the ORR. We further test this correlation through manipulating the transition metal valence and oxide electronic structure via substitution of  $\text{La}^{3+}$  with  $\text{Sr}^{2+}$  in the series  $\text{La}_{(1-x)}\text{Sr}_x\text{MnO}_3$ , exploring the relation between band structure and work function with activity and wetting.

For some oxides, the interaction with water and associated ions can be observed by well-defined redox peaks, such as  $\text{RuO}_2$ —one of the most active catalysts of the OER.[6] We have studied the redox features of oriented  $\text{RuO}_2$  films, where the unique surface structures dictate the interaction with water and its ions ( $\text{H}^+$ ,  $\text{OH}^-$ ), as well as the ability of the active Ru sites to change valence state. The ease and extent of Ru redox impacts the specific OER activity of different crystallographic orientations,[7] motivating further work on in situ spectroscopy and theory to understand and design more active catalyst surfaces.

The insights obtained from study of these epitaxial surfaces build fundamental understanding of the mechanisms of oxygen electrocatalysis, as well as guide the rational design of high surface area oxide catalysts for electrochemical conversion and storage.

## References

- [1] J. Suntivich, K.J. May, H.A. Gasteiger, J.B. Goodenough, Y. Shao-Horn, *Science* 334 (2011) 1383-1385.
- [2] G.E. Brown, V.E. Henrich, W.H. Casey, D.L. Clark, C. Eggleston, A. Felmy, D.W. Goodman, M. Grätzel, G. Maciel, M.I. McCarthy, K.H. Nealson, D.A. Sverjensky, M.F. Toney, J.M. Zachara, *Chem. Rev.* 99 (1998) 77-174.
- [3] J.K. Nørskov, J. Rossmeisl, A. Logadottir, L. Lindqvist, J.R. Kitchin, T. Bligaard, H. Jonsson, *J. Phys. Chem. B* 108 (2004) 17886-17892.
- [4] G. Ketteler, S. Yamamoto, H. Bluhm, K. Andersson, D.E. Starr, D.F. Ogletree, H. Ogasawara, A. Nilsson, M. Salmeron, *M. J. Phys. Chem. C* 111 (2007) 8278-8282.
- [5] K.A. Stoerzinger, W.T. Hong, G. Azimi, L. Giordano, Y.-L. Lee, E.J. Crumlin, M.D. Biegalski, H. Bluhm, K.K. Varanasi, Y. Shao-Horn, Submitted (2015).
- [6] J. Rossmeisl, Z.-W. Qu, H. Zhu, G.-J. Kroes, J.K. Nørskov, *J. Electroanal. Chem.* 607 (2007) 83-89.
- [7] K.A. Stoerzinger, Q. Liang, M.D. Biegalski, Y. Shao-Horn, *J. Phys. Chem. Lett.* 5 (2014) 1636-1641.

# CO<sub>2</sub> electroreduction products and intermediates in organic solvents

Marta C. Figueiredo, Marc T. M. Koper  
Leiden Institute of Chemistry, Leiden University,  
PO Box 9502, 2300 RA Leiden, Netherlands  
*m.c.costa.figueiredo@lic.leidenuniv.nl*

CO<sub>2</sub> amounts are increasing continuously in the atmosphere generating an issue of global concern, as CO<sub>2</sub> is known to be one of the major contributors to the greenhouse effect [1]. Several methods for CO<sub>2</sub> sequestration [2] (capture and storage) have been studied and developed in the last decades but this technology still divides the scientific opinion around the world, as the storage of CO<sub>2</sub> in container under sea water do not look as an appealing long term solution [3]. In this sense, the electrochemical conversion into something useful (like fuels or chemicals) is probably of one the most promising options.

The electrochemical reduction of CO<sub>2</sub> has, in fact, been studied intensively over the last decades [4]. It is known that its products depend on the many factors like supporting electrolyte, electrode material, applied potential. In aqueous solutions the possible products are CO, formic acid and hydrocarbons such as methane, ethane and ethylene [5]. However, in water, CO<sub>2</sub> reduction has as competing reaction the hydrogen evolution that occurs in the same potential range. Yet, in organic solvents hydrogen evolution can be avoided. Organic solvents also present other important advantages when compared with aqueous media such as higher solubility of CO<sub>2</sub>, larger cathodic potential window and stabilization of important reaction intermediates such as CO<sub>2</sub> anion radical [6, 7]. It has been described that in non-aqueous solvents, the CO<sub>2</sub> electroreduction mechanism follows three different paths: by self-coupling of the anion radical with the formation of oxalate; through oxygen-carbon coupling of CO<sub>2</sub><sup>•-</sup> with CO<sub>2</sub> having CO and CO<sub>3</sub><sup>2-</sup> as products and, and CO<sub>2</sub><sup>•-</sup> protonation by residual water to yield formate as main reaction product [6]. Despite all the efforts on this subject, the real nature of the intermediates and the mechanism of the CO<sub>2</sub> reduction on non-aqueous solvents is not fully understood and a wide range of information can be found in the literature [8, 9].

In this work, we persecute a further understanding on the reduction mechanism of CO<sub>2</sub> in acetonitrile at copper electrodes. Copper electrodes were chosen due to their known reactivity for CO<sub>2</sub> in aqueous media [10]. The experiments were performed by using in situ Fourier Transformed infra-red spectroscopy (FTIR) in order to get insights on the products and intermediates of the reaction and its dependence on the applied potential. The results show that carbonates are the main product of this reaction and, for the first time, CO was identified by FTIR in acetonitrile media. Water contents and the solvent decomposition are shown to heavily influence the reaction mechanism and the nature of the products.

## References:

- [1] S. Pacala, et al, *Science*, 305 (2004) 968-972.
- [2] G.H. Rau, *Environ. Sci. & Technol.*, 45 (2010) 1088-1092.
- [3] K.S. Lackner, *Science*, 300 (2003) 1677-1678.
- [4] J. Qiao, et al, *Chem. Soc. Reviews*, 43 (2014) 631-675.
- [5] Y. Hori, *Electrochemical CO<sub>2</sub> Reduction on Metal Electrodes*, in: C. Vayenas, R. White, M. Gamboa-Aldeco (Eds.) *Modern Aspects of Electrochemistry*, vol. 42, Springer New York, 2008, pp. 89-189.
- [6] C. Amatore, et al, *J. Am. Chem. Soc.*, 103 (1981) 5021-5023.
- [7] S. Ikeda, et al, *Bull. Chem. Soc. Japan*, 60 (1987) 2517-2522.
- [8] J. Desilvestro, et al, *J. of Electroanal. Chem.*, 267 (1989) 207-220.
- [9] P.A. Christensen, et al., *J. Electroanal. Chem.*, 288 (1990) 197-215.
- [10] K.J.P. Schouten, et al, *Chem. Sci.*, 2 (2011) 1902-1909.

# Observation of Gas Structures at the Interface between a Hydrophobic Electrode and Water Using Atomic Force Microscopy

Yi-Hsien Lu, Chih-Wen Yang, Chung-Kai Fang, Hsien-Chen Ko and Ing-Shouh Hwang  
*Institute of Physics, Academia Sinica,  
Taipei 11529, Taiwan  
zonslan@gmail.com*

The microscopic picture at the vicinity of the electrode-solution interface is of fundamental and extreme importance to the electrochemical processes. The dissolved gases, with only  $\sim 0.8$  mM equilibrium concentration in water (standard conditions), have been attracted only limited attention. However, experimental evidence is growing in support of the critical role of dissolved gases at water interfaces, and particularly for hydrophobic/water interfaces.

In this work, we use high sensitivity atomic force microscopy (AFM) modes, including the frequency modulation (FM) and the PeakForce (PF) modes, to investigate the interface between water and a common hydrophobic electrode, highly ordered pyrolytic graphite (HOPG). We show that dissolved gas can accumulate and form an ordered layer at HOPG/water interface, even when the gas concentration is well below the saturation level<sup>[1-3]</sup>. When the gas concentration is high, various gas structures can be observed, including ordered adlayer(s), disordered pancake-like layer, and cap-shaped structures (nanobubbles). Since some of the common used electrode, such as gold, and graphite, have a certain degree of hydrophobicity, the effect of dissolved gas at the interface should be taken into account in electrochemical systems.

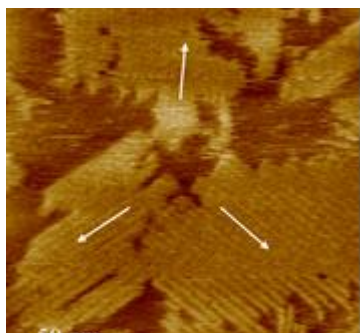


Figure 1 An AFM image of the HOPG/water interface showing an ordered layer of gas molecules when the gas concentration is low.

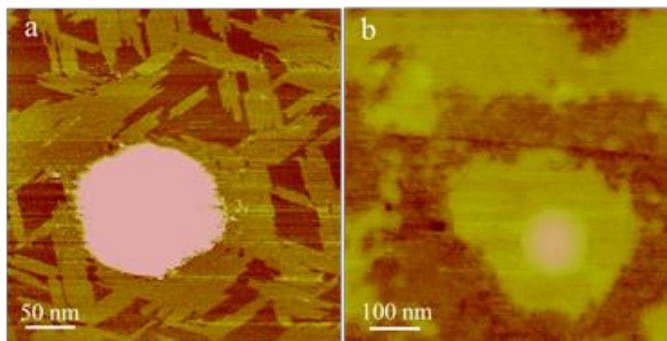


Figure 2 AFM Images of HOPG-water interfaces after the nitrogen (a) and oxygen (b) supersaturated water is deposited.

## References

- [1] Y. H. Lu, C. W. Yang and I. S. Hwang, *Langmuir* 2012, **28**, 12691.
- [2] Y. H. Lu, C. W. Yang and I. S. Hwang, *Appl. Surf.Sci.* 2014, **304**, 56.
- [3] Y. H. Lu, C. W. Yang, C. K. Fang, H. C. Ko, and I. S. Hwang, *Sci. Rep.* 2014, **4**, 7189.

# **Glow Discharge Optical Emission Spectroscopy Used for Film Formation studies on Graphite Electrodes**

Niloofer Ghanbari, Thomas Waldmann, Michael Kasper, Peter Axmann, Margret Wohlfahrt-Mehrens  
*Zentrum für Sonnenenergie- und Wasserstoff-Forschung, Baden-Württemberg,  
Helmholtzstrasse 8, D-89081 Ulm, Germany  
niloofer.ghanbari@zsw-bw.de*

Glow discharge optical emission spectroscopy (GD-OES) was introduced by Grimm in 1968<sup>1</sup>. It provides an elemental depth profile analysis of solid samples. Sensitivity to light elements such as Li and H, mitigated lattice damage, fast analysis, quantification of the recorded elemental intensity and the possibility to perform high resolution depth profiling as deep as ~100µm gives GD-OES some specific strengths compared with similar analytical methods (SIMS, XPS, and AES). Therefore, it is considered as a powerful tool in analyzing Li-ion battery electrodes since it presents a more clear view of “surface” and bulk and allows also a quantified analysis of surface inhomogeneities.

A more detailed understanding of the contribution of individual electrode reactions to the ageing of complete lithium ion batteries is absolutely necessary, in order to optimize both cell chemistry as well as battery management systems.<sup>2</sup> Post mortem analysis of lithium ion cells provides an insight into aging phenomena under different operation conditions, and leads to improving cell design and ensuring safe operation. Li deposition (plating) on graphite electrodes, which could take place upon anode polarization at low temperature and/or high cycling rate, is a crucial phenomenon with intense impact on cell capacity fading and safety. The study aims on the analysis of the film formed on graphite anodes under Li deposition conditions based on quantified depth profile analysis using GD-OES.

The GD-OES method is developed for graphite-based electrodes and calibrated for selected elements using lab coated samples. Beside model graphite electrodes, which have been cycled under well controlled conditions, electrode samples from “fresh” and aged commercial graphite/NMC cells have been investigated. The commercial cells have been aged at different C rates and low and high temperature (5°C and 45°C). The depth profile analysis shows low carbon and high Li content in the first ~10µm from the surface. These two elements help defining a border between “surface film” and “bulk”. The GDOES analysis shows significant differences in the depth profiles for lithium, carbon and phosphorous content. The results of various electrodes aged at different conditions are compared with a fresh graphite electrode of the same cell type and model electrodes for better comparison. This detailed analysis accompanied by electrochemical data, SEM imaging and data from conventional post mortem analysis reveals different mechanisms and localization of Li deposition on graphite during cycling with high C-rates at low and high temperatures.

1. Grimm, W. *Spectrochimica Acta Part B: Atomic Spectroscopy* **23**, 443–454 (1968).
2. Vetter, J. *et al. Journal of Power Sources* **147**, 269–281 (2005).

# **Spectroelectrochemical characterization of a salicylidene Ni(II) redox conducting polymer for supercapacitors**

Kamila Łepicka,<sup>1</sup> Piotr Pieta,<sup>1</sup> Paweł Borowicz,<sup>1</sup> Alexey Popov,<sup>3</sup> and Włodzimierz Kutner,<sup>1,2</sup>

*1. Institute of Physical Chemistry, Polish Academy of Sciences,  
Kasprzaka 44/52, 01-224 Warsaw, Poland*

*2. Faculty of Mathematics and Natural Sciences, School of Science, Cardinal Stefan Wyszyński University  
in Warsaw, Wóycickiego 1/3, 01-815 Warsaw, Poland*

*3. Leibniz Institute for Solid State and Materials Research Dresden (IFW Dresden) Dep. 14  
(Electrochemistry and Conducting Polymers), Helmholtzstrasse 20  
D-01069 Dresden, Germany*

*e-mail address:* [klepicka@ichf.edu.pl](mailto:klepicka@ichf.edu.pl)

A redox conducting poly[*meso-N,N'*-Bis-(salicylidene)-2,3-butanediaminonickel(II)] was synthesized by electrochemical polymerization. The resulting polymer film was highly conducting and stable with respect to potential multicycling under cyclic voltammetry conditions. The properties of the polymer were very promising for devising a new electrode material for supercapacitors. The UV-visible, FT-IR-ATR, and low-temperature ESR in situ spectroelectrochemical experiments unraveled both the charge transfer and polymerization mechanism of this polymer. With the low-temperature ESR measurements short-living paramagnetic transient species were detected and identified as bisphenolic radical cations. Moreover, structures responsible for the charge transfer in the polymer film were modeled with the quantum chemistry calculation method using density functional theory (DFT). The neutral polymer, bisphenolic dication, and bisphenolic radical cation were simulated as basic polymer building blocks consisting of two monomer units. Geometry of these structures in the ground state was DFT optimized with the B3LYP functional and the 6-31G basis. The excited state parameters were calculated on the ab-initio level by the time-dependent DFT (T-D DFT) method. Similarly as for the geometry optimization, the same B3LYP functional and basis set were applied. All the methods used were implemented in the Gaussian 09 software package [1].

[1] M.J. Frisch, et al., Gaussian 09, Gaussian, Inc., Wallingford, CT, USA, 2009.

***Ab initio* lattice stability of the  $x\text{Li}_2\text{MnO}_3 \cdot (1-x)\text{Li}(\text{Ni}_{1/3}\text{Mn}_{1/3}\text{Co}_{1/3})\text{O}_2$   
composite-layered cathode materials for lithium-ion batteries**

Yu-cheng Chuang<sup>a</sup>, Ping-chun Tsai<sup>a</sup> and Shih-kang Lin<sup>a,b,c,d,\*</sup>

<sup>a</sup>Department of Materials Science and Engineering, National Cheng Kung University, Tainan 70101, Taiwan; <sup>b</sup>Promotion Center for Global Materials Research, National Cheng Kung University, Tainan 70101, Taiwan; <sup>c</sup>Research Center for Energy Technology and Strategy, National Cheng Kung University, Tainan 70101, Taiwan; <sup>d</sup>Center for Micro/Nano Science and Technology, National Cheng Kung University, Tainan 70101, Taiwan

\*Corresponding author: E-mail: linsk@mail.ncku.edu.tw; Tel: +886-6-2757575 ext. 62970

**Abstract**

With today's great demand for energy, energy storage and its materials have become one of the most important technologies. Lithium ion batteries (LIBs) have high energy density and low environmental impact, and thus have drawn the most attentions among various energy storage technologies. Developing high capacity LIBs is the key for commercializing electrical vehicles and smart grids. The lithium-rich composite-layered oxide,  $x\text{Li}_2\text{MnO}_3 \cdot (1-x)\text{LiM}'\text{O}_2$ , where  $\text{M}'$  is transition metals, is a promising cathode material with high capacity. However, it has some native fatal weaknesses, including: (1) high initial irreversible capacity, (2) quick capacity fading, and (3) low rate capability, which greatly limit its range of applications. In this work, *ab initio* calculations based on density function theory were employed to simulate the lattice stability of  $x\text{Li}_2\text{MnO}_3 \cdot (1-x)\text{Li}(\text{Ni}_{1/3}\text{Mn}_{1/3}\text{Co}_{1/3})\text{O}_2$  composite-layered cathode materials. The atomistic models based on both monoclinic (C2/m) and rhombohedral (R3m) for the pristine  $\text{Li}_2\text{MnO}_3$  and  $\text{Li}(\text{Ni}_{1/3}\text{Mn}_{1/3}\text{Co}_{1/3})\text{O}_2$  phases were built. In addition, the atomistic models of composite-layered oxide with combinations of different individual structures and compositing ratios were examined. The optimized composite-layered oxide exhibits pseudo-rhombohedral or monoclinic-like structure, which agrees closely with experiments. The calculated X-ray diffraction patterns based the optimized structure also agrees closely with experiments. These findings clearly identify the fact that the major mechanism of capacity fading is lattice distortion. Finally, the convex hull calculation of lithiated composite-layered oxides was also performed to investigate the mechanism of Li-ion intercalation during charging/discharging. This paper proposes fundamental understandings of the  $x\text{Li}_2\text{MnO}_3 \cdot (1-x)\text{LiM}'\text{O}_2$  composite-layered oxides based on theoretical computations, which can provide guidance for developing novel high capacity cathode materials.

# In-situ monitoring of metal dissolution during anodisation of Al and Ti

J. P. Kollender<sup>1</sup>, A. I. Mardare<sup>1</sup>, A. W. Hassel<sup>1,2</sup>

<sup>1</sup>*Institute for Chemical Technology of Inorganic Materials*

<sup>2</sup>*CD-Laboratory for Combinatorial Oxide Chemistry*

*Johannes Kepler University Linz*

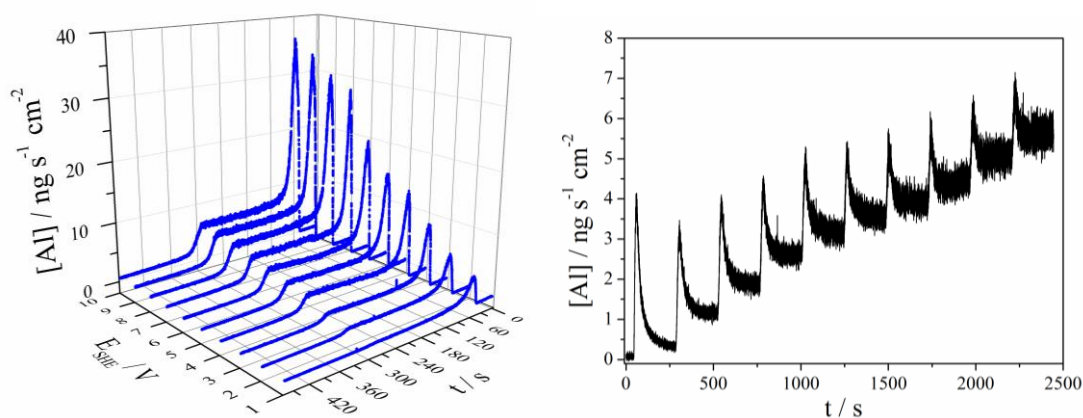
*Altenbergerstraße 69, 4040 Linz, Austria*

*jan.kollender@jku.at*

Aluminum and titanium are non-noble metals which are spontaneously reacting with water or oxygen forming aluminum oxide ( $\text{Al}_2\text{O}_3$ ) and titanium dioxide ( $\text{TiO}_2$ ). These thin passive layers are protecting the metals from further corrosion. The thickness of the passive layers can be artificially increased for improved corrosion and wear resistance using an electrochemical process called anodisation.

Many aspects of the oxide growth process during anodisation of Al and Ti have been investigated in the past. The most widely used model for description of the oxide growth mechanism during anodisation is the high field model [1]. One parameter that cannot be described by the high field model or any other existing model is the metal dissolution during oxide growth. Until now the metal dissolution during anodisation has also never been experimentally observed or quantified. To investigate this phenomenon a flow-type scanning droplet cell microscope (FT-SDCM) [2] which is directly coupled to inductively coupled plasma mass spectrometry (ICP-MS) was developed. This technique allows time resolved in-situ analysis of metal dissolution during anodisation.

Using this technique we investigated the time and potential dependent dissolution of Al during anodisation on individual spots (see left image) and during stepwise potential growth on a single addressed spot (see right image). During all experiments it was observed that an overshoot in Al dissolution occurs during the initial stage of oxide growth. After the initial oxide growth the dissolution rate stabilized into a constant plateau (transpassive dissolution) for all investigated potentials. It was further observed that the transpassive dissolution rate in case of Al linearly depends on the applied potential. In case of Ti an overshoot in metal dissolution during initial oxide growth was also observed, but at a significantly lower rate. Unlike Al, Ti showed no significant transpassive dissolution, indicating a much higher stability of titanium dioxide compared to aluminum oxide.



[1] M. M. Lohrengel, *Mater. Sci. Eng. R.* **11** (1993) 243

[2] J. P. Kollender, A.I. Mardare, A. W. Hassel et al., *J. Electroanal. Chem.* **740** (2015) 53

# ATR-SEIRAS and Electrochemical Study of the Tautomeric Equilibrium of Adsorbed Thymine on Gold Electrodes

Manuela Rueda<sup>(a)</sup>, Francisco Prieto<sup>(a)</sup>, Julia Alvarez-Malmagro<sup>(a)</sup>, Jose M. Ors<sup>(b)</sup>

a) Department of Physical Chemistry University of Seville

c/ Profesor García González 2. 41012 Seville. Spain

b) Department of Physical Chemistry and Institute of Electrochemistry.

University of Alicante. Ap. 99, E-03080, Alicante. Spain

marueda@us.es

The combination of electrochemical methods with modern in-situ Fourier infrared techniques can provide microscopic information about the orientations and interactions of adsorbed molecules on electrode surfaces [1]. The adsorption of thymine on electrodes is interesting because as a DNA base (complementary of adenine) this molecule plays important roles in genetic expression and replication in well organised biological interfaces, which presents similar characteristics as the electrode interfaces. The molecule can adopt different tautomeric forms, depending on the pH of the solution but the preponderance of them at the interfaces can be affected also by the electric field. The study of the influence of pH and electric potential on the tautomeric equilibrium can have epigenetic implications because it is known that unstable tautomeric forms can induce unpaired bases interactions which seem to be related with some illness.

Thymine adsorption on gold electrodes has previously been studied and different electric potential regions were identified at which physical or chemical adsorptions take place. Under some conditions characteristic transition of phase peaks were observed delimiting potential regions with different organised surface structures [2,3]. It was proposed that thymine gets deprotonated when adsorbed on the electrode, even at low pH values. It is known that in solution two thymine forms are related by one acid-base equilibrium ( $pK_a$  value 9.5) but each of them can present also enol-imino tautomeric forms [4].

In this communication, the advantages of the ATR-SEIRAS technique to determine the structures at electrode surfaces are exploited in order to establish the nature of the different organisations of thymine on gold electrodes as a function of pH and potential. Experiments have been performed in the pH range 1 to 12 in perchlorate and either perchloric acid/or sodium hydroxide solutions, using  $H_2O$  and  $D_2O$  as solvents. Thin-film gold electrodes prepared by sputtering were used as working electrodes and some complementary electrochemical and SNIPTIRS experiments have been performed using Au(111) electrodes.

The analysis of the characteristic bands in the  $1200$  to  $1800\text{ cm}^{-1}$  spectral region is used to identify the two tautomers of the deprotonated molecule. The assignments of the most stable tautomers are confirmed by DFT calculations that optimise the geometry of the adsorbed molecule on Au(111) surfaces. A semi-quantitative analysis of the orientation of each tautomer as a function of potential has also been performed on the base of the ratio between two characteristic stretching signals in the  $2500$  to  $3500\text{ cm}^{-1}$  spectral region. The results are discussed in relation to the effect of the electric field on the permanent dipole of the tautomeric adsorbed forms.

## References

- 1.- M. Osawa, in: C. Alkire, D. Kolb, J. Lipkowski, P.N. Ross (Eds.), *Diffraction and Spectroscopic Methods in Electrochemistry*, vol. 9, Wiley-VCH, Weinheim, 2006, pp. 269–314.
- 2.- B. Roelfs, E. Bunge, C. Schröter, T. Solomun, H.Meyer, R.J. Nichols, H. Baumgärtel; *J. Phys.Chem. B* 101 (1997) 754
- 3.- W. Haiss, B. Roelfs, S.N. Port, E. Bunge, H. Baumgärtel, R.J. Nichols; *J. Electroanal. Chem.* 454 (1998) 107.
- 4.- G. N. Ten and V. I. Baranov; *J. Struct. Chem.* 50 (1) (2009) 90.



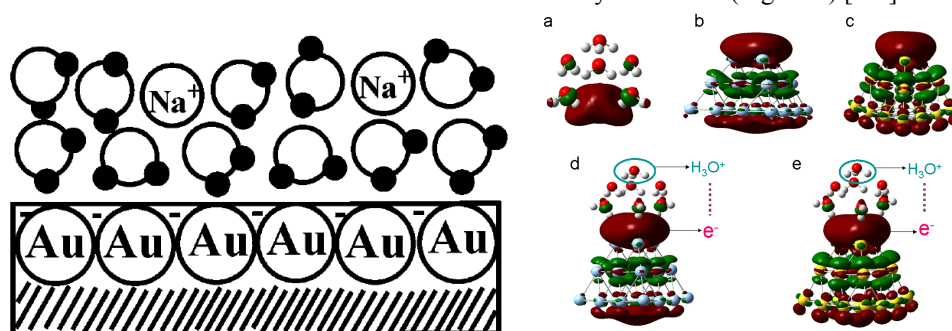
# Adsorption and Photocatalytic Hydrogen Evolution Reactions of Water on Silver and Gold Cathodes: DFT and SERS Study

Ran Pang, De-Yin Wu, Zhong-Qun Tian

*State Key Laboratory for Physical Chemistry of Solid Surfaces, Xiamen University, Xiamen 361005, China; College of Chemistry and Chemical Engineering, Xiamen University  
Siming Nanlu 422, Xiamen 361005, China  
dywu@xmu.edu.cn*

To study water in electrochemical interfaces plays important roles not only the most usual solvent but also energy source and environment fields. Hydrogen evolution reaction is one of the most fundamental electrochemical reactions in electrode/aqueous solution interfaces and strongly depends on experimental conditions, such as electrode materials, light irradiation, and containing organic molecules electrolytes [1]. The reaction mechanisms elucidated before are all based on the two-step mechanism of Volmer, and Tafel or Heyrovsky reactions so far. Nanoscale noble metals display special catalyst in light splitting water reaction for its high efficiency and environment friendly and the surface plasmon resonance in the visible region.

In this paper, we proposed a novel intermediate for photocatalytic hydrogen evolution reaction on silver and gold cathodes by a combining study of surface spectroscopy and quantum chemical calculations with the density functional theoretical methods and metallic cluster models. Water and hydronium ion adsorbs on metal cathodes with an embedded layer of water (Figure 1) [2-4].



According to the calculated results, water molecules approach to metal cathodes by the hydrogen atoms. As for hydrated protons, the surface electron-hydronium ( $e^- \cdots H_3O^+$ ) ion pair can be formed on the metal cathodes. Under the irradiation of light, the surface bound electrons are excited and devote to the reduction reaction, with a structural relaxation from Eigen-type proton to hydrated hydrogen atoms, i.e., a stepwise pathway as Eigen  $\rightarrow$  Zundel  $\xrightarrow{+e^-}$  H. The relaxation process of the  $e^- \cdots H_3O^+$  ion pair happens in the solution side rather than hydrogen directly at adsorbed sites on the surface of silver/gold nanoparticles. Finally they recombined to hydrogen molecules. Additionally, we calculated surface-enhanced Raman scattering (SERS) spectra of adsorbed water molecules and the interfacial  $e^- \cdots H_3O^+$  ion pairs, indicating the SERS spectroscopy is a powerful technique to characterize surface species in photocatalytic hydrogen evolution reactions.

## References

1. D. Y. Wu, J. F. Li, B. Ren, Z. Q. Tian, *Chem. Soc. Rev.*, 2008, 37, 1025.
2. J. F. Li, Y. F. Huang, S. Duan, R. Pang, D. Y. Wu, B. Ren, X. Xu, Z. Q. Tian, *Phys. Chem. Chem. Phys.* 2010, 12, 2493.
3. D. Y. Wu, S. Duan, X. M. Liu, Y. C. Xu, Y. X. Jiang, B. Ren, X. Xu, S. H. Lin, Z. Q. Tian, *J. Phys. Chem. A*, 2008, 112, 1313.
4. R. Pang, L. J. Yu, D. Y. Wu, B. W. Mao, Z. Q. Tian, *Electrochim. Acta*, 2013, 101, 272.

**Acknowledgement(s)** Financial supports from National Science Foundation of China (Nos. 21373172 and 21321062 and 91027009) are highly acknowledged.

# Electrochemical Tip-Enhanced Raman Spectroscopy (EC-TERS)

Bin Ren, Zhi-Cong Zeng, Sheng-Chao Huang, Teng-Xiang Huang, Jin-Hui Zhong, Mao-Hua Li, Xiang Wang

*State Key Laboratory of Physical Chemistry of Solid Surface, Collaborative Innovation Center of Chemistry of Energy Materials (iChEM), Department of Chemistry, College of Chemistry and Chemical Engineering, Xiamen University, Xiamen 361005, China  
E-mail: bren@xmu.edu.cn*

Tip-enhanced Raman spectroscopy (TERS) can not only provide very high sensitivity but also high spatial resolution, and has found applications in various fields, including surface science, materials, and biology. Most of previous TERS studies were performed in air or in the ultrahigh vacuum. If TERS study can be performed in the electrochemical environment, the electronic properties of the surface can be well controlled so that the interaction of the molecules with the substrate and the configuration of the molecules on the surface can also be well controlled.

However, the EC-TERS is not just a simple combination of electrochemistry with TERS, or the combination of EC-STM with Raman. It is a merge of STM, electrochemistry and Raman spectroscopy, and the mutual interference among these techniques makes the EC-TERS particularly challenge: the light distortion in EC system, the sensitivity, the tip coating to work under EC-STM and retain the TERS activity and cleanliness.

We designed a special spectroelectrochemical cell to eliminate largely the distortion of the liquid layer to the optical path. We have been able to obtain TER spectra of reasonably good signal to noise ratio for surface adsorbed molecules under electrochemical potential control. For example, potential dependent TERS signal have been obtained for adsorbed aromatic thiol molecule, and much obvious signal change compared with SERS has been found, manifesting the importance of EC-TERS to reveal the interfacial structure of an electrochemical system. Furthermore, we are able to detect the potential dependent surface photochemical reaction on the single crystal surface. More systems will be discussed during the talk.

The success in constructing the EC-TERS offers us an opportunity for investigation of electrochemical interfaces by vibrational spectroscopy with unprecedented spatial resolution and molecular fingerprints.

Acknowledgement: Financial supports from MOST (2011YQ03012406) and NSFC (21227004 and 21321062), and MOE (IRT13036) are highly acknowledged.

# Electrochemical interrogation of the structure of self-assembled monolayers on nanofabricated metallic nanowires

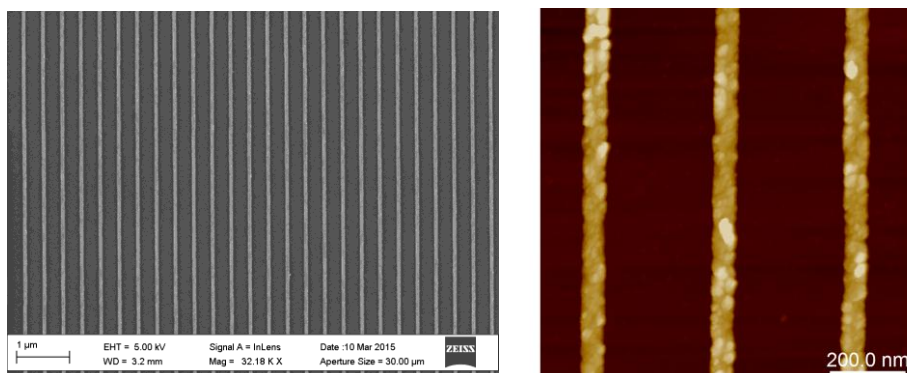
D. William A. Morton, A. Giles Davies, Christoph Wälti  
*School of Electronic and Electrical Engineering, University of Leeds*  
*Woodhouse Lane, Leeds LS2 9JT, UK*  
*mt09dwm@leeds.ac.uk*

With the recent advancement of ultrahigh-resolution patterning techniques, such as electron beam and extreme ultraviolet lithography, now enabling the fabrication of devices with typical feature sizes significantly less than 100 nm, nanostructured metallic structures are becoming increasingly important in a number of areas. Such structures have proven to be particularly popular as interfaces between solid-state devices and molecular or biological molecules. The nanostructured electrodes are often functionalized with self-assembled monolayers (SAMs), for instance to attach biological molecules. Very popular examples where such functionalized metallic nanostructures are employed are nanowire-based biosensors.

While the fabrication of the nanostructures as well as their electronic properties are relatively well understood, the understanding of the influence of the nanostructure on the structure and order of the SAM is still in its infancy. Any inconsistency in the properties of the SAM, such as increased leakage current due to disorder in the SAM, will be significant, and hence it is essential to understand the impact of the nanostructure on the assembly and structure of SAMs.

To establish a more detailed understanding of the impact these nanostructures have, we have fabricated arrays of gold nanowires of different dimensions using electron beam lithography (EBL) (nanowire widths 40 – 100 nm, array spacings 300 nm – 3 µm). These nanowire arrays were functionalized with well-packed SAMs of mercapto-alkanes of varying length. Through careful definition of the width and height of the nanowires, the impact of the edges of the metallic structures (the “edge effect”), which induce disorder in the SAM as the SAM formed on sharp topological features of the structures is not well-packed, can be maximized. Electrochemical analytical techniques are very well suited to interrogate this disorder in the SAM. We used a combination of cyclic voltammetry (CV), electrochemical impedance spectroscopy (EIS) and chronoamperometry (CA) in Faradaic solutions to understand qualitatively the level of disorder in the monolayer as a function of nanowire dimensions and SAM molecule length. In addition, we used atomic force microscopy (AFM) and scanning electrochemical microscopy (SECM) to image directly and quantitatively analyze this disorder.

We found that the greatest disorder was induced in the SAM on the smallest fabricated nanowires (40 nm wide and 30 nm high), where edge effects are most prominent. This was established through equivalent circuit, such as Randles circuit, analysis, where a greater disorder was associated with a higher concentration of pinhole-like defects in the SAM, manifested in increasing leakage current. We found the shortest SAM molecule studied ( $\text{CH}_3(\text{CH}_2)_8\text{SH}$ ) exhibited the greatest disorder on all nanowire dimensions, and the leakage current was found to decrease with increasing SAM molecule length. Negligible leakage current was measured for SAMs formed from molecules with lengths above a certain threshold. These findings are corroborated by AFM and SECM imaging.



SEM and AFM image of an array of EBL patterned nanowires.

# Electrochemical Adsorption and Surface-Enhanced Raman Spectroscopy on Nanostructured Electrodes

De-Yin Wu, Yuan-Fei Wu, Zhong-Qun Tian

*State Key Laboratory for Physical Chemistry of Solid Surfaces, Xiamen University, Xiamen 361005, China; College of Chemistry and Chemical Engineering, Xiamen University  
Siming Nanlu 422, Xiamen 361005, China  
dywu@xmu.edu.cn*

Surface-enhanced Raman spectroscopy (SERS) with high detection sensitivity is a powerful tool for characterization of probe molecules on electrode surfaces. High quality Raman signals provide not only adsorption orientation but also chemical bonding interaction between molecules and electrode surfaces with applied potentials. In electrochemical interfaces, the photo-driven charge transfer can happen at the proper excitation light to significantly enhance Raman intensities along selectively vibrational modes. Thus the SERS signals of these specific vibrational probes can be used to explore low-lying excited states and the complex interaction between electrode surfaces and different lights under applied potentials. Pyridine is one of the best typical modeling molecules in electrochemical SERS fields. In previous studies, we have investigated the SERS of pyridine adsorbed on silver and gold and other transition metal electrodes dependent on the potential energy surface of excited charge transfer states. There are four vibrational modes display strongly potential-dependent SERS effect on the surface electronic structures and chemical adsorptions. For example, when pyridine adsorbed on a silver electrode, there are four strong Raman peaks at 1008, 628, 1590, and 1215  $\text{cm}^{-1}$  arising from the ring breathing mode ( $\nu_1$ ), the ring deformation ( $\nu_{6a}$ ), and the ring C-C stretching vibration ( $\nu_{8a}$ ) and the C-H in-plane bending vibration ( $\nu_{9a}$ ) at -0.6 ~ -0.8 V vs SCE.

To understand the photo-driven charge transfer mechanism in electrochemical SERS, we have calculated the potential energy curves of the low-lying excited states on the basis of density functional theoretical (DFT) method. Specifically, the hybrid functional approach B3LYP was combined with the basis sets of 6-311+G\*\* for elements C, N, O, S and H, as well as LANL2DZ pseudopotential basis set for silver and gold. The time-dependent DFT (TDDFT) was used to calculate the excited states, which chemically contribute to the Raman intensity enhancement. The charge transfer enhanced mechanism also depends on metal property, such as silver and gold electrodes and the electric field in double electric layers. We discuss the electric and vibrational Stark effect on the Raman signal. Next, we further explore the anchor group effect on the charge transfer enhancement mechanism in 4-mercaptopyridine adsorbed on silver electrodes. Our result showed that the charge transfer direction from the probe molecule to silver surfaces when 4-mercaptopyridine binds to silver through its thiol sulfur. However, when pyridine ring nitrogen also approaches to the silver surfaces. The charge transfer energy significantly decreases to ~2.0 eV, matching to the photonic energy used in usual SERS measurements. In the case, the charge transfer mechanism may be switched from surface silver to pyridine ring moiety. Therefore, we suggested the electrochemical SERS can be used to explore some excited states related to the photo-driven charge transfer process.

**Acknowledgement(s)** Financial supports from National Science Foundation of China (Nos. 21373172 and 21321062 and 91027009) are highly acknowledged.

## References

- [1] M. T. Lee, D. Y. Wu, Z. Q. Tian, S. H. Lin, *J. Chem. Phys.*, 122 (2005) 094719.
- [2] D. Y. Wu, X. M. Liu, S. Duan, X. Xu, B. Ren, S. H. Lin, Z. Q. Tian, *J. Phys. Chem. C*, 112 (2008) 4195.
- [3] S. Tao, L. J. Yu, R. Pang, Y. F. Huang, D. Y. Wu, Z. Q. Tian, *J. Phys. Chem. C*, 117(2013) 18891.
- [4] D. Y. Wu, X. M. Liu, Y. F. Huang, B. Ren, X. Xu, Z. Q. Tian, *J. Phys. Chem. C* 113(2009) 18212.

# Self-Organized TiO<sub>2</sub> Nanotubes: Influence of Ti substrates

J.M. Macak<sup>\*,a</sup>, P. Knotek<sup>b</sup>, H. Söpha<sup>a</sup>, M. Krbal<sup>a</sup>, J. Subrt<sup>c</sup>, M. Klementova<sup>c</sup>

<sup>a</sup> Center of Materials and Nanotechnologies, Faculty of Chemical Technology, University of Pardubice  
Nam. Cs. Legii 565, 530 02 Pardubice, Czech Republic

<sup>b</sup> Dep. of General and Inorganic Chemistry, Faculty of Chemical Technology, University of Pardubice  
Studentska 573, 532 10 Pardubice, Czech Republic

<sup>c</sup> Institute of Inorganic Chemistry of AS CR, Husinec-Rez 1001, 25068 Rez, Czech Republic  
<sup>\*</sup>jan.macak@upce.cz

Synthesis of highly-ordered nanostructures of valve metal oxides has recently attracted huge scientific and technological interest motivated by their possible use in many applications. The nanoporous Al<sub>2</sub>O<sub>3</sub> – most established member of this group of materials – has been prepared by anodic oxidation of Al under suitable electrochemical conditions two decades ago into perfectly ordered, honeycomb-like porous structures (1). Owing to the flexibility of the pore diameter/length and the relative ease of the Al<sub>2</sub>O<sub>3</sub> dissolution, its porous membranes have been since then widely used as template material of the choice for a range of materials (2-4).

It is the TiO<sub>2</sub> that has received the highest attention after Al<sub>2</sub>O<sub>3</sub> motivated by its range of applications, including photocatalysis, water splitting, solar cells and biomedical uses. Very significant research efforts have led to reproducible synthesis of self-organized TiO<sub>2</sub> nanotube layers by means of anodic oxidation, during which the starting Ti substrate is converted into highly-ordered nanotubular layer by anodization in suitable electrolytes (5-7). Although advancements in the anodic synthesis of self-organized TiO<sub>2</sub> nanotube layers have been presented over past years (8), as shown in Fig. 1a, the degree of ordering has not reached so far the level known from porous alumina (1). Numerous factors influence the ordering and the homogeneity of the TiO<sub>2</sub> nanotube layers.

In the presentation, we aim to demonstrate significant advancements in the ordering of anodic TiO<sub>2</sub> nanotubes compared to known state-of-art. Utilizing AFM, SEM and optical measurements, we will show how to obtain via tailored anodization protocols a very decent degree of uniformity and homogeneity of the nanotube layers, as shown on Fig. 1b (9). Moreover, based on SEM, EBSD and TEM measurements, we will demonstrate how the Ti grain structure influences the lateral uniformity of the nanotube layers (10).

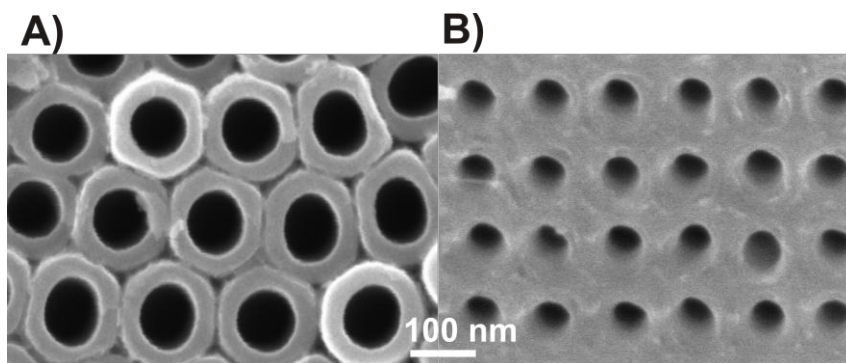


Fig. 1 Anodic TiO<sub>2</sub> nanotube layers ordered on a smaller (a) and larger (b) scale.

## References

1. H. Masuda, K. Fukuda, Science, 268 (1995) 1466.
2. K. Nielsch, F. Müller, A.-P. Li, U. Gösele, Adv. Mater. 12 (2000) 582
3. H. Asoh et al., J. Electrochem.Soc. 148 (2001) B152.
4. J. Kolar, J. M. Macak, K. Terabe, T. Wagner, J. Mater. Chem. C, 2 (2014) 349.
5. J. M. Macak, H. Tsuchiya, P. Schmuki, Angew. Chem. Int. Ed. 44 (2005) 2100.
6. J.M. Macak et al., Curr. Opin. Solid State Mater. Sci. 1-2 (2007) 3.
7. K. Lee, A. Mazare, P. Schmuki, Chem. Rev. 114 (2014) 9385
8. J.M. Macak, S. P. Albu, P. Schmuki, Phys. Stat. Sol. (RRL) 1 (2007) 181.
9. J. M. Macak et al., Electrochim. Acta, to be submitted.
10. J. M. Macak et al., J. Electroanal. Chem., to be submitted.



# Tailoring properties of Pt nanoparticles electrocatalysts towards ethanol oxidation: surface-structure, particles dispersion and pH effect

Carlos Busó-Rogero, Jose Solla-Gullon, Francisco J. Vidal-Iglesias, Enrique Herrero, Juan M. Feliu  
*Instituto de Electroquímica, Universidad de Alicante*  
*Apdo. 99, E-03080 Alicante, Spain*  
*carlos.buso@ua.es*

Nowadays, ethanol has an increasing interest for its use as a fuel in the fuel cell technology, due to some environmental and energetic advantages respect to similar small alcohols molecules. In addition, the higher activity for ethanol oxidation observed in alkaline solutions together with the appearance of new alkaline membranes have triggered the studies at higher pHs with the aim of improve the selectivity to CO<sub>2</sub>. As a catalyst, platinum presents the best behavior among pure metals this reaction. However, the higher cost of the material has induced the use of nanoparticles, which optimizes the active area of catalyst using lower amounts of platinum.

It is well-known the dependence of ethanol oxidation reaction with the surface structure orientation of platinum. In acidic solutions, (100) surfaces favors the C-C bond scission producing the complete oxidation to CO<sub>2</sub>, in spite of the CO formation that poison the catalytic surface. In (111) domains, only the incomplete oxidation to acetic acid is observed [1]. These tendencies are also observed for preferentially oriented platinum nanoparticles [2]. To promote the CO<sub>2</sub> formation and to facilitate the oxidation of CO, foreign atoms are adsorbed on the Pt surface, transferring to the CO molecule the oxygen group necessary to complete the oxidation until CO<sub>2</sub> [3]. Additionally, if larger loadings of nanoparticles are confined in a small support, aggregation problems can occur, which leads to lower catalytic activities [4]. For this reason, it is important control the nanoparticles dispersion around the support for ensure the correct behavior of the catalyst.

In this communication, the ethanol oxidation reaction is studied in shape-controlled platinum nanoparticles with several adsorbed atoms, trying to obtain the better combination nanoparticle orientation/adatom for achieving the highest activity at lower potentials. In addition, the dispersion of nanoparticles is also controlled for prevent aggregation problems. Electrochemical techniques (cyclic voltammetry and chronoamperometry) are used for characterize the reactivity for the ethanol electrooxidation.

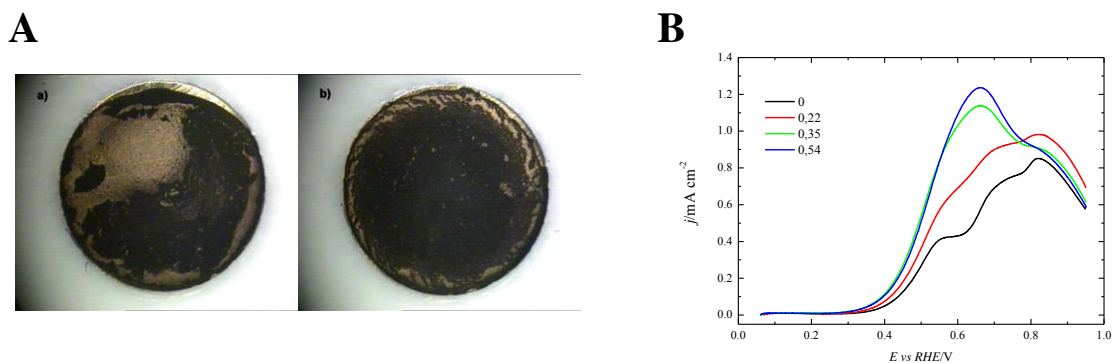


**Figure 1:** (A) Difference between a non-disperse (a) and disperse (b) nanoparticles deposit in a gold support. (B) Cyclic voltammetry response for (111) Pt nanoparticles with different Sn coverage in 0.2 M ethanol + 0.5 M H<sub>2</sub>SO<sub>4</sub> at 0.02 V s<sup>-1</sup>.

## References

- [1] F. Colmati *et. al.*, Faraday Discuss., 140 (2008) 379.
- [2] C. Buso-Rogero *et. al.*, Journal of Materials Chemistry A, 1 (2013) 7068.
- [3] V.P. Santos *et. al.*, Electrochim. Acta, 52 (2007) 2376.
- [4] S. Chumillas *et. al.*, Electrochem. Commun., 13 (2011) 1194.

# Potential-Dependent Structure of [BMIM]<sub>(1-x)</sub>Li<sub>x</sub>[FSA] on a Gold Electrode: A Surface-Enhanced Infrared Study

K. Uchida<sup>1</sup>, K. Motobayashi<sup>1</sup>, K. Minami<sup>2</sup>, N. Nishi<sup>2</sup>, T. Sakka<sup>2</sup>, and M. Osawa<sup>1</sup>

<sup>1</sup>Catalysis Research Center, Hokkaido University

Sapporo 001-0021, Japan

<sup>2</sup>Graduate School of Engineering, Kyoto University

Kyoto 615-8510, Japan

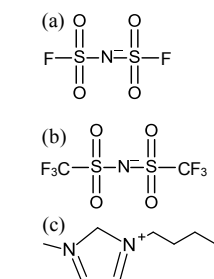
kmotobayashi@cat.hokudai.ac.jp

Room temperature ionic liquids (RTILs) are promising electrolyte materials for Li ion batteries and other electrochemical devices due to high ionic conductivity and wide electrochemical windows. It has been reported that the cathodic decomposition potential of the FSA-based RTIL is less negative than that of TFSA-based RTIL when Li salt is added,<sup>1</sup> despite the similar chemical structures of FSA and TFSA anions (Fig.1). A mechanism for stabilization of the FSA-based RTIL on the electrode involving an interfacial structure of the RTIL has been proposed;<sup>1</sup> however, direct observation using spectroscopic techniques is required to understand the details. Surface-enhanced infrared absorption spectroscopy (SEIRAS) that can selectively probe solid/liquid interfaces is suited for this purpose as represented in our recent studies on the potential-dependent behavior of a pure TFSA-based RTIL on an Au electrode using this method.<sup>2</sup> In the present work, we investigated the effect of Li ion on the potential-dependent structure of [BMIM][FSA] (Fig.1) on an Au electrode by using SEIRAS as a function of Li<sup>+</sup> concentration.

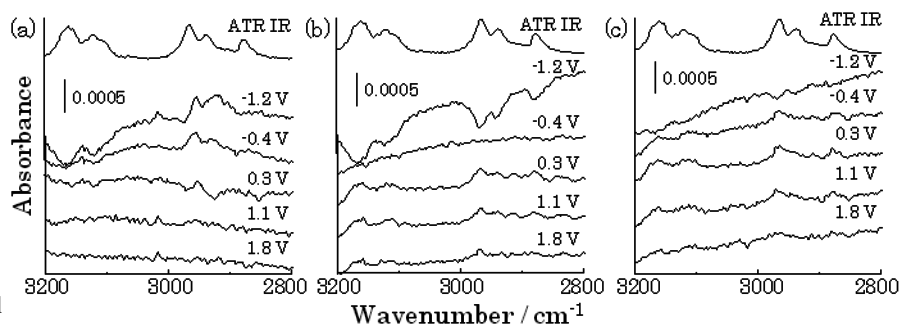
SEIRAS experiments have been performed on an Au thin film electrode chemically deposited on a Si prism in a vacuum-compatible glass cell. The electrode potential was controlled by a potentiostat against a Pt quasi-reference electrode and corrected by the redox potential of Fc/Fc<sup>+</sup> couple. LiFSA is added to [BMIM][FSA] to control the concentrations of Li<sup>+</sup>. SEIRAS measurements have been performed during potential scans where the deposition of Li does not occur.

Figure 2 shows potential-dependent SEIRA spectra of the [BMIM][FSA]/Au electrode at various Li concentrations. For pure [BMIM][FSA] (Fig. 2a), negative absorption bands at 3200-3000 cm<sup>-1</sup> assigned to C-H stretch modes of imidazolium ring of the cation  $\nu(\text{CH})_{\text{ring}}$  and positive bands at 3000-2840 cm<sup>-1</sup> assigned to those of alkyl group  $\nu(\text{CH})_{\text{alkyl}}$  are observed at negative potentials. This indicates, as reported previously for [BMIM][TFSA],<sup>2</sup> that the orientation of the imidazolium ring changes from a perpendicular orientation to a more flat one on the basis of the surface selection rule in SEIRAS: the vibrations that yield oscillating dipoles perpendicular to the surface are selectively observable. For [BMIM][FSA] with 10 % Li salt (Fig. 2b), on the other hand, negative absorption bands of both  $\nu(\text{CH})_{\text{ring}}$  and  $\nu(\text{CH})_{\text{alkyl}}$  are observed at negative potentials, suggesting that BMIM cations move further away from the electrode although electrode is negatively charged. A possible interpretation is that decomposition products of [BMIM][FSA] formed at negative potentials inhibit cations from approaching to the electrode and dissolve at positive potentials. For [BMIM][FSA] with 20 % Li salt (Fig. 2c), very small absorption bands of  $\nu(\text{CH})_{\text{ring}}$  and  $\nu(\text{CH})_{\text{alkyl}}$  suggest that BMIM cations exist much further away from the electrode than in the case of 10 %. Potential-dependent behavior of anions and solvation of Li<sup>+</sup> will be also reported in the presentation.

<sup>1</sup>M. Yamagata et al., *Electrochim. Acta* 110, 181 (2013). <sup>2</sup>K. Motobayashi et al., *J. Phys. Chem. Lett.* 4, 3110 (2013).



**Figure 1.** The chemical structures of (a) [FSA], (b) [TFSA], and (c) [BMIM].



**Figure 2.** SEIRA spectra of [BMIM][FSA]/Au at Li molar ratio of (a) 0, (b) 10, and (c) 20 % recorded during the negative-going potential scans at 2 mV/s. The reference spectra were recorded at 1.8 V vs Fc/Fc<sup>+</sup> for each concentration.



# Electrocatalysis of Formic Acid Oxidation on Gold and Platinum: Where Does the Crucial Activity Difference Come From?

Momo Yaguchi<sup>1</sup>, Marc T. M. Koper<sup>2</sup> and Masatoshi Osawa<sup>1</sup>

<sup>1</sup>Catalysis Research Center, Hokkaido University, Sapporo 001-0021 Japan

<sup>2</sup>Leiden Institute of Chemistry, Leiden University, 2300 RA Leiden, The Netherlands  
myaguchi@cat.hokudai.ac.jp

## I. Introduction

The electrocatalytic oxidation of formic acid has been the subject of intense investigations due to its importance in understanding the oxidation of small organics utilized as fuels in low-temperature fuel cells. It is widely accepted that formic acid is oxidized through the so-called ‘dual-pathway’ mechanism; the direct pathway via a reactive intermediate, and the indirect pathway via CO. The reaction kinetics and the chemical nature of the reactive intermediates, however, have been remained uncertain. Joo et al.<sup>[1]</sup> was the first to investigate the formic acid oxidation on Pt over various electrolyte pH, from acid through alkaline, and demonstrated that formate ion is the dominant reactant even in acidic media (note that the  $pK_a$  of formic acid is 3.75). Au is less active than Pt and thus the formic acid/formate oxidation takes place moderately, which allows us to study the reaction mechanism more in detail with no interference from the poisoning species (CO). In this work, we have systematically examined the formic acid oxidation on Au under wide range of electrolyte pH by cyclic voltammetry and *in-situ* attenuated total reflection-surface enhanced infrared absorption spectroscopy (ATR-SEIRAS) with aiming for identifying the nature of the reactive intermediates. The results are compared with those obtained on Pt, which would help reveal the origin of the difference in catalytic activity.

## II. Experimental

All electrochemical and ATR-SEIRAS measurements were carried out in conventional three-electrode glass cells at room temperature. Phosphate buffer solutions were used as the supporting electrolytes. The working electrodes were the polycrystalline Au and Pt disk electrodes for the RDE experiments and the chemically deposited polycrystalline Au and Pt thin-film electrodes for the ATR-SEIRAS experiments. A large platinum foil served as the counter electrode, and the reference electrode was the silver/silver chloride electrode (Ag/AgCl/sat. KCl). All potentials were converted to RHE scale.

## III. Results and Discussion

On Au, an oxidation peak was observed at  $\sim 1.0$  V in both the forward and the following backward scans. An additional peak was also observed at  $\sim 1.5$  V as a shoulder only in the forward scan. In Fig. 1, the current densities (at 1.0 V in the backward scan) for the oxidation of 0.5 M formic acid/formate in 0.1M phosphate buffer solutions are plotted against the electrolyte pH. It exhibits a volcano-shaped dependence and the maximum current density is achieved at pH  $\sim 5$ . In the ATR-SEIRA spectra, the band attributed to the adsorbed bridge-bonded formate (b-HCOO<sub>ads</sub>) was observed at  $1330\text{ cm}^{-1}$ . The integrated intensity of this band displayed similar pH dependence to Fig.1. The drastic reduction of current density in alkaline region seems to be related to the strong adsorption of  $\text{HPO}_4^{2-}$ . Considering the effect of anion adsorption from the electrolyte, other buffer solutions composed of weakly adsorbed anions were employed. It was found that the point where the current density or the band intensity of b-HCOO<sub>ads</sub> starts to decrease was extended toward higher pH region. Overall, it turns out that the current density is associated with the b-HCOO<sub>ads</sub> band intensity, suggesting that, unlike on Pt<sup>1</sup>, the adsorbed bridge-bonded formate plays a significant role as a reactive intermediate or a promotor in the dominant reaction pathway on Au, which eventually would result in the difference between Au and Pt as a catalyst.

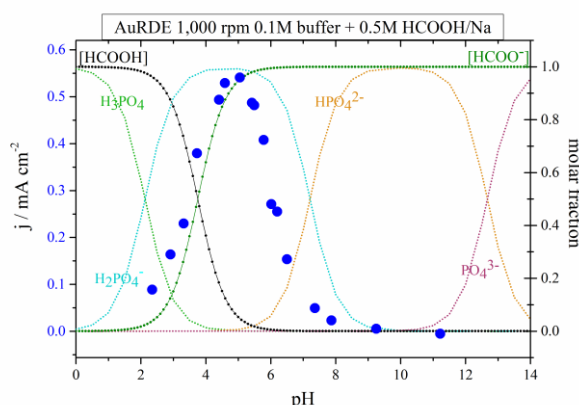


**Fig.1.** pH dependence of the current density for formic acid/formate oxidation on a gold RDE in phosphate buffer solution.

[1] J. Joo, T. Uchida, A. Cuesta, M.T.M. Koper, M. Osawa, Importance of acid-base equilibrium in electrocatalytic oxidation of formic acid on platinum, J. Am. Chem. Soc. 135 (2013) 9991.

# ***In Situ* X-ray Absorption Fine Structure Spectroscopy of Dinuclear Copper Catalyst under Oxygen Reduction Reaction Conditions**

Masaru Kato,<sup>1</sup> Ken'ichi Kimijima,<sup>2</sup> Mari Shibata,<sup>2</sup> Hideo Notsu,<sup>2</sup> Kazuya Ogino,<sup>2</sup> Kiyoshi Inokuma,<sup>2</sup>  
Narumi Ohta,<sup>2</sup> Hiromitsu Uehara,<sup>1</sup> Yohei Uemura,<sup>1</sup> Nobuhisa Oyaizu,<sup>1</sup> Tadashi Ohba,<sup>1</sup> Satoru  
Takakusagi,<sup>1</sup> Kiyotaka Asakura,<sup>1</sup> Ichizo Yagi<sup>1</sup>  
<sup>1</sup>Hokkaido University and <sup>2</sup>FC-Cubic TRA  
<sup>1</sup>N10W5, Kita-ku, Sapporo 060-0810, Japan and <sup>2</sup>2-3-26 Aomi, Koto-ku, Tokyo, 135-0064, Japan  
masaru.kato@ees.hokudai.ac.jp

The oxygen reduction reaction (ORR) occurs at the cathode in polymer electrolyte fuel cells (PEFCs) and its sluggish kinetics is one of the limiting factors for the performance of PEFCs. Although platinum-based ORR catalysts are used in the state-of-the-art PEFCs, they still have high overpotential (>200 mV). In nature, on the other hand, it is known that enzymes such as multi-copper oxidases catalyze ORR with almost no overpotential (ca. 20 mV), where a catalytic active center with a multinuclear copper complex is found.<sup>[1-2]</sup> Although these enzymes show such high ORR activity, enzymes are not suitable for use in practical PEFCs since enzymes are easily denatured and their footnotes are large, resulting in low stability and low current density output, respectively. Thus, it is highly desirable to design and develop robust artificial ORR catalysts with electrocatalytic properties that are similar to those of the enzymes.<sup>[3]</sup>

Here, we present our *in situ* X-ray absorption fine structure (XAFS) spectroscopic studies on a dinuclear copper(II) complex of 3,5-diamino-1,2,4-triazole, Cu-Hdatrz (Figure 1)<sup>[4,5]</sup> under catalytic conditions. Cu-Hdatrz is one of the most active copper-based catalysts for ORR in basic solution<sup>[5]</sup> and its mechanistic studies would allow us to gain insights into designing highly active bio-inspired catalysts. Our *in situ* XAFS measurements revealed that the electron transfer from a Cu<sup>I</sup> species to O<sub>2</sub> was faster under basic conditions than that under the neutral condition.<sup>[6]</sup> This result indicated that deprotonation occurred in the triazole ligand and then a highly active ORR species was formed under basic conditions. The deprotonated structure of the Cu<sup>I</sup> active species may be a key to understand the high ORR activity of Cu-Hdatrz or to design bio-inspired catalysts based on multinuclear copper complexes.

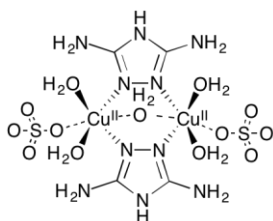


Figure 1. Molecular structure of Cu-Hdatrz.

## **References**

- [1] N. Mano, V. Soukharev, A. Heller, *J. Phys. Chem. B*, **110**, 11180 (2006)
- [2] M.S. Thorum, C.A. Anderson, J.J. Hatch, A.S. Campbell, N.M. Marshall, S.C. Zimmerman, Y. Liu, A.A. Gewirth, *J. Phys. Chem. Lett*, **1**, 2251 (2010)
- [3] C.H. Kjargaard, J. Rossmeisi, J.K. Norskov, *Inorg. Chem.*, **49**, 3567 (2010)
- [4] E. Aznar, S. Ferrer, J. Borrás, F. Lloret, M. Liu-Gonzalez, H. Rodriguez-Prieto, S. Garcia-Granda, *Eur. J. Inorg. Chem.*, **2006**, 5115 (2006)
- [5] M.S. Thorum, J. Yadav, A.A. Gewirth, *Ang. Chem. Int. Ed.*, **48**, 165 (2008)
- [6] M. Kato, K. Kimijima, M. Shibata, H. Notsu, K. Ogino, K. Inokuma, N. Ohta, H. Uehara, Y. Uemura, N. Oyaizu, T. Ohba, S. Takakusagi, K. Asakura and I. Yagi, *Phys. Chem. Chem. Phys.*, **17**, 8638-8641 (2015).

# Nanoparticle-assisted electrochemical formation of ferrocenethiol-monolayer nanodots

Yuma Takeuchi<sup>1,2</sup>, Kohei Uosaki<sup>1,2</sup>, Kei Murakoshi<sup>1</sup>, Katsuyoshi Ikeda<sup>2,3,\*</sup>

<sup>1</sup>Department of Chemistry, Faculty of science, Hokkaido University, Sapporo 060-0810 JAPAN

<sup>2</sup>Global Research Center for Environment and Energy based on Nanomaterials Science (GREEN), National Institute for Materials Science (NIMS) Tsukuba 305-0044 JAPAN

<sup>3</sup>Graduate School of Engineering, Nagoya Institute of Technology, Nagoya 466-8555 JAPAN

Email: [y-take@mail.sci.hokudai.ac.jp](mailto:y-take@mail.sci.hokudai.ac.jp), [kikeda@nitech.ac.jp](mailto:kikeda@nitech.ac.jp)\*

## Introduction

Nanofabrication of functional molecular layers has recently attracted much interest in various research fields such as molecular electronics. Although self-assembled monolayers (SAMs) of thiol molecules have been extensively studied due to their simple fabrication process, it is still difficult to form two-dimensional nano-structures. Recently, we fabricated monolayer nanodots of methylbenzenethiols on Au(111) surfaces using Au nanoparticle (AuNP) assisted electrochemical reductive desorption of thiols. In this work, we constructed monolayer nanodots of ferrocene-terminated alkanethiols on Au(111) electrodes. The electrochemical behavior of the ferrocenethiols was examined by cyclic voltammogram (CV).

## Experimental

A mixed SAM of 11-ferrocenyl-1-undecanethiols (FcC11SH) and decanethiols (C10SH) was formed by immersing of an Au(111) electrode in ethanol solution of the thiols at 1 mM total thiol concentration. For monolayer nanodots, a uniform monolayer was firstly prepared using ethanol solution of 1 mM FcC11SH. AuNPs were then deposited on top of the SAM by soaking the SAM-covered electrode in colloidal gold solution. The electrochemical potential was applied to the electrode in KOH solution, at which SAMs were reductively desorbed from the Au(111) surface but remain intact within AuNP-@Au(111) gaps. Finally, C6SH were introduced in the nanodot-formed electrode in a similar manner.

## Results and Discussions

Figures (a) and (b) show schematic illustrations of the mixed SAM and monolayer nanodots with FcC11SH. When the surface density of ferrocene is low enough in the mixed SAM, each ferrocene is expected to be isolated from others. This is indeed supported by CV of the SAM in the red line of Fig. (c); a pair of sharp redox peaks at +0.25 V vs. Ag/AgCl is similar to that of free ferrocene molecules. On the other hand, the CV of the nanodots exhibited an additional redox peak at around +0.40 V, as shown in the blue line of Fig. (c). It is known that the highly ordered SAM of ferrocenethiols shows positively shifted redox peaks because the interaction between ferrocene moiety and counter anions is sterically hindered. Therefore, the observed electrochemical behavior strongly suggests that FcC11SH were indeed packed with island forms in the monolayer.

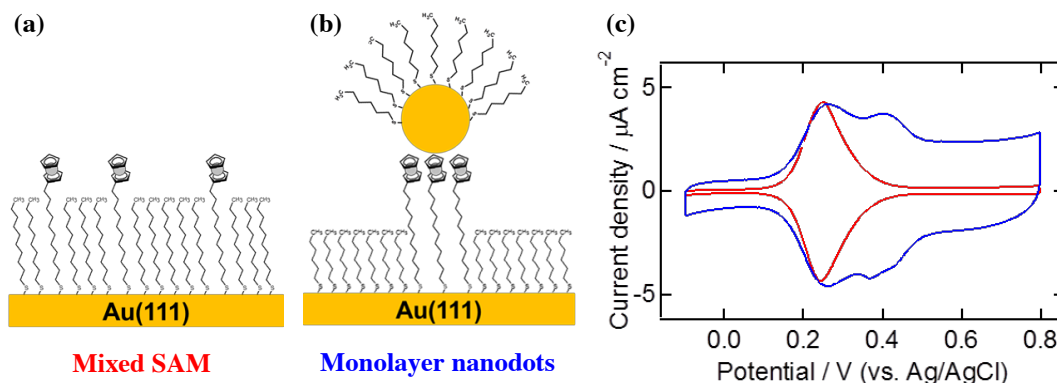


Figure. Schematic illustrations of (a) the mixed SAM and (b) monolayer nanodots. (c) CVs of the mixed SAM (red line) and monolayer nanodots (blue line).

# X-ray spectroscopic analyses of electronic states on quinone-based cathode materials for Li-ion batteries

<sup>1</sup>Yuta Kitada, <sup>2</sup>Naoka Nagamura, <sup>1</sup>Ryosuke Taniki, <sup>1</sup>Itaru Honma

<sup>1</sup>IMRAM, Tohoku Univ., Japan, <sup>2</sup>NIMS, Japan

<sup>1</sup>2-1-1, Katahira, Aoba-ku, Sendai, Miyagi, Japan

<sup>2</sup>1-2-1, Sengen, Tsukuba, Ibaraki, Japan

kitada@mail.tagen.tohoku.ac.jp

There is now an increasing demand of secondary batteries with a low cost and high energy density for large-scaled applications such as electric vehicles and peak load leveling installations. Recently, redox-active organic materials are attracting many attentions as an alternative to conventional active materials, LiCoO<sub>2</sub>, LiFePO<sub>4</sub> and LiNiO<sub>2</sub>, due to their advantages such as low costs, low environmental loads and flexibility of molecular design<sup>[1]</sup>. Quinone-based molecules have been studied as promising candidates for cathode materials, since a quinone skeleton shows a multi-electron redox reaction<sup>[2]</sup>. It is essential for a proper molecular design to understand a relation between electronic states and electrochemical characteristics. Spectroscopic analysis is a powerful tool for observing electronic states of organic active materials, whereas there are few reports. In this study, electronic states of quinone-based active materials in electrochemically discharged states were investigated by X-ray photoelectron spectroscopy (XPS) and X-ray absorption spectroscopy (XAS).

We used 9,10-anthraquinone (AQ), 1-chloro-9,10-anthraquinone (1-ClAQ), 1,5-dichloro-9,10-anthraquinone (1,5-diClAQ), 5,12-naphthacenequinone (NCQ) and 6,13-pentacenequinone (PCQ) as cathode materials. Figure 1 shows a half-reaction of AQ. Electrochemically reduced quinone compounds (reduced-quinone lithium compounds) were obtained by galvanostatic discharge tests at 0.2C until -2.0V vs Ag<sup>+</sup>/Ag by a three electrode beaker cell, followed by drying in a vacuum. XAS measurements were carried out at the soft-X-ray beamline BL-7A at Photon Factory in High Energy Accelerator Research Organization.

Figure 2 shows XAS spectrum of AQ pristine (AQ) and electrochemically reduced AQ Li compound (AQ-Li). Peaks at 285.0 and 287.0 eV and a peak at 286.0 eV appear only in AQ and AQ-Li, respectively. These results indicate that electronic states of not only the C-O bonding but the aromatic ring in a quinone skeleton dynamically change between the oxidized and reduced states.

In the presentation, detailed analyses of ab initio calculation, FT-IR, XPS and XAS for 1-ClAQ, 1,5-diClAQ, NCQ and PCQ will be reported with a comparison discussion.

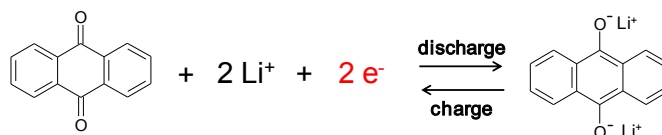


Fig.1 A half-reaction of AQ

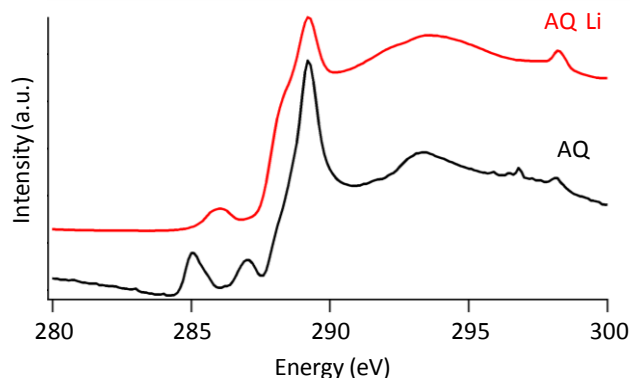


Fig.2 XAS spectrum of AQ powder (black line) and AQ Li powder (red line)

## [Reference]

[1] M. Yao *et al.*, *Journal of Power Sources*, 195, (2010) 8336-8340

[2] Y.Hanyu *et al.* *SCIENTIFIC REPORTS*, 2 (2012) 453

# On the origin of the greatly different kinetics of the hydrogen electrode reactions on Pt in acid and alkaline media

Junxiang Chen, Shengli Chen\*

Department of Chemistry, Wuhan University, Wuhan, China  
slchen@whu.edu.cn

The hydrogen electrode reactions, including the hydrogen evolution and oxidation reactions (HER and HOR), have long served as the model reactions in electrochemical kinetics. Besides, they are key reactions in hydrogen energy technologies. Pt is so far the best metal electrocatalysts for the HER and HOR. Although having been extensively and intensively studied for decades, there remain numerous questions standing in the electrocatalysis of HER and HOR on Pt-based materials. One question that has received considerable recent attentions, due to the increasing interest in alkaline fuel cells, is why the HER and HOR exhibit much slower kinetics on Pt in alkaline media than in acidic media, although in both conditions Pt is the best metal electrocatalyst.[1] The answer to this question should help designing the hydrogen electrode catalysts for alkaline fuel cells and water electrolysis. In this study, we investigate the pH effect on the hydrogen electrode kinetics on Pt(111) surface by combining the density functional theory (DFT) calculation and micro kinetic model analysis. The results lead to two main conclusions.

**1. The hydrogen electrode reactions on Pt should follow the Volmer-Heyrovsky instead of Volmer-Tafel mechanism, with the Heyrovsky reaction being the rate-determining step (*rds*).** Considering the highly reversible hydrogen adsorption and desorption behaviors indicated in the cyclic voltammogram (CVs) in both acid and alkaline media, the Volmer reaction ( $\text{H}^+ + \text{e}^- + * \leftrightarrow \text{H}^*$  and/or  $\text{H}_2\text{O} + \text{e}^- + * \leftrightarrow \text{H}^* + \text{OH}^-$ ) can be approximately considered being in equilibrium. Therefore, it should not be the *rds* regardless of pH. For the Tafel and Heyrovsky reaction, the exchange current density  $j_0$  are derived as

$$j_0^{\text{Tafel}} = 2Fk_0^{\text{T}}\theta_{\text{H}^*}(1-\theta_{\text{H}^*})(c_{\text{H}_2})^{0.5} \quad (1)$$

$$j_0^{\text{Heyrovsky}} = 2Fk_0^{\text{H}}\theta_{\text{H}^*}(1-\theta_{\text{H}^*})(c_{\text{H}^+}c_{\text{H}_2})^{0.5} \quad (2)$$

where  $k_0^{\text{T}}$  and  $k_0^{\text{H}}$  refer to the standard rate constants of the Tafel and Heyrovsky reactions;  $\theta_{\text{H}^*}$  is the coverage of  $\text{H}^*$  at the equilibrium electrode potential;  $c_{\text{H}^+}$  and  $c_{\text{H}_2}$  are the concentrations of  $\text{H}^+$  and  $\text{H}_2$  in the solution. For the Tafel reaction, pH may alter the  $j_0$  mainly by changing the  $\theta_{\text{H}^*}$  (eq. 1). Our DFT calculation results show that the  $\theta_{\text{H}^*}$  in acid solution (pH=1) is about 1.3 times lower than that in alkaline solution (pH=13), which, according to eq. 1, would predict a larger  $j_0$  in the alkaline solution. This obviously contradicts to the much lower  $j_0$  in alkaline media observed in experiments [1]. As indicated by eq.2, the  $j_0$  for the Heyrovsky reaction is affected by the  $\theta_{\text{H}^*}$  and  $c_{\text{H}^+}$ . Therefore, large pH effect could occur if the Heyrovsky reaction is the *rds*.

**2. The Heyrovsky reaction proceeds in different ways in acid and alkaline media.** The Heyrovsky reaction may proceed in two ways, namely,  $\text{H}^* + \text{H}^+ + \text{e}^- \leftrightarrow \text{H}_2 + *$  (H1) and  $\text{H}^* + \text{H}_2\text{O} + \text{e}^- \leftrightarrow \text{H}_2 + \text{OH}^- + *$  (H2) respectively. The two types of reaction paths should have different kinetics due to that different proton donors and acceptors are involved. By using the DFT-calculated  $\theta_{\text{H}^*}$  and the values of  $c_{\text{H}^+}$ , eq. 2 predicts  $j_0$  values that differ ca. 7 order of magnitude in acid (pH=1) and alkaline (pH=13) if the same  $k_0^{\text{H}}$  is used, which is also against that observed in experiments. Therefore, we think that the Heyrovsky reaction proceeds mainly through H1 in acid solution, while the H2 is the major reaction path in alkaline solution. By fitting the experimental polarization curves for the HER and HOR obtained in different media, the standard reaction constants for the Heyrovsky reactions in solutions of pH=1 and pH=13 are found to be  $1 \times 10^{-4} \text{ s}^{-1}$  and  $4 \times 10^{-7} \text{ s}^{-1}$ , respectively.

## Reference

[1] Strmcnik D, Uchimura M, et al., Nature chemistry, 2013, 5(4): 300-306.

# In Situ DRIFTS Analysis of SEI formation over Cathodes at Elevated Temperature

Minbale Admas Teshager, Shawn D. Lin\*, Bing Joe Hwang\* and Yaw-Terng Chern  
Department of Chemical Engineering, National Taiwan University of Science and Technology, Taipei,  
Taiwan 106, R.O.C.

\*E-mail: [sdlin@mail.ntust.edu.tw](mailto:sdlin@mail.ntust.edu.tw) (S. D. Lin) and [bjh@mail.ntust.edu.tw](mailto:bjh@mail.ntust.edu.tw) (B. J. Hwang)

The thermal and electrochemical instability of conventional  $\text{LiPF}_6$ -organocarbonate electrolytes hinder the integration of large-scale lithium ion batteries (LIBs) for high powered electric vehicles (EVs), hybrid electric vehicles (HEVs), plug-in hybrid electric vehicles (PHEVs) and smart grids [1]. Its thermal decomposition has been considered as the main challenge at moderately elevated temperature (60-85°C) and result in catastrophic failure of the battery. Wilken et al. [2] and Yang et al. [3] reported the thermal decomposition of  $\text{LiPF}_6$ -based electrolyte using ex situ techniques such as NMR, GC-MS, and on-line-TGA-FTIR. They found fluorinated organic and inorganic species as decomposition products. However, the decomposition products of electrolyte at elevated temperature and solid electrolyte interface (SEI) formation in the real battery system is still a debating issue, due to the lack of direct evidence from in-situ analysis. In situ diffuse reflectance infrared Fourier-transformed spectroscopy (DRIFTS) is proved a convenient technique for SEI analysis[4]and will be used in this study at elevated temperature.

Another important issue is electrochemical stability of electrolyte, for which new Li-salt electrolyte with large redox window is persistently required. Very recently Chern et al. [5] reported, a new cyano-substituted benzimidazole derivative Li-salt,  $(\text{Li}[5\text{-CNTFBI}(\text{BF}_3)_2])$ , for high temperature and high potential application of LIBs. However, complicated interaction occurs between Li salt, solvent, additive, and electrode surface within a cell wherein the change of only one electrolyte component would require reconsideration of SEI chemistries of the electrodes. Perhaps therefore, studies of new electrolytes are few in number and in general new Li-salts are hardly investigated and developed in LIBs.

Here, we report in-situ DRIFTS analysis at elevated temperature (65°C) during electrochemical cycling using a commercial electrolyte ( $\text{LiPF}_6/\text{EC}+\text{DEC}$ ) and the new electrolyte of cyano-benzimidazole derivative Li-salt ( $\text{Li}[5\text{-CNTFBI}(\text{BF}_3)_2]/\text{EC}+\text{DEC}$ ) over two cathode materials (Li-rich LLNMO and commercial  $\text{LiCoO}_2$ ). Fig.1 illustrates the DRIFTS difference spectra using the commercial electrolyte,  $\text{LiPF}_6/\text{EC}+\text{DEC}$  (a) and  $\text{Li}[5\text{-CNTFBI}(\text{BF}_3)_2]/\text{EC}+\text{DEC}$  (b) over Li-rich LLNMO cathode. In the case of  $\text{LiPF}_6$  system (Fig.1a), absorbance bands indicating decomposition product of  $\text{LiPF}_6$  along with EC adsorption were detected at a lower potential of 3.8 V than that at room temperature [6]. With the new electrolyte (Fig.1b), there is no indication of decomposition product other than EC adsorption at below 4.4V, suggesting that the new electrolyte is promising for high temperature application of LIBs. SEI species observed above the mentioned onset potential were somewhat different for the two electrolyte systems. The identified species and their possible formation mechanism will be discussed and compared to that observed at room temperature and over commercial  $\text{LiCoO}_2$  cathode.

**Acknowledgement:** We are grateful to Ministry of Economic Affairs of Taiwan, ROC (103-EC-17-A-08-S1-183) for the financial support.

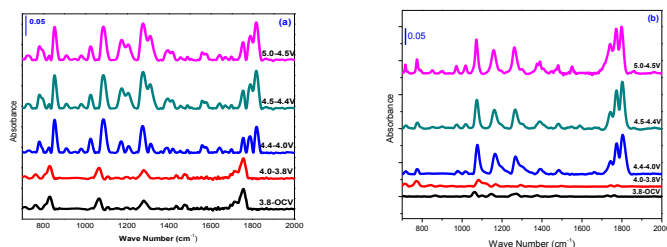


**Fig.1** DRIFTS difference spectra of using  $\text{LiPF}_6/\text{EC}+\text{DEC}$  (a) and  $\text{Li}[5\text{-CNTFBI}(\text{BF}_3)_2]/\text{EC}+\text{DEC}$  (b) electrolyte over LLNMO during electrochemical charging at elevated temperature (65°C).

## References

- [1] S. Tan, Y.J. Ji, Z. R. Zhang, and Y. Yang, *ChemPhysChem*, 15 (2014) 1956-1969.
- [2] S. Wilken, M. Treskow, J. Scheers, P. Johansson and P. Jacobsson, *RSC Adv.*, 3(2013) 16359-16364.
- [3] H. Yang, G. V. Zhuang, P.N. Ross Jr., *J. Power Sources* 161 (2006) 573-579.
- [4] A. M. Haregewoin, T.-D. Shie, S. D. Lin, B.-J. Hwang, F.-M. Wang, *ECS Trans.* 53 (2013) 23-32.
- [5] Y.-T. Chern, J.-L. Jeng, S.-Y. Chen, A.-S. Wei, B.-J. Hwang, *US Patent Appl.* 2014/0178771 A1,
- [6] M. A. Teshager, S. D. Lin, B. J. Hwang, F.-M. Wang, S. Hy, A. M. Haregewoin, *Electrochimica Acta* (submitted).

# Optical Force Applied to Molecules at Nanogap of Metal Nanodimer

Yumi Wakisaka, Mai Takase, Hiro Minamimoto, Satoshi Yasuda, Kei Murakoshi

*Department of Chemistry, Hokkaido University*

*Sapporo, Hokkaido, 060-0810, Japan*

*kei@sci.hokudai.ac.jp*

Optical manipulation of molecules at room temperature is a key for sophisticated nanotechnology in future. We have developed the system to segregate molecules using the steep gradient of the chemical potential at metal nanogap less than 100 nm in width [1]. Our results demonstrated that the force of <fN applied to a single molecule is enough to control molecular 2D diffusion at room temperature [2]. Several innovative findings on optical manipulation for molecules are available both on experiment and theory [3]. Optical trapping of molecule at room temperature, however, has not been achieved yet. Recently, it has been shown that highly localized anisotropic electromagnetic field generated by plasmon resonance of metal nanodimer emerge very characteristic phenomena of the alternation of selection rule at the optical excitation [4], and the change in Raman scattering due to strong coupling between plasmons and molecule excitons [5]. Such huge gradient of the field could be used to generate optical force in the order of sub-pN for controlling molecule motions [3]. In the present work, possibility of the molecule trapping at the gap of metal nanodimer is discussed based on the observation of the signal evolution of surface-enhanced Raman scattering reflecting the increment of the number of molecules in the plasmon field. The orientation of molecules adsorbed on the surface of metal is controlled by electrochemical potential to estimate the effect of the anisotropy of the electromagnetic field to polarize molecules.

## References

- [1] H. Nabika *et al.*, *J. Am. Chem. Soc.*, **2005**, 127 16786-16787; *Anal. Chem.*, **2008**, 81, 699-704.
- [2] B. Takmoto *et al.*, *Nanoscale*, **2010**, 2, 2591-2595.
- [3] L. Novotny *et al.*, *Phys. Rev. Lett.* **1997**, 79, 645-648; H. Xu and M. Käll, *Phys. Rev. B*, **2002**, 89, 246802.
- [4] M. Takase *et al.*, *Nat. Photo.*, **2013**, 7, 550-554.
- [5] F. Nagasawa *et al.*, *J. Phys. Chem. Lett.*, **2014**, 5, 14-19.



# Electrochemical behaviour of new 3-aminopyrazine-2-carboxylate Fe(III)-complexes

Armando J.L. Pombeiro,<sup>a</sup> Anirban Karmakar,<sup>a</sup> Luísa M.D.R.S. Martins,<sup>a,b</sup> M. Fátima C. Guedes da Silva,<sup>a</sup> Susanta Hazra<sup>a</sup>

<sup>a</sup>Centro de Química Estrutural, Instituto Superior Técnico, Universidade de Lisboa, Av. Rovisco Pais, 1049-001, Lisbon, Portugal.

<sup>b</sup>Chemical Engineering Department, ISEL, R. Conselheiro Emídio Navarro, 1959-007 Lisboa, Portugal.  
[pombeiro@tecnico.ulisboa.pt](mailto:pombeiro@tecnico.ulisboa.pt)

Three new mononuclear Fe(III) complexes with ligands derived from 3-amino-2-pyrazinecarboxylic acid, [H(EtOH)][FeCl<sub>2</sub>(L)<sub>2</sub>] (**1**) [L = 3-amino-2-pyrazinecarboxylate], [H<sub>2</sub>bipy]<sub>1/2</sub>[FeCl<sub>2</sub>(L)<sub>2</sub>].DMF (**2**) and [FeCl<sub>2</sub>(L)(2,2'-bipy)] (**3**) (Figure 1) were prepared and characterized.

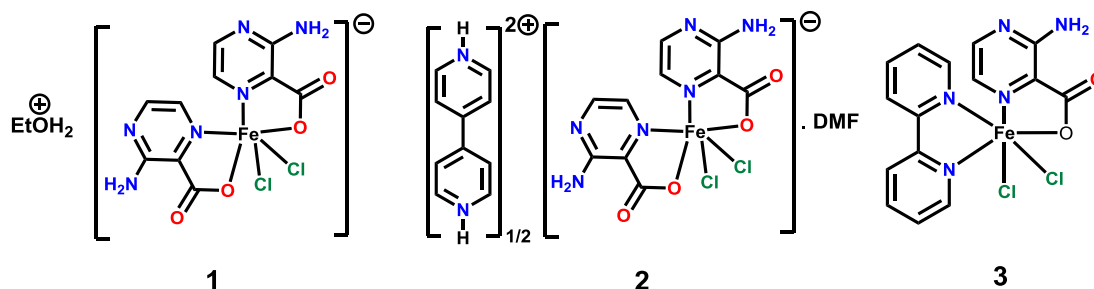


Figure 1

The electrochemical behaviours of complexes **1-3**, as well as of 3-amino-2-pyrazinecarboxylic acid (HL), doubly protonated 4,4'-bipyridine [(H<sub>2</sub>bipy)Cl<sub>2</sub>] and 2,2'-bipyridine, were investigated by cyclic voltammetry (CV) and controlled potential electrolysis (CPE), at a platinum working electrode at room temperature in a 0.2 M [<sup>n</sup>Bu<sub>4</sub>N][BF<sub>4</sub>]/NCMe solution.

Complexes **1-3** exhibit a first single-electron (as measured by CPE) reversible cathodic wave at *ca.* 0.06 V vs. SCE, assigned to the Fe(III) to Fe(II) reduction (wave I<sup>red</sup>). A second irreversible cathodic wave (II<sup>red</sup>) in the -0.62 to -1.12 V vs. SCE range is also observed, which involves the L<sup>-</sup> ligand. A typical cyclic voltammogram is exemplified for **3** in Figure 2.

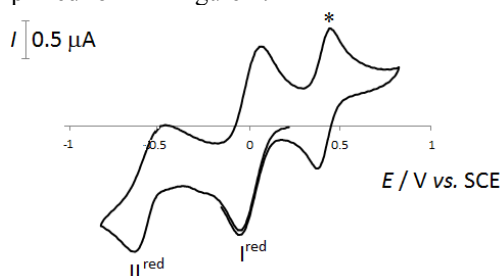


Figure 2 - Cyclic voltammogram, initiated by the cathodic sweep, of **3** in a 0.2 M [<sup>n</sup>Bu<sub>4</sub>N][BF<sub>4</sub>]/NCMe solution, at a Pt disc working electrode (*d* = 0.5 mm), run at a scan rate of 200 mVs<sup>-1</sup>. \* [Fe(η<sup>5</sup>-C<sub>5</sub>H<sub>5</sub>)<sub>2</sub>]<sup>0/+</sup>.

The electrochemical study provided a valuable tool to establish the structures of complexes **1** and **2**.

The values of the Fe<sup>II/III</sup> redox potential of our complexes also allowed to estimate, for the first time, the value of the Lever *E<sub>L</sub>* electrochemical ligand parameter for the 3-amino-2-pyrazinecarboxylate ligand, on the basis of the Lever linear relationship (eq. 1).

$$E = S_M (\Sigma E_L) + I_M \quad (1)$$

## Acknowledgements

This work has been supported by the Fundação para a Ciência e a Tecnologia (FCT), Portugal (project UID/QUI/00100/2013). Authors A. Karmakar and S. Hazra express their gratitude to the FCT for post-doctoral fellowships (Ref. Nos. SFRH/BPD/76192/2011 and SFRH/BPD/78264/2011).



# In-Situ Monitoring the Electrocatalytic Reaction Processes at Platinum Single Crystal Electrode Using SHINERS

Jin-Chao Dong, Du-Hong Chen, Yue Li, Jin-Hui Meng, Yang Zhao, Chao-Yu Li, Jian-Feng Li\*  
*College of Chemistry and Chemical Engineering, Xiamen University, Xiamen 361005, China*  
*E-mail: Li@xmu.edu.cn*

Raman spectroscopy, as a vibrational spectroscopy technique, can provide detail structural information about the probed molecules, however, the signal intensity is too weak. The discovery of surface-enhanced Raman scattering (SERS) paved way for sensitive detection of target analytes even down to single molecule level, but the applications of the SERS are limited by a lack of substrate generality and its high surface selective performance. Since our group invented “shell isolated nanoparticle-enhanced Raman spectroscopy” (SHINERS) in 2010, it received more and more attention by many research groups. SHINERS entails metal nanoparticles with thin inert silica shell and the inner Au NPs are treated as “signal amplifiers” which can enhance the Raman signal of target molecules due to its strong electromagnetic field. The ultrathin silica shells can effectively isolate the “signal amplifiers” from the ensemble, and also avoid aggregation of nanoparticles. The SHINERS technique offsets the long-standing limitations of SERS such as substrate and morphology generality to a certain extent. It has been widely accepted by different fields such as electrochemistry, surface science, analytical science, and especially applied at atomically flat single crystal electrode surfaces.

From the perspective of catalytic materials and energy fields, the platinum and platinum alloy owned the best catalyst activity in fuel cells, so the electrocatalytic reactions, which using platinum as working electrodes, get lots of concerns. Currently, there are many studies on the electrochemical properties of the platinum electrodes, however, in-situ monitoring the electrocatalytic reaction processes at single crystal platinum electrodes using Raman spectroscopy has not been reported. We employ in-situ EC-SHINERS technique to in-situ monitor the electrocatalytic processes of CO, methanol, formic acid oxidation, and oxygen reduction at Pt single crystal electrodes and systematically evaluate the influence of different factors, such as crystallographic orientations, anions and pH, during reaction processes.

## References:

1. J. F. Li et al. *Nature* **464** (2010) 392.
2. J. F. Li et al. *J. Am. Chem. Soc.* **137** (2015) 2400.
3. P. Rodriguez, Y. Kwon, Marc T. M. Koper *Nat. Chem.* **4** (2012) 177.
4. V. Climent, J. M. Feliu *J. Solid State Electrochem.* **15** (2011) 1297.

# Application of an Ultra-high Resolution Optical Microscopy ~Imaging of Fast Reactions with Single Atomic Step Resolution~

M.Azhagurajan<sup>1</sup>, Takashi Itoh<sup>2</sup> and K. Itaya<sup>1</sup>.

<sup>1</sup>Institute of Multidisciplinary Research for Advanced Materials, Tohoku University,

<sup>2</sup>Frontier Institute for Interdisciplinary Sciences, Tohoku University

[itaya@atom.chem.tohoku.ac.jp](mailto:itaya@atom.chem.tohoku.ac.jp)

## 1. Introduction

It is shown in our previous papers that the Au deposition occurs mainly at atomic steps resulting the layer-by-layer growth at potentials near the onset of cathodic currents over the entire area (ca.  $100 \times 100 \mu\text{m}^2$ ). New small islands with a monatomic height were also observed on atomically flat terraces during the deposition. These islands expanded in the lateral direction, resulting the formation of new layers. A laser confocal microscope combined with a differential interference contrast microscope (LCM-DIM) used to observe the electrochemical dynamic processes.

LCM-DIM provides direct images of dynamics in the electrochemical deposition of Au with an atomic layer resolution [1,2]. It is also demonstrated that LCM-DIM can be applied for other reactions such as upd processes of Ag, Cu on Au electrodes and Si(100)[4]. More recently, it has been found that the intercalation reaction of Li ions [3] into layered material such as transition metal chalcogenides can be imaged by our new technique. Here, we show unique capability of the new optical microscopy.

## 2. Experiment

The apparatus of our LCM-DIM was constructed and improved using an optical system (FV300, Olympus Optical Co. Ltd.) with a super-luminescent diode (Amonics Ltd., Model ASLD68-050-G-FA:680 nm) to eliminate interference fringes. We usually used a mode with data points ( $512 \times 512$  points), in which the speed of 4 frames/s can be achieved. It was necessary to prepare ultra-flat surfaces with terrace widths greater than several micrometers, because the lateral resolution of the LCM-DIM method was limited in the range of 0.2–0.3  $\mu\text{m}$  by the wavelength of the monitoring light as in the conventional optical microscopy.  $\text{MoS}_2$  surface was prepared by cleaving method. Ionic liquid used as electrolyte solution (EMI-FSI) containing 0.32 mol/kg lithium (LiTFSI). Lithium foil used as reference and counter electrode.

## 3. Result and Discussion

It has been shown that the Au deposition occurs mainly at atomic steps resulting the layer-by-layer growth at potentials near the onset of cathodic currents over the entire area (ca.  $100 \times 100 \mu\text{m}^2$ ). New small islands with a monatomic height were also observed on atomically flat terraces during the deposition. These islands expanded in the lateral direction, resulting the formation of new layers. LCM-DIM provides direct images of dynamic growth modes in the electrochemical deposition of Au with an atomic layer resolution [2].

Recently, it has been demonstrated for the first time that in situ imaging of the dynamic processes of Li ions intercalation reactions into  $\text{MoS}_2$  single crystal electrodes with an atomic layer resolution is now possible in an ionic liquid, using LCM-DIM as shown in Fig.1(a-c). It can be concluded that the intercalation reaction occurs in the two phases forming undoped and doped domains. Newly formed intercalated Li ions, push away to all previously intercalated all Li ions to the inner part of undoped  $\text{MoS}_2$  phase as illustrated in Fig.1(d)

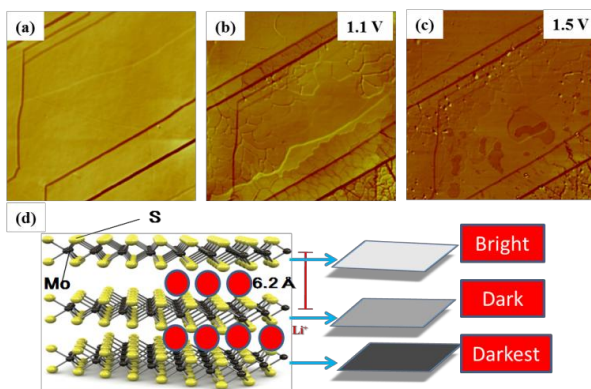


Figure1. The Li intercalation and de-intercalation(a-c) process into  $\text{MoS}_2$  and (d) schematic illustration of intercalation process.

## References

- 1) R. Wen, A. Lahiri, M. Azhagurajan, S. Kobayashi and K. Itaya, J. Am. Chem. Soc. 132 (2010) 13657.
- 2) M. Azhagurajan, R. Wen, A. Lahiri, Y. G. Kim, T. Itoh, and K. Itaya. J Electrochem Soc., 160 (9) (2013) D361.
- 3) T. Stephenson, Z. Li, B. Olsen and D. Mitlin, *Energy Environ. Sci.*, 2014, 7, 209–231
- 4) S. Kobayashi, Y. G. Kim, R. Wen, K. Yasuda, H. Fukidome, T. Suwa, R. Kuroda, X. A. Teramoto, T. Ohmi and K. Itaya, Electrochemical and Solid-State Letters, 14 (2011) H351.

# The Redox Behaviour of Graphene Oxide: A Spectroelectrochemical Study

Martin Pfaffeneder-Kmen, Günter Trettenhahn  
*Department of Physical Chemistry, University of Vienna*  
*Währinger Straße 42, A-1090, Vienna*  
*guenter.trettenhahn@univie.ac.at*

Since 2004, when Novoselov and Geim published their groundbreaking work about the preparation and characterization of graphene,[1] great interest in this material developed. Very soon there was the demand for new synthesis methods, because the method, which was described in this paper, was only suitable for research. Starting with this motivation, graphene oxide (GO) was proposed to be a possible precursor to graphene.[2] GO is now known since more than 150 years as graphitic acid,[3] but it is state-of-the-art and many possible applications have been published in the past few years.[4,5]

The exact structure of GO is still under discussion, but the Lerf-Klinowski model is generally accepted.[6] It says that the single sheets in graphite are decorated with the most different oxygen containing groups, mostly alcohols, epoxides and at the sheet edges carboxylic acid groups. The structure is completely non-ordered and a recent electrochemical study showed, that the final GO product depends even on the synthesis method.[7] The oxygen containing groups decrease the hydrophobicity of the sheets and make the dispersion of GO and the exfoliation to single nanosheets in water (depending on the pH)[8] and other solvents possible.[9] The electrochemical reduction [10] is favored, because, structural defects can be healed [4] and aggressive reductants can be avoided. In the literature it was published as green method.[11]

Therefore the reduction mechanism and the structure of the final product are of great interest. In this study the GO/electrolyte interface was investigated by in-situ ATR FTIR spectroscopy. The very fundamental reduction behavior of GO is described, as well as the possible oxidation of the reduced form. Although there are no reversible redox processes, the reduced form can be electrochemically re-oxidized. This work describes the formation and degeneration of oxygen containing groups during cathodic reduction. In situ FTIR data obtained in aqueous and D<sub>2</sub>O solutions elucidated the reduction reaction of GO.

- [1] K.S. Novoselov, A.K. Geim, S. V. Morozov, D. Jiang, Y. Zhang, S. V. Dubonos, et al., Electric field effect in atomically thin carbon films., *Science*. 306 (2004) 666–669.
- [2] S. Gilje, S. Han, M. Wang, K.L. Wang, R.B. Kaner, A Chemical Route to Graphene for Device Applications, *Nano Lett.* 7 (2007) 3394–3398.
- [3] B.C. Brodie, On the Atomic Weight of Graphite, *Philos. Trans. R. Soc. Lond.* 149 (1859) 249–259.
- [4] S. Pei, H.-M. Cheng, The reduction of graphene oxide, *Carbon N. Y.* 50 (2012) 3210–3228.
- [5] A. Chavez-Valdez, M.S.P. Shaffer, A.R. Boccaccini, Applications of graphene electrophoretic deposition. A review., *J. Phys. Chem. B.* 117 (2013) 1502–1515.
- [6] A. Lerf, H. He, M. Forster, J. Klinowski, Structure of Graphite Oxide Revisited, *J. Phys. Chem. B.* 102 (1998) 4477–4482.
- [7] A.Y.S. Eng, A. Ambrosi, C.K. Chua, F. Šaněk, Z. Sofer, M. Pumera, Unusual inherent electrochemistry of graphene oxides prepared using permanganate oxidants, *Chem. - A Eur. J.* 19 (2013) 12673–12683.
- [8] S.A. Hasan, J.L. Rigueur, R.R. Harl, A.J. Krejci, I. Gonzalo-Juan, B.R. Rogers, et al., Transferable graphene oxide films with tunable microstructures., *ACS Nano.* 4 (2010) 7367–7372.
- [9] J.I. Paredes, S. Villar-Rodil, A. Martínez-Alonso, J.M.D. Tascón, Graphene oxide dispersions in organic solvents., *Langmuir.* 24 (2008) 10560–4.
- [10] M. Pfaffeneder-Kmen, G. Trettenhahn, W. Kautek, An in situ FTIR and in situ QMB study of the Electrochemistry of Graphene Oxide on Platinum, *J. Phys. Chem. C.* submitted (n.d.).
- [11] H. Guo, X. Wang, Q. Qian, F. Wang, X. Xia, A Green Approach to the Synthesis of Graphene Nanosheets, *ACS Nano.* 3 (2009) 2653–2659.

## Potentiostatic pulse technique to investigate the hydrogen diffusion and trapping into subsurface of nickel single crystal (100)

X. Feaugas, C. Lekbir, E. Conforto, J. Creus, R. Sabot

*LaSIE UMR 7356 CNRS, Université de la Rochelle, Av. Michel Crépeau, 17042 La Rochelle, France.*

*Email addresses : [xavier.feaugas@univ-lr.fr](mailto:xavier.feaugas@univ-lr.fr)*

A potentiostatic double-step technique was applied to unstrained (US), strained with suppression of strain bands (SWB) and strained (S) Ni (100) single crystal surfaces in sulphuric acid medium to characterize hydrogen diffusion and trapping in relation with the different effects of plastic strain [1]. In these potentiostatic pulse experiments, the hydrogen atoms are generated at a constant cathodic potential  $E_C$  for a time  $t_C$  in the range of 2 to 1200s. During this charging period a proportion of the hydrogen atoms diffuse into the electrode interior. At the end of the charging period the potential is stepped to a more positive value  $E_0$  (a few millivolts negative of its corrosion potential  $E_C$ ) resulting in an anodic current transient and charge  $q_A$  associated with the re-oxidation of hydrogen atoms. Diffusion and trapping parameters:  $\langle F.C_S.(D/\pi)^{1/2} \rangle$  and  $\langle k_T \rangle$  are determined by fitting the experimental current transients to the theoretical solution of an appropriate model [2]. For US Ni (100) surfaces, the effect of trapping on the diffusion of hydrogen is not taken into account and show that the residual dislocation densities present in metal is negligible with respect to the trapping. Two domains can be distinguished, that of the subsurface and that of the bulk of the sample. For all mechanical states studied we observe that the diffusion coefficient near the surface (subsurface) seems to be much higher than that obtained in the bulk of the metal, and that the density of trapping sites decrease around the surface. According to thermodynamic framework the origin of both results is analysed and possible implication on hydrogen embrittlement is discussed.

[1] Lekbir, C., Creus, J., Sabot, R., Feaugas, X., Mater. Sci. and Eng. A, 578, (2013) 24-34.

[2] McKibben, R., Sharp R.M., Harrington, D.A., Pound, B.G., Wright, G.A., Acta Metall. 35 (1987) 253-262.

These instructions are an example of what a properly prepared meeting abstract should look like. Proper column and margin measurements are indicated.

The abstract **should not exceed ONE PAGE** of text, references, tables and figures. Abstracts exceeding this limit may be cut without consideration of content after the first page.

Type the title single-spaced in 14-point Times Roman bold, upper and lower case and NOT in ALL CAPITAL letters.

Type the author(s) name(s) single-spaced in 10-point Times Roman regular.

Type the affiliation(s) and address(es) single-spaced in 10-point Times Roman italic.

Type the body of the abstract text (including references and tables) single-spaced in 10-point Times Roman regular.

**Paper Size: A4 (21.0 x 29.7 cm)**

**Margins**

Top: 30.0 mm

Bottom: 30.0 mm

Sides: 30.0 mm

- Processus de corrosion des nano
- Diffusion de H en subsurface : techniques pulsées
- Perméation électrochimique appliquée à l'étude de la diffusion de H dans le nickel
-

# Imaging of electrocatalytical activities of mixed transition metal oxides for oxygen reduction reaction with scanning electrochemical microscopy

Fei Li, Li Ma, Han Zhou, Shuli Xin, Chunhui Xiao and Shujiang Ding

Department of Chemistry, School of Science, Xi'an Jiaotong University, Xi'an 710049, P.R. China  
feili@mail.xjtu.edu.cn

Looking for cheap and commercially available materials to replace the precious and nondurable Pt catalysts to facilitate the sluggish oxygen reduction reaction (ORR) is a key issue in fuel cells. In recent years, various alternative catalysts based on non-precious metals have been developed, in which the mixed valence oxides of transition metals have attracted much attention due to their considerable advantages of low cost, environmental friendliness, prominent ORR activity and stability. In this work, the  $\text{ZnCo}_2\text{O}_4$  nanosheets@CNT ( $\text{ZnCo}_2\text{O}_4$  NSs@CNT) and the  $\text{Co}_3\text{O}_4$  nanosheets@CNT ( $\text{Co}_3\text{O}_4$  NSs@CNT) composites with hierarchical and sheet-like structure were successfully synthesized on the CNT covered with sulfonated polystyrene layer by virtue of sulfonated gel medium. Their catalytic activities for ORR measured by cyclic voltammetry show that the  $\text{ZnCo}_2\text{O}_4$  NSs@CNT composite exhibits the highest ORR catalytic activity compared with  $\text{ZnCo}_2\text{O}_4$  NSs, CNT alone, the physically mixed  $\text{ZnCo}_2\text{O}_4$  and CNT and the  $\text{Co}_3\text{O}_4$  NSs@CNT, which could contribute to the unique “cable” structure of  $\text{ZnCo}_2\text{O}_4$  NSs@CNT providing large surface area and great electron conductivity for catalyzing oxygen reduction, and the synergetic effect between  $\text{Zn}^{2+}$  and  $\text{Co}^{3+}$ . And the presence of CNT as support could provide sufficient electric conductivity for the rapid electron transfer and form an efficient and well-connected structure with  $\text{ZnCo}_2\text{O}_4$ . The simultaneous investigation and comparison of the catalytic activities of these catalysts at a same GCE in one single experiment were also achieved by scanning electrochemical microscopy (SECM). The obtained SECM results agree well with the CV results and additionally provide the differences in the local catalytic activities of these catalysts at different sample potentials. The better catalytic performance of  $\text{ZnCo}_2\text{O}_4$  nanosheets@CNT than that of the cobalt-based oxides ( $\text{Co}_3\text{O}_4$ ) shows promising as a new non-Pt, mixed transition metal oxides ORR catalyst for future fuel cell applications.

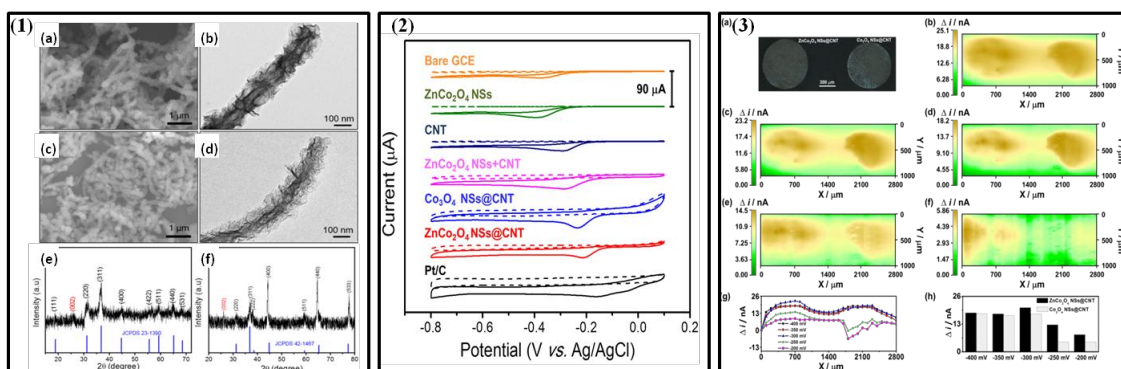


Fig. 1. (1) The morphology and composition characterizations of the prepared (a,b,e)  $\text{ZnCo}_2\text{O}_4$  NSs@CNT and (c,d,f)  $\text{Co}_3\text{O}_4$  NSs@CNT; (2) Cyclic voltammograms in  $\text{O}_2$ -saturated (solid curves) or  $\text{N}_2$ -saturated (dashed curves) 0.1 M KOH solution; (3) (a) Photograph of  $\text{ZnCo}_2\text{O}_4$  NSs@CNT (left) and  $\text{Co}_3\text{O}_4$  NSs@CNT (right) spots modified on a GCE and (b-f) the corresponding SECM images in  $\text{O}_2$  saturated 0.1 M KOH solution at different sample potentials: (b)  $-0.400$  V, (c)  $-0.350$  V, (d)  $-0.300$  V, (e)  $-0.250$  V and (f)  $-0.200$  V; (g) Background-subtracted RC-SECM x-line scans along the most active areas of the two catalysts at different sample potentials; (h) Bar diagram of the reduction current derived from (g).

## References

- [1] C. Z. Yuan, H. B. Wu, Y. Xie, X. W. Lou, *Angew. Chem. Int. Ed.* 2014, 53, 1488.
- [2] Z. H. Pu, Q. Liu, C. Tang, A. M. Asiri, A. H. Qusti, A. O. Al-Youbi, X. P. Sun, *J. Power Sources*, 2014, 257, 170.
- [3] J. L. Fernandez, D. A. Walsh, A. J. Bard, *J. Am. Chem. Soc.* 2005, 127, 357.
- [4] T. C. Nagaiah, A. Maljusch, X. X. Chen, M. Bron, W. Schuhmann, *ChemPhysChem*, 2009, 10, 2711.

# Noise and ac impedance analysis of ion transfer kinetics at the micro liquid/liquid interface

Vladimír Mareček, Oksana Josypčuk, Karel Holub  
J. Heyrovský Institute of Physical Chemistry of the CAS, v.v.i.  
Dolejšková 2155/3, 182 23 Prague 8, Czech Republic  
vladimir.marecek@jh-inst.cas.cz

Fluctuation analysis was utilized to determine the TEA ion transfer kinetics across the water/1,2-dichloroethane interface. The obtained data were compared with those derived from electrochemical impedance spectroscopy experiments using the same electrolytic cell. A two electrode cell with the liquid/liquid interface supported at the tip of a silanised microcapillary with an open circuit potential of 0 V was used throughout:

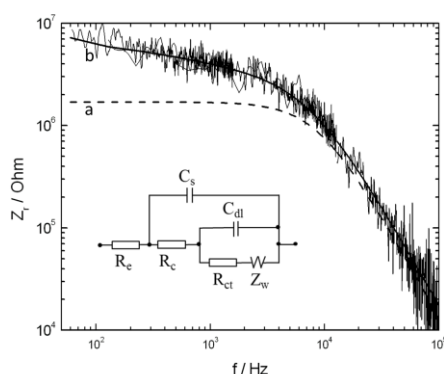
Ag/AgCl/x mM LiCl + 0.5 mM TEACl(w)/x mM TBATPB + 0.5 mM TEADCC(o)/x mM LiCl + 0.5 mM TEACl(w)/AgCl/Ag (1)

where  $x = 10$  or  $20$ . The capillary with orifice diameter of approximately  $18\ \mu\text{m}$  was prepared similarly as previously reported [1]. Home-made low noise - high impedance input preamplifier equipped with a high-pass filter was constructed using operational amplifiers INA116 and OPA 2227 (Texas Instruments). The preamplifier output was connected to the Dynamic Signal Analyzer HP 35665A (Hewlett Packard). FFT data were obtained in three frequency spans 0-1.6; 0-12.8 and 0-102.4 kHz, each with the 800 lines resolution. The square of the noise mean amplitude  $V(f)$  is related to the real part of impedance  $Z_r$  by the Nyquist formula  $V(f)^2 = 4kTZ_r\Delta f$ .

The noise analysis data of the cell (1) for  $x = 10$  are shown in Fig. 1. The curve *a* represents a fit to the noise data measured for the cell only filled with the aqueous phase, i.e. without a liquid/liquid interface. The electrical equivalent circuit used in a fitting procedure is composed of a parallel combination of the cell resistance  $R$  and capacitance  $C$ . At low frequencies below 3 kHz, the value of  $Z_r$  is constant and represents resistance of the cell  $R = 1.7\ \text{M}\Omega$ . The  $Z_r$  decrease at high frequencies is caused by a parallel capacitance  $C$  which amounts to 10 pF. It comprises the input capacitance of the preamplifier  $C_i = 5\ \text{pF}$  and a stray capacitance of the cell  $C_s$ .

The thick full line in Fig. 1 represents a fit to the noise data *b* measured in the presence of a liquid/liquid interface. The noise data were fitted using a real part of the impedance  $Z_r$  of the equivalent circuit shown in the inset of Fig. 1. In contrast to the line *a*, the real part of the impedance is not constant at low frequencies, but increases with decreasing the frequency below 3 kHz. The impedance decrease at high frequencies, similar to line *a*, is analogously due to the parallel capacitance  $C$ , amounting in this case to 5.4 pF only.

Ac impedance of the cell was determined before and after the noise measurement. The purpose



of these ac impedance measurements was to check the electrolytic cell stability and to compare the ac impedance data with those derived from the noise measurement. The ac impedance data obtained before and after the noise measurement are almost identical, which proves stability of the electrolytic cell.

Kinetic parameters derived from the ac impedance and the noise data are in a very good agreement. The average rate constant value  $k_s = 0.37\ \text{cm s}^{-1}$  corresponds to the value obtained previously [1] with the ac impedance spectroscopy technique. It is therefore evident that the ac impedance technique utilizing a small amplitude perturbation signal is comparable with a noise analysis and the both methods provide reasonable data on

the ion transfer kinetics. Application of a method employing a small perturbation signal prevents polarization of the inner capillary surface by current flowing through the cell [2]. The induced polarization of the capillary can affect ion concentration at the interface due to electroosmosis and thus make the kinetics data evaluation difficult or erroneous.

References: 1. B.R. Silver, K. Holub, V. Mareček, J. Electroanal. Chem. 731 (2014) 107-111.  
2. B.R. Silver, K. Holub, V. Mareček, Electrochim. Acta 156 (2015) 316-320.

We gratefully acknowledge funding from the Czech Science Foundation (project number 13-04630S).



# Modeling of quasi-stationary process at the Platinum anode in the KF–NaF–AlF<sub>3</sub>–Al<sub>2</sub>O<sub>3</sub>

O.V. Limanovskaya<sup>a,b</sup>, V.N. Nekrasov<sup>a</sup>, A.V. Suzdaltsev<sup>a</sup>, A.P. Khramov<sup>a</sup>, Yu.P. Zaikov<sup>a,b</sup>

<sup>a</sup>*Institute of High Temperature Electrochemistry*

<sup>b</sup>*Urals Federal University*

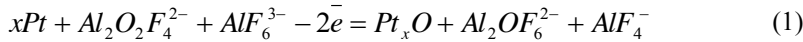
<sup>a</sup>*Yekaterinburg, 620990, Russia,*

<sup>b</sup>*Yekaterinburg, 620002, Russia*

*o.v.limanovskaia@urfu.ru*

The non-stationary behavior of platinum anode in the KF–NaF–AlF<sub>3</sub>–Al<sub>2</sub>O<sub>3</sub> melt has been studied by means of voltammetry and chronopotentiometry in previously our work [1]. The pre-peak near the oxygen oxidation peak is found to be on the almost all experimental cyclic voltammetry curves. Although it was suggested that the nature of the process corresponding with that pre-peak has non diffusion nature, the mechanism of this process is still not clear. This work presents the mathematical model of this process and comparing of calculation and experimental results.

It was proposed [1] that the pre-peak caused by dynamical forming and decomposition of platinum oxide compound on the platinum surface. Therefore the following reactions may be assumed:



The partial currents of these processes may be written as follow:

$$i_1 = i_{01} \cdot \left\{ \frac{X}{X_0} \cdot \frac{1-\Theta}{1-\Theta_0} \cdot e^{\frac{2\alpha NuF}{RT}} - \frac{Y}{Y_0} \cdot \frac{\Theta}{\Theta_0} \cdot e^{\frac{-2(1-\alpha)NuF}{RT}} \right\} \quad (3)$$

$$i_2 = i_{02} \cdot \left\{ \frac{\Theta}{\Theta_0} - \left( \frac{C_{O_2}}{C_{O_2}^0} \right)^{\frac{1}{2}} \frac{1-\Theta}{1-\Theta_0} \right\} \quad (4),$$

where  $i_{01}$ ,  $i_{03}$  – exchange current of (1) and (2),  $X$ ,  $X_0$  – local and initial concentration of  $Al_2O_2F_4^{2-}$  ions,  $Y$ ,  $Y_0$  – local and initial concentration of  $Al_2OF_6^{2-}$  ions,  $\theta$ ,  $\theta_0$  – local and initial value of surface filling degree,  $Nu$  – potential,  $F$ – Faraday,  $R$ – Gas constant,  $T$  – temperature,  $C_{O_2}$ ,  $C_{O_2}^0$  – local and initial concentration of oxygen.

The expressions (3) and (4) were used as base for modeling calculations with follow assumption. As far the pre-peak has non-diffusion nature changing of concentration of  $Al_2O_2F_4^{2-}$  and  $Al_2OF_6^{2-}$  ions have been ignored. The changing of oxygen concentration has been ignored too because oxygen concentration so large that it's changing is negligible. Figure 1 shows the results of modeling calculations.

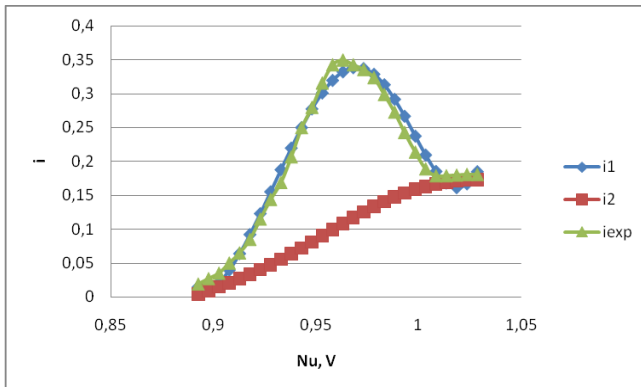


Fig. 1 Comparing modelling and experimental results

As seen in Figure 1, the modeling and experimental results appeared to be considerable matching.





# Ligand Induced Self-Assembly for High Efficiency Quantum Dot Sensitized Cells

Xinhua Zhong

School of Chemistry and Molecular Engineering, East China University of Science and Technology  
Shanghai 200237, China  
e-mail: zhongxh@ecust.edu.cn

A higher surface coverage of QD sensitizers on the oxide substrate is a “must” to improve the efficiencies of quantum dot sensitized solar cells (QDSCs). Due to the big size and lack of anchoring site on colloidal QD surface, the deposition of colloidal QD on  $\text{TiO}_2$  film electrode has been a bottleneck in the construction of high efficiency QDSCs. A ligand-induced self-assembly approach, wherein QDs capped with bifunctional linker ligands such as mercaptopropionic acid (MPA) are immobilized on  $\text{TiO}_2$  prompted by the affinity between carboxyl group and  $\text{TiO}_2$ , has been developed to achieve fast, uniform, and dense deposition of colloidal QD on  $\text{TiO}_2$  electrode.<sup>[1-3]</sup> Meanwhile, alloyed and type-II core/shell structured QD sensitizers with features of wide absorption range and high conduction band edge have been designed and prepared.<sup>[4-7]</sup> Furthermore, the potential charge recombination inside QD, and at  $\text{TiO}_2/\text{QD}/\text{electrolyte}$  interfaces is substantially suppressed with the use of a double inorganic coating treatment, consisting of a novel optimized  $4\text{ZnS}/\text{SiO}_2$  recipe onto QD sensitized  $\text{TiO}_2$  electrodes.<sup>[7,8]</sup> With the combination of high-quality QD sensitizers, effective deposition technique, and suppressed charge recombination, the power conversion efficiency (PCE) of QDSCs under simulated AM 1.5, full 1 sun illumination has been improved steadily from the level of 4-5% to a certified value of 9.0%.<sup>[1-9]</sup> We believe that through optimizing the electrolyte and counter electrode, the PCE of QDSCs will break through 10% (the threshold for commercial applications) in the near future.

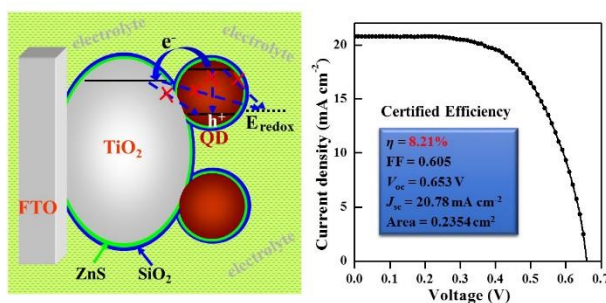


**Figure.** (left) Schematic illustration of charge recombination suppressed by the ZnS/SiO<sub>2</sub> energetic barrier layers; (right) Certified efficiency of 8.21% based on CdSeTe QDSC.

## References:

- (1) Pan, Z.; Zhang, H.; Chen, K.; Hou, Y.; Hua, J.; Zhong, X. *ACS Nano* **2012**, 6, 3982.
- (2) Li, W.; Zhong, X. *J. Phys. Chem. Lett.* **2015**, 6, 798.
- (3) Zhang, H.; Chen, K.; Hou, Y.; Fang, Z.; Pan, Z.; Wu, W.; Hua, J.; Zhong, X. *Chem. Commun.* **2012**, 48, 11235.
- (4) Wang, J. Mora-Sero, I.; Pan, Z.; Zhao, K.; Zhang, H.; Feng, Y.; Yang, G.; Zhong, X.; Bisquert, J. *J. Am. Chem. Soc.* **2013**, 135, 15913.
- (5) Pan, Z.; Zhao, K.; Wang, J.; Zhang, H.; Feng, Y.; Zhong, X. *ACS nano* **2013**, 7, 2115.
- (6) Jiao, S.; Shen, Q.; Mora-Sero, I.; Wang, J.; Pan, Z.; Zhao, K.; Kuga, Y.; Zhong, X.; Bisquert, J. *ACS Nano* **2015**, 9, 908.
- (7) Pan, Z.; Mora-Sero, I.; Shen, Q.; Zhang, H.; Li, Y.; Zhao, K.; Wang, J.; Zhong, X.; Bisquert, J. *J. Am. Chem. Soc.* **2014**, 136, 9203.
- (8) Zhao, K.; Pan, Z.; Mora-Seró, I.; Cánovas, E.; Wang, H.; Song, Y.; Gong, X.; Wang, J.; Bonn, M.; Bisquert, J.; Zhong, X. *J. Am. Chem. Soc.* **2015**, 137, 5602.
- (9) Z. Wen, J. Wang, Z. Pan, X. Zhong, submitted.

## Methodologies for 20% Efficient Perovskite Solar Cells

Nam-Gyu Park

*School of Chemical Engineering and Department of Energy Science*

*Sungkyunkwan University, Suwon 440-746, Korea*

*npark@skku.edu*

Since the groundbreaking report on long-term durable solid-state perovskite solar cell based on organolead halide in 2012, perovskite solar cell has been considered as a promising and potential alternative to silicon or CIGS solar cells due to low-cost and superb performance. In this talk, methodologies will be presented to achieve perovskite solar cells with power conversion efficiency approaching 20%. Morphology of  $\text{CH}_3\text{NH}_3\text{PbI}_3$  (MAPbI<sub>3</sub>) perovskite can be controlled from 3-dimensional (3D) to 1-dimensional (1D) nanostructures. 3D nanocuboids were prepared by two-step spin-coating method, where cuboid size was controlled by engineering solution concentration. Light harvesting efficiency, hole mobility rate and charge extraction were significantly dependent on the nanocuboid size. I-V hysteresis was also found to be affected by nanocuboid size. Piezoresponse force microscopic studies confirmed that polarization behavior was strongly affected by the size. 1D nanowire MAPbI<sub>3</sub> was prepared by means of local dissolution of the PbI<sub>2</sub> layer in two-step procedure. Reduction in dimensionality resulted in the hypsochromic shift of both absorption and fluorescence spectra, indicative of more localized exciton states in nanowires. 1D structure showed better lateral conductivity and charge separation at HTM interface than 3D nanocuboid. The power conversion efficiency (PCE) of ~17% and ~15% was achieved from 3D nanocuboids and 1D nanowire, respectively. Processing is critical to have high quality perovskite film, where we have developed reproducible method for 20% efficiency perovskite solar cell via acid-base chemistry. We have also tried to fabricate perovskite solar cell under high relative humidity (RH) outside glove box and attained PCE over 15% from the device prepared at 50% RH. Preliminary results on long-term stability of perovskite solar cell will be also discussed.

# Graphene Oxide Quantum Dots for Photon Energy Conversion

Hsisheng Teng, Te-Fu. Yeh, Liang-Che Chen, Chiao-Yi Teng

*Department of Chemical Engineering and Research Center for Energy Technology and Strategy, National Cheng Kung University, Tainan 70101, Taiwan*  
*hteng@mail.ncku.edu.tw*

Graphene oxide (GO) is a semiconductor that can absorb light to generate electron-hole pairs. The electronic properties of GO can be tuned by varying its size and embedding different functional groups. Doping nitrogen on GO by ammonia treatment can convert p-type GO to an n-type semiconductor. The size effect resulting from quantum confinement also influences the electronic structures of GO. Introducing nitrogen into GO quantum dots has resulted in the coexistence of p- and n-type conductivities in the nitrogen-doped GO quantum dots (NGOQDs) [1]. Under irradiation the photogenerated electron-hole pairs in NGOQDs undergo recombination for photoluminescence or separation for photocatalysis. The function of NGOQDs, as a phosphor or photocatalyst, depends on the defect-state density on the NGOQD surface.

The NGOQDs have a band gap of approximately 2.3 eV. The Pt-deposited NGO-QDs effectively catalyzed H<sub>2</sub> evolution from an aqueous solution containing triethanolamine as a sacrificial electron donor. The quantum yield for H<sub>2</sub> evolution reached a value as high as 13 % under irradiation at 420 nm [2].

Surface-passivated NGOQDs suspended in water or other solvents exhibit strong emission at  $\lambda = 530$  nm, irrespective of the excitation wavelength. Excitation at 470 nm yields a maximum photoluminescence quantum yield. Electron relaxation from the graphene anti-bonding  $\pi$  orbital to the non-bonding oxygen state may be responsible for this emission [3].

## References

- [1] T.F. Yeh, C.Y. Teng, S.J. Chen, H. Teng, *Advanced Materials* 26 (2014) 3297.
- [2] T.F. Yeh, S.J. Chen, H. Teng, *Nano Energy* 42 (2015) 476.
- [3] C.Y. Teng, T.F. Yeh, K.I. Lin, S.J. Chen, M. Yoshimura, H. Teng, *J. Mater. Chem. C* 3 (2015) 4553.

# **Impedance Spectroscopic Analysis of Organic-Inorganic Hybrid Perovskite Solar Cell under Different Architectures**

Yu-Tung Yin and Liang-Yih Chen\*

*Department of Chemical Engineering, National Taiwan University of Science and Technology  
No.43, Sec. 4, Keelung Rd., Da'an Dist., Taipei 106, Taiwan  
sampras@mail.ntust.edu.tw*

The organic-inorganic hybrid perovskite ( $\text{CH}_3\text{NH}_3\text{PbI}_3$ ) solar cell with spiro-MeOTAD as a hole transport material (HTM) was investigated via electron impedance spectroscopy (EIS). A model has been established to analysis the frequency response of the perovskite based solar cell, which was derived from the existing models used for the liquid and solid-state dye-sensitized solar cells. The benefit of structure layer existence has been demonstrated in this study. Furthermore, the influence of ferroelectric characteristic of perovskite would also be investigated. On the extraction of fitting EIS parameters, the interfacial electric carriers transport/transfer properties inside perovskite solar cell were studied and correlated with the overall performance of devices. In particular, the features in the EIS responses could be attributed to the ionic and electronic transport properties of the perovskite. The ferroelectric characteristic was strongly correlated with the flatness on the interface of perovskite. The key issues on maintain high performance of perovskite solar cell respect to the EIS analysis were studied.

# Photoelectrochemical characterization of ZnLaTaON based electrodes for water oxidation reaction

Abdullah AlMayouf<sup>a</sup>, Mohamed Ali Ghanem<sup>a</sup>, Maged Naji Shaddad<sup>a</sup>, Prabhakarn Arunachalam<sup>a</sup>, Mansour AlHoshan<sup>b</sup>, Mark T Weller<sup>c</sup>, Frank Marken<sup>c</sup>

<sup>a</sup>Department of Chemistry, College of Science, King Saud University, Riyadh, KSA. amayouf@ksu.edu.sa

<sup>b</sup>Department of Chemical Engineering, College of Engineering, King Saud University, Riyadh, KSA.

<sup>c</sup>Department of Chemistry and Centre for Sustainable Technologies, University of Bath, UK.

The development of an efficient semiconductor photocatalysts for direct conversion of solar energy into chemical energy is one of the most potential approaches to meet the environmental and energy demands.<sup>1</sup> Photoelectrochemical water splitting is promising approach for utilizing solar energy to generate oxygen and hydrogen.<sup>2</sup> It is challenging to develop a semiconductor that has both suitable conduction and valence band for H<sub>2</sub> and O<sub>2</sub> production and narrow band gap (< 3 eV) for visible light absorption. Tantalum oxynitrides (TaON) based materials have that potential for water splitting reaction under visible light reaction.<sup>3</sup> In the present work, we investigated in alkaline medium, the photoelectrochemical properties of Zn<sub>0.5</sub>La<sub>0.5</sub>TaO<sub>1.5</sub>N<sub>1.5</sub>, LaTaON<sub>2</sub> and TaON particles coated onto ITO glass by electrophoretic deposition method.. Also the photoelectrochemical characterizations of Zn<sub>0.5</sub>La<sub>0.5</sub>TaO<sub>1.5</sub>N<sub>1.5</sub> for water oxidation reactions was performed by loading co-catalyst of cobalt phosphate (CoPi). The nanostructured photoanodes are characterized with a range of electrochemical techniques, such as cyclic voltammetry (CV) and electrochemical impedance spectroscopy. Zn<sub>0.5</sub>La<sub>0.5</sub>TaO<sub>1.5</sub>N<sub>1.5</sub> based photoanodes retain its crystalline structure and it possess the band gap of < 2.6 eV. The oxygen production on the photoanodes is evidenced by sensing oxygen concentration in alkaline solution and under illumination condition. Figure 1a shows the CVs characteristics of Zn<sub>0.5</sub>La<sub>0.5</sub>TaO<sub>1.5</sub>N<sub>1.5</sub> and CoPi/Zn<sub>0.5</sub>La<sub>0.5</sub>TaO<sub>1.5</sub>N<sub>1.5</sub> photoanodes in dark and under illumination and it evidences the potential shift towards the lower potential regions with the additions of CoPi co-catalysts. In addition, photocurrent density of 2 mA/cm<sup>2</sup> was observed for the Zn<sub>0.5</sub>La<sub>0.5</sub>TaO<sub>1.5</sub>N<sub>1.5</sub> photoanodes and it is further enhanced to 5 mA/cm<sup>2</sup> by loading CoPi co-catalyst. Fig. 1b shows the oxygen evolution measurement in a sulphate solution (pH 13) in a two compartment cell under visible light (> 450 nm) with the corresponding chronoamperometric measurements of the photoanodes. The use of photodeposited CoPi co-catalyst on ZnLaTaON together with sulphate solutions significantly increased the photocurrent and enabled us to produce O<sub>2</sub> from water under visible light irradiation at a potential of (1.2 V vs SCE).

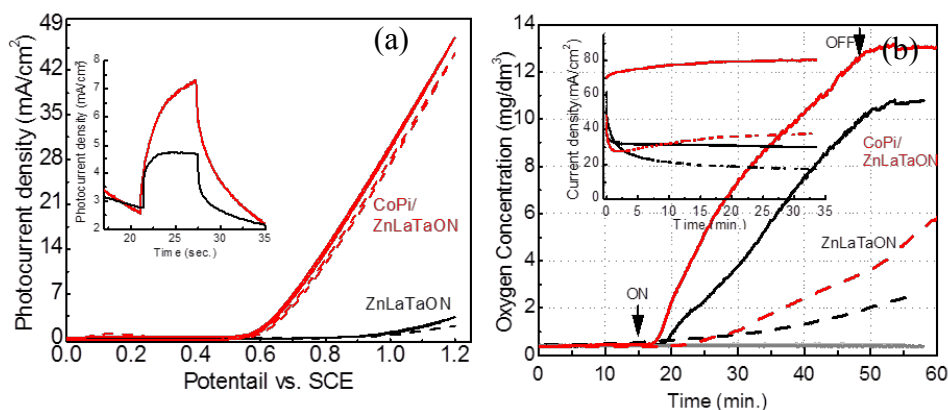


Figure 1: (a) CVs and (b) Oxsense measurements of oxygen at ZnLaTaON with and without CoPi at 1.2 V vs SCE. Dashed line-dark; solid line: light (Inset corresponding CA of the photoanodes).

## References:

- 1- A. Kudo, Y. Miseki, Materials Letters, 148,155(2015).
- 2- A. Fujishima, K. Honda, Nature 238, 37 (1972).
- 3-M. Higashi, K. Domen, R. Abe, 134, 6968 (2012).

**Acknowledgments:** This project was supported by King Saud University, Deanship of Scientific Research, College of Science Research center.

# Nano-Impacts – Studying Magnetic Field Effects on Single Magnetite Nanoparticles in Solution

Kristina Tschulik, Richard G. Compton

Physical and Theoretical Chemistry Laboratory, Department of Chemistry, University of Oxford, South Parks Road, Oxford, OX1 3QZ, UK  
*Tschulik.Kristina@gmail.com*

Magnetite nanoparticles ( $\text{Fe}_3\text{O}_4$  NPs) have widespread application in magnetic field-based medical treatments, for instance in Magnetic Resonance Imaging (MRI) for diagnostics or in future therapies like targeted drug delivery or hyperthermia. Inferring information on the effects of the applied magnetic fields on nanoparticle agglomeration and thus biodegradation, e.g. in the human body, is therefore an important analytical task.

Two electrochemical ‘nano-impact’ methodologies Anodic (APC) and Cathodic Particle Coulometry (CPC) are presented herein to address these tasks. They enable the detection and sizing of magnetite nanoparticles in a solution on a single particle basis and in the presence or the absence of a magnetic field. Particle Coulometry measures the charge transferred when a particle impacts an electrode that is held at a potential high enough to either reduce (CPC) or oxidize (APC) the impacting particle (Fig. 1). The charge transferred per impact provides the number of atoms in each nanoparticle and thus individual particle sizes and agglomeration states can be determined [1]. For mixed oxides like  $\text{Fe}_3\text{O}_4$  both APC and CPC can be applied complementarily [2]. While the used superparamagnetic  $\text{Fe}_3\text{O}_4$  nanoparticles were found to be stable against agglomeration even in the presence of electrolytes of high ionic strength (0.2 M phosphate buffer), the application of a magnetic field of 0.3 T induced individual nanoparticles to agglomerate to larger clusters in the same electrolyte solution [3]. Furthermore, the dissolution of  $\text{Fe}_3\text{O}_4$  nanoparticles was found to be strongly slowed down in the presence of a magnetic field. This effect is attributed to the high magnetic field gradients established at the nanoparticles’ surface and the associated local action of a magnetic field gradient force retarding the dissipation of the formed paramagnetic  $\text{Fe}^{2+}$  ions from the nanoparticle surface.

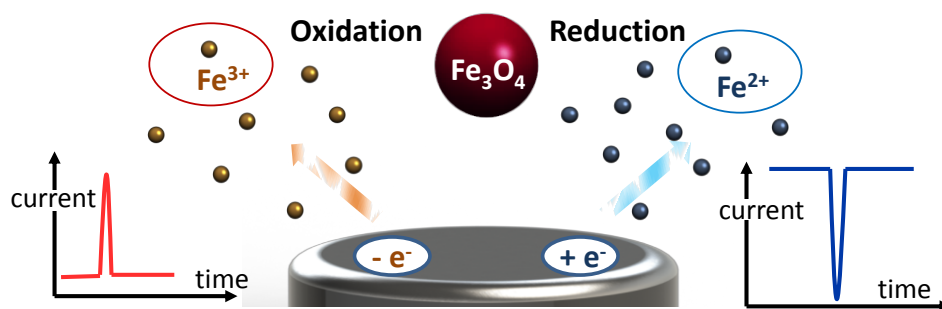


Fig. 1: Schematic drawing showing the principle of nanoparticle impact based sizing of individual magnetite nanoparticles via Anodic (left) and Cathodic Particle Coulometry (right).

## References:

- [1] Y.-G. Zhou, N.V. Rees, R.G. Compton, *Angew. Chem. Int. Ed.* 50 (2011) 4219–4221.
- [2] K. Tschulik, B. Haddou, D. Omanović, N.V. Rees, R.G. Compton, *Nano Res.* 6 (2013) 836–841.
- [3] K. Tschulik, R.G. Compton, *Phys. Chem. Chem. Phys.* 16 (2014) 13909–13913.

# Scanning Electrochemical Microscopy for Probing the Properties of 2D Materials

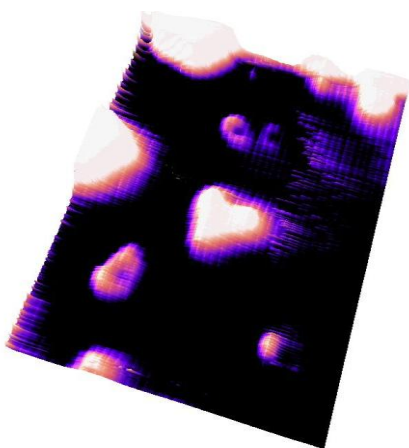
Stefania Rapino,<sup>a</sup> Emanuele Treossi,<sup>b</sup> Vincenzo Palermo,<sup>b</sup> Massimo Marcaccio,<sup>a</sup> Francesco Zerbetto,<sup>a</sup> and Francesco Polucci<sup>a</sup>

<sup>a</sup> *Dipartimento di Chimica, Università di Bologna, Via Selmi 2, I-40126 Bologna, Italy*

<sup>b</sup> *ISOF-CNR, Via Gobetti 101, I-40129 Bologna, Italy*

*e-mail: stefania.rapino3@unibo.it*

Graphene oxide (GO) has attracted much attention as a water soluble, highly tunable platform for applications in composites,[1] sensors[2] and biomaterials.[3] The hydrophilic structure of GO is given by epoxy bridges, hydroxyl and carboxyl groups and allows the preparation of aqueous solutions, mainly formed by single layer GO sheets, which can be processed on different substrates,[4] and possibly reduced to obtain conductive reduced graphene oxide (RGO).[5] The complex structure of GO and the large variety of chemical groups present in it require specific techniques to study its properties at the single sheet level. Scanning electrochemical microscopy (SECM) can image GO flakes on insulating and



A SECM image of GO sheet on gold.

conducting substrates. The contrast between GO and the substrate is controlled by the electrostatic interactions that are established between the charges of the molecular redox mediator and the charges present in the sheet. SECM also allowed quantitative measurements of the charge transfer kinetics between single monolayer sheets and redox mediator molecules. By using different redox mediators and different substrates we show the effect of single layer coating on the electrochemical processes that take place on a surface. The charges present on the surface of a monoatomic layer can hinder the SECM current or enhance it. The final contrast is indicative of the state of the sheets and of the electrostatic interactions between the molecular redox mediator and the charges of the sheet surface. [6]

This approach will likely allow to study – with nano/microscale resolution – the electrochemical properties and processes of monoatomic sheets of other 2D materials

such as BN and MoS<sub>2</sub>, in both water and other liquids.

## References

- [1] M. Cano, U. Khan, T. Sainsbury, A. O'Neill, Z. Wang, I. T. McGovern, W.K.Maser, A.M. Benito and J. N. Coleman, *Carbon*, 2013, 52, 363–371.
- [2] S. Borini, R. White, D. Wei, M. Astley, S. Haque, E. Spigone, N. Harris, J. Kivioja and T. Ryhanen, *ACS Nano*, 2013, 7, 11166–11173.
- [3] D. Depan, B. Girase, J. S. Shah and R. D. Misra, *Acta Biomater.*, 2011, 7, 3432–3445.
- [4] E. Treossi, M. Melucci, A. Liscio, M. Gazzano, P. Samori and V. Palermo, *J. Am. Chem. Soc.*, 2009, 131, 15576–15577.
- [5] A. Liscio, G. P. Veronese, E. Treossi, F. Suriano, F. Rossella, V. Bellani, R. Rizzoli, P. Samori and V. Palermo, *J. Mater. Chem.*, 2011, 21, 2924–2931.
- [6] S. Rapino, E. Treossi, V. Palermo, M. Marcaccio, F. Paolucci, F. Zerbetto, *Chem. Commun.*, 2014, 50, 13117–13120



# Preparation, Characterization, and Electrochemical Properties of Monolith Glass-like Carbon-Silica Composites

Jane Karla F.B. Machado<sup>1</sup> and Herenilton P. Oliveira<sup>2</sup>

<sup>1</sup>Universidade de Franca, Av. Dr. Armando Salles Oliveira, 201, Franca (SP), Brazil

<sup>2</sup>Universidade de São Paulo, FFCLRP, Av. Bandeirantes, 3900, Ribeirão Preto (SP), Brazil  
e-mail: herepo@ffclrp.usp.br

Polymeric glassy carbon/silica composites were prepared by carbonizing cured pre-polymers from phenolic resins and silica xerogel. The idea behind this study is to obtain a composite electrode through simultaneous polymerization of phenol formaldehyde oligomers and tetraethoxysilane or methyltriethoxysilane monomers forming an interpenetrating hybrid polymer network using soft chemistry approach, followed by controlled heating up to 1200 °C in an oxygen-free environment. The proposed methodology enables to obtain isotropic and monolithic glass-like carbon/silica composite electrodes with high carbon amount (the resultant glassy ceramic composites consist of up to 85 mass% of glassy carbon and 15 mass% of silica) based on phenol-formaldehyde thermosetting resin (Figure 1), and their application as working electrode and as support to chemically modified electrodes. The characterization of the as-synthesized monoliths was carried out by thermal analysis, scanning electron microscopy, X-ray dispersive energy spectroscopy, X-ray powder diffraction, infrared and Raman spectroscopies, and the electrochemical properties were evaluated by cyclic voltammetry as well impedance. X-ray dispersive energy mapping indicates that the silica (presence confirmed by X-ray diffraction patterns) is homogeneously dispersed in the glassy carbon matrix. The electrochemical properties were characterized in NaOH and H<sub>2</sub>SO<sub>4</sub> solution by cyclic voltammetry at different sweep rates in the potential range between the hydrogen and oxygen evolution. The electrode surfaces were evaluated for their electron transfer with Fe(CN)<sub>6</sub><sup>3-/4-</sup> system in aqueous electrolyte (Figure 2), as well as the effects of the different silica precursors on electrochemical properties. Finally, the adopted procedure minimizes the formation of bubbles, cracks and distortions in the material, as well as it is possible to assemble electrodes of different sizes and shapes depending on the geometry of the mold.

Acknowledgments : FAPESP and CNPq



Figure 1: Photography of the composite GPC/Si.

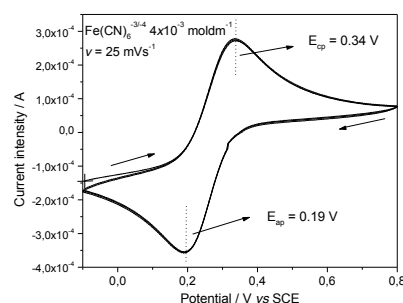


Figure 2: Cyclic voltammetry of Fe(CN)<sub>6</sub><sup>3-/4-</sup> system in KCl 0.05 molL<sup>-1</sup> using GPC with 7.5 % TEOS.

# Observation of Charge Transfer Cascade in $\alpha$ -Fe<sub>2</sub>O<sub>3</sub>/IrO<sub>2</sub> Photoanodes by In-Operando X-Rays Absorption Spectroscopy

Alessandro Minguzzi,<sup>a</sup> Elisabetta Achilli,<sup>b</sup> Francesco D'Acapito,<sup>c</sup> Alberto Naldoni,<sup>d</sup> Francesco Malara,<sup>d</sup> Cristina Locatelli,<sup>a</sup> Alberto Vertova,<sup>e</sup> Paolo Ghigna<sup>b</sup>

<sup>a</sup> Dipartimento di Chimica and ISTM, Università degli Studi di Milano, Via Golgi 19, 20133 Milano, Italy

<sup>b</sup> Università di Pavia, Dipartimento di Chimica, Via Taramelli 16, 27100, Pavia, Italy

<sup>c</sup> Consiglio Nazionale delle Ricerche, Istituto Officina dei Materiali, Operative Group in Grenoble, c/o European Synchrotron Radiation Facility, B.P. 220, 38043 Grenoble, France

<sup>d</sup> Consiglio Nazionale delle Ricerche, Istituto di Scienze e Tecnologie Molecolari, Via C. Golgi 19, 20133 Milano, Italy

<sup>e</sup> Dipartimento di Chimica, ISTM and CNR-ISTM Università degli Studi di Milano, Dipartimento di Chimica, Via Golgi 19, 20133 Milano, Italy  
alessandro.minguzzi@unimi.it

In this work we show the direct observation, by means of spectro-photoelectrochemical experiments, of charge transfer between a semiconductor ( $\alpha$ -Fe<sub>2</sub>O<sub>3</sub>) and a metal oxide overlayer (hydrous IrO<sub>x</sub>) as a photoanode architecture in photoelectrochemical water splitting.<sup>1</sup> The aim is to clarify the ambiguous role of oxygen evolving catalysts used as overlayers on top of photoanodes in photoelectrochemical water splitting cells. Previous literature suggested that the real benefit of covering hematite with overlayers like iridium or cobalt oxides is not due to an increase of reaction kinetics but the decrease of the electron density in the hematite<sup>2</sup> or the storage of photogenerated holes.<sup>3</sup> These effects are likely more important when hydrous overlayer, that can act as adapting catalysts,<sup>4</sup> are considered. All these hypothesis can explain the observed improved hole lifetime and reduce recombination with electrons.

The present experimental approach is similar to the one that allowed our recent disclosure of the oxidation states assumed by hydrous IrO<sub>x</sub> as catalyst for water oxidation.<sup>5</sup> In the present case, FEXRAV<sup>6</sup> and XANES have been used to probe changes in the charge state of Ir while the hematite was illuminated with 410nm radiation. Thanks to this *in-operando* setup, we were able to observe an increase of the density of empty Ir 5d states during hematite illumination and in correspondence of water spitting in the photoelectrochemical cell. The main conclusion is that a charge (hole) transfer between hematite and iridium occurs only when the hematite is illuminated. Hydrous iridium oxide is therefore capable of withdrawing holes from the semiconductor thus increasing the probability of interface reaction rather than charge recombination.

<sup>1</sup> Minguzzi A., Lugaresi O., Achilli E., D'Acapito F., Naldoni A., Malara F., Locatelli C., Vertova A., Rondinini S., Ghigna P., *In preparation*

<sup>2</sup> Badia-Bou L., Mas-Marza E., Rodenas P., M. Barea E., Fabregat-Santiago F., Gimenez S., Peris E., Bisquert J., *J. Phys. Chem. C*, **2013**, 117, 3826–3833

<sup>3</sup> Lin F., Boettcher S.W. *Nature Materials*, **2014**, 13, 81-86

<sup>4</sup> Barroso M., Mesa C.A., Pendlebury S.R., Cowana A.J., Hisatomi T., Sivula K., Grätzel M., Klug D.R., Durrant J.R. *PNAS*, **2012**, 109, 15640–15645

<sup>5</sup> Minguzzi A., Lugaresi O., Achilli E., Locatelli C., Vertova A., Ghigna P., Rondinini S., *Chem. Sci.*, **2014**, 5, 3591-3597

<sup>6</sup> Minguzzi, A.; Lugaresi, O.; Locatelli, C.; Rondinini S.; d'Acapito, F.; Achilli, E.; Ghigna, P. *Anal. Chem.* **2013**, 85, 7009-7013.

# DFT-MD Study on Formation Processes of Solid Electrolyte Interphase at Negative Electrode Interfaces in Lithium-Ion Battery

Yoshitaka Tateyama<sup>†,§</sup>, Keisuke Ushirogata<sup>†,¶</sup>, Keitaro Sodeyama<sup>†,§</sup>, Yukihiro Okuno<sup>†,¶</sup>

<sup>†</sup>International Center for Materials Nanoarchitectonics (MANA), National Institute for Materials Science (NIMS), 1-1 Namiki, Tsukuba, Ibaraki 305-0044, Japan. <sup>§</sup>Elements Strategy Initiative for Catalysts & Batteries, Kyoto University, Goryo-Ohara, Nishikyo-ku, Kyoto 615-8245, Japan. <sup>¶</sup>Research and Development Management Headquarters, FUJIFILM Corporation, 210 Nakanuma, Minamiashigara, Kanagawa 250-0193, Japan.  
TATEYAMA.Yoshitaka@nims.go.jp

Lithium-Ion Battery (LIB) applications for electric vehicles, smart grids etc. have recently attracted much attention. For this purpose, a new class of LIBs with larger capacities and power density as well as higher reliability is quite demanded. It is well known that most of those properties are governed by the quality of solid electrolyte interphase (SEI) film formed on the interface between negative electrode and organic electrolyte. However, the reaction mechanisms around electrolyte-electrode interfaces have not been fully understood yet on the atomic scale due to the difficulty in experimental in-situ observation. Then, we have addressed such unresolved issues by using DFT-MD sampling with sufficient accuracy.

The SEI formation is initiated by the electrochemical decomposition of the electrolyte molecules such as solvents, additives, and Li-salt anions. Slight change of the electrolyte component often exhibits a large impact on the SEI quality. We first examined the reductive decomposition of the electrolyte molecules at charging, namely under reductive environment, using a representative LIB system with ethylene carbonate (EC) solvents and vinylene carbonate (VC) additives on a graphite electrode. We carried out DFT-MD free energy calculations with a cutting-edge Blue-moon ensemble technique for the possible reductive decomposition pathways, together with DFT-MD samplings of probable metastable states. We then found that VC passivation to EC anion radical, a product of one-electron reductive decomposition of EC, is more appropriate mechanism than the conventional scenario with sacrificial reductive decomposition of VC (Fig. (a)) [1]. This novel mechanism can explain the decrease of irreversible capacity and the CO<sub>2</sub> evolution with a small amount of VC additives observed experimentally, and the concept has been supported by subsequent studies.

Next, we extracted stable SEI film components (SFCs) from the products of the reductive decompositions of the electrolyte molecules. We then investigated the characteristic of the SFC monomers as well as the probable SFC amorphous aggregates on the adhesion to the graphite electrode and the interfacial electronic states. The results showed that the SFC aggregates are characterized by “unstable adhesion” to the graphite surface (Fig. (b)) and “high electronic insulation”. With these results, we discussed the mechanism how the SFC aggregates are formed toward the SEI film formation [2]. These new findings will contribute to the development of more efficient and reliable LIBs.

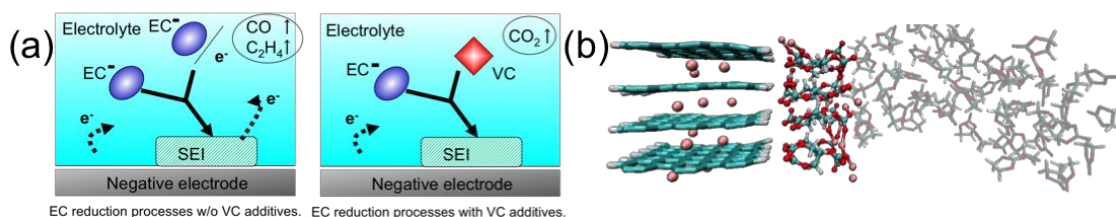


Figure (a) Schematic mechanisms of the initial reductive decompositions in the electrolyte with EC solvents only and the EC solvents with VC additives. (b) A snapshot of the adhesion of SFC aggregate to the graphite electrode.

## Acknowledgement:

The calculations in this work were carried out on the K computer at the RIKEN AICS through the HPCI System Research Projects (Proposal Numbers hp140071 and hp140232).

## Reference:

- [1] K. Ushirogata, K. Sodeyama, Y. Okuno, Y. Tateyama, J. Am. Chem. Soc. **135**, 11967-11974 (2013).
- [2] K. Ushirogata, K. Sodeyama, Z. Futera, Y. Tateyama, Y. Okuno, submitted.

# Photoelectrochemical Response of Hetero-layer Films Composed of Redox-active Ru Complexes: Charge Trapping and Memory Effect

Masa-aki Haga, Takumi Nagashima, Hiroaki Ozawa

Department of Applied Chemistry, Chuo University, 1-13-27 Kasuga, Bunkyo-ku, Tokyo 112-8551, Japan  
E-mail: mhaga@kc.chuo-u.ac.jp

Sequential layer-by-layer assembly by coordination bond is of great scientific and practical importance due to a promising method for the construction of well-ordered layered structures on a solid surface. Combining with two components with different redox potentials, many layer structures with different potential gradients can be constructed. Here, two dinuclear Ru complexes, Ru-NP and Ru-CP, were selected as shown in Fig 1, in which the oxidation potentials are  $E_{1/2} = +0.84$  and  $+1.06$  V vs  $\text{Fc}^{0/+}$  for Ru-NP, and  $E_{1/2} = -0.40$  and  $0.07$  V for Ru-CP, respectively.[1] The structure of the multilayers is described as  $\text{ITO}||(\text{Ru-NP})_n(\text{Ru-CP})_m$ , where the subscript “n or m” represents the number of Ru layers connected by the Zr layer. Two heterolayer films were chosen: i.e., one structure was  $\text{ITO}||(\text{Ru-NP})_n(\text{Ru-CP})_m$ , and the other was  $\text{ITO}||(\text{Ru-CP})_n(\text{Ru-NP})_m$ . In the hetero-layer films of  $\text{ITO}||(\text{Ru-NP})_4(\text{Ru-CP})_4$ , cyclic voltammogram showed a typical catalytic wave, resulting from the rectification of electron transfer due to the large potential difference between Ru-NP and Ru-CP, and the charge was trapped in the outer layers. This charge trapping process in the outer Ru-CP layer was proved by the observation of the intervalence charge transfer (IVCT) band at 1140 nm in the thin-layer film spectroelectrochemistry. Under photocurrent measurements on the  $\text{ITO}||(\text{Ru-NP})_4(\text{Ru-CP})_4$  film, the direction of photocurrent was governed by the charging state of the outer Ru-CP layers; i.e., when the Ru-CP layer possessed the discharging Ru(III)-Ru(III) state, a *cathodic photocurrent* was observed, but once the Ru-CP layer became charged as a mixed-valent Ru(II)-Ru(III) state, the photocurrent direction was changed to anodic. Since the charging/discharging of the outer Ru-CP layer was controlled by altering the potential from -0.5 V to 0.7 V, the present hetero-layered films acts as a memory device. (See Fig 2) When the sequence of the layers was inverted from  $\text{ITO}||(\text{Ru-NP})_4(\text{Ru-CP})_4$  to  $\text{ITO}||(\text{Ru-CP})_4(\text{Ru-NP})_4$ , the photocurrent response became reverse as an *anodic photocurrent*. Therefore, the molecular sequence plays an important role in the hetero-layer films composed of the Ru complexes.

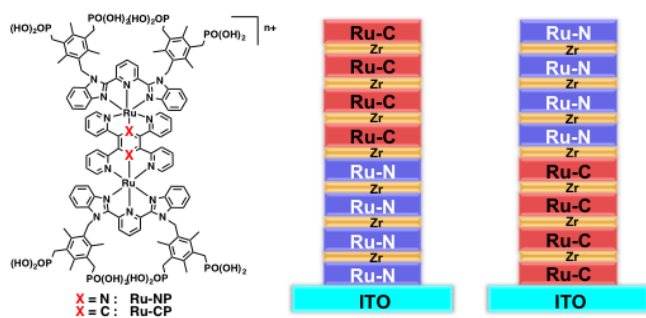


Fig1. Chemical Structures of two Ru complexes, Ru-NP and Ru-CP, and schematic drawings for two different hetero-layer structures linked by Zr ion: i.e.,  $\text{ITO}||(\text{Ru-NP})_4(\text{Ru-CP})_4$  (left)  $\text{ITO}||(\text{Ru-CP})_4(\text{Ru-NP})_4$  (right side).

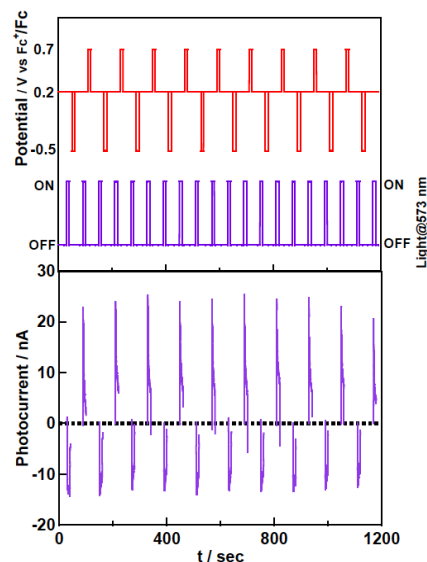


Fig 2. Potential pulse pattern (red line) and concomitant photoirradiation pattern (violet line) and resulting photocurrent response on heterolayer  $\text{ITO}||(\text{Ru-NP})_4(\text{Ru-CP})_4$ .

[1] T. Nagashima, et al, *Organometallics* **33**, 4893(2014)

# Electrocatalytic Oxidation of Biologically Active Compounds on MoS<sub>2</sub> Nanopetal Stacks Decorated with Carbon or Gold Nanoparticles

Joanna Dolinska<sup>a</sup>, Arunraj Chidambaram<sup>b</sup>, Zahra Taleat<sup>b</sup>, Witold Adamkiewicz<sup>a</sup>, Wojciech Lisowski<sup>a</sup>,  
Michalina Iwan<sup>a</sup>, Barbara Palys<sup>c</sup>, Volodymyr Sashuk<sup>a</sup>, Tomasz Andryszewski<sup>a</sup>, Marcin Opallo<sup>a</sup>, Liza  
Rassaei<sup>b</sup>

*a/Institute of Physical Chemistry, Polish Academy of Sciences, ul. Kasprzaka 44/52, 01-224 Warszawa,  
Poland*

*b/Organic Materials and Interfaces, Department of Chemical Engineering, Delft University of  
Technology, Delft, Netherlands*

*c/Faculty of Chemistry, University of Warsaw, Pasteura 1 Str. 02-093 Warsaw, Poland*

*jdolinska@ichf.edu.pl*

Two dimensional layer-structured transition metal dichalcogenides has recently received much attention, due to their specific optical, electronic and mechanical properties resulting from their unique structures [1,2]. This is related to their physicochemical characteristics resulting from the specific structure consisting covalently bonded metal atoms sandwiched between chalcogen layers [2]. MoS<sub>2</sub> is the most extensively studied material from this class and its application in lithium ion batteries [3] and as hydrogen evolution catalyst [4] was reported. The limitations of electrochemical applications of this material were also pointed out [5]. MoS<sub>2</sub> can be decorated with other nanomaterials, for example gold nanoparticles. Such hybrid material was reported to exhibit electrocatalytic synergy in dioxygen reduction reaction [6] or oxidation of ascorbic acid, dopamine and uric acid oxidation for selective sensing [7].

Here we will report preparation and characterisation of MoS<sub>2</sub> nanopetal stacks decorated with carbon and gold nanoparticles and the application of these materials in electrocatalysis of biologically active compounds. The decoration of MoS<sub>2</sub> with negatively and/or positively charged carbon nanoparticles was performed in suspension of both substrates by sonication and the obtained material was characterised by dynamic light scattering. The hybrid material was deposited on the electrode (glassy carbon) by drop casting. On the other hand MoS<sub>2</sub> nanopetal stacks decorated with positively charged Au nanoparticles were directly formed on the electrode (ITO) surface by alternate dropcasting of both components suspension. The films of both hybrid materials were characterised by scanning electron microscopy, X-ray photoelectron spectroscopy and Fourier transformed infrared spectroscopy.

Cyclic voltammetry reveals that modification of the electrode substrate produce an increase of electrochemically active surface and increase electronic conductivity of MoS<sub>2</sub>. The decoration of MoS<sub>2</sub> with carbon nanoparticles produces material with electrocatalytic activity towards neurotransmitters as epinephrine or dopamine. In turn the hybrid material consisting MoS<sub>2</sub> nanopetals stacks decorated with Au nanoparticles exhibits electrocatalytic activity towards cysteine, glutathione and glucose. This activity depends also on the functionalisation of Au nanoparticles used for decoration.

- [1] Y. Sun, S. Gao, F. Lei, C. Xiao, and Yi Xie, *Acc. Chem. Res.* 48 (2015) 3.
- [2] R. Lv, J.A. Robinson, R.E. Schaak, D. Sun, Y. Sun, T. E. Mallouk, M. Terrones, *Acc. Chem. Res.* 48 (2015) 56.
- [3] Y. Liu, Y. Zhao, L. Jiao, J. Chen. *J. Mater. Chem. A*, 2014, 2, 13109. |
- [4] D. Voiry, M. Salehi, R. Silva, T. Fujita, M. Chen, T. Asefa, V. B. Shenoy, G. Eda, M. Chhowalla, *Nano Lett.* 2013, 13, 6222.
- [5] M. Zafir M. Nasir, Z. Sofer, A. Ambrosi, M. Pumera, *Nanoscale*, 2015, 7, 3126.
- [6] T. Wang, J. Zhuo, Y. Chen, K. Du, P. Papakonstantinou, Z. Zhu, Y. Shao, M. Li, *ChemCatChem* 6 (2014) 1877.
- [7] H. Sun, J. Chao, X. Zuo, S. Su, X. Liu, L. Yuwen, C. Fanab, L. Wang, *RSC Adv.* 4 (2014) 27625.

# Co-axial Nanostructures for CO<sub>2</sub> Conversion: Synergic Effects between Carbon Nanotubes and Metal Oxides

Giovanni Valenti,<sup>a</sup> Alessandro Boni,<sup>a</sup> Tiziano Montini,<sup>b</sup> Massimo Marcaccio,<sup>a</sup> Stefania Rapino,<sup>a</sup> Paolo Fornasiero,<sup>b</sup> Maurizio Prato,<sup>b</sup> and Francesco Paolucci.<sup>a</sup>

<sup>a</sup> Department of Chemistry “G. Ciamician” University of Bologna, via Selmi 2, 40126 Bologna, Italy

<sup>b</sup> Department of Chemical and Pharmaceutical Sciences, Center of Excellence for Nanostructured Materials (CENMAT), University of Trieste, Italy  
e-mail: g.valenti@unibo.it

The growing need for energy on global scale and the realization that the so called oil-based economy cannot sustain our world anymore, prompted researchers to find new ways to “power” the planet.<sup>1</sup> In particular a lot of efforts have been done in the field of chemical energy conversion, that remains very challenging because of the requirement for higher efficiencies.<sup>2</sup> Over the last decades the continuous increase of carbon dioxide in the biosphere has been recognised as one of the main causes for the global warming. The conversion of carbon dioxide into chemical fuels is a topic of great interest and recently a lot of different approaches for the electrochemical reduction of this powerful greenhouse gas to more useful products have been reported.<sup>3</sup>

In this context our group recently focused the attention on the study of catalytic systems for the splitting of water.<sup>4</sup> Our last efforts have been done in the design and development of new nanostructured material that synergistically combine the unique properties of multiwall carbon nanotubes (MWCNTs), metal oxides (CeO<sub>2</sub>) and Pd nanoparticles (Pd NPs).<sup>5</sup> The MWNT@Pd/CeO<sub>2</sub> nanomaterial have been designed and evaluated as electrocatalyst for the CO<sub>2</sub> conversion.

This nanohybrid exhibit very good performances and efficiencies, showing physical and chemical properties that differ to those expected from the simple sum of the individual building blocks. Finally, we shed light on the role of the Pd NPs in terms of their influence on the electrocatalytic activities.



## References

- [1] Armaroli, V. Balzani, *Angew. Chem. Int. Ed.* **2007**, 46, 52-66.
- [2] G. Centi, S. Perathoner, *ChemSusChem*, **2010**, 3, 195-208.
- [3] X. Min, M. W. Kanan, *J. Am. Chem. Soc.* **2015**, 137, 4701-4708.
- [4] a) F. Toma, A. Sartorel, M. Iurlo *et al.*, *Nature Chemistry* **2010**, 2, 826-831. b) G. Valenti, M. Cargnello, A. Boni *et al.* *submitted*
- [5] M. Cargnello *et al.*, *J. Am. Chem. Soc.* **2012**, 134, 11760-11766.

# Shape-Controlled and Size-Controlled Synthesis of Metal Nanocrystals and Their Electrochemical Applications

Guobao Xu<sup>\*1</sup>, Jianping Lai<sup>1,2</sup>, Wenxin Niu<sup>1,2</sup>, Ling Zhang<sup>1,2</sup>

<sup>1</sup> State Key Laboratory of Electroanalytical Chemistry, Changchun Institute of Applied Chemistry, Chinese Academy of Sciences, P. R. China;

<sup>2</sup> Graduate University of the Chinese Academy of Sciences.

E-mail: [guobaoyu@ciac.ac.cn](mailto:guobaoyu@ciac.ac.cn)

The electrochemical properties of noble-metal nanocrystals strongly depend on their shapes and sizes. Therefore, shape-controlled and size-controlled syntheses of noble-metal nanocrystals have been extensively studied.<sup>1,2</sup> We introduce here some methods, such as seed-mediated growth methods, hydrothermal methods and diazonium methods, for the synthesis of high-quality noble metal nanocrystals, such as rhombic dodecahedral, cubic, and octahedral gold and palladium nanocrystals, as well as many derivatives with varying degrees of edge- and corner-truncation,<sup>3,4</sup> convex hexoctahedral palladium@gold core-shell nanocrystals with {431} high-index facets,<sup>5</sup> platinum highly concave cube with one leg on each vertex,<sup>6</sup> and porous PtM (M=Cu, Ni) nanowires<sup>7</sup> developed during the past few years. The electrocatalytic properties of the as-prepared nanostructures toward alcohol oxidation and electrochemiluminescent reactions will be demonstrated.<sup>8</sup>

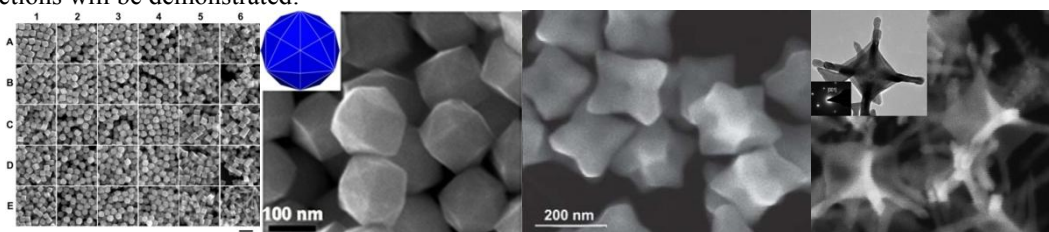


Figure 1. Images of some synthesized metal nanocrystals.

**Acknowledgement.** We gratefully acknowledge support from the National Natural Science Foundation of China (No. 21475123, 21175126 and 20875086).

## References:

- [1] W. X. Niu, G. B. Xu, *Nano Today*, 2011, 6, 265.
- [2] J. P. Lai, W. X. Niu, R. Luque, G. B. Xu, *Nano Today*, DOI: 10.1016/j.nantod.2015.03.001
- [3] W. X. Niu, L. Zhang, G. B. Xu, *ACS Nano*, 2010, 4, 1987.
- [4] W. X. Niu, S. L. Zheng, D. W. Wang, X. Q. Liu, H. J. Li, S. Han, J. A. Chen, Z. Y. Tang, G. B. Xu, *J. Am. Chem. Soc.*, 2009, 131, 697.
- [5] L. Zhang, W. X. Niu, W. Y. Gao, L. M. Qi, J. P. Lai, J. M. Zhao, G. B. Xu, *ACS Nano*, 2014, 8, 5953.
- [6] J. P. Lai, W. X. Niu, W. J. Qi, J. M. Zhao, S. P. Li, W. Y. Gao, R. Luque, G. B. Xu, *ChemCatChem*, DOI: 10.1002/cctc.201403042.
- [7] J. P. Lai, L. Zhang, W. J. Qi, J. M. Zhao, M. Xu, W. Y. Gao, G. B. Xu, *ChemCatChem*, 2014, 6, 2253.
- [8] Z. Y. Liu, W. J. Qi, G. B. Xu, *Chem. Soc. Rev.*, 2015, DOI: 10.1039/c5cs00086f.



# Electrochemical Synthesis of Red Fluorescent Graphene Quantum Dots for the Bioimaging Platform

Louzhen Fan\*, Xiaoyun Tan, Ruihua Guo

Department of Chemistry, Beijing Normal University, Beijing, China, 100875

lfan@bnu.edu.cn

Graphene quantum dots (GQDs) have attracted much recent attention due to their ultrafine dimensions, tunable surface functionalities and economical synthetic routes. The stable photoluminescence (PL) and low toxicity make them outstanding as an alternative to organic dyes and inorganic quantum dots (QDs) in biological applications.<sup>1</sup> On the other hand, due to the auto-fluorescence and light scattering background of biological specimens in the short-wavelength region, fluorescent materials of choice are expected to emit in the long-wavelength region in order to provide a deeper light penetration into the specimens, resulting in a higher imaging contrast. To date, most of the reported GQDs emit the blue to green fluorescence, which usually exhibits excitation wavelength dependence<sup>2</sup>. Herein, we report the facile electrochemical exfoliation of graphite in  $K_2S_2O_8$  solution for the synthesis of uniform small-sized red fluorescent GQDs (RF-GQDs) without any chemical modification, which has been used for cellular imaging.<sup>2</sup>

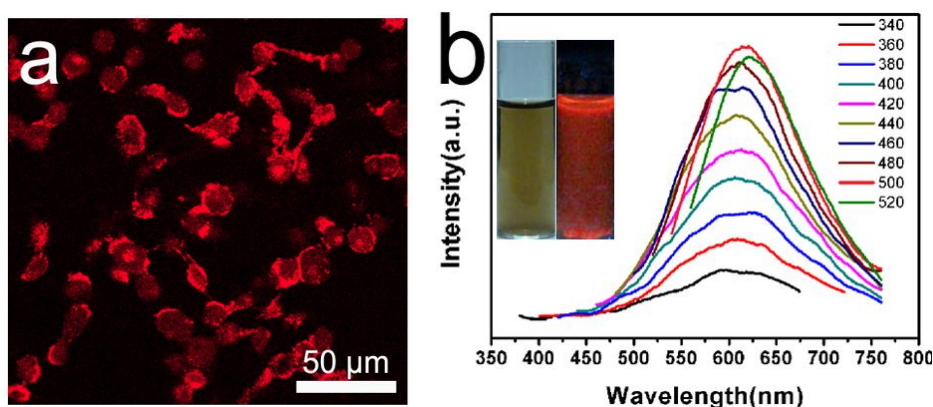


Figure 1. (a) Confocal fluorescence microscopy images of HeLa cells with RF-GQDs incorporated at the excitation wavelength of 488 nm, (b) Spectra of RF-GQDs aqueous solution. The inset of (b) is the photograph of the RF-GQDs solution under day light and 365 nm illumination.

**Acknowledgement:** This work is supported by NSFC (21073018), the Major Research Plan of NSFC (21233003), the Fundamental Research Funds for the Central Universities, Key Laboratory of Theoretical and Computational Photochemistry

## Reference:

- (a) S. N. Baker, G. A. Baker, *Angew. Chem. Int. Ed.* 2010, **49**, 6726-6744; (b) J. Shen, Y. Zhu, C. Chen, X. Yang, C. Li, *Chem. Commun.* 2011, **47**, 2580; (c) K. Habiba, V. I. Makarov, J. Avalos, M. J. F. Guinel, B. R. Weiner, G. Morell, *Carbon* 2013, **64**, 341.
- (a) Z. Fan, Y. Li, X. Li, L. Fan, S. Zhou, D. Fang, S. Yang, *Carbon* 2014, **70**, 149; (b) M. Zhang, L. Bai, W. Shang, W. Xie, H. Ma, D. Fang, H. Sun, L. Fan, L.; Han, M.; Liu, C.; Yang, S., *J. Mater. Chem.* 2012, **22**, 7461.



# **Development of Multifunctional Materials Composed of Selected Noble Metal and Metal Oxide Nanostructures for Efficient Electrocatalytic Oxidation of Small Organic Molecules**

Iwona A. Rutkowska\*, Pawel J. Kulesza

*Faculty of Chemistry, University of Warsaw, Pasteura 1, PL-02-093 Warsaw, Poland.*

*\*ilinek@chem.uw.edu.pl*

Certain organic fuels that include formic acid, methanol, dimethyl ether or ethanol are presently considered as alternatives to hydrogen for application in low-temperature fuel cells. Although all of them can be ideally oxidized to carbon dioxide, their actual electrooxidation mechanisms can significantly differ and may result in distinct electrocatalytic efficiencies and final reaction products. There is a need to develop multifunctional electrocatalytic systems exhibiting specific reactivity and capability to induce the slow reaction steps at ambient conditions.

Platinum or palladium-based nanoparticles have been recognized as the most active catalytic systems towards oxidation of small organic molecules at low and moderate temperatures. Noble metal nanoparticles are readily poisoned by the strongly adsorbed CO-type intermediate species requiring fairly high overpotentials for their removal. For example, to enhance activity of Pt-based catalysts toward the ethanol oxidation, additional metal or metal oxide nanostructures (rhodium, iridium, tin or molybdenum and tungsten oxides) will be intentionally introduced to the electrocatalytic interface. We are also going to demonstrate that catalytic activity of platinum-based nanoparticles towards electrooxidation of ethanol can be significantly enhanced through their interfacial modification with ultra-thin monolayer-type films of mixed metal oxo species of tungsten, titanium, cerium or zirconium. Remarkable increases of electrocatalytic currents measured under voltammetric and chronoamperometric conditions have been observed. The most likely explanation takes into account possibility of specific interactions of noble metals with transition metal oxide species as well as existence of active hydroxyl groups in the vicinity of catalytic noble metal sites. It is noteworthy that certain metal and mixed-metal oxides can generate –OH groups at low potentials: they induce oxidation of passivating CO adsorbates (e.g. on Pt) or breaking C-H bonds (e.g. during oxidation of methanol or dimethyl ether). When combined with dispersed Rh or Ir, they tend to weaken C-C bonds during ethanol oxidation.

# Simultaneous Covalent Assembling of Two Different Organic Films on Glassy Carbon Using Bipolar Electrochemistry

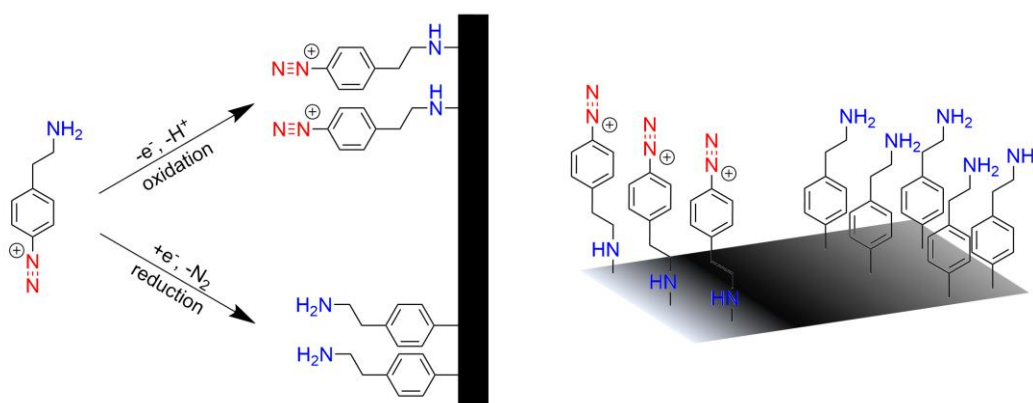
Line Koefoed,<sup>1</sup> Kyoko Shimizu,<sup>1</sup> Steen Utrup Pedersen,<sup>1</sup> Kim Daasbjerg,<sup>1</sup> Alexander Kuhn,<sup>2</sup> Dodzi Zigah<sup>2</sup>

<sup>1</sup>Department of Chemistry and iNANO, Aarhus University, Denmark

<sup>2</sup>Université de Bordeaux, CNRS, ISM, UMR 5255, France  
line88@chem.au.dk

Bipolar electrochemistry is a well-established technique which, recently, has attracted renewed interest in various fields, including fabrication of Janus particles.<sup>[1]</sup> The versatility of this technique allows several kind of surface modifications to be carried out, including direct reduction of metal ions to form the corresponding metal deposit,<sup>[2]</sup> fabrication of both gradient and patterned polymer brushes,<sup>[3]</sup> and oxidation of monomers to electrogenerate polymer films.<sup>[4]</sup>

In this study a novel methodology is reported, which for the first time allows simultaneous deposition of two different organic films at each end of a glassy carbon substrate ( $1 \times 1 \text{ cm}^2$ ). The approach is based on the use of an organic bifunctional molecule, i.e., 4-(2-aminoethyl)benzenediazonium, which may be reductively and oxidatively grafted at the same time using bipolar electrochemistry (Scheme 1). The reduction process goes through the diazonium group while the oxidation proceeds via the primary amine. The double functionalized plates are investigated by ellipsometry, cyclic voltammetry, condensation imaging, x-ray photoelectron spectroscopy, and time-of-flight secondary ion mass spectrometry. Post-modification of one of the anchoring layers illustrates the versatility of the system, pointing to its potential use in fields going from molecular electronics to targeted drug delivery. Furthermore, it is shown that the new technique is not limited to glassy carbon as substrate, but that it works equally well for, e.g., transferred graphene.



**Scheme 1.** Simultaneous grafting of two different organic films on glassy carbon using bipolar electrochemistry.

<sup>[1]</sup> S.E. Fosdick, K.N. Knust, K. Scida, R.M. Crooks, Bipolar Electrochemistry, *Angew. Chem. Int. Ed.* (2013), 10438-10456.

<sup>[2]</sup> C. Warakulwit, T. Nguyen, J. Majimel, M.-H. Delville, V. Lapeyre, P. Garrigue, V. Ravaine, J. Limtrakul, A. Kuhn, Dissymmetric Carbon Nanotubes by Bipolar Electrochemistry, *Nano Lett.* (2008), 500-504.

<sup>[3]</sup> N. Shida, Y. Koizumi, H. Nishiyama, I. Tomita, S. Inagi, Electrochemically Mediated Atom Transfer Radical Polymerization from a Substrate Surface Manipulated by Bipolar Electrolysis: Fabrication of Gradient and Patterned Polymer Brushes, *Angew. Chem. Int. Ed.* (2015), 3922-3926.

<sup>[4]</sup> S. Kong, O. Fontaine, J. Roche, L. Bouffier, A. Kuhn, D. Zigah, Electropolymerization of Polypyrrole by Bipolar Electrochemistry in an Ionic Liquid, *Langmuir* (2014), 2973-2976.

# Spectroelectrochemistry in the Course of Oxidative Electrolysis as a Tool to Determine the Molecular Structure of Electroactive Polymer Based on Mg(II) Porphine

D.V. Konev<sup>a,b</sup>, O.I. Istakova<sup>a,b</sup>, O.A. Sereda<sup>c</sup>, M.A. Shamraeva<sup>c</sup>, C.H. Devillers<sup>d</sup>, M.A. Vorotyntsev<sup>a,b,c,d</sup>

<sup>a</sup> *Institute for Problems of Chemical Physics of the Russian Academy of Sciences, Chernogolovka, Russia*

<sup>b</sup> *D. I. Mendeleev University of Chemical Technology of Russia, Moscow, Russia*

<sup>c</sup> *M. V. Lomonosov Moscow State University, Moscow, Russia*

<sup>d</sup> *ICMUB - UMR 6302 CNRS - Université de Bourgogne, Dijon, France*

*mivo2010@yandex.com*

Electroactive materials containing the porphine macrocycle in their structure are actively studied in view of their applied prospects in electrocatalysis, photocatalysis, sensors, solar energy conversion, non-linear optics, etc. Porphine unit is present in most systems in its monomeric form, e.g. as a pendant group of a polymer chain. There are a few examples of copolymers possessing a well-defined molecular structure of alternating porphyrin and (hetero)aromatic units which are mostly synthesized by organometallic catalysis. On the contrary, molecular structures of polymer films deposited by direct oxidation of substituted porphyrins on electrode surface were not determined.

Our team succeeded in synthesis of the first homopolymer (pMgP-I) on the basis of non-substituted Mg(II) porphine (MgP, Fig. 1a) [1]. This polymer has been characterized by combination of methods of electrochemistry, spectroscopy and microscopy which demonstrated that it represents a typical electroactive material, i.e. it can be charged and discharged in a quasi-reversible manner by means of the potential variation (within certain limits), this variation of the oxidation state being accompanied by the drastic change of its redox, conductive and spectroscopic properties. IR spectra, XPS and electrochemistry data [1] testify in favor of conservation of both the porphine macrocycle as monomer unit and Mg cation inside this material. However, the way of their bonding in the polymer was unclear.

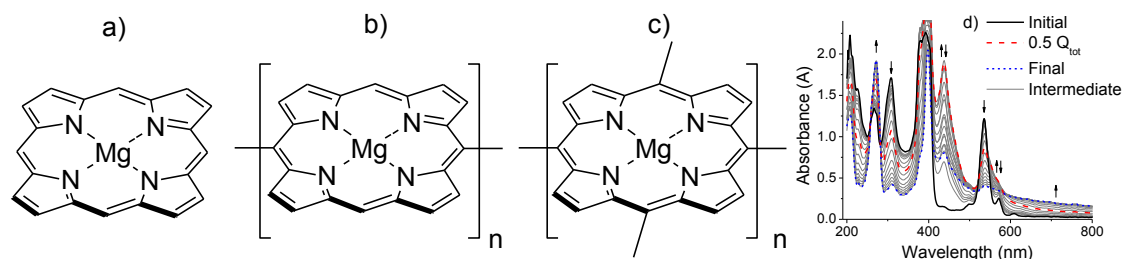


Fig.1. Mg(II) porphine (a) and hypothetic structures of its polymer: linear chain (b) or 2D structure (c). Evolution of the UV-visible spectrum of MgP solution in the course of its oxidative electrolysis (d).

The goal of the actual study has been to get direct information on the average number of bonds inside this polymer, which are formed by each porphine species in the course of its oxidative transformation from the monomeric state in solution to the monomer unit inside the polymer. Our approach is based on fundamental principles of electrochemical polymerization processes, in particular, those resulting in deposition of electroactive polymer films on electrode surface, which relate the amounts of the consumed monomeric reactant, of the reaction product(s) and of the electric charge spent for this process via **stoichiometric** relations. Reliable experimental determination of their parameters may be used both to get conclusions on the molecular structure of the polymer and to estimate the current efficiency of the polymer film formation as well as the maximal degree of the polymer oxidation.

The amount of oxidized monomer species may be determined from the temporal evolution of the spectrum of the electrolyzed solution in the UV-visible range (Fig. 1d). Its relation to the passed electric charge has been used to calculate the number of chemical bonds that a monomer porphine unit inside the polymer/oligomer structure forms with neighboring monomer units (Fig. 1b vs. Fig. 1c). Conclusion on the chain structure of the Mg(II) polyporphine has been made on the basis of these data.

1. M. A. Vorotyntsev, D. V. Konev, C. H. Devillers, I. Bezverkhyy, O. Heintz, *Electrochim. Acta*, 2010, 55, 6703-6714

# Deposition of Ag Nanostructures on Ni-based 3D Electrodes and their Application as Electrocatalysts

Enrico Verlato<sup>1</sup>, Simona Barison<sup>1</sup>, Wenyan He<sup>2,3</sup>, Didier Floner<sup>2</sup>, Florence Fourcade<sup>3</sup>, Abdeltif Amrane<sup>3</sup>, Florence Geneste<sup>2</sup>, Marco Musiani<sup>1</sup>

*1. IENI CNR - Corso Stati Uniti 4 – 35124 Padova Italy*

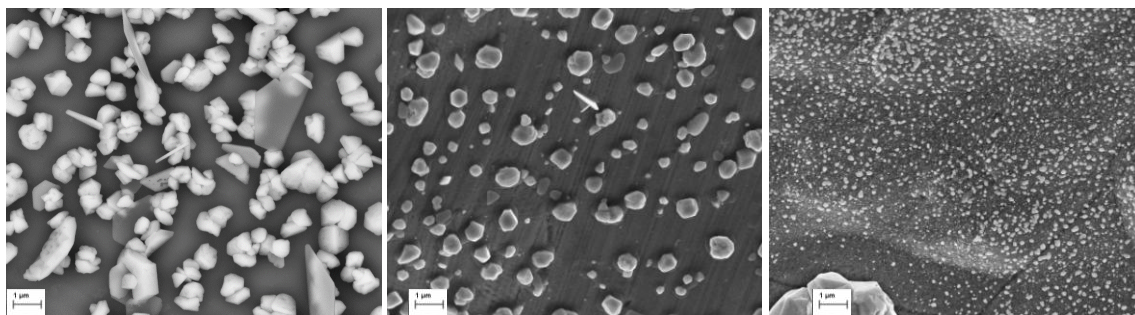
*2. Université de Rennes 1, CNRS, UMR 6226, Equipe Matière Condensée et Systèmes Electroactifs, Campus de Beaulieu, 35042 Rennes Cedex, France*

*3. Ecole Nationale Supérieure de Chimie de Rennes / Université de Rennes 1, CNRS, UMR 6226, 11 allée de Beaulieu, CS 50837, 35708 Rennes cedex 7, France  
[enrico.verlato@ieni.cnr.it](mailto:enrico.verlato@ieni.cnr.it)*

Galvanic displacement reaction (GDR) is potentially one of the most efficient methods to decorate 3D porous electrodes with noble metal nanoparticles. In the last few years, we studied GDR processes and we applied it to modify several 3D substrates, including Ni porous layers, Ni foams, FeCrAlloy foams, with noble metals like Pt, Pd, Rh [1].

In the present communication, we describe the use of galvanic displacement reactions for the deposition of Ag nanostructures onto two substrates: (i) commercial Ni foams and (ii) high surface area 3D Ni electrodes obtained by the electrodeposition of thin Ni layers on carbon felts [2]. Several experimental variables, like bath composition, temperature, chemical activation of the Ni surface, and reactant diffusion, influence the GDR, yielding deposits with different characteristics. These variables must be accurately selected to optimize the surface/loading ratio of silver.

The Ag deposits shown in the SEM images below were obtained, from left to right, from a thiosulfate bath, from a thiocyanate bath without Ni activation and from a thiocyanate bath after Ni activation in 1M HNO<sub>3</sub>. Clearly, a strong correlation was observed between silver complexing agents and nanostructures morphology. Reactant diffusion affected the homogeneity of distribution of Ag nanoparticles on inner/outer parts of 3D electrodes.



Since Ag is an active cathode for dehalogenation of organic compounds [3], e.g. pesticides, Ag-modified electrodes were tested as electrocatalysts for the dechlorination of organic pollutants. Cyclic voltammetries in aqueous and organic media were performed to underline the electrocatalytic activity of the modified electrodes toward dehalogenation. Electrolyses were performed in a flow cell in aqueous medium. Preliminary results showed an improved conversion for Ag modified 3D Ni electrodes over unmodified electrodes.

## References:

- [1] M. Musiani, S. Cattarin, S. Cimino, N. Comisso, L. Mattarozzi, L. Vazquez-Gomez, E. Verlato *J. Appl. Electrochem.* DOI 10.1007/s10800-015-0808-1.
- [2] D. Floner, F. Geneste, *Electrochem. Commun.* 9 (2007) 2271.
- [3] S. B. Rondinini, P.R. Mussini, F. Crippa, G. Sello, *Electrochem. Commun.* 2 (2000) 491.

# Tuning the electrocatalytic properties of Cu<sub>2</sub>O nanoparticles by controlling size and geometry

Susana I. Córdoba de Torresi, Fabian A. Cerda Pastrian, Anderson Marques, Pedro H. C. Camargo  
*Instituto de Química, Universidade de São Paulo. C.P. 26077, 005513-970 São Paulo (SP), Brazil.*  
*storresi@iq.usp.br*

We report the use of Cu<sub>2</sub>O nanoparticles synthesized from simple and cheap copper salts as effective catalyst for electrochemical reactions of great interest, such as water and glucose oxidation. These nanostructured materials with varying shapes (spheres, cubes and octahedrons) but the same size, Figure 1, were prepared by a facile method in the presence of sodium dodecyl sulfate (SDS) surfactant and hydroxylamine.

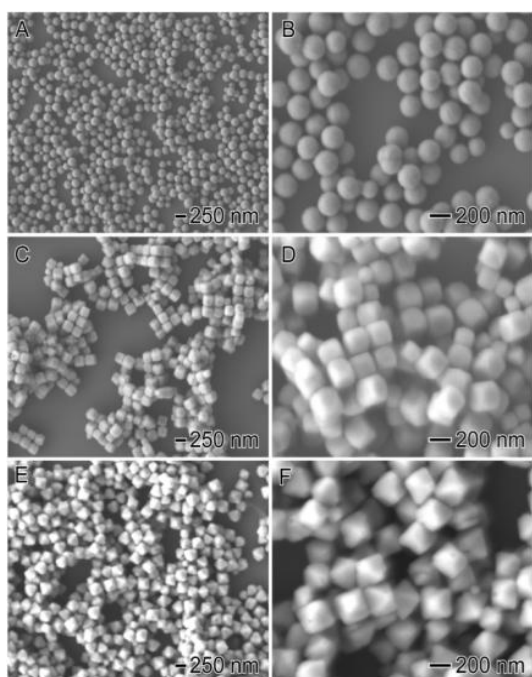


Figure 1

The nanoparticles were characterized by X-Ray powder diffraction (XRD), scanning electron microscopy (SEM) and Atomic force microscopy (AFM).

The nanoparticles were deposited by casting onto vitreous carbon electrodes, taking care to maintain the same amount of copper, measured by ICP-OES, in each electrode.

All three different shaped Cu<sub>2</sub>O materials showed catalytic activity for both, glucose and water oxidations. The influence of different shapes and sizes on the catalytic activity of both reactions is analyzed.

In the case of glucose oxidation, it was observed a much higher catalytic activity for octahedrons than the other forms but this activity was different for water electrolysis, at different pHs.

The very controlled geometry of these nanoparticles expose different crystallographic planes which could be selectively active for different electrochemical reactions.

Figure 2 shows the X-Ray diffraction patterns of different nanoparticles where it can be observed that

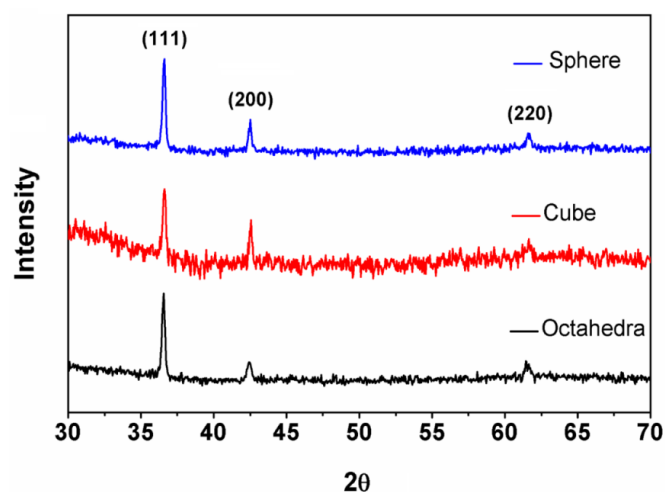


Figure 2

the geometry define the structure of each nanomaterial. The importance of controlling the synthetic parameters for obtaining well-designed catalysts is emphasized in this work.

# Evaluation of bifunctional electrocatalysts for oxygen reduction and evolution by means of scanning electrochemical microscopy (SECM)

Xingxing Chen<sup>1,2</sup>, Justus Masa<sup>2</sup>, Alexander Botz<sup>2</sup>, Daniela Wintrich<sup>2</sup>,  
Wolfgang Schuhmann<sup>2</sup>

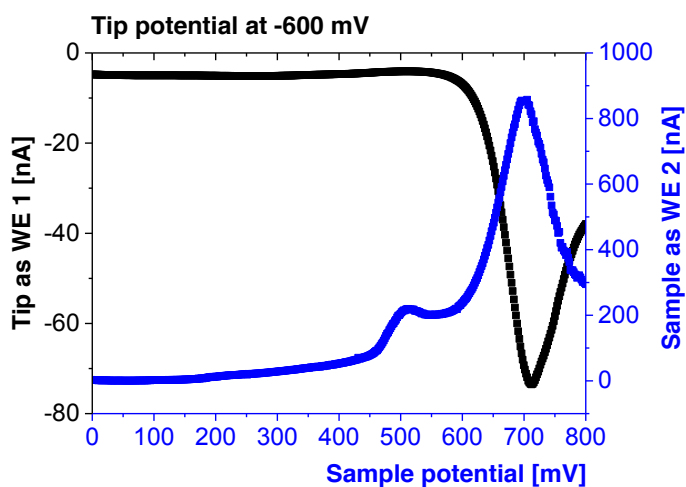
<sup>1</sup> School of Chemical Engineering, University of Science and Technology Liaoning, Qianshan Road 185,  
114051 Anshan, China

<sup>2</sup> Analytical Chemistry - Center for Electrochemical Sciences (CES), Ruhr-Universität Bochum,  
Universitätsstr. 150, 44780 Bochum, Germany  
email: xingchenstar79@163.com

The development of electrocatalysts that can reversibly reduce oxygen and oxidize water are of prime importance for the advancement of new emerging electrochemical energy storage and conversion systems, especially in rechargeable metal-air batteries and reversible fuel cells. Rotating disc electrode (RDE) and rotating ring-disc electrode (RRDE) voltammetry are the most commonly used techniques for studying the kinetics and selectivity of oxygen reduction and oxygen evolution catalysts. However, these techniques suffer from drawbacks when applied to non-flat or non-smooth catalytic surfaces due to non-defined flow of the electrolyte through the catalyst film, the prevalence of local turbulences and dissimilarity between the effective electrocatalytically active surface area and the geometric area of the electrode, which lead to inaccurate kinetic and mechanistic assumptions, particularly, the quantity of hydrogen peroxide generated and the average number of electrons transferred. This drawback can be circumvented by applying scanning electrochemical microscopy (SECM) to study the selectivity of ORR, where the tip of the SECM is brought in close proximity to the electrocatalytic surface, to serve as a sensor for O<sub>2</sub> in the redox competition mode of SECM (RC-SECM), or for H<sub>2</sub>O<sub>2</sub> detection in the sample generation-tip collection (SG-TC) mode.

We present the application of scanning electrochemical microscopy (SECM) for characterization of bifunctional catalysts. By using model bifunctional catalysts based on oxides of cobalt (Co<sub>x</sub>O<sub>y</sub>) and nickel (Ni<sub>x</sub>O<sub>y</sub>) embedded in nitrogen-doped carbon (NC), we specifically show the unique ability to determine most of the important electrocatalytic parameters including the selectivity of the oxygen reduction reaction (ORR).

The initial mechanistic steps during the oxygen evolution reaction (OER), and the onset potential for both ORR and OER can be reliably determined in a single SECM experiment. We were able to directly observe that prior to oxygen evolution, local depletion of oxygen occurs at the SECM tip during redox transition accompanying metal oxyhydroxide formation thus enabling direct *in-situ* observation of the initial mechanistic steps of the OER. This is critical for the assessment and development of new generations of bifunctional oxygen electrodes for energy applications.



Example of the response of the SECM tip current during the OER at a Ni<sub>x</sub>O<sub>y</sub>/NC sample.



# Effect of Electrode Surface-State Change on Electrogenenerated Chemiluminescence from a Ruthenium-Doped Silica Nanoparticle

Kenta Imai, Giovanni Valenti, Elena Villani, Massimo Marcaccio, Luca Prodi and Francesco Paolucci  
*Department of Chemistry "G. Ciamician", University of Bologna*  
*Via Selmi 2, 40126 Bologna, Italy*  
*E-mail: kenta.imai2@unibo.it*

## 1. Introduction

Electrogenenerated chemiluminescence (ECL) is widely studied due to its high performance in analytical applications and complicated reaction mechanism. It has been recently reported that Ru(bpy)<sub>3</sub><sup>2+</sup>-doped silica nanoparticles (Ru-DSNPs) generate efficient ECL by applying anodic potentials under the presence of tripropylamine (TPA) [1]. Numerical modeling is a powerful tool to clarify complicated reaction mechanism. In this study, we investigated numerical modeling of ECL from a Ru-DSNP in TPA-containing buffer, focusing on electrode surface-state change caused by the anodic potential application.

## 2. Experimental

We used COMSOL Multiphysics® (version 3.5a) for our modeling mainly considering the Butler-Volmer equation and Fick's law of diffusion. A Ru-DSNP with a diameter of 18 nm was placed on the center of a working electrode with a diameter of 0.5 mm. Representative modeling parameters are shown in Table 1 [1-3]. Electrochemical measurements were carried out with the Bio-Logic SP-300 potentiostat.

## 3. Results and discussion

Figure 1 shows simulated ECL behaviors as a function of applied potential. First we carried out simulations using two constants suggested in the related studies; however, we could not well simulate rapid ECL decay at >0.9 V vs. Ag|AgCl observed in the experimental study. Chen et al. have suggested that the deprotonation of TPA radical cation on working electrode become faster after oxidizing the electrode surface [4]. On the other hand, our electrochemical measurements indicated Ru-DSNPs would be detached and then the electrode surface would be oxidized at >0.9 V. Considering these findings, we made the deprotonation equilibrium of TPA radical cation dependent on the applied potential to simulate the dynamic electrode surface-state change. Finally, we found out the ECL behavior for the Ru-DSNP was well simulated by increasing forward rate constant for the equilibrium during potential application.

## 4. Conclusion

This study suggests that electrode surface-state change during potential application should be carefully considered in analysis for ECL generation.

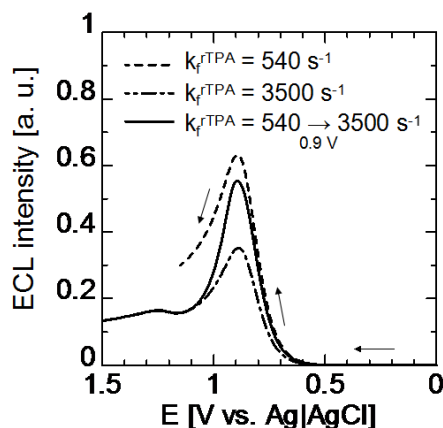
Table 1. Representative modeling parameters.

	reaction	modeling parameters
1	$\text{TPA} \rightarrow \text{TPA}^{++} + \text{e}^-$	$k_s^{\text{TPA}} = 10 \text{ cm s}^{-1}$ $E_{\text{TPA}}^0 = 0.88 \text{ V}$
2	$\text{TPA}^{++} \leftrightarrow \text{TPA}^{\bullet+} + \text{H}^+$	$k_f^{\text{TPA}} = 540 - 3500 \text{ s}^{-1}$ $k_b^{\text{TPA}} = 1.08 \times 10^6 \text{ M}^{-1} \text{ s}^{-1}$
3	$\text{TPA}^{\bullet+} + \text{Ru}(\text{bpy})_3^{2+} \rightarrow \text{P1} + \text{Ru}(\text{bpy})_3^{3+}$ (P1: $\text{Pr}_2\text{N}^+\text{C}=\text{HCH}_2\text{CH}_3$ )	$k_f^1 = 10^{10} \text{ M}^{-1} \text{ s}^{-1}$
4	$\text{TPA}^{++} + \text{Ru}(\text{bpy})_3^{3+} \rightarrow \text{TPA} + \text{Ru}(\text{bpy})_3^{2+*}$	$k_f^2 = 10^6 \text{ M}^{-1} \text{ s}^{-1}$
5	$\text{Ru}(\text{bpy})_3^{2+*} \rightarrow \text{Ru}(\text{bpy})_3^{2+} + \text{ECL}$	$k_f^{\text{ECL}} = 10^{7.2} \text{ s}^{-1}$

## 5. References

- [1] Zanarini, S. et al., J. Am. Chem. Soc. 131 (2009) 2260.
- [2] Wightman, R. M. et al., J. Phys. Chem. 108 (2004) 19119.
- [3] Klymenko, O. V. et al., ChemPhysChem 14 (2013) 2237.
- [4] Chen, Z. et al., J. Phys. Chem. C 112 (2008) 16663.

Fig. 1. Simulated ECL for a Ru-DSNP.



# The Impact of Short-Range Electronic Interactions on the Electrochemical Activity of Single- and Few- Layer Graphene

J. Hui; R. Bhargava; X. Zhou; A.J. Chinderle and J. Rodríguez-López  
Department of Chemistry, University of Illinois at Urbana-Champaign  
600 S Mathews Avenue, Urbana, IL, 61801, P: +1(217) 300 7354, F: 217-265-6290  
[joaquinr@illinois.edu](mailto:joaquinr@illinois.edu)

Symposium 14:

Modeling, Design and Characterization of Nanostructured, Electroactive and Multifunctional Materials

Bulk and surface electrochemical reactivity converge on ultrathin electrochemical interfaces such as single layer graphene (SLG) the world's thinnest electrode, and few layer graphene (FLG).[1] We will demonstrate that these materials enable unique chemical interactions that operate at scales coincident with their thickness. These electronic and chemical interactions result in enhanced rates of electron transfer for electrocatalytic processes. Thus, beyond its superior electronic properties, ultra-thin carbons permit a wide array of chemistries that enable new interactions in electrocatalysis.

We will discuss our results on the electrochemistry of  $\text{cm}^2$ -large SLG and FLG with a well-controlled morphology produced via chemical vapor deposition in our laboratory. This material yields electrode surfaces that are easy to transfer and to address electrochemically in aqueous and nonaqueous electrolytes, with a well-defined area and clean contacts [2,3]. Using scanning electrochemical microscopy (SECM), we demonstrate unambiguously that SLG electrodes deposited over micro-patterned metallic substrates exhibit facilitated electron transfer to mediators in solution. For instance, the reaction of the ferri/ferrocyanide redox pair which is notoriously slow on pristine SLG [3] is dramatically accelerated on Au/SLG spots as shown in **Figure 1** via feedback SECM measurements. These interactions were further used to tune the reactivity of molecular adsorbates on SLG for the oxygen reduction reaction (ORR). Our results indicate that the nature of the underlying metal has a profound impact on the electrochemical potential for the ORR and its mechanism. These observations strongly suggest that SLG and FLG used as carbon supports, far from a role as spectator materials, might engage actively by facilitating electrocatalytic reactions on a larger area than the nominal metal/graphene interaction. The strategy presented here suggests new methods by which metal-molecule interactions can be stabilized by ultra-thin carbons. For instance, metals prone to corrosion or prone to poisoning can be protected while permitting some degree of interaction with the electrolyte. The new strategies will be critical in the creation of new bulk materials with tailored properties.

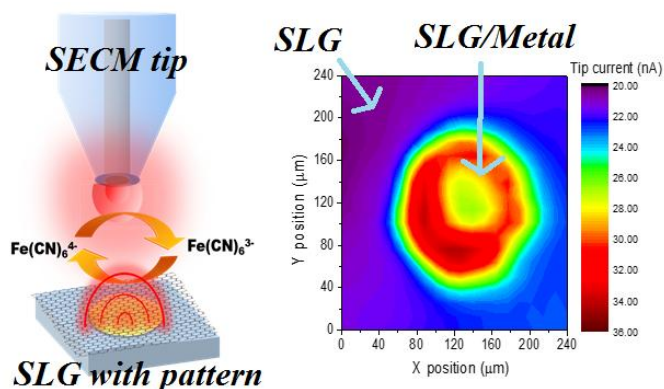


**Figure 1.** SECM imaging of enhanced redox kinetics on metal-supported SLG.

- [1] A.K. Geim. Graphene: Status and Prospects. *Science* 324 (2009) 1312.
- [2] T.C. Cristarella, A.J. Chinderle, J. Hui, J. Rodríguez-López. Single-Layer Graphene as a Stable and Transparent Electrode for Nonaqueous Radical Annihilation Electrogenenerated Chemiluminescence. *Langmuir*, In Press.
- [3] N.L. Ritzert, J. Rodríguez-López, C. Tan, H.D. Abruña. Kinetics of Interfacial Electron Transfer at Monolayer Graphene Electrodes in Aqueous and Non-Aqueous Solutions. *Langmuir* 29 (2013) 1683.



# Electrical Characteristics of Raw Si-based Powders for Li-ion Electrode by Kelvin Probe Force Microscopy (KPFM) and Electrostatic Force Microscopy (EFM)

Jing-Ting Liao(廖敬庭), Sin-Syu Liao(廖信旭), Bernard HaoChih Liu(劉浩志)†

*Department of Materials Science and Engineering, National Cheng Kung University, Taiwan*

*†Corresponding author, Tel : (06)2757575#62926 , E-mail address: hcliu@mail.ncku.edu.tw*

As there are many components in a Li-ion battery system, such as electrode materials, binders and additives, it is hard to analyze the individual contribution of raw materials to the battery performance. In this research, we utilized scanning probe microscopy (SPM) to analyze raw Si-based powders for electrode materials directly. We used Kelvin probe force microscopy (KPFM) and electrostatic force microscopy (EFM) to measure microscopic electrical properties and topography at nanoscale simultaneously. The preliminary measurement results are shown below, and we will discuss the relation among work function, particle size and roughness of raw materials. The aim is to evaluate the advantages and disadvantages of electrode materials before battery assembling and reduce the complexity of the whole battery analysis. This approach will assist manufacturers in the control of raw material quality as well as that of the production lines.

**Keywords:** raw electrode materials, Kelvin probe force microscopy, electrostatic force microscopy, microscopic electrical property

Figure.1 EFM (a) Topography (b) Phase image of silicon powder

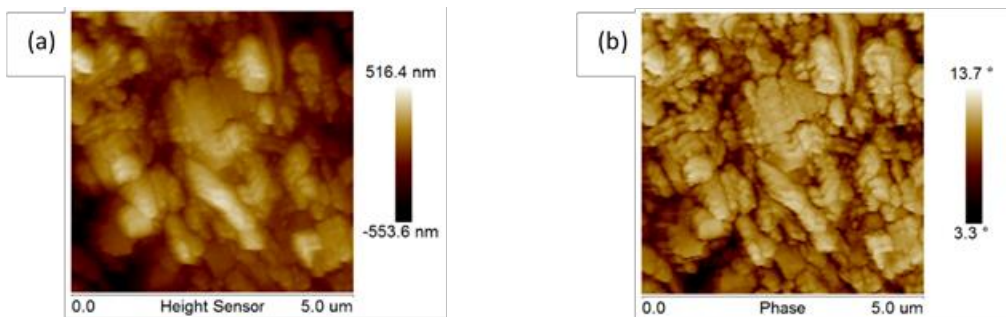
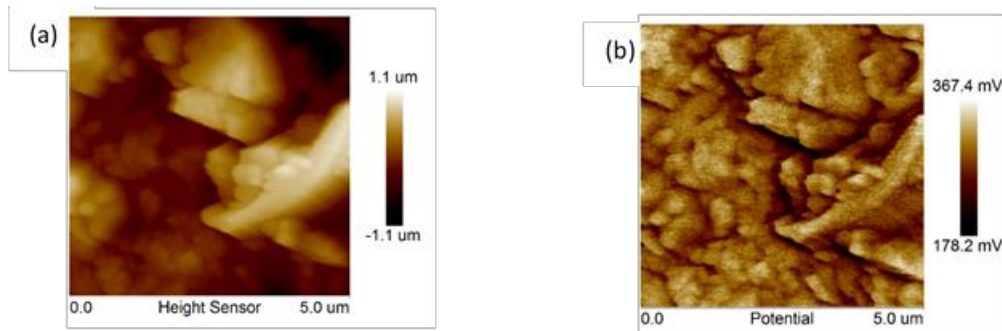


Figure.2 KPFM (a) Topography (b) Surface potential of silicon powder



# An Electrochromic Copolymer with One-dimensional Nanowire Arrays

Lu-Hsiang Yin<sup>1</sup>, Sheng-Yuan Kao<sup>1</sup>, Chung-Wei Kung<sup>1</sup>, Ting-Hsiang Chang<sup>1</sup>, Kuo-Chuan Ho<sup>1,2,\*</sup>

<sup>1</sup> Department of Chemical Engineering, National Taiwan University, Taipei, Taiwan,

<sup>2</sup> Institute of Polymer Science and Engineering, National Taiwan University, Taipei, Taiwan,

\*E-mail: kcho@ntu.edu.tw

Conducting polymers have been extensively investigated in the field of electrochemistry, particularly involving electrochromism. Among these conducting polymers, polyaniline (PANI) has been regarded as a promising material for electrochromic thin films due to its low cost, excellent redox reversibility and facile synthesis. However, it still possesses undesirable features such as poor cycling stability and long coloration time.

Several strategies have been proposed to improve the electrochemical performance of the PANI-based thin films. Recently, Wang *et al.* synthesized the one-dimensional (1-D) nanorods of a cross-linked copolymer constructed from aniline, triphenylamine (TPA), and p-phenylenediamine (PPDA) [1]. Thin films of the obtained copolymer were found to exhibit a better electrochemical stability due to the cross-linked nature, thus can be applied for supercapacitors. However, the reported thin film was prepared by physically depositing the PANI-based nanorods onto the underlying electrode with random orientation. Since the 1-D nanowire arrays of an electrochromic material have been proved to shorten the coloration time through easier ion diffusion [2], it is reasonable to consider that the 1-D nanorod arrays of such PANI-based cross-linked copolymers chemically grown on conducting substrates may exhibit both the stable electrochemical performance and fast redox switching.

Herein, 1-D nanorod arrays of a cross-linked PANI-based copolymer (c-PANI) were grown on the conducting glass by using an *in-situ* chemical polymerization in the solution containing aniline, TPA and PPDA (Fig. 1(a)). The self-assembled monolayer (SAM) was utilized to chemically bond the conducting glass and the c-PANI thin film, which is expected to further enhance the stability of the electrode and reduce the charge-transfer resistance at the interface. A higher utility in redox reaction was thus obtained by the c-PANI thin film compared to the electropolymerized flat PANI thin film (Fig. 1(b)). Interestingly, a significant difference in spectroelectrochemical response was observed, which indicates that the c-PANI film has a higher absorbance below 400 nm and a lower absorbance in the visible range (Fig. 1(c)); this observation is attributed to the existence of TPA and PPDA. The higher absorbance change of the c-PANI thin film between 0 and -0.6 V at around 450 nm (Fig. 1(c)) offers the potential application of the c-PANI thin film for electrochromic devices.

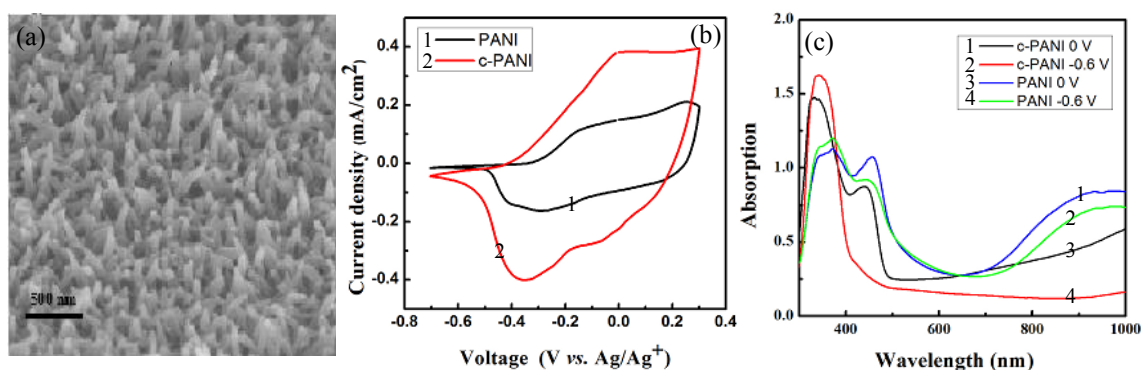


Figure 1 (a) Electron microscopic image of the nanorod arrays of c-PANI. (b) Cyclic voltammograms of the flat PANI and c-PANI measured in LiClO<sub>4</sub>/propylene carbonate. (c) UV-vis spectra of the PANI and c-PANI measured at 0 V and -0.6 V.

## Reference:

1. X. Wang, J. Deng, X. Duan, D. Liu, J. Guo, P. Liu, J. Mater. Chem. A 2014, 2, 12323–12329.
2. N. R. Chiou, C. M. Lui, J. J. Guan, L. J. Lee, A. J. Epstein, Nat. Nanotechnol. 2007, 2, 354–357.

# Electrical Heating Effect of Carbon Nanoparticles as Electrodes in the Charging Process

C. Y. Ho<sup>1</sup>, B. C. Chen<sup>2</sup>, M. Y. Wen<sup>3</sup>, Y. H. Tsai<sup>1</sup>, H. H. Ku<sup>4</sup>

<sup>1</sup>Department of Mechanical Engineering, Hwa Hsia University of Technology, Taipei 235, Taiwan

<sup>2</sup>Department of Chinese Medicine, Buddhist Dalin Tzu Chi General Hospital, Chiayi 622, Taiwan

<sup>3</sup>Department of Mechanical Engineering, Cheng Shiu University, Kaohsiung 833, Taiwan

<sup>4</sup>Department of Computer Science & Information Engineering, Hwa Hsia University of Technology, Taipei 235, Taiwan

hcy2182@yahoo.com.tw

Hollow carbon nanoparticles with uniform and interconnected pore networks are considered as promising candidates for supercapacitor electrodes since they can provide excellent capacitive performance owing to their high surface area, large pore volume and uniform pore size distribution. Working as candidates for supercapacitor electrodes, hollow carbon nanoparticles needs high specific capacitance, long cycle life, high power density, short charge/discharge time. Consequently, a high current density through hollow carbon nanoparticles may occur due to short charge/discharge time. If the high current density-induced heat in hollow carbon nanoparticles does not be well released, it will result in temperature rise of hollow carbon nanoparticles and reduce the performance of electrode. Therefore this project will investigate the electrical heating effects in hollow carbon nanoparticles with high current density in charge/discharge process of electrode. The nanoscale thermal transport models will be employed to analyze the high current density-induced electrical heating effects in hollow carbon nanoparticles. The effects of various parameters on electrical heating in hollow carbon nanoparticles will be also discussed.

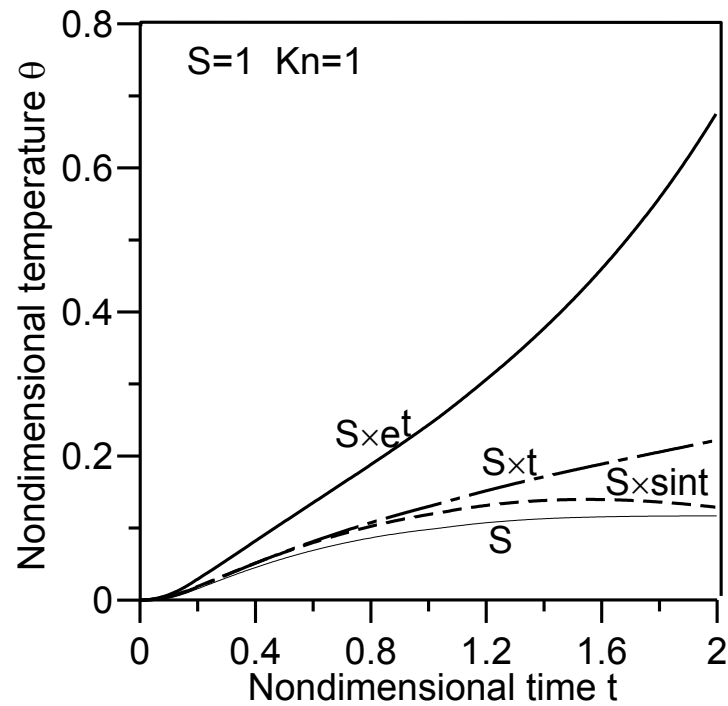


Fig. Temperature variation with time in different charging processes

# Glassy Polymeric Carbon/ $\text{Fe}_x\text{C}_y$ and Carbon/ $\text{Co}_x\text{C}_y$ Nanocomposites: Electrochemical and Magnetic Properties

Laura Santos Novais<sup>1</sup>, Raíssa P. Camargo<sup>1</sup>, Paulo Noronha L. Filho<sup>2</sup>, and Herenilton P. Oliveira<sup>1</sup>

<sup>1</sup>Universidade de São Paulo, FFCLRP, Av. Bandeirantes, 3900, Ribeirão Preto (SP), Brazil

<sup>2</sup>Universidade Estadual Júlio de Mesquita Filho – Departamento de Física – Grupo de materiais avançados – UNESP, Avenida Engenheiro Luiz Edmundo Carrijo Coube, 1000, Bauru – SP – Brazil  
e-mail: lauranovais@hotmail.com

It is described the synthesis, magnetic and electrical properties of a new iron oxide/polymeric glassy carbon nanocomposite formed by means of a carefully heating of a premodelled polymeric phenol-formaldehyde resin matrix with iron ion dispersed in a citric acid-polyethylene glycol resin in a nitrogen atmosphere. The obtained specimens were analyzed by magnetic measurements using a Quantum Design MPMS-5S SQUID Magnetometer. It is shown that structural characterization by X-ray diffraction reveals the presence of magnetite, Fe and CoC phases dispersed in the glassy carbon matrix. SEM, EDS, FT-IR, AFM, TGA/DTA were used to characterize the composite. For magnetization as function of applied field ( $M$  vs  $H$ ) taken at 10 K a ferromagnetic response was observed with a coercive field ( $H_r$ ) close to 725 Oe and saturation magnetization ( $M_s$ ) around 0.036 emu. In addition, for measurements at 300 K an enhancement of an antiferromagnetic signal was observed with a coercive field ( $H_c$ ) close to 265 Oe. Further, the response of magnetic iron oxide-polymeric glassy carbon nanocomposite to the external magnetic field can also be visualized, thus providing that the iron oxide phase would lead to higher magnetization. The electrochemical behavior of both materials by using hexacyanoferrate and ferrocene systems is quite similar to glassy carbon, as evaluated by cyclic voltammetry and chronoamperometry experiments. In addition, the obtained nanocomposite is thermally stable under air atmosphere up to 600 °C and decomposes slightly up to 1050 °C under inert condition. In conclusion, these materials present thermal stability, robustness, mechanical strength, electrical conductivity, large potential range as well as magnetic properties. Besides, glassy polymeric carbon matrix maintains functional surface groups such as carboxyl and hydroxyl. In fact, these set of experiments were profitable, and they indicate new possibilities to modify the properties leading to multifunctional materials as well as explore new applications.

Acknowledgments: FAPESP and CNPq



Figure 1: Photography of the composite GPC/ $\text{Fe}_x\text{C}_y$ .

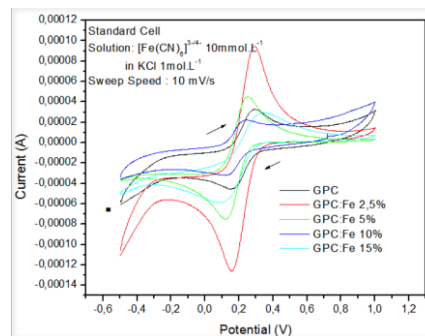


Figure 2: Cyclic voltammograms in 10 mmol/L ferrocyanide solution in 1 mol/L KCl for the GPC/ $\text{Fe}_x\text{C}_y$  electrodes.

# Study of Effect of Various Solvents on the Electropolymerization Process of Mg(II) Porphine and Electroactive Properties of Polyporphine Films

D.V. Konev<sup>a,b</sup>, O.I. Istakova<sup>a,b</sup>, D.K. Khayrullina<sup>b</sup>, M.A. Vorotyntsev<sup>a,b,c,d</sup>

<sup>a</sup> Institute for Problems of Chemical Physics of the Russian Academy of Sciences, Chernogolovka, Russia

<sup>b</sup> D. I. Mendeleev University of Chemical Technology of Russia, Moscow, Russia

<sup>c</sup> M. V. Lomonosov Moscow State University, Moscow, Russia

<sup>d</sup> ICMUB - UMR 6302 CNRS - Université de Bourgogne, Dijon, France

mivo2010@yandex.com

Electroactive materials produced by introduction of porphyrin macrocycle into conjugated polymer film as a counter ion or by covalent bonding with active groups of the polymer are of great practical interest. A new high-efficiency method of Mg(II) porphine (**MgP**) synthesis has recently been developed [1] and homopolymers of Mg(II) porphine (**pMgP**) with original optical and electrical properties were obtained [2].

The goal of this research is the investigation of the influence of various solvents on the electropolymerization process of MgP and properties of electroactive polyporphine films deposited on electrode surface.

Acetonitrile, dichloromethane and dimethyl sulfoxide were used as the solvent for electropolymerisation bath. The process of MgP-electrodeposition was carried out in potentiostatic regime at low values of oxidation potential with transmission of the constant number of electricity - 120  $\mu\text{C}$  (Fig. 1a). CVA within the narrow and wide potential intervals was used for polymer films characterization (Fig. 1b-c).

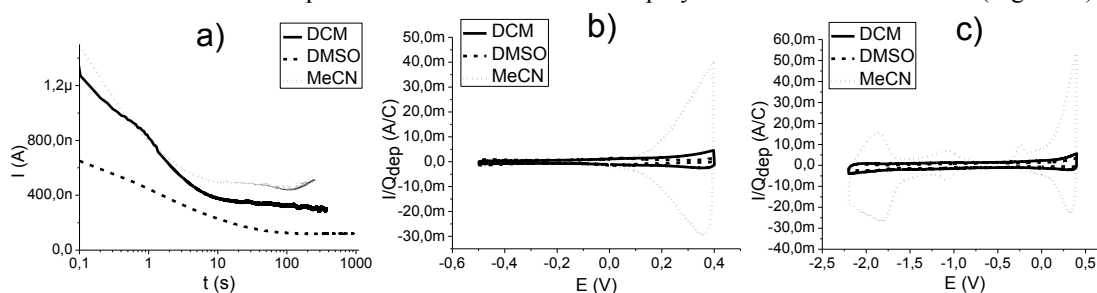


Fig.1. Chronoamperometric curves of MgP electrooxidation in acetonitrile, dichloromethane, dimethyl sulfoxide (a). CV-responses of pMgP films in monomer-free solution (MeCN + TBAPF<sub>6</sub>) within the narrow (b) and wide (c) potential intervals.

Among three studied solvents with low content of water, acetonitrile is especially well suited for the electropolymerization of MgP because in acetonitrile solutions the thickness of the polymer film on the electrode surface uniformly increases in potentiostatic regime.

Polymer films, obtained in acetonitrile solutions at low values of oxidation potential show stable CV-response in monomer-free acetonitrile solution within the narrow and wide potential intervals and including large negative values of the potential.

The electropolymerization of MgP in dichloromethane solutions leads to the slow growth of the polymer film on the electrode surface. Moreover, the CV-response of such films in monomer-free solution is unstable and varies during execution of multiple cycling. Polymer films, obtained in dimethyl sulfoxide solutions have a small thickness and therefore low current response. All these films have a completely different redox-properties. pMgP films deposited in DMSO and DCM reveal less intensive current response due to following reasons: 1) partial blocking of the surface of electrode for-electronic transport 2) formation more stable and soluble intermediates (cation-radicals, oligomers etc.) during electropolymerization leading to decrease of its efficiency.

1. D. K. Dogutan, M. Ptaszek, J. S. Lindsey, J. Org. Chem., 2007, 72, 5008 – 5011

2. M. A. Vorotyntsev, D. V. Konev, C. H. Devillers, I. Bezverkhyy, O. Heintz, Electrochim. Acta, 2010, 55, 6703 - 6714

# Pyro-Synthesis of Functional Nanocrystals

Jinju Song, Jihyeon Gim, Sungjin Kim, Jeonggeun Jo, Baboo Joseph Paul, Seokhun Kim, Sohyun Park, Dongyun Kim and Jaekook Kim\*

Department of Materials Science and Engineering, Chonnam National University  
Room no.214, Building 6th, Engineering college, Chonnam National University, Gwangju, South Korea  
Email: jaekook@chonnam.ac.kr

Despite nanomaterials with unique properties playing a vital role in scientific and technological advancements of various fields including chemical and electrochemical applications, the scope for exploration of nano-scale applications is still wide open. The intimate correlation between material properties and synthesis in combination with the urgency to enhance the empirical understanding of nanomaterials demand the evolution of new strategies to promising materials. Herein we introduce a rapid pyro-synthesis that produces highly crystalline functional nanomaterials under reaction times of a few seconds in open-air conditions. The versatile technique may facilitate the development of a variety of nanomaterials and, in particular, carbon-coated metal phosphates with appreciable physico-chemical properties benefiting energy storage applications. The present strategy may present opportunities to develop “design rules” not only to produce nanomaterials for various applications but also to realize cost-effective and simple nanomaterial production beyond lab-scale limitations.

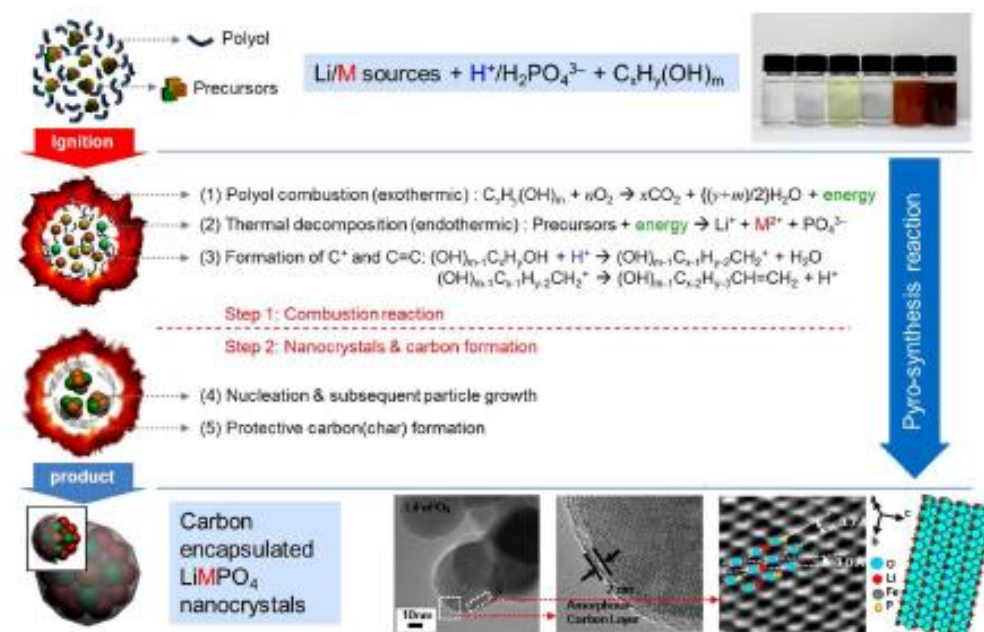


Figure 1. Rapid pyro-synthesis mechanism that explains typical production of carbon-encapsulated nanoparticles. The combustion of polyol with oxygen provides thermochemical energy for the pyrolytic decomposition of the precursors to finally yield nanoparticles under oxygen-limited condition, during which the rate of pyrolysis is much faster than the diffusion of oxygen.

- [1] Burda, C., Chen, X., Narayanan, R. & El-Sayed, M. A. Chemistry and properties of nanocrystals of different shapes. Chem. Rev. 105, (2005)1025–1102.
- [2] Rao, C. N. R., Kulkarni, G. U., Thomas, P. J. & Edwards, P. P. Size-dependent chemistry: Properties of nanocrystals. Chem. Eur. J. 8, (2002) 28–35.
- [3] Ma, R. & Sasaki, T. Nanosheets of oxides and hydroxides: ultimate 2D chargebearing functional crystallites. Adv. Mater. 22, (2010) 5082–5104.

# Amino-Silica Modified Nafion Membrane for Vanadium Redox Flow Battery

Chien-Hong Lin, Heng-Wei Chiang, Chao-Yen Kuo  
*Chemistry Division, Institute of Nuclear Energy Research, Longtan, Taiwan*  
*E-mail address: chlin0805@iner.gov.tw (C.-H. Lin).*

A hybrid membrane of Nafion/amino-silica (amino-SiO<sub>2</sub>) for vanadium redox flow battery (VRB) systems is prepared via the sol-gel method to improve the selectivity of the Nafion membrane, to reduce the crossover of vanadium ions, and to decrease water transfer across the membranes. The sulfonated pores of the pristine Nafion membrane are filled with amino-SiO<sub>2</sub> nanoparticles localized by electrostatic interaction. The permeability of vanadium ions through the Nafion/amino-SiO<sub>2</sub> hybrid membrane is determined by electrometric titration. The results indicate the crossover of vanadium ions through the hybrid membrane is 26.8% of the pristine Nafion membrane. The presence of amino-SiO<sub>2</sub> in the hybrid membrane is verified by X-ray photoelectron spectroscopy (XPS). Nafion/amino-SiO<sub>2</sub> hybrid membrane exhibits through plane conductivity about the same as the pristine Nafion membrane. The ion exchange capacity (IEC) of the hybrid membrane is 9.4% higher than that of the pristine Nafion membrane. In addition, Nafion/amino-SiO<sub>2</sub> hybrid membrane exhibits a higher coulombic efficiency (CE), voltage efficiency (VE), and energy efficiency (EE) over a range of current densities from 20 to 80 mA cm<sup>-2</sup>. The performance of VRB with Nafion/amino-SiO<sub>2</sub> hybrid membrane varies little around a charge-discharge current density of 80 mA cm<sup>-2</sup> for 150 cycles. Thus, the Nafion/amino-SiO<sub>2</sub> hybrid membrane can suppress the vanadium ions crossover in VRB.



# Electrochemical shape transformation of Pt nanocrystals with high-index facets

Na Tian\*, Jia-Huan Du, Shi-Gang Sun\*

College of Chemistry and Chemical Engineering and School of Energy Research, Xiamen University, Xiamen, 361005, China

\*e-mail address: tnsd@xmu.edu.cn, sgsun@xmu.edu.cn

To observe shape evolution of nanoparticles is helpful for shape-controlled synthesis of nanocrystals and understanding growth mechanism of the nanocrystals. A variety of growth conditions can influence the final shapes or surface structure of the nanocrystals. Previously, we developed an electrochemical square-wave potential (SWP) method to synthesize Pt-group metal nanocrystals with high-index facets, and found that surface structures can be tuned by the electrode potentials. The upper ( $E_U$ ) potential controls the oxygen species adsorption that can induce the formation of high-index facets, and etching Pt surface atoms. The lower ( $E_L$ ) potential enables the desorption of oxygen species, and mediates the growth of nanocrystals. The final surface structure of the obtained nanocrystals is the balance of these interactions.

As for Pt nanocrystals, we observed previously the shape evolution from  $\{hk0\}$ -faceted tetrahexahedron (THH) to  $\{hkl\}$ -faceted hexoctahedron (HOH) and finally to  $\{hkk\}$ -faceted trapezohedron (TPH) by increasing the  $E_U$  or  $E_L$  of SWP, if these nanocrystals directly grow from  $H_2PtCl_6$  plating solution [1]. Here, we found that the growth habits of Pt nanocrystals depend on starting materials. If preformed THH Pt nanocrystals are further subjected to the SWP treatment, they are not converted into HOH as expected, but into truncated ditetragonal nanoprisms (DTPs), as shown in Fig. 1. Both THH and DTP are enclosed by  $\{hk0\}$  facets, but crystal symmetries are different. The former has 24 facets, while the latter has 12 facets. The relationship between them is like that between octahedron and tetrahedron. Clearly, DTP has short edge length totally. This shape transformation occurs through elongation of tetragonal pyramid, resulting in the gradual disappearance of two facets. The driving force of this shape transformation may be attributed to reduce the high energy vertices at pyramid and cube. The study provides a new insight into growth habits of Pt nanocrystals under electrochemical conditions, and will contribute to surface structure controls of Pt nanocrystals.

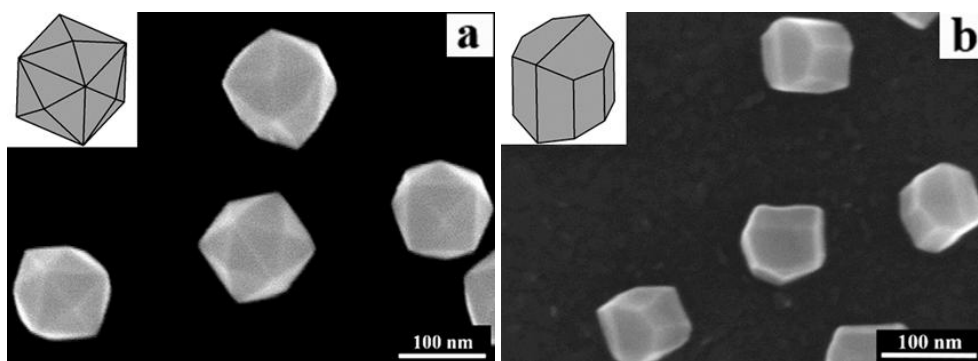


Fig.1 SEM images of Pt tetrahexahedral nanocrystals (a) and truncated ditetragonal nanoprisms (b).

## References:

- (1) Xiao J.; Liu S.; Tian, N.; Zhou, Z. Y.; Liu H. X; Xu B. B.; Sun, S. G. *J. Am. Chem. Soc.*, **2013**, 135, 18754.

**Acknowledgements:** This work was supported by NFSC (21222310).



# Mesocellular Carbon based Electrodes for High-Performance Vanadium Redox Flow Battery

Jooyoung Jeong<sup>a</sup>, Seongbeen Kim<sup>a</sup>, Yongchai Kwon<sup>b,\*</sup>, Jinwoo Lee<sup>a,\*</sup>

<sup>a</sup> *Department of Chemical Engineering*

*Pohang University of Science and Technology (POSTECH), Pohang, Republic of Korea*  
*jinwoo03@postech.ac.kr*

<sup>b</sup> *Graduate School of Energy and Environment,*

*Seoul National University of Science and Technology, Seoul, Republic of Korea*  
*kwony@seoultech.ac.kr*

Redox flow batteries (RFBs), one of the promising candidates for energy storage system (ESS), require two separated and dissolved redox couples with standard reduction potential difference. Among them, vanadium redox flow battery (VRFB) has an advantage of low cross-contamination and long lifetime. However, sluggish cathode reaction ( $\text{VO}^{2+}/\text{VO}_2^+$ ) activity lowers the efficiencies of VRFB; thus, using catalysts in the cathode is essential for improving VRFB performance. Herein, we use new catalysts including large pore sized mesocellular carbon foam (MSU-F-C and Pt/MSU-F-C) to enhance the slow cathode reaction. Compared to materials including commercial carbon black (Vulcan XC-72 and Pt/Vulcan XC-72), MSU-F-C-based catalysts show higher energy efficiency, lower cathode overpotential, and lower internal resistance in single cell tests. These improved results are due to mostly of MSU-F-C having high surface area, large opened mesopores, and large ratio of hydroxyl groups which are active sites for  $\text{VO}^{2+}/\text{VO}_2^+$  redox reaction, and partly of Pt nanoparticles supported on the MSU-F-C.

# Advanced Anode Material with Bubble-Nanorod-Structured Metal Oxide-Carbon Composite Nanofibers

Jung Sang Cho, Young Jun Hong, and Yun Chan Kang

Department of Materials Science and Engineering, Korea University, Anam-Dong, Seongbuk-Gu, Seoul 136-713, Republic of Korea

jjj777@snu.ac.kr

A novel structure denoted as a “bubble–nanorod composite” is synthesized by introducing the Kirkendall effect into the electrospinning method. Bubble–nanorod-structured metal oxide–C composite nanofibers, which are composed of nanosized hollow metal oxide spheres uniformly dispersed in an amorphous carbon matrix, are synthesized. The post-treatment of the electrospun precursor nanofibers at 500 °C under 10% H<sub>2</sub>/Ar mixture gas atmosphere produces metal–carbon composite nanofibers. The post-treatment of the metal–carbon composite nanofibers at 300 °C under air atmosphere produces the bubble–nanorod-structured metal oxide–C composite nanofibers. The solid metal nanocrystals formed by the reduction are converted into hollow metal oxide nanospheres during the further heating process by the well-known Kirkendall diffusion process. The discharge capacities of the bubble–nanorod-structured Fe<sub>2</sub>O<sub>3</sub>–C composite nanofibers and hollow bare Fe<sub>2</sub>O<sub>3</sub> nanofibers for the 300<sup>th</sup> cycles at a current density of 1.0 A g<sup>−1</sup> are 812 and 285 mA h g<sup>−1</sup>, respectively, and their capacity retentions measured from the second cycle are 84 and 24 %, respectively. The hollow nanospheres accommodate the volume change that occurs during cycling. The unique structure of the bubble–nanorod-structured Fe<sub>2</sub>O<sub>3</sub>–C composite nanofibers results in their superior electrochemical properties by improving the structural stability during long-term cycling.

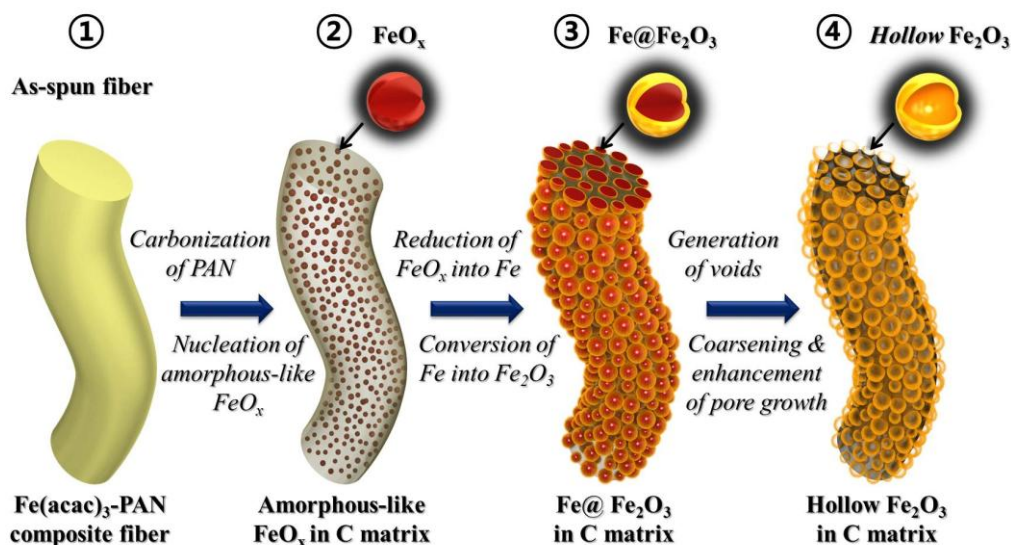


Figure 1. Formation mechanism of bubble-nanorod-structured Fe<sub>2</sub>O<sub>3</sub>-C composite nanofiber by Kirkendall-type diffusion.

## REFERENCES

- (1) Aldinger, F. Controlled Porosity by an Extreme Kirkendall Effect. *Acta Metall. Mater.* **1974**, *22*, 923-928.
- (2) Fan, H. J.; Knez, M.; Scholz, R.; Hesse, D.; Nielsch, K.; Zacharias, M.; Gösele, U. Influence of Surface Diffusion on the Formation of Hollow Nanostructures Induced by the Kirkendall Effect: The Basic Concept. *Nano Lett.* **2007**, *7*, 993-997.

# Fabrication of 3D Micro/Nano-Polymer and Metal Structures in Room-Temperature Ionic Liquid by Electron Beam Irradiation

Hiro Minamimoto<sup>1†</sup>, Haruyasu Irie<sup>1</sup>, Taro Uematsu<sup>1,2</sup>, Tetsuya Tsuda<sup>1</sup>, Akihito Imanishi<sup>3</sup>,  
Shu Seki<sup>1‡</sup> and Susumu Kuwabata<sup>1</sup>

<sup>1</sup>Department of Applied Chemistry, <sup>2</sup>Frontier Research Base for Global Young Researchers, Graduate School of Engineering, Osaka University, 2-1 Yamada-oka, Suita, Osaka 565-0871, Japan

<sup>3</sup>Department of Materials Engineering Sciences, Graduate School of Engineering, Osaka University 1-3 Machikaneyama, Osaka 560-8531, Japan

e-mail address : minamimoto@sci.hokudai-u.ac.jp

Room-temperature ionic liquids (RTILs), which are liquid salts consisting only of cation and anion, fascinate many researchers in various fields because of their unique physicochemical properties. Among them, negligible vapor pressure of RTILs is one of the most important features for the researches that use RTILs under vacuum conditions. Our research group developed several new technologies by combining RTIL with vacuum technology, i.e., electron microscope [1]. In the investigations, we have established a completely new method to fabricate micro/nano-sized polymer structures by irradiating focused ion beam onto a polymerizable RTIL layer [2]. This technique can build various 3D polymer structures with complicated shapes by simple raster scanning irradiation. In this study, in order to extend our previous method, we employed an electron beam (EB) writing system for the micro/nano fabrications of polymer and metal structures from RTILs.

The fabrications of 3D polymer structures from 1-Allyl-3-ethylimidazolium bis(trifluoromethanesulfonyl)amide ([AllylEtIm][Tf<sub>2</sub>N]) were demonstrated in the form of drawing some images and characters. Figure 1 shows SEM images of the polymers deposited by EB irradiation onto the [AllylEtIm][Tf<sub>2</sub>N] layer that was spun on a Si substrate. The fine structures were obtained according to the irradiation design with a uniform thickness. One of the important points for our present technique is that we can make any shapes of deposits precisely by a single raster writing of images. Even if the total area exceeds 50  $\mu\text{m}^2$ , the obtained structure had a resolution of several tens of nanometers.

In order to establish the fabrication method for silver structures, we used an aliphatic type of RTIL; trimethyl-propylammonium bis(trifluoromethanesulfonyl)amide ([N<sub>1,1,1,3</sub>][Tf<sub>2</sub>N]) which contained 390 mM Ag[Tf<sub>2</sub>N]. Figure 2 shows the SEM image of the obtained silver structures. The images reveal that the reduction reaction of silver ions occurred selectively in the part where electron beam was irradiated and this technique can fabricate silver structures having desired shapes with a high resolution. More detailed information about each fabrication method will be given in our presentation.

## References

[1] T. Torimoto et al., *Adv. Mater.*, 0871 (2010) 1196

[2] S. Kuwabata and H. Minamimoto et al., *Sci. Rep.*, 4 (2014) 3722

**Present addresses:** <sup>†</sup>Department of Chemistry, Faculty of Science, Hokkaido University, Sapporo, Hokkaido 060-0810 Japan

<sup>‡</sup>Department of Molecular Engineering, Graduate School of Engineering, Kyoto University, Nishikyo-ku, Kyoto 615-8510, Japan

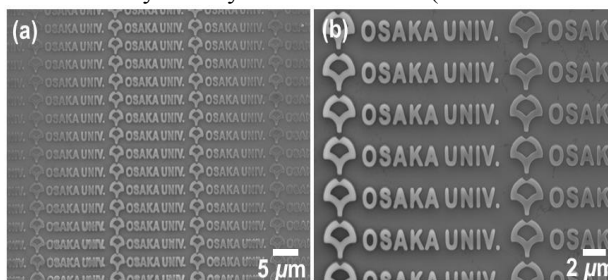


Figure 1. SEM images of polymer structures prepared by EB irradiation to [AllylEtIm][Tf<sub>2</sub>N]; (a) “OSAKA UNIV.” characters prepared in the area of 50  $\mu\text{m}^2$ , (b) the magnified image of (a).

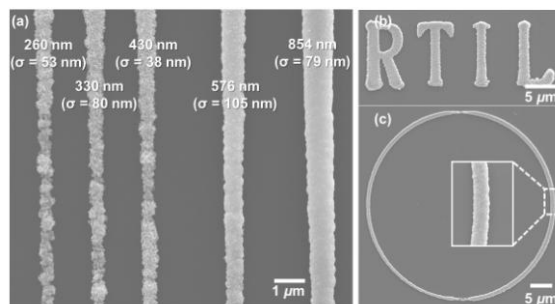


Figure 2. SEM images of deposited silver patterns prepared by EB irradiation to [N<sub>1,1,1,3</sub>][Tf<sub>2</sub>N] containing Ag[Tf<sub>2</sub>N]: (a) line structures prepared from the irradiation design of 80, 90, 100, 200, and 300 nm widths from left to right. The average line widths and standard deviations for each deposited line in (a). (b) Micro-sized alphabets, and (c) circular structure.

# Electrochemical Reaction of Single Nanoparticle

Shuo Liu, Li Liu, Na Tian\*, Zhi-You Zhou, Shi-Gang Sun\*

College of Chemistry and Chemical Engineering and School of Energy Research, Xiamen University, Xiamen, 361005, China

\*e-mail address: [tnsd@xmu.edu.cn](mailto:tnsd@xmu.edu.cn); [sgsun@xmu.edu.cn](mailto:sgsun@xmu.edu.cn)

Metal nanoparticles (NPs) find widespread application due to their unique physical and chemical properties. NPs have generated considerable interest in catalysis<sup>1</sup> and electrocatalysis<sup>2</sup>, where they provide a high surface area to mass ratio and can be tailored to promote particular reaction pathways. Significant research efforts have devoted to a definitive understanding of the effect of shape and size of NP properties. The activity of NPs can be analyzed especially well using electrochemistry, which probes interfacial chemistry directly. Electrochemical techniques are especially interesting, particularly when electrochemical characteristics can be related directly to other properties of the NPs. The challenge of ultimately measuring the electrochemical behavior of individual NPs is leading to imaginative experiments that have an impact on electrochemistry in general, as well as broader surface and colloid science.

Although the electrochemical properties of a single crystal nanoparticle have been previously studied by visualizing at ultramicroelectrode<sup>3</sup>, the current is randomness and may come from several nanoparticles impacted electrode. Herein, we developed a new method to place a nanocrystal in a marked hole and can find it with microscope easily. The current of the

nanocrystal was determined by using a scanning electrochemical cell microscopy (SECCM)<sup>4</sup>. As observed in Fig.1, the current of double-layer recorded on the single nanocrystal in 0.1M H<sub>2</sub>SO<sub>4</sub> is similar with that on the hole. However, the hydrogen evolution current on the single nanocrystal is much larger than that on the hole. It is clear that the single nanocrystal is contributed to the increased current. The results demonstrated that it is electrically conductive between the particle and substrate and our new method is effective and practical.

The developed method has thrown a new insight into study electrochemical reaction of a single nanocrystal and even a crystal plane on it in combination with STM.

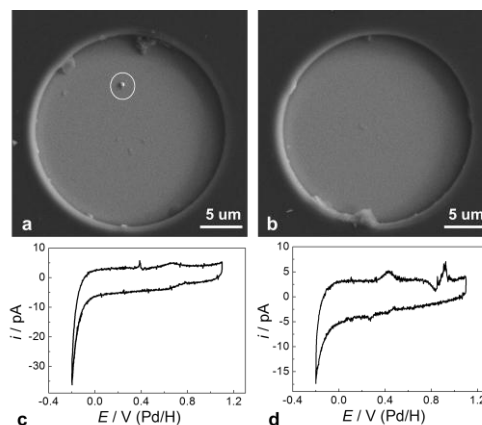


Fig 1. The SEM of the single particle (a) and blank hole (b). The current of them (c,d) in 0.1M H<sub>2</sub>SO<sub>4</sub>. Scan rate: 100 mV·s<sup>-1</sup>. The single particle is marked with a white circle.

## References:

- (1) Bell, A. T. *Science* **2003**, 299, 1688.
- (2) Tian, N.; Zhou, Z. Y.; Sun, S. G.; Ding, Y.; Wang, Z. L. *Science* **2007**, 316, 732.
- (3) Kim, J.; Kim, B.-K.; Cho, S. K.; Bard, A. J. *J. Am. Chem. Soc.* **2014**, 136, 8173.
- (4) Lai, S.; Patel, A. N.; McKelvey, K.; Unwin, P. R. *Angewandte Chemie* **2012**, 124, 5501.

# A Finite Element Simulation of the Electrochemical growth of single nanoparticle

Mesfin Haile Mamme<sup>1\*</sup>, El Amine Mernissi Cherigui<sup>1</sup>, Olga Dolgikh<sup>1</sup>, Jon Ustarroz<sup>1</sup>,  
Herman Terryn<sup>1</sup>, Johan Deconinck<sup>1</sup>

<sup>1</sup>Research Group Electrochemical and Surface Engineering, Vrije Universiteit Brussel, Pleinlaan 2, 1050  
Brussels, Belgium

mesfin.haile.mamme@vub.ac.be

The early stage of Electrochemical nucleation and growth process is one of the most important and interesting phenomena in nanoparticle electrodeposition. However, for many systems the process is not fully understood. In this work, we introduce a new modeling approach to study the growth of single hemispherical nucleus: Multi-Ion Transport and Reaction Model (MITReM) [1]. This approach takes into account the transport driven by diffusion and migration of all species in the electrolyte together with the electrochemical reactions at the electrode boundary. The Finite Element Method (FEM) is used to solve the balance equations for the concentration of all the active species and the electrolyte potential. In this work, we consider silver deposition in acetonitrile solution with 0.1M LiClO<sub>4</sub> as a supporting electrolyte. The simulation results confirm that, the initial stage of growth of a 10 nm single hemispherical silver nucleus always starts under kinetic control, regardless of concentration and overpotential. The reason is that, initially, the nucleus size is so small that diffusion is large enough. Secondly, it is noted that the growth of a single hemispherical silver nucleus will always show a transition from kinetic control to diffusion control. The time of transition depends on the imposed concentration and overpotential. To our knowledge, these combined phenomena have not yet been reported in other numerical approaches. In addition, the simulations clearly show that the deposition time and the rate of growth is easily affected by the imposed concentration and overpotential, as it has been proven experimentally in countless occasions. Furthermore, the simulation definitely shown the effect of nucleus size (10 nm, 20 nm, 30 nm and 50 nm) on the growth process (Figure 1(a) and (b)).

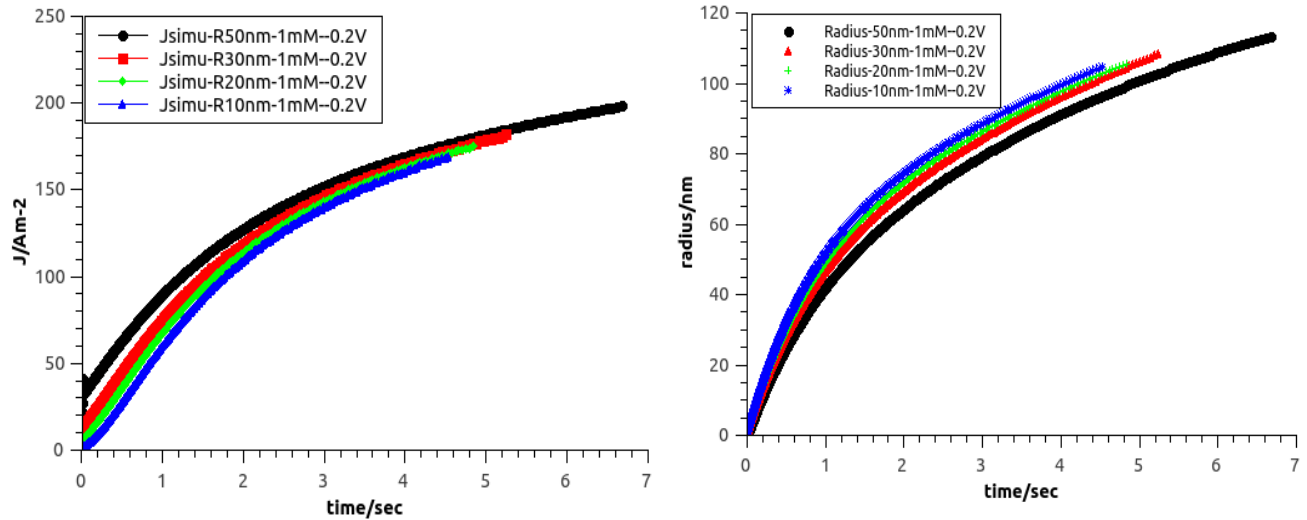


Figure 1. The current transient and the radius evolution of the hemispherical silver nucleus of different nucleus size (10 nm, 20 nm, 30 nm and 50 nm) at -200 mV (a) and (b) respectively. The solution contains 1mM of Ag<sup>+</sup> in acetonitrile solution with 1M LiClO<sub>4</sub> electrolyte.

- [1]. L. Bortels, J. Deconinck, and B. Van Den Bossche, J. Electroanal. Chem. 404, no. 1 (1996): 15-26.

# Activity and Stability of Pt Clusters supported on Au(111) for Electro-oxidation of Formic Acid

Hongjiao Li<sup>1</sup>, Yunchang Liang<sup>2,3</sup>, Wenbo Ju<sup>2,3</sup>, Marian D. Rötzer<sup>1</sup>, Florian F. Schweinberger<sup>1</sup>, Ulrich Stimming<sup>2</sup>, Ueli Heiz<sup>1</sup>, Oliver Schneider<sup>2</sup>

<sup>1</sup>Lehrstuhl für Physikalische Chemie, Catalysis Research Center and Chemistry Department, Technische Universität München, Lichtenbergstr. 4, 85748 Garching, Germany; <sup>2</sup>Institut für Informatik VI, Technische Universität München Schleißheimerstr. 90a, 85748 Garching Germany <sup>3</sup>Physik-Department, James-Frank-Str.1, Technische Universität München  
h.li@tum.de, oliver\_m.schneider@tum.de

Pure platinum as an electrocatalyst for the oxidation of formic acid is well known to be poisoned by CO, generated as surface intermediate in the indirect oxidation pathway<sup>1</sup>. Previous reports on Pt-Au alloys<sup>2</sup>, Pt decorated Au nanoparticles<sup>3</sup> and Pt-Au core-shell nanoparticles<sup>4</sup> demonstrated both advanced activity and stability compared to Pt. Despite these achievements, there is still a strong need for further study of the catalysis at the bimetallic systems and especially for exploring the underlying reaction mechanism.

In this work, unselected Pt<sub>n</sub> (n>35 atoms) clusters generated in a laser-ablation cluster source with an average surface area of 0.92 nm<sup>2</sup> per cluster were deposited on Au(111) under soft-landing conditions in an ultra-high vacuum (UHV) system<sup>5,6</sup>. As this technique provides a uniform distribution and an accurate size-control of the Pt clusters, the role of Au(111) on the oxidation of formic acid can be studied by varying the surface coverage of deposited Pt. For a sample with a high coverage of 1.16 clusters per nm<sup>2</sup>, the scanning tunneling microscopy (STM) image in Figure 1a elucidates the surface morphology. The image confirms that the landed clusters are around 1 nm high and form a uniform deposit. The electrochemical performance tests shows that the as prepared Pt<sub>n>35</sub>@Au(111) is much more active than Pt and further increases upon cycling. STM imaging of the sample after 50 cycles indicated no obvious agglomeration of the Pt particles. The enhanced activity and stability of our Pt<sub>n>35</sub>@Au(111) is attributed to the active boundaries of the Pt clusters and the Au substrate. With decreasing Pt coverage, the potential of the main oxidation peak shifts to higher values. The results clearly indicated that Au plays an important role in the Pt-Au bimetallic catalyst for electro-oxidation of formic acid.

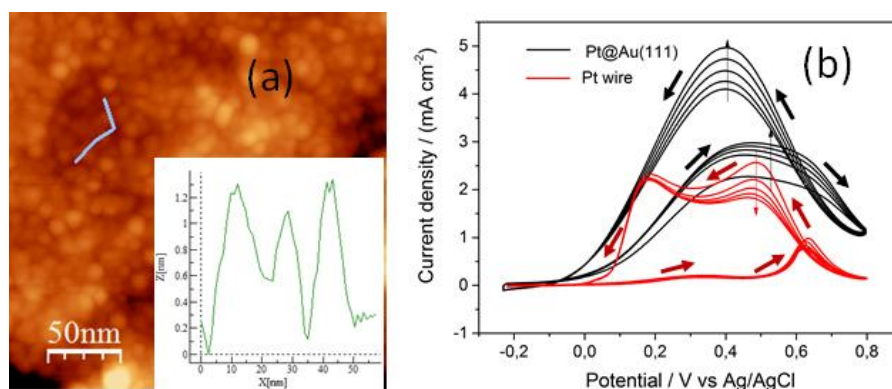


Figure 1. (a) STM image of Pt<sub>n>35</sub> clusters on Au(111). Inset: Height profile along blue line. (b) Cyclic voltammetry of two catalyst materials in 0.1 M HClO<sub>4</sub> + 0.5 M HCOOH at 50 mV s<sup>-1</sup>. The current is normalized to the actual Pt area as determined from H<sub>UPD</sub>.

## References

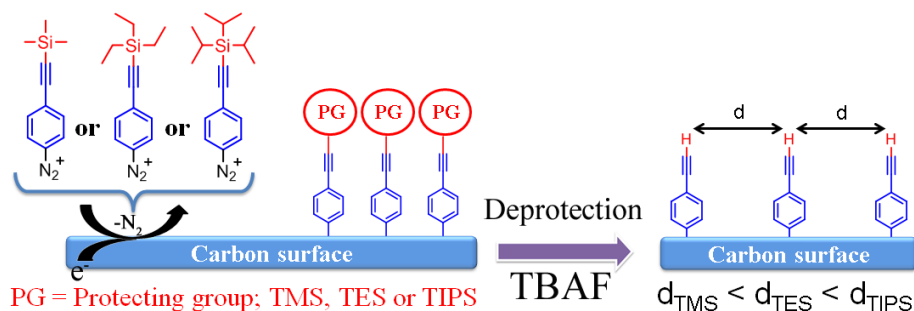
- (1) Gao, W.; Keith, J. A.; Anton, J.; Jacob, T. *J Am Chem Soc* **2010**, *132*, 18377.
- (2) Zhang, S.; Shao, Y. Y.; Liao, H. G.; Liu, J.; Aksay, I. A.; Yin, G. P.; Lin, Y. H. *Chem Mater* **2011**, *23*, 1079.
- (3) Zhang, S.; Shao, Y. Y.; Yin, G. P.; Lin, Y. H. *Angew Chem Int Edit* **2010**, *49*, 2211.
- (4) Xu, D.; Bliznakov, S.; Liu, Z. P.; Fang, J. Y.; Dimitrov, N. *Angew Chem Int Edit* **2010**, *49*, 1282.
- (5) Schweinberger, F. F.; Berr, M. J.; Dobliger, M.; Wolff, C.; Sanwald, K. E.; Crampton, A. S.; Ridge, C. J.; Jackel, F.; Feldmann, J.; Tschurl, M.; Heiz, U. *J Am Chem Soc* **2013**, *135*, 13262.
- (6) Kunz, S.; Hartl, K.; Nesselberger, M.; Schweinberger, F. F.; Kwon, G.; Hanzlik, M.; Mayrhofer, K. J.J.; Heiz, U.; Arenz, M. *Phys Chem Chem Phys* **2010**, *12*, 10288.

# Nanostructured Monolayers on Carbon Substrates.

Yann R. Leroux, Philippe Hapiot

*Institut des Sciences Chimiques de Rennes, CNRS, Université de Rennes I  
263, avenue du Général Leclerc, Campus de Beaulieu, Bat 10C, Rennes, 35042 France  
yann.leroux@univ-rennes1.fr*

The electro-generation of aryl radicals from protected aryl diazonium salts combined with protection-deprotection steps<sup>1</sup> was evaluated to design functional monolayers on carbon substrates with a well-controlled organization of the modifier at the molecular scale. The influence of the size of different silyl protecting groups on resulting covalently bounded films were investigated. Three different protecting groups were considered: trimethylsilyl (TMS), triethylsilyl (TES) and tri(isopropyl)silyl (TIPS). When the active function was introduced on para position of the aryl ring, a robust ethynylaryl monolayer is obtained after deprotection whatever the substituent. Electrochemical and structural analyses show that the organization of the attached monolayer is totally governed by the size of the protecting group. Properties of the monolayer (charge transfer, permeation of molecules through the layer, density of functional groups) were examined in combination of the performances for post-functionalization taken an alkyl-ferrocene derivative as an example of immobilized species. As a remarkable feature, all layers present large density of active alkyne terminations that remain totally available for further “click chemistry” coupling.<sup>2</sup>



## References:

- (1) Y. R. Leroux, H. Fei, J.-M. Noël, C. Roux, P. Hapiot, Efficient Covalent Modification of a Carbon Surface: Use of a Silyl Protecting Group To Form an Active Monolayer *J. Am. Chem. Soc.* 132 (2010) 14039.
- (2) Y. R. Leroux, P. Hapiot, Nanostructured Monolayers on Carbon Substrates Prepared by Electrografting of Protected Aryldiazonium Salts. *Chem. Mater.* 25(3) (2013) 489.



# Understanding Proton Conductivity within Porous Organic Cage Networks

L.J. Hardwick\*, S. Lewis, M. Liu, L. Chen, I. Aldous, M. Little, S. Chong, A.I. Cooper  
Department of Chemistry, University of Liverpool, Liverpool, L69 7ZF, UK  
\*hardwick@liverpool.ac.uk

Organic molecular cage salts containing protonated secondary amine groups show promise as proton conducting electrolytes due to their high water uptake, intrinsic porosity and appreciable ionic conductivity. Herein we report the proton conductivity of reduced amine cage salts with conductivities in the range  $10^{-3}$ – $10^{-2}$  S cm $^{-1}$ , at temperatures up to 80°C. These cages are formed from reversible imine bond formation and packing of discrete, rigid cage molecules results in a defined microporous structure <sup>[1, 2]</sup>. Proton conductivity was investigated using the 2-probe AC method of impedance spectroscopy under varying humidity and temperature for various cage systems. The determined activation energies of ca. 0.3 eV indicate a mixed Grotthuss and vehicular method of proton transport and suggest high intrinsic proton transport for some cage materials (Figure 1) <sup>[3]</sup>. Proton transference number was measured to be 0.71 via chronoamperometry using an H-cell containing equimolar concentrations of acidic and basic media, indicated that the counter ion was not the major charge carrying species. Comprehensive simulation studies and structural characterisation using powder XRD, solid state NMR and water uptake measurements suggests that water molecules form clusters within the voids of the charged cage cations and as a result, become polarised which facilitates proton transport. Both molecular dynamic simulation and transference number studies suggest that the anionic moieties investigated (for example Cl $^{-}$  and SO $_4^{2-}$ ) are too large to be mobile and remain fixed around each cage cation.

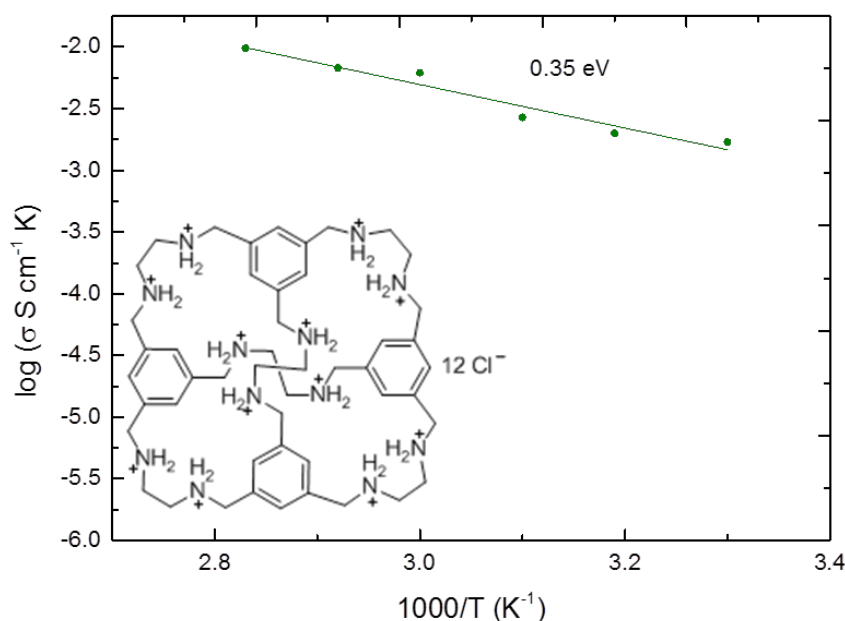


Figure 1: Arrhenius plot showing conductivity range with temperature for reduced cage 1 chloride salt (RCC1.Cl, shown inset). The activation energy indicates a mixed mechanism of proton transport.

1. Hasell, T. *et al.* Triply interlocked covalent organic cages. *Nat. Chem.* **2**, 750–5 (2010).
2. Tozawa, T. *et al.* Porous organic cages. *Nat. Mater.* **8**, 973–8 (2009).
3. Liu M. *et al.* 3D protonic conductivity within porous organic cage networks. *submitted* (2015).

# First principles study of thermal stability of LiNiO<sub>2</sub> materials coated with ultrathin amorphous Al<sub>2</sub>O<sub>3</sub> layer

Joonhee Kang<sup>1</sup>, Byungchan Han<sup>2,\*</sup>

<sup>1</sup>*Department of Energy Systems Engineering, DGIST, Daegu, 711-873, Republic of Korea*

<sup>2</sup>*Department of Chemical and Biomolecular Engineering, Yonsei University, Seoul, 120-749, Republic of Korea*

[calmbird@dgist.ac.kr](mailto:calmbird@dgist.ac.kr), [bchan@yonsei.ac.kr](mailto:bchan@yonsei.ac.kr)

Development of materials with outstanding energy capacity and structural durability is especially of paramount importance in Li-ion batteries. The bi-functional properties have been seriously challenged to high Ni cathodes via unfavorable electrochemical and thermal instability when exposed to liquid organic-phase electrolytes or under ambient environment above room temperature.

Conformal ultrathin Al<sub>2</sub>O<sub>3</sub> coating by atomic layer deposition (ALD) has been mostly employed to enhance the electrochemical stability of the cathodes. However, atomistic understanding of thermal stability issue still remains.

In this presentation, we extensively utilize first principles density functional theory (DFT) calculations to identify the thermal stabilities of Al<sub>2</sub>O<sub>3</sub> coated LiNiO<sub>2</sub> (LNO) (012) surface. First, the interface structures between LNO and varying Al<sub>2</sub>O<sub>3</sub> coating layers increased from 0.20 nm ~ 0.88 nm were calculated. We identify that phase transformation of Al<sub>2</sub>O<sub>3</sub> from ordered into amorphous structure as the thickness reach about 0.88 nm, at which the cathode shows exceptional thermal durability with suppressed oxygen evolution. Second, thermal stability of LNO (012) facet with and without Al<sub>2</sub>O<sub>3</sub> coating layer are predicted at higher than ambient temperature (T = 400 K) using ab-initio molecular dynamics (AIMD). Finally, by calculating electron density distributions we characterize chemical bonding natures of Li-O and Al-O to understand underlying mechanism providing such high thermal stability.

# GO/rGO Microelectrode Arrays with Adjustable Electrochemical Activity and Biocompatibility for Highly Sensitive Detection of Hydrogen Peroxide Released by Living Cells

Aiping Liu, Ming Zhao, Panju Xu, Guodong Qian

Center for Optoelectronics Materials and Devices, Zhejiang Sci-Tech University  
Hangzhou, Zhejiang Province 310018, China  
liuaiping1979@gmail.com

Cell secretions detection is of very importance in disease diagnosis and precaution. Especially, hydrogen peroxide ( $\text{H}_2\text{O}_2$ ), as the stable and common reactive oxygen species (ROS) among intracellular signaling molecules is being proved to play a vital role in physiological signaling pathways of healthy cells through mainly regulating DNA damage, cell apoptosis and protein synthesis. Electrochemical biosensors based on noble metals have been developed for  $\text{H}_2\text{O}_2$  detection due to their rapid response, good simplicity and sensitivity [1]. However, it is almost inevitable that the release of metal ions and endocytosis of nanoparticles will affect the cell metabolism in living systems.

In this paper, a catalyst-free and multi-functional graphene-based microelectrode array (MEA) is fabricated on arbitrary substrates by an electrochemistry-assisted microstructuring process [2]. The dimension of special-shaped rGO microarrays localized in an insulating GO matrix is effectively adjusted by changing GO reduction time without multi-mask patterning. When the pheochromocytoma cells (PC12) are seeded on the GO/rGO MEA, PC12 prefer to migrate and grow on the GO surfaces, exactly distribute along the interface of GO and rGO with filopodia fixed on rGO surface, which favors the highly sensitive detection of  $\text{H}_2\text{O}_2$  released by the stimulated living cells at the nanomolar level. The present MEA would have a potential application in next generation electronic and electrochemical devices.

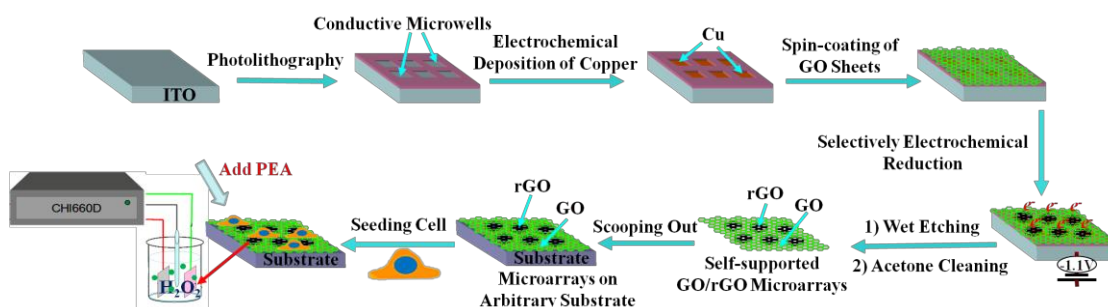


Figure 1. Schematic illustration of GO/rGO MEA fabrication of  $\text{H}_2\text{O}_2$  detection released by living cell.

## References:

- [1] Aiping Liu, et al. *Electrochimica Acta* 2010, 55(6):1971-1977.
- [2] Ming Zhao, Aiping Liu\*, et al. *Electrochemistry Communications* 2014, 48: 86-90.

# Nucleation and Growth of PEDOT on the Surface of Horizontally Aligned Carbon Nanotubes

Katarzyna Krukiewicz<sup>a</sup>, John S. Bulmer<sup>b</sup>, Dawid Janas<sup>b</sup>, Krzysztof K.K. Koziol<sup>b</sup>, Jerzy K. Zak<sup>a</sup>  
<sup>a</sup> *Department of Physical Chemistry and Technology of Polymers, Silesian University of Technology,  
M. Strzody 9, 44-100 Gliwice, Poland*  
<sup>b</sup> *Department of Materials Science and Metallurgy, University of Cambridge,  
27 Charles Babbage Road, Cambridge CB3 0FS, United Kingdom  
katarzyna.krukiewicz@polsl.pl*

When spun directly and continuously from gas phase as an aerogel, carbon nanotubes (CNTs) are able to form high-performance fibers [1]. These macrostructures can be successfully applied as wires in electrical transformers, fillers for composites with superior erosive wear resistance and materials for electromagnetic shielding and electrostatic dissipation applications. The properties of CNT fibers can be further enhanced by covering them with conjugated polymers (CPs). Highly conductive CPs are expected to enhance the direct charge transfer with electron hopping effects on intertube conductivity, leading to further decrease in resistivity of CNT material [2].

Poly(3,4-ethylenedioxythiophene), PEDOT, exhibits superior chemical and electrochemical stability as compared to other CPs. When electrodeposited on the surface of horizontally aligned carbon nanotube (HA-CNT) electrode, it is able to cover the surface of each HA-CNT individually. The mechanism of the nucleation process highly depends on the reaction environment. The presence of a surfactant or non-aqueous medium favors the progressive nucleation in which the polymer growth is homogeneous over the large area of the electrode. Because of the non-uniform in respect of conductivity area of HA-CNT, the application of overpotential is necessary to generate radical cations and cause relatively fast growth of polymer layer [3].

*K.K.K. acknowledges the European Research Council (under the Seventh Framework Program FP7/2007–2013, ERC Grant Agreement No. 259061) and the Royal Society for the financial support.*

## References:

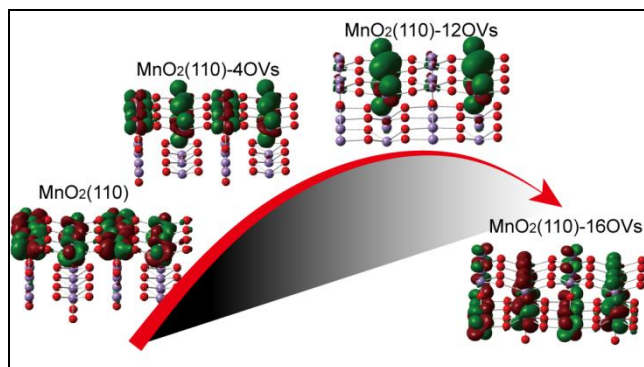
1. K. Koziol, J. Vilatela, A. Moisala, M. Motta, P. Cuniff, M. Sennett, A. Windle, High-performance carbon nanotube fiber, *Science* 318 (2007) 1892.
2. L. Fu, A.M. Yu, Carbon nanotubes based thin films: fabrication, characterization and application, *Rev. Adv. Mater. Sci.* 36 (2014) 40.
3. K. Krukiewicz, J.S. Bulmer, D. Janas, K.K.K. Koziol, J.K. Zak, Poly(3,4-ethylenedioxythiophene) growth on the surface of horizontally aligned MWCNT electrode, *Appl. Surf. Sci.* 335 (2015) 130.

# Insight into the effect of oxygen vacancy concentration on the catalytic performance of MnO<sub>2</sub>

Li Li,\* Yao Nie, Siguo Chen, Wei Ding, Xueqiang Qi, Feng Shi, Zidong Wei\*

Chongqing Key Laboratory of Chemical Process for Clean Energy and Resource Utilization, School of Chemistry and Chemical Engineering, Chongqing University, Chongqing, 400044; China  
zdwei@cqu.edu.cn; liliracial@cqu.edu.cn

Oxygen vacancies (OVs) are important for changing the geometric and electronic structures as well as the chemical properties of MnO<sub>2</sub>. In this study, we performed a DFT+U calculation on the electronic structure and catalytic performance of a  $\beta$ -MnO<sub>2</sub> catalyst for oxygen reduction reaction (ORR) with different numbers and extents of OVs. Comparing to the experimental XRD analysis, we determined that OVs produce a new crystalline phase of  $\beta$ -MnO<sub>2</sub>. Changes in the electronic structure (Bader charges, band structure, partial density of states (PDOS), local density of states (LDOS), and frontier molecular orbital), proton insertion and oxygen adsorption in  $\beta$ -MnO<sub>2</sub> (110) were investigated as a function of the bulk OVs. The results show that a moderate concentration of bulk OVs reduced the band gap, increased the Fermi and HOMO levels of the MnO<sub>2</sub> (or MnOOH), and elongated the O-O bond of the adsorbed O<sub>2</sub> and co-adsorbed O<sub>2</sub> with H. These changes substantially increase the conductivity of MnO<sub>2</sub> for the catalysis of ORR. However, an excessively high concentration of OVs in  $\beta$ -MnO<sub>2</sub> (110) will work against the catalytic enhancement of MnO<sub>2</sub> for ORR. The DFT+U calculation reveals that a moderate concentration of OVs induced a large overlap of the surface Mn orbitals and thus introducing an extra donor level at the bottom of the conductive band (CB), which increased the conductivity of  $\beta$ -MnO<sub>2</sub> (110). Such a curvilinear change of the catalytic activity and electronic structure as a function of the oxygen vacancy concentration suggests that the  $\beta$ -MnO<sub>2</sub> with moderate concentration OVs exhibits the highest conductivity and catalytic activity for ORR. Therefore, the electronic structure and catalytic performance of  $\beta$ -MnO<sub>2</sub> can be effectively modulated by regulating the oxygen vacancy concentration.



- [1] Wei, Z. D.; Huang, W. Z.; Zhang, S. T.; Tan, J. *J Appl Electrochem* 2000, **30**, 1133.
- [2] Tompsett, D. A.; Parker, S. C.; Islam, M. S. *J Am Chem Soc* 2014, 136, 1418.
- [3] Cheng, F.; Zhang, T.; Zhang, Y.; Du, J.; Han, X.; Chen, J. *Angew Chem Int Ed Engl* 2013, **52**, 2474.
- [4] Tang, Q. W.; Jiang, L. H.; Liu, J.; Wang, S. L.; Sun, G. Q. *Acs Catal* 2014, **4**, 457-463.

# Electrochemical properties of nano functionalized iron oxyhydroxide: strategies for the corrosion protection of rusted steels

Emmanuel ROCCA<sup>1\*</sup>, Hadri FAIZ<sup>1</sup>, François MIRAMBET<sup>2</sup>, Solenn REGUER<sup>3</sup>

<sup>1</sup>*Institut Jean Lamour – UMR CNRS 7198, Université de Lorraine, BP70239 Vandoeuvre les Nancy, 54506, France.*

<sup>2</sup>*C2RMF - Palais du Louvre –14, quai François Mitterrand - 75001 Paris 54518, France.*

<sup>4</sup>*DiffAbs beamline, Synchrotron Soleil, L'Orme des Merisiers, Saint-Aubin, BP48 Gif sur Yvette, 91192, France.*

\**emmanuel.rocce@univ-lorraine.fr*

Since several ten years, a large number of heritage collections are related to the technical and industrial field because society wishes to preserve those materials which constitute traces of our industrial development. The diagnosis of the conservation state and the choice of the restoration treatment are important questions, that have to be solved by curators to avoid expensive restoration works on numerous objects or important buildings as U4 blast furnace in Uckange in France.

Previous studies [1] have demonstrated that the electrochemical properties of some iron(III) oxyhydroxide phases constituting the rust layers play an important role in the corrosion processes during wet and dry periods, and can increase the corrosion rate of the underlying metal.

The purpose of this study is to functionalize the surface of iron oxyhydroxide constituting the rust layers to freeze or block the electrochemical activity of these complex systems in order to lower the degradation rate of structures, without applying thick organic coatings as paints or varnishes.

The surface functionalization is based on a dip treatment in linear aliphatic carboxylic acid solutions [2] to form by a self-organization process a nanometric layer of iron carboxylate, constituted by the “ferric wheel” cluster.

The electrochemical activity of the functionalized oxyhydroxide iron compounds was characterized by cyclic voltamperometry in a carbon paste electrode, and the behavior of the whole “metal/rust layer” system after functionalization was described by recording electrochemical impedance spectroscopy in aqueous corrosive media in function of immersion time.

In-situ x-ray absorbance spectroscopy (XAS) measurements [3] allow confirming the formation of the “ferric wheel” cluster from the iron oxyhydroxide during the treatment, with a chemical formulae  $[\text{Fe}_3\text{O}(\text{C}_n\text{H}_{2n+1}\text{O}_2)_6(\text{H}_2\text{O})_3]^+$  ( $n$  = carbon number of aliphatic chain). So, the EIS analysis coupled with the analysis of the oxides surfaces (SEM, X-ray diffraction, Raman spectroscopy) show that the application of the functionalization treatment has a positive effect on both the dissolution of iron species, then their chemical diffusion in the pores network of the rust layer, and the electrical conductivity of the oxide system. So, the electrochemical reactivity of the iron oxide phases is drastically reduced.

From those experiments, it turns out that these functionalization solutions represent an interesting alternative of new environmentally safe treatments for corroded steels as iron artefacts.

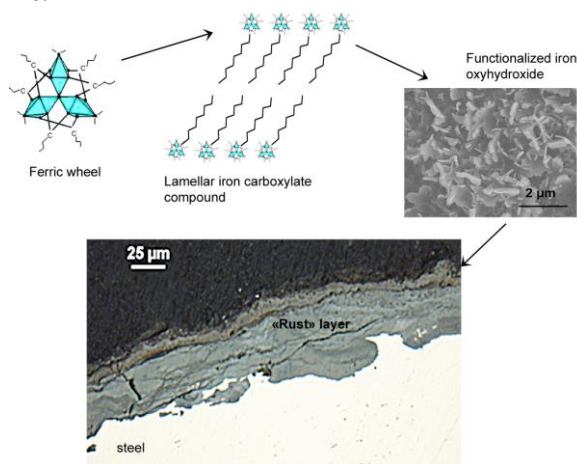


Fig 1 : Principle of functionalization of oxyhydroxide iron layer – From the “Ferric wheel” to a functionalized surface

## References:

- [1] J. Monnier, L. Legrand, L. Bellot-Gurlet, E. Foy, S. Reguer, E. Rocca, P. Dillmann, D. Neff, F. Mirambet, S. Perrin, I. Guillot, *Journal of Nuclear Materials*, 379 (2008) 105
- [2] E. Rocca, C. Rapin, F. Mirambet, *Corrosion Science*, 46(3) (2004) 653
- [3] F. Mirambet, S. Reguer, E. Rocca, S. Hollner, D. Testemale, *Applied Physics A-Material Science & Processing*, 99(2) (2010) 341

# Electropolymerized carbazole-containing ionic liquid

Kirankumar.R<sup>a</sup>, Po-Yu Chen<sup>a,b\*</sup>.

<sup>a</sup>Department of Medicinal and Applied Chemistry, Kaohsiung Medical University, Kaohsiung City 80708, Taiwan

<sup>b</sup>Department of Chemistry, National Sun Yat-sen University, Kaohsiung City 80424, Taiwan

\*Corresponding author. Tel.: +886 7 3121101x2587; fax: +886 7 3125339.  
E-mail address: [pyc@kmu.edu.tw](mailto:pyc@kmu.edu.tw) (P.-Y. Chen).

## Abstract:

In this study, a new class of polymerizable ionic liquids were synthesized and modified upon conductive surfaces to enhance the sensitivity and/or selectivity of the electrodes, which were used for electroanalytical and electrochromic application. At suitable conditions, the poly-ionic liquids were liquid and soluble in some organic solvents.

Ionic liquids (ILs) have shown the advantages on electroanalysis if they can be modified on electrode surface. Electropolymerization might be a good approach for the modification of ILs on conductive surface. Various carbazole-based ILs (Figure 1) were synthesized in this study and they were electropolymerized on indium tin oxide (ITO) electrodes by cyclic voltammetry in ILs BMP-TFSI, Bu<sub>3</sub>MeN-TFSI and etc., as well as in conventional solvents (Acetonitrile, methanol) <sup>[1]</sup>. Electrochemical oxidation of the carbazole pendant units affords a conjugated polymer network (CPN) film of polycarbazole and the polymer is expected to have good conductivity on the conducting surface<sup>[2]</sup>. The electrodes with electropolymerized ILs will be used for the determination of various bio-molecules, such as uric acid (UA) and also in the field of electrochromic devices.

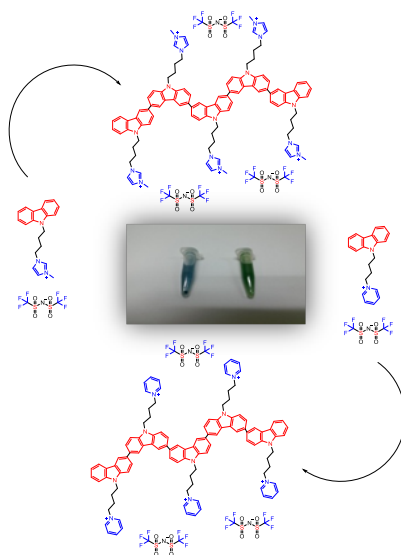


Figure 1: The solvanochromic behaviour of the polymerized carbazole-containing ionic liquids

## Reference:

<sup>[1]</sup> D.-X. Zhuang,, P.-Y. Chen, Journal of Electroanalytical Chemistry, **2009**, **626**: 197–200.

<sup>[2]</sup> Antonio F. Frau, Nicel C. Estillore and Rigoberto C. Advincula, ACS Appl. Mater. Interfaces, **2010**, **2**: 3726–3737.

# The pH effect on the electrochemical reduction of carbonate species over metal oxide electrodes

Seunghwa Lee<sup>a</sup>, Hansaem Jang<sup>a</sup>, Jaeyoung Lee<sup>a,b</sup>

<sup>a</sup>Electrochemical Reaction and Technology Laboratory, School of Environmental Science and Engineering, Gwangju Institute of Science and Technology (GIST), Gwangju, 500-712, South Korea.

<sup>b</sup>Ertl Center for Electrochemistry and Catalysis, Research Institute for Solar and Sustainable Energies, GIST, Gwangju, 500-712, South Korea.

Gwangju Institute of Science and Technology (GIST), Gwangju, 500-712, South Korea.  
jaeyoung@gist.ac.kr

Carbon dioxide (CO<sub>2</sub>) emission from the fuel combustion and other human activities are of great interest due to its adverse effects on climatic change and ecosystem. In terms of reducing atmospheric CO<sub>2</sub>, the CO<sub>2</sub> utilization for synthesizing useful chemicals attracts a significant attention as an alternative method compared to capture and sequestration techniques [1]. In particular, electrochemical reduction of CO<sub>2</sub> has been studied using metal oxide catalysts which are reported as the superior catalysts very recently [2-3]. Furthermore, from our recent study, it was demonstrated that stannic oxide (SnO<sub>2</sub>) can efficiently catalyze formate production (HCOO<sup>-</sup>) from CO<sub>2</sub> and oxygen-evacuated cuprous oxide (Cu<sub>2</sub>O) enhance the product selectivity towards ethylene from CO<sub>2</sub> at lower overpotential [4-5]. In this report, we study the electrochemical reduction of carbonate species on the both two types of metal oxide catalysts under the various pH conditions. The electrolyte pH is an important indicator regarding the CO<sub>2</sub> equilibria in aqueous system [6]. With this recognition, considering the distribution of dissolved CO<sub>2</sub>, bicarbonate (HCO<sub>3</sub><sup>-</sup>) and carbonate (CO<sub>3</sub><sup>2-</sup>) which are functioning as a CO<sub>2</sub> reservoir, catalytic activity, selectivity and stability for CO<sub>2</sub> electroreduction are evaluated using SnO<sub>2</sub> and Cu<sub>2</sub>O electrode.

## References

- [1] J. Lee, Y. Kwon, R. L. Machunda, H. J. Lee, Electrocatalytic Recycling of CO<sub>2</sub> and Small Organic Molecules, *Chem. Asian J.*, **4** (2009) 1516.
- [2] Y. Chen, M. W. Kanan, Tin Oxide Dependence of the CO<sub>2</sub> Reduction Efficiency on Tin Electrodes and Enhanced Activity for Tin/Tin Oxide Thin-Film Catalysts, *J. Am. Chem. Soc.*, **134** (2012) 1986.
- [3] C. W. Li, M. W. Kanan, CO<sub>2</sub> Reduction at Low Overpotential on Cu Electrodes Resulting from the Reduction of Thick Cu<sub>2</sub>O Films, *J. Am. Chem. Soc.*, **134** (2012) 7231.
- [4] D. Kim, S. Lee, J. D. Ocon, B. Jeong, J. K. Lee, J. Lee, Insights into autonomously formed oxygen-evacuated Cu<sub>2</sub>O electrode for the selective production of C<sub>2</sub>H<sub>4</sub> from CO<sub>2</sub>, *Phys. Chem. Chem. Phys.*, **17** (2015) 824.
- [5] S. Lee, J. D. Ocon, Y. Son, J. Lee, Alkaline CO<sub>2</sub> Electrolysis toward Selective and Continuous HCOO<sup>-</sup> Production over SnO<sub>2</sub> Nanocatalysts, *J. Phys. Chem. C*, **119** (2015) 4884.
- [6] K. J. P. Schouten, E. P. Gallent, M. T. M. Koper, The influence of pH on the reduction of CO and CO<sub>2</sub> to hydrocarbons on copper electrodes, *J. Electroanal. Chem.*, **716** (2014) 53.



# A multi-scale model to account for the electrochemical response of the oxygen reduction reaction on highly active graphene nanosheets in alkaline conditions

Guadalupe Ramos-Sanchez<sup>a</sup>, Jorge Vazquez-Arenas<sup>b</sup> and Alejandro A. Franco<sup>c</sup>

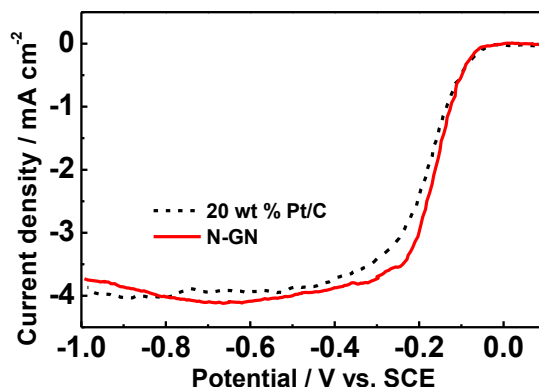
Departamento de Química, Universidad Autónoma Metropolitana, Av. San Rafael Atlixco No. 186 Col. Vicentina México, D.F., 09340 México

<sup>a</sup>gramossa@conacyt.mx

<sup>b</sup>jorge\_gva@hotmail.com

<sup>c</sup> Laboratoire de Réactivité et Chimie des Solides (LRCS) - Université de Picardie Jules Verne & CNRS, UMR 7314 – 33 rue Saint Leu, 80039 Amiens Cedex, France

A multi-scale modeling framework is used to describe polarization curves collected for the oxygen reduction reaction (ORR) performed on highly active graphene nanosheets in alkaline conditions. Density functional theory (DFT), and electrode kinetics with transport phenomena are respectively utilized to compute the inputs at the different scales. The framework extracts *ab initio* information of the chemical contributions to the activation energies for the elementary reaction steps involving the multiple adspecies generated within the mechanism at the atomic level. This information is subsequently connected with a mesoscale-level Mean Field model, which integrates the current density of the elementary steps along with the chemical data obtained from quantum mechanics.<sup>1</sup> In order to enhance the influence of the catalyst properties on the ORR mechanism, a sensitivity analysis is conducted to compare the multi-scale and single mesoscale-level models. Likewise, the electrochemical parameters are determined by fitting the experimental data to each model, to determine the deviations existing in sole scale models (e.g. mesoscale, macroscopic). The surface coverage on the cathode material and the catalytic nitrogen bonding (e.g. pyridinic, pyrrolic, and quaternary) are also evaluated to determine their influence upon the activation energy of the elementary steps.



ORR polarization curves (900 RPM) recorded on Pt/C and Graphene nanosheets in O<sub>2</sub>-saturated KOH electrolytes.

<sup>1</sup> Rodrigo Ferreira de Morais, Philippe Sautet, David Loffreda, Alejandro A. Franco, *Electrochimica Acta* 56 (2011) 10842– 10856.

# Multi-scale Computational Design of Multi-functional Catalyst Materials for Fuel Cells Beyond Conventional Bulk Pt

Byungchan Han<sup>1</sup>, Seunghyo Noh<sup>2</sup>

<sup>1</sup>Department of Chemical and Biomolecular Engineering, Yonsei University  
Seoul, 120-749, Republic of Korea

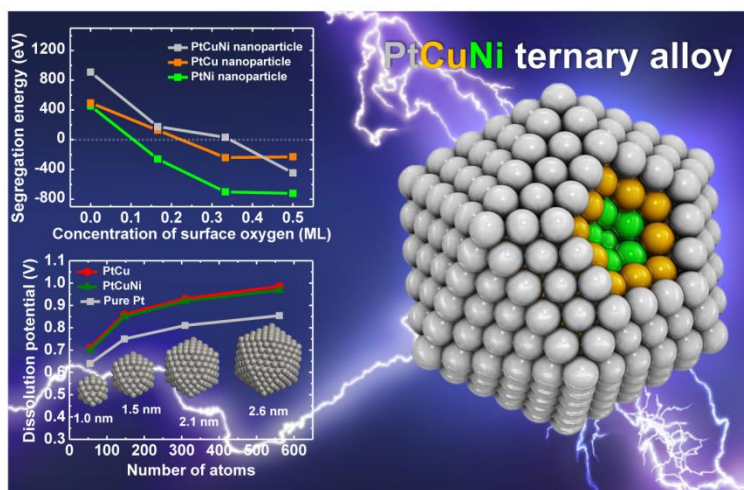
<sup>2</sup>Department of Electronic Chemistry, Interdisciplinary Graduate School of Science and Engineering,  
Tokyo Institute of Technology, 4259-G1-5 Nagatsuta, Midori-ku, Yokohama, 226-8502, Japan

bchan@yonsei.ac.kr

Using density functional theory (DFT) calculations and statistical formalisms we rationally design metallic nanocatalyst with ternary transition metals for oxygen reduction reaction (ORR) in fuel cell application. We surround binary core-shell nanoparticles with a Pt skin layer. To overcome surface segregation problem of the core 3-d transition metal we identified a binary alloy  $\text{Cu}_{0.76}\text{Ni}_{0.24}$ , having strongly attractive atomic interactions by computationally screening 158 different alloy configurations using energy convex hull theory. The Pt-skin- $\text{Cu}_{0.76}\text{Ni}_{0.24}$  nanoparticle shows better electrochemical stability and higher ORR activity than bulk Pt at approximately 3 nm. We propose that underlying mechanisms of the results are originated from favorable compressive strain on Pt for ORR catalysis and atomic interactions between the nanoparticle shells for electrochemical stability. Our results will contribute to accurate identification and innovative design of promising nanomaterials for renewable energy systems.

We also demonstrate that Cu@N-C catalysts are promising catalysts with enhanced ORR activity and durability by experiments and computations. The active Cu@N-C catalyst is synthesized by  $\text{CO}_2$  treatment. Carbon dioxide gas at high temperature induces the dramatically enhanced ORR activity by the oxidation of the surface carbon atoms. We expect that  $\text{CO}_2$  treatment could be employed in a variety of carbon encapsulation structures such as metal@N-C, metal carbide@N-C, metal oxide@N-C to control the thickness of carbon layers.

These two results are outstanding examples showing how to screen desired materials with more than single properties using combined multi-scale computations, which are often validated by experimental measurements.



# Boosting Lithium Air Batteries from a Multiscale Modeling Approach

Yinghui Yin,<sup>1,2,3</sup> Guillaume Blanquer,<sup>1,2,3</sup> Matias A. Quiroga,<sup>1,2,3</sup> and Alejandro A. Franco<sup>1,2,3</sup>

<sup>1</sup>Laboratoire de Réactivité et Chimie des Solides (LRCS) - Université de Picardie Jules Verne & CNRS, UMR 7314 – 33 rue Saint Leu, 80039 Amiens Cedex, France

<sup>2</sup>Réseau sur le Stockage Electrochimique de l'Energie (RS2E), FR CNRS 3459, France

<sup>3</sup>ALISTORE-ERI European Research Institute, FR CNRS 3104, 80039 Amiens Cedex, France.

[yin.yinghui@u-picardie.fr](mailto:yin.yinghui@u-picardie.fr)

Li Air Batteries (LABs) can theoretically provide a capacity significantly higher than conventional Lithium Ion Batteries<sup>1</sup>. However, there are still a significant amount of challenges in the way of bringing LABs to practicality. For instance, resulted from its insulating and insoluble nature, the discharge product  $\text{Li}_2\text{O}_2$  would bring in hindrance to charge transfer as well as mass transport limitations in the cathode by insulator film formation and pore clogging.

It is reported that the passivation of carbon surface could be delayed when high donor number solvents were employed, which give rise to the formation of toroidal  $\text{Li}_2\text{O}_2$  through a solution phase reaction mechanism.<sup>2</sup> But the origin of this mechanism, whether from the existence of water<sup>3</sup> or the solubility of  $\text{Li}^+\text{-O}_2^-$  pair<sup>2</sup>, is still under debating. Besides, the pore clogging problem stays unsolved and even becomes more serious at high rate discharging conditions, leading to inactivation of effective surface inside the choked pore. Hence, to improve the performance of LABs, it is illuminating to bypass the above inherent limitations by designing and optimizing the cathode architecture.

Following a multiscale computational modeling approach being developed by us,<sup>4</sup> here we extend our previous discharge model for  $\text{Li-O}_2$  batteries<sup>5,6</sup> in order to investigate the influence of different innovative cathode architectures onto the overall cell performance. Architectures explored include porosity gradients along the cathode thickness as well as implanting pipe-like channels with different volume densities within cathode, aiming to facilitate the oxygen transport especially at high discharge rates. Furthermore, by using three-dimensional mesoscale simulations at the pore level<sup>7</sup>, the competition of thin-film mechanism and solution phase mechanism are studied to elucidate the effects of the local cathode microstructure on the details of the reaction mechanisms.

The modeling results are discussed in comparison with state-of the-art data, and allow establishing a single comprehensive theoretical framework explaining multiple experimental observations. Practical implications of our approach towards the design of the next generation of LABs are finally discussed.

[1] P. G. Bruce, S. A. Freunberge, L. J. Hardwick and J.-M. Tarascon, *Nature Materials*, **11** (2012) 19.

[2] L. Johnson, C. Li, Z. Liu, Y. Chen, S. A. Freunberger, P. C. Ashok, B. B. Praveen, K. Dholakia, J.-M. Tarascon and P. G. Bruce, *Nature Chemistry*, **6** (2014) 1091.

[3] Alan C. Luntz · Bryan D. McCloskey, *Chem. Rev.*, **114** (23) (2014) 11721.

[4] A. A. Franco, *RSC Advances*, **3** (32) (2013) 13027.

[5] K.-H. Xue, T.-K. Nguyen and A. A. Franco, *Journal of the Electrochemical Society* **161** (2014) E3028.

[6] K.-H. Xue, E. McTurk, L. Johnson, P. G. Bruce and A. A. Franco, *Journal of the Electrochemical Society.*, **162** (2015) A614.

[7] M.A. Quiroga, A.A. Franco, *J. Electrochem. Soc.*, **162** (7) (2015) E73.

# **Water Management in Proton Exchange Membrane Fuel Cells by Materials Design and Engineering**

Trung Van Nguyen

*University of Kansas*

*Department of Chemical & Petroleum Engineering, Lawrence, Kansas, USA*

*cptvn@ku.edu*

## **Abstract**

Proton-exchange-membrane fuel cells (PEMFCs) depend on proper water management to obtain high power density and energy efficiency. Proper water management also plays a major role in the durability of the membrane-electrode assemblies. Traditionally, water management has been addressed by system design and engineering. That is, by adding auxiliary systems to the basic fuel cell system to provide humidification to the anode and to remove water from the cathode. This approach adds significant complexities and costs and reduces the overall efficiency of the PEMFC system. Development of new materials and better understanding of the functions of these materials have led to a paradigm shift as to how water management can be implemented in a PEMFC system. Theoretical calculations have shown that if materials with the right properties are used in the membrane and electrodes such that zero-net-water transport across the membrane could be achieved, then water management in a PEMFC system could be attained with no or minimal external-water requirement. If this objective could be achieved, the PEM fuel cell system and its operation would be greatly simplified, and its cost would be greatly reduced. This presentation will discuss some of the approaches that could be used to achieve the zero-net-water transport condition across the membrane.

## **Acknowledgement**

The work presented was funded by NSF through grant numbers CBET-0651758 and CBET-1518755.

# Combined Finite Element Modelling and EIS Studies for SoC Indication in Rechargeable Li-Ion Batteries

Daniel Brandell, Shruti Srivastav, Matthew J Lacey  
*Department of Chemistry- Ångström Laboratory, Uppsala University*  
*Box 538, 751 21 Uppsala, Sweden*  
*Daniel.Brandell@kemi.uu.se*

Battery modelling is a key technique for the understanding of electrochemical processes in the cell in context of the inherent morphological conditions and different loss mechanisms. At the same time, electrochemical impedance spectroscopy (EIS) is as a fast, non-destructive and reliable method to determine battery state of charge (SoC) [1,2]. Impedance studies are known to provide several important parameters such as charge-transfer resistance, double-layer capacitance, etc. These parameters are seminal to: (1) derive information on the optimum utilization of the storage batteries; (2) understand the modes of the cell failures; and (3) determine SoC [3]. Finite Element Methodology (FEM) studies have proved very fruitful for Li-ion battery (LiB) modelling in recent years. However, these studies have generally not yet been used for exploring the different factors affecting the LiB SoC. This work attempts to utilize the possibilities of correlating cell impedance with the FEM modelling for SoC prediction. The objective is to extract electrical parameters which vary continuously as a function of the battery SoC from the impedance spectra [4]. In short, the following impedance components will be examined computationally and experimentally as functions of the SoC: a) Ohmic resistance of the battery ( $R_{\Omega}$ ); b) constant phase element (CPE) corresponding to the high frequency capacitive semicircle; c) parallel charge-transfer resistance ( $R_{ct}$ ); d) CPE corresponding to the low-frequency capacitive semicircle; e) frequency maximum and corresponding real as well as imaginary components of the impedance spectra; f) phase angle at several frequencies.

## References

- [1] F. Huet, J. Power Sources 70 (1998) 59-69.
- [2] S. Rodrigues, N. Munichandraiah, A.K. Shukla, J. Power Sources 87 (2000) 12-20.
- [3] S. Rodrigues, N. Munichandraiah, A.K. Shukla, J. Solid State Electrochem. (1999) 3: 397-405.
- [4] H. Blanke, O. Bohlen, S. Buller, R. W. De Doncker, B. Fricke, A. Hammouche, D. Linzen, M. Thele, D. U. Sauer, J. Power Sources 144 (2005) 418-425.

# Arrays of microwells equipped with a recessed ring nanoelectrode and a disk microelectrode for nanoelectrochemistry investigations

F. Sekli Belaïdi<sup>1</sup>, W. Tiddi<sup>1</sup>, M. Polverel<sup>1</sup>, G. Lemerrier<sup>1</sup>, V. S. R Vajrала<sup>2</sup>, D. Zigah<sup>2</sup>, N. Sojic<sup>2</sup>,  
J. Launay<sup>1</sup>, P. Temple-Boyer<sup>1</sup> and S. Arbault<sup>2</sup>

<sup>1</sup>LAAS-CNRS; Université de Toulouse, F-31400 Toulouse, France

<sup>2</sup>Univ. Bordeaux, CNRS UMR 5255, ISM, NSysA, ENSCBP, 33607 Pessac, France

The increasing interest in miniaturized analytical systems involving small-volume samples induces to the development of “Nanoelectrochemistry”, which combines the advantages of nanotechnology and electroanalysis. As a result, several research works attempted to miniaturize complete electrochemical cells. This is an important challenge because of the necessity to minimize the sample volume when dealing with toxic waste, or precious body fluids, expensive reagents, or to precisely trap single cells. Microwells with recessed ring nanoelectrodes are a novel kind of electrochemical devices that attract big attention. Similar to ultra-microelectrodes, they exhibit high current density, fast response time, reduced charging current and high signal to noise ratio. In addition, their small volumes make them well suited for the detection of low concentrations or for the analysis of individual cells. In the current study, recessed platinum ring nanoelectrodes (RNE) and disk ultramicroelectrodes (DME) (surface:  $21\ \mu\text{m}^2$  and  $64\ \mu\text{m}^2$ , respectively) into microwells (diameter:  $9\ \mu\text{m}$ , depth:  $5.2\ \mu\text{m}$ ) were realized using silicon-based technology (Figure 1). These electrochemical devices were characterized by cyclic voltammetry with different redox probes (ex. ferrocene methanol:  $\text{Fc}(\text{MeOH})$ ) using a single well or arrayed configurations, and optimised compared to COMSOL<sup>TM</sup> simulations. Steady-state sigmoidal responses were evidenced for the DME devices in agreement with theoretical studies. Similar results were obtained for the RNE ones and validated by our theoretical model (Figure 2). To check the confinement effects within microwells, devices were used in generator-collector mode. Chronoamperometry (Figure 3) was used to quantify the amplification and collection factors: around 1.3 and 0.67, respectively. All these results demonstrate that such microsystems could be effectively used for the electrochemical analysis of single cells.

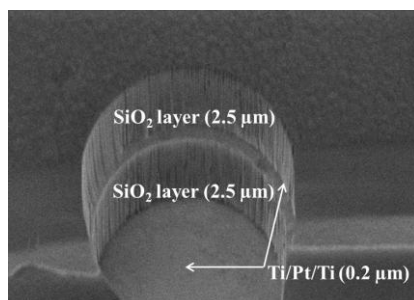


Figure 1: SEM image of  $9\ \mu\text{m}$  diameter  $\text{SiO}_2$  microwell showing the bottom layer recessed DME and the middle layer RNE devices

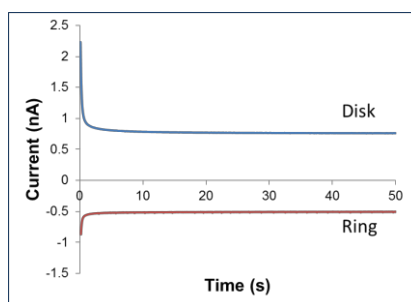


Figure 3: Chronoamperograms for recessed disk/ring electrodes in 1 mM  $\text{Fc}(\text{MeOH})$  solution (respective electrical bias: 0.4 and 0V).

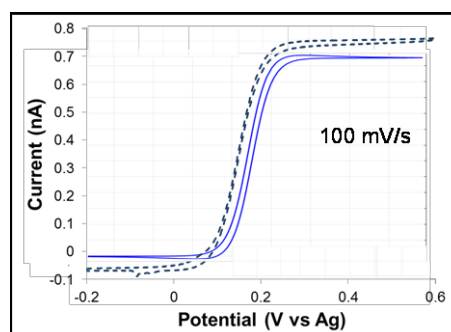
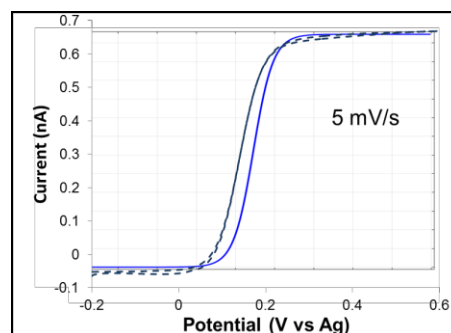


Figure 2: Comparison between simulated (solid line) and experimental (dotted line) cyclic voltammograms detected in 1 mM  $\text{Fc}(\text{MeOH})$  solutions with the platinum ring nanoelectrodes in microwells

## Solid electrolyte interphase formation in dye-sensitized solar cells: where experimental ends and modeling could start

Frédéric Sauvage\*, Miguel Flasque, Albert Nguyen Van Nhien  
*Laboratoire de Réactivité et Chimie des Solides, LRCS CNRS UMR7314, Université de Picardie Jules Verne, 33 Rue St-Leu, 80039 Amiens Cedex, France*  
*Frederic.sauvage@u-picardie.fr*

Further strengthened by the recent achievement of 13 % power conversion efficiency (PCE)<sup>[1]</sup>, the credibility of DSC for day-to-day utilization has never been as unequivocal as today. Beside such a record efficiency, establishing once again its reliable place in the photovoltaic panorama, to see it a light of day successfully introduced into the market, this last phase will now depend on how to make it more stable while preserving low-cost and sufficient PCE. Towards such objectives, two approaches are actually opposed: introduction of new materials by somehow playing at the naval battle vs. understanding the high complexity of the different chemical/electrochemical interactions between the DSC components, especially under temperature and/or light stresses. By simply looking at the actual scientific production in the domain, this top-down approach is much marginalized.

For long time, dye and sealant was culprit to account for the lack of stability. For instance, it is often answered that if the electrolyte leaks at a sudden moment it is because of poor sealing or if the performance is dropping upon ageing, it stems from the dye stability. Our principal research is actually focused on better understanding the chemical/electrochemical reactions which can take place in the cell upon ageing according to IEC61646 protocol. The objectives are to gather different experimental data to propose *in fine* a realistic mechanism accounting for the performance failure at elevated temperatures, to bring a beginning of an answer to the frequent speculations raised in the literature such as on the origin of iodine consumption or on why electrolyte leaks swiftly > 60°C whereas MPN boiling point is *ca.* 165°C.

Against the general preconceived idea, we will highlight during this presentation that one of the most stable DSC constituent, TiO<sub>2</sub>, plays in reality a significant role on the electrolyte degradation<sup>[2]</sup>. For first time, we have demonstrated this latter to be responsible of (i) the formation of highly volatile compounds including gas evolution driven by the temperature and (ii) we revealed the growth of a conformal solid electrolyte interphase (SEI) layer wrapping not only TiO<sub>2</sub> but also the Pt catalyst at the counter-electrode. The chemical composition of this SEI will be described. The collateral implication of this SEI formation on both the electrolyte composition and charge transfer kinetic into the device will be discussed. This experimental observation, which will govern the device lifetime, paves the way not only to new development of more robust chemicals but also call for modeling at multiscale to offer predictive directions to help the experimentalists in the quest of highly durable dye-sensitized solar cells development and also to deepen our understanding on the impact of SEI growth versus the multifaceted device complexity in terms of mass transport into the mesopores, charge transport, dynamic of recombinations and dye regeneration.

[1] S. Mathew, A. Yella, P. Gao, R. Humphry-Baker, B.F.E. Curchod, N. Ashari-Astani, I. Tavernelli, U. Rothlisberger, Md. K. Nazeruddin, M. Graetzel, *Nat. Chem.* 2014, 6(3), 242-247

[2] M. Flasque, A. Nguyen Van Nhien, J. Swiatowska, A. Seyeux, C. Davoisne, F. Sauvage, *ChemPhysChem* **2014**, 15(6), 1126-1137

# Catalyzing Innovation in Organic Battery Electrodes from Computational Modelling

C. Frayret\*, D. Tomerini, C. Gatti, Y. Danten

\* LRCS-CNRS UMR 7314, Université de Picardie Jules Verne, 33, Rue Saint-Leu, 80039 Amiens, France, Phone: +33(0)3.22.82.75.86, Fax: +33(0)3.22.82.75.90  
christine.frayret@u-picardie.fr

The increase in the importance of eco-friendly considerations in the field of energy supply currently motivates the need to identify new strategies for the development of alternatives to commercial inorganic lithium-ion battery. The desired emergence of sustainable technologies thus pushes research towards new directions. Electroactive organic battery electrodes (containing no scarce metal resources) continue gaining attention mainly due to their benefit in terms of environmental benignity combined with a decreased cost (along with the potential extraction from biomass). Energy efficiency will be key in the possible advent of manufacturing for such new set-ups. Taking advantage of the possible fine tuning of redox potential provided by this kind of materials, one should ideally design low-weight electrodes exhibiting high cell voltage (*i.e.* high/low redox potential for positive/negative electrodes) and being completely devoid of solubility issues. Yet, several barriers might still inhibit such objective. For instance, tackling difficulties in achieving electronic conduction in these materials still remain a major concern. Experimental sequences improve most of the time one of the required features while they may be detrimental or inactive with respect to other specifications. Moreover, they involve iterative, costly and time consuming trial and error approaches. As a complementary tool, new theoretical paradigms are likely to facilitate or accelerate the production of suited organic electrodes. Simulation can be situated directly upstream or downstream of the relevant experiments, involving investigations at various scales (*e.g.* molecular/materials modelling) and as support of the characterization methods.

First, a work of prospection and engineering can correspond to the initial and most significant milestone in designing advanced materials. The emergence of strategies for lead candidates' identification requires the establishment of property-based guidelines. Improvement of success rates for innovation therefore relies on the ability to rationally understand the quantitative structure-activity relationship. Spin density maps, electronic delocalization indices or energy stabilization decomposition, ... clearly constitute powerful local indicators that enable to distinguish molecular compounds, especially regarding their ranking in terms of electrochemical features. In particular, fine dissection of these data can give the opportunity to discover subtleties regarding the role played by each parameter within various sets of combined effects of functionalization/heteroatom substitution/nature of backbone, ... that could not be disentangled easily otherwise. Recent studies in this area outline lessons originating from the consideration of both systematic screening of existing compounds modulated through various effects and hypothetical novel candidates [1]. By exploring various invention possibilities, the ultimate goal of such investigations is to engineer a few potentially attracting new compounds.

Beyond design problematics through molecular modelling, computational studies can be beneficial as well for the direct consideration of the material (through *e.g.* periodic DFT simulation). For instance, due to the possible partial lack of accurate structural knowledge of either one or various (lithiated/delithiated) phase(s), guess of lithium positioning may become crucial to fully understand the electrochemical process [2]. In link with the peculiar difficulties arising from the large extent of relative orientation of molecules/lithium ions, the set of relevant tools for achieving this purpose can be broader than pure DFT computations and may involve multi-scale modelling. Additionally, spectroscopic simulations may eventually complement the experimental characterization and play a part in the full interpretation of the structural changes occurring during the electrochemical process.

Based on our recent theoretical studies, an overview of the potentialities of modelling approaches will be provided with a specific focus on the way to contribute to the conceptual knowledge of these compounds for paving the road towards improved organic electrode materials development.

[1]: see *e.g.*: D. Tomerini, C. Gatti, C. Frayret, *Phys. Chem. Chem. Phys.*, **17**, 8604 (2015).

[2]: see *e.g.*: G. Bonnard, A.-L. Barrès, Y. Danten, D.G. Allis, O. Mentré, D. Tomerini, C. Gatti, E.I. Izgorodina, P. Poizot, C. Frayret, *RSC Adv.*, **3**, 19081 (2013).



# Electrochemistry with Nanobioconjugates and Soft Interfaces for Sensing Applications

Hye Jin Lee

*Department of Chemistry and Green-Nano Materials Research Center, Kyungpook National University,  
80 Daehakro, Buk-gu, Daegu, 702-701, Republic of Korea  
hyejinlee@knu.ac.kr*

Over the last decade, numerous efforts have been made on creating highly sensitive and selective electrochemical biosensing platforms for a wide range of biological, food and environmental science applications. In this talk, we will highlight our recent efforts on developing amperometric biosensors utilizing two distinct electrochemical interfaces: gold nanobioconjugates and soft interfaces between two immiscible electrolyte solutions. The first part of my talk includes the combined use of nanobioconjugates and surface enzyme reactions for the development of highly sensitive and selective amperometric biosensing platforms that can be usefully employed for food science and medical diagnostics. For example, a layer by layer assembly of oppositely charged Au nanocubes, polyelectrolytes and enzymes on a screen printed carbon electrode (SPCE) was developed for the selective and sensitive detection of catechol compounds in various tea samples [1]. The second part of my presentation will be on amperometric ion selective sensing platforms featuring a single micro-hole interface supported on a thin polymer substrate between water and gelified organic phases for water quality control and pharmaceutical applications. Amperometric responses upon the transfer of anticancer drug molecules [2] and Cu(II) ions [3] across the polarized microhole supported soft interface were utilized to create a selective and sensitive detection platform.

## References

- [1] MD. N. Karim, J. E. Lee, H. J. Lee, *Biosensors and Bioelectronics*, **2014**, *61*, 147-151.
- [2] H. R. Kim, C. M. Pererira, H. Y. Han, H. J. Lee, *Analytical Chemistry*, **2015**, in press.
- [3] S. H. Lee, J. Sumranjit, P. Tongkate, B. H. Chung, H. J. Lee, *Electrochimica Acta*, **2014**, *123*, 198-204.

# Theoretical Study of Lithium-Sulfur Battery Cathodes

Payam Kaghazchi

*Institut für Chemie und Biochemie, Freie Universität Berlin*

*Takustr. 3, 14195 Berlin, Germany*

*payam.kaghazchi@fu-berlin.de*

In this talk, I will present our recent efforts to model Li-S battery cathodes. Theoretical studies on the electronic and atomic structure as well as Raman spectra of intermediate and final products of discharge process will be discussed. I will first present our results for intermediate  $\text{Li}_2\text{S}_x$  polysulfide species. By comparing our theoretical Raman spectra to the experimental spectra we study the mechanism of lithiation of sulfur. It is found that  $\text{Li}_2\text{S}_x$  molecules bind strongly to each other, forming crystal-like  $\text{Li}_2\text{S}_2$  structures. The crystallization is driven by strong electrostatic interactions between  $\text{Li}^{+\delta}-\text{S}^{-\delta}$  dipoles of  $\text{Li}_2\text{S}_x$  molecules. Afterwards, the interaction of  $\text{Li}_2\text{S}_x$  with graphene and the possibility of inhibiting the shuttle effect will be discussed. Finally, I will present our results for  $\text{Li}_2\text{S}$  which is the final product of lithiation of sulfur. It is found that  $\text{Li}_2\text{S}$  particles consist of  $\{111\}$  facets which are metallic at low concentrations of surface Li atoms.

# Toward efficient electrochemical conversion of CO<sub>2</sub>: catalyst design accelerated by simulation-based screening

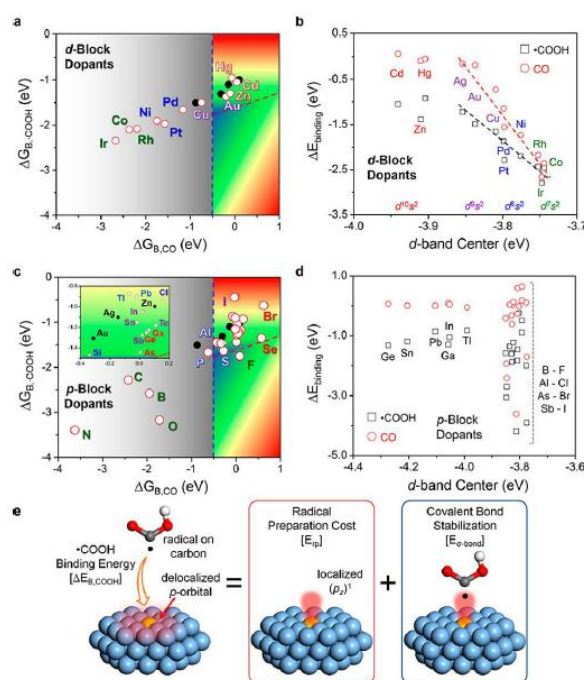
Hyungjun Kim, Hyung-Kyu Lim, and Hyeyoung Shin

Graduate School of EEWS, Korea Advanced Institute of Science and Technology

291 Daehak-ro, Yuseong-gu, Daejeon 305-701, KOREA

linus16@kaist.ac.kr

CO<sub>2</sub> conversion is an essential technology to develop a sustainable carbon economy for the present and the future. Many studies have focused extensively on the electrochemical conversion of CO<sub>2</sub> into various useful chemicals. However, there is not yet a solution sufficiently high enough efficiency and stability to demonstrate practical applicability. A key obstacle here is mostly due to the limited performance of the catalysts in terms of activity, stability, etc. To improve and tailor the catalytic properties, it is thus required to understand the operational mechanism of the various possible CO<sub>2</sub> reduction pathways and identify the mechanistic role of catalysts. In this talk, we use high-throughput quantum mechanics (QM) catalyst screening (coupled with continuum description of solvation effects) to discover new catalysts expected improve the performance of the electrochemical CO<sub>2</sub>-to-CO conversion by decreasing the overpotential by 0.4-0.5 V. We discovered the covalency-aided electrochemical reaction (CAER) mechanism in which *p*-block dopants have a major effect on the modulating reaction energetics by imposing partial covalency into the metal catalysts, thereby enhancing their catalytic activity well beyond modulations arising from *d*-block dopants [1]. We expect this work to provide useful insights to guide the development of a feasible strategy to overcome the limitations of current technology for electrochemical CO<sub>2</sub> conversion.



[1] H.-K. Lim, H. Shin, W. A. Goddard, Y. J. Hwang, B. K. Min, and H. Kim, *J. Am. Chem. Soc.*, 2014, **136**, 11355-11361.

# Modelling, Simulation and Characterization of Electrochemical Oxygen Reduction on Cr-modified Ni Surfaces

Ivan Kondov<sup>1</sup>, Patrick Faubert<sup>2</sup>, Claas Müller<sup>2</sup> and Holger Reinecke<sup>2</sup>

<sup>1</sup>Steinbuch Centre for Computing, Karlsruhe Institute of Technology,  
Hermann-von-Helmholtz-Platz 1, 76344 Eggenstein-Leopoldshafen, Germany, [ivan.kondov@kit.edu](mailto:ivan.kondov@kit.edu)

<sup>2</sup>University of Freiburg, Department of Microsystems Engineering – IMTEK,  
Laboratory for Process Technology, Georges-Köhler-Allee 103, 79110 Freiburg, Germany

Oxygen reduction reaction (ORR) is an important process on the cathode of polymer electrolyte fuel cells [1]. Crucial for the cost-effective exploitation of these devices in future is to use a precious-metal-free material as catalyst. Recent development of alkaline polymer electrolytes [2] has opened up possibilities to use nickel as alternative cathode catalyst. Particularly interesting application of Ni/Cr material is the alkaline polymer electrolyte fuel cells which have been increasingly recognized as a solution to overcome the dependence on noble metal catalysts. The key challenge is to increase the exchange current density of chromium decorated nickel electrodes by enhancement of the active surface area of the electrode itself. While ORR on Pt has been investigated using modelling in great detail [3] there are sparse studies [4; 5] on Ni in alkaline environment. Comparing to Pt and Ag, Hansen et al. [5] have found too high surface reactivity combined with electrode stability limited in small ranges of pH and electrode potentials.

In the present contribution, we study the mechanisms and the kinetics of the electrocatalytic ORR on pure Ni(111) surfaces and on Ni(111) surfaces decorated or doped by Cr. Using density functional theory and transition state theory we elucidate possible routes of the ORR and calculate the reaction rates in cell operation conditions, i.e. at presence of solvent, finite temperature and electrode potential. First we devise and optimize several atomistic model structures varying Cr surface doping and Cr surface coverage and applying multiple constraints from x-ray photoelectron spectroscopy (XPS) data. A sample model structure is depicted in Figure 1. For the resulting structures we investigate all possible surface elementary processes, such as adsorption and desorption, surface diffusion, hydrogen transfer, and O–O cleavage, for the cathode half reaction  $\frac{1}{2} \text{O}_2 + 2\text{e}^- + \text{H}_2\text{O} \rightarrow 2\text{OH}^-$ . In addition, we vary the surface coverage and consider the influence of spectator co-adsorbates (O, OH).

We show that modifications of the Ni surface with Cr as well as different surface coverages lead to strong variation of the elementary ORR rates and thus to various ORR routes, indicating qualitative different behavior of the catalyst. In the discussion we rationalize the findings with cyclic voltammetry (CV). Furthermore, we systematically derive a design strategy for improving the performance on the device level based on the full reaction kinetics simulation based on the calculated rates. The acquired data will be used in a holistic device-level approach, for example by coupling the kinetic model with mass/charge transport in fuel cell.

**Acknowledgements:** This work was performed on the computational resource bwUniCluster funded by the Ministry of Science, Research and the Arts Baden-Württemberg and the Universities of the State of Baden-Württemberg, Germany, within the framework program bwHPC and supported by the Berthold Leibinger Stiftung as a carrier of the Fritz-Hüttinger scholarship. Support for laser processing by the Karlsruhe Nano Micro Facility (KNMF, <http://www.knmf.kit.edu>) a Helmholtz research infrastructure at the Karlsruhe Institute of Technology is gratefully acknowledged.

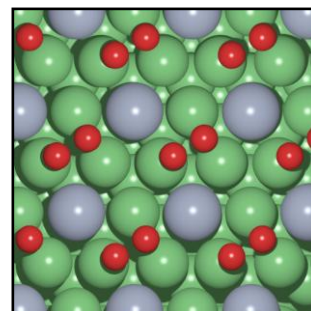


**Figure 1: Structure of a Cr-doped Ni(111) surface with adsorbed O<sub>2</sub> at 1/2 ML O coverage.**

[1] M. Eikerling, and A. Kulikovskiy, Polymer Electrolyte Fuel Cells: Physical Principles of Materials and Operation, Taylor & Francis, 2014.

[2] S. Lu, J. Pan, A. Huang, L. Zhuang, and J. Lu, Alkaline polymer electrolyte fuel cells completely free from noble metal catalysts. Proceedings of the National Academy of Sciences 105 (2008) 20611-20614.

[3] J.A. Keith, G. Jerkiewicz, and T. Jacob, Theoretical Investigations of the Oxygen Reduction Reaction on Pt(111). ChemPhysChem 11 (2010) 2779-2794.

[4] Z. Shi, J. Zhang, Z.-S. Liu, H. Wang, and D.P. Wilkinson, Current status of ab initio quantum chemistry study for oxygen electroreduction on fuel cell catalysts. Electrochimica Acta 51 (2006) 1905-1916.

[5] H.A. Hansen, J. Rossmeisl, and J.K. Nørskov, Surface Pourbaix diagrams and oxygen reduction activity of Pt, Ag and Ni(111) surfaces studied by DFT. Phys. Chem. Chem. Phys. 10 (2008) 3722-3730.

# Discover a Role of Ionic-Liquid in Electrochemical CO<sub>2</sub> Reduction by Using QM/MM Method

Hyung-Kyu Lim, Hyungjun Kim\*

*Graduate School of EEWS (Energy, Environment, Water and Sustainability)*

*Korea Advanced Institute of Science and Technology, 291 Daehak-ro, Yuseong-gu, Daejeon 305-701, Korea*

*zinnia7@kaist.ac.kr*

For the mitigation of global-warming problems and the sustainable development of the inevitable carbon-based economy, carbon dioxide (CO<sub>2</sub>) conversion technology has been regarded as one of the most important and urgent current scientific issues. Many researchers anticipate the efficient transformation of CO<sub>2</sub> from various emission sources into more valuable chemicals and fuels. Among the various ongoing attempts, which are categorized as biochemical, thermochemical, electrochemical, and photo-assisted electrochemical processes, the electrochemical method has certain merits in terms of high reactivity at ambient conditions and good extensibility from small to large-scale processes. Also, the possibility of direct integration with renewable electric sources adds more potential to the electrochemical method as a promising route for CO<sub>2</sub> conversion. A number of studies have been performed to improve performance of electrochemical CO<sub>2</sub> reduction on various catalyst and electrolyte systems, however it still has many scientific and engineering issues to be elucidated and improved, to achieve commercial-level technology. In 2011, the promising effect of ionic-liquid on the electrochemical CO<sub>2</sub> reduction performance have been reported that the mixture electrolyte contains ionic-liquid (18 mol% Emim-BF<sub>4</sub>) and water lowers the over-potential of CO<sub>2</sub> to CO reduction process on silver electrode as only 0.17 V from the equilibrium potential as well as suppress the competitive hydrogen evolution reaction effectively.[1] Further experimental studies have been tried to figure out the mechanism of lowering over-potential with ionic-liquid water mixture electrolyte,[2, 3] but the detailed understanding of complex electrochemical system has not been achieved. In our research, we developed the new grid-based QM/MM (Quantum Mechanics/Molecular Mechanics) methodology which can effectively handle the complex electrostatic interaction between catalyst and mixed electrolyte, and theoretically figured out the main role of ionic-liquid and water mixture electrochemical CO<sub>2</sub> reduction system.

## [ References ]

- [1] B.A. Rosen, A. Salehi-Khojin, M.R. Thorson, W. Zhu, D.T. Whipple, P.J.A. Kenis, R.I. Masel, Ionic Liquid-Mediated Selective Conversion of CO<sub>2</sub> to CO at Low Overpotentials, *Science*, 334 (2011) 643-644.
- [2] B.A. Rosen, J.L. Haan, P. Mukherjee, B. Braunschweig, W. Zhu, A. Salehi-Khojin, D.D. Dlott, R.I. Masel, In Situ Spectroscopic Examination of a Low Overpotential Pathway for Carbon Dioxide Conversion to Carbon Monoxide, *J Phys Chem C*, 116 (2012) 15307-15312.
- [3] B.A. Rosen, W. Zhu, G. Kaul, A. Salehi-Khojin, R.I. Masel, Water Enhancement of CO<sub>2</sub> Conversion on Silver in 1-Ethyl-3-Methylimidazolium Tetrafluoroborate, *J Electrochem Soc*, 160 (2013) H138-H141.

# A flexible framework for solving transport in lithium sulfur batteries

Kan-Hao Xue,<sup>1,2,3</sup> Youcef Mammeri,<sup>4</sup> Claude Guéry,<sup>1,2,3</sup> Patrik Johansson,<sup>1,3,5</sup> Mathieu Morcrette,<sup>1,2,3</sup> and Alejandro A. Franco<sup>1,2,3</sup>

<sup>1</sup>Laboratoire de Réactivité et Chimie des Solides (LRCS) - Université de Picardie Jules Verne & CNRS, UMR 7314 – 33 rue Saint Leu, 80039 Amiens Cedex, France

<sup>2</sup>Réseau sur le Stockage Electrochimique de l'Energie (RS2E), FR CNRS 3459, France

<sup>3</sup>ALISTORE-ERI European Research Institute, FR CNRS 3104, 80039 Amiens Cedex, France

<sup>4</sup>Laboratoire Amiénois de Mathématiques Fondamentales et Appliquées (LAMFA) - Université de Picardie Jules Verne & CNRS, UMR 7352 – 33 rue Saint Leu, 80039 Amiens Cedex, France

<sup>5</sup>Department of Applied Physics, Chalmers University of Technology, SE-412 96 Göteborg, Sweden  
[alejandro.franco@u-picardie.fr](mailto:alejandro.franco@u-picardie.fr)

The lithium sulfur (Li-S) battery is currently receiving much attention due to its supreme energy density, i.e., estimated to *ca.* 500 to 700 Wh/kg at the prototype cell level. Although it is a relatively “old” technology, world-wide interest came first when hierarchical carbon cathodes were used to improve the capacity retention.<sup>1,2</sup> In this scheme, sulfur is loaded in the micropores or mesopores of carbon particles, while the carbon particles themselves are immersed in the surrounding electrolyte, creating a liquid phase in between. To better understand the discharge mechanisms, especially the benefits of applying the hierarchical carbon cathode scheme, theoretical modeling is a powerful tool. Unfortunately, none of the current Li-S battery models take into account the hierarchical microstructure of the carbon cathode.

We here propose a physical discharge model for Li-S batteries, taking in consideration the cathode carbon microstructure through a multi-scale simulation approach.<sup>3</sup> In this model, solved within our MS LIBER-T computational framework,<sup>4</sup> the transport of species such as lithium cations ( $\text{Li}^+$ ), anions such as TFSI, native sulfur  $\text{S}_8$  and various polysulfides  $\text{S}_y^{2-}$  (5 different species) across the cell occurs in the liquid electrolyte. Additionally, species are also allowed to shuttle locally between the liquid phase and the electrolyte within micropores/mesopores. Electrochemical and chemical reactions may occur in both regions. Solid species precipitation, especially  $\text{Li}_2\text{S}$ , consume the active surface area of the carbon particles as well as of the pore surfaces. All these factors add to the complexity of the model, thus numerical efficiency is also a significant factor for practical use.

There are generally three theories for transport in electrolytes: the Poisson-Nernst-Planck equation, the dilute solution theory, and the concentrated solution theory. The Poisson equation is relatively unstable and may cause numerical convergence problems. The dilute solution theory requires the definition of an electrostatic potential in the solution, which may increase the computational load and most battery electrolytes are far from dilute. The concentrated solution theory is rather complicated apart for the binary electrolyte case, and in the Li-S batteries there are numerous charged species necessary to address. Hence, in order to compute the species transport in an efficient way, we here use a different approach, where the concentration profile of the anion in the liquid phase is self-adjusted to meet the charge neutrality condition, while the transport equations of all other species;  $\text{Li}^+$ ,  $\text{S}_8$ , and polysulfides, are solved. At the same time, fluxes of species between the various pores and the liquid phase electrolyte are obtained. Since long chain polysulfides are generated and consumed by reduction during discharge and dissolved into the electrolyte, the diffusion coefficients of all species are updated over time according to the altered electrolyte viscosity. In more detail, both  $\text{S}_8$  and long chain polysulfides affect the viscosity by their volume fraction applying Einstein's theory for viscosity. A finite volume method is implemented for the conservation of mass, resulting in simulation times typically less than one hour on a standard PC. The efficiency of our algorithm is discussed and exemplified by some realistic Li-S battery test cases.

1. X. Ji, K. T. Lee and L. F. Nazar, *Nat. Mater.* **8**, 500–506 (2009).
2. C. Liang, N. J. Dudney and J. Y. Howe, *Chem. Mater.* **21**, 4724–4730 (2009).
3. A. A. Franco, *RSC Adv.* **3**, 13027–13058 (2013).
4. <http://modeling-electrochemistry.com/ms-liber-t/>

# Multiparadigm Simulation of Electrochemical Energy Devices: the Fuel Cell Membrane Degradation

Matias A. Quiroga<sup>1,2,3</sup>, Yinghui Yin<sup>1,2,3</sup> and Alejandro A. Franco<sup>1,2,3</sup>

<sup>1</sup>Laboratoire de Réactivité et Chimie des Solides (LRCS) - Université de Picardie Jules Verne & CNRS,  
UMR 7314 – 33 rue Saint Leu, 80039 Amiens Cedex, France

<sup>2</sup>Réseau sur le Stockage Electrochimique de l'Energie (RS2E), FR CNRS 3459, France

<sup>3</sup>ALISTORE-ERI European Research Institute, FR CNRS 3104, 80039 Amiens Cedex, France.

[alejandro.franco@u-picardie.fr](mailto:alejandro.franco@u-picardie.fr)

A multiparadigm simulation tool is reported here in the frame of electrochemical energy conversion and storage devices. The tool is based on a new methodology able to couple on-the-fly two of our in house computational codes: the Kinetic Monte Carlo (KMC) code called MESSI<sup>1</sup> (*Monte Carlo Electrochemical Software for System Innovation*) with the simulation package MS LIBER-T (*Multiscale Simulator of Lithium Ion Batteries and Electrochemical Reactor Technologies*).<sup>2,3</sup> This coupling is achieved thanks to an algorithm we have recently developed and called Electrochemical-Variable Step Size Method (E-VSSM) allowing KMC simulations to communicate on-the-fly with continuum models.

An application example is illustrated here, concerning the investigation of Perfluorinated Sulfonic Acid Polymer Electrolyte Membrane (PEM) degradation in PEM Fuel Cells.<sup>4</sup> The electrochemical reactions in the electrodes are simulated by the KMC code, in a similar fashion we reported in Ref. 1. Reactions described include the Hydrogen Oxidation Reaction in the anode, the H<sub>2</sub>O<sub>2</sub> formation in the anode and in the cathode, and the Oxygen Reduction Reaction in the cathode. The crossover of H<sub>2</sub>/O<sub>2</sub> through the PEM, the species transport and elementary reactions responsible of the H<sub>2</sub>O<sub>2</sub> decomposition catalyzed by Fenton's cations and the side-chains detachment due to OH<sup>•</sup> and OOH<sup>•</sup> radicals attack, are described through coupled partial/ordinary equations solved with MS LIBER-T following a fully continuum-based scheme originally proposed by us<sup>5,6</sup> and later followed by other authors.<sup>7,8</sup> In our approach, these equations have as boundary conditions the chemical potentials and reaction rates calculated by the KMC code. Furthermore, the instantaneous feedback between the PEM degradation and the conductivity evolution (impacting the cell performance) is described. In such a way, the overall model is able to resolve the competitive processes at multiple temporal scales and predict performance decay over long simulated times (> 500 h). Results obtained for multiple operation conditions (imposed current density, temperature, Fenton's cations injection rates...) are discussed in comparison with experimental data.

1. M.A. Quiroga, A.A. Franco, *J. Electrochem. Soc.*, **162** (7) (2015) E73.
2. A. A. Franco, *RSC Adv.* **3** (2013) 13027.
3. M. A. Quiroga, K.H. Xue, T.K. Nguyen, H. Huang, M. Tulodziecki, A.A. Franco, *J. Electrochem. Soc.*, **161** (8) (2014) E3302.
4. M.A. Quiroga, K. Malek and A.A. Franco (in preparation).
5. R. Coulon, W. Bessler, A.A. Franco, *ECS Transactions*, **25** (35) (2010) 259.
6. R. Coulon. Modélisation de la dégradation chimique de membranes dans les piles à combustibles à membrane électrolyte polymère. Université de Grenoble, France (2012).
7. K. H. Wong, E. Kjeang, *ChemSusChem*, **8** (6) (2015) 1072.
8. K. H. Wong, E. Kjeang, *Journal of The Electrochemical Society*, **161**(9) (2014) F823.



# Electrochemical Studies at an Interface between Two Immiscible Electrolyte Solutions for CO<sub>2</sub> Reduction

Hye Youn Han, Farhana Sharmin Diba and Hye Jin Lee\*

*Department of Chemistry and Green-Nano Materials Research Center, Kyungpook National University,  
80 Daehakro, Buk-gu, Daegu, 702-701, Republic of Korea  
hyejinlee@knu.ac.kr*

In this poster, we demonstrate an electrochemical approach utilizing an interface between two immiscible electrolyte solutions (ITIES) for the reduction of CO<sub>2</sub>. An electrochemical H-cell was designed to contain water and 1,2-dichloroethane electrolyte solutions interfaced with Nafion 115 membrane. The aqueous electrolyte composed of potassium bicarbonate placed at an anode providing protons which can then pass through the Nafion 115 membrane reaching to 1,2 DCE phase where CO<sub>2</sub> reduction occurs at a gold working electrode (surface area of 1 cm<sup>2</sup>). Two different hydrophobic organic supporting electrolytes in 1,2-DCE were investigated including tetraoctylammonium perchlorate and tetrabutylammonium perchlorate and their performance in improving CO<sub>2</sub> reduction efficiency were compared. Linear sweep voltammetry (LSV) was performed to verify the CO<sub>2</sub> reduction reaction at the ITIES under N<sub>2</sub> only and in the presence of CO<sub>2</sub> in 1,2-DCE phase. Also the CO<sub>2</sub> purging time, concentration of organic supporting electrolytes alongside applied voltage for the efficient CO<sub>2</sub> reduction were studied. Immediately after the reduction of CO<sub>2</sub> via applying -1.5 V (vs Ag/AgCl) for 1 h using chronoamperometry under the condition of purging CO<sub>2</sub> at room temperature, the catholyte solution were analyzed using UV-vis spectrometry and high performance liquid chromatography. Our preliminary results show that formic acid can be produced via CO<sub>2</sub> reduction at the ITIES and further quantitative analysis is underway.

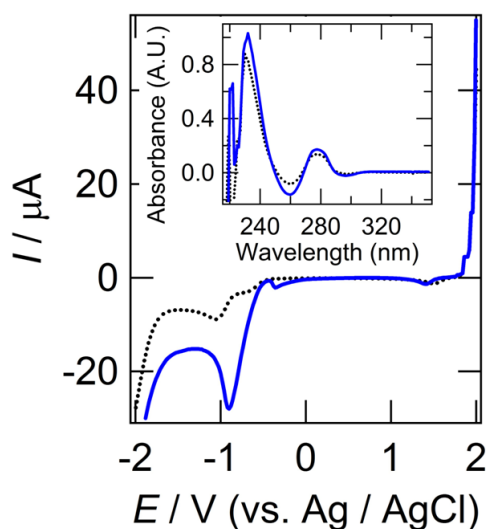


Fig.1 Representative LSVs for the reduction of CO<sub>2</sub> at an interface between water and 1,2-DCE electrolyte solutions. Scan rate = 20 mV/s. Solid line represents the LSV result obtained after applying -1.5 V (vs Ag/AgCl) for 1 h under CO<sub>2</sub> purging. Dotted line is the LSV data for only N<sub>2</sub> purging in 1,2-DCE electrolyte solution in the absence of CO<sub>2</sub>. Inset shows the UV-vis spectrum for the analysis of catholytes.



# Synthesis of High Ionic Conductive $\text{Li}_7\text{La}_3\text{Zr}_2\text{O}_{12}$ Solid Electrolyte by a Sol-gel Process

Changbin Im<sup>1</sup>, Jae Kwang Lee<sup>1</sup>, Jaeyoung Lee<sup>1,2</sup>

<sup>1</sup> Ertl Center for Electrochemistry and Catalysis, Research Institute for Solar and Sustainable Energies (RISE), Gwangju Institute of Science and Technology (GIST), Gwangju 500-712, Korea

<sup>2</sup> Electrochemical Reaction and Technology Laboratory, School of Environmental Science and Engineering, GIST, Gwangju 500-712, Korea  
jaeyoung@gist.ac.kr

Lithium batteries with high energy density are required for the rapidly growing markets of electric vehicles and mobile electronic devices. High-voltage battery system is one of the ways to achieve high energy lithium batteries [1]. However the practical use of high-voltage lithium batteries is hampered by the intrinsic problems of the conventional batteries: narrow electrochemical window and poor cycle stability of liquid electrolyte [2]. Furthermore safety issues are the greatest concern for conventional lithium-ion batteries. All-solid-state lithium batteries with solid electrolyte can play a key role to overcome these problems. All-solid-state batteries have problems, however, their low energy densities compared with liquid electrolyte lithium batteries resulting from the low ionic conductivity of the solid electrolyte and the electrolyte/electrode interfacial resistance [3]. The garnet-type solid electrolyte lithium lanthanum zirconium oxide,  $\text{Li}_7\text{La}_3\text{Zr}_2\text{O}_{12}$  (LLZO), has been reported lithium as superionic conductors performing high ionic conductivity of  $2 \times 10^{-4} \text{ S cm}^{-1}$  at room temperature, high voltage window beyond 5 V with excellent stability [4-5]. In this study, garnet-type LLZO solid electrolyte was prepared by sol-gel based Pechini method [6] and their electrochemical properties were characterized. The cubic phase stability of LLZO and their ionic conductivity were investigated with voltage beyond 5 V. We would like to acknowledge the financial support from the R&D Convergence Program of NST (National Research Council of Science & Technology) of Republic of Korea.

## References

- [1] V. Thangadurai, S. Narayanan, D. Pinzaru, Garnet-type solid-state fast Li ion conductors for Li batteries: critical review, *Chem. Soc. Rev.* 43 (2014) 4714.
- [2] N. Kamaya, K. Homma, Y. Yamakawa, M. Hirayama, R. Kanno, M. Yonemura, T. Kamiyama, Y. Kato, S. Hama, K. Kawamoto, A. Mitsui, A lithium superionic conductor, *Nature Materials* 10 (2011) 682.
- [3] M. Haruta, S. Shiraki, T. Suzuki, A. Kumatani, T. Ohsawa, Y. Yakagi, R. Shimizu, T. Hitosugi, Negligible “Negative Space-Charge Layer Effects” at oxide-electrolyte/electrode interfaces of thin-film batteries, *Nano Lett.*, 15 (2015) 1498.
- [4] R. Murugan, V. Thangadurai, W. Weppner, Fast lithium ion conduction in garnet-type  $\text{Li}_7\text{La}_3\text{Zr}_2\text{O}_{12}$ , *Angew. Chem., Int. Ed.* 46 (2007) 7778.
- [5] N. J. Dudney, Solid-state thin-film rechargeable batteries, *Mater. Sci. Eng.:B* 116 (2005) 245.
- [6] N. Rosenkiewitz, J. Schuhmacher, M. Bockmeyer, J. Deubener, Nitrogen-free sol-gel synthesis of Al-substituted cubic garnet  $\text{Li}_7\text{La}_3\text{Zr}_2\text{O}_{12}$  (LLZO), *J. Power Sources* 278 (2015) 104.

# Combined Experiment and DFT Investigations of Catalytic Activities into Pt-based electrocatalysts for Fuel Cell Applications

Hung-Lung Chou

Graduate Institute of Applied Science and Technology, National Taiwan University of Science and  
Technology 106 Taiwan  
HLCHOU@mail.ntust.edu.tw

## ABSTRACT

To make direct methanol fuel cell technology commercially viable, the principle drawbacks, namely high anode and cathode Pt-loadings and the sluggish kinetics of the anodic methanol oxidation reaction (MOR) need to be addressed. Several important investigations, related to the design and development of electrode configurations, have shown that the reaction kinetics of the MOR depend strongly on the surface's structure and size, together with the amount and degree of dispersion of the catalytic nanoparticles, as well as the nature of the support materials. To fully comprehend the functional effect of these controlling parameters on the electrochemical reactions an understanding of the relationship between the structural features and the corresponding reaction kinetics is necessary. Experimentally determined relationships can then be connected with theoretical considerations to achieve a deeper understanding, thus providing us with the knowledge to improve the catalysts performance. This lecture presents our recent work combining systematic experimental electrochemical measurements with a density functional theory (DFT) computational approach, directed towards the investigation of two key issues, namely: (1) the nano-size effect of Pt catalysts on the catalyst-size-dependent surface coverage of  $\text{OH}_{\text{ads}}$ ,  $\text{CO}_{\text{ads}}$  and its relationship to the energetics of the MOR, (2) the catalytic activities of ternary  $\text{Fe}_{1-x}\text{PtRu}_x$  nanocrystals in enhanced MOR. Our investigations into methanol oxidation show that, in contrast to bulk Pt, a relatively higher  $\text{CO}_{\text{ads}}$  coverage on the nano-sized Pt catalyst is observed from the *in situ* EC-FTIR investigations. Surface coverage models for the electrocatalytic MOR on bulk and nano-sized Pt catalysts are proposed using the combined knowledge gained from *in situ* EC-FTIR and DFT computational results. The chemical transformation reaction of binary FePt nanocrystals (NCs) in solution phase was used to synthesize a series of  $\text{Fe}_{1-x}\text{PtRu}_x$  NCs. The size, structures, compositions and alloying extents of the NCs were analyzed by transmission electron microscopy (TEM), X-ray diffraction (XRD) and X-ray absorption spectroscopy (XAS). Measurements of the catalytic activity of ternary  $\text{Fe}_{35}\text{Pt}_{40}\text{Ru}_{25}$ ,  $\text{Fe}_{31}\text{Pt}_{40}\text{Ru}_{29}$ ,  $\text{Fe}_{17}\text{Pt}_{40}\text{Ru}_{43}$ , binary  $\text{Fe}_{58}\text{Pt}_{42}$  and PtRu NCs showed that  $\text{Fe}_{31}\text{Pt}_{40}\text{Ru}_{29}$  NCs had the highest alloy extent and the lowest onset potential for the methanol oxidation reaction (MOR) among the ternary NCs. Furthermore, the ternary  $\text{Fe}_{1-x}\text{PtRu}_x$  NCs showed a superior ability to withstand CO poisoning compared to binary  $\text{Fe}_{58}\text{Pt}_{42}$  and PtRu NCs. The origin for the anti-CO poisoning was investigated by determining the adsorption energy of CO on the NCs surfaces and the charge transfer from Fe/Pt to Pt using a simulation based on density function theory. The results suggested that with the addition of a new metal into binary PtRu/PtFe NCs, the ability of ternary  $\text{Fe}_{1-x}\text{PtRu}_x$  NCs to withstand CO poisoning in the MOR can be greatly enhanced because the bonding of CO-Pt on the NC's surface was weakened. Overall, our results have opened a simple route for the discovery of new metal alloyed catalysts for fuel cell applications. The proposed models that we have derived show reasonably corroboration with the observed electrochemical measurements.

## Acknowledgements:

We thank the NCHC and NTUST for providing massive computing time. Financially support from the MOST (103-2221-E-011-041) is gratefully acknowledged.

# Lyotropic cubic phase gels and nanoparticles for drug delivery: tuning drug diffusion and sustained release from the mesophase

Renata Bilewicz<sup>a</sup>, Ewa Nazaruk<sup>a</sup>, Monika Szlezak<sup>a</sup>, Ehud M. Landau<sup>b</sup>

<sup>a</sup>University of Warsaw, Faculty of Chemistry

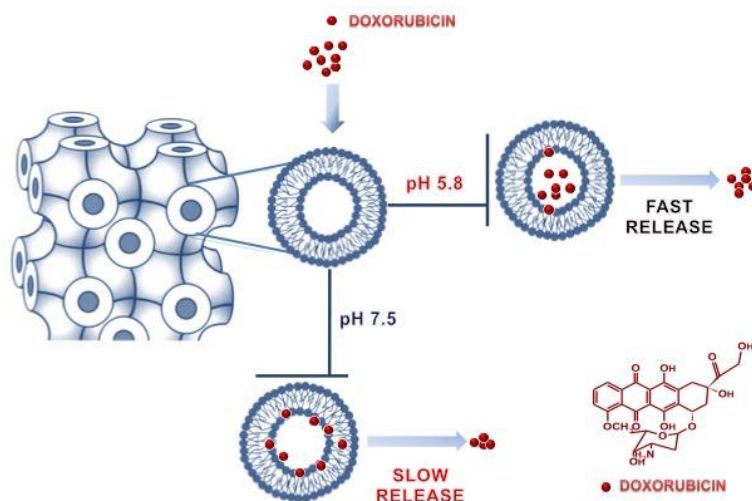
Pasteura St 1, 02093 Warsaw, Poland

<sup>b</sup>Department of Chemistry, University of Zürich

Winterthurerstrasse 190, 8057 Zürich (Switzerland)

[bilewicz@chem.uw.edu.pl](mailto:bilewicz@chem.uw.edu.pl)

Lyotropic liquid crystalline systems are excellent carriers for drugs due to their biocompatibility, stability in aqueous environment and well defined structure that allows hosting significantly larger amounts of drugs, as compared to other carriers e.g. liposomes or gold nanoparticles. Holding the drug inside the mesophase gel or cubosome/hexosome nanoparticle may decrease its toxic effects towards healthy cells while appropriate mechanisms can stimulate the release of the drug from the carrier when it approaches the cancer cell environment [1-4]. Drug diffusion and kinetics of release from the mesophase depend among other factors on the nanostructure and aqueous channels sizes which are defined by the amphiphilic molecules used for the formation of the liquid crystalline phase. The channels diameters can be also increased by adding hydration increasing surfactants to the main lipid forming the mesophase [2]. Here we present the electrochemical studies of drug transport and sustained drug release in lyotropic cubic phases and cubosomes. Using chronocoulometry and voltammetry at micro and large electrodes we show the dependence of diffusion coefficients of an electroactive drug on the size of the channels. Moreover, we demonstrate that profiles of drug release may depend on pH, since the liquid crystalline phase may change with pH. or drug interactions with the lipidic bilayers forming the channel walls in the mesophase can be modified. Interactions between the drug and the cubic phase can be modified by using acidic additives that are incorporated into the cubic phase structure.



## References:

1. Caboi F., Nylander T., Razumas V., Talaikyte Z., Monduzzi M., Larsson K., Langmuir 1997, 13, 5476.
2. Negrini R., Mezzenga R., Langmuir 2011, 27, 5296.
3. Nazaruk E., Szlezak M., Górecka E., Bilewicz R., Osornio Y., Uebelhart P., Landau E.M, Langmuir 2014, 30, 1383.
4. Rahanyan-Kagi N., Aleandri S., Speziale C., Mezzenga R., Landau E.M, Chem. Eur. J., 2015,21, 1873.



# Application of New Conjugate of Cyclodextrin and Lipoic Acid in pH-Sensitive, Multifunctional Drug Carriers

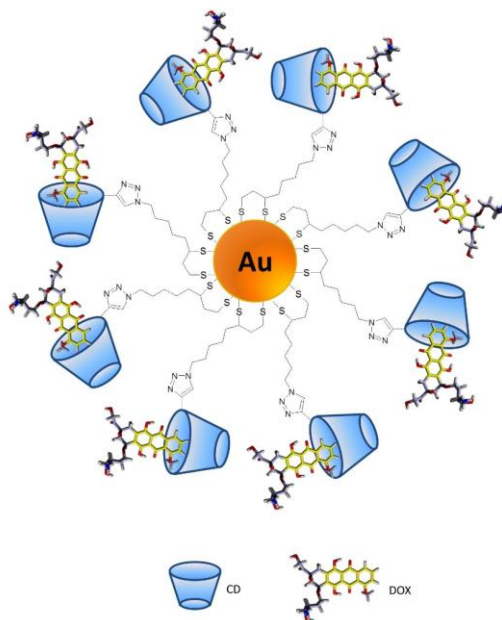
Olga Swiech<sup>a</sup>, Ewelina Kurowicka<sup>a</sup>, Agata Krzak<sup>a</sup>, Maciej Majdecki, Marcin Kruszewski<sup>b</sup>, Renata Bilewicz<sup>a</sup>

<sup>a</sup>University of Warsaw, Faculty of Chemistry, Poland, Pasteura 102-093 Warsaw

<sup>b</sup>Institute of Nuclear Chemistry and Technology, Dorodna 16, Warsaw, Poland  
oswiech@chem.uw.edu.pl

Over the past decade, metallic nanoparticles, especially gold nanoparticles (AuNPs) have been investigated extensively as they possess unique electronic, optical, and catalytic properties.<sup>1</sup> AuNPs can be used as multifunctional platforms for biomedical applications such as contrast and imaging agents for diagnostic purposes and gene or drug delivery.<sup>2</sup> Several targeting ligands such as monoclonal antibodies, sugars, hormones, peptides, vitamins, or other small organic molecules can be used for specific biological recognition. An alternative (and novel) functionalization strategy is to use host-guest cyclodextrin (CD) inclusion complexes to assemble targeting functionality.<sup>3</sup>

We synthesized the new conjugate of  $\beta$ -cyclodextrin and lipoic acid with pH-sensitive triazole linker to immobilize the oligosaccharide on the gold electrode or gold nanoparticles surface, Figure 1. We investigated their usefulness as carriers for anthracycline drugs. The formation of CD-drug complex and the release of doxorubicin and daunorubicin at various pH were studied using chronoamperometry and compared with cyclic voltammetry technique. The immobilization of anticancer drugs on the gold nanoparticles by creation of pH sensitive inclusion complex improves the efficiency and selectivity of the drugs and helps to prevent multi-drug resistance. In addition, the using of appropriately modified cyclodextrin (CD) protects not only against cardiotoxic effects of the drugs, but also allows the release of the drug in the tumor environment. Electrochemical studies were confirmed by MTT cytotoxicity tests and visualized by confocal microscope.



1. A. N. Shipway, E. Katz, I. Willner, *ChemPhysChem* **2000**, 1, 18.
2. D. A. Giljohann, D. S. Seferos, A. E. Prigodich, P. C. Patel, C. A. Mirkin, *J. Am. Chem. Soc.* **2009**, 131, 2072.
3. F. van de Manakker, T. Vermonden, C. F. van Nostrum, W. E. Hennink, *Biomacromolecules*, **2009**, 10, 3157.

This work was supported by grant DEC 2014/13/B/ST5/04117 from NSC

# Application of Natural Cationic Peptides as Potential Antibacterial Agents

Joanna Juhaniewicz<sup>1</sup>, Dorota Konarzewska<sup>1</sup>, Michał Jamroz<sup>2</sup>, Sławomir Sek<sup>1</sup>

1. Faculty of Chemistry, Biological and Chemical Research Centre, University of Warsaw, Zwirki i Wigury 101, 02-089, Warsaw, Poland

2. Faculty of Chemistry, University of Warsaw, Pasteura 1, 02-093 Warsaw, Poland  
e-mail: [jjuhaniewicz@chem.uw.edu.pl](mailto:jjuhaniewicz@chem.uw.edu.pl)

The discovery of antibiotics was a milestone in the human fight against infectious diseases and has led to the substantial increase in quality of human's life. However, rapidly increasing number of multi-drug resistance pathogens resulted in a continuous need for new active compounds with strong activity. One of the most promising groups of compounds includes antimicrobial peptides (AMPs) [1,2]. These are small naturally occurring peptides with molecular mass less than 10 kDa and usually positively charged. Antimicrobial peptides are functional substances in the innate immune system of virtually all forms of life and they constitute a first line of defense against pathogens [3]. They display a broad range of activity on bacteria, fungi and parasites as well as on several cancer cell lines. Therefore, they have enormous potential as novel therapeutic agents.

Here we present the results of our studies on interactions of two natural antimicrobial peptides: cecropin B (from the hemolymph the giant silkworm *Hyalophora cecropia*) and anoplin (from the venom of the solitary wasp *Anoplius samariensis*) with model lipid membranes. The biomimetic lipid films were composed of: a) phosphatidylcholine and cholesterol, b) phosphatidylethanolamine and phosphatidylglycerol, reflecting the eukaryotic and bacterial cell membrane, respectively. Firstly, the influence of peptides on the behavior of lipid membranes was examined by means of surface pressure and Brewster Angle Microscopy. The experiments performed using Langmuir trough allowed us to determine the affinity of peptides to particular lipid components of the cell membranes. To better mimic the natural membrane, we prepared lipid bilayers by transferring the lipids on solid support using the combination of Langmuir-Blodgett and Langmuir-Schaefer techniques. The action of antimicrobial peptides was investigated by means of Cyclic Voltammetry, Electrochemical Impedance Spectroscopy and Atomic Force Microscopy. We have also employed the molecular modeling methods to determine structural details of peptide-lipid interactions.

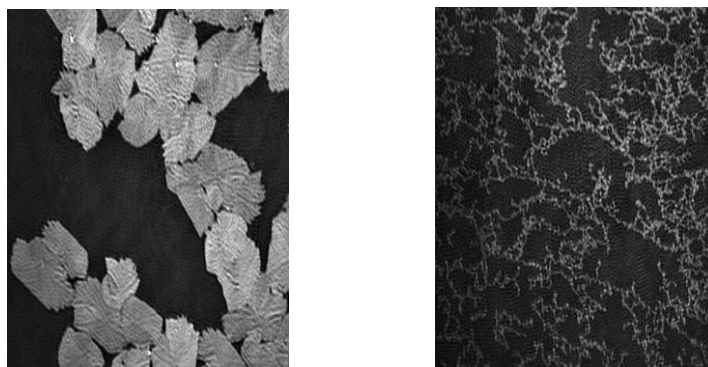


Figure 1. Exemplary BAM images of zwitterionic lipid - phosphatidylethanolamine (left) and cecropin B (right) monolayers at the air-water interface.

## References:

- [1] R.E.W. Hancock, Expert Opinion on Investigational Drugs 9 (2000) 1723.
- [2] J. Juhaniewicz, S. Sek, Electrochimica Acta, 162 (2015) 53.
- [3] Y. Li, Q. Xiang, Q. Zhang, Y. Huang, Z. Su, Peptides 37 (2012) 207.

Acknowledgement: The project was financially supported by National Science Centre (NCN Grant Opus No. 2014/13/B/ST5/04117).

# Electrocatalytic glucose oxidation in suspension and film consisting charged Au and Pt nanoparticles

Marcin Opallo, Joanna Dolinska, Palanisamy Kannan, Volodymyr Sashuk, Janusz W Sobczak, Zbigniew Kaszukur, Wojciech Lisowski, Martin Jonsson Niedziolka

*Institute of Physical Chemistry, Polish Academy of Sciences, Warszawa, Poland  
mopallo@ichf.edu.pl*

It is generally understood that the neighboring surface atoms of different elements of alloys participate in the electrocatalytic reaction of the same molecule, contributing to the synergistic effect [1]. It has been also demonstrated, that electrocatalytic synergy results from close proximity of the different bulk metals surfaces [2]. One may expect that the film consisting of nanoparticles of different metals may exhibit synergistic effect in certain electrocatalytic reactions. Here, we tested this hypothesis with glucose electrooxidation on Au and Pt nanoparticles. This is because this reaction was earlier studied on films consisting Au-Pt alloy nanoparticles and synergistic effect was reported [3-5]. We extended our study to suspension of Au and Pt nanoparticles as electrocatalysis is observed on inert electrodes immersed in suspension of electrocatalytic nanoparticles [6,7]. These studies were so far restricted to suspensions of single type of nanoparticles in quiescent conditions.

The nanoparticulate film electrodes were prepared by layer-by-layer technique or by droplet deposition from suspensions of oppositely charged Au and Pt nanoparticles on ITO substrate. They were covered by 1-(11-mercaptoundecyl)-ammonium (positively charged) or 11-mercaptoundecanoate (negatively charged) functionalities. The bimetallic film is formed (as seen by Scanning Electron Microscopy) due to electrostatic interactions. The presence of both Au and Pt nanoparticles in film was identified by X-ray Powder diffraction and X-ray photoelectron spectroscopy. The shape of voltammetric curves in glucose alkaline solution is different than observed on electrodes modified only with Au or Pt nanoparticles. Most importantly, the significant shift of onset potential as compared to electrodes prepared only from platinum (ca. 0.45 V) or gold (ca. 0.6 V) nanoparticles, indicating synergistic effect. Significant increase of the voltammetric current is also seen,

For experiments in suspension Au and Pt nanoparticles of the same charge (citrate functionalized) were employed. Having like charges prevents nanoparticles from aggregating and precipitating. The experiments were performed at rotating glassy carbon electrode with methodology described earlier [8]. The voltammetric current density in bimetallic suspension is approximately fourfold larger than measured for Pt nanoparticles in suspension and three orders of magnitude larger than observed for a suspension of Au nanoparticles. The features of voltammograms are classically different from voltammograms obtained for suspensions of Au or Pt nanoparticles under the same conditions. They also indicate synergistic effect. The most significant voltammetric signal arises mainly from the electrocatalytic oxidation of glucose at nanoparticles adsorbed on the glassy carbon electrode as confirmed by the increase of the voltammetric current during experiment and X-ray photoelectron spectroscopy performed after voltammetric experiment.

1. M. T. M. Koper, *Surf. Sci.* 2004, 548, 1.
2. L. Zhuang, J. Jin, H. D. Abruna, *J. Am. Chem. Soc.* 2007, 129, 11033.
3. M. Tominaga, T. Shimazoe, M. Nagashima, H. Kusuda, K. Hideaki, K. Atsushi, Y. Kuwahara, I. Taniguchi, *J. Electroanal. Chem.* 2006, 590, 37.
4. A. Habrioux, E. Sibert, K. Servat, W. Vogel, B. Kokoh, N. Alonso-Vante, *J. Phys. Chem. B* 2007, 111, 10329.
5. A. Habrioux, W. Vogel, M. Guinel, L. Guetaz, K. Servat, B. Kokoh, N. Alonso-Vante, *Physical Chemistry Chemical Physics*, 2009, 11, 3573.
6. X. Xiao, A. J. Bard, *J. Am. Chem. Soc.* 2007, 129, 9610.
7. Y.-G. Zhou, E. J. E. Stuart, J. Pillay, S. Vilakazi, R. Tshikhudo, N. V. Rees, R. G. Compton, *Chem. Phys. Lett.* 2012, 551, 68.
8. J. Dolinska, M. Jonsson-Niedziolka, V. Sashuk, M. Opallo, *Electrochem. Commun.* 2013, 37, 100.

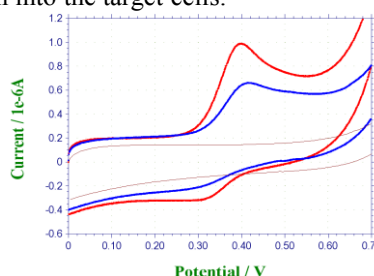
# Magnetic Nanoparticles and Magnetoliposomes as Anticancer Drug Carriers

Paweł Krysiński, Dorota Nieciecka, Aleksandra Joniec

<sup>1</sup> Faculty of Chemistry, University of Warsaw, 02-093 Warsaw, Poland)

Superparamagnetic iron oxide nanoparticles (SPIONs) have attracted wide attention due to magnetic properties and the ability to chemically modify their surfaces. Therefore it appears that SPIONs could be ideal candidates as carrier platform in targeted drug delivery, where the drug/carrier conjugate can be guided to the specific site with an aid of external magnetic field. Magnetic nanoparticles have been focusing an increasing interest especially due to the possibility of limiting the adverse side-effects of traditional therapy, elongated time of drug release, increased efficiency, as well as an improvement in drug activity towards malignant cells and tissues.

We synthesized nanoferrites and modified their surface by adsorptive or covalent binding of doxorubicin (DOX) – a potent anti-cancer drug. We also incorporated hydrophobic SPIONs into the lipid bilayer of liposomes loaded with the same drug. For both cases the drug load, efficiency and release under the effect of pH, temperature and alternating magnetic field were monitored by means of spectroscopic and electrochemical techniques.<sup>1,2,3,4</sup> The development of such conjugate systems as reported here, can result in much more efficient targeting of disease tissues and a substantial reduction of the required therapeutic dosage of a drug, thereby minimizing its adverse side effects. In addition, the superparamagnetic core can itself be used therapeutically for the creation of localized magnetic hyperthermia, enhancing also the drug release. In our research we have focused also on the interaction of nanoparticle/drug conjugates with biomimetic membrane systems and cancer cell lines. The mechanism of SPION crossing through the lipid bilayer in cells is still unknown. Therefore it is very important to study the transport of nanoparticles and their permeation into the target cells.



Left: Magnetoliposomes with DOX accumulated with a magnet at the wall of a vial (B – liposomes without SPIONs). Right: CV of DOX released from magnetoliposomes under temperature stress.

## References

- Nawara, K., Romiszewski, J., Kijewska, K., Szczytko, J., Twardowski, A., Mazur, M., Krysiński, P., *J. Phys. Chem. C.*, **2012**, 116, 5598-5609.
- Nowicka, A.M., Kowalczyk, A., Jarzebinska, A., Donten, M., Krysiński, P., Stojek, Z., Augustin, E., Mazerska, Z., *Biomacromolecules*, **2013**, 14, 823-833.
- Nieciecka, D., Nawara, K., Kijewska, K., Nowicka, A.M., Mazur, M., Krysiński, P., *Bioelectrochem.*, **2013**, 93, 2-14.
- Nieciecka D., Królikowska A., Krysiński P., *Electrochim. Acta*, **2015**, 165, 430-442.



# Artificial protein architectures on electrodes

S. Feifel<sup>1</sup>, R. McGovern<sup>2</sup>, P. Crowley<sup>2</sup>, R. Ludwig<sup>3</sup>, F. Lisdat<sup>1</sup>

*1 Biosystems Technology, Institute of Applied Life Sciences, Technical University Wildau,  
15745 Wildau, Germany,*

*2 - School of Chemistry, National University of Ireland Galway, Galway, Ireland,*

*3 – Food Biotechnology Laboratory, University of Natural Resources and Life Sciences, Vienna, Austria  
e-mail: flisdat@th-wildau.de*

Considerable progress has been achieved in constructing artificial signal chains which follow natural examples. One approach is based on the construction of protein arrangements using the redox protein cytochrome *c* (cyt *c*) and exploiting its self-exchange capabilities [1].

Originally the layer-by-layer adsorption technique has been used for a defined biomolecule arrangement. Different building blocks are applied including polyaniline derivatives, DNA and nanoparticles. Furthermore, the construction of bi-protein assemblies with catalytic properties have been demonstrated, e.g. with sulfite oxidase [2]. These architectures allow the adjustment of the electrode response to the respective substrate by the numbers of deposited layers without using any soluble shuttle molecule.

Based on these results a more complex tri-protein architecture has been created on a modified gold electrode [3]. Here two signal chains can be established within an unseparated matrix and switched on and off by the electrode. For this purpose cellobiose dehydrogenase and laccase have been co-immobilised within the layered cyt *c* structure. Enzyme molecules in different distances to the electrode can be addressed. The redox state of cyt *c* can be used for tuning the activity of the biocatalysts. Whereas the CDH allows lactose detection, the activity of laccase is determined by the oxygen content of the solution.

Recent investigations demonstrate that such defined electron transfer chains can not only be obtained in protein assemblies, but also within a protein crystal with more defined positions of every redox center within the structure [5]. Such investigations are based on findings of an improved protein crystallization by means of a small molecule – a calixarene [4]. Consequently the procedure has been adopted to electrochemical studies and cyt *c* was co-crystallized with *p*-sulfonato-calix[4]arene on a modified gold electrode. Although only a part of the electrode surface was covered by the crystals a well-defined and rather large electrochemical response has been found. This has been investigated kinetically and compared with the behavior of cyt *c* multilayer structures prepared by the LbL technique. Obviously efficient electron pathways exist within the crystals which can be rationalized by the structural data.

Such an approach represents an interesting aspect in the developments of systems confining biological electron transfer cascades to technical devices by fixing protein-protein reactions to electrodes in the immobilized state and may open up the door to new functional systems.

[1] Lisdat et al., Chemical Communications 3 (2009) 274

[2] Dronov et al., JACS 130 (4) (2008) 1122.

[3] Feifel et al. Angew. Chemie 53(22) (2014) 5782.

[4] McGovern et al. Nature Chem. 4 (2012) 527.

[5] McGovern et al. Angew. Chemie 2015 (in press)

# Lipid-Membrane Modified Electrodes to Study Respiratory Membrane Enzymes and their Complexes in a Native-Like Lipid Environment

Lars J. C. Jeuken<sup>1</sup>, Theodoros Laftsoglou<sup>1</sup>, George Heath<sup>1</sup>, Valentin Radu<sup>1</sup>, Antony Blake<sup>2</sup>, Julea N. Butt<sup>2</sup>, Stefan Frielingsdorf<sup>3</sup>, Oliver Lenz<sup>3</sup>

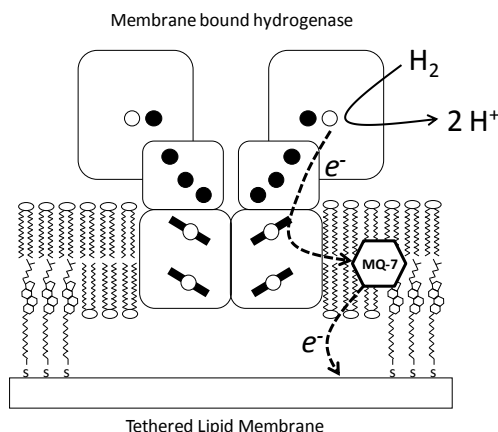
<sup>1</sup>*School of Biomedical Sciences and the Astbury Centre, University of Leeds, Leeds LS2 9JT, United Kingdom*

<sup>2</sup>*Centre for Molecular and Structural Biochemistry, School of Chemistry, and School of Biological Sciences, University of East Anglia, Norwich Research Park, Norwich NR4 7TJ, United Kingdom*

<sup>3</sup>*Institut für Chemie, Sekretariat PC14, Technische Universität Berlin, 10623 Berlin, Germany*  
*L.J.C.Jeuken@leeds.ac.uk*

Bioelectrochemistry has been extremely valuable in elucidating the catalytic mechanism of respiratory redox enzymes, although in almost all cases only globular enzymes or water-soluble subcomplexes have been investigated. In biology, however, many respiratory reactions are catalysed by redox enzymes that reside in the lipid membrane, where they play a major role in almost all metabolic processes, including photosynthesis and biochemical processes such as the nitrogen cycle. The relative lack of bioelectrochemical studies of membrane proteins are due to their amphiphilic nature, which make them difficult to handle experimentally, especially in sensitive electrochemical experiments where proteins are prone to denaturation on the electrode surface.

By modifying ultra-flat electrode surfaces with so-called tethered bilayer lipid membranes (tBLMs), supramolecular platforms can be constructed that enable the electrochemical characterisation of membrane-bound redox enzymes contained within the tBLM. In this presentation, two examples will be discussed in which tBLM systems have elucidated respiratory processes. In the first example, the inner membrane architecture of *Shewanella oneidensis* was mimicked by incorporating the menaquinone-7 (MQ-7) dehydrogenase, CymA, within the tBLM. Quartz-crystal microbalance with dissipation (QCM-D) is used to detect the binding of CymA to globular partner proteins from the periplasm and with cyclic voltammetry the electron transfer from MQ-7 to CymA and then to the partner proteins is monitored. In the second example, a membrane-bound [NiFe]-hydrogenases (MBH), which has been extensively studied for applications in hydrogen–oxygen fuel cells, was incorporated in the tBLM. The MBH of *Ralstonia eutropha* was used in this study as compared to other MBHs it is relatively insensitive to deactivation by oxygen. Previous bioelectrochemical studies with the water soluble subcomplex of MBH, lacking the membrane-bound subunit, showed that this MBH is inactivated at high potentials, especially in the presence of oxygen. In contrast, cyclic voltammetry and chronoamperometry experiments show that MBH, when in equilibrium with the quinone pool in the tBLM, does not inactivate under oxidative redox conditions. Furthermore, although the MBH in the tBLM is still inactivated by O<sub>2</sub>, reactivation was found to be fast even under oxidative redox conditions. We propose that this enhanced resistance to inactivation is due to the fact that MBH is in a more native-like environment in the tBLM.

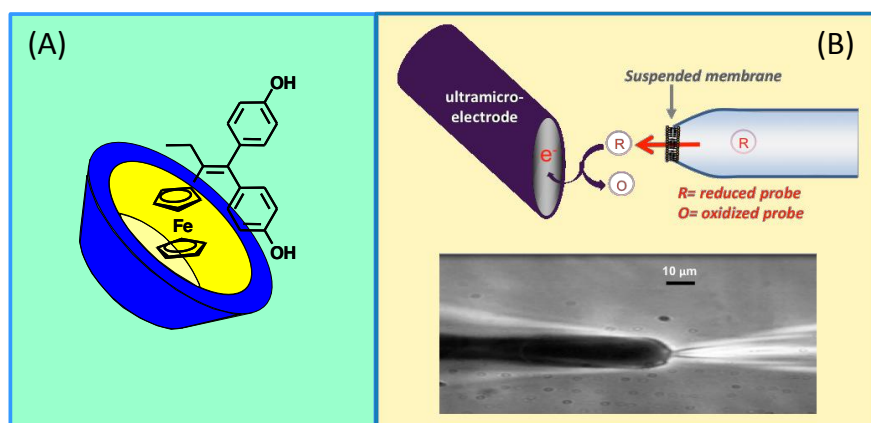


# Contribution of Electrochemistry to Investigate the Solubilization and Transport Through Suspended Membranes of Redox Active Molecules

O. Buriez

*Ecole Normale Supérieure, Département de Chimie, UMR ENS-CNRS-UPMC 8640 « PASTEUR,  
24 rue Lhomond, 75231 Paris cedex 05, France.  
olivier.buriez@ens.fr*

Drug delivery is a central issue for the success of many pharmaceutical strategies. In this context, electrochemistry has been used as a tool to monitor solubilization and transport of biomolecules [1]. For instance, it was demonstrated that cyclodextrins can be used to solubilize ferrocene-based anti-cancer drug candidates in water without changing their biological activity (Figure A) [2]. On the other hand, we have used two complementary approaches to electrochemically probe both the interactions and the crossing of these valuable redox molecules in the presence of supported and suspended pure lipid membranes, respectively [3-5]. Supported membranes were obtained via the polarization of a glassy carbon electrode whereas solvent-free pure lipid suspended membranes were originally obtained by excision of giant vesicles (20 - 50  $\mu\text{m}$  in diameter). In the latter case, novel integration of patch-clamp and amperometry provided a powerful mean for quantifying, in real time, fluxes of molecules across real cell and artificial membranes (Figure B) [5].



(A) Solubilization of a ferrocene-based anti-cancer drug candidate. (B) Electrochemical detection of molecular species crossing suspended membranes.

- [1] Y. G. de Paiva, F. da Rocha Ferreira, T. L. Silva, E. N. da Silva Jr., E. Labbé, O. Buriez, C. Amatore, M. O. F. Goulart. *Curr. Top. Med. Chem.* 15 (2015) 136-162.
- [2] O. Buriez, J.M. Heldt, E. Labbé, A. Vessièrès, G. Jaouen, C. Amatore. *Chem. Eur. J.* 14 (2008) 8195.
- [3] O. Mertins, P. Messina, E. Labbé, V. Vivier, S. Arbault, F. Lemaître, O. Buriez, C. Amatore. *Inorg. Chim. Acta.* 374 (2011) 59.
- [4] O. Mertins, O. Buriez, E. Labbé, P.P. Fang, E.A. Hillard, A. Vessièrès, G. Jaouen, Z.Q. Tian, C. Amatore. *J. Electroanal. Chem.* 635 (2009) 13.
- [5] P. Messina, F. Lemaître, F. Huet, K. A. Ngo, V. Vivier, E. Labbé, O. Buriez, C. Amatore. *Angew. Chem. Int. Ed.* 53 (2014) 3192.

# Imidazolium-Based Supramolecular Ionic Material and Its Application in Biosensing and Electronic Device

Ping Yu, Lanqun Mao

*Beijing National Laboratory for Molecular Sciences, Key Laboratory of Living Biosystems, Institute of Chemistry, the Chinese Academy of Sciences, Beijing 100190, China.  
Tel: 86-10-62646525. E-mail: yuping@iccas.ac.cn, lqmao@iccas.ac.cn*

Over the past two decades, functional supramolecular materials prepared with noncovalent interactions have attracted enormous attention because of their unique applications in electronics, photonics, light-energy conversion, biosensing, and catalysis. Recently, supramolecular materials with water-stability and adaptive encapsulation properties have become particularly attractive especially in biosensor development since most biological processes take place in aqueous environments and biological molecules such as proteins and enzymes are generally active in water. Moreover, the ability to encapsulate functional molecules in supramolecular networks enables the materials to hold great promise in tailoring and improving their functions for target-oriented applications. So far, several kinds of water-stable and adaptive materials have been developed, mainly based on metalcoordination interactions. As a result, it is imperative to explore other kinds of noncovalent interactions for the development of water-stable and adaptive materials with excellent properties.

Ionic interaction between oppositely charged species represents one of the strongest noncovalent interactions and has been widely used in self-assembly, typically as electrostatic self-assembly in solid state and ionic self-assembly in solution. All this work suggests that Coulombic interaction could be used as the noncovalent interaction to form supramolecular materials by self-assembly. While wide availability of charged species and the simplicity of their synthesis allow the ionic interactions to be used in synthesis of various functional materials, it remains a great challenge to utilize this kind of interaction to develop functional supramolecular materials with water stability and adaptive encapsulation property. This is because, on one hand, most of the charged species could easily dissolve in water because of the high dielectric constant of water ( $\epsilon = 78.5$ , at 25 °C) and thus the electrostatic interactions become significantly weakened in water. On the other hand, the large lattice energy in ionic compounds essentially limits their encapsulation property. Very recently, this interaction was utilized to create supramolecular ionic networks and supramolecular polymers by using multiple electrostatic bonds. This implies that ionic interaction could potentially provide the possibility to form water-stable and adaptive supramolecular materials by rationally designing the structure of the building blocks. However, such potential has not been explored so far.

Herein, we demonstrate a series of water-stable, adaptive, and electroactive supramolecular ionic materials (SIM) that is formed from the aqueous solutions of imidazolium-based dication and dianionic through ionic self-assembly. The formed SIM not only shows good thermostability and unique optical and electrochemical properties that are raised from precursors of the SIM, but also exhibits good water-stability, salt-stability, and adaptive encapsulation properties toward some heterocyclic cationic dye molecules. Firstly, we systematically studied the self-assembly behavior based on different carbon chains in imidazolium dications and its structure. Secondly, we found these SIM bears good adaptive inclusion property towards organic dyes and inorganic salt. Based on this, some kinds of biosensors including fluorescence and electrochemistry have been developed. Finally, the electronic property of this kind of SIM was investigated. And we found its electric conductivity was strongly dependent on the humidity. Based on this property, the solid electronic device with high sensitivity and stability was developed. The present study not only opens a new avenue to the preparation of the supramolecular materials, but also provides a versatile platform for (bio)sensing and electronic devices.

# First-Passage Statistics in Nanoelectrochemistry: Applications to Nano-Impacts

Enno Kätelhön, Shaltiel Eloul, Christopher Batchelor-McAuley, Kristina Tschulik,  
and Richard G. Compton

*Department of Chemistry, Physical and Theoretical Chemistry Laboratory, University of Oxford  
South Parks Road, Oxford, OX1 3QZ (United Kingdom)  
enno.kaetelhoe@chem.ox.ac.uk*

Stochastic processes play a crucial role in electroanalytical measurements near the theoretical limit of detection as well as in a variety of nanoelectrochemical set-ups, where the dimensions of the electrode are of the order of the average spacing of electroactive species. While classic electrochemical systems can be well described through locally-averaged analyte concentrations and Fick's laws, processes in the aforementioned systems are often determined by the stochastics of each individual analyte's Brownian motion [1]. Measured results may hence depend on a number of different first passage problems: When does a species hit an electrode for the first time? What is the probability that this species reacted at a particular other electroactive site beforehand? Or what is the average residence time in a zone of electron transfer?

Aside from applications in the investigation of biological membranes, single-molecule detection, molecular recognition, and many others, first-passage statistics are of particular interest in the fastly-developing field of nano-impacts. In nano-impact measurements, an electrode is exposed to a solution of freely diffusing nanoparticles, which, by virtue of their Brownian motion, will stochastically impact on the electrode. During collisions, they may either react due to their intrinsic electrochemical properties or catalytically enable a reaction between the electrode and electroactive species in solution [2,3]. Impacts can be observed as spikes in the measured electrode current, which provides insight into the detected particles' electrochemical properties and their sizing. As individual particles can be detected, a number of first-passage effects directly affect the measured currents in terms of the frequency of spikes, their magnitude, and shape.

In this talk, we discuss general aspects of first-passage statistics in the context of nanoelectrochemistry and demonstrate an analysis of a nanoparticle's average time of residence within the zone of electron transfer at a planar electrode. Additionally considering the effect of near-wall hindered diffusion, we find that nanoparticles generally experience hydrodynamic adsorption at surfaces, which can be quantified in great detail via a first-passage approach [4]. As our findings are generally applicable to systems that comprise of freely diffusing nanoparticles, the effect of hydrodynamic adsorption has wide implications on nanoparticle research.

## References:

- [1] Shaltiel Eloul, Enno Kätelhön, Christopher Batchelor-McAuley, Kristina Tschulik, and Richard G. Compton, '*Diffusional Nano-Impacts: The Stochastic Limit*', **to be published**, 2015.
- [2] Yi-Ge Zhou, Neil V. Rees, and Richard G. Compton, '*The Electrochemical Detection and Characterization of Silver Nanoparticles in Aqueous Solution*', **Angewandte Chemie International Edition**, 2011, Volume 50, Issue 18, Pages 4219–4221.
- [3] Wei Cheng, Xiao-Fei Zhou, and Richard G. Compton, '*Electrochemical Sizing of Organic Nanoparticles*', **Angewandte Chemie International Edition**, 2013, Volume 52, Issue 49, Pages 12980–12982.
- [4] Enno Kätelhön and Richard G. Compton, '*Understanding Nano-Impacts: Impact Times and Near-Wall Hindered Diffusion*', **Chemical Science**, 2014, Volume 5, Issue 12, Pages 4592–4598.

# One-step Supramolecule Assembly of N-(aminobutyl)-N-(ethylisoluminol) Functionalized Gold Nanodots on Multiwalled Carbon Nanotubes and Their Applications to Sensors

H. Cui, H. L. Zhang, Z. L. Han

*Department of Chemistry, University of Science and Technology of China,  
Hefei, Anhui 230026, P.R. China  
hcui@ustc.edu.cn*

Based on the remarkable electronic, optical, thermal, high surface area properties, carbon nanotubes (CNTs) have been extensively investigated for chemical and biological application. Gold nanomaterials (AuNMs) are considered as the most common building blocks for current nanoscience due to the unique properties, including stability, biocompatibility and ease of self-assembly property. Take advantages of both CNTs and AuNMs, the combination of them could give rise to novel AuNMs–CNTs hybrid nanomaterials. Recently, in our group,<sup>1</sup> N-(aminobutyl)-N-(ethylisoluminol) (ABEI) functionalized gold nanodots (ABEI-GNDs) were successfully assembled onto the sidewalls of chitosan-modified multiwalled CNTs (cs-MWCNTs) via the reduction of HAuCl<sub>4</sub> with ABEI in the presence of cs-MWCNTs by virtue of covalent and noncovalent interactions. The proposed one-step strategy is green, simple and highly effective. The obtained hybrid nanomaterial exhibited excellent chemiluminescence (CL) and electrochemiluminescence (ECL) properties. Based on the excellent ECL performance of the novel hybrid nanomaterials, an ECL immunosensor was developed for the determination of N-terminal pro-brain natriuretic peptide (NT-proBNP).<sup>2</sup> The hybrid nanomaterials were coated onto the surface of ITO electrode via their film-forming property. Then, anti-NT-proBNP antibody was attached to the surface of modified electrode by virtue of amide reaction via glutaraldehyde. Finally, when NT-proBNP was captured by its antibody via immunoreaction, the ECL intensity decreased, which were used for the determination of NT-proBNP. The proposed ECL immunosensor demonstrated a quite wide linear range of 0.01–100 pg/mL and achieved low detection limit of 3.86 fg/mL, which was about 3 orders of magnitude lower than that obtained with electrochemistry method reported previously.<sup>3–4</sup> The present immunosensor is highly sensitive, simple, fast, selective, stable and reliable. It has been successfully applied to the determination of NT-proBNP in practical plasma samples. Furthermore, the proposed strategy might be used for the detection of other important clinically biomarkers. This work revealed that the as-prepared hybrid nanomaterial could be used as ideal nanointerface to fabricate sensitive biosensors.

The support of these researches by the National Natural Science Foundation of P. R. China (Grant No. 21475120 and 21173201) is gratefully acknowledged.

1. H. L. Zhang, H. Cui, *Nanoscale*, 2014, 6, 2563–2566.
2. H. L. Zhang, Z. L. Han, X. Wang, F. Li, H. Cui, D. Yang, Z. P. Bian, *ACS Appl. Mater. Inter.*, DOI: 10.1021/am509094p.
3. W. B. Liang, Y. Li, B. Zhang, Z. J. Zhang, A. Chen, D. L. Qi, W. J. Yi, C. M. Hu, *Biosens. Bioelectron.*, 2012, 31, 480–485.
4. Y. Zhuo, W. J. Yi, W. B. Lian, R. Yuan, Y. Q. Chai, A. Chen, C. M. Hu, *Biosens. Bioelectron.*, 2011, 26, 2188–2193.

# Supramolecular Biological Assemblies for Biosensors and Biofuel Cells

Cosnier Serge

*Département de Chimie Moléculaire UMR CNRS 5250  
Grenoble Alpes University, BP-53, 38041 Grenoble Cedex 9, France  
Serge.Cosnier@ujf-grenoble.fr*

With the aim to improve the performance of biomaterials, 3D structures were designed to create an oriented biomolecule monolayer or a high density of biological entity at the transducer surface. Owing to their high conductivity, inertness and electroactive surface area, graphene and carbon nanotube are widely used for the design of biosensors and biofuel cells [1,2].

In this context, we report the functionalization of a single graphene layer on a thin gold film by copper coordinated nitrilotriacetic acid attached to graphene via  $\pi$ - $\pi$  interactions with pyrene derivatives and the subsequent immobilization of biotinylated cholera toxin antigen. With the amplification of the SPR signal by graphene, a detection limit of 4 pg mL<sup>-1</sup> was obtained for the antibody anticholera toxin [3]. Carbon nanotube coatings were also functionalized with 4-aminonaphtoic acid. These carboxylated nanotubes exhibited an efficient direct wiring of hydrogenase allowing H<sub>2</sub> oxidation and hence the elaboration of a hydrogen/oxygen biofuel cell [4].

Increased attention has been also given to the functionalization of electrode and SPR surfaces by the combination of carbon nanotube coating with graphene, polypyrrole, polyacrylonitrile or polynorbornene films. For instance, deposition on carbon nanotube electrodes of reduced graphene oxide nanosheets functionalized by anthraquinone groups allows excellent electron transfer properties. Laccases were immobilized on the nanostructured electrode by the interaction between the anthraquinone moiety and the laccase hydrophobic pocket leading to efficient bioelectrocatalytic oxygen reduction [5]. The combination of carbon nanotube coating and an electropolymerized polypyrrole film of a protein: concanavalin A is also an original strategy for the non-covalent immobilization of glycoproteins via specific interactions with polymerized concanavalin A [6,7]. Finally, another approach concerns the fabrication of fiber tissue electrode from nanosized fibers containing carbon nanotubes. The latter were produced by electrospinning from a solution containing nanotubes and polyacrylonitrile. The biofunctionalization of the nanofiber electrodes was exemplified by chemical grafting of an enzyme model, polyphenol oxidase, onto the nanofiber tissue [8].

1. S. Cosnier, M. Holzinger. *Chem Soc. Reviews* 40 (2011) 2146-2156.
2. M. Holzinger, A. Le Goff, S. Cosnier. *Electrochim. Acta*, 82 (2012) 179-190
3. M. Singh, M. Holzinger, M. Tabrizian, S. Winters, N. Berner, S. Cosnier, G. Duesberg. *J. Am. Chem. Soc.*, 137 (2015) 2800-2803
4. N. Lalaoui, A. de Poulpiquet, R. Haddad A. Le Goff, M. Holzinger, S. Gounel, M. Mermoux, N. Mano, E. Lojou, S. Cosnier. *Chem. Commun.*, in press.
5. N. Lalaoui, A. Le Goff, M. Holzinger, M. Mermoux, S. Cosnier. *Chem. Eur. J.*, 21 (2015) 3198-3201.
6. V. Papper, K. Elouarzaki, K. Gorgy, A. Sukharaharja, S. Cosnier, R. Marks. *Chem. Eur. J.*, 20 (2014) 13561-13564.
7. K. Elouarzaki, M. Bourourou, M. Holzinger, Alan Le Goff, R. S. Marks, S. Cosnier. Submitted.
8. M. Bourourou, M. Holzinger, F. Bossard, F. Hugenell, A. Maaref, S. Cosnier. *Carbon*, 87 (2015) 233-238.

# Interactions of Anticancer Drug and Adducts of the Drug with Carbon Nanotubes with Model Biological Membranes – Langmuir-Blodgett and Electrochemical Studies.

Dorota Matyszewska<sup>1,2</sup>, Jan F. Biernat<sup>3</sup>, Renata Bilewicz<sup>2</sup>

<sup>1</sup>Biological and Chemical Research Centre, University of Warsaw, Żwirki i Wigury 101, 02089 Warsaw, Poland

<sup>2</sup>Faculty of Chemistry, University of Warsaw, ul. Pasteura 1, 02093 Warsaw, Poland

<sup>3</sup>Chemical Faculty, Gdansk University of Technology, ul. Narutowicza 11/12, 80233 Gdansk, Poland  
dorota.matyszewska@chem.uw.edu.pl

Daunorubicin (DNR) is an anthracycline antitumour drug, which finds application in the treatment of various types of cancer including leukemia, breast cancer, ovarian cancer, lung carcinoma, as well as several sarcomas [1]. However, the usage of this drug in the treatment is limited because of serious side effects including drug-induced heart failure. Therefore, numerous studies focus on the application of different drug delivery systems (DDS) such as for example carbon nanotubes to transport daunorubicin to cancer cells [2]. The influence of both free drug and drug adducts with single-walled carbon nanotubes (SWCNTs) as potential drug carriers on model biological membranes was investigated first using Langmuir technique. The model membranes were composed of 1,2-dipalmitoyl-*sn*-glycero-3-phosphothioethanol (DPPTE). Our previous studies revealed that application of the thiolipid allows one to transfer the layers onto solid support by means of both Langmuir-Blodgett method and self assembly and electrochemical methods such as chronocoulometry along with STM studies proved that the organization and structure of the transferred layers strongly depend on the mode of transfer [3].

Results of Langmuir studies show that daunorubicin easily incorporates into the DPPTE layers during their formation increasing significantly the area per molecule and causing immense fluidization of the layers. The observed changes depend on the concentration of the drug in the subphase [4]. Additionally, the dominating type of the driving forces responsible for the interactions (electrostatic or hydrophobic) depends on the organization of the layers. Cyclic voltammetry experiments revealed that DNR incorporation is easier into supported layers transferred by LB method than into SAMs because LB layers are less compact and hydrophobic interactions between the acyl chains of the thiolipid and hydrophobic anthraquinone part of DNR are facilitated. In the next step, the results of the interactions of the free drug with model membranes were compared with the results obtained for DNR attached to the SWCNTs by forming hydrazone with the nanotubes, which provides covalent bonding either at the ends or sides of the nanotubes [5]. Langmuir studies of mixed monolayers showed that even at the highest investigated content of the nanotubes in the monolayer, the changes in the properties of DPPTE monolayers were not as significant as in case of the incorporation of free drug, while electrochemical studies revealed that in the same time the surface concentration of DNR in supported monolayers is comparable to the reported surface concentration of the free DNR incorporated into supported DPPTE monolayers. Therefore, it may be concluded that the application of carbon nanotubes as potential DNR carrier allows for the incorporation of comparable amount of the drug into model membranes with simultaneous decrease in the negative changes in the membrane structure and organization, which is an important aspect in terms of side effects of the drug.

## References:

- [1] H. Cortes-Funes, C. Coronado, *Cardiovasc Toxicol*, **2007**, 7, 56–60.
- [2] P. Ma, R.J. Mumper, *Nano Today*, **2013**, 8, 313–331.
- [3] D. Matyszewska, S. Sęk, R. Bilewicz, *Langmuir*, **2012**, 28, 5182–5189.
- [4] D. Matyszewska, R. Bilewicz, *Electrochim. Acta*, **2015**, doi:10.1016/j.electacta.2015.01.032
- [5] Y.J. Gu, J. Cheng, J. Jin, S. H. Cheng, W.-T. Wong, *Int. J. Nanomed.*, **2011**, 6, 2889.



# On the Synthesis of Zinc-Tetrapyrridylporphine Complex for the Electrochemical Recognition of Bilirubin in Serum

Mei-Jywan Syu\*, Yao-Wei Hsu

Department of Chemical Engineering, National Cheng Kung University

No. 1, University Rd., Tainan, Taiwan 701

syumj@mail.ncku.edu.tw syumei2014@gmail.com

The aim of this work is to synthesize a metal-tetrapyrridylporphine complex with the inclusion ability for bilirubin. The metal-tetrapyrridylporphine complex thus prepared is a kind of stimulated-responsive gel. It owns regularity from its repeated and symmetric structure while, on the other hand, it also owns softness for the inclusion of the guest molecules into its flexible framework once the stimulation is applied. Via tuning the structure of the metal-organic complex with the stimulation, different applications could be expected. In this work, 5,10,15,20-tetra(4-pyridyl)-21H,23H-porphine (TPyP), a compound of porphyrin series is used as the precursor for the synthesis of the metal-organic complex. A basic unit scheme of the metal complex from TPyP precursor is shown in Fig. 1. The feasibility on the formation of the metal-organic gel with zinc(II) and ferrous(II), via the coordination of TPyP with a metal ion with the valence number of two, were studied. The formation of the metallic organic gel could be the consequence of not only via the hydrogen bonds, but also via the  $\pi$  interaction of the porphyrin plane donated from the electron pairs of the pyridyl groups laid on the four tops. The geometric symmetry of the TPyP is an essential feature contributed to the formation of the metallic organic crystal. The Zn(II)TPyP is further analyzed by a UV/Vis spectrophotometer and an FTIR (Figures 2(a), 2(b)) to confirm the characteristic peak and major bonds from the stretching and bending vibrations. The Zn(II)TPyP crystal is then fabricated onto the Au substrate for the electrochemical uptake of bilirubin. The results confirm the successful calibration of bilirubin concentration in the available clinical range with a sensitivity of  $0.336 \pm 0.021$  ( $\mu\text{A}/\text{cm}^2$ )/(mg/dL) by using this inclusion material.

Keywords: TPyP, porphyrin, pyridyl group, bilirubin, coordination

The grant from NSC100-2815-C-006-017-E and NSC99-2221-E-006-094-MY3 for the accomplishment of this work is deeply appreciated.

1. OM Yaghi, et al, Nature 378(6558), 703 (1995).
2. M Kondo, et al, Angew Chem Int Ed 36(16), 1725 (1997).

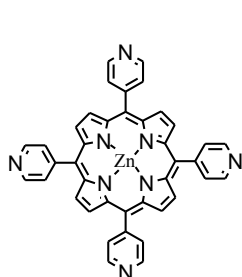


Fig. 1 Sketch of a Zn(II)TPyP.

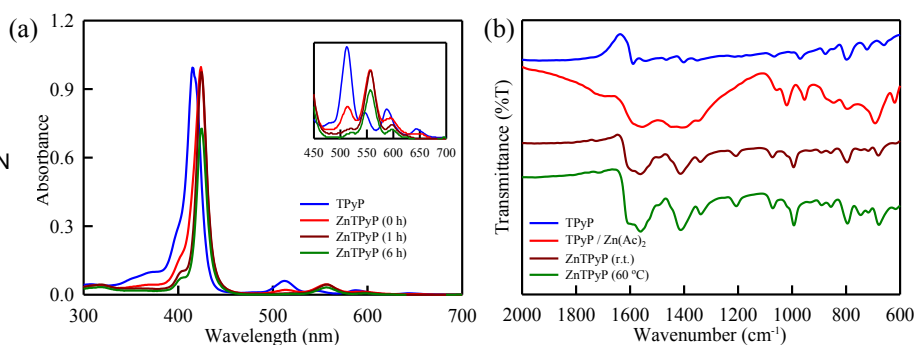


Fig. 2 Analysis of the Zn(II)TPyP by a UV/ Vis spectrophotometer and an FTIR. (a) UV/Vis spectrophotometer; (b) FTIR.

# DNA Bases Co-Adsorption at Gold Electrodes. An in-situ FT-IR Spectro-Electrochemical Study

Manuela Rueda, Julia Alvarez-Malmagro, Francisco Prieto  
*Department of Physical Chemistry University of Seville.*  
*c/ Profesor Garcia Gonzalez 1. 41012 Seville. SPAIN*  
*tfn. +34955421003*  
*marueda@us.es*

The interactions between complementary DNA bases play a significant role in genetic expression and replication. The co-adsorptions of these bases on solid substrates are important to understand the interactions of complementary bases interactions and the non-complementary bases interactions, that can induce genetic modifications, in organised interfaces similar to the biological interfaces. Moreover, the co-adsorptions of DNA bases are interesting in relation to technological processes as the manufacturing of biosensors with capabilities to detect epigenetic modifications or the design of nano-platforms for drug delivery.

In this respect, we have already started a systematic study of the co-adsorption of DNA bases on gold electrodes by combining modern in-situ FTIR techniques that provide chemical specificity and high sensitivity with electrochemical methods. Thus, the co-adsorption of thymine and adenine on gold thin-film electrodes from acid solutions has been previously studied by surface-enhanced infrared absorption spectroscopy in the attenuated total reflection mode (ATR-SEIRAS) [1]. The results suggest a rearrangement of both molecules on the electrode surface in a cooperative process in order to facilitate the Watson–Crick (W–C) and/or Hoogsteen (HG) interactions between the bases, as the atoms involved in these interactions are also the most probably sites of interactions with the metal. On the other hand, recent studies about the influence of pH on adenine adsorption on gold electrodes have shown that the two acid-base equilibriums of adenine are modified at the electrode interfaces [2, 3]. Moreover, our results about thymine adsorption on gold show that different tautomers can be stabilised on the electrode surface depending on the pH of the solution and of the electric potential.

In this communication the co-adsorption of the complementary DNA bases adenine-thymine and of guanine-cytosine on gold thin-film electrodes are studied in a wide pH range (from pH 1 to 12) by combination of ATR-SEIRAS and electrochemical experiments. They have been performed in perchlorate and either perchloric acid or hydroxide solutions, using H<sub>2</sub>O and D<sub>2</sub>O as solvents. Thin-film gold electrodes prepared by sputtering were used as working electrodes and electrochemical and some complementary SNIFTIRS experiments have been performed using Au(111) electrodes.

The spectrums of co-adsorbed bases are analysed as a function of potential at each pH value and are compared to the spectrums of each adsorbed base in the same experimental conditions. Different concentrations of each base are assayed in the sub-monolayer range. In this way the interactions between the different acid-bases and/or tautomeric forms of each DNA complementary base are determined. In the case of adenine-thymine co-adsorption the cooperative rearrangement of both molecules is confirmed and discussed based on  $\pi$ -stacking and dipole-dipole interactions among the different tautomeric and acid-base forms. In the case of guanine-cytosine the co-adsorption study is limited to basic media in order to achieve the simultaneous chemical adsorption of the two molecules in the same potential range and to avoid guanine oxidation. Guanine adsorption is stronger and induces the rearrangement of cytosine on the surface, even at lower concentrations.

## References

- 1.- M. Rueda, F. Prieto, J. Alvarez-Malmagro, A. Rodes, *Electrochem. Commun.* 35 (2013) 53.
- 2.- M. Rueda, F. Prieto, A. Rodes and J.M. Delgado, *Electrochim. Acta*, 82 (2012) 534.
- 3.- J. Alvarez-Malmagro, F. Prieto, M. Rueda, A. Rodes, *Electrochim. Acta*, 140 (2014) 476.

# Ultrasensitive Electrochemical Detection of the Cancer Biomarker CA19.9

Flavio Maran,<sup>1</sup> Anna Pellattiero,<sup>1,2</sup> Federico Polo,<sup>1</sup> Giuseppe Toffoli,<sup>2</sup>  
Aline S. C. Fabricio,<sup>2,3</sup> Massimo Gion<sup>3</sup>

<sup>1</sup> *Department of Chemistry, University of Padova  
via Marzolo 1, 35131 Padova, Italy*

<sup>2</sup> *Experimental and Clinical Pharmacology Unit, Centro di Riferimento Oncologico  
National Cancer Institute*

*Via Franco Gallini 2, 33081 Aviano (PN), Italy*

<sup>3</sup> *Regional Center for Biomarkers, Department of Clinical Pathology, Azienda ULSS12  
Campo SS Giovanni e Paolo 6777, 30122 Venice, Italy  
flavio.maran@unipd.it*

Cancer antigen 19.9 (CA19.9) is the reference biomarker for pancreatic cancer, one of the most aggressive malignant tumors and leading cause of cancer-related deaths worldwide.<sup>1</sup> The determination of CA19.9 in pancreatic cyst fluid might improve diagnostic performance. In the framework of point-of-care testing, however, measuring CA19.9 during the endoscopy is a very challenging task, particularly when the biomarker concentration is very low. We focused on implementing electrochemical nanotechnologies suitable to detect CA19.9 with very high sensitivity and very low detection limits. Electrodes were modified with functionalized gold nanoparticles that were then modified with an antibody specifically tailored to bind CA19.9. Magnetic particles capped with a redox label (horseradish peroxidase, HRP) and a second antibody completed the immunosensor. Biorecognition was granted by the strong affinity between the antigen and the two antibodies. The sandwich-like immunosensor was integrated into a microfluidic device. Activation of the HRP labels with H<sub>2</sub>O<sub>2</sub> causes an amperometric-current transient proportional to the protein concentration. This immunosensor strategy successfully detects CA19.9 concentrations that are typically one order of magnitude lower than those obtained using the ELISA assay, and with a much higher sensitivity.

1. <http://www.cancer.org/research/cancerfactsfigures/cancerfactsfigures/cancer-facts-figures-2013>.

# A Rapid Detection of Biomarkers Applied by Electrochemical Biosensor Accelerated with an AC Electrokinetic Manipulation

Yu Cheng, Tzu-Ying Wu, and Hsien-Chang Chang\*

Department of BioMedical Engineering, Cheng Kung University, Tainan, Taiwan  
hcchang@mail.ncku.edu.tw

## Abstract

Fluorescent labelling and chromogenic reactions that are commonly used in conventional immunoassays typically utilize diffusion dominated transport of analytes, which is limited by slow reaction rates and long detection times. By integrating alternating current (AC) electrokinetics and electrochemical impedance spectroscopy (EIS), we construct an immunochip for rapid, sensitive, and label-free detection. AC electroosmosis (ACEO) and positive dielectrophoresis (DEP), induced by a biased AC electric field, can rapidly convect and trap the analyte onto an EIS working electrode within a few minutes (Fig. 1). We apply this system for the detection of the tumor marker, Alpha-feto protein (AFP,  $\alpha$ -fetoprotein). After AFP containing sample injected and reacted with antibody of AFP (Anti-AFP) will allow the change of electron-transfer resistance ( $R_{et}$ ) caused by the antibody-antigen (Anti-AFP-AFP) binding to be measured and quantified in real time (Fig. 2). The detection limit is able to reach 150 ng/ml of AFP (Fig. 3).

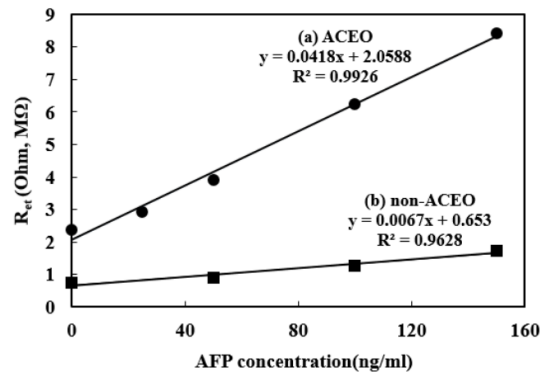


Fig.1. Comparison between the detection effect of the ACEO and non-ACEO

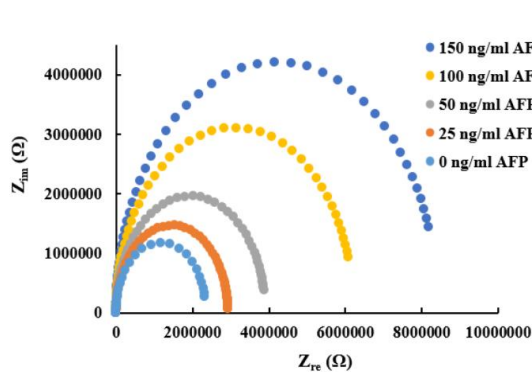


Fig.2. The Nyquist Plot of AFP

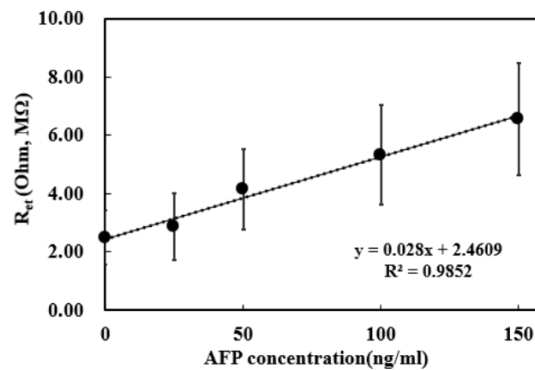


Fig.3. The calibration curve of AFP

Keywords: AC electroosmosis (ACEO), electro- chemical impedance spectroscopy (EIS),  $\alpha$ -fetoprotein

# Application of GroEL Complexes as Nano-sized Cargo

Hiromi Yoda, Ayumi Koike-Takeshita

Department of Applied Chemistry and Bioscience, Graduate School of Engineering,  
Kanagawa Institute of Technology, 1030 Shimo-Ogino, Atsugi, Kanagawa 243-0292, Japan

E-mail: koike@bio.kanagawa-it.ac.jp, Tel/Fax: +80-46-2913326

## Introduction

Chaperonin GroEL and co-chaperonin GroES are related to intracellular protein folding in *Escherichia coli*. GroEL is constructed by two heptameric rings of 57 kD subunits, and these rings are stacked back to back. GroES is a single heptameric ring of 10 kD subunits. GroEL binds a wide variety of substrate proteins in non-native states. After GroEL catches the substrate, GroEL binds ATP and GroES to form GroEL/GroES complex which has about 5 nm cavity for the encapsulation of substrates.

GroEL<sup>D52/398A</sup> is extremely defective in ATP hydrolysis [1][2]. In the presence of GroES and ATP, GroEL<sup>D52/398A</sup> produces a symmetric 1:2 GroEL-GroES complex (the “football”-shaped complex) in which both GroEL rings encapsulated substrate protein. Notably, the symmetric complex of GroEL<sup>D52A/D398A</sup> was extremely stable, with a half-time of ~150 h (~6 days). Furthermore, the two rings of GroEL<sup>D52/398A</sup> can be controlled individually to close the cavities by using nucleotide differences. In ADP, GroEL<sup>D52/398A</sup> can bind GroES to form a stable 1:1 GroEL-GroES complex in which one of GroEL rings contains an encapsulated substrate protein. This 1:1 GroELGroES complex (the “bullet”-shaped complex) is converted into the symmetric 1:2 GroEL-GroES complex when GroES is supplied in ATP.

The property of the GroEL<sup>D52/398A</sup> looks beneficial not only for folding the polypeptide but dispersing aggregatable nanoparticles and hydrophobic compounds. So, we tried to encapsulate a few varieties of the nanoparticles in the GroEL<sup>D52/398A</sup>.

## Experiments

Pt (Average  $\phi$  2 nm), FePt ( $\phi$  4 nm), CdSe/ZnS ( $\phi$  7nm), Au ( $\phi$  10 nm) and Ag ( $\phi$  5 nm) were used to encapsulate in GroEL as metal nanoparticles. In the case of nanoparticle encapsulation in one side of GroEL<sup>D52/398A</sup> cavities, 0.1-1.0  $\mu$ M GroEL<sup>D52/398A</sup>, 0.2-2.0  $\mu$ M GroES (2-fold mol of GroEL), and 1mM ATP were added to the sonicated nanoparticle solution. For two different nanoparticle encapsulation in both sides of GroEL<sup>D52/398A</sup> cavities, GroEL<sup>D52/398A</sup> which is bound to first nanoparticle was added to the same molar of GroES and 5mM ADP. The bullet-shaped GroEL<sup>D52/398A</sup> encapsulating first nanoparticle was mixed with the second nanoparticle solution for 1 minute, then, GroES and 1mM ATP were added to form the football-shaped complex. The specimen was stained with 0.5-1 % phosphotungstic acid (pH 4.0) and observed with an electron microscope (JEM-2000EX or JEM 2100, JEOL).

## Results and discussion

TEM images showed GroEL<sup>D52/398A</sup>/GroES complexes encapsulating several types of nanoparticles. In the absence of nanoparticles, holes of GroEL<sup>D52/398A</sup>/GroES were looked white. In contrast, nanoparticle encapsulating GroEL<sup>D52/398A</sup>/GroES caught black ~ gray colored dot in their cavities. Interestingly, GroEL<sup>D52/398A</sup>/GroES could encapsulate one FePt and two pt nanoparticles in each cavity of the complex (Fig. 1f). These results suggest GroEL<sup>D52/398A</sup>/GroES can encapsulate a variety types of nanoparticles (particle size ~10 nm).

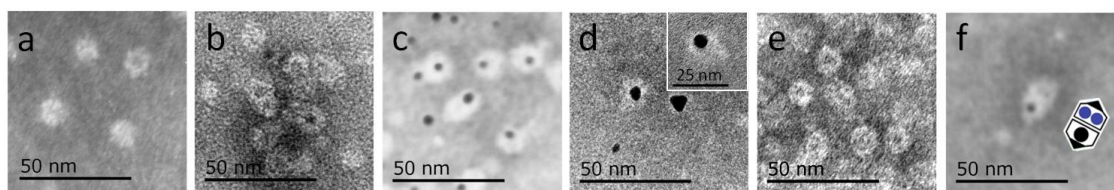


**Fig. 1.** TEM images of metal nanoparticles encapsulated in the GroEL<sup>D52/398A</sup> football-shaped complex. (a) No nanoparticles, (b)  $\phi$  7 nm CdSe/ZnS, (c)  $\phi$  4 nm FePt, (d)  $\phi$  10 nm Au, (e)  $\phi$  5 nm Ag, (f) FePt and  $\phi$  2 nm Pt.

[1] A. Koike-Takeshita, T. Arakawa, H. Taguchi, T. Shimamura, *J. Mol. Biol.* 2014, **426**, 3634.

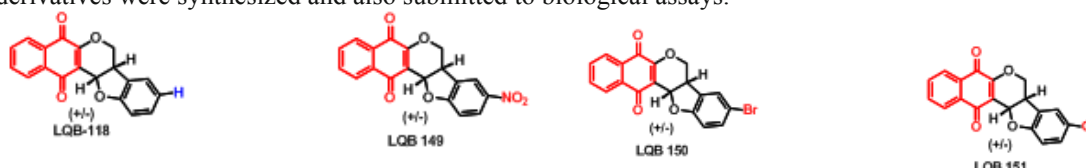
[2] A. Koike-Takeshita, K. Mitsuoka, H. Taguchi, *J. Biol. Chem.* 2014, **289**, 30005.

# The Yin-Yang Nature of Biologically Active Pterocarpanquinones: ROS Release and Alkylating Ability also Revealed by Electrochemistry

Marilia O. F. Goulart,<sup>a</sup> Thaissa L. Silva,<sup>a</sup> Camila C. de Vasconcelos,<sup>a</sup> Fabricia R. Ferreira,<sup>a</sup>  
Chaquip D. Netto,<sup>b</sup> Paulo R.R. Costa<sup>b</sup>

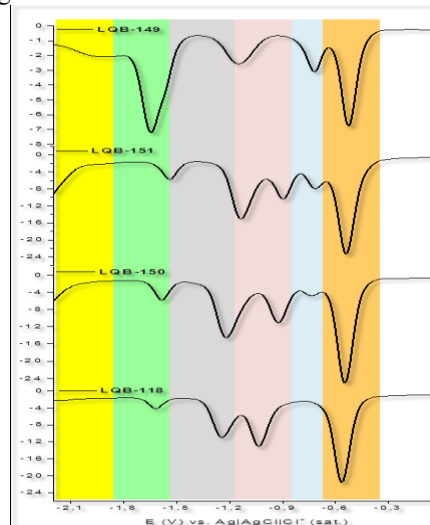
*Instituto de Química e Biotecnologia, UFAL, Maceió, Alagoas, Brazil*  
*Núcleo de Pesquisa em Recursos Naturais, UFRJ, Rio de Janeiro, Brazil*  
*mariliaofg@gmail.com*

LQB-118, a pterocarpanquinone, promotes apoptosis in *Leishmania amazonensis* promastigotes through the formation of ROS, which cause oxidative stress, mitochondrial membrane depolarization and DNA fragmentation <sup>[1]</sup>. Furthermore, it inhibited the proliferation and induced apoptosis in leukemic cells, via activation of caspases-3 <sup>[2]</sup>. The *para*-quinone moiety can participate in the redox cycle in the cell, acting as a precursor of ROS and leading to oxidative stress. Alternatively, LQB 118 can be activated in situ by reduction, leading to conjugated intermediates, which are powerful alkylating agents <sup>[1,2]</sup>. Some derivatives were synthesized and also submitted to biological assays.



We investigated the electrochemical behavior of LQB-118 and derivatives in aprotic media, in the absence and presence of oxygen in order to obtain data regarding its reduction mechanism, reactivity with oxygen, the analysis of the stability of the electrogenerated intermediate and interactions with biological targets, like DNA. An electrochemical cell with three electrodes was used: Ag/AgCl (KCl saturated) (reference), platinum wire (auxiliary) and glassy carbon as working electrode was used.

CV and DPV for LQB-118 and derivatives in aprotic medium (Figure 1) display, at least, 4 waves, the first two related to the usual reduction of the quinone moiety. The presence of additional waves suggests the cleavage of the heterocyclic rings and the generation of additional reducible systems <sup>[2]</sup>. Further, electrochemical experiments were carried out in the presence and absence of oxygen to verify the reactivity with oxygen, after the reduction of LQB-118, with positive results. Studies with dsDNA biosensor, in buffered aqueous medium showed no interaction between LQB-118 and reduction product with dsDNA after 15 min of contact, differently from the behavior in presence of ssDNA, in solution. The interaction with oxygen and the generation of ROS partly explains the cytotoxic action of the quinone in studied cancer cells. It is another case of successful pharmacoelectrochemical investigation. Further studies on substituted pterocarpanquinones will be also described. CNPq, CAPES, FAPEAL, INCT-Bioanalítica.



## References

- [1] MAIA R.C. et al., *Invest New Drugs*, 29, 2011, 1143–1155.
- [2] NETTO C.D. et al., *Bioorganic & Medicinal Chemistry*, 18, 2010, 1610–1616.
- [3] RIBEIRO, G. A. et. al., *Journal of Antimicrobial Chemotherapy*, 3, 2013, 1-11.

# Local Delivery of Biologically Active Compounds Based on Conjugated Polymer Matrices

Katarzyna Krukiewicz<sup>a</sup>, Tomasz Jarosz<sup>a</sup>, Barbara Bednarczyk-Cwynar<sup>b</sup>, Piotr Ruszkowski<sup>b</sup>, Jerzy K. Zak<sup>a</sup>  
*Silesian University of Technology, M. Strzody 9, 44-100 Gliwice, Poland*  
*Poznan University of Medical Sciences, Fredry 10, 61-701 Poznan, Poland*  
katarzyna.krukiewicz@polsl.pl

Local delivery is an innovative approach of medical treatment introduced to decrease the toxicity of therapeutics against healthy tissues by optimization of their concentrations during extended drug exposure time. This is of a significant importance when strong drugs, especially antibiotics and anti-cancer agents, are used. The concept of localized drug delivery may be realized by means of conjugated polymers – biocompatible, highly conducting materials able to undergo reversible redox reactions. In contrast to the physical entrapment, conjugated polymers allow highly controlled, reversible electrostatic immobilization of a wide range of biologically active compounds [1,2]. Change in their reduction-oxidation state as a result of electrical stimulation is followed by the release of a precise amount of drug [3].

Betulin is a naturally abundant triterpene significantly inhibiting viability in cervix carcinoma HeLa cells, lung adenocarcinoma A549 cells and breast cancer MCF-7 cells [4]. In this study, conducting poly(3,4-ethylenedioxypyrrole) matrix was used to serve as a nano-reservoir of disuccinyl derivative of betulin (Fig.1). The process of immobilization was realized with the use of electrochemical techniques, cyclic voltammetry and chronoamperometry. The efficiency of electrically-triggered release was studied in-situ by means of UV/Vis spectrophotometry. Raman spectroscopy and scanning electron microscopy were used to analyze structural and surface properties of polymer matrices.

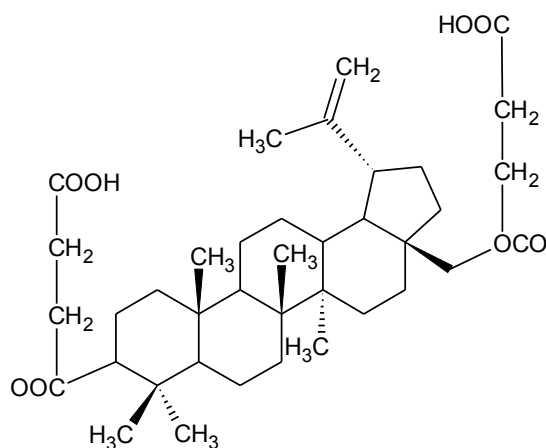


Fig.1. Chemical structure of disuccinyl derivative of betulin.

*The authors would like to thank the Polish National Science Centre (PRELUDIUM, 2012/07/N/ST5/01878), Foundation for Polish Science together with European Social Fund (INTER'2015, 30/UD/SKILLS/2015).*

## References:

1. R. Wadhwa, C.F. Lagenaur, X.T. Cui, Electrochemically controlled release of dexamethasone from conducting polymer polypyrrole coated electrode, *J. Control. Release* 110 (2006) 531.
2. K. Krukiewicz, J.K. Zak, Conjugated polymers as robust carriers for controlled delivery of anti-inflammatory drugs, *J. Mater. Sci.* 49 (2014) 5738.
3. N. Alizadeh, E. Shamaeli, Electrochemically controlled release of anticancer drug methotrexate using nanostructured polypyrrole modified with cetylpyridinium: Release kinetics investigation, *Electrochim. Acta* 130 (2014) 488.
4. Y. Li, K. He, Y. Huang, D. Zheng, C. Gao, L. Cui, Y.H. Jin, Betulin induces mitochondrial cytochrome c release associated apoptosis in human cancer cells, *Mol. Carcinog.* 49 (2010) 630.



# Combined Ionic Diffusion and Faradaic Reactions in Electrodeposited Highly Hydrated Amorphous Iridium Oxide by in-operando Dispersive XAS Investigation

Sandra Rondinini,<sup>a</sup> Paolo Ghigna,<sup>b</sup> Elisabetta Achilli,<sup>b</sup> Alberto Vertova,<sup>a</sup> Cristina Locatelli,<sup>c</sup> Francesco D'Acapito<sup>d</sup>

<sup>a</sup>Department of Chemistry, ISTM and CNR-ISTM Università degli Studi di Milano,  
Via Golgi 19, 20133 Milano, Italy

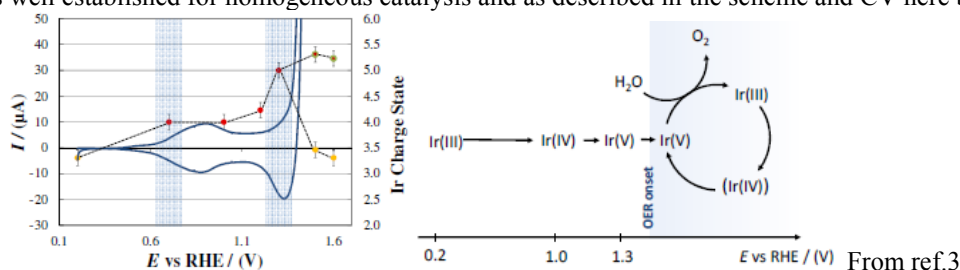
<sup>b</sup>Università di Pavia, Dipartimento di Chimica, Via Taramelli 16, 27100, Pavia, Italy

<sup>c</sup>Department of Chemistry and ISTM, Università degli Studi di Milano,  
Via Golgi 19, 20133 Milano, Italy

<sup>d</sup>Consiglio Nazionale delle Ricerche, Istituto Officina dei Materiali, Operative Group in Grenoble, c/o  
European Synchrotron Radiation Facility, B.P. 220, 38043 Grenoble, France  
sandra.rondinini@unimi.it

Electrodeposited amorphous Iridium Oxide (EIROF) pertains to a class of highly hydrated transition metal oxides with a set of peculiar properties (e.g. low density), bound to their deposition conditions identifying the kinetically most accessible, rather than thermodynamically most stable, form [1].

Quite recently, EIROF was used as electrode material in a series of investigations centered on disclosing the mechanism of oxygen evolution reaction (OER) in combination with in-situ X-Ray Absorption techniques, by taking advantage of the high accessibility of its electrocatalytic sites [2,3]. In particular, it could be proved that for  $E > 1.3$  V (vs RHE), Ir assumes two distinct oxidation states, namely (III) and (V). This is in line with the participation of Ir sites, in the heterogeneous Ir oxide catalyst, to the catalytic cycle as well established for homogeneous catalysis and as described in the scheme and CV here below.



This effect comes not only from the easy accommodation of different oxidation states in IrOx nanoparticles [4], but also from the facilitated ionic transport within the hydrous oxide layer during electron and charge transfer processes.

In the present contribution the behaviour of electrodeposited EIROF nanoparticles, as observed by in-situ dispersive XAS in the pseudo-capacitance region at different pH's and for different polarisation steps, is presented and discussed.

[1] L.D. Burke, M. E. G. Lyons, "Electrochemistry of Hydrous Oxide Films", in Modern Aspects Of Electrochemistry, R. E. White, J. O'M. Bockris, B. E. Conway, 1986 Plenum Press, New York]

[2] A. Minguzzi, O. Lugaresi, C. Locatelli, S. Rondinini, F. D'Acapito, E. Achilli, and P. Ghigna, "Fixed Energy X-ray Absorption Voltammetry", Anal. Chem. 2013, 85, 7009–7013

[3] A. Minguzzi, O. Lugaresi, E. Achilli, C. Locatelli, A. Vertova, P. Ghigna and S. Rondinini "Observing the Oxidation State Turnover in Heterogeneous Iridium-Based Water Oxidation Catalysts", Chem. Sci. 2014, 5, 3591-3597 DOI: 10.1039/C4SC00975D, open access

[4] A. Minguzzi, C. Locatelli, O. Lugaresi, E. Achilli, G. Cappelletti, M. Scavini, M. Coduria, P. Masala, B. Sacchi, A. Vertova, P. Ghigna, S. Rondinini, "Easy Accommodation of Different Oxidation States in Iridium Oxide Nanoparticles With Different Hydration Degree as Water Oxidation Electrocatalysts", ACS Catalysis, submitted



# Electrochemical Surface-Enhanced Raman Microscopy (EC-SERM)

Bin Ren, Cheng Zong, Chanjun Chen, Meng Zhang

*State Key Laboratory of Physical Chemistry of Solid Surface, Collaborative Innovation Center of Chemistry of Energy Materials (iChEM), Department of Chemistry, College of Chemistry and Chemical Engineering, Xiamen University, Xiamen 361005, China*  
E-mail: bren@xmu.edu.cn

Recent development of electrochemistry requires techniques with higher temporal and spatial resolution. Conventional electrochemical methods can only obtain the total current response of the electrode, which cannot fulfill the increasing request to detect the local electrochemical information. Scanning electrochemical microscopy is the most widely used electrochemical technique that is able to obtain the spatial electrochemical information of heterogeneous electrode surfaces. However, the point-scan mode limits its imaging rate. Recently, the combination of high resolution optical imaging techniques such as surface plasmon resonance, fluorescence and dark field scattering with electrochemical methods are receiving increasing interest. However, all these optical methods lack of molecular signature, which can hardly be used in a complex system containing multiple electrochemical active components due to the poor chemical identification and low selectivity.

To address the aforementioned challenges, we developed an electrochemical surface-enhanced Raman microscopy (EC-SERM), which allows us to simultaneously monitor the local electrochemical process with the fingerprint molecular information. We used the intensity of surface-enhanced Raman spectroscopy (SERS) signals of molecule of interest to deconvolute the local faradic current during cyclic voltammetric measurement. The method allowed us to simultaneously monitor the redox process of a mixture, Nile blue and viologen, on a Ag NPs electrode, and successfully reconstructed the independent electrochemical current of these two molecules. In addition, by using line-shape laser, we have been able to obtain the local electrochemical response at different position of the electrode surface. EC-SERM enables local electrochemical measurements with high spatial and temporal resolution, which will be particularly important for the investigation of non-uniform surfaces widely used in some energy-related electrochemical systems.

Acknowledgement: We acknowledge support from NSFC (21227004, 21321062, and J1310024), MOST (2013CB933703 and 2011YQ03012406) and MOE (IRT13036).

# ***operando* synchrotron X-ray analysis for investigation of electrode property of lithium ion battery cathode**

Yoshiharu Uchimoto\* and Yuki Orikasa\*, Zempachi Ogumi\*\*

\*Graduate School of Human and Environmental Studies, Kyoto University

\*\*office of Society-Academia Collaboration for Innovation, Kyoto University  
Kyoto University, Yoshida, Kyoto, 606 Japan  
uchimoto.yoshiharu.2n@kyoto-u.ac.jp

*operando* synchrotron X-ray analysis enables us to clarify the reaction mechanism at lithium ion cathode. In this study, *operando* techniques by using synchrotron X-ray method and its application to lithium battery cathode analysis using their measurement characteristics are demonstrated.

## 1. Dynamics of the phase transition behavior of cathode materials<sup>1-2)</sup>

*operando* analysis enables us to observe dynamic behavior occurring in an operating battery without touching its components and so actual processes associated with charging/discharging can be elucidated. Recently the measuring probes have been much improved and observation at practical charging/discharging rate to 50 C is now available. In this study, in situ techniques by using synchrotron X-ray method and its application to lithium battery analysis using their measurement characteristics are demonstrated.

The (dis)charge reaction of  $\text{LiFePO}_4$  proceeds through a two phase behavior between Li-rich  $\text{Li}_{1-x}\text{FePO}_4$  (LFP) and Li-poor  $\text{Li}_x\text{FePO}_4$  (FP). Phase transition mechanism is analyzed by time-resolved X-ray diffraction (TR-XRD) measurements at various temperatures. For  $\text{LiFePO}_4$  electrodes, we tracked the phase transition behavior under 1C rate charging conditions and figured out that there are various intermediate states between the LFP (discharged) and FP (charged) phases that have not been clarified with ex situ analysis.<sup>1)</sup> The smaller the particle size was, the greater the intermediate states changes until it reached to the thermodynamically stable FP phase. At much higher rate of 10 C, we found a new metastable crystalline phase “ $\text{Li}_x\text{FP}$ ”<sup>2)</sup>. This result shows that such a metastable phase can be a kinetically favorable intermediate when a strong motive force (large polarization) exists. Under high rate cycling, we revealed the formation of a metastable phase of  $\text{Li}_x\text{FePO}_4$  ( $x = 0.6\text{--}0.75$ ) ( $\text{L}_x\text{FP}$ ) which acts as a buffer layer between LFP and FP.<sup>2)</sup>

## 2. *operando* X-ray Absorption Spectroscopic Study on Stability at Electrode / Electrolyte Interface<sup>3-4)</sup>

Lifetimes of lithium-ion batteries are often affected by deterioration of positive electrodes. It is well-known that the deterioration of the positive electrodes can be reduced by using electrolyte additives; however, the mechanism underlying this cyclability improvement needs to be clarified. In this study, we investigate electronic structure at the electrode/electrolyte interface using in situ total-reflection fluorescence X-ray absorption spectroscopy to elucidate the mechanism underlying the cyclability improvement of a  $\text{LiCoO}_2$  electrode. We also clarify the effect of electrolyte addition of vinylene carbonate (VC) to the electrolyte. The results indicate that the reduction of cobalt ions at the surface of the  $\text{LiCoO}_2$  electrode, which occurs upon soaking in the electrolyte in the absence of VC, is suppressed by the presence of the VC additive. The VC additive also suppresses irreversible change in the electronic structure of the cobalt ions at the  $\text{LiCoO}_2$  surface during successive charge/discharge processes. The effects of the VC additive can be attributed to the formation of a layer of decomposed VC molecules at the  $\text{LiCoO}_2$ /electrolyte interface, which plays an important role in the suppression of the irreversibility at the  $\text{LiCoO}_2$  surface during the charge/discharge processes.

## References

- 1) Y. Orikasa, T. Maeda, Y. Koyama, H. Murayama, K. Fukuda, H. Tanida, H. Arai, E. Matsubara, Y. Uchimoto, Z. Ogumi, *Chem. Mater.*, 2013, 25, 1032 – 1039
- 2) Y. Orikasa, T. Maeda, Y. Koyama, H. Murayama, K. Fukuda, H. Tanida, H. Arai, E. Matsubara, Y. Uchimoto, Z. Ogumi, *J. Am. Chem. Soc.*, 2013, 135, 5497 – 5500
- 3) Daiko Takamatsu, Yuki Orikasa, Shinichiro Mori, Takayuki Nakatsutsumi, Kentaro Yamamoto, Yukinori Koyama, Taketoshi Minato, Tatsumi Hirano, Hajime Tanida, Hajime Arai, Yoshiharu Uchimoto and Zempachi Ogumi, *J. Phys. Chem. C*, 2015, accepted,
- 4) Kentaro Yamamoto, Taketoshi Minato, Shinichiro Mori, Daiko Takamatsu, Yuki Orikasa, Hajime Tanida, Koji Nakanishi, Haruno Murayama, Titus Masese, Takuya Mori, Hajime Arai, Yukinori Koyama, Zempachi Ogumi, Yoshiharu Uchimoto, *J. Phys. Chem. C*, 2014, 118, 18, 9538 – 9543

# Electrooxidation mechanism of NH<sub>3</sub> on Pt by in situ FTIR reflection spectroscopy

**Zhi-You Zhou\***, Yu-Hao Hong, Tian Sheng, Jian-Long Lin, Ji Ren, Sheng-Pei Chen, Shi-Gang Sun  
*State Key Laboratory of Physical Chemistry of Solid Surfaces, Department of Chemistry, College of Chemistry and Chemical Engineering, Xiamen University, Xiamen 361005, China*

\*e-mail address: [zhouzy@xmu.edu.cn](mailto:zhouzy@xmu.edu.cn)

Ammonia contains high percentage of hydrogen, and is considered as a potential fuel molecule for fuel cells. Electrooxidation of ammonia on Pt surface is a complex reaction, since it involves a series of possible adsorbed species (NH<sub>2,ad</sub>, NH<sub>ad</sub>, N<sub>ad</sub>), and their couple to form N<sub>2</sub> finally. Although a general reaction mechanism has been proposed as early as 1970 by Gerischer and Mauzerer<sup>[1]</sup>, the spectroscopic evidences of adsorbates are very limitted.

In this presentation, I will talk about our recent studies about NH<sub>3</sub> electrooxidation on Pt by in situ FTIR spectroscopy. We used square-wave electrodeposition to prepare dendritic Pt nanostructure that shows high significantly enhanced infrared absorption for adsorbed species. On such dendritic Pt nanostructure, we successfully detected N-coupled adsorbed species (N<sub>2</sub>H<sub>x,ad</sub>), a key intermediate to form N<sub>2</sub> for NH<sub>3</sub> electrooxidation on Pt. The IR band of this species locates at ~1250 cm<sup>-1</sup> with a Stark tuning rate of 55 cm<sup>-1</sup> V<sup>-1</sup>, and <sup>14</sup>N-<sup>15</sup>N isotopic shift of 2 ~ 3 cm<sup>-1</sup>, indicating it is adsorbed species and contains N-H. DFT calculation shows that NH<sub>2,ad</sub> and NH<sub>ad</sub> have no vibration peaks near 1200 cm<sup>-1</sup>, but N<sub>2</sub>H<sub>x</sub> (x=2-4) species have vibration peaks between 1200 and 1300 cm<sup>-1</sup>. According to calculated free energy diagram of NH<sub>3</sub> oxidation on Pt(100), this species is likely to be N<sub>2</sub>H<sub>x</sub> (x=2, 4). In addition to adsorbed species, a series of solution species, such as N<sub>2</sub>, NO, N<sub>2</sub>O, and NO<sub>2</sub><sup>-</sup> were also detected by in situ FTIR spectroscopy and online electrochemical mass spectrometry (OLEMS). This study is of importance for understanding electrooxidation mechanism of NH<sub>3</sub>.

## References:

[1] H. Gerischer, A. Mauzerer, *J. Electroanal. Chem. Interf. Electrochem.*, 1970, 25, 421.

**Acknowledgements:** This work is supported by NSFC (21373175) and Program for New Century Excellent Talents in University (NECT-11-0301).

# In situ NMR for Electrochemistry

Eric G. Sorte, YuYe J. Tong  
Georgetown University, Department of Chemistry  
37<sup>th</sup> and O Streets NW, Washington DC 20057  
eric.sorte@georgetown.edu

We have developed two novel and potentially groundbreaking new *in situ* methodologies for applications of nuclear magnetic resonance (NMR) spectroscopy to the current research in the fields relevant to electrochemical (EC) energy generation (fuel cells) and storage (Li/Na/Al- ion batteries). NMR features unmatched chemical specificity and accessibility to most elements in the periodic table, and its exquisite technical versatility (i.e., non-invasiveness, applicability to various forms of matters, ability to see the buried interfaces, and access to both static and dynamic information) has made it the spectroscopic method of choice for studying many systems. However, technical incompatibilities between good NMR detection and the presence of conducting materials indispensable to electrochemistry have hampered efforts to apply the full power of NMR to investigations of EC systems. While a handful research groups have been constantly working in this niche of frontier research with well-known technical challenges,<sup>1,2</sup> the last decade has witnessed only incremental progress in the *in situ* applications of NMR to investigating fundamental chemical processes involved in the EC energy generation and storage. Both of our new methods of *in situ* EC-NMR lay the groundwork for bringing the entirety of NMR measurement and imaging power to investigations of electrochemical systems.

## 1. Interdigitated stripshield EC-NMR

The first method employs an **interdigitated electrode stripshield** design that can be realized in a rather straightforward fashion, and is ideal for measuring high-resolution liquid NMR during electrolysis in standard commercial facilities, as no modifications to commercially available NMR equipment is required. Identifying and quantifying electrocatalytic-reaction-generated solution species is highly desirable in terms of understanding the associated mechanisms of a given reaction. We report a straightforward implementation of *in situ* solution electrochemical <sup>13</sup>C and <sup>1</sup>H NMR spectroscopy that for the first time enables *in situ* NMR studies of catalyzed reactions during electrolysis. Using ethanol oxidation reaction (EOR) and bromoanthracene reduction as reaction examples, we demonstrate <sup>13</sup>C and <sup>1</sup>H NMR during electrochemical experiments using our interdigitated gold electrode stripshield EC-NMR design. In addition to demonstrating the feasibility and power of our system, we report new discoveries in EOR on Pt and PtRu black commercial catalysts using our new EC-NMR design.

## 2. Stripline EC-NMR

The second method is based on an **electrically floating stripline** detector, and is well suited to air-sensitive battery and supercapacitor research where the elements of interest are not necessarily in the liquid state. *In situ* NMR studies of metal-ion batteries are traditionally very challenging, and require the use of sophisticated and expensive equipment.<sup>3,4</sup> This EC-NMR design is intended to simplify and improve *in situ* NMR measurements on electrodes and electrolytes of Li, Na, or other metal-ion batteries. We present our design for the stripline EC-NMR probe and demonstrate its utility and simplicity in battery measurements. We show also the feasibility of multi-pulse experiments, which may allow for *in situ* imaging of the storage devices during operation. This method allows the observation and quantification of the growth of metallic microstructures (which can cause short circuits and battery failure), and can be utilized to identify conditions that promote malicious dendrite formation.

[1] Webster, R. D., Anal. Chem. 2004, 76, 1603-1610.

[2] Klod, S., Ziegls, F., Dunsch, L. Anal. Chem. 2009, 81, 10262–10267.

[3] Grey, C. P., Dupre, N. Chem. Rev. 2004, 104, 4493–4512.

[4] Key, B., Bhattacharyya, R., Morcrette, M., Seznec, V., Tarascon, J-M., Grey, C.P. J. Am. Chem. Soc. 2009, 131, 9239–9249.

# ***In situ* visualization of Li<sub>2</sub>O<sub>2</sub> decomposition for a Li–O<sub>2</sub> battery using electrochemical atomic force microscopy (ECAFM)**

Misun Hong,<sup>1,2</sup> Hee Cheul Choi,<sup>2</sup> Hye Ryung Byon<sup>1\*</sup>

<sup>1</sup> Byon Initiative Research Unit (IRU), RIKEN, 2-1 Hirosawa, Wako, Saitama 351-0198, Japan

<sup>2</sup> Center for Artificial Low Dimensional Electronic Systems, Institute for Basic Science (IBS), and Department of Chemistry, Pohang University of Science and Technology (POSTECH), 77 Cheongam-Ro, Nam-Gu, Pohang 790-784, South Korea  
misun.hong@riken.jp, hrbyon@riken.jp

The lithium–oxygen (Li–O<sub>2</sub>) battery has suffered from huge charge polarization ( $> 4.0$  V) due to sluggish oxidation of insulating Li<sub>2</sub>O<sub>2</sub> ( $2\text{Li}^+ + \text{O}_2 + 2\text{e}^- \rightleftharpoons \text{Li}_2\text{O}_2(\text{s})$ ), which accompanies degradation of electrolyte solution and carbonaceous electrode.[1, 2] Understanding the decomposition process of Li<sub>2</sub>O<sub>2</sub> is therefore of important to circumvent low round-trip efficiency in the Li–O<sub>2</sub> battery. However, there is little knowledge for detailed oxidation process. Here, we present *in situ* imaging observation of Li<sub>2</sub>O<sub>2</sub> decomposition during oxidation using electrochemical atomic force microscopy (ECAFM). In a Li–O<sub>2</sub> model cell, highly oriented pyrolytic graphite (HOPG) was used as the working electrode in an O<sub>2</sub> gas-saturated glyme-based electrolyte, which was performed with metallic lithium as the counter and reference electrodes.[3] The AFM probe scanned the surface of HOPG during potential-controlled reduction and oxidation process. During reduction, the Li<sub>2</sub>O<sub>2</sub> film is uniformly formed with  $\sim 3$  nm thickness at 2.2 V (vs. Li/Li<sup>+</sup>). The subsequent oxidation was conducted via anodic linear sweep voltammetry (LSV) at a potential sweep rate of 0.2 mV/s or 0.5 mV/s.

The oxidation process can be separated to two distinct processes at low-potential ( $< \sim 3.7$  V) and high-potential ( $\sim 3.7$ – $4.5$  V) regimes. In the low-potential regime, slow decomposition occurs from thinner spots of Li<sub>2</sub>O<sub>2</sub> film, which results in sparse holes on the film. Further decomposition takes place at the edge of holes. However, its sluggish process restricts the decomposition at local spots, which cannot propagate to the entire Li<sub>2</sub>O<sub>2</sub> film. At the high potential, bulk decomposition of Li<sub>2</sub>O<sub>2</sub> occurs. The total thickness Li<sub>2</sub>O<sub>2</sub> film is promptly decreased and the film completely disappears at  $\sim 4.2$  V.

The high potential required for the bulk oxidation can be curtailed by the addition of a redox mediator. Representatively, the redox mediator of TEMPO ((2,2,6,6-tetramethylpiperidin-1-yl)oxyl)[4] in electrolyte solution is oxidized to TEMPO<sup>+</sup> at a potential of 3.75 V (vs. Li/Li<sup>+</sup>), which then functions as electron acceptor thus chemically triggering the decomposition of Li<sub>2</sub>O<sub>2</sub>. By using the ECAFM imaging during anodic LSV at 0.2 mV/s, we observe that the Li<sub>2</sub>O<sub>2</sub> film is completely decomposed at around 3.76 V with 10 mM of TEMPO, demonstrating decrease in bulk-oxidation potential and fast electron-transfer reaction between TEMPO<sup>+</sup> and Li<sub>2</sub>O<sub>2</sub>. Detailed ECAFM study of Li<sub>2</sub>O<sub>2</sub> decomposition process at the low- and high-potential regimes will be discussed in the presentation.

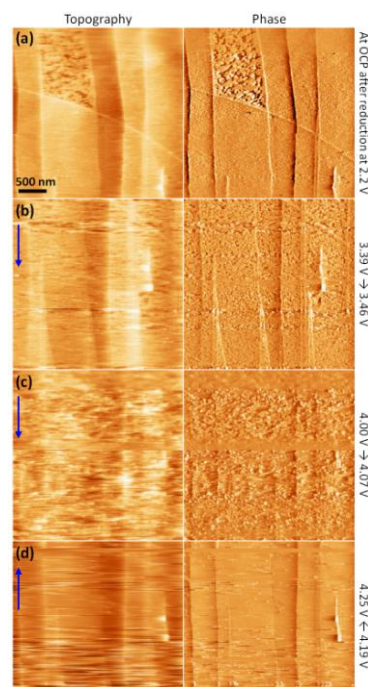


**Figure 1.** *In situ* ECAFM images obtained (a) after reduction at 2.2 V, and (b–d) during anodic LSV at 0.2 mV/s sweep rate. Blue arrows indicate AFM scanning direction. Topography and phase images cover the contrast in the range of 5 nm and 1 deg, respectively.

## References

- [1] B.D. McCloskey, D.S. Bethune, R.M. Shelby, T. Mori, R. Scheffler, A. Speidel, M. Sherwood, A.C. Luntz, Limitations in rechargeability of Li–O<sub>2</sub> batteries and possible origins, *J. Phys. Chem. Lett.*, 3 (2012) 3043–3047.
- [2] M.M. Ottakam Thotiyl, S.A. Freunberger, Z. Peng, P.G. Bruce, The carbon electrode in nonaqueous Li–O<sub>2</sub> cells, *J. Am. Chem. Soc.*, 135 (2013) 494–500.
- [3] R. Wen, M. Hong, H.R. Byon, *In situ* AFM imaging of Li–O<sub>2</sub> electrochemical reaction on highly oriented pyrolytic graphite with ether-based electrolyte, *J. Am. Chem. Soc.*, 135 (2013) 10870–10876.
- [4] B.J. Bergner, A. Schurmann, K. Peppler, A. Garsuch, J. Janek, TEMPO: a mobile catalyst for rechargeable Li–O<sub>2</sub> batteries, *J. Am. Chem. Soc.*, 136 (2014) 15054–15064.

# Multi-scale tomographic analysis of fuel cells, batteries and electrolyzers

*Simon Thiele, Lukas Zielke, Riko Moroni, Severin Vierrath, Matthias Klingele and Roland Zengerle*  
Laboratory for MEMS Applications, IMTEK - Department of Microsystems Engineering, University of  
Freiburg Address: Georges-Köhler-Allee 103, 79110 Freiburg, Germany  
e-mail address: [simon.thiele@imtek.de](mailto:simon.thiele@imtek.de)

Electrochemical systems such as batteries, fuel cells, or electrolyzers typically exhibit performance-relevant morphological features on different length scales (e. g. nano and micro porosity in battery electrodes, Figure 1 A) [1–3]. Imaging on these length scales is covered by various tomographic techniques, such as X-ray tomography (Xt), focused ion beam / scanning electron microscopy tomography (FIB/SEMt), transmission electron microscopy tomography (TEMt) and atom probe tomography (APT) (Figure 1 B).

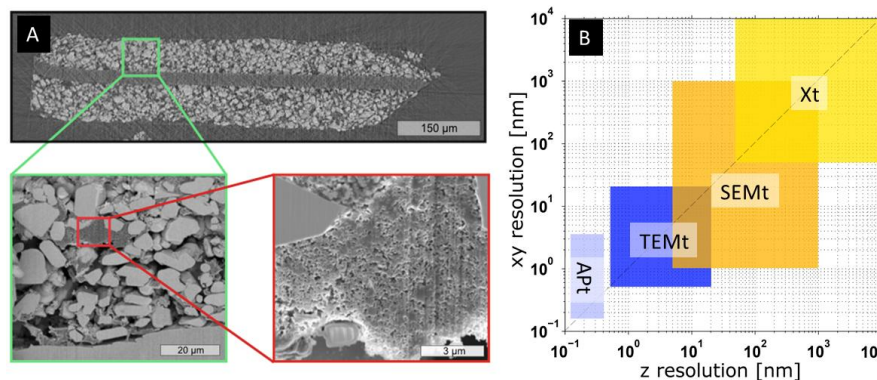


*Figure 1 A) Top-down images of the three-phase configuration of a  $\text{LiCoO}_2$  battery electrode (X-ray tomogram and two scales of FIB-SEM imaging). Each imaging approach reveals different morphological features of the battery. B) shows lateral resolution (x- and y-direction) and z-resolution of various tomographic approaches. For a specific resolution only a limited number of tomographic methods can be used.*

For hierarchical structures on multiple length scales, the use of different tomographic approaches is usually necessary, resulting in multi-scale analysis. However, a variety of challenges arises with the use of tomographic approaches: i) Transport parameter calculation is not straight forward, as physically correct solvers are often either not available or too costly by means of calculation time. ii) The validation of results obtained by tomographic imaging is essential to enable correct interpretation. In many cases, this can solely be performed virtually by inverse approaches (e.g. [4]). iii) To combine information from different length scales, additional tools are necessary (e. g. spatio-statistical modeling [1]).

Within this talk, multi-scale tomographic approaches and challenges for various electrochemical systems are discussed: i) For Lithium-metal-oxide electrode reconstruction we show that multi-scale approaches are necessary if transport parameters extracted from tomographic reconstructions are supposed to be meaningful. ii) For polymer electrolyte membrane (PEM) fuel cells we demonstrate that multi-scale reconstruction is not only important for the whole cell, but also already for their individual components, such as catalyst layers. iii) For PEM electrolyzers, we show first results for tomographic reconstructions and place emphasis on the importance of future works on multi-scale reconstruction.

## References

- [1] S. Thiele, T. Fürstenhaupt, D. Banham, T. Hutzenlaub, V. Birss, C. Ziegler, R. Zengerle, J. Power Sources 228 (2013) 185–192.
- [2] L. Zielke, A. Fallisch, N. Paust, R. Zengerle, S. Thiele, RSC Adv 4 (2014) 58888–58894.
- [3] L. Zielke, T. Hutzenlaub, D.R. Wheeler, C.-W. Chao, I. Manke, A. Hilger, N. Paust, R. Zengerle, S. Thiele, Adv. Energy Mater. 5 (2015) n/a.
- [4] M. Klingele, R. Zengerle, S. Thiele, J. Power Sources 275 (2015) 852–859.



# A Long Duration Experiment Facility for the Study of Battery Materials Using In Situ Synchrotron X-Ray Powder Diffraction

Sarah Day<sup>1</sup>, Annabelle Baker<sup>1</sup>, Chiu Tang<sup>1</sup>, Claire Murray<sup>1</sup>, Stephen Thompson<sup>1</sup>

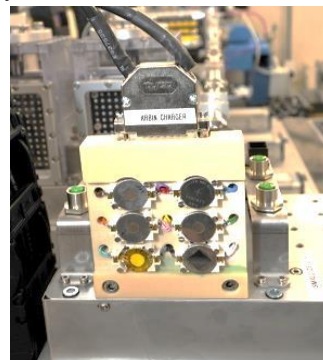
<sup>1</sup>*Diamond Light Source*

*Harwell Science and Innovation Campus, Didcot, Oxfordshire, OX11 0DE*

[sarah.day@diamond.ac.uk](mailto:sarah.day@diamond.ac.uk)

The use of in-situ X-Ray Powder diffraction for the study of new battery materials has grown in recent years and has proven to be an extremely useful technique for the in operando study of new battery materials, providing an insight into the complex processes that take place during charge/discharge cycling. Typical in situ experiments using existing facilities are, however, often limited to short periods of time, from a few hours up to a few (2-3) days, and therefore only allow one long cycle or multiple very fast cycles to be observed. The result is that the material characteristics may be well understood for the first cycle but little is known about the long term processes that ultimately lead to failure of the cell over longer timescales.

The Long Duration Experiment (LDE) Facility on Beamline I11 at Diamond Light Source (UK) is the first of its kind, housing experiments that require periodic, in-situ monitoring over periods of months to years. With a specially designed coin cell holder (right) and a dedicated multi-channel battery charger, it is an ideal facility for the long term study of both existing and next generation battery materials. This setup allows data to be collected over many hundreds of cycles at more realistic rates, without the need for accelerated cycling, therefore better simulating battery use under real-life conditions.



Previous in-situ diffraction experiments of battery materials have generally involved using unconventional battery cells - loading battery materials into capillaries or Swagelok cells, for example, and while these are effective and excellent for fundamental research, they are not real batteries and are not desirable for long duration experiments. We have therefore modified standard coin cells to allow the transmission of X-rays, while also remaining impermeable to air and moisture for long periods of time. Preliminary data from the modified cells, confirming their suitability for long duration, in-situ experiments will be presented, along with further details of the LDE facility and its suitability for the study of battery materials.

# From Quantitative Differential Electrochemical Mass Spectrometry Experiments to Electrochemical Surface Reaction Models

Fabian Kubannek, Ulrike Krewer

TU Braunschweig

Franz-Liszt-Str. 35, Braunschweig, Germany

f.kubannek@tu-braunschweig.de, u.krewer@tu-braunschweig.de

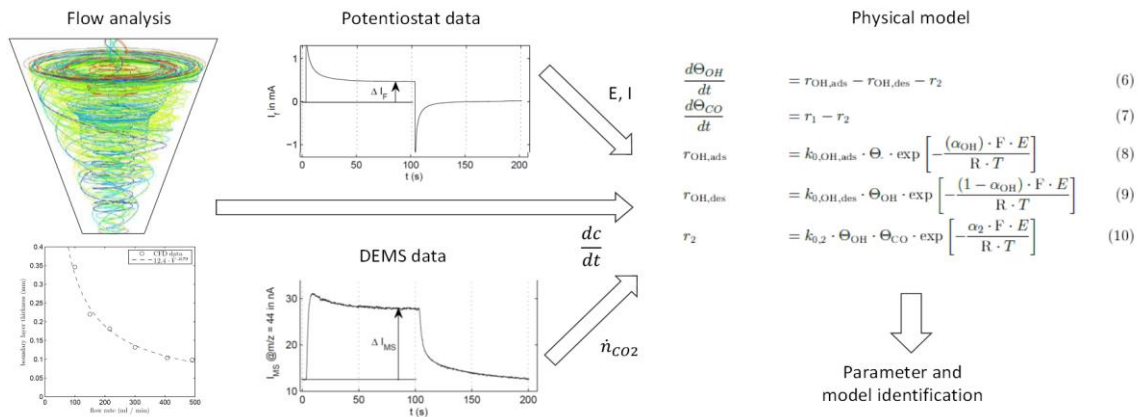
Understanding the micro- and makrokinetics of electrochemical reactions in detail is essential for the development, model-based analysis, and optimization of electrocatalysts and devices such as fuel cells and batteries. Physical modelling is a tool which is often employed to better understand reaction kinetics and determine rate constants by fitting model parameters to experimental data. However, since physical models often require numerous parameters to be determined, monitoring potential and current only – for example during a CV – provide only restricted insight and limited reliability of the fitted parameters. In this work we present how to produce more reliable quantitative models of electrochemical surface reactions by using Differential Electrochemical Mass Spectrometry (DEMS) to monitor in situ not only electric quantities but also product and intermediate formation rates.

Quantitative modeling and analysis of reaction kinetics requires to minimize response times of the DEMS. Moreover, the reactant flow within the electrochemical cell and the concentration distribution over the electrode need to be defined and well-known so that mass transfer effects can be taken into account. We designed a new cell, a DEMS cyclone flow cell, for quantitatively detecting products of electrochemical reactions with a low response time.

The newly designed cell features a well-defined flow regimen and response times of well below one second, enabling dynamic DEMS measurements. While quantitative DEMS studies in the past (eg. [1]) have mostly assessed conversion efficiencies for different products in steady state or during CVs at low scan rates we combined for the first time dynamic measurements such as potential step response measurements and impedance techniques with DEMS to better resolve different timescales.

The new cyclone flow cell and the DEMS setup are presented along with calibration results, and the influence of reactant concentration on the calibration constants for reaction products is analyzed. In order to extract kinetic data from measurements, mass transfer and kinetic effects need to be separated. Thus, the concentration distribution in the cell is analyzed closely. CFD simulations and experimental analysis of electrolyte flow and mass transfer in the cyclone flow cell are presented. We obtain a nearly homogeneous concentration boundary layer over 75% of the electrode surface and demonstrate how to use this information to set up a physical model that describes the concentration in the concentration boundary layer. The physical model furthermore contains differential equations for the surface coverages of adsorbed species, adsorption and desorption steps as well as reaction steps. Rate constants are obtained by fitting simulated faradaic currents and product formation rates to measured currents and DEMS data using the oxidation of small organic molecules as example reactions.

Our work expands the scope of DEMS to dynamic measurements and opens up a way to fit model parameters more reliably to experimental data by in situ monitoring of product formation rates. Thus, our approach provides a valuable tool for analyzing reaction kinetics, setting up and parameterizing physical models, and determining rate constants.





# In-situ $^{13}\text{C}$ NMR spectroscopy study of ethanol electro-oxidation on Pt and PtRu

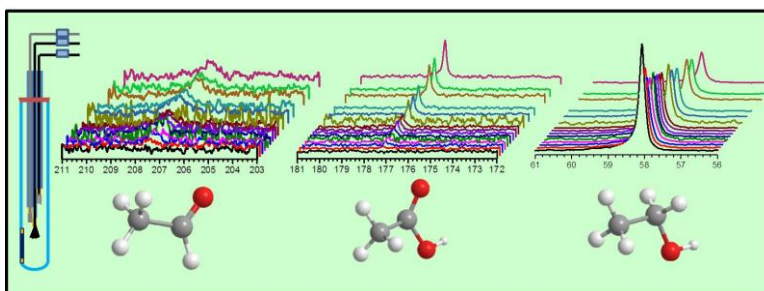
Long Huang,<sup>ab</sup> Eric G. Sorte,<sup>b</sup> YuYe Tong<sup>\*b</sup> and Shi-gang Sun<sup>\*a</sup>

<sup>a</sup>Departments of Chemistry and State Key Laboratory for Physical Chemistry of Solid Surfaces, Xiamen University, Xiamen 361005, P. R. China. E-mail: [sgsun@xmu.edu.cn](mailto:sgsun@xmu.edu.cn)

<sup>b</sup>Department of Chemistry, Georgetown University, 37th & O Streets,NW, Washington, DC 20057, USA. E-mail: [yyt@georgetown.edu](mailto:yyt@georgetown.edu)

Nuclear magnetic resonance (NMR) spectroscopy is powerful in identifying and quantifying chemical species, especially for those containing carbon and hydrogen atoms, and is prevalingly used in organic chemistry. However, it has rarely been applied to electrochemistry due largely to the intrinsic incompatibility between NMR detection coil and the electrical conduction necessary for electrochemical reactions. Recently, Dunsch et al. studied electrochemical redox reaction by acquiring in-situ sampling  $^1\text{H}$  NMR spectra through designing a novel combined electrochemical-NMR (EC-NMR) cell configuration and adopting carbon fiber as working electrode.<sup>[1]</sup>

By slightly modifying the Dunsch's configuration, we carried out, for the first time, an in-situ  $^{13}\text{C}$  NMR spectroscopic study of ethanol electrooxidation reaction (EOR). An ampule containing a known amount of  $^{13}\text{C}$ -label octanethiol was used as an internal reference for quantitative analysis. The position of the carbon fiber with respect to the NMR detection coil is critical to the NMR measurements. Placing the end the carbon fiber just above the detection coil was found to be the best compromise between NMR detection and electrochemical operation. By physical deposition of commercial (Johnson Matthey) platinum black (Pt black-JM) and platinum ruthenium black (PtRu black-JM) onto the carbon fiber, EOR at 250mV vs a Ag/AgCl wire was followed by  $^{13}\text{C}$  NMR over a period of 24 hours during which the spectra were recorded with a time interval of 1 hour before and of 2 hours after 8-hour mark. The peak at 58ppm is assigned to carbon atoms bound to the hydroxy group of ethanol, which diminished as the EOR continued, indicating a consumption of ethanol. Simultaneously, acetic acid ( $\text{CH}_3^*\text{COOH}$ ) at 177ppm and acetaldehyde ( $\text{CH}_3^*\text{CHO}$ ) at 208ppm were detected respectively. By quantitative analysis of the time-resolved  $^{13}\text{C}$  NMR spectra recorded during EOR on Pt black and PtRu black, we discovered that (1) the complete oxidation of ethanol to  $\text{CO}_2$  only took place dominantly at the very beginning of a potentiostatic chronoamperometric (CA) measurement, and (2) the PtRu black has a much higher activity in catalyzing oxygen insertion reaction that leads to acetic acid.



**Acknowledgements.** This work was supported by NSFC (21229301 and 21321062), DOE-BES (DE-FG02-07ER15895), Xiamen University Graduate School and Georgetown College and graduate School.

## References

- [1] S. Klod, F. Ziegls, L. Dunsch, *Analytical Chemistry* **2009**, *81*, 10262-10267.

# ***In-situ* identification of electrochemical oxidation of Pt(111) and Pt(100) by Raman spectroscopy assisted by DFT calculation**

Yi-Fan Huang and Marc T. M. Koper

*Leiden Institute of Chemistry, Leiden University, Einsteinweg 55, P.O. Box 9502, 2300 RA Leiden, The Netherlands*

*E-mail: y.huang.13@chem.leidenuniv.nl*

Towards the fundamental understanding of the mechanism of degradation of Pt catalysts in electrochemical oxygen reduction reaction, we employed *in-situ* shell-isolated nanoparticles-enhanced Raman spectroscopy to identify the intermediate stages of the electrochemical oxidation of Pt(111) and Pt(100) single crystal at the molecular level. DFT calculations were carried out to assist in assigning the experimental Raman spectra by simulating the vibrational frequencies of possible intermediates and products.

Figure 1a represents a cyclic voltammogram of Pt(111) in 0.1 mol/L HClO<sub>4</sub> electrolyte. The oxidation of Pt(111) can be divided into different three stages, according to the characteristic peaks. Figure 1b shows typical Raman spectra acquired in these stages. A single band with a frequency of 922 cm<sup>-1</sup> can be seen at 0.8 V, whose frequency is closed to that of symmetric stretching of Cl-O of ClO<sub>4</sub><sup>-</sup>. Thus, the adsorption of ClO<sub>4</sub><sup>-</sup> appears to be involved in the formation of OH species on surface at the potential span between 0.5 V and 0.9V. When the potential is stepped to 1.0 V, the bands at 240 cm<sup>-1</sup>, 956 cm<sup>-1</sup> and 1169 cm<sup>-1</sup> replace the stretching of Cl-O. To the best of our knowledge, this is the first report of these bands. Thus, we relied on the DFT calculation of possible surface species. We found the superoxo-like species represent quite similar vibration frequency of stretching modes of O-O and Pt-O (not shown), as shown in figure 1c. It has been found the Raman intensity stretching mode of O-O is usually strong. Therefore, we propose a superoxo-like 2D surface oxide form at the potentials between 1.0 V and 1.2 V. At the potentials above 1.3 V, a new broad band at *ca.* 600 cm<sup>-1</sup> appears. According to the normal Raman spectra of PtO<sub>2</sub> and hydrated PtO<sub>2</sub>, the new band can be assigned to the amorphous 3D PtO<sub>2</sub> species. Our measurements elucidate the entire process of the electrochemical oxidation of Pt single crystals corresponding to cyclic voltammogram. We will include results and discussions on Pt(100) and polycrystalline Pt.

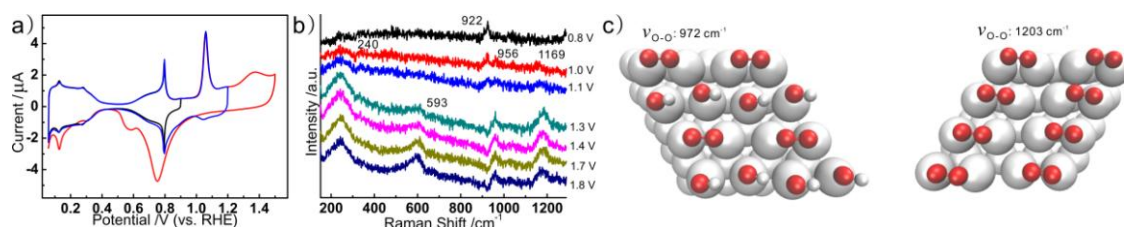


Figure 1 a) Cyclic voltammogram of Pt(111) in 0.1 mol/L HClO<sub>4</sub>; b) Potential dependent Raman spectra of Pt(111) covered by Au@SiO<sub>2</sub> nanoparticles in 0.1 mol/L HClO<sub>4</sub>; c) Superoxo-like surface oxide on Pt(111) surface simulated by DFT calculation.

## **Acknowledgement:**

This work was supported by The Dutch National Research School Combination Catalysis Controlled by Chemical Design (NRSC-Catalysis) and European Commission Horizon 2020 - Research and Innovation Framework Programme (Marie Skłodowska-Curie actions Individual Fellowship)

## **Reference:**

Y. F. Huang, M. T. M. Koper, *in preparation*.

# Complementary operando XPS and Raman spectroscopy of graphite cycled in ionic liquids

D. Streich, P. Novák, M. El Kazzi  
 Paul Scherrer Institut, Electrochemistry Laboratory,  
 CH-5232 Villigen PSI, Switzerland  
 mario.el-kazzi@psi.ch

It was recently demonstrated that the reversibility of the graphite cycling is significantly improved in presence of bis(fluorosulfonyl)imide ([FSI]<sup>-</sup>) [1]. In order to understand the origin of this beneficial effect, Raman [2] and XPS [3] analyses were employed as two complementary operando techniques to monitor structural changes in the bulk and the evolution of the chemical surface composition, respectively. Graphite particles and HOPG were used as model electrodes for Raman and XPS, respectively. These were cycled in 1-ethyl-3-methylimidazolium / bis(trifluoromethanesulfonyl)imide ([EMIM][TFSI]) ionic liquid electrolyte with either 1 M LiTFSI or 1 M LiFSI salt. The Raman outcomes show that [EMIM]<sup>+</sup> competes strongly with Li<sup>+</sup> for intercalation sites in graphite so that Li<sup>+</sup> intercalation only takes place at a detectable level in presence of [FSI]<sup>-</sup> (Figure 1.a). The in situ XPS measurement at the interface IL/electrode indicates that both [TFSI]<sup>-</sup> and [EMIM]<sup>+</sup> undergo reductive decomposition reactions during cycling and form a solid surface layer (Figure 1.b). Based on these results a model describing the mechanism behind the cycling improvement in presence of FSI<sup>-</sup> will be presented.

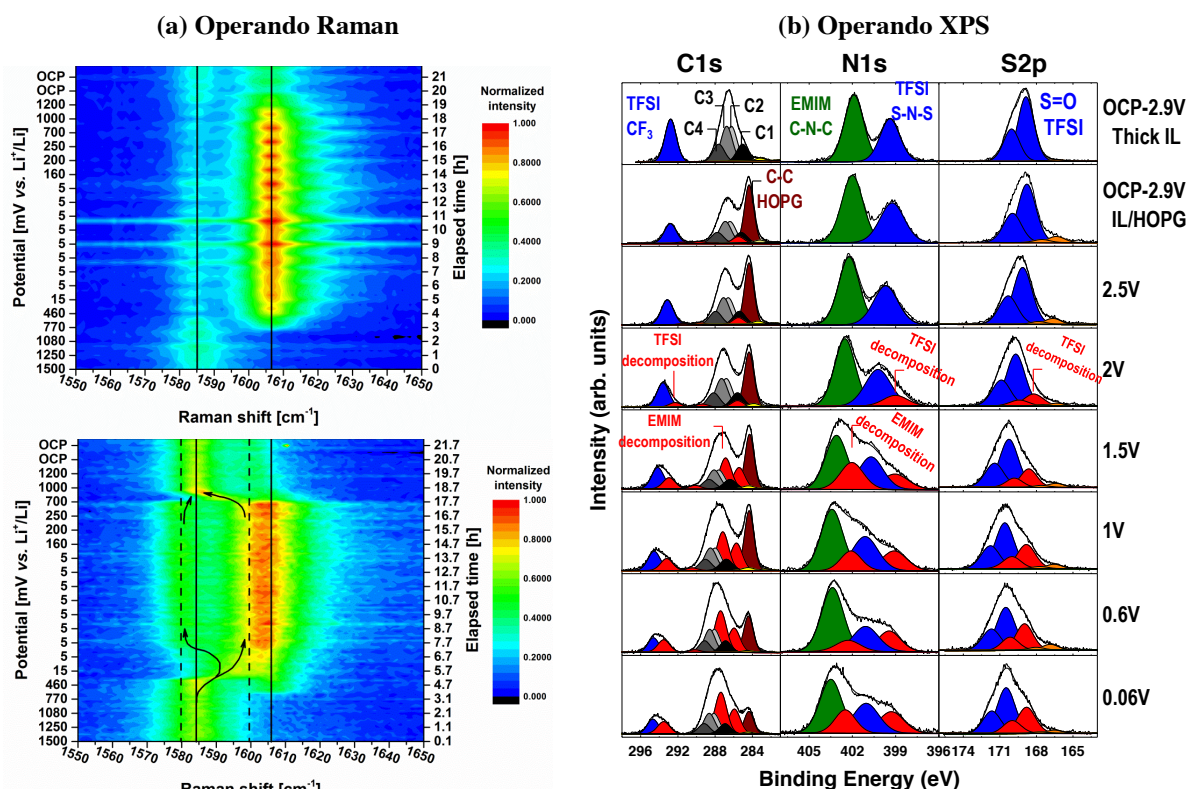


Figure 1: (a) Operando Raman characterization of a graphite particle cycled in discrete potential steps against Li metal in 1 M LiTFSI / [EMIM][TFSI] (top) and 1 M LiFSI / [EMIM][TFSI] (bottom). (b) Operando XPS spectra acquired at the interface electrolyte/electrode during the first reduction of HOPG against Li metal in 1 M LiTFSI / [EMIM][TFSI].

- [1] M. Ishikawa, et al, *Journal of Power Sources* **162**, 658-662 (2006)
- [2] P. Lanz, P. Novák, *J. Electrochem. Soc.* **161**, 10, A1555-A1563 (2014)
- [3] D. Weingarh, A. Foelske-Schmitz, A. Wokaun, R. Kötz, *Electrochem. Commun.* **11**, 619-622 (2011)

# The time and current-resolved evolution of sodium location and distribution in electrodes of sodium-ion batteries

Neeraj Sharma

UNSW Australia

School of Chemistry, UNSW Australia, Sydney NSW 2052 Australia

[Neeraj.sharma@unsw.edu.au](mailto:Neeraj.sharma@unsw.edu.au)

Electrochemical energy storage devices in the form of batteries are ubiquitous in society providing portable power solutions. There is a continuous drive for the improvement of batteries. A large proportion of the function of batteries arises from the electrodes, and these are in turn mediated by the atomic-scale perturbations or changes in the crystal structure during an electrochemical process (e.g. battery use). Therefore, a method to both understand battery function and improve their performance is to probe the crystal structure evolution *in situ* or *operando* - while an electrochemical process is occurring inside a battery.

Our work has used the benefits of *in situ* X-ray diffraction to probe structural-electrochemical evolution of different batteries types, such as primary lithium and ambient temperature rechargeable sodium-ion batteries. For sodium-ion batteries we are able to literally track the time-resolved evolution of sodium in cathode materials such as  $\text{Fe}[\text{Fe}(\text{CN})_6]_{1-x} \cdot y\text{H}_2\text{O}$ ,  $\text{FeCo}(\text{CN})_6$ , and  $\text{Na}_3\text{V}_2\text{O}_{2x}(\text{PO}_4)_2\text{F}_{3-2x}$  (Figure 1). In these systems, we have been able to directly relate electrochemical properties such as capacity, battery history, electrolyte influence and asymmetry in the charge/discharge potential profiles to the content, distribution and evolution of sodium in the cathode crystal structure.

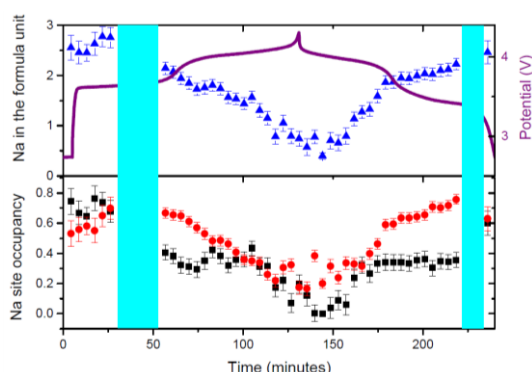


**Figure 1.** Evolution of the occupancy of the Na(1) (red circles) and Na(2) (black squares) sites and total sodium content (blue triangles) in  $\text{Na}_3\text{V}_2\text{O}_{2x}(\text{PO}_4)_2\text{F}_{3-2x}$   $x = 0.8$ . Shaded regions are two phase regions.

Additionally, we have used neutron diffraction which shows good sensitivity towards lithium, to probe the evolution of electrodes in rechargeable lithium-ion batteries. Again, we are able to track lithium evolution during battery function (Figure 2).

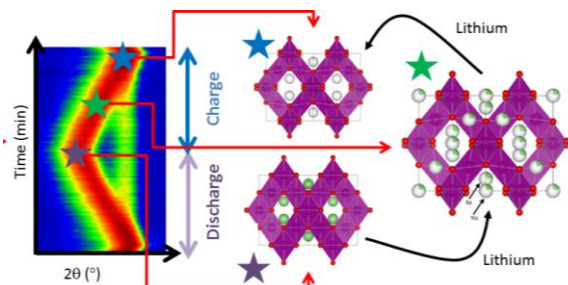


**Figure 2.** A (left) selected reflection of the cathode (dark red) evolving as a function of time, correlated to the charge and discharge process in the battery. Snapshots (right) of the cathode crystal structure at various potentials during charge. Lithium is shown in green with shading indicating lithium occupancy and  $\text{MnO}_6$  octahedra are purple.

*In situ* experiments that probe the time-resolved structural evolution during charge/discharge provide unparalleled insight into how electrodes evolve. Using this information a comprehensive atomic-scale picture of battery functionality can be created and permutations can be made to the electrodes that optimize battery performance. This talk will showcase some of our recent results on electrode structural evolution with respect to electrochemistry in fully functioning batteries.

# Investigation of Solid Electrolyte Interface of Silicon Electrode in Li-ion Batteries by Dual-Electrode Scanning Probe

Chen-Yuan Lu(盧鎮遠), Yu-Lun Cheng(鄭毓倫), Bernard HaoChih Liu(劉浩志)<sup>†</sup>

Department of Materials Science and Engineering, National Cheng Kung University, Taiwan

<sup>†</sup> Corresponding author, Tel : (06)2757575#62926 ; E-mail address: [hcliu@mail.ncku.edu.tw](mailto:hcliu@mail.ncku.edu.tw)

Silicon electrode in Li-ion batteries is an attractive material because of its high theoretical specific capacity ( 4200 mAh/g ) as compared to that of the commercial graphitic carbons ( 372 mAh/g ). However, the large charge-discharge volume change of silicon makes it very challenging to form a stable solid electrolyte interface (SEI), whose stability has strong influence on the cycle life of Li-ion battery.. As it is difficult to observe *in-situ* status of SEI, a new method to characterize and analyze the condition of SEI is very much desired. In this study, we have developed a dual-electrode scanning probe (DESP) by microfabrication (Fig. 1). The two probes of DESP confine the electric current on the surface of silicon electrode. We also combined the micromanipulators and the electrochemical impedance spectroscopy (EIS) to establish *in-situ* measurement of the microscopic electrical property of SEI on the silicon electrode (Fig. 2). The DESP can measure the impedance in a single particle due to the micro scale of this special probe. With different degree of discharge time and charge-discharge cycles, the EIS results can help us to understand the forming mechanism of SEI on the Si electrode in more detail (Fig.3).

**Keywords:** silicon electrode, solid electrolyte interface, dual-electrode scanning probe, electrochemical impedance spectroscopy, microscopic electrical property, in situ

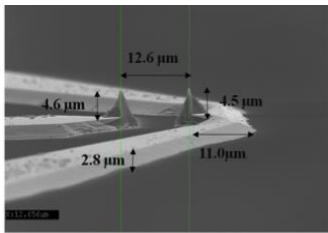


Fig.1 dual-electrode scanning probe. (Patent applications in progress)

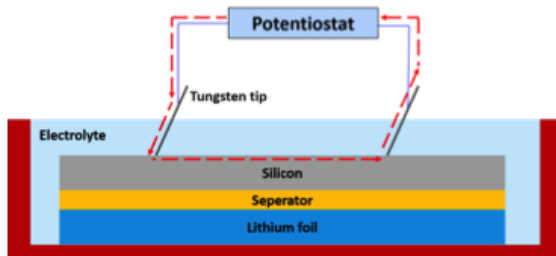


Fig.2 Schematic representation of “exposed cell” assembling with micro-dual-electrode scanning probe.

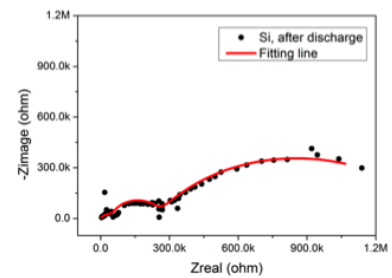


Fig. 3 EIS of backside Si electrode after discharge and its equivalent circuit.



# Effects of Alkali Metal Cation on the Phase Transformation of $\alpha$ -Ni(OH)<sub>2</sub> by Electrochemical Quartz Crystal Microbalance and *in situ* Raman Spectroscopy

Tzu-Ho Wu<sup>†,‡</sup>, Jia-Cing Chen<sup>†</sup>, Chun-Tsung Hsu<sup>†</sup>, Laurence J. Hardwick<sup>\*,‡</sup>, and Chi-Chang Hu<sup>\*,†</sup>

<sup>†</sup> Department of Chemical Engineering, National Tsing Hua University, Hsin-Chu, 30013 TAIWAN

<sup>‡</sup> Department of Chemistry, Stephenson Institute for Renewable Energy, The University of Liverpool, Crown Street, Liverpool, L69 7ZD, UK

\*E-mail: [hardwick@liverpool.ac.uk](mailto:hardwick@liverpool.ac.uk); \*E-mail: [cchu@che.nthu.edu.tw](mailto:cchu@che.nthu.edu.tw);

Cation effects on the phase transformation and redox retention of  $\alpha$ -Ni(OH)<sub>2</sub> are demonstrated through the electrochemical quartz crystal microbalance (EQCM) and *in situ* Raman spectroscopy in LiOH, NaOH, and KOH.  $\alpha$ -Ni(OH)<sub>2</sub> was synthesised by cathodic deposition. From the literature [1,2], the redox mechanism of  $\gamma$ -NiOOH/ $\alpha$ -Ni(OH)<sub>2</sub> involves alkali and hydroxyl ions intercalation/de-intercalation, while  $\beta$ -NiOOH/ $\beta$ -Ni(OH)<sub>2</sub> only involves proton. Mass change (Fig. 1) related to cation intercalation can be clearly observed in LiOH for 10 cycles, while in KOH, it involves proton during the charge/discharge process. The strong A<sub>1g</sub> mode around 3580 cm<sup>-1</sup> is the signature of  $\beta$ -Ni(OH)<sub>2</sub>. *In situ* Raman spectra (Fig. 2) demonstrated the fast phase transformation from  $\alpha$ -Ni(OH)<sub>2</sub> to  $\beta$ -Ni(OH)<sub>2</sub> in KOH. The order of cations with respect to inducing the phase transformation is: K<sup>+</sup> > Na<sup>+</sup> > Li<sup>+</sup>. Due to the unstable  $\gamma$ -NiOOH structure with insufficient intercalated K<sup>+</sup>, the rapid phase transformation to a predominant phase of  $\beta$ -Ni(OH)<sub>2</sub> with severe structure deformation is obtain in KOH. In LiOH, Li<sup>+</sup> forms a larger size of hydrated ion in  $\gamma$ -NiOOH structure, which retains the water molecules in the inter-slab space to perform  $\gamma$ -NiOOH/ $\alpha$ -Ni(OH)<sub>2</sub> redox reaction. This work emphasizes the important electrolyte design for Ni(OH)<sub>2</sub> in its wide range of applications; e.g., the rechargeable batteries, supercapacitors, oxygen reduction reaction, and electrochromic devices.

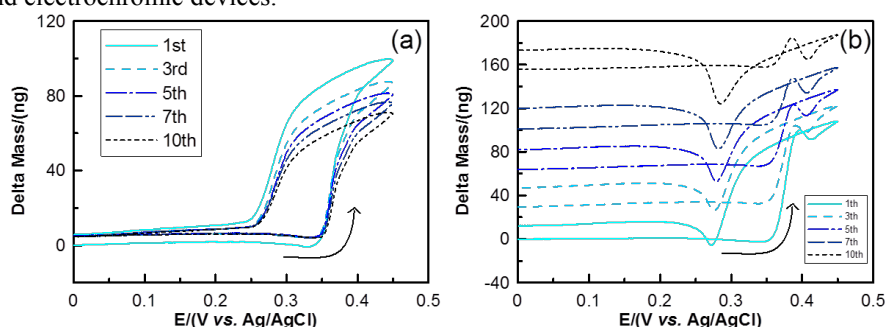


Fig. 1 EQCM  $\Delta m$  - E curves of  $\alpha$ -Ni(OH)<sub>2</sub> in 1 M (a) LiOH and (b) KOH for 10 cycles at 10 mV s<sup>-1</sup> after 10 preceding cycles at 5 mV s<sup>-1</sup>.

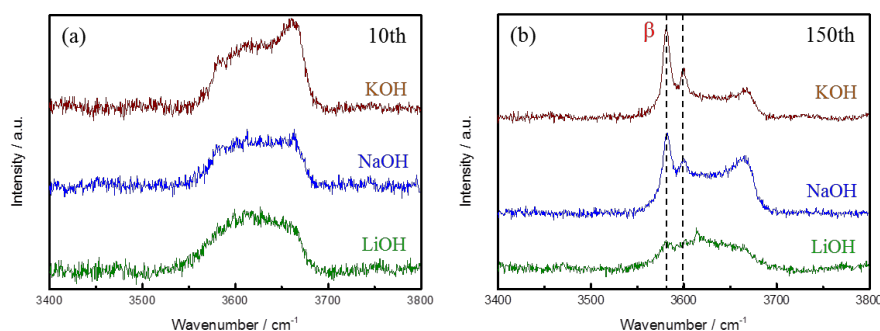


Fig. 2 *In situ* Raman spectra recorded after (a) 10 and (b) 150 CV cycles at 10 mV s<sup>-1</sup> in LiOH, NaOH, and KOH.

[1] M.S. Kim, K.B. Kim, *J. Electrochem. Soc.*, 145 (1998) 507-511.

[2] S.I. Cordoba-Torresi, C. Gabrielli, A. Hugot-Le Goff, R. Torresi, *J. Electrochem. Soc.*, 138 (1991) 1548-1553.

# Analysis of the Surface Structure and Catalytic Behavior of Cr-modified Ni Surfaces for Fuel Cells

Patrick Faubert<sup>1</sup>, Ivan Kondov<sup>2</sup>, ~~and~~ Claas Müller<sup>1</sup>, Holger Reinecke<sup>1</sup>, Peter Smyrek<sup>3</sup>, Johannes Proell<sup>3</sup>,  
~~and~~ Wilhelm Pfleging<sup>3</sup>

<sup>1</sup>University of Freiburg, Department of Microsystems Engineering – IMTEK,  
Laboratory for Process Technology, Georges-Köhler-Allee 103, 79110 Freiburg, Germany

<sup>2</sup>Steinbuch Centre for Computing, Karlsruhe Institute of Technology,

Hermann-von-Helmholtz-Platz 1, 76344 Eggenstein-Leopoldshafen, Germany, [ivan.kondov@kit.edu](mailto:ivan.kondov@kit.edu)

<sup>3</sup>Karlsruhe Institute of Technology KIT, Institute for Applied Materials,  
D-76344 Eggenstein-Leopoldshafen, Germany

One appealing form of integrated energy storage is the use of H<sub>2</sub>/air, a so-called fuel cell type (FC) battery. Such devices promise very high volumetric energy densities of more than 2000 Wh/l. Consequently, this type of battery has recently attracted more attention and primary as well as secondary cells have been realized. Oxygen reduction reaction (ORR) is an important process on the cathode of polymer electrolyte fuel cells [1]. ~~Particularly interesting is employing an alkaline polymer electrolyte fuel cell which brings the possibility to use non-noble metals as catalysts. Pickrahn et al. have used active MnO<sub>2</sub> electrocatalysts prepared by atomic layer deposition (ALD) for OER and ORR and oxygen evolution reaction (OER) [2].~~ Further improvements for these kinds of fuel cells have to be reached with respect to high power.

To this end, a promising approach is to increase the skin surface of porous chromium decorated nickel electrodes for enhancement of exchange current density by forming three-dimensional (3D) microstructures directly into the electrode. A novel laser structuring process was applied using ultrashort laser pulses. Ultrashort laser processing of complex multi-material systems for energy storage allow for precise material removal without changing the material properties. By applying this novel laser-based structuring technique, 3D microstructures could be formed permitting shortened diffusion lengths between the electrolyte and the electrode surface being necessary for increased exchange current densities (see Fig. Figure 1-1 Fig.1). The catalytic activity determines the exchange current density which is limiting factor of the whole cell performance. Modelling of the reactive surface at the atomistic scale is essential for understanding the effects of Cr on catalytic activity and optimizing the device function. Nevertheless, constructing adequate atomistic models for the oxygen reduction reaction on the cathode requires ~~determination of that~~ the composition, i.e. the amount and distribution of Cr on the surface and/or in the topmost layers at the surface, as well as ~~elucidation of~~ the structure of the surface ~~have to be elucidated~~. In this contribution, we combine x-ray photoelectron spectroscopy (XPS) data ~~of from the~~ experimental investigations of the Cr-modified Ni electrode with core-level shifts computed using density functional theory in order to estimate the amount and ~~determine the chemical~~ oxidation state of Cr on the catalyst surface, and ~~thus~~ develop atomistic models commensurate with the distribution of Cr on the surface and in the topmost atomic layers. In addition, the XPS data allow estimates of the locations and surface coverage by atomic oxygen. Amount of surface atomic oxygen O is known to be important not only for the catalytic activity but also for the stability of the electrode. These data enable modelling of the reaction rates under cell operating conditions which in turn allows deriving a design strategy for cell performance enhancements and creates an essential bridge between theory and experiment.

**Acknowledgements:** This work was supported by the Berthold Leibinger Stiftung as a carrier of the Fritz-Hüttinger scholarship. Support for laser processing by the Karlsruhe Nano Micro Facility (KNMF, <http://www.knmf.kit.edu>) a Helmholtz research infrastructure at the Karlsruhe Institute of Technology is gratefully acknowledged. ~~Simulations were performed on the computational resource bwUniCluster funded by the Ministry of Science, Research and the Arts Baden-Württemberg and the Universities of the State of Baden-Württemberg, Germany, within the framework program bwHPC.~~



**Figure 1: 3D structured Cr-doped Ni(111) surface.**

Mis en forme : Police :11 pt

Mis en forme : Soulignement ,  
Allemand (Allemagne)

Mis en forme : Allemand (Allemagne)

Mis en forme : Allemand (Allemagne)

Mis en forme : Allemand (Allemagne)

[1] M. Eikerling and A. Kulikovsky, Polymer Electrolyte Fuel Cells: Physical Principles of Materials and Operation, Taylor & Francis (2014).  
[2] K. L. Pickrahn, S. W. Park, Y. Gorlin, H. B. R. Lee, T. F. Jaramillo, S. F. Bent, Adv. Energy Mat. 10, 1269–1277 (2012).

[1] M. Eikerling, A. Kulikovsky, Polymer Electrolyte Fuel Cells: Physical Principles of Materials and Operation, Taylor & Francis, 2014.  
[2] K.L. Pickrahn, S.W. Park, Y. Gorlin, H.-B.-R. Lee, T.F. Jaramillo, S.F. Bent, Advanced Energy Materials, 2 (2012) 1269-1277.

Mis en forme : Police :9.5 pt

Mis en forme : Justifié

Mis en forme : Police :9.5 pt



# A Study on the Hollow Cubic SnO<sub>2</sub> as Anode Material for Lithium-ion Battery by Transmission X-ray Microscopy

Ju-Hsiang Cheng<sup>a,†</sup>, Ming-Hsien Lin<sup>a,†</sup>, Chun-Yi Wu<sup>a</sup>, Chun-Chieh Wang<sup>b</sup>, Yen-Fang Song<sup>b</sup>, Bing-Joe Hwang<sup>a,b,\*</sup>

<sup>a</sup> Department of Chemical Engineering, National Taiwan University of Science and Technology  
43 Keelung Road, Section 4, Taipei 106, Taiwan, ROC

<sup>b</sup> National Synchrotron Radiation Research Center, Hsin-Chu, Taiwan 30076

<sup>†</sup>These authors contributed equally to this work.

Corresponding author: bjh@mail.ntust.edu.tw

Sn-based material with higher theoretical capacity than commercial graphite has been seen as a potential material used in lithium-ion battery application. However, it suffers from huge capacity fading during the cycling due to its large volume expansion while lithium inserts/extracts. In order to overcome this problem, many efforts have been reported[1], such as porous/hollow structure and nano-composite, which could play a role as buffer zone and maintain its own structure. Recently, the synthesis of hollow cubic SnO<sub>2</sub> has been developed and effectively reduce the capacity fading of SnO<sub>2</sub>. [2] It is interesting to understand its mechanism for the capacity retention. Many characterization techniques have been intensively used to probe the structure change of SnO<sub>2</sub>, such as XRD, SEM and TEM. However, the study on the shape transformation of lithiated SnO<sub>2</sub> is still difficult to access. Synchrotron-based Transmission X-ray Microscopy (TXM) could be an useful tool to directly observe the shape change. [3]

The hollow cubic SnO<sub>2</sub> has been synthesized by selective leaching method[2]. SEM image of hollow cubic SnO<sub>2</sub> is shown in Figure 1(a), uniform hollow cubic SnO<sub>2</sub> could be observed and the average size of the cubic is around 2  $\mu\text{m}^3$ . Meanwhile, those particles are observed by TXM, shown in Figure 1(b), an image of square with black frame and white center has been obtained and the average size of the square frame is also around 2  $\mu\text{m}^3$  as well. This result indicates the cubic is hollow with the wall thickness around 300 nm. The various lithiated state of hollow cubic SnO<sub>2</sub> has also been studied. It could be found that as the lithium content increases, the size of the cubic enlarges but still remains in its cubic shape.

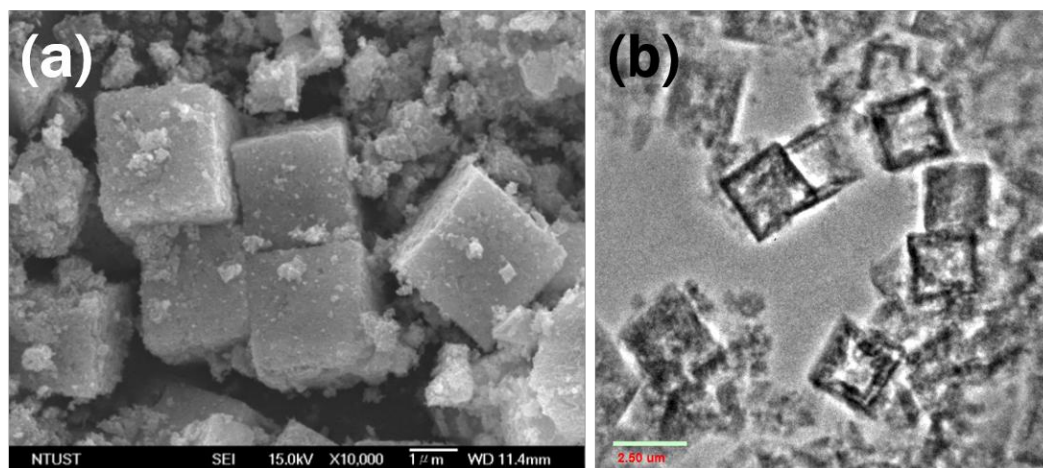


Figure 1. (a) SEM image and (b) TXM image of hollow cubic SnO<sub>2</sub>

## Reference

1. Goriparti, S., et al., *Review on recent progress of nanostructured anode materials for Li-ion batteries*. Journal of Power Sources, 2014. **257**(0): p. 421-443.
2. Zhang, L., et al., *Formation of porous SnO<sub>2</sub> microboxes via selective leaching for highly reversible lithium storage*. Energy & Environmental Science, 2014. **7**(3): p. 1013-1017.
3. Chao, S.-C., et al., *A study on the interior microstructures of working Sn particle electrode of Li-ion batteries by in situ X-ray transmission microscopy*. Electrochemistry Communications, 2010. **12**(2): p. 234-237.

# In-situ monitoring of elastic properties of common binders in Lithium ion batteries via electrochemical quartz microbalance with dissipation and dilatometry

Nicolas Jäckel,<sup>1,2</sup> Nethanel Shpigel,<sup>3</sup> Sergey Sigalov,<sup>3</sup> Mikhael D. Levi,<sup>3</sup> Daniel Weingarth,<sup>1</sup>  
Doron Aurbach,<sup>3</sup> Volker Presser<sup>1,2</sup>

<sup>1</sup> INM – Leibniz Institute for New Materials, 66123 Saarbrücken, Germany

<sup>2</sup> Saarland University, 66123 Saarbrücken, Germany

<sup>3</sup> Department of Chemistry, Bar-Ilan University, Ramat-Gan 52900, Israel

[nicolas.jaekel@inm-gmbh.de](mailto:nicolas.jaekel@inm-gmbh.de)

The cycling performance of composite LIB electrodes is strongly influenced by the significant dimensional changes (deformation) of the electrode material during reversible lithium ion intercalation and deintercalation. [1, 2]. Typical LIB composite cathodes are composed of an active material with conductive additives and a polymeric binder. [you can add here your Adv. Energy Mat. paper?] Lithium manganese oxide (LMO) is a commercial grade active material with its inexpensive synthesis and a long lifetime.[3, 4] Until recently, dimensional changes in intercalation-type electrodes such as LiFePO<sub>4</sub> were characterized by quartz-crystal microbalance measurements assuming that the polymeric binder remains in its completely rigid form during cycling [5,6] However, dimensional changes in the active material apply stress on the binder which reacts with a strain dependent on its viscoelastic properties. [1] Here we combine a non-invasive in-situ monitoring of the dimensional changes via electrochemical quartz-crystal microbalance with dissipation monitoring (EQCM-D) [1] and electrochemical dilatometry.[6]

The monitoring of elastic properties of three different polymeric binders, namely polyvinylidene fluoride (PVdF), polytetrafluoroethylene (PTFE), and sodium carboxymethylcellulose (Na-CMC), was carried out in an aqueous electrolyte (0.1 M LiSO<sub>4</sub>) and in an aprotic electrolyte (1 M LiPF<sub>6</sub> in EC/DMC 1:1). While monitoring EQCM-D response from single/a few layer thick intercalation particles translated by a hydrodynamic admittance model [5] to average changes of the geometric characteristics of the composite electrode layer [1, 6] this information is supplemented by dilatometric measurements in the same electrodes of significantly larger thickness. In this way, we can track an average effect of the whole bulk electrode, which results in dimensional changes less than 1 % for rigid binder types and more than 10 % for soft ones. We find the combination of both, EQCM-D and dilatometry, as a unique tool to track the structural behavior of the binder in-situ and non-invasive during intercalation and deintercalation of Li ions into LMO composite electrodes.

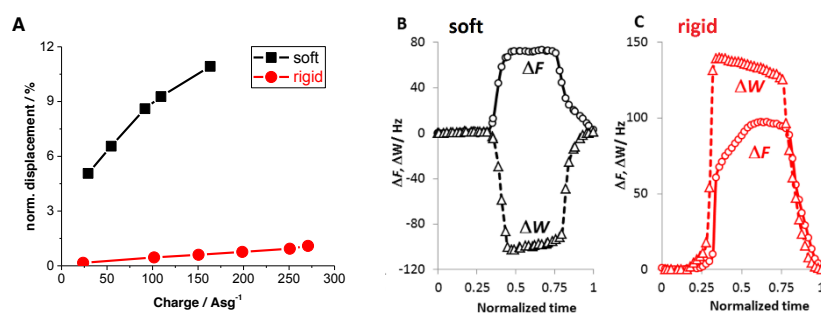


Figure 1: Different behavior of soft and rigid binder types in aqueous and non-aqueous electrolytes. (A) Dilatometry measurements shows varied expansion with soft or rigid binder and (B)+(C) EQCM-D data shows different change in frequency shift and dissipation.

- Shpigel, N., et al., *Non-Invasive In Situ Dynamic Monitoring of Elastic Properties of Composite Battery Electrodes by EQCM-D*. Angewandte Chemie – International Edition, 2015. DOI: 10.1002/anie.201501787
- Thackeray, M.M., *Manganese oxides for lithium batteries*. Progress in Solid State Chemistry, 1997. **25**(1-2): p. 1-71.
- Miller, J.R., *Valuing Reversible Energy Storage*. Science, 2012. **335**(6074): p. 1312-1313.
- Aurbach, D., et al., *Design of electrolyte solutions for Li and Li-ion batteries: a review*. Electrochimica Acta, 2004. **50**(2-3): p. 247-254.
- Daikhin, L., et al., *Quartz crystal impedance response of nonhomogenous composite electrodes in contact with liquids*. Analytical Chemistry, 2011. **83**(24): p. 9614-21.
- Levi, M.D., et al., *In Situ Tracking of Ion Insertion in Iron Phosphate Olivine Electrodes via Electrochemical Quartz Crystal Admittance*. The Journal of Physical Chemistry C, 2013. **117**(3): p. 1247-1256.

# ***In situ* and *ex situ* NMR observation of delithiation/lithiation behavior of $\text{LiNi}_{0.5}\text{Mn}_{1.5}\text{O}_4$**

Keiji Shimoda, Miwa Murakami, Hideyuki Komatsu, Hajime Arai, Yoshiharu Uchimoto, Zempachi Ogumi

Office of Society-Academia Collaboration for Innovation, Kyoto University  
Gokasho, Uji, Kyoto 611-0011, Japan  
k-shimoda@saci.kyoto-u.ac.jp

Lithium ion rechargeable batteries (LIBs) have been widely used as a power source for portable devices and now are available for applications to electric vehicles (EVs), which demand high-power, high-energy, inexpensive and safe batteries. A nickel-substituted lithium manganese spinel  $\text{LiNi}_{0.5}\text{Mn}_{1.5}\text{O}_4$  has been extensively studied as a preferred candidate of high-voltage positive electrode materials because it shows a wide potential plateau at  $\sim 4.7$  V vs.  $\text{Li/Li}^+$  with a theoretical capacity of 146.7 mAh/g. This material shows two distinct cubic structures depending on the Ni and Mn distribution. In the Ni/Mn ordered structure,  $\text{Ni}^{2+}$  and  $\text{Mn}^{4+}$  ions occupy the  $4b$  and  $12d$  Wyckoff positions in the space group  $P4_332$ , respectively, while these ions randomly occupy the  $16d$  position in the Ni/Mn disordered  $Fd\bar{3}m$  structure. The delithiation of the  $P4_332$  spinel basically proceeds in separate two-phase reactions between  $\text{LiNi}_{0.5}\text{Mn}_{1.5}\text{O}_4$  ( $\text{Li}_{1.0}$  phase) and  $\text{Li}_{0.5}\text{Ni}_{0.5}\text{Mn}_{1.5}\text{O}_4$  ( $\text{Li}_{0.5}$ ) at  $\sim 4.70$  V, and between  $\text{Li}_{0.5}\text{Ni}_{0.5}\text{Mn}_{1.5}\text{O}_4$  and  $\text{Ni}_{0.5}\text{Mn}_{1.5}\text{O}_4$  ( $\text{Li}_{0.0}$ ) at  $\sim 4.74$  V. On the other hand, the  $Fd\bar{3}m$  spinel shows a single-phase reaction (solid solution behavior) on going from the  $\text{Li}_{1.0}$  phase to  $\text{Li}_{0.5}$  phase [1].

Solid-state nuclear magnetic resonance (NMR) spectroscopy is a useful technique for investigating the chemical environments on a specific element in the battery materials. In particular, the  $^{6,7}\text{Li}$  NMR has been widely applied for the chemical structure characterization of the pristine and delithiated positive electrode materials, because it gives direct information about mobile Li ions. Previous studies reported the difference in Li local environments between the ordered and disordered  $\text{LiNi}_{0.5}\text{Mn}_{1.5}\text{O}_4$  [2]. We here examine the delithiation and lithiation behavior of ordered and disordered  $\text{LiNi}_{0.5}\text{Mn}_{1.5}\text{O}_4$  by using *in situ* (*in operando*)  $^7\text{Li}$  NMR and *ex situ*  $^6\text{Li}$  MAS NMR spectroscopy. The *in situ*  $^7\text{Li}$  monitoring of the ordered spinel revealed a clear appearance and subsequent disappearance of a new signal from  $\text{Li}_{0.5}\text{Ni}_{0.5}\text{Mn}_{1.5}\text{O}_4$ , suggesting the two-phase reaction processes among  $\text{Li}_{1.0}$ ,  $\text{Li}_{0.5}$ , and  $\text{Li}_{0.0}$  phases in agreement with the *in situ* XRD studies (See figure). High-resolution  $^6\text{Li}$  MAS NMR spectra, which give information about the Li environment in details for the disassembled samples, suggested that the nominal Li-free phase  $\text{Li}_{0.0}\text{Ni}_{0.5}\text{Mn}_{1.5}\text{O}_4$  can accommodate a small amount of Li ions in its structure. The tetragonal phase  $\text{Li}_{2.0}\text{Ni}_{0.5}\text{Mn}_{1.5}\text{O}_4$ , which was formed when the cell was discharged down to 2.0 V, was very different in Li environment between the ordered and disordered spinels. It is found that  $^{6,7}\text{Li}$  NMR is highly sensitive not only to the Ni/Mn ordering in  $\text{Li}_x\text{Ni}_{0.5}\text{Mn}_{1.5}\text{O}_4$  but also to the delithiation/lithiation process during charge-discharge cycle.

This work was supported by the Research and Development Innovative for Scientific Innovation of New Generation Battery (RISING) project from New Energy and Industrial Technology Development Organization (NEDO), Japan.

## References

[1] Manthiram, A. *et al.*, *Energy Environ. Sci.* **2014**, 7, 1339. [2] Cabana, J. *et al.*, *Chem. Mater.* **2012**, 24, 2952.

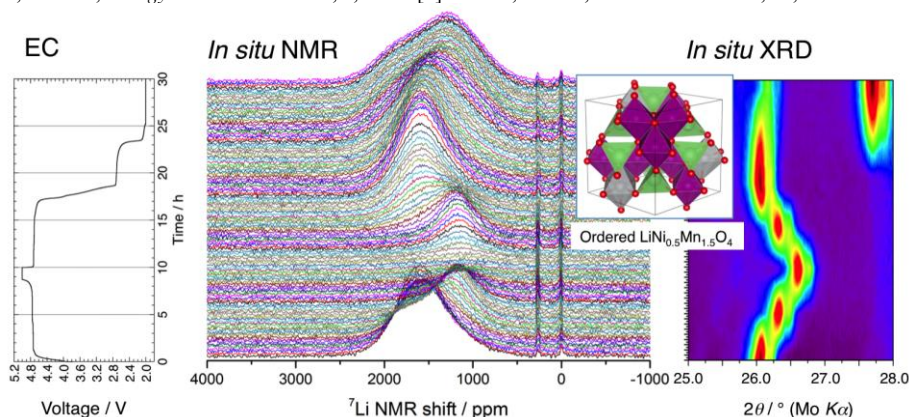


Figure. *In situ*  $^7\text{Li}$  NMR spectra of  $\text{Li}/\text{LiNi}_{0.5}\text{Mn}_{1.5}\text{O}_4$  (ordered) cell along with electrochemical profile (C/10 rate, CC-CV mode, and a voltage window of 5.0 – 2.0 V) and *in situ* XRD contour plot.

# Electrodeposition of Cu-Sn Hexagonal Tubes from Room Temperature Ionic Liquid and its In-Situ Scanning Electron Microscopy Study

Yi-Ting Hsieh<sup>1</sup>, I-Wen Sun<sup>1\*</sup>, Tetsuya Tsuda<sup>2</sup>, Susumu Kuwabata<sup>2</sup>,

<sup>1</sup>Department of Chemistry, National Cheng Kung University, Taiwan

<sup>2</sup>Department of Applied Chemistry, Graduate School of Engineering, Osaka University, Japan

Address: No.1, University Road, Tainan City 701, Taiwan

e-mail address: ytshirley0303@gmail.com

Copper-tin alloy is a useful material for corrosion resistance and soldering<sup>1</sup>. Electrodeposition is a relatively inexpensive technique is not practical for the production of CuSn alloy in the aqueous solution because the electrode potentials for Cu and Sn depositions are far apart.

Room-temperature ionic liquids (RTILs) composed of organic cations and various anions are liquid salts staying as a liquid phase even at room temperature. Most RTILs have unique properties such as nonflammability, negligible vapor pressure, high conductivity, wide electrochemical window. We have succeeded in electrodeposition of various pure metals and alloys, which cannot be produced in aqueous solutions, in the RTILs. Recently we found that Cu-Sn alloy tubes can electrochemically be obtained in the 1-ethyl-3-methylimidazolium dicyanamide (EMI-DCA) containing Cu(I) and Sn(II) without any templates<sup>2</sup>. In this paper, we report the template-free electrodeposition of Cu-Sn alloy tube and in-situ SEM observation of the alloy electrodeposition process.

The electrolytes were prepared by dissolution of proper amounts of anhydrous CuCl and SnCl<sub>2</sub> into the EMI-DCA. All electrochemical experiments were carried out in a three-electrode cell. Cu spiral wire was used as a counter electrode and a Pt wire immersed in a melt solution containing ferrocene/ferrocenium (50/50mol%) in a fritted glass tube was used as a reference electrode. Ni foils were used as the substrate for electrodeposition. For in-situ SEM observation study a specially-manufactured sandwich cell was used. A 100 mesh Ni sheet as used as a working electrode for metal deposition; Cu foil and wire were used as counter and reference electrodes, respectively. The glass fiber membrane was used as the separator between each electrode.

The electrochemical behavior of the individual copper<sup>3</sup> and tin<sup>4</sup> in EMI-DCA has been studied previously. Based on these reports, electrodeposition of Cu-Sn alloys was conducted under different conditions. Figure 1 shows hollow tubes<sup>2</sup> obtained at a low current density of  $-0.4 \text{ mA cm}^{-2}$  from EMI-DCA containing (A) 33mM Cu(I)- 16.5mM Sn(II) at 40°C. According to the XRD results, while Cu<sub>10</sub>Sn<sub>3</sub> hollow tubes could be obtained from Cu(I)-rich solution. Although we proposed a plausible formation mechanism for the alloy deposits in our previous paper<sup>2,5</sup>, still it is not clear. Here, we attempted to visually investigate the growth mechanism by using an in-situ scanning electron microscope (SEM) observation method established in our laboratory. A part of the deposition process was successfully observed in real time shown in Figure 2.

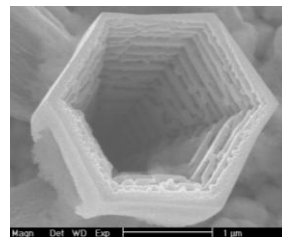


Fig.1. SEM images of Cu-Sn alloy electrodeposit at  $-0.4 \text{ mA cm}^{-2}$  in EMI-DCA containing (A) 33mM Cu(I)- 16.5mM Sn(II) at 40°C

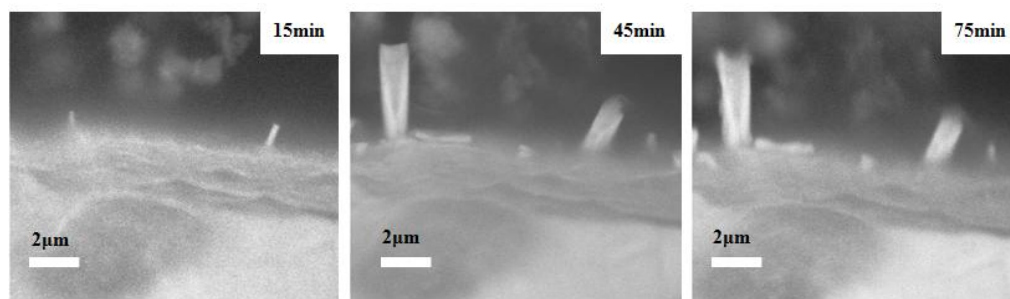


Fig. 2 SEM images of the sample observed during the deposition for 15, 45, and 75min.



# Single ion activity, pH, liquid junction potential, and the essence of electrochemistry: in response to “A pH centenary” by Robert de Levie

Takashi Kakiuchi<sup>1,2</sup>, Masahiro Yamamoto<sup>1</sup>

1. CREST-JST, Department of Chemistry of Functional Molecules, Konan University, 8-9-1 Okamoto, Kobe 658-8501, Japan
2. pH Science and Technology Laboratory, Kinomoto 1058, Wakayama 640-8453, Japan  
kakiuchi.takashi.55e@st.kyoto-u.ac.jp

An article published last year, “A pH centenary,” by Robert de Levie [1] is not simply a scholarly and elaborative essay on history of pH, but is a provocative proposition of his opinion that pH or the scale of acidity of an electrolyte solution should be based on the concentration, rather than the single ion activity, of hydrogen ion. His reasoning is “the activity (or, more precisely, the corresponding activity coefficient) of a single ionic species is a supposedly thermodynamic concept, introduced by G. N. Lewis. However, it cannot be defined thermodynamically, and therefore does not have a physical existence and cannot be measured” [2].

The thermodynamically immeasurable nature of the single ion activity has been the subject of discussion over nearly one hundred years [3] and supposed to be well understood. However, that some discussions on this issue, including the de Levie’s essay [1], among electrochemists have continued to date suggests that a certain important point has been overlooked in those preceding discussions and polemics. In fact, both sides, de Levie and Bates [4] (or IUPAC2002 recommendations [5]) seem to have a common understanding that the cell voltage of the cell,  $\text{Pt}|\text{H}_2(\text{g}), \text{aq. HCl}||\text{AgCl}|\text{Ag}$ , i.e., the so-called “Harned cell”, provides the thermodynamically defined mean activity coefficient of HCl. This background unfortunately seems to make their arguments unnecessarily involved and complicated.

A hidden nonthermodynamic assumption in use of the “Harned cell” is the negligible diffusion potential existing, however small, across the liquid junction that must be present somewhere within the cell [6], which in fact is inevitable in any electrochemical cells by nature. As is well known or too obvious, any galvanic cell consists of two redox couples that are placed separately in the cell to minimize direct redox reactions between them, and, hence is intrinsically nonthermodynamic [7]. In this respect, an approach, “thermodynamic properties...by means of cells without liquid junctions” [8] promoted by R. S. Harned might have dazzled many textbooks of electrochemistry, despite the warning by MacInnes[6], by depicting the cell as if thermodynamic properties are obtainable through “equilibrium cell voltage.” If we start with the premise that a liquid junction is an important player in any electrochemical cell but the liquid junction potential may be made negligibly small by use of a salt bridge or otherwise, we will be able to obtain a good estimate of the magnitude of hydrogen ion activity, undoubtedly a non-thermodynamic quantity, with the extent of the uncertainty determined by the residual liquid junction potential. Unfortunately, the performance of a salt bridge of a concentrated aqueous KCl solution or similar ones, which have been used over more than a hundred years, is not necessarily satisfactory. However, a new salt bridge that consists of a moderately hydrophobic ionic liquid (ILSB) [9-11] has been shown to reduce the liquid junction potential between aqueous HCl solutions of different concentrations to as low as 0.5 mV[12], which demonstrates that it is possible by use of an ILSB to narrow down the pH based on hydrogen ion activity within  $\pm 0.01$ . By simply using a better salt bridge, it is thus possible to have a good estimate of “thermodynamically immeasurable” single ion activity of hydrogen and other ions. Starting with an intrinsically nonthermodynamic electrochemical cell and a nonthermodynamic assumption which is inevitably required for any type of electrochemical cell, we may obtain non-thermodynamic quantities that can be useful for better understanding of the relevant thermodynamic properties. My (T.K.’s) essay on de Levie’s view on measurability of single ion activity written before publication of [1] is available [13]; a full version in response to [1] is in preparation.

## References

- [1] R. de Levie, *Electrochim. Acta*, **135**, 604-639 (2014). [2] Ref.1, p.636. [3] Ref.1, p.605-608. [4] R. G. Bates, “Determination of pH,” 2<sup>nd</sup> ed., Wiley (1973). [5] R. G. Buck, et al., *Pure Appl. Chem.*, **74**, 2169-2200 (2002). [6] D. A. MacInnes, “The Principles of Electrochemistry,” Dover (1961), p.246. [7] H. Reiss, *J. Electrochem. Soc.*, **135**, 247C-258C (1988). [8] H. S. Harned, B. B. Owen, *Chem Rev.*, **25**, 31-65 (1939). [9] T. Kakiuchi, T. Yoshimatsu, *Bull. Chem. Soc. Jpn.*, **79**, 1017-1024 (2006) [10] H. Sakaida, Y. Kitazumi, T. Kakiuchi, *Talanta*, **83**, 663-666 (2010). [11] T. Kakiuchi, H. Sakaida, *J. Phys. Chem. B*, **115**, 13222-13226 (2011). [12] T. Kakiuchi, *Electrochem. Commun.*, **45**, 37-39 (2014). [13] T. Kakiuchi, *Rev. Polarogr.*, **60**, 99-109 (2014), (in Japanese); English translation is available upon request.

# Wire Beam Electrode Technique for Investigation Galvanic Corrosion Behavior between Zinc and Carbon Steel

ZHANG Dalei<sup>1</sup>, Guan Xiaorui<sup>2</sup>, Jin Youhai<sup>2</sup>, LI Yan<sup>1</sup>

<sup>1</sup> College of Mechanical and Electronic Engineering, China University of Petroleum

<sup>2</sup> College of Chemical Engineering, China University of Petroleum

Qingdao 266580, P. R. China

Phone: +86 18325429329. E-mail: cupguanxiaorui@126.com

Submit to the Symposium 18: General session

Three kinds of wire beam electrodes(WBE) composed by zinc and mild steel wires were developed, which was used to simulate hot-dip galvanized steel with spot coating defect in different dimension, to obtain the spatial distributions of potential and current density and their variations with time during the galvanic corrosion. The electrochemical characteristics among these WBEs were also investigated. The results showed that zinc wires within the WBEs could provide enough cathodic protection to steel wires after immersed in seawater, with surface area ratio of zinc wires versus steel wires as 1:120, 9:112, and 25:76, respectively. The potential and current density distributions were found to be inhomogeneous among zinc wires; firstly, main anodic areas shifted randomly among the zinc wires adjacent to steel wires, then transferred to the direction away from steel wires, and finally occurred on the zinc wires farther. The similar heterogeneous phenomenon also appeared on steel wires surface on which hydrogen evolution might take part in the cathodic process occurred. The current density of water molecule reduction reaction, along with dissolved oxygen reduction reaction, decreased with the ratio of the surface area of steel wires versus zinc wires rising.

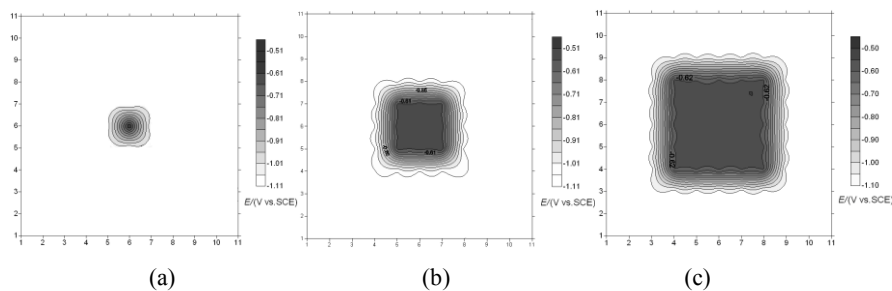


Fig.1 Spatial open circuit potential distribution of zinc/steel-WBE after immersed in seawater for 0.5 h:

(a) WBE-1×1S; (b) WBE-3×3S; (c) WBE-5×5S

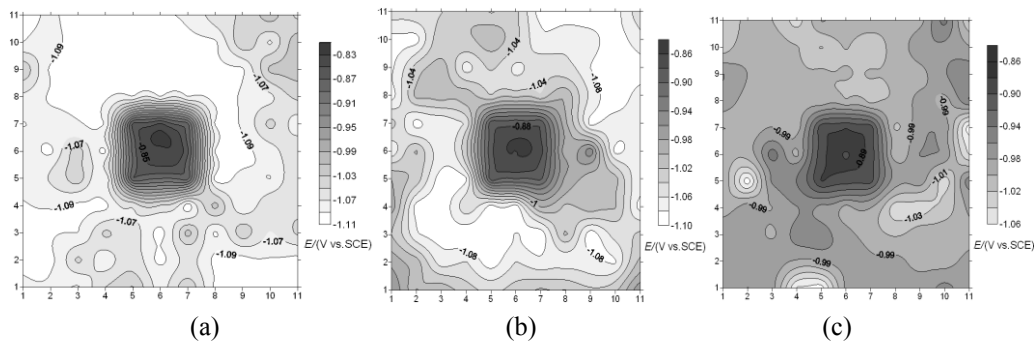


Fig.2 Spatial electrochemical distributions of WBE-3×3S after being coupled: potential distribution for 0.5h (a), potential distribution for 4 h (b); and potential distribution for 24h (c)

# Dynamics of Interfacial Oxide Formation during Anodization of Valve Metal Superimposed Ultra-Thin Films

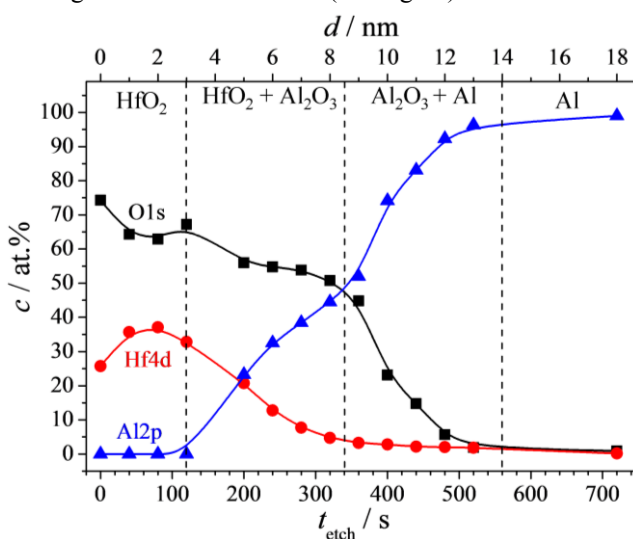
Andrei Ionut Mardare<sup>1</sup>, Christian M. Siket<sup>2</sup>, Cezarina Cela Mardare<sup>1</sup>, Siegfried Bauer<sup>2</sup>,  
Achim Walter Hassel<sup>1</sup>

<sup>1</sup> Christian Doppler Laboratory for Combinatorial Oxide Chemistry at the Institute for Chemical  
Technology of Inorganic Materials, Johannes Kepler University Linz, 4040 Linz, Austria

<sup>2</sup> Soft Matter Physics, Johannes Kepler University Linz, 4040 Linz, Austria  
andrei.mardare@jku.at

Anodization of superimposed valve metals has been in the focus of the electrochemical community due to the necessity of better understanding the anodic oxide formation in such cases with direct applications in capacitors, high-k materials and MOS-based devices or sensors. In particular, superimposed layers containing Al are highly relevant due to its abundance, high band-gap and already implemented industrial processing. Both early theoretical and experimental studies revealed that if the underlying metal forms a lower ionic resistivity oxide as compared to the outer  $\text{Al}_2\text{O}_3$ , "fingers" of the inner metal oxide may penetrate into the outer oxide layer [1-3]. The anodic oxide mixing during the anodization is based on an inherent competition for oxygen between different valve metal ions regulated by their individual ionic transport numbers [4, 5]. However, even though a principally correct theoretical prediction describing the formation of a layered anodic oxide when the underlying film has a high ionic resistivity (e.g. Al) was formulated [1], studies on the metals interfacial anodization are scarce in spite of their tremendous importance for the overall anodic oxide properties. Moreover, the oxide-oxide interface remains unexplored. Hafnium is an excellent candidate for such studies due to its extremely low ionic transport number combined with its amorphous nature when deposited at room temperature [6].

In the present work, the anodization behavior of Hf and Al stacked thin films, sequentially deposited from vapor phase without breaking vacuum, was investigated using scanning droplet cell microscopy. The effect of the ultra-thin nature of the superimposed film on the final oxide properties was studied. Surface microstructure and crystallographic analysis revealed the formation of highly textured and compact films for Hf thicknesses above 7.5 nm. Cyclic voltammetry suggested the formation of discrete anodic layers when Hf was superimposed on Al starting with pure  $\text{HfO}_2$  on the surface, a mixture of  $\text{HfO}_2$  and  $\text{Al}_2\text{O}_3$  as an intermediate layer and pure  $\text{Al}_2\text{O}_3$  in depth of the films. The finding of a mixed interfacial oxide layer completes the initial Pringle's theory which predicted a full oxide segregation [1]. Coulometric investigations revealed oxide formation factors of  $2.2 \text{ nm V}^{-1}$  for  $\text{HfO}_2$  while for pure  $\text{Al}_2\text{O}_3$  a maximum of  $1.4 \text{ nm V}^{-1}$  was measured. Electrochemical impedance spectroscopy performed for various Hf thicknesses and different final anodization potentials revealed almost ideal dielectrics formed from mixed  $\text{HfO}_2/\text{Al}_2\text{O}_3$ , permittivities up to 26 being measured for the anodized Hf/Al films. Surface analytical investigations and depth profiling confirmed the discrete anodic layer growth together with the mixing of both anodic oxides (see Figure).



[1] J.P.S. Pringle, *Electrochim. Acta* **25** (1980) 1423

[2] P. Skeldon, K. Shimizu, G.E. Thompson, G.C. Wood, *Philos. Mag. B* **61** (1990) 927

[3] L. Iglesias-Rubianes, P. Skeldon, G.E. Thompson, H. Habazaki, K. Shimizu, *J. Electrochem. Soc.* **149** (2002) B23

[4] A.I. Mardare, A. Ludwig, A. Savan, A.W. Hassel, *Electrochim. Acta* **140** (2014) 366

[5] A.I. Mardare, A. Ludwig, A. Savan, A.W. Hassel, *Sci. Technol. Adv. Mater.* **15** (2014) 015006

[6] A.I. Mardare, C.M. Siket, A. Gavrilovic-Wohlmuther, C. Kleber, S. Bauer, A.W. Hassel, *J. Electrochem. Soc.* **162** (2015) E30

# Ferrocenium triiodide ionic liquids: Synthesis, electron transfer and their (thermo)electrochemical waste heat harvesting properties

Leigh Aldous<sup>1</sup>, Wuan Xin Teh<sup>1</sup>, Trang Quynh To<sup>1</sup>, Sean Cadogan<sup>2</sup>

<sup>1</sup>The University of New South Wales, Sydney, NSW 2052, Australia

<sup>2</sup>The University of New South Wales Canberra, Canberra, BC 2610, Australia

*l.alldous@unsw.edu.au*

Ionic liquids (ILs) are essentially pure electrolytes, being composed of unsolvated cations and anions. As such they can behave as excellent electrolytes, both dissolving compounds and facilitating electron transfer. This talk will describe a new family of ionic liquids which are themselves formed by reversible electron transfer; referred to as redox ionic liquids (RILs). In particular, this talk will focus upon ferrocene/iodine-based ionic liquids (Figure 1), and will give an overview of their physiochemical electrochemical and properties.

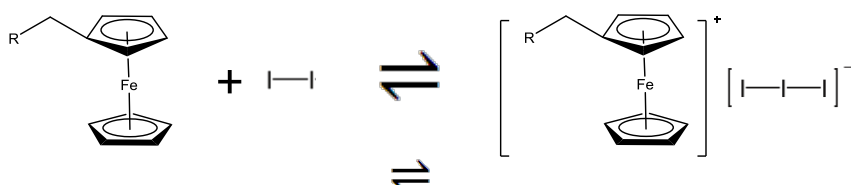


Figure 1. Ferrocene + iodine

Ferrocenium triiodide ionic liquid

As equilibrium ionic liquids, the position of the (electron transfer) equilibrium is temperature and potential dependent, making them both distillable and electrochemically switchable electrolytes. As 100% of the liquid is redox active they represent potential ‘high power density’ electrolytes for electrochemical processes such as supercapacitor and redox flow batteries. This talk will focus upon the application of their temperature-sensitive redox equilibrium for excellent waste heat harvesting in thermoelectrochemical cells, via which a temperature difference can be directly converted into an electric current (Figure 2(a)).

The ionicity of the RILs was found to depend upon the relative redox potentials of the component parts and the stoichiometry of their composition. Such RILs are either inherently “super” ionic electrolytes, or are easily made “super” ionic by altering the stoichiometry (Figure 2(b)). This stems from polyiodide chains (Grotthuss mechanism) and potentially ferrocene-ferrocenium electron propagation.

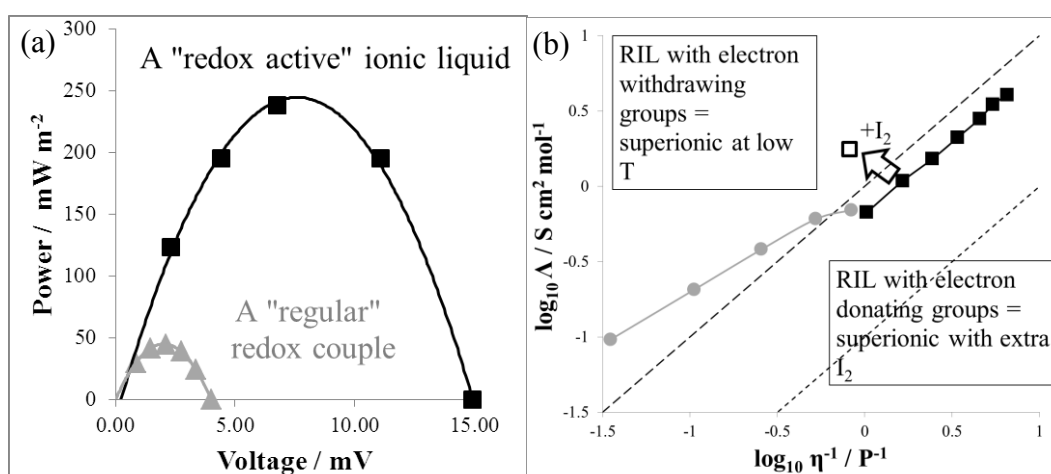


Figure 2(a) Superior power harvesting of an RIL using a simple battery casing as a thermoelectrochemical cell (temperature difference of 30 K), and (b) Walden plot displaying the “good” ionicity of [DiButylFc][I<sub>3</sub>] (■), the “super” ionicity of [DiBuFc][I<sub>3</sub>] (□) and temperature-dependent ionicity of [DiButyryl][I<sub>3</sub>] (●).



# Thermal membrane potential – Application to thermoelectric power generation

Miikka Jokinen<sup>a</sup>, José A. Manzanares<sup>b</sup>, Kyösti Kontturi<sup>a</sup>, Lasse Murtomäki<sup>a</sup>

*a) Department of Chemistry, Aalto University, PO Box 16100, FI-00076 AALTO, Finland.*

*b) Dept. of Thermodynamics, Fac. Physics, University of Valencia, E-46100 Burjasot, Spain.  
miikka.jokinen@aalto.fi*

Thermoelectric materials offer a means for converting thermal energy directly into electricity, with a plethora of possible applications [1]. However, poor efficiency and high price of the materials are still hindering the commercialization of thermoelectric semiconductors, which has generated interest in other forms of thermoelectricity [2,3]. Ion-exchange membranes have been suggested as an alternative to semiconductors in terms of thermoelectricity [3], as they can provide larger voltage per temperature difference [4,5], lower fabrication costs and low thermal conductivity [3]. However, to the best of our knowledge, no measurements on the thermoelectric power production with thermogalvanic cells and ion-exchange membranes have been made.

In this work we evaluate the thermal membrane potential in various 1-1 electrolytes and apply the thermally generated potential difference to electric power generation. The left panel of Figure 1 shows a sketch of the measurement cell of uniform electrolyte concentration, with one hot stream flanked by commercial anion and cation-exchange membranes. The temperature difference creates an electric potential difference, with the positive electrode adjacent to the hot stream. Connecting the cell to a load allows the transport of ions through the membranes, which in turn drives electrochemical reactions at the electrodes (e.g. Ag/AgCl).

We evaluate theoretically the thermal membrane potential taking into account the concentration dependence of the ionic heats of transport, the thermal polarization [6] and the concentration polarization caused by the Soret effect [7] in the boundary layers adjacent to the membrane surfaces. The theoretical predictions are compared to the measured values for different electrolytes and concentrations. We also show that it is possible generate electric power with the proposed cell, and measure how the power output behaves as a function of temperature difference (Figure 1, right panel) and concentration. The theory shows good agreement with the experimental results for both thermal membrane potential and power in various electrolytes and concentrations, and enables comparison and prediction of the potential with different membranes and electrolytes in different cell designs. Although still at the proof-of-concept level, the maximum power is already similar to that of other emerging thermoelectric materials [2].

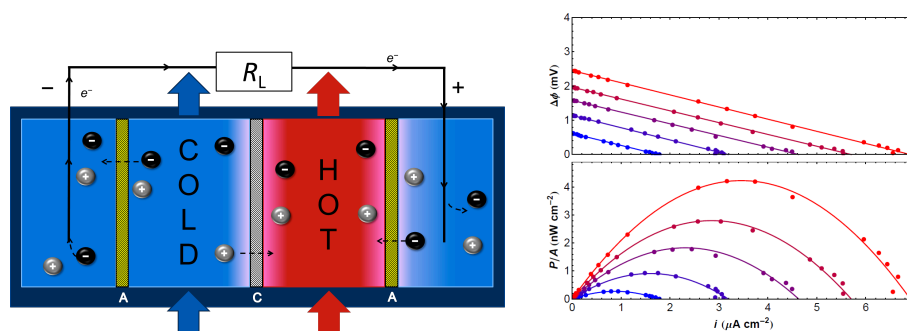


**Fig 1.** Left: Sketch of the measurement cell with anion-exchange (A) and cation-exchange membranes (C). Electrode reactions are driven by the thermal electrodiffusion of ions; the positive electrode is the one closer to the hot stream. Right: Thermally generated voltage  $\Delta\phi$  and power output vs. current density measured for 0.1 mol/L NaCl with different temperature differences: 5.4 K (blue), 9.3 K, 13.3 K, 16.5 K, and 20.5 K (red).

- [1] T. Chang, *et al.* *Electrochim. Acta* 161 (2015) 403-407.
- [2] O. Bubnova, *et al.* *Nat. Mater.* 10 (2011) 429-433.
- [3] K.D. Sandbakk, A. Bentien, S. Kjelstrup, *J. Membr. Sci.* 434 (2013) 10-17.
- [4] M. Tasaka, *Pure & Appl. Chem.* 58 (1986) 1637-1646.
- [5] J.R. Szczech, J.M. Higgins, S. Jin, *J. Mater. Chem.* 21 (2011) 4037-4055.
- [6] V.M. Barragán, C. Ruiz-Bauzá, *J. Membr. Sci.* 125 (1997) 219-229.
- [7] P.N. Snowdon, J.C.R. Turner, *Trans. Faraday Soc.* 56 (1960) 1812-1819.

- [3] K.D. Sandbakk, A. Bentien, S. Kjelstrup, J. Membr. Sci. 434 (2013) 10-17.
- [4] M. Tasaka, Pure & Appl. Chem. 58 (1986) 1637-1646.
- [5] J.R. Szczech, J.M. Higgins, S. Jin, J. Mater. Chem. 21 (2011) 4037-4055.
- [6] V.M. Barragán, C. Ruiz-Bauzá, J. Membr. Sci. 125 (1997) 219-229.
- [7] P.N. Snowdon, J.C.R. Turner, Trans. Faraday Soc. 56 (1960) 1812-1819.

# Amperometric Detection of Hemoglobin A1c using a Poly(3-aminophenylboronic acid) Thin Film with Binding-Induced Ion Flux Blocking

Jen-Yuan Wang<sup>a,\*</sup>, Tse-Chuan Chou<sup>b</sup>, Lin-Chi Chen<sup>c</sup>, Kuo-Chuan Ho<sup>d</sup>

<sup>a</sup>Physics Division, Institute of Nuclear Energy Research, Taoyuan 325, Taiwan

<sup>b</sup>Department of Chemical Engineering, National Cheng Kung University, Tainan 701, Taiwan

<sup>c</sup>Department of Bio-Industrial Mechatronics Engineering, National Taiwan University, Taipei 10617, Taiwan

<sup>d</sup>Department of Chemical Engineering, National Taiwan University, Taipei 10617, Taiwan

E-mail: [b90209004@ntu.edu.tw](mailto:b90209004@ntu.edu.tw)

This study reports a novel enzyme-free, label-free amperometric method for direct detection of hemoglobin A1c (Hb<sub>A1c</sub>), a potent biomarker for diabetes diagnosis and prognosis. The method relies on an electrode modified with poly(3-aminophenylboronic acid) (PAPBA) nanoparticles (20-50 nm) and a sensing scheme named “binding-induced ion flux blocking.” The PAPBA nanoparticles were characterized by FT-IR, XPS, TEM, and SEM. Being a polyaniline derivative, PAPBA showed an ion-dependent redox behavior, in which insertion or extraction of ions into or out of PAPBA occurred for charge balance during the electron transfer process. The polymer allowed Hb<sub>A1c</sub> selectively bound to its surface via forming the *cis-diol* linkage between the boronic acid and sugar moieties. Voltammetric analyses showed that Hb<sub>A1c</sub> binding decreased the redox current of PAPBA; however, the binding did not alter the redox potentials and the apparent diffusivities of ions. This suggests that the redox current of PAPBA decreased due to an Hb<sub>A1c</sub> binding-induced ion flux blocking mechanism, which was then verified and characterized through an *in situ* electrochemical quartz crystal microbalance (EQCM) study. Assay with Hb<sub>A1c</sub> by differential pulse voltammetry (DPV) indicates that the peak current of a PAPBA electrode has a linear dependence on the logarithm of Hb<sub>A1c</sub> concentration ranging from 0.975 to 156  $\mu$ M. The Hb<sub>A1c</sub> assay also showed high selectivity against ascorbic acid, dopamine, uric acid, glucose and bovine serum albumin. This study has demonstrated a new method for developing an electrochemical Hb<sub>A1c</sub> biosensor and can be extended to other label-free, indicator-free protein biosensors based on a similar redox polymer electrode.

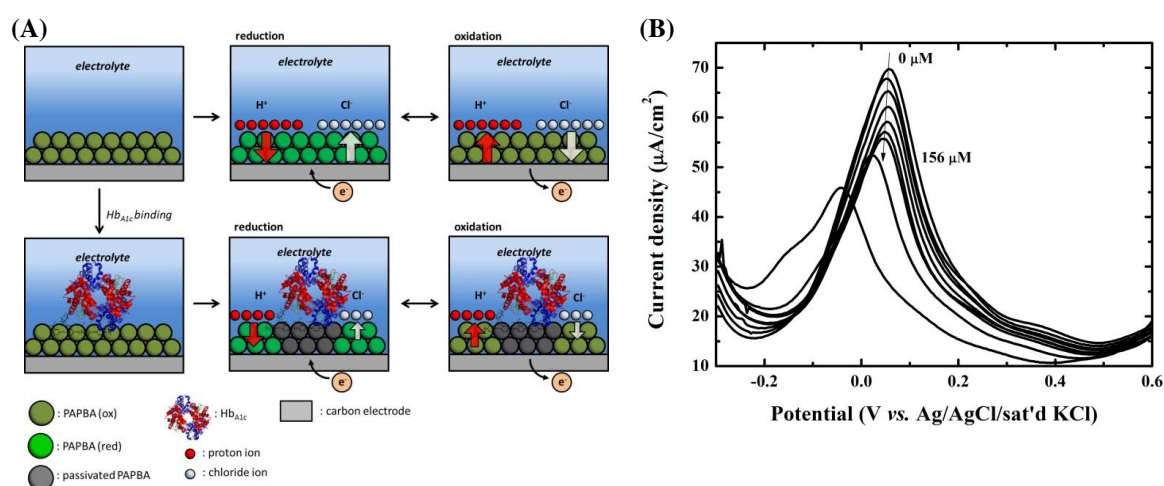


Figure 1 (A) The proposed mechanism of the ion fluxes change of PAPBA nanoparticles with Hb<sub>A1c</sub> binding. (B) DPVs of the PAPBA/SPCE reacted with Hb<sub>A1c</sub> samples with different concentrations.

# Functionalization of Conductive Carbon Supports at Water/Oil Interfaces with Non-Precious Metal Hydrogen Evolution Catalysts

Micheál D. Scanlon,\* Andrés Molina Osorio

University College Cork

Department of Chemistry & Tyndall National Institute, University College Cork, Cork, Ireland

\*micheal.scanlon@ucc.ie

Generation of molecular hydrogen ( $H_2$ ) by the electrochemical reduction of water is key to developing several clean-energy technologies (e.g.,  $H_2$  fuel cells). While noble metals, such as Pt, effectively facilitate the electrochemical  $H_2$  evolution reaction (HER), cheaper, earth-abundant, non-precious metal containing  $H_2$  evolution catalysts (HECs) are required to make the clean-energy technologies economically viable. In this regard, significant research has been devoted to their development and lead candidates include transition metal dichalcogenides ( $MoS_2$ ), carbides ( $Mo_2C$ ), borides ( $MoB$ ) and metal phosphides ( $Ni_2P$ ).<sup>(1)</sup> Furthermore, a HECs activity can be markedly improved by nanoscale deposition onto conductive materials (such as graphene). The latter both increases the HECs surface-to-volume ratio, exposing more active sites, and improves electron transport between the reducing agent and catalyst (the conductive support acts as an “electron superhighway”).<sup>(2)</sup>

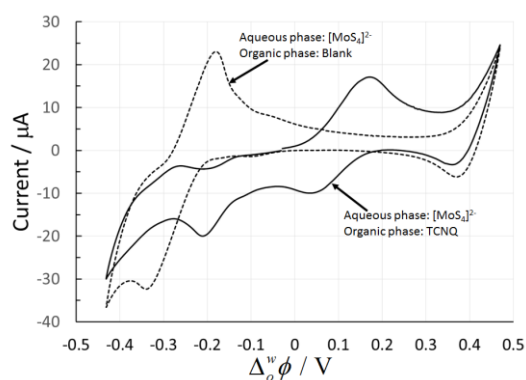


**Fig. 1:** Cyclic voltammetry of the ion transfer (IT) responses for a biphasic system containing  $[MoS_4]^{2-}$  in the aqueous phase both in the absence and presence of an oxidizing agent (TCNQ) in the organic phase. Additional IT responses with TCNQ indicate a biphasic reaction has taken place.

The interface between two immiscible electrolyte solutions (or ITIES) offers a unique platform at which to deposit nanoscale HECs onto conductive materials free-floating at the water/oil interface. These experiments are performed under ambient conditions and without the use of traditional solid-electrodes, allowing ease of recovery of the resultant advanced functionalized materials. Initial studies in this field involved the *in situ* deposition of Pt and Pd nanoparticles at the water/oil interface by reducing an aqueous metallic salt (e.g.,  $[PdCl_4]^{2-}$ ) using a lipophilic electron donor (decamethylferrocene; DMFc) via interfacial electron transfer (IET).<sup>(3)</sup> Depending on the reduction potentials of the species in the respective phases, IET can occur spontaneously or be controlled electrochemically by varying the interfacial Galvani potential difference ( $\Delta_o^w\phi$ ).

Recently, Dryfe’s group introduced an elegant approach to functionalize graphene at the water/oil interface by transferring graphene, grown on a polymer by CVD, onto the interface. In this instance, metallic (Pd and Au) nanoparticle deposition occurred preferentially on the graphene rather than at the bare interface with IET occurring via the conductive graphene.<sup>(4)</sup>

Herein, we investigated the biphasic deposition of transition metal dichalcogenide nanoparticles onto graphite and CNTs adsorbed at the water/oil interface from aqueous  $[MoS_4]^{2-}$ . Both the oxidative (Equation 1 and Figure 1) and reductive (Equation 2) pathways were considered, using lipophilic electron acceptors (tetracyanoquinodimethane; TCNQ) and donors (DMFc), respectively.



The catalytic activity of the resulting  $MoS_x$ /graphite and  $MoS_x$ /CNT materials towards the HER were characterized by linear polarization curves and electrochemical impedance spectroscopy.

- References:** (1) H. Fei, Y. Yang, Z. Peng, G. Ruan, *et al.*, *ACS Appl. Mater. Interfaces*, (2015), **7**, 8083.  
 (2) X. Bian, M.D. Scanlon, S. Wang, L. Liao, *et al.*, *Chem. Sci.*, (2013), **4**, 3432.  
 (3) J.J. Nieminen, I. Hatay, P. Ge, M.A. Méndez, *et al.*, *Chem. Commun.*, (2011), **47**, 5548.  
 (4) P.S Toth, Q.M. Ramasse, M. Velicky and R.A.W. Dryfe, *Chem. Sci.*, (2015), **6**, 1316.

## A glance at the photoelectrochemical response of nanoporous carbon/semiconductor electrodes

Alicia Gomis-Berenguer<sup>1\*</sup>, Verónica Celorrio<sup>2</sup>, David J. Fermín<sup>2</sup>, Jesús Iniesta<sup>3</sup>, Conchi O. Ania<sup>1</sup>  
<sup>1</sup>*Instituto Nacional del Carbón (INCAR, CSIC), 33011 Oviedo, Spain,* <sup>2</sup>*School of Chemistry, University of Bristol, Bristol BS8 ITS, UK,* <sup>3</sup>*Dept. Química Física e Instituto de Electroquímica, Universidad de Alicante, E-03080 Alicante, Spain.*  
\**alicia.gomis@incar.csic.es*

The semiconductor-mediated photochemical reactions are an attractive tool for the degradation of pollutants as the excitation of electronic molecular states at energies corresponding to the ultraviolet light may induce easier chemical bond breaking. However, the low photonic efficiency of most semiconductors is still a challenge that calls out for a research to be conducted to optimize the optical features of semiconductor materials, or to explore the use of novel materials in this kind of applications. [1] The incorporation of carbon materials as additives to semiconductor has long proved to be an interesting strategy to improve the performance of such carbon/semiconductor composites in several fields. However, despite the superior performance of the hybrid photocatalysts, the exact role of the carbon phase remains rather unclear. [2,3]

To throw some light on the mechanisms of the photoinduced processes occurring in such hybrid carbon/semiconductor catalysts, we have investigated the photoelectrochemical response of thin film electrodes under different conditions of illumination (UV-vis light source and monochromatic light). Several nanoporous carbon materials and inorganic semiconductors (TiO<sub>2</sub>, WO<sub>3</sub>, Bi<sub>2</sub>WO<sub>6</sub>) have been examined for the preparation of the hybrid photocatalysts.

As a first step, spectroscopic techniques have been applied to investigate the structural and optical properties of the carbon/semiconductor composites compared to the intrinsic characteristics of the unsupported semiconductor. The second approach consisted in the preparation of thin film electrodes to explore the photoinduced reactions at the interface under illumination and bias potential.

Our results point out that beyond the beneficial effect of the porosity, the carbon matrix does play an important role in the photo-induced reactions, hence different mechanisms have been postulated and will be discussed considering the characteristics of the carbon material. Moreover, our data showed a strong dependence of the photoelectrochemical response of the hybrid catalysts with the origin and structure of the carbon phase, the composition of the inorganic semiconductor and the irradiation source.

[1] Serpone N, Pelizzetti E (Eds) in Photocatalysis: fundamental and applications, New York: Wiley Interscience; 1989.

[2] Ania CO, Velasco LF, Valdes-Solis T. Photochemical behavior of carbon adsorbents, in Novel Carbon Adsorbents, Chapter 17 (Ed: JMD Tascón), Elsevier, London, 2012 pp. 521.

[3] Haro M, Velasco LF, Ania CO, Carbon mediated photoinduced reactions as a key factor in the photocatalytic performance of C/TiO<sub>2</sub>, Catal. Sci Technol. 2012;2:2264.

# Conductive mesoporous carbon electrodes for biosensing applications

Alicia Gomis-Berenguer<sup>1</sup>, Naiara Hernández-Ibañez<sup>2</sup>, Jesús Iniesta<sup>2</sup>, Conchi O. Ania<sup>1\*</sup>

<sup>1</sup>*Instituto Nacional del Carbón (INCAR, CSIC), 33011 Oviedo, Spain,* <sup>2</sup>*Dept. Química Física e Instituto de Electroquímica, Universidad de Alicante, E-03080 Alicante, Spain.*

\*conchi.ania@incarcsic.es

The diversity of carbon materials used as electrodes in electrochemical applications stands from the varied bulk and surface properties (such as the structural polymorphism, chemical stability, rich surface chemistry and electronic conductivity) among the members of the carbon family, which depend on the spatial arrangement of the carbon atoms [1]. Besides carbon allotropes (graphite, graphene, carbon nanotubes), the use of nanoporous carbon materials having large surface areas (ranging between 500-2500 m<sup>2</sup>/g) as electrodes, has opened up new opportunities in electrochemistry [2].

Although most of them have limited electronic conductivity derived from a poor structural order [3], the main advantage of nanoporous carbon electrodes in electrochemical application relies on the increased adsorption and diffusion derived from the surface area (provided the adequate distribution of pore sizes); such properties may bring about an enhancement in the sensitivity of an electrochemical sensor, or favour direct electron transfer reactions at the electrode surface. However, to effectively take advantage of the textural features of carbon electrodes leading to an enhanced contact between the electrode surface and the target molecule, the internal structure (porosity) of the carbon must be accessible.

In this work we have explored the electrochemical features of highly mesoporous carbon electrodes prepared from sol-gel polycondensation reactions and nanocasting procedures [4,5] as porous substrates for the immobilization of cytochrome c (Cyt-c) and glucose oxidase (GOx). Immobilization of Cyt-c and GOx was optimized according to protein concentration, buffer ionic strength solution, temperature, adsorption time and nature of nanoporous carbons. The pseudo peroxidase activity of Cyt-c and the response of GOx to the detection of glucose.

Our results showed that the nanoconfinement in the porosity of the carbon increased the electron transfer rate and electrical contact. This demonstrates the critical role of matching the molecular dimensions of the target molecule with the mean pore size of the carbon electrode for an optimal and efficient molecular orientation minimizing the random distribution at non-efficient positions. Additionally, surface functionalization of the nanoporous carbon electrode is also important as it may control the conductivity, wettability and hydrophobicity, creating favorable/unfavorable interactions with the immobilized molecule that end up controlling the electrochemical response.

[1] Series of Chemistry and physics of Carbon, CRC Press, Taylor and Francis Group, volumes 1-30, 1966-2012. <http://www.crcpress.com/browse/series/CRCCHEPHYCAR>

[2] R.L. McCreery, Advanced Carbon Electrode Materials for Molecular Electrochemistry, Chem. Rev. 2008;108: 2646–2687.

[3] B. Dyatkin, Y. Gogotsi, Effects of structural disorder and surface chemistry on electric conductivity and capacitance of porous carbon electrodes, Faraday Discuss, 2014;172:139-162.

[4] Macias C, Haro M, Rasines G, Parra JB, Ania CO. Carbon-black directed synthesis of mesoporous aerogels, Carbon 2013;63: 487-497.

[5] Rasines G, Lavela P, Macias C, Zafra MC, Tirado JL, Parra JB, Ania CO. N-doped monolithic carbon aerogel electrodes with optimized features for the electrosorption of ions, Carbon 2015;83:262-274.

# Locally Self-induced “electro-click” onto self-assembled monolayer: Evidence for surface self-catalysis propagation

Sébastien Lhenry<sup>a</sup>, Yann R. Leroux<sup>a</sup>, Christophe Orain<sup>b</sup>, Françoise Conan<sup>b</sup>, Nathalie Cosquer<sup>b</sup>, Nicolas Le Poul<sup>b</sup>, Yves Le Mest<sup>b</sup>, O. Reinaud<sup>b</sup>, Philippe Hapiot<sup>a</sup>

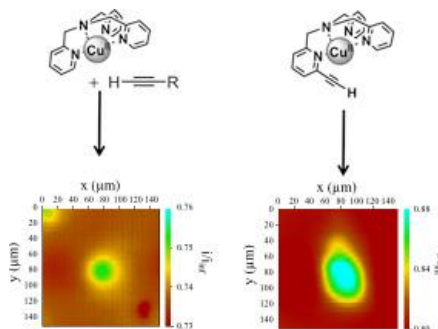
<sup>a</sup>*Institut des Sciences Chimiques de Rennes, CNRS, Université de Rennes 1*

<sup>b</sup>*CEMCA, Université de Bretagne Occidentale, Brest*

<sup>c</sup>*LCBPT, Université Paris Descartes, France*

yann.leroux@univ-rennes1.fr

In this communication, observation of a 2D self-propagation catalytic reaction on surfaces is described. Huisgen 1,3-dipolar cycloaddition, known as click chemistry<sup>1</sup>, is one of the most used catalytic reaction nowadays as it is a highly versatile and fast coupling reaction. It can be used as well with biological samples in water or in classic organic synthesis. In parallel, interest in chemically modified surfaces has been growing for several decades due to their many applications in various scientific areas. Among many methods to chemically modified surfaces, click chemistry coupling is also often used for its efficiency and its great selectivity. This coupling reaction between an azido and a free alkyne is catalyzed by Cu(I) which can be generated chemically or electrochemically, leading to “electro-click chemistry reaction” in the latter case. Recently, using Scanning Electrochemical Microscopy (SECM), localized electro-click chemistry reactions were successfully performed.<sup>2</sup> “Self-induced” electro-click chemistry reaction can be achieved when using a molecule that is at the same time a reactant and the catalyst.<sup>3</sup> In this communication, we will specifically study local self-induced electro-click chemistry reaction onto self-assembled monolayers by SECM. It will be demonstrated that using this specific class of molecule (see scheme), catalytic properties can be transferred to the surface and that 2D self-propagation of the catalytic reaction on the surface can be seen. Particular attention will be paid to the determination of the experimental conditions needed to perform and monitor these experiments in unbiased conditions (the substrate is not electrically connected).<sup>4</sup>



[1] V. V. Rostovtsev, L. G. Green, V. V. Fokin, K. B. Sharpless. A Stepwise Huisgen Cycloaddition Process: Copper(I)-Catalyzed Regioselective “Ligation” of Azides and Terminal Alkynes, *Angew. Chem., Int. Ed.* 41 (2002) 2596.

[2] D. Quinton, A. Maringa, S. Griveau, T. Nyokong, F. Bedioui, Surface patterning using scanning electrochemical microscopy to locally trigger a “click” chemistry reaction, *Electrochem. Com.* 31 (2013) 112.

[3] A. Gomila, N. Le Poul, N. Cosquer, J.-M. Kerbaol, J.-M. Noël, M. T. Reddy, I. Jabin, O. Reinaud, F. Conan, Y. Le Mest, Self-induced “electroclick” immobilization of a copper complex onto self-assembled monolayers on a gold electrode, *Dalton Trans* 39 (2010) 11516.

[4] S. Lhenry, Y. R. Leroux, C. Orain, F. Conan, N. Cosquer, N. Le Poul, O. Reinaud, Y. Le Mest, P. Hapiot, Locally Induced and Self-Induced “electro-click” onto Self-Assembled Monolayer: Writing and Reading with SECM under Unbiased Condition, *Langmuir* 30 (2014) 4501–4508.



# New Strategies to Manufacture Low-cost Thin-film MicroElectrode Arrays for Electroanalysis

Ana Fernández-la-Villa\*, Diego F. Pozo-Ayuso, Mario Castaño-Álvarez  
MicruX Technologies. Severo Ochoa Bldg. Julián Clavería s/n, Floor -1, Room 4 & 6, 33006 Oviedo  
(Asturias) SPAIN.

\*[anafv@micruxfluidic.com](mailto:anafv@micruxfluidic.com)

Electroanalysis is a very important analytical field that has demonstrated its potential for solving real-life analytical problems by understanding of the fundamentals of electrode reactions and the principles of electrochemical methods. The high performance, small size, low power requirements and low cost of electrochemical sensors has led to many important detection systems.

In this sense, thin-film microtechnologies enable the fabrication of metal-based electrodes with high precision and resolution in a cost-effective way. Besides, these technologies allow the fabrication of microelectrodes which show at least one dimension not greater than 25  $\mu\text{m}$ . Microelectrodes provide unique electrochemical properties such as small capacitive-charging currents, reduced ohmic ( $iR$ ) drop, and steady-state diffusion currents. Moreover, the small size of the microelectrodes enables measurements on very limited solution volumes.

Thus, microelectrodes are currently available on different materials, geometric shapes and configurations. In this work, new **microelectrode arrays** (MEA) based on pinholes with a honeycomb microstructure have been designed and manufactured on a metal working single-electrode. Microelectrode arrays overcome the extremely large current densities yet very small absolute currents of a single microelectrode and have both helpfully high current densities and satisfactory output signals. The basic layout of two microelectrode arrays is shown in **Figure 1**.

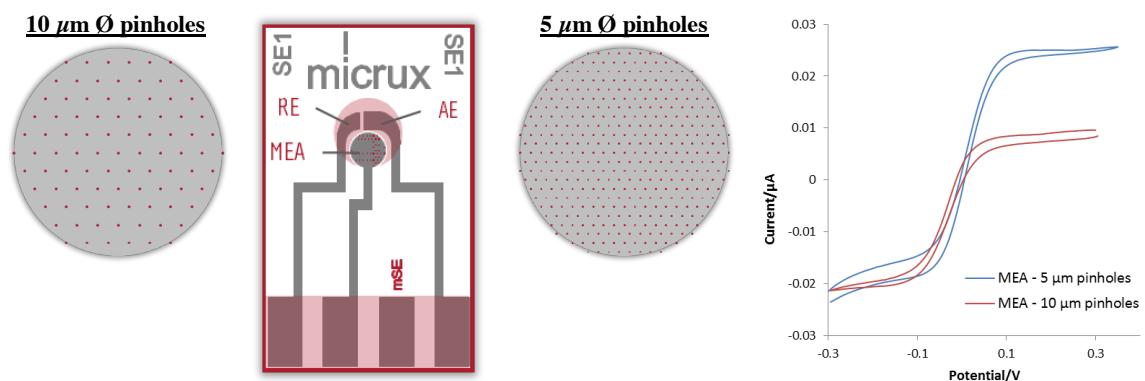


**Figure 1.** Basic layout of the microelectrode arrays and typical cyclic voltammograms for redox compounds

The new electrochemical sensors are based on a three-electrode (working – WE, reference – RE and auxiliary – AE) approach. The metal structure of electrodes is fabricated by a photolithographic process. A SU-8 resin layer is used to delimit the electrochemical cell as well as define the microstructure of the array. Thus, the working electrode (1 mm diameter) consists of a metal surface (platinum or gold) coated with the SU-8 layer (3–4  $\mu\text{m}$  thickness) in which is defined different pinholes with a honeycomb microarray structure, all in the same photolithographic process. Two different microstructures were achieved, one based on ninety 10- $\mu\text{m}$  diameter pinholes with 100- $\mu\text{m}$  pitch each other and another based on five hundred 5- $\mu\text{m}$  diameter pinholes with 50- $\mu\text{m}$  pitch each other. In **Figure 1** is shown the typical microelectrode behavior for both structures reaching the steady-state in a short time.

Microelectrodes offer a very suitable analytical tool in applications such as the study of electrochemical reaction mechanisms and kinetics, trace electrochemical analysis, electrochemical reactions in solutions of very high resistance, in-vivo measurements on biological objects, multichannel (bio)sensors as well as detection in flowing liquids (FIA, HPLC, CE...).

*This work has been supported by EU (M-ERA.NET), IDEPA (IDE/2013/000028) and the Spanish Ministry of Economy and Competitiveness (RTC-2014-1496-1)*

# Validating a Central Approximation in Theories of Regular and Random Electrochemical Electrode Arrays

O. Sliusarenko, A. Oleinick, I. Svir, C. Amatore  
CNRS UMR 8640 PASTEUR, Ecole Normale Supérieure-PSL Research University,  
Département de Chimie, Sorbonne Universités, UPMC Paris 6  
24, rue Lhomond, 75005 Paris, France  
*christian.amatore@ens.fr; irina.svir@ens.fr*

Regular electrode arrays generally possess a symmetry which (under certain conditions) allows to reduce their mathematical description to consideration of a single electrode of this array within the laterally bounded domain (known as ‘unit cell’ or ‘diffusion domain’) [1, 2]. In this case by multiplying the simulated current of the single cell by the number of electrodes in the array one would obtain an electrochemical response of the whole array. The electrodes in arrays are generally ordered in a hexagonal or square patterns, which result in hexagonal or square cross-sections of the unit cells, respectively. A straightforward approach to the mass-transport problem in such cells would require complex and time-consuming 3D simulations. Therefore almost always an approximation is made in simulations by replacing the original cross-section with the circular one of the same surface area. At one hand, this greatly facilitates the simulations due to the possibility to formulate the mass-transport problem in two dimensions (2D). On the other hand, although this approach was proven to be effective in practice, the error introduced by this approximation, to the best of our knowledge, was never been studied or even estimated.

The error associated with the approximation is based on the fact that it is impossible to pave the plane with non-intersecting circles contrary to the perfect plane paving with hexagons or squares as well as due to the different possible diffusion pathways within the single cells with different cross-sections. In order to assess quantitatively this approximation we performed 3D Brownian motion simulations for the single cells of square, hexagon and circular cross-sections equipped with disk electrode. Moreover the situations with inlaid, recessed and protruding electrodes were also considered for each cross-section shape. Notwithstanding the completely different diffusion patterns observed in these systems, the obtained results showed that the approximation gives rise to an experimentally indistinguishable error (less than 5%) for all considered systems [2]. The only exception (i.e. when the error is larger than 5%) was the case when the electrode radius was extremely close to the characteristic size of the cross-section, i.e. the situation when the neighbouring electrodes in the array almost touch each other. The latter situation is of low experimental interest and in addition such systems exhibit the same behavior as a planar electrode with the surface area of the whole array (except of the initial times of the experiment).

With the same idea in mind, to check the validity of the circular diffusion domain approximation, the random arrays were considered. We dealt with 2D Gaussian (i.e. centered) and space uniform distributions of the electrodes in array. The electrochemical response of the array can be obtained by the following procedure: (i) construct the diffusion domains of each electrode (via Voronoi tessellation); (ii) build up the histogram of diffusion domains surface areas; (iii) using circular approximation of the diffusion domain simulate the current with for each bin (i.e. different values of the single cell surface area) in the histogram; (iv) sum up the responses for each bin with an appropriate weight taken from the histogram. This approach was compared with similar approach where distribution of the domain surfaces areas was described analytically (i.e. fit of the histogram) and heuristic analytical expressions were used for a domain with a given surface area. The reference for these two approaches was a simulation of the whole randomly generated array. The outcome of these simulations reveal that any of the weighting procedures works perfectly for initial and intermediate times of the experiment, however, may lead to a discrepancies of about 5-10% at larger times. The latter occurs due to the presence of the domains with very large surface area as well as compelled asymmetry of such domains [3].

## References:

- [1] C. Amatore, J.-M. Savéant, D. Tessier, *J. Electroanal. Chem.* 1983, 147, 39.
- [2] O. Sliusarenko, A. Oleinick, I. Svir, C. Amatore, *Electroanal.* 2015, in press.
- [3] O. Sliusarenko, A. Oleinick, I. Svir, C. Amatore, in preparation.

# Thin Layer Ionophore-Based Membranes Electrochemically modulated by Poly(3-octylthiophene) for Multianalyte Detection

Maria Cuartero, Gaston Crespo and Eric Bakker

Department of Inorganic and Analytical Chemistry, University of Geneva, Quai Ernest-Ansermet 30, CH-1211 Geneva, Switzerland.

Email address: Maria.Cuartero@unige.ch

We report here on the selective voltammetric transfer of lithium and calcium into an ionophore-based polymeric thin layer membrane back side contacted with electropolymerized poly(3-octylthiophene) (POT), an anion exchanger conducting polymer. It has been demonstrated that POT permits to modulate the ion-transfer process across the membrane/sample interface by its oxidation.<sup>1,2</sup> The additional incorporation of either calcium or lithium ionophore into the thin membrane permits the discrimination between background electrolyte (10 mM NaCl) and primary analytes (Figure 1a). The peak displayed in the cyclic voltammogram is gradually displaced to positive values with increasing activity of the corresponding cation, which follows precisely the Nernst equation. In contrast to other techniques, for instance rotating electrode stripping voltammetry, these electrodes exhibit a linear range suitable for biomedical and environmental applications ( $10^{-5}$ - $10^{-2}$  M).

An interesting selectivity characteristic is observed when both ionophores are incorporated simultaneously in the same membrane. Applying a linear sweep potential, each cation shows its own peak in a distinct potential range (Figure 1b). These peaks follow a Nernst shift with increasing concentrations of lithium and calcium. With this new approach both cations can be easily determined in the presence of 10 mM NaCl. To the best of our knowledge, this is the first time such selective multianalyte analysis is demonstrated with an ion transfer electrochemical technique.

Current efforts in our laboratory to further improve this approach include the use of thin layer samples to develop exhaustive processes and extending the detection to other systems such as polyion sensors.

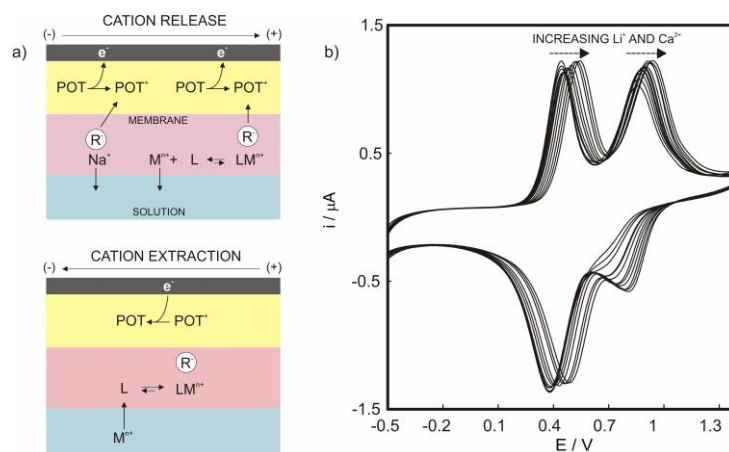


**Figure1.** a) Scheme of the electrochemical process ( $R^-$ =cation exchanger,  $M^{n+}$ = $Li^+$  and/or  $Ca^{2+}$ ,  $L$ =ionophore). b) Cyclic voltammograms obtained for increasing equimolar concentrations of lithium and calcium. (Scan rate of  $100\text{ mVs}^{-1}$ ).

## References:

1. Y. Kim, P.J. Rodgers, R. Ishimatsu, S. Amemiya, *Anal. Chem.* 2009, 81, 7262-7270.
2. P. Si, E. Bakker, *Chem. Comm.* 2009, 5260-5262.

# Surface-Initiated Enzymatic Polymerization Based Signal Amplification Strategies for Sensitivity Improvement of Electrochemical DNA Sensors

Ying Wan, Pengjuan Wang, Yan Su\*

School of Mechanical Engineering, Nanjing University of Science and Technology  
Xiaolingwei Street 200, Nanjing, Jiangsu, 210094, China  
wanying@njust.edu.cn

Electrochemical DNA (E-DNA) sensors have great potential in point-of-care diagnosis because of their ability to produce a simple, accurate and inexpensive platform for DNA sensing. However, it is difficult to detect extremely low abundance of DNA biomarkers in clinical samples. Thus different signal amplification methods have been developed to improve the sensitivity of E-DNA sensors. We have developed a serial of signal amplifying E-DNA sensors based on terminal deoxynucleotidyl transferase (TdT) mediated surface-initiated enzymatic polymerization (SIEP). The first one was simply constructed by a capture probe to recognize target and the TdT catalyzed elongation of target DNA. We developed an ultrasensitive E-DNA sensor based on the signal amplification efficiency of nanoprobe and surface-initiated enzymatic polymerization (SIEP). In this method, a sandwich-type hybridization structure was formed by capture probe, target and signal probe. Capture probe was immobilized onto gold electrode and signal probe was immobilized onto gold nanoparticles (AuNPs). Upon hybridization, AuNPs modified with signal probe DNA were bound to the electrode and then subjected to terminal deoxynucleotidyl transferase (TdT)-mediated SIEP. During the extension reaction, biotin labels are incorporated into the SIEP-generated long single-stranded DNA (ssDNA). As there are hundreds of DNA probes on the nanoprobe, one hybridization event would generate hundreds of long ssDNA. Then specific binding of Av-HRP to the biotin label leads to an enzyme turnover-based signal transduction. By employing nanoprobe and TdT, we aim to provide a novel E-DNA sensor with high femtomolar sensitivity and excellent differentiation ability for even single mismatches.

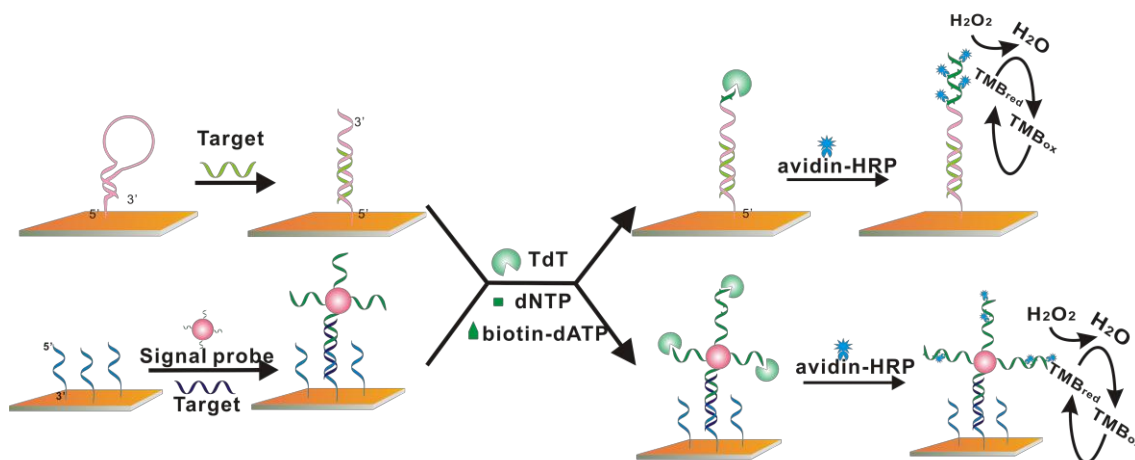


**Figure 1** Strategy of surface-initiated enzymatic polymerization (SIEP) amplified E-DNA sensor.

1. "A Surface-Initiated Enzymatic Polymerization Strategy for Electrochemical DNA Sensors"Y. Wan, H. Xu, Y. Su, X. Zhu, S. Song, C. Fan, *Biosens. Bioelectron.* **2013**, 41(1): 526-531.
2. "Ultrasensitive electrochemical DNA sensor based on the target induced structural switching and surface-initiated enzymatic polymerization"Y. Wan, P. Wang, Y. Su, X. Zhu, S. Yang, J. Lu, J. Gao, C. Fan, Q. Huang, *Biosens. Bioelectron.* **2014**, 55(1): 231-236.

# Electrochemical Characterization of Gold-Coated Magnetic Nanoparticles as ‘Dispersible Electrodes’

Saimon Moraes Silva, Roya Tavallaie, Muhammed Alam, J. Justin Gooding

School of Chemistry and Australian Centre for NanoMedicine, The University of New South Wales  
Sydney 2052, Australia

[s.silva@student.unsw.edu.au](mailto:s.silva@student.unsw.edu.au), [justin.gooding@unsw.edu.au](mailto:justin.gooding@unsw.edu.au)

The ‘Dispersible Electrodes’ concept was previously introduced in our group by Goon *et. al.* as an electrochemical approach to detect extreme low concentration of analyte in large samples volumes in a reasonable time frame.<sup>1, 2</sup> In this concept, the electrochemical sensor is subdivided in minute pieces by using conducting gold coated magnetic nanoparticles (Au@MNPs) as active element in the selective capture and direct electroanalytical quantification of the species of interest.<sup>1</sup> The Au@MNPs are dispersed in solution,

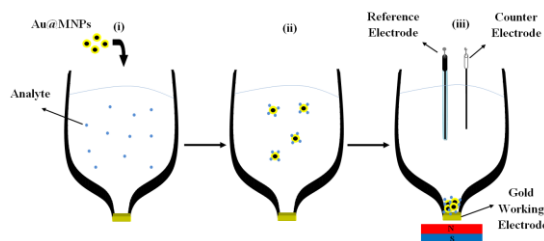


**Figure 1** – Outline of the basics steps necessary for the measurement of a target analyte using the Dispersible Electrodes.

once the capturing process has completed a magnetic field is applied and brings the nanoparticles to the sensing interface to the electrochemical measurements (Figure 1). So far, the Au@MNPs that has been used in this approach is on average 150 nm in size and exquisite results have been achieved with them.<sup>3</sup> However, with a view to obtain improved monodispersity and stability against aggregation, the present work evaluates the synthetic route and the electrochemical properties of different types of Au@MNPs for its application as ‘Dispersible Electrodes’. The obtaining of stable, monodisperse, well-defined, and nanoparticles that are fully coated with gold are crucial to understand how the particles assemble in the sensor interface and how they interact with the analyte. The Au@MNPs proposed in our group by Goon *et. al.* was used as the model particles, this kind of particles have a ill-defined shape but exhibited excellent magnetic properties.<sup>3</sup> A second type of spherical particles was studied, which are henceforth referred to as Gao-Au@MNPs because the synthesis was performed according to a procedure reported by Gao and co-workers.<sup>4</sup> The third kind of particles was synthesized according to a procedure reported by Freitas *et. al.*,<sup>5</sup> so called Freitas-Au@MNPs. Finally, cubic Au@MNPs (Cubic-Au@MNPs) were obtained by using the iron oxide cores coated with polyethylenimine according to procedure reported by Goon and co-workers<sup>3</sup> and the gold nanoshell was formed by reducing gold chloride with a reducing agent. The four types of particles were characterized morphologically by using Transmission Electron Microscopy, Scanning Electron Microscopy and X-Ray Photoelectron Spectroscopy. The success of the fully gold coating of the different Au@MNPs was accessed by using cyclic voltammetry in 50 mM H<sub>2</sub>SO<sub>4</sub> solution in comparison to a polycrystalline gold electrode. All the four types of particles were stable in the acid medium even after 100 scans. The kinetics of electron transfer and how the Au@MNPs assemble in the bulk electrode were investigated by using techniques such as cyclic voltammetry and impedance and also different electrochemical probes such as potassium ferricyanide, ruthenium hexamine and cobalt-phenanthroline. The four types of particles presented different behaviours that is discussed in this current work and each of them presents positive and negatives features for its applications as ‘Dispersible Electrodes’. We are still looking for improvements in the synthesis of the Au@MNPs so we can have a better defined system to investigate.

1. I. Y. Goon, L. M. H. Lai, M. Lim, R. Amal and J. J. Gooding, *Chem Commun*, 2010, **46**, 8821-8823.
2. L. M. H. Lai, I. Y. Goon, M. Lim, A. B. Hibbert, R. Amal and J. J. Gooding, *J Electroanal Chem*, 2011, **656**, 130-135.
3. I. Y. Goon, L. M. H. Lai, M. Lim, P. Munroe, J. J. Gooding and R. Amal, *Chem Mater*, 2009, **21**, 673-681.
4. Y. D. Jin, C. X. Jia, S. W. Huang, M. O'Donnell and X. H. Gao, *Nat Commun*, 2010, **1**.
5. M. Freitas, S. Viswanathan, H. P. A. Nouws, M. B. P. P. Oliveira and C. Delerue-Matos, *Biosens Bioelectron*, 2014, **51**, 195-200.

# Volume Synthesis of Calcareous Deposit on Carbon Steel in Natural Seawater: Effect of Two-Step Applied Potential Waveform

Dan Nguyen Dang<sup>a,b</sup>, Stéphanie Gascoin<sup>b</sup>, Cosmelina G. Da Silva<sup>a,b</sup>, Richard Retoux<sup>b</sup>, Benoît Riffault<sup>a</sup>, Daniel Chateigner<sup>b</sup>, Otavio Gil<sup>a</sup>

<sup>a</sup> Laboratoire Aliments Biotechnologies Toxicologie et Environnement (ABTE), EA 4651 – IUT de Caen – Univ. Caen Basse-Normandie, France

<sup>b</sup> Laboratoire de Cristallographie et Sciences des Matériaux (CRISMAT) UMR6508 CNRS – Ensicaen – IUT de Caen – Univ. Caen Basse-Normandie, France

[dang-dan.nguyen@unicaen.fr](mailto:dang-dan.nguyen@unicaen.fr); [stephanie.gascoin@ensicaen.fr](mailto:stephanie.gascoin@ensicaen.fr); [richard.retoux@ensicaen.fr](mailto:richard.retoux@ensicaen.fr);  
[cosmelina.goncalves-dasilva@unicaen.fr](mailto:cosmelina.goncalves-dasilva@unicaen.fr); [benoit.riffault@unicaen.fr](mailto:benoit.riffault@unicaen.fr);  
[daniel.chateigner@ensicaen.fr](mailto:daniel.chateigner@ensicaen.fr); [otavio.gil@unicaen.fr](mailto:otavio.gil@unicaen.fr)

In seawater, cathodic protection (CP) of metallic structures leads to the formation of calcareous deposits. This phenomenon depends on a lot of parameters, which have given origin to numerous researches for several years: applied potential, substrate nature, flow rate, temperature, pH, pressure or seawater composition influences have been extensively studied in artificial and natural seawaters. Recently, a new method based on an innovative adaptation of cathodic protection technique has been developed in order to synthesise in volume the calcareous structures in natural seawater. Our objective, in the context of the Research National Agency (ANR) EcoCorail project, is to favour conditions to a rapid 3D deposit growth, predominantly composed of  $\text{CaCO}_3$ . This calcareous conglomerate could be used as “natural cement” linked with sand, shells, marine sediments, etc. to create a natural concrete. This method needs to apply more cathodic potentials than those used in CP, corresponding to the range of potential of hydrogen evolution, in order to prevent the cathode blocking, and to induce pH increased far away from the electrode.

The influence of applied potential and temperature on properties of calcareous deposit has previously been studied [1]. It was shown that brucite is predominantly observed ( $> 90$  at%) with high deposition rate for high cathodic potentials ( $-1.2$ ;  $-1.3$  V vs.  $\text{Ag}|\text{AgCl}_{\text{sat}}$ ) and acts as an aragonite's growth inhibitor. A temperature decrease deactivates hydrogen evolution and reduces the pH favouring aragonite formation. For less negative potentials ( $-1.0$ ;  $-1.1$  V vs.  $\text{Ag}|\text{AgCl}_{\text{sat}}$ ), deposit growth is very low. In all experiments, calcite is only present at very small ratio, typically lower than a few percent.

The present study focuses on the influence of the two-step applied potentials on the deposition and structure of calcareous formed. Experiments are designed to form volume calcareous deposits on immersed carbon steel grids in natural seawater with deposition time varied from 2 to 30 days. In order to simulate a natural environment, experiments are led with natural seawater directly pumped from the sea into a  $0.9 \text{ m}^3$  tank at the Marine Station of Luc-sur-Mer (Channel coast of France). The temperature is fixed at  $20^\circ\text{C}$ . Four different series were carried out with a first step of applied potential  $E_1$  fixed at  $-1.3$  V vs.  $\text{Ag}|\text{AgCl}_{\text{sat}}$ . The second step of applied potential ( $E_2$ ) is fixed successively at  $-1.1$ ;  $-1.0$ ;  $-0.9$  V vs.  $\text{Ag}|\text{AgCl}_{\text{sat}}$  or open circuit potential–OCP for each experiment. Different periods for both steps were tested.

Two-step potential waveform influences the chronoamperometric curves. Deposit weights, structures and microstructures are followed using electrochemical impedance spectroscopy (EIS), scanning electron microscopy (SEM), transmission electron microscopy (TEM) and X-ray diffraction. XRD patterns analysed using the combined analysis methodology allow the quantitative determination of phase fractions, cell parameters, atomic positions and mean anisotropic crystallite sizes for each phase. Our results show that the two-step potential waveform permits to maintain a high rate of calcareous deposition and so favours to form rapidly the 3D calcareous deposits. The second step  $E_2$  (especially at  $-0.9$  V vs.  $\text{Ag}|\text{AgCl}_{\text{sat}}$ ; OCP) plays an important role to increase significantly the proportion of  $\text{CaCO}_3$  present in the deposit to about 30-50 at%.

## References:

[1] Volume synthesis of calcareous deposit on carbon steel in natural seawater: effect of applied potential and temperature, D. Nguyen Dang, B. Kabbadj, S. Gascoin, B. Riffault, R. Sabot, M. Jeannin, D. Chateigner, O. Gil, Eurocorr2015, Graz – Austria, September 2015.

# Conductive Ceramics as O<sub>2</sub>-Evolving Anodes for Electrolytic Reduction of Metal Oxides

Sung-Wook Kim, Eun-Young Choi, Wooshin Park, Hun Suk Im, and Jin-Mok Hur  
*Nuclear Fuel Cycle Process Development Group, Korea Atomic Energy Research Institute*  
989-111 Daedeok-daero, Yuseong-gu, Daejeon 305-353, Republic of Korea  
swkim818@kaeri.re.kr

An electrolytic reduction process has been developed to produce pure metals from their oxides through an electrochemical reaction using molten salt electrolyte [1]. An electrolytic reduction is essential in pyroprocessing, in which the spent oxide fuels used in current nuclear reactors are recycled into metallic fuels for the next-generation fast reactors [2]. High-temperature O<sub>2</sub> gas is evolved in the anode during the electrolytic reduction, and therefore, the anode material should be stable in this highly oxidizing atmosphere. Pt is the common anode material owing to its excellent oxidation resistance. However, Pt can be damaged during the electrochemical reaction in a LiCl-Li<sub>2</sub>O electrolyte, which is widely used in the electrochemical reduction of UO<sub>2</sub> in the pyroprocessing [3].

In this study, we investigated the feasibility of conductive ceramics as O<sub>2</sub>-evolving anodes because they are considered to be more stable than metals or their alloys in an oxidizing atmosphere. Several conductive ceramics were able to electrochemically reduce UO<sub>2</sub> into metallic U with an O<sub>2</sub> evolution, showing the potential of conductive ceramic anodes.

[1] G. Z. Chen, D. J. Fray, T. W. Farthing, *Nature* 407 (2000) 361.

[2] H. Lee, G.-I. Park, K.-H. Kang, J.-M. Hur, J.-G. Kim, D.-H. Ahn, Y.-Z. Cho, E. H. Kim, *Nucl. Eng. Technol.* 43 (2011) 317.

[3] S. M. Jeong, H.-S. Shin, S.-H. Cho, J.-M. Hur, H. S. Lee, *Electrochim. Acta* 54 (2009) 6335.



# Does a link between multiple oxidation peaks of gold oxide formation and exposed crystal planes exist on polycrystalline gold?

C. Jeyabharathi, P. Ahrens, U. Hasse and F. Scholz

*Institute of Biochemistry, University of Greifswald,  
Felix-Hausdorff-Str.4, 17487 Greifswald, Germany  
E-mail: chinnayaj@uni-greifswald.de*

## ABSTRACT

Though monolayer oxidation on single crystal gold surfaces are well studied and crystal planes can be distinguished based on the peak potential of oxide formation, to the best of our knowledge, no paper relates the multiple oxide peaks on polycrystalline gold to crystal planes. In this work, we cycled the gold electrode in  $\text{H}_2\text{SO}_4$  and hydrochloric acid solutions and tried to link the CV features to crystal planes. Electrochemically cycling of gold electrode in 0.1 M  $\text{H}_2\text{SO}_4$  shows that the as-polished gold surface has a broad peak centered at 1.33 V vs Ag/AgCl (3 M KCl), whereas the surface after electrochemical cycling for 50 runs exhibited three distinct peaks in the monolayer-oxide region, those could be related to the oxide formation on different crystal planes. However, cycling in 0.1 M hydrochloric acid solution shows a sharp peak at 1.35 V initially, and a highly intense peak at 1.12 V during consequent potential cycles at the cost of a peak at 1.35 V (Fig 1a). These features can be ascribed to the preferential orientation or faceting of the gold surface during dissolution and re-deposition cycles. The activity of the surface to the ORR is less in terms of half-wave potential ( $E_{1/2}$ ) when the peak current at 1.35 V is higher than that of the one at 1.12 V. After prolonged cycling, the shift of ORR peak to more positive  $E_{1/2}$  values (Fig 1b) is observed, when the peak at 1.12 V gets larger than the one at 1.35 V. Such a transition can be attributed to changes in the surface structure. When comparing with the peak potentials of monolayer oxidation on single crystal electrodes [J.Phys.Chem.C, 2007, 111, 13197], we can attribute the peak at 1.35 V to the (111) plane and the one at 1.12 V to the (100) plane. The observed ORR activity is also in accordance with the trend given in literature: (100) > (110) > (111). The changes in the double layer capacitance due to reconstruction of the surface and its lifting in addition with the above results suggest that there is a clear link between the oxide formation peaks on polycrystalline gold to single crystal planes.

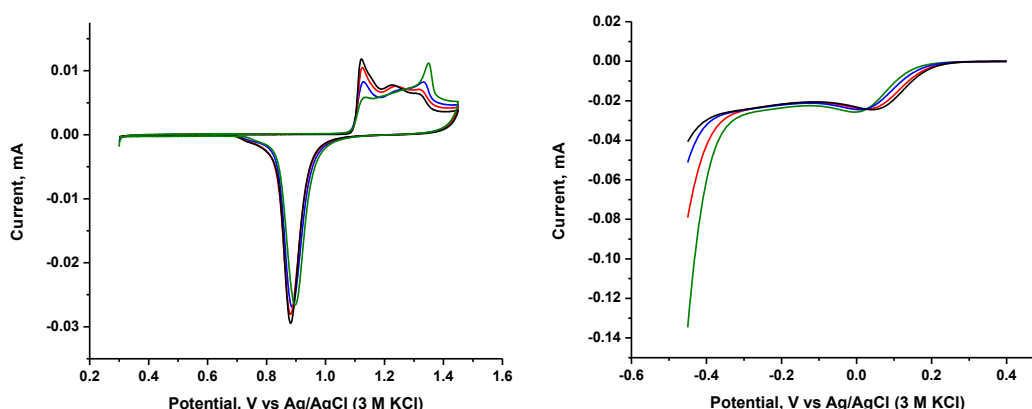


Fig 1. (a) Cyclic voltammograms of gold electrode treated in HCl solution; (b) corresponding linear sweep voltammograms of ORR



# Concentration Rectification in Nanofluidic Transducers

Jin Cui, Klaus Mathwig, Serge G. Lemay  
MESA+ Institute for Nanotechnology, University of Twente  
Enschede, The Netherlands  
j.cui-1@utwente.nl

We are incorporating microfluidic fluid flow control with redox-cycling based nanogap bioelectrochemical transducers. This allows deterministic mass transport across multiple transducers located downstream for each other, even near or at the single-molecule limit. We introduced earlier electrical cross-correlation spectroscopy to detect molecule-number fluctuations in nanofluidic channels by cross-correlating steady-state electrochemical signals between pairs of electrodes located upstream and downstream from each other.<sup>1</sup> Surprisingly, the transient change in signal at a downstream electrode pair in response to switching of the potential at an upstream electrode cannot be explained exclusively in terms of processes taking place at the upstream electrode.<sup>2</sup> This effect persists in the presence of high concentrations of supporting electrolyte and is thus not purely electrostatic in nature. We argue that it instead results from concentration enhancement-depletion effects tied to unequal effective diffusion coefficients for the analyte molecules in different redox states.<sup>3</sup> The observed nonlocality is thus closely related to so-called rectifying behavior in nanofluidic diodes,<sup>4</sup> with the added element that here redox chemistry provides the required breaking of symmetry between cation and anion flow. The experiments can be understood qualitatively in terms of the Péclet number in the nanochannel, and lead to new insights into the effect of longitudinal diffusion under fluid flow in electrochemical nanofluidics.

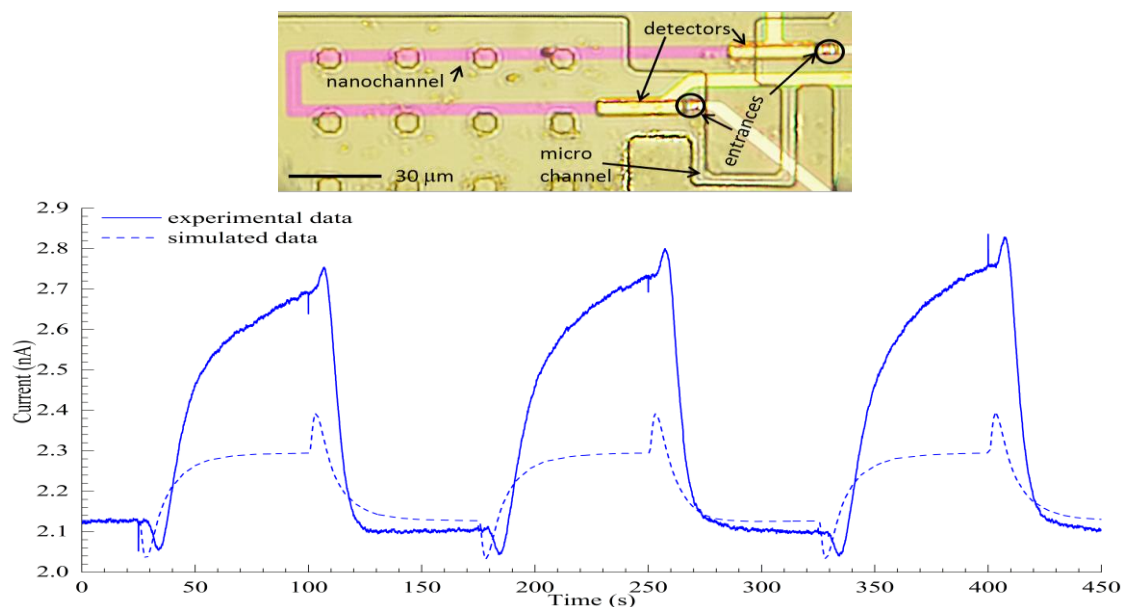


Figure 1 (Top) two nanogap transducers coupled via a microchannel and a nanochannel connected in parallel. (Bottom) The solid line represents the experimental amperometric signal from a downstream transducer in response to stepping the potential of the upstream electrode. Surprisingly, the downstream steady-state current is influenced by the remote upstream electrodes. The dashed line is a simulated result obtained by solving the coupled equations for convection of the solvent and diffusion of the redox species. The simulation, which assumes bulk values for the diffusion constants of reduced and oxidized molecules ( $6.7 \times 10^{-10} \text{ m}^2/\text{s}$  and  $5.36 \times 10^{-10} \text{ m}^2/\text{s}$ , respectively) captures the main features of the experimental observations.

- 1 Klaus Mathwig, Dileep Mampallil, Shuo Kang, and Serge G. Lemay, *Physical Review Letters* **109** (11) (2012).
- 2 Klaus Mathwig and Serge G. Lemay, *Electrochimica Acta* **112**, 943 (2013).
- 3 Dileep Mampallil, Klaus Mathwig, Shuo Kang, and Serge G. Lemay, *Analytical chemistry* **85** (12), 6053 (2013).
- 4 Hirofumi Daiguji, *Chemical Society Reviews* **39** (3), 901 (2010).

# Electrical Current-Induced Thermal Characteristics in a Carbon Nanotube

B. C. Chen<sup>1</sup>, C. Y. Ho<sup>2</sup>, H. H. Ku<sup>3</sup>, M. Y. Wen<sup>4</sup>, W. C. Wu<sup>5</sup>, Y. H. Tsai<sup>2</sup>

<sup>1</sup> Department of Chinese Medicine, Buddhist Dalin Tzu Chi General Hospital, Chiayi 622, Taiwan

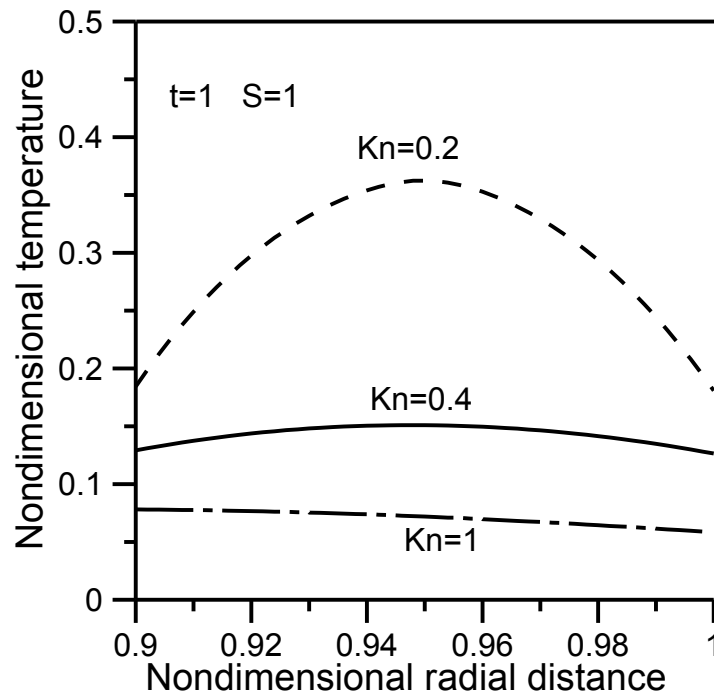
<sup>2</sup> Department of Mechanical Engineering, Hwa Hsia University of Technology, Taipei 235, Taiwan

<sup>3</sup> Department of Computer Science & Information Engineering, Hwa Hsia University of Technology, Taipei 235, Taiwan

<sup>4</sup> Department of Mechanical Engineering, Cheng Shiu University, Kaohsiung 833, Taiwan

<sup>5</sup> Department of Digital Media Design, Hwa Hsia University of Technology, Taipei 235, Taiwan  
hcy2182@yahoo.com.tw

There are special heat transfer properties in carbon nanotube due the high aspect of surface area to volume. Carbon nanotube can be used as the filling stuff of composite materials or nanofluid to enhance their thermal performances. This paper investigates the difference of heat transfer characteristics of carbon nanotube from bulk material to improve the thermal transport performance. Using nanoscale thermal transport model, this paper analyzes heat transfer characteristics of carbon nanotube and compares the predicted result with the available experimental data. The effects of parameters on heat transfer characteristics in the carbon nanotube are also discussed.



Temperature profile along the nanotube for different Knudsen numbers

# Multilayer Deposition of Iridium Oxide for Biocompatible Stimulating Electrode Application

<sup>a</sup>Pu-Wei Wu, <sup>a</sup>Chai-Wei Chung, <sup>a</sup>Yong-Min Chen, <sup>b</sup>Po-Chun Chen\*

<sup>a</sup>*Department of Materials Science and Engineering, National Chiao Tung University, Hsinchu 300, Taiwan, R.O.C.*

<sup>b</sup>*Biomedical Electronics Translational Research Center, National Chiao Tung University, Hsinchu 300, Taiwan, R.O.C.*

[\\*pcchen@g2.nctu.edu.tw](mailto:pcchen@g2.nctu.edu.tw)

Iridium oxide has received substantial attention in recent years because of its unique ability to inject electric charge and its resistance to corrosion. Moreover, this metal oxide is formed with ionic bonds and the hybridized s orbitals are fully occupied with electrons, which lead to notable stability in both thermal and chemical properties. In this study, we carry out a multilayer deposition of IrO<sub>2</sub> film via chemical bath process. IrO<sub>2</sub> film (CIROF) is successfully fabricated via multi-step deposition with heat treatment, and it is expected to be used as a biocompatible stimulating electrode. The multilayer CIROF is characterized its morphology, composition, crystallinity, surface roughness by SEM, XPS, XRD, and contact angle, respectively. In addition, the conductivity and stimulating performance of the CIROF are employed by Hall Effect and electrochemical measurements following ISO-10993.

# Manufacturing of Micro Probe Tip through Ni Alloys Electroplating

Joo-Yul Lee, Yongsoo Jeong

*Korea Institute of Materials Science*

*797 Changwondaero, Seongsangu, Changwon, Gyeongnam, 642-831, Korea*

*leeact@kims.re.kr*

Electroplating through thick photoresist made it possible to manufacture three dimensional metallic features precisely for the electronic parts. The most popular metallic microstructure is made of nickel sulfamate bath. However, the strength of the as-plated nickel is insufficient, and needs to be hardened through alloying with other elements such as Mn, Co, B, P and so on followed by post-annealing process. We developed new nickel alloy plating solutions to cope with the necessity for monitoring the electrical characteristics of more precise metallic circuits and architecture with narrow line and space. We manufactured photoresist mold on the silicon wafer surface after the shape of micro probe tip array using spin coating and some semiconductor fabrication unit process. Probe tip was electroplated at different alloy composition and additives, and underwent annealing process in the oxygen free atmosphere at 300°C for one hour to endow hard surface characteristics. We also observed the effect of surface modification on the electrical properties of probe tips.

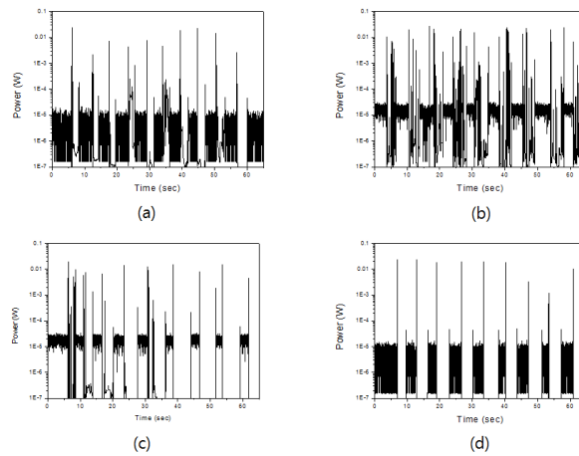


[Fig.1] Electrostatic properties of Ni alloy probe Tips

# Electrochromic Copolymer Film Deposition for Visualization of Latent Fingerprints on Stainless Steel Surfaces

A. Robert Hillman, Rachel M. Sapstead, Natalie Corden and Emma J. R. Palin  
University of Leicester, Leicester LE1 7RH, UK  
e-mail: arh7@le.ac.uk

The pattern of friction skin ridges on the fingertips of an individual is unique. Contact between the finger and an object results in the transfer of material between the finger and the surface in a manner determined by this fingerprint ridge pattern, thereby unambiguously demonstrating that the individual was in that location (for a fixed entity, such as a fixture in a building) or handled that object (in the case of a moveable entity, such as a weapon or tool). This principle is widely exploited in criminal investigations to link people, objects and locations.

In cases where the transferred material is coloured – including blood, ink, paint or foodstuff – the image is immediately visible, irrespective of whether transfer is from the finger to the surface (creating a positive image) or from the surface to the finger (leaving a negative image). Such images are readily seen by the individual and thus commonly removed ("wiped"). However, even in the absence of such foreign substances, there is transfer of fingerprint sweat to the surface, resulting in a non-visible fingerprint image. These *latent* marks are the predominant source of fingerprint evidence at a crime scene: the challenge is to make them visible. Innumerable procedures and reagents (powders, dyes, cyanoacrylate) have been developed to interact with the *fingerprint residue*, but their utility is limited by loss of residue due to environmental exposure. For the case of metallic objects, we have adopted a complementary strategy, in which the fingerprint residue acts as a template to direct electrochemically generated reagent to the *bare surface* between the deposited ridges.

The basic templating concept was recently demonstrated using electrodeposited polyaniline [1] and PEDOT [2] films. These materials have electrochromic properties so, after transfer to background electrolyte, the applied potential can be used to vary the optical properties (simplistically "colour") of the films to optimize visual contrast with the substrate. Here we extend the concept to copolymer films, with the aim of expanding the range of colours available. Building upon the previous polyaniline study [1], we use co-monomers based on aniline and pyrrole. As substrate, we consider stainless steel, a material of forensic relevance in terms of weapons (e.g. knife crime) and tools.

The first stage is establishment of relative growth rates under different conditions (potential, control function, electrolyte). In the case of polypyrrole, new homopolymer enhanced latent fingerprint images are acquired, complementing those available for polyaniline enhancement [1]. The ability of polypyrrole to reveal fingermarks on surfaces subject to a range of environmental conditions (notably heat and water exposure) is promising. Based on these data for the homopolymers, we identify compromise conditions and co-monomer concentration ratios under which co-polymers containing significant fractions of both monomers can be deposited and for which the films are stable.

Spectroelectrochemical characterization of the resulting co-polymers and fingerprint images was then pursued at two levels. Digital optical images were split into their *RGB* components; this is a simple procedure giving improved visualization without complex instrumentation. More detailed FTIR spectroscopic analysis of poly(pyrrole-co-aniline) is complicated by the presence of similar functionalities in the two monomers. We therefore explored the polymerization of 1-(2-cyanoethyl)pyrrole and of a dansyl-functionalised aniline. The former provided a characteristic cyano functionality, readily identified in the FTIR spectrum, and the latter holds the prospect – to be exploited – of a fluorescent electrochromic material.

[1] A.R. Hillman, and A. Beresford, *Anal. Chem.*, 2010, **82**, 483.

[2] R.M. Brown and A.R. Hillman, *Phys. Chem. Chem. Phys.*, 2012, **14**, 8653.

# Minimal instrumentation electroanalytical experimental approach

Arturo García-Mendoza, Adrián de Santiago, Alejandro Baeza\*  
Departamento de Química Analítica, Facultad de Química, UNAM  
Ciudad Universitaria, 04510, Mexico. D.F.  
baeza@unam.mx

Nowadays commercial instruments are becoming increasingly more sophisticated and the user interfaces are simpler and sleeker, leading many teachers to believe that the essential or professional educational objective is to know how to “insert” a sample, learn the instrument software and how performing many assays in few time. Regrettably many instruments have become in “black boxes” that frequently students never appreciate because of they do not realize the real physicochemical principle of the technique, the practical limitations over the instrument design and data acquisition nor the aspects that influence the significance or quality of the data.

In our laboratory we have developed low cost equipment with local materials to perform potentiometric, conductimetric, coulometric, electrochemical and photocolormetric measurements to teach Instrumental Analytical Chemistry focusing in the principles of each technique, the minimal instrumentation necessary and the data acquisition details using available digital low cost devices [1-3] Good analytical results have been achieved in undergraduate and graduate courses in most of Chemistry Colleges in México, some ones in Center and South America or even Europe, in a period of at least eleven years. In some of the latter universities, the methodology presented has given them their first opportunity to achieve electrochemical experimental approach.

Fig. 1 shows the minimal instrumentation equipment built with low-cost local available materials to perform, (a) ISE potentiometric, (b) conductimetric, (c) voltammetric and (d) photocolormetric determinations in several applied fields as clinic, foods analyses, environmental and pharmaceutical, with statistically acceptable analytical results. Fig. 2 shows typical plots obtained with our equipment.

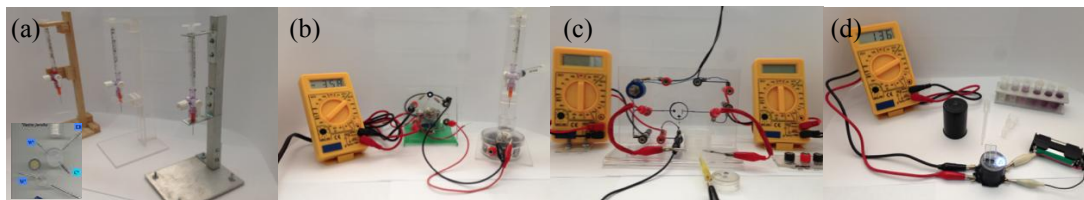


**Fig. 1** Low cost minimal instrumentation designed in our laboratory.

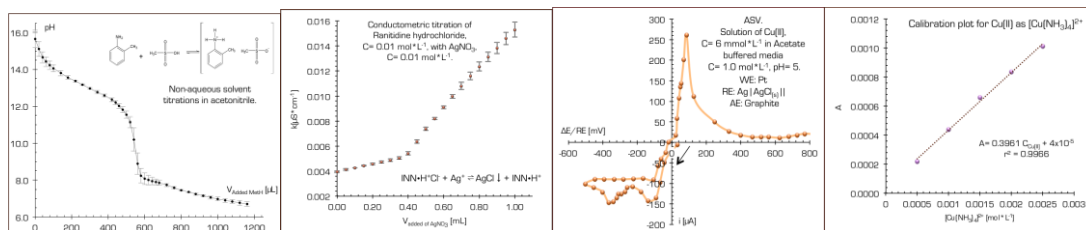


**Fig. 2** Typical records obtained with low-cost equipment. Assay specifications are displayed as inserts.

## References

- [1] A. Baeza, Workshop in the 3rd International Microscale Chemistry Symposium. Mexico City. (2005)
- [2] L. Vierna, A. García-Mendoza, A. Baeza, J. Mod. Edu. Rev. 2 (2012) 243-251.
- [3] A. Marin, A. García-Mendoza, A. De Santiago, A. Baeza, Rev. Cub. Quím. 2 XXVI (2014) 126-136.

# Construction and evaluation of reference electrodes for imidazolium-based ionic liquids. An analytical description.

Arturo García-Mendoza, Julio C. Aguilar

*Departamento de Química Analítica, Facultad de Química, UNAM*

*Ciudad Universitaria, 04510, Mexico. D.F.*

*julioca@unam.mx*

Notwithstanding the increasing importance of ionic liquids (IL) in electrochemical studies and applications, true reference electrodes (RE) are not readily available for its use in these media, and potential scales in IL are scarce. Furthermore, electrochemical assays with quasireference electrodes are not suitable for establishing such scales, since the quasireference electrode potential greatly depends on the composition of the sample and on the state of its surface [1].

In this study, the construction of twelve RE for the aprotic ionic liquids (AIL) [C<sub>2</sub>mim][NTf<sub>2</sub>], [C<sub>3</sub>mim][NTf<sub>2</sub>] and [C<sub>2</sub>mmim][NTf<sub>2</sub>], as well as eight RE for the protic ionic liquid (PIL) [C<sub>2</sub>Him][NTf<sub>2</sub>] (C<sub>2</sub>mim = 1-ethyl-3-methylimidazolium, C<sub>3</sub>mim = 1-propyl-3-methylimidazolium, C<sub>2</sub>mmim = 1-ethyl-2,3-dimethylimidazolium, C<sub>2</sub>Him = 1-ethylimidazolium, NTf<sub>2</sub> = bis(trifluoromethanesulfonyl)imide), is reported and the stability of their electrode potential values for at least nine months was determined by cyclic voltammetry (CV) of the cobaltocenium cation, Cc<sup>+</sup>, and ferrocene, Fc. The electrode potential stability studies were carried out on gold, platinum and glassy carbon working electrodes (WE). The cobaltocenium/cobaltocene redox couple, Cc<sup>+0</sup>, is an important redox system commonly used as internal standard for calibration of RE in IL. The ferricenium/ferrocene couple, Fc<sup>0/+</sup>, commonly used as a standard redox system, was only used when Cc<sup>+0</sup> was not suitable for analysis, since some experimental drawbacks have been previously reported [2], related with the chemical stability, volatility and to the concentration dependence of the diffusion coefficient of ferrocene [2,3].

The RE Ag|AgCl|[C<sub>2</sub>mim][Cl] (IL)|| were prepared following in glass tubes sealed with Vycor® glass. The RE were filled with an internal solution of [C<sub>2</sub>mim][Cl] in each IL giving different concentration of chloride, and then they were stored for five days before their first use. All measurements were performed under N<sub>2(g)</sub> in a glass cell. A Pt wire was used as a counter electrode and each IL was dried for 24 hours at 90° C. The water content in the IL after drying was determined by cathodic stripping square wave voltammetry (CSSWV) at a gold electrode and it was usually found < 180 ppm for all three AIL and > 350 ppm for the PIL. The time evolution of the potential of the RE was followed using [Cc][PF<sub>6</sub>], in all three AIL, or Fc, in the PIL, as internal standards. Individual CV studies of the Cc<sup>+</sup> ion in any of the RE regardless showed a reversible behaviour, following a linear proportional relationship to both the square root of the scan rate and concentration. Diffusion coefficients were calculated with the Randles-Sevcik relationship, and their values are comparable to previously reported data [4]. The standard electron transfer rate constant, k<sup>0</sup>, was also estimated by an alternative method [5]. In order to describe the process associated to the electrode potential in the interphase metal-solution, potentiometric assays in solutions of [C<sub>2</sub>mim]Cl or Ag[NTf<sub>2</sub>] were carried out. A Nernstian relationship was found for Ag or Ag|AgCl electrodes in a cell using the best RE previously described. These results suggest the formation of [AgCl<sub>n</sub>]<sup>1-n</sup> species in these IL.

## References

- [1] G.A. Snook, A.S. Best, A.G. Pandolfo, A.F. Hollenkamp, *Electrochem. Commun.* 8 (2006) 1405–1411.
- [2] E.I. Rogers, D.S. Silvester, D.L. Poole, L. Aldous, C. Hardacre, R.G. Compton, *J. Phys. Chem. C.* 112 (2008) 2729–2735.
- [3] M.A. Vorotyntsev, V.A. Zinovyeva, D.V. Konev, M. Picquet, L. Gaillon, C. Rizzi, *J. Phys. Chem. B.* 113 (2009) 1085–1099.
- [4] S.K. Sukardi, J. Zhang, I. Burgar, M.D. Horne, A.F. Hollenkamp, D.R. MacFarlane, et al., *Electrochem. Commun.* 10 (2008) 250–254.
- [5] I. Lavagnini, R. Antiochia, F. Magno, *Electroanalysis.* 16 (2004) 505–506.

# Physical and Electrochemical Properties of Quaternary Ammonium Compounds in Highly Concentrated Solutions

Shohei Suzuki, Masaru Ogasawara, and Noritoshi Nambu  
 Department of Life Science and Sustainable Chemistry,  
 Faculty of Engineering, Tokyo Polytechnic University  
 1583 Iiyama, Atsugi, Kanagawa 243-0297, Japan  
 nanbu@chem.t-kougei.ac.jp

Electric double-layer capacitor (EDLC) is an energy storage device that accumulates electric charges in an interphase between an activated carbon electrode and an electrolyte. Tetraethylammonium tetrafluoroborate (TEABF<sub>4</sub>) or triethyltetraethylammonium tetrafluoroborate (TEMABF<sub>4</sub>) is commonly used as the single electrolyte for EDLCs. Propylene carbonate (PC) is commonly used as the single solvent for EDLCs. The use of moderately high concentrations of electrolytes can improve both the concentration of charge carriers and the availability of pores. There are two approaches to the realization of highly concentrated and conductive solutions containing electrolytes: designs for electrolytes and solvents. The solubility of tetramethylammonium difluoro(oxalato)borate (TMADFOB) in PC was 2 M (M = mol dm<sup>-3</sup>) or more at 25 °C. In contrast, the solubility of tetramethylammonium tetrafluoroborate (TMABF<sub>4</sub>) is as low as 0.1 M at 25 °C. The solubility of TEABF<sub>4</sub> in PC is about 1.1 M at 25 °C, whereas that of TEMABF<sub>4</sub> is 2.2-2.3 M at 25 °C. The maximal electrolytic conductivity of a TMADFOB solution in PC was observed at about 1.6 M at 25 °C.

The determination of double-layer capacitance is essential for the evaluation of the performance of EDLCs. The potential-time plot resulting from a current step gives a straight line for a simple RC series circuit. One can roughly estimate the double-layer capacitance from the reciprocal of the slope of the similarity line. However, the experimental data for the charge and discharge of EDLCs do not follow the straight lines, but show slightly curved ones.

We have derived theoretical equation for a constant-current (CC) charge or discharge. The equivalent circuit of the average pore of an activated carbon electrode is represented by use of a transmission-line network of finite length. The theoretical treatment involves double-layer capacitances at the opposite end of the pore as well as on the electrode surface. The equation we derived has enough flexibility to show the effect of double-layer capacitance on the length and shape of a single pore.

$$-\Phi_{\text{max}}(\tau) = -\Phi_1 + 1 + \frac{\gamma^2}{6(\theta^2 + \gamma^2(1 + \zeta^2))} [6(\theta^2 + \gamma^2(1 + \zeta^2)) \tau + 3(\theta^2 + \gamma^2(1 + \zeta^2))(\theta^2 + 2\gamma^2\zeta^2) - \{6\gamma^4\zeta^2 + \theta^4 + 3\gamma^2\theta^2(1 + \zeta^2)\}] \quad (1)$$

$$\tan \alpha_n + \frac{\gamma^2\theta^2\alpha_n(1 + \zeta^2)}{\theta^4 - \gamma^4\zeta^2\alpha_n^2} = 0 \quad (2)$$

$$-2\gamma^2\theta^2 \sum_{n=1}^{\infty} \frac{\alpha_n^2}{\alpha_n^4 \{[-\gamma^4\zeta^2\alpha_n^2 + \theta^4 + \gamma^2\theta^2(1 + \zeta^2)] \cos \alpha_n - \alpha_n \{ \gamma^2\theta^2(1 + \zeta^2) + 2\gamma^4\zeta^2 \} \sin \alpha_n \}} \exp\left(-\frac{\alpha_n^2 \tau}{\theta^2}\right)$$

Here  $\theta^2 (= R_l C_l^2 / R_s C_s)$  denotes the time constant ratio of a pore to an electrode surface.  $\gamma^2 (= R_l / R_s)$  stands for the resistance ratio of a pore to the bulk of a solution.  $\zeta^2 (= C_e / C_s)$  represents the double-layer capacitance ratio of the closed end of a single pore to an electrode surface. Accordingly,  $(\theta / \gamma)^2 (= C_l / C_s)$  and  $\zeta^2 (= C_e / C_s)$  show the effect of the double-layer capacitance on the length and shape of a single pore, respectively.  $\zeta^2 = 1$ ,  $\zeta^2 = 0$ , and  $\zeta^2 \gg 1$  may correspond to a cylinder, a cone, and a reverse cone, respectively.

The theoretical cell voltage-time curves were fitted to experimental data for the discharge of EDLCs. Figure 1 compares theoretical and experimental cell voltage ( $U_{\text{cell}}(t)$ )–time ( $t$ ) behavior resulting from a CC discharge. The initial electric-potential difference between an electrode and a solution phases ( $E_i$ ) was taken as 2.5 V. The experimental discharge curves of 2025-type coin cells were obtained by use of (a) 1.6 M TMADFOB and (b) 1.6 M TEMABF<sub>4</sub> solutions in PC. They were used as single electrolytes. Current and cut-off voltage during the CC discharge were set to 1.33 mA ( $= I_{\text{appl}}$ ) (1 mA cm<sup>-2</sup>) and 0 V, respectively. The increase in the concentration of the electrolyte resulted in the increase in the capacitance. The capacitance and resistance found for TMADFOB ( $C_l = 0.80$  F and  $R_l = 100$  Ω) was slightly higher than that for TEMABF<sub>4</sub> ( $C_l = 0.77$  F and  $R_l = 83$  Ω). A very small distance between activated carbon electrodes in the coin cell can compensate for the lower ionic mobility of TMADFOB in the bulk of a PC solution. Furthermore, TMA<sup>+</sup> and DFOB<sup>-</sup> may more closely approach the electrode in a compact double layer.

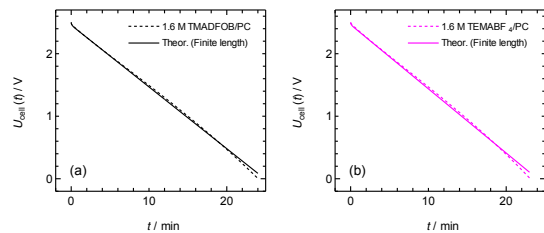


**Fig. 1** Comparison of theoretical and experimental cell voltage-time behavior resulting from a current step.



# Electrochemical CO<sub>2</sub> Reduction in EMIM-TFSI Ionic Liquid

Kazuhisa Azumi, Hayato Yoshikawa, Kazunori Suetake  
Graduate School of Engineering, Hokkaido University  
N13W8, Kitaku, Sapporo, Japan  
azumi@eng.hokudai.ac.jp

Reduction of CO<sub>2</sub> gas using natural energy resource to produce useful chemicals has been an important issue to establish the sustainable society. Some of ionic liquid such as 1-ethylimidazoliumbis(trifluoromethylsulfonyl)imide (EMIM-TFSI) ionic liquid (I.L.) is known to absorb CO<sub>2</sub> gas and thus considered as a medium for CO<sub>2</sub> gas separation. In this study EMIM-TFSI was used for electrolyte solution in which CO<sub>2</sub> gas is electrochemically reduced to form, for example, methane. EMIM-TFSI is also an hydrophobic liquid and thus water content is limited to be low level. This means that the sub-reaction of electrochemical CO<sub>2</sub> reduction such as water decomposition can be suppressed. In the experiments a small two-compartment electrochemical cell composed of a room filled with I.L. and another room filled with KCl solution was used (**Fig.1**). Two rooms were separated with a Nafion membrane to allow proton transportation between two rooms. CO<sub>2</sub> gas was bubbled in the I.L. bath and cathodically reduced on Cu working electrode (WE). The ambient gas in the cell was then induced to gas sensors to analyze the reduction products. In the another room the counter reaction of water decomposition (oxygen evolution reaction) was proceeded on a Pt-counter electrode (CE). The protons were formed in this reaction and supplied to the I.L. room *via* proton conducting Nafion membrane. If a single compartment cell was used, I.L. was decomposed on the CE in the water-poor medium. **Fig. 2** shows change in voltammogram of Cu-WE in the EMIM-TFSI-I.L. bath as a function of water content and CO<sub>2</sub> gas injection. Fig. 2 shows clearly that both of water and CO<sub>2</sub> gas were necessary to cause CO<sub>2</sub> reduction reaction at the potential lower than -1.4 V. Cathodic current showed clear response to changing the flow gas between Ar and CO<sub>2</sub> as shown in **Fig. 3**. Gas analysis using gas chromatography revealed that the optimized water content for efficient CO<sub>2</sub> reduction to form methane was ca. 5000 ppm.

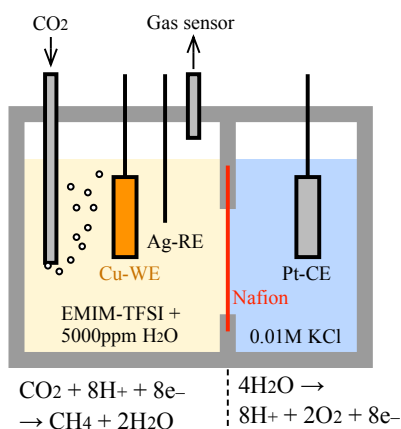


**Fig. 1.** Two compartment cell used for electrochemical CO<sub>2</sub> reduction.

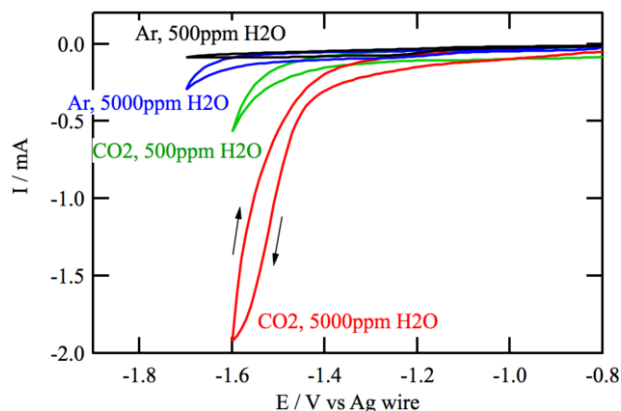


**Fig. 2.** Dependence of CV curves of Cu-WE in EMIM-TFSI I.L. bath as a function of CO<sub>2</sub> gas and water content.

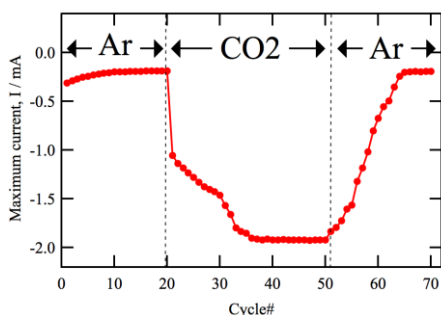


**Fig. 3.** Transition of cathodic current at -1.6 V in the CV changing with flow gas between Ar and CO<sub>2</sub>.

# Relative Permittivities of Binary Solvent Mixtures

Masaru Ogasawara, Shohei Suzuki, and Noritoshi Nambu  
*Department of Life Science and Sustainable Chemistry,  
 Faculty of Engineering, Tokyo Polytechnic University  
 1583 Iiyama, Atsugi, Kanagawa 243-0297, Japan  
 nanbu@chem.t-kougei.ac.jp*

Binary solvent mixtures exist as liquids over a wide range of temperatures and pressures. For the rational use of the solvent mixtures it is essential to know their physical and chemical properties as functions of their composition and the ambience. Relative static permittivity ( $\epsilon_r$ ) reflects the ease of dielectric polarization. The relative permittivity is a measure of the solvent's ability to insulate opposite charges from each other and has a very significant effect on the strength of the interactions between ions especially in dilute solutions. Electrostatic attractions and repulsions between ions are smaller in solvents with higher relative permittivities.

Assuming the triangular configurations ( $ijk$ ) in a liquid state and a first approximation for the number of molecular configurations, we have derived the equation for the dependence of relative permittivity ( $\epsilon_{r \text{ soln}}$ ) on the composition of a binary solvent mixture ( $x_2$ ).

$$\epsilon_{r \text{ soln}} \approx \epsilon_{r111}(1-x_2) + \epsilon_{r222}x_2 + 3\Delta\epsilon_{r112}\bar{\zeta}_t + 3\Delta\epsilon_{r122}\bar{\zeta}_t \quad (1)$$

$$\bar{\zeta}_t = \frac{x_2}{\eta_t^{2-\alpha} \rho_t^2 + 2\rho_t + 1} = \frac{\rho_t(1-x_2)}{\eta_t^{2\alpha-1} + 2\rho_t + \rho_t^2} \quad (2)$$

$$\rho_t = \frac{\bar{\zeta}_t}{\zeta_t} \quad (3)$$

Based on the random distribution of the solvent molecules, the equation (1) can be simplified in the following manner.

$$\epsilon_{r \text{ soln}} \approx \epsilon_{r111}(1-x_2) + \epsilon_{r222}x_2 + 3x_2(1-x_2)\{\Delta\epsilon_{r112}(1-x_2) + \Delta\epsilon_{r122}x_2\} \quad (4)$$

Here  $\Delta\epsilon_{r112}$  and  $\Delta\epsilon_{r122}$  may be related to the dipole moments, the polarizabilities, and the angular correlations between the dipoles. The equation (4) is similar to an empirical representation of relative permittivity with polynomials of the molar fraction.

Figure 1 shows the relative permittivities ( $\epsilon_{r \text{ soln}}$ ) of a binary mixture of ethylene carbonate (EC) and 2-fluoroethyl methyl carbonate (2FEMC) and a binary mixture of EC and ethyl methyl carbonate (EMC) at 25 °C as a function of composition. The symbol  $x_2$  denotes the molar fraction of a low-viscosity solvent (2FEMC or EMC). EC is a cyclic carbonate, whereas 2FEMC and EMC are linear carbonates. EC and EMC are commonly used as high-polarity and low-viscosity solvents for lithium-ion batteries, respectively. The equation for the composition dependence of the relative permittivity fitted experimental data. The relative permittivity of the EC–2FEMC binary mixture was higher than that of the EC–EMC counterpart. The value of  $\Delta\epsilon_{r122}$  found in the EC–2FEMC binary solvent system (–14.0) was less negative than that in the EC–EMC binary solvent system (–16.5). These findings suggest that dipole moments associated with 2FEMC molecules add vectorially to larger values and that linear but short chain structures predominate in the solution containing a large amount of 2FEMC. The attraction of 2FEMC molecules can be based on nonconventional weak intermolecular hydrogen bonding ( $\text{CF-H}\cdots\text{O=C}$  or  $\text{C-H}\cdots\text{F-C}$ ) as well as conventional dipole-dipole interactions. The weak hydrogen-bonding system does not exchange its proton and therefore it is no more a genuine hydrogen bond; it is an electrostatic attraction of positive charge on the hydrogen and negative charge on the organic fluorine or the organic oxygen.

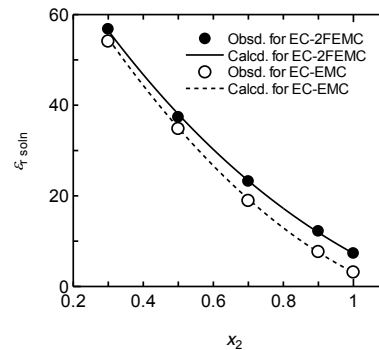


**Fig. 1** Relative permittivities ( $\epsilon_{r \text{ soln}}$ ) of EC–2FEMC and EC–EMC binary mixtures at 25 °C as a function of composition. The symbol  $x_2$  represents the molar fraction of a low-viscosity solvent (2FEMC or EMC).

# Reverse Electrodialysis (RED) as a New Electrical Power Source for a Drug Delivery System

Seung-Ryong Kwon, Sung Yul Lim, and Taek Dong Chung\*

*Department of Chemistry, Seoul National University*

*Gwanak-ro 599, Gwanak-gu, Seoul 151-747, Korea*

*tdchung@snu.ac.kr*

Reverse electrodialysis (RED) is one of the promising technologies for generating eco-friendly electrical power from renewable energy resources. In the early 1950s, Pattle demonstrated the production of electrical power by mixing the fresh water with sea water which are continual resources at estuaries for the first time [1]. When a semi-permeable membrane presents between solutions with different salinity concentrations (e.g., sea and river water), a defined voltage can be gained as a result of selective transports of ions from higher concentration to lower one. However, this process had not been fairly considered as a potential alternative to conventional power sources before we seriously faced the depletion crisis of natural resources. Recently, a couple of European countries, including Netherland, Italy, and Norway, have been interested in development of the electricity production systems based on salinity gradient. Meanwhile, some scientists paid attention eco-friendly and readily combinable RED systems with other technologies for unique applications. Logan group at Pennsylvania State University showed an interesting strategy for the greatly increased electricity production ( $5.6 \text{ W/m}^2$ ) with simultaneous waste water purification using the hybrid system of RED and microbial cell [2]. They also demonstrated the hydrogen production process using the generated electricity in the same combinations [3]. In this presentation, a drug delivery system based on RED as a new electrical power source is introduced and discussed.

- [1] R.E. Pattle, Production of electric power by mixing fresh and salt water in the hydroelectric pile, *Nature* 174 (1954) 660.
- [2] R.D. Cusick, Y. Kim, B.E. Logan, Energy capture from thermolytic solutions in microbial reverse-electrodialysis cells, *Science* 335 (2012) 1474-1477.
- [3] Y. Kim, B.E. Logan, Hydrogen production from inexhaustible supplies of fresh and salt water using microbial reverse-electrodialysis electrolysis cells, *Proc. Natl. Acad. Sci. U. S. A.* 108 (2011) 16176-16181.



# Synthesis of nanoparticle-type new proton conductor made from d-glucose by a hydrothermal method

Masahiro Kobayashi<sup>1</sup>, Hidenobu Shiroishi<sup>1\*</sup>, Masahiko Kijima<sup>2</sup>, Yumi Tanaka<sup>2</sup>, Jun Kuwano<sup>2</sup>  
Tokyo National College of Technology<sup>1</sup>, Tokyo University of Science<sup>2</sup>  
<sup>1</sup>Kunugida 1220-2, Hachioji, Tokyo, 193-0997, JAPAN, <sup>2</sup>12-1 Ichigayafunagawara-cho, Shinjuku,  
Tokyo 162-0826, JAPAN  
<sup>1\*</sup>[h-shiroishi@tokyo-ct.ac.jp](mailto:h-shiroishi@tokyo-ct.ac.jp)

## 1. Introduction

A new low-cost electrolyte is expected to be developed for polymer electrolyte fuel cells (PEFCs) because conventional perfluorosulfonate polymers (e.g. Nafion<sup>®</sup>) with high proton conductivity ( $0.1 \text{ S cm}^{-1}$ ) and excellent chemical stability are expensive. In this report, nano particle-type new proton conductors (NPPCs) has been synthesized by a hydrothermal method with a d-glucose solution followed by the introduction of sulfonic acid groups.

## 2. Experimental

50 mL of 0.5 M d-glucose aqueous solution was hydrothermally-treated at 193°C for 6 h to produce nano-carbon particles, followed by washing with acetone and Milli-Q water and drying in vacuum. The obtained powders were refluxed in 9-18 M  $\text{H}_2\text{SO}_4$  aqueous solution for 7.5-24 h to introduce sulfonic acid groups; the following washing with Milli-Q water and drying in vacuum produced NPPCs powders (sample names were denoted by "NPPC-[reflux time]-[concentration of sulfuric acid]"). The NPPCs powders were characterized by FE-SEM (Quanta 250 FEG, FEI), acid base titration, and TG/DTA (TG-DTA2500, NETZSCH)-GC/MS (GCMS-QP2010 Ultra, SHIMADZU). The bulk proton conductivity of NPPC pellets sputtered with Au electrode, which was prepared by pressing NPPC powders mixed with 25 wt% PTFE powder (TFW3000F, Seishin Enterprise) at 46 MPa, was measured with AC impedance analyzer (4192A, HP); the frequency and temperature were varied between 5 Hz-13 MHz and 80-200°C, respectively, with an applied voltage of 0.05 V under 10 mol%  $\text{H}_2\text{O-N}_2$  atmosphere.

## 3. Results and Discussion

The yield of nano-carbon particles was about 29% after the hydrothermal treatment. Fig. 1 shows the typical SEM image of NPPC powders. The average particle size of the NPPS powders was  $360 \pm 95 \text{ nm}$ , which was independent of synthesizing condition.

Arrhenius plots for the proton conductivity of 25 wt% PTFE-NPPC pellets are shown in Fig. 2. The maximum conductivities reached over  $8.6 \times 10^{-4} \text{ S cm}^{-1}$  at 80°C using NPPC-24 h-9 M. The proton conductivity of the NPPCs decreased with the increase in temperature. The TG/DTA-GC/MS measurements clarified that water content in the electrolytes decrease with increasing temperature below 130°C, which probably caused the depression of proton hopping and the diffusion of  $\text{H}_3\text{O}^+$  in the electrolytes. Sulfonic acid groups on NPPCs decomposed above 130°C to decrease the proton conductivity.

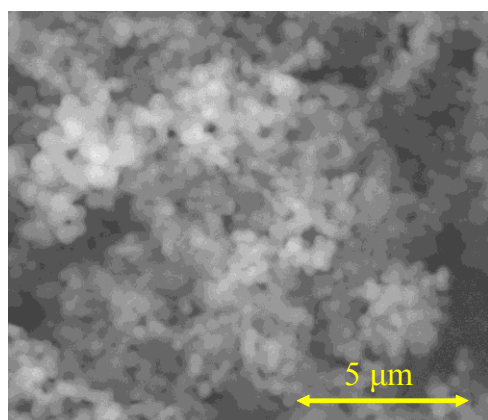


**Fig. 1.** SEM image of a NPPC synthesized by the hydrothermal method.

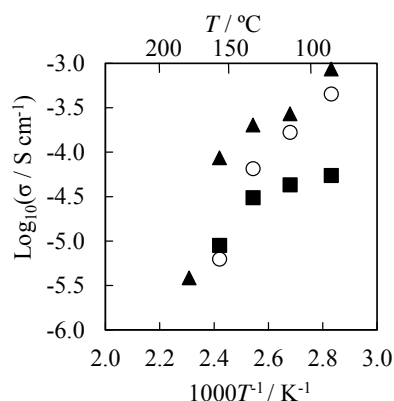


**Fig. 2.** Temperature dependence of the proton conductivity of NPPC under 10 mol%  $\text{H}_2\text{O-N}_2$  atmosphere. NPPC-24 h-9 M ( $\blacktriangle$ ), NPPC-7.5 h-18 M ( $\circ$ ) and NPPC-7.5 h-12 M ( $\blacksquare$ ).

# Characteristics of an intermediate-temperature fuel cell using proton conductive $\text{ZrO}_2\text{-1.6P}_2\text{O}_5$ -doped $\text{ZnO-2P}_2\text{O}_5$ hybrid electrolyte

Kayato Ooya<sup>1</sup>, Hidenobu Shiroishi<sup>1\*</sup>, Morihiro Saito<sup>2</sup>, Yumi Tanaka<sup>3</sup>

<sup>1</sup>Tokyo National college of Technology, <sup>2</sup>Tokyo University of Agriculture and Technology

<sup>3</sup>Tokyo University of Science

<sup>1</sup>1220-2, Hachioji, Tokyo, 193-0997, JAPAN, <sup>2</sup>2-24-16 Nakacho, Koganei, Tokyo 184-8588, JAPAN,

<sup>3</sup>12-1 Ichigayafunagawara-cho, Shinjuku, Tokyo 162-0826, JAPAN

<sup>1\*</sup>[h-shiroishi@tokyo-ct.ac.jp](mailto:h-shiroishi@tokyo-ct.ac.jp)

## 1. Introduction

$\text{ZrO}_2\text{-1.6P}_2\text{O}_5$  has high proton conductivity ( $10^{-1.0}$  to  $10^{-1.5}$  S / cm) at a temperature range of 75°C to 250°C, but poor water resistance. In this study,  $\text{ZrO}_2\text{-1.6P}_2\text{O}_5$  doped  $\text{ZnO-2P}_2\text{O}_5$  hybrid electrolyte has been synthesized by heat treatment with the mixture of  $\text{ZrO}_2\text{-1.6P}_2\text{O}_5$  and  $\text{ZnO-2P}_2\text{O}_5$  for the development of a high proton conductive electrolyte with high water resistivity and low hydrogen gas permeability.

## 2. Experimental

$\text{ZrO}_2\text{-1.6P}_2\text{O}_5$  doped  $\text{ZnO-2P}_2\text{O}_5$  hybrid electrolyte was prepared as follows: A mixture of  $(\text{NH}_4)_2\text{HPO}_4$  (Junsei Chemical Co.) and  $\text{ZrCl}_2\text{O} \cdot 8\text{H}_2\text{O}$  (Wako Pure Chemical Industries) was heated at 500°C for 2 h under 10 mol%  $\text{H}_2\text{O}$  to synthesize  $\text{ZrO}_2\text{-1.6P}_2\text{O}_5$ . In order to synthesize  $\text{ZnO-2P}_2\text{O}_5$ , after a desired amount of Zn powder (Wako Pure Chemical Industries) and CaO (Kishida Chemical Co.) were dissolved in 86 wt%  $\text{H}_3\text{PO}_4$  (Kishida Chemical Co.) and the obtained solution was heat-treated at 900°C and quenched on a copper plate. The resultant  $\text{ZnO-2P}_2\text{O}_5$  glass was powdered by an agate mortar and was mixed with the desired amount of  $\text{ZrO}_2\text{-1.6P}_2\text{O}_5$ . The mixture heat-treated at a temperature range of 300°C to 900°C. Then, the sample was quenched on a copper plate to produce  $\text{ZrO}_2\text{-1.6P}_2\text{O}_5$  doped  $\text{ZnO-2P}_2\text{O}_5$  hybrid electrolytes (abbreviated as  $(\text{ZnO-2P}_2\text{O}_5\text{-0.3M CaO})\text{-}x$  wt% ( $\text{ZrO}_2\text{-1.6 P}_2\text{O}_5$ )).

## 3. Results and Discussion

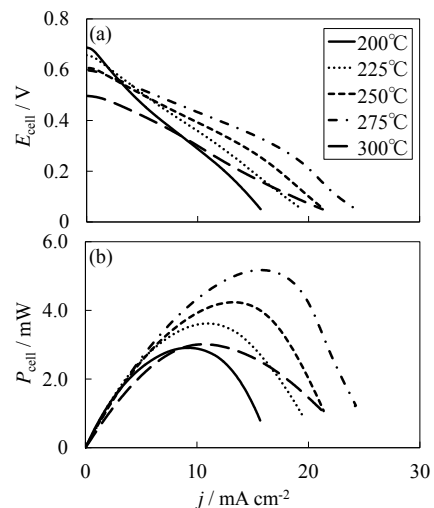
The increase in the heat treatment temperature during the preparation process of the electrolytes caused the improvement of water resistance and the decrease in the proton conductivity of the electrolytes. The trade-off relationship between the water resistance and the proton conductivity became prominent with increasing ratio of  $\text{ZrO}_2\text{-1.6P}_2\text{O}_5$  in the hybrid electrolytes. Thus, the acceptable trade-off condition was heat treatment at 500°C and 30 wt%  $\text{ZrO}_2\text{-1.6P}_2\text{O}_5$  for the water resistance and the proton conductivity of the electrolytes. From the data of XRD measurements and SEM-EDX mappings, it was confirmed the core structure ( $\text{ZrP}_2\text{O}_7$ ) of  $\text{ZrO}_2\text{-1.6P}_2\text{O}_5$  was maintained and the  $\text{ZrO}_2\text{-1.6P}_2\text{O}_5$  was uniformly dispersed in the  $\text{ZnO-2P}_2\text{O}_5$ . The proton conductivity of the hybrid electrolyte showed almost the same level as that of  $\text{ZrO}_2\text{-1.6P}_2\text{O}_5$ . The water resistance and the hydrogen gas permeability of the hybrid electrolyte were 3 times and 1/80 times higher than those of  $\text{ZrO}_2\text{-1.6P}_2\text{O}_5$ , respectively.

Fig. 1 shows the single cell performance of an intermediate temperature fuel cell (ITFC) using the hybrid electrolyte. The OCV of the ITFC decreased with increasing operating temperature, suggesting the gas crossover through the electrolyte. The proton conductivity increased with an increase in the operating temperature, and the power density reached the maximum value of 5.2 mW at 275°C.

## 4. References

1) D.E. Priyant, H. Shiroishi, S. Tanimoto, S. Hirukawa, M. Saito and J. Kuwano, *Key Eng. Mater.*, **421-422**, 471 (2010).

**Acknowledgement:** This study was partially supported by a Grant-in-Aid for Young Scientists (B) (No. 26820321) from Japan Society for the Promotion of Science.



**Fig. 1.** Single cell performances for  $\text{H}_2/\text{O}_2$  fuel cells with the  $(\text{ZnO-2P}_2\text{O}_5\text{-0.3M CaO})\text{-30 wt\%}$  ( $\text{ZrO}_2\text{-1.6P}_2\text{O}_5$ ) hybrid electrolytes (area:  $0.196 \text{ cm}^2$ , thickness :  $0.796 \text{ mm}$ ) using a spray method ( $2.86 \text{ mg cm}^{-2}$  Pt / C) under dry  $\text{N}_2$ . (a)  $j - V$  curve and (b) power density.

# **Determination of optimal design parameters for preparing ion-exchange membranes for efficient redox flow batteries**

Yu-Jin Kim, Do-Hyeong Kim, Jin-Soo Park, Moon-Sung Kang  
*Department of Environmental Engineering, Sangmyung University*  
*300 Anseo-dong, Dongnam-gu, Cheonan-si, Chungnam 330-720, Republic of Korea*  
*solar@smu.ac.kr*

Ion-exchange membranes (IEMs) have been widely developed for the efficient separation processes of ionic substances such as electrodialysis, electrodeionization, diffusion dialysis, and water-splitting electrodialysis and so on. Recently, there has also been much attention towards IEMs for the applications in the energy generation and storage systems such as fuel cells (FCs) and redox flow batteries (RFBs). IEMs are one of the key components dominating the overall performances of the processes. Low ion transport resistance through membrane, excellent chemical and mechanical stability, high permselectivity, and low cross-over rate of undesirable components are required for the successful applications of the IEMs in the processes. The low cost of the membranes is also very important for the practical and commercial uses. In this work, we have successfully prepared high performance IEMs using engineering polymers, such as poly(2,6-dimethyl-1,4-phenylene oxide) (PPO) and polyetheretherketone (PEEK) as the based materials. In addition, the optimization of membrane design parameters has been systematically investigated using the membranes via various electrochemical analyses.

## **Acknowledgements**

This work was supported in part by the Basic Science Research Program through the National Research Foundation of Korea (NRF) funded by the Korea government (MSIP) (No. 2012013811) and the Material Technology Development Program funded by the Ministry of Trade, industry & Energy (MOTIE) (No. 10047796).

# Electrochemical Redox Behavior of Cobaltocenium in Imidazolium-based Ionic Liquids with Various Alkyl Chain Length

Hiroyuki Ueda<sup>a</sup>, Katsuhiko Nishiyama<sup>a,b</sup>, Soichiro Yoshimoto<sup>b,c</sup>

<sup>a</sup> Graduate School of Science and Technology, Kumamoto University

2-39-1 Kurokami, Chuo-ku, Kumamoto 860-8555, Japan

<sup>b</sup> Kumamoto Institute for Photo-Electro Organics (Phoenix)

3-11-38, Higashi-machi, Higashi-ku, Kumamoto 862-0901, Japan

<sup>c</sup> Priority Organization for Innovation and Excellence, Kumamoto University

2-39-1 Kurokami, Chuo-ku, Kumamoto 860-8555, Japan

so-yoshi@kumamoto-u.ac.jp

Ionic liquids (ILs) are promising materials for rechargeable batteries and capacitors because of their negligible vapor pressure, high thermal stability, and wide electrochemical potential window [1]. The most different feature of ILs compared with water and organic solvents is that ILs are composed of cations and anions only. Owing to these features, it was reported that the diffusion of metallocenes in ILs is not determined by the Stokes-Einstein equation [2]. In this study, we report the electrochemical redox behavior of cobaltocenium ( $\text{Cc}^+$ ) in imidazolium-based ILs to understand the effect of the alkyl chain length of cation on the activation energy for the diffusion and the Stokes radius of  $\text{Cc}^+$  in ILs.

10 mM  $\text{Cc}^+$  in  $[\text{C}_n\text{mim}][\text{TFSI}]$  ( $n = 2, 4, 6, 8, \text{ or } 10$ ) were prepared. The diffusion of  $\text{Cc}^+$  was investigated in each IL by using cyclic voltammetry (CV) and chronoamperometry (CA) at 20–70 ( $\pm 1$ ) °C. The Au(111) electrode was used as the working electrode. The potential values were calibrated to the ferrocene/ferrocenium ( $\text{Fc}/\text{Fc}^+$ ) reference electrode. The diffusion coefficients of  $\text{Cc}^+$  obtained from the Cottrell equation were utilized to estimate the activation energy for the diffusion by Arrhenius plots. The Stokes radius of  $\text{Cc}^+$  was estimated by the following equation [2]:

$$D = k_B T / (\theta \pi \eta \alpha), \quad \theta = 6 (1 + 2\eta/\beta\alpha) / (1 + 3\eta/\beta\alpha) \quad (\text{Eq. 1})$$

where  $D$  is the diffusion coefficient of  $\text{Cc}^+$ ,  $k_B$  is the Boltzmann constant,  $T$  is the temperature in Kelvin,  $\eta$  is the viscosity of an IL,  $\alpha$  is the Stokes radius of  $\text{Cc}^+$ ,  $\beta$  is the coefficient of sliding friction ( $0 \leq \beta \leq \infty$ ), and  $\theta$  is the Sutherland coefficient ( $4 \leq \theta \leq 6$ ).

Fig. 1 shows typical cyclic voltammograms of 10 mM  $\text{Cc}^+$  in  $[\text{C}_2\text{mim}][\text{TFSI}]$ . A reversible one-electron redox couple was observed. Similar voltammograms were obtained in the other  $[\text{C}_n\text{mim}][\text{TFSI}]$  ( $n = 4, 6, 8, \text{ or } 10$ ), but the peak currents for the reduction of  $\text{Cc}^+$  at various scan rates and temperatures were smaller when the alkyl chain length of  $[\text{C}_n\text{mim}]^+$  increased. Table 1 shows the activation energies for the diffusion and the Stokes radii of  $\text{Cc}^+$  in  $[\text{C}_n\text{mim}][\text{TFSI}]$ . The activation energy for the diffusion of  $\text{Cc}^+$  increased with the increase in the alkyl chain length of  $[\text{C}_n\text{mim}]^+$ , indicating that the viscosity of the medium affects the activation energy for the diffusion of  $\text{Cc}^+$ . On the other hand, the lowest Stokes radius of  $\text{Cc}^+$  was estimated in  $[\text{C}_4\text{mim}][\text{TFSI}]$  when the same Sutherland coefficient was used in each IL. This result indicates that  $\theta\alpha$  depends on  $[\text{C}_n\text{mim}]^+$  although  $\text{Cc}^+$  seems to attract  $[\text{TFSI}]^-$  by the electrostatic interaction. Our result suggests that Eq. 1 is more appropriate than the Stokes-Einstein equation for describing the diffusion of  $\text{Cc}^+$  in  $[\text{C}_n\text{mim}][\text{TFSI}]$ .

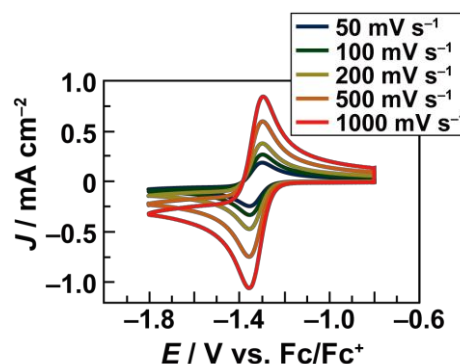


Fig. 1. CV profiles of 10 mM  $\text{Cc}^+$  in  $[\text{C}_2\text{mim}][\text{TFSI}]$  at 20 °C.

Table 1. The activation energies for the diffusion ( $E_a$ ) and the Stokes radii of  $\text{Cc}^+$  ( $\alpha$ ) in  $[\text{C}_n\text{mim}][\text{TFSI}]$ .

IL	$E_a$ [kJ mol <sup>-1</sup> ]	$\alpha$ [Å]	
		$\theta = 6$	$\theta = 4$
$[\text{C}_2\text{mim}][\text{TFSI}]$	28.2	3.1	4.6
$[\text{C}_4\text{mim}][\text{TFSI}]$	34.5	1.8	2.7
$[\text{C}_6\text{mim}][\text{TFSI}]$	32.0	1.9	2.8
$[\text{C}_8\text{mim}][\text{TFSI}]$	39.1	2.5	3.8
$[\text{C}_{10}\text{mim}][\text{TFSI}]$	45.7	3.1	4.6

[1] P. Hapiot, C. Lagrost, *Chem. Rev.* **2008**, *108*, 2238.

[2] M.A. Vorotyntsev, V.A. Zinovyeva, M. Picquet, *Electrochim. Acta* **2010**, *55*, 5063.



# **Development of Novel Bipolar Membranes for Efficient Electro-Adsorptive Deionization**

Eun-Hye Jang, Do-Hyeong Kim, Jin-Soo Park, Moon-Sung Kang  
*Department of Environmental Engineering, Sangmyung University*  
*300 Anseo-dong, Dongnam-gu, Cheonan-si, Chungnam 330-720, Republic of Korea*  
*solar@smu.ac.kr*

Recently, electro-membrane processes using ion-exchange membranes have gained increased industrial importance. The electro-membrane processes are considered to be environment-friendly as well as energy efficient, since the generation of salt wastes can be minimized in these processes. Bipolar membranes in which the anion- and cation-exchangeable layers are adjoined together in series easily split water molecules into protons and hydroxyl ions under a reverse bias condition. It is expected that water-splitting electro dialysis using bipolar membrane can make zero-emission possible and be applied as a clean technology without the production of undesirable by-products. Very recently, an efficient electrochemical desalination process employing bipolar membranes with large ion-exchange area is being developed (so-called 'electro-adsorptive deionization'). In this process, ions dissolved in a feed solution can be removed through an ion-exchange mechanism under a strong electric field (a forward bias condition). The membranes can also be regenerated without the use of additional chemicals by the water-splitting reactions which occur at the bipolar junction of membranes (a reverse bias condition). The process performances, such as desalination efficiency and power consumption are largely dependent upon the properties of bipolar membranes. In this work, we have developed novel bipolar membranes containing iron oxide/hydroxide catalysts for efficient electrochemical water-splitting. Especially, new methods for the synthesis and immobilization of iron oxide/hydroxide catalysts have been developed to enhance the water-splitting efficiency of the membranes. In addition, the ion-exchange capacities of the bipolar membranes have been largely enlarged by embedding finely powdered ion-exchange resins.

## **Acknowledgements**

This work was supported by the Material Technology Development Program funded by the Ministry of Trade, industry & Energy (MOTIE) (No. 10047796).

# Optimization of Ionomer Membrane Characteristics for High Performance Reverse Electrodialysis

Do-Hyeong Kim, Eun-Hye Jang, Yu-Jin Kim, Jin-Soo Park, Moon-Sung Kang  
*Department of Environmental Engineering, Sangmyung University*  
*300 Anseo-dong, Dongnam-gu, Cheonan-si, Chungnam 330-720, Republic of Korea*  
*solar@smu.ac.kr*

Reverse electrodialysis (RED) is one of the promising processes for generating electricity from the salt concentration gradient between river and sea water. A RED stack contains alternately arranged anion and cation exchange membranes (AEMs and CEMs, respectively) which separate salt solutions of different concentrations. The power generation performance of RED significantly depends on the characteristics of ion exchange membranes (IEMs), which are selective for cations or anions. When the IEMs with different polarities are stacked alternately, with compartments for seawater or river water in between, the Donnan potentials over each membrane result in a voltage that can be used for electricity generation. The important membrane properties dominating the power generation in RED processes are ion-exchange capacity, water swelling degree, electrical resistance, permselectivity, membrane thickness, and surface morphology etc. In this work, we have successfully prepared high performance IEMs using engineering polymers, such as poly(2,6-dimethyl-1,4-phenylene oxide) (PPO) and polyetheretherketone (PEEK) as the based materials. In addition, the optimization of membrane design parameters has been systematically investigated using the membranes via various electrochemical analyses.

## Acknowledgements

This work was supported by the Material Technology Development Program funded by the Ministry of Trade, industry & Energy (MOTIE) (No. 10047796).

# (Electro)catalysis at Room Temperature Ionic Liquid|Water Interface: H<sub>2</sub>O<sub>2</sub> Generation

Marcin Opallo<sup>a</sup>, Justyna Jedraszko,<sup>a</sup> Wojciech Nogala,<sup>a</sup> Wojciech Adamiak,<sup>a</sup> Saustin Dongmo,<sup>b</sup>  
Gunther Wittstock,<sup>b</sup> Hubert H. Girault<sup>c</sup>

<sup>a</sup>*Institute of Physical Chemistry, Polish Academy of Sciences, Warszawa, Poland*

<sup>b</sup>*Department of Chemistry, Center of Interface Science. School of Mathematics and Science, Carl von Ossietzky University of Oldenburg, Germany.*

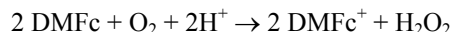
<sup>c</sup>*LEPA, Ecole Polytechnique Federale de Lausanne, Lausanne, Switzerland.*

*mopallo@ichf.edu.pl*

Biphasic systems with room temperature ionic liquid (RTIL)|water interfaces are crucial constituents of an increasing number of physicochemical systems including advanced materials [1,2]. Extraction and phase separation of RTIL and aqueous solution are intensively studied [3,4], whereas the application of RTIL–water systems in synthesis has been limited so far [5,6].

When the aqueous phase containing considerable amount of ionic species is in direct contact with a RTIL, the efficiency and pathway of interfacial processes involving charged reactants depends on the Galvani potential difference across the interface, controlled externally by means of a potentiostat or by the composition and concentration of ions in both phases [7-9]. Polarisation control of the liquid|liquid interface may provide favourable conditions for chemical reactions generating hydrogen or hydrogen peroxide [10]. It has been shown that H<sub>2</sub>O<sub>2</sub> can be obtained from dissolved dioxygen at the interface between water and an organic solvent immiscible with water (1,2-dichloroethane, trifluorotoluene) using a strong electron donor such as decamethylferrocene (DMFc) dissolved in the organic phase [11,12]. So far, these studies were restricted to interfaces formed by aqueous solutions of acids and salt solutions in nonaqueous polar solvents.

Here, we will demonstrate that by using the same methodology hydrogen peroxide can be generated at a RTIL|water interface:



The product was detected by, colorimetric substrate depletion, scanning electrochemical microscopy (SECM) and optical readout with fluorogenic substrate [13]. The experiments with carbon paste electrode with DMFc solution in hydrophobic ionic liquid demonstrated that electron donor can be regenerated electrochemically. This increases the flux of produced hydrogen peroxide as detected by SECM.

1. M.V. Fedorov, A.M. Kornyshev, *Chem. Rev.*, 2014, **114**, 2978.
2. M. Opallo, A. Lesniewski, *J. Electroanal. Chem.*, 2011, **656**, 2.
3. X. Sun, H. Luo, S. Dai, *Chem. Rev.*, 2012, **112**, 2100.
4. J.H. Zhang, H. Gao, Y.B. Li, Z.Q. Zhou, *J. Separation Sci.*, 2011, **34**, 3178.
5. V. Ladnak, N. Hofmann, N. Brausch, *Adv. Synth. & Cat.*, 2007, **349**, 719.
6. M. Petkovich, K.R. Seddon, *Chem. Soc. Rev.*, 2011, **40**, 1383.
7. Z. Samec, J. Langmaier, T Kakiuchi, *Pure Appl. Chem.*, 2009, **81**, 1473.
8. Y. Wang, T. Kakiuchi, Y. Yasui, M.V. Mirkin, *J. Am. Chem. Soc.*, 2010, **132**, 16945.
9. T. Kakiuchi, *Anal. Chem.*, 2007, **79**, 6442.
10. M. A. Mendez, R. Partovi-Nia, I. Hatay, B. Su, P. Ge, A. Olaya, N. Younan, M. Hojeij and H. H. Girault, *Phys. Chem. Chem. Phys.*, 2010, **12**, 15163.
11. B. Su, R. NiaPartovi, F. Li, M. Hojeij, M. Prudent, C. Corminboeuf, Z. Samec. H.H. Girault, *Angew. Chem. Int. Ed.*, 2008, **47**, 4675.
12. W. Adamiak, J. Jedraszko, O. Krysiak, W. Nogala, J. Hidalgo-Acosta,, H. H. Girault and M. Opallo, *J. Phys. Chem. C*, 2014, **118**, 23154.
13. M. Burchardt and G. Wittstock, *Langmuir*, 2013, **29**, 15090.

# Evaluation of oxygen reduction properties by ring-disk flow electrode

Masakuni Takahashi<sup>1</sup>, Hidenobu Shiroishi<sup>1\*</sup>, Genichiro Nakamura<sup>1</sup>, Tatsuhiro Okada<sup>2</sup>

<sup>1</sup>Tokyo National College of Technology, <sup>2</sup>Tsukuba Fuel Cell Laboratory, Inc.

<sup>1</sup>Kunugida 1220-2, Hachioji, Tokyo, 193-0997, JAPAN, <sup>2</sup>Shimotakatsu 2-14-3, Tsuchiura, Ibaraki, 300-0812, JAPAN

*h-shiroishi@tokyo-ct.ac.jp*

## 1. Introduction

Rotating ring-disk electrode (RRDE) is one of the most popular electrochemical tools, which enables quantitative analyses of electrode processes by controlling the mass transfer rate in the solution. However, the RRDE method, which needs a rotor-electrode system, glassy carbon-Pt ring electrode and an electrochemical cell equipped with a water jacket for temperature controls, becomes complex and of high cost. Moreover, the closed cell may cause the accumulation of interfering materials during the electrochemical reaction. We here propose a new handy electrochemical method named as "Ring disk flow cell (RDFC) method" that features advantages of both of the RRDE and the channel flow electrode. In this report, basic research has been performed including a comparison between the RRDE method and the new method, using a commercially available fuel cell catalyst.

## 2. Experimental

2.00 mg of 20 wt% Pt/XC72(E-TEK) was suspended in the 1 mL of 0.1 wt% Nafion<sup>®</sup>-methanol solution by a shaker at 1000 rpm for 1 h, then an aliquot of 7  $\mu$ L was cast on a glassy carbon (GC) disk electrode (5 mm $\phi$ ) of the RDFC, and was allowed to dry for 1 h at room temperature. Fig. 1 shows the scheme of a RDFC apparatus. The electrolyte solution was circulated from the reservoir to the electrochemical cell at desired flow rate controlled by a peristaltic tube pump (SMP-21S, EYELA). The electrochemical cell was equipped with the working electrode and a Nafion<sup>®</sup>115|EC-E20-10-07(1.0 mgPtcm<sup>-2</sup>)|H<sub>2</sub> membrane-electrode assembly, functioning as both the counter and the reference electrodes. Electrochemical measurements were carried out in 0.1 M HClO<sub>4</sub> with a multi potentiostat (PS-08, Toho Tech.) connected to a function generator (FG-02, Toho Tech.). Cathodic current of oxygen reduction reaction (ORR) was derived by subtracting the blank current measured under N<sub>2</sub> from the current under O<sub>2</sub>.

## 3. Results and discussion

Fig. 2 shows the ORR polarization curves on GC disk electrodes supporting 20 wt% Pt/XC72 (E-TEK) with 0.1  $\mu$ M Nafion<sup>®</sup>, measured by RRDF and RRDE methods. The less steep current decrease towards the diffusion limiting current observed in the RDFC as compared with the RRDE, indicates the IR drop due to the contact resistance of the working electrode. To overcome this problem, the reduction of contact resistance in the RDFC is now attempted in several ways.

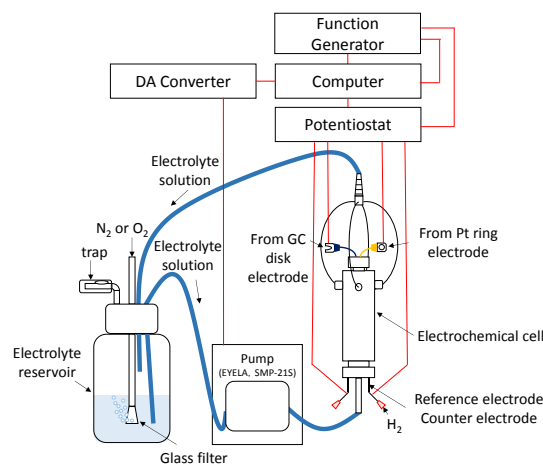


Fig. 1. Scheme of a ring-disk flow cell apparatus.

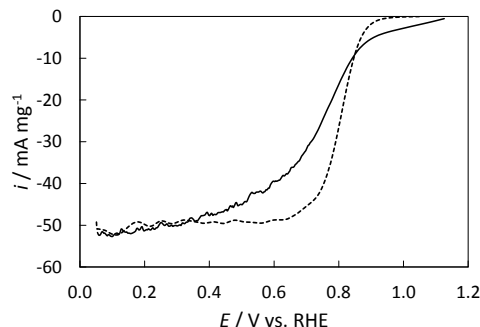


Fig. 2. Polarization curves for oxygen reduction on GC|20 wt% Pt/C(E-Tek) with 0.1  $\mu$ M Nafion<sup>®</sup> during positive going scan in 0.1 M HClO<sub>4</sub> under 1 atm O<sub>2</sub> at 20°C. — : ring-disk flow electrode (8 mL min<sup>-1</sup>); .....: RRDE (600 rpm).

# Effects of constant on-off current pulse on the properties of $\text{Cu}_2\text{O}$ films fabricated by electrochemical deposition method

Leo Chau-Kuang Liao\*, Po-Chin Tseng, and Jia-Lin Jhan

Department of Chemical Engineering and Materials Science, Yuan Ze University, Chung-Li 32003, Taoyang city, Taiwan

\*e-mail: lckliau@saturn.yzu.edu.tw

Cuprous oxide ( $\text{Cu}_2\text{O}$ ) is a direct band-gap semiconductor material which is abundant and nontoxic and considered in the development and application of the recent optoelectronic technology.<sup>1</sup> Optoelectronic devices, such as  $\text{Cu}_2\text{O}$ -based solar cells,<sup>2,3</sup> were designed and produced to take advantages of the unique properties of  $\text{Cu}_2\text{O}$ . However, the properties of  $\text{Cu}_2\text{O}$  films were greatly affected by the fabrication methods. In this study, the effects of constant on-off current pulse processes on the properties of  $\text{Cu}_2\text{O}$  films fabricated using electrochemical deposition (ECD) were investigated. The  $\text{Cu}_2\text{O}$  films were prepared using a ECD solution, mixed of Copper (II) acetate ( $\text{Cu}(\text{OOCCH}_3)_2 \cdot \text{H}_2\text{O}$ ) with acetic acid to adjust pH = 4.9 at 70 °C. The ECD process was carried out under the control of different on-off periods of the current pulse. Results showed that the morphologies of the  $\text{Cu}_2\text{O}$  particles were greatly affected by the ECD parameters, such as voltage and current setup. The particle shapes change from dendritic (Figure 1(a)), cubic (Figure 1(b)), to faceted (Figure 1(c)), for the operating conditions setup at constant voltage, constant current, and constant on-off current pulse approaches, respectively. The particle sizes of the respective samples were 2.0  $\mu\text{m}$ , 5.0  $\mu\text{m}$ , and 0.35  $\mu\text{m}$  evaluated from Figures 1(a) – 1(c). Additionally, the particle sizes of the ECD samples can also be varied by different on-off periods of current pulse according to the SEM image data. The crystalline sizes of all these samples were similar and analyzed to be 47 nm from the analysis of the XRD spectral data. The electronic properties of the films were determined using the Mott-Schottky analysis and current-voltage (I-V) tests. The properties of the  $\text{Cu}_2\text{O}$  films using constant current pulse in different on-off periods were also discussed in this work.

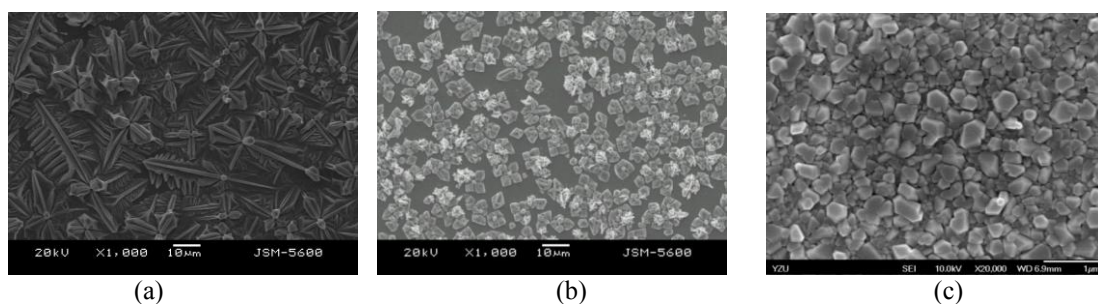


Figure 1 SEM morphologies of the  $\text{Cu}_2\text{O}$  particles using ECD processing setup for (a) constant voltage, (b) constant current, and (c) constant on-off current pulse methods.

## References

1. Meyer, B.K. ; Polity, A. ; Reppin, D. ; Becker, M. ; Hering, P. ; Klar, P. J. ; Sander, Th. ; Reindl, C. ; Benzl, J. ; Eickhoff, M. et al. Binary Copper Oxide Semiconductors: From Materials Towards Devices. *Phys. Status Solidi B* **2012**, 249, 1487-1509.
2. Nishi, Y.; Miyata, T.; Minami, T. The Impact of Heterojunction Formation Temperature on Obtainable Conversion Efficiency in n-ZnO/p-Cu<sub>2</sub>O Solar Cells. *Thin solid films* **2013**, 528, 72-76.
3. Ruhle, S.; Anderson, A. Y.; Barad, H.-N.; Kupfer, B.; Bouhadana, Y.; Rosh-Hodesh, E.; Zaban A. All-oxide photovoltaics. *J. Phys. Chem. Lett.* **2012**, 3, 3755-3764.

# Preparation and Physicochemical Properties of Room-Temperature Phosphonium Ionic Liquids Based on Tetracyanoborate Anion

Keiichi Nishihata<sup>1</sup>, Katsuhiko Tsunashima<sup>1</sup>, Masahiko Matsumiya<sup>2</sup>

<sup>1</sup> National Institute of Technology, Wakayama College

77 Noshima, Nada-cho, Gobo, Wakayama 644-0023, Japan

<sup>2</sup> Graduate School of Environment and Information Sciences, Yokohama National University

79-2 Tokiwadai, Hodogaya-ku, Yokohama 240-8501, Japan

E-mail: tsunashima@wakayama-nct.ac.jp (K. Tsunashima)

Room-temperature ionic liquids (RTILs) have been regarded as potential electrolytes for various electrochemical systems. From this point of view, RTILs based on nitrogen-based cations have been considerably reported in recent years; however, RTILs based on phosphonium cations have been rarely investigated. On the other hand, interests in a tetracyanoborate ( $\text{B}(\text{CN})_4^-$ , TCB) anion based ILs have been increasing for their electrochemical application due to the fact that the TCB-based ILs exhibited remarkably high transport property [1]. In this work, we report the preparation and physicochemical properties of novel ILs based on quaternary phosphonium cations [2] together with the TCB anion (Fig. 1).

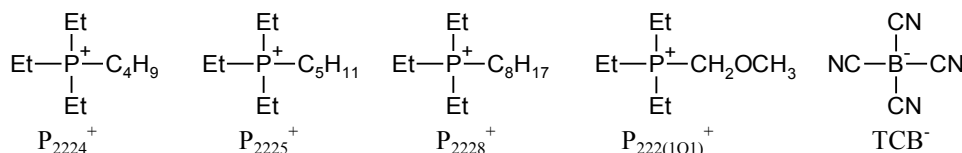


Fig. 1 Ionic components of phosphonium ILs in this work.

The preparation of the phosphonium ILs was performed by aqueous ion exchange reactions of precursor phosphonium halides with sodium tetracyanoborate ( $\text{Na-TCB}$ ). Residual metal and halide ions in the crude ILs were removed by a silica gel column. The physicochemical and electrochemical properties such as conductivity, viscosity, density, melting point, thermal decomposition temperature and electrochemical window were measured under argon atmosphere.

The combination of the asymmetric phosphonium cations with TCB anion successfully gave liquids at ambient temperature.

As shown in Fig. 2, it was found that phosphonium ILs based on TCB anion showed relatively high conductivity when compared to the corresponding ammonium IL, which were similar to those observed in bis(fluorosulfonyl)amide (FSA)-based and bis(trifluoromethylsulfonyl)amide (TFSA)-based phosphonium ILs. This result might be due to the charge distribution on the TCB anion.

Fig. 3 suggests that the thermal decomposition temperature of TCB-based phosphonium ILs were more than approximately 400°C, indicating their higher thermal stability than those of the other ILs.

## Reference

- [1] M. Marszalek, et al, Inorg. Chem. 50 (2011) 11561.
- [2] K. Tsunashima, et al, Electrochem. Commun. 9 (2007) 2353.

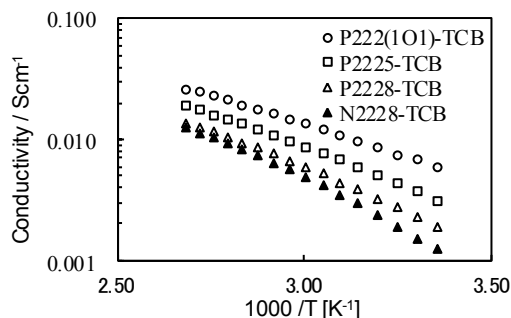


Fig. 2 Arrhenius plots of conductivity for TCB-based phosphonium ILs.

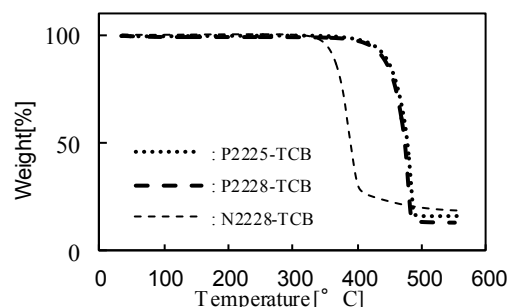


Fig. 3 Thermogravimetric traces for TCB-based phosphonium ILs.

# **Fabrication of AuNPs Array on ITO electrode via Nanospheres Lithography and its DNA Sensing Applications**

Ching-Hsiang Chen<sup>a,\*</sup>, Agnes Purwidyantri<sup>b</sup>, Bing-Joe Hwang<sup>c,d</sup>, Ya-Chung Tian<sup>e</sup>, Chi-Hui-Cheng<sup>f,g</sup>,  
Chao-Sung Lai<sup>h,i,\*</sup>

<sup>a</sup>*Graduate Institute of Applied Science and Technology, National Taiwan University of Science and Technology, Taipei, Taiwan*

<sup>b</sup>*Biomedical Engineering, Chang-Gung University, Taoyuan, Taiwan*

<sup>c</sup>*Department of Chemical Engineering, National Taiwan University of Science and Technology, Taipei, Taiwan*

<sup>d</sup>*National Synchrotron Radiation Research Center, Hsinchu, Taiwan*

<sup>e</sup>*Kidney Research Center, Department of Nephrology, Chang Gung Memorial Hospital, Taoyuan, Taiwan*

<sup>f</sup>*Department of Pediatrics, Division of Pediatric Nephrology, Chang Gung Children's Hospital, Chang Gung Memorial Hospital, Taoyuan, Taiwan*

<sup>g</sup>*Department of Medicine, Chang Gung University, Taoyuan, Taiwan*

<sup>h</sup>*Department of Electronic Engineering, Chang-Gung University, Taoyuan, Taiwan*

<sup>i</sup>*Biosensor Group, Biomedical Engineering Research Center, Chang Gung University, Taoyuan, Taiwan*

*[bluse.chen@gmail.com](mailto:bluse.chen@gmail.com); [cslai@mail.cgu.edu.tw](mailto:cslai@mail.cgu.edu.tw)*

Nanopatterning of AuNPs on ITO electrode is reported in this abstract. The nanospheres lithography (NSL) encompassed the deposition of monolayered Polystyrene (PS) via drop casting protocol onto the ITO substrate that further acted as the mask for the gold nanoparticles (AuNPs) assembly. Results show that AuNPs spin coating allowed AuNPs to follow the contour and stick around the PS nanospheres. The final products after etching of PS generated a highly-ordered AuNPs array on ITO substrate. This hexagonal AuNPs array on ITO electrode provided greater surface area and successfully enhanced the peak current of electrochemical measurement and was used in the detection of DNA hybridization. As compared with the non-templated AuNPs structure, the patterned AuNPs array on ITO electrode contributed an optimum sensitivity improvement in the DNA hybridization detection by 20%. The high specificity of this distinguished structure was also achieved in the hybridization measurement of multi-analyte pathogens. Findings indicate that PS nanosphere lithography with its inexpensive and simple fabrication has effectively generated uniform patterned AuNPs array on ITO which provides greater surface area to optimize electrochemical performance of the DNA biosensor.

# Simultaneous Determination of Ascorbic acid, Norepinephrine and Uric acid by Differential Pulse Voltammetry on a Disposable Pencil Graphite Electrode in the Pharmaceutical Formulations and Human Urine Samples

Abdulkadir Levent, Günay Önal

Batman University, Health Services Vocational College, 72100 Batman, Turkey

E-mail: [leventkadir@hotmail.com](mailto:leventkadir@hotmail.com)

Norepinephrine (NE) is a very important neurotransmitter in the mammalian central nervous system and mechanical pressure to excite sensory nerve endings in the skin, chemical neurotransmitters to transmit signals from one neuron to the next in the brain, and electrical current to transmit signals between successive muscle cells in the heart and intestine [1]. Ascorbic acid (AA) and Uric acid(UA) are important analytes that present in many biological fluids. A large number of papers in the literature involve the use of modified electrodes [2,3].

In this study, the electrochemical behaviors of AA, NE and UA on the pencil graphite electrode (PGE) were investigated by cyclic voltammetry (CV) and differantial pulse voltammetry (DPV) at different supporting solutions (acetate, phosphate and Britton-Robinson). By simultaneously changing the concentrations of these three molecules, their electrochemical oxidation peaks appeared at +0.16, 0.41 and 0.54 V, respectively (Figure 1). The peak currents were found to vary linearly with their concentrations in the range of 250-850 nM, 40-160 nM and 60-180 nM for AA, NE and UA, respectively. The proposed electrochemical method was successfully applied for quantification AA and NE individually in commercial pharmaceutical formulations, and AA and NE plus UA in spiked human urine samples. The prepared electrode showed several advantages, such as a modified electrode method, high sensitivity and low detection limits.

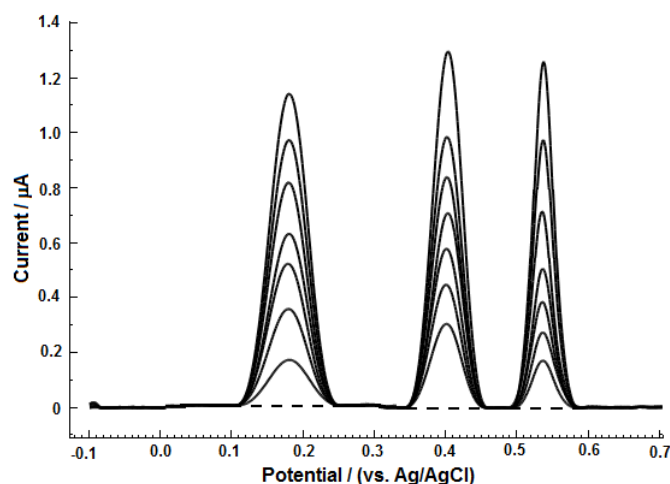


**Figure 1.** DP voltammograms of AA, NE and UA in BR buffer at pH 4.0 at PGE, DPV parameters: Step Potential, 1 mV; Modulation amplitude, 40 mV; Modulation Time, 0.03 s, Interval Time 0.4 s.

## Reference

- [1] Guyton, A. and Hall, J., Textbook of Medical Physiology, 11th edition, Philadelphia: Elsevier Inc., 2006.
- [2] Atta, N.F., El-Kady, M.F., Galal, A. Analytical Biochemistry 400 (2010) 78–88.
- [3] Ma, X., Chao, M., Chen, M. Russian Journal of Electrochemistry, 50 (2014), 154-161.



# Synthesis and Electrochemical FTIR Study of Nanoporous Palladium-Based Bimetallic Catalysts

Aicheng Chen<sup>\*</sup>, Suresh Konda, Cassandra Ostrom, Brian Adams, Robert Asmussen  
*Department of Chemistry, Lakehead University*  
955 Oliver Road, Thunder Bay, Ontario P7B 5E1, Canada  
achen@lakeheadu.ca

Palladium is well known for its high affinity to hydrogen, which enables the use of palladium nanomaterials as a primary catalyst over a wide variety of applications [1-3]. In view of the inherent limitations of current portable technology energy sources, the implementation of micro fuel cells is becoming increasingly appealing. This has generated a great interest in the development of direct formic acid micro fuel cells. In this presentation, we report on the synthesis and comparative study of nanoporous palladium-based bimetallic catalysts for formic acid oxidation.

Five Pd-based nanoporous catalysts (Pd, PdCd, PdPb, PdIr, and PdPt) with controlled compositions were synthesized and examined for their electrocatalytic activity in the oxidation of formic acid. For each of the bimetallic catalysts with 10 at.% additive metal, the hydrothermal synthesis method resulted in the formation of alloys between Pd and the additional metal, as determined by XRD. Several electrochemical techniques, including linear sweep voltammetry and chronoamperometry, were utilized to compare the activity of the catalysts toward the oxidation of formic acid. The chronoamperometric measurements showed that the current responses at 0.10 V attained the highest values within 0.8 s, which were relatively close for all five of the nanoporous Pd-M electrodes, indicating that the initial electrode performance toward formic acid oxidation was independent of the alloying materials (Cd, Ir, Pd, and Pt). In contrast, the ratio of the steady state current measured at 500 s gave rise to the following order: PdIr (1.97) < PdPt (2.44) < PdCd (3.91) < Pd (4.62) < PdPb (5.26), showing that the second incorporated metal strongly affected the stability of the Pd-based electrocatalysts. With the aid of in situ ATR-FTIR spectroscopy, the mechanisms of formic acid oxidation were investigated for the Pd-based nanoporous catalysts. Formic acid oxidation on the nanoporous Pd, PdCd, and PdPb catalysts proceeded predominantly through the direct mechanism; whereas the indirect mechanism was observed for the PdIr and PdPt catalysts. The incorporation of even small amounts of Pt and Ir was found to inhibit the oxidation of formic acid, with the generation of large volumes of CO, which caused a rapid decay in catalytic activity. In contrast, the addition of inexpensive Pb still promoted the direct mechanism, which might facilitate further increase of the activity and decrease in the cost of Pd-based catalysts.

## References:

- [1] B. Adams, A. Chen, *Mater. Today* 14 (2011) 282-289.
- [2] C. K. Ostrom, A. Chen, *J. Phys. Chem. C* 117 (2013) 20456-20464.
- [3] B. Adams, R. Asmussen, C. K. Ostrom, A. Chen, *J. Phys. Chem. C* 118 (2014) 29903-29910.

# Electrochemical Characterization and Molecular Dynamics Simulation on Corrosion Inhibition of Quinoline

Guan Xiao-rui<sup>1</sup>, Zhang Da-lei<sup>2</sup>, Jin You-hai<sup>1</sup>, Wang Jian-jun<sup>1</sup>

<sup>1</sup> College of Chemical Engineering, China University of Petroleum

<sup>2</sup> College of Mechanical and Electronic Engineering, China University of Petroleum  
Qingdao 266580, P. R. China

Phone: +86 18325429329. E-mail: cupguanxiaorui@126.com

Submit to the Symposium 18: General Session

Vapor phase inhibitor is needed to control the top of line corrosion (TLC) in wet gas pipeline. The corrosion inhibition of 2-(1-methyl-nonyl)-quinoline in CO<sub>2</sub>-saturated standard NACE solution was studied by electrochemical measurements, SEVT, molecular dynamics method and surface analysis techniques. It is found that, the adsorption of quinoline inhibitor on X80 steel surface obeys Langmuir adsorption isotherm and has a characteristic of parallel adsorption. The inhibitor film prevents the corrosion media from reacting with the steel. The inhibition efficiency increases with the temperature from 30°C to 50°C and pH from 4.15 to 5.76. The inhibition efficiency is 97.25% when the concentration of quinoline is 0.0282mol/l. The X80 steel surface was divided into two parts, in which the part from x=0 μm to 3500μm was covered with inhibitor film and the other part was without inhibitor. The SEVT results show the obvious difference of current densities in the absence and presence of quinoline. The part with quinoline was cathode region and the average current density of the other part is about 2 times than the cathode region. The SEM pictures show that X80 steel immersed with quinoline is covered with inhibitor film. The pitting corrosion exists when the X80 steel is without inhibitor.

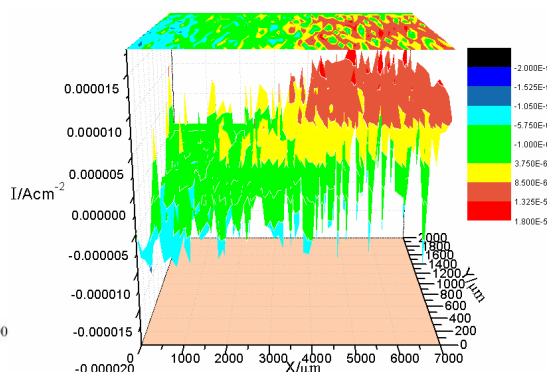
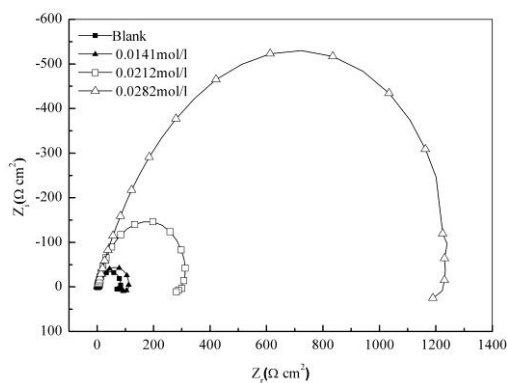


Fig.1 Nyquist diagrams with and without inhibitor at different concentrations

Fig.2 The obvious difference of current densities in the absence and presence of quinoline

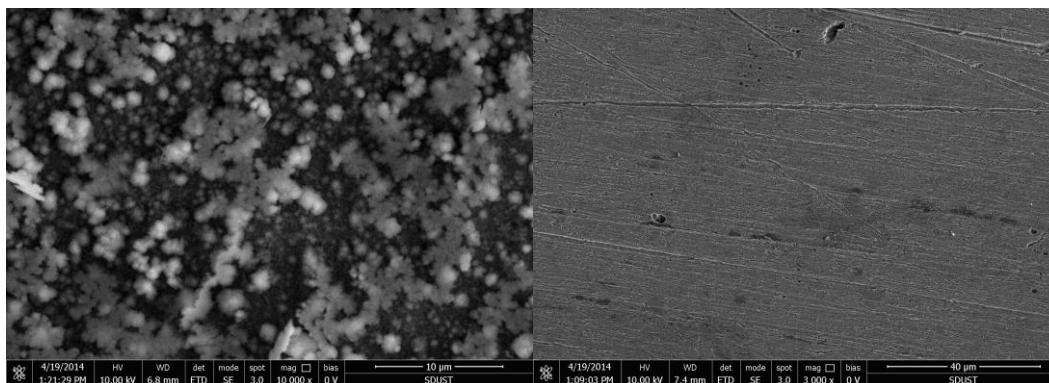


Fig.3 SEM of X80 steel after immersion in CO<sub>2</sub>-saturated standard NACE solution (a) with inhibitor; (b) without inhibitor

# Electrochemistry of Transition Metal Dichalcogenides: Dependence on Composition and Exfoliation Method

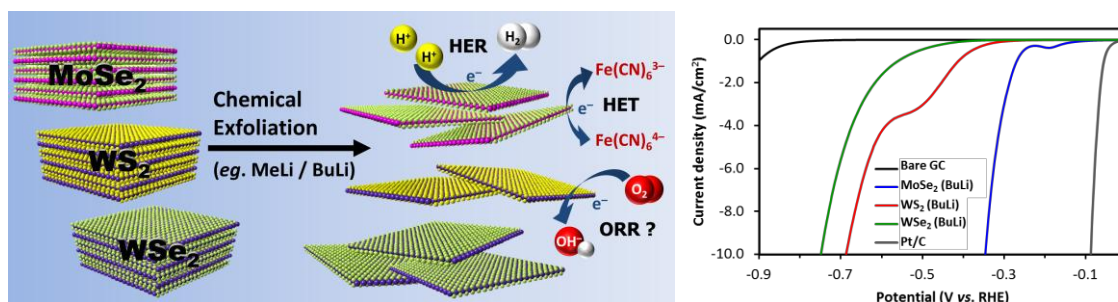
Alex Yong Sheng Eng,<sup>a</sup> Adriano Ambrosi,<sup>a</sup> Zdeněk Sofer,<sup>b</sup> Petr Šimek,<sup>b</sup> Martin Pumera<sup>\*a</sup>

<sup>a</sup> Division of Chemistry & Biological Chemistry, School of Physical and Mathematical Sciences, Nanyang Technological University, Singapore 637371.

<sup>b</sup> Institute of Chemical Technology, Department of Inorganic Chemistry, Technická 5, 166 28 Prague 6, Czech Republic.

ENGY0008@e.ntu.edu.sg

Beyond MoS<sub>2</sub> as the first transition metal dichalcogenide (TMD) to gain recognition as an efficient catalyst for the hydrogen evolution reaction (HER), interest in other TMD nanomaterials is also beginning to proliferate. Various electrochemical applications have been proposed, ranging from catalysis to supercapacitors and solar cells. Despite this rise, current understanding of their intrinsic electrochemical characteristics is especially lacking with few prior studies conducted [1,2]. We examine the inherent electroactivity of various chemically exfoliated TMDs (MoSe<sub>2</sub>, WS<sub>2</sub>, WSe<sub>2</sub>) and discuss their implications for sensing, catalysis of the hydrogen evolution, and oxygen reduction reactions (ORR) [3]. TMDs studied are found to possess distinctive inherent electroactivity. Together with their catalytic effects for the HER these strongly depend on the chemical exfoliation route and metal-to-chalcogen composition particularly in MoSe<sub>2</sub>. Inherent MoSe<sub>2</sub> electrochemistry shows the most variation depending on the exfoliation extent, but is also the most efficient HER catalyst with a low overpotential of -0.36 V vs RHE (at 10 mA cm<sup>-2</sup> current density) and reasonably low Tafel slope of ~65 mV/dec after BuLi exfoliation. It also demonstrates an improved heterogeneous electron transfer rate towards the ferro/ferricyanide redox couple, as compared to conventional glassy carbon electrodes. Knowledge of TMD electrochemistry is essential for the rational development of future applications since inherent TMD activity may potentially limit certain usages.



## References:

1. J. Bonde, P.G. Moses, T.F. Jaramillo, J.K. Nørskov, I. Chorkendorff, Faraday Discuss. 140 (2008) 219–231.
2. A. Ambrosi, Z. Sofer, M. Pumera, Small 11 (2015) 605–612.
3. A.Y.S. Eng, A. Ambrosi, Z. Sofer, P. Šimek, M. Pumera, ACS Nano 8 (2014) 12185–12198.

# A Flexible all-solid-state Electrochromic Device with Polymeric Crystal Composite Electrolyte and WO<sub>3</sub>/NiO Complementary System

Jen-Yuan Wang<sup>a,\*</sup>, Min-Chuan Wang<sup>a</sup>, Hsin-Fu Yu<sup>b</sup>, Der-Jun Jan<sup>a</sup>, Kuo-Chuan Ho<sup>b</sup>

<sup>a</sup>Physics Division, Institute of Nuclear Energy Research, Taoyuan 325, Taiwan

<sup>b</sup>Department of Chemical Engineering, National Taiwan University, Taipei 10617, Taiwan

E-mail: b90209004@ntu.edu.tw

A flexible all-solid-state electrochromic device (ECD), assembled with a polymeric crystal composite electrolyte and tungsten oxide/nickel oxide (WO<sub>3</sub>/NiO) complementary system, is demonstrated in this study. The polymeric crystal composite electrolyte, which is composed of a UV-cured ethoxylated trimethylolpropane triacrylate (ETPTA), succinonitrile (SN) and 2,2,6,6-tetramethyl-1-piperidinyloxy (TEMPO), is used as the electrochromic material and electrolyte in the flexible all-solid-state ECD. The optimal composition ration of this composite is at the weight ratio of 20/80 for ETPTA/SN with 1 M LiBF<sub>4</sub>. For the cathodic electrochromic electrode, a flexible polyethylene terephthalate (PET) is used as the substrate, and indium–tin–oxide (ITO) and WO<sub>3</sub> are deposited sequentially on the PET by sputtering. A NiO/ITO/PET electrode prepared by sputtering is used as the anodic coloring electrode. The thickness of ITO, WO<sub>3</sub> and NiO film is 110, 70 and 60 nm, respectively. This flexible all-solid-state ECD fabricated with the polymeric crystal composite electrolyte shows an optical contrast of *ca.* 33.7% at 550 nm. The optical transmittance of the ECD at 550 nm can be reversibly modulated from 59.7% (bleached) to 26.0% (darkened), by applying potentials of 1 and -2.5 V, respectively.

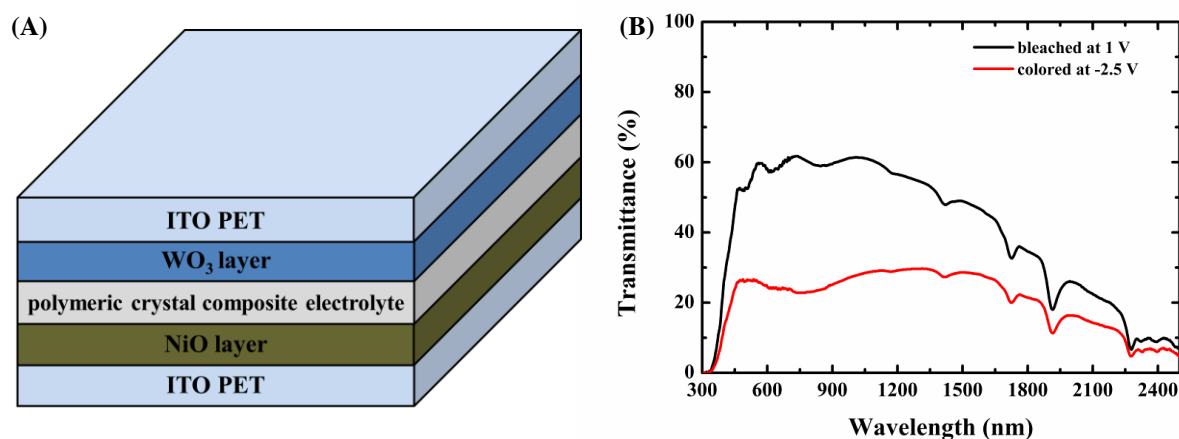


Figure 1 (A) The Schematic diagram of the flexible all-solid-state ECD. (B) The optical transmittance spectra of the ECD recorded under different applied potentials at -2.5 and 1 V.

# Simultaneous Determination of Ascorbic Acid, Epinephrine and Uric Acid by Differential Pulse Voltammetry on a Disposable Pencil Graphite Electrode

Abdulkadir Levent<sup>1</sup>, Günay Önal<sup>1</sup>, Yavuz Yardım<sup>2</sup>, Zühre Şentürk<sup>3</sup>

<sup>1</sup>Batman University, Health Services Vocational College, 72100 Batman, Turkey

<sup>2</sup>Yüzüncü Yıl University, Faculty of Pharmacy, Department of Analytical Chemistry, 65080 Van, Turkey

<sup>3</sup>Yüzüncü Yıl University, Faculty of Science, Department of Analytical Chemistry, 65080 Van, Turkey

E-mail: [leventkadir@hotmail.com](mailto:leventkadir@hotmail.com)

Ascorbic acid (AA), epinephrine (EP), and uric acid (UA) are important human body compounds that play determining role in metabolism; hence, monitoring their concentration in biologic fluids such as blood and urine may prevent and control many diseases. Since these compounds are all electroactive, it is possible to develop voltammetric analysis for their determination. However, they are oxidized at similar oxidation potentials at most solid electrodes which results in rather poor selectivity. So the ability to selectively detect AA, EP, and UA has been a matter of great interest to bioelectrochemists, electroanalytical chemists and neuroscientists. A large number of papers in the literature involve the use of modified electrodes [1-3]. The present study is intended to investigate the electrochemical behaviors of AA, EP and UA on single-use disposable pencil graphite electrode (PGE) by cyclic voltammetry (CV) and differential pulse voltammetry (DPV).

After optimization of analytical conditions employing this electrode, well-defined oxidation peaks for AA, EP, and UA were obtained at pH 4.0 in Britton-Robinson buffer solution (0.1 M) using DPV. By simultaneously changing the concentrations of these three molecules, their electrochemical oxidation peaks appeared at +0.17, 0.37 and 0.51 V, respectively (Figure 1). The peak currents were found to vary linearly with their concentrations in the range of 300-900 nM, 50-150 nM and 75-195 nM for AA, EP and UA, respectively. The proposed electrochemical method was successfully applied for quantification AA and EP individually in commercial pharmaceutical formulations, and AA and EP plus UA in spiked human urine samples.

The remarkable analytical sensitivity of the PGE, together with its simplicity and being low cost which enables its use without applying any series of chemical modification steps for electrode preparation, makes this electrode very promising for determination of AA, EP and UA in their mixture.

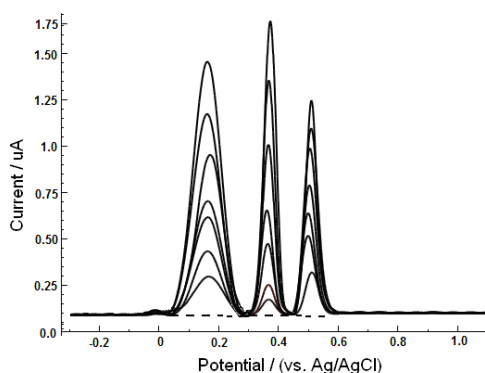


Figure 1. DP voltammograms of AA, EP and UA (from left to right) in Britton-Robinson buffer, pH 4.0 at PGE.

## References

- [1] Taei, M.; Jamshidi, M., J. Solid State Electrochem., 18, 673, 2014.
- [2] Chen, M.F.; Ma, X.Y.; Russian J. Appl. Chem., 87, 200, 2014.
- [3] Ç.C. Koçak, Dursun, Z., J. Electroanal. Chem., 694, 94, 2013.

## Acknowledgements

This research was funded by the Scientific Research Projects Presidency of Batman University (2011-FED-11).

# Development of New Electrochemical Evaluation Method for Antioxidant Capacity with Polyoxometalates as Potential Probes

Tadaharu Ueda,<sup>a</sup> Takashi Okumura,<sup>a</sup> Yukino Tanaka,<sup>a</sup> Saki Akase,<sup>a</sup> Mina Taniguchi,<sup>a</sup> Tomoko Shimamura,<sup>b</sup> Hiroyuki Ukeda<sup>b</sup>

<sup>a</sup> Department of Applied Science, Faculty of Science, Kochi University, Kochi, 780-8520, Japan

<sup>b</sup> Department of Agriculture, Faculty of Agriculture, Kochi University, Kochi, 783-8502, Japan

E-mail address: chuji@kochi-u.ac.jp

Many people live under oxidative stress, defined as the imbalance between reactive oxygen and nitrogen species and antioxidant defence. To decrease the risk of developing pathology from oxidative stress, extensive attention has been devoted to the intake of dietary antioxidants such as polyphenolic compounds, vitamins, and carotenoids from natural products. Thus, many people are interested in knowing the antioxidant capacities of foods and beverages. Many methods have been developed for evaluating the antioxidant capacity of foods and beverages; these methods are mostly based on spectrophotometric measurements such as UV-Vis spectrophotometry and fluorescence spectrophotometry. Such spectrophotometric evaluation methods of antioxidant capacity require skills to obtain correct values with high precision, and spectrophotometers are very expensive, implying that it is difficult for many people to evaluate antioxidant capacity for foods and beverages by themselves.

Polyoxometalates (POMs), which consist of molybdenum, tungsten and oxygen in the framework, and phosphorus and silicon at the center of POMs (Fig. 1), exhibit excellent electrochemical properties rather than general metal-complexes.

In this study, a new electrochemical method was developed for evaluating antioxidant capacity based on the redox properties of POMs. Antioxidant capacity was estimated from an equilibrium potential shift of POMs reduced partially by antioxidants (Fig. 2). The antioxidant capacities of gallic acid, ellagic acid, catechin, quercetin, morin, *trans*-ferulic acid, sesamol,  $\alpha$ -tocopherol,  $\delta$ -tocopherol and L-ascorbic acid, which are major antioxidants contained in foods and beverages, were potentiometrically evaluated under the optimised conditions. The observed potential shifts ( $\Delta E$ ) were compared with the spectrophotometrically evaluated antioxidant capacities. In addition, the antioxidant capacities of some types of beverages such as tea, juice and wine, were evaluated.

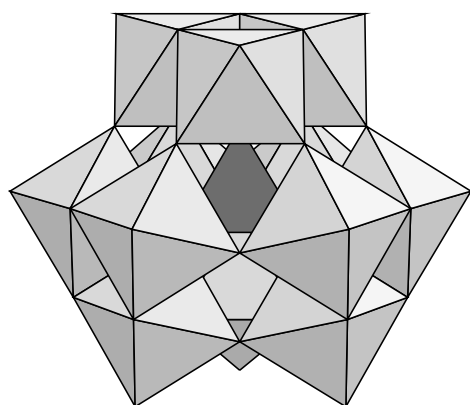


Fig. 1 Structure of Keggin-type polyoxometalates

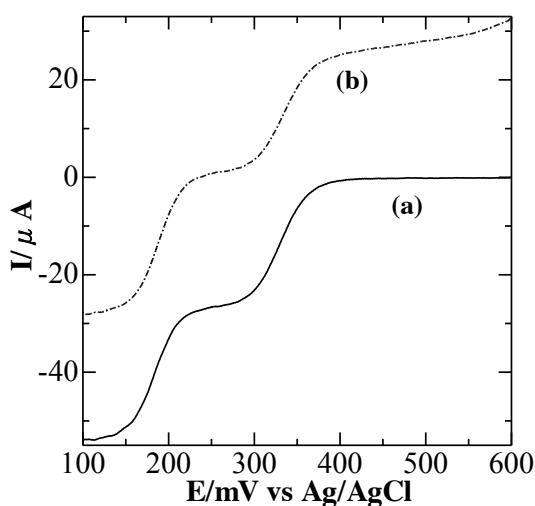


Fig. 2 Linear-sweep hydrodynamic voltammograms of  $[\text{PMo}_{12}\text{O}_{40}]^{3-}$  that form *in situ* in a Mo(VI) – P(V) – HCl – EtOH system in the absence (a) and in the presence (b) of ascorbic acid.



# Significant cation mixing in the transition-metal layer of $\text{Li}_2\text{MnO}_3$

Toshiyuki Matsunaga, Hideyuki Komatsu, Keiji Shimoda, Taketoshi Minato, Masao Yonemura, Takashi Kamiyama, Shunsuke Kobayashi, Takeharu Kato, Tsukasa Hirayama, Yuichi Ikuhara, Hajime Arai, Yoshio Ukyo, Yoshiharu Uchimoto, and Zempachi Ogumi

Office of Society-Academia Collaboration for Innovation, Kyoto University, Gokasho, Uji,  
Kyoto 611-0011, Japan

Neutron Science Laboratory, Institute of Materials Structure Science, High Energy Accelerator Research Organization, 1-1 Oho, Tsukuba, Ibaraki 305-0801, Japan

Nanostructures Research Laboratory, Japan Fine Ceramics Center, 2-4-1 Mutsuno, Atsuta,  
Nagoya 456-8587, Japan

t-matsunaga@rising.saci.kyoto-u.ac.jp

In recent years, lithium-rich  $\text{Li}_2\text{MO}_3$  compounds (M: transition metals) such as  $\text{Li}_2\text{MnO}_3$  have been extensively investigated because they or their solid solutions with  $\text{LiMO}_2$  (widely used in current as cathode materials) show higher specific capacities than the  $\text{LiMO}_2$  compounds alone. Therefore, many structural examinations of these  $\text{Li}_2\text{MO}_3$  compounds have hitherto been performed. Of these  $\text{Li}_2\text{MO}_3$  compounds, the structure of  $\text{Li}_2\text{MnO}_3$  is reported to have a monoclinic structure ( $C2/m$ ), in which Li, transition metal (TM), and O layers are ABC-stacked the same as in the  $\text{LMO}_2$  crystals (Strobel model [1]). However, the TM-layers in the former crystals are occupied also by lithium atoms ( $2b$  site) together with Mn atoms ( $4g$  site) unlike in the latter crystals [Fig. 1(a)]. It has been believed that this  $\text{Li}_2\text{MnO}_3$  structure is maintained from low temperatures just after the solid-phase reaction for its compound synthesis to high temperatures near the melting point. Our present x-ray powder diffraction analysis of  $\text{Li}_2\text{MnO}_3$  materials synthesised at various temperatures, however, revealed that the  $2b$  site is occupied mainly not by lithium atoms, but by manganese atoms, and that the  $4g$  site is occupied by approximately 50% lithium and 50% manganese atoms [see Fig. 1(b)]. This Li and Mn atomic configuration at the TM layer can be regarded as having the opposite order to that of the Stroble model. This Li/Mn arrangement found in low-temperature calcined materials, however, changed as a function of the synthesis temperature; and gradually approached that of the Strobel model as the heat treatment temperature increased. This newly found structure was also confirmed by neutron and synchrotron joint analyses; in addition, we further performed the HAADF-STEM direct observations on single crystallites in low-temperature-calcined  $\text{Li}_2\text{MnO}_3$  and ensured the presence of the new structure in them. Ionic conduction of Li atoms in solid substances is considered to be caused by their hopping from one Li atomic site to other neighboring Li sites. In the atomic configuration of the Strobel model, i.e. perfectly ordered model,  $\text{Mn}^{4+}$  ions are always located close to the hopping paths and inhibit the  $\text{Li}^+$  ion conduction without exception. However, in the newly found crystal structure of  $\text{Li}_2\text{MnO}_3$  with significant cation mixing in the TM layers, the formation of three-dimensional chains with only low Coulomb potential barriers becomes possible by random replacement of the obstacle Mn ions with the favorable Li ions, which can shape smooth lithium ion diffusion (percolation) paths in the crystal. Here, note that the Coulomb potential barrier of the favorable  $\text{Li}^+$  ion is far lower than that of the obstacle  $\text{Mn}^{4+}$  ion [2]. This work received the support of the Research and Development Innovative for Scientific Innovation of New Generation Battery (RISING) project of the New Energy and Industrial Technology Development Organization (NEDO), Japan.

- [1] Strobel, P. and Lambert-Andron, B. J.; *Solid State Chem.* **1988**, 75, 90.  
[2] Lee, J. et. al.; *Science* **2014**, 343, 519.

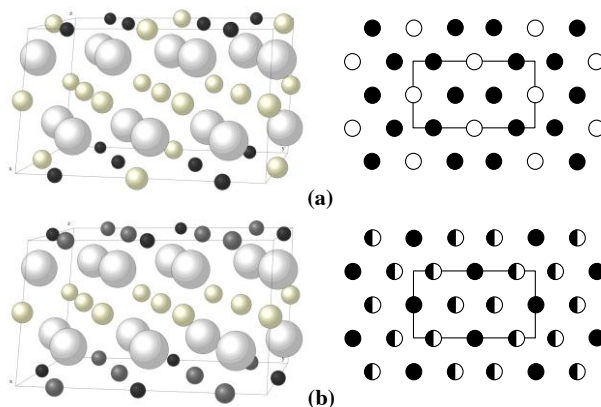


Fig. 1: Structure models for ideally ordered  $\text{Li}_2\text{MnO}_3$ . a) Currently reported structure (Li: small white, O: large white, Mn: small black) and b) new structure proposed for specimens synthesised at low temperatures (Li/Mn: dark grey). The unit cells of these crystals consist of cubic-stacked, TM, oxygen, lithium, and oxygen layers. To the right of the models, the atomic configurations of both TM layers are illustrated (open circles: Li, filled circles: Mn, and half-filled circles: Mn/Li). Rectangles represent the  $a$ - $b$  unit cells.

# Quinone Based Polypyrroles for Energy Storage Materials

Hao Huang<sup>a</sup>, Christoffer Karlsson<sup>a</sup>, Rikard Emanuelsson<sup>a</sup>, Maria Strømme<sup>a</sup>,  
Adolf Gogoll<sup>b</sup>, Martin Sjödin<sup>a</sup>

<sup>a</sup> Nanotechnology and Functional Materials, Department of Engineering Sciences, The Ångström  
Laboratory, Uppsala University

<sup>b</sup> Department of Chemistry - BMC, Biomedical Centre, Uppsala University  
Box 534, SE-751 21 Uppsala, Sweden  
Hao.Huang@angstrom.uu.se

Quinones, which are naturally occurring redox active organic compounds, have been proposed as cathode materials in lithium ion batteries for their high theoretical specific capacities and more environmentally friendly manufacturing compared to conventional inorganic cathode materials. However, many of them suffer from poor kinetics as well as capacity loss due to dissolution.<sup>1</sup> In our work, by attaching quinones as pendant moieties onto conducting polymers, e.g. polypyrroles, we have composed conducting redox polymers, which are expected to decrease problems with resistance and dissolution while retaining capacity and cyclability.<sup>2</sup> A series of monomeric compounds incorporating pyrrole and quinone units were synthesized and polymerized electrochemically. The resulting polymers were studied by in-situ spectro-electrochemical techniques as well as by EQCM to elucidate the redox chemistry of the quinone units as well as the kinetics of polymer redox performance.

## Reference

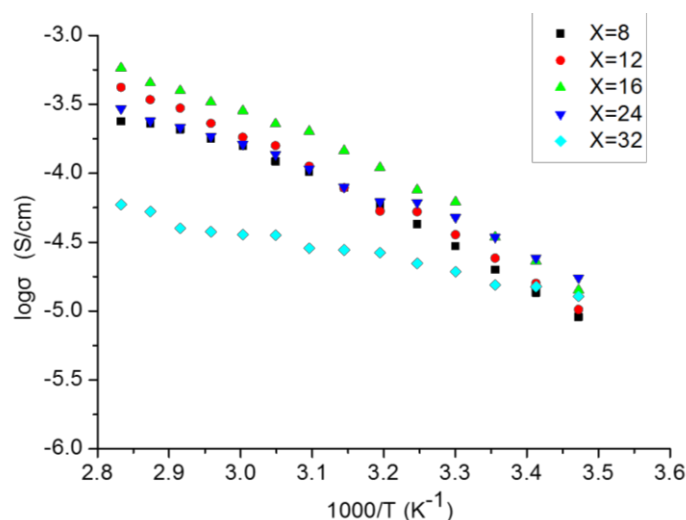
- [1] a) M. Yao, S.-i. Yamazaki, H. Senoh, T. Sakai, T. Kiyobayashi, *Mater. Sci. Eng., B* **2012**, 177, 483-487.  
b) Y. Liang, P. Zhang, J. Chen, *Chem. Sci.* **2013**, 4, 1330-1337.
- [2] a) C. Karlsson, H. Huang, M. Strømme, A. Gogoll, M. Sjödin, *J. Phys. Chem. C* **2013**, 117, 23558-23567. b) C. Karlsson, H. Huang, M. Strømme, A. Gogoll, M. Sjödin, *J. Phys. Chem. C* **2014**. c) C. Karlsson, H. Huang, M. Strømme, A. Gogoll, M. Sjödin, *J. Electroanal. Chem.* **2014**, 735, 95-98.



# Synthesis, Structure Characterization, Electrical and Thermodynamic Properties of Comb Structured Organic-Inorganic Hybrid Solid Polymer Electrolytes

Kwo-Wei Lou, Hsueh-Ming Liu, Diganta Saikia, Hsien-Ming Kao\*  
*Department of Chemistry*  
*National Central University, Chung-Li, 32054, Taiwan, R.O.C.*  
*E-mail: achem\_liu@hotmail.com; hmkao@cc.ncu.edu.tw*

Solid polymer electrolytes (SPEs) have long been the subject of intense research because of their potential electrochemical applications in solid-state rechargeable lithium batteries, dye-sensitized solar cells, chemical sensors, data storage and electrochromic devices [1-3]. In the present study, a new type of comb-branched organic-inorganic hybrid electrolyte based on the reaction of polymethylhydrosiloxane, allytriethoxysilane, poly(propylene glycol)-*block*-poly(ethylene glycol)-*block*-poly(propylene glycol) bis(2-aminopropyl ether), and 3-(glycidyloxypropyl)trimethoxysilane has been prepared by varying the LiClO<sub>4</sub> concentration. <sup>13</sup>C CPMAS NMR and Fourier transform infrared spectroscopy (FTIR) results provide the information about the successful synthesis of the hybrid membrane. The hybrid electrolyte exhibits semi-crystalline to amorphous structure with the increase in salt concentration. A maximum ionic conductivity of  $6.2 \times 10^{-5} \text{ S cm}^{-1}$  is obtained at 30 °C for the solid hybrid electrolyte with a [O]/[Li] ratio of 16. The good value of electrochemical stability window (~ 4V) makes the hybrid electrolyte promising for electrochromic devices and sensors applications.



Temperature dependence ionic conductivity of organic-inorganic hybrid electrolyte with different [O]/[Li] ratios, X.

## References:

1. Y. Xing, Y. Wu, H. Wang, G. Yang, W. Li, L. Xu, X. Jiang, *Electrochim. Acta* 136 (2014) 513–520.
2. J.R. MacCallum and C.A. Vincent, in: *Polymer Electrolyte Reviews 1 and 2*, Elsevier, London, 1987 and 1989.
3. F.M. Gray, *Solid Polymer Electrolytes: Fundamentals and Technological Applications*, VCH Publishers, New York, 1991.

# Synthesis and Characterization of Polyether Diamine based Organic-Inorganic Hybrid Solid Electrolyte for Electrochromic Devices

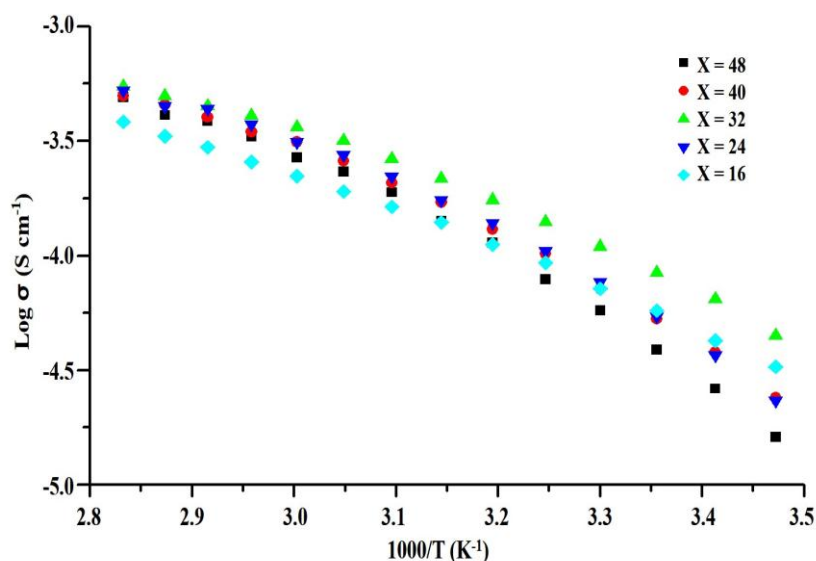
Hsueh-Ming Liu, Cheng-Gang Wu, Diganta Saikia, Hsien-Ming Kao\*

Department of Chemistry

National Central University, Chung-Li, 32054, Taiwan, R.O.C.

E-mail: achem\_liu@hotmail.com; hmkao@cc.ncu.edu.tw

Polymer electrolyte is one of the promising research areas that attracted ever-increasing interests due to its potential applications in electrochemical devices, such as rechargeable lithium-ion batteries, dye-sensitized solar cells, electrochromic devices, etc. [1–3]. In this study, a new type of highly conductive organic–inorganic hybrid polymer electrolytes has been synthesized based on polymerization of poly(propylene glycol)-block-poly(ethylene glycol)-block-poly(propylene glycol) bis(2-aminopropyl ether) (ED2003), 2,4,6-trichloro-1,3,5-triazine (cyanuric chloride, CC) and alkoxysilane precursor (3-isocyanatopropyl)triethoxysilane (ICPTES), followed by doping various amounts of  $\text{LiClO}_4$  salt. The  $^{13}\text{C}$  and  $^{29}\text{Si}$  solid-state NMR and Fourier transform infrared spectroscopy results reveal the successful synthesis of the organic–inorganic hybrid structure. The solid hybrid electrolyte exhibits a maximum ionic conductivity of  $1.1 \times 10^{-4} \text{ S cm}^{-1}$  at  $30^\circ\text{C}$  for the  $[\text{O}]/[\text{Li}]$  ratio of 32. The hybrid electrolyte possesses a good electrochemical stability window of 4.0 V. The prototype electrochromic device with such a solid hybrid electrolyte demonstrates exceptionally high coloration efficiency value of  $732 \text{ cm}^2 \text{ C}^{-1}$ . The present organic–inorganic hybrid electrolytes hold promise for applications in electrochromic devices and lithium ion batteries.



Temperature dependence ionic conductivity of organic-inorganic hybrid electrolyte with different  $[\text{O}]/[\text{Li}]$  ratios, X.

## References:

1. Q. Lu, J. Yang, W. Lu, J. Wang, Y. Nuli, *Electrochim. Acta* 152 (2015) 489–495.
2. W. Kwon, Y.J. Chang, Y.C. Park, H.M. Jang, S.W. Rhee, *J. Mater. Chem.* 22 (2012) 6027–6031.
3. C.A. Nguyen, S. Xiong, J. Ma, X. Lu, P.S. Lee, *Phys. Chem. Chem. Phys.* 13 (2011) 13319–13326.

# Inadvertent contamination of graphene materials: Synthetic routes introduce a whole spectrum of unanticipated metallic elements

Colin Hong An Wong<sup>a</sup>, Zdeněk Sofer<sup>b</sup>, Marie Kubešová<sup>c</sup>, Jan Kučera<sup>c</sup>, Stanislava Matějková<sup>d</sup>, Martin Pumera<sup>a</sup>

<sup>a</sup>*Division of Chemistry & Biological Chemistry, School of Physical and Mathematical Sciences, Nanyang Technological University, Singapore 637371, Singapore*

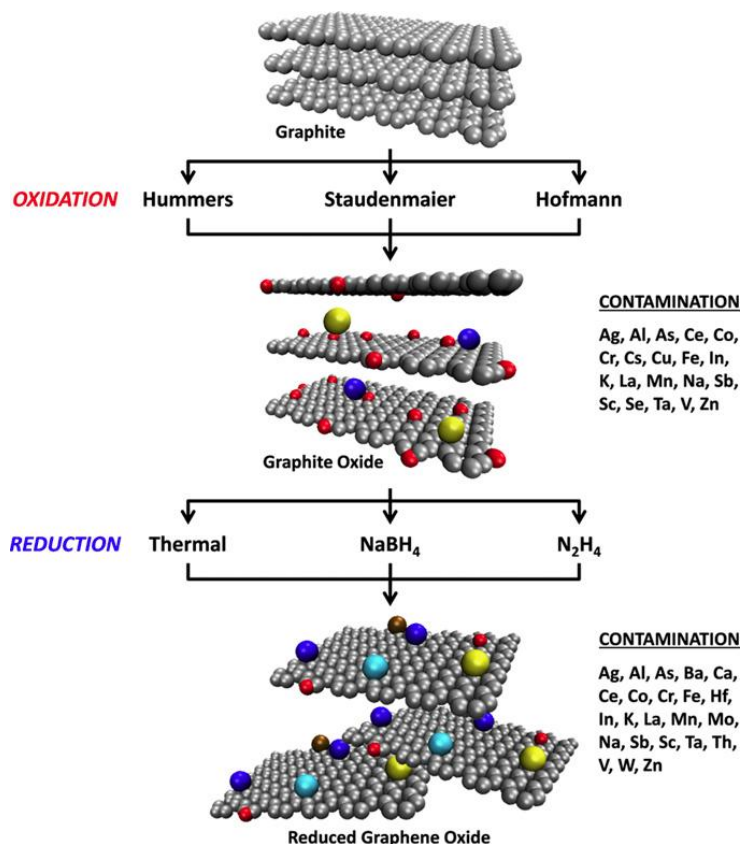
<sup>b</sup>*Department of Inorganic Chemistry, Institute of Chemical Technology, Technická 5, 166 28 Prague 6, Czech Republic*

<sup>c</sup>*Nuclear Physics Institute of the ASCR, v.v.i., Husinec-Řež 130, 250 68 Řež, Czech Republic*

<sup>d</sup>*Institute of Organic Chemistry and Biochemistry ASCR, v.v.i., Flemingovo náměstí 2, 166 10 Prague 6, Czech Republic*

WONG0804@e.ntu.edu.sg

The synthesis of graphene materials is typically carried out by oxidizing graphite to graphite oxide, followed by a reduction process. Numerous methods exist for both the oxidation and reduction steps, which causes unpredictable contamination from metallic impurities into the final material. These impurities are known to have considerable impact on the properties of graphene materials. We synthesized several reduced graphene oxides from extremely pure nuclear graphite using several popular oxidation and reduction methods, and tracked the concentrations of metallic impurities at each stage of synthesis. We demonstrate that different combinations of oxidation and reduction introduce varying types as well as amounts of metallic elements into the graphene materials, and their origin can be traced to impurities within the chemical reagents used during synthesis. These metallic impurities are able to alter the graphene materials' electrochemical properties significantly, and have wide-reaching implications on the potential applications of graphene materials.



## References

[1] C. H. A. Wong, Z. Sofer, M. Kubešová, J. Kučera, S. Matějková and M. Pumera, *Proc. Natl. Acad. Sci. USA*, 2014, **111**, 13774–13779.

# Molybdenum Disulfide (MoS<sub>2</sub>) Nanoflakes as Inherently Electroactive Labels for DNA Hybridization Detection

Adeline Huiling Loo, Alessandra Bonanni, Adriano Ambrosi and Martin Pumera

*Division of Chemistry & Biological Chemistry, School of Physical and Mathematical Sciences, Nanyang Technological University  
21 Nanyang Link, Singapore 637371, Singapore  
S120022@e.ntu.edu.sg*

The detection of specific DNA sequences plays a critical role in the areas of medical diagnostics, environmental monitoring, drug discovery and food safety. This has therefore become a strong driving force behind the ever-increasing demand for simple, cost-effective, highly sensitive and selective DNA biosensors. In this study, we report for the first time, a novel approach for the utilization of molybdenum disulfide nanoflakes, a member of the transition metal dichalcogenides family, in the detection of DNA hybridization. Herein, molybdenum disulfide nanoflakes serve as inherently electroactive labels, with the inherent oxidation peak exploited as the analytical signal. The principle of detection is based on the differential affinity of molybdenum disulfide nanoflakes towards single-stranded DNA and double-stranded DNA. The employment of transition metal dichalcogenides nanomaterials for sensing and biosensing purposes represents an upcoming research area which holds great promise. Hence, our findings are anticipated to have significant contributions towards the fabrication of future DNA biosensors.

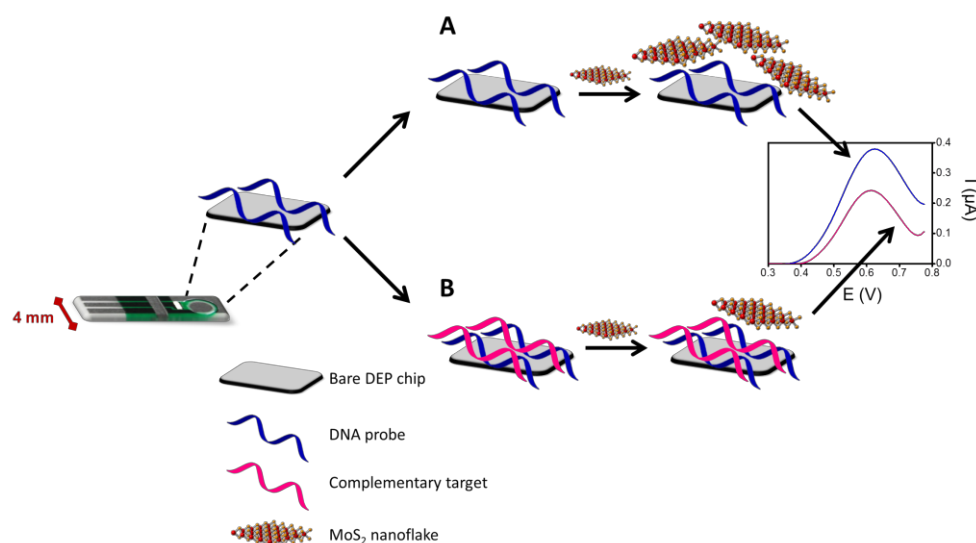


**Figure 1. Schematic illustration of the experimental approach.**

## Reference

[1] A.H. Loo, A. Bonanni, A. Ambrosi, M. Pumera, *Nanoscale*, (2014).

# **Fate of silver nanoparticles in natural waters; integrative use of conventional and electrochemical analytical techniques**

Wei Zhe Teo, Martin Pumera

*Division of Chemistry & Biological Chemistry, School of Physical and Mathematical Sciences,  
Nanyang Technological University  
21 Nanyang Link, Singapore 637371  
TEOW0051@e.ntu.edu.sg*

The rapid emergence of commercially available products containing silver nanoparticles (AgNPs) in recent years is worrying, as the widespread use of these items could lead to hazardous silver pollution to our environment waters. When released into the environment, AgNPs' toxicity and transport in water is ultimately dependent on its transformation. Therefore, the study on AgNPs' transformation in different aqueous environments is important in predicting the damage that will be incurred by the accumulation of AgNPs in natural waters. In this paper, we investigated the AgNPs speciation in three types of aqueous media (ultrapure water, lake water and seawater) after one week of dispersion using analytical techniques such as inductively coupled plasma mass spectrometry (ICP-MS), and X-ray photoelectron spectroscopy (XPS). The amount of Ag ions measured in the AgNPs–seawater suspension was found to be one order of magnitude higher than the amount measured in the AgNPs–ultrapure water suspension, hence indicating that the extent of transformation of Ag<sup>0</sup> to ionic Ag in AgNPs is very different. Furthermore, the data acquired from XPS analysis showed that the metallic state of silver prevailed after dispersion in all three types of water, suggesting that the AgNPs did not undergo any reactions that resulted in the formation of silver containing compounds. Cyclic voltammetry (CV) was also performed for the study of the transformation of AgNPs. The trend gathered from the magnitudes of the AgNPs oxidation peak (0.52  $\mu$ A, 12.2  $\mu$ A and 49.2  $\mu$ A for AgNPs–seawater, AgNPs–lake water and AgNPs–ultrapure water suspensions respectively) exhibited a positive relationship with that attained from the ICP-MS and XPS results, demonstrating the likelihood of employing this technique as a simple and rapid alternative in future work in this field.

# A study on Supercritical Electrolytic Polishing Process for Stainless steel substrates

Jau-Kai Wang, Yan-Ru Wang, Ying-Ting Wang  
School of Environmental & Life Science, Fooyin University,  
151 Chin-Hsueh Rd, Ta-Liao Hsiang, Kaohsiung City, 831 Taiwan, R.O.C.  
sc104@fy.edu.tw

## Abstract

The polishing technique is an important surface treatment method used in both conventional and electronic industry. Traditionally, there are three main skills included (1) mechanic polishing (2) electrolytic polishing (3) chemical polishing. However, all of them could not deal with complex parts with higher aspect ratio and serious environmental problem with labor cost. In this work, we have explored a new polishing method which applies principles of electro-chemistry and electro-physics to treat the surface of stainless substrate under the supercritical carbon dioxide fluid. It used to get rid of oxides on it and to increase its smoothness as well as brightness. The various kinds of golf head were selected as the investigated system. The roughness of sample can be upgraded to nano-metered size ( $\sim 200\text{nm}$ ) and the it's brightness of mirror also be obtained (reflectivity  $> 95\%$ ). It is highlighted that the new supercritical polishing method is a green process without polluting environments and it is suitable to complex work pieces and simple operation with high efficiency.

**Keywords :** polishing, gold head, brightness, roughness

The Austenite type of stainless were the investigated samples included SUS 303, 304 and 316. The applied electrical field was controlled at 280 volts and operating temperature setted at  $75^\circ\text{C}$ . The dependence of process time on roughness and brightness of substrates were shown in Figure 1 and Figure 2, respectively. The results indicate that the optimal roughness and brightness were achieved after 10 minutes. Smooth finish of substrates can be increased 2-3 grades after polishing and the roughness,  $R_a$ , less than  $0.1\mu\text{m}$  as well as brightness,  $r$ , larger than 95%. The data also show that the polishing effect have the following order: SUS 316 > SUS 304 > SUS 303.

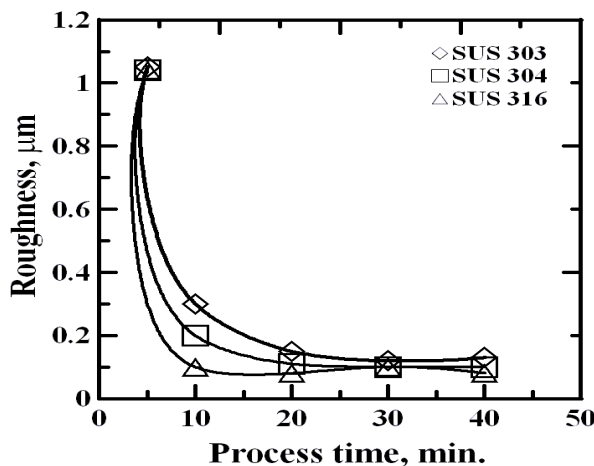


Figure 1 Polishing effect on roughness .

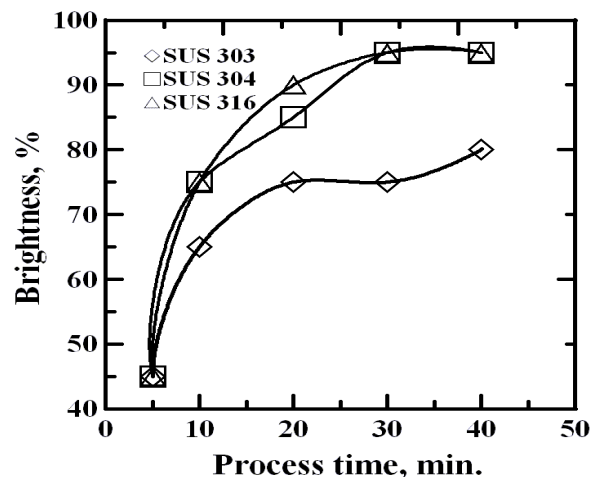


Figure 2 Polishing effect on brightness.

## References :

1. J-K Wang, ROC Patent 538146 (2005).
2. J-K Wang, ROC Patent I404826 (2013).
3. T. Fritz, et. al., Electrochim. Acta, 47, 55(2001).
4. G. Nelissen, et. al., Galvanotechnik, 4, 970(2000).
5. D. de Kubber, et. al., Electrochim Acta, 47, 91(2001).
6. S. C. Hung, et. al., Microelectro. Rel., 41, 677(2001).

# Quantifying Surface Diffusion by Nanoelectrode

Wei Wang, Fang-Fang Wang, Jie Zhang, Bao-Fa Su, Dong-Ping Zhan\*, Zhong-Qun Tian  
*Department of Chemistry, College of Chemistry and Chemical Engineering, and State Key Laboratory of  
Physical Chemistry of Solid Surfaces, Xiamen University, Xiamen 361005, China.*  
*E-mail: dpzhan@xmu.edu.cn*

The mobility of adsorptive atoms and molecules on catalyst surface is one of the most fundamental issues in solid surface science. It plays a pivotal role in myriad physiochemical processes, especially in thin-film deposition and heterogeneous catalysis. To quantify the surface mobility will aid in deeply understanding the mechanism of these processes. Therefore, numerous methods have been developed for measuring surface diffusion coefficient, and many systematic investigations have been performed on solid surfaces in vacuum or atmospheric environment.

However, studying surface mobility on solid surface in liquid environment, especially in electrochemical system, still faces challenges both in experiment and theory. The reason mainly lies in that most of the techniques adopted for surface diffusion traditionally don't work at the solid/liquid interfaces. Moreover, the coadsorption of the water molecules or electrolyte ions and the presence of strong electric fields make it extremely complicated at the electrochemical interface. Nevertheless, information on the transport and interaction of atoms or molecules on electrode surfaces is badly needed for gaining insights into many electrochemical interface processes, such as electrodeposition and electrocatalysis. These processes are directly related to electrochemical energy conversion, metal electrode processes as well as other electrocatalytic domains.

The surface diffusion of hydrogen adatoms on Pt nanoelectrodes along Pt/SiO<sub>2</sub> boundary in acidic solution has been observed directly in our previous work.<sup>1</sup> Here, we present a method based on Fick's second law to further prove the existence of surface diffusion of adsorbates and quantitatively separate the Faraday adsorption area and surface diffusion area on Au or Pt nanoelectrodes. The surface diffusion coefficients of the oxygen-containing adsorbates on Au or Pt surface were obtained.

## References

1. Zhan, D.; Velmurugan, J.; Mirkin, M. V., Adsorption/Desorption of Hydrogen on Pt Nanoelectrodes: Evidence of Surface Diffusion and Spillover. *J Am Chem Soc* 2009, 131 (41), 14756-14760.

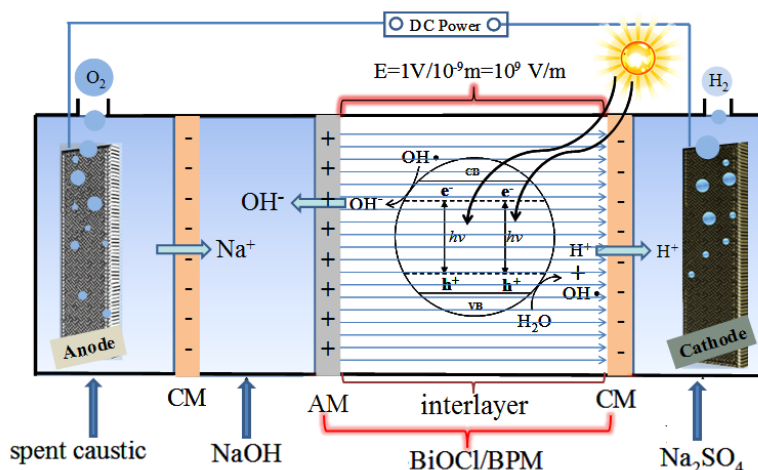
# A Novel Photoelectrocatalytic Approach for Regenerating NaOH by a BiOCl/bipolar Membrane Sandwich Structure

Zhenhai Liang\*, Xian Liu, Xuan Jian, Yang huimin  
*College of Chemistry and Chemical Engineering, Taiyuan University of Technology*  
*No.79 west Yingze street, Taiyuan, Shanxi, China, 030024*  
*e-mail: liangzhenh@sina.com; liangzhenhai@tyut.edu.cn*

A novel photoelectrocatalytic approach for regenerating NaOH through a BiOCl/bipolar membrane (BiOCl/BPM) sandwich structure with photoelectro-synergistic catalysis is proposed in this study. This distinctive BiOCl/BPM sandwich structure presents four advantages. (1)The high-electric field at the interlayer contributes in separating photo-induced electron-hole pairs, thereby improving water splitting into protons and hydroxide ions. (2) In a high-electric field,  $H^+$  and  $OH^-$  are generated at the interlayer of the BiOCl/BPM, and migrate into the cathode and the central chambers, respectively, thereby decreasing the reverse reaction of the as-formed  $H^+$  and  $OH^-$  to form  $H_2O$  again. (3)The membrane impedance of the BiOCl/BPM decreased under the sunlight irradiation, which reduced energy consumption. (4) This technique not only makes full use of the recyclable bases, but also limits the usage of acids.

The BiOCl/BPM was prepared using a paste method. The anode chamber was fed with the spent caustic (200 mL), the cathode chamber was fed with 0.3mol/L  $Na_2SO_4$  (200 mL) as the supporting electrolyte solution, and the central chamber was fed with 0.1mol/L NaOH solution (200 mL). The anode was a Pt electrode, and the cathode was a Pd electrode. A 350W xenon lamp with 350–760 nm filters as simulative sunshine.

The principle is shown in Scheme 1. The BiOCl/BPM sandwich structure with consists of an anion-exchange membrane layer (AM), a cation-exchange membrane layer (CM) and a BiOCl catalyst layer (i.e. interlayer). The interlayer has a nano-size thickness ( $10^{-7}$  m to  $10^{-9}$  m); thus, the electric field intensity at the interlayer reaches from  $10^7$  V  $m^{-1}$  to  $10^9$  V  $m^{-1}$  when 1 V is applied.  $H^+$  and  $OH^-$  are generated at the interlayer of the BPM using a high-electrical field and solar irradiation. Sodium ion ( $Na^+$ ) in the spent caustic migrates through the CM to the base compartment, where it combines with  $OH^-$  produced by the BiOCl/BPM to generate sodium hydroxide (NaOH).



**Scheme 1** Schematic diagram of operating principle for NaOH recovering from spent caustic liquor

- [1] R.Y. Chen, Z. Chen, X. Zheng, X. Chen, S.Y. Wu, Preparation and characterization of mSA/mCS bipolar membranes modified by CuTsPc and CuTAPc, *J. Membr. Sci* 355 (2010) 1-6.
- [2] N.M.V. Barbosa, G.M. Geise, M.A. Hickner, T.E. Mallouk, Assessing the utility of bipolar membranes for use in photoelectrochemical water-splitting cells, *ChemSusChem* 7(2014) 3017-3020.
- [3] X. Liu, H. Yang, H. Dai, X. Mao, Z. Liang, A novel photoelectrocatalytic approach for water splitting by an I-BiOCl/bipolar membrane sandwich structure, *Green Chem.* 17(2015) 199-203.



# Synthesis and Electrochemical Performances of Hollow Spherical $\text{Li}_4\text{Ti}_5\text{O}_{12}$ for Lithium Ion Batteries

Yingbin Lin, Zhigao Huang

Fujian Provincial Key Laboratory of Quantum Manipulation and New Energy Materials  
Fujian Normal University (Qishan Campus), Minhou District, Fuzhou, Fujian, 350117 China.  
yblin@fjnu.edu.cn

Hollow spherical  $\text{Li}_4\text{Ti}_5\text{O}_{12}$  anode powders were synthesized by spray drying under low vacuum level, followed by the calcination at  $800^\circ\text{C}$  for 12, 16 and 20 h respectively. The structure, morphology, and texture of the as-prepared composites were characterized with XRD, Raman, TG-DTA and SEM techniques. The electrochemical properties of the as-prepared composites were investigated systematically by charge/discharge testing, cyclic voltammograms and AC impedance spectroscopy, respectively. It is found that all as-prepared powders show hollow spherical structure. In comparison, the sample calcined for 16 h exhibited best electrochemical performances. Analysis from the electrochemical measurements revealed that the sample calcined for 16 h had the lowest charge-transfer resistances and highest lithium diffusion rate.

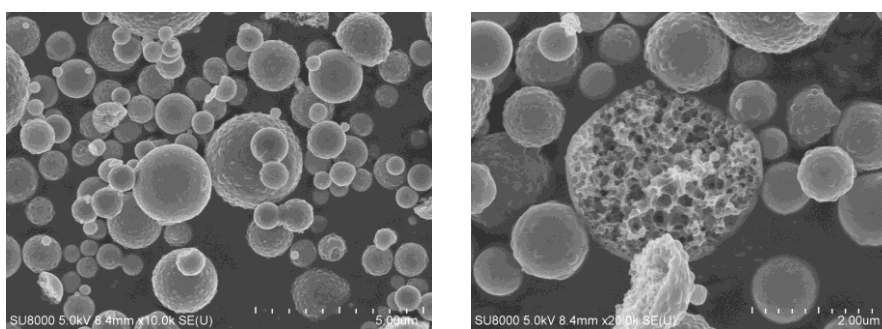


Figure 1 SEM images of the precursor

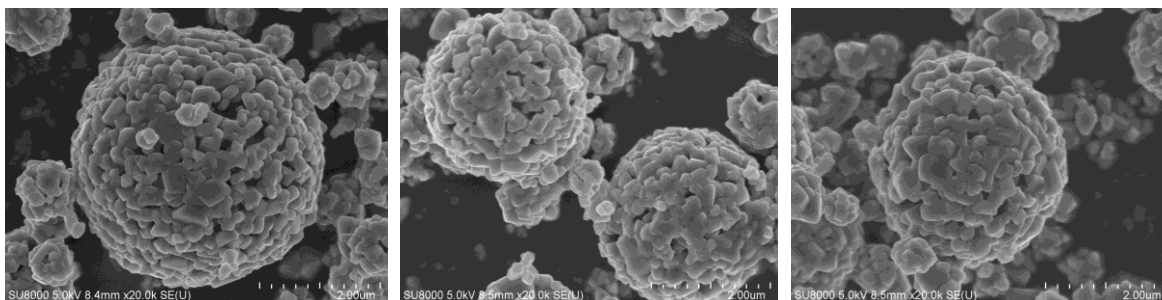


Figure 2 SEM images of the as-prepared  $\text{Li}_4\text{Ti}_5\text{O}_{12}$  calcined at  $800^\circ\text{C}$  for (a) 12 h, (b) 16 h and (c) 20 h

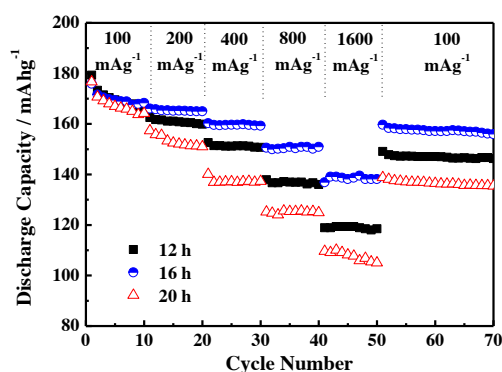


Figure 3 Rate performances of  $\text{Li}_4\text{Ti}_5\text{O}_{12}$

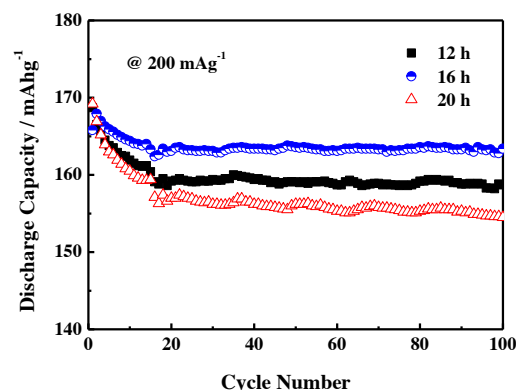


Figure 4 Cycle stability of  $\text{Li}_4\text{Ti}_5\text{O}_{12}$  at  $200\text{mA g}^{-1}$

# Actinide Recovery using Anode-Liquid Cathode Module for Pyroprocessing

Gha-Young Kim, Jisun Shin, Si-Hyung Kim, Do-Hee Ahn, Seungwoo Paek  
*Korea Atomic Energy Research Institute (KAERI)*  
*Daedeok-daero 989-111, Yuseong-gu, Daejeon 305-353, Republic of Korea*  
*gkim@kaeri.re.kr*

The accumulated spent nuclear fuel (SNF) from current nuclear power plants remains a formidable challenge despite the wide use of nuclear energy. One of the promising solutions is to reduce the spent oxide fuel and recycle it as metal fuel for fast neutron reactors through pyroprocessing. This enables increasing the uranium (U) usage efficiency and decreasing both the radiotoxicity and the amount of radioactive waste generated, thereby increasing the safety and economic efficiency. Pyroprocessing based on molten salt involves the reduction of spent oxide fuel into a metal through an electrolytic reduction process and the recovery of the fuel components by means of an electrorefining process. The actinide metal oxide is reduced to metal in the electrolytic reduction process operated in a  $\text{Li}_2\text{O}$ - $\text{LiCl}$  molten salt medium at 650 °C. Then, the metallic product is used as an anode for the electrorefining process. In the electrorefining process, the actinide metals are electrochemically dissolved and transported to the bulk  $\text{LiCl}$ - $\text{KCl}$ - $\text{UCl}_3$  molten salt at 500 °C, whereas high purity U metal is deposited on a solid cathode. Subsequently, the cathode is changed with a liquid cadmium and the transuranic elements (TRUs) as well as U remaining in the salt are simultaneously deposited onto a liquid cadmium cathode (LCC). In a flow diagram of pyroprocessing in KAERI, an inert anode (graphite) is used instead of actinide metal in LCC electrorefining to increase the recovery of TRUs. To increase the metal recovery of the electrorefining process, multiple electrode pairs have been employed in the electrorefiner [1, 2]. Previously, we reported an anode-liquid cathode module (ALCM) having a compact structure to increase the efficiency of group actinide recovery by adopting multiple modules in an electrolyte bath [3]. The present work aims at investigating the performance of ALCM in molten  $\text{LiCl}$ - $\text{KCl}$ - $\text{UCl}_3$  (3.1 wt.%) -  $\text{NdCl}_3$  (2.6 wt.%) salt and identifying the ratio of U : Nd in the recovered metal product. When current-controlled electrolysis (50  $\text{mA}/\text{cm}^2$ ) was conducted, the passed charge was 0.51 A·hr, which is consistent with 1.4 wt% U/Cd. The cathode potential was maintained as -1.5 to -1.55 V, while the anode potential was 1.8 to 1.9 V, indicating a chlorine gas evolution. After the termination of the electrolysis, the metal deposits (U and Nd) were separated in a Cd distiller and then dissolved in nitric acid for an elemental analysis. The metal recovery efficiency was over 82 % and the U:Nd ratio in the product was determined to be 95:5. This work was supported by a grant from the Nuclear Research & Development Program of NRF funded by the MSIP, Republic of Korea.

## References

1. Westphal BR, Mariani RD, Vaden D, Sherman SR, Li SX, Keiser DD, Recent advances during the treatment of spent EBR-II fuel. Proc. ANS 4<sup>th</sup> Topical Meeting on DOE Spent Nuclear Fuel and Fissile Material Management, San Diego, CA, Jun. 4-8, 2000
2. Iizuka M, Uozumi K, Ogata T, Omori T, Tsukada T, Nucl Sci Tech 46 (2009) 699.
3. Kim GY, Kim TJ, Kim SH, Paek S, Radioanal Nucl Chem 300 (2014) 1261.